

# TMS2010

139th Annual Meeting & Exhibition

February 14-18, 2010 • Washington State Convention & Trade Center • Seattle, Washington USA



***“Going for the Gold in  
Materials Technology”***

Includes:  
Meeting Information  
Floor Plans  
Exhibition Directory  
Technical Program

**FINAL PROGRAM**

LEARN • NETWORK • ADVANCE

When it comes to professional development and networking, there is nothing like a face-to-face connection with colleagues. TMS provides members with numerous opportunities for advancing research and collaborating on the latest technology through a series of diverse conferences. Take advantage of these engaging events for the materials science and technology community.

### **ICMOVPE 2010**

Incline Village, NV..... May 23-28..... Hyatt Regency Lake Tahoe

### **2010 Electronic Materials Conference (EMC10)**

Notre Dame, IN..... June 23-25..... University of Notre Dame

### **Lead-Zinc 2010** (in conjunction with Conference of Metallurgists (COM 2010))

Vancouver, BC, Canada..... October 3-6..... Hyatt Regency Vancouver

### **7th International Symposium on Superalloys 718 & Derivatives 2010**

Pittsburgh, PA ..... October 10-13..... Marriott Pittsburgh City Center

### **Materials Science & Technology 2010 (MS&T)**

Houston, TX..... October 17-21..... George R. Brown Convention Center

### **2011 TMS Annual Meeting & Exhibition**

San Diego, CA..... February 27-March 3..... San Diego Convention Center

### **Co-sponsored Meetings**

#### **Copper 2010**

Hamburg, Germany ..... June 6-10..... Congress Center Hamburg

#### **1st TMS-ABM International Materials Congress 2010** (To be held in conjunction with the 65th Annual Congress of ABM and the 18th IFHTSE Congress)

Rio de Janeiro, Brazil..... July 26-30 ..... International Rio Hotel

#### **7th Pacific Rim International Conference on Advanced Materials and Processing 2010 (PRICM-7)**

Cairns, Australia ..... August 1-5 ..... Cairns Convention Centre

#### **Uranium 2010 Conference**

Saskatoon, SK, Canada ..... August 15-18 ..... Delta Bessborough & Sheraton Cavalier





# TMS 2010

139th Annual Meeting & Exhibition

February 14-18, 2010

Washington State Convention & Trade Center

Seattle, Washington USA

## Welcome to the TMS 2010 Annual Meeting & Exhibition!



Dear Colleagues and Friends:

It is wonderful to have all of our esteemed members, exhibitors and guests assembled here in Seattle for the 139th annual meeting of The Minerals, Metals & Materials Society. Your attendance at this annual forum is a testament to the dedication of our members and the steadfast support of industry experts from the materials field. This network of professional exchange will keep the society a global thought leader and move materials science forward.

Please take advantage of these invaluable offerings during the conference:

**Technical & Poster Sessions** – Nearly 60 symposia will focus on the pioneering efforts of some of the world’s brightest and most promising minds. Sessions are offered in dynamic technical areas including aluminum and magnesium, advanced characterization and modeling, electronic materials, high performance structural materials, materials and society, materials processing and production, and nanoscale and amorphous materials.

**Continuing Education** – Knowledge is the power that fuels developments in research and builds careers. TMS 2010 features 7 compelling courses and workshops designed to enhance your conference experience through education.

**Networking** – Simply put, there is nothing like being here. Your presence at TMS 2010 offers one of the greatest benefits – connecting with colleagues from around the world! Enjoy casual conversations or attend one of our 11 technical receptions. On Sunday evening, gather with professionals in your field, or join us at the President’s Welcoming Reception on Monday and Happy Hour on Tuesday, both held in the exhibit hall.

**Special Lectures** – One of the hallmarks of the TMS annual meeting is the series of special lectures presented by prestigious professionals in the materials field. Here is this year’s agenda: Extraction & Processing/Materials Processing & Manufacturing Joint Lecture; Extraction & Processing Division Distinguished Lecturer; Light Metals Division Lecture, and the Young Leaders Tutorial Lecture. See page 15 for speakers.

**Awards Presentation** – Celebrating the accomplishments of fellow colleagues builds our society. The TMS and AIME Awards Dinner is a must-attend event on Tuesday evening. See page 16 for a preview.

**Exhibition** – The movers and shakers in the technology solutions field shine at this all-encompassing showcase. Among the noteworthy exhibitors available to answer questions and demonstrate their wares is the Automobili Lamborghini Advanced Composite Structures Laboratory, Department of Aeronautics & Astronautics, from the University of Washington, which will feature an actual Lamborghini sports car.

**Student Events** – The future of TMS is alive in its student members. The annual meeting offers budding scientists and engineers the opportunity to network with peers, as well as learn from the pros. Visit the Student Poster Contest and see what students are working on, and enjoy their competitive spirit at the Materials Bowl sponsored by Alcoa. Details are on page 18.

So, how do we possibly summarize all the great things TMS and the annual meeting have to offer? Perhaps our **TMS, MSE & Me Video Contest** participants can show us. See what’s on their minds at the winners’ announcement, Sunday at 8 p.m. in Room 6C of the convention center.

Get ready to experience TMS 2010. It all starts now!

Sincerely,

Ray D. Peterson  
2009 TMS President

### Table of Contents

Presidential Welcome .....	1	Lectures, Luncheons & Receptions ....	14	TMS 2010 Leadership .....	20
Meeting Policies.....	2	Awards Banquet .....	16	Exhibit Directory .....	21
Floor Plans .....	3-8	Student Events .....	18	Technical Program.....	37
Schedule of Events.....	9-13	Proceedings.....	19		

---

# Meeting Perks and Policies

## Full Conference Registration

Your full conference badge provides you admission to each of these premier events!

1. Technical & Poster Sessions
2. Exhibition
3. President's Welcoming Reception in the Exhibit Hall
4. Symposia-Related Networking Receptions
5. Hosted Exhibit Hall Reception
6. Young Leaders Tutorial Lecture<sup>+</sup>
7. Women in Science Breakfast Lecture<sup>\*</sup>
8. Student Poster Contest
9. Student Materials Bowl

<sup>+</sup>Young Leaders lecture is free. Lunch requires preregistration.

<sup>\*</sup>Breakfast is free; preregistration required.

## Internet Options

Free wireless access will be available to attendees on the 4th and 6th floors of the Washington State Convention & Trade Center.

## Policies

### Badges

All attendees must wear registration badges at all times during the conference to ensure free admission to events included in the paid fee such as technical sessions, exhibition and receptions. "Exhibit Only" badges provide exclusive admittance to the show floor for events in the exhibit hall. "Guest" badges are for spouses or companions of registered attendees and used as identification only. "Guest" and "Exhibit Only" may not attend technical sessions.

### Refunds

The deadline for all refunds was January 15, 2010. No refunds will be issued at the conference. Fees and tickets are nonrefundable.



### Americans With Disabilities Act

TMS strongly supports the federal Americans with Disabilities Act (ADA) which prohibits discrimination against, and promotes public accessibility for those with disabilities. In support of, and in compliance with, ADA, we ask those requiring specific equipment or services to contact TMS Meeting Services in advance.

### Cell Phone Use

In consideration of attendees and presenters, TMS kindly requests your cooperation in minimizing disturbances which may occur during technical sessions due to cell phone use. Please place cell phones or other electronic devices in "silent mode" while you are in meeting rooms.

### Audio/Video Recording

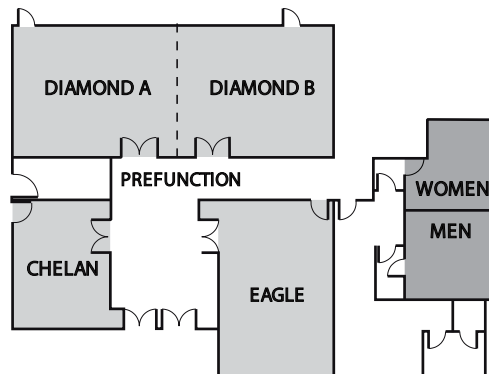
TMS reserves the right to all audio and video reproduction of presentations at TMS sponsored meetings. Recording of sessions (audio, video, still photography, etc.) intended for personal use, distribution, publication, or copyright without the express written consent of TMS and the individual authors is strictly prohibited. Contact TMS Technical Programming at (724) 776-9000, ext. 212, to obtain a copy of the waiver release form.

### Photography Notice

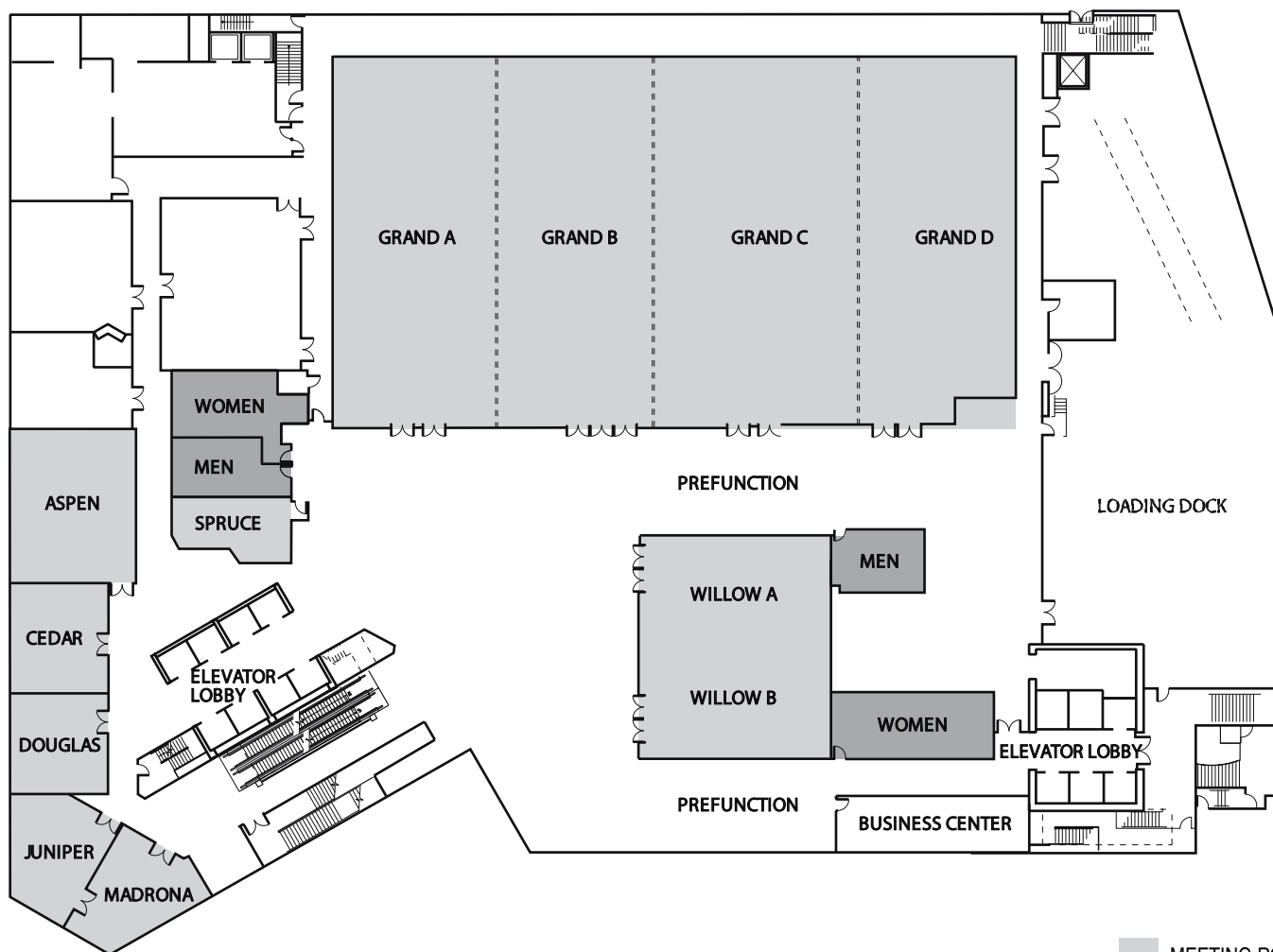
By registering for the meeting, all attendees acknowledge that they may be photographed by TMS personnel while at events. Photos may be used for promotional purposes in print and online.

## Sheraton Seattle Hotel Floor Plans

### LEVEL 1



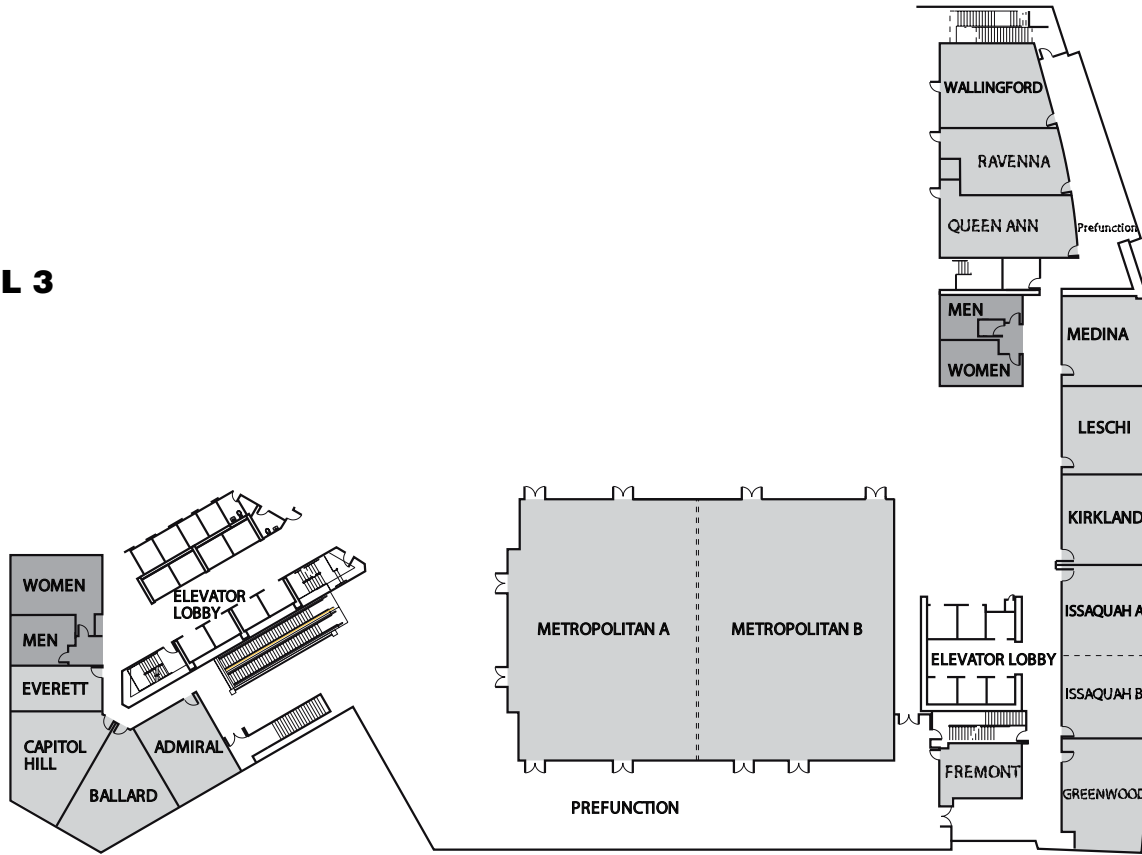
### LEVEL 2



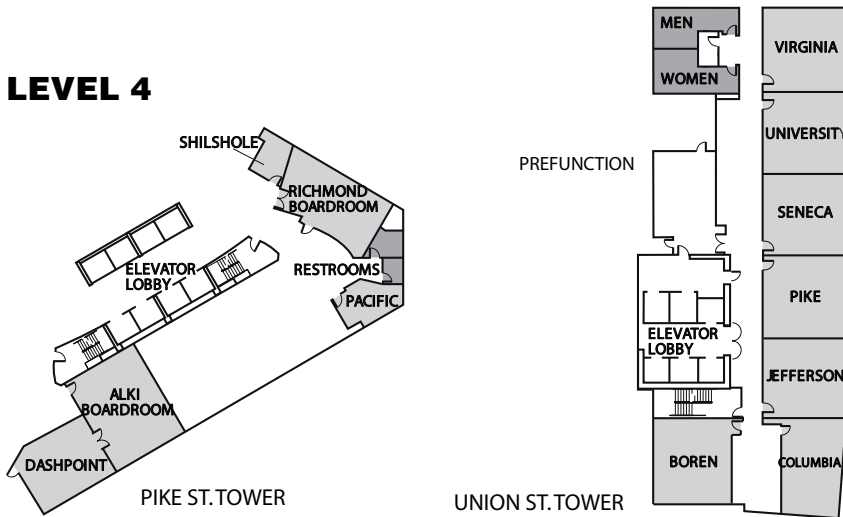
MEETING ROOMS  
RESTROOMS

# Sheraton Seattle Hotel Floor Plans

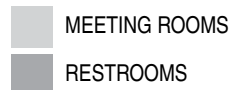
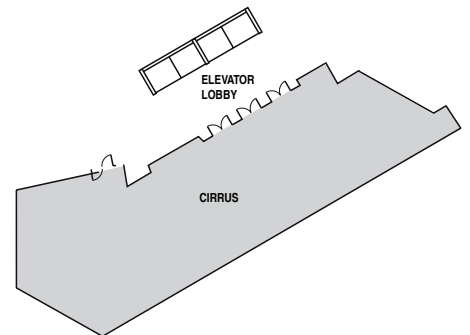
## LEVEL 3



## LEVEL 4

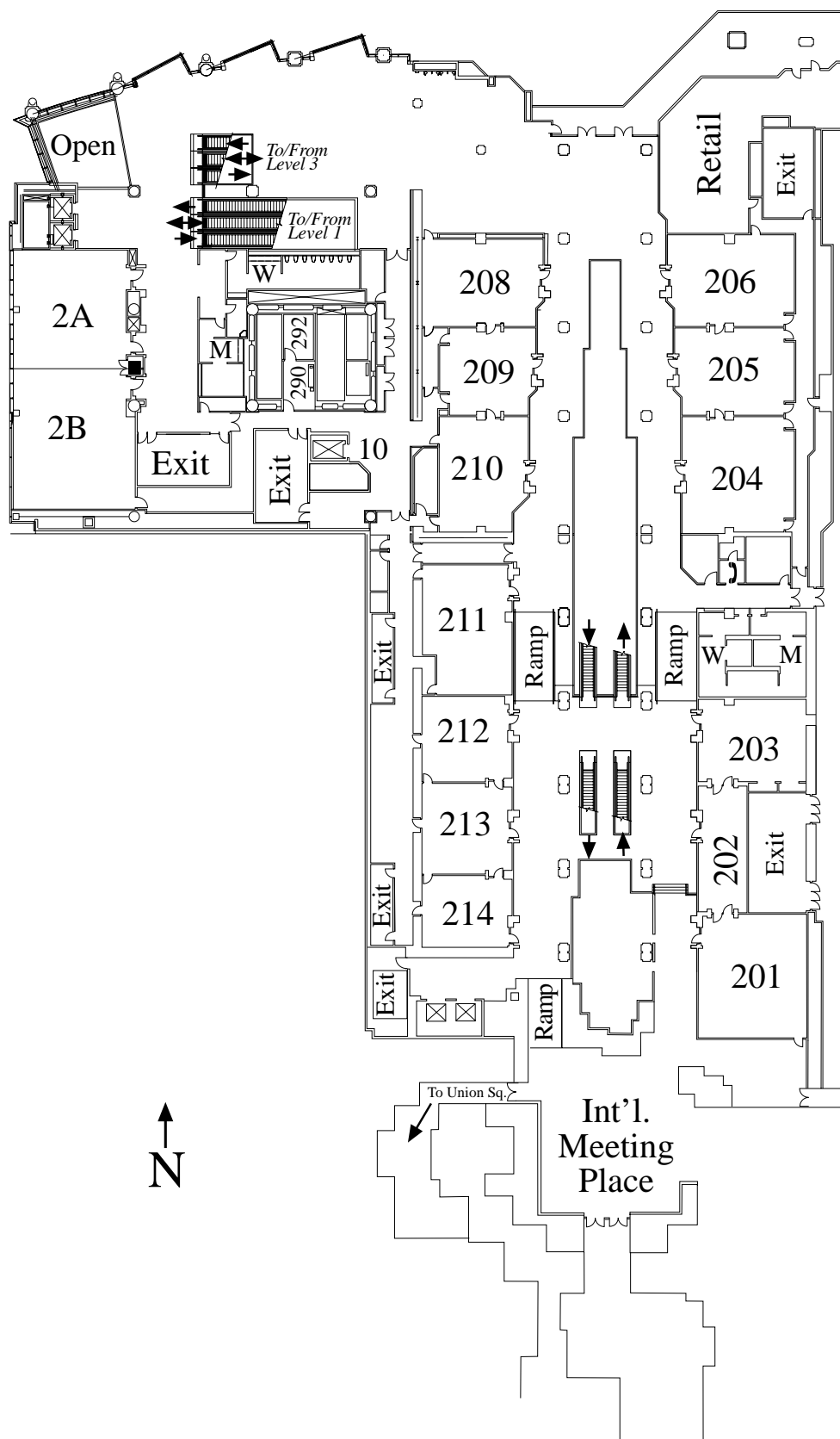


## LEVEL 35



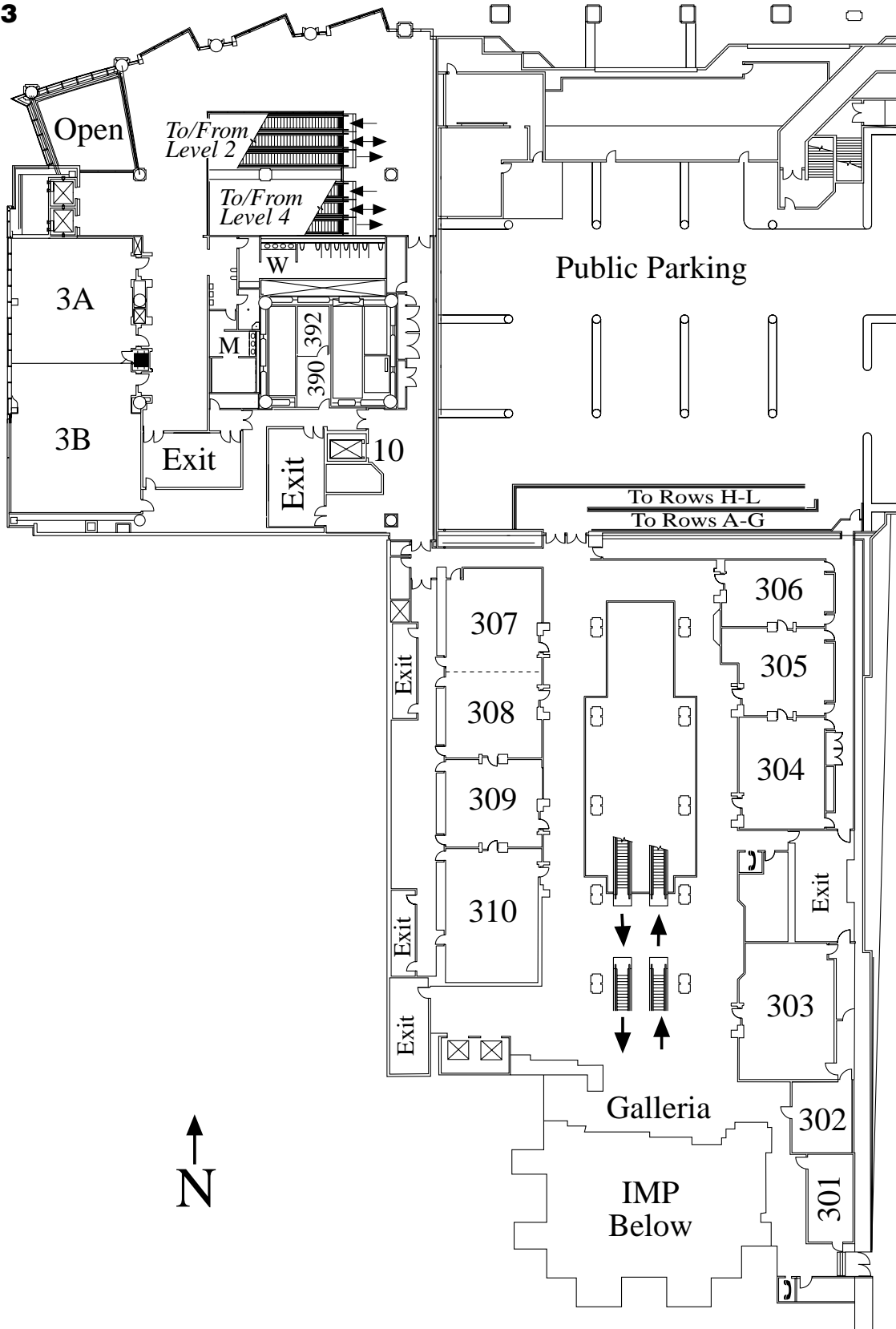
## Convention Center Floor Plans

### LEVEL 2



# Convention Center Floor Plans

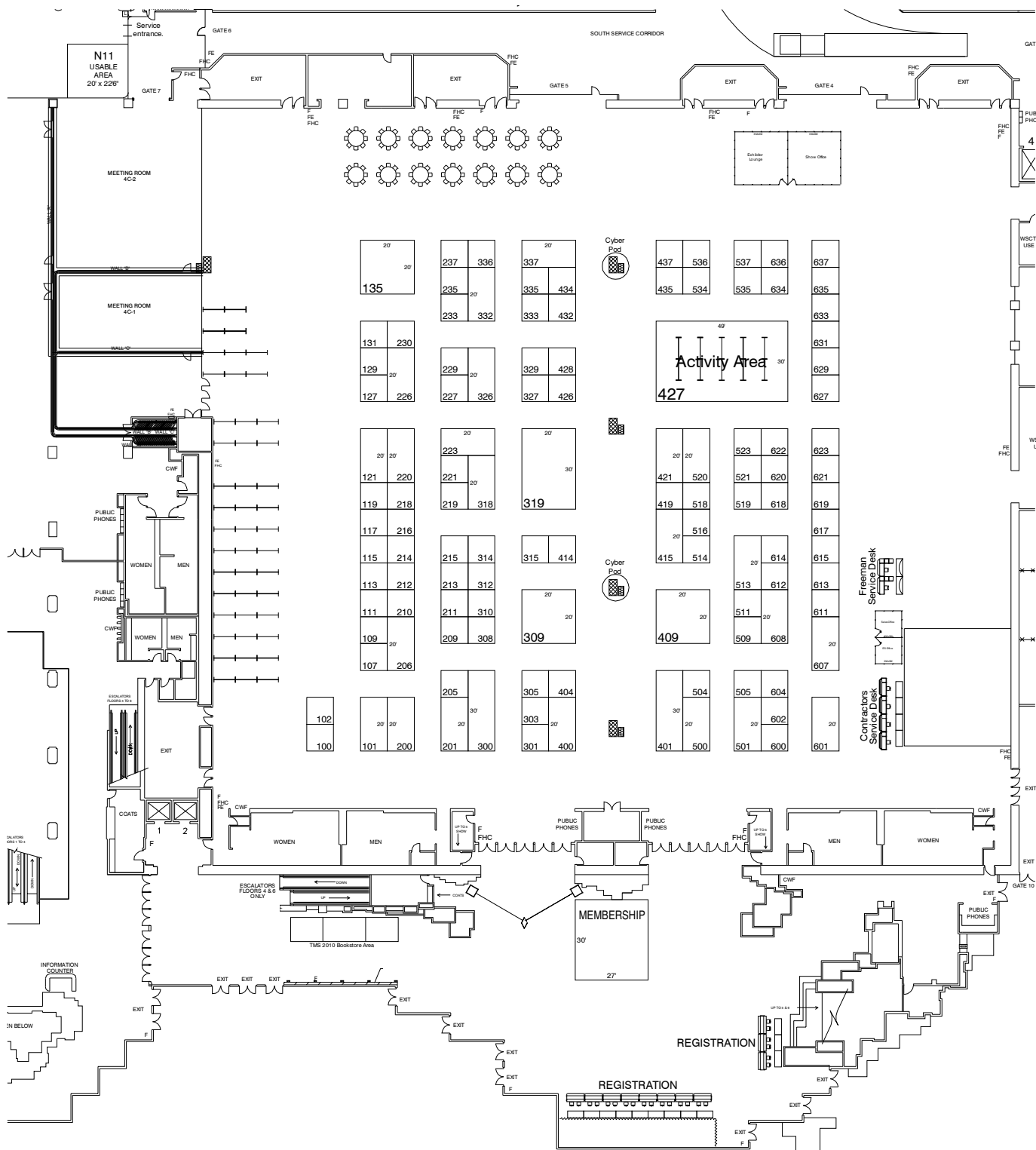
## LEVEL 3



## Convention Center Floor Plans

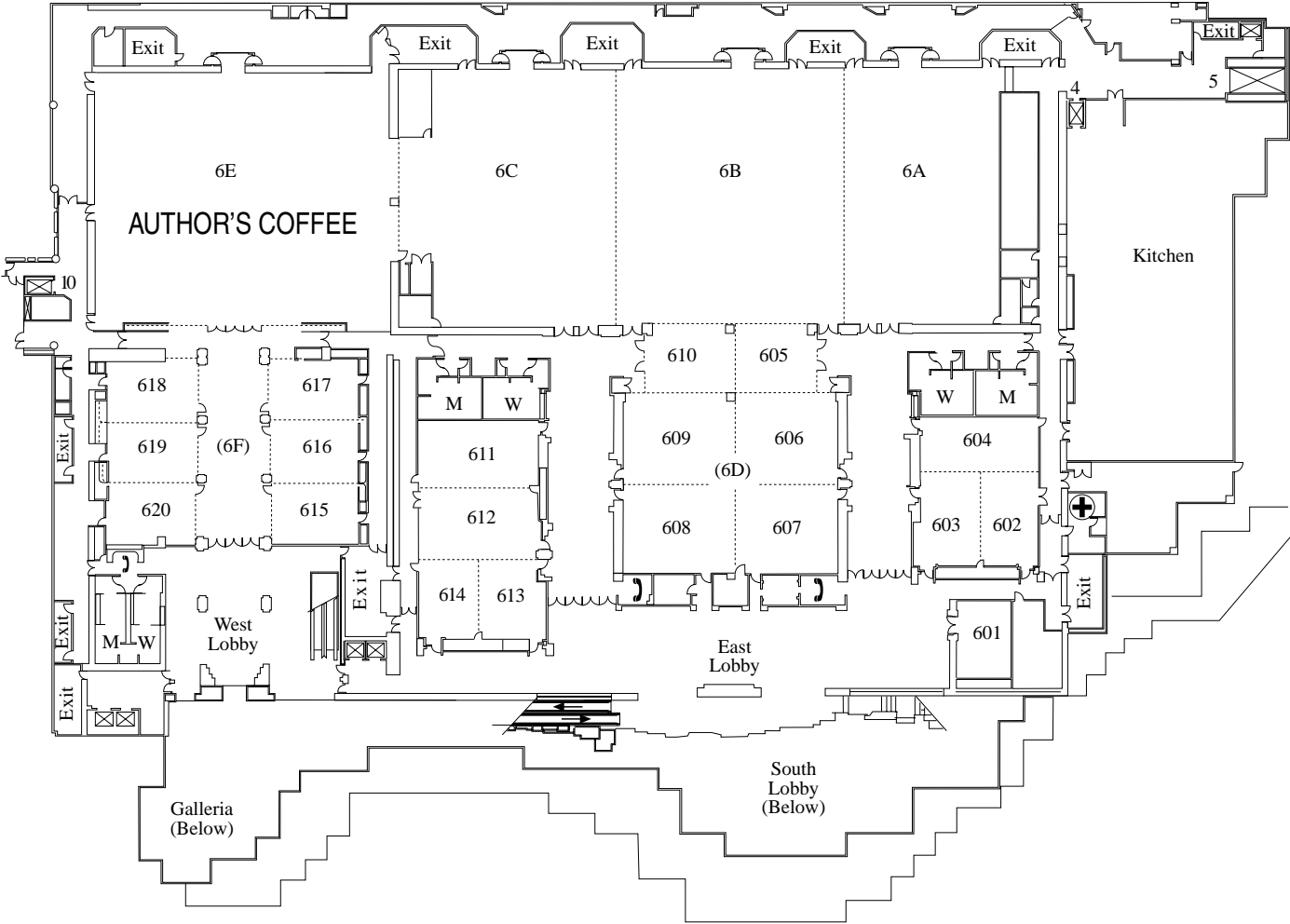
### EXHIBIT HALL

#### LEVEL 4



# Convention Center Floor Plans

## LEVEL 6



## Schedule of Events *(as of 1/20/10)*

TMS Meetings and Events are scheduled for the following dates, times, and locations:

Key: C = Washington State Convention & Trade Center

S = Sheraton Seattle Hotel

### SATURDAY, FEBRUARY 13

FUNCTION	TIME	LOCATION	ROOM
<b>COMMITTEE MEETINGS</b>			
Professional Registration Workshop.....	9 a.m. to 3 p.m.....	S.....	Ravenna
Professional Registration Committee Meeting.....	3 to 5 p.m.....	S.....	Ravenna

### SUNDAY, FEBRUARY 14

FUNCTION	TIME	LOCATION	ROOM
<b>REGISTRATION</b> .....	11 a.m. to 7:30 p.m.....	C.....	4th Floor, South Lobby
<b>TMS MEMBER WELCOME CENTER</b> .....	11 a.m. to 7:30 p.m.....	C.....	4th Floor, South Lobby
<b>TMS, MSE &amp; ME VIDEO CONTEST ANNOUNCEMENT</b> .....	8 to 8:30 p.m.....	C.....	Room 6C
<b>WORKSHOPS, SHORT COURSES, FORUMS &amp; TUTORIALS</b>			
Lead Free Solder Technology 2010.....	8:30 a.m. to 5 p.m.....	C.....	Rooms 2A/2B
Managing Smelter Operations in Turbulent Times.....	8:30 a.m. to 5 p.m.....	C.....	Room 4C 2
Materials in Nuclear Power Plant Construction .....	8:30 a.m. to 5 p.m.....	C.....	Room 4C 1
Process Modeling Short Course.....	8:30 a.m. to 5 p.m.....	C.....	Room 4C 4
Shutdown and Restart of Potlines .....	8:30 a.m. to 5 p.m.....	C.....	Room 4C 3
<b>ANSWER Tutorial Series: Neutron &amp; Synchrotron</b>			
Scattering 101 .....	1 to 4:30 p.m.....	C.....	Room 401
<b>STUDENT EVENTS</b>			
Materials Bowl.....		C.....	Room 6C
Elimination Rounds.....	noon to 4 p.m.....	C.....	Room 6C
Championship Round.....	8:30 p.m.....	C.....	Room 6C
Student Networking Mixer .....	9 to 11 p.m.....	C.....	Ballroom 6B
<b>SOCIAL FUNCTIONS</b>			
Fellows & Invited Guests Reception.....	4:30 to 6 p.m.....	S.....	Aspen
Young Leader/New Member Reception .....	5 to 6 p.m.....	S.....	Douglas
2009 Functional & Structural Nanomaterials: Fabrication, Aluminum Alloys: Fabrication, Characterization &			
Applications Networking Reception.....	6 to 8 p.m.....	C.....	Room 615
Biological Materials Science Reception.....	6 to 8 p.m.....	C.....	Room 205
Characterization of Minerals, Metals, & Materials			
Reception .....	6 to 8 p.m.....	C.....	Room 307
Computational Thermodynamics & Kinetics Networking Reception.....	6 to 8 p.m.....	C.....	Room 308

# Schedule of Events

FUNCTION	TIME	LOCATION	ROOM
Global Innovations in Manufacturing of Aerospace Materials: The 11th MPMD Global Innovations Symposium Networking Reception.....	6 to 8 p.m.....	C.....	Room 306
Light Metals Networking Reception.....	6 to 8 p.m.....	C.....	Room 608
Magnesium Technology 2010 Networking Reception.....	6 to 8 p.m.....	C.....	Room 612
Pb-Free Solders and Emerging Interconnect & Packaging Technologies Networking Reception.....	6 to 8 p.m.....	C.....	Room 204
Vasek Vitek Honorary Symposium on Crystal Defects, Computational Materials Science and Applications Networking Reception.....	6 to 8 p.m.....	C.....	Room 603
Ultrafine Grained Materials – 6th International Symposium Networking Reception.....	6 to 8 p.m.....	C.....	Room 606
<b>COMMITTEE MEETINGS</b>			
Financial Planning Committee.....	7:30 to 8:30 a.m.....	S.....	Greenwood
Professional Registration Leadership Committee.....	9 to 11 a.m.....	S.....	Everett
TMS Board of Directors Orientation & Briefing.....	9 a.m. to 1:30 p.m.....	S.....	Aspen
Recycling & Environmental Technologies Committee.....	noon to 1:30 p.m.....	C.....	Room 208
Young Leader Committee Business Meeting.....	12:30 to 2 p.m.....	S.....	Issaquah
Accreditation Committee.....	12:30 to 2:30 p.m.....	S.....	Wallingford
Pyrometallurgy Committee.....	1 to 2:30 p.m.....	C.....	Room 210
Magnesium Committee.....	1:30 to 3:15 p.m.....	C.....	Room 304
Nominating Committee.....	2 to 3 p.m.....	S.....	Kirkland
Thin Films & Interfaces Committee.....	3 to 4 p.m.....	C.....	Room 211
Aluminum Committee.....	2:30 to 4 p.m.....	C.....	Room 305
Public & Government Affairs Committee.....	3 to 4:30 p.m.....	S.....	Everett
Materials Characterization Committee.....	3 to 5 p.m.....	C.....	Room 203
Program Committee.....	3 to 5 p.m.....	C.....	Room 208
ABET Training Session.....	3 to 5 p.m.....	S.....	Greenwood
Electrode Subcommittee.....	4 to 5 p.m.....	C.....	Room 305
ICME Committee.....	4 to 5:30 p.m.....	C.....	Room 304
Nanomaterials Committee.....	4 to 5 p.m.....	C.....	Room 309
Publications Coordinating Committee.....	4 to 5:30 p.m.....	S.....	Cedar
LMD Council Meeting.....	4:30 to 6 p.m.....	C.....	Room 209
Global Innovations Committee.....	5 to 5:45 p.m.....	C.....	Room 301
Hydrometallurgy and Electrometallurgy Committee.....	5 to 6:30 p.m.....	C.....	Room 210
Nanomechanical Materials Behavior Committee.....	5:45 to 6:45 p.m.....	C.....	Room 211
Mechanical Behavior of Materials Committee.....	7 to 8:30 p.m.....	C.....	Room 203
Alloy Phases Committee.....	7:30 to 9 p.m.....	C.....	Room 210
Phase Transformations Committee.....	7:30 to 9:30 p.m.....	C.....	Room 208

## TMS, MSE & Me Video Contest Awards Ceremony

Nine creative TMS members have produced short film adaptations of their lives in materials science for the "TMS, MSE & Me Video Contest." The top three winners of \$2,010, \$750 and \$250 will be announced during a special presentation of all submissions on Sunday, February 14th at 8 p.m. prior to the Materials Bowl Championship Round at the Washington State Convention & Trade Center, Room 6C. Come and enjoy the show!



# TMS2010

139th Annual Meeting & Exhibition

Key: C = Washington State Convention & Trade Center

S = Sheraton Seattle Hotel

## MONDAY, FEBRUARY 15

FUNCTION	TIME	LOCATION	ROOM
<b>AUTHORS' COFFEE</b> .....	7:30 to 8:30 a.m. ....	C.....	Ballroom 6E
<b>REGISTRATION</b> .....	7 a.m. to 6 p.m.....	C.....	4th Floor, South Lobby
<b>TMS MEMBER WELCOME CENTER</b> .....	7 a.m. to 6 p.m.....	C.....	4th Floor, South Lobby
<b>GENERAL POSTER SESSION</b> .....	5 to 6:30 p.m.....	C.....	Exhibit Hall
<b>2010 TMS EXHIBITION</b>			
Exhibit Hours .....	noon to 6:30 p.m.....	C.....	4th Floor
President's Welcoming Reception .....	5 to 6:30 p.m.....	C.....	Rooms 4A/4B
<b>TECHNICAL DIVISION STUDENT POSTER CONTEST</b> .....	5 to 6:30 p.m.....	C.....	Exhibit Hall
<b>SOCIAL FUNCTIONS</b>			
Women in Science Breakfast/Lecture.....	7 to 8 a.m. ....	S.....	Grand Ballroom A
Guest Hospitality .....	7 to 10 a.m. ....	S.....	Greenwood
Past Presidents' Brunch.....	9:30 to 11 a.m. ....	S.....	Douglas
California Polytechnic State University Alumni Reception.....	6:30 to 9 p.m.....		Offsite
Colorado School of Mines Alumni Reception .....	7 to 8 p.m.....	S.....	Aspen
<b>COMMITTEE MEETINGS</b>			
PbZn 2010 Planning Meeting .....	7 to 8:30 a.m. ....	S.....	Everett
Met Trans "A" Board of Review .....	7 to 8 a.m. ....	S.....	Issaquah
Met Trans Joint Commission.....	8 to 10:30 a.m. ....	S.....	Issaquah
Process Technology and Modeling Committee.....	8 to 9 a.m. ....	C.....	Room 210
Superconducting & Magnetic Materials Committee.....	8 to 9 a.m. ....	C.....	Room 208
Membership & Student Development Committee.....	8:45 to 9:45 a.m. ....	S.....	Wallingford
EPD Council Meeting .....	noon to 2 p.m.....	S.....	Room 208
Seven Springs Int'l Symposium on Superalloys Program Committee .....	noon to 2 p.m.....	S.....	Cedar
Graduate Student Advisory Council .....	noon to 1:30 p.m.....	S.....	Wallingford
MetSoc/TMS Leadership Meeting .....	12:15 to 1:45 p.m.....	S.....	President's Suite
EMPMD Council Meeting .....	12:30 to 2 p.m.....	C.....	Room 210
TMS Executive Committee .....	2 to 4 p.m.....	S.....	President's Suite
Seven Springs Int'l Symposium on Superalloys General Organizing Committee .....	5 to 7 p.m.....	S.....	Cedar
Advanced Characterization, Testing & Simulation Cmt.....	5:30 to 6:30 p.m.....	C.....	Room 401
Chemistry & Physics of Materials Committee.....	5:30 to 6:30 p.m.....	C.....	Room 208
Surface Engineering Committee.....	5:30 to 6:30 p.m.....	C.....	Room 604
Nuclear Materials Committee .....	5:30 to 7 p.m.....	C.....	Room 310
Composite Materials Committee .....	5:45 to 6:45 p.m.....	C.....	Room 305
Biomaterials Committee .....	6 to 7 p.m.....	C.....	Room 210
Solidification Committee .....	6 to 7 p.m.....	C.....	Room 601
Technical Division Board .....	6 to 8 p.m.....	C.....	Room 301
Materials & Society Committee .....	7 to 9 p.m.....	S.....	Issaquah
Computational Materials Science & Engineering Committee.....	8 to 9 p.m.....	C.....	Room 208

# Schedule of Events

TUESDAY, FEBRUARY 16

FUNCTION	TIME	LOCATION	ROOM
<b>AUTHORS' COFFEE</b> .....	7:30 to 8:30 a.m. ....	C.....	Ballroom 6E
<b>REGISTRATION</b> .....	7 a.m. to 6 p.m.....	C.....	4th Floor, South Lobby
<b>TMS MEMBER WELCOME CENTER</b> .....	7 a.m. to 6 p.m.....	C.....	4th Floor, South Lobby
<b>GENERAL POSTER SESSION</b> .....	10:30 a.m. to 6 p.m.....	C.....	Exhibit Hall
<b>2010 TMS EXHIBITION</b>			
Exhibit Hours.....	10:30 a.m. to 6 p.m.....	C.....	4th Floor
Happy Hour Reception.....	5 to 6 p.m.....	C.....	Exhibit Hall
<b>TECHNICAL DIVISION LUNCHEON &amp; LECTURE</b>			
EPD/MPMD Luncheon.....	noon to 1:30 p.m.....	C.....	Room 6C
Extraction & Processing Division Distinguished Lecture.....	1:45 to 2:15 p.m.....	C.....	Room 6C
<b>STUDENT EVENTS</b>			
Technical Division Student Poster Awards.....	noon to 2:30 p.m.....	C.....	Exhibit Hall
Student Career Forum.....	3 to 5 p.m.....	C.....	Rooms 4C3
<b>TUTORIAL LECTURE/LUNCHEON</b>			
Young Leaders Tutorial Lecture/Luncheon.....	noon to 2 p.m.....	S.....	Douglas
<b>WORKSHOPS, SHORT COURSES, FORUMS &amp; TUTORIALS</b>			
Reliability Excellence Workshop.....	8 a.m. to 4:30 p.m.....	C.....	Room 4C 1
Furnace Systems Technology 2010 Workshop.....	8:30 a.m. to 5 p.m.....	C.....	Room 4C 2
<b>TMS-AIME ANNUAL AWARDS BANQUET</b>			
Reception.....	6:30 to 7:15 p.m.....	S.....	Grand Ballroom (Pre-Function)
Dinner and Awards.....	7:15 to 10 p.m.....	S.....	Grand Ballroom B, C & D
<b>SOCIAL FUNCTIONS</b>			
Guest Hospitality.....	7 to 10 a.m. ....	S.....	Greenwood
Acta Materialia, Inc. Board of Governors Luncheon.....	noon to 1 p.m.....	S.....	Aspen
<b>COMMITTEE MEETINGS</b>			
Electronic Packaging & Interconnection Committee.....	7 to 8 a.m. ....	C.....	Room 204
Met Trans "B" Board of Review.....	7 to 8 a.m. ....	S.....	Issaquah
MPMD Council Meeting.....	7 to 9 a.m. ....	C.....	Room 210
Acta Materialia, Inc. Board of Governors Meeting.....	7:30 a.m. to 6 p.m.....	S.....	Cedar
Fellows Award Committee.....	7:30 to 9 a.m. ....	S.....	Kirkland
Hume-Rothery/ACTA Met Awards Committee.....	7:30 to 9 a.m. ....	S.....	Kirkland
IOM/Mehl Awards Committee.....	7:30 to 9 a.m. ....	S.....	Kirkland
Copper 2010 IOC Meeting.....	8 to 10 a.m. ....	S.....	Everett
Honors & Professional Recognition Award Committee.....	9 to 10 a.m. ....	S.....	Kirkland
ASM/TMS Leadership Meeting.....	noon to 1:30 p.m.....	S.....	President's Suite
SMD Council Meeting.....	noon to 2 p.m.....	C.....	Room 210
Powder Materials Committee.....	12:30 to 2 p.m.....	C.....	Room 208
Women in Materials Science & Engineering Committee.....	3 to 4:30 p.m.....	S.....	Everett
PRICM-7 International Organizing Committee.....	4 to 6 p.m.....	S.....	Wallingford
Education Committee.....	5 to 6:30 p.m.....	S.....	Issaquah

# TMS2010

139th Annual Meeting & Exhibition

Key: C = Washington State Convention & Trade Center

S = Sheraton Seattle Hotel

FUNCTION	TIME	LOCATION	ROOM
Energy Committee	5 to 6 p.m.	C	Room 209
Energy Conversion & Storage Committee	5 to 6 p.m.	C	Room 210
Refractory Metals & Materials Committee	5:30 to 6:30 p.m.	C	Room 3B
High Temperature Alloys Committee	5:30 to 7 p.m.	C	Room 212
Titanium Committee	6 to 7 p.m.	C	Room 618
Shaping & Forming Committee	6 to 8 p.m.	C	Room 208
Corrosion & Environmental Effects Committee	6:30 to 7:30 p.m.	C	Room 213

## WEDNESDAY, FEBRUARY 17

FUNCTION	TIME	LOCATION	ROOM
<b>AUTHORS' COFFEE</b>	7:30 to 8:30 a.m.	C	Ballroom 6E
<b>REGISTRATION</b>	7 a.m. to 5 p.m.	C	4th Floor, South Lobby
<b>TMS MEMBER WELCOME CENTER</b>	7 a.m. to 5 p.m.	C	4th Floor, South Lobby
<b>GENERAL POSTER SESSION</b>	10:30 a.m. to 2:30 p.m.	C	Exhibit Hall
<b>2010 TMS EXHIBITION</b>			
Exhibit Hours	10:30 a.m. to 3 p.m.	C	4th Floor
<b>TECHNICAL DIVISION LUNCHEON</b>			
Light Metals Division Luncheon	noon to 2:15 p.m.	C	Room 6C
<b>WORKSHOPS, SHORT COURSES, FORUMS &amp; TUTORIALS</b>			
Furnace Systems Technology 2010 Workshop	8:30 a.m. to 5 p.m.	C	Room 4C 2
<b>SOCIAL FUNCTIONS</b>			
Guest Hospitality	7 to 10 a.m.	S	Greenwood
<b>COMMITTEE MEETINGS</b>			
TMS Board of Directors Meeting	7:30 a.m. to noon	S	Issaquah
Aluminum Processing Committee	6:30 to 8 p.m.	C	Room 210

## THURSDAY, FEBRUARY 18

FUNCTION	TIME	LOCATION	ROOM
<b>AUTHORS' COFFEE</b>	7:30 to 8:30 a.m.	C	Ballroom 6E
<b>REGISTRATION</b>	7 to 10 a.m.	C	4th Floor, South lobby
<b>TMS MEMBER WELCOME CENTER</b>	7 to 10 a.m.	C	4th Floor, South lobby
<b>COMMITTEE MEETINGS</b>			
Light Metals Subject Chair Breakfast	7 to 8:30 a.m.	C	Room 209
Worcester Polytechnic Institute Alumni Reception	5:30 to 8 p.m.	S	Everett
FCRD Advanced Materials Development Workshop Planning Meeting	1 to 5 p.m.	S	Aspen

## Lectures & Luncheons



### Women in Science Breakfast Lecture

*“ADVANCing Women in Engineering”*

**Monday • 7 to 8 a.m. • Sheraton Seattle, Grand Ballroom A**

Speaker: **Eve A. Riskin**, associate dean of academic affairs, professor of electrical engineering and director of the ADVANCE Center for Institutional Change, *University of Washington, USA*

About the Topic:

ADVANCE is an initiative of the National Science Foundation intended to improve the climate for success of women in science/technology/engineering/mathematics (STEM) at universities in the United States. At the University of Washington, the program has been in effect since 2001, focusing on faculty recruitment and retention as well as leadership development. Riskin, director of the university's ADVANCE Center for Institutional Change, will discuss the program and highlight some of its successes. Also addressed will be interventions that can improve chances that women STEM faculty will succeed in their careers.



### Extraction & Processing/ Materials Processing & Manufacturing Joint Division Luncheon Lecture

*“Titanium: Its Attributes, Characteristics and Applications”*

**Tuesday • Noon to 1:30 p.m. • Washington State Convention & Trade Center, Room 6C**

Speaker: **Rodney Boyer**, Boeing Commercial Airplanes, *Seattle, Washington, USA*

About the Topic:

This presentation will focus on the desirable and unique attributes of this alloy system, the types of applications which result from these unique characteristics and a general overview of some of the approaches being taken to reduce the cost, some of which could have an impact on non-aerospace industries. These include techniques such as solid-state and fusion welding, roll-forged shapes, SPF and SPF/DB, new alloys and powder metallurgy.



### Extraction & Processing Division Distinguished Lecture

*“Alloy Formation during Electrochemical Cementation Reactions”*

**Tuesday • 1:45 to 2:15 p.m. • Washington State Convention & Trade Center, Room 6C**

Speaker: **J. Brent Hiskey**, associate dean, *University of Arizona, USA*

About the Topic:

Metal displacement (cementation) reactions have been important to many hydrometallurgical processes for centuries. For the most part, these reactions involve rather straight-forward electrochemical steps. The deposition of unique alloys by this technique has been reported for several systems. This paper describes these systems and provides an explanation for this phenomenon.



### Young Leaders Tutorial Luncheon Lecture

*“Energy Materials – Past, Present, and Future”*

**Tuesday • Noon to 2 p.m. • Sheraton Seattle, Douglas Room**

Speaker: **Xingbo Liu**, professor of mechanical & aerospace engineering, *West Virginia University, USA*

About the Topic:

This presentation focuses on the history of pursuing improved materials for the need of production and efficient consumption of energy. Discussed will be primary sources of energy prior to the 18th century; how advances in technology, beginning with James Watt's invention of the steam engine, led to coal and other resources being dominant sources of energy; today's energy resources; how the demand of energy has been tremendously increased in recent years with the development of the world's economy; and those of the foreseeable future.

## Lectures & Luncheons Cont.



### Light Metals Division Luncheon Lecture

*"Aluminum – Are We There Yet?"*

**Wednesday • Noon to 2:15 p.m. • Washington State Convention & Trade Center, Room 6C**

Speaker: **Wayne Hale**, executive vice president and CEO, *Century Aluminum, USA*

#### About the Topic:

With the recession and the associated impact on commodities, industry consultants and pundits continually prognosticate the future of the aluminum industry. The future of a commodity is an uncertain proposition, but usually there is a general consensus on the future trends of the market. For aluminum, the uncertainty of the market continues to generate debate. With a surplus of aluminum on world markets and the current global economic slowdown, the uncertainty regarding the future of the aluminum market has become a strong point of discussion. Optimism of a global recovery, the massive monetary and fiscal liquidity injected worldwide and the strong growth in emerging nations could lead to a surge in demand and an increase in prices. Others believe that the world of high inventories and increasing production will limit the upside. Review of the industry's current position, the necessary milestones and the potential bumps along the way will help answer the vexing question.... "Are we there yet?"

## Award Winning Speakers

### William Hume-Rothery Award Lecture/Symposium

*"How Hume-Rothery's Work Led to Computational Thermodynamics"*

**Monday • 8:30 a.m. to 9:15 p.m. • Washington State Convention & Trade Center, Room 212**

Speaker: **Didier de Fontaine**, Professor Emeritus, *University of California, USA*

### Institute of Metals/Robert Franklin Mehl Lecture

*"Nature-Inspired Structural Materials" — Biological Materials Science Symposium*

**Tuesday • 8:35 a.m. to 9:15 a.m. • Washington State Convention & Trade Center, Room 205**

Speaker: **Robert Ritchie**, Chua Distinguished Professor of Engineering, *University of California, USA*

### Vittorio de Nora Prize Lecture

*"Designing Crushing and Grinding Circuits for Improved Energy Efficiency"*

**Wednesday • 9:50 a.m. to 10:15 a.m. • Washington State Convention & Trade Center, Room 2B**

Speaker: **Zeljka Pokrajcic**, *WorleyParsons Services Pty Ltd – Minerals and Metals, Australia*

### JIM International Scholar Award Lecture

*"Development of Coherent X-Ray Diffraction Microscopy and Its Application in Materials Science"*

**Wednesday • 12:50 p.m. to 1:05 p.m. • Washington State Convention & Trade Center, Room 303**

Speaker: **Yukio Takahashi**, *Osaka University, Japan*

## Spotlight Event

### TMS Lunch and Learn

*"Carbon Fiber Composites Research and Development at Automobili Lamborghini"*

**Monday • 12:30 p.m. to 1:45 p.m. • Washington State Convention & Trade Center, Room 4C2**

Speakers: **Paolo Feraboli, Ph.D.**, assistant professor of Aircraft Materials and Structures and Director, *Automobili Lamborghini Advanced Composite Structures Laboratory, Department of Aeronautics & Astronautics, University of Washington, USA*; **Dr. Luciano DeOto**, senior manager of composites activities for Automobili Lamborghini S.p.A., Italy



# Awards Banquet

## 139th TMS and AIME Awards Presentation

With Installation of the 2010 TMS President

Tuesday, February 16 • Reception: 6:30 to 7:15 p.m.

Dinner and Awards: 7:15 to 10 p.m. • Sheraton Seattle, Grand Ballroom B, C & D

Tickets may be purchased at the TMS registration desk



Ray Peterson  
2009 TMS President



George T. "Rusty" Gray III  
2010 TMS President



Ian Sadler  
2009 AIME President

### About the 2010 TMS President

George T. "Rusty" Gray III is laboratory fellow at Los Alamos National Laboratory in Los Alamos, New Mexico, and a member of the National Materials Advisory Board of the U.S. National Academies. Gray has served as team leader of the Dynamic Materials Properties section, where he promoted dynamic structure/property research on materials within the U.S. Department of Energy.

Gray earned his B.S. and M.S. in Metallurgical Engineering from South Dakota School of Mines and Technology and his Ph.D. in metallurgical engineering from Carnegie Mellon University in Pittsburgh. Prior to joining Los Alamos, Gray held a postdoctoral fellowship at the Technische Universitaet Hamburg-Harburg in Germany. His research interests include the substructure evolution and mechanical response of metals, alloys, intermetallics, and composites as a function of microstructure and applied test conditions.

Gray is a member of the TMS Titanium and Mechanical Metallurgy committees and has served as the Structural Materials Division representative to the TMS Program Committee. Gray is also a member of ASM International, the American Physical Society, and the International Scientific Advisory Board of DYMAT Journal.

## Society Awards

### TMS Fellow Class of 2010

- Jeff DeHosson, *University of Groningen, Netherlands*
- James W. Evans, *Wireless Industrial Technologies, California, USA*
- Easo P. George, *Oak Ridge National Laboratory, Tennessee, USA*
- Richard Hoagland, *(Retired) Los Alamos National Laboratory, New Mexico, USA*
- Phillip J. Mackey, *Xstrata Process, Canada*

### Alexander Scott Distinguished Service Award

Brajendra Mishra, *Colorado School of Mines, USA*

### Application to Practice Award

Carol Handwerker, *Purdue University, Indiana, USA*

### Bruce Chalmers Award

Cristoph Beckermann, *University of Iowa, USA*

### Champion H. Mathewson Award

Guillaume Reinhart, *Université Paul Cézanne, France*

### Early Career Faculty Fellow Award

Xingbo Liu, *West Virginia University, USA*

### Educator Award

John Moore, *Colorado School of Mines, USA*

### Institute of Metals/Robert Franklin Mehl Award

Robert Ritchie, *University of California, USA*

### John Bardeen Award

Eugene Haller, *Lawrence Berkeley National Laboratory, California, USA*

### Leadership Award

Donald Gubser, *Naval Research Laboratory, California, USA*

### Robert Lansing Hardy Award

Diana Lados, *Worcester Polytechnic Institute, Massachusetts, USA*

### William Hume-Rothery Award

Didier de Fontaine, *University of California, USA*

### Shri Ram Arora Award

Apu Sarkar, *Bhabha Atomic Research Center, India*

### Vittorio de Nora Prize for Environmental Improvements in Metallurgical Industries

Zeljka Pokrajcic, *WorleyParsons, Australia*

## Division Awards

### Electronic, Magnetic & Photonic Materials Division

**Distinguished Scientist/Engineer Award**  
Brent Fultz, *California Institute of Technology*

**Distinguished Service Award**  
Elizabeth Holm, *Sandia National Laboratories, California, USA*

### Extraction & Processing Division

**Distinguished Lecturer Award**  
J. Brent Hiskey, *University of Arizona, USA*

**Distinguished Service Award**  
Patrick Taylor, *Colorado School of Mines, USA*

**Science Award**  
Stanko Nikolic, *Xstrata Technology, Canada*  
Peter C. Hayes, *University of Queensland, Australia*  
Hector Henao, *University of Queensland, Australia*  
Evgueni Jak, *University of Queensland, Australia*

**Technology Award**  
Gabriel Riveros, *Universided de Chile*  
Andrzej Warczok, *Universided de Chile*  
Daniel Smith, *ENAMI, Chile*  
Ariel Balocchi, *ENAMI, Chile*

### Light Metals Division

**Distinguished Service Award**  
Neale Neelameggham, *US Magnesium LLC, Utah, USA*

**Aluminum Reduction Award**  
Patrice Doiron, *Alcoa Inc., Canada*  
Stephen Lindsay, *Alcoa Inc., Canada*

**Electrode Technology for Aluminum Production Award**  
Jeremie Lhuissier, *Rio Tinto Alcan, Canada*  
Lailah Bezmanifary, *Rio Tinto Alcan, Canada*  
Magali Gendre, *Rio Tinto Alcan, Canada*  
Marie-Josée Chollier, *Rio Tinto Alcan, Canada*

**Light Metals Award**  
Anthimos Xenidis, *National Technical University of Athens, Greece*  
Charalabos Zografidis, *National Technical University of Athens, Greece*  
Ioannis Kotsis, *National Technical University of Athens, Greece*  
Dimitrios Boufounos, *Aluminium of Greece*

**Light Metals Division JOM Best Paper Award**  
Barry Welch, *Welbank Consulting, New Zealand*  
Martin Iffert, *Trimet Aluminum AG, Germany*  
Maria Skyllas-Kazacos, *University of South Wales*

**Magnesium Application Award**  
Ozgur Duygulu, *TUBITAK Marmara Research Center, Turkey*  
Onuralp Yucel, *Istanbul Technical University, Turkey*  
Selda Ucuncuoglu, *TUBITAK Marmara Research Center, Turkey*  
Gizem Oktay, *TUBITAK Marmara Research Center, Turkey*  
Ali Arslan Kaya, *Mugla University, Turkey*  
Deniz Sultan Temur, *Tubitak, Turkey*

**Magnesium Fundamental Research Award**  
Alok Singh, *National Institute for Materials Science, Japan*  
Julian M. Rosalie, *National Institute for Materials Science, Japan*  
Somekawa Hidetoshi, *National Institute for Materials Science, Japan*  
Toshiji Mukai, *National Institute for Materials Science, Japan*

**Technology Award**  
Douglas Granger, *Gras Inc., Pennsylvania, USA*

**Warren Peterson Cast Shop for Aluminum Production Award**  
Marc Badowski, *Hydro Aluminium Deutschland GmbH, Germany*  
Werner Droste, *Hydro Aluminium Deutschland GmbH, Germany*

### Material Processing & Manufacturing Division

**Distinguished Service Award**  
John Smugeresky, *Sandia National Laboratories, California, USA*

**Distinguished Scientist/Engineer Award**  
Yuntian Zhu, *North Carolina State University, USA*

### Structural Materials Division

**Distinguished Scientist/Engineer Award**  
Reinhold Dauskardt, *Stanford University, California, USA*

**Distinguished Service Award**  
Dallis Hardwick, *U.S. Air Force*

**Structured Materials Division JOM Best Paper Award**  
Marc A. Meyers, *University of California, USA*  
Sirirat Traiviratana, *University of California, USA*  
V.A. Lubarda, *University of California, USA*  
David J. Benson, *AMSRD-CER-NV-ST-IFT, USA*  
Eduardo M. Bringa, *Lawrence Livermore National Laboratory, USA*

### Other Awards

**AIME Honorary Membership**  
Y. Austin Chang, *University of Wisconsin, Madison, USA*

**AIME 2009 Rossiter W. Raymond Memorial Award**  
Rajen S. Sidhu, *Intel, Arizona, USA*  
Nikhilesh Chawla, *Arizona State University, USA*

**AIME Robert Earl McConnell Award**  
Diran Apelian, *Worcester Polytechnic Institute, Massachusetts, USA*

**AIME James Douglas Gold Medal**  
James C. Williams, *Ohio State University, USA*

# Student Events

TMS 2010 features a number of activities designed to captivate and educate young materials science minds. Registered student attendees may participate in any of the following events.

## Sunday

**Sponsored by** **2010 Materials Bowl**  
 Elimination Rounds.....noon to 4 p.m..... Washington State Convention & Trade Center, Room 6C  
 Championship Round .....8:30 p.m..... Washington State Convention & Trade Center, Room 6C



Twelve student teams will not only compete for cash prizes, but will vie for the right to take home the traveling trophy emblazoned with their school name after conquering three rounds of intense, materials science-based trivia questions. In its fourth year, this game show-like event is always a crowd favorite.

**Student Networking Mixer** .....9 to 11 p.m..... Washington State Convention & Trade Center, Room 6B

The TMS Graduate Student Advisory Council (GSAC) invites TMS members to attend the student mixer! As students, we are eager to meet professionals from industry and academia to learn about their experiences in the real world. The student mixer has a welcoming atmosphere that is ideal for informally meeting new people and having friendly conversations. We sincerely hope that members will stop by and attend the mixer

## Monday

**Poster Judging**.....5 to 6:30 p.m..... Washington State Convention & Trade Center, Exhibit Hall

Undergraduate and graduate students will vie for cash prizes at the annual Student Poster Contest sponsored by the five technical divisions of TMS – Electronic, Magnetic & Photonic Materials; Extraction & Processing; Light Metals; Materials Processing & Manufacturing, and Structural Materials.

Participants in this dynamic and interactive event compete for a \$500 prize in each division for the best undergraduate and best graduate poster. A top prize of \$1,000 will be awarded for the “Best of Show” poster.

## Tuesday

**Poster Awards Presentation**.....Noon..... Washington State Convention & Trade Center, Exhibit Hall

**Student Career Forum**.....3 to 5 p.m..... Washington State Convention & Trade Center, Room 4C3  
 Organized by the TMS Young Leader Committee, this session will feature speakers hailing from a variety of materials science backgrounds and career stages who discuss how to navigate a career path to ultimate goals. Speaker schedule:

**Introduction of Forum and Careers in Policy and Funding Agencies**  
 Speaker: Eric N. Brown, *Los Alamos National Laboratory*. ..... 3 p.m.  
**Careers in Academia: Public**  
 Speaker: Dallas Trinkel, *University of Illinois at Urbana-Champaign*. ..... 3:15 p.m.  
**Careers at National Laboratories**  
 Speaker: Brad Boyce, *Sandia National Laboratory*. ..... 3:30 p.m.  
**Careers in Industry**  
 Speaker: Amy Clarke, *Caterpillar, Inc.* ..... 3:45 p.m.  
**Careers in Academia: Private**  
 Speaker: Julia Greer, *California Institute of Technology*. ..... 4 p.m.  
**Q&A with Speakers** ..... 4:15 p.m.  
**TMS Leadership**  
 Speaker: George T. Gray III (2010 TMS Vice President), *Los Alamos National Laboratory*.... 4:45 p.m.

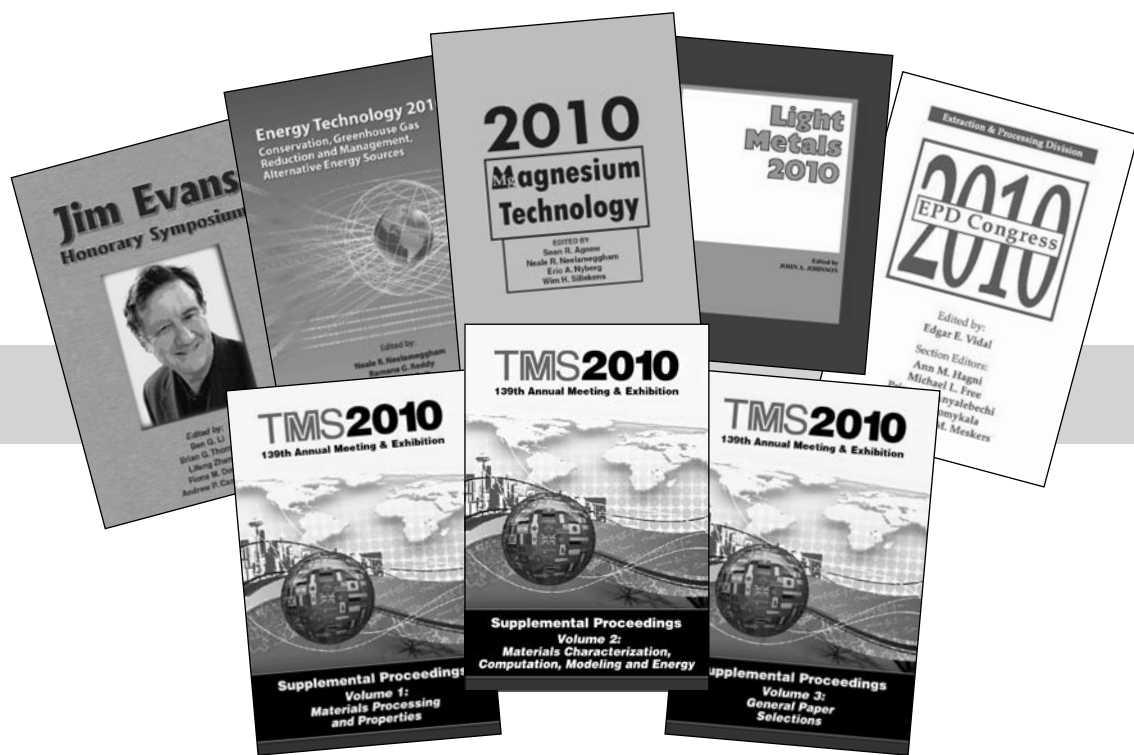


## Proceedings

These new TMS 2010 Annual Meeting books may be purchased on-site at the TMS Bookstore area.

- Magnesium Technology 2010
- Light Metals 2010
- EPD Congress 2010
- Energy Technology 2010: Conservation, Greenhouse Gas Reduction and Management, Alternative Energy
- Jim Evans Honorary Symposium
- Supplemental Proceedings: Volume 1: Materials Processing and Properties
- Supplemental Proceedings: Volume 2: Materials Characterization, Computation, Modeling and Energy
- Supplemental Proceedings: Volume 3: General Paper Selections

Or order online in the TMS Knowledge Resource Center at <http://knowledge.tms.org>.  
TMS members receive a discount!



### Collected Proceedings CD-ROM

A collected proceedings CD-ROM containing all TMS 2010 symposia proceedings is available free of charge for all full conference registrants. This valuable resource offers endless use for future research and educational purposes.

Additional copies of the Collected Proceedings CD-ROM may be purchased in the bookstore and on the registration form and will not be available after the meeting. The cost is \$150, with a special student rate of \$75. All CD-ROMS must be picked up at the meeting. Shipping is not available.

# TMS 2010 Leadership

## TMS 2009-10 Board of Directors

### Executive Committee

#### President:

Ray D. Peterson, *Aleris International Inc.*

#### Past President:

Diran Apelian, *Worcester Polytechnic Institute*

#### Vice President:

George T. "Rusty" Gray III, *Los Alamos National Laboratory*

Garry Warren, *University of Alabama-Tuscaloosa (incoming)*

#### Financial Planning Officer

Stanley Howard, *South Dakota School of Mines and Technology*

### Functional Area Directors

#### Professional Development:

David Shifler, *Office of Naval Research*

#### Membership Student Development

Ellen Cerreta, *Los Alamos National Laboratory*

#### Programming

Hani Henein, *University of Alberta*

#### Public & Government Affairs

Kevin J. Hemker, *Johns Hopkins University*

#### Publications

Elizabeth Holm, *Sandia National Laboratories*

### Technical Division Directors

#### Electronic, Magnetic & Photonic Materials

Zi-Kui Liu, *The Pennsylvania State University*

#### Extraction & Processing

Thomas P. Battle, *Midrex Technologies*

#### Light Metals

John N. Hryn, *Argonne National Laboratory*

#### Materials Processing & Manufacturing

James W. Sears, *South Dakota School of Mines & Technology*

#### Structural Materials

Eric M. Taleff, *University of Texas*

Dennis M. Dimiduk, *Air Force Research Laboratory (incoming)*

## TMS 2010 Annual Meeting Technical Program Committee

### Director/Chairperson:

Hani Henein, *University of Alberta*

### Past Chairperson:

James C. Foley, *Los Alamos National Laboratory*

### Electronic, Magnetic & Photonic Materials

#### Division Representatives:

Long Qing Chen, *The Pennsylvania State University*

Sung K. Kang, *IBM*

Mark A. Palmer, *Kettering University*

### Extraction & Processing

#### Division Representatives:

Boyd R. Davis, *Kingston Process Metallurgy*

Jian Li, *Natural Resources Canada*

### Light Metals

#### Division Representatives:

Alan A. Luo, *General Motors Corp.*

Eric A. Nyberg, *Pacific Northwest National Laboratory*

### Materials Processing & Manufacturing

#### Division Representatives:

Corbett C. Battaile, *Sandia National Laboratories*

Thomas R. Bieler, *Michigan State University*

Amit Misra, *Los Alamos National Laboratory*

### Structural Materials

#### Division Representatives:

Robert J. Hanrahan, Jr., *National Nuclear Security Administration*

Eric Allen Ott, *GE Aviation*

Judy Schneider, *Mississippi State University*



# TMS2010

## 139th Annual Meeting & Exhibition

February 14-18, 2010 • Washington State Convention Center • Seattle, Washington USA



### Exhibition Hours

Monday • noon to 6:30 p.m.  
Tuesday • 10:30 a.m. to 6 p.m.  
Wednesday • 10:30 a.m. to 3 p.m.

### Table of Contents

Exhibiting Companies.....	22
Products and Services Index.....	23
Exhibition Floor Plan.....	25
Company Descriptions .....	26
Sponsors .....	Inside back cover

# EXHIBIT DIRECTORY

# Exhibiting Companies

Exhibiting Companies (as of January 20, 2010)

Company	Booth	Company	Booth
ABB Bomem.....	513	Metallurgical Society of CIM (MetSoc) .....	315
Advanced Dynamics Corporation, Ltd.....	115	Microtrac.....	629
Agilent Technologies.....	404	Mid-Mountain Materials, Inc .....	101
Almeq Norway AS.....	200	Momentum Press .....	221
Aluminum Times.....	511	Nalco .....	516
Aluminium International Journal.....	601	National Institute of Standards & Technology .....	604
ATR National Scientific User Facility.....	623	NIST Technology Innovation Program .....	602
B&P Process Equipment.....	401	NFC.....	421
Brochot.....	337	OKAYA, (USA) Inc.....	218
Buss AG.....	631	OLI Systems, Inc.....	504
BUSS Chem Tech.....	226	Olympus America, Inc.....	210
C A Picard Intl.....	314	Opsis.....	514
CIMM Group Co., Ltd.....	618	Outotec.....	319
Claudius Peters Projects Gmb.....	213	Precimeter.....	201
Colt International.....	434	Proto Manufacturing, Inc.....	519
Computherm.....	428	Riedhammer GmbH.....	215
Coperion GmbH.....	520	Rio Tinto Alcan.....	309
CSM Instruments.....	239	Sente Software, Ltd.....	414
Cytec Industries, Inc.....	332	Shanghai Zhengyu Special Alloys Co., Ltd.....	208
Dantherm Filtration, Inc.....	222	Shimadzu Scientific Instruments, Inc.....	633
DesignMecha Co., Ltd.....	627	STAS.....	509
ECL.....	308	Sunstone.....	230
EDAX, Inc.....	209	Techmo Car S.p.A.....	310
Eirich Machines, Inc.....	312	Thermo-Calc Software, Inc.....	100
ELSEVIER.....	109	Thermo Scientific.....	523
FLSmidth Minerals.....	227	Thermo Scientific Niton Analyzers.....	622
Five Solios.....	409	Windhoff Bahn-und Anlagentechnik GmbH.....	521
Gillespie & Powers, Inc.....	300		
GLAMA.....	318		
Gouda Refractories B.V.....	428		
Harbin Dongshen Metal Co., Ltd.....	535		
Hencon.....	432		
Hertwich Engineering.....	423		
Hydro Aluminum Hycast AS.....	608		
Hysitron.....	400		
Impec AS.....	205		
Innovathem.....	336		
Innov – X Systems.....	209		
International Magnesium Association.....	235		
Jervis B. Webb Company.....	326		
Kabert Industries, Inc.....	435		
Kempe Engineering.....	223		
Life Cycle Engineering.....	534		
Light Metal Age.....	233		
L.P. Royer, Inc.....	505		
Magnesium Elektron.....	437		
Major.....	301		



## Products and Services Index

### Advanced Materials

Compu Therm  
Hysitron  
Magnesium Elektron  
Mid Mountain Materials, Inc.  
NIST Technology Innovation Program  
Proto Manufacturing, Inc.  
Sente Software, Ltd.

### Advanced Processing

Cytec Industries, Inc.  
DesignMecha Co., Ltd.  
FL Smidth Minerals  
Innovatherm  
Momentum Press  
Nalco  
NIST Technology Innovation Program  
Olympus America, Inc.  
Proto Manufacturing, Inc.  
Rio Tinto Alcan  
Sente Software, Ltd.  
Thermal Technology LLC

### Aluminum

Advanced Dynamics Corporation, Ltd.  
Almeq Norway AS  
*ALUMINIUM International Journal*  
*Aluminium Times*  
*Aluminum International Today*  
B&P Process Equipment  
China Nonferrous Metal Industry's Foreign  
Engrg & Construction Co., Ltd. (NFC)  
Claudius Peters Projects GmbH  
ECL  
Farra Engineering, Ltd.  
Fives Solios  
FLSmidth Minerals  
Gouda Refractories B.V.  
Harbin Dongsheng Metal Co., Ltd.  
Hencon  
Hydro Aluminum Hycast AS  
Impec AS  
Industrial Initiatives and Projects  
Jervis B Webb Co.  
Kempe Engineering  
Life Cycle Engineering  
*Light Metal Age*  
LP Royer, Inc.  
Metallurgical Society of CIM (MetSoc)  
Mid Mountain Materials, Inc.  
National Institute of Standards  
and Technology  
OKAYA, (USA) Inc

Opsis  
Outotec Canada, Ltd.  
Riedhammer GmbH  
Rio Tinto Alcan  
Techmo Car SpA  
Thermo Scientific  
Thermo Scientific Niton Analyzers  
Thermo-Calc Software Inc.

### Aqueous Processing

FLSmidth Minerals  
Nalco

### Ceramics

Eirich Machines, Inc.  
Gouda Refractories B.V.  
Hysitron  
National Institute of Standards  
and Technology

### Characterization

CSM Instruments  
Hysitron  
Innov - X Systems  
Micro Materials, Ltd.  
Momentum Press  
Proto Manufacturing, Inc.  
Thermo Scientific  
Thermo Scientific Niton Analyzers

### Composites

Hysitron

### Computer Applications and Process Control

ABB Inc  
Innovatherm  
ProQuest  
Thermo-Calc Software, Inc.

### Copper Nickel and Cobalt

Advanced Dynamics Corporation, Ltd.  
China Nonferrous Metal Industry's Foreign  
Engrg & Construction Co., Ltd. (NFC)  
Metallurgical Society of CIM (MetSoc)  
National Institute of Standards  
and Technology  
Techmo Car SpA  
Thermo Scientific Niton Analyzers  
Thermo-Calc Software, Inc.

### Education

Initiatives Et Projets Industriels SARL  
Life Cycle Engineering  
Momentum Press  
Olympus America, Inc.  
Thermo-Calc Software, Inc.

### Electrometallurgy

ABB Inc  
Industrial Initiatives and Projects  
National Institute of Standards  
and Technology  
Proto Manufacturing, Inc.

### Electronic Materials

ABB, Inc.  
National Institute of Standards  
and Technology

### Energy

Compu Therm  
Life Cycle Engineering  
Nalco  
NIST Technology Innovation Program  
Olympus America, Inc.

### Environmental Effects

ECL  
Nalco  
Opsis  
Rio Tinto Alcan

### Environmental Issues

ECL  
Eirich Machines, Inc.  
Industrial Initiatives and Projects  
Innov - X Systems  
Innovatherm  
Metallurgical Society of CIM (MetSoc)  
Mid Mountain Materials, Inc.  
Nalco  
National Institute of Standards  
and Technology  
Opsis

### Experimental Methods

Hysitron  
Thermal Technology LLC  
Thermo Scientific

# Products and Services Index

## **Extraction and Processing**

B&P Process Equipment  
FL Smidth Minerals  
Kempe Engineering  
Nalco  
Rio Tinto Alcan  
Thermo-Calc Software, Inc.

## **Fundamentals**

Industrial Initiatives and Projects

## **High-Temperature Materials**

Compu Therm  
Gouda Refractories B.V.  
Kabert Industries, Inc.  
Mid Mountain Materials, Inc.  
National Institute of Standards  
and Technology  
Sente Software, Ltd.

## **Iron and Steel**

Advanced Dynamics Corporation, Ltd.  
Hysitron  
Life Cycle Engineering  
Metallurgical Society of CIM (MetSoc)  
National Institute of Standards  
and Technology  
OKAYA (USA), Inc.  
Sente Software, Ltd.  
Thermo Scientific  
Thermo-Calc Software, Inc.

## **Joining**

Thermo-Calc Software, Inc.

## **Lead Zinc and Tin**

Advanced Dynamics Corporation, Ltd.  
China Nonferrous Metal Industry's Foreign  
Engrg & Construction Co., Ltd. (NFC)  
National Institute of Standards  
and Technology  
Techmo Car SpA

## **Lightweight Materials**

ABB Inc  
Advanced Dynamics Corporation, Ltd.  
International Magnesium Association  
*Light Metal Age*  
Magnesium Elektron  
National Institute of Standards  
and Technology  
Sente Software, Ltd.

## **Magnesium**

Advanced Dynamics Corporation, Ltd.  
International Magnesium Association  
*Light Metal Age*  
Magnesium Elektron  
Techmo Car SpA

## **Manufacturing and Markets**

Advanced Dynamics Corporation, Ltd.  
Almeq Norway AS  
C A Picard Intl  
Claudius Peters Projects GmbH  
Coperion GmbH  
CSM Instruments  
DesignMecha Co., Ltd.  
Gouda Refractories B.V.  
Harbin Dongsheng Metal Co., Ltd.  
Hencon  
Industrial Initiatives and Projects  
Innovatherm  
Kempe Engineering  
Life Cycle Engineering  
National Institute of Standards  
and Technology  
NIST Technology Innovation Program  
Olympus America, Inc.  
Outotec Canada, Ltd.  
Rio Tinto Alcan  
SunStone

## **Mechanical Properties**

CSM Instruments  
DesignMecha Co., Ltd.  
Hysitron  
Micro Materials, Ltd.  
Sente Software, Ltd.

## **Minerals**

China Nonferrous Metal Industry's Foreign  
Engrg & Construction Co., Ltd. (NFC)  
Claudius Peters Projects GmbH  
Coperion GmbH  
Cytec Industries, Inc.  
FL Smidth Minerals  
Hencon  
Innov - X Systems  
OKAYA (USA), Inc.

## **Modeling and Simulation**

Advanced Dynamics Corporation, Ltd.  
Compu Therm  
ECL  
NIST Technology Innovation Program  
Thermo-Calc Software, Inc.

## **Molten Metal and Solidification**

Advanced Dynamics Corporation, Ltd.  
Harbin Dongsheng Metal Co., Ltd.  
Hencon  
Hydro Aluminum Hycast AS  
Outotec Canada, Ltd.  
Thermo-Calc Software, Inc.

## **Nanotechnology**

CSM Instruments  
Hysitron  
Micro Materials, Ltd.  
Momentum Press  
National Institute of Standards  
and Technology  
NIST Technology Innovation Program

## **Nontechnical Topics**

DesignMecha Co., Ltd.

## **Nuclear Materials**

National Institute of Standards  
and Technology

## **Other Nonferrous**

Cytec Industries, Inc.  
International Magnesium Association  
OKAYA (USA), Inc.  
Outotec Canada, Ltd.

## **Physical Properties**

Hysitron  
Micro Materials, Ltd.  
National Institute of Standards  
and Technology  
Proto Manufacturing, Inc.  
Sente Software, Ltd.

## **Polymers**

Cytec Industries, Inc.  
Hysitron  
Momentum Press  
Nalco  
National Institute of Standards  
and Technology

## Powder Technology

B&P Process Equipment  
 Claudius Peters Projects GmbH  
 Coperion GmbH  
 Magnesium Elektron  
 Thermal Technology LLC

## Precious Metals

Eirich Machines, Inc.  
 Innov - X Systems

## Process Mineralogy

Claudius Peters Projects GmbH  
 Cytec Industries Inc.

## Pyrometallurgy

China Nonferrous Metal Industry's Foreign  
 Engng & Construction Co. Ltd. (NFC)  
 Metallurgical Society of CIM (MetSoc)

## Recycling and Secondary Recovery

Eirich Machines, Inc.  
 Hencon  
 Kempe Engineering  
 Nalco  
 Thermo Scientific Niton Analyzers

## Shaping and Forming

Gouda Refractories B.V.

## Surface Modification and Coatings

DesignMecha Co., Ltd.  
 Micro Materials, Ltd.  
 Olympus America, Inc.

## Synthesis and Processing

NIST Technology Innovation Program  
 Thermal Technology LLC

## Titanium

Innov - X Systems  
 National Institute of Standards  
 and Technology  
 Techno Car SpA  
 Thermo Scientific  
 Thermo Scientific Niton Analyzers  
 Thermo-Calc Software, Inc.

# Floor Plan

## New on the Exhibit Floor!

### TMS Student Poster Competition

*Exhibit Hall Booth 427*

View posters during the President's  
 Welcoming Reception

Winners will be announced Tuesday at noon.

### General Poster Session

*Exhibit Hall Aisle 100*

During Exhibit Hours

### Lamborghini Viewing

*Exhibit Hall Booth 135*

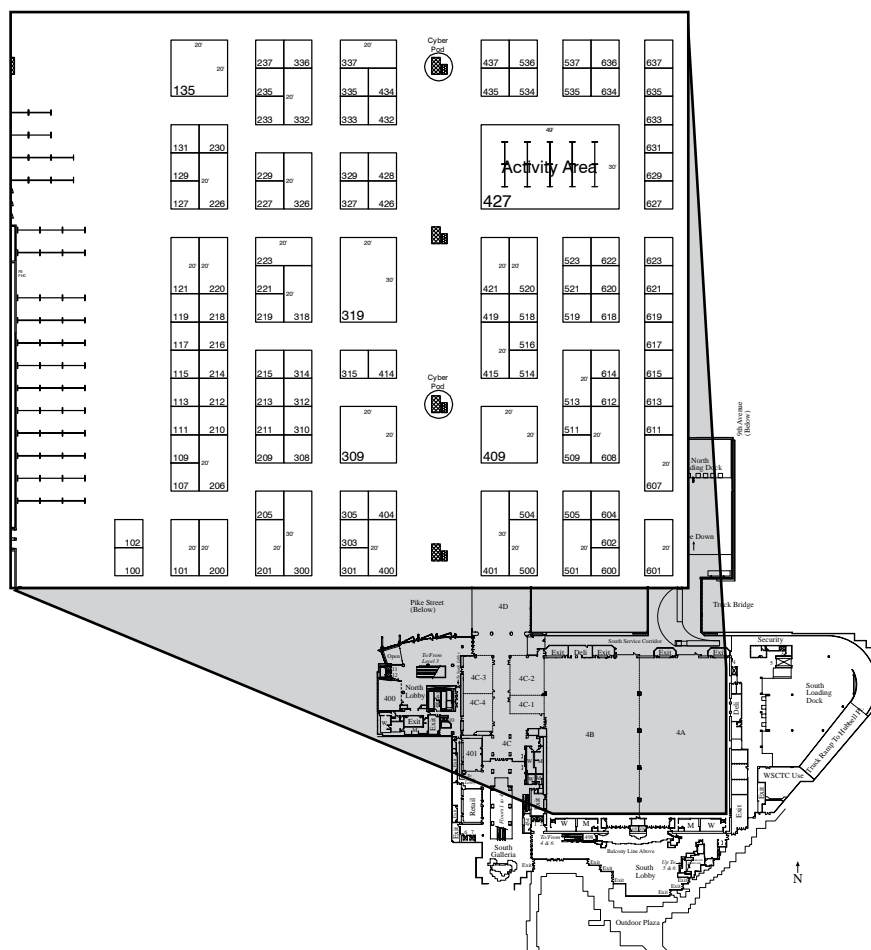
During Exhibit Hours

### President's Welcoming Reception

*Monday from 5 to 6:30 pm*

### Exhibit Hall Happy Hour

*Tuesday from 5 to 6 pm*



# Company Descriptions

**ABB, Inc.** (Quebec, QC Canada)

**Booth # 513 • [www.abb.com/analytical](http://www.abb.com/analytical)**

ABB Analytical Business Unit designs, manufactures and markets high-performance analytical system solutions and spectroradiometers for petroleum, chemical, life science, semiconductor, metallurgy and remote sensing/aerospace markets. Building on its 37 years of experience in analytical instrumentation, the company, through a dedicated team of engineers, offers you the best solutions with its complete range of reliable analytical instruments for inclusions and dissolved hydrogen measurement: AISCAN, LiMCA II, LIMCA CM, Prefil®-Footprinter, PoDFA and Metallographic Analysis Service.

**Advanced Dynamics Corporation, Ltd.** (St. Bruno, QC Canada)

**Booth #426 • [www.advanceddynamics.com](http://www.advanceddynamics.com)**

For over four decades, Advanced Dynamics (ADCL) has supplied our global customer base with state-of-the-art material handling systems for carbon plants and cast houses. Our handling technology includes fully automated or semi-automated equipment for anode handling and cleaning, aluminum ingot and T-Bar handling, sawing and packaging systems. We also have experience in specialty systems for the magnesium, copper, zinc, steel and lead industries.

ADCL is a one-stop shop for your material handling needs, including mechanical and controls engineering, fabrication, assembly, test and commissioning. Whether you need a new system, or upgrades to existing systems, or simply individual pieces of equipment, we can help improve your company's productivity. Remember "our ingenuity delivers productivity" – when you think of ADCL for your next project.

**Agilent Technologies** (Chandler, AZ)

**Booth #404 • [www.agilent.com/fina/nano](http://www.agilent.com/fina/nano)**

**Almeq Norway AS** (Langhus, Norway)

**Booth #200 • [www.almeq.com](http://www.almeq.com)**

ALMEQ Norway AS is an engineering, marketing and production company offering a wide range of equipment to the primary aluminium industry. The focus is on crucible and potshell repair shops. In addition to its own designed equipment, ALMEQ is an exporter and marketing partner for other renowned suppliers.

Among the equipment engineered and produced in Norway are the Crucible Cleaning Machine, Tube Cleaning Machine, Pot Lining Machine, Electric Cathode Preheater, electric drying and preheating systems for crucibles and various potroom equipment.

At TMS 2010, ALMEQ will focus on the Cathode Preheating system and Potlining Machine. We will also display our 3D construction tools, which enable us to show specific details of our equipment.

**Aluminium Times** (Shoreham By Sea, Great Britain)

**Booth #511**

Aluminium Times publishes five times a year, serving primary and secondary aluminium producers, rolling mills and extruders throughout the world. The magazine is free to aluminium operators involved in the purchase chain of equipment and materials.

Aluminium Times promotes, through its editorial pages, the aluminium equipment and consumable supplier with editorial features. Each issue contains news, views, features and both company and people profiles. Aluminium Times publishes the industry wall maps and directories. The Aluminium Primary Smelter Map and Directory, for example, is published each July. Published by Modern Media Communications Limited, two sister magazines are Cast Metal & Diecasting Times and Iron & Steel Today.

**ALUMINIUM International Journal** (Germany)

**Booth #601 • [www.giesel-verlag.de](http://www.giesel-verlag.de)**

**Aluminium International Today** (Great Britain)

**Booth #212 • [www.aluminiumtoday.com](http://www.aluminiumtoday.com)**

ALUMINIUM International, journal for industry, research and applications, is the leading international journal (bilingual: German/English) for more than 80 years. It covers everything that concerns the material, its extraction, processing, recycling and applications. Matters of economics and the ecological consequences of using aluminium are also considered. The scope of the month-by-month reporting includes scientific contributions and condensed information about new technologies and applications. The journal addresses aluminium producers, semis manufacturers, foundries, processors, metal and semis traders and, not least, research institutes concerned with aluminium. ALUMINIUM is circulated in over 40 countries worldwide – made in Germany, distributed to the world.

**ATR National Scientific User Facility** (Idaho Falls, ID)

**Booth #623 • [www.inl.gov](http://www.inl.gov)**

## **B&P Process Equipment** (Saginaw, MI)

**Booth #401 • [www.bpprocess.com](http://www.bpprocess.com)**

B&P Process Equipment (manufacturers of Baker Perkins machinery) is a supplier of specialized process equipment for the production of carbon paste, energetic materials, plastics, industrial chemicals, and for chemical separation. Many pieces built since the 1930s are still in service. In 1952, the aluminum industry production requirements grew, and the continuous kneader became the preferred method of manufacturing carbon paste. Today, our batch mixers and continuous kneaders are used worldwide in the production of carbon paste. B&P also offers a complete line of continuous pusher centrifuges for liquid/solid separation. B&P also has a joint venture with Battaglion S.R.L., headquartered in Bergamo, Italy, for a broad line of mixing equipment.

## **Brochot** (Tremblay-en-France Cedex, France)

**Booth #337 • [www.brochot.fr](http://www.brochot.fr)**

## **Buss AG** (Pratteln, Switzerland)

**Booth #631 • [www.busscorp.com](http://www.busscorp.com)**

## **BUSS ChemTech** (Prattein 1, Switzerland)

**Booth #226 • [www.buss-ct.com](http://www.buss-ct.com)**

## **C A Picard Intl** (Remscheid, Germany)

**Booth #314 • [www.capicard.com](http://www.capicard.com)**

Carl Aug Picard International specializes in the manufacture of high quality wear parts for continuous kneaders for the manufacture of green anodes used in the primary aluminum industry. Picard manufactures kneading teeth, wearing plates/liners and screw flights out of different, highly wear-resistant qualities.

## **China Nonferrous Metal Industry's Foreign Engrg & Construction Co. Ltd. (NFC)** (Beijing, China)

**Booth #421 • [www.nfc.com.cn](http://www.nfc.com.cn)**

Founded in 1983, China Nonferrous Metal Industry's Foreign Engineering & Construction Co., Ltd. (NFC) is a state-owned holding company listed on Shenzhen Stock Exchange. As a leading Chinese enterprise engaged in general contracting of overseas nonferrous metal (particularly in aluminum, copper, zinc and etc.) projects and resources development, it covers a wide spectrum from technical assistance, engineering design, equipment manufacturing, construction, supervision, installation and training to mining, beneficiation, smelting, processing, etc. It has also been listed on ENR as one of the top 225 international contractors and the top 200 international design firms for consecutive years. In 2007, NFC was awarded ISO 9001 Quality Management System certification. In 2008, NFC was awarded ISO 14001 EMS and OHSMS 28001 certification. With competitive edges in technology and rich experience in EPC contracting, NFC has consistently been dedicated to the global nonferrous metal industry, based on long-standing commitment to good faith and innovation, in the pursuit of excellence. NFC is capable and willing to work with world partners by providing a portfolio of services including technologies, equipment supply and project management.

## **CIMM Group Co., LTD** (DaLian, China)

**Booth #618 • [www.cimmuk.com](http://www.cimmuk.com)**

CIMM GROUP is a professional manufacturer, international trade and service provider, and an EPC company engaged in the field of Aluminum, Iron & Steel, Mining and Beneficiation, Petrochemical industry. Our key products are: Aluminum Fluoride, Prebaked Anode, Copper Mould Tube and Material Handling System etc.

### VISION

Based on technology, engineering and EPC project, we envision strengthening energy and resource businesses, integrating business sectors of science, industry and trading, to build up a multinational enterprise group of the first class in the world; embracing the great power of love and friendship, making our contributions to the happier homes of prosperity and peace for mankind.

### MISSION

Let the world share the first-class equipment, technology and services of China; let China share the first-class equipment, technology and services of the world; let the world share the progress and civilization of mankind; let mankind share the peace and prosperity of the world.

## **Claudius Peters Projects GmbH** (Buxtehude, Germany)

**Booth #213 • [www.claudiuspeters.com](http://www.claudiuspeters.com)**

Claudius Peters Projects GmbH, is headquartered in Buxtehude, near Hamburg, Germany, own manufacturing and R&D, with regional offices in the Americas, Europe, China and the Far East. Claudius Peters Projects offers technologies in the field of material handling and processing, together with turnkey and semi-turnkey systems to a wide range of industries such as aluminium, cement, gypsum and other bulk industries and coal grinding plants, coal pulverizing and injection systems for the global steel industry. Claudius Peters Projects GmbH is a wholly subsidiary of Langley Holdings plc, a privately controlled U.K. engineering group.

# Company Descriptions

**Colt International** (Cuijk, Netherlands)

**Booth #434 • [www.coltgroup.com](http://www.coltgroup.com)**

**COLT : YOUR SPECIALIST IN GRAVITY VENTILATION**

Colt is a global supplier and manufacturer of natural and mechanical ventilation systems.

The principal activity of Colt is the supply of specialist products and systems in the field of building services with particular emphasis on gravity ventilation and the environmental control of industrial and commercial buildings. Specially for the aluminium industries, Colt is supplier of Static roof Ventilators and air intake louvers for potroom buildings, anode bake buildings and cast houses.

**Compu Therm** (Madison, WI)

**Booth #428 • [www.compu therm.com](http://www.compu therm.com)**

CompuTherm, LLC, expertise in thermodynamics and kinetics, develops computational tools for industrial applications in the broad field of materials science and engineering. In addition, we provide consulting services to materials industries and collaborate with other institutions working on challenging programs. Current products include Pandat, PanEngine, PanOptimizer, PanPrecipitation, PanAl, PanTi, PanNi, PanFe, PanNb, and PanMg. Pandat is a robust, user-friendly software package for multi-component phase diagram calculations. PanEngine is the engine of Pandat, which can be integrated with user's codes to create custom applications. PanOptimizer is used to optimize thermodynamic, kinetic and thermo-physical model parameters from known experimental or calculated data. PanPrecipitation is a kinetic module designed for simulating precipitation kinetics during heat treatment processes. The last six products are multi-component thermodynamic databases for Al, Ti, Ni, Fe, Nb, and Mg, respectively.

**Coperion GmbH** (Weingarten, Germany)

**Booth #520 • [www.coperion.com](http://www.coperion.com)**

Coperion GmbH is the competent partner for all bulk materials handling solutions around and within the smelter. The company offers solutions to the aluminium producing industry that have proven to be extremely efficient and reliable. The company supports its customers from the first project concept through a wide range of services for realization and the start-up of bulk materials plants. Those services include retrofit solutions and valuable after-sales support. Coperion has the necessary expertise for every process stage along the entire process chain in manufacturing of primary alumina. In each process step, the challenges demand plenty of experience, specialist competence and flexibility.

**CSM Instruments** (Needham, MA)

**Booth #239 • [www.csm-instruments.com](http://www.csm-instruments.com)**

CSM Instruments has been a leader in the development of instruments for advanced materials testing for over 30 years. Our products include hardness testers, scratch testers, and tribometers of varying load ranges. 3D-imaging options are available with the ConScan or AFM objective.

Our focus on research and development helps us to continue our tradition of cutting edge technology and superior performance specifications. We manufacture testing modules that can be configured alone or combined together on a testing platform for a single instrument capable of multiple analysis modes.

In the design of our instruments, we integrate the testing module(s) with imaging module(s) for a seamless testing and imaging process. The modules and microscopes are positioned and synchronized so the instrument automatically moves the point of interest under the appropriate imager with a single click. It also allows us to correlate an optical coating failure (like cracks) to the exact force, depth, and frictional force... that was occurring at that time.

Additionally, we have a thorough sample testing service laboratory.

**Cytec Industries Inc.** (Prairieville, LA)

**Booth #332 • [www.cytec.com](http://www.cytec.com)**

Cytec collaborates with alumina companies to optimize their operations through the delivery of innovative chemical technologies. We utilize our superior application expertise to develop solutions based on our customer's specific needs. We offer technologies that:

- Decrease the cost of operations
- Allow the processing of problematic bauxites
- Prevent or limit employee's exposure to hazards
- Optimize the use of natural resources
- Minimize waste and re-tooling
- Do not require on-staff scientists or engineers

Cytec is committed to partnering with our customers to meet their needs. Our network of technical staff provides on-site technical assistance worldwide. We are dedicated to on-time delivery, even to the worlds harder to reach areas. Our unique approach to servicing our customers has made Cytec the leading provider of reagents to the mining industry.

**DesignMecha Co., LTD** (Asan, Korea South)

**Booth #627 • [www.designmecha.co.kr](http://www.designmecha.co.kr)**

**ECL** (Ronchin, France)

**Booth #308 • [www.ecl.fr](http://www.ecl.fr)**

With more than 60 years experience, ECL is the world leading smelter equipment manufacturer and is 100% dedicated to the Aluminium Industry. ECL offers complete solutions for the smelter's reduction, carbon, and metal sectors.

From design, manufacturing and erection, through training, maintenance, audit, and refurbishment, ECL provides products and services adapted to the needs and demands of its customers for any reduction technology.

A high level of innovation and an unmatched expertise allow ECL to offer solutions for single machines or complete turnkey projects, which help aluminium smelters in their productivity and EHS efforts.

**EDAX Inc.** (Mahwah, NJ)

**Booth #209 • [www.edax.com](http://www.edax.com)**

EDAX provides Results with the Greatest Confidence. EDAX has led the industry as the technical innovator and the world's largest supplier of EDS, EBSD and WDS systems. EDAX integrates these latest technologies in its Trident system. Accurate analytical results require solid foundations and EDAX is the only company to achieve this through Expert ID and the Genesis EDS Apex system. The new Genesis Apex microanalysis system offers superior performance using fundamental physics, rule-based element identification and automated background calculation. EDAX's EBSD Data Collection provides a powerful, easy to use environment for acquiring EBSD data in the SEM. The EBSD Analysis has virtually unlimited potential for interrogating the wealth of information contained in EBSD data. EDAX offers detector solutions to meet all your EBSD needs. The Hikari Detector is a completely integrated CCD-based detector optimized for high speed data collection. Combined with the power of WDS to enhance qualitative and quantitative analysis, EDAX provides today's scientists with the ultimate materials characterization solution, offering vastly improved speed and accuracy.

**Eirich Machines Inc** (Gurnee, IL)

**Booth #312 • [www.eirich.com](http://www.eirich.com)**

Eirich Machines Inc. of Gurnee, Illinois, is a manufacturer of the Eirich Intensive Mixer, noted for the many advantages it provides the metallurgy industries. Eirich has been providing machines and complete plants to the carbon industry for more than 30 years. A constantly growing number of renowned manufacturers of carbon products all over the world are currently using Eirich equipment.

We offer the latest state-of-the-art technology for coke heating, mixing and re-mixing/cooling of pre-bake and Söderberg anode paste. The capacities of our batchwise and continuous systems range from 10 to nearly 60 tons/hour in a single line. Our latest development is the Eirich Intensive Mixing Cascade (EMC) for the all-intensive preparation of anode paste at the lowest cost and the highest efficiency. For more information on our capabilities, please visit us in booth #312.

**ELSEVIER** (New York, NY)

**Booth #327 • [www.elsevier.com](http://www.elsevier.com)**

As the world's leading publisher of science and health information, Elsevier serves more than 30 million scientists, students and health & information professionals worldwide. Elsevier is committed to making genuine contributions to the science and health communities by providing: World-Class Information: Elsevier publishes trusted, leading-edge Scientific, Technical and Medical (STM) information; Global Dissemination: Elsevier disseminates and preserves STM literature to meet the information needs of the world's present and future scientists and clinicians - linking thinkers with ideas; Innovative Tools: Elsevier develops electronic tools that demonstrably improve the productivity and outcomes of those we serve; Working Together: Elsevier works in partnership with the communities we serve to advance scholarship and improve lives. Visit the Elsevier booth #109 to meet our representatives and learn more about our products. For the latest from Elsevier's Materials Science research publications, download our Materials Science RSS feed at: [www.elsevier.com/materials](http://www.elsevier.com/materials).

**Fives Solios** (St Germain En Laye, France)

**Booth #409 • [www.fivesgroup.com](http://www.fivesgroup.com)**

As a leading manufacturer, Fives Solios designs and supplies process equipment and turnkey plants for main aluminum producers worldwide for these areas: Reduction area: gas treatment centers and bath processing plants—Fives Solios is well known for providing high quality equipment in terms of performance, reliability, and ease of maintenance. Carbon area: green anode plants including carbon butts processing and pitch fume treatment systems, pitch storage and processing, and firing systems and fume treatment centers for anode baking furnaces—Fives Solios has also developed innovative solutions such as Rhodax for dry material preparation, IMC for paste preparation, Xelios for anode forming, and Eolios for pitch fume treatment. Cast house area: melting and holding furnaces including water cooling systems as well as integration of downstream casting machines and heat treatment furnaces for rolling mills and associated control systems. For more information on Fives Solios, visit [www.fivesgroup.com](http://www.fivesgroup.com).

# Company Descriptions

**FLSmidth Minerals** (Salt Lake City, UT)

**Booth #415 • [www.flsmidthminerals.com](http://www.flsmidthminerals.com)**

FLSmidth is your major equipment supplier from bauxite mining and refining through calcination and smelting. Every day, worldwide, our equipment crushes, conveys, grinds, digests, clarifies, precipitates, stores, and calcinates bauxite to produce alumina. Combining the respected brand names of MÖLLER, KOCH-MVT, FULLER-TRAYLOR, WEMCO, EIMCO, DORR-OLIVER, PNEUMAPRESS, KREBS, ABON, RAHCO, CEntry, Conveyor Engineering and EXCEL, FLSmidth offers a broad range of equipment and processes while increasing recoveries, lowering energy consumption, and providing proven reliability. We also offer metallurgical testing utilizing the expertise of FLSmidth Dawson's metallurgical laboratories. FLSmidth is your "One Source, One Partner" providing integrated solutions that will save valuable time on project schedules!

**Gillespie & Powers Inc** (St Louis, MO)

**Booth #300 • [www.gillespiepowers.com](http://www.gillespiepowers.com)**

**GLAMA** (Gladbeck, Germany)

**Booth #318 • [www.glama.de](http://www.glama.de)**

**Gouda Refractories B.V.** (Gouda, Netherlands)

**Booth #305 • [www.goudarefractories.com](http://www.goudarefractories.com)**

Gouda Refractories is an innovative refractory producer (refractory bricks, castables, mortar, self-flowing castables, complex pre-cast shapes) with global experience and a long track record of supplying superior quality refractories all over the world, combined with innovative installation technology for more than 100 years. Gouda Refractories develops, manufactures, sells and installs top quality refractory linings. Gouda's solutions play an important role in non-ferrous metal (mainly aluminium), petrochemical, environmental and energy industries. Based on an industry-oriented structure and highly competent employees, Gouda Refractories guarantees an optimal support, which results in efficiency and reduction of refractory cost. Gouda Refractories supplies total solutions to customers which are cost effective, state of the art, and reliable. Gouda's R&D department is conducted in close co-operation with its customers and renowned research institutes. Gouda's quality assurance is based on the international ISO 9001 standard.

**Harbin Dongsheng Metal Co., Ltd.** (Harbin, China)

**Booth #535 • [www.sinodongsheng.com](http://www.sinodongsheng.com)**

We focus on producing aluminium alloying material (hardener) in the aluminium castinghouse. Our products are as follows: Alloying Tablets and Mini-tablet, for the precise compositional adjustment of Mn, Fe, Ti, Cr, Cu and Ni additions to the aluminium bath; Fast Melting Silicon; ALTi,ALV;other Master Alloy. We are the designers of China National Standard of Alloying Tablet. We also have three plants, already one of the biggest alloying tablets producers in China. We are the long term supplier of these famous aluminium companies. Finally, we have the honor to be the raw material supplier of China Shenzhou airship man-in-space flight project.

**Hencon** (Ulft, Netherlands)

**Booth #432 • [www.hencon.nl](http://www.hencon.nl)**

HENCON: Your Global Partner

Backed by more than 50 years of experience, Hencon is a worldwide supplier of services and mobile processing equipment for potroom and cast house. In addition to our main plant located in the Netherlands, Hencon has production and service facilities in South Africa, Mozambique, Russia and India. The delivery program covers the complete range of vehicles and vacuum technology equipment needed in potroom and cast houses. In our booth, you will find our new developments with regards to vehicles that reach the latest HSE standards and contribute to the efficiency of primary smelters and cast houses. You will also find our new product line of vacuum technology solutions (mobile and stationary) for the recovery of valuable materials in processing plants and mines. Our services include the support of (start up) customers complete with know-how, repairs and parts geared to specifics for the maintenance of industrial vehicles in an aluminium production environment. Within the group, Hencon Alumina, along with its partners Alcor Technology and Alfa Laval, is producer and supplier of M2M-Unit, which enables alumina refineries to recover remaining alumina values from bauxite residue.

**Hertwich Engineering** (Toledo, OH)

**Booth #423 • [www.hertwich.com](http://www.hertwich.com)**

**Hydro Aluminum Hycast AS** (Sunndalsora, Norway)

**Booth #608**

Hycast is a subsidiary of Hydro Aluminium. Hycast's principle task is to ensure a leading edge for Hydro Aluminium in melt refining and casting technology. The annual turnover for Hycast approximates USD 16-20 mill. Hycast has extensive expertise in aluminium cast house technology. Key competencies include project management, as well as metallurgical, mechanical and electrical (automotive and process control) engineering. Activities within these areas are performed internally, while supplementary services are recruited from selected external partners. Experience has been gained over several years through collaboration not only with Hydro but also with other aluminium companies in numerous projects world-wide. Many involved turnkey supplies, with Hycast being responsible for supervision, installation, commissioning and testing of all equipment and systems supplied. Technology development projects in cooperation with Hydro's R&D and Cast House Support Departments resulted in further competitive advantages. Beginning in November 2009, Hycast's technology and expertise are also available to customers outside Hydro Aluminium.

**Hysitron** (Eden Prairie, MN)

**Booth #400 • [www.hysitron.com](http://www.hysitron.com)**

As world leader in nanomechanical testing, Hysitron is dedicated to providing testing solutions for nanoscale mechanical characterization. Hysitron's nano-mechanical test instruments provide high-speed in-situ SPM imaging in addition to the quantitative measurement of many mechanical properties, including hardness, modulus, fracture toughness, and wear resistance. Our instruments feature advanced techniques such as nanoDMA<sup>®</sup> for time dependent and viscoelastic materials, Modulus Mapping for quantitative large area property mapping, and nanoECR<sup>®</sup> enabling simultaneous electrical and mechanical property measurements. We are excited to demonstrate the TI 950 Tribolndenter<sup>®</sup> nanomechanical test system featuring 25x faster feedback, a nanoNewton to Newton force range, and an unprecedented <30nN noise floor. Stop by our booth to see how the TI 950 redefines the world of nanomechanical testing. Hysitron will also be showcasing the PI 95 and PI 85 Picolndenter<sup>®</sup>, the truly quantitative depth-sensing indenters capable of direct-observation testing inside a TEM and SEM.

**Impec AS** (Ovre Ardal, Norway)

**Booth #205 • [www.impec.no](http://www.impec.no)**

Impec AS is an innovative supplier of equipment for rodding shops and pot rooms. For more than 30 years, Impec has proven to be a reliable partner for aluminium smelters in operation, maintenance and supplies. We use our experience and process knowledge to design new products based on established technology. This ensures our equipment is designed to fulfill all aspects of rodding shop: process optimization; high quality, reliable products with long lifetimes; low costs in operation and maintenance. Impec has developed and improved a number of new machines all in operation in smelters showing good operation and focus on maintenance. Impec is situated in Norway just outside a Hydro Aluminium smelter. We work on a daily basis with the aluminium industry in Norway, and we are familiar with the industry's demands and needs. The company has so far performed a number of successful projects in the aluminium industry. IMproving Process EffiCiency, the IMPEC way.

**Industrial Initiatives and Projects** (LA BUISSE, France)

**Booth #419**

**Innov - X Systems** (Woburn, MA)

**Booth #206**

Stop by to check out our handheld XRF with automated GPS-XRF. Handhelds (4W) come equipped with weather-proof, ultra-rugged integrated PC control or our classic removable PDA. Optional vacuum (light element) or camera attachments are available. Our Portable Closed-beam X-50 (10W) operates at up to 25 times the power of most handhelds for solids or liquids. Our handhelds and X-50's are available with Si Pin diode or Si Drift detectors. Applications: Geology, Environmental, Metals & Mining, RoHS & Consumer Regulations (Pb, Hg, As, Cr, Cd) and More. Learn about our Academic Relations Grant program. Innov-X: Home of portable XRF for on-site, in-situ analysis of Mg-U; ppm to 100%.

**Innovatherm** (Butzbach, Germany)

**Booth #336 • [www.innovatherm.com](http://www.innovatherm.com)**

**International Magnesium Association** (Wauconda, IL)

**Booth #235 • <http://www.intlmag.org/index.cfm>**

Founded in 1943, the International Magnesium Association (IMA) is the global voice of the magnesium industry. Its mission is to promote the use of the metal magnesium and to educate both manufacturers and consumers about the numerous options and benefits metal magnesium provides. IMA's members consist of: primary producers of the metal and its alloys, recyclers, foundries, fabricators, end users and suppliers. The IMA serves the industry and its membership through its Annual World Magnesium Conference and other workshops and seminars held worldwide. Other services include: industry advocacy, statistical programs and publications.

**Jervis B Webb Co** (Farmington, MI)

**Booth #326 • [www.jerviswebb.com](http://www.jerviswebb.com)**

Webb Aluminium Group, an alliance comprised of Jervis B. Webb Worldwide Company, Webb Australia and Webb-India, has more than 50 years experience providing turnkey systems for aluminium carbon plant production. Our global workforce and advanced technology has made us a leading provider for aluminium companies such as Alcoa, BHP Billiton, Norsk Hydro, Rio Tinto and more. Whether you're constructing a new facility or upgrading an existing plant, Webb Aluminium Group will work with you to design a system that meets your specific needs. We offer cost-effective products and services for your entire carbon plant - from the paste plant to the baking furnace to the rodding shop. Webb Aluminium Group is your single-source supplier for carbon plant production systems.

**Kabert Industries Inc** (Villa Park, IL)

**Booth #435 • [www.kabert.com](http://www.kabert.com)**

# Company Descriptions

## **Kempe Engineering** (Geelong, VIC Australia)

**Booth #223 • [www.kempe.com.au](http://www.kempe.com.au)**

Kempe is the largest provider of asset and maintenance services in the aluminium smelting industry. Kempe has the most extensive product range for the aluminium smelting industry and is one of the top five global suppliers. Kempe works for 30 smelters in 20 countries across 7 regions - Australasia, Middle East, Africa, Asia, Europe, North America and South America. Kempe has in-house manufacturing in Australia, China, UAE & Mozambique and in-house construction crews & equipment. With 2,000 employees globally, Kempe supplies products and turnkey projects for Anode Handling & Cleaning, Rodding Shops, Butt Cleaning (hot & cold), Bath Cooling & Processing, plus other Carbon, Potroom & Casthouse equipment.

## **Life Cycle Engineering** (Charleston, SC)

**Booth #534 • [www.lce.com](http://www.lce.com)**

Life Cycle Engineering (LCE) is a leading provider of reliability consulting, engineering services and applied technology solutions that help both government and private enterprises achieve sustainable success. Widely recognized as the premier provider of innovative and successfully executed reliability and maintenance solutions worldwide, areas of focus for LCE include: design and engineering, logistics support, information technology applications, program management, change management, education, and holistic implementations of Reliability Excellence (Rx). Founded in 1976, LCE is headquartered in Charleston, South Carolina, with offices across North America. For more information, please visit our Web site at [www.LCE.com](http://www.LCE.com) or call (843) 744-7110.

## **Light Metal Age** (South San Francisco, CA)

**Booth #233 • [www.lightmetalage.com](http://www.lightmetalage.com)**

Light Metal Age is the pre-eminent magazine of the light metal world. For over 68 years, Light Metal Age has covered primary production and semifabrication of the light metals. The majority of editorial coverage is of aluminum processing and production, but also includes magnesium and titanium. Circulation is international and goes to primary and secondary smelters; casthouses; extrusion operations; rolling mills; sheet, rod, and wire mills; and foundries. Recipients are executives, general managers, plant managers, technicians, metallurgists, chemists, and engineers responsible for fabrication, production, and operations. Some of the editorial topics covered in Light Metal Age include: anode plant; potline technology; smelter/casthouse expansions; secondary aluminum processing and recycling; metallurgy; plant upgrades; metal quality; die design and simulation; rolling mill technology; energy, sustainability, and the environment; and markets and applications. For more information, visit Light Metal Age on the web at: [www.lightmetalage.com](http://www.lightmetalage.com).

## **LP Royer, Inc.** (Lac-Drolet, QC Canada)

**Booth #505 • [www.lproyer.com](http://www.lproyer.com)**

For all workers in the metallurgical industry, L.P. Royer, celebrating its 75th anniversary, is your "one stop" supplier for specialized and innovative safety footwear. L.P. Royer's specialized safety footwear, including our renowned smelter boots, are designed for ultimate performance in the multiple environment of your industry. The XPAN® soling technology, unique to L.P. Royer in North America, adds to the mix to bring you a lighter dual density rubber sole that protects from heat and extreme cold and offer superior traction, shock absorption and durability. With our wide range of adapted protection, including internal and external metatarsal protection, men and ladies styles, plus extra wide, you will find the best style for you. L.P. Royer products meet CSA ASTM quality standards and CE Marking.

## **Magnesium Elektron** (Madison, IL)

**Booth #437 • [www.magnesium-elektronusa.com](http://www.magnesium-elektronusa.com)**

Magnesium Elektron is a leading supplier of high performance magnesium wrought alloys, sand casting and die casting alloys, powders for numerous applications, recycling services and light metal-related technologies. A division of the Luxfer Group, Magnesium Elektron has 7 manufacturing sites located in North America and Europe and supplies the aerospace, military, commercial and transportation markets. Magnesium Elektron's alloy innovation and collaboration with the US Army has recently led to the establishment of the first Magnesium Armor/Ballistic Plate specification (MIL-DTL-32333). Magnesium Elektron will be promoting several new magnesium alloys in various forms including casting alloy Elektron 21, and wrought alloys WE43 and Elektron 675 in rolled form.

## **Metallurgical Society of CIM (MetSoc)** (Montréal, QC Canada)

**Booth #315 • [www.metsoc.org](http://www.metsoc.org)**

## **Microtrac** (Montgomeryville, PA)

**Booth #629 • [www.microtrac.com](http://www.microtrac.com)**

## **Mid Mountain Materials Inc** (Vancouver, WA)

**Booth #101 • [www.mid-mountain.com](http://www.mid-mountain.com)**

**Momentum Press** (Bahama, NC)

**Booth #221 • [www.momentumpress.net](http://www.momentumpress.net)**

Momentum Press was founded in 2007 on the principle of providing the very best information and knowledge on today's advancements in science, engineering, and applied technology. Its aim is to reach practitioners, researchers, educational faculty, and students in engineering, science, and industry with both traditional print media, as well as new, innovative electronically-delivered content. Momentum Press intends to reach those goals by offering its authors and customers a happy alternative to the often impersonal publishing environment so often encountered among today's ever-larger media conglomerates. Momentum Press publishes original scientific and engineering content, with a focus on the North-American, English language market, but with distribution and market presence worldwide. We have sales offices throughout the world, with a particularly strong presence in Asia, North America, and Latin America, as well as Europe and the Middle East.

**Nalco** (Naperville, IL)

**Booth #516 • [www.nalco.com](http://www.nalco.com)**

As the global leader in Process & Water Treatment, Nalco Company provides essential expertise to the Alumina / Aluminum industry with technically, economically and environmentally sustainable solutions from mine-to-mill. Nalco's on-site, trained engineers help our customers achieve their goals by selecting and implementing optimal water and process technologies to increase recoveries and improve finished product quality, while providing the lowest overall total cost of operation.

**National Institute of Standards and Technology** (Gaithersburg, MD)

**Booth #604 • [www.nist.gov/srm](http://www.nist.gov/srm)**

**NFC** (Beijing, China)

**Booth #607 • [www.nfc.com.cn](http://www.nfc.com.cn)**

**NIST Technology Innovation Program** (Gaithersburg, MD)

**Booth #602 • <http://nist.gov/tip>**

The Technology Innovation Program (TIP), at the National Institute of Standards and Technology, supports, promotes, and accelerates innovation in the United States by funding high-risk, high-reward research in areas of critical national need. TIP was established as an early stage innovation cost-shared R&D funding program to assist U.S. businesses and institutions of higher education or other organizations, such as national laboratories and nonprofit research institutions, pursue transformational research in areas of critical national need identified by TIP. These areas need government attention because the magnitude of the problem is large and societal challenges are not being sufficiently addressed. Single company projects may receive up to \$3 million of TIP funding and Joint Venture projects up to \$9 million. Subject to funding, TIP anticipates issuing a call for proposals in early 2010. More information about TIP may be found on the web at <http://nist.gov/tip>.

**OKAYA (USA) Inc** (Rosemont, IL)

**Booth #218 • <http://www.okayausa.com/>**

We specialize in producing all kinds of alloying tablets. We are continuing to improve, modernize and expand our company's production capacity in order to increase productivity and efficiency. This year, we obtained one of the biggest Mn ore mines in Jingxi County, Guangxi province of China. The capacity of this Mn ore mine is more than 3 million tons and our new production line of Mn flakes has also been completed. The new capacity is 30,000 tons per year. By combining the development of these programs with our state-of-the-art production management, technologies and facilities, we can guarantee enough raw material supply at very competitive prices, while also maintaining our high level of quality. Information about our partners: Okaya (U.S.A.), Inc., is an international trading house that provides representation in North America for Chongqing Runji Alloy Company, LTD. This partnership is an example of Okaya's expansion of our business domain from its core area of iron and steel to various related fields of business. We can also perform marketing, logistics and processing functions to fulfill our role as the "Best Global Sourcing Partner." As an independent trading company with a high level of flexibility, Okaya will continue to propose insightful and creative business opportunities by looking at various areas with a broad perspective. Also visit us online at [www.okaya.co.jp/en](http://www.okaya.co.jp/en)

**OLI Systems, Inc.** (Morris Plains, NJ)

**Booth #504**

**Olympus America Inc.** (Orangeburg, NY)

**Booth #210 • [www.olympusamerica.com](http://www.olympusamerica.com)**

Olympus Scientific Equipment Group - Industrial Microscopes Olympus is a leader in industrial microscopy, with its recognized innovation, optical quality, customer support and training. Olympus industrial microscopes and metrology systems play a vital role in precision R&D, engineering and manufacturing applications in fields as diverse as the aerospace, automotive, electronics, materials science/metallurgy, medical device, photovoltaics, and semiconductor arenas. A newly expanded nationwide service, training and support network enhances the company's dedication to client partnership, helping customers achieve even greater success. Olympus systems are designed and manufactured according to rigorous ISO 9001 and ISO 14001 international standards, demonstrating a commitment to offering the highest quality products and services, with minimal environmental impact. Visit us at [www.olympusamerica.com/industrialmicroscopes](http://www.olympusamerica.com/industrialmicroscopes)

# Company Descriptions

**Opsis** (Furulund, Sweden)

**Booth #514 • [www.opsis.se](http://www.opsis.se)**

Opsis is a worldwide supplier of gas monitoring systems for industrial emissions and process applications and ambient air and industrial fence line monitoring applications. For 20 years, Opsis has provided the aluminium smelter industry automatic monitoring systems for potroom and duct measurements of Hydrogen Fluoride (HF) and also other components such as sulfur dioxide, nitrogen dioxide, carbon monoxide, carbon dioxide, VOC's and others. Opsis systems use open path UV, FTIR and TDL technologies. Monitoring solutions are provided as integrated systems including gas measurements, additional sensors such as flow and temperature and software applications for reporting and networking. For open path measurements in the potroom roof vent, potroom instability can cause alignment issues. The Opsis monitoring technology features optional automatic alignment function of the telescopes that will keep the optical paths optimized at all times. Opsis has a worldwide network of technically skilled distributor companies.

**Outotec Canada Ltd** (Burlington, ON Canada)

**Booth #319 • [www.outotec.com](http://www.outotec.com)**

**PreciMeter** (Tempe, AZ)

**Booth #201 • [www.precimeter.com](http://www.precimeter.com)**

**Proto Manufacturing Inc.** (Ypsilanti, MI)

**Booth #519 • [www.protoxrd.com](http://www.protoxrd.com)**

**Riedhammer GmbH** (Nuernberg, Germany)

**Booth #215 • [www.riedhammer.de](http://www.riedhammer.de)**

Since 1925, the company has specialized in the design, construction and commission of highly productive, state-of-the-art Ring Pit Furnaces for baking of first quality anodes and cathodes for the aluminum industry as well as electrodes for the steel industry: more than 185 baking furnaces, in 25 different countries were built or modernized based on this concept. Our reference list includes the major players in the production of primary aluminum with pre-baked technology as well as the top suppliers of electrodes for the steel industry. Beginning in 2004, the Italian Group SACMI acquired 90% of the Riedhammer shares (subsequently increased to 95%). One essential consequence of this association was the development of important synergies between both companies, increasing our technical potentialities and strengthening the financial backup necessary for facing increasing market demands. With the acquisition of the Alesa Anode Baking technology in 2005, Riedhammer continues to advance towards technological maturity and market consolidation to become the only independent supplier worldwide capable to implement anode baking plants with both open and closed top furnaces.

**Rio Tinto Alcan** (Montreal, QC Canada)

**Booth #309 • [www.riotintoalcan.com](http://www.riotintoalcan.com)**

Building on more than a century of experience and expertise, Rio Tinto Alcan is the global leader in the aluminium industry. We supply high quality bauxite, alumina and aluminium worldwide and our AP smelting technology is the industry benchmark. Our enviable hydroelectric power position delivers significant competitive advantages in today's carbon-constrained world. Rio Tinto Alcan is the aluminium product group of Rio Tinto, a leading international business involved in each stage of metal and mineral production. The Group is listed on the London Stock Exchange and Australian Securities Exchange under the symbol RIO. Rio Tinto's major products are aluminium, copper, diamonds, coal, iron ore, uranium, gold and industrial minerals.

**Sente Software Ltd** (Guildford, Surrey Great Britain)

**Booth #414 • [www.sentesoftware.co.uk](http://www.sentesoftware.co.uk)**

**Shimadzu** (Columbia, MD)

**Booth #633 • [www.ssi.shimadzu.com](http://www.ssi.shimadzu.com)**

**STAS** (Chicoutimi, QC Canada)

**Booth #509 • [www.stas.com](http://www.stas.com)**

**SunStone** (Beijing, China)

**Booth #230 • <http://www.sun-stone.com>**

SunStone was established in 1998 and is registered with independent corporate status. The headquarters is in Beijing, but there are branch agencies in Tianjin, in Kunshan Jiangsu Province, and Tehran, Iran. Sun Stone also has sister companies in Korea, India and Turkey. We focus on import & export business, domestic business and processing business of Prebaked Carbon Anode and other raw materials and equipments of Aluminum Smelter.

**Techmo Car SpA** (Limena Padova, Italy)

**Booth #310 • [www.techmo.it](http://www.techmo.it)**

Techmo is an Italian independent company focused in the engineering and production of special mobile and stationary equipment for the aluminium and nonferrous metals industry. The full range of purpose designed machines covers different types of equipment performing a large number of operations in pot-rooms, rodding shops and cast-houses. The Company's aim is to provide the most innovative, rational, cost effective and user friendly technical solutions. Among the most significant families of mobile equipment are the Multipurpose Anode Changers, Tapping Vehicles, Crust Breakers, Anode Transporters, Crucible Transporters and Tilters, Alumina/ AlF<sub>3</sub> Feeding Vehicles, Furnace Charging Vehicles and Furnace Tending Vehicles. Beside its line of purposed designed vehicles, Techmo provides a number of stationary equipment such as Crucible Cleaning Machines, the Crucible Tilting stations and the Anode Butts Cleaning Stations.

**Thermo Scientific** (Madison, WI)

**Booth #523 • [www.thermofisher.com](http://www.thermofisher.com)**

**Thermo Scientific Niton Analyzers** (Billerica, MA)

**Booth #622 • [www.thermo.com/niton](http://www.thermo.com/niton)**

When it comes to the accurate analysis of metal alloys, Thermo Scientific Niton XRF analyzers set the industry standard. With a unique library of 400-plus alloy grades, our handheld XRF instruments provide immediate, nondestructive chemical analysis of aluminum, titanium, and nickel alloys, as well as superalloys, stainless steel, and other metals. These analyzers deliver superior performance in the form of faster analysis, lower detection limits and unparalleled analytical precision. This can mean decreased potential for material mix-ups, as well as instant recovery of lost traceability. Using the Niton® XL3 with GOLDD technology, you not only gain rapid grade identification and lab-quality composition, but also improvements in light element detection, overall sensitivity, and measurement times.

**Thermo-Calc Software Inc** (McMurray, PA)

**Booth #100 • [www.thermocalc.com](http://www.thermocalc.com)**

Thermo-Calc Software is a leading developer of software and databases for calculations involving computational thermodynamics and diffusion controlled simulations. Thermo-Calc is a powerful tool for performing thermodynamic calculations for multi-component systems. Calculations are based on thermodynamic databases produced by expert evaluation of experimental data. Databases are available for steels, Ti, Al, Ni-superalloys and other materials. Programming interfaces are available which enable Thermo-Calc to be called directly from in-house developed software or MatLab. DICTRA is used for accurate simulations of diffusion in multi-component alloys. Applications include: homogenization of alloys, microsegregation during solidification, coarsening of precipitates, and welding.

**Windhoff Bahn-und Anlagentechnik GmbH** (Rheine, Germany)

**Booth #521 • [www.windhoff.de](http://www.windhoff.de)**





# SIMPLIFIND

Tap into the incredible network of **The Minerals, Metals & Materials Society** with The Minerals, Metals & Materials Society Marketplace. Powered by MultiView, the Guide gives materials and metallurgy professionals a faster and easier way to find great vendors.

Simplifind your search today at  
[tmsmarketplace.com](http://tmsmarketplace.com).

**TMS**



# TMS2010

## 139th Annual Meeting & Exhibition

February 14-18, 2010 • Washington State Convention Center • Seattle, Washington USA



# TECHNICAL PROGRAM

### Table of Contents

Program-at-a-Glance.....	2
Sunday PM.....	10
Monday AM.....	33
Monday PM.....	82
Tuesday AM.....	133
Tuesday PM.....	183
Wednesday AM.....	237
Wednesday PM.....	283
Thursday AM.....	333
Posters.....	375
Index.....	397



Page	Room	Sun.		Mon.		Tue.		Wed.		Thur.	
		AM	PM	AM	PM	AM	PM	AM	PM	AM	PM
<b>2010 Functional and Structural Nanomaterials: Fabrication, Properties, Applications and Implications</b>											
283	214								X		
33	214		X								X
333	214										
82	214		X	X	X	X	X	X	X	X	X
10	214		X	X	X	X	X				
133	214										
183	214						X				
237	214							X			
<b>Advanced Materials and Fuels Enabling Future Fusion, Fission and Hybrid Reactor Systems</b>											
285	3A								X		
334	3A										X
<b>Advances in Composite, Cellular and Natural Materials</b>											
83	305				X						
286	305								X		
238	305							X			
134	305					X					
185	305						X				
34	305		X								
11	305	X	X	X	X	X	X	X	X	X	X
<b>Alternative Energy Resources for Metals and Materials Production Symposium</b>											
239	310								X		
<b>Alumina and Bauxite</b>											
336	611										X
287	612								X		
84	611				X						
135	611					X					
288	611								X		
186	611										
240	611								X		
<b>Aluminum Alloys: Fabrication, Characterization and Applications</b>											
35	615									X	
289	615										X
241	615								X		
187	615									X	
85	615					X					
11	615	X	X	X	X	X	X	X	X	X	X
136	615						X				

# At-A-Glance

Page	Room	Sun.		Mon.		Tue.		Wed.		Thur.	
		AM	PM	AM	PM	AM	PM	AM	PM	AM	PM
<b>Aluminum Reduction Technology</b>											
86	608			X							
87	609			X							
188	608					X					
290	608							X			
243	608							X			
244	614							X			
336	608									X	
138	608					X					
337	615										X
<b>Aluminum Rolling</b>											
Session I											
<b>Biological Materials Science</b>											
37	205										
89	205			X							
338	205										X
139	205					X					
190	205							X			
245	205									X	
13	205		X	X	X	X	X	X	X	X	X
291	205										X
<b>Bulk Metallic Glasses VII</b>											
140	213					X					
191	213						X				
246	213							X			
339	213										X
292	213									X	
38	213			X							
90	213					X					
<b>Carbon Dioxide and Other Greenhouse Gas Reduction Metallurgy - 2010</b>											
142	310						X				
<b>Carbon Management and Carbon Dioxide Reduction</b>											
294	310								X		
<b>Cast Shop for Aluminum Production</b>											
295	609									X	
248	609								X		
193	609							X			
143	609						X				
341	609										X



Page	Room	Sun.		Mon.		Tue.		Wed.		Thur.	
		AM	PM	AM	PM	AM	PM	AM	PM	AM	PM
<b>Characterization of Minerals, Metals and Materials</b>											
144	307					X					
296	307								X		
194	307						X				
40	307			X							
92	307				X						X
342	306								X		
349	307										X
343	307										X
15	307		X		X		X		X		X
<b>Coatings for Structural, Biological, and Electronic Applications</b>											
93	309				X						
196	309								X		
146	309						X				
41	309			X							
<b>Computational Thermodynamics and Kinetics</b>											
43	308			X							
94	308				X						
251	308								X		
19	308		X		X		X		X		
147	308						X				
197	308								X		
<b>Cost-Affordable Titanium III</b>											
252	618								X		
297	618									X	
96	618				X						
44	618			X							
148	618						X				
198	618							X			
<b>Electrode Technology for Aluminum Production</b>											
298	616									X	
253	616								X		
97	616				X						
149	616						X				
344	616										X
200	616							X			
<b>Electrometallurgy - General Session</b>											
98	310				X						
<b>Energy Conservation in Metals</b>											
201	310							X			
<b>Failure of Small-Scale Structures</b>											
99	206				X						
150	206						X				
202	206								X		
45	206			X							

# At-A-Glance

Page	Room	Sun.		Mon.		Tue.		Wed.		Thur.	
		AM	PM	AM	PM	AM	PM	AM	PM	AM	PM
<b>Federal Funding Workshop</b>											
<b>General Abstracts: Electronic, Magnetic and Photonic Materials Division</b>											
299	602							X			
300	308							X			
345	308									X	
346	310									X	
<b>General Abstracts: Light Metals Division</b>											
254	607					X					
301	607							X			
347	607									X	
<b>General Abstracts: Materials Processing and Manufacturing Division</b>											
349	606										X
256	601						X				
302	601								X		
46	611		X								
<b>General Abstracts: Structural Materials Division</b>											
350	601										X
203	3A						X				
48	608		X						X		
257	3A										
<b>General Poster Session</b>											
375	Exhibit Hall				X	X	X	X	X		
<b>Global Innovations in Manufacturing of Aerospace Materials: The 11th MPMD Global Innovations Symposium</b>											
151	306					X					
100	306				X						
304	306									X	
258	306								X		
205	306						X				
49	306		X								
21	306		X	X	X	X	X	X	X		
<b>Heterogeneous Nucleation and Initial Microstructure Evolution in Alloys and Colloids</b>											
153	614						X				
206	614							X			
50	614		X								
102	614				X						
<b>Hume-Rothery Symposium: Configurational Thermodynamics of Materials</b>											
52	212		X								
103	212			X							
154	212				X						
207	212					X					
260	212							X			
305	212								X		



Page	Room	Sun.		Mon.		Tue.		Wed.		Thur.	
		AM	PM	AM	PM	AM	PM	AM	PM	AM	PM
<b>Hydrometallurgy - General Session</b>											
Session I											
52	310		X								
<b>International Symposium on High-Temperature Metallurgical Processing</b>											
Ceramics and Intermetallics					X						
104	619			X							
Innovations in Ironmaking							X				
53	619										
Secondary Processing											
155	619										
Smelting and Reduction Processes											
208	619										
<b>Jim Evans Honorary Symposium</b>											
Beyond Berkeley Times											X
352	620										
Cast Shop Aluminum Production Joint Session: Flow and Solidification Phenomena in Nonferrous Casting					X						
105	620										
Electrochemical Phenomena											X
306	619										
Flow Phenomena in Steel Continuous Casting			X								
55	620										
Flow, Solidification, and Inclusion Behavior in Casting Processes							X				
156	620										
Metal Flow, Bubbles, and Inclusions Behavior in Refining and Reduction Vessels											X
210	620										
Modeling											X
307	620										
Poster Session		X	X	X	X	X	X	X	X	X	X
22	620										
Primary and Secondary Production of Metals											X
261	620										
<b>Magnesium Technology 2010</b>											
Cast Alloys, Casting, and Grain Refinement											X
262	613										
Coatings and Corrosion							X				
157	612										
Creep, Relaxation, Recovery, and Recrystallization							X				
159	613										
Deformation Mechanisms											X
263	612										
Effects of Heat Treatment and Casting Process											X
308	613										
Fatigue, Failure, and Wear											X
211	613										
Forming and Welding											X
353	613										
ICME I (Integrated Computational Materials Engineering)					X						
106	612										
ICME II and Biomedical Applications											X
354	612										
Magnesium - Rare Earth Alloys											X
212	612										
Plenary Session			X								
56	612										
Poster Session		X	X	X	X	X	X	X	X	X	X
22	612										
Primary Production and Flammability Issues											X
108	613										
<b>Materials in Clean Power Systems V: Clean Coal, Hydrogen Based-Technologies, Fuel Cells, and Materials for Energy Storage</b>											
Batteries and Others											
356	212										X
Materials for Clean Coal Power and CCS Systems I			X								
57	211										
Materials for Clean Coal Power and CCS Systems II					X						
109	211										
Materials for Hydrogen Production, Storage, and Distribution							X				
160	211										
PEM and Batteries											X
357	211										
SOFC I											X
214	211										
SOFC II											X
265	211										
SOFC, PEM and DMFC											X
310	211										
<b>Materials Processing Fundamentals</b>											
Deformation Processing and Heat Treatment											
110	601										
Process Modeling and Measurements										X	
162	601										
Smelting, Refining, Aqueous and Liquid Processing											X
215	601										
Solidification and Casting											X
58	601										

# At-A-Glance

	Page	Room	Sun.		Mon.		Tue.		Wed.		Thur.	
			AM	PM	AM	PM	AM	PM	AM	PM	AM	PM
<b>Mechanical Performance for Current and Next-Generation Nuclear Reactors</b>												
Advances in Mechanical Testing	60	201			X							
Advances in Modeling for Reactor Conditions	163	201				X						
Ensuring Lifetime and Reliability	112	201			X							
Microstructure and Nanostructure in Reactor Environments	216	201					X					
<b>Modeling of Multi-Scale Phenomena for Batteries</b>												
Session I	266	604							X			
<b>Modeling, Simulation, and Theory of Nanomechanical Materials Behavior</b>												
Nanindentation and Contact Mechanics	358	304									X	
Nanotubes, Soft Materials and Biomedical Applications	218	304					X					
Physics of Defects, Dislocation Nucleation and Fracture I	267	304							X			
Physics of Defects, Dislocation Nucleation and Fracture II	311	304								X		
Plasticity and Strength of Nanostructured and Nanoscale Materials I	61	304		X								
Plasticity and Strength of Nanostructured and Nanoscale Materials II	113	304		X								
Plasticity and Strength of Nanostructured and Nanoscale Materials III	165	304				X						
<b>Neutron and X-Ray Studies of Advanced Materials III</b>												
2D Materials Science from Diffraction	114	303			X							
Applications of Line Profile Analysis	219	303				X						
Diffraction Analysis of Alloys	359	303									X	
Diffuse Scattering I	166	303					X					
Diffuse Scattering II	312	303								X		
Poster Session	25	303	X	X	X	X	X	X	X	X	X	X
Strain and Dislocation Gradients from Microdiffraction I	62	303		X								
Strain and Dislocation Gradients from Microdiffraction II	268	303							X			
Structure from Diffraction	64	613		X								
<b>Nuclear Energy: Processes and Policies</b>												
Characterization	314	201								X		
Material Behavior	270	201							X			
Material Development	362	201									X	
<b>Pb-Free Solders and Emerging Interconnect and Packaging Technologies</b>												
Alloy Development	271	204								X		
Electromigration	66	204			X							
Mechanical Behavior, Failure Mode	116	204				X						
Microstructure, Intermetallics, Whisker (I)	363	204									X	
Microstructure, Intermetallics, Whisker (II)	315	204								X		
Poster Session	25	204	X	X	X	X	X	X	X	X	X	X
Reliability (I)	168	204					X					
Reliability (II)	221	204						X				
<b>Phase Stability, Phase Transformations, and Reactive Phase Formation in Electronic Materials IX</b>												
Session I	68	203			X							
Session II	117	203				X						
Session III	170	203					X					
Session IV	223	203						X				



Page	Room	Sun.		Mon.		Tue.		Wed.		Thur.	
		AM	PM	AM	PM	AM	PM	AM	PM	AM	PM
<b>Polymer Nanocomposites</b>											
272	309							X			
364	309								X		
317	309									X	
<b>Processing Materials for Properties</b>											
69	617		X								
171	617				X						
119	617			X							
274	617						X				
224	617					X					
366	617									X	
318	617								X		
<b>Recycling General Sessions</b>											
275	206							X			
320	206								X		
<b>Refractory Metals 2010</b>											
172	2A					X					
70	2A		X								
120	2A			X							
<b>Solar Cell Silicon: Production and Recycling</b>											
71	2B			X							
<b>Solid-State Interfaces: Toward an Atomistic-Scale Understanding of Structure, Properties, and Behavior through Theory and Experiment</b>											
72	602			X							
226	602						X				
173	602					X					
227	602						X				
321	602				X						
122	602									X	
<b>Stochastic Methods in Materials Research</b>											
322	614									X	
367	614										X
<b>Surface Engineering for Amorphous, Nanocrystalline-, and Bio-Materials</b>											
27	604		X	X	X	X	X				
74	604			X							
123	604				X						
175	604					X					
227	604						X				

# At-A-Glance

	Page	Room	Sun.		Mon.		Tue.		Wed.		Thur.	
			AM	PM	AM	PM	AM	PM	AM	PM	AM	PM
<b>Sustainable Materials Processing and Production</b>												
Measuring Sustainability	229	2B						X				
Motivating Sustainability I	124	2B			X							
Motivating Sustainability II	176	2B				X						
Sustainability in Education	323	2B							X			
Sustainable Technologies I	276	2B							X			X
Sustainable Technologies II	369	2B										
<b>The Aluminium Industry – Perspectives on our Future</b>												
Session I	75	Ballrm. 6A			X							
<b>The Vasek Vitek Honorary Symposium on Crystal Defects, Computational Materials Science and Applications</b>												
Computational Materials Science I	76	603			X							
Computational Materials Science II	125	603			X							
Crystal Defects and Mechanical Properties	324	603							X			
Dislocations I	177	603				X						
Dislocations II	327	604							X			
Grain Boundaries and Grain Boundary Engineering	370	604									X	
Grain Boundaries and Interface Structure and Properties: Joint Session with Solid-State Interfaces	278	603							X			
Grain Boundaries, Dislocations and Mesoscopic Modeling	372	603									X	
Mechanical Properties	230	603					X					
Poster Session	27	603	X	X	X	X	X	X	X	X	X	X
<b>Thermo-Mechanical Response of Molecular Solids: Multi-Resolution Theory, Simulations, and Experiments</b>												
Molecular Solids I	328	203								X		
Molecular Solids II	373	203									X	
Polymers and Composites	279	203							X			
<b>Three-Dimensional Materials Science VI</b>												
3D Representative Volume Elements and Simulated Microstructures	232	401						X				
Applications of 3D Microstructural Data	179	401				X						
Novel Tools for 3D Data Acquisition and Analysis - Part I	280	401					X			X		
Novel Tools for 3D Data Acquisition and Analysis - Part II	330	401								X		
Processing and Analysis of Large 3D Datasets	127	401				X						
Three-Dimensional Crystallography and Grain Boundary Analysis	77	401			X							
<b>Ultrafine Grained Materials – Sixth International Symposium</b>												
Applications and Transitions	331	606								X		
Characterization and Computational Modeling	233	607						X				
Deformation and Processing Mechanics	180	607					X					
Mechanical Response	128	606				X						
Microstructural Evolution	235	606						X				
Poster Session	29	606	X	X	X	X	X	X	X	X	X	X
Processing Technologies	130	607										
Processing-Microstructure-Properties I	78	606			X							
Processing-Microstructure-Properties II	80	607			X							
Stability	182	606					X					
Young Scientist	281	606								X		



### 2010 Functional and Structural Nanomaterials: Fabrication, Properties, Applications and Implications: Poster Session

Sponsored by: The Minerals, Metals and Materials Society, TMS Electronic, Magnetic, and Photonic Materials Division, TMS: Nanomaterials Committee

Program Organizers: David Stollberg, Georgia Tech Research Institute; Nitin Chopra, University of Alabama; Jiyoung Kim, University of Texas - Dallas; Seong Jin Koh, University of Texas at Arlington; Navin Manjooan, Siemens Corporation; Ben Poquette, Keystone Materials; Jud Ready, Georgia Tech

Sun PM-Thurs AM Room: 214  
February 14, 2010 Location: Washington State Convention Center

**Functional Materials with Shape Memory Effect at the Nanoscale:** Arteni Irzhak<sup>1</sup>; Victor Koledov<sup>1</sup>; Vladimir Shavrov<sup>1</sup>; Peter Lega<sup>1</sup>; Alexander Shelyakov<sup>1</sup>; Veronika Afonona<sup>1</sup>; Kristina Akatyeva<sup>1</sup>; Vladimir Kalashnikov<sup>1</sup>; Pnina Ari-Gur<sup>2</sup>; <sup>1</sup>Kotelnikov<sup>1</sup> Institute of Radioengineering and Electronics of RAS (Moscow); <sup>2</sup>Western Michigan University

Shape Memory Alloys (SMA) demonstrate unique potential of application in such fields as space technology and surgical implants. The present report outlines their micro- and nanomechanical applications, where nanotools made from SMA may help resolve presently unresolved problems, such as 3D manipulation of real nano-sized objects including single wall carbon nanotubes, graphene layers or living cells and viruses. In the present experiments the actuating structures made from Ti<sub>2</sub>NiCu SMA have been constructed and tested in an environment of vacuum camera of scanning ion microscope, with an active layer thickness in the range of 800 – 70 nm. The shape memory strains of the structures controlled by laser radiation were measured. (See video demonstration on the web: [www.smwsm.org/11/micropincer.html](http://www.smwsm.org/11/micropincer.html)).

**Mechanical Properties and Consolidation of Binderless Nanocrystalline Niobium Carbide by Rapid Sintering:** In-Jin Shon<sup>1</sup>; Kee-Do Woo<sup>1</sup>; In-Yong Ko<sup>1</sup>; Kee-Seok Nam<sup>2</sup>; Byung-Ryang Kim<sup>1</sup>; <sup>1</sup>Chonbuk University; <sup>2</sup>Korea Institute of Materials Science

Niobium carbide has a very important and promising properties, such as outstanding hardness, high melting point (3610°C), good resistance to chemical attack, good catalyst and excellent electronic conductivity. So it can find applications in many fields, such as mechanical, chemical, and microelectronic industries. The rapid sintering of NbC hard materials in a short time was investigated with a focus on the manufacturing potential of pulsed current activated sintering process. A dense pure NbC hard material with a relative density of up to 98% was produced with simultaneous application of 80 MPa pressure within 2 minutes. The mechanical properties and density of NbC increased with decrease in initial particle size of NbC. The fracture toughness and hardness values obtained from 10 hrs milled powder were 5.6 MPa.m<sup>1/2</sup> and 2134 kg/mm<sup>2</sup>, respectively under 80 MPa pressure and an applied current of 2800 A.

**Microstructure and Nanocrystalline Film of Fe- Mn Vs Fe-Ni Films:** Bassey Udofot<sup>1</sup>; <sup>1</sup>NASA/Goddard Space Flight Center

Electrodeposition of nanocrystalline material structure such as Fe, Ni, Mn and their alloys such as Fe-Mn and Fe-Ni in solvent systems that are aqueous onto substrate such as ceramic insulators or glass have wide spread technological uses. The hysteresis loop of the nanocrystalline alloy films being characterized under a vibratory Sample magnetometry shows the films to have a high magnetic permeability, low coreceivity, good for industrial applications. These films could also be produced by thermal means but such process is expensive usually requiring the use of high temperature and high energy conditions. The novel electrochemical cell processing technique designed by the present Author to electro-deposit microstructures and nanocrystalline films different from those produced by thermal means.

**Nanocomposites of Brazilian Organophilic Clays with Natural Rubber:** Guillermo Martín-Cortés<sup>1</sup>; Fabio Esper<sup>1</sup>; Adriana Silva<sup>2</sup>; Alexandre Dantas<sup>2</sup>; Wildor Hennies<sup>1</sup>; Francisco Valenzuela-Díaz<sup>1</sup>; <sup>1</sup>Polytechnic School-University of São Paulo; <sup>2</sup>BENTONISA – Bentonita do Nordeste S.A

Organophilic clays (OC) and polymers produce a new type of nanocomposites. Technological, economical, and environmental properties of polymers are enhanced. At Brazil several laboratories of public and private entities are researching many works on this line. Between them, the Non-Metallic and Particulate Solid Materials Laboratory (LMPSOL – PMT-EPUSP), of the Metallurgical and Materials Engineering Department - Polytechnic School - University of São Paulo research some variants of the organophilic clays production with Smectites from Brazil and other countries seeking enhance quality, efficiency and productivity. Lately is researching OC/ rubber nanocomposites, where small amount of OC substitutes the carbon black, maintaining or improving properties of the end product. This paper presents a case study inside these research lines.

**Photochemical Solution Phase Engineering of TiO<sub>2</sub> - Based Amphiphilic Nanocrystals:** Gianvito Caputo<sup>1</sup>; Davide Cozzoli<sup>1</sup>; <sup>1</sup>University of Salento

In the past years, the ability to rapidly and efficiently transfer nanocrystals from their growing environment into diverse liquids is crucial in the fields that require careful balance of the hydrophilic and hydrophobic components on a nanostructured surface, exploitable for example in biomedicine, and waste treatment. Three main general strategies have been pursued to transfer as-prepared nanocrystals in different liquids, but they suffer from several major drawbacks, such as tedious functionalization steps, and aggregation phenomena. Here, we demonstrate that the UV-driven TiO<sub>2</sub> hydrophilicization mechanism can be extended to processing of nanostructures in the liquid phase, devising a simple photochemical technique by which the solubility behaviour of organic-capped TiO<sub>2</sub> nanocrystals can be reversibly switched in solvents of dissimilar polarity and solvation ability. Our approach offers a way of beating the metastability of UV-hydrophilicized TiO<sub>2</sub> surfaces, paving the way to a new class of solution-processable TiO<sub>2</sub> nanostructures with “surfactant-like” amphiphilic properties.

**Properties and Consolidation of Nanostructured MoSi<sub>2</sub>-Si<sub>3</sub>N<sub>4</sub> from Mechanically Reacted Powder by Rapid Sintering:** In-Jin Shon<sup>1</sup>; Na-Ra Park<sup>1</sup>; Jin-Kook Yoon<sup>2</sup>; In-Yong Ko<sup>1</sup>; Kee-Seok Nam<sup>3</sup>; Na-Ri Kim<sup>1</sup>; <sup>1</sup>Chonbuk University; <sup>2</sup>Korea Institute of Science and Technology; <sup>3</sup>Korea Institute of Materials Science

MoSi<sub>2</sub> has been investigated as potential material for high temperature structural applications and for application in the electronics industry. Its properties provide a desirable combination of a high melting temperature (2020°C), high modulus (440 GPa), good oxidation resistance in air, a relatively low density (6.24 g/cm<sup>3</sup>), and the ability to undergo plastic deformation above 1200°C. Combined with good thermal and electric conductivities, these properties have led to the utilization of MoSi<sub>2</sub> as a heating element material in high-temperature furnaces operating in air up to about 1700°C. However, as in the case of many such compounds, the current concern about these materials focuses on their low fracture toughness below the ductile-brittle transition temperature. To improve on the mechanical properties of these materials, the fabrication of nanostructured composite material has been found to be effective. A dense nanostructured MoSi<sub>2</sub>-Si<sub>3</sub>N<sub>4</sub> was sintered by the high-frequency induction heating method within 2 minutes from mechanically synthesized powder of MoSi<sub>2</sub>-Si<sub>3</sub>N<sub>4</sub>. Highly dense MoSi<sub>2</sub>-Si<sub>3</sub>N<sub>4</sub> with relative density of up to 96% was produced under simultaneous application of a 80 MPa pressure and the induced current. The average grain sizes of MoSi<sub>2</sub> and Si<sub>3</sub>N<sub>4</sub> were about 52 nm and 440 nm, respectively. The hardness and fracture toughness values obtained were 1403 kg/mm<sup>2</sup> and 5.9 MPa.m<sup>1/2</sup>, respectively. These fracture toughness and hardness values of nanostructured MoSi<sub>2</sub>-Si<sub>3</sub>N<sub>4</sub> composite are higher than those (fracture toughness; 2.58 MPa.m<sup>1/2</sup> hardness; 8.7Mpa) of monolithic MoSi<sub>2</sub>.

# Technical Program

**Synthesis and Characterization of Nano-Structured Silica from Rice Husk and Its Application as a Heterogeneous Catalyst:** *Harini Pattabhiraman<sup>1</sup>; Gopalakrishnan Ramalingam<sup>1</sup>; Sajan Mittal<sup>1</sup>; Shuvarthi Bhattacharjee<sup>1</sup>; Sachin Mandavgane<sup>1</sup>; Jatin Bhatt<sup>1</sup>; Dilip Peshwe<sup>1</sup>;* <sup>1</sup>Visvesvaraya National Institute of Technology

In the present investigation potential of rice husk as a source of high purity nano-structured silica is evaluated. The rice husk is subjected to a chemical pre-treatment with HCl followed by incineration in a tubular furnace in a controlled flowing oxygen atmosphere at 900°C with a constant heating rate of 200C/min. The effect of oxygen flow rate on the morphology, particle size and surface area are investigated. The increased surface area, pore size and pore volume makes the nano-structured silica suitable for its use in catalytic applications. The present study considers a different approach to the two major problems of heterogeneous catalysis viz. the high cost and the low interphase-mass transfer rate for immiscible liquid-liquid reactions like hydrolysis, esterification and trans-esterification. The novel amphiphilic properties of silica as heterogeneous acid catalysts produced from rice husk will be discussed.

**Synthesis of Nanowires-Enhanced Bulk TE Nanocomposite for High-Efficiency Power Generation:** *Wei Luo<sup>1</sup>; Jiye Fang<sup>1</sup>; Timothy Lin<sup>1</sup>;* <sup>1</sup>Aegis Technology Inc.

There are great interest in developing high-efficiency thermoelectrical (TE) materials for power generation. Significant improvements in a few TE material systems have been realized in thin film through the incorporation of nanoscale structures, there still exists a formidable difficulty in synthesizing the quantum-confined materials into a bulk material, which is essential to form a practical TE system capable of producing sufficiently strong power generation or energy harvesting. This presentation is on the development of low-cost, nanowires-enhanced bulk TE nanocomposites for high-efficiency, compact TE devices. With the support from one ongoing DoE SBIR program on this project, Aegis has established the capability in the development and large scale production of high performance nanostructured TE materials. The latest results including the establishment of a cost-effective scalable process, the influence of key processing parameters, and the characterizations of the bulk TE nanocomposites are presented.

## Advances in Composite, Cellular and Natural Materials: Poster Session

*Sponsored by:* The Minerals, Metals and Materials Society, TMS Structural Materials Division, TMS/ASM: Composite Materials Committee

*Program Organizers:* Yuyuan Zhao, The University of Liverpool; David Dunand, Northwestern University

Sun PM-Wed PM Room: 305  
February 14, 2010 Location: Washington State Convention Center

**Effects of Particle Sizes of Titanium Hydride on Cell Structures for Al Foams:** *Lei Wang<sup>1</sup>; Guangchun Yao<sup>1</sup>; Hongjie Luo<sup>1</sup>; Lisi Liang<sup>1</sup>; Jia Ma<sup>1</sup>;* <sup>1</sup>Zhongsheng Hua<sup>1</sup>; <sup>1</sup>Northeastern University

Al foams made by powder metallurgy route have been prepared with Al powder, Mg powder and TiH<sub>2</sub> powder as raw materials. Decomposition characteristics of TiH<sub>2</sub> powder with different pre-treating temperatures and different particle sizes and distribution with particle sizes were investigated; Effects of TiH<sub>2</sub> powder with different particle sizes on change of cell structures were analyzed. The results show that temperatures of endothermic peaks within DSC curves of TiH<sub>2</sub> powder increase with the rise of pre-treating temperatures while those increase slowly with different particle sizes. Cell sizes and thicknesses of Al foams increase with particle sizes in the identical foaming process.

**Nanocrystalline Al<sub>4</sub>Si<sub>3</sub>C<sub>6</sub> Formed in Low Temperature Sinter Processing:** *Li Xiaodan<sup>1</sup>; Zhai Yuchun<sup>1</sup>; Qiu Feng<sup>1</sup>; Zhang Haixin<sup>1</sup>;* <sup>1</sup>Institute of Materials and Metallurgy, Northeastern University

During sinter process of the preparation of Al/SiC MMCs, nanocrystalline Al<sub>4</sub>Si<sub>3</sub>C<sub>6</sub> was formed unexpectedly. Size distribution, particle shape and phase structure of samples were investigated by means of laser particle size distribution, scanning electron microscope(SEM), and X-ray diffractometry (XRD). The results show that particles size and its distribution range for mixture powders decrease with increase of the milling time. When the milling

time is up to 24h, the average particle size is 1.1969 μm, and crystalline grain of Al is about 1nm. The nanocrystalline Al<sub>4</sub>Si<sub>3</sub>C<sub>6</sub> is obtained using the mixture powders treated by high energy milling for 24h as the sinter materials, when the sinter temperature is conducted at 520° sinter in argon for 20min. This suggested that the nanocrystalline Al<sub>4</sub>Si<sub>3</sub>C<sub>6</sub> could be formed in low temperature under the particular processing conditions.

**On Closed-Cell Aluminum Foam Used as Train Floor and Side Plate:** *Lisi Liang<sup>1</sup>; Guangchun Yao<sup>1</sup>; Yongliang Mu<sup>1</sup>; Lei Wang<sup>1</sup>;* <sup>1</sup>Institute of Materials and Metallurgy, Northeastern University

The feasibility analysis of closed-cell aluminum foam sandwich panels used as train floor and acoustic side-lining was conducted and a comparison was made with other train floor and acoustic side-lining, according to the noise frequency characteristic curve inside the train, Sound insulation characteristic curve and vibration isolation performance test results. The purpose is to reduce the noise and the vibration inside the carriages. The results show that the noise reduction capacity and damping capacity of closed-cell aluminum foam panels with a density of 0.5g/cm<sup>3</sup> and a thickness of 15-20mm is superior to wood materials and aluminum honeycomb, which shows a great development prospect.

**Research on Aluminum Foam Railway Noise Barrier:** *Lisi Liang<sup>1</sup>; Guangchun Yao<sup>1</sup>; Lei Wang<sup>1</sup>; Yongliang Mu<sup>1</sup>; Zhongsheng Hua<sup>1</sup>; Jia Ma<sup>1</sup>;* <sup>1</sup>Institute of Materials and Metallurgy, Northeastern University

Frequency ranges of train noises are concentrated between 500 and 2000Hz according to frequency spectrum of noise generated through running trains. Sound absorption properties of the absorbing boards made up of the closed-cell Al foams are measured. The results show that absorption effects of Al foams are good during the frequency range of 500-2000Hz. Sound absorption efficiency may reach up to 60-90%, corresponding to the two peak values of 800Hz and 1600Hz respectively. The sound absorption features of noise barriers made up of Al foams are investigated and are compared with fiber glass and open Al foams. The results show that noise barriers of Al foams have a better developing trend in noise reduction of railways.

**Preparation of Aluminum Matrix Composites Reinforced with Nano-SiC Particles by Stir Casting Technique:** *Li Xiaodan<sup>1</sup>; Zhai Yuchun<sup>1</sup>; Qiu Feng<sup>1</sup>; Zhang Haixin<sup>1</sup>;* <sup>1</sup>Institute of Materials and Metallurgy, Northeastern University

Aluminum metal matrix composites were processed by stir casting technique with commercially pure aluminum as the matrix material and nano-SiC (40nm) particles as the reinforcement. Since it is extremely difficult to obtain uniform dispersion of nano-SiC particles in molten metal, we designed the experimental setup consists of fusion, vacuum and stir parts. Aluminum matrix nano-composites with various weight percentages of nano-SiC particles were fabricated. For comparison, samples of 0 wt% SiCp were prepared. Microstructural study was carried out with an optical microscope, SEM, and EDS mapping. It validates that the Al-SiCp composites of below 0.5 wt% SiCp can be added to the melt without agglomeration and clustering by stir casting. It also indicates that the samples show uniform distribution of particles after 1h thermostatic processing at 750°. Mechanical properties of the samples have been improved and the strengthening mechanism is major attributes to the higher dislocation density.

## Aluminum Alloys: Fabrication, Characterization and Applications: Poster Session

*Sponsored by:* The Minerals, Metals and Materials Society, TMS Light Metals Division, TMS: Aluminum Processing Committee

*Program Organizers:* Subodh Das, Phinix LLC; Steven Long, Kaiser Aluminum Corporation; Tongguang Zhai, University of Kentucky

Sun PM-Wed PM Room: 615  
February 14, 2010 Location: Washington State Convention Center

**A Mechanism-Based Constitutive Model for Alloy IC10:** *Hongjian Zhang<sup>1</sup>; Weidong Wen<sup>1</sup>; Haitao Cui<sup>1</sup>; Ying Xu<sup>1</sup>;* <sup>1</sup>Nanjing University of Aeronautics and Astronautics

IC10 is a newly developed Ni<sub>3</sub>Al-based superalloy, with its nominal composition(wt%):0.07-0.12%C11.5-12.5%Co6.5-7.5%Cr5.6-6.2%Al4.8-5.2%W1.0-2.0%Mo6.5-7.5%Ta1.3-1.7%Hf0.01-0.02%B and Bal.Ni. As



IC10 exhibit unusual thermo-mechanical flow behaviors, a mechanism-based constitutive model was developed to describe the features of IC10. In this model, two assumes were proposed: (1) the yield and hardening of IC10 are the net effect of point obstacles opposing the motion of mobile dislocations. (2) The mobility of dislocation is connected to its superkink heights. So, the evolution of the mobile dislocation density can be developed based on the evolution of whole dislocation density and the distribution of their superkink heights. And the evolution of obstacles density can be derived from the evolution of the mobile dislocation density. The model was used to simulate flow behaviors of IC10 under different experiment conditions. The results show that it is valid.

**Analysis of Metal Flow Behavior during Friction Welding of Tube to Tube Plate Using an External Tool:** *S. Muthukumaran*<sup>1</sup>; *S. Senthil Kumaran*<sup>1</sup>; <sup>1</sup>National Institute of Technology

Friction welding of tube to tube plate using an external tool is an innovative friction welding process which is capable of producing leak proof high quality weld joints. In the present study, tube to tube plate welds have been performed and metal flow analysis has been carried out by radiography test and brass insertion technique. Based on the results obtained, the metal flow pattern and the principle behind joint formation are explained.

**Effect of Age Hardening on Corrosion Behavior of Friction Stir Welded AA 2024 Aluminum Alloy:** *Muna Abbass*<sup>1</sup>; <sup>1</sup>University of Technology

This work aims to study the effect of age hardening heat treatment on the corrosion behavior of friction stir welded joint of AA2024 aluminum alloy. The microstructure and corrosion behavior of the welds and base alloy were studied before and after age hardening which includes solution heat treatment at 510°C and aging at 190°C for 3hrs. The friction stir welding was carried out by using CNC milling machine at constant tool rotational speed (1000 rpm) and welding speed (20mm/min). Corrosion current was found using potentiostatic polarization measurements of all samples in 3.5%NaCl solution at a temperature 30°C. It was found that the corrosion rate of welds was higher than that of base metal before age treatment. Post weld aging treatment leads to reduce the corrosion current of welds because of precipitation homogeneity occurring in the microstructures of various welding regions.

**Effect of Alloying Elements on the Electrochemical Behavior of Al-Si-Mg alloys in Aqueous Solutions:** *Maximo Pech-Canul*<sup>1</sup>; *Martin Pech-Canul*<sup>2</sup>; *Marbella Echeverría*<sup>1</sup>; *Euler Coral-Escobar*<sup>1</sup>; *Miguel Montoya-Davila*<sup>2</sup>; <sup>1</sup>Cinvestav-Merida; <sup>2</sup>Cinvestav-Saltillo

High volume fraction SiCp/Al composites are attractive for different structural and electronic packaging applications. Fabrication by pressureless infiltration is promising; however inadequate wetting and the potential attack of SiC by molten aluminum represent two major drawbacks. These can be overcome by adequately controlling alloy chemistry, processing time and temperature, preform porosity and particle size. In particular high levels of Si and Mg are required (e.g. 9% Mg, 13.5% Si). In this work the electrochemical behavior of plain Al-Si-Mg alloys (with varying concentrations of Si and Mg) is investigated in near-neutral solutions by means of potentiodynamic polarization measurements. The role of alloying elements on the resistance to pitting corrosion of such alloys in chloride containing solutions is discussed by comparing the results to those for pure aluminum. The Mg<sub>2</sub>Si intermetallic has a determining effect on the electrochemical behavior of these alloys since it behaves anodic with respect to the matrix.

**Effect of Friction Stir Processing (FSP) on Particle Erosion Resistance of Casting A384 Aluminum Alloy:** *Chung-Wei Yang*<sup>1</sup>; *Truan-Sheng Lui*<sup>1</sup>; *Li-Hui Chen*<sup>1</sup>; *Yun-Han Chang*<sup>1</sup>; <sup>1</sup>National Cheng Kung University

Al-Si-(Mg) alloys are used in the main carrier of wind turbines, which is often encountered particle erosion. This study is to explore the effect of friction stir processing (FSP) with artificial aging on erosion characteristics. The full-annealed A384 was used as base metal (BM). Si particles,  $t_1$  (Al<sub>3</sub>FeNi),  $\nu$ 98 (Al<sub>3</sub>CuNi) and Q (Al<sub>5</sub>Cu<sub>2</sub>Mg<sub>8</sub>Si<sub>6</sub>) precipitate phases were observed in the A384 alloy. It generally had high erosion rate at oblique impact angles. After FSP, the refined and uniformly distributed second phases can help to increase the erosion resistance. The Si and  $\nu$ 98 phases were found with brittle fracturing at the end of erosion grooves. The  $t_1$  phase was easily removed by the impact of erodent particles. It was inferred that Si and  $\nu$ 98 were beneficial, whereas  $t_1$  phase was detrimental to the erosion resistance. The hardness and deformation resistance were increased, and the maximum erosion rate was decreased after peak-ageing treatments.

**Effect of Welding Parameters on Microstructure and Properties of 6005A Aluminum Alloy:** *Kai Ji*<sup>1</sup>; *Guangchun Yao*<sup>1</sup>; *Guoyin Zu*<sup>1</sup>; *Jianchao Shi*<sup>1</sup>; <sup>1</sup>School of Materials & Metallurgy, Northeastern University

Through 12mm thick 6005A-T6 aluminum alloy was welded with ER5356 wire by Semi-automatic MIG welding, the effects of the main welding parameters on the tensile properties and weld configurations were investigated by orthogonal testing method. The result shows that the descending order of factors influencing tensile strength is as follows: welding current, welding voltage, welding speed and preheat temperature, in which the former two affected it obviously; the descending order of factors influencing weld configurations is as follows: preheat temperature, welding current, welding voltage and welding speed. The preferable welding parameters are reached as: welding current 150A, welding voltage 16.5V, welding speed of 26cm/min, preheat temperature 210°. The heataffected zone (HAZ) of alloy side less than 20um without any abnormal structure, the tensile strength of Welded joints up to 270 MPa, and the fractograph exhibited typical ductile dimple fracture pattern.

**Microstructure and Wear Characterization of HyperEutectic Al-Si FGM:** *Kiran Aithal*<sup>1</sup>; *N. Narendranath*<sup>2</sup>; *Vijay Desai*<sup>2</sup>; *P. G. Mukunda*<sup>1</sup>; <sup>1</sup>Nitte Meenakshi Institute of Technology; <sup>2</sup>NITK

The work investigates Functionally Graded Material (FGM) fabricated using Al / 17wt% Si alloy for the effects of Rotating speed (G Force) and mold temperature on the microstructure, hardness and wear. A modified centrifugal technique has been used specially designed for the purpose. The cast test samples were evaluated using optical microscope, Scanning electron microscope and Hardness test. The hardness decreased from Upper end to the lower end. This was confirmed by the structure of this alloy varying from enriched Hyper-Eutectic at upper end through to Hypoeutectic at the lower end. The wear behavior of the FGM was evaluated under dry condition using Pin-on-Disk configurations. The surface morphologies of the FGM sample after wear experiment were examined by SEM. The test showed wear resistance was more on the upper hyper eutectic region and less on the lower region of the cast sample as expected.

**Modification of Hypereutectic Al-17.5%Si Alloy by Nd:** *Weixi Shi*<sup>1</sup>; *Bo Gao*<sup>1</sup>; *Ganfeng Tu*<sup>1</sup>; *Yi Hao*<sup>1</sup>; *Shiwei Li*<sup>1</sup>; <sup>1</sup>Northeastern University

In this paper, modification of hypereutectic Al-17.5%Si alloy by Nd was investigated. The modification mechanism was studied by OM, SEM and XRD. The results of OM and SEM analysis showed that pure Nd could effectively refine primary and eutectic silicon in hypereutectic Al-17.5%Si alloy. When Nd addition was 0.3%, the average grain size of primary silicon reached its minimum. The average grain size of primary silicon was reduced from 40~60µm to 10~30µm after modification. XRD patterns showed that no new phase formed after Nd modification. The results of mechanical properties test showed that whole properties of modified samples were significantly improved. When Nd addition was 0.3%, tensile strength of the alloy reached its maximum. Tensile strength was increased about 35.8% from 120MPa to 163MPa. Elongation was increased about 175% from 0.8% to 2.2%. The improvement of mechanical properties should attribute to fine primary and eutectic silicon after modification.

**Non-Corrosion-Flux-Assisted Wetting and Spreading of Al-Si-Cu-Based Brazing Alloy on 6063 Aluminum:** *Yefeng Bao*<sup>1</sup>; *Guowei Zhang*<sup>1</sup>; *Yongfeng Jiang*<sup>1</sup>; <sup>1</sup>Hohai University

The K-Al-F-Cs-flux-assisted spreading of Al-Si-Cu-based brazing alloy on 6063 aluminum, at temperatures up to 560°, in N<sub>2</sub> has been studied. The effect of different heating rate on spreading was studied. Intermetallic compounds formed at brazing alloy/ substrate interface were investigated by means of SEM and EDS. Experimental results show that: As temperature rising, KAIF<sub>4</sub> in flux melted firstly, removed part of the oxide film of substrate and resulted in a shiny appearance. Then, other components of the flux melted, dissolved oxide film and provided a locally protective atmosphere by covering over the surface of substrate and brazing alloy. Under the liquid flux, melted brazing alloy spreaded spontaneously and instantaneously. The contact angle of samples rapidly heated was about 3°, whereas that slowly heated was about 25°. A large number of bone-like CuAl<sub>2</sub> eutectic and rich silicon intermetallic compounds formed inside brazing alloy and extended to substrate.

**Optimization of Ingate Velocity via Gate Design:** *Pongsak Dulyapraphant<sup>1</sup>; Prarop Kritboonyarit<sup>1</sup>; <sup>1</sup>National Metals and Materials Technology Center*

A gating system is one of the major factors directly affecting quality of castings in High Pressure Die Casting (HPDC) processes. In this study, the effect of gate design to the ingate velocity is studied. The real gating system used in the production of an automotive part is used as a case study and a commercial casting process simulation is used as a tool. The experimental results show that, by changing only the gate design but still use the same runner system and process parameters setup, ingate velocity can be increased by 10 percent. The increased of ingate velocity would benefit in reducing the use of high plunger velocity, which results in less machine power, lower tool wear, less flash, and higher injection pressure.

**Prediction of Bake Hardenability of Aluminum Alloys Al6110 and Al7075 Using Neural Network:** *Niloofer Kamkar Zahmatkesh<sup>1</sup>; Kamran Dehghani<sup>1</sup>; <sup>1</sup>Amirkabir University of Technology*

Using artificial neural network (ANN), the effect of composition on bake hardenability of two aluminum alloys 7075 and 6110 was studied and verified based on experimental data. Following these, the bake hardening and final yield stress values were predicted. Samples were prepared from the as received sheets. They were then subjected to different aging conditions in temperature range of 150-250°C, following different amounts of pre-straining for 15-30 minutes. Test results show that the bake hardenability increased with increasing ageing time and temperature and prestrain amount, as well as Zn content. By comparing the predicted values with the experimental data, it is demonstrated that the ANN model is a useful and practical tool for prediction of bake hardenability and mechanical properties of these two alloys.

**Preparation of Al-Ti-C Master Alloys from TiO<sub>2</sub>:** *Dali Cao<sup>1</sup>; Jikun Wang; Zhongning Shi<sup>1</sup>; Zhaowen Wang<sup>1</sup>; Yi Liu<sup>1</sup>; <sup>1</sup>University of Shenyang Chemical Technology*

Al-Ti-C master alloys used as grain refiners of aluminum and its alloys with different titanium and carbon contents have been prepared by excess aluminum, graphite powder and titanium dioxide in the presence of cryolite flux. The phenomenon that Al-Ti-C alloys creep up along the inner wall of the crucible when the TiO<sub>2</sub> content in the flux comparatively excess aluminum content has been found. The influence of various process parameters on Al-Ti-C master alloy has been studied in detailed. Microstructure and phase structure indicate that TiC and TiAl<sub>3</sub> are the two secondary phases, and content of TiAl<sub>3</sub> and TiC formed depends on the TiO<sub>2</sub> content and Ti/C mass ratio in the master alloy.

**Process Design and Characterization of Bulk Nanostructured Aluminium Alloy by Equal Channel Angular Pressing (ECAP):** *Prasad Shanmugasandaram<sup>1</sup>; Narayani Narasimhan<sup>1</sup>; Balasivananda Prabhu<sup>1</sup>; Hariharan Raja<sup>1</sup>; <sup>1</sup>Anna University*

The paper involves developing nanostructured Al6061 particles and characterizing their unique mechanical properties and microstructure. Equal Channel Angular Pressing (ECAP), a discontinuous process for Severe Plastic Deformation (SPD) is used. The Ultra Fine Grain microstructure of the material is characterized by TEM, SEM and XRD to identify their high angle strain, low angle strain and other strength related properties. A split die of required dimensions to produce maximum possible strain without causing failure is used for the process. The resulting Aluminium 6061 alloy material can be widely used in aerospace industries where the proposed increase in density and toughness will make a very big impact. Sports, yacht construction, automotive industries also stand to gain out of this project. The characterization will give researchers and industrialists better insight into the mechanical behaviour and properties of Al 6061 processed through ECAP. Suggestions relating to more optimized die design and lubrication aims at making ECAP a more efficient and effective production process for bulk materials.

**Review of Solidification of Al-Si Alloy under Superhigh Pressure:** *Guozhi Zhang<sup>1</sup>; <sup>1</sup>Northeastern University*

The paper reviews solidification of Al-Si alloy at under 5.5GPa high pressure, the effects of high pressure on structure and solidification process were analysed. The microstructure of hypo-eutectic Al-9.21wt.%Si alloy and hyper-eutectic Al-26.6wt.%Si alloy solidified under 5.5GPa high pressure was studied. The nonequilibrium microstructures of the hyper-eutectic Al-26.6wt.%Si alloy solidified under 5.5GPa pressure is an intergrowth structure of a+b+(a+b) eutectic with large amount of primary  $\alpha$  phase. The primary  $\alpha$  phase is an extended solid

solution. The solid solubility of Si in  $\alpha$  phase and the solid solubility of Al in  $\beta$  phase increase largely. For hypoeutectic Al-9.21wt.%Si alloy solidified under 5.5MPa pressure, the growth mode of a phase is cellular. The cellular growth mechanism of the  $\alpha$  phase is interpreted in term of the decrease of the diffusivity and the extended solid solution under high pressure. The effect of high pressure on stability of solid-liquid interface were discussed.

**Study on Al/P Diffusion Couples at Lower Temperature:** *Danqing Yi<sup>1</sup>; Ying Zhang<sup>1</sup>; <sup>1</sup>Central South University*

Be added into hypereutectic Al-Si alloys, Phosphorus can create nucleus of AlP that cause modification effect. However the condition of the reaction is seldom expatiated. References indicated that it is easy to synthesize AlP whenever through adding phosphorus to melted aluminum or being calcined the mixture of Al and compounds containing phosphorus, although the limits of reaction temperature is not mentioned. In this paper, used powders as raw materials, diffusion couple of Al and P at lower reaction temperature is studied. Scanning electronic microscope, X-ray diffraction, Energy-dispersive spectroscopy and optical microscopy are used to detect the reactants. The results show gasified phosphorus can react to solid aluminum at a few centigrade higher than etherealization temperature but almost not under it. The results agree with thermodynamics calculations.

**Study on Recrystallization Behaviors of Alloy IC10 at Elevated Temperature:** *Hongjian Zhang<sup>1</sup>; Weidong Wen<sup>1</sup>; Haitao Cui<sup>1</sup>; Ying Xu<sup>1</sup>; <sup>1</sup>Nanjing University of Aeronautics and Astronautics*

IC10 is a newly developed Ni<sub>3</sub>Al-based superalloy. In order to investigate its recrystallization behaviors, tensile experiments were conducted over a wide range of strain rates (10<sup>-4</sup>-10<sup>-2</sup>s<sup>-1</sup>) at 900° on a material testing system (MTS809). Experiments show that:(1) the flow stress is sensitive to the strain rate while the stress-strain curve at various strain rate exhibits similar features;(2)the flow stress, critical stress and critical strain increase with strain rates. And the mechanisms of these properties are studied based on the examinations of TEM and SEM. In order to capture the flow features of IC10, a new phenomenological constitutive equation is developed. The effectiveness of this newly developed model is verified by extensive experiments on IC10. The results show that it is valid.

**Vacuum Thermal Extract Lithium with Coarse Ferrosilicon-Aluminum Alloy Produced by Electro Thermal Process:** *Di Yuezhong<sup>1</sup>; Dong Weiwei<sup>1</sup>; Feng Naixiang<sup>1</sup>; <sup>1</sup>Northeastern University*

Abstract: In present paper, the coarse ferrosilicon-aluminum alloy containing 28.83% aluminum and 41.10% silicon is used as reductant to extract metal lithium from Lithia obtained by the thermal decomposition of lithium carbonate. The thermal decomposition rate of lithium carbonate and reduction rate of Lithia by coarse ferrosilicon-aluminum alloy are investigated under different experiment conditions. The result shows that the decomposition rate of lithium carbonate is up to 99.86% when the reaction temperature and time is 1173K and 100min, the reduction rate of Lithia with coarse ferrosilicon-aluminum alloy can reach 95.26% when the reduction temperature, the reaction time and excessive coefficient of reductant is 1273K, 180min and 25%.

## Biological Materials Science: Poster Session

*Sponsored by:* The Minerals, Metals and Materials Society, TMS Structural Materials Division, TMS: Biomaterials Committee, TMS/ASM: Mechanical Behavior of Materials Committee

*Program Organizers:* John Nychka, University of Alberta; Jamie Kruzic, Oregon State University; Mehmet Sarikaya, University of Washington; Amit Bandyopadhyay, Washington State University

Sun PM-Thurs AM Room: 205  
February 14, 2010 Location: Washington State Convention Center

**Design and Fabrication of Implants for Amputation Prosthesis:** *Paul DeVasConcellos<sup>1</sup>; Vamsi Balla<sup>1</sup>; Susmita Bose<sup>1</sup>; Amit Bandyopadhyay<sup>1</sup>; William Dernel<sup>2</sup>; <sup>1</sup>BRC, Washington State University; <sup>2</sup>College of Veterinary Medicine, Washington State University*

It is now widely accepted that 'fit' and 'fill' of the bone canal is critical to the success of cementless load bearing metal implants and there exists a wide variation to the size and shape of this canal within the population. This study



presents designing and fabricating a unitized Ti-based metal implant closely resembling the natural bone for amputation prostheses based on a computed tomography scan of the patient's joint. The custom designed implant showed a maximum of 94% fill of bone cavity. The efficient fill and porous structure at appropriate location of the implant has potential to improve load transfer from the prosthesis to the bone, the bone in-growth, and reduce premature loosening, thus decreasing the rehabilitation period for the amputees. The primary disadvantage of custom implants – the cost, is also addressed by the use of rapid manufacturing technology; for quick and economical fabrication of custom implant components.

**Electro-Thermally Polarized Hydroxyapatite (HAp) Ceramics: Influence of MgO, ZnO, and SrO Dopants:** *Subhadip Bodhak*<sup>1</sup>; Susmita Bose<sup>1</sup>; Amit Bandyopadhyay<sup>1</sup>; <sup>1</sup>Washington State University

The objective of this work is to investigate the influence of doping of trace elements (Mg<sup>2+</sup>, Zn<sup>2+</sup>, and Sr<sup>2+</sup>) on polarization behavior of sintered HAp pertinent to biomedical applications. For this purpose, commercially procured phase pure HAp was doped with MgO, SrO, and ZnO in single, binary, and ternary compositions. All samples were sintered at 1200°C for 2h and subsequently electro-thermally polarized via application of an external d.c. field (2 kVcm<sup>-1</sup>) at 400°C. Thermally stimulated depolarization current (TSDC) results demonstrate that SrO and MgO dopants increase the polarizability and charge storage ability (2.37 and 3.84  $\mu\text{C}/\text{cm}^2$ , respectively) of sintered undoped HAp (1.81  $\mu\text{C}/\text{cm}^2$ ) by enhancing the structural stability of HAp while ZnO has minimal influence. Our research findings establish that combined influence of dopants and polarization can potentially assist in designing of a bone graft material that can permit accelerated mineralization and rapid tissue in-growth for faster healing.

**Electrochemical Corrosion Behavior of Gamma TiAl Alloy Modified by Means of Plasma Electrolytic Oxidation:** *Laura Lara*<sup>1</sup>; Paul Sundaram<sup>1</sup>; Nannette Difffoot-Carlo<sup>1</sup>; <sup>1</sup>University of Puerto Rico

The emerging need to enhance the biological performance of titanium alloys (extensively used in biomedical industry) has led to the development of techniques to modify its surface using ceramic coatings. Plasma electrolytic oxidation (PEO) has been recently applied to cp-Titanium and Ti6Al4V, improving the coating adhesion and allowing the calcium and phosphorous inclusion into the coating. Additionally and due to different studies regarding the cytotoxic effects of vanadium, research is directed to explore different titanium alloys with similar mechanical properties but without the side effects of vanadium. In this study, GammaTiAl is modified by means of PEO using a calcium/Phosphorous electrolyte under different current density and time conditions. Morphological features and thickness are examined and measured respectively by SEM, in order to be related to electrochemical parameters. Open circuit potential, Cyclic polarization and electrochemical impedance spectroscopy test were performed using SBF in order to establish favorable conditions for the coating.

**Fatigue Behavior of Laser Processed Porous Nitinol:** *Sheldon Bernard*<sup>1</sup>; Vamsi Balla<sup>1</sup>; Susmita Bose<sup>1</sup>; Amit Bandyopadhyay<sup>1</sup>; <sup>1</sup>Washington State University

Porous implants are known to promote cell adhesion and have low elastic modulus, a combination that can significantly increase the life of an implant. However, porosity can significantly reduce the fatigue life of porous implants, and very little work has been reported in this area. In our work, we have studied low cycle and high cycle fatigue behavior of porous Nitinol structures. Nitinol (NiTi) is an equiatomic intermetallic compound of nickel and titanium whose unique mechanical properties contribute to its increasing use as a biomaterial. The purpose of this study is to determine the fatigue behavior of porous Nitinol. Using Laser Engineering Net Shaping (LENS<sup>TM</sup>) porous Nitinol sample were fabricated ranging from 10 to 30 volume% porosity. These samples were tested under low cycle compression and high cycle rotating bending fatigue conditions. This presentation will focus on fatigue deformation of porous nitinol under cyclic compression and rotary bending loading conditions.

**Fatigue of EBM-Processed Cellular Titanium for Biomedical Applications:** *Nikolas Hrabec*<sup>1</sup>; Burkhard Fuchs<sup>2</sup>; Peter Heinl<sup>2</sup>; Carolin Koerner<sup>2</sup>; Rajendra Bordia<sup>1</sup>; <sup>1</sup>University of Washington; <sup>2</sup>University of Erlangen-Nuremberg

Cellular titanium has the potential to reduce stress shielding in load-bearing bone replacement implants through a reduction of the elastic modulus with decreasing relative density. The implant is subjected to cyclic loading, providing motivation for this work. Cellular titanium has been fabricated over a range of relative densities (0.14-0.34) using electron beam melting (EBM) and found to display mechanical properties approximately within the range of cortical and cancellous bone. For all relative densities tested, the compression-compression fatigue strength at 1 million cycles was found to be rather low (approximately 20% of the yield strength). The effects of simulated body fluid and infiltration of a simulated bone material on monotonic and fatigue properties will also be presented. This talk will include a discussion on the proposed deformation mechanisms based on results from nanoindentation, scanning electron and optical microscopy, and micro-computed x-ray tomography.

**In Vitro Wear of Compositionally and Structurally Graded CoCrMo Ti6Al4V Structures:** *Stanley Dittrick*<sup>1</sup>; Vamsi Balla<sup>1</sup>; Susmita Bose<sup>1</sup>; Amit Bandyopadhyay<sup>1</sup>; <sup>1</sup>Washington State University

Common hip implants have a metal ball with an UHMWPE liner in which wear is a serious problem because of microscopic wear particles that can lead to osteolysis. CoCrMo alloy is common as femoral head because of its excellent wear resistance and Ti6Al4V alloy as stem due to its excellent biocompatibility. Laser Engineered Net Shaping (LENS) was used to combine the favorable properties of each of these alloys in a functionally graded structure without creating any unwanted intermetallics. CoCrMo-Ti6Al4V gradient samples with varying concentrations of CoCrMo between 100% and 50% were fabricated. These samples were tested in simulated body fluids under a 5N load for 1 and 3 kilometer sliding distance for wear performance against UHMWPE and CoCrMo substrates. The wear rates, coefficient of friction, and Co, Cr and Ti metal-ion concentrations were determined. This presentation will focus on in vitro wear characteristics of these graded structures.

**Resorbable Tricalcium Phosphates for Bone Tissue Engineering: Influence of SrO Doping:** *Ken DeVoe*<sup>1</sup>; Shashwat Banerjee<sup>1</sup>; Amit Bandyopadhyay<sup>1</sup>; Susmita Bose<sup>1</sup>; <sup>1</sup>Washington State University

Tricalcium phosphate (TCP) ceramics are widely used for implant applications because of their bioresorbable and osteoconductive nature in a physiological environment. However, metal oxide dopants are needed to control the properties of TCP. The objective of this research is to determine the biological and mechanical effects of SrO dopants on a TCP matrix at concentrations of 0.5, 2 and 5 mol% SrO. The SrO doped TCP was synthesized through a wet precipitation method and then processed and sintered. The synthesized powder was analyzed via X-ray Diffraction. Archimedes principle was used to determine the density of the samples. Compressive strength of the samples was also determined using a mechanical testing machine (Instron). Biological degradation and cell proliferation was determined using Simulated Body Fluid (SBF) and cell culture studies. The presentation will describe synthesis, processing, mechanical and biological properties of doped TCP matrix.

**Tissue Development in Arabidopsis: 3D Shape Analysis for Detection of Cell Type:** *Fatma Uyar*<sup>1</sup>; Begum Gulsoy<sup>1</sup>; Jean Christophe Palauqui<sup>2</sup>; Marc De Graef<sup>1</sup>; Anthony Rollett<sup>1</sup>; <sup>1</sup>Carnegie Mellon University; <sup>2</sup>Institut Jean-Pierre Bourgin

Tools developed to study microstructures in metal and ceramic polycrystals have been adapted to investigate biological tissues. Optical sections of an Arabidopsis cotyledon were obtained using confocal laser scanning microscopy. The cotyledon was reconstructed digitally using two different approaches to segment the individual cells, namely, 3D seeded watershed transform and Expectation Maximization/Maximization of Posterior Marginals segmentation. The 3D marching cubes method was then employed on the segmented data to reconstruct the tissue structure as a triangular mesh. The digital mesh was smoothed with the Constraint Line Smoothing technique and the cell shapes were evaluated with respect to volume, area, mean width and second order moment invariant measures. A combination of gene marking techniques and measurements of cell shapes can improve our understanding of cell differentiation and can be used to train Neural Networks to automate cell type detection.

## Characterization of Minerals, Metals and Materials: Poster Session

*Sponsored by:* The Minerals, Metals and Materials Society, TMS Extraction and Processing Division, TMS Structural Materials Division, TMS/ASM: Composite Materials Committee, TMS: Materials Characterization Committee

*Program Organizers:* Ann Hagni, Geoscience Consultant; Sergio Monteiro, State University of the Northern Rio de Janeiro - UENF; Jiann-Yang Hwang, Michigan Technological University

Sun PM-Thurs AM Room: 307  
February 14, 2010 Location: Washington State Convention Center

### Atom Probe Tomography Investigation of a Commercial Dual Precipitation Martensitic Steel: *F. Danoix*<sup>1</sup>; R. Danoix<sup>1</sup>; J. Akre<sup>1</sup>; D. Delagnes<sup>2</sup>; A. Grelier<sup>3</sup>;

<sup>1</sup>Université de Rouen; <sup>2</sup>Ecole des Mines d'Albi-Carmaux; <sup>3</sup>Aubert & Duval

The microstructural evolution of an industrial Fe-1C-10Co-2.5Cr-1Mo-14Ni-2Al (composition in at.%) secondary hardening martensitic steel during ageing from room temperature to several hours at 500°C has been studied by atom probe tomography. A complex precipitation sequence is evidenced. During the heating stage from room temperature to 500°C, two types of iron carbides, including Fe<sub>3</sub>C cementite, have been observed. During isothermal ageing at 500°C, secondary M<sub>2</sub>C type carbides and NiAl rich particles are shown to develop simultaneously, since the first seconds of ageing. The precipitation sequence, as well as the changes in the solute distribution between precipitates and matrix is investigated. After holding times prolonged up to 100 hours, very fine scale elongated particles of reverted austenite are also observed, and chemically analysed. Particular attention is paid to understand the synergetic aspects of these different precipitation stages. These researches were conducted under ANR grant 05-RNMP-008.

### Characterization of a Greensand Slate from Abaeté – Brazil to the Synthesis of a Potassium Thermophosphate: *Adriana da Silva*<sup>1</sup>; João Sampaio<sup>2</sup>; Francisco Garrido<sup>1</sup>; Marta Medeiros<sup>1</sup>; <sup>1</sup>UFRJ; <sup>2</sup>CETEM

Brazil has a large agricultural potential and the success of the production is related to the chemical and physical soil characteristics. Therefore, the demand in the use of a great quantity of fertilizers to compensate the low amount of nutrients in the soil include about 40% of food production costs. In order to develop economical alternatives to the traditional fertilizers, rocks with potential use in agriculture will be studied. In this work potassium rocks, such as a greensand slate and a phlogopite, will be chemically and structurally characterized for the development of a potassium thermophosphate. This alternative fertilizer will be obtained based in a fusion of a pondered mixture of potassium, magnesium and phosphate rocks to be applied in the Brazilian agriculture. Preliminary characterization results indicate that the greensand slate presents high percentage of glauconite and illite whereas the phlogopite presents basically phlogopite and talcum.

### Characterization of High Carbon Equivalent Cast Iron Using Thermal Analysis Curves: *Wenbin Zhou*<sup>1</sup>; Yongshen Yan<sup>1</sup>; Dengke Zheng<sup>1</sup>; Qin Hua<sup>1</sup>; Qijie Zhai<sup>1</sup>; <sup>1</sup>Shanghai University

In this paper the mechanical properties of high carbon equivalent cast iron for automobile brake discs were analyzed through thermal analysis curves. Experiment results show that the mechanical properties have a strong correlation with thermal analysis curves and an effective way to predict the mechanical properties of high carbon equivalent cast iron was proposed based on the features of thermal analysis curves.

### Characterization of Mechanochemically Synthesized ZrO<sub>2</sub>-B<sub>2</sub>O<sub>3</sub>-Mg System by Thermogravimetry/Differential Thermal Analyses and X-Ray Diffraction Studies: *Duygu Agaogullari*<sup>1</sup>; Fikret Aynibal<sup>1</sup>; Osman C. Demirhan<sup>1</sup>; Ismail Duman<sup>1</sup>; <sup>1</sup>Istanbul Technical University

Two different high-energy ball-mills (planetary ball-mill and Spex 8000 D mixer/mill) were used to mill the powder mixtures containing stoichiometric amount of zirconium dioxide (ZrO<sub>2</sub>), boron oxide (B<sub>2</sub>O<sub>3</sub>) and magnesium (Mg) with different durations (up to 100 hours). After the XRD analysis of the as-blended and milled powders, 25 mg of them were placed in a platinum crucible and heated up to 1200°C by 10°C.min<sup>-1</sup> under flowing Argon atmosphere for TG/DTA analysis. The powder mixtures were placed in alumina boats through

tube furnace under Argon atmosphere and heated up to the phase formation temperatures with a rate of 10°C.min<sup>-1</sup>. Then it was cooled rapidly to the room temperature by externally circulating ethanol-water mixture. The temperature ranges which exothermic peaks occur were examined for phase formations. The heated products were characterized by XRD in order to indicate and compare the certain phases form in both milling systems.

### Early-Stage Formation of Copper Nanoclusters in Model Reactor Pressure Vessel Steel: *Wei Wang*<sup>1</sup>; Bangxin Zhou<sup>1</sup>; Mindong Lin<sup>1</sup>; <sup>1</sup>Institute of Materials, Shanghai University

The formation of copper nanoclusters can cause hardening and embrittlement of nuclear reactor pressure vessel steels. Our work centered on achieving the composition evolution during the early-stage formation of copper nanoclusters. Cu nanoclusters are observed to form from high nickel regions. The data indicate that Cu segregates into the nanoclusters and Ni segregates to interface from the central cores with increasing Cu-Cu atom congregate. Based on experimental results, the effect of solute atoms on the early-stage formation of copper nanoclusters is discussed.

### Effect of Melt Superheat on Structure of Unsteady-State Unidirectionally Solidified Duplex Stainless Steel: *Z.J. Li*<sup>1</sup>; Xiang-ru Chen<sup>1</sup>; Qijie Zhai<sup>1</sup>; <sup>1</sup>Shanghai University

An experimental study with respect to the effect of melt superheat on the unidirectional solidified structure of duplex stainless steel is reported. The results show that the melt superheat causes distinct modifications of both macrostructure and microstructure of duplex stainless steel. For macrostructure of duplex stainless steel, the columnar to equiaxed transition is observed at different melt superheats. The length of equiaxed zone increases and the equiaxed grain size decrease with melt superheat decreasing. For microstructure of duplex stainless steel, there are significant differences in the morphology of the austenite at each location. In the interior of ferrite grains, the austenite appears primarily as acicular morphology. Nevertheless, the austenite takes on a Widmanstätten side plate appearance at the ferrite grain boundaries. In addition, the austenite content increases with melt superheat decreasing. Keywords: Melt superheat; Solidified structure; Duplex stainless steel; Widmanstätten

### Effect of Mg, Cu and Ni as Alloying Elements on the Dendritic Growth in an Al-7Si Cast Alloy: *Aline Hernandez-Garcia*<sup>1</sup>; Alejandro Garcia-Hinojosa<sup>1</sup>; Francisco Esteves-Alcazar<sup>1</sup>; Yvan Houbaert<sup>2</sup>; <sup>1</sup>UNAM; <sup>2</sup>Gent University

The properties of aluminum alloys in cast conditions could be increased if adequate alloying elements are added. One factor that defines the properties of the cast alloys is the plane or direction of dendritic growth, because this is done anisotropy. In the case of the A356 alloy (Al-7Si) in casting conditions, not only the eutectic Si determines the direction of preferential growth, it is also important the presence of alloying elements. This work studied the effect of the Cu, Mg and Ni alloying elements added to A356 alloy in the dendritic growth. Experimental alloys were analyzed using thermal analysis, optical metallography and figures poles by DRX. The better properties (more anisotropy) were reached for the Al-7Si-1.5Cu-1Mg-0.5Ni cast alloy.

### Effect of the Aged Heat Treatment on Al-Zn-Mg Alloys, in Texture, Microstructure and Properties of Corrosion: *Aline Hernandez-Garcia*<sup>1</sup>; Bernardo Campillo-Illanes<sup>1</sup>; Francisco Esteves-Alcazar<sup>1</sup>; Sergio Serna<sup>2</sup>; <sup>1</sup>UNAM; <sup>2</sup>CIICAP-UAEM

The light alloys have great application and demand in the industry. This work studies how the aging treatment takes part in the distribution and microstructural changes, as well on the texture of the Al-alpha phase. These is associated with the change in the corrosive properties of the new propose alloys Al-Zn-Mg. Being observed that it exists changes in the corrosive mechanism of reaction that have beginning in complex phases of Al<sub>x</sub>Mg<sub>y</sub>Zn<sub>z</sub>. Occurring optimal results in sample of 5 hours of treatment. These results are observed by tests of impedance, curves of polarization, metallography and figures of poles (DRX).

### Effects of Dolomite on Reduction Swelling Properties of Iron Ore Pellets: *Bin Xu*<sup>1</sup>; Tong Hou<sup>1</sup>; Xu-Ling Chen<sup>1</sup>; Qian Li<sup>1</sup>; Tao Jiang<sup>1</sup>; <sup>1</sup>Central South University

The effect of MgO on reduction swelling properties of oxide pellets was studied by adding different dosages of magnesium oxide. Results showed that the reduction swell index (RSI) reduce from 13.35% to 4% and the porosities of pellets were increased from 35% to 40% with the dosage increasing from 0.43% to 2.4%. High melting temperature magnesium ferrite was increased and



then Fe<sub>3</sub>O<sub>4</sub> was stabilized with the MgO contents increasing. Because there has no stage of  $\alpha$ -Fe<sub>2</sub>O<sub>3</sub> reducing to  $\gamma$ -Fe<sub>2</sub>O<sub>3</sub>, the RSI was reduced. As the porosities increased, it could absorb some of the volume swell due to crystal transfer and could decrease the diffusion resistance of the air, so it reduced the pressure of air volume expansion. Besides, dissociative quartz was reduced and formed calcium silicate, and magnesium solved into calcium silicate system, which stability its phase transition, so the RSI was improved.

**Embrittlement of Low Carbon Low Alloy Steel Occurring in the Austenite and  $\gamma$ -Ferrite Regions:** Xingjian Gao<sup>1</sup>; Dengfu Chen<sup>1</sup>; Mujun Long<sup>1</sup>; Liwei Song<sup>1</sup>; Jian Zhang<sup>1</sup>; Yanyan Bi<sup>1</sup>; Xianguang Zhang<sup>1</sup>; <sup>1</sup>Chongqing University

The mechanical properties of a low carbon low alloy steel in the austenite and  $\gamma$ -ferrite regions during continuous casting have been analyzed through the thermal-tensile tests using Gleeble-1500D system at temperatures in the range 600°C to 1300°C and a strain rate of 10<sup>-3</sup>/s. The yield strength and tensile strength of steel decreased with increasing test temperature and the embrittlement zone occurred in the temperature range 800°C to 970°C. In the embrittlement zone, the fracture surfaces and microstructures of the tensile specimens were examined by SEM. The results showed that the cause of the embrittlement at 950°C with the minimum %R of A around 36% is the second phase particle precipitated along the  $\gamma$  grain boundary during deformation leading to intergranular brittle fracture.

**FIB-Based Experimental Technique to Determine Phase Fractions of Two-Phase  $\gamma$  Titanium Aluminides:** Dennis Peter<sup>1</sup>; Martin Wagner<sup>1</sup>; Gunther Eggeler<sup>1</sup>; <sup>1</sup>Ruhr University Bochum

The properties of two-phase  $\gamma$ -TiAl alloys strongly depend on their microstructural constitution. An accurate quantitative microstructural characterization is therefore quite important. The present work introduces special preparation procedures utilizing the focused ion beam (FIB) technique to generate high contrast ion-induced secondary electron images. Two-phase structures, e.g. fine-lamellar colonies in  $\gamma$ -TiAl, can be imaged in high resolution with respect to individual phases, which allow to quantify the  $\alpha_2/\gamma$  phase fractions by conventional image analysis. To validate these data, we compare the FIB results to those obtained by phase determination using the electron backscatter diffraction (EBSD) method. The FIB technique generally provides higher  $\alpha_2$ -fractions, due to an improved lateral resolution near grain boundaries and interfaces compared to EBSD. Our results indicate that the FIB technique is a simple, fast and more exact way to characterize microstructural features with respect to different phase constitutions in TiAl.

**High Resolution Analysis of the Microstructure and Chemistry of a High-Strength Al-Zn-Mg-Cu Alloy:** Yi-Yun Li<sup>1</sup>; Libor Kovarik<sup>2</sup>; Wen-Hsiung Wang<sup>1</sup>; Yung-Fu Hsu<sup>3</sup>; Shan Trong<sup>4</sup>; Michael Mills<sup>2</sup>; <sup>1</sup>National Taiwan University; <sup>2</sup>The Ohio State University; <sup>3</sup>National Taipei University of Technology; <sup>4</sup>Chung-Shan Institute of Science and Technology

The microstructure and chemistry of the metastable phases (GP zones and  $\eta'$ ) in Al-Zn-Mg-Cu alloys are controversial issues despite many previous efforts devoted to their understanding. The role of copper, which is believed to have a significant contribution to the early stage of age hardening, is still unknown, but especially important to understand. In this study, we use HRTEM, HAADF, and EELS to characterize the metastable precipitates. From these careful microscopic observations and chemical analyses, the crystallographic aspect of the metastable structures has been revealed for the first time. The results enable us to gain more understanding of the effect of Cu on the hardening rate, precipitation sequence, precipitate coarsening, and morphology. The results will also be compared with previous work in the literature.

**Investigation of Life Prediction in Notched Specimens Subjected to Thermomechanical Loadings:** Justin Karl<sup>1</sup>; <sup>1</sup>University of Central Florida

Life prediction for components in gas turbines subjected to cyclic, non-isothermal, variable mechanical loading conditions, known as thermomechanical fatigue, is a complex problem with added difficulty introduced by complex shapes, particularly in the blades of the turbines. Turbine blade geometries offer a direct analog to notched test specimens with stress concentrations. To date, researchers have been unable to develop accurate life prediction models for notched parts that undergo thermomechanical conditions. This research details experimentation and analysis performed to extend data obtained from smooth and variably notched specimens to existing notched life prediction models. The experimental setup involves strain range cycling up to 2%, and thermal cycling in the range of 250-450 degrees Celsius of generic super-clean rotor steel used

primarily in steam turbines. The insight provided by these results will enable researchers to more expediently develop accurate life predictions in intricately designed components subjected to thermomechanical cycling.

**Investigation of Surface Area Change of Bauxite Particle in Digesting Process by Nitrogen Adsorption:** Li Bao<sup>1</sup>; Ting'an Zhang<sup>1</sup>; Guozhi Lv<sup>1</sup>; Zhihe Dou<sup>1</sup>; Yongnan Guo<sup>1</sup>; Xujian Wu<sup>1</sup>; Peiyuan Ni<sup>1</sup>; Jia Ma<sup>1</sup>; <sup>1</sup>Northeastern University

The microstructure properties of red mud particles produced by bauxite digesting in sodium aluminate solution in autoclave have been investigated. Nitrogen adsorption at boiling temperature (77 K) which represents the most widely used technique to determine particle surface area and to characterize its porous texture was employed to measure the surface area, pore volume and pore size of red mud particle performing on Micromeritics ASAP 2020 (America). Based on nitrogen adsorption-desorption isotherm, BET method and Langmuir method were discussed respectively. On the theoretical analysis and experimental data, both methods are suitable to determine the surface area of red mud particle, but BET method is better than Langmuir method. The measured data of Chinese diaspora particle digesting under different digestion temperatures and times reflect the digestion performance.

**Magnetic and Transport Properties of Half Doped Manganites:** Nitta Swamy<sup>1</sup>; R. Singh<sup>1</sup>; <sup>1</sup>MATS University, Raipur (C.G)

The manganites and Multiferroic materials have potential technological applications in the magnetic sensors, computer hard drive reader, logic devices, magnetic refrigeration, magnetic memory storage, electric motors, loudspeakers, transformers, automobiles, magnetic resonance devices and a diverse range of scientific instruments from large particle-accelerators to tiny multimeters. The continuous evolution is taking place in the field of magnetic materials which are important components of the modern technologies. Often classes of magnetic materials are discovered with new interesting functionality, which stimulates the growth of newer technology. The recent research activities pertaining to important class of manganites and multiferroic materials narrated below provide a platform to discuss such emerging science and technology involving newer class of functional magnetic materials.

**Mechanical Behavior of Epoxy Composites Reinforced with Acetylation-Treated Coir Fibers:** Helvio Santafe<sup>1</sup>; Lucas Costa<sup>1</sup>; Ruben Jesus Rodriguez<sup>2</sup>; Felipe Lopes<sup>1</sup>; Sergio Monteiro<sup>1</sup>; <sup>1</sup>State University of the Northern Rio de Janeiro - UENF

The coir fiber extracted from the husk of the coconut has been extensively used as polymer composite reinforcement in a variety of industrial applications ranging from civil construction to automobile seat cushions. The hydrophilic coir fiber does not act as an effective reinforcement owing to its low interfacial strength with hydrophobic polymers. As a consequence, coir fiber composites display relatively low mechanical strength. The objective of this work was to investigate the effect of an acetylation treatment of the coir fiber surface on the mechanical behavior of epoxy composites with amounts of fibers up to 30% in volume. Coir fibers were immersed in an acid solution of acetic anhydride for one hour, washed and dried, before mixing with DGEBA/TETA epoxy to fabricate the composites. Flexural mechanical properties were obtained by bend tests. The results showed significant differences to similar composites with alkali treated coir fibers that have been previously investigated.

**Microstructural Evolution and Tensile Behavior in Heat-Treated Ti-5111 Alloy:** Vikas Dixit<sup>1</sup>; John Sosa<sup>1</sup>; Daniel Huber<sup>1</sup>; Peter Collins<sup>1</sup>; Hamish Fraser<sup>1</sup>; <sup>1</sup>The Ohio State University

Ti-5Al-1V-1Zr-1Sn-0.8Mo (Ti-5111) alloy is relatively unexplored 'near alpha' titanium alloy. In this work, a database for a statistics based neural network relating tensile properties with a wide range of microstructural variations in terms of both, size and morphology has been developed. Preliminary results will be discussed that establish the features that are relevant to controlling tensile properties. These features have been quantified using traditional 2-D stereological methods, as well as advanced 3-D techniques such as DualBeam™ FIB/SEM and Robomet.3D. It will be shown that for some features, the stereological methods provide reasonable approximations of what is directly obtained in 3D, while such methods fail for others.

**Microstructural Evaluation of Mullite as a Function of the Parameters of Sintering with Microwave:** *Maria Brasileiro<sup>1</sup>; Daniele Cavalcante<sup>2</sup>; Elieber Bezerra<sup>1</sup>; Romualdo Menezes<sup>1</sup>; Gelmires Neves<sup>1</sup>; Heber Ferreira<sup>1</sup>; Lisiane Santana<sup>1</sup>;* <sup>1</sup>Universidade Federal de Campina Grande; <sup>2</sup>Universidade Federal da Paraíba

In recent years, the use of microwave energy in the processing and acquisition of materials, has attracted special interest from different areas of knowledge such as materials of engineering. This interest is directly connected to its simple usage, besides reducing the number of steps in many syntheses, improved physical properties in ceramic technology and be combined with energy saving / time achieved in the processing of many materials. In this study, compositions containing residue of kaolin and alumina were sintered in a microwave oven home in order to obtain the mullite. The samples were produced by uniaxial pressing at pressure of 35 MPa and sintered in powers of 80 and 90% with times of 10, 15 and 20 min. The samples were analyzed by SEM and XRD. It was observed that with the increase of the processing variables of the peak intensity of mullite phase increased.

**Novel Techniques for the Investigation of the Mechanical Properties of Single Crystal Iridium:** *Douglas Stauffer<sup>1</sup>; Ryan Major<sup>2</sup>; William Gerberich<sup>1</sup>;* <sup>1</sup>University of Minnesota; <sup>2</sup>Hysitron, Inc.

Iridium allows the unique opportunity to study the deformation of a high-modulus FCC metal devoid of a surface oxide at room temperature. Here, a single-crystal, electropolished, sample of Iridium oriented in the <100> is examined by indentation and scratch techniques. Depth sensing indentation, normally used to obtain hardness and modulus, is used to determine the activation volume for dislocation nucleation by stress relaxation and dislocation wall spacing. Conductive probe indentation, using Hysitron's nanoECR™, gives insight into incipient plasticity, as well as demonstrating electrical contact behavior without an interfering oxide layer. Fracture testing by the scratch method pulls the material into tension behind the tip, while compressing the material in front during loading in both the x and z direction. The singularity occurring under the tip provides the necessary stress to nucleate cracks, and a linear, first-order, elasticity fracture solution gives the value for  $K_{IC}$ .

**On the Precipitation of the Omega Phase in the Beta Matrix of Titanium Alloys:** *Arun Devaraj<sup>1</sup>; Robert Williams<sup>2</sup>; Soumya Nag<sup>1</sup>; Srinivasan Rajagopalan<sup>2</sup>; Srinivasan Srivilliputhur<sup>1</sup>; Hamish Fraser<sup>2</sup>; Rajarshi Banerjee<sup>1</sup>;* <sup>1</sup>University of North Texas; <sup>2</sup>The Ohio State University

The precipitation of the omega phase in beta titanium alloys influence the beta to alpha phase transformation and the final mechanical properties of these alloys. Understanding of beta to alpha phase transformation in beta titanium alloys will enable us to predict and control microstructural development via heat treatments. In this work advanced characterization techniques such as 3D atom probe tomography and probe corrected high-resolution scanning transmission electron microscopy will be employed in combination with first principle calculations using Vienna Ab initio Simulation Package (VASP) to understand the atomic scale structure, chemistry, and energetics associated with the precipitation of omega phase in pure titanium and Ti-9at% Mo. The energetics of beta to omega transformation path, proposed by De. Fontaine et al (Acta Metallurgica, vol. 19, p 1153 (1971)), will be determined using VASP. This will complement our experimental results and provide insight into the omega precipitation in beta titanium alloys.

**Onset of Void Coalescence Studied by X-Ray Computed Tomography:** *Akihide Hosokawa<sup>1</sup>; David Wilkinson<sup>1</sup>; Eric Maire<sup>2</sup>;* <sup>1</sup>McMaster University; <sup>2</sup>INSA-Lyon

Ductile fracture in metals occurs after significant amount of plastic deformation, involving the three progressive processes namely, nucleation, growth and coalescence of voids. To study the behaviors of internal voids, X-ray computed tomography (XCT) seems quite useful due to its capability to visualize internal defects (e.g. cracks). In fact, a rather newer technique called fast tomography was recently developed. This novel technique made it possible to record a series of tomograms in non-stop deformation. In this study, fast tomography coupled with in-situ tensile deformation was performed at ESRF ID15 (white X-ray from wigglers) to study the void growth and coalescence in a class of model materials in which an arbitrary artificial void array is embedded in copper matrix. The onset of void coalescence was successfully visualized. The measurement of the void diameters along principal stress directions allowed us to capture the void growth and its termination by coalescence quantitatively.

**Phase Equilibria in the  $La_{1-x}Ca_xFeO_{3-d}$  System:** *Patrick Price<sup>1</sup>; Ellen Rabenberg<sup>1</sup>; David Thomsen<sup>1</sup>; Darryl Butt<sup>1</sup>;* <sup>1</sup>Bosie State University

Lanthanum calcium ferrite (LCF) materials are non-stoichiometric complex oxide ceramics with the general chemical formula  $La_{1-x}Ca_xFeO_{3-d}$ . The end members  $LaFeO_3$  and  $Ca_2Fe_2O_7$  have a perovskite and brownmillerite structure, respectively. Previous investigations have shown that temperature, oxygen partial pressure, and synthesis methods all have an impact on the resulting LCF structure and properties. Presently, a comprehensive phase diagram does not exist for the ternary  $LaO_{1.5}$ - $CaO$ - $FeO_{1.5}$  or pseudo binary  $La_{1-x}FeO_{3-d}$ - $Ca_2FeO_{3-d}$  systems at more than one temperature. In this study we have synthesized  $La_{1-x}Ca_xFeO_{3-d}$  materials for  $0 \leq x \leq 1$  using solid state reaction methods. Pellets of select compositions, initially sintered at 1250 °C, were annealed, quenched, and subsequently characterized with x-ray diffraction and electron microscopy. Compositions which exist as a single phase at elevated temperatures decompose into at least 2 phases at lower temperatures. A novel pseudo binary phase diagram mapping this multiple phase region has been proposed.

**Precipitate Characterization in a NiAl-Strengthened Ferritic Steel:** *Zhenke Teng<sup>1</sup>; Michael Miller<sup>2</sup>; Peter Liaw<sup>1</sup>; Chain Liu<sup>1</sup>;* <sup>1</sup>University of Tennessee, Knoxville; <sup>2</sup>Oak Ridge National Laboratory

NiAl-strengthened ferritic steels are potential steam turbine materials. In this system, B2-ordered NiAl precipitates may form having a coherent-coplanar orientation with the BCC Fe matrix. This microstructure exhibits good creep resistance at high temperatures. However, the structure, morphology, and composition of the NiAl precipitates have not been fully identified. Atom probe tomography has been used to study the NiAl precipitates, and revealed that the microstructure of an aged NiAl-strengthened ferritic steel (Fe-12.7%Al-9%Ni-10.2%Cr-1.9%Mo) contains primary Ni<sub>41.2</sub>Al<sub>41.6</sub>Fe<sub>12.7</sub>Cr<sub>0.8</sub>Mo<sub>1.4</sub> precipitates and hyperfine secondary Ni<sub>26.3</sub>Al<sub>41.6</sub>Fe<sub>26.9</sub>Cr<sub>3.3</sub>Mo<sub>1.7</sub> precipitates. The existence of the secondary precipitates together with the large amount of Al remaining in the matrix contributes to the poor room temperature ductility. This project is sponsored by the U.S. Department of Energy, Office of Fossil Energy. Research at the Oak Ridge National Laboratory SHaRE User Facility was sponsored by the Scientific User Facilities Division, Office of Basic Energy Sciences, U.S. Department of Energy.

**Semi-Automated Characterization of the Gamma Prime Phase in Ni-Based Superalloys via High-Resolution Backscatter Electron Imaging, Segmentation, and Stereology:** *Eric Payton<sup>1</sup>; Patrick Phillips<sup>1</sup>; Michael Mills<sup>1</sup>;* <sup>1</sup>Ohio State University

Quantitative characterization of materials microstructure is required for the development and calibration of models of microstructural evolution. Automated analysis of metallographic images is desired for rapid quantitative characterization of microstructure. The size distribution of second-phase particles can play a significant role in microstructural evolution, so it is of substantial importance to be able to measure such size distributions. The backscatter signal in the scanning electron microscope yields images that are more readily segmented with image processing algorithms than other signals, but the interaction volume complicates stereology of such images. This imaging bias has been modeled using monte carlo techniques to develop stereological corrections, such that backscatter imaging can be used for semi-automated characterization of the gamma prime phase in Ni-based superalloys. The methods developed have been applied to the study of the dissolution of the gamma prime phase, which plays an important role in grain coarsening during heat treatment.

**Surface Characterization of Single and Mixed Mineral Systems Using Sedimentation Potential:** *Salah Uddin<sup>1</sup>; Mitra Mirnezami<sup>1</sup>; James Finch<sup>1</sup>;* <sup>1</sup>McGill University

An integrated device has been developed to measure sedimentation potential, conductivity and pH simultaneously of particulate systems. Maxwell's model was used to calculate volume fraction of solid from the conductivity data. In this approach, since all system variables are known, zeta potential can be calculated from Smoluchowski's equation. Zeta potential variation with pH is presented for alumina and silica suspension and compared with electrophoresis measurements. Mixed alumina/silica systems were studied with this technique. Sufficient column height was maintained along with size difference between two minerals to allow gravity separation during settling. Sedimentation potential was measured with time. XRD was performed to identify the composition of the samples collected from the column in different times. Results indicated



correlation between surface charge and sample composition. This is a step towards characterizing surface charge of mixed systems of interest in mineral processing.

**Synthesis of Lanthanum Orthophosphate and Polyphosphate in Condensed Phosphoric Acid Solutions:** *Naoyuki Hatada*<sup>1</sup>; Yoshitaro Nose<sup>1</sup>; Tetsuya Uda<sup>1</sup>; <sup>1</sup>Kyoto University

Lanthanum orthophosphate,  $\text{LaPO}_4$ , and lanthanum polyphosphate,  $\text{LaP}_3\text{O}_9$ , are considered as potential solid electrolytes in fuel cells. They exhibit relatively high proton conductivities when doped with alkaline earth metals. For practical use, however, further enhancement of the conductivities is necessary while the proton conductivity mechanism has not been understood. For example, it is unknown whether the bulk conduction or grain boundary conduction is dominant. To determine it, we aimed at measuring proton conductivities using samples with different grain sizes. However, the synthesis method of these compounds with sufficiently large grains has not been established. In this study, we examined synthesis conditions of large crystals of lanthanum phosphates in condensed phosphoric acid solutions. We also investigated the solubility of dopant Sr, and the relationship between the amount of Sr and the proton conductivities.

**Temperature and Orientation Dependence of the Plastic Flow Behavior of Tantalum:** *Zhi Duan*<sup>1</sup>; Andrea Hodge<sup>1</sup>; <sup>1</sup>University of Southern California

The plastic flow behavior of single crystal bcc tantalum with different orientations was studied at various temperatures ranging from 25 to 200° using nanoindentation. The shape of the load-displacement curves showed correlations to crystal orientations as well as temperatures. The discontinuities in p-h curves (pop-ins) in tantalum were observed in different forms including single large pop-in at room temperature, which is considered as a major feature of bcc materials, as well as multiple pop-ins at elevated temperatures, usually observed in fcc materials. Detailed studies revealed this variation was related to the onset of dislocation activities and not to oxide layer and/or thermal drift.

**The Development of Databases Relating Microstructure and Mechanical Properties in Ti-5Al-5Mo-5V-3Cr-0.5Fe (Timetal 555):** *John Foltz*<sup>1</sup>; Brian Welk<sup>1</sup>; Peter Collins<sup>1</sup>; James Williams<sup>1</sup>; Hamish Fraser<sup>1</sup>; <sup>1</sup>The Ohio State University

Thermal and thermo-mechanical processing metastable  $\beta$ -Ti alloys, such as Timetal 555, can result in a rich variety of microstructures that affect mechanical properties. Until recently, limited data was available for Timetal 555 relating the size and distribution of microstructural features to properties such as yield strength and fatigue life. We are developing such a knowledge base using sub-scale tension tests and four-point bend fatigue tests on material that was thermally processed in a Gleeble® 1500 thermo-mechanical simulator. The microstructural features of these  $\beta$  solutionized and aged treatments have been characterized at the TEM, SEM and optical length scales. The influence of microstructure on yield strength, elongation to failure and tensile strength has been identified using neural networks. Preliminary results to establish a similar neural network relating fatigue life and microstructure will also be presented.

**The Effect of Y on the Refinement of Cast and Rapidly Solidified TiAl Alloys:** *Zhiguang Liu*<sup>1</sup>; Lihua Chai<sup>1</sup>; Yuyong Chen<sup>1</sup>; <sup>1</sup>Harbin Institute of Technology, China

The effect of rare earth element Y (0-1.0at.%) on the microstructure of TiAl alloys in the as cast and rapidly solidified conditions has been investigated. The results show that the addition of yttrium greatly refined the microstructure of TiAl alloys in the both conditions. The refinement is more significantly with increasing the content of yttrium. The mechanism of the refinement of Y in the cast alloys is that the yttrium rich phase as ribbon-shaped locating on the grain boundaries impedes the grain growth during the solidification process. But in the rapidly solidified alloys, yttrium rich phase as global particles dispersing uniformly on the matrix became the heterogeneous nucleation site which increasing the rate of nucleation of the  $\gamma$  phase during the  $\alpha$  to  $\gamma$  phase transformation, a refined initial microstructure formed during the solidification process. And the higher cooling rate can restrict the grain growth during further cooling.

**The Microstructure and Mechanical Behavior of  $\text{Fe}_{30}\text{Ni}_{20}\text{Mn}_{30}\text{Al}_{20}$  Alloys:** *Xiaolan Wu*<sup>1</sup>; Ian Baker<sup>1</sup>; Hong Wu<sup>1</sup>; Micheal Miller<sup>2</sup>; Kaye Russell<sup>2</sup>; <sup>1</sup>Thayer School of Engineering, Dartmouth College; <sup>2</sup>Materials Science and Technology Division, Oak Ridge National Laboratory

High strength, near equiatomic FeNiMnAl alloys have recently been discovered. Characterization by transmission electron microscopy, scanning electron microscopy and atom probe tomography has revealed that arc-melted and drop-cast  $\text{Fe}_{30}\text{Ni}_{20}\text{Mn}_{30}\text{Al}_{20}$  alloys exhibit different microstructures - a periodic spinodal structure of b.c.c and B2 phases aligned along  $\langle 100 \rangle$  directions and a lamellar eutectic structure. The hardness of the as-arc-melted alloy increased from 454 to 657 HV after annealing for 67 h at 823 K. However, no significant difference in the hardness ( $\sim 230$  HV) was found in the drop-cast alloy. The results of tensile tests performed at different strain rate on the as-drop-cast alloy will be reported. The relationship between the mechanical properties and the microstructures of these alloys will be discussed. Research supported by DOE Award #DE-FG02-07ER46392; the ORNL SHaRE User Facility which was sponsored by the Scientific User Facilities Division, Office of Basic Energy Science, U.S. Department of Energy.

**Thermodynamic Research of the Dissolving of Chrysocolla ( $\text{CuSiO}_3 \cdot \text{H}_2\text{O}$ ) in the Ammonia-Ammonium Chloride-Water System:** *Liu Wei*<sup>1</sup>; Tang Motang<sup>1</sup>; Tang Zhaobo<sup>1</sup>; He Jing<sup>1</sup>; Yang Jianguang<sup>1</sup>; Yang Shenghai<sup>1</sup>; <sup>1</sup>Central South University

In order to make clear the dissolving characteristic of the chrysocolla ( $\text{CuSiO}_3 \cdot \text{H}_2\text{O}$ ) in the ammonia-ammonium chloride solution, a thermodynamic model of the chrysocolla ( $\text{CuSiO}_3 \cdot \text{H}_2\text{O}$ )-ammonia-ammonium chloride-water system is established using the exponential computation method based on both mass balance and charge balance equations. The equation group of the thermodynamic model is solved by the MATLAB Soft on PC. The condition which is favorable for dissolving high concentration of copper in solution is making out. The stable area of chrysocolla ( $\text{CuSiO}_3 \cdot \text{H}_2\text{O}$ ) and the condition of chrysocolla ( $\text{CuSiO}_3 \cdot \text{H}_2\text{O}$ ) converting to atacamite ( $\text{Cu}(\text{OH})_{1.5}\text{Cl}_{0.5}$ ) is also studied. A group of experiments are designed to validate the veracity of the results of the thermodynamic calculation.

**Three-Dimensional Atom-Probe Tomography of High-Strength Low-Carbon Steels Containing Multiple Phases:** *Mike Mulholland*<sup>1</sup>; David Seidman<sup>1</sup>; <sup>1</sup>Northwestern University

Laser-assisted local-electrode atom-probe (LEAP) tomography is an excellent tool for obtaining three-dimensional nanoscale spatial and compositional information from a wide-range of materials. This makes it highly useful for the characterization of BA160, which is a high strength, low-carbon steel strengthened by nanoscale copper and M2C carbide precipitation. Laser-assisted LEAP tomography permits significantly larger datasets to be collected than voltage-pulsed LEAP tomography, which produces smaller datasets due to tip fracture. However, significantly lower copper concentrations within copper precipitates are observed by laser-pulsed LEAP tomography as compared to voltage-pulsed LEAP tomography. A procedure is developed to produce usable precipitate size distributions (PSDs) and volume fractions from laser-pulsed LEAP tomography using a correction based on voltage-pulsed LEAP tomographic experimental data. The differences between M2C carbide evaporation behavior when using laser-pulsed LEAP or voltage-pulsed LEAP are also compared in detail. This approach is extremely important for obtaining quantitatively correct concentrations in this complex steel.

**Ultrasonic Characterization of Copper using Wavelet Analysis:** *Prasad Shanmugasandaram*<sup>1</sup>; Narayani Narasimhan<sup>1</sup>; Kalayappan Srinivasan<sup>1</sup>; Praveen Selvaraj<sup>1</sup>; <sup>1</sup>Anna University

The effectiveness of ultrasonic velocity measurements and attenuation of the propagating pulse was evaluated as a means of Non-Destructive characterization of cold worked and annealed copper. Commercial copper is subjected to mechanical working such as forging, rolling and thermal treatment to induce re-crystallization. The microstructural changes that occur in copper and variations in its mechanical properties are subjected to analysis using the ultrasonic technique. The signal processing is carried out using the wavelet analysis technique. The features of wavelet analysis namely localization in space and presence of infinite set of basis functions allows removing noise from the time series and components of a non-stationary signal to be analyzed and also proves to be increasingly effective and notably time saving procedure.

# Technical Program

This is seen to improve the accuracy of the results obtained from the ultrasonic technique in the case of copper, which has distinct coarse grains that are difficult to inspect due to backscattering from grain boundaries

## Computational Thermodynamics and Kinetics: Poster Session

*Sponsored by:* The Minerals, Metals and Materials Society, TMS Electronic, Magnetic, and Photonic Materials Division, TMS Materials Processing and Manufacturing Division, TMS Structural Materials Division, TMS: Chemistry and Physics of Materials Committee, TMS/ASM: Computational Materials Science and Engineering Committee  
*Program Organizers:* Jeffrey Hoyt, McMaster University; Dallas Trinkle, University of Illinois at Urbana-Champaign

Sun PM-Wed AM Room: 308  
February 14, 2010 Location: Washington State Convention Center

### Atomistic Modeling of Solid-Liquid Interfaces Subject to Lateral Stresses: T. Frolov<sup>1</sup>; Y. Mishin<sup>1</sup>; <sup>1</sup>George Mason University

We present results of atomistic computer simulations of solid-liquid interfaces when the solid is subject to non-hydrostatic stresses. The methodology includes molecular dynamics simulations, the semi-grand canonical Monte Carlo method and embedded-atom potentials. A generalized adsorption equation and various thermodynamic integration schemes are applied to study the effect of applied lateral stresses (uniaxial, biaxial, tension, compression, etc.) on the interface stress, interface free energy, segregation and other thermodynamic properties. As expected from thermodynamic relations, the shift of the solid-liquid equilibrium temperature is found to be quadratic in non-hydrostatic components of the stress tensor in the solid. At a critical value of the lateral compression stress, the interface loses stability and triggers rapid crystallization into stress-free solid, leaving a relatively sharp stressed/unstressed solid/solid interface behind.

### Atomistic Simulation of Segregation Coefficient of High Concentration Ni-Cu Alloys: Harith Humadi<sup>1</sup>; Jeff Hoyt<sup>1</sup>; Mark Asta<sup>2</sup>; Yang Yang<sup>3</sup>; <sup>1</sup>McMaster University; <sup>2</sup>University of California, Berkeley; <sup>3</sup>East China Normal University

The segregation coefficient,  $k(V)$ , and its dependency on the solidification rate has been modeled by Aziz and subsequently by Sobolev. Recently, molecular dynamics (MD) simulations have been performed on dilute systems to test the validity of these models. However, there is no real understanding of the effect of higher concentration(s) on the segregation coefficient. In this work, MD simulations of different concentration(s) have been performed on a model alloy of the Ni-Cu system using the embedded atom method. The solute trapping behavior at different concentrations will be compared in terms of their driving forces and trapping velocities.

### Developing Reliable Interatomic Potentials for HCP Mg-Li Alloys from Ab Initio and Experimental Data: Alex Welcing<sup>1</sup>; <sup>1</sup>University of North Texas

Ultralight hexagonal close packed (HCP) Mg-Li alloys have potential transportation related applications if we can overcome fundamental issues such as instability of its room temperature mechanical properties. This talk will summarize our efforts to develop an interatomic potential for HCP Mg-Li alloys using a modified embedded atom method approach (MEAM) derived from a database of ab initio and experimental data (when available). Ab initio calculations are used to determine single crystal elastic constants, vacancy and interstitial formation and migration energies of 10 HCP Mg-Li alloys. From these, engineering properties such as the ratio of bulk modulus over shear modulus (B/G) and the ratio of Young's modulus over mass density ( $Y/\rho$ ) are calculated. B/G and  $Y/\rho$  values of HCP Mg-Li alloys are compared with those of BCC Mg-Li alloys. An Ashby map of  $Y/\rho$  versus B/G is generated to determine whether or not it is possible to increase both  $Y/\rho$  and B/G by changing only the Li composition.

### Development of Reliable Interatomic Potentials for HCP Mg-Li Alloys from Ab Initio and Experimental Data: Alex Welcing<sup>1</sup>; Srinivasan Srivilliputhur<sup>1</sup>; M. Baskes<sup>2</sup>; Alfredo Caro<sup>3</sup>; <sup>1</sup>University of North Texas; <sup>2</sup>Los Alamos National Laboratory; <sup>3</sup>Lawrence Livermore National Laboratory

Ultralight hexagonal close packed (HCP) Mg-Li alloys have many potential applications if we can overcome issues including instability of their room temperature properties. We summarize our efforts to develop a modified embedded atom method approach (MEAM) interatomic potential for HCP Mg-Li alloys using an ab initio and experimental database. Ab initio calculations are used to determine single crystal elastic constants, vacancy and interstitial formation and migration energies of 10 HCP Mg-Li alloys. From these, engineering properties such as the ratio of bulk modulus over shear modulus (B/G) and the ratio of Young's modulus over mass density ( $\gamma/\rho$ ) are calculated. B/G and  $\gamma/\rho$  values of HCP Mg-Li alloys are compared with those of BCC Mg-Li alloys. An Ashby map of  $\gamma/\rho$  versus B/G is generated to determine whether or not it is possible to increase both  $\gamma/\rho$  and B/G by changing only the Li composition.

### Diffusion on Al-Type Sites in Intermetallic Phases Having the Tetragonal Al<sub>4</sub>Ba Structure: Gary Collins<sup>1</sup>; Randal Newhouse<sup>1</sup>; Samantha Cawthorne<sup>1</sup>; <sup>1</sup>Washington State University

The Al<sub>4</sub>Ba structure is very common. It has two inequivalent Al-sites, each with two atoms per formula unit. Each site is surrounded by atoms of the other site, so that diffusion carries atoms between the two sublattices. Due to differing, but collinear, electric field gradients (EFG) at the two sites, the EFGs at jumping atoms fluctuate in magnitude. For large jump frequencies, this leads to motional averaging of quadrupole interaction frequencies that we have studied in many phases using perturbed angular correlation spectroscopy (PAC). At low temperature, one observes two quadrupole interaction frequencies. With increasing temperature, the apparent frequencies approach and then merge, above which temperature one observes only a single signal. The jump frequency at the temperature of merge is approximately equal to the difference in the static quadrupole interaction frequencies. An overview of results for many phases and their interpretation will be given.

### Effects of Tempering on Fe-Atom Vibrations in Martensitic Steel: Lisa Mauger<sup>1</sup>; Brent Fultz<sup>1</sup>; <sup>1</sup>California Institute of Technology

Martensitic steels have non-equilibrium distributions of carbon atoms, and the rearrangements of carbon atoms upon tempering are responsible for major changes in mechanical properties. We studied how the phonon dynamics and vibrational entropy of AISI 1095 steel and quenched Fe-C alloys are changed by tempering. Measurements with inelastic nuclear resonant scattering of synchrotron radiation showed that the quenched martensite had a broadened phonon spectrum that sharpened with tempering towards that of pure bcc Fe. Large changes to the phonon spectra occurred after tempering at only 125 C. The vibrational entropy of the quenched material was approximately 0.1 k<sub>B</sub>/atom larger than that of the tempered alloys, although the vibrational spectra of carbon atoms remains to be obtained. The implications to the thermodynamic stability of martensite seem to be modest.

### First-Principles Calculations on Impurity Substituted Cementite: Chaitanya Krishna Ande<sup>1</sup>; Marcel Sluiter<sup>2</sup>; <sup>1</sup>Materials Innovation Institute, Delft University of Technology; <sup>2</sup>Delft University of Technology

So far, most steel research has been based on time consuming, expensive experimental work and thermodynamic models made to fit experimental data. To overcome this, considerable effort is being made to incorporate first-principles calculations. As a first step, we study the energetics of partitioning of alloying elements between the cementite and ferrite phases in steel. Cementite is the most commonly formed carbide phase in steel. It's stability can be altered by the alloying elements used in steel. We show how T=0 K first-principles calculations can be at variance with experiments and how magnetism plays an important role in explaining the differences. Effects of the alloying elements on the nearest neighbor distribution, total magnetization, and finite size effects of the supercells will also be presented.



**Grain Boundary and Interfacial Energy Database for Fe in a Suitable Form for Simulation of Microstructure Evolution:** *Hyun-Kyu Kim*<sup>1</sup>; Seong Gyoon Kim<sup>2</sup>; Byeong-Joo Lee<sup>1</sup>; <sup>1</sup>POSTECH; <sup>2</sup>Kunsan National University

Meso-scale simulations such as Phase Field or Monte Carlo are widely used for prediction of microstructure evolution in polycrystalline materials. Since the results are highly sensitive to the grain boundary or interfacial energy given as input data, realistic values of misorientation and energy (especially their misorientation dependency) for grain boundaries or interfaces are necessary for realistic simulations. In the present work, a method how to identify a grain boundary (or interface) between two arbitrarily oriented grains and how to arrange all possible grain boundaries (or interfaces) to construct a grain boundary property database will be proposed.  $\alpha/\alpha$ ,  $\gamma/\gamma$  grain boundary and  $\alpha/\gamma$  interfacial energy databases for Fe obtained using a molecular statics calculation will also be presented. Then it will be shown that the constructed grain boundary (or interface) property database can be successfully implemented in meso-scale simulation codes for prediction of microstructure evolution based on realistic grain orientations.

**Grain Growth Stagnation due to Grain Boundary Roughening:** *Elizabeth Holm*<sup>1</sup>; Stephen Foiles<sup>1</sup>; <sup>1</sup>Sandia National Laboratories

The thermodynamic equilibrium state of crystalline materials is a single crystal; however, polycrystalline grain growth almost always stops before this state is reached. While typically attributed to solute drag, stagnation occurs even in high purity materials. Molecular dynamics (MD) simulations indicate that boundaries undergo thermal roughening associated with an abrupt mobility change. At typical annealing temperatures polycrystals will contain both smooth (slow) and rough (fast) boundaries. When the roughening transition is included in a mesoscale grain growth model, even small fractions of smooth, slow boundaries stop grain growth, with the final grain size dependent on the smooth boundary fraction. In MD simulations of atomic-scale polycrystals, grain radius initially increases with the square root of time and then slows dramatically at a characteristic grain radius, in quantitative agreement with the mesoscale model predictions. We conclude that grain boundary roughening provides an alternate stagnation mechanism that applies even to high purity materials.

**Kinetics of ALN Precipitation in the Ferrite Phase Field of Microalloyed (HSLA) Steels:** *Rene Radis*<sup>1</sup>; Ernst Kozeschnik<sup>1</sup>; <sup>1</sup>Vienna University of Technology

In the present work, the thermodynamic information on aluminium nitride formation and experimental precipitation kinetics data are reviewed. Using the software package MatCalc and a revised expression for the Gibbs energy of AlN, computer simulations of AlN precipitation kinetics are performed and compared to several independent experimental results. For this purpose a new model for precipitation at grain boundaries is used, which takes into account fast short-circuit diffusion along grain boundaries as well as the slower bulk diffusion of atoms from inside the grain to the grain boundaries. Furthermore the precipitation of randomly distributed precipitates at dislocations is considered, taking into account the volumetric precipitate/matrix mismatch. Apart from the grain size, all simulations are performed with one set of input parameters. Depending on chemical composition, grain size and annealing temperature a predominant precipitation at grain boundaries or at dislocations is observed as well as the combination of both precipitate types.

**Kinetics of Corrosive Defects Formed on Au Substrates Accompanied by Alkanethiol Monolayer Assembly in the Presence of Oxygen:** *Zhong Cao*<sup>1</sup>; Pu-Ni Zeng<sup>1</sup>; Xiao-Chuan He<sup>1</sup>; Dao-Chang Huang<sup>1</sup>; Ling Zhang; <sup>1</sup>Changsha University of Science and Technology

The mechanism and kinetics of corrosive defects formed on Au substrates accompanied by alkanethiol monolayer assembly in the presence of oxygen have been investigated by using in situ quartz crystal microbalance (QCM) and atomic force microscopy (AFM). The gold lost from the in situ QCM could be well explained by the AFM image, which evidently shows the corrosive defects or holes produced on the corresponding Au surface. The initial corrosion rate on gold was calculated to be  $9.2 \times 10^{11}$  Au atoms  $\text{cm}^{-2} \text{s}^{-1}$ . For a long-term Au corrosion occurred during alkanethiol assembled process, the kinetics behavior has been determined with an atomic absorption spectroscopy (AAS). The corrosion rate on the long-term Au dissolution on Au plates was calculated to be  $1.3 \times 10^8$  Au atoms  $\text{cm}^{-2} \text{s}^{-1}$ . Both corrosive kinetics equations obtained with QCM and AAS show a consistent corrosion trend on Au substrates.

**Local Interface Phenomenon on the Coalescence Kinetics in Ni-Base Alloys:** *Youhai Wen*<sup>1</sup>; Jeff Simmons<sup>2</sup>; Chris Woodward<sup>2</sup>; <sup>1</sup>UES, Inc; <sup>2</sup>AFRL The high coalescence rate in modeling gamma-prime microstructural evolution becomes serious in simulations with high volume fractions of gamma prime precipitate (e.g. higher than 60%). While the out-of-phase domains that come into contact tend to maintain a thin layer of gamma matrix phase between them due to favorable APB/interfacial energy considerations, the in-phase domains tend to coalesce into one single domain to remove the extra matrix layer and reduce the interfacial energy. In phase field simulations of this latter process the simulated coalescence rate is extremely high compared with experimental observations. We identified that this is a result of ignoring the local phenomenon in the gamma and gamma prime interface regions in all major simulation methods. Reasonable coalescence rate is achieved by properly addressing this local phenomenon. This implies that local phenomenon in the interface region has a strong effect on controlling the coalescence kinetics and corresponding microstructural evolution.

**Modeling of Cementite Formation in Extra and Ultra Low Carbon Steels:** *Jong Min Choi*<sup>1</sup>; *Bong June Park*<sup>1</sup>; *Sung Il Kim*<sup>2</sup>; *Kyung Sub Lee*<sup>1</sup>; *Kyung Jong Lee*<sup>1</sup>; <sup>1</sup>Hanyang University; <sup>2</sup>POSCO

The solute carbon content in ferrite is a very important factor to obtain good formability in interstitial free steels. Although most of carbons are consumed by formation of grain boundary cementite during coiling after hot-rolling, the carbon content of final state after coiling is much more than that of equilibrium. In this study, the effects of total carbon content and cooling rate on grain boundary cementite formation are modeled by classical nucleation and growth. As results of simulation, the reason of sluggish kinetics of grain boundary cementite is a lateral growth of thickening toward ferrite grain interior. Also, the carbon content in ferrite increases as total carbon content increase, it is a good agreement of trend with experimental results from literatures.

**Modeling of Phase Transformation Behaviors by Cementite Formation at Isothermal Bainite Transformation Region in TRIP-Assisted Steels:** *Bong June Park*<sup>1</sup>; *Jong Min Choi*<sup>1</sup>; *Sung Il Kim*<sup>2</sup>; *Kyung Jong Lee*<sup>1</sup>; <sup>1</sup>Hanyang University; <sup>2</sup>POSCO

It is a major factor that the retained austenite fraction to determine mechanical properties of cold rolled TRIP-assisted steels. To obtain the maximum retained austenite, cementite is retarded by addition of Si, Al at isothermal bainite transformation heat treatment (IBT). In this study, carbide free bainitic-ferrite and cementite transformation behaviors are simulated by classical nucleation and growth model, and it is predicted that complex transformation behavior as the formation of cementite during carbide free bainitic-ferrite transformation at IBT. The effect on bainite transformation behavior as Si, Al contents is investigated by dilatometric and XRD experiments, results which are compared with the modeling are analyzed.

**Monte Carlo Simulation of Multiferroic BiFeO<sub>3</sub>:** *Yang Yang*<sup>1</sup>; *Jiangyu Li*<sup>1</sup>; <sup>1</sup>University of Washington

Magnetoelectric multiferroics such as BiFeO<sub>3</sub> (BFO), which simultaneously possess magnetic and ferroelectric orders, are of great interest to both fundamental studies and practical applications because of the promising coupling between magnetic and electric order parameters. In this work, a lattice model of multiferroic BFO is developed. We consider a two-dimensional square lattice of three-dimensional dipoles and magnetic spins, with dipoles ferroelectrically coupled and spins antiferromagnetically coupled. Furthermore, the spins are indirectly coupled with dipoles through the ferroelastic interactions. The electric, magnetic, and elastic energies of the lattice are evaluated, and the equilibrium distribution of dipoles and spins are realized through the Monte Carlo simulation. The coupled ferroelectric and antiferromagnetic domains are observed, and the electric switching of magnetic spins are investigated.

**Multiscale Modelling of Grain Growth in Nanocrystalline Iron:** *Tomasz Wejrzanowski*<sup>1</sup>; *Krzysztof Kurzydowski*<sup>1</sup>; <sup>1</sup>Warsaw University of Technology

In the present paper two scales are addressed in order to study microstructural aspects of grain growth in nanometals. The motion of individual grain boundaries (GBs) was modelled at atomic scale by molecular dynamics. The results of this calculations were transferred to the MonteCarlo model with population of grain boundaries (GB) represented by nanostructures differ in grain size homogeneity. The mesoscopic model enable also for simulation of the effect of fraction of low-angle grain boundaries on the grain growth process. The results shows that grain size distribution and grain boundary properties has an important impact

# Technical Program

on stability of nanometals. The results of simulations are discussed with respect to experimental investigations performed on nanometals obtained by Severe Plastic Deformation methods.

**Phase Field Modeling of Grain Size Dependent Particle Pinning:** *Sina Shahandeh*<sup>1</sup>; Matthias Militzer<sup>1</sup>; <sup>1</sup>University of British Columbia

In polycrystalline materials, triple lines and quadruple points have a more disordered atomic structure than grain boundary faces. Therefore a stronger interaction between second phase particles and grain boundaries is expected when particles coincide with these special grain boundary sites. Phase field modelling has been extended to simulate pinning at these special grain boundary locations. For this purpose, an additional energy term is implemented into the phase field energy functional to account explicitly for the interaction of particles and triple lines. Simulation of microstructural evolution in 2D systems shows grain size dependent pinning when particle spacing and grain size are comparable. In this situation, abnormal grain growth can be initiated and the conditions leading to abnormal growth have been quantified with the simulations.

**Phase Field Modelling of Austenite Formation from a Ferrite-Carbide Lamella Structure:** *Hamid Azizi-Alizamini*<sup>1</sup>; Matthias Militzer<sup>1</sup>; Warren Poole<sup>1</sup>; <sup>1</sup>UBC

In this study, austenite formation from a lamella ferrite-carbide structure in a plain C-Mn steel was simulated using a phase field approach in two- and three-dimensional space. The model quantitatively describes the kinetics of austenite formation during continuous heating of a lamella ferrite-carbide aggregate to form a fully austenite structure. Simultaneously, it is also capable of capturing spheroidization of carbide lamella during heating. The model can resolve the interlamellar spacing of about 500 nm to mimic the morphological complexity of microstructural features during austenite formation. The interface mobility was used as a fitting parameter to obtain agreement between the simulation results and experimental data for the transformation kinetics.

**Phase Field Simulations of Growth and Coarsening of Electrocatalyst Particles:** *Megna Shah*<sup>1</sup>; Scott Barnett<sup>1</sup>; Peter Voorhees<sup>1</sup>; <sup>1</sup>Northwestern University

Catalyst particles are critical to the performance of sensors and fuel cells. One method of forming the particles is to dope the ceramic substrate with the desired catalytic element. Under operating conditions, the dopant will diffuse out of the bulk to form metal electrocatalyst particles on the surface of the ceramic. The performance is directly related to how much surface area is available for catalysis, and therefore it is important to know the stability of the microstructure over time. We employ a phase field model to describe the growth and coarsening of the electrocatalyst particles. A ternary alloy model is used to describe the interactions between vacancies, the metal catalyst and the ceramic substrate. Using this model, we examine the effects of varying levels of bulk and surface diffusion on the growth and coarsening of the particles. The results of the simulations are compared to experimental results.

**Simulation of Austenite-Martensite Interface and Hysteresis in Microstructures:** *Chi Hou Lei*<sup>1</sup>; <sup>1</sup>University of Washington

We utilize the nonconventional multivariant model to simulate the Austenite-Martensite interface in microstructure. Separation of length scales between the Austenite-Martensites and the twinned-Martensites is critical here. An innovated algorithm, the multiscale simulation, has been introduced to deal with the problem. Microstructures in common crystal systems are generated to explore its over the conventional modal. We then attempt to examine and verify the hypothesis in microstructure raised by R.D. James on whether the middle eigenvalue being zero is a critical criterion in the linearized theory. Other alternative conditions affecting hysteresis are also studied. We also analyze the appropriate parameters involved to guarantee the existence of patterned, laminated structures. A rigorous theory with numerical analysis is being deduced to one-dimensional problem, as an insight to the choices of parameters in general. Thermal, mechanical, electric and magnetic effects are also considered in the evolution of various structures for optimal design.

**The Effect of Quenched-in Vacancies on the Kinetics of Coherent Cu-Precipitation in Fe-Cu Alloys:** *Ivan Holzer*<sup>1</sup>; Ernst Kozeschnik<sup>2</sup>; <sup>1</sup>Graz University of Technology; <sup>2</sup>Vienna University of Technology

In the present work, the effect of quenched-in vacancies on the kinetics of coherent Cu precipitation in alpha-iron is investigated. It is shown that, especially in the early stages of precipitation, quenched-in vacancies strongly accelerate the kinetics of the precipitation reaction. It has been observed previously that several experimental results from literature can only be explained if this effect is accounted for. In order to analyze the effect of quenched-in vacancies quantitatively, TTP-plots are calculated for an Fe-1.4wt.% Cu alloy in the temperature range between 400°C and 750°C and compared with the corresponding experimental data reported in literature. It is shown that the TTP curves for Cu-precipitation can only be consistently reproduced if the quenched-in vacancy effect is duly considered.

## Global Innovations in Manufacturing of Aerospace Materials: The 11th MPMD Global Innovations Symposium: Poster Session

*Sponsored by:* The Minerals, Metals and Materials Society, TMS Materials Processing and Manufacturing Division, TMS Structural Materials Division, TMS: Shaping and Forming Committee, TMS: High Temperature Alloys Committee

*Program Organizers:* Deborah Whitis, General Electric Company; Thomas Bieler, Michigan State University; Michael Miles, BYU

Sun PM-Wed PM Room: 306  
February 14, 2010 Location: Washington State Convention Center

**Deformation in Two-Phase Titanium Alloys Studied by Surface Strain Mapping Techniques:** R. Sandala<sup>1</sup>; J. Quinta da Fonseca<sup>1</sup>; *Michael Preuss*<sup>1</sup>; <sup>1</sup>University of Manchester

Two-phase titanium alloys are light weight materials, exhibiting very high strength at temperatures up to 600°C, and are widely used in the aerospace industry. In order to develop physically based lifing models, an improved understanding of the dominating deformation mechanisms in these alloys is necessary. Particularly, the study of deformation at the surface of these alloys is critical as cracks initiate at the surface and thus affects the fatigue life of the material and the life expectancy of the component. In situ loading experiments with DIC (Digital Image Correlation) are used to develop a detailed understanding of the deformation mechanisms in Ti6246 alloys. Images are taken before, during and after loading experiments and DIC is used to correlate the strain fields. The strain maps of these microstructures are subsequently related to corresponding EBSD (Electron Backscatter Diffraction) maps which assist in understanding how the behaviour of slip at the  $\alpha/\beta$  interface depends on the crystallographic orientation relationship of the two phases. Detailed TEM analysis will be carried out in the future to focus mainly on the movement of dislocations and further understanding of the deformation by slip in these alloys.

**Delamination in Al-Li Alloys:** *Armand Beaudoin*<sup>1</sup>; Roy Crooks<sup>2</sup>; Sean Hamel<sup>1</sup>; Mark Hernquist<sup>1</sup>; Russell McDonald<sup>1</sup>; Wes Tayon<sup>1</sup>; <sup>1</sup>University of Illinois at Urbana-Champaign; <sup>2</sup>National Institute of Aerospace

The use of lightweight Al-Li alloys in aerospace application is increasing. However, these alloys are often quite susceptible to delamination. Design considerations relating to fracture and fatigue prompt the need for sound understanding of the mechanisms leading to delamination. In the present work, fracture toughness and fatigue studies are carried out. Digital Image Correlation is employed in mechanical testing to identify the onset of plastic localization. EBSD mapping methods are used in the characterization of sectioned samples. Collectively, this data is applied to pose detailed models of a delamination in the presence of a primary crack. Both "crack divider" and "crack arrestor" delaminations are studied. Results indicate the key role of slip incompatibility. Parametric study considering the toughness ratio and strength ratio between the primary crack and the delamination crack serve to illustrate the key mechanical parameters integral to the development of delamination.



### In-Situ 3D Observation of Short Crack Propagation in Titanium Alloys:

*Soran Biroscala*<sup>1</sup>; J. Y. Buffiere<sup>2</sup>; M. Preuss<sup>1</sup>; <sup>1</sup>University of Manchester; <sup>2</sup>Universite de Lyon

In the present study, crack propagation was imaged non-destructively in 3 dimensions during in-situ fatigue loading of Ti-6246 using X-ray microtomography on beamline ID19 at the European Synchrotron Radiation Facility (ESRF). Different microstructures including fully lamellar, equiaxed and bimodal structures were investigated to ascertain exact structure/property relationship in such alloys. Phase contrast enabled the visualization of the two-phase microstructure in 3D but in order to obtain the crystallographic orientation of individual grains along the crack path a 3D EBSD volume was recorded subsequently. By combining both techniques it was possible to relate the crystallographic orientation of grains to crack arrest and accelerated crack propagation. It is shown that the prior  $\beta$  and  $\alpha$  grains orientation and microstructure have a great influence on the crack behavior and growth. In addition, crack resistance property of the alloy is investigated by means of EBSD grain characterisation methodology, orientation and misorientation data evaluations. In the light of this 3D study, the postulation and modeling of crack shape and its related phenomenon are critically reviewed.

### Kinetics Aspects of Phase Transformation in a Ti-Al-Nb Gamma+Sigma Alloy:

*Sonalika Goyal*<sup>1</sup>; Michael Kesler<sup>1</sup>; Orlando Rios<sup>1</sup>; Damian Cupid<sup>2</sup>; Hans Seifert<sup>2</sup>; Fereshteh Ebrahimi<sup>1</sup>; <sup>1</sup>University of Florida; <sup>2</sup>Freiberg University of Mining and Technology

A high Nb Ti-Al-Nb alloy that solidifies as a single beta phase and has potential application in aerospace jet engines was studied. Thermodynamic calculations indicated that the alloy exhibits a gamma+sigma microstructure at low temperatures. DTA studies were performed to evaluate the transformation temperatures and design heat treatments to investigate the phase evolution. On cooling, Widmanstätten laths of the gamma phase nucleated at the beta grain boundaries. However, further cooling, including furnace cooling, failed to form sigma phase in the microstructure. XRD analysis in conjunction with TEM studies revealed that the microstructure upon slow cooling consisted of gamma, beta and metastable phases. Aging treatments of the as-quenched microstructure, however, resulted in an equilibrium microstructure. This paper discusses the factors affecting the nucleation of the sigma phase including the stabilization of the beta phase by the formation of metastable phases. This work has been supported by NSF/AFOSR (DMR-0605702 and DMR-0856622).

### Jim Evans Honorary Symposium: Poster Session

*Sponsored by:* The Minerals, Metals and Materials Society, TMS Extraction and Processing Division, TMS Light Metals Division  
*Program Organizers:* Ben Li, University of Michigan; Brian G. Thomas, University of Illinois at Urbana-Champaign; Lifeng Zhang, Missouri University of Science and Technology; Fiona Doyle, University of California, Berkeley; Andrew Campbell, WorleyParsons

Sun PM-Thurs AM Room: 620  
February 14, 2010 Location: Washington State Convention Center

*Session Chair:* Jae-Chun Lee, Korea Institute of Geoscience and Mineral Resources

### A Novel Process for Separating Silver from Waste Lead-Free Solder:

*Byung-Su Kim*<sup>1</sup>; Jae-chun Lee<sup>1</sup>; <sup>1</sup>Korea Institute of Geoscience and Mineral Resources (KIGAM)

Significant amounts of waste lead-free solder have been generated from electric and electronic industry. In general, the waste lead-free solder is generated from the step to affix components to printed circuit boards, which contains 2–4% of silver and 90–93% of tin. In this work, a novel process to separate silver from waste lead-free solder using a metal solvent has been developed. The process uses zinc as the metal solvent which selectively forms metallic compounds with silver, and zinc is also recovered through the volatilization separation step to reuse as the metal solvent. Up to 90% of the silver in the waste lead-free solder was separated in the dross phase from the proposed process. This paper is only concerned with the results for the separation of silver from waste lead-free solder using zinc as the metal solvent.

### Separation of Ag and Cu from Waste Pb-Free Tin Solder by Nitric Acid

*Leaching:* *Kyoungeun Yoo*<sup>1</sup>; Jae-chun Lee<sup>1</sup>; Soo-kyoung Kim<sup>1</sup>; Jinki Jeong<sup>1</sup>; <sup>1</sup>Korea Institute of Geoscience and Mineral Resources (KIGAM)

The nitric acid leaching of waste Pb-free tin solder has been performed to separate Ag and Cu, which are major alloying elements in Pb-free tin solder. Batch experiments were carried out to investigate the leaching behavior of metals such as Ag, Cu, and Sn etc. in nitric acid solution. Various parameters, viz. nitric acid concentration, leaching temperature and time, agitation speed have been studied to establish the optimum conditions for separating Ag and Cu from waste Pb-free tin solder. The leaching of Sn was found to be negligible regardless of the leaching conditions. XRD results identified that the leaching residues consisted of stannic dioxide (SnO<sub>2</sub>). These results suggest that Sn could be selectively recovered as sparingly soluble stannic dioxide precipitate by leaching out Ag and Cu from waste Pb-free tin solder in nitric acid solution.

### Magnesium Technology 2010: Poster Session

*Sponsored by:* The Minerals, Metals and Materials Society, TMS Light Metals Division, TMS: Magnesium Committee  
*Program Organizers:* Sean Agnew, University of Virginia; Eric Nyberg, Pacific Northwest National Laboratory; Wim Sillekens, TNO; Neale Neelameggham, US Magnesium LLC

Sun PM-Thurs AM Room: 612  
February 14, 2010 Location: Washington State Convention Center

### Assessing Data in Support of Structure-Processing-Property Relationships

*in Mg-Alloy Design:* *Kim Ferris*<sup>1</sup>; Dumont Jones<sup>2</sup>; <sup>1</sup>Pacific Northwest National Laboratory; <sup>2</sup>Proximate Technologies, LLC

While challenges remain in force for Mg-alloy design, a preliminary problem is to assure that the existing data, as stored in data repositories, is suitable in scope and consistency for Structure-Processing-Property Relationships (SPPRs) construction. Starting with a Mg-alloy property repository database, we have assembled algorithms to test the consistency and scope of property measurements as a basis for SPPR model development. Consistency problems, such as divergent properties for systems with similar database structure-processing representations, have been observed. Data scope is assessed by observing the quality of associations between available structure-processing information and end properties. Gaps in consistency and scope do not preclude the possibility of SPPR-design—but suggest that existing alloy-property repositories be augmented with new details for optimal SPPR support in the future. One of the goals of this effort is to offer guidance for this knowledge augmentation.

### Complex Microstructure Consisting Precipitates and Long Periodic

*Stacking (LPS) Phases in Mg<sub>97</sub>Zn<sub>1</sub>Y<sub>2</sub>-X (Ce, Nd, Sm)X Alloys:* *JongBeom Lee*<sup>1</sup>; Toyohiko J Konno<sup>2</sup>; Kenji Hiraga<sup>2</sup>; <sup>1</sup>Tohoku University; <sup>2</sup>Institute for Materials Research, Tohoku University

Mg-Zn-Y alloys exhibit excellent mechanical properties due mainly to the long periodic stacking (LPS) phases. We recently reported that  $\alpha$ -Mg matrix of Mg<sub>97</sub>Zn<sub>0.7</sub>Y<sub>1.4</sub> alloy quenched from high temperature of 520° results in a simple supersaturated solution without forming LPS phases [1]. In order to improve their mechanical strength by post-annealing, therefore, we must optimize the formation of the LPS phases and other precipitates by controlling the aging conditions. In this study, we prepared Mg-Zn-Y alloy samples with rare earth elements (RE) such as Ce, Nd and Sm, and examined their precipitation behaviors using transmission electron microscope (TEM). After annealing the samples at 200° for 100 hr, their hardness increased. Our TEM observations suggested that their precipitation behaviors, i.e., the formation of GP-zones, LPS phases and inter-metallic precipitates, are strongly influenced by the addition of RE elements. [1] J.B. Lee et al.: Mater. Trans. 50 (2009) 222

### Effect of CaO and Al Contents on Tensile Properties of Creep Resistant

*Eco-Mg Alloys:* *Jung ho Seo*<sup>1</sup>; Shae K. Kim<sup>1</sup>; <sup>1</sup>Korea Institute of Industrial Technology

Creep resistant Eco-Mg alloys of CaO added Mg-Al alloys have been researched and developed. The purpose of present paper is to investigate the influence of CaO and Al on room and high temperature tensile properties of CaO added Mg-Al alloys and ultimately to make foundation of developing low-cost creep resistant Eco-Mg alloys. To optimize CaO and Al contents, varying

amounts of CaO(0.8, 1.0, 1.5 and 2.0wt.%) and Al(5, 6 and 7wt.%) were added into pure Mg and the prepared alloys were gravity-cast into a metallic mold. The optimization of CaO and Al contents is not only for creep resistance but also high castability without hot tearing and die-soldering. Each alloy will be characterized in terms of microstructure, hardness, phase analysis and tensile properties at room temperature and 150° and the results will be compared with those of Ca added Mg-Al alloys containing the same Ca and Al contents.

**Effect of Microstructure and Texture on Property of Friction Stir Processed Magnesium Alloy AZ31B:** *Wei Yuan*<sup>1</sup>; Rajiv Mishra<sup>1</sup>; <sup>1</sup>Missouri University of Science and Technology

Friction stir processing improves the mechanical properties of metals by refining the grains to micron and even submicron scale. Previous results indicate anisotropy in tensile properties of friction stir processed magnesium alloy AZ31B, which exhibits higher tensile strength and ductility in transverse direction as compared to the longitudinal direction for both single pass and two-pass friction stir processing. However, the two-pass processed material shows finer grained microstructure with higher tensile strength and ductility. In this study, the effect of processing parameters and multiple passes (two and three passes) with same or reverse processing direction on microstructure and texture of magnesium alloy AZ31B has been evaluated. The influence of textured microstructure on tensile property will be discussed.

**Effect of Zr Addition on Microstructural Evolution and Mechanical Properties of Mg-Zn-Y Alloy:** *JoonSeok Kyeong*<sup>1</sup>; WonTae Kim<sup>2</sup>; DoHyang Kim<sup>1</sup>; <sup>1</sup>Yonsei University; <sup>2</sup>Cheongju University

Recently, it has been reported that Mg-Zn-Y ternary system exhibits a good combination of strength and ductility due to low energy interface between icosahedral phase particles and a-Mg matrix. In the present study, the effect of Zr addition on microstructure evolution and mechanical properties of Mg-Zn-Y alloy have been investigated. The alloy sheets have been fabricated by pre-extrusion process followed by conventional hot rolling process. When compared with the ternary Mg-Zn-Y alloy, the Zr containing alloy exhibits a more refined microstructure, i.e. the icosahedral phase particles are distributed more uniformly in the a-Mg matrix. The Mg-Zn-Y-Zr alloy exhibits superior mechanical properties to ternary Mg-Zn-Y alloy. In particular, the mechanical properties of rolled sheets are significantly affected by microstructure evolution during the annealing treatment. For example, rolled sheet annealed at 400°C for 30 min shows an excellent combination of strength and ductility, i.e. 373.8 MPa in strength and 26.4% in total elongation.

**Experimental and Computational Simulation of the Post-Warm Forming Constitutive Behavior of AZ31:** *Frederick Polesak*<sup>1</sup>; Babak Raeisina<sup>1</sup>; Sean Agnew<sup>1</sup>; <sup>1</sup>University of Virginia

There has been a world-wide interest in exploring, and indeed improving, the warm sheet formability of magnesium alloys. One issue that has not been extensively investigated is the effect of such warm forming on the properties of magnesium alloys. In this study, we compare the room temperature tensile properties (strength, ductility, and anisotropy) of as-received O-tempered sheets of alloy AZ31 (continuously cast and direct chill cast) with those previously deformed in tension at temperatures typical of warm forming operations. The evolution of grain size and texture, which occurs during the warm deformation is incorporated into the analysis. The possibility that the strength and anisotropy may be predicted provided information regarding the microstructure evolution is explored using a viscoplastic self-consistent model initially calibrated using the properties and microstructure of the as-received material.

**Experiments and Modeling of Fatigue in an Extruded Magnesium Alloy:** *J. Gibson*<sup>1</sup>; J. Jordan<sup>1</sup>; M. Horstemeyer<sup>1</sup>; <sup>1</sup>Mississippi State University

The objective of this study is to experimentally investigate the fatigue behavior of an extruded AZ61 magnesium alloy. Experiments were performed in the extruded and transverse directions under low and high cycle fatigue conditions. The cyclic behavior of this alloy displayed varying degrees of cyclic hardening based on the strain amplitude and the specimen orientation. The fracture surfaces of the fatigued specimens were analyzed using a scanning electron microscope with the intent to develop structure-property relations with respect to microstructural features. Direct correlations between particle size, nearest neighbor distance, and grain size as a function of failure cycles were determined. Lastly, a multistage fatigue model based on the structure-property relations determined in this study was employed to capture the anisotropic fatigue damage of Magnesium AZ61.

**Fatigue Crack Propagation Behavior of Wrought Mg-Zn Alloys:** *Kyosoo Song*<sup>1</sup>; Hwa Chul Jung<sup>1</sup>; Kwang Seon Shin<sup>1</sup>; <sup>1</sup>Seoul National University

There have been limited studies on fatigue crack propagation behavior of magnesium alloys, particularly in the near-threshold region. In the present study, fatigue crack propagation behavior of wrought Mg-Zn alloys was investigated. Fatigue crack propagation experiments were carried out on a fatigue test machine under the constant load amplitude with a sinusoidal frequency 20Hz in laboratory air at ambient temperature. The effects of stress ratio on fatigue crack propagation behavior were examined in conjunction with crack closure phenomena which were determined using the compliance method. The  $\Delta K_{th}$  values, which were defined as the  $\Delta K$  at  $da/dN$  below  $10^{-10}$ m/cycle in the present study, of Mg-Zn alloys were affected by the change in stress ratio. The  $\Delta K_{th}$  value decreased with increasing the stress ratio. The effect of heat treatment was also examined.

**Finite Element Simulation of Mg Warm Sheet Forming Operations:** *Babak Raeisina*<sup>1</sup>; Louis Hector<sup>2</sup>; Paul Krajewski<sup>2</sup>; Sean Agnew<sup>1</sup>; <sup>1</sup>University of Virginia; <sup>2</sup>GM

There is world-wide interest in improving the warm sheet formability of magnesium alloys. To this end, the influences of forming process parameters (e.g., temperature, blank holder pressure, friction) and characteristics of the selected material constitutive model on the forming behavior are explored using PamStamp2G finite element simulations. Two types of constitutive model are examined: i) a simple viscoplastic model due to Sellars and Tegart, which captures the temperature and rate sensitivity of the flow stress and was calibrated to experimental data obtained from continuously cast alloy AZ31 sheet; and ii) an empirical, dynamic recrystallization model by Liu et al., that introduces both strain hardening and softening. The latter model is used, in particular, to examine the influence of strain softening on the formability. The simulation results are compared with separately published results of experimental warm forming trials.

**Generic Materials Property Data Storage and Retrieval for Alloy Material Applications:** *Dumont Jones*<sup>1</sup>; Kim Ferris<sup>2</sup>; <sup>1</sup>Proximate Technologies, LLC; <sup>2</sup>Pacific Northwest National Laboratory

Informatics-based design of alloys establishes patterns of behavior across materials systems, and depends upon the development of a robust database of materials properties. The fundamental basis for developing these patterns lies in the information content of the materials property database. However, the accuracy and integrity of the knowledge base are often affected by information loss due to incomplete entry and loss of context. We describe methods for materials property data storage and retrieval, in support of lightweight alloy development for automotive applications. Analysis-ready data representations vary with each materials design problem, and are often inconsistent with accurate generic property storage. We propose a simple, strongly-typed generic storage approach for as-measured properties, with retrieval tools for assessing as-measured properties and converting them to analysis-ready representations. This process simplifies the task of property data stewardship, and allows fine control over data fusion, system characterization, and property representations employed in property-estimation models.

**In-Situ Scanning Electron Microscopy Comparison of Deformation Behavior between AZ31 and WE43 Magnesium Alloys:** *Tomoko Sano*<sup>1</sup>; Bruce Davis<sup>2</sup>; Richard DeLorme<sup>2</sup>; Kyu Cho<sup>1</sup>; <sup>1</sup>US Army Research Lab; <sup>2</sup>Magnesium Elektron North America Inc.

In-situ tensile testing in the scanning electron microscope was used to investigate the quasi-static deformation behavior and fracture mechanism of AZ31 and WE43 magnesium alloys. The AZ31 alloy with aluminum and zinc additives is known for ductility and strength, but also for its superplasticity at elevated temperatures. The WE43 alloy, which contains the rare earth elements yttrium and neodymium, is known for its high strength, corrosion, and creep resistance. The goal of this research was to determine the effects of precipitates and grain boundary morphology on crack nucleation and propagation, and characterize other deformation behavior such as slip and twins. The in-situ tensile experiments were conducted at room temperature at a constant crosshead speed of 0.5 mm / min. The microstructure and resulting microcracks, voids, and slip lines comparison between these alloys pre, during, and post deformation will be discussed.



**Microstructure and Corrosion Properties of Rapidly Solidified Mg-Zn-Y-X Alloys:** S.W. Nam<sup>1</sup>; Do H. Kim<sup>1</sup>; H.K. Lim<sup>1</sup>; W. T. Kim<sup>1</sup>; D.H. Kim<sup>1</sup>; <sup>1</sup>Cheongju University

The Microstructures and corrosion properties of melt spun Mg-Zn-Y-X (X=Sn, Ca) alloys have been studied by using scanning electron microscopy, transmission electron microscopy, X-ray diffractometry and dynamic polarization test. The melt spun ribbon specimens exhibits in-situ composites, consisted of homogeneously distributed icosahedral phase (I-phase) in an alpha-Mg matrix. With increasing the volume fraction of I-phase, corrosion resistance tested in 3.5wt% NaCl solution remarkably increases due to the inherent corrosion potential of I-phase (open circuit potential -1.10 V). The finely distributed I-phase acted as a corrosion barrier reducing corrosion rate. Addition of small amount of Sn further increases its corrosion resistance. However, the addition of Ca was not as effective as Sn in improving corrosion resistance.

**Phase Structures and Phase Relationships of the Alloys of Mg-Zn-La System at 400°:** *Mingli Huang*<sup>1</sup>; <sup>1</sup>School of Materials and Metallurgy, Northeastern University

The structure, the composition and the phase relationships of the intermetallics formed in the Mg-(0-37)at.%Zn-5at.%La alloys have been identified at 400° using electron probe microanalysis with energy dispersive X-ray spectroscopy and transmission electron microscopy. The results show that there was a linear ternary compound (T) in Mg-Zn-La ternary system. The T phase has a C-centered orthorhombic structure unreported by the others. The range of the two phase range of Mg + T was also identified clearly at 400°. And the three-phase region of Mg + Liquid phase(Mg-29at%Zn)+T at 400° were identified. The isothermal section of Mg-Zn-La system in the Mg-rich corner at 400° are established completely.

**Recovery and Static Recrystallization of Magnesium Alloy AZ31:** *Zohreh Keshavarz*<sup>1</sup>; Aiden Beer<sup>1</sup>; <sup>1</sup>Deakin University

The restorative mechanisms operative during the annealing of cold worked magnesium alloy AZ31 were examined. It was found that recovery was the main restorative mechanism at low strains, low annealing temperatures and times. This was characterised by a decrease in the hardness of the deformed material with no obvious change in the corresponding optical micrographs. However, after annealing at 300°C and above, recrystallization was observed to occur. Recrystallization was enhanced with higher strains and annealing temperatures and was found to mainly nucleate in regions associated with twins. Interestingly, it was also found that at the highest strain examined, recrystallization led to a refinement of the microstructure. This was related to the development of a higher frequency of twins, which increased the number of nucleation sites for recrystallization.

**Role of Quasicrystalline Phase in Mechanical Properties of Mg-Sn-Zn-Al Alloys:** *Young Kyun Kim*<sup>1</sup>; Do Hyung Kim<sup>1</sup>; Joon Seok Kyeong<sup>1</sup>; Won Tae Kim<sup>2</sup>; Do Hyang Kim<sup>1</sup>; <sup>1</sup>Yonsei University; <sup>2</sup>Cheongju University

We report in the present study on the role of quasicrystalline (approximant) phase in microstructural evolution and mechanical properties of Mg-Sn-Zn(-Al) alloys. As-cast microstructure of Mg-Sn-Zn(-Al) alloys consists of a-Mg dendrite and interdendritic eutectic of a-Mg, Mg<sub>2</sub>Sn and quasicrystalline (approximant) phases. Solidification sequence for interdendritic eutectic is as follow: binary eutectic solidification between a-Mg and Mg<sub>2</sub>Sn phase followed by ternary eutectic solidification of a -Mg, Mg<sub>2</sub>Sn and quasicrystalline(approximant) phases. The quasicrystalline phase reinforced Mg-Sn-Zn-Al alloy rolled sheets exhibit a good combination of mechanical properties; high ultimate strength, large elongation to failure, and good formability at high temperature. In particular, enhanced mechanical properties have been achieved due to precipitation of fine quasicrystalline phase particles in the Mg-Sn-Zn-Al alloy rolled sheets.

**Texture and Anisotropy of Continuous Cast(CC) and Direct Chill Cast (DC) AZ31 Magnesium Sheets:** *SooHo Kim*<sup>1</sup>; Raja Mishra<sup>1</sup>; Jon Carter<sup>1</sup>; <sup>1</sup>GM R&D Center

This study compares the microstructure and mechanical properties of low-cost continuous cast (CC) and direct chill (DC) cast AZ31 sheets. In the O-temper condition, the grain sizes are homogeneous through the sheet thickness and the CC sheet has a finer grain size than the DC material. The CC sheet also contains center-line-segregation besides dispersion of second phase particles through the sheet thickness. The c-axes of grains in both materials lie normal to the sheet surface with the prism planes distributed nearly randomly. The yield strength values are nearly the same in both materials in the rolling direction (RD) and

increases from RD to TD (transverse direction) by 26%. The ultimate tensile strengths are independent of in-plane orientation and elongation of CC sheet decreases from RD to TD. The talk will discuss the correlation between the texture and properties of the CC and DC sheets and correlate this to formability.

**Thermo-Mechanical Processing Design of Mg Alloys with High Strength and Formability via Twin-Roll Casting:** G.T. Bae<sup>1</sup>; D. Li<sup>1</sup>; H. Garmestani<sup>1</sup>; K.-H. Kim<sup>2</sup>; J.H. Bae<sup>2</sup>; Nack J. Kim<sup>2</sup>; <sup>1</sup>Georgia Institute of Technology; <sup>2</sup>Pohang University of Science and Technology

Mg alloys have great potential in transportation systems mainly due to their low density and high specific strength. Recent development of twin-roll casting technology has shown that it can efficiently produce low cost, high performance wrought Mg alloy sheets. For the successful application of twin-roll cast Mg alloys, however, further improvement in strength and formability is still needed to substitute Fe and Al alloys. The present research is aimed at developing a materials design framework to optimize thermo-mechanical processing of Mg alloy to achieve high strength and improved formability. It is based on the prediction of texture and grain size evolution based on processing path model with the capability to capture texture evolution during mechanical treatment. This new theory will act as a cornerstone in materials design to build up a streamline grid presenting microstructure evolution during rolling and annealing.

**Ultra Light Metallic Armor (ULMA)- Magnesium Hard Alloys as the Defense against Modern Warfare Threats:** *Rick Delorme*<sup>1</sup>; Bruce Davis<sup>1</sup>; Kyu Cho<sup>2</sup>; Jonathan Montgomery<sup>2</sup>; <sup>1</sup>Magnesium Elektron North America; <sup>2</sup>Army Research Laboratory

The Ultra Lightweight Metallic Armor (ULMA) program sets out to develop a new generation of armor materials that surpass the current capabilities of traditional light alloys, while offering significant weight savings. This is being achieved by the development of new wrought magnesium alloys and processing methods to fabricate plate products with enhanced ballistic and blast properties. The work program can be divided into three categories: Casting; Thermomechanical Processing- Rolling; and Heat treatment. Optimization of these aspects of materials production, as well as joining and high strain rate testing, are being carried out in partnership with the Edison Welding Institute, University of Virginia, Johns Hopkins University, and University of Missouri Science and Technology. This paper reviews the activity of this program and highlights the benefits of light weight magnesium armor plate.

**Void Nucleation and Growth Behavior of Mg Alloy: A Study by X-Ray Microtomography and Finite Element Analysis:** *Ji Hoon Yoo*<sup>1</sup>; Dae Ha Lim<sup>1</sup>; Jae-Hong Lim<sup>1</sup>; Jung Ho Je<sup>1</sup>; Hyoung Seop Kim<sup>1</sup>; <sup>1</sup>Postech

Ductile fracture behavior of metallic materials expressed by the Gurson's damage model is governed by the nucleation, growth and coalescence of micro voids in hydrostatic tensile stress regions. The aim of this study is to systematically obtain necessary parameters for the Gurson's ductile fracture model of Mg alloys in conjunction with the finite element method (FEM) analysis. In order to predict plastic deformation behavior with neck onset and post necking in tensile testing of the Mg alloy by the FEM analysis, void nucleation and growth behavior is examined by a microtomography technique with synchrotron X-rays. First, we prepare tensile testing samples at several tensile strain stages. Three dimensional (3D) void structure of each sample in its strain stage is obtained by the tomography technique. By measuring the void volume fraction of each sample from the 3D structure, a quantitative relationship between stress, strain and void nucleation is achieved. The parameters of the Gurson's damage model that are obtained from the relationship are used for FEM simulations.

## Neutron and X-Ray Studies of Advanced Materials III: Poster Session

*Sponsored by:* The Minerals, Metals and Materials Society, ASM International, TMS Structural Materials Division, TMS/ASM: Mechanical Behavior of Materials Committee, TMS: Titanium Committee  
*Program Organizers:* Rozaliya Barabash, Oak Ridge National Laboratory; Jaimie Tiley, Air Force Research Laboratory; Erica Lilleodden, GKSS Research Center; Peter Liaw, University of Tennessee; Yandong Wang, Northeastern University

Sun PM-Thurs AM Room: 303  
February 14, 2010 Location: Washington State Convention Center

### X-Ray Characterization of the a-Si/HfO<sub>2</sub> Interface: Sandeep Kohli<sup>1</sup>; <sup>1</sup>Colorado State University

Chemical and physical properties of the interface formed between amorphous silicon and hafnium oxide were investigated using X-ray reflectivity (XRR) and X-ray photoelectron spectroscopy (XPS). XRR showed that the interface layer formed between the a-Si and HfO<sub>2</sub> layer had a thickness of  $0.7 \pm 0.3$  nm and a density of  $4.4 \pm 0.2$  g/cm<sup>3</sup>. Based on the XPS results, the interface is comprised hafnium oxide, silicon oxide and hafnium silicate phases. Hafnium silicide was also found and likely formed as a result of the differential sputtering of HfO<sub>2</sub> film. High-temperature annealing led to the conversion of elemental silicon and non-stoichiometric silicate into silicon dioxide phases. This reaction was also accompanied by the reduction of hafnium oxide phase. High-temperature annealing also led to the crystallization of 10nm hafnium oxide films into the high-pressure orthorhombic phase of HfO<sub>2</sub>, versus the ambient monoclinic phase.

### Pb-Free Solders and Emerging Interconnect and Packaging Technologies: Poster Session

*Sponsored by:* The Minerals, Metals and Materials Society, TMS Electronic, Magnetic, and Photonic Materials Division, TMS: Electronic Packaging and Interconnection Materials Committee  
*Program Organizers:* Kwang-Lung Lin, National Cheng Kung University; Sung Kang, IBM; Jenq-Gong Duh, National Tsing-Hua University; Laura Turbini, Research In Motion; Iver Anderson, Iowa State University; Fu Guo, Beijing University of Technology; Thomas Bieler, Michigan State University; Andre Lee, Michigan State University; Rajen Sidhu, Intel Corporation

Sun PM-Thurs AM Room: 204  
February 14, 2010 Location: Washington State Convention Center

*Session Chairs:* Iver Anderson, Iowa State University; Fu Guo, Beijing University of Technology

### Characterization of Metal Whisker Growth in Sn-Based Solders: Guangchen Xu<sup>1</sup>; Dongyue Zhang<sup>1</sup>; Hu Hao<sup>1</sup>; Mengke Zhao<sup>1</sup>; Yaowu Shi<sup>1</sup>; Fu Guo<sup>1</sup>; <sup>1</sup>Beijing University of Technology

Metal whiskers are small crystals that grow from the surface of metals, resulting in reliability issues such as electrical short circuit or debris for equipment manufacturers and users. In order to reveal the basic mechanism for the growth of metal whiskers and evaluate its physical properties, accelerated test was employed by adding the rare earth elements into the Sn-based solder alloys. The ultimate results illustrate the rapid growth of metal whiskers with various morphologies at the surface of rare earth oxide phase. The correlation among ambient temperature, different rare earth additives, and isothermal aging time were achieved to quantify the unique morphology of metal whiskers. What's more, focus ion beam (FIB) was assisted to analyze the fast diffusion channel at the root of metal whiskers. In addition, a preliminary attempt was carried out to investigate the capacity of carrying electric current by the metal whiskers.

### Impression Creep of Pb: Fuqian Yang<sup>1</sup>; Rong Chen<sup>1</sup>; <sup>1</sup>University of Kentucky

The impression creep behavior of Pb was investigated using a flat-ended, cylindrical punch, over an impression stress range of 11.1-34.6 MPa and in a temperature range of 343-443 K. A steel punch of 0.3 mm in diameter was used in the tests. A steady state creep was observed for low stresses. Recrystallization was observed for high stresses with a sudden jump on the impression time-depth curves. The steady state impression velocity of Pb followed the power-law stress dependence. For temperature less than 403 K, the stress exponent was in the range of 2.1-3.9 at low stress region, which was due to grain boundary sliding. For high stress region, the stress exponent is 7.5-9.0 controlled by dislocation climb. For temperature higher than 403 K, the stress exponent was 5.6-6.6.

### Interfacial Reaction and Joint Reliability of Electrodes Bonded with Transverse Ultrasonic: Jong-Bum Lee<sup>1</sup>; Jong-Gun Lee<sup>1</sup>; Seung-Boo Jung<sup>1</sup>; <sup>1</sup>Sungkyunkwan University

In this study, the electrodes on the flexible printed circuit board (FPCB) and rigid PCB (RPCB) were bonded using transverse ultrasonic system. The surface finishes of the electrodes of FPCB and RPCB were fixed as electroless Ni/electroless Pd/immersion gold (ENEPIG) and electroless Ni/immersion gold (ENIG), respectively. Dipping method was used for the ENEPIG surface finish on Cu electrodes of the FPCB. Peel tests of the joints were carried out with increasing bonding time and pressure to optimize the bonding condition. The interfacial reaction layer was observed by transmission electron microscopy (TEM). Thin intermetallic compound (IMC) was formed on ENEPIG surface finish that showed stable electrical resistance during reliability test.

### Mechanical Properties of Intermetallic Properties in Lead-Free Solder Materials: Chandra Rao Bhesetti<sup>1</sup>; K.Y. Zeng<sup>2</sup>; V. Kripesh<sup>3</sup>; <sup>1</sup>National University of Singapore, Department of Mechanical Engineering - and - A\*STAR (Agency for Science, Technology and Research), Institute of Microelectronics; <sup>2</sup>National University of Singapore, Department of Mechanical Engineering; <sup>3</sup>A\*STAR (Agency for Science, Technology and Research), Institute of Microelectronics

In this work, we have measured mechanical properties of Intermetallic properties using nanoindentation and correlated measured mechanical properties variation with texture, grain size, thickness and substrate effects. EBSD and EPMA techniques has been used for microstructural and compositional analysis.

### Microvoid Formation at Solder-Copper Interfaces during Annealing: A Systematic Study of the Root Cause: Santosh Kumar<sup>1</sup>; Carol Handwerker<sup>1</sup>; Joseph Smetana<sup>2</sup>; David Love<sup>3</sup>; James Watkowski<sup>4</sup>; Richard Parker<sup>5</sup>; <sup>1</sup>Purdue University; <sup>2</sup>Alcatel-Lucent; <sup>3</sup>Sun Microsystems, Inc.; <sup>4</sup>MacDermid Inc; <sup>5</sup>Delphi Electronics & Safety

The electrodeposition conditions that may contribute to microvoid formation during isothermal aging of Pb-free solder-electrodeposited copper are evaluated in a systematic series of experiments. We first show that the Kirkendall effect alone does not explain the observed microvoids at Cu-Cu<sub>3</sub>Sn interface and in Cu<sub>3</sub>Sn phase using classic solid-solid diffusion couple experiments. Then, we report the results of 2<sup>k</sup> full factorial Design of Experiment to study the effect of pre-screened electroplating parameters such as brighteners, wetting agent, bath age and current density on the propensity of microvoiding at solder-copper interface after annealing at 125°C for 40 days. It was found that amount of microvoiding is greatly affected by brighteners, wetting agent, bath age and their interactions. Time of Flight - Secondary Ion Mass Spectroscopy and Glow Discharge Mass Spectroscopy allowed us to establish a correlation between impurities incorporated in copper during electroplating and microvoiding at the solder-copper interface.

### Observations of IMC Formation for Au Wire Bonds to Al Pads: John DeLucca<sup>1</sup>; John Osenbach<sup>1</sup>; Frank Baiocchi<sup>1</sup>; <sup>1</sup>LSI Corporation

A materials investigation of Au wire bonds to Al pads revealed the evolution of a multi-phase system that resembles a pseudo-binary diffusion couple in which the phase evolution proceeds through several intermediate phases before reaching its final state. STEM/EDS and electron diffraction data that sheds light on the phase evolution will be presented.



**Optimization of Solutions to Electrodeposit Sn-Based Pb-Free Solders:** *Neda Dalili*<sup>1</sup>; Anqiang He<sup>1</sup>; Qi Liu<sup>1</sup>; Douglas Ivey<sup>1</sup>; <sup>1</sup>University of Alberta

The authors have been developing simple and "green" solutions for the electrodeposition of lead-free solders (e.g., Au-Sn, Sn-Cu and Sn-Ag-Cu) for microelectronic and MEMS packaging applications. Eutectic and near-eutectic alloys of these systems can be deposited with good composition and thickness control; however, details of solution chemistry, solute interactions and deposition mechanisms are not well known. A novel technique, employing cryogenic X-ray photoelectron spectroscopy (XPS) will be used to study the solutions in order to determine the identity and concentrations of the chemical species in solution. Electron microscopy and X-ray diffraction techniques will be used to characterize deposit microstructures and compositions. These results will be correlated to thermodynamic calculations in order to optimize the types and concentrations of additives with respect to the useful shelf-life of the solutions, electrodeposition rates and deposit morphology.

**Orientation Imaging Studies of Sn<sub>3.0</sub>Ag<sub>0.5</sub>Cu Solder Joint with Various Ni Doping after Aging:** *Tae-Kyu Lee*<sup>1</sup>; Kuo-Chuan Liu<sup>1</sup>; Kai-Jheng Wang<sup>2</sup>; Jo-Mei Wang<sup>2</sup>; Chien-Fu Tseng<sup>2</sup>; Jenq-Gong Duh<sup>2</sup>; <sup>1</sup>CISCO; <sup>2</sup>National Tsing Hua University

SnAgCu solder has been widely used in the electronic package. However, the Sn grain size of SnAgCu solder is easily grown with slow cooling rate and aging. Coefficient of thermal expansion (CTE) along the c-axis of Sn is two times larger than that along a-axis. Larger Sn grain increases CTE mismatch and induces more stress at the grain-boundary region. In this study, the Sn<sub>3.0</sub>Ag<sub>0.5</sub>Cu-xNi solder balls were aged at 100 and 150 C for 500 h, respectively. The orientation images of solder balls were acquired by electron backscattered diffraction (EBSD), and correlated with the microstructure and composition evaluated by FE-EPMA. Besides, the Sn<sub>3.0</sub>Ag<sub>0.5</sub>Cu-xNi solder ball was jointed with Ni/Au UBM for identifying the substrate effect on the size and orientation of Sn grain.

**Polycrystalline Sn Whisker Growth:** *Aleksandra Dimitrovska*<sup>1</sup>; Radovan Kovacevic<sup>1</sup>; <sup>1</sup>SMU

Sn whisker growth is a very significant reliability issue of electronic components. Research over the past several decades has agreed on some the fundamental characteristics of Sn whisker growth: 1) Sn whisker is usually single crystal 2) Sn whisker grows in variety of shapes and dimensions from electroplated Sn surface when exposed to various environmental influence and 3) compressive stress is the primary driving force for Sn whisker formation. Different environmental conditions such as humidity and elevated temperatures can accelerate Sn whisker growth and produce whiskers with complex morphology. In this study samples with pure Sn film electrodeposited on a brass substrate were monitored under three environmental conditions: ambient temperature, 95% humidity, and elevated temperature of 60°C for period of six months. Experimental results demonstrated that whiskers grown from samples exposed to controlled environment can also have polycrystalline morphology and not only single crystalline as usually known.

**Solidification of the Sn-Cu-Ag Eutectic Alloy:** *Yoshiko Takamatsu*<sup>1</sup>; Hisao Esaka<sup>1</sup>; Kei Shinozuka; <sup>1</sup>National Defense Academy

At present Sn-Ag-Cu alloy is an important candidate for use as a Pb-free solder. In order to understand solidification process of Sn-Ag-Cu alloy, Sn-3.5Ag-0.5Cu and Sn-3.5Ag-1.5Cu have been prepared in this study. The specimens were quenched during solidification at a cooling rate of 3 K/min. In the case of Sn-3.5Ag-0.5Cu alloy, the Sn-Ag<sub>3</sub>Sn binary eutectic started to grow just after primary β-Sn dendrites nucleated. After growing of binary eutectic, Sn-Ag<sub>3</sub>Sn-Cu<sub>6</sub>Sn<sub>3</sub> ternary eutectic formed, though the volume fraction of Ag<sub>3</sub>Sn in ternary eutectic was small. It was found that the large undercooling was not necessary for Sn-Ag<sub>3</sub>Sn-Cu<sub>6</sub>Sn<sub>3</sub> ternary eutectic. In the case of Sn-3.5Ag-1.5Cu alloy, no undercooling for primary Cu<sub>6</sub>Sn<sub>3</sub> and Ag<sub>3</sub>Sn was found, even though they were facet phases. However, there was a large undercooling for formation of β-Sn. Volume fraction of ternary eutectic was small compared with the estimation from equilibrium phase diagram.

**Study of Emerging New Interconnect Methods: How Far SMT Will Go:** *Idelcio Cardoso*<sup>1</sup>; Josineto Costa<sup>1</sup>; <sup>1</sup>INDT

Electronic products continuously evolve in terms of embedded functions and miniaturization, a challenge to deal with at industrial scale. Reduced sizes make components mechanically and electrically sensitive, as well as soldering them to the PWB is increasingly difficult. Perhaps miniaturization of resistors,

capacitors and diodes is close to the physical limit, so integration is a solution. But even integrated circuits are becoming smaller, which is easy to verify when 0,3mm pitch and even less are being introduced. These small solder interconnects bring metallurgical difficulties and requires new technologies for solder paste deposition, as stencils are not suitable. This paper aims at study some materials applicable to ultrafine pitch interconnects and how to bring the dispensing technology at the scale required by the cell phone industry, discussing about a proposal for a stable and high yield process capable of attending the future of SMT.

**Study of UBM Consumption in Flip Chip Solder Joints with Local Temperature Control:** *Ting-Li Yang*<sup>1</sup>; Y. L. Lin<sup>1</sup>; H. Y. Chuang<sup>1</sup>; C. Robert Kao<sup>1</sup>; <sup>1</sup>National Taiwan University

A temperature control system, employing forced fluid convection, was adopted to separate thermomigration and electromigration effect in flip chip solder joints. With this temperature control system, the die temperature can be precisely fixed at 50±1°C under the current stressing of 5.03 × 10<sup>4</sup> A/cm<sup>2</sup>. The temperature gradient through the joint can be minimized to 330°C/cm, and experimental evidence suggests that thermomigration effect can be neglected. When the temperature control system is not used, the temperature gradient is as high as 3000°C/cm across the solder joints. Under this circumstance, our observation suggests that both the thermomigration and electromigration effect are important.

**Study on Paste Printing for Electronics:** Rafael Mancosu<sup>1</sup>; Ocildeide Silva<sup>1</sup>; Renato Bonadiman<sup>1</sup>; <sup>1</sup>Nokia Technology Institute

Paste printing is a cost efficient and well-controlled volume production method with current component selection to dose solder paste. However, the future trends in electronics will raise new demands for interconnection methods used in miniaturized assemblies. This work goals to overview the evolution of paste printing processes to attend the new demands of the market. In this sense, the new paste printing composition and manufacturing methods are also evaluated. According to this study paste printing when incremented with new compositions and methodologies can be considered an important technology to be applied in large industrial scale.

**The Effect of Temperature on the Critical Cu Concentration in SnCu/Ni Reaction:** *Pei-Hsuan Wu*<sup>1</sup>; C. Robert Kao<sup>1</sup>; <sup>1</sup>National Taiwan University

The reaction product(s) at the interface between SnCu and Ni are very sensitive to the Cu concentration in solders. This critical Cu concentration required for formation of (Cu,Ni)<sub>6</sub>Sn<sub>5</sub> depends on temperature according to thermodynamic calculation by Kivilahti and co-workers. In this study, it is experimentally verified that this critical Cu concentration indeed decreases with decreasing temperature.

**Thermal and Electrical Evaluation of GaAs Flip-Chip after Thermal Reliability Test:** *Young-Chul Lee*<sup>1</sup>; Jong-Woong Kim<sup>1</sup>; Kwang-Seok Kim<sup>1</sup>; Seung-Boo Jung<sup>1</sup>; <sup>1</sup>Sungkyunkwan University

Currently, compound semiconductors such as GaAs and GaN were used for optoelectronic components and high-frequency applications. The difference in the coefficient of thermal expansion (CTE) of GaAs, the carrier or substrate, and the package material can cause mechanical stresses in the die that may result in device failure. Since the CTE of the GaAs (about 5.6 ppm/K) differed from PCB (about 20ppm/K) substrate, thermal shock test may cause die cracking and delamination. Reliability test vehicles comprise a GaAs chip which was flip chip soldered on a PCB substrate. Assembled test vehicles were subjected to a thermal shock reliability test. The condition for the TS test is -40 ~ 125° (JESD22-A106-A) for 1000 cycles. The four-point probe method was used to measure the resistance change after thermal shock test. For analysis of the fracture mode transition in TS test, finite element modeling was conducted.

## Surface Engineering for Amorphous-, Nanocrystalline-, and Bio-Materials: Poster Session

Sponsored by: The Minerals, Metals and Materials Society, TMS Materials Processing and Manufacturing Division, TMS: Surface Engineering Committee

Program Organizers: Sandip Harimkar, Oklahoma State University; Arvind Agarwal, Florida International University; Sudipta Seal, University of Central Florida; Narendra Dahotre, University of Tennessee

Sun PM-Tues PM Room: 604  
February 14, 2010 Location: Washington State Convention Center

**Pulse Electrodeposition of Bio-Coatings:** *Tushar Borkar*<sup>1</sup>; Sandip Harimkar<sup>1</sup>; <sup>1</sup>Oklahoma State University

Pulse electrodeposition brings a new era in improving the surface properties of metals. It is associated with many advantages such as reduction in porosity, low level of inclusions, and higher deposition rate compared to direct current deposition process. There is much more flexibility in varying three basic parameters which are pulse peak current density, on time and off time in pulse electrodeposition resulting into unique composition and microstructure of coating being deposited. In the present work, pulse electrodeposition technique has been used for synthesizing hydroxyapatite coatings on titanium substrates. Evolution of mechanical and bio-properties of the coatings will be discussed with emphasis on electrodeposition processing parameters and resultant microstructure of the coatings.

## The Vasek Vitek Honorary Symposium on Crystal Defects, Computational Materials Science and Applications: Poster Session

Sponsored by: The Minerals, Metals and Materials Society, TMS Materials Processing and Manufacturing Division, TMS/ASM: Computational Materials Science and Engineering Committee

Program Organizers: Mo Li, Georgia Institute of Tech; David Srolovitz, Institute for High Performance Computing, Agency for Science, Technology and Research, Singapore; Adrian Sutton, Imperial College London; Vaclav Paidar, Institute of Physics AS CR vvi; Jeff De Hosson, University of Groningen

Sun PM-Thurs AM Room: 603  
February 14, 2010 Location: Washington State Convention Center

Session Chairs: Mo Li, Georgia Institute of Tech; David Srolovitz, Institute for High Performance Computing, Agency for Science, Technology and Research, Singapore; Adrian Sutton, Imperial College London; Vaclav Paidar, Institute of Physics AS CR vvi

**A Molecular Dynamics Study of a Deformation Behavior of Nanocrystalline Palladium:** *Dmitriy Bachurin*<sup>1</sup>; Peter Gumbsch<sup>1</sup>; <sup>1</sup>University of Karlsruhe

Modern parallel computing platforms allow to simulate three-dimensional nanocrystalline structures with grain sizes of the same order as can be achieved experimentally. The study presents a molecular dynamics investigation of deformation mechanisms in nanocrystalline palladium structures with mean grain size of 10 nm at room temperature. Detailed analysis of atomic configurations revealed no dislocation activity in the range of 0% and 3% strain during both tensile and compressive straining. Plastic regime in this range is found to be controlled by grain boundary accommodation processes and by formation of dislocation embryos. The intergranular cracking was discovered at later stages of tensile straining. Nanocrystalline palladium sample shows a plastic response including a motion of extended partial dislocations emitted from the grain boundaries in the range of 3% and 5% of compressive strain. With further increase of compressive strain the deformation mechanism involves full dislocations and twinning.

**A Multi-Scale Approach in Understanding Grain Boundary (GB) Effects on Fatigue Crack Initiation from the Energies of Slip-GB Interactions:** *Michael Sangid*<sup>1</sup>; Huseyin Sehitoglu<sup>1</sup>; <sup>1</sup>University of Illinois, Urbana-Champaign

Excessive scatter is observed in the fatigue response of a nickel-based superalloy, U720, which is partly attributed to the variability in the microstructure. There is great interest in linking the microstructure to fatigue properties using a multi-scale approach that focuses on integrating the results of atomic simulations to the continuum level. This work focuses on MD simulations to characterize the slip transmission across the GB in a bicrystal and obtain quantitative values for the energy barriers necessary for slip to penetrate the GBs. This information along with expressions for dislocation interactions and pile-ups is used to create an energy balance for a persistent slip band (PSB). Through this methodology the PSB energy is calculated as a function of the mis-orientation angles, texture, and (small to large) grain size. A micro-mechanical model incorporates the PSB energy and its stability, which can be used to predict fatigue crack initiation in the material.

**Ab Initio Study of the Core Structure and Kinks of Screw Dislocations in Fe and W:** *Lisa Ventelon*<sup>1</sup>; François Willaime<sup>1</sup>; Emmanuel Clouet<sup>1</sup>; Mihai-Cosmin Marinica<sup>1</sup>; <sup>1</sup>CEA

Dislocation properties in bcc metals are closely related to the dislocation core structure, which itself is quite sensitive to details in the interatomic interactions. We have investigated the properties of [111] screw dislocations in iron and tungsten, using ab initio electronic structure techniques, primarily in the periodic dipole approach. In both cases the core is non-degenerate and we evidence a significant core dilatation effect, which can be successfully accounted for by an anisotropic elasticity model [Clouet et al., PRL 102, 055502 (2009)]. The Peierls potential is single humped i.e. there is no metastable configuration at halfway position, at variance with predictions from EAM potentials [Ventelon and Willaime, JCAMD 14, 85 (2007)]. The methodology for constructing tri-periodic cells with one kink per dislocation line has been developed. Results obtained with empirical potentials and preliminary DFT calculations are presented for the Peierls stress and kinked dislocations [Ventelon et al., JNM 386-388, 26 (2009)].

**Accurate Description of Elastic Properties of Random Alloys with Minimum Supercell Sizes:** *Johann von Pezold*<sup>1</sup>; Alexey Dick<sup>1</sup>; Martin Friák<sup>1</sup>; Jörg Neugebauer<sup>1</sup>; <sup>1</sup>Max-Planck-Institut für Eisenforschung GmbH

While special-quasi-random structures (SQS) have been shown to accurately reproduce the total energy of random alloys, their performance with respect to elastic properties has not been systematically studied so-far. We determined the elastic constants of AlTi solid solutions over the entire concentration range, using both 32-atom-fcc SQS and supercells containing a randomly generated distribution of Ti solutes within the Al matrix consisting of up to 4000 atoms. The elastic constants were calculated using EAM-type potentials together with a suitable averaging procedure. It was found that the SQS reproduce the elastic properties of the random alloys across the entire concentration range significantly more accurately than the equivalent 32-atom cell containing a randomly generated distribution of impurity atoms, making them an ideal choice in connection with ab initio calculations.

**Computer Simulation of the Two-Nanoparticles Agglomeration:** *Ilya Karkin*<sup>1</sup>; Yuri Gornostyrev<sup>1</sup>; Lidia Karkina<sup>1</sup>; <sup>1</sup>Institute of Metal Physics

We present the results of the investigation of the kinetics of transformations during the two particles agglomeration at temperatures from RT to  $T=0,6T_m$  of melting temperature  $T_m$  by the molecular dynamic method with the use of the realistic well approved EAM potential for Ni (by Voter and Chen). We studied nanoparticles with the number of atoms  $N=1505$  or 17117 (diameter of the agglomerated particles  $d=2,8$  or 6,7 nm). One particle was misoriented relative to another and they came into contact at a distance of the first coordination sphere. The atomic structural transformations during elementary sintering step are studied. The microscopic mechanism of the spontaneity agglomeration was studied in details in dependence on temperature and misorientations of particles. We show that size of particles is important factors which control the powder sintering.



### **Dislocation-Based Modeling of Yield Strength of Multilayer Thin Films with Nanoscale Microstructures:** *Qizhen Li*<sup>1</sup>; <sup>1</sup>University of Nevada, Reno

The yield strength of multilayer thin films increases to the gigapascal level when the layer thickness decreases to the nanometer scale. A three-dimensional dislocation based model is used to simulate the yielding of metallic multilayer thin films with nanoscale microstructures under biaxial tensile loading. In the model, the films are composed of two alternating types of single crystal layer phase with FCC structure and (001) epitaxy. The two phases have different stress-free lattice parameters and the same elastic moduli. Multilayer thin film systems with different layer thickness ratios are investigated to identify the effect on yield strength of the systems. The result will contribute to the understanding of strengthening mechanism of the studied systems.

### **Effect of Chemical Composition and Applied Stresses on the Martensitic Transformation in NiAl:** *G. P. Pun*<sup>1</sup>; *Y. Mishin*<sup>1</sup>; <sup>1</sup>George Mason University

We apply molecular dynamics and semi-grand canonical Monte Carlo simulations to study the B2-L10 martensitic transformation in NiAl. The transformation displays a significant hysteresis with the martensite-start and austenite-finish temperatures strongly depending on the chemical composition and applied stresses. We find that the mechanism of the transformation and the obtained martensitic structure both depend on the sign of the stress. Under tensile stresses, the transformation follows the Bain path and results in large single-crystalline areas with the L10 structure. Compressive stresses redirect the transformation along a different path involving a shuffling of close packed planes. This produces heavily nano-twinned martensitic structures similar to those observed in experiments. The effect of microstructural elements such as dislocations, anti-phase boundaries and open surfaces on the transformation has also been studied.

### **Evaluation of Phason Elastic Constants from HRTEM Image of a Dislocation in Icosahedral Quasicrystals:** *Yeong-Gi So*<sup>1</sup>; *Yasushi Kamimura*<sup>1</sup>; *Keiichi Edagawa*<sup>1</sup>; <sup>1</sup>Institute of Industrial Science, University of Tokyo

Originating in the quasiperiodic translational order, quasicrystals have a special type of elastic degrees of freedom, termed as phason degrees of freedom. Phason elasticity is a key to elucidate the physical origin of why the quasicrystalline structural order is formed. So far, experimental evaluations of phason elastic constants have been done only by neutron and X-ray diffuse scattering measurements. In this study, we propose the method for evaluating the phason elastic constants by measuring displacement fields around a dislocation by high resolution transmission electron microscopy (HRTEM). Hytch's method for a quantitative evaluation of displacement fields from HRTEM images is generalized to quasicrystals that are accompanied by two types of displacement fields: phonon and phason ones. The application of the method to displacement fields around a dislocation in an icosahedral quasicrystal is formulated. It is demonstrated that the ratio of the two phason elastic constants can be evaluated by this method.

### **Molecular Dynamics Simulation of Reactions Forming Ni-Al Nanoparticles:** *Alexander Evteev*<sup>1</sup>; *Elena Levchenko*<sup>1</sup>; *Daniel Riley*<sup>2</sup>; *Irina Belova*<sup>1</sup>; *Graeme Murch*<sup>1</sup>; <sup>1</sup>The University of Newcastle; <sup>2</sup>The University of Melbourne

Alloying reactions of a Ni-coated Al nanoparticle, Al-coated Ni nanoparticle as well as separate Ni and Al nanoparticles with the f.c.c. structure, equi-atomic fractions and diameter of 4.5 nm are studied by means of molecular dynamics simulation of isochronal heating as well as thermal explosion under adiabatic conditions (self-heating). The interatomic interactions are described by an embedded atom method potential developed by Mishin et al. (2002). In particular, it is shown that the product after thermal explosion in Ni-coated Al nanoparticle and Al-coated Ni nanoparticle is a nanoparticle with the B2-NiAl ordered structure, while thermal explosion during sintering of separate Ni and Al nanoparticles results in a liquid Ni-Al solution. However, it is demonstrated that in all cases studied the intermixing of the components at the first stage of the reactions is accompanied by solid state amorphization of the f.c.c. structure in the vicinity of the interface.

### **New Tools and Methods for Analyzing Deformed Materials:** *Woosong Choi*<sup>1</sup>; *Yong Chen*<sup>1</sup>; *Stefanos Papanikolaou*<sup>1</sup>; *James Sethna*<sup>1</sup>; <sup>1</sup>Cornell University

There are a remarkable number of experimental tools for analyzing the morphology evolution of deformed materials. EBSD, X-ray and neutron diffraction, TEM, extensometry -- all provide different windows into the evolution of grain size and orientations, dislocation patterns, and cell wall structures. We describe tools for analyzing two and three-dimensional data sets,

applicable both to our simulations of grain boundary and cell wall evolution and to experimental data sets. We present real-space observers for orientations, strain, dislocation; morphology observers for automatically identifying and analyzing cells and cell walls, Fourier-space observers mimicking X-ray diffraction patterns and line shapes, and correlation function analysis of self-similar and complex morphologies.

### **Partitioning and Site Preference of Rhenium or Ruthenium in Model Ni-Based Superalloys: An Atom-Probe Tomographic and First-Principles Study:** *Yang Zhou*<sup>1</sup>; *Zugang Mao*<sup>1</sup>; *Christopher Booth-Morrison*<sup>1</sup>; *David Seidman*<sup>1</sup>; <sup>1</sup>Northwestern University

The partitioning behavior and sublattice site preference of Re or Ru in Ni<sub>3</sub>Al (L1<sub>2</sub>) gamma-prime-precipitates of model Ni-Al-Cr alloys are investigated utilizing atom-probe tomography (APT) and first-principles calculations, employing the Vienna ab initio simulation package (VASP). Rhenium and Ru are experimentally observed to partition to the gamma (fcc)-phase aged at 1073 K, which is consistent with the smaller values of the gamma-matrix Re and Ru substitutional energies determined by first-principles calculations. APT measurements of the gamma-prime-precipitates composition indicate that Re and Ru occupy the Al sublattice-sites of the Ni<sub>3</sub>Al (L1<sub>2</sub>) phase. The preferential site substitution of Re and Ru at Al sublattice-sites is confirmed by first-principles calculations.

### **Pd<sub>2</sub>Ni Surface-Sandwich Ordering at the Nanoscale: Atomistic Simulations and First-Principles Calculations:** *Elena Levchenko*<sup>1</sup>; *Alexander Evteev*<sup>1</sup>; *Irina Belova*<sup>1</sup>; *Graeme Murch*<sup>1</sup>; <sup>1</sup>The University of Newcastle

Using molecular dynamics simulation with the embedded atom method we predict Pd<sub>2</sub>Ni surface-sandwich ordering, which allows the efficient minimization of the surface energy of Pd<sub>100-x</sub>Ni<sub>x</sub> (x 8776 33%) nanostructures. In the surface ordering, the Ni atoms mostly accumulate in a layer just below the surface. They are located in the centers of interpenetrating icosahedra and generate a subsurface layer as a Kagomé net. Meanwhile, the Pd atoms occupy the vertices of the icosahedra and cover this Ni layer from inside and outside with two Pd layers, which can be obtained by splitting of a close packed f.c.c. (111) layer. These findings open up a range of opportunities for the synthesis of new kinds of Pd-Ni nanostructures. For example, of interest for nanotechnology would be success in synthesizing a five-layer Pd<sub>2</sub>Ni nanofilm from which a Pd<sub>2</sub>Ni nanotube might be fabricated. First-principles calculations confirm the stability of the five-layer Pd<sub>2</sub>Ni nanofilm.

### **Quantitative Analysis and CPFEM Simulation of Deformation System Activity in Commercial Purity Ti Deformed in Tension:** *Yiyi Yang*<sup>1</sup>; *Leyun Wang*<sup>1</sup>; *Philip Eisenlohr*<sup>2</sup>; *Yunjo Ro*<sup>2</sup>; *Thomas Bieler*<sup>1</sup>; *Martin Crimp*<sup>1</sup>; <sup>1</sup>Michigan State University; <sup>2</sup>Max-Planck-Institut für Eisenforschung GmbH

The anisotropic plastic deformation of polycrystalline commercial purity Ti has been studied by comparing the experimentally observed dislocation behavior in patches of microstructure with crystal plasticity finite element models (CPFEM) based on the same microstructural patches. Prior to deformation, the microstructure was characterized using orientation-imaging microscopy (OIM). Plastic deformation was experimentally characterized in selected regions at the surface of 4-point bending specimens. Active deformation systems were identified and quantified using trace analysis based on OIM, backscattered electron images, and atomic force microscopy to measure shear displacements from slip bands and deformation twins. Based on initial OIM maps, meshes of local microstructure patches were generated and their uniaxial deformation was simulated with CPFEM. The experimental observations were used to assess the accuracy of the simulations in predicting the slip and twinning activity, leading to modifications in the modeling paradigm. This project was supported by NSF grant DMR-0710570 and DFG grant EI681/2-1.

### **Role of Artificial Neural Networks in Materials Science Research:** *N. S. Reddy*<sup>1</sup>; *Jae Sang Lee*<sup>1</sup>; *Y.M. Koo*<sup>1</sup>; <sup>1</sup>GIFT, POSTECH, Pohang, Korea

The application of artificial neural networks (ANN) in materials science is a rapidly growing field. This proposed presentation reviews some of the recent advances in implementation of ANN modeling in various fields of materials science. The advent of powerful computing facilities and the rapid growth in applications of ANN methods in materials science has stimulated new research initiative with the aim of bringing these two areas together. ANN approach allows specification of multiple input criteria, and no assumption is made regarding the form of the functions relating the input and output variables. ANN, like people, is a very logical approach that learns by example.

# Technical Program

This presentation begins with an introduction to ANN and contains various techniques available, implementation details of models to materials science problems and the presentation concludes with an outline of the main features and possible avenues for future research.

## **Sliding Behavior of Favoured and Non-Favoured Boundaries in Zinc:** *Askar Sheikh-Ali<sup>1</sup>; <sup>1</sup>Kazakh-British Technical University*

High-temperature deformation in zinc bicrystals with symmetric tilt boundaries coincidence and far off-coincidence misorientations has been studied. The coupled behavior of boundary sliding and migration as well as sliding and intragranular slip was observed for the coincidence boundary. In contrast, no regular boundary migration during sliding was observed for non-coincidence boundaries. At lower applied stresses, only pure sliding took place whereas at higher stresses there were a combination of pure and slip induced sliding components. The obtained results enable to make a distinct difference between sliding behavior of favoured and non-favoured boundaries.

## **Structure and Energetics of the Stacking Faults in Austenitic FeMn Alloys Studied by First Principles Calculations:** *Alexey Dick<sup>1</sup>; Tilmann Hickel<sup>1</sup>; Jörg Neugebauer<sup>1</sup>; <sup>1</sup>Max-Planck-Institut für Eisenforschung GmbH*

An in-depth understanding of the physical processes that may influence the stacking fault energy (SFE) is necessary for an effective optimization and control of mechanical properties of high-Mn-steels [ISIJ Int. 43, 438 (2003)]. We have performed a first principles study of SFE in Fe<sub>1-x</sub>Mn<sub>x</sub>-alloys, which are prototype structures for realistic high-Mn-steels. The relevant atomic configurations have been identified by the cluster-expansion method and the concept of special quasirandom structures together with density functional theory calculations. Employing either the axial interaction model and/or explicit calculations of the generalized SFE surfaces we show that the value of the SFE sensitively depends on the chemical and magnetic ordering in the system and can be changed not only by varying the composition of the alloy and the temperature, but also by controlling local strain fields.

## **The Influence of Substitutional Solute on Nucleation of Dislocations from Cracktips in Alpha-Fe:** *Peter Gordon<sup>1</sup>; Neeraj Thirumalai<sup>1</sup>; <sup>1</sup>ExxonMobil Research and Engineering*

We employ atomistic modeling to examine the influence substitutional solutes have on the activated process of nucleating dislocations from cracktips in Fe. We demonstrate a strong correspondence between the energy landscape of the solute during an idealized block-like sliding process and the influence on the activation energy barrier for dislocation emission near a idealized cracktip. Using a series of solute potentials developed with input from ab initio calculations, these models predict that Cu and Ni both lower the activation energy barriers for emission, while solutes such as Mo and W raise the barriers. For solutes that raise or lower the emission barriers, the implications for the overall nucleation frequency turn out to be very different.

## **Thermodynamic Study of the Neptunium-Zirconium System:** *Saurabh Bajaj<sup>1</sup>; Andres Garay<sup>2</sup>; Raymundo Arroyave<sup>1</sup>; Cem Sevik<sup>1</sup>; Tahir Cagin<sup>1</sup>; Patrice Turchi<sup>3</sup>; <sup>1</sup>Texas A&M University; <sup>2</sup>CINVESTAV Queretaro; <sup>3</sup>Lawrence Livermore National Laboratory*

In fast breeder nuclear reactors, high "burn-up rates" lead to fissioning of trans-uranium elements, thus solving the problems of waste disposal and spent nuclear fuel recycling. Zr is alloyed with such metals so as to increase their melting points and suppress inter-diffusion between the nuclear fuel and cladding. In this work, we study one such metal actinide alloy fuel, Np-Zr, on which little and contrasting prior information is available. A detailed ab-initio study, implemented with the L(S)DA+U formalism, is performed to better approximate such a localized and strongly correlated system. Also, a thermodynamic model is developed using the CALPHAD method. In this method, the Gibbs energies of all the phases that are likely to take part in equilibrium are described based on empirical models. The thermodynamic model is found to be in close proximity with experimental results.

## **Ultrafine Grained Materials – Sixth International Symposium: Poster Session**

*Sponsored by:* The Minerals, Metals and Materials Society, TMS Materials Processing and Manufacturing Division, TMS Structural Materials Division, TMS/ASM: Mechanical Behavior of Materials Committee, TMS: Nanomechanical Materials Behavior Committee, TMS: Shaping and Forming Committee

*Program Organizers:* Suveen Mathaudhu, U.S. Army Research Laboratory; Mathias Goeken, University Erlangen--Nürnberg; Terence Langdon, University of Southern California; Terry Lowe, Manhattan Scientifics, Inc.; S. Semiatin, Air Force Research Laboratory; Nobuhiro Tsuji, Kyoto University; Yonghao Zhao, University of California - Davis; Yuntian Zhu, North Carolina State University

Sun PM-Wed PM Room: 606  
February 14, 2010 Location: Washington State Convention Center

*Session Chair:* Terry Lowe, Manhattan Scientifics, Inc.

## **Anisotropy of the Fracture Behaviour of Severely Deformed Iron and Pearlitic Rail Steel:** *Anton Hohenwarter<sup>1</sup>; Christoph Kammerhofer<sup>1</sup>; Reinhard Pippan<sup>1</sup>; <sup>1</sup>Erich Schmid Institute of Materials Science, Austrian Academy of Sciences*

High Pressure Torsion (HPT) is a well known technique for producing submicro- and nanocrystalline materials. Due to the limited dimensions of HPT-deformed metals little is known about their fracture and fatigue properties. A distinctive increase of the sample size enabled to extend fracture tests to HPT processed materials. In the study presented here the fracture toughness of SPD deformed iron and of a SPD deformed pearlitic steel was investigated. The measurements were performed with respect to different crack plane orientations and as a function of the temperature. The study shows that there is a strong mechanical anisotropy with respect to the different loading directions ranging from ductile to brittle fracture at room temperature for both materials. Additionally an enhanced toughness compared to coarse grained iron at cryogenic temperature was found. Reasons for the pronounced mechanical anisotropy will be discussed.

## **Crystal Plasticity Simulation of Equal Channel Angular Pressing of Aluminium Single Crystals with Different Initial Orientations:** *Guanyu Deng<sup>1</sup>; Cheng Lu<sup>2</sup>; Lihong Su<sup>1</sup>; Xianghua Liu<sup>3</sup>; Kiet Tieu<sup>2</sup>; <sup>1</sup>University of Wollongong and Northeastern University; <sup>2</sup>University of Wollongong; <sup>3</sup>Northeastern University*

Equal channel angular pressing (ECAP) has attracted much attention during last decade due to its capability of significant grain refinement. Texture in ECAP dominates many aspects of material behavior, such as strength, grain refinement, and plastic anisotropy. Effects of die angles, passes and routes have been widely investigated, while the good understanding of influence of initial orientation on texture is still lacking. In this paper, a crystal plasticity finite element model has been developed for the first time to analyze the texture evolution during ECAP of aluminium single crystal with different initial orientations: (-1 -1 2) [-3 30 14] and (-1 -1 2) [-8 18 5]. Textures predicted by the developed model are in good agreement with experimental observations. The simulation results indicate the inhomogeneous orientation distributions in the samples for both initial orientations. However, the orientation rotation patterns are different. The first initial orientation exhibits a higher rotation around the transverse direction than the second one.

## **Deformation and Microstructure of Ferrous Alloy Processed by Continuous Shear Drawing:** *Chul Won Lee<sup>1</sup>; Young Gun Ko<sup>2</sup>; Seung Namgung<sup>1</sup>; Kang Min Lee<sup>1</sup>; Dong Hyuk Shin<sup>1</sup>; <sup>1</sup>Hanyang University; <sup>2</sup>Yeungnam University*

Although equal-channel angular pressing has been a promising method over the past decade to produce ultrafine grained materials, actual applications were limited by the discontinuous nature of processing itself. To alleviate the problem associated with industrialization, this study suggested continuous shear drawing (CSD) by simply designing the geometrical shape of the die and thereby investigated deformation behavior of ferrous alloys after deforming the same. Additionally, influence of the subcritical annealing treatment following CSD was investigated in terms of spheroidization of the pearlitic cementite phases.



**Deformation Characteristics Evaluation of Modified Equal Channel Angular Pressing Processes:** *Ji Hoon Yoo*<sup>1</sup>; Seung Chae Yoon<sup>1</sup>; Anumalasetty Venkata Nagasekhar<sup>2</sup>; Hyoung Seop Kim<sup>1</sup>; <sup>1</sup>POSTECH; <sup>2</sup>The University of Queensland

In current studies, equal channel angular pressing process (ECAP) and modified ECAP processes are simulated under ideal conditions to compare the deformation characteristics. The deformation behaviour is more complicated and the strain induced during the processes is highly non-uniform in the modified ECAP processes except in the equal channel multi-angular pressing (ECMAP) process with Route C. The strain homogeneity is more of a possibility with ECAP and ECMAP with Route C processes. The deformation stress state is highly tensile in nature in modified ECAP processes. In addition, the load requirements are also higher in modified ECAP processes with that of the ECAP process.

**Deformation Twinning in Boron Carbide Particles:** *Ying Li*<sup>1</sup>; Yonghao Zhao<sup>1</sup>; Wei Liu<sup>1</sup>; Zhihui Zhang<sup>1</sup>; Rustin Vogt<sup>1</sup>; Enrique Lavernia<sup>1</sup>; Julie Schoenung<sup>1</sup>; <sup>1</sup>University of California Davis

The crystal plasticity deformation mechanism known as twinning has been widely documented for metallic systems. In the case of ceramics, however, only a few reports of twinning have been documented. In this study, we report on the observation of twinning in B<sub>4</sub>C particles in a nanostructured metal matrix composite. The mechanism is documented using TEM analysis, and a possible atomic displacement mechanism is proposed.

**Equal Channel Angular Pressing of Al-Mg Bimetal:** *Sapthagireesh Subbarayan*<sup>1</sup>; Hans Roven<sup>1</sup>; <sup>1</sup>NTNU

Severe plastic deformation (SPD) seems to be an interesting alternative for preparing bimetals considering the problems and cost issues involved in processing through conventional methods. The present work deals with a study applying ECAP on Al and Mg based bimetal. The effects of interface on structure and properties have been investigated together with crystallographic texture development. The literature has considered the mechanism of diffusion of Mg in Al, however no reports have been published for short time, high strain diffusion in the submicrometer regime. In this work, submicrometer diffusion of Mg into Al rich regions has been investigated using scanning auger microprobe (SAM) analysis. Electron microscopy studies were engaged in order to investigate possible dynamic precipitation due to SPD at or close to the interfaces. Nano- and microhardness profiles were applied to reveal local properties. Further, the microstructure was correlated to the texture evolution and the macroscopic mechanical properties.

**Evaluation of Ultra-Fine Grained Magnesium Alloy - AZ31 Processed through Constrained Groove Pressing Severe Plastic Deformation Technique:** *BalaSivanandha Prabhu*<sup>1</sup>; *D. Sathish Kumar*<sup>1</sup>; Preethi Balan<sup>1</sup>; Jayanthi Shanmugam<sup>1</sup>; A. Sekar<sup>1</sup>; <sup>1</sup>Anna University

Magnesium alloys have become one of the most widely used non ferrous alloys in the engineering applications. Their light weight, low cost and considerable strength have favored their use in automotive and aerospace industries. The simplest of the Mg alloy AZ31, having larger grain size, is subjected to severe plastic deformation using the Constrained Groove Pressing technique (CGP) at elevated temperature so that the cracking of the magnesium alloy is averted. This results in a microstructure having ultra-fine grains. The Specimens are deformed in two steps of viz., Groove Pressing and Straightening. The process cycle is repeated until a homogeneous distribution of ultra-fine grains is obtained through out the specimens. Selected ultra-fine grained materials thus obtained are subjected to mechanical testing and is found to have enhanced hardness and tensile strength. The resulting microstructure is investigated with light microscopy and Scanning Electron Microscopy.

**Experimental and Finite Analyses of Pressure Effect on the Plastic Deformation and Microstructural Evolution of Copper during High Pressure Torsion:** *Eun Yoo Yoon*<sup>1</sup>; Soo Hyun Joo<sup>1</sup>; Chong Soo Lee<sup>1</sup>; Hyoung Seop Kim<sup>1</sup>; <sup>1</sup>POSTECH

Severe plastic deformation processing by high pressure torsion (HPT) is becoming definite as an important and simple procedure for the production of ultrafine or even nanocrystalline grained metallic materials. A shear stress by twisting of the specimen under high pressure by dies in HPT allows the process to generate extremely high strains without sample fracture by instability generally occurring in simple torsion. In this study, disk shape samples of commercial purity copper were processed by HPT at room temperature under

different conditions of imposed pressure. Quantitative as well as qualitative measurements were taken of microhardness distributions, tensile tests and microstructural observations of the HPT processed copper. Also, finite element analyses of the plastic deformation behavior of purity copper during the HPT processing are presented. The simulated results of deformed geometries, microstructure and hardness evolutions are compared with experiment ones under different conditions of the applied pressure.

**Experimental Studies of Subsurface Strains and Microstructures in Severe Plastic Deformation by Machining:** *Yang Guo*<sup>1</sup>; Matthew Hudspeth<sup>1</sup>; Srinivasan Chandrasekar<sup>1</sup>; <sup>1</sup>Purdue University

It has been demonstrated that the subsurface strains resulting in the creation of a machined surface are large and result in a substantial refinement of the microstructure. In this study, measurements of these sub-surface strains have been made with high-speed imaging by tracking asperities on the workpiece and applying a technique known as Particle Image Velocimetry (PIV). These observations are supported by transmission electron microscopy, electron backscatter diffraction and nano-indentation measurement of these regions, all together providing a high resolution mapping of macroscopic deformation fields to mechanical/microstructure properties. Changes in the strain introduced into the chip, as well as the extent of the strained sub-surface, are realized by modifying the machining parameters (e.g., rake angle and depth of cut). Attempts towards establishment of a quantifiable relationship between the microstructure observations, strength characteristics and macro-level deformation parameters are presented.

**Fabrication of Nanostructured Bulk Copper with High Strength and High Conductivity (HSHC): Microstructure and Properties:** *Timothy Lin*<sup>1</sup>; <sup>1</sup>Aegis Technology Inc.

Demanding requirement in dimension shrinking of microelectronic components such as connectors and interconnects has imposed a pressing need in advanced Cu materials that possess both good electrical conductivity for high energy efficiency, and high mechanical strength. Commercial Cu has high electrical conductivity but relatively low mechanical strength. Recent investigations suggested the formation of a special class of nanocrystalline microstructure in Cu would provide the opportunity to achieve both high strength and high conductivity, in contrast with conventional nanocrystalline Cu that is featured with high strength but low electrical conductivity. Recently Aegis Technology has demonstrated the fabrication of a novel class of nanostructured bulk high-strength, high-conductivity (HSHC) Cu material by using a cost-effective scalable process, which was funded through an U.S. Army Small Business Innovative Research (SBIR) project. In this presentation, we will report the microstructure, processing, and properties of this HSHC Cu material.

**Finite and Experimental Analyses of Ultrafine Microstructure Evolution and Plastic Deformation of Copper under Various Pressures by High Pressure Torsion:** *Eun Yoo Yoon*<sup>1</sup>; Soo Hyun Joo<sup>1</sup>; Dong-Wook Kim<sup>1</sup>; Nack J. Kim<sup>2</sup>; Chong Soo Lee<sup>1</sup>; Hyoung Seop Kim<sup>1</sup>; <sup>1</sup>POSTECH; <sup>2</sup>Center for Advanced Aerospace Materials

Severe plastic deformation is important for producing ultrafine grained metallic materials and be used to solve problems where high deformation of material is involved. High pressure torsion (HPT) is becoming definite as an important and simple procedure because it leads both to smaller grains and to a higher fraction of high-angle grain boundaries. In this research, commercial purity copper of disk shape samples were processed by HPT at room temperature under different conditions of imposed pressure. Quantitative as well as qualitative measurements were taken of microhardness distributions, tensile tests and microstructural observations of the HPT processed copper. Also, finite element analyses of the plastic deformation behavior of purity copper during the HPT processing are presented. The simulated results of deformed geometries, microstructure and hardness evolutions are compared with experiment ones under different conditions of the applied pressure.

**Finite Element Analyses of Plastic Deformation Behavior on the Geometry Effect during High Pressure Torsion:** *Soo Hyun Joo*<sup>1</sup>; Chong Soo Lee<sup>1</sup>; Hyoung Seop Kim<sup>1</sup>; <sup>1</sup>POSTECH

Severe plastic deformation (SPD) has been widely used for producing bulk metallic materials with ultrafine-grained microstructures. High pressure torsion (HPT) has become an especially attractive process among various SPD processes because it produces ultrafine or even nanometer scaled grain sizes with high angles of grain boundary misorientation, compared to the other SPD processes.

Nevertheless, little works have been done on the plastic deformation related to material flow during HPT. In this research, we investigate plastic deformation behavior of workpieces, experimentally and theoretically in terms of the die geometry effect. The numerical simulations deal with a phenomenological constitutive model based on microstructure and dislocation density evolutions during the HPT process. The FEM is employed to predict pressure and cycling effects. The simulation results of hardness and deformed geometries of the workpiece are compared with experimental ones. Through this investigation, we expect to shed light on better understanding of the HPT processing.

**Forced Atomic Mixing of Immiscible Ternary Alloys during Severe Plastic Deformation:** *Nhon Vo*<sup>1</sup>; Robert Averback<sup>1</sup>; Thuy Nguyen<sup>2</sup>; Michael Campion<sup>1</sup>; Shankar Sivaramakrishnan<sup>1</sup>; Brad Stumph<sup>1</sup>; Pascal Bellon<sup>1</sup>; <sup>1</sup>University of Illinois, Urbana-Champaign; <sup>2</sup>Hanoi University of Technology

Ni and Ag67Cu33 homogeneous alloy powders were ball milled together at room temperature (RT) with average Ni atomic concentration of 4, 9, 15, and 25%. X-ray diffraction and Molecular Dynamics (MD) simulations indicated formation of a Ni/Cu core/shell structure where Cu atoms diffuse out of the Ag matrix to coat the Ni particles. High Resolution Transmission Electron Microscopy (HRTEM) showed that the grain size of the Ag matrix and the particle size of Ni/Cu particles were as small as ~6 nm and ~4 nm respectively. The core/shell structure formation is discussed in terms of shear induced atomic mobility at particle interfaces, even at RT. The fine particle sizes, in comparison to those observed with binary alloy systems, is discussed in terms of suppressed particle coalescence due to the Cu coating layer. The very small Ag grain size is attributed to grain boundary pinning at triple junctions.

**Geometry Effect Study on Plastic Deformation Behavior during High Pressure Torsion with Finite Element Method:** *Soo Hyun Joo*<sup>1</sup>; Chong Soo Lee<sup>1</sup>; Hyoung Seop Kim<sup>1</sup>; <sup>1</sup>POSTECH

Severe plastic deformation (SPD) has been a widely used procedure for producing bulk metallic materials with ultrafine-grained microstructures. High pressure torsion (HPT) has become an attractive process because of ultrafine or even nanometer scaled grain sizes with high angles of grain boundary misorientation, compared to the other SPD process. Nevertheless, less works have been done on relation between plastic deformation behavior and material flow during HPT. This research deals with experimental and theoretical plastic deformation behavior of workpieces in terms of the die geometry effect. The numerical simulation is conducted with a phenomenological constitutive model based on microstructure and dislocation density evolutions. The FEM is employed to predict pressure and cycling effects. These simulation results of hardness and deformed workpieces are compared with experimental ones. Through this investigation, we expect to shed light on better understanding of the HPT processing.

**Improving Strength and Ductility of Ultra-Fine Grained 5052 Al Alloy by Cryogenic and Warm Rolling:** *Ui Gu Kang*<sup>1</sup>; Jong Chul Lee<sup>1</sup>; Shin Woong Joong<sup>1</sup>; Won Jong Nam<sup>1</sup>; <sup>1</sup>Kookmin University

The formation of ultra-fine grains through severe plastic deformation process, usually enhances high strength in Al alloys, with the deficiency of ductility. Thus, a number of works have been performed to improve ductility without the sacrifice of tensile strength. As one of these efforts, an effective approach of achieving high strength and high ductility in Al alloys was suggested in this study. The combination of cryogenic rolling with warm rolling had effectively increased tensile strength without the decrease of ductility through the formation of ultra-fine grains with dynamic recovery in 5052 Al alloy. And static annealing, as a post heat treatment, enhanced the improvement of ductility through recovery. Therefore, ultra-fine grained 5052 Al alloy with high strength and a moderate level of ductility could be made by the combination of cryogenic rolling with warm rolling and the additional static annealing process.

**Interstitial-Assisted Strengthening Mechanism of Ultrafine Grained Pure Aluminium Processed by ECAP:** Lihong Su<sup>1</sup>; Cheng Lu<sup>2</sup>; Guanyu Deng<sup>1</sup>; Lizi He<sup>2</sup>; Xudong Sun<sup>3</sup>; Kiet Tieu<sup>2</sup>; <sup>1</sup>University of Wollongong and Northeastern University; <sup>2</sup>University of Wollongong; <sup>3</sup>Northeastern University

Commercial purity aluminium AA1050 has been subjected to equal channel angular pressing (ECAP) at room temperature to obtain ultrafine grained structure. A total strain up to 8 was introduced to the materials. Tensile tests of ECAPed samples show an increase in both strength and ductility as the number of processing passes increases. The strength also increases with post heat treatment temperature from 80°C to 110°C, and then decreases at 150°C. X-ray

diffraction profile analysis shows that lattice parameters of ECAPed samples decrease with increasing passes. After tensile failure, the lattice parameters restored to the initial value of the materials before ECAP. An interstitial-assisted deformation mechanism, demonstrated by a molecular dynamics simulation, has been proposed to explain the phenomena observed. Our results indicate that in addition to the shear strain, the hydrostatic pressure during ECAP also plays an important role in the strength enhancement of the ECAPed samples.

**Microstructure and Properties of Ultrafine-Grained Steel Produced by Warm Compression of Martensite:** *Xin Zhao*<sup>1</sup>; <sup>1</sup>Zhengzhou Institute of Aeronautics

Specimens of medium carbon steel were quenched and warm-compressed on a Gleeble 3500 Machine. The microstructure of the specimens was studied by using an optical microscope and a transmission electron microscopy. And the properties were investigated by using tensile tests and hardness tests. Results show that the starting microstructure was lath martensite with a small amount of flake martensite. After 50% compression at 550-700°C, ultrafine grains can be obtained in the specimens. The microstructure of the specimens compressed at 600°C was equiaxed ultrafine ferrite grains + nano-carbides. And the hardness was 233.81HV. The tensile strength and total elongation were 861MPa and 19.1%, respectively.

**Nanostructured Commercially Pure Titanium Prepared via Cryomilling and High Pressure Torsion (HPT):** *Osman Ertorer*<sup>1</sup>; Ying Li<sup>1</sup>; Yonghao Zhao<sup>1</sup>; Ruslan Valiev<sup>2</sup>; Enrique Lavernia<sup>1</sup>; <sup>1</sup>University of California - Davis; <sup>2</sup>Ufa State Aviation Technical University

Several plastic deformation (SPD) methods are known to be effective for production of bulk nanostructure alloy systems. In this study, multiple SPD methods (i.e. cryomilling + HPT) were performed for obtaining bulk nanostructured titanium. Microstructure and microhardness studies were made in order to investigate the deformation on different sections of the specimen. Results were compared discussed in means of defect structures and microhardness.

**Reported Ductilities in Ultrafine Grain Metals and Confusion Regarding Measurement:** *Kaoru Yamamoto*<sup>1</sup>; *Amit Ghosh*<sup>1</sup>; <sup>1</sup>University of Michigan

Measurement of tensile ductility is generally based on elongation to failure in a tensile test. Elongation measurement methods, well established in the handbooks of American Society for Materials Testing, require a fixed gauge length into which new material is not continuously fed in during test. For testing strain rate sensitive materials, the importance of fixing gauge length have been extensively discussed in the literature. With great emphasis on ultrafine grain materials research at this time, however, the importance of fixing the gauge length during test has been overlooked in many cases, resulting in unreliable results for such materials. The roles of microstructure produced by different SPD processes, test temperatures and strain rates on material behavior could be overly exaggerated when attention is not paid to such details. The purpose of this talk is to reemphasize proper material testing techniques to test these materials.

**Spheroidization of High-Carbon Steel Processed by Equal Channel Angular Pressing:** *Seung Namgung*<sup>1</sup>; *Chul Won Lee*<sup>1</sup>; *Dong Hyuk Shin*<sup>1</sup>; *Jae Sik Lee*<sup>2</sup>; *Young Gun Ko*<sup>2</sup>; <sup>1</sup>Hanyang University; <sup>2</sup>Yeungnam University

The paper demonstrates the spheroidization behavior of pearlitic cementite in high-carbon steel processed by equal channel angular pressing. The influences of strain, post-ECAP annealing temperature, and time on morphological change of cementite are investigated. Intense plastic straining triggers the kinetics of spheroidization during annealing. It is found that the cooling rate after the annealing is also important in reducing the size of cementite phase. Thus, an appropriate condition to obtain the fully spheroidized microstructure of high-carbon steel is suggested. In addition, mechanical properties after spheroidization are examined.

**Strain Hardening Behavior of Ultra-Fine Grained 5083 Aluminum Alloy:** *Troy Topping*<sup>1</sup>; Ying Li<sup>1</sup>; Zhihui Zhang<sup>1</sup>; Enrique Lavernia<sup>1</sup>; <sup>1</sup>University of California, Davis

Aluminum alloys with nanocrystalline and ultra-fine grain (UFG) size are of interest because of their high strength – typically more than 30% stronger than conventionally processed alloys. For this study, the microstructure and mechanical behavior of UFG Al 5083 plate, produced by quasi-isostatic forging and rolling of cryomilled powder, has been investigated and compared to coarse-grained Al 5083 - in particular, the ability to strengthen the UFG material further by strain hardening. Plate material was cold rolled up to 50% without cracking. It is found that the UFG structure accommodates dislocations differently than coarse grained materials, but significant strength gains can be achieved. Microstructural

evidence shows dislocation forests in UFG Al, while conventional Al forms cells or subgrains. Dislocation densities are quantified in an effort to explain their contribution to the overall strength of the alloy. Analysis of tensile data shows changes in the work hardening rate after cold rolling.

**Texture and Microstructure Evolution in Ultrafine Grained AZ31 Processed by EX-ECAP:** *Milos Janecek*<sup>1</sup>; Sangbong Yi<sup>2</sup>; Radomir Kuzel<sup>1</sup>; Jitka Vratna<sup>1</sup>; Karl Kainer<sup>2</sup>; <sup>1</sup>Charles University; <sup>2</sup>GKSS Research Centre

Direct extruded commercial magnesium wrought alloy AZ31 was processed by ECAP up to 12 passes. Texture and microstructure evolutions as a function of strain imposed by ECAP were observed using EBSD and X-ray diffraction. ECAP pressing up to 4 passes resulted in the formation of a new texture component which corresponds to the bimodal structure, in terms of the texture as well as grain size, observed in this specimen. Relatively large grains (larger than 10  $\mu\text{m}$ ) exhibit the orientation change with c-axes tilted by approximately 60° from the press direction and formed a new texture component. The relatively fine grains with the average size of 1  $\mu\text{m}$  kept their original orientation, i.e. their c-axes perpendicular to the press direction. Further ECAP pressing (up to 12P) resulted in a complete refinement of the microstructure and the corresponding orientation changes of all grains and the strengthening of the new texture component.

**The Effect of Friction Stir Welding on the Microstructure and Mechanical Behavior of Continuously Equal-Channel Angular Pressed (CECAP) A5052 Alloy Sheets:** *Nilesh Kumar*<sup>1</sup>; Rajiv Mishra<sup>1</sup>; Gaurav Mohanty<sup>2</sup>; Santosh Karthik<sup>2</sup>; Krishna Rajan<sup>2</sup>; <sup>1</sup>Missouri University of Science & Technology; <sup>2</sup>Iowa State University

In this study, CECAP processed ultra-fine grained (UFG) A5052 sheets were used. Such materials possess very high strength and moderate ductility. Fusion welding techniques are not suitable for retaining UFG microstructure and properties. Friction stir welded UFG A5052 exhibited either a very little decrease in strength or superior mechanical properties than that of the parent materials. For CECAP material, main source of superior strength is high dislocation density and very fine grain size. Friction stir welding led to lower dislocation density, but a further refinement of grains. Transmission electron microscopy and electron back-scattered diffraction have been used to characterize the microstructure. These results have been used to predict the strength of the alloy using the existing strengthening models. Mini tensile testing was carried out to evaluate the predictive capability of the strengthening models.

# Technical Program

## 2010 Functional and Structural Nanomaterials: Fabrication, Properties, Applications and Implications: Electrical Properties of Nanomaterials

Sponsored by: The Minerals, Metals and Materials Society, TMS Electronic, Magnetic, and Photonic Materials Division, TMS: Nanomaterials Committee

Program Organizers: David Stollberg, Georgia Tech Research Institute; Nitin Chopra, University of Alabama; Jiyoung Kim, University of Texas - Dallas; Seong Jin Koh, University of Texas at Arlington; Navin Manjoran, Siemens Corporation; Ben Poquette, Keystone Materials; Jud Ready, Georgia Tech

Monday AM Room: 214  
February 15, 2010 Location: Washington State Convention Center

Session Chair: Jud Ready, Georgia Tech; Seung H. Kang, Qualcomm Inc

### 8:30 AM Introductory Comments

#### 8:35 AM Invited

**Schottky Diodes on Nanowires of Cadmium Telluride and Copper Indium Diselenide Embedded in Porous Alumina Templates:** *Vijay Singh*<sup>1</sup>; <sup>1</sup>University of Kentucky

Nanowires of copper indium diselenide (CuInSe<sub>2</sub> or CIS) and cadmium telluride (CdTe) are of interest in solar cells of relatively high efficiency that can be produced inexpensively. These nanowires were electrodeposited inside porous alumina templates and characteristics of Al/CIS and Au/CdTe nanowire Schottky diodes were studied. The X-ray diffraction of the nanowires showed nanocrystalline cubic phase structures with the grain size equal to the diameter of the pores. The EDX analysis confirmed that both  $\alpha$  and  $\beta$ -phases of CdTe were present. For CIS, analysis of the current-voltage characteristics of these devices yielded diode ideality factor and reverse saturate current density values similar to those reported in the literature for bulk CIS/Al junctions. For CdTe, Analysis of Schottky diodes yielded a diode ideality factor of 10 in the dark and under "one sun" illumination. Reverse saturation current density was 34.9  $\mu$ A/cm<sup>2</sup> in the dark and 39.7  $\mu$ A/cm<sup>2</sup> under illumination.

#### 8:55 AM

**Electronic Transfer in Molecular Nanostructures:** *Karel Kral*<sup>1</sup>; <sup>1</sup>Inst. Phys. ASCR, v.v.i.

The transfer of electrons or holes between states localized on individual molecules is considered theoretically. The mechanism considered can apply to molecular crystals, polymer solids, DNA molecule, etc. The electronic transfer is studied within a model with inter-molecular electron tunnelling accompanied by the coupling of charge carriers to intra-molecular vibrations. The multiple electronic scattering on phonons is taken into account in the self-consistent Born approximation to the nonequilibrium Green's function self-energy. The corresponding kinetic equation shows the diffusion mechanism of electrons along the molecular solid. This mechanism will be compared to the well-known Marcus theory of electronic transfer. Using the above mechanism we shall discuss earlier experimental data on photoconductivity in charge-transfer crystals, recent data on electric conduction of DNA molecules and also the electric conduction in polymers.

#### 9:15 AM

**Effect of the Nanocrystalline Structure of Metallic Cathodes on the Efficiency of Ion-Induced Electron Emission:** *Radik Mulyukov*<sup>1</sup>; Rinat Khisamov<sup>1</sup>; Konstantin Nazarov<sup>1</sup>; Yulai Yumaguzin<sup>2</sup>; Ayrat Nazarov<sup>1</sup>; <sup>1</sup>Institute for Metals Superplasticity Problems, Russian Academy of Sciences; <sup>2</sup>Bashkiria State University

Cold cathodes which are based on ion-induced electron or secondary electron emission are widely used in vacuum and discharge devices, optical quantum generators, displays, ion sources etc. Lowering their work function is an important fundamental task. Traditionally it is solved by a variation of the chemical composition of cathodes, coating, and giving a special shape for the improvement of emission characteristics. Recent investigations have shown that the work function of metals can be lowered by their nanostructuring. On an example of pure nickel and Al-6%Mg alloy it will be shown that nanostructuring results in a decrease of the work function by 0.4 to 0.8 eV and enhancement of the ion-induced electron emission current by 30% and more. This allows

an increase of the efficiency of ion sources by using nanocrystalline materials as cold cathodes. Prospects of application of nanocrystalline materials for manufacturing highly effective cold cathodes will be outlined.

#### 9:35 AM

**Electrical Conductance of Single TiO<sub>2</sub> Nanotube Devices:** *Jie Huang*<sup>1</sup>; Dongkyu Cha<sup>1</sup>; Mingun Lee<sup>1</sup>; Moon Kim<sup>1</sup>; Jiyoung Kim<sup>1</sup>; <sup>1</sup>University of Texas at Dallas

Titanium dioxide (TiO<sub>2</sub>) nanotubes attract increasing attention because of their wide range of potential applications: photocatalysts, gas sensors, solar cells and bio-sensors, etc. In our research, TiO<sub>2</sub> nanotubes were fabricated using atomic layer deposition (ALD) combining with an anodic aluminum oxide (AAO) template technique. Materials characterization was done by both XRD and TEM. Single nanotube devices were made by focus ion beam (FIB) as well as e-beam lithography. As fabricated TiO<sub>2</sub> nanotubes with different wall thicknesses were annealed either in vacuum or O<sub>2</sub> with various temperatures in order to control the oxygen vacancy doping rate. Conductivity was measured by both four-probe measurements and in-situ characterization in TEM. In this presentation, we will also propose a potential conduction mechanism. This research was supported by a grant (code #: 2009K000469) from 'Center for Nanostructured Materials Technology' under '21st Century Frontier R&D Programs' of the Ministry of Education, Science and Technology, Korea.

#### 9:55 AM

**Enhancing Electrical Performance of Solution Processed Doped ZnO Film by Nanowire Alignment:** *Sujay Phadke*<sup>1</sup>; Jung-Yong Lee<sup>1</sup>; Jack West<sup>2</sup>; Alberto Salleo<sup>1</sup>; <sup>1</sup>Stanford University; <sup>2</sup>Stanford University/Sequoia High School

ZnO is a wide band gap semiconductor with potential to replace ITO as transparent electrode material. Low cost ZnO thin films can be fabricated by depositing ZnO nanowires synthesized using low temperature solution based processes. To improve the conductivity of intrinsic ZnO, it is n-doped with Gallium atoms during synthesis. In order to study the electrical properties of ZnO nanowire films, the effect of directional alignment of doped ZnO nanowires on film sheet resistance was studied. Nanowires are aligned by shearing a nanowire dispersion between two silicon wafers. Directional sheet resistances of ZnO films have been measured with a four point probe. The sheet resistance observed in the direction of alignment is lower than that observed perpendicular to that. Computer simulations used in conjunction with sheet resistance measurements on aligned films are used to quantitatively determine the effect of inter-wire contact on conductivity of ZnO nanowire mat films.

#### 10:15 AM Break

#### 10:25 AM

**3D Carbon Nanotube Based Photovoltaic Devices:** *Jack Flicker*<sup>1</sup>; Jud Ready<sup>2</sup>; <sup>1</sup>Georgia Institute of Technology; <sup>2</sup>Georgia Tech Research Institute

Although photovoltaic technology has been around for over fifty years, the use of a nanostructured, three dimensional morphology in these types of devices has occurred only relatively recently. We introduce a three dimensional photovoltaic device with carbon nanotube pillars coated with photoactive materials to create a solar cell. The extra dimensionality of this cell added by the nanotubes has been theorized to increase the relative energy generated over planar cells by up to four times. The energy increase is due to an increase in the interactions between photons and the photoactive material as the sun is at an off normal angle to the cell substrate. Prototypes of these cells have been made and, although suffering from a low overall efficiency, do show an increased energy production in the same manner that theory predicts when the light source is at an off normal angle.

#### 10:45 AM

**CuO Nanowire-Co<sub>3</sub>O<sub>4</sub> Nanoparticle Heterostructures for the Development of Multi-Functional Photocatalyst:** *Wenwu Shi*<sup>1</sup>; *Nitin Chopra*<sup>1</sup>; <sup>1</sup>The University of Alabama

Heterostructures comprising of nanowires and nanoparticles with controlled compositions are critical for the development of future devices. In this regard, nanostructured CuO and Co<sub>3</sub>O<sub>4</sub> are significantly important because of their semiconducting and catalytic properties. Here, we report a simple method to synthesize CuO nanowire-Co<sub>3</sub>O<sub>4</sub> nanoparticle heterostructures and study these novel materials as photocatalysts. Our synthetic approach couples chemical vapor deposition (CVD) growth of CuO nanowires (diameters ~78.3±17.9 nm) with wet-chemistry method to result narrow size distribution Co<sub>3</sub>O<sub>4</sub>



nanoparticles (diameter  $\sim 7.0 \pm 1.5$  nm) uniformly decorated on CuO nanowires. A series of characterization steps (SEM, HRTEM, XRD and EDX) are undertaken to observe size, morphology, phases, and composition of heterostructures. The absorption spectrum of as-prepared materials is collected by UV-vis-NIR spectrometer. It has been found that after nanoparticles decoration, absorption in visible region enhanced greatly. Experiments of using them as photocatalyst under visible light show photocatalytic properties have been improved by  $\sim 4.5$  times.

### 11:05 AM

**CNT Based Thermoelectric Devices for Energy Harvesting:** *David Lashmore*<sup>1</sup>; Tom VanVechten<sup>1</sup>; Jennifer Mann<sup>1</sup>; Cory Timoney<sup>1</sup>; Ian Wilson<sup>1</sup>; <sup>1</sup>Nanocomp

Carbon nanotube sheets can be doped to create n and p type regions with Seebeck coefficients from  $+60 \mu\text{V/k}$  for p type and  $-50 \mu\text{V/k}$  for n type. Devices fabricated from these sheets will be described along with optimization of thermoelectric performance along with ZT, Watts/gram, Watts/m<sup>2</sup> and Dollars per Watt. Two parameters limiting thermoelectric behavior are electrical conductivity, which can be made very high,  $\sim 2 \times 10^6$  S/m, and the thermal conductivity which can be made very as low as 10 W/m oK. Thermal conductivity and electrical conductivity can be independently controlled. Direct solar conversion to electricity, a kind of thermoelectric solar cell, will be described. Carbon nanotube material acts much like a black body from near UV to almost 12 microns so that 98% of the solar radiation can very efficiently be converted to heat.

### 11:25 AM

**Synthesis of Tin Filled Carbon Nanotubes and Their Application to Lithium Ion Batteries:** Raj Das Gupta<sup>1</sup>; Carsten Schwandt<sup>1</sup>; *Derek Fray*<sup>1</sup>; <sup>1</sup>University of Cambridge

There is a need to increase the charge capacity of the anodes in lithium ion batteries and this can be achieved by using tin, aluminium or silicon particles but the particles decrepitate, due to the large volume changes on charging and discharging. In order to overcome this problem, carbon nanotubes were filled with tin by placing graphite electrodes into a bath of molten lithium chloride – tin chloride and applying a slow altering current. It was found that the yield of carbon nanotubes was high and the majority were filled with tin. Anodes were made from this material and it was found that the charge capacity levelled off at 430 mAh/g after about 400 charge-discharge cycles at which point it became constant. TEM examination of the used anode showed that the nanotubes had expanded due to the volume changes of the tin but still encapsulated the tin particles.

### 11:45 AM

**Radar Absorption Properties of Radar Absorbing Structures Composite Filling with Carbon Nanotubes:** *Zhengquan Zhang*<sup>1</sup>; Tiehu Li<sup>1</sup>; <sup>1</sup>Northwestern Polytechnical University

The developments of evading radar detection have become increasingly more important. By reducing the radar cross section, they could evade radar detection. Radar absorbing structures are the structure that has both the function of load bearing and the EM energy absorbing capability. The construction of polymeric composite RAS could be achieved by regulating the electric property or magnetic property of material. Nowadays studies on investigating RAS using fiber reinforced polymeric composite materials are becoming popular research field. In the study, Radar absorbing structures laminate composites composed of glass fibers, carbon fibers and epoxy resin filled with carbon nanotubes, were fabricated in a press mould. The absorbing properties were simulated based on electromagnetic theory. Two optimal double-layered radar absorbing structure and one three-layered radar absorbing structure was obtained. Reflection loss of a three-layered radar absorbing structure was less -10dB in whole frequency range of 8.2-12.4GHZ and has double absorbing peaks.

### 12:05 PM

**Study of the AC Conductivity Affected by Crystallization and CNFs for PVDF/CNF Composite Thin Films:** *Lili Sun*<sup>1</sup>; Bin Li<sup>1</sup>; Weihong Zhong<sup>1</sup>; Yan Zhao<sup>2</sup>; <sup>1</sup>Washington State University; <sup>2</sup>Beihang University

Poly (vinylidene fluoride) (PVDF) is an important ferroelectric polymer with complicated phase behaviors and the polar functional group, -C-F-. In this paper, carbon nanofiber (CNFs) filled PVDF thin films were prepared via a solution casting method. The effects of CNFs on the crystallization of PVDF and the AC conductivity of CNF/PVDF nanocomposites were investigated. The

results revealed that the introduction of CNFs not only affected the conductivity directly, but also caused indirect effects to the conductivity through influencing the size of crystal grains, the degree of crystallinity and the crystal phase transformation of PVDF. In particular, a phase transformation from  $\alpha$ -phase to  $\beta$ -phase in PVDF was found to affect conductivity of the nanocomposites due to the increment of CNF concentration in the nanocomposites.

### 12:25 PM Concluding Comments

## Advances in Composite, Cellular and Natural Materials: Natural Materials and Polymer Matrix Composites

*Sponsored by:* The Minerals, Metals and Materials Society, TMS Structural Materials Division, TMS/ASM: Composite Materials Committee

*Program Organizers:* Yuyuan Zhao, The University of Liverpool; David Dunand, Northwestern University

Monday AM

Room: 305

February 15, 2010

Location: Washington State Convention Center

*Session Chairs:* Lorna Gibson, Massachusetts Institute of Technology; Amy Johnson, University of Illinois at Urbana-Champaign

### 8:30 AM

**Alpha-helical Protein Networks Are Self-Protective and Flaw-Tolerant:** *Markus Buehler*<sup>1</sup>; <sup>1</sup>Massachusetts Institute of Technology

Alpha-helix based protein networks as they appear in intermediate filaments in the cell's cytoskeleton and the nuclear membrane robustly withstand large deformation of up to several hundred percent strain, despite the presence of structural imperfections or flaws. Here we report a series of molecular simulations with a coarse-grained multi-scale model of alpha-helical protein domains, explaining the structural and mechanistic basis for this observed behavior. We find that the characteristic properties of alpha-helix based protein networks are due to the particular nanomechanical properties of their protein constituents, enabling the formation of large dissipative yield regions around structural flaws, effectively protecting the protein network against catastrophic failure. We show that the key for these self-protecting properties is a geometric transformation of the crack shape that significantly reduces the stress concentration at corners. Our findings help to explain the ability of cells to undergo large deformation without failure while providing significant mechanical resistance.

### 8:50 AM

**Mechanical Behavior of Natural Sisal Fibers:** Flavio Silva<sup>1</sup>; *Nik Chawla*<sup>1</sup>; Romildo Toledo Filho<sup>2</sup>; <sup>1</sup>Arizona State University, School of Mechanical, Aerospace, Chemical, and Materials Engineering; <sup>2</sup>Civil Engineering Department, COPPE, Universidade Federal do Rio de Janeiro

Environmental awareness and an increasing concern with the greenhouse effect have resulted in the development of sustainable materials in construction, automotive, and packing industries. Natural fibers are a good alternative since they are ready available in fibrous form and can be extracted from plant leaves at a very low costs. They are also biodegradable materials. In this work we present a systematic experimental investigation on the mechanical performance of sisal fibers. Tensile tests were performed at four different gage lengths. The measured Young's modulus was corrected for machine compliance. Weibull statistics were used to quantify the degree of variability in fiber strength, at the different gage lengths. Fatigue tensile tests were performed at stress-levels between 80 to 400 MPa. The failure mechanisms will be described and discussed in terms of the fiber microstructure as well as the defect population in the fibers.

### 9:10 AM

**Development of Eco-Friendly Brake Friction Composites:** *Yafei Lu*<sup>1</sup>; Baoting Suo<sup>1</sup>; Hui Wang<sup>1</sup>; Yimei Lu<sup>1</sup>; <sup>1</sup>Beijing University of Chemical Technology

Eco-friendly brake friction composites with good friction performance were developed. The raw materials utilized were selected according to eco-friendly criterion that natural products should be preferably chosen. The formulations are composed of plant flax, mineral basalt, and wollastonite fibers as reinforcements, natural graphite as solid lubricant, zircon as abrasive, vermiculite and baryte as

# Technical Program

functional and space fillers, and cardanol based benzoxazine toughen phenolic resin as binder. To enhance the heat resistance of flax fiber, chemical and physical methods including drying, room temperature alkaline solution, acid steam, high temperature alkaline solution were performed and after the treatments, microfibrils were formed. A new cardanol based benzoxazine was synthesized by the reactions among cardanol, aniline, and formaldehyde. The effects of the content of treated flax fiber and friction temperature on friction performance, friction coefficient and specific wear rate, of the composites were evaluated.

## 9:30 AM

**Energy Attenuation Capability of Woven Natural Silk (WNS)/Epoxy Composites Plates Subjected to Drop-Weight Impacts:** *Albert Uchenna Ude<sup>1</sup>; Che Husna Azhari<sup>1</sup>; Kamauzzaman Sopian<sup>1</sup>; <sup>1</sup>The National University of Malaysia (UKM)*

The impact energy attenuation and damage characterisation of woven natural silk (WNS)/epoxy laminated composite plates were evaluated. The samples which were prepared in configurations of sandwich WNS/epoxy/honeycomb, WNS/epoxy/coremat WNS/epoxy/foam and reinforced WNS/Epoxy laminate plates were subjected to low velocity impact loading at energy level of 32J, 48J and 64J respectively. Impact parameters like load-deflection, load-time and absorbed energy-time behaviour were measured for evaluating the impact performance in terms of load bearing capabilities, energy absorption and failure modes. Evaluations of the results showed WNS/epoxy/coremat as possessing better load bearing capability qualities. In general energy absorption decreases as impact energy increases in all the composite samples; WNS/epoxy/foam was seen as better energy absorber. Damage areas increases as impact energy increases while time decreases with increase in impact energy in all the configurations. SEM micrographs show mode of failure as matrix crack, delamination and fibre breakage.

## 9:50 AM

**Strain Rate Effects on the Deformation Behavior of Particles in Epoxy-Based Composites:** *Bradley White<sup>1</sup>; Jonathan Spowart<sup>2</sup>; Jennifer Jordan<sup>3</sup>; Naresh Thadhani<sup>1</sup>; <sup>1</sup>Georgia Institute of Technology; <sup>2</sup>AFRL/RXLMD; <sup>3</sup>AFRL/RWME*

The micromechanical mechanisms controlling stress transfer between particles and matrix in a composite are fairly well understood. However, the influence of microstructural details on the amount of local stress/strain the individual particles experience and the strain rate dependence of the stress transfer are not well understood. In order to determine the bulk material-particle deformation relationship for particulate composites, particle strain measurements were carried out on cast epoxy-based materials containing metal particles that were subjected to compressive loads across a large range of strain rates ( $10^{-4}$  -  $10^4$ ). These composite materials varied by particle loading fraction (10-50 Vol%), size (5-50  $\mu$ m), and type (Al or Al+Ni) to produce microstructures with varied distributions of particle reinforcement. Individual particle deformations were evaluated, and correlated with quantitative characteristics of the distribution of reinforcement phase(s) within the matrix. In this presentation the approach as well as current findings and results will be discussed.

## 10:10 AM Break

## 10:30 AM

**Reactive Polymeric Nanocomposites:** *Christopher Crouse<sup>1</sup>; Christian Pierce<sup>1</sup>; Jonathan Spowart<sup>1</sup>; <sup>1</sup>Air Force Research Laboratory*

Metal nanoparticles have attracted much interest over the past decade as fuel sources for energetic materials due in part to their high surface areas and large energy densities. In combination with the appropriate oxidizer component, or secondary metal, these mixtures are capable of liberating energy through either a thermite process or intermetallic formation, respectively. Without a strong interface between the component metal particles, these composites are typically very brittle, and offer little in terms of structural integrity. To this end, we have pursued monomer functionalization of the particles subsequently followed by an in situ polymerization to integrate a polymeric component (i.e. binder) into these systems. This approach affords a tunable energetic response through manipulation of the particle content and polymer selection. A detailed assessment of the chemistry employed to develop these composites along with an evaluation of their energetic performance will be presented.

## 10:50 AM Invited

**B/SiO<sub>x</sub> Nanonecklace Reinforced Nanocomposites by Unique Mechanical Interlocking Mechanism:** *Xinyong Tao<sup>1</sup>; Jie Liu<sup>1</sup>; Goutam Koley<sup>1</sup>; Xiaodong Li<sup>1</sup>; <sup>1</sup>University of South Carolina*

We demonstrate that nanonecklaces with SiO<sub>x</sub> beads on boron strings can be synthesized via a facile and environment-friendly method under atmospheric pressure. The continuous crystalline boron strings possess a thousand times higher electrical conductivity than bulk boron. The SiO<sub>x</sub> beads demonstrate good compatibility with the epoxy resin matrix. Due to the mechanical interlocking between the SiO<sub>x</sub> beads and the surrounding matrix, the reinforcement effect of this kind of nanonecklaces in epoxy nanocomposites is even better than normal carbon nanotubes. The marriage of boron strings and SiO<sub>x</sub> beads in the form of nanonecklaces is expected to exhibit unique electrical and mechanical properties for constructing nanodevices and nanocomposites. These nanonecklace fiber reinforcement concepts are expected to have significant applications in the design and optimization of intricate nanostructures and nanocomposites with superior mechanical properties.

## 11:10 AM

**A Review of Fiber Waviness and Its Effect on Material Properties:** *Bryan Allison<sup>1</sup>; Jeff Evans<sup>1</sup>; <sup>1</sup>University of Alabama in Huntsville*

Fiber waviness is a common defect in fiber reinforced polymer (FRP) composites. Waviness is generally created during the manufacturing process. It negatively affects the material properties in most cases, particularly the ultimate compressive strength. This reduction has been reported to be over 80% in certain cases. This is not always the case, however. One case where waviness can actually increase the strength is buckling. This presentation is a review of how fiber waviness affects the mechanical properties of FRP, and a look at what future work might be on the horizon.

## 11:30 AM

**Structure and Capability of TiB<sub>2</sub>/UHMWPE Composite Shielding Material for Nuclear Radiation:** *Xiaozhou Cao<sup>1</sup>; Xiangxin Xue<sup>1</sup>; Ting'an Zhang<sup>1</sup>; Xianwei Hu<sup>1</sup>; <sup>1</sup>Northeastern University*

A new style TiB<sub>2</sub>/UHMWPE Composite Shielding Material for Nuclear Radiation was prepared by hot pressing method. The microstructure, mechanical property and radiation shielding of composite material were analyzed. The results indicate that each component was distributed continuously and evenly and the interface was combined closely. Hardness and tensile strength of the composite improved with TiB<sub>2</sub> content increased. The absorption ration for thermal neutron increased with the thickness of composite increased.

## Aluminum Alloys: Fabrication, Characterization and Applications: Development and Application

*Sponsored by:* The Minerals, Metals and Materials Society, TMS Light Metals Division, TMS: Aluminum Processing Committee

*Program Organizers:* Subodh Das, Phinix LLC; Steven Long, Kaiser Aluminum Corporation; Tongguang Zhai, University of Kentucky

Monday AM

Room: 615

February 15, 2010

Location: Washington State Convention Center

*Session Chair:* John Chinella, U.S. Army Research Laboratory

## 8:30 AM

**High Strength and High Temperature Aluminum Alloys for High Performance Applications:** *Awadh Pandey<sup>1</sup>; Jonathan Spowart<sup>1</sup>; <sup>1</sup>Pratt & Whitney Rocketdyne*

New high strength and high temperature aluminum alloy has been developed to provide weight reduction benefit for rocket engines. The present aluminum alloy is based on a novel Al-Sc based alloy system. Aluminum-scandium alloy forms Al<sub>3</sub>Sc based precipitate that has an L1<sub>2</sub> structure which is strong and thermally stable up to very high temperatures. This material was made by a powder metallurgy technique consisting of ingot fabrication, powder production, compaction and extrusion. The proposed alloy has demonstrated very high strength for a range of temperatures up to 600F. High cycle fatigue and creep tests of these alloys were also conducted. Fatigue result of this alloy showed good endurance limit at room temperature. Creep resistance of this alloy was found to be significantly superior to the existing aluminum alloys. The



dominant strengthening mechanisms in this alloy is grain size strengthening, Orowan strengthening and antiphase boundary energy strengthening.

**8:50 AM**

**Scandium/Zirconium Modified Aluminum Alloys for Improved Mechanical and Corrosion Properties:** *Jennifer Gaies*<sup>1</sup>; <sup>1</sup>NSWC Carderock Division

Due to the need for high speed, lightweight ships there is an increased use of aluminum alloys in ship construction. These applications require materials with the following combination of properties: high welded strength, ductility and elongation, corrosion resistance, and fatigue and corrosion fatigue resistance. The most commonly used aluminum alloy families in marine applications are the Al-Mg (5XXX series) alloys which derive their strength from work hardening and are not heat-treatable. Reduced as-welded strengths limit their practical structural applications. The high temperatures introduced during the welding process reverse some of the effects of the strengthening mechanisms so aluminum alloys which can retain the greatest amount of post-welded strength are, therefore, greatly desired. Small additions of Sc and Zr have been shown to improve mechanical and corrosion properties of aluminum alloys and their effect as additions to commercial 5XXX alloys are investigated.

**9:10 AM**

**TRIMAL 52@ - A New Aluminium Alloy for High Performance Spaceframe Construction:** *Marcel Rosefort*<sup>1</sup>; Horst Gers<sup>2</sup>; Thomas Koehler<sup>1</sup>; Jana Ehrke<sup>1</sup>; Dirk Schnapp<sup>2</sup>; Hubert Koch<sup>1</sup>; <sup>1</sup>Trimet Aluminium AG; <sup>2</sup>Honsel AG

Aluminium especially extrusions of the 6xxx series have considerable potential to make cars lighter and thus more economical. Trimet Aluminium AG has been supplying aluminium and services for the aluminium industry since 1988. TRIMET Essen is producing aluminium billets for high performance profiles especially in automotive applications since 1994. Over the time requirements has been changed to higher strength for profiles with lower wall thickness including better energy absorbing behaviour. Therefore TRIMET and Honsel started an innovative alloy and process development to give these profiles a considerably greater strength and better folding behaviour under load compared to other alloys available. Extrusions made out of this new alloy, trimal@-52, fulfil the highest demands of the OEMs. This paper describes the most important aspects of the production chain of aluminium for spaceframe application from the alloy development to the casting process and at last to test results of the final product.

**9:30 AM**

**High-Temperature Fatigue Deformation Behavior of Heat-Resistant Aluminum Alloy for Automobile Parts:** Jong-Soo Park<sup>1</sup>; Si-Young Sung<sup>2</sup>; Bum-Suk Han<sup>2</sup>; Chang-Yeol Jung<sup>3</sup>; *Kee-Ahn Lee*<sup>4</sup>; <sup>1</sup>Center for Advanced Green Materials Technology, Andong National University; <sup>2</sup>Korea Automotive Technology Institute; <sup>3</sup>Korea Institute of Industrial Technology; <sup>4</sup>Department of Advanced Material Science and Engineering, Andong National University

In this study, fatigue samples were processed from cylinder head parts that are actually used in domestic and foreign automobiles; high-temperature, high-cycle, and low-cycle fatigue characteristics were then evaluated and compared. The result of the tensile strength test on material B at 250° was higher by 15.9MPa compared to material A. On the other hand, elongation was 9.5% higher for material A. At 130°, material B exhibited high fatigue life given high-cycle fatigue under high stress, whereas material A showed high fatigue life when stress was lowered. With regard to the low-cycle fatigue result (250°) showing higher fatigue life as ductility is increased, material A demonstrated higher fatigue life. Through the observation of the differences in microstructure and the fatigue fracture surface, an attempt to explain the high-temperature fatigue deformation behavior of the materials was made.\* supported by Fundamental R&D Program for Core Technology of Materials, Korea

**9:50 AM Break**

**10:05 AM**

**Optimized Heat Treatment Sequence for AA 6061:** *Christian Zelger*<sup>1</sup>; Josef Schnitzlbaumer<sup>1</sup>; Ramona Prillhofer<sup>1</sup>; Josef Enser<sup>1</sup>; Carsten Melzer<sup>1</sup>; <sup>1</sup>AMAG Rolling

Increasing material requirements regarding formability and mechanical properties sometimes force customers to apply either 5xxx alloys for better formability or 2xxx/7xxx alloys for higher strength in cases where standard 6xxx alloys and heat treatment processes fail. In this paper optimized heat treatment processes are presented, which allow to (i) form parts in T4 temper

and reduce the subsequent time-consuming and costly artificial ageing step, or (ii) reach strength levels >10% above standard T6 temper or (iii) combine these two benefits. The advanced heat treatment processes enable 6xxx alloys to reach T6 temper within <1 hour compared to about 12 hours in standard processes. For the costumers this means significant time-, energy- and cost savings. Additionally a new heat treatment sequence allows reaching strength levels, which reduce the gap between known mechanical property levels of 6xxx alloys and 2xxx/7xxx alloys, without reducing high formability and corrosion resistance.

**10:25 AM**

**Microstructure, Mechanical Characterization and Hot Tensile Behaviour of Al-Zn-Mg Modified Alloys:** *Paola Leo*<sup>1</sup>; *Emanuela Cerri*<sup>1</sup>; Hugh J. McQueen<sup>2</sup>; <sup>1</sup>University of Salento; <sup>2</sup>Concordia University

Two Al-Zn-Mg alloys (Zr modified and not) were investigated by optical microscopy, hardness and tensile tests. The alloys were solutionized (2h at 490°C) and artificial aged at 130, 160, 190 and 220°C. Tensile tests were performed at room temperature on as-cast, solutionized and peak aged and the deformed samples annealed at 500°C. Tensile tests at 250°C-350°C and 10-5s-1 to 10-3s-1 were run on as-cast alloys. For both the alloys at room temperature, the solutionized samples exhibited the best ductility, the peak aged the highest strength and the as-cast alloy the highest strain-hardening rate. Hot tensile behaviour of both alloys is similar. The higher average grain size of the Zr alloy leads to lower hardness both in the as-cast and heat treated state and to lower peak stresses during room temperature tensile tests. Recrystallization of Zr-modified alloy is incomplete and not homogeneous as compared with unmodified alloy.

**10:45 AM**

**Cast Aluminum Housings in Electrical Fires:** *Joel Liebesfeld*<sup>1</sup>; <sup>1</sup>Countermeasure Security, Inc.

Cast aluminum and its alloys are often used as enclosures for electrical appliances and similar devices. Electrical faults can often be analyzed by the melting patterns of aluminum and its alloys. The properties of the various types of cast aluminum can assist the forensic investigator/engineer/scientist in forming accurate hypotheses that can be used for adherence to the "scientific method" standards needed for the proper procedural de-layering processes called for in loss analysis. The deployment of appropriate metallurgical test techniques and evaluations lends great credibility to the needed conformance to the scientific method. Aluminum castings are usually combined with other materials with differing melting temperatures and properties as components within enclosures, however in electrical applications the aluminum housing may have higher relevance as aluminum is an excellent electrical conductor and frequently used as an integral electrical grounding path for the subject encasements.

**11:05 AM**

**Influence of the Grain Size on the IGC, Crack Propagation and Fracture Toughness Behaviour of Aa2024-T3 Sheet Material:** *Josef Berneder*<sup>1</sup>; Reinhard Rachlitz<sup>1</sup>; Carsten Melzer<sup>1</sup>; Helmut Antrekowitsch<sup>2</sup>; Peter Uggowitzer<sup>3</sup>; <sup>1</sup>AMAG Rolling; <sup>2</sup>University of Leoben; <sup>3</sup>ETH Zürich

The alloy AA2024 is the most important sheet material for aerospace applications. Alloy AA2024 sheet material in T3 temper with variations in grain size and grain shape was produced on industrial practice. A significant difference between globular fine grain and in rolling direction elongated coarse grain material was observed regarding intergranular corrosion resistance (IGC) as well as fatigue crack propagation behaviour. In the present work we (i) describe the appropriate rolling procedures aiming at variations in grain's shape and size, (ii) investigate the secondary precipitates present at the grain boundaries after solution heat treatment and water quenching by means of transmission electron microscopy (TEM), and (iii) discuss the TEM results in view of IGC behaviour, fatigue crack propagation, and fracture toughness behaviour.

**11:25 AM**

**Microstructure and Mechanical Properties of Age-Hardening Al-Li-Sc-Yb, Al-Li-Sc, and Al-Sc Alloys:** *Matthew Krug*<sup>1</sup>; David Seidman<sup>1</sup>; David Dunand<sup>1</sup>; <sup>1</sup>Northwestern University

Three Al-based alloys were cast, homogenized, and aged producing strengthening L12 precipitates. A quaternary Al-5.31 Li-0.0448 Sc-0.0089Yb (at %) alloy was aged at 325°C, yielding core-shell Al<sub>3</sub>(Li,Sc,Yb) precipitates with a Yb-rich core and a Sc-rich shell, which confer strength at ambient and

Mon. AM

# Technical Program

elevated temperatures (>300°C). This was followed by an aging treatment at 170°C, resulting in precipitation of an Al<sub>3</sub>Li shell on the Al<sub>3</sub>(Li,Sc,Yb) precipitates. The additional shell yielded a large increase in volume fraction and strength. Precipitation-strengthened Al-2.90 Li-0.106 Sc (at %) and Al-0.106 Sc (at %) alloys were also aged at 325 °C, allowing direct investigation of the effect of Li addition on the mechanical properties and microstructural development of the Al-Sc alloy. Room-temperature Vickers microhardness measurements and compression creep of the three alloys at 300°C were interpreted on the basis of strengthening and creep models informed by microstructural observations by atom-probe tomography and TEM.

## Biological Materials Science: Bio-inspired Materials Design and Processing I: Macromolecular Concepts and Applications

*Sponsored by:* The Minerals, Metals and Materials Society, TMS Structural Materials Division, TMS: Biomaterials Committee, TMS/ASM: Mechanical Behavior of Materials Committee

*Program Organizers:* John Nychka, University of Alberta; Jamie Kruzic, Oregon State University; Mehmet Sarikaya, University of Washington; Amit Bandyopadhyay, Washington State University

Monday AM                      Room: 205  
February 15, 2010              Location: Washington State Convention Center

*Session Chair:* John Nychka, University of Alberta

### 8:30 AM Introductory Comments by John A. Nychka, 2010 Lead Organizer

#### 8:35 AM Keynote

#### From Materials Science to Medicine Using Genetically Engineered Peptides: Mehmet Sarikaya<sup>1</sup>; <sup>1</sup>University of Washington

With the recent developments of nanoscale engineering in physical and chemical sciences and the advances in molecular biology, molecular biomimetics is combining genetic tools and biological evolutionary approaches with synthetic nanoscale constructs to create a new hybrid methodology, genetically designed peptide-based molecular materials. Following the fundamental principles of biology-based design, molecular recognition, and self-assembly in nature, we can now use recombinant DNA technologies to design single or multifunctional peptides and peptide-based molecular constructs. These GEPIs, genetically engineered peptides for inorganics, have been making significant impact as inorganic material synthesizers, nano-particle linkers, and molecular assemblers, simply as molecular building blocks, in a wide range of fields from chemistry to materials science to medicine with practical implementations in biosensing, targeted assembly, hard tissue regeneration, probe and implant materials. This review presents a synopsis of the developments, current challenges, and future prospects. The research supported by NSF-MRSEC, -BioMat, and -IRES programs.

#### 9:15 AM

#### Electronic Transport through Solid-Binding Peptides: Yuhei Hayamizu<sup>1</sup>; Marketa Hnilova<sup>1</sup>; Ersin Emre Oren<sup>1</sup>; Chao Zhong<sup>1</sup>; Candan Tamerler<sup>1</sup>; Marco Rolandi<sup>1</sup>; Mehmet Sarikaya<sup>1</sup>; <sup>1</sup>University of Washington

Genetically engineered peptides for inorganics (GEPIs) could be used as novel bio-molecular linkers in bioelectronic devices because of their materials-specific binding properties. We characterized their electronic transport using scanning tunneling microscopy and atomic force spectroscopy. As typical platforms, gold binding peptides (AuBPs) and ITO (indium-tin-oxide) binding peptides (ITOBPs) with specific binding affinity to gold and ITO surfaces, respectively, are used. The electronic transport properties of AuBPs, which were self-assembled and immobilized on the Au (111) surface, were investigated. Similarly, ITOBPs assembled on a highly smooth ITO were investigated. Several types of peptides which have different sequence of amino acids were used. The binding versus transport characteristics were studied using AuBPs on ITO and ITOBPs on Au (111) substrate to quantitatively investigate binding versus electron conductivity of these dodecapeptides. The research was supported by Genetically Engineered Materials Science and Engineering Center (GEMSEC), an NSF-MRSEC at the UW and an NSF-BioMat grant.

#### 9:35 AM

#### Computational Biomimetic Design of Materials Specific Peptides: Ersin Emre Oren<sup>1</sup>; Ram Samudrala<sup>1</sup>; John S. Evans<sup>2</sup>; Malcolm L. Snead<sup>3</sup>; Martha J. Somerman<sup>1</sup>; Candan Tamerler<sup>4</sup>; Mehmet Sarikaya<sup>1</sup>; <sup>1</sup>University of Washington; <sup>2</sup>New York University; <sup>3</sup>University of Southern California; <sup>4</sup>Istanbul Technical University

Solid/protein interactions are at the heart of biology-inspired materials engineering, biomineralization, and bionanotechnology. Adaptations of biological principles relies on our ability to manipulate peptide/solid interfaces. Recently adapted biocombinatorial techniques permit isolation of peptides recognizing inorganic solids that are used as key molecules in the synthesis, assembly and formation of functional inorganics. To explore propensity rules connecting sequence and function that play major role in peptide/solid interaction, we developed a bioinformatics approach that further enables us to design novel peptides with specific affinities and multiple functionalities, e.g., peptides capable of binding to only silica or gold, both or neither. These peptides have utility in developing surface engineering of solids, combining several nanoentities, or molecular erectors when conjugated to other proteins, or to each other via a linker. Experimental verifications of designed peptides confirm our predictions with high accuracies. Supported by GEMSEC an NSF-MRSEC at the University of Washington, and NSF-BioMater Program.

#### 9:55 AM

#### Bridging Inorganic Nanoparticles and Biomolecules via Genetically Engineered Peptides: Turgay Kacar<sup>1</sup>; Marketa Hnilova<sup>1</sup>; Banu Taktak<sup>2</sup>; Yuhei Hayamizu<sup>1</sup>; Ersin Emre Oren<sup>1</sup>; John Evans<sup>3</sup>; Candan Tamerler<sup>1</sup>; Mehmet Sarikaya<sup>1</sup>; <sup>1</sup>University of Washington; <sup>2</sup>Istanbul Technical University; <sup>3</sup>New York University

Genetically engineered peptides for inorganics (GEPIs), isolated through biocombinatorial approaches, were used for nanoparticle and protein immobilization on inorganic surfaces. Gold binding (AuBP) and quartz binding (QBP) peptide sequences were chemically linked, constituting bi functional GEPIs. The assembly of silica and gold nanoparticle was successfully carried out on gold and glass substrates, respectively, that were each functionalized with bi-GEPIs. Also, AuNPs were attached to the larger silica NPs yielding an optically active platform that enabled detection of a target biomolecule, i.e. Anti-Maltose Binding Protein (Anti-MBP), using AuBP-MBP as probe. Our results demonstrate that GEPIs can be an attractive approach for immobilization of inorganic NPs and proteins on a given solid substrate provided that the appropriate solid-specific peptide is used in the bifunctional entity. The novel molecular bi-GEPI platform including their protein fusion products have enormous potential in practical applications in nanobiotechnology. Supported by NSF-MRSEC and -IRES programs at the UW.

#### 10:15 AM Break

#### 10:25 AM

#### Peptide-Mediated Formation of Hybrid Metallic Nanostructures: Marketa Hnilova<sup>1</sup>; Hanson Fong<sup>1</sup>; Banu Taktak<sup>2</sup>; Turgay Kacar<sup>1</sup>; Candan Tamerler<sup>1</sup>; Mehmet Sarikaya<sup>1</sup>; <sup>1</sup>University of Washington; <sup>2</sup>Istanbul Technical University

Syntheses of metallic nanostructures mediated by combinatorially selected peptides and carried out at ambient conditions are potentially appealing as environmental- and bio-friendly alternatives to conventional chemical syntheses methods. We specifically probe gold-binding peptide (AuBP)-mediated gold crystal growth morphologies and kinetics in solution. We find that both AuBP sequences catalyze gold crystal growth in aqueous solution resulting in formation of stable and dispersed peptide-capped gold-nanoparticles in a single reaction step. Additionally, we use novel recombinant maltose-binding proteins genetically fused to inorganic-binding peptides i.e., AuBPs, and demonstrate formation of multifunctional water-dispersible metallic nanostructures via gold-binding sequence motif. The peptide-based biomimetic approaches of synthesis metallic nanostructures described here have implications in a wide range of potential practical applications such as controlled bottom-up assembly of hybrid nanostructures, nanobiophotonic and biosensing platforms. The research was supported by GEMSEC, an NSF-MRSEC at UW, NSF-BioMat grant, and NSF-IRES, TUBITAK-NSF Joint Project, TR-SPO at MOBGAM-ITU.



10:45 AM

**In Situ Biomineralization Using Peptides via SPR and QCM:** *Brandon Wilson*<sup>1</sup>; Eugene Ngai<sup>1</sup>; James Park<sup>1</sup>; Mustafa Gungormus<sup>1</sup>; Marketa Hnilova<sup>1</sup>; Candan Tamerler<sup>2</sup>; Mehmet Sarikaya<sup>1</sup>; <sup>1</sup>University of Washington; <sup>2</sup>Istanbul Technical University

There is an ever increasing interest in the understanding of mechanism of hydroxyapatite (HA) formation in both biological and synthetic environments. Practical methods are sought for synthesizing HA with controlled structures using a variety approaches. Here we use bifunctional peptide to mineralize a HA film on a titanium substrate. The experiments were carried by a combining titanium-binding peptide (TiBP) and HA-binding peptide, HABP, sequences into a bi-functional construct. Biomineralization was catalyzed by immobilized in various solution conditions. The kinetics of the biomineralization process was monitored by liquid-mode QCM. Scanning electron microscopy (SEM) was used to examine the film morphology. The results will be discussed in enzymatic and morphogenesis effects of the peptide. The process developed here may be used in wide ranging applications in biotechnology from tissue engineering to creating biocompatible surfaces. This research is supported by GEMSEC, and NSF-MRSEC at the University of Washington, NSF-IRES, and NSF-BioMat programs.

11:05 AM

**Self-Mineralized/Self Assembled Peptide-based Hydrogels as Scaffolds for Tissue Regeneration:** *Mustafa Gungormus*<sup>1</sup>; Monica Branco<sup>2</sup>; Hanson Fong<sup>1</sup>; Candan Tamerler<sup>1</sup>; Joel Schneider<sup>2</sup>; Mehmet Sarikaya<sup>1</sup>; <sup>1</sup>University of Washington; <sup>2</sup>University of Delaware

We developed an in situ forming, self assembling peptide hydrogel for hard tissue-engineering with a high, inherent propensity for calcium phosphate mineralization. The hydrogel possesses a genetically engineered hydroxyapatite binding peptide (HABP). In vitro solution and cell mineralization studies demonstrated that the HABP retains the mineralization capability when attached to the hydrogel resulting in a hybrid scaffold with an inherent ability to regulate the HA formation. The mineral deposited on the hybrid hydrogel was elongated, biological-like apatite while poorly crystalline calcium phosphate was deposited on the native hydrogel. This study demonstrates that inorganic-binding peptides conjugated to self assembling peptide hydrogels participate in the biomineralization process similar to a native extra cellular matrix. The ability to engineer such three-dimensional assemblies with spatial control and programmed functions may find substantial use in tissue engineering applications for successful restoration or regeneration. The research supported by NSF-MRSEC and-IRES programs at the University of Washington.

11:25 AM

**Peptide-Based Biofunctionalization of Implant Materials:** *Dmitry Khatayevich*<sup>1</sup>; Mustafa Gungormus<sup>1</sup>; Christopher So<sup>1</sup>; Sibel Cetinel<sup>2</sup>; Hong Ma<sup>1</sup>; Alex Jen<sup>1</sup>; Candan Tamerler<sup>2</sup>; Mehmet Sarikaya<sup>1</sup>; <sup>1</sup>University of Washington; <sup>2</sup>Istanbul Technical University

Genetically engineered peptides for inorganics (GEPs) offer unique advantages for biomaterials functionalization over the conventional molecular immobilization methods. They require no hostile environments to bind, are specific to their materials, can be adapted to carry various active entities, and are unlikely to exhibit toxicity. In this study we used peptides selected for gold, platinum and glass to modify surfaces with Poly(ethylene glycol) anti-fouling polymer and RGD integrin binding sequence. Using this approach we imparted anti-fouling properties to gold and platinum via 3GBP1 and PtBP1 binding sequences. We also induced a 2.5 fold increase in the number and a 4 fold increase in the spreading of osteoblast cells on glass using the QBP1-RGD construct. Work is ongoing to take advantage of GEPI selectivity for simultaneous functionalization of multi-material substrates. The research was supported by Genetically Engineered Materials Science and Engineering Center (GEMSEC), an NSF-MRSEC at the UW and an NSF-BioMat grant.

11:45 AM

**Directed Assembly and Fabrication by Materials Selective Fusion Protein-Peptides:** *Candan Tamerler*<sup>1</sup>; Mehmet Sarikaya<sup>2</sup>; <sup>1</sup>Istanbul Technical University; <sup>2</sup>University of Washington

Bio-based building blocks are explored for establishing novel routes to develop new performance materials, manufacturing processes and novel biological materials. In our approach, we design, and utilize peptides and multifunctional proteins as molecular tools. Current biotechnological applications such as

biosensors, protein arrays and microchips require oriented immobilization of enzymes. The characteristics of recognition, self-assembly and ease of genetic manipulation make inorganic binding peptides an ideal molecular tool for site-specific enzyme immobilization. Here, we provide examples on the use of peptides as fusion partners to different proteins in creating biocompatible nanomaterials, self immobilization on material surfaces, and formation of scaffolds for tissue restoration and regeneration. Among them, hydroxyapatite binding peptide linked to green fluorescence protein to target biomineralization, and laccase fused with gold and silica binding peptides as biosensors and as a biocathode for fuel cell application will be discussed. Research Supported by GEMSEC-UW, NSF-MRSEC, NSF-BIOMAT and TUBITAK-NSF Joint Project, TR-SPO

### Bulk Metallic Glasses VII: Structures and Mechanical Properties I

*Sponsored by:* The Minerals, Metals and Materials Society, TMS Structural Materials Division, TMS/ASM: Mechanical Behavior of Materials Committee

*Program Organizers:* Peter Liaw, The University of Tennessee; Hahn Choo, The University of Tennessee; Yanfei Gao, The University of Tennessee; Gongyao Wang, University of Tennessee

Monday AM

Room: 213

February 15, 2010

Location: Washington State Convention Center

*Session Chairs:* Takeshi Egami, University of Tennessee; Peter Liaw, University of Tennessee

8:30 AM Keynote

**Mechanical Failure and Glass Transition:** *Takeshi Egami*<sup>1</sup>; Pengfei Guan<sup>2</sup>; Mingwei Chen<sup>2</sup>; <sup>1</sup>University of Tennessee; <sup>2</sup>WPI-AIMR, Tohoku University

It is not easy to elucidate the properties of metallic glasses based upon the atomic structure. In the absence of the established theory many use the free-volume model to explain the experimental results, even though it does not work well for metallic liquids. We developed an alternative theory based upon the concept of atomic level stresses to explain the glass transition and the glass transition temperature. We now expand the theory to account for mechanical yield and failure. We see failure as the glass transition induced by shear stress, and explain it in terms of percolation of the atomic sites made topologically unstable by applied stress. We also relate the stress sensitivity of the glass transition to the shear thinning phenomenon in supercooled liquids. We show the formation of shear bands and local heating as consequences of the stress-induced glass transition, not the cause.

9:00 AM

**Embrittlement of Bulk Metallic Glasses:** *Golden Kumar*<sup>1</sup>; Dale Conner<sup>2</sup>; Jan Schroers<sup>1</sup>; <sup>1</sup>Yale University; <sup>2</sup>California State University

Embrittlement of bulk metallic glasses (BMGs) was studied after annealing at temperatures below and above T<sub>g</sub>, for time scales comparable to structural relaxation and crystallization. The effect of annealing on the bending ductility, the isoconfigurational elastic constants, the structure, and the thermal stability is examined. The embrittlement during sub-T<sub>g</sub> annealing originates from structural relaxation and can be reversed by subsequently annealing above T<sub>g</sub>. The embrittlement kinetics correlate with the structural relaxation. However, only a fraction of relaxation time at a given temperature (below T<sub>g</sub>) is sufficient to significantly embrittle the Zr-based BMGs. Above T<sub>g</sub>, plasticity is retained for annealing far beyond the relaxation time but instead embrittlement is caused by crystallization. The values of  $\nu$  and  $\mu/B$  during annealing-induced embrittlement remain well above and below the respective critical values (0.31 for  $\nu$  and 0.41 for  $\mu/B$ ) previously proposed to denote the transition from a tough to brittle behavior.

9:10 AM Invited

**Anelastic Deformation of a Metallic Glass:** *Michael Atzmon*<sup>1</sup>; Jong Doo Ju<sup>1</sup>; Dongchan Jang<sup>2</sup>; <sup>1</sup>University of Michigan; <sup>2</sup>Caltech

We report on our ongoing studies of anelastic deformation in amorphous Al<sub>86.8</sub>Ni<sub>3.7</sub>Y<sub>9.5</sub>. Using a combination of bend stress relaxation and nanoindenter cantilever measurements, time scales ranging from 10 to 10<sup>7</sup> s were probed. We had previously reported on multiple time constants for anelastic

# Technical Program

relaxation for this alloy. Recent improvements in precision have allowed us to refine our results, with attention to the state of relaxation and deformation history. While plastic deformation and annealing are generally assumed to have opposite effects on the atomic structure of metallic glasses, our results indicate that they affect the anelastic response at short time scales in a similar manner. This suggests that both deformation and annealing lead to removal of similar deformation sites. In separate experiments, using surface profiling, we observe time-dependent flow at shear bands.

## 9:30 AM

**In situ X-Ray Diffraction Investigations of Cu-Zr Bulk Metallic Glasses under Applied Stress:** *Norbert Mattern*<sup>1</sup>; *Jozef Bednarcik*<sup>2</sup>; *Gang Wang*<sup>1</sup>; *Juergen Eckert*<sup>1</sup>; <sup>1</sup>IFW Dresden; <sup>2</sup>DESY Hamburg

The structural behaviour of Cu<sub>64.5</sub>Zr<sub>35.5</sub>, Cu<sub>50</sub>Zr<sub>45</sub>Al<sub>5</sub>, Cu<sub>50</sub>Zr<sub>45</sub>Ti<sub>5</sub> bulk metallic glasses was investigated in situ under compressive stress by means of high energy X-ray synchrotron diffraction. The changes of the structure factor in reciprocal space and in the atomic pair correlation function in real space were analyzed in detail upon loading and unloading. The components of the elastic strain tensor were determined by the shift of the position of first maximum of the structure factor as well as by the higher order maxima of the atomic pair correlation function. The obtained elastic moduli agree qualitatively with those measured macroscopically. The atomic pair correlation functions indicate changes of the nearest neighbourhood under stress even in the elastic regime. The number density of Cu-Zr and Zr-Zr nearest neighbour atomic pair becomes oriented along the loading direction, pointing to changes in topological and chemical short-range order. Possible mechanism will be discussed.

## 9:40 AM Invited

**Structure – Property Relationship in Bulk Metallic Glasses:** *Evan Ma*<sup>1</sup>; <sup>1</sup>Johns Hopkins University

For monolithic BMGs that are completely and invariably amorphous, an understanding of how the internal structures influences strength, ductility, relaxation dynamics remains elusive. Here we resolve the structure of typical BMG-forming Zr-Cu, and Zr-Cu-Al [PRL (2009)], in relationship with the properties [PRB (2008)]. We identify the structural disordering processes responsible for the initiation of shear flow [Acta Mater. (2008)] and localization [Acta Mater. (2009)], and the fertile and resistant sites for carrying shear transformations. The composition-dependent and processing (cooling rate)-dependent local order is monitored in a quantitative manner, in lieu of arguments based on free volume. This structural perspective offers an explanation to the reported (e.g., Zr-rich) BMGs with large plasticity, and allows the prediction of ductile BMGs [Acta Mater. (2009)]. We also illustrate the apparent correlation between the elastic constants (such as G, B) and the behavior of BMGs [Acta Mater. (2009)], in terms of the structural origin.

## 10:00 AM Break

## 10:10 AM Invited

**Defects and Plastic-Deformation Modes of Bulk-Metallic Glasses:** *Yuri Petrusenko*<sup>1</sup>; *Alexander Bakai*<sup>1</sup>; *Ivan Neklyudov*<sup>1</sup>; *Igor Mikhailovskij*<sup>1</sup>; *Sergij Bakai*<sup>1</sup>; *Peter K. Liaw*<sup>2</sup>; *Lu Huang*; *Tao Zhang*<sup>3</sup>; <sup>1</sup>National Science Center - Kharkov Institute of Physics and Technology; <sup>2</sup>Department of Materials Science and Engineering, The University of Tennessee; <sup>3</sup>Department of Materials Science and Engineering, Beijing University of Aeronautics and Astronautics

This report describes the results of theoretical and experimental investigations of mechanisms of the plastic deformation of bulk-metallic glasses (BMGs) by taking into account of their heterogeneous polycluster structures. It will be shown that the intercluster boundaries and vacancies are the most important defects of BMGs controlling the small-scale creep processes, shear-band formation, and diffusion-viscous flow. The boundary structure determines initial slipping processes under shear stresses. The boundary structure can be changed under repeating loading-unloading processes or ultrasonic vibrations (USV). The impact of USV on the Kaiser effect is chosen as a tool for studying the boundary-slip initiation and effect of vibrations on the boundary structure. The generation and stability of vacancies under the electron irradiation in BMGs are investigated. The map of the plastic-deformation states of metallic glasses is studied and discussed.

## 10:30 AM Invited

**Structural Features of BMG under Mechanical Deformation:** *Wojciech Dmowski*<sup>1</sup>; *Andrew Chuang*<sup>1</sup>; *Peter Liaw*<sup>1</sup>; *Yang Ren*<sup>1</sup>; *Jon Almer*<sup>1</sup>; *Takeshi Egami*<sup>1</sup>; <sup>1</sup>University of Tennessee

We investigated changes in the atomic structure in metallic glasses that had been deformed in a homogeneous and inhomogeneous way and in the elastic regime. We attempted to resolve elastic, inelastic and anelastic contributions. We examined structural changes induced by high temperature creep followed by high temperature recovery. The X-ray diffraction was carried in-situ during loading, after creep and recovery. The data was analyzed by expanding the scattering function and PDF in terms of Legendre polynomials. We observed the development of a bond anisotropy that supported apparent macroscopic shear strain after high temperature creep. High temperature recovery reduced bond anisotropy; however, some plastic strains were irreversible. We compare changes in the atomic structure of BMG due to different modes of deformation: homogeneous creep, inhomogeneous plastic deformation and elastic deformation. Work was supported by the U.S. DOE under DE-AC05-00OR-22725 and NSF-DMR-0906744.

## 10:50 AM

**(Fe,Co)-Based BMGs with Small Cu Additions:** *Mihai Stoica*<sup>1</sup>; *Ran Li*<sup>1</sup>; *Stefan Roth*<sup>1</sup>; *Jürgen Eckert*<sup>1</sup>; *Gavin Vaughan*<sup>2</sup>; *Alain Yavari*<sup>3</sup>; <sup>1</sup>IFW Dresden; <sup>2</sup>ESRF Grenoble; <sup>3</sup>INP Grenoble

Recently, (Fe-Co)-B-Si-Nb bulk metallic glasses (BMGs) were produced. Such BMGs exhibit high glass-forming ability (GFA) as well as good mechanical and magnetic properties. These alloys combine the advantages of functional and structural materials. The soft magnetic properties can be enhanced by nanocrystallization. To force the nanocrystallization, small content of Cu was added to the starting composition. In this paper,  $\{[(\text{Fe}_{0.5}\text{Co}_{0.5})_{0.75}\text{Si}_{0.05}\text{B}_{0.20}]_{0.9}\text{Nb}_{0.04}\}_{100-x}\text{Cu}_x$  glassy alloys ( $x = 1, 2$  and  $3$ ) were chosen for investigation. The GFA and the thermal stability of these alloys were evaluated. The effects of crystallization during heat-treatment processes on the phase evolution, the kinetic parameters and the magnetic properties, including  $M_s$ ,  $H_c$  and  $T_c$ , in these alloys were investigated. The phase analyses were done with the help of the X-ray diffraction patterns recorded in-situ by using the synchrotron radiation in transmission configuration.

## 11:00 AM Invited

**Irreversible Structural Changes with Cyclic Loading in Zr Based Amorphous Alloys:** *Despina Louca*<sup>1</sup>; *Peng Tong*<sup>1</sup>; *Gongyao Wang*<sup>2</sup>; *Peter Liaw*<sup>2</sup>; *Yoshihiko Yokoyama*<sup>3</sup>; <sup>1</sup>University of Virginia; <sup>2</sup>University of Tennessee; <sup>3</sup>Tohoku University

Bulk amorphous metallic alloys possess unique mechanical properties, suitable in a wide range of engineering applications. However, they tend to exhibit low ductility and are particularly vulnerable to fatigue damage as irreversible changes occur through the formation of shear bands during the deformation process. The physical mechanism leading to failure under fatigue-loading conditions is currently not well understood. To determine the deformation behavior at the microscale, the local atomic structure of Zr-based glasses subjected to cyclic fatigue tests is investigated. In order to provide a direct description of the three-dimensional structure and associate the atomic environment to physical properties, the pair density function analysis of neutron and X-ray diffraction data is used. Our results indicate that the cyclic-fatigue effects are not elastic. At the same time, Zr glasses show improved ductility upon cooling and the results from the local structure analysis will be additionally presented.

## 11:20 AM

**Effect of Plastic Deformation History on the Subsequent Mechanical Behavior of a Bulk-Metallic Glass: A High-Energy Synchrotron X-Ray Scattering Study:** *Feng Jiang*<sup>1</sup>; *Dongchun Qiao*<sup>1</sup>; *Yang Ren*<sup>2</sup>; *Wojtek Dmowski*<sup>1</sup>; *Gongyao Wang*<sup>1</sup>; *Yangdong Wang*<sup>3</sup>; *Takeshi Egami*<sup>1</sup>; *Peter Liaw*<sup>1</sup>; *Hahn Choo*<sup>1</sup>; <sup>1</sup>University of Tennessee; <sup>2</sup>Argonne National Laboratory; <sup>3</sup>Northeastern University

The elastic-strain tensors of a (Zr<sub>55</sub>Cu<sub>30</sub>Al<sub>10</sub>Ni<sub>5</sub>)<sub>99</sub>Y<sub>1</sub> bulk metallic glass with and without deformation history have been studied at ambient temperature by using high-energy synchrotron x-ray diffraction facility with an in-situ mechanical loading device. The results show that the specimens with plastic deformation history, introduced by performing four-point bending fatigue, exhibits more compliant elastic behavior than the specimen without plastic



deformation history. Furthermore, more pronounced changes in the diffraction peak widths were observed in the elastic-scattering intensity,  $I(q)$ , of the specimen with the deformation. The results will be discussed in terms of the increases in the residual-stress and/or free-volume during the plastic deformation and their roles in the subsequent deformation behavior of the BMG alloys.

### 11:30 AM Invited

**Atomic-Scale Mechanisms of Tension-Compression Asymmetry in a Metallic Glass:** Lianyi Chen<sup>1</sup>; B. Z. Li<sup>1</sup>; X. D. Wang<sup>1</sup>; Feng Jiang<sup>2</sup>; H. Franz<sup>3</sup>; Ren Yang<sup>4</sup>; Peter Liaw<sup>2</sup>; *Jianzhong Jiang*<sup>1</sup>; <sup>1</sup>Zhejiang University; <sup>2</sup>University of Tennessee; <sup>3</sup>HASYLAB at DESY; <sup>4</sup>Argonne National Laboratory

Materials exhibit tension-compression asymmetry in terms of plasticity and/or strength. This phenomenon is usually interpreted by continuum mechanics, which neglects the stress-induced structure change. Here we investigated the structure change of a metallic glass of Cu<sub>45</sub>Zr<sub>46</sub>Al<sub>7</sub>Ti<sub>2</sub> under both the tension and compression stresses by in-situ loading high-energy X-ray diffraction. A correlation of the stress-induced structure change with the extraordinary tension-compression asymmetry in the metallic glass will be discussed. The results obtained in this work might provide a new perspective on the tension-compression asymmetry from the structural aspect, which is useful for understanding the deformation mechanisms of metallic glasses and may guide the development of plastic metallic glasses.

### 11:50 AM

**Thermomechanical Behavior of Cu<sub>50</sub>Hf<sub>41.5</sub>Al<sub>8.5</sub> Bulk Metallic Glass Following Cyclic and Static Elastic Compression in Different Loading Directions:** Arif Mubarak<sup>1</sup>; *Rainer Hebert*<sup>1</sup>; <sup>1</sup>University of Connecticut

Recent temperature-modulated thermomechanical analyses have demonstrated that cyclic deformation of bulk metallic Cu<sub>50</sub>Hf<sub>41.5</sub>Al<sub>8.5</sub> glass tends to reduce the non-reversible length decrease during heating while static elastic compression for the same amount of time as the cyclic testing and at the peak stress of the cyclic test enhanced the length decrease in the supercooled liquid region. As a continuation of the static and cyclic elastic tests, cubic-shaped bulk metallic Cu<sub>50</sub>Hf<sub>41.5</sub>Al<sub>8.5</sub> samples were exposed to static and cyclic elastic compression tests, followed by thermomechanical analysis to determine the isotropy of the length changes relative to the compression direction and the axial direction of the initial cast bar. Anisotropic thermomechanical behavior was observed for the as-cast samples compared to the structurally relaxed samples that reveal isotropic thermomechanical behavior. Sustained elastic deformation emerges as a novel approach for changing the level of structural relaxation of metallic glasses and imparting directionality on the thermomechanical behavior.

### 12:00 PM

**Static and Dynamic Observation of Shear Bands in Metallic Glasses:** *Eun Soo Park*<sup>1</sup>; Frans Spaepen<sup>2</sup>; <sup>1</sup>Seoul National University; <sup>2</sup>Harvard University

Understanding how shear bands form and propagate in amorphous metals is essential for the eventual use of these materials in structural applications. However, only little quantitative information has been collected on their dynamics. Furthermore, the structure and density of these shear bands has been studied mostly after the fact. In the present study, using self-designed experimental setup, nucleation and density of shear bands depending on strain rate has been clearly observed in bend test on thin ribbons. We will compare the static and dynamic observation results for shear bands in mainly iron-based metallic glasses.

### 12:10 PM

**Effect of Stress State on Flow at Bulk Metallic Glass Interfaces:** *Nicholas Hutchinson*<sup>1</sup>; Dan Campbell<sup>1</sup>; Katharine Flores<sup>1</sup>; <sup>1</sup>The Ohio State University

Plastic deformation in metallic glasses is a dilatational process that depends on both the shear and normal stress on the flow plane. It is therefore interesting to consider the effect of stress state on material mixing and mechanically assisted diffusion across an interface as a mechanism for solid state joining. We evaluate the effect of interface orientation relative to the loading axis on material flow and joint formation via a thermo-mechanical joining technique. Post-test characterization of the interfaces was conducted using X-ray diffraction (XRD), scanning electron microscopy (SEM) and transmission electron microscopy (TEM). Surprisingly, although plastic flow is commonly considered to be a shear driven process, preliminary experiments with 45° interfaces indicate that the addition of shear stresses actually impedes joint formation relative to that observed for pure compression. This suggests that normal stress-driven

diffusion plays a much larger role in joint formation than shear stress-driven mechanical mixing.

## Characterization of Minerals, Metals and Materials: Characterization of Iron and Steel I

*Sponsored by:* The Minerals, Metals and Materials Society, TMS Extraction and Processing Division, TMS Structural Materials Division, TMS/ASM: Composite Materials Committee, TMS: Materials Characterization Committee

*Program Organizers:* Ann Hagni, Geoscience Consultant; Sergio Monteiro, State University of the Northern Rio de Janeiro - UENF; Jiann-Yang Hwang, Michigan Technological University

Monday AM Room: 307  
February 15, 2010 Location: Washington State Convention Center

*Session Chairs:* Jiann-Yang Hwang, Michigan Technological University; Donato Firrao, Politecnico di Torino

### 8:30 AM Introductory Comments

#### 8:35 AM

**Nano-Scale Characterization of Carbon Partitioning from Supersaturated Plates of Ferrite:** *Francisca Caballero*<sup>1</sup>; Mike Miller<sup>2</sup>; Carlos Garcia-Mateo<sup>1</sup>; <sup>1</sup>CENIM-CSIC; <sup>2</sup>ORNL

A new processing concept has been proposed for designing ductile steels. The 'quenching and partitioning' process involves quenching austenite below the martensite-start temperature, followed by a partitioning treatment to enrich the remaining austenite with carbon, thereby stabilizing it to room temperature. It is important to understand the partitioning of carbon from supersaturated plates of ferrite. Carbon partitioning is also critically relevant for fundamental reasons associated with the bainite transformation mechanisms. In these processes, the supersaturation must be relieved either through precipitation of carbides, or by partitioning to austenite. This atom probe tomography study investigated the redistribution of carbon during the bainite formation and during subsequent tempering in a nanocrystalline steel that transforms at abnormally low temperatures and exhibits extremely slow transformation kinetics. Research at the Oak Ridge National Laboratory SHaRE User Facility was sponsored by the Scientific User Facilities Division, Office of Basic Energy Sciences, U.S. Department of Energy.

#### 8:55 AM

**Nondestructive Characterization of Microstructure and Properties of Steel Products:** *Jagdish Pandey*<sup>1</sup>; Manish Raj<sup>1</sup>; Nikhiles Bandyopadhyay<sup>1</sup>; <sup>1</sup>Tata Steel Ltd.

The paper highlights the experimental investigations to characterize texture and plastic strain ratio  $r$ -Bar in auto grade steel sheets by ultrasonic measurements, whereas attempts were made to characterize interlamellar spacings in pearlite, tensile stresses and torsional properties in prestressed concrete wires by eddy current measurements. Good correlations were obtained between the testing parameters (such as ultrasonic attenuation and velocity in case of steel sheets as well as eddy current out put voltage and phase angle in case of steel wires) and the materials properties (such as texture, plastic strain ratio  $r$ -Bar, interlamellar spacings in pearlite, tensile stresses and torsional properties). 15 MHz normal direct contact and 20 MHz delay line normal shear wave probes were used for ultrasonic measurements. Eddy current measurements were done using an absolute coil probe with variable frequency selection. The experimental results show the possibility of nondestructive on line measurement of the above microstructures and properties.

#### 9:15 AM

**Role of Microstructure and Composition in Resisting Hydrogen Embrittlement of Fastener Grade Steels:** *Nicholas Nanninga*<sup>1</sup>; Lloyd Heldt<sup>2</sup>; Karl Rundman<sup>2</sup>; <sup>1</sup>NIST; <sup>2</sup>Michigan Technological University

The degree of hydrogen embrittlement for several fastener grade steels has been determined. The technique used to assess the resistance to hydrogen embrittlement of the steels was the rising step load test on notched tensile specimens. While microstructural alteration resulted in some improvement in resistance to hydrogen embrittlement, the overriding factor contributing to susceptibility of the steel was strength. The susceptibilities of the microstructures

# Technical Program

to hydrogen embrittlement, ranked in decreasing order, are as follows: tempered martensite, bainite, fine pearlite. The effect of alloying was also assessed by comparing rising step load results from different fastener grade steels with similar microstructures. In most cases, the alloy chemistry had little effect on rising step load results, presumably due to trap saturation associated with this testing technique.

**9:35 AM**

**2D Imaging of Nano-Hardness and Phase Characterization in Steel by Noncontact Optical Photodeflection Microscopy:** *Nelida Mingolo*<sup>1</sup>; Oscar Martínez<sup>2</sup>; Ulises Crossa Archiropoli<sup>2</sup>; <sup>1</sup>Universidad de Buenos Aires; <sup>2</sup>Tolket SRL

We describe a technique that allows rapid imaging of the thermal diffusivity of the sample by a modified photo-thermal technique. The thermal diffusivity in hardened steels strongly correlates to the hardness. Hence in a noncontact manner and with optical microscope resolution, a 2D map exhibiting the crystallographic phases and hardness of the sample can be retrieved. Two almost collinear laser beams scan the surface, one as a modulated pump and a second as a CW probe. The deflection of the probe carries information on the thermal expansion of the sample and with it, on the thermal diffusivity. It is shown that a single determination of the time delay of the modulation of the probe beam can be used to retrieve the thermal diffusivity.

**9:55 AM**

**Characterization of AISI 4340 Steel Formed by Direct Metal Deposition Process:** *Jyotirmoy Mazumder*<sup>1</sup>; Sudip Bhattacharyya<sup>1</sup>; <sup>1</sup>University of Michigan

Materials generated by Direct Metal Deposition, a rapid prototyping technique for manufacturing near-net shape components, usually have very fine microstructure and residual stresses due to extremely high cooling rates. AISI 4340 is extensively used in many applications including submarine connecting rods. In this investigation microstructure of 4340 steel deposited on a mild steel substrate using a 6 kW continuous CO<sub>2</sub> laser was investigated using optical, scanning electron microscopy (SEM) and x-ray diffraction (XRD) techniques. Ferrite, martensite and cementite phases were determined by XRD. Transmission electron microscopy (TEM) corroborated the findings and change in crystal structure e.g. lattice parameters due to fine microstructure and residual stresses. Bright field TEM images and corresponding selected area diffraction (SAD) patterns confirmed the ferrite and cementite phases and show that there is an approximately 0.5-2% reduction in the lattice parameters of these phases. No retained austenite phase was found in either XRD or TEM results.

**10:15 AM**

**Classification and Rating of Inclusions in a High Carbon Steel:** M. Faraji<sup>1</sup>; R. Thackray<sup>1</sup>; I. Todd<sup>1</sup>; P. Tsakirooulos<sup>1</sup>; <sup>1</sup>The University of Sheffield

Inclusions formed in a high-carbon, manganese-silicon killed plain steel (Fe-0.77C wt%) were studied. Various techniques were used to characterize the inclusions, and the latter were classified according to their chemical composition, size and morphology. The main constituent elements entering the inclusions were Mn, S, Al, and oxygen. Alongside MnS and some Al<sub>2</sub>O<sub>3</sub> inclusions many non-metallic inclusions appeared in complex forms, consisting of silicates, sulphides and oxides. Duplex oxy-sulphides, mainly MnS combined with Al<sub>2</sub>O<sub>3</sub>, or SiO<sub>2</sub> were the most common complex multiphase inclusions in this steel. The nanoindentation technique was used to assess and rate different types of inclusions and data of the hardness and elastic modulus of individual inclusions at room temperature are presented.

**10:35 AM**

**Inspecting and Analyzing Microstructural Homogeneity in Grey Cast Iron:** *M. David Hanna*<sup>1</sup>; <sup>1</sup>General Motors R&D Center

There is a great deal of emerging evidence that microstructural homogeneity of grey cast iron has significant effects on mechanical and physical properties that are directly influenced by the amount, size, and morphology of graphite flakes present throughout the casting. The large mismatch in physical and mechanical properties between graphite flakes and the iron matrix is significant. Hence, it has become important to analyze and inspect microstructural homogeneity in grey cast iron used for many applications with one fundamental motivation being to obtain a uniform microstructure. In this study a wide range of grey irons having different compositions and casting mold designs were analyzed using an image analyzer to reveal the extent of graphite flake size (GFS) homogeneity. A review of the literature and published work concerning homogeneity of

the microstructure was conducted and information about effects on physical properties was gathered.

**10:55 AM**

**An Approach for Graphite Nodules Detection in Ductile Cast Iron:** *Ali-Reza Kiani-Rashid*<sup>1</sup>; S.A. Rounaghi<sup>1</sup>; <sup>1</sup>Ferdowsi University of Mashhad

The present study has been conducted to the as-cast samples. The aim of this work is to acquire the structural information about graphite detection in experimental cast iron so there is no doubt between this kind of phases with foreign particles such as inclusions and impurities which are reported occasionally instead of graphite in Metallography of cast irons. In this paper the problem of identification and characterization of the graphite nodules have been considered and a novel qualitative analysis procedure has been developed based on a chemical etchant technique. This is a kind of methodology for image analysis of the material metallographic specimen's pictures that provide a reliable and efficient separation of the elements of interest from the background and the evaluation of their morphological characteristics.

**11:15 AM**

**As-Cast Microstructures of Aluminum Containing Ductile Cast Irons:** *Ali-Reza Kiani-Rashid*<sup>1</sup>; A. Shayesteh-Zeraati<sup>2</sup>; H. Naser-Zoshki<sup>3</sup>; M.R. Yousef-Sani<sup>1</sup>; <sup>1</sup>Ferdowsi University of Mashhad; <sup>2</sup>Sharif University of Technology; <sup>3</sup>Iran University of Science and Technology

In this paper, the effect of aluminum content on the formation mechanism, volume fraction, morphology and particle size distribution of graphite has been investigated. Addition of aluminum on ductile iron causes some fundamental changes in iron-carbon phase-diagram and as a result, improves the graphite formation during eutectic transformation. The results reveals that aluminum compounds have been formed in the core of graphite nodules, thus aluminum plays an important role in the formation of graphite nodules. Furthermore, it is indicated that an increase in the aluminum content also leads to an increase in the number of graphite nodules and a decrease in the nodules size. By using EPMA, the segregation of aluminum and silicon between graphite nodules has been studied.

**11:35 AM Concluding Comments**

**11:40 AM Question and Answer Period**

---

## Coatings for Structural, Biological, and Electronic Applications: Processing Techniques and Characterization

*Sponsored by:* The Minerals, Metals and Materials Society, TMS Electronic, Magnetic, and Photonic Materials Division, TMS Structural Materials Division, TMS: Biomaterials Committee, TMS: Thin Films and Interfaces Committee

*Program Organizers:* Nuggeshalli Ravindra, New Jersey Institute of Technology; Gregory Krumdick, Argonne National Laboratory; Roger Narayan, Univ of North Carolina & North Carolina State Univ; Choong-un Kim, University of Texas at Arlington; Nancy Michael, University of Texas at Arlington

Monday AM

Room: 309

February 15, 2010

Location: Washington State Convention Center

*Session Chair:* Gregory Krumdick, Argonne National Labs

---

**8:30 AM Introductory Comments**

**8:35 AM Invited**

**Morphological Evolution during the Annealing and Growth of Polycrystalline Films:** *Ramanathan Krishnamurthy*<sup>1</sup>; Mikko Haataja<sup>2</sup>; <sup>1</sup>Purdue University; <sup>2</sup>Princeton University

Polycrystalline films are commonly used in materials applications; however, growth models rarely include time-dependent lateral grain size effects. We employ a thermodynamics-based method to effectively handle grain grooving / lateral grain growth. We model the annealing of a film (zero deposition flux) with polydisperse grain sizes and successfully predict several experimental observations on surface-diffusion dominated grooving and boundary motion (ghost lines, groove asymmetry effects). We also predict experimentally observed, grain aggregate behavior, such as the non-monotonous time-variation



of film roughness. We discuss simulation results vis-a-vis the assumed values for surface diffusivity / grain mobility. For film growth (non-zero deposition flux), the greater chemical potential driving grooving when a large average deposition flux (compared to surface diffusivity / grain mobility) is employed results in enhanced film grooving / impeded grain growth. We discuss the effects of spatially varying deposition fluxes on film growth, with a form chosen to simulate electrodeposition.

**9:05 AM**

**Synthesis of Amorphous Al-Co-Ce Alloys via Atomization and Mechanical Milling:** *Zhihui Zhang*<sup>1</sup>; Ying Li<sup>1</sup>; Yizhang Zhou<sup>1</sup>; Enrique Lavernia<sup>1</sup>; <sup>1</sup>University of California Davis

Amorphous Al-Co-Ce coatings have demonstrated unique protection capability when applied to a high-strength Al substrate. These coatings can serve as a protection barrier, sacrificial anode, and reservoir to supply inhibitor ions to protect any defect sites, due to the structural amorphicity and chemical composition. In this study, the glass forming ability of Al<sub>86</sub>Co<sub>10</sub>Ce<sub>4</sub> and Al<sub>89</sub>Co<sub>7</sub>Ce<sub>4</sub> alloys, produced via gas atomization, were systematically investigated by varying atomization parameters (superheat 175-340°C, atomization pressure 1.4-6.9 MPa) and using helium as atomization gas. The results showed that it was difficult to suppress the crystallization of the intermetallic compounds Al<sub>9</sub>Co<sub>2</sub> and Al<sub>11</sub>Ce<sub>3</sub> even when the powder particle size was separated down to <10 μm. Alternatively, complete amorphization of the Al<sub>9</sub>Co<sub>2</sub> and Al<sub>11</sub>Ce<sub>3</sub> compounds was achieved by mechanical milling the atomized powder. The effect of initial amorphicity and chemical composition in the starting powder on the amorphization kinetics during mechanical milling is discussed in detail.

**9:25 AM Invited**

**Microstructure and Mechanical Properties of Vanadium Oxide-Based Coatings on Steel Substrates Prepared by Pulsed Laser Deposition:** Andreas Jahja<sup>1</sup>; *Paul Munroe*<sup>2</sup>; <sup>1</sup>Materials Science and Engineering; <sup>2</sup>Materials Science and Engineering, University of New South Wales

A range of vanadium oxide coatings were deposited on a H13 tool steel substrate via pulsed laser deposition as a function of processing conditions. The coatings were subject to detailed microstructural characterization, including cross-sectional TEM studies. It was shown that the pressure of the oxygen reactive gas during deposition was critical to the quality and performance of the coating. That is, more compact and resilient coatings were prepared at lower oxygen concentrations. Further, high oxygen pressures promoted the formation of iron oxide on the substrate prior to deposition. These iron oxide layers promoted delamination of the vanadium oxide. Mechanical behaviour was assessed through nanoindentation using a spherical indenter. The coatings exhibited high hardness values and significant resistance to cracking. Examination of the indented layers revealed intercolumnar cracks within the coatings, together with shear steps at the coating-substrate interface, whilst inclined cracks were observed at the periphery of the indentations.

**9:55 AM Break**

**10:10 AM Invited**

**Method of Characterizing Pore Structure in Porous Coating Layer Using a Simple Voltammetry:** *Nancy Michael*<sup>1</sup>; Woong-Ho Bang<sup>1</sup>; Choong-Un Kim<sup>1</sup>; <sup>1</sup>University of Texas at Arlington

Porous thin films are used in various applications, including the coating for biomaterials and energy storage materials, as they provide unique electrical, structural and chemical properties that are not available at the bulk. Characterization of pore structure is typically done by a direct observation of pores using microscope, but such techniques only visualize limited volume of the film. The need for new characterization techniques is growing, especially because the use of thin films with extremely small pore size, is expanding. A new technique that can characterize the pore structure without limitations of microscopy is developed in our research. This technique is based on a simple voltammetry that uses ions in electrolyte as pore size tracer and found to work even with nanoscale pores. This paper introduces theoretical background and experimental examples of the technique.

**10:40 AM**

**The Effect of Aging Time on the Properties of Sol-Gel Derived Nanostructure Fluorapatite Powder and Coating:** *Ehsan Mohammadi Zahrani*<sup>1</sup>; M. H. Fathi<sup>2</sup>; Akram Alfantazi<sup>1</sup>; <sup>1</sup>The University of British Columbia; <sup>2</sup>Isfahan University of Technology

The effect of aging time on the formation and phase purity of nanostructure fluorapatite (FA:Ca<sub>10</sub>(PO<sub>4</sub>)<sub>6</sub>F<sub>2</sub>) powder and coating was evaluated in this work. Fluorapatite nanostructure powder and coating were prepared by sol-gel method using calcium nitrate tetrahydrate, phosphorous pentoxide and hexafluorophosphoric acid as starting materials. Precursor sols were dip coated onto the pure 316L stainless steel substrate. The coated plates were aged at different aging times and dried. Finally samples were calcinated at 600°C. Thermal behaviour, phase formation, size and morphology of nanoparticles, surface morphology and also interfacial coherency of the coating as well as functional groups were investigated by thermogravimetry analysis, x-ray diffraction, transmission electron microscopy, scanning electron microscope and fourier transform infrared spectroscopy, respectively. Results showed that a solution aging time of at least 18-24 hr was required to achieve monophasic nanostructure FA powder and coating. The nanoparticles size was increased as a result of aging time increasing.

**11:00 AM Invited**

**Microstructure and Mechanical Properties of Ytria-stabilized Zirconia Coatings Produced By Electrophoretic Deposition and Microwave Sintering:** *Wei Wang*<sup>1</sup>; Shiqiang Qian<sup>1</sup>; <sup>1</sup>Shanghai University of Science Engineering

The coatings of Y<sub>2</sub>O<sub>3</sub>-stabilized zirconia have been deposited on superalloy K17 substrates at room temperature by electrophoretic deposition technique followed by two different sintering methods. Scanning electron microscopy (SEM), X-ray diffraction (XRD) and indentation techniques have been employed to characterize morphological, structural and mechanical properties of the coatings. Finer and more uniform microstructures were observed in the microwave sintered coatings when compared to the conventional sintered samples. Nanohardness indentation tests of the coatings exposed (1500 W) to microwave have shown hardness of 4.3 GPa with elastic modulus of 172.7 GPa compared to the conventional sintered coatings of 3.1 GPa with elastic modulus of 83.5 GPa. For the conventional sintered coatings, the monoclinic phase was observed. The microwave sintered coatings of Y<sub>2</sub>O<sub>3</sub>-stabilized zirconia contain mainly cubic/tetragonal phases with some metastable phase present. Such coatings have potential in being used as thermal barrier coatings on superalloy substrates.

**11:30 AM Invited**

**Carrier Concentration Tuning and Enhanced Photoelectrochemical Response of Bandgap-Reduced Cu and Ga Co-Doped P-Type ZnO Films:** *Sudhakar Sher*<sup>1</sup>; Kwang-Soon Ahn<sup>2</sup>; Heli Wang<sup>1</sup>; Todd Deutsch<sup>1</sup>; Nuggehalli Ravindra<sup>3</sup>; Yanfa Yan<sup>1</sup>; John Turner<sup>1</sup>; Mowafak Al-Jassim<sup>1</sup>; <sup>1</sup>National Renewable Energy Laboratory; <sup>2</sup>Yeungnam University; <sup>3</sup>New Jersey Institute of Technology

The synthesis of p-type ZnO films with similar bandgaps but with varying carrier concentrations through co-doping of Cu and Ga is studied. The ZnO:(Cu,Ga) films were synthesized by RF magnetron sputtering in O<sub>2</sub> gas ambient at room temperature and then annealed at 500°C in air for 2 hours. We found that the bandgap reduction and p-type conductivity are caused by Cu incorporation. The tuning of carrier concentration is realized by varying the Ga concentration. It was found that the carrier concentration tuning does not significantly change the bandgap and crystallinity of the ZnO:Cu films. However, it can optimize the carrier concentration and thus dramatically enhance PEC response for the bandgap-reduced p-type ZnO thin films. Our studies suggest that carrier concentration tuning by acceptor-donor co-doping is an important approach to enhance the PEC performance of electrodes

**12:00 PM**

**Research on Nano Fe<sub>2</sub>O<sub>3</sub> Film Coated on Surface of 3D-Meshwork SiC by Sol-Gel Method:** *Yu Liang*<sup>1</sup>; Wu Yanjun<sup>1</sup>; Ru Hongqiang<sup>1</sup>; Yue Xinyan<sup>1</sup>; Li Jingyang<sup>1</sup>; <sup>1</sup>Texture of Materials, Ministry of Education, College of Materials and Metallurgy, Northeastern University,

This paper represented the preparation process of nano ferric oxide thin film coated on three-dimensional meshwork silicon carbide by the sol-gel method, in which Fe(NO<sub>3</sub>)<sub>3</sub>·9H<sub>2</sub>O and CO(NH<sub>2</sub>)<sub>2</sub> were used as raw material, water

Mon. AM

# Technical Program

as solvent. Concentration of  $\text{Fe}(\text{NO}_3)_3 \cdot 9\text{H}_2\text{O}$  and  $\text{CO}(\text{NH}_2)_2$ , temperature of hydrolyze, mechanism of desiccation, temperature of heat treatment were controlled. X-ray diffraction (XRD), scanning electronic microscope (SEM) were used to study the component, microstructure and phase constitution of the film. Infra-red spectrometry (IR), differential scanning calorimetry (DSC) and thermogravimetry (TG) were used to study the change of the ferric oxide precursor. The investigation clearly showed that a- $\text{FeOOH}$  sol solution in which concentration of  $\text{Fe}^{3+}$  was 0.167mol/L and be hydrolyzed in the order under 50°C and 80°C was perfect. With vacuum impregnation and step desiccation methods, and sintered at 480°C, the ideal densification nano ferric oxide thin film coated on three-dimensional meshwork silicon carbide can be prepared.

## Computational Thermodynamics and Kinetics: Diffusion and Defects

*Sponsored by:* The Minerals, Metals and Materials Society, TMS Electronic, Magnetic, and Photonic Materials Division, TMS Materials Processing and Manufacturing Division, TMS Structural Materials Division, TMS: Chemistry and Physics of Materials Committee, TMS/ASM: Computational Materials Science and Engineering Committee  
*Program Organizers:* Jeffrey Hoyt, McMaster University; Dallas Trinkle, University of Illinois at Urbana-Champaign

Monday AM Room: 308  
February 15, 2010 Location: Washington State Convention Center

*Session Chair:* To Be Announced

### 8:30 AM Invited

**Controlling Diffusion in Semiconductor Nanostructures by Size and Dimensionality:** *James Chelikowsky*<sup>1</sup>; <sup>1</sup>University of Texas

The ability to control the diffusion of dopants or impurities is a controlling factor in the functionalization of materials used in devices both at the macro- and nano-scales. At the nanoscale, manipulating diffusion of dopants is complicated by a number of factors such as the role of quantum confinement and the large surface to volume ratio. Here I will examine Li in Si nanowires as atoms with low atomic mass such as Li can be used as a carrier for energy storage with high specific energy capacity. Specifically, Li-ion batteries with specific energy capacity as high as 4200 mAh/g using Si nanowires as anodes have been achieved. Using ab initio calculations, we determine how the factors of size and dimensionality can be used to achieve an optimal diffusion of Li atoms in Si nanowires.

### 9:00 AM Invited

**Compositional Point Defect Evaluation Using Diffusion Multiples:** *Ji-Cheng Zhao*<sup>1</sup>; Xuan Zheng<sup>2</sup>; David Cahill<sup>2</sup>; <sup>1</sup>The Ohio State University; <sup>2</sup>University of Illinois at Urbana-Champaign

Compositional point defects such as vacancies and anti-sites have a significant effect on the properties of alloys and intermetallic compounds. For instance, point defects in NiAl result in orders of magnitude change in diffusion coefficients. Two indirect ways to find the formation of compositional point defects in alloys and intermetallics using diffusion couples and diffusion multiples will be discussed. The first involves micron-scale thermal conductivity mapping over a wide range of compositions. A sharp change in thermal conductivity in a very narrow range of composition is indicative of compositional point defect formation. Thermal conductivity measurements can also be used to study the site preference / elemental substitution in intermetallic compounds. The second method looks at the shape of the diffusion profiles and the dependence of diffusivity on composition. Examples will be used to illustrate these methodologies. Both methods are sufficient, but not necessary tests of the compositional point defects.

### 9:30 AM Invited

**Diffusion in Alloys and Intercalation Compounds from First Principles:** *Anton Van der Ven*<sup>1</sup>; <sup>1</sup>University of Michigan

Diffusion in substitutional alloys and solids containing high concentrations of mobile interstitial elements is a complex kinetic process that depends on the nature of intrinsic defects, the energetically most favorable hop mechanisms and the degree of short and long-range order among the constituents of the solid. In this talk, I will describe how these factors can be rigorously accounted for in

a first-principles prediction of diffusion coefficients in non-dilute alloys. The approach relies on the evaluation of Kubo-Green expressions, which provide the link between macroscopic diffusion coefficients and atomic trajectories sampled in kinetic Monte Carlo simulations. A first-principles description of the thermodynamics of short and long-range order in multi-component solids is achieved with the cluster expansion formalism. I will describe recent work on the prediction of diffusion coefficients in intermetallic compounds and Li ion battery electrode materials.

### 10:00 AM

**Ab Initio Modeling of Interstitial Diffusion in bcc Fe:** *Marcel Sluiter*<sup>1</sup>; <sup>1</sup>TU Delft

The role of diffusion of interstitial species such as carbon in bcc iron with minor additions of other common alloying elements such as aluminum, silicon, manganese, niobium and others are studied using ab initio techniques. It is shown that interactions between C and substitutional alloying elements in bcc Fe is not trivially guessed from carbon affinity as derived from carbide formation tendencies. Generally, kinetic Monte Carlo simulations show that substitutional elements reduce the carbon diffusivity.

### 10:20 AM Break

### 10:30 AM Invited

**First-principles Approach to Transition States of Diffusion:** *Zi-Kui Liu*<sup>1</sup>; <sup>1</sup>The Pennsylvania State University

In recent publications, we predicted self- and impurity diffusion coefficients through first-principles calculations based on the transition state theory [1] and a five-frequency model [2]. The free energy of vacancy formation and vacancy impurity binding is obtained through total energy and phonon calculations. Various jump frequencies are evaluated from phonon vibrational frequencies at the equilibrium and transition states when the vacancy is present. More recently, we proposed a new first-principles approach to treat the unstable vibrational mode of transition states [3]. It particularly allows one to determine the entropy of migration and the characteristic vibrational frequency, along with their temperature dependences. In this presentation, above results will be discussed.  
1. Mantina et al., "First-principles calculation of self-diffusion coefficients," Phys. Rev. Lett., Vol.100, 2008, 215901. 2. Mantina et al., "First-Principles Impurity Diffusion Coefficients", Acta Mater., (accepted, May 2009) 3. Mantina et al. "First-principles Approach to Transition States of Diffusion," submitted

### 11:00 AM

**Quantifying the Strength of Point Defect Based Hydrogen Traps in bcc and fcc Iron:** *William Counts*<sup>1</sup>; Chris Wolverton<sup>1</sup>; Ron Gibala<sup>2</sup>; <sup>1</sup>Northwestern University; <sup>2</sup>University of Michigan

Hydrogen embrittlement of iron and steels is a classic but still unresolved problem in metallurgy. While hydrogen can freely move through the Fe lattice, its diffusion is hindered by lattice imperfections. Experimentally quantifying the binding energy of hydrogen to these defects has proven to be difficult. Fortunately, computational tools are ideally suited to study defect trapping because it is possible to isolate individual traps. Density function theory was used to quantify the binding energy of hydrogen to a number of point defects in both bcc and fcc Fe. In bcc Fe, vacancies are the strongest hydrogen trap with a binding energy of 0.57 eV. The binding energies of common alloying elements are significantly less and range between -0.08 - 0.20 eV. Using a number of different anti-ferromagnetic configurations to model the paramagnetic state in fcc Fe, we found the hydrogen-vacancy binding energy to be between 0.20-0.36 eV.

### 11:20 AM

**Island Shape Controls Magic Size Effect for Heteroepitaxial Diffusion:** *Henry Wu*<sup>1</sup>; Dallas Trinkle<sup>1</sup>; <sup>1</sup>University of Illinois at Urbana-Champaign

Low temperature in situ STM studies of Cu islands on Ag(111) by Weaver at UIUC observed anomalously fast diffusion for specific sizes of small monolayer islands (magic size effect). To computationally study the dynamics of Cu island diffusion, we use ultrasoft pseudo-potential GGA calculations to optimize an embedded atom method (EAM) potential. The optimized EAM calculates diffusion barriers of Cu islands up to 14-atoms. Previous work by Hamilton for 1D and 2D heteroepitaxial island diffusion found a magic size effect associated with collective glide dislocation-mediated mechanism. For Cu/Ag(111) we find--in addition to collective glide--lower diffusion barriers for the reptation dislocation-mediated mechanism. The reptation mechanism is



limited by bond-breaking considerations that result from the 2D island shape. By grouping islands according to the number of [110] rows affected by the diffusion dislocation, the 2D diffusion barriers follow trends seen in the 1D magic size effect.

### 11:40 AM

**Effects of Spin Transition on Diffusion of Fe<sup>2+</sup> in Ferroperricite in Earth's Lower Mantle:** Saumitra Saha<sup>1</sup>; Dane Morgan<sup>1</sup>; Amy Bengtson<sup>2</sup>; <sup>1</sup>University of Wisconsin-Madison; <sup>2</sup>University of Michigan

Diffusion plays a fundamental role for many processes in Earth's mantle involving chemical, isotopic and advective mass transfer, homogenization of mantle materials, grain growth, electrical conductivity and communication between elements in core and mantle. Recent studies have established that iron undergoes an electronic spin transition in ferroperricite ((Mg,Fe)O) in the lower part of the mantle. However, due to the challenges of diffusion experiments at lower mantle pressures and temperatures, the effect of the spin transition of Fe<sup>2+</sup> on diffusion in ferroperricite is unknown. In the present study we combine first principles methods with the five-frequency statistical model to compute the Fe<sup>2+</sup> diffusivity. The results are compared with existing experimental diffusion data and changes in the diffusion rate are interpreted in terms of the changes in electronic structure with the spin transition. Finally, possible implications of the spin crossover for the lower mantle properties are discussed.

### 12:00 PM

**Molecular Dynamics Simulation of Self-Diffusion in bcc Metals:** Mikhail Mendeleev<sup>1</sup>; <sup>1</sup>Ames Laboratory

It is widely accepted that the vacancy mechanism governs the self-diffusion in fcc metals. We used molecular dynamics (MD) simulation to check whether this is the case for bcc metals. We determined the point defect formation and migration energies and found that both interstitial and vacancy formation energies strongly depend on temperature and the sum of the interstitial formation and migration energies can be smaller than the same quantity for vacancies. Next we used MD simulation to determine the equilibrium point defect concentration and found that at high temperatures the interstitial concentration can be comparable with the vacancy concentration. Finally we calculated diffusivities in both vacancy and interstitial mechanisms and found that in bcc Zr, vacancy and interstitial mechanisms give about the same contribution in the self-diffusivity. Work at the Ames Laboratory was supported by the Department of Energy, Office of Basic Energy Sciences, under Contract No. DE-AC02-07CH11358.

## Cost-Affordable Titanium III: Overview and Low Cost Processing

*Sponsored by:* The Minerals, Metals and Materials Society, TMS Structural Materials Division, TMS: Titanium Committee  
*Program Organizers:* M. Ashraf Imam, Naval Research Lab; F. H. (Sam) Froes, University of Idaho; Kevin Dring, Norsk Titanium

Monday AM Room: 618  
February 15, 2010 Location: Washington State Convention Center

*Session Chairs:* Henry Rack, Clemson University; James Sears, Quad City Manufacturing Laboratory

### 8:30 AM

**Cost Affordable Developments in Titanium Technology and Applications:** F. H. (Sam) Froes<sup>1</sup>; M. Ashraf Imam<sup>2</sup>; <sup>1</sup>Institute for Materials and Advanced Processes; <sup>2</sup>Naval Research Lab

Titanium is the "wonder" metal, which makes sense as the material of choice for a wide variety of applications. However, because of its relatively high price-a result of extraction and processing costs- it is used basically only when it is the only choice; with the caveat that titanium has a bright "image" which can lead to use even when the economics are unfavorable. The major thrust in the area of titanium development has been aimed at achieving cost reduction rather than the developing alloys with enhanced properties. This paper will overview the potential areas, which are amenable to the cost reduction for developments in titanium technology and applications.

### 8:55 AM

**The FFC-Cambridge Process for Titanium Metal Winning:** Carsten Schwandt<sup>1</sup>; Derek Fray<sup>1</sup>; Gregory Doughty<sup>1</sup>; <sup>1</sup>University of Cambridge

The FFC-Cambridge Process is a molten salt electro-deoxidation method that was invented at the University of Cambridge one decade ago. It is a generic technology that allows direct conversion of metal oxides into the corresponding metals through cathodic polarisation of the oxide in molten calcium chloride. The process has wide applicability, and numerous studies on metals, semi-metals, alloys and intermetallics have since been performed at Cambridge and worldwide. The electro-winning of titanium metal is a particularly rewarding target because of the disadvantages of present extraction methods. This presentation summarises the research performed on the FFC-Cambridge Process with a focus on electro-winning titanium metal from titanium dioxide. Topics addressed encompass the investigation of the key process parameters, the identification of the reaction pathway, and the derivation of an optimised set of process parameters. The presentation also discusses some aspects of technology transfer and development activities undertaken to date.

### 9:20 AM

**Direct Electrochemical Reduction of Titanium Dioxide in Molten Salts:** Kevin Dring<sup>1</sup>; <sup>1</sup>Norsk Titanium

Electrochemical methods and electrowinning of titanium have been promoted, unsuccessfully, for many years as a replacement for the current Kroll process, which has not achieved the same economies of scale as other light metals (eg. Al, Mg) have. One such method is the direct electrochemical reduction of titanium dioxide, which encompasses a range of processes involving the electrolysis of a molten salt and the subsequent reduction of titanium via the metal of the salt cation. Norsk Titanium AS, in a collaboration with Norsk Hydro and NTNU through a Norwegian Research Council grant, has been actively involved in the development of such a process and the focus of this presentation is to give a summary of the research activities. Particular emphasis will be given to the fundamental reactions underlying the process.

### 9:45 AM

**The Production of Ti Alloy Powder from Chloride Precursors:** James Withers<sup>1</sup>; J. Laughlin<sup>1</sup>; Y. Elkadi<sup>1</sup>; J. DeSilva<sup>1</sup>; R. Loutfy<sup>1</sup>; <sup>1</sup>MER Corporation

It has long been a goal to produce Ti Alloy powder directly to eliminate the standard processing of melting sponge, alloying, producing a billet/ingot and then reducing to powder by one of several techniques. The batch Kroll process where reaction occurs at the reactor wall interface from TiCl<sub>4</sub> vapor and molten magnesium, limits the potential to directly form alloys. Any batch processing has the limitation of alloy compositional control from batch to batch. A unique continuous processing approach permits the gaseous mixing of chloride precursors with metallothermic reduction that directly produces an alloy powder in a size that is useable for standard powder metallurgy. Discussion will include producing Ti-6Al-4V and other alloy powder.

### 10:10 AM Break

### 10:25 AM

**Quantitative X-Ray Synchrotron Analysis of the FFC Cambridge Process:** Rohit Bhagat<sup>1</sup>; David Dye<sup>2</sup>; Ben Jackson<sup>2</sup>; Seema Raghunathan<sup>2</sup>; Douglas Inman<sup>2</sup>; Richard Dashwood<sup>1</sup>; <sup>1</sup>The University of Warwick; <sup>2</sup>Imperial College London

This paper demonstrates how in-situ synchrotron analysis has been used to obtain the first unequivocal description of the reduction pathway for the electrochemical production of titanium via the FFC Cambridge process. In previous studies of this process, phase identification was carried out ex-situ and this has resulted in erroneous and conflicting reduction pathways being proposed. By performing in-situ synchrotron, it was found that the reduction pathway proceeded sequentially through TiO<sub>2</sub>, sub-stoichiometric TiO<sub>2</sub> phases, Ti<sub>2</sub>O<sub>3</sub>, cubic TiO and hexagonal titanium. CaTiO<sub>3</sub> formed from the sub-stoichiometric TiO<sub>2</sub> phases. CaTi<sub>2</sub>O<sub>4</sub> formed by a comproportionation reaction in the inner layers of the pellet. CaO was also observed, indicating that for some interval the electrolyte was locally saturated with oxide ions. TiC formed at the latter stages of reduction on the pellet surface. The occurrence of the individual phases was dependent on location, with the transformations shifting to longer times away from the surface.

# Technical Program

## 10:50 AM

**New Methods for Low-Cost Titanium Production:** *Ana Maria Martinez<sup>1</sup>; Karen Osen<sup>1</sup>; Egil Skybakmoen<sup>1</sup>; Ole Kjos<sup>2</sup>; Geir Martin Haarberg<sup>2</sup>; Kevin Dring<sup>3</sup>; <sup>1</sup>SINTEF; <sup>2</sup>NTNU; <sup>3</sup>Norsk Titanium AS*

Metallurgical reduction is, at the moment, the only commercially available process for the industrial production of titanium sponge (Kroll process). Although the apparatus and procedures have improved over the past 50 years, it is still difficult to recover the waste heat from the individual steps and the total efficiency of titanium production is worse than that in continuous steelmaking. Therefore, alternative processes to produce low-cost titanium are desirable. These methods should possess the same requisites as the Kroll process, in terms of metal quality, as well as continuous operation and energy effective. The present work deals with the investigation of a titanium production method that uses TiO<sub>2</sub> enriched titania slag as raw material. The process involves two steps: i) carbothermal reduction of the slag to form titanium oxycarbide (TiOxCy) powder; and ii) electrolysis in molten chlorides using a TiOxCy consumable anodes.

## 11:15 AM

**A Continuous Process to Produce Titanium Utilizing Metallurgical Chemistry:** *James Withers<sup>1</sup>; J. Laughlin<sup>1</sup>; Y. Elkadi<sup>1</sup>; J. DeSilva<sup>1</sup>; R. Loutfy<sup>1</sup>; <sup>1</sup>MER Corporation*

In the standard Kroll process reaction between the TiCl<sub>4</sub> and Mg is at the reactor wall interface that limits the potential to design a continuous process. Many alternatives have been investigated over the past 70 years to engineer a continuous process utilizing metallurgical reduction of TiCl<sub>4</sub>. Approaches utilizing burner type architectures for continuous processing result in unacceptable very fine Ti powder. A unique process that operates continuously and produces controlled size powder that can be directly utilized in standard powder metallurgy, rapid manufacturing, or substituted for sponge will be discussed.

## 11:40 AM

**The Electrolytic Production of Ti from a TiO<sub>2</sub> Feed (The DARPA Sponsored Program):** *James Withers<sup>1</sup>; J. Laughlin<sup>1</sup>; Y. Elkadi<sup>1</sup>; J. DeSilva<sup>1</sup>; R. Loutfy<sup>1</sup>; <sup>1</sup>MER Corporation*

DARPA instituted an Initiative in Titanium in 2003 to produce titanium, alternatively to the Kroll process, in a billet form for under \$4/lb. This DARPA sponsored program has gone into Phase II consisting of utilizing ore/TiO<sub>2</sub> as a feed. The TiO<sub>2</sub> is carbothermally reduced to a suboxide-carbide (Ti<sub>3</sub>O<sub>2</sub>C) which is used anodically to resupply the titanium content in an electrolysis process that deposits titanium in a powder morphology. The deposited powder is uniquely stripped from the cathodes and harvested in a separate stream that permits continuous electrolytic processing to produce titanium at an estimated cost about 1/2 the Kroll process. Oxygen contents less than 500 ppm are achievable with particle sizes in the desired range for powder metallurgy applications. The process has been demonstrated on a continuous basis and is in the stage of scaling-up to 500 lbs/day. Approved for Public Release, Distribution Unlimited

## 12:05 PM

**The FFC Cambridge Process for Production of Low Cost Titanium and Titanium Powders:** *Mark Bertolini<sup>1</sup>; Lee Shaw<sup>1</sup>; Lucy England<sup>1</sup>; Kartik Rao<sup>1</sup>; James Dean<sup>1</sup>; James Collins<sup>1</sup>; <sup>1</sup>Metalysis*

The current status and recent advancements in the use of the FFC Cambridge process for the production of low cost titanium and titanium powders is presented. This will include an overview of the process, current and future process equipment and recent results in terms of chemistry, structure and properties of powder and consolidated product. The future direction and activities for the FFC Cambridge process will also be briefly discussed.

## Failure of Small-Scale Structures: Nanowire Behavior

*Sponsored by:* The Minerals, Metals and Materials Society, TMS Materials Processing and Manufacturing Division, TMS Structural Materials Division, TMS/ASM: Mechanical Behavior of Materials Committee, TMS: Nanomechanical Materials Behavior Committee  
*Program Organizers:* Marian Kennedy, Clemson University; Brad Boyce, Sandia National Laboratory; Reinhold Dauskardt, Stanford; Zhiwei Shan, Hysitron Inc

Monday AM Room: 206  
February 15, 2010 Location: Washington State Convention Center

*Session Chairs:* Brad Boyce, Sandia National Laboratories; Molly Kennedy, Clemson University

## 8:30 AM Invited

**Insights from Nanomechanical Testing: Nanoengineering Surfaces, Thin Films, and Nanowires:** *Christopher Muhlstein<sup>1</sup>; <sup>1</sup>The Pennsylvania State University*

Our ability to engineer nanomaterials for mechanical applications hinges on a fundamental understanding of how they accumulate damage and fail. In this presentation we will review a series of experiments conducted on surfaces, thin films, and nanofilaments that challenge generally accepted nanoengineering strategies. Specifically, nanoindentation and fatigue crack growth experiments conducted on nanograin platinum films show that the films are extremely susceptible to time and cycle-dependent degradation. In contrast, tensile testing results demonstrate that individual nanowires can appear to have anomalous deformation behavior that is an artifact of the testing methodology.

## 8:55 AM Invited

**Mechanical Behavior of Au Nanowires:** *Cynthia Volkert<sup>1</sup>; B. Roos<sup>1</sup>; B. Kapelle<sup>1</sup>; G. Richter<sup>2</sup>; A. Sedlmayr<sup>3</sup>; D.S. Gianola<sup>4</sup>; R. Mönig<sup>3</sup>; <sup>1</sup>Institute for Materials Physics, University of Göttingen; <sup>2</sup>Max Planck Institute for Metals Research; <sup>3</sup>Institute for Materials Research-II, Forschungszentrum Karlsruhe; <sup>4</sup>Formerly at the Institute for Materials Research-II, Forschungszentrum Karlsruhe, currently at the Department of Materials Science and Engineering, University of Pennsylvania*

The mechanical behavior of single crystal Au nanowires with diameters between 40 and 100 nm have been investigated by in-situ tensile loading in the TEM and by instrumented testing using a nanoindenter. The nanowires are grown by physical vapour deposition onto W substrates and are initially dislocation-free. Preliminary observations of the nanowires in the TEM reveal that numerous dislocations are nucleated uniformly along the length of the nanowire during tensile loading. These dislocations remain in the wire, possibly influenced by a surface Pt layer formed during transfer in the SEM, before they exit the nanowire on further loading. The wire eventually fails by ductile fracture. Neither the site of fracture nor the dislocation structure in the fracture area show any distinguishing features. Tensile tests with a nanoindenter and instrumented tensile testing in an SEM show that the strengths of the Au nanowires are in good agreement with those measured in nanoporous Au ligaments and in Au micro-compression columns of the same diameters, and support the widely observed trend of increasing strength with decreasing size.

## 9:20 AM

**In-Situ Tensile Deformation of Silver Nanowires:** *Junhang Luo<sup>1</sup>; Jian Yu Huang<sup>2</sup>; Catherine Murphy<sup>3</sup>; Scott Mao<sup>1</sup>; <sup>1</sup>University of Pittsburgh; <sup>2</sup>Sandia National Laboratories; <sup>3</sup>University of South Carolina*

Using a unique transmission electron microscopy (TEM) - scanning tunneling microscopy (STM) platform, in-situ tensile tests combined with high resolution TEM (HRTEM) observations have been performed successfully on silver nanowires. A uniform plastic elongation without necking was achieved with an elongation more than 19% in the bicrystalline Ag nanowires. In-Situ HRTEM observations and fast Fourier transform (FFT) analysis showed that a lot of stacking faults were formed during the tensile test to accommodate the plastic deformation. Interestingly, the stacking faults are not induced by Shockley partial dislocations but by the frank loops formation and expansion.



9:35 AM

**In-Situ TEM Studies of Nanomechanics and Fracture in Nanowires and Nanotubes:** *Reza Shahbazian-Yassar*<sup>1</sup>; Hessam Ghasemi<sup>1</sup>; Anahita Pakzad<sup>1</sup>; Kasra Momeni<sup>1</sup>; Anjana Ashtana<sup>1</sup>; Yoke Yap<sup>1</sup>; <sup>1</sup>Michigan Technological University

One-dimensional nanomaterials including nanotubes, nanowires, and nanofibers are building blocks for constructing various complex nanodevices. In this work, deformation of individual nanotubes and nanowires will be performed inside a high-resolution transmission electron microscope (TEM) using a piezo-driven atomic force microscope (AFM) and scanning tunneling microscope (STM)-TEM holder. The electrical and mechanical properties of individual nanotubes/nanofibers are obtained from the experimentally recorded I-V and force-displacement curves. Failure and deformation of various nanostructures including ZnO nanowires, BN nanotubes, carbon nanotubes, and cellulose nanocrystals show distinct behavior.

9:50 AM Break

10:05 AM Invited

**Fracture and Deformation in Metallic Nanowires:** *Scott Mao*<sup>1</sup>; A. Cao<sup>2</sup>; Y. Wei<sup>2</sup>; <sup>1</sup>University of Pittsburgh; <sup>2</sup>Institute of Mechanics

The mechanical behavior of bulk metals is usually characterized as smooth continuous plastic flow following by yielding. Here we show, by using molecular dynamics simulations and in-situ experiment that the mechanical deformation behaviors of single-crystalline nickel and copper nanowires are quite different from their bulk counterparts. Correlation between the obtained stress-strain curves and the visualized defect evolution during deformation processes clearly demonstrates that a sequence of complex dislocation slip processes results in dislocation starvation, involving dislocation nucleation, propagation and finally escaping from the wire system, so that the wires deformed elastically until new dislocation generated. This alternating starvation of dislocations is unique in small-scale structures. Furthermore, the magnitude of yield stress of these nanowires is strongly dependent of the wire size.

10:30 AM Invited

**In-Situ Atomic Scale Nanomechanics Revealed by a TEM-SPM Platform:** *Jianyu Huang*<sup>1</sup>; Junhang Luo<sup>2</sup>; He Zheng<sup>2</sup>; Scott Mao<sup>2</sup>; Nan Li<sup>3</sup>; Jian Wang<sup>3</sup>; Xinghang Zhang<sup>4</sup>; Armit Misra<sup>5</sup>; Yang Lu<sup>5</sup>; Jun Lou<sup>6</sup>; Erik Bitzek<sup>6</sup>; Ju Li<sup>6</sup>; <sup>1</sup>Sandia National Laboratories; <sup>2</sup>University of Pittsburgh; <sup>3</sup>Los Alamos National Laboratories; <sup>4</sup>Texas A&M University; <sup>5</sup>Rice University; <sup>6</sup>University of Pennsylvania

By integrating scanning tunneling microscopy (STM) probes, atomic force microscopy (AFM) probes, and nanoindentors into a transmission electron microscope (TEM), novel deformation and failure mechanisms of individual carbon nanotubes, nanowires, and graphene were revealed at an atomic-scale. In NaCl nanowires, unusual fast diffusion rather than dislocation mediated superplasticity was observed. Silica glass nanowires were ductile at room temperature, with surprisingly large tensile plastic elongations. These ductile glass nanowires also possess high flow strengths. The unexpected ductility is due to the development of a surface affected zone in the nanowires, which enhances ductility. Detwinning, the reverse process of twinning, is an important deformation mechanism in face-centered-cubic metals. In graphene, fractal sublimation patterns and sp<sup>2</sup>-edge reconstructions were observed, indicating that bilayer rather than monolayer graphene is more realistic candidate for device applications. Future directions of applying the TEM-SPM techniques to studying batteries, thermal and thermoelectric energy-related materials will be discussed.

10:55 AM

**An In Situ Scanning Electron Microscopy Study of Size Dependent Mechanical Behaviors of Metallic Nanowires:** *Cheng Peng*<sup>1</sup>; Yang Lu<sup>1</sup>; Yogi Ganesan<sup>1</sup>; Yongjie Zhan<sup>1</sup>; Jun Lou<sup>1</sup>; <sup>1</sup>Rice University

Metallic nanowires are of great technological importance due to their current and potential applications in miniaturized electronic, optical, thermal and electromechanical systems. This talk presents some of our recent efforts to study the size dependent mechanical behavior of metallic nanowires. We have developed a simple micro-device that allows in situ quantitative mechanical characterization of metallic nanowires, in scanning electron microscope chamber equipped with a quantitative nanoindenter. The unique design of this device makes it possible to convert compression from nanoindentation to uni-axial tension at the sample stages. Finite element analysis is employed

to model the device behavior under mechanical loading and compared with experiments. Ni, Cu and Au nanowires with different diameters ranging from tens of nanometers to hundreds of nanometers were fabricated by template-assisted electro-chemical deposition and hydrothermal synthesis. Finally, main results on size effects in deformation and fracture behavior of Ni, Cu and Au nanowires will be discussed.

11:10 AM Invited

**Deformation Mechanisms in Quasi-1D Nanostructures: In Situ Observations and Measurements during Tensile Testing in Electron Microscopes:** *Daniel Gianola*<sup>1</sup>; <sup>1</sup>University of Pennsylvania

The mechanical behavior of single crystalline metals has been known to be size dependent for decades, but the details of the underlying deformation mechanisms have seen only recent attention. Escape to free surfaces and nucleation of new dislocations are expected to trump interactions between dislocations, precluding the operation of bulk hardening mechanisms. However, the real strength and rate controlling mechanisms at sub-micrometer length scales are still elusive. In the present work, we describe quantitative *in situ* tensile experiments on quasi-1D nanostructures in a dual-beam SEM and FIB. Complementary *in situ* TEM studies of dislocation multiplication and shearing processes in sub-micrometer Al fibers were also conducted. The detailed operation and nature of the sources have been systematically analyzed and compared to their crystal dimensions. The influence of pre-existing defects and flaws in these nanostructures, which is critically linked to the materials synthesis route, is discussed.

11:35 AM Invited

**Statistical Effects on Material Strength at Small Length Scales:** Shyam Keralavarma<sup>1</sup>; *Ahmed Benzerga*<sup>1</sup>; <sup>1</sup>Texas A&M University

One of the characteristic features of available experimental data for the mechanical strength of materials at small length scales is the increased scatter resulting from the statistical nature of discrete dislocation events. From a design point of view, it is important to characterize this observed feature of material behavior in order to improve the reliability of the mechanical components at the nano scale. In this work, we employ two-dimensional discrete dislocation dynamics (DD) simulations of the homogeneous deformation of single crystals under compressive loads to study the statistical effects on material response as a function of size. Some examples of non-homogeneous deformation such as discrete dislocation effects on micro-void growth under plane strain conditions will also be considered. The results are compared to available experimental results, such as the micro-pillar compression experiments.

### General Abstracts: Materials Processing and Manufacturing Division: Welding

*Sponsored by:* The Minerals, Metals and Materials Society, TMS Materials Processing and Manufacturing Division, TMS/ASM: Computational Materials Science and Engineering Committee, TMS: Global Innovations Committee, TMS: Nanomechanical Materials Behavior Committee, TMS/ASM: Phase Transformations Committee, TMS: Powder Materials Committee, TMS: Process Technology and Modeling Committee, TMS: Shaping and Forming Committee, TMS: Solidification Committee, TMS: Surface Engineering Committee  
*Program Organizers:* Thomas Bieler, Michigan State University; Corbett Battaile, Sandia National Laboratories

Monday AM

Room: 611

February 15, 2010

Location: Washington State Convention Center

*Session Chair:* To Be Announced

8:30 AM

**High Brightness Nd:YAG Laser Welding of Aluminum 5754:** *Jyotirmoy Mazumder*<sup>1</sup>; Leslie Pipe<sup>1</sup>; Yi Liu<sup>1</sup>; David Roessler<sup>1</sup>; <sup>1</sup>University of Michigan

Bead-on-plate keyhole welds were made in aluminum alloy Al-5754, (a popular alloy in auto industry for weight reduction) using a pumped solid-state diode-laser with 500W average power and high-brightness, operating at a 20% duty cycle and argon as the shielding gas. The welding parameters included laser beam pulse width, repetition rate, focusing lens optics and traverse speed. Besides penetration depth data, spectral lines from Al I transitions were examined with a spectrometer and an Intensity Charge Coupled Device. At laser

# Technical Program

power of 400 W, full penetration of 3-mm sheets was possible with a traverse speed-focal length combination of 0.85 cm/s and 150-mm or 0.21 cm/s and 200-mm. Emission spectroscopy revealed the temperature of the vapor plume between 8,000-10,000 K at the workpiece surface and increasing over the first millimeter of height. Plume temperatures seem to be higher with longer laser pulses, shorter focal lengths and higher welding traverse speeds.

## 8:50 AM

### **Robotic Welding of Large Floor Panels Made of Light Aluminum Extrusions:** *Michel Guillor<sup>1</sup>*; <sup>1</sup>Laval University

Gaz metal arc welding is commonly used for joining large assemblies and is increasingly preferred for welding thin wall components despite some limitations. In this paper, several parameters of the GMAW process and robot motion are investigated for joining AL6061-T6 and AL6063-T6 extrusions of floor panels. Based on welding tests carried out on flat stock samples, the effect of several parameters like GMAW and robot settings, joint preparation, wire diameters, alloys and feed are studied and optimized for weld quality as well as for higher welding speed. In the second and main part of the paper the best settings are implemented for joining complex extrusions of a floor panel used typically in a 53ft semi-trailer. The geometric and positioning errors of the components mounted in the fixture and the distortion after welding several 2.4m long extrusions on both sides are studied. The weld quality is tested at different locations in the floor panel. Several improvements are experimented to optimize even further the welding performances.

## 9:10 AM

### **Effects of Novel Processing Techniques on the Fatigue Crack Growth Behavior of 6061 Alloys:** *Brendan Chenelle<sup>1</sup>*; Christopher Lammi<sup>1</sup>; Diana Lados<sup>1</sup>; <sup>1</sup>Worcester Polytechnic Institute

Friction stir welding and coldspray are solid-state processes that could be beneficially used for joining and repair in transportation and defense applications. Understanding fatigue crack propagation is necessary to use these processes in critical structural applications. In this study, tensile properties and fatigue crack growth mechanisms in friction stir welded and coldspray 6061 alloys were investigated. Fatigue crack growth testing of the base and processed materials was conducted on compact tension specimens in ambient conditions using a constant stress ratio,  $R=0.1$ . Tests parallel and normal to the friction stir weld traverse direction and to the coldspray consolidation direction were conducted. The microstructures after processing were characterized and the resulting residual stresses were examined using fracture mechanics techniques. Individual and combined effects of residual stresses, microstructural changes, and reinforcements of the processed regions were related to the fatigue crack growth response of the materials and will be presented and discussed.

## 9:30 AM

### **Numerical and Experimental Analyses for Effect of Welding Speeds on Cooling Rates in Manual Metal Arc Welding(MMAW):** *Muna Abbass<sup>1</sup>*; *Jalal M. Jali<sup>1</sup>*; Abbas Sh. Alwan<sup>1</sup>; <sup>1</sup>University of Technology, Baghdad

Abstract Manual Metal Arc Welding (MMAW) is carried out for low carbon steel (AISI 1015) for plate of thickness 8mm. Experimentally, cooling rates are determined for the fusion zone at different welding speeds(1.7, 2.3 and 3.2) mm/s with constant welding current at (100 Amp). Numerical analysis by using the Control Volume Method (CVM), applied to three-dimensional heat transfer model to determine the cooling rate in fusion zone. Cooling rates models are helping in prediction the microstructure and microhardness distribution in weld metal and heat affected zone. The comparison of cooling curves between numerical and experimental work have a good agreement, so that deviation was in range (6%-21%) (which is confirming the capability and reliability of the proposed numerical heat transfer model in manual metal arc welding. The best result for cooling rates when applying mathematical model is at welding speed 1.7mm/s.

## 9:50 AM

### **The Effect of Welding Speed on the Crystallographic Texture Observed in Friction Stir Welding of Near-Alpha Titanium:** *Richard Fonda<sup>1</sup>*; Keith Knippling<sup>1</sup>; <sup>1</sup>Naval Research Laboratory

In a series of experiments performed at different welding speeds, friction stir welds in a near- $\alpha$  Ti-5111 titanium alloy exhibit different crystallographic textures. The crystallographic orientations produced at slower weld speeds, which allow more heat to accumulate in the weld, indicate that the weld-induced deformation occurs primarily while the material is in the low-temperature a

phase. The faster, cooler welds exhibit a texture indicative of transformation in the high-temperature  $\beta$  phase. This apparent contradiction indicates that friction stir welds of this titanium alloy are influenced less by the heat generated during welding than by the speed at which the rotating tool is retreating from the deposited weld. The accelerated cooling at faster weld speeds quenches-in the initial high-temperature deformation structure, while slower weld speeds allow for a more efficient transfer of the stirring deformation into the cooler material behind the tool.

## 10:10 AM Break

## 10:30 AM

### **Spot Welding of Automotive Steels and Light Metals by Friction Bit Joining:** *Michael Miles<sup>1</sup>*; K. Kohkonen<sup>1</sup>; Zhili Feng<sup>2</sup>; <sup>1</sup>BYU; <sup>2</sup>Oak Ridge National Lab

Resistance spot welding (RSW) of steels and light metals in automotive manufacturing is difficult, because of incompatibility of these alloys during fusion. Self piercing riveting (SPR) can be done to join dissimilar alloys, but if the strength of the steel is very high this is difficult. It can also be difficult to form magnesium sheets around the rivet using SPR. A new process, called friction bit joining (FBR), was used to weld several high strength steels and light metals, where very good joint strength was obtained, even when joining a very hard alloy like DP 980 to a very soft alloy like AA 5754. Joint properties and microstructures will be presented and compared to current technologies like RSW and SPR.

## 10:50 AM

### **Ultrasonic Welding a Novel Approach to Friction Spot Welding Dissimilar Aluminum to Steel Automotive Sheets:** *Farid Haddadi<sup>1</sup>*; Philip Prangnell<sup>1</sup>; Dimitrios Bakavos<sup>1</sup>; <sup>1</sup>The University of Manchester

High power Ultrasonic Spot Welding (USW) has recently been developed as an alternative technique for friction joining aluminum automotive panels. USW can produce high quality joints in gauges up to 3 mm, with a lower energy requirement than resistance spot welding and a shorter weld cycle than FSSW. However, to date USW has not been studied for applications in joining dissimilar automotive materials, where the rapid weld cycle should be beneficial in preventing bond line embrittlement. In the present research, the optimization of the USW technique has been studied for joining aluminum to steel. Effects of different welding parameters, such as pressure and weld energy, on weld quality was assessed for two types of galvanized and un-galvanized steel. The Mechanical properties of the welds were examined and correlated to the weld parameters and interface microstructures. Results are also presented on the defects present and stages of bond formation.

## 11:10 AM

### **Computational Welding Mechanics: Hardening Models in Welding Simulation:** *Amir Masoud Akbari Pazooki<sup>1</sup>*; <sup>1</sup>TU Delft

Dual phase steel is used in automotive industries because of good strength and formability. Major problems in the welding process for this type of steel are residual stress and distortion. FEM is a very straightforward strategy for prediction of residual stress and distortion in welding engineering nowadays. Many models have been developed for prediction of residual stress and distortion in an accurate way. Most of these models use an isotropic hardening model. This paper presents isotropic, chaboche and kinematic hardening models in simulation of welding process for DP600 steel. The predicted results have been compared with the experimental measurements. It is concluded that different hardening models predict longitudinal residual stresses dissimilarly while the maximum distortion predictions are very close.

## 11:30 AM

### **Thermo-Mechanical-Metallurgical Simulation of DP600 Steel during Welding:** *Amir Masoud Akbari Pazooki<sup>1</sup>*; <sup>1</sup>TU Delft

In this paper a 2D thermo-mechanical-metallurgical simulation of DP600 steel plate during GTAW process is presented. The first part of the paper deals with the thermal analysis and then in the second part the microstructural evaluation during heating and cooling cycles (in welding process) is shown. Finally the thermal and microstructural results are used as input files in mechanical analysis. The predicted results of residual stress and distortion during welding of this type of steel are compared with experiments.



11:50 AM

**Correlation between Shoulder Flow Zone Quality and Material Flow Quantity during Friction Stir Welding of Thick Aluminum Section Using Scroll Shoulder Tool:** *David Yan*<sup>1</sup>; Zhan Chen<sup>1</sup>; Guy Littlefair<sup>1</sup>; <sup>1</sup>AUT University

Scroll tool offers advantages of eliminating the tilted tool axis and performing non-linear thick section FSW with a simple machine. However, the correlation between its weld quality and material flow quantity remains unrevealed. A novel scroll tool was used to FSW thick aluminium plates at a range of welding parameters. These were followed by quantifying the mass of pick up material (PUM), and then evaluating the effect of welding parameters and PUM on the shoulder flow zone formation and weld quality. It was found that there is a positive linear relationship between the mass of PUM and shoulder flow zone weld quality. In order to obtain a defect-free weld produced by scroll tool, the scroll groove not only needs to be fully filled up with PUM before tool starts to travel, but also needs to be filled in with a sufficient amount of PUM per tool revolution during tool travelling.

12:10 PM

**Distortion Assessment of a Direct Cast Uranium - 6 wt. % Niobium Cylinder:** *Hunter Swenson*<sup>1</sup>; Rob Aikin<sup>1</sup>; <sup>1</sup>Los Alamos National Laboratory

A homogenization and quenching cycle generates complex thermal histories where components experience thermal and phase transformation-induced volume changes. The residual stress profile and resulting geometric changes are established by the interaction and timing of these competing factors. This work details the process history, material characterization, and distortion analysis of vacuum induction melted and direct cast U-6 wt. % Nb component. The parts evaluated are a 13 kg hollow cylinder (tube) with a 120 mm diameter, an 8.5 mm wall thickness and a length of 250 mm. The cylinders were homogenized in a vacuum furnace 1000°C, cooled and stabilized to 850°C, and then quenched in cold oil bath. The high temperature gamma structure is converted to an alpha martensite during the quench. Dimensional data obtained from a coordinate measuring machine allowed for direct geometric comparison before and after heat treatment. Microstructure characterization was performed at various locations on the cylinder.

### General Abstracts: Structural Materials Division: Materials Characterization and Shock Loading

*Sponsored by:* The Minerals, Metals and Materials Society, TMS Structural Materials Division, TMS: Advanced Characterization, Testing, and Simulation Committee, TMS: Alloy Phases Committee, TMS: Biomaterials Committee, TMS: Chemistry and Physics of Materials Committee, TMS/ASM: Composite Materials Committee, TMS/ASM: Corrosion and Environmental Effects Committee, TMS: High Temperature Alloys Committee, TMS/ASM: Mechanical Behavior of Materials Committee, TMS/ASM: Nuclear Materials Committee, TMS: Refractory Metals Committee, TMS: Titanium Committee  
*Program Organizers:* Eric Ott, GE Aviation; Robert Hanrahan, National Nuclear Security Administration; Judith Schneider, Mississippi State University

Monday AM Room: 608  
February 15, 2010 Location: Washington State Convention Center

*Session Chair:* To Be Announced

8:30 AM

**Characteristics of High Interstitially Alloyed 18Cr-10Mn Stainless Steels:** *Chang-Seok Oh*<sup>1</sup>; Tae-Ho Lee<sup>1</sup>; Heon-Young Ha<sup>1</sup>; Sung-Joon Kim<sup>1</sup>; <sup>1</sup>Korea Institute of Materials Science

Some results of characterizations on Cr-Mn stainless steels with combined addition of carbon and nitrogen are presented, where high nitrogen alloyed steels having same compositions of Cr and Mn were chosen for reference. High nitrogen alloyed steels (HNS) of 18Cr-10Mn-(0.4-0.7)N and high interstitially alloyed steels (HIA) of 18Cr-10Mn-0.38C-0.38N and 18Cr-10Mn-0.42N-0.15C were manufactured by a VIM process under the nitrogen atmosphere. Regardless of kind of interstitial elements, tensile and yield strengths of annealed specimens were increased with increasing amount of interstitial elements. The deformed microstructures of HNS alloys were changed from planar dislocation

glide, strain induced martensitic transformation and to deformation twinning at higher strain, whereas no deformation induced transformation was not observed in HIA alloys. The electrochemical polarization response in chloride solution revealed that simultaneous alloying of carbon and nitrogen enhanced pitting corrosion resistance, which was confirmed by galvanostatic reduction test, Mott-Schottky analysis and XPS measurement.

8:50 AM

**Research on the Thermal Plasticity of the 18Mn-18Cr-0.77N-2Mo High Nitrogen Austenitic Stainless Steel:** *Li Wanming*<sup>1</sup>; Li huabing<sup>1</sup>; Jiang Zhouhua<sup>1</sup>; <sup>1</sup>Northeastern University

Hot compression tests of the 18Mn-18Cr-0.73N-2Mo high nitrogen austenitic stainless steel were performed on a GLEEBLE-2000 thermomechanical simulator under different deformation temperatures and strain rates. The microstructure of the compression samples were also observed by optical microscope. The model of the resistance to deformation was built, and the recrystallization activation energy, stress exponent and other parameters were obtained through analyzing the experimental data. The dynamic recrystallization model was established, and the distribution map of the dynamic recrystallization critical condition was given. The microstructure of the compression samples show that there are equiaxed grains on the edge of the samples and recrystallization grains in the core. Under same strain rate, the dynamic recrystallization becomes more sufficient under higher deformation temperature. But the grain coarsens and the plastic plasticity decreases when the temperature is above 1150°C. The recrystallization grain size is bigger and the amount becomes more under lower strain rate.

9:10 AM

**An Overview of the Microstructures of High-Strength Two-Phase near-Equi-Atomic FeNiMnAl Alloys:** *I. Baker*<sup>1</sup>; Y. Liao<sup>1</sup>; X. Wu<sup>1</sup>; H. Wu<sup>1</sup>; M.K. Miller<sup>2</sup>; K.F. Russell<sup>2</sup>; P.R. Munroe<sup>3</sup>; <sup>1</sup>Dartmouth College; <sup>2</sup>Oak Ridge National Laboratory; <sup>3</sup>University of New South Wales

This presentation will discuss the microstructures of several high strength alloys that have been discovered in the Fe-Ni-Mn-Al alloy system at near equi-atomic compositions. The microstructures of the alloys have been characterized using a combination of transmission electron microscopy, including X-ray mapping and convergent beam electron diffraction, and atom probe tomography. The highest strength alloys appear to have formed by spinodal decomposition and have very fine (10-90 nm wavelength) microstructures consisting of b.c.c. and B2 or L21 phases. Several alloys in this system that formed by eutectic decomposition still have very fine microstructures (0.1-1 μm) but consist of f.c.c. and B2 phases. The latter alloys can show significant tensile ductility. Research supported by NSF grants DMR-0505774 and DMR-0905229, DOE Award #DE-FG02-07ER46392 and the ORNL SHaRE User Facility which is sponsored by the Scientific User Facilities Division, Office of Basic Energy Science, U.S. Department of Energy.

9:30 AM

**Quantitative Measurement of Crack Initiation and Propagation in High Explosives and Mocks:** *Carl Cady*<sup>1</sup>; Cheng Liu<sup>1</sup>; Philip Rae<sup>1</sup>; Manuel Lovato<sup>1</sup>; <sup>1</sup>Los Alamos National Laboratory

Cracking is the most dominating mechanical failure mechanism in high explosives and cracks could affect both safety and performance of high explosive materials. However, one of the major challenge in studying fracture and failure of high explosives and their mock materials, is that physical cracks can exist that are not distinguishable by eye before they have grown large enough. A technique was developed to quantitatively describe macroscopic cracks, both their location and extent, in heterogeneous high explosive and mock material. By combining such a technique with the displacement field measurement using digital image correlation (DIC), we can describe, in detail, quantities that characterize material fracture process, like the crack-opening displacement and crack-opening angle. Results of this investigation will provide insights and validation data for the development of material failure models. In this presentation, properties like damage nucleation, crack initiation and extension, and crack-opening displacement will be quantitatively described.

9:50 AM

**Was There a Bomb on Mattei's Aircraft?:** *Donato Firrao*<sup>1</sup>; Graziano Ubertalli<sup>1</sup>; <sup>1</sup>Politecnico di Torino

Enrico Mattei, the President of the Italian oil conglomerate, was about to land in Milan Linate Airport, when his airplane crashed on the ground due to

Mon. AM

# Technical Program

a then unexplained accident. The investigation, reopened more than 30 years later, implied complete re-examining of the theories on macroscopic and lattice deformations under high velocity waves emanating from a small charge explosion. At the microstructural level multiple slip bands or mechanical twins, induced from the pressure wave caused by an explosion, can be observed, depending on the type of metal, the pressure and the strain rate. Different situations regarding stainless steels, aluminium, copper and gold alloys are analysed. Calculations and results of field explosion experiments are incorporated into the evaluation of microstructural signs possibly induced on metal targets by an unknown explosive event. Revisited theories were applied to this forensic case, reaching the conclusion that the aircraft had fallen following an ...

## 10:10 AM Break

### 10:20 AM

**The Response of Aluminium Alloys to Shock Loading:** *Jeremy Millett*<sup>1</sup>; Neil Bourne<sup>1</sup>; Ming Chu<sup>2</sup>; Ian Jones<sup>2</sup>; George Gray III<sup>3</sup>; Gareth Appleby-Thomas<sup>4</sup>; <sup>1</sup>AWE; <sup>2</sup>University of Birmingham; <sup>3</sup>Los Alamos National Laboratory; <sup>4</sup>Cranfield University

Like most materials, the response of aluminium alloys to shock loading is strongly influenced by a number of factors such as chemistry, microstructure and processing. In this work, we examine the response of the aluminium alloys, 6061 and 5083, in particular, the evolution of lateral stress and shear strength behind the shock front. In 6061, the alloy is investigated in the solution treated (T0) and fully aged conditions (T6). Stress rise times and equilibration behind the shock front are observed to be quicker in T0 than T6, and has been attributed to fine Mg<sub>2</sub>Si particles inhibiting dislocation generation and motion in T6. In 5083, strength has also been observed to be relatively stable behind the shock front. In this case, the alloy was received in the H32 state, with the material previously worked by ca. 20%. Full one-dimensional recovery experiments have also been performed, confirming the above observations.

### 10:40 AM

**Deformation Behavior of U-6wt%Nb Following Shock Loading:** *Adam Farrow*<sup>1</sup>; Heather Volz<sup>1</sup>; George Gray III<sup>1</sup>; Ellen Cerreta<sup>1</sup>; Donald Brown<sup>1</sup>; Carl Cady<sup>1</sup>; Mike Lopez<sup>1</sup>; Ann Kelly<sup>1</sup>; Pallas Papin<sup>1</sup>; <sup>1</sup>Los Alamos National Laboratory

Uranium-6wt%Niobium samples in two different temper conditions were shocked with a high-explosive plane-wave lens and tested in compression. The suppression of the Shape-Memory effect typical of artificially aged Uranium-Niobium alloys appears to have been removed following shock loading. Metallography, scanning electron and ion microscopy, X-ray diffraction, and neutron diffraction techniques were applied to characterize the deformation mechanisms. Texture evolution during compressive deformation evaluated via neutron diffraction in both temper conditions is discussed in comparison to the texture evolution normally observed in non-shocked Uranium-Niobium Shape-Memory Alloys, as is the role of retained high-pressure phases on the subsequent deformation behavior. Additionally, the shear-banding behavior is investigated via the "top-hat" forced-shear specimen geometry. Metallography is presented to reveal the twinning local to the shear-banding.

### 11:00 AM

**Mechanical and Computational Investigation of Ni-Al Laminates of Laser-Shock Compression and Spalling:** *Chung-Ting Wei*<sup>1</sup>; Vitali Efreml<sup>1</sup>; David Benson<sup>1</sup>; Brian Maddox<sup>1</sup>; Timothy Weihs<sup>1</sup>; Adam Stover<sup>1</sup>; Marc Meyers<sup>1</sup>; <sup>1</sup>University of California, San Diego

Ni-Al laminates with two different bilayer thicknesses, 5 and 30 μm, were subjected to high intensity laser-shock. The initial pressures of the laser-shock vary from 25 to 333 GPa. The cross-sections of recovered samples, analyzed by SEM and the 2-dimensional simulation RAVEN, show the consistencies between the SEM observations and the computational simulations. The morphologies of fragments, which were expelled by laser-shock wave compression and reflection from the spall surface, reveal that fragments from thinner bilayer sample have non-layered morphology, which is distinct from the fragments of thicker bilayer samples. The as-prepared Ni-Al laminates were subjected to quasi-static extension test and Vickers hardness test. The fracture toughness of thinner and thicker bilayer samples are 75 and 130 MPa, respectively. The measurements of the Vickers hardness are 1.51 and 1.92 GPa as well as the yield strength are 502 and 641 MPa for 5 and 30 μm bilayer samples, respectively.

### 11:20 AM

**Improvement of Charpy Impact Properties in Heat Affected Zones of API X80 Linepipe Steels Containing Complex Oxides:** *Hyo Kyung Sung*<sup>1</sup>; Sang Yong Shin<sup>1</sup>; Woo-Yeol Cha<sup>2</sup>; Kyungshik Oh<sup>2</sup>; Sunghak Lee<sup>1</sup>; <sup>1</sup>POSTECH; <sup>2</sup>POSCO

This study is concerned with the improvement of Charpy impact properties in heat affected zones (HAZs) of API X80 linepipe steels containing complex oxides. The steels were fabricated by adding Mg and O<sub>2</sub> to form complex oxides, and their microstructures and Charpy impact properties were investigated. The number of complex oxides increased as the excess amount of Mg and O<sub>2</sub> was included in the steels. After the HAZ simulation test, the steel having many oxides contained a considerable amount of acicular ferrite, together with bainitic ferrite and granular bainite. The volume fraction of acicular ferrite increased as the amount of complex oxides increased and the heat input decreased, and thus Charpy impact properties of the oxide-containing steel HAZs were greatly improved. These findings suggested that the active nucleation of acicular ferrite in the oxide-containing steel HAZs was associated with the great improvement of Charpy impact properties of the HAZs.

### 11:40 AM

**Microstructural Analysis of Separations Occurring during Charpy Impact Test of Linepipe Steels:** *Seokmin Hong*<sup>1</sup>; Sang Yong Shin<sup>1</sup>; Jin-ho Bae<sup>2</sup>; Kisoo Kim<sup>2</sup>; Sunghak Lee<sup>1</sup>; Nack J. KIM<sup>3</sup>; <sup>1</sup>POSTECH; <sup>2</sup>POSCO; <sup>3</sup>POSTECH GIFT

The microstructural investigation was conducted on separations occurring during Charpy impact tests of linepipe steels. Particular emphasis was placed on roles of microstructural phases such as acicular ferrite, bainite, and hard secondary phases. The microstructural analysis of fractured impact specimens revealed that the band structure of bainite elongated along the rolling direction worked as prior initiation sites for separations, and that the number and length of separations increased with increasing bainite. Tearing-shaped separations were found in the steels having high work hardenability because the hammer-impacted region was seriously hardened during the impact test, which led to the reduction in the impact toughness. According to the analysis on the effect of separations on Charpy toughness, the energy transition temperature increased as the length of separations increased. This was because brittle fracture occurring at low temperatures reduced the ratio of ductile fracture, while the increased separations further decreased ratio of ductile fracture.

## Global Innovations in Manufacturing of Aerospace Materials: The 11th MPMD Global Innovations Symposium: Perspectives from Government and Industry

*Sponsored by:* The Minerals, Metals and Materials Society, TMS Materials Processing and Manufacturing Division, TMS Structural Materials Division, TMS: Shaping and Forming Committee, TMS: High Temperature Alloys Committee

*Program Organizers:* Deborah Whitis, General Electric Company; Thomas Bieler, Michigan State University; Michael Miles, BYU

Monday AM

Room: 306

February 15, 2010

Location: Washington State Convention Center

*Session Chairs:* Deb Whitis, GE Aviation; Rollie Dutton, AFRL-RX

### 8:30 AM Invited

**Future Materials and Process Needs for Commercial Jet Transports: The 21st Century Challenge:** *Alan Miller*<sup>1</sup>; <sup>1</sup>Boeing

Despite the recent economic turnaround and its effects on the commercial aviation industry, the long term prognosis for future aircraft demand is still robust with demand for approximately 29,000 new airplanes through 2028. Recent twin aisle airplanes have dramatically increased the amount of carbon fiber reinforced materials used in the airframe which changes the proportions of different materials used in the airplanes. Looking to future airplane design opportunities, we can visualize multiple development paths which drive varying combinations of materials for future airplanes. One scenario would address more polymer composite applications while other scenarios could envision significant alloy improvements which drive more metallic airplane structures. Looking beyond structures we can also see the demand for novel



materials for systems and propulsion applications. The fusion of design properties into integrated material systems (e.g., structural, electrical, acoustic, thermal conductivity, thermal stability, etc.) offers unique design solutions to be developed and matured. The international market economics will continue to drive more performance for less cost so that integrated manufacturing processes, production systems, and fleet support technologies will need to be designed commensurate with design enhancements. Overarching all of this development work are progressive environmental requirements that will drive substantial reductions in emissions, hazardous materials, waste streams, and overall environmental effects. There has never been a time when the combined technical challenges have been higher for performance, cost, and environmental factors – these challenges will take all of us working together across industry, government and academia to find solutions that work.

### 9:00 AM Invited

**Realizing Advances in Aerospace Materials: ONR Perspective:** *Julie Christodoulou*<sup>1</sup>; <sup>1</sup>Office of Naval Research

The Office of Naval Research supports basic and applied research in advanced materials and processing for numerous applications that support the needs of naval aviation and sea-launched defensive and strike systems. Our role is to ensure that essential and unique requirements imposed by operations in the marine environment can be met, reliably and affordably. Examples of current programs include, environmental/thermal barrier coating systems and environmentally resistant monolithic materials for turbine engines; novel approaches to materials systems for hypersonic vehicles that must operate at high Mach number near sea level; environmentally insensitive high strength steels for landing gear; and concepts for integrating thermal management capability into load bearing structures. Transitioning these advancing into competitive systems and platforms is never trivial. However, recent efforts to capture understanding into tools for design and life prediction provide a forum for the transfer of knowledge that has proven to be agile and efficient.

### 9:30 AM Invited

**Modeling in Aerospace Materials and Manufacturing in AFRL:** *Mary Kinsella*<sup>1</sup>; Howard W. Sizel<sup>1</sup>; <sup>1</sup>United States Air Force, Air Force Research Laboratory

The development of computational tools to model materials processing and manufacturing has been long supported by the Air Force Research Laboratory and its predecessor. This rich tradition continues today with the Materials and Manufacturing Directorate's support of projects to develop computational tools to advance the state of modeling to support the Department of Defense's needs. This presentation will provide a brief background on past developments supported by the Air Force as well as ongoing efforts in computational materials and manufacturing science. The manufacturing and process modeling needs of the Air force as they modeling of manufacturing processes and needs of the Air Force will also be discussed.

### 10:00 AM Break

### 10:20 AM Invited

**Innovations in Aerospace Materials and Manufacturing Process Development:** *Robert Schafrik*<sup>1</sup>; <sup>1</sup>GE Aviation

High temperature structural materials, such as nickel-based superalloys and titanium alloys, have contributed immensely to societal benefit. These materials provide the backbone for many applications in the aerospace industry. Many challenges, technical and otherwise, were overcome to achieve successful applications. This presentation will highlight some of the key developments in nickel and titanium alloy technology, from the perspective of aeronautical applications. In the past, it was not unusual for development programs to stretch out 10 to 20 years as the materials and processing technology was developed, followed by the development of engineering practice, and lengthy production scale-up. Today, new classes of materials, such as intermetallics and ceramics are challenging traditional superalloys and titanium alloys for key applications. A new development paradigm is described that emphasizes creativity, development speed, and customer value that will enable continued innovations in concurrent material and manufacturing process development.

### 10:50 AM Invited

**Global Innovations in Manufacturing Aerospace Materials: A Rolls-Royce Perspective:** *Malcolm Thomas*<sup>1</sup>; <sup>1</sup>Rolls-Royce

The aerospace industry has provided a number of materials challenges and opportunities relative to the unique temperature, strength, weight and safety requirements that apply to aero applications. Global design and materials communities have responded to these challenges with many innovations to enable continued enhancement of capabilities. Unprecedented improvements in fuel in fuel efficiency coupled with efforts to reduce the environmental impact of aero engines are being achieved. To support the theme of this symposium, this presentation will review a number of materials technology innovations and initiatives that have occurred globally, and their impact on future technology directions. As an example, global aerospace collaboration efforts have become commonplace with new materials technologies and manufacturing efforts supported by organizations throughout the world. Additionally, universities and government research laboratories are also linking with industry to jointly work on opportunities that emerging composite, hybrid and smart materials can offer the aerospace industry, and the challenges that increased performance and environmental issues present.

### 11:20 AM Invited

**The DARPA/DSO Perspective on Materials Science:** *Leontios Christodoulou*<sup>1</sup>; <sup>1</sup>Defense Advanced Research Agency

DARPA's Defense Sciences Office (DSO) pursues and exploits fundamental science and innovation for national security. Materials programs range from developing physics- and chemistry-based models that allow for the design of novel material systems and possessing for radically improved or new properties, to innovative technologies that dramatically reduce the cost of producing titanium metal and its alloys. Mathematical and characterization tools are being generated to enable rapid design and development of new armor systems. Biologically inspired approaches to material synthesis and design are pervasive in many of the DARPA DSO initiatives. Future investments will continue to explore the frontiers of material science, which include new science-based tools for the development of new materials, novel materials for energy and water harvesting, new mechanical designs that exploit or challenge new materials and material systems, and innovative electromagnetic materials that will revolutionize the field of electronics. This aggressive vision to pursue the development of radically new materials and material systems is producing the critical technologies that will allow for the next generation of high-performance military platforms.

---

### Heterogeneous Nucleation and Initial Microstructure Evolution in Alloys and Colloids: Simulation I

*Sponsored by:* The Minerals, Metals and Materials Society, TMS Electronic, Magnetic, and Photonic Materials Division, TMS Materials Processing and Manufacturing Division, TMS Structural Materials Division, TMS: Alloy Phases Committee, TMS/ASM: Phase Transformations Committee

*Program Organizers:* Rainer Schmid-Fetzer, Clausthal University of Technology; Heike Emmerich, RWTH Aachen University; Frans Spaepen, Harvard University; Martin Glicksman, University of Florida; John Perepezko, University of Wisconsin, Madison

Monday AM                      Room: 614  
February 15, 2010              Location: Washington State Convention Center

*Session Chairs:* Yunzhi Wang, Ohio State University; Frans Spaepen, Harvard School of Engineering and Applied Sciences

---

### 8:30 AM Invited

**Molecular Dynamics Simulation of Two-Dimensional Nucleation in the Context of Crystal Growth:** *Dorel Buta*<sup>1</sup>; *Mark Asta*<sup>1</sup>; *Jeff Hoyt*<sup>2</sup>; <sup>1</sup>University of California, Davis; <sup>2</sup>McMaster University

We present results of molecular dynamics (MD) simulations of crystal growth from the melt, mediated by two-dimensional terrace nucleation at a faceted crystal-melt interface. The work focuses on the well-characterized Stillinger-Weber model of Si, where the (111) oriented crystal-melt interface is faceted. An analysis of equilibrium crystalline fluctuations is used to extract step free energies. The steps are diffuse in nature and have a free energy considerably

# Technical Program

smaller in magnitude than that measured at crystal-vacuum interfaces in the same system. We will also present results of non-equilibrium MD growth simulations as a function of system size. The results are consistent with a two-dimensional nucleation and growth mechanism for undercoolings up to approximately 30 K. An analysis of the kinetics at 20 K undercooling is used to extract the lag time and steady-state island nucleation rates. The results will be compared to available classical theories of two-dimensional terrace nucleation kinetics.

## 8:55 AM

**Molecular Dynamics Simulation of Nucleation Process:** *Ramanarayan Hariharaputran*<sup>1</sup>; David Wu<sup>1</sup>; <sup>1</sup>Institute of High Performance Computing, Singapore

Phase transformation is exploited in designing and processing materials for various applications. In most phase transformations, nucleation process plays a significant role in controlling the final microstructure. In the study of nucleation, insights from experimental results are limited due to finite resolution of the observation tools, while theories such as classical nucleation theory (CNT) are handicapped by its assumptions. In this talk, we present our studies of nucleation using molecular dynamics (MD) simulation. Due to length and time scale limitations in equilibrium MD, traditionally the nucleation process is studied at very high driving forces which induces artifacts into the simulation. We propose non-equilibrium corrections to the MD methodology in order to cure these artifacts arising from high driving forces. In this talk, we present our results from simulation of nucleation in unary systems using this modified MD. These results are also compared with the predictions of CNT.

## 9:15 AM

**Prefreezing and Heterogeneous Nucleation at the Cu/Pb Solid-Liquid Interface: A Molecular-Dynamics Simulation Study:** *Jesus-Pablo Palafox-Hernandez*<sup>1</sup>; Mark Asta<sup>2</sup>; Brian Laird<sup>1</sup>; <sup>1</sup>University of Kansas; <sup>2</sup>University of California at Davis

We report results of molecular-dynamics simulations of the Cu/Pb solid-liquid interface. We employ Embedded Atom Method (EAM) potentials to study this interface at temperatures between the melting points of Pb (618K for this model) and Cu (1279K). The two interfacial orientations studied (Cu [111] and [100]) are characterized through the calculation of the density, energy, orientational order, stress and diffusion constant as functions of distance normal to the interface. Our results at 625K (slightly above the melting temperature of Pb) for the Cu [111] interface show the complete "wetting" of the Cu/Pb interface by a layer of (metastable) crystalline Pb, leading to rapid heterogeneous nucleation of crystalline Pb when this system is quenched below the Pb melting temperature. For the Cu [100] orientation at the same temperature, no such wetting layer is observed, and heterogeneous nucleation at this interface is not observed when undercooled.

## 9:35 AM

**Computer Simulation of Solid-Liquid Interfaces in Metals:** *Roberto E. Rozas*<sup>1</sup>; Juergen Horbach<sup>1</sup>; <sup>1</sup>German Aerospace Center

Key parameters for the description of nucleation phenomena are solid-liquid interfacial free energies. Using molecular dynamics (MD) computer simulation, interfacial properties of crystal-liquid interfaces are investigated for Ni and Ti. Potentials of the embedded atom type are employed. We show that these models lead to a realistic description in terms of melt properties and the crystallization process. Inhomogeneous systems are simulated where the crystal phase in the middle of an elongated simulation box is surrounded by the liquid phase and separated by two interfaces (due to periodic boundary conditions in all Cartesian directions). The melting temperature and crystal growth coefficients are determined. At coexistence, we demonstrate how one can accurately obtain interfacial free energies from a detailed analysis in the framework of capillary wave theory, using both the broadening of the solid-liquid interface with increasing lateral system size and the capillary wave spectrum as input.

## 9:55 AM

**Dissolutive and Reactive Wetting:** *James Warren*<sup>1</sup>; Daniel Wheeler<sup>1</sup>; William Boettinger<sup>1</sup>; <sup>1</sup>NIST

The analysis a solid nuclei wetting and/or reacting with an impurity in a melt provides the basis for classical models of nucleation. Conversely, models of a liquid melt dissolving into/reacting with a solid substrate provide insight into phenomena as diverse as VLS growth and soldering. In this talk I will explore current efforts to model dissolutive and reactive wetting using phase field models of wetting and spreading and explore some of the new metrics

that might provide better predictive power in understanding these systems. Particular attention will be paid to the computational and theoretical challenges in achieving realistic experimental simulations, as well as the outstanding issues towards complete models of a liquid-solid system.

## 10:15 AM Break

## 10:35 AM Invited

**Entropy in Crystal Nucleation of Hard Spheres:** *Eli Sloutskin*<sup>1</sup>; Peter Lu<sup>1</sup>; David Weitz<sup>1</sup>; <sup>1</sup>Harvard University

Crystal nucleation is among the most important and fundamental processes in materials science. Yet this process is poorly understood, even in a system as simple as hard spheres. We characterize crystal nucleation in a model system of colloidal hard spheres, using confocal microscopy to individually resolve each sphere. The hard-sphere crystal nuclei are neither compact solids nor tenuous fractals, but instead adopt a wide range of morphologies. We account for these morphologies with a simple empirical model that describes our experimental size distributions of the nuclei and exactly reproduces our measured nucleation rates. We use the same model to account for size distribution of nuclei in copper and find quantitative agreement with computer simulations; this indicates that our approach may be applicable to other systems.

## 11:00 AM

**Analysis of Cluster Statistics in Homogeneous and Heterogeneous Nucleation:** *David Wu*<sup>1</sup>; Ramanarayan Hariharaputran<sup>1</sup>; <sup>1</sup>Institute of High Performance Computing

In nucleation studies of conventional materials, precritical clusters of the stable phase are normally too small to observe directly; thus the nucleation rate is inferred from counting large clusters that are formed via a subsequent growth stage. In colloid systems and in computer models, however, very small clusters are routinely observed in situ. We survey existing methods for interpreting the statistics of small clusters and conclude that they are either inaccurate or are impractical due to the amount of data required. We propose a new method to analyze cluster statistics and show that parameters such as the critical size and the Zeldovich factor can be obtained. These parameters can give insight to the nucleation process that is not obtainable from measured nucleation rates alone.

## 11:20 AM

**Phase Behavior and Microstructure of Binary Colloidal Mixtures:** *Nina Lorenz*<sup>1</sup>; Hans-Joachim Schöpe<sup>1</sup>; Holger Reiber<sup>1</sup>; Thomas Palberg<sup>1</sup>; Patrick Wette<sup>2</sup>; Ina Klassen<sup>2</sup>; Dirk Holland-Moritz<sup>2</sup>; Dieter Herlach<sup>2</sup>; Tsuneo Okubo<sup>3</sup>; <sup>1</sup>University of Mainz; <sup>2</sup>German Aerospace Center; <sup>3</sup>Institute for Colloidal Organization

We report a systematic study of the phase behavior of charged colloidal binary mixtures of different size and charge ratio. We find that with decreasing size ratio  $\Gamma = a_s/a_L$  (where  $a$  refers to the particle radius and  $S$  and  $L$  refer to the small and large particles, respectively) the miscibility decreases substantially. Accordingly, phase diagrams of spindle-, lower acetropo- and eutectic-type are observed as well as fluid-fluid phase separation for low  $\Gamma$ . The influence of the charge ratio  $\Lambda = Z_s/Z_L$  shows no systematic behavior. The observed trends bear great resemblance to the behavior of binary metal systems and colloidal hard sphere systems. As compared to the latter, the phase boundary is located at much lower freezing densities and compound formation is only rarely seen. For selected samples we discuss interesting morphologies observed after heterogeneous nucleation.

## 11:40 AM

**Wall-Induced Structures in Heterogeneous Nucleation:** *Fathollah Varnik*<sup>1</sup>; Markus Gross<sup>1</sup>; Suvendu Mandal<sup>1</sup>; <sup>1</sup>ICAMS, Ruhr University Bochum

Via event driven molecular dynamic simulations, we study the effect of atomic structure of the wall on heterogeneous nucleation. A particular focus is the effect of mismatch between the crystalline structure emerging from the undercooled melt and the wall structure. We observe a complex time evolution through structures with a relatively long but finite life time as intermediate steps towards the final crystalline order.



### Hume-Rothery Symposium: Configurational Thermodynamics of Materials: Session I

*Sponsored by:* The Minerals, Metals and Materials Society, TMS Electronic, Magnetic, and Photonic Materials Division, TMS Structural Materials Division, TMS: Alloy Phases Committee, TMS: Chemistry and Physics of Materials Committee

*Program Organizers:* Chris Wolverton, Northwestern University; Mark Asta, University of California, Davis; Gerbrand Ceder, Massachusetts Institute of Technology (MIT)

Monday AM Room: 212  
February 15, 2010 Location: Washington State Convention Center

*Session Chair:* To Be Announced

#### 8:30 AM Plenary

**William Hume-Rothery Award Winner: How Hume-Rothery's Work Led to Computational Thermodynamics:** *Didier De Fontaine*<sup>1</sup>; <sup>1</sup>University of California

As an undergraduate student of metallurgy in Belgium, I became acquainted with Hume-Rothery's textbooks, and I was particularly intrigued by the question: why could the Cu-Au phase diagram not be reproduced by the Bragg-Williams approximation? The answer came much later with the Cluster Variation Method of Ryo Kikuchi, which was able to handle the problem of frustration on the fcc lattice. Clusters of lattice points, rather than mere pairs, led Juan Sanchez to formulate a cluster expansion (CE) whose cluster functions formed a complete orthonormal set with which solid solutions could be analyzed rigorously. The resulting cluster algebra could then be used in conjunction with first-principles LDA electronic structure calculations to provide a veritable "computational thermodynamics of alloys", a very active field today, as will be apparent from the many applications of it to be presented at this symposium.

#### 9:15 AM Invited

**Deconstructing the Cluster Expansion:** *Juan Sanchez*<sup>1</sup>; Alejandro Diaz-Ortiz<sup>2</sup>; <sup>1</sup>University of Texas at Austin; <sup>2</sup>Max Planck Institute for Metals Research

The cluster expansion (CE), initially introduced in the late seventies to describe the configuration of finite clusters will be reviewed. In particular, the presentation will focus on distinguishing between the ability of the CE to accurately parametrize a set of configurationally dependent quantities, e.g. the energy of a binary alloy, and the physical meaning, or lack thereof, of the fitting parameters, e.g. the effective cluster interactions (ECI). Several examples will be presented, such as expansions giving concentration-dependent ECIs and the application of the method to the electronic density of states of binary alloys. Finally, the structure of the CE that emerges from density functional theory will be explored and discussed in the context of numerous efforts over the last 20 years to map the energy of alloys into a relatively small set of ECIs.

#### 9:45 AM Invited

**The Existence of a Multi-Phase Critical Point in Metastable fcc Ordering Phase Diagrams and Its Influence on Phase Diagram Features, Interfacial Energies and Alloy Properties:** *John Cahn*<sup>1</sup>; <sup>1</sup>University of Washington

Analysis of the puzzling four-phase critical point computed for the fcc (CuAu) ordering phase diagram by the Bragg-Williams approximation suggests that it should persist in an altered form as a metastable feature of real phase diagrams at the composition along the ordering spinodal where the cubic term in the free energy expansion changes sign. Properties that are still affected when the point is metastable are heats of ordering, some curves on the phase diagrams, and some interfacial energies. These in turn should affect the concentration dependences of gamma prime nucleation, coarsening rates, and mechanical properties.

#### 10:15 AM Break

#### 10:45 AM Invited

**What's New in Cluster Expansion?:** *Gus Hart*<sup>1</sup>; Rodney Forcade<sup>1</sup>; Tobias Kerscher<sup>2</sup>; Richard Taylor<sup>1</sup>; Lance Nelson<sup>1</sup>; Alejandro Diaz-Ortiz<sup>3</sup>; <sup>1</sup>Brigham Young University; <sup>2</sup>University of Erlangen; <sup>3</sup>Max-Planck Institute for Metals

The cluster expansion has evolved significantly in the last several decades and has become an extraordinarily accurate method. What started out as conceptually simple, qualitative approach has become a complex method where practitioners

achieve accuracies approaching that of first-principles methods. Despite the maturity of the method, there are still some fundamental questions that remain elusive. In this talk I will discuss some of the unanswered questions and some recent developments: representation of derivative structures, fitting approaches, parallelization of CE-based MonteCarlo simulations, understanding the effects of noisy data, etc.

#### 11:15 AM Invited

**Cluster Expansions from Bond-Order Potentials:** *Ralf Drautz*<sup>1</sup>; David Pettifor<sup>2</sup>; <sup>1</sup>Ruhr-Universität Bochum; <sup>2</sup>University of Oxford

Cluster expansion coefficients are calculated routinely by interpolating density functional total energy data. The cluster expansions obtained in this way may be used to predict accurately thermodynamic and kinetic properties of the system at hand. For complex lattices or multi-component systems it may be useful to estimate the cluster expansion coefficients from coarse grained models of the electronic structure and to predict the systematics of the expansion coefficients as a function of crystal structure and alloy constituents. In our contribution to Didier de Fontaine's Hume-Rothery Symposium, we show how cluster expansion coefficients may be obtained for arbitrary lattices from the analytic Bond-Order Potentials by decomposing the local moments of the atomic density of states into occupation dependent clusters and occupation independent reference contributions.

#### 11:45 AM Invited

**Application of Continuous Displacement Cluster Variation Method to Phase Equilibria Calculations:** *Tetsuo Mohri*<sup>1</sup>; <sup>1</sup>Hokkaido University

Cluster Variation Method (CVM) has been recognized as one of the most reliable theoretical tools to incorporate wide range of atomic correlations. By combining CVM with electronic structure total energy calculations, first-principles phase equilibria calculations have been extensively attempted. One of the deficiencies of the conventional CVM, however, is the fact that the local lattice distortion is not efficiently introduced. Hence, various inconveniences such as the overestimation of an order-disorder transition temperature or an underestimation of a single phase field have resulted in the calculated phase diagram. In order to circumvent such inconveniences, Kikuchi and his coworkers developed Continuous Displacement Cluster Variation Method. It is demonstrated that the additional freedom introduced by the local atomic displacement further decreases the free energy of a system and a resultant phase diagram is significantly improved.

### Hydrometallurgy - General Session: Session I

*Sponsored by:* The Minerals, Metals and Materials Society, TMS Extraction and Processing Division, TMS: Aqueous Processing Committee

*Program Organizer:* Michael Free, University of Utah

Monday AM Room: 310  
February 15, 2010 Location: Washington State Convention Center

*Session Chair:* Michael Free, University of Utah

#### 8:30 AM

**Highly Selective Oxygen Evolution Anodes for Electrowinning of Metal:** *Masatsugu Morimitsu*<sup>1</sup>; Kana Uno<sup>1</sup>; Naoyuki Oshiumi<sup>1</sup>; <sup>1</sup>Doshisha University

This paper presents our recent development on the oxide coated titanium electrode, which is highly active for oxygen evolution and has an excellent selectivity to oxygen evolution against unwanted side reactions such as manganese or cobalt oxides deposition on the anode used in zinc or cobalt electrowinning. The electrode consists of a mixture of amorphous IrO<sub>2</sub> and Ta<sub>2</sub>O<sub>5</sub> on a titanium substrate by thermal decomposition method. The results demonstrate that the amorphous oxide coating is effective to reduce the electric power consumption of electrowinning process and can suppress the deactivation of the anode's surface during continuous operation.

#### 8:50 AM

**Characteristics of Cathodic Reduction of Oxygen on Gold Electrode:** *Yongbin Yang*<sup>1</sup>; Tao Jiang<sup>1</sup>; Qian Li<sup>1</sup>; Yu-feng Guo<sup>1</sup>; <sup>1</sup>CSU

Cathodic reduction of oxygen is a process involved in many fields. As is well known, the mechanism of oxygen reduction usually varies considerably

Mon. AM

# Technical Program

with electrode substrates. In this paper, cathodic reduction of oxygen on gold electrode was studied by linear sweep voltammetry with regards to cyanide leaching of gold. As the results showed, the electron transfer number increased as potential shifted negatively and decreased as pH value increased. Besides, the increment of electron transfer number as a function of potential decreased when pH value increased. When pH increased to 13.0, the volt-ampere curve exhibited an approximate plateau with currents approximate to the limiting current of an 2e process. By varying dissolved oxygen concentration, the electron transfer number was measured for pH 11.0 at different potentials, the results being 1.894e, 2.387e, 2.732V, 2.982V, and 3.227V at -0.30V, -0.35V, -0.40V, -0.45V, and 0.50V, respectively.

## 9:10 AM

**Dissolution of Precious Metal Alloys Containing Zinc in Acid Solution:** *Hideaki Sasaki*<sup>1</sup>; Takashi Nagai<sup>1</sup>; Masafumi Maeda<sup>1</sup>; <sup>1</sup>Institute of Industrial Science, The University of Tokyo

Dissolution of precious metals in aqueous solutions can be enhanced by alloying with other metals. Taking the advantage of the phenomena, a new recovery process for precious metals from scraps was proposed. The process incorporates an exposure of precious metals to the vapor of Zn prior to acid leaching. Precious metals form alloys with zinc and become easy to dissolve. In this study, dissolution of precious metal alloys containing zinc (Pt-Zn, Au-Zn, Rh-Zn) was examined quantitatively by electrochemical measurement. Anodic dissolution rates of precious metals and zinc from the alloys were measured separately by channel flow double electrode (CFDE). Potential dependencies and time variations of the dissolution were observed.

## 9:30 AM

**Extraction of Copper from Sulfate Leach Solution Containing Minor Metallic Constituents in Mixer Settler Unit:** *Vinay Kumar*<sup>1</sup>; Manis Kumar Jha<sup>1</sup>; Manoj Kumar<sup>1</sup>; Jinki Jeong<sup>2</sup>; Jae-chun Lee<sup>2</sup>; <sup>1</sup>National Metallurgical Laboratory; <sup>2</sup>Korea Institute of Geosciences and Mineral Resources (KIGAM)

The present investigation describes R & D studies carried out for recovery of copper from the sulfate solution expected from the leaching of e-wastes in presence of minor constituents such as cadmium, zinc and nickel using solvent extraction process. In order to extract copper in continuous mode in mixer settler unit (MSU), basic studies have been made to optimize the optimum condition using 5%LIX84 in kerosene. Subsequently, the solvent extraction of copper was made in MSU maintaining leach solution flow rate 4.0 L/h and A/O ratio 1. The results showed complete extraction (~97%) of copper in three stages at A/O ratio 1 from the aqueous solution containing 1.98g/L Cu at pH 1.91 in presence of impurities. Loaded metal was completely stripped after scrubbing with 10% sulfuric acid in two stages. The stripped solution could be used for metal/ salt recovery by electrolysis/ crystallization.

## 9:50 AM

**Gold and Silver Recovery by Electrocoagulation:** *Jose Parga*<sup>1</sup>; Jesus L. Valenzuela<sup>2</sup>; <sup>1</sup>Technology Institute of Saltillo; <sup>2</sup>University of Sonora

In Mining operations, cyanidation is the predominant method by which gold and silver are recovered from their ores and it is recognized that the Merrill-Crowe, Carbon in Pulp process are used to recovery gold and silver. Among several options available for recovery precious metals from cyanide solutions, Electrocoagulation (EC) is a very promising electrochemical treatment technique that does not require high concentrations of gold and silver in solutions. First, this study will provide an introduction to the fundamental concepts of the EC method for recovery precious metals from cyanide solutions. In this study, Powder X-ray Diffraction, Scanning Electron Microscopy and Transmission Mössbauer Spectroscopy were used to characterize the solid products formed at iron electrodes during the EC process. The results suggest that magnetite particles and amorphous iron oxyhydroxides present in the EC products remove gold and silver in 5 minutes with an efficiency of more than 99% from cyanide solutions.

## 10:10 AM Break

## 10:20 AM

**Pressure Leaching of Enargite-Pyrite Concentrates:** *Maria Ruiz*<sup>1</sup>; Maria Vera<sup>1</sup>; Rafael Padilla<sup>1</sup>; <sup>1</sup>University of Concepcion

Enargite rich copper concentrates cannot be treated by conventional smelting/converting technology and thus nonconventional methods such as leaching must be used. Since enargite (Cu<sub>3</sub>As<sub>4</sub>) is a hard to dissolve mineral

in acidic solutions, pyrite, a common impurity in copper concentrates, could be used to increase the enargite dissolution rate. On this matter, we present in this work experimental data on the pressure leaching of a mixed enargite-pyrite concentrate in H<sub>2</sub>SO<sub>4</sub>-O<sub>2</sub>. The results show that the dissolution of enargite from the mixed concentrate is considerably faster than the dissolution of pure enargite mineral. The leaching rate increases significantly with temperature. Over 95% of enargite was dissolved in leaching 64 micron size particles at 200 °C and 100 psi of partial pressure of oxygen in just 30 minutes. A change in the partial pressure of oxygen from 50 to 150 psi showed also a large influence in the leaching rate.

## 10:40 AM

**The Rate-Enhancing Role Provided to Oxygen by Nitrite (N(III)) in Acidic Aqueous Oxidation-Processes:** *Gerard Martins*<sup>1</sup>; O. Solak-Gok<sup>1</sup>; <sup>1</sup>Colorado School of Mines

During the past three decades since the discovery of the "catalytic" role of nitrite in these processes (e.g. leaching of refractory gold ores), the mechanism by which nitrogen species (N(IV) and N(II)) provide a cyclic pathway for the enhancement of oxidation by oxygen gas has been tackled, for the most part, from a qualitative or semi-quantitative, euphemistic, perspective. The work conducted recently in the Metallurgical and Materials Engineering Department at the Colorado School of Mines has now provided an insight (as best as we are able to determine) hitherto not published in the open literature. A Rate Model that incorporates the simultaneous homogeneous-reactions participating in the oxidation of ferrous to ferric in a sulfuric-acid electrolyte has been developed. The Model includes the prominent nitrogen species that are constituents in the system: HNO<sub>2</sub>, N<sub>2</sub>O<sub>3</sub>, NO, NO<sub>2</sub>NO<sub>2</sub>, NO<sup>-3</sup> and [Fe(NO)]<sup>2+</sup> and provides time trajectories of their concentrations during the conversion of Fe<sup>2+</sup> to Fe<sup>3+</sup>. Laboratory-scale experiments have also been performed to address "calibration" characteristics of the Model simulations relative to the data acquired from the experiments.

## 11:00 AM

**Halide Chlorine Leaching for Malachite and Chrysocolla Mineral Copper from Western Utah Copper Concentrate Company:** *Edgar Blanco*<sup>1</sup>; Mark Dotson<sup>1</sup>; <sup>1</sup>Western Utah Copper Company

The production of oxide copper flotation concentrates found a lack of sulfur content necessary to get exothermic reaction in smelter operations. A Malachite and Chrysocolla dissolution is achieved by sulfuric acid leachant (pH: 1.5) and the oxide and precious metals remained in the ore are attacked by halide reaction oxidants. The results show the dissolution of malachite and chrysocolla is greater than 93%. The behavior of precious metals dissolution during the process was investigated. The PLS generated were 22 g/L. The copper can be displaced from PLS by a lesser noble iron element. The main factor to achieve that extraction was a fast reaction by the halide oxidant in acidic media.

## International Symposium on High-Temperature Metallurgical Processing: Innovations in Ironmaking

*Sponsored by:* The Minerals, Metals and Materials Society, TMS Extraction and Processing Division, TMS: Pyrometallurgy Committee  
*Program Organizers:* Jaroslav Drellich, Michigan Technological University; Jiann-Yang Hwang, Michigan Technological University; Tao Jiang, Central South University; Jerome Downey, Montana Tech

Monday AM

Room: 619

February 15, 2010

Location: Washington State Convention Center

*Session Chair:* Jaroslav Drellich, Michigan Technological University

## 8:30 AM Introductory Comments

## 8:35 AM Keynote

**Development of a Novel Gas-Suspension Ironmaking Technology with Greatly Reduced Energy Consumption and CO<sub>2</sub> Emission:** *Hong Yong Sohn*<sup>1</sup>; Moo Eob Choi<sup>1</sup>; <sup>1</sup>University of Utah

A novel alternative ironmaking technology based on direct gaseous reduction of iron ore concentrate is under development. The process is based on the flash reduction of concentrate particles in hydrogen or syngas with drastically reduced CO<sub>2</sub> emission. The direct use of the concentrates, bypassing agglomeration



and cokemaking, greatly decreases the energy requirement for ironmaking, by about 40% of a typical blast furnace operation. The process is expected to be sufficiently intensive to give a production rate comparable to a modern blast furnace with a much smaller furnace volume. The kinetic feasibility tests in lab- and bench-scale reactors demonstrated sufficiently rapid flash reduction of the concentrates in pure hydrogen or syngas at 1200–1500°C within 2–10 seconds residence time. Process design and simulation has been performed using the METSIM software with several process flowsheets composed of a flash reactor, heat recovery system, water removal and recycle of hydrogen.

9:15 AM

**Thermal Equilibrium Calculation and Application of Microwave Heated Ignition (MHI) for Iron Ore Sintering:** *Yuanbo Zhang*<sup>1</sup>; Xiaoming Mao<sup>1</sup>; Zhucheng Huang<sup>1</sup>; Guanghui Li<sup>1</sup>; Tao Jiang<sup>1</sup>; <sup>1</sup>Central South University

As well-known, conventional sintering ignition has many disadvantages, such as low energy utilization rate, much waste gas, etc. To develop a clean and efficient sintering ignition technology is significant to the Iron & Steel industry. Central South University and Bao-steel have put forward a novel process of microwave heated ignition (MHI) for iron ore sintering. In this investigation, the thermal equilibrium of MHI is firstly calculated. Providing that ignition time is 90s, the ignition temperature required is no less than 639°C, and the lowest heat quality for ignition is 25625 kJ/m<sup>2</sup>. The pilot-scale sintering experiments using MHI have been done in a 1260mm×320mm×300mm sintering pot, and the optimal conditions are obtained. Compared with the former findings, the energy consumption of MHI is only 25.65 MJ/m<sup>2</sup>, far less than that of coal gas ignition (CGI) of 185.13MJ/m<sup>2</sup>.

9:35 AM

**Coal-Based Direct Reduction of Iron Concentrate Pellets by Microwave Heating:** Wang Xia<sup>1</sup>; *Huang Zhucheng*<sup>1</sup>; <sup>1</sup>Central South University

In this paper, direct reduction of iron concentrate pellets in continuous shaft furnace by microwave heating is studied. Fe<sub>2</sub>O<sub>3</sub> and fixed carbon in coke has a strong capacity to absorb microwave, the material can quickly reach the required temperature. However, gangue minerals remain lower temperature because of their weak microwave absorbing capacity, so that selective heating of pellets can be realized. In this investigation, the oxidized pellet with TFe of 64.24% is studied. The results show that under the condition of carbon to iron ratio of 0.32 heated by microwave, the temperature of materials can rapidly rise up with the increasing of microwave output power. The metallization rate of pellets is up to 90% when direct reduction time more than 50 minutes and reduction temperature higher than 950°.

9:55 AM

**Effects of Composite Binder (CB) on Oxidation Behavior of Iron Ore Pellets:** *Tao Jiang*<sup>1</sup>; Youming Hu<sup>1</sup>; Yanfang Huang<sup>1</sup>; Guanghui Li<sup>1</sup>; Guihong Han<sup>1</sup>; Yuanbo Zhang<sup>1</sup>; <sup>1</sup>School of Minerals Processing and Bioengineering, Central South University

Organic binders are found superior to bentonite in improvement of iron grade of pellet. As an organic binder, Funa, has been developed and used in the reduced pellets production in China. In this work, a comparative investigation on the oxidation behaviors of various binder pellets is carried out in order that Funa is applied in production of oxidative pellets. Results show FeO content of bentonite pellets decreases obviously with the increase of roasting temperature from 550° to 1050°, but increases slightly from 1050° to 1250° due to formation of double-layer structure. Meanwhile, the minimal FeO content of Funa pellets appears at 950°, and then the FeO content increases sharply from 950° to 1250°. Polarizing microscope and XRD analysis indicate that reduction reaction occurs inside of Funa pellets, leading to the rise of FeO content of pellets.

10:15 AM

**Study on Direct Reduction-Separation of Limonite by Microwave Heating:** *Zhu-cheng Huang*<sup>1</sup>; Lili Lv<sup>1</sup>; <sup>1</sup>Central South University

As well-known, there are a large number of limonite ores all over the world and they are still not completely utilized. It can be separated by physical separation and magnetic roasting technology but the effect is not ideal, iron concentrate grade can't meet the production requirements. In this paper the direct reduction-separation of carbon-containing limonite pellets by microwave heating is studied. The results show that the metallization rate of reduced pellets is up to 91.03% when under the condition of microwave output power at 1.0kw, roasting temperature reaches to 1150° from room temperature in 90 minutes. The concentrate of iron content 75.95% and iron recovery 91.45% can be

obtained under the condition of grinding time 20min, magnetic field intensity 0.15T. The new process possesses a promising prospect.

10:35 AM Break

10:50 AM

**Preparation of Metallized Pellets and Recovery of Tin and Zinc from Tin, Zinc-Bearing Complex Iron Concentrates:** Dan Huang<sup>1</sup>; Yuanbo Zhang<sup>1</sup>; Guihong Han<sup>1</sup>; Guanghui Li<sup>1</sup>; *Tao Jiang*<sup>1</sup>; <sup>1</sup>School of Minerals Processing and Bioengineering, Central South University

The tin, zinc-containing iron ores are typical complex and intractable ones, and great reserves of them are found in China. At present, they have not been efficiently utilized. Based on the thermodynamic analysis of iron, tin and zinc oxides reduction by CO, technological conditions of metallized pellets preparation from the complex iron concentrates (containing 0.30% Sn, 0.21% Zn and 65.42% Fe) by one-step direct reduction process are studied and a new comprehensive utilization process is developed in this investigation. Volatilization of 90% tin and 95% zinc are obtained under the optimum conditions, and metallization of iron is above 94%. The compression strength of roasted pellet is more than 1800 N/P. The residual tin and zinc in the finished pellets is below 0.03%. The metallized pellets can be used as steelmaking burdens.

11:10 AM

**Researches on Magnetic Roasting-Separation of Coal-Containing Limonite Pellets by Microwave Heating:** Hu Bing<sup>1</sup>; *Huang Zhucheng*<sup>1</sup>; <sup>1</sup>Central South University

Limonite ores is difficult to obtain ideal indexes by traditional physical processes. In this investigation, the limonite with TFe of 48.92% is studied. The experimental results show the conventional heating takes a long reduction time, easily leads to cold center and over reduction, and even forms fayalite. Magnetic roasting-separation of limonite by microwave heating under the conditions of output power 1.0kw at 35min achieves the concentrate of iron content 61.15% and recovery of 88.35% while the concentrate of iron content 60.55% and recovery of 74.06% is obtained under the optimal conditions for 60min at 800° following conventional heating. The whole pellet is heated simultaneously, which gives priority to heat coal particles and iron minerals, and accelerate the transformation of limonite into magnetite. Meanwhile, gangue minerals remain lower temperature due to their weak microwave absorbing capacity, and thus it greatly restrains the formation of fayalite.

11:30 AM

**Mathematical Modeling for Side-Blow Combustion Region in Iron Bath Reactor with H<sub>2</sub>-C Mixture Reduction:** *Zhang Bo*<sup>1</sup>; Hong Xin<sup>1</sup>; <sup>1</sup>Shanghai University

The basic idea of H<sub>2</sub>-C mixture reduction reflexes using hydrogen as main reductor and carbon as main heat generator in iron bath smelt reduction reactors on purpose to cut down total energy consumption and CO<sub>2</sub> emission. The author applied the methods of modeling for separating regions and complex integration to research the kinetics behavior of this new metallurgical reactor. Important one among separating regions was side-blow region where the changes of temperature and substance concentration field in multiple-phase mixture of solid, liquid and gas were coupled integrating models including shrinking core of granulated carbon, carbon-oxygen combustion and heat absorption of slag drops etc. Besides inlet flux of injecting oxygen and carbon, the boundary and initial conditions included substance and energy exchanges in boundaries between the region and other reaction regions. After dispersion treatment with Control-Volume-Method, the model was programmed as software for digital simulation of combustion procedure in side-blow region.

11:50 AM

**Al-Fe Separation from High Aluminium Content Limonite Ores by Salt-Added Reduction Roasting Process:** *Tao Jiang*<sup>1</sup>; Mudan Liu<sup>1</sup>; Na Sun<sup>1</sup>; Guanghui Li<sup>1</sup>; <sup>1</sup>School of Minerals Processing and Bioengineering, Central South University

Large reserves of high aluminium content limonite ores are widely found all over the world. Traditional processes are found invalid to remove aluminium from the ores due to the close combination of aluminium with iron minerals. Sodium salt-added reduction roasting followed by magnetic separation is developed in this study. A metallic iron concentrate with the total iron grade of 91.00% and aluminium content of 1.36% is achieved in laboratory for a sample

# Technical Program

of 48.92% iron and 8.16% Al<sub>2</sub>O<sub>3</sub>, and the recovery of iron is greater than 90%. SEM and XRD investigations on microstructures of reduced pellets indicate that, aluminium and iron minerals combine closely without additives, and added sodium salts destroy the complex substitution relationship between iron and aluminium and accelerate the growth of metallic iron granules remarkably.

## 12:10 PM

**A Study on Beneficiation of Low Grade High-Phosphorus Iron Ore:** Zhu Deqing<sup>1</sup>; Chun Tiejun<sup>1</sup>; Pan Jian<sup>1</sup>; Wei Xuemei<sup>1</sup>; <sup>1</sup>Central South University

The reduction roasting-magnetic separation-acid leaching of low grade high-phosphorus iron ores was studied. The process parameters of acid leaching were optimized with rougher iron ore concentrate which was obtained by reduction roasting-magnetic separation of ROM ores. Effects of various factors on upgrading iron and dephosphorization were discussed in acid leaching. The result showed that the iron ore concentrate, assaying 62.35% iron and 0.20% phosphorus content were achieved at the overall iron recovery rate of 90.54% and dephosphorization rate of 87.42% under the conditions of leaching for 2 hours, at 2.5 liquid-to-solid ratio, 50kg/t sulphuric acid and 500 r/min agitating speed after the ROM ore with 47.28% iron and 1.59% phosphorus content was pretreated by reduction roasting-magnetic separation. It is important to decrease the feedstock of acid leaching by the preconcentration technology of reduction roasting-magnetic separation for saving investment and reducing operation cost.

## Jim Evans Honorary Symposium: Flow Phenomena in Steel Continuous Casting

*Sponsored by:* The Minerals, Metals and Materials Society, TMS Extraction and Processing Division, TMS Light Metals Division  
*Program Organizers:* Ben Li, University of Michigan; Brian G. Thomas, University of Illinois at Urbana-Champaign; Lifeng Zhang, Missouri University of Science and Technology; Fiona Doyle, University of California, Berkeley; Andrew Campbell, WorleyParsons

Monday AM                      Room: 620  
February 15, 2010              Location: Washington State Convention Center

*Session Chair:* Brian Thomas, University of Illinois at Urbana-Champaign

## 8:30 AM

**Jim Evans: A Reflection on his Impact:** *Fiona Doyle*<sup>1</sup>; <sup>1</sup>University of California, Berkeley

The Jim Evans Honorary Symposium was organized to pay tribute to a true giant in the field of extractive and process metallurgy. This opening talk briefly discusses how Jim's approach to technical problems has paved the way for new developments in the production of materials, and inspired fruitful work in a much broader arena. But Jim's impact goes far beyond his technical influence; many of Jim's colleagues, collaborators and students (former and present) are here because of the friendship and mentorship that Jim has warmly offered over the years. As discussed here, Jim's love of life and inimitable sense of humor are inextricably interwoven with his lasting technical legacy.

## 8:55 AM

**Liquid Metal Modelling of Continuous Steel Casting:** *Gunter Gerbeth*<sup>1</sup>; Sven Eckert<sup>1</sup>; Klaus Timmel<sup>1</sup>; Xincheng Miao<sup>1</sup>; <sup>1</sup>Forschungszentrum Dresden-Rossendorf

Model experiments with low melting point liquid metals are an important tool to investigate the flow structure and related transport processes in melt flows relevant for metallurgical applications. We present the new experimental facility CONCAST for modelling the continuous casting process of steel using the alloy SnBi at temperatures of 200-400C. The possibilities for flow investigations in tundish, submerged entry nozzle and mould will be discussed. In addition, experimental results will be presented on the impact of a steady magnetic field on the outlet flow from the nozzle, obtained at a smaller-scale set-up working with the room-temperature alloy GaInSn. Local velocities in both facilities are measured by Ultrasound Doppler Velocimetry and contactless inductive flow tomography. The latter is attractive also for real-scale steel casting.

## 9:20 AM

**Experimental and Numerical Simulation of the Mold Region of a Steel Continuous Caster:** *Koullis Pericleous*<sup>1</sup>; Zacharias Kountouriotis<sup>1</sup>; Georgi Djambazov<sup>1</sup>; Francois Domgin<sup>2</sup>; Pascal Gardin<sup>2</sup>; <sup>1</sup>University of Greenwich; <sup>2</sup>ArcelorMittal

We present the development and validation (using an oil/water system) of a FV computer model of the steel continuous casting process. The emphasis is on hydrodynamics and particularly the dynamic behavior of the metal/slag interface. Instability and wave action encourage inclusion entrainment into the melt affecting product quality. To track the interface between oil and water a new implicit algorithm was developed, the Counter Diffusion Method. To prevent excessive numerical damping, a time-filtered version of the k-ε turbulence model was used. Air sparged through the Submerged Entry Nozzle simulates experimentally argon in a real process. Air bubbles disturb the oil water layer and affect its dynamics. This effect is modeled using a Lagrangian particle tracking scheme. Integral gas concentration in each computational cell alters the fluid density, as a feedback mechanism between gas and liquid. The simulations are compared against LDA velocity measurements for mean value, turbulence and frequency content.

## 9:45 AM

**Effect of Stopper-Rod Misalignment on Asymmetric Flow and Vortex Formation in Steel Slab Casting:** *Seong-Mook Cho*<sup>1</sup>; Go-Gi Lee<sup>2</sup>; Seon-Hyo Kim<sup>1</sup>; Rajneesh Chaudhary<sup>3</sup>; Oh-Duck Kwon<sup>4</sup>; Brian G Thomas<sup>3</sup>; <sup>1</sup>Pohang University of Science and Technology; <sup>2</sup>Research Institute of Industrial Science and Technology; <sup>3</sup>University of Illinois at Urbana-Champaign; <sup>4</sup>POSCO

Vortices forming near the slag-steel interface in the mold can entrap inclusions and cause defects in continuous casting of steel slabs. Lab experiments employing a 1/3 scale water model were performed to quantify the effects of stopper rod asymmetry on vortex formation. Three stopper-rod placements (aligned, front-misaligned and left-misaligned) were considered. Vortex formation was visualized with a high speed camera by placing sesame-seed tracer on the surface, which enables counting the number and detecting the location of vortices with time. Impeller flow probes were adopted to measure velocity profiles near the surface. Misaligning the stopper-rod placement induces asymmetric flow, resulting in asymmetric surface velocity, velocity variations, and turbulent kinetic energy. These factors influence vortex frequency and location among four zones near the SEN. Most vortices form at the left regions beside the SEN with a left-misaligned stopper-rod. Vortices form more preferentially at outside regions with a front-misaligned stopper-rod.

## 10:10 AM Break

## 10:30 AM

**Slag Infiltration and Initial Solidification Mechanisms during Continuous Casting:** *Pavel Ramirez Lopez*<sup>1</sup>; Peter Lee<sup>1</sup>; Kenneth Mills<sup>1</sup>; <sup>1</sup>Imperial College London

An integrated model able to simulate the metal flow, heat transfer and solidification inside the continuous casting mould is presented. The model calculates direct slag infiltration and its effects on shell formation during mould oscillation. Extremely fine meshes in the meniscus corner (~100/956m) were required to characterise the pressure, velocity and temperature through the slag layers in the shell-mould gap, allowing the prediction of the heat transfer between shell and mould. Results show excellent agreement with physical models for features such as slag film thicknesses and heat flux evolution during an oscillation cycle whereas, predicted shell thicknesses and powder consumption are also in good agreement with plant measurements. Results also describe how variations in shell and slag layer thicknesses are decisive on the formation of typical defects such as oscillations marks and transverse cracks, which are a major source of defects in the casting practice.

## 10:55 AM

**Control of Fluid Flow, Heat Transfer and Inclusions in Continuous Casting: CFD and Neural Network Studies:** *Petri Vayrynen*<sup>1</sup>; Shenqiang Wang<sup>1</sup>; Jukka Laine<sup>1</sup>; Seppo Louhenkilpi<sup>1</sup>; <sup>1</sup>Helsinki University of Technology

Fluid flow and heat transfer calculations have been carried out in tundish and mould including different kind of submerged entry nozzles. The effect of different kind of tundish dams have been studied in a bloom tundish in steady state and transient conditions. Many different CFD parameters, like turbulence models and mesh density, were tested. CFD calculations were also carried out to study the effects of swirling flow inside the SEN as well as different kind on



SEN nozzles on mould flow phenomena. Different kind of criteria for the ideal mould flow were derived. Neural network model was developed to predict and control the tundish temperature from process parameters and casting time.

### 11:20 AM

**Turbulent Instabilities in a Thin Slab Mold:** *Rodolfo Morales<sup>1</sup>*; Saul Hernandez-Garcia<sup>1</sup>; <sup>1</sup>IPN

Mathematical simulations are employed to describe short and large scale flow distortions observed in a water model of a thin slab casting mould using a two-port SEN located at deep and shallow positions for two casting speeds of 5 and 7 m/min. Two types of oscillations are identified high frequency and low frequency; the first have short length scales and long life while the length scale of the second involves the whole mould length and have short life. Through turbulent flow principles it was found that the high frequency of the discharging jets is the same as those of the oscillating meniscus. Therefore the discharging jets transfer vibrating momentum, at frequencies of 1.1-5 Hz, to the two upper roll flows during long periods of time inducing meniscus oscillations. Large-scale, short-life oscillations induce a dynamic distortion of the flow which forms deep meniscus depressions.

### 11:45 AM

**Numerical Investigation of the Flow and Steel/Slag Interface Behaviors in Slab Continuous Casting Mold with Electromagnetic Brake and Argon Gas Injection:** *Miaoyong Zhu<sup>1</sup>*; Haiqi Yu<sup>1</sup>; <sup>1</sup>Northeastern University

A new 3-D code for modelling the flow and interface fluctuation behaviours was developed in this paper, with fully taking into account the effects of flow-control-mold (FC-mold) EMBR, argon gas injection and the double actions of two means. The finite element code ANSYS was used to calculate the magnetic induction intensity distribution that produced by the EMBR device. The finite volume code FLUENT was used to calculate the coupled solution for the magnetic field, turbulence model, VOF model and discrete phase model on the basis of imposing the magnetic field data files of the mold region calculated by the ANSYS in a certain data format on the corresponding nodes of the mold geometry model by its own magneto-hydrodynamics (MHD) module. So the simulation results of the magnetic field distribution and the coupled calculation of multi-physics fields are more in line with the actual production situation and more accurate.

## Magnesium Technology 2010: Plenary Session

*Sponsored by:* The Minerals, Metals and Materials Society, TMS Light Metals Division, TMS: Magnesium Committee

*Program Organizers:* Sean Agnew, University of Virginia; Eric Nyberg, Pacific Northwest National Laboratory; Wim Sillekens, TNO; Neale Neelameggham, US Magnesium LLC

Monday AM Room: 612  
February 15, 2010 Location: Washington State Convention Center

*Session Chairs:* Sean Agnew, University of Virginia; Wim Sillekens, TNO Science and Industry

### 8:30 AM Introductory Comments

#### 8:35 AM

**Magnesium Alloys in Aerospace Applications - Flammability Testing and Results:** *Bruce Gwynne<sup>1</sup>*; <sup>1</sup>Magnesium Elektron

Current Federal Aviation Administration regulations and other restrictions prohibit magnesium alloy for use in internal aircraft applications that would benefit greatly from its light weighting advantages. This paper reviews magnesium alloy uses in past and potentially new aerospace applications, and then focuses on the regulatory environment and magnesium fire testing evaluations in an effort to have these restrictions modified or eliminated. Flammability experiments conducted with the FAA using laboratory oil burner type bench testing have found that rare earth containing magnesium alloys had a tendency to either not ignite or self extinguish. This is in contrast to traditional aluminum containing magnesium alloys that do not perform as well due to the lack of a protective oxide film. Actual in-aircraft full-scale flammability testing of traditional aluminum alloy and magnesium alloy aircraft seat structure components will be shown and discussed.

### 9:00 AM Keynote

**A Possible Route to Making Magnesium Fit for Hydrogen Storage in Automotive Applications:** *Vladimir Skripnyuk<sup>1</sup>*; Eugene Rabkin<sup>1</sup>; *Yuri Estrin<sup>2</sup>*; Rimma Lapovok<sup>2</sup>; <sup>1</sup>Technion; <sup>2</sup>Monash University

The high hydrogen storage capacity of magnesium, coupled with the reversibility of hydrogen absorption/desorption, give it an advantage over other metallic systems. However, a high hydrogen release temperature is an obstacle to its mobile hydrogen storage applications. Attempts to reduce this temperature below the desired level of 200 °C have been unsuccessful. While nanostructuring does improve the storage kinetics, the temperature dependence of hydrogen pressure cannot be controlled in this way. We proposed a novel approach to Mg processing using equal channel angular pressing, which changes both the kinetics and the thermodynamics of hydrogen storage. ECAP produces a long-lived non-equilibrium microstructure characterized by ultrafine grains, enhanced vacancy concentration and excess volume. These factors induce thermodynamic shifts in a desired way. Future efforts will be directed at ECAP optimization in order to reach the temperature and pressure levels required for use of magnesium as a hydrogen storage material for automotive applications.

### 9:30 AM Keynote

**Precipitation Strengthening in Magnesium Alloys Containing Rare Earth Elements:** *Xiaoqin Zeng<sup>1</sup>*; Wenjiang Ding<sup>1</sup>; Yujuan Wu<sup>1</sup>; Liming Peng<sup>1</sup>; Alan Luo<sup>2</sup>; <sup>1</sup>National Engineering Research Center of Light Alloy Net Forming, Shanghai Jiao Tong University; <sup>2</sup>Materials and Processes Laboratory, General Motors Research and Development Center

Rare earth (RE) elements, gadolinium (Gd), yttrium (Y), and neodymium (Nd), have been studied for their effects on the room- and elevated-temperature properties of magnesium alloys. Phase identification and microstructure analysis of RE-containing magnesium alloys have been conducted using optical microscopy (OM), scanning electron microscopy (SEM), X-ray diffraction (XRD) and transmission electron microscopy (TEM) techniques. Tensile and creep properties of the alloys have also been tested at room and elevated temperatures. The results have shown significant aging hardening responses in these alloys and revealed the precipitation sequences and the crystal orientation relationships of the RE-containing strengthening phases. It has been demonstrated that the primary strengthening mechanism in these RE-containing magnesium alloys is the formation of meta-stable phases during aging treatment. Long period stacking order (LPSO) has been observed when zinc (Zn) is added to the RE-containing magnesium alloys, which provides further strengthening to the alloys.

### 10:00 AM Keynote

**Thermodynamics and Constitution of Mg-Zn-Ce Alloys:** *Chen-nan Chiu<sup>1</sup>*; Artem Kozlov<sup>2</sup>; Joachim Groebner<sup>2</sup>; *Rainer Schmid-Fetzer<sup>2</sup>*; <sup>1</sup>National Tsing Hua University; <sup>2</sup>Clausthal University of Technology

This is a first report in our series of ongoing studies of ternary Mg-Zn-RE systems. Cerium is a major component of misch-metal and thus considered as the most important part in these industrially used rare earth (RE) additions. Therefore, the Mg-Zn-Ce ternary system plays a prominent role among the Mg-Zn-RE systems and precise knowledge of the phase diagram and thermodynamic properties of the Mg-Zn-Ce system is necessary for a better understanding of alloy design. It is also a key system for extending our multicomponent Mg-alloy database. The Mg-rich part of the ternary Mg-Zn-Ce system was experimentally investigated (DTA, DSC, SEM/EDS) by key samples to determine the primary crystallization, invariant reactions and solid solubilities. A consistent thermodynamic model of the ternary Mg-Zn-Ce system is developed by using the Calphad method. This work is supported by the German Research Foundation (DFG) in the Priority Programme "DFG-SPP 1168: InnoMagTec"

### 10:30 AM Break

### 10:50 AM Keynote

**Modeling Temperature and Strain Rate Dependent Inelastic Deformation and Recrystallization in Mg Alloys:** *Douglas Bammann<sup>1</sup>*; Esteban Marin<sup>1</sup>; Kiran Solanki<sup>1</sup>; <sup>1</sup>Mississippi State University

The thermodynamics of Coleman and Gurtin are employed with respect to the natural to ensure satisfaction of the second law of thermodynamics and to derive a consistent thermal balance equation including both internal and external work as source terms. Evolution equations for the state variables are determined from the physics of the defects they represent. For example, Kocks-Mecking dislocation storage and recovery for SSDs and the Cocks-Ashby

Mon. AM

# Technical Program

evolution for void growth in a steady state creeping material. In addition, kinematic expressions (plastic stretching, plastic spin...) are required, consistent with the degrees of freedom introduced by the multiplicative decomposition of the deformation gradient. The volume fraction of recrystallized grains is also introduced to describe both static and dynamic recrystallization. Grain size dependence of the kinetics of plastic flow, mean free path of the SSDs and GNDs, and grain evolution are also considered in the model.

## 11:20 AM

**Magnesium Alloys in Army Applications: Past, Current and Future Solutions:** *Suveen Mathaudhu*<sup>1</sup>; Eric Nyberg<sup>2</sup>; <sup>1</sup>U.S. Army Research Laboratory; <sup>2</sup>Pacific Northwest National Laboratory

As early as the 1940's Magnesium-alloys have been used for military applications, from aircraft components to ground vehicles. The drive for usage was largely availability and lightweighting of military systems. But the promise of widespread usage has not been met. With recent fuel costs and logistical burdens has come increased recognition of the need to develop and implement lightweighting strategies for the full range of weapons platforms (land, sea, and air) without a loss in platform functionality. The potential for significant improvements in the mechanical and physical properties of lightweight metals will drive design of ultralightweight metal structures and components, thus reducing large logistical burdens, minimizing operational constraints and liabilities, and reducing vulnerabilities. This lecture will cover past, present and potential future Mg-alloy applications with a focus on scientific barriers relevant to integration of Mg-alloy, and solutions which are currently being developed to address these issues.

## 11:45 AM

**MagForming - Development of New Magnesium Forming Technologies for the Aeronautics Industry:** *Bruce Davis*<sup>1</sup>; Amir Fein<sup>2</sup>; Wolfgang Entelmann<sup>3</sup>; Elke Hombergmeier<sup>4</sup>; <sup>1</sup>Magnesium Elektron North America; <sup>2</sup>Palbam-AMTS; <sup>3</sup>Airbus-Deutschland; <sup>4</sup>EADS Deutschland GmbH

MagForming was a European Union Framework Six Priority 4 Aeronautics and Aerospace funded program. Its purpose was to advance the state of the art in forming methods for a range of magnesium alloys in extruded, forged, sheet and plate forms using aerospace prototypes as demonstrators. The program was a collaboration between 12 partners including material manufacturers, tier 1 aerospace suppliers, OEMs, and academic institutes. The program targeted specific areas of forming, including forging, superplastic forming, roll bending, pad forming, deep drawing, and creep forming. The aim was to develop best practices for all of these methods via the production of aerospace prototype parts. This not only acted to demonstrate the forming process and its application to magnesium alloys, but also resulted in the production of useful parts for testing, potentially leading to the use of magnesium in the system and structure areas from which the parts had been taken.

## Materials in Clean Power Systems V: Clean Coal-, Hydrogen Based-Technologies, Fuel Cells, and Materials for Energy Storage: Materials for Clean Coal Power and CCS Systems I

*Sponsored by:* The Minerals, Metals and Materials Society, TMS Electronic, Magnetic, and Photonic Materials Division, TMS Structural Materials Division, TMS/ASM: Corrosion and Environmental Effects Committee, TMS: Energy Conversion and Storage Committee  
*Program Organizers:* Xingbo Liu, West Virginia University; Zhenguo Yang, Pacific Northwest National Lab ; K. Weil, Pacific Northwest National Lab ; Mike Brady, Oak Ridge National Lab; Jay Whitacre, Carnegie Mellon University; Ayyakkannu Manivannan, National Energy Technology Laboratory; Zi-Kui Liu, Penn State University

Monday AM

Room: 211

February 15, 2010

Location: Washington State Convention Center

*Session Chair:* Xingbo Liu, West Virginia University

## 8:30 AM Keynote

**Development and Implementation of Materials to Enable Clean Coal Technologies:** *Cynthia Powell*<sup>1</sup>; <sup>1</sup>Office of Research and Development, National Energy Technology Laboratory, US Department of Energy

A growing realization that the environmental impact of energy production must be reduced on a global scale, combined with an increased desire in this country to reduce dependence on foreign energy sources, is driving significant change in the way the United States will derive and produce power in the future. While renewable energy resources will continue to grow in importance, environmentally responsible fossil energy production will be necessary to provide a bridge to the next energy revolution. The practical result is a requirement for affordable, high-performance materials and materials systems capable of withstanding increasingly severe operating environments to enable these next-generation fossil energy systems. This talk will focus on the research being performed at the National Energy Technology Laboratory to identify and meet the requirements for high performance structural materials for advanced combustion and gasification power systems.

## 9:10 AM Invited

**Ageing and Corrosion in CO<sub>2</sub> Rich Flue Gases and Their Influence on the Creep and Fatigue Properties of Superheater Materials:** *Axel Kranzmann*<sup>1</sup>; Jürgen Olbricht<sup>1</sup>; Daniela Hünert<sup>1</sup>; Diana Marcano<sup>1</sup>; Wencke Schulz<sup>1</sup>; Werner Österle<sup>1</sup>; Romeo Saliwan-Neumann<sup>1</sup>; Hellmut Klingelhöffer<sup>1</sup>; Gabriele Oderl<sup>1</sup>; Ingrid Urban<sup>1</sup>; Birgit Skrotzki<sup>1</sup>; <sup>1</sup>Federal Institute for Materials Research and Testing

Oxyfuel Power Plants combined with Carbon Capture and Sequestration produce flue gases with high CO<sub>2</sub> and H<sub>2</sub>O partial pressures. Commercial steel tubes for steam heaters and super heaters were annealed for up to 1000 h in atmospheres of 70 mol% CO<sub>2</sub>, 30 mol% H<sub>2</sub>O and a variation with 29 mol% H<sub>2</sub>O and 1 mol% O<sub>2</sub>. Temperatures between 500°C and 650°C and surface stress were applied. The reaction with CO<sub>2</sub> during annealing caused significant material loss due to oxidation and, carburization of the base material. Oxidation and carburization may affect the lifetime of plant components by embrittlement, mechanical interaction of thick oxide scales and base material, or rapid local attacks when cracks are induced by mechanical loads. Mechanical testing in oxyfuel atmospheres, involving static creep and cyclic low cycle fatigue loading, was carried out to demonstrate the environmental effect on the mechanical performance of super heater materials.

## 9:50 AM

**Designing Amine-Based CO<sub>2</sub> Sorbents - A Computational and Experimental Study:** *John Kitchin*<sup>1</sup>; <sup>1</sup>Carnegie Mellon University

Atmospheric CO<sub>2</sub> concentrations are increasing by 1-2 ppmv/year due to CO<sub>2</sub> emissions from the combustion of fossil fuels for power generation and transportation. Efficient methods for separating CO<sub>2</sub> from flue gas are needed to make the capture cost-effective and technologically viable. We are developing a sorbent-based approach to CO<sub>2</sub> capture in which molecular amines are supported on porous substrates. We have used experimental methods to probe the role of moisture in the capture mechanism of CO<sub>2</sub>, the role of the support in parasitic moisture sorption and the capture capacity of two amidines, DBU and



DBN. We have also used quantum mechanical calculations to explore the range of CO<sub>2</sub> capacities that might be possible from functionalized amidines. These functional groups modify the electronic and geometric environment around the CO<sub>2</sub> binding site through steric hindrance, hydrogen bonding and electron withdrawing/donating effects.

### 10:10 AM Break

### 10:40 AM Invited

#### Deployment of New High Temperature Alloys for Power Generation Systems: *Bruce Pintl*<sup>1</sup>; <sup>1</sup>Oak Ridge National Laboratory

Two Fe-base alloys developed at ORNL, alumina-forming austenitic (AFA) steel and cast austenitic CF8C-Plus, are in the process of moving from invention to application. A considerable effort is required to move an alloy from laboratory heats to commercial products. AFA steels were developed to bridge the gap between high strength austenitics and oxidation-resistant alumina-forming alloys. They are being considered for applications such as high-temperature, thin-walled heat exchangers, boiler and petrochemical tubing, and non-stack fuel cell applications where they are expected to produce minimal Cr poisoning. Decades of alloy strengthening knowledge developed for fission and fusion applications was used to rapidly develop cast CF8C-Plus, which is already used in heavy-duty commercial diesel engines. New applications being considered are in additional automotive applications, turbine casings and boilers. Examples will be given about the deployment process for these alloys and the program required to support these efforts.

### 11:20 AM

#### Density Functional Theory Study of Grain Boundary Properties in Ni-Base Superalloys: *Kuiying Chen*<sup>1</sup>; *Wei-Di Cao*<sup>1</sup>; <sup>1</sup>ATI Allvac

Traditionally, impurities phosphorus was treated as a detrimental element in the development of Ni-base superalloys. However, the experimental works conducted at ATI Allvac demonstrated that the effect of phosphorus in Ni-base superalloys is quite complex. Within a certain range of concentrations, phosphorus has a positive effect on stress rupture / creep resistance of all wrought Ni-base alloys. The rupture life was increased, not decreased, by the addition of phosphorus. This positive effect of phosphorus is alloy-dependent with the largest effect observed in Fe-containing Ni-base alloys and much weaker in alloys without significant Fe addition such as Waspaloy and Rene 220. The mechanisms responsible for the above phenomena are not clear. Therefore it is proposed to investigate the effect of phosphorus on Σ5 (012) grain boundary (GB) properties with Fe-containing and Fe-free Ni-base superalloys using ab initio density functional theory calculations. The study will (1) reveal why and how phosphorus at the GB of Fe-containing and Fe-free Ni-base superalloys affect the GB strength as a function of phosphorus content; (2) to examine how boron at the GB of Fe-containing and Fe-free Ni-base superalloys affect the GB strength as a function of boron content; (3) to study the interaction between phosphorus and boron in Fe-containing and Fe-free Ni-base superalloys in terms of effect on GB strength with an aim of providing reasonable explanations for experimental results; (3) on the basis of (1) and (2), find the critical phosphorus composition  $C_p$ , where phosphorus or boron starts to weaken GB strength. The research will provide a comprehensive understanding on impurity such as phosphorus or boron complex effect on GB strength.

### 11:40 AM

#### Materials Selection for Steam Turbine Components in Advanced Ultra Supercritical Power Plants: *Jeffrey Hawk*<sup>1</sup>; <sup>1</sup>U.S. Department of Energy

In order to reduce greenhouse gas emissions to combat global warming, the efficiency of pulverized coal steam power plants must be increased. Raising the temperature is the primary way to do this, but to significantly increase efficiency, temperatures in excess of 700C are needed. Above 700C, wrought nickel alloys are needed for steam turbine component parts such as the rotor, blades and valve internal parts. Most wrought nickel alloys were designed primarily for aerospace applications or where excellent resistance to corrosion is needed. In many instances high temperatures are experiences but the life of the component is considerably less than the 100,000 hours minimum needed for steam turbine parts. This paper will explore candidate selection criteria for the European AD700 initiative and the DOE 1400F steam turbine program. Phase stability, mechanical behavior, and microstructural stability will be discussed with respect to steam turbine components.

## Materials Processing Fundamentals: Solidification and Casting

*Sponsored by:* The Minerals, Metals and Materials Society, TMS Extraction and Processing Division, TMS: Process Technology and Modeling Committee

*Program Organizer:* Prince Anyalebechi, Grand Valley State University

Monday AM

Room: 601

February 15, 2010

Location: Washington State Convention Center

*Session Chair:* Prince Anyalebechi, Grand Valley State University

### 8:30 AM

#### Fe-Mn-Al-C Austenitic Steels Treated by Ca and Ce: *Simon Lekakh*<sup>1</sup>; *Von Richards*<sup>1</sup>; *Angella Schulte*; *David Van Aken*<sup>1</sup>; <sup>1</sup>MST

Phosphorus segregated at grain boundaries during solidification and heat treatment dramatically decreases low temperature toughness of precipitation hardened Fe-Mn-Al austenitic steel. Thermo-dynamical analysis was performed for evaluation of the possibility of decreasing P grain boundary segregation by Ce- and Ca-additives in the melt. It was shown that the predicted probability of P containing compound formation depends on melt composition and treatment sequence. Experimental heats were performed and the several micro- and macro-structural effects of Ce- and Ca-additives were recognized by using automated inclusion analyzer technique. Increasing low temperature toughness in austenitic steel by complex Ca-wire injection followed by Cemishmetal additions was achieved.

### 8:50 AM

#### Strong Magnetic Field Induced Phase Alignment during Solidification: *Zhi Sun*<sup>1</sup>; *Muxing Guo*<sup>1</sup>; *Jef Vleugels*<sup>1</sup>; *Omer Van der Biest*<sup>1</sup>; *Bart Blanpain*<sup>1</sup>; <sup>1</sup>Katholieke Universiteit Leuven

Imposing a strong magnetic field is considered as an attractive method to prepare materials with aligned or textured structures due to its intrinsic properties, e.g. non-contact and easily adjustable. However, the nature of strong magnetic field effect still remains unclear and further research is needed. In the present paper, the effect of a strong magnetic field on the solidification of a hypereutectic Al-Cu alloy was investigated. After magnetic field treatment, the primary theta phase was aligned parallel to the magnetic field direction. Meanwhile, the eutectic micro-structural constituent became elongated and thinner. A theoretical analysis was conducted to have a better understanding of the phenomena. During solidification, the magnetic Faraday force and dipole-dipole interaction force are considered to decrease the solute pile-up in front of the solid-liquid interface and increase the theta phase formation. The alignment of the theta phase is due to the shape magnetic anisotropy and crystal magnetic anisotropy.

### 9:10 AM

#### Experimental Analysis of Thermal, Tensile and Microhardness Properties in Directional Solidified ZA, Zn-Ag and ZINAG Alloys: *Alicia Ares*<sup>1</sup>; *Sergio Gueijman*<sup>2</sup>; *Carlos Schvezov*<sup>1</sup>; <sup>1</sup>CONICET/FCEQyN-UNaM; <sup>2</sup>FCEQyN-UNaM

The family of Zn-Al (ZA) and Zn-Al-Ag (ZINAG) alloys offers high mechanical properties, ease of finishing, the advantage of low energy and pollution-free melting. Also, present alternatives to the well developed alloy systems, such as brasses, bronzes, cast irons and aluminum alloys. The main objective of this paper is to measure thermal parameters in ZA and ZINAG hypoeutectic and hypereutectic alloys directionally solidified which present columnar, equiaxed and columnar to equiaxed transition structures (CET). Also, estimate the mechanical properties, such as microhardness and tensile parameters and correlate these with the thermal and structural parameters (grain size and dendritic spacing). The different types of structures were analyzed with optical and scanning electron microscopy. The results show that bulk alloys have greater microhardness values than those directionally solidified. Also, alloys with equiaxed structures presented a better tensile resistance than the columnar and CET zones. The results of the present investigation are compared with previous experiments. Keywords: Thermal parameter, tensile parameters, microhardness, ZA and ZINAG alloys, directional solidification.

# Technical Program

## 9:30 AM

**Effects of Solidification Rate and Alloy Composition on the Cast Microstructure of Aluminum Alloy 5182:** *Prince Anyalebechi*<sup>1</sup>; <sup>1</sup>Grand Valley State University

The effects of solidification rate (0.4-26.1 K/s) and alloying elements on the cast microstructure of aluminum alloy (AA) 5182 have been investigated with directionally cooled laboratory-size ingots. The alloying elements examined included Mg (3.8-4.66 wt.%), Mn (0.35-0.75 wt.%), Fe (0.11-0.42 wt.%), Cu (0.03-0.25 wt.%), and Si (0.11-0.26 wt.%). These reflect the chemical compositions of AA 5182 end stocks with high recycled used beverage container (UBC) content. For a given chemical composition, the average dendrite cell and second phase particle size decreased with increase in average solidification rate. In general, within the levels investigated, Mg did not have a significant effect on the types, volume fractions, and average sizes of the second phase particles. However, increase in Mn, Si, Fe, and Cu increased average sizes and volume fractions of the second phase particles. These effects appear to depend on the maximum solid solubility of the element in aluminum.

## 9:50 AM Break

## 10:10 AM

**Elaboration and Nanoscale Characterization of a Fe-Y<sub>2</sub>O<sub>3</sub> Nanocomposite Prepared by Reactive Ball-Milling and Annealing:** *Mathilde Brocq*<sup>1</sup>; Fabrice Legendre<sup>1</sup>; Bertrand Radigue<sup>2</sup>; Mathieu Couvrat<sup>1</sup>; Fabien Cuvilly<sup>2</sup>; Philippe Pareige<sup>2</sup>; Jean-Marie Lebreton<sup>2</sup>; <sup>1</sup>SRMP - CEA; <sup>2</sup>GPM-Université de Rouen

Reactive high energy ball-milling has known an increasing interest from both fundamental and applied point of view. We studied the properties of this technique through the study of a metal-oxide nanocomposite. It was synthesized by ball-milling YFe<sub>3</sub> and Fe<sub>2</sub>O<sub>3</sub> in the stoichiometric proportions of the following chemical reaction: 2YFe<sub>3</sub> + Fe<sub>2</sub>O<sub>3</sub> → 8Fe + Y<sub>2</sub>O<sub>3</sub>. Then it was briefly annealed. The material was characterized at different steps of the process by X-Ray Diffraction, Mössbauer Spectroscopy and Atom Probe Tomography. We will present the different stages of the process – mixing of reactants, propagation of chemical reaction and refinement of the microstructure during ball-milling followed by composition change and phase coarsening during annealing. It will be explained with the concept of competition between thermal and forced processes. We will also identify the processing parameters which control it.

## 10:30 AM

**The Effect of Boron Addition on the Wear Resistance of High Chromium White Cast Iron:** *Cenk Saglam*<sup>1</sup>; Selim Ozavar<sup>2</sup>; Onuralp Yucel<sup>1</sup>; <sup>1</sup>Istanbul Technical University; <sup>2</sup>UMIT Casting

In this study, mechanical properties and wear resistance of high chromium white cast irons were investigated with varying boron concentration. Fe-Cr-C-Si-Mo-B alloys with varying boron concentration from 0.0 to 0.56 wt.% were prepared by pilot scale induction melting furnace. Effects of alloying elements and heat treatment methods on wear resistance were studied. For every chemical composition, a specimen for metallographic research was prepared. Microstructure of the specimens was studied by optical microscope. Quantitative elemental analysis was performed by using XRD, XRF, EPMA and AAS. Moreover, micro hardness measurements were made on different cross-section areas and wear resistance of the specimens was measured by using ball-cratering methods. It has been concluded that with the increasing of boron content, the hardness increases and the tensile strength decreases. The wear resistance is improved up to 0.1 wt.% B concentration. Above 0.1 wt.% B, there is a decrease in wear resistance.

## 10:50 AM

**Novel Current Activated Tip-Based Sintering (CATS) of Advanced Materials:** *K. Morsi*<sup>1</sup>; K. Moon<sup>1</sup>; S. Kassegne<sup>1</sup>; R. Ugle<sup>1</sup>; M. Patel<sup>1</sup>; <sup>1</sup>San Diego State University

This paper discusses the Current-activated Tip-based Sintering (CATS) of intermetallic and metallic powder-based materials. In CATS electric current is applied to a powder bed/compact using a small stationary or moving conductive tip to selectively sinter macro- or micro-scale features. The effect of processing variables on the microstructure and properties of metallic and shape memory alloy (TiNi) are discussed.

## 11:10 AM

**Comparison of Microstructural Evolution of Nickel during Conventional and Spark Plasma Sintering:** Matthew Luke<sup>1</sup>; Darryl Butt<sup>1</sup>; Megan Frary<sup>1</sup>; <sup>1</sup>Boise State University

Spark plasma sintering (SPS) is a rapid powder consolidation technique that uses pulsed electric current to directly heat the powder. A comparison was made between the microstructural evolution of pure polycrystalline nickel powder processed by conventional (press and sinter) and SPS routes. The sintering temperature, dwell time, applied pressure and ramp rate were varied to affect the densification and microstructural evolution of the powders. Characterization of grain size, morphology, grain boundary character, and crystallographic texture was performed on SPS and traditionally-processed specimens using electron backscatter diffraction. The microstructure of SPS nickel was observed to vary between one that resembles a green body with some grain coarsening to one that is indistinguishable from a wrought nickel microstructure except for some porosity. Grain size distributions in press and sintered nickel were much wider than those for SPS nickel. SPS nickel has increased porosity at the edges, evidence of processing temperature variations.

## 11:30 AM

**Secondary Cooling Technology for Casting of Hypo-Peritectic Steels:** Jian Zhang<sup>1</sup>; Chen Dengfu<sup>1</sup>; Long Mujun<sup>1</sup>; Wang Shuigen<sup>1</sup>; Bi Yanyan<sup>1</sup>; <sup>1</sup>Chongqing University

From the standpoint of quality, surface cracks normally pose more of a problem than internal cracks. Hypo-peritectic steel grades are well known for their proneness to surface longitudinal cracking during continuous casting. This study analyzed the influences of chemical composition, technique parameter and secondary cooling on the surface longitudinal cracks. Based on the optimized the first and secondary cooling zone water distribution in the process of continuous casting, low cooling water distribution at solidification initial stages and uniform cooling at secondary cooling zone were suggested, which can be use to effectively control the surface longitudinal cracks.

## 11:50 AM

**Investigation of a “Swirling” Phenomenon in Tungsten Carbide-Cobalt during Laser Deposition Using In-Situ Thermal Imaging:** *Yuhong Xiong*<sup>1</sup>; William Hofmeister<sup>2</sup>; John Smugeresky<sup>3</sup>; Jonathan Nguyen<sup>1</sup>; Jean-Pierre Delplanque<sup>1</sup>; Julie Schoenung<sup>1</sup>; <sup>1</sup>University of California; <sup>2</sup>University of Tennessee Space Institute; <sup>3</sup>Sandia National Laboratories

Laser deposition is used for the fabrication of net shapes from a broad range of materials, including tungsten carbide-cobalt (WC-Co) cermets (composites composed of a metallic phase and a hard refractory phase). The thermal behavior of WC-Co cermets during the Laser Engineered Net Shaping (LENS<sup>®</sup>) process was studied using an in-situ high-speed thermal imaging system. An interesting “swirling” phenomenon was observed in the molten pool, and was not present when the bottom of the sample was being built. To provide fundamental insight into this phenomenon for cermets, the thermal behavior of pure Co during the LENS<sup>®</sup> process was investigated for comparison. Temperature gradients and cooling rates in the vicinity of the molten pool for both material systems were analyzed. Their unique physical properties, such as wettability, emissivity, and viscosity at high temperature were considered to determine the source of the observed differences.



### Mechanical Performance for Current and Next-Generation Nuclear Reactors: Advances in Mechanical Testing

*Sponsored by:* The Minerals, Metals and Materials Society, TMS Materials Processing and Manufacturing Division, TMS Structural Materials Division, TMS/ASM: Mechanical Behavior of Materials Committee, TMS: Nanomechanical Materials Behavior Committee, TMS/ASM: Nuclear Materials Committee

*Program Organizers:* Dylan Morris, NIST; Greg Oberson, Nuclear Regulatory Commission; Nicholas Barbosa, National Institute of Standards & Tech; Wolfgang Hoffelner, Paul Scherrer Institute

Monday AM Room: 201  
February 15, 2010 Location: Washington State Convention Center

*Session Chairs:* Nicholas Barbosa, National Institute of Standards and Technology; Peter Hosemann, LANL

### 8:30 AM Invited

#### Small Specimen Test Techniques for Evaluating Properties of Irradiated Materials: *Mikhail Sokolov*<sup>1</sup>; <sup>1</sup>ornl

Small specimens are playing the key role in evaluating properties of irradiated materials. The use of small specimens provides several advantages for researchers. Typically, only small volume of material can be irradiated in a reactor at desirable conditions in terms of temperature, neutron flux, and dose. Small volume of irradiated material may also allow for easier handling of specimens. However use of small specimens imposes variety of challenges as well. These challenges are associated with proper accounting for size effects and transferability of small specimen data to the real structures of interest. In this presentation variety of small specimens techniques will be reviewed. Main interest will be focused but not limited on tensile, fracture toughness, creep, and Charpy impact tests.

### 9:00 AM

#### Micro and Macro Scale Mechanical Testing and Characterization on Irradiated Structural Materials for Nuclear Application: *Peter Hosemann*<sup>1</sup>; Manuel Pouchon<sup>2</sup>; Yong Dai<sup>2</sup>; Stuart Maloy<sup>1</sup>; <sup>1</sup>LANL; <sup>2</sup>Paul Scherrer Institute

Testing of reactor irradiated materials for nuclear applications (fission and fusion) are cost and labor intensive tasks. Large scale materials testing means that large amounts of highly radioactive materials must be handled. Using small scale materials testing can reduce the amount of active material and allow for relatively inexpensive lower energy irradiations. Here we present micro compression testing and nanoindentation results performed on spallation source (neutron) and ion beam irradiated engineering materials such as HT-9 (12Cr ferritic/martensitic) and F82H (8Cr 2W ferritic/martensitic). It was found that the trend of radiation induced hardening measured with small scale techniques is the same as observed with large scale tensile testing. Measurements performed on nanostructured ODS alloys such as MA957 (14Cr ODS alloy) and PM2000 (20Cr 5Al ODS alloy) show that the yield strength measured using small scale techniques is equal to data obtained with large scale testing techniques.

### 9:20 AM

#### Microscale Methods for Evaluating Mechanical Behavior of Ion Irradiated Metals at High Damage Levels: *Luke Brewer*<sup>1</sup>; Khalid Hattar<sup>1</sup>; Brad Boyce<sup>1</sup>; Joseph Michael<sup>1</sup>; <sup>1</sup>Sandia National Laboratories

Next generation nuclear power reactors will push materials to radiation damage levels beyond 100 displacements per atom. It is vital to understand how the mechanical behavior of structural metals changes at these damage levels. High energy, heavy ion accelerators are able to produce these damage levels in metals, but only in small volumes. In this talk we will extend current and introduce new microscale methods for assessing the change in micromechanical behavior of metals irradiated by high energy, heavy ions. We will present data that extends the recent work using micropillar compression of ion irradiated metals, including work on copper single crystals which is allowing an examination of the accuracy and precision of these methods. These results will be compared to spherical indentation experiments on the same materials. In addition, we will present novel in situ experiments to monitor swelling by using an SEM attached to a tandem accelerator.

### 9:40 AM Invited

#### Small Specimen and in situ Mechanical Test Methods in the US Fusion Reactor Materials Program: *Roger Stoller*<sup>1</sup>; G. Robert Odette<sup>2</sup>; Richard Kurtz<sup>3</sup>; Mikhail Sokolov<sup>1</sup>; Yutai Katoh<sup>1</sup>; Thak Sang Byun<sup>1</sup>; Anton Moeslang<sup>4</sup>; <sup>1</sup>Oak Ridge National Laboratory; <sup>2</sup>University of California; <sup>3</sup>Pacific Northwest National Laboratory; <sup>4</sup>FZK Karlsruhe

The development of small specimens for mechanical testing has been a priority for the US Fusion Materials Program for several practical reasons. High-flux volume available for materials irradiation is relatively limited, and a large number of specimens is required to map a material's response to irradiation. Smaller specimens reduce the amount of radioactive material, minimizing personnel exposures and waste disposal. Notably, design-relevant data for fusion must ultimately be obtained in a prototypical 14 MeV neutron source such as the International Fusion Materials Irradiation Facility. The high-flux volume of IFMIF will be limited, leading the international community to devote considerable effort to refining experimental matrices using small specimens. The history and status of this and related work will be discussed, including a comparison of small and conventional specimens to demonstrate their validity and value to the development of advanced reactors.

### 10:10 AM Break

### 10:25 AM Invited

#### Mechanical Testing of Core Fast Reactor Materials for the Advanced Fuel Cycle Initiative: *Stuart Maloy*<sup>1</sup>; Tobias Romero<sup>1</sup>; Mychailo Toloczko<sup>2</sup>; Thak-sun Byun<sup>3</sup>; <sup>1</sup>Los Alamos National Laboratory; <sup>2</sup>PNNL; <sup>3</sup>ORNL

The Advanced Fuel Cycle Initiative is investigating methods of burning minor actinides in a transmutation fuel. To achieve this goal, the core fast reactor materials (cladding and duct) must be able to withstand significant radiation damage (greater than 200 dpa). Developing these radiation tolerant materials requires high dose irradiation effects data on relevant materials. These data should include tensile, fracture toughness and creep data after irradiation to doses greater than 200 dpa at irradiation temperatures of 350-600°C. To obtain this data in the near term, tensile, fracture toughness, Charpy specimens and in-reactor creep specimens of traditional ferritic/martensitic alloys (HT-9 and T91) previously irradiated in the Fast Flux Test Facility (FFTF) to doses up to 210 dpa at irradiation temperatures from 350-700°C are being tested and analyzed. This includes analysis of a duct made of HT-9 after irradiation to a total dose of 155 dpa at temperatures from 370 to 510°C.

### 10:55 AM

#### Damage Related Information Contained in Small Material Volumes of Advanced Nuclear Plants: *Wolfgang Hoffelner*<sup>1</sup>; Manuel Pouchon<sup>1</sup>; Jiachao Chen<sup>1</sup>; Maria Samaras<sup>1</sup>; <sup>1</sup>Paul Scherrer Institute

Condition based residual life assessments are important for plants and operating conditions where not enough service experience exists. This will be also the case for advanced nuclear power plants. Investigations on service exposed material (taken either directly from a component or from surveillance coupons) are considered as one possible option particularly for damage types where current NDE methods are not accurate enough (creep, cyclic softening, microstructural changes etc.). Advanced micro-sample testing (indentation, micro-pillars, indentation creep, punch test etc.) together with microstructural analyses and materials modeling can help to increase the accuracy of damage and residual life assessments. The paper will discuss possibilities of getting damage related information from small sample volumes for advanced nuclear plants. Test results from micro-samples and its interpretation will be shown.

### 11:15 AM

#### Studying the Effect of Carbon on DU-Mo Foil Fabrication Using Small-Scale Specimen Testing: *Ramprashad Prabhakaran*<sup>1</sup>; Douglas Burkes<sup>1</sup>; Amy DeMint<sup>2</sup>; Jack Gooch<sup>2</sup>; Dennis Keiser<sup>1</sup>; Daniel Wachs<sup>1</sup>; Indrajit Charit<sup>3</sup>; <sup>1</sup>Idaho National Laboratory; <sup>2</sup>Y-12 National Security Complex; <sup>3</sup>University of Idaho

In support of the Reduced Enrichment for Research and Test Reactors (RERTR) program, efforts are ongoing to develop and validate a monolithic depleted uranium molybdenum (DU-Mo) foil fabrication process adaptable for a potential implementation in a manufacturing environment. Efforts are ongoing to study the effect of carbon (source material impurity) on DU-Mo foil fabrication. Carbon is of particular interest due to its potential effects on the metalworking process. Hence, DU-10Mo test foils were fabricated with different carbon levels (150-400 ppm). Small-scale specimen testing (Sub-size tensile, shear punch and microhardness testing) along with optical metallography, SEM and XRD are

# Technical Program

being conducted to understand the effect of carbon on the fabrication reliability and process yields. Thus, this study would help in finding out a tolerable limit of carbon content in the alloy.

**11:35 AM**

**Mechanical Properties of Fresh and Irradiated Monolithic U-Mo Fuels:** *Ramprashad Prabhakaran*<sup>1</sup>; Douglas Burkes<sup>1</sup>; Dennis Keiser<sup>1</sup>; Daniel Wachs<sup>1</sup>; Adam Robinson<sup>1</sup>; Jan-Fong Jue<sup>1</sup>; Indrajit Charit<sup>2</sup>; <sup>1</sup>Idaho National Laboratory; <sup>2</sup>University of Idaho

The Reduced Enrichment for Research and Test Reactors (RERTR) program was initiated to develop new nuclear fuels to enable research and test reactors to use low-enriched uranium instead of high-enriched uranium fuels without significant loss in performance. This has led to a pursuit of developing high uranium density monolithic fuel that possesses the greatest possible uranium density in the fuel region. Hot-isostatic pressing and friction bonding are being investigated to encapsulate fuel foils in Al alloy cladding. The fabrication technique significantly affects the mechanical properties of the foil and it also dominates the overall plate mechanical behavior. Sub-size tensile and microhardness testing are being performed to evaluate the mechanical properties of the fresh fuel and fuel irradiated at the Advanced Test Reactor. Efforts are ongoing to standardize the shear punch testing procedure so that the tensile behavior can be predicted using small volumes of material and at reduced irradiation costs.

**11:55 AM**

**Structural Modifications and Mechanical Degradation of Ion Irradiated Glassy Polymer Carbon:** *Malek Abunaemeh*<sup>1</sup>; Mohammad Seif<sup>1</sup>; Lumin Wang<sup>2</sup>; Ibidapo Ojo<sup>1</sup>; Young Yang<sup>3</sup>; Claudiu Muntele<sup>1</sup>; Abdulla Elsamadicy<sup>4</sup>; Daryush ILA<sup>1</sup>; <sup>1</sup>Alabama A&M University; <sup>2</sup>University of Michigan; <sup>3</sup>University of Wisconsin; <sup>4</sup>University of Alabama in Huntsville

The TRISO fuel consists of UOx coated in several layers of materials with different functions. Here we are looking at ion irradiation induced structural modifications of glassy polymeric carbon (GPC) and the effect on mechanical and physical properties. GPC is one material considered as a potential replacement for pyrolytic carbon coatings, with a function of diffusion barrier for the fission products. Here we irradiated GPC with 5 MeV Ag and Au. The fission fragment mass distribution has two maxima around mass 98 and 137 that would best fit Rb and Cs, respectively. However, both ions are hard to produce from our SNICS source, therefore we chose Ag and Au as best replacements. We used scanning electron microscopy, transmission electron spectroscopy, and nano-indentation for characterization. We were able to correlate the imaging results with SRIM simulations of ion range and distribution, energy loss, and damage to the GPC material.

## Modeling, Simulation, and Theory of Nanomechanical Materials Behavior: Plasticity and Strength of Nanostructured and Nanoscale Materials I

*Sponsored by:* The Minerals, Metals and Materials Society, TMS Materials Processing and Manufacturing Division, TMS/ASM; Computational Materials Science and Engineering Committee, TMS; Nanomechanical Materials Behavior Committee

*Program Organizers:* Thomas Buchheit, Sandia National Laboratories; Sergey Medyanik, Washington State Univ.; Douglas Spearot, University of Arkansas; Lawrence Friedman, Penn State University; Edmund Webb, Sandia National Laboratories

Monday AM Room: 304  
February 15, 2010 Location: Washington State Convention Center

*Session Chairs:* Douglas Spearot, University of Arkansas; Stephen Foiles, Sandia National Laboratories

**8:30 AM Invited**

**Molecular Dynamics Simulation of the Deformation of an Equilibrated Nanograined Metal:** *Stephen Foiles*<sup>1</sup>; <sup>1</sup>Sandia National Laboratories

Molecular dynamics (MD) simulations of grain growth of nanograined metals indicate the presence of a high density of twin boundaries in the resulting microstructure. This is consistent with experimental observations of the post-annealing structure of pulsed laser deposited Ni. In this work, an initial structure

is obtained via the annealing of an initial nano-scale grain structure. The tensile deformation of this system is then computed via MD simulations. The resulting deformation mechanisms are examined to elucidate the influence of the twin boundaries on the deformation mechanism. Sandia is a multi-program laboratory operated by Sandia Corporation, a Lockheed Martin Company, for the United States Department of Energy's National Nuclear Security Administration under contract DE-AC0494AL85000.

**9:00 AM**

**Analysis of Dislocation Twin-Interaction in Deformed Nanocrystalline fcc Metals:** *Karsten Albe*<sup>1</sup>; Alexander Stukowski<sup>1</sup>; Diana Farkas<sup>2</sup>; <sup>1</sup>TU Darmstadt; <sup>2</sup>VirginiaTech

The strengthening effect of twins in nanocrystalline metals has been reported both in experiment and simulation. While twins are mostly considered as effective barriers to slip transfer of dislocations, they can also provide nucleation sites for dislocations or migrate during the deformation process, contributing to plasticity. Here we present a comparative atomistic study of the effect of twins on the deformation behavior of nanocrystalline Cu, Al and Pd. A new analysis method based on an automated Burgers circuit is applied, which allows to analyze the dislocation interaction with twin planes and grain boundaries. While Cu shows hardening from the twins, Pd and Al show the opposite effect. The results provide evidence how the dissociation widths affect the slip transfer across the twin boundary and why twin planes provide additional dislocation sources, which is the main reason for softening of these samples as compared to identical nanocrystals without twins.

**9:20 AM**

**Dislocation Nucleation and Starvation in Metallic Nanowires:** *Scott Mao*<sup>1</sup>; A. Cao<sup>2</sup>; Y Wei<sup>2</sup>; <sup>1</sup>University of Pittsburgh; <sup>2</sup>Institute of Mechanics

The mechanical behavior of bulk metals is usually characterized as smooth continuous plastic flow following by yielding. Here we show, by using molecular dynamics simulations that the mechanical deformation behaviors of single-crystalline nickel and copper nanowires are quite different from their bulk counterparts. Correlation between the obtained stress-strain curves and the visualized defect evolution during deformation processes clearly demonstrates that a sequence of complex dislocation slip processes results in dislocation starvation, involving dislocation nucleation, propagation and finally escaping from the wire system, so that the wires deformed elastically until new dislocation generated. This alternating starvation of dislocations is unique in small-scale structures. Furthermore, the magnitude of yield stress of these nanowires is strongly dependent of the wire size.

**9:40 AM**

**Dislocation Nucleation from Grain Boundaries in Nanocrystalline Pd and Pd-Au Studied by Molecular Dynamics Simulations:** *Jonathan Schaefer*<sup>1</sup>; Alexander Stukowski<sup>1</sup>; Karsten Albe<sup>1</sup>; <sup>1</sup>TU Darmstadt

Molecular dynamics simulations on the nucleation and absorption of dislocations at grain boundaries are presented for nanocrystalline Pd and Pd-Au with grain sizes exceeding 15nm. Initial structures are generated with the Voronoi tessellation method and alloyed systems are created via a Monte-Carlo simulation in the semi-grand-canonical ensemble. A novel approach that allows to identify dislocation lines within the grains and grain boundaries from atomistic data is introduced and applied. Nucleation processes are analyzed with respect to the local stresses, grain boundary structure, alloy composition and relaxation state of the initial structure.

**10:00 AM**

**Orientation Dependent Plasticity in Metal Nanowires under Torsion:** *Christopher Weinberger*<sup>1</sup>; Wei Cai<sup>1</sup>; <sup>1</sup>Stanford University

Plasticity at small scales is more heterogeneous and intermittent than in the bulk which may lead to the limitation of plastic metal forming at the micro- and nanoscales. In order to better understand the plastic response of metals at these scales and the effects of strain gradients, we investigate the orientation dependent plasticity in pristine metal nanowires under torsion using molecular dynamics and dislocation dynamics simulations. When the wires are oriented along the <110> direction, coaxial dislocations nucleate, creating a homogeneous plastic deformation which is similar to the Eshelby twist problem. However, in the <111> and <100> direction, plasticity occurs through the formation of twist boundaries, which localizes the plastic deformation. These results illustrate that plastic deformation in the presence of strain gradients can be strongly influenced by crystal orientation.



### 10:20 AM Break

### 10:40 AM Invited

**Slip Transmission Mechanisms for Glide Dislocations across Dissimilar Metallic Interfaces:** *Jian Wang*<sup>1</sup>; Richard Hoagland<sup>1</sup>; John Hirth<sup>1</sup>; Amit Misra<sup>1</sup>; <sup>1</sup>LANL

Using atomistic modeling and anisotropic elastic theory, we have studied slip transmission for glide dislocations across dissimilar metallic interfaces in a model Cu-Nb system. The Cu-Nb interfaces have relatively low shear strength and are referred to as 'weak' interfaces. Our work shows that such interfaces are very strong traps for glide dislocations and thus, effective barriers for slip transmission, because the weak interface is readily sheared under the stress field of an impinging glide dislocation, resulting in an attractive force on the glide dislocation and leading to the absorption of dislocation in the interface. Besides the trapping of dislocations in weak interfaces, we also discuss geometric factors such as the crystallographic discontinuity of slip systems across the Cu/Nb interfaces, which contribute to the difficulty of dislocation transmission across an interface. The implications of these findings to the unusually high strengths experimentally measured in Cu/Nb nanolayered composites are discussed.

### 11:10 AM

**Molecular Mechanics Simulation of Plastic Deformation in Nanoscale FCC-BCC Multilayered Metallic Composites:** *Shuai Shao*<sup>1</sup>; Sergey Medyanik<sup>1</sup>; <sup>1</sup>Washington State University

A significant increase in strength can be often observed in multilayered metallic composites when the individual layer thickness is decreased from microscale to nanoscale. Recently, a number of atomistic simulation studies have been conducted to investigate nanoscale metallic bilayers with different types of interfaces. However, the case with incoherent interfaces focused mainly on studying the interaction of single artificially introduced dislocations with the interface under two-dimensional loading conditions. In this work, molecular mechanics simulations are applied to study dislocation nucleation and propagation in a Cu-Nb bilayer with an incoherent FCC-BCC interface under three-dimensional loading conditions due to indentation. Indenter is applied to generate dislocations at and near the surface from each side of the bilayer (in separate simulations). The role which incoherent interfaces play in the strengthening of multilayered metallic composites is explored. Mechanisms of interactions between gliding dislocations and the incoherent interface are identified and studied in detail.

### 11:30 AM

**Shock Response of Cu-Nb Nanolayer Composites:** *Timothy Germann*<sup>1</sup>; Shengnian Luo<sup>1</sup>; Nathan Mara<sup>1</sup>; <sup>1</sup>Los Alamos National Laboratory

Large-scale classical molecular dynamics (MD) simulations and laser-driven shock wave experiments (both direct laser drive and laser-launched minifyler plates) have been used to study the response of Cu-Nb nanolayered composites to shock compression. At a layer thickness of 5 nm, the hardness of such metallic multilayers (as measured by quasistatic indentation or compression tests) reaches a maximum due to the difficulty of dislocation transmission across the interfaces. We observe a similar strengthening effect under dynamic shock loading, both in the MD simulations and in post mortem examinations of shock-recovered samples subjected to ~20 GPa shock loading. The MD simulations provide insight into the dislocation nucleation and transmission processes that occur under compression, as well as the subsequent annihilation upon release.

### 11:50 AM

**Yield Strength in Nanocrystalline Cu during High Strain Rate Deformation:** *Nhon Vo*<sup>1</sup>; Robert Averback<sup>1</sup>; Pascal Bellon<sup>1</sup>; Alfredo Caro<sup>2</sup>; <sup>1</sup>University of Illinois, Urbana-Champaign; <sup>2</sup>Lawrence Livermore National Laboratory

We observe in molecular dynamics a nearly linear relationship between the yield strength in nanocrystalline Cu during high strain rate deformation and the fractional grain boundary (GB) volume. Specimens were prepared with grain sizes between 2.5 to 20 nm and with different grain configurations. They were subsequently annealed to reduce the fraction of grain boundary volume, but without significantly changing their grain sizes. The yield strengths of the samples were then calculated for uniaxial compression at strain rates of  $1 \times 10^8$  1/s and  $1 \times 10^9$  1/s. For each strain rate, the observed strength was found to scale with the fractional number of GB atoms in the sample. This observation suggests a new scaling behavior for the onset of plasticity in nanocrystalline materials, controlled not by the grain size alone, but by a combination of both

grain size and degree of GB relaxation, as measured by the grain boundary volume.

### 12:10 PM

**A Quantized Crystal Plasticity Model for Nanocrystalline Metals: Dislocation Source Strengths and Internal Stress:** Lin Li<sup>1</sup>; Myoung-Gyu Lee<sup>2</sup>; *Peter Anderson*<sup>1</sup>; Steven Van Petegem<sup>3</sup>; Helena Van Swygenhoven<sup>3</sup>; <sup>1</sup>The Ohio State University; <sup>2</sup>Korea Institute of Materials Science; <sup>3</sup>Paul Scherrer Institute

A quantized crystal plasticity (QCP) model is used to study several distinctive deformation features of nanocrystalline (NC) metals [1]. A key model feature is that the average plastic strain evolves in a stepwise fashion, as seen in MD simulations involving dislocation slip across grains. The model reproduces several experimental features of NC metals, including an enhanced flow stress, an extended elasto-plastic transition, large recoverable strain and reversible peak broadening upon unloading, and even the evolution of lattice strains with deformation. These successful predictions occur when the grain-to-grain distribution of source strengths for plasticity has certain features, and only for certain pre-deformation histories. The experiment-model comparison therefore provides an approach to determine some fundamental deformation characteristics of NC metals.[1] Li L, et. al.. Acta Materialia 2009;57:812.

## Neutron and X-Ray Studies of Advanced Materials III: Strain and Dislocation Gradients from Microdiffraction I

*Sponsored by:* The Minerals, Metals and Materials Society, ASM International, TMS Structural Materials Division, TMS/ASM: Mechanical Behavior of Materials Committee, TMS: Titanium Committee  
*Program Organizers:* Rozaliya Barabash, Oak Ridge National Laboratory; Jaimie Tiley, Air Force Research Laboratory; Erica Lilleodden, GKSS Research Center; Peter Liaw, University of Tennessee; Yandong Wang, Northeastern University

Monday AM Room: 303  
February 15, 2010 Location: Washington State Convention Center

*Session Chairs:* Rozaliya Barabash, ORNL; Hongbin Bei, Oak Ridge National Laboratory

### 8:30 AM Keynote

**Imaging Methods for Mapping Orientations, Plastic Strain and Stresses in Grains:** *Henning Poulsen*<sup>1</sup>; <sup>1</sup>Risoe DTU

3DXRD microscopy is an emerging technique for characterizing individual grains in 3D. In favorable cases, the position, shape, orientation and stress state of thousands of grains can be determined in situ during processing. The status of the technique is outlined and four new functionalities are highlighted: 1) mapping of type-II stresses 2) orientation imaging of deformed materials 3) combined tomography-3DXRD techniques and 4) 3D maps of the local slip amplitudes. Examples of use are presented from the areas of polycrystal deformation, nucleation, recrystallisation, and grain growth.

### 9:00 AM Invited

**Using High Energy X-Ray Experiments and Crystal-Based Simulations to Understand Micromechanical Deformation Behavior of Metallic Polycrystals:** *Matthew Miller*<sup>1</sup>; Paul Dawson<sup>1</sup>; Christos Efstathiou<sup>1</sup>; Donald Boyce<sup>1</sup>; Ulrich Lienert<sup>2</sup>; <sup>1</sup>Cornell University; <sup>2</sup>Advanced Photon Source

The mechanical behavior of a crystal within a loaded aggregate is complicated by anisotropic properties and complex microscale loading conditions. Our approach for understanding this behavior consists of high fidelity micromechanics-based simulations together with a new class of synchrotron x-ray diffraction experiments to determine mechanical properties and performance measures for polycrystalline structural alloys. The stress determination experiments are part of the High Energy Diffraction Microscopy (HEDM) suite of capabilities at the Advanced Photon Source (APS) beamline 1-IDC. The polycrystal model begins with anisotropic elasticity and restricted slip plasticity. Each crystal is discretized with finite elements. The initial orientations are specified by matching the measured crystallographic texture. This talk describes experiments and simulations on beta 21s, a bcc titanium alloy. Measured lattice strains are compared to simulation results. Since no

# Technical Program

results exist in the literature, the first step in the analysis was the determination of the single crystal elastic moduli.

## 9:20 AM Invited

**Three Dimensional X-Ray Scanning Micro/Nano-Diffraction Probe for High-Pressure Research:** *Wenjun Liu<sup>1</sup>; Ho-kwang Mao<sup>2</sup>; Wenge Yang<sup>2</sup>; Yang Ding<sup>2</sup>; Lin Wang<sup>2</sup>; Przemyslaw Dera<sup>2</sup>; Gene Ice<sup>3</sup>; Paul Zschack<sup>1</sup>;* <sup>1</sup>Argonne National Laboratory; <sup>2</sup>Carnegie Institution of Washington; <sup>3</sup>Oak Ridge National Laboratory

During the past decade, substantial progress has been made in the research and development of x-ray focusing optics at synchrotron facilities. Submicron focused beams are now in routine operation and sub-hundred nanometer spots have been achieved. However, these advances have not yet been well applied to high-pressure research. We now have the opportunity for major breakthroughs that will fundamentally change the diamond anvil cell (DAC) technology using this more than order-of-magnitude improvement of beam size. 3D x-ray diffraction microscopy developed at 34-ID beamline at the Advanced Photon source has been proved to be a powerful tool for providing detailed local crystal structural information of crystallographic orientation, strain tensor, and lattice structure in materials, as well as materials at high-pressure. Preliminary experiments on adopting DAC at submicron focused beamline for structure determination by single-crystal diffraction are presented. Related instrumentation issues to high-pressure research problems will be also discussed.

## 9:40 AM

**A Facility for  $\mu$ XRD,  $\mu$ XRF and  $\mu$ XAS at the Canadian Light Source:** *Renfei Feng<sup>1</sup>; Morgan Bradford<sup>1</sup>; Stewart McIntyre<sup>2</sup>;* <sup>1</sup>Canadian Light Source; <sup>2</sup>University of Western Ontario

VESPERs is a newly commissioned beamline at the Canadian Light Source. It is a hard X-ray microprobe beamline dedicated to X-ray micro-diffraction ( $\mu$ XRD), X-ray micro-fluorescence ( $\mu$ XRF), and micro X-ray absorption spectroscopy ( $\mu$ XAS) studies. The beamline offers four widely differing bandwidths,  $\sim 0.01\%$ ,  $\sim 1.6\%$ ,  $\sim 10\%$ , and fully polychromatic beam, to simplify the Laue diffraction analysis, to optimize XRF excitation, and to enable X-ray absorption spectroscopy measurement. The energy range provided by the beamline covers 6-30 keV. The beamline and its current status will be described and some applications will be presented.

## 9:55 AM Invited

**Size Effects in Plasticity Investigated by In Situ Laue Diffraction:** *Steven Van Petegem<sup>1</sup>; Helena Van Swygenhoven<sup>1</sup>;* <sup>1</sup>Paul Scherrer Institut

Microcompression of micron-sized pillars is a promising tool which allows evaluating mechanical properties of materials via specimens with sizes in the range of micrometers. In order to investigate the microstructural evolution during deformation a new in-situ testing technique was developed at the Swiss Light Source. Here, micron-sized single crystal pillars are illuminated by a micron-sized pink x-ray beam during continuous deformation. The evolution of the position and shape of the diffraction spots is directly linked to changes in local crystallographic orientation and strain gradients. Remarkable differences in the initial microstructure of single crystal micropillars prepared from the same bulk material were found. Furthermore we show that initial plastic deformation is controlled by the boundary constraints of the test. It is anticipated that this new in situ technique has great potential to gain insight into the deformation mechanisms in more complex structures, providing essential input for predictive plasticity models.

## 10:15 AM Invited

**Residual Stress Effects on the Phase-Specific Strains in Directionally-Solidified NiAl-Mo Composite under Thermal and Mechanical Loading:** *Hongbin Bei<sup>1</sup>; R Barabash<sup>2</sup>; Easo George<sup>2</sup>; Gene Ice<sup>1</sup>;* <sup>1</sup>Oak Ridge National Laboratory; <sup>2</sup>Oak Ridge National Laboratory and University of Tennessee

Neutron diffraction measurements and model calculations suggest that, in directionally-solidified NiAl-Mo composites, stresses develop between the NiAl and Mo phases because of thermal expansion mismatch. It is known that such residual stresses play important roles in the thermal and mechanical responses of individual phases in a composite material. In this study, three-dimensional (3D) spatially resolved strain distributions in the NiAl matrix and the  $\sim 550$ – $1000$  nm Mo fibers of a NiAl–Mo eutectic were investigated by microbeam x-ray diffraction. For embedded Mo fibers, the measured elastic strain is consistent with the predicted thermal mismatch strain between the NiAl and Mo phases. However, when the NiAl matrix is etched the d-spacing of

the exposed Mo micropillars, increases to that of unconstrained Mo, indicating release of the residual strain in the Mo fibers. We will discuss how the residual stress influences the phase-specific strain response in a NiAl–Mo composite under thermal and mechanical loading.

## 10:35 AM Break

## 10:45 AM

**X-Ray Micro Beam Probing Pre-Strain Effects on Dislocation and Strain Gradients in the NiAl-Mo Composite:** *Rozaliya Barabash<sup>1</sup>; H Bei<sup>2</sup>; Y. Gao<sup>1</sup>; G. Ice<sup>2</sup>; E. George<sup>1</sup>;* <sup>1</sup>Oak Ridge National Laboratory and the University of Tennessee, Knoxville; <sup>2</sup>Oak Ridge National Laboratory

3D spatially-resolved polychromatic microdiffraction was applied to probe the depth-dependent dislocation density and strain gradients in separate phases of a NiAl–Mo composite. Dislocation density and strain gradients are investigated as a function of pre-strains. It is found that pre-strain changes the stress state as compared to the as grown composite. In as grown composites, due to the thermal expansion mismatch, the Mo phase is under compression and the NiAl phase is in tension. After pre-straining, the Mo phase is in tension and NiAl matrix is under compression, which can be understood from their mismatch in yield strain and the elastic constraints during unloading. The dislocation density in both phases is found to grow with increased pre-straining. These measurements provide dislocation information to recent directional solidified Mo micro-pillar testing.

## 11:00 AM Invited

**Synchrotron X-Ray Microdiffraction for the Study of Micromechanics of Materials at Nanoscale:** *Nobumichi Tamura<sup>1</sup>; Martin Kunz<sup>1</sup>; Kai Chen<sup>1</sup>;* <sup>1</sup>Lawrence Berkeley National Lab.

The dedicated x-ray microdiffraction beamline BL12.3.2 at the Advanced Light Source is opened to the user community since 2007 while additional commissioning has been completed in 2008. Providing both monochromatic and polychromatic focused x-ray beam from a superbend source in the energy range of 5–22 keV, the beamline is especially well suited for spatially resolved measurements of strain in micro-devices and phase identification in heterogeneous samples. The sample can be scanned under the focused beam and 2D x-ray diffraction patterns as well as fluorescence data are collected at each step in an automated fashion to provide for grain orientation, phase distribution and strain/stress distribution map of the sample with micron to submicron resolution. We will review some of the applications from this beamline including measurements of stress in copper interconnects and lead-free solder joints, study of tin whisker growth, compression test in nanopillars and domain switching in ferroelectric materials.

## 11:20 AM Invited

**Spatially Resolved Elastic Strains within Bulk Dislocation Cell Structures: What Next?:** *Lyle Levine<sup>1</sup>; Bennett Larson<sup>2</sup>; Peter Geantl<sup>3</sup>; Jon Tischler<sup>2</sup>; Michael Kassner<sup>2</sup>; Wenjun Liu<sup>4</sup>;* <sup>1</sup>National Institute of Standards and Technology; <sup>2</sup>Oak Ridge National Laboratory; <sup>3</sup>University of Southern California; <sup>4</sup>Advanced Photon Source

Over the past several years, we have used depth-resolved, submicrometer X-ray beams to directly measure the axial elastic strains within dislocation cell interiors and cell walls in plastically deformed copper single crystals. Although these studies have settled long-standing questions about the long-range stresses in heavily deformed metals, other critical issues remain both unresolved and largely unaddressed in the literature. For example, the usual picture of high dislocation density cell walls surrounding dislocation-free cell interiors comes primarily from TEM measurements of thin foils, even though it is well established that a substantial fraction of the dislocation content is lost during sample thinning. Also, most work on stresses within dislocation cell structures, including our own, looks only at axial stresses and doesn't address the full tensorial nature of the elastic strain. We will discuss our progress in tackling both of these problems using depth resolved submicrometer X-ray diffraction.

## 11:40 AM Invited

**In-situ X-Ray Diffraction of Brittle and Ductile Nanostructured Materials:** *Ralph Spolenak<sup>1</sup>;* <sup>1</sup>ETH Zurich

The combination of several in-situ methods can shed additional light on deformation and failure mechanisms in nanostructured materials. In the current study in-situ X-ray diffraction studies at synchrotron light sources are combined with in-situ SEM and Raman spectroscopical observations. In



Mon. AM

this context the scaling behavior in fracture and delamination of Ta thin films on polyimide substrates, the fracture of natural zirconia on Zr alloys and the fracture of ductile Au and Al thin film alloys is studied. Both brittle and ductile crack patterns can be correlated to the corresponding stress transfer between substrate and thin film. A further extension of this concept is presented when Raman spectroscopy is utilized to locally measure the stress evolution in nacre, a natural nanocomposite, and correlating it to the macroscopic deformation behavior as obtain by diffraction. Fracture toughness and strength is correlated to the microstructure of different sea shells.

**12:00 PM Invited**

**Real, Orientation and Reciprocal Space Coverage of 3DXRD at the APS 1-ID Beamline:** *Ulrich Lienert*<sup>1</sup>; <sup>1</sup>ANL

The three-dimensional x-ray diffraction (3DXRD) technique employs high energy synchrotron radiation and area detectors for the structural characterization of polycrystalline bulk materials. The 'tomographic' data acquisition provides the temporal resolution for in situ investigations. Within the high energy diffraction microscopy (HEDM) program at the APS 1-ID beamline near-, farfield, and high reciprocal space resolution variants of the technique are developed. Unique capabilities of these variants are grain boundary mapping, high strain sensitivity, and dislocation structure sensitive peak profile measurements, respectively. By combining these techniques the real, orientation and reciprocal space coverage can be significantly extended. The status, future plans, and limitations will be presented and illustrated by selected case studies.

**12:20 PM**

**Inverse Analysis of Engineering Neutron Diffraction Data:** *Seung-Yub Lee*<sup>1</sup>; *Youngshin Kim*<sup>1</sup>; *Hyuntae Na*<sup>1</sup>; *Ersan Ustundag*<sup>1</sup>; <sup>1</sup>Iowa State University

Integration of engineering neutron diffraction (ND) data analysis and solid mechanics modeling offers a powerful approach to deduce in-situ constitutive behavior of materials. The basic approach is to perform an inverse analysis of ND data so that experimental strains fit predictions of the model by optimizing the model parameters that define the constitutive law. This presentation will outline recent results from the use of finite element analysis (FEA) and self-consistent modeling (SCM) in the interpretation of ND data. Various optimization algorithms (including least-square and artificial neural network analyses) were employed. The latter also allowed the study of the relative influence of various model parameters and yielded suggestions on optimum experiment design.

**12:35 PM**

**Compositional Effects on the Superelasticity of Gum Metal:** *Russell Talling*<sup>1</sup>; *David Dye*<sup>1</sup>; <sup>1</sup>Imperial College

The deformation mechanisms of the bcc Ti alloy, Gum metal (Ti-36Nb-2Ta-3Zr-0.3O, wt.%) have recently been the focus of much attention. This alloy possesses high strength, high elastic strain, low Young's modulus and high ductility. We have identified that Gum metal deforms via a reversible stress-induced phase transformation to the  $\alpha''$  phase. This work has focuses on the effect of O and Sn on the micromechanics. In-situ synchrotron X-ray diffraction has been used to infer the shear modulus  $C'$ , which gives an indication of the susceptibility of the bcc phase to transform. The texture of the martensite and bcc parent phase has been reconstructed at various points during tensile tests. We have also witnessed shape memory type loading behaviour in some Gum metal compositions, with evidence of martensite self-accommodation within the plateau region of the stress strain curve.

**12:50 PM**

**First ex-situ/in-situ Measurements of Strains/Stresses at Engineering Diffractometer VULCAN at SNS:** *Ke An*<sup>1</sup>; *H.D. Skorpenske*<sup>1</sup>; *A.D. Stoica*<sup>1</sup>; *Dong Ma*<sup>1</sup>; *Ercan Cakmak*<sup>2</sup>; *Hahn Choo*<sup>2</sup>; *X.L. Wang*<sup>1</sup>; <sup>1</sup>Oak Ridge National Laboratory; <sup>2</sup>The University of Tennessee

The engineering diffractometer VULCAN at the SNS started commissioning since June 26th in 2009. This instrument is designed for materials science and engineering studies. With VULCAN, users can not only conduct mapping of residual stresses, chemistry, microstructure and texture but also measure dynamically mechanical deformation response, material chemical properties change and microstructure evolution under dynamic loading (e.g. fatigue) or severe material processing (e.g., welding). With special sample environments, such as the vacuum furnace and unique multi-axial tension-torsion load frame,

etc., VULCAN extends neutron scattering studies to broader areas of material science and engineering mechanics.

**Neutron and X-Ray Studies of Advanced Materials III: Structure from Diffraction**

*Sponsored by:* The Minerals, Metals and Materials Society, ASM International, TMS Structural Materials Division, TMS/ASM: Mechanical Behavior of Materials Committee, TMS: Titanium Committee  
*Program Organizers:* *Rozaliya Barabash*, Oak Ridge National Laboratory; *Jaimie Tiley*, Air Force Research Laboratory; *Erica Lilleodden*, GKSS Research Center; *Peter Liaw*, University of Tennessee; *Yandong Wang*, Northeastern University

Monday AM

Room: 613

February 15, 2010

Location: Washington State Convention Center

*Session Chairs:* *Emil Zolotoyabko*, Technion

**8:30 AM Invited**

**Atomic Structure and Nano-Structure of Natural Bio-Composites:** *Emil Zolotoyabko*<sup>1</sup>; <sup>1</sup>Technion

Biom mineralization process within living organisms results in producing the organic/inorganic composite materials with superior characteristics. This field continues to attract a lot of attention of many research groups worldwide. Organic macromolecules, supplied by organisms according to genetic program, play a crucial role in this sophisticated "processing". Our studies using high-resolution x-ray and neutron powder diffraction show a complexity of bio-minerals on the atomic and nano-scale due to interaction of organic macromolecules with ceramic crystallites. Based on systematic studies of natural calcium carbonate structures, we indicate three main structural features of biogenic crystals (as compared to their geological counterparts): anisotropic distortions of unit cells; bond lengths differences; unusual diminishing under annealing of the sizes of crystallite blocks which coherently scatter X-rays. All this is the result of local forces imposed on mineral crystallites by intra-crystalline organic macromolecules, the forces being strongly affected by mild annealing at 200-300 C.

**8:50 AM Invited**

**In-Situ Study of Time and Thickness Dependence of Crystallization of Amorphous TiO<sub>2</sub> Thin Films and Powders:** *Radomir Kuzel*<sup>1</sup>; *Lea Nichtova*<sup>1</sup>; *Zdenek Matej*<sup>1</sup>; *Jindrich Musil*<sup>2</sup>; <sup>1</sup>Charles University in Prague, Faculty of Mathematics and Physics; <sup>2</sup>University of West Bohemia in Pilsen

Numerous interesting properties of titanium dioxide, in particular photocatalytic activity, strongly depend on crystallization and phase composition. Annealing temperatures were selected below 220°C where fast crystallization appears. Then the slow process allowed detailed time XRD in-situ investigations in laboratory conditions. Strong dependence of crystallization kinetics on the film thickness was found. The process could be well described by the Avrami equation modified by initial time of crystallization. The crystallization starts later and it is slow for very thin films (below 300 nm). Evolution of preferred orientation was observed, the (001) crystallites grow first but after complete crystallization the texture was usually weak. Line broadening was constant and small from the beginning of observable crystallization which was due to the rapid growth of a few crystallites. Tensile residual stresses were developed slowly during the crystallization and confirmed by detailed measurements at room temperature. They increase rapidly with decreasing film thickness.

**9:10 AM**

**Lattice Distortion Formations by Low Energy Ar<sup>+</sup> Bombardment of Epitaxial Thin Films Grown on Silicone (100):** *Paul Rozenak*<sup>1</sup>; <sup>1</sup>Hydrogen Energy Batteries LTD

Transmission electron microscopy (TEM) and X-ray characterization of lattice distortion forms, caused by low energy Ar<sup>+</sup> bombardment of grown thin silicon films on silicon (001) substrate were studied. The isotropic case (of spherical distortions) takes place in epitaxial silicon "as grown" processes. The intensity distribution consists of two maxima, one from the distorted layer and the other from original un-effected silicon lattice. The significant changes in the 2θ location, peak broadening and integrated intensity from the (004)\* reflections were obtained as the function of aging temperatures. First, aging

# Technical Program

heat treatment, affects the distribution of distortions obtained from local regions at the “as grown” layer, which changes to a special topography of continued distortions at higher aging temperatures. At aging temperatures above 650°C, this extra diffraction peak disappears. The TEM observations reveal the appearance of dislocation lines, with dark and bright contrasts around the lines and inter-dislocation strain contrasts.

## 9:25 AM Invited

**Voyaging around Nacre with the X-Ray Shuttle: From Bio-Mineralisation to Prosthetics via Mollusc Phylogeny:** *Daniel Chateigner*<sup>1</sup>; M. Morales<sup>1</sup>; L. Lutterotti<sup>1</sup>; <sup>1</sup>Ecole Nationale Supérieure d'Ingénieurs de Caen (ENSICAEN)

Bobbio (1970) analysed Maya cranes exhibiting nacre teeth with antemortem character, demonstrating the oldest signature of human implantology, using natural mollusc shells! The possibility of their osteointegration in human bone was born, in dentistry and prosthetics in general. Lopez (1980) promoted this idea further, demonstrating that natural nacles are not only biocompatible but osteoinductive. These two fascinating discoveries gave rise to tremendous research developments at the interfaces of several scientific disciplines opening the following questionings: - are all natural shells implantable? can we use shell spares from mollusc farming? - can we detect which shell microstructures, structures ... are the best appropriated to a given medical application? can we detect some differences between natural nacles? - can we synthetically reproduce biogenic-like nacre? - can we produce nacre-like bulks or cover prostheses? can we implant them? We illustrate these questionings using x-ray investigations.

## 9:45 AM Invited

**Materials Characterization Using the Hard X-Ray Nanoprobe Beamline at Argonne National Laboratory:** *Jörg Maser*<sup>1</sup>; Martin V. Holt<sup>1</sup>; Robert P. Winarski<sup>1</sup>; Volker Rose<sup>1</sup>; Peter Fuesz<sup>1</sup>; Gregory Brian Stephenson<sup>1</sup>; <sup>1</sup>Argonne National Laboratory

The Center for Nanoscale Materials' Hard X-ray Nanoprobe (HXN) at the Advanced Photon Source is designed to characterize composition and structure of nanoscale materials and devices with high spatial resolution [1]. The HXN uses hard x-rays with a photon energy between 3 and 30 keV, taking advantage of the good penetration of hard X-rays to study buried structures and interfaces, and perform trace element analysis of elemental constituents of the sample with high sensitivity. X-ray diffraction is used to identify crystallographic phase, strain and structure in novel materials and devices. In addition, the HXN integrates a tomographic full-field transmission mode that is used to characterize the 3-dimensional structure of complex systems and devices. All operation modes can be changed in-situ. The HXN takes advantage of the good penetration of hard X-rays to study buried structures and interfaces. The HXN uses diffractive optics to allow specimen characterization at high spatial resolution. In scanning probe mode, an incident, spatially coherent wave front is focused by a Fresnel zone plate to a diffraction limited probe with a size of 50 nm and below. X-ray excited x-ray fluorescence photons and scattered photons are collected by energy dispersive and area detectors. In full-field transmission mode, the sample is illuminated using a capillary condenser system; a magnified image of the sample with a spatial resolution of 30 nm is created by an imaging zone plate downstream of the sample. 3-D images are obtained by rotating the sample for tomographic data acquisition. The HXN is optimized for the study of novel materials, such as ferroelectrics, complex oxides, thin films with novel structural and electronic/magnetic properties, and devices that utilize these properties. Typical applications include Si-based materials and devices, as well as novel materials and materials systems for potential use in energy applications, actuation, switching. The high trace element sensitivity is also useful for characterizing metal distributions in biological systems such as cells and tissues. We will give an overview of the HXN system and its characterization capabilities, and will present initial scientific applications. References: [1] J. Maser, G.B. Stephenson, D. Shu, B. Lai, S. Vogt, A. Khounsary, Y. Li, C. Benson, G. Schneider, “Conceptual design for a hard x-ray nanoprobe beamline with 30 nm resolution,” AIP Conf. Proc., 705, AIP (2004), 470 - 473. [2] H. Kang, H. Yan, R. P. Winarski, M. Holt, J. Maser, C. Liu, R. Conley, S. Vogt,

A. T. Macrander, G. B. Stephenson. “Focusing of hard x-rays to 16 nanometers with a multilayer Laue lens”. Appl. Phys. Lett. 92, 221114-1-221114-3 (2008).

## 10:05 AM Invited

**In-Situ Characterization of Creep-Damage by X-Ray Microtomography:** Krzysztof Dzieciol<sup>1</sup>; Federico Sket<sup>1</sup>; Thomas Buslaps<sup>2</sup>; Marco di Michiel<sup>2</sup>; *Andras Borbely*<sup>1</sup>; Anke Pyzalla<sup>3</sup>; <sup>1</sup>Max-Planck Institut für Eisenforschung; <sup>2</sup>European Synchrotron Radiation Facility; <sup>3</sup>Helmholtz Zentrum für Materialien und Energie

In-situ tomography based on its nondestructive nature has opened new possibilities for studying the kinetics of damage during high temperature creep. Application of accurate image processing algorithms to three-dimensional reconstructions series characterizing consecutive stages of damage offers an excellent opportunity to characterize the deterministic nature of the process. In contrast to metallographic techniques, where damage evolution results from statistical considerations by averaging over cavities of different sizes, in situ tomography allows studying the more appropriate evolution of single cavities, which is in accordance with the theoretically predicted volume dependence of cavities growth-rate. The new approach delivered for the first time accurate experimental data that can be compared with theoretical predictions. Experimental results for copper confirm the theoretically predicted proportionality between cavity growth-rate and cavity volume as well as between growth-rate and strain-rate. The real growth-rates, however, are larger by a factor of about 10 compared to theoretical predictions.

## 10:25 AM Break

## 10:35 AM

**In Situ X-Ray Synchrotron Observations of Steel Phase Transformation under Non-Equilibrium Conditions:** *Wanchuck Woo*<sup>1</sup>; Eliot Specht<sup>2</sup>; Zhili Feng<sup>2</sup>; Wei Zhang<sup>2</sup>; Xunli Wang<sup>2</sup>; <sup>1</sup>Korea Atomic Research Institute; <sup>2</sup>Oak Ridge National Laboratory

Non-equilibrium solid-state phase transformation in cold-rolled carbon steels was investigated using an X-ray synchrotron beam line of the Advanced Photon Source. A programmable electric resistance heating device was used to heat the steel specimens up to 1300 °C (fully austenitized) under vacuum environment. Different heating rates (1, 3, 10, 30 °C/s) were used to study the non-equilibrium phase transformation kinetics. A fast CCD detector with time resolution of 1 second was used to collect the diffraction patterns from the surface of the specimen during the experiment. The phase transformation starting and finishing temperatures ( $T_{A1}$ ,  $T_{A3}$ ) and the relative volume fractions of austenite and ferrite phases were obtained from the diffraction peak analysis. The experiments revealed unexpected transformation behavior including reduced  $T_{A1}$  temperature and increased volume fraction of the austenite phase at increased heating rate. The experimental details and the observed phase transformation behavior will be presented and discussed.

## 10:50 AM

**Characterization of Hydride Phase Stability in Zirconium Alloys as a Function of Yield Stress with Synchrotron X-Ray Diffraction:** *Eric Tulk*<sup>1</sup>; Matthew Kerr<sup>2</sup>; Mark Daymond<sup>1</sup>; <sup>1</sup>Queen's University; <sup>2</sup>US Nuclear Regulatory Commission

Zirconium alloys find application world wide as a structural material in nuclear reactors. The mechanical properties of zirconium components degrade in-service as a result of hydride embrittlement. While some aspects of the mechanics of embrittlement are well characterized, there is significant disagreement in the literature regarding hydride phase stability during thermo-mechanical processing. It has been suggested that zirconium yield stress is the dominate factor associated with hydride phase stability, but no comprehensive database was available to test this hypothesis (previous studies examined only a narrow range of alloy compositions and processing conditions). This work uses synchrotron x-ray diffraction to characterize the hydride phase formed in zirconium alloys under a wide range of zirconium alloy compositions and processing conditions. The surprising result is that zirconium yield stress is only one parameter effecting hydride phase stability, a result that may explain the wide variation reported for hydride phase stability in the literature.



11:05 AM

**Growth of Anti-Phase Domains in Ternary FeCo Alloys under Various Annealing Treatments and Cooling Processes:** *Ralph Gilles<sup>1</sup>*; Michael Hofmann<sup>1</sup>; Yan Gao<sup>2</sup>; Frank Johnson<sup>2</sup>; Debashis Mukherji<sup>3</sup>; Christoph Hugenschmidt<sup>1</sup>; Philip Pikart<sup>1</sup>; <sup>1</sup>TU Muenchen; <sup>2</sup>GE Global Research; <sup>3</sup>TU Braunschweig

Recent years have seen a reawakened interest in Fe-Co alloys due to the increased demands of modern electrical power generation and distribution equipment. For industrial application the challenge involves increasing the tensile strength and ductility of FeCo alloys. The effects of alloying FeCo with Pt, Pd, Mn, Ir, and Re have been investigated as part of this work by neutron diffraction. In the composition range of about 30%-70% Co, FeCo alloys undergo a continuous order-disorder phase transformation in the temperature range of 615±30°C [1]. Whereas the T<sub>c</sub> temperature is independent of the thermal history, the microstructure of ordered domains is sensitively dependent on thermal history and on the kinetics of the order/disorder transition. As a complementary method positron measurements have been performed to describe the nucleation of domains with the correlation to the defect density. Reference:[1] R. Gilles et al., Metall. Mat. Trans. A, 2009, in print.

11:20 AM

**Effects of Shot Peening Aluminum Alloy A356.2 Cast Plate with Steel and Glass Shot on the through-Thickness Residual Stresses:** A. Ritter<sup>1</sup>; B. Kuhr<sup>1</sup>; C. Hubbard<sup>2</sup>; T. R. Watkins<sup>2</sup>; *Carl Boehlert<sup>1</sup>*; X. Niu<sup>3</sup>; <sup>1</sup>Michigan State University; <sup>2</sup>Oak Ridge National Laboratory; <sup>3</sup>Magna Cosma International

Shot peening forms a compressive residual stress on the surface which can favorably increase fatigue life. The goal of this study was to gain an understanding of the residual stresses formed after shot peening a cast automotive aluminum alloy A356.2. The residual stresses were measured using X-ray diffraction for near surface and neutron diffraction for through thickness residual stresses. Using the Neutron Residual Stresses Mapping Facility in the High Flux Isotope Reactor at Oak Ridge National Laboratory the residual stresses were measured in the longitudinal, transverse and normal direction as a function of depth from the surface. The d-spacings and strain free d-spacing, obtained by careful measurement of a stress free coupon, were used to calculate the residual strains and derive the residual stresses using Young's modulus and Poisson's ratio. The results indicated that the greatest compressive residual stress existed within 20 µm from the surface and the compressive residual

11:35 AM

**Residual Stress Analysis of Resistance Spot Welding, FE Modeling and Neutron Diffraction Measurement:** *Liang Wang<sup>1</sup>*; Sergio Felicelli<sup>2</sup>; Camden Hubbard<sup>3</sup>; Douglas Bammann<sup>1</sup>; <sup>1</sup>Center For Advanced Vehicular Systems, Mississippi State University; <sup>2</sup>Mechanical Engineering Department, Mississippi State University; <sup>3</sup>Oak Ridge National Laboratory

A finite element model was developed based on the welding software SYSWELD in order to calculate and analyze the residual stress distribution in the resistance spot welding process. The model takes into account the electrical-thermal, thermal-metallurgical, and thermo-metallurgical-mechanical aspects of the process. The model was employed to calculate the temperature history, nugget size growth, and the residual stress field during different stages of resistance spot welding. The effects of welding parameters such as current, pressure, and weld cycles on residual stress distribution were investigated. The predicted nugget shape and size agree well with experimental data. To validate the predicted stresses, neutron diffraction residual stress mapping was used to characterize the through-thickness stresses and surface stresses in a spot welded steel joint. The origin of the residual stress distribution is discussed based on the thermal histories of the samples, and the calculated stresses are compared with measurements obtained by neutron diffraction mapping.

11:50 AM

**Deformation Behavior of Nanocrystalline Co Measured by High-Energy X-Ray Diffraction:** *Ryan Ott<sup>1</sup>*; Morris Wang<sup>2</sup>; Matthew Besser<sup>1</sup>; Jon Almer<sup>3</sup>; Matthew Kramer<sup>1</sup>; <sup>1</sup>Ames Laboratory (USDOE); <sup>2</sup>Lawrence Livermore National Laboratory; <sup>3</sup>Argonne National Laboratory

Unlike most nanocrystalline (nc) metals, nc-Co exhibits large tensile plasticity prior to failure. Previous molecular dynamics simulations have shown that plastic deformation in nc-Co is characterized by an hcp-fcc phase transformation while bulk mechanical tests have suggested that mechanical twinning is responsible for the enhanced ductility. We have examined the

deformation behavior of nc-Co subject to cycled loading at different strain rates using in situ X-ray diffraction. From these experiments we do not see any evidence of a strain-induced phase transformation, but instead we find distinct changes in the crystal orientations during plastic flow. The relationship between the texture changes and mechanical twinning and slip are discussed.

### Pb-Free Solders and Emerging Interconnect and Packaging Technologies: Electromigration

*Sponsored by:* The Minerals, Metals and Materials Society, TMS Electronic, Magnetic, and Photonic Materials Division, TMS: Electronic Packaging and Interconnection Materials Committee

*Program Organizers:* Kwang-Lung Lin, National Cheng Kung University; Sung Kang, IBM; Jenq-Gong Duh, National Tsing-Hua University; Laura Turbini, Research In Motion; Iver Anderson, Iowa State University; Fu Guo, Beijing University of Technology; Thomas Bieler, Michigan State University; Andre Lee, Michigan State University; Rajen Sidhu, Intel Corporation

Monday AM

Room: 204

February 15, 2010

Location: Washington State Convention Center

*Session Chairs:* Sung Kang, IBM Corp.; K. N. Subramanian, Michigan State University

8:30 AM **Introductory Comments by K. L. Lin**

8:35 AM **Invited**

**Thermomigration and Creep in Pb-Free Flip Chip Solder Joints:** *King-Ning Tu<sup>1</sup>*; <sup>1</sup>University of California, Los Angeles

Due to joule heating powered by AC, thermomigration was observed in Pb-free flip chip solder joints. Motion of indented markers indicated that Sn had moved from the cold end to the hot end, and hillocks of Sn were found at the hot end. Hillock formation means that creep has occurred. We have used irreversible processes to analyze the interaction between thermal force and chemical force. To do so, we have included temperature as a variable in the chemical force. Comparing to the interaction between electromigration and creep at constant temperature, we have not found a critical length in thermomigration. Both experimental and theoretical analyses will be presented.

9:00 AM

**Effect of Initial Microstructure on Electromigration Behavior of Eutectic Sn-Pb Solder Joints:** *Andre Lee<sup>1</sup>*; Yi-Chih Lee<sup>1</sup>; K.N. Subramanian<sup>1</sup>; <sup>1</sup>Michigan State University

Atom/ion migration from current stressing a multi-phase alloy should depend on the size, shape, and distribution of phases present since they will affect the number and orientation of phase boundaries encountered by migrating species. In order to gain a better understanding of the role of microstructure on material movement resulting from current stressing, electromigration studies were carried out on eutectic Sn-Pb solder joints subjected to various isothermal aging treatments. These studies characterized the development of surface topography and evolution of microstructural features resulting from electromigration. Results of this study indicate that electromigration in two-phase alloys will be significantly influenced by the initial microstructural features.

9:15 AM

**Effects of Reinforcements Addition on Microstructural Evolution in Eutectic SnBi Solder Joints under Current Stressing:** *Ruihong Zhang<sup>1</sup>*; Mengting Han<sup>1</sup>; Fu Guo<sup>1</sup>; Guangchen Xu<sup>1</sup>; <sup>1</sup>Beijing University of Technology

Composite approaches have been efficient in enhancing the reliability of lead-free solder joints in many aspects. However, the effects of reinforcement particles on solder joints under current stressing have been paid little attention. In this study, eutectic SnBi solder was used as the matrix soldering material to examine the effects of reinforcements addition on the microstructural evolution in solder joints under current stressing. Such electromigration features were compared with non-composite SnBi solder joints from our earlier studies. Polyhedral oligomeric silsesquioxanes (POSS<sup>®</sup>), Cu, and Ni particles with different volume fractions were chosen as reinforcements for the eutectic SnBi solder. The electromigration behavior of the composite solder joints were investigated under the current density of 1.0×10<sup>4</sup>A/cm<sup>2</sup> at 50°C and 80°C. Our

# Technical Program

first-stage study reveals that the POSS particles can slow down the separation of Bi- and Sn-rich phases and retard the solder depletion at the cathode of joints.

## 9:30 AM

**Electromigration Study of Flip Chip Packages under Extra-High Current Density Tests with Temperature Control:** *Jia-Hong Ke*<sup>1</sup>; Yu-Wei Lin<sup>1</sup>; C. R. Kao<sup>1</sup>; <sup>1</sup>Department of Materials Science and Engineering, National Taiwan University

Electromigration phenomenon in flip chip solder joints under high temperature conditions has been widely studied. However, electromigration tests were seldom carried out under proper temperature control. In this study, a cooling system with a PID controller was applied in order to maintain the chip temperature at 60 degree C, and different extra-high current densities ( $5.5 \times 10^4$  A/cm<sup>2</sup>,  $5.0 \times 10^4$  A/cm<sup>2</sup>, and  $4.5 \times 10^4$  A/cm<sup>2</sup>) were used. The objective of this study is to investigate the effects of controlled temperature and extra-high current density on flip chip solder joints. The results showed that low controlled temperature could retard void formation in solder joints even under extra-high current density tests. Instead, substantial IMC dissolution at the cathode and IMC accumulation at the anode was observed.

## 9:45 AM

**Interaction between Electromigration and Diffusionally Accommodated Interfacial Sliding at Hetero-Interfaces:** *Praveen Kumar*<sup>1</sup>; Indranath Dutta<sup>1</sup>; <sup>1</sup>WSU

Thin film structures in microelectronic devices can deform via unusual, scale-sensitive phenomena due to thermo-mechanical loads sustained during service. In particular, large shear stresses may develop at interfaces during thermo-mechanical excursions, allowing the interface to slide via diffusionally accommodated processes (i.e., creep). Such interfacial creep can be further augmented by superimposed electric currents (via electromigration) as the thin film features shrink to the nanometer regime in modern microelectronic devices, potentially causing severe reliability problems. In this paper, we present experimental evidence of the interaction between electromigration and interfacial sliding, based on a model Pb-Si system. It was noted that sliding rates were enhanced at interfaces where the shear stress was in the same direction as electron flow, and less at interfaces where stress and electron flow opposed each other. The kinetics of these interactions and their importance in microelectronics are assessed using a new constitutive law for electromigration-assisted interfacial sliding.

## 10:00 AM Break

## 10:15 AM

**Microstructures and Crystal Orientation of  $\beta$ -Sn for Sn-Ag and Sn-Cu Solder Joints under Electromigration:** *Sun-Kyoung Seo*<sup>1</sup>; Sung K. Kang<sup>2</sup>; Moon Gi Cho<sup>1</sup>; Hyuck Mo Lee<sup>1</sup>; <sup>1</sup>KAIST; <sup>2</sup>IBM T.J. Watson Research Center

Recently, it is known that the anisotropic properties of the  $\beta$ -Sn phase in Pb-free solders strongly affect the reliability of solder joints. Especially, under electrical current, the  $\beta$ -Sn grain orientation could be an important factor to determine the lifetime of solder joints because the diffusion rates of Cu, Ni and Ag atoms in  $\beta$ -Sn are very different depending on Sn grain directions. It is also found that the Sn grain orientation is strongly influenced by solder alloys, Sn-Ag vs. Sn-Cu, as well as by the substrate pad metallurgy, such as Cu/OSP vs. Ni(P)/Au. In this study, the changes in the microstructures and the  $\beta$ -Sn crystal orientation to occur during electromigration are investigated with Pb-free solder joints. The electromigration test is conducted at 150°C under a constant current density, with two solder joints of Ni(P)/Sn-Cu/Cu and Ni(P)/Sn-Ag/Cu. The electromigration lifetime is compared for the two joint systems.

## 10:30 AM

**Direct Measurement of Back Stress in Tin Strips under Electromigration by Synchrotron Radiation X-Ray:** *Yang Yi Lin*<sup>1</sup>; Albert T. Wu<sup>1</sup>; <sup>1</sup>National Central University

This paper presents in situ measurements of stress evolution in tin strips under DC electromigration using synchrotron radiation X-ray. The back stress gradients at various testing conditions were directly detected by the shift of diffraction peaks. The kinetic parameters were deduced. Samples were also subjected to alternating polarity of current. The effect of Joule heating was observed and the increase in temperature was determined. The protective oxide layer on the surfaces is considered to influence critically the kinetics of stress evolution.

## 10:45 AM

**Discussion on the Mechanism of Electromigration from the Perspective of Electromagnetism:** *Peng Zhou*<sup>1</sup>; William Johnson<sup>2</sup>; <sup>1</sup>UC Irvine; <sup>2</sup>MSE, University of Virginia

From the perspective of electromagnetism, conservation of both momentum and energy in the electro-magnetic fields can show that the effective charge number has a linear dependence on the current density. It is suggested that at low temperatures, the momentum of the electro-magnetic fields, instead of the momentum of the drifting electrons, is transferred to the crystal defects to give rise to the polarity effects; while at high temperatures the momentum of the electro-magnetic fields is progressively transferred to the vibrating atoms and causes the "stressing effect" of the lattice, which can be the origin of the decrease of activation energy for diffusion at high temperatures. A tentative failure analysis will give an equation similar to the Black's equation with an extra  $J^2$ -dependent exponential term to take into account the "stressing effect" at high temperatures.

## 11:00 AM

**Critical Conditions of Electromigration-Induced Cu Dissolution in Pb-Free Solder Joints:** *Jung Kyu Han*<sup>1</sup>; King-Ning Tu<sup>1</sup>; <sup>1</sup>UCLA

One of the most serious reliability problems in solder joints technology still remains on current crowding region. In order to reduce current crowding effect, thick Cu under-bump-metallization (UBM) or Cu column structure has been investigated. If the thickness of Cu is not thick enough, it could not effectively eliminate current crowding. If Cu is too thick, however, it may cause the increase of thermal-mechanical stress. Therefore, kinetics under electromigration to study how fast Cu dissolves into the solder is of interest. The thickness of intermetallic compounds (IMC) shrinks first and reaches dynamic equilibrium. Once it reaches the dynamic equilibrium, Cu starts to dissolve into solder very fast. Experiment of several different conditions was carried out and the kinetic model is proposed to predict Cu dissolution rate at given temperature and current density. This study also shows critical conditions to stimulate fast Cu dissolution.

## 11:15 AM

**TEM Characterization of the Porous Structure Induced by High Current Density in the Flip-Chip Solder Joint:** *Ming-Yen Tsai*<sup>1</sup>; Yen-Liang Lin<sup>1</sup>; C. Robert Kao<sup>1</sup>; <sup>1</sup>National Taiwan University

Owing to the combined effects of current crowding and local Joule heating during electromigration, asymmetrical consumption of the Ni(V) layer in UBM was initiated near the edge of passivation where the electrons entered into the solder joint. Afterward this consumed Ni(V) layer transformed to a porous structure. This porous structure was non-conductive and eventually propagated all over the Ni(V) layer to make the joint fail. In this study TEM technique was used to analysis the porous structure in detail. Many voids were observed near the interface of Ni(V)/(Cu,Ni)<sub>6</sub>Sn<sub>5</sub> in the porous structure. EDX analysis on TEM showed that almost no Ni signal was detected in the Ni(V) layer except for the interface of Ni(V)/Al. The result of SADP verification of the porous structure showed that Cu<sub>6</sub>Sn<sub>5</sub> and V<sub>2</sub>Sn<sub>3</sub> fine grains distributed in the amorphous Ni(V) matrix. A very thin layer of Ni<sub>3</sub>Sn<sub>4</sub> fine grains formed at the interface of Ni(V)/Al.

## 11:30 AM

**The Enhanced Growth of Sn Whisker on High Melting Temperature Sn-Pb Solder Joint by Current Stressing:** *Yng-Ta Chiu*<sup>1</sup>; Kwang-Lung Lin<sup>1</sup>; Yi-Shao Lai<sup>2</sup>; <sup>1</sup>Department of Materials Science and Engineering, NCKU; <sup>2</sup>Central Labs, Advanced Semiconductor Engineering, Inc., Kaohsiung

In this study, the Sn whisker formation behavior of 95Pb5Sn/63Sn37Pb composite solder joint was investigated. The test samples were stressed with a current density of  $5 \times 10^3$  A/cm<sup>2</sup> at 150°C for 100, 200 and 300 hours and then were kept under 50% RH at 24°C for 38 days. The results reveal that no Sn whiskers were found on the polished surface of 95Pb5Sn/63Sn37Pb composite solder joint after current stressing. However, Sn whisker formed on the surface of the high-Pb matrix after treatment at 24°C with 50% RH for 38 days. The interesting phenomenon is that the length of Sn whisker increases as the current stressing time increases. It is believed that the Sn whisker formation on the surface of high-Pb matrix is resulted from the residual compressive stress relieved after annealing for 38 days. The mechanism of the growth of Sn whisker was discussed in this present work.



11:45 AM

**Study of Joule Heating Effects in Lead-Free Solder Joints under Various Current Densities Using Infrared Thermography:** *Guangchen Xu*<sup>1</sup>; Fu Guo<sup>1</sup>; Andre Lee<sup>2</sup>; K.N. Subramanian<sup>2</sup>; Neil Wright<sup>2</sup>; <sup>1</sup>Beijing University of Technology; <sup>2</sup>Michigan State University

Temperature distribution in the eutectic Sn-Bi solder joints that does not exhibit thin-thick divergence associated with current crowding issues was investigated using the non-contact infrared thermography technique. These studies evaluated the role of imposed current density and the associated increases in temperature at different regions of solder joint. Findings of this study indicate that the existing temperature differences between center and end region of these solder joints are based on thermal conductivity issues, in spite no having current crowding in the joint geometry employed. These differences arise based on the thermal conduction issues rather than current crowding issues. Implications of these findings on thermal migration, which is believed to be of importance in inter-connects will be discussed.

### Phase Stability, Phase Transformations, and Reactive Phase Formation in Electronic Materials IX: Session I

*Sponsored by:* The Minerals, Metals and Materials Society, TMS Electronic, Magnetic, and Photonic Materials Division, TMS Structural Materials Division, TMS: Alloy Phases Committee

*Program Organizers:* Chih-ming Chen, National Chung Hsing University; Srinivas Chada, Medtronic; Sinn-wen Chen, National Tsing-Hua University; Hans Flandorfer, University of Vienna; A. Lindsay Greer, University of Cambridge; Jae-ho Lee, Hongik University; Kejun Zeng, Texas Instruments; Yee-wen Yen, National Taiwan University of Science and Technology; Wojciech Gierlotka, AGH University of Science and Technology; Chao-hong Wang, National Chung Cheng University

Monday AM Room: 203  
February 15, 2010 Location: Washington State Convention Center

*Session Chairs:* Chih-ming Chen, National Chung Hsing University; Yee-wen Yen, National Taiwan University of Science and Technology

8:30 AM Invited

**Evaluation of Current Mode and Additives in Copper Via Filling:** Jin-Yong Sim<sup>1</sup>; In-Kyu Lee<sup>2</sup>; *Jae-Ho Lee*<sup>1</sup>; <sup>1</sup>Hongik University; <sup>2</sup>Korea Aerospace University

Copper via filling by electroplating method became a common technology for interlayer metallization in 3D SiP and then it has been extensively studied. The void free copper via can be obtained with varying the additives of the electrolytes and, the current density and mode. The effects of current mode and additives on the copper via filling were investigated. The acid copper electrolytes containing additives such as PEG, SPS, JGB and PEI were examined to fill 5~20 $\mu$ m via hole without void. The different sized vias were successfully filled with copper varying current density and mode after fixing additive conditions. The effect of pulse duty cycle on via filling was also investigated.

8:55 AM

**Carbon Nano Tube and Nickel Alloys Composite Electroplating:** Ho-Kyung Um<sup>1</sup>; Heung-Yeol Lee<sup>2</sup>; Tai-Hong Yim<sup>2</sup>; *Jae-Ho Lee*<sup>1</sup>; <sup>1</sup>Hong Ik University; <sup>2</sup>Korea Institute of Industrial Technology

Nickel alloys have been extensively used in packaging and electronic industries. Ni-Fe alloy, was used as shadow mask for its low coefficient of thermal expansion. Even Ni-Fe alloy has high yield stress and hardness, its values are reduced after heat treatment. CNT is one of the eminent nanomaterial and has many advantages in electrical conductivity, yield stress, thermal stability and etc. If CNT is coexisted in Ni-Fe matrix, the disadvantages of Ni-Fe alloy can be reduced. CNT were agglomerated and tangled each other and then their surface needs to be modified to be suspended in the electrolytes. CNT was grinded and pulverized in the ball mill and followed by acid digestion. Surface modified CNT was suspended in the Ni-Fe electrolytes and then CNT and Ni-Fe alloy was codeposited. The optimum condition for the CNT suspension was investigated. The electrical and mechanical properties of composite coating were also investigated.

9:15 AM

**A Study on the Microstructure Evolution of Cu/Sn/Cu Bonding Stacks during Bonding and Their Mechanical Properties for the Applications of 3D Packaging:** *Byunghoon Lee*<sup>1</sup>; Sang-Su Ha<sup>1</sup>; Jeong-Won Yoon<sup>1</sup>; Hoo-Jeong Lee<sup>1</sup>; Seung-Boo Jung<sup>1</sup>; <sup>1</sup>Sungkyunkwan University

For 3D packaging, in which multiple chips are stacked and bonded vertically for a higher level of integration, searching for bonding materials with high mechanical and electrical reliabilities is a key issue. In this study, we chose Sn as a bonding layer and examined the phase evolution process that occurred between Cu and Sn during the bonding process. We also carried out lap-shear tests on the samples bonded at different temperatures and different pressures to investigate how the microstructure changes (such as the formation of different intermetallic compounds) affect the mechanical properties of the bonded samples. Our analysis discloses that the molten Sn aggressively reacted with the Cu to form Cu<sub>6</sub>Sn<sub>5</sub> and then Cu<sub>3</sub>Sn intermetallic compounds and that the formation of the IMC phases substantially enhances the strength of the bonds.

9:35 AM

**Effect of Wet Chemical Pretreatment Conditions on Cu-Cu Bonding Characteristics for 3-D IC Stacks:** *Jae-Won Kim*<sup>1</sup>; Eun-Jung Jang<sup>1</sup>; Myeong-Hyeok Jeong<sup>1</sup>; Seungmin Hyun<sup>2</sup>; Hak-Joo Lee<sup>2</sup>; Young-Bae Park<sup>1</sup>; <sup>1</sup>Andong National University; <sup>2</sup>Korea Institute of Machinery and Materials

Cu to Cu direct bonds for 3-D IC stacks have several advantages such as low electrical resistivity, high electrical reliability, and reduced interconnect signal delay. However, the process temperature is limited up to 400<sup>o</sup> to prevent CMOS devices from being thermally damaged. High temperature bonding is one of the key bottlenecks for 3D ICs applications due to a deadly impact on device reliability. In this work, the effect of wet chemical pretreatments on quantitative interfacial adhesion energy of Cu to Cu direct bond was systematically analyzed by using 4-point bending test. The interfacial adhesion energy was evaluated for various pretreatment times with HF and HCl pre-treatments. Surface and delaminated interface were characterized by the scanning electron microscope and X-ray photoelectron spectroscopy. The interfacial adhesion energy was systematically dependent on the wet pre-treatment time. Dependence of interfacial adhesion energy on the cleaning chemicals and times will be discussed in detail.

9:55 AM Break

10:15 AM Invited

**Tin Whisker Growth in Vacuum Thermal Cycling:** *Katsuaki Saganuma*<sup>1</sup>; Alongheng Baated<sup>1</sup>; Seong-Jun Kim<sup>1</sup>; Keun-Soo Kim<sup>1</sup>; Norio Nemoto<sup>2</sup>; Tsuyoshi Nakagawa<sup>3</sup>; <sup>1</sup>Osaka University; <sup>2</sup>JAXA; <sup>3</sup>Nippon Avionics Co., Ltd.

The aerospace electronics have specific requirements as compared with consumer electronics. Reliability is one of the most key facets that the mechanic designers must think of in the first place. Nevertheless, there have been the electronics failures of the satellites caused by Sn whiskers and Sn whisker failure is one of the most serious concerns for the space electronics. This work is the first report on the vacuum influence on Sn whiskers. In the space, surely Sn whiskers will grow under temperature cycling even in vacuum. 42 alloy lead-frames and ceramic chip capacitors with Sn plating were tested both in the vacuum and in air up to 2000 cycles. There are apparent differences in Sn whisker growth. The width of Sn whiskers is the most significant. Vacuum whiskers are thinner than air whiskers. The whisker growth mechanism in vacuum will be discussed.

10:40 AM

**Growth and Orientation of Tin Whiskers on an Electrodeposited Tin Thin Film under Three-Point Bending:** *Chih-ming Chen*<sup>1</sup>; Yu-jeen Chen<sup>1</sup>; <sup>1</sup>National Chung Hsing University

Tin (Sn) whisker/hillock growth is a result of release of compressive stress in a Sn thin film. Filamentary Sn whiskers were formed on an electrodeposited Sn thin film aged at room temperature, while Sn hillocks were formed as the aging temperature was raised to 80 and 150<sup>o</sup>. A three-point bending test was performed on an electrodeposited Sn layer to investigate the Sn whisker growth under mechanically applied tensile stress. Sn whisker growth was mitigated on the Sn layer subjected to a tensile stress in bending. This mitigation growth suggests that part of the compressive stress in the Sn thin film was neutralized by the mechanically applied tensile stress. The growth orientation of the Sn whiskers formed on the high tensile stress region was random but directional on the low tensile stress region.

Mon. AM

# Technical Program

11:00 AM

**Synthesis of Nanostructured Carbon Materials Using Commercial Paper Phenolic Board:** *Yi-Wei Lin*<sup>1</sup>; Chih-ming Chen<sup>1</sup>; <sup>1</sup>National Chung Hsing University

Owing to possess the characteristics of low cost and easy fabrication, printed circuit boards (PCBs) have been widely manufactured and used in a variety of electronic products. But the lifetime of consumer electronic products is usually very short. So, they become out-of-date very quickly and then are abandoned. Unfortunately, this produces large amounts of waste PCBs which might have detrimental effects on the environment. In this poster, two potential methods are demonstrated to recycle PCBs and use them as the carbon source to synthesize highly valuable carbon nanomaterials.

---

## Processing Materials for Properties: Advanced Materials Processing

*Sponsored by:* The Minerals, Metals and Materials Society, TMS Extraction and Processing Division

*Program Organizers:* Brajendra Mishra, Colorado School of Mines; Akio Fuwa, Waseda University; Paritid Bhandhubanyong, National Metal and Materials Technology Center

Monday AM Room: 617  
February 15, 2010 Location: Washington State Convention Center

*Session Chairs:* Akio Fuwa, Waseda University; Tonya Wolfe, University of Alberta

---

8:30 AM Keynote

**Materials Science for the Next Generation:** *David Olson*<sup>1</sup>; Brajendra Mishra<sup>1</sup>; <sup>1</sup>Colorado School of Mines

Advanced materials, with their interfaces, steep gradients and very small dimensional microstructural features require more comprehensive analytical treatments. Future chemical, physical, and mechanical analyses and implementations need further refinement, such as incorporation of the non-linear behavior associated with interfaces and gradients. The use of electronic, magnetic, and elastic assessments to evaluate the material state will be an everyday practice, including the establishment of electronic metallography practices. The application of wave mechanics with wave-perturbing nondestructive tools and practices to assess more than one property measurement should enable a more comprehensive understanding of the material state.

9:00 AM

**Increase Production and Quality Improvement of Electrolytic Copper at Tank House in Naoshima Smelter and Refinery:** *Hideki Zen*<sup>1</sup>; Tatsuo Ishida<sup>1</sup>; Makoto Takagi<sup>1</sup>; <sup>1</sup>Mitsubishi Materials Corporation

Operation of copper tank house in Naoshima Smelter & Refinery started in 1969. Increase of electrolytic copper production had been mainly carried out in the past by installing more tank house cells and raising current density of commercial cells. However this time increase of production and improvement of quality was achieved without big amount of capital investment, as follows. 1)22 cells which were used for lead refinery were converted to starter sheet cells for copper refinery. 2)To improve verticalness of starter sheets, electrolysis time for starter sheets was changed from 24hours to 48 hours. 3)Starter sheet preparation machine was modified. 4)Flow amount of electrolyte was controlled at commercial cells. 5)Current efficiency of commercial cells was kept over 96.5%. As a result, production of electrolytic copper was increased by 750 T/M and tank house capacity reached to 19,500 T/M.

9:20 AM

**Damage of Surface by Impact of Nitrogen Jet under Pressure and Low Temperature:** *Hicham Laribou*<sup>1</sup>; Claude Fressengeas<sup>1</sup>; Denis Entemeyer<sup>1</sup>; Véronique Jeanclaude<sup>1</sup>; Abdel Tazibt<sup>2</sup>; <sup>1</sup>Laboratoire de Physique et Mécanique des Matériaux; <sup>2</sup>CRITT TJF&U

Processing surfaces with nitrogen jet at low temperature is an environmentally friendly and innovating technology. It has been introduced by NITROCISION® for industrial applications since 2003. The process consists in projecting onto the surface a nitrogen jet at 3000bars and -150°C. Several effects are combined. Reducing the temperature fragilizes the material, the thermal shock induces traction waves through the material, depressurization of the cryogenic fluid

during vaporization induces a blasting effect promoting plastic deformation or lifting the material from the substrate, cavitation of gas inclusions in droplets induces high impact pressures. The process does not generate additional waste and it releases neutral gas into the atmosphere. It can be used in a range of industrial applications, including surface treatment, cutting, drilling, striping and cleaning. This work aims at understanding the mechanisms of surface removal as well as the modes of action of the jet on metallic materials.

9:40 AM

**Non-Linear Analytical Practices for Interfacial Phenomena and Nano-Size Microstructural Properties and Behavior:** *John Roubidoux*<sup>1</sup>; J.E. Jackson<sup>2</sup>; B. Mishra<sup>1</sup>; D.L Olson<sup>1</sup>; <sup>1</sup>Colorado School of Mines; <sup>2</sup>Generation 2 Materials Technology LLC

When the microstructural dimension approaches nano size and/or the interfacial boundary achieves space-charging behavior, the traditional linear driving force and mobility terms become insufficient to describe physical observations. This situation involves non-linear and higher order phenomena, which if properly analyzed can provide new insights and allow better predictions of small dimensional phenomena. Elastic and electronic wave measurements and practices can be used to assess thin films, nano-structure, surface layers, and other steep gradient potentials driven in materials. This paper presents the analytical basis for these nano microstructural property measurement correlations with elastic and electric wave property measurements. In addition, specific examples will be given which demonstrate the differences between linear and non-linear behavior.

10:00 AM

**Modernization Project of Onahama Smelter with New "O-SR Process":** Osamu Iida<sup>1</sup>; *Teruyuki Matsutani*<sup>1</sup>; Kenji Kiyotani<sup>2</sup>; <sup>1</sup>Mitsubishi Materials Corporation; <sup>2</sup>Onahama Smelting and Refining Company

Onahama Smelter has been maintained its profitability with overcoming several high energy price period over 40 years by developing innovatory technology, while it employs conventional process, such as huge energy-consuming reverberatory furnaces (RFs) and conventional PS-converters. New development of combustible waste material treatment in RFs was commenced in 1990's, which realized drastic fuel saving and accompanying metal recovery. In December 2007, installation of new S-furnace of the Mitsubishi Process was completed. For copper concentrates smelting, S-furnace is solely used, which is directly laundered to two RFs to deliver melts continuously and automatically. RFs are dedicated to slag/matte separation and combustible waste material treatment. This new "O-SR Process" realized not only higher copper production and more flexibility for various kinds of raw materials, but also more combustible waste material treatment and less fuel consumption in RFs. This paper introduces good example of old-fashioned smelter revived and recent operating status.

10:20 AM

**Evaluation of Stress Corrosion Cracking Susceptibility of Drill Pipe Steels in CO<sub>2</sub> Saturated Aqueous Solutions:** *Arshad Bajvani Gavanluei*<sup>1</sup>; Bhola Shailly<sup>1</sup>; B Mishra<sup>1</sup>; D. Olson<sup>1</sup>; <sup>1</sup>Colorado School of Mines

Constant extension rate test (CERT), or slow strain rate test (SSRT), has been conducted to investigate the stress corrosion cracking (SCC) susceptibility of high strength low alloy (HSLA) steels in CO<sub>2</sub> containing aqueous environments. G-105 and S-135 grades of drill pipe steels have been used to study the effect of temperature and solution chemistry on the stress corrosion cracking behavior of these steels, using a high temperature and high pressure one liter autoclave. SCC susceptibility of HSLA steels has been evaluated by comparing the results of the experiments conducted in an inert environment (air) and various corrosive solutions at different temperatures from ambient temperature to 200°C, based on the NACE TM0198-2004 standard. Using EDS and XRD techniques, corrosion products have been identified. It has been shown that the SCC susceptibility increased with increasing temperature and maximum occurred at 160°C.

10:40 AM Break

10:50 AM

**Promotion of Recyclable Material Treatment at Mitsubishi Prpcess in Naoshima Smelter and Refinery:** Tetsuro Sakai<sup>1</sup>; Norio Usami<sup>1</sup>; *Masayuki Kawasaki*<sup>1</sup>; <sup>1</sup>Mitsubishi Materials Corporation

The recyclable materials including valuable metals such as copper and precious metals had been treated at Mitsubishi Continuous Copper Smelting

Mon. AM



Furnace (Mitsubishi Process) in Naoshima Smelter and Refinery since the start of furnace operation. Early stage of recyclable material treatment was mainly focused on treating the copper bearing materials which did not contain inflammable materials due to a restriction on capacity of furnace waste heat boilers. As the environmental conservation awareness had been rapidly raised in recent years, establishing treatment systems for wide range of recyclable materials was demanded. To cope with the demand, Naoshima Smelter & Refinery started the operation of incinerating and melting plant of recycle waste in 2003. All of produced slag-metal generating from incinerating and melting plant of recycle waste is treated at Mitsubishi Process. Consequently new treatment system is established without secondary industrial waste by uniting two processes.

### 11:10 AM

**A Novel Process on Production of Thin Wall Austempered Ductile Iron Heat-Treated in the Mold:** *Ali-Reza Kaini-Rashid<sup>1</sup>; Abolfazl Babakhani<sup>1</sup>; Mohammad Reza Ziaei<sup>1</sup>; <sup>1</sup>Ferdowsi University of Mashhad*

In this study, the production of thin wall austempered ductile iron, heat treated in the mold and in the presence of Ni and Mo was investigated. The base iron was melted in an induction furnace and treated at 1450°C by plunging and sandwich methods. Ductile irons were cast in two molds: one was a strip metallic mold with the thickness of 3mm and another cylindrical mold with diameter of 2.5cm. After casting, the specimens were austempered at 350°C for 1hr. Then the microstructures of the specimens were examined by optical microscopy. Results indicated that the ausferrite microstructure can be achieved by the control of the cooling rate within temperature range between 280-400°C. Austempering time about 1hr resulted in no trace of martensite and the structure was only composed of bainitic-ferrite and retained austenite.

### 11:30 AM

**Remarkable Oxidation Resistance of Nanocrystalline Fe-Cr Alloys:** *Raman Singh<sup>1</sup>; Prabhakar Singh<sup>2</sup>; <sup>1</sup>Monash University; <sup>2</sup>University of Connecticut*

The paper will present a review of the fundamentals of likely oxidation mechanism of nanocrystalline metallic materials with examples, and validation of the hypothesis that it may be much easier to develop a protective film on nanocrystalline Fe-Cr alloys. A nanocrystalline Fe-10%Cr alloy has been found to possess in excess of an order of magnitude superior oxidation resistance than its microcrystalline counterpart of same composition. Validation of the hypothesis may have highly attractive economic/industrial implications, for example for high temperature components in solid oxide fuel cells.

### 11:50 AM

**Discrete Element Simulation: An Efficient Tool for Optimizing Powder Processes from the Sintering Stage to the Final Properties:** *Christophe Martin<sup>1</sup>; Xiaoxing Liu<sup>1</sup>; Jean-Jacques Kadjo<sup>1</sup>; Didier Bouvard<sup>1</sup>; <sup>1</sup>Grenoble-INSP*

The modeling of processes involving powder materials needs taking into account the particulate nature of the materials involved. The Discrete Element Method (DEM) is well suited for this task. It allows the macroscopic behavior of an assembly of particles to be calculated from the contact forces generated between each particle. Originally devised for geomaterials, we show that DEM simulations have great potential for powder processes in materials science. Using the example of a thin partially sintered ceramic electrode, we first model the process stages from powder packing to sintering to generate a realistic microstructure. This numerical microstructure is then used to compute macroscopic characteristics such as electrochemical or mechanical properties. In particular, the elastic and fracture properties of the electrodes are calculated as a function of pertinent microstructural properties. The DEM simulations are finally used to propose novel microstructures to optimize the electrochemical performance of an electrode for electrochemical applications.

### 12:10 PM

**Cold Gas Dynamic Spraying of Titanium: A Reliable and Environmentally Friendly Coating Deposition Process:** *Wilson Wong<sup>1</sup>; Stephen Yue<sup>1</sup>; Eric Irissou<sup>2</sup>; Jean-Gabriel Legoux<sup>2</sup>; <sup>1</sup>McGill University; <sup>2</sup>National Research Council Canada*

Cold gas dynamic spray is a solid state high kinetic energy coating and free-form technique. Micrometres-scaled metallic powders are projected onto substrates at supersonic velocities to form a coating. This technique has initiated major interest in the aerospace industry due to its potential to manufacture aerospace engine components with minimal material waste, estimated with a

capability to reduce waste of up to 90% compared to conventional fabrication methods. On account of the severe requirements in producing these components, cold sprayed coatings must prove themselves reliable to earn recognition in the industry. Thus, in this study, mechanical properties such as the bond strength of cold sprayed titanium coatings were evaluated. Various particle impact velocities were achieved by altering process conditions (temperature and pressure). Substrates of different surface roughness and hardness were investigated (aluminum alloy, pure titanium, and steel). Additionally, the coating properties were studied via scanning electron microscopy and microhardness testing.

## Refractory Metals 2010: Processing and Properties I

*Sponsored by:* The Minerals, Metals and Materials Society, TMS Structural Materials Division, TMS: Refractory Metals Committee  
*Program Organizers:* Brian Cockeram, Bechtel-Bettis; Gary Rozak, H.C. Stark

Monday AM

Room: 2A

February 15, 2010

Location: Washington State Convention Center

*Session Chairs:* Brian Cockeram, Bechtel Marine Propulsion Corporation; Gary Rozak, H. C. Starck, Inc.

### 8:30 AM

**Surface Processing of an Iridium Alloy:** *Evan Ohriner<sup>1</sup>; George Ulrich<sup>1</sup>; Roger Miller<sup>1</sup>; Wei Zhang<sup>1</sup>; <sup>1</sup>Oak Ridge National Laboratory*

The effects of surface processing on the microstructure and properties of DOP-26 iridium alloy (Ir-0.3% W-0.006% Th-0.005% Al) are investigated. The surface treatments include pulse laser heating, grit-blasting with tungsten carbide media, and mechanical surface deformation by manual scribing. The effects of processing parameters on surface morphology, grain structure, and optical emissivity are evaluated. The results are compared to those from numerical modeling of surface processing and material grain growth behavior. Recrystallization and grain growth is evaluated for both as-treated surfaces and following post-treatment annealing as a method to estimate plastic strains associated with surface processing. Laser surface processing results are compared to those for mechanical surface processing. This research was sponsored by the Office of Radioisotope Power Systems, U. S. Department of Energy, under Contract DE-AC05-00OR22725 with UT-Battelle, LLC.

### 8:55 AM

**Effect of Tantalum on the Tensile Impact Ductility and Fracture Behavior of Iridium:** *E. P. George<sup>1</sup>; C. Carmichael<sup>1</sup>; A. Gali<sup>1</sup>; E. Ohriner<sup>1</sup>; <sup>1</sup>Oak Ridge National Laboratory*

Iridium has a high melting point (2450C) and excellent corrosion resistance making it ideal for certain refractory applications. Trace elements can have beneficial (e.g., Th, Ce and W) and deleterious (e.g., Si) effects on the mechanical properties of iridium. Here, we investigate the effects of Ta (0.1 to 0.5 wt.%) on an iridium alloy referred to as DOP-26 in the literature (Ir-0.3W-0.006Th-0.005Al). Tensile impact tests were performed using a gas-powered gun at strain rates of ~1000/second and temperatures of ~1000C. Tantalum additions as low as 0.1 wt.% were found to severely embrittle the DOP-26 iridium alloy, with tensile ductility decreasing to ~5%, which is a factor of 3~5 lower than that of the Ta-free alloy. Possible mechanisms for the embrittlement, including grain growth, grain boundary segregation, and formation of low-melting eutectics, are investigated and discussed. Research sponsored by the Office of Radioisotope Power Systems, U.S. Department of Energy.

### 9:20 AM

**Effects of Thermo-Mechanical Processing on Texture and Microstructure of Pure Molybdenum Plates for Optimum Sputtering Performance:** *Gary Rozak<sup>1</sup>; Peter Jepson<sup>1</sup>; <sup>1</sup>HC Starck Inc*

Crystallographic texture and uniform microstructure are important characteristics for sputtering targets in order to produce a uniform thin film. Texture and microstructure develop in Molybdenum plates as a result of the processing methods. Powder metallurgy and arc cast molybdenum samples were produced via various thermo-mechanical processing (TMP) techniques, e.g., hot rolling, extruding or forging. The subsequent texture was evaluated with electron back scattering diffraction (EBSD) analysis and the microstructure was recorded with standard optical techniques. This presentation will report the

# Technical Program

effects of TMP conditions on the subsequent microstructure and crystallographic texture.

**9:45 AM**

**The Role of Stress State and Wrought Processing on the Fracture Toughness and Toughening Mechanisms of Wrought Unalloyed Molybdenum, TZM Molybdenum, ODS Molybdenum, and Molybdenum Alloys:** *Brian Cockeram*<sup>1</sup>; *Bechtel-Bettis*

The ductile laminate toughening mechanism observed for wrought molybdenum results from a lower toughness in the short-transverse orientation that leads to splitting of the microstructure along grain boundaries in the regions of stress concentration. In this work, commercially available molybdenum, molybdenum alloys, and ODS molybdenum are rolled to thinner sheet and then subject to tensile and fracture toughness testing and examination of the microstructure and toughening mechanism. The finer grain size, finer precipitate size, and state of plane stress achieved for the thinner sheet specimens appears to enhance the ductile laminate toughening observed for wrought molybdenum alloys to improve the fracture toughness. The detrimental effect of crack initiation from brittle carbides, oxides, and second phases is diminished under a state of plane stress to result in higher fracture toughness and lower DBTT values. The impact of stress-state and grain size on the toughening mechanism and resulting properties is discussed.

**10:10 AM Break**

**10:25 AM**

**Plastic Strain Concentration at Grain Boundaries in a 50Mo-50Re Alloy:** *Tongguang Zhai*<sup>1</sup>; *Jianhui Xu*<sup>2</sup>; <sup>1</sup>University of Kentucky; <sup>2</sup>Smith International

A 50Mo-50Re alloy was stretched at room temperature in air at a range of strain rates between 10<sup>-6</sup>s<sup>-1</sup> and 1s<sup>-1</sup>. It was found that the alloy exhibited brittle fracture at slow strain rates while it became ductile at a fast strain rate. Cracks were predominantly initiated from grain boundaries and triple junctions. Peaks of misorientation gradient were observed close to grain boundaries and triple junctions in the deformed alloy with EBSD. Misorientation maps were then calculated from the measured orientation maps using EBSD, indicating that indeed misorientation gradient peaked around grain boundaries and triple junctions in the deformed alloy. This was consistent with the TEM observation of bend contours around grain boundaries in the alloy. The results from the EBSD experiments demonstrated that there was stress concentration around grain boundaries and triple junctions during plastic deformation, thereby leading to crack initiation at grain boundaries or triple junctions in this alloy.

**10:50 AM**

**Processing and Properties of Tungsten-25%Rhenium with and without Hafnium Carbide:** *Todd Leonhardt*<sup>1</sup>; *James Ciulik*<sup>2</sup>; <sup>1</sup>Rhenium Alloys, Inc.; <sup>2</sup>The University of Texas at Austin

Historically, tungsten-25% rhenium alloy has been produced into wire for the thermocouple market, but recent demands for high temperature structural components and high-temperature friction stir welding tooling has forced the development of novel processing techniques for tungsten-rhenium and tungsten-rhenium with hafnium carbide. With a melting point of 3050°C, a recrystallization temperature near 1900°C, and a ductile-to-brittle transitional temperature (DBTT) of -50°C, tungsten-25% rhenium is a high-temperature alloy with high strength, high toughness, and low erosion properties needed for friction stir welding tooling. The addition of hafnium carbide substantially improves the strength of this alloy at elevated temperatures, although it makes deformation processing of it into useful shapes more challenging. The processing and microstructures of tungsten-25% rhenium and tungsten-25% rhenium with hafnium carbide will be discussed, as well as the effects of different processing conditions on the mechanical properties of the alloys at ambient temperature, 1371°C, and 1926°C.

**11:15 AM**

**Fracture Behavior of Polycrystalline Tungsten:** *Bernd Gludovatz*<sup>1</sup>; *Stefan Wurster*<sup>1</sup>; *Andreas Hoffmann*<sup>2</sup>; *Reinhard Pippan*<sup>1</sup>; <sup>1</sup>Erich Schmid Institute of Materials Science / Austrian Academy of Sciences; <sup>2</sup>Plansee Metall GmbH

Tungsten and tungsten alloys show the typical change in fracture behavior from brittle at low temperatures to ductile at high temperatures, however the parameters influencing the brittle fracture behavior are not well understood. Using techniques like electron backscatter diffraction (EBSD) and Auger electron spectroscopy (AES) parameters like grain size, texture and grain boundary

segregation were investigated. EBSD was used to record the crack propagation path, which shows transgranular and intergranular fracture. Depending on temperature and alloying content, different sizes of plastically deformed areas were observed along the crack path. The crack propagation was additionally recorded using the potential method which showed an R-curve behavior for these materials. To improve the understanding of the influence of impurities on the cleavage resistance of grain boundaries different microstructured materials were investigated by AES. The effect of the different microstructural features on the fracture behavior and the ductile to brittle transition will be discussed.

**11:40 AM**

**Study the Activated Sintering of Tungsten as a Function of Heating Mode:** *Avijit Mondal*<sup>1</sup>; *Kranti V. Reddy*<sup>1</sup>; *Anish Upadhyaya*<sup>1</sup>; *Dinesh Agrawal*<sup>1</sup>; <sup>1</sup>Indian Institute of Technology, Kanpur

Tungsten is an excellent material for many industrial applications due to its attractive properties. However, its potential of being an excellent high temperature structural material is hindered because of poor sinterability. Usually the consolidation of a conventional microcrystalline W powder is difficult and requires very high temperature in electrical resistance sintering under hydrogen atmosphere. Activated sintering of tungsten metals through addition of selected transition metals such as Ni, Fe, Co, Cu has been critically discussed in this paper. The general observations and theoretical treatments have led to the identification of beneficial activators by studying the binary phase diagrams of the metal and the activator element. Microwave processing has been emerging as an innovative sintering method for consolidation of particulate metals. The 2nd part of this study describes recent research findings wherein W, W-1Ni, W-1Fe, W-1Co and W-1Cu have been successfully consolidated using microwave heating which resulted in further acceleration in densification.

## Solar Cell Silicon: Production and Recycling: Session I

*Sponsored by:* The Minerals, Metals and Materials Society, TMS Extraction and Processing Division, TMS Light Metals Division, TMS: Recycling and Environmental Technologies Committee, TMS: Energy Conversion and Storage Committee  
*Program Organizers:* Anne Kvithyld, SINTEF; Gregory Hildeman, Solar Power Industries

Monday AM

Room: 2B

February 15, 2010

Location: Washington State Convention Center

*Session Chair:* Anne Kvithyld, SINTEF

**8:30 AM**

**Electrochemical Production of Affordable Solar Grade Silicon:** *Antony Cox*<sup>1</sup>; *Derek Fray*<sup>1</sup>; <sup>1</sup>University of Cambridge

Photovoltaic technology has the potential to offer unlimited pollution-free renewable energy. A major barrier in the commercialisation and acceptance of this technology is the high cost of silicon. There are alternatives to silicon but they are less efficient and degrade rapidly. Current methods to extract silicon also produce substantial amounts of CO<sub>2</sub>, operate at very high temperatures and involve several stages with the use of expensive and highly toxic chemicals. An alternative electrochemical method is discussed which involves electro-deoxidizing inexpensive silica feedstock in a molten salt electrolyte to produce 99.90wt% silicon which is then electrorefined in the same electrolyte to remove trace impurities such as C, Fe, P, B, Ti, Ni, Mn and remaining O to deposit silicon of 99.9999wt% purity. The process consumes less energy than current methods and with the use of inert anodes the only by-product is oxygen.

**8:55 AM**

**Electrorefining of Metallurgical Grade Silicon in Molten Salts:** *Geir Martin Haarberg*<sup>1</sup>; *Shuihua Tang*<sup>1</sup>; *Karen Osen*<sup>2</sup>; *Henrik Gudbrandsen*<sup>2</sup>; *Sverre Rolseth*<sup>2</sup>; *Ole Edvard Kongstein*<sup>2</sup>; *Shulan Wang*<sup>3</sup>; <sup>1</sup>Norwegian University of Science and Technology; <sup>2</sup>SINTEF; <sup>3</sup>Northeastern University

Electrochemical studies of the behaviour of silicon were carried out in molten salt electrolytes. Electrorefining of metallurgical grade silicon was done in molten chloride and fluoride electrolytes at temperatures from 700 – 850°C. Electrochemical studies such as voltammetry showed that silicon can be anodically dissolved and cathodically deposited from molten salts. Silicon deposits of good quality was obtained by electrorefining in molten KF-



LiF-K<sub>2</sub>SiF<sub>6</sub> at 760°C. High current densities of ~0.5 A/cm<sup>2</sup> could be used, but inclusions of fluorides represent a challenge in this electrolyte. The use of a liquid alloy anode of silicon and copper was found to be beneficial in molten CaCl<sub>2</sub> (80 mol%) - with NaCl, CaO, and dissolved Si. Promising electrorefining results for some impurity elements such as aluminium and titanium were obtained in recent experiments. However, the contents of phosphorus and boron were still too high for solar cell applications.

9:20 AM

**Preparation of High Purity Silicon by Electrolysis-Vacuum Distillation:** *Jidong Li*<sup>1</sup>; Mingjie Zhang<sup>2</sup>; Yiyong Wang<sup>1</sup>; <sup>1</sup>School of Materials Science and Engineering; University of Science and Technology Liaoning; <sup>2</sup>School of Metallurgy, Northeastern University

In this paper, Mg-Zn-Si alloys were prepared by electrolysis in electromagnetic stirring using high purity silicon dioxide as raw material and high purity silicon obtained was separated from Mg-Zn-Si alloys by vacuum distillation. The conditions such as current density, electrolysis time and electromagnetic stirring effecting on back electromotive force, silicon content and current efficiency were well investigated. Finally, at 1000°C, magnetic field intensity of 28mT, the silicon content of 35.7% (mass fraction) in Mg-Zn-Si alloy can be obtained by electrolyzing for 4h in the current density of 0.56A.cm<sup>-2</sup>. Then, at 1050°C, the high purity silicon of 99.98% was obtained by vacuum distillation for 3h.

9:45 AM Break

10:20 AM

**Hierarchy of Slurry Recycling Options:** *Walter Radeker*<sup>1</sup>; <sup>1</sup>CRS Reprocessing Services LLC

When considering the wire slicing process for cutting PV silicon wafers, recycling slurry is an economic requirement. There are, however, meaningful variations in recycling choices. By exploring these choices, we can help companies make the right choices for them. In general the options are no recycling of the slurry components, use of self-managed on-site systems, or using an outside vendor to manage the reprocessing system, either on-site or off-site. Within this range of offerings, there is a hierarchy designed to satisfy desires that drives how firms think when considering how best to recycle. This hierarchy includes satisfying the desire for risk management, cost improvement, stable process control, and direct process management. Customer data and industry experience tells us that these are all important drivers that can be arranged in a way to determine the best recycling method for a customer.

10:45 AM

**Wetting Properties of Molten Silicon with Graphite Materials:** *Arjan Cifjija*<sup>1</sup>; Merete Tangstad<sup>2</sup>; Thorvald Engh<sup>2</sup>; <sup>1</sup>SINTEF; <sup>2</sup>Norwegian University of Science and Technology

The wetting behavior of molten-silicon/refractory-materials system is important in refining and casting of silicon with respect to production of low cost solar cells. Here we study the wetting properties of molten silicon with several graphite materials used in the PV industry. The sessile drop method is employed to measure the contact angles. Initially molten silicon does not wet graphite materials. The initial contact angles measured are approximately 120°. As soon as the silicon melts, it starts to react with C to form SiC. Equilibrium wetting angles of 0 – 31° are measured. With increasing surface roughness the equilibrium wetting angles decrease. Infiltration of molten silicon is also studied. The results show that infiltration depth of molten silicon increases with the average pore size of graphite materials.

11:10 AM

**Mechanical Properties of Fine Grained Polysilicon Grown in Fluidized Bed Reactors:** *Mohamad Zbib*<sup>1</sup>; David Bahr<sup>1</sup>; Wayne Osborne<sup>2</sup>; Grant Norton<sup>1</sup>; <sup>1</sup>Washington State University; <sup>2</sup>REC Solar Grade Silicon LLC

A new method of growing polycrystalline silicon for solar applications is the fluidized bed reactor, which produces a fine grained granular bead from chemical vapor deposition. The beads vary from a few millimeters to a centimeter in diameter. During handling this material may crack; therefore, there is an interest in understanding the toughness and hardness of the material. Using nanoindentation and indentation fracture testing the mechanical properties as a function of grain size and annealing conditions were measured. Post grown annealing does not change the hardness of the beads (9.5 GPa), but does alter the toughness from between 1.1 MPa m<sup>0.5</sup> at 1050°C to 2.3 MPa m<sup>0.5</sup> at 600°C. The grain sizes and small voids within the sample due to the growth

mechanisms did not affect the typical fracture path, suggesting that porosity at this scale is not the dominant feature controlling the fracture of this material.

11:35 AM Panel Discussion

**Recycling Needs led by Gregory Hildeman, Solar Power Industries**

### Solid-State Interfaces: Toward an Atomistic-Scale Understanding of Structure, Properties, and Behavior through Theory and Experiment: Atomic-Level Structure and Composition

*Sponsored by:* The Minerals, Metals and Materials Society, TMS Electronic, Magnetic, and Photonic Materials Division, TMS Structural Materials Division, TMS: Chemistry and Physics of Materials Committee

*Program Organizers:* Michael Demkowicz, Massachusetts Institute of Technology; Douglas Medlin, Sandia National Laboratories; Emmanuelle Marquis, University of Oxford

Monday AM

Room: 602

February 15, 2010

Location: Washington State Convention Center

*Session Chairs:* Michael Demkowicz, Massachusetts Institute of Technology; Emmanuelle Marquis, University of Oxford

8:30 AM Invited

**Atomic-Scale STEM-EELS Mapping of Structure, Chemistry, Bonds and Electronic Properties across Functional Interfaces:** *Christian Colliex*<sup>1</sup>; <sup>1</sup>CNRS

Aberration corrected STEMs now deliver and raster angstrom-size electron probes on cross-sectional foils with solid-state interfaces parallel to the incident beam. Bright and annular dark field images deliver views of the structural arrangement of the atomic columns across such interfaces. In parallel, EELS spectroscopy has demonstrated its efficiency for mapping with a high level of spatial resolution, the electronic response of the irradiated specimen. It thus provides maps, atomic column by atomic column, of the nature of the atoms across interfaces between artificially grown layers for electronics, spintronics or oxitronics components. This diagnosis is now extended to the determination of their bonding states through the monitoring of the spectral fine structures which modulate the characteristic edges. Various practical examples will be shown to demonstrate recent successes and present limitations of these new potentialities, claiming for further developments in theory and modelling in order to optimize the information thus accessible.

9:00 AM

**Atomic Scale Structure and Composition across G/G' Interfaces in Ni-Base Superalloys:** *Srinivasan Rajagopalan*<sup>1</sup>; J.Y. Hwang<sup>2</sup>; Soumya Nag<sup>2</sup>; A. Singh<sup>2</sup>; G.B. Viswanathan<sup>3</sup>; J. Tiley<sup>4</sup>; Rajarshi Banerjee<sup>2</sup>; Hamish Fraser<sup>1</sup>; <sup>1</sup>The Ohio State University; <sup>2</sup>University of North Texas; <sup>3</sup>UES Inc.; <sup>4</sup>Air Force Research Laboratory

The interface between the ordered  $\gamma'$  and the disordered  $\gamma$  phase in Ni-base superalloys plays a significant role in determining physical and mechanical properties. Using advanced characterization techniques such as aberration-corrected HRSTEM, EELS and 3DAP Tomography, the nature of the order-disorder and compositional transitions across the  $\gamma/\gamma'$  interface have been investigated in Rene' 88 DT, a multicomponent Ni-base superalloy. The variation of the interface width for different types of  $\gamma'$  precipitates (primary and secondary) has also been studied as a function of cooling rate and aging time. Using measurements based upon HRSTEM and 3DAP observations, the mechanism of  $\gamma'$  coarsening in Rene' 88 DT is rationalized, based upon existing models. Finally, the implications of the observations on the nucleation and evolution of different generations of  $\gamma'$  precipitates are discussed.

9:20 AM

**Chemomechanical Analysis of Metal Nanoparticle Interfaces under Extreme Environments via Molecular Dynamics Simulations:** *Hansohl Cho*<sup>1</sup>; Krystyn Van Vliet<sup>1</sup>; <sup>1</sup>Massachusetts Institute of Technology

Metal nanoparticles, capable of exothermic reactions upon mechanical mixing, can offer new means of controlled reactions under extreme environments. Forced mixing of nickel and aluminum via mechanical stress input results in extensive energy dissipation with extreme deformation and alloying reactions.

# Technical Program

Here, we present our study of the chemomechanical behavior of the Ni and Al nanoparticles under mechanical impact, up to the point of shock loading, using nonequilibrium molecular dynamics simulations. We find that the interfacial mixing and alloying are accompanied by rapid thermal energy release. Thus, kinetic energy dissipation can be achieved in the extreme mechanical stress states at the nanoscale Ni/Al interface via high speed impact loading. We discuss the effect of nanoparticle radius on the extent of this effect. Finally, we consider the effects of impact loading conditions and boundary conditions that affect the extent and duration of energy dissipation within the Ni and Al nanoparticles.

**9:40 AM**

**Measurement of the Interface Width by Atom Probe Tomography:** *Michael Miller<sup>1</sup>; Ai Serizawa<sup>1</sup>; <sup>1</sup>ORNL*

Accurate measurements of solute gradients at interfaces, precipitate concentrations, and interface widths are important for understanding materials properties. In this study, the interface width was estimated from the distance between the 10 and 90% points of the solute concentrations in the precipitates and the matrix in the proximity histogram. Simulations indicate that a minimum interface width of ~0.15 nm may be obtained under optimum conditions. However, artifacts, such as the overestimation of concentrations, are generated under some data analysis conditions. The accuracy of these measurements will be demonstrated with a combination of simulations and experimental data from reactor pressure vessel steels and nanostructured ferritic alloys. This research was sponsored by the U.S. Department of Energy, Division of Materials Sciences and Engineering; research at the Oak Ridge National Laboratory SHaRE User Facility was sponsored by the Scientific User Facilities Division, Office of Basic Energy Sciences, U.S. Department of Energy.

**10:00 AM Break**

**10:20 AM Invited**

**Structure and Chemistry of Nanometer-Thick Intergranular Films at Au-Al<sub>2</sub>O<sub>3</sub> Interfaces:** *Wayne Kaplan<sup>1</sup>; Mor Baram<sup>1</sup>; <sup>1</sup>Technion - Israel Institute of Technology*

The existence of nanometer-thick intergranular equilibrium films at metal-ceramic interfaces has been experimentally verified for the Au-Al<sub>2</sub>O<sub>3</sub> system. The films were formed by equilibrating thin Au films on a sapphire substrate which was previously partially wetted with drops of anorthite glass (CaO-2SiO<sub>2</sub>-Al<sub>2</sub>O<sub>3</sub>). The process resulted in sub-micron equilibrated Au particles residing on glass drops and on the sapphire substrate adjacent to the glass drops. The interfaces between the Au particles and the sapphire substrates were characterized using a monochromated and aberration corrected TEM (Titan 80-300 S/TEM). The thickness of the films was determined from quantitative HRTEM and the composition was determined from combined energy filtered TEM and energy dispersive spectroscopy (EDS). The use of aberration corrected HRTEM proved the existence of structural order within the films, which serves as part of the entropy term balancing the positive and relatively large Hamaker coefficients for the interface.

**10:50 AM**

**The Structure of Uranium Dioxide Grain Boundaries and its Influence on Fission Gas Segregation:** *Pankaj Nerikar<sup>1</sup>; Chris Stanek<sup>1</sup>; Blas Uberuaga<sup>1</sup>; Susan Sinnott<sup>2</sup>; <sup>1</sup>Los Alamos National Laboratory; <sup>2</sup>Department of Materials Science and Engineering, University of Florida*

In many materials, defects preferentially segregate to grain boundaries often resulting in a profound effect on the properties of the material. This is especially important for xenon (Xe) segregation in uranium dioxide. It is well known that Xe migrates to grain boundaries, where bubbles may form resulting in fuel swelling. Atomistic simulations often reveal phenomena that are necessary to fully understand material behavior. The atomic structures of symmetric S5 tilt, S5 twist, and amorphous grain boundaries in uranium dioxide are explored in this work using empirical potentials and density functional theory. We have found that for both the S5 tilt and S5 twist boundary, there is an unsymmetrical structure that is lower in energy than the symmetric structure. Xe segregation to these boundaries is also investigated in this work. Our simulations predict the segregation energy to be sensitive to the local atomic environment of the solute atom in the host.

**11:10 AM**

**Spatially Resolved Compositional Measurements across Interfaces, Phase Separations, and Non-Conservative Faults in Complex Oxides:** *Srinivasan Rajagopalan<sup>1</sup>; G.B. Viswanathan<sup>2</sup>; David McComb<sup>3</sup>; Jan Ringnald<sup>4</sup>; Hamish Fraser<sup>1</sup>; <sup>1</sup>The Ohio State University; <sup>2</sup>UES Inc.; <sup>3</sup>Imperial College London; <sup>4</sup>FEI Company*

Complex oxides have been the subject of intense study in the recent past. Of particular interest is the ability to characterize interfaces and faults in nanometer-scale thin films and multilayered versions of these materials, requiring structural and compositional resolutions at or near to the atomic scale. An advantageous technique involves the aberration-corrected (scanning) transmission electron microscope; when the spherical aberration of probe is corrected, compositional information can be determined with very high spatial resolution. This paper presents the results of an assessment of the ability to perform spatially resolved measurements of compositional variations across phase separations and faults in strontium titanate thin films, and interfaces between strontium and barium titanate multilayered couples. The role of intrinsic and extrinsic factors affecting these measurements will be discussed. Support from the National Science Foundation for the Materials Research Science and Engineering Center (MRSEC) under contract number DMR-0820414 is gratefully acknowledged.

**11:30 AM**

**Nanoscale Characterization of a Nanostructured Fe-Y<sub>2</sub>O<sub>3</sub> Composite Material:** *Mathilde Brocq<sup>1</sup>; Bertrand Radigue<sup>2</sup>; Fabrice Legendre<sup>1</sup>; Fabien Cuvilly<sup>2</sup>; Philippe Pareige<sup>2</sup>; Jean-Marie Lebreton<sup>2</sup>; <sup>1</sup>SRMP - CEA; <sup>2</sup>GPM-Université de Rouen*

To be able to understand nanostructured materials microstructure, a set of nanoscale characterization techniques able to complement each other are needed. A special attention has to be paid on interface since those materials, by definition, contain a significant proportion of interfaces. An iron based material reinforced by nanometric yttrium oxide precipitates was studied because of its interest for ODS (Oxide Dispersion strengthened) steels considered for future nuclear reactors. It was synthesized by reactive ball-milling and annealing. It was then characterized in the as-milled and as-annealed state by Electron Probe Micro-Analysis (EPMA), X-Ray Diffraction (XRD), Mössbauer spectroscopy (MS) and Atom Probe Tomography (APT). Matching results give a precise and reliable description of the two phases of the material and of their evolution during the process. On the other hand, comparison of MS and APT results reveals an aberration in APT reconstruction of interface which will be presented in detail.

**11:50 AM**

**Chemical Interface Width and Triple Line Transport in Metallic Multilayers:** *Guido Schmitz<sup>1</sup>; Patrick Stender<sup>1</sup>; Constantin Ene<sup>2</sup>; Henning Galinski<sup>1</sup>; <sup>1</sup>Westf. Wilhelms-Universität; <sup>2</sup>Universität Göttingen*

Based on the thermodynamics of inhomogeneous systems, it is expected that the chemical transition at interfaces, even between two immiscible materials, cannot be atomically sharp. We could demonstrate by atom probe tomography that the width of interfaces in stable metallic multilayers varies systematically with temperature. Systems Ag/Cu, Cu/NiFe and Fe/Cr were analyzed using a wide-angle tomographic atom probe (WATAP). Owing to the outstanding resolution of this instrument, a broadening of interfaces can be demonstrated on a depth scale between 0.4 and 1.5 nm. Since these metallic systems are immiscible from a thermodynamic point of view, Cahn-Hilliard theory is used to explain the observed temperature dependence. In addition, the large volume of analysis of modern atom probes allows statistically significant observation of atomic transport along one-dimensional defects lines, which are interpreted as triple lines of the grain structure. Mobility of individual triple lines, diffusion coefficients and segregation behaviour are determined.



### Surface Engineering for Amorphous-, Nanocrystalline-, and Bio-Materials: Session I

Sponsored by: The Minerals, Metals and Materials Society, TMS Materials Processing and Manufacturing Division, TMS: Surface Engineering Committee

Program Organizers: Sandip Harimkar, Oklahoma State University; Arvind Agarwal, Florida International University; Sudipta Seal, University of Central Florida; Narendra Dahotre, University of Tennessee

Monday AM Room: 604  
February 15, 2010 Location: Washington State Convention Center

Session Chair: Narendra Dahotre, University of Tennessee

#### 8:30 AM Introductory Comments

#### 8:35 AM Invited

##### Development of Multi-Functional Nanostructured and Composite Coatings for Tribological Applications: Ali Erdemir<sup>1</sup>; <sup>1</sup>Argonne National Laboratory

During last decade or so, great strides have been made in the development and utilization of nanostructured and composite coatings for a wide range of engineering applications. These coatings are much more robust and multi-functional than their earlier predecessors and are well-suited for demanding mechanical and tribological applications. In this paper, the primary focus will be on the design, synthesis, and mechanical and tribological characterization of a new generation of super-hard nanocomposite coatings that can have great application potentials in the transportation and manufacturing sectors. Specifically, we will introduce a crystal-chemical model that can help identify the specific coating ingredients that are needed to form these nanocomposite coatings that will attain ultra-low friction and wear under dry and lubricated sliding conditions. These designer coatings provide friction coefficients of less than 0.05 under severe boundary lubricated sliding conditions and they cannot be scuffed under the heaviest loadings that are available in reciprocating and block-on-ring type test machines. Because of their extreme resistance to wear and scuffing, they are well-suited for a wide range of engine applications as well as machining and manufacturing applications that require high precision and durability in molds, dies, and tools. Recent test results from bench-top and fired engine tests will be presented to illustrate the much superior tribological properties for these designer coatings over a broad range of sliding conditions. A variety of surface analytical tools are also used to understand the fundamental tribological mechanisms of these coatings after tests under severe conditions.

#### 9:00 AM Invited

##### The Tribological Behaviour of Graded Nanocrystalline Nickel Coatings: Sundararajan G<sup>1</sup>; Nitin Wasekar<sup>1</sup>; <sup>1</sup>ARCI

Pulsed electrodeposition technique is ideally suited to deposit thick, nanocrystalline coatings on a variety of substrates. By controlling the pulse parameters it is possible to obtain coatings which are graded in terms of grain size. In this study, thick Ni coatings have been deposited on a mild steel substrate using pulsed electrodeposition so as to obtain a grain size grading along the thickness direction. At one extreme, the grain size increased from 25 nm at the coating surface continuously to 500 nm at the coating-substrate interface. At the other extreme, the grain size decreased from a value of 500 nm at the coating surface to 25 nm at the coating-substrate interface. A number of intermediate variants within the above two extremes were also obtained. The sliding wear and solid particle erosion behaviour of all these variants were evaluated and the results will be presented and analysed.

#### 9:25 AM Invited

##### Evolution of Microstructure in Laser Clad Coatings Studied by Orientation Imaging Microscopy: Václav Ocelík<sup>1</sup>; Ivan Furár<sup>1</sup>; Jeff De Hosson<sup>1</sup>; <sup>1</sup>University Groningen/M2i

Laser powder deposition of thick metallic coatings is one of the surface engineering techniques which provide resistant against high loading impact, severe wear and corrosion at high temperatures. In this work Orientation Imaging Microscopy (OIM) based on Electron Back Scatter Diffraction in a Scanning Electron Microscope was employed as a very powerful instrument for the study of the relationship between processing parameters and the microstructure of individual and overlapping laser tracks at different processing speeds. OIM

provided new insights into the microstructure of laser clad coatings and very useful information concerning the directional grow of individual grains, the solidification texture and the shape of solidification front during laser processing. Strong correlations between the microstructure, processing parameters as well as mechanical performance were discovered.

#### 9:50 AM

**Residual Stresses in PS 304 Tribological Coating:** Pnina Ari-Gur<sup>1</sup>; Simon Narasimhan<sup>1</sup>; Mark Croft<sup>2</sup>; Zhong Zhong<sup>3</sup>; Thomas Gnäupel-Herold<sup>4</sup>; Malcolm K. Stanford<sup>5</sup>; Christopher DellaCorte<sup>5</sup>; Phillip B. Abel<sup>5</sup>; <sup>1</sup>Western Michigan University; <sup>2</sup>Rutgers University; <sup>3</sup>Brookhaven National Laboratory; <sup>4</sup>National Institute of Standards and Technology; <sup>5</sup>National Aeronautics and Space Administration

Oil-free turbomachinery need high-temperature hard coatings to withstand the harsh conditions. The PS<sub>3</sub>O<sub>4</sub> coating was developed by NASA for that purpose. It is a composite of Ni-Cr, Cr<sub>2</sub>O<sub>3</sub>, eutectic BaF<sub>2</sub>-CaF<sub>2</sub>, and Ag, and is applied by plasma spray. It can be deposited on variety of substrates. One of the metrics for performance is the cohesive strength of the coating. The best cohesive strength is achieved via heat treatment in air. The goal now was to analyze the residual stresses developed following stages of the process (plasma spray, heat treatment, and surface grinding). Stresses with spatial resolution of 0.1 mm were measured, allowing depth profiling of the coatings and into the substrate near the interface. Consistently the coatings exhibit compressive stresses in the circumferential direction and tensile stresses in the axial direction. There is a modest stress relaxation in the coating near the substrate interface. The substrate stresses are generally low.

#### 10:10 AM

**Microstructural Assessment Associated with Micropitting in Rolling Contact Fatigue:** Fang Cao<sup>1</sup>; Peter Jacobs<sup>1</sup>; Martin Webster<sup>1</sup>; <sup>1</sup>ExxonMobil Research and Engineering

Micropitting is a surface fatigue phenomenon encountered in bearings and gears under lubricated conditions, which leads to their premature failure. The failure mechanisms of micropitting are complicated by the nature of the tribological contact where a number of factors such as load, speed, sliding, specific film thickness, and lubricant chemical composition can play a critical role. In this study, experiments have been carried out in a three-contact roller disc machine to assess the influence of these factors on micropitting of roller samples made from AISI52100 bearing steel. The formation of micropitting under different test conditions was studied in detail by metallographic investigation of the roller samples in both plain-view and cross-section, with an emphasis on the changes of microstructure and chemical compositions associated with the top surface layer of the sample. Possible mechanisms for micropitting formation and alleviation remedies will be discussed based on these experimental results.

#### 10:30 AM Break

#### 10:45 AM

**Engineering Non-Stick, Pro-Stick/Adhesion and Anti-Corrosion Surfaces with Self-Assembled Monolayer of Phosphonate (SAMP) Technology:** Eric Bruner<sup>1</sup>; <sup>1</sup>Aculon, Inc.

Self-Assembled Monolayer of Phosphonates (SAMP) were developed as a technology platform. SAMP coating solutions have formulated for numerous markets including optical, display, electronics, and industrial coatings. These coatings outperform all known alternatives in characteristics such as adhesion, stain resistance, and scratch resistance. Surface treatments must be mechanically and chemically stable under conditions experienced in the intended area of use. SAMPs can impart any of these properties to metals, metal oxides and even some polymer surfaces by drawing on its library of structurally tailored phosphonic acids. The key is covalent bonding, which creates a uniquely strong attachment between the SAMP and substrate. The SAMP is one approximately 1.5 nm thick. It completely covers the material to which it is applied, and assures total surface coverage regardless of the type or texture of that material. The composition of the SAMP determines the properties that it imparts to its substrate.

# Technical Program

11:05 AM

**Anisotropic Nanaofriction Behavior of Aligned Carbon Nanotube Carpet:** Jiangnan Zhang<sup>1</sup>; Yuekai Sun<sup>1</sup>; Lijie Ci<sup>1</sup>; P.M. Ajayan<sup>1</sup>; Jun Lou<sup>1</sup>; <sup>1</sup>Rice University

The adhesion and frictional properties of surfaces coated with vertically and transversely aligned multi-walled carbon nanotube (MWCNT) carpet was investigated in ambient, around 10% RH humidity and nitrogen condition by atomic force microscope (AFM). The measured friction forces are higher for vertically aligned CNT carpet than for transversely aligned CNT carpet in all above environments. The friction force was found to be critically influenced by the relative humidity, with the decreasing relative humidity the friction force drops. The adhesive force data which was determined from force-displacement curves shows the adhesion forces are lower for transversely aligned CNT carpet than for vertically aligned CNT carpet while the adhesion forces drop as the relative humidity was decreased.

11:25 AM

**Dry Sliding Wear of Nanocrystalline Al - 12.6 at. % Si:** I. Baker<sup>1</sup>; M. Gwaze<sup>1</sup>; Y. Sun<sup>1</sup>; A.T. Dohner<sup>1</sup>; A. Grosse<sup>1</sup>; T. Tran<sup>1</sup>; F.E. Kennedy<sup>1</sup>; P.R. Munroe<sup>2</sup>; <sup>1</sup>Dartmouth College; <sup>2</sup>University of New South Wales

Wear resistance of many materials has been found to be proportional to their hardness. Thus, one might expect wear resistance to increase with decreasing grain size and nanocrystalline alloys to show exceptionally good wear resistance. Since sliding wear has been shown to refine the near-surface grain structure, it could be argued that nanoscale grains would not significantly affect wear behavior. This presentation will describe the results of a study designed to determine whether the wear rates of nanocrystalline eutectic Al-Si, produced by cryomilling followed by compaction using backpressure-assisted equal channel angular extrusion, are lower than material of the same composition produced by drop casting. Pin on disc wear tests were performed in air and argon against a Y-stabilized ZrO<sub>2</sub> counterface. Scanning electron microscopy and transmission electron microscopy, including energy dispersive X-ray mapping, were used to examine the worn pin surfaces. Work supported by U.S. NSF Grant CMMI 0651642.

11:45 AM

**Wear Resistance and Adherence of TiO<sub>2</sub> Sol-Gel Thin Films:** Miguel Alterach<sup>1</sup>; Pablo Favilla<sup>1</sup>; Mario Rosenberger<sup>1</sup>; Alicia Ares<sup>1</sup>; Carlos Schvezov<sup>1</sup>; <sup>1</sup>Universidad Nacional de Misiones - CONICET

The wear resistance and adherence of TiO<sub>2</sub> films was studied; the films were synthesized by the sol-gel dip-coating technique on a grade 5 titanium alloy. Monolayer and multilayer films were deposited by varying: dip-coating velocity, aging time of sol and the heat treatment parameters. These process conditions had influence on the color (thickness) of the film and the cracks formation. The wear resistance was measured on a ball-on-flat machine using a rotating glass ball as counterface. The worn films were evaluated by the size of the superficial scars, which can be noted by the change of color on the surface. The adherence was measured on a scratch test machine and examined by optical microscope to determine the adherent critical load. The best wear resistance and adherence of the films was measured on a trilayer film fabricated with a heat treatment at 500°C for 1h for each layer.

12:05 PM

**Fretting Corrosion Behaviour of Untreated and Surface Engineered Ti-6Al-4V Alloy:** Satendra Kumar<sup>1</sup>; Sankara Narayanan TSN<sup>1</sup>; Ganesh Sundara Raman S<sup>2</sup>; Seshadri S.K.<sup>2</sup>; <sup>1</sup>National Metallurgical Laboratory, Madras Centre; <sup>2</sup>Indian Institute of Technology Madras

Fretting corrosion is one of the major modes of failures observed in hip and knee implants which lead to a reduction in life-time of prosthesis. Surface engineering is a viable option to improve the fretting corrosion behaviour of these implants. The present paper will address the fretting corrosion behaviour of surface engineered Ti-6Al-4V alloy in Ringer's solution and compared with that of the untreated one. The methods used for surface modification are thermal and anodic oxidation. The change in free corrosion potential (FCP) measured as a function of time with the onset of fretting, during fretting and after stopping off the fretting motion is used to evaluate the fretting corrosion behaviour. Thermally oxidized Ti-6Al-4V alloy exhibit a better fretting corrosion resistance than the anodized and untreated one. The study concludes that thermal oxidation is a suitable surface engineering method for improving the fretting corrosion resistance of Ti-6Al-4V alloy.

## The Aluminium Industry – Perspectives on our Future: Session I

Sponsored by: The Minerals, Metals and Materials Society, TMS Light Metals Division, TMS: Aluminum Committee  
Program Organizer: Geoff Bearn, Rio Tinto Alcan

Monday AM Room: Ballroom 6A  
February 15, 2010 Location: Washington State Convention Center

Session Chair: Geoff Bearn, Rio Tinto Alcan

### 8:30 AM Introductory Comments

#### 8:35 AM Plenary

**The Challenges that Aluminium Faces as Material of Choice:** Frank Field<sup>1</sup>; <sup>1</sup>Massachusetts Institute of Technology; <sup>2</sup>CRU International Ltd  
Abstract not available.

#### 9:05 AM Plenary

**The Strategic Impact of Changing Energy Markets on the Aluminum Industry:** Robin Adams<sup>1</sup>; Kelly Driscoll<sup>2</sup>; <sup>1</sup>CRU Strategies; <sup>2</sup>CRU International Ltd

Aluminum is the most energy-intensive of the major commodity metals and the industry's smelting strategy has always been driven by the search for cheap power. In the past 5 years there have been clear signs of a structural change in energy prices, both for primary energy and electricity. What does this mean for the aluminum industry? In particular how will it affect the competitive structure of existing alumina refineries and aluminum smelters, the locations where new projects are constructed and the long-run equilibrium price for both alumina and metal? The paper will explore recent structural changes in global markets for oil, gas and coal as well as the state of play regarding carbon taxes and climate change. It will examine how these, along with regulatory changes around the world, are impacting on the price of thermal energy in regions with competitive bauxite-alumina potential and on the price power available to the aluminum industry. It will include a special evaluation of the changing situation in China. On this basis it will develop the competitive implications for today's refineries and smelters, the likely locations for tomorrow's successful projects and the all-important impact on long-term price levels in the industry.

#### 9:35 AM Plenary

**The Impact of Economic Highs and Lows on Aluminium Smelter Construction:** Cesar Inostroza<sup>1</sup>; <sup>1</sup>SNC-Lavalin Inc.

Since 1990, SNC-Lavalin has been a major player in 17 of the 28 largest aluminium smelter projects globally (outside China and Russia). Currently, SNC-Lavalin is engaged in the design and construction of 5 major aluminium smelter projects - Emal, Dubal, Qatalum, Boyne Smelter Upgrade and the Jonquiere Pilot Plant. The cyclical nature of this commodity-driven business is characterized by inherent risks that have an impact on decision making on aluminium smelter construction. The business case for new projects has also demanded the need to look at more difficult and complex projects, which are located in more remote regions, with limited access to a skilled labour force and operating under tighter environmental standards. This presentation will present an overview of the impact of the economic cycles on the main drivers in smelter construction cost, and will attempt to provide mechanisms to mitigate these impacts.

#### 10:05 AM Break

#### 10:25 AM Plenary

**Challenges and Opportunities Relative to Increased Usage of Aluminum within the Automotive Industry:** Mark W. Verbrugge<sup>1</sup>; Paul E. Krajewski<sup>1</sup>; Anil K. Sachdev<sup>1</sup>; James G. Schroth<sup>1</sup>; David R. Sigler<sup>1</sup>; Blair E. Carlson<sup>1</sup>; <sup>1</sup>General Motor Research and Development Center

The various alloys and processes associated with the use of aluminum within the automotive industry are overviewed, and key issues and challenges that stand in the way of increased aluminum use are highlighted.

Mon. AM



### 10:55 AM Plenary

#### Aluminum's Sustainability Strategy: *Steve Williamson*<sup>1</sup>; <sup>1</sup>ARCO Aluminum

Lightweight, corrosion resistant and ease of fabrication have been Aluminum's value proposition for over 100 years. With the advent of green-marketing, Aluminum is updating its Sustainability profile accordingly. Tasked by the Aluminum Association's Board of Directors in 2008, the member companies mandated a re-staffing and re-focus of the Association's efforts on a consolidated Sustainability Strategy. The Association had successfully delivered relevant product and end-use segment recycling, safety and productivity activities for decades. Through the traditional product and market focus, the packaging, transportation, and the building and construction markets were served and promoted. Now, staffed with experienced Sustainability managers, the Aluminum Association is embarking on a two-lane approach to a comprehensive Sustainability Strategy. The first objective is to build a robust data set that will enable each product and segment committee to respond to their respective downstream consumers. Simultaneously, the Association is creating a communications plan that will tell Aluminum's Sustainability story to key stakeholders and policy makers. Just a year into the initiative, and a year fraught with significant macroeconomic turmoil, the Aluminum Association's Sustainability Strategy has taken shape and is gaining traction.

### 11:25 AM Plenary

#### Aluminum Recycling in a Carbon-Constrained World: Observations and Opportunities: *Subodh Das*<sup>1</sup>; <sup>1</sup>Phnix LLC

This presentation will discuss the key aspects of aluminum recycling for several market sectors such as transportation, packaging, aerospace and building and construction in light of existing and anticipated debate on climate changes, carbon trading, carbon constraints and sustainability enhancement. The specific topics to be presented will be in the areas of commercialization of recycling-friendly alloys, development of recycling indices and carbon foot print of various aluminum alloys, and some thoughts and suggestions on enhancing recycling rates and use of recycled materials for developing new aluminum markets and products.

### 11:55 AM Concluding Comments

## The Vasek Vitek Honorary Symposium on Crystal Defects, Computational Materials Science and Applications: Computational Materials Science I

*Sponsored by:* The Minerals, Metals and Materials Society, TMS Materials Processing and Manufacturing Division, TMS/ASM; Computational Materials Science and Engineering Committee  
*Program Organizers:* Mo Li, Georgia Institute of Tech; David Srolovitz, Institute for High Performance Computing, Agency for Science, Technology and Research, Singapore; Adrian Sutton, Imperial College London; Vaclav Paidar, Institute of Physics AS CR vvi; Jeff De Hosson, Univ of Groningen

Monday AM Room: 603  
February 15, 2010 Location: Washington State Convention Center

*Session Chairs:* Adrian Sutton, Imperial College London; David Pope, University of Pennsylvania

### 8:30 AM Introductory Comments

#### 8:35 AM Charles McMahan

#### 8:50 AM David Pettifor

### 9:00 AM Keynote

#### Atomistic Modeling of Defects through the Ages: *Vasek Vitek*<sup>1</sup>; <sup>1</sup>University of Pennsylvania

We discuss the long-term development of the atomic level modeling of defects in materials and relation to our understanding of their mechanical behavior. The three major themes are: Understanding of atomic bonding and the limits this imposes on what can be studied by modeling, interpretation of the results and relation between calculations and experiments. First we discuss the development starting from pair-potentials through many-body central-force potentials, tight-binding methods up to the DFT based calculations and show for each significant contributions albeit on different levels. In interpretation

we are particularly interested in paths towards development of theoretical analyses enabled by modeling. Finally, we emphasize that the link with experiment is crucial for both validation of the studies and for motivation of new investigations. Such experiments need to involve all levels, starting with atomic, such as HREM, up to macroscopic, such as studies of orientation dependencies of yielding in single and polycrystals.

### 9:25 AM Invited

#### Challenges in Modelling TCP Phase Formation in Ni-Based Superalloys: *David Pettifor*<sup>1</sup>; Bernhard Seiser<sup>1</sup>; Thomas Hammerschmidt<sup>2</sup>; Aleksey Kolmogorov<sup>1</sup>; Ralf Drautz<sup>2</sup>; <sup>1</sup>University of Oxford; <sup>2</sup>ICAMS

Modelling topologically close-packed (TCP) phase formation in Ni-based superalloys is a challenging task with only the semi-empirical PHACOMP and NewPHACOMP schemes providing some guidance. In this talk we develop a microscopic understanding of the factors that control TCP phase stability by coarse-graining the electronic structure from density functional theory (DFT) to tight-binding (TB) to bond-order potentials (BOPs). These many-body interatomic BOPs are unique in that they depend explicitly on the electron per atom ( $e/a$ ) ratio, so that they predict the structural sequence from bcc to sigma to hcp that is found, for example, across the W-Re system. The observed stability of the mu and Laves phases requires the additional contribution of size and electronegativity differences. Remaining challenges in modelling TCP phase formation are briefly discussed.

### 9:50 AM Invited

#### Dislocation-Based Simulation of the Migration of Low-Angle Grain Boundaries: *David Srolovitz*<sup>1</sup>; Adele Lim<sup>2</sup>; Mikko Haataja<sup>2</sup>; <sup>1</sup>Yeshiva University; <sup>2</sup>Princeton University

Understanding the mechanisms of grain boundary migration are complicated by the complexity of the structure of general boundaries, the high dimensionality of the boundary parameter space and the large number of dynamic degrees of freedom in the system. We, therefore, focus on low angle grain boundaries, the structure and dynamics of which can be described in terms of lattice dislocations and their glide, climb, and reactions. We perform a series of 2 and 3-dimensional simulations of stress driven migration of low angle grain boundaries where the dynamical variables are the location and Burgers vectors of the dislocations. We investigate the effect of dislocation climb mobility, boundary inclination, and misorientation on the mechanisms and mobilities of such boundaries. Next, we develop analytical models for boundary mobility that are in excellent agreement with both simulation and experimental results.

### 10:15 AM Break

### 10:40 AM Invited

#### Discrete Dislocation and Multi-Scale Analyses of Fatigue Crack Growth: *Alan Needleman*<sup>1</sup>; <sup>1</sup>University of North Texas

Processes at a variety of scales play a role in the fatigue crack growth of crystalline metals. The mesoscale, where discrete dislocation effects need to be accounted for, plays a central role in mediating between atomic scale effects and macroscale dissipation processes that can be modeled appropriately using conventional continuum descriptions. The organized dislocation structures near a crack tip give rise to much higher stress levels to drive atomic scale processes than are predicted by conventional continuum plasticity. Some discrete dislocation plasticity predictions for fatigue crack growth will be discussed along with some recent steps taken to carry out multi-scale analyses of fatigue crack growth in metal single crystals.

### 11:05 AM Invited

#### Displacive Processes in Systems with BCC Parent Lattice: *Vaclav Paidar*<sup>1</sup>; <sup>1</sup>Institute of Physics AS CR vvi

The changes of sample shape are caused by plastic deformation or by martensitic phase transformations. In both cases the mechanisms of atomic rearrangements are based on collective displacements of atomic aggregates. The internal structure of dislocations, carriers of plastic deformation, can be examined using the energies of generalized stacking faults displayed by so called  $\gamma$ -surfaces calculated for bcc metals by Prof. Vitek already more than forty years ago. This approach can be extended to the shuffling of atomic planes that plays a crucial role in martensitic phase transformations. Similarities and differences between displacive processes of local lattice shearing and atomic plane alternate shuffling will be discussed.

# Technical Program

## 11:30 AM Invited

**Coupling of the Continuum Theory of Dislocations and Structural Phase Transformations at the Mesoscale:** *Roman Groger*<sup>1</sup>; Turab Lookman<sup>2</sup>; <sup>1</sup>Academy of Sciences of the Czech Republic; <sup>2</sup>Los Alamos National Laboratory

Collective motion of dislocations often gives rise to correlated dislocation domains and to spatially inhomogeneous microstructure with unconventional mechanical properties. In multiphase materials the evolution of crystal structure can be studied using well-developed concepts such as the mean-field Landau theory. However, theoretical studies of plasticity in multiphase materials are rather scarce owing to a complicated coupling of the dislocation density and the underlying microstructure. In this talk, we propose a self-consistent scheme in which the coupling of the order parameter field with the dislocation density is accomplished using a set of incompatibility constraints. When these physical constraints are incorporated into the Landau free energy functional, one arrives at a mesoscopic model of phase transformations mediated by dislocations. This model serves to bridge the length scales by allowing for the systematic incorporation of data from both atomistic simulations and macroscopic experimental measurements.

## Three-Dimensional Materials Science VI: Three-Dimensional Crystallography and Grain Boundary Analysis

*Sponsored by:* The Minerals, Metals and Materials Society, ASM International, TMS Structural Materials Division, TMS: Advanced Characterization, Testing, and Simulation Committee, ASM-MSCTS: Texture and Anisotropy Committee, TMS/ASM: Phase Transformations Committee

*Program Organizers:* Alexis Lewis, Naval Research Laboratory; Anthony Rollett, Carnegie Mellon University; David Rowenhorst, Naval Research Lab; Jeff Simmons, AFRL; Stuart Wright, EDAX Inc-TSL

Monday AM Room: 401  
February 15, 2010 Location: Washington State Convention Center

*Session Chairs:* David Rowenhorst, U S Naval Research Laboratory; Stuart Wright, EDAX-TSL

## 8:30 AM Invited

**Deriving the Grain Boundary Character Distribution and Relative Grain Boundary Energies from Three Dimensional EBSD Data:** *Gregory Rohrer*<sup>1</sup>; <sup>1</sup>Carnegie Mellon University

The proliferation of the dual-beam focused ion-beam scanning electron microscope has allowed for more routine collection of data from calibrated serial sections. Combining this technique with electron back-scatter diffraction (EBSD) allows for a complete description of the complete description of the crystallography of all of the grain boundaries within a polycrystal. The grain boundary character distribution (GBCD) is an important description of the grain boundary network that is thought to be a significant indicator of materials properties. Serial sections of EBSD data have been collected and reconstructed in 8% yttria-stabilized zirconia, yttria, SrTiO<sub>3</sub>, and nickel. Different methods for calculating the GBCD from 3D reconstructed microstructures are compared with a more established stereological analysis of 2D data. Implications of the results on our understanding of relative grain boundary energies and the structure of grain boundary networks in polycrystals will be discussed.

## 9:00 AM

**Deriving the Relative Grain Boundary Areas and Energies in Nickel from Three Dimensional EBSD Data:** *Jia Li*<sup>1</sup>; Gregory Rohrer<sup>1</sup>; Shen Dillion<sup>2</sup>; <sup>1</sup>Carnegie Mellon University; <sup>2</sup>University of Illinois at Urbana-Champaign

The three dimensional interfacial network of grain boundaries in polycrystalline nickel has been characterized using a combination of electron backscatter diffraction mapping and focused ion beam serial sectioning. These data have been used to determine the relative areas of different grain boundary types, categorized on the basis of lattice misorientation and grain boundary plane orientation. Using the geometries of the interfaces at triple lines, relative grain boundary energies have also been determined as a function of lattice misorientation and grain boundary plane orientation. Grain boundaries comprised of (111) planes have, on average, lower energies than

other boundaries. Asymmetric tilt grain boundaries with the S9 misorientation also have relatively low energies. The grain boundary energies and areas are inversely correlated.

## 9:20 AM

**Calculation of Grain Boundary Angles at Triple Junctions in 3D Digitized Microstructures:** *Michael Chandross*<sup>1</sup>; Elizabeth Holm<sup>1</sup>; <sup>1</sup>Sandia National Laboratories

Digitized microstructures are generated in both simulations and experiments. Because of the discrete nature of digitized grain boundaries, it is difficult to measure dihedral angles at triple junctions in these microstructures. We recently developed a method that utilizes linear fits to grain boundaries followed by a comparison of correlation coefficients to accurately calculate triple junction angles (TJAs) in digitized microstructures. We use this method to analyze cross-sections of 3D simulated microstructures as well as various experimental micrographs. Histograms of TJAs show the expected peak about 120 degrees. Simulated microstructures agree well with experiment. Details of the angle distribution indicate the accuracy of grain growth simulations (lattice effects, faceting) or the distribution of grain boundary energies in experimental systems (anisotropy). Further, we note specific peaks that can be used to determine the microstructural dimensionality (i.e. columnar vs. equiaxed) from a 2D cross-section.

## 9:40 AM Break

## 10:10 AM Invited

**Three-Dimensional Grain Boundary Networks: Modeling and Connections to Experimental Data:** *Megan Frary*<sup>1</sup>; <sup>1</sup>Boise State University

The grain boundary network that makes up a microstructure plays an important role in determining the properties of the material. These networks are well-studied in two dimensional systems; however, most microstructures are inherently three dimensional, so an understanding of the role microstructure plays in determining properties must account for the full 3D microstructure. Here, percolation-based models are applied to 3D grain boundary networks with both regular and irregular grain shapes. The microstructures are characterized in terms of the cluster size distribution, mean cluster size, and radius of gyration; grain boundary area must be accounted for when calculating these properties in 3D. The analytical tools developed to characterize simulated microstructures can be applied to experimentally-determined data sets to extract the same metrics from those microstructures. Developing an understanding of 3D connectivity in real microstructures may elucidate the role of grain boundary character distribution on property improvement observed during grain boundary engineering.

## 10:40 AM

**Three Dimensional Analysis of Grain Curvature and Crystallography:** *David Rowenhorst*<sup>1</sup>; Alexis Lewis<sup>1</sup>; George Spanos<sup>1</sup>; Gregory Rohrer<sup>2</sup>; Anthony Rollett<sup>2</sup>; <sup>1</sup>US Naval Research Laboratory; <sup>2</sup>Carnegie Mellon University

The state of serial sectioning has now allowed for statistically relevant structures to be analyzed, often containing thousands of objects within the sampling volume. We will briefly present our methodology for serial sectioning, including crystallographic orientations from EBSD in a single phase, beta-titanium alloy. The resultant reconstruction contains over 4300 grains, within the 200 sections taken. In the results, we will present the analysis of the grain boundary curvature and use this as a measure of the grain growth rate. Furthermore the correlation between boundary curvature to the crystallographic interface of the grain boundary will be examined.

## 11:00 AM

**Synthesizing Annealing Twins in Three-Dimensional Voxel-Based Microstructures:** *Lisa Chan*<sup>1</sup>; Anthony Rollett<sup>1</sup>; Gregory Rohrer<sup>1</sup>; <sup>1</sup>Carnegie Mellon University

In face-centered cubic metals, Grain Boundary Engineering typically involves maximizing the density of high symmetry boundaries to improve grain boundary dependent properties, such as the resistance to intergranular corrosion and fatigue cracking. These high symmetry boundaries are denoted by low sigma values for Coincident Site Lattice relationships. In the studies of increasing the fraction of low sigma boundaries, twinning events have been found to be very effective in introducing low sigma boundaries. In this study, annealing twins are added into a digitally simulated microstructure such that the number fractions and twin cluster statistics match with the values observed



in experimental structures. The resulting texture and grain boundary character distribution are also compared against the experimental measurements.

**11:20 AM**

**Crystallographic Orientation Determined from the Pattern of Solidified Structure:** *Hisao Esaka*<sup>1</sup>; Kei Shinozuka<sup>1</sup>; <sup>1</sup>National Defense Academy

Solidified structure is complex, since the growth directions of dendrites are not in accordance with the observed plane. Many ghost lines are observed. Dendrite of cubic metals has been simplified with rod and four plates with the same thickness. Then, the ghost lines have been analyzed applying the solid analytical geometry. In order to characterize the solidified pattern, angles and the ratio of width of ghost lines have been formulated using the angles, which determine the orientation of dendrite. The computer program has been developed to determine the spatial orientation of dendrite from the characteristic parameters of ghost lines. Applying this computation, it was found that the cross sections of dendrite model performed by 3D-CAD agreed well with the solidified structure. Furthermore, the crystallographic orientation estimated from the solidified pattern agreed with EBSD data of the cast specimen of Al-20 mass% Cu alloy.

**11:40 AM**

**3D Monte-Carlo Simulation of Microstructural Evolution upon Heating of Deformed LCB Titanium Alloy:** *Sergii Shevchenko*<sup>1</sup>; Orest Ivasishin<sup>1</sup>; Elena Pereloma<sup>2</sup>; Azdiar Gazder<sup>2</sup>; <sup>1</sup>Institute for Metal Physics; <sup>2</sup>University of Wollongong

The evolution of microstructure, texture and grain boundary statistics during thermal treatment of deformed LCB titanium alloy was modeled using a 3D Monte Carlo (Potts) approach. The initial microstructure, texture (ODF), spatial distribution of the stored energy of deformation (cold drawn, 70%). The modeling technique allowed to compare how differences in nucleation mechanisms and kinetics affect recrystallization kinetics and microstructure and texture evolution. It was shown that oriented nucleation led to formation of recrystallization texture, which, however, smeared during subsequent grain growth. Also, oriented nucleation resulted in slower recrystallization rate in comparison with the case of not oriented nucleation. Results of the MC Potts modeling were verified experimentally by analysis of textures and microstructures (EBSD orientation maps) at different stages of recrystallization and grain growth.

**Ultrafine Grained Materials – Sixth International Symposium: Processing-Microstructure-Properties I**

*Sponsored by:* The Minerals, Metals and Materials Society, TMS Materials Processing and Manufacturing Division, TMS Structural Materials Division, TMS/ASM: Mechanical Behavior of Materials Committee, TMS: Nanomechanical Materials Behavior Committee, TMS: Shaping and Forming Committee

*Program Organizers:* Suvreen Mathaudhu, U.S. Army Research Laboratory; Mathias Goeken, University Erlangen--Nürnberg; Terence Langdon, University of Southern California; Terry Lowe, Manhattan Scientifics, Inc.; S. Semiatin, Air Force Research Laboratory; Nobuhiro Tsuji, Kyoto University; Yonghao Zhao, University of California - Davis; Yuntian Zhu, North Carolina State University

Monday AM Room: 606  
February 15, 2010 Location: Washington State Convention Center

*Session Chairs:* S. Lee Semiatin, U.S. Air Force Research Laboratory; En (Evan) Ma, Johns Hopkins University; Xavier Sauvage, University of Rouen, CNRS; Henry Rack, Clemson University

**8:30 AM Introductory Comments**

**8:35 AM Invited**

**Superior Properties of Ultrafine-Grained Metals Produced by SPD Processing:** *Ruslan Valiev*<sup>1</sup>; <sup>1</sup>Ufa State Aviation Technical University

Over the last years there appeared a number of observations stating that ultrafine-grained (UFG) metals and alloys produced by severe plastic deformation can exhibit unique and extraordinary mechanical and physical properties that differ fundamentally from their conventional, coarse-grained counterparts. The present report considers several new examples of that

kind - effect of superstrength revealed in several nanostructured light alloys, appearance of super-ductility in UFG Al alloy already at room temperature and a number of other unique features of physical and mechanical behaviour of nanometals. Findings of such unusual properties are of high scientific interest as these properties are attributed to novel physics of deformation and phase transformations in UFG materials. Practical importance of these works arises from the development of metallic materials of new generation. These aspects are considered and discussed in the report with the emphasis on the phenomena origin and strategies for achievements.

**8:55 AM**

**Nanostructures and Magnetic Properties of FePd Alloys Processed by Severe Plastic Deformation:** *Xavier Sauvage*<sup>1</sup>; Abdelahad Chbhihi<sup>1</sup>; Didier Blavette<sup>1</sup>; Dmitry Gunderov<sup>2</sup>; A.G. Popov<sup>3</sup>; <sup>1</sup>University of Rouen, CNRS; <sup>2</sup>Ufa State Aviation Technical University; <sup>3</sup>Institute of Metal Physics

The intermetallic FePd alloy was processed by severe plastic deformation (high pressure torsion) both in the ordered and the disordered state. The resulting materials are nanostructured with a grain size smaller than 100nm. Using x-ray diffraction, transmission electron microscopy and magnetic properties measurements some strain induced disordering was revealed. The ordering kinetics during post deformation aging treatment was also investigated. In the optimum state, nanoscaled ordered domains give rise to a record coercivity of about 1400 Oe.

**9:10 AM Invited**

**High Tensile Strength and Ductility in Nanocrystalline and Ultrafine-Grained HCP Cobalt:** *Xiaolei Wu*<sup>1</sup>; Yuntian Zhu<sup>2</sup>; <sup>1</sup>Institute of Mechanics, Chinese Academy of Sciences; <sup>2</sup>North Carolina State University

Tensile property and work hardening behavior were investigated in both nanocrystalline (NC) and ultrafine-grained (UFG) cobalt produced by the surface mechanical attrition treatment. The yield strength of UFG Co and NC Co is around 3 and 5 times higher than that of the coarse-grained counterpart, with the uniform plastic strains being as high as 8.6% and 6.1% respectively. In particular, the annealing results in a significant increase in ductility and work hardening rate as compared with their deformed states, with plastic strains reaching 13.8% and 8.3% respectively. TEM observations show the presence of basal stacking faults of high density in both UFG and NC grains. The successive formation of SFs and their interplay with dislocations, together with the formation of NC grains during tension enhances the work hardening and uniform ductility.

**9:30 AM**

**Effect of Strain Path and Texture on Grain Refinement in Severe Plastic Deformed Copper:** *Chengfan Gu*<sup>1</sup>; Laszlo Tóth<sup>2</sup>; Rimma Lapovok<sup>1</sup>; Chris Davies<sup>1</sup>; <sup>1</sup>Monash University; <sup>2</sup>Université Paul Verlaine de Metz

OFHC copper were obtained by ECAP, route Bc, up to four passes and cold rolled to a thickness reduction of 97.5% (total true strain of 4.26) respectively. The crystallographic textures and microstructure of obtained samples were measured by X-ray diffraction and EBSD. It has been found that the microstructure in the ECAPed copper was much more refined with respect to the rolling case (at same equivalent strain) leading to smaller grain sizes in ECAP. The grain refinement between ECAP and rolling can be interpreted by the model based on lattice distortion of crystals due to the constraining effects of their neighbors in the polycrystal [Tóth L.S. et al, ICSMA15, 2009]. The model produces subgrains in orientations controlled by the orientation of the grain boundaries and by the rate of lattice rotation. It is applied in this study to reproduce the differences in grain sizes and the texture developments.

**9:45 AM**

**Superior Grain Refinement via Intelligent ECAE Processing of Materials:** *Suvreen Mathaudhu*<sup>1</sup>; Laszlo Kecskes<sup>1</sup>; Jae-Taek Im<sup>2</sup>; David Foley<sup>2</sup>; Majid Al-Maharbi<sup>3</sup>; Ibrahim Karaman<sup>2</sup>; K. Ted Hartwig<sup>2</sup>; <sup>1</sup>U.S. Army Research Laboratory; <sup>2</sup>Texas A&M University; <sup>3</sup>Sultan Qaboos University

Severe plastic deformation (SPD) by equal channel angular extrusion/pressing (ECAE/ECAP), has been recognized as a premier processing tool for obtaining ultrafine grained or nanocrystalline (UFG/NC) microstructures in bulk metal samples. While the progress in grain refinement capabilities has been significant, the majority of results have been demonstrated on metals and alloys with f.c.c. crystal structures, and relatively fine starting grains sizes and homogeneous textures. In this paper, we will present results which show that factors such as texture, chemistry, and starting grain size play a significant

Mon. AM

# Technical Program

role on the grain refinement potential of all metallic systems, including h.c.p. and b.c.c. crystal structures. Examples of enhanced grain refinement will be given for b.c.c. Ta, Nb and W, h.c.p. Mg- and Ti- alloys, and hexagonal Bi<sub>2</sub>Te<sub>3</sub>. The results presented will demonstrate concrete examples of superior grain refinement by incorporation of unconventional rotation routes, chemical homogenization, and pre-processing.

## 10:00 AM Invited

**High Pressure Torsion of Pure Metals for Universal Plot:** Kaveh Edalati<sup>1</sup>; Zenji Horita<sup>1</sup>; <sup>1</sup>Kyushu University

Several pure metals such as Al, Ag, Au, Cu, Ni, Pt and Fe are processed by high-pressure torsion (HPT). Hardness first increases with an increase in strain and then saturates to a steady state when plotted against equivalent strain. The hardness increase is more rapid as the pressure increases but the saturation levels are the same under different pressures. When the plotting is made with the equivalent strain multiplied by pressure and divided by shear modulus, it is shown that all data points under different pressures fall on a single curve. It is also shown that when the hardness is normalized by shear modulus with an inclusion of the homologous temperature for HPT operation, a universal plot is obtained for all data points of different pure metals covered in this study except for Al where recovery is very fast.

## 10:20 AM Break

## 10:35 AM Invited

**Nanostructures, Grain Refinement and Mechanical Properties in Al-Mg Alloys Subjected to High Pressure Torsion:** Hans Roven<sup>1</sup>; Manping Liu<sup>2</sup>; Maxim Murashkin<sup>3</sup>; Ruslan Valiev<sup>3</sup>; Tamas Ungár<sup>4</sup>; Levente Balogh<sup>4</sup>; <sup>1</sup>Norwegian University of Science and Technology (NTNU); <sup>2</sup>Shanghai Jiao Tong University; <sup>3</sup>Ufa State Aviation Technical University; <sup>4</sup>Eötvös University

Recent results on nanostructures, grain refinement and mechanical properties in Al-Mg alloys subjected to high pressure torsion will be reviewed. Typical nanostructures of non-equilibrium grain boundaries, full dislocations and Shockley partials, deformation microtwins and stacking faults, as well as hexagonal and rhombic shaped nanostructures have been identified using high-resolution transmission electron microscopy. Grain size distributions and dislocation densities and densities of planar defects were quantified by X-ray diffraction (XRD) and high-resolution XRD line profile analysis. Microhardness and tensile properties of the Al-Mg alloys were comparatively investigated. The major part of the presentation will focus upon the formation mechanisms of the typical nanostructures, the refinement and strengthening mechanisms associated with the typical nanostructures and faults. A possible formation process of the hexagonal and rhombic shaped nanostructures will be proposed based on molecular-dynamics simulations. The role of Mg solute on the formation, refinement and strengthening mechanisms will also be considered.

## 10:55 AM

**Crystal Size Influences the Propensity for Deformation Twinning:** Evan Ma<sup>1</sup>; Ju Li<sup>2</sup>; Qian Yu<sup>2</sup>; Zhiwei Shan<sup>4</sup>; Jun Sun<sup>3</sup>; <sup>1</sup>Johns Hopkins University; <sup>2</sup>University of Pennsylvania; <sup>3</sup>Xi'an Jiaotong University; <sup>4</sup>Hysitron Inc.

Deformation twinning (DT) in crystals is a highly correlated inelastic shearing process which controls the mechanical behavior of many engineering materials. It is known that deformation twinning can become more difficult in small grains and crystals. Using micro-compression and in situ nano-compression experiments, we find that deformation twinning in a Ti-5at%Al alloy is overtaken by less correlated, ordinary dislocation plasticity (ODP), when its physical dimension *d* is reduced to below a critical *d<sub>c</sub>* ~ 1 micrometer. A phenomenological stimulate-slip model has been developed to explain the strong crystal/grain size dependence for DT. The large transition size is far above that (~ 20 nm) for the switch of deformation mechanisms in nanocrystalline materials and easily accessible in experiments, making our findings highly relevant for practical applications.

## 11:10 AM

**Enhanced Strain Hardenability of Uniform, Submicrocrystalline Dual-Phase Steel Processed via Equal Channel Angular Pressing and Intercritical Annealing:** Young Gun Ko<sup>1</sup>; C.W. Lee<sup>2</sup>; S. Namgung<sup>2</sup>; D.H. Shin<sup>2</sup>; <sup>1</sup>Yeungnam University; <sup>2</sup>Hanyang University

Tensile deformation behavior is investigated of submicrocrystalline dual-phase steel (DPS) via equal channel angular pressing (ECAP) accompanied by heat treatment in an intercritical region, with a specific focus on strain hardening

behavior. A fully martensite structure is used as a preform microstructure because easy dissolution of carbon atoms during ECAP leads to a uniform distribution of each constituent phase (martensite + ferrite) during intercritical annealing treatment. From tension tests, the submicrocrystalline DPS exhibits greater strain hardenability than what submicrocrystalline steels behave, resulting in a tensile strength of ~ 1 GPa with a total elongation of ~ 20 pct. The strain hardening behavior is here analyzed based on strain gradient model.

## 11:25 AM Invited

**Superplasticity in Nanocrystalline Metallic and Ceramic Materials:** Amiya Mukherjee<sup>1</sup>; <sup>1</sup>University of California

Significant differences, including higher flow stresses and enhanced strain hardening rates in nanocrystalline structure, have been observed in the deformation characteristics of nanocrystalline materials at elevated temperatures as compared to their microcrystalline counterparts. Conventional understanding of elevated temperature crystalline plasticity cannot explain these observations. Cooperative grain boundary sliding (CGBS) in superplasticity has shown to account for the majority of macroscopic strain in microcrystalline materials. In this work, nanocrystalline Ni<sub>3</sub>Al produced via High Pressure Torsion is deformed superplastically in the TEM. In-situ tensile testing shows the nature of CGBS at the nanoscale through direct observation of this phenomenon. The second part of this presentation is devoted to demonstrating the potential of using spark plasma sintering to consolidate nanocrystalline powder and the subsequent superplastic deformation of the compact to near-finished shape. This procedure has provided one of the lowest temperature, high strain rate superplastic formings of nanocrystalline ceramics to date.

## 11:45 AM

**ECAE Processing of Pure and Mg Alloy Powders: Effect of Confinement, Route, and Temperature:** Laszlo Kecskes<sup>1</sup>; Kristopher Darling<sup>1</sup>; Micah Gallagher<sup>2</sup>; Suveen Mathaudhu<sup>1</sup>; David Foley<sup>3</sup>; Robert Barber<sup>2</sup>; Karl Hartwig<sup>3</sup>; <sup>1</sup>US Army Research Laboratory; <sup>2</sup>Dynamic Science, Inc.; <sup>3</sup>Texas A&M University

Severe plastic deformation processing by ECAE has been applied to coarse-grained ZK-60 Mg alloy powders. The effects of confinement, route, and temperature were studied to elucidate the break-down of the prevailing, intermetallic-inclusion-interposed, laminar structure of rolled ZK-60 alloy plate. We relied on routes A, C, or E, at a range of temperatures up to 300°C, to explore inherent limitations of dispersion and homogenization in solid, as-received ZK-60 alloy rods. At the same time, to examine potential improvements to the ZK-60 alloy microstructure, we side-by-side extruded prealloyed ZK-60 powders and co-milled blends of Mg, Zr, and Zn powders with the nominal ZK-60 composition. Scanning electron microscopy, texture measurements, energy dispersive x-ray analysis, and microhardness measurements were applied to characterize the resultant extrudates. A comparison of extrudates from both top-down and bottom-up approaches are discussed.

## 12:00 PM

**Shape Memory Characterization of Aged Ti-50.6Ni:** Henry Rack<sup>1</sup>; Astrid Mueller<sup>1</sup>; Erica Sampson<sup>1</sup>; Ruslan Valiev<sup>2</sup>; <sup>1</sup>Clemson University; <sup>2</sup>Ufa State Aviation Technical University

This presentation will present the results of a study which has examined the shape memory response of ultra-fine grained Ti-50.6 Ni aged at temperatures between 400 and 550°C for times to 100 hrs. These results will be contrasted with solution treated and aged Ti-50.6Ni with the variations in shape memory transformations temperatures and latent heats of reaction being described in terms of the microstructure observed utilizing x-ray, scanning and transmission electron microscopy.

## 12:15 PM Invited

**The Brittle-To-Ductile Transition in Severely Deformed Low Carbon Steel:** Masaki Tanaka<sup>1</sup>; Kenji Higashida<sup>1</sup>; Tomotsugu Shimokawa<sup>2</sup>; <sup>1</sup>Kyushu University; <sup>2</sup>Kanazawa University

The brittle-to-ductile transition (BDT) behavior was investigated in low carbon steel deformed by an accumulative roll-bonding (ARB) process. The temperature dependence of its fracture toughness was measured by conducting four-point bending tests at various strain rates. The fracture toughness increased while the BDT temperature decreased in the specimens deformed by the ARB process. Arrhenius plots between the BDT temperatures and the strain rates indicated that the activation energy for the BDT did not change due to the deformation with the ARB process. It indicated that the decrease in the BDT



temperature by grain refining was not due to the reduction in the dislocation mobility with respect to short-range barriers. Quasi-three-dimensional simulations of discrete dislocation dynamics indicated that the decrease in the number of dislocation sources decreases in the DBT temperature. The roles of grain boundaries will be also discussed in order to explain the decrease in the BDT temperature.

### Ultrafine Grained Materials – Sixth International Symposium: Processing-Microstructure-Properties II

*Sponsored by:* The Minerals, Metals and Materials Society, TMS Materials Processing and Manufacturing Division, TMS Structural Materials Division, TMS/ASM: Mechanical Behavior of Materials Committee, TMS: Nanomechanical Materials Behavior Committee, TMS: Shaping and Forming Committee

*Program Organizers:* Suveen Mathaudhu, U.S. Army Research Laboratory; Mathias Goeken, University Erlangen-Nürnberg; Terence Langdon, University of Southern California; Terry Lowe, Manhattan Scientifics, Inc.; S. Semiatin, Air Force Research Laboratory; Nobuhiro Tsuji, Kyoto University; Yonghao Zhao, University of California - Davis; Yuntian Zhu, North Carolina State University

Monday AM Room: 607  
February 15, 2010 Location: Washington State Convention Center

*Session Chairs:* Donald Lesuer, Lawrence Livermore National Laboratory; Megumi Kawasaki, University of Southern California; Challapalli Suryanarayana, University of Central Florida; Zenji Horita, Kyushu University

#### 8:30 AM Introductory Comments

##### 8:35 AM Invited

**Flow Stress Anisotropy and Tension-Compression Asymmetry in Ultrafine Grained AZ31B Magnesium Alloy:** *Ibrahim Karaman*<sup>1</sup>; Majid Al-Maharbi<sup>1</sup>; David Foley<sup>1</sup>; Irene Beyerlein<sup>2</sup>; K.Ted Hartwig<sup>1</sup>; Suveen Mathaudhu<sup>3</sup>; Laszlo Kecskes<sup>2</sup>; <sup>1</sup>Texas A&M University; <sup>2</sup>Los Alamos National Laboratory; <sup>3</sup>U.S. Army Research Laboratory

AZ31B Magnesium alloy has been processed at 150-200°C using equal channel angular extrusion (ECAE) up to four passes following four different routes. The flow stress anisotropy and tension-compression (T/C) asymmetry along the three orthogonal directions of the ECAE billet were monitored. The texture evolution during ECAE was measured and predicted using a viscoplastic self-consistent crystal plasticity model. The initial grain orientations with respect to the ECAE die greatly influence the type of deformation modes during ECAE and hence resultant texture and grain morphology. If basal planes are oriented perpendicular to ECAE shear plane, non-basal slip systems are activated which suppresses dynamic recrystallization during ECAE. Flow stress anisotropy and T/C asymmetry after ECAE are highly dependent on crystallographic texture. It is demonstrated that controlling starting texture, ECAE temperature, route and number of passes provide some control over resulting texture, grain size and morphology, and thus, flow stress anisotropy and T/C asymmetry.

##### 8:55 AM

**Role of Ultrafine Grain Size in the HCP - FCC Allotropic Transformation in Ti, Zr, and Hf:** *Uma Seelam*<sup>1</sup>; Gagik Barkhordarian<sup>2</sup>; *C. Suryanarayana*<sup>1</sup>; <sup>1</sup>University of Central Florida; <sup>2</sup>GKSS Research Center

Allotropic HCP - FCC transformations were observed in mechanically milled Ti, Zr, and Hf powders. While the transformation was observed in powders milled under regular milling conditions, no such phase transformation was observed when the powders were milled in an ultra-high purity environment by placing the mill inside an argon-filled glove box. From a critical analysis of the width and intensity of X-ray diffraction peaks and chemical analysis of the milled powders, it was inferred that the transformation was associated with the formation of nanocrystals in the milled powder. It was also concluded that the HCP - FCC phase transformation was, at least partially, due to pick-up of interstitial impurities by the powder during milling of these powders to the nanocrystalline state. Isothermal equation of state was used to estimate the stability of the FCC phase in the Group IV B metals.

##### 9:10 AM

**Ultra-High Strength of Nanocrystalline Iron-Based Alloys Produced by High Pressure Torsion:** *Tadahiko Furuta*<sup>1</sup>; Shigeru Kuramoto<sup>1</sup>; Tetsu Osuna<sup>1</sup>; Zenji Horita<sup>2</sup>; <sup>1</sup>Toyota Central R & D Labs., Inc.; <sup>2</sup>Kyusyu University

Elastic and plastic deformation behaviors were investigated in a nanocrystalline Fe-19%Ni-34%Co-8%Ti (in at%) alloy produced by High Pressure Torsion (HPT) at room temperature with a rotating speed of 1 rpm under a pressure of 6 GPa. Applying the HPT process, the average grain size appears to be 20-50 nm with high density crystal defects and such an intense grain refinement have never been reported in bulk iron alloy. The alloy shows ultimate tensile strength (UTS) of about 2.75 GPa and Young's modulus (E) of about 150 GPa with the total tensile elongation of 8 - 10 %. As a result, the ratio of UTS/E for the present alloy is ~0.02, which is substantially higher than conventional metallic materials. It is inferred from this high value of UTS/E that the dislocation motion, which governs the plastic deformation behavior of metallic materials, is inhibited by the grain refinement up to ultra-high stress level.

##### 9:25 AM Invited

**Fatigue Behavior of Friction Stir Processed Ultrafine Grained Aluminum and Magnesium Alloys:** *Rajiv Mishra*<sup>1</sup>; Partha De<sup>1</sup>; Rajeev Kapoor<sup>1</sup>; Wei Yuan<sup>1</sup>; <sup>1</sup>Missouri University of Science and Technology

The fundamental micromechanism of fatigue deformation changes from microcrystalline to ultrafine grained (UFG) materials. The well proven concepts of persistent slip bands and extrusion/intrusion features in microcrystalline alloys do not apply directly to UFG materials because of the grain length scale and change in the dislocation micromechanisms. In the recent years, friction stir processing is emerging as a convenient tool for producing very fine grained and UFG materials with high fraction of high angle boundaries. Additionally it results in refinement and homogenization of constituent particles in commercial aluminum alloys. Initial results indicate that the UTS normalized fatigue stress for 10<sup>7</sup> cycles increases significantly for commercial aluminum and magnesium alloys. An overview of the S-N curves and the changes in micromechanisms will be presented and discussed. A conceptual dislocation dynamics-microstructural length scale framework has been developed to rationalize the enhancement in fatigue strength.

##### 9:45 AM

**Influence of Grain Boundary Character and Strain Rate on the Ductility of Ultrafine Grained AA 5052:** *Rajeev Kapoor*<sup>1</sup>; Nilesh Kumar<sup>1</sup>; Rajiv Mishra<sup>1</sup>; <sup>1</sup>Missouri University of Science and Technology

Presented here is a study of ultrafine grained AA 5086 (a solid solution hardening Al-2.5%Mg alloy) obtained by two methods, one through friction stir processing and the other through the continuous equal channel angular pressing technique for four different conditions of 1, 2, 3 and 4 passes. The microstructure and fraction of high angle grain boundaries for the different conditions of materials is determined using electron backscattered diffraction (EBSD) in a SEM-OIM. Tensile tests on miniature size samples are carried out at room temperature at strain rates ranging from 10<sup>-2</sup> to 10<sup>-4</sup> s<sup>-1</sup>. The effect of decreasing strain rate on the total and uniform elongation is studied and compared with earlier work of Sabirov et al. (2008). The work-hardening behavior and its relation to strain localization is compared for the different differently processed UFG materials. The effect of strain rate on the interaction of microshear-bands with grain boundaries and their influence on both uniform and total elongation is investigated. The influence of increasing fraction of high angle boundaries on both ductility and uniform elongation is presented and compared with earlier works.

##### 10:00 AM

**Fatigue Crack Growth Behaviour of Ultrafine Grained Copper:** *Jelena Horky*<sup>1</sup>; Golta Khatibi<sup>1</sup>; Brigitte Weiss<sup>1</sup>; Michael Zehetbauer<sup>1</sup>; <sup>1</sup>Faculty of Physics, University of Vienna

Previous literature on the fatigue crack growth behaviour of ultrafine grained and nanocrystalline metals processed by electrodeposition or cryomilling shows enhanced crack growth rates compared to coarse grained metals especially in the near threshold regime related to a less tortuous crack path (see e.g. T. Hanlon et. al., Int. J. Fatigue 27 (2005) 1147). First investigations on SPD processed materials show the same tendency. The aim of the current work was to shed more light on crack propagation behavior of SPD processed metals, at the example of Cu. HPT processing has been chosen since it achieves a broader range of grain sizes than e.g. ECAP. A number of experiments were carried out

# Technical Program

on specimens which were subjected to a certain thermal treatment after HPT processing. The results show correlations between the microstructure, crack propagation rate and ductility of HPT copper.

## 10:15 AM

**Implications of Deformation under Constraint in Development of UFG Microstructure in an Austenitic Stainless Steel:** Chiradeep Gupta<sup>1</sup>; J. B. Singh<sup>1</sup>; Swetha Mulki<sup>2</sup>; R. Kapoor<sup>3</sup>; Apu Sarkar<sup>1</sup>; I. Samajdar<sup>2</sup>; J. K. Chakravarty<sup>1</sup>; <sup>1</sup>Bhabha Atomic Research Centre; <sup>2</sup>Indian Institute of Technology, Powai; <sup>3</sup>Department of Materials Science and Engineering, Missouri University of Science and Technology

The widely used methods of production of ufg microstructure rely on the application of SPD by either ECAP or high pressure torsion. These methods essentially are based on the application of shear deformation on the sample to obtain the refinement in microstructure. In metastable austenitic stainless steels however, application of deformation leads to formation strain induced martensite, which may hinder the extent of refinement achievable by SPD. In this work the effects of application of constrained deformation is explored and compared with those carried out without constraint for the propensity for strain induced martensite formation. Preliminary results indicate that constrained deformation, as using plane strain compression, suppress the formation of strain induced martensite. The effect of application of ultra high deformation in both cases are explored in terms of changes in microstructure characterized by TEM and SEM-EBSD and changes in mechanical properties by compression tests at room temperature.

## 10:30 AM Break

## 10:45 AM Invited

**The Ambient-Temperature Mechanical Properties of UFG Ag with Nanotwins Using Microshear Tests:** Michael Kassner<sup>1</sup>; Andrea Hodge<sup>1</sup>; <sup>1</sup>USC

The mechanical properties of ultrafine grained (UFG) 150  $\mu\text{m}$  silver interlayers prepared by planar magnetron sputtering were studied using microshear torsion tests. The interlayers have very high ductility in pure shear, comparable to conventional grain sizes, and show a mechanical steady-state. The Hall-Petch behavior at 1.25  $\mu\text{m}$  is consistent with other earlier work. The hardening rates (ds/de) are substantially higher in the UFG Ag. The saturation stress and strain-rate sensitivity at this stress are identical to coarse-grained silver.

## 11:05 AM

**Formation of Ultrafine Grains during Friction Stir Processing of Ti-6Al-4V:** Adam Pilchak<sup>1</sup>; James Williams<sup>2</sup>; <sup>1</sup>Universal Technology Corporation; <sup>2</sup>The Ohio State University

Friction stir processing was applied to modify the surface of an investment cast and hot isostatically pressed titanium alloy. In a single pass, the fully lamellar microstructure was refined to sub-micron sized globular  $\alpha$  grains when the peak temperature was kept below the  $\beta$ -transus. The microstructure was examined with electron microscopy and electron backscatter diffraction. The stir zone was found to be free from microtexture, which is prevalent in  $\alpha+\beta$  forged products, and is detrimental to fatigue properties. Analysis of the transition zone between the unaffected base material and the stir zone revealed that grain refinement revealed that the sub-micron grains formed by deformation induced lattice rotations within individual  $\alpha$  lamellae. Due to the plastic anisotropy of the  $\alpha$ -phase, a significant orientation dependence was noted. This talk will describe the grain refinement mechanisms operative during friction stir processing of cast Ti-6Al-4V and discuss them in terms of crystal plasticity theory.

## 11:20 AM

**Coarsening-Induced Fatigue-Crack Initiation in Several Nanocrystalline Nickel Alloys:** Henry Padilla<sup>1</sup>; Brad Boyce<sup>1</sup>; Paul Kotula<sup>1</sup>; Elizabeth Holm<sup>1</sup>; <sup>1</sup>Sandia National Labs

Nanocrystalline nickel alloys exhibit impressive fatigue-life performance, even beyond that associated with Hall-Petch strengthening. Fatigue-crack initiation resistance appears to be the key to their enhanced performance, since crack propagation proceeds with ease. Microstructural analysis using Focused Ion Beam dissection of several nanocrystalline Ni alloys (Ni, Ni-Mn, Ni-Fe) reveals regions of coarsened grains at the crack initiation zone. This fatigue-induced coarsening is thought to be a necessary precursor for fatigue crack initiation. Therefore, for these nanocrystalline alloys, grain-boundary stabilization is a pathway towards improved fatigue performance.

Interestingly, alloys which are stable against thermally-induced coarsening are not necessarily stable against fatigue-induced coarsening. A Potts model provides insight into the role of Zener pinning and solute drag on thermally- and mechanically-induced grain growth.\* Sandia is a multi-program laboratory operated by Sandia Corporation, a Lockheed Martin Company, for the United States Department of Energy's National Nuclear Security Administration under Contract No. DE-AC04-94AL85000.

## 11:35 AM Poster Preview

**Texture and Microstructure Evolution in Ultrafine Grained AZ31 Processed by EX-ECAP:** Milos Janecek<sup>1</sup>; <sup>1</sup>Charles University

## 11:40 AM

**Effect of Strain Reversals on Processing by High-Pressure Torsion:** Megumi Kawasaki<sup>1</sup>; Byungmin Ahn<sup>1</sup>; Terence Langdon<sup>1</sup>; <sup>1</sup>University of Southern California

Processing by high-pressure torsion (HPT) is a continuous operation in which the sample remains within the HPT facility so that, unlike equal-channel angular pressing (ECAP), it is difficult to develop different processing methods. However, reversing the direction of torsional straining is available in HPT after straining in the forward direction. Experiments were conducted on pure Al using either monotonic-HPT (m-HPT) or cyclic-HPT (c-HPT) for totals of 1 to 4 turns at room temperature under an applied pressure of 6.0 GPa. Detailed observations were taken to evaluate the microstructural damage introduced by reversal straining on the surface of each disk. Microhardness values were measured both along diameters in each disk and over the complete surfaces in order to construct color-coded contour maps of the hardness distributions. Additional microstructural analyses permit an evaluation of the significance of strain reversal during processing by HPT.

## 11:55 AM Invited

**Strengthening Mechanisms in Deformed and Annealed Nanostructured Metals:** Xiaoxu Huang<sup>1</sup>; Naoya Kamikawa<sup>2</sup>; Niels Hansen<sup>1</sup>; <sup>1</sup>Risø National Laboratory for Sustainable Energy, Technical University of Denmark; <sup>2</sup>Tohoku University

The yield strength of nanostructured metals processed by plastic deformation to ultrahigh strain has been analyzed by using the boundary spacing as the strengthening parameter in a Hall-Petch equation. However, the deformed microstructure is composed of different structural features such as dislocation boundaries, high angle boundaries and loose dislocations between boundaries. It follows that several strengthening mechanisms may contribute to the yield stress and that a strength-structure relationship might include more structural parameters than just the boundary spacing. In the present study the relative contribution to the yield stress from different strengthening mechanisms are varied by annealing deformed samples to different stages of recovery and recrystallisation followed by a quantification of structural (strengthening) parameters. The structure-strength relationships are then analyzed and it is found that not only dislocation and grain boundary hardening contribute to the yield stress but also mechanisms such as precipitation hardening and dislocation source hardening.

## 12:15 PM

**Composition and Structure of Nitrogen-Containing Dispersoids in Tri-Modal Metal Matrix Composites:** Clara Hofmeister<sup>1</sup>; Bo Yao<sup>1</sup>; Yongho Sohn<sup>1</sup>; Timothy Delahanty<sup>2</sup>; Mark van den Bergh<sup>3</sup>; Kyu Cho<sup>4</sup>; <sup>1</sup>University of Central Florida; <sup>2</sup>Pittsburgh Materials Technologies, Inc.; <sup>3</sup>DWA Aluminum Composites; <sup>4</sup>U.S. Army Research Laboratory

Aluminum tri-modal composite reinforced with B4C particulates has been fabricated successfully, and exhibited an extremely high yield strength and tailorable ductility. The fabrication of this composite starts from the cryomilling of 5083 Al alloy powders with B4C particles, which yields agglomerates containing sub-micron B4C particles solidly bonded with nanocrystalline Al (NC-Al) grains. These agglomerates are then blended with coarse grain Al powders, and consolidated to form the bulk composite. In this study, secondary ion mass spectrometry was employed to determine the composition of Nitrogen that linearly varied a function of cryomilling time. Crystalline and amorphous dispersoids containing Nitrogen and other constituents were documented by analytical transmission electron microscopy. The influence of composition and structure of the dispersoids on the strength of the composite will be discussed.



12:30 PM

**Nano-Scale Strengthening from Grains, Sub-Grains and Particles in Fe-C Alloys:** *Donald Lesuer*<sup>1</sup>; Chol Syn<sup>1</sup>; Oleg Sherby<sup>2</sup>; <sup>1</sup>Lawrence Livermore National Laboratory; <sup>2</sup>Stanford University

The nano-scale grain-size strengthening effect has been studied relative to the strengthening influence of other microstructural features such as sub-grains, particles and solid solution additions. In Fe-C alloys these microstructural features can result from phase transformation and deformation processes. The formation of lath and plate martensite during quenching and severe plastic deformation will be shown to result in very high strengths (4600 MPa) which can be correlated with nano-scale grain sizes and interparticle spacing. The development of a nano-scale grain size in the Fe-C alloys will be shown to be controlled by the inter-related influence of deformation, transformation products and ultra-fine particles. Particles, grains and subgrains will be shown to provide significantly higher strengthening than contributions from solid solution effects.

### 2010 Functional and Structural Nanomaterials: Fabrication, Properties, Applications and Implications: Nano-Sensors and Magnetic Properties

*Sponsored by:* The Minerals, Metals and Materials Society, TMS Electronic, Magnetic, and Photonic Materials Division, TMS: Nanomaterials Committee

*Program Organizers:* David Stollberg, Georgia Tech Research Institute; Nitin Chopra, University of Alabama; Jiyoung Kim, University of Texas - Dallas; Seong Jin Koh, University of Texas at Arlington; Navin Manjooran, Siemens Corporation; Ben Poquette, Keystone Materials; Jud Ready, Georgia Tech

Monday PM Room: 214  
February 15, 2010 Location: Washington State Convention Center

*Session Chair:* Seong Jin Koh, University of Texas at Arlington; Nitin Chopra, The University of Alabama

### 2:00 PM Introductory Comments

### 2:05 PM Invited

**Gold Nano-Engineered Mercury Sensor for Alumina Refineries:** *Suresh Bhargava*<sup>1</sup>; <sup>1</sup>MIT University

The toxicity of mercury remains a threat to the environment and public health despite a number of efforts by government bodies world-wide. Mercury is a common environmental pollutant that is neurotoxic and bioaccumulative. Currently, mercury sensors which are primarily based on ultraviolet techniques are plagued by cross-sensitivity issues. However, when the humble Quartz Crystal Microbalance (QCM) is combined with well formed gold nano-engineered surfaces these cross-sensitivity issues can be overcome without compromising sensitivity. Using a single step electrochemical approach, a QCM loaded with nano-engineered gold structures has an increase in sensitivity of approximately 340% to 180% towards 1 to 10mg/m<sup>3</sup> of Hg vapor over non-modified sensors when operating at 89°C, respectively. What is more promising is that over many months of continuous testing in the presence of ammonia and high humidity contaminated simulated streams, the sensor showed a maximum of ±6.6% in response magnitude towards the tested concentrations.

### 2:25 PM

**Fundamental Studies and On-Chip Integration of Nanoporous Energetic Silicon:** *Collin Becker*<sup>1</sup>; Luke Currano<sup>2</sup>; Wayne Churaman<sup>2</sup>; Conrad Stoldt<sup>1</sup>; <sup>1</sup>University of Colorado; <sup>2</sup>U.S. Army Research Lab

Porous silicon (PS) is a widely studied material and holds great potential in the realization of novel Microelectromechanical systems (MEMS). When impregnated with any one of a number of oxidizers, porous silicon can function as an energetic material. Because silicon is widely used in micromachining and CMOS processes, PS can be integrated on-chip alongside a MEMS sensor. This new class of energetic can be used for applications requiring on-chip power, propulsion, and fuzing. The strength of the energetic reaction, which is comparable to traditional energetics, is controlled by altering processing parameters to tune PS thickness, porosity, specific surface area, and surface terminations. Currently, the correlation between PS morphology and energy

release rate is unclear. Here we characterize the structure of the PS prior to ignition, using Fourier transform infrared spectroscopy, Raman spectroscopy, and scanning electron microscopy. This characterization is coupled with calorimetry data. Lastly, on-chip energetic PS devices are presented.

### 2:45 PM

**Gas Sensing Behavior of Nanostructured CoSb<sub>2</sub>O<sub>6</sub> Prepared by a Colloidal Method:** *Hector Guillen-Bonilla*<sup>1</sup>; Carlos Michel<sup>2</sup>; Juan Moran-Lazaro<sup>2</sup>; Juan Reyes-Gomez<sup>3</sup>; Dario Pozas-Zepeda<sup>3</sup>; <sup>1</sup>Centro de Enseñanza Tecnica Industrial; <sup>2</sup>Universidad de Guadalajara; <sup>3</sup>Universidad de Colima

Nanostructured powders of CoSb<sub>2</sub>O<sub>6</sub>, possessing the trirutile-type structure, were synthesized by a colloidal method in ethyl alcohol. Microwave radiation was used to evaporate the solvent. The sample heated at 200°C was observed by SEM, revealing the presence microspheres having an average diameter of 2µm. The thermal decomposition at 700°C in air produced hollow nanostructured spheres having abundant nanoporosity; this observation was made by TEM. X-ray powder diffraction was used to identify the crystal structure. To test CoSb<sub>2</sub>O<sub>6</sub> as a gas sensor material, the powder calcined at 700°C was deposited on alumina as thick films. DC and AC electrical characterization was performed in air, O<sub>2</sub> and CO<sub>2</sub>. Polarization curves were recorded to obtain quantitative information about CO<sub>2</sub> and O<sub>2</sub> detection. The results indicate that CoSb<sub>2</sub>O<sub>6</sub> detects changes in the surrounding atmosphere, at a temperature as low as 250°C.

### 3:05 PM

**Carbon Dioxide Gas Sensing Properties of CoSb<sub>2</sub>O<sub>6</sub> Prepared by a Colloidal Method:** *Hector Guillen-Bonilla*<sup>1</sup>; Carlos Michel<sup>2</sup>; Juan Moran<sup>2</sup>; Juan Reyes<sup>3</sup>; Dario Pozas<sup>3</sup>; <sup>1</sup>Centro de Enseñanza Tecnica Industrial; <sup>2</sup>Universidad de Guadalajara; <sup>3</sup>Universidad de Colima

CoSb<sub>2</sub>O<sub>6</sub> has a significant response in gas detection (CO<sub>2</sub>). In order to improve its gas sensing properties it is necessary to have a better control on the size and shape of the particles. The colloidal methods are effective to control the microstructure inorganic materials. In this work CoSb<sub>2</sub>O<sub>6</sub> was synthesized by the colloidal method. Single-phase CoSb<sub>2</sub>O<sub>6</sub> was obtained after a calcination at 600°C in air; the crystal structure was identified by XRD. By SEM the formation of microcolumns was observed. These particles had a length between 10 to 29 µm. CoSb<sub>2</sub>O<sub>6</sub> thick-films were tested as gas sensors. The electrical characterization was performed in alternating current (AC) in air and CO<sub>2</sub>, at frequencies: 100 Hz, 1 kHz and 100 kHz. At 200°C, the change of the magnitude of the impedance (Z) was 246 to 249 KO. The results indicated that CoSb<sub>2</sub>O<sub>6</sub> would be a CO<sub>2</sub> gas sensing material.

### 3:25 PM

**Multi-Walled Carbon Nanotube Sensor Devices for Gas Sensing Applications:** *Raghu Mangu*<sup>1</sup>; *Suresh Rajaputra*<sup>1</sup>; *Srikanth Durgamahanty*<sup>1</sup>; *Dali Qian*<sup>1</sup>; *Rodney Andrews*<sup>1</sup>; *Vijay Singh*<sup>1</sup>; <sup>1</sup>University of Kentucky

Multi Walled Carbon Nanotubes (MWCNTs) based device configurations studied as part of this research work were simple and did not require any manipulation of individual or bundles of tubes, through techniques such as e-beam or photolithography. MWNTs grown inside the pores of insulating AAO matrix by a chemical vapor deposition (CVD), without the use of catalyst, was the first design. MWNTs grown as thick films on Si/SiO<sub>2</sub> substrates via CVD process using Ferrocene as a catalyst was the second design. Both device configurations were integrated into resistance sensing devices. Steady state sensitivities as high as 5% and 10% for 100 ppm of NH<sub>3</sub> and NO<sub>2</sub> respectively were observed. Variations in sensor resistance with exposure to oxidizing and reducing gases were explained on the basis of charge transfer between the analyte and the MWCNTs, the latter behaving as p-type semiconductors.

### 3:45 PM Break

### 3:55 PM

**Electromechanical Coupling Behaviors of Suspended Low Dimensional Materials and Applications to Sensing:** *Hao Lu*<sup>1</sup>; Li Song<sup>1</sup>; P.M. Ajayan<sup>1</sup>; Jun Lou<sup>1</sup>; <sup>1</sup>Rice University

Electrical properties of suspended graphene and nanowires will be studied with coupling of stress induced by AFM (Atomic Force Microscope). Sample behavior will be probed both in air and different liquids. We'll investigate response of the suspended structures with respect to different environments and discuss the possibility of using it as a sensing mechanism.

Mon. PM

# Technical Program

4:15 PM

**Functionalization of Single TiO<sub>2</sub> Nanotubes for Bio-Sensor Applications:** *Mingun Lee*<sup>1</sup>; Dongkyu Cha<sup>1</sup>; Jie Hunang<sup>1</sup>; Hyunjung Shin<sup>2</sup>; Moon J. Kim<sup>1</sup>; Jiyoung Kim<sup>1</sup>; <sup>1</sup>University of Texas at Dallas; <sup>2</sup>Kookmin University

Nanoscale structures have been widely investigated for emerging applications such as chemical and biological sensors. Thanks to their nontoxicity, large surface to volume ratio and hollow structure, single TiO<sub>2</sub> nanotube devices hold great promise in that role. TiO<sub>2</sub> nanotubes fabricated by combining ALD with nanotemplates method behave like an n-type semiconductor, where the noticeable shift of their electrical conductance upon exposure to certain chemicals provides a means of detecting the targeted material. To achieve good selectivity between different biomaterials, a critical concern for biosensors, inner and outer surfaces of the nanotubes were functionalized by chemical compounds including biotin. In this study, we will present effects of TiO<sub>2</sub> nanotube functionalization in bio-sensor applications. This research has been supported by a grant (code #: 2009K000469) from 'Center for Nanostructured Materials Technology' under '21st Century Frontier R&D Programs' of the Ministry of Education, Science and Technology, Korea

4:35 PM

**Enhanced Irreversibility Field and Critical Current Density in Superconducting NbC Integrated with Aligned Carbon Nanotubes:** *Guifu Zou*<sup>1</sup>; Hongmei Luo<sup>2</sup>; Scott Baily<sup>1</sup>; Yingying Zhang<sup>1</sup>; Junyi Zhai<sup>1</sup>; Jie Xiong<sup>1</sup>; Quanxi Jia<sup>1</sup>; <sup>1</sup>Los Alamos National Laboratory; <sup>2</sup>New Mexico State University

We report a novel chemical solution approach to integrate the superconducting NbC with oriented carbon nanotubes (CNTs). The NbC:CNTs composite shows improved irreversibility field (~ 5 T at 4.2 K), far greater than reported 1.2 T at 4.2 K. In addition, very high critical current densities 10<sup>5</sup> A/cm<sup>2</sup> are achieved at 3 T and 6 K. To the best of our knowledge, both the irreversibility field and the critical current density of the NbC composite are the highest reported in the literature. We believe that the aligned CNTs play a key role in the enhancement of pinning of vortex lines to increase the performance of superconducting NbC. Our results suggest that the incorporation of CNTs into superconductors has potential for high-field applications.

4:55 PM

**Nanoparticles with Double Perovskite La<sub>2</sub>BB'O<sub>6</sub> Composition:** *Yuanbing Mao*<sup>1</sup>; <sup>1</sup>Washington State University

Magnetic semiconductors with near room temperature ferromagnetism have attracted much attention due to their broad potential applications. For example, double perovskite La<sub>2</sub>NiMnO<sub>6</sub> exhibits a ferromagnetic order with T<sub>c</sub> of ~280 K and large magnetic-field-induced changes in the resistivity and dielectric properties. Most previous studies were performed in bulk ceramic and thin film forms and proved that synthetic conditions determine the atomic order of the B-site sublattice and, as a result, the ferromagnetic properties of La<sub>2</sub>BB'O<sub>6</sub> (B = Ni and Co; B' = Mn). Here, we first report the successful synthesis of La<sub>2</sub>BB'O<sub>6</sub> nanoparticles with size ranging from 15-50 nm in diameter. These nanoparticles are characterized by power x-ray diffraction, transmission electron microscopy and Raman spectroscopy. The microstructure of these multifunctional nanostructured materials is investigated by analytical high-resolution TEM. To better understand their processing-structure-property relation, these results are combined with the measurements of their magnetic and electronic properties.

5:15 PM **Concluding Comments**

## Advances in Composite, Cellular and Natural Materials: Cellular and Porous Materials

*Sponsored by:* The Minerals, Metals and Materials Society, TMS Structural Materials Division, TMS/ASM: Composite Materials Committee

*Program Organizers:* Yuyuan Zhao, The University of Liverpool; David Dunand, Northwestern University

Monday PM

Room: 305

February 15, 2010

Location: Washington State Convention Center

*Session Chairs:* David Dunand, Northwestern University; Markus Buehler, Massachusetts Institute of Technology

2:00 PM **Keynote**

**Cellular Materials in Nature:** *Lorna Gibson*<sup>1</sup>; Michael Ashby<sup>2</sup>; <sup>1</sup>MIT; <sup>2</sup>Cambridge University Engineering Department

Cellular materials are widespread in nature. Wood and cork have a honeycomb-like structure with cells that are roughly hexagonal prisms. Trabecular bone, plant parenchyma, adipose tissue, coral and sponge all have a foam-like structure, with polyhedral cells. Natural structures often have a cellular component: skulls and leaves of monocotyledon plants are sandwich structures, with dense outer skins separated by a foam-like core; animal quills and plant stems are nearly fully dense cylindrical shells supported by a foam-like core; and palm and bamboo stems are cylinders with radial density gradients. This talk provides an overview of cellular materials in nature and illustrates how the cellular structure gives rise to increased mechanical performance.

2:40 PM

**Multi-Scale Osteointegration of Biphasic Calcium Phosphate Bone Scaffolds:** *Amy Wagoner Johnson*<sup>1</sup>; <sup>1</sup>University of Illinois at Urbana-Champaign

In engineering porous ceramics for bone regeneration, most studies focus on optimizing the macroarchitecture. The few that focus on microstructure use it to enhance osteoconductivity. While microporosity improves bone growth in macropores, we are the first to show osteocytes embedded in bone within micropores <10µm in size. Biphasic calcium phosphate (BCP)/macroporous scaffolds with microporous rods were implanted in swine mandibular defects. Cells migrated into the interconnected micropores and bone formed throughout the rods, creating a co-continuous BCP/bone composite. Here we characterize the bone growth using several imaging modalities and show the first truly osteointegrated scaffold with integration at both the macro and the micro length scales, leaving no "dead space" or discontinuities of bone. The bone-filled micropores increase the bone-scaffold interface by orders of magnitude compared to bone that is limited to the macropores, and has important implications for the efficacy of such scaffolds in load bearing defects.

3:00 PM

**Shape-Memory NiTi Foams:** *David Dunand*<sup>1</sup>; <sup>1</sup>Northwestern University

NiTi (Nitinol) foams with shape-memory or superelastic properties are of interest for biomedical implants and for actuators. Here, we present various processes to create these foams based on sintering of NiTi powders together with space-holders which are removed to create porosity. The spaceholder can be fugitive, e.g. NaCl evaporating during the sintering operation, or ice which is freeze-dried before sintering. The spaceholder can also remain during the sintering operation, leading to a NiTi/spaceholder composite. The spaceholder is then removed by chemical dissolution (e.g. NaF) or by electrochemical dissolution (e.g. steel). Microstructure and mechanical properties of these various foams, with equiaxed or elongated porosity (depending on the type of spaceholder), are also reported, focusing on the superelastic and shape-memory effect.

3:20 PM

**Mechanical and Biological Properties of Titanium Syntactic Foams:**

*Xiaobing Xue*<sup>1</sup>; Victoria Kearns<sup>1</sup>; Rachel Williams<sup>1</sup>; *Yuyuan Zhao*<sup>1</sup>; <sup>1</sup>The University of Liverpool

Titanium syntactic foam is a novel composite material with hollow ceramic microspheres embedded in titanium matrix. This paper reports on the preliminary studies on the mechanical and biological properties of Ti syntactic foam manufactured by powder metallurgy. The density and porosity



were measured. The compression, three-point bending, indirect and direct contact cell culture tests were conducted. The density and porosity varied with compaction pressure. However, higher pressure resulted in a large number of crushed microspheres. The apparent modulus, compressive and flexural strength increased with increasing sintering temperature or sintering time. Indirect cell contact tests demonstrated that the titanium syntactic foams were non-cytotoxic. In direct cell contact tests the cells attached and spread well on the surface of titanium syntactic foams. These data suggest that this material warrants further investigation in bone replacement applications.

### 3:40 PM Break

### 4:00 PM

**Mechanical Behavior of Nanoporous Pt:** *Antonia Antoniou*<sup>1</sup>; Dhriti Bhattacharyya<sup>2</sup>; Pat Dickerson<sup>2</sup>; Nathan Mara<sup>2</sup>; <sup>1</sup>Georgia Institute of Technology; <sup>2</sup>Los Alamos National Laboratory

Nanoporous Pt (np-Pt) is synthesized by electrochemical dealloying of co-sputtered Pt-Si-x amorphous films. The deposition and dealloying conditions were varied. As the Pt fraction in the amorphous alloy increases, Si dissolution is favored along pre-existing features of the amorphous film (i.e. column boundaries, surface asperities). The morphology of the resulting np-Pt depends on the manner in which silicon is preferentially removed. In addition to the expected isotropic open cell structure, anisotropic structures are also observed such as columnar and radial-type foam. The foam is found to be polycrystalline with 5 nm grains, and voids and ligaments range between 20-30 nm. Mechanical behavior has been examined by nanoindentation and micropillar compression.

### 4:20 PM Invited

**Elastic Modulus Study of Nanoporous Au Foams:** *Andrea Hodge*<sup>1</sup>; Monika Biener<sup>2</sup>; Juergen Biener<sup>2</sup>; <sup>1</sup>University of Southern California; <sup>2</sup>LLNL

The effect of Ag and the relative density on the elastic properties of nanoporous Au (np-Au) foams will be presented for partially as well as fully dealloyed np-Au samples with various ligament sizes. Additionally, Ag coated np-Au samples were synthesized by immersing np-Au in a 1 M Ag nitrate solution, followed by drying and thermal decomposition of the deposited Ag nitrate salt to Ag and NO<sub>2</sub> and O<sub>2</sub>. Cross-sectional analysis revealed that this method yields a homogeneous Ag distribution, and that the Ag concentration can be adjusted within the range of 0-20 at.%. Mechanical testing was performed by depth-sensing nanoindentation. It was observed that the effect of the relative density on the elastic properties of np-Au seems to be much stronger than predicted by the Gibson and Ashby relationship. The elastic modulus of np-Au seems to be independent of the ligament size.

### 4:40 PM

**Effect of Partial Filling of Cells on Mechanical Strength of WBK Cores under Compression and Shear:** *Ki-Ju Kang*<sup>1</sup>; Jong-Sun Park<sup>1</sup>; <sup>1</sup>Chonnam National University

Among various fabrication methods for cellular metals, a technique based on 3 dimensional wire-weaving, known as Wire-woven Bulk Kagome (WBK), has taken attention because WBK can be useful for fabricating multilayered Kagome truss-type cellular metal. WBK has been proved that it has high strength-per-weight. Recently, a new idea for strengthening WBK even further was introduced, that is, filling tetrahedron-like cells in its interior space suppress the elastic buckling of struts which is a typical failure mechanism of truss type PCM (periodic cellular metals). In this work, first, theoretical studies using elementary mechanics of material are presented to estimate the strength under out-of-plane compression and shear. And the results are compared with those measured by experiments which were performed with specimens with various slenderness ratios of struts. It has been found that the partially filled WBK exhibited high specific stiffness and strength, absorption of energy in comparison with ordinary WBK.

### 5:00 PM

**Influence of Porosity and Microstructure on Thermal Properties of Laser Processed Ni and Ti6Al4V Alloy:** *Felix Espana*<sup>1</sup>; Vamsi Krishna Balla<sup>1</sup>; Susmita Bose<sup>1</sup>; Amit Bandyopadhyay<sup>1</sup>; <sup>1</sup>Washington State University

Thermal properties of metals and alloys depend on various parameters including composition, microstructure and surface topography. In this study we have fabricated Ni and Ti6Al4V alloy samples with varying porosity between 5 and 20 vol. % using Laser Engineered Net Shaping (LENS<sup>TM</sup>) and tested

their thermal properties and performance. It was found that porosity influences thermal performance, in terms of thermal conductivity, conductive and convective heat transfer. However, the finer microstructural features, formed as a result of rapid cooling rates associated with LENS<sup>TM</sup>, prevented degradation of thermal conductivity of these materials. This microstructural influence on thermal properties has been confirmed by post-fabrication heat treatment studies. This presentation focuses on influence of porosity and microstructure of Ni and Ti6Al4V alloy on their thermal performance.

### 5:20 PM

**Mechanical Properties of LCS Porous Steel: Comparison between the Dissolution and Decomposition Routes:** *Miao Lu*<sup>1</sup>; Yuyuan Zhao<sup>1</sup>; <sup>1</sup>The University of Liverpool

Porous metals have many potential applications because of higher strength, stiffness and energy absorption capacity than polymer foams. This paper studied the porous steels produced by the lost carbonate sintering (LCS) process. The LCS porous steels had different mechanical properties when they were produced by the decomposition or dissolution route. The effects of the two routes on the mechanical behavior of the porous steels with different porosities (from 75% to 60%) and pore sizes (from 250µm to 1500µm) were compared. The compression strength and elastic modulus of the porous steel produced by the decomposition route were higher than those of the porous steel produced by the dissolution method. However, the differences became smaller at higher porosities and larger pore sizes. The study provided useful information for tailoring the mechanical properties of LCS porous steels.

## Alumina and Bauxite: Bayer Process Chemistry and Alumina Quality I

*Sponsored by:* The Minerals, Metals and Materials Society, TMS Light Metals Division, TMS: Aluminum Committee, TMS: Aluminum Processing Committee

*Program Organizers:* Carlos Suarez, Hatch Associates Inc; Everett Phillips, Nalco Company

Monday PM Room: 611  
February 15, 2010 Location: Washington State Convention Center

*Session Chair:* Fred Williams, CMIS Corporation

### 2:00 PM Introductory Comments

### 2:10 PM

**Development of Particle Breakdown and Alumina Strength during Calcination:** *Benny Raahauge*<sup>1</sup>; Claus Jensen-Holm<sup>1</sup>; Susanne Wind<sup>1</sup>; <sup>1</sup>FLSmidth Denmark

Since the replacement of rotary kilns with stationary calciners, the impact from hydrate properties and calcination technology on the quality of Smelter Grade Alumina (SGA) have been studied frequently. F.L.Smith are studying the complex interaction between calcining conditions, particle breakdown and development of alumina particle strength in both bench - scale and full scale calcination units using conventional analytical techniques. The bench - scale unit is simulating the pre-calcination step at 320 - 380°C, common to all stationary calciners and the final calcination stage at 1075°C in Gas Suspension Calciners without Holding Vessel. The calcining capacity of the full scale units are ranging from 2200 - 4500 tpd of SGA and covers stationary calciners with and without Holding Vessel. Representative hydrate samples are calcined and compared from more than eight (8) different alumina refineries. The first results of the above work will be presented with focus on how the calcining conditions impacts the properties of calcined industrial hydrates with respect to particle strength and particle breakdown.

### 2:40 PM

**Effect of Environmental Light on the Raman Spectrum of Sodium Aluminate Liquors:** *Jianguo Yin*<sup>1</sup>; Wangxing Li<sup>1</sup>; Zhonglin Yin<sup>1</sup>; Zhanwei Liu<sup>1</sup>; Zhaohui Su<sup>1</sup>; <sup>1</sup>Zhengzhou Research Institute Aluminum Corporation of China Limited

Raman spectroscopy is a useful instrument to character the structure of sodium aluminate liquors. As the spectrum of sodium aluminate liquors is not very strong, some environmental factors may affect the spectrum and hinder

Mon. PM

# Technical Program

us from attaining good results. Effect of environmental light on the Raman spectrum of sodium aluminate liquors was investigated. It is concluded that sunlight affects the spectrum of sodium aluminate liquors the most and almost masks it. For the light of fluorescence, it shows strong signal of light in the spectrum. But for the light of desk lamp and display screen, they have a little effect on the spectrum. To attain a good Raman spectrum of sodium aluminate liquors, the optimum operation condition is in a darkroom, or only let weak desk lamp on if necessary.

## 3:10 PM Break

## 3:30 PM

**Effect of Na<sub>2</sub>O on Alumina Leaching and Self-Disintegrating Property of Calcium Aluminate Slag:** *Sun Huilan*<sup>1</sup>; Wang Bo<sup>1</sup>; Bi Shiwen<sup>2</sup>; <sup>1</sup>Hebei University of Science and Technology; <sup>2</sup>Northeastern University

Effect of Na<sub>2</sub>O content on Al<sub>2</sub>O<sub>3</sub> leaching rate and self-disintegrating rate of calcium aluminate slag are studied by adding Na<sub>2</sub>O into pure calcium aluminate slag. And the reaction mechanism is also discussed by XRD analysis initially. The results indicate that Lattice distortion and the weakness of bond energy which is asymmetry in Molecular are caused by the solid solution of Na<sub>2</sub>O into 12CaO·7Al<sub>2</sub>O<sub>3</sub>. And this make Na<sub>2</sub>CO<sub>3</sub> and H<sub>2</sub>O easy to penetrate into 12CaO·7Al<sub>2</sub>O<sub>3</sub> crystal, and improve the reaction speed and degree. So the existence of Na<sub>2</sub>O will improve the leaching property of calcium aluminate slag. But the self-disintegrating property of slag will be decreased because a great amount of β-2CaO·SiO<sub>2</sub> is formed when the content of Na<sub>2</sub>O is higher than 2.5%. Considering from the property of calcium aluminate slag only, the largest allowable content of Na<sub>2</sub>O is 2.0~2.5% in slag and 1.2~1.5% in materials.

## 4:00 PM

**Improvement of Product Quality in Circulating Fluidized Bed Calcination:** *Cornelis Klett*<sup>1</sup>; Michael Missalla<sup>1</sup>; Roger Bligh<sup>2</sup>; <sup>1</sup>Outotec GmbH; <sup>2</sup>Outotec (Australasia) Pty. Ltd.

Until the introduction of Circulating Fluidized Bed (CFB) Calciners by Outotec (formerly Lurgi) in 1961 rotary kilns were the standard technology for the calcination of alumina. Since then, stationary calciners such as CFBs are the preferred technologies for new installations due to their superior energy efficiency despite their higher generation in fines. Over the last years Outotec researched ways to minimize particle breakage in its CFB calciners. Particle breakage is strongly dependent on the properties of the hydrate such as the hydrate shrinking behavior. Nevertheless other major influences like mechanical stress are a direct function of the calcining technology. Recent installed calciners and measurements from these have shown that Outotec has made a significant leap forward to reduce the particle breakage close to the level of rotary kilns whilst maintaining their enhanced operating performance and energy efficiency. The results of the recent achievements will be presented in this paper.

## Aluminum Alloys: Fabrication, Characterization and Applications: Numerical Modeling

*Sponsored by:* The Minerals, Metals and Materials Society, TMS Light Metals Division, TMS: Aluminum Processing Committee  
*Program Organizers:* Subodh Das, Phinix LLC; Steven Long, Kaiser Aluminum Corporation; Tongguang Zhai, University of Kentucky

Monday PM Room: 615  
February 15, 2010 Location: Washington State Convention Center

*Session Chair:* Zhengdong Long, Kaiser Aluminum

## 2:00 PM

**Constitutive Relations for Plastic Deformation in a 5754 Sheet:** *Lin Hu*<sup>1</sup>; Stephen Banovic<sup>2</sup>; Tim Foecke<sup>2</sup>; Mark Iadicola<sup>2</sup>; Anthony Rollett<sup>1</sup>; <sup>1</sup>Carnegie Mellon University; <sup>2</sup>National Institute of Standards and Technology

Constitutive equations for the multiaxial stress-strain behavior of aluminum alloy 5754 sheet have been developed, based on crystal plasticity. Both a Taylor-based polycrystal plasticity code (LApp) and a self-consistent viscoplastic code (VPSC) have been used to fit a single slip system hardening law to the available data for tension, plane strain and equibiaxial stretching. The fitting procedure yields good agreement with the monotonic stress-strain data. When the developed hardening law is used to model tests involving strain path changes,

however, the agreement is less good. Furthermore, the simulated texture evolution is too rapid when compared to the experiments. These discrepancies motivate the further development of the constitutive relations to include such effects as grain-to-grain interactions and latent hardening.

## 2:20 PM

**Modeling Processing and Performance of an Al-Zn-Mg Alloy:** *John Chinella*<sup>1</sup>; <sup>1</sup>U.S. Army Research Laboratory

This study evaluates an Al-4.5Zn-1.2Mg-alloy 7020 armor. Microstructures of alloys 7039 and 7020 are shown. Computational thermodynamic modeling predicts: phase structures, equilibrium states, process temperatures, and manufacturing advantages. An artificial age study was conducted to modify the initial T651 condition to T7 tempers. The ageing study determines the hardness levels in response to holding periods of time-temperature. Aging parameters can help establish alloy 7020 processing factors to optimize and meet requirements for resistance to penetration by projectiles, or fragments, and fracture from stress corrosion cracking (SCC) or blast. The 7020-T651 ballistic test results versus armor piercing projectiles reveal protection levels superior to 5083-H131 aluminum and equivalent to Class 1, penetration-resistant rolled homogeneous armor (RHA). Results suggest a 7020-T7 material may be optimized to resist blast fracture and SCC, with levels of fragment protection that exceeds any RHA performance and penetration protection levels of shock-resistant RHA Class 2 armor.

## 2:40 PM

**Perturbed Bi-Particle Model of Deformation of Commercial Aluminum Alloys:** *Yansheng Liu*<sup>1</sup>; Xiyu Wen<sup>2</sup>; Ranall Bowers<sup>1</sup>; Xiaoxuan Li<sup>1</sup>; Shridas Ningilieri<sup>2</sup>; <sup>1</sup>SECAT Inc; <sup>2</sup>University of Kentucky

Commercial aluminum alloys contain particles either as impurities or designated components. Bi-particle model is used in the current simulation by ABAQUS software. Perturbation is introduced in order to accommodate random distribution of particles. The model is applied to continuous cast ((CC) aluminum alloy under uniaxial tensile deformation. The behavior of particles and surrounding matrix during deformation is discussed. The result is helpful in understand the effect of particle distribution on the failure of CC aluminum alloys and in improvement of the mechanical properties of the materials. It is concluded that particles with larger effective cross section being perpendicular to tensile axial have more detrimental effect on elongation.

## 3:00 PM

**Modeling the Solidification under Pressure Casting Process for Aluminum Alloys:** *Edward Druschitz*<sup>1</sup>; Alan Druschitz<sup>1</sup>; Robin Foley<sup>1</sup>; <sup>1</sup>University of Alabama at Birmingham

Applying isostatic pressure during solidification has been shown to improve the mechanical properties of aluminum castings due to a reduction in the size of porosity. Existing equations appear to adequately describe the effect of pressure on gas pore size but do not describe the effect of pressure on dendrite arm spacing or cell size. In this paper, microstructural data (pore size, dendrite arm spacing, cell size) are compared for aluminum alloys solidified under 10 MPa pressure and at atmospheric pressure. The measured differences in microstructure are then compared to the relevant equations available in the literature. A model accounting for applied isostatic pressure during solidification is proposed.

## 3:20 PM

**An Integrated Computational Tool for Precipitation Simulation of Multi-Component Aluminum Alloys:** *Weisheng Cao*<sup>1</sup>; Kaisheng Wu<sup>1</sup>; Fan Zhang<sup>1</sup>; Shuanglin Chen<sup>1</sup>; Ying Yang<sup>1</sup>; Y. Austin Chang<sup>2</sup>; Jianzheng Guo<sup>3</sup>; Mark Samonds<sup>3</sup>; <sup>1</sup>CompuTherm LLC; <sup>2</sup>University of Wisconsin - Madison; <sup>3</sup>ESI Group

Modeling of microstructure and mechanical property during precipitation process plays a critical role in understanding the behavior of materials and thus accelerating the development cycles of materials. Nevertheless, an integrated computational tool coupling reliable thermodynamic calculation, kinetic simulation and property prediction of multi-component systems for industrial applications is rarely available. In these regards, a software package named as PanPrecipitation is being developed. It is seamlessly integrated with the thermodynamic calculation engine—PanEngine, which provides accurate thermodynamic properties and mobility data necessary for precipitation simulation. The generic system design together with multi-level kinetic and hardening models enable a range of applications. Its functionalities and advantages will be demonstrated by simulation of a number of aluminum



alloys. In addition, the integration of PanPrecipitation with ProCAST for pre-process or/and post-process simulation will be also discussed.

### 3:40 PM Break

### 3:55 PM Invited

**2010 LMD Young Leader Professional Development Award Winner: Ultrasonic Welding of Aluminum Wires for Cables Harnesses in the Automotive Industry:** Frank Balle<sup>1</sup>; Guntram Wagner<sup>1</sup>; Dietmar Eifler<sup>1</sup>; <sup>1</sup>University of Kaiserslautern, Institute of Materials Science and Engineering

The cable harness of a modern upper class car, actually made of copper wires, has a weight of about 50 kg. The application of aluminum wires will be a promising method to reduce significantly the weight of cable harnesses in the range of about 40% with a simultaneous reduction of material costs. The ultrasonic metal welding process is already well established in the automotive industry to join copper wires. The challenge to substitute copper by aluminium is the affinity of aluminium to adhere at the ultrasonic welding tools during the solid state joining process. In this work suitable welding parameters were determined and special surface coatings for the ultrasonic welding tools were developed to ensure a reproducible manufacturing of joints between aluminum wires or between Al-wires and Al-connectors. Mechanical and electrical properties of ultrasonic welded Al-wires-joints as well as microstructural investigations of the joining zone by using computer tomography and electron microscopy will be discussed.

### 4:15 PM

**Phase-Field Simulations of Microstructure Formation in A356 during Casting:** Markus Apel<sup>1</sup>; Antoine Carre<sup>1</sup>; Bernd Böttger<sup>1</sup>; <sup>1</sup>Access e. V.

Today the phase field method emerges as a tool which can be applied to simulate the phase formation and solidification morphologies in technical alloys. In this presentation we present a combined study, sand casting experiments using a pure Al7%Si0.3%Mg alloy, accompanied by phase-field simulations of the microstructure formation during solidification. By calibrating the heat extraction rate, the simulations can be adjusted to yield approx. the same cooling curves as they are measured for the real castings. The simulated microstructures are in good agreement with the experimental ones. In addition, we will discuss the solidification path predicted by the phase-field simulation in comparison to Scheil-Gulliver type calculations. Further simulations take Fe and Cu impurities into account. The microsegregation pattern of Si, Mg and of the impurity elements will be discussed with respect to further heat treatments.

### 4:35 PM

**Modeling Non-Isothermal Annealing in Precipitate Hardening Aluminum Alloys: Microstructural Simulation:** Panthea Seppehrband<sup>1</sup>; Shahrzad Esmaili<sup>1</sup>; Haiou Jin<sup>2</sup>; <sup>1</sup>University of Waterloo; <sup>2</sup>Novelis Global Technology Centre

A new approach is introduced for computational modeling of microstructural evolution during non-isothermal annealing in cold-rolled precipitate hardening aluminum alloys. Microstructural states are simulated using a Monte Carlo technique and on the basis of a competition between recovery and recrystallization for reduction of stored energy. The initial amount of stored energy, which is related to the level of deformation, is distributed inhomogeneously within the deformed grains, as dictated by the microstructural inhomogeneities and the grain structure. The effects of deformation-induced and pre-existing inhomogeneities, as well as precipitate coarsening and grain boundary pinning on the competitive recovery-recrystallization process are included in the algorithm of simulation. The method is implemented to predict the microstructural evolution during a non-isothermal annealing process that leads to fine-grained AA6xxx sheets. A good quantitative agreement is observed comparing the model predictions with the results from a comprehensive set of microstructural characterization experiments.

### 4:55 PM

**Prediction of Microstructure and Mechanical Properties in Aluminum Castings after Heat Treatment:** Jianzheng Guo<sup>1</sup>; Weisheng Cao<sup>2</sup>; Sam Scott<sup>3</sup>; Tony Kronenberger<sup>4</sup>; Joe Hirvela<sup>4</sup>; <sup>1</sup>ESI US R&D; <sup>2</sup>CompuTherm LLC; <sup>3</sup>ESI Group NA; <sup>4</sup>CPP-Minneapolis

A comprehensive numerical model is being developed for the calculation of the final microstructure and mechanical properties of aluminum casting alloys after heat treatment. After specifying the alloy chemical composition, solidification process, and heat treatment parameters, the model predicts the microstructure

and potential defects through various stages of the component lifecycle: casting and heat treatment. The model takes into account the relationship between the different input parameters and the link to basic metallurgical features. Such a model can be used for tailoring mechanical properties and component performance with the correct choice of chemical composition and manufacturing process parameters. The effects of cooling history during casting and heat treatment processes are numerically and experimentally investigated. The microstructure and mechanical properties are predicted and compared with experimental measurements.

### 5:15 PM

**Study of a Geometrically Necessary Dislocations Field near the Interface of a Deformed Aluminum Bicrystal:** Alankar Alankar<sup>1</sup>; Ioannis Mastorakos<sup>1</sup>; David Field<sup>1</sup>; <sup>1</sup>Washington State University

We reiterate the study by Sun et al. (2000) on a lattice curvature field near the interface of a deformed aluminum bicrystal using our crystal plasticity finite element method (CPFEM) model. The CPFEM model shows evolution of statistically and geometrically necessary dislocations (GND) on all the octahedral slip systems in FCC material. The evolution of statistical dislocations is modeled in form of loops comprising pure edge and pure screw dislocations. Geometric character of dislocations is modeled using divergence of the flux of dislocations. In the simulation, a bicrystal with specific crystallite orientations is deformed in a channel die compression with thickness reduction perpendicular to the common interface. The model results show that due to lattice incompatibility at the interface, GNDs are created with high field density near the interface which tends to diminish away from the interface. The results are compared with the work presented in the above reference.

## Aluminum Reduction Technology: Aluminium Smelter: Environment, Health and Safety

*Sponsored by:* The Minerals, Metals and Materials Society, TMS Light Metals Division, TMS: Aluminum Committee, TMS: Aluminum Processing Committee

*Program Organizers:* Charles Mark Read, Bechtel Corporation; Gilles Dufour, Aluminerie de Deschambault

Monday PM Room: 608  
February 15, 2010 Location: Washington State Convention Center

*Session Chairs:* Bob McCulloch, Bechtel Corporation; Robert Baxter, Bechtel Corp

### 2:00 PM Introductory Comments

### 2:05 PM

**Modern Potline Gas Treatment Technology for High Amperage Pots - The Alcoa Fjardaal Experience:** Alain Moras<sup>1</sup>; Neal Dando<sup>1</sup>; Bernard Cloutier<sup>2</sup>; Philippe Dumortier<sup>2</sup>; Hugues Vendette<sup>2</sup>; <sup>1</sup>Alcoa; <sup>2</sup>Solios Environnement Inc.

Alcoa's latest greenfield smelter at Fjardaal, Iceland has a fluoride emission permit of 0.35 kg F/T Al which is about half the future (2010) European standard of 0.6 kg F/T. To facilitate meeting this requirement, the potline gas treatment centers (GTCs) were designed with dual pot suction systems to double pot extraction flow rate during pot work periods with balancing outlet dampers and venturi flowmeters and an alumina feed calibration system. Both GTCs have been in full operation since Q1 2008 with the following performance: GTC HF emission in the range of 0.2 -0.3 mg per Nm<sup>3</sup> at an alumina wt% fluoride loading ~1.7%. No bags have been changed (23000 bags in total for the 2 GTCs), indicating there are no zones of high velocity within the filter casings. Additional design and control features will be presented and performance data will be discussed.

### 2:30 PM

**Heat Recovery from the Exhaust Gas of Aluminum Reduction Cells:** Martin Flerl<sup>1</sup>; Odd-Arne Lorentsen<sup>2</sup>; William Harvey<sup>3</sup>; Halldor Palsson<sup>4</sup>; Gudrun Saevarsdottir<sup>3</sup>; <sup>1</sup>Reyst, Reykjavik Energy School of Sustainable Systems; <sup>2</sup>Norsk Hydro; <sup>3</sup>Reykjavik University; <sup>4</sup>University of Iceland

Waste heat losses from aluminum smelting processes are around half of the total energy input and have the potential to be harnessed for useful purposes. The heat loss is by several paths of which the exhaust gas carries the second largest energy amount and is the most accessible. An experimental analysis of

Mon. PM

# Technical Program

the exhaust gas was conducted at the 270,000 tpy Nordural aluminum smelter in Iceland. The district heating potential of heat recovery from the exhaust gas was assessed for at the local community of Akranes. For this smelter the potential is up to 60 MWt. The chemical composition and dew point of the exhaust gas was analyzed. Particulates were isokinetically sampled and analyzed for chemical properties and size distribution. Scale buildup on a fouling probe was similarly examined. Data and commentary are presented that illustrate the difficulties and considerations for waste heat recovery from exhaust gas streams

## 2:55 PM

**Increased Energy Efficiency and Reduced HF Emissions with New Heat Exchanger:** *Anders Sorhuus*<sup>1</sup>; Geir Wedde<sup>1</sup>; Ketil Rye<sup>2</sup>; Gaute Nyland<sup>2</sup>; <sup>1</sup>Alstom; <sup>2</sup>Alcoa Mosjøen

The first full scale heat exchanger has now successfully demonstrated several months of stable operation at a smelter in Norway. Potentially 100 GWh per year can be recovered from this smelter alone for use in the district heating system. In hot climates recovered energy may be used to produce fresh water in desalination plants which may be equally beneficial. A sharp rise in fluoride emissions (HF) is seen as pot gas temperatures exceed 100°C. Dilution of the pot gas with ambient air is used to achieve acceptable GTC gas temperatures (110-115°C) and emission levels. In these cases installing the heat exchanger will not only reduce the size of the GTCs, but also large savings in the power consumption and reductions in HF emissions are obvious. On top of this the value of the recovered energy can justify the heat exchanger installation by itself.

## 3:20 PM

**Reduction Line-5 DC Electrical Hazard:** *Mohsen Shukralla*<sup>1</sup>; <sup>1</sup>Aluminium Bahrain (Alba)

Two of Reduction line-5 employees got slight electrical sensation while doing their routine jobs on the pots; the first one was on April while the second was on May 2009. Despite the fact that no body was injured in both accidents, the issue of electrical shock was taken very seriously. In both cases, the measurements showed the operating floor, which was supposed to be on Floating potential, is on Earth potential. After extensive measurements, checks and taken corrective actions, the hazardous areas were contained in a zone of 3 slabs which accounts for 9 pots. Danger zone notification was raised on the affected areas and all the safety precautionary measures were taken to safe guard all the employees. This paper shall describe the problem of electrical Dc hazard in pot line-5 and actions taken to resolve it. The detailed shock test measurements along with safety precautions taken are also discussed.

## 3:45 PM Break

## 3:55 PM

**2008 Global Anode Effect Survey Results:** *Jerry Marks*<sup>1</sup>; Chris Bayliss<sup>2</sup>; <sup>1</sup>J. Marks & Associates; <sup>2</sup>International Aluminium Institute

The International Aluminium Institute (IAI) conducts annual surveys of global primary aluminum producers on various performance parameters. Anode effect performance data has been collected annually since 2000. Prior to 2000 periodic surveys were conducted covering anode effect performance back to 1990. The current paper discusses progress toward a new 2020 PFC reduction objective. In addition other primary aluminum production survey statistics will be discussed on parameters such as energy consumption, fluoride emissions and safety performance.

## 4:20 PM

**The Applicability of Carbon Capture and Sequestration in Primary Aluminium Smelters:** *Stephan Broek*<sup>1</sup>; Sanjiv Save<sup>1</sup>; <sup>1</sup>Hatch Ltd

Climate Change is affecting every industry including the Primary Aluminium industry. The International Energy Agency has developed several strategies how to abate GHG emissions on large industrial scale. One of the tools identified to abate CO<sub>2</sub> emissions from large sources is carbon capture and sequestration (CCS). Earlier papers have touched on the topic of using CCS in primary smelters and in this paper further details are shown of technological aspects of CCS, but also on some of the specific conditions that have to be dealt with when applied in primary aluminium smelters. Conclusions are presented.

## 4:45 PM

**Application of a Method for the Determination of PFC Emissions during Aluminum Pot Startup:** *Jean-Nicolas Maltais*<sup>1</sup>; Josette Ross<sup>1</sup>; Alain Marcoux<sup>1</sup>; <sup>1</sup>Rio Tinto Alcan

Because of their global warming effect, PFC emissions are a major focus for the aluminum industry. The significant reductions achieved in the main source of PFCs, anode effects, had led to questions about the quantification of PFC emissions beyond anode effects. Rio Tinto Alcan has developed a precise industrial method for analysing PFC emissions. It uses active sampling through sorbent material and analysis by a system which includes thermal desorption, gas chromatography and mass spectroscopy. Measurement campaigns have been carried out on P155 and AP30 pots, in partnership with Environment Canada, to define the rate and quantity of PFC emissions during the startup high voltage period. This paper compares results with those from anode effects in the same smelters, and with pot start up measurements from other smelters. The wide variability of measured emission slopes highlights that pot startup practices have an impact on the PFC emissions rate.

## 5:10 PM

**Aluminum Fluoride – A Users Guide:** *Stephen Lindsay*<sup>1</sup>; <sup>1</sup>Alcoa, Inc.

Aluminum fluoride is an important raw material that is primarily manufactured via reactions of aluminum hydrate with fluorspar or with fluosilicic acid. Impurities generally have a minor impact upon smelting processes and metal products, but there can be exceptions. Likewise there are some physical properties of concern with this raw material. In this paper the author illustrates the important factors to consider when selecting and using sources of AlF<sub>3</sub>.

## 5:35 PM

**Dissolution Behavior of Aluminum Dross in Aluminum Electrolyte:** *Wei Qin Fu*<sup>1</sup>; Zhaowen Wang<sup>1</sup>; Youjian Yang<sup>1</sup>; *Xianwei Hu*<sup>1</sup>; <sup>1</sup>Northeastern University

Aluminum dross generated during electrolytic refining process of aluminum could be added into aluminum electrolysis cells for recycling because of its high aluminum contents. In this paper, the constituents and compositions of the aluminum dross were determined by X-ray and chemical analyses and AlN and Al<sub>2</sub>O<sub>3</sub> were proved to be the main constituents. On that basis, the phenomena of dissolution process of AlN and the aluminum dross in cryolite-based salt melts were observed through a transparent quartz cell. It was found that AlN was dispersed into the melts as small flocculent aggregate, and then dissolved into the melts gradually. The solubility of AlN was estimated to 2.0-2.5wt% at 1258 K. The aluminum dross was observed to form agglomerates on the bath surface, and then dissolved into the melts by chemical reaction with the adjacent electrolyte. Keywords: aluminum dross; dissolution behavior; solubility; transparent cell

## 5:55 PM Concluding Comments

## Aluminum Reduction Technology: Aluminium Smelter: Equipment

*Sponsored by:* The Minerals, Metals and Materials Society, TMS Light Metals Division, TMS: Aluminum Committee, TMS: Aluminum Processing Committee

*Program Organizers:* Charles Mark Read, Bechtel Corporation; Gilles Dufour, Aluminerie de Deschambault

Monday PM

Room: 609

February 15, 2010

Location: Washington State Convention Center

*Session Chairs:* Kevin Watson, Bechtel Corporation; John (Jack) Judson, Bechtel Corporation

## 2:00 PM Introductory Comments

## 2:05 PM

**Improving Heat Dissipation and Cell Life of Aged Reduction Lines at Aluminium Bahrain (Alba):** *Abdulla Ahmed*<sup>1</sup>; K.S.R. Raghavendra<sup>1</sup>; Barry Welch<sup>2</sup>; <sup>1</sup>Aluminium Bahrain (Alba); <sup>2</sup>University of New South Wales (UNSW) & Welbank, Consulting Limited

The side worked end-on-end pre-bake anode technologies installed at beginning of 1970's gave pot life of 1600 days. During the early nineties, the potlines were retrofitted from side-break to point-fed, which was accompanied



by an increase of 8% in line current. The retrofits included gas collection system, changing anode setting pattern and installation of Alumina and Aluminium-fluoride feeders. However, pot life reduced to 1350 days due to increase of heat input by 5%. After introducing certain remedies, the pot life increased to above 2000 days. As the cells were still not operating at their full potential, a heat balance study was conducted in 2005. Several modifications were introduced in collector bar design, use of Silicon Carbide and Carbon composite inserts. Following this development a study has been made on the potential of applying the well-established principles of air-cooling in selective location around the pot shell to improve sidewall ledge protection.

### 2:30 PM

**Update on the Evaluation of HF Emission Reduction Using Covered Anode Trays:** *Jean-Pierre Gagne*<sup>1</sup>; Rene Minville<sup>1</sup>; Neal R Dando<sup>2</sup>; Gilles Dufour<sup>3</sup>; Mike Gershenzon<sup>2</sup>; Pierre Champoux<sup>3</sup>; Alain Moras<sup>3</sup>; <sup>1</sup>STAS; <sup>2</sup>Alcoa Technical Center; <sup>3</sup>Alcoa Canada

During the production of aluminum from conventional prebake Hall-Héroult electrolysis, carbon anodes have to be replaced on a regular basis. The anode butts are usually placed on uncovered trays for transportation and cooling, a practice that contributes to overall hydrogen fluoride (HF) emission from the smelter. In 2000, special anode tray covers developed by Alcoa Deschambault were implemented to significantly reduce fluoride emissions. In 2004, the Alcoa-STAS R&D team developed a second generation of anode tray covers for the new Alcoa Fjardaal plant. In 2009, the Alcoa STAS R&D Team designed and fabricated an experimental setup which allows the accurate full-scale measurement of temporal HF emissions from cooling anode trays. This paper presents a description of the setup, a summary of the procedure and an update of the results obtained with the use of the anode tray covers.

### 2:55 PM

**Automated Anode Gauging:** Said Al Maqbal<sup>1</sup>; C. Smith<sup>1</sup>; J. Raman<sup>1</sup>; M. Angirash<sup>1</sup>; S. Abdullah<sup>1</sup>; S. Thirunavukkarasu<sup>1</sup>; R. Kulkarni<sup>1</sup>; P. Marchand<sup>2</sup>; S. David<sup>2</sup>; P. Boucher<sup>2</sup>; <sup>1</sup>Sohar Aluminium Company; <sup>2</sup>ECL<sup>TM</sup>

Anode change is one of the most critical operations of the reduction process. A continuous improvement project was conducted by Sohar Aluminum in collaboration with ECL to evaluate and optimize the laser based auto gauging system developed by ECL on Pot Tending Machines (PTM). This has eliminated risks to the operator from the hot butts being moved by the PTM as well as exposure to the radiant heat of the open pot. It also reduced the time taken for changing the anodes by 25%. From a process point of view, it reduced improper anode settings by 40%. The process capability (based on mV reading 24 hours after the anode change) increased from a Cpk of 0.47 with manual gauging to 0.62 with laser auto gauging, resulting in better current distribution in the anodes and hence, better smelting efficiency.

### 3:20 PM

**Keeping the Pace of Continuous Improvement by Retrofitting Pot Tending Machines:** *José Barry*<sup>1</sup>; Fidiás Roriguez<sup>1</sup>; Jesus Imery<sup>1</sup>; <sup>1</sup>CVG Venalum

Pot tending machines play a key role in the productivity of smelters, and as aluminium companies are squeezing any aspect of their processes to improve profits, in many cases old pot tending machines can not cope with new requirements. Hence, companies have to evaluate either retrofitting or installing new pot tending machines to carry on with their global improvement strategies. CVG-Venalum tackled this issue by developing its own pot tending technology; some of the improvements implemented are an enhanced design of the tool trolley, an automated anode height measurement, PLC and VFD based control system, electronically controlled clamp-tightening torque, and weight measurement modules integrated to the new control and supervisory system. The low cost of the two prototypes constructed at local workshops, as well as their enhanced performance, boosted this project, so CVG-Venalum management decided to carry on the retrofitting of the twenty original pot tending machines serving 720 pots

### 3:45 PM Break

### 3:55 PM

**New Concepts for Bulk Materials Plants for the Aluminium Producing Industry – From Raw Material Receiving to Electrolysis Cells:** *Stefan Skirde*<sup>1</sup>; <sup>1</sup>Coperion GmbH

Today's new smelters are often built at remote places with ever increasing plant capacity. The various plant layouts require different solutions for an

economic bulk material handling system from ship to cell for a continuous production. A very common way for the receipt of raw material delivered by ships such as alumina and petrol coke is with a vacuum ship unloader. The product is conveyed at high capacities with a pipe conveyor directly to a storage silo, which can hold at least one complete shipload. Alumina quality will be maintained with an Anti-Segregation system. Further transports can be of pneumatic or mechanical nature depending on its best suitability. The electrolysis cell is the core element of the smelter where the raw material is transformed to valuable metal and requires an automatic and reliable feed of alumina in a dense mode.

### 4:20 PM

**Alfeed, a New Alumina Feeding System to Aluminium Pots:** *Sivert Ose*<sup>1</sup>; Anders Sorhuus<sup>1</sup>; Odd Bjarno<sup>1</sup>; Geir Wedde<sup>1</sup>; <sup>1</sup>Alstom

A new alumina distribution and feed system to the pots, Alfeed, has been developed and is now installed at one of the largest aluminium smelters in the world. At this smelter alone, more than one million ton of alumina per year will be distributed in more than 15 km of transport airslides. The Alfeed system contains several new features which are improvements above existing systems:

- Slim design - making retrofit easy
- Completely enclosed and self regulating system
- Keep pot hoppers automatically topped up all the time
- Recycles fines back to the pots
- Transports coarse material to the pot
- Minimal attrition, segregation or scaling of the material.

The Alfeed has been developed during several years. With the successful delivery to one of the world largest smelters, Alfeed has now evolved into a commercial product using standard integrated design and robotic production methods.

### 4:45 PM

**Electrolysis Pot J Hooks New Design: Positive Impacts on Performance and Environment:** *Nicolas Dupas*<sup>1</sup>; *Damien Rose*<sup>1</sup>; <sup>1</sup>ECL

J hooks are crucial elements of modern aluminium smelting. Their task is to support and ensure the anode rods clamping by the anode clamps, and guide the pot tending machines extraction tool during the anode changing phase. Although they appear as simple components, their performances are critical to a successful production process. For 40 years, their design has almost remained unchanged, their simplicity and criticality making measurable improvements difficult to obtain. To create the new design, finite elements studies and computer assisted production methods have been used. The new concept's validation and its fine tuning has been performed on specially designed test benches, taking into account normal and abnormal conditions of use, and also during extensive field test with collaborating smelters. By working on the structural design, materials and shape of the J hooks, it has been possible to improve their performances and reduce their overall impact on the environment.

### 5:10 PM

**Cleaning and Maintenance of Crucibles and Siphons/Tubes:** *Dominique Prive*<sup>1</sup>; *Pascal Côté*<sup>1</sup>; Robin Boulianne<sup>1</sup>; <sup>1</sup>STAS

To optimise metal transportation from the potroom to the cast house, crucibles and siphons/tubes must be regularly cleaned and maintained to remove metal/bath deposits that accumulate inside, reducing the crucible capacity after several operations. Cleaning after cooling to room temperature is quite common but has time and cost implications. Moreover, heating cycles and cleaning operations in crucibles with improper equipment may damage the refractory. It is now possible to clean hot crucibles within a very short period of time, thus minimising the time when they are out of service. At the same time, siphon/tube cleaning and preheating are carried out and usually conducted in a common location with the crucible cleaning operation in the smelter. All those operations are automated and require minimum activities from an operator. This paper presents the latest available technologies in a fully integrated solution for the cleaning and maintenance of crucibles and siphons/tubes.

### 5:35 PM

**Erosion of Ferrous Alloys by Liquid Aluminum:** *Mandeep Sidhu*<sup>1</sup>; Milo Kral<sup>1</sup>; <sup>1</sup>University of Canterbury

Cast iron and/or cast steel pipes, which are commonly used to transfer molten aluminum, degrade by material loss and cracking. This is a problem for the aluminum production industry because of the cost of replacing pipes. Service conditions are severe, not only because liquid aluminum can react with nearly all metals and their oxides but also because of cycles of steep thermal gradients. The scope of this research was therefore to investigate the degradation of ferrous alloys under the demands of liquid metal transfer conditions. Pipe alloys

Mon. PM

# Technical Program

currently employed in service were selected as benchmarks for comparison with candidate alloys. Two specialized experiments were developed to expose candidate materials to erosive and thermal conditions similar to actual service. The various samples of ferrous alloys were compared by their erosive weight loss (by exposure to flowing aluminum) and response to thermal cycling (by cyclic exposure to static aluminum). Electron microscopy was used to characterize the reaction interfaces and microstructural changes to shed light upon the erosion and thermal fatigue mechanisms. The main outcome of this work is to recommend the best candidate material for the service conditions.

## 5:55 PM Concluding Comments

## Biological Materials Science: Bio-inspired Materials Design and Processing II: Bioceramics and Biomineralization

*Sponsored by:* The Minerals, Metals and Materials Society, TMS Structural Materials Division, TMS: Biomaterials Committee, TMS/ASM: Mechanical Behavior of Materials Committee

*Program Organizers:* John Nychka, University of Alberta; Jamie Kruzic, Oregon State University; Mehmet Sarikaya, University of Washington; Amit Bandyopadhyay, Washington State University

Monday PM Room: 205  
February 15, 2010 Location: Washington State Convention Center

*Session Chairs:* Amit Bandyopadhyay, Washington State University; Mehmet Sarikaya, University of Washington

## 2:00 PM Invited

**Novel Sol-Gel Bioactive Glasses for Tissue Engineering:** John Mitchell<sup>1</sup>; <sup>1</sup>Oregon Health and Science University

The interaction of biological fluids with certain compositions of glass materials has been shown to promote the crystallization of new mineral phases on the glass surfaces. Novel glasses synthesized in our laboratory, by sol-gel fabrication methods, have been shown to promote such biomimetic deposition in as little as 4 hours after immersion. The resulting materials are biocompatible and bioactive, inducing favorable cell and tissue reactions in vivo. This presentation will provide an overview of these amorphous materials and present examples of our investigations into their potential use in a myriad of situations, including: the prevention of dental hypersensitivity; the prevention of bone loss and the promotion of new bone growth; the enhancement of dental restorative materials; and the delivery of therapeutic compounds in vivo.

## 2:30 PM

**Factors Affecting the Dissolution of Resorbable Bioactive Glasses:** Satadru Kashyap<sup>1</sup>; Hamidreza Pirayesh<sup>1</sup>; John Nychka<sup>1</sup>; Ding Li<sup>2</sup>; Fuqian Yang<sup>2</sup>; <sup>1</sup>University of Alberta; <sup>2</sup>University of Kentucky

Bioactive glasses used in bone replacement therapy can be made to be entirely resorbable (e.g., bioactive glass 45S5). Factors affecting dissolution are numerous: residual stress, composition, crystallinity, immersion medium, and surface morphology. Here we present results on effects of residual stress, crystallinity, and manufacturing method on the dissolution behaviour of glasses with fixed overall composition (i.e., 45S5).

## 2:50 PM

**Mechanical and Biological Characterization of Dense Nanocrystalline HA Consolidated by Field-Assisted Sintering:** Tien Tran<sup>1</sup>; James Shackelford<sup>1</sup>; Joanna Groza<sup>1</sup>; <sup>1</sup>University of California, Davis

As the main inorganic component of bone, hydroxyapatite (HA) should ideally be a premier candidate in the selection of biomaterials. When grain sizes are restrained to the nanoscale regime, protein adsorption and cell adhesion are enhanced, while strength, hardness, and wear resistance are improved. Unfortunately, low phase stability, poor sinterability, and a tendency towards exaggerated grain coarsening challenge full densification of nanocrystalline HA by conventional sintering techniques. The field-assisted sintering technique (FAST) is capable of heating rates up to 1000°C/min, minimizing the time powders are exposed to sub-densification temperatures when some coarsening may occur. Transparent nanocrystalline specimens greater than 99% dense have been sintered in less than 20 min. Simulated body fluid immersion tests were conducted to probe the effects of sintering-related dehydroxylation on surface

apatite deposition. Fracture toughness values in the range of 1.4-1.9 MPa√m were measured by single-edge v-notch bend.

## 3:10 PM Invited

**Nanoscale Calcium Phosphates in Bone Implants and Drug Delivery:** Susmita Bose<sup>1</sup>; <sup>1</sup>Washington State University

Synthetic calcium phosphates (CaPs) have been used in orthopedics and dentistry because of their excellent biocompatibility and chemical similarity with bone. Most commonly used synthetic CaPs are bioactive hydroxyapatite (Hap, Ca<sub>10</sub>(PO<sub>4</sub>)<sub>6</sub>(OH)<sub>2</sub>) and bioresorbable tricalcium phosphate (TCP, Ca<sub>3</sub>(PO<sub>4</sub>)<sub>2</sub>). These nanoscale inorganic ceramics can be used as both bone implant as well as a drug delivery vehicle, especially for bisphosphonate based drugs, which is a common drug being used to treat osteoporosis. In our research we have shown that both nanoscale feature as well as addition of dopants can influence biological and mechanical properties of CaP based bone graft material. This invited presentation will discuss nanoscale CaP processing, mechanical, biological property characterization as well as their use in bisphosphonate based drug delivery. Keywords: calcium phosphate, bioceramics, bone graft, drug delivery, processing

## 3:40 PM Break

## 3:50 PM Invited

**Crab Shell Osteogenesis:** Otto Wilson<sup>1</sup>; <sup>1</sup>Catholic University of America

There is a kinship that exists among biologically derived hard tissues. This inter-relatedness is expressed via comparable mechanisms for organic matrix organization and biomineralization processes. The ability to use biogenic hard tissues such as coral and nacre in augmentation of damaged bone tissue further attests to the unique bonds which are shared by hard tissues in nature. Crab shell cuticle is another candidate material for enhancing the healing and remodeling of bone. Extensive work has been performed utilizing crab shell component chitin and its chemical derivative chitosan. However, whole crab shell poses some interesting possibilities for use in bone tissue engineering due to similarities with bone tissue. A comparison of the unique chemical and physical characteristics of bone and crab shell with a focus on the respective organic matrices and mineral phases will serve as the focus for this talk. (This work was supported by NSF grant DMR-0645675).

## 4:20 PM

**Unveiling the Formation Mechanism of Pseudo Single-Crystal Aragonite Platelets in Nacre:** Xiaodong Li<sup>1</sup>; Zaiwang Huang<sup>1</sup>; <sup>1</sup>University of South Carolina

We demonstrate direct evidence that a single-crystal-like aragonite platelet is essentially assembled with aragonite nanoparticles. The aragonite nanoparticles are readily oriented and assembled into pseudosingle-crystal aragonite platelets via screw dislocation and amorphous aggregation, which are two dominant mediating mechanisms between nanoparticles during biomineralization. These findings will advance our understanding of nacre's biomineralization process and provide additional design guidelines for developing biomimetic materials.

## 4:40 PM

**Osteoinductive Potential of Biphasic Calcium Phosphate Scaffolds with Multi-Scale Porosity:** Amy Wagoner Johnson<sup>1</sup>; <sup>1</sup>University of Illinois at Urbana-Champaign

Calcium phosphates are synthetic biomaterials that are used in a wide range of dental and orthopedic applications to replace or restore bone because of their excellent bioactivity and osteoconductivity. Here we evaluate the effect of the growth factor BMP-2 on multi-scale osteointegration for biphasic calcium phosphate scaffolds with multi-scale porosity. Results show osteoinductive effects for scaffolds with and without BMP-2, as evidenced by cell migration and bone formation in micropores less than 10μm in size with average interconnection size of 2μm. Scaffolds with BMP-2 had significantly more cells in pores at 3, 6, and 12, but not 24 weeks. There is no effect of BMP-2 on the volume of bone formed within macropores in this defect model. Data suggest that osteoinductivity is imparted to the scaffolds via in vivo modifications related to the microporosity. These mechanisms have yet to be resolved, but possible mechanisms will be discussed.



### 5:00 PM

**Growth of Nacre in Abalone:** *Maria Lopez*<sup>1</sup>; P.Y. Chen<sup>1</sup>; K. Chumbimuni-Torres<sup>2</sup>; J. Wang<sup>1</sup>; J. McKittrick<sup>1</sup>; M.A. Meyers<sup>1</sup>; <sup>1</sup>UCSD

The processes of aggregation of minerals to the growing surfaces in red abalone (*Haliotis rufescens*) are analyzed. Flat pearl implantation method is used to observe the transient phases of calcium carbonate and the steady-state growth of aragonite tiles. Calcium-Ion Selective Electrode is used to monitor the variation of concentration of Ca<sup>++</sup> between the extrapallial layer of mantle and the shell. These results are correlated with the growth of tiled aragonite. The morphology of the organic interlayer is characterized by scanning electron microscopy and atomic force microscopy. Its response to mechanical stresses is evaluated by means of nanoindentation. The nanoscale holes in the organic interlayer are measured. These measurements enable a realistic modeling of the formation of the terraced cones that comprise the principal biomineralization mechanism in this gastropod. Research support: NSF Biomaterials Program (DMR 0510138).

### 5:20 PM

**Bioinspired Synthetic Laminates:** *Gustavo Hirata*<sup>1</sup>; Sandra Diaz<sup>1</sup>; Po-Yu Chen<sup>2</sup>; Marc Meyers<sup>2</sup>; Joanna McKittrick<sup>2</sup>; <sup>1</sup>Center for Nanoscience and Nanotechnology; <sup>2</sup>UC San Diego

Bioinspired by the abalone shell microstructure, we have fabricated inorganic/polymer multistacked layers by combining pulsed laser ablation and magnetron sputtering. Smooth thin polymer (PMMA) films were grown by laser ablation and alternatively inserted between inorganic layers deposited by DC or RF magnetron sputtering in order to fabricate multi-layers of several biocompatible materials: CaCO<sub>3</sub> (aragonite), ZrO<sub>2</sub> ZrN and TiO<sub>2</sub>. The inorganic films are composed of nanocrystalline or amorphous particles with different degrees of porosity as observed by TEM and AFM. High resolution TEM analysis at the inorganic/organic interface revealed well formed inorganic films which are separated by the polymeric layer (10-50 nm). The hardness values showed an increase for the inorganic film/polymer stacked system as compared with the single film. A more detailed analysis of the results together with AFM/nanoindentation measurements will be presented. This research is supported by ARO Grant W911F-08-1-0461 and NSF Grant DMR 0510138.

## Bulk Metallic Glasses VII: Structures and Mechanical Properties II

*Sponsored by:* The Minerals, Metals and Materials Society, TMS Structural Materials Division, TMS/ASM: Mechanical Behavior of Materials Committee

*Program Organizers:* Peter Liaw, The University of Tennessee; Hahn Choo, The University of Tennessee; Yanfei Gao, The University of Tennessee; Gongyao Wang, University of Tennessee

Monday PM Room: 213  
February 15, 2010 Location: Washington State Convention Center

*Session Chairs:* A. Greer, University of Cambridge; Dan Miracle, Air Force Research Laboratory

### 2:00 PM Keynote

**Anisotropy in Metallic Glasses:** *A. Greer*<sup>1</sup>; <sup>1</sup>University of Cambridge

Metallic glasses when fully relaxed are expected to be isotropic. However, they can be anisotropic as a result of their production method (for example, melt-spun ribbons appear to be strongly anisotropic), or anisotropy can be induced by various treatments such as annealing under stress or in a magnetic field. Examples of anisotropy will be reviewed and its structural origins will be considered, linking with anelasticity and viscous flow. The potential anisotropy of metallic glasses is often ignored, and this can lead to misleading conclusions. On the other hand, anisotropy can be also be useful.

### 2:30 PM

**Condensed Bond Enthalpies in Metallic Elements, Alloys and Compounds:** *Dan Miracle*<sup>1</sup>; James Dahlman<sup>2</sup>; Amanda Dahlman<sup>2</sup>; Garth Wilks<sup>3</sup>; <sup>1</sup>Air Force Research Laboratory; <sup>2</sup>SOCHÉ; <sup>3</sup>General Dynamics, Inc.

Bond dissociation energy and bond enthalpy are widely used measures of the energy contained in a bond between atoms in molecular gases. We propose a new quantity, the condensed bond enthalpy, to specify the energy contained in a bond between elements in the condensed state. We develop an

approach for determining the condensed bond enthalpy in metallic elements, alloys and compounds using readily available bulk thermodynamic quantities and crystallographic data. The usefulness of these values is demonstrated by application to a range of problems in physics and materials science.

### 2:40 PM Invited

**Investigation of Homogeneous and Inhomogeneous Plastic Flow in Metallic Glasses:** *Katharine Flores*<sup>1</sup>; Wendelin Wright<sup>2</sup>; Wolfgang Windl<sup>1</sup>; <sup>1</sup>The Ohio State University; <sup>2</sup>Santa Clara University

As metallic glasses mature and are implemented, understanding the relationship between their atomic structure and plastic deformation mechanisms is increasingly relevant for both manufacturing and reliability. We have examined the mechanical behavior of a Zr-based BMG at the micro- and sub-microscale and observed a tendency towards more stable shear band behavior and mixed homogeneous-inhomogeneous flow at the smallest length scales. Shear band stability shows a strong dependence on the relative stiffness of the specimen. Implications of such stiffness and length-scale dependant behavior for the design of micro-scale devices and BMG composites will be discussed. These observations are discussed in light of structural changes observed in molecular dynamics simulations of Zr-Cu binary glasses during deformation under different stress state conditions. In these simulations, we characterize local density fluctuations and the coordination of the surrounding atoms as a means of describing the structure at points of incipient failure.

### 3:00 PM

**Aging and Plastic Flow in Metallic Glasses: Monte Carlo Simulations Based on the Activation-Relaxation Technique:** *David Rodney*<sup>1</sup>; Christopher Schuh<sup>2</sup>; <sup>1</sup>Grenoble Institute of Technology; <sup>2</sup>Massachusetts Institute of Technology

The yield stress in disordered solids marks a transition between aging at low applied stresses and plastic flow at higher stresses. The transition involves thermally-activated processes that are difficult to account for at the atomic scale because they occur on long timescales. Here, we overcome this limitation through Monte Carlo simulations in which the elementary thermally-activated events are determined using the activation-relaxation technique. We show that aging increases the stability of the glass, both thermodynamically (the internal energy decreases) and dynamically (the aged glass is surrounded by higher energy barriers). By contrast, plastic flow brings the glass into a high internal energy state only marginally stable, being surrounded by a high density of low-energy barriers. The strong influence of plastic deformation on the glass state is also shown through a polarization of the microstructure, evidenced by an asymmetry of the distribution of thermally-activated plastic strains in glasses after shear deformation.

### 3:10 PM Invited

**Inhomogeneous to Homogeneous Transition in an Au-Based Metallic Glass during Microcompression at Elevated Temperatures:** *Shuangxi Song*<sup>1</sup>; *T.G. Nieh*<sup>1</sup>; J.C. Huang<sup>2</sup>; J.S.C. Jang<sup>3</sup>; <sup>1</sup>The University of Tennessee; <sup>2</sup>National Sun Yet-sen University; <sup>3</sup>National Central University

Transition from inhomogeneous to homogeneous deformation was characterized in Au<sub>49</sub>Ag<sub>5.5</sub>Pd<sub>2.3</sub>Cu<sub>26.9</sub>Si<sub>16.3</sub> metallic glass pillars under compression at 373.1 – 384.2 K or 0.93 – 0.96T<sub>g</sub>. Localized shear bands were formed well before macroscopic yielding at low temperatures. High-temperature compression were conducted on these pillar samples near the glass transition temperature to investigate the homogeneous deformation behavior. In contrast to local shear at low temperatures, samples were observed to deform uniformly. The strength was observed to decrease with increasing temperature and decreasing strain rate. Plastic flow behavior can be described by a shear transition zone (STZ) model. The activation energy and the size of the basic flow unit were both deduced and compared favorably with the free volume theory.

### 3:30 PM Break

### 3:40 PM Invited

**Deformation and Fracture Behavior of Metallic Glassy Alloys and Glassy-Crystal Composites:** *Dmitri Louzguine*<sup>1</sup>; Alexei Vinogradov<sup>2</sup>; Alain Reza Yavari<sup>3</sup>; Guoqiang Xie<sup>4</sup>; Akihisa Inoue<sup>1</sup>; <sup>1</sup>WPI-AIMR, Advanced Institute for Materials Research, Tohoku University; <sup>2</sup>Department of Intelligent Materials Engineering, Faculty of Engineering; <sup>3</sup>Institut National Polytechnique de Grenoble; <sup>4</sup>Institute for Materials Research, Tohoku University

The present work demonstrates the deformation behaviour of Zr-Cu-Ni-Al bulk glassy alloys as well as Ni-Cu-Ti-Zr crystal-glassy composites. Fracture

Mon. PM

# Technical Program

of Zr<sub>60</sub>Cu<sub>16</sub>Ni<sub>14</sub>Al<sub>10</sub> bulk glassy alloy is featured by nearly equal fraction areas of cleavage-type and vein-type relief. The observed pattern of alternating cleavage-like and vein-type patterns illustrates a result of dynamically self-organizing shear propagation at the final catastrophic stage. One can suppose that the presence of a small volume fraction of eutectic colonies imposing a heterogeneity into a glassy Zr-Ni-Cu-Al matrix may help to block the plastic slip events. We also present a Ni-Cu-Ti-Zr crystal-glassy composite material having a superior strength paired with a considerable ductility of 15%. The metastable crystalline phase promotes a strain-induced martensitic transformation leading to enhanced plasticity at room temperature. Underlying mechanisms of plastic deformation are discussed in terms of the interplay between dislocation slip in the crystalline phase and shear deformation in the glassy matrix.

## 4:00 PM

**Effects of Hydrogen on Structural and Mechanical Behavior of Zr-Based Bulk-Metallic Glasses:** *Chih-Pin Chuang*<sup>1</sup>; Wojciech Dmowski<sup>1</sup>; Yun Liu<sup>2</sup>; Terry Udovic<sup>2</sup>; Yang Ren<sup>3</sup>; Peter Liaw<sup>1</sup>; Jaihung Huang<sup>4</sup>; <sup>1</sup>University of Tennessee; <sup>2</sup>NIST Center for Neutron Research; <sup>3</sup>Advanced Photon Source, Argonne National Lab.; <sup>4</sup>National TsingHua University

We report the hydrogen-induced phase transformation of Zr-based bulk metallic glasses (BMGs) and their effect on mechanical behavior. The hardness of hydrogen-charged alloys was increased, but was accompanied by the significant reduction in the toughness and strength. The changes of the local atomic structures of amorphous alloys were investigated by the radial-distribution-function (RDF) analysis using high-energy X-ray scattering. The results showed only the increase of the Zr-Zr inter-atomic distance, rather than the expansion of the whole amorphous matrix. Inelastic neutron scattering was used to determine the hydrogen-occupation site in amorphous alloys. The hydrogen optical frequency exhibits a very broad band (~70meV FWHM) at around 142 meV, and only shows the consistency of hydrogen atoms being occupied at the tetrahedral-like site. The observation from the X-ray scattering and inelastic neutron scattering suggests the existence of a stable, amorphous hydride phase, which could be responsible for the embrittlement of Zr-based BMGs.

## 4:10 PM Invited

**Flow and Fracture Studies on Bulk Metallic Glasses:** *John Lewandowski*<sup>1</sup>; <sup>1</sup>Case Western Reserve University

The effects of changes in pressure on the flow stress have been determined in both tension and compression with pressures up to 9 GPa. The dependence of the flow stress on the pressure will be compared to the pressure dependence of the elastic constants in order to rationalize the behavior observed. In addition, work continues on determining the effects of changes in elastic constants on both the compressive plasticity and toughness. Results will be presented for a number of different metallic glass systems.

## 4:30 PM

**Structural Defects in Metallic Glass Structures as Shear Transformation Zones:** *Dan Miracle*<sup>1</sup>; Garth Wilks<sup>2</sup>; Amanda Dahlman<sup>3</sup>; <sup>1</sup>Air Force Research Laboratory; <sup>2</sup>General Dynamics, Inc.; <sup>3</sup>SOCHÉ

Beyond simple estimates of the size and general nature of shear transformation zones (STZs) responsible for the initiation of deformation in metallic glasses, specific details regarding the atomic structural characteristics, frequency and distribution of STZs are presently unavailable. The purpose of this paper is to explore structural defects within the efficient cluster packing (ECP) model as possible STZs. Two specific point defect pairs will be developed in detail. The size of the candidate defect pairs will be determined, the energy associated with a defect pair will be used to estimate the frequency with which these defects may occur, and the free volume associated with these defect pairs will be calculated. The characteristics of these defect pairs will be compared with other theoretical and experimental studies regarding expectations for STZs in metallic glasses.

## 4:40 PM Invited

**Structure of Ca-Mg-Zn Bulk Metallic Glasses:** *Oleg Senkov*<sup>1</sup>; Daniel Miracle<sup>1</sup>; Emma Barney<sup>2</sup>; <sup>1</sup>Air Force Research Laboratory; <sup>2</sup>ISIS, Rutherford Appleton Laboratory

Amorphous structure of ternary Ca<sub>60</sub>Mg<sub>10-X</sub>Zn<sub>30-X</sub> metallic glasses (X = 0, 5, 10, and 15 at.%) was studied using neutron scattering and Reverse Monte Carlo (RMC) techniques. The scattered neutron intensities were measured in the scattering vector range Q from 0.1 to 100 Å<sup>-1</sup> and the total structure factors, S(Q), and the radial distribution function, G(r), were determined for each of the

tested specimens. The RMC method was used to model the amorphous structure of the metallic glasses, which has the best fit to the experimental S(Q) and G(r). The computed amorphous structures were then analyzed and the Mg and Zn – centered atomic clusters were identified as the main features of these structures. Atom pair distances and partial coordination numbers were determined as functions of the alloy compositions and the results were compared with recently proposed cluster packing models.

## 5:00 PM

**Shear Bands Evolution in Cold-Rolled Bulk Metallic Glasses:** Q.P. Cao<sup>1</sup>; J.W. Liu<sup>1</sup>; L.Y. Chen<sup>1</sup>; X.D. Wang<sup>1</sup>; *Jianzhong Jiang*<sup>1</sup>; <sup>1</sup>International Center for New-Structured Materials (ICNSM)

Two bulk metallic glasses have been rolled at room temperature with different thickness reduction. Shear band evolution has been monitored during cold-rolling process. The dependences of microstructure and tensile mechanical property on the strain and rolling directions have been investigated. It is revealed that deformation-induced transformation does not occur up to 92% in thickness reduction except for shear bands. Shear band formation in conjugated directions is achieved in the specimen rolled in two directions, while rolling in one direction induces shear band formation only in one single direction. The efficient intersection of shear bands in conjugated directions results in work-hardening behavior and obvious plastic strain in tensile tests, which is further confirmed by in-situ SEM observation. Based on the experimental results, it is deduced that normal-stress-modified maximum shear stress criterion rather than shear plane criterion can describe the conditions for the formation of shear bands in uniaxial tension.

## 5:10 PM Invited

**Sample Size Dependent Deformation in Amorphous Metals:** Dominik Tönnies<sup>1</sup>; *Cynthia Volkert*<sup>1</sup>; <sup>1</sup>University of Göttingen

Recent studies show that sample size can have a strong influence on the deformation behaviour of metallic glasses. Below a critical dimension on the order of several hundred nanometers, some metallic glasses change from deforming by shear band formation to deforming by apparent homogeneous flow. This transition will be discussed in detail for the case of nanoindentation and micro-compression testing of amorphous Pd<sub>80</sub>Si<sub>20</sub>. In this alloy, samples with diameters larger than 400 nm deform by shear band formation at stresses consistent with the behaviour of bulk specimens, whereas smaller samples undergo homogenous deformation and strain softening. The transition in deformation mode with sample size will be discussed in terms of the available energy for shear band formation and will consider results from measurements of shear band spacing, offset, and overlap in small volumes.

## 5:30 PM

**Understanding Microstructure-Induced Ductility in Porous Bulk Metallic Glasses via Molecular Dynamics Simulations:** *Yunfeng Shi*<sup>1</sup>; <sup>1</sup>Rensselaer Polytechnic Institute

Bulk metallic glasses (BMGs) have excellent strength, processibility and resistance to corrosion for load-bearing applications. However, most monolithic BMGs are intrinsically brittle in unconfined loading conditions. One promising method for achieving ductility is to introduce porous microstructures into the BMGs. The precise mechanistic details of the confinement effect of pores on shear band development are still poorly understood. Here we present a simulation study focusing on the early-stage plasticity of porous BMGs. We will investigate possible toughening mechanisms including proliferation of shear band initiation, blunting the sharp shear off-sets at the pore surfaces and restriction of the shear band propagation from pore confinement. The relevance of various mechanisms depends on the pore size, shape and spacing. This study will also shed lights on designing porous microstructure that optimize both the ductility and strength.

## 5:40 PM

**Viscous Flow and Superplastic Deformation Behavior of Pt-, Pd- and Au-Based Bulk Metallic Glasses:** Jinn Chu<sup>1</sup>; *Yen-Chen Chen*<sup>1</sup>; Jason Shian-Ching Jang<sup>2</sup>; Tsong-Ru Tsai<sup>3</sup>; Hidemi Kato<sup>4</sup>; <sup>1</sup>National Taiwan University of Science and Technology; <sup>2</sup>National Central University; <sup>3</sup>National Taiwan Ocean University; <sup>4</sup>Tohoku University

Viscous flow and superplastic deformation behaviors of bulk metallic glasses (BMGs) in the supercooled liquid region (SCLR) are interesting to study, because BMGs are readily flowed under an applied pressure. The relative displacement as a function of temperature is obtained with the thermomechanical analyzer



(TMA) for the  $Pt_{40}Ni_{20}P_{40}$  BMG rod with various compressive stresses at the heating rate of 10K/min. The viscosity under different stresses is thus computed from TMA results. The superplastic deformation behavior of Pd- and Au-based BMGs are examined in the SCLR at various strain rates in air. In addition, we demonstrate that various micro patterns of BMGs can be imprinted from mold in air. The forming component is characterized by scanning electron microscope and its optical property is further evaluated. The results show the BMGs exhibit excellent flowability and have potential micro/nano-device application.

### 5:50 PM

#### Indentation Size Effect of Bulk Metallic Glass: A New Observation: *Jae-il Jang*<sup>1</sup>; Byung-Gil Yoo<sup>1</sup>; Jun-Hak Oh<sup>1</sup>; Yong-Jae Kim<sup>1</sup>; <sup>1</sup>Hanyang University

Since the popular models for indentation size effect (ISE) are mainly based on dislocation strengthening, one might imagine that the models do not hold valid for bulk metallic glasses (BMGs) which do not contain crystalline defects. Despite the expectation of the size-independent hardness or strength in BMGs due to the absence of the dislocation, some experiential indentation studies reported the possible ISE. Additional controversy over the size effect of BMGs arose in recent studies performing microcompression tests: While some suggested 'smaller is softer,' 'smaller is stronger' is reported by others. Also, very recent micro-pillar test showed that the BMG strength is size-independent. To shed light on this dispute, we systematically analyzed the ISE of BMG through nanoindentations with various three-sided pyramidal indenters having different indenter angles. The purpose of this presentation is to report our recent experimental results, which led us to somewhat surprising observation on the issue.

#### Characterization of Minerals, Metals and Materials: Characterization of Iron and Steel II

*Sponsored by:* The Minerals, Metals and Materials Society, TMS Extraction and Processing Division, TMS Structural Materials Division, TMS/ASM: Composite Materials Committee, TMS: Materials Characterization Committee

*Program Organizers:* Ann Hagni, Geoscience Consultant; Sergio Monteiro, State University of the Northern Rio de Janeiro - UENF; Jiann-Yang Hwang, Michigan Technological University

Monday PM Room: 307  
February 15, 2010 Location: Washington State Convention Center

*Session Chairs:* Jian Li, CANMET-MTL; Jaroslav Drelich, Michigan Technological University

### 2:00 PM Introductory Comments

### 2:05 PM

#### Mechanisms of Composite Agglomeration of Fluoric Iron Concentrates: You-ming Hu<sup>1</sup>; *Qian Li*<sup>1</sup>; Guang-hui Li<sup>1</sup>; Yong-bin Yang<sup>1</sup>; Yuan-bo Zhang<sup>1</sup>; Tao Jiang<sup>1</sup>; <sup>1</sup>Central South University

It is well-known that fluoric iron ores are very difficult for sintering and pelletizing. The yield and quality of sinter are greatly improved when using the composite agglomeration process (CAP) assisted with heat airflow, enhancing MgO contents and so on. For traditional sinter of fluoric iron concentrate, there is lower viscosity of binding phase and higher fluidity of liquid phase, the sinter is formed with large thin-walled holes and strength of sinter is deteriorated consequently. The novel process forms composite agglomerate in which acid pellets are embedded in basic sinter. The pellets are solid phase bonding and there forms Fe<sub>2</sub>O<sub>3</sub> and Fe<sub>3</sub>O<sub>4</sub> interconnect crystal. For basic sinter, after adding MgO, the viscosity are increased and fluidity decreased, and there form complex calcium ferrites (SFCA) and magnesium ferrite, they are crystallized perfectly and the sinter microstructure is very well.

### 2:30 PM

#### On Plastic Notch Effects in Quenched and Tempered Steels: Pasquale Russo Spena<sup>1</sup>; *Donato Firrao*<sup>1</sup>; Paolo Matteis<sup>1</sup>; <sup>1</sup>Politecnico di Torino

In 1971, Firrao and Spretnak performed a large experimental campaign to assess the plastic stress concentration factor at fracture as a function of the elastic stress concentration factor and of the tempering temperature, by using 25.4 mm wide, 1.14 mm thick AISI 4340 steel sheet tensile specimens with variable tip radius central notches. The availability of finite element methods allows now

to re-examine those results and overcome the simplifying assumptions that were originally used to evaluate notch stresses. The elastic stress concentration factors are obtained by three-dimensional solutions, which also evidence the gradual evolution from plane-stress to plane-strain that occurs by decreasing the notch radius while keeping the thickness constant. Moreover, both the actual stress state and the stress concentration factor in the notch immediately before the failure are evaluated by elastic-plastic solutions. Finally, the original conclusions on the notch sensitivity of the examined steel are re-assessed and re-interpreted.

### 2:50 PM

#### Calculating Model Establishing and Application of Nitriding and Denitriding to 304 Stainless Steel in AOD: *Chunfei Shen*<sup>1</sup>; Qiao-lei Shi<sup>1</sup>; Yang Li<sup>2</sup>; Zhou-hua Jiang<sup>2</sup>; <sup>1</sup>Baoshan Iron and Steel Co., LTD; <sup>2</sup>Northeastern University

Nitriding and denitriding behavior of 304 stainless steel melts was researched in AOD refining process. Nitrogen solubility behavior of nitriding was mainly controlled by interphase reaction, and nitrogen solubility behavior of denitriding was controlled by both liquid phase transferring and interphase reaction. And the calculation models of nitriding and denitriding were established. Meanwhile, the comparisons of measured values and model calculation of nitrogen contents were also done. The results of AOD nitriding model showed that 85% of these comparisons had absolute error less than 100×10<sup>-4</sup> % after removal of outlying data points. The same level of absolute error was achieved by 80% of the comparisons in AOD denitriding model in reduction period and desulfurization period. After removal of outliers, 90% of the comparisons achieved the level after desulfurization period of AOD.

### 3:15 PM

#### Cyclic Deformation Behavior of a Medium Carbon Steel in the VHCF Range: *Dietmar Eifler*<sup>1</sup>; Michael Koster<sup>1</sup>; Guntram Wagner<sup>1</sup>; <sup>1</sup>University of Kaiserslautern

An ultrasonic testing system (UTS) for the fatigue assessment of steels in the very high cycle fatigue (VHCF) range was developed. The UTS allows to measure characteristic data to de-scribe the cyclic deformation behaviour of medium carbon steels at ultrasonic frequencies. Cyclic loading leads to a defined change of process parameters of the UTS like generator power, dissipated energy and specimen temperature, indicating that irreversible changes in the materials microstructure occur. The measured data, strongly depend on the microstructure of the material. Specimen failure can be predicted with the applied technique in an early state. The very sensitive measuring methods indicate irreversible microstructural changes by a significant rise of process parameters before final failure occurs. In SEM investigations subsurface fatigue cracks emanating from phase boundaries between ferrite and cementite were observed in the VHCF range. Koster Michael, Wagner Guntram, Eifler Dietmar

### 3:40 PM

#### Methods to Characterize Very Thin Passive Film Formed in SCW Corrosion Tests: *Jian Li*<sup>1</sup>; D. Guzonas<sup>2</sup>; Wenyue Zheng<sup>1</sup>; <sup>1</sup>CANMET-MTL; <sup>2</sup>Atomic Energy of Canada Limited

Developing the Generation IV nuclear reactor is an international collaborative effort. One of the most important Gen IV nuclear reactor designs is the supercritical water (SCW) concept, in which the water coolant runs at about 625oC at the outlet. Under this temperature and high pressure condition, the cooling water is at supercritical state, which could pose significant demand for in-core materials. High-temperature mechanical properties, corrosion resistance and radiation damage are some of the key challenges. At present, no single commercial material can meet all the requirements of the severe SCWR in-core conditions. Corrosion experiments performed under SCW condition yields various kinds of corrosion modes, some pose great challenge to characterize using conventional techniques. A combination of various advanced characterization techniques proved to be necessary to understand the root cause of materials failure.

### 4:05 PM

#### Mechanical Properties of Heat Treated HSLA Bolt Steels: *Hamed Fathi Doost*<sup>1</sup>; Ali Nazari<sup>1</sup>; <sup>1</sup>Islamic Azad University (Saveh Branch)

Tensile properties, Fracture toughness and Charpy impact energy of four types of HSLA steels which are used in 10/9 and 12/9 grade bolts has been studied. All of the four groups has been annealed at 850 degree of centigrade, water- and oil-cooled and then tempered at 500, 550 and 600 degree of centigrade. The

Mon. PM

# Technical Program

best heat treating cycle has been optimized and metallographic studies has been conducted to investigate the created structures. Scanning electron microscope fractography also used to verify fracture mode. Some empirical relations have been proposed for prediction fracture toughness of HSLA steels using tensile properties and Charpy impact energy data.

## 4:30 PM

**Effect of Stacking Fault Probability and  $\epsilon$  Martensite on Damping Capacity of Fe-16%Mn-2% Si Alloy:** *Girish Bm<sup>1</sup>; Satish Bm<sup>2</sup>; K. Mahesh<sup>2</sup>; <sup>1</sup>MVJ College of Engineering ; <sup>2</sup>East Point College of Engineering and Technology*

The Damping capacity of a Fe-16%Mn-1%Mg-2%Si (wt. %) alloy has been studied with respect to cold rolling and annealing after cold rolling. The damping capacity of 8% cold rolled specimen is much higher than 0% cold rolled specimen. In the 0% rolled specimen, the stacking faults are responsible for the damping capacity characterized by the large amplitude dependence. The improvement in damping capacity by cold rolling is attributed to the formation of  $\epsilon$  martensite. As the temperature increases, the damping capacity improves, reaching its maximum around 1000°C. A further increase in the temperature, however, degrades the damping capacity. The area of the  $\gamma/\epsilon$  boundaries is the major factor for damping capacity. Heat treatment at 1100°C lessens the number of  $\epsilon$  martensite plates, leading to area reduction of  $\gamma/\epsilon$  boundaries despite an increase in amount of  $\epsilon$  martensite.

## 4:55 PM

**Study of Pre-Strain Effect on Indentation Fracture Toughness of HSLA Steel Using Continuum Damage Mechanics:** *Sabita Ghosh<sup>1</sup>; Mita Tarafder<sup>1</sup>; Goutam Das<sup>1</sup>; Soumitra Tarafder<sup>1</sup>; <sup>1</sup>National Metallurgical Laboratory*

Since last three decades Ball Indentation Technique (BIT) has been used to evaluate mechanical properties like ultimate tensile test, yield strength, strain hardening exponent, strength coefficient and true stress-true strain curve of various engineering materials. BIT can be used when a tensile test cannot be performed: on welded joints or components under service. There has been an urge among the researchers to get an idea about the fracture toughness (KJC) value non-destructively. Various models have been developed to estimate KJC using indentation flow curve. The present work highlights the study about the effect of pre strain on indentation KJC of HSLA steel from the flow curve using continuum damage model. To establish the damage model for the evaluation of KJC under compression, attempt has been made to simulate the ball indentation experimentation to find stress triaxiality just beneath the indenter. ABAQUS software package has been used for finite element simulation.

## 5:20 PM

**The Influence of Different Heat Treatment Cycles on Controlled Surface Graphitization in CK45 Steel:** *Ali-Reza Kiani-Rashid<sup>1</sup>; Y Hamed<sup>2</sup>; H.R. Shishegar<sup>2</sup>; <sup>1</sup>Ferdowsi University of Mashhad; <sup>2</sup>Sharif University of Technology*

Controlled graphitization has become known as a practical method for improvement of wear resistance and machining properties in steels. In this paper, the effect of heat treatment on microstructure of Ck45 steel has been investigated. Austenitising was carried out at 920°C for 5 hours. Besides, isothermal transformation was conducted at 750°C in the time range of 1-20 hours. The microstructure of the steel considerably changes by this heat treatment process which exhibits the effects of temperature, appropriate austenitising duration and isothermal transformation. Conducted experiments show a suitable distribution of semi-spherical graphite particles especially on the surface of the steel. Also, analyses demonstrate that the amount of formed graphite in the austenitising temperature 920°C is more than graphite in single heat treatment temperature of 750°C.

## 5:45 PM Concluding Comments

## 5:50 PM Question and Answer Period

## Coatings for Structural, Biological, and Electronic Applications: Applications of Coatings I

*Sponsored by:* The Minerals, Metals and Materials Society, TMS Electronic, Magnetic, and Photonic Materials Division, TMS Structural Materials Division, TMS: Biomaterials Committee, TMS: Thin Films and Interfaces Committee

*Program Organizers:* Nuggehalli Ravindra, New Jersey Institute of Technology; Gregory Krumdick, Argonne National Laboratory; Roger Narayan, Univ of North Carolina & North Carolina State Univ; Choong-un Kim, University of Texas at Arlington; Nancy Michael, University of Texas at Arlington

Monday PM Room: 309  
February 15, 2010 Location: Washington State Convention Center

*Session Chair:* Nancy Michael, University of Texas

## 2:00 PM Introductory Comments

### 2:10 PM Invited

**A Load-based Depth-sensing Micro-Indentation Technique for Spallation Detection of Thermal Barrier Coatings:** *Bruce Kang<sup>1</sup>; Jared Tannenbaum<sup>1</sup>; Mary Anne Alvin<sup>2</sup>; <sup>1</sup>West Virginia University; <sup>2</sup>National Energy Technology Lab*

In this research, we present a micro-indentation technique for NDE spallation detection of thermal barrier coating (TBC) materials. Based on a multiple-partial unloading procedure during indentation, stiffness responses of TBC coupons subjected to thermal cyclic loadings were found to correlate well with morphology changes and increase of residual out-of-plane stress at the bond coat/TGO/top coat interfacial region. A TBC thermal exposure test plan was carried out where time-series cross-sectional microstructural analyses of damage accumulation and spallation failure associated with the evolution of the bond coat/TGO/top coat composite were evaluated and correlated with the measured stiffness responses at various thermal cycles. The results show that prior to the large-scale TBC spallation, the micro-indentation method is capable of identifying TBC spallation site(s). This technique can be viewed as a viable NDE technique for as-manufactured and process-exposed TBCs. A portable instrument for on-line spallation detection/prediction of industrial-size TBC turbine components is also developed.

### 2:40 PM

**Temperature and Scale Dependent Deformation and Creep Behavior of Polymer Derived Si-C-O Ceramics:** *Ming Gan<sup>1</sup>; Vikas Tomar<sup>1</sup>; <sup>1</sup>Purdue University*

Due to their high thermal resistance and outstanding mechanical strength under elevated temperatures, Si-C-O polymer derived ceramics (PDCs) have a wide application in thermal barrier coatings. Effect of temperature and length scale on the elastic modulus and creep strength a Si-C-O based PDC was investigated by nano and micro-scale tests from room temperature up to 750°C. The results showed that elastic modulus of the material first decreases as a function of temperature up to 100°C and then increases with further increase in temperature at both nano- and micro length scales. The modulus showed reduction by one tenth while switching from the nanoscale to the microscale. During nanoscale and microscale creep experiments, effects of peak load, loading rate, and holding time on the creep behavior were investigated. A strong size effect was observed at initiation stage of creep, which leads to higher stress exponents under all testing conditions.

### 3:05 PM Break

### 3:20 PM Invited

**Surface Modification of Nanostructured Materials for Functional Medical Devices:** *Roger Narayan<sup>1</sup>; Nancy Monteiro-Riviere<sup>2</sup>; Robin Brigmon<sup>3</sup>; Michael Pellin<sup>4</sup>; Jeffrey Elam<sup>4</sup>; <sup>1</sup>University of North Carolina & North Carolina State University; <sup>2</sup>North Carolina State University; <sup>3</sup>Savannah River National Laboratory; <sup>4</sup>Argonne National Laboratory*

Nanoscale materials may play a leading role in treatment of chronic disease (e.g., controlled release of chemotherapeutic agents for treatment of cancer). Nanoporous alumina provides several advantages over conventional polymeric materials for use in functional medical applications. In this study, atomic layer



deposition was used to coat all the surfaces of nanoporous alumina membranes in order to improve the biocompatibility and reduce the pore size in a controlled manner. In vitro studies revealed that titanium oxide-coated nanoporous alumina membranes did not exhibit statistically lower viability compared to the uncoated control materials. 20 nm pore size titanium oxide-coated nanoporous alumina membranes exposed to ultraviolet light exhibited activity against *Escherichia coli* and *Staphylococcus aureus* bacteria. Nanostructured materials prepared using atomic layer deposition may be used to delivering a pharmacologic agent at a precise rate within the body. These materials may also serve as the basis for orthopedic implants or self-sterilizing medical devices.

### 3:50 PM

**Preparation of the Biomimetic Calcium Phosphate Coating on CoCrMo Implant Alloys via an Effective Chemical Activation:** *Luning Wang*<sup>1</sup>; Jingli Luo<sup>1</sup>; <sup>1</sup>University of Alberta

An ion adsorption based chemical method was applied to generate calcium phosphate coatings on CoCrMo implants. The surface was fully covered by calcium phosphate nucleation crystallites after immersion in supersaturated calcium solution (SCS) for 1 h at room temperature, rinsing by water and completely dry in air. The treated specimen was readily for growing calcium phosphate coatings once it immersed in SCS at 37°C. A homogenous calcium phosphate coating formed on the surface after 2 hrs immersion. It shows that the coating mainly contains octacalcium phosphate phase with minor hydroxyapatite. The coating layer is about 4 μm thickness and with high bonding strength (26.2 ± 1.2 MPa). The in vitro electrochemical characterization also indicates that the coated specimen shows higher corrosion resistance and more noble corrosion potential than the uncoated CoCrMo implants. This method shows an efficient way to prepare a bioactive CoCrMo surface for medical application.

### 4:15 PM Invited

**Molecular-Scale Surface and Interfacial Coatings Utilizing Self-Assembled Monolayer of Phosphonates (SAMP) Technology:** *Eric Bruner*<sup>1</sup>; <sup>1</sup>Aculon, Inc.

Nanoscale thick Self-Assembled Monolayer of Phosphonates (SAMP) coatings can be classified into three functional areas; non-stick, pro-stick/adhesion, and anti-corrosion. Coating solutions and processes were engineered for numerous markets including optical, display, electronics, and industrial coatings. These coatings outperform all known alternatives in characteristics such as adhesion, stain resistance, and scratch resistance. SAMP treatments can be used for a variety of applications including imparting hydrophobicity, adhesion, or corrosion inhibition to numerous substrates. Aculon's proprietary methodology can impart any of these properties on metals, metal oxides and even some polymer surfaces by drawing on its library of structurally tailored phosphonic acids. The SAMP is one approximately 1.5 nm thick, and it completely covers the material to which it is applied, and assures total surface coverage regardless of the type or texture of that material. The composition of the SAMP determines the properties that it imparts to its substrate.

### 4:45 PM

**Piezoelectric Measurements and Microstructural Characterization of 'Smart' AlN Thin Films Fabricated by Pulsed Closed Field Unbalanced Magnetron Sputtering:** *Masood Hasheminasari*<sup>1</sup>; J. Lin<sup>1</sup>; J.J. Moore<sup>1</sup>; B. Mishra<sup>1</sup>; <sup>1</sup>Colorado School of Mines

A 'Smart' die coating based on AlN piezoelectric thin film sensor embedded into a tribological coating system is been investigated in this research. Thin film sensor design and its overall incorporation within the coating system are explained briefly. Piezoelectric AlN thin film with highly preferred (002) orientation has been deposited by pulsed closed field unbalanced magnetron sputtering (P-CFUBMS) system using Cr as the electrode/adhesion layer. The effect of working pressure on residual stress and (002) orientation of AlN thin film is discussed together with gas ratio effect on the piezoelectric measurements. The piezo-responses of AlN thin films were characterized by a lock-in-amplifier, which measures the output piezo-voltage of AlN thin film under cyclic loading conditions using a micro-actuator.

### 5:10 PM

**Plasma Spray Coatings for Aerospace Applications:** *David Koch*<sup>1</sup>; D.M. Fell<sup>1</sup>; David Field<sup>1</sup>; <sup>1</sup>Washington State University

While plasma-spray coatings have been vital process for application of high technology, high performance coatings in aerospace engines, etc., application has been limited to most metals, and a few ceramics. Research to apply

various oxides, borides, carbides, nitrides, and couple silicides powders as high temperature coatings appear to have positive results after the plasma system was modified with a reactive-atmospheric-processing (RAP) apparatus and techniques. Zirconium Carbide (highest known melting point material at 6400°F {3540°C}), Titanium Carbide, and Titanium Boride coatings were applied with Plasma-RAP variations, with each coating chemistry XRD confirmed and discussed. Further characterization to discuss includes SEM, EDX, porosity content, coating thickness; plus microhardness and abrasion/wear testing.

### 5:35 PM

**Using Artificial Neural Network to Optimize Thickness and Hardness of TiN Layers Deposited by PACVD Method:** *Mohammad Sadegh Mahdipoor*<sup>1</sup>; Farzad Mahboubi<sup>1</sup>; *Niloofer Kamkar Zahmatkesh*<sup>1</sup>; Mahdi Raoufi<sup>1</sup>; <sup>1</sup>Amir Kabir University

Recently, TiN coating deposited by different methods especially plasma-assisted chemical vapor deposition (PACVD) is used to protect tools from wear. The parameters of used methods for deposition of layers can be so effective on their final characteristics. The aim of this study was to investigate the effective parameters of PACVD method on the final thickness and hardness of TiN coatings and predicting these values in different situations using Artificial Neural Network (ANN). The deposition temperature, deposition time and duty cycle were investigated. The experimental data was used for training of ANN and a multilayer cascade forward back-propagation neural network was designed. The optimization was performed by minimizing the generalized interval between the predicted values and the optimized ones that were obtained experimentally. The predicted values obtained from the trained ANN are found to be in close agreement with the experimental results.

## Computational Thermodynamics and Kinetics: Grain Growth

*Sponsored by:* The Minerals, Metals and Materials Society, TMS Electronic, Magnetic, and Photonic Materials Division, TMS Materials Processing and Manufacturing Division, TMS Structural Materials Division, TMS: Chemistry and Physics of Materials Committee, TMS/ASM: Computational Materials Science and Engineering Committee  
*Program Organizers:* Jeffrey Hoyt, McMaster University; Dallas Trinkle, University of Illinois at Urbana-Champaign

Monday PM Room: 308  
February 15, 2010 Location: Washington State Convention Center

*Session Chair:* To Be Announced

### 2:00 PM Invited

**Abnormal Grain Growth in the Presence of a Static Particle Dispersion:** *Elizabeth Holm*<sup>1</sup>; Todd Hoffmann<sup>1</sup>; Anthony Rollett<sup>2</sup>; Christopher Roberts<sup>2</sup>; <sup>1</sup>Sandia National Laboratories; <sup>2</sup>Carnegie Mellon University

Dispersions of second phase particles are often used to inhibit grain growth in polycrystalline metals, so it stands to reason that they might also prevent abnormal grain growth. We used mesoscale grain growth simulations to test this hypothesis for two cases: an initially unpinned polycrystal, and an initially pinned polycrystal. When we added inert, static second phase particles to an initially unpinned structure, abnormal grain growth occurred as if in the absence of particles; only when the abnormal grains impinged and began to grow normally did particle pinning occur. When we induced pinning by placing inert, static second phase particles along grain boundaries, abnormal grain growth occurred even in systems that did not grow abnormally in the absence of particles. We explain this particle-assisted abnormal grain growth in terms of boundary fluctuations and mobility advantage. These results have important implications for designing microstructures that are resistant to abnormal growth.

### 2:30 PM Invited

**Effect of Stresses on Grain Boundary Thermodynamics: Theory and Atomistic Simulations:** T. Frolov<sup>1</sup>; Y. Mishin<sup>1</sup>; <sup>1</sup>George Mason University

Thermodynamic properties of grain boundaries (GBs) are usually described in terms of the Gibbs absorption equation which was originally derived for fluid-fluid and solid-fluid interfaces. By contrast to such systems, GBs can support elastic shear stresses applied parallel to the GB plane. We derive a generalized

Mon. PM

# Technical Program

adsorption equation that includes additional terms representing the effect of the applied shear stresses and the excess strains conjugate to them. These new terms permit computation of the tensor of excess elastic compliances of GBs and can give rise to stress-strain, stress-segregation and other types of cross-effects. The new thermodynamic relations are applied to atomistic simulation of GBs in Cu and Cu-Ag alloys under applied tensile, compressive and shear stresses. We study the effect of such stresses on GB free energy, interface stress, solute segregation and other thermodynamic properties.

## 3:00 PM

**Controlling Crystal Structure in Phase Field Crystal Modeling:** *Michael Greenwood*<sup>1</sup>; *Nikolas Provatas*<sup>2</sup>; *Joerg Rottler*<sup>1</sup>; <sup>1</sup>University of British Columbia; <sup>2</sup>McMaster University

The phase field crystal (PFC) method has emerged as a promising candidate for modeling materials with atomistic resolution on mesoscopic time scales. With the currently available (phenomenological) free energy functionals, however, only lattices with triangular (2D) or bcc (3D) symmetries can be studied. We extend the free energy functionals through classical density functional theory to generate a broader class of crystalline structures in both 2D and 3D. Specifically, the correlation functions in these energies are constructed using from the desired lattice and basis structure and the probability densities of the atomic positions within these lattices. We apply this method to crystallization from the liquid state and structural solid-solid transformations.

## 3:20 PM Break

## 3:30 PM Invited

**Molecular Dynamics Simulation of Grain Growth in 3D Nanograined Ni:** *Stephen Foiles*<sup>1</sup>; *Elizabeth Holm*<sup>1</sup>; <sup>1</sup>Sandia National Laboratories

Grain growth is one of the fundamental phenomena in materials processing. There is current interest in potential differences in grain growth in nanograined materials compared to conventional materials. Molecular dynamics simulations of the grain growth in a fully 3D nanocrystalline sample have been performed at a variety of temperatures and system sizes. It is observed that a high density of twin boundaries is formed during the growth process consistent with recent experimental findings. The grain growth kinetics are observed to obey the conventional parabolic time dependence until a temperature dependent stagnation is observed. The origin of this stagnation is discussed. Sandia is a multi-program laboratory operated by Sandia Corporation, a Lockheed Martin Company, for the United States Department of Energy's National Nuclear Security Administration under contract DE-AC0494AL85000.

## 4:00 PM Invited

**Evolving Microstructures in Lipid Bilayers: Novel Insights from Materials Science:** *Mikko Haataja*<sup>1</sup>; <sup>1</sup>Princeton University

Lipid bilayer membranes are semi-permeable, two-dimensional fluid-like sheets which control the exchange of matter and information between living cells and their surroundings. Far from being a featureless mixture of lipids and proteins, compositional lipid microdomains within these membranes are believed to facilitate many important cellular processes. The physical mechanisms which control the sizes and lifetimes of these spatially-extended domains ("membrane microstructure") are rather poorly understood at the moment. In this talk I will argue that a combination of thermodynamics of immiscible systems (driving phase separation) and incorporation of active cellular lipid transport mechanisms to and from the membrane impeding phase separation (analogous to irradiation effects in immiscible binary alloys) provides a compelling physical picture of the spatio-temporal microstructure of the membrane. In more general terms, I will argue that tools from materials science can provide important and novel insight into complex "microstructural evolution" phenomena in biophysics.

## 4:30 PM

**Twinning Nucleation Mechanisms in Hexagonal-Close-Packed Crystals:** *Jian Wang*<sup>1</sup>; *John Hirth*<sup>1</sup>; *Carlos Tome*<sup>1</sup>; <sup>1</sup>LANL

We have studied mechanisms for (-1012) twinning in hexagonal-close-packed crystals at an atomic scale using topological analysis and atomistic simulations. Two twinning mechanisms were found: a normal-twinning mechanism in which a stable twin nucleus is created by simultaneous nucleation of multiple twinning dislocations, and a zonal-twinning mechanism in which a stable twin nucleus is created by simultaneous nucleation of a partial dislocation and multiple twinning dislocations. Atomistic simulations, using density-function-theory for Mg, Zr and Zn and an empirical potential for Mg, were performed to study

the kinetics and energetics associated with the two twinning mechanisms. The results show that the zonal-twinning mechanism is energetically favorable relative to the normal-twinning mechanism because the zonal dislocation has a smaller Burgers vector.

## 4:50 PM

**Phase Field Modelling of Austenite Grain Growth in the Heat Affected Zone:** *Morteza Toloui*<sup>1</sup>; *Matthias Militzer*<sup>1</sup>; <sup>1</sup>UBC

Austenite grain growth in the heat affected zone (HAZ) of girth welds in a microalloyed linepipe steel is simulated using phase field modelling. The steep temperature gradient in the HAZ leads to thermal pinning that can adequately be replicated with the phase field approach. An effective grain boundary mobility has been determined from experimental grain growth studies during rapid continuous heating tests thereby accounting for pinning of TiN and NbCN as well as solute drag when Nb particles dissolve. Using the effective mobility austenite grain growth has been predicted in the HAZ employing typical time-temperature profiles and the resulting thermal gradients as a function of the position from the fusion line. Predicted grain structures have been compared with the grain structures observed in the HAZ.

## 5:10 PM

**Affinities for Grain Contacts in 3D Grain Growth:** *Burton Patterson*<sup>1</sup>; *Alan Sprague*<sup>1</sup>; *Veena Tikare*<sup>2</sup>; *Cristina Cardona*<sup>3</sup>; *Daniel Chappell*<sup>1</sup>; *Robert T. DeHoff*<sup>4</sup>; <sup>1</sup>University of Alabama at Birmingham; <sup>2</sup>Sandia National Laboratories, New Mexico; <sup>3</sup>San Diego State University; <sup>4</sup>University of Florida

The tendencies for preferred contact among grains of different numbers of faces is quantified using an affinity term describing the actual frequency of occurrence of grain pairs relative to the frequency expected from random contact. Thus, the affinity term describes these tendencies as multiplicative factors of occurrence greater or less than the random state. Data from 3D Monte Carlo simulations shows preferred contact between grains with high and low numbers of faces, with affinities as high as 8 times random. Mid-class grains of approximately 14 faces show merely random contact, i.e., no preference or avoidance, with grains of higher and lower numbers of faces. Affinities also have been determined for different topological characteristics on separated grains. These affinity characteristics provide insight into the topological mechanism of grain growth.

## 5:30 PM

**Atomistic Comparison of Volume-Dependent Melt Properties from Four Models of Aluminum:** *Chandler Becker*<sup>1</sup>; *Matthew Kramer*<sup>2</sup>; <sup>1</sup>Materials Science and Engineering Laboratory, National Institute of Standards and Technology; <sup>2</sup>Materials and Engineering Physics, Ames Laboratory

With the increasing use of simulations in materials research and design, it is important to quantify differences between, and accuracy of, models used in these simulations. Here we present the results of such a comparison for four embedded-atom models of aluminum that were optimized to have good liquid properties, particularly the melting temperatures. The effects of temperature and volume are systematically examined in the melts for bulk thermodynamic quantities, pair correlation functions and structure factors, and diffusion coefficients for each interatomic potential. Where possible, these are then compared with experimental values. We find quantitative differences in the properties determined from the various interatomic potentials despite the fact that they were fit with similar sets of data.



### Cost-Affordable Titanium III: Low Cost Materials and Processing

Sponsored by: The Minerals, Metals and Materials Society, TMS Structural Materials Division, TMS: Titanium Committee

Program Organizers: M. Ashraf Imam, Naval Research Lab; F. H. (Sam) Froes, University of Idaho; Kevin Dring, Norsk Titanium

Monday PM Room: 618  
February 15, 2010 Location: Washington State Convention Center

Session Chairs: F. H.(Sam) Froes, University of Idaho; M. Ashraf Imam, Naval Research Laboratory

#### 2:00 PM

**Applications of the FFC Cambridge Process:** *Richard Dashwood*<sup>1</sup>; Rohit Bhagat<sup>1</sup>; Ben Jackson<sup>2</sup>; Randhir Singh<sup>2</sup>; Peter Lee<sup>2</sup>; Douglas Inman<sup>2</sup>; David Dye<sup>2</sup>; Martin Jackson<sup>3</sup>; <sup>1</sup>The University of Warwick; <sup>2</sup>Imperial College London; <sup>3</sup>The University of Sheffield

The FFC Cambridge is a potential alternative to the Kroll process and, when a mixed oxide precursor is used, is a low-cost method for producing alloy powder. This paper will demonstrate the relative ease with which novel and challenging alloy compositions such as Ti-Mo, Ti-W, and Ni-Ti, or complex geometries, such as titanium foams, can be produced. Highly alloyed compositions (i.e. 50 wt.%Mo) can be produced with homogenous chemistry, refined microstructure and low oxygen content (as low as 600 ppm in equiatomic Ni-Ti). Another benefit of the process derives from the nature of the oxygen removal in that the geometry of the cathode precursor is unaltered through to the metal product, albeit with some shrinkage. By combining a novel precursor manufacturing route with the FFC Cambridge process, open cell titanium foams have been produced. The foams possess good mechanical properties and high permeability, making them especially attractive for biomedical applications.

#### 2:25 PM

**Very Low Cost Manufacturing of Titanium Alloy Components:** James Withers<sup>1</sup>; R. Storm<sup>1</sup>; V. Shapovalov<sup>1</sup>; D. Myers<sup>1</sup>; R. Loutfy<sup>1</sup>; <sup>1</sup>MER Corporation

MER has developed a new process for the manufacture of near net shape components of titanium alloys at a cost significantly lower than conventional manufacturing. Based on the MER plasma transferred arc (PTA) rapid additive manufacturing process, the low cost route is a single melt process that utilizes very low cost raw materials, and has been demonstrated with Ti-6Al-4V. The melt processing of the PTA manufacturing results in fully dense structures without the need for post HIPping. The cost of near net shape manufactured components of Ti-6Al-4V is projected to be <\$16/lb, compared to >\$125 for ram graphite castings or >\$50/lb for flat sheet. The mechanical properties obtained for the low cost material will be reviewed, and examples of shapes produced will be shown. The low cost route is expected to find major usage in both commercial and defense applications where light weight, high strength, and corrosion resistance are important.

#### 2:50 PM

**Development of High Strength Titanium Alloy Bar Stock from TiH<sub>2</sub> Powder:** *Curt Lavender*<sup>1</sup>; Elizabeth Stephens<sup>1</sup>; Eric Nyberg<sup>1</sup>; Vladimir Moxson<sup>2</sup>; Volodymyr Duz<sup>2</sup>; <sup>1</sup>Battelle - Pacific Northwest National Laboratory; <sup>2</sup>ADMA Products Inc.

A new low-cost method to produce TiH<sub>2</sub> for use in blended elemental powder metallurgy has been under development and has been synthesized into many alloys. This paper reports on the results of use of the TiH<sub>2</sub> powder for the production of the Ti6Al4V and the difficult to cast Ti1Al8V5Fe alloys via cold iso-static pressing, sintering and rod rolling. Static and dynamic mechanical properties of the as rolled and heat treated materials were characterized by room temperature tensile, compression and fatigue tests. Elastic constants were determined by ultrasonic techniques. This paper will summarize the characterization of the material and discuss the suitability for use in automotive suspension applications.

#### 3:15 PM

**Titanium Reduction through Carbothermic Reduction and Molten Salt Electrolysis:** Xiaohui Ning<sup>1</sup>; Chengjun Gao<sup>1</sup>; Shuqiang Jiao<sup>1</sup>; *Hongmin Zhu*<sup>1</sup>; <sup>1</sup>University of Science and Technology Beijing

Titanium dioxide can be reduced by carbon to form oxycarbide TiCxOy. In a certain range of components, titanium oxycarbide is an electronic conductor, and is able to be dissolved into molten salts through anodic electrolysis. During the anodic electrolysis of the titanium oxycarbide, titanium dissolves as an ion of titanium, while carbon and oxygen leave the anode as carbon oxide. By controlling the conditions of carbothermic reduction, and molten salt electrolysis, pure titanium can be obtained on the cathode.

#### 3:40 PM Break

#### 3:55 PM

**High Temperature Electrolysis of Ti and Its Alloys with a DC-ESR Unit:** *Toshihide Takenaka*<sup>1</sup>; Hidetaka Matsuo<sup>1</sup>; Mitsuru Sugawara<sup>1</sup>; Akihiro Matsuyama<sup>1</sup>; Masahiro Kawakami<sup>1</sup>; <sup>1</sup>Toyohashi University of Technology

Direct electro-winning of Ti metal above its melting point should bring the simplification of its production process. From this viewpoint, high temperature electrolysis of Ti and its alloys has been investigated by using a direct current electro-slag remelting (DC-ESR) unit. Liquid Ti, Ti-Al and Ti-Fe were obtained by this method in a CaF<sub>2</sub>-CaO-TiO<sub>2</sub>, CaF<sub>2</sub>-CaO-TiO<sub>2</sub>-Al<sub>2</sub>O<sub>3</sub> and CaF<sub>2</sub>-CaO-TiO<sub>2</sub>-FeO bath, respectively. It was shown that Ti deposition was strongly affected by the state of the Ti ion in the bath and by the heat generation during the electrolysis. Strong influence of the bath composition on the Ti content in the Ti-Al was not seen, whereas Ti-Fe alloy was deposited only in the CaF<sub>2</sub>-CaO-TiO<sub>2</sub>-FeO bath of a limiting composition.

#### 4:20 PM

**Development of Novel Alloying Techniques for Cost-Affordable Titanium:** *Peter Collins*<sup>1</sup>; Santhosh Koduri<sup>2</sup>; John Sosa<sup>2</sup>; Hamish Fraser<sup>2</sup>; Jim Sears<sup>1</sup>; <sup>1</sup>Quad Cities Manufacturing Lab; <sup>2</sup>The Ohio State University

As the means of producing cost-affordable titanium powder mature, there exists simultaneously the need to advance fundamental understandings regarding microstructure-property relationships in Ti-powder and opportunities to develop novel techniques for alloy development. Thus, an overview of the need will be given with an emphasis of the emerging models which incorporate composition and microstructure into property predictions. Regarding the latter, two techniques for alloy development will be described. The first makes use of LENS<sup>TM</sup>, an additive manufacturing technique where it is possible to deposit composition gradients among Ti alloys using either pre-alloyed or element blends of powder, and thereby tailor the properties and microstructures to achieve local design minimums. The second exploits Kinetic Metallization to produce alloys from elemental blends. An overview of these techniques and current research will be given, specifically as related to the Quad Cities Manufacturing Lab – a fully integrated titanium powder processing facility.

#### 4:45 PM

**Thermal Plasma Synthesis of Titanium Diboride:** *Muralidharan Ramachandran*<sup>1</sup>; Sutham Niyomwas<sup>2</sup>; Ramana Reddy<sup>1</sup>; <sup>1</sup>The University of Alabama; <sup>2</sup>Prince of Songkla University

A novel processing technique using thermal plasma was used to investigate the production of fine TiB<sub>2</sub> particles. The thermodynamic feasibility of the powder production process and the equilibrium composition were calculated using thermodynamic software. The yield of TiB<sub>2</sub> as a function of molar ratio of CH<sub>4</sub> was calculated using a constant molar ratio of TiO<sub>2</sub>:B<sub>2</sub>O<sub>3</sub> = 1:1. Results showed that the maximum yield was obtained at a molar ratio of TiO<sub>2</sub>:B<sub>2</sub>O<sub>3</sub>:CH<sub>4</sub> = 1:1:6. Experiments were conducted using the thermal plasma reactor with varying molar ratios of CH<sub>4</sub>. At the molar ratio of TiO<sub>2</sub>:B<sub>2</sub>O<sub>3</sub>:CH<sub>4</sub> = 1:1:5, highest yield of TiB<sub>2</sub> was obtained. Effect of process parameters such as the feed rate and the plasma input power for the production of TiB<sub>2</sub> powders were investigated.

#### 5:10 PM

**Electrochemical Production of Titanium from Oxycarbide Anodes:** *Ole Kjos*<sup>1</sup>; Geir Haarberg<sup>1</sup>; Ana Martinez<sup>2</sup>; <sup>1</sup>Norwegian University of Science and Technology; <sup>2</sup>SINTEF Materials and Chemistry

The use of titanium metal is increasing worldwide, but the high cost of metal production is limiting its use. This high cost is mainly due to the complicated and inefficient existing production method, the Kroll process. A new production

Mon. PM

# Technical Program

route is therefore desired, and an electrochemical approach would seem like a sensible way to go. Due to the properties of titanium, no existing electrochemical process is suitable. This work has focused on investigating the use of titanium oxycarbide anodes as a source of titanium ions in an electrolytic production process from a molten salt. The anodes were manufactured from a purified TiO<sub>2</sub>-rich slag, which was heated with carbon to form a TiC-TiO solid solution. These anodes were then used in electrolysis experiments in different molten chloride and fluoride electrolytes. The anode reacts to CO-gas and form Ti<sup>3+</sup> ions in the melt.

## Electrode Technology for Aluminum Production: Cathodes - Materials and Operation

*Sponsored by:* The Minerals, Metals and Materials Society, TMS Light Metals Division, TMS: Aluminum Committee

*Program Organizers:* Ketil Rye, Alcoa Mosjøen; Morten Sorlie, Alcoa Norway; Barry Sadler, Net Carbon Consulting Pty Ltd

Monday PM                      Room: 616  
February 15, 2010              Location: Washington State Convention Center

*Session Chair:* Manfred Banek, SGL Carbon GmbH

### 2:00 PM Introductory Comments

#### 2:05 PM

**Carburation Phenomenons at the Cathode Block/Metal Interface:** Martin Lebeuf<sup>1</sup>; Marc-André Coulombe<sup>1</sup>; Patrice Chartrand<sup>2</sup>; Benedicte Allard<sup>3</sup>; Gervais Soucy<sup>1</sup>; <sup>1</sup>Université de Sherbrooke; <sup>2</sup>École Polytechnique de Montréal; <sup>3</sup>Carbone Savoie

The industrial cathode blocks wear more rapidly with increasing current density and bath acidity, the current trend in the aluminium industry. The importance to understand, measure and control the degradation mechanisms is obvious when considering the cost of replacing such potlines. One of the accepted wearing mechanisms is the aluminium carbide formation and dissolution process. Six experiments were performed to study this mechanism and the effect of current density, time and electrolyte exposition of the surface on the amount of aluminium carbide produced. The aluminum carbide formation has been studied using XPS, SEM-EDS, as well as XRD. The bath chemistry, before and after electrolysis, was characterized by XRD and XRF. Increasing current density, time, and surface unexposed to the electrolyte enhance the accumulation of aluminium carbide in the few first millimeters in the cathode block. The relation between the aluminium carbide formation and the final bath chemistry will be discussed.

#### 2:25 PM

**Erosion Measurements of High Density Cathode Block Samples through Laboratory Electrolysis with Rotation:** Yoshinori Sato<sup>1</sup>; Pascal Lavoie<sup>2</sup>; Prethesh Patel<sup>3</sup>; <sup>1</sup>SEC CARBON LTD.; <sup>2</sup>Light Metals Research Center, University of Auckland; <sup>3</sup>The Light Metals Research Centre, University of Auckland

The increasing trend in line current over recent years has seen the erosion rate of graphitized cathode blocks also increasing, which has led to the problem of decreasing trends in the pot life. This has led some smelters to adopt cathode blocks with high density, especially pitch impregnated cathode blocks as an anti-erosion measure. SEC CARBON and the Light Metals Research Center tried to evaluate the erosion of high density cathode block samples with by using an apparatus which was designed with a rotating cathode to promote physical erosion and electrochemical erosion at the same time. Results have shown that pitch impregnated materials were found to have no benefit in regards to erosion resistance. This paper will primarily discuss the impact of formulation, pitch impregnation and processing techniques on the electrochemical erosion resistance of graphitized materials.

#### 2:45 PM

**Thermo-Mechanical Characterisation of Graphitic and Graphitized Carbon Cathode Materials Used in Aluminium Electrolysis Cells:** Donald Picard<sup>1</sup>; Wadii Bouzemmî<sup>1</sup>; Bénédicte Allard<sup>2</sup>; Houshang Alamdari<sup>1</sup>; Mario Fafard<sup>1</sup>; <sup>1</sup>Aluminium Research Centre - REGAL; <sup>2</sup>Carbone-Savoie

In the conventional Hall-Héroult electrolysis process, both the carbon anode and cathode operate at up to 980°C under a very corrosive environment. Since

the lifetime expectancy is an important economic point to take into consideration it is imperative that all process related phenomena present in the cells be well understood, e.g. the thermo-mechanical behaviour of carbon cathode materials used into the cell linings. To do so, an experimental program based on uniaxial compressive tests, for a temperature range from 25°C to 1000°C, has been conducted on graphitic and graphitized cathodes. The Young's modulus, compressive strength and damaging coefficients at various temperatures are examples of measured properties. The properties of both cathode block types were compared and analysed. Mainly, the damaging at high temperature can be neglected in the graphitic cathode block but not in the graphitized one. The Young's modulus evolution with temperature also differs from the two materials.

#### 3:05 PM

**Electrical Resistance of Graphitic and Graphitized Cathode Materials at Elevated Temperatures:** Jilai Xue<sup>1</sup>; Jun Zhu<sup>1</sup>; Yunxia Song<sup>1</sup>; <sup>1</sup>University of Science and Technology Beijing

Electrical resistance is of great importance for cathode performance and energy consumption in aluminum reduction cells. The values of the electrical resistance for the cathodes are material and temperature dependent. The electrical resistance of graphitic and graphitized cathode materials before and after electrolysis was also measured at temperatures from 30°C to 965°C. An increase in electrical resistance was found with all samples after the electrolysis under identical conditions, and the graphitized one had the lowest resistance value among the testing samples. SEM inspection showed more salt penetration and micro-cracking in the semi-graphitized cathode than in the graphitized one, which may be the causes for the change in electrical resistance after electrolysis. Higher graphitization and lower porosity can reduce the electrical resistance of the cathodes. The electrical resistance of TiB<sub>2</sub>-carbon composite material exhibited a higher value than those of graphitic and graphitized cathodes at elevated temperatures.

#### 3:25 PM

**Development of High Density Graphitized Cathode Blocks for Aluminium Electrolysis Cells:** Sten Yngve Larsen<sup>1</sup>; Xian-An Liao<sup>1</sup>; Hermann Gran<sup>1</sup>; Stian Madhus<sup>1</sup>; Johan Arnold Johansen<sup>1</sup>; <sup>1</sup>Elkem Carbon AS

New types of coke were successfully introduced one decade ago for production of semigraphitic (E-30), graphitic (E-100) and especially graphitized (E-G) cathode blocks. Compared to cokes historically used for production of cathode blocks, these cokes are different in both structure and chemical composition. The present paper mainly describes the characteristics of E-G blocks. Compared to the graphitized cathode blocks based on traditional cokes, E-G blocks have been found to be denser, less porous, more resistant to wear in aluminium electrolysis as well as having a slightly higher sodium expansion rate and a higher coefficient of thermal expansion. An average apparent density in excess of 1.72 g/cm<sup>3</sup> was achieved without pitch impregnation. In addition E-G blocks have more evenly distributed properties in different directions than the traditional graphitized cathode blocks. These characteristics are expected to contribute to a longer pot life and a more stable pot operation.

#### 3:45 PM Break

#### 4:00 PM

**Sodium Diffusion in Cathode Lining in Aluminium Electrolysis Cells:** Zhaohui Wang<sup>1</sup>; Jørn Rutlin<sup>2</sup>; Tor Grande<sup>1</sup>; <sup>1</sup>Norwegian University of Science and Technology (NTNU); <sup>2</sup>Norsk Hydro Aluminium AS

A qualitative understanding of the diffusion of sodium into the cathode lining in aluminium electrolysis cells, including the carbon cathode, the ceramic sidelining and refractory lining, is important for the improvement of cathode cell design and performance. In this paper, a mathematical model is used to describe sodium diffusion and reaction behavior through the entire cathode lining. In addition to the degradation mechanisms in different lining materials, a mass balance of sodium consumption in a typical cell is considered and used for the verification of the model. The simulation gives additional insight into the transport of sodium in the carbon cathode and demonstrates that sodium transport in the cathode goes through solid state diffusion. The model is also used to simulate the consequences of changes in the carbon materials in the cathode lining.



4:20 PM

**Characterization of Sodium Expansion of Industrial Graphitic and Graphitized Cathodes:** *Jilai Xue*<sup>1</sup>; Liancheng Wu<sup>2</sup>; Qingsheng Liu<sup>1</sup>; Qingren Niu<sup>2</sup>; Wei Wang<sup>1</sup>; Xin Hou<sup>2</sup>; Jun Zhu<sup>1</sup>; Hua He<sup>2</sup>; <sup>1</sup>University of Science and Technology Beijing; <sup>2</sup>Ningxia Qingtongxia Energy Aluminium Group, China Power Investment Corporation

A series of experiments with various industrial cathodes ranging from 35% to 100% graphitic and fully graphitized carbons were carried out using a modified Rapoport apparatus. Sodium expansion during aluminum electrolysis was measured against time at 960°C. For a higher cryolite ratio, the cathodes with lower graphitic carbons exhibited more sodium expansion than the fully graphitized carbon, while for a lower cryolite ratio, such a difference become less profound among the tested samples. XRD characterization shows that the d002 value of all types of the cathode samples increases after aluminum electrolysis, and the increased graphitization (p002) in the cathode carbons can reduce the sodium expansion. SEM-EDS inspection reveals that the sodium and fluorides penetration within the cathode samples has different patterns for varying graphitization of the carbon materials. The results can provide useful information for operational evaluation of the industrial cathode products as well as for improvement in cathode performance.

4:40 PM

**Electrochemical Investigation of Potassium Intercalation into Graphite:** Dongren Liu<sup>1</sup>; *Wangxing Li*<sup>2</sup>; Zhanhong Yang<sup>1</sup>; Shilin Qiu<sup>2</sup>; Yingtao Luo<sup>2</sup>; <sup>1</sup>Central South university; <sup>2</sup>Zhengzhou Research Institute of Chalco

Electrochemical intercalation of potassium into graphite in molten KF was investigated by means of cyclic voltammetry, chronoamperometry, galvanostatic electrolysis and open-circuit potential measurements. It was found that potassium intercalated into graphite proceeding via the mechanism of intercalation between graphite layers. The intercalation compound formed in graphite matrix in molten KF was quite unstable. The intercalation process was found to be governed by both the diffusion of potassium ion in graphite bulk and the phase transition kinetics. The transfer coefficient of the intercalation reaction was calculated according to the parameters resulting from nonlinear fitting of the current-time transient curves with a quasi-reversible equation. Analysis with scanning electron microscope analyses shows graphite was severely eroded by intercalation of potassium. These findings could provide a deeper understanding of the basic mechanism of potassium interaction with cathodic carbon block in the Hall-Héroult process when potassium cryolite would be used as low temperature electrolyte.

5:00 PM

**Corrosion Resistance of Cathode to NaF-KF-ALF<sub>3</sub>-Based Electrolyte:** *Hengwei Yan*<sup>1</sup>; Wangxin Li<sup>2</sup>; Shilin Qiu<sup>2</sup>; Ji Li<sup>1</sup>; <sup>1</sup>Central South University; <sup>2</sup>Zhengzhou Research Institute of Chalco

The KF-AIF<sub>3</sub>-based electrolyte is a kind of promising bath in low-temperature aluminum reduction, but it has strong corrosion to cathode material. In this paper, the cathode expansion rate in KF-AIF<sub>3</sub>-based electrolyte was tested for semi-graphite cathode and graphitization cathode, after electrolysis, the cathodes were analyzed by SEM-EDS. The experimental results show that when KF content is higher than 7wt.%, the semi-graphite cathode were corroded seriously after electrolysis, but for graphitization cathode, despite KF content in electrolyte reach 20wt.%, the expansion rate still keep in an acceptable level. The result suggest that the graphitization cathode can be used with KF-AIF<sub>3</sub>-based electrolyte in aluminum reduction process.

5:20 PM

**Development Status of Processing Technology for Spent Potlining in China:** *Xiping Chen*<sup>1</sup>; <sup>1</sup>Zhengzhou Research Institute of Chalco

With the development of Chinese aluminum industry, wastes from smelters are severely restricted by the government. Different processing technologies for spent potlining (short as SPL) have been developed in the past five years. Main SPL processing technologies are Detoxifying with limestone, coal cinder by Pyro-process, Detoxifying with bauxite in Aluminum Sintering Process and Floatation of SPL. Three typical technologies were put into industrial application in Pingguo Smelter, Shangdong Smelter and Yichun Smelter, respectively. SPL plant in Pingguo which adopts Pyro-process has a capacity of 15000 metric tons per year. SPL-bauxite Sintering Process used in Shangdong can treat 6000 metric tons SPL every year. Floatation of SPL was put into industrial test in Yichun this year and the test scale is 1000 metric tons SPL per year. Different

products which were received from three processes can meet national standard, at the same time SPL can be sufficiently detoxified after processing.

### Electrometallurgy - General Session: Session I

*Sponsored by:* The Minerals, Metals and Materials Society, TMS Extraction and Processing Division, TMS: Aqueous Processing Committee

*Program Organizer:* Michael Free, University of Utah

Monday PM

Room: 310

February 15, 2010

Location: Washington State Convention Center

*Session Chair:* Michael Free, University of Utah

2:00 PM

**A Sandwich Structure Lead-Based Composite Porous Anode for Zinc Electrowinning:** Jiang Liangxing<sup>1</sup>; *Lv Xiaojun*<sup>1</sup>; Lai Yanqing<sup>1</sup>; Li Jie<sup>1</sup>; Liu Yexiang<sup>1</sup>; <sup>1</sup>Central South University

In order to improve the electric conductivity and mechanical performance of lead-based porous anode (PA) for zinc electrowinning, a sandwich structure composite porous anode (CPA) was prepared by counter-gravity infiltration and its structure was optimized. SEM observation shows that under the optimized infiltration conditions, the core and foam outside can integrate together. The results of anodic polarization show that the pore diameter and thickness of foam influence the anodic potential, and the optimized value of them is 1.43-1.6mm and 2mm, respectively. Mechanical performance measurements show that pore diameter and thickness of foam has negligible effect on tensile strength, but the thickness of core metal has great effect on it. According to the practice in zinc electrowinning, the thickness of core metal was designed to 2mm, and the tensile strength is about 8MPa, which is 3 times of PA. With the optimized structure, the electric conductivity is 2 times of PA.

2:25 PM

**Constant and Pulse Voltage Applications in CaWO<sub>4</sub> Reduction:** Orhan Goksu<sup>1</sup>; Ishak Karakaya<sup>1</sup>; *Metehan Erdogan*<sup>1</sup>; <sup>1</sup>Middle East Technical University

It has been shown that metallic tungsten powder can be obtained by electrochemical reduction of solid CaWO<sub>4</sub> in molten CaCl<sub>2</sub>-NaCl eutectic mixture at 600°C. In this study, constant and pulse voltage electrolysis experiments were performed to optimize electroreduction kinetics and to obtain information about the mechanism of above process. It was found that pulse voltage applications yield faster reduction rates when average voltage of pulse voltage application was the same as constant voltage application. In addition, analysis of the current vs. time graphs of constant and pulse voltage electrolysis studies showed that reduction occurs at potential differences higher than 2.25 V between CaWO<sub>4</sub> cathode and graphite rod anode. Cyclic voltammetry studies and thermodynamic computations were performed to support above result.

2:50 PM

**Electrochemical Formation of Mg-Li-Y Alloys at Solid Magnesium Electrode from LiCl-KCl-YCl<sub>3</sub> Melts:** *Pengkai Wang*<sup>1</sup>; Huimin Lu<sup>1</sup>; Feng Shi<sup>1</sup>; <sup>1</sup>Beihang University

In this paper, the electrochemical formation of Mg-Li-Y alloys from LiCl-KCl-YCl<sub>3</sub> melts at 823K was conducted with solid Magnesium cathode. The cyclic voltammetry, chronopotentiometry and chronoamperometry were used to study the electroreduction mechanism and controlling step of Li and Y electrodeposition on Mg cathode. The results indicated that Li(I) and Y(III) could be reduced at -2.1V(Vs.Mo) and -1.1V(Vs.Mo), the electroreduction processes of Li and Y were quasi-reversible diffusion controlled reactions including one and three electrons transfer respectively. The X-ray diffraction and scanning electron microscopy analyses also showed Mg-Li-Y alloys could be obtained by potentiostatic electrolysis at 3.2V, formation of Mg-Li-Y alloys controlled by applied current, and Lithium and Yttrium contents by electrolysis time. At this moment, the cathodic density was 2A/cm<sup>2</sup>; Li and Y could co-deposit and diffuse into the Mg cathode to form the Mg-Li-Y alloys.

Mon. PM

# Technical Program

3:15 PM

## Electrochemistry of Tantalum Pentachloride in the Room Temperature Ionic Liquid 1-Butyl-3-Methylimidazolium Hexafluorophosphate: Xiaoxiang Zhang<sup>1</sup>; Huimin Lu<sup>1</sup>; Tao Zhang<sup>1</sup>; <sup>1</sup>Beihang University

Electrochemical behavior of 0.25M tantalum chloride on platinum substrate was investigated in the 1-butyl-3-methylimidazolium hexafluorophosphate ([Bmim]PF<sub>6</sub>) by cyclic voltammetry, chronopotentiometry and chronoamperometry. Cyclic voltammograms of tantalum pentachloride in the employed ionic liquid at 100°C exhibit four reduction peaks, the first reduction peak contributes to the reduction of trichloride anion (Cl<sub>3</sub><sup>-</sup>) at -0.4V vs. Pt, the second corresponds to the reduction of the tantalum (V) to tantalum (III) at -0.9V vs. Pt, the third is attributed to the reduction of the tantalum (III) to tantalum metal at -1.25V vs. Pt and the fourth is the formation of various tantalum subchlorides at -1.6V vs. Pt. The results have shown that the electrodeposition of tantalum from tantalum pentachloride in [Bmim]PF<sub>6</sub> is quite complicated process, but tantalum can be electrodeposited in thin layers.

3:40 PM Break

3:50 PM

## ZrB<sub>2</sub> Produced with Molten Salt Electrolysis: Selda Özkın<sup>1</sup>; Servet Timur<sup>1</sup>; Mustafa Urgan<sup>1</sup>; <sup>1</sup>ITU Metallurgical and Materials Engineering Department

In this study, a combination of cathodic arc physical vapor deposition (PVD) and molten salt electrolysis methods were used to obtain ZrB<sub>2</sub> layers on AISI 304 grade stainless steel surface. Prior to boriding, steel surface was coated with metallic zirconium via cathodic arc PVD method and then the zirconium coated steel was borided by molten salt electrolysis. Well adherent, dense, ZrB<sub>2</sub> layers are formed on the substrates. The thickness of the ZrB<sub>2</sub> layer showed dependence on the thickness of the metallic Zr coating layer and the time of boriding. During the boriding process the alloying elements of the substrate also took part in the coating structure depending on their diffusion characteristics.

4:15 PM

## Effects of Ultrasound on Cell Voltage of Aluminum Electrolysis in Cryolite-Alumina Melts: Jilai Xue<sup>1</sup>; Shao Hua<sup>1</sup>; Jun Zhu<sup>1</sup>; <sup>1</sup>University of Science and Technology Beijing

Aluminum electrolysis aided with ultrasound was carried out in cryolite-alumina melts in a laboratory cell, and a layer CO<sub>2</sub> gas bubbles was formed on the anode. Cell voltage varied as the bubbles generated on the anodes surface, and reduced by applying ultrasound on the anode. The effects of ultrasound frequency and anodic current density were investigated with ultrasound on and off, alternatively during the electrolysis process. The cell voltage can be lowered by 5% with ultrasound, which demonstrate the potential energy saving for aluminum reduction process.

4:40 PM

## Evaluation of the Corrosion Behavior of Laser Welded and GTAW Welded Austenitic Stainless Steel 316L in Lithium Bromide and Comparing the Inhibition Effect of Chromate, Bromate and Molybdate on the Corrosion Behavior of Austenitic Stainless Steel 316L in Lithium Bromide: Ahmad Momtaz<sup>1</sup>; <sup>1</sup>German University in Cairo

The corrosion behavior of ASS 316L laser welded and GTAW welded in lithium bromide concentrations of 0.05, 0.1, 0.5, 1, 3, 4.6, 6, 8.06 and 9.79 M was evaluated using electrochemical methods and optical microscopy. The inhibitors used were: sodium chromate, sodium bromate and sodium molybdate. Optical microscopy showed that ferrite was formed in the austenite matrix exhibiting austenite ferrite solidification. Open circuit potential showed that laser welded had more noble potentials than GTAW welded at most of the concentrations. The laser welded showed lower corrosion currents and corrosion rates than GTAW welded. Moreover, laser welded showed better pitting resistance than GTAW welded, while GTAW welded showed better repassivation behavior than laser welded. The sodium chromate appeared to be the most efficient inhibitor. Moreover, laser welded is inhibited more efficiently by the three types of inhibitors than GTAW welded. Laser welding is better than GTAW welding for ASS 316L.

## Failure of Small-Scale Structures: Deformation and Failure

Sponsored by: The Minerals, Metals and Materials Society, TMS Materials Processing and Manufacturing Division, TMS Structural Materials Division, TMS/ASM: Mechanical Behavior of Materials Committee, TMS: Nanomechanical Materials Behavior Committee  
Program Organizers: Marian Kennedy, Clemson University; Brad Boyce, Sandia National Laboratory; Reinhold Dauskardt, Stanford; Zhiwei Shan, Hysitron Inc

Monday PM

Room: 206

February 15, 2010

Location: Washington State Convention Center

Session Chair: Reinhold Dauskardt, Stanford University

2:00 PM Invited

## SIZE MATTERS: Nano-Scale Mechanical Properties of Single Crystals, Nanocrystalline Metals, and Amorphous Metallic Glasses: Julia Greer<sup>1</sup>; Ju-Young Kim<sup>1</sup>; Dongchan Jang<sup>1</sup>; Michael Burek<sup>2</sup>; <sup>1</sup>California Institute of Technology; <sup>2</sup>University of Waterloo

When microstructural or external sizes of materials are reduced to nano-scale, they exhibit unique behaviors. We fabricate nanopillars with different initial microstructures ranging from 50 nm to 1 micron by using Focused Ion Beam and E-beam lithography/electroplating approaches. Their strengths in uniaxial compression and tension are subsequently measured in in-situ mechanical deformation instrument, SEMentor. We discuss nano-mechanical behavior in three distinct material classes: single crystals, nano-crystalline metals, and metallic glasses. We observe SMALLER is STRONGER phenomenon in single crystals while nano-crystalline metals exhibit SMALLER is SOFTER trend. Metallic glasses show both strength increase and ductility when reduced to nano-scale. Unlike in bulk, nano-scale materials also exhibit numerous discrete strain bursts. We attribute these dissimilarities to free surface effects, leading to unique dislocation behavior in crystals, grain-boundary activity in nano-crystalline solids, and shear transformation zones in metallic glasses, serving as fundamental reason for observed failure and plasticity mechanisms.

2:25 PM

## The Role of Grain Boundaries in the Creep of Sub-Micrometer Thick Cu and Cu/Si<sub>3</sub>N<sub>4</sub> Microbeams at 300 K: Robert Klassen<sup>1</sup>; Yong Liu<sup>2</sup>; <sup>1</sup>The University of Western Ontario; <sup>2</sup>Eaton Corporation

Constant-load creep tests were performed at 300 K on 250 μm long cantilever microbeams of Cu and Cu/Si<sub>3</sub>N<sub>4</sub> containing a sputter-deposited Cu layer between 200 and 1300 nm thick. A nano-indentation tester was used to apply the load and to measure the displacement of the microbeams during the creep tests. The internal stress and strain rate within the microbeams was determined by FE modelling incorporating user-defined material constitutive expressions. The reduced average grain diameter within the thinnest Cu microbeams was found to enhance the contribution from grain boundary diffusional creep and reduce the contribution from obstacle-limited dislocation glide. The activation energy and the athermal flow stress were found to be larger for Cu/Si<sub>3</sub>N<sub>4</sub> than for the free-standing Cu microbeams of the same thickness. This suggests that the presence of the Si<sub>3</sub>N<sub>4</sub> layer invokes a higher dislocation density which results in stronger obstacles to dislocation glide.

2:40 PM Invited

## Competing Roles of Deformation and Void Formation during Rapid Thermal Cycling of Metal Interconnects: Robert Keller<sup>1</sup>; David Read<sup>1</sup>; Roy Geiss<sup>1</sup>; <sup>1</sup>NIST

Development of methods for testing the thermomechanical reliability of metal interconnects has led to the observation of a transition in material response during rapid thermal cycling, as induced by alternating electric current cycling at 100 Hz. In tests of partially encapsulated copper lines in vacuum, thermal cycling over temperature ranges of approximately 250°C and higher resulted in the formation of damage largely consistent with dislocation slip due to thermomechanical fatigue. Thermal cycling over temperature ranges of approximately 225°C and lower resulted in the formation of damage consistent with diffusive mechanisms, i.e., voids. This observed range of transition temperature appears to be similar to the optimum hold temperatures seen for the formation of stress voids in highly constrained interconnects. We discuss

Mon. PM



this transition in terms of local conditions of stress, temperature, constraint, heating/cooling rates, and localized variations in microstructure.

### 3:05 PM

**Visualization of Failure Mechanisms in Nanocrystalline Thin Films:** Krishna Jonnalagadda<sup>1</sup>; John Sharon<sup>1</sup>; Kevin Hemker<sup>1</sup>; *Kaliat Ramesh*<sup>1</sup>; <sup>1</sup>Johns Hopkins University

One of the main reasons for early failure of nanocrystalline metals is the presence of voids. The mechanical behavior of nanocrystalline metals with voids was investigated via in-situ optical and scanning electron microscope tensile experiments. The 200 nm thick, electron transparent, nanocrystalline aluminum films were patterned with small 5-10 micron holes to understand failure via void growth. Under tensile loading, the void size increased, becoming elliptical, and a small crack nucleated normal to the loading direction. Under displacement controlled loading the crack growth was slow until complete failure of the film. Experiments are also conducted in which the crack growth is arrested and the deformation mechanisms are investigated with TEM. Due to high stress concentration at the crack tip both grain growth and void nucleation are expected along the crack front. Furthermore, the void growth rate and its change in shape are modeled considering 2D plane stress in the film.

### 3:20 PM

**Tuning the Mechanical Properties of a Nanoporous Gold:** *Hai-Jun Jin*<sup>1</sup>; Lilia Kurmanaeva<sup>1</sup>; Jörg Weissmüller<sup>1</sup>; <sup>1</sup>Forschungszentrum Karlsruhe GmbH

Conventional approach towards tailoring the mechanical properties of materials is to manipulate their atomic structure or microstructure. However, instead of these “permanent” changes, here we introduce a new concept to develop “smart” materials which allows prompt and reversible variation of its mechanical properties. We demonstrate in bulk nanoporous gold samples prepared by dealloying, with very small structure size and large surface area, that both the yield stress and the brittleness can be “tuned” in an electrochemical environment. Compression tests were performed in situ with samples immersed in the electrolyte and with potentiostatic control. Potential changes allow a reversible variation of the flow stress by as much as the factor two. Furthermore, the samples are obviously more brittle at positive potential. The underlying mechanisms will be discussed in terms of surface dislocation nucleation and dislocation motion concerning the roles of the surface stress, surface energy and even the surface diffusivity.

### 3:35 PM Break

### 3:50 PM Invited

**Failure of Protein Materials in Extreme Conditions and Disease:** *Markus Buehler*<sup>1</sup>; <sup>1</sup>Massachusetts Institute of Technology

Biological protein materials feature hierarchical structures, ranging through the atomistic, molecular to macroscopic scales, forming functional biological tissues as diverse as spider silk, tendon, bone, skin, hair or cells. Here I will present computational studies, focused on how protein materials deform and fail due to extreme mechanical conditions, disease and injuries. Based on a multi-scale atomistic simulation approach that explicitly considers the architecture of proteins including at the chemistry level, we have developed predictive models of protein materials, validated through quantitative comparison with experimental results. This bottom-up approach enables us to extract fundamental physical concepts that control the properties of protein materials. I will present studies of several major classes of protein materials, including cellular alpha-helix rich protein networks, beta-sheet structures as found in spider silk and amyloids, as well as collagenous tissues that form tendon and bone. Materials failure in the contact of genetic diseases will be discussed.

### 4:15 PM

**Deformation and Fracture in Human Skin:** *Kemal Levi*<sup>1</sup>; Victoria Hsiao<sup>1</sup>; Ruijiang Jia<sup>1</sup>; Reinhold Dauskardt<sup>1</sup>; <sup>1</sup>Stanford University

The outermost layer of human skin, the stratum corneum (SC), is a critical small-scale biological structure with important chemical barrier and mechanical properties. The tissue is 10-25 μm thick and has cellular and intercellular components that vary from tens of microns to submicrons in size. We describe micromechanical techniques to probe the biomechanical properties of the SC together with optical and atomic force microscopy integrated with digital image correlation. We demonstrate how environmental, enzymatic and chemical treatments influence SC components and their resulting mechanical properties. We also describe novel thin-film methods to probe the resistance to

intercellular delamination and the stresses that arise naturally in SC as a result of treatment or environmental conditions. Finally, a biomechanics framework to account for the SC drying stress as a mechanical driving force for dry skin damage is presented. This research presents a new approach to characterize the fundamental biomechanics of human SC.

### 4:30 PM Invited

**Size Dependent Deformation in Polymers - Experiments and Theory:** *Chung-Souk Han*<sup>1</sup>; <sup>1</sup>North Dakota State University

Similar to the size-dependent deformation observed in metals at length scale ranges from microns down to nanometers, many polymers exhibit size dependent deformation at these length scales as well. While for metals such size dependent deformation phenomena are commonly attributed to geometrically necessary dislocation densities, this notion can not be applied to polymers and a sound theory explaining these phenomena in polymers seems not to be available. Experimental investigations where such size dependent deformation has been observed are reviewed here and include microbeams, indentation testing, and foam and composite materials. In addition a related micromechanically motivated higher gradient theory incorporating a Frank energy type component to the deformation potential is suggested for the prediction and rationalization of such size dependent deformation in polymers. This theory is discussed with respect to the reviewed experiments and it is found that it is capable to link some molecular properties of the polymer to its size dependent deformation.

## Global Innovations in Manufacturing of Aerospace Materials: The 11th MPMD Global Innovations Symposium: Innovations in Casting Technologies

*Sponsored by:* The Minerals, Metals and Materials Society, TMS Materials Processing and Manufacturing Division, TMS Structural Materials Division, TMS: Shaping and Forming Committee, TMS: High Temperature Alloys Committee

*Program Organizers:* Deborah Whitis, General Electric Company; Thomas Bieler, Michigan State University; Michael Miles, BYU

Monday PM Room: 306  
February 15, 2010 Location: Washington State Convention Center

*Session Chairs:* Chris Woodward, AFRL-RX; John Miller, TBD

### 2:00 PM Invited

**Advances in the Solidification of Single Crystal Superalloys:** *Tresa Pollock*<sup>1</sup>; Clinique Brundidge<sup>1</sup>; Jonathan Madison<sup>1</sup>; Jonathan Miller<sup>2</sup>; <sup>1</sup>University of Michigan; <sup>2</sup>Air Force Research Laboratory

Recent challenges in the solidification of superalloy single crystals include new creep resistant alloys, the need for physically large single crystals for power generation turbines and the linkage of solidification process models to mechanical property models. Recent developments in high gradient processing and techniques for quantifying solidification structure and defects will be discussed. Key features of the high gradient liquid metal cooling (LMC) process for solidifying superalloy single crystals will be quantified. New insights to defect formation that arise from fluid flow studies performed on 3-D dendritic structures obtained by serial sectioning will be presented. Finally, the aspects of solidification structure that influence creep and fatigue will be discussed along with the needs for linkage of process models to property models.

### 2:30 PM

**Direct Digital Manufacturing of Airfoils:** *Suman Das*<sup>1</sup>; John Halloran<sup>2</sup>; Wil Baker<sup>3</sup>; <sup>1</sup>Georgia Institute of Technology; <sup>2</sup>University of Michigan; <sup>3</sup>Honeywell Aerospace

Direct Digital Manufacturing (DDM) of airfoils is a concept that disrupts the current state-of-the-art investment casting process for manufacturing superalloy airfoils. DDM of airfoils will be achieved by processing photocurable ceramic resins through a new technology known as Large Area Maskless Photopolymerization (LAMP). LAMP combines layered manufacturing of complex three-dimensional objects with the fine-feature resolution and high throughput of massively parallel scanning maskless lithography to achieve a disruptive breakthrough in part build speed and feature definition. DDM of airfoils will eliminate nearly all the tooling, handling, and associated causes for scrap in the investment casting process. Thus, it will disrupt not only the cost

Mon. PM

# Technical Program

structure of conventional investment castings, but also the speed with which components can be fabricated. This presentation will highlight progress made to date on development of LAMP technology. This work is sponsored by DARPA grant HR0011-08-1-0075.

## 2:50 PM

**Experimental and Mathematical Modeling Progress on Scanning Laser Epitaxy: A Technique for Growing Single Crystal Superalloys:** Michael Kirka<sup>1</sup>; Rohan Bansal<sup>1</sup>; *Suman Das*<sup>1</sup>; <sup>1</sup>Woodruff School of Mechanical Engineering, Georgia Institute of Technology

We present recent progress on scanning laser epitaxy, a laser additive manufacturing technique under development for producing single crystal growth in nickel-based superalloys. Experimental investigations have been performed on the single-crystal capable nickel alloy CMSX-4. Additionally, mathematical models have been coupled with analytical information obtained from experiments to understand the scanning laser epitaxy process and the requirements to achieve monolithic deposits on like chemistry single-crystal nickel superalloy substrates. Presentation of microstructure development and need of process control in the context of the laser generated melt pool will be discussed from the view-point of repairing high-value single-crystal turbine engine components. This work is funded by the Office of Naval Research contract #N00173-07-1-G012.

## 3:10 PM

**Modeling of Grain Selection during Directional Solidification of Superalloy Single Crystal Turbine Blade Casting:** Dong Pan<sup>1</sup>; Qingyan Xu<sup>1</sup>; *Baicheng Liu*<sup>1</sup>; Jiarong Li<sup>2</sup>; Hailong Yuan<sup>2</sup>; Haipeng Jin<sup>2</sup>; <sup>1</sup>Tsinghua University; <sup>2</sup>Beijing Institute of Aeronautical Materials

Superalloy single crystal turbine blade are nowadays widely used as key parts in gas turbine engines. The single crystal turbine blade casting properties are quite sensitive to the grain orientation determined directly by the grain selection behavior of the grain selector. A mathematical model was proposed for the grain selection during directional solidification of turbine blade casting. Based on heat transfer model during directional withdrawing process, the competitive grain growth within the start block and the spiral part were simulated by using cellular automaton method (CA). Validation experiments were carried out, and the measured results were compared quantitatively with the predicted results. It is indicated that the model could be used to reproduce the grain morphology and the competitive grain evolution during solidification, together with the distribution of grain orientation of primary <001> dendrite growth direction, with respect to the longitudinal axis of the turbine blade casting.

## 3:30 PM Break

## 3:50 PM

**Prediction of As-Cast Grain Size Distribution from a Model of Equiaxed Solidification with Free Dendrite Transport:** *Wajira Mirihanage*<sup>1</sup>; David Browne<sup>1</sup>; <sup>1</sup>University College Dublin

As-cast microstructure is one of the essential engineering concerns for aerospace materials. Movement of equiaxed dendrites during solidification has a significant influence on the final microstructure of shape cast components. The authors have developed a predictive model of equiaxed solidification which treats dendrite transport in the solidifying alloy melt, at low computational cost. The non-equilibrium model considers nucleation from industrial inoculants, growth and movement of dendrites. The motion of free dendrites is computed as the combined effects of sedimentation settling of denser dendrites and transport of small dendrites by liquid flow due to natural convection. When free dendrites become coherent at the latter stage of solidification, the resultant equiaxed mush of coherent dendrites is assumed to have become a porous medium until it becomes completely solid. Simulations are used to establish the sensitivity of the as-cast structure of Al-Si shape castings to the magnitude of mould material heat transfer coefficients.

## 4:10 PM

**Damage Tolerant Cast Alloy Ti-5Al-5Mo-5V-3Cr for Aerospace Applications:** *Edward Chen*<sup>1</sup>; L.W. Weihmuller<sup>2</sup>; D.R. Bice<sup>1</sup>; G.D. Hall<sup>2</sup>; W.A. Thomas<sup>2</sup>; <sup>1</sup>Transition45 Technologies, Inc.; <sup>2</sup>Bell Helicopter Textron

It is well established that aerospace systems would benefit greatly from the development and application of high strength titanium alloys with improved durability and damage tolerance. Current and future commercial and military aircraft in particular have requirements for such alloys, particularly if near-

net shape components can be manufactured as castings for affordability. The application of a higher strength titanium alloy versus the industry workhorse Ti-6Al-4V also allows direct conversion of forged titanium parts to titanium castings without sacrificing strength and durability or increasing weight. This presentation covers work performed to evaluate the emerging high strength titanium alloy Ti-5Al-5Mo-5V-3Cr-0.5Fe (Ti-5553) as castings. The microstructure-properties of this alloy including tensile strength, toughness, and damage tolerance under different thermo-mechanical processing conditions will be reviewed in depth. These results will be discussed in light of the potential applicability of cast Ti-5553 to aerospace structures. This work was supported by the Naval Air Warfare Center.

## 4:30 PM

**Coupling Computational Thermodynamics with Experimental Study for Accelerated Development of Mo-Si-B Based Alloys:** *Ying Yang*<sup>1</sup>; Hongbin Bei<sup>2</sup>; Easo George<sup>2</sup>; Jaimie Tiley<sup>3</sup>; Y. Chang<sup>4</sup>; <sup>1</sup>CompuTherm LLC; <sup>2</sup>Oak Ridge National Laboratory; <sup>3</sup>Air Force Research Laboratory; <sup>4</sup>University of Wisconsin-Madison

Recent advance in computational thermodynamics using the CALPHAD (CALculation of PHase Diagram) approach has enabled us to rapidly obtain multi-component phase diagrams with significantly reduced experimental effort. In this presentation, the stable region of the three-phase (Mo)+Mo<sub>3</sub>Si+Mo<sub>5</sub>SiB<sub>2</sub> equilibrium in the Mo-Si-B-X (X=Ti, Zr, Hf) system was rapidly established by coupling computational thermodynamics with guided experiments. Computational thermodynamics helps not only identifying critical alloy compositions for experimental study, but also understanding the complex microstructures in multi-component alloys. The results show that additions of Zr and Hf much limit the stable region of the three-phase (Mo)+Mo<sub>3</sub>Si+Mo<sub>5</sub>SiB<sub>2</sub> equilibrium because of the formation of the ternary phases MoSiZr(Hf), while Ti addition leads to a much larger one. This work is an essential building block for developing high-performance Mo-Si-B based Refractory Metal Intermetallic Composites (RMICs) for ultra-high temperature applications (T>1200°C).

## 4:50 PM

**Mechanical Properties of TiAl-Based Alloys for High Temperature Applications:** *Fereshteh Ebrahimi*<sup>1</sup>; Michael Kesler<sup>1</sup>; Sonalika Goyel<sup>1</sup>; Orlando Rios<sup>1</sup>; Damian Cupid<sup>2</sup>; Hans Seifert<sup>2</sup>; <sup>1</sup>University of Florida; <sup>2</sup>Freiberg University of Mining and Technology

There is a need to reduce the weight of the turbine engines used in aircrafts. Two-phase TiAl+Ti<sub>3</sub>Al alloys have recently been employed in the low temperature section of the turbine engines. In order to extend the applicability of TiAl-based alloys to higher temperatures we have designed alloys based on the TiAlNbCrMo system. These alloys solidify as solid solution beta phase which could be retained upon fast cooling to room temperature. Stable microstructures consisting of gamma (TiAl) phase with different volume fractions of the sigma (Nb<sub>2</sub>Al) phase were obtained by aging treatments. The results of this study elucidate that fracture at the prior beta grain boundaries limits the ductility of these alloys. In this paper the optimization of low temperature ductility and high temperature strength is discussed in terms of the volume fraction of the phases and their distribution. This work has been supported by NSF/AFOSR (DMR-0605702 and DMR-0856622).

## 5:10 PM

**Development of Ni-Mn-Based Braze Alloys for the Fast Epitaxial Braze Repair of Wide Cracks in Single-Crystalline Nickel-Base Superalloys:** *Britta Laux*<sup>1</sup>; Joachim Rösler<sup>1</sup>; <sup>1</sup>Technische Universität Braunschweig

Diffusion brazing is a widely-used technology for the repair of cracks in hot section turbine components, mostly fabricated from single-crystalline nickel-based superalloys. Typically, braze alloys similar to the base material, enhanced by fast diffusing melting point depressants like B, are used. In case of single-crystalline components, an epitaxial healing can be achieved, however, the filling of wide cracks in the range of 100-300 μm is difficult, due to the precipitation of brittle secondary phases. New Ni-Mn-based braze alloys enhanced by Al, Cr and Ti were developed, which allow a very fast epitaxial healing of wide cracks (300 μm). As B is replaced by Mn, the repair process can be significantly shortened since the epitaxial solidification is no longer completely diffusion controlled. Improved brazing cycles for the minimization of porosity, heat treatments producing a γ/γ'-microstructure very similar to the parent material as well as results from mechanical testing will be presented.



### Heterogeneous Nucleation and Initial Microstructure Evolution in Alloys and Colloids: Simulation II

Sponsored by: The Minerals, Metals and Materials Society, TMS Electronic, Magnetic, and Photonic Materials Division, TMS Materials Processing and Manufacturing Division, TMS Structural Materials Division, TMS: Alloy Phases Committee, TMS/ASM: Phase Transformations Committee

Program Organizers: Rainer Schmid-Fetzer, Clausthal University of Technology; Heike Emmerich, RWTH Aachen University; Frans Spaepen, Harvard University; Martin Glicksman, University of Florida; John Perepezko, University of Wisconsin, Madison

Monday PM Room: 614  
February 15, 2010 Location: Washington State Convention Center

Session Chairs: Dieter Herlach, DLR; Martin Glicksman, University of Florida

#### 2:00 PM Invited

**Heterogeneous Nucleation as a Deterministic Process:** *A. Green*<sup>1</sup>; <sup>1</sup>University of Cambridge

Heterogeneous nucleation in a wide variety of cases is likely to be deterministic, rather than stochastic. An example is the athermal heterogeneous nucleation of freezing, in which the number of nuclei generated is dependent on temperature and not on time, in contrast to many conventional analyses of nucleation rates. A correct analysis of the kinetics is essential for prediction of microstructure evolution. Accurate prediction may be facilitated when the nucleation is deterministic. Examples of such behaviour will be analysed and compared. They include not only cases from materials science, but also from biological systems.

#### 2:25 PM

**Heterogeneous Nucleation on Spherical and Flat Catalysing Surfaces:** *Ma Qian*<sup>1</sup>; <sup>1</sup>The University of Queensland

Fletcher's spherical substrate model is a basic model for understanding heterogeneous nucleation in nature. This work presents an analysis of this model using a novel analytical approach. It is revealed that when a special geometrical angle (pseudo-contact angle) were chosen for thermodynamic descriptions, the first derivatives of the free energy change with respect to embryo radius would be identical for nucleation on spherical and flat surfaces. It is further shown that there exists a local maximum in the difference between the equivalent contact angles for nucleation on spherical and flat surfaces. The negative spherical substrate size effect occurs primarily when  $R < 5r^*$  ( $R$ : substrate radius) and diminishes rapidly when  $R > 5r^*$ . Ultrapure water that freezes at  $-39.1^\circ\text{C}$  or below contains particles of  $R < 5r^*$  while that freezes at  $-38.0^\circ\text{C}$  or above includes particles of  $R > 5r^*$ . The freezing of liquid metals was discussed as well.

#### 2:45 PM

**A Phase-Field Simulation Study on Heterogeneous Nucleation in Ti-Al-B Alloys:** Janin Eiken<sup>1</sup>; Victor Witusiewicz<sup>2</sup>; Ulrike Hecht<sup>1</sup>; *Markus Apel*<sup>1</sup>; <sup>1</sup>Access e. V.

During directional solidification of TiAl based alloys with Al contents around 45at.% the peritectic  $\alpha$ -Ti phase usually nucleates on properitectic  $\beta$ -Ti dendrites. Adding boron to the melt may lead to the formation of  $\text{TiB}_2$  particles. Depending on the Al and B content,  $\text{TiB}_2$  appears in the melt prior to the nucleation of the  $\alpha$ -Ti phase. In this case,  $\text{TiB}_2$  particles may act as nucleation sites for  $\alpha$ -Ti in the interdendritic melt. This scenario was observed in Bridgman experiments and being confirmed by thermodynamic calculations. Here, we present a phase-field simulation study which elucidates the effect of the Al content on the dendritic growth morphology and the effect of the boride particle size distribution on the heterogeneous nucleation of  $\alpha$ -Ti. The simulation results agree with experimental observations and reveal the influence of the different parameters on grain refinement.

#### 3:05 PM

**A Precipitate Growth Model Based on a Variational Approach:** *Qiang Du*<sup>1</sup>; Warren Poole<sup>1</sup>; Mary Wells<sup>2</sup>; <sup>1</sup>University of British Columbia; <sup>2</sup>University of Waterloo

In this paper, a new precipitate growth model is proposed for multi component alloys. The model is based on the approximate solution to the mass transfer diffusion equation by Ritz method (a variational approach) with a quadratic shape function. Using the model a number of case studies are investigated for binary systems with various extents of super-saturation as well as multi-component systems where the disparity in the diffusivities of the alloying elements exists. The proposed model appears to capture the precipitate growth kinetics well for these systems. It is concluded that the proposed model could replace the one widely used in a "conventional" Particle Size Distribution (PSD) model.

#### 3:25 PM

**Effect of Local Stress on Nucleation and Variant Selection during Solid-State Transformation with Symmetry Reduction:** *Rongpei Shi*<sup>1</sup>; *Ning Zhou*<sup>1</sup>; *Yunzhi Wang*<sup>1</sup>; <sup>1</sup>Ohio State University

Microstructural features developed during solid-state reactions such as phase transformation, plastic deformation and fracture are often influenced by elastic strain fields associated with existing structural and compositional nonuniformities. A rigorous treatment of nucleation in solids requires a self-consistent description of the interactions between nuclei and an arbitrary pre-existing microstructure without any a priori assumptions. Taking advantage of the generality of phase-field total free energy functional and, in particular, its ability to describe arbitrary nonuniformities in the presence of long-range interactions, we study the effect of local stress and grain boundary in a polycrystalline aggregate on variant selection during nucleation and growth of a low-symmetry product phase from a high symmetry parent phase. The spatial distribution of different variants of the product phase is found to correlate strongly with the stress distribution in the polycrystalline sample. Under certain circumstances, certain variants may percolate through the entire sample, leading to micro-texturing.

#### 3:45 PM Break

#### 4:05 PM Invited

**Phase-Field Crystal Modeling of Nucleation, Patterning, and Early-Stage Growth in Colloidal Systems in Two and Three Dimensions:** *Laszlo Granasy*<sup>1</sup>; *Gyorgy Tegze*<sup>1</sup>; *Gyula Toth*<sup>1</sup>; *Frigyes Podmaniczky*<sup>1</sup>; *Tamas Pusztai*<sup>1</sup>; <sup>1</sup>Research Institute for Solid State Physics and Optics

Using a simple dynamical density functional approach (the phase-field crystal model), we address nucleation and morphology evolution during colloidal crystal aggregation. In single component systems, we observe a diffusion controlled growth mechanism at low supersaturations that switches to a diffusionless mechanism at high supersaturations, a behavior often seen in colloidal systems. We present a morphology map that contains transitions between compact, dendritic and fractallike structures, we investigate the change of growth anisotropy, polycrystalline aggregation, and study crystal aggregation in the presence of foreign matter represented by appropriate potentials. In 3D we use large scale-simulations of  $\sim 3$  million particles to address various aspects of freezing the single component liquid into bcc, fcc and hcp structures, including dendritic solidification.

#### 4:30 PM

**Nucleation and Successive Microstructure Evolution via Phasefield and Phasefield Crystal Method:** *Heike Emmerich*<sup>1</sup>; *Ricardo Siquieri*<sup>1</sup>; <sup>1</sup>RWTH Aachen

It is well known, that the mechanical material properties of a material sample after solidification are strongly tied to its microstructure structure. Nevertheless, the precise laws governing the initial stage of this structuring process, i.e. nucleation and the successive transient microstructure evolution scenarios, are still far from being fully understood. Here we show - after a thorough overview on the phasefield method and its relation to the phasefield crystal method - that the phase field method, which originally established itself to tackle the free boundary problem given by microstructure evolution, can also be employed to investigate the energetics of heterogenous nucleation in a solidifying sample. Moreover it is demonstrated, how the phasefield crystal method can shade more light in open questions regarding a quantitative formulation of nucleation statistics to thereby simulate the phase transition phenomena in solidification from nucleation to crystallization in larger domains thoroughly.

# Technical Program

4:50 PM

**Ab Initio Determination of Phase-Field Parameters Needed for Scale-Bridging Studies of Nucleation and Microstructure Formation in the Ti-Fe Eutectic System:** *Martin Friak*<sup>1</sup>; Juergen Hubert<sup>2</sup>; Heike Emmerich<sup>2</sup>; Antje Schlieter<sup>3</sup>; Uta Kuehn<sup>3</sup>; Juergen Eckert<sup>3</sup>; Joerg Neugebauer<sup>1</sup>; <sup>1</sup>Max Planck Institute for Iron Research; <sup>2</sup>RWTH Aachen University; <sup>3</sup>Institute for Complex Materials at the Leibniz-Institute for Solid State and Materials Research

Ti-based alloys have been suggested for commercial applications with a great potential due to their high strength (~1000 MPa) and good corrosion resistance. The strength of these materials can be even further increased if bulk nano-structured eutectic alloys are produced. In our study we focus on the effects that local lattice strains in the nano-structured eutectics have on the thermodynamic phase stability, elastic properties, and kinetics during the initial stages of microstructure evolution. To achieve this goal a joint approach, where ab initio determined parameters are used in phase-field simulations and systematically cross-checked against experimental data, is adopted. In particular, the free energies of both stable and metastable phases, the elastic constants, local elastic strains due to lattice-constant mismatch between different inter-facing phases, and selected gamma-surface energies and kinetics energy-barriers in FeTi and beta-Ti phases obtained employing density functional calculations will be presented.

## Hume-Rothery Symposium: Configurational Thermodynamics of Materials: Session II

*Sponsored by:* The Minerals, Metals and Materials Society, TMS Electronic, Magnetic, and Photonic Materials Division, TMS Structural Materials Division, TMS: Alloy Phases Committee, TMS: Chemistry and Physics of Materials Committee

*Program Organizers:* Chris Wolverton, Northwestern University; Mark Asta, University of California, Davis; Gerbrand Ceder, Massachusetts Institute of Technology (MIT)

Monday PM Room: 212  
February 15, 2010 Location: Washington State Convention Center

*Session Chair:* To Be Announced

2:00 PM Invited

**High Energy X-Ray Scattering Studies of Ordering and Phase Separation in Binary Metallic Alloys:** *Harald Reichert*<sup>1</sup>; <sup>1</sup>ESRF

Using high energy x-ray scattering we have developed experimental tools in order to reveal details in the energetics of binary alloys with very high accuracy. With this technique we have collected 2-dimensional scattering patterns for many binary alloy systems. In the time-resolved mode the technique can be used to monitor the evolution of diffuse scattering signals to Bragg-like peaks in the diffraction pattern. This allows one to follow phase transformations in-situ. Parallel to improvements in the data collection it is of equal importance to extract the maximum amount of information encoded in the diffuse scattering distribution. To this end we have developed a reciprocal space description in a single unified model which allows one to analyze the diffuse scattering data in terms of a few physically motivated parameters. As examples, details of ordering and phase separation in Au-Ni, Ti-V, N-Pd, Cu-Au, Ni-W, and Mo-Ta alloys are presented.

2:30 PM Invited

**Phase Separation in Al(Sc)-Based Alloys on a Nanoscale:** *David Seidman*<sup>1</sup>; David Dunand<sup>1</sup>; <sup>1</sup>Northwestern University

Phase separation is studied in Al(Sc)-based alloys utilizing atom-probe tomography and transmission electron microscopy, where the precipitating phase consists of coherent precipitates of Al<sub>3</sub>Sc(L1<sub>2</sub> structure). The effects of transition metal (TM) and/or rare earth (RE) and/or lithium additions on the temporal evolution of Al<sub>3</sub>(Sc1-xTMx or REx) is determined for a range of concentrations of TMs and/or REs. The time dependencies of the mean radius, number density, and supersaturations in the matrix and coherent precipitates are determined, during the coarsening regime, and used to extract alpha-Al/Al<sub>3</sub>(Sc1-xTMx or REx) interfacial free energies, solute diffusivities, solute solubilities in alpha-Al. The measured interfacial free energies are compared with first-principles calculations, using the Vienna ab initio simulation package (VASP), wherever possible. The relevance of this research to the use of

these Al(Sc) based alloys for high temperature structural applications is also discussed. Research supported by DOE.

3:00 PM

**First-Principles Cluster Expansions for Predicting Surface Reconstructions:** Wei Chen<sup>1</sup>; *Chris Wolverton*<sup>1</sup>; William Schneider<sup>2</sup>; <sup>1</sup>Northwestern University; <sup>2</sup>University of Notre Dame

The cluster expansion (CE), pioneered by the work of Prof. de Fontaine, has become a remarkably ubiquitous and useful tool for studying problems involving states of configurational order/disorder. Here, we use a CE approach to study the "missing-row" reconstructions of (110) surfaces of transition metals. It is well-known that Au and Pt undergo a (1×2) missing-row reconstruction, while clean surfaces of Cu and Ag do not. We have used density functional calculations with a CE to study (110) surfaces as a 2D system of metal atoms and vacancies. The CE correctly demonstrates the (1×2) missing-row structure is stable for the (110) surface of Au and Pt, but not for Cu and Ag. The finite temperature properties of the missing-row surfaces were also studied by a CE+Monte Carlo approach, and we find transition temperatures, step energy anisotropy, and equilibrium shapes for the reconstructed surface in good agreement with experimental results.

3:20 PM

**Effects of Temperature and Chemical Order on Phonons in Fe-V Alloys:** *Jorge Munoz*<sup>1</sup>; Matthew Lucas<sup>2</sup>; Brent Fultz<sup>1</sup>; <sup>1</sup>California Institute of Technology; <sup>2</sup>Oak Ridge National Laboratory

Inelastic neutron scattering spectra were measured from 300 to 773 K on B2 ordered FeV, and on A2 disordered solid solutions of bcc Fe-V alloys of different compositions. A substantial softening of the phonons upon ordering was observed, so a higher vibrational entropy stabilizes the ordered phase. Generalized phonon density of states (GDOS) curves were obtained from these data and a general cluster expansion was employed to extract interaction generalized phonon DOS (IGDOS) functions from the disordered alloys. The long-range order parameter was obtained at each temperature. The reconstruction of the ordered FeV GDOS from the IGDOS functions is in qualitative agreement with the measurements, and predicts a change in vibrational entropy with ordering of about +0.2 kB/atom.

3:40 PM Break

4:10 PM Invited

**Modeling Ni-C Alloys to Study the Growth of Carbon Nanotubes and Graphene Sheets:** *François Ducastelle*<sup>1</sup>; Hakim Amara<sup>1</sup>; Christophe Bichara<sup>2</sup>; <sup>1</sup>LEM CNRS-ONERA; <sup>2</sup>CINaM-CNRS

We have developed a tight binding model for Ni-C alloys to study the catalytic nucleation and growth of graphene sheets or of single wall carbon nanotubes (1). The model describes the total energy of the system as a sum of atomic contributions, and is coupled to Monte Carlo simulations in different thermodynamic ensembles. Using grand canonical conditions, we calculate the adsorption isotherms and the corresponding configurations of C atoms on Ni surfaces as well as on crystalline or amorphous Ni clusters. At low concentration carbons atoms interact strongly with nickel. At higher concentration carbon segregates and self-organize to form sp<sup>2</sup> graphitic structures which no longer interact with nickel atoms. This accounts for the catalytic properties of Ni but also of Fe and Co in the formation of these structures. (1) H. Amara, C. Bichara and F. Ducastelle, Phys. Rev. B 79, 014109 (2009).

4:40 PM

**Equilibria among R<sub>n</sub>CoIn<sub>2+3n</sub> Phases (R= La, Ce, Dy) Having Ho<sub>n</sub>CoGa<sub>2+3n</sub> Structures:** *Randal Newhouse*<sup>1</sup>; Gary Collins<sup>1</sup>; <sup>1</sup>Washington State University

Recent experiments showed high diffusional jump frequencies of Cd probes on the In-sublattice in RIn<sub>3</sub> phases of L1<sub>2</sub> structure (R= rare-earth) [Phys. Rev. Lett. 92, 225901 (2004); 102, 155901 (2009)]. Jump frequencies were determined from measurements of nuclear quadrupolar relaxation using perturbed angular correlation spectroscopy. Here, related ternary phases R<sub>n</sub>CoIn<sub>2+3n</sub> (R= La, Ce, Dy) were studied that are formed by periodic replacement of mixed In-R layers with layers of transition-metal atoms (prototypes Ho<sub>n</sub>CoGa<sub>2+3n</sub>). Hyperfine interaction signals were observed that are consistent with Cd probes on In-sites in either type n=1 or n=2 phases or in a disordered mixture of type n=1 and 2 layers. Jumping was detected only at much higher temperatures than in L1<sub>2</sub> phases. The evolution of signals during annealing and also up to temperatures where the phases disappear will be presented and discussed.



5:00 PM

**First Principles Shape Memory Alloy Design: Ni-Ti-X (Pt, Pd) Ternary Systems:** *Nicholas Hatcher*<sup>1</sup>; *Oleg Kontsevoi*<sup>1</sup>; *Arthur Freeman*<sup>1</sup>; <sup>1</sup>Northwestern University

We investigate ternary additions on the martensitic behavior of NiTi by applying ab initio calculations using the highly precise FLAPW method to the Ni-Ti-X(Pt, Pd; 0-30%) system. We determine ternary site preferences, pair interaction energies, and the energy hierarchy among the phases, finding that Pd and Pt atoms replace Ni and decorate the lattice at second and third nearest neighbors from one another, respectively. We calculate the cleavage and planar generalized stacking fault energetics of the {001}, {011}, and {112} shear planes to determine shear and brittle/ductile behavior and identify a high resistance to {001} shear. Detailed elastic properties are calculated and analyzed in connection with the martensitic transformation, and we show that the  $C'$  elastic constant becomes unstable with increased alloying. Finally, we explain the effect of these additions on the NiTi transformation path. These results provide further inputs for multiscale approaches to SMA design. \*Supported by AFOSR (FA9550-07-1-0174)

5:20 PM

**Gamma-Gamma' Interfacial Free Energy through In-Silico Nucleation Experiments:** *Stefano Angioletti-Uberti*<sup>1</sup>; *Mark Asta*<sup>2</sup>; *Christopher Woodward*<sup>3</sup>; *Axel van de Walle*<sup>4</sup>; *Peter Lee*<sup>1</sup>; *Mike Finnis*<sup>1</sup>; <sup>1</sup>Imperial College London; <sup>2</sup>University of California Davis; <sup>3</sup>Air Force Research Laboratory; <sup>4</sup>California Institute of Technology

By modeling the energetics of the system through a cluster expansion formalism, we perform in-silico nucleation experiments in a Ni-Al alloy at the gamma-gamma+gamma' phase boundary. From these simulations we obtain the probability of formation for clusters of different sizes and thus their free energy. We interpret our results using classical nucleation theory, and from these assumptions we derive the gamma/gamma' interfacial free energy. The results compare well with separate calculations of the interfacial free energy for planar interfaces in the same system, based on the same cluster expansion. Additionally, we obtain qualitative and quantitative information on the size dependence of the interfacial free energy, which is found to be an important correction to include when modelling the energetics of nanosized clusters

5:40 PM

**Multi-Scale Modeling of Martensite Formation in Fe-Based Solid Solutions:** *Alexander Udyansky*<sup>1</sup>; *Johann von Pezold*<sup>1</sup>; *Jörg Neugebauer*<sup>1</sup>; <sup>1</sup>Max-Planck-Institut für Eisenforschung GmbH

Martensitic phases refer to tetragonal states of interstitial Fe-based solid solutions containing carbon, nitrogen or oxygen. We study such dilute phases by combining atomistic modeling with the microscopic elasticity theory (MET), which allows us to account for long-ranged elastic interactions between impurities. The short-range chemical interactions, as well as the parameters entering the MET are obtained atomistically employing density functional theory (DFT). This approach allowed us to compute phase diagrams and provided a direct insight into the stability and formation of martensite: specifically, tetragonal states are predicted to be preferred also at low C concentrations due to a thermodynamically driven orientational ordering of carbon interstitials. The critical concentration for the cubic-tetragonal transition at room temperature is found in excellent agreement with experimental data. This methodology allows to study long-range elastic interactions even with rather modest supercell sizes making it an ideal tool in combination with modern DFT approaches.

### International Symposium on High-Temperature Metallurgical Processing: Ceramics and Intermetallics

*Sponsored by:* The Minerals, Metals and Materials Society, TMS Extraction and Processing Division, TMS: Pyrometallurgy Committee  
*Program Organizers:* Jaroslaw Drellich, Michigan Technological University; Jiann-Yang Hwang, Michigan Technological University; Tao Jiang, Central South University; Jerome Downey, Montana Tech

Monday PM

Room: 619

February 15, 2010

Location: Washington State Convention Center

*Session Chair:* Jerome Downey, Montana Tech

2:00 PM Keynote

**Process Development: Challenges and Driving Forces for Change:** *Karl Forwald*<sup>1</sup>; <sup>1</sup>Elkem AS Solar

The set-back in the global economy has left us in a stand-still in a large part of the high temperature processing industry. For many of us this may also be a time for long term thinking: What are the challenges for high temperature processing of materials? Do we need new materials and processes? Can we identify some main driving forces for new development? Who is in a position to decide on what development directions to follow: Shall we lean on international declarations, government regulations or board room and management decisions? Or will "the market" eventually give us the feed-back we need in order to set the course? These and other questions will be discussed from the authors point of view.

2:40 PM

**Glass Coating for Iron-Based Powder Metallurgy Components:** *Adele Garkida*<sup>1</sup>; *Jiann-Yang Hwang*<sup>2</sup>; *Xiaodi Huang*<sup>2</sup>; *Allison Hein*<sup>2</sup>; *Zhiwei Peng*<sup>2</sup>; <sup>1</sup>Ahmadu Bello University; <sup>2</sup>Michigan Technological University

Die-pressed Fe-1wt% C powder metallurgy compacts having theoretical densities ranging from 75%-85% were used as coating substrates. The glass slurries used for coating was prepared by stirring pulverized acustar untempered glass into butanol. Copper oxide, iron oxide and cobalt oxide were evaluated as transition metal oxide additives to promote adherence of the glass to the ferrous substrate. Likewise Borax and Boron oxide were evaluated as boron additives. Initially samples were coated by brushing the slurry onto the compact, later samples were coated by spraying the slurry onto the compact. These were sintered in vacuum at 1120°C with 1 hour holding time. The coating composition adopted consisted of 70 wt% pulverized glass, 25 wt% boron oxide and 5 wt% cobalt oxide and its potential durability was characterized using an optical metallography. This can be employed as a wear-resistant coating for iron-based PM components used in automotive applications.

3:00 PM

**Thermodynamic Measurement of Al<sub>2</sub>O<sub>3</sub>-B<sub>2</sub>O<sub>3</sub> System by Double Knudsen Cell Mass Spectrometry:** *Takashi Nagai*<sup>1</sup>; *Masafumi Maeda*<sup>1</sup>; <sup>1</sup>The University of Tokyo

Thermodynamic information on Al<sub>2</sub>O<sub>3</sub>-B<sub>2</sub>O<sub>3</sub> system is important for various high temperature processes in ceramics, glass, and metallurgical industries, but the information is extremely limited. Recently, a process to produce solar cell grade Si from metallurgical grade Si by slag refreshing has been studied. In previous study, the possibility of the removal of B from Si using flux containing Al<sub>2</sub>O<sub>3</sub> was reported although B is one of the most difficult elements to remove from Si. In this study, vapor pressure of B<sub>2</sub>O<sub>3</sub> in equilibrium with Al<sub>2</sub>O<sub>3</sub>-B<sub>2</sub>O<sub>3</sub> compounds or melts in Al<sub>2</sub>O<sub>3</sub>-B<sub>2</sub>O<sub>3</sub> system were measured by double Knudsen cell mass spectrometry. The Gibbs energy of formation of Al<sub>11</sub>B<sub>4</sub>O<sub>33</sub> was estimated from the vapor pressure in equilibrium with a mixture of Al<sub>11</sub>B<sub>4</sub>O<sub>33</sub> and Al<sub>2</sub>O<sub>3</sub> at 1573 to 1673 K. And activities of B<sub>2</sub>O<sub>3</sub> in two phase region Al<sub>11</sub>B<sub>4</sub>O<sub>33</sub> and B<sub>2</sub>O<sub>3</sub>-rich liquid, and Al<sub>2</sub>O<sub>3</sub>-B<sub>2</sub>O<sub>3</sub> melts were obtained at 1373 to 1423 K.

Mon. PM

# Technical Program

3:20 PM

**Bonite - A New Raw Material Alternative for Silica-Free High Strength Aluminum Metal Refractories:** Dale Zacherl<sup>1</sup>; Andreas Bühr<sup>2</sup>; Dagmar Schmidtmeier<sup>2</sup>; Robert McConnell<sup>1</sup>; <sup>1</sup>Almatis, Inc; <sup>2</sup>Almatis GmbH

Refractory castables in the aluminum industry as well as chemical and petrochemical industries typically see much lower temperatures than in the steel industry. The maximum temperature is very often in the range of 800 – 1200 °C. Nevertheless these applications can also be very demanding regarding mechanical strength, abrasion resistance, and chemical stability. Mechanical strength of refractory linings is of particular interest at the intermediate temperatures, which do not provide sufficient energy for strong sintering reactions. This paper discusses raw material concepts for high purity silica-free castables for demanding aluminum or petrochemical applications. Bonite, a new dense calcium hexaluminate (CA6) refractory aggregate is introduced for low wettability, high temperature stability and low thermal conductivity of aluminum refractories.

3:40 PM Break

3:55 PM

**On Line Monitoring and Process Parameters Estimation of Multiple Passes Laser Phase Transformation Hardening by Using High-Power Direct Diode Laser:** Soundarapandian Santhanakrishnan<sup>1</sup>; Radovan Kovacevic<sup>1</sup>; <sup>1</sup>Southern Methodist University

A component treated by a laser beam especially during multiple passes needs on line monitoring and process parameter optimization to achieve the required surface properties and mechanical properties. In this work, a coupled non-contact monitoring and estimation technique is developed. This technique is based on a laser-assisted infrared pyrometer and an infrared camera to monitor the laser treated surface temperature in real time. A laser-assisted infrared pyrometer is used to measure the emissivity and surface temperature of the laser treated zone. The measured emissivity is used as an input required for the infrared camera. An infrared camera is used to measure the temperature distributions across the laser treated surface in real time. A polynomial fitting method is used to obtain a relationship between the process parameters and the surface hardness for multiple passes laser hardening.

4:15 PM

**Phase Transformation of Andalusite-Mullite and Its Fiber Reinforcement to Refractory Ceramics:** Bowen Li<sup>1</sup>; Jiann-Yang Hwang<sup>1</sup>; Wayne Bell<sup>1</sup>; <sup>1</sup>Michigan Technological University

Andalusite (Al<sub>2</sub>SiO<sub>5</sub>) is a widely distributed industrial mineral. When heated to 1200-1400°C, andalusite will be rapidly decomposed into mullite and vitreous silica, a phase transformation process usually referred as mullitization. The phase transformation from andalusite to mullite can be different from a common crystal transition from a parent crystal to a product crystal. An individual andalusite crystal can be divided into thousands of fiber-shaped crystals of mullite. The finer the particle of andalusite is, the smaller the mullite fibers are produced. In this study, it was found that when fine particles of andalusite were dispersed among refractory aggregates in green body, cross-linked networks of mullite fibers were produced in sintered refractory bricks. This can increase the mechanical strength of refractory ceramics significantly.

4:35 PM

**Thermodynamic Measurement of Rare Earth Metal Systems by Knudsen Cell Mass Spectrometry:** Sho Shirai<sup>1</sup>; Takashi Nagai<sup>1</sup>; Masafumi Maeda<sup>1</sup>; <sup>1</sup>Institute of Industrial Science, University of Tokyo

RE metals are used as various functional materials, such as Nd-Fe-B magnet, electrode materials of batteries, hydrogen storing alloy and so on. Thermodynamic properties of RE metal system are very important to produce and recycle the materials. The properties can not be, however, estimated easily by traditional methods, because chemical affinities of RE metal with oxygen are very strong. Using double Knudsen cell mass spectrometry, vapor pressure of RE metals in equilibrium with the alloys can be measured without effect of oxygen, because this measurement is run under high vacuum condition. In this study, we investigated thermodynamic properties of Nd-Fe systems by this method. Vapor pressure of Nd in Nd-Fe was measured and the activities of Nd and Fe in Nd-Fe at 1373 to 1523K were revealed in complete composition domain. Gibbs free energy of formation of Nd<sub>2</sub>Fe<sub>17</sub>, intermetallic compound of Nd-Fe, was estimated.

4:55 PM

**A Technique to Measure Heat of Reaction in TiB<sub>2</sub> Reinforced Intermetallic Matrix Composites:** Andrew Baker<sup>1</sup>; S.L. Kampe<sup>1</sup>; Tony Zahrah<sup>2</sup>; <sup>1</sup>Michigan Tech; <sup>2</sup>Matsys, Inc

Reaction synthesis is a technique to produce ceramics, intermetallics, and in-situ composite materials. The technique, and the resulting microstructures of the product, rely upon a large enthalpy reduction during the reaction, and also the relatively high temperatures that are characteristic of the process. This research focuses on a technique to measure the heat of reaction of a series of TiB<sub>2</sub>-reinforced titanium aluminide composites. To overcome the kinetic constraints and achieve ignition in these formulations, a boron (B)/potassium nitrate (KNO<sub>3</sub>) initiation aid was incorporated within the blended reactant compact and placed in an unmodified bomb calorimeter. A design of experiments matrix was created to determine the enthalpy of reaction and the associated sensitivity to a variety of process variables including volume relative proportions of product phases, reactant particle size, B/KNO<sub>3</sub> fraction, gas environment and initial bomb pressure. This research was sponsored by the Office of Naval Research under grant N0014-07-1-1055.

5:15 PM

**Microwave Synthesis of Nano-Boron Carbide Powder:** Liang Hu<sup>1</sup>; Huimin Lu<sup>1</sup>; Yi Liu<sup>1</sup>; <sup>1</sup>Beihang University

Boron Carbide (B<sub>4</sub>C) is a light weight material and has many fine performances, such as high melt point, high hardness, low density, and good abilities of neutron absorption and anti-chemical corrosion, so widely applied in some domains such as refractory, project ceramics, nuclear industry, and astronavigation and so on. This paper describes the synthesis process of the nano-boron carbide powder with the microwave carbothermal reduction method. The experiments showed that the microwave synthesis temperatures of nano-boron carbide were controlled in the 1600~1700°C range and the time in 60min. The energy consumption of this method has been reduced by about 70% as compared with traditional heating methods. The prepared powder has high purity and particle size in 30~90nm range, which is a very good raw material for sintering boron carbide products with high performances. In the meantime, the thermodynamics and kinetics of the microwave synthesizing nano-boron carbide were systematically studied.

## Jim Evans Honorary Symposium: Cast Shop Aluminum Production Joint Session: Flow and Solidification Phenomena in Nonferrous Casting

*Sponsored by:* The Minerals, Metals and Materials Society, TMS Extraction and Processing Division, TMS Light Metals Division  
*Program Organizers:* Ben Li, University of Michigan; Brian G. Thomas, University of Illinois at Urbana-Champaign; Lifeng Zhang, Missouri University of Science and Technology; Fiona Doyle, University of California, Berkeley; Andrew Campbell, WorleyParsons

Monday PM Room: 620  
February 15, 2010 Location: Washington State Convention Center

*Session Chair:* Lifeng Zhang, Missouri University of Science and Technology

2:00 PM Introductory Comments

2:10 PM

**Coupled Multi-Physics Modeling of Continuous Casting of Steel and DC Casting of Aluminum:** Philippe Thevoz<sup>1</sup>; Olivier Ludwig<sup>1</sup>; Marco Aloe<sup>1</sup>; <sup>1</sup>Calcom ESI

As the product quality requirements are ever increasing and the gains in productivity are a must to sustain the competition, numerical modeling is now an essential tool to reach these targets. Due to the complexity of continuous and DC casting processes, a coupled multi-physics approach is required to capture all the important phenomena. This paper will present a fully coupled thermal-flow-transport-stress 3D modeling of continuous casting processes, with illustrations on continuous casting of steel and DC casting of aluminum. The influence of fluid flow, using different nozzle designs, on the first solidified shell will be investigated, together with the stress build-up and the air gap formation. Such coupling is achieved using a novel technique recently developed based upon the Mixed Lagrangian-Eulerian method (MiLE) implemented in the Finite Element



software ProCAST. Finally, results of microporosity, hot tearing, grain structure and solid state transformations, based upon further multi-physics coupling, will be presented.

### 2:35 PM

#### **Metal Flow and Heat Transfer in Wagstaff® Rapidfill™ Metal Distribution Systems for Billet DC Casting:** *Bin Zhang*<sup>1</sup>; <sup>1</sup>Wagstaff Inc

Modelling of fluid flow and heat transfer in Wagstaff® Classic and RapidFill™ metal distribution systems for billet DC casting were conducted during the start-up and casting phases. Results clearly show the effect of different designs in the two systems on metal fill/flow and heat loss. The Wagstaff® RapidFill™ system allows metal to fill casting positions almost simultaneously. Total metal fill time is greatly reduced compared to the Classic system. The hold time difference between casting positions is also significantly decreased in the RapidFill™ system. It is shown that the metal heat loss in a RapidFill™ system is ~3-10°C less than that of a Classic system during the start-up phase and ~3°C less when casting approaches steady state. Details on metal flow and temperature variation during the start-up phase are presented for comparison at strategic locations. Results were verified through field measurements.

### 3:00 PM

#### **Thermal-Fluid-Compositional Model of Electron Beam Casting of Ti-6Al-4V:** Riley Shuster<sup>1</sup>; Daan Maijer<sup>1</sup>; *Steven Cockcroft*<sup>1</sup>; Tao Meng<sup>1</sup>; Denis Favez<sup>1</sup>; David Tripp<sup>2</sup>; Stephen Fox<sup>3</sup>; <sup>1</sup>The University of British Columbia; <sup>2</sup>TIMET Morgantown; <sup>3</sup>TIMET Henderson

Two of the principle concerns during the final stage of the semi-continuous ingot casting process associated with Electron Beam Cold Hearth Remelting/Melting of titanium alloys are the formation of shrinkage voids and the evaporation of volatile species. The presence of voids or loss of chemistry control requires ingot cropping before further downstream processing. Raising the shrinkage void location can be achieved through hot topping, where the top surface is heated after steady state casting is complete. However, hot topping increases selective evaporation. A mathematical model of the final transient stage has been developed to assist in reducing the associated production losses during casting of Ti-6Al-4V ingots and slabs. The model, developed within a commercial software platform, solves the coupled thermal-fluid flow problem including solute conservation and evaporation. Plant trial measurements including sump depth, pool profile, and compositional analysis are used to validate the model predictions under various hot topping conditions.

### 3:25 PM

#### **The Effect of SF<sub>6</sub> on the Surface Tension of AZ91D Magnesium Alloy:** Steven Roach<sup>1</sup>; *Hani Henein*<sup>2</sup>; <sup>1</sup>Vale INCO Ltd.; <sup>2</sup>University of Alberta

A new draining crucible technique was used to measure the effect of SF<sub>6</sub> on the surface tension of magnesium. This technique is based on the relationship between the height of metal in a crucible and the outgoing flowrate. This relationship is obtained from a model where the surface tension, viscosity and density of a melt are simultaneously determined. Experiments performed with molten magnesium at temperatures from 923 to 1173K indicate under Argon the surface tension (N/m) and density (kg/m<sup>3</sup>) are [0.62 – 2.13 e-4 (T-T<sub>m</sub>)] and [1651 – 0.16 (T-T<sub>m</sub>)], which is within 6.5pct. and 2.5pct., respectively, of values reported in the literature. The viscosity (Nsm<sup>-2</sup>) has been determined to range from 8.46e-4 at 8K superheat to 2.93e-4 at 250K superheat. SF<sub>6</sub> reduces the surface tension (N/m) of AZ91D to [0.491 – 7.44e-4 (T-T<sub>m</sub>)].

### 3:50 PM Break

### 4:05 PM

#### **Application of Computational Fluid Flow and Experimentations to Improve Horizontal Casting Process Performance at Rio Tinto Alcan:** *André Larouche*<sup>1</sup>; <sup>1</sup>Rio Tinto Alcan

Over the last decade computational fluid dynamic has been increasingly used in the aluminum industry in order to understand, analyze and improve various processes in reduction, raw material and casting. Improved computer performances and user friendliness of CFD software has allowed reducing design cycle time, hence improving applicability of CFD in an industrial context. This paper describes the successful application of numerical modeling capabilities in conjunction with experimental approaches to understand and improve the horizontal direct chilled (HDC) casting of T-ingot. Several examples of fluid flow and thermal analysis such as metal feeding, casting speed increase, and alloy transfer are brought and described to highlight the contribution of CFD

to the development and successful implementation of practical solutions in plants.

### 4:30 PM

#### **DC Casting of Aluminum Alloys — Importance of Mold Boundary Conditions:** *Amir Baserinia*<sup>1</sup>; Harry Ng<sup>1</sup>; David Weckman<sup>1</sup>; Mary Wells<sup>1</sup>; <sup>1</sup>University of Waterloo

Accurate thermofluids models of DC casting of aluminum ingots must be capable of solving the heat transfer equation within the ingot with realistic external thermal boundary conditions. These boundary conditions are typically separated into two zones: primary cooling, which occurs inside the water-cooled mold, and secondary cooling, where a film of water directly contacts the ingot surface. In this study, a simple yet comprehensive model is developed for the primary cooling region of the steady-state DC casting process. First the mold and its water-cooling were modeled using a commercial CFD package and the heat transfer coefficient was determined. A simple density-based model was then used to predict the added effect on the primary cooling of ingot shrinkage and the formation of a gap between the ingot and mold. Simulations using this model suggest that remelting of the primary shell and liquid metal exudation can be predicted.

### 4:55 PM

#### **Measurement of As-Cast Residual Stresses in an Aluminium Alloy AA6063 Billet Using Neutron Diffraction:** *Jean-Marie Drezet*<sup>1</sup>; Alexander Evans<sup>2</sup>; Christophe Jaquero<sup>3</sup>; André Phillion<sup>1</sup>; <sup>1</sup>Ecole Polytechnique Federale Lausanne; <sup>2</sup>Paul Scherrer Institut, Villigen; <sup>3</sup>Alcan Aluminium Valais, Sierre

Machining and sawing Aluminium DC cast products without a stress relief treatment can lead to uncontrolled distortion, crack formation, and significant safety concerns due to the development of thermally-induced residual stresses within the casting. Numerical models have been developed to compute these residual stresses and only validated against measured surface distortions. In the present contribution, the variation in residual strains and stresses as a function of radius has been measured using neutron diffraction in an AA6053 grain-refined cylindrical billet. A thermomechanical finite element model was used to determine the minimum section-length which can be sawed from the billet without significantly relaxing the residual stresses while conforming to the requirements of the neutron diffractometer. The results of these measurements, particularly the depth at which the axial and hoop stresses change sign, can be used for validation of the numerical models and provide insight into the development of residual stresses within castings.

## Magnesium Technology 2010: ICME I (Integrated Computational Materials Engineering)

*Sponsored by:* The Minerals, Metals and Materials Society, TMS Light Metals Division, TMS: Magnesium Committee

*Program Organizers:* Sean Agnew, University of Virginia; Eric Nyberg, Pacific Northwest National Laboratory; Wim Sillekens, TNO; Neale Neelameggham, US Magnesium LLC

Monday PM

Room: 612

February 15, 2010

Location: Washington State Convention Center

*Session Chairs:* John Allison, Ford Motor Company; Alan Luo, General Motors Corporation

### 2:00 PM

#### **Integrated Computational Materials Engineering (ICME) for Magnesium: An International Pilot Project:** *John Allison*<sup>1</sup>; Baicheng Liu<sup>2</sup>; Kevin Boyle<sup>3</sup>; Lou Hector<sup>4</sup>; Robert McCune<sup>5</sup>; <sup>1</sup>Ford Motor Company; <sup>2</sup>Tsinghua University; <sup>3</sup>CanMET Materials Technology Laboratory; <sup>4</sup>General Motors R&D Center; <sup>5</sup>Robert C. McCune and Associates

This talk will provide an overview and progress report for an international collaborative project developing an ICME infrastructure for magnesium for use in automotive body applications. Quantitative processing-microstructure-property relationships are being developed for extruded magnesium alloys, sheet-formed magnesium alloys and high pressure die cast magnesium alloys. These relationships are captured in computational models which are then linked with manufacturing process simulation and used to provide constitutive models for component performance analysis. The long term goal is to capture

Mon. PM

# Technical Program

this information in efficient computational models and in a web-centered knowledge base. The work is being conducted at leading universities, national labs and industrial research facilities in the US, China and Canada. This project is sponsored by the U.S. Department of Energy, the U.S. Automotive Materials Partnership (USAMP), Chinese Ministry of Science and Technology (China) and Natural Resources Canada (Canada).

## 2:20 PM Keynote

**Thermodynamic and Elastic Properties of La-X (X=Al,Mg) Intermetallic Compounds from First Principles Calculations:** *Louis Hector Jr<sup>1</sup>*; Jan Wrobel<sup>2</sup>; Krzysztof Kurzydowski<sup>2</sup>; <sup>1</sup>GM R&D Center; <sup>2</sup>Warsaw University of Technology

The La-X (X=Al,Mg) intermetallic compounds are a scientifically interesting class of materials with broad technological relevance. Some occur as precipitates in certain magnesium alloys while others are considered to be potential hydrogen storage materials. Using first principles density functional theory, we computed thermodynamic and elastic properties of LaAl, LaAl<sub>2</sub>, LaAl<sub>3</sub>, LaAl<sub>4</sub>, La<sub>3</sub>Al<sub>11</sub>, La<sub>3</sub>Al, La<sub>16</sub>Al<sub>13</sub>, LaMg, LaMg<sub>2</sub>, LaMg<sub>3</sub>, La<sub>2</sub>Mg<sub>17</sub> and La<sub>5</sub>Mg<sub>41</sub>. Specifically, lattice parameters, thermodynamic functions from phonon calculations based upon the direct method for lattice dynamics, and enthalpies of formation at 0 and 298K, were calculated for each compound with the generalized gradient approximation. Components of the elasticity tensor, C<sub>ij</sub>, were computed with a least squares fitting method using a set of sequential strains to improve the accuracy of each calculation. Polycrystalline moduli based on the Hill criteria were calculated from the C<sub>ij</sub>. A new La<sub>3</sub>Al structure was identified from a soft mode in the phonon dispersion curves.

## 2:50 PM

**Numerical Simulation of Direct Extrusion of Magnesium Alloys:** *Wojciech Misiolek<sup>1</sup>*; Luigi DePari<sup>1</sup>; <sup>1</sup>Lehigh University

An existing flow stress model was examined with as-cast AZ31 compression test data from literature for a range of temperatures (250-450 deg C) and strain rates (0.001-30 s<sup>-1</sup>) to evaluate its applicability to direct extrusion of AZ31. The model was successful in predicting the hardening region of the flow stress curve but was unable to simulate the sizable recovery portion of the flow stress curve that Mg alloys tend to exhibit before failure. In order to correct for this shortcoming, an empirical recovery expression was developed for the model with the same range of temperatures and strain rates. This modified flow stress model has then been implemented into the finite element software package DEFORMTM 3-D to predict the state variables of hot-direct extrusion of Mg alloy automobile structural components manufactured with an port-hole extrusion die.

## 3:10 PM Keynote

**On Modeling the Extrusion Process of Magnesium Alloys:** *Esteban Marin<sup>1</sup>*; Stephen Horstemeyer<sup>1</sup>; Clemence Bouvard<sup>1</sup>; Douglas Bammann<sup>1</sup>; Haitham El Kadiri<sup>1</sup>; Paul Wang<sup>1</sup>; <sup>1</sup>Mississippi State University

The work presents the lab-scale extrusion experiments being performed on magnesium alloy AZ61, the numerical modeling of the process using an Eulerian / ALE approach, and the constitutive modeling framework characterizing the material's mechanical response. The lab-scale experiments have been planned to learn about the extrusion process (material microstructure, material flow, processing parameters) as well as to be used as a benchmark case to validate the modeling and simulation tools. The experiments have been modeled using HyperXtrude, an Eulerian finite element code suitable to represent deformation processes where severe plastic deformation occurs, as in the case of extrusion. Two particular material modeling frameworks have been employed to model the process: a macroscopic internal state variable (ISV) model and a crystal plasticity model. Predictions from the numerical tools (finite element code and material models) are compared with experiments to show the predictive capability of the modeling approach.

## 3:40 PM Break

## 4:00 PM

**Transmutation and Accommodation Effects by Glide Twinning:** *Andrew Oppedal<sup>1</sup>*; Haitham El Kadiri<sup>1</sup>; <sup>1</sup>Mississippi State University

Magnesium is being intensively integrated in large mechanical structures for energy savings due to its favorable strength / stiffness to weight ratio. This industrial renaissance is reviving attention to the complex fundamentals of deformation twinning in metallic double-lattice structures. Significant

advances were made to integrate deformation twinning in polycrystal plasticity simulations, but constitutive models are still unable to capture significant hardening mechanisms unique to deformation twinning identified and studied in the late 1950s through the 1970s. This spurs the need to recall and analyze major mechanisms relevant to hardening in double lattice metals. In this work, we emphasize the effect of parent dislocation "transmutation" upon their incorporation within a twin, and effects related to slip and kinking accommodations of twinning deformation. A model routine is formulated for these mechanisms within the framework of a dislocation-density based constitutive model put forward by Beyerlein and Tomé (2008).

## 4:20 PM

**Plasticity in a Rod-Textured Extruded Mg AM30 Alloy:** *Q. Ma<sup>1</sup>*; H. El Kadiri<sup>1</sup>; <sup>1</sup>Mississippi State University

When a sharp-textured hcp metal is loaded under an orientation whereupon twinning or detwinning is profuse, the stress-strain curve is sigmoidal with a critical inflection point. Authors unarguably attributed the dramatic stress increase in the lower-bound vicinity of the inflection point to a combined effect of i) Hall-Petch mechanism correlated to grain refinement by twinning, and ii) twinning-induced reorientation requiring activation of hard slip modes. Accordingly, these two mechanisms cast the driving approach for determination of appropriate strain hardening model parameters in polycrystal plasticity simulations, namely the Visco-Plastic Self Consistent (VPSC) model developed by Molinari (1987) and implemented by Lebensohn and Tome (1993). Predominantly, the Hall-Petch extent needed to fit the sigmoidal curve corresponded to a latent hardening rate of twinning on other active slip modes 400% to 3500% higher than the slip-slip self-hardening rates. In this paper, we experimentally and numerically demonstrate that these two mechanisms alone cannot consistently explain the effect of profuse twinning on the hardening rate in textured hcp metals. We argue based on adopting various mechanistic approaches in hardening model correlations. These correlations are motivated by available literature and carefully analyzed twinning-induced texture evolution upon strain. We mainly focus on the extended formulation of Voce hardening model most commonly used in the polycrystal VPSC simulations. The hcp material is exemplified by a rod-textured AM30 alloy whereupon twinning readily impinges the entire structure under a suitable compression orientation. We suggest the parent dislocation transmutation mechanism upon incorporation within the twin lamella as to play a major role in the increasing hardening rate induced by profuse twinning in the lower-bound range of the inflection point.

## 4:40 PM

**Effect of Grain-Matrix Interaction Stiffness on Slip System Hardening Parameters of a Viscoplastic Self-Consistent Polycrystal Model:** *Babak Raeesinia<sup>1</sup>*; Sean Agnew<sup>1</sup>; <sup>1</sup>University of Virginia

The flow curves and Lankford coefficients of a rolled AZ31 magnesium alloy deformed under different uniaxial strain paths are simulated using a viscoplastic self-consistent polycrystal model. The experiments are modeled while the rigidity of the interaction between the individual grains and the surrounding polycrystalline aggregate is systematically varied from a stiff (nearly iso-strain) to a compliant (nearly iso-stress) interaction. The simulated critical resolved shear stress (CRSS) for the prismatic slip system is insensitive to the type of interaction used, consistent with the notion that the flow stress in magnesium alloys is controlled by the strength of the prismatic slip mode. This is in contrast to the trend observed for the basal slip system where the model CRSS rises appreciably as more compliant interactions are used. Simulated CRSS ratios of non-basal slip to basal slip are closest to those reported in the literature for single-crystals in the stiff interaction regime.

## 5:00 PM

**Extracting Post-Uniform Constitutive Behavior from High Temperature Tensile Test Data:** *Cyrus Dreyer<sup>1</sup>*; Louis Hector<sup>1</sup>; Sean Agnew<sup>1</sup>; <sup>1</sup>University of Virginia

Constitutive model development for the simulation of hot forming operations is traditionally conducted using hot compression or torsion data, yet neither is possible for thin sheet metal due to sample buckling. It is widely recognized to be difficult to extract constitutive behavior from tensile test data at strain levels adequate for simulating metal forming. However, at the temperatures required for warm forming of magnesium alloys, the strain rate sensitivity can be sufficient to delay the onset of catastrophic localized necking instability to significant strain levels. This permits the extraction of true stress-true strain data even in



cases where modest strain softening, e.g., due to dynamic recrystallization has occurred. A protocol involving on-sample measurements of the strain within a localized region and invoking the Marciniak-Kucinski approach for describing the development of plastic instability is used to constrain the parameters of an internal state variable model due to Bammann, Chelsea, and Johnson.

### 5:20 PM

#### Strain Field Measurement during Bending of Extruded Magnesium Alloys:

Adi Ben-Artzy<sup>1</sup>; Louis Hector<sup>2</sup>; Paul Krajewski<sup>2</sup>; <sup>1</sup>Rotem Ind.; <sup>2</sup>GM

Tensile and compressive deformation of magnesium alloys AZ31, AZ61, AM50 and ZM21 were investigated with a digital image correlation (DIC) algorithm. Three and four-point bending tests of rectangular bars at selected orientations relative to the extrusion direction were conducted in a miniature screw-driven stage. Four-point bending was designed to give a plane strain state between the fixture pivots. Displacement and load data were acquired with external controller electronics and custom data acquisition software. High resolution digital images of one surface of each bar were recorded during deformation with a variable framing rate high speed digital camera. Post-processing of the image data with the DIC algorithm resulted in strain contour maps from which the evolution of tensile and compressive strains in both bending schemes was quantified. Bending strains were found to be sensitive to Mg alloy composition and orientation, and tensile bending data was in good agreement with uniaxial tensile tests.

### 5:40 PM

#### Cyberinfrastructure for Integrated Computational Material Engineering:

Tomasz Haupt<sup>1</sup>; <sup>1</sup>Mississippi State University

The goal of the cyberinfrastructure for ICME is to exploit the recent transformative research in material science involving multiscale physics-based predictive modeling, multiscale experiments and design. More specifically, the creation of the cyberinfrastructure will result in the development of "community of practice" portal that allows development and integration of multiscale physics-based materials models for selected properties and processes. This presentation demonstrates the use of the modern information infrastructure based on AJAX-based rich user interfaces, Service Oriented Architecture (SOA), Web Services and Grid computing streamlining of the process of gathering experimental results, and deriving the material properties (using online model calibration tools) for a particular material model (e.g., Damage Fit or Multistage Fatigue Fit) and employing the material model in finite element analysis in the process of building validated metamodels and design optimizations to support the Magnesium Front-End Three Nation Pilot Program.

## Magnesium Technology 2010: Primary Production and Flammability Issues

Sponsored by: The Minerals, Metals and Materials Society, TMS Light Metals Division, TMS: Magnesium Committee

Program Organizers: Sean Agnew, University of Virginia; Eric Nyberg, Pacific Northwest National Laboratory; Wim Sillekens, TNO; Neale Neelameggham, US Magnesium LLC

Monday PM Room: 613  
February 15, 2010 Location: Washington State Convention Center

Session Chairs: Neale Neelameggham, US Magnesium LLC; Adam Powell, Opennovation

### 2:00 PM

#### The Magnesium Industry Today: A Global Perspective: Greg Patzer<sup>1</sup>; <sup>1</sup>International Magnesium Association

This document/presentation will present the current situation in the global magnesium industry in 2009 and Ytd. 2010. World demand for magnesium continues to remain subdued, succumbing to the global recessionary period as well as intra-industry pressures. The industry has seen marked changes in the sources of supply for primary and alloyed magnesium in recent years. The current state and trends in the production side of the magnesium industry will be examined. The immediate past industry changes will be assessed as to the impact that is being realized today, while also examining those developing factors, which will impact the industry's future. Particular attention will be focused upon current production, capacity utilization and potential capacity

coming on line. Historical pricing as compared to production cost factors will be examined. Factors affecting future demand will be discussed as well as potential trends.

### 2:20 PM

#### Magnesium: Bridging Diverse Metal Markets: Susan Slade<sup>1</sup>; <sup>1</sup>US Magnesium LLC

Magnesium consumption crosses a multitude of metal industries as both a structural material and a chemical unit. Magnesium's superior strength to weight ratio and ductility enhances aluminum alloys and provides lightweighting opportunities in automotive, electronic and aerospace components. Its diverse chemical properties make magnesium important in the production of low-sulfur steel and ferroalloys, as a reducing agent for transition metals and organic chemistry, in electrochemical applications and finally pyrotechnic applications for the military. Growing environmental pressures and the global economic recession impact each of these consuming industries differently. The same pressures impart a long-term bearing on the supply side of the magnesium industry as well. The future impact of the convergence of the unique pressures on both the supply and demand of magnesium will be described.

### 2:40 PM

#### Development of Recyclable Mg-Based Alloys: Nathan Reade<sup>1</sup>; Jerry Sokolowski<sup>1</sup>; Adam Gesing<sup>2</sup>; Carsten Blawert<sup>3</sup>; Daniel Fechner<sup>3</sup>; Norbert Horst<sup>3</sup>; <sup>1</sup>University of Windsor; <sup>2</sup>GCI; <sup>3</sup>GKSS

The formation of phases during solidification and their disappearance during melting of Mg alloys with recyclable composition was studied with the help of macro thermal analysis using UMSA. Solidification rates were chosen to simulate the conditions encountered in conventional commercial magnesium shape casting processes. Distribution, quantity and composition of phases in the resultant microstructure were used to understand the measured mechanical and corrosion properties of these recyclable alloys.

### 3:00 PM

#### Preparation of Al-Mg Alloys from MgO by Molten Salt Electrolysis

Method: Sh Yang<sup>1</sup>; Fl Yang<sup>1</sup>; Xianwei Hu<sup>2</sup>; Zhaowen Wang<sup>2</sup>; Zhongning Shi<sup>2</sup>; Bingliang Gao<sup>2</sup>; <sup>1</sup>Jiangxi University of Science and Technology; <sup>2</sup>Northeastern University

Aluminum-magnesium alloys were prepared from magnesium oxide by molten salt electrolysis method. MgF<sub>2</sub>-BaF<sub>2</sub>-LiF was taken as electrolysis. Current efficiency was more than 80%, the maximum was 89.4%. Effect of temperature on electrolysis was great. The process of electrolysis was controlled together by electrochemical polarization and concentration polarization at 850°, but at 870° and 890°, the process was controlled only by electrochemical polarization. The results showed that electrolytic temperature had little effect on electrolytic process if about 7% KCl as additive was in electrolyte, and the electrolytic process was controlled by electrochemical polarization.

### 3:20 PM

#### Effect of KCl on Conductivity of BaF<sub>2</sub>-LiF-MgF<sub>2</sub> Molten Salts: Sh Yang<sup>1</sup>;

Fl Yang<sup>1</sup>; Guocheng Wang<sup>1</sup>; Xianwei Hu<sup>2</sup>; Zhaowen Wang<sup>2</sup>; Zhongning Shi<sup>2</sup>; Bingliang Gao<sup>2</sup>; <sup>1</sup>Jiangxi University of Science and Technology; <sup>2</sup>Northeastern University

Conductivity of molten salt was studied by continuously varying cell constant method. It was proved that the method was reliable and accurate by experiments. Cell impedance was measured by electrochemical instrument of a PGSTAT 30 and a BOOSTER 20A. The results were shown that effect of KCl on conductivity of molten salt was great for MgF<sub>2</sub>-BaF<sub>2</sub>-LiF electrolyte. Electrical conductivity was increased with content of KCl in electrolyte. Electrical conductivity could be increased 0.58s/cm with content of KCl in electrolyte from 0wt% to 11wt%. Also, Electrical conductivity could be increased 0.2-0.3s/cm if temperature was increased 40°. Activation energy of conductance was obtained by the experimental results.

### 3:40 PM

#### Powder Metallurgy of Magnesium: Is it Feasible?: Paul Burke<sup>1</sup>; Georges Kipouros<sup>1</sup>; <sup>1</sup>Dalhousie University

Magnesium and its alloys are attractive materials for use in automotive and aerospace applications because of the low density and good mechanical properties. However, difficulty in forming magnesium and the limited number of available commercial alloys limit their use. Powder Metallurgy (P/M) can be used to alleviate the formability problem through near-net-shape processing,

Mon. PM

# Technical Program

and also allows unique chemical compositions that can lead to new alloys with novel properties. A surface layer forms on Mg powders through reactions with the atmosphere, and this layer acts as a barrier to diffusion making traditional press and sinter processing problematic. Previously, attempts have been made to circumvent the issue with novel approaches to powder production, powder consolidation and sintering techniques. Discussion of the performance and applicability of these methods is provided. This work also presents an in-situ layer disruption mechanism by the use of Ca, which can utilize traditional press and sinter P/M technology.

## 4:00 PM Break

## 4:20 PM

**Fireproof Evaluation of CaO Added Mg-3Al, Mg-6Al, and Mg-9Al Mg Cast Products:** *Jin-Kyu Lee*<sup>1</sup>; Shae K. Kim<sup>1</sup>; <sup>1</sup>Korea Institute of Industrial Technology

Mg products are easily oxidized and burned when they are exposed to high temperature or fire by accident. The fireproof solution has been developed by adding CaO in Mg alloys. The fireproof was evaluated by three methods: quantitative DTA for small sphere specimen, furnace ignition test for burrs and machined chips, and torch ignition test for products. DTA was carried out for obtaining quantitative ignition temperature data with respect to specimen geometry and test environment; the furnace test for burr and chip ignition temperature data; and the torch test for ignition temperature data about manufactured products. This paper will discuss the results of fireproof properties of 1wt.% and 1.5wt.% CaO added Mg-3Al, Mg-6Al and Mg-9Al Mg alloys compared with other high temperature Mg alloys. Fireproof Eco-Mg alloy will be low-cost Mg alloys for airplane and train applications in terms of preventing poisonous gas generation, inhalation burn, and ignition generation.

## 4:40 PM

**Effect of Ca(OH)<sub>2</sub> on Oxidation and Ignition Resistances of Pure Mg:** *Dong-In Jang*<sup>1</sup>; Shae K. Kim<sup>1</sup>; <sup>1</sup>Korea Institute of Industrial Technology

CaO added Eco-Mg alloy has the potential to maximize the environmental benefits provided by lightweight, unlimited, and recyclable Mg alloy by eliminating global warming SF<sub>6</sub> or other protective gases as well as Be addition. It is possible to ensure the safety during manufacturing and application, especially without sacrificing process abilities and mechanical properties and increasing the cost of Mg alloy. However, only one problem of CaO is prone to moisture absorption during storage. Instead of CaO, it is attempted to use Ca(OH)<sub>2</sub>, which does not absorb moisture during storage, for Eco-Mg alloy. This paper will discuss the effect of Ca(OH)<sub>2</sub> on oxidation and ignition resistances of pure Mg and to compare the results with them of CaO addition. Pure Mg was used instead of Mg alloys to minimize the effects of other elements.

## 5:00 PM

**Research on the Oxidation Behavior of AZ91D-Based Magnesium Alloys:** *Hongjie Luo*<sup>1</sup>; <sup>1</sup>Northeastern University

Magnesium alloys are easily to be ignited and oxidized during heating and melting, especially in high temperature, so their applications are limited by these problems. In this study, some anti-ignition magnesium alloys were prepared by adding Ca, Ce mischmetal and Sb into molten AZ91D magnesium alloy and their oxidation behavior at high temperature were also measured. Meanwhile, the phase compositions of oxidation film were analyzed and the microstructure of these alloys was observed. The results showed that the antioxidant capacity of AZ91D-based alloys has been improved significantly after the elements of Ca, Ce mischmetal and Sb were added into them. The phenomenon of oxidation weight increase on the alloy's surface happens nearly at 700° when Ca, Ce mischmetal and Sb content are 1wt. %, 1 wt. % and 0.4 wt.%, respectively. The curves of oxidation weight increase of the above alloy are coincident closely when heated at 500° or 600°.

## 5:20 PM

**Low-Cost Zero-Emission Primary Magnesium Production by Solid Oxide Membrane (SOM) Electrolysis:** *Adam Powell*<sup>1</sup>; Uday Pal<sup>2</sup>; Steve Derezhinski<sup>1</sup>; <sup>1</sup>Metal Oxygen Separation Technologies, Inc.; <sup>2</sup>Boston University

Solid Oxide Membrane (SOM) Electrolysis is a new low-cost process for direct extraction of magnesium oxide to pure magnesium and oxygen gas. It is a high-temperature molten salt process with a solid oxide ion-conducting membrane separating the liquid electrolyte from the anode. This both protects the anode from the molten salt, significantly expanding the range of anode

material candidates, and also leads to high purity oxygen production. Unlike the Hall Cell, operating above the boiling point of magnesium effectively adds in-line distillation, making the product much purer than the raw material. The absence of chlorine and carbon anywhere in the process makes it emission-free. A Department of Energy cost modeling study concluded that this process has lower cost than any other existing or proposed primary magnesium process. This talk will discuss challenges and opportunities involved in scaling SOM Electrolysis to meet the growing magnesium needs of the automotive industry.

## 5:40 PM

**Corrosion Resistance of Graphite Anode for Magnesium Electrolyzers:** *Bing Li*<sup>1</sup>; Jingwei Lou<sup>1</sup>; Can Zhan<sup>1</sup>; Jianguo Yu<sup>1</sup>; <sup>1</sup>East China University of Science and Technology

Graphite is used as an inert anode material due to its stability in a molten chloride salt electrolyte. But during the magnesium electrolysis, there is a gradual wearing of the anodes, which increases cell resistance and hinders hydrodynamics of cell. In this paper, several graphite electrodes, made of different ingredients such as a needle coke, a composite of needle coke and petroleum coke, a fine petroleum coke and a high-purity petroleum coke were employed as anodes for magnesium electrolyzers. The electrolysis experiments were conducted from a molten chloride salt electrolyte with current density of 1A/cm<sup>2</sup> at 750° under air to accelerate the corrosion of graphite anode. After electrolysis, SEM was used to examine the morphology of graphite anode and analyze the corrosion resistance of graphite anode. Results showed the corrosion resistance of graphite anode was related to the graphite purity, grain size, apparent porosity and oxidative stability in air.

## Materials in Clean Power Systems V: Clean Coal-, Hydrogen Based-Technologies, Fuel Cells, and Materials for Energy Storage: Materials for Clean Coal Power and CCS Systems II

*Sponsored by:* The Minerals, Metals and Materials Society, TMS Electronic, Magnetic, and Photonic Materials Division, TMS Structural Materials Division, TMS/ASM: Corrosion and Environmental Effects Committee, TMS: Energy Conversion and Storage Committee  
*Program Organizers:* Xingbo Liu, West Virginia University; Zhenguo Yang, Pacific Northwest National Lab; K. Weil, Pacific Northwest National Lab; Mike Brady, Oak Ridge National Lab; Jay Whitacre, Carnegie Mellon University; Ayyakkannu Manivannan, National Energy Technology Laboratory; Zi-Kui Liu, Penn State University

Monday PM

February 15, 2010

Center

Room: 211

Location: Washington State Convention

*Session Chairs:* David Alman, National Energy Technology Laboratory; Bruce Pint, Oak Ridge National Laboratory

## 2:00 PM Invited

**Competing Fatigue Failure Modes in Structural Alloys and the Implications for Life-Management Approaches:** *Michael Caton*<sup>1</sup>; S. K. Jha<sup>2</sup>; J. M. Larsen<sup>1</sup>; <sup>1</sup>US Air Force Research Laboratory; <sup>2</sup>Universal Technology Corporation

Recent fatigue studies of numerous aerospace alloys have revealed competing failure modes under relevant loading conditions contributing to dual-fatigue lifetime distributions. It has been observed that inherent fatigue life variability is often composed of a population of life-limited specimens that experience immediate crack initiation and a population of long-life specimens that demonstrate a significant crack initiation period. Recognizing the competition of these distinctly different mechanisms enables reduced uncertainty in life prediction methods and has significant implications for damage prognosis and life-management practices for fracture-critical components. Alloys demonstrating this phenomenon include Ni-base superalloys, Ti alloys, Al alloys, and  $\gamma$ -TiAl. While these studies have focused on aerospace applications, the observations have relevance for the design and life management of any fracture-critical structure, including power generation systems. A generic framework for applying probabilistic life prediction methods will be presented.



### 2:40 PM Invited

**Addressing Materials Processing Issues for USC Steam Turbines: Cast Versions of Wrought Ni-Based Superalloys:** *Paul Jablonski<sup>1</sup>*; Christopher Cowen<sup>1</sup>; Phillip Maziasz<sup>2</sup>; Neal Evans<sup>2</sup>; Yuki Yamamoto<sup>2</sup>; <sup>1</sup>National Energy Technology Laboratory; <sup>2</sup>Oak Ridge National Laboratory

The proposed steam inlet temperature to the Advanced Ultra Supercritical (A-USC) steam turbine is high enough (760°C) that traditional turbine casing and valve body materials such as ferritic/martensitic steels will not work due to temperature limitations of this class of materials. In this presentation we will explore cast versions of seven traditionally wrought Ni-based superalloys in order to evaluate their application as casing or valve components for the next generation of Industrial Steam Turbines. The full size castings are quite substantial: ~4in thick, several feet in diameter and weigh 5-10,000lb each half. Our castings were quite a bit smaller, but section size was retained and cooling rate controlled in order to produce relevant microstructures. We developed a multi-step homogenization heat treatment in order to better deploy the alloy constituents. These castings were subsequently evaluated by characterizing their microstructure as well as their mechanical performance (tensile and creep).

### 3:20 PM

**Assessing Cast Alloys for Use in Advanced Ultra-Supercritical Steam Turbines:** *Neal Evans<sup>1</sup>*; Yukinori Yamamoto<sup>2</sup>; Philip Maziasz<sup>2</sup>; Paul Jablonski<sup>3</sup>; <sup>1</sup>University of Tennessee, Knoxville; <sup>2</sup>Oak Ridge National Laboratory; <sup>3</sup>National Energy Technology Laboratory

Cast forms of traditionally wrought Ni-base precipitation-strengthened superalloys are being considered for service in the ultra-supercritical conditions of next-generation steam turbines (760°C, 35MPa). In this study, small (~10 kg) castings of Nimonic 105, Nimonic 263, Haynes 282, and Inconel 740 were produced under conditions designed to mimic the casting conditions of full-size components, where slow cooling rates and segregation may impact materials properties. A multi-step homogenizing, solutionizing and heat treating schedule was used to eliminate segregation and develop the strengthening  $\gamma'$  phase. For comparison, wrought forms of these alloys were obtained and heat treated to develop the strengthening  $\gamma'$  phase. Microstructures developed in both forms of these alloys were examined via SEM; phase identification and chemistry are being confirmed by TEM. This presentation will discuss microstructures observed in both forms of these alloys and assess the suitability of using these traditionally wrought alloys in cast form.

### 3:40 PM Break

### 3:50 PM Invited

**High Temperature Corrosion of Fe-Cr, Fe-Al, Fe-Si and Fe-Si-Al Alloys in CO<sub>2</sub>-H<sub>2</sub>O Gases:** *David Young<sup>1</sup>*; Jianqiang Zhang<sup>1</sup>; Thomas Gheno<sup>1</sup>; Huan Li<sup>1</sup>; <sup>1</sup>University of New South Wales

Iron and model alloys containing 2.25, 9, and 20 wt% Cr, 2, 4 and 6 wt% Al, 1, 2 and 3 wt% Si, and dilute Fe-Si-Al ternaries were reacted in dry and wet CO<sub>2</sub> gases at 800°C. External chromia scales grew on Fe-20Cr according to slow, linear kinetics in dry CO<sub>2</sub>. Additions of H<sub>2</sub>O accelerated the reaction until steady-state parabolic kinetics were achieved. Lower Cr alloys developed thicker iron oxide scales, featuring cavities, cracks and poor adherence, and sustained internal oxidation. The presence of H<sub>2</sub>O led to even higher oxidation rates. Aluminium additions to iron of up to 4 wt% had no effect, but 6 wt% significantly slowed oxidation. Silicon additions had little effect. However, simultaneous alloying with aluminium and silicon strongly depressed corrosion rates. The effectiveness of different alloy additions is discussed, along with the effects of water vapour, in the context of oxyfuel combustion technology.

### 4:30 PM

**Phase Stability of Cast and Wrought IN 740 at Ultra Supercritical Boiler Temperatures:** *Christopher Cowen<sup>1</sup>*; Paul Jablonski<sup>1</sup>; Xingbo Liu<sup>2</sup>; <sup>1</sup>United States Department of Energy; <sup>2</sup>West Virginia University

The nickel-based superalloy IN 740 has gained much attention recently as a candidate material for use as tubing in Ultra Super Critical (USC) power plant applications. The ultimate USC goal is a coal-fired power plant that operates utilizing steam at pressures up to 35 MPa and temperatures up to 760°C. The microstructural stability of IN 740 at USC temperatures has been shown to be an issue through observations of gamma prime coagulation, transformation of gamma prime to eta phase, and also through the formation of G phase. In this work, we evaluate the effect of nominal Al content on the microstructural

stability of wrought IN 740 at USC temperatures for times up to 2000 hours. We also provide a comparison of the microstructural stability of both wrought and cast versions of IN 740 evaluated under these conditions.

### 4:50 PM

**Development of Friction Stir Welding Technology for Coal and Nuclear Power Applications:** *K. Scott Weil<sup>1</sup>*; Glenn Grant<sup>1</sup>; Yuri Hovanski<sup>1</sup>; Curt Lavender<sup>1</sup>; Jens Darsell<sup>1</sup>; <sup>1</sup>Pacific Northwest National Lab

Most ferritic/martensitic steels used in coal and nuclear plant applications are limited to operating temperatures of <600°C due to degradations in tensile and creep strength. While the addition of insoluble, nanoscale oxide dispersoids greatly improves their high-temperature mechanical properties of these alloys, it can also make them more difficult to join into large-scale componentry. Liquid phase methods of joining such as brazing and fusion welding lead to regions within the joints that are devoid of the dispersoids and the associated strengthening effects, making the joined components susceptible to failure by creep. Friction stir welding is a solid-state joining technique that has shown promise in joining hard-to-weld materials such as ODS alloys in coupon-size specimens. Our work is focused on translating the technology to larger scale plate and pipe joining, evaluating possible tools for thick section welds, and developing methods of weld qualification based on in-situ measurements of weld tool force.

### 5:10 PM

**Interaction of Mechanical Performance and Environmental Compatibility:** *Sebastien Dryepondt<sup>1</sup>*; Bruce Pint<sup>1</sup>; <sup>1</sup>Oak Ridge National Laboratory

Several preliminary studies are being conducted to study the effect of environment on high temperature mechanical properties, including the effect of environmentally-resistant coatings. Earlier work suggested that in-situ measurements would be superior to measuring mechanical properties of specimens after exposure to a simulated environment such as steam or exhaust gas. Examples include Fe- and Ni-base alloys for boiler applications, Ni-base alloys for valves and Al-rich coatings for these alloys. The effect of internal oxidation on mechanical properties is an initial objective. One concern about oxidation-resistant coatings is the potential for detrimental effects on substrate mechanical properties including creep strength and fatigue resistance. In component design, the coating layer is commonly assumed to have no creep strength. However, a coating that reduces component fatigue life is not a practical solution. The coating ductile-to-brittle transition temperature may determine its applicability for some applications.

## Materials Processing Fundamentals: Deformation Processing and Heat Treatment

*Sponsored by:* The Minerals, Metals and Materials Society, TMS Extraction and Processing Division, TMS: Process Technology and Modeling Committee

*Program Organizer:* Prince Anyalebechi, Grand Valley State University

Monday PM

Room: 601

February 15, 2010

Location: Washington State Convention Center

*Session Chair:* Prince Anyalebechi, Grand Valley State University

### 2:00 PM

**Mechanical Properties and Their Dependence on Microstructure in Hot-Rolled 3rd Generation Advanced High Strength Steels:** *Meghan McGrath<sup>1</sup>*; Dave Van Aken<sup>1</sup>; Von Richards<sup>1</sup>; <sup>1</sup>Missouri University of Science and Technology

A new third generation advanced high strength steel is based on duplex microstructures of acicular ferrite and retained austenite. Good combinations of strength and ductility can be achieved in these duplex steels by suppressing cementite formation and transformation induced plasticity from the retained austenite. This paper compared the mechanical properties of two hot-rolled alloys with duplex microstructures. The two compositions used were: (1) 0.14%C, 13.87%Mn, 1.42%Si, and 3.51%Al; and (2) 0.06%C, 14.2%Mn, 1.85%Si, and 2.38%Al. Addition of aluminum reduces density along with inhibiting formation of cementite. These steels were cast, homogenized, and hot rolled at 900°C to obtain a refined microstructure with ultimate tensile strengths of 865 MPa and 1,217 MPa with elongations of 39% and 28%, respectively.

Mon. PM

# Technical Program

The amount of metastable austenite in both compositions decreased after tensile testing from 58% and 28% to 6% and 0%, respectively. Microstructures were characterized using optical microscopy, scanning electron microscopy, and x-ray diffraction.

## 2:20 PM

**Influence of Direct Aged Treatment on Creep Behaviors of Hot Continuous Rolling GH4169 Superalloy:** *Sugui Tian*<sup>1</sup>; Zhenrong Li<sup>1</sup>; Zhonggang Zhao<sup>1</sup>; Liqing Chen<sup>2</sup>; Xianghua Liu<sup>2</sup>; <sup>1</sup>Shenyang University of Technology; <sup>2</sup>Northeast University

By direct aged treatment, creep properties measurement and microstructure observation, the influences of the direct aged treatment on the creep behaviors of Hot Continuous Rolling GH4169 Superalloy are investigated. Results show that the creep resistance of Hot Continuous Rolling GH4169 Superalloy may be obviously improved by directly aged treatment. Under the applied stress of 700MPa at 660°, the creep life of the alloy is enhanced to 126h from 60h. During hot rolling, the deformation features of the alloy are the twinning and the double orientations slipping of the dislocation activated within the twinning regions. And the alloy displays a smaller grain size. After direct aged treatment, the finer  $\gamma'$  phase is dispersedly precipitated in the matrix of the alloy, which is a main reason of enhancing creep life of the alloy.

## 2:40 PM

**The Effect of Carburizing on the Fatigue Life of 4130 Steel:** *Roselita Fragoudakis*<sup>1</sup>; Anil Saigal<sup>1</sup>; <sup>1</sup>Tufts University

AISI 4130 (25Cr-4Mo) steel is a medium carbon Cr-Mo steel used in automotive, aeronautic and other general-purpose industries. In this study, 4130 steel fatigue specimens were carburized at 1700°F to enhance the carbon content in the steel, raising it from approximately 0.3% wt (non-carburized) to 0.9% wt (carburized, oil quenched and tempered). Rotating bending fatigue tests were performed on the R. R. Moore Rotating Beam Fatigue Testing System, in order to determine the high cycle fatigue (HCF) life of 4130 steel and plot the corresponding S-N diagrams. A comparison of the results of carburized and non-carburized specimens shows that carburizing of steel: a) doubles the surface hardness and b) improves the fatigue strength of the steel by at least an order of magnitude.

## 3:00 PM

**Cast and Wrought Tensile Properties of a 2nd Generation Advanced High Strength Steel (AHSS):** *Tracy Frick*<sup>1</sup>; Dave Van Aken<sup>1</sup>; Ryan Howell<sup>1</sup>; <sup>1</sup>Missouri University of Science and Technology

Second generation AHSS include an age hardening austenitic alloy known as TRIPLEX. These steels are duplex, austenite and ferrite, when solution treated and are hardened by aging at 550°C to obtain ultimate tensile strengths greater than 1,500 MPa. An austenitic grade with composition Fe-30Mn-9Al-1Si-0.9C-0.5Mo has been developed for lightweight, cast military armor. The addition of 9 wt.% aluminum reduces the density by 13% over traditional steel chemistries. The current study examines the same alloy after hot rolling and recrystallization at 900°C. Specimens were water quenched to produce an equiaxed, 10 to 20  $\mu$ m grain diameter with a hardness of Rockwell C27 after recrystallization. The rolled microstructure contained less than 1% ferrite, which appeared as small discrete islands aligned parallel to the principal rolling direction. Aging at 530°C for 10 and 30 hours produced a hardness of Rockwell C30 and Rockwell C37, respectively.

## 3:20 PM Break

## 3:40 PM

**Microstructure and Mechanical Properties of Multiphase Steel after Quenching and Partitioning:** *Thomas Rieger*<sup>1</sup>; Oliver Buelters<sup>2</sup>; Jian Bian<sup>3</sup>; <sup>1</sup>Department of Ferrous Metallurgy, RWTH Aachen University; <sup>2</sup>Institute for Metal Forming, RWTH Aachen University; <sup>3</sup>ThyssenKruppSteel

The 'quenching and partitioning' process has been developed to produce high strength steel. After austenitisation and interrupted quenching the austenite transforms partly to martensite. The remaining austenite is stabilised by carbon partitioning from martensite. After final quench the tempered martensite gives a high strength level. The TRIP-assisted local strain hardening assures satisfying ductility. The process design is limited by reactions competing against the carbon partitioning, i. e. carbide precipitation and isothermal bainite transformation. For a given chemical composition the vast scope of adjustable mechanical properties is investigated as function of the process parameters. The

corresponding microstructure is characterised by light and electron microscopy and XRD measurements. Supplementary information on the process kinetics is obtained by dilatometry. Silicon shows more effective in retarding cementite precipitation than aluminium. Retained austenite occurs in filmy constitution between bcc laths as well as in blocky grains. The authors are grateful for support by ThyssenKruppSteel.

## 4:00 PM

**Ag Exudation during Internal Oxidation in Various Contact Materials:** *Gunther Schimmel*<sup>1</sup>; Bernd Kempf<sup>2</sup>; Markus Rettenmayr<sup>1</sup>; <sup>1</sup>Friedrich-Schiller-University Jena; <sup>2</sup>Umicore AG & Co. KG

Internally oxidized Ag alloys are frequently used as contact materials in high-energy switching operations. During internal oxidation, diffusion of Ag atoms towards the sample surface is commonly observed. This leads to the formation of external and internal layers that consist of essentially pure Ag. In the present work, results of high temperature bending tests of already oxidized specimens and targeted oxidation experiments accompanied by FEM simulation calculations are presented. There is no correlation between internal stresses and the amount of Ag in the exuded layers. The diffusion direction of Ag atoms is shown to be dependent on the direction of oxygen diffusion. It is concluded that exudation is dependent on the oxygen concentration gradient that generates a difference in the chemical potential of the Ag atoms. The gradient in oxygen concentration between sample surface and internal oxidation front is identified as main driving force for the Ag diffusion.

## 4:20 PM

**Effects of Phosphorous on the Precipitation Kinetics of  $\kappa$ -carbides in the Fe-30%Mn-9%Al-1%Si-0.9%C-0.5%Mo Alloy System:** *Laura Bartlett*<sup>1</sup>; David Van Aken<sup>1</sup>; Kent Peaslee<sup>1</sup>; Ryan Howell<sup>2</sup>; <sup>1</sup>Missouri University of Science and Technology; <sup>2</sup>Army Research Lab

Recent studies on the age-hardenable Fe-30%Mn-9%Al-1%Si-0.9%C-0.5%Mo alloy have shown that small increases in the amount of phosphorous, 0.001 to 0.043 wt%, corresponded to an increase in hardness for all aging times tested in the temperature range of 530 to 600°C. As phosphorous increased, the time to achieve peak hardness was also found to decrease by 50% for specimens aged at 530°C and 60% for specimens aged at 600°C. Avrami kinetic analysis suggests that phosphorous lowers the activation energy for the precipitation of fine  $\kappa$ -carbide, (Fe,Mn)<sub>3</sub>AlC, from 301 kJ/mol to 204 kJ/mol as the phosphorous level is increased from 0.001 to 0.043 wt%. Microstructural changes as a function of aging time, temperature, and phosphorous content were characterized by optical microscopy as well as scanning electron microscopy (SEM). Phosphorous was found to segregate to interdendritic grain boundaries and promote both the precipitation and size of the  $\kappa$ -carbide on the grain boundaries.

## 4:40 PM

**A Study on Heat Transfer Coefficient Distribution in High Pressure Hydrogen Quenching:** *Bowang Xiao*<sup>1</sup>; Gang Wang<sup>1</sup>; Yiming Rong<sup>1</sup>; <sup>1</sup>Worcester Polytechnic Institute (WPI)

Recently more and more attentions are paid to High pressure hydrogen quenching (HPHQ) for its advantages such as environmental friendliness, low distortion, etc, compared to oil and water quenching. In practice, heat transfer coefficient (HTC) usually varies from part surface to surface because of the variation of gas velocity around the part. This article studies the effect of HTC distribution on part distortion and microstructure after HPHQ and shows that Finite Element simulations considering HTC distribution predict different distortion from these without considering HTC distribution. It is also pointed out in this article that HTC distribution can be optimized by adjusting part orientation and HPHQ condition so that part distortion is minimized.

## 5:00 PM

**Evolution of Graphite Phase Morphology during Graphitization Process in Hypereutectoid Steels:** *Amin Rounaghi*<sup>1</sup>; Payam Shayesteh<sup>1</sup>; Ali-Reza Kiani-Rashid<sup>1</sup>; <sup>1</sup>Ferdowsi University

Graphitization process in steels is referred to the decomposition of cementite phase to graphite and ferrite during prolonged time. Graphite presence in the final microstructure is identified as one of the best solid lubricants that significantly improves wear resistance, machinability and self-lubricating of ferrous alloys. In addition, investigations show effect of graphite shape and morphology on mentioned properties. In this matter, we can refer to magnesium edition in molten iron for production ductile cast iron with spherical graphites and its



better strength rather than other similar kinds such as gray cast iron with flake graphites. In present research, effect of graphite stabilizer alloying elements on morphology, size and distribution of graphite particles has been studied during graphitization process in hypereutectoid steels.

irradiation embrittlement and the susceptibility to environmentally assisted cracking.

### 3:20 PM

#### **Effects of Common Alloying Additions on Solidification Cracking of Zirconium Alloys:** *Micah Hackett*<sup>1</sup>; George Young<sup>1</sup>; <sup>1</sup>KAPL

Zirconium alloys are commonly welded for nuclear applications, but they can be susceptible to solidification cracking. In this work the role of minor alloying additions on the weldability and solidification cracking behavior of zirconium alloys is explored using transverse v restraint testing with gas tungsten arc welding (GTAW). The alloy compositions vary in the content of Fe, Cr, Sn and Nb in order to measure the effect of composition on solidification cracking susceptibility. Solidification cracking resistance was assessed as a function of welding speed and heat input. Gleeble testing was used to determine the solidus temperature to better understand the effects of alloying elements on solidification range.

### 3:40 PM

#### **Effect of Neutron Radiation Exposure on Low Cycle Fatigue of 304SS:** *Korukonda Murty*<sup>1</sup>; Indrajit Charit<sup>2</sup>; <sup>1</sup>North Carolina State University; <sup>2</sup>University of Idaho

We review here the tensile and fatigue characteristics of Type 304 SS from hexagonal cans of EBR-II guide tubes before and after irradiation to a fast fluence of  $\sim 8 \times 10^{26}$  n/m<sup>2</sup>. The mechanical properties were evaluated at room temperature and 598K. Typical radiation hardening is noted along with ductility loss while the work hardening parameter decreased following radiation exposure. Symmetrical strain reversal fatigue tests at 0.1 cps were performed at varied strains from  $\sim 1\%$  to 2.4% with number of cycles varying from 500 to 40,000. While a slight decrease in fatigue life is noted at high strains, the data clearly revealed improved fatigue life at low strains or high cycles. Predictive model equation developed based on Universal Slopes concept using tensile data is noted to predict the fatigue behavior of both unirradiated and irradiated materials at room temperature and 598K. This work is supported by the Department of Energy grant #DE-AC07-05ID14517.

### 4:00 PM Break

### 4:15 PM Invited

#### **When the Turtle Can't Get There and the Rabbit Gets Lost: Predicting Low Flux High Fluence RPV Embrittlement:** *G. Robert Odette*<sup>1</sup>; Takuya Yamamoto<sup>1</sup>; <sup>1</sup>University of California, Santa Barbara

Nuclear plant life extension will require accurate predictions of irradiation-induced ductile-brittle transition temperature shifts (TTS) in RPV steels at high fluence, far outside the existing surveillance database. Progress in mechanistic understanding of irradiation embrittlement has led to physically motivated TTS correlation models that provide excellent statistical fits to the surveillance database. However, these models cannot reliably extrapolate TTS predictions, since 99% of the existing surveillance data is less than half the maximum extended life fluence. High flux can access high fluence, but such TTS data is under-predicted by current models that do not properly account for dose rate effects. We describe a systematic effort to develop a mechanism database on dose rate effects in support building physically based models to reliably predict TTS for low flux high fluence conditions, that also account for possible embrittlement by delayed formation of "late blooming phases" in low copper steels.

### 4:45 PM Invited

#### **Materials Issues Potentially Impacting Long-Term Safe Operations:** *C. E. Carpenter*<sup>1</sup>; <sup>1</sup>U.S. Nuclear Regulatory Commission

Existing nuclear power plants (NPPs), which were originally designed for operating lives of 30 to 40 years, are being considered for extended operating periods, of perhaps 80 or more years. The U.S. Nuclear Regulatory Commission (NRC) has enacted a process for plant safety assessments to enable license renewal from 40 to 60 years, and 54 such license extensions has been granted to date; and, it is expected that more than 90 percent of current plants will seek at least an initial license renewal period (e.g., 40 to 60 years). The NRC is initiating research to determine what are the key technical and regulatory issues that require attention by the nuclear industry to enable a second, and subsequent, renewal period, to 80 years and potentially longer. This presentation will address the key material aging-related degradation issues that are under consideration by the NRC at this time.

## **Mechanical Performance for Current and Next-Generation Nuclear Reactors: Ensuring Lifetime and Reliability**

*Sponsored by:* The Minerals, Metals and Materials Society, TMS Materials Processing and Manufacturing Division, TMS Structural Materials Division, TMS/ASM: Mechanical Behavior of Materials Committee, TMS: Nanomechanical Materials Behavior Committee, TMS/ASM: Nuclear Materials Committee

*Program Organizers:* Dylan Morris, NIST; Greg Oberson, Nuclear Regulatory Commission; Nicholas Barbosa, National Institute of Standards and Technology; Wolfgang Hoffelner, Paul Scherrer Institute

Monday PM Room: 201  
February 15, 2010 Location: Washington State Convention Center

*Session Chairs:* Greg Oberson, U.S. Nuclear Regulatory Commission; Matthew Kerr, US Nuclear Regulatory Commission

### 2:00 PM Invited

#### **Ensuring the Performance of Nuclear Reactor Pressure Vessels for Long Time Service:** *Randy Nanstad*<sup>1</sup>; <sup>1</sup>Oak Ridge National Laboratory

Structural integrity of the reactor pressure vessel is a critical element in demonstrating the capability of light water reactors for operation to at least 80 y. The Light Water Reactor Sustainability Program is a collaborative program between the U.S. Department of Energy and the private sector directed at extending the life of the present generation of nuclear power plants to enable such long-time operation. Given that the current generation of light water reactors were intended to operate for 40 y, there are significant issues that need to be addressed to reduce the uncertainties in regulatory application. The neutron dose to the vessel will at least double, and the database for such high dose levels under the low flux conditions in the vessel is nonexistent. Associated with this factor are uncertainties regarding flux effects, effects of relatively high nickel content, and uncertainties regarding application of fracture mechanics.

### 2:30 PM Invited

#### **Experience of the Fossil Industry with the Creep-Strength Enhanced Ferritic Steels:** *Jeffrey Henry*<sup>1</sup>; <sup>1</sup>Energy Solutions Group

The Creep Strength Enhanced Ferritic Steels, such as Grade 91, have been selected by design engineers for use in the fossil power industry because of their superior elevated temperature properties when compared to more "traditional" alloys, such as Grade 22. In many cases the selections have been made without regard to the ability of OEMs and constructors to satisfy the more demanding process requirements of these steels. In this presentation we will review the numerous problems that were encountered in the fossil industry when Grade 91 was introduced on a large scale and will discuss the reason for those problems. In addition, we will look at the steps that were taken by the ASME Code to address some of the more critical issues that were encountered in an effort to minimize the risk of component failure.

### 3:00 PM

#### **Comparative Plant Performance of Stabilized and Non-Stabilized Austenitic Stainless Steels:** *Raul Rebak*<sup>1</sup>; <sup>1</sup>GE Global Research

Austenitic stainless steels core internals components in light water reactors may be susceptible to stress corrosion cracking and irradiation assisted stress corrosion cracking. One of the effects of irradiation is the hardening of these materials and a change in the dislocation distribution in the alloy. Irradiation also alters the local chemistry of the alloys, for example in the vicinity of grain boundaries which may increase their susceptibility to environmentally assisted cracking. In the United States the nuclear power plants internals are mostly made using 304/304L, in Japan the nuclear industry prefers 316L and in Europe (e.g., Germany) mostly the stabilized 347/321 versions of stainless steels. An open literature review has been conducted to compare the relative performance of these austenitic stainless steels under operation conditions. The review will cover, among other things, the sensitization behavior during welding, the

Mon. PM

# Technical Program

## 5:15 PM Invited

**Safety Evaluation Challenges for NNGP VHTR Materials of Construction and Components:** *Makuteswara Srinivasan*<sup>1</sup>; Amy Hull<sup>1</sup>; Shah Malik<sup>1</sup>; <sup>1</sup>U.S. Nuclear Regulatory Commission

A variety of specialty metallic alloys, nuclear graphite, ceramic insulation, and ceramic matrix composites, will be used in the design and construction of components for the very high temperature gas cooled reactor (VHTR) next generation nuclear plant (NNGP). Several challenges exist in the safety evaluation of these components for design certification and licensing review. The component performance reliability estimate depends on the robustness of several models which provide technical bases, data, and analyses methods. These models address environment-assisted material degradation, component inspection, structural integrity estimation, and risk assessment. Aspects of these models are inter-connected and influence risk information. A technical decision exercise has provided prioritization guidance on research areas needed for construction of the above models. Consensus design codes and standards need to address performance acceptance criteria, surveillance and in-service inspection requirements, and component degradation management program and procedure to assess its efficacy.

## 5:45 PM

**Gen IV Materials (ASME-DOE Project):** *James Ramirez*<sup>1</sup>; <sup>1</sup>ASME

To facilitate the commercialization (licensing, construction, operations and maintenance, etc) of Generation IV reactors, ASME Standards Technology, LLC (ASME ST-LLC) has been working with major stakeholders from industry, government, and academia to develop and compile material research required to update and build the next set of ASME codes and standards that will directly support commercialization of Gen IV reactors. This paper will focus on providing a summary of the projects results currently being developed under the ASME ST-LLC and DOE materials project and more specifically will address the following areas: operating conditions for allowable stress values, ASME Code considerations for IHX, creep and creep-fatigue crack growths at structural discontinuities and welds, improving ASME Subsection NH, and new materials such as Inconel 617, Haynes 230, and Hastelloy XR. ASME ST-LLC utilizes an "early involvement approach" where stakeholders review and comment on the projects conclusions early on.

## Modeling, Simulation, and Theory of Nanomechanical Materials Behavior: Plasticity and Strength of Nanostructured and Nanoscale Materials II

*Sponsored by:* The Minerals, Metals and Materials Society, TMS Materials Processing and Manufacturing Division, TMS/ASM; Computational Materials Science and Engineering Committee, TMS; Nanomechanical Materials Behavior Committee

*Program Organizers:* Thomas Buchheit, Sandia National Laboratories; Sergey Medyanik, Washington State Univ.; Douglas Spearot, University of Arkansas; Lawrence Friedman, Penn State University; Edmund Webb, Sandia National Laboratories

Monday PM Room: 304  
February 15, 2010 Location: Washington State Convention Center

*Session Chairs:* Jian Wang, LANL; Edmund Webb, Sandia National Laboratories

## 2:00 PM Invited

**Discrete Dislocation Modeling of the Relaxation of Intrinsic Stress in Thin Films:** Can Ayas<sup>1</sup>; *Erik Van der Giessen*<sup>1</sup>; <sup>1</sup>University of Groningen

Deposition techniques for (sub-)micron thick metallic films generally leave intrinsic stresses. They arise as a consequence of the Volmer--Weber mechanism. Island growth and coalescence lead to a tensile stress in the film, which can be relaxed by the diffusion of material into the grain boundary, or by plasticity inside the grains, or by a combination of both. We present a framework to analyze these relaxation processes --during or after growth-- based on discrete dislocations. The approach builds on an existing method to describe plastic deformation at (sub-)micron size scales in terms of dislocations treated as line singularities in an elastic solid. Within the same framework, grain boundary diffusion is represented by the 'climb' motion of edge dislocations along grain boundaries, with a mobility that is determined by the diffusion coefficient.

In addition to the separate relaxation mechanisms, we analyze the coupling between diffusion and dislocation plasticity.

## 2:30 PM

**A Further Step in Understanding the Plasticity Size-Dependency: 3D Modelling of Solid and Annular Micropillars:** *Jaafar El-Awady*<sup>1</sup>; Satish Rao<sup>2</sup>; Christopher Woodward<sup>3</sup>; Dennis Dimiduk<sup>3</sup>; <sup>1</sup>AFRL/UTC; <sup>2</sup>AFRL/UES; <sup>3</sup>AFRL

In this work, we conduct three-dimensional dislocation dynamics simulations of solid and annular cylindrical Ni single-crystals under compression. The simulations are performed using the parametric dislocation dynamics coupled with the boundary element method. We investigate various boundary conditions and loading techniques as well as the trapping of dislocations within the micropillar due to the presence of FIB damage or due to a coating with a higher strength material. It is observed that the the FIB damage as well as the coatings will raise the stored dislocation density by a couple of orders of magnitude. Annular micropillars are observed to exhibit a size effect similar to solid micropillars. The flow strength obeys a power law relationship with the effective radius of the annular pillar (i.e.  $R_{out} - R_{in}$ ). Finally, the results of the annular micropillar simulations are compared to the plastic deformation of freestanding thin films.

## 2:50 PM

**Modeling the Statistics of Yield Behavior in Nanopillar Compression and Nanoindentation:** *James Morris*<sup>1</sup>; Hongbin Bei<sup>1</sup>; George Pharr<sup>2</sup>; Easo George<sup>1</sup>; <sup>1</sup>Oak Ridge National Laboratory; <sup>2</sup>University of Tennessee

Strengths of materials at small length scales approach theoretical values, due to the absence of defects in the probed volumes. These strengths may be an order of magnitude larger than those measured in the bulk. When the probed volume contains few dislocations or other defects, the mechanical properties are inherently statistical, with a wide variation in the yield and flow behavior. A statistical model is presented to capture the change in behavior from the defect-free case to the bulk limit, with a focus on capturing the wide variability of the intermediate regime. The model is compared to both nanoindentation and pillar experiments. Both the average potency and the distribution of dislocations and pinning points are included. We also present molecular dynamics simulations examining the effects of pre-existing dislocation networks on subsequent plastic behavior. This research was sponsored by the Division of Materials Sciences and Engineering, U.S. Department of Energy.

## 3:10 PM Invited

**Modeling the Mechanical Properties of Gum Metal:** *Daryl Chrzan*<sup>1</sup>; Matthew Sherburne<sup>1</sup>; Yuranan Hanlumyuang<sup>1</sup>; Tianshu Li<sup>2</sup>; J. W. Morris, Jr.<sup>1</sup>; <sup>1</sup>University of California, Berkeley; <sup>2</sup>University of California, Davis

The remarkable mechanical properties of Gum Metal, a Ti-Nb based alloy developed recently by Toyota, are considered within the context of ideal strength and dislocation core structures. The hypothesis that these alloys deform at stresses approaching their ideal strength is examined. It is suggested that the elastic anisotropy of these materials enables the dislocations to be pinned easily by nanoscale defects even at stresses approaching the ideal shear strength of the bulk alloy. Further, ab initio electronic structure total energy calculations indicate that the dislocation core structures are spread significantly, a feature that may also lead to pinning of dislocations. This work is supported by the National Science Foundation, and Toyota Motor Corporation.

## 3:40 PM Break

## 4:00 PM

**Tensile Deformation of Gold Nanowires: Structural Transitions during Elongation and Breaking Mechanisms:** *Francesca Tavazza*<sup>1</sup>; Lyle Levine<sup>1</sup>; Anne Chaka<sup>1</sup>; <sup>1</sup>National Institute of Standards and Technology

Semistatic density functional theory is used to explore the evolution of gold nanowires during tensile deformation under a wide range of conditions. Large structural changes are observed, resulting in the formation of locally ordered intermediate structures with interesting electronic properties. A rich diversity of deformation pathways is also uncovered, that converge to only two final local configurations with reproducible breaking strengths, in agreement with experimental results



4:20 PM

**Atomic-Scale Analysis of the Mechanical Behavior of Gold Nanofoams:** Kedarnath Kolluri<sup>1</sup>; Michael Demkowicz<sup>1</sup>; <sup>1</sup>Massachusetts Institute of Technology

We present atomic-scale analysis of a model Au nanofoam (nf-Au) using an EAM potential. A model nf-Au structure forms spontaneously upon relaxing a random distribution of atoms with a density of 20% of perfect crystalline FCC Au. The relaxed microstructure is polycrystalline and contains numerous defects in both the nanofoam ligaments and nodes. Annealing using Molecular Dynamics (MD) at 300 K for ~ 1 ns causes the nanofoam to coarsen. During volume conserving uniaxial compression of the nf-Au, ligaments are in a combined state of tension, shear, bending, and torsion. Peaks and valleys of the stress-strain curves after initial elastic loading correlate with the necking and pinch-off, respectively, of nanofoam ligaments. Similar mechanisms are found to operate during nanofoam coarsening.

4:40 PM

**Molecular Dynamics Simulations of Uniaxial Compression of Silicon Nanoparticles:** Lucas Hale<sup>1</sup>; William Gerberich<sup>1</sup>; Roberto Ballarini<sup>1</sup>; Neville Moody<sup>2</sup>; Xiaowang Zhou<sup>2</sup>; Jonathan Zimmerman<sup>2</sup>; <sup>1</sup>University of Minnesota; <sup>2</sup>Sandia National Laboratories

Molecular dynamics has been used to study the uniaxial compression of silicon nanospheres based upon both Stillinger-Weber and Tersoff potentials. The mechanical behavior of the particles is found to be sensitive to sphere size, temperature, crystallographic orientation, and the interatomic potential. Plastic deformation is found to be accompanied by nucleation and migration of dislocation when the particle size and temperature exceed some critical values. The critical particle size for the dislocation deformation mechanism is larger for the Tersoff potential than for the Stillinger-Weber potential. During compression along the [100] crystallographic direction using the Tersoff potential, a diamond-cubic to  $\beta$ -Sn phase transformation occurs. Similar transformation is not found for the Stillinger-Weber potential. An alternate yielding and hardening mechanism is also observed. These results provide comprehensive understanding of the unique mechanical properties of silicon nanoparticles.

5:00 PM

**Reaction Rate Theory Prediction of Dislocation Nucleation in Aluminum at Room Temperature:** Linh Nguyen<sup>1</sup>; Derek Warner<sup>1</sup>; <sup>1</sup>Cornell University

The limited time domain directly accessible to atomistic simulations of plasticity has long hindered their predictive capability. For nano-structured and/or nano-dimensioned metals, this shortcoming is exacerbated due to the high strain rate sensitivity of the controlling deformation mechanisms, such as dislocation nucleation. One viable means of overcoming this challenge is to view plasticity within a thermally activated reaction rate context. In this work, we use the finite temperature string method to calculate the most probable path for dislocation nucleation in a nano-wire and nano-void at room temperature. By parallelizing the samples trajectory along this path we can calculate directly the rate of nucleation at experimental loads. Sampling along the reaction path yields the free energy of activation, and thus, allows for a systematic assessment of the transition state theory prediction and the validity of other simplifying approximations common to recent efforts.

### Neutron and X-Ray Studies of Advanced Materials III: 2D Materials Science from Diffraction

*Sponsored by:* The Minerals, Metals and Materials Society, ASM International, TMS Structural Materials Division, TMS/ASM: Mechanical Behavior of Materials Committee, TMS: Titanium Committee  
*Program Organizers:* Rozaliya Barabash, Oak Ridge National Laboratory; Jaimie Tiley, Air Force Research Laboratory; Erica Lilleodden, GKSS Research Center; Peter Liaw, University of Tennessee; Yandong Wang, Northeastern University

Monday PM  
February 15, 2010

Room: 303  
Location: Washington State Convention Center

*Session Chairs:* Karen Pantleon, Denmark Technical University; Carol Thomson, NIU

### 2:00 PM Keynote

**In Situ X-Ray Scattering Studies of the Polarization Structure of Ultrathin Ferroelectric Films:** Gregory Stephenson<sup>1</sup>; Matthew Highland<sup>1</sup>; Dillon Fong<sup>1</sup>; Timothy Fister<sup>1</sup>; Paul Fuoss<sup>1</sup>; Jeffrey Eastman<sup>1</sup>; Stephen Streiffer<sup>1</sup>; Carol Thompson<sup>2</sup>; <sup>1</sup>Argonne National Laboratory; <sup>2</sup>Northern Illinois University

Ferroelectric thin films are both fascinating and useful because their polarization structure depends sensitively on the nature of the charge compensation at their interfaces. We have been using in situ surface x-ray scattering to monitor film growth and observe the polarization structure of ultrathin epitaxial PbTiO<sub>3</sub> films as a function of thickness and environmental conditions. Recently we discovered that in coherent PbTiO<sub>3</sub> / SrRuO<sub>3</sub> heterostructures on SrTiO<sub>3</sub> (001) substrates, the direction of polarization can be switched by changing the oxygen partial pressure (pO<sub>2</sub>) in equilibrium with the surface. Here we present results on the equilibrium polarization phase diagram and stability limits as a function of temperature, pO<sub>2</sub>, and film thickness. Results will be compared with a model for the interaction of surface chemistry with the ferroelectric phase transition. Work supported under contract DE-AC02-06CH11357 between UChicago Argonne LLC and the Dept. of Energy.

### 2:30 PM Invited

**Nucleation, Coarsening, and Coalescence during Layer-by-Layer Growth via Pulsed Laser Deposition: Time-Resolved, Diffuse X-Ray Scattering Studies:** Joel Brock<sup>1</sup>; John Ferguson<sup>1</sup>; Hui-Qiong Wang<sup>1</sup>; Arthur Woll<sup>1</sup>; <sup>1</sup>Cornell University

We report real-time x-ray diffuse scattering studies of the structure of the growth surface of complex oxide thin films during pulsed laser deposition in the layer-by-layer growth mode. These measurements provide detailed information on the in-plane growth kinetics on the relevant time and length scales. Empirically, it is necessary to monitor both the in-plane length scale,  $L$ , and the characteristic relaxation time,  $\tau$ , as a function of temperature, to obtain the diffusivity,  $D$ . For both homo- and hetero-epitaxy, island nucleation and coalescence under supersaturated conditions followed by coarsening of the resulting island distribution are key fundamental growth processes. The time-dependent pair distribution function,  $G(r,t)$ , obtained by Hankel transforming the experimental data, is used to characterize both the island size distribution and the near neighbor separations as a function of time and coverage.

### 2:50 PM Invited

**The Growth and Formation of Nanostructures at Surfaces: In Situ X-Ray Scattering Studies:** Paul Miceli<sup>1</sup>; Shawn Hayden<sup>1</sup>; Michael Gramlich<sup>1</sup>; Chinkyo Kim<sup>2</sup>; Edward Conrad<sup>3</sup>; <sup>1</sup>University of Missouri-Columbia; <sup>2</sup>Kyunghee University; <sup>3</sup>Georgia Institute of Technology

The surfaces of metal crystals are a useful laboratory for studying atomic-scale processes that control the growth and formation of nanostructures. Many of these processes depend on structure that lies below the surface. Because it is sensitive to both the surface and the subsurface of a sample, x-ray scattering possesses unique capabilities for investigating buried defects and subsurface strains that are not observed by conventional "surface-only" tools. This talk will discuss recent results from our ongoing research program that explores vacancy clusters, surface strains and quantum size effects in the epitaxial crystal growth of metals. These are in-situ studies which utilize the surface scattering

Mon. PM

# Technical Program

facility that we developed at Sector 6 at the Advanced Photon Source. Financial support is gratefully acknowledged from NSF and DOE.

## 3:10 PM Invited

**Time-Resolved X-Ray Studies of Materials Processing at Surfaces and Interfaces - Present and Future:** *Carol Thompson*<sup>1</sup>; <sup>1</sup>Northern Illinois University

The development of surface and interface x-ray scattering and spectroscopy techniques has led to seminal in-situ measurements of materials as they are synthesized and processed or interact with their target environments. Researchers have applied these techniques to study fundamentals of advanced materials, e.g., deposition, catalysis, electrochemistry, phase transitions, oxidation, corrosion, and biological activity. At the x-ray synchrotrons, several new user facilities have been proposed for in-situ and real-time materials processing. As these dedicated facilities come into operation within the next few years, they will provide increased user access and offer flexible designs for experiments. This enhances the opportunities for new communities of materials researchers to exploit these techniques successfully for their materials systems and questions. Using examples from the current literature and from our own research, we describe the strengths and weaknesses of these x-ray techniques for studying materials synthesis and processing in real-time at surfaces and interfaces.

## 3:30 PM Invited

**Two-Dimensional X-Ray Diffraction for Advanced Materials Analysis:** *Bob He*<sup>1</sup>; <sup>1</sup>Bruker AXS

Two-dimensional x-ray diffraction is the ideal, non-destructive, analytical method for examining samples of all kinds, such as metals, polymers, ceramics, semiconductors, and biomaterials, especially materials with anisotropic, nanoscale, composite or heterogeneous structures. This presentation introduces the geometry convention, data collection strategy, data interpretation, and data analysis in two-dimensional X-ray diffraction for various applications, including phase identification, crystal size, stress and texture measurements. Based on the matrix transformation between diffraction space, detector space and sample space, the unit diffraction vector can be expressed in the sample space corresponding to all the geometric parameters and Bragg conditions. The fundamental equations for crystal size, stress and texture measurement are developed from the unit diffraction vector expressed in sample space. The experimental examples in crystal size, stress and texture analysis for various samples, including friction stir weldment, magnetron sputter-deposited Cu films and micro-arc oxidation generated TiO<sub>2</sub> films, are given in this presentation.

## 3:50 PM Invited

**In-Situ X-Ray Diffraction Studies of Microstructure Evolution in Electrodeposits at Room Temperature and Elevated Temperatures:** *Karen Pantleon*<sup>1</sup>; <sup>1</sup>Technical University of Denmark

The thermodynamic non-equilibrium state of electrodeposited layers causes changes of the microstructure as a function of time and/or temperature. For Cu- and Ag-layers, self-annealing occurs already at room temperature, whereas Ni-layers evolve only at elevated temperatures. (Self-)annealing affects the functionality and reliability of electrodeposited components, which can be beneficial, e.g. increased electrical conductivity of interconnect lines, or detrimental, e.g. reduced strength in MEMS applications. Applying X-ray diffraction with conventional and synchrotron radiation, the kinetics of microstructure evolution has been investigated in-situ as a function of time at room temperature and during isothermal and isochronal annealing up to temperatures of 800 K. Time-resolved line profile analysis and crystallographic texture analysis during the course of (self-)annealing have revealed orientation dependent growth of the as-deposited nanocrystalline grains and drastic changes of preferred grain orientations. Quantification of the kinetics allowed conclusions on the mechanisms of microstructure evolution.

## 4:10 PM Break

## 4:20 PM Invited

**Strain Profiling in Group-III-Nitride Based Multilayer Systems on Silicon:** *Alois Krost*<sup>1</sup>; *Rainer Clos*<sup>1</sup>; *Juergen Blaessing*<sup>1</sup>; <sup>1</sup>Otto-von-Guericke University Magdeburg

The epitaxial growth of crack free group-III Nitrides on large size silicon substrates is a promising way towards large scale production of, e.g. high-brightness LEDs for general lighting. However, the growth of thick layers is hindered by a huge thermal mismatch between GaN and Si inducing tensile

stress. This problem can be overcome by a proper strain management during growth by the insertion of low-temperature AlN interlayers allowing for the growth of group-III Nitride layers exceeding 7 micrometer in thickness on 6 inch substrates. The impact of strain compensating (Al,Ga)N is evaluated by in situ curvature measurements and ex situ x-ray measurements. The strains and stresses of such multilayers are calculated analytically and compared to experimental results.

## 4:40 PM Invited

**Real Time Reciprocal Space Mapping of Nano-Islands Induced by Quantum Confinement:** *Hawoong Hong*<sup>1</sup>; *Aaron Gray*<sup>2</sup>; *T.-C. Chianng*<sup>2</sup>; <sup>1</sup>Argonne National Lab; <sup>2</sup>University of Illinois at Urbana-Champaign

The effects of the quantum confinement have been observed pronouncedly in the island morphology in the Pb thin films. The evolution of these nano-islands on Si (111)-(7x7) and sapphire (001) surfaces has been studied. A CCD camera was used to collect the 2/3-D maps of the x-ray reflectivity in real time. Large ranges of the reflectivity curves, and the rocking curves at every point on the reflectivity curves could be continuously measured. The abundance of information from 2-D k-space maps reveals clear changes in growth modes of thin Pb films. With the 3-D extension of this method, it was possible to observe the ordering of the islands and their coarsening. The islands coarsen and order, maintaining a nearly uniform inter-island distance but without angular correlation. Over a wide temperature range, the inter-island ordering is well correlated with the development of "magic" island heights caused by quantum confinement.

## 5:00 PM

**Dependence of the Preferred Growth Directions of GaN Nanorods on Polytypism:** *Sanghwa Lee*<sup>1</sup>; *Yuri Sohn*<sup>1</sup>; *Chinkyoo Kim*<sup>1</sup>; *Dong Ryeol Lee*<sup>2</sup>; *Hyun-Hwi Lee*<sup>3</sup>; <sup>1</sup>Kyung Hee University; <sup>2</sup>Soongsil University; <sup>3</sup>Pohang Accelerator Lab

Reciprocal-space-mapping with a 2-dimensional (2-D) area detector in a grazing incidence geometry is applied to determine crystallographic orientations of GaN nanostructures epitaxially grown on a sapphire substrate. By using both unprojected and projected reciprocal space mapping with a proper coordinate transformation, the crystallographic orientations as well as the preferred growth directions of GaN nanostructures with respect to that of a substrate were unambiguously determined. In particular, polytypism is found to play an important role in determining the preferred growth directions and preferred orientations of GaN nanorods.

## 5:15 PM

**Roentgenographic Determination of Residual Stresses in Carbonitrided Layers:** *Angel Zumbilev*<sup>1</sup>; *Iliya Zumbilev*<sup>1</sup>; <sup>1</sup>Technical University of Sofia, Plovdiv Branch

The aim of the present investigation is to examine the influence of carbonitriding in low temperature plasma over forming macro-residual stresses on the surface of the materials. Particular modes of ion carbonitriding are considered, in which layers of different depth and different surface micro-hardness are obtained. The residual stresses in the carbonitride layers are determined by the method of  $\sin^2\psi$ . The results show that at different modes of ion carbonitriding residual macro-stresses with different sizes are obtained and they depend on the mode of treatment (ammonia pressure, temperature of carbonitriding, duration of treatment) and the depth of the carbonitride zone.

## 5:25 PM Invited

**High-Energy X-Ray Measurements of Layered Systems for Energy Applications:** *Jonathan Almer*<sup>1</sup>; *Di-Jia Liu*<sup>2</sup>; *B. Harder*<sup>3</sup>; *K. Faber*<sup>3</sup>; <sup>1</sup>Argonne National Laboratory, X-Ray Science Division; <sup>2</sup>Argonne National Laboratory, Chemical Technology Division; <sup>3</sup>Northwestern University, Materials Science and Engineering Department

Microfocused high-energy x-rays are used to investigate two layered systems relevant for energy applications: solid-oxide fuel cells and thermal barrier coatings. The combination of an undulator source, brilliance preserving optics and focusing lenses at Sector 1 of the Advanced Photon Source provides high-energy x-rays (E~80 keV) with transverse beamsizes on the micron-level. In addition to their high penetration power, a key feature of high-energy x-rays is their forward scattering geometry, which when combined with area detectors allows for efficient mapping of microstructural gradients. Both x-ray diffraction and radiography are used to map the areal distribution of phases, internal strain, lattice parameter and integrated porosity of solid-oxide fuel cell (SOFC) stacks.



This information is used to better understand SOFC degradation mechanisms in the presence of reactive Cr, as well as further general understanding of SOFC processing-structure relationships. Figure 1 illustrates the lattice parameter distribution of the  $\text{La}_x\text{Sr}_{1-x}\text{MnO}_{3-\delta}$  phase from a deactivated SOFC, obtained from GSAS-refinement of diffraction data. The changes in lattice parameter in the vicinity of the electrolyte/anode and electrode/cathode interfaces are discussed with respect to processing, electro-chemical activity and related Cr-species accumulation. High-energy diffraction is also used to study phase and strain distributions of thermal barrier coatings (TBCs). When applied to turbine blades, TBCs permit higher engine operating temperatures, with concomitant increases in energy efficiency. However, the high temperatures are often combined with harsh operating environments, which have led to challenges for these coating systems. Accordingly, we examine the microstructural evolution of TBCs upon exposure to high temperatures and relevant reactive materials, to improve understanding of potential degradation mechanisms.

### Pb-Free Solders and Emerging Interconnect and Packaging Technologies: Mechanical Behavior, Failure Mode

*Sponsored by:* The Minerals, Metals and Materials Society, TMS Electronic, Magnetic, and Photonic Materials Division, TMS: Electronic Packaging and Interconnection Materials Committee

*Program Organizers:* Kwang-Lung Lin, National Cheng Kung University; Sung Kang, IBM; Jenq-Gong Duh, National Tsing-Hua University; Laura Turbini, Research In Motion; Iver Anderson, Iowa State University; Fu Guo, Beijing University of Technology; Thomas Bieler, Michigan State University; Andre Lee, Michigan State University; Rajen Sidhu, Intel Corporation

Monday PM  
February 15, 2010  
Room: 204  
Location: Washington State Convention Center

*Session Chairs:* Laura Turbini, Research In Motion; Jenq-Gong Duh, National Tsing Hua University

#### 2:00 PM

**Effects of POSS on Impact Behavior of Thermomechanically Fatigued Lead-Free Solder Joints:** *Takayuki Kobayashi*<sup>1</sup>; *Andre Lee*<sup>1</sup>; *K.N. Subramanian*<sup>1</sup>; <sup>1</sup>Michigan State University

Polyhedral oligomeric silsesquioxanes (POSS) addition to lead-free electronic solders have shown to considerably increase the residual shear strength and reliability of thermomechanically fatigued solder joints. In this study, impact tests on joints made with SAC305 and SAC105 solders, with and without POSS, were carried out. Realistic studies to evaluate the reliability of electronic devices after impact should be carried out after they have experienced different extents of thermal influences during service. Hence, impact studies on these solder joints were performed after subjecting them to different extents of thermomechanical fatigue (TMF) in (-15°C to 150°C), and (-55°C to 125°C) temperature ranges. Roles of the microstructural features and IMC morphologies that result from the imposed TMF treatments and their influences on the impact responses of SAC305 and SAC105 solder joints, with and without POSS, will be discussed.

#### 2:15 PM

**Influence of Interface Reaction on Out-of-Plane Displacements during Thermal Cycling of Copper-Silicon Bond with an Indium Interlayer:** *Daniel Gruber*<sup>1</sup>; *Nagaraj Chelliah Machavallavan*<sup>1</sup>; *Jia Liu*<sup>2</sup>; *Indranath Dutta*<sup>2</sup>; *Rishi Raj*<sup>1</sup>; <sup>1</sup>University of Colorado; <sup>2</sup>Washington State University

Out of plane displacement field on the surface of a silicon wafer bonded to a thick copper substrate with a thin indium layer is measured as a function of the shape of the heating and cooling cycle. The largest bending strains are measured when cooling down from the elevated temperature. The shear lag model is employed to understand the relaxation of strains induced by the difference in the thermal expansion of copper and silicon. The time dependent propagation of the shear relaxation from the edge of the silicon wafer is analyzed and correlated with the experiments. The influence of the a reaction between copper and indium, which forms intermetallics, on the stress relaxation behavior is reported.

#### 2:30 PM

**The Fracture Behavior of Aged Sn-Ag-Cu Solder Joints during High-Strain Rate Loading:** *Taecheon You*<sup>1</sup>; *Heylim Choi*<sup>1</sup>; *Eunsik Kim*<sup>2</sup>; *Jungtak Moon*<sup>2</sup>; *Heeman Choi*<sup>1</sup>; <sup>1</sup>Kookmin University; <sup>2</sup>MK Electron

Lead-free solders, particularly Sn-Ag-Cu, are becoming more and more popular in the electronic packaging industry, due to the environmental concerns associated with lead. However, the fact that they are stiffer and more brittle also makes them more prone to brittle failure during impact loading, which is frequently encountered in microelectronic packages for handheld electronic devices. This study assesses the reliability of eutectic Sn-Pb, Sn-1.0Ag-0.5Cu, Sn-3.0Ag-0.5Cu and Sn-4.0Ag-0.5Cu solder balls with and without an aging treatment at 150°C for various times; this study focuses primarily on how the pad surface finish and solder alloy composition affects the reliability of solder joints using a high-speed ball pull test method. Also investigated is the effect of selected rare-earth dopants on the pull strength of a Sn-1.0Ag-0.5Cu solder joint under a high-strain rate condition with and without aging treatment. The fracture forces and failure mechanisms are also examined.

#### 2:45 PM

**Synchrotron Microdiffraction Study of Localized Stress and Surface Evolution in Sn-Cu System:** *Nitin Jadhav*<sup>1</sup>; *Eric Buchovecky*<sup>1</sup>; *Wenjun Liu*<sup>2</sup>; *Jon Tischler*<sup>3</sup>; *Gene Ice*<sup>3</sup>; *Allan Bower*<sup>1</sup>; *Eric Chason*<sup>1</sup>; <sup>1</sup>Brown University; <sup>2</sup>Argonne National Laboratory; <sup>3</sup>Oak Ridge National Lab

It is generally understood that whiskers are the result of compressive stress build up in Sn layers on Cu, but the stress distribution within the Sn layer and how it relaxes due to whisker formation are not clear. We have done in-situ studies on the Sn-Cu system using synchrotron X-ray microdiffraction to develop an atomic-level understand of the relationship among the IMC growth, stress and whisker formation. Spatially-resolved Sn and Cu fluorescence maps quantify the local rate of IMC formation and whisker development. By overlaying the IMC and Sn stress maps we can see the effect of IMC formation on localized stress in the Sn layer and the dependence of whisker nucleation on Sn grain orientation and localized stress. Based on insight developed, we present results of finite-element simulations that include stress relaxation in the Sn due to both plastic deformation and through Sn diffusion along Sn grain boundary.

#### 3:00 PM

**Effect of Zn-Containing Flux on the Joint Strength and Microstructure of Sn-3.5Ag Soldering on an Electroless Ni-Au Surface Finish:** *Hitoshi Sakurai*<sup>1</sup>; *Youichi Kukimoto*<sup>2</sup>; *Katsuaki Suganuma*<sup>1</sup>; <sup>1</sup>Osaka University; <sup>2</sup>Harima Chemicals, Inc.

The joint strength and microstructure for Sn-3.5Ag soldering on an electroless Ni-Au pad by using the new flux containing Zn(II) stearate were investigated. The content of the zinc compound in a flux varies from 0 wt.% to 50 wt.%. The results of a bump pull test showed that the Zn-containing flux gave higher joint strength than did a conventional flux without Zn compound. The study of the interfacial microstructure revealed that the thickness of the interfacial intermetallics layer became thinner with increasing Zn content in a flux. In addition to this, the new flux gave a thinner P-rich layer at the interface than that seen with the conventional flux. It is assumed that Zn derived from a flux affects an interfacial reaction which correlates with the suppression of P-rich layer, and this may contribute to the improvement of the joint strength obtained by using the Zn-containing flux.

#### 3:15 PM Break

#### 3:30 PM

**Electrochemical Corrosion Behavior of High Temperature Pb-Free Solders:** *Chi-Hang Tsai*<sup>1</sup>; *Jenn-Ming Song*<sup>1</sup>; <sup>1</sup>National Dong Hwa University

This study aims to investigate the electrochemical corrosion behavior of the potential Pb-free solders, Bi-11wt%Ag and Zn-40wt%Sn, in 3.5% NaCl solution using the potentiodynamic polarization method with the scanning range from -2000mV to +2000mV. Pb-5wt%Sn alloy is also examined for comparison. Experimental results show that the corrosion potential (E<sub>corr</sub>) decreases in turns from Bi-11Ag, Pb-5Sn, Zn-40Sn to Zn-40Sn-0.5Al. Bi-11Ag exhibits the highest current density (I<sub>corr</sub>), and that for Pb-5Sn is the lowest. The Pb-5Sn samples have a much extended passive region compared to Bi-11Ag, while the Zn-40Sn samples show no passive behavior. According to the XPS data, the corrosion products are PbCl<sub>2</sub> and PbO for Pb-5Sn, BiOCl, AgCl<sub>2</sub>, and Bi<sub>2</sub>O<sub>3</sub> for Bi-11Ag, and ZnCl<sub>2</sub>, ZnO, SnO, SnO<sub>2</sub> for Zn-40Sn. Furthermore, it is found that a small amount of Al addition improved the corrosion resistance of Zn-40Sn.

Mon. PM

# Technical Program

3:45 PM

**Joint Strength Enhancement by CNT Inserted Sn3.5Ag Solder Balls:** *Youn-Ki Ko*<sup>1</sup>; *Yoon-Ki Sa*<sup>1</sup>; *Jung-Hwan Bang*<sup>1</sup>; *Jeong-Han Kim*<sup>1</sup>; *Chang-Woo Lee*<sup>1</sup>; *Sehoon Yoo*<sup>1</sup>; <sup>1</sup>KITECH/Micro-Joining Center

CNTs were inserted onto the surface of Sn-3.5Ag solder balls by using simple ball milling process. Sn-3.5Ag solder balls with diameter of 450  $\mu\text{m}$  were mixed in the CNT dispersed solution. Ball mill times were varied with 6, 12, 24, and 36 hours. Even after 24hrs of ball milling, the shape and size of Sn-3.5Ag solder balls were not changed. The amount of surface-inserted CNTs increased as the ball mill time increased. CNT-inserted Sn-3.5Ag solder balls were attached on ENIG finished copper pads by reflow process. Intermetallic compound layer thickness of CNT-inserted solder balls were not different from that of non-mixed solder balls. Shear strength of CNT inserted Sn3.5Ag solder balls increased by 10 % after 24 hour-ball mill process. From the fracture surface observation after the shear test, fracture occurred at solder region, not at the intermetallic layer.

4:00 PM

**Intermetallic Compounds and Mechanical Properties of Sn-3Ag-0.5Cu and Sn-1Ag-0.5Cu-0.06Ni-0.01Ge Solder Ball Grid Array Packages with ENIG Surface Finish:** *Chin-Liang Chen*<sup>1</sup>; *Jim Wang*<sup>2</sup>; *Tung-Han Chuang*<sup>1</sup>; <sup>1</sup>National Taiwan University; <sup>2</sup>SHENMAO Technology Inc.

Due to concerns about the material costs of Sn-3Ag-0.5Cu (SAC305) solder, the Ag content of this alloy should be decreased; thus, a Sn-1Ag-0.5Cu-0.06Ni-0.01Ge (SAC105) has been suggested. Tensile tests show that the SAC105 alloy possesses lower ultimate strength and greater elongation in comparison to SAC305 alloy. Further studies on the reflowed and aged solder joints in BGA packages with Au/Ni/Cu pads using both alloys indicate that the (Cu, Ni)<sub>6</sub>Sn<sub>5</sub> interfacial intermetallics layers in SAC105 specimens are twice as thick as those in SAC305, and that the morphology of the latter is continuous, in contrast to the coarse scallop-shape of the former. For evaluation of the bonding strength of solder joints with this solder, the ball shear test (BS), high speed ball shear test (HS-BS), and ball pull test (BP) were employed. The fractography of specimens after BS and BP tests revealed ductile fractures through the solder balls and the HS-BS tests resulted in brittle fractures along the solder/pad interfaces, and the bonding strengths of SAC105 solder joints in all cases were lower than those of SAC305.

4:15 PM

**Internal Strain Evolution during Thermal Cycling in a Row of Lead-Free Solder Joints in a Flip Chip Ball Grid Array Package:** *Bite Zhou*<sup>1</sup>; *Thomas Bieler*<sup>1</sup>; *Guilin Wu*<sup>2</sup>; *Stefan Zaeferrer*<sup>2</sup>; *Tae-Kyu Lee*<sup>3</sup>; *Kuo-Chuan Liu*<sup>3</sup>; <sup>1</sup>Michigan State University; <sup>2</sup>Max-Planck Institut für Eisenforschung; <sup>3</sup>Cisco Systems, Inc.

In-situ measurement of transmission diffraction patterns during thermal cycling of a single row from a 44x44 flip chip ball grid array package were analyzed to characterize internal strain evolution. The analyzed joints were in the ball grid array with a 1 mm pitch and an 18x18 mm die. The as-assembled package on its printed circuit board was sliced to provide a row that went through the center of the package. A thermal cycling stage was placed in a synchrotron beamline so that patterns could be measured periodically during a thermal cycle, in about 20% single, 40% bi-, and 40% tri-crystals (the method was confirmed with serial sectioning on other samples). Due to the different orientations in each joint, the effect of the anisotropic expansion coefficient on strain history in each in each of the crystal orientations is analyzed to identify how crystal orientations affect strain history during a thermal cycle.

4:30 PM

**Mechanical Shock of Environmentally-Benign Pb-Free Solders:** *Kyle Yuzzie*<sup>1</sup>; *Huiyang Fei*<sup>1</sup>; *Jason Williams*<sup>1</sup>; *Dallas Kingsbury*<sup>1</sup>; *Hanqing Jiang*<sup>1</sup>; *Pedro Peralta*<sup>1</sup>; *Nik Chawla*<sup>1</sup>; <sup>1</sup>Arizona State University, School of Mechanical, Aerospace, Chemical, and Materials Engineering

Pb-free solder alloys are subjected to mechanical shock and drop conditions in service. A fundamental understanding of intermediate strain rate behavior (10-50 s<sup>-1</sup>) is lacking. Existing methods developed to probe this strain-rate regime do not provide a direct and local measurement of strain in the solder. Quantifying the contributions of intermetallic thickness and solder microstructure to the mechanical shock behavior of the solder specimen is extremely important and needs to be studied. In this study the mechanical behavior of pure Sn and Sn-3.5Ag-0.7Cu solders was systematically quantified at strain-rates of 0.001 s<sup>-1</sup> to

30 s<sup>-1</sup>. Digital image correlation was used in conjunction with high-speed video to measure global and local strain fields. A novel mirror configuration was used to measure the instantaneous cross-sectional area for the measurement of true stress-true strain. Multiscale modeling of the complex stress state experienced by solder during mechanical shock was conducted and will be presented.

4:45 PM

**Fatigue-Creep Interaction Damage Theory Based Thermal Fatigue Life Prediction Model for SnAgCu Solder Joints:** *Yan Chang*<sup>1</sup>; *Li Yan*<sup>1</sup>; *Liu Na*<sup>1</sup>; <sup>1</sup>Beijing University of Technology

SnAgCu solder is fast becoming a reality in electronic manufacturing during to marketing and legislative pressure. This paper studies thermal fatigue life prediction model for SnAgCu solder on basis of classic continuous damage mechanism (CDM). In order to imitate the service condition of chip, the single point model coupling temperature and creep is adopted. The value of resistance is defined as the damage variable. As the value of stress or strain is difficult to be measured, FEM is applied to calculate the value of stress and strain. Then the constant in damage model is fitted by the experiment data. Base on the damage evolution equation, the life of solder joint is calculated and the result is compared to actual life of solder joint. It can be seen that difference between the prediction life and tests is no more than 10.2%.

## Phase Stability, Phase Transformations, and Reactive Phase Formation in Electronic Materials IX: Session II

*Sponsored by:* The Minerals, Metals and Materials Society, TMS Electronic, Magnetic, and Photonic Materials Division, TMS Structural Materials Division, TMS: Alloy Phases Committee

*Program Organizers:* Chih-ming Chen, National Chung Hsing University; Srinivas Chada, Medtronic; Sinn-wen Chen, National Tsing-Hua University; Hans Flandorfer, University of Vienna; A. Lindsay Greer, University of Cambridge; Jae-ho Lee, Hongik University; Kejun Zeng, Texas Instruments; Yee-wen Yen, National Taiwan University of Science and Technology; Wojciech Gierlotka, AGH University of Science and Technology; Chao-hong Wang, National Chung Cheng University

Monday PM

Room: 203

February 15, 2010

Location: Washington State Convention Center

*Session Chairs:* Jae-Ho Lee, Hongik University; Chao-hong Wang, National Chung Cheng University

2:00 PM Invited

**Interfacial Reactions in the Sn-Co/Ni and Sn-Cu-Co/Ni Couples:** *Yu-kai Chen*<sup>1</sup>; *Sinn-wen Chen*<sup>1</sup>; <sup>1</sup>National Tsing Hua University

Sn-Cu-Co alloys are promising Pb-free solders, and Ni is the most commonly used barrier layer. Interfacial reactions in the Sn-Co/Ni and Sn-Cu-Co/Ni couples are examined. Ni<sub>3</sub>Sn<sub>4</sub> and (Ni, Co)Sn<sub>4</sub> phases are formed in the early stage in the Sn-yCo/Ni couples reacted at 250°C where y varies from 0.06wt% to 0.4wt%. The Sn concentrations in the (Ni, Co)Sn<sub>4</sub> phase decrease with longer reaction time, and it becomes (Ni, Co)Sn<sub>4-x</sub>. With even longer reaction time, the (Ni, Co)Sn<sub>4-x</sub> phase cracks and detaches from the interface, and the Ni<sub>3</sub>Sn<sub>4</sub> phase becomes the stable reaction product. There are at least two different competing reactions in the Sn-Cu-Co/Ni couples. For example, the interfacial reactions in the Sn-0.7wt%Cu-0.05wt%Co/Ni couples are similar to those in the Sn-0.7wt%Cu/Ni couples, and the  $\eta$ -Cu<sub>6</sub>Sn<sub>5</sub> is the reaction phase. The reaction phases in the Sn-0.3wt%Cu-0.05wt%Co/Ni are Ni<sub>3</sub>Sn<sub>4</sub> and (Ni, Co)Sn<sub>4-x</sub>, and the results are similar to those in the Sn-Co/Ni couples.

2:25 PM

**Interfacial Reactions of Co/Sn/Cu Sandwich Structure:** *Chao-hong Wang*<sup>1</sup>; *Chun-yi Kuo*<sup>1</sup>; <sup>1</sup>National Chung Cheng University

In flip-chip packaging, Sn-based solder bumps are used to connect integrated circuit (I.C.) chip and Cu pad substrate. Co and Co-based alloys are the potential materials for under bump metallurgy (UBM) of I.C. chip. Thus, the designed experiments are conducted in this study to investigate the interfacial reactions of Co/Sn/Cu sandwich structure. The Co/Sn/Cu couples were electroplated on Cu substrates at various Sn layer thicknesses of 75  $\mu\text{m}$  to 600  $\mu\text{m}$ . The reactions

Mon. PM



were carried out at various temperatures, 150°C and 200°C, respectively. For the Sn/Cu interface,  $\text{Cu}_6\text{Sn}_5$  and  $\text{Cu}_3\text{Sn}$  are formed, which is similar to those of Sn/Cu interfacial reactions without Co layer. For the Co/Sn interface, two reaction phases,  $\text{Co}_3\text{Sn}$  and  $(\text{Cu},\text{Co})_6\text{Sn}_5$ , are simultaneously observed. Remarkably, the  $\text{Co}_3\text{Sn}$  reaction layer is much thinner than that of Sn/Co couple without Cu layer. The results in the present study indicate the  $\text{Co}_3\text{Sn}$  growth is significantly inhibited in Co/Sn/Cu sandwich couple.

### 2:45 PM

**Effects of Mechanically Applied Stress on Solid-State Sn/Cu Interfacial Reaction:** *Chi-pu Lin*<sup>1</sup>; Chih-ming Chen<sup>1</sup>; <sup>1</sup>National Chung-Hsing University

Plastic boards have been widely employed as the substrates for flexible printed-circuit board (PCB) due to their flexibility. The flexible PCB is usually bended in order to reduce the packaging volume, which makes the solder joints subjected to tensile or compressive stress. Sn is the primary element of Pb-containing and Pb-free solders and Cu is commonly used as a metallization layer for flexible PCB. In this study, Sn layer was electrodeposited on a thin Cu foil and solid-state interfacial reactions of the Sn/Cu joints subjected to tensile or compressive stress were investigated. The samples were bended upward or downward to apply tensile or compressive stress on the joint interface, respectively. Formation and growth behavior of the reaction products at the Sn/Cu interface were investigated and the correlation with the mechanically applied stresses was also discussed.

### 3:05 PM

**Stress Effect Study on Sn-Cu Intermetallic Formation by Four Point Bending Method:** Chuo-Cheng Yang<sup>1</sup>; *Ya-Chi Cheng*<sup>1</sup>; Chi-Jia Tong<sup>1</sup>; Ming Tzer Lin<sup>1</sup>; <sup>1</sup>National Chung Hsing University

In microelectronics, the fabrication of a reliable solder joint plays a very important role. In order to obtain better understanding on the effect of stress state related to interfacial IMC layer growth, custom design four point bend experiments had been conducted. Double polished silicon wafers were cut into strips with 27mm in length and 5mm in width as test samples. Electroplate 10um copper layer on silicon and deposit 30um tin layer on top of it. During the experiment, a set of samples were put into furnace for 168 hours at 200°C and relatively low levels of in-plane bending stress were applied on the samples under tensile, compressive stress and without stress. The results on intermetallic formation affected by different stress levels (10MPa, 20MPa and 50MPa) were presented. Both tensile and compressive stresses effects on the Cu-Sn intermetallic formation were observed and increased with increased the amplitude of the stress.

### 3:25 PM

**Correlation between Solder Wettability and Surface Properties of Deformed Cu Foils:** *Yu-Hsiang Hsiao*<sup>1</sup>; Chengyi Liu<sup>1</sup>; <sup>1</sup>National Central University

Typically, a so-called hardening surface layer would form on the Cu foil after mechanical process. This thin surface layer has very different properties from the bulk Cu foil. With different degrees of mechanical process, such as, cold-roll, the surface layers exhibit various properties. Nano-indentor and GIXRD were used to analyze the properties on the surface of Cu foils with different cold-roll percentages. We found that the hardening surface layer thickens with the cold-roll percentage. With the aid of the nano-indentor and GIXRD analysis, we can correlate the results of the surface properties of the cold-rolled Cu substrates with the solder wettability. According to the preliminary results, we found that the mechanical property of the very surface layer of the cold-rolled Cu foil has a strong influence on the solder wettability. In this talk, the detail relationship between solder wettability and Cu surface properties will be presented.

### 3:45 PM Break

### 4:05 PM Invited

**Suppressing the Sn-Patch Growth in Ti/Ni(V)/Cu under Bump Metallization with SnAgCu Solder after Aging:** Kai-Jheng Wang<sup>1</sup>; *Jenq-Gong Duh*<sup>1</sup>; <sup>1</sup>National Tsing Hua University

The sputtered Ti/Ni(V)/Cu under bump metallization (UBM) is widely used in flip chip technology, owing to the non-magnetic metals and low consumption rate. It was noted that V did not react with solders and intermetallic compounds (IMC) during reflow and aging, yet a Sn-patch would form in the Ni(V) layer. However, the Sn-patch growth may cause the IMCs detaching from the interface of solder joints. In this study, the Sn<sub>3.0</sub>Ag<sub>0.5</sub>Cu solder was reflowed on the Ti/

Ni(V)/Cu UBM with various Cu thickness at 250 C for 60 s, and then aged at 150 C for various periods of duration. It was revealed that the Sn-patch growth could be controlled by Cu thickness in the Ti/Ni(V)/Cu UBM. Therefore, a feasible approach to suppress the Sn-patch formation was discussed and proposed.

### 4:30 PM

**Interfacial Reactions of Sn-0.7Cu, Sn-9Zn and Sn-58Bi Lead-Free Solders with the Au/Ni/SUS304 Substrate:** *Yee-wen Yen*<sup>1</sup>; Kuen-da Chen<sup>1</sup>; Wei-kai Liou<sup>1</sup>; <sup>1</sup>National Taiwan University of Science and Technology

This study investigates the interfacial reactions between three kinds of lead-free solders, Sn-0.7 wt%Cu (SC), Sn-58 wt%Bi (SB) and Sn-9 wt%Zn (SZ), and Au/Ni/SUS 304 substrates. According to experimental results, only the (Cu, Ni)<sub>6</sub>Sn<sub>5</sub> phase with a hexagonal-type structure was formed in the SC/Au/Ni/SUS 304 couples. It should be the. When the Ni layer was completely consumed, the massive spalling of the (Cu, Ni)<sub>6</sub>Sn<sub>5</sub> phase was found in the solder. When the (Cu, Ni)<sub>6</sub>Sn<sub>5</sub> phase was spread over the interface, the SUS304 substrate surface could directly contact the SC solder and then the FeSn<sub>2</sub> phase with a platy-type layer was formed at the interface. In the SB/Au/Ni/SUS304 couple, only the Ni<sub>3</sub>Sn<sub>4</sub> phase with a needle type layer was found at the SB/Au/Ni/SUS 304 interface. The Ni<sub>5</sub>Zn<sub>21</sub> phase with a layered structure was formed at the SZ/Au/Ni/SUS 304 interface.

### 4:50 PM

**Influence of Palladium Thickness on the Solderability between Sn3Ag0.5Cu and Au/Pd/Ni(P) Surface Finish:** *Wei-Hsiang Wu*<sup>1</sup>; S. P. Peng<sup>1</sup>; C. H. Lin<sup>1</sup>; C. E. Ho<sup>1</sup>; <sup>1</sup>Yuan Ze University

Electroless nickel/immersion gold (ENIG) process has been widely accepted for depositing a viable surface finish over the Cu, providing a reliable soldering and wire-bonding pads in the high-end applications. However, the galvanic hyper-corrosion of the electroless nickel induced by the gold plating process will cause the so-called "black pad", which might embrittle the interfacial strength and deteriorate the overall reliability of one package. In order to solve this problem completely, modifications to ENIG by plating one additional Pd layer in-between, preventing the gold plating bath to attack Ni, are being considered and adopted by industry. The present study was conducted to evaluate the solderability of Sn<sub>3</sub>Ag<sub>0.5</sub>Cu with Au/Pd/Ni(P) having various Pd thicknesses (0-0.3 microns). The reliability of the joints was examined using a high-speed ball shear test with a shear speed of 2 m/s. The correlation between the interfacial strength and various Pd thicknesses will be presented in this study.

### 5:10 PM

**Electroless Nickel Plating on Porous Medium:** So-Young Chun<sup>1</sup>; Young-Mok Rhym<sup>2</sup>; *Jae-Ho Lee*<sup>1</sup>; <sup>1</sup>Hongik University; <sup>2</sup>Korea Institute of Materials Science

Electroless nickel plating is widely used technique in solder and packaging industries. In most cases, electroless nickel plating was applied on the open metallic surfaces and the rate of deposition was controlled with temperature and time. However, when the electroless plating is applied on the porous medium, the rate of deposition is also dependent on the activation process and mass flow of electrolyte prior to the electroless plating. In this research, electroless nickel plating on the porous medium was investigated. The carbon/polymer was selected as the substrate. Hydrophobic surface prevented the penetration of solution into the porous medium. Wettability of the substrate was improved by surface treatment prior to the activation process. The concentration of activating solution was varied to give the uniform palladium seeds. The optimum concentration of activating solution was also investigated. The rate of deposition in the porous medium was investigated with time and reducing agent concentration.

Mon. PM

# Technical Program

## Processing Materials for Properties: Agglomerates and Composite Materials Processing

Sponsored by: The Minerals, Metals and Materials Society, TMS Extraction and Processing Division

Program Organizers: Brajendra Mishra, Colorado School of Mines; Akio Fuwa, Waseda University; Paritub Bhandhubanyong, National Metal and Materials Technology Center

Monday PM Room: 617  
February 15, 2010 Location: Washington State Convention Center

Session Chairs: David Olson, Colorado School of Mines; Greg Oberon, U.S. Nuclear Regulatory Commission

### 2:00 PM Keynote

#### Innovations in Processing of Lightweight Metal Matrix Composites: Ramana Reddy<sup>1</sup>; <sup>1</sup>The University of Alabama

Newly emerging chemical in situ process is economical and energy efficient for large scale manufacturing of particulate metal matrix composites compared to the conventional (physical ex situ) processes. This presentation concentrates on some of the key examples from the author's experience and others, application of engineering fundamentals on the in situ processing of nanoparticulates of discontinuously reinforced Al and Mg alloys metal matrix composites. Aluminum and Magnesium alloys were reinforced with AlN nanoparticles using chemical in situ process. Thermodynamic analyses were made to identify the conditions for the in situ formation of the AlN in Al and Mg alloys. Effect of experimental processing parameters (i.e. time of gas injection, concentration of ammonia, and temperature of the melt) on the formation of AlN nanoparticles in alloy was determined. The AlN quantities in the composites varying from 5 to 51 wt % were produced. Increase in either injection time or flow rate of the ammonia gas increased the nitride content. AlN particles with an average size of 400 nm were produced. The measured Vickers hardness of the composites formed increased with increasing AlN content. The amount of AlN experimentally formed is in good agreement with the thermodynamically predicted data. A kinetic rate equation of in situ formation of AlN nanoparticulates in lightweight metal matrix composites was developed. A possible reaction mechanism of AlN formation was proposed. The industrial applications of this in situ manufacturing of composites by molten metal technology were discussed.

### 2:30 PM

#### Surface Peening Morphology Evaluation in Anodized Aluminum Alloy Rotors: M. Bilal Khan<sup>1</sup>; <sup>1</sup>SCME NUST

Correspondence between photoelastic stress and stress bearing capacity by shot peening on the tip of a light weight turbine rotor. SEM investigates the treated tip and the bulk of the rotor. EDS reveals the coarse features of silicon shots reinforced Al-alloy at the tip with anodized Al sealed with hot water in the bulk of the rear profile. AFM measures 3D flake surface topography of the treated tip. The hole-drill method predicts the distribution of stresses at the profile. Measurements are performed on an aerodynamic guide module under static pressure. High tensile residual stress in pressure die cast LM24 alloy convert to compressive mode by similar treatment. Pro Cast predicts the stress across the fin portion of the cast part. Radiography shows that Level 4 porosity exists in the thicker portion of the cast part due to the steep temperature gradient accompanied by the drastic dimensional changes, (~3.0-10 mm).

### 2:50 PM

#### Processing of Mullite and Mullite-Zirconia Composites Via Microwave Sintering: Subhadip Bodhak<sup>1</sup>; Susmita Bose<sup>1</sup>; Amit Bandyopadhyay<sup>1</sup>; <sup>1</sup>Washington State University

The objective of this research is to evaluate microwave sintering as a viable option to process high strength mullite and mullite-zirconia composites utilizing reduced time and energy. Mullite samples were sintered using a 3 KW, 2.45 GHz microwave furnace. With an increase in sintering temperature from 1400°C to 1500°C, the porosity decreased from 30 to 13% and the compressive strength increased from 128±18 MPa to 387±21MPa when 1wt% MgO was added as a sintering aid to mullite. Furthermore, yttria stabilized tetragonal zirconia (YTZP) was incorporated (up to 20wt%) to prepare zirconia toughened mullite composites. A maximum hardness of 10.24±0.61 GPa, compressive strength of

740±38 MPa and indentation fracture toughness of 3.65±0.43 MPam<sup>1/2</sup> was obtained for Mullite with 1wt% MgO and 10wt% ZrO<sub>2</sub> composites sintered at 1500°C in microwave furnace. Microwave sintering data, when compared with those of conventional sintering, reveal that localized heating of microwaves significantly enhanced the mechanical properties.

### 3:10 PM

#### SHS Synthesized Aluminum-Titanium Carbide MMC Die Casting Alloys: William Garrett<sup>1</sup>; Cosan Unuvar<sup>1</sup>; John Moore<sup>1</sup>; <sup>1</sup>Colorado School of Mines

Self-propagating High-temperature Synthesis utilizes the local heat of an energetic solid-state reaction to propagate the reaction through a mixed chemical body. For aluminum-titanium carbide composites the SHS process forms titanium carbide from elemental titanium and carbon powders as they are added to an aluminum melt which is then die cast. The SHS synthesis of TiC in aluminum increases the workable volume fraction of TiC (30-60 Vol%) in the aluminum alloy and reduces oxide impurities at the Al/TiC interface. The engineered properties design target is to match the wear, hardness, and compression strength properties of cast iron with the Al/TiC composite. Reducing the ignition temperature of the titanium/carbon reaction is done by adding low ignition temperature, chemical oven reactants to the elemental Ti and C powders and is important to reducing the cost of the manufacturing process and equipment and adapting the process for magnesium/TiC composites.

### 3:30 PM

#### Compaction Behavior of Aggregated and Agglomerated Nano-Powder Using Discrete Element Method: Avinash Balakrishnan<sup>1</sup>; Christophe Martin<sup>1</sup>; <sup>1</sup>Grenoble-INP

Why are powders made of nano-particles so difficult to compact? We attempt to answer this question using 3-D discrete simulations in which the adhesive forces linked to van der Waals interactions are explicitly taken into account at the particle length scale. Our simulations show that indeed, there is a significant effect of particle size and interparticle friction on the macroscopic stress necessary to attain a given relative density. The homogeneity of the compacted microstructure is also greatly affected by size effects. We show that aggregates exhibit a brittle to plastic transition in their crushing behavior as the particle size decreases. We demonstrate that both normal and tangential interparticle contact forces are affected by adhesive effects and that their coupling is responsible for the difficulty to compact these powders. Finally, we investigate the effect of compaction pressure and particle size on the tensile strength of green compacts made of sub-micronic particles.

### 3:50 PM

#### Effects of Particle Size, Deformation and Heat Treatment Processing on Strength and Ductility of Aluminum-Iron Composite: Samson Adeosun<sup>1</sup>; Sanambo Balogun<sup>1</sup>; Fidelia Ocholor<sup>1</sup>; Wasiu Ayoola<sup>1</sup>; Olatunde Sekunowo<sup>1</sup>; <sup>1</sup>University of Lagos, Akoka

This paper presents new evidence for enhancement of strength and ductility of aluminum 1200 alloy through the addition of steel particles. Iron particles of sizes 106,181,256,362.5 and 512.5 μm were added to the aluminum alloy. The samples produced were homogenized at 4200C for 10 hours and further processed through upset forging at 320C and annealed at 4700C for 8 hours. Tensile strength of 280MPa and ductility of 1.75 were achieved in the aluminum alloy with coarse particles of Fe (106μm) at 10% reduction when forged and subsequently annealed. With 50% reduction and finer-sized particles of Fe, strength dropped to 160MPa without significant decrease in ductility (1.7). The presence of fine Fe particles at grain boundaries after annealing with most of the particles in solid solution is responsible for the drop in strength. Keywords: Iron particle, forging, annealing, strength and ductility, aluminum alloy.

### 4:10 PM

#### Features of a Structure and Properties of the Agglomerates Obtained from Rich Ores: Sereda Borys<sup>1</sup>; Irina Kruglyak<sup>1</sup>; Aleksandr Zherebtsov<sup>1</sup>; <sup>1</sup>ZSEA

Structural - textural features of agglomerate structure obtained from rich ores deposits have been described in this work. The formation and cross-feeding of different structures (brecciated, porphyry, eutectic type) of sintered agglomerates have been described. The mechanism of structures changes in the block of fluxed agglomerate from periphery to the center at different fuel content has been considered. Influence of original sintering composition on a structure and properties of obtained agglomerates has been established. It is determined that durability and reducibility is depended from good crystallization, structural



porosity homogeneity at basicity rate 1.8 – 2.0. At low basicity and large fuel content in ore mixture the high durability of agglomerates is observed too.

### 4:30 PM

**In situ Neutron Diffraction Study of Solvent-Free Fabrication of Ferromagnetic Core-Shell Fe<sub>3</sub>O<sub>4</sub>-Carbon Nanocomposite:** *Sven Vogel*<sup>1</sup>; Vilas Pol<sup>2</sup>; Luke Daemen<sup>1</sup>; George Chertkov<sup>1</sup>; <sup>1</sup>Los Alamos National Laboratory; <sup>2</sup>Argonne National Laboratory

The synthesis of nanomaterials is the subject of intense current research since the nanoparticles of interest to applications are only prepared in the laboratory and are difficult to produce in a monodisperse form. Most of the current processes are complex and synthesize nanomaterials to varying degrees of commercially-viable quantities. Pol et al. developed a completely new facile synthesis approach called RAPET [Reaction under Autogenic Pressure at Elevated Temperature] for the nano-synthesis of metals, oxides, carbides, phosphides, sulfides etc. However, it has always remained a challenge to understand the exact dissociation stage of the chemical precursor under autogenic pressure at elevated temperature and the exact arena of segregation or formation of nanostructures. Using neutron diffraction, we could study the thermolysis of a single deuterated precursor, Fe<sub>3</sub>(CH<sub>3</sub>COO)<sub>6</sub>(OH)<sub>2</sub>CH<sub>3</sub>COO, in a closed reactor in situ at temperatures up to 700/176C. The reaction produced ferromagnetic core-shell Fe<sub>3</sub>O<sub>4</sub>-carbon nano-composite without need for a solvent or catalyst.

### 4:50 PM

**Thermal Properties of Advanced Diamond - Metal Matrix Composites:** *Vikas Sinha*<sup>1</sup>; Jessica Remmert<sup>2</sup>; Sabyasachi Ganguli<sup>3</sup>; Robert Wheeler<sup>1</sup>; Jonathan Spowart<sup>4</sup>; <sup>1</sup>UES, Inc.; <sup>2</sup>UTC; <sup>3</sup>UDRI; <sup>4</sup>Air Force Research Laboratory

A reliable operation as well as further improvements in performance of advanced electronic components requires a credible thermal management strategy. A high thermal conductivity and a tailorable coefficient of thermal expansion are important attributes of candidate substrate/ packaging materials for high power density electronic components. Several diamond containing metal matrix composites have been developed to generate this combination of properties. Diamond-metal matrix composites were fabricated and variables included metal matrix chemistry as well as volume % of diamond. The thermal conductivity for different material conditions was measured via laser flash techniques. Attempts were also made to directly measure the interface thermal conductance via time-domain thermoreflectance techniques. To aid in improved understanding of interfacial thermal transport, microstructural characterization of interface region was also carried out. The chemistry changes near the interface were evaluated via energy dispersive spectroscopy and/ or electron energy loss spectroscopy techniques in a transmission electron microscope.

### 5:10 PM

**Effect of Process Parameters on Powering Characteristics of Galvannealed Materials:** *Ram Janam Singh*<sup>1</sup>; Khursid Khan<sup>2</sup>; Shantanu Chakrabarti<sup>2</sup>; <sup>1</sup>NIT Jamshedpur; <sup>2</sup>Tata Steel

Globally, the use of metallic coated steel sheets in the automobile industry is increasing. The sheet should have excellent formability, weldability, paintability and corrosion resistance. Since bare cold rolled steel sheets have certain limitations, application of galvanized steel sheets is steadily expanding. Galvannealed steel sheet fulfills all requirements and has become of major interest in the automobile industry. The success of Galvannealed (GA) steels in the body-in-white depends upon material design and parameters of various processes involved, like cold rolling, continuous annealing, hot dipping and galvannealing. In the present work, powdering resistance, one of the important product characteristics of GA, has been studied and a relation is established between the process parameters and the powdering value. The product obtained through optimisation of the process parameters has been successfully used by major automotive producers without any powdering problem, for internal as well as external automotive applications.

### 5:30 PM

**Porous Superelastic NiTi Produced by Sintering with NaCl Space-Holders:** *Ampika Bansiddhi*<sup>1</sup>; David Dunand<sup>2</sup>; <sup>1</sup>Kasetsart University; <sup>2</sup>Northwestern University

Porous NiTi with ~30-40% porosity was fabricated by densification of NiTi powder with temporary NaCl space-holders. The porosity and pore characteristics (pore size, shape and connectivity) were controllable through the initial volume fraction and geometry of the space holders. The NiTi

foams exhibited shape recovery behavior at room temperature and at body temperature. High compressive yield strength with low stiffness and large recovery strain were observed. Simple, cost-effective processing and post-processing procedures were demonstrated to achieve a desired porous structure, and hence a desired mechanical and shape recovery behavior. By combining the unique properties of NiTi with an adjustable foam architecture, NiTi foams can be custom-designed for multi-functional applications such as impedance-matching connectors between structural parts, energy-absorbing structures, actuators, and bone implants.

### 5:50 PM

**Experimental Investigations of the Ti-Fe- Eutectic System Needed for the Further Understanding of the Microstructural Evolution in an Eutectic Alloy at Different Cooling Rates:** *Antje Schlieter*<sup>1</sup>; Uta Kühn<sup>1</sup>; Martin Friak<sup>2</sup>; Juergen Hubert<sup>3</sup>; Heike Emmerich<sup>3</sup>; Joerg Neugebauer<sup>2</sup>; Juergen Eckert<sup>1</sup>; <sup>1</sup>IFW Dresden; <sup>2</sup>MPI Düsseldorf; <sup>3</sup>RWTH Aachen

Ti-based alloys have been suggested for commercial applications with a great potential due to their high strength (~1000 MPa) and good corrosion resistance. The strength of these alloys can be further increased by producing a nano/ ultrafine grained and lamella structured Ti-eutectic. In this paper we focused on the influence of the different cooling rates due to the several casting techniques (arc melting, cold crucible, tilt casting, injection casting and Bridgeman technic) on the Ti-Fe-eutectic alloy. The evolution of the microstructure, the phase constituents, the chemical composition linked to the mechanical properties and elastic constants depending on lamellar growth with multiple orientation will be presented. To achieve this goal a joint approach, where the detected experimental data are systematically cross-checked against the phase-field simulations with parameters determined from ab initio calculations, is adopted.

## Refractory Metals 2010: Processing and Properties II

*Sponsored by:* The Minerals, Metals and Materials Society, TMS Structural Materials Division, TMS: Refractory Metals Committee  
*Program Organizers:* Brian Cockeram, Bechtel-Bettis; Gary Rozak, H.C. Stark

Monday PM Room: 2A  
February 15, 2010 Location: Washington State Convention Center

*Session Chairs:* Brian Cockeram, Bechtel Marine Propulsion Corporation; Gary Rozak, H. C. Starck, Inc.

### 2:00 PM

**Tantalum Plates with Controlled Texture:** *Dincer Bozkaya*<sup>1</sup>; Peter Jepson<sup>1</sup>; <sup>1</sup>H.C. Starck Inc.

Texture control of tantalum plates used as sputtering targets is crucial for the uniformity of thin films as the sputtering rate at a given location is a strong function of grain orientation. In addition, texture of plates and sheets may also be critical in other applications such as forming. In this paper, a new grade of tantalum plate with improved uniformity of texture radially and through thickness is introduced. The thermomechanical processes utilized for breaking up the ingot structure of electron-beam melted tantalum are described. A novel rolling process for obtaining the desired, uniform texture in final plates and sheets is explained.

### 2:25 PM

**Analysis of Tantalum Taylor Impact Specimens:** *Joel House*<sup>1</sup>; John Bingert<sup>2</sup>; Philip Flater<sup>1</sup>; James O'Brien<sup>3</sup>; William Hosford<sup>4</sup>; Robert DeAngelis<sup>5</sup>; Richard Harris<sup>1</sup>; <sup>1</sup>Air Force Research Laboratory; <sup>2</sup>Los Alamos National Laboratories; <sup>3</sup>O'Brien and Associates; <sup>4</sup>University of Michigan; <sup>5</sup>University of Florida

Taylor impact experiments were conducted on commercially pure Ta subjected to thermo-mechanical processing including Equal Channel Angular Processing (ECAP), forging and annealing. The microstructures were characterized by optical microscopy and Electron-Backscattered Diffraction (EBSD) before and after the impact experiments. Specimens of the material were tested in the cold worked and recrystallized conditions. The final geometry of recovered specimens was obtained to characterize the plastic anisotropy. The EBSD data sets from the recovered impact specimens revealed the texture evolution in the specimen as measured along the axial length. These data show the evolution of the <111>, and <100> texture components as they rotate toward the compression

Mon. PM

# Technical Program

axis of the sample. The final specimen geometry, optical microscopy and EBSD characterization reveal the affect of processing history on the high strain rate deformation in the Taylor impact experiment.

## 2:50 PM

**Comparison of Optimized Finite Element Crystal Plasticity Model and Tensile Tests of Niobium Single Crystals:** *Derek Baars*<sup>1</sup>; *Payam Darbandi*<sup>1</sup>; *Chris Compton*<sup>2</sup>; *Wenjun Liu*<sup>3</sup>; *Rozaliya Barabash*<sup>4</sup>; *Thomas Bieler*<sup>1</sup>; <sup>1</sup>Michigan State University; <sup>2</sup>National Superconducting Cyclotron Laboratory; <sup>3</sup>Advanced Photon Source Argonne National Laboratory; <sup>4</sup>Oak Ridge National Laboratory

Manufacturing superconducting radio frequency (SRF) cavities from single or multi-crystal niobium is being investigated as an alternative to using polycrystalline niobium, as single crystal sheets may be cut directly from a purified ingot, eliminating the cost of forging and rolling ingots into polycrystalline sheet. Simulation of deformation of single or multi-crystal parts is desirable, but the data needed to develop single crystal constitutive models are lacking. Selected crystal orientations to resolve shear stress on specific slip systems during uniaxial tension are used to identify orientation dependent critical resolved shear stresses and work hardening parameters. Active slip systems are identified using orientation imaging microscopy, electron channeling contrast imaging, and depth resolved 3-D x-ray measurements. These specimens develop shape changes that reflect activated slip system and work hardening phenomena, so optimized constitutive models can be developed to predict shape changes and observed activated slip systems.

## 3:15 PM

**Deformation Mechanism for Polycrystal Niobium at Cryogenic Temperature:** *Payam Darbandi*<sup>1</sup>; *Derek Baars*<sup>2</sup>; *Saravan Chandrasekaran*<sup>3</sup>; *Farhang Pourboghrat*<sup>3</sup>; *Tom Bieler*<sup>2</sup>; *Chris Compton*<sup>4</sup>; <sup>1</sup>Michigan State University; <sup>2</sup>Department of Chemical Engineering and Materials Science, Michigan State University; <sup>3</sup>Department of Mechanical Engineering, Michigan State University; <sup>4</sup>National Superconducting Cyclotron Laboratory, Michigan State University

Niobium has been used in superconducting cavities for several years. The cavities operate at 4.2K, as niobium becomes superconducting at temperatures below 9.2 K. Since the deformation mechanisms of niobium at 4.2 K are not completely understood, tensile testing was done at 4.2 K in liquid helium. Serrated flow of the material was observed in the stress-strain curve which literature of similar tests suggests that it is caused by twinning and not by dislocation slip alone. Orientation imaging microscopy of the polished cross-section of the specimen revealed evidence of twinning. Tensile tests were also done at 77 K in liquid nitrogen, with no serration in the stress-strain curve. Serration has been reported in similar literature, though at lower strain rates than the present test. Strain rate affects the deformation mechanism, affecting the serration behavior. The effect of strain rate on serrated flow will be discussed.

## 3:40 PM Break

## 3:55 PM

**Mechanical Properties and Constitutive Modeling of Some Refractory Metals:** *Shuh Rong Chen*<sup>1</sup>; *G.T. (Rusty) Gray III*<sup>1</sup>; <sup>1</sup>Los Alamos National Laboratory

The high density and high melting temperature of several refractory metals make them attractive candidates for defense applications. The mechanical properties of these metals are very sensitive to deformation temperature, strain rate, and the impurity contents due to its more open crystallographic structure (bcc) with a higher intrinsic barrier (Peierls stress) to dislocation movement. We will present constitutive properties on Ta, Mo, W, V, Nb, and Re obtained by compressing samples as a function of temperature from 77 to 1273K, and strain rate from 0.001/s to 3000/s. We will also present the development of more physically-based constitutive models to describe the mechanical responses of these metals to large strains. And finally we will validate the models and their corresponding parameters using high velocity Taylor cylinder impact tests by comparing results from the post-mortem plastic deformation profiles and the finite element calculations. \*Work supported jointly by the U.S. Department of Energy and Department of Defense

## 4:20 PM

**Chromium Alloys for More Efficient Fossil Energy Conversion Technologies:** *Omer Dogan*<sup>1</sup>; *Michael Gao*<sup>1</sup>; *Paul King*<sup>1</sup>; <sup>1</sup>DOE National Energy Technology Laboratory

In order to improve efficiency and reduce environmental emissions in fossil energy conversion systems, new technologies such as oxy-fuel gas turbines, hydrogen turbines, and syngas turbines are being developed. These technologies will require new materials that can withstand higher temperatures. Even the state-of-the-art nickel based superalloys cannot meet these demands as they are unsuitable for use above 1150°C. Accordingly, alloys based on refractory metals such as Nb, Mo, Cr and W are being investigated as potential solutions. The materials community has been interested in Cr based alloys since 1950's due to (i) their relative low cost, (ii) relative low density and (iii) good high temperature strength. However, low ductility and fracture toughness of Cr and its alloys around room temperature kept them from a major structural application. We will review the historical data on mechanical properties and take a close look at the recent research on the Cr alloys.

## 4:45 PM

**Strength and Oxidation Resistance of Mo-Si-B Alloys Produced by Reaction Synthesis:** *Michael Middlemas*<sup>1</sup>; *Joe Cochran*<sup>1</sup>; *P. Jain*<sup>2</sup>; *K. S. Kumar*<sup>2</sup>; <sup>1</sup>Georgia Institute of Technology; <sup>2</sup>Brown University

Mo-Si-B alloys are a leading candidate for next generation of jet turbine engine blades and have the potential to increase the service temperature of the base metal 200-300°C higher than nickel-based superalloys. The alloys form a composite microstructure of the molybdenum solid solution (Mo<sub>ss</sub>) and two intermetallic phases, Mo<sub>3</sub>Si and Mo<sub>5</sub>SiB<sub>2</sub>, where the Mo<sub>ss</sub> phase increases ductility and the intermetallic phases enhance strength and provide oxidation resistance. The properties of the alloys are highly dependent on the morphology of the microstructure. A powder processing approach has been developed in which the three-phase alloys are produced through the reaction of molybdenum, Si<sub>3</sub>N<sub>4</sub> and BN powders. The resulting microstructures are a fine dispersion of the intermetallic phases in a Mo<sub>ss</sub> matrix. The strengths of the alloys produced by this method have been examined by tensile testing between 1000 and 1300°C and the oxidization resistance was examined using cyclic oxidation tests.

## 5:10 PM

**Cyclic Deformation Behavior of Commercially Pure Mo and a Mo-Si-B Solid Solution Alloy:** *X Yu*<sup>1</sup>; *K.S. Kumar*<sup>1</sup>; <sup>1</sup>Brown University

Monotonic tensile deformation behavior of Mo and a Mo-Si-B alloy has been previously examined and it was shown that in both these materials, dynamic strain aging(DSA)occurs for specific strain rate-temperature combinations. Therefore,it was thought necessary to understand the cyclic deformation behavior of these materials,particularly in the regime where DSA is prevalent. In this presentation, we will discuss our results on the cyclic deformation response(tension-tension, R=0.1)of commercially pure Mo in the fully recrystallized condition in the temperature range 300K-873K using various levels of maximum stress.The resulting fracture surfaces have been analyzed and will be compared to those obtained from monotonic loading. A similar parallel study is currently underway on a Mo-Si-B solid solution alloy to understand the contribution of the Si in solid solution(since B is thought to have negligible solubility)to the cyclic loading response. Results from these studies will be presented and compared, and the underlying deformation mechanism will be discussed.

## 5:35 PM

**Tensile Creep of Mo-Si-B Alloys:** *P. Jain*<sup>1</sup>; *Sharvan Kumar*<sup>1</sup>; <sup>1</sup>Brown University

The elevated temperature uniaxial tensile response at a nominal strain rate of 10<sup>-4</sup> s<sup>-1</sup> and the tensile creep response at constant load between 1000°C and 1300°C of a (i) single-phase solid solution (Mo-3.0Si-1.3B in at.%), (ii) two-phase alloy containing ~35 vol.% of the T2 phase (Mo-6Si-8B in at.%), and (iii) three-phase alloy with ~50 vol.% of T2 + Mo<sub>3</sub>Si phases (Mo-8.6Si-8.7B in at.%) were evaluated. The results confirm that Si in solid solution significantly enhances both the yield strength and the creep resistance of these materials. A Larson-Miller plot of the creep data showed improved creep resistance of the two-and three-phase alloys in comparison to Ni-based superalloys. A stress exponent of ~5 for the solid solution alloy and ~7 at 1200°C for the two multiphase alloys suggests dislocation climb to be the controlling mechanism. Grain boundary precipitation of the T2 phase during creep deformation is



observed and the precipitation kinetics appears to be affected by the test temperature and applied stress.

### Solid-State Interfaces: Toward an Atomistic-Scale Understanding of Structure, Properties, and Behavior through Theory and Experiment: Thermodynamics and Morphological Stability

Sponsored by: The Minerals, Metals and Materials Society, TMS Electronic, Magnetic, and Photonic Materials Division, TMS Structural Materials Division, TMS: Chemistry and Physics of Materials Committee

Program Organizers: Michael Demkowicz, Massachusetts Institute of Technology; Douglas Medlin, Sandia National Laboratories; Emmanuelle Marquis, University of Oxford

Monday PM Room: 602  
February 15, 2010 Location: Washington State Convention Center

Session Chairs: Douglas Medlin, Sandia National Labs; Wayne Kaplan, Technion - Israel Institute of Technology

#### 2:00 PM Invited

#### Gamma/Gamma Prime Interfacial Free Energies in Nickel-Based Alloys: Atom-Probe Tomographic Experiments and First-Principles Calculations:

David Seidman<sup>1</sup>; <sup>1</sup>Northwestern University

We determine  $\gamma(\text{f.c.c.})/\gamma\text{-prime(L12)}$  interfacial free energies in Ni-Al-Cr and Ni-Al alloys by studying the coarsening kinetics of gamma-prime precipitates, which permits us to determine the rate constants associated with the temporal evolution of the mean radius and number density of the precipitates, and the matrix supersaturation, employing 3D atom-probe tomography. The interfacial free energies for the Ni-Al-Cr alloys are extracted employing a continuum formalism for ternary alloys, Kuehmann-Voorhees, where all requisite quantities are experimentally measured except for the second derivatives of the free-energy surfaces w.r.t. concentration, which come from thermodynamic data bases. For the Ni-Al alloys we use an approach developed by Ardell that does not require a value of the diffusivity. In parallel with the experiments we employ first-principles calculations (VASP) to calculate interfacial energies, which are compared with the experimental values. It is concluded that the dominant quantity affecting the interfacial free energy is chemical (electronic) in origin.

#### 2:30 PM

#### Atomic Scale Characterization of Deformation Induced Interfacial Mixing

in a Nanostructured Cu/V Composite Wire: Xavier Sauvage<sup>1</sup>; Cécile Genevois<sup>1</sup>; Gérald Da Costa<sup>1</sup>; Victor Pantsyrny<sup>2</sup>; <sup>1</sup>University of Rouen, CNRS; <sup>2</sup>Bochvar Institute of Inorganic Materials

The nanoscaled structure of a Cu/V composite wire was investigated by HR-STEM (HAADF) and Atom Probe Tomography (APT). Some deformation induced interfacial mixing was clearly observed. Mixed layers are typically 2nm wide vanadium gradients in the fcc Cu phase. This mechanical mixing leads to the local fragmentation and dissolution of the filaments where their thickness is less than 5nm. Thus, the material contains locally a significant amount of vanadium super saturated solid solutions in fcc Cu.

#### 2:50 PM

Heterogeneous Nucleation of NiSi<sub>2</sub> Epitaxial Growth in Si Nanowires: Yi-Chia Chou<sup>1</sup>; Wen-Wei Wu<sup>2</sup>; Lih J. Chen<sup>3</sup>; K. N. Tu<sup>1</sup>; <sup>1</sup>University of California Los Angeles; <sup>2</sup>National Chiao Tung University; <sup>3</sup>National Tsing Hua University

We report the heterogeneous nucleation of NiSi<sub>2</sub> epitaxial growth in Si nanowires observed by in situ high resolution TEM. Heterogeneous nucleation of NiSi<sub>2</sub> with Si nanowires was achieved by forming steps in the interface of NiSi<sub>2</sub> and Si, which resulted in two silicide/Si interfaces in TEM observation. The lattices between the two interfaces are partially transformed to NiSi<sub>2</sub>. Moreover, the third interface was observed to move repeatedly from the silicide-rich interface to the Si-rich interface. Line scan EDX analysis indicated the stepwise distribution of Ni and Si concentration profile between the two interfaces. The steps served as kinks for heterogeneous nucleation which required lower supersaturation than homogeneous nucleation. Incubation time

of forming one NiSi<sub>2</sub> nucleus was measured shorter, and thus the growth rates were faster by heterogeneous nucleation than by homogeneous nucleation.

#### 3:10 PM

#### Metastability and Competition in Grain Boundary Complexion Transitions:

Shen Dillon<sup>1</sup>; Gregory Rohrer<sup>2</sup>; <sup>1</sup>University of Illinois at Urbana-Champaign; <sup>2</sup>Carnegie Mellon University

Grain boundaries may undergo structural and compositional transitions that are analogous to grain boundary 'phase' transitions. These transitions are termed complexion transitions and their behavior significantly affects microstructural evolution and materials properties. The relative energy of boundaries of different complexion is quantified to determine their stability. The results indicate the importance of an activation barrier and metastability. Like other processes subject to phase selection, both the equilibrium thermodynamics and the activation barrier will impact complexion transitions. This suggests that complexion transitions should compete with processes like precipitation for partitioning excess solute. Relative interfacial energies between the host and various precipitates are measured experimentally and correlated with the propensity for complexion transitions. The results indicate a new criterion for additive selection to control grain boundary complexions and microstructural evolution.

#### 3:30 PM

#### Influence of Grain Boundary Chemistries in Mix-Mobility Thin Film Growth: Bianzhu Fu<sup>1</sup>; Gregory Thompson<sup>1</sup>; <sup>1</sup>University of Alabama

Thin films exhibit compressive-tensile-compressive stress states during the nucleation of islands, coalescence of islands and post-coalescence stages of growth. Using an in situ wafer curvature measurement technique, the stress evolution in Fe-Pt and Fe-Cu systems has been investigated. The stresses were shown to be compositionally dependent. In general, the tensile or compressive stress for the various binary compositions was associated with whichever element enriched the grain boundaries. Under specific growth conditions, a 'zero-stress' state could be achieved. The as-deposited alloy stress states do not show significant stress recovery upon ceasing the deposition. In contrast, in situ annealing resulted in significant changes in stress recovery which is believed to be the enhanced migration of atoms from the boundaries because of the phase state of the film. TEM, AFM and atom probe tomography have been employed to quantify the boundaries as they relate to the preferential segregation and thin film stress.

#### 3:50 PM Break

#### 4:10 PM Invited

#### Thermodynamics of Solid-Fluid Interfaces with Non-Hydrostatically Stressed Solids: T. Frolov<sup>1</sup>; Y. Mishin<sup>1</sup>; <sup>1</sup>George Mason University

While thermodynamics of solid-fluid interfaces is well understood for hydrostatic systems, the case of non-hydrostatically stressed solids remains less studied. We present thermodynamic relations for the free energy, interfaces stress, segregation and other excess properties of interfaces between fluids and non-hydrostatically stressed solid phases in multi-component systems. These relations lead to various thermodynamic integration schemes and are presented in forms convenient for atomistic simulations. These relations are illustrated by several examples of calculation of interface thermodynamic properties in solid-liquid coexistence systems using Monte Carlo and molecular dynamics methods with embedded-atom potentials.

#### 4:40 PM

#### Grain Boundary Misorientation Instabilities: W. Craig Carter<sup>1</sup>; <sup>1</sup>MIT

Grain boundary energies are, among other things, a function of misorientation. Such misorientation-energy functions typically have cusps at particular misorientations. It is demonstrated that such functions, including some reported in the literature, possess instabilities with respect to the creation of an additional misorientation.

#### 5:00 PM

#### On the Thermodynamic Stabilization of Defects in the Framework of a Defactant Concept: Reiner Kirchheim<sup>1</sup>; <sup>1</sup>University of Göttingen

Gibbs treatment of surfactants is extended to include other crystalline defects besides interfaces, because there is an analogy between surfactants in liquids stabilizing structures with large surface areas like foams or microemulsions, and components in a crystalline solid stabilizing grain boundaries, dislocations and vacancies. These components are called defactants (defect acting agents). Thus

Mon. PM

# Technical Program

solutes may reduce the defect formation energies given by Gibbs as  $d\gamma = -\Gamma d\mu$ , where  $\mu$  is the chemical potential of solute,  $\Gamma$  is the excess solute and  $\gamma$  is now the defect energy. In this context conditions and consequences are discussed where defect energies become zero or negative leading to metastable equilibrium or instable crystalline phases. First principle calculations of (i) the surface energy of small alumina particles with excess hydrogen, (ii) the grain boundary energy of copper with bismuth excess and (iii) the vacancy formation energy in iron with excess hydrogen all yield negative defect formation energies.

## 5:20 PM

**Interfacial Structure and Morphological Evolution of Platinum Nano-Precipitates Embedded in Sapphire:** *Melissa Santala*<sup>1</sup>; Velimir Radmilovic<sup>2</sup>; Raquel Guilian<sup>3</sup>; Mark Ridgway<sup>3</sup>; Andreas Glaeser<sup>1</sup>; Ronald Gronsky<sup>1</sup>; <sup>1</sup>University of California; <sup>2</sup>National Center for Electron Microscopy; <sup>3</sup>Australian National University

Platinum nano-precipitates (<100nm diameter) were formed in sapphire by high-energy ion implantation followed by thermal annealing. The morphology of the precipitates depends on the orientation relationship of the precipitates within the sapphire and can be either partially or almost fully faceted. Atomically flat faceted interfaces coinciding with low index planes of sapphire were observed with high-resolution transmission electron microscopy (HRTEM). Prominent planar interfaces form for interfacial relationships with (111)<sub>Pt</sub> planes parallel to low-index planes of sapphire. Some specimens were annealed at 1600°C for 100h, a time and temperature expected to result in full morphological equilibration for precipitates <100nm in diameter, if the evolution were purely diffusion-limited. For precipitates with an orientation relationship (0001)<sub>sapphire</sub> || (111)<sub>Pt</sub>; [10-10]<sub>sapphire</sub> || [1-10]<sub>Pt</sub>, the presence of atomically flat interfaces parallel to the (0001) basal plane of sapphire frustrates the expected morphological equilibration.

## Surface Engineering for Amorphous-, Nanocrystalline-, and Bio-Materials: Session II

*Sponsored by:* The Minerals, Metals and Materials Society, TMS Materials Processing and Manufacturing Division, TMS: Surface Engineering Committee

*Program Organizers:* Sandip Harimkar, Oklahoma State University; Arvind Agarwal, Florida International University; Sudipta Seal, University of Central Florida; Narendra Dahotre, University of Tennessee

Monday PM Room: 604  
February 15, 2010 Location: Washington State Convention Center

*Session Chairs:* Arvind Agarwal, Florida International University; Roger Narayan, North Carolina State University; Narendra Dahotre, University of Tennessee

## 2:00 PM Introductory Comments

### 2:05 PM Invited

**Assessment of Microbial Biofilm Growth on Nanocrystalline Diamond Coatings Using a CDC Biofilm Reactor:** J. S. Lewis<sup>1</sup>; S. D. Gittard<sup>1</sup>; Roger Narayan<sup>1</sup>; C. J. Berry<sup>2</sup>; Robin Brigmon<sup>2</sup>; R. Ramamurti<sup>3</sup>; R. N. Singh<sup>3</sup>; <sup>1</sup>University of North Carolina & North Carolina State University; <sup>2</sup>Savannah River National Laboratory; <sup>3</sup>University of Cincinnati

Nanostructured materials may play a major role in next generation medical devices. In this work, atomic layer deposition was used to deposit titanium oxide coatings on all the surfaces of nanoporous alumina membranes in order to reduce pore size in a controlled manner. The titanium oxide coating serves several purposes, including: (1) maintaining a narrow pore size distribution, (2) reducing pore size in a controlled manner, (3) preventing aluminum ions from leaching into tissues, and (4) creating a biocompatible membrane/tissue interface. Staphylococcus aureus and Escherichia coli were used to evaluate the antimicrobial properties of TiO<sub>2</sub>-coated nanoporous alumina membranes. Nanostructured materials prepared using atomic layer deposition may be used in "smart" drug delivery devices or self-sterilizing medical devices.

### 2:30 PM

**Wetting Behavior of Laser Synthetic Surface Micro Textures on Ti-6Al-4V for Bioapplication:** *Sameer Paital*<sup>1</sup>; Wei He<sup>1</sup>; Claus Daniel<sup>2</sup>; Narendra Dahotre<sup>1</sup>; <sup>1</sup>The University of Tennessee; <sup>2</sup>Oak Ridge National Laboratory

Wettability at the surface of an implant material play a key role in its success as it modulate the protein adsorption and thereby influences cell attachment and tissue integration at the interface. Hence, surface engineering of implantable materials to enhance wettability to physiological fluid under in vivo conditions is an area of active research. In light of this, in the present work a laser based optical interference and direct melting techniques were used to develop synthetic micro textures on Ti-6Al-4V alloys and their effects on wettability were systematically studied. Improved wettability to simulated body fluid and distilled water was observed for the Ca-P coatings obtained by direct melting technique. The effect of physical texture and wetting on biocompatibility of laser processed Ca-P coating was evaluated in the preliminary efforts on culturing of mouse MC3T3-E1 osteoblast cells.

### 2:50 PM

**Corrosion of the Implant Alloy Ti-45wt.%Nb in Simulated Physical Media:** *Daniela Zander*<sup>1</sup>; <sup>1</sup>TU Dortmund

Titanium and titanium alloys, especially Ti-6Al-4V, are used for various medical applications, e.g. endoprosthesis. There is evidence that metallic dissolution into surrounding tissue can cause complications with the implant and the environment. This research focuses on investigating the electrochemical surface properties of Ti-45wt.%Nb in simulated physiological media. In order to verify the influence of the radical reaction by free oxygen and the interaction with hyaluronic acid by potentiodynamic polarization and electrochemical impedance spectroscopy were conducted in PBS solution without and with H<sub>2</sub>O<sub>2</sub> and hyaluronic acid in comparison to titanium. The surface topography and passive layer was studied by X-ray diffraction, SEM and TEM. DC and AC measurements showed a strong influence of OH<sup>o</sup>-radicals and hyaluronic acid on the passive current and the passivation mechanisms. The results obtained by electrochemical measurements are correlated with microstructural investigations, e.g. the formation of a porous passive layer due to the influence of H<sub>2</sub>O<sub>2</sub>.

### 3:10 PM

**Corrosion Behaviour Evaluation of Fluoridated Hydroxyapatite/Niobium Filler-Matrix Composite Coating for Hard Tissue Implant:** *Ehsan Mohammadi Zahrani*<sup>1</sup>; M. H. Fathi<sup>2</sup>; Akram Alfantazi<sup>1</sup>; <sup>1</sup>The University of British Columbia; <sup>2</sup>Isfahan University of Technology

Need to reduce cost in public health services has compelled use of 316L stainless steel as the most economical alternative for hard tissue implants because of its relatively low cost and reasonable corrosion resistance. However, this material is prone to localized attack in long-term application due to the aggressive biological effects. In this study fluoridated hydroxyapatite/niobium (FHA/Nb) coatings with 0 and 100% degree of fluoridation was deposited on 316L SS substrate by using nanostructure FHA powders, produced by mechanical alloying technique, to improve the corrosion properties and biocompatibility of implant. XRD and SEM techniques were utilized to investigate the effect of fluoridation on morphology of the coatings. Electrochemical polarization tests were carried out in ringer and normal solution in order to determine the corrosion behaviour of coated specimen as an indication of biocompatibility. The results confirmed that fluoridation could improve the corrosion resistant and phase stability of the plasma-sprayed coating.

### 3:30 PM

**Surface Engineering of Titanium Alloy Modified by Plasma-Based Low-Energy Ion Implantation:** *M.K. Lei*<sup>1</sup>; Z.L. Wu<sup>1</sup>; Y.X. Ou<sup>1</sup>; T.K. Song<sup>1</sup>; Q. Zhou<sup>1</sup>; <sup>1</sup>Dalian University of Technology

Plasma-based low-energy ion implantation, including plasma source ion nitriding/carburizing and plasma source low-energy ion enhanced deposition, has emerged as a low-temperature surface engineering technique for metal and alloy. In this work, the biomedical titanium alloy samples were modified by plasma source ion nitriding at a low temperature ranging from 500°C to 650°C, and sequentially by physical vapor deposition of the titanium nitride films. The TiN films deposited on the plasma source ion nitrided titanium alloy surface which consisted of TiN and Ti<sub>2</sub>N possessed an improvement in wear and corrosion properties. The tribological behavior of the modified titanium alloy samples were investigated on a ball-on-disc tribometer against AISI 52100



bearing steel. The electrochemical polarization measurement was measured in 1% NaCl solution using a standard three electrodes system. It can be found that plasma-based low-energy ion implantation of titanium alloy provides a potential application in biomedical devices.

### 3:50 PM Break

### 4:05 PM

**Surface Nitriding of Ti-6Al-4V for Bio-Implant Application:** *Jyotsna Dutta Majumdar*<sup>1</sup>; <sup>1</sup>Indian Institute of Technology Kharagpur

Ti-6Al-4V alloy is widely used as an implant material because of its high strength, superior corrosion resistance and bio-compatibility. However, a poor wear resistance causes restriction over prolonged use of the component as bio-implant. In the present study titanium nitride layer has been formed on Ti-6Al-4V substrate by cathodic arc evaporation and laser gas alloying process. The effect of surface nitriding on the characteristics and properties (microhardness, wear, corrosion resistance and bio-compatibility) of the surface has been studied in details. Titanium nitrided layer formed by physical vapor deposition is homogenous and defect-free with an improved hardness to 650 VHN as compared to 260 VHN of as-received Ti-6Al-4V. Wear resistance of the physical vapor deposited surface is also improved significantly. Corrosion resistance against simulated body fluid is marginally improved in titanium nitride coated surface as compared to as-polished Ti-6Al-4V substrate.

### 4:25 PM

**Nanostructured Bio-Scaffold for Bone Implants, Stents: A Biomedical Evolution:** *Shampa Aich*<sup>1</sup>; Chandra Shekhar<sup>1</sup>; Mrinal Mishra<sup>1</sup>; <sup>1</sup>Indian Institute of Technology

Multifunctional nanostructured bio-scaffolds were fabricated on biocompatible titanium and Nitinol surfaces through a simple, inexpensive, easy scale-up, one-step hydrothermal reaction of alkali (NaOH) with the metal and alloy surfaces without using any seeds, templates, TiO<sub>2</sub> powder, or stabilizers. The structure and morphologies of the bio-scaffold were investigated using electron microscopy and glancing angle X-ray diffraction techniques. The nano-scaffold seems to root firmly inside the Ti and NiTi substrates and grow on top to eventually self assemble into macroporous (~ 0.5-1.0 μm in diameter) scaffolds. The effects of alkali concentration, reaction time on the bio-scaffold morphologies were investigated. The maximum bio-scaffold thickness of 987 nm was observed at NaOH conc. 2.85 M for 3 hours treatment time. Thus-formed scaffolds on the metal implant or stent surfaces, mimicking the natural extracellular matrix in structure, can promote good cellular compatibility, mechanical toughness and proliferation and perform controlled on-site drug release and photocatalytic sterilization.

### 4:45 PM

**The Effect of Processing Parameters on Surface Properties of Ti6Al7Nb Alloys:** *Mert Günyüz*<sup>1</sup>; Murat Baydoğan<sup>1</sup>; Huseyin Cimenoglu<sup>1</sup>; Eyup Sabri Kayali<sup>1</sup>; <sup>1</sup>Istanbul Technical University

In this study, the effect of micro arc oxidation process on surface morphology of Ti6Al7Nb alloy was investigated. Micro arc oxidation was performed by using an AC power supply operating in constant voltage mode between 450-600 V using two different electrolytes. Mechanical and physical properties were evaluated on the surface including hardness, contact angle and surface roughness of the oxide film. Rockwell C testing was used to compare the relative adhesion characteristics of the oxide film. The surface oxide layer was examined by an X-ray diffractometer. Mechanical and physical properties of the samples were discussed on the basis of micro arc oxidation parameters such as applied voltage and electrolyte composition.

### 5:05 PM

**Electrodeposition of Hydroxyapatite on Magnesium for Biodegradable Implant Applications:** *Satendra Kumar*<sup>1</sup>; M. Jamsheh<sup>1</sup>; Sankara Narayanan TSN<sup>1</sup>; <sup>1</sup>National Metallurgical Laboratory, Madras Centre

Development of biodegradable Mg based implants and stent materials assumed significance in recent years. Higher corrosion rate, generation of large volume of hydrogen gas and, increase in local pH value of body fluid, are the major limiting factors in using Mg as a biodegradable implant material. The present work aims to engineer the surface of Mg by electrodeposition of hydroxyapatite to control the rate of corrosion and to solve the associated problems. The corrosion behaviour of hydroxyapatite coated Mg in Ringer's solution was evaluated by electrochemical impedance spectroscopy and its

corrosion protective ability was compared with that of the untreated one. The study reveals that deposition of hydroxyapatite coating on Mg decreased the rate of corrosion. Being a bioactive coating, it will also enable bone in-growth. The study concludes that electrodeposition of hydroxyapatite coating is a useful surface engineering approach in the development of biodegradable Mg based biomaterials.

### 5:25 PM

**Fabrication and Characterization of TiO<sub>2</sub> Films on Ti-6Al-4V by Anodic Oxidation:** *Maria Vera*<sup>1</sup>; Alicia Ares<sup>1</sup>; Mario Rosenberger<sup>1</sup>; Diego Lamas<sup>2</sup>; *Carlos Schvezov*<sup>1</sup>; <sup>1</sup>CONICET-UNaM; <sup>2</sup>CONICET-CITEDEF

In contact with air, a protective titanium dioxide (TiO<sub>2</sub>) film normally covers the surface of titanium and its alloys, which is 2 to 7 nm in thick. Artificial TiO<sub>2</sub> films can be produced on Ti-6Al-4V substrates by anodic oxidation. In this study, TiO<sub>2</sub> films were produced on Ti-6Al-4V substrates by anodic oxidation technique, using a H<sub>2</sub>SO<sub>4</sub> solution as electrolyte at different voltages (from 10V to 100V). The morphology, thickness and phase composition of the films were determined by scanning electron microscopy, X-ray reflectometry and X-ray diffraction, respectively. TiO<sub>2</sub> films of different colors were obtained, with thickness ranging from 20 to 200 nm depending on the applied voltage. Relationships among voltage, color and thickness were confirmed. The film roughness is of the order of the substrate roughness. At voltages higher than 70V, two crystalline phases of TiO<sub>2</sub> were obtained, anatase and rutile. For lower voltages the coating is amorphous.

### 5:45 PM

**Effect of Laser Surface Treatment on Tribological Behavior and Bioactivity of ASTM F-75 Cobalt Base Alloy:** *J.L. Davila*<sup>1</sup>; F. Cepeda Rodriguez<sup>2</sup>; M.F. Trejo Aguirre<sup>1</sup>; <sup>1</sup>Corporación Mexicana De Investigación En Materiales

A biomedical ASTM F-75 cobalt base alloy specimen was subjected to laser surface treatment using pulsed Nd-YAG laser equipment. Laser surface treated and untreated discs specimens were tested on Pin-on-disk tribometer to evaluate the wear resistance following the ASTM G99 standard. The laser surface treatment was beneficial, the treated specimen present considerably minor wear than the untreated one, and also increased surface microhardness of 325 to 445 Vickers at remelted zone due to grain refinement and solid solution strengthening. For the Bioactivity evaluation, the laser surface treated and untreated samples were immersed in simulated body fluid (SBF) for 15 days, later the metallic surface were analyzed by Optical Microscopy (OM), Scanning Electron Microscopy (SEM), Energy Dispersive X-Ray analysis (EDX) and Infrared Spectroscopy (IR). The results show presence of P-O stretching band, that indicating formation of apatite.

## Sustainable Materials Processing and Production: Motivating Sustainability I

*Sponsored by:* The Minerals, Metals and Materials Society, TMS Extraction and Processing Division, TMS Light Metals Division, TMS: Recycling and Environmental Technologies Committee, TMS: Education Committee

*Program Organizers:* Christina Meskers, Umicore; Randolph Kirchain, Massachusetts Institute of Technology; Diana A. Lados, Worcester Polytechnic Institute; Markus Reuter, Ausmelt Limited

Monday PM

Room: 2B

February 15, 2010

Location: Washington State Convention Center

*Session Chairs:* Markus Reuter, Ausmelt Ltd.; Iver Anderson, Ames Laboratory

### 2:00 PM Introductory Comments by Iver Anderson

### 2:10 PM Plenary

**A Framework and a New Paradigm for Sustainable Materials Development and Engineering: The Status Quo is not Sustainable!** *Diran Apelian*<sup>1</sup>; <sup>1</sup>Worcester Polytechnic Institute

Though there is much discussion on the subject of sustainable development for the 21st Century, the Materials Science and Engineering (MSE) community has not responded nor provided a roadmap as to how we respond to the global issues regarding material resource scarcities. Inorganic materials are non-renewable; one would expect that appropriate design, life-cycle analysis, judicious material

Mon. PM

# Technical Program

selection as well as recovery and recycling be the keystones of a new paradigm. The status quo is not sustainable. A framework is presented and discussed in an effort to have material development and material engineering be sustainable in the 21st Century.

## 2:35 PM Plenary

**The Sustainable Organization: Fostering the Capacity for Change:** *Leith Sharp*<sup>1</sup>; <sup>1</sup>Harvard University

For the last 18 years Leith Sharp has worked with a wide variety of universities around the world. Most recently Leith founded and directed Harvard's Green Campus Initiative (now the Office for Sustainability) for nine years, successfully placing Harvard at the forefront of the green campus movement. In this presentation Leith will provide a detailed overview of the organizational requirements for achieving deep, lasting and ongoing transformation towards sustainability. Using the Harvard University case study, Leith will provide a variety of insights, strategies and examples touching upon aspects of leadership, finance and accounting, human resources, governance, communication and more. The purpose of the presentation is to assist the audience in leading their own organizations to take the greatest possible strides towards sustainability.

## 3:00 PM Plenary

**Building a Sustainability Strategy into a Consumer Products Business:** *Leon H. Bruner*<sup>1</sup>; *Peter White*<sup>1</sup>; <sup>1</sup>The Procter & Gamble Company

This paper presents a case study describing how a global consumer products company with 138,000 employees that markets over 300 brands in 180 countries is building sustainability into the rhythm of its business. This strategy extends beyond social investment programs by incorporating sustainability into the fabric of product design, manufacturing operations, employee engagement and stakeholder partnerships. During the implementation of this program it has been necessary to be explicit about sustainability and its importance to the business, to broadly define sustainability, to ensure that sustainability is not added work, to eliminate trade-offs between performance, value and sustainability and to implement programs to ensure that sustainability is incorporated into the DNA of the company. Our program continually emphasizes the importance of making no tradeoffs between consumer acceptance of sustainable products and sustainability investments. We also work diligently to overcome the challenges of engaging employees around the world to implement a single coherent sustainability strategy that delivers great results.

## 3:25 PM Plenary

**Practicing Informed Substitution of Restricted Materials in Electronic Products: Knowing Whether Replacements are Better for the Environment and Human Health:** *Helen Holder*<sup>1</sup>; <sup>1</sup>Hewlett-Packard Company

When a substance is targeted for restriction, often all unregulated substances are treated as equally suitable replacements. This practice has several disadvantages, most significantly that alternatives may be equally bad or worse than the substances they replace. A much better approach to material selection is to practice informed substitution when transitioning out of chemicals of concern such that the environmental and human health impacts of alternatives are considered in order to ensure that the new materials represent a move to safer chemicals or nonchemical alternatives. In order to practice informed substitution, a framework for assessing competing options is needed. A promising tool to support informed substitution is a hazard-based assessment method called the Green Screen, which was created by Clean Production Action, an environmental non-profit dedicated to advancing green chemistry, sustainable materials and environmentally preferable products. This talk will discuss the Green Screen as a tool for alternatives assessment as a part of informed substitution, and how this tool is being used to inform material selection decisions for replacing restricted substances in electronic products.

## 3:50 PM Break

## 4:05 PM Plenary

**Sustainability, a Strategic Opportunity for Umicore:** *Mark Caffarey*<sup>1</sup>; <sup>1</sup>Umicore, USA

How does one turn a historically burdened industrial company into a flagship of sustainability? How does one, literally and figuratively, come clean with a less than sustainable past? With a clear vision and keeping its sights on the future, Umicore has cleared the decks of all its past inheritance. New policies have been laid down, based on eco-efficiency and social responsibility. The outcome is a company that is re-energized believing in a future that is just as

sustainable as profitable. Ten years ago, Umicore made fundamental choices by concentrating on two activities, i.e. the development of high quality materials with extensive technology content and the recycling of precious and rare metals, which form the basis of many of these high-tech materials. As the materials provider for rechargeable batteries, catalytic converters, solar cells and other high tech applications and as the recycler of end-of-life materials from these same technologies, Umicore has been able to illustrate and effectively close the material loop. Today, over half of Umicore turnover and profits is derived from this wide range of Clean Technologies. This illustrates the success sustainability as a strategy is having for Umicore.

## 4:30 PM Plenary

**Title Not Available:** *John Allison*<sup>1</sup>; <sup>1</sup>Ford

**Abstract not available.**

## 4:55 PM Plenary

**Energy (to be confirmed)**

**5:20 PM Concluding Comments by Markus Reuter**

## The Vasek Vitek Honorary Symposium on Crystal Defects, Computational Materials Science and Applications: Computational Materials Science II

**Sponsored by:** The Minerals, Metals and Materials Society, TMS Materials Processing and Manufacturing Division, TMS/ASM: Computational Materials Science and Engineering Committee  
**Program Organizers:** Mo Li, Georgia Institute of Tech; David Srolovitz, Institute for High Performance Computing, Agency for Science, Technology and Research, Singapore; Adrian Sutton, Imperial College London; Vaclav Paidar, Institute of Physics AS CR vvi; Jeff De Hosson, Univ of Groningen

Monday PM Room: 603  
February 15, 2010 Location: Washington State Convention Center

**Session Chairs:** David Srolovitz, Institute for High Performance Computing, Agency for Science, Technology and Research, Singapore; David Pettifor, University of Oxford

## 2:00 PM Invited

**Atomic Level Stresses:** *Takeshi Egami*<sup>1</sup>; <sup>1</sup>University of Tennessee

When V. Vitek joined Penn in 1978 I was starting to think that the stress could be defined at the atomic level, and would be quite helpful in characterizing the local structure of metallic glasses. The trouble was I had no idea how to calculate it. But Vasek knew exactly how to do it, and we right away entered one of my most productive and enjoyable collaborations. David Srolovitz and Adrian Sutton just joining Penn as students also helped the development. The origin of the atomic level stresses is geometrical and topological fluctuation in the atomic environment. Since it has the dimension of energy (per volume), it can readily be related to the local energy landscape, and to various local properties. I will discuss how this concept helped advanced the understanding of glass and glass transition, and helped unlock one of the few remaining deep mysteries in solid state theories.

## 2:25 PM Invited

**Molybdenum at High Pressure and Temperature: Melting from Another Solid Phase:** *Shao-Ping Chen*<sup>1</sup>; *Leonid Burakovsky*<sup>1</sup>; *A. B. Belonoshko*<sup>2</sup>; <sup>1</sup>Los Alamos National Laboratory; <sup>2</sup>The Royal Institute of Technology

The Gibbs free energies of bcc and fcc Mo are calculated from first principles in the quasiharmonic approximation in the pressure range from 350 to 850 GPa at room temperatures up to 7500 K. It is found that Mo, stable in the bcc phase at low temperatures, has lower free energy in the fcc structure than in the bcc phase at elevated temperatures. Our density-functional-theory-based molecular dynamics simulations demonstrate that fcc melts at higher than bcc temperatures above 1.5 Mbar. Our calculated melting temperatures and bcc-fcc boundary are consistent with the Mo Hugoniot sound speed measurements. We find that melting occurs at temperatures significantly above the bcc-fcc boundary. This suggests an explanation of the recent diamond anvil cell experiments, which find a phase boundary in the vicinity of our extrapolated bcc-fcc boundary.



Other possible phases will also be discussed. Phys. Rev. Lett., 100, 135701 (2008); 101, 049602 (2008).

### 2:50 PM Invited

**Analytic Bond-Order Potentials Including Magnetism:** *Ralf Drautz*<sup>1</sup>; David Pettifor<sup>2</sup>; <sup>1</sup>Ruhr-Universität Bochum; <sup>2</sup>University of Oxford

Simulations of mechanical properties of materials require interatomic potentials that can predict interatomic interactions in stacking faults or dislocation cores, for example. In iron and ferritic steels the magnetic contribution to the binding energy depends strongly on the local atomic environment. We have developed an analytic interatomic bond-order potential (BOP) for non-magnetic transition metals that depends explicitly on the valence of the transition metal element and describes the structural trend from hcp to bcc to hcp to fcc across the transition metal series. This potential may be extended to include magnetic contributions within the 3d series. We show that the resulting magnetic interatomic potential displays the experimental trend from anti-ferromagnetic to ferromagnetic order across the 3d transition metal series. For iron, the potential correctly predicts a large magnetic energy for the alpha phase whereas the close-packed gamma and epsilon phases exhibit only a small magnetic contribution to the binding energy.

### 3:15 PM Invited

**Irradiating Point Defects in bcc Transition Metals and Alloys: A Multi-Scale Modeling Review:** *Duc Nguyen-Manh*<sup>1</sup>; <sup>1</sup>UKAEA

Body centered cubic (bcc) transition metals, especially tungsten alloys and ferritic-martensitic steels, are the leading candidate materials for fusion-power-plant applications. A quantitative understanding of point defects under neutron irradiations is essential for modeling the micro-structural evolution of these materials. Our recent systematic and multi-scale studies based on density functional theory (DFT) calculations of self-interstitial atom (SIA) defects, spanning the entire group of bcc metals, reveal that the SIAs adopt a linear <111> crowdion configuration in all non-magnetic bcc transition metals whereas in ferromagnetic bcc-Fe the most stable SIA configuration has the <110> orientation. The predicted SIA formation energy in bcc-W has been recently confirmed experimentally. Combining DFT calculations with the analytic expression for the Peierls potentials, a very small migration energy barrier has been obtained for crowdion in agreement with resistivity recovery measurements. The interactions between crowdion with impurities and other defects in bcc alloys are being investigated.

### 3:40 PM Break

### 4:05 PM Invited

**Deformations in Nanosized Metallic Glass Systems:** *Jeff De Hosson*<sup>1</sup>; C. Chen<sup>1</sup>; Y. Pei<sup>1</sup>; Vasek Ocelik<sup>1</sup>; Dave Matthews<sup>1</sup>; <sup>1</sup>University of Groningen

Size effect, or the lack thereof, during deformation of metallic glasses (MGs) has recently drawn great attention. After the computer modeling approach by Vasek Vitek and collaborators significant progress has been made in the understanding of deformation of amorphous metals. An intriguing question is why and how nucleation and propagation of shear bands are affected by the size of the system, and would it be possible to suppress brittleness and enhance ductility by changing the size of the samples? Our quantitative in-situ TEM deformations of metallic glass pillars with diameters ranging from 50 nm to 500 nm reveal that the deformation is controlled by nucleation of shear bands in larger pillars but becomes propagation controlled in smaller pillars. A micromechanical model based on quantitative description of shear banding events explains the size-dependent deformation behavior. Implications of our findings for applications in nanosized systems will be illustrated.

### 4:30 PM Invited

**Recent Advances and Ongoing Challenges in Accelerated Molecular Dynamics Methods:** *Arthur Voter*<sup>1</sup>; <sup>1</sup>Los Alamos National Laboratory

Many important materials processes take place on time scales that vastly exceed the nanoseconds accessible to molecular dynamics simulation. Typically, this long-time dynamical evolution is characterized by a succession of thermally activated infrequent events involving defects in the material. Over the last decade, we have been developing a new class of methods, accelerated molecular dynamics, in which the known characteristics of infrequent-event systems are exploited to make reactive events take place more frequently, in a dynamically correct way. For certain processes, this approach has been remarkably successful, offering a view of complex dynamical evolution on time

scales of microseconds, milliseconds, and sometimes beyond. Examples include metallic surface diffusion and growth, radiation damage annealing in ceramics, and carbon nanotube dynamics. After an introduction to these methods, I will present some recent advances and results, and then describe the major ongoing challenges and our current thinking on how to overcome them.

### 4:55 PM Invited

**Bond-Order Potential for Iron:** *Matous Mrovec*<sup>1</sup>; Duc Nguyen-Manh<sup>2</sup>; Christian Elsaesser<sup>1</sup>; Peter Gumbsch<sup>1</sup>; David Pettifor<sup>3</sup>; <sup>1</sup>Fraunhofer Institute for Mechanics of Materials; <sup>2</sup>EURATOM/UKAEA Fusion Association; <sup>3</sup>Oxford University

Development of reliable interatomic potentials for atomistic simulations of lattice defects in iron and iron-based materials presents a significant challenge. Energetics and structural stability of magnetic materials is strongly influenced by magnetic effects and details of the Fermi surface. These materials therefore cannot be described adequately by common many-body central-force potentials, which are only density dependent. In this work we constructed a bond-order potential (BOP) for iron, which is based on a tight-binding bond representation. This model is not only able to capture the directional character of bonds present in transition metals but includes also a description of magnetic effects within the Stoner model of itinerant magnetism. A high reliability and predictive power of the constructed BOP will be demonstrated in studies of point defects, dislocations, and grain boundaries in iron.

### 5:20 PM

**Core Structure and Kinks of Screw Dislocations in Fe and W from First-Principles:** *Lisa Ventelon*<sup>1</sup>; François Willaime<sup>1</sup>; Emmanuel Clouet<sup>1</sup>; Mihai-Cosmin Marinica<sup>1</sup>; <sup>1</sup>CEA

Dislocation properties in bcc metals are closely related to the dislocation core structure, which itself is quite sensitive to details in the interatomic interactions. We have investigated the properties of [111] screw dislocations in iron and tungsten, using ab initio electronic structure techniques, primarily in the periodic dipole approach. In agreement with previous calculations, we find a compact structure of the core, but we also evidence a significant core dilatation effect, which can be successfully accounted for by an anisotropic elasticity model. The Peierls potential is single humped i.e. there is no metastable configuration at halfway position, at variance with predictions from EAM potentials. The methodology for constructing tri-periodic cells with one kink per dislocation line has been developed. Results obtained with empirical potentials and preliminary DFT calculations are presented for the Peierls stress and kinked dislocations.

### 5:35 PM

**Core Traction Contribution to the Elastic Energy of a Dislocation:** *Emmanuel Clouet*<sup>1</sup>; <sup>1</sup>CEA Saclay

The elastic energy of a straight dislocation can be decomposed into two contributions: one corresponding to an integration along the dislocation cut of the work necessary to create the dislocation; the other arising from the work done by the tractions exerted on the tube which isolates the dislocation core. This last contribution is often forgotten although it is necessary for the elastic energy being a state variable consistent with the work of the Peach–Koehler forces. We derive an expression of this contribution within linear anisotropic elasticity theory [1]. The obtained expression is then used to extract dislocation core energies from atomistic simulations. This is illustrated by calculating core energies of edge dislocation in bcc iron, where we show that dislocations gliding in {110} planes are more stable than those gliding in {112} planes.[1] E. Clouet, Philos. Mag. 89, p. 1565 (2009).

### 5:50 PM

**Ab Initio Study of Extreme Loading Conditions in Transition-Metal Disilicides with the C40 Structure:** *Martin Friak*<sup>1</sup>; Dominik Legut<sup>2</sup>; Mojmir Sob<sup>3</sup>; <sup>1</sup>Max Planck Institute for Iron Research; <sup>2</sup>Institute of Physics of Materials, Academy of Sciences of the Czech Republic; <sup>3</sup>Faculty of Science, Masaryk University

The ideal tensile test in transition metal disilicides NbSi<sub>2</sub>, TaSi<sub>2</sub>, CrSi<sub>2</sub>, and VSi<sub>2</sub> with the hexagonal C40 structure is simulated by ab initio electronic structure calculations. The theoretical tensile strength for the [0001] loading direction is determined and compared with that of (i) MoSi<sub>2</sub> and WSi<sub>2</sub> disilicides crystallizing in the C11b tetragonal structure and (ii) NbSi<sub>2</sub>, TaSi<sub>2</sub>, CrSi<sub>2</sub>, and VSi<sub>2</sub> with C11b structure. A full relaxation of both external and internal structural parameters is performed and their response to the tensile loading is

Mon. PM

# Technical Program

analyzed. The changes in the electronic structure induced by loading conditions far from equilibrium are demonstrated on the comparison of the densities of states in the ground state and at the limit of mechanical stability.

**6:05 PM**

**Modeling the Synergetic Interactions between Creep and the Growth of Thermal Scales:** *David Wilkinson*<sup>1</sup>; Somaradi Khiev<sup>1</sup>; Andi Limarga<sup>2</sup>; <sup>1</sup>McMaster University; <sup>2</sup>Harvard University

The growth rate of oxide and nitride scales can be considerably affected by the application of stress when the underlying substrate creeps. We have developed a model to calculate the residual stress induced in growing scales which demonstrates that the applied stress causes the metallic substrate and overlying scale to creep at different rates leading to the accumulation of a large stress in the thin scale layer. This influences the diffusional flux of anions towards the metal/nitride interface, controlling the scale growth kinetics. The model is applied to the growth of TiN scales on  $\gamma$ -TiAl in a pure N<sub>2</sub> atmosphere as well as to oxidation in an Fe-based intermetallic. The scale growth rate is dependent on the sign and magnitude of the applied stress wherein a tensile stress accelerates the growth process and vice versa. The model predicts experimental results in TiN bars following flexural creep.

---

## Three-Dimensional Materials Science VI: Processing and Analysis of Large 3D Datasets

*Sponsored by:* The Minerals, Metals and Materials Society, ASM International, TMS Structural Materials Division, TMS: Advanced Characterization, Testing, and Simulation Committee, ASM-MSCTS: Texture and Anisotropy Committee, TMS/ASM: Phase Transformations Committee

*Program Organizers:* Alexis Lewis, Naval Research Laboratory; Anthony Rollett, Carnegie Mellon University; David Rowenhorst, Naval Research Lab; Jeff Simmons, AFRL; Stuart Wright, EDAX Inc-TSL

Monday PM                      Room: 401  
February 15, 2010              Location: Washington State Convention Center

*Session Chairs:* Jeff Simmons, U S Air Force Research Laboratory; Marc De Graef, Carnegie Mellon University

---

**2:00 PM Invited**

**Archival Storage of Three-Dimensional Data:** Mike Jackson<sup>1</sup>; Jeff Simmons<sup>2</sup>; *Marc De Graef*<sup>3</sup>; <sup>1</sup>Bluequartz Software; <sup>2</sup>Air Force Research Laboratory; <sup>3</sup>Carnegie Mellon University

The ever-expanding capability of 3-D characterization tools has led to the development of high quality multimodal data sets. The vast majority of these are currently managed in an ad-hoc fashion on individual computers, a practice which runs a significant risk of data loss through random events; long-term storage is hence a non-trivial problem. We have developed a new file format suitable for the archival storage of 3D data. The Multidimensional eXtensible Archive (MXA) format is built on the robust open source Hierarchical Data Format (HDF-5), and provides a means of storing multidimensional data along with meta-data in a single file. The format is flexible and relies on Document Type Definition and eXtensible Markup Language files. A C++ library along with documentation is provided at <http://mxa.web.cmu.edu>. We will illustrate both the file format and its use by means of 3D microstructure examples.

**2:30 PM**

**Data Fusion by Means of Mutual Information and Image Entropy:** *Begum Gulsoy*<sup>1</sup>; Jeff Simmons<sup>2</sup>; Marc De Graef<sup>1</sup>; <sup>1</sup>Carnegie Mellon University; <sup>2</sup>Air Force Research Laboratory

For years, the materials community has been developing experimental techniques that allow for the characterization of different aspects of materials, resulting in multi-modal data sets. When information from different detectors, such as scanning electron microscopy images and orientation imaging maps, needs to be fused together to obtain a more complete microstructural understanding, the data fusion process is not always straightforward. Mutual information, a concept borrowed from the field of information theory, is an entropy-based measure of how similar two pieces of information are. It is an easily implemented approach that can be used for general affine multi-modal image registration problems, and proves to be especially useful for cases where

the traditional cross-correlation approach does not work. We will provide an introduction to this concept and show applications of image registration in nickel-based superalloys as well as two-phase titanium alloys.

**2:50 PM**

**Using Moment Invariants to Assess the Realism of Digitally Constructed Microstructures:** Patrick Callahan<sup>1</sup>; Mike Groeber<sup>2</sup>; *Marc De Graef*<sup>1</sup>; <sup>1</sup>Carnegie Mellon University; <sup>2</sup>AFRL/UTC

Digitally constructed microstructures can be generated from a combination of microstructural descriptors, such as grain size, aspect ratio, and number of neighbors, which are determined from experimental microstructures. Usually, a synthetic microstructure is compared qualitatively to the experimental microstructure. It is important to remove any user bias inherent in qualitative comparisons and obtain objective comparisons by using quantitative descriptors. Synthetic microstructures can be compared quantitatively to experimental microstructures using coordinate independent quantities such as moment invariants. We will define moment invariants and then use them in combination with other shape parameters, such as volume and surface area, to compare quantitatively experimental microstructures with synthetic microstructures. The synthetic reconstructions are generated starting with ellipsoids and superellipsoids as the initial grain shapes. Our work shows that moment invariants provide a tool for assessing the accuracy and realism of digitally constructed microstructures, and can validate or compare reconstructions produced using different models.

**3:10 PM Break**

**3:30 PM Invited**

**Acquisition and Analysis of Gigabyte-Scale Tomographic Spectral Images:** *Paul Kotula*<sup>1</sup>; Lysle Serna<sup>1</sup>; <sup>1</sup>Sandia National Laboratories

Spectral imaging where a complete spectrum is acquired from each of an array of points has been extended to 3D volume analysis via serial sectioning with FIB [1] and metallography. With the advent of automated data acquisition software for FIB in particular, the scale of data sets that can be acquired easily exceeds a gigabyte. This talk will describe both data acquisition strategies and robust multivariate statistical analysis methods of tomographic spectral images. The result is an unbiased and compact representation of the data in terms of correlated elemental contrast. Examples from corrosion, brazing, and thin-film analysis will be presented. [1] P.G. Kotula et al., *Microsc. Microanal.* 12, pp.36-48, 2006. Sandia is a multi-program laboratory operated by Sandia Corporation, a Lockheed Martin Company, for the United States Department of Energy's National Nuclear Security Administration under Contract DE-AC04-94AL85000.

**4:00 PM**

**Application of Novel Techniques to the Three-Dimensional Characterization of Microstructural Features in Alpha+Beta Titanium Alloys:** *John Sosa*<sup>1</sup>; Santhosh Koduri<sup>1</sup>; Vikas Dixit<sup>1</sup>; Peter Collins<sup>1</sup>; Hamish Fraser<sup>1</sup>; <sup>1</sup>The Ohio State University

Advanced three-dimensional data collection techniques such as Robo.Met-3D™ has led to rapid acquisition of robust datasets on optical length scales. Implementation of such datasets may improve the accuracy of neural networks and phase-field models. However, the accurate statistical representation of three-dimensional microstructural features is challenging and thus requires further improvement to analytical methods. This work addresses the serial two-dimensional collection of datasets containing microstructural features such as prior-beta grain size, and equiaxed-alpha particle size/distribution in alpha+beta titanium alloys. Subsequent reconstruction and quantitative analysis has been facilitated by the development of a MATLAB-based toolkit. Furthermore, comparisons have been made between two-dimensional stereological measurements and their three-dimensional extensions. Additionally, crystallographic orientation data has been incorporated into Robo.Met-3D™ datasets via EBSD maps collected at regular intervals.

**4:20 PM**

**Prior Information for Segmentation of Large Serial Section Image Datasets:** *Jeff Simmons*<sup>1</sup>; Mary Comer<sup>2</sup>; Ilya Pollak<sup>2</sup>; Marc De Graef<sup>2</sup>; <sup>1</sup>AFRL; <sup>2</sup>Purdue University; <sup>3</sup>Carnegie Mellon University

Currently, segmented images are used to build inputs for property simulations. With image segmentation, pixels are classified according to two factors: (1) signal strength (the image) and (2) interpretation within a materials context.

Mon. PM



Classical image processing extensively utilizes algorithms that process the observed signal, but are generally blind to knowledge of material behavior. Incorporation of "prior information," i.e. information that is known prior to the microscope observation can further aid in segmentation. While prior information has been used for segmentation in Materials Science [e.g. Krill and Chen, *Acta Mater.* 50, p. 3057, (2002)], the vast majority of segmentation only uses observation information. A wealth of prior information is available in Materials Science, examples being capillarity (boundary smoothing), diffusion (equalizing intensity), and particle size distributions. This presentation gives some examples of the use of prior information for developing segmentation algorithms that promise to reduce the necessary human interaction for this purpose.

4:40 PM

**Characterization of Complex Three-Dimensional Interconnected Microstructures via the Level-Set Method:** *Victor Chan*<sup>1</sup>; Katsuyo Thornton<sup>1</sup>;

<sup>1</sup>University of Michigan, Ann Arbor

While the characterization of microstructures containing particles is mostly straightforward, characterizing complex, interconnected microstructures (those present in fuel cell and battery materials) poses a major challenge. Yet, the optimization of microstructures is an essential task toward improving the performance of these materials. We present a new method for characterizing complex three-dimensional microstructures, which utilizes the level-set method and topological measures such as the genus, the number of independent bodies, and the number of handles. The analysis provides the channel width distribution, similar to the particle size distribution for particulate systems. This type of characterization can lead to understanding of the microstructural effect on bulk transport in composite materials. The utility of the method will be illustrated by its application to complex, interconnected structures that form as a consequence of spinodal decomposition (Cahn-Hilliard dynamics) and interfacial motion by mean curvature (Allen-Cahn dynamics), for which composite transport properties have been determined.

5:00 PM

**Processing of 3D Data Sets from X-Ray Micro-Tomography of Impulse Atomized Powders:** Denise Thornton<sup>1</sup>; Jon Johansson<sup>1</sup>; *Arash Ilbagi*<sup>2</sup>; Hani Henein<sup>1</sup>; <sup>1</sup>University of Alberta

Avizo®, ImageJ and MATLAB® were used to create mask files for large data sets obtained from X-ray microtomography of impulse atomized powders. This is an essential step in analyzing the 3D microstructure of the samples since the mask file enables the user to distinguish between the interior and the exterior of the particles. Creating the mask file using Avizo® software required almost continuous user involvement and was time consuming. However, it was used as benchmark against other approaches. The mask file created using the ImageJ software was found to be less time consuming but did not preserve the outer surface details. It was found that MATLAB was the most efficient way to create the mask files. The feasibility to remove the x-ray artifacts in the large dataset will also be discussed.

### Ultrafine Grained Materials – Sixth International Symposium: Mechanical Response

*Sponsored by:* The Minerals, Metals and Materials Society, TMS Materials Processing and Manufacturing Division, TMS Structural Materials Division, TMS/ASM: Mechanical Behavior of Materials Committee, TMS: Nanomechanical Materials Behavior Committee, TMS: Shaping and Forming Committee

*Program Organizers:* Suveen Mathaudhu, U.S. Army Research Laboratory; Mathias Goeken, University Erlangen–Nürnberg; Terence Langdon, University of Southern California; Terry Lowe, Manhattan Scientifics, Inc.; S. Semiatin, Air Force Research Laboratory; Nobuhiro Tsuji, Kyoto University; Yonghao Zhao, University of California – Davis; Yuntian Zhu, North Carolina State University

Monday PM

Room: 606

February 15, 2010

Location: Washington State Convention Center

*Session Chairs:* Josef Zmík, Comtes FHT Ltd.; Jingtao Wang, Nanjing University of Science and Technology; Buyang Cao, Johns Hopkins University; Y.G. Ko, Yeungnam University

2:00 PM

**Deformation Behavior during Tensile Straining of Nano/Ultrafine-Grained Structures Formed by Reversion in Metastable Austenitic Steels:** Pavan Venkatasurya<sup>1</sup>; Venkata Ramuni<sup>1</sup>; *Sachin Mali*<sup>1</sup>; Jinesh Shah<sup>1</sup>; Sashank Nayak<sup>1</sup>; Devesh Misra<sup>1</sup>; Mahesh Somani<sup>2</sup>; Pentti Karjalainen<sup>2</sup>; <sup>1</sup>University of Louisiana; <sup>2</sup>University of Oulu

The deformation behavior of nano/ultrafine-grained structures during tensile deformation has been examined by transmission electron microscopy in metastable austenitic steels. Special fine-grained structures were obtained by controlled reversion annealing of strain-induced martensite. Proper gradual strain hardening by the formation of ultra-fine martensite results in excellent tensile strength-ductility property combination.

2:15 PM

**Deformation Behavior of Nanocrystalline Pd-10 At.% Au Alloy Investigated in Compression Mode at Different Temperatures:** *Lilia Kurmanaeva*<sup>1</sup>; Yulia Ivanisenko<sup>1</sup>; Elena Tabachnikova<sup>2</sup>; Hans-Jörg Fecht<sup>3</sup>; <sup>1</sup>Institute für Nanotechnologie, Forschungszentrum Karlsruhe; <sup>2</sup>B. Verkin Institute for Low Temperatures Physics and Engineering, National Academy of Science of Ukraine; <sup>3</sup>Institute of Micro and Nanomaterials

Mechanical behaviour (strength, ductility, mechanisms of deformation, strain hardening) of nanomaterials is one of the key topics of modern material science. Here, we present investigation of mechanical properties of nanocrystalline (nc) Pd-10 at.% Au prepared by inert gas condensation. This method allows to produce nc samples having uniform equiaxed microstructure with the mean grain size of 5-10 nm, and of very high purity. The specimens' microstructure was analysed by means of XRD analysis and TEM. Miniature nc samples with a gauge section of 1 mm was tested in compression mode in temperature range between 4.2 and 300 K. Conventional compression tests showed that samples demonstrate high strength (the yield strength was 1.1 and 2.1 GPa at room temperature and 4.2 K, respectively). Strain-rate jump compression tests revealed high strain rate sensitivity. The obtained results of microstructure and mechanical properties are discussed.

2:30 PM Invited

**Fatigue Behavior of Highly Nanotwinned Copper:** Carla Shute<sup>1</sup>; Benjamin Myers<sup>1</sup>; Sujing Xie<sup>1</sup>; Troy Barbee<sup>2</sup>; Andrea Hodge<sup>3</sup>; *Julia Weertman*<sup>1</sup>; <sup>1</sup>Northwestern University; <sup>2</sup>Lawrence Livermore National Laboratory; <sup>3</sup>University of Southern California

Nanotwinned metals combine the high strength of nanocrystalline materials with much improved elongation to fracture and good microstructural stability. While stress-strain curves have been reported little is known of the fatigue properties of such material. Tension-tension fatigue tests have been carried out on high-purity Cu specimens made by magnetron sputtering that are comprised of adjacent aligned nanotwinned columns. The average spacing between twin interfaces is around 35-40 nm but individual values vary over a wide range. Cycling in the LCF range leads to increased regions where de-nanotwinning occurs and some secondary twinning is seen. De-nanotwinned regions close to the surface are associated with extended surface depressions that turn into

# Technical Program

fatigue cracks. Much of this work was performed in the EPIC facility of the NUANCE Center at Northwestern University. It was partially supported by DOE contract DE-AC52-07NA27344 at LLNL.

## 2:50 PM

**Influence of Stacking Fault Energy on Microstructures and Mechanical Properties of fcc Metals by Equal Channel Angular Pressing:** Yue Zhang<sup>1</sup>; *Jing Tao Wang*<sup>1</sup>; Jin Qiang Liu<sup>1</sup>; <sup>1</sup>Nanjing University of Science and Technology

In the present work 99.98% commercial pure copper, 99.6% commercial pure nickel and 99.6% commercial pure aluminum samples were processed to high strain levels of ~24, ~12 and ~44 by equal channel angular pressing (ECAP) via route Bc, respectively. Microstructures and mechanical properties are investigated by TEM observations, tensile tests and microhardness tests. It shows that grain sizes of pure copper, pure nickel and pure aluminum has been severely refined from several tens of microns into several hundreds of nanometers after ECAP processing, however, microstructure of copper are mainly consisted of equiaxed (sub) grains with illegible grains/ subgrains boundaries after a true strain level of ~8 by ECAP; while it is featured as lamellar boundaries in that of pure nickel and as elongated grains in that of pure aluminum after same ECAP processed to 8 passes. Different trends of mechanical properties upto ECAP strain levels is observed for different metals.

## 3:05 PM

**Microstructure and Tensile Properties of Ultrafine Grained, TRIP-Aided Low-Carbon Steel:** *Young Gun Ko*<sup>1</sup>; C.W. Lee<sup>2</sup>; S. Namgung<sup>2</sup>; D.H. Shin<sup>2</sup>; <sup>1</sup>Yeungnam University; <sup>2</sup>Hanyang University

Transformation-induced plasticity (TRIP)-aided carbon steels have been regarded as one of the promising candidates for automotive applications due to its good mechanical properties. Thus, the present study investigates microstructure and mechanical properties of the ultrafine grained, TRIP-aided low-carbon steel subjected to equal channel angular pressing and isothermal heat treatment. In tension tests at room temperature, the ultrafine grained, TRIP-aided steel shows much excellent combination of strength and ductility as compared to the coarse-grained counterpart due to its fine grain size of each constituent phase despite nearly same volume fraction. This result can be explained by concept of enhanced plasticity associated with strain-induced transformation during tension deformation.

## 3:20 PM

**Ultra-High Strength Aluminum Nanocomposites:** *Julie Schoenung*<sup>1</sup>; <sup>1</sup>University of California, Davis

Over the last several years, work has been ongoing to prepare and characterize bulk nanocrystalline metal matrix materials consisting of aluminum and boron carbide. These materials, fabricated by means of cryomilling to produce the nanostructured aluminum matrix and clean metal-ceramic interface, followed by powder metallurgy based consolidation methods (including isostatic pressing, extrusion and forging), have demonstrated compressive strengths of over 1000 MPa, which is extremely high for an aluminum alloy system. Furthermore, these materials exhibit high elastic strain when deformed at high strain rates. The microstructural features observed within these materials, which have been studied in great detail using a wide range of techniques, provide insight into the uniqueness of these materials and the properties they exhibit. Select modeling techniques have also been applied to further explain the observed behavior. This paper will present an overview of these research activities.

## 3:40 PM Break

## 3:55 PM Invited

**Grain Size Effects on Rate Sensitivity of FCC Metals:** *K. Ramesh*<sup>1</sup>; Emily Huskins<sup>1</sup>; Buyang Cao<sup>1</sup>; <sup>1</sup>Johns Hopkins University

Processes such as severe plastic deformation, E-beam evaporation, and cryomilling have become increasing popular techniques for producing ultrafine grained (UFG) materials. These materials show a significant increase in strength as compared to their coarse grain counterparts; however, grain size effects extend beyond just strengthening. In UFG materials a new length scale, the grain size, is introduced which limits the available space within grains for dislocation motion. Therefore, both the deformation mechanisms and the strain rate sensitivity of the material experience grain size effects. This talk focuses specifically on UFG FCC metals including high purity aluminum, commercially pure aluminum, and an aluminum alloy. The dynamic response of the UFG

materials is investigated in both compression ( $10^3$  s<sup>-1</sup>) and shear ( $10^5$ - $10^6$  s<sup>-1</sup>) experiments.

## 4:15 PM

**Microstructures and Mechanical Properties of Ultrafine Grained Medium Carbon Steel Processed By HPT at Increased Temperature:** *Jozef Zrnik*<sup>1</sup>; Reinhard Pippan<sup>2</sup>; Stephan Scheriau<sup>2</sup>; Libor Kraus<sup>1</sup>; <sup>1</sup>Comtes FHT Ltd.; <sup>2</sup>Austrian Academy of Sciences

High pressure torsion method at increased temperature of 400°C was applied to refine microstructure in AISI 1045 steel. Deformation behavior of the steel was executed under different shear deformation and constant pressure of 7 GPa. The shear stress evolution and measurement of the torque were recorded. Transmission electron microscopy was used to characterize the microstructure development. Grain refinement was observed after the first turn at disc periphery. In disc centre, the structure had moderately deformed features. The effective strain increase, set an equilibrium between the fragmentation cementite phase and new grains restoration processes, led to saturation of the refinement process. Upon tensile testing, the yield strength and ultimate strength increased with increasing  $\epsilon_{eq}$ . A small decrease in the hardness across the disc was measured after execution of 4 turns, which may be related to formation of fine grain structure in the disc and structure recovery in disc centre.

## 4:30 PM

**Mechanical Evaluation of Heavily Drawn Fe-Ni-Mn Martensitic Steel:** Hadi Ghasemi-Nanasa<sup>1</sup>; *Mahmoud Nili Ahmadabadi*<sup>1</sup>; Hassan Shirazi<sup>1</sup>; <sup>1</sup>University of Tehran

Fe-10wt%Ni-7wt%Mn martensitic steel categorized as a high strength steel which has excellent age hardenability. The steel shows a very good ductility in non-aged martensitic condition which means, it is a suitable material for severe plastic deformation (SPD) at room temperature. To study the effect of SPD on the mechanical properties of steel heavy cold rolling and wire drawing were used. Total strain in this process was about  $\epsilon \sim 7$ . A sample with cross section of 22×8 mm was used which finally deformed to wires with 0.6 and 0.45 mm in diameters. After wire drawing process, x-ray diffraction pattern showed some peaks of austenite in the microstructure while before SPD process, the x-ray shows austenite free specimen. Microhardness results showed the hardness of thinner wire is lower than thicker one and formation of austenite after SPD was studied and mechanical properties of different wire were also measured.

## 4:45 PM Invited

**Mechanical Properties of Nanocrystalline Tantalum within a Wide Range of Strain Rates:** Zhiliang Pan<sup>1</sup>; Weihua Yin<sup>1</sup>; Xiaolei Wu<sup>2</sup>; Brian Schuster<sup>3</sup>; Laszlo Kecskes<sup>3</sup>; *Qiuming Wei*<sup>1</sup>; <sup>1</sup>University of North Carolina at Charlotte; <sup>2</sup>Institute of Mechanics, CAS; <sup>3</sup>US Army Research Lab

We have investigated the mechanical properties of nanocrystalline tantalum within a wide range of strain rates: from quasi-static rate ( $\sim 10^{-3}$  s<sup>-1</sup>) to dynamic rate ( $\sim 10^3$  s<sup>-1</sup>). Grain size below 40 nm has been achieved through high-pressure torsion, and is thus free of artifacts associated with bottom-up processing routes. The microstructure of the NC tantalum is characterized by equi-axed grains of high angle grain boundaries. Grain interiors are decorated with high density dislocations revealed by HRTEM. Quasi-static mechanical behaviors have been evaluated by means of nanoindentation at different loading rates, and by microcompression of pillars fabricated by focused ion beam technique. Quasi-static stress-strain curves show elastic-nearly perfect plastic behavior. Dynamic uniaxial compression via Kolsky bar technique is used to examine the high rate deformation and failure behavior of the NC tantalum. Experimental results are compared with those of other bcc metals such as W, V and Fe with various microstructures.

## 5:05 PM

**Deformation Twinning in High-Strain-Rate Sheared Nanocrystalline Aluminum:** *Buyang Cao*<sup>1</sup>; Bin Li<sup>1</sup>; Nitin Daphalapurkar<sup>1</sup>; En Ma<sup>1</sup>; K. Ramesh<sup>1</sup>; <sup>1</sup>The Johns Hopkins University

Nanocrystalline aluminum films with grain sizes of 50 nm to 100 nm were made through E-beam evaporation. The films were then subjected to high-rate shearing deformations with strain rates of  $10^5$ - $10^6$  s<sup>-1</sup>. The experimental configuration is a compression-torsion Kolsky bar, where the specimen is a thin film on a silicon wafer ring. Strain rates during the shearing are determined from the measured shear waves in the bars. Deformed regions are observed on the sample surface by SEM. Site-specific TEM samples are prepared using Focused Ion Beam micromachining to investigate the regions of large plastic



deformation. Deformation twins and stacking faults are found to develop under the high-strain-rate shearing. The formation of twinning in pure aluminum with comparatively large grain sizes and the high-strain-rate promotion of twinning are discussed. The interactions of stacking faults/twins were also observed. Based on HREM observation, possible deformation mechanisms are proposed.

### 5:20 PM

**Methods for Improving Ductility in Nanostructured Titanium Prepared via Powder Metallurgical Routes:** *Osman Ertorer<sup>1</sup>; Troy Topping<sup>1</sup>; Ying Li<sup>1</sup>; Yonghao Zhao<sup>1</sup>; Wes Moss<sup>2</sup>; Enrique Lavernia<sup>1</sup>; <sup>1</sup>University of California - Davis; <sup>2</sup>Toyota Racing Development*

Bulk nanostructured metals are very well known for their high strength. Recent studies in the field aim to provide high strength without sacrificing ductility for advanced engineering applications. Current study focuses on the methods for improving ductility of cryomilled titanium. Several strategies presented are based on experimental results using a comparative approach. Accordingly, influence of cryomilling media, consolidation methods, addition of coarse grains and heat treatments were discussed.

### 5:35 PM

**Strain Rate Sensitivity of Ultrafine Grained Boron Carbide Reinforced Aluminum Metal Matrix Composites:** *Rustin Vogt<sup>1</sup>; Zhihui Zhang<sup>1</sup>; Troy Topping<sup>1</sup>; Enrique Lavernia<sup>1</sup>; Julie Schoenung<sup>1</sup>; <sup>1</sup>University of California, Davis*

Boron carbide particulate reinforced cryomilled aluminum alloy composites produced through various consolidation methods exhibit significant differences in microstructural and mechanical performance. The microstructural differences such as grain sizes and their distribution were characterized in detail, and the relationships between grain size and work hardening rate and strain rate sensitivity were studied in the characteristic length scale 150-2000 nm. The role of geometrically necessary dislocations (e.g., due to thermal expansion mismatch strain) on the mechanical behavior was investigated for select microstructures.

## Ultrafine Grained Materials – Sixth International Symposium: Processing Technologies

*Sponsored by:* The Minerals, Metals and Materials Society, TMS Materials Processing and Manufacturing Division, TMS Structural Materials Division, TMS/ASM: Mechanical Behavior of Materials Committee, TMS: Nanomechanical Materials Behavior Committee, TMS: Shaping and Forming Committee

*Program Organizers:* Suveen Mathaudhu, U.S. Army Research Laboratory; Mathias Goeken, University Erlangen-Nürnberg; Terence Langdon, University of Southern California; Terry Lowe, Manhattan Scientifics, Inc.; S. Semiatin, Air Force Research Laboratory; Nobuhiro Tsuji, Kyoto University; Yonghao Zhao, University of California - Davis; Yuntian Zhu, North Carolina State University

Monday PM Room: 607  
February 15, 2010 Location: Washington State Convention Center

*Session Chairs:* M. Ravi Shankar, University of Pittsburgh; Sergey Dobatkin, A.A. Baikov Institute of Metallurgy and Materials Science of RAS; Gencaga Purcek, Karadeniz Technical University; Deliang Zhang, The University of Waikato

### 2:00 PM Invited

**A New Biaxial Extrusion Method to Create Sheets of Ultrafine Grain Size:** *Amit Ghosh<sup>1</sup>; Rick Lee<sup>1</sup>; <sup>1</sup>University of Michigan*

A new method of extruding a billet into sheet containing fine grain size is reported. This method permits extrusion of billet in 360 degree direction rather than extruding one direction at a time as used in some Severe Deformation Processes. This process helps achieve effective grain refinement without requiring a repetitive process. However, the extrusion die has flexibility to introduce multi-step extrusion with biaxial stretching within the same process and helps eliminate multiple steps. Grain sizes of 0.5 micron has been achieved with Ti alloy and Mg alloys. This is work-in-progress, reported under a new US Patent application in 2009, and in the talk we will report process details and mechanical properties. (work supported by Boeing Airplane Co.)

### 2:20 PM

**Ideal Engineering Materials by High Rate Severe Plastic Deformation:** *M. Ravi Shankar<sup>1</sup>; Shashank Shekhar<sup>1</sup>; Jiazhao Cai<sup>1</sup>; <sup>1</sup>University of Pittsburgh*

Traditionally, severe plastic deformation at small strain rates has been used to create nanostructured metals. These nanostructures are strengthened by incoherent high angle grain boundaries that are unfortunately typified by poor ductility and stability. Here, we demonstrate opportunities for engineered interface structures in fine grained metals by High-Rate Severe Plastic Deformation (HRSPD) to achieve a much more optimal balance of strength, ductility and stability. HRSPD under large strain but high strain-rate conditions was explored within the prototypical framework of large strain machining in an array of metal alloys including Cu, 70-30 brass and Inconel 718. These studies illustrate opportunities for creating, in a single deformation pass, fine-grained metals that are either multimodal nanostructure distributions or densely nanotwinned or composed of low-energy, low-mobility dislocation structures, each offering intriguing property combinations. The creation of these nanostructures is traced to the peculiar thermomechanical conditions inherent to HRSPD.

### 2:35 PM

**Mechanical and Dry Sliding Wear Behavior of Ultrafine-Grained AISI1024 Steel Processed Using Multi Axial Forging:** *Aditya Padap<sup>1</sup>; Gajanan Chaudhari<sup>1</sup>; S.K. Nath<sup>1</sup>; <sup>1</sup>IIT Roorkee*

AISI1024 steel was severely deformed by using warm (500°C) multi-axial forging (MAF) technique using up to 9 MAF passes. The initial coarser grains of average 17 μm size subdivided into submicron sized grains. Grain refinement is confirmed using TEM. After warm MAF, the strength related properties improved significantly, although total elongation values decreased with increasing strain steps. In present study, the tribological properties of ultrafine-grained low carbon steel produced by multi-axial forging have been investigated. Dry sliding was carried out against the counter face of a hardened and polished disk made of En-32 steel (HRC 62 to 65 hardness) in ambient environment and at varying load and constant sliding speed. The wear test results showed that the strengthening of AISI1024 steel by MAF processing does not lead to the improvement of wear resistance at least for the load and the sliding speed used in this study.

### 2:50 PM Invited

**Nanostructured Materials by Mechanical Alloying: New Results on Property Enhancement:** *Carl Koch<sup>1</sup>; Ronald Scattergood<sup>1</sup>; Khaled Youssef<sup>1</sup>; Ethan Chan<sup>1</sup>; Yuntian Zhu<sup>1</sup>; <sup>1</sup>North Carolina State University*

Mechanical alloying or milling – the ball milling of powders-is an effective and well studied method for the synthesis of nanostructured materials. Of the severe plastic deformation methods, it is the most consistent in preparing materials with the smallest nanocrystalline grain sizes. This talk will focus on recent results from our laboratory and the literature in the preparation of materials with property enhancement due to their nanocrystalline microstructures. The results of nanocrystalline Mg-based alloys with very high strength will be presented. A ternary nanocrystalline Cu-Al-Zn low stacking fault energy alloy with high strength and good ductility will also be discussed. Finally, attempts to enhance the thermoelectric behavior of p-type (Bi<sub>2</sub>Te<sub>2.7</sub>Se<sub>0.3</sub>) and n-type (Bi<sub>0.4</sub>Sb<sub>1.6</sub>Te<sub>3</sub>) thermoelectric materials will be presented.

### 3:10 PM

**Microstructure and Mechanical Properties of IF-Steel Sheets after Equal-Channel Angular Sheet Extrusion (ECASE) and Subsequent Annealing:** *Gencaga Purcek<sup>1</sup>; Onur Saray<sup>1</sup>; Ibrahim Karaman<sup>2</sup>; <sup>1</sup>Karadeniz Technical University; <sup>2</sup>Texas A&M University*

The conventional ECASE has disadvantages for commercial applications, such as limited scalability and low uniformly deformed material yield. Also, long sheets are not available due to the discontinuity of the extrusion process. Therefore, several attempts have been made to overcome these problems and to transform ECASE into a continuous process. We have recently developed an ECASE tool called “equal-channel angular sheet extrusion (ECASE)” for processing of IF-steel sheets. IF-steel sheets were processed using ECASE system to various passes. After processing, the microstructure and mechanical properties were investigated. Moreover, the deformed sheets were annealed to enhance the formability of IF-steel sheets. Continuous shear deformation of the sheets successfully refined the grain size down to submicron upon multi-pass ECASE. As a result, abnormal improvement in yield strength exceeding 150%

Mon. PM

# Technical Program

was noted with remarkable increase in tensile strength. Annealing of the sheets after multi-pass ECASE led to improvement in formability of them.

## 3:25 PM

**Severe Plastic Deformation of a Pearlitic Steel by Wire Drawing:** *Reiner Kirchheim*<sup>1</sup>; Shoji Goto<sup>1</sup>; Christine Borchers<sup>1</sup>; <sup>1</sup>University of Göttingen

Cold drawing of pearlitic steel wires with total strains of up to 6 leads to a fiber like structure of ferrite and cementite lamella with thicknesses of a few tens of nanometers or a few nm, respectively. Maximum flow stresses of up to 6 GPa are obtained this way. Atom probe analysis reveals that the carbon concentration in cementite is reduced whereas the carbon concentration within the ferrite may reach a few at. %. In addition, the cementite becomes amorphous and, therefore, will contribute remarkably to the strength of the material. Further plastic deformation during ball milling leads to a total dissolution of cementite and yields nanocrystalline Fe-C alloys, where carbon is partitioned between saturated grain boundaries and ferrite grains. The formation of defects (vacancies, dislocations and grain boundaries) during severe plastic deformation and their interaction with carbon atoms is discussed based on the presently available experimental data.

## 3:40 PM Break

## 3:55 PM Invited

**Strength-Ductility Combination of Nanostructured 316L Stainless Steel Processed by Means of Dynamic Plastic Deformation (DPD):** G.Z. Liu<sup>1</sup>; N.R. Tao<sup>1</sup>; K. Lu<sup>1</sup>; <sup>1</sup>SYNL, Institute of Metal Res. CAS

316L stainless steel was processed by means of dynamic plastic deformation (DPD, i.e., plastic deformation at high strain rates). Single-phased (austenite) bulk nanostructured stainless steel specimens were prepared, consisting of nano-sized grains embedded with nano-scale twin bundles. Tensile properties of the as-prepared DPD samples with different amounts of nano-twin bundles and grain sizes have been systematically investigated to reveal the effects of grain size and twin density on strength and ductility. Subsequent thermal annealing results in partial recrystallization of the nanostructured steel, forming a mixture structure of coarse-grains embedded with nano-twin bundles. Strength and ductility of the stainless steels with different structure characteristics are analyzed with emphasis of optimization of the strength-ductility combinations.

## 4:15 PM

**Structure, Texture, and Mechanical Properties of Copper and a Mg-Al-Zn-Mn Alloy after Constrained Groove Pressing:** *Sergey Dobatkin*<sup>1</sup>; Vladimir Serebryany<sup>1</sup>; Jozef Zrník<sup>2</sup>; <sup>1</sup>A.A. Baikov Institute of Metallurgy and Materials Science of RAS; <sup>2</sup>COMTES FHT

The structure, texture, and mechanical properties of copper and a Mg-Al-Zn-Mn alloy after by constrained groove pressing (CGP) at room temperature to a true strain of ~7 (for copper) and at temperatures of 300–400°C to a true strain of ~2.3 (for Mg alloy) have been studied. The CGP of copper leads to the formation of submicrocrystalline structure, increases the strength characteristics (YS up to 350 MPa). The final structure of the Mg-Al-Zn-Mn alloy is determined by the competition of the fragmentation processes and the dynamic processes of recovery and recrystallization. The maximum yield strength (YS = 216 MPa) was obtained after CGP at 350°C. The Hall–Petch relationship in the Armstrong approximation is shown that, as the orientation factor N for the prismatic slip increases, the activity of prismatic slip and the plasticity decrease, and the strength increases. This effect was confirmed experimentally.

## 4:30 PM

**Improvement of Strength and Wear Resistance of Cp-Ti by ECAE and MAO Processes:** *Akgun Alsanar*<sup>1</sup>; Gencaga Purcek<sup>1</sup>; Yenel Vangolu<sup>1</sup>; Onur Saray<sup>1</sup>; <sup>1</sup>Ataturk University

Pure titanium are used in many applications ranging from biomedical to aerospace. However, the low strength and very poor wear resistance of CP-Ti limits its use in biomedical applications. In this study, CP-Ti (grade-2) was processed via multi-pass equal-channel angular extrusion (ECAE) using route-Bc in order to improve its strength and subsequently the processed samples were coated by micro-arc oxidation (MAO) for enhancing their wear resistance. The microstructural evolution, and tensile and wear properties of the processed and coated materials were investigated. It was found that ECAE-processed CP-Ti exhibited a significant increase in strength with a slight decrease in ductility. This process did not lead to any improvement in its wear resistance. However, the MAO process after ECAE resulted in a considerable increase in wear

resistance of CP-Ti without decreasing its bulk strength. Consequently, high strength CP-Ti with improved wear resistance was produced by combining the ECAE and MAO processes.

## 4:45 PM Invited

**Severe Plastic Deformation Processes for Thin Samples:** *Rimma Lapovok*<sup>1</sup>; Arnaud Pougis<sup>2</sup>; Dmitry Orlov<sup>1</sup>; Laszlo Toth<sup>3</sup>; Yuri Estrin<sup>4</sup>; <sup>1</sup>Monash University; <sup>2</sup>CSIRO; <sup>3</sup>Université Paul Verlaine-Metz; <sup>4</sup>Monash University / CSIRO

Among the known severe plastic deformation techniques, one group can be defined as SPD processing of thin samples. Their distinctive feature is that one of the sample dimensions, namely the thickness, is much smaller than the other two dimensions. The well-known process of High Pressure Torsion, as well as the less-known Cone-on-Cone Method and the High Pressure Tube Twisting process are all in this category of SPD techniques. For all of them, a severe shear strain is imposed within the thickness of the sample due to the difference in magnitude of the material flow velocities at two large surfaces, rather than by a change in the velocity direction. The microstructure, texture and mechanical properties of copper samples deformed by all three SPD processes mentioned will be reported and compared with those obtained by equal-channel angular pressing as a reference bulk forming SPD technique.

## 5:05 PM

**Tailoring Materials Properties of Aluminium Alloys by Sandwich-like Structures with Accumulative Roll Bonding:** *Tina Hausöl*<sup>1</sup>; Heinz Werner Höppel<sup>1</sup>; Mathias Göken<sup>1</sup>; <sup>1</sup>Friedrich-Alexander-University Erlangen-Nürnberg

Accumulative roll bonding (ARB) is used to produce ultrafine-grained materials with extraordinary mechanical properties. In this work ARB is used to tailor the material's properties by producing sandwich-like structures. The high strength aluminium alloy AA5754, after 4 ARB cycles (N4), is used as the core material. To achieve high corrosion resistance and good visual properties, it is clad with commercial purity aluminium AA1050 (N4) at room temperature and alternatively with AA6014 (N4) at 230 °C. All materials show an ultrafine-grained microstructure and satisfactory bonding between the layers of the different aluminium alloys. Nanoindentation measurements reveal that there is a sharp transition in hardness at the interface. The yield and tensile strength of the core material are fully retained in the case of the AA6014/AA5754 sandwich material. The strength of the AA1050/AA5754 sandwich material is slightly reduced compared to the core material but still twice as high as the clad material.

## 5:20 PM

**Comparison of the Mechanical Properties for Equally Strained Ultrafine Grained Al 99.5 Produced by Accumulative Roll Bonding and Equal Channel Angular Pressing:** *Andreas Böhrner*<sup>1</sup>; Verena Maier<sup>2</sup>; Heinz Höppel<sup>1</sup>; Mathias Göken<sup>1</sup>; <sup>1</sup>University of Erlangen-Nuernberg; <sup>2</sup>ZMP

Significantly increased strain rate sensitivity (SRS) in ultrafine-grained (UFG) metals it is commonly observed. It is also widely accepted that the enhanced SRS is the key issue for improved ductility of UFG metals. In order to evaluate the influence of the process - equal channel angular pressing (ECAP) or accumulative roll bonding (ARB) - on the mechanical properties, UFG aluminium of technical purity (Al 99.5) was produced using these methods. For this purpose quite similar total deformation strains of eARB=6.4 and eECAP=6.3 were selected. For both conditions the microstructure and the mechanical properties were investigated. For the same testing geometry significant differences in the ductility of the ARB and ECAP material are observed. The results will be discussed in terms of microstructural differences, texture effects and damaging mechanisms.

## 5:35 PM

**Synthesis of Bulk Nanostructured and Ultrafine Structured Metallic Materials by Thermomechanical Consolidation of Nanostructured Powders:** *Deliang Zhang*<sup>1</sup>; Aamir Mukhter<sup>1</sup>; Amro Gazawi<sup>1</sup>; Vijay Nadakuduru<sup>1</sup>; <sup>1</sup>The University of Waikato

Nanostructured metallic powders including nanostructured metal matrix composite powders can be effectively produced by high energy mechanical milling (HEMM). However, consolidation of such powders to produce high quality bulk nanostructured and ultrafine structured metallic materials which are highly desirable for numerous practical applications is high challenging. We take the challenge by utilising thermomechanical powder consolidation techniques such as powder compact forging and powder compact extrusion

which are also combined with rapid powder compact heating. A number of experiments on Cu, Al, and Ti based metallic materials have been done along this line, and some very interesting and informative results have been obtained. Theoretical considerations on the mechanisms and scientific principles underlying the thermomechanical consolidation of nanostructured metallic powders have also been developed to guide the experimental work. This talk is to present and discuss the major findings from the experimental study and theoretical thinking.

**5:50 PM**

**Preliminary Investigation of Novel Micro-Scale Current Activated Tip-Based Sintering ( $\mu$ -CATS):** A. El-Desouky<sup>1</sup>; S. Chang<sup>1</sup>; S. Kassegne<sup>1</sup>; K. Moon<sup>1</sup>; K. Morsi<sup>1</sup>; <sup>1</sup>San Diego State University

Spark Plasma Sintering (SPS) has emerged as a process with unique advantages such as lower sintering temperatures and shorter holding times than conventional sintering, in addition to the production of materials with unique microstructures and properties. However, the process has been largely limited to the production of bulk materials with simple geometries on the macro-scale. In this paper preliminary experimental and modeling results on novel current activated tip-based sintering (CATS) of ultrafine and nano-nickel powder are presented. CATS enables the selective sintering of micro-scale features using a moving or stationary (electrically conductive) tip configuration. A finite element model was also developed to investigate current and temperature distributions under typical CATS conditions.

## 2010 Functional and Structural Nanomaterials: Fabrication, Properties, Applications and Implications: Synthesis of Nanomaterials I

Sponsored by: The Minerals, Metals and Materials Society, TMS Electronic, Magnetic, and Photonic Materials Division, TMS: Nanomaterials Committee

Program Organizers: David Stollberg, Georgia Tech Research Institute; Nitin Chopra, University of Alabama; Jiyoung Kim, University of Texas - Dallas; Seong Jin Koh, University of Texas at Arlington; Navin Manjorran, Siemens Corporation; Ben Poquette, Keystone Materials; Jud Ready, Georgia Tech

Tuesday AM Room: 214  
February 16, 2010 Location: Washington State Convention Center

Session Chair: Navin Manjorran, Siemens AG; Jud Ready, Georgia Tech

### 8:30 AM Introductory Comments

#### 8:35 AM Invited

#### Oxide Nanostructures: Synthesis, Characterization and Properties Evaluation: *Avanish Srivastava*<sup>1</sup>; <sup>1</sup>National Physical Laboratory

Important findings pertaining to ZnO, TiO<sub>2</sub> and WO<sub>3</sub> on novel growth morphologies and related spectroscopic, optical and electrochemical performance are elucidated. Moreover certain fundamental concerns on oxide nanostructures dealing with their preparation and correlating the ensuing microstructure with luminescence and electrochemical activity have been tackled to resolve queries of (i) effect of processing on size and morphologies, (ii) consequences of microstructures on optical performance and (iii) correlation of magnetic resonance and Raman spectroscopic measurements with fine scale microstructures and potential applications. A detailed correlation between nanostructures, their growth parameters, microstructural characterization and their property evaluation will be presented and discussed. References: 1.A.K.Srivastava, K.N.Sood, K.Lal, R.Kishore., Patent Filed Ref. No. 0773DEL2005 Dated 31st March, 2005. 2.A.K.Srivastava, N.Gupta, K.Lal, K.N.Sood, R.Kishore, J Nanosci Nanotech 7,1941 (2007). 3.M.Deepa, A.K.Srivastava, K.N.Sood, S.A.Agnihotry, Nanotechnology 17, 2625 (2006). 4.A.K.Srivastava, M.Deepa, S.Bhandari, H.Fuess, Nanoscale Res.Lett. (2009) in press.

#### 8:55 AM

#### Effect of Processing Parameters on the Physical, Thermal, and Combustion Properties of Plasma-Synthesized Metallic Nanopowders: *Chris Haines*<sup>1</sup>; *Darold Martin*<sup>1</sup>; *Joseph Paras*<sup>1</sup>; *Ryan Carpenter*<sup>1</sup>; *Deepak Kapoor*<sup>1</sup>; <sup>1</sup>US Army ARDEC

US Army ARDEC has employed inductively-coupled inert gas condensation to synthesize a wide range of nanopowders. This paper focuses on metallic systems; specifically the effects of processing parameters on the particle size, thermal characteristics, and combustion behavior of these materials. A design of experiments was conducted which varied the plasma power, feed rate, system pressure, and quench gas conditions while holding all other parameters constant. The powders were characterized by X-ray diffraction, BET, FE-SEM, TGA/DSC, and bomb calorimetry. The role of each processing parameter on the various properties will be discussed and summarized with effects plots. The consistency of these effects across a number of material systems will be shown. Lastly, the concept of *tunability* will be discussed.

#### 9:15 AM

#### Synthesis and Characterization of Single Crystalline Metal Nanowire Rings: *Yongjie Zhan*<sup>1</sup>; *Hao Lu*<sup>1</sup>; *Yang Lu*<sup>1</sup>; *Cheng Peng*<sup>1</sup>; *Jiangnan Zhang*<sup>1</sup>; *Jun Lou*<sup>1</sup>; <sup>1</sup>Rice University

In this paper, we reported a simple and effective solvothermal route to prepare copper and silver nanowire ring structures, demonstrating new possibility through hydrothermal/solvothermal route to prepare novel nanostructures. Single crystalline copper and silver nanowire rings with wire diameters from tens to hundreds of nanometers and ring diameters around 15-40 $\mu$ m were synthesized through solvothermal process, in which cuprous chloride was used as copper resource and polyvinyl alcohol (PVA) used as reducing agent, and N-methyl-2-pyrrolidone (NMP) used to provide a water/NMP mixture reaction system was believed to be the key factor to form the novel closed structure. A

growth-stress induced bending mechanism was suggested to explain the possible formation mechanism. The single crystallinity and perfectly closed structure of copper nanowire rings could potentially be explored for many interesting applications in the fields of nanoelectronics, nanophotonics and nanomechanics. Preliminary results on mechanical, optical and electrical characterizations of such nanostructures were also discussed.

#### 9:35 AM

#### Spontaneous Growth of Novel Hexagonal Mn Nanowhiskers from Hydrogen Activated Laves Phase Alloys: *Erdong Wu*<sup>1</sup>; *Xiumei Guo*<sup>1</sup>; *Wuhui Li*<sup>1</sup>; <sup>1</sup>Institute of Metal Research, Chinese Academy of Science

Spontaneous growth of metal whiskers is a well-established phenomenon. Owing to its significant importance either as a hidden peril for electronic devices or a potential fabrication technique for complex microstructures, the phenomenon has been extensively studied for decades. However, only the whiskers of soft metals with relatively low melting points, such as Sn, Cd and Zn and primarily in a micrometer diameter scale, can spontaneously grow at room temperature. With the aid of activation of repeated hydrogenation/dehydrogenation, the crystalline whiskers of transition metal Mn in the shape of nanorod can segregate and grow spontaneously from the crystals of Zr<sub>1-x</sub>Ti<sub>x</sub>MnCr Laves phase alloys at room temperature. Moreover, the Mn atoms in the nanowhiskers form a novel hexagonal structured allotrope, which is the first non-cubic allotrope found for the Mn element. The morphology and structure of the Mn nanowhiskers are exhibited, and the mechanism and potential applications of the phenomenon are discussed.

#### 9:55 AM

#### Geometry Dependence of the Strain-Driven Self-Rolling of Semiconductor Nanotubes: *Ik Su Chun*<sup>1</sup>; *Huan Li*<sup>1</sup>; *Archana Challa*<sup>1</sup>; *K. Jimmy Hsia*<sup>1</sup>; *Xiuling Li*<sup>1</sup>; <sup>1</sup>University of Illinois at Urbana-Champaign

Semiconductor nanotube is an emerging material system that has caught limited attention, yet possesses the potential to provide a wide range of functionalities (X. Li, J. Phys. D. 41, 193001, 2008). It is formed by a combination of bottom-up and top-down approaches through self-rolling of residually strained thin-films that are epitaxially grown and lithographically defined. This allows feasible large area assembly and integration with existing semiconductor technologies while maintaining control of tube size and heterojunction formation in the tube wall. The tube diameter is determined by the total layer thickness and the mismatch strain in the epitaxial layers. The self-rolling direction is controlled by the anisotropy of the Young's moduli and, for crystallographically equivalent directions, depends on the feature geometry of the thin film. In this presentation, we report on the experimental observations and FEM simulations of the geometry dependence of the self-rolling behavior of In<sub>x</sub>Ga<sub>1-x</sub>As - GaAs semiconductor nanotubes.

#### 10:15 AM Break

#### 10:30 AM

#### Mesoscale Simulations of Self-Assembly of Arbitrarily-Shaped Particles in Bulk and at Fluid-Fluid Interfaces: *Paul Millett*<sup>1</sup>; *Yu Wang*<sup>2</sup>; <sup>1</sup>Idaho National Laboratory; <sup>2</sup>Michigan Tech

Recent advances in the ability to experimentally control the size, shape, and composition of nanoparticles have significantly broadened the possibilities to create novel mesoscale structures as a result of their "bottom-up" assembly. Here, we present a novel mesoscale simulation approach that utilizes diffuse interface fields to capture and investigate the dynamic assembly processes for arbitrarily shaped particles with arbitrary charge density and/or dipole moment. Illustrative results demonstrating the method's ability to predict a wide variety of colloidal crystal structures, with a particular focus on binary lattices consisting of positively- and negatively-charged particles, will be presented. Furthermore, this mesoscale approach has also been extended to include the capillary forces experienced by particles segregated at fluid-fluid interfaces. We will present simulations of the complex evolutions of multi-phase fluid mixtures in which particle absorption to the interfaces significantly alters the dynamics of system.



10:50 AM

**Morphological Evolution and Coarsening Process of a Strained Heteroepitaxial Thin Film during Constant Deposition:** *Solmaz Torabi*<sup>1</sup>; Steve Wise<sup>2</sup>; Peng Zhou<sup>1</sup>; John Lowengrub<sup>1</sup>; <sup>1</sup>University of California Irvine; <sup>2</sup>University of Tennessee, Knoxville

Self-assembly semiconductor nanostructures such as quantum-dots are a promising inexpensive and effective approach to manufacture novel nanoscale electronic devices. Producing such quantum-dot-based devices, however, is still challenging. Consequently, we need to have a fundamental understanding of the self-organization process (nucleation, growth and coarsening) during epitaxial growth. So we study the morphological evolution of a strained heteroepitaxial thin film, during continuous mass deposition, on a substrate. Here, we use our new approach for modeling strongly anisotropic crystal and epitaxial growth using regularized, anisotropic Cahn-Hilliard-type equations. In order to model the misfit strains, we add the elastic energy to our diffuse model. Adding elastic energy modifies the equilibrium shape and in particular affects the shape of the corners. We can predict different Qdot shapes, such as pyramids and domes, based on the strength of the elastic interactions. We present 2D and 3D numerical results using an adaptive, nonlinear multigrid finite-difference method.

11:10 AM

**Development and Characterization of Nanoporous Carbon Coated ZnO Powders Prepared by Pyrolysis of Spray Dried ZnO-PVA Mixtures:** *Burak Özkal*<sup>1</sup>; Seyma Duman<sup>1</sup>; Osamu Yamamoto<sup>2</sup>; <sup>1</sup>ITU; <sup>2</sup>Akita University

It is known that some carbons remain as residue during inert atmosphere pyrolysis of polymers and type and polymerization degree of the polymer are very important parameters leading different final properties. Starting from homogeneous polymer and powder mixtures, it is possible to produce composite powders and structures where the outer phase is amorphous carbon. This coating layer is very attractive especially for nanopowders and nanofibers where encapsulation is necessary. In this study, development and characterization of the nanoporous carbon coated ZnO powders were performed consecutive processes of spray drying and polymer pyrolysis technics. For this purpose spray drying process conditions of ZnO powders having different amounts of PVA were optimized and final products were characterized via advanced powder characterization technics. Spray dried powders were subjected to polymer pyrolysis under protective atmosphere and then integrity of ZnO granules and properties of nanoporous carbon coating were characterized.

11:30 AM

**Low-Temperature Synthesis of NiFe<sub>2</sub>O<sub>4</sub> Spinel Nanopowder via Solid-State Reactions:** *Zhigang Zhang*<sup>1</sup>; Guangchun Yao<sup>1</sup>; Jia Ma<sup>1</sup>; Zhongsheng Hua<sup>1</sup>; Lei Wang<sup>1</sup>; <sup>1</sup>Northeastern University

Nickel ferrite (NiFe<sub>2</sub>O<sub>4</sub>) nanopowder was successfully synthesized via solid-state reactions at low temperature. The precursors prepared by rubbing FeSO<sub>4</sub>·7H<sub>2</sub>O, NiSO<sub>4</sub>·6H<sub>2</sub>O, NaOH and dispersant sufficiently at room temperature were calcined at different temperature for different holding time. Effects of content of dispersant, calcining temperature and holding time on morphology and grain size of nanopowder were researched by orthogonal experiment. Single factor experiment was carried out successively according to range analysis. The phase, surface morphology and grain size were characterized using X-ray diffraction (XRD), scanning electron microscopy (SEM) and laser particle analyzer. The solid-state reaction mechanism was discussed according to the XRD analysis of the precursors. The results indicated the NiFe<sub>2</sub>O<sub>4</sub> spinel nanopowder prepared by adding 20wt% NaCl (dispersant) in the rubbing process and calcining at 800° for 1.5 hour was of pure cubic spinel structure with the grain size about 40-70 nm.

11:50 AM Concluding Comments

### Advances in Composite, Cellular and Natural Materials: Metal Foams

*Sponsored by:* The Minerals, Metals and Materials Society, TMS Structural Materials Division, TMS/ASM: Composite Materials Committee

*Program Organizers:* Yuyuan Zhao, The University of Liverpool; David Dunand, Northwestern University

Tuesday AM

Room: 305

February 16, 2010

Location: Washington State Convention Center

*Session Chairs:* Antonia Antoniou, Georgia Institute of Technology; Ki-Ju Kang, Chonnam National University

8:30 AM

**Fabrication of Ti-6Al-4V Open-Cellular Foams by Additive Manufacturing Using Electron Beam Melting:** *L. Murr*<sup>1</sup>; S. Gaytan<sup>1</sup>; F. Medina<sup>1</sup>; E. Martinez<sup>1</sup>; L. Martinez<sup>1</sup>; R. Wicker<sup>1</sup>; <sup>1</sup>University of Texas at El Paso

Methods to fabricate Ti or Ti-alloy foams suffer from their high melting point issues, extreme chemical affinity with atmospheric gases, and other reactivity issues. In this work, we have utilized computerized tomography (CT) scans of more common aluminum alloy foams to develop build elements in CAD models from which Ti-6Al-4V prototypes have been fabricated by electron beam melting (EBM). This strategy has allowed a wide variation of open-cellular foams of Ti-6Al-4V to be fabricated in density or porosity variations and associated low stiffnesses. Complex, monolithic arrays have been fabricated composed of various density regimes and including solid, fully dense components. These prototypes have been characterized by optical and electron microscopies. Applications in biomaterials implant areas and aeronautics and aerospace will be illustrated. While this program is specific to Ti-6Al-4V as a precursor powder, any metal or alloy prototype may be fabricated.

8:50 AM

**Compression-Compression Fatigue of LENS-Processed Cellular Titanium:** *Nikolas Hrabe*<sup>1</sup>; B. Vamsi Krishna<sup>2</sup>; Amit Bandyopadhyay<sup>2</sup>; Rajendra Bordia<sup>1</sup>; <sup>1</sup>University of Washington; <sup>2</sup>Washington State University

Cellular titanium is a candidate material for a range of biomedical and aerospace applications. It has been fabricated over a range of relative densities (0.53-0.73) using laser-engineered net shaping (LENS) and found to display monotonic mechanical properties suitable for the intended application of load-bearing bone replacement implants. For all relative densities tested, the compression-compression fatigue strength at 1 million cycles was found to be rather high (approximately 150% of the yield strength). This talk will include a correlation of monotonic and fatigue results to the Gibson-Ashby model for cellular solids as well as a discussion on the proposed deformation mechanism based on results from scanning electron and optical microscopy, and micro-computed x-ray tomography.

9:10 AM

**Properties of Energetic Materials Reinforced by Open-Cell Metal Foams:** *Dmitriy Kiselkov*<sup>1</sup>; Ravi Yakushev<sup>1</sup>; <sup>1</sup>Institute of Technical Chemistry

One of the most challenging ways of improving the energetic materials performance is reinforcement of energetic polymer composition by heat conducting elements. Widely used methods of filling the energetic material by different types of metallic components (fibers, wires, meshes, cells, bars etc) have considerable disadvantages including impossibility of uniform distribution of the elements. Thus the idea of using open-cell metal foams as heat conducting elements seems to be very challenging. The aim of this work is to study the influence of characteristics (porosity, cell size) and chemical structure of the open-cell metal foams on energetic and ballistic properties of energetic materials. The results of this study can be used for the development of energetic materials with required characteristics.

9:30 AM

**Microstructural Characterization of PORVAIR Metal Foams:** *S. Raj*<sup>1</sup>; Jacob Kerr<sup>2</sup>; <sup>1</sup>NASA Glenn Research Center; <sup>2</sup>Pennsylvania State University

Metal foams are being studied for use in future aircraft engines to control environmental noise. The development of acoustic and structural models require an understanding of the complex foam microstructures and their role in noise reduction. Details of quantitative microstructural analyses of PORVAIR metal

# Technical Program

foams are reported. The present results revealed that 57% of the cell faces were pentagonal in nature while the quadrilateral and hexagonal faces were 25 and 15%, respectively. These observations reveal that the Kelvin tetrakaidecahedron with six (43%) flat quadrilateral faces and eight (57%) curved hexagonal faces cannot adequately describe the PORVAIR cellular microstructure. Instead, it is suggested that the PORVAIR cells have 11 or 12 faces consisting of 3 quadrilateral, 2 hexagonal and either 6 or 7 pentagonal faces, respectively.

## 9:50 AM

**Formation and Disappearance of Crack-Like Pores for Al Foams Made by PM Route:** *Lei Wang*<sup>1</sup>; Guangchun Yao<sup>1</sup>; Xiaoming Zhang<sup>1</sup>; Yihan Liu<sup>1</sup>; Jia Ma<sup>1</sup>; <sup>1</sup>Northeastern University

Aluminum foams have been fabricated by powder metallurgy technology. The reason for formation of crack-like pores formed during early foaming stage and mechanism of their disappearance are analyzed systematically. The model for disappearance of crack-like pores has been put forward for the first time. Stress generated within compacted precursors is caused by particle interaction in the presence of high compaction pressure and is the main reason of formation of crack-like pores. The results show that pressure difference  $\Delta P$  between initial round pores and crack-like pores is the drive force of disappearance of crack-like pores. The rapid reduction of  $\Delta P$  is attributed to the decomposition characteristic of TiH<sub>2</sub> powder.

## 10:10 AM Break

## 10:30 AM

**Open Celled Bulk Metallic Glass Foam Using Equal Channel Angular Pressing:** *Marie Cox*<sup>1</sup>; David Dunand<sup>1</sup>; Suveen Mathaudhu<sup>2</sup>; <sup>1</sup>Northwestern University; <sup>2</sup>U.S. Army Research Laboratory

Bulk metallic glasses (BMGs) have very high specific strength but lack room-temperature plasticity and fail catastrophically from highly localized shear bands [1]. Shear band arrest can be achieved by pores, leading to improved compressive ductility in porous BMGs [2]. Here, we present BMG foams with a relative densities of 30-55% produced by consolidating a powder mixture of Zr<sub>58.5</sub>Nb<sub>2.8</sub>Cu<sub>15.6</sub>Ni<sub>12.8</sub>Al<sub>10.3</sub> (Vitreloy 106a) and tungsten using different warm equal channel angular extrusion (ECAE) routes (1A, 2A, 2B, 2C) followed by the dissolution of the tungsten fugitive phase. The foam morphology was investigated using a variety of imaging techniques and uniaxial compression testing was performed to determine the effect of porosity and ECAE route on the materials mechanical properties. [1] C.A. Schuh, T.C. Hufnagel, and U. Ramamurty: *Acta Materialia*, 2007, vol. 55, pp. 4067-4109. [2] A.H. Brothers and D.C. Dunand: *Advanced Materials*, 2005, vol. 17, pp. 484-846.

## 10:50 AM

**Mechanical Damping Properties of Al-Si Closed-Cell Aluminum Foam:** *Yong Liang Mu*<sup>1</sup>; Guang Chun Yao<sup>1</sup>; Hong Jie Luo<sup>1</sup>; <sup>1</sup>Northeastern University

The mechanical damping properties of Al-Si closed-cell aluminum foam with various porosities were measured using the cantilevered beam mount based on a modified sample geometry. The measured loss factor shows that Al-Si closed-cell aluminum foam have a damping capacity which is independent of frequency and increases with increasing porosity when the cell size is kept constant. There is a critical strain amplitude  $\epsilon_c$ . When strain amplitude is less than  $\epsilon_c$ , the loss factor does not change with strain amplitude. When strain amplitude exceeds  $\epsilon_c$ , the loss factor increases remarkably with increasing strain amplitude. A Voigt two-parameter model was introduced to explain the damping behavior of Al-Si closed-cell aluminum foam.

## 11:10 AM

**Sound Absorption of Closed-Cell Aluminum Foam Fabricated by Melt Foaming Route:** *Lisi Liang*<sup>1</sup>; Yongliang Mu<sup>1</sup>; Lei Wang<sup>1</sup>; Zhongsheng Hua<sup>1</sup>; Jia Ma<sup>1</sup>; *Guangchun Yao*<sup>1</sup>; <sup>1</sup>Institute of Materials and Metallurgy, Northeastern University

Closed-cell aluminum foam was fabricated by molten body transitional foaming process. The sound absorption coefficient  $\alpha$  was measured by standing-wave method in the frequency range up to 2000Hz. The relationship between  $\alpha$  and pore structure of aluminum foam was studied. The results show that there is an optimal porosity with which aluminum gives the best sound absorption. Moreover, the influence of perforation rate and cavity thickness on  $\alpha$  was investigated. The sound absorption coefficient increases remarkably when the perforation rate reaches 1.5%. However, when the perforation rate exceeds 2.5%  $\alpha$  is lower than that of as received sample. Moreover, the highest sound

absorption coefficient shows the trend of traveling to low-frequency region with increasing the cavity thickness.

## 11:30 AM

**Study on Compressive Properties of Aluminum Foams Reinforced with Short Copper-Coated Carbon Fibers:** *Jinjing Du*<sup>1</sup>; Guangchun Yao<sup>1</sup>; Zhuokun Cao<sup>1</sup>; <sup>1</sup>Northeastern University

The closed-cell aluminum foams reinforced with 1.7 vol.% copper-coated short carbon fibers (Al/Cf) were manufactured by melt foaming method using TiH<sub>2</sub> as blowing agent. The distributions of the short fibers in the composite foams observed by scanning electron microscopy (SEM) and the quasi-static compressive properties of Al/Cf foams have been investigated. The compression test indicated that Al/Cf foams show better compressive properties than pure aluminum foams. The compressive curves of the composite foams exhibit a smooth and no dentate collapse plateau region; the compressive yield stress and energy absorption capacity of the composite foams increase more rapidly than those of pure aluminum foams with increasing density.

## 11:50 AM

**The Influence of Cell Shape Anisotropy on the Compressive Property of Closed-Cell Al-Si Alloy Foam:** *Yong Liang Mu*<sup>1</sup>; Guan Chun Yao<sup>1</sup>; <sup>1</sup>Northeastern University

Closed-cell Al-Si alloy foams have been prepared by melt route. The cell shape anisotropy ratio of Al-Si alloy foams specimens in relative density range of 0.11-0.39 were measured. The quasi-static compressive tests show that Al-Si alloy foams have higher plastic collapse stress in the longitudinal direction than in the transverse direction. The plastic collapse stress ratio increases with cell shape anisotropy ratio, which is basically in agreement with Gibson&Ashby model. Moreover, energy absorption capacity of Al-Si alloy foams was investigated. The results show that the energy absorption capacity in the longitudinal direction is higher than that in the transverse direction.

## Alumina and Bauxite: Bayer Process Chemistry and Alumina Quality II

*Sponsored by:* The Minerals, Metals and Materials Society, TMS Light Metals Division, TMS: Aluminum Committee, TMS: Aluminum Processing Committee

*Program Organizers:* Carlos Suarez, Hatch Associates Inc; Everett Phillips, Nalco Company

Tuesday AM Room: 611  
February 16, 2010 Location: Washington State Convention Center

*Session Chair:* Pat Clement, Alcoa - Point Comfort Operations

## 8:30 AM Introductory Comments

## 8:40 AM

**Segregation of Alumina – The Challenge for the Aluminium Industry:** *Andreas Wolf*<sup>1</sup>; Peter Hilgraf<sup>1</sup>; <sup>1</sup>Claudius Peters Projects GmbH

The possible segregation during filling of alumina into storage silos causes substantial problems in the further aluminium production chain. For example accumulation of finenesses < 45  $\mu\text{m}$  leads to sludge formation inside the electrolysis cells which can result in anode effects. The present paper reports on the performance, functional and operational experiences with the Anti-Segregation Technology (ASS). The primary advantage of the air-locked ASS is feeding the alumina into the silos with an unchanged grain size distribution between inlet and outlet of the silo. This paper describes how to integrate ASS Technology and how to use the optimization potential of this technology in several installations up to 50000 tons storage capacity engineered by Claudius Peters.

## 9:10 AM

**Unique High-Temperature Facility for Studying Organic Reactions in the Bayer Process:** *Allan Costine*<sup>1</sup>; Joanne Loh<sup>1</sup>; Robbie McDonald<sup>1</sup>; Greg Power<sup>1</sup>; <sup>1</sup>CSIRO Minerals

CSIRO's new autoclave facility at Waterford features safe, continuous monitoring of oxygen and hydrogen concentrations in the headspace of a 2 L Parr reactor. The system can be operated up to 280°C and 1125 psi, enabling investigations over the full range of Bayer unit operations. The facility is



particularly suitable for the study of wet oxidation. Results from commissioning tests including detection response times, purge times and limits of detection for the O<sub>2</sub> and H<sub>2</sub> electrochemical sensors are provided. Preliminary results from the treatment of individual organics under Bayer digestion conditions are reported. The system will be used for both fundamental investigations and to solve specific problems for individual industry clients.

### 9:40 AM Break

### 10:00 AM

#### Technology Solutions to Increase Alumina Recovery from Aluminogothitic

**Bauxites:** *Andrey Panov*<sup>1</sup>; *Alexander Suss*<sup>1</sup>; *Alexander Fedyayev*<sup>1</sup>; <sup>1</sup>RUSAL VAMI

High grade lateritic bauxites from tropical regions have iron minerals largely represented by hematite and aluminogothite. The latter can contain upto 33 molar % alumina substituted in the goethite crystalline lattice, resulting 0.5 to 3.5% alumina being predominantly not recoverable even under high temperature digestion conditions. Finding the way of extracting this alumina can substantially enhance economics of alumina refineries, specially processing imported bauxites. The paper describes technological solutions developed in RUSAL VAMI and enhancing extraction of alumina from aluminogothite. Ways of industrial implementation of the technology are discussed.

### 10:30 AM

#### New Polymers for Improved Flocculation of High DSP-Containing

**Muds:** *Matthew Davis*<sup>1</sup>; *Qi Dai*<sup>1</sup>; *H.-L. Tony Chen*<sup>1</sup>; *Matthew Taylor*<sup>1</sup>; <sup>1</sup>Cytec Industries

The production of alumina from bauxite requires effective solid-liquid separation in gravity thickeners to generate liquor containing low amounts of suspended solids. As global resources of high quality bauxite are depleted and efforts are made to exploit lower quality deposits which contain increased levels of reactive silica, this separation becomes more difficult. This is an expected consequence of increased levels of desilication product (DSP) and other silica-derived mineral species in the mud residue which are poorly flocculated by conventional polymeric flocculants. It has been discovered that polymers incorporating silane functionality show improved flocculation of suspended DSP solids when added to the slurry in combination with hydroxamated polyacrylamide (HXPAM). Recent developments will be presented to demonstrate the utility of these new molecules for improved clarification of red mud-containing slurries generated in the Bayer Process.

### 11:00 AM

#### Some Aspects of Tricalcium Aluminate Hexahydrate Formation on the

**Bayer Process:** *Silvia Franca*<sup>1</sup>; *Paulo Braga*<sup>1</sup>; *Jorge Aldi Lima*<sup>2</sup>; *Juarez Moraes*<sup>2</sup>; *Americo Borges*<sup>2</sup>; <sup>1</sup>CETEM; <sup>2</sup>Alunorte

Tricalcium aluminate hexahydrate (TCA) - Ca<sub>3</sub>Al<sub>3</sub>(OH)<sub>12</sub> - is used in the Bayer process as a filter aid during the pregnant liquor polishing. The filtration efficiency depends on some TCA characteristics, such as particle size distribution and morphology and how these particles are formed by physical-chemical reactions that take place during the alumina production. To reach a high performance in the filtration step, it is important to understand the influence of variables like source of calcium - CaO or Ca(OH)<sub>2</sub> - residence time, stirring speed and temperature in the TCA formation. This study is being developed as partnership CETEM/ Alunorte - Alumina do Norte do Brasil S.A., using liquor from the plant streams, to evaluate the efficiency of their process. Preliminary results shown that the formation of TCA particles begins partially, in the first minutes of reaction, and that its morphology and particle size distribution can change, during the experiment, depending on the particle size distribution of lime and impurities, which play an important role in the lime reactivity and in the kinetic of the TCA formation.

### Aluminum Alloys: Fabrication, Characterization and Applications: Processing and Texture

*Sponsored by:* The Minerals, Metals and Materials Society, TMS Light Metals Division, TMS: Aluminum Processing Committee  
*Program Organizers:* Subodh Das, Phinix LLC; Steven Long, Kaiser Aluminum Corporation; Tongguang Zhai, University of Kentucky

Tuesday AM

Room: 615

February 16, 2010

Location: Washington State Convention Center

*Session Chair:* Tongguang Zhai, University of Kentucky

### 8:30 AM

#### Concurrent Precipitation in Continuous Cast AlAlloys: Q. Zeng<sup>1</sup>; Tongguang Zhai<sup>1</sup>; <sup>1</sup>University of Kentucky

Continuous cast AA3004 Al alloy hot band was annealed at 420°C for 4 hours followed by cold rolling of 70% in reduction and full recrystallization at 399°C. The alloy showed a strong P texture. EBSD and TEM were used to study nucleation and growth of the P oriented grains, and dislocation structures in the alloy. It was found that the P oriented grains were preferably nucleated around coarse particles, especially in the regions where plastic strain was over a critical value. P oriented grains grew faster than grains with other orientations. P orientation was likely to be formed by lattice rotation from brass orientation. The transition from brass to P orientations might be caused by sudden release of a large number of dislocations which were pinned by fine precipitates around particles.

### 8:50 AM

#### Characterization of Novel Microstructures in Al-Ag-Cu Ternary Eutectic: Amber Genau<sup>1</sup>; Lorenz Ratke<sup>1</sup>; Markus Köhler<sup>1</sup>; <sup>1</sup>German Aerospace Center

While binary eutectics have been extensively studied and are generally well understood, the dynamics of three phases developing from a liquid make ternary eutectics far more complex. Samples at the ternary eutectic composition in the AlAgCu system were directionally solidified with relatively low growth velocities between 0.2 to 4.0 microns/sec in a thermal gradient of 3 K/mm to insure fully coupled growth. The structures produced in these samples were extensively studied using SEM, EDX and EBSD. Cross sectional and longitudinal images will be used to demonstrate the types of microstructures which form and the varying degrees of organization they exhibit. Several attempts are made to quantify these non-trivial structures, such as the distribution of nearest neighbor phases and the distribution of interphase spacings. We also analyze the effects of solid state diffusion on the volume fraction and composition of the phases, and present information on the crystal orientation relationships.

### 9:10 AM

#### Evaluation of Process Speed Effect in Aluminium Extrusion by Experiment and Simulations: Barbara Reggiani<sup>1</sup>; Lorenzo Donati<sup>1</sup>; Luca Tomesani<sup>1</sup>; <sup>1</sup>University of Bologna

In order to analyse metal forming processes and to avoid expensive trial-and-error experiments, finite element simulations are commonly utilized to investigate the material flow, temperature distribution and many other process-related issues. Nevertheless, the crucial role of experimental tests is still recognized due to difficulties encountered in achieving accuracy in the simulation of complex processes like hot aluminium extrusion. With this aim a periodical meeting between extruders and developers of FE tools was organized and a special benchmark session was set. The extrusion of 4 L-shaped profiles made by AA6082 aluminium alloy were investigated at two ram speed (0.5 and 5 mm/s respectively) through a die designed with different concepts for each extrusion orifices. This work presents the comparison between experimental data recorded during the benchmark trials and two FE codes in terms of maximum process load, final profiles lengths, profile distortions and exit temperatures.

### 9:30 AM

#### Processing of Forgings with Fine Crystalline Structure out of Commercial Aluminum Alloys: Vadim Trifonov<sup>1</sup>; <sup>1</sup>Institute for Metals Superplasticity Problems, Russian Academy of Sciences

Processing of fine crystalline structure in metallic materials provides improved mechanical properties. However, hot die forgings with fine crystalline structures are not used widely. Fine crystalline structure processing of hot deformed

Tue. AM

materials occurring at annealing from static recrystallization is connected with high strains at low temperatures and is very labor intensive. The advisability of fine crystalline structure processing in forgings out of commercial aluminum alloys in terms of labor intense has been analyzed and ways of its reduction are proposed. The paper considers various schemes of fine crystalline structure processing including a combined process of static and dynamic recrystallization, and also gives examples of practical use of hot die fine crystalline forgings for production of specific parts. The paper shows features of fine crystalline structure transformation occurring in forgings depending on temperature-strain rate regimes of their following hot processing.

## 9:50 AM Break

### 10:05 AM

**Growth Morphology of Eutectic under Unidirectional Solidification in Al-13%Si Alloys Containing Strontium and Magnesium:** Hengcheng Liao<sup>1</sup>; Wanru Huang<sup>1</sup>; Shengqing Wu<sup>1</sup>; Mingdong Cai<sup>2</sup>; Qigui Wang<sup>3</sup>; <sup>1</sup>Southeast University; <sup>2</sup>Exova - Houston Laboratory; <sup>3</sup>Advanced Materials Engineering, GM Powertrain

Effect of addition of Sr and Mg in the alloy, solidification velocity and thermal gradient on growth morphology of eutectic in Al-13%Si alloy under unidirectional solidification was discussed in this paper. It was found that growth morphology of eutectic changed from planar into cellular, cellular/columnar and afterwards equiaxed in nonfacet-facet Al-Si system with increase in addition of Sr and Mg in the alloy. Solidification velocity and thermal gradient have an important influence on evolution of eutectic growth morphology in Al-Si system. Under unidirectional solidification, different morphologies of eutectic growth, such as planar interface, cellular, cellular/columnar and equiaxed eutectic, could be obtained by tailoring Sr and Mg contents in the alloy, solidification velocity and thermal gradient. The third solute content (Sr and Mg), solidification velocity and thermal gradient together determine the stability of eutectic growth interface, consistent with the classical constitutional supercooling theory on planar interface stability of eutectic growth.

### 10:25 AM

**Influence of Cold Rolling and Equal-Channel Angular Extrusion on the Microstructural and Mechanical Behaviors of Al-40Zn Alloy:** Gencaga Purcek<sup>1</sup>; Onur Saray<sup>1</sup>; Ibrahim Karaman<sup>2</sup>; <sup>1</sup>Karadeniz Technical University; <sup>2</sup>Texas A&M University

Al-40Zn alloy was subjected to cold rolling, and equal-channel angular extrusion (ECAE) up to four passes via route-A at 200°C with and without successive cold-rolling. The microstructural evolution and mechanical properties of the alloy were investigated. Rolling of the as-cast alloy to 50% thickness reduction resulted in a banded microstructure with mainly elongated grains. ECAE processing alone led to the elimination of the as-cast microstructure and formed a structure consists of elongated, ribbon shaped alpha-phase. Additional rolling after ECAE to 75% thickness reduction brought about further reduction in microstructure. Rolling of the as-cast alloy increased the strength in the expense of ductility. ECAE alone decreased the yield strength (from 239MPa to 231MPa after 4A) of the alloy but resulted in an exceptionally high elongation to failure (from 13% to about %34 after 4A). Additional rolling after ECAE increased both strength and ductility of the alloy as compared to identical rolling.

### 10:45 AM

**Experimental Investigations on Influence of Process Parameters on Weld Strength of Friction Stir Welded Aluminium Alloy:** Krishnaiah Arkanti<sup>1</sup>; Syed Yousuf Haq<sup>2</sup>; <sup>1</sup>Osmania University; <sup>2</sup>Steel Authority of India Limited

The effect of the welding speed on the microstructure, mechanical properties of friction stir welded joints has been investigated in the IS 737 aluminium alloy. The functional behavior of weldments is substantially determined by the nature of the weld strength characterized by the tensile strength, metallurgical behaviour, surface roughness, weld hardness and micro hardness. This project attempts to determine and evaluate the influence of the process parameters of FSW on the weldments. The Tensile strength, Vicker hardness and microstructure are considered for investigation by varying tool speed, tool feed and maintaining constant depth of penetration of weld. Experiments were conducted on IS 737 Aluminium alloy in a Vertical axis CNC milling machine by programming for every experiment. Results show strong relation and robust comparison between the weldment strength and process parameters.

### 11:05 AM

**Optimization of Baking Hardening of Al 5052 Sheet by a Response Surface Method:** Atiye Nekahi<sup>1</sup>; Kamran Dehghani<sup>1</sup>; Mohammad Ali Mohammad Mirzaie<sup>2</sup>; Niloofar Kamkar Zahmatkesh<sup>1</sup>; <sup>1</sup>Amirkabir University of Technology; <sup>2</sup>Modares University

In this study, the bake-hardenability of Al5052 was investigated. The specimens were subjected to different baking treatments according to the design experiments of response surface method. A model based on response surface method was designed to predict the optimal combination of baking parameters. Then, the tests were carried out according to the levels predicted by the model. The optimal baking parameters predicted were baking at 285°C for 35 min with 9% pre-strain. maximum bake hardening was 92 MPa which is in close agreement with the predicted results. The counter plots were obtained to study the interaction of process variables. The elliptical counter plots indicate that the variables exhibit strong interaction during the baking of. The multiple correlation coefficient (R<sup>2</sup>) of the regression models was about 0.98. This implies that more than 98% of the variability in the response can be explained by the model confirming the excellent accuracy of the model.

### 11:25 AM

**Orientation Distribution Plots in a Cold-Rolled Heat-Treated Specimen of Aluminum Alloy 6061:** Samuel Adedokun<sup>1</sup>; Victor Ojo<sup>2</sup>; <sup>1</sup>University of Lagos, Akoka-Yaba, Lagos, Nigeria; <sup>2</sup>Ladoke Akintola University of Technology

Aluminum alloy 6061 is used for applications such as structural application. A 10-mm thick sample of aluminum alloy 6061 was given 85% deformation by cold rolling. The rolling was carried out through a multi-step process until the 85% deformation was achieved. Samples from the rolled specimen were cut and heat treated at 200°C, 310°C, 350°C, 400°C, 450°C and 500°C at 10, 30, 60 and 100 minutes for each of the temperatures. Pieces of heat treated samples were cut, cold mounted in epoxy resin and polished to 3micron surface finish. Thereafter, the samples were scanned by a x-ray diffractometer equipped with texture goniometer and texture measurements were carried on the samples. Orientation plots of the samples were generated after analysis of the results. Results indicated that texture variations were according to the changes in temperature and time of the heat treatment.

### 11:45 AM

**Comparison of Textures and Microstructures between AA3XXX Hot Bands from Three Different Casting Processes:** Xiyu Wen<sup>1</sup>; Yansheng Liu<sup>2</sup>; Ningileri Shridas<sup>2</sup>; Tongguang Zhai<sup>1</sup>; Zhong Li<sup>3</sup>; <sup>1</sup>University of Kentucky; <sup>2</sup>Secat, Inc.; <sup>3</sup>Aleris International Inc.

Textures in AA3xxx hotbands made from three different casting routes respectively (twin belt casting (CC), the proprietary pellet cast process (HPC) and direct chill (DC) casting) were measured using XRD and EBSD, separately. The microstructures of these hot bands were also studied using optical and scanning electronic microscopies. It was found that the differences in texture and microstructure. In the CC hot band, there is a typical rolling texture with a well-developed  $\beta$  fiber. From surface to more  $\frac{1}{4}$  depth of HPC hot band, it was found that there is a strong  $\{001\}\langle 110\rangle$  shear texture. In the DC hot band sample, there is a high volume fraction of cube texture component compared to other two processes.



### Aluminum Reduction Technology: Hall-Héroult Cell: Technology

Sponsored by: The Minerals, Metals and Materials Society, TMS Light Metals Division, TMS: Aluminum Committee, TMS: Aluminum Processing Committee

Program Organizers: Charles Mark Read, Bechtel Corporation; Gilles Dufour, Aluminerie de Deschambault

Tuesday AM Room: 608  
February 16, 2010 Location: Washington State Convention Center

Session Chair: Alton Tabereaux, Consultant

### 8:30 AM Introductory Comments

8:35 AM

**Development of the AP39: The New Flagship of AP Technology:** Olivier Martin<sup>1</sup>; Laurent Fiot<sup>1</sup>; David Munoz<sup>1</sup>; Xavier Berne<sup>1</sup>; Claude Ritter<sup>1</sup>; <sup>1</sup>Rio Tinto Alcan

A new milestone has been achieved with AP30 technology. During the summer of 2009, the AP39 cell has been fully demonstrated at Saint-Jean de Maurienne (France). This new cell combines very high productivity (at 385 kA) with a high level of process performance (anode effect frequency, current efficiency and energy consumption) and has the potential to go beyond 400 kA. After the modelling and design phase, three years of testing has enabled the development of a reliable cell with appropriate process control parameters. Several measurement campaigns have confirmed the cell thermal, electrical and MHD equilibrium. However, in order to achieve world class performance, a very efficient process from pre-feasibility study to start-up and operation is also required. Along with the AP39 technology results, this paper describes the overall support provided to smelter projects throughout the world and the latest smelter project performances obtained.

9:00 AM

**DX Pot Technology Powers Green Field Expansion:** Ali Al Zaroumi<sup>1</sup>; Marc Zelicourt<sup>1</sup>; Maryam Al Jallaf<sup>1</sup>; Kamel Alaswad<sup>1</sup>; Arvind Kumar<sup>1</sup>; Abdulla Al Reyami<sup>1</sup>; Vijay Kumar<sup>1</sup>; Dinesh Bakshi<sup>1</sup>; Jose Blasques<sup>1</sup>; Ibrahim Baggash<sup>1</sup>; <sup>1</sup>DUBAL

Dubal's potline 8 was commissioned in the year 2008 with DX pot technology. The present potline amperage is 370 kA, current efficiency has exceeded 95.5% and energy consumption is less than 12.95 kWh/kg of aluminium. Anode effect frequency is well below 0.02. This has been achieved through a balanced electrical, thermal and magneto-hydrodynamic cell design, implementation of optimal controllers and sound operating practices. The design has low investment cost per tonne of aluminium produced, lower instrumentation and automation cost and better fume capture efficiencies. Dubal's in house developed pot controller unit, a web based monitoring system for pots and an ORACLE data base for historical data complement the DX technology. The technology has been at the forefront of the 1.5 million tonne green field smelter coming up in Abu Dhabi (U.A.E). It is expected to be commissioned in December 2009.

9:25 AM

**New Logistic Concepts for 400 and 500 kA Smelters:** Maarten Meijer<sup>1</sup>; <sup>1</sup>Hencon

With today's scenario tools it is possible to de-bottle operational issues and as a benefit lower the cost per ton. In this presentation key stone technology's that influences the success and performance of this new operational approaches are presented. With the introduction of cells that run above 300kA new challenges are introduced in the reduction logistic of modern smelters. So far the amperage increase showed a logical trend of up scaling in auxiliary equipment like transporters and cranes. The latest products used in High Amperage smelters shows the dawn of an area where alternatives come available. The implementation of this new products resulted in the need for better tools in order to predict how this new operation perform. High Amperage operations give room for Smart cost saving production if you re-engineer the production chain. This leads to surprising new and innovative solutions for every day problems.

9:50 AM

**The Pot Technology Development in China:** Zhu Jia ming<sup>1</sup>; Yang Xiaodong<sup>1</sup>; Sun Kangjian<sup>1</sup>; <sup>1</sup>SAMI

Starting from 1996, the Shenyang Aluminium & Magnesium Engineering & Research Institute (SAMI) developed a series of prebaked pot technologies ranging from 160kA, 190/200kA, 230/240kA 280kA, 300kA, 350kA to 400kA pots. All of them have been applied to the industry field, which gives rise to total capacity of 12Mt of aluminium. These pot technologies were developed through effective numerical simulation modelling and by learning the success and failure of the engineering and operation of previous pot technologies. Numerical modelling, pot design, pot measurements and process control will be described in this article. The SY series pot technology has been validated for its technical performance and economy. SAMI is launching a new campaign to reduce more investment and improve pot performance.

10:15 AM Break

10:20 AM

**The Newly Advancement of SY400 Pot:** Sun Kangjian<sup>1</sup>; <sup>1</sup>Shenyang Aluminum and Magnesium Engineering and Research Institute

The newly advancement of SY400 pot Kangjian Sun Hongwu Hu Shenyang Aluminum & Magnesium Engineering & Research Institute Keywords: pot technology, technical improvements, Energy consumption, SY400 pot Abstract: Starting from 2002, the Shenyang Aluminum & Magnesium Engineering & Research Institute (SAMI) developed SY350 pot technologies, after optimize the SY350 pots and increase the current to the 400kA without increase the anode dimension. These pot technologies were developed through effective numerical simulation modeling and by learning the success and failure of the engineering and operation of these pot technologies. SAMI optimize the SY350/400 technology and have been applied to the industry field and there are 17 new 400kA potlines are designed or constructed, 2 potlines in operation. The SY 400 pot technology has been validated for its technical performance and economy and become one of best availability pot technology in the world.

10:45 AM

**Successful Commercial Operation of NEUI400 Potline:** Xiquan Qi<sup>1</sup>; <sup>1</sup>Northeastern University Engineering and Research Institute, Co., Ltd

Development of large aluminum reduction technology is a complex system engineering. While overcoming the core technologies, more attentions shall be paid to structure optimization, environmental protection and energy saving. As a professional engineering and research institute in light metals industry, NEUI has overcome successfully, by carrying out self-developing and joint collaboration, some bottle-neck technologies which affect the development of high amperage reduction cells, such as the simulation of MHD stability, 3-D thermoelectric field, stress and rigidity status both in superstructure and potshell, gas fluid dynamics inside the cell, etc. Simulated and optimized with multi-advanced software, NEUI400 (I) reduction cells have been put into normal operation rapidly after startup, and the technical parameters are close or over the design indices. Thus, all the simulation technologies of NEUI are proved to be mature and reliable. Here, the development process of NEUI400(I) is presented and comparison is done with measurement data.

11:10 AM

**Continues Advancement in Lanzhou Smelter:** Sun Kangjian<sup>1</sup>; Jun Chen<sup>2</sup>; <sup>1</sup>Lanzhou Branch CHALCO; <sup>2</sup>Shenyang Aluminum and Magnesium Engineering and Research Institute

Lanzhou smelter is one of the first primary aluminum producers in china which found in 1958, the development of Lanzhou smelter is the epitome of china alumina primary aluminum industry. Various china typical technologies were in operation last 51 Years. Now only the typical pots technology SY200 and SY350/SY400 pot were operation, this two potline were build in last ten years. Lanzhou has make technical improvements using optimum practice include optimization of operational, optimization of process control system and application of slotted anodes as well as improvement of anode quality.

# Technical Program

11:35 AM

## **Baking Start-up and Operation Practices of 400kA Prebaked Anode Pots:**

*Yungang Ban*<sup>1</sup>; Xiquan Qi<sup>1</sup>; Dingxiong Lv<sup>1</sup>; Jihong Mao<sup>1</sup>; Yu Mao<sup>1</sup>; Zhaowen Wang<sup>1</sup>; Zhongning Shi<sup>1</sup>; Bingliang Gao<sup>1</sup>; Xianwei Hu<sup>1</sup>; <sup>1</sup>Northeastern University Engineering and Research Institute Co. Ltd

This paper introduces the important points concerned with baking start-up and operation management of 400kA pots in China. The smelter was designed by Northeastern University Engineering & Research Institute Co., Ltd (NEUI), and adopted in modernization project of ZhongFu Industry Co. Ltd. The performance of NEUI400 pots have been continuously improved since the start-up in August of 2008. The pots are currently operating at 403kA and have been in operation successfully for more than 10 months. Good performance obtained from the NEUI400 pots with high current efficiency, low energy consumption and low anode effect frequency.

12:00 PM **Concluding Comments**

## **Biological Materials Science: Mechanical Behavior of Biological Materials I: Nature-inspired Materials**

*Sponsored by:* The Minerals, Metals and Materials Society, TMS Structural Materials Division, TMS: Biomaterials Committee, TMS/ASM: Mechanical Behavior of Materials Committee  
*Program Organizers:* John Nychka, University of Alberta; Jamie Kruzic, Oregon State University; Mehmet Sarikaya, University of Washington; Amit Bandyopadhyay, Washington State University

Tuesday AM Room: 205  
February 16, 2010 Location: Washington State Convention Center

*Session Chairs:* John Nychka, University of Alberta; Jamie Kruzic, Oregon State University

8:30 AM **IOM Mehl Award Winner Announcement for Rob Ritchie**

8:35 AM **Keynote**

*Institute of Metals/Robert Franklin Mehl Award Winner: Nature-Inspired Structural Materials:* Robert Ritchie<sup>1</sup>; <sup>1</sup>University of California Berkeley

The structure of materials invariably defines their mechanical behavior. However, in most materials, specific mechanical properties are controlled by structure at widely differing length scales. Nowhere is this more apparent than with natural materials. Bone and nacre, for example, are sophisticated composites whose unique combination of mechanical properties derives from an architectural design that spans nanoscale to near-macroscopic dimensions; few engineering materials have such hierarchy of structure and properties. Unlike engineering composites where properties are invariably governed by the "rule of mixtures", the mechanical properties of many natural composite materials are generally far greater than their constituent phases. However, actually making such materials synthetically has proved to be extremely difficult, particularly in bulk form. Here we describe an approach, involving processing by ice-templating, to developing bulk ceramic-polymer nacre/bone-like structural materials with unprecedented strength/toughness properties. Indeed, we believe that these materials represent the highest toughness ceramics reported to date.

9:15 AM

**Mechanical Properties of Saxidomus Purpuratus Shells:** Yang Wen<sup>1</sup>; Zhang Guangping<sup>2</sup>; Li Xiaowu<sup>1</sup>; Marc Andre Meyers<sup>3</sup>; <sup>1</sup>Northeastern University; <sup>2</sup>Institute of Metal Research Chinese Academy of Science; <sup>3</sup>University of California, San Diego

The strength and fracture behavior of Saxidomus purpuratus biological shells were investigated by means of three-point bending and compression tests. It was found that the bending strength and fracture mode are a function of lamella thickness and angles between lamellae. The flexure strength of the shell ranges from 51 to 128 MPa, whereas the compressive strength ranges from 42 to 151 MPa. Weibull statistical analysis yielded mean yielding moduli of 5.45 and 3.97, and the mean characteristic stresses of ~101 MPa and ~72.76 MPa for bending and compression, respectively. The lamellar configurations are correlated with the strength to understand the orientational and positional effects on the mechanical properties of the shell. The distribution of bending strengths and fracture modes as a function of the position of the specimens taken from the

whole shell was also examined. The relation between mechanical properties and microstructures of the shell was elucidated.

9:35 AM

**Structure and Mechanical Properties of Armadillo Armor:** Irene Chen<sup>1</sup>; Y. S. Lin<sup>1</sup>; P.-Y. Chen<sup>1</sup>; Marc Meyers<sup>1</sup>; J. McKittrick<sup>1</sup>; <sup>1</sup>University of California, San Diego

The armadillo has a unique protective shell-like armor, called the osteoderm. It has a bony components to result in distinctive mechanical properties. The pectoral and pelvic shields of the osteoderm have polygonal (hexagonal) tiles with diameters of 5 mm; the banded and tail shields have rectangular shapes. Optical microscopy reveals that laterally oriented osteons are found in the papillary region within the skin layer of 2 mm in depth and are mainly collagen fibers. The surface layer of the epidermis is approximately 200 μm and is composed of keratin. The collagen network within the layer provides mechanical toughness to the entire structure. The tough and highly mineralized polygonal tiles are bridged with a network of collagen fibers which give resilience to the whole structure. The mechanical properties (tensile, flexure, impact) will be discussed of the different shell components. Research support: NSF Biomaterials Program (Grant DMR0510138).

9:55 AM

**Battle in the Amazon: Araipamas (Pirarucu) vs. Serrasalmus (Piranha):** Marc Meyers<sup>1</sup>; Y. S. Lin<sup>1</sup>; P.-Y. Chen<sup>1</sup>; E. A. Olevsky<sup>2</sup>; J. McKittrick<sup>1</sup>; <sup>1</sup>University of California, San Diego; <sup>2</sup>San Diego State University

The Araipamas is a large fish (up to 200 kg) living primarily in Amazon basin lakes. It is covered with scales having up to 10 cm length that provide protection against the piranha, the principal predator. The scales are highly mineralized and are a laminate composite that can undergo significant non-elastic deformation prior to failure, providing significant toughness. We performed mechanical tests on the scales and teeth and characterized both. The piranha teeth form triangular arrays creating a guillotine action that is highly effective in slicing through muscle. The cutting and puncturing ability of the piranha teeth are evaluated and it is demonstrated that they cannot penetrate the Araipamas scales. Research funded by NSF DMR Biomaterials program (Grant DMR 0510138).

10:15 AM **Break**

10:25 AM **Invited**

**Biological Materials, Biomaterials and Biomimetics:** Ulrike Wegst<sup>1</sup>; <sup>1</sup>Drexel University

Biological materials have exceptional mechanical properties which still cannot easily be emulated by man-made materials. With an informed evaluation of their hierarchical structure, properties and function we wish to identify their principles of optimisation and to apply these in the development of novel and improved man-made materials. Illustrated will be how the mechanical efficiency of biological materials can be evaluated and compared with engineering materials. A variety of methods for the structural and mechanical characterisation of biological materials, ranging from synchrotron-based X-ray microtomography with phase-contrast to methods for in situ mechanical testing in SEM or FIB, will be presented. It will further be shown how, by collating principles of optimisation and function, a software-based design tool, the Biomimetic Design Guide, can be created to aid bio-inspired engineering and a systematic knowledge transfer from nature to technology. Finally, an example for biomimetic material design will be shown to illustrate this approach.

10:55 AM

**What it Takes to be Light as a Feather:** Sara Bodde<sup>1</sup>; Joanna McKittrick<sup>1</sup>; Marc Meyers<sup>1</sup>; <sup>1</sup>University of California, San Diego

Feathers are the most distinguishable feature of all modern Aves, and they are considered to be the most complex of integumentary appendages of all vertebrata. We have observed structural hierarchy from mesoscale to nanoscale. The primary shaft, or rachis, and secondary structures, barbs, are foam-filled having cellular solid cores. Because flight feathers play a role in the generation of thrust and lift forces, we have focused on fitness of remiges, wing feathers, and retrices, tail feathers. We have conducted tensile tests of the rachis cortex, flexure tests of intact rachis sections, and compression tests of foam sections of rachis in order to assess optimization of structural adaptations for feeding ecology of selected species. Research support: N.S.F. Biomaterials Program (Grant DMR 0510138)



11:15 AM

**Microstructural Features that Toughen Horn:** *Katya Novitskaya*<sup>1</sup>; Ana Castro-Ceseña<sup>2</sup>; Luca Tombolato<sup>1</sup>; Po-Yu Chen<sup>1</sup>; Steven Lee<sup>1</sup>; Gustavo Hirata<sup>3</sup>; Joanna McKittrick<sup>1</sup>; <sup>1</sup>University of California, San Diego; <sup>2</sup>Centro de Investigación Científica y de Educación Superior de Ensenada; <sup>3</sup>Center for Nanoscience and Nanotechnology

Horns from the family bovidae are tough biological materials containing crystalline  $\alpha$ -keratin nanofibers embedded in an amorphous keratin matrix. The horn structure is a laminated structure, with the laminates stacked from the dorsal to the ventral side of the horn. Optical microscopy images showed that the horn structure is composed of aligned empty tubules with diameter of 12-14  $\mu\text{m}$  and 100-125  $\mu\text{m}$  length. TEM analysis revealed the existence of  $\alpha$ -keratin intermediate filaments, 12 nm in diameter, that bridge the laminates, which aids in resisting delamination. Deformation mechanisms such as microbuckling of the laminates, tubule closure, crack deflection and nanoscale filament bridging, provides the horn with its extraordinary toughness. Quasi-static and dynamic property behavior will be discussed. This research is supported by ARO Grant W911F-08-1-0461 and NSF Grant DMR 0510138.

11:35 AM

**Structural Investigations on Demineralized and Deproteinized Bone:** *Ana Castro-Ceseña*<sup>1</sup>; Po-Yu Chen<sup>2</sup>; Gustavo Hirata<sup>3</sup>; Damon Toroian<sup>2</sup>; Paul Price<sup>2</sup>; Joanna McKittrick<sup>2</sup>; <sup>1</sup>Centro de Investigación Científica y de Educación Superior de Ensenada; <sup>2</sup>University of California, San Diego; <sup>3</sup>Center for Nanoscience and Nanotechnology

Investigations of the microstructural and mechanical properties of elk antler and bovine femur bone were carried out on demineralized and deproteinized samples. Small pieces of compact and cancellous bone were demineralized or deproteinized at different degrees by aging in various solvents. Structural, chemical, and mechanical properties of demineralized and deproteinized antler and bone were studied by micro-CT, SEM, HR-TEM, IR, Raman spectroscopy and AFM. Both the demineralized and deproteinized bones appeared identical at the macro-scale. At the micro-scale, SEM images showed that the minerals are aligned in a coherent manner, forming a continuous network. The chemical composition change at different degrees of demineralization and deproteinization and their relation to mechanical properties were also examined. This research is supported by the National Science Foundation grant DMR 0510138.

11:55 AM

**Arthropod Cuticle: A Biological Multifunctional Composite Used As Template for Multidisciplinary Nano-To-Macro-Scale Hierarchical Modeling:** *Martin Friak*<sup>1</sup>; Michal Petrov<sup>1</sup>; Svetoslav Nikolov<sup>1</sup>; Christoph Sachs<sup>1</sup>; Helge Fabritius<sup>1</sup>; Pavlina Elstnerova<sup>1</sup>; Duancheng Ma<sup>1</sup>; Liverios Lymparakis<sup>1</sup>; Dierk Raabe<sup>1</sup>; Sabine Hild<sup>2</sup>; Andreas Ziegler<sup>3</sup>; Joerg Neugebauer<sup>1</sup>; <sup>1</sup>Max Planck Institute for Iron Research; <sup>2</sup>Johannes Kepler University Linz; <sup>3</sup>University of Ulm

Biological structural materials receive increasing attention by material science because they have been optimized during evolution and they are therefore ideally suited to study the efficiency of nature's design principles. These materials differ fundamentally from most man-made structural materials in being structurally heterogeneous by combining different in/organic constituents into composites with hierarchical organization. We propose a hierarchical model for the prediction of the elastic properties of a mineralized arthropod cuticle using ab initio calculations to find the elastic properties at the nanoscale and hierarchical homogenization performed in a bottom-up order to find the cuticle properties at all hierarchy levels. Our results suggest that the mineral-protein matrix possesses a microstructure (so-called symmetric cell material) which exhibits extremal properties in terms of stiffness. We also discuss the role of chitin and the multifunctional optimization of the cuticle in terms of trade off between stiffness and transport capacity of the pore canal system.

### Bulk Metallic Glasses VII: Alloy Development and Application I

*Sponsored by:* The Minerals, Metals and Materials Society, TMS Structural Materials Division, TMS/ASM: Mechanical Behavior of Materials Committee

*Program Organizers:* Peter Liaw, The University of Tennessee; Hahn Choo, The University of Tennessee; Yanfei Gao, The University of Tennessee; Gongyao Wang, University of Tennessee

Tuesday AM Room: 213  
February 16, 2010 Location: Washington State Convention Center

*Session Chairs:* J. Eckert, IFW Dresden; Marios Demetriou, California Institute of Technology

8:30 AM Invited

**Strengthening of Ti-Base Glass-Forming Alloys by Microstructure Design:** *J. Eckert*<sup>1</sup>; <sup>1</sup>IFW Dresden

Ti-alloys have potential use for automotive, aerospace, and biomedical applications due to the low density of the Ti and high corrosion resistance but their strength only slightly exceeds 1000 MPa with plastic strain to failure of 10-15%. The strength of these conventional alloys is quite low compared to the strength (~2000MPa) of Ti-bulk glassy/nanostructured alloys. The amorphous/nanostructured alloys usually lack ductility, and an additional toughening phase is needed in the microstructure to improve plasticity. Therefore, it is of strong interest to develop composite microstructures. Using different Ti-base alloy systems as examples, we demonstrate the beneficial effect of composite microstructures on the mechanical performance of the alloys. We emphasize the possibilities to tailor different types of composite microstructures in favor of either strength or ductility, or a combination of both, and also discuss the ability to synthesize in situ composite microstructures in bulk form through inexpensive processing routes.

8:50 AM

**Novel Semi-Solid Processing Techniques for Metallic Glass Matrix Composites:** *Douglas Hofmann*<sup>1</sup>; Henry Kozachakov<sup>2</sup>; Hesham Khalifa<sup>3</sup>; Joseph Schramm<sup>2</sup>; Marios Demetriou<sup>2</sup>; Kenneth Vecchio<sup>2</sup>; William Johnson<sup>2</sup>; <sup>1</sup>Liquidmetal Technologies; <sup>2</sup>California Institute of Technology; <sup>3</sup>University of California, San Diego

Bulk metallic glasses (BMGs) are a unique class of materials known for their high strengths, large elastic limits and amorphous microstructure. As structural materials however, BMGs lack tensile ductility, exhibit low fracture toughness and have poor fatigue life, limiting their potential uses. Recently, it has been shown that semi-solidly processed BMG matrix composites can have mechanical properties equaling or surpassing the best crystalline materials. Unfortunately, due to the higher viscosity of semi-solid liquids, these alloys are difficult to die cast. In this work, we develop new processing techniques which allow us to create complex net-shapes from highly-toughened BMG matrix composites. We expect that this work will provide a foundation for future commercialization of structural BMG components.

9:00 AM Invited

**High Performance Structures Made of Ductile-Phase Reinforced Metallic Glass:** *Marios Demetriou*<sup>1</sup>; Joseph Schramm<sup>1</sup>; Douglas Hofmann<sup>1</sup>; William Johnson<sup>1</sup>; <sup>1</sup>California Institute of Technology

Ductile-phase reinforced metallic glasses with optimized microstructures are found to exhibit mechanical properties such as strength, ductility, and toughness on par with the highest-performance engineering materials like ferrous metals and titanium alloys. Unlike traditional engineering metals however, ductile-phase reinforced metallic glasses have a relatively low melting point which enables fabrication of high precision parts directly from the melt. In this presentation, periodic cellular (honeycomb) structures made of ductile-phase reinforced metallic glass will be introduced. Structures of different architectures and various relative densities will be presented, and structure-property relations will be discussed and compared to conventional steel honeycombs. For a given relative density and structure design, the present cellular structures outperform steel honeycombs in terms of strength and energy absorption by a factor of about 4, a consequence of the high yield strength and large process-zone size of

Tue. AM

# Technical Program

the ductile-phase reinforced metallic glass enabling large plastic deformability at high plateau stresses.

## 9:20 AM

**Applications for Amorphous Metals in Reactive Materials:** *Alan Brothers*<sup>1</sup>; <sup>1</sup>Mainstream Engineering

Amorphous metals have been considered for a wide variety of applications, ranging from solar wind catchers to cellular phone housings. This presentation will evaluate amorphous metals for a new application – reactive materials. Their effects on the key characteristics of reactive materials, such as energy density, energy release rate, processing and handling safety, and mechanical properties, will be discussed. The effects will then be illustrated using experimental data from a reactive Al-based amorphous metal matrix composite material, including calorimetric heats of reaction, flame speeds, sensitivity to electrostatic discharge and impact, and microhardness.

## 9:30 AM Invited

**Thermodynamics and Stability of Nanoglasses with Tunable Atomic Structure: Basic Ideas and First Results:** *Hans Fecht*<sup>1</sup>; <sup>1</sup>Ulm University

Nanoglasses can be considered as highly disordered non-crystalline materials with a tuneable atomic structure. They can be generated by introducing interfaces into metallic glasses on a nanometer scale. Interfaces in metallic glasses delocalize upon annealing close to  $T_g$  so that the free volume associated with these interfaces spreads throughout the entire volume of the glass. In fact, by controlling the spacing between the interfaces introduced as well as the degree of their delocalization the atomic structures and density (and hence all structure/density dependent properties) of nanoglasses may be controlled. First results using BMG type materials will be presented. The material here is produced either by (i) inert gas condensation and full compaction of non-crystalline clusters and (ii) by production of primary and secondary shear bands using extreme plastic deformation methods such as high pressure torsion.

## 9:50 AM

**Nanofabrication with Metallic Glasses:** *Golden Kumar*<sup>1</sup>; *Shiyang Ding*<sup>1</sup>; *Jan Schroers*<sup>1</sup>; <sup>1</sup>Yale University

Homogeneous and isotropic nature of metallic glasses makes them ideal candidates for nano-scale applications. The ability to form metallic glasses on the nanoscale (<100 nm) has been limited. This is because of enormous repulsive capillary forces which need to be overcome. We have recently shown that manipulation of metallic glasses on nanometer scale is controlled by the wetting of the metallic glass on the mold. Wetting can be controlled by the mold-metallic glass combination. In this study we evaluated the wetting behavior and capillary forces between different metallic glasses and mold materials. For some metallic glass mold combinations features as small as 13 nm with an aspect ratio exceeding 20 can be imprinted on the metallic glass. The unusual softening behavior of metallic glasses can be utilized for a versatile toolbox for nanofabrication. Applications of nanofabrication with metallic glasses are discussed and examples given.

## 10:00 AM Break

## 10:10 AM Invited

**Development of Bulk Metallic Glasses with High Plasticity Using the Surface Nano-Crystallization:** *Jian Lu*<sup>1</sup>; *Ji Tang Fan*<sup>1</sup>; *Qing Wang*<sup>1</sup>; *Yuan Hao Huang*<sup>1</sup>; *Hao Jiang*<sup>1</sup>; <sup>1</sup>The Hong Kong Polytech University

The enhancement of the plastic deformation capacity is a critical issue for the development of the bulk metallic glasses (BMG). This presentation summarizes the recent research works carried out in the field of high plasticity BMG using the surface nano-crystallization. A novel route to form the BMG with high plasticity property by subjecting the metallic glass to the surface mechanical attrition treatment (SMAT) will be presented. A structural gradient consisting of submicron-scale crystallization on the top surface to inside fully amorphous metallic glass matrix was obtained. Its compression plasticity was thus greatly improved compared to that of the as-cast metallic glasses. For example, the maximum compression strain of the treated BMG may reach a level of 10% for a Zr-Cu-Al based BMG without major sacrifice of the strength. The effect of the formation of nanograins and the compressive residual stresses on the compression plasticity will be discussed.

## 10:30 AM

**Bulk Metallic Glasses and the Composites Fabricated by Microwave-Induced Heating and Sintering:** *Guoqiang Xie*<sup>1</sup>; *Song Li*<sup>1</sup>; *Dmitri V. Louzguine-Luzgin*<sup>1</sup>; *Motoyasu Sato*<sup>2</sup>; *Akihisa Inoue*<sup>1</sup>; <sup>1</sup>Tohoku University; <sup>2</sup>National Institute for Fusion Science

Microwave (MW)-induced heating and sintering process has attracted increasing attention due to its significant advantages in material processing. MW radiation causes internal heating of the materials, and it is a volumetric heating, so that the lower temperatures and shorter times can be used compared to those applied at conventional heating processes. In this study, we investigated sintering behavior of Cu-, Ni-, and Fe-based glassy alloy powders, as well as their mixed powders blended with crystal or polymer powders, using MW-induced heating and sintering process in a single mode 915 MHz MW applicator in a separated electric (E) field and magnetic (H) field. These powders could be heated well in the H-field, but not heated enough in the E-field. The bulk sintered specimens with retention of a glassy phase were obtained. Addition of Sn particles reduced the sintering temperature, and promoted the densification of the sintered glassy alloy specimens.

## 10:40 AM Invited

**Formation and Properties of New Au-Based Bulk Glassy Alloys with Ultralow Glass Transition Temperature:** *Wei Zhang*<sup>1</sup>; *Hai Guo*<sup>2</sup>; *Mingwei Chen*<sup>3</sup>; *Yasunori Saotome*<sup>1</sup>; *Chunling Qin*<sup>3</sup>; *Akihisa Inoue*<sup>4</sup>; <sup>1</sup>Institute for Materials Research, Tohoku University; <sup>2</sup>Graduate School, Tohoku University; <sup>3</sup>WPI, Advanced Institute for Materials Research, Tohoku University; <sup>4</sup>Tohoku University

It has been reported that Au-based Au-Cu-Si-Ag-Pd bulk glassy alloys (BGAs) exhibited high glass-forming ability (GFA), low glass transition temperature ( $T_g$ ) of about 130°C, large supercooled liquid region ( $\Delta T_x$ ), and good processibility. Recently, we developed new Au-based BGAs with lower Au contents of 35-45 at.%, which had large  $\Delta T_x$ , low  $T_g$ , higher GFA with sample critical diameters (dc) of 2-6 mm, and high fracture strength over 1000 MPa. More recently, we investigated the thermal stability and GFA of the alloys with higher Au contents of 60-75 at.% in quaternary Au-Cu-Si-Ag (Pd) systems. It was found that the glassy alloys show ultralow  $T_g$  of 66-98°C, large  $\Delta T_x$  of 36-55°C, and high GFA with dc of 2-5 mm. The BGAs exhibited good mechanical properties, excellent corrosion resistance in 1N HCl and H<sub>2</sub>SO<sub>4</sub> solutions, high stability at room temperature, strong oxidation resistance, and excellent thermoplastic formability at temperature below 100°C.

## 11:00 AM

**Nanoglass Formation and Properties Studied by Molecular Dynamics Simulations:** *Daniel Soppa*<sup>1</sup>; *Karsten Albe*<sup>1</sup>; *Herbert Gleiter*<sup>2</sup>; <sup>1</sup>TU-Darmstadt; <sup>2</sup>Research Center Karlsruhe

Nanoglasses are a new class of material which can be synthesized by consolidating glassy nanoparticles. Molecular dynamics simulations are presented which provide a detailed picture of nanoglass formation. The results prove the existence of interfaces in the nanoglass. By comparing simulations for covalently bonded Ge nanoglass and metallic CuZr nanoglass, the delocalization of the interfacial free volume is analyzed. Initially, the interface relaxation is driven by homogeneous plastic flow depending on the materials flow strain. Using pressure dependent diffusion coefficient calculated from MD simulations we further estimate the times scales needed for delocalization driven by thermally activated diffusion. In addition, we investigate the phonon density of states and the related thermal properties of nanoglasses and compare to bulk amorphous and nanocrystalline samples. Our results suggest that the density distribution within a nanoglasses can be adjusted by the initial particle size and chemical composition as well as by the annealing conditions.

## 11:10 AM

**Fabrication and Mechanical Characterization of Zr-Based Bulk-Metallic-Glass-Matrix Composites:** *Junwei Qiao*<sup>1</sup>; *Yong Zhang*<sup>1</sup>; <sup>1</sup>USTB

A series of Zr-Ti-Cu-Be-Nb bulk-metallic-glass-matrix composites were fabricated by the Bridgman solidification with different withdrawal velocities. By adjusting the withdrawal velocities, the scale and the volume fraction of dendrites dispersed in the glass matrix were optimized effectively. Under the withdrawal velocity of 1.0 mm/s, the composite materials exhibited the large compressive plasticity and the high fracture strength upon quasi-static loading. Additionally, the deformation and fracture behavior of the composites upon dynamic compressive loading were investigated.



11:20 AM

**Synthesis of  $\text{Cu}_{50}\text{Zr}_{50}$  Bulk Metallic Glasses Composites by Spark Plasma Sintering:** *Zhihui Zhang*<sup>1</sup>; Troy Topping<sup>1</sup>; Ying Li<sup>1</sup>; Yizhang Zhou<sup>1</sup>; Enrique Lavernia<sup>1</sup>; <sup>1</sup>University of California, Davis

Annealing induced embrittlement often represents a challenge to synthesize bulk metallic glasses (BMGs) with enhanced ductility using powder metallurgy techniques. Spark plasma sintering (SPS) uniquely provides a fast heating rate (400 °C/min) and accurate temperature control to study the effects of structural relaxation and partial crystallization on the mechanical properties of BMGs. In this study, the crystallization behavior during SPS and the corresponding mechanical properties of  $(\text{Cu}_{100-x}\text{Zr}_{100-x}\text{Al}_x)$  ( $x=0, 2.5, 5, 7.5$  and  $10$ ) BMGs were investigated. In the supercooled liquid region, the SPS consolidated  $(\text{Cu}_{100-x}\text{Zr}_{100-x}\text{Al}_x)$  alloys undergo partial crystallization. The  $\text{Cu}_{50}\text{Zr}_{50}$  binary alloy crystallized into  $\text{CuZr}_2$  and  $\text{Cu}_{10}\text{Zr}_7$  while the Al-containing alloys crystallized into  $\text{CuZr}_2$ ,  $\text{CuZr}$  and  $\text{AlCu}_2\text{Zr}$ . However, below the glass transition temperature, fcc-Cu nanocrystals formed in the SPS consolidated  $\text{Cu}_{50}\text{Zr}_{50}$  alloy. The results showed that the fracture strength and ductility were enhanced due to the precipitation of fcc-Cu nanocrystals. The fracture behavior of the  $(\text{Cu}_{100-x}\text{Zr}_{100-x}\text{Al}_x)$  alloys was discussed.

11:30 AM

**Synthesis of Amorphous/Amorphous and Amorphous/Crystalline Composites in Phase Separating Gd-Ti-Al-(Co/Cu) Alloys:** *Sung Woo Sohn*<sup>1</sup>; Wan Yook<sup>1</sup>; Hye Jeong Chang<sup>2</sup>; Won Tae Kim<sup>3</sup>; Do Hyang Kim<sup>1</sup>; <sup>1</sup>Yonsei University; <sup>2</sup>Oak Ridge National Laboratory; <sup>3</sup>Cheongju University

In the multi-component systems exhibiting high glass forming ability, the difference in the heat of mixing between some binary combinations can be large, possibly leading to phase separation onto two glass phases. In the present study, results on the phase separation in Gd-Ti-Al-(Co/Cu) alloys where Gd have positive heat of mixing with Ti will be presented, showing that phase separating metallic glass system can offer a unique opportunity for designing composites with hierarchical microstructure. The existence of miscibility gap and spinodal decomposition curve was examined by thermodynamic calculation using CALPHAD method. Based on these thermodynamic calculation results, metastable pseudo-binary liquid phase diagram including miscibility gap and spinodal decomposition curve could be obtained. Considering the liquid phase diagram, we could predict and control the microstructure. Furthermore, the deformation behavior of interconnected-type phase separated alloys has been investigated, emphasizing that the different length-scale plays a role in the mechanical properties.

11:40 AM Invited

**Air-Oxidation of a  $(\text{Zr}_{55}\text{Cu}_{30}\text{Al}_{10}\text{Ni}_5)\text{98Er}_2$  Bulk Metallic Glass at 350-500°C:** *Wu Kai*<sup>1</sup>; P.C. Kao<sup>1</sup>; I.F. Ren<sup>1</sup>; P.C. Lin<sup>1</sup>; Z.H. Hsiao<sup>1</sup>; D.W. Xing<sup>2</sup>; P.K. Liaw<sup>3</sup>; <sup>1</sup>Institute of Materials Engineering, National Taiwan Ocean University; <sup>2</sup>Department of Materials Science, Harbin Institute of Technology; <sup>3</sup>Department of Materials Science and Engineering, The University of Tennessee, Knoxville

The oxidation behavior of a  $(\text{Zr}_{55}\text{Cu}_{30}\text{Al}_{10}\text{Ni}_5)\text{98Er}_2$  bulk metallic glass (Zr-2Er BMG) was studied over the temperature range of 350-500°C in dry air. In general, the oxidation kinetics of the Zr-2Er BMG followed a two-to-three-stage parabolic-rate law, and the parabolic-rate constants ( $k_p$  values) fluctuated with increasing temperature. It was found that the oxidation rates of the Zr-2Er BMG are faster than those of the Er-free glassy alloy, indicative of a poor oxidation resistance. Very likely, the addition of 2% Er increased the concentration of oxygen vacancies in the defective  $\text{ZrO}_2$ -lattice, which in turn enhanced inward diffusion of oxygen, thereby leading to the faster oxidation rates of the Zr-2Er BMG. The scales formed on the Zr-2Er BMG were strongly temperature-dependent, consisting exclusively of tetragonal  $\text{ZrO}_2$  (t- $\text{ZrO}_2$ ) at 350°C, while minor amounts of monoclinic  $\text{ZrO}_2$  (m- $\text{ZrO}_2$ ),  $\text{CuO}$ ,  $\text{Al}_2\text{O}_3$ , and  $\text{Er}_2\text{O}_3$  were detected at  $T > 400^\circ\text{C}$ .

12:00 PM

**Artificial Microstructures as a Tool Box to Study Shear Band Stabilization in BMG Composites:** Golden Kumar<sup>1</sup>; *Jan Schroers*<sup>1</sup>; <sup>1</sup>Yale University

The current understanding in mechanical properties of BMG composites is that the interaction between shear bands and heterogeneities plays a critical role in stabilizing shear bands and preventing crack formation. The crack tip plastic zone size was suggested to be a crucial length scale influencing shear band interaction with the second phase. However, the properties of the heterogeneities—their size, distribution, and spacing—can also have an

effect on this length scale and therefore on the resulting tensile ductility and toughness. With current BMG composite synthesis techniques, it is difficult to control size, shape, distribution, and spacing of heterogeneities independently. However, our recent progress in thermoplastic forming allows fabricating artificial microstructures from BMGs where the dimensional aspects of the heterogeneities can be varied—controllably and independently. The results from tensile tests on samples with a different size and distribution of second phase are reported.

## Carbon Dioxide and Other Greenhouse Gas Reduction Metallurgy - 2010: Session I

*Sponsored by:* The Minerals, Metals and Materials Society, TMS Extraction and Processing Division, TMS Light Metals Division, TMS: Energy Committee

*Program Organizers:* Neale Neelameggham, US Magnesium LLC; Ramana Reddy, The University of Alabama; Jiann-Yang Hwang, Michigan Technological University; Jean-Pierre Birat, Arcelor Mittal; Kotaro Ogura, Yamaguchi University

Tuesday AM

Room: 310

February 16, 2010

Location: Washington State Convention Center

*Session Chairs:* Mahesh Jha, US Dept of Energy; Lifeng Zhang, Missouri University

8:30 AM Introductory Comments

8:35 AM Invited

**Overview of Removal Methods for CO<sub>2</sub> and Other Greenhouse Gases and Details of the Method Using Non-Thermal Plasma:** *Marcela Morvová*<sup>1</sup>; *Imrich Morva*<sup>1</sup>; Mario Janda<sup>1</sup>; <sup>1</sup>Comenius University

The possibilities of greenhouse gas mitigation using various methods are brought out. The special case of utilization of mixture of CO<sub>2</sub> with other greenhouse gases in synergistic way inside non-thermal plasma based system is described in details. Measurements on pilot system comprising pyrolysis chamber as alternative energy system (production of hydrogen and liquid tar) were made for various biomass and waste as the input material. The exhaust from this system was treated with non-thermal plasma gap suitable for up to 650Nm<sup>3</sup>/hour of exhaust gas flow. Condensed portion of exhaust is liquefied in distillation unit, produced hydrogen is on-line stored inside nanosized carbon of our own production. The CO<sub>2</sub> removal efficiency varies depending on exhaust composition between 45 to 98%. Other oxides as CO, NO<sub>x</sub>, SO<sub>x</sub> and several hydrocarbons and VOC are also removed. The main product connected with CO<sub>2</sub> removal is solid powder of proteinoid nature.

9:15 AM

**DOE's Industrial Energy Efficiency Grand Challenge Solicitation to Support Development of Technologies to Reduce Energy Intensity and Greenhouse Gas Emissions:** *Mahesh Jha*<sup>1</sup>; Bhima Sastri<sup>1</sup>; <sup>1</sup>U. S. Department of Energy

U. S. industry consumes approximately 32 quadrillion Btu of energy, almost a third of all energy used in the country, and emits about 1.6 billion metric tons of CO<sub>2</sub> per year. One of the mission of Energy Efficiency and Renewable Energy (EERE) division of U.S. Department of Energy (DOE) is to strengthen America's energy security, environmental quality and economic viability by enhancing the energy efficiency and productivity of the industrial sector. In support of this mission, the Industrial Technologies Program (ITP) issued "Industrial Energy Efficiency Grand Challenge" solicitation to seek, select and fund cost-shared development of transformational industrial processes and technologies that can reduce the energy intensity and greenhouse gas emissions from energy-intensive industries. This paper briefly describes the solicitation and selection process and presents a summary of the selected technologies to be developed.

# Technical Program

9:40 AM

**Sunshine to Petrol: A Metal Oxide-Based Thermochemical Route to Solar Fuels:** *James Miller*<sup>1</sup>; Richard Diver<sup>1</sup>; Nathan Siegel<sup>1</sup>; Eric Coker<sup>1</sup>; Andrea Ambrosini<sup>1</sup>; Daniel Dedrick<sup>1</sup>; Mark Allendorf<sup>1</sup>; Gary Kellogg<sup>1</sup>; Roy Hogan<sup>1</sup>; Ellen Stechel<sup>1</sup>; Ken Chen<sup>1</sup>; <sup>1</sup>Sandia National Laboratories

Converting carbon dioxide and water to hydrocarbons is an attractive option for storing solar energy and impacting atmospheric CO<sub>2</sub> concentrations. Thermochemical approaches for this conversion are potentially highly efficient as they avoid the inherent limitations of photosynthesis and also sidestep the solar-to-electric conversion necessary to drive electrolytic reactions. Solar-driven two-step metal oxide-based thermochemical cycles for producing the components of syngas, CO and H<sub>2</sub>, from CO<sub>2</sub> and H<sub>2</sub>O are the basis of the "Sunshine to Petrol" project. Multi-cycle production of both H<sub>2</sub> and CO has been demonstrated over several iron- and cerium-based compositions fabricated into monolithic pieces both in the laboratory and at the National Solar Thermal Test Facility. Progress in advancing the chemistry, understanding, and fabrication of materials for this application will be reported. Additionally, systems analysis and progress towards further demonstrating the reactions in a unique and continuous solar-driven reactor, the counter-rotating-ring receiver reactor recuperator or CR5, will be reported.

10:05 AM Break

10:15 AM

**Synthetic Fuel Production Utilizing CO<sub>2</sub> Recycling as an Alternative to Sequestration:** *Joseph Hartvigsen*<sup>1</sup>; S Elangovan<sup>1</sup>; Lyman Frost<sup>1</sup>; Carl Stoots<sup>2</sup>; James O'Brien<sup>2</sup>; J. S. Herring<sup>2</sup>; Manohar Sohal<sup>2</sup>; Grant Hawkes<sup>2</sup>; <sup>1</sup>Ceramatec Inc; <sup>2</sup>Idaho National Laboratory

Ceramatec, Inc and the Idaho National Laboratory are applying solid oxide fuel cell (SOFC) technology to syngas production by high temperature co-electrolysis of CO<sub>2</sub> and steam. This technology utilizes SOFC stacks to electrochemically extract oxygen from steam and CO<sub>2</sub>, leaving hydrogen and carbon monoxide suitable for fuel synthesis. The product H<sub>2</sub> to CO ratio of can be controlled to match the desired type of synthetic fuel product by varying the feed ratio. The resultant synthesis gas has been used to produce methane and Fischer-Tropsch liquid fuels. Concentrated industrial emitters of CO<sub>2</sub>, such as metallurgical reduction furnaces, cement kilns and fossil power plants can provide a valuable feedstock for a synthetic fuels industry, which incorporates energy from nuclear, solar, wind and hydropower sources. Widespread implementation of synfuel production will enable a greater reliance on intermittent renewable energy than can be accommodated by conventional electric demand profiles, while increasing our energy security.

10:40 AM

**Development of Self-Reduction as the Future of Metals-Making Technology:** *Jose Noldin*<sup>1</sup>; D'Abreu Jose<sup>2</sup>; <sup>1</sup>Tecno-Logos S/A; <sup>2</sup>Catholic University (PUC-Rio)

This paper will discuss the role of self-reduction as the technology of choice for metals production in the future. The main characteristics and fundamentals of this promising technological route will be presented, followed by a discussion on existing and developing technologies, potential impacts on raw materials requirements and economical and environmental benefits, with special focus on the reduction of CO<sub>2</sub> emissions during metals production.

11:05 AM

**Synthesis of Zeolitic Imidazolate Frameworks for Adsorbing Carbon Dioxide:** *Jinghua Zou*<sup>1</sup>; *Huimin Lu*<sup>1</sup>; Min Li<sup>1</sup>; <sup>1</sup>Beihang University

Zeolitic imidazolate frameworks (ZIFs) are new type of porous materials, form inerratic polyhedral in three-dimensional with large cages and small apertures, and appear structural diversity. Their hole size can be adjusted. These materials have high selective adsorption capacity to carbon dioxide. In this paper, zeolitic imidazolate frameworks were synthesized by solvothermal synthesis method with dimethylformamide (DMF) as solvent and structure-directing agent, divalent metallic ions as cation, and imidazole as ligand. The crystals were characterized with XRD, SEM for their crystal structures and physical properties, the adsorption of the crystals for carbon dioxide was also tested, and the result suggests that these porous materials have a capacity of 1.35ml/g for storing carbon dioxide at 273 Kelvin under ambient pressure.

11:30 AM

**Photochemical and Photo Electrochemical Conversion of Carbon Dioxide to Methanol Using Nanotubular TiO<sub>2</sub>:** *Manoranjan Misra*<sup>1</sup>; S. Mohapatra<sup>1</sup>; <sup>1</sup>University of Nevada

Global warming due to the emission of CO<sub>2</sub> is a serious environmental concern. The atmospheric concentration of CO<sub>2</sub> is about 384 ppm by volume and 3.0 × 10<sup>2</sup> tonnes by weight. This paper discusses the potential of converting the CO<sub>2</sub> into alternate fuels. CO<sub>2</sub> feedstocks can be converted into fuels using band-gap engineered TiO<sub>2</sub> nanotubes as a catalyst in the presence of solar light. Since no external energy is required, the energy saving would be in the order of 0.1-0.24 kwh/mole of CO<sub>2</sub> as compared to electrolytic conversion.

## Cast Shop for Aluminum Production: Grain Refinement, Alloying, Solidification and Shape Casting

*Sponsored by:* The Minerals, Metals and Materials Society, TMS Light Metals Division, TMS: Aluminum Committee, TMS: Aluminum Processing Committee

*Program Organizers:* John Grandfield, Grandfield Technology Pty Ltd; Pierre Le Brun, Alcan Voreppe Research Center

Tuesday AM

Room: 609

February 16, 2010

Location: Washington State Convention Center

*Session Chair:* Rein Vainik, Swerea KIMAB

8:30 AM

**On the Mechanism of Grain Refinement by Ultrasonic Melt Treatment in the Presence of Transition Metals:** *Dmitry Eskin*<sup>1</sup>; Tetyana Atamanenko<sup>2</sup>; Liang Zhang<sup>2</sup>; Laurens Katgerman<sup>2</sup>; <sup>1</sup>Materials Innovation Institute; <sup>2</sup>Delft University of Technology

Ultrasonic melt treatment is known to induce grain refining in aluminum alloys. The degree of grain refinement is strongly linked to the stage of solidification when the treatment is applied and on the alloy composition. In the latter case the presence of grain refiners is important. In this paper it is shown that very strong grain refining can be achieved in aluminum and its commercial alloys when the ultrasonic treatment is combined with the introduction of Zr and Ti. Ultrasonic processing is performed in the temperature range of the primary solidification of an intermetallic phase, i.e. normal casting temperatures of aluminum alloys. Dual mechanism is discussed involving (1) the dispersion and refinement of primary intermetallic particles that act as solidification sites and (2) growth restriction by the transition metal(s) that are present in the liquid phase.

8:55 AM

**Impurities in Al-5Ti-1B (wt.%) Grain Refiner Rod:** *Brian McKay*<sup>1</sup>; Georg Nunner<sup>1</sup>; Georg Geier<sup>2</sup>; *Peter Schumacher*<sup>1</sup>; <sup>1</sup>University of Leoben; <sup>2</sup>Austrian Foundry Institute

A "standard" and a "poor" Al-5Ti-1B (wt.%) grain refiner rod have been examined using computed tomography (CT) and scanning electron microscope (SEM) equipped with an energy dispersive x-ray (EDX) spectrometer. The refining potency of each rod was checked using the TP1 test. CT and SEM results from the "poor" refiner rod revealed the presence of Al<sub>3</sub>Ti agglomerates and residual unspent salts. These findings are indicative of an inefficient, non-optimal manufacturing process. Results from the TP1 test showed the "standard" rod to be more effective in promoting refinement, as expected. The quality of the grain refiner rod used in industrial practice is therefore vital as the grain size, feedability, cleanliness, uniformity of microstructure and integrity of the as-cast part may all be deleteriously affected. Moreover, a well controlled manufacturing process is important for the production of cleaner grain refiner as this can indirectly improve the quality of castings.

9:20 AM

**Experience with Production Scale Usage of Optifine – A High Efficiency Grain Refiner:** *John Courtenay*<sup>1</sup>; Rein Vainik<sup>2</sup>; <sup>1</sup>MQP Limited; <sup>2</sup>Swerea KIMAB

Optifine is a new grain refiner developed to give maximum grain refinement together with high consistency and good cleanliness. Laboratory tests, in combination with full scale trials, have shown that this grain refiner generally is at least twice as efficient than the standard grain refiners used today. This means



that at least two times more nuclei are active during the nucleation process and a fine grain can be obtained in the final cast with a much lower addition rate. This has now been demonstrated in full scale at Hulamin cast house in South Africa, where Optifine is used for all casts.

### 9:45 AM

**Effects of Cooling Rate on Microstructure in En-Ac43000 Gravity Castings and Related T6 Mechanical Properties:** *Ivan Todaro*<sup>1</sup>; Rosario Squatrito<sup>1</sup>; Alessandro Morri<sup>1</sup>; Luca Tomesani<sup>1</sup>; <sup>1</sup>University of Bologna

The aim of this work is to assess a correlation law between local cooling rate and SDAS for the EN AC43000 cast alloy. Bars 200 mm long with a double T cross section (suitable for tensile testing) were sand cast under controlled processing conditions. Chillers of different dimensions and materials, including water cooled ones, were placed at one side of the casting in order to obtain mono-dimensional heat flux and different cooling rates throughout the casting length. Thermocouples were used to acquire local cooling curves. A campaign of FE simulations was run to fine tune boundary conditions and to obtain a reliable cooling rate distribution throughout the whole casting. A correlation between experimental SDAS and simulated cooling rates was assessed. Finally, mechanical properties from extracted specimens in T6 condition were related to local SDAS and cooling rate.

### 10:10 AM

**Evaluation of Transient Heat Transfer Coefficient Evolution in EN43000 Gravity Castings towards Steel Chills with Different Interface Conditions:** Rosario Squatrito<sup>1</sup>; Ivan Todaro<sup>1</sup>; Luca Tomesani<sup>1</sup>; <sup>1</sup>University of Bologna

Heat exchange phenomena in foundry processes are governed by the heat resistance through contact interfaces between metal and casting tools. As known, physical and geometrical aspects play a fundamental role on the heat transfer conditions during the solidification process. This high dependence of heat transfer coefficient (HTC) by process variables determines the experimental method as the only way for a correct evaluation of heat fluxes during the cooling phase. The evolution of HTC between EN43000 aluminum alloy and H11 steel chills was investigated with different shapes of interface by means of an experimental gravity casting device and by developing an inverse method based on numerical analysis. The behavior of HTC as a function of time and casting temperature was evaluated with different treatment conditions of the chills surfaces (presence of coatings, knurling or smooth surface) to obtain correlations between HTC efficiency and manufacturing conditions.

### 10:35 AM

**In Situ Synchrotron Quantification of Fe-Rich Intermetallic Formation in Al-Si-Cu-Fe Alloys:** *Chedtha Puncreobutr*<sup>1</sup>; Junsheng Wang<sup>1</sup>; Peter Lee<sup>1</sup>; <sup>1</sup>Imperial College London

Iron uptake occurring during aluminum recycling can alter an alloy's castability while limiting the final component's fatigue life because of large Fe-rich intermetallic formation. To better understand these intermetallics, *in situ* synchrotron x-ray radiography was performed on an Al-7.5Si-3.5Cu-Fe(wt.%) alloy for two Fe levels and for different cooling rates. The intermetallic growth was quantified using image analysis. Nucleation temperatures were estimated by extrapolating growth back to zero size. The results illustrate that nucleation of the  $\beta$ -intermetallics is a function of both Fe level and cooling rate. The  $\beta$ -intermetallics nucleate between  $\alpha$ -Al dendrites and grow rapidly until they impinge on surrounding  $\alpha$ -Al dendrites. As the cooling rate increased, finer and closer packed  $\alpha$ -Al grains form, limiting intermetallic plate growth. The results are compared to prior analytical and numerical models and discussed in terms of their influence on both alloy castability and component life.

## Characterization of Minerals, Metals and Materials: Characterization of Alloys

*Sponsored by:* The Minerals, Metals and Materials Society, TMS Extraction and Processing Division, TMS Structural Materials Division, TMS/ASM: Composite Materials Committee, TMS: Materials Characterization Committee

*Program Organizers:* Ann Hagni, Geoscience Consultant; Sergio Monteiro, State University of the Northern Rio de Janeiro - UENF; Jiann-Yang Hwang, Michigan Technological University

Tuesday AM                      Room: 307  
February 16, 2010              Location: Washington State Convention Center

*Session Chairs:* Sergio Monteiro, State University of the Northern Rio de Janeiro - UENF; Donato Firrao, Politecnico di Torino

### 8:30 AM

**Detection of Creep Damage in a Nickel Base Super-Alloy by Nondestructive Means:** *Hector Carreon*<sup>1</sup>; <sup>1</sup>UMSNH

By using eddy current images, it was shown that the eddy current technique could be used to monitor creep damage in a nickel base super-alloy. The eddy current results also show a significative variation in the electrical conductivity on the creep damage zone with respect to the background zone in nickel-base super-alloy samples. The absolute thermoelectric power coefficient show a strong dependence associated with creep damage in nickel base super-alloy samples using a copper hot tip reference. The eddy current and thermoelectric power techniques seems to show promise as nondestructive evaluation tools for monitoring the level of creep damage in metallic alloys.

### 8:50 AM

**Microstructural, Mechanical and Fatigue Properties of Cobalt Alloys:** Giorgio Scavino<sup>1</sup>; Paolo Matteis<sup>1</sup>; Giovanni Mortarino<sup>1</sup>; *Donato Firrao*<sup>1</sup>; <sup>1</sup>Politecnico di Torino

Cobalt alloy samples (wt.% composition: Cr 25, W 5, C 1.2, "stellite 6" type) were produced either by casting or by sintering (hot isostatic pressing) and subjected to microstructural examination and to fatigue tests performed at 250 or 500°C, with the staircase method, to determine the 2 million cycles fatigue limit. Cast samples exhibit coarse dendrites, with lamellar carbides in the interdendritic (eutectic) regions, whereas sintered samples exhibit spheroidal carbides dispersed in a fine-grained matrix; these microstructures are not detectably modified by the test temperatures. The cast material shows similar fatigue behaviors at 250 and 500°C. The sintered material (tested at 500°C only) exhibits comparatively better tensile and fatigue properties. The microscopic mechanisms for the fatigue crack nucleation and growth and for the overload fracture, as evidenced by fractographic investigations, are different in the two materials and are clearly dictated by their different microstructures and defect population.

### 9:10 AM

**Reconstruction and Visualization of Multi-Phase Three-Dimensional Microstructure of a Cast Al-Si Base Alloy:** *Arun Gokhale*<sup>1</sup>; Harpreet Singh<sup>1</sup>; Yuxiong Mao<sup>1</sup>; Asim Tewari<sup>2</sup>; Anil Sachdev<sup>2</sup>; <sup>1</sup>Georgia Institute of Technology; <sup>2</sup>General Motors Co.

This contribution reports reconstruction of the multi-phase multi-scale 3D microstructure of a permanent mold cast unmodified Al-12wt%Si-1wt%Ni base alloy containing eutectic Si platelets, coarse primary polyhedral Si particles, Fe-rich script intermetallic particles, and pores. These constituents are segmented, reconstructed, rendered, and characterized in three dimensions. The estimated 3D microstructural attributes include distribution of eutectic platelet thickness; mean volume, mean surface area, and mean thickness of the eutectic Si platelets; mean volume and mean surface area of the polyhedral primary Si particles; and mean number of faces, edges, and corners on the polyhedral primary Si particles.

### 9:30 AM

**Phase Separation in Fe-20%Cr-6%Al-0.5%Ti ODS Alloy:** *Carlos Capdevila-Montes*<sup>1</sup>; Michael Miller<sup>2</sup>; Felix Lopez<sup>1</sup>; Jesus Chao<sup>1</sup>; Kaye Russell<sup>2</sup>; <sup>1</sup>CENIM-CSIC; <sup>2</sup>ORNL

The temporal evolution of the microstructure resulting from phase separation of an Fe-20%Cr-6%Al-0.5%Ti ODS alloy at temperatures between 708 and

Tue. AM

# Technical Program

748 K has been analyzed by atom probe tomography (APT), thermoelectric power measurements (TEP), and differential scanning calorimetry (DSC). The roles of Al and Ti during the decomposition process have been investigated. Proximity histogram analysis revealed significant partitioning of Al and Ti, which is consistent with theoretical calculations. TEP measurements describe the macroscopic evolution of the process, which can be correlated with the kinetic equations obtained from atomic scale measurements obtained by APT. Finally, the activation energy of the process of phase separation is obtained by DSC. These results indicate that simultaneous phase separation into Fe-rich, Cr-rich and Fe-Ti-Al phases occurs. Research at the Oak Ridge National Laboratory SHaRE User Facility was sponsored by the Scientific User Facilities Division, Office of Basic Energy Sciences, U.S. Department of Energy.

## 9:50 AM

**Development of a High-Temperature Micro-Indentation Technique for Material Mechanical Property Evaluation up to 1200°C:** Jared Tannenbaum<sup>1</sup>; Brody Conklin<sup>1</sup>; Bruce Kang<sup>1</sup>; Mary Anne Alvin<sup>2</sup>; <sup>1</sup>West Virginia University; <sup>2</sup>National Energy Technology Lab

A depth-sensing micro-indentation technique is developed for evaluating material mechanical properties at elevated temperatures (to 1200°C). The depth-sensing micro-indentation system is capable of determining Young's modulus and creep strength of test materials with flat, tubular or curved architectures from room to 1200°C under either air or controlled gaseous environments. Calibration tests were conducted on a 1-in x 1-in 0.25-in H13 Tool Steel specimen from room to 600°C. Test results were in excellent agreement with literature values. Mechanical property evaluations of single crystal René N5 and Haynes 230 alloys were performed from room to 1100°C in air, inert gas, or in air with controlled moisture content. Post test microstructural analyses were conducted to correlate the effect of oxidation and moisture on the measured mechanical properties. Micro-indentation tests were conducted on MA 956 and PM 2000 ODS alloys at 1200°C. Preliminary test results will be presented and discussed.

## 10:10 AM

**Characterization and Properties of a Stoichiometric NiTiPt High Temperature Shape Memory Alloy:** Fan Yang<sup>1</sup>; Libor Kovarik<sup>1</sup>; Anita Garg<sup>2</sup>; Michael Kaufman<sup>3</sup>; Santo Padula<sup>2</sup>; Ronald Noebe<sup>2</sup>; Michael Mills<sup>1</sup>; <sup>1</sup>The Ohio State University; <sup>2</sup>NASA Glenn Research Center; <sup>3</sup>Colorado School of Mines

There has been a growing demand to achieve higher transformation temperatures than the commercial NiTi alloys can offer. Pt additions (greater than 10 at%) to the NiTi binary system is more potent in raising the Ms temperature than any other ternary element tested so far. For the stoichiometric alloy Ti<sub>50</sub>Ni<sub>29</sub>Pt<sub>21</sub>, the best shape memory response is obtained after aging at 500°C, during which a fine precipitate phase forms. Their unique structure and coherency have been characterized by conventional and high resolution scanning transmission electron microscopy. For the same alloy, aging at higher temperature introduces much coarser lath-like precipitates. The role of these phases in improving the work output and minimizing the permanent strain will be discussed.

## 10:30 AM

**Estimation of Three-Dimensional Mean Dihedral Angle in a W-Ni-Fe Alloy Liquid-Phase Sintered in Microgravity:** Maneel Bharadwaj<sup>1</sup>; Arun Gokhale<sup>1</sup>; William Goodwin<sup>2</sup>; <sup>1</sup>Georgia Institute of Technology; <sup>2</sup>University of Tennessee

The three-dimensional mean dihedral angle of impinging tungsten grains is estimated in a 50%W-35%Ni-15%Fe alloy liquid-phase sintered (LPS) in microgravity at 1500°C for times ranging from 1 to 600 minutes using unbiased stereology and automated image analysis. The estimated mean dihedral angles are in the range of 50 ± 3 degrees. The mean dihedral angle does not vary significantly with the liquid-phase sintering time although the mean intercept size of the tungsten grains increases almost by a factor of 5.

## 10:50 AM

**Microscopic Analysis of Ni-Cr Alloy Produced by Single Roll Strip Casting:** Sanjeev Das<sup>1</sup>; J. B. Seol<sup>1</sup>; Y.C. Kim<sup>2</sup>; C. G. Park<sup>1</sup>; <sup>1</sup>POSTECH; <sup>2</sup>Research Institute of Industrial Science and Technology

In the present investigation the microstructure and some mechanical properties of Ni-Cr alloy prepared by single roll strip casting (SRSC) were studied. The top surface (surface not in contact with the roll) of the as received sample was rough and lusterless. The grain size of the top surface was significantly larger compared to that of the bottom surface. Grain interior showed dendritic morphology. Etch

pits, formed by dislocation were observed on the top and bottom surfaces of the sample. Scanning electron microstructure revealed continuous corroded region along the grain boundaries. X-ray diffraction (XRD) study confirms the formation of chromium carbide at the grain boundary, which depletes Cr near the grain boundary. SEM EBSD of the alloy in as-cast, homogenized, cold rolled, and annealed conditions were evaluated to observe the orientation of the grains. Twins were observed in cold rolled annealed sample.

## 11:10 AM

**Influence of TCP Phase on Enduring Property of Single Crystal Nickel-Based Superalloys:** Tian Sugui<sup>1</sup>; Qian Benjiang<sup>1</sup>; Li Tang<sup>1</sup>; Wang Minggang<sup>1</sup>; Xie Jun<sup>1</sup>; <sup>1</sup>Shenyang University of Technology

By means of the measurement of the enduring property and microstructure observation, an investigation has been made into the influences of the element Re and TCP phase on the enduring property of the single crystal nickel base superalloys. Results show that the strip-like TCP phase is precipitated along the <110> orientation on {111} planes in the containing/free Re superalloys during the aging, and the TCP phase is identified as  $\mu$  phase, and the precipitated  $\mu$  phase in 4.5%Re alloy is gradually spheroidized during aging. Thereinto, the strip-like  $\mu$  phase may obviously decrease the enduring lifespan of the superalloys due to the consumption of the refractory elements and the effect of the stress concentration. But the stress concentration is not easily generated in the regions near the spheroidized  $\mu$  phase, this is main reason of reducing to a small extent the creep lifespan of the 4.5%Re alloy.

## 11:30 AM

**Structure and Properties of Melt-Spun Ni-Ti Shape Memory Alloy:** Walman Castro<sup>1</sup>; Carlos Araújo<sup>1</sup>; George Anselmo<sup>1</sup>; <sup>1</sup>Universidade Federal de Campina Grande

Many physical properties of melt-spun ribbons as well as their microstructures sensitively depend on the values of the processing parameters such as the wheel speed, gas pressure, melt temperature and nozzle-wheel gap, etc. In the present study, the shape memory behavior of Ti-49 at.%Ni alloy ribbons fabricated at different cooling rates by the melt spinning and the influence of rapidly solidified on shape memory behavior was studied. When the ribbon is produced at a higher wheel velocity in melt spinning, the degree of undercooling becomes high because of its thinner thickness. Therefore, the amount of crystalline layer decreases with wheel velocity. The B2-B19 transformation occurs in ribbons fabricated at the wheel velocity of 30 m/s, while only B19 martensite transformation occurs in ribbons fabricated at the wheel velocity of 50 m/s.

## 11:50 AM

**The Modeling and Processes Research of Titan Aluminides Structurization Received by SHS Technology:** Sereda Borys<sup>1</sup>; Aleksandr Zhrebtsov<sup>1</sup>; Yuriy Belokon<sup>1</sup>; <sup>1</sup>ZSEA

As it is known the creation and development of new titanic alloys has been problematic up to now. They can be used in aircraft and vehicle construction, shipbuilding and as materials for keeping static loadings in high-temperature environments. In this work the synthesis of various titan aluminides is investigated. Mathematical model of structurization process was done. On the base of retrieved model the mechanisms of structurization in systems Ti + Al and Ti + 3Al was determined. The method of retrieving compacted products combusted in SHS conditions (SHS-compacting) was used to gain these intermetallic compounds. It is established that the SHS-compacting technology is fully capable of supervising the process of structurizations with the whole complex of advantages and can be applied for receiving qualitative titan aluminides with the set of chemical-physical properties.

## 12:10 PM

**Influence of Preparing Technologies on Microstructure and Creep Behavior of GH4169 Alloy:** Tian Sugui<sup>1</sup>; Li Zhenrong<sup>1</sup>; Zhao Zhonggang<sup>1</sup>; Chen Liqing<sup>2</sup>; Liu Xianghua<sup>2</sup>; <sup>1</sup>Shenyang University of Technology; <sup>2</sup>Northeast University

Influence of the preparing technology on the microstructure and creep behaviour of the alloy is investigated by means of the creep curves measurement of the forged and hot continuous rolled (HCR) GH4169 alloy. Results show that the deformed features of the alloy during HCR are the twinning and dislocation activated within twinning, and HCR alloy displays a better creep resistance. During creep, the twinning occurs only the forged alloy, but the deformed features of HCR alloy is the twinning and dislocation activated within the twins. Thereinto, "pre-dislocation" in HCR alloy promote the multi-systems slipping of dislocation activated within the twins, and releasing the stress concentration,



which is thought to be a main reason of improving creep resistance of the alloy. In the later period of creep, the fact that the micro-cracks are formed and expanded along the boundaries is the fracture mechanism of the alloy during creep.

layer prepared by a direct current plating. The ultrasonic agitation during pulse plating resulted in increasing neutral salt fog spray life and wear resistance that is related to smaller crack size and more broad size distribution of the trivalent chromium. A model of nucleation and growth was proposed to describe deposition rate and microstructure of the pulse plating.

### Coatings for Structural, Biological, and Electronic Applications: Metallic Coatings

*Sponsored by:* The Minerals, Metals and Materials Society, TMS Electronic, Magnetic, and Photonic Materials Division, TMS Structural Materials Division, TMS: Biomaterials Committee, TMS: Thin Films and Interfaces Committee

*Program Organizers:* Nuggehalli Ravindra, New Jersey Institute of Technology; Gregory Krumdick, Argonne National Laboratory; Roger Narayan, Univ of North Carolina & North Carolina State Univ; Choong-un Kim, University of Texas at Arlington; Nancy Michael, University of Texas at Arlington

Tuesday AM Room: 309  
February 16, 2010 Location: Washington State Convention Center

*Session Chair:* Roger Narayan, University of North Carolina

#### 8:30 AM Introductory Comments

#### 8:40 AM

**Evaluation of Thermal and Intrinsic Stress in Copper and Tantalum Sputtered Films:** *Anahita Navid*<sup>1</sup>; Eric Chason<sup>2</sup>; Andrea Hodge<sup>1</sup>; <sup>1</sup>University of Southern California; <sup>2</sup>Brown University

The thermal stress contribution to the total film's residual stress is presented for copper and tantalum films deposited by magnetron sputtering on Si substrates using a uniform power at various pressures. The in-situ stress was measured using a Multibeam Optical Stress Sensor (MOSS) system while the ex-situ stress was measured by stylus profilometry. Results show that the thermal stress contribution is quite significant and can be as large as the intrinsic stress and might change the stress state on the film after deposition. The deposition temperature was also examined as a function of sputtering pressure, in order to relate to the thermal stress. It was determined that as the pressure increases, the deposition temperature decreases; this was related to the calculated total energy of the sputtered atoms and gas neutrals which also decreased with increasing pressure.

#### 9:05 AM

**Surface Modification of Steel Substrate by Pulsed Laser Deposition Technique:** *Shampa Aich*<sup>1</sup>; Saket Ahuja<sup>1</sup>; Lakpathi Banoth<sup>1</sup>; Indranil Manna<sup>1</sup>; <sup>1</sup>Indian Institute of Technology

A series of bi-layer and multi-layer coatings of Ti/TiB<sub>2</sub>, Ti/TiN, Cr/CrN and Ti/TiN/Cr/CrN were successfully deposited over austenitic stainless steel substrate using pulsed laser deposition technique. The X-ray diffraction patterns reveal the coatings to be crystalline and compositional micro-analysis suggests that titanium atoms diffuse into the substrate to form strong bond between film and substrate. The Ti/TiB<sub>2</sub> coatings were developed in varying thicknesses from 55 nm to 550 nm, with the maximum thickness at 500°C. For the nitride bi-layer and multi-layer coatings, the optimum coatings (~ 600 nm) were produced at 300°C to obtain excellent surface properties. The multi-layered metal/nitride coatings improved resistance to scratching and helped in arresting the crack propagation. In terms of mechanical properties, double bi-layer (Ti/TiN/Cr/CrN) performs the best followed by Ti/TiN/Ti and then Cr/CrN/Cr. While the bi-layer of Ti/TiB<sub>2</sub> shows the best followed by single TiB<sub>2</sub> and then single Ti layers.

#### 9:30 AM

**A Nucleation and Growth Model for Pulse Plated Trivalent Chromium Deposition:** *Yong Choi*<sup>1</sup>; Sik C. Kwon<sup>2</sup>; <sup>1</sup>Sunmoon University; <sup>2</sup>KIMS

eco-friendly trivalent chromium layers were prepared in modified chromium chloride and sulfate baths by pulse plating with ultrasonic agitation to replace hexavalent hard chromium coating in industrial fields. Deposition rates of the chromium layers by ultrasonic pulse plating was in the range of 300-350 nm/min. Micro-hardness of the ultrasonic pulse plating is lower than those of pulse plating and direct current plating. Wear resistance of the trivalent chromium layer prepared by ultrasonic pulse plating is higher than that of the chromium

#### 9:55 AM Break

#### 10:10 AM

**An Investigation on Phase Formations and Microstructures of Ni-Rich NiTi Shape Memory Alloy Thin Films:** *B. Geetha Priyadarshini*<sup>1</sup>; Shampa Aich<sup>1</sup>; Madhusudan Chakraborty<sup>1</sup>; <sup>1</sup>Indian Institute of Technology

Ni-rich NiTi alloy thin film of 40 at. % Ti was fabricated by RF/DC magnetron sputtering using elemental Ni and Ti as sputter targets. Si (100) was chosen as substrate which was either held at room temperature or at 300 °C during the deposition. The 380 nm thick films were characterized by Field Emission Scanning Electron Microscopy, Energy Dispersive Spectroscopy, Grazing Angle X-ray Diffraction, Atomic Force Microscopy and High-Resolution Transmission Electron Microscopy. The results showed that due to lack of surface mobility of the adatoms the room temperature deposited films were smooth, amorphous, with a grain size of 20-25 nm accompanied with porous microstructure. At higher substrate temperatures, increase in the surface diffusion leads to formation of partially crystalline, rougher films with denser, compact, fibrous grains without void boundaries. Formation of Ni-rich precipitates such as: Ni<sub>4</sub>Ti<sub>3</sub>, Ni<sub>2</sub>Ti and Ni<sub>3</sub>Ti along with small amount of the NiTi phase were also confirmed.

#### 10:35 AM

**Effect of Heat Treatment on the Microstructure and Mechanical Properties of Ti-Mo-N Coating Films:** *Shoko Komiyama*<sup>1</sup>; Yuji Sutou<sup>1</sup>; Junichi Koike<sup>1</sup>; <sup>1</sup>Tohoku University

TiN coatings are widely used in cutting tools and medical implants. Recently, it has been reported that the addition of Mo is effective to enhance the wear resistance of TiN coatings [1]. In this study, the effects of heat treatment on the mechanical properties of (TiMo)<sub>1-x</sub>N<sub>x</sub> films were investigated. The (TiMo)<sub>1-x</sub>N<sub>x</sub> films were deposited on AISI304 steel by reactive RF sputtering using a Ti50Mo50 target. To deposit the nitrides, the mixture of Ar (7.5ccm) and N<sub>2</sub> (0-2.0ccm) gases was introduced. The obtained films were heat treated at various temperatures in Ar atmosphere. It was found that the microhardness of the (TiMo)<sub>1-x</sub>N<sub>x</sub> films showed a maximum value of about 30GPa at N<sub>2</sub>=0.3ccm, which was increased further to 35 GPa after heat treatment at 1000° Q. The maximum hardness was due to the formation of a fine grain structure. [1] Q. Yang et al. Wear 261 (2006) 119.

#### 11:00 AM

**PVD Coated Hot Work Tool Steels for Tooling Applications in Semi-Solid Processing of Steels:** *Duygu Isler*<sup>1</sup>; Yucel Birol<sup>2</sup>; Mustafa Urgan<sup>1</sup>; <sup>1</sup>Istanbul Technical University; <sup>2</sup>TUBITAK

Semi-solid processing of metals combines the advantages of forging and casting while shaping of metallic components. Having already matured into an industrial practice for Al and Mg alloys, this technology could upgrade the market for forged steel parts. However, the surface-to-interior temperature differentials in steel thixoforming dies are much larger than with Al and Mg. Combined with the chemical, tribological and thermal interactions between die and formed material confer very specific requirements on tool materials. Hot work tool steel dies are inadequate due to the limited temper resistance of the commercially available grades. Physical Vapour Deposition (PVD) coatings, shown to have beneficial impact on the lifetime of pressure die casting tools, could offer a solution. X32CrMoV3-3 hot work tool steel was coated with AlTiN and AlTiON utilizing cathodic arc PVD technique in the present work. The performance of the coated samples was tested under thermal fatigue and erosive wear conditions.

Tue. AM

# Technical Program

## Computational Thermodynamics and Kinetics: Wetting Phenomena I

*Sponsored by:* The Minerals, Metals and Materials Society, TMS Electronic, Magnetic, and Photonic Materials Division, TMS Materials Processing and Manufacturing Division, TMS Structural Materials Division, TMS: Chemistry and Physics of Materials Committee, TMS/ASM: Computational Materials Science and Engineering Committee  
*Program Organizers:* Jeffrey Hoyt, McMaster University; Dallas Trinkle, University of Illinois at Urbana-Champaign

Tuesday AM Room: 308  
February 16, 2010 Location: Washington State Convention Center

*Session Chair:* To Be Announced

### 8:30 AM Invited

**Grain Boundary Premelting: Insights from Order Parameter Models:** *Alain Karma*<sup>1</sup>; Ari Adland<sup>1</sup>; Robert Spatschek<sup>2</sup>; <sup>1</sup>Northeastern University; <sup>2</sup>Ruhr-University

The presence of liquid films at grain boundaries below the bulk melting point can alter macroscopic properties of polycrystalline solids and dramatically reduce their resistance to shear stresses. This talk will discuss recent progress made in understanding grain boundary premelting using both atomic-scale and coarse-grained order parameter models. New fundamental insights that will be reported stem from detailed numerical surveys of those models over a wide range of parameters, analyses in tractable limits, and critical quantitative comparisons with molecular dynamics simulations in bcc and fcc elemental systems.

### 9:00 AM Invited

**Molecular Dynamics Simulations of Brazing:** *Edmund Webb*<sup>1</sup>; Jeff Hoyt<sup>2</sup>; <sup>1</sup>Sandia National Laboratories; <sup>2</sup>McMaster University

Brazing is a relatively high temperature joining process important to a range of metallurgical technology. Brazing depends upon good wettability between constituent materials; furthermore, reactions between solid and liquid are often observed. Understanding fundamental phenomena in high temperature reactive wetting bears potential for impact on technology but also on theoretical descriptions of capillarity. Molecular dynamics (MD) simulations are a useful counterpart to experiment in describing fundamental wetting mechanisms. This talk will review MD simulations of high temperature wetting for metals in a braze geometry. Infiltration of molten metal into a solid pore is simulated for a system where the solid simultaneously dissolves into the liquid. Simulations reveal a regime where the dissolution reaction is aggressive enough to alter the kinetics of infiltration. MD simulations are coupled with Monte Carlo calculations to draw quantitative connections between the free energy of the dissolution reaction and the kinetics of pore infiltration.

### 9:30 AM

**A Hybrid Phase-Field and ALE Model for Reactive Wetting in Metal/Metal Systems:** *Shun Su*<sup>1</sup>; Bruce Murray<sup>2</sup>; Ying Sun<sup>1</sup>; <sup>1</sup>Drexel University; <sup>2</sup>Binghamton University

Reactive wetting refers to a liquid drop spreading on a substrate with reaction or dissolution. In order to model the dissolutive wetting process, fluid flow, species transport and phase change must be coupled. In this work, the phase-field method along with the Arbitrary Lagrangian-Eulerian (ALE) technique is used to simulate the evolution of an alloy drop on a metal substrate while the process is assumed to be isothermal. The liquid-vapor interface of the drop is tracked by a phase-field variable while the evolution of the solid-liquid interface is determined by the ALE method. The shape of the dissolution boundary and the extent of spreading are investigated as a function of initial solute concentration. The triple junction kinetics is studied in relation to the model assumptions. The simulations are performed on a millimeter scale and the results are compared with experimental data for a Sn-Bi system.

### 9:50 AM Break

### 10:00 AM Invited

**Modeling Grain Boundaries: Wetting, Vacancies and Creep:** *James Warren*<sup>1</sup>; William Boettinger<sup>1</sup>; <sup>1</sup>NIST

The challenges in developing a robust macroscopic model of grain boundaries that describes the majority of processes of interest to the materials processor are substantial. In this work I will describe the ongoing efforts to synthesize several different efforts in grain boundary modeling with classical models developed by Larche and Cahn into a coherent picture. It is hoped that such models will provide substantial insights into the mechanical properties of materials, and, in particular, insights into vacancy diffusion mediated creep (either in the bulk or grain boundaries) of materials with residual stress. The back-coupling of these phenomena to grain boundary wetting should also prove interesting.

### 10:30 AM Invited

**Atomistic Behavior Driving High Temperature Contact Line Advancement:** *Ying Sun*<sup>1</sup>; Edmund Webb<sup>2</sup>; <sup>1</sup>Drexel University; <sup>2</sup>Sandia National Laboratories

Atomic scale phenomena driving contact line advancement during wetting of a solid by a liquid are investigated via molecular dynamics simulations of Ag(l) drops spreading on Ni substrates. For homologous temperature ~5% above melting for Ag, essentially non-reactive wetting is observed with relatively high spreading velocity. Delivery of material to the contact line occurs preferentially along the L/V interface. New material transported into the drop edge near the L/V interface displaces existing edge material. Atoms forming the droplet edge at a given instant are preferentially constrained near the S/L interface as the droplet advances across the substrate. While contact line advancement appears dominated by rapid flow along the L/V interface, evidence emerges that molecular kinetic mechanisms play a role as some atoms move with the contact line, desorbing and re-adsorbing between neighboring sites at the S/L interface. Results illustrate specific mechanisms underlying wetting and spreading behavior at high temperature.

### 11:00 AM

**Diffusivity in Al-Cu and Cu-Zr Liquids:** *Shihuai Zhou*<sup>1</sup>; Ralph E. Napolitano<sup>2</sup>; <sup>1</sup>Ames Laboratory; <sup>2</sup>Department of Materials Science and Engineering, Iowa State University

A high-temperature thin tube liquid diffusion couple method is employed to determine the composition dependent diffusivity in binary Al-Cu and Cu-Zr alloys. Composition profiles are measured in quenched thin-tube specimens and analyzed in conjunction with assessed solution thermodynamic models. Experimental methods and results are presented, and composition-dependent atomic mobility and thermodynamic factors are discussed. This research is supported by the U.S. Dept. of Energy Office of Science through Ames Laboratory contract No. DE-AC02-07CH11358.

### 11:20 AM

**A Study of the Te Melting Line and Solid-Liquid Transitions:** *Chuck Henager*<sup>1</sup>; Fei Gao<sup>1</sup>; John Jaffe<sup>1</sup>; <sup>1</sup>PNNL

Te-particles that form during the growth of CdZnTe (CZT) single crystals are a macroscopic defect with apparent origin in the CZT melt. As the freezing point for CdTe is 1365 K and that of Te is 722 K it is important to understand the mechanisms by which presumably I-Te(Cd)-particles form within the CZT solid. A new interatomic potential (IAP) for Te has been developed based on a modified Stillinger-Weber form as was done previously for Se by others in order to study large systems more suited to crystal growth modeling. The IAP is used to study Te melting and the Te melting line via molecular dynamics. Results for density changes, enthalpy of melting, and Te liquid structures will be presented and compared to ab initio and literature results. The use of the new IAP for Te in developing an improved IAP for CdTe is discussed.

### 11:40 AM

**Compositional Patterning and Morphological Evolutions in Binary and Ternary Alloys Driven by Irradiation:** *Pascal Bellon*<sup>1</sup>; Anoop Damodaran<sup>1</sup>; Daniel Schwen<sup>1</sup>; Robert Averback<sup>1</sup>; <sup>1</sup>University of Illinois

The dynamical competition between irradiation-induced atomic mixing and thermally activated decomposition can induce the self-organization of the composition field into patterns. Analytical modeling and atomistic simulations works showed that a key requirement for this self-organization is that the forced mixing takes place at a finite range exceeding the characteristic range of diffusional jumps. We extend past kinetic Monte-Carlo approaches to



multi-component alloy systems, and we investigate the effects of composition-dependent atomic mobility. In the case of slow solute mobility, it is shown that precipitates stabilized by irradiation may develop a “cherry-pit” structure. In the case of ternary and quaternary alloys, we show that, compared to binary alloys, several new nanostructures can be stabilized, in particular core-shell precipitates. These results will be contrasted with available experimental results.

### 12:00 PM

**Irradiation Induced Re-Resolution and Growth of Xenon Nano-Bubbles Simulated by First Passage Monte Carlo:** *Daniel Schwen*<sup>1</sup>; Robert Averback<sup>1</sup>; <sup>1</sup>University of Illinois

With the development of generation IV reactor technology, the impact of intragranular fission gas on the performance of UO<sub>2</sub> fuels has gained considerable concern. Gaseous fission products and their precipitation as nano-scale fission gas bubbles are known to adversely influence the thermal and mechanical properties of fuels. To study the gas diffusion and bubble population evolution we developed a first passage based fast Monte Carlo software. First passage Monte Carlo dramatically accelerates simulation times for dilute systems of diffusing particles, such as fission gas in fuel matrices, by analytically describing the temporal behavior of random walkers and thus removing the need to compute single atomic jumps. In contrast to mean field theories spatial correlations arising from re-resolution distances and proximity to grain boundaries (sinks) can be readily incorporated. A variety of gas re-resolution scenarios and diffusion models are explored and compared to existing data.

### Cost-Affordable Titanium III: Powder Consolidation and Properties I

*Sponsored by:* The Minerals, Metals and Materials Society, TMS Structural Materials Division, TMS: Titanium Committee  
*Program Organizers:* M. Ashraf Imam, Naval Research Lab; F. H. (Sam) Froes, University of Idaho; Kevin Dring, Norsk Titanium

Tuesday AM Room: 618  
February 16, 2010 Location: Washington State Convention Center

*Session Chairs:* James Withers, Materials and Electrochemical Research Corporation; Derek Fray, University of Cambridge

### 8:30 AM

**Equations for the Compaction of Titanium Powders:** *Stephen Gerdemann*<sup>1</sup>; Paul Jablonski<sup>1</sup>; <sup>1</sup>NETL

Accurate modeling of powder densification has been an area of active research for more than 60 years. The earliest efforts were focused on linearization of the data since computers were not readily available which made curve fitting difficult. In this work several lots of titanium powders ranging in size, shape and chemistry were cold pressed in a single acting die instrumented to collect stress and deformation data during compaction. From this data the density of each button was calculated and then plotted as a function of pressure. The results show that densification of all the powders, regardless of particle size, shape or chemistry, can be very accurately modeled as the sum of an initial density plus the sum of a particle shape term and a powder densification term. These last two terms are found to be a function of applied pressure and take the form an exponential rise.

### 8:55 AM

**Making Titanium Powder Metallurgy a Viable Alternative to Wrought for Manufacturing:** *James Sears*<sup>1</sup>; <sup>1</sup>South Dakota School of Mines and Technology

An overview of the current and developing production sources for Titanium powder are given along with a review of the potential applications and new opportunities being pursued. It has long been known that titanium would enter many new markets if production and manufacturing costs could be reduced. It is also known that making components directly from Titanium Alloy powder circumvents many of the production costs associated with wrought Titanium manufacturing. The hurdle that prevents Titanium Powder Metallurgy (PM) for becoming a viable alternative to wrought manufacturing is the high costs associated with Titanium powder production. An evaluation of the processes that currently produce Titanium powder is presented along with the methods that are being employed to reduce the associated costs of Titanium powder

production. An overview of the National Center of Excellence for Titanium Powder Metallurgy will be given.

### 9:20 AM

**Development of an Affordable Supply Chain for Meltless Titanium Alloys:** *Eric Ott*<sup>1</sup>; Andy Woodfield<sup>1</sup>; Jon Blank<sup>1</sup>; Michael Peretti<sup>1</sup>; David Linger<sup>1</sup>; <sup>1</sup>GE Aviation

The advent of new technologies for conversion of Ti-bearing raw materials to metal powder forms, and particularly the capability of some processes to produce titanium alloys directly provides a path to make titanium alloy products without incurring the expense, energy, and time associated with melting processes. This “meltless” titanium technology can substantially decrease the number of major processing steps and provide large improvements in product yield, energy utilization and emissions. Near-net-shape processing provides further material yield improvements for complex, machining intensive geometries. A disruptive, efficient and stable supply chain that takes advantage of these improvements is needed and new strategies must be developed to ensure sufficient production capacity as well as a competitive environment. This paper will establish technical, cost and capacity benefits of the meltless titanium technology, will propose criteria for development of a robust supply chain, and will discuss key requirements for aerospace and non-aerospace commercial implementation.

### 9:45 AM

**Consolidation Process in Near Net Shape Manufacturing of Armstrong CP-Ti/Ti-6Al-4V Powders:** *Yukinori Yamamoto*<sup>1</sup>; Jim Kiggans<sup>1</sup>; Michael Clark<sup>1</sup>; Stephan Nunn<sup>1</sup>; Adrian Sabau<sup>1</sup>; William Peter<sup>1</sup>; <sup>1</sup>Oak Ridge National Laboratory

This presentation summarizes our recent efforts to develop the manufacturing technologies of consolidated net-shape components by using new low-cost commercially pure titanium (CP-Ti) and Ti-6Al-4V alloy powders made by Armstrong process. Net-shape components have been fabricated by pressing and sintering, cold isostatic pressing (CIP), hot isostatic pressing (HIP), pneumatic isostatic forging (PIF), and/or adiabatic compaction. The press-and-sinter processing of the powders in the as-reduced condition were evaluated systematically in terms of theoretical density and microstructure as functions of time, pressure, and temperature. Up to 96.4% theoretical density has been achieved with the press-and-sinter technology. A consolidation modeling is also under development to interpret the powder deformation during processing. The detailed experimental results in conjunction with future plan will be discussed. This research was sponsored by the U.S. DOE, ORNL, under Contract DE-AC05-00OR22725 with UT-Battelle, LLC. Additional funding and collaboration with the SHaRE User Facility at ORNL is also acknowledged.

### 10:10 AM Break

### 10:25 AM

**Technical Challenges and Solutions for Cost-Efficient Manufacturing of Complex Shape Parts from Ti Alloys via PM HIP:** *Victor Samarov*<sup>1</sup>; <sup>1</sup>Synertech PM Inc.

Innovative developments in HIP technology provide novel answers to the old challenges of processing complex shape parts from Ti alloys: -very low material yield during processing of complex shape parts; -dominating costs of machining to the final geometry; -high cost on initial materials, including alloyed powders; -increasing technical difficulties and cost with larger parts; -eternal fight for the appropriate micro-structure and properties in large forgings. These new developments are based on the selectively net shape computer controlled HIP processing of alloyed powders atomized with high solidification rates and enable -to cut substantially the material losses and increase the “buy-to-fly” ratio several times; -to improve machinability of Ti parts; -to provide uniformity and homogeneity of complex shape parts -to build the material properties above the level of wrought. Various examples of developed parts and processes illustrate these novel solutions.

### 10:50 AM

**Cost-Effective Production and Thermomechanical Consolidation of Titanium Alloy Powders:** *Deliang Zhang*<sup>1</sup>; Stiliana Raynova<sup>1</sup>; Vijay Nadakuduru<sup>1</sup>; Peng Cao<sup>1</sup>; Brian Gabbitas<sup>1</sup>; Barry Robinson<sup>2</sup>; <sup>1</sup>The University of Waikato; <sup>2</sup>South Auckland Forging Engineering Ltd

This talk has two parts: (i) an introduction of the TiPro process which has been recently developed at the University of Waikato for cost-effectively producing titanium alloy powders from low cost TiO<sub>2</sub> and Al powders and

# Technical Program

other reactants such as calcium granules; and (ii) an overview of major recent findings from our research on thermomechanical consolidation of titanium and Ti-6wt%Al-4wt%V alloy powders. The TiPro process includes several steps: solid-liquid separation, crushing, powder purification and by-product treatment. The thermomechanical consolidation of titanium and titanium alloy powders involves open-die forging of powder compacts, extrusion of powder compacts, and rolling of forged disks and extruded billets. In the talk, the materials science principles underlying the powder production steps and the different thermomechanical powder consolidation processes will also be discussed based on the experimental results from microstructural characterisation of samples produced under different conditions.

**11:15 AM**

**The Impact of Diffusion on Synthesis of High-Strength Titanium Alloys from Elemental Powder Blends:** *Orest Ivasishin*<sup>1</sup>; *Vadym Bondarchuk*<sup>1</sup>; *Dmytro Savvak*<sup>1</sup>; <sup>1</sup>G.V. Kurdyumov Institute for Metal Physics, NAS of Ukraine

High strength alpha plus beta and near-beta titanium alloys are being increasingly used in industry due to their excellent combination of properties. Blended elemental powder metallurgy (BEPM) allows producing the above alloys and parts from them in a cost-effective manner. However, the alloy synthesis is complicated by a big amount (up to 20 wt.%) of alloying elements which diffusional redistribution between alloying particles and titanium matrix has a strong impact on microstructure evolution. In this paper synthesis of the high-strength alloys from the powder blends based on either titanium or hydrogenated titanium was compared. It was found that hydrogen strongly affects diffusion controlled processes upon synthesis, such as chemical homogenization, densification and grain growth through its influence on phase composition and defect structure of the blends. Optimization of the processing parameters allowed to produce uniform, nearly-dense alloys with reduced grain size, which mechanical properties met the requirements of corresponding specifications.

**11:40 AM**

**In-situ Compression and Sintering of CP-Ti Powder Made by Armstrong Process:** *Wei Chen*<sup>1</sup>; *Yukinori Yamamoto*<sup>2</sup>; *William Peter*<sup>2</sup>; <sup>1</sup>Michigan State University; <sup>2</sup>Oak Ridge National Lab

This work used *in-situ* technique to investigate the pressing and sintering processes of the commercially pure (CP) Ti powder made by Armstrong process. Ti powders were uniaxially pre-pressed at designated pressures up to 100 ksi to form disk samples with different theoretical densities. Compression tests were performed in an SEM at different temperatures to obtain the mechanical properties and deformation behavior of these samples. *In-situ* sintering was also performed in an SEM to record the morphology change of the porosities on the sample surface during the sintering process. The results will provide valuable information for optimizing the manufacturing process of high-density near net shape Ti components. This research was sponsored by the U.S. Department of Energy, Oak Ridge National Laboratory, under Contract DE-AC05-00OR22725 with UT-Battelle, LLC. Additional funding and collaboration with the SHaRE User Facility at ORNL is also acknowledged.

## Electrode Technology for Aluminum Production: Non-Carbon Materials in Cathodes

*Sponsored by:* The Minerals, Metals and Materials Society, TMS Light Metals Division, TMS: Aluminum Committee  
*Program Organizers:* Ketil Rye, Alcoa Mosjøen; Morten Sorlie, Alcoa Norway; Barry Sadler, Net Carbon Consulting Pty Ltd

Tuesday AM Room: 616  
February 16, 2010 Location: Washington State Convention Center

*Session Chair:* Arne Ratvik, NTNU

### 8:30 AM Introductory Comments

**8:35 AM**

**Lower Aluminium Production Cost through Refractory Material Selection:** *Ole-Jacob Siljan*<sup>1</sup>; *Steinar Slagnes*<sup>2</sup>; *Anton Sekkingstad*<sup>2</sup>; *Egil Furu*<sup>1</sup>; *Sigurd Aaram*<sup>1</sup>; *Asbjørn Solheim*<sup>3</sup>; <sup>1</sup>Hydro Aluminium AS; <sup>2</sup>North Cape Minerals; <sup>3</sup>SINTEF

Hydro Aluminium and North Cape Minerals have jointly developed olivine-based refractories for use in the cathode lining in aluminum electrolysis cells. This type of material has turned out to be thermally stable and cost efficient, and more than 400 cells have been started with olivine-based linings since the first installation at the SU3 prebake potline at Sunndalsøra in 1999. Operational data from SU3 indicate that cells with olivine-based lining have higher current efficiency than similar cells with traditional lining. This seems to be due to a combination of factors, as analyzed in the present paper. The introduction of olivine was accompanied by conversion to a much larger brick format, resulting in shorter pot turn-around time and reduced relining costs. Based on the positive experience from the Norwegian plants, the olivine-based refractory material Alubrick 2092 will now be installed in 60% of the cells in the Qatalum smelter.

**9:00 AM**

**Chemical Degradation Map for Sodium Attack in Refractory Linings:** *Kati Tschöpe*<sup>1</sup>; *Tor Grande*<sup>1</sup>; *Jørn Rutlin*<sup>2</sup>; <sup>1</sup>NTNU; <sup>2</sup>Hydro Aluminium AS

Here we show by autopsies of spent pot linings that the degradation of refractory linings in aluminum reduction cells is governed by sodium transport into the lining. The chemical reactions caused by sodium infiltration are qualitatively explained by the construction of a chemical degradation map. The degradation map corresponds to a predominance phase diagram showing the stable compounds present as a function of SiO<sub>2</sub>/Al<sub>2</sub>O<sub>3</sub> ratio in the refractory lining and the amount of sodium infiltrated in the lining. We demonstrate that the degradation map is a useful tool for the evaluation of autopsies of spent pot linings and the prediction of the mineralogical composition of the spent pot lining.

**9:25 AM**

**Reactions in the Bottom Lining of Aluminium Reduction Cells:** *Asbjørn Solheim*<sup>1</sup>; *Christian Schøning*<sup>1</sup>; *Egil Skybakmoen*<sup>1</sup>; <sup>1</sup>SINTEF

The bottom lining in aluminium cells deteriorates due to chemical reactions with sodium vapour as well as with molten bath that penetrates the cathode carbon. The supposedly most important reactions in the system were studied, both theoretically and by experiments. The phase diagram for the system SiO<sub>2</sub>-Al<sub>2</sub>O<sub>3</sub>-Na<sub>2</sub>O was supplied with numbers for the equilibrium pressure of sodium as well as vectors showing the change in oxide composition during attack. It could be predicted that chamotte ends up as mainly nepheline. By exposing samples of firebricks to a fluoride melt at 950°C ("cup test") as well as to sodium vapour at 800°C, it was found that materials high in silica were less deteriorated than materials rich in alumina. The reason is probably that the silica-rich materials formed larger amounts of a viscous glass phase. Some observations concerning the "lens" formed in industrial cells are also reported.

**9:50 AM**

**Sidewall Materials for the Hall-Heroult Process:** *Reiza Mukhlis*<sup>1</sup>; *Muhammad Rhamdhani*<sup>1</sup>; *Geoffrey Brooks*<sup>1</sup>; <sup>1</sup>Swinburne University of Technology

The performance of current sidewall materials (such as carbon and silicon carbide-based materials) in an aluminum smelter in the Hall-Heroult process rely on the existence of a frozen electrolyte layer on the sidewall, which contributes to the high energy requirement of the process. If the overall heat required to be



dissipated with the process were lowered through improvements in anode and cathode design, it maybe possible to decrease the heat flux through the sidewalls and move to a low heat loss operating regime. This study will consider new sidewall materials that can resist the corrosive, reductive and oxidative nature of molten cryolite, molten aluminum and air, respectively, that would need to be developed in order to avoid the necessity of the frozen layer formation. This paper will review previously proposed and current sidewall materials, and details materials selection, design and process criteria for identifying viable alternative solutions to the problem.

### 10:15 AM Break

### 10:30 AM

#### Excellent Cryolite Resistance and High Thermal Conductivity SiC Sidewall Material for High-Amperage Aluminium Reduction Cells: *Zhigang Huang*<sup>1</sup>; <sup>1</sup>LIRR

With the development of the aluminium reduction cell towards high current and large-scale, the performance of the sidewall materials are expected to be even better. To meet the requirements of this technical trend, new sidewall material which contains SiC up to 95% has been developed. After testing cryolite corrosion resistance which was conducted by simulating the erosion environment of the aluminium reduction cell, the new material presents much better cryolite corrosion resistance nearly twofold of the traditional Si<sub>3</sub>N<sub>4</sub>-SiC material. In addition, the thermal conductivity of the new developed sidewall material is about 30% higher than that of traditional Si<sub>3</sub>N<sub>4</sub>-SiC material. High thermal conductivity is favorable to quick formation of the frozen ledge and can therefore improve the service life of the cells. The other properties are equivalent to those of Si<sub>3</sub>N<sub>4</sub>-SiC material. Therefore, the new developed material has been considered as a promising sidewall material for large-scale Aluminium reduction cell.

### 10:55 AM

#### Structure Design and Deformation Measurements of C/TiB<sub>2</sub> Function Gradient Materials for Aluminum Reduction Cathode: *Jilai Xue*<sup>1</sup>; *Baisong Li*<sup>1</sup>; *Jun Zhu*<sup>1</sup>; <sup>1</sup>University of Science and Technology Beijing

Carbon/TiB<sub>2</sub> Function Gradient Materials (FGM) were tested for use as aluminum reduction cathode materials, where a 10mm thick TiB<sub>2</sub>-rich layer was on the top as an Al-wettable surface, the C-TiB<sub>2</sub> layers in the middle as a transition interface and the carbon on the bottom as a base. ANSYS simulations suggest that the C/TiB<sub>2</sub> FGM cathode with the layers number n = 3 and the gradient coefficient = 0.6 can offer lower thermal strain and sodium expansion. Cathode deformations (creep and sodium expansion), were measured in a modified Rapoport apparatus. During aluminum electrolysis, the 3-layer FGM samples showed lower sodium expansion than the 2-layer one, while the later exhibited smaller creep deformation than the former. Both the creep and sodium expansion varied with changing in operating temperature, melt composition and current density. The obtained data can be used for cathode design and cell construction using the C/TiB<sub>2</sub> FGM cathode materials.

### 11:20 AM

#### Electrolysis Expansion Performance of TiB<sub>2</sub>-C Composite Cathode in [K<sub>3</sub>AIF<sub>6</sub>/Na<sub>3</sub>AIF<sub>6</sub>]-AlF<sub>3</sub>-Al<sub>2</sub>O<sub>3</sub> Melts: *Fang Zhao*<sup>1</sup>; *Lu Xiao-jun*<sup>1</sup>; *Li Jie*<sup>1</sup>; *Lai Yan-qing*<sup>1</sup>; *Tian Zhong-liang*<sup>1</sup>; <sup>1</sup>School of Metallurgical Science and Engineering, Central South University

Electrolysis expansion of pitch, furan, phenolic aldehyde and epoxy based TiB<sub>2</sub>-C composite cathodes in [K<sub>3</sub>AIF<sub>6</sub>/Na<sub>3</sub>AIF<sub>6</sub>]-AlF<sub>3</sub>-Al<sub>2</sub>O<sub>3</sub> melts were tested, and the morphology and element distribution of cut sections of specimens after electrolysis were studied. The results show that pitch based TiB<sub>2</sub>-C composite cathode has the maximal electrolysis expansion, while epoxy based TiB<sub>2</sub>-C composite cathode has the minimal electrolysis expansion. Moreover, each binder has the optimum addition, corresponding to its own minimum electrolysis expansion. The optimum addition of pitch, furan, phenolic aldehyde and epoxy are 16%, 18%, 14% and 12% respectively. At this circumstance, electrolysis expansion of TiB<sub>2</sub>-C composite cathodes are 1.49%, 1.26%, 1.18% and 0.92% severally. SEM and EDS analysis suggest that no matter what kind of binder used, TiB<sub>2</sub>-C composite cathodes have good wettability by molten aluminum. K and Na penetrate into cathodes from exterior to interior gradually, and K has stronger penetrating ability than Na.

### Failure of Small-Scale Structures: Deformation Events in Pillars, Films and Other Structures

*Sponsored by:* The Minerals, Metals and Materials Society, TMS Materials Processing and Manufacturing Division, TMS Structural Materials Division, TMS/ASM: Mechanical Behavior of Materials Committee, TMS: Nanomechanical Materials Behavior Committee  
*Program Organizers:* Marian Kennedy, Clemson University; Brad Boyce, Sandia National Laboratory; Reinhold Dauskardt, Stanford; Zhiwei Shan, Hysitron Inc

Tuesday AM Room: 206  
February 16, 2010 Location: Washington State Convention Center

*Session Chair:* Zhiwei Shan, Hysitron Inc.

### 8:30 AM Invited

#### Prestraining and Annealing of Gold Micropillars: Strengthening and Weakening Turned Upside Down: *William Nix*<sup>1</sup>; *Seok-Woo Lee*<sup>1</sup>; <sup>1</sup>Stanford University

When soft metals are plastically deformed, they get stronger, mainly because the dislocation density increases dramatically. Correspondingly, annealing of strain-hardened metals commonly leads to softening because the annealing causes the dislocation density to decrease. Recent experiments with gold micropillars have shown that metals behave very differently at the sub-micrometer scale. At that scale plastic deformation leads to softening and annealing leads to hardening, just the opposite of what occurs in bulk metals. These results suggest that plasticity at the sub-micrometer and nanometer scale is controlled not by the elastic interactions of dislocations, as in bulk metals, but by the operation of dislocation sources. The evidence for source-controlled plasticity is reviewed and a model to describe the corresponding size effects and the unusual effects of prestraining/annealing is described. The model is inspired by Johnston and Gilman's dislocation dynamics approach to plasticity and celebrates the 50th anniversary of that classic work.

### 8:55 AM Invited

#### In-situ Micromechanical Testing: *Johann Michler*<sup>1</sup>; <sup>1</sup>EMPA, Swiss Federal Laboratories for Materials Testing and Research

The presentation will first review in-situ SEM micromechanical testing techniques (micro-compression, nanoindenter, atomic force microscope, nano-tensile MEMS device). In the second part different case studies will be presented: 1) The compressive fracture strength of micron-sized Si and GaAs pillars increases with decreasing pillar diameter, but submicrometer pillars were found to deform plastically in uni-axial compression. TEM observations suggest that single partial dislocations are the carriers of plasticity in GaAs and that the critical size for ductile - brittle transition can be predicted from the fracture mechanics of pillar splitting. 2) The yield strength of rectangular micro-pillars of monocrystalline tungsten is shown to scale with the smallest dimension of the structure, whereas micro-pillars of amorphous metals exhibit the macroscopic yield strength down to diameters of 300nm. 3) The strength of both monocrystalline silicon and Rhenium nanowires is found to be close to the theoretical strength, in contrast to nanocrystalline nanowires.

### 9:20 AM

#### Investigation of the Deformation Mechanism of Gum Metal by In Situ TEM Nanocompression Testing: *Elizabeth Withey*<sup>1</sup>; *Andrew Minor*<sup>1</sup>; *Shigeru Kuramoto*<sup>2</sup>; *Daryl Chrzan*<sup>1</sup>; *John Morris*<sup>1</sup>; <sup>1</sup>University of California, Berkeley; <sup>2</sup>Toyota Central R&D Laboratories, Inc.

Gum Metal is a set of β-Ti alloys, which appear to deform near ideal strength. Recent work has suggested that Gum Metal deforms by a stress-induced martensitic transformation to the orthorhombic α' phase. In order to better investigate the roll of this martensitic deformation in the overall deformation behavior of Gum Metal, nanopillars of solution-treated and cold-worked Gum Metal were compressed in situ in a quantitative compression stage in a transmission electron microscope. By performing these tests in diffraction mode it is possible to follow the evolution of the crystal structure as deformation occurs and correlate it to a quantitative load-displacement curve. Results from these tests showed that the martensitic phase transformation sometimes occurred, but did not appear to be a significant cause of deformation.

Tue. AM

# Technical Program

## 9:35 AM Invited

**A Combined Experimental and Simulation Study to Examine Lateral Constraint Effects in Ni Superalloy Microcrystals:** Paul Shade<sup>1</sup>; Robert Wheeler<sup>2</sup>; Yoon-Suk Choi<sup>2</sup>; *Michael Uchic*<sup>3</sup>; Dennis Dimiduk<sup>3</sup>; Hamish Fraser<sup>4</sup>; <sup>1</sup>Universal Technology Corporation; <sup>2</sup>UES, Inc.; <sup>3</sup>Air Force Research Laboratory; <sup>4</sup>The Ohio State University

We have used a custom in-situ SEM mechanical testing system to study the deformation behavior of single-slip oriented Rene N5 microcrystals. Two different types of platens were used to explore the effect of lateral stiffness on the resultant mechanical response in both tension and compression, which approximated either a rigid or extremely compliant lateral constraint. The change in the lateral constraint of the test system had a demonstrable effect on many aspects or attributes of plastic flow: the yield stress and strain-hardening behavior, the intermittency of strain bursts, the spatial distribution of slip bands, and the development of internal crystal rotations. Finite element modeling of the experiments using an anisotropic crystal plasticity framework provided insight regarding changes in the internal stress field and resultant activity of slip systems. The experimental findings are rationalized based on these simulation results.

## 10:00 AM Break

## 10:15 AM Invited

**Interface Fracture and Fatigue of Thin Metallic Films on Substrates:** *Gerhard Dehm*<sup>1</sup>; Megan Cordill<sup>1</sup>; Walther Heinz<sup>2</sup>; Kurt Matoy<sup>3</sup>; F. Dieter Fischer<sup>4</sup>; <sup>1</sup>University of Leoben, Materials Physics; <sup>2</sup>Austrian Academy of Sciences, Erich Schmid Institute of Materials Science; <sup>3</sup>Kompetenzzentrum Automobil- und Industrie-Elektronik GmbH; <sup>4</sup>University of Leoben, Institute for Mechanics

In this overview two methods to obtain the interfacial energy release rates are discussed and an outlook on thermo-mechanical fatigue of metallic films on substrate is provided: (I) In order to study the critical energy release rate for crack initiation at silicon oxide/metal interfaces, miniaturized fracture mechanic specimens are employed. Bi-material cantilevers were fabricated by FIB milling which enables high spatial resolution mechanical characterization of buried interfaces. (II) For metallic films on polymers the energy release rate is estimated from a post-buckling analysis which considers the strain energy of the buckled configuration and the energy necessary for delamination. Based on a thermodynamical model the driving force for delamination is evaluated, which allows to calculate the delamination energy release rate. (III) Finally, the influence of film microstructure for thermal fatigue damage is elaborated by comparing epitaxial and polycrystalline Al films which were cycled up to 10.000 times between 373 and 723K.

## 10:40 AM

**Buckle Driven Delamination in Thin Gold Film-Compliant Substrate Systems:** *Neville Moody*<sup>1</sup>; John Yeager<sup>2</sup>; E. David Reedy<sup>1</sup>; Edmundo Corona<sup>1</sup>; Marian Kennedy<sup>3</sup>; Megan Cordill<sup>4</sup>; David Adams<sup>1</sup>; David Bahr<sup>2</sup>; <sup>1</sup>Sandia National Laboratories; <sup>2</sup>Washington State University; <sup>3</sup>Clemson University; <sup>4</sup>Erich Schmid Institute

Film durability is a primary factor governing the use of emerging thin film flexible substrate devices where compressive stresses can lead to delamination and buckling. It is of particular concern in gold film systems found in many submicron and nanoscale applications. We are therefore studying these effects in gold on PMMA systems using compressively stressed tungsten overlayers to force interfacial failure and simulations employing cohesive zone elements to model the fracture process. Delamination and buckling occurred spontaneously following deposition with buckle morphologies that differed significantly from existing model predictions. Moreover, use of thin adhesive interlayers had no discernable effect on performance. In this presentation we will use the observations and simulations to show how substrate compliance and yielding affects the susceptibility to buckling of gold films on compliant substrates. This work was supported by Sandia National Laboratories under USDOE Contract DE-AC04 94AL85000.

## 10:55 AM

**Strain Rate Sensitivity Effects on the Failure of Metal Films on Compliant Substrates:** *Megan Cordill*<sup>1</sup>; *Gerhard Dehm*<sup>1</sup>; <sup>1</sup>University of Leoben

Polymer substrates are used in a variety of new technically advanced flexible electronics and sensors where the devices flex and stretch. Mechanical properties and interfacial phenomena of thin films on compliant substrates

are important to understand in order to design reliable flexible electronic devices. These responses are commonly measured with little discussion of the viscoelastic behavior and strain rate sensitivity of the polymer substrate. Using an in-situ tensile device inside a SEM the effects of strain rate on the mechanical and interfacial properties are determined. Thin films of Cr on PET and Cr on PI systems will be examined for their use as adhesion layers. The strain of initial failure and subsequent delamination are retarded when slow rates are used, thus increasing the lifetime of the components. Other factors of the polymer substrate, such as crystallite orientation effects of the PET, will also be discussed.

## 11:10 AM

**Fracture Properties of Fuel Cell Membranes:** *Ruiliang Jia*<sup>1</sup>; Kemal Levi<sup>1</sup>; Takuya Hasegawa<sup>2</sup>; Jiping Ye<sup>3</sup>; Reinhold Dauskardt<sup>1</sup>; <sup>1</sup>Stanford University; <sup>2</sup>Nissan Motor Co., Ltd; <sup>3</sup>Nissan ARC LTD.

Perfluorosulfonic acid (PFSA) polymer membranes are widely used as the electrolyte thin films to transport protons in fuel cells. These thin membranes (thickness ~ 100 μm) represent critical small-scale components in PEM fuel cells. The fracture of the membrane including pinhole formation and micro crack propagation, is a common failure mode that limits the operational life of the cells. In the present work, we adapt thin film testing methods to assess the fracture properties of PFSA membranes under mixed-mode loading conditions in simulated fuel cell operational environments. Moreover, the microstructure of PFSA polymers is studied, which provides us with the knowledge to examine the different mechanical and fracture behaviors of Nafion and its nanocomposite membranes. This study not only reveals some significant factors that influence the fracture properties of current Nafion membranes, but also investigates the methods to improve their thermo-mechanical reliability in fuel cells.

## 11:25 AM

**Exploiting Delamination to Fabricate Microcontact-Printed MEMS:** *Corinne Packard*<sup>1</sup>; Vladimir Bulovic<sup>1</sup>; <sup>1</sup>Massachusetts Institute of Technology

In standard silicon-based MEMS, delamination due to residual stresses from high temperature processing and stiction from surface tension of drying solvents are two common failure mechanisms limiting yield and reliability. We have developed a method for fabricating MEMS which avoids these limitations in a room-temperature, solvent-free process that relies on intentional, controlled delamination of thin films in a microcontact printing-based process. Release of metal membranes from a carrier substrate is assisted by a nanoscale molecular organic adhesion-reduction layer, allowing suspension of crack-free films over pre-patterned supports on a target substrate. This process is additionally capable of conformal coating of curved or flexible surfaces as well as large areas, since it is not limited by wafer-scale photolithography. Contrary to silicon-based MEMS fabrication practices where poor interfacial adhesion and thin film delamination are avoided, we demonstrate that these features can instead be exploited to fabricate functional MEMS sensors and actuators.

## Global Innovations in Manufacturing of Aerospace Materials: The 11th MPMD Global Innovations Symposium: Innovations in Additive Manufacturing

*Sponsored by:* The Minerals, Metals and Materials Society, TMS Materials Processing and Manufacturing Division, TMS Structural Materials Division, TMS: Shaping and Forming Committee, TMS: High Temperature Alloys Committee

*Program Organizers:* Deborah Whitis, General Electric Company; Thomas Bieler, Michigan State University; Michael Miles, BYU

Tuesday AM  
February 16, 2010  
Center

Room: 306  
Location: Washington State Convention Center

*Session Chairs:* Michael Peretti, GE Aviation; Patrick Martin, AFRL-RX

## 8:30 AM Invited

**Additive Manufacturing's Role in Fabrication and Repair of Aerospace Components:** *James Sears*<sup>1</sup>; <sup>1</sup>South Dakota School of Mines and Technology  
Additive Manufacturing (AM) for component repair and manufacturing offers some unique solutions for Aerospace applications. Additive Manufacturing comprises technologies that add material to existing structures for function



or performance enhancement. AM is a CAD/CAM solid freeform fabrication technology that uses metal powder and fusion for repairing or manufacturing of components. Fusion can be invoked through laser, electron beam, plasma, or ultrasonic energy sources. Inherent to AM is the ability to add material for repair or manufacture of critical GTE components with minimal heat affect to the under lying material. Also, due to the nature of AM, hard coatings can be achieved without heat treatment allowing for repair of heat-treated steels. In some cases AM repair can be used to replace hard chrome or carburized surfaces. An overview of AM developments over the years will be provided along with details of repair and manufacturing several Aerospace components.

### 9:00 AM

**Advanced Gas Atomization Processing for Ti and Ti Alloy Powder Manufacturing:** *Iver Anderson*<sup>1</sup>; James Sears<sup>2</sup>; David Byrd<sup>3</sup>; Joel Rieken<sup>4</sup>; Andrew Heidloff<sup>5</sup>; Mike Glynn<sup>6</sup>; Mark Ward<sup>7</sup>; <sup>1</sup>Ames Laboratory; <sup>2</sup>South Dakota School of Mines and Technology; <sup>3</sup>n/a; <sup>4</sup>Iowa State University

The feasibility of a precision ceramic pouring tube has been demonstrated for efficient production of large quantities of fine spherical powders of pure Ti and Ti alloys by an advanced gas atomization method during initial trials of Ti alloy pouring and free-fall gas atomization. The experiments at University of Birmingham utilized a novel ceramic/metal composite tundish/pour tube and existing bottom pouring cold wall crucible induction melting capability, with pouring stream temperatures measured by a 2-color pyrometer. Minimal reaction/dissolution of both pour tubes was verified by microscopic and micro-analytical examination. The trials produced a chill cast ingot and spherical powder of Ti-6Al-4V (wt.%) and the composition and microstructure of both also were analyzed. Progress on close-coupled gas atomization studies at Iowa State University also will be reported. Work supported by Iowa State University Research Foundation and the Grow Iowa Values Fund and performed at Ames Lab under contract no. DE-AC02-07CH11358.

### 9:20 AM

**Cold Spray Characteristics of Ti-6Al-4V Coating:** *Ahmad Rezaeian*<sup>1</sup>; Eric Irissou<sup>2</sup>; Steve Yue<sup>1</sup>; <sup>1</sup>McGill University; <sup>2</sup>National Research Council Canada (NRC)

Cold spray process is a novel technique used to consolidate particles in order to manufacture complex parts or additive features with minimal waste. The advantages of this technology as compared with conventional thermal spraying techniques have been motivation for the recent investigations. Despite FCC structured materials such as Ni and Cu, aerospace materials such as Titanium alloys exhibited limited deformation upon impact which is key parameter to obtain dense coatings. In this work, Ti-6Al-4V powder was cold sprayed on steel and Ti-6Al-4V substrates using CGT 4000 gun. Gas temperature, pressure and stand-off distance were calibrated to achieve the maximum particle velocity. The gun traverses speed as well substrate thickness /material were varied in order to evaluate the effect of heat introduced during spray on the powder deformability and therefore the coating properties. Deposition efficiency, fracture features and microstructural changes were investigated by optical microscopy, XRD, SEM, and microhardness.

### 9:40 AM

**Additive Manufacturing of Gamma Titanium Aluminide Parts by Electron Beam Melting:** *Silvia Sabbadini*<sup>1</sup>; Oriana Tassa<sup>2</sup>; Paolo Gennaro<sup>3</sup>; *Ulf Ackelid*<sup>4</sup>; <sup>1</sup>Avio SpA; <sup>2</sup>Centro Sviluppo Materiali S.p.A; <sup>3</sup>ProtoCast S.r.l.; <sup>4</sup>Arcam AB

In recent years, Electron Beam Melting (EBM) has matured as a technology for additive manufacturing of dense metal parts. The parts are built by additive consolidation of thin layers of metal powder using an electron beam. With EBM, it is possible to create parts with geometries too complex to be fabricated by other methods, e.g. fine network structures and internal cavities. The process is run in vacuum, which makes it well suited for materials with a high affinity to oxygen, e.g. titanium compounds. We present material data from a recently developed EBM process for gamma titanium aluminide, Ti-48Al-2Cr-2Nb, including a microstructure investigation and a high temperature study of tensile and creep properties.

### 10:00 AM Break

### 10:20 AM

**Properties of Ti-5Al-5Mo-5V-3Cr Samples Produced via Powder Hot-Isostatic-Pressing:** *Nick Wain*<sup>1</sup>; Xinjiang Hao<sup>1</sup>; Ravi Swamy<sup>1</sup>; Xinhua Wu<sup>1</sup>; <sup>1</sup>The University of Birmingham

Hot-isostatic-pressing ("HIPping") of powder is an effective manufacturing technique: it allows the production of complex parts to very near net-shape and is therefore highly material-efficient. In this work, Ti-5Al-5Mo-5V-3Cr ("Ti-5553"), a high-strength metastable beta Ti alloy, was HIPped from powder to produce monolithic parts. The effects of powder production route, alloy composition and HIPping conditions on the microstructure and properties of the HIPped Ti-5553 were assessed. The difference between gas atomised powders and PREPed (plasma-rotating-electrode processed) powders has been studied, together with the influence of minor carbon addition on HIPped microstructure. Mechanical testing showed the effect of these different microstructures on tensile strength, fatigue and fracture toughness. Mechanical properties were often found to be comparable to those of Ti-5553 alloy produced from ingot. The significance of the results on the viability of HIPped beta Ti alloys is discussed.

### 10:40 AM

**The Influence of Thermal History on the Microstructure of Laser-Additive-Manufactured Ti-6Al-4V Samples:** *Xinhua Wu*<sup>1</sup>; Laura Qian<sup>1</sup>; Junfa Mei<sup>1</sup>; <sup>1</sup>The University of Birmingham

The microstructure and mechanical property of laser-additive manufactured Ti64 have been assessed. A 3D-transient finite element model has been developed for predicting the temperature history of laser-fabricated Ti6Al4V thin wall samples. The model has been validated by direct measurements of thermal history throughout the height of fabricated samples. The effects of location, laser scanning speed and laser power on the thermal profile have been modelled and compared with temperatures measured. The microstructures in direct laser fabricated Ti-6Al-4V under most conditions are dominated by columnar grains which contain martensites and this is consistent with those expected on the basis of the measured and predicted thermal histories of the different samples and for the different regions within samples.

### 11:00 AM

**Fabrication and Characterization of Reticulated, Porous Mesh Arrays and Foams for Aerospace Applications by Additive Manufacturing Using Electron Beam Melting:** *Sara Gaytan*<sup>1</sup>; L.E. Murr<sup>1</sup>; F. Medina<sup>1</sup>; E. Martinez<sup>1</sup>; L. Martinez<sup>1</sup>; R.B. Wicker<sup>1</sup>; <sup>1</sup>UTEP

Various non-isotropic arrays of reticulated mesh geometries and isotropic foam structures of Ti-6Al-4V have been fabricated by additive manufacturing (AM) using electron beam melting (EBM). These arrays consist of complex, monolithic prototypes which include various mesh geometries and foam structures with a range of densities, including fully dense geometries. Density and stiffness variations have been fabricated for aeronautics/aerospace applications and these complex arrays provide unique energy or impact absorption features, thermal management, stiffness and strength in sandwich cores, and excellent corrosion resistance. These monolithic mesh arrays have been fabricated using geometrical unit cells whose bases and size variations can allow density, porosity, stiffness, and strength tailoring to fabricate multifunctional materials prototypes while foam components have been fabricated from CAD models based on CT-scans of common aluminum alloy foams. The microstructures of these prototypes have been characterized by optical and electron microscopy.

### 11:20 AM

**Properties and Microstructure of Net Shape HIPped Ti6Al4V Components:** *Kun Zhang*<sup>1</sup>; Junfa Mei<sup>1</sup>; *Xinhua Wu*<sup>1</sup>; <sup>1</sup>The University of Birmingham

The microstructures and mechanical properties of HIPped (Hot Isostatically Pressed) Ti6Al4V have been assessed on samples which have been manufactured from PREP powder. In preliminary experiments the HIPping conditions have been varied in order to identify the optimum HIPping parameters and a detailed study has been made on optimally HIPped samples. Test samples have been manufactured where the as-HIPped surface is retained and others where the as-HIPped surface has been removed by machining or electropolishing before testing. It has been shown that HIPped samples, manufactured using conventional HIPping, have rough surfaces on the scale of the powder diameter which leads to poor fatigue properties. A new HIPping procedure has been developed in which this surface roughness is eliminated and the fatigue properties correspondingly

# Technical Program

improved. Details of the microstructure of the HIPped PREP powder will be presented and correlated with the tensile, fatigue and fracture toughness.

**11:40 AM**

**Influence of Powder Particle Size on the Microstructure and Properties of HIPped Ti Alloy Powders:** *Kun Zhang*<sup>1</sup>; Junfa Mei<sup>1</sup>; Xinhua Wu<sup>1</sup>; <sup>1</sup>The University of Birmingham

Two alloy powders (Ti-6Al-4V and Ti-25V-15Cr-2Al-0.2C (wt%)) have been Hot Isostatically Pressed (HIPped) and the influence of particle size on the microstructure and mechanical properties assessed. The individual powders have very different microstructures with the Ti6Al4V being martensitic and the Ti-25V-15Cr-2Al-0.2C being retained beta and hence the response of these two different microstructures to HIPping is very different. The size range of the supplied powders was from 50–400 μm. Powders were sieved to produce batches with sizes of 50–150 μm, 250–400 μm and 50–400 μm and these together with a batch using the whole size range were HIPped for both alloys. The properties of samples HIPped using the whole size range (50–400 μm) powder were superior to those made using individual size fractions. For both alloys the smallest particle size fraction had lower ductility and smoother fracture surfaces than the large particle size. These observations are discussed in terms of the microstructures developed during HIPping and of the factors which influence the properties of HIPped powders.

## Heterogeneous Nucleation and Initial Microstructure Evolution in Alloys and Colloids: Experiment I

*Sponsored by:* The Minerals, Metals and Materials Society, TMS Electronic, Magnetic, and Photonic Materials Division, TMS Materials Processing and Manufacturing Division, TMS Structural Materials Division, TMS: Alloy Phases Committee, TMS/ASM: Phase Transformations Committee

*Program Organizers:* Rainer Schmid-Fetzer, Clausthal University of Technology; Heike Emmerich, RWTH Aachen University; Frans Spaepen, Harvard University; Martin Glicksman, University of Florida; John Perepezko, University of Wisconsin, Madison

Tuesday AM Room: 614  
February 16, 2010 Location: Washington State Convention Center

*Session Chairs:* David StJohn, University of Queensland; Heike Emmerich, RWTH Aachen

**8:30 AM Invited**

**Heterogeneous Nucleation in Peritectic Systems:** *Rohit Trivedi*<sup>1</sup>; Jongho Shin<sup>1</sup>; John Perepezko<sup>2</sup>; <sup>1</sup>Iowa State University; <sup>2</sup>University of Wisconsin-Madison

Heterogeneous nucleation is investigated through directional solidification experiments in the Sn-Cd peritectic system in which nucleation plays a key role in the formation of repeated bands of primary and peritectic phases. Nucleation undercooling for each phase is determined through the measurements of temperature and composition at the location where each band nucleates. Nucleation is found to occur at the ampoule wall-liquid-solid triple junction, and nucleation undercooling for each phase is found to be very small, from a fraction of a degree to about one degree. Relevant contact angles have been measured and it is shown that experimental nucleation undercooling values for the two phases are orders of magnitude smaller than those predicted by the classical nucleation theory. A mechanism of heterogeneous nucleation is proposed to explain the experimental results.

**8:55 AM**

**Heterogeneous Nucleation in Charged Colloidal Model Systems Induced by Seeds of Various Shape and Structure:** *Hans Joachim Schöpe*<sup>1</sup>; Patrick Wette<sup>2</sup>; Andreas Engelbrecht<sup>1</sup>; Markus Franke<sup>1</sup>; <sup>1</sup>University of Mainz; <sup>2</sup>Deutsches Zentrum für Luft- und Raumfahrt

Understanding the process that drives an undercooled fluid to the crystal state is still a challenging issue for condensed matter physics and plays a key role designing new materials. Crystallization undergoes crystal nucleation, growth and ripening. The crystallization kinetics and the resulting polycrystalline morphology are given by a complex interplay of these mechanisms. A great deal of progress has been made in recent years using colloidal suspensions as

model system studying crystallization. Close analogies to atomic systems are observed which can be exploited to address questions not accessible in atomic solidification. We here present systematic measurements of the crystallization kinetics of a charged colloidal model system adding small amounts of seeds using time resolved scattering techniques. We report how the seeds size, structure and concentration affect crystal nucleation and growth as function of meta stability giving the possibility to control the crystallization process and the resulting microstructure of the polycrystal.

**9:15 AM**

**Colloids as Model Systems for Undercooled Metallic Melts:** *Ina Klassen*<sup>1</sup>; Patrick Wette<sup>1</sup>; Dirk Holland-Moritz<sup>1</sup>; Thomas Palberg<sup>2</sup>; Dieter M. Herlach<sup>1</sup>; <sup>1</sup>German Aerospace Center; <sup>2</sup>Johannes Gutenberg Universität Mainz

We present investigations of short-range order (SRO) of charged colloidal suspension by applying Ultra-Small-Angle X-ray Scattering using synchrotron radiation at DESY Hamburg. The colloidal system is shear melted, subsequently, it is in a liquid state far from equilibrium. The development of the structure factor is measured as a function of time after shear melting. The deviation from equilibrium is determined by the difference of the chemical potential between solid and liquid state. The structure factors as measured are analysed within a cluster model. The results reveal the preference of icosahedral SRO in the metastable liquid colloidal system. With decreasing deviation from equilibrium the icosahedral SRO is reduced and eventually vanishes at equilibrium. The SRO of the stable liquid state is determined to be fcc like. The results obtained from the colloidal suspensions are compared with previous investigations of SRO in undercooled melts of pure metals studied by elastic neutron diffraction.

**9:35 AM**

**Competition between Heterogeneous and Homogeneous Nucleation near a Flat Wall:** Patrick Wette<sup>1</sup>; Hans-Joachim Schöpe<sup>2</sup>; Ina Klassen<sup>1</sup>; *Dieter Herlach*<sup>1</sup>; <sup>1</sup>German Aerospace Center; <sup>2</sup>Johannes Gutenberg Universität Mainz

The competition between heterogeneous and homogeneous nucleation of a charged colloidal suspension is studied close to container walls. Colloidal crystals were shear melted and a metastable melt left to solidify afterwards. The crystallization kinetics was monitored using time resolved Ultra Small Angle X-ray Scattering (USAXS) at different degrees of metastability. Whereas at high metastability the homogeneous nucleation dominates the solidification scenario leading to a small amount of oriented wall based crystals. At lower metastability the homogeneous nucleated crystals do crystallize first while the crystallization of the wall crystal is delayed. When the amount of solid crystallized near the wall shows its fastest increase the amount of polycrystalline crystal decreases indicating that the randomly oriented polycrystal is converted into a wall crystal finally resulting in a large amount of oriented wall based material. Our experiments demonstrate the complexity of the crystallization process of colloidal suspension close to container walls.

**9:55 AM**

**Preliminary Investigation of the Nucleation of Si in Entrained Droplets in High Purity Al Alloys:** Muhammad Zarif<sup>1</sup>; Brian McKay<sup>1</sup>; *Peter Schumacher*<sup>1</sup>; <sup>1</sup>University of Leoben

An Al-5wt%Si master-alloy was produced using super purity Al 99.99 wt% and Si 99.999 wt% materials in an arc melter under a 200 mbar reduced Ar atmosphere. Using a melt-spinner the master alloy was melt-spun by ejecting the melt with an ejection pressure of 100 mbar, at a temperature of 750 °C onto a Cu wheel, rotating at a circumferential wheel speed of 15 ms<sup>-1</sup>. This resulted in the production of a ribbon ~3 mm in width and ~80 μm thick. Using optical microscopy entrained droplets of Al-Si eutectic within Al grains and at Al grain boundaries were observed. Differential scanning calorimetry and transmission electron microscopy techniques were subsequently employed to investigate the effect of Sr additions on eutectic undercoolings and to examine nucleation phenomenon, respectively.

**10:15 AM Break**

**10:35 AM Invited**

**Study of Heterogeneous Nucleation in High Purity Al-Si Alloys with Sr Addition:** *Peter Schumacher*<sup>1</sup>; <sup>1</sup>University of Leoben

Metallic glasses give a unique opportunity to study nucleation as the glass forming ability of the alloys slows nucleation kinetics sufficiently down to observe individual nucleation events. These may occur above the glass transition temperature and are subsequently quenched in or alternatively



nucleation is triggered below the glass transition by e.g. annealing. In particular the deliberate addition of particles into glasses permit to study their effect on heterogeneous nucleation of crystals. Extensive studies of particles used in grain refining of Al alloys such as Al<sub>3</sub>Ti and TiB<sub>2</sub> have been investigated in Al based glasses. Thereby, it was possible to distinguish between nucleation events occurring in both metallic glasses and conventional Al- alloys and growth effects dominating grain refinement in conventional alloys. This paper gives an overview on nucleation phenomena observed on added heterogeneous nucleation sites in Al based metallic glasses and their relevance to industrial casting practice.

### 11:00 AM

**Embryonic Crystallization in Al-Based Marginal Glass Forming Alloys:** *Eren Kalay*<sup>1</sup>; Matthew Kramer<sup>2</sup>; Scott Chumbley<sup>1</sup>; Iver Anderson<sup>1</sup>; Ralph Napolitano<sup>1</sup>; <sup>1</sup>Ames Laboratory

The Al-rich Al-RE and Al-TM-RE (TM: transition metals; RE: rare earth elements) marginal glass-forming alloys have attracted much attention due to unique devitrification products with a very high number density of nuclei on order of 10<sup>20</sup> to 10<sup>24</sup>m<sup>-3</sup>. A mechanism to explain such high nanocrystal densities has not been identified to date. In this study Al-Sm and Al-Tb systems were chosen to investigate this unusual nucleation phenomenon in marginal glass forming alloys. Both liquid and as-quenched structures were analyzed using a combined study of high energy X-ray diffraction (HEXRD), 3-D atom probe tomography and transmission electron microscopy (TEM). The transformation kinetics and microstructural evolution during initial crystallization was investigated using differential scanning calorimetry, and TEM. A new nucleation model based on the existence of the RE-rich clusters in the as-quenched state promoting high nucleation density of fcc-Al nanocrystals will be discussed. Research supported by U.S. DOE-OS, Ames Laboratory contract No.DE-AC02-07CH11358.

### 11:20 AM

**Intrinsic Heterogeneous Nucleation in Eutectic Systems:** *Joachim Bokeloh*<sup>1</sup>; Gerhard Wilde<sup>1</sup>; <sup>1</sup>Universität Münster

Experimental studies on nucleation kinetics in metallic systems are often impaired by the unknown identity of the nucleant phase and by the convoluting contributions of different nucleation mechanisms that might be active simultaneously in droplet ensembles. With respect to these issues, the solidification pathway of near-eutectic alloys offers the opportunity to study the kinetics of heterogeneous nucleation on intrinsic nucleant phases. If the melt is cooled below its liquidus, the first crystalline phase can form. Upon cooling the specimen below the solidus line, this first crystalline phase can then serve as pre-defined heterogeneous nucleant for the nucleation of the second crystalline phase. Moreover, analyzing repeated freezing cycles on single droplets prevents the convoluting contributions from different mechanisms in droplet populations. A statistically relevant data set for this reaction in the Ag-Cu system obtained by repeated differential thermal analysis cycles is presented and the kinetics of the nucleation reaction is evaluated.

## Hume-Rothery Symposium: Configurational Thermodynamics of Materials: Session III

*Sponsored by:* The Minerals, Metals and Materials Society, TMS Electronic, Magnetic, and Photonic Materials Division, TMS Structural Materials Division, TMS: Alloy Phases Committee, TMS: Chemistry and Physics of Materials Committee

*Program Organizers:* Chris Wolverton, Northwestern University; Mark Asta, University of California, Davis; Gerbrand Ceder, Massachusetts Institute of Technology (MIT)

Tuesday AM Room: 212  
February 16, 2010 Location: Washington State Convention Center

*Session Chair:* To Be Announced

### 8:30 AM Invited

**Ab Initio Modeling of the Lattice Stability of W in the Presence of Interstitials:** *Marcel Sluiter*<sup>1</sup>; <sup>1</sup>TU Delft

In recent years the ab initio study of alloy phase stability, as pioneered by Prof. de Fontaine, has found wide application. Especially in the area of phase

diagram modeling ab initio studies have rapidly advanced. Here we examine the W-rich side of the W-O phase diagram. It has long been known that oxygen can stabilize the so-called beta-W structure, now better known as the Cr<sub>3</sub>Si prototype. So far it has remained unclear how oxygen affects the lattice stability of W. Here ab initio methods are used to examine the various ways in which oxygen can, or cannot be, present in W. A model for O in W is proposed which explains several phenomena observed in W thin films.

### 9:00 AM Invited

**Alloy Thermodynamics without Lattice Stability?:** *Axel van de Walle*<sup>1</sup>; <sup>1</sup>Caltech

Both the cluster expansion and the CALPHAD formalisms are implicitly based on the assumption that some well-defined lattice(s) (e.g. bcc, fcc, hcp) remain at least metastable throughout the whole composition range of an alloy system. However, this assumption is clearly violated in a number of systems (e.g. Ti-Al, Cu-Fe, etc.). This conundrum is generally addressed by viewing the free energies of unstable phases as merely convenient extrapolations without a physical meaning. We describe a more rigorous way to handle this issue, based on the idea that the (classical) partition function of the system can be cleanly factored as nested sums over lattices, over configurations and over displace degrees of freedom. In this approach, a well-defined free energy can be assigned to mechanically unstable phases by constraining the domain of the integration traditionally employed to obtain free energies in lattice dynamics calculations, based on the geometrical features of the lattices involved.

### 9:30 AM Invited

**DFT, CE, CALPHAD and Phase Field, Cooperative Phenomena Powered by DDF:** *Suzana Fries*<sup>1</sup>; <sup>1</sup>ICAMS, Ruhr University Bochum

There are a series of methods for treating special features of materials which were independently developed in the last 60 years. A magnification of understanding is achieved by the combination of these methods. Because they extend from first-principles calculations to the processing of real alloys their link is not straightforward requiring a global vision of the studied event. This is possible only by an investigator carrying a certain scientific culture. Once this culture is transmitted the combination of these methods becomes more and more creative, and as a quality inherent to the culture, the development keeps tracing the subject as a whole. These phenomena will be exemplified by the achievements obtained by a large group of researchers which were touched by the DDF culture

### 10:00 AM Break

### 10:30 AM Invited

**First-Principles Calculations of Free Energies of Unstable Phases:** *Vidvuds Ozolins*<sup>1</sup>; <sup>1</sup>University of California, Los Angeles

Ab initio density-functional theory molecular dynamics simulations are used to solve the long-standing problem of calculating free energies of harmonically unstable phases, such as fcc W. We find that fcc W is mechanically unstable with respect to long-wavelength shear at all temperatures considered (T>2500 K), while the short-wavelength phonon modes are anharmonically stabilized. The calculated fcc/bcc enthalpy and entropy differences at T=3500 K (308 meV and 0.74 kB per atom, respectively) agree well with recent values derived from CALPHAD analysis of experimental data. Our results for Zr show that even harmonically stable phases (such as fcc and hcp Zr) become dynamically unstable at high temperatures. The proposed methods are expected to be useful for modeling the thermodynamic properties of solid phases and thermodynamic driving forces for structural transformations in pure elements and alloys using first-principles density-functional theory techniques.

### 11:00 AM

**Another View of Phase Diagrams:** *John Morral*<sup>1</sup>; Ximiao Pan<sup>1</sup>; <sup>1</sup>Ohio State University

With improved software and databases that predict phase diagrams there is need for new, user-friendly ways to view ternary and higher order phase diagrams. Two dimensional (2D) sections are well known ways to view information about phase stability, even when multiple components and phases are present. Three dimensional projections of ternaries are well known, too, especially liquidus projections. These are available for a variety of ternary systems. Liquidus and other projections in the literature are a series of lines that border single phase regions. On 2D phase fraction charts these are lines where the fraction equals one. However another type of diagram can be drawn using

Tue. AM

# Technical Program

lines where the phase fraction is zero. An example of such a diagram will be given in which the Q-phase stability in Al-Si-Cu-Mg alloys can be viewed as a function of three solute concentrations. The diagram is a polyisopleth projection at the solutionizing temperature.

## 11:20 AM Invited

### The Kinetics of Diffusional and Structural Phase Transformations from First Principles: *Anton Van der Ven*<sup>1</sup>; <sup>1</sup>University of Michigan

While much progress has been made in the first-principles prediction of the thermodynamics of multi-component solids, predicting the kinetics of solid-state phase transformations remains a major challenge. A large class of phase transformations in multi-component solids involves a redistribution of its constituents, which requires atomic diffusion. Other phase transformations are characterized by structural changes at the crystallographic level. First-order phase transformations require the passage of interfaces separating new phases from old phases. One approach to simulate first-order phase transformations from first-principles is through parameter passing, whereby kinetic coefficients describing atomic diffusion and interface mobilities are implemented in a continuum description. In this talk I will describe first-principles approaches to predict coefficients of kinetic rate equations in multi-component alloys and intercalation compounds used in Li-ion batteries. Kubo Green expressions for rate coefficients are evaluated by applying kinetic Monte Carlo simulations to first-principles parameterized effective Hamiltonians.

## 11:50 AM Invited

### Vibrational Thermodynamics at High Temperatures: *Brent Fultz*<sup>1</sup>; <sup>1</sup>California Institute of Technology

Differences between the vibrational entropies of alloy phases have become much better understood over the past decade. Our understanding is best for low temperatures, where it is often possible to use the harmonic approximation. Vibrational entropy at elevated temperatures is a bigger challenge. Only part of the story is provided by the quasiharmonic approximation, where vibrational frequencies are reduced as a crystal expands against its bulk modulus. Existing phonons alter the energy to excite other phonons (phonon-phonon interaction, PPI), and electronic excitations interact with vibrational excitations (electron-phonon interaction, EPI). It has been a surprise that the EPI in metals can be important thermodynamically at temperatures of 1000 K. One of the more prominent effects of the PPI is the lifetime broadening of phonon spectra, which highlights other risks of the quasiharmonic approximation. Nevertheless, systematic trends for the PPI in fcc and other structures will be reported.

## International Symposium on High-Temperature Metallurgical Processing: Secondary Processing

*Sponsored by:* The Minerals, Metals and Materials Society, TMS Extraction and Processing Division, TMS: Pyrometallurgy Committee  
*Program Organizers:* Jaroslav Drellich, Michigan Technological University; Jiann-Yang Hwang, Michigan Technological University; Tao Jiang, Central South University; Jerome Downey, Montana Tech

Tuesday AM Room: 619  
February 16, 2010 Location: Washington State Convention Center

*Session Chair:* Jiann-Yang Hwang, Michigan Technological University

## 8:30 AM Keynote

### Overcoming the Final Challenges to Initiating Production Treatment of EBR-II Spent Fuel at Idaho National Laboratory: *Michael Simpson*<sup>1</sup>; <sup>1</sup>Idaho National Laboratory

Since its successful demonstration for DOE from 1996 to 1999, the Experimental Breeder Reactor-II Spent Fuel Treatment Process has been used to treat a total of 2.6 metric tons of fuel in addition to the 1.1 MT treated during the demonstration. And a number of evolutionary-type improvements have been made in the process to improve efficiency and minimize waste. Idaho National Laboratory is now on the cusp of initiating production operations at up to 3.4 MT/year. Key pre-requisites for such a production level include funding to support 24-hour operations. And key technology issues must be resolved including electrorefiner (ER) oxidant production, improving design of the ER anode-cathode module, developing a process for treating dross, scaling-up and qualifying the ceramic waste process, and renovating the mass tracking system

that is currently used for material control and accountability. Each of these areas is currently being worked, and progress is rapidly being made.

## 9:10 AM

### Recovery of Iron and Zinc from Electric Arc Furnace Dust Using a Microwave Processing Method: *Jiann-Yang Hwang*<sup>1</sup>; Xiang Sun<sup>1</sup>; Xiaodi Huang<sup>1</sup>; <sup>1</sup>Michigan Technological University

In the United States, there are approximately 700,000 to 800,000 tonnes of Electric Arc Furnace dusts generated each year. This material is rich in the oxides of iron, zinc, lead and chromium. It has been classified as a hazardous material and requires special disposal. A microwave processing method was investigated in this study. This method employs the mixtures of dust and powders of reductant under microwave for heating while the air is prevented from the system to cause the oxidation of the products. The products are the iron and zinc metals that can be easily recycled.

## 9:30 AM

### Reduction Behavior of Chromium Oxide in Molten Stainless Steel Slag with Graphite: *Qiuju Li*<sup>1</sup>; <sup>1</sup>Shanghai University

To recover chromium in stainless steel slag, the direct smelting reduction of chromium oxide in molten slag was investigated by small furnace experiments. Graphite was used as reductant under conditions of 1823-1873K. The distribution ratio of chromium was addressed by investigating the thermodynamic equilibrium between the liquid iron and CaO-MgO-SiO<sub>2</sub>-Al<sub>2</sub>O<sub>3</sub>-CrOx-FeO stainless steel slag. Effects of temperature, slag basicity and composition on the reduction of chromium and iron oxides in the slag were investigated. The slag basicity had a significant effect on the reduction behavior. Increasing Al<sub>2</sub>O<sub>3</sub> content from 0 to 10mass% in initial slag, reduction results showed that Al<sub>2</sub>O<sub>3</sub> content in slag increased, the content of chromium and iron decreased in slag.

## 9:50 AM

### A Novel Process for Preparing Ferronickel Powder from Laterite Ores: *Guanghui Li*<sup>1</sup>; Mingjun Rao<sup>1</sup>; Tao Jiang<sup>1</sup>; Yuanbo Zhang<sup>1</sup>; Qian Li<sup>1</sup>; <sup>1</sup>(School of Minerals Processing and Bioengineering, Central South University

The traditional pyrometallurgical and hydrometallurgical processes for nickel recovery from laterite ores are characterized as either great energy consumption or low efficiency. In this paper, reduction roasting-magnetic separation process with addition of composite additive was developed to process the ores. Ferronickel powders with 6.5% to 8.0% Ni content, and 80% to 86% total iron grade were obtained from a sample of laterite ore with 1.58% Ni and 22.07% total iron grade; the recovery of nickel and iron is 80%~91% and 60%~74% respectively. The reduction behaviors and the function of composite additive were primarily involved. It was shown that composite additive not only promotes metallic iron grain growth but also reacts with gangues in the laterite to form non-magnetic or weak-magnetic matters, which are easily removed by low intensity magnetic separation. Key Words: Laterite, Composite additive, Direct reduction, Ferronickel

## 10:10 AM

### Phase Equilibria in Ferrous Calcium Silicate Slags: Stanko Nikolic<sup>1</sup>; Hector Hena<sup>2</sup>; Peter Hayes<sup>2</sup>; Evgueni Jak<sup>2</sup>; <sup>1</sup>Xstrata Technology; <sup>2</sup>University of Queensland

Ferrous calcium silicate slags (described by the FeO-Fe<sub>2</sub>O<sub>3</sub>-CaO-SiO<sub>2</sub> system) form the basis of many non ferrous slags used in primary and secondary metallurgical processes. Despite the industrial and scientific importance of this system, the phase equilibria have not been fully investigated over the range of process conditions encountered in industrial practice. This is on the one hand surprising but also understandable because of the inherent difficulties of undertaking accurate measurements of the system under controlled conditions. Characterization of this slag system is necessary to improve the optimization of existing metallurgical processes and to design new technologies. Sophisticated new experimental methods have been developed to investigate the phase equilibria of these slags. Using these techniques liquidus and solidus data can now be obtained for all primary phase fields in this system. Experimental data obtained to date have revealed interesting trends and some unexpected and important findings about the slag chemistry.



### 10:30 AM Break

### 10:45 AM

#### Decomposition/Volatilization of Enargite in Nitrogen-Oxygen Atmosphere: *Rafael Padilla*<sup>1</sup>; *Alvaro Aracena*<sup>1</sup>; *Maria Ruiz*<sup>1</sup>; <sup>1</sup>University of Concepcion

Enargite (Cu<sub>3</sub>As<sub>3</sub>S<sub>9</sub>) occurs as impurity in most Chilean copper sulfide minerals. However, when enargite content in copper concentrates is high (>1.5%), smelting of such a concentrate produces pollution problems and contamination of the final copper with arsenic. Thus understanding the behavior of enargite at high temperatures is crucial. In this paper, research data is discussed on the decomposition/volatilization of natural enargite mineral in nitrogen and oxygen-containing atmospheres by thermogravimetry and DTA analyses. The results indicated that enargite decomposes in nitrogen through intermediate tenantite to form Cu<sub>2</sub>S in the range 600-900°C. However, in the presence of oxygen, enargite reacts forming CuO as final product. Temperature affects significantly the arsenic volatilization rate in inert and oxidizing atmospheres. At 900°C in pure nitrogen, 95% arsenic volatilized in 15 min, while in the presence of 1% oxygen, 95% of arsenic volatilized in 6 min. At higher oxygen concentration, the rate is even faster.

### 11:05 AM

#### Influence of Additives on Dephosphorization of Oolitic Hematite by Direct Reduction Process: *Guanghai Li*<sup>1</sup>; *Chaoming Xie*<sup>1</sup>; *Yuanbo Zhang*<sup>1</sup>; *Qian Li*<sup>1</sup>; *Tao Jiang*<sup>1</sup>; <sup>1</sup>School of Minerals Processing and Bioengineering, Central South University

With the rapid development of iron and steel industry in the world, the demand and consumption of iron ores increase continuously. Large reserves of high phosphorus content hematite resources have been found in China, but traditional separation methods are found invalid to treat the ore due to high phosphorus content (0.4%~1.0%), low total iron grade (35%~50%) and fine dissemination size of iron-oxide grain. Based on the investigation of mineralogy of oolitic hematite ore, additive aided direct reduction-magnetic separation process is developed to process the ore in this study. The effects of additives, parameters of reduction and magnetic separation are tested. The metallic iron concentrate with total iron grade of 93.84% and phosphorous content of 0.083% has been obtained in laboratory for an ore sample with total iron grade of 48.96%, phosphorous content of 1.61%; the iron recovery is 93.0%, and dephosphorization reaches 96.74%.

### 11:25 AM

#### Thermodynamic Analysis and Experimental Test of primary Al-Si Alloy Prepared by Carbothermal Reduction of Bauxite Tailings: *Yang Dong*<sup>1</sup>; *Di Yuezong*<sup>1</sup>; <sup>1</sup>Northeastern University

The thermodynamic analysis on the carbothermal reduction of bauxite tailings was carried out. The carbothermal reduction process, effect of Fe<sub>2</sub>O<sub>3</sub> addition on the reduction reaction and the composition of products were studied by various methods such as TG/DTA, XRD, XRF, SEM-EDS. It was found that Fe<sub>2</sub>O<sub>3</sub> could not only reduce the reaction temperature and the yield of SiC, but also improve the reduction ratio of Al<sub>2</sub>O<sub>3</sub>. The proper temperature was 1900° in the carbothermal reduction of bauxite tailings. The carbothermal reduction process could be divided into 4 stages, and the key stage was the formation and decomposition of carbides stage. Besides Al-Si-Fe phases, there were residual Al<sub>2</sub>O<sub>3</sub> and carbides phases in the products.

### 11:45 AM

#### Thermodynamic Study on the Recovery of Vanadium from Low-Vanadium Hot Metal: *Xuemei Qing*<sup>1</sup>; *Bing Xie*<sup>1</sup>; *Qingyun Huang*<sup>1</sup>; *Jianping Xiao*<sup>1</sup>; <sup>1</sup>Chongqing University

Thermodynamic calculation software FactSage was used to calculate the thermodynamics of the oxidation reaction of carbon/silicon/vanadium etc in low-vanadium hot metal, the oxidation behavior of the elements in hot metal and the valencies of vanadium and iron in vanadium slag were analyzed. The vanadium slag which was obtained by simulating the reaction of vanadium recovery in laboratory were analyzed by x-ray diffraction technique and spectral analysis technique to verify the theoretical derivation results, and the effects of ferrous oxide contents on the grade of vanadium slag were also studied. Meanwhile, the effects of temperature on the equilibrium distribution ratios of carbon/silicon/vanadium etc were studied by the thermodynamic equilibrium experiments.

### 12:05 PM

#### Effect of Damp Grinding on Preparation of Oxidized Pellet from Pyrite Cinders Concentrates: *Jianchen Li*<sup>1</sup>; *Guohua Bai*<sup>1</sup>; *Guanghai Li*<sup>1</sup>; *Xiaoping Zhou*<sup>1</sup>; <sup>1</sup>School of Minerals Processing and Bioengineering; Central South University

Pyrite cinders (PyCs) are by-products of sulphuric acid production, and they usually contain variable iron oxides; therefore, PyCs are regarded as a kind of iron bearing resources. Many investigations have been carried out to produce oxidized pellet with PyCs concentrates after beneficiation in lab, but its industrial application encounters embarrassment due to inferior ballability and low induration strength of fired pellet. In this study, damp grinding was adopted to enhance the pelletization of PyCs concentrates. It is shown that strength of green ball is able to be increased obviously when PyCs concentrates are ground for 4min at 10% moisture. The roasting experiments in small scale and pilot scale indicate that the compression strength of fired pellet is also able to be increased after damp grinding, their strength go up to 3332N/P, which meets requirements of blast furnace.

### Jim Evans Honorary Symposium: Flow, Solidification, and Inclusion Behavior in Casting Processes

*Sponsored by:* The Minerals, Metals and Materials Society, TMS Extraction and Processing Division, TMS Light Metals Division  
*Program Organizers:* Ben Li, University of Michigan; Brian G. Thomas, University of Illinois at Urbana-Champaign; Lifeng Zhang, Missouri University of Science and Technology; Fiona Doyle, University of California, Berkeley; Andrew Campbell, WorleyParsons

Tuesday AM Room: 620  
February 16, 2010 Location: Washington State Convention Center

*Session Chair:* Vaughan Voller, University of Minnesota

### 8:30 AM Introductory Comments

### 8:40 AM

#### Inclusion Motion and Removal in a Steel Slab Continuous Casting Strands under EMBr: *Lifeng Zhang*<sup>1</sup>; *Yufeng Wang*<sup>1</sup>; <sup>1</sup>Missouri University of Science and Technology

In current study, a 3-D numerical model is built to investigate the effect of a local type ElectroMagnetic Brake (EMBr) on the fluid flow, heat transfer and inclusion motion in slab continuous casting strands. The results indicate that the magnetic force affects the jet characteristics, including jet angle, turbulent kinetic energy and its dissipation rate. In order to reduce the top surface velocity and stabilized the top surface, the magnetic flux intensity should larger than a critical value. With a 0.39 T magnetic flux intensity, the top surface velocity and its fluctuation can be well controlled, and less slag is entrained. The motion of argon bubbles is also studied. More bubbles, especially >2.0 mm bubbles, escape from the top surface between the mold Submerged Entry Nozzle (SEN) and ¼ width for the case with a 0.39 T EMBr. This may push the top slag away and create an open "eye" on the top slag. Small bubbles (=1mm) tend to escape from one side of wide face no matter with or without EMBr, which is induced by the swirl flow from the SEN outport. EMBr has a little effect on the overall removal fraction of inclusions; however, it affects the local distribution of inclusion in the slab. With EMBr, more inclusions accumulate the region just below the surface, thus a worse subsurface quality, while the inner quality of the slab is better than that without EMBr. For heat transfer in the mold, the heat flux on the narrow face and the area of possible break-out zones can be reduced by using EMBr. Prevention of bias flow and/or asymmetrical flow in mold by EMBr is also concluded.

### 9:05 AM

#### A General Enthalpy Method for Molding Solidification Phenomena: *Vaughan Voller*<sup>1</sup>; <sup>1</sup>University of Minnesota

The development of fast, accurate, and robust computation methods is crucial to the modeling of fluid flow and solidification in continuous casting. A basic solidification modeling approach, nearing 60 years of use, is the enthalpy formulation; an approach that is able to provide numerical solutions on fixed grids. Enthalpy methods work well when the solid/liquid interface

# Technical Program

is at a constant phase-change temperature. In a general solidification system, however, the phase change temperature may be a function of (i) the curvature of the interface, (ii) the speed of the interface, and (iii) the redistribution of solute phases. In this paper it is first shown that the modest enthalpy method can be easily and straightforwardly modified to model all of three of these situations. This modified approach is then verified by comparison with available analytical solutions and alternative more sophisticated front tracking approaches.

## 9:30 AM

**Modelling of Mould Filling in Open Mould Conveyor Ingot Casting:** *Vu Nguyen*<sup>1</sup>; Patrick Rohan<sup>1</sup>; John Grandfield<sup>2</sup>; Kevin Naidoo<sup>3</sup>; Kurt Oswald<sup>3</sup>; <sup>1</sup>CSIRO; <sup>2</sup>Grandfield Technology; <sup>3</sup>o.d.t. Engineering

This paper describes the modelling procedure and compares the predicted flow patterns during mould filling with those obtained from casting trials for CASTfill - a patented low dross filling system used in open mould chain conveyor ingot casting machines. The results showed the predicted flow patterns were in good agreement with those observed during casting trials. The effects of flow patterns and the predicted aluminium oxide generation on ingot appearance are also discussed.

## 9:55 AM

**Influence of a Plunging Liquid Jet on a Dual Alloy Casting:** *Autumn Fjeld*<sup>1</sup>; Abdellah Kharicha<sup>1</sup>; Andreas Ludwig<sup>1</sup>; <sup>1</sup>University of Leoben

In casting processes with an impinging jet pouring stream high levels of turbulence, mixing and entrained phases are introduced into the molten metal. For very large scale castings the impinging jet approaches 6 m long, reaching high velocities with high impact force. The impact of such a pouring stream creates highly turbulent zone at depths up to 1.5 m below the surface of the molten metal. The intensity of this impact driven flow is of particular interest in the case of dual alloy castings in which one alloy is cast into a precast shape of another alloy. This results in a remelting of the precast alloy and subsequent solidification of a mixed bonding zone between the two alloys. Investigations with a numerical model have shown that understanding the interaction between the impinging jet, flow patterns and melting is critical to ensuring optimal amount of remelting and bonding between the alloys.

## 10:20 AM Break

## 10:35 AM

**Centrifugal Casting of Complex Geometries: Computational Modelling and Validation Experiments:** *Diane McBride*<sup>1</sup>; Nick Croft<sup>1</sup>; D. Shevchenko<sup>2</sup>; N. Humphreys<sup>2</sup>; P. Withey<sup>3</sup>; N. Green<sup>2</sup>; Mark Cross<sup>1</sup>; <sup>1</sup>Swansea University; <sup>2</sup>The University of Birmingham; <sup>3</sup>Roll Royce Plc

Centrifugal casting offers one route through to high quality products in difficult to cast high temperature low superheat alloys. The coupling of free surface flows and complex rotating geometries, results in significant centrifugal forces; combined with rapid heat transfer and solidification this yields a significant computational modelling challenge. The objective of the work reported here is to develop a comprehensive computational model of centrifugal casting that can reliably predict the macro-defects that arise from the process. In this contribution we describe: • The development of the computational model yielding simulations which involve of the order of a million elements with thousands of time steps on large parallel clusters • Experimental data to validate the model, and • The configuration of a full scale computational model capturing all the important macro-phenomena.

## 11:00 AM

**Integration of CFD Simulation and Virtual Reality Visualization for Iron and Steel Making:** *Chenn Zhou*<sup>1</sup>; <sup>1</sup>Purdue University Calumet

Computational Fluid Dynamics (CFD) has become a powerful simulation technology used in many industrial applications for process design and optimization to save energy, improve environment, and reduce costs. In order to better understand CFD results and more easily communicate with non-CFD experts, advanced virtual reality (VR) visualization is desired for CFD post-processing. Efforts have recently been made at Purdue University Calumet to integrate VR with CFD to visualize complex data in three dimensions in an interactive, virtual environment. The virtual engineering environment greatly enhances the value of CFD simulations and allows engineers to gain much needed process insights for the design and optimization of industrial processes. Examples of a number of applications to iron and steel making will be presented.

## 11:25 AM

**Surface Tension and Temperature Effect on Ar Bubbles Behavior at the Solid/Liquid Interface of the Steel:** *Sang-min Lee*<sup>1</sup>; Sang-joon Kim<sup>1</sup>; Hae-geon Lee<sup>1</sup>; <sup>1</sup>GIFT POSTECH

In order to clarify the entrapment behavior of bubbles onto the solidifying front of molten steel, the effect of surface tension gradient induced force was investigated. During the solidification of steel, the surface tension gradient due to the concentration gradient is developed in addition to the temperature gradient by the mold cooling. In view of the bubble movement in the vicinity of the solidification front, therefore, the effect of the gradient of solutal surface tension must be taken into consideration together with the thermal gradient effect. The order of magnitude analysis shows that the thermal Marangoni force is comparable to the solutal Marangoni force especially for the larger size of bubbles. The temperature dependency of surface tension ( $ds/dT$ ) of Fe-S binary system is also considered with varying concentration of sulfur. At the critical concentration the sign of  $ds/dT$  is changed and hence the thermal Marangoni effect so generated may act as either pushing or pulling force to the bubble in the vicinity of solid/liquid interface.

## 11:50 AM

**Water Model Experiments for Hydrodynamic Forces Acting on Inclusion Particles in Molten Metal under Turbulent Condition:** *Takuya Kato*<sup>1</sup>; Shin-ichi Shimasaki<sup>1</sup>; Shoji Taniguchi<sup>1</sup>; <sup>1</sup>Tohoku University

On the metal manufacturing processes, the inclusion particles in molten metal cause the crucial problems to metal products. In recent years, the inclusion removal processes are improved based on numerical simulations of inclusion particles behavior. However, it sometimes provides an inaccurate result because the hydrodynamic forces acting on particle in turbulent condition, especially lift force, has not been clarified yet. Among various hydrodynamic forces, the drag force always influences largely to particle trajectory. On the other hand, the lift force acts an important role only in high shear rate condition such as wall vicinity. Its prediction model, however, is needed for numerical simulations about inclusion particle behaviors of adhesion to wall and entrapment to interface. Thus, we aimed to evaluate the drag and the lift force acting on small particle in turbulent shear flow by means of water model experiments and numerical simulations.

## Magnesium Technology 2010: Coatings and Corrosion

*Sponsored by:* The Minerals, Metals and Materials Society, TMS Light Metals Division, TMS: Magnesium Committee  
*Program Organizers:* Sean Agnew, University of Virginia; Eric Nyberg, Pacific Northwest National Laboratory; Wim Sillekens, TNO; Neale Neelameggham, US Magnesium LLC

Tuesday AM Room: 612  
February 16, 2010 Location: Washington State Convention Center

*Session Chairs:* Susan Slade, US Magnesium LLC; Robert C. McCune, Robert C McCune & Associates LLC

## 8:30 AM

**Galvanic Corrosion and Stress Corrosion Cracking of Steel and Aluminum Bolts in Magnesium Die Cast Alloy AZ91:** *Gerhard Gerstmayr*<sup>1</sup>; Gregor Mori<sup>2</sup>; Wilfried Eichlseder<sup>1</sup>; <sup>1</sup>Chair of Mechanical Engineering, University of Leoben; <sup>2</sup>University of Leoben

This paper discusses the applicability of selected steel and high-strength aluminum bolts AW 6056 and AW 7075 in magnesium die cast alloy AZ91 regarding corrosion. All aluminum bolts in magnesium parts reveal superior corrosion properties compared to galvanized steel bolts with respect to galvanic corrosion. No aluminum bolt AW 7075 failed in magnesium due to stress corrosion cracking (SCC). Even aluminum bolts in T6 condition can be used for automotive applications when compressive residual stresses introduced by thread rolling are present.



8:50 AM

**Characterization of Multilayer Coating Prepared by Combining Plasma Electrolyte Deposition and Electroless Copper and BTA Passivity on Magnesium Alloy:** *Yongfeng Jiang*<sup>1</sup>; *Yefeng Bao*<sup>1</sup>; <sup>1</sup>Hohai University

Anovel multilayer coating was prepared to produce pore-free copper coatings on AZ91 magnesium alloy combining the methods of plasma electrolytic oxidation (PEO) pre-treatment, electroless copper plating and benzotriazole(BTA), which are examined using scanning electron microscopy (SEM) equipped with energy dispersive analysis of X-rays (EDX). Electrochemical characterizations methods are employed to evaluate corrosion protection of the coating to substrate in 5% NaCl solution. It is indicated that electroless copper process produces a rough interface between the electroless copper layer and the ceramic layer. And the corrosion potential shifts to the positive direction significantly and the current density decreases by more than one order of magnitude. There is no noticeable galvanic corrosion pits on the surface of the duplex coating combination PEO and electroless copper after 168 h neutral salt spray testing. The color of copper after BTA immersion could be hold above 60 days.

9:10 AM

**Enhanced Corrosion Resistance of AZ91 Mg Alloy by Plasma Electrolytic Oxidation with KMnO<sub>4</sub>:** *Dong H. Shin*<sup>1</sup>; *In J. Hwang*<sup>1</sup>; *Ki R. Shin*<sup>1</sup>; *Kang M. Lee*<sup>1</sup>; *Bongyoung Yoo*<sup>1</sup>; <sup>1</sup>Hanyang University

The plasma electrolytic oxidation(PEO) process in AZ91 alloy was studied with a electrolyte containing potassium permanganate(KMnO<sub>4</sub>). Potassium permanganate in the electrolyte affected film thickness, surface morphology and microstructure of oxide layers obtained by the PEO process. Oxide layers on AZ91 Mg alloy by the PEO process was confirmed as a mixture of MgO, MgF<sub>2</sub> and Mn<sub>2</sub>O<sub>3</sub>. The corrosion resistance of this sample was superior to that of the sample processed in the bath without KMnO<sub>4</sub> due to the presence of manganese oxide in the oxide layer.

9:30 AM

**Laser Surface Alloying of a Creep Resistant Magnesium Alloy MRI 230D with Al and Al<sub>2</sub>O<sub>3</sub>:** *G. Rapheal*<sup>1</sup>; *S. Kumar*<sup>1</sup>; *C. Blawert*<sup>2</sup>; *Narendra B. Dahotre*<sup>3</sup>; <sup>1</sup>Indian Institute of Science; <sup>2</sup>GKSS Research Centre; <sup>3</sup>The University of Tennessee

A creep resistant magnesium alloy MRI 230D was laser surface alloyed (LSA) with Al and (Al+Al<sub>2</sub>O<sub>3</sub>) using Nd:YAG laser at four different scan speeds. The coating comprised of fine dendritic and cellular structure, and interfacial bonding was good. A few solidification cracks reaching down to substrate were observed. The LSA alloy exhibited an improvement in wear resistance due to the presence of ultra-hard Al<sub>2</sub>O<sub>3</sub> particles and increased solid solubility of Al in the coating owing to rapid solidification. The LSA alloy with Al exhibited a poorer corrosion resistance, while a two step coating with Al and (Al+Al<sub>2</sub>O<sub>3</sub>) exhibited a slightly better corrosion resistance, than the substrate. This is attributed to the increased coating thickness and closure of solidification cracks in second coating. The corroded surface of the LSA alloy revealed a highly localized corrosion. The laser scan speed did not exhibit a monotonic trend either in wear or corrosion resistance.

9:50 AM

**Corrosion Phenomenon Evaluation of Mg Alloys Using Surface Potential Difference Measured by SKPFM:** *Rei Takei*<sup>1</sup>; *Hiroyuki Fukuda*<sup>1</sup>; *Hisashi Imai*<sup>1</sup>; *Junko Umeda*<sup>1</sup>; *Katsuyoshi Kondoh*<sup>1</sup>; <sup>1</sup>Osaka University

One of weak points of magnesium alloys used as the structural materials is lack of corrosion resistance. That is because magnesium is low in standard electrode potential, and results in the galvanic corrosion when contacting the other metals. The electro-chemical evaluation of Mg alloys is often applied to investigate the corrosion phenomena. However, it is essential to clarify the Volta potential at the interface between  $\alpha$ -Mg and dispersoids or precipitates in the discussion of the corrosion behavior. This study suggests the quantitative evaluation of the local surface potential difference (SPD) at the interface by using Scanning Kelvin Probe Force Microscope (SKPFM) system. This equipment serves the contact potential difference (CPD) between sample metal and the needle (PtIr5) of cantilever. Furthermore, the effects of additives such as iron (Fe), copper (Cu) and carbon nanotube (CNT) of Mg alloys, strongly causing the corrosion phenomena, on the CPD are discussed in detail.

10:10 AM Break

10:30 AM

**A Study of Corrosion Film Growth on Pure Magnesium and a Creep-Resistant Magnesium Alloy in an Automotive Engine Coolant:** *Zhiming Shi*<sup>1</sup>; *Pankaj Mallick*<sup>1</sup>; *Robert McCune*<sup>2</sup>; *S. Simko*<sup>3</sup>; *F. Naab*<sup>4</sup>; <sup>1</sup>University of Michigan-Dearborn; <sup>2</sup>Robert C. McCune and Associates; <sup>3</sup>Ford Research Laboratory, Ford Motor Co.; <sup>4</sup>Ion Beam Laboratory, University of Michigan

In recent years, several creep resistant magnesium alloys have been developed which has created a great interest in using magnesium in automotive engine components, such as the engine block. One major technical concern in using magnesium for engine blocks is its corrosion performance in the presence of engine coolant that flows through its cooling passages. The principal objective of this study was to determine the effects of engine coolant parameters, such as the engine coolant composition, presence of sodium chloride, time and temperature, on the corrosion film growth on pure magnesium and a creep resistant magnesium alloy. The film thickness and composition were determined using both Auger Electron Spectroscopy (AES) and Rutherford Backscattering Spectrometry (RBS). A design of experiments approach was used to determine the main effects of these parameters and their interactions on the corrosion film growth.

10:50 AM

**Electroless Nickel Phosphorus Plating on AZ31:** *Georges Kipourou*<sup>1</sup>; *Khalid Shartal*<sup>1</sup>; <sup>1</sup>Dalhousie University

A nickel – boron coating placed on a nickel – phosphorus coating which in turn is placed on a phosphate-permanganate conversion coating layer produced on the magnesium alloy AZ31. This work reports on the determination of optimum kinetic parameters to produce a coherent nickel – phosphorus coating using an electroless procedure phosphate-permanganate conversion coating layer. Measurements of the plating rate as a function of the experimental variables such as the compositions of the plating bath constituents, the temperature and the pH using the weight gain method were implemented and the phosphorus content of the electroless nickel-phosphorus coatings was measured using EDS analysis. The surface morphology of the coating was examined using SEM, and XRD. The deposition rate of electroless nickel-phosphorus coating increases by increasing the deposition temperature, the concentration of free nickel ions, and the concentration of hypophosphite ions in the plating bath.

11:10 AM

**Improving Corrosion Performance of AZ31B Mg Alloy Sheet by Surface Polishing:** *Guang-Ling Song*<sup>1</sup>; *Zhenqing Xu*<sup>2</sup>; <sup>1</sup>GM R&D; <sup>2</sup>Meda Limited Engineering and Technical Service

AZ31B Mg alloy sheets in the as-received and polished conditions were compared in terms of their corrosion behavior. It was found that the as-received surface has significantly poorer corrosion performance than the polished surface. It is strongly suggested that a surface cleaning treatment should be conducted for AZ31B parts in production. A preliminary analysis of the improvement by polishing was carried out. Iron contamination of the as-received surface is thought to be responsible for its poor corrosion performance. However, the detailed mechanism of the detrimental effect of the iron-contaminant on corrosion is unclear according to a theoretical analysis of the polarization behavior of steel in the same corrosion environment. It appears that in addition to metallic iron particles, iron oxides and carbonates on the surface could also deteriorate the corrosion performance of the AZ31B sheet.

11:30 AM

**Microstructure and Corrosion of AZ91D with Small Amounts of Cerium:** *Daniela Zander*<sup>1</sup>; *Meredith Heilig*<sup>2</sup>; *Norbert Hort*<sup>3</sup>; *Gerald Klaus*<sup>4</sup>; *Andreas Buehrig-Polaczek*<sup>4</sup>; *Joachim Gröbner*<sup>5</sup>; *Rainer Schmid-Fetzer*<sup>5</sup>; <sup>1</sup>TU Dortmund; <sup>2</sup>Colorado School of Mines; <sup>3</sup>GKSS Research Centre; <sup>4</sup>Foundry-Institute of RWTH Aachen; <sup>5</sup>TU Clausthal

Recent investigations of magnesium-aluminum alloys revealed a strong influence of mainly four microstructural parameters on corrosion: porosity, volume fraction, distribution and Al-content of Al<sub>12</sub>Mg<sub>17</sub>. Further an improved corrosion resistance was observed by the addition of rare earth elements. The influence of cerium on casting skin, inner microstructure and corrosion of sand- and die-cast AZ91D with 0.5-2.0 wt.% cerium was investigated by SEM and TEM before and after potentiodynamic measurements or electrochemical impedance spectroscopy in pH8 and pH11. Cerium significantly improved the corrosion resistance by the formation of a passive layer. A strong influence

Tue. AM

# Technical Program

of cerium on the average grain size, changes in morphology and/or volume fraction of Al12Mg17 and formation of a cerium-rich intermetallic phase was observed. Therefore, not only the chemical composition but also the change of microstructure influences the local corrosion mechanism and passive layer formation of AZ91D with cerium. This was supported by DFG (Za 426/3-1).

## 11:50 AM

**Effect of Neodymium Addition on Corrosion Resistance of Mg-Li Alloy:** *Min Li<sup>1</sup>; Guang Chun Yao<sup>1</sup>; Yi Han Liu<sup>1</sup>; Hai Bin Ji<sup>1</sup>; <sup>1</sup>Northeastern University*

Effect of neodymium addition on corrosion resistance of Mg-Li alloy was investigated using the metallographical observation, scanning electron microscope (SEM), X-ray diffraction (XRD) and polarization curve method. The results indicate that 0.5-2 wt. % neodymium in Mg-Li alloy can significantly reduce the corrosion current density, and Mg-Li-2 wt. % Nd alloy has better corrosion resistant performance, the corrosion current density reached 36 $\mu$ A/cm<sup>2</sup>, which is lower than that of traditional AZ91D (54.50 $\mu$ A/cm<sup>2</sup>) obviously. The reason for increasing corrosion resistance is attributed to grain refinement due to the addition of neodymium, which lead to the weak cathodic polarization behavior and the decrease of corrosion current density. Moreover, the denser corrosion film of Mg-Li alloy was formatted due to the addition of neodymium, which can increase the corrosion potential alloy.

## Magnesium Technology 2010: Creep, Relaxation, Recovery, and Recrystallization

*Sponsored by:* The Minerals, Metals and Materials Society, TMS Light Metals Division, TMS: Magnesium Committee

*Program Organizers:* Sean Agnew, University of Virginia; Eric Nyberg, Pacific Northwest National Laboratory; Wim Sillekens, TNO; Neale Neelameggham, US Magnesium LLC

Tuesday AM  
February 16, 2010  
Center

Room: 613  
Location: Washington State Convention

*Session Chairs:* Xiaoqin Zeng, Shanghai Jiao Tong University; Eric Nyberg, Pacific Northwest National Laboratory

## 8:30 AM

**Effect of Aluminum Addition on the Strengthening and High Temperature Deformation Behavior of Mg-3Sn-2Ca Alloy:** *Pitcheswara Kamineni<sup>1</sup>; Y.V.R.K. Prasad<sup>1</sup>; Norbert Hort<sup>2</sup>; Karl Kainer<sup>2</sup>; <sup>1</sup>City University of Hong Kong; <sup>2</sup>GKSS Research Centre*

The hot working behavior of Mg-3Sn-2Ca-0.4Al alloy has been investigated in compression in the temperature range 300–500°C and strain rate range 0.0003–10 s<sup>-1</sup>, with a view to evaluate the strengthening effect of aluminum. The stress-strain curves exhibited steady state behavior at strain rates lower than 0.01 s<sup>-1</sup> and at temperatures higher than 350°C and flow softening occurred at higher strain rates. There has been some strengthening due to aluminum addition particularly at lower temperatures compared to that of the base alloy Mg-3Sn-2Ca. Standard kinetic rate equation is obeyed in two different temperature and strain rate regimes and an analysis yielded apparent activation energy values of 175 and 195 kJ/mole in the two regimes. These are higher than that for self-diffusion in magnesium suggesting that the strengthening due to aluminum and the large volume fraction of intermetallic particles CaMgSn present in the matrix generate considerable back stress.

## 8:50 AM

**Atomistic Simulation of Grain Boundary Sliding in Mg during High Temperature Deformation:** *Hao Zhang<sup>1</sup>; <sup>1</sup>University of Alberta*

A better understanding of superplastic deformation mechanisms in wrought magnesium alloys at high temperature will allow us to better control the processes so that material properties can be optimized. In this work, a series of molecular dynamics simulations were performed to study grain boundary sliding of three types of [10-10] tilt grain boundaries in a magnesium bicrystal at elevated temperature. Simulations showed that grain boundary sliding did not occur over the stress range applied; instead, coupled shear motion (grain boundary sliding induced boundary migration) was dominant. While the measured coupling coefficient, the ratio of boundary tangential displacement to boundary normal displacement, was in good agreement with theoretical prediction, the detailed

shear behavior was different, depending on types of grain boundary, magnitude of applied shear stress and temperature. It was also noted that grain boundary twinning was the predominant mechanism that allowed the coupled shear motion to occur in HCP magnesium.

## 9:10 AM

**Grain Size Effect on the Dome-Forming Limit and Deformation Mechanism of AZ31B Magnesium Alloy Sheets:** *HyungLae Kim<sup>1</sup>; WonKyu Bang<sup>2</sup>; YoungWon Chang<sup>1</sup>; <sup>1</sup>POSTECH; <sup>2</sup>RIST*

The deformation behaviour of AZ31 Mg alloy has been studied in relation to temperature. The rolled sheet with 50mm thickness was homogenized at 400°C for 4 hrs. The specimens were then prepared in the directions of the rolling direction (RD). A series of tensile tests was then carried out under the strain rate of 10<sup>-2</sup> /s at RT, 100°C, 200°C and 300°C together with the load relaxation tests to obtain flow curves in terms of stress and strain rate. The flow curves were found to consist of the usual GMD (grain matrix deformation) curve, GBS (grain boundary sliding) and an additional term due to friction stress as was prescribed by an internal variable theory. Especially, friction stress term in low homologous temperature and GBS term in high homologous temperature was shown.

## 9:30 AM

**Approaching Bolt Load Retention Behaviour of AS41 through Compliance and Creep Deformation:** *Okechukwu Anopuo<sup>1</sup>; Yuanding Huang<sup>1</sup>; Norbert Hort<sup>1</sup>; Hajo Dieringa<sup>1</sup>; Karl Kainer<sup>1</sup>; <sup>1</sup>GKSS Research Centre*

Bolt load retention (BLR) test is a practical way to quantify the degree of fastener clamp load retained at bolted joint in an engineering assembly. This is especially important for automotive power train applications working at elevated temperatures above 100°C. BLR behaviour, creep and microstructure are important to achieve more heat resistant Mg-alloys for automotive power train application. In this study, these methods of investigation were used to analyse the elevated temperature properties of permanent mould cast AS41. Investigations were carried out at temperatures between 100°C and 175°C and stresses of 40-90 MPa. Stress exponent values of ~ 2 at low stress regions of 40 and 55 MPa, and between 4-6 at high stress regions of 70 and 90 MPa suggest grain boundary sliding and dislocation climb. The prediction of the BLR behaviour and experimental results are in good agreement.

## 9:50 AM

**Grain Boundary Sliding Characteristics of AZ31 Alloy Sheet:** *Yong-Nam Kwon<sup>1</sup>; <sup>1</sup>Korea Institute of Materials Science*

In the present study, commercially rolled AZ31 alloy sheets were used to investigate grain boundary sliding characteristics with temperature. Microstructural observation showed that grain boundary sliding occurs in the case of smaller grained alloy while dislocation slip is dominantly operating for larger grains. Deformation assisted grain growth becomes evident at superplastic temperature of AZ31 alloy. Also, cavitation started at the very low level of strain under superplastic deformation condition. Initial strong basal texture remained after deformation irrespective of temperature. Therefore, it might be concluded that poor accommodation for grain boundary sliding of AZ31 alloy results from a limited slip systems even at the high temperature where grain boundary sliding becomes very active. Also, grain growth and compatibility problems during grain boundary sliding are discussed.

## 10:10 AM Break

## 10:30 AM

**Elevated Temperature Tensile Behavior of Extruded Magnesium Sheets:** *Pawl Krajewski<sup>1</sup>; Adi Ben-Artzy<sup>2</sup>; <sup>1</sup>General Motors; <sup>2</sup>Rotem Industries Ltd*

The elevated temperature tensile behavior of AZ31, AM50, ZM21, ZK10, and ZK30 magnesium alloys was investigated using direct extruded sheets. Uniaxial tensile testing to failure and step strain rate testing were performed at 400C and 450C to determine the effect of alloy composition and microstructure on elevated temperature ductility, strain rate sensitivity, cavitation and fracture behavior. Ductilities of almost 300% were observed in the as-extruded material with the ZK alloys giving the highest ductility at temperature. The high ductility of the ZK materials was due, in part, to their ability to maintain a relatively fine grain size throughout tensile testing. The stress exponent, n, for dislocation creep was affected by aluminum content as was the amount of grain boundary sliding. These results will be discussed in the context of designing improved alloys for elevated temperature forming processes.



### 10:50 AM

**Elevated-Temperature Tensile Behavior of a Rapidly Solidified and Reverse Extruded Mg-Zn-Y-Ce-Zr Alloy:** *Jon Carter*<sup>1</sup>; Paul Krajewski<sup>1</sup>; Dan Shechtman<sup>2</sup>; <sup>1</sup>General Motors R&D; <sup>2</sup>Technion-Israel Institute of Technology

The elevated-temperature tensile behavior of a rapidly solidified and reverse extruded Mg-6% Zn-4.2%Y-1.2%Ce-0.66%Zr alloy was studied. The material was prepared as plates, from which sheet-like tensile bars were extracted using wire EDM. The grain size was 0.7 microns. Testing was performed at 300C, 400C, and 450C using both constant strain rate (0.001, 0.01, 0.1 s<sup>-1</sup>) tests to failure, and step strain rate tests. The material showed very high elongations at 400C and 450C, with a maximum of 800%. The peak in ductility occurred at the intermediate strain rate of at both temperatures. The effect of grain size on tensile behavior was investigated by annealing some samples to coarsen the grains to two microns prior to testing, and by testing AZ31 sheet having a grain size of 10 microns.

### 11:10 AM

**Microstructure, Tensile Properties and Creep Resistance of Binary Mg-Rare Earth Alloys:** *Mark Gibson*<sup>1</sup>; Suming Zhu<sup>1</sup>; Mark Easton<sup>1</sup>; Jian-Feng Nie<sup>1</sup>; <sup>1</sup>CAST CRC

This paper investigates the microstructure and its relationship to tensile properties and creep resistance of binary Mg-rare earth (RE) alloys. Alloys with 0.5-5wt.% additions of La, Ce or Nd were produced by high pressure die casting (HPDC). The intermetallic phase formed in the eutectic was identified to be Mg<sub>12</sub>La, Mg<sub>12</sub>Ce and Mg<sub>3</sub>Nd in the Mg-La, Mg-Ce and Mg-Nd alloy systems, respectively. In tensile tests, the alloys showed an increase in yield strength but a decrease in elongation with an increase in the addition of RE element. The creep resistance was found to be significantly influenced by the choice and the amount of the RE element, with the Mg-La alloys being the least creep-resistant and the Mg-Nd alloys the most creep-resistant. The tensile properties and creep resistance are analysed based on microstructural observations.

### 11:30 AM

**The Role of Strain on the Recrystallization Behaviour of Hot Worked and Annealed Magnesium Alloy Mg-3Al-1Zn:** *Aiden Beer*<sup>1</sup>; <sup>1</sup>Deakin University

The present work examines the microstructure that evolves during the hot deformation and subsequent annealing of magnesium alloy AZ31. In particular, the role of strain on the progression of dynamic recrystallization (DRX) and post-deformation recrystallization is investigated. It is found that for the smallest strain examined, the percentage of DRX is low and that, upon subsequent annealing, post-deformation recrystallization results in a slightly larger grain size. With larger deformation strains, the percentage of DRX is increased and finer annealed grain sizes are obtained. However, when the percentage of DRX is above approximately 40%, strain appears to have no influence on both the kinetics of post-deformation recrystallization and the fully annealed grain size developed. Increasing strain alters the texture of the hot deformed microstructure (for the deformation mode examined) and the texture developed during post-deformation recrystallization is found to be similar to that of the dynamically recrystallised microstructure prior to annealing.

### 11:50 AM

**The Relationships between Grain Boundary Sliding and Grain Orientation in AZ31 Magnesium Alloys at Room Temperature:** *Daisuke Ando*<sup>1</sup>; Yuji Sutou<sup>1</sup>; Junichi Koike<sup>1</sup>; <sup>1</sup>Tohoku University

Recently we reported the occurrence of grain boundary sliding (GBS) at room temperature in AZ31 Mg alloy, and proposed that GBS was induced by plastic anisotropy. Since then, additional papers on GBS have been published by others, but the detailed mechanism remains unclear. The purpose of this study is to find a quantitative correlation between GBS and plastic anisotropy. On the chemically polished surface of rolled AZ31 samples, a grid pattern was drawn by a focus ion beam system. The same area was examined by EBSD to obtain crystallographic information. These samples were tensile-tested along the rolling direction at room temperature to a 10% elongation. The deformation of the grid pattern was compared with the expected deformability from the EBSD data. The obtained results provide qualitative understanding of the origin of the GBS at room temperature.

### 12:10 PM

**Texture Change in Pure Mg and Mg-1.5wt%Mn Casting Alloy during Compressive Creep-Deformation:** Mert Celikin<sup>1</sup>; D. Sediako<sup>2</sup>; *Mihriban Pekguleruz*<sup>1</sup>; <sup>1</sup>McGill University; <sup>2</sup>Canadian Neutron Beam Centre, NRC

Most Mg alloys undergo creep under the service conditions of the engine block (50-100MPa, 175-200°C). Texture studies on creep-tested pure Mg and Mg-1.5wt%Mn casting alloys were performed via Neutron Diffraction (ND) and XRD. Analysis of cast pure Mg, before creep testing, indicated that preferential orientation exists with the HCP prismatic planes normal to the growth direction of columnar grains due to directional solidification. Following compressive creep testing (15MPa, 175°C, 150hrs.), the maximum intensity of the texture in pure Mg dropped notably, indicating a slight rotation of basal-plane normals. No significant change in the maximum intensity of texture was observed in Mg-1.5%Mn samples creep tested at 15 MPa at temperatures up to 175°C. Creep tests conducted at higher loads (above the yield strength - 50MPa, 150°C) on both pure Mg and Mg-1.5%Mn samples resulted in the rotation of the basal plane normals towards the compression axis.

## Materials in Clean Power Systems V: Clean Coal-, Hydrogen Based-Technologies, Fuel Cells, and Materials for Energy Storage: Materials for Hydrogen Production, Storage, and Distribution

**Sponsored by:** The Minerals, Metals and Materials Society, TMS Electronic, Magnetic, and Photonic Materials Division, TMS Structural Materials Division, TMS/ASM: Corrosion and Environmental Effects Committee, TMS: Energy Conversion and Storage Committee  
**Program Organizers:** Xingbo Liu, West Virginia University; Zhenguang Yang, Pacific Northwest National Lab; K. Weil, Pacific Northwest National Lab; Mike Brady, Oak Ridge National Lab; Jay Whitacre, Carnegie Mellon University; Ayyakkannu Manivannan, National Energy Technology Laboratory; Zi-Kui Liu, Penn State University

Tuesday AM Room: 211  
February 16, 2010 Location: Washington State Convention Center

**Session Chairs:** Jason P. Trembly, Center for Energy Technology, RTI International; Richard Ricker, NIST

### 8:30 AM Invited

**Co-Production of Pure Hydrogen and Electricity from Coal Syngas via the Steam-Iron Process Using Promoted Iron-Based Catalysts Sub-Pilot Plant Based Studies:** *Jason P. Trembly*<sup>1</sup>; Brian S. Turk<sup>1</sup>; Raghubir P. Gupta<sup>1</sup>; <sup>1</sup>Center for Energy Technology, RTI International

RTI with funding from the U.S. Department of Energy has successfully developed a novel iron-based catalyst for using the iron redox cycle to produce high purity high pressure hydrogen from syngas. This novel iron-based catalyst was based on nanostructured crystalline phases which allowed significantly higher hydrogen production at significantly lower temperatures compared to the state-of-art iron-based redox systems. A preliminary techno-economic analysis of RTI's steam-iron process using this catalyst for co-production of hydrogen and power in an IGCC plant showed cost benefits over a commercial pressure swing adsorption process for hydrogen production. RTI is continuing the development of this steam-iron process technology focusing on scaling up production of the novel iron-based catalyst and design and fabrication of a circulating dual fluidized bed reactor system. Catalyst and process scale-up activities have been initiated producing catalyst batches up to 100 lbs and fabricating a 50kwth system capable of operating at 550°C.

### 9:10 AM

**High Permeability Ternary Palladium Alloy Membranes with Improved Sulfur and Halide Tolerances:** *Kent Coulter*<sup>1</sup>; J. Douglas Way<sup>2</sup>; David Sholl<sup>3</sup>; Bill Pledger<sup>4</sup>; Gokhan Alptekin<sup>5</sup>; <sup>1</sup>Southwest Research Institute; <sup>2</sup>Colorado School of Mines; <sup>3</sup>Georgia Institute of Technology; <sup>4</sup>IdaTech LLC; <sup>5</sup>TDA Research

A three year Department of Energy (DOE) funded project has focused on developing robust, poison-tolerant, hydrogen selective free standing membranes. Extensive DFT calculations have been performed for H in the bulk of Pd, Pd<sub>96</sub>Ag<sub>4</sub>, Pd<sub>96</sub>Au<sub>4</sub>, Pd<sub>96</sub>Cu<sub>4</sub>, Pd<sub>96</sub>Ni<sub>4</sub>, Pd<sub>96</sub>Pt<sub>4</sub>, Pd<sub>96</sub>Rh<sub>4</sub>, Pd<sub>96</sub>Y<sub>4</sub>, Pd<sub>74</sub>Cu<sub>26</sub>, Pd<sub>70</sub>Cu<sub>30</sub>, Pd<sub>70</sub>Cu<sub>26</sub>Ag<sub>4</sub>, Pd<sub>70</sub>Cu<sub>26</sub>Au<sub>4</sub>, Pd<sub>70</sub>Cu<sub>26</sub>Ni<sub>4</sub>,

Tue. AM

# Technical Program

Pd70Cu26Pt4, and Pd70Cu26Y4. In the last two years, over 50 freestanding foils of binary and ternary Pd alloys have been deposited. Pure gas permeation tests with the binary and ternary alloy membranes have been completed and to date PdCuAu and PdCuPt membranes have exhibited equivalent performance at temperatures in the range of 423-773°C with their performance correlating well with the theoretical predictions. Multiple membranes have been tested under the National Energy Technology Laboratory (NETL) Test Protocol with initial promising results from Au containing foils. In this presentation the modeling, fabrication and performance data for these novel membranes will be presented and the challenges discussed.

## 9:30 AM

### **Palladium-Hydrogen Interaction in Dislocations: Trapping and Diffusion:** *Hadley Lawler*<sup>1</sup>; Dallas Trinkle<sup>1</sup>; <sup>1</sup>University of Illinois, Urbana-Champaign

Palladium has a high hydrogen solubility, and a high diffusivity due to low binding energy in the bulk. However, experiments have shown that additional binding sites are available in single-crystal Pd with much higher binding energy, effectively storing residual H in the crystal after removal from high pressure H. The storage of H is believed to occur in dislocation cores, which act as nanoscale H traps. Electronic-structure calculations of an isolated Pd dislocation core using flexible boundary conditions, to accurately couple to the long-range elasticity solution, determine the binding energy of H to a dislocation core, the changes in local geometry and electronic structure. Local vibrational modes of H give information about dynamics and compare with neutron scattering measurements; together with energy barrier calculations, H pipe diffusion is compared with bulk diffusivity. These calculations help elucidate the physical ingredients to design more energetically favorable hydrogen storage traps in materials.

## 9:50 AM

### **Materials Metrology for a Hydrogen Distribution Infrastructure:** *Richard Ricker*<sup>1</sup>; Thomas Siewert<sup>1</sup>; Andrew Slifka<sup>1</sup>; David McColskey<sup>1</sup>; David Pitchure<sup>1</sup>; <sup>1</sup>NIST

Hydrogen is a very promising energy transfer and storage medium. However, hydrogen can be absorbed into and alter the fracture resistance of metals and alloys. An infrastructure for the safe and economical use of hydrogen requires codes and standards for the design and construction of pressure chambers, equipment, and pipelines that will not fail and endanger the public. The ability of these codes and standards to economically protect public safety will be depend on the quality of the available data and the ability of the measurement methods to accurately represent service conditions. This paper will present and discuss the NIST program to meet these needs through the construction of a high-pressure hydrogen gas testing facility and the development and evaluation of testing methods. The prioritization of the research and the coordination with other national metrology institutes and agencies will be discussed.

## 10:10 AM Break

## 10:20 AM

### **Influence of Activation Process on the Hydrogen Storage Properties of Carbon Materials:** *Vinay Bhat*<sup>1</sup>; Cristian Contescu<sup>1</sup>; Nidia Gallego<sup>1</sup>; Frederic Baker<sup>1</sup>; <sup>1</sup>Oak Ridge National Lab

Storing large amount of hydrogen near ambient temperature in safe, economic and portable manner is the challenge that poses obstacles in path of commercializing the fuel cell vehicles. Till now, none of the explored materials or technologies meets the requirements set by DoE. Activated carbon materials can adsorb and store large amount of hydrogen, but at cryogenic temperatures. Recent investigations demonstrate that, even at room temperature, a significant amount of hydrogen could be stored on activated carbons if the pores are tuned between 5 to 7 Å. Here, we present how the method of activation influences the hydrogen storage properties of carbon materials. The results support that creation of nano-pores using chemical activation is more effective than physical activation in enhancing the hydrogen storage capacity of carbon materials. In addition, we also explore how catalyst addition further influences the storage capacity and kinetics of activated carbon materials.

## 10:40 AM

### **Hydrogen Storage Using Electric Field Enhanced Adsorption:** *Jiann-Yang Hwang*<sup>1</sup>; Shangzhao Shi<sup>1</sup>; Xiang Sun<sup>1</sup>; Stephen Hackney<sup>1</sup>; Xuan Li<sup>2</sup>; <sup>1</sup>Michigan Technological University; <sup>2</sup>University of Science and Technology Beijing

Hydrogen adsorption capacity has been low for the effective use of hydrogen fuel cell in automobile applications. Efforts have been attempted by many researchers to develop the material that can meet the target of the Department of Energy. The weak van der Waals force between the hydrogen molecule and the sorbent is a fundamental barrier for high adsorption capacity. In an effort to increase the attractive force between the hydrogen molecule and the sorbent, an electric field was applied. The results are presented in this paper.

## 11:00 AM

### **Effect of Hydrogen on the Mechanical Behavior of AISI 4340 and SA372 Steels:** Anil Saigal<sup>1</sup>; Junior Aguaze<sup>2</sup>; Gary Leisk<sup>1</sup>; Chris San Marchi<sup>3</sup>; *Douglas Matson*<sup>1</sup>; <sup>1</sup>Tufts University; <sup>2</sup>Boeing Co.; <sup>3</sup>Sandia National Laboratory

This work addresses selection of candidate materials for use as pipelines and storage tanks at distribution systems to support developing the infrastructure necessary to promote sustainable energy management via the hydrogen economy. Air and vacuum-melted 4340 and SA372 Grade J Class 70 steels, which were first copper plated and annealed, were analyzed to study the effects of hydrogen charging on its mechanical properties. Hydrogen charging increases the stiffness of 4340 steels by 3.4 to 7.8% and decreases the stiffness of SA372 alloy steel by 5.2%. Hydrogen charging results in decrease in strength of air-melted 4340 steel, increase in strength of vacuum-melted 4340 steel, and no significant change in the strength of SA372 steel; while it always leads to reduced ductility. Copper-plating has the ability to retain hydrogen concentration within the specimen. Finally, air-melted 4340 steel was found to hold maximum amounts of hydrogen followed by vacuum-melted 4340 and SA372 steels.

## 11:20 AM

### **Ni<sub>3</sub>Al Foil Catalysts for Hydrogen Production from Methanol:** *Ya Xu*<sup>1</sup>; Dong Hyun Chun<sup>2</sup>; Jun Hyuk Jang<sup>3</sup>; Masahiko Demura<sup>1</sup>; Dang Moon Wee<sup>3</sup>; Toshiyuki Hirano<sup>1</sup>; <sup>1</sup>National Institute for Materials Science; <sup>2</sup>Korea Institute of Energy Research; <sup>3</sup>Korea Advanced Institute of Science and Technology

Hydrogen is attracting much attention as a clean and efficient energy source. It is highly necessary to develop efficient, low-cost catalysts for hydrogen production. Ni<sub>3</sub>Al intermetallic compound has been known as a promising high-temperature structural material because of its excellent high temperature strength and corrosion/oxidation resistance. Recently, we have successfully fabricated Ni<sub>3</sub>Al cold-rolled thin foil. In this study, we investigated the catalytic properties of the Ni<sub>3</sub>Al foil for hydrogen production from methanol decomposition in the temperature range of 713-793 K. The Ni<sub>3</sub>Al foil showed high catalytic activity and selectivity for methanol decomposition by spontaneous formation of fine Ni particles during the reaction. The results indicate that the Ni<sub>3</sub>Al foil can be used both as catalyst and as structural material of microreactors for hydrogen production.

## 11:40 AM

### **Interfacial Fracture Toughness of $\alpha$ -Al<sub>2</sub>O<sub>3</sub>(0001)/ $\beta$ -NiAl(110):** *Kuiying Chen*<sup>1</sup>; I. Ofzidani<sup>2</sup>; L. Zhao<sup>3</sup>; <sup>1</sup>National Research Council Canada; <sup>2</sup>University of Ottawa; <sup>3</sup>National Research Council Canada

Interfacial fracture toughness  $K_{IC}^{int}$  of thermally growth oxide (TGO)  $\alpha$ -Al<sub>2</sub>O<sub>3</sub>(0001)/ $\beta$ -NiAl(110) bond coat is one of key parameters in assessing the lifing of thermal barrier coating (TBC) in aerospace gas turbine components. This research reports on a systematic study of interfacial fracture toughness of  $\alpha$ -Al<sub>2</sub>O<sub>3</sub>(0001)/ $\beta$ -NiAl(110) using a combination of ab initio density functional theory (DFT) calculations with fracture mechanics. The interfacial fracture toughness model considers the contribution of both elastic and plastic deformations in the crack tip energy rate formulate. By means of the calculated surface energies  $\gamma_s$ , the work of adhesion  $W_{ad}$ , Peierls-Nabarro (P-N) barrier energy  $U_{P-N}$  and a generalized fault energy  $\gamma_F$ , the interfacial fracture toughness  $K_{IC}^{int}$  has been evaluated. The effect of interfacial embrittlement sulphur and potential interfacial enhancer alloying elements such as Pt and Hf on  $K_{IC}^{int}$  has been examined, and a comparison was made on interfacial fracture toughness between the clean and doped interfaces with a purpose to reveal a possible atomic mechanism that may suppress sulphur detrimental effect in terms of electronic structures.



## Materials Processing Fundamentals: Process Modeling and Measurements

Sponsored by: The Minerals, Metals and Materials Society, TMS Extraction and Processing Division, TMS: Process Technology and Modeling Committee

Program Organizer: Prince Anyalebechi, Grand Valley State University

Tuesday AM Room: 601  
February 16, 2010 Location: Washington State Convention Center

Session Chair: Prince Anyalebechi, Grand Valley State University

### 8:30 AM

**Finite Element Modeling of the Twin-Roll Strip Casting Process: Application to an AZ31 Magnesium Alloy:** *Youliang He*<sup>1</sup>; Elhachmi Essadiqi<sup>1</sup>; <sup>1</sup>Natural Resources Canada

Twin-roll casting is an integrated casting and rolling process that involves the continuous solidification of a melt and the plastic deformation of the solidified metal between two rotating rolls. Computer modeling is a valuable tool to help engineers understand the metallurgical process during twin-roll casting. However, commercially available software can only model either the fluid flow/heat transfer of the melt or the plastic deformation of the solid, but not both. In this study, an object-oriented finite element program was developed to simulate the steady-state fluid flow, solidification and plastic deformation of an AZ31 alloy in a horizontal twin-roll caster. The melt, the mush zone and the solid were treated as a generalized Newtonian flow in an Eulerian frame and different constitutive equations were employed to describe the material behaviours. The effect of operational parameters on the solidification process was discussed based on the simulation results.

### 8:50 AM

**A Thermodynamic Model and Database for Gaseous Species Dissolved in Molten Multicomponent Slags:** *Youn-Bae Kang*<sup>1</sup>; Arthur Pelton<sup>1</sup>; <sup>1</sup>Ecole Polytechnique de Montreal

A thermodynamic model has been developed in the framework of the Modified Quasichemical Model in the quadruplet approximation in order to permit the calculation of solubilities of various gaseous species (sulfide, sulfate, nitride, carbide, water, etc.) in molten oxide slags. The model calculates the solubilities solely from existing databases of the thermodynamic activities of the component oxides and the Gibbs energies of the pure components (oxide, sulfide, sulfates etc.). In particular, solubilities of sulfide in the Al<sub>2</sub>O<sub>3</sub>-CaO-FeO-Fe<sub>2</sub>O<sub>3</sub>-MgO-MnO-Na<sub>2</sub>O-SiO<sub>2</sub>-TiO<sub>2</sub>-Ti<sub>2</sub>O<sub>3</sub> multi-component slag, predicted with no additional adjustable model parameters, were found to be in good agreement with all available experimental data. The model applies at all compositions from pure oxides to pure sulfides, sulfates, etc., and from basic slags to acidic slags. By coupling this database with other evaluated databases for molten metal and gas phases, practically important slag/metal/gas equilibria can be computed such as the S-distribution ratio and gas impurity pick-up levels in molten steel.

### 9:10 AM

**Stress Analysis and Deformation Prediction of a Heavy Hydraulic Turbine Blade Casting in Heat Treatment Process:** *Jinwu Kang*<sup>1</sup>; <sup>1</sup>Tsinghua University

The hydraulic turbine blade of the austenitic stainless steel (Cr13%, Ni5%, Mo1%) is a kind of large and curved shape, which is susceptible to deformation in both casting and heat treatment processes. The coupling analysis of heat transfer, phase transformation and stress in heat treatment process of the turbine blade for Three Gorges Project is carried out by using Deform-3D software. Its temperature fields, phase fields and stress fields in heat treatment process are obtained. And its deformation is predicted. In the cooling process of normalizing, the blade exhibits relatively large deformation. Based on the stress analysis and deformation prediction in heat treatment process, an algorithm for the determination of reverse deformation of the blade casting in heat treatment process is presented. And the reverse deformation distribution of blade is obtained.

### 9:30 AM

**Discrete Particle Simulation of Solid Flow in a Blast Furnace:** *Hun-je Jung*<sup>1</sup>; Jong-in Park<sup>1</sup>; <sup>1</sup>Inha University

Burden distribution control is an important technology by which iron is efficiently reduced from iron-bearing particles. This paper reports a numerical study of solid flow in blast furnace by discrete element model (DEM). The results demonstrate that the DEM approach shows trajectory of the particle and stock line profile without global assumptions. The applicability of the proposed DEM approach is validated from its good agreement with the experiment in terms of solid flow patterns.

### 9:50 AM

**Ultrasound Removing Oxygen Gas Bubbles on Anode and Reducing Cell Voltage during Pb Electrodeposition:** *Jilai Xue*<sup>1</sup>; Yifang Zheng<sup>1</sup>; Jiegang Li<sup>1</sup>; <sup>1</sup>University of Science and Technology Beijing

Oxygen gas bubbles generate on anode during Pb electro-deposition process in PbSiF<sub>6</sub>-H<sub>2</sub>SiF<sub>6</sub> aqueous solutions at room temperature. Cell voltage varies as the bubbles formed on the anodes surface. The bubble layer on the anode surface makes a voltage drop that consumes energy in the Pb process and can decrease by applying ultrasound on the anode. The effects of ultrasound frequency and anodic current density were investigated with ultrasound on and off, alternatively during the Pb electrode-position process. The removing of the gas bubbles were recorded with a drop in the cell voltage. The cell voltage can be lowered by 5% with ultrasound, which demonstrates potential energy saving in Pb production.

### 10:10 AM Break

### 10:20 AM

**Lorentz Force Velocimetry: Fundamentals and Application:** *Christian Karcher*<sup>1</sup>; Yuri Kolesnikov<sup>1</sup>; Vitaly Minchenya<sup>1</sup>; Andre Thess<sup>1</sup>; <sup>1</sup>Ilmenau University of Technology

Lorentz force velocimetry (LFV) is a non-contact measuring technique to determine the flow-rate in high-temperature liquid metals. Physically, this technique exploits the basic principles of magnetofluidynamics. Here, by Ohm's law, eddy currents are generated within an electrically conducting fluid that moves through an externally applied magnetic field. The interaction of these currents and the magnetic field induces Lorentz forces in the melt that break the flow. In turn, by Newton's 3rd law, the Lorentz forces exert an accelerating force on the magnet system. These reaction forces are proportional to the flow-rate and can be measured precisely by high-performance digital strain gauges. At Ilmenau University of Technology we have designed and constructed various prototypes of such Lorentz force flowmeters. Moreover, we have tested the prototypes in industrial environment during the production of secondary aluminum. The paper presents the theory of LFV as well as results of the industrial test measurements.

### 10:40 AM

**The Studying of Nonstoichiometric Pyrrhotites Heat Capacity:** *Tatyana Chepushtanova*<sup>1</sup>; Vladimir Lukanov<sup>1</sup>; Brajendra Mishra<sup>2</sup>; <sup>1</sup>Kazakh National Technical University; <sup>2</sup>CSM

Basing on literary data complicated phase relations in pyrrhotites area of Fe-S system throw with different thin properties of high-temperature solid solution structure. To present day the heat capacity of pyrrhotites from Fe<sub>0.885</sub>S until Fe<sub>0.90</sub>S in reference books is absent. In this work represent the results of studying phase transitions at Neel temperature in pyrrhotites, the dependence of heat capacity from temperature at 320 – 303°C, 600 – 783°C. Was established that heat capacity of pyrrhotites Fe<sub>0.855</sub>S – Fe<sub>0.888</sub>S practically is not depend from structure and equal at 550°C 73,30 J/mole•°C, at 740, 750, 783°C – 71,50 J/mole•°C.

### 11:00 AM

**Multi-Scale Solidification Model for Laser Engineered Net Shaping (LENS) Process:** *Hebi Yin*<sup>1</sup>; Sergio Felicelli<sup>1</sup>; <sup>1</sup>Mississippi State University

A two-dimensional multi-scale solidification model was developed to study the heat transfer, fluid flow, and grain growth occurring in the molten pool during the LENS process. This model coupled the finite element method to calculate mass, energy and momentum transport in the macroscale with the cellular automaton technique to calculate liquid/solid phase change at the microscale. The validation of the model was performed by comparing the simulation results with experimental data from previously published works, showing

Tue. AM

# Technical Program

good agreement in temperature distribution and the dendrite morphology. The simulation results showed that Marangoni convection played a critical role in determining the flow pattern in the molten pool and exerted influence on the pool size and shape. It was also found that columnar dendrites can be formed, with dendrite arm spacings as fine as a few microns. In addition, the influence of fluid flow on the dendrite growth in the pool was discussed.

**11:20 AM**

## **Multitechnique Characterization and Prediction of Phase Diagram Topology:** *Marcelle Gaune-Escard*<sup>1</sup>; <sup>1</sup>Ecole Polytechnique, CNRS UMR 6595

Complex phase equilibria in lanthanide halide-alkali metal halide systems are characterized by the existence of several stoichiometric compounds. Their stability depends both on the nature of cations (lanthanide, alkali) and of the halide. A simple scheme for classifying phase diagram topology, with predictive capability, is presented.

**11:40 AM**

## **High-Strength Spring Steel:** *S.A.J. Forsik*<sup>1</sup>; Sangwoo Choi<sup>2</sup>; P.E.J. Rivera-Diaz-del-Castillo<sup>3</sup>; Sybrand van der Zwaag<sup>1</sup>; <sup>1</sup>Delft University of Technology; <sup>2</sup>POSCO Lab.; <sup>3</sup>University of Cambridge

Latest developments in automobile spring steels demand an ultimate tensile strength (UTS) exceeding 2400 MPa along with an area reduction (AR) in excess of 25 %. This requirement was achieved via austenitisation followed by oil-quenching and tempering at various temperatures (ranging from 250 to 450°C). The present work shows the influence of both heat treatment parameters in achieving  $\approx 2450$  MPa UTS and  $\approx 27$  % AR. These properties are achieved via a fine lath martensite microstructure on which vanadium,  $\epsilon$  and  $\theta$  carbides precipitate in various proportions at the tempering stage. These are identified via X-ray and transmission electron microscopy. The experimental evidence suggests  $\epsilon$  carbides to be responsible for such properties, as they display dimensions in the range of 30 nm and a spacing lower than 60 nm. Our attempts to model the precipitation sequence so as to further improve the mechanical properties are presented.

**12:00 PM**

## **High Temperature Oxidation of Fe-Cu-Sn Alloys for Surface Hot Shortness:** *Lan Yin*<sup>1</sup>; Sridhar Seetharaman<sup>1</sup>; <sup>1</sup>Carnegie Mellon University

Steel produced in an electric arc furnace (EAF) contains a high amount of copper that causes a surface cracking phenomenon called surface hot shortness. It is known that tin can exacerbate hot shortness problem but the precise causes are yet to be elucidated. A series of Fe-0.3 wt%Cu-x wt%Sn alloy samples with Sn contents ranging from 0.03 to 0.15 wt% were oxidized in air at 1150 °C for 5 minute and 10 minutes using Thermogravimetry (TG). Scanning electron microscopy (SEM) investigations show that: (i) The oxide/metal interface is planar; (ii) Sn leads severe penetration of liquid-Cu into grain boundaries; (iii) cracks and iron oxides were found beneath the oxide/metal interface. A numerical model was developed to explain the planar interface morphology in the Fe-Cu-Sn ternary system. Focused ion beam (FIB) serial sectioning technique was used to reveal 3-D structure of the penetrated liquid-Cu and cracks beneath the oxide/metal interface.

## **Mechanical Performance for Current and Next-Generation Nuclear Reactors: Advances in Modeling for Reactor Conditions**

*Sponsored by:* The Minerals, Metals and Materials Society, TMS Materials Processing and Manufacturing Division, TMS Structural Materials Division, TMS/ASM: Mechanical Behavior of Materials Committee, TMS: Nanomechanical Materials Behavior Committee, TMS/ASM: Nuclear Materials Committee  
*Program Organizers:* Dylan Morris, NIST; Greg Oberson, Nuclear Regulatory Commission; Nicholas Barbosa, National Institute of Standards & Tech; Wolfgang Hoffelner, Paul Scherrer Institute

Tuesday AM  
February 16, 2010

Room: 201  
Location: Washington State Convention Center

*Session Chairs:* Ioannis Mastorakos, Washington State University; Dylan Morris, NIST

**8:30 AM Invited**

## **Atomic-Scale Modeling of the Dislocation - Radiation Obstacle Interactions Responsible for Mechanical Property Changes in Irradiated Metals:** *Brian Wirth*<sup>1</sup>; Hyon-Jee Lee<sup>1</sup>; <sup>1</sup>University of California, Berkeley

In the early stages of deformation of irradiated materials, dislocations emitted from grain boundaries and localized regions of stress concentration interact with and destroy radiation-induced defects, creating defect-free channels. Although the presence of channels in a wide range of materials is well documented, the atomistic processes responsible for defect annihilation are not yet well established. In this presentation, we describe our recent atomic-scale molecular dynamics simulation results to investigate the motion and interaction of screw, edge and mixed dislocations in fcc Cu and bcc Fe-Cu and Fe-Cr alloys. The simulations have been performed to investigate the dislocation interaction and detachment mechanisms with a variety of obstacles, including dislocation loops, stacking fault tetrahedron, voids and helium bubbles, as well as coherent precipitates. These observations provide insight into irradiation hardening and defect interaction and annihilation mechanisms, as well as interaction rules for larger-scale modeling, and are compared with available experimental results.

**9:00 AM**

## **Multiscale Modeling of Amorphous-Fe and Fe-Ni Systems Used in Extreme Environments such as Nuclear Reactors:** *Ioannis Mastorakos*<sup>1</sup>; N. Le<sup>1</sup>; H.M. Zbib<sup>1</sup>; M. Khaleel<sup>2</sup>; <sup>1</sup>Washington State University; <sup>2</sup>Pacific Northwest National Laboratory

The development of fusion as a viable energy source depends on ensuring structural materials integrity. Structural materials in fusion reactors operate in harsh radiation conditions coupled with high levels of hydrogen and helium production, thus experiencing severe degradation of mechanical properties. The development of structural materials for use in such a hostile environment is predicated on understanding the underlying physical mechanisms responsible for microstructural evolution along with corresponding dimensional instabilities and mechanical property changes. The purpose of this work is to study the behavior of a-Fe and Fe-Ni systems under irradiation using both Molecular Dynamics (MD) and Dislocation Dynamics (DD) simulations. The approach is to pass critical information from the atomistic scale (MD) to the microscale (DD) in order to study the behavior of the material at higher scales. In particular, information pertaining the dislocation-defects (such as voids, helium bubbles and prismatic loops) interactions is obtained from MD simulations. Then this information is used by DD to simulate large systems with high dislocation, and defect densities.

**9:20 AM**

## **Influence of Hydrostatic Stress on Primary Defect Generation during Displacement Cascade in a-Fe:** *Kevin Boyle*<sup>1</sup>; Ronald Miller<sup>2</sup>; <sup>1</sup>CANMET-MTL; <sup>2</sup>Carleton University

Materials for next generation nuclear reactors must be able to withstand more severe operating conditions as compared to current reactors. Advanced steels are being considered for various reactor components due to their thermo-mechanical stability. Although there have been numerous computational studies of primary defect generation in a-iron, few have considered the influence of

Tue. AM



stress. The current study investigates the influence of hydrostatic pressure on the statistics of primary displacement cascade defect generation in  $\alpha$ -iron using molecular dynamics. Both compressive and tensile hydrostatic pressures (0-1000 MPa) are investigated for a range of primary-recoil energies (1-20 keV). Although hydrostatic pressure is found to have a relatively small influence on defect formation energy, it is found to have a relatively large influence on the total number of defects produced. The results are rationalized in terms of the influence of hydrostatic pressure on defect formation energy and mobility and the molten cascade core.

### 9:40 AM

**Phase-Field Simulation of Void and Fission-Gas Bubble Evolution in Irradiated Polycrystalline Materials:** *Paul Millett<sup>1</sup>; Anter El-Azab<sup>2</sup>; Michael Tonks<sup>1</sup>; Srujan Rokkam<sup>2</sup>; Dieter Wolf<sup>1</sup>; <sup>1</sup>Idaho National Laboratory; <sup>2</sup>Florida State University*

The interactive evolution of both polycrystalline microstructure and irradiation-induced defects such as voids and fission gas-filled bubbles in nuclear fuels and structural alloys is complex and critically important to the long-term performance of fission reactors. Here, the phase-field technique is used to model the evolution of multiple point-defect species (vacancies, self-interstitials, and gas atoms), generated randomly in space and time to represent collision cascade events, thus allowing spatially-resolved simulations of void and gas bubble nucleation and growth both within grain interiors and at grain boundary interfaces (which are shown to be heterogeneous nucleation sites). Illustrative results including the formation of void denuded zones and void peak zones adjacent to grain boundaries, the interlinkage of intergranular gas bubbles leading to fission gas release, and the effects of temperature and stress gradients will be presented. This work was supported by the DOE-BES Computational Materials Science Network (CMSN).

### 10:00 AM

**Modeling the Effect of Stress on Defect Migration and Void Formation Using the Phase Field Method:** *Michael Tonks<sup>1</sup>; Anter El-Azab<sup>2</sup>; Paul Millett<sup>1</sup>; Dieter Wolf<sup>1</sup>; <sup>1</sup>Idaho National Laboratory; <sup>2</sup>Florida State University*

Microstructural defects play an important role in determining the internal stress in materials. They can also alter the applied stress distribution, e.g. stress concentrations due to voids. The internal stress, in turn, affects the defect dynamic within the material. In this work, we model the internal stresses in irradiated materials, taking into consideration the intrinsic defect stress as well as their interactions with each other and with the applied stress, all within the framework of phase field simulation. We then apply the combined approach to the problem of point defect diffusion and microstructure evolution in irradiated materials. The stress models are first verified against analytical expressions. They are then used to investigate the effect of an applied load on point defect migration and void formation in irradiated materials.

### 10:20 AM Break

### 10:35 AM

**Modelling Steels Used in Nuclear Energy Applications:** *Maria Samaras<sup>1</sup>; Maximo Victoria<sup>1</sup>; Wolfgang Hoffelner<sup>1</sup>; <sup>1</sup>Paul Scherrer Institute*

Materials under the extreme conditions present in nuclear energy facilities are degraded by their exposure to conditions such as high temperatures, irradiation and a corrosive environment. Life-time assessments still follow simple concepts. To go beyond the current state-of-the-art methodologies, an understanding of the materials' physical phenomena on a scale ranging from the microscopic level all the way up to macroscopic effects is necessary. Multiscale modelling is emerging as a complement to experimental work and is intended to enhance and speed up the assessments of the expected life-time of materials. Model validation through experiments needs to be included in modelling schemes to accurately describe materials phenomena and to enable extrapolation to longer time frames. It is hoped that such paths of research will eventually lead to a predictive methodology, which will not only provide lifetime predictions but also tools for alloy development. Such modelling strategies will be presented in this talk.

### 10:55 AM

**Universal Scaling of Work Hardening Parameters in Type 316L(N):** *Isaac Edwin<sup>1</sup>; B. K. Choudhary<sup>2</sup>; <sup>1</sup>Pohang University of Science and Technology; <sup>2</sup>Indira Gandhi Centre for Atomic Research*

The tensile flow behaviour of Type 316L(N) austenitic steel had been well described in terms of Hollomon and Ludwigson relations over the wide range of test temperatures and strain rates. The work hardening parameters obtained from the Hollomon and Ludwigson relations yielded interesting inter-relations: all the strength coefficients and the transition stress values exhibited a linear variation with the respective strength exponents and transition strains. The observed linear relation was found to extend over the temperature and strain regions where the flow behaviour was dominated by various micro mechanisms such as cross slip, dynamic strain ageing, recovery etc. The inter-relation exhibited could be correlated with the linear relation reported between tensile strength and uniform strain for the alloy. This suggests that there exists a universal scaling of all the strength parameters and strain parameters with the tensile strength and uniform strain respectively.

### 11:15 AM

**Experimental Analysis and Computational Modeling of Temperature Dependent Cyclic Plastic Hardening and Strain Controlled Ratcheting:** *Koen Janssens<sup>1</sup>; <sup>1</sup>Paul Scherrer Institute*

Cyclic temperature shock induced low cycle fatigue can play a role in the safety of the primary cooling system of nuclear reactor power plants. As the yield stress varies with temperature, a thermal shock leads to a sudden local change in the mechanical properties, which may induce unrealistic strain localization and local ratcheting in an elasto-plastic finite element model. We present an experimental analysis of the temperature dependent cyclic hardening of AISI 316L stainless steel, and report on the influence of ratcheting as observed in strain-controlled fatigue experiments. An evaluation of the performance of an implementation of the experimental data into a temperature-dependent, cyclic plastic hardening model is given in the context of a case study of notched ring specimens submitted to cyclic thermal shocks.

### 11:35 AM

**Intergranular Thermal Residual Strain in Rolled and Texture-Free  $\alpha$ -Uranium:** *Don Brown<sup>1</sup>; James Wollmershauser<sup>2</sup>; Bjørn Clausen<sup>1</sup>; Thomas Sisneros<sup>1</sup>; <sup>1</sup>Los Alamos National Laboratory; <sup>2</sup>University of Virginia*

Uranium is known to undergo pronounced thermal ratcheting due to very anisotropic and strongly temperature dependent coefficients of thermal expansion and elastic stiffness. This intrinsic phenomenon can cause unpredictable mechanical behaviors during thermo-mechanical processing and industry utilization, such as in nuclear reactors, effectively wasting resources and/or endangering process stability or efficiency. In this study, the intergranular thermal residual strains are determined from crystallographic lattice parameters in solid polycrystalline rolled and texture-free  $\alpha$ -uranium measured by neutron diffraction during cooling. Elasto-plastic self-consistent modeling serves to assist in the identification of the initiation and degree of activity of plastic deformation, such as slip and twinning, during the cooling process. Temperature dependence of single crystal elastic constants and coefficients of thermal expansion specific to  $\alpha$ -uranium are uniquely allowed in the employed model. The measured and predicted internal strains and their relationship with the micro-mechanics of deformation and the development of back stresses are discussed.

### 11:55 AM

**Evolution of the Thermo-Mechanical Response of Nitride and Oxide Nuclear Fuels through Microstructurally Explicit Models:** *Manuel Parra Garcia<sup>1</sup>; Kirk Wheeler<sup>1</sup>; Kenneth McClellan<sup>2</sup>; Pedro Peralta<sup>1</sup>; <sup>1</sup>Arizona State University; <sup>2</sup>Los Alamos National Laboratory*

A two-dimensional (2D) thermo-mechanical finite element model of a cylindrical fuel pellet, seen from the longitudinal plane, that includes degradation of its mechanical and thermal properties with temperature and burnup has been used to investigate variability of the thermo-mechanical response (stress and strain fields, grain boundary interactions, temperature distributions, creep and swelling responses) due to microstructure heterogeneity within a Representative Volume Element (RVE). Microstructural information was obtained from sintered ZrN, as a surrogate for (Pu,Zr)N, processed under conditions similar to those used in actinide bearing fuels. The 2-D RVE obtained from microstructural characterization, which includes pore and grain

# Technical Program

geometry as well as grain orientation, is surrounded by “effective material” and located at different positions in the model to evaluate the effect of stress, strain, and temperature gradients on local fields. The same techniques are used to analyze UO<sub>2</sub> fuels to establish a comparison. Work supported under DOE/NE Agreement # DE-FC07-05ID14654

**12:15 PM**

**First Principles Study of Defects in Uranium:** *Nikolas Antolin<sup>1</sup>; Oscar Restrepo<sup>1</sup>; John Morral<sup>1</sup>; Wolfgang Windl<sup>1</sup>; <sup>1</sup>Ohio State University*

With renewed interest in development of nuclear power, studies of nuclear materials are increasingly important. In particular, previously unstudied properties of uranium metal are relevant in development of metallic fuels, which are being examined by the Global Nuclear Energy Partnership as a potential replacement for oxide fuels. Ab-initio calculations have been successful in providing the necessary input for continuum-level diffusion-reaction models such as parameters and processes to include, and thus are primary candidates to build models for metallic-fuel performance. However, application of ab-initio methods is problematic in modeling the body-centered cubic phase of uranium, because it is mechanically unstable, similar to bcc phases of other metals including Zr and Hf. We use first principles calculations to examine defect energies of uranium while addressing problems of phase instability. Using defect energies, favorable defects in uranium metal can be determined, allowing subsequent calculation of diffusion mechanisms relevant in design of nuclear fuels.

## Modeling, Simulation, and Theory of Nanomechanical Materials Behavior: Plasticity and Strength of Nanostructured and Nanoscale Materials III

*Sponsored by:* The Minerals, Metals and Materials Society, TMS Materials Processing and Manufacturing Division, TMS/ASM; Computational Materials Science and Engineering Committee, TMS; Nanomechanical Materials Behavior Committee

*Program Organizers:* Thomas Buchheit, Sandia National Laboratories; Sergey Medyanik, Washington State Univ.; Douglas Spearot, University of Arkansas; Lawrence Friedman, Penn State University; Edmund Webb, Sandia National Laboratories

Tuesday AM Room: 304  
February 16, 2010 Location: Washington State Convention Center

*Session Chairs:* Thomas Buchheit, Sandia National Laboratories; Sergey Medyanik, Washington State University

**8:30 AM**

**Effects of Vacancies on Dislocation Nucleation in Metals – An Atomistic Simulation Study:** *Sergey Medyanik<sup>1</sup>; Iman Salehina<sup>1</sup>; <sup>1</sup>WSU*

As strength of crystalline materials strongly depends on their ability to nucleate new dislocations or move the existing ones, a proper knowledge of factors that play major role at the first stages of plastic deformation is highly desirable. However, fundamental understanding of the role of point defects, such as vacancies or inclusions, on the onset of plastic deformation in otherwise defect free solids is still lacking. In this work, atomistic simulations are applied to study the role of vacancies in the inception of plasticity in metals. In particular, the effect of one vacancy and its position on dislocation nucleation in nickel during nano-indentation is explored. Furthermore, the effect of the vacancies density on the onset of plastic deformation is also investigated.

**9:00 AM**

**On Homogeneous Nucleation of Dislocation Loops in Nanocrystalline Materials:** *Yuri Estrin<sup>1</sup>; Vincent Lemiale<sup>2</sup>; Rob O'Donnell<sup>2</sup>; Laszlo Toth<sup>3</sup>; <sup>1</sup>Monash University; <sup>2</sup>CSIRO; <sup>3</sup>Universite de Metz*

Dislocation glide as a mechanism of plasticity of nanocrystalline materials has been debated for quite some time. While the occurrence of dislocations in nanosized grains has been often questioned, molecular dynamics simulations suggest that dislocations can be generated at a grain boundary, traverse the grain and get absorbed at the opposite grain boundary. Further work has suggested that dislocations can be nucleated within nanograins. In this talk we consider homogeneous nucleation of dislocation loops in individual nanoparticles and also in nanosized grains in a polycrystal. An emphasis is put on the role of image

forces, which in this situation act to promote thermally activated nucleation of dislocation loops. On the basis of estimates of the activation energy for this process, it will be shown that image-force assisted homogeneous nucleation is possible in polycrystalline nanomaterials, albeit for a special case of very small grain size.

**9:20 AM**

**Real Space Dislocation Dynamics Model Using the Phase Field Approach:** *Siu Sin Quek<sup>1</sup>; Rajeev Ahluwalia<sup>1</sup>; David Srolovitz<sup>2</sup>; <sup>1</sup>Institute of High Performance Computing Singapore; <sup>2</sup>Yeshiva University*

We describe a dislocation dynamics model in an elastically anisotropic crystal using the phase-field approach and solve it in real space so that realistic boundary conditions can be prescribed readily. This model allows us to study size and boundary effects on mechanical properties and serves as a basic framework to couple dislocation plasticity with phase transformation in materials (e.g. spinodal decomposition, martensitic transformation etc.). We apply the model to study the interplay between binary alloy phase separation and dislocation dynamics. The lattice mismatch that results from the phase separation can influence the dynamics of defects like dislocations, while the long range elastic fields induced by the dislocations can in turn affect the phase separation. The coupling between the phase transformation and the dislocation dynamics is simulated in a single phase-field framework and the resulting microstructure evolution in the system is analyzed.

**9:40 AM Break**

**10:00 AM Invited**

**Dislocation Dynamics Simulations of Thin Film Nanoimprinting:** *Yunhe Zhang<sup>1</sup>; Erik Van der Giessen<sup>2</sup>; Lucia Nicola<sup>1</sup>; <sup>1</sup>Delft University of Technology; <sup>2</sup>University of Groningen*

Metal nanoimprinting is of great technological interest due to its current as well as its potential applications in miniaturized systems. The objective of this study is to investigate numerically the capability of metal films to retain imprints when indented by an array of rigid bodies of various shapes, size and spacings. The challenge originates from the size dependent plastic properties at sub-micron size scales, which causes a non-trivial interaction of the plastic zones underneath the indenters. The approach used in this study is 2D discrete dislocation plasticity, where plasticity in the metal film originates from the collective motion of discrete dislocations. The simulations track the evolution of the dislocation structure during loading, unloading and relaxation and provide an detailed description of the metal surface profile and the residual stresses.

**10:30 AM**

**Microstructural Aspects of Material Strength in Small Volumes:** *Amine Benzerga<sup>1</sup>; P. J. Guruprasad<sup>1</sup>; <sup>1</sup>Texas A&M University*

There is abundant experimental evidence that the plastic behavior of crystals changes at micro-scales in a way that is not necessarily captured by state-of-the-art models. In this paper, plasticity length scale effects are analyzed by means of direct numerical simulations that resolve the scale of the carriers of plasticity, i.e., the dislocations. A computationally efficient, atomistically informed dislocation dynamics framework which has the capability of reaching high dislocation densities and large strains at moderately low strain rates in finite volumes is recalled. Using this framework, a new type of size effect in the hardening of crystals under compression is discovered. In light of such findings, behavior transitions in the space of meaningful structural parameters, from forest-hardening dominated regime to an exhaustion hardening dominated regime are discussed. Various scalings of the flow stress with crystal size emerge in the simulations, which are compared with experimental data on micro- and nano-pillars.

**10:50 AM**

**Temporal Statistics in the Framework of Kinetic Theory of Crystal Dislocations:** *Jie Deng<sup>1</sup>; Mamdouh Mohamed<sup>1</sup>; Anter El-Azab<sup>1</sup>; <sup>1</sup>Florida State University*

Theoretical modeling and numerical simulation of temporal statistics of dislocation ensembles is presented. A hierarchy of kinetic equations is established to describe the evolution of dislocation density, in which the source terms are governed by the rates of dislocation cross slip, annihilation and junction reactions. Stochastic point process and time series theories are used to model the spatial and temporal dependence of these processes and to model the associated rate terms in the kinetic equation. The statistical properties of these



processes, in both time and frequency domain, are analyzed in conjunction with dislocation dynamics simulations. The moving average technique is applied to remove the trend and keep all the processes stationary. Numerical simulation of the autocorrelation function and spectrum provides the preferred frequencies of different types of processes, which, together with their dependence of dislocation density, provide better understanding of the temporal nature of those processes.

### 11:10 AM

**Multiscale Simulation of Crystals, Defects and Deformation Using the Phase Field Crystal Model:** *Zhi Huang*<sup>1</sup>; Jonathan Dantzig<sup>1</sup>; <sup>1</sup>University of Illinois at Urbana-Champaign

Bridging atomic and continuum length and time scales is an important computational challenge. The phase field crystal (PFC) model approaches this problem by minimizing a continuum-based free energy functional to describe processes at the atomic length scale and diffusive time scale. Previous work demonstrated that the combination of an amplitude formulation of the PFC equation with adaptive mesh refinement enables efficient simulation of systems up to micron length scale. However, the amplitude formulation does not represent accurately the behavior near high-angle grain boundaries and other defects. We present a hybrid algorithm that couples the amplitude equations in the crystal bulk to the original PFC equation near defects. A wavelet decomposition scheme is used to couple the two descriptions. Several examples are given to demonstrate the approach, and we also examine the role of deformation in the movement of dislocations and grain boundaries.

### Neutron and X-Ray Studies of Advanced Materials III: Diffuse Scattering I

*Sponsored by:* The Minerals, Metals and Materials Society, ASM International, TMS Structural Materials Division, TMS/ASM: Mechanical Behavior of Materials Committee, TMS: Titanium Committee  
*Program Organizers:* Rozaliya Barabash, Oak Ridge National Laboratory; Jaimie Tiley, Air Force Research Laboratory; Erica Lilleodden, GKSS Research Center; Peter Liaw, University of Tennessee; Yandong Wang, Northeastern University

Tuesday AM Room: 303  
February 16, 2010 Location: Washington State Convention Center

*Session Chairs:* Zahirul Islam, Argonne National Laboratory; Jan Ilavsky, Argonne National Laboratory

### 8:30 AM Keynote

**X-Ray and Neutron Scattering for the Examination of Micro- and Nanostructured Materials:** *Gernot Kostorz*<sup>1</sup>; <sup>1</sup>ETH Zurich

Diffraction and scattering experiments, possibly complemented by electron microscopy, are often decisive for the understanding and control of materials properties. X-rays and neutrons have served as probes for the study of microstructures in materials for a long time. The availability and continuous improvement of suitable facilities at neutron and synchrotron radiation sources have been very useful to materials scientists and favored the realization of increasingly sophisticated experiments. Some recent applications of neutron and X-ray scattering – diffraction, diffuse and small-angle scattering – will be discussed where the limits of spatial and temporal resolution of both types of radiation or their unique or complementary properties were fully exploited. With the combination of appropriate tools, the structure, shape and size characteristics of spatial inhomogeneities and their evolution can be studied with great accuracy, in the bulk and at or near surfaces, and even on single objects.

### 9:00 AM Invited

**X-Ray Scattering Investigation of Semiconductor Magnetic Composite Materials:** *Vaclav Holy*<sup>1</sup>; Guenther Bauer<sup>2</sup>; Rainer Lechner<sup>2</sup>; <sup>1</sup>Charles University in Prague; <sup>2</sup>J. Kepler University

Semiconductor magnetic composites represent a promising route for fabrication of room-temperature magnetic semiconductors. The magnetic properties of these materials substantially depend on the sizes, positions, and on the atomic structure of magnetic inclusions embedded in a non-magnetic semiconductor matrix. For the characterization of composite GeMn and GaFeN systems we

used both x-ray diffraction and x-ray spectroscopy methods. The former class of x-ray methods gives information on the size, and crystallographic nature of the inclusions as well as on elastic strains in the semiconductor matrix around the inclusions. Anomalous x-ray diffraction performed for the photon energies close to the absorption edge of the magnetic ions makes it possible to study the positions of the magnetic ions dissolved in the semiconductor lattice. X-ray spectroscopy methods like EXAFS or DAFS are used for the determination of the magnetic ion positions in magnetic inclusions.

### 9:20 AM Invited

**Depth Dependent Ordering, Two Length Scale Phenomena and Crossover Behavior in a Defective Skin Layer of V<sub>2</sub>H:** *Kevin Bassler*<sup>1</sup>; Charo Del Genio<sup>1</sup>; Johann Trenkler<sup>2</sup>; Aleksandr Korzhenevskii<sup>3</sup>; Rozaliya Barabash<sup>4</sup>; Simon Moss<sup>1</sup>; <sup>1</sup>University of Houston; <sup>2</sup>Carl Zeiss SMT AG; <sup>3</sup>Institute of Problems of Mechanical Engineering; <sup>4</sup>Oak Ridge National Laboratory

Structural defects in a crystal can alter its ordering behavior. Such defects are responsible for the “two length scale” phenomena in which a sharp central peak is superimposed over a broad peak in critical diffuse X-ray scattering. In a defective skin layer crystal of V<sub>2</sub>H, X-ray diffuse scattering shows unusual two length scale phenomena. Defect-free bulk V<sub>2</sub>H has a strong first-order structural transition, but the defective skin has a weak first-order transition and a continuous transition with critical properties that crossover from one universality class to another. We explain this with a theory in which order preferentially occurs in cylindrically shaped regions near edge dislocations. As temperature is reduced, the crossover occurs as order spreads from individual cylinders through a network of cylinders until the correlation length in the network diverges. Reducing the temperature further causes a weak first-order transition in the remaining portions of the crystal.

### 9:40 AM Invited

**Using X-Ray Correlation Spectroscopy to Test Dynamical Scaling:** *Mark Sutton*<sup>1</sup>; <sup>1</sup>McGill University

Many of the properties of a material depend more on its microstructure than its atomic structure. X-ray photon correlation spectroscopy (XPCS) is an ideal way to study temporal fluctuations of these structures. By extending PCS to x-rays, allows one to study opaque materials and to probe much shorter length scales, as required, for example, by binary alloys. Furthermore, XPCS has been extended to study fluctuations in non-equilibrium systems where it measures a two-time correlation function. This ability to measure two-time correlation functions has been used to study dynamical scaling in first order phase transitions of both conserved and non-conserved order parameter systems. Since XPCS measurements reflect fluctuations of the order around its instantaneous value, XPCS results in a new kind of test of the general concept of dynamical scaling. The presented measurements are compared to a theory of dynamical scaling and agree remarkably well with its predictions.

### 10:00 AM Invited

**Pair Distribution Function of Relaxed Se-Clusters inside a Zeolite Structure:** *M. Castro-Colin*<sup>1</sup>; T. Baruah<sup>1</sup>; R. Zope<sup>1</sup>; A. Abeykoon<sup>2</sup>; W. Donner<sup>3</sup>; M. Brunelli<sup>4</sup>; S. Moss<sup>2</sup>; A. Jacobson<sup>2</sup>; <sup>1</sup>University of Texas at El Paso; <sup>2</sup>University of Houston; <sup>3</sup>Technische University Darmstadt; <sup>4</sup>ESRF

Zeolites have a rigid aluminosilicate porous structure that present an excellent template for allocation of nanoclusters, and due to their morphologies, provide the means to vary their bulk counterpart properties. Selenium was introduced into the pores of a faujasite, where Sodium was removed by ionic exchange to increase its adsorption capability. Selenium atoms are then constrained to form structures within the nanometer-sized sodalite cages, on the one hand integrating themselves to the zeolite structure and contributing to the Bragg intensities, which can be studied via Rietveld refinement, but on the other hand giving rise to diffuse scattering where the pair-distribution function technique is most useful. To understand the structural origin of the diffuse signal a comparison was made between structures generated using ab-initio molecular dynamics and those produced by further relaxation, through a Monte Carlo procedure. A comparison is made of those results.

Tue. AM

# Technical Program

## 10:20 AM Invited

**Quantification of Void Network Architectures of Suspension Plasma Sprayed Yttria-Stabilized Zirconia Coatings Using Ultra-Small Angle Scattering (USAXS):** Jan Ilavsky<sup>1</sup>; Ghislain Montavon<sup>2</sup>; Alain Denoirjean<sup>2</sup>; Stéphane Valette<sup>2</sup>; Pierre Fauchais<sup>2</sup>; <sup>1</sup>APS, Argonne National Laboratory; <sup>2</sup>Université de Limoges

Suspension plasma spraying is novel process to form 20 to 100  $\mu\text{m}$  thick ceramic coatings from a suspension of nanometer-sized (50 nm diameter) feedstock. The resulting unique void (pore) network architecture is challenge to characterize and quantify using most techniques due to small sizes involved. Nevertheless, the discrimination of these pore architectures in terms of size and shape distribution, anisotropy, specific surface area, etc., is critical for the understanding of processing, microstructure, and properties relationships. Number of different microstructures, as deposited and annealed, was studied. Total void content of varied between 13 to 20% with most pores being smaller than 30 nm. Only one-tenth to one-third of voids volume was found to be accessible by intrusion. Pore sizes changed during annealing even at temperatures as low than 850°C. Combination of USAXS and Helium pycnometry, combined with scanning electron microscopy was found to provide sufficient detail for these challenging microstructures.

## 10:40 AM Invited

**Near-Surface and Bulk Microstructure: A Comparative Study for Ni-Pt and Pt-Rh:** Bernd Schoenfeld<sup>1</sup>; <sup>1</sup>ETH Zurich

Diffuse scattering of alloys offers access to short-range order and, if states of thermal equilibrium are present, to effective pair interaction parameters. Differences in the local atomic arrangement between the bulk and the near-surface microstructure might occur due to relaxation, segregation profile and reconstruction, but they were barely investigated till now in a quantitative way. Here, results of such a comparative study of Ni-23 at.% Pt and Pt-47 at.% Rh solid solutions will be reported, employing synchrotron radiation under grazing incidence for the near-surface microstructure. Differences in local order were found for Pt-Rh between the (111) and (110) surfaces where only the latter surface gave diffuse maxima at  $1/20$  positions as in the bulk. For Ni-Pt(111), Ni-Pt(110) and the bulk sample, diffuse maxima are always located at the 100 positions of the  $L1_2$  superstructure. The presence of the segregation profile is repeatedly seen in the near-surface microstructure.

## 11:00 AM Invited

**Complex Intermetallics – The Decisive Role of Weak Reflections:** Walter Steurer<sup>1</sup>; Thomas Weber<sup>1</sup>; Miroslav Kobas<sup>2</sup>; <sup>1</sup>ETH Zurich; <sup>2</sup>Dectris Ltd.

Increasing structural complexity is reflected in an increasing amount of weak and very weak diffraction intensities. Without including them in a structure analysis the results would poorly reflect the actual complex ordering phenomena, if at all. The decisive role of weak reflections will be discussed on two examples. The first example deals with the Bragg reflection density as a function of synchrotron radiation exposure time of a high-quality icosahedral quasicrystal in order to see how perfect a quasicrystal can be. In the second example, the crucial role of weak reflections is shown for the structure analysis of the largest known intermetallic structure so far, with more than 23,000 atoms per unit cell. In both cases diffraction data within an intensity range of ten orders of magnitude was collected at the Swiss Light Source (SLS) employing the novel, noise-free, single-photon-counting X-ray pixel detector, PILATUS 6M.

## 11:20 AM Break

## 11:30 AM Invited

**Mapping Phonon Dispersions and Anomalies with X-Ray Thermal Diffuse Scattering:** Tai Chiang<sup>1</sup>; Ruqing Xu<sup>1</sup>; Hawoong Hong<sup>2</sup>; <sup>1</sup>University of Illinois; <sup>2</sup>Argonne National Laboratory

X-ray thermal diffusion scattering (TDS) has proven to be a powerful method for studying phonon dispersion relations and phonon anomalies related to phase transitions. The intensity of TDS at a given momentum transfer is determined by the corresponding phonon frequencies and thermal populations. Thus, measurements of the TDS intensity as a function of momentum transfer and temperature under selected polarization configurations provide a means for extracting the phonon properties. In this talk, we will review recent advances in the development of the methodology including two new approaches: one based on calorimetric determination of the phonon frequency, and the other based on direct intensity comparison between TDS and Compton scattering. Results will be presented of recent studies of various prototypical systems including Cu (a

simple metal), SrTiO<sub>3</sub> (a prototypical complex oxide), Pu (a 5f metal with a complex electronic response), and Cr (a spin density wave system).

## 11:50 AM Invited

**X-Ray Studies of Structural Effects Induced by Pulsed (30 Tesla), High Magnetic Fields at the Advanced Photon Source:** Zahirul Islam<sup>1</sup>; <sup>1</sup>Argonne National Laboratory

A portable 30 Tesla pulsed-magnet system for materials studies in high magnetic fields is presented. A split-pair magnet (Tohoku design) cooled on a closed-cycle cryostat is used for scattering studies. This system is unique because it uses two closed-cycle cryostats, implemented on a standard diffractometer. Such a scheme allows the sample to be cooled near the liquid helium temperature and the magnet to its operating temperature, independently, in a cryogen-free environment. Pulsed magnetic fields (~ 1 ms in total duration) are generated by discharging a configurable bipolar capacitor bank into the magnet coils. Time-resolved scattering data are typically collected using a multi-channel scaler and an oscilloscope, respectively. Seminal work on structural effects in pulsed fields of a geometrically frustrated system has been performed revealing strong magneto-strictive effects in the spin-liquid state. Use of the APS is supported by the DOE, Office of Science, Contract No. DE-AC02-06CH11357.

## 12:10 PM

**Investigation of the Nanoscale Nial Precipitates in the Ferritic Superalloy by USAXS:** Shenyan Huang<sup>1</sup>; Xin Li<sup>2</sup>; Gautam Ghosh<sup>3</sup>; Jan Ilavsky<sup>4</sup>; Zhenke Teng<sup>1</sup>; Morris E. Fine<sup>3</sup>; Emily Liu<sup>2</sup>; Peter Liaw<sup>1</sup>; <sup>1</sup>University of Tennessee; <sup>2</sup>Rensselaer Polytechnic Institute; <sup>3</sup>Northwestern University; <sup>4</sup>Argonne National Laboratory

Ultra-small-angle X-ray scattering (USAXS) technique was employed to measure the nanoscale NiAl B2-type precipitates in a ferritic superalloy for elevated temperature applications. Alloys annealed with various aging times and post-creep alloys as a function of applied stress and composition were investigated. A theoretical model on the absolute intensity scale was developed to quantitatively predict the precipitate size distribution, inter-particle spacing, and volume fraction. Complementary TEM characterization was performed to compare and evaluate the microstructural information obtained from the small-angle scattering analysis.

## 12:20 PM Invited

**Studies Phase Evolution of Triblock Copolymer Solutions by Small Angle Neutron and X-Ray Scattering: Effects of Molecular Weight, Temperature, Pressure and Salt:** Lixin Fan<sup>1</sup>; Liang Guo<sup>2</sup>; Papanan Thiyagarajan<sup>3</sup>; <sup>1</sup>Rigaku Innovative Technologies; <sup>2</sup>Argonne National Laboratory; <sup>3</sup>Office of Basic Energy Sciences, U.S. Department of Energy,

We have investigated the self-assembly and phase behavior of 5 wt% aqueous solutions of triblock copolymers of PEO and PPO, Pluronic F38, F68, F88, F98 and F108, at different temperatures and sodium carbonate concentrations by using small angle neutron and X-ray scattering. The pressure-induced phase transition of 5 wt% F108 was studied and its phase diagram as function of pressure and temperature is obtained. We determined the thermodynamic parameters of micellization by measuring the critical micellization temperature as a function of F108 concentration in the presence of sodium carbonate. We obtained information on the size of the core and corona, inter-micelle distance, aggregation number and the volume fraction of the micelles. The mechanisms of micellization and spherical-to-cylindrical micelle transformation are interpreted to be gradual dehydration of the copolymer chains and progressive insertion of PEO segments from the corona into the core upon the increase in either temperature and/or salt concentration.

## 12:40 PM

**Role of External Stimuli on Phase Transformation in Ferromagnetic Shape-Memory Alloys and Related Properties:** Yandong Wang<sup>1</sup>; Yang Ren<sup>2</sup>; Zhihua Nie<sup>1</sup>; Gang Wang<sup>3</sup>; Ru Lin Peng<sup>4</sup>; Sten Johanson<sup>4</sup>; Daoyong Cong<sup>5</sup>; Stefan Roth<sup>5</sup>; Tomoyuki Terai<sup>6</sup>; Tomoyuki Kakeshita<sup>6</sup>; Dennis Brown<sup>7</sup>; <sup>1</sup>Beijing Institute of Technology; <sup>2</sup>Argonne National Laboratory; <sup>3</sup>Northeastern University; <sup>4</sup>Linköping University; <sup>5</sup>IFW Dresden; <sup>6</sup>Osaka University; <sup>7</sup>Northern Illinois University

Materials that can reversibly change their dimension upon the application of external fields, such as magnetic or electric fields, have been used as actuators or sensors in many applications. Among them are magnetic-driven shape-memory alloys (SMAs), which can be stimulated by a magnetic field. The possibility of a magnetic-field control of the shape-memory effect has been demonstrated



in the ferromagnetic alloys, such as Ni-Mn-Ga, and antiferromagnetic alloy such as Ni-Co-Mn-In and CoO. Here we used the synchrotron high-energy X-ray diffraction technique and EBSD method to study the selection of martensite variants with ferromagnetic or antiferromagnetic state under the external (magnetic and stress) fields. Some important progresses on the in-situ investigations of the phase transformation behavior will be presented in many aspects, including the principle of variant selections in both ferromagnetic and antiferromagnetic alloys and the mechanism of 'magnetic field' and 'stress' training in the advanced metallic materials.

### Pb-Free Solders and Emerging Interconnect and Packaging Technologies: Reliability (I)

*Sponsored by:* The Minerals, Metals and Materials Society, TMS Electronic, Magnetic, and Photonic Materials Division, TMS: Electronic Packaging and Interconnection Materials Committee

*Program Organizers:* Kwang-Lung Lin, National Cheng Kung University; Sung Kang, IBM; Jenq-Gong Duh, National Tsing-Hua University; Laura Turbini, Research In Motion; Iver Anderson, Iowa State University; Fu Guo, Beijing University of Technology; Thomas Bieler, Michigan State University; Andre Lee, Michigan State University; Rajen Sidhu, Intel Corporation

Tuesday AM Room: 204  
February 16, 2010 Location: Washington State Convention Center

*Session Chairs:* Thomas Bieler, Michigan State University; Fu Guo, Beijing University of Technology

#### 8:30 AM Invited

**The Interaction between Imposed Current and Creep of Idealized SnAgCu Solder Interconnects:** *John Morris*<sup>1</sup>; Christopher Kinney<sup>1</sup>; Xio Linares<sup>1</sup>; Tae-Kyu Lee<sup>2</sup>; <sup>1</sup>University of California - Berkeley; <sup>2</sup>Cisco Systems

The work reported here concerns the effect of an imposed current on the creep of simple SnAgCu interconnects. Both double-shear and multiple-ball samples were tested in shear with and without current, and with various thermal histories. These tests consistently yield two unexpected results. First, the relative increase in creep rate with current is nearly the same over a range of temperatures and variety of starting microstructures. Second, when tests are done at the same temperature (including the effect of Joule heating) the rate of creep is lower under current than under isothermal conditions. These results have a fairly straightforward, quantitative interpretation. Given constant temperature and a microstructure that includes interfacial voids, the current depletes the joint of vacancies, lowering the average creep rate, and introducing observable heterogeneities in the creep pattern.

#### 8:55 AM

**Analysis of Simple Shear of Lead-Free Solder Joints to Examine Heterogeneous Strain and Slip System Activity:** Bite Zhou<sup>1</sup>; Thomas Bieler<sup>1</sup>; Tae-Kyu Lee<sup>2</sup>; Kuo-Chuan Liu<sup>2</sup>; <sup>1</sup>Michigan State University; <sup>2</sup>Cisco Systems, Inc.

Simple shear deformation at a strain rate of about 3x10<sup>-6</sup>/s was imposed on several 4x4 sections of a plastic ball grid array package having different aging conditions. One side was polished before deformation and characterized using OIM (orientation imaging microscopy) before deformation so that changes in crystal orientation could be measured after deforming to a shear of about 0.5. Strain was concentrated on the side closer to the package having a smaller cross sectional area. Some joints showed a strongly defined shear band where crystal orientations rotated to a softer orientation very close to the package side (often showing topographic features), and others showed a much more diffuse region of deformation. A ranking of slip system facility was identified from analysis of surface topography and changes in crystal orientation, based upon the hypothesis that more easily activated slip systems would lead to a greater amount of homogeneous deformation.

#### 9:10 AM

**Bending and Strain/Stress Distribution on Flip Chips Measured by Using Synchrotron X-Ray Laue Microdiffraction:** *Kai Chen*<sup>1</sup>; Nobumichi Tamura<sup>1</sup>; Wei Tang<sup>2</sup>; Martin Kunz<sup>1</sup>; King-Ning Tu<sup>2</sup>; <sup>1</sup>LBNL; <sup>2</sup>UCLA

The thermal expansion coefficient mismatch of the Si and the substrate material, such as FR-4, induces residual strain / stress into the flip chips, and thus causes serious reliability issues for semiconductor industry. In this study, the bending of Si chips was measured at both room temperature and enhanced temperature by applying the technique of scanning synchrotron polychromatic X-ray Laue microdiffraction with micro-scale spatial resolution and 0.01 degree angular resolution. The Si chip surface was scanned by dedicatedly focused polychromatic X-ray beam and a two-dimensional Laue pattern was taken by a CCD detector at each sample position. The orientation was analyzed at each spot on the surface of the Si chip, so that the bending angle was measured. The topography of the Si chip was mapped by this technique, and furthermore the strain / stress distribution was calculated based on a simple model.

#### 9:25 AM

**Wafer Bonding Using an Amorphous Si-Au Eutectic Structure:** *Maryam Abouie*<sup>1</sup>; Qi Liu<sup>1</sup>; Douglas G. Ivey<sup>1</sup>; <sup>1</sup>University of Alberta

MEMS typically involve the integration of mechanical elements, sensors, actuators and electronics on a common silicon substrate, through the utilization of micro-fabrication technologies. Packaging is crucial to the function of MEMS devices, as it is key in determining the cost, size and reliability of the device. To reduce the costs, either the package must provide functionality or its cost must be significantly reduced. Wafer-level packaging using eutectic bonding, which was originally developed for the microelectronics industry, can provide a cost effective alternative for MEMS device packaging. In this work, the Au-Si eutectic system (363°C and 3.16 wt% Si) is investigated, whereby amorphous Si is bonded with electrodeposited Au, in order to produce a more structurally sound bond. To optimize the process, bonding temperature, pressure and duration are altered. Microstructural and mechanical property characterization are done using electron microscopy and X-ray diffraction techniques, as well as shear testing and ultrasonic testing.

#### 9:40 AM

**Effect of Pb Addition on Creep and Tensile Behavior of SAC 305 Solder:** *Jonathon Tucker*<sup>1</sup>; Carol Handwerker<sup>1</sup>; Ganesh Subbarayan<sup>1</sup>; <sup>1</sup>Purdue University

Comprehensive characterization of the mechanical behavior of Pb-mixed SAC solders is necessary to understand the reliability of reworked legacy components and mixed assemblies. Three alloys of 1, 5 and 20 weight percent Pb were selected so as to represent reasonable ranges of Pb contamination expected from different Sn-Pb components reworked with Sn3.0Ag0.5Cu. Monotonic and creep tests were performed on specially designed assemblies at temperatures of 25°C, 75°C, and 125°C using a double lap shear test setup that ensures a nearly homogeneous state of plastic strain at the joint interface. The observed changes in creep and tensile behavior with Pb addition were related to phase equilibria and microstructure differences observed through DSC and SEM cross section analysis. With increasing Pb content, the steady state creep strain rates increased while primary creep decreased. The experimental data were used to fit for the parameters of the rate-dependent constitutive models.

#### 9:55 AM

**Impact Testing of Sn3.0Ag0.5Cu Solder with Ti/Ni(V)/Cu under Bump Metallization after Aging at 150 C:** *Kai-Jheng Wang*<sup>1</sup>; Jenq-Gong Duh<sup>1</sup>; Bob Sykes<sup>2</sup>; Dirk Schade<sup>2</sup>; <sup>1</sup>National Tsing Hua University; <sup>2</sup>XYZTEC bv

Non-magnetic Ni(V) metal and low consumption rate with solders are the advantages of sputtered Ti/Ni(V)/Cu under bump metallization (UBM). Sn-patch composed of Sn and V would form in the Ni(V) layer after reflow and aging. In the lead-free solder, Sn-patch was formed and grown more quickly than that in SnPb solder. Thus, the effect of Sn-patch formation on the reliability of solder joint becomes critical. In this study, the Sn3.0Ag0.5Cu solder was reflowed with Ti/Ni(V)/Cu UBM at 250 C for 60 s, and then aged at 150 C for various periods of duration. The high-speed impact test was used to determine the reliability of solder joints. After impact test, the more Sn-patch, the more brittle fracture of solder joint. The correlation between Sn-patch and the reliability of solder joint was discussed and proposed.

Tue. AM

# Technical Program

## 10:10 AM Break

### 10:25 AM

**Modeling of Pb-Free BGA Solder Joint Fatigue Life during Random Vibration:** *Fengjiang Wang*<sup>1</sup>; Matthew O'Keefe<sup>1</sup>; <sup>1</sup>Missouri University of Science and Technology

Development of a vibration fatigue life model to predict solder joint reliability in Pb-free ball grid array (BGA) electronic packages as a function of components location, the number and size of the solder joints, mechanical clamping positions, and the vibration Power Spectral Density (PSD) during random vibration has been investigated. Assessing solder joint reliability under these conditions is especially important for harsh environments such as space, military and automobile applications. A 3-D global/local finite element modeling technique is used to simulate the random vibration responses of different size BGAs soldered onto a polyimide printed circuit board (PCB) and to determine the stresses/strain of BGA solder joints. A vibration fatigue life model based on the Miner's cumulative damage index (CDI) and the derived solder effective strain is then used to predict the BGA solder joint reliability.

### 10:40 AM

**Improved Reliability of Sn-Ag-Cu-In Solder Joint by the Addition of Trace Elements:** A-Mi Yu<sup>1</sup>; Mok-Soon Kim<sup>1</sup>; Jong-Hyun Lee<sup>2</sup>; Jeong-Han Kim<sup>3</sup>; *Jun Ki Kim*<sup>3</sup>; <sup>1</sup>Inha University; <sup>2</sup>Seoul National University of Technology; <sup>3</sup>Korea Institute of Industrial Technology

Among the various Pb-free solder alloys, Sn-3.0Ag-0.5Cu has been an industrial standard in consumer electronics due to its moderate wetting behavior and reliability in thermal fatigue. Recently, however, its high material cost and low reliability in drop impact condition resulted in the use of Sn-0.3Ag-0.7Cu and the development of Sn-1.2Ag-0.7Cu-0.4In solder alloys. Authors have reported that the Sn-1.2Ag-0.7Cu-0.4In showed as good wettability as Sn-3.0Ag-0.5Cu and load drop reliability as Sn-1.0Ag-0.5Cu. It was believed that the small addition of In could make up for the large reduction of Ag with the material cost benefit of about 20%. It was also noteworthy that the load drop reliability of Sn-1.2Ag-0.7Cu-0.4In could be improved beyond Sn-1.0Ag-0.5Cu by the small addition of some elements. In this study, effects of the trace elements, such as Mn and Pd, on the load drop reliability of board-level CSP and failure mechanism in solder joint were investigated.

### 10:55 AM

**Improvement of Heat Dissipation in High-Power Light-Emitting Diodes Using Highly Heat Conductive Die-Attach Material:** *Chia-ju Chen*<sup>1</sup>; Chih-ming Chen<sup>1</sup>; <sup>1</sup>National Chung Hsing University

In recent years, applications of high-power light-emitting diodes (HP LED) have constantly increased. HP LED requires high current drives than before and then generates much heat. Only 15~20% of the input power converts to light and the rest converts to heat. The heat generated by LED chip must be dissipated to the environment effectively in order to maintain the thermal stability of the LED devices. In this poster, we proposed a novel composite die-attach material for LED packaging. This composite die-attach material is prepared by adding proper amounts of nanosized diamond particles into commercial Sn-3wt.%Ag-0.5wt.%Cu (SAC305) solder paste. Since diamond is a highly heat conductive material with an excellent heat conductivity of 2300 W/mk, its incorporation into the SAC305 solder paste (~ 20 W/mk) can promote greatly the heat conductive capacity of the die attach materials and thereby dissipates heat more effectively.

### 11:10 AM

**Mechanism of Microstructure Evolution and Fatigue Failure in Lead Free Solder Joint:** *Jeong Min Kim*<sup>1</sup>; Woong Ho Bang<sup>1</sup>; Choong-Un Kim<sup>1</sup>; Tae-Kyu Lee<sup>2</sup>; Hongtao Ma<sup>2</sup>; Kuo-Chuan Liu<sup>2</sup>; <sup>1</sup>University of Texas at Arlington; <sup>2</sup>Cisco System Inc.

There have been extensive studies on the microstructural characteristics on the solder joint and their evolution with thermal history. Such studies are motivated by anticipation that fracture reliability is keenly affected by solder joint microstructure, and in fact identifies several potential contributing factors including Sn phase texture, grain size, IMC thickness, its morphology and interface composition. However, the exact mechanism by which such factors become influential to fracture reliability is not well understood. Spurred by this, we have conducted series of experiments that 1) track the microstructural evolution of lead-free solder joint with aging and 2) correlate the result to fracture reliability by conducting cyclic fatigue testing. This paper discusses

the major findings of our research and shows 1) fracture resistance and even fracture location changes greatly with aging and 2) such change can only be explained by consideration on changes in mechanical constraints collectively induced by all contributing factors.

### 11:25 AM

**Effect of Joule Heating on Thermo-Electromigration Induced Failure in Lead-Free Solder:** *Di Xu*<sup>1</sup>; Luhua Xu<sup>1</sup>; Shih-Wei Liang<sup>2</sup>; Stephen Gee<sup>3</sup>; Luu Nguyen<sup>3</sup>; Marshall Andrews<sup>4</sup>; K.N. Tu<sup>1</sup>; <sup>1</sup>UCLA; <sup>2</sup>National Chiao Tung University, Taiwan; <sup>3</sup>National Semiconductor Corporation; <sup>4</sup>High Density Packaging User Group international, Inc

Electromigration tests have been performed on lead-free solders for wafer level chip scale package (WL-CSP). It has been found that under current stressing, joule heating introduces temperature increase in solders and creates a thermal gradient from chip side to substrate side. Electromigration in the solder joints is thus accompanied by thermo-migration. Statistical failure analysis of the combined effect has been studied by multichannel time to failure (TTF) recording and Weibull distribution. By analyzing TTF data for several different current densities and temperatures, we are able to calculate the activation energy (Ea) and the current density exponent (n) in Black's Mean Time to Failure (MTTF) equation. The effect of joule heating on the increase of temperature has been considered in Black's equation. It is believed that the joule heating plays an important role in void nucleation and growth process thus has a dominant influence on the value of n.

### 11:40 AM

**Effect of Minor Alloying on the Performance of Snagcu Solder Joints under Ball Impact Test:** *Yao-Ren Liu*<sup>1</sup>; Jenn-Ming Song<sup>1</sup>; Yi-Shao Lai<sup>2</sup>; Ying-Ta Chiu<sup>2</sup>; <sup>1</sup>National Dong Hwa University, Taiwan; <sup>2</sup>Advanced Semiconductor Engineering, Inc.

In this study, the effect of minor alloying on interfacial reaction products and the ball impact reliability of SAC solder joints was investigated. The solders selected were SAC305, SAC105, SAC105RE and SAC105Mn. The substrates included OSP/Cu and electroplated Ni/Au. There were 3 kinds of fracture modes for the BITed joints. They were the S-mode with ductile fracturing, the I-mode with completely brittle fracturing and the M-mode with the mixed ductile-brittle fracturing. The impact performance for the Ni/Au samples was better than those with Cu for as-mounted joints. For the aged Ni/Au joints, the SAC105RE joints possessed a high S-mode fracturing proportion and thus superior impact toughness under high impact rate. As for aged Cu joints, the performance of the SAC105Mn samples was greater, which may due to the higher thickness ratio of Cu3Sn/Cu6Sn5 at interface. It was demonstrated that Cu3Sn had a better fracture toughness than Cu6Sn5.

### 11:55 AM

**Uncovering the Driving Force for Massive Spalling:** *Wei-Ming Chen*<sup>1</sup>; Su-Chun Yang<sup>1</sup>; C. Robert Kao<sup>1</sup>; <sup>1</sup>National Taiwan University

The phenomenon that intermetallic compounds spall massively from the interface during soldering reaction is both technologically important and scientifically interesting. To verify that the driving force for the spalling phenomenon is purely thermodynamic in nature, well designed experiments were carried out. Copper-doped solder was reacted with Ni to form the Sn(Cu) / (Cu,Ni)6Sn5 / Ni structure first; the original Sn(Cu) solder was then removed and replaced with pure Sn. The swapping of Sn(Cu) with Sn caused the massive spalling of (Cu,Ni)6Sn5. A layer of (Ni,Cu)3Sn4 formed at the solder / Ni interface. The results of this study unequivocally prove that the massive spalling here was driven by thermodynamics.



### Phase Stability, Phase Transformations, and Reactive Phase Formation in Electronic Materials IX: Session III

*Sponsored by:* The Minerals, Metals and Materials Society, TMS Electronic, Magnetic, and Photonic Materials Division, TMS Structural Materials Division, TMS: Alloy Phases Committee

*Program Organizers:* Chih-ming Chen, National Chung Hsing University; Srinivas Chada, Medtronic; Sinn-wen Chen, National Tsing-Hua University; Hans Flandorfer, University of Vienna; A. Lindsay Greer, University of Cambridge; Jae-ho Lee, Hongik University; Kejun Zeng, Texas Instruments; Yee-wen Yen, National Taiwan University of Science and Technology; Wojciech Gierlotka, AGH University of Science and Technology; Chao-hong Wang, National Chung Cheng University

Tuesday AM                      Room: 203  
February 16, 2010                Location: Washington State Convention Center

*Session Chairs:* Sinn-wen Chen, National Tsing Hua University; Alexandre Kodentsov, Eindhoven University of Technology

#### 8:30 AM Invited

**New Challenges and Solutions for Metal-Semiconductor Contacts:** *Suzanne Mohney*<sup>1</sup>; <sup>1</sup>Pennsylvania State University

The requirements for ohmic contacts for many state-of-the-art transistors have become more stringent in recent years due to aggressive scaling of the devices, which places limitations on both contact size (necessitating even lower specific contacts resistances) and process integration. In this presentation, three examples of studies that address these issues are described. First, the development of low-resistance selective ohmic contacts to p-InGaAs using electroless deposition is described. These contacts are suitable for the base of self-aligned heterojunction bipolar transistors. Next, the phase transformations that occur in ohmic contacts for low-power antimonide-based compound semiconductor field effect transistors are described, and the role of interfacial reactions in determining the contact resistance is discussed. Finally, nickel silicide formation in wrap-around-gate silicon nanowire field effect transistors is examined. An intriguing dependence of the identity of the nickel silicide that forms on the original silicon nanowire growth direction is highlighted.

#### 8:55 AM Invited

**Reaction Diffusion in GaSb/Co Metallization Contacts during Thermal Processing:** *Alexandre Kodentsov*<sup>1</sup>; <sup>1</sup>Eindhoven University of Technology

The utility of thermodynamic potential diagrams in predicting the diffusion zone morphology developed in the GaSb/Co metallization contacts during thermal processing is demonstrated. A number of experiments were designed to test the model. These are aimed at determining phase equilibria in the Ga-Sb-Co system and studying the microstructural evolution of the reaction zone in bulk as well as thin-film diffusion couples. Interfacial reactions between cobalt and single-crystal (001) GaSb have been investigated at 500 C. No ternary phases exist in the system at this temperature. The cubic CoGa and CoSb<sub>3</sub> phases were observed to be dominant growing compounds in the semi-infinite bulk as well as in thin-film reaction couples, the latter intermetallic being formed next to the GaSb-substrate. When Co-film is consumed by the reaction, the final configuration of the metallization layer GaSb/CoSb<sub>3</sub>/CoGa was found. This information is important in designing uniform, stable contacts for the metallization of gallium antimonide.

#### 9:20 AM

**Development of Advanced Barrierless Interconnect Using Novel Cu Alloy Seed:** *Chon-Hsin Lin*<sup>1</sup>; Jinn P. Chu<sup>2</sup>; C.H. Wu<sup>2</sup>; W.K. Leau<sup>3</sup>; <sup>1</sup>Chin-Min Institute of Technology/Environmental Engineering; <sup>2</sup>National Taiwan University of Science and Technology/Graduate Institute of Materials Science and Technology; <sup>3</sup>National Taiwan Ocean University/Institute of Materials Engineering

Copper metallization can be used to manufacture nanoscale interconnects. Although Cu is widely used as an interconnect material in Si-based devices, it diffuses rapidly into the Si layer, deteriorating the device properties. To prevent device failure, a diffusion barrier must be inserted between Cu and Si. However, these barriers make device miniaturization difficult. Herein, we propose a novel alloy seeding technique for barrier-free Cu metallization. The Cu seed layer—

which acts as a barrier that minimizes Cu/Si interdiffusion—was alloyed with small amounts of insoluble substances, e.g., VN and ReN. The seed layer was characterized by X-ray diffraction, focused ion beam microscopy, secondary-ion mass spectroscopy, and transmission electron microscopy, and by film resistivity and current-voltage measurements. The reliability of the seed layer in copper interconnects was assessed by studying the time-dependent dielectric breakdown in MOS structures. The results revealed enhanced thermal stability of the Cu film.

#### 9:40 AM

**The Effect of Arsenic Dopant in Nickel Silicide Formation:** *S.Y. Tan*<sup>1</sup>; Yi-Lun Hsia<sup>1</sup>; Hsing-Hung Chen<sup>1</sup>; Ming-Yuan Wu<sup>1</sup>; <sup>1</sup>Chinese Culture University

The thermal stability of fully silicided NiSi with arsenic dopant on a different dielectric (SiO<sub>2</sub>, HfSiO, and HfO<sub>2</sub>) was investigated. It was found that arsenic-incorporation demonstrated some improvement in both morphology and phase stability of NiSi films at high processing temperatures regardless underlying gate dielectrics. Furthermore, the modulation of the workfunction (WF) of Ni fully silicided gates by arsenic doping is presented, comparing the effects of dopant (As) on the WF for different dielectrics (SiO<sub>2</sub>, HfSiO, and HfO<sub>2</sub>) and silicide phases (NiSi and NiSi<sub>2</sub>). We confirmed also that the work function of NiSi can be tuned by implanting As dopant, which segregate to the silicide/oxide interface.

#### 10:00 AM Break

#### 10:20 AM Invited

**Thermal Stability of Advanced Gate Stacks for Microelectronic Devices—the Case of Pt/Gd<sub>2</sub>O<sub>3</sub>/Si:** *Moshe Eizenberg*<sup>1</sup>; Eran Lipp<sup>1</sup>; <sup>1</sup>Technion

In order to realize future metal/oxide/semiconductor devices, the currently used SiO<sub>2</sub> gate oxide and poly-Si gate electrode should be replaced by a high dielectric-constant (high-k) material and a metal electrode, respectively. Gd<sub>2</sub>O<sub>3</sub> is a promising high-k material for future devices, offering a sufficiently high k-value and low leakage currents. Pt is considered as a high-workfunction metal for Gd<sub>2</sub>O<sub>3</sub>-based devices. In this work, the stability of Pt/epitaxial Gd<sub>2</sub>O<sub>3</sub>/Si stacks is studied after annealing in forming-gas or in vacuum. It is found that stack instability, which is observed after annealing at temperatures above 550°C, is caused by out-diffusion of Gd through Pt grain-boundaries. The out-diffusion kinetics has been quantified and will be reported. Gd diffusion is enhanced and is accompanied by Si out-diffusion and formation of PtSi clusters when the annealing is in vacuum. The better stability in forming-gas is correlated with the content of oxygen in the Pt during the treatment.

#### 10:45 AM

**Observations on the Melting of Metallic Nanoparticle Deposites via In-situ Synchrotron Radiation X-Ray Diffraction:** Tzu-Hsuan Kao<sup>1</sup>; *Jenn-Ming Song*<sup>2</sup>; In-Gann Chen<sup>1</sup>; Teng-Yuan Dong<sup>3</sup>; Weng-Sing Hwang<sup>1</sup>; <sup>1</sup>National Cheng Kung University, Tainan; <sup>2</sup>National Dong Hwa University, Hualien, Taiwan; <sup>3</sup>National Sun Yat-Sen University, Kaohsiung, Taiwan

Through monitoring the evolution of the Au (111) diffraction peak, the low temperature melting of Au nanoparticles, as well as the transient nanosize induced liquid-solid low temperature alloying behavior, were demonstrated via in-situ synchrotron radiation X-ray diffraction. Upon heating, the broad diffraction peak of nanosized Au particles with the average diameter of 2.5nm was suppressed at around 200°C and soon became sharp due to melting and the following solidification. If the test was performed on a Ni film, an unstable intermetallic compound, Au<sub>3</sub>Ni, appeared with well crystallized Au, which resulted from the reaction between the supercooled liquid of Au and Ni substrate. However, it decomposed when the heating temperature reached 275°C.

#### 11:05 AM

**Control of the Interface Traps in Hf-Based Gate Dielectric Films on Silicon:** *S.Y. Tan*<sup>1</sup>; Yi-Lun Hsia<sup>1</sup>; Ming-Yuan Wu<sup>1</sup>; Hsing-Hung Chen<sup>1</sup>; <sup>1</sup>Chinese Culture University

The continuous scaling of the dimensions of CMOS transistors has caused the thickness of the silicon dioxide to decrease below 1.6nm. The replacement oxides must satisfy various requirements as satisfactory gate oxides. (i) thermodynamically stable in contact with the Si (ii) Oxygen diffusion (iii) form a high quality interface with Si. Hafnium based oxide films have potential to form a silicon oxide comparable interface with the Si. In order to fully understand the origins of the interface trap generation and deep oxide traps in Hf-based films, we introduced two unique process to control the deep trap centers in Hf-based/Si. A

Tue. AM

# Technical Program

combined approach of (i) Thermal annealing treatment (ii) Different Hf contents in HfO<sub>2</sub> (iii) Incorporating N atom into HfO<sub>2</sub> (iv) Electrical characterization—C-V and J-V, to study the effect of the thermal annealing and Hf contents on the interface charge and oxide charge densities. It is the first time, two unique process techniques are employed to control of the deep interface traps in Hf-based gate dielectric films on Silicon.

**11:25 AM**

**Phase Stability and Phase Transformations, in the Ternary Cd-Sb-Zn: Application to the Growth of a Thermoelectric Material:** *Jean Claude Tedenac*<sup>1</sup>; Ya Liu<sup>1</sup>; <sup>1</sup>ICG

High performance thermoelectric materials are obtained by a good knowledge of the systems involved in their fabrication. The phase transformations and phase stabilities of such new materials are still unknown; consequently, a thermodynamic study of these systems is needed. The development of thermodynamic and kinetic databases of such practical materials is important for the microstructural evolution of the materials during processing and service for improving the knowledge. In this paper we will present the results obtained in the study of the ternary Cd-Sb-Zn in a general Calphad procedure. This system contains a well known intermetallic material Zn<sub>4</sub>Sb<sub>3</sub> showing a high conversion factor. Crystal growth of such ternary material is study at the light of a phase diagram analysis. The phase stability of such intermetallic compound is particularly important in this system. It has been studied in the whole range composition.

**11:45 AM**

**Mechanical Properties of (Ni, Cu)<sub>3</sub>Sn<sub>4</sub> Ternary Crystal Structure Using First-Principle Calculation:** *Feng Gao*<sup>1</sup>; Jianmin Qu<sup>1</sup>; <sup>1</sup>Northwestern University

In electronic packaging, a ternary (Ni, Cu)<sub>3</sub>Sn<sub>4</sub> intermetallic compound (IMC) is often found at the interface of solder joints due to the Cu present in Sn-Ag-Cu solders. The IMC compromises the solder joint reliability due to the brittle properties if present in excessive amounts. However, data on mechanical properties of (Ni, Cu)<sub>3</sub>Sn<sub>4</sub> IMC are sparse and fall in a broad range. We report the Cu solubility effect on the mechanical properties of Ni<sub>3</sub>Sn<sub>4</sub>-based crystal structure using first-principle calculation. Based on the calculated single crystal stiffness, the Young's modulus and Poisson's ratio of polycrystalline are extracted. Moreover, the anisotropic elasticity of (Ni, Cu)<sub>3</sub>Sn<sub>4</sub> is explored by computing the electronic structures, such as band structure and density of states (DOS), when the single crystal structure is subjected to a principle strain along different directions.

## Processing Materials for Properties: Advanced Steel Processing

*Sponsored by:* The Minerals, Metals and Materials Society, TMS Extraction and Processing Division

*Program Organizers:* Brajendra Mishra, Colorado School of Mines; Akio Fuwa, Waseda University; Paritub Bhandhubanyong, National Metal and Materials Technology Center

Tuesday AM                      Room: 617  
February 16, 2010              Location: Washington State Convention Center

*Session Chairs:* Florian Kongoli, FLOGEN Technologies Inc; Sven Vogel, Los Alamos National Laboratory

**8:30 AM Keynote**

**Control Microstructures in Iron-Based Alloys by Directional Recrystallization:** *Z. W. Zhang*<sup>1</sup>; G. Chen<sup>1</sup>; H. Bei<sup>2</sup>; G. L. Chen<sup>3</sup>; C. T. Liu<sup>4</sup>; <sup>1</sup>Nanjing University of Science and Technology; <sup>2</sup>Oak Ridge National Laboratory; <sup>3</sup>USTB; <sup>4</sup>Auburn University

Microstructure with controlled grain structures can improve and/or enhance material properties. Directional recrystallization technique matches the requirement of simultaneously producing directional microstructure and enhancing material properties. For example, Directional recrystallization of an Fe-6.5wt%Si alloy was investigated by changing hot zone temperatures and growth rates. Elongated (columnar) grains with an aspect ratio more than 10 can be produced when growth parameters are carefully adjusted. In this study, we show a kinetic approach to model the growth of the columnar grains for Fe-

based alloys. The aspect ratio of the columnar grains predicted by our model is in good agreement with experimental observation. The mechanism of the columnar grain growth essentially can be described as selective growth of grains or competitive migration of the grain boundaries.

**9:00 AM**

**Casting Practice for High-Carbon Nitrogen-Alloyed Chromium-Manganese Austenitic Stainless Steels:** *Meredith Heilig*<sup>1</sup>; *Brajendra Mishra*<sup>1</sup>; Manuel Marya<sup>2</sup>; David Olson<sup>1</sup>; <sup>1</sup>Colorado School of Mines; <sup>2</sup>Schlumberger Reservoir Completion Center

A development regarding carbon additions in nitrogen-alloyed stainless steels presents intriguing possibilities for the future of chromium-manganese based stainless steels. With proper levels of carbon and nitrogen, a cast material can be made that will not form carbides or nitrides, alleviating concern over localized corrosion. The metallurgical requirements to achieve enhanced properties will be considered. Work has been done to economically produce austenitic stainless steel alloys with improved mechanical properties and corrosion resistance. The combination of a series of casting practices is crucial in manufacturing high-carbon nitrogen-alloyed austenitic stainless steel castings with minimal inclusions. The practices to economically produce these castings at atmospheric pressure will be discussed. Alloys of moderate to high nitrogen and carbon concentrations have been produced and examined in comparison to commercially available stainless steels. A review of melting trials, microstructural features, and the results of mechanical testing and corrosion resistance assessment will be presented.

**9:20 AM**

**The State of the Indian Steel Industry:** *Sanak Mishra*<sup>1</sup>; <sup>1</sup>Arcelor Mittal India

Year 2007 was one of the most exciting periods in the history of Indian steel industry; the capacity utilization was more than 85%, with a production of 53 MT of finished steel, corresponding to 7% growth over 2006 and the profitability had reached a peak. However, in 2008, due to the unprecedented global economic meltdown, it mustered only a marginal growth of 3.7%. Consumption had declined, in fact, from July 2008 onwards. To de-stock the inventory, integrated steel producers had announced up to 30% production cut from the beginning of November 2008. Most interestingly, though, the year 2009 was a year of great resilience and recovery for the Indian steel industry. The expansion projects bounced back on track and production ramp-up started from as early as March. India moved to third position in the world steel production arena, after China and Japan, during the first six months of the year 2009. Indian steel industry took gainful advantage of the price correction in iron ore, coke and freight and this helped in reducing the per ton cost of production by about 30% from September 2009. The events of the last few months in fact suggest that Indian steel producers were, on the whole, better equipped to deal with market turbulence due to relatively stronger domestic demand, their competitive position in respect of cost of production, primarily on account of higher levels of capacity utilization, and growing competence of human resource working in the industrial sector in India. In this paper a forecast of the Indian steel industry in the coming five years will also be presented.

**9:40 AM**

**Processing and Electrochemical Corrosion Resistance of a Nanocrystalline Fe-20Cr Alloy:** *Rajeev Gupta*<sup>1</sup>; *Raman Singh*<sup>1</sup>; Carl Koch<sup>2</sup>; <sup>1</sup>Monash University; <sup>2</sup>North Carolina State University

It was hypothesized that it may be much easier to develop a protective film on nanocrystalline Fe-Cr alloys. However, successful processing of nanocrystalline alloy samples suitable for oxidation/corrosion testing proved to be a non-trivial task. This paper will present description of the processing of nanocrystalline Fe-Cr alloy powders by mechanical alloying. Powders thus produced were successfully compacted and sintered to nearly 100% density while retaining nanocrystalline structure. When oxidation and aqueous corrosion resistance of nanocrystalline and microcrystalline alloys of same composition were compared, the nanocrystalline structure was found to provide in excess of an order of magnitude superior oxidation/corrosion resistance.



### 10:00 AM Break

### 10:10 AM

**Towards Modelling of Phase Transformation and Mechanical Properties in Hot Rolled Dual Phase Steel:** *Piyada Suwanpinij<sup>1</sup>*; Krishnendu Mukherjee<sup>1</sup>; Marcel Graf<sup>1</sup>; Ulrich Prahl<sup>1</sup>; Wolfgang Bleck<sup>1</sup>; Rudolf Kawalla<sup>2</sup>; <sup>1</sup>RWTH Aachen University; <sup>2</sup>Institute for Metal Forming (IMF), Freiberg University of Mining and Technology

The excellent combination of mechanical properties of dual phase (DP) steels arises from the distribution of hard martensite islands in the soft ferrite matrix. Hot rolling is a potential route for commercial production of flat DP steel products in which the present work systematically studies the rolling schedule and run out table cooling strategy. All the processing parameters: rolling temperature and strain, interpass time, temperature control on the run-out-table and the quenching time before coiling were simulated by deformation dilatometer and transferred to a 4-stand pilot rolling mill. The recrystallization behaviour during rolling has been investigated by a hot compression simulator. The morphology, phase fraction, and distribution of ferrite are found to be dependent on the run-out-table cooling condition. The mechanical properties of the sheet were determined by tensile test. The influence of different alloying concepts and the interrelationship between the resulting microstructure and mechanical properties will be investigated.

### 10:30 AM

**A Novel Asymmetric Rolling Method for Controlling Texture of Plates and Sheets:** *Dincer Bozkaya<sup>1</sup>*; Peter Jepson<sup>1</sup>; <sup>1</sup>H.C. Starck Inc.

Crystallographic texture of plates and sheets produced by conventional rolling is not uniform through the thickness due to non-uniformity of shear strain distribution induced during rolling. No shear strain is introduced at mid-thickness while shear strain is non-zero elsewhere. Texture non-uniformity through thickness can be eliminated by improving the shear strain distribution. In this paper, a novel asymmetric rolling method, named tilt-rolling, is introduced. Coupling of finite element models (FEM) and crystal plasticity models employed to develop the tilt-rolling process will be explained. Texture results of tantalum plates produced by tilt rolling will be demonstrated. The advantages of tilt-rolling in comparison to other asymmetrical rolling methods such as rolls with different diameters and speeds will be discussed.

### 10:50 AM

**Laser Surface Modification of AISI 410 Stainless Steel with Brass for Enhanced Thermal Properties:** *Felix Espana<sup>1</sup>*; Susmita Bose<sup>1</sup>; Amit Bandyopadhyay<sup>1</sup>; <sup>1</sup>Washington State University

Brass coating was applied to AISI 410 stainless steel substrate using high power laser in a Laser Engineered Net Shaping (LENS<sup>TM</sup>) system. Laser deposition resulted in a diffused and sound interface between metallurgically incompatible brass coating and AISI 410 stainless steel substrate. The thermal conductivity of AISI 410 steel increased from 27 W/mK to a maximum of 37 W/mK depending on the coating thickness, almost a 50% gain. The absence of sharp interface between the coating and the substrate, as a result of laser processing, resulted in low interfacial thermal contact resistance. Based on thermal performance tests, the brass coating found to enhance not only the heat transfer by conduction but also the convective heat transfer rate. These results show that novel and efficient feature based coatings can be created by exploiting the capabilities of laser based coating approach and advanced manufacturing technologies for various industrial applications.

### 11:10 AM

**Development of Ferritic Steels with Increased Strength and Ductility:** *Semyon Vaynman<sup>1</sup>*; Monica Kapoor<sup>1</sup>; Dieter Isheim<sup>1</sup>; Gautam Ghosh<sup>1</sup>; Morris Fine<sup>1</sup>; Yip-Wah Chung<sup>1</sup>; <sup>1</sup>Northwestern University

A high yield strength of 1600 MPa and elongation-to-fracture up to 25% was achieved in ferritic steels by addition of Cu, Ni, Mn and Al for precipitation strengthening. It was demonstrated that the strength of the steel is proportional to the total amount of these alloying elements; thus, the strength of the steel can be tailored to a specific application by changing the amount of these elements. Atom probe studies demonstrate that two types of coherent slightly misfitting nanosized precipitates are formed in the steel: Cu-rich and NiAl-type. The interaction of these precipitates with the matrix locally lowers the Peierls stress for dislocation motion thus improving dislocation mobility and hence ductility in these steels.

### 11:30 AM

**Effect of Deformation Ratio and Cooling Rate on Mechanical Properties and Microstructure of 0.08wt% C HSLA Steel Microalloyed with Nb and Mo:** *Taher El-Bitar<sup>1</sup>*; *Ahmed Zaky Farahat<sup>1</sup>*; Almosilhy Almosilhy<sup>1</sup>; Ahmed Hegazy<sup>1</sup>; <sup>1</sup>Central Metallurgical Research and Development Institute

A low carbon steel microalloyed with Nb and Mo is thermomechanically processed. The effect of two important parameters; deformation percent and post deformation cooling rate; is studied. It was found that increasing amount of hot deformation decreases strength and increases elongation in C-Mn-Nb-Mo steel till a definite value then increases strength appreciably and decreases elongation with a less amount. This is due to the refinement of grain size. Moreover, water quenched specimen had higher strength and lower ductility than air cooled ones. This is due to the smaller grain size and higher amount of hard phases like acicular ferrite and bainite. However, the effect of cooling rate weakens with increasing amount of deformation. This can be attributed to mechanisms.

### 11:50 AM

**Influence on Non-Metallic Inclusions and Magnetic Properties by Deoxidation Method in Non-Oriented Electrical Steel:** *Zhang Feng<sup>1</sup>*; Li Guang-qiang<sup>2</sup>; Chen Xiao<sup>1</sup>; <sup>1</sup>Silicon Steel Department, Baoshan Iron and Steel Co. Ltd; <sup>2</sup>Wuhan University of Science and Technology

The magnetic properties mainly lie on the grain size, crystal texture and non-metallic inclusions in non-oriented electrical steels. Especially the inclusions, their exist will restrain grain growth, accelerate crystal lattice aberrance and block magnetic domain movement. Thus the inclusions in non-oriented electrical steels must be constrained vigorously. In this paper the distribution, variety, shape and size of inclusions and the magnetic properties were investigated under different deoxidation method in two typical non-oriented electrical steel grades. The results showed, there were distinct differences on variety, size, removal speed and magnetic properties under Si-Al and Al-Si deoxidation method, and the magnetic properties will be suffered more salient after the second annealing. The main variety of inclusions were FeO•SiO<sub>2</sub>, FeO•Al<sub>2</sub>O<sub>3</sub>, the complex of FeO•Al<sub>2</sub>O<sub>3</sub> and MnS under Si-Al deoxidation method, and AlN, Al<sub>2</sub>O<sub>3</sub>, FeO•SiO<sub>2</sub>, FeO•Al<sub>2</sub>O<sub>3</sub>, the complex of FeO•Al<sub>2</sub>O<sub>3</sub> and MnS, the complex of FeO•Al<sub>2</sub>O<sub>3</sub> and AlN under Al-Si deoxidation method, separately.

## Refractory Metals 2010: Oxidation of Alloys and Coatings

*Sponsored by:* The Minerals, Metals and Materials Society, TMS Structural Materials Division, TMS: Refractory Metals Committee  
*Program Organizers:* Brian Cockeram, Bechtel-Bettis; Gary Rozak, H.C. Stark

Tuesday AM Room: 2A  
February 16, 2010 Location: Washington State Convention Center

*Session Chairs:* Brian Cockeram, Bechtel Marine Propulsion Corporation; Gary Rozak, H. C. Starck, Inc.

### 8:30 AM

**Development of Oxidation Protective Coatings for Molybdenum Alloys:** *Ridwan Sakidja<sup>1</sup>*; Travis Sossaman<sup>1</sup>; *John Perepezko<sup>1</sup>*; <sup>1</sup>University of Wisconsin-Madison

Molybdenum alloys including TZM and Mo-rich Mo-Si-B alloys have great potential for high temperature structural applications due to their high melting point and high temperature strength. The main limitation has been their high temperature oxidation resistance. In previous work Mo disilicide coatings were used for oxidation protection. However, the CTE mismatch between the coatings and Mo alloys and the loss of coating by Si diffusion into the substrate are two main challenges. In the current study, we evaluated the synthesis and performance of two types of Mo-based coatings: borosilicide and aluminosilicide. The borosilicide coating is comprised of a three layer structure: borosilicate, Mo-rich silicide and Mo-rich borosilicide, whereas the aluminosilicide coating is composed of Al-saturated Mo silicide and Mo-aluminide. The new coatings exhibit a significant improvement in the oxidation protection for Mo alloys over the conventional disilicide coatings under various oxidation conditions. The financial support from ONR(N00014-07-1-1083) is greatly appreciated.

Tue. AM

# Technical Program

8:55 AM

**Refractory Metal Alloys for Ultra High Temperature Applications:** *Panayiotis Tsakiroopoulos*<sup>1</sup>; <sup>1</sup>The University of Sheffield

The search for new materials to replace Ni based superalloys in gas turbine engines has included alloys of refractory metals, in particular Mo and Nb based alloys. Alloys selected from Nb-Si-X-Y (X=sd element(s), Y=sp element(s) or metalloid) systems can provide a good combination of high strength, adequate toughness and creep as well as high melting temperature. This presentation will concentrate on the development of such alloys with emphasis on processing, phase selection and phase stability. Alloys based on Mo-Si-Y (Y as above) systems offer opportunities to exploit multiphase microstructures with good oxidation resistance. This presentation will also concentrate on alloys of the Mo-Si-Al system as a basis for providing environmental protection to refractory metal alloys.

9:20 AM

**Microstructures and High Temperature Oxidation Behavior of Mo-Ni-Al Alloys:** *Pratik Ray*<sup>1</sup>; Travis Brammer<sup>1</sup>; Mufit Akinci<sup>1</sup>; Matthew Kramer<sup>2</sup>; <sup>1</sup>Iowa State University; <sup>2</sup>Ames Laboratory

Discovery of high temperature materials that go beyond current state-of-the-art Ni based alloys has proven to be an extreme challenge. Based on the body of research available on silicides and Ni based alloys, we attempt to design an alloy that will combine the ultra-high temperature phase stability of the silicides with adequate ductility and oxidation resistance. The first criterion in the choice of the alloy system is high melting temperature. Additionally, there is the need for an oxidation resistant as well as relatively ductile high temperature phase (which is usually a refractory metal based solid solution). The experimental design is to closely couple the semi-empirical methodologies to ab initio methods to assess the best candidate for high temperature alloy design. The architectural framework for our material's design is a refractory base metal with a high temperature intermetallic which provides both high temperature rigidity and a source of oxidatively stable elements.

9:45 AM

**Comparison of the Oxidation Behavior of Nb-20Mo-15Si-25Cr and Nb-20Mo-15Si-25Cr-5B Alloys from 700 to 1300°C:** *Benedict Portillo*<sup>1</sup>; Shailendra Varma<sup>1</sup>; <sup>1</sup>The University of Texas at El Paso

Nb-20Mo-15Si-25Cr and Nb-20Mo-15Si-25Cr-5B alloys have been subjected to oxidation in air from 700 to 1300°C. Weight gain per unit area as a function of time has been used for the estimation of the oxidation resistance of these two alloys. There is a noticeable improvement in the resistance for the alloys containing B. Both alloys can withstand the oxidation for 24 hours up to 1300°C. However, alloys without B are susceptible to extensive pitting at 900°C. As cast structure in both alloys contains Laves, Nb based solid solution and silicide phases. Their relative proportions influence the oxidation resistance in the range of temperature used in this study. Results from EDS, XRD and TGA characterization will be discussed.

10:10 AM Break

10:25 AM

**Effect of Al on the Oxidation Behavior of Nb-Si-Cr Alloys in Air from 700 to 1300°C:** *Clemente Parga*<sup>1</sup>; *David Alvarez*<sup>1</sup>; Shailendra Varma<sup>1</sup>; <sup>1</sup>The University of Texas at El Paso

Nb-10Si-20Cr-5Al, Nb-10Si-30Cr-5Al, Nb-30Si-10Cr-5Al, and Nb-30Si-20Cr-5Al alloys (compositions are in atomic percent) have been subjected to oxidation in air from 700 to 1300°C. Oxidation resistance of these alloys has been monitored using weight gain per unit area as a function of time isothermally. Static heating for 24 hours and cyclic heating of 4 and 24 hours of cycles up to 24 and 168 hours, respectively, at a given temperature has been used to compare the oxidation characteristics. The observed microconstituents have been compared with those predicted by the isotherms calculated by PandatTM software program. The oxide scale identification has been performed by EDS in SEM and BSE imaging, and XRD. The effect of Al on the oxidation behavior can then be determined by comparing the results with the reported work from earlier studies.

10:50 AM

**General Chemical Solution Deposition to Epitaxial Growth of Transition Metal (Ti, Nb, V, Ta, etc.) Carbide Films:** *Guifu Zou*<sup>1</sup>; Haiyan Wang<sup>2</sup>; Nathan A. Mara<sup>1</sup>; Quanxi Jia<sup>1</sup>; <sup>1</sup>Los Alamos National Laboratory; <sup>2</sup>Texas A&M University

Transition metal carbides possess a number of useful properties including exceptional hardness, high-temperature stability, low electrical resistivity, and corrosion and oxidation resistance. Due to high performance, their films/coatings are widely interesting for materials scientists. This work shows the epitaxial growth of some metal carbide films on the sapphire substrates by general chemical solution deposition. Both X-ray diffraction analyses and HRTEM images shows the epitaxial growth of carbides films with high quality. The electron transports of TiC and NbC films have the properties of semiconductor and superconductivity, respectively. The transition temperature of NbC is close to 10.5 K. Furthermore, these carbides films show strong hardness in the nanomechanical tests. The hardness and Young's modulus of TiC are achieved to ~ 23 and 420 GPa, respectively.

---

**Solid-State Interfaces: Toward an Atomistic-Scale Understanding of Structure, Properties, and Behavior through Theory and Experiment: Mechanical Properties and Interaction with Dislocations**

*Sponsored by:* The Minerals, Metals and Materials Society, TMS Electronic, Magnetic, and Photonic Materials Division, TMS Structural Materials Division, TMS: Chemistry and Physics of Materials Committee

*Program Organizers:* Michael Demkowicz, Massachusetts Institute of Technology; Douglas Medlin, Sandia National Laboratories; Emmanuelle Marquis, University of Oxford

Tuesday AM

Room: 602

February 16, 2010

Location: Washington State Convention Center

*Session Chairs:* Sylvie Aubry, Stanford University; Kedarnath Kolluri, Massachusetts Institute of Technology

8:30 AM Invited

**TEM Analysis of the Structure and Deformation Behavior of an Incommensurate Grain Boundary in Gold:** *Ulrich Dahmen*<sup>1</sup>; Jia Ye<sup>1</sup>; Andy Minor<sup>1</sup>; Tamara Radetic<sup>1</sup>; Damien Caliste<sup>2</sup>; Frederic Lancon<sup>2</sup>; <sup>1</sup>NCEM; <sup>2</sup>CEA

The atomic structure of an incommensurate grain boundary in gold has been characterized by high resolution electron microscopy and compared with atomistic simulations. Local relaxation of the boundary near the surface leads to a chevron-like defect of whose size and stability is related to the stacking fault energy. Simulations predict that such local relaxations play a dominant role during deformation of finite-sized bicrystals because the surfaces act as defects in the incommensurate structure of the infinite boundary, which is expected to deform by superglide. We have tested these predictions by compressing bicrystalline nanopillars of gold using a nanoindenter inside an electron microscope. A detailed analysis of the observed structure and deformation behavior is in good agreement with atomistic simulations.

9:00 AM

**Coupling between Grain Boundary Sliding and Migration: Analysis of Possible Mechanisms:** *Askar Sheikh-Ali*<sup>1</sup>; <sup>1</sup>Kazakh-British Technical University

The coupling between grain boundary sliding and migration has been established for boundaries with coincidence misorientations in metals and ceramics. However, the exact mechanism of this process remains unclear. In the present investigation the behavior coincidence and near-coincidence symmetric tilt boundaries in zinc bicrystals subjected to high-temperature deformation have been studied. Sliding-migration ratio and direction of boundary migration have been determined. The obtained results are analyzed in terms of two possible mechanisms: the glide of extrinsic DSC dislocations and motion of secondary grain boundary dislocations.

Tue. AM



9:20 AM

**Structure and Hardness of V/Ag Multi-Layers:** *Qiangmin Wei*<sup>1</sup>; Amit Misra<sup>1</sup>; <sup>1</sup>Los Alamos National Lab

Microstructure and hardness of polycrystalline V/Ag multilayers with different individual thickness ranging from 1nm to 50 nm were investigated. It was found that, with decreasing individual layer thickness, interface structure changes from incoherent to semicoherent, accompanied by the decrease of defect density. For individual layer thickness less than 5 nm, although the interface exhibits considerable variation, close packed planes of face centered cubic (FCC) and body centered cubic (BCC) connect each other at the interface and as a consequence Bain orientation was generated. When layer thickness is 1 nm, semicoherent interface was observed in which most of Ag becomes BCC structure. The role of interfaces and layer thickness on the structure and hardness of V/Ag multilayers is discussed. This research is funded by the US DOE, Office of Basic Energy Sciences.

9:40 AM

**Atomic-Scale Study of Nanoindentation in FCC Crystal with Internal Interface:** *Yury Osetskiy*<sup>1</sup>; Anna Serra<sup>2</sup>; Roger Stoller<sup>1</sup>; <sup>1</sup>ORNL; <sup>2</sup>UPC

We present results of an extensive molecular dynamics study of material deformation during the nanoindentation process of an fcc crystal containing an internal interface. As a first example, we have used Al and Cu and elementary twin boundary in the  $\frac{1}{2}\{111\}$  plane. The indentation process was simulated by spherical or cylindrical indenters with diameter up to 40 nm moving at a constant speed of 10 or 2 m/s. Features of plastic deformation made by spherical and cylindrical indenters, formation of different glissile microstructures and their interactions with twin boundary were studied and the effects of indenter type, size and rate as well as material, i.e. low stacking fault energy Cu versus high stacking fault energy Al, were observed and will be discussed.

10:00 AM

**Simulations of Dislocation Pile-up at Asymmetric Tilt Boundary in Aluminum:** *Steven Valone*<sup>1</sup>; Timothy Germann<sup>1</sup>; Richard Hoagland<sup>1</sup>; Authur Voter<sup>1</sup>; Danny Perez<sup>1</sup>; Zhiqiang Wang<sup>1</sup>; <sup>1</sup>Los Alamos National Laboratory

Problems in materials deformation processes are becoming approachable for the first time through the largest available computers that implement both conventional and accelerated molecular dynamics. In one deformation process, dislocation pile-up at a grain boundary, a greater understanding is required as to how dislocations are either transmitted through grain boundaries, cause plastic deformation in an adjoining grain, or cause the grain boundary to fail. Here dislocation pile-ups in an aluminum bicrystal with an asymmetric tilt grain boundary are simulated at several levels of resolution of the pile-up, gradually introducing effects of dislocation interactions beyond linear elastic ones. The observed responses as functions of the number of explicitly modeled dislocations and the magnitude of the applied stress are discussed. Longer-time responses are examined more fully through accelerated molecular dynamics simulations, thereby allowing more realistic applied stresses, strain rates, and mechanisms to be modeled.

10:20 AM Break

10:40 AM Invited

**Ductility, Interfacial Shear, and Fracture of Cu/Nb Nanolayered Composites:** *Nathan Mara*<sup>1</sup>; Dhriti Bhattacharyya<sup>1</sup>; Pat Dickerson<sup>1</sup>; Richard Hoagland<sup>1</sup>; Amit Misra<sup>1</sup>; <sup>1</sup>Los Alamos National Laboratory

Cu/Nb nanoscale multilayered composites have shown ultra-high strength as well as high ductility in a variety of mechanical test methods (nanoindentation, tensile testing, and micropillar compression). Individual layer thicknesses tested range from 100 nm to 5 nm, with flow stresses of nearly 3 GPa (5 nm Cu/Nb case), and deformation in excess of 20% during micropillar compression. It is found that the relatively low Cu/Nb interfacial shear strength leads to localization of deformation at the interface when loaded directly in shear. When the material is loaded perpendicular to the interface, homogeneous deformation of over 10% true strain is evident at individual layer thicknesses as low as 5 nm, followed by shear band formation. TEM evaluation of the microstructure within the shear band exhibits large plastic deformation and grain rotation relative to the compression axis, and the layered structure remains continuous even after local strains in excess of 70%.

11:10 AM

**Computer Simulation of Boundary – Dislocation and Boundary – Loop Interactions in the {10-12} Twin in Alpha-Zirconium:** *Anna Serra*<sup>1</sup>; David Bacon<sup>2</sup>; <sup>1</sup>Technical University of Catalonia; <sup>2</sup>The University of Liverpool

The development of a method that allows an interface containing a disconnection line to be simulated with periodic boundary conditions in the interface plane has allowed to investigate the interaction of a moving {10-12} twin boundary with two types of crystal defect, namely, a straight  $\frac{1}{3}\langle 11-20 \rangle$  (0001) dislocation lying perpendicular to the direction of the twinning shear and a periodic row of perfect dislocation loops. Boundary reactions with crystal dislocations are likely to be important for assisting the twinning process by providing a simple mechanism for twin growth/shrinkage. The boundary attracts both vacancy and interstitial dislocation loops with inclined Burgers vector but is not transparent to them as the complete loop is swept along its glide prism by the moving interface. The results indicate that twinning is efficient at sweeping loops from the microstructure when their density is low and is suppressed by loops when their density is high.

11:30 AM

**Flexible Boundary Condition Methods for Interfaces: Dislocation/Twin-Boundary Interactions:** *Maryam Ghazisaeidi*<sup>1</sup>; Dallas Trinkle<sup>1</sup>; <sup>1</sup>University of Illinois at Urbana-Champaign

Flexible boundary condition methods couple an isolated defect to bulk through the bulk lattice Green's function. Application of such methods to materials involving an interface requires the computation of interfacial lattice Green's functions. We present a method to compute the lattice Green's function for a planar interface with arbitrary interactions. The interface is coupled to two different semi-infinite bulk regions, and the Green's function for interface-interface, bulk-interface and bulk-bulk interactions are computed individually. The elastic bicrystal Green function and the bulk lattice Green function give the interaction between bulk regions. Direct inversion of the force constant matrix using a partial Fourier transform to account for translational invariance provides the interface terms. The general method makes no assumptions about the atomic interactions or crystal orientations. We simulate a screw dislocation interacting with a (10-12) twin boundary in Ti using flexible boundary conditions, and compare with previous results.

11:50 AM

**The Behavior of  $\Sigma 11, \langle 110 \rangle \{252\} \{414\}$  Grain Boundary in Aluminum under Shock Loading by Molecular Dynamics Simulations:** *Chiara Pozzi*<sup>1</sup>; Timothy Germann<sup>2</sup>; *Donato Firrao*<sup>1</sup>; Richard Hoagland<sup>2</sup>; <sup>1</sup>Politecnico di Torino; <sup>2</sup>Los Alamos National Laboratory

Metastable configurations can be obtained for the  $\Sigma 11 \langle 110 \rangle \{252\} \{414\}$  asymmetric grain boundary (GB) in aluminum by varying the reciprocal positions of the two grains before relaxing the initial structure. Molecular Dynamics (MD) simulations were performed in order to study the behavior of some of these GB configurations under shock loading. For different shock strengths and EAM potentials, observed plastic deformation modes include the emission of perfect and partial dislocations from the GB and, in some cases, the formation of nanotwins. These features and their nucleation mechanisms, as related to the shock strength and direction, the GB arrangement, the size of the model, and the material properties (via comparison of different EAM potentials) will be discussed on the basis of our MD simulation results.

12:10 PM

**Microstructural Stability and Plastic Deformation in Nanocrystalline Copper Doped with Antimony: Experiments and Molecular Dynamics Simulations:** *Douglas Spearot*<sup>1</sup>; Rahul Rajgarhia<sup>1</sup>; Ashok Saxena<sup>1</sup>; <sup>1</sup>University of Arkansas

Experimental and simulation results have provided a wealth of information on the behavior of pure metallic materials with nanocrystalline microstructures. However, the influence of alloying elements at the grain boundaries in nanocrystalline materials is still unknown. In this work, the microstructural stability and plastic deformation of a nanocrystalline Cu-Sb alloy is evaluated via experiments and molecular dynamics (MD) simulations. MD simulations are used to study grain boundary stability and dislocation activity in nanocrystalline Cu with antimony (0.0-2.0 at.%Sb) at the grain boundaries. Microhardness and microtensile test experiments are performed on nanocrystalline Cu with 0.2 and 0.5 at.%Sb located predominantly at the grain boundaries. Results show that small concentrations of Sb can retard grain growth mechanisms, raising the

Tue. AM

# Technical Program

potential service temperature of nanocrystalline Cu. MD simulations also show that small concentrations of Sb at the grain boundaries increase the flow stress of nanocrystalline Cu, in agreement with the experimental results.

## Surface Engineering for Amorphous-, Nanocrystalline-, and Bio-Materials: Session III

*Sponsored by:* The Minerals, Metals and Materials Society, TMS Materials Processing and Manufacturing Division, TMS: Surface Engineering Committee

*Program Organizers:* Sandip Harimkar, Oklahoma State University; Arvind Agarwal, Florida International University; Sudipta Seal, University of Central Florida; Narendra Dahotre, University of Tennessee

Tuesday AM Room: 604  
February 16, 2010 Location: Washington State Convention Center

*Session Chairs:* Indranil Manna, Indian Institute of Technology; Ramki Kalyanaraman, University of Tennessee

### 8:30 AM Introductory Comments

#### 8:35 AM Invited

**Materials Research in the Materials and Surface Engineering Program at the National Science Foundation:** *Clark Cooper*<sup>1</sup>; <sup>1</sup>National Science Foundation

Materials research is supported by several programs at the National Science Foundation (NSF), including the Materials and Surface Engineering (MSE) program. While submissions to NSF programs typically focus on the advancement of fundamental science, most proposals identify application areas that are expected to be underpinned through successful execution of the proposed research. Examples of increasingly important application areas for proposals submitted to myriad programs at NSF, including MSE, are (1) energy and sustainability and (2) life sciences and biomedicine. This presentation will provide an overview of the MSE program, including funding opportunities and the identification of program foci, and will highlight exciting recent advances that have been achieved through NSF research grants from this program. Also to be underscored in this presentation is the importance of modeling and simulation, experimentation, theory development, and their interplay to advance frontiers in the fundamental understanding of materials.

#### 9:00 AM Invited

**Glass-Forming Metallic Films for Enhancing Mechanical Property of Structural Materials:** *Cheng-min Lee*<sup>1</sup>; *Jinn P. Chu*<sup>1</sup>; *Peter K. Liaw*<sup>2</sup>; *T. G. Nieh*<sup>2</sup>; <sup>1</sup>Nation Taiwan University of Science and Technology; <sup>2</sup>The University of Tennessee

Metallic glass-forming materials show desirable properties, including good surface finishes and high strength in the thin film form, thus making them ideal candidates for coating materials to improve mechanical properties, especially fatigue properties of structural materials. Zr- and Cu-based glass-forming metallic films were deposited on stainless steels, using magnetron sputtering. Four-point-bending fatigue tests were conducted on these coated materials. The fatigue life and the fatigue-endurance limit were considerably improved, depending on the different films and the maximum applied stresses. Fractographic studies indicated the good adhesion between the glass-forming film and the substrate. The surface-roughness measurements showed the improved surface conditions due to the film deposition. Analyses showed that the high strength and the moderate bending ductility of the glass-forming metallic films might play beneficial roles, revealing the deposition of glass-forming metallic films on structural materials as a potentially novel and effective method to enhance fatigue properties of structural materials.

#### 9:25 AM Invited

**Surface and Bulk Nanostructures for Optical Absorption Enhancement in Thin Si Films:** *Ritesh Sachan*<sup>1</sup>; *J. Strader*<sup>1</sup>; *A.W. Paradies*<sup>1</sup>; *W. Yueying*<sup>1</sup>; *H. Uk*<sup>1</sup>; *H. Garcia*<sup>2</sup>; *P.D. Rack*<sup>1</sup>; *G. Duscher*<sup>1</sup>; *R. Kalyanaraman*<sup>1</sup>; <sup>1</sup>University of Tennessee-Knoxville; <sup>2</sup>Southern Illinois University

Crystalline thin film Si is considered as an important photovoltaic material for sustainable solar energy harvesting applications. However, Si has an inherent limitation due to its poor light absorption in the visible wavelengths. In the

present study, this drawback is addressed by utilizing optical materials design models to guide the preparation of surface or embedded metallic nanostructures with Si thin films. Various metals and silicides have been prepared by sputtering, pulsed laser deposition and laser-induced self-organization routes. The resulting structure, morphology and interfaces have been investigated using electron and scanning probe microscopies and EELS analysis in TEM. Optical and electrical studies of various structures integrated with Si show promise for enhancing these functional characteristics. From such studies, we expect to identify the composition and nanoscale morphologies that could be relevant towards increasing the absorption of visible light in thin film solar devices.

#### 9:50 AM

**Formation of Amorphous Metallic Coatings by the LENS™ Process:** *Hongqing Sun*<sup>1</sup>; *Katharine Flores*<sup>1</sup>; <sup>1</sup>The Ohio State University

Direct laser deposition is a useful technique to create coatings and large-scale components with amorphous or uniquely tailored, non-equilibrium microstructures. We use the Laser Engineered Net Shaping (LENS™) process to deposit Zr-based metallic glass forming powders on both amorphous and crystalline substrates. In both cases, amorphous melt zones are observed surrounded by crystalline heat-affected zones (HAZs). The microstructures of the deposited layers and underlying substrates were characterized as functions of the processing parameters. Optimization of the heat input results in the formation of a continuous amorphous layer without crystallization in the HAZ. However, multilayer deposition results in devitrification of previously deposited material. To better describe the thermal history of the glassy melt zone and underlying substrate material, finite element modeling analysis was performed and compared to in-situ thermal imaging measurements. The crystalline HAZ is found to occur only in regions reaching temperatures more than 100 K above the crystallization temperature.

#### 10:10 AM Invited

**Fe-Cr-Mo-Y-B-C Bulk Metallic Glass Coating on AISI 4340 Steel by Laser Surface Cladding:** *Indranil Manna*<sup>1</sup>; *S. Harimkar*<sup>2</sup>; *Jyotsna Dutta Majumdar*<sup>1</sup>; *Manoj Debnath*<sup>1</sup>; *N. Dahotre*<sup>3</sup>; <sup>1</sup>Indian Institute of Technology Kharagpur; <sup>2</sup>Oklahoma State University; <sup>3</sup>University of Tennessee

In the present study, Fe<sub>48</sub>Cr<sub>15</sub>Mo<sub>14</sub>Y<sub>2</sub>C<sub>15</sub>B<sub>6</sub> bulk metallic glass has been laser surface cladded on AISI 4340 steel substrate to develop an amorphous coating. Due to solute redistribution within the clad zone and across the clad-substrate interface, complete amorphous surface microstructure has not been observed. The incident laser power and interaction time controls the thickness of coating. The thickness of the clad layer was found to increase with increase in applied power and decreases with increasing scan speed. XRD profiles shows  $\alpha$ -Fe, iron carbide (Fe<sub>7</sub>C<sub>3</sub>), chromium carbide (Cr<sub>7</sub>C<sub>3</sub>), iron boride (Fe<sub>2</sub>B), Molybdenum boride (Mo<sub>2</sub>B) and yttrium boride (YB<sub>12</sub>) phases. The microhardness of the clad layer is significantly improved (to as high as 1100 VHN) as compared to the substrate hardness (240 VHN). Laser surface cladding has also improved wear resistance. The microhardness and wear resistance properties of the clad zone were found to vary with laser parameters and depth.

#### 10:35 AM Break

#### 10:50 AM

**Spark Plasma Sintering of Amorphous Coatings on Metallic Substrate:** *Ashish Singh*<sup>1</sup>; *Sandip Harimkar*<sup>1</sup>; <sup>1</sup>Oklahoma State University

There is increasing commercial and scientific interest in developing metallic glass coatings due to their enhanced mechanical properties. However, deposition of dense and amorphous coating is still a challenge by using conventional thermal processing methods like thermal spray coatings. Spark plasma sintering is an emerging technology and is used to compact nano ceramics, bulk metallic glass, and functionally graded materials at comparatively low temperature and pressure. In the present work, we will discuss the results of deposition of amorphous coatings on metallic substrates using spark plasma sintering method. The influence of spark plasma sintering processing parameters on the degree of coating amorphosity, coating density, and strength of coating/substrate interface will be discussed.



11:10 AM

**Surface Amorphization in “Chromium-on-Silicon” System Resulted by Compression Plasma Action:** *Vladimir Uglov*<sup>1</sup>; Nikolai Kvasov<sup>2</sup>; Yuri Petukhou<sup>2</sup>; Valiantsin Astashynski<sup>3</sup>; Anton Kuzmitski<sup>3</sup>; <sup>1</sup>Belarusian State University; <sup>2</sup>Belarusian State University of Informatics and Radioelectronics; <sup>3</sup>B.I. Stepanov Institute of Physics, National Academy of Sciences of Belarus

The results of studies of pre-surface layers structure, phase and elemental composition of plasma-intermixed “chromium-on-silicon” system are reported. Plasma intermixing was carried out by quasi-stationary compression plasma flows. Power density absorbed by target varied from 0,8 to 1,3 GW/cm<sup>2</sup>, pulse duration about 100 μs. XRD-studies revealed the formation of amorphous phase and crystalline hexagonal chromium disilicide CrSi<sub>2</sub>. Coordination sphere radius of amorphous phase estimates about 0,95 nm and increases with power density. SEM-studies showed amorphous phase to locate in the pre-surface layer (about 1 μm thickness). In accordance with XMA results it contains about 65 at.% of chromium and 35 at.% of silicon. Thermal stability of amorphous phase after 400°C and 600°C anneal is discussed.

11:30 AM

**Laser and E-Beam Generated Micro-Nanostructures on the Surface of Amorphous Chalcogenide Layers:** *Sandor Kokenyesi*<sup>1</sup>; Viktor Takats<sup>2</sup>; Istvan Chernovich<sup>1</sup>; Mihail Trunov<sup>3</sup>; Attila Csik<sup>2</sup>; Csaba Cserhati<sup>1</sup>; <sup>1</sup>University of Debrecen; <sup>2</sup>ATOMKI; <sup>3</sup>Uzhgorod National University

Holographic gratings and optical waveguide structures are important in optoelectronics. They can be rather easily created by optical or e-beam recording in special materials due to the stimulated changes of their optical and other parameters. Last time special interest is increasing to the direct, one step recording processes, especially connected with surface modulation at micro- and nanoscales. In a wide class of functional materials amorphous chalcogenides are interesting because of the complex of light- and e-beam induced effects like giant surface deformations. These data show on the prospects of direct, one-step recording process which may be especially useful for prototyping optical, photonic elements, but the correlations with composition of the material and experimental conditions are not clear yet. It was a reason of our detailed investigations on the surface deformation processes in amorphous layers made from different As-S(Se) chalcogenide glasses and some nanolayered films.

11:50 AM

**A High Throw Bright Acid Copper for Rack Plating of Printed Circuit Boards:** *Xiao Faxin*<sup>1</sup>; Shen Xiaoni<sup>1</sup>; <sup>1</sup>Henan University of Science and Technology of China

A novel acid copper plating process produces a bright deposit with excellent throwing power from a sulfate system. Particular attention is placed on the effect of phenyl poly disulfide propane sulfonate, PEG and 2-Mercapto benzimidazole on the copper coating and the appropriate concentration of these additives is 20 mg/L, 60 mg/L and 0.6mg/L, respectively. The bright smooth copper layer may be deposited at 1-5 A/ dm<sup>2</sup> and 20-45° in this solution. The throwing power can reach 91.5% and the deepening plating ability of hole with L/d of 5 is 100%, which shows that this process may be used for rack plating applications of printed circuit board. The corruption rate of the coating is 0.0548g/(m<sup>2</sup>·h) in 5%NaCl solution. The XRD results show that the crystal face is mainly assigned to the (112) crystal face on the deposits. The SEM results show that the appearance is uniform and the grain is superfine.

12:10 PM

**Electroless Cu Metallization of Carbon Fiber by Precious-Metal Free Process:** *Che Dehui*<sup>1</sup>; Yao Guangchun<sup>1</sup>; Liu Kai<sup>1</sup>; Cao Zhuokun<sup>1</sup>; <sup>1</sup>Institute of Materials and Metallurgy, Northeastern University

The paper introduces the new technique of electroless copper deposition on the carbon fibers under absence of precious-metal as catalyzer. Cu layer were electrolessly deposited on the surface of carbon fiber without having to use the conventional palladium or silver catalyst to initiate the redox reaction leading to metallization. This new technique showed that Ni seeds can serve as excellent catalyst, which expedite the re-deoxidation reactions. Through experiment, the activation temperature, concentration, the PH value, were optimized, and a orbicular copper plating layer of carbon fiber in copper sulfate salt-based conventional electroless solution was obtained. The Surface morphology of copper coating was characterized by scanning electron microscope (SEM) and X-ray diffraction (XRD). The results indicate that uniform and smooth copper

coating could be obtained by the new precious-metal free activation process. The whole copper coating thickness is about 1 micron.

### Sustainable Materials Processing and Production: Motivating Sustainability II

*Sponsored by:* The Minerals, Metals and Materials Society, TMS Extraction and Processing Division, TMS Light Metals Division, TMS: Recycling and Environmental Technologies Committee, TMS: Education Committee

*Program Organizers:* Christina Meskers, Umicore; Randolph Kirchain, Massachusetts Institute of Technology; Diana A. Lados, Worcester Polytechnic Institute; Markus Reuter, Ausmelt Limited

Tuesday AM Room: 2B  
February 16, 2010 Location: Washington State Convention Center

*Session Chairs:* Christina Meskers, Umicore Precious Metals Refining; Elsa Olivetti, MIT

### 8:30 AM Introductory Comments

#### 8:35 AM Keynote

**Title Not Available:** *Guido Sonnemann*<sup>1</sup>; <sup>1</sup>United Nations Environmental Program (UNEP)

Abstract not available.

#### 9:00 AM Keynote

**Title Not Available:** *Jim Puckett*<sup>1</sup>; <sup>1</sup>Basel Action Network

Abstract not available.

### 9:25 AM

**European Recycling Platform – Experiences from a New Venture:** *Hans Korfmacher*<sup>1</sup>; <sup>1</sup>The Procter & Gamble Company

Product take-back regulations implemented in Europe have presented significant challenges to the consumer electronic product and battery industries. Initially companies established single compliance organisations within individual Member States. These programs met business needs but were inefficient and costly. They were protected from pressures of marketplace competition and could not leverage economies of scale. In order to address these problems P&G, Hewlett Packard, Sony and Electrolux conceived a pan-European compliance organisation to collect waste electronic equipment Europe-wide. This organization, called the European Recycling Platform (ERP), operates in competition with existing national compliance systems. Since 2002 ERP has collected 700,000+ tons of waste electronic products and delivered millions of dollars in cost savings. This presentation reviews the steps needed to establish successful competitive collection organizations that provide sustainable recycling at the lowest cost.

### 9:50 AM Break

### 10:05 AM Invited

**Scarce Metals and Emerging Technologies: Strategies towards a Sustainable Governance:** *Patrick Wüger*<sup>1</sup>; Daniel Lang<sup>2</sup>; <sup>1</sup>Empa; <sup>2</sup>ETH Zürich

Emerging technologies such as photovoltaics or information and communication technologies (ICT) play an increasingly important role in our society. For several of these technologies it is claimed that they significantly contribute to a transition towards a more sustainable society. As many of these technologies are based on scarce metals, a scholarly and societal discussion has emerged regarding, the questions if (i) the accessibility to the scarce metals might restrict the diffusion of emerging technologies and (ii) the increasing demand for scarce metals might counterbalance the positive effects expected from these technologies in view of sustainable development. Scarce metals supply is governed by a multitude of geological, geopolitical, technological, ecological and other factors. The identification of options for a more sustainable scarce metals supply hence requires the application of an integrative, systemic perspective that considers existing uncertainties as well as the partly diverging interests of different societal actor groups (e.g. state, company or individuals). In our contribution we will derive major challenges with respect to a more sustainable supply of scarce metals, sketch a framework of possible approaches to cope with these challenges and illustrate the approaches with selected examples. The framework is intended to be a first step towards sustainable

# Technical Program

governance of scarce metals, which, in addition to supply issues also will have to consider the demand side.

## 10:30 AM

### Lithium-Ion Batteries: Examining Material Demand and Recycling Issues:

Linda Gaines<sup>1</sup>; Paul Nelson<sup>1</sup>; <sup>1</sup>Argonne National Laboratory

Use of vehicles with electric drive, which could reduce our oil dependence, will depend on lithium-ion batteries. But is there enough lithium? Will we need to import it from a new cartel? Are there other materials with supply constraints? We project the maximum demand for lithium and other materials if electric-drive vehicles expanded their market share rapidly, estimating material demand per vehicle for four battery chemistries. Total demand for the United States is based on market shares from an Argonne scenario that reflects high demand for electric-drive vehicles, and total demand for the rest of the world is based on a similar International Energy Agency scenario. Total material demand is then compared to estimates of production and reserves, and the quantity that could be recovered by recycling, to evaluate the adequacy of supply. Finally, we identify producing countries to examine potential dependencies on unstable regions or future cartels.

## 10:55 AM

### Critical and Strategic Failure of Rare Earth Resources: James Kennedy<sup>1</sup>;

<sup>1</sup>Wings Enterprises, Inc.

Rare Earths: Understanding The United States complete failure of status and relevance in Rare Earth Oxides, Elements and Alloys. Although rare earth oxides are strategic and critical in their own right, elements and alloys are even more important for the development of "Green Technologies" and advanced weapons systems. America does not have an active domestic source of rare earth oxides. America does not have any Heavy Rare Earth Elemental or Alloy capabilities. The magnitude of this failure continues to become more apparent as the manufacture of REO based electronics and magnetic components moves eastward towards China. China has succeeded in outmaneuvering The United States and the world in its quest to control the Rare Earth Oxides, Elements and Alloys, and the many industries dependent upon REO. What can be done?

## 11:20 AM

### Motivating Sustainable Material Use through Industry-Level Simulation

Modeling of Platinum Stocks and Flows: Elisa Alonso<sup>1</sup>; Richard Roth<sup>1</sup>; Frank Field<sup>1</sup>; Randolph Kirchain<sup>1</sup>; <sup>1</sup>MIT

Manufacturing firms who rely on finite resources have a stake in ensuring sustainable materials use. Higher material prices and uncertain material supply, consequences associated with scarcity, can be damaging to firms. Firms have a number of options to improve material sustainability including dematerialization, material substitution and recycling. However, these options require technological capability, capital investments and supply-chain infrastructure and firms may decide to only make such investments if material prices increase. Once decisions are made, there are further delays before changes can be implemented, delays that may harm the slower-to-react firms. The impact of these delays on firms facing material scarcity was examined for the case of different platinum-using industries. It was found that these delays are particularly problematic for firms when limited material availability leads to volatile market conditions. Industries can benefit especially if they ensure supply diversity by using recycled materials as well as primary.

## 11:45 AM

### A Collaborative Tool for Waste Management in the Industry: Marisa

Borges<sup>1</sup>; Humberto Riella<sup>1</sup>; Paulo Janissek<sup>2</sup>; <sup>1</sup>Universidade Federal de Santa Catarina; <sup>2</sup>Positivo University

The industry needs to reach environmental patterns, technological innovations and demands of the productive sector, is covered by this study. The environmental care, responsibility in the industry activities and the necessary cultural changes for companies and entities is also emphasized. A collaborative tool was developed to help all partners involved in the environmental administration. This tool is focused on the essential interaction among residue generators belonging to the all productive chain. It was addressed to the industrial unit of a vehicle assembler company, with additional support of entities or institutions with emphasis in the research, development and innovation. To find the best environmental solution it is necessary an expertise and capacity to develop new applications and products, as well as reuse, recycling and reduction of waste generated on industrial processes. The aim of this work is to establish a tool for socio-environmental management.

## 12:10 PM Concluding Comments

### The Vasek Vitek Honorary Symposium on Crystal Defects, Computational Materials Science and Applications: Dislocations I

Sponsored by: The Minerals, Metals and Materials Society, TMS Materials Processing and Manufacturing Division, TMS/ASM; Computational Materials Science and Engineering Committee  
Program Organizers: Mo Li, Georgia Institute of Tech; David Srolovitz, Institute for High Performance Computing, Agency for Science, Technology and Research, Singapore; Adrian Sutton, Imperial College London; Vaclav Paidar, Institute of Physics AS CR vvi; Jeff De Hosson, University of Groningen

Tuesday AM

Room: 603

February 16, 2010

Location: Washington State Convention Center

Session Chairs: Roman Groger, Academy of Sciences of the Czech Republic; Jeff De Hosson, University of Groningen

## 8:30 AM Invited

### First Principles Study of Dislocation Cores and Solute Interactions:

Christopher Woodward<sup>1</sup>; Dallas Trinkle<sup>2</sup>; Louis Hector<sup>3</sup>; <sup>1</sup>Air Force Research Laboratory; <sup>2</sup>University of Illinois, Champaign Urbana; <sup>3</sup>General Motors Research and Development Center

The local strain field around a dislocation, the dislocation core, can have a strong influence on local and macroscopic deformation behavior in both FCC and BCC metals. This presentation will review the variety of dislocation cores that have been derived using density functional theory coupled with a flexible boundary condition method. These include  $a/2\langle 111 \rangle$  screw dislocations in Mo, Ta, and Fe, and  $a/2\langle 110 \rangle$  screw dislocations in fcc Al, Ir, and L10 TiAl. In the BCC transition metals, contrary to classical central-force potentials, this first principles method always produces a screw dislocation with an isotropic core. First principles methods have also been used to reassess solution softening in Mo-Re and Mo-Pt alloys. Finally, we have been calculating the solute dislocation interactions of  $a/2\langle 110 \rangle$  edge dislocations with Mg, Si, Cr, and Ge solutes in FCC Al. Progress towards understanding solute diffusion effects in the core region will be reviewed.

## 8:55 AM Invited

### Multiscale Modeling of Cross-Slip: Knowns and Unknowns: Ladislav

Kubin<sup>1</sup>; Benoit Devincere<sup>1</sup>; <sup>1</sup>CNRS

The impact of cross-slip on dislocation microstructures and the mechanical response of fcc crystals is discussed from two examples. 1 - In stage I, mesoscale observations and atomistic simulations indicate that screw dipoles are annihilated by athermal cross-slip, which leads to the formation of superjogs. Dislocation dynamics simulations show that the interactions of superjogs with primary dislocations lead to the observed microstructures containing bundles of elongated prismatic loops. From these results the strain hardening rate can be estimated. 2 - During the dynamic recovery stage III, the thermally activated annihilations of screw dislocations can be described as involving the formation of screw dipoles and their annihilation in a complex local stress field. The incorporation of cross-slip events into dislocation-based continuum models and the reasons why current atomistic simulations or elastic models cannot provide sufficient information for a parameter-free modeling of strain hardening during stage III are discussed.

## 9:20 AM

### Dislocation Nucleation and Re-Ordering of Bicrystal Interfaces: Garritt

Tucker<sup>1</sup>; David McDowell<sup>1</sup>; <sup>1</sup>Georgia Institute of Technology

Nanostructured materials produced by severe plastic deformation techniques contain a higher percentage of grain boundaries of high-angle character in a non-equilibrium or energetically metastable state. Excess free volume associated with this metastable state modifies fundamental attributes of grain boundaries such as atomic mobility, energy, and mediation of dislocations. Atomistic simulations with importance sampling are used to construct representative non-equilibrium bicrystalline grain boundaries in both copper and aluminum using an embedded atom method potential. The excess free volume results in changes to the initial atomic composition and deformation response under both uniaxial



tension and simple shear at low homologous temperature. Uniform and gradient free volume distributions are used to investigate the free volume redistribution and atomic reordering within the grain boundary plane during straining. A detailed comparison between copper and aluminum is provided with regard to boundary strength, deformation mechanisms, and stress-assisted free volume migration during both tensile and shear simulations.

### 9:35 AM

**Thermally-Activated Glide of Dislocations at the Atomic Scale in High Peierls Stress Crystals:** *David Rodney*<sup>1</sup>; Laurent Proville<sup>2</sup>; <sup>1</sup>Grenoble Institute of Technology; <sup>2</sup>Commissariat à l'Energie Atomique

The thermally-activated glide of dislocations in crystals such as BCC and HCP metals is difficult to account for at the atomic scale because the nucleation of kink pairs on dislocation lines occurs on timescales long compared to those accessible to molecular dynamics. So far, thermally-activated glide has been modeled only the case of mesoscale Dislocation Dynamics simulations, using phenomenological laws fitted on macroscopic experiments. Here, in a multi-scale approach, we employ 2 saddle-point search methods, the Nudged Elastic Band method and the Activation-Relaxation Technique, to determine in different atomic systems the activation enthalpy for kink-pair nucleation as a function of applied shear stress. The validity of these static enthalpies is proved by comparison with molecular dynamics and we show that the enthalpy-stress curve can be predicted from a simple line tension model if one accounts for a shear-stress dependence of the Peierls potentials evidenced by the atomic scale simulations.

### 9:50 AM Invited

**Dislocations and Phase Transformations in Energetic Molecular Crystals:** *Marc Cawkwell*<sup>1</sup>; <sup>1</sup>Los Alamos National Laboratory

Despite their extreme brittleness, plastic deformation mediated by dislocations and/or phase transformations is thought to control many of the properties of energetic molecular crystals. I will review recent computational and experimental work toward a rigorous characterization of the mechanisms for plastic flow in orthorhombic cyclotrimethylene trinitramine (RDX) single crystals under shock and quasi-static loading conditions. Owing to the low symmetry of these crystals and their degrees intramolecular freedom it will be demonstrated that a surprisingly large number of deformation mechanisms are possible which depend sensitively on orientation and strain rate. Finally, contradictory results from recent nanoindentation experiments will be clarified using the calculated structure of the core of the [100] screw dislocation in RDX.

### 10:15 AM Break

### 10:35 AM Invited

**Determination of Dislocation Type by X-Ray Line Profiles:** *Geza Tichy*<sup>1</sup>; <sup>1</sup>Eotvos University, Budapest

The width of diffraction profiles of Bragg reflection is not monotonous function of the diffraction angle. This behaviour is caused by the anisotropic contrast effect of dislocations. The broadening of the line is characterized by the contrast factor. The calculation of the anisotropic contrast factor is based on the elastic field of dislocation determined by Stroh formalism. The effect is illustrated by examples of severely deformed polycrystalline materials

### 11:00 AM

**Thermally Activated Glide of Partial Dislocations in Nickel Based Superalloys:** Libor Kovarik<sup>1</sup>; Raymond Unocic<sup>1</sup>; Ning Zhou<sup>1</sup>; Yunzhi Wang<sup>1</sup>; *Michael Mills*<sup>1</sup>; <sup>1</sup>The Ohio State University

A rich variety of deformation processes can operate in Ni-based superalloys depending on the deformation condition and the nature of the  $\gamma/\gamma'$  microstructure. In the temperature range of 600-800°C, and for low stress and strain rate conditions, the deformation mechanisms include microtwinning, a[112] dislocation ribbon and superlattice intrinsic and superlattice extrinsic stacking fault formation. Complex arrangements of Shockley partial dislocations are responsible for the operation of these mechanisms, as revealed by high-resolution STEM imaging and ab-initio calculations of the fault configurations. It is found that while these mechanisms are distinct, they are all controlled by the same thermally activated process of chemical reordering in the  $\gamma'$  precipitates after shearing. In addition to reordering, other factors such as segregation of heavy elements have been identified as a simultaneous process. Professor Vitek's

pioneering work on dislocation cores in L12 compounds will be discussed in connection to these mechanisms in the two-phase microstructures.

### 11:15 AM

**Predicting Dislocation Mobility from Explicit Atomistic Details: A Kinetic Monte Carlo Study:** *Mukul Kabir*<sup>1</sup>; Timothy Lau<sup>1</sup>; David Rodney<sup>2</sup>; Sidney Yip<sup>3</sup>; Krystyn Van Vliet<sup>1</sup>; <sup>1</sup>Department of Materials Science and Engineering, Massachusetts Institute of Technology; <sup>2</sup>Science et Ingenierie des Materiaux et Procédés, Grenoble Institute of Technology; Department of Materials Science and Engineering, Massachusetts Institute of Technology; <sup>3</sup>Department of Nuclear Science and Engineering and Department of Materials Science and Engineering, Massachusetts Institute of Technology

We report kinetic Monte Carlo simulations of dislocation climb at elevated temperatures for heavily deformed body-centered cubic or alpha iron. This approach explicitly incorporates energy barriers associated with iron vacancy-dislocation interactions as determined from atomistic calculations, and enables observations of self-diffusivity and climb over experimentally relevant timescales. We find that, as vacancies approach the edge dislocation cores, the energy barriers to vacancy migration rapidly decrease and consequently, the diffusivity is accelerated in the vicinity of dislocation cores. We also find that the climb velocity to be a complex function of applied stress through the corresponding dislocation density and vacancy supersaturation density as well. The calculated macroscopic creep rates at elevated temperatures are in quantitative agreement with available experiments in terms of the so-called creep stress exponent of power law creep, and in qualitative agreement with our calculated dependence of activation barriers on applied stress.

### 11:30 AM

**Short Range and Long Range Spatial Correlation Effects on Dislocation Distributions:** *Juliette Chevy*<sup>1</sup>; Claude Fressengeas<sup>2</sup>; Mikhail Lebyodkin<sup>2</sup>; Vincent Taupin<sup>2</sup>; Pierre Bastie<sup>3</sup>; Paul Duval<sup>4</sup>; <sup>1</sup>University of Illinois; <sup>2</sup>Université Paul Verlaine-Metz-France; <sup>3</sup>Institut Laue Langevin; <sup>4</sup>Laboratoire de Glaciologie et Géophysique de l'Environnement

Ice single crystals deformed in torsion at different strain levels were analyzed by hard X-ray diffraction. Because of the very strong viscoplastic anisotropy of this material and the geometry of the tests, this technique enabled obtaining from the diffracted intensity the local geometrically necessary dislocation densities along the samples. The local density distribution appeared to be heterogeneous and characterized by a complex scale invariance, which was analyzed by means of a multifractal technique. The analysis revealed that the dislocation density distribution is controlled by different kinds of interactions depending on the strain level. Whereas long range elastic interactions between dislocations are responsible for scale invariance at low strain level, short range interactions inherent to dislocation multiplication mechanisms progressively prevail as deformation proceeds. A field dislocation dynamics model taking into account interactions linked to both long range elastic stresses and dislocation transport was used to support this interpretation.

### 11:45 AM

**Fractals versus Scaling: Self-Similarity in Dislocation Cell Wall Simulations:** Yong Chen<sup>1</sup>; Woosong Choi<sup>1</sup>; Stefanos Papanikolaou<sup>1</sup>; *James Sethna*<sup>1</sup>; <sup>1</sup>Cornell University

Some experiments of dislocation cell wall structures evolving in deformed metals have observed fractal structures; others have been analyzed in terms of distributions of cell sizes and misorientations that appear non-fractal, but scale with increasing deformation. We analyze a continuum simulation of geometrically necessary dislocations, relaxing in time. In the absence of climb, we observe self-similar (fractal) cell-wall structures, which we exhibit with a visual real-space renormalization group and analyze in terms of critical exponents for correlation functions of dislocation density, orientation, and plastic distortion. For the same simulation, we analyze the distribution of cell sizes and cell wall misorientations, and compare to the corresponding experiments. In the presence of climb (roughly simulating grain boundary polygonization) we observe non-fractal scaling.

Tue. AM

# Technical Program

## Three-Dimensional Materials Science VI: Applications of 3D Microstructural Data

*Sponsored by:* The Minerals, Metals and Materials Society, ASM International, TMS Structural Materials Division, TMS: Advanced Characterization, Testing, and Simulation Committee, ASM-MSCTS: Texture and Anisotropy Committee, TMS/ASM: Phase Transformations Committee

*Program Organizers:* Alexis Lewis, Naval Research Laboratory; Anthony Rollett, Carnegie Mellon University; David Rowenhorst, Naval Research Lab; Jeff Simmons, AFRL; Stuart Wright, EDAX Inc-TSL

Tuesday AM                      Room: 401  
February 16, 2010              Location: Washington State Convention Center

*Session Chairs:* Anthony Rollett, Carnegie Mellon University; Andrew Geltmacher, U S Naval Research Laboratory

### 8:30 AM Invited

**3D Characterisation of Fatigue Cracks Using X-Ray Tomography: From Synchrotron to Laboratory Sources:** *Jean-Yves Buffiere*<sup>1</sup>; Nathalie Limodin<sup>1</sup>; Julien Rethore<sup>1</sup>; Wolfgang Ludwig<sup>1</sup>; Anthony Gravouil<sup>1</sup>; François Hild<sup>2</sup>; Stéphane Roux<sup>2</sup>; <sup>1</sup>Universite de Lyon INSA LYON; <sup>2</sup>LMT, ENS-Cachan / CNRS / UPMC / PRES UniverSud Paris

3D images of fatigue cracks in metals are obtained using X-ray micro-tomography. The presentation is twofold. First, synchrotron phase contrast imaging and a small voxel size are used to achieve a high spatial resolution. Results obtained in a fine grain alloy are shown to illustrate the quantitative use of 3D data for modelling propagation through finite element calculations. In a second part, it is shown that laboratory X-ray tomography can also be used quantitatively. Although voxel sizes are somewhat higher, and the beam is incoherent and non-monochromatic, 3D image correlation compensates those weaknesses. This technique provides the 3D morphology and front location of the crack as well as the displacement fields within the specimen. Crack opening displacement maps are obtained in the whole sample cross-section and stress intensity factors are measured all along the crack front. They allow for a quantitative estimation of crack closure/opening.

### 9:00 AM Invited

**Three-Dimensional Validation of Deformation Simulations:** *Corbett Bataille*<sup>1</sup>; Luke Brewer<sup>1</sup>; Remi Dingreville<sup>2</sup>; <sup>1</sup>Sandia National Laboratories; <sup>2</sup>Polytechnic Institute of New York University

Many approaches exist to simulate the deformation of engineering materials, but most are based on, and therefore tuned to, macroscopic observables produced by collective phenomena. The fidelity of the material's micro-scale behavior, however, is not guaranteed, especially when the material's internal structure, and therefore its response, is inhomogeneous (e.g. in a polycrystal). We have used electron backscatter diffraction to characterize the microstructure-scale deformation of pure, polycrystalline nickel and brass in tension. We employ both conventional, two-dimensional characterization of the surface; and in-situ, three-dimensional focused ion beam milling to enable volumetric analysis. These data serve as both input (via microstructure morphology and texture) to, and validation of, finite element simulations of the experiments. We will discuss the approaches used to ensure registry between the experimental and simulation datasets, and the implications of the validation for the micro-scale fidelity of deformation simulations in cases where meso- and macro-scale agreement is established.

### 9:30 AM

**Finite Element Analysis of Large Three-Dimensional Microstructural Datasets:** *Alexis Lewis*<sup>1</sup>; M. A. Qidwai<sup>2</sup>; Surya Kalidindi<sup>3</sup>; Stephen Niezgod<sup>3</sup>; Andrew Geltmacher<sup>1</sup>; <sup>1</sup>Naval Research Laboratory; <sup>2</sup>SAIC; <sup>3</sup>Drexel University

Advances in three-dimensional Materials Science have resulted in the availability of large microstructural datasets representing real materials whose mechanical response can be simulated using advanced Finite Element (FE) codes. Due to the computationally intensive nature of most FE codes, however, the volumes that can be incorporated into FE models often do not contain a statistically significant number of grains. Using n-point correlation algorithms to select statistical volume elements from a large 3D reconstruction of a single-phase beta-Ti, we have simulated the mechanical response of a representative

sample of sub-volumes. Using appropriate weighting factors based on grain orientation and boundary crystallography, the data from these simulations is combined to investigate the relationship between microstructure, applied load, and mechanical response on the level of individual grains as well as nearest-neighbor interactions. A correlation between the alignment of individual grains with the loading direction and their plastic response is observed.

### 9:50 AM

**Stagnation of Thin Film Grain Growth under the Effect of Stress:** *Fatma Uyar*<sup>1</sup>; Myrjam Winning<sup>2</sup>; Anthony Rollett<sup>1</sup>; <sup>1</sup>Carnegie Mellon University; <sup>2</sup>Max Planck Institute für Eisenforschung

A three-dimensional curvature driven moving finite element model has been adapted to account for the effect of stress field on grain growth in thin films. In this analysis, grain boundaries are treated as dislocation structures and net Burgers vectors have been calculated using the misorientation information and boundary inclinations. Then using Peach-Koehler relation, additional forces due to stress field are calculated. For this study, an experimental thin film texture has been fit to a microstructure represented by 3D digital mesh. The microstructures were allowed evolve under curvature driving forces only and then with an additional stress field. Grain growth dynamics are slowed down by the stress field under certain circumstances. Alternate methods will be also employed to further investigate the stagnation effect.

### 10:10 AM Break

### 10:30 AM Invited

**Permeability Determination via 3D Reconstruction of the Mushy Zone of Nickel-Base Single Crystals:** *Jonathan Madison*<sup>1</sup>; Jonathan Spowart<sup>2</sup>; Dave Rowenhorst<sup>3</sup>; Katsuyo Thornton<sup>1</sup>; Tresa Pollock<sup>1</sup>; <sup>1</sup>The University of Michigan; <sup>2</sup>Air Force Research Laboratory; <sup>3</sup>Naval Research Laboratory

Convective flow at the solid-liquid interface within directionally solidified superalloys can result in the formation of freckles and misoriented grains. These defects can result in reductions in performance and component life. Predictions for the onset of convective flow have primarily employed the Rayleigh number, which is sensitive to the permeability of the mushy zone. Permeability varies with fraction liquid and the geometry of the dendritic array and is difficult to measure experimentally. This research utilizes 3D dendritic reconstructions from solid-liquid interfaces of a model ternary nickel alloy and commercial nickel-base superalloy as direct inputs to fluid flow simulations. These models yield permeability and permit analysis of the role of dendrite morphology and interfacial surface area on flow processes. Permeabilities determined from modeling will be compared to Kozeny-Carmen and modified Blake-Kozeny empirical models and implications for improved directional solidification processing will be discussed.

### 11:00 AM

**A Phase Field Model of Dual-Phase Multi-Grain Material Applied to Duplex Steel with Experimental Verification:** *Stefan Poulsen*<sup>1</sup>; Peter Voorhees<sup>2</sup>; Erik Lauridsen<sup>1</sup>; Wolfgang Ludwig<sup>3</sup>; Richard Fonda<sup>4</sup>; Dorte Jensen<sup>1</sup>; <sup>1</sup>Risø DTU; <sup>2</sup>Northwestern University; <sup>3</sup>European Synchrotron Radiation Facility; <sup>4</sup>U.S. Naval Research Laboratory

A phase field model for the microstructural evolution of a binary dual-phase system, where both phases are polycrystalline, has been developed. The model handles both the long-range diffusion processes driving the coarsening and growth of the two phases, and the short-range ordering processes driving the growth of grains. The model has specifically been used to predict the evolution of the microstructure of a duplex stainless steel, which is a material attracting increasing attention due to its strength and corrosion resistance. The phase field simulation employs the microstructure measured using X-ray tomography, holotomography for the phase information and diffraction contrast tomography for the crystallographic information, as an initial condition. Since X-ray tomography is non-destructive we have the unique ability to compare the computed microstructure to that taken experimentally following an ex-situ anneal.



11:20 AM

**Anisotropic 3D Phase Field Simulations of Grain Growth: A Comparison between Simulation and Experiment:** *Ian McKenna*<sup>1</sup>; Mogadala Gururajan<sup>2</sup>; Stefan Poulsen<sup>3</sup>; Dave Rowenhorst<sup>4</sup>; Erik Lauridsen<sup>3</sup>; Peter Voorhees<sup>1</sup>; <sup>1</sup>Northwestern University; <sup>2</sup>Indian Institute of Technology - Delhi; <sup>3</sup>Risø; <sup>4</sup>Naval Research Laboratory

We employ phase field simulations to study the evolution of grains in polycrystalline materials. Many materials undergoing grain growth exhibit anisotropic grain structures. Thus, one of the challenges of performing accurate simulations is to develop a robust model capable of handling systems with varying levels of anisotropy in the grain boundary energy and mobility. We have developed such a model which incorporates all five macroscopic degrees of freedom of the grain boundary energy. To validate our model we utilize two different experimental datasets as initial conditions: a serial sectioned sample and an in-situ X-ray tomography sample. Since the X-ray tomography data is taken in-situ it is possible to compare the morphology of individual grains computed using the phase field method with that observed experimentally. Despite the relatively isotropic appearance of the grain structures that are measured experimentally, the one-to-one comparison between simulation and experiment reveals clear evidence of anisotropy.

11:40 AM

**Modeling the Effect of Eutectic Nucleation Behavior on Permeability during Solidification of Al-19.5wt%Cu:** *Ehsan Khajeh*<sup>1</sup>; Daan Maijer<sup>1</sup>; <sup>1</sup>The University of British Columbia

The nucleation and growth behavior of eutectic phase and the resulting distribution of eutectic colonies within the mushy zone can have a significant influence on interdendritic permeability. Therefore, it will also significantly affect the amount and distribution of feeding related defects. In the present study, 3D geometry of eutectic/primary phases obtained by X-ray microtomography (XMT) has been used to generate a computational domain in which the eutectic transformation takes place. By applying conventional theory of eutectic nucleation and the Monte Carlo technique for simulating the growth of eutectic colonies, the evolution of interdendritic channels has been modeled. The mushy zone permeability during eutectic evolution has then been calculated by solving the full Navier-Stokes equation on the evolving microstructures. The calculated permeability shows the impact of the eutectic solidification behavior.

12:00 PM

**Dealloying and Coarsening Behavior of Nanoporous Gold by X-Ray Nanotomography:** *Yu-chen Chen*<sup>1</sup>; JaeMock Yi<sup>2</sup>; Wah-Keat Lee<sup>2</sup>; Ian McNulty<sup>2</sup>; Peter Voorhees<sup>1</sup>; David Dunand<sup>1</sup>; <sup>1</sup>Northwestern University; <sup>2</sup>Advanced Photon Source of Argonne National Lab.

Nanoporous gold has novel mechanical, optical, and chemical properties leading to potential applications for sensors, actuators, catalysts, and fuel cell electrodes. Its nanoporous structure is formed by dealloying and can be coarsened by subsequent annealing. The 3D morphology has been studied by TEM tomography. However, the kinetics underlying structural evolution have not been fully resolved and morphological evolution during dealloying and coarsening has not been directly measured in 3D. Here, by using 3D X-ray nanotomography, we reconstructed the structural evolution of nanoporous gold during both dealloying and coarsening. We have observed a dealloying front progressing within the Ag-Au alloy and quantified the relationship between dealloying distance and time. We have also quantified the nanostructure by creating probability maps for the surface curvature and surface normal during coarsening. These results will advance our understanding of the diffusion mechanism of 3D in a complex nanoporous metallic structure.

12:20 PM

**Microstructures Simulation of Magnesium-Based Alloys during Solidification by Phase-Field Method:** *Tao Jing*<sup>1</sup>; Mingyue Wang<sup>1</sup>; <sup>1</sup>Tsinghua University

An expression is proposed for the anisotropic function of crystal-melt interfacial free energy for hexagonal metals, based on the combination of experiments and crystal structure. The phase field model of alloys, whose density free energy is built on the basis of thermodynamic extended substitutional-regular-solution approximation, incorporated into anisotropic function reflecting hexagonal symmetry, is established. Numerical computations of primary hcp-Mg phase dendritic growth in the freezing process of magnesium-based alloys melts are implemented. The three-dimensional dendritic morphologies of magnesium

alloys microstructures, whose hierarchical branches can be seen clearly, are obtained, which have been well in agreement with experimental results and are obviously different from that of would be usually expected.

### Ultrafine Grained Materials – Sixth International Symposium: Deformation and Processing Mechanics

*Sponsored by:* The Minerals, Metals and Materials Society, TMS Materials Processing and Manufacturing Division, TMS Structural Materials Division, TMS/ASM: Mechanical Behavior of Materials Committee, TMS: Nanomechanical Materials Behavior Committee, TMS: Shaping and Forming Committee

*Program Organizers:* Suveen Mathaudhu, U.S. Army Research Laboratory; Mathias Goeken, University Erlangen--Nürnberg; Terence Langdon, University of Southern California; Terry Lowe, Manhattan Scientifics, Inc.; S. Semiatin, Air Force Research Laboratory; Nobuhito Tsuji, Kyoto University; Yonghao Zhao, University of California - Davis; Yuntian Zhu, North Carolina State University

Tuesday AM

Room: 607

February 16, 2010

Location: Washington State Convention Center

*Session Chairs:* Gerhard Wilde, University of Muenster; Rainer Hebert, University of Connecticut; Yulia Ivanisenko, Forschungszentrum Karlsruhe; Matthias Hockauf, Chemnitz University of Technology

8:30 AM

**Plasticity and Grain Boundary Diffusion at Small Grain Sizes:** *Gerhard Wilde*<sup>1</sup>; Nancy Boucharat<sup>2</sup>; Sergiy Divinsky<sup>1</sup>; Joern Leuthold<sup>1</sup>; Gerrit Reglitz<sup>1</sup>; Harald Roesner<sup>1</sup>; <sup>1</sup>University of Muenster; <sup>2</sup>Research Center Karlsruhe

Bulk nanostructured - or ultrafine-grained materials are often fabricated by severe plastic deformation to break down the grain size by dislocation accumulation. Underlying the often observed property enhancement is a modification of the volume fraction of the grain boundaries. Yet, along with the property enhancements, several important questions arise concerning the accommodation of external stresses if dislocation-based processes are not longer dominant at small grain sizes. One such factor are so-called "non-equilibrium" grain boundaries that have been postulated to form during severe deformation and that might be of importance not only for the property enhancement known already today, but also might serve as internal transport pathways offering new applications in the context of e.g. gas permeation or fast matter transport for self-repairing structures. This contribution addresses the underlying issues by combining quantitative microstructure analysis at high resolution with grain boundary diffusion measurements. Funding by DFG (FG714) is gratefully acknowledged.

8:50 AM

**Twist Extrusion - Technique for Bulk Ultrafine- and Nanomaterials Obtaining:** *Viktor Varyukhin*<sup>1</sup>; Yakov Beygelzimer<sup>1</sup>; Sergey Synkov<sup>1</sup>; <sup>1</sup>Donetsk Institute for Physics and Engineering of NASc of Ukraine

Twist extrusion (TE) is the severe plastic deformation technique for bulk ultrafine- and nanomaterials manufacture. We present an experimental study of the kinematics of TE and show that TE has the following properties: • The mode of deformation in twist extrusion is simple shear. There are two shear planes; one of them is perpendicular and the other is parallel to the specimen axis. • The following processes are present during twist extrusion: vortex-like flow with large strain gradient, stretching and mixing of metal particles. We argue that due to these properties, TE opens possibilities for investigating and forming new structures. It has already been successfully used to obtain ultrafine and nanostructure with good properties in Al, Cu and Ti alloys.

9:05 AM

**Plastic Instability during Accumulative Roll Bonding (ARB) of Metallic Multilayers:** *Rainer Hebert*<sup>1</sup>; Jyothi Suri<sup>1</sup>; Girija Marathe<sup>1</sup>; <sup>1</sup>University of Connecticut

A common conception is that the flow stress differences between individual layers of multilayers determine if layers codeform or respond with plastic instabilities during cold-rolling. Following this conception Cu-Ni multilayers were prepared with different initial flow stress levels of the Cu and Ni foils to test if codeformation can be extended to higher strain levels during ARB processing for a particular set of work-hardening levels. Microstructure analyses

Tue. AM

# Technical Program

demonstrate, however, that the plastic instability behavior of the Ni layers is not significantly affected by the choice of the initial thermomechanical treatment of the Cu and Ni foils and thus the flow stress ratio. The experimental results are compared with predictions for plastic instabilities during rolling of multilayers from continuum mechanics models. The comparison shows that additional factors such as shear stresses, texture formation, stress partitioning, or shear band formation have to be considered to rationalize the experimental results.

## 9:20 AM Invited

**Role of Dislocations during Processing and Deformation of Nanocrystalline Materials:** *Farghalli Mohamed*<sup>1</sup>; <sup>1</sup>University of California, Irvine

Nanocrystalline (nc) materials are characterized by a unique substructural feature: grain sizes are less than 150 nm. Recent research activities have demonstrated that dislocation activity can play a key role not only in processing nc-materials via severe plastic deformation (SPD) but also in accounting for their mechanical behavior. Various aspects of this role will be presented.

## 9:40 AM

**How do Partially Multiply to Produce Deformation Twins in Nanocrystalline fcc Metals?:** *Yuntian Zhu*<sup>1</sup>; <sup>1</sup>North Carolina State University

Deformation twins are often observed in nanocrystalline face-centered cubic (fcc) metals and alloys. However, since the conventional twin growth mechanisms such as the pole mechanism no longer operate in nanocrystalline materials, there has been a puzzle on how the partials multiply to glide on consecutive slip planes. It is statistically improbable for a partial to exist on every slip plane. Here I review several recently proposed mechanisms for the nucleation and growth of four different single and multifold twins. These mechanisms provide continuous generation of twinning partials for the growth of the twins after nucleation. Relatively high-stress or high strain rate is needed to activate these mechanisms, making them more prevalent in nanocrystalline materials than in their coarse-grained counterparts. Experimental observations that support the proposed mechanisms are presented.

## 9:55 AM Break

## 10:10 AM Invited

**Deformation Mechanisms in Multiscale Nanostructured Materials:** *Yonghao Zhao*<sup>1</sup>; *Ying Li*<sup>1</sup>; *Troy Topping*<sup>1</sup>; *Xiaozhou Liao*<sup>2</sup>; *Yuntian Zhu*<sup>3</sup>; *Ruslan Valiev*<sup>4</sup>; *Enrique Lavernia*<sup>1</sup>; <sup>1</sup>University of California-Davis; <sup>2</sup>The University of Sydney; <sup>3</sup>North Carolina State University; <sup>4</sup>Ufa State Aviation Technical University

Multiscale nanostructured materials containing multimodal grain size distributions can be engineered to display unusual balance of properties, such as strength and ductility. Despite well documented reports of enhanced ductility in multiscale nanostructured materials, systematic identification of the underlying deformation mechanisms has not been accomplished. In this work, we selected high-purity Cu and commercial pure Ti as a model material system in an effort to elucidate the underlying mechanisms. The multimodal Cu and Ti were prepared by equal-channel-angular pressing (ECAP) and subsequent annealing. In situ atomic force microscopy (AFM) in combination with tensile testing and ex situ transmission electron microscopy (TEM) are used to characterize the deformation mechanisms and mechanical behavior.

## 10:30 AM

**Information on Deformation Mechanisms in nc Pd-10% Au Inferred from Texture Analysis:** *Yulia Ivanisenko*<sup>1</sup>; *Werner Skrotzki*<sup>2</sup>; *Robert Chulist*<sup>2</sup>; *Lilia Kurmanaeva*<sup>1</sup>; *Hans-Jörg Fecht*<sup>3</sup>; <sup>1</sup>FZK; <sup>2</sup>Technische Universität Dresden; <sup>3</sup>Universität Ulm

There is still a lack of understanding of deformation mechanisms in nanocrystalline (nc) materials. We have studied microstructures formed in nc Pd-10% Au (grain size about 15nm) after high pressure torsion, and have revealed signatures of various deformation processes as cooperative grain boundary sliding, shear banding, dislocation slip and twinning. In order to establish contributions of these processes to total strain, we compared torsion textures formed in nc and coarse grained (cg) samples after identical shear strain. The textures were measured with synchrotron radiation. Intensities of characteristic components of the shear texture are two times stronger in the cg sample than in the nc one, indicating that dislocation slip is less significant in the nc sample. Furthermore, distribution of intensities between different shear texture components presumably points to the contribution of deformation twinning in the nc sample in agreement with microstructure investigations.

## 10:45 AM Invited

**Extending Kocks' Equation for Work Softening in UFG Materials:** *Tamás Ungár*<sup>1</sup>; *Li Li*<sup>2</sup>; *Géza Tichy*<sup>1</sup>; *Hahn Choo*<sup>2</sup>; *Peter Liaw*<sup>2</sup>; <sup>1</sup>Eötvös University Budapest; <sup>2</sup>University of Tennessee

When the grain size is reduced to below about 20 nm and dislocation density is larger than about  $10^{16} \text{ m}^{-2}$  plastic deformation may cause grain growth and reduction of dislocation density. It is shown that the equation of Kocks describing stage-III deformation can account for the above mentioned behavior by appropriate selection of materials constants. The kind of grain growth, often called "abnormal grain growth" along with the reduction of dislocation density produced by plastic deformation can be considered perfectly "normal" within the frame of the extended Kocks' equation.

## 11:05 AM

**Plastic Deformation in Nanocrystalline and Ultrafine Carbon Steel:** *Rodolfo Rodríguez-Baracaldo*<sup>1</sup>; *Jose Antonio Benito Páramo*<sup>2</sup>; *José María Cabrera Marrero*<sup>2</sup>; <sup>1</sup>Universidad Nacional de Colombia; <sup>2</sup>Universitat Politècnica de Catalunya

This work is focused on the evaluation of plastic deformation of near fully dense nanostructured and ultrafine grained bulk samples of carbon steel (0.55% C). The specimens were obtained by warm static pressing from mechanically milled powder. Compaction parameters and annealing treatments were selected to promote a relatively wide range of the grain sizes (15 nm to 2.8  $\mu\text{m}$ ). Hardness, compression and nanoindentation test were performed at room temperature. It was found that the nanocrystalline grained steel samples presented very high strength with low ductility, as the ferritic grain size was increased, the amount of strain hardening and total plastic strain increased and the maximum strength diminished. A constant decrease of strain rate sensibility parameter ( $m$ ) was found as the grain size decreases in the ultrafine regime. On the contrary, in the nanocrystalline regime as the grain size decreases a slight increase of  $m$  was observed.

## 11:20 AM

**Microstructure and Creep Properties of Nanocrystalline Oxide Dispersion Strengthened Fe-18Cr-8Ni-2W-0.25Y2O3 Austenitic Steel Synthesized by High Energy Ball Milling and Vacuum Hot Pressing:** *P. Susila*<sup>1</sup>; *D. Sturm*<sup>2</sup>; *M. Heilmaier*<sup>3</sup>; *B. S. Murty*<sup>1</sup>; *Vadlamani Subramanya Sarma*<sup>4</sup>; <sup>1</sup>Indian Institute of Technology Madras; <sup>2</sup>Otto-von-Guericke University Magdeburg; <sup>3</sup>TU Darmstadt; <sup>4</sup>Indian Institute of Technology Madras and North Carolina State University

Materials for future power plants require enhanced creep resistance, corrosion resistance and oxidation resistance. Austenitic stainless steels (ASS) have good corrosion and creep resistance. The creep properties of the ASS can be further enhanced through oxide dispersion strengthening (ODS). There is limited knowledge base on the microstructure-properties correlations in nanostructured ODS alloys. High energy ball milling is considered to be a better technique to synthesize large quantities of nanostructured materials and well suited to produce ODS alloys. In this presentation, we report the results of studies on microstructure and mechanical properties of nanostructured (Fe-18Cr-8Ni-2W-0.25Y2O3) austenitic ODS alloy. The nanostructured base and ODS alloys were synthesized by mechanical alloying of elemental powders. The mechanically alloyed ODS powders were characterized by X-ray diffraction (XRD) analysis and transmission electron microscopy (TEM). The results show that fcc phase formation is accelerated in the ODS alloy in comparison to the base alloy and a crystallite size of 10 nm is achieved in ODS alloy after 25 h of milling. The ODS alloy powders have a hardness of 1800 HV and this is significantly higher than the hardness of 1200 HV reported for nanostructured ferritic ODS alloy powders. The powders are consolidated to near theoretical density by vacuum hot pressing (VHP). The grain size following VHP is about 75 nm in the ODS alloy. The creep properties will be evaluated and an attempt is made to quantitatively assess the impact of particle as well as grain size strengthening on the high temperature strength.

## 11:35 AM Invited

**Plastic Flow Stability and Detwinning in Cu with Nanoscale Growth Twins:** *Amit Misra*<sup>1</sup>; *X. Zhang*<sup>2</sup>; *J. Wang*<sup>1</sup>; *N. Li*<sup>3</sup>; *O. Anderoglu*<sup>3</sup>; *J. Huang*<sup>4</sup>; *R. Hoagland*<sup>1</sup>; *J. Hirth*<sup>1</sup>; <sup>1</sup>LANL; <sup>2</sup>Texas A&M University; <sup>3</sup>Texas A&M University & LANL; <sup>4</sup>Sandia National Laboratories

Nanotwinned Cu, with a very fine scale structure consisting of twin lamellae with an average thickness of 5 nm, exhibited stable plastic flow with no shear

localization or fracture, even at thickness reduction of over 50% in room temperature rolling. The {111} fiber texture was retained after rolling indicating insignificant out-of-plane rotation of the columnar grains and is interpreted in terms of a symmetric slip model. No significant change in the average twin lamellae thickness was seen even at thickness reduction of over 50%, suggesting that some twin boundaries were annihilated during deformation. The detwinning of nanotwins was also shown via in situ indentation experiments in a transmission electron microscope. Molecular dynamics simulations show that de-twinning is accomplished via a collective glide of multiple twinning dislocations and that de-twinning becomes the dominant deformation mechanism when the thickness of twins is on the order of a few nanometers.

11:55 AM

**Processing and Oxidation Resistance of Nanocrystalline Fe-Cr Alloys:** Rajeev Gupta<sup>1</sup>; Raman Singh<sup>1</sup>; Carl Koch<sup>2</sup>; <sup>1</sup>Monash University; <sup>2</sup>North Carolina State University

For their unique physico-mechanical properties and exciting industrial applications, nanostructured materials are the most widely investigated materials research topic of recent times. However, corrosion of nano materials has received very limited research attention, even though the materials will be required to demonstrate acceptable corrosion resistance in most potential applications. This paper will present a review of the fundamentals of likely corrosion mechanism of nanocrystalline metallic materials with examples. The paper will present description of the processing of nanocrystalline Fe-Cr alloys by mechanical alloying. The paper will also discuss the most recent findings to address the hypothesis that it may be much easier to develop a protective film on nanocrystalline alloys. Validation of the hypothesis will have highly attractive economic/industrial implications.

## Ultrafine Grained Materials – Sixth International Symposium: Stability

*Sponsored by:* The Minerals, Metals and Materials Society, TMS Materials Processing and Manufacturing Division, TMS Structural Materials Division, TMS/ASM: Mechanical Behavior of Materials Committee, TMS: Nanomechanical Materials Behavior Committee, TMS: Shaping and Forming Committee

*Program Organizers:* Suveen Mathaudhu, U.S. Army Research Laboratory; Mathias Goeken, University Erlangen–Nürnberg; Terence Langdon, University of Southern California; Terry Lowe, Manhattan Scientifics, Inc.; S. Semiatin, Air Force Research Laboratory; Nobuhiro Tsuji, Kyoto University; Yonghao Zhao, University of California - Davis; Yuntian Zhu, North Carolina State University

Tuesday AM Room: 606  
February 16, 2010 Location: Washington State Convention Center

*Session Chairs:* Kristopher Darling, U.S. Army Research Laboratory; Brady Butler, U.S. Army Research Laboratory; Christopher Saldana, Purdue University; Jane Adams, U.S. Army Research Laboratory

8:30 AM Invited

**Thermal Stability of SPD Microstructures:** Günter Gottstein<sup>1</sup>; Xenia Molodova<sup>1</sup>; <sup>1</sup>RWTH Aachen University

The annealing of plastically deformed crystals generally causes softening processes, recovery and/or recrystallization, to occur. During severe plastic deformation pronounced cellular microstructures of submicron dimensions develop which convey beneficial properties to such materials. Since softening processes are usually accompanied by microstructural coarsening they may be detrimental to the mechanical performance of the processed material, though. On the other hand an increasing strain leads to the transformation of the cellular dislocation structure to a granular arrangement with a large fraction of high angle grain boundaries that may resist recovery and recrystallization. We will present results of investigations into the thermal stability of ECAP generated microstructures of Cu and Al alloys, identify the softening mechanisms and propose strategies to improve the resistance to coarsening and softening during annealing of SPD materials.

8:50 AM

**Mechanical Properties of Nanocrystalline Aluminum Stabilized with Dimonoids:** Khinlay Maung<sup>1</sup>; Ali Yousefiani<sup>2</sup>; Farghalli Mohamed<sup>1</sup>; James Earthman<sup>1</sup>; <sup>1</sup>UCI; <sup>2</sup>The Boeing Company

Nanocrystalline aluminum stabilized with either 1 wt% diamantane, 5 wt% diamantane, or 7 wt% of diamantane nanoparticles were processed by cryomilling. The as-cryomilled powders containing diamantane had an average grain size of 22 nm. Thermal stability analysis shows that the average grain size for 1% diamantane and 5% diamantane were not significantly different and the average grain sizes for these samples annealed at 500°C for 10hr were well under 100 nm. The cryomilled alloy powders were consolidated by hot isostatic pressing (HIP) followed by extrusion. The average grain size of as HIP'd samples are slightly larger than the powders heat treated at the same temperature range. This effect will be discussed in terms of stress assisted grain growth model. Mechanical properties of the three different compositions will also be presented.

9:05 AM

**Characterization of Thermally Stable Nanocrystalline Nickel Powders:** Brady Butler<sup>1</sup>; Kristopher Darling<sup>1</sup>; Bradley Klotz<sup>1</sup>; Matthew Kelly<sup>1</sup>; Micah Gallagher<sup>1</sup>; Eric Klier<sup>1</sup>; <sup>1</sup>U.S. Army Research Laboratory

The development of nanocrystalline and ultra-fine grained bulk materials through powder metallurgy processes has long been constrained by the thermal stability of nanostructures. Many difficulties arise due to the fact that grain growth and densification occur within the same temperature regime. Additionally, the mechanisms supporting densification require some degree of grain coarsening in order to achieve full density. This study outlines the development of a thermally stable nanocrystalline nickel powder and discusses the influence of this grain size stability on the overall densification rate during pressureless sintering in hydrogen atmosphere. Furthermore, the activation energy of sintering is calculated to determine whether the mechanisms of grain growth and densification can be decoupled through the addition of thermal grain stabilizers.

9:20 AM Invited

**Room Temperature Instability of Super Saturated Solid Solution in a Nano Crystalline Al-4Cu Alloy Produced by SPD:** Phil Prangnell<sup>1</sup>; Joe Robson<sup>1</sup>; Yan Huang<sup>1</sup>; <sup>1</sup>The University of Manchester

The reduction in grain size achievable and long term stability of severely deformed aluminium has been investigated when copper in solution is used to inhibit recovery. It is shown that copper is more effective than magnesium in inhibiting dynamic recovery. A grain width of only 70 nm was obtained in an Al-4wt%Cu alloy, after processing by ECAE to a strain of  $\epsilon_{eff} \sim 15$ , resulting in a lamellar nano-grain structure. However, post-processing the severely deformed solid solution was found to be unstable at room temperature and copious precipitation of  $\theta$  occurred at new grain boundaries within the deformed state, leading to recovery of the deformation structure and a loss of strength. The solute level fell to equilibrium within  $\sim 9$  months. The precipitation kinetics were shown to occur at many orders of magnitude higher than can be predicted by classical theory. The reasons for this discrepancy are discussed.

9:40 AM

**Characterizing Ultrafine Grained Ti-6Al-4V Thermal Stability with Long-Term High-Resolution EBSD:** Andrew Deal<sup>1</sup>; Radhakrishna Bhat<sup>1</sup>; Richard DiDomizio<sup>1</sup>; Judson Marte<sup>1</sup>; PR Subramanian<sup>1</sup>; <sup>1</sup>GE Global Research

A near-isothermal multi-axis forging (MAF) process was used to produce ultra-fine grained (UFG) Ti-6Al-4V alloys. To better understand the coarsening kinetics of the primary alpha, the thermal stability of the material was evaluated at temperatures well below the beta transus. Both static and dynamic coarsening were examined using heat treatments and hot compression tests, respectively. To precisely quantify the alpha grain size as a function of time and temperature, a FEG-SEM equipped with EBSD was enclosed to isolate it from thermal oscillations inherent to HVAC systems. The isolation chamber kept the short-term temperature fluctuations of the microscope below  $\pm 0.1^\circ\text{C}$  and long-term temperature drift below  $1^\circ\text{C}$ . This, in combination with appropriate EBSD protocols, achieved a stable 60nm resolution for periods up to 60 hours. Such long periods of stability enabled more statistically meaningful regions of the UFG Ti-6Al-4V to be characterized with EBSD to study primary alpha coarsening.

# Technical Program

## 9:55 AM Invited

**Microstructural Stability and Damage Evolution in Ultra-Fine Grained Alloys under Cyclic Loading:** *Thomas Niendorf*<sup>1</sup>; Hans Maier<sup>1</sup>; Ibrahim Karaman<sup>2</sup>; <sup>1</sup>University of Paderborn; <sup>2</sup>Texas A&M University

In the present study the mechanical behavior of ultra-fine grained alloys, e.g. interstitial-free steel and niobium-zirconium alloy, under cyclic loading is investigated and correlated to the microstructural evolution of the materials tested. All materials were processed by ECAP, employing different processing routes in order to obtain microstructures with significant different characteristics. The results obtained in the current study revealed that in addition to the grain size and impurity content the grain boundary characteristic and the grain size distribution have significant influence on the fatigue response of the materials tested. Thorough microscopical observation in combination with the digital image correlation technique allowed for the investigation of the early stages of damage evolution, i.e. crack initiation. By means of EBSD it was found that elongated grain structures dominated by low-angle grain boundaries were the reason for early crack initiation, independent of the ECAP route.

## 10:15 AM Break

## 10:30 AM Invited

**Stability of Nanocrystalline Alloys:** *Christopher Schuh*<sup>1</sup>; <sup>1</sup>MIT

Through alloying, it is possible to dramatically increase the thermal stability of nanocrystalline metals, even without the introduction of secondary phases. Solid solutions are potentially more stable in nanocrystalline form than are pure metals, owing to the possibility of solute segregation to intergranular regions. Segregation provides a deep metastable state for grain boundaries that is both thermodynamically and dynamically more stable. This talk summarizes our modeling efforts on nanocrystalline alloys, which permit the evaluation of structural stability with respect to grain coarsening, phase separation, and chemical ordering. Such models provide guidelines for the design of alloys that are sufficiently stable for use at ambient or even elevated temperatures.

## 10:50 AM

**Thermal Stability of Ultra-Fine Grained Ti-6Al-4V Alloys Processed via Multi-Axis Forging:** *Radhakrishna Bhat*<sup>1</sup>; Andrew Deal<sup>1</sup>; Richard Didomizio<sup>1</sup>; Judson Marte<sup>1</sup>; P.R. Subramanian<sup>1</sup>; <sup>1</sup>GE Global Research Center

A near-isothermal multi-axis forging (MAF) process was used to produce ultra-fine grained (UFG) Ti-6Al-4V alloys. The thermal stability of the resulting ultra-fine grained structure was evaluated at low temperatures below the beta transus under both static and dynamic conditions in order to investigate the coarsening kinetics of the alpha grains in the alpha+beta phase field. Specimens were heat-treated for varying durations at different temperatures within the alpha+beta phase field for the static studies, while hot compression tests were conducted at different strain rates to evaluate the thermal stability under dynamic conditions. The results of a new characterization technique, namely electron back scattered diffraction (EBSD) line-scans, optimized for quantitative image analysis of ultrafine alpha and beta grains will be presented. The coarsening mechanisms and thermal stability of the ultra-fine grain Ti-6Al-4V will be discussed, especially in the context of using UFG Ti-6Al-4V for producing near-net shape Ti components via superplastic deformation.

## 11:05 AM

**Grain Growth Kinetics of Thermally Stabilized Nanocrystalline Fe-Alloys:** *Kris Darling*<sup>1</sup>; Brian Schuster<sup>1</sup>; Brady Butler<sup>1</sup>; Suveen Mathaudhu<sup>1</sup>; Laszlo Kecskes<sup>1</sup>; <sup>1</sup>ARL

Interfacial energy reduction has been suggested to be a superior method to prevent grain growth in nanocrystalline materials. Recently, examples of thermally stabilized nanocrystalline alloys have emerged showing dramatic high temperature stability owing to grain boundary segregation of solutes and the associated interfacial energy reduction. Such samples are typically synthesized through high energy non equilibrium processes and therefore limited to small product geometries such as particles. Furthermore, the very same mechanism responsible for the high thermal stability can often lead to frustrated atomic diffusion and hinder the densification required for production of bulk samples. The primary objective of this study was to delineate the grain growth kinetics of thermally stabilized Fe based nanocrystalline alloys by use of differential scanning calorimetry. Knowledge of such grain growth kinetics will establish the appropriate consolidation parameters for successful densification in the future.

## 11:20 AM Invited

**Elemental Redistribution Induced by High-Pressure Torsion in Alloys:** *Xiaozhou Liao*<sup>1</sup>; Song Ni<sup>1</sup>; Yanbo Wang<sup>1</sup>; Gang Sha<sup>1</sup>; Simon Ringer<sup>1</sup>; Terence Langdon<sup>2</sup>; Yuntian Zhu<sup>3</sup>; <sup>1</sup>The University of Sydney; <sup>2</sup>University of Southern California; <sup>3</sup>North Carolina State University

Severe plastic deformation techniques including high-pressure torsion have been widely used to refine materials for superior mechanical properties. Complex structural evolutions occur during severe plastic deformation, which include not only grain refinement but also composition redistribution for alloys. The composition redistribution is expected to affect significantly the mechanical properties and structural thermal stability of the alloys. This presentation discusses the effect of high-pressure torsion on the compositional distribution in two materials systems. The starting materials are both solid solutions – one in an equilibrium state and the other in a supersaturated non-equilibrium state. The composition distribution was investigated using transmission electron microscopy and atom probe tomography.

## 11:40 AM

**Engineering Stored Energy in Ultra Fine Grained Metals Created by Severe Plastic Deformation:** M. Ravi Shankar<sup>1</sup>; *Shashank Shekhar*<sup>1</sup>; Jiazhao Cai<sup>1</sup>; <sup>1</sup>University of Pittsburgh

Severe plastic deformation (SPD) induces very high density of dislocations and other defects in material systems. The storage of these defects results in nanostructured interfaces which are characterized by a finite stored energy. This energy offers a component of the driving force for thermally-induced coarsening which leads to softening, and therefore directly influences microstructure stability. Here, we demonstrate means for manipulating the stored interfacial energy for achieving tunable stability as well as mechanical property combinations. It is demonstrated that by manipulating strain, strain-rate and temperature of severe plastic deformation, it is possible to engineer fine microstructures with subdued stored interfacial energy, low enough so that the as prepared material remains stable over a relatively larger range of temperature, but still retain high strength and sometimes, even enhanced ductility.

## 2010 Functional and Structural Nanomaterials: Fabrication, Properties, Applications and Implications: Synthesis of Nanomaterials II

*Sponsored by:* The Minerals, Metals and Materials Society, TMS Electronic, Magnetic, and Photonic Materials Division, TMS: Nanomaterials Committee

*Program Organizers:* David Stollberg, Georgia Tech Research Institute; Nitin Chopra, University of Alabama; Jiyoung Kim, University of Texas - Dallas; Seong Jin Koh, University of Texas at Arlington; Navin Manjorran, Siemens Corporation; Ben Poquette, Keystone Materials; Jud Ready, Georgia Tech

Tuesday PM Room: 214  
February 16, 2010 Location: Washington State Convention Center

*Session Chair:* Jiyoung Kim, University of Texas - Dallas; David Stollberg, Georgia Tech Research Institute

## 2:00 PM Introductory Comments

## 2:05 PM Invited

**Nanowires of Phase Change Materials for Memory Applications:** Jeong-Soo Lee<sup>1</sup>; Chan Hoon Park<sup>1</sup>; Jung Hyun Cho<sup>1</sup>; Ki Hyun Kim<sup>1</sup>; Yoon-Ha Jeong<sup>1</sup>; *Meyya Meyyappan*<sup>2</sup>; <sup>1</sup>National Center for Nanomaterials Technology; <sup>2</sup>NASA Ames Research Center

Nanoscale memory technologies providing an alternative to flash memory have been receiving much attention in recent years. Among them, phase change random access memory (PCRAM) has shown considerable promise in terms of endurance, programming current and other metrics and therefore is ready for market. But continued scalability, density and reduction in current for many more generations to come will have unique challenges. The nanowire (NW) form of the same phase change materials such as germanium telluride (GeTe), GeSbTe (GST) and indium selenide provides an alternative to tackle future challenges. First, the NW memory cell volume is inherently smaller in size thus driving the thermal budget down. Second, it is well known that nanomaterials



exhibit a lower melting point relative to their bulk counterparts, which will also help to reduce the thermal budget. Other thermal properties are also favorable in the nanowire form. These aspects together will reduce the programming current needs. We have grown nanowires of the above phase change materials using a vapor-liquid-solid approach and characterized them extensively. This presentation will provide details of growth results, characterization, evidence of melting point reduction and preliminary device results for programming current and switching ratio between SET/RESET.

### 2:25 PM

**Effects of Process Parameters of ALD on High-k Dielectric Deposition on HOPG for Graphene Based Nanoelectronics:** *Greg Mordí<sup>1</sup>; Bongki Lee<sup>1</sup>; Jiyoung Kim<sup>1</sup>; <sup>1</sup>University of Texas at Dallas*

Graphene, a single layer of graphite with 2-D honeycomb structure, has been the center of attention as an emerging material for novel nanoelectronics, thanks to its unique electronic properties and potential applications. In order to realize high performance nanoelectronic devices, it is required to build localized gate structures on a graphene layer. Atomic layer deposition (ALD) is expected to be a suitable technique to deposit conformal thin high-k dielectric films while avoiding damages on the graphene layer. Unfortunately, chemical inertness of a pristine graphene layer causes an additional challenge for high-k dielectric deposition. Process conditions of ALD such as dielectric deposition temperature, type of oxidant, oxidant exposure dose, the dielectric material used and its growth rate must be carefully understood and controlled to achieve a high quality and conformal gate dielectric deposition while limiting any process induced defects. In this work, we extensively and systematically examine the effects of temperature and oxidant exposure dose on highly ordered pyrolytic graphite (HOPG), a chemically inert surface of 3-D bulk form of graphite that accurately mimics graphene and characterize the surface before and after ALD process using atomic force microscope, Raman spectroscopy and high resolution transmission electron microscopy (HRTEM) in order to optimize a standard for dielectric deposition. We also investigate electrical characteristics of the dielectric.

### 2:45 PM

**Dual-Gated Graphene Devices with High-k Dielectric Using Ozone-Based Atomic Layer Deposition (ALD):** *Bongki Lee<sup>1</sup>; Greg Mordí<sup>1</sup>; Jiyoung Kim<sup>1</sup>; <sup>1</sup>University of Texas at Dallas*

Graphene, a recently discovered single sheet of carbon atoms, stands out as an outstanding material that possesses a unique band structure as well as a high electronic mobility, which allows for fundamental studies in condensed-matter physics and potential applications in nanoelectronic devices. In order to realize graphene-based devices, many challenging issues must be overcome. One of the challenges is the absence of a high quality dielectric layer on graphene required for local gate application due to its chemically inert surface. We have reported a facile process that allows for a conformal deposition of ALD dielectric on HOPG (highly oriented pyrolytic graphite) by using O<sub>3</sub> treatment. In this study, we will present an O<sub>3</sub>-based atomic layer deposition process to deposit high-quality of gate dielectrics on single layer graphene for localized gate applications. The performance of a top-gated graphene device utilizing an O<sub>3</sub>-based Al<sub>2</sub>O<sub>3</sub> dielectric in a dual-gated structure will be presented.

### 3:05 PM

**The Interface Characteristics and the Electrical Properties of ZnO/ITO/ZnO Nano Thin Films:** *Fei-Yi Hung<sup>1</sup>; K. J. Chen<sup>2</sup>; S. J. Chang<sup>2</sup>; Z. S. Hu<sup>2</sup>; Y. T. Chen<sup>1</sup>; <sup>1</sup>Institute of Nanotechnology and Microsystems Engineering, Center for Micro/Nano Science and Technology, National Cheng Kung University; <sup>2</sup>Institute of Microelectronics and Department of Electrical Engineering; Center for Micro/Nano Science and Technology, National Cheng Kung University*

ZnO film has the advantage of thermal stabilization while ITO film plays an important role in electrical conductivity. The present ZnO/ITO/ZnO tri-layer thin films were designed and fabricated by RF sputtering. The results showed that increasing the thickness of the ITO interlayer had no obvious effect on the optical transmittance. Notably, a 13 nm ITO interlayer, the ZnO/ITO(13nm)/ZnO thin film possessed better crystallized structures and electrical properties. Also, the interfacial characteristics of the ZnO/In/ZnO thin film was studied to confirm the contribution of the ITO interlayer on the electrical properties of the ZnO/ITO/ZnO thin film. Under the thermal effect, the indium atoms in the ITO film had migrated into the ZnO matrix and improved the conductivity of the thin film.

### 3:25 PM

**Nanotube Grafting on Porous Solids for Multifunctional Applications:** *Sharmila Mukhopadhyay<sup>1</sup>; <sup>1</sup>Wright State University*

Recent investigation in this group allows grafting of strongly bonded carbon nanotubes (CNT) in porous cellular materials for creating robust structures with very high surface to volume ratio. These form multi-scale hierarchical surfaces similar to those in hair and capillary type structures abundantly seen in biological systems. Once the core substrate is created, the increased surface area can be modified for functional applications such as porous electrodes, catalysts, filters, thermal radiators, tissue scaffolds etc. This paper will discuss the nucleation-growth mechanisms involved in the two-step fabrication technique that makes such structures possible. The effectiveness of CNT-grafted porous structures fabricated so far have been found to be very promising in the following areas, and will be discussed: (i) Porous supports for nano-catalyst particles such as Pd, (ii) Scaffolds for cell and protein growth, (iii) Thermal management devices, and (iv) Core support for structural composites.

### 3:45 PM Break

### 4:00 PM

**Synthesis and Surface Roughening of CoSb<sub>3</sub> Nanowires by Electrochemical Methods:** *Dat Quach<sup>1</sup>; Ruxandra Vidu<sup>1</sup>; Pieter Stroeve<sup>1</sup>; Joanna Groza<sup>1</sup>; <sup>1</sup>University of California, Davis*

Cobalt antimonide (CoSb<sub>3</sub>) belongs to a group of materials called skutterudites that possess promising thermoelectric properties. While most studies on CoSb<sub>3</sub> have been focused on the so-called phonon-glass / electron-crystal approach in order to increase the material's figure of merit, the low dimensional materials approach is rarely discussed due to difficulties involved in the processing of nanostructured CoSb<sub>3</sub>. In this work the synthesis of CoSb<sub>3</sub> nanowires by electrodeposition is investigated under different deposition conditions. Surface roughening of such nanowires is also applied via electrochemical treatment in order to further enhance materials properties. Characterizations of the nanowires by electron microscopy and x-ray diffraction are also discussed.

### 4:20 PM

**Intermediate Composition of at wt. % Mn/Ni in Amorphous, Nano or Microcrystalline Alloy Films of Fe-Mn or Fe-Ni Deposited from Aqueous Solution of Simple Salt Bath:** *Bassey Udofo<sup>1</sup>; <sup>1</sup>NASA/Goddard Space Flight Center*

Fe-Mn as well as that of Fe-Ni alloy films are can be deposable by electrochemical means from reducing aqueous solution or thermally reducing vacuum or furnace atmospheres on insulator, semiconductor or conductive substrate surfaces. These alloy films is soft ferromagnetic materials possessing low residual induction, low hysteresis loop and low coercive force, maximum permeability and low thermal coefficient of thermal expansion useful for various applications. Thermally produced films are thinner with limited crystalline structures ranging from nano to polycrystalline or amorphous film structures. Electrochemically produced film are cheap requiring low temperature applications and the films produce ranges from nano to polycrystalline structures, amorphous and other forms of microstructures that could not be produced by thermal means. These are soft ferromagnetic films that could become antiferromagnetic materials when combined as multilayer alloys. Intermediate composition of these alloy depositions are possible requiring good knowledge of electrochemistry of metallurgy, thermodynamic and kinetic reactions.

### 4:40 PM

**Controlling Composition at the Individual FePt Nanoparticle Level:** *Chandan Srivastava<sup>1</sup>; David Nikles<sup>1</sup>; Gregory Thompson<sup>1</sup>; <sup>1</sup>University of Alabama*

The self assembly of FePt nanoparticles is proposed as a candidate architecture for achieving ultra high magnetic storage. An outstanding issue is the compositional and size variation between individual nanoparticles. This research will demonstrate that a two-step nucleation process of Pt seeds with the subsequent heterogeneous nucleation of Fe from organo-metallic or salt precursors can significantly reduce the composition and size distribution between individual nanoparticles. This two-step process, and the narrowing of these distributions, has been demonstrated in two separate FePt synthesis techniques: the thermal decomposition of Fe(CO)<sub>5</sub> or reduction of FeCl<sub>2</sub> with Pt(acac) precursors. The results are explained in terms of a Monte Carlo free energy simulation. Individual nanoparticle chemistry has been quantified using STEM-EDX analysis. The results demonstrate how mechanistic nucleation and growth control can be used to tune multi-component nanoparticles.

# Technical Program

5:00 PM

**Chemical Vapour Synthesis of Boron Modified Nanocrystalline Anatase Titania for Photocatalytic Applications:** *Imteyaz Mohammad*<sup>1</sup>; Subramshu Bhattacharya<sup>1</sup>; Horst Hahn<sup>2</sup>; <sup>1</sup>IIT Madras; <sup>2</sup>Technische Universität Darmstadt

Titania is a popular wide bandgap semiconductor with high potential for diverse catalytic applications. Of the three well-known polymorphs of titania, anatase is the most effective catalyst for the degradation of many organic and inorganic pollutants. However, anatase is metastable and irreversibly transforms to rutile on heating. Further, the bandgap of anatase lies in the ultra-violet region, which reduces its efficiency under ambient light. Modification of nanocrystalline anatase with boron could result in improved high temperature stability and lower bandgap energy. In the present study, boron modified nanocrystalline anatase was synthesized in a single step by a chemical vapour synthesis (CVS) route. The powders were characterized by x-ray diffraction, nitrogen adsorption and Fourier transform infrared spectroscopy. Analysis revealed the presence of boron in  $\text{BO}_4$  co-ordination in the titania structure. Studies on the photocatalytic degradation of rhodamine dye under UV radiation confirmed faster degradation in case of the boron modified powders.

5:20 PM **Concluding Comments**

---

## Advances in Composite, Cellular and Natural Materials: Metal Matrix Composites

*Sponsored by:* The Minerals, Metals and Materials Society, TMS Structural Materials Division, TMS/ASM: Composite Materials Committee

*Program Organizers:* Yuyuan Zhao, The University of Liverpool; David Dunand, Northwestern University

Tuesday PM                      Room: 305  
February 16, 2010              Location: Washington State Convention Center

*Session Chairs:* Xiaodong Li, University of South Carolina; T. Venkatesh, Stony Brook University

---

2:00 PM

**Fabrication of Al6061-SiC Composite by a Novel Semisolid Powder Processing:** Yufeng Wu<sup>1</sup>; *Gap-Yong Kim*<sup>1</sup>; Iver Anderson<sup>2</sup>; Thomas Lograsso<sup>2</sup>; <sup>1</sup>Iowa State University; <sup>2</sup>Ames Laboratory of US DOE

Metal matrix composites (MMCs) offer advantages such as improved strength, stiffness and electrical properties to provide weight or performance benefits. In this study, we investigated fabrication of Al6061-SiC composite by particle-based semisolid processing (pSP), which combines the advantages of semisolid forming and powder metallurgy. High wt% SiC (>50%) particle reinforced Al6061 were fabricated by pSP. Effects of the processing parameters (SiC volume fraction and pressure) on the microstructures and mechanical properties of the composite were investigated. Composites with high wt% SiC were successfully formed. Observed microstructures indicate the SiC was uniformly distributed within the matrix. Microhardness test showed that the composite strength was significantly improved by the addition of SiC particles. The hardness increased as the SiC fraction and pressure increased. Test results show that the process has the potential to synthesize and fabricate final part simultaneously in MMCs at low cost and with high efficiency.

2:20 PM

**Compressive Properties of Closed-Cell Aluminum Foams Reinforced with Fly Ash Particles:** *Yong Liang Mu*<sup>1</sup>; Guang Chun Yao<sup>1</sup>; Hong Jie Luo<sup>1</sup>; <sup>1</sup>Northeastern University

The closed-cell aluminum foam reinforced by 1.5wt.% and 3.0wt.% fly ash particles were manufactured by molten body transitional foaming process. The quasi-static compression tests were conducted. Results show that the plateau stress of Al/Fly ash foams increases nearly linearly with relative density. Moreover, the addition of fly ash particles improves the plateau stress. Also, the energy absorption property of Al/Fly ash foams increase with relative density and fly ash content, which can be attributed to the reinforced cell walls by fly ash particles and the existence of sliding between fly ash and matrix.

2:40 PM

**Fabrication of Carbon Nano-Fiber (CNF) Reinforced Aluminum Matrix Composites by Pressureless Infiltration: Effect of Aluminum Coatings on Infiltration Behavior:** *Fumio Ogawa*<sup>1</sup>; Tatsuya Hirakawa<sup>2</sup>; Minoru Oda<sup>1</sup>; Chitoshi Masuda<sup>3</sup>; Toshiyuki Nishimura<sup>4</sup>; <sup>1</sup>Graduate School of Waseda University; <sup>2</sup>Waseda University; <sup>3</sup>Kagami Memorial Institute for Materials Science and Technology, Waseda University; <sup>4</sup>National Institute for Materials Science

Recently, CNF reinforced aluminum matrix composites are considered to be used as brake disc rotor of automobile or thermal management device due to their high specific strength, modulus and thermal conductivity. In general, CNF is not easily wetted by molten aluminum. So, since it is hard to infiltrate molten aluminum into CNF preform, fabrication of composites by casting is difficult. In this study, aluminum or its compounds are coated on CNF by chemical vapor deposition to enhance wetting. Pressureless infiltration of aluminum is studied and effects of aluminum coating and magnesium content in preform on infiltration behavior are investigated. Optimum condition for fabrication of composites is studied. Mechanical and physical constants such as elastic modulus, hardness, strength, and thermal conductivity are measured and compared with those of composites fabricated by powder metallurgy method.

3:00 PM

**Un-Bundled Carbon Nanotubes Reinforced Titanium Composites via Powder Metallurgy Process:** *Katsuyoshi Kondoh*<sup>1</sup>; Thotsaphon Threujirapapong<sup>1</sup>; Hisashi Imai<sup>1</sup>; Junko Umeda<sup>1</sup>; Bunshi Fugetsu<sup>2</sup>; <sup>1</sup>Osaka University; <sup>2</sup>Hokkaido University

Zwitterionic surfactant solution process was applied to prepare titanium powders coated with un-bundled multi-wall carbon nanotubes (MWCNTs). They were consolidated by spark plasma sintering (SPS) and subsequently hot extrusion process. The microstructures and mechanical properties of titanium composites reinforced with CNTs were evaluated. The distribution of CNTs and in-situ formed titanium carbide (TiC) compounds during sintering was investigated by XRD, optical and scanning electron microscopy (SEM) equipped with EDS analyzer. The mechanical properties of TMC were significantly improved by the additive of CNTs. For example, when employing the pure titanium composite powder coated with CNTs of 0.35 mass%, the increase of tensile strength and yield stress of the extruded TMC was 157 MPa and 169 MPa, respectively, compared to those of extruded titanium materials with no CNT additive. Fractured surfaces showed uniform distribution of CNTs and TiC particles, being effective for the dispersion strengthening of the composites.

3:20 PM

**Fabrication of High Strength Pure Ti Matrix Composite Reinforced with Carbon Black Particle via Wet Process:** *Thotsaphon Threujirapapong*<sup>1</sup>; Katsuyoshi Kondoh<sup>2</sup>; Hisashi Imai<sup>2</sup>; Junko Umeda<sup>2</sup>; Bunshi Fugetsu<sup>3</sup>; <sup>1</sup>Graduate School of Engineering, Osaka University; <sup>2</sup>Osaka University; <sup>3</sup>Hokkaido University

A titanium matrix composite reinforced with carbon black was prepared by spark plasma sintering (SPS) and hot extrusion. Carbon black particles were added for the in situ formation of TiC dispersoids during the SPS process. Sponge and fine Ti powders were coated with carbon black particles via a wet process using a zwitterionic solution containing carbon black spheres. The morphology and distribution of the in situ TiC phases were investigated using optical microscopy and SEM with an EDS analyzer. The mechanical properties of these composites were remarkably improved by adding a small amount of carbon black at 0.07 ~ 0.16 wt.%. The increases in the yield stress of the extruded sponge and fine Ti were 70.0 and 291 MPa, while the tensile strength increases were 67 and 231 MPa, respectively, compared to those of extruded pure Ti with no reinforcement. The advantages of the wet process are discussed in detail.



### 3:40 PM Break

### 4:00 PM

**Load Partitioning in Al<sub>2</sub>O<sub>3</sub>-Al Composites with Three-dimensional Periodic Architecture:** *Marcus Young*<sup>1</sup>; *Ranjeet Rao*<sup>2</sup>; *Jon Almer*<sup>3</sup>; *Dean Haefner*<sup>3</sup>; *Jennifer Lewis*<sup>2</sup>; *David Dunand*<sup>1</sup>; <sup>1</sup>Department of Materials Science and Engineering, Northwestern University; <sup>2</sup>Department of Materials Science and Engineering, University of Illinois at Urbana-Champaign; <sup>3</sup>Advanced Photon Source, Argonne National Laboratory

Interpenetrating Al<sub>2</sub>O<sub>3</sub>/Al composites were created by liquid-metal infiltration of 3-D periodic ceramic preforms with simple tetragonal and face-centered tetragonal symmetry produced by direct-write assembly. Volume-averaged lattice strains in the ceramic phase of the composite were measured by synchrotron X-ray diffraction for various levels of uniaxial compression. Load transfer is found to occur from the metal phase to the ceramic phase and is in general agreement with simple rule-of-mixture models and in better agreement with more complex, 3-D finite-element models that account for metal plasticity and details of the geometry of both phases. Spatially resolved diffraction measurements show variations in load transfer at two different positions within the composites. Lastly, the effects of Al<sub>2</sub>O<sub>3</sub> symmetry on load partitioning in Al<sub>2</sub>O<sub>3</sub>/Al composites are discussed.

### 4:20 PM

**Bulk Metallic Glass Composites: A New High-Performance Structural Material:** *Douglas Hofmann*<sup>1</sup>; *Maximilien Launey*<sup>2</sup>; *Robert Ritchie*<sup>3</sup>; *William Johnson*<sup>4</sup>; <sup>1</sup>Liquidmetal Technologies; <sup>2</sup>Lawrence Berkeley National Laboratory; <sup>3</sup>University of California Berkeley; <sup>4</sup>California Institute of Technology

Bulk metallic glasses (BMGs) are well-known for having high strengths and nearly negligible ductility in unconfined loading conditions. However, when properly designed and processed, BMG matrix composites can have mechanically properties equally or surpassing the best crystalline materials. These composites exhibit >10% ductility in tension at yield strengths between 1-2 GPa, fracture toughness in excess of 150 MPa√m and endurance fatigue limits of ~30% of the tensile yield strength. In this talk, we will discuss recent collaborative efforts towards improving design, manufacturing, and mechanical properties of these new composites. This work will encompass alloy development, semi-solid processing, fracture toughness and fatigue measurements, novel manufacturing strategies, and the successful demonstration of complex net-shapes.

### 4:40 PM

**Creep and In-situ TEM Investigations of Short Fiber Reinforced Metal Matrix Composites:** *Deniz Kurumlı*<sup>1</sup>; *Marcus Young*<sup>1</sup>; *Antonin Dlouhy*<sup>2</sup>; *Gunther Eggeler*<sup>1</sup>; <sup>1</sup>Ruhr Universitaet; <sup>2</sup>Institute of Physical Metallurgy, Academy of Sciences of the Czech Republic

Short fiber reinforced metal matrix composites (MMCs), consisting of an AlZn11Mg0.2 alloy matrix reinforced with 15 vol. % Saffil fibers, were produced by squeeze casting. Miniature creep specimens were examined during creep under uniaxial tensile loading at temperatures ranging from 573 K to 648 K. The fiber reinforcement is found to decrease the creep rate and creep ductility and increase the creep strength. Moreover, the fiber reinforcement changes the characteristics of the stress and temperature dependence of the overall creep process. Microstructural processes, which control the creep behavior, were examined using TEM during uniaxial loading and during heating and cooling. A considerable increase in the dislocation density towards the fiber was observed in the crept material.

### 5:00 PM

**Creep Behavior of Aluminum Based Nanocomposites Reinforced with Multi-Walled Carbon Nanotubes:** *Hyunjoo Choi*<sup>1</sup>; *Jaehyuck Shin*<sup>1</sup>; *Donghyun Bae*<sup>1</sup>; <sup>1</sup>Yonsei University

Reinforcing effects of multi-walled carbon nanotubes (MWNTs) on the creep behavior of aluminum-based nanocomposites were investigated. The composites were produced by hot rolling of the ball-milled mixture of aluminum powders and MWNTs. During the specially controlled milling process, each of the MWNTs was uniformly dispersed and fully packed with aluminum atoms, providing the perfectly sticking interface between the MWNTs and the matrix. The creep behavior of the composites at high and low stress levels was examined in the temperature range from 150° to 250°. MWNTs can effectively block both thermal diffusion of aluminum atoms and dislocation movement; the composites exhibit significantly reduced thermal diffusivity and remarkably enhanced strength at elevated temperatures. The operative creep mechanism

was also predicted based on the stress exponent and activation energy for creep and evaluated using transmission electron microscope (TEM) images after creep.

### 5:20 PM

**Microstructural Evaluation of ZrC Reinforced Al-Cu Matrix Alloy Composites Fabricated by Mechanical Alloying and Vacuum Hot Pressing:** *Hulya Kaftelen*<sup>1</sup>; *Necip Unlu*<sup>1</sup>; *Mustafa Ovecoglu*<sup>1</sup>; *Hani Henein*<sup>2</sup>; <sup>1</sup>Istanbul Technical University; <sup>2</sup>University of Alberta

In this work, Al-4wt.%Cu composites comprising two differently sized ZrC reinforcing particles (157 μm and 8 μm) were fabricated by high energy ball milling and vacuum hot pressing. Vacuum hot pressing experiments were carried out at 550°C under a pressure of 70 MPa on Al-4wt. %Cu composite powders ball milled for 3h. Effects of reinforcement size on the microstructural and physical properties of the composites were investigated by X-ray diffraction (XRD), scanning electron microscopy (SEM) with energy-dispersive spectrometry (EDS) techniques. Following vacuum hot pressing, approximately relative density values of 98 % were achieved for all hot pressed Al-4wt.%Cu composites. Highest microhardness values were measured for the hot pressed Al-4wt.%Cu composites containing the smallest sized ZrC reinforcing particles (8 μm). On the basis of analysis, in addition to the Al, ZrC and Al<sub>2</sub>Cu phase reflections, a tetragonal Al<sub>7</sub>Cu<sub>2</sub>Fe phase was formed due to iron contamination from balls and/or vial in the metal matrix composite during MA process.

## Alumina and Bauxite: Process Improvements and Experiences - Red Side I

*Sponsored by:* The Minerals, Metals and Materials Society, TMS Light Metals Division, TMS: Aluminum Committee, TMS: Aluminum Processing Committee  
*Program Organizers:* Carlos Suarez, Hatch Associates Inc; Everett Phillips, Nalco Company

Tuesday PM Room: 611  
February 16, 2010 Location: Washington State Convention Center

*Session Chair:* Austin Mooney, Sherwin Alumina

### 2:00 PM Introductory Comments

### 2:10 PM

**Study on Ore Dressing and Characterization of Different Granulometric Fractions that Compound Bauxite from Pará/Brazil:** *Fernanda Silva*<sup>1</sup>; *Rachel Santos*<sup>1</sup>; *João Sampaio*<sup>2</sup>; *Francisco Garrido*<sup>3</sup>; *Marta Medeiros*<sup>3</sup>; <sup>1</sup>IQ/UFRJ - CETEM; <sup>2</sup>CETEM; <sup>3</sup>IQ/UFRJ

Bauxite from Northeast of Pará/Brazil was ore dressed and characterized by XRD, XRF, chemical and thermal analysis. XRD was performed to determine the mineral content. Such bauxite is essentially gibbsitic and has been associated with kaolinite, aluminum-goethite, goethite and iron and titanium compounds. XRF analysis was carried out in order to determine the sample's chemical composition and how its content varied after ore dressing. However, the chemical content of Al<sub>2</sub>O<sub>3</sub>available and SiO<sub>2</sub>reactive was determined by back titration and flame atomic absorption. The results found for the Bayer Process sample were 47.2% and 5.3%, respectively. Thermal analysis was performed as a supplemental technique to observe the bauxite decomposition in the mineralogical phases. Thus, based on stoichiometric relations of the bauxite components decomposition and the mass loss observed in the thermal analysis, it was possible to confirm the following phases: gibbsite, aluminum-goethite and kaolinite.

### 2:40 PM

**Autoclave Desilication of Digested Bauxite Slurry in the Flashing Circuit:** *Andrey Panov*<sup>1</sup>; *Alexander Suss*<sup>1</sup>; *Irina Paromova*<sup>1</sup>; *Alexander Damaskin*<sup>1</sup>; <sup>1</sup>RUSAL VAMI

Bauxite digestion conditions should provide not only the maximum alumina recovery from raw material into liquor, but also the required desilication rate to produce further alumina of high quality. Several desilication equipment circuits are common for alumina industry, namely low temperature predesilication of crude and digested slurry, Sumitomo process. These processes as a rule involve heavy process equipment. The proposed option of autoclave desilication in the

Tue. PM

# Technical Program

flashing circuit of the bauxite slurry allows implementation of the process at higher temperature enhancing chemical reactions of green liquor desilication. This stimulation gives an opportunity to reduce the retention time from 8-10 to 1-2 hours, facilitates reduction in the balanced silica content and increases alumina to silica ratio in the liquor up to 300. The mud produced after digestion and desilication has better sedimentation properties as compared to that obtained as a result of low temperature desilication.

## 3:10 PM

**Bauxite Grinding Practices and Options:** Anthony Filidore<sup>1</sup>; John Hadaway<sup>1</sup>; <sup>1</sup>FLSmith Minerals

Grinding of bauxite as feed to alumina refineries is undertaken in a variety of grinding circuit types utilizing a range of mill types such as Rod, Rod/Ball and Ball Mills both in open circuit and closed circuit systems. This paper considers the selection criteria in terms of the objectives of the grinding process and reviews the range of options available particularly those used in recent installations. The advantages and disadvantages of these options are discussed. Important evaluation criteria such as product size distribution, specific power consumption and costs are considered, summarised and compared with the design objectives.

## 3:40 PM Break

## 4:00 PM

**The Effect of Anatase and Lime on the Transformation of Sodalite to Cancrinite in Bayer Digestion at 250°C:** Bingan Xu<sup>1</sup>; Peter Smith<sup>1</sup>; Christine Wingate<sup>1</sup>; Lynette De Silva<sup>1</sup>; <sup>1</sup>CSIRO Minerals

Sodalite (SOD) and cancrinite (CAN) are important desilication products in the refining of high silica bauxites by the Bayer process. SOD, usually formed at pre-desilication or low temperature digestion, is transformed to CAN under high temperature digestion. CAN provides opportunities to minimize soda loss and reduce both silica contamination of product and silicate scaling. This paper reports the influence of anatase and types of lime on the transformation. It was found that the rate of transformation is greatly increased by lime, but when anatase is also present, the rate is suppressed by a coating of sodium titanate on SOD. Reducing sodium titanate by forming calcium-containing titanates was critical for the transformation. The efficiency of calcium titanate formation depended on lime charge and type. Calcite as calcium source was more efficient than CaO, enhancing the formation of CAN and promoting the formation of more stable perovskite. The underlying mechanisms are discussed.

## 4:30 PM

**Study on the Rheological Behavior of Crystallized and Crystallized - Amorphous Bauxites:** Carla Barbato<sup>1</sup>; Silvia França<sup>2</sup>; Marcio Nele<sup>3</sup>; <sup>1</sup>UFRJ/CETEM; <sup>2</sup>Cetem; <sup>3</sup>EQ/UFRJ

The Bauxite of Northern Brazil is characterized by a geological profile with five different layers: nodular, crystallized nodular, crystallized, crystallized - amorphous and amorphous. The crystallized bauxite is used for alumina production by the Bayer process. Although the mining process is selective, this layer is removed with a certain amount of crystallized-amorphous bauxite. The ore-dressed bauxite pulp is transported through pipelines to the plant where alumina is produced. It is important to predict the pulp's behavior during its transportation through the pipeline. It is necessary to study the rheology and understand their rheological properties in the pumping. Due the difference in the ore typology it is important to verify the influence of crystallized-amorphous bauxite in the rheological behavior of crystallized bauxite pulps, different concentrations of crystallized-amorphous and crystallized bauxite pulps were studied. It was verified that the increase on the crystallized-amorphous bauxite concentration resulted on viscosity increase and thixotropy decrease.

## Aluminum Alloys: Fabrication, Characterization and Applications: Materials Characterization

**Sponsored by:** The Minerals, Metals and Materials Society, TMS Light Metals Division, TMS: Aluminum Processing Committee  
**Program Organizers:** Subodh Das, Phinix LLC; Steven Long, Kaiser Aluminum Corporation; Tongguang Zhai, University of Kentucky

Tuesday PM Room: 615  
February 16, 2010 Location: Washington State Convention Center

**Session Chair:** Zhengdong Long, Kaiser Aluminum

## 2:00 PM

**Structure Evolution and Recrystallization in 7xxx Series Al Alloys:** Jameson Root<sup>1</sup>; David Field<sup>1</sup>; <sup>1</sup>Washington State University

Recrystallization of hot-rolled 7xxx series aluminum alloy plates can vary greatly due to grain size, texture, varying solute concentration, and second phase particle distribution. The purpose of this study is to observe recrystallization during hot-rolling of a 7xxx series alloy. Hot deformation experiments were performed at various temperatures and strain rates to simulate the hot rolling process. The specimens were subsequently annealed in salt baths for various times at given temperatures. The evolution of microstructure and recrystallization behavior of these specimens were observed with electron backscatter diffraction and optical microscopy. These data are used as a basis for developing a model that tracks recrystallization behavior during hot rolling.

## 2:20 PM

**Quantification of Marine Aluminum Alloy Sensitization Based upon Thermal Loading:** William Golumbfskie<sup>1</sup>; Catherine Wong<sup>2</sup>; <sup>1</sup>Naval Surface Warfare Center, Carderock Division; <sup>2</sup>NAVSEA

In recent years, structural aluminum alloys have become more popular in marine applications, with the shipbuilding industry looking to reduce weight. The 5xxx series is an ideal candidate, combining high specific strength, corrosion resistance, and weldability. Of particular concern is that it becomes sensitized in service. Aluminum becomes sensitized when beta phase ( $Al_3Mg_2$ ) is precipitated at the grain boundaries, which may lead to stress corrosion cracking. The ASTM G67 mass loss test is being used to quantify the extent of sensitization as a function of different thermal loading conditions. Temperature recording devices have been installed on two ships to determine the amount of in-service thermal loading. The objective of this work is to interpret the sensitization and thermal loading data into a quantitative tool that can aid in determining the degree of sensitization for in-service 5xxx alloys and estimate the lifetime until the material has fully sensitized.

## 2:40 PM

**Influence of Grain Boundary Sliding on the Ductility of Ultrafine-Grained Al:** Yonghao Zhao<sup>1</sup>; John F. Bingert<sup>2</sup>; Ying Li<sup>1</sup>; Peiling Sun<sup>3</sup>; Xiaozhou Liao<sup>4</sup>; Yuntian Zhu<sup>5</sup>; Enrique Lavernia<sup>1</sup>; <sup>1</sup>University of California-Davis; <sup>2</sup>Los Alamos National Lab; <sup>3</sup>Feng Chia University; <sup>4</sup>The University of Sydney; <sup>5</sup>North Carolina State University

Early reports on nanostructured materials predicted that grain boundary (GB) sliding should enhance the ductility of nanostructured materials. However, review of the literature shows that direct evidence for this mechanism is still lacking. In this work, we report on post mortem analyses of tensile fractured specimens using atomic force microscopy (AFM) and scanning electron microscopy (SEM), as a means to provide direct evidence for the influence of GB sliding on ductility. Specifically, ultrafine grained (UFG) Al was prepared by equal-channel-angular pressing (ECAP) and annealed at 250°C for 20 min. Transmission electron microscopy (TEM) and electron back-scattering diffraction (EBSD) analyses indicate that annealing changes statistically stored dislocations to low-energy dislocation walls, without significantly affecting grain size or other microstructural parameters. Tensile testing shows an evidently enhanced ductility after annealing. AFM and SEM analyses indicate that the enhanced ductility stems from the much finer micro-deformation bands formed during extensive GB sliding.



### 3:00 PM

**Transmission Electron Microscopic Investigation of Sensitized Al-5083:** *Ramasis Goswami*<sup>1</sup>; George Spanos<sup>2</sup>; Peter Pao<sup>2</sup>; Ronald Holtz<sup>2</sup>; <sup>1</sup>SAIC/Naval Research Laboratory; <sup>2</sup>Naval Research Laboratory

Microstructure of Al-5083 (H-131) sensitized at 175°C for 1, 10, 25, 50, 100, 240, 500 and 1000 hours has been investigated using transmission electron microscopy (TEM) to study the evolution of  $\beta$  phase (Al<sub>3</sub>Mg<sub>2</sub>) at grain boundaries and on existing particles. The  $\beta$  precipitates formed at grain boundaries thicken faster than the rate estimated assuming volume diffusion controlled growth of planar interfaces. It is suggested that pipe diffusion through dislocations contributes to the enhanced growth rate of  $\beta$ , consistent with TEM observations of a high dislocation density both in the aluminum matrix in the as-received material, and in the matrix surrounding the particles in the annealed material. The temporal distribution and the grain boundary coverage of  $\beta$  will be discussed.

### 3:20 PM

**Microstructure Evolution of Pre-Strained 3xxx Aluminum Alloys during Annealing:** *Payman Babaghorbani*<sup>1</sup>; Nick Parson<sup>2</sup>; Mary Wells<sup>3</sup>; Warren Poole<sup>1</sup>; <sup>1</sup>The University of British Columbia; <sup>2</sup>Rio Tinto Alcan, Arvida Research and Development Centre; <sup>3</sup>University of Waterloo

Room temperature deformation is often the final stage in the processing route for 3xxx aluminum alloys which are used in heat exchanger applications and cooling systems. The deformation can be low (1-5%) for sizing applications or relatively large for example in the case of tube drawing. Often the parts are annealed either as a separate processing step or in conjunction with the brazing operation. The current study examines the annealing behavior in AA3xxx alloys for different levels of pre-strain, ranging from a few percent to 80% and with different homogenization treatments which modify the dispersoid distribution. The microstructures were characterized by optical microscopy and EBSD. Preliminary observations indicate that there is a strong interaction between the homogenization treatment, the level of pre-strain and the final microstructure and corresponding mechanical properties.

### 3:40 PM

**Characterization of Hypereutectic Al-19%Si Alloy Solidification Process Using In-Situ Neutron Diffraction and Thermal Analysis Techniques:** *Wojciech Kasprzak*<sup>1</sup>; Dimitry Sediako<sup>2</sup>; Mahi Sahoo<sup>1</sup>; Michael Walker<sup>1</sup>; <sup>1</sup>CANMET Materials Technology Laboratory; <sup>2</sup>National Research Council Canada

The objective of this publication is to evaluate the effect of alloying elements on structural and mechanical properties of hypereutectic Al-Si alloy used for light weight automotive applications. Simultaneous application of the in-situ thermal analysis and neutron diffraction (source: NRU nuclear reactor in Chalk River, ON) was used to evaluate the melt characteristics using the non-equilibrium solidification analysis. Some of the factors controlling microstructural modification are melt and pouring temperatures as well as solidification rate. The alloy "dissecting" approach was used to evaluate the contributions of individual alloying elements (Si, Cu, Mg and P) and to determine their effect on alloy and casting parameters including liquid metal processing as well as heat treatment. This outcome will help to better understand the solidification and heat treatment processing of the Al-Si hypereutectic alloys used for the HPDC and LPPM cast components.

### 4:00 PM Break

### 4:15 PM

**Characterization of the Spacing Selection in AlCu Alloys:** *Sebastian Gurevich*<sup>1</sup>; Morteza Amoozezaei<sup>1</sup>; Nikolas Provatas<sup>1</sup>; <sup>1</sup>McMaster University

We study the relationship between growth conditions and the resulting microstructure of cast alloys in industrially relevant conditions. We directionally solidify AlCu alloys under upward unsteady-state solidification conditions utilizing a range of cooling rates, and perform phase field simulations of directional solidification, including varying the growth conditions dynamically. To address the influence of the transient states and growth history on the resulting primary spacing we apply a power spectral analysis. We find that the resulting spacing is not uniquely determined by the cooling conditions but does fall within a specific, reproducible band. This consolidates the hypothesis of a band of accessible spacings for a given growth conditions rather than one unique spacing, consistent with previous works by Warren and Langer, Trivedi

and Hun and Huang et al, as well as the notion of a predictable statistical scaling theory of primary spacing selection of Greenwood et al.

### 4:35 PM

**Development of Al-Si Alloy by Optimizing Modifiers and Grain Refiners:** *Saeed Farahany*<sup>1</sup>; Ali Ourdjini<sup>1</sup>; Mohd Hasbullah Idris<sup>1</sup>; <sup>1</sup>UTM University

We studied interaction of modifiers and grain refiners in hypoeutectic aluminum-silicon alloys, Al-6.5% Si- 0.3 Mg-Cu 2% to obtain optimum microstructure. Control of grain size and morphology of eutectic are major steps to achieve desired properties in these alloys. We used ingot pure aluminum; Al-Ti-B and Al-Sr master alloys and melt them in induction furnace. We used scanning electron microscope (SEM) and image analyzer software to study microstructure and measure grain size according to ASTM standard E112-88. Microstructural observations showed that by adding modifier, such as sodium, antimony and strontium to hypoeutectic aluminum-silicon alloys coarse flake of eutectic silicon converted to fine particles. Also titanium and boron created fine grain size that improves ductility. Optimum composition for sodium, strontium and antimony in hypoeutectic Al-Si alloys is 0.001% - 0.003%, 0.01%-0.015% and 0.10% -0.15% respectively. These elements can be compatible together or have reverse effects. Antimony is not compatible with other modifying elements

### 4:55 PM

**Patterning Surface Precipitation in Al-Cu Alloys via Localized Loading:** *Jack Franklin*<sup>1</sup>; Jennifer Lukes<sup>1</sup>; <sup>1</sup>University of Pennsylvania

A new method for patterning precipitates at the surface of aluminum rich copper alloys is investigated. In this method, micron-scale patterned loading devices are used to apply constant localized loading to a mechanically polished surface as the samples are cooled below the solvus line from solid solution. Precipitates grow preferentially underneath the loaded regions for slowly cooled samples but for quickly cooled samples precipitate growth is suppressed. Examples and causes for the observed precipitate patterns will be discussed.

### 5:15 PM

**Refinement of Hypereutectic Al-Si Alloy by Ca<sub>3</sub>P<sub>2</sub>:** Ying Zhang<sup>1</sup>; Wangxing Li<sup>1</sup>; Danqing Yi<sup>2</sup>; Zhiseng Ren<sup>1</sup>; Xianghui Cang<sup>1</sup>; *Jianhong Yang*<sup>1</sup>; <sup>1</sup>Zhengzhou Research Institute of CHALCO; <sup>2</sup>Central South University

Refinements of hypereutectic Al-Si alloy were studied by adding calcium phosphide, which were always carried out with phosphorus or phosphides with low melting points and so on, through optical microscopy, scanning electronic microscope and chemical analysis. The results showed that adding phosphide of alkaline earth metals with higher melting points, such as calcium phosphide, could replace phosphorus modifier used to modify silicon phases and decrease the releasing of poisonous gas at the same time. Orthogonal experiments gave the optimized operational parameter.

## Aluminum Reduction Technology: Hall-Héroult Cell: Energy Conservation Through Cell Design and Process Improvements

*Sponsored by:* The Minerals, Metals and Materials Society, TMS Light Metals Division, TMS: Aluminum Committee, TMS: Aluminum Processing Committee

*Program Organizers:* Charles Mark Read, Bechtel Corporation; Gilles Dufour, Aluminerie de Deschambault

Tuesday PM

Room: 608

February 16, 2010

Location: Washington State Convention Center

*Session Chair:* William Imrie, Bechtel Corporation

### 2:00 PM Introductory Comments

### 2:05 PM

**Wettable Athodes: An Update:** *Rudolf Pawlek*<sup>1</sup>; <sup>1</sup>TS+C

This overview covers the development of aluminium wettable cathodes for the primary aluminium industry in the period 2000 to 2009. It continues a review of TiB<sub>2</sub>-C/composites, including their physical and mechanical properties. This overview also includes the development of binders, the manufacture of the composites, their application on the cathode surface, and their resistance to sodium penetration into the cathode lining. Mathematical modelling has

Tue. PM

# Technical Program

been introduced for the drained slope, the cathode current distribution, the flow of anode gas bubbles and the heat balance. Practical tests involved not only laboratory and bench scales, but also use in big electrolysis cells operated at more than 160 kA. Aluminium wettable cathode coatings appear advantageous for future multi-cell designs and for new electrolysis cell designs rather than for revamping existing Hall-Héroult aluminium electrolysis cells.

## 2:30 PM

**Wettability of Liquid Aluminum on Carbon/Graphite/TiB<sub>2</sub> Composite Cathode Materials:** *Jilai Xue*<sup>1</sup>; Xing Chen<sup>1</sup>; <sup>1</sup>University of Science and Technology Beijing

Wettability of liquid aluminum on the cathode is of great importance for metal stability and cathode service life in aluminum reduction cells. Cathode material for today's reduction cells is carbon with poor wettability by Al, while emerging cathode materials are the carbon/graphite/TiB<sub>2</sub> composites with potential better Al-wettability and cell sustainability. In this paper, a modified sessile drop method was applied to determine the contact angles for various testing materials, in which a newly formed fresh metal drop came into contact with the testing materials when the temperature was reached. The wetting process was recorded against operating time from the beginning of the Al-cathode contact. The TiB<sub>2</sub> addition is found to improve the Al-wettability. The graphite aggregates can make better Al-wettability with a limited addition. The obtained information can be used in improve cathode stability and cell sustainability.

## 2:55 PM

**Study on the New Reduction Technology for Energy Saving:** *Fengqin Liu*<sup>1</sup>; Songqing Gu<sup>1</sup>; <sup>1</sup>Chalco

A new aluminum reduction technology for energy saving recently developed in China is outlined in this paper. It is feasible to reduce ACD and to save energy by changing the properties and structures of the cathodes and lining materials in the reduction cells, which leads to minimizing impacts of magnetic field in the cells on molten metal fluctuation. The industrial tests for the cells with new structure have been conducted recently in China. The test results show that by using the new type cells the reduction operation can be kept steady at lower ACD, while the energy efficiency will be increased. The characteristics, existing problems and future development of various types of the new energy saving cells are reviewed in this paper.

## 3:20 PM

**Effect of Atmosphere-Changing Sintering on the Corrosion Resistance of 17Ni/(10Ni<sub>0</sub>-NiFe<sub>2</sub>O<sub>4</sub>) Cermet Inert Anode:** Liu Kai<sup>1</sup>; Tian Zhongliang<sup>1</sup>; Li Jie<sup>1</sup>; Lai Yanqing<sup>1</sup>; Zhang Hongliang<sup>1</sup>; *Lü Xiao-jun*<sup>1</sup>; <sup>1</sup>School of Metallurgical Science and Engineering, Central South University

A new method termed atmosphere-changing sintering was adopted to prepare 17Ni/(10Ni<sub>0</sub>-NiFe<sub>2</sub>O<sub>4</sub>) cermet inert anode for aluminum reduction. Its corrosion resistance against Na<sub>3</sub>AlF<sub>6</sub>-Al<sub>2</sub>O<sub>3</sub> melts was compared with that of anodes prepared by traditional method through electrolysis tests. The results revealed that the anodes prepared by atmosphere-changing sintering method had better corrosion resistance against the melts. The wear rate of the anodes decreased from 3.12 cm/y to 1.10 cm/y due to the application of atmosphere-changing sintering. According to the SEM pictures of anodes after electrolysis tests, a 200 μm corroded layer can be noted in the outer zone of anodes made by atmosphere-changing sintering method, which was 220 μm thinner than that of anodes fabricated by traditional method.

## 3:45 PM Break

## 3:55 PM

**Liquidus Temperatures of Cryolite Melts with Low Cryolite Ratio:** Alexei Apisarov<sup>1</sup>; Alexander Dedyukhin<sup>1</sup>; *Elena Nikolaeva*<sup>1</sup>; Pavel Tin'ghev<sup>1</sup>; Olga Tkacheva<sup>1</sup>; Alexander Redkin<sup>1</sup>; Yurii Zaikov<sup>1</sup>; <sup>1</sup>Institute of High Temperature Electrochemistry

Multi-component fluoride mixtures are the only possible media for the development of new ecologically clean and energy saving technologies for aluminum production. The radical decrease of operating temperature is impossible in the frame of existing technology in which sodium cryolite is a basic component of electrolyte. In order to obtain essential decrease of the electrolyte liquidus temperature potassium cryolite can be used as a basic component of electrolyte. Sodium and lithium cryolite additions are necessary in this case. Liquidus temperatures for the ternary KF-LiF-AlF<sub>3</sub> and quaternary KF-NaF-CaF<sub>2</sub>-AlF<sub>3</sub> systems have been determined by means of cooling curves.

There are two minimums in the quasi-binary system (KF-AlF<sub>3</sub>)-(LiF-AlF<sub>3</sub>) at CR 1,3 and 1,5. The calcium fluoride solubility in the KF-NaF-AlF<sub>3</sub> system rises with cryolite ratio and NaF content.

## 4:20 PM

**Industrial Test of Low-Voltage Energy-Saving Aluminum Reduction Technology:** Li Jie<sup>1</sup>; *Lü Xiao-jun*<sup>1</sup>; Lai Yan-qing<sup>1</sup>; Xie Chang-chun<sup>2</sup>; Zhang Hong-liang<sup>1</sup>; Xiao Jin<sup>1</sup>; Ding Feng-q<sup>1</sup>; Liu Shi-wen<sup>3</sup>; Guo Qi-feng<sup>3</sup>; Li Yun-long<sup>3</sup>; <sup>1</sup>School of Metallurgical Science and Engineering, Central South University; <sup>2</sup>Hunan Zhongda Yexiang Technology Co., Ltd; <sup>3</sup>Qiya Aluminum (Group) Co, Ltd

It is main way to save energy through reducing electrolysis temperature and/or cell-voltage for the present aluminum electrolysis industry. On 300kA pre-baked cells at Qiya aluminum smelter, low-temperature and low-voltage technology was achieved with the optimization of control algorithm, bath components and process parameter. The industrial tests results for about one year show that the electrolysis temperatures and cell-voltages are about 925° and 3.80V respectively for test cells, and decrease of 30° and 0.3V compared to the reference cells. The bath superheats for test cells range from 10° to 12°. The current efficiencies reach about 92%, which remain the same as those of the reference cells. The energy consumptions for test cells are 12300kWh/t•Al, and decrease of 900 kWh/t•Al compared to the potline cells.

## 4:45 PM

**New Cathodes in Aluminum Reduction Cells:** *Feng Naixiang*<sup>1</sup>; Tian Yingfu<sup>2</sup>; Peng Jianping<sup>1</sup>; Wang Yaowu<sup>1</sup>; Qi Xiquan<sup>3</sup>; Tu Ganfeng<sup>3</sup>; <sup>1</sup>Northeastern University; <sup>2</sup>Chongqing Tiantai Aluminum Industry Co., Ltd.; <sup>3</sup>Northeastern University Engineering and Research Institute Co. Ltd.

Three aluminum electrolysis cells with a novel uneven cathode bottom are being operated successfully in Chongqing Tiantai Aluminum Industry Co., Ltd., China. More and more aluminum smelters are using the model cathode structure. In the past year the three 168 kA cells have produced steadily with low cell voltages of 3.70 V to 3.75 V, and the current efficiency (CE) has been improved by at least 1% in comparison with 127 traditional model cathode cells in the same potline. The technical characteristics of the cells are described in this paper and the fluctuation of metal pad in the cells is measured.

## 5:10 PM

**Calculation of the Aluminum Flow Field at the Interface of Molten Aluminum and Electrolyte in the New Cathode Aluminum Cells:** Jiang Yanli<sup>1</sup>; Peng Jianping<sup>1</sup>; *Feng Naixiang*<sup>1</sup>; Wang Yaowu<sup>1</sup>; Qi Xiquan<sup>2</sup>; <sup>1</sup>Northeastern University; <sup>2</sup>Northeastern University Engineering and Research Institute Co. Ltd.

The mathematical model of electromagnetic field and the aluminum flow field in the 168 kA conventional cells and the new model cathode cells were numerically calculated with the commercial software ANSYS. The calculated results show that the voltage drop in the electrolyte of the new model cathode cells was reduced by 0.38 V, which indicates that the new model cathode cells have the potential for significant energy savings. Furthermore, the velocity of liquid aluminum and molten electrolyte at the aluminum/electrolyte interface in the new model cathode cells is lower than that of the conventional cells.

## 5:30 PM Concluding Comments



## Biological Materials Science: Mechanical Behavior of Biological Materials II: Hard Tissues and their Replacement Materials

*Sponsored by:* The Minerals, Metals and Materials Society, TMS Structural Materials Division, TMS: Biomaterials Committee, TMS/ASM: Mechanical Behavior of Materials Committee

*Program Organizers:* John Nychka, University of Alberta; Jamie Kruzic, Oregon State University; Mehmet Sarikaya, University of Washington; Amit Bandyopadhyay, Washington State University

Tuesday PM Room: 205  
February 16, 2010 Location: Washington State Convention Center

*Session Chair:* To Be Announced

### 2:00 PM Invited

#### Structural Mechanisms for the Inelastic Deformation of Haversian Bone:

*Rizhi Wang*<sup>1</sup>; Vincent Ebacher<sup>1</sup>; <sup>1</sup>University of British Columbia

Biological tissues such as bone and teeth are known for their well-controlled ultra-structure and extraordinary mechanical performance. Bone has high fracture resistance because of its capability to undergo significant inelastic deformation. Understanding the detailed process and structural mechanisms of inelastic deformation thus hold the key to bone mechanics. In this presentation, we will report our latest experimental progress on bone structure, deformation and fracture. The emphasis will be on the most well-known hierarchical structure in human cortical bone, the Haversian system or secondary osteon. It will be shown that the inelastic deformation happens through the multiple microcrack nucleation and propagation processes, which are obviously governed by the unique structure of the osteonal lamellae and the distribution of the Haversian systems within the cortical bone. Such a unique and stable microcracking process eliminates the detrimental stress concentration effect of the Haversian canals and makes Haversian bones highly resistant to catastrophic failure.

### 2:30 PM

#### The Mixed-Mode Fracture of Human Cortical Bone: *Elizabeth Zimmermann*<sup>1</sup>; Maximilien Launey<sup>1</sup>; Holly Barth<sup>1</sup>; Robert Ritchie<sup>1</sup>; <sup>1</sup>Lawrence Berkeley National Laboratory and The University of California at Berkeley

Previous studies on the toughness of human cortical bone have primarily been focused on mode-I (tensile-opening) loading; however, bones *in vivo* are invariably loaded multiaxially. Consequently, an understanding of mixed-mode fracture is necessary to determine whether a mode-I fracture-toughness test provides the appropriate information to accurately quantify fracture risk. We have found that, in a transversely-oriented crack, the competition in crack paths between the maximum mechanical driving force (applied by means of an asymmetric load) and “weakest” microstructural path surprisingly cause the mode-II (shear-loaded) toughness to be ~25% less than the mode-I toughness in human cortical bone. This implies that in the transverse (breaking) orientation, bones are easier to fracture in shear than in tension. This intriguing result is further investigated by characterization of the mixed-mode (crack-initiation) toughness in the longitudinal orientation, and specifically by analyzing how a growing mixed-mode crack interacts with the hierarchical microstructure of bone.

### 2:50 PM

#### Looking at the Effects of Radiation Doses on the Fracture Toughness of Human Cortical Bone: *Holly Barth*<sup>1</sup>; Alastair MacDowell<sup>2</sup>; Maximilien Launey<sup>2</sup>; Robert Ritchie<sup>1</sup>; <sup>1</sup>Lawrence Berkeley National Laboratory and University of California, Berkeley; <sup>2</sup>Lawrence Berkeley National Laboratory

This study is designed to show that both strength and toughness of human cortical bone deteriorates with an increase in exposure to radiation. Bone is a complex hierarchical composite structure of mineral and collagen. Indeed, the toughness of bone is a result of a multi-scale suite of potent extrinsic (shielding) mechanisms, coupled with an additional role of intrinsic toughening due to the significant “plasticity” in the material. Our three control groups contain one group with no radiation exposure, one group with clinically relevant exposure and a third group with high dose exposure. Specimens were fractured and the toughening mechanisms were identified via *in situ* Environmental Scanning Electron Microscope (ESEM) and synchrotron-based x-ray computed tomography (SR $\mu$ CT). *In situ* ESEM mechanical testing allows visualizing the

crack growth in real time and gaining information on the salient toughening mechanisms. The SR $\mu$ CT allows for non-destructive three-dimensional imaging of the microstructure and crack path.

### 3:10 PM

#### Microscale Uniaxial Compression Testing of Bone Tissue Specimens: *Katrina Altman*<sup>1</sup>; *Stacey Vansickle*<sup>1</sup>; *Elise Morgan*<sup>2</sup>; *Katharine Flores*<sup>1</sup>; <sup>1</sup>The Ohio State University; <sup>2</sup>Boston University

Bone is an anisotropic, hierarchically structured material, and as a result, its mechanical behavior is highly statistical in nature. It has been shown for other engineering materials that uniaxial testing at the microscale enables characterization of individual microstructural components in an effort to understand their role in the macroscopic mechanical behavior. The application of such microscale compression testing to bone will permit modeling of the aggregate material to predict effects of age, disease, or injury on the mechanical properties. The present work analyzes the mechanical behavior of 20- and 30 $\mu$ m nominal diameter compression pillars prepared by a femtosecond laser micromachining technique. Pillars are selectively machined within regions of interest on the bone specimen surface (i.e. within osteons). Modulus, strength, and modes of deformation are compared as functions of specimen size and anatomic position. In addition, the effects of water loss on mechanical properties are studied using the microcompression technique.

### 3:30 PM

#### Nanomechanics of Tropocollagen and Hydroxyapatite Biomaterials with an Account of Collagen Mutations and Varied Hydroxyapatite Textures: *Devendra Dubey*<sup>1</sup>; *Vikas Tomar*<sup>1</sup>; <sup>1</sup>Purdue University

In hierarchical nanocomposite materials (eg. bone, nacre), interfacial interactions between the organic phase (eg. tropocollagen (TC)) and the mineral phase (eg. calcium hydroxyapatite (HAP)) as well as the structural effects arising due to the staggered arrangement, TC mutations, and varied HAP textures significantly affect the strength of such biomaterials. In the present investigation, different idealizations of TC-HAP composite biomaterial system under tensile and compressive loadings are analyzed using explicit three dimensional (3-D) molecular dynamics (MD) simulations to develop an understanding of these factors. Analyses show that maximizing the contact area between the TC and HAP phases result in higher interfacial strength as well as higher fracture strength. Analyses based on strength scaling as a function of structural hierarchy reveal that while peak strength follows a multiscaling relation, the fracture strength does not. The peak strain for failure was found to be independent of the level of structural hierarchy.

### 3:50 PM Break

### 4:00 PM Invited

#### Fracture Processes and Mechanisms of Crack Growth Resistance in Human Enamel: *D Bajaj*<sup>1</sup>; *Dwayne Arola*<sup>1</sup>; <sup>1</sup>University of Maryland Baltimore County

Enamel of the human tooth is the hardest and highly mineralized tissue of the body. Despite the high mineral content, recent experimental evaluations of the fracture behavior using incremental crack growth have shown that this tissue undergoes a substantial rise in toughness with crack extension. In fact, the crack growth toughness of enamel (1.13 MPam<sup>0.5</sup>/mm to 3.93 MPam<sup>0.5</sup>/mm) exceeds that of human bone and dentin, tissues with much lower mineral content. Optical observations indicate crack growth toughening in enamel is achieved by a host of mechanisms operating across a range of length scales, and that these mechanisms are most active within the inner enamel. The predominant mechanisms appear to be crack deflection and twist, crack-bridging by unbroken ligaments of prism bundles and organic tethers, and microcracking about the protein-rich prism boundaries. This presentation will review the fracture properties of human enamel and discuss the mechanisms responsible for its exceptional behavior.

### 4:30 PM

#### Interfacial Failure of Dentin Adhesively Bonded to Quartz-Fiber Reinforced Epoxy: *Renata Melo*<sup>1</sup>; *Nima Rahbar*<sup>2</sup>; *Wole Soboyejo*<sup>1</sup>; <sup>1</sup>Princeton University; <sup>2</sup>University of Massachusetts Dartmouth

The aim of this study is to measure the fracture toughness and investigate the mechanisms of failure at the interfaces dentin/resin cement/ quartz-fiber reinforced epoxy. Rectangular slices of dentin from the pulp chamber were acid etched and covered with bonding agent. The slices of dentin were sandwiched by

Tue. PM

# Technical Program

two half-circle quartz-fiber discs covered with bonding agent, and bonded with dental cement to make Brazil-nut sandwich specimens for interfacial toughness testing. The interfacial fracture surfaces were examined using SEM and EDX to determine the failure modes when loading angles changed. Based on SEM/EDX analyses of the two halves, the crack was initiated and continued at the resin cement/quartz fiber substrate for loading angles 1 through 10°, whereas for loading angle 15° the crack was initiated at the top of the hybrid layer and continued there for the most part. The dentin/cement appears to be tougher than the resin cement/quartz-fiber reinforced epoxy.

**4:50 PM**

**Structure and Mechanical Properties of Cementum Biocomposites:** *Hanson Fong*<sup>1</sup>; *Mustafa Gungormus*<sup>1</sup>; *Biran Foster*<sup>1</sup>; *Martha Somerman*<sup>1</sup>; *Candan Tamerler*<sup>1</sup>; *Mehmet Sarikaya*<sup>1</sup>; <sup>1</sup>University of Washington

Enamel, dentin and cementum are biocomposites with unique mechanical properties and hierarchical structures that, working together, make up a mechanically functional tooth. Focus of this study is to understand the structure and mechanical properties of cementum to provide a foundation for cementum regeneration for clinical applications. Teeth from normal mice and mice with mutation or deletion of 'ank' gene which produced excessive but functional cementum, revealed similar mechanical properties in cementum and dentin, as analyzed by nanoindentation. TEM analysis revealed, while similar in mineral crystal size and collagen matrix structure, a distinct orientation difference in mineralized collagen fibers between dentin and cementum, adding overall strength isotropy to the tooth, analogous to off-angle lay-up laminate composites. Current research effort is focusing on fabricating cementum-like layers with similar structural and mechanical properties using genetically engineered hydroxyapatite binding peptides (HABP) created in our lab. Supported by NIDCR/NIH DE015109/DE09532 and GEMSEC (NSF-MRSEC at UW).

**5:10 PM**

**Fabrication and Mechanical Properties of Calcium Phosphate Cements (CPC) for Bone Substitution:** *Jingtao Zhang*<sup>1</sup>; *Franck Tancret*<sup>1</sup>; *Jean-Michel Bouler*<sup>1</sup>; <sup>1</sup>Université de Nantes

Calcium phosphate cements have been used in medical and dental applications for many years. However, their low strength and their high brittleness prohibit their use in many stress-bearing locations, which would require an improvement in mechanical properties. The influence of microstructural parameters on the latter have nevertheless barely been investigated in a systematic manner. In this aim, apatite cements have been fabricated using powders based on  $\alpha$ -TCP ( $\alpha$ -tricalcium phosphate), and their mechanical properties have been measured (compressive strength, Young's modulus and fracture toughness), as a function of various parameters (particle size; liquid-to-powder ratio; amount and morphology of porosity, including macropores created by porogens). This should allow, in the end, to improve mechanical properties by controlling the microstructure, and to find a compromise between strength and biological behaviour.

**5:30 PM**

**Tricalcium Phosphates with Strontium Oxide and Zinc Oxide Dopants for Resorbable Bone Grafts:** *Johanna Feuerstein*<sup>1</sup>; *Shashwat Banerjee*<sup>1</sup>; *Susmita Bose*<sup>1</sup>; *Amit Bandyopadhyay*<sup>1</sup>; <sup>1</sup>Washington State University

Tricalcium phosphate (TCP) ceramics have recently gained a lot of attention for their chemical similarity to bone. However, they show poor mechanical strength. The purpose of this research is to develop a ceramic material with proper strength degradation kinetics and biocompatibility to be used as bone implants. In this study, four different (TCP)-based compounds were studied: (i) 0.25 wt% ZnO, (ii) 1 wt% SrO, (iii) binary dopants with 0.25wt% ZnO and 1 wt% SrO, and (iv) undoped TCP Control. Following wet mixing and pressing, the compounds were sintered at 1250° C. Sintered densities for both undoped TCP and the binary composition were above 95% of theoretical density. All compositions exhibited strengths above 200 MPa before being placed in simulated body fluid (SBF). The binary dopant seems to be the most bioactive as it has the most HCA formation. The presentation will discuss processing and characterization including in-vitro strength degradation analysis.

**5:50 PM**

**Biomimetic Chitosan-Based Nanocomposite Scaffolds for Bone Tissue Engineering:** *Wah Wah thein-Han*<sup>1</sup>; *Devesh Misra*<sup>1</sup>; <sup>1</sup>University of Louisiana

In the development of bone tissue engineering, three-dimensional biomimetic nanostructured composites composed of organic and inorganic materials are

of significant interest to mimic natural bone. We describe here biodegradable chitosan-based nanocomposite scaffolds with improved mechanical, physico-chemical, and biological properties compared to pure chitosan scaffolds for bone tissue engineering. The influence of the properties of chitosan such as degree of deacetylation (DD) and molecular weight (MW) were examined. The nanocomposite scaffolds were characterized by desired porous structure. Furthermore, DD and MW had influence on physico-chemical properties of the scaffolds. Favorable biological response of pre-osteoblast (MC 3T3-E1) on nanocomposite scaffolds included improved cell adhesion, higher proliferation, and well spreading morphology in relation to pure chitosan scaffold. The study underscores chitosan-based nanocomposite as a potential scaffold material for bone regeneration.

---

## Bulk Metallic Glasses VII: Alloy Development and Application II

*Sponsored by:* The Minerals, Metals and Materials Society, TMS Structural Materials Division, TMS/ASM: Mechanical Behavior of Materials Committee

*Program Organizers:* Peter Liaw, The University of Tennessee; Hahn Choo, The University of Tennessee; Yanfei Gao, The University of Tennessee; Gongyao Wang, University of Tennessee

Tuesday PM

Room: 213

February 16, 2010

Location: Washington State Convention Center

*Session Chairs:* Katharine Flores, The Ohio State University; Jan Schroers, Yale University

---

**2:00 PM Invited**

**Processing of Bulk Metallic Glass:** *Jan Schroers*<sup>1</sup>; <sup>1</sup>Yale University

The sluggish crystallization kinetic of bulk metallic glass results in two fundamentally different processing opportunities. BMG can be directly cast. But even for BMGs with low critical cooling rates geometries with high aspect ratio are particularly challenging since during casting cooling and filling of the mold must occur simultaneously. This limits the complexity of the geometries that can be cast even when processing parameters are carefully balanced. Alternatively, BMG can be thermo plastically formed in the supercooled liquid region. In this case the required fast cooling and forming are decoupled. The BMG is formed in a high viscous state where it behaves very similar to plastics when compared by processing temperature and forming pressure. A measure for the formability of BMGs will be introduced. Processing potentials and challenges will be discussed and various examples will be given including blow-molding, miniature fabrication, and nano-patterning.

**2:20 PM**

**Development of Ti-Based Bulk Glassy Matrix Composites with Excellent Mechanical Performance:** *Jin Man Park*<sup>1</sup>; *Norbert Mattern*<sup>1</sup>; *Ka Ram Lim*<sup>2</sup>; *Do Hyang Kim*<sup>2</sup>; *Jürgen Eckert*<sup>1</sup>; <sup>1</sup>Leibniz Institute for Solid State and Materials Research Dresden; <sup>2</sup>Yonsei University

Recently, highly toughened glassy matrix composites with different length scale heterogeneity have been developed in Zr-, Ti-, La-based glassy alloys. These heterostructured composites exhibit improved macroscopic plasticity by controlling the shear band formation and preventing the rapid propagation of major shear bands. In this study, we developed ductile dendrite reinforced composites in the Ti-Zr-Be-Cu-Ni-(Nb, Ta, V) system. Although in-situ composites were successfully formed by optimizing the alloy composition and cooling rate, ductility does not necessarily occur. When the size, the distribution and elastic constants of the dendrites are properly controlled, i.e. coarsened dendrites with lower shear modulus homogeneously distributed in the glassy matrix, large plasticity can be obtained. By optimization of the microstructure, Ti-based bulk glassy matrix composites with excellent mechanical performance (high yield strength of ~1.7 GPa and large plasticity of ~20 %) could be achieved.



### 2:30 PM Invited

**Towards a New Class of Biodegradable Implants: Mg-Based Glasses with No Hydrogen Evolution:** Jörg Löffler<sup>1</sup>; Peter Uggowitzer<sup>1</sup>; Bruno Zberg<sup>1</sup>; <sup>1</sup>ETH Zurich

Magnesium alloys are being increasingly studied for biodegradable implant applications because they show good biocompatibility and a suitable degradation rate. However, unfavorable hydrogen evolution during degradation has so far prevented their use in larger implants. In this context, Mg-based glasses show great promise because their degradation characteristics may be tailored by large amounts of alloying elements integrated into the glass structure. Here I will report on the dramatic reduction or complete cessation of hydrogen evolution during the degradation of MgZnCa glasses. Above a particular Zn-alloying threshold, a Zn- and oxygen-rich passivating layer forms on the alloy surface which can be explained by a model based on the Pourbaix diagram of Zn in simulated body fluid. Animal studies confirm the absence of hydrogen evolution and reveal tissue compatibility as good as that observed for crystalline Mg alloys. Thus these MgZnCa glasses show great potential for a new generation of biodegradable implants.

### 2:50 PM

**Solute Substitution Induced Changes in Structure and Nucleation in an Al-Based Metallic Glass:** Feng Yi<sup>1</sup>; Paul Voyles<sup>1</sup>; Seth Imhoff<sup>1</sup>; John Perepezko<sup>1</sup>; <sup>1</sup>UW-Madison

Fluctuation microscopy measurements have shown that strong Al crystal-like nanoscale order is a potential nucleation site for primary crystallization in high Al-like content metallic glasses. We have recently found that substitution of 1% of Cu for Fe in Al<sub>88</sub>Y<sub>7</sub>Fe<sub>5</sub> causes a dramatic change in the nanocrystal density after primary crystallization, in the delay time for the onset of crystallization, and in the order measured by fluctuation microscopy. Variable resolution STEM fluctuation electron microscopy results, interpreted in the light of computer simulations of Al-based metallic glasses, will shed new light on the size and density of the nanoscale ordered regions in this system.

### 3:00 PM Invited

**Formation and Characterization of Individual Metallic Glassy Nanowire:** Koji Nakayama<sup>1</sup>; Yoshihiko Yokoyama<sup>1</sup>; Takahito Ono<sup>1</sup>; Mingwei Chen<sup>1</sup>; Kotone Akiyama<sup>1</sup>; Toshio Sakurai<sup>1</sup>; Akihisa Inoue<sup>1</sup>; <sup>1</sup>Tohoku University

Metallic glasses have exciting potential for structural, chemical, and magnetic applications with the sizes ranging from micrometer to centimeter, but the fabrication and characterization down to nanoscale remains an important challenge. Progress has been hindered by the lack of bottom-up methodologies to produce amorphous nanostructures. Recently, we show the self-organized amorphous nanowires that are formed on the fracture surfaces of bulk metallic glasses [Nakayama et al., Nano Lett. 8, 516-519 (2008)]. However, it is difficult to control their morphologies because they were created by instantaneous fracture processes. Here we first report the controlled formation and mechanical characterization of individual amorphous nanowires. We find that they have a high strength with the excellent flexibility where the elastic modulus is much smaller than that of the bulk owing to the hyper-excess free volume in nanowire.

### 3:20 PM Invited

**Role of Ductile  $\beta$ -Phase Dendrite in Optimizing Mechanical Properties of Ti-Based Bulk Metallic Glass Composites:** Ka Ram Lim<sup>1</sup>; Jin Man Park<sup>1</sup>; Won Tae Kim<sup>2</sup>; Do Hyang Kim<sup>1</sup>; <sup>1</sup>Yonsei University; <sup>2</sup>Cheongju University

Recently, highly toughened bulk metallic glass (BMG) composites with mechanical properties comparable to high performance crystalline alloys have been reported in Zr-based system. Ductile-phase-reinforced BMG composites show enhanced global plasticity and more graceful failure since soft crystalline inclusions stabilize the glass against the catastrophic failure associated with unlimited extension of a shear band. In the present study, role of ductile  $\beta$  phase dendrite in optimizing the mechanical properties of Ti-rich Ti-Zr-Be-Cu-Ni-Nb BMG composites. Metastable equilibrium condition for  $\beta$  phase and glass matrix is established, therefore, the combination of strength and plasticity is optimized by tailoring relative volume fraction and morphology of  $\beta$  phase and glass matrix. It is considered that the presence of Nb assists the enhancement of glass forming ability as well as plasticity of the composites. In addition, possibility for ductile phase reinforced Be-free Ti-based bulk metallic glass composites will be discussed.

### 3:40 PM Break

### 3:50 PM Invited

**Ductile Hypoeutectic Zr-Cu-Al and Zr-Ni-Cu-Al Bulk Glassy Alloys:** Y. Yokoyama<sup>1</sup>; K. Fujita<sup>2</sup>; T. Yamasaki<sup>3</sup>; A. Yavari<sup>4</sup>; P. Liaw<sup>5</sup>; A. Inoue<sup>1</sup>; <sup>1</sup>Institute for Materials Research; <sup>2</sup>Department of Mechanical Engineering; <sup>3</sup>School of Engineering; <sup>4</sup>LTPcSIMAP-CNRS; <sup>5</sup>The University of Tennessee

Ductility of metallic glasses is probably originated from the flexibility of the metallic bond and open volume in random structures. The glass-transition temperature ( $T_g$ ) has large positive correlation coefficients against Young's modulus (E) and Vickers hardness (HV). Ultimately, we found that only the Zr-enriched hypoeutectic composition exhibits low values of  $T_g$  and E and a high value of Poisson's ratio. Especially, hypoeutectic Zr-Cu-Al bulk glassy alloys exhibit high-fracture toughness equivalent to tool steels, and also do not show the remarkable embrittlement after annealing below  $T_g$ . In this presentation, we will talk about ductile mechanical properties of cast glassy ternary Zr-Cu-Al and quaternary Zr-Ni-Cu-Al alloys in hypoeutectic composition. Especially, the hypoeutectic Zr70Ni16Cu6Al8 bulk glassy alloy with extremely a low Young's modulus (70 GPa) and high Poisson's ratio (0.39) reveals the distinct tensile plastic elongation at room temperature, and the plastic strain depends on the strain rate.

### 4:10 PM

**On Interfacial Bonding in Mg-Cu-Gd Metallic Glass during Spark Plasma Sintering Processing:** Baolong Zheng<sup>1</sup>; Troy Topping<sup>1</sup>; Yizhang Zhou<sup>1</sup>; Chi Y.A. Tsao<sup>2</sup>; Enrique Lavernia<sup>1</sup>; <sup>1</sup>University of California, Davis; <sup>2</sup>National Cheng Kung University

Metallic glasses (MGs) show superplastic behavior in the super-cooled liquid region. This provides a pathway for MG powder consolidation via powder metallurgy processes. The nature of the interface between particles critically influences the mechanical properties of consolidated bulk MGs, whereas the low atomic diffusivity, characteristic of MG, hinders diffusion bonding. In this work, Mg-Cu-Gd amorphous powder was consolidated by Spark Plasma Sintering (SPS), while cast Mg-Cu-Gd rods were used to simulate conditions that are analogous to those present during powder sintering. The SPS studies provided insight into the phenomena of atomic diffusion and interfacial bonding during MG powder consolidation. The microstructural evolution of the bond interface of Mg-Cu-Gd powders and bulk materials was investigated as a function of processing parameters using SEM, XRD, DSC, and TEM. In addition, interfacial bond formation, mechanical response and the underlying mechanisms are discussed in an effort to provide insight into fundamental phenomena in MGs.

### 4:20 PM

**Effect of Heat Treatment at Semisolid Region on Zr-Based Metallic Glass Matrix Composites:** Takuya Tamura<sup>1</sup>; Advenit Makaya<sup>1</sup>; Kenji Miwa<sup>1</sup>; <sup>1</sup>National Institute of Advanced Industrial Science and Technology (AIST)

It was reported that micrometer-sized ductile crystalline phases can improve the ductility of Zr-based bulk metallic glasses. However, it is known to be difficult that the sample, for which the crystal particles are dispersed into the metallic glass phase, is prepared by Cu mold casting, because the cooling rate is different between the outside and the inside. The present authors reported that heat treatment at semisolid region is effective in forming uniform dispersed crystalline particles. Thus, this study aims to investigate effect of heat treatment at semisolid region on Zr-based metallic glass matrix composites.

### 4:30 PM Invited

**Improving the Deformation Ability of Bulk Metallic Glasses by Different Approaches:** Ke-Fu Yao<sup>1</sup>; Sheng-Bao Qiu<sup>1</sup>; Yang Li<sup>1</sup>; Hong-Yu Ding<sup>1</sup>; <sup>1</sup>Tsinghua University

Bulk metallic glasses (BMGs) have attracted tremendous attentions due to their excellent properties and potential applications. But lack of whole plasticity is a road block which needs to be overcome before their real application, especially in structural application. Then developing possible way for improving the plasticity of BMGs is important and meaningful. Here, we report that the deformation ability of BMGs can be significantly improved by both outside treatment and inside structural relaxation. It has been found that when the surface of a BMG sample is coated with a thin crystalline metallic layer its global plasticity can be effectively enhanced. On the other hand, the global plasticity of BMGs can also be increased greatly by treating them with high-density pulsing current, which could result in obvious structural relaxation

Tue. PM

# Technical Program

of the glassy alloys. The present results indicate that the global plasticity of BMGs can be enhanced by different ways.

**4:50 PM**

**Thermodynamic Optimization of the Cu-Zr-Ag System and Its Applications to Amorphous Alloy Development:** *Dae Hoon Kang*<sup>1</sup>; In-Ho Jung<sup>1</sup>; <sup>1</sup>McGill University

Recently a great amount of research has been carried out to understand the characteristics of the Cu-Zr-Ag amorphous alloys. However, the thermodynamics and phase diagram information of the system is still poorly investigated. In the present study, all available thermodynamic and phase diagram data of ternary Cu-Zr-Ag system as well as its sub-binary systems have been critically evaluated and optimized to obtain one set of model parameters which can reproduce all the reliable experimental data. The ternary phase diagram of the Cu-Zr-Ag was properly calculated for the first time. In particular, the existence of wide stable liquid miscibility gap was predicted in the ternary system. The roles of the metastable liquid miscibility gap and spinodal decomposition to the Cu-Zr-Ag amorphous alloys with nano Ag particles will be discussed.

**5:00 PM Invited**

**Study of Microscopic Deformation Behaviors of Bulk Metallic-Glasses:** *Yong Yang*<sup>1</sup>; J. Lu<sup>1</sup>; J.C. Ye<sup>1</sup>; <sup>1</sup>The Hong Kong Polytechnic University

In this talk, we present a summary of our recent experimental findings in the deformation behaviors of bulk metallic-glasses (BMGs) at the microscopic scale, which comprise the results from the micro-compression, micro-bending and two-dimensional nanoindentation at room temperature. The outcome of the micromechanical study of BMGs reveals the possible intrinsic mechanisms of shear-band nucleation, propagation and ductile-to-brittle transition in the metallic amorphous structures.

**5:20 PM Invited**

**Cooling Process and Cast Structure of Zr-Al-Ni-Cu-Based Bmgs Produced in Various Atmospheres:** *Junji Saida*<sup>1</sup>; Albertus Setyawan<sup>1</sup>; Hidemi Kato<sup>1</sup>; Mitsuhide Matsushita<sup>2</sup>; Akihisa Inoue<sup>1</sup>; <sup>1</sup>Tohoku University; <sup>2</sup>JEOL Co., Ltd

A different dependence of apparent glass-forming ability on casting atmosphere pressure is observed in a Zr-Al-Ni-Cu-Pd alloy system. Results of a measurement of alloy temperature during casting indicate an enhancement of the cooling effect in the low-temperature region of undercooled-liquid in the high chamber pressure. However, it has not a significant difference in the high-temperature region against a chamber pressure. The cooling mechanism may change from a direct heat transfer between the cast alloy and mold in the high-temperature region into that via cavity between them in the low-temperature region. We investigate that cooling is significant in the high chamber pressure due to the existence of gas in the cavity. Such a control of cooling process by a chamber pressure brings new BMGs formation by the suppression of the metastable phase precipitation. The method is recognized as a new and simple technique for the fabrication and structure control of BMGs.

**5:40 PM Invited**

**Recent Progress in High-Entropy Alloys:** *Jien-Wei Yeh*<sup>1</sup>; *Ming-Hung Tsai*<sup>1</sup>; <sup>1</sup>National Tsing Hua University

It has been considered that alloys consisting of a greater number of principal elements will form complicated and brittle microstructures. Hence research regarding such alloys has received little attention. To overcome this misunderstanding high-entropy alloys (HEAs) have been proposed and explored since 1995. With the high mixing entropy HEAs tend to have simplified microstructures with solid-solution phases. This new alloy concept generates numerous alloys and activates a new research area beyond traditional alloys. In addition to high entropy effect, sluggish diffusion, severe lattice distortion, and cocktail effects are significant in affecting the structures and properties of HEAs. HEAs have been found to possess a wide spectrum of microstructures and properties, and hence provide a number of promising applications. This presentation reviews the recent progress in HEAs and also forecasts the future trend.

## Cast Shop for Aluminum Production: Furnace Technology and Melt Handling

*Sponsored by:* The Minerals, Metals and Materials Society, TMS Light Metals Division, TMS: Aluminum Committee, TMS: Aluminum Processing Committee

*Program Organizers:* John Grandfield, Grandfield Technology Pty Ltd; Pierre Le Brun, Alcan Voreppe Research Center

Tuesday PM

Room: 609

February 16, 2010

Location: Washington State Convention Center

*Session Chair:* Peter Whiteley, Munimula

**2:00 PM**

**Influence of Heating Technology on Melt Quality in Ladles for Road Transportation of Liquid Aluminum Casting Alloys during Holding:** *Bernd Prillhofer*<sup>1</sup>; Jens Knaack<sup>1</sup>; <sup>1</sup>AMAG Casting GmbH

Due to the increasing demand for liquid metal deliveries from refiners to shape casting foundries, melt quality topics, which are well known from the aluminum wrought alloy sector, are becoming more and more important. Long distance transportation of liquid metal alloys requires superheating to compensate temperature loss and to avoid any solidification. After arrival, the transport ladles sometimes replace holding furnaces or have to wait for metal transfer into the holder. Therefore the liquid metal must be heated at destination. Foundry managers can choose between gas burners and ceramic immersion heaters. So far, there hasn't been a detailed scientific investigation of the influence of both heating technologies on melt quality criteria. This paper examines the influence of heating technologies at constant holding temperature on inclusion and hydrogen content, density index, as well as chemical composition. The experimental work has been carried out on the alloy AISi7Mg and AISi9Cu3(Fe).

**2:25 PM**

**Degreasing of Aluminium Turnings and Implications for Solid-State Recycling:** *Jirang Cui*<sup>1</sup>; *Anne Kvithyld*<sup>2</sup>; Hans Roven<sup>1</sup>; <sup>1</sup>Norwegian University of Science and Technology; <sup>2</sup>SINTEF Materials and Chemistry

With the global warming being of concern, recycling of aluminium by new solid-state recycling techniques instead of conventional remelting and subsequent refining processing has been taken into account. Solid-state recycling processes such as extrusion and compaction at room or moderate temperature can result in significant energy savings. However, as aluminium scrap is normally contaminated by oil and/or organic coatings, decoating of scrap is an essential step for the solid-state recycling process. In the present study, degreasing of aluminium turnings with or without cold compaction was investigated by thermal methods and chemical treatment. Thermo-gravimetric furnace coupled with mass spectroscopy was utilised to understand the decomposing of machine oil on aluminium turnings in oxidising atmospheres. For further comparison, degreasing of turnings by acetone followed by solid-state processing was also studied in laboratory. The results may be used to choose a suitable pre-treatment method for solid state recycling of aluminium scrap.

**2:50 PM**

**Retrofitting Aluminum Melting Furnaces:** *Tom Schmidt*<sup>1</sup>; <sup>1</sup>Otto Junker

The average service life of aluminium melting and holding furnaces is several decades. As a result of that, many aluminium casthouses operate with equipment of an older generation. The drawback of this is that these production tools not always meet the current standards on the fields of: Emissions, machine safety, fuel economics, Ergonomics, Process control. Unless forced by authorities or unions, it is not an easy decision if a modernization of an old furnace makes sense. Cost of a complete modernization, combined with new refractory lining takes almost the same investment as installing a new furnace. This paper will address this subject in order to make a well balanced decision on whether modernization of aluminum melting furnace is a desired option.



3:15 PM

**Establishing Operational Parameters of AL-EMS Using Numerical Simulations to Promote Energy Efficiency during Final Heating in Aluminium Furnaces:** *Robert Stal*<sup>1</sup>; Ulf Sand<sup>1</sup>; Olof Hjortstam<sup>1</sup>; <sup>1</sup>ABB AB

In aluminum melting and holding furnaces, electromagnetic stirring (AL-EMS) is a well established technology used to achieve enhanced thermal and chemical homogeneity, reduced cycle time, reduced energy consumption and reduced dross generation. In the present work, on site measurements and numerical simulations using a CFD-model (Computational Fluid Dynamics) have been conducted for an installed reverberatory melting furnace operating with ABB AL-EMS. Simulated and measured values of the time needed for melt temperature homogenization (homogenization time) are compared and good agreement has been found. Using the CFD-model, a parametric study is conducted for the relation between the strength of the AL-EMS and the energy efficiency in the furnace. The study clearly illustrates how the use of AL-EMS drastically reduces the homogenization time and improves the heat pick-up. A discussion of how the CFD-model can be used to optimize the strength of the AL-EMS for a given application is also presented.

3:40 PM

**Energy Efficiency in Casthouse Furnaces:** *Robert Voyer*<sup>1</sup>; Francis Caron<sup>2</sup>; <sup>1</sup>Hatch; <sup>2</sup>Alcoa

More than ever, the high cost of fuels and the need to reduce carbon emissions are forcing changes in casthouse equipment choices and shop practices. Some smelters have already started moving in this direction and have set in place energy tracking programs, while others are considering making these changes. Before implementing any project for reducing energy consumption, there is a need to assess the actual state of consumption, rate it with respect to technically achievable targets, and monitor the consumption in order to have a record of improvements. Continued monitoring is also essential in order to maintain the new standards. This presentation provides an overview of the status of energy consumption in typical casthouse furnaces. It quantifies the potential for reducing fuel consumption, as well as reducing carbon emissions, and proposes a cost efficient solution for reducing the fuel consumption and carbon emissions.

4:05 PM

**Implementation of a Global Casthouse Furnace Energy Efficiency Program at Rio Tinto Alcan:** *Mathieu Roy*<sup>1</sup>; Vincent Goutiere<sup>1</sup>; Claude Dupuis<sup>1</sup>; <sup>1</sup>Rio Tinto Alcan

Over the past several years, energy has been subjected to variable but sustained price increase. During the same time, climate change awareness has become more and more a concern for our society with the result that energy efficiency is now an environmental as well as an economic priority for all businesses. In the context of sustainable development, energy efficiency has always been a strong priority at Rio Tinto Alcan. In 2005, a global casthouse energy efficiency program was initiated to significantly reduce the consumption in all furnaces and put in place the means to maintain and improve on a continuous basis. This paper describes the key elements of this program and its successful implementation through practical examples of key operating practices and process parameters.

4:30 PM

**Crucible Transfer by Siphoning: A Review of the Benefits and the Latest Technology:** *Jerry Locatelli*<sup>1</sup>; Guangwei Liu<sup>2</sup>; *Andrew North*<sup>2</sup>; <sup>1</sup>Millennium Metals Pty Ltd; <sup>2</sup>Major Furnace Australia Pty Ltd

Siphoning has long been recognised as a method of transferring molten aluminium from reduction crucibles to Casthouse holding furnaces which generates the least amount of dross. This paper reviews some data on dross generation and melt loss, which compares the transfer of metal from crucibles by traditional cascade pouring with that of siphoning. The substantial difference between the two techniques is highlighted when the melt loss is viewed in terms of the amount of energy involved in producing the lost aluminium. It also becomes clear that the change from cascade pouring to siphoning represents the largest single energy reduction initiative which can be made in the Casthouse. This paper also presents examples of the latest automated siphon transfer systems which are finding application in installations ranging from the largest smelters to the smallest foundries.

4:55 PM

**Heating and Melting of Single Al Ingots in an Aluminium Melting Furnace:** *Jørgen Furu*<sup>1</sup>; Andreas Buchholz<sup>2</sup>; Trond Harald Bergstrøm<sup>3</sup>; Knut Marthinsen<sup>1</sup>; <sup>1</sup>NTNU; <sup>2</sup>Hydro Aluminium Deutschland GmbH; <sup>3</sup>SINTEF Materials and Chemistry

The efficiency of aluminium recycling and remelting processes is becoming increasingly important due to the tremendous growth of energy costs in recent years. Modeling the heating and melting behaviour of aluminium can help to better understand the interaction of different heat transfer mechanisms and the limiting factors for the heat exchange in a conventional reverberatory furnace. In the present work heating and melting experiments were carried out in a 500 kg test furnace with a conventional air-fuel burner. Small blocks of aluminium were equipped with thermocouples and insulated on all sides but one to approximate 1-dimensional heat transfer. Numerical heat transfer calculations were compared with the experimental results along with CFD modeling to investigate the contribution of various parameters to the heat transfer into the aluminium ingot.

5:20 PM

**Optimised Re-Melting by the Use of Low-Temperature Oxyfuel at Hydro Aluminium's Primary Aluminium Casthouse, Øvre Årdal, Norway:** *Henrik Gripenberg*<sup>1</sup>; Ken Torvanger<sup>2</sup>; Johannes Lodin<sup>1</sup>; <sup>1</sup>Linde Gases Division; <sup>2</sup>Hydro Aluminium

Hydro Aluminium Årdal produces primary foundry alloys of mainly AA4000 series. The capacity is 130 000 tonne per year. The four furnaces at the cast house are charged with a mix of pot-room metal and commodity metal. In 2007 the Söderberg pot-room was closed and the re-melting of solid metal had to be increased by 60% to keep up the production from the cast house. This meant that the fraction of solid metal in the casting furnace batch had to be increased. The goal had to be reached using the same furnaces and casting equipment. Therefore the furnaces were converted from air-fuel to Low-temperature Oxyfuel burners from Linde. The paper will discuss how the melting process was optimized. Further how the energy efficiency depend on the fraction of solid metal in the batch and results of productivity, dross, and economy. The Low-temperature Oxyfuel technology will be described.

### Characterization of Minerals, Metals and Materials: Characterization of Grain Size, Morphology, Transmittance, and Tomography

*Sponsored by:* The Minerals, Metals and Materials Society, TMS Extraction and Processing Division, TMS Structural Materials Division, TMS/ASM: Composite Materials Committee, TMS: Materials Characterization Committee

*Program Organizers:* Ann Hagni, Geoscience Consultant; Sergio Monteiro, State University of the Northern Rio de Janeiro - UENF; Jiann-Yang Hwang, Michigan Technological University

Tuesday PM Room: 307  
February 16, 2010 Location: Washington State Convention Center

*Session Chairs:* Shadia Ikhmayies, University of Jordan; Mingdong Cai, Exova

### 2:30 PM Introductory Comments

2:35 PM

**A Statistical Study of Grain Size, Grain Orientation, and Grain Boundary Misorientation Effects on Deformation Twinning:** *Rodney McCabe*<sup>1</sup>; Irene Beyerlein<sup>1</sup>; Laurent Capolungo<sup>2</sup>; Peter Marshall<sup>2</sup>; Carlos Tome<sup>1</sup>; <sup>1</sup>Los Alamos National Laboratory; <sup>2</sup>Georgia Tech

A statistical analysis is carried out to examine correlations between deformation twinning and grain size, grain orientation, and grain boundary misorientation. The analysis uses large data sets generated using electron backscatter diffraction (EBSD) of magnesium, zirconium, and uranium. Similarities and differences between metals of the same crystal structure (hcp versus hcp) and the different crystal structures (hcp versus orthorhombic) are examined.

Tue. PM

# Technical Program

3:00 PM

**An Automated Approach for Prior Austenite Grain Size Measurement by EBSD:** *Ning Ma*<sup>1</sup>; Russell Mueller<sup>1</sup>; Timothy Anderson<sup>2</sup>; Raghavan Ayer<sup>1</sup>; <sup>1</sup>Corporate Strategic Research, ExxonMobil Research and Engineering Company; <sup>2</sup>ExxonMobil Upstream Research Company

Although prior austenite grain size has significant influence on the mechanical properties of steels, its determination has historically been a challenge. The present work describes the development of a robust and computationally efficient approach to determine prior austenite grain size from EBSD patterns in steels. The method is based on the crystallographic orientation relationships between the elevated temperature face centered cubic austenite and the body centered transformation products that form upon cooling to room temperature. The details of the procedure, such as the EBSD step width optimization and noise reduction, will be emphasized. Since the approach relies on the crystallography of the phase transformation, it is independent of the process history of the steels and it can be applied to a wide range of steels, including the grain size determination in heat affected zones in weldments.

3:25 PM

**Linear Measures for Estimating Grain Growth Rates:** *Martin Glicksman*<sup>1</sup>; Paulo Rios<sup>2</sup>; Daniel Lewis<sup>3</sup>; <sup>1</sup>University of Florida; <sup>2</sup>Universidade Federal Fluminense; <sup>3</sup>Rensselaer Polytechnic Institute

Average caliper,  $C$ , introduced by Minkowski in 1903, was generalized for polyhedral grains by Cahn and DeHoff in 1967. Recently, mean width,  $L$ , a linear measure applicable to non-convex objects, was introduced by MacPherson and Srolovitz, 2007, and by Le and Duc, 2009. These measures correlate geometric properties of polyhedral grains, including their areas, volumes, and curvatures, and permit prediction of curvature-mediated growth rates. Linear measures provide connections among growth rate, grain size, topological class, and shape.  $C$  and  $L$  for polyhedral grains were calculated using an exact topological representation of space-filling grains. Calculations confirmed by independent Surface Evolver computations yield relations among  $C$  and  $L$ , the geometric properties, and the growth kinetics of polycrystals during normal grain growth. In addition, easily applied formulae were found to estimate linear measures accurately, knowing the number of grain faces, plus any metrically-based measure such as grain size, volume, or grain boundary area.

3:50 PM

**Serial Sectioning, X-Ray Tomography, and EBSD Analyses of Martensitic Alloys:** *George Spanos*<sup>1</sup>; David Rowenhorst<sup>1</sup>; Richard Fonda<sup>1</sup>; Keith Knipling<sup>1</sup>; Richard Everett<sup>1</sup>; Greg Olson<sup>2</sup>; Stephanie Chan<sup>2</sup>; <sup>1</sup>Naval Research Laboratory; <sup>2</sup>Northwestern University

This talk presents investigations of microstructure and damage/defects in two alloy systems: (1) a commercial 4330 steel, and (2) model Fe - 20wt%Ni - 5-6wt% Mn alloys. A combination of serial sectioning and X-ray tomography were employed to reconstruct and study in three dimensions (3D) the inclusions, cracks, and voids (and their interrelationship) in compact tension specimens of a Ti-modified 4330 steel. Emphasis will be placed on the methodology employed, including a comparison of the 3D data between the two techniques (serial sectioning and X-ray tomography). A brief discussion will also be presented on how these experimental results are used by our collaborators for validation and input in 3D multiscale fracture models. Secondly, Electron Backscatter Diffraction (EBSD) analyses of martensite in Fe - 20wt%Ni - 5-6wt% Mn alloys will be presented, along with a discussion of possible avenues for examining these structures in three dimensions.

4:15 PM

**Computed Tomography of Titanium Friction Stir Welds:** *Jennifer Wolk*<sup>1</sup>; Richard Everett<sup>2</sup>; Lourdes Salamanca-Riba<sup>3</sup>; <sup>1</sup>Naval Surface Warfare Center; <sup>2</sup>Naval Research Laboratory; <sup>3</sup>University of Maryland

This work focuses on using x-ray computed tomography to assist in understanding defect formation and material flow in Ti-5111 friction stir welds. Tomographic techniques have been previously utilized to determine void geometries in ferrous and non-ferrous materials. A transverse cross-section of friction stir welded Ti-5111 containing defects was scanned using a Skyscan tomography system. Volume rendered images of the reconstructed data were revealed the internal void structures. This analysis showed a distinct void substructure on an advancing side defect. The substructure shows material bands that are unrelated to the friction stir welding tool design. The peak-to-peak distance appears to be approximately same as the forward advance

per revolution. Analysis of the void formation at the bottom of the stir zone shows a complex substructure indicative of wormhole formation and material consolidation. The x-computed tomography is correlated to transverse electron backscatter diffraction scans and selected transmission electron microscopy analysis.

4:40 PM

**Aberration-Corrected Vector Field Electron Tomography of Magnetic Nano-Structures:** Charudatta Phatak<sup>1</sup>; Emma Humphrey<sup>1</sup>; Amanda Petford-Long<sup>2</sup>; *Marc De Graef*<sup>1</sup>; <sup>1</sup>Carnegie Mellon University; <sup>2</sup>Argonne National Laboratory

Nanoscale magnets are used for a variety of applications, including spintronic devices and sensors, magnetic memory applications, and biomedical applications. To improve the functionality of these devices, it is necessary to characterize not only the particle/layer shapes and relative locations, but also the magnetostatic interactions between them. Therefore, the magnetic field distribution in and around the nano-scale magnets must be determined quantitatively. The electron-optical phase shift of electrons in a transmission electron microscope (TEM) can be expressed in terms of tomographic projections which, in combination with vector field electron tomography, can be used to reconstruct the 3D magnetic vector potential as well as the 3D magnetic induction in and around the magnetic particles. Results obtained for patterned magnetic structures will be demonstrated. The improvement due to aberration correction in the TEM, along with the development of an iterative technique for 3D reconstructions to minimize reconstruction errors will also be discussed.

5:05 PM

**Using Transmittance Measurements to Investigate the Interdiffusion through the SnO<sub>2</sub>/CdS and CdS/CdTe interfaces in SnO<sub>2</sub>/CdS/CdTe Solar Cells:** *Shadia Ikhmayies*<sup>1</sup>; Riyad Ahmad-Bitar<sup>1</sup>; <sup>1</sup>University of Jordan

The SnO<sub>2</sub>/CdS/CdTe thin film solar cells were fabricated on glass substrates by using the spray pyrolysis (SP) technique for the deposition of the SnO<sub>2</sub> and CdS layers and vacuum evaporation for the CdTe layer. The transmittance curves were used to investigate the interdiffusion in the two interfacial regions SnO<sub>2</sub>/CdS and CdS/CdTe by taking the first derivative of the absorbance as a function of wavelength. The appearance of new bandgaps around the bandgaps of SnO<sub>2</sub>:F, CdS:In and CdTe layers is a strong evidence on the interdiffusion in the two interfacial regions and/or the formation of quantum dots.

5:30 PM

**The Effect of Aluminum Content on Morphology, Size, Volume Fraction and Number of Graphite Nodules in Ductile Cast-Iron:** *Ali-Reza Kiani-Rashid*<sup>1</sup>; A Shayesteh-Zeraati<sup>2</sup>; H Naser-Zoshki<sup>3</sup>; <sup>1</sup>Ferdowsi University of Mashhad; <sup>2</sup>Sharif University of Technology; <sup>3</sup>Iran University of Science and Technology, Tehran,

In this paper, we have investigated the effect of aluminum content on the formation mechanism, volume fraction, morphology and particle size distribution of graphite. Addition of aluminum to ductile iron causes some fundamental changes in iron-carbon phase-diagram and as a result, improves the graphite formation during the eutectic transformation. The results reveal that aluminum compounds have been formed in the core of graphite nodules; thus aluminum plays an important role in the formation of graphite nodules. Furthermore, it is indicated that an increase in the aluminum content also leads to an increase in the number of graphite nodules and a decrease in the nodules size. By using EPMA, the segregation of aluminum and silicon between graphite nodules has been studied.

5:55 PM

**Characterization of the Deep Interface Traps in Hf-Based/Si Gate Stacks:** *S.Y. Tan*<sup>1</sup>; Yi-Lun Hsia<sup>1</sup>; Ming-Yuan Wu<sup>1</sup>; Hsing-Hung Chen<sup>1</sup>; <sup>1</sup>Chinese Culture University

The continuous scaling of the dimensions of CMOS transistors has caused the thickness of the silicon dioxide to decrease below 1.6nm. The replacement oxides must satisfy various requirements as satisfactory gate oxides. (i)thermo dynamically stable in contact with the Si (ii)Oxygen diffusion(iii)form a high quality interface with Si. Hafnium based oxide films have potential to form a silicon oxide comparable interface with the Si. In order to fully understand the origins of the interface trap generation and deep oxide traps in Hf-based films, we introduced two unique process to control the deep trap centers in Hf-based/Si. A combined approach of (i)Thermal annealing treatment(ii)Different Hf contents in HfO<sub>2</sub> (iii)Incorporating N atom into HfO<sub>2</sub>(iv)Electrical characterization-

Tue. PM



C-V and J-V, to study the effect of the thermal annealing and Hf contents (v) Physical characterization - TEM, XPS, and SIMS. It is the first time, two unique process techniques are employed to control of the deep interface traps in Hf-based gate dielectric films on Silicon.

### 6:15 PM

**Arsenic Dopant Effect in Nickel Silicide Formation for NiSi/Hf-Based/Si Gate Stacks:** *S.Y. Tan*<sup>1</sup>; <sup>1</sup>Chinese Culture University

The thermal stability of fully silicided NiSi with arsenic doping on silicon was investigated. The aims of the work were to investigate the Ni silicide phase-related issues associated with arsenic dopant and thermal annealing on Ni-FUSI/HfO<sub>2</sub>/Si and Ni-FUSI/HfSiO<sub>2</sub>/Si gate stacks. It was found that arsenic-incorporation demonstrated some improvement in both morphology and phase stability of nickel silicided films at high processing temperatures regardless underlying gate dielectrics. The correlations of Ni-Si phase transformation and arsenic dopant with their electrical and physical changes were established by sheet resistance measurements, XRD, AFM, and X-ray photoelectron spectroscopy (XPS) analysis. Furthermore, the modulation of the work function (WF) of Ni fully silicided gates by arsenic impurity is presented, comparing the effects of dopant (As) on the WF and silicide phases (NiSi and NiSi<sub>2</sub>). It confirmed that the work function of NiSi can be tuned by implanting arsenic dopant, but it ineffective for NiSi<sub>2</sub> phase.

6:35 PM Concluding Comments

6:40 PM Question and Answer Period

## Coatings for Structural, Biological, and Electronic Applications: Applications of Coatings II

Sponsored by: The Minerals, Metals and Materials Society, TMS Electronic, Magnetic, and Photonic Materials Division, TMS Structural Materials Division, TMS: Biomaterials Committee, TMS: Thin Films and Interfaces Committee

Program Organizers: Nugehalli Ravindra, New Jersey Institute of Technology; Gregory Krumdick, Argonne National Laboratory; Roger Narayan, Univ of North Carolina & North Carolina State Univ; Choong-un Kim, University of Texas at Arlington; Nancy Michael, University of Texas at Arlington

Tuesday PM Room: 309  
February 16, 2010 Location: Washington State Convention Center

Session Chair: Nugehalli Ravindra, NJIT

2:00 PM Introductory Comments

2:10 PM Invited

**Experimental Study of Ternary Cobalt Spinal Oxides for Photoelectrochemical Hydrogen Production:** *Sudhakar Sher*<sup>1</sup>; Kwang-Soon Ahn<sup>2</sup>; Heli Wang<sup>1</sup>; Nugehalli Ravindra<sup>3</sup>; Yanfa Yan<sup>1</sup>; John Turner<sup>1</sup>; Mowafak Al-Jassim<sup>1</sup>; <sup>1</sup>National Renewable Energy Laboratory; <sup>2</sup>YeungNam University; <sup>3</sup>New Jersey Institute of Technology

In this study, we present an experimental study of ternary cobalt spinal oxides for solar driven hydrogen production. Co<sub>1-x</sub>Al<sub>x</sub>O<sub>4</sub> (X = Al, Ga, In) thin films were deposited using RF magnetron reactive co-sputtering system. All the thin films were deposited on silver/stainless steel and quartz substrates, because of the high temperature (800°C) oxide growth. We found that these thin films show excellent stability in solution and good visible light absorption. However, their performance as photoelectrochemical catalyst is limited by the poor transport properties induced by small polaron mobility.

2:40 PM

**Effect of Superficially Applied Y<sub>2</sub>O<sub>3</sub> Coating on High Temperature Corrosion Behaviour of Ni-Base Superalloys:** *Gitanjali G*<sup>1</sup>; *Harpreet Singh*<sup>2</sup>; *Satya Prakash*<sup>2</sup>; *Surendra Singh*<sup>2</sup>; <sup>1</sup>National Institute of Technology; <sup>2</sup>Indian Institute of Technology

Effect of Y<sub>2</sub>O<sub>3</sub> on high temperature corrosion of Superni 718 and Superni 601 superalloys was investigated in Na<sub>2</sub>SO<sub>4</sub>-60%V<sub>2</sub>O<sub>5</sub> environment at 900°C for 50 cycles. Y<sub>2</sub>O<sub>3</sub> was applied as a coating on the surfaces of the specimens. Superni 601 was found to be having better corrosion resistance in comparison with Superni 718 in the Na<sub>2</sub>SO<sub>4</sub>-60%V<sub>2</sub>O<sub>5</sub> environment. The Y<sub>2</sub>O<sub>3</sub> superficial

coating was successful in decreasing the reaction rate for both the superalloys. In the oxide scale of the alloy Superni 601, Y & V were observed to co-exist thereby indicating the formation of a protective YVO<sub>4</sub> phase. There was a distinct presence of protective Cr<sub>2</sub>O<sub>3</sub> rich layer just above the substrate/scale interface in the alloy. Whereas, Cr<sub>2</sub>O<sub>3</sub> was present with Fe and Ni in the scale of Superni 718. Y<sub>2</sub>O<sub>3</sub> seemed to be contributing to better adhesion of the scale as comparatively lesser spalling was noticed in the presence of Y<sub>2</sub>O<sub>3</sub>.

3:00 PM

**Semiconductor Device Integration Utilizing Magnetic Films:** *Rene Rivero*<sup>1</sup>; *Michael Booty*<sup>1</sup>; *Anthony Fiory*<sup>1</sup>; *Nugehalli Ravindra*<sup>1</sup>; <sup>1</sup>New Jersey Institute of Technology

Semiconductor device integration utilizing magnetic films is described here. In particular, Indirect Template Magnetic Field Assisted Assembly (IT-MFAA), a parallel processing technique, is presented. IT-MFAA is designed to assemble devices onto substrates through a versatile and scalable methodology, which is capable of adjusting to manufacturing situations and producing 100% yields with error correction. This paper discusses existing serial and parallel techniques and compares them to IT-MFAA. It demonstrates that IT-MFAA circumvents drawbacks present in other techniques, and outlines a model of IT-MFAA.

3:20 PM

**Crystallization and Thermal Stability of Amorphous and Nanocrystalline TiO<sub>2</sub> Magnetron-Deposited Thin Films Studied by X-Ray Diffraction:** *Radomir Kuzel*<sup>1</sup>; *Zdenek Matej*<sup>1</sup>; *Lea Nichtova*<sup>1</sup>; *Jindrich Musil*<sup>2</sup>; <sup>1</sup>Charles University in Prague, Faculty of Mathematics and Physics; <sup>2</sup>University of West Bohemia, Faculty of Applied Sciences

Photocatalytic and other remarkable properties of titanium dioxide depend on phase composition (rutile, anatase, brookite) and on the crystallinity. Various sets of films with different thickness were studied by X-ray scattering. Reflectivity showed increase of surface roughness with annealing time and film thickness. Depth profiling of nanocrystalline films by varying angle of incidence revealed a gradient of phase composition (rutile - anatase). While amorphous films crystallized quickly above 220°C depending on the film thickness (slow crystallization for very thin films), the nanocrystalline films (about 10 nm) showed microstructural stability up to about 500°C. This was evaluated with the aid of newly-developed software for total XRD pattern fitting which also confirmed the presence of tensile residual stresses arising during crystallization of amorphous films and increasing with the decreasing film thickness. They were also measured independently. Best film hydrophilicity was usually found for nanocrystalline anatase and/or mixed nanocrystalline anatase+rutile films.

3:40 PM Break

3:55 PM Invited

**Spin Coated Er-Doped SiO<sub>2</sub> for High Efficiency Waveguide Optical Amplifiers:** *Sufjan Abedrabbo*<sup>1</sup>; *Bashar Lahlouh*<sup>1</sup>; *Anthony T. Fiory*<sup>2</sup>; *Nugehalli Ravindra*<sup>2</sup>; <sup>1</sup>University of Jordan; <sup>2</sup>NJIT

Erbium doped fiber amplifiers (EDFAs) and erbium doped waveguide amplifiers (EDWAs) have been studied extensively due to their enormous importance in optical communications networks. Although expenses in optical communications systems have been decreasing over time, device processing remains a significant cost component. This work describes a cost-effective process for fabricating Er-doped SiO<sub>2</sub> thin films deposited on silicon substrates by spin coating of a sol-gel containing Er and silica precursors. The process includes thermal annealing to form Er doped SiO<sub>2</sub> films. Optical activity of Er was determined by photoluminescence as a function of the excitation wavelength, and the optical constants of the processed films were determined by near infrared (NIR) absorption techniques and Fourier transform infrared (FTIR) spectroscopy.

4:25 PM

**Stellite Coatings on Hot Work Tool Steels for Tooling Applications in Semi-Solid Processing of Steels:** *Agca Kayihan*<sup>1</sup>; *Yucel Biro*<sup>1</sup>; *Kemal Demirci*<sup>2</sup>; <sup>1</sup>Tubitak Mam; <sup>2</sup>Kobatek Surface Treatment Industry

Semi-solid processing of metals combines the advantages of forging and casting while shaping metallic components. Having already matured into an industrial practice for Al and Mg alloys, this innovative forming technology could upgrade the market and provide lightweighting for forged steel parts. However, with process temperatures above 1250°C, the surface-to-interior

Tue. PM

# Technical Program

temperature differentials in steel thixoforming dies are much larger than with Al and Mg. Combined with the erosive wear caused by abrasion, the impact of already solid particles in the slurries and high temperature oxidation of the die surface, these cyclic thermal stresses confer very specific requirements on tool materials. X38CrMoV5 hot work tool steel widely used in the manufacture of conventional forging dies was coated with a series of stellite coatings in the present work. The performance of the coated samples was subsequently tested under thermal fatigue and erosive wear conditions encountered in the thixoforming of steels.

## 4:45 PM

**Phase Change Materials – An Overview:** Maneesh Merwade<sup>1</sup>; Vishal K. Singh<sup>1</sup>; Arun Ramadass<sup>1</sup>; Nugehalli Ravindra<sup>1</sup>; <sup>1</sup>New Jersey Institute of Technology

Phase Change Materials (PCM) have found wide spread applications in the field of materials science and technology due to their interesting properties. High latent heat of fusion and low melting point of Phase Change Materials make them very good candidates for thermal management systems. Phase Change Materials have been widely used as thermal storage units (in direct and indirect contact), for removal of excess heat from systems/devices, in scenarios where increase in the operating temperature of these devices would be detrimental to their performance. The ability to store thermal energy in PCM (paraffins) has been employed for effective use of solar energy in buildings for air-conditioning purposes. Phase change materials have also been utilized very successfully in memory technology wherein the transition in state of materials is from amorphous to crystalline state. Phase Change Materials offer many potential applications. This paper describes some of the recent applications.

## 5:05 PM Invited

**Organic Coatings to Prevent Molten Metal Explosions:** Alex Lowery<sup>1</sup>; Joe Roberts<sup>2</sup>; <sup>1</sup>Wise Chem LLC; <sup>2</sup>Pyrotek Inc.

Over 60 years ago, the first reported molten metal explosion from a bleed-out during direct chill casting in an aluminium mill was reported. Soon thereafter testing was performed to determine the root cause of the explosion. Upon determination of the root cause, an investigation to determine if any preventive measures could be instituted to prevent the explosions was conducted. Results found that a specific organic coating (e.g., Wise Chem E-212-F) prevented molten metal explosions, whereas some specific organic coatings initiated the explosions. Fifteen years ago the U.S. Department of Energy in conjuncture with the Aluminum Association reinvestigated the root cause of the molten metal explosions. Testing revealed that an initiation or trigger had to be present for a molten metal explosion to occur. Testing identified three additional coatings that could afford protection.

## 5:35 PM

**Diaphragm Coatings to Enhance Performance of Fabry-Perot Sensors:** Ivan Padron<sup>1</sup>; Anthony Fiory<sup>1</sup>; Nugehalli M Ravindra<sup>1</sup>; <sup>1</sup>NJIT

The performance of sensors based on Fabry-Perot (FP) interferometry is determined by optical reflection and transmission at the FP cavity interfaces. In the extrinsic FP sensor considered here, one of the cavity surfaces is the terminus of an optical fiber, the other is a flat surface of a silicon diaphragm, and the cavity contains a fluidic or gaseous medium. Dielectric or metallic coatings and surface texturing can be used to optimize the sensitivity of the FP interference signal to the displacement of the diaphragm. Optical modeling and simulation techniques are used to determine the optimal properties of coatings and surface treatments. Experimental data and analysis for FP pressure sensors are presented.

## Computational Thermodynamics and Kinetics: Wetting Phenomena II

*Sponsored by:* The Minerals, Metals and Materials Society, TMS Electronic, Magnetic, and Photonic Materials Division, TMS Materials Processing and Manufacturing Division, TMS Structural Materials Division, TMS: Chemistry and Physics of Materials Committee, TMS/ASM: Computational Materials Science and Engineering Committee  
*Program Organizers:* Jeffrey Hoyt, McMaster University; Dallas Trinkle, University of Illinois at Urbana-Champaign

Tuesday PM Room: 308  
February 16, 2010 Location: Washington State Convention Center

*Session Chair:* To Be Announced

## 2:00 PM Invited

**Prefreezing at Heterogeneous Solid-Liquid Interfaces:** Brian Laird<sup>1</sup>; Ruslan Davidchack<sup>2</sup>; <sup>1</sup>University of Kansas; <sup>2</sup>University of Leicester

Through the accurate calculation of surface and interfacial free energies, we determine the thermodynamic driving forces governing the wetting of the hard-sphere-fluid/hard-wall interface by a thin layer of (metastable) fcc crystal in a [111] orientation. Because this phenomenon occurs at densities below the equilibrium freezing density of hard spheres, it is an example of prefreezing. We discuss the relationships of these findings with other recently observed prefreezing phenomena in chemically heterogeneous solid-liquid interfaces.

## 2:30 PM Invited

**Thinning, Instability and Rupture of Thin Liquid Films in Metal Foam:** Lucien Brush<sup>1</sup>; <sup>1</sup>University of Washington

Thinning and rupture of thin liquid films in metallic foam can occur rapidly since there are no surfactants available to slow these processes. A matched asymptotic analysis is used to derive laws governing the capillary-suction driven thinning of very thin films in metallic foams. After an initial transient, films settle into one over time-squared behavior. The thinning films are tested for instabilities that arise from van der Waals forces. The effects of the Plateau borders and the flow in the lamella are seen to stabilize the thinning films. The critical film thickness denoting the onset of instability scales as the cube root of the Sheludko number. The results show instabilities may be localized near the edges of the film lamellae when there is a drainage flow. Linear instability initiates the rupture process of a film and the effect of flow on the rupture of the film is discussed.

## 3:00 PM

**Simulating Surface Energy Anisotropy Using Extended Cahn-Hilliard Model:** Solmaz Torabi<sup>1</sup>; ZhengZheng Hu<sup>1</sup>; John Lowengrub<sup>1</sup>; <sup>1</sup>University of California Irvine

We study the influence of surface and strain energies on heteroepitaxial thin-film growth. We propose an alternate way of simulating anisotropy for the surface energy by using the higher order terms in the free energy. To the second order, the system only have isotropic properties. We can produce different anisotropy by adding higher order terms to the energy. By choosing the right parameters, we can study the behavior SiGe/Si thin film. This type of extended Cahn-Hilliard model has been previously studied to the 4th order, but to our knowledge no one has ever implemented all the terms in this system. One advantage of this energy is that it has the intrinsic regularization. We present numerical results using an adaptive, nonlinear multigrid finite-difference method. Finally, in order to model the misfit strains, we add the elastic energy to our diffuse model to predict different Qdot shapes, such as pyramids and domes.

## 3:20 PM Break

## 3:30 PM Invited

**Nanoscale Quasi-Liquid Interfacial Films: The Interplay of Premelting, Prewetting and Multilayer Adsorption:** Jian Luo<sup>1</sup>; <sup>1</sup>Clemson University

Nanoscale quasi-liquid intergranular films have been observed in various ceramic materials (Crit. Rev. Solid State Mater. Sci. 2007, 32:67), as well as in metals such as W-Ni (Acta Mater. 2007, 55:3131) and Mo-Ni (APL 2009, 94:251908). Several thermodynamic models are presented and discussed. First, using CALPHAD data, a premelting type model predicts onset grain boundary



disordering at as low as 60-85% of the bulk eutectic/peritectic temperatures (APL 2008, 92:101902). This model quantitatively explains mysterious subsolidus activated sintering in refractory metals. Second, a systematical spectrum of interfacial phenomena, including prewetting/premelting, critical points, multilayer adsorption, layering/roughening, and complete wetting/drying, are predicted by combining diffuse-interface and lattice-gas models and incorporating colloidal type interfacial forces. This model also produces a series of grain boundary phases (complexions) with character similar to those observed by Dillon and Harmer. Finally, analogous phenomena at free surfaces and their thermodynamic models are reviewed (Annu. Rev. Mater. Res. 2008, 38:227).

#### 4:00 PM

**Influence of Local Interface Phenomenon on Coalescence Kinetics Models in Ni-Base Alloys:** *Youhai Wen*<sup>1</sup>; Jeff Simmons<sup>2</sup>; Chris Woodward<sup>2</sup>; <sup>1</sup>UES, Inc; <sup>2</sup>AFRL

The high coalescence rate in modeling gamma-prime microstructural evolution becomes especially serious in simulations with high volume fractions of gamma prime precipitate (e.g. higher than 60%). While the out-of-phase domains that come into contact tend to maintain a thin layer of gamma matrix phase between them due to favorable APB/interfacial energy considerations, the in-phase domains tend to coalesce into one single domain to remove the extra matrix layer between them and reduce the interfacial energy. In phase field simulations of this latter process the simulated coalescence rate is extremely high compared with experimental observations. We identified that this is a result of ignoring the local phenomenon in the gamma and gamma prime interface regions in all major simulate methods. Reasonable coalescence rate is achieved by properly addressing this local phenomenon. This implies that local phenomenon in the interface region has a strong effect on controlling the coalescence kinetics and corresponding microstructural evolution.

#### 4:20 PM

**Microstructure Engineering via Throttled Nucleation:** *David Wu*<sup>1</sup>; Jerry Quek<sup>1</sup>; Kevin Chu<sup>1</sup>; <sup>1</sup>Institute of High Performance Computing

We consider the crystallization of a thin film via interface-limited growth and throttled nucleation – a transient nucleation schedule in which the nucleation rate is turned off before the sample is fully transformed. This schedule can be readily realized by two stages of isothermal anneals, where the throttling time is parameterized by the area fraction transformed when throttling occurs. The limits of throttling are simultaneous and continuous nucleation, which produce the Poisson-Voronoi and Johnson-Mehl structures, respectively. We use an efficient level set method to generate microstructure, which is subsequently used to study a crystal's geometric properties. We find that throttling produces significant differences in the distributions of grain area, grain perimeter, and number of grain edges. Our results suggest a possible way to easily engineer certain types of microstructures via isothermal annealing stages.

#### 4:40 PM

**Phase Field Modeling of Void Microstructure Evolution in Irradiated Metals:** *Srujan Rokkam*<sup>1</sup>; Santosh Dubey<sup>1</sup>; Anter El-Azab<sup>1</sup>; Paul Millett<sup>2</sup>; Dieter Wolf<sup>2</sup>; <sup>1</sup>Florida State University; <sup>2</sup>Idaho National Laboratory

We present a phase field model for void nucleation and growth in irradiated metals. The point defects generated due to cascades are modeled using the concept of stochastic point process in space and time. The kinetics of point defects is obtained using a Cahn-Hilliard type description of vacancy and interstitial concentration fields. The void microstructure is obtained in terms of the evolution of a non-conserved order parameter, whose evolution is prescribed by a phenomenological Allen-Cahn type equation. We illustrate model capabilities using 2D and 3D examples for the case of pure metals. Void nucleation and growth is investigated in the presence of interacting point defects, defects interaction with lattice sinks, thermal fluctuations and cascade damage. Finally, the effect of spatially resolved defect sinks (such as dislocations) on void nucleation and growth is investigated.

#### 5:00 PM

**Monte Carlo Potts Simulation of Strain Induced Sub-Grain Structure Formation:** *Corentin Guebels*<sup>1</sup>; Tien Tran<sup>1</sup>; Phi Thanh<sup>1</sup>; Joanna Groza<sup>1</sup>; Jean-Pierre Delplanque<sup>1</sup>; <sup>1</sup>University of California, Davis

The prediction of microstructural evolution and abnormal grain growth phenomena during high-temperature deformation requires an accurate description of recrystallization. A recovery model is presented and contributes to

Monte Carlo Potts simulations for recrystallization phenomena. This approach describes the creation of low angle boundaries in the grain interior from stored strain energy, which produces a sub-grain structure. This novel recovery model investigates the often-ignored incubation period prior to a static recrystallization cycle. The model provides a flexible, physics-based methodology to investigate the initiation of recrystallization through competing sub-grain growth. The simulation results clarify the influence of the advantageous growth of a few sub-grains on recrystallization kinetics.

#### 5:20 PM

**Using Size Distributions for Determining Growth Mechanisms of Grain Boundary Precipitates:** *Shirley Northover*<sup>1</sup>; <sup>1</sup>The Open University

In the past various single parameters such as the mean, mode or maximum of the precipitate size distribution have been used in experiments to determine growth mechanisms. In the present study the observed development with aging time of the size and shape distributions of bcc precipitates at grain boundaries in an fcc material (Co-20Fe at 1003°K) have been compared with various possible theoretical models to determine the rate controlling process. The growth of these precipitates is initially well described by the grain boundary dependent collector plate mechanism of Brailsford and Aaron. As the precipitates grow low energy facets are formed which can move only by the propagation of ledges and growth becomes interface controlled. The precipitates' diffusion fields soon overlap and coarsening occurs with interface control. The results demonstrate that this would not have been revealed using simpler measures of precipitate size.

#### 5:40 PM

**Genetic Alloy Design by Nanoprecipitate Control: Stainless Steels and Aluminium Alloys:** *Pedro Rivera-Diaz-del-Castillo*<sup>1</sup>; <sup>1</sup>University of Cambridge

Alloy designers usually encounter a myriad of possibilities when engineering and optimising existing and new alloys. Thermochemical databases have recently become increasingly reliable, covering now a widespread number of phases, and can now be used for high-performance alloy design; however, the alloy designer encounters typically at least 5 relevant alloying elements combined with various heat treatment stages, temperatures and times. Due to computational time, thermodynamic and kinetic calculations for all possibilities are unfeasible. The present work describes a methodology to optimise properties such as strength, ductility and/or corrosion resistance in stainless steels and aluminium alloys. The key parameter to control is the formation of nanoprecipitates. Strategies to deal with meta-stable phases for which energetics may be estimated from first principle calculations are introduced. Genetic algorithms are employed as a means to minimise the computational time to devise an optimal alloy composition and its corresponding heat treatment.

### Cost-Affordable Titanium III: Powder Consolidation and Properties II

*Sponsored by:* The Minerals, Metals and Materials Society, TMS Structural Materials Division, TMS: Titanium Committee  
*Program Organizers:* M. Ashraf Imam, Naval Research Lab; F. H. (Sam) Froes, University of Idaho; Kevin Dring, Norsk Titanium

Tuesday PM Room: 618  
February 16, 2010 Location: Washington State Convention Center

*Session Chairs:* Ramana Reddy, University of Alabama; Kevin Dring, Norsk Titanium AS

#### 2:00 PM

**Microwave Sintering and Melting of Titanium Powder for Low-Cost Processing:** *Ralph Bruce*<sup>1</sup>; Arne Fliflet<sup>2</sup>; Hugo Huey<sup>3</sup>; Chad Stephenson<sup>1</sup>; M. Ashraf Imam<sup>2</sup>; <sup>1</sup>Bethel College; <sup>2</sup>Naval Research Laboratory; <sup>3</sup>HWave, LLC

The emerging reduction technologies for titanium from ore produce powder instead of sponge. Conventional methods for sintering and melting of titanium powder are costly, as they are energy intensive and require high vacuum since titanium acts as a getter for oxygen at high temperature, adversely affecting mechanical properties. Other melting processes such as plasma arcs have the additional problem of electrode consumption, and direct induction heating of the titanium powder is problematic. Microwave sintering or melting in

Tue. PM

# Technical Program

an atmospheric pressure argon gas environment is potentially cost effective and energy efficient due to the possibility of direct microwave heating of the titanium powder augmented by hybrid heating in a ceramic casket. We are investigating this approach at the Naval Research Laboratory using an S-Band microwave system. Evaluation of the product metal is underway and results will be discussed. Acknowledgment: This work is supported by the Office of Naval Research.

**2:25 PM**

**Microwave Sintering of Titanium:** *Ma Qian*<sup>1</sup>; Shudong Luo<sup>1</sup>; Ming Yan<sup>1</sup>; Graham Schaffer<sup>1</sup>; <sup>1</sup>The University of Queensland

Effective sintering of titanium requires use of a high sintering temperature (> 1200°C) in high vacuum (<10<sup>-2</sup> Pa). Consequently, sintering of titanium has been normally pursued in high vacuum ceramic tube furnaces, mostly on a laboratory scale. This confines the heating and cooling rates to typically about 4°C/min, thereby leading to lengthy processing. This work presents an assessment of microwave sintering of titanium. Elemental titanium powders of < 20 µm; 45-63 µm; and 100-150 µm were used to make green samples at 400 MPa. Sintering was conducted at 1200°C for 2 hrs in a 3 kW high vacuum microwave furnace with a 2.45 GHz multimode cavity under a vacuum of 2-5×10<sup>-3</sup> Pa. In all cases studied, the MW-sintered densities compare favorably or at least equally with the conventionally sintered densities. HRTEM examination of the MW-sintered interfaces revealed excellent bonding. Microwave sintering shows significant cost-effectiveness for processing of titanium.

**2:50 PM**

**Reaction Assisted Ultrasonic Consolidated TiNi:** *Henry Rack*<sup>1</sup>; Mykola Kulakov<sup>1</sup>; Erica Sampson<sup>1</sup>; <sup>1</sup>Clemson University

This presentation will describe the results of an investigation that was designed to examine the feasibility of fabricating near-net shape components containing TiNi shape memory constituents by combining the attributes of ultrasonic consolidation and reaction heat treatment. An optimization design of experiment was conducted to determine the ultrasonic consolidation control parameters, e.g., sonotrode rotational velocity, amplitude and normal force, which would result in the maximum weld quality as defined by the linear weld density. Subsequent thermal treatment of the consolidated compact resulted in the formation of a graded Ti-TiNi-Ni microstructure, the thickness of each constituent depending upon the exposure time and temperature.

**3:15 PM**

**Properties of Conventionally Alloyed and Powder Alloyed Nano-Crystalline Titanium Consolidated Via Spark Plasma Sintering:** Christopher Melnyk<sup>1</sup>; Steven Schroeder<sup>1</sup>; David Grant<sup>1</sup>; *Robert Gansert*<sup>2</sup>; <sup>1</sup>California Nanotechnologies; <sup>2</sup>Advanced Materials and Technology Services

Nano, near-nano, and multi-modal grained materials show great potential for application in many commercial industries. The Hall-Petch relationship cites the strengthening of materials by reducing the average crystallite size. A study is proposed to investigate the increase in mechanical properties provided by nano, near-nano as well as multi-modal grained powders used in powder metallurgical applications. Consolidations of processed materials will be produced using Spark Plasma Sintering (SPS). Nano-crystalline titanium, and titanium alloy powders and will be processed via cryogenic milling. The mechanical properties of the nano, near-nano and multi-modal crystalline materials will be compared to conventional materials of the same composition. Initial testing of titanium based materials indicates an increase in strength and hardness by 2 to 3 times from the use of nano and near nano crystalline structures. Cryo milled powders and the consolidated forms of these powders will be examined using microstructural analysis and mechanical testing.

**3:40 PM Break**

**3:55 PM**

**Fabrication of Ultrafine/Nanostructured Ti-TiN/TiC Matrix Composites Using Low-Temperature Back Pressure Equal Channel Angular Pressing:** Wei Xu<sup>1</sup>; Xiaolin Wu<sup>1</sup>; Haowen Xie<sup>1</sup>; Jizhong Li<sup>1</sup>; *Kenong Xia*<sup>1</sup>; <sup>1</sup>University of Melbourne

Fully dense nanostructured Ti-TiN/TiC composites have been synthesized by consolidating ball-milled mixtures of pure Ti and TiN/TiC particles (up to 10 vol.%) using back pressure equal channel angular pressing (BP-ECAP) for up to 6 passes at temperatures between 500-550°C which is much lower than that of conventional sintering. Microstructure analysis indicated that nanoscale

reinforcing phases of several tens of nanometers were distributed mainly at grain boundaries and partially within the interior of ultrafine Ti grains (< 1 µm). The presence of nanoscale reinforcing particles was attributed to ball milling whereas the refinement of Ti matrix was ascribed to both ball milling and BP-ECAP. As a result, yield strength up to 1260 MPa and Vickers microhardness up to 5000 MPa have been attained with noticeable compressive plastic strain. It implies that the strategy of employing both ball milling and BP-ECAP is feasible to produce high-performance nanostructured Ti matrix composites.

**4:20 PM**

**Stress-Corrosion Cracking and Fatigue Crack Growth Behavior of Ti-6Al-4V Plates Consolidated from Low Cost Powders:** *Peter Pao*<sup>1</sup>; M. Ashraf Imam<sup>1</sup>; Robert Bayles<sup>1</sup>; C.R. Feng<sup>1</sup>; <sup>1</sup>Naval Research Laboratory

Ti-6Al-4V plates, consolidated from low cost powders, manufactured from Armstrong-process and also from hydride-process were studied. The yield strengths of these plates of Ti-6Al-4V are comparable and are about 920 MPa. The plate from hydride-process has higher oxygen content compared to the plate from the Armstrong-process (0.3 vs. 0.2 wt%). To remove the prior history of consolidation, the plates are beta annealed and the test results are compared with as received condition. Fatigue crack growth study indicates that, in the as-received condition, the fatigue crack growth threshold stress intensities of Armstrong-process and hydride-process Ti-6Al-4V approaches to that of the conventional Ti-6Al-4V. The stage II fatigue crack growth rates of hydride-process of Ti-6Al-4V are substantially higher than that of the Armstrong-process and the conventional cast-ingot-cast. The mechanism of the fatigue crack growth rates difference, fracture toughness, and stress-corrosion cracking resistance of Ti-6Al-4V will be discussed.

**4:45 PM**

**Sintering Behavior of TiH<sub>2</sub> for Manufacturing of Titanium Alloys and Products:** *Zhigang Fang*<sup>1</sup>; Hongtao Wang<sup>1</sup>; Shuming Fang<sup>2</sup>; Jiamin Zhang<sup>2</sup>; <sup>1</sup>University of Utah; <sup>2</sup>CYMCO

Powder Metallurgy (PM) is an effective cost-saving approach for production of titanium parts due to the advantage of near net shape (NNS) capability of PM techniques. However, the traditional powder metallurgy approach for making titanium alloys faces a number of challenges with respect to issues related to contamination, porosity, and cost when highly alloys powders and high pressure consolidation processes are used. In recent years, a new process technology is emerging by which titanium and titanium alloys can be made by sintering titanium hydride (TiH<sub>2</sub>) and its mixture with alloying elements. The feasibility of this manufacturing approach has been demonstrated fully from powder to sintering and from microstructure to mechanical properties. However, to date there is little published information on fundamentals of this manufacturing technology. In this investigation, the basic chemical and physical properties of TiH<sub>2</sub> are examined through literature as well as experiments. The behavior of TiH<sub>2</sub> powder during compaction and sintering is reported.

**5:10 PM**

**Structure Formation during Preparation of Variable Porosity Ti Foams by Solid State Replication:** Yu. Orlova<sup>1</sup>; K. Maekawa<sup>1</sup>; *Henry Rack*<sup>2</sup>; <sup>1</sup>Kyoto University; <sup>2</sup>Clemson University

Fabrication of variable porosity titanium foams through incorporation of sacrificial sodium chloride powder has been investigated. While the solid foam skeleton was formed during high temperature sintering of the host commercial purity titanium powder particles, with faceting of the powder surface being noted throughout, the three-dimensional pore structure contained macro- (200-400µm), micro- (5-10µm) and sub-micropores (< 1.5µm). The largest macropores had a cubical topography representative of the sodium chloride powder, this having been left following vaporization of the sacrificial powder. Formation of the smaller micro-pores appeared to have occurred during the compaction process and having been kept in the specimen's body due to incomplete sintering of the host powder. Finally formation of the smallest sub-micropores was associated with high temperature gas evolution occurring during sodium chloride vaporization.

**5:35 PM**

**Production of a Low-Cost DMD Wire Feedstock by Direct Consolidation of Ti Sponge:** *Kevin Dring*<sup>1</sup>; Martin Lefstad<sup>2</sup>; Ola Jensrud<sup>3</sup>; <sup>1</sup>Norsk Titanium; <sup>2</sup>SINTEF - Materials and Chemistry; <sup>3</sup>Sintef Raufoss Manufacturing

Direct Metal Deposition (DMD) and other additive manufacturing techniques have received significant interest amongst end users of titanium



in recent years. Promises of dramatically reduced machining to obtain a final titanium component, while retaining mechanical properties approaching wrought material have engaged a broad spectrum of industries. The cost of such manufacturing processes may be prohibitively high when expensive feedstocks such as titanium powder are used. Norsk Titanium, in collaboration with SINTEF and NTNU through a Norwegian Research Council grant, has investigated the production of a low-cost wire feedstock that was produced by direct, non-melt consolidation of titanium. By eliminating the melting and primary working of titanium, significant cost-savings may be realised. The titanium wire was characterised for chemical composition and has demonstrated oxygen levels of 1500 ppm. Test specimens were built up from the wire feedstock and these were analysed for mechanical properties and compositional conformance to relevant standards.

### Electrode Technology for Aluminum Production: Traditional and Inert Anode Materials

*Sponsored by:* The Minerals, Metals and Materials Society, TMS Light Metals Division, TMS: Aluminum Committee  
*Program Organizers:* Ketil Rye, Alcoa Møsjøen; Morten Sorlie, Alcoa Norway; Barry Sadler, Net Carbon Consulting Pty Ltd

Tuesday PM Room: 616  
 February 16, 2010 Location: Washington State Convention Center

*Session Chair:* Jilai Xue, University of Science and Technology Beijing

#### 2:00 PM Introductory Comments

##### 2:05 PM

**Higher Softening Point Pitch as Anode Binder Pitch:** *Robert Wombles*<sup>1</sup>; *Stacey McKinney*<sup>1</sup>; *Thomas Golubic*<sup>1</sup>; *Kathryn Sickels*<sup>1</sup>; *Koppers Inc.*

In recent years several authors have discussed the use of higher softening point pitches as anode binder pitches. Several drivers exist to encourage movement from the use of the traditional 110°C softening point pitch as anode binder pitch to pitches with higher softening points. Some of these include the movement to higher amperage pots, the concern for employee exposure to coal tar pitch volatiles and polynuclear aromatic hydrocarbons, and the never ending search for improved anode performance. This paper will discuss several aspects of high softening point pitch including their production; physical, chemical and composition properties, and the potential for their use to improve the quality of anodes produced. In addition, the effect of their use on coal tar pitch volatile and polynuclear aromatic hydrocarbon emissions will be discussed.

##### 2:25 PM

**Study of Resistivity – Real Density Correlation in CPC Calcination Control:** *Oscar Mascarenhas*<sup>1</sup>; *Arun Mathur*<sup>1</sup>; *Jose Botelho*<sup>1</sup>; *Goa Petcoke Consultancy Services*

Petroleum Coke calcination process control relies on testing the Electrical Resistivity of the output product. This resistivity test is in lieu of the Real Density requirement in the Calcined Petroleum Coke quality specifications, as it takes lesser time for analysis instead of the standard methods for Real Density. The correlation between Real Density and Resistivity is suitably linear, however the correlation is affected when there is significant variation in the green coke in terms of particle size distribution or variation in proportion of multiple green cokes used. This paper presents details of an on field study and analysis of the Resistivity – Real Density correlation and suggests methods to use Resistivity as a more effective predictor of Real Density in a production run, including dynamically set Resistivity targets leading to better calcination control and optimization of production costs.

##### 2:45 PM

**The Comparison between Vertical Shaft Furnace and Rotary Kiln for Petroleum Coke Calcination:** *Yi Sun*<sup>1</sup>; *Haifei Xu*<sup>1</sup>; *Yubin Wang*<sup>1</sup>; *Yinhe Cui*<sup>1</sup>; *Chaodong Liu*<sup>1</sup>; *Shenyang Aluminum and Magnesium Engineering and Research Institute*

At present, the petroleum coke is mainly calcined by vertical shaft furnace or rotary kiln to meet the requirement of prebaked anode used for Aluminum reduction in China. Vertical shaft furnace for calcination is quite different from rotary kiln for calcination in the principle of calcination process, calcined coke

quality, product availability, production capacity, energy consumption, operation cost, environmental issues and especially in the properties of calcined coke on real density, air reactivity, CO<sub>2</sub> reactivity and ignition temperature which are closely related to the consumption of anode for aluminum reduction. Therefore, calcination of coke used for aluminum reduction by vertical shaft furnace is more competitive based on the existing quality of the green petroleum coke and the supply thereof.

##### 3:05 PM

**Prebaked Anode from Coal - Utilization of Coal Extract as a Coke Feedstock:** *Maki Hamaguchi*<sup>1</sup>; *Noriyuki Okuyama*<sup>1</sup>; *Nobuyuki Komatsu*<sup>1</sup>; *Jiro Koide*<sup>2</sup>; *Keisuke Kano*<sup>2</sup>; *Kobe Steel, Ltd.*<sup>1</sup>; *Sumitomo Corporation*

Preparation of prebaked anode utilizing coal solvent extraction technology will be reported. In the prebaked anode industry, it is recognized that the quality of anode coke has continuously declined, namely, higher sulfur and impurities, higher volatile matter content, and lower density, mostly due to the deterioration of crude oil quality. We at Kobe Steel, Ltd., have been developing a new non-hydrogenative solvent extraction process for coal with the aim of applying the coal-extract to metallurgical coke making. We named this process and the product (the ash-free coal-extract), a HYPER-COAL (HPC). In this paper, we will describe fabrication of prebaked anode test specimen using HPC as a feedstock of coke. It was demonstrated that prebaked anodes prepared from HPC coke have various advantages such as extremely low impurities such as Sulfur, Vanadium and Nickel, high apparent density, and low air- and CO<sub>2</sub>-reactivity compared to those from anode grade calcined petroleum coke.

##### 3:25 PM

**Charcoal in Anodes for Aluminium Production:** *Bodil Monsen*<sup>1</sup>; *Arne Ratvik*<sup>1</sup>; *Lorentz Lossius*<sup>2</sup>; *SINTEF Materials and Chemistry*<sup>1</sup>; *Hydro Aluminium - PM Technology*

Carbon anodes used in aluminium production are made from petroleum coke and coal tar pitch. Substituting some of the petroleum coke with charcoal have the potential to reduce the environmental footprint of the aluminium production, as CO<sub>2</sub> from renewable sources are not considered a greenhouse gas. However, since charcoal is more porous and have a different reactivity towards air and CO<sub>2</sub> than pet coke, charcoal may have adverse effects on anode properties. Pilot anodes, substituting part of the petrol coke with charcoal, have been produced and evaluated based on typical anode properties, e.g. apparent density, air-, and CO<sub>2</sub>-reactivity. Industrial charcoals, as used in the production of silicon, and pure charcoals, produced from maple and spruce, have been tested. In an attempt to reduce the effect of the porous charcoal, only the finer fractions of the anode dry mix were substituted. Substitutions based on both weight and volume are examined.

##### 3:45 PM Break

##### 4:00 PM

**Ball-Milled Materials as Inert Anodes for Aluminum Production in KF-AlF<sub>3</sub> Low-Temperature Electrolyte:** *Sébastien Helle*<sup>1</sup>; *Benoit Brodru*<sup>1</sup>; *Boyd Davis*<sup>2</sup>; *Daniel Guay*<sup>1</sup>; *Lionel Roue*<sup>1</sup>; *INRS EMT*<sup>1</sup>; *Kingston Process Metallurgy Inc.*

High-energy ball milling is well-known to be a powerful and simple technique to produce fine-grained and highly homogeneous materials with unique chemical, physical and mechanical properties for various applications. In this study, various nanostructured materials including Cu-Ni-Fe, Cu-Al-Ni-Fe based alloys and (Cu-Ni-Fe + MO<sub>x</sub>) composites were prepared by ball milling, consolidated to form dense electrodes and then evaluated as inert anodes for aluminum production in low-temperature (700°C) KF-AlF<sub>3</sub> electrolyte. Their morphological, structural and chemical characteristics were studied at different stages during their preparation and after 20 h of electrolysis. Some of these ball-milled materials were identified as promising inert anodes for producing aluminum with a good purity.

##### 4:20 PM

**Corrosion Behaviors of NiFe<sub>2</sub>O<sub>4</sub>-NiO-Co<sub>3</sub>O<sub>4</sub> Inert Anodes Materials in Na<sub>3</sub>AlF<sub>6</sub>-Al<sub>2</sub>O<sub>3</sub> Melts:** *Jilai Xue*<sup>1</sup>; *Tao Zeng*<sup>1</sup>; *Jun Zhu*<sup>1</sup>; *University of Science and Technology Beijing*

Inert anodes for aluminum electrolysis were fabricated in laboratory by solid-state sintering of NiFe<sub>2</sub>O<sub>4</sub>-NiO-Co<sub>3</sub>O<sub>4</sub> mixtures with varying composition. The microstructures of the materials, before and after electrolysis, were characterized using XRD, SEM-EDS and EPMA. The corrosion tests were systematically performed in Na<sub>3</sub>AlF<sub>6</sub>-Al<sub>2</sub>O<sub>3</sub> melts under different operating

Tue. PM

# Technical Program

parameters. It was found that the Co<sub>3</sub>O<sub>4</sub> addition up to 3% in mass improved the material density and conductivity, and lowered its porosity as well, due to more chemically stabilized microstructure formed with the NiFe<sub>2</sub>O<sub>4</sub>-NiO-Co<sub>3</sub>O<sub>4</sub> mixture than the NiFe<sub>2</sub>O<sub>4</sub>-NiO. The corrosion rate reduced with adding Co<sub>3</sub>O<sub>4</sub>, but increased again with the addition above 4%. The major contributing factor to the corrosion was the metallic Al dissolved in the melts, but this could be counteracted partly by oxygen gas generated in electrolysis with the appropriate current density about 0.4 A/cm<sup>2</sup>. The chosen materials show good corrosion resistance with potential for further application.

## 4:40 PM

**Effect of Sintering Parameters on Properties of 18NiO-17(Cu-Ni)-65NiFe<sub>2</sub>O<sub>4</sub> Composite Ceramic Anode:** *Jia Ma*<sup>1</sup>; Yao Guang Chun<sup>1</sup>; Bao Li<sup>1</sup>; Zhang Xiao<sup>1</sup>; Ma Jun Fei<sup>1</sup>; <sup>1</sup>Northeastern University

Cold-pressing sintering is adopted to prepare 18NiO-17(Cu-Ni)-65NiFe<sub>2</sub>O<sub>4</sub> composite ceramic inert anodes for aluminum electrolysis. The morphology, grain size and phases were investigated by scanning electron microscopy (SEM), energy dispersive spectroscopy (EDS) and X-ray diffraction (XRD), respectively. The effect of temperature and pressure on the relative density, porosity, grain size, electrical conductivity and bending strength was studied. The results show that temperature and pressure can significantly improve the properties of 18NiO-17(Cu-Ni)-65NiFe<sub>2</sub>O<sub>4</sub> composite ceramic. The relative density of the specimens increases with temperature and pressure. The grain size increases with increase of the temperature, while it decreases with the increase of the pressure. The electrical conductivity increases with the decrease of grain size and porosity. The bending strength increasing with temperature and pressure then decreasing with temperature and pressure.

## 5:00 PM

**Research on Preparation and Properties of 18NiO-NiFe<sub>2</sub>O<sub>4</sub> Composite Ceramic Inert Anodes:** *Jia Ma*<sup>1</sup>; Yao Guangchun<sup>1</sup>; Bao Li<sup>1</sup>; Zhang Xiao<sup>1</sup>; Ma Junfei<sup>1</sup>; <sup>1</sup>Northeastern University

In order to improve the properties of NiFe<sub>2</sub>O<sub>4</sub> ceramic inert anodes, two-step sintering process was adopted to prepare and reinforce 18NiO-NiFe<sub>2</sub>O<sub>4</sub> composite ceramic inert anodes by solid-state reaction, with 18wt% excess NiO. 18NiO-NiFe<sub>2</sub>O<sub>4</sub> spinel matrix material was prepared firstly with NiO and Fe<sub>2</sub>O<sub>3</sub> as the raw materials. The material prepared above was crushed to different sizes grains, and then blended together by cold-pressing sintering method. The effect of temperature on the relative density, porosity, electrical conductivity and bending strength was studied. The results show that temperature can significantly improve the properties of NiFe<sub>2</sub>O<sub>4</sub> composite ceramic. The relative density of the samples increases from 69.59% to 98.28%, the porosity decreasing from 30.41% to 1.72% and the bending strength increasing from 14.62MPa to 71.94MPa, with temperature increasing from 1423 K to 1673K.

## 5:20 PM

**Effect of Adding Ni-Fe on Properties of Inert Anodes of NiFe<sub>2</sub>O<sub>4</sub> Based Cermet:** *Zhongsheng Hua*<sup>1</sup>; Guangchun Yao<sup>1</sup>; Lei Wang<sup>1</sup>; Zhigang Zhang<sup>1</sup>; Lisi Liang<sup>1</sup>; <sup>1</sup>Northeastern University

To study the effect of metal addition on the properties of inert anodes of NiFe<sub>2</sub>O<sub>4</sub> based cermet, Ni-Fe-NiFe<sub>2</sub>O<sub>4</sub> cermet inert anodes were prepared by adding Ni and Fe powders into raw materials. The phase compositions, the micro-structures, and the bending strength were investigated by X-ray diffraction (XRD) and scanning electron microscopy (SEM), INSTRON4206-006 electron mechanical experimental machine, respectively, and the bulk density and porosity were characterized by Archimedes drainage. The results showed that the cermets were consisted of NiFe<sub>2</sub>O<sub>4</sub> and Ni-Fe, Ni-Fe distributed uniformly in the matrix. The bending strength increased with increasing Ni-Fe content, but the bulk density decreased, the porosity increased. Also the reasons leading to this phenomenon were analyzed.

## Energy Conservation in Metals: Session I

*Sponsored by:* The Minerals, Metals and Materials Society, TMS Extraction and Processing Division, TMS Light Metals Division, TMS: Energy Committee

*Program Organizers:* Cynthia Belt, Superior Industries International; Mark Cooksey, CSIRO; Donald Whipple, Bloom Engineering Co Inc; Russell Hewertson, Air Products and Chemicals Inc

Tuesday PM Room: 310  
February 16, 2010 Location: Washington State Convention Center

*Session Chairs:* Mark Cooksey, CSIRO; Russell Hewertson, Air Products and Chemicals Inc

## 2:30 PM Introductory Comments

### 2:35 PM

**Five Low Cost Methods to Improve Energy Efficiency on Reverberatory Furnaces:** *Cynthia Belt*<sup>1</sup>; Ray Peterson<sup>2</sup>; Dave Bequette<sup>1</sup>; <sup>1</sup>Superior Industries International; <sup>2</sup>Aleris International

One important way to cut production costs in the metals industry is through implementation of energy efficiency improvements. Energy improvements can be found by reviewing furnace equipment systems and operating practices so as to operate the melting and holding process at the highest efficiency. A number of the changes can be implemented with minimal expense or capital investment. This paper will review several low cost methods to optimize energy efficiency on reverberatory melting or holding furnaces. These five methods (furnace utilization, idle procedures, fire rate, controls, and furnace pressure) will be explained along with information to implement these changes. Included are several rules-of-thumb and benchmarks for aluminum reverberatory furnaces.

### 2:55 PM

**Energy Saving in the Foundry Industry by Using the CRIMSON Single Shot up Casting Process:** *Mark Jolly*<sup>1</sup>; <sup>1</sup>University of Birmingham

Instead of using the traditional batch casting process, the CRIMSON (Constrained Rapid Induction Melting Single Shot Up-Casting) method employs a high-powered furnace to melt just enough metal to fill a single mould in a closed crucible. The crucible is transferred to a station for computer-controlled counter gravity filling of the mould for optimum filling and solidification. The CRIMSON method therefore holds the liquid aluminium for a minimum of time drastically reducing the energy losses attributed to holding the metal at temperature. With the rapid melting times achieved, of the order of minutes, there isn't a long time at temperature for hydrogen to be absorbed or for thick layers of oxide to form. The metal is never allowed to fall under gravity and therefore any oxide formed is not entrained within the liquid. Thus higher quality castings are produced leading to a reduction in scrap rate and reduced overall energy losses.

### 3:15 PM

**Energy and Emissions with Oxyfuel:** *Thomas Niehoff*<sup>1</sup>; <sup>1</sup>Linde Gas

Oxyfuel combustion systems are state of the art for many melting operations. Airfuel systems have been stepwise modified to oxygen enrichment, oxygen lancing and oxyfuel. Every change of the melting process will have consequences with regards to emissions and energy usage. The uniqueness of many operations requires unique skills to resolve potential issues. This paper will give some examples of how airfuel systems can be successfully converted to oxyfuel.

### 3:35 PM

**Industrial Application Experiences with Microporous Calcium Hexaluminate Insulating Material SLA-92:** *Dale Zacherl*<sup>1</sup>; Rainer Kockegey-Lorenz<sup>2</sup>; Andreas Buhr<sup>2</sup>; <sup>1</sup>Almatis, Inc; <sup>2</sup>Almatis GmbH

The microporous calcium hexaluminate insulating material SLA-92 has been introduced as an alternative to refractory ceramic fiber and other insulating refractory materials. Key properties associated with this product include: high chemical purity, long term high temperature stability up to 1500°C, low thermal conductivity up to 1500°C and high thermal shock resistance. The properties of this material and various applications in the steel and ceramic industries have been reported in previous papers. The current paper summarizes the industrial application experiences with innovative refractories based on SLA-



92 and discusses potential new applications in various manufacturing as well as energy-related industries.

**3:55 PM**

**Identifying Some Potential Future Hydrometallurgical Processes in Treatment of Nickel Laterites:** *Sarveswara Rao Katragadda*<sup>1</sup>; <sup>1</sup>Institute of Minerals and Materials Technology

Existing technologies that currently produce nickel worldwide utilize only about half of the nickel laterite deposits. So, there is a need for a new processing route to recover nickel and cobalt from the remaining laterite ores that are otherwise unutilized. Accordingly, an overview of different existing types of nickel resources and economical processes based on laterite horizons, consumption of energy and reagents and environmental concerns is made in this paper, along with a summary of metallurgical and engineering challenges to be overcome when implementing new technologies and concepts with regard to base metal extraction and sulfur removing efficiency. The paper also compiles and analyses a range of data concerning energy and greenhouse emissions pertaining to nickel technology.

**4:15 PM Concluding Comments**

### Failure of Small-Scale Structures: Device Failure and Fatigue

*Sponsored by:* The Minerals, Metals and Materials Society, TMS Materials Processing and Manufacturing Division, TMS Structural Materials Division, TMS/ASM: Mechanical Behavior of Materials Committee, TMS: Nanomechanical Materials Behavior Committee  
*Program Organizers:* Marian Kennedy, Clemson University; Brad Boyce, Sandia National Laboratory; Reinhold Dauskardt, Stanford; Zhiwei Shan, Hysitron Inc

Tuesday PM Room: 206  
February 16, 2010 Location: Washington State Convention Center

*Session Chair:* Molly Kennedy, Clemson University

**2:00 PM Invited**

**Nitinol Fatigue – A Review:** *Xiao-Yan Gong*<sup>1</sup>; Jixi Zhang<sup>2</sup>; Yanyao Jiang<sup>2</sup>; <sup>1</sup>Medical Implant Mechanics LLC; <sup>2</sup>University of Nevada, Reno

Stent is a metal mesh used as a medical implantable device to open the blocked artery or as a structural device supports the prosthetic flexible heart valve leaflets. Typical cross-section of a Nitinol self-expanding stent is on the order of several hundred microns. Recently, there is an increasing interest in understanding the fatigue of Nitinol owing to a hard lesson learned from using self-expanding stents treating the superficial femoral arteries. Fracture occurrences of up to 50% have been reported in some stents after one year follow-up. These stent fractures are due to in vivo cyclic displacements. As such, this presentation provides a review of Nitinol fatigue from over seventy published articles. It summarizes the key findings, identifies important challenges and provides a perspective for future work.

**2:25 PM**

**Failure of Micron-Scale Polysilicon MEMS: Fatigue and Wear Mechanisms:** *Daan Hein Alsem*<sup>1</sup>; Robert Ritchie<sup>2</sup>; <sup>1</sup>Lawrence Berkeley National Laboratory; <sup>2</sup>Lawrence Berkeley National Laboratory/University of California at Berkeley

Adhesion, wear, fatigue and fracture are all potential failure modes for MEMS devices. We focus on failure mechanisms in micron-scale polycrystalline silicon using on-chip testing and explain these phenomena in terms of the physical mechanisms using analytical transmission electron microscopy. With fatigue shown to occur via moisture-assisted sub-critical cracking within a cyclic stress-assisted thickened nano-scale oxide layer until the crack reaches a critical size to cause device failure, the sidewall morphology quantitatively determines fatigue and fracture behavior. Wear in ambient air is shown to involve a short adhesive wear regime, followed by an abrasive wear regime, where <100 nm silicon debris is created by fracture through silicon grains. These particles oxidize while plowing, leaving abrasive grooves associated with cracking rather than plastic deformation. Wear rates were orders of magnitude smaller than expected from macro-scale studies. This work illustrates that large surface-to-volume ratios in micron-scale systems can markedly alter mechanical behavior.

**2:40 PM**

**Finite Element Simulation of Galvanic Corrosion in Silicon Microsystems:** *Collin Becker*<sup>1</sup>; Conrad Stoldt<sup>1</sup>; David Miller<sup>2</sup>; <sup>1</sup>University of Colorado; <sup>2</sup>National Renewable Energy Laboratory

Many microsystems fabrication technologies currently employ a metallic overlayer, such as gold, in electrical contact with silicon (Si) structural layers. During postprocessing in hydrofluoric acid based solutions, a galvanic cell is created between the silicon and the metallic layer. As a consequence, autonomous corrosion (etching) of the silicon layer occurs and mechanical and electrical properties of structural Si are degraded. We present a finite element simulation to model electrochemical corrosion in MEMS. The model uses a heat transfer analogy to electrical conduction and predicts electrochemical kinetics with the Tafel equation. Focused ion beam milling of micron scale silicon resistive probes with metallic overlayers verifies the model accurately predicts corrosion in MEMS. Specifically, modeling results reproduce the current limited trend resulting from the surface area ratio (SAR) of metal to silicon.

**2:55 PM**

**Size-Scale Effects in the Fracture of Polycrystalline Silicon for Microsystems:** *Brad Boyce*<sup>1</sup>; E. David Reedy<sup>1</sup>; James Foulk<sup>1</sup>; <sup>1</sup>Sandia National Labs

In polycrystalline silicon used for microelectromechanical systems (MEMS), fracture is governed by the relationships between the size of the native flaws and the size of the microstructure, the size of geometric features (corners, notches, etc.), and the size of the device itself. In this study, we investigate the influence of these four length scales on resulting reliability using a recently developed high-throughput sequential tensile test structure which permits rapid collection of 1000's of microscale tests for robust extreme-value statistical analysis. Each of these four factors are shown to have a pronounced effect, sometimes reducing the strength by a factor of two or more. Cohesive zone and finite element modeling are employed to gain insight into these length scale effects.\* Sandia is a multi-program laboratory operated by Sandia Corporation, a Lockheed Martin Company, for the United States Department of Energy's National Nuclear Security Administration under Contract No. DE-AC04-94AL85000.

**3:10 PM**

**Theta-like Specimens to Determine Tensile Strength at the Micro Scale:** *Michael Gaither*<sup>1</sup>; Frank DelRio<sup>1</sup>; George Quinn<sup>1</sup>; Richard Gates<sup>1</sup>; Robert Cook<sup>1</sup>; <sup>1</sup>National Institute of Standards and Technology

Components of micro- and nano-electromechanical systems are typically formed via lithographic and etching processes that are known to leave residual surface features, stresses, and chemistry that ultimately control component strength and thus device performance and reliability. In order to measure how these surface characteristics interact with applied loads and deformations to induce failure and truncate lifetime, mechanical test structures are required to measure mechanical properties at ultra-small length scales. Here we describe a new "theta-like" geometry for micro-scale tensile strength measurement that allows for direct assessment of surface effects on strength. Specimens were formed from silicon-on-insulator wafers via deep reactive ion etching (DRIE) and tested with an instrumented indenter. The experimental results were interpreted via finite element models to extract fracture strength. Fracture strengths as great as 3 GPa were observed, with fracture initiating at DRIE etch pits. Statistical and fractographic analyses verified the existence of two processing-induced flaw populations.

**3:25 PM**

**Fracture Behavior of Partially-Sintered Ceramics for Electrochemical Cell Applications:** *Xiaoxing Liu*<sup>1</sup>; Christophe Martin<sup>1</sup>; Gerard Delette<sup>2</sup>; <sup>1</sup>Grenoble-INP; <sup>2</sup>CEA-Grenoble

The discrete nature of the fracture behavior of partially sintered ceramic powders is addressed using 3D Discrete Element Method simulations (DEM). Small samples, typically 30 μm thick, which are typical of electrochemical cell applications, are first prepared numerically by partially sintering around 20,000 micronic particles. Solid contacts formed during sintering are then modeled as brittle elastic bridges that may break under tension or shear. The numerical samples obtained from this sintering stage are submitted to tensile and compressive tests up to failure to obtain the fracture strength as a function of porosity and pertinent microstructural features at the particle length scale. Using these tests, we also investigate the effect of large pores on fracture. The formation and propagation of cracks originating from the thermal mismatch between the porous ceramic and a dense substrate is finally treated. Whenever

Tue. PM

# Technical Program

possible, simulation results are compared to experimental data from the literature.

## 3:40 PM

**Failure Analysis of Audio Connectors Component Using X-Ray 3D Technology:** *Daniele Rolim*<sup>1</sup>; *Iramylson Freitas*<sup>1</sup>; *Idelcio Cardoso*<sup>1</sup>; *Ocilide Silva*<sup>1</sup>; <sup>1</sup>Nokia Institute of Technology

This work proposes to investigate a critical assembly problem in audio connectors using non destructive method with both 2D and 3D X-Ray and destructive method with SEM. The main trouble when 2D analysis is used is the material overlay. This can induce to incorrect conclusions. Analysis in x-ray with 3D image can take a too long time during process of image acquisition but the result shows better precision to distinguish components interconnections. Each sample has taken around 40 minutes to acquire using 120kV and 60μA for tension and current respectively. It was detected that proximity of some wires with solder of another connection can produce a friction between them, so the risk of short circuit arises, as some wires that composed one out of four connections are worn and/or broken. The complimentary analysis with SEM detected that either the wires insulating layer or most of the whole connection was damaged.

## 3:55 PM Break

## 4:10 PM Invited

**Mitigation of Wear-Induced Failure of Microsystems by Vapor Phase Lubrication:** *Michael Dugger*<sup>1</sup>; <sup>1</sup>Sandia National Laboratories

Since their inception about twenty years ago, microelectromechanical systems (MEMS) have been plagued with failures attributable to the interaction of moving surfaces. Designers have learned to avoid surfaces that touch or slide in order to maximize the reliability of their structures. While chemisorbed monolayers of organic molecules and non-liquid-based release processes have enabled successful fabrication of compliant structures, these approaches are not sufficiently robust to permit long term operation of devices with impacting and sliding surfaces. A recent advance in MEMS surface modification relies upon vapor phase lubrication. Using this approach, surface passivation is maintained via adsorption of a desired molecule from a low concentration source in the vapor phase. Unprecedented improvements in operating life result from maintaining surface passivation, and the elimination of wear particle generation. This presentation will discuss recent advances in MEMS lubrication and ongoing research aimed at developing a mechanistic understanding of vapor phase lubrication.

## 4:35 PM

**In-Situ Microscale Fatigue Study to Determine the Effect of Microstructural Neighborhoods on Crack Initiation Mechanisms and Lifetimes:** *Christopher Szczepanski*<sup>1</sup>; *Sushant Jha*<sup>1</sup>; *Bob Wheeler*<sup>2</sup>; *James Larsen*<sup>3</sup>; <sup>1</sup>UTC/AFRL; <sup>2</sup>UES/AFRL; <sup>3</sup>AFRL

Recent studies of fatigue crack-initiation mechanisms and their relationship to lifetime variability in bulk samples of Ti-6Al-2Sn-4Zr-6Mo has revealed that crack initiation results from a few different characteristic microstructural arrangements. These microstructural configurations, which vary in size and local crystallographic texture, can be ranked based on their frequency of occurrence and ultimately correlated with lifetime to failure. This paper will focus on a micro-scale fatigue study where micro-samples were machined in specific microstructural neighborhoods with textures that are believed to enhance their susceptibility to specific crack initiation mechanisms. A focused ion beam (FIB) microscope was used to machine micro-scale fatigue specimens containing microstructural arrangements of interest, as determined from the original study on bulk specimens. These specimens were then fatigued, in-situ, in a scanning electron microscope chamber. A study of deformation modes active in these specimens and correlation of microstructural arrangements to fatigue lifetime will be presented.

## General Abstracts: Structural Materials Division: Fatigue and Fracture

*Sponsored by:* The Minerals, Metals and Materials Society, TMS Structural Materials Division, TMS: Advanced Characterization, Testing, and Simulation Committee, TMS: Alloy Phases Committee, TMS: Biomaterials Committee, TMS: Chemistry and Physics of Materials Committee, TMS/ASM: Composite Materials Committee, TMS/ASM: Corrosion and Environmental Effects Committee, TMS: High Temperature Alloys Committee, TMS/ASM: Mechanical Behavior of Materials Committee, TMS/ASM: Nuclear Materials Committee, TMS: Refractory Metals Committee, TMS: Titanium Committee  
*Program Organizers:* Eric Ott, GE Aviation; Robert Hanrahan, National Nuclear Security Administration; Judith Schneider, Mississippi State University

Tuesday PM Room: 3A  
February 16, 2010 Location: Washington State Convention Center

*Session Chair:* To Be Announced

## 2:00 PM

**Fatigue Crack Growth Mechanisms of Long and Small Cracks in Structural Materials:** *Anastasios Gavras*<sup>1</sup>; *Christopher Lammi*<sup>1</sup>; *Diana Lados*<sup>1</sup>; <sup>1</sup>Worcester Polytechnic Institute

Fatigue crack growth mechanisms of long and small cracks were investigated in cast and wrought aluminum and titanium alloys (as-cast A535, 6061-T6, and Ti-6Al-4V) with various microstructures. The effects of microstructure and bulk residual stresses on the fatigue crack growth response of each material were evaluated. Bulk residual stresses were introduced in the testing specimens through quenching. Long crack growth data were generated on compact tension specimens tested at low and high stress ratios ( $R=0.1$  and  $R=0.7$ ). Small crack growth testing was performed on surface flaw tension specimens at low stress ratio ( $R=0.1$ ). Closure and microstructurally small crack growth mechanisms in samples with low and high residual stress levels were identified and related to the characteristic features of the materials. Corrective techniques compensating for residual stress, closure, and microstructural effects on fatigue crack growth data will be presented and discussed.

## 2:20 PM

**Novel Methods for Microstructure-Sensitive Probabilistic Fatigue Notch Factor:** *William Musinski*<sup>1</sup>; *David McDowell*<sup>1</sup>; <sup>1</sup>Georgia Institute of Technology

Traditional fatigue analysis schemes used for geometries with stress gradient fields (such as notches) have required extensive experimentation, estimation of fatigue failure distributions, and characterization of the notch effect via a notch root fatigue strength reduction factor, often called the fatigue notch factor,  $K_f$ . These experimental results are beneficial for life prediction of a given geometry and microstructure, but do not offer predictive insight into the underlying physical mechanisms that explain fatigue variability, size effects, and local gradient effects on fatigue damage. These notch effects are depicted through probability distributions of slip and small crack initiation processes that are informed by computational crystal plasticity simulations performed on realistic microstructures of materials used for aircraft gas turbine engines. Finally, the concept of a probabilistic, microstructure-sensitive fatigue notch factor,  $K_f^{956}$ , is introduced that considers effects of nonlocal notch root plasticity, microstructure variability, and the probability of crack formation.

## 2:40 PM

**Effect of Low-Temperature Overload on Fatigue Crack Growth Retardation:** *Sai Kumar*<sup>1</sup>; *Jyoti Mohanty*<sup>1</sup>; *Bipin Verma*<sup>1</sup>; *Prabal Ray*<sup>1</sup>; <sup>1</sup>National Institute of Technology, Rourkela

Exponential model can be used to model fatigue crack growth predict the a-N curve to calculate residual life without integration of fatigue crack growth rate curve. In the present investigation an attempt has been made to estimate the fatigue life and retardation parameters of aluminium alloy components subjected to spike overload at subzero temperature using an Exponential Model. The specific growth rate in the model changes with loading condition and crack length. It has been expressed through dimensionless groups ( $\Delta K/K_C$ ), ( $K_{max}/K_C$ ) and ( $\sigma_y/E$ ), and correlated with overload temperature. It is concluded that (i) an Exponential model can be effectively used to determine fatigue life,



(ii) overload at low temperature enhances retardation effect, (iii) presence of a large number of secondary cracks in the overload affected tear zone due to low temperature environment may be responsible for enhancing the retardation effect by reducing the available  $\Delta K$  for primary crack extension.

### 3:00 PM

**A Physical Interpretation of Basquin Relation:** *Partha De*<sup>1</sup>; Wei Yuan<sup>1</sup>; Rajiv Mishra<sup>1</sup>; <sup>1</sup>Missouri University of Science and Technology

Basquin's empirical relation expresses  $\sigma_a$  the stress amplitude in a fully reversed fatigue test as an explicit function of  $N_f$  the number of load reversals to failure. The relation involves two parameters: ' $\sigma_f$ ' the fatigue strength coefficient and 'b' the fatigue strength exponent. The fatigue strength coefficient strongly correlates to true fracture strength of the material in monotonic tensile test, while b generally varies within a small range of -0.05 to -0.12. Using friction stir processing a range of microstructures were produced with different combinations of strength leading to corresponding changes in S-N characteristics. The change of fatigue constants at different length scales of microstructure and variation in strengthening mechanism is utilized to give a physical significance to Basquin relation.

### 3:20 PM

**Effect of Hydrogen on Crack Nucleation in 316 Stainless Steel under Rotating Beam Fatigue Loading Conditions:** *Douglas Matson*<sup>1</sup>; Christian Skipper<sup>1</sup>; Gary Leisk<sup>1</sup>; Anil Saigal<sup>1</sup>; <sup>1</sup>Tufts University

Alloy 316 stainless steel samples were tested using a rotating beam fatigue test machine. Samples were either as-machined (uncharged) or precharged in hydrogen gas to obtain a concentration of 109 ppm. Cumulative damage was determined by counting the number and size distribution of cracks following sample fatigue failure using dye-penetrant and sample sectioning. Hydrogen precharged specimens have fewer and longer cracks than non-charged specimens for each alloy. The average number of cracks per specimen at the 500 MPa stress level was  $14.67 \pm 2.08$  for non-charged specimens and  $5 \pm 1$  for hydrogen-charged specimens. Total crack surface area was also determined by summing the cumulative area of all cracks in a sample for both precharged and non-charged condition and this damage area at failure was on the order of the gage area. These results are consistent with previous results showing hydrogen retards crack nucleation but accelerates crack growth for this alloy system.

### 3:40 PM Break

### 3:50 PM

**S-N Fatigue and Fatigue Crack Propagation Behaviors of High Manganese Steels:** *Jaeki Kwon*<sup>1</sup>; Sanguk Jin<sup>1</sup>; Sangshik Kim<sup>1</sup>; <sup>1</sup>Gyeongsang National University

Austenitic manganese steels with more than 13% manganese addition have been gathering a great interest particularly in ship-building and architectural industries due their excellent mechanical properties and weldability. Despite the interest, fatigue behavior of high manganese steels, including microstructural influences and fatigue crack initiation mechanism, have not been well established. In this study, uniaxial S-N fatigue and fatigue crack propagation (FCP) behaviors of high manganese steels were studied and the results were compared to those of TMCP steels with similar yield strengths. The present high manganese steels showed enhanced resistances to FCP in low stress intensity factor regime. Abnormally high resistance to S-N fatigue was observed for the high manganese steels in high and intermediate stress ranges probably due to extremely high strain hardening. Mechanism(s) associated FCP and S-N fatigue for high manganese steels were discussed based on detailed SEM micrographic and fractographic observations.

### 4:10 PM

**Effect of Ca, Mg and Ti-Mg Addition on the Impact Toughness of Heat Affected Zone in Low Carbon Steel:** *Jianghua Ma*<sup>1</sup>; Dongping Zhan<sup>1</sup>; Zhouhua Jiang<sup>1</sup>; Jin Yu<sup>1</sup>; Jicheng He<sup>1</sup>; Haijun Shen<sup>2</sup>; <sup>1</sup>Northeastern University; <sup>2</sup>Baoshan Iron & Steel Co., Ltd.

In order to understand the effects of deoxidants such as calcium, magnesium and titanium on the impact toughness of heat affected zone, three low carbon steels deoxidized by Ca, Mg and Ti-Mg were obtained respectively. After smelting, forging, rolling and welding simulation, the effects of Ca, Mg and Ti-Mg addition were studied. The inclusion characteristics of samples before welding and the fracture pattern of the specimens after the Charpy-type test were respectively analyzed using optical microscope and scanning electron

microscopy. The following results were found. The density of inclusion is raised and the average diameter is decreased after adding alloys, especially when the Ca and Ti-Mg alloys were added, but the density adding Ca decreases 71.8% after 1 hour. The addition of Ti-Mg can enhance the impact toughness of the HAZ after welding simulation. The maximal value of the impact toughness is 66.5J/cm<sup>2</sup>. And the enhancing mechanism is discussed.

### 4:30 PM

**Development of Layer-Integrated Steels with Superior Strength-Ductility Combination:** *Shoichi Nambu*<sup>1</sup>; Masato Michiuchi<sup>1</sup>; Junya Inoue<sup>1</sup>; Toshihiko Koseki<sup>1</sup>; <sup>1</sup>The University of Tokyo

Variety of extraordinary high strength-ductility combinations, tensile strength above 1.3GPa and uniform elongation above 20%, could be achieved by layer-integration method using commercial steels. Multilayered (layer-integrated) steel composites consisting alternating layer of martensitic steel and austenitic steels were fabricated by controlling layer thickness and volume fraction of each component. Type 420J2 stainless steel, which shows ultra high strength in as-quenched condition was prepared for martensite layer, and three types of austenitic stainless steels, Type 304, 304N2 and 301 which have different work hardening exponent and yield strength, were prepared for austenite layer. The fracture toughness of Type 420J2 was controlled by heat treatment. It was demonstrated that variety of extraordinary high strength-ductility combinations could be obtained by controlling the geometrical and materials parameters, such as fracture toughness of martensite, work hardening exponent of austenite and strength ratio between components.

### 4:50 PM

**Fatigue Crack Growth Behavior in a Monocrystalline Ni-Based Superalloy:** *Clarissa Yablinsky*<sup>1</sup>; Katharine Flores<sup>1</sup>; Michael Mills<sup>1</sup>; James Williams<sup>1</sup>; <sup>1</sup>The Ohio State University

Historically, Ni-based monocrystal superalloy turbine blades have been limited by creep resistance. With modern airfoil designs and longer service times, fatigue resistance can also be a limiting factor. We examined the fatigue crack growth characteristics of monocrystalline Ni-based superalloy René N5. Test temperature was varied in order to examine the effects of deformation mode, plastic zone size, recovery, and other time dependent processes. The crack path observed at 550°C was highly faceted on the macro-scale, but the facets were smooth and mirror-like. In contrast, the crack path at 850°C was flat, consistent with an increase in crack growth rate with temperature, but with significant surface roughness. Scanning electron microscopy was used to determine crack path, fracture topography, and  $\gamma/\gamma'$  morphology along the crack wake and in the bulk material. Dislocation arrangements were examined via transmission electron microscopy in order to characterize the mechanisms of damage accumulation during fatigue crack growth.

### 5:10 PM

**The Role of Non-Planar Deformation in Cyclic Softening Following Low Cycle Fatigue of a Ni-Based Superalloy:** *Patrick Phillips*<sup>1</sup>; Raymond Unocic<sup>1</sup>; Libor Kovarik<sup>1</sup>; Dan Wei<sup>2</sup>; David Mourer<sup>2</sup>; Michael Mills<sup>1</sup>; <sup>1</sup>Ohio State University; <sup>2</sup>GE Aviation

Cyclic softening is a common material response during low cycle fatigue (LCF) over a wide range of testing temperatures. The polycrystalline Ni-based superalloy explored in this study exhibits this softening behavior, but only at elevated temperatures. This tendency is likely a result of activating new deformation modes depending on time and temperature. Using transmission electron microscopy characterization methods, the evolution of damage mechanisms was studied on specimens interrupted after a limited number of cycles. Both fine and coarse precipitate microstructures were examined, corresponding to a fast or slow cool, respectively, from the gamma prime solvus temperature. The operative deformation mechanisms are correlated with the precipitate structure, number of cycles, and testing temperature. The observed deformation modes include paired APB shearing, intense dislocation bands on {111} planes, and eventual cross-slipping processes between {111} and {100} planes. A rationale for the observed mechanisms in terms of time-dependent damage processes will be discussed.

Tue. PM

# Technical Program

6:00 PM

## Computational Thermodynamics, Neural Networks and Genetic Algorithms: Tools to Design Creep Resistant and Weldable Superalloys:

*Franck Tancret*<sup>1</sup>; <sup>1</sup>Université de Nantes

One drawback of many nickel-base superalloys is their poor weldability. In particular, cracking can occur in the mushy zone during solidification, in the so-called Brittle Temperature Range (BTR). Another type of cracking is due to the formation of intergranular liquid films, by the liquation of low melting point phases like carbides and/or intermetallics. In this work, computational thermodynamics (Thermo-Calc) is used to predict the occurrence of these types of cracking, and to design Ni base alloys by minimizing both the BTR and the risk of  $\gamma'$  liquation cracking, while keeping a good phase stability and good mechanical properties in the expected service temperature range. Optimized alloy compositions are determined by an automated maximization of stability and weldability, using genetic algorithms. Also, the creep rupture resistance is estimated through the regression of existing data, using neural networks. Predictions are then used to propose new weldable and creep-resistant superalloys.

## Global Innovations in Manufacturing of Aerospace Materials: The 11th MPMD Global Innovations Symposium: Innovations in Primary and Secondary Forming - Titanium

*Sponsored by:* The Minerals, Metals and Materials Society, TMS Materials Processing and Manufacturing Division, TMS Structural Materials Division, TMS: Shaping and Forming Committee, TMS: High Temperature Alloys Committee

*Program Organizers:* Deborah Whitis, General Electric Company; Thomas Bieler, Michigan State University; Michael Miles, BYU

Tuesday PM Room: 306  
February 16, 2010 Location: Washington State Convention Center

*Session Chairs:* Dan Sanders, Boeing Corporation; Lee Semiatin, AFRL-RX

2:00 PM Invited

## Severe-Plastic Deformation and Superplasticity of Two-Phase Titanium

*Alloys:* *Lee Semiatin*<sup>1</sup>; G. A. Sargent<sup>2</sup>; A. K. Ghosh<sup>3</sup>; G. A. Salishchev<sup>4</sup>; C. S. Lee<sup>5</sup>; <sup>1</sup>US Air Force Research Laboratory; <sup>2</sup>UES, Inc.; <sup>3</sup>University of Michigan; <sup>4</sup>Belgorod State University; <sup>5</sup>Pohang University of Science and Technology

A number of severe-plastic-deformation (SPD) methods have been developed to impart an ultrafine grain size during cold or warm primary processing of metallic materials. These techniques include high-reduction flat rolling, redundant or multi-directional forging, and multi-pass equal-channel angular extrusion. The microstructures developed in single-phase materials by such means and their effect on secondary superplastic (SP) forming will be summarized. With this as background, the balance of the talk will focus on the nature of the microstructure developed via SPD of two-phase titanium alloys, such as Ti-6Al-4V, and the effect of such microstructures on subsequent low-temperature SP deformation. The importance of controlling the size of alpha-particles (versus that of the alpha grains within each particle) in order to optimize low-temperature SP flow during forging or sheet forming will be discussed. It will be shown that microstructure evolution via static coarsening, dynamic coarsening, or dynamic spheroidization can each have a major effect on SP flow behavior. The specific role played by each mechanism depends on the microstructure developed in billet or sheet during primary processing via SPD.

2:30 PM

## Processing, Structure and Properties of Safety Critical Titanium - An Engineering Perspective: *David Rugg*<sup>1</sup>; D. Furrer<sup>2</sup>; M. Glavicic<sup>2</sup>; <sup>1</sup>Rolls-Royce Plc; <sup>2</sup>Rolls-Royce Corporation

Advanced experimental techniques are available that allow scientists to routinely assess intergranular strain evolution, interface structures and mechanical properties at length scales of a few microns. Similarly, physically based models are reaching a level of maturity that allow use for niche industrial application. This paper reviews the industrial need for fundamental research of this type in the areas of processing, microstructural characterisation and

mechanical behaviour. An overview of key future requirements in terms of measurement, representation and modelling will also be presented. Safety critical components will be used as a case study representing a combination of advanced manufacturing routes and complex load regimes in service.

2:50 PM

## The Effect of Macrozone Formation during Thermo-Mechanical Processing on the Fatigue Response of Commercial Ti-6Al-4V Products: *M.R. Bache*<sup>1</sup>; C. Pleydell-Pearce<sup>1</sup>; <sup>1</sup>Swansea University

The development of regions of common crystallographic orientation during thermo-mechanical processing of  $\alpha/\beta$  titanium alloys is now recognised as a major controlling factor for subsequent mechanical properties. In particular, a process of stress redistribution driven by inhomogeneous plasticity acts as a key mechanism behind fatigue crack initiation. Recent efforts have focussed on the identification of effective structural units (ESUs) in commercially processed products and their role during the fatigue process. Various product forms of the same alloy, Ti-6Al-4V, will be assessed to identify differences in texture and associated fatigue performance, utilising a variety of plain and notched specimen designs. Implications for service applications will be discussed.

3:10 PM

## In Situ Observation of Texture Evolution during Rolling and Recrystallisation of Ti-6Al-4V: *Jonathan Warwick*<sup>1</sup>; R. J. Talling<sup>2</sup>; M. Preuss<sup>2</sup>; D. Dye<sup>1</sup>; <sup>1</sup>Imperial College London; <sup>2</sup>Manchester University

A fine primary microstructure is produced in bimodal Ti-6Al-4V by the recrystallisation of material that has previously been deformed in the  $\alpha+\beta$  field, i.e. by recrystallisation (RX) of deformed laths. Here we track the evolution of texture and microstructure during RX by using in situ hot stage backscatter electron imaging and in situ synchrotron X-ray diffraction, both with  $\sim 1$ s time resolution. These measurements are complemented by ex situ texture measurements and EBSD. The understanding generated of the evolution of these microstructures allows conclusions about process optimisation and the effect of RX on texture to be drawn.

3:30 PM

## The Effect of Beta Grain Growth on Alpha Variant Selection in Ti-6Al-4V: G. Obasi<sup>1</sup>; S. Biroscu<sup>1</sup>; *Michael Preuss*<sup>1</sup>; <sup>1</sup>University of Manchester

In the current study, the texture evolution and the role of  $\beta$  grain growth on variant selection in Ti-6Al-4V have been investigated. Three samples from different processing routes (Conventional Ingot Metallurgy (IM), Powder Metallurgy (PM) and Ti-6Al-4V with 0.39wt%Y) were uni-directionally rolled at 950°C, followed by recrystallization for 8h and cooled at 1°C/min to produce similar equiaxed microstructures and textures for the three alloys. The recrystallized samples were subsequently heat treated above beta transus temperature and then cooled at 1°C/min to allow diffusional transformation. The microstructural analysis including beta grain reconstruction indicates the largest beta grain growths for the PM material followed by the IM and Yttrium containing alloy. Electron back scatter diffraction (EBSD) texture analysis shows that the major texture component in all recrystallized samples were the  $\{11-20\} \langle 0001 \rangle$ . However, the PM material showed the most significant difference in terms of measured texture intensity compared to the calculated on a basis of equal variant probability followed by the IM material and the Ti-6Al-4V with 0.39wt%Y. The results suggest that variant selection can be related to grain growth and possibly the development of specific beta grain boundaries with a common (110) normal direction.

3:50 PM

## The Relevance of Twinning during Deformation of Ti-6Al-4V: D.G. Leo Prakash<sup>1</sup>; R. J. Moat<sup>1</sup>; R. Ding<sup>2</sup>; I. Jones<sup>2</sup>; P. Withers<sup>1</sup>; J. Quinta da Fonseca<sup>1</sup>; *Michael Preuss*<sup>1</sup>; <sup>1</sup>University of Manchester; <sup>2</sup>University of Birmingham

A detailed study has been carried aimed at providing unambiguous evidence of twinning in Ti-6Al-4V during moderate (4 - 14%) uniaxial compression deformation at room temperature using a slow strain rate ( $10^{-6}$  s<sup>-1</sup>). This is achieved by generating a strongly textured and recrystallised microstructure with strong basal texture components in the transverse and normal direction but none in the rolling direction. By subsequently compressing the material along the rolling direction dramatic texture changes were found after only 6% plastic deformation with a strong basal texture component in the rolling direction. Even though electron channelling contrast imaging and transmission electron microscopy were able to provide direct evidence of tensile and compression twins in the deformed material it was also evident that the fraction of twins



appeared far too low to explain the dramatic texture change during deformation. Detailed orientation mapping using EBSD identified an increasing number of entire grains having their c-axis aligned with the loading direction in the deformed material. The root cause for such complete grain rotation can only be speculated at the moment but it is suggested that individual grains require high activation energy for twinning but a low energy for the growth of the twin. It is further speculated that such twinning of entire grains might act as a recovery process of grains.

#### 4:10 PM Break

#### 4:20 PM

**Dislocation Transmission through Interphase Boundaries in Ti-6Al-4V:** R. Ding<sup>1</sup>; J. Gong<sup>2</sup>; A.J. Wilkinson<sup>2</sup>; I. P. Jones<sup>1</sup>; <sup>1</sup>University of Birmingham; <sup>2</sup>Oxford University

Dislocation transmission through interphase boundaries in Ti-6Al-4V has a significant effect on mechanical properties. Triangular cross-section microcantilevers have been machined using FIB from a commercially processed Ti-6Al-4V ingot and deformed using a nanoindenter. Each cantilever contains several alpha lamellae separated by thin fillets of beta. Slip occurs as well defined slip bands, which cross the beta fillets. TEM specimens in various orientations with respect to the cantilever (and slip bands) have been machined (again using FIB) from the deformed cantilever and the processes of slip nucleation and transmission examined.

#### 4:40 PM

**The Application of Fine Grain Titanium 6Al-4V for Superplastic Forming and Superplastic Forming and Diffusion Bonding of Aerospace Products:** Larry Hefti<sup>1</sup>; <sup>1</sup>The Boeing Company

Superplastic Forming (SPF) of titanium 6Al-4V, with a standard grain size of about 8 μm, is typically performed at around 1650° to 1700°F (900° to 920°C). VSMPO in Russia has developed a fine grain version of the 6-4 alloy, with a grain size of about 1 μm, which is able to be superplastically formed at around 1425°F (775°C). Since this material diffusion bonds to itself as well as other standard grain size titanium alloys at this temperature, Superplastically Formed and Diffusion Bonded (SPF/DB) hardware can be produced. There are several advantages to using this lower forming temperature including a smaller amount of alpha case is developed on parts so there is less to remove, longer press platen and heater life, and less oxidation of the tool surface. In order to take advantage of these improvements, this material is currently being used in the production of SPF and SPF/DB aerospace components.

#### 5:00 PM

**Manufacturing of β-Titanium Ti-10V-2Fe-3Al Spin-Extruded Hollow Shafts for High Strength Power Train Applications in Aerospace and Automotive Industries:** Christian Machai<sup>1</sup>; Dirk Biermann<sup>1</sup>; <sup>1</sup>Technische Universität Dortmund

The aerospace and automobile sector strives to increase the efficiency of turbines and internal combustion engines. Fuel efficient engines demand components with a good combination of low mass and appropriate mechanical properties of the material used. Components which consist of a spin-extruded hollow shaft made of β-titanium alloy offer high specific strength in addition to good fatigue and corrosion resistance. The presented process route for manufacturing the hollow β-titanium shaft consists of a complex incremental forming-process followed by a turning operation to remove surface damages induced by the preceding forming processes. The machining operation of the undeformed titanium raw material and the deformed near-net-shape hollow shaft is investigated to identify the optimum process route for manufacturing an undamaged workpiece. Therefore, for different tool materials and machining strategies the static and dynamic process forces, tool wear, surface quality and metallographic samples of the undeformed and deformed peripheral workpiece area are analyzed.

#### 5:20 PM

**Superplastic Forming and Diffusion Bonding Process Design for Aerospace Component:** Yong-Nam Kwon<sup>1</sup>; <sup>1</sup>Korea Institute of Materials Science

Main interest in modeling superplastic forming (SPF) and diffusion bonding (DB) process is to predict an optimum pressurization schedule to control strain rate and to predict a resulting thickness distribution of forming parts. Finite element method (FEM) could be a useful guide to optimize SPF/DB processes. FEM is used to model the SPF/DB process of box and sandwich type

structures to predict the pressure-time curve. Also, other process variables were investigated for process optimization. In order to eliminate defects of the part such as folding or excessive thinning, a new pressurization scheme is proposed. Contrary to the conventional one-step pressurization, which causes the folding, two-step pressurization can eliminate the folding. SPF/DB process was carried out with Ti-6Al-4V sheet. SPF/DB formed part was cut down into pieces to check various features like dimensional accuracy, check thickness profile, hydrogen contamination, microstructure evolution and tensile properties.

#### 5:40 PM

**Application of Statistical Continuum Mechanics to Guide Processing of Aerospace Materials:** Dongsheng Li<sup>1</sup>; Hamid Garmestani<sup>1</sup>; <sup>1</sup>Georgia Institute of Technology

To guide processing of aerospace materials, inverse materials design manage the information flow from design to properties to microstructure to processing. Using a new representation method to characterize statistical correlation in microstructure, a set of spherical harmonics weight is utilized to represent microstructures in our work. Multi scale modeling including statistical continuum mechanics is used to predict microstructure evolution during processing. We also developed statistical continuum mechanics models to calculate microstructure determined properties, including elastic, plastic, electronic, transfer and magnetic properties of aerospace materials. The relationship among microstructure, properties and processing is established using statistical continuum mechanics. Explicit mathematical solution may be calculated to solve detailed processing steps on how to achieve target microstructure with desired properties. Examples on titanium and magnesium alloys will be presented to demonstrate the capability of statistical continuum mechanics on manufacturing of aerospace materials.

### Heterogeneous Nucleation and Initial Microstructure Evolution in Alloys and Colloids: Experiment II

**Sponsored by:** The Minerals, Metals and Materials Society, TMS Electronic, Magnetic, and Photonic Materials Division, TMS Materials Processing and Manufacturing Division, TMS Structural Materials Division, TMS: Alloy Phases Committee, TMS/ASM: Phase Transformations Committee

**Program Organizers:** Rainer Schmid-Fetzer, Clausthal University of Technology; Heike Emmerich, RWTH Aachen University; Frans Spaepen, Harvard University; Martin Glicksman, University of Florida; John Perepezko, University of Wisconsin, Madison

Tuesday PM

Room: 614

February 16, 2010

Location: Washington State Convention Center

**Session Chairs:** Ma Qian, University of Queensland; John Perepezko, University of Wisconsin - Madison

#### 2:00 PM Invited

**Grain Formation: The Interdependence between Grain Growth and Nucleation:** David StJohn<sup>1</sup>; Ma Qian<sup>1</sup>; Mark Easton<sup>2</sup>; <sup>1</sup>CAST CRC, University of Queensland; <sup>2</sup>CAST CRC, Monash University

A description of grain formation is presented that links the initial growth of a grain to its heterogeneous nucleation during the initial transient. It is proposed that, when potent nucleant particles are present, each nucleation event occurs very early in the initial transient. The grain size is determined by two components: (1) the distance a previously nucleated grain must grow in order to establish sufficient constitutional undercooling to be able to nucleate the next grain and (2) the additional distance to the most potent available nucleant particle that actually nucleates the new grain. The relative significance of these two components is illustrated by comparing magnesium and aluminium alloy systems. It will be further shown that the initial growth of a grain is spherical and that further nucleation events usually occur before growth breaks down to globular and dendritic morphologies. The factors affecting the limit of spherical growth are explored.

Tue. PM

# Technical Program

## 2:25 PM Invited

### **Modeling Transient Growth of Undercooled Solid Nuclei in the Melt:** *Markus Rettenmayr*<sup>1</sup>; Marcel Fink<sup>1</sup>; <sup>1</sup>Friedrich-Schiller-University Jena

The growth conditions of undercooled solid nuclei in a liquid are hardly accessible experimentally due to the involved small length scale and the initial rapid growth velocity. However, some insight can be obtained through modeling. Standard solidification models applying continuum theory can describe growth only starting from the point where local equilibrium is reached, since off-equilibrium models generally assume a steady-state which is not applicable for the growth of undercooled nuclei. Early stages of growth can be described with a continuum model that incorporates recent progress in the description of interfacial thermodynamics. Such a model is applied in the present study on binary aluminum alloys. It is shown that depending on the initial undercooling a nucleus can theoretically start growing with velocities in the order of m/s. Local equilibrium is reached after a time span in the order of microseconds. Further details regarding growth conditions, nucleus size etc. will be discussed.

## 2:50 PM

### **Investigation of Heterogeneous Nucleation of the Beta Phase in the System Ti-Al:** *Daniel-Hendrik Gosslar*<sup>1</sup>; Christian Hartig<sup>1</sup>; Robert Guenther<sup>1</sup>; Ulrike Hecht<sup>2</sup>; Ruediger Bormann<sup>1</sup>; <sup>1</sup>Hamburg University of Technology; <sup>2</sup>Access e.V.

The alloy system Ti-Al, in the composition range of 43 to 46 at.% Al, is suitable to study heterogeneous nucleation from the melt. Recent experiments proved directly heterogeneous nucleation of the alpha phase on in-situ formed borides. Additionally, from these experiments heterogeneous beta nucleation on ex-situ added borides is strongly suggested. The aim of this work is to investigate heterogeneous nucleation of the beta phase in more detail. For this purpose inoculation experiments are carried out for the Ti-45Al at.% alloy at different cooling rates. As appropriate inoculants titanium diboride particles are used. The resulting grain size in the as cast microstructures will be compared to free growth model calculations of the beta grain size. This comparison and atomic mismatch calculations in view of nucleation barrier are used to understand the microstructure evolution under the influence of heterogeneous beta nucleation.

## 3:10 PM

### **Heterogeneous Nucleation and Microstructure Formation in Peritectic Al-Ni Alloys:** Evelyn Doernberg<sup>1</sup>; Ricardo Siquieri<sup>2</sup>; Hailin Chen<sup>1</sup>; Heike Emmerich<sup>2</sup>; *Rainer Schmid-Fetzer*<sup>1</sup>; <sup>1</sup>Clausthal University of Technology; <sup>2</sup>RWTH Aachen

The Al-Ni system is an important model system for investigating heterogeneous nucleation and microstructure formation during peritectic solidification. Peritectic reactions with both types II and III are systematically investigated by a close coupling of phase-field (PF) simulation, thermodynamic modeling, and various experimental methods. Microstructure evolutions during directional solidification were experimentally studied and parameters including the secondary dendrite arm spacing, the thickness of the peritectic envelope, and the volume percent of each phase were semi-quantitatively estimated. All the experimental results were reasonably reproduced by simulations. Using the internal droplet technique and precise calorimetric experiments, together with the PF calculation, nucleation undercooling, nucleation rates and mechanisms of nucleation will be preliminarily evaluated. The role of peritectic transformation and direct precipitation of the peritectic phase for both types of peritectic reactions is discussed. This work is supported by the German Research Foundation (DFG) in the Priority Program "DFG-SPP 1296".

## 3:30 PM

### **Heterogeneous Nucleation in Liquid Immiscible Alloys:** *Markus Koehler*<sup>1</sup>; Lorenz Ratke<sup>1</sup>; <sup>1</sup>German Aerospace Center

Alloys being immiscible in the liquid state decompose into two liquid phases during cooling through the miscibility gap. In contrast to solidification where the solid phase is generally nucleated at inoculants or container walls, liquid immiscible alloys are thought to decompose via homogeneous nucleation. The process is badly investigated. Therefore we study heterogeneous nucleation in Al-base immiscible alloys (Al-Pb, Al-Bi) induced by inoculants like TiB<sub>2</sub>, TiC and ZrO<sub>2</sub>. We present experimental results on Al-Pb alloys cooled with different amounts of TiB<sub>2</sub> and ZrO<sub>2</sub> through the miscibility gap. The microstructure is analysed in 2D with SEM and light microscopy and also in 3D using x-ray tomography. The experiments show a pronounced effect of the inoculants. The average Pb drop size changes as well as the size distribution.

The experimental results are discussed with respect to classical theories of heterogeneous nucleation and newer models of nucleation and growth by Greer and co-workers.

## 3:50 PM Break

## 4:10 PM

### **Characterization of the Initial Stages of Phase Separation by Atom Probe Tomography:** *Michael Miller*<sup>1</sup>; Ai Serizawa<sup>1</sup>; <sup>1</sup>ORNL

The changes that occur in the solute distributions during homogeneous or heterogeneous nucleation growth and during spinodal decomposition may be characterized by atom probe tomography in model and complex engineering alloys. Statistical analysis of the distribution of the solute atoms in the three-dimensional data with the maximum separation envelope method and simulations enables clusters and embryos as small as 5 atoms to be detected, and their size, composition, morphology and number density to be estimated as the microstructure evolves. In this study, the initial phases of phase separation of the remarkably stable Ti-O-Y nanoclusters in a nanostructured ferritic steel will be discussed. This research was sponsored by the U.S. Department of Energy, Division of Materials Sciences and Engineering; research at the Oak Ridge National Laboratory SHaRE User Facility was sponsored by the Scientific User Facilities Division, Office of Basic Energy Sciences, U.S. Department of Energy.

## 4:30 PM

### **Nucleation of Strengthening Dispersions in a High-Strength Low-Carbon Steel:** *Mike Mulholland*<sup>1</sup>; David Seidman<sup>1</sup>; <sup>1</sup>Northwestern University

Steels often rely on the precipitation of several phases to derive their mechanical properties, which results in very complex microstructures. Blast Alloy (BA) 160 is a high-strength low-carbon steel that relies on the precipitation of copper and M<sub>2</sub>C carbide precipitates in a martensitic matrix for its high yield strength of 160 ksi. Since the copper and M<sub>2</sub>C precipitates are less than 5 nm in radius, 3-D local-electrode atom-probe (LEAP) tomography is employed to study their precipitation as a function of time. The majority of the copper and M<sub>2</sub>C carbides are co-located spatially at peak aging times and beyond, suggesting the heterogeneous nucleation of M<sub>2</sub>C precipitates on copper precipitates. The nucleation behavior of both copper precipitates and M<sub>2</sub>C carbides is investigated to determine whether or not this is the case.

## **Hume-Rothery Symposium: Configurational Thermodynamics of Materials: Session IV**

*Sponsored by:* The Minerals, Metals and Materials Society, TMS Electronic, Magnetic, and Photonic Materials Division, TMS Structural Materials Division, TMS: Alloy Phases Committee, TMS: Chemistry and Physics of Materials Committee

*Program Organizers:* Chris Wolverton, Northwestern University; Mark Asta, University of California, Davis; Gerbrand Ceder, Massachusetts Institute of Technology (MIT)

Tuesday PM Room: 212  
February 16, 2010 Location: Washington State Convention Center

*Session Chair:* To Be Announced

## 2:00 PM Invited

### **Chasing Exotic Binary Alloy Compounds: The Necessary Synergy of Cluster Expansion and High-Throughput Methods:** *Stefano Curtarolo*<sup>1</sup>; Gus Hart<sup>2</sup>; Ohad Levy<sup>3</sup>; <sup>1</sup>Duke University; <sup>2</sup>Brigham Young University; <sup>3</sup>NRCN

Predicting the stable crystal structures of alloys from their components is a major challenge of current materials research. Ab initio methods explore the phase stability landscape of binary alloys by calculating the formation enthalpies of a large number of structures, and identifying the minima at various component concentrations. Major methods of this type are cluster expansion (CE) and high-throughput ab initio calculations (HT). The CE explores structures on specific types of lattices while the HT method explores experimentally-known structures representing all crystal systems. The CE may find derivative superstructures missed by the HT but is not applicable off-lattice. Combining and reciprocally informing both methods resolve their respective drawbacks. We demonstrate this in a several technologically important Hf, Rh alloy systems. These results emphasize the complementary strengths of the CE and HT methods and the need for using both in searching for new stable compounds in metallic systems.



## 2:30 PM

**Informatics Applications to Electronic Structure Calculations:** *Krishna Rajan*<sup>1</sup>; Scott Broderick<sup>1</sup>; Tao Wang<sup>1</sup>; <sup>1</sup>Iowa State University

This presentation provides a demonstration of the types of classification and prediction possible when linking statistical learning methods with electronic structure calculations. Examples include the development of new methods to model the density of states and to explore methods of establishing correlations between crystal structure and crystal chemistry from data mining from DFT calculations.

## 2:50 PM

**The Prediction of Crystal Structure by Combining Machine Learning Knowledge Methods with First Principles Energy Methods:** *Gerbrand Ceder*<sup>1</sup>; <sup>1</sup>Massachusetts Institute of Technology (MIT)

De Fontaine's key work in cluster expansions enabled the ab initio prediction of structures with common underlying lattice. Finding ground states in topologically unconstrained space is still very difficult due to the complexity and high dimensionality of the coordinate space. As an efficient solution to this problem we have developed machine learning approaches that extract knowledge from a large set of experimental and computed information, and used these to rapidly direct accurate quantum mechanical techniques to the lowest energy crystal structure of a material. Knowledge is captured in a Bayesian probability network that relates the probability to find crystal structure at a given composition to structure and energy information at other compositions. We show that this approach is highly efficient in finding the ground states of binary metallic alloys and can be easily generalized to more complex systems. Using this approach we have already identified more than 400 new compounds.

## 3:10 PM Invited

**Predicting Solid - Aqueous Equilibria for Materials Design:** *Kristin Persson*<sup>1</sup>; <sup>1</sup>LBNL

Ab initio methods have proven very powerful in accurately predicting solid, surface and nano-scale properties. However, many technological problems involve materials in equilibrium with liquids, which are less straightforward to describe from first principles. We have addressed this issue for aqueous environments in an efficient manner by combining experimental data with ab initio calculations through a common point of reference system. We will briefly outline the method and show several examples of applications. In the first example we develop nanoparticle Pt Pourbaix diagrams to study size-dependent dissolution, relevant for fuel cell degradation mechanisms. Furthermore, we apply the formalism to the olivine LiFePO<sub>4</sub> to predict the change of particle shape under different pH and potential conditions in order to facilitate targeted synthesis by hydrothermal methods. Finally, we map out solid state stability for oxides, in order to identify rules of stabilization under severe corrosive aqueous conditions.

## 3:40 PM Break

## 4:10 PM Invited

**Transfer Matrix Approach to Quasi-1D Nanostructures with Cluster Interatomic Interactions:** *Vasyl Tokar*<sup>1</sup>; *Hugues Dreyssé*<sup>2</sup>; <sup>1</sup>Institute of Magnetism of NAS and MES; <sup>2</sup>Universite de Strasbourg, CNRS

Two types of epitaxial nanostructures (ENS) can be described in the framework of the lattice gas model: the ENS consisting of atoms of the same kind and filling some region on the surface in a submonolayer coverage regime or the ENS composed of a monolayer-thick binary alloy. ENS of this type include, in particular, such technologically important structures as nanowires (continuous quasi-1D ENS) and quasi-1D chains of magnetic islands for potential use in memory devices. Because of the quasi-1D character of the structures, they can be treated exactly within the transfer matrix approach (TMA) recently developed in the theory of protein folding and generalized by us to the theory of strained epitaxy. An important advance with respect to the traditional TMA is that cluster interactions within contiguous atomic chains of arbitrary length as well as the solid on solid restriction can be treated exactly within this approach.

## 4:30 PM

**Towards a First-Principles Understanding of the Iron Phase Diagram:** *Fritz Körmann*<sup>1</sup>; Alexey Dick<sup>1</sup>; Blazej Grabowski<sup>1</sup>; Tilmann Hickel<sup>1</sup>; Jörg Neugebauer<sup>1</sup>; <sup>1</sup>Max-Planck-Institut für Eisenforschung

Accurate tools for the theoretical prediction of material properties, such as the specific heat capacity or free energy, become increasingly important for a computational design of new materials. Density functional theory has emerged as one of the most powerful tools for such predictions. While originally developed and applied as a groundstate (T=0 K) theory, the combined concepts of DFT and finite temperature models evolved nowadays to a state making reliable and accurate predictions of a wide range of materials properties possible. In this talk we discuss the thermodynamic concepts capturing the vibrational, electronic, and magnetic excitations from DFT. To describe the magnetic contributions new methodologies based on the Heisenberg model were developed allowing for the first time an ab initio based quantitative prediction of the magnetic free energy [PRB 78, 033102 (2008)]. The predictive power of the proposed theoretical framework is verified by comparison with experimental data.

## International Symposium on High-Temperature Metallurgical Processing: Smelting and Reduction Processes

*Sponsored by:* The Minerals, Metals and Materials Society, TMS Extraction and Processing Division, TMS: Pyrometallurgy Committee  
*Program Organizers:* Jaroslaw Drelich, Michigan Technological University; Jiann-Yang Hwang, Michigan Technological University; Tao Jiang, Central South University; Jerome Downey, Montana Tech

Tuesday PM Room: 619  
February 16, 2010 Location: Washington State Convention Center

*Session Chair:* Tao Jiang, Central South University

## 2:00 PM

**Industrial Operation of JAE Nickel Smelting Technology at Jinchuan Nickel Smelter:** Min Zhou<sup>1</sup>; Aidong Wan<sup>1</sup>; Guang Li<sup>1</sup>; *Ross Baldock*<sup>2</sup>; Harry Li<sup>2</sup>; <sup>1</sup>Jinchuan Non Ferrous Metals Corp.; <sup>2</sup>Ausmelt Ltd

A commercial nickel smelter using JAE nickel smelting technology has been successfully commissioned and put into the smooth operation at Jinchuan Non-ferrous Metals Corporation China since August 2008, after 2.5 years design and construction works. The paper provides details of this nickel smelting project, including the technical evaluation, demonstration plant investigation, engineering design, plant commissioning and operation. Emphasis has been given in comparison between the design targets and actual performance of the plant.

## 2:20 PM

**Arc Plasma Smelting of Niobium Pentoxide towards Production of Nb Metal:** *Bijan Nayak*<sup>1</sup>; Barada Mishra<sup>1</sup>; <sup>1</sup>IMMT

Smelting of niobium pentoxide was carried out in an extended arc plasma reactor using carbon as reductant. Carbon in the form of graphite was used as the reducing agent in the smelting. Niobium pentoxide powder with 98.5% purity and grain size below 63 micron, was taken as the starting raw material. Smelting of the charge (taken in the form of a mixture of oxide and carbon) was carried out in an arc plasma reactor at 100g scale for 15-20 min. The smelted product obtained in the form of chunk was characterized by XRD for identification of Nb and other impurity phases. Optical microscopy, SEM, EDS and micro Raman spectroscopy were employed to study the morphology and corroborate the occurrence of Nb. Chemical analysis of the product was done by ICPS and was found to contain 97.5% Nb with 86% maximum recovery.

## 2:40 PM

**Carbothermic Reduction of Niobium Concentrate:** *Joao Ferreira Neto*<sup>1</sup>; Flavio Beneduce Neto<sup>1</sup>; Cyro Takano<sup>2</sup>; <sup>1</sup>Institute for Technological Research - IPT; <sup>2</sup>University of Sao Paulo

Ferro Niobium is produced by aluminothermic reduction of the niobium concentrate. However, the niobium concentrate has impurities, such as phosphorus, lead and tin, which can contaminate the Ferro Niobium. Therefore, the niobium concentrate must be refined before aluminothermy. The carbothermic reduction of niobium concentrate was investigated as a method to promote the

Tue. PM

# Technical Program

impurities removal. The carbothermic reduction of niobium concentrate was investigated in self-reducing briquettes in temperatures between 1100 and 1250°C, aiming to promote the reduction of impurities, mainly phosphorus. The reduction was carried out using graphite as carbonaceous material. After reduction, the briquettes were evaluated in scanning electronic microscope. It was observed that the iron oxide of the niobium concentrate was simultaneously reduced with oxides of phosphorus, lead and tin, producing an alloy Fe-Sn-P, with phosphorus content up to 20%. Based on the results it was obtained an apparent activation energy of 296,3 +/- 29 kJ/mol.

## 3:00 PM

**Volatilization of Antimonite in Nitrogen-Oxygen Atmospheres:** *Rafael Padilla*<sup>1</sup>; Gustavo Ramirez<sup>1</sup>; Alvaro Aracena<sup>1</sup>; Maria Ruiz<sup>1</sup>; <sup>1</sup>University of Concepcion

The vaporization of antimonite (Sb<sub>2</sub>S<sub>3</sub>) was investigated in the temperature range 600-900°C in a conventional thermogravimetric apparatus. The study was conducted in inert (N<sub>2</sub>) and oxidizing (N<sub>2</sub> - O<sub>2</sub>) atmospheres under various gas flow rates. The results indicated a linear behavior of vaporization of the sample at temperatures above 700°C. Thus by using the vaporization kinetic constants, activation energy of 124 kJ/mol was determined for the vaporization in nitrogen gas. On the other hand, the weight loss due to volatilization of antimonite in the presence of oxygen occurs up to a certain extent depending on the temperature and partial pressure of oxygen. 20% of total vaporization occurred at 700°C while at 900°C the total vaporization was about 60%. The incomplete volatilization of antimonite is due to the formation of non-volatile oxides since the weight loss increases with a decrease in partial pressure of oxygen.

## 3:20 PM

**The Optimization of the Coke and Agglomerate Quantity in Lead Production in "Water-Jacket" Furnace:** *Ahmet Haxhijaj*<sup>1</sup>; Egzon Haxhijaj<sup>2</sup>; <sup>1</sup>University of Prishtina; <sup>2</sup>American University in Kosovo

Paper contains the analysis of technological process depending on the composition of lead (Pb) in agglomerate, and the theoretical and real rapport of coke consumption per tone of technical lead produced. The findings are based in the work of "Water-jacket" furnace in Trepça. Paper brings the results of theoretical and experimental studying, along with analytical and graphical analyses of regional thermal balance depending on the composition of lead, and the coke quantity in load. While analyzing the technological process of technical lead production we have been searching for the growth of technical lead quantity produced depending on lead percentage in agglomerate and the air that is enclosed in the furnace. Moreover, we aimed to optimize the percentage of lead in agglomerate and the parameters of the process. Simultaneously, keeping the attention to the growth of technical lead produced, the minimization of energy consumption, and the minimization of environment pollution.

## 3:40 PM Break

## 3:55 PM

**Influences of MgO on Roasting Properties of Iron Ore Oxidized Pellets:** *Xiaohui Fan*<sup>1</sup>; Min Gan<sup>1</sup>; Tao Jiang<sup>1</sup>; Xuling Chen<sup>1</sup>; Lishun Yuan<sup>1</sup>; <sup>1</sup>Central South University

The roasting properties of iron ore oxidized pellets, such as the mechanical strength, the suitable roasting temperature and the remnant contents of FeO, are affected by adding MgO. As the contents of MgO increased, the strength of roasted pellets is decreased, the range of suitable roasting temperature is narrowed, and the remnant FeO of pellets roasted in high temperature is increased. According to the analysis of spectrum and microstructure, and combining the theory of solid reaction and the phase diagram, the main two reasons that affecting the roasting properties of pellets are that MgO dissolves in magnetite, and MgO reacts with Fe<sub>2</sub>O<sub>3</sub> to form magnesium ferrite.

## 4:15 PM

**Research on the Intensifying Reduction Technology Based on Mechanically Activated Ilmenite Ore:** *Yufeng Guo*<sup>1</sup>; Hemei Liu<sup>1</sup>; Tao Jiang<sup>1</sup>; Guanzhou Qiu<sup>1</sup>; <sup>1</sup>Central South University

This text regarded Panzhihua ilmenite as the research object, systematically studied the influence law of reductive iron oxide affected by the ultra-fine ilmenite powder which was prepared from one part of raw material. The research showed that reduction process of ilmenite was accelerated by adding super-fines. The degree of metallization was investigated, and a metallization rate of

88.30% was obtained under the condition of superfine powder fineness 80%-0.010mm, Superfine powder /Ore 3:97, whereas no super-fines was 84.30%. The growth of reduction iron crystal in ilmenite iron oxide was investigated by light microscopy and scanning electron microscopy. Through the analysis, it was found that the metal iron content and micro-pore in reduced ilmenite which was added super-fines significantly increased compared with the control (without super-fines addition).

## 4:35 PM

**Study on Reduction Roasting and Separation of Nickeliferous Laterite by Microwave Heating:** *Yi Lingyun*<sup>1</sup>; *Huang Zhucheng*<sup>1</sup>; <sup>1</sup>Central South University

Nickeliferous laterite is difficult to achieve ideal indexes by conventional physical process. In this paper, the reduction roasting-magnetic separation of coal-containing nickeliferous laterite briquette was carried out by microwave heating and traditional roasting. The results show that traditional roasting has many difficulties such as needs higher temperature, longer roasting time and easily leads to lower reduction of the center. Reduction roasting by microwave radiation can heat the whole pellet simultaneously and give priority to heat coal particles and nickel minerals, which is conducive to the form of nickel-iron grains. The electromagnetic field effect of microwave can also improve the growing up and movement of Ni-Fe grains. The reduction roasting by microwave heating for 45min at power of 2kw can obtain the concentrate of 5.21% nickel and recovery of 72.01% while using traditional roasting for 150min at 1150°, the concentrate of 2.24% nickel and 30.96% recovery can be got.

## 4:55 PM

**Study on Preparation of Titanium-Rich Material From Ilmenite by Reduction-Magnetic Separation Process:** *Yufeng Guo*<sup>1</sup>; Dan Huang<sup>1</sup>; Guangzhou Qiu<sup>1</sup>; Tao Jiang<sup>1</sup>; <sup>1</sup>School of Minerals Processing and Bioengineering, Central South University

The preparation of Ti-rich material from Panzhihua-Xichang ilmenite in China was investigated by solid-state reduction-magnetic separation. The results indicated that high metallization of reduction product could be obtained by adding alkali metal additives under low reducing temperature, which realized the effective separation of iron and titanium. The ilmenite was added 3% additives and roasted at 1100° for 180 min, a Ti-rich material with 75% TiO<sub>2</sub> and 90% recovery could be obtained by grinding-magnetic separation. Compared with no alkali metal additives, the reducing temperature was decreased from 1250°~1280° to 1100° and TiO<sub>2</sub> grade increased by about 10%. The mechanism research indicated that the additive had the function of strengthening solid diffusion and could reduce the effect of Mg<sup>2+</sup> on the stability of Fe<sub>2</sub>TiO<sub>5</sub>, which had realized the reduction of iron oxidation in the ilmenite and the crystal grain growth of metal iron under low temperature.

## 5:15 PM

**The Kinetics of Oxidation of Tellurium Sulfide Concentrate:** *Edgar Blanco*<sup>1</sup>; <sup>1</sup>Western Utah Copper Company

A thermodynamic and kinetics investigation of the oxidation of tellurium in sulfide concentrate to TeO<sub>2</sub> at high temperature was carried out as part of a new process to extract tellurium from its sulfide ore. The kinetics of the reaction was determined by measuring the weight change of a sample with time at temperatures between 700-1100°C. The reaction rate followed the Shrinking-Unreacted-Core model under chemical reaction control. While most base metals remained with the calcine during the oxidation, almost all tellurium was volatilized in agreement with thermodynamic analysis.



### Jim Evans Honorary Symposium: Metal Flow, Bubbles, and Inclusions Behavior in Refining and Reduction Vessels

*Sponsored by:* The Minerals, Metals and Materials Society, TMS Extraction and Processing Division, TMS Light Metals Division  
*Program Organizers:* Ben Li, University of Michigan; Brian G. Thomas, University of Illinois at Urbana-Champaign; Lifeng Zhang, Missouri University of Science and Technology; Fiona Doyle, University of California, Berkeley; Andrew Campbell, WorleyParsons

Tuesday PM Room: 620  
 February 16, 2010 Location: Washington State Convention Center

*Session Chair:* Stavros Argyropoulos, University of Toronto

#### 2:30 PM Introductory Comments

#### 2:40 PM

**Plume Characteristics in Gas Stirred Ladles:** *Piotr Scheller*<sup>1</sup>; *Olena Volkova*<sup>1</sup>; *Dmitri Ryabov*<sup>1</sup>; <sup>1</sup>Freiberg University

In our investigations trials in water models were performed as well as in the industrial process in the 30t ladles. In water models the phenomenology of plume formation and development was investigated and some characteristic parameter estimated. In the industrial trials the evolution of the geometry of the "eye" with gas flow rate was measured as a function of Ar flow rate. Using this basic information the flow velocity in the plume and its geometry as well as the bubble size were estimated for usual industrial process conditions. Using the dimension analysis the similarity criterion for the plume flow in the water model and in liquid steel is developed. The experimental results from water model are compared with the industrial one. The results obtained give a solid basis for the development of process models and establish the similarity criterion.

#### 3:05 PM

**Development of Online Sensors for Bubble Stirred Vessels:** *Geoffrey Brooks*<sup>1</sup>; *Xiaodong Xu*<sup>1</sup>; *William Yang*<sup>2</sup>; <sup>1</sup>Swinburne University of Technology; <sup>2</sup>CSIRO Minerals

Bubbling is commonly used in pyrometallurgical vessels to enhance mass and heat transfer. These processes can be difficult to monitor because of the severe operating conditions associated with these processes. In this paper, we describe the development of techniques for simultaneously analysing image, sound and vibration signals associated with bubbling in vessels using multivariate statistical analysis to form new "latent" variables from the combined signals to control the process. This approach has been tested over a range of conditions for a bottom stirred cold model with two liquid layers (to simulate metal and slag) and the effect of combining different signals (e.g. sound and image, vibration and sound) has also been analysed. These results are examined in terms of what the signals tells us about bubbling but also with the view of developing practical online sensors for pyrometallurgical processes.

#### 3:30 PM

**Fluid Flow and Inclusion Behavior in a Continuous Billet Casting Tundish:** *Qinglin He*<sup>1</sup>; *Geoff Evans*<sup>1</sup>; <sup>1</sup>University of Newcastle

The fluid flow and inclusion behaviour in a continuous billet casting tundish was studied by oil/water modeling. Oil content and droplet size distribution were measured at different locations in the tundish under various casting conditions, using high speed videoing technology in conjunction with a flow-through optical cell. Focus of this study was, in particular, placed on the behavior of macro size inclusions (>100µm), which are detrimental to the mechanical properties of steel. It was found that inclusion removal efficiency was affected by a number of factors, such as ladle stream condition, casting rate, initial inclusion concentration, tundish depth, ladle change, flow control device and shroud type. Tundish depth had the most significant effect on inclusion removal in the tundish. However, there is a critical tundish depth, beyond which it had no effect on inclusion removal.

#### 3:55 PM

**Physical Modeling of Slab Caster Tundish to Improve Yield and Quality of Steel:** *Dipak Mazumdar*<sup>1</sup>; <sup>1</sup>Indian Institute of Technology-Kanpur

To minimize the volume of tundish skull (residual liquid left behind at the end of a sequence casting) in two different slab casting tundishes, an extensive

water modeling investigation has been carried out. On the basis of such, appropriate modifications in the existing tundish designs (i.e. in terms of tundish floor, dam and pouring box) required to improve skull losses were derived and implemented in the shop floor. Full scale industrial trials show almost 60 to 70% reductions in tundish skull at the end of a sequence casting. Parallel to such, Residence Time Distribution measurements and microscopic examination of steel samples (collected from shroud, mono block regions and solidified slab) confirmed that modified and original tundish designs have similar inclusion floatation efficiency. Modified tundish designs have since been implemented in the two steel melt shops and practiced regularly in sequence casting.

#### 4:20 PM Break

#### 4:35 PM

**Time Dependent MHD Models for Aluminium Reduction Cells:** *Valdis Bojarevics*<sup>1</sup>; *Koulis Pericleous*<sup>1</sup>; <sup>1</sup>University of Greenwich

The time dependent MHD or stability problems for the aluminium reduction cells are typically restricted to the mathematical developments without the inclusion of the electrolyte channels. However, according to the well known Evans-Moreau model, the presence of electrolyte channels in the stationary case increases very significantly the interface deformation. The theory and numerical model of the reduction cell can be extended to the cases of variable bottom of aluminium pad and the variable thickness of the electrolyte with the presence of the channels. We present instructive analysis of different physical coupling factors affecting the magnetic field, electric current, velocity and wave development with animated examples for the high amperage cells. The results indicate that the 'rotating wave' instability is dominant in the absence of the channels, while the channels exert a stabilizing effect with a 'sloshing' parametrically excited MHD wave development in the aluminium production cells.

#### 5:00 PM

**Modeling on Multiphase Fluid Flow in Aluminum Electrolysis Cell:** *Yufeng Wang*<sup>1</sup>; *Lifeng Zhang*<sup>1</sup>; <sup>1</sup>Missouri University of Science and Technology

Water modeling and mathematical modeling were established to study the fluid flow related phenomena in an aluminum electrolysis cell. The VOF multiphase fluid flow modeling was developed and validated by the water modeling - Laser Doppler Velocimeter (LDV) measurement in a full scale water model. Effects of the slot design and the tilted angle of the anode on the behavior of bubbles under the anode were studied. The slot under anode facilitates the escape of bubbles. With flat bottom anode, the slot is the main releasing path for bubbles. Without slot, a thicker gas film forms under the anode and this cause great energy consumption and induce violent fluctuation in the slot. By increasing the tilted angle of the anode, bubbles have multi-paths to escape, from the slot or moving along the tilted anode bottom and escaping from the curved end of the anode.

#### 5:25 PM

**Research and Development of Three-Dimensional Electrochemical Reactors at UC Berkeley and ICPF Prague – Overview:** *Vladimir Jiricny*<sup>1</sup>; *James Evans*<sup>2</sup>; <sup>1</sup>Institute of Chemical Process Fundamentals, ASCR, v.v.i.; <sup>2</sup>University of California

The contribution is focused on the research and development of three-dimensional (fluidized and spouted bed) electrochemical reactors conducted at Berkeley and ICPF Prague. The overview of principles, experimental results on electrowinning of metals and organic synthesis and the reactor design will be presented. Some excursion to applications of these results will be shown.

#### 5:50 PM

**Importance of Microexothermicity in the Assimilation and Recovery of Additions in Liquid Metals:** *Zhi Li*<sup>1</sup>; *Stavros Argyropoulos*<sup>1</sup>; <sup>1</sup>University of Toronto

Whenever exothermicity takes places during the course of assimilation of additions in liquid metals, two types have been identified, namely, Macroexothermicity and Microexothermicity. The former type of exothermicity is exhibited when a relatively small amount of addition is immersed into a large quantity of liquid metal; the latter type, on the other hand, is displayed when a powder mixture compacts consisted of different elements reacts exothermically to form intermetallics. The impact of Microexothermicity in the assimilation and recovery of compacted powder additions in liquid metals will be examined. Experimental work involving cylindrical compacted powder additions in liquid

Tue. PM

# Technical Program

Aluminum and liquid Magnesium will be presented. The additions used in this experimental work include Mn-Al,Zr-Zn and Zr-Al cylindrical powder compacts. The Microexothermicity, assimilation, and recovery data of these additions in liquid metals such as Aluminum and Magnesium will be compared. In addition, various ramifications of these comparisons in different liquid metal operations will be presented.

## Magnesium Technology 2010: Fatigue, Failure, and Wear

*Sponsored by:* The Minerals, Metals and Materials Society, TMS Light Metals Division, TMS: Magnesium Committee

*Program Organizers:* Sean Agnew, University of Virginia; Eric Nyberg, Pacific Northwest National Laboratory; Wim Sillekens, TNO; Neale Neelameggham, US Magnesium LLC

Tuesday PM Room: 613  
February 16, 2010 Location: Washington State Convention Center

*Session Chairs:* Michele Manuel, University of Florida; Anumalasetty Nagasekhar, The University of Queensland

### 2:00 PM

**Effect of Shot Peening on High Cycle Fatigue Performance of Mg-10Gd-3Y-0.5Zr Magnesium Alloy:** Wencai Liu<sup>1</sup>; Jie Dong<sup>1</sup>; Ping Zhang<sup>2</sup>; Li Jin<sup>1</sup>; Wenjiang Ding<sup>1</sup>; <sup>1</sup>Shanghai Jiao Tong University; <sup>2</sup>BTU-Cottbus

The effect of shot peening on high cycle fatigue performance of four states Mg-10Gd-3Y-0.5Zr magnesium alloy which named as as-cast, cast-T6, as-extruded and extruded-T5 GW103 were investigated. The glass bead with an average diameter of 0.35mm was adopted for shot peening and Almen intensity was arranged from 0.05 to 0.60mmN. The surface characteristics as roughness, microhardness and residual stresses produced by shot peening were measured. The microstructures of deformation layer of the peened specimens were observed by TEM and fracture surfaces were analyzed using SEM. The results show that the optimum Almen intensities of the four alloys are 0.40, 0.50, 0.10 and 0.10 mmN, respectively. The fatigue strengths of the four states peened specimens with the optimum Almen intensities were 30, 20, 65 and 75 MPa stronger than those of the reference unpeened specimens, the improvement of about 35%, 19%, 43% and 45% have been achieved, respectively.

### 2:20 PM

**Monotonic and Multiaxial Cyclic Behavior of the Extruded AZ31B Magnesium Alloy:** Jafar Albinmousa<sup>1</sup>; Hamid Jahed<sup>1</sup>; Steve Lambert<sup>1</sup>; <sup>1</sup>University of Waterloo

Recently, focus has been directed towards using magnesium alloys as a material for automobile vehicle structural components. In automotive applications, load bearing components are subjected to multiaxial fatigue loading. Thus, a better understanding of multiaxial fatigue behavior is a necessary step in the fatigue design of these components. This paper focuses on the monotonic and uniaxial and multiaxial cyclic behavior of extruded AZ31B magnesium alloy. Flat or tubular specimens were machined from large AZ31B extrusion sections. Two loading modes were considered for multiaxial tests: tensile and shear. All tests were performed at standard laboratory and in as-received conditions. Cyclic axial test results indicate that AZ31B exhibit asymmetrical cyclic behavior due to twinning. In contrast, cyclic torsional behavior was found to be symmetric. Energy, as a fatigue parameter, has been used to correlate the test results.

### 2:40 PM

**Fatigue Evaluation of Friction Stir Spot Welds in Magnesium Sheets:** J. Jordan<sup>1</sup>; M. Horstemeyer<sup>1</sup>; Jenna Grantham<sup>1</sup>; <sup>1</sup>Mississippi State University

In this study, the fatigue crack growth rate of magnesium AZ31 in friction stir spot welded is experimentally determined. Interrupted load control cyclic tests were conducted on single weld lap-shear coupons to determine fatigue crack growth rates. The coupons were stopped at regular intervals and the crack length was measured via an optical microscope. In addition, fractured coupons were examined under a scanning electron microscope with the intent to correlate striation spacing to the interrupted crack growth tests. The interrupted tests also revealed the percentage of initiation life associated with the friction stir spot weld joint. The crack growth rates conducted in this study were used

to validate a long crack growth approach employed to predict the fatigue life of the friction stir spot weld coupons.

### 3:00 PM

**Atomistic Simulations of Fatigue Crack Growth and the Influence of Temperature on Fatigue Behavior in Magnesium Crystals:** Tian Tang<sup>1</sup>; Sungho Kim<sup>1</sup>; Mark F. Horstemeyer<sup>1</sup>; <sup>1</sup>Mississippi State University

The fatigue behavior of magnesium single crystals at various temperature and the fatigue crack growth in magnesium bicrystals has been computational simulated at nanoscale. The computational method used in this study is Embedded Atom Method (EAM), potentials. Five crystal orientation of initial crack, orientation C-(10<sup>-10</sup>)[0001], orientation D-(1<sup>-210</sup>)[0001]orientation F-(0001)[1<sup>-210</sup>], orientation G (10<sup>-11</sup>)[<sup>-1012</sup>], and orientation I (10<sup>-12</sup>)[10<sup>-11</sup>] were analyzed for verifying the influence of temperature on fatigue behavior. The critical values of maximum strains at which the cracks start growing for different orientation increase with increasing temperature. The maximum strain \949max of cyclic loading was chosen as 0.8 of the critical value determined in uniaxial tension test. The fatigue crack growth rate of different orientation decrease with increasing temperature. In order to verify the effects of grain boundary, the mechanism of fatigue propagation was also investigated in several bicrystal model.

### 3:20 PM

**Structure-Property Evaluation of Fatigue Damage in a Magnesium AM30 Alloy:** J. Bernard<sup>1</sup>; J. Jordan<sup>1</sup>; M. Horstemeyer<sup>1</sup>; H. El Kadiri<sup>1</sup>; <sup>1</sup>Center for Advanced Vehicular Systems, Mississippi State University

The purpose of this study is to experimentally evaluate the fatigue characteristics of an extruded AM30 magnesium alloy in regards to structure-property relations. Fully-reversed, strain control fatigue tests were conducted in the extruded direction. Specimens were machined from locations with varying grain size and texture gradients. Using scanning electron microscopy, the fracture surfaces of the fatigued specimens were analyzed in order to develop relationships between the microstructure and the fatigue behavior of this material. Parallels between microstructural features such as particle size, grain size, Taylor factor, nearest neighbor distance and the number of cycles to failure were determined. These results were then used to develop a microstructure-based multistage fatigue model (MSF) employed to predict the variability of the fatigue results.

### 3:40 PM Break

### 4:00 PM

**Very High Cycle Fatigue Property of Magnesium Alloy in Axial Loading and Rotating Bending:** Tatsuo Sakai<sup>1</sup>; Yosuke Nakamori<sup>1</sup>; Noriyuki Ninomiya<sup>1</sup>; Mitsuji Ueda<sup>2</sup>; <sup>1</sup>Ritsumeikan University; <sup>2</sup>KS TECHNOS

Lightness and low value of Young's modulus are typical characteristics for Magnesium alloy when they are applied to the mechanical components in the engineering application. Fatigue property of this alloy is also important factor in order to ensure the reliability of the mechanical structures. Especially, the fatigue property in the long life region should be clarified for the fundamental design data to provide the safety of the mechanical structures in the long term use. From this point of view, fatigue tests were performed for the magnesium alloy(AMCa602) in axial loading and rotating bending. Such fatigue tests were carried out up to gigacycle regime to examine the very high cycle fatigue characteristics. S-N properties obtained in both loading types are compared to each other. Fracture surfaces of failed specimens were observed by means of SEM and fracture mechanisms of this alloy was discussed from view points of fractography and fracture mechanics.

### 4:20 PM

**Numerical Modeling of Failure in Magnesium Alloys during Crush Simulations:** Jonathan Rossiter<sup>1</sup>; Kaan Inal<sup>1</sup>; Raja Mishra<sup>2</sup>; <sup>1</sup>University of Waterloo; <sup>2</sup>General Motors R&D Center

Numerical modeling of failure of magnesium tubes during crush simulations is performed for commercial AZ31 magnesium alloy. LS-DYNA material model MAT\_124 along with experimental stress-strain data from tensile and compression tests of the extruded tube have been used to capture the asymmetry in the tension and compression response over a range of strain and strain rates. A combination of three different failure criteria, consistent with observations of fractured components, has been implemented in the finite element simulations to accurately reproduce the experimental observations during axial



compression tests of round tubes. The presentation will include simulations of failure of magnesium tubes with both round and rectangular cross-sections and with different initial texture and tension/compression asymmetry. The predicted numerical responses of these tubes will be compared to experimental observations.

**4:40 PM**

**Dry Sliding Wear Behavior of AE44 Magnesium Alloy Reinforced with Saffil Alumina Fibers:** Bin Hu<sup>1</sup>; Liming Peng<sup>1</sup>; Bob Powell<sup>2</sup>; Michael Lukitsch<sup>2</sup>; Anil Sachdev<sup>2</sup>; Xiaojin Zeng<sup>1</sup>; <sup>1</sup>Shanghai Jiao Tong University; <sup>2</sup>General Motors Corporation

The effect of 15 volume percent short alumina fibers for improving the wear resistance of the creep-resistant magnesium alloy AE44 was determined by pin-on-disk test under dry sliding wear conditions. The alumina fiber-reinforced AE44 composites were prepared by squeeze casting. Their wear behavior was determined for variations in sliding speed, applied load, and test temperature. Under all conditions the fibers improved wear resistance although the degree was influenced by fiber orientation and the nature of the binder (alumina or silica) used in the alumina fiber preforms.

**5:00 PM**

**Influence of Cerium on Stress Corrosion Cracking in AZ91D:** Meredith Heilig<sup>1</sup>; Daniela Zander<sup>2</sup>; David Olson<sup>1</sup>; Brajendra Mishra<sup>1</sup>; Norbert Hort<sup>3</sup>; Gerald Klaus<sup>4</sup>; Andreas Buehrig-Polaczek<sup>4</sup>; Joachim Gröbner<sup>5</sup>; Rainer Schmid-Fetzer<sup>5</sup>; <sup>1</sup>Colorado School of Mines; <sup>2</sup>TU Dortmund; <sup>3</sup>GKSS Research Centre; <sup>4</sup>Foundry-Institute of RWTH Aachen; <sup>5</sup>TU Clausthal

Applications of Mg-Al alloys are continually increasing, prompting the need to understand the corrosion behavior of these materials in loading conditions. This paper considers the effect of cerium additions on the stress corrosion cracking in the Mg-Al-Zn alloy AZ91D. The two dominant phases in the AZ91D microstructure are intermetallic Mg<sub>17</sub>Al<sub>12</sub> precipitates interspersed within the Mg-rich matrix. The addition of cerium is thought to improve the corrosion performance of AZ91 alloys through microstructural modifications. Formation of Ce-Al intermetallics appear to minimize the volume fraction of Mg<sub>17</sub>Al<sub>12</sub>, thereby increasing the aluminum content of the Mg-rich matrix. Electrochemical impedance spectroscopy is used to characterize and compare the oxide films formed in AZ91D with varying amounts of cerium added. Immersion, potentiostatic polarization, and slow strain rate testing (SSRT) of AZ91D and AZ91D+Ce alloys were used to explore the influence of cerium on stress corrosion cracking behavior and passive film properties of AZ91D.

**5:20 PM**

**In-situ Fracture Investigations of YAl<sub>2</sub> Reinforced Magnesium Matrix Composite:** Zhaohua Ling<sup>1</sup>; Guoqing Wu<sup>1</sup>; Jianku Shang<sup>2</sup>; Sujie Wang<sup>1</sup>; Zheng Huang<sup>1</sup>; <sup>1</sup>Beihang University; <sup>2</sup>University of Illinois, Urbana-Champaign

A novel kind of magnesium matrix composites reinforced with YAl<sub>2</sub> intermetallic particles was prepared by stir-casting. The microstructure of the composite was observed by optical microscope and scanning electron microscope (SEM). The fracture process was in-situ investigated by the SEM during dynamic tensile test. The results show that the microcracks initiate both in the alloy matrix and interfaces, and then propagate continuously in the alloy matrix or along the interfaces. The YAl<sub>2</sub> particles can impede propagation of microcracks during the fracture process. The dominant crack mainly propagates along the boundary of the particle-dense area and particle-rare area and which finally leads to the failure of the composite. The matrix failure plays a significant role in the failure mechanisms of this kind of composite materials.

### Magnesium Technology 2010: Magnesium - Rare Earth Alloys

*Sponsored by:* The Minerals, Metals and Materials Society, TMS Light Metals Division, TMS: Magnesium Committee  
*Program Organizers:* Sean Agnew, University of Virginia; Eric Nyberg, Pacific Northwest National Laboratory; Wim Sillekens, TNO; Neale Neelameggham, US Magnesium LLC

Tuesday PM Room: 612  
February 16, 2010 Location: Washington State Convention Center

*Session Chairs:* Sean Agnew, University of Virginia; Jian-Feng Nie, Monash University

**2:00 PM**

**Development of High Ductility Magnesium-Zinc-Cerium Extrusion Alloys:** Alan Luo<sup>1</sup>; Raj Mishra<sup>1</sup>; Anil Sachdev<sup>1</sup>; <sup>1</sup>General Motors Corporation

It has been shown in a previous study that the ductility of Mg-0.2%Ce alloy extrusion is higher than that of magnesium and other known magnesium alloys. However, the yield and tensile strengths of the Mg-0.2%Ce alloy remain low. In this paper, it is found that a small addition of zinc (around 2%) can significantly improve the strength of the Mg-0.2%Ce alloy (96% in yield strength and 32% in ultimate tensile strength) with only a slight reduction in elongation (27.4% vs. 31%). The microstructure of Mg-Zn-Ce alloys at various extrusion speeds is characterized using optical metallography, electron probe micro-analysis (EPMA), and electron backscattered diffraction (EBSD) techniques. It is concluded that while Zn provides strength through solid solution strengthening, Ce increases the ductility of the Mg-Zn-Ce alloys via improved texture.

**2:20 PM**

**Effect of Extrusion Temperature on Microstructure and Mechanical Properties of Mg-8.5Gd-2.3Y-1.8Ag-0.4Zr Alloy Solid State Recycled by Hot Extrusion:** Qudong Wang<sup>1</sup>; Jie Chen<sup>1</sup>; Tao Peng<sup>1</sup>; Zheng Zhao<sup>1</sup>; Wenjiang Ding<sup>1</sup>; <sup>1</sup>National Engineering Research Center of Light Alloy Net Forming, Shanghai Jiao Tong University

The effect of extrusion temperature on microstructure and mechanical properties of Mg-8.5Gd-2.3Y-1.8Ag-0.4Zr (wt.%) alloy solid state recycled by hot extrusion was investigated. The recycled specimens have very fine microstructure due to dynamic recrystallization during extrusion. Higher extrusion temperature tends to coarsen grains, especially when extruded at 773K. The age hardening response as well as UTS of recycled samples are remarkably improved with increased extrusion temperature. Better metallurgical bonding and reduced extrusion precipitation with increased extrusion temperature are responsible for the improvements. However, elongation decreases rapidly to 1.3% for the sample recycled at 773K probably because of coarsened grains and excessive cavitations. The sample recycled at 723K shows the best combination of strength and elongation after ageing treatment, whose TYS, UTS and elongation reach 346MPa, 390MPa and 4.2%. Therefore, it is necessary to extrude at lower temperature while ensure fully metallurgical bonding of chips to obtain excellent strength and elongation of recycled samples.

**2:40 PM**

**Structure of  $\beta_1$  precipitates in Mg-Zn based alloys: Co-Existence of MgZn<sub>2</sub> and Mg<sub>4</sub>Zn<sub>7</sub> Phases:** Alok Singh<sup>1</sup>; Julian Rosalie<sup>1</sup>; Hidetoshi Somekawa<sup>1</sup>; Toshiji Mukai<sup>1</sup>; <sup>1</sup>National Institute for Materials Science

Although the rod-like  $\beta_1$  precipitate is among the most important in magnesium alloys, its crystal structure is not yet clear. Its structure has been believed to be based on the Lave's phase MgZn<sub>2</sub>, but recently reported to be of monoclinic Mg<sub>4</sub>Zn<sub>7</sub> phase. We have studied the structure of these precipitates by high resolution TEM in a Mg-Zn-Y alloy. It was found that domains of Mg<sub>4</sub>Zn<sub>7</sub> phase coexist with Laves phase MgZn<sub>2</sub> within the precipitates. Structural units of the Mg<sub>4</sub>Zn<sub>7</sub> phase characterized by icosahedral coordination rearrange to form the MgZn<sub>2</sub> structure with the orientation relationship with the matrix reported earlier. The crystallographic relationship between the phases is described. Axially, these phases are related to each other and the matrix as  $[1-210]_{\text{MgZn}_2} \parallel [010]_{\text{Mg}_4\text{Zn}_7} \parallel [0001]_{\text{Mg}}$ . The  $\{10-10\}$  planes of MgZn<sub>2</sub> correspond to  $\{003\}$  and  $\frac{1}{2}\{023\}$  planes of the Mg<sub>4</sub>Zn<sub>7</sub> phase.

# Technical Program

## 3:00 PM

**Rheological Behavior of Semi-Solid Mg-Y Alloys:** *Qiuming Peng*<sup>1</sup>; Yuanding Huang<sup>1</sup>; Norbert Hort<sup>1</sup>; Karl Ulrich Kainer<sup>1</sup>; <sup>1</sup>MagIC – Magnesium Innovation Centre

The knowledge of the rheological behaviour of Mg-RE suspensions is an important issue in semi-solid processes of Mg alloys containing RE. Therefore, rheological experiments like step-change in shear rate tests, shear stress ramps and oscillation experiments have been carried out to characterise the flow behaviour of Mg-RE alloys exemplarily Mg-Y and Mg-Nd alloys. The microstructures, solid fraction and viscosity of the alloys at different solidified temperatures are investigated. The materials exhibit a yield stress and shows shear-thinning and thixotropic flow behaviour, which are strongly influenced by the solid traction, the particle shape and size and the degree of particle agglomeration. All experiments were carried out in a Couette rheometer. The experimentally gained data are similar to a model approach, which consists of a modified Herschel-Bulkley law. These databases provide an implication for the development of Mg-RE alloys.

## 3:20 PM

**The Use of Computer Modeling for Producing DC Cast WE43 Magnesium Alloy Slab:** *Mark TurSKI*<sup>1</sup>; John Grandfield<sup>2</sup>; Tim Wilks<sup>1</sup>; Bruce Davis<sup>3</sup>; Rick DeLorme<sup>3</sup>; <sup>1</sup>Magnesium Elektron; <sup>2</sup>Grandfield Technology Pty Ltd; <sup>3</sup>Magnesium Elektron North America

During direct chill casting, significant stresses can develop within the material leading to cracking within the cast slab. The situation is made worse for higher strength magnesium alloys, such as WE43, which also exhibits high strength at elevated temperatures. Consequently, the temperature and stress field must be well understood during the casting process. ALSIM is a fully coupled thermo-mechanical finite element modeling code capable of simulating the DC casting process. ALSIM was used to simulate vertical DC casting of 870 x 315 mm WE43 slab. Validation of the model was carried out by the use of thermocouples and post mortem sectioning of cast slabs containing cracks. Good agreement has been found between modeling predictions and thermocouple measurements and post-mortem examination of cast material. The use of this validated model has allowed optimized casting parameters to be developed to produce crack free WE43 slab.

## 3:40 PM Break

## 4:00 PM

**Effects of Extrusion Conditions on the Microstructure and Properties of Mg-Zn-Y-RE Alloys:** *Jonghyun Kim*<sup>1</sup>; Yoshihito Kawamura<sup>2</sup>; <sup>1</sup>Kumamoto Technology & Industrial Foundation; <sup>2</sup>Kumamoto University

Magnesium alloys are known for their light weight and specific stiffness which are greatly attractive to the automotive and aerospace industries. They are usually supplied as the flat sheets or profiled products processed by metal working. Extrusion process is a prevailing shape forming procedure of magnesium products. In the present study, the authors conducted hot extrusion of Mg-Zn-Y-RE alloys billets and investigated the effects of extrusion conditions on the microstructure and mechanical properties of the extruded products. The extrusion in the Mg-Zn-Y-RE alloys led to grain refinement through dynamic recrystallization. Extrusion at the lower ram speed of 3.7 mm\*s<sup>-1</sup> resulted in a larger average grain size and higher elongation than at 2.5 mm\*s<sup>-1</sup>. The yield strength of the Mg-Zn-Y-RE alloys after extrusion at 3.7 mm\*s<sup>-1</sup> was lower than that of the alloy extruded at 2.5 mm\*s<sup>-1</sup>.

## 4:20 PM

**Effect of Cerium on the Deformation Behavior of Two Mg-Ce Alloys:** *Lan Jiang*<sup>1</sup>; Xavier Queleenne<sup>1</sup>; John Jonas<sup>1</sup>; Raja Mishra<sup>2</sup>; <sup>1</sup>McGill University; <sup>2</sup>GM

The effect of cerium on the formability of Mg alloy tubes was investigated by means of uniaxial tension and uniaxial compression testing. The tests were carried out at ambient temperature and 200°C at strain rates of 0.1/s and 0.001/s. Samples were cut from extruded tubes containing two different levels of Ce addition. Specimens deformed to increasing strain levels were examined by optical microscopy and electron backscattered diffraction (EBSD) techniques. At both test temperatures, higher tensile ductilities were observed in the Mg-0.5%Ce material than in the Mg-0.2%Ce, especially at the higher strain rate. However, at 200°C/0.001s<sup>-1</sup>, the Mg-0.2%Ce displayed better formability than the Mg-0.5%Ce. The differences can be attributed to the effects of initial texture, particle concentration and distribution, and grain size.

## 4:40 PM

**Structural Relationships between Monoclinic and Laves Phase Precipitates in Mg-Zn-Y Alloys:** *Julian Rosalie*<sup>1</sup>; Hidetoshi Somekawa<sup>1</sup>; Alok Singh<sup>1</sup>; Toshiji Mukai<sup>1</sup>; <sup>1</sup>National Institute for Materials Science

The response of textured Mg-Zn and Mg-Zn-Y alloys to controlled pre-ageing deformation has been examined in detail. Samples subjected to c-axis tension developed both deformation twins and some dislocations, while c-axis compression resulted in more extensive dislocation multiplication. Rod-like  $\beta_1'$  phase (Mg<sub>2</sub>Zn<sub>3</sub>) formed on dislocations while irregular precipitates of similar composition (and of the MgZn<sub>2</sub> Laves phase) formed on twin boundaries. The ageing response was accelerated by precipitation on both types of defect, but was more sensitive to the number of dislocations present. Higher dislocation densities also resulted in a more refined distribution of  $\beta_1'$  precipitates, which was not observed when the predominant defects were twins. The results highlight the sensitivity of Mg-Zn alloys to the nature of pre-ageing deformation and the importance of texture control in developing heat treatments for wrought Mg alloys.

## 5:00 PM

**Exploiting Low Levels of Rare Earth Addition in Mg Extrusion Alloys:** *Matthew Barnett*<sup>1</sup>; A.G. Beer<sup>1</sup>; N. Stanford<sup>1</sup>; <sup>1</sup>Deakin University

The benefit of adding rare-earth alloying elements to wrought magnesium alloys is well known. How these elements act to alter the mechanical performance is less understood. The present article presents some experimental results that shed light on this effect. It is also shown that low levels of their addition can lead to notable improvements in performance without the deterioration in extrudability seen with other alloying elements. It is demonstrated that the texture changes rapidly with small levels of addition. However, there is a limited operating window within which favourable textures arise. It is argued in agreement with previous suggestions that the key to understanding the role of rare earth elements at low levels is twofold. One effect relates to the influence exerted on the homogeneity of the deformation, which is also manifest in dynamic strain aging phenomena. The other relates to the retardation of recrystallization, which allows a characteristic deformation structure to develop during hot working.

## 5:20 PM

**Thermodynamic Database Development of Mg Alloys with RE Elements and Its Applications to Mg Alloy Design:** *Youn-Bae Kang*<sup>1</sup>; Liling Jin<sup>1</sup>; In-Ho Jung<sup>2</sup>; Arthur D. Pelton<sup>1</sup>; Patrice Chartrand<sup>1</sup>; Carlton D. Fuerst<sup>3</sup>; <sup>1</sup>Ecole Polytechnique de Montreal; <sup>2</sup>McGill University; <sup>3</sup>General Motors

Rare earth (RE) elements are often added to Mg-based alloys in order to improve creep resistance and strength at elevated temperature by forming stable precipitates with Al (AlxREy) or Zn (ZnxREy). Thermodynamic models and databases can provide invaluable information to elucidate the complex precipitation behaviors involving RE. In the present study, recent progresses of Mg alloy database development with FactSage toward adding RE elements, including the systems of Mg-RE and Al-RE (RE = La, Ce, Pr, Nd, Y, Sc, ...), and a number of Mg-Al-RE and Mg-Zn-RE (RE = La, Ce, Y, Sc), will be presented. The applications of the newly developed database to the Mg alloy design will be also presented.



## Materials in Clean Power Systems V: Clean Coal-, Hydrogen Based-Technologies, Fuel Cells, and Materials for Energy Storage: SOFC I

*Sponsored by:* The Minerals, Metals and Materials Society, TMS Electronic, Magnetic, and Photonic Materials Division, TMS Structural Materials Division, TMS/ASM: Corrosion and Environmental Effects Committee, TMS: Energy Conversion and Storage Committee  
*Program Organizers:* Xingbo Liu, West Virginia University; Zhenguo Yang, Pacific Northwest National Lab; K. Weil, Pacific Northwest National Lab; Mike Brady, Oak Ridge National Lab; Jay Whitacre, Carnegie Mellon University; Ayyakkannu Manivannan, National Energy Technology Laboratory; Zi-Kui Liu, Penn State University

Tuesday PM Room: 211  
 February 16, 2010 Location: Washington State Convention Center

*Session Chairs:* Teruhisa Horita, AIST; Harry Finklea, West Virginia University

### 2:00 PM Invited

**Degradation of SOFC Anodes and SOFC Performance in Coal Syngas Containing Phosphine:** Harry Finklea<sup>1</sup>; Oktay Demircan<sup>1</sup>; John Zondlo<sup>1</sup>; Chunchuan Xu<sup>1</sup>; <sup>1</sup>West Virginia University

Coal syngas, a potential fuel for solid oxide fuel cells in large scale power generation, may contain ppm levels of phosphine as well as other impurities. In this presentation, we report studies of anode-supported solid oxide fuel cells (Ni/YSZ anode) exposed to 10 ppm levels of phosphine in a synthetic syngas mixture of hydrogen, water, carbon monoxide and carbon dioxide. Cell power degrades immediately at high rates (on the order of mW/cm<sup>2</sup>/hr) upon introduction of 10 ppm into the syngas. Operation for over hundred hours results in substantial migration of nickel to the surface of the anode and into voids in the anode as nickel phosphide phases. The rate of degradation is significant over a range of operating voltages of the SOFC. The mechanism of phosphine-induced degradation will be discussed, along with suggestions on how to mitigate the degradation.

### 2:40 PM

**Effects of Phosphine on Solid Oxide Fuel Cell Performance and Related Anode Surface Temperature Measurement:** Huang Guo<sup>1</sup>; Gulfam Iqbal<sup>1</sup>; Bruce Kang<sup>1</sup>; <sup>1</sup>West Virginia University

The degradation effects of phosphine (PH<sub>3</sub>) contaminant on the solid oxide fuel cells (SOFCs) performance are investigated under hydrogen and simulated coal syngas environment with and without steam. The related anode surface temperature measurements, as a function of applied current densities, are also carried out via our in-situ experimental technique. The experimental results indicate that the Ni-cermet-based SOFC anode is more susceptible to degradation due to PH<sub>3</sub> in wet hydrogen than in dry hydrogen condition. Combining the results from post experiment characterization, such as SEM, EDX, XPS, the poisoning effect and degradation mechanism of PH<sub>3</sub> on the SOFCs performance are discussed.

### 3:00 PM

**Fabrication and Characterization of Thin Film La<sub>0.6</sub>Sr<sub>0.4</sub>Co<sub>0.2</sub>Fe<sub>0.8</sub>O<sub>3-δ</sub> (LSCF) and La<sub>0.6</sub>Sr<sub>0.4</sub>Co<sub>0.2</sub>Fe<sub>0.8</sub>O<sub>3-δ</sub> - Ce<sub>0.8</sub>Gd<sub>0.2</sub>O<sub>1.9</sub> (CGO) Composite Cathodes:** Bainye Angoua<sup>1</sup>; Elliot Slamovich<sup>1</sup>; <sup>1</sup>Purdue University

Due to their high electrocatalytic activity for oxygen reduction, LSCF cathodes improve the performance of solid oxide fuel cells at intermediate temperatures (500-700°C). In this study, thin (<500 nm) dense LSCF and LSCF-CGO cathodes are produced by spray pyrolysis. Solutions of nitrate salts dissolved in a mixture of ethanol, butyl carbitol and methyl carbitol were atomized onto dense 8YSZ substrates between 230-240°C, followed by subsequent crystallization in air at 700-900°C. The effect of sintering temperature on film morphology and electrical conductivity was investigated to determine an optimum firing temperature with respect to cathode electrical resistance and formation of reaction products between 8YSZ and LSCF. Microstructure evolution of the raw films as a function of firing temperature was followed via SEM, FIB sections and EDS. Electrical characterization was performed by impedance spectroscopy on cathodes deposited symmetrically across the 8YSZ substrate. The effect of a thin CGO buffer layer was also investigated.

### 3:20 PM

**Sintering Performance of YSZ Ceramics with Transition Metal Oxide Sintering Aid:** Stephen Sofie<sup>1</sup>; M.L. Lifson<sup>1</sup>; C. Law<sup>1</sup>; <sup>1</sup>Montana State University

The effect of NiO additions in YSZ was examined to provide a means to tailor the sintering behavior of both fully and partially stabilized YSZ. YSZ powders of micro size scale were mixed with 0.1, 0.5, and 1.0 mol% NiO. Pellets were characterized from 1200C to 1400C with a 1 hour dwell. Undoped micro 8YSZ and 3YSZ powders sintered at 1300C for one hour yielded 79.5% and 67.6% theoretical density, respectively. At the same temperature profile, the 8YSZ powder with 1.0mol% nickel oxide reached 95% theoretical density and the 3YSZ micro powder with 1.0mol% nickel achieved 96.7% theoretical density. Dilatometry revealed that the onset of sintering decreased and maximum rate of sintering increased with increasing nickel oxide concentration.

### 3:40 PM Break

### 3:50 PM

**Modeling of Total and Topologically Connected Triple Phase Boundaries in Composite Cathodes for Solid Oxide Fuel Cells:** Arun Gokhale<sup>1</sup>; Shenjia Zhang<sup>1</sup>; <sup>1</sup>Georgia Institute of Technology

Analytical and numerical modeling of three-phase microstructures of LSM/YSZ composite cathodes is carried out for prediction of the geometric characteristic of the YSZ-LSM-Pore triple phase boundaries (TPB). The analysis predicts total and topologically connected TPB length per unit volume (LTPB) from volume fractions and characteristics of initial powder populations of YSZ and LSM. The parametric analysis reveals that (1) non-equiaxed plate-like, flake-like, and needle-like YSZ/LSM particle shapes can yield substantially higher LTPB; (2) mono-sized YSZ/LSM powders lead to higher LTPB as compared to the powders having wide size distributions; (3) LTPB is inversely proportional to the mean sizes of YSZ and LSM particles; (4) high value of LTPB is obtained at the lowest porosity volume fraction that permits sufficient connectivity of the pores for gas permeability; and (5) LTPB is not sensitive to the relative proportion of YSZ and LSM phases in the regime of interest in composite cathode applications.

### 4:10 PM

**Modeling Solid Oxide Fuel Cells with Mixed Conducting Electrolytes and Anode Functional Layers:** Keith Duncan<sup>1</sup>; Eric Wachsman<sup>1</sup>; <sup>1</sup>University of Florida

Recent research at the University of Florida has shown that the inclusion of an anode functional layer (AFL) significantly increases the maximum power density of ceria electrolyte solid oxide fuel cells (SOFCs). Here, results from the latest development of AFL-equipped SOFCs are presented. Accordingly, a continuum-level analytical model was developed to accurately describe and predict the performance of SOFCs, in general, and to better explain the electrochemical impact of the AFLs on SOFC performance. The model was derived by coupling the Nernst-Planck and Butler-Volmer equations, while employing defect thermodynamics for boundary values. This approach allowed the usual assumptions of reversible electrodes and linear potential gradients to be removed; thereby allowing a non-ohmic response in the mixed conducting electrolyte. The model was validated through successful fits to experimental data from SOFCs with acceptor-doped ceria electrolytes. Finally, the model was used to predict open-circuit voltage dependence on electrolyte thickness.

### 4:30 PM

**Modelling the Effect of Dopant Concentration on Lattice Strain and Ionic Conductivity in Fluorite Oxides:** Keith Duncan<sup>1</sup>; Eric Wachsman<sup>1</sup>; <sup>1</sup>University of Florida

Scientists have searched intensely for oxides with high ionic conductivity for use in SOFCs. In oxides, ionic conduction is by point defect migration, so management of point defect population is a key strategy for maximizing conductivity. Research on doping strategies revealed that, for each host oxide, there exists optimal dopants and dopant concentrations, which are largely determined by minimizing the tradeoff between mobile defects, defect association and lattice strain. Though increasing dopant concentration increases the concentration of defects, it also increases defect association while decreasing mobility—both are deleterious to ionic conductivity. In the presentation, this phenomenon will be articulated in a continuum-level framework to formulate the relationship between dopant concentration, lattice strain, defect association and ionic conductivity. Excellent fits of the model were obtained for (CeO<sub>2</sub>)<sub>1-</sub>

Tue. PM

# Technical Program

x(SmO<sub>1.5</sub>)x at various temperatures with only two adjustable parameters. Further analysis of the results reproduces empirical trends and relationships previously reported in the literature.

## 4:50 PM

**Simulation of Oxygen Ion Transport in Mixed-Conducting Solid Oxide Fuel Cell Cathode with Complex Microstructure:** *Hsun-Yi Chen*<sup>1</sup>; Hui-Chia Yu<sup>1</sup>; Cortney Kreller<sup>2</sup>; James Wilson<sup>3</sup>; Scott Barnett<sup>3</sup>; Stuart Adler<sup>2</sup>; Katsuyo Thornton<sup>1</sup>; <sup>1</sup>University of Michigan; <sup>2</sup>University of Washington; <sup>3</sup>Northwestern University

LaSrCoO<sub>3</sub> (LSC) is a mixed ionic-electronic conductor and is considered a promising material for solid oxide fuel cell (SOFC) cathodes. Understanding oxygen transport mechanisms in LSC can provide insights that could lead to the rational design of the cathode microstructure. Electrochemical impedance spectroscopy (EIS) measurements combined with theoretical modeling and simulation can be employed to elucidate oxygen reduction mechanisms. We developed a numerical approach to simulate the electrochemical response of a mixed-conducting cathode with complex microstructures. The method was demonstrated for a cathode with simple structures. Simulations were also performed using a three-dimensional LSC microstructures constructed using images obtained by focused ion beam-scanning electron microscopy (FIB-SEM). The current-voltage relation and impedance are calculated for various rate limiting cases.

## 5:10 PM

**Reliability Model for Different Configurations of Planar-SOFC Anode under Syngas Contaminants:** *Gulfam Iqbal*<sup>1</sup>; *Huang Guo*<sup>1</sup>; *Bruce Kang*<sup>1</sup>; <sup>1</sup>West Virginia University

An anode material reliability model developed for solid oxide fuel cell (SOFC) button cell is adapted for the planar-SOFC configurations: co-flow, counter-flow and cross-flow. The model accounts for thermo-mechanical and fuel gas contaminants effects on the anode material to predict its structural life. The temperature field and contaminant concentration on planar-SOFC anode are interpreted from DREAM-SOFC, a multi-physics solver. Due to larger active areas, planar-SOFC configurations exhibit greater spatial and temporal temperature gradients compared to button cells, which lead to higher thermo-mechanical degradation. For the co-flow configuration, anode thermo-mechanical degradation is severe at the anode-electrolyte interface and it starts near the fuel outlet whereas the fuel gas contaminants effects on the anode microstructure begin at the fuel inlet and propagate through the anode thickness and along the fuel flow. The knowledge obtained from this research will be useful to establish control parameters to achieve desired service life of SOFC stacks.

## Materials Processing Fundamentals: Smelting, Refining, Aqueous and Liquid Processing

*Sponsored by:* The Minerals, Metals and Materials Society, TMS Extraction and Processing Division, TMS: Process Technology and Modeling Committee

*Program Organizer:* Prince Anyalebechi, Grand Valley State University

Tuesday PM                      Room: 601  
February 16, 2010                Location: Washington State Convention Center

*Session Chair:* Prince Anyalebechi, Grand Valley State University

## 2:30 PM

**A Comparative Electrochemical Study of Arsenic Removal from Organic and Inorganic Sources Using Various Sacrificial Electrodes:** *Jewel Gomes*<sup>1</sup>; Sanoar Rahman<sup>1</sup>; Srikanth Varma<sup>1</sup>; Kamol Das<sup>1</sup>; David Cocks<sup>1</sup>; <sup>1</sup>Lamar University

Arsenic is considered as one of the toxic materials being controlled by Environmental Protection Agencies in several developed and developing countries. In nature, it occurs in the soil, minerals and in various organic forms. It enters the air, water, and land from wind-blown dust and gets into water from runoff, leaching, soil erosion and anthropogenically from chemicals used for wood preservation, insecticides, medicine, military purpose, pigments, and electronic circuitries. There are several techniques available for removal of arsenic, such as coagulation/filtration, ion exchange, reverse osmosis, and

electrochemical. Electrocoagulation has been found as one of the most efficient techniques to remove inorganic arsenic with >99% efficiency. Here we present our work on electrochemical treatment of both inorganic and organic arsenic from water using various sacrificial electrode materials, i.e., iron, aluminum, copper, titanium and combination of them. The floc produced has been characterized using XRD, SEM/EDS, FTIR, and cyclic voltammetry.

## 2:50 PM

**Characterization of Sodium and Bath Penetration in Industrial Graphitic and Graphitized Cathodes:** *Jilai Xue*<sup>1</sup>; Liancheng Wu<sup>1</sup>; Gangqiang Jiang<sup>1</sup>; Qingren Niu<sup>1</sup>; Qingsheng Liu<sup>1</sup>; Hou Xin<sup>1</sup>; Jun Zhu<sup>1</sup>; He Hua<sup>1</sup>; <sup>1</sup>University of Science and Technology Beijing

Experiments with various industrial cathodes ranging from 35% to 100% graphitic and fully graphitized carbons were carried out in a laboratory aluminum electrolysis cell. Sodium and bath penetration into the cathode samples was measured by XRD and SEM-EDS analysis. For a higher cryolite ratio, the cathodes with lower graphitic carbons exhibited more sodium penetration than the fully graphitized. XRD characterization shows that the increased graphitization (p002) in the cathode carbons can reduce the sodium penetration. SEM-EDS inspection reveals that the sodium and fluorides penetration within the cathode samples has different patterns for varying graphitization of the carbon materials. The porosity of the cathode materials did not demonstrate the importance in correlation with the penetration process as expected before. The results can provide useful information for quality evaluation of the industrial cathode products as well as for improvement in cathode performance.

## 3:10 PM

**Analysis and Identification Minerals Present in Rock Samples:** *Andrew Appaji*<sup>1</sup>; <sup>1</sup>Noorul Islam University

Abstract Rocks and Minerals are inseparable. The area of our investigation in placed at the southern horn of India – Velimalai Hills, where still no great mineralogical surveys are done. This study is the first of its kind of analyzing the presence of different minerals in these rocks. The Rocks samples are collected and they are subjected to X ray diffraction study and Fourier Transform Infra Red Studies. The minerals are analyzed. Their presence is confirmed. The study was carried out for 3 samples; other samples are also to be studied.

## 3:30 PM

**Preparation and Degradation Organic of TiO<sub>2</sub> Coated on Light Ceramic Surface:** *Ju Hua*<sup>1</sup>; <sup>1</sup>Harbin Institute of Technology

TiO<sub>2</sub> photocatalyst could degrade the organic pollutants from the surface. This process has many advantages, including low energy consumption, simple techniques, mild reaction conditions, and less secondary pollution. However, the granular TiO<sub>2</sub> is so tiny that it is difficult to precipitate, it loses its active constituents, and difficult to recycle. Thus, the granular state greatly limits its practical application. In order to resolve these problems, in the thesis we studied and produced the TiO<sub>2</sub>-coated light weight ceramic material. Because the TiO<sub>2</sub>-coated light weight ceramic's specific gravity is close to the water's, it can be floated on the water. Also it increases the interface with water and illuminating area, which enhances the capability of photocatalysis.

## 3:50 PM

**Fe-Ni Alloys Formation in Carbothermal Reduction Process using Laterite Nickel Ore:** *Jilai Xue*<sup>1</sup>; Luxing Feng<sup>1</sup>; Jun Zhu<sup>1</sup>; <sup>1</sup>University of Science and Technology Beijing

Fe-Ni alloys can be used as raw material in making of stainless steel and laterite nickel ore is one of resources. In this work, a mixture of laterite ore and coal was set in a furnace at 900°C and then reduced to form Fe-Ni alloys at 1550-1620°C through direct carbothermal reduction process. The targeted contents of Ni in the alloys were investigated against various parameters. The ratio of the laterite to coal was found as a major factor in forming the alloy with targeted nickel content. A higher temperature can make better separation between the metal and the slag, and is in favor of producing high content of nickel. The slag contained relative higher Mg and Si, and can make some processing difficulties.



### 4:10 PM Break

### 4:30 PM

**Active Zinc Oxide Production from Waste Zinc Powder:** *Cem Colakoglu*<sup>1</sup>; Onuralp Yucel<sup>1</sup>; <sup>1</sup>Istanbul Technical University

Active zinc oxide has a high surface area (approximately 35-60 m<sup>2</sup>/g) and also has 10 times less particle size than that of zinc oxide. In this study, various quality of active zinc oxides containing up to 98 wt.% ZnO were produced by hydrometallurgical process from waste zinc powder (blue zinc powder). In the first step of the experiments, waste zinc powder containing 95 wt.% Zn and 0.5 wt.% Fe was reacted with sulphuric acid solution then hydrogen peroxide was added to remove Fe from the system. In the second step, obtained zinc sulphate solution was reacted with the addition of sodium carbonate solution. Resulting zinc carbonate was first be dried at 100°C then calcined at different temperatures and time to set the alternative quality of active zinc oxide. Elemental analysis of the waste zinc powder and active zinc oxide was performed by using XRD, XRF, BET and AAS.

### 4:50 PM

**Preparation of MgO Whisker from Magnesite Tailings:** *Li Yue-yuan*<sup>1</sup>; Cui Hong-Xu<sup>1</sup>; Chen Min<sup>1</sup>; <sup>1</sup>Northeastern University

China has abundant magnesite resource, but the low-grade and powder ores have always been rejected, which influences the comprehensive utilization of resource and often causes circumstance problems. The present work investigated the preparation of magnesia whisker using magnesite tailings as starting materials by preparation magnesium carbonate whisker as precursor firstly in the route of calcination, hydration, carbonation and pyrolysis, follows by second calcination of the precursor. The influence of pyrolysis conditions and additives on morphology of magnesium carbonate crystal as well as the influence of calcination conditions on morphology of magnesia whisker was investigated. The results showed that thermal decomposition products was MgCO<sub>3</sub>·3H<sub>2</sub>O. Magnesium carbonate whisker with length of 10-60 μm and the length-to-diameter ratio of 10-20 was prepared when soluble magnesium salt was added. While temperature was elevated at 1°C·min<sup>-1</sup>, magnesia whisker with length of 10-60μm was obtained.

### 5:10 PM

**Remediation of Chicken Processing Wastewater Using Electrochemically Produced Layered Double Hydroxides:** *Jewel Gomes*<sup>1</sup>; Daniel Atambo<sup>1</sup>; Manish Rahate<sup>1</sup>; Kamol Das<sup>1</sup>; George Irwin<sup>1</sup>; Hector Moreno<sup>2</sup>; David Cocke<sup>1</sup>; <sup>1</sup>Lamar University; <sup>2</sup>Instituto Tecnológico de la Laguna

Green rust (GR) are Layered Fe(II)-Fe(III) Double Hydroxides (LDH), having a pyroaurite-type structure consisting of positively charged hydroxide layers and hydrated anions in interlayers. This special feature of GR is very efficient for wastewater treatment as the pollutants are easily taken in or exchanged with the anions in the interlayers. It can be very simply and cost-effectively produced by electrocoagulation (EC). Chicken processing plant (CPP) produces large amount of wastewater containing variety of readily biodegradable organic compounds, fats and proteins. The possible re-use of properly treated CPP wastewater would be economic and environment friendly. In this study, we present our work on treatment of CPP wastewater using EC. Analysis of the EC-treated water for reuse in the same plant is discussed considering the U.S. EPA regulations. Two types of EC-reactors were used for this purpose. To better understand the treatment mechanism, EC-floc was also characterized using XRD, SEM-EDS, and FTIR.

### 5:30 PM

**Carbon-Thermal Reduction Process for Making Al-Si Alloys from Al<sub>2</sub>O<sub>3</sub>-SiO<sub>2</sub> Containing Industrial Wastes:** *Jilai Xue*<sup>1</sup>; Yunxia Song<sup>1</sup>; Jun Zhu<sup>1</sup>; <sup>1</sup>University of Science and Technology Beijing

Industrial solid wastes containing 40%-50% Al<sub>2</sub>O<sub>3</sub> and 30-50% SiO<sub>2</sub> have potential to be an alternative resource for Al-Si alloys production. Spent potlining materials from aluminum reduction cells and coal flyash from electrical power plants were tested in laboratory to make Al-Si alloys using carbonthermal reduction process. A mixture of anthracite and petroleum coke was used as reducing agency. One of the most important operations was to prepare the briquettes made of different raw materials with varying contents of Al<sub>2</sub>O<sub>3</sub> and SiO<sub>2</sub>. The effects of briquette porosity, Al/Si ratio, the amount of carbon reducing agency, on the reduction process and the resulting alloy quality were investigated. The results are useful for further development of an

alternative technology for Al-Si alloy production, and for waste treatment in recycling metals from the industrial solid wastes containing Al<sub>2</sub>O<sub>3</sub> and SiO<sub>2</sub>.

### Mechanical Performance for Current and Next-Generation Nuclear Reactors: Microstructure and Nanostructure in Reactor Environments

*Sponsored by:* The Minerals, Metals and Materials Society, TMS Materials Processing and Manufacturing Division, TMS Structural Materials Division, TMS/ASM: Mechanical Behavior of Materials Committee, TMS: Nanomechanical Materials Behavior Committee, TMS/ASM: Nuclear Materials Committee  
*Program Organizers:* Dylan Morris, NIST; Greg Oberson, Nuclear Regulatory Commission; Nicholas Barbosa, National Institute of Standards & Tech; Wolfgang Hoffelner, Paul Scherrer Institute

Tuesday PM Room: 201  
February 16, 2010 Location: Washington State Convention Center

*Session Chair:* Wolfgang Hoffelner, Paul Scherrer Institute

### 2:00 PM Invited

**Irradiation Effects in Thin Metal Films – Texture Control and Mechanical Properties:** *Ralph Spolenak*<sup>1</sup>; <sup>1</sup>ETH Zurich

Thin metal films can serve as model systems for radiation effects in nuclear materials or are under study for application in fusion reactors. The current study focuses on the effects of the interaction between radiation-induced defects in thin metal films and their grain-boundaries. Frenkel pairs as well as stacking fault tetrahedra are induced by high energy ions (argon or self ions). Energy minimization leads to a selective grain-growth of the undamaged grains and converts a fiber textured thin films (driven by surface energy minimization) into a “single-crystal”. The interaction of ions with grain boundaries renders the process nearly athermal. In spite of the growth of “undamaged” grains, ion-induced hardening is observed by local mechanical probes. In addition to observations by TEM and EBSD the interaction of defects and grain-boundaries is observed in-situ at the JANNUS facility at Orsay, Paris.

### 2:30 PM

**Elevated-Temperature Compression Testing and Characterization of Deformation and Fracture in Sintered ZrN Pellets as Surrogates for PuN Fuels:** *Kirk Wheeler*<sup>1</sup>; Pedro Peralta<sup>1</sup>; Kenneth McClellan<sup>2</sup>; <sup>1</sup>Arizona State University; <sup>2</sup>Los Alamos National Laboratory

ZrN was studied as a possible surrogate for PuN under the Global Nuclear Energy Partnership (GNEP) program. In particular, this work addresses the mechanical properties and fracture behavior of sintered ZrN pellets at elevated temperatures and relates this behavior to its initial microstructure. Uniaxial compression testing was performed in an ultra-high purity Argon atmosphere at both intermediate (800°C) and high (1200°C) temperatures. Post-mortem fractography was performed via scanning electron microscopy (SEM) on pyramidally shaped fracture pieces produced as a result of localized shear bands that developed during high temperature tests and lattice rotations typical of plastic deformation were discovered at the tips of cracks that were arrested at grain boundaries using Electron Backscatter Diffraction (EBSD). Applicability of the results to the understanding of the structural reliability of nitride fuel pellets at working as well as thermal overload temperatures is discussed. Work supported under DOE/NE Agreement # DE-FC07-05ID14654.

### 2:50 PM

**High Temperature Oxidation Behavior of Grain-Refined Inconel 617 for VHTRs:** *Tae Sun Jo*<sup>1</sup>; Jeong Hun Lim<sup>1</sup>; Dae-gun Kim<sup>1</sup>; *Young Do Kim*<sup>1</sup>; <sup>1</sup>Hanyang University

In this study, the effect of grain size on high temperature oxidation of Inconel 617 alloy was investigated by exposure at 950°C for 1000 h in air atmosphere. The grain-refined Inconel 617 was obtained by recrystallization after cold rolling of 50%. The grain size was refined from 71μm to 5.2μm. The as-received and grain-refined alloys were oxidized with forming external oxide layer as Cr<sub>2</sub>O<sub>3</sub> and with forming internal oxide as Al<sub>2</sub>O<sub>3</sub>·2O<sub>3</sub> along the grain boundary. The formation of Cr<sub>2</sub>O<sub>3</sub> caused the Cr-depleted zone below the external oxide scale. The Cr-depleted zone of grain-refined alloy was thicker than that of the as-received one, while the depth of internal oxide of grain-

Tue. PM

# Technical Program

refined one was shallower. By prolonging the exposure time, the area of internal oxide of grain-refined alloy was gradually decreased. However, as-received one was constantly increased. The internal oxide at the grain-refined alloy had a more homogeneous microstructure.

## 3:10 PM

**Hot Steam Corrosion Behavior of Ni-Based Superalloys at High Temperature Steam Environments:** *Donghoon Kim*<sup>1</sup>; Minu Kim<sup>1</sup>; Hyun Min Lee<sup>1</sup>; Daejong Kim<sup>1</sup>; Changheui Jang<sup>1</sup>; Duk-Joo Yoon<sup>2</sup>; <sup>1</sup>KAIST; <sup>2</sup>KEPRI

A high temperature steam electrolysis (HTSE) is one of the promising ways of the massive hydrogen production using the very high temperature gas cooled reactor (VHTR). During the operation of the HTSE-VHTR system, structural material such as intermediate heat exchanger (IHx) are exposed to high temperature steam condition. Thus the corrosion resistance of the heat exchanger materials is critical to the safety and performance of the system. In this study, the corrosion behaviors of several Ni-based superalloys were investigated in steam environments at 900° with and without hydrogen gas. Corrosion kinetics was studied by weight change per unit surface area and oxide layer and microstructure change were analyzed using a scanning electron microscope (SEM), energy-dispersive X-ray spectroscopy (EDX), and X-ray diffractometer (XRD). Also, the effects of alloying elements on steam corrosion resistance were investigated. Finally, the results were compared with those at high temperature air and helium conditions.

## 3:30 PM

**The Cause of Dynamic Strain Aging in Zirconium Alloys:** *Young Suk Kim*<sup>1</sup>; Sung Soo Kim<sup>1</sup>; <sup>1</sup>Korea Atomic Energy Research Institute

Tensile tests were conducted from RT to 400°C using the tensile specimens taken from the tangential (TD) and longitudinal directions (LD) of a Zr-2.5Nb tube with a strong tangential texture. The yield stress plateau (YSP), representing dynamic strain aging (DSA) of zirconium alloys, appeared from 150°C for the TD specimens but from 250°C for the LD specimens. To understand the cause of the YSP, the deformation mode was determined by measuring a textural change with temperature in the TD and LD specimens before and after the tensile tests using an X-ray method. It is found that the YSP for the TD and LD specimens is due to the operation of different deformation modes with orientation: twinning in the TD and <c+a> slip in the LD, respectively. Furthermore, negative temperature dependence of ductility from 200°C to 350°C is caused by the operation of <c+a> slip.

## 3:50 PM Break

## 4:05 PM

**The Thermal Stability and Weldability of a Lean Grade of Duplex Stainless Steel:** *Julie Tucker*<sup>1</sup>; George Young<sup>1</sup>; <sup>1</sup>Knolls Atomic Power Laboratory

Duplex stainless steels are desirable for use in power generation systems due to their attractive combination of strength, corrosion resistance, and cost. However, thermal embrittlement at high temperature (~1300°F) can complicate fabrication and embrittlement at low temperatures (≤800°F) limits the service temperature for many applications. New lean grade alloys may improve the manufacturing margin and potentially increase the upper service temperature of these alloys. The present work assesses the weldability and thermal stability of lean grade AL2003. Weldability was assessed by the transverse restraint test. Thermal stability was investigated via a series of isothermal agings between 550°F and 1300°F for times between 1 and 10,000 hours. The thermal stability of the aged samples was characterized by changes in hardness, Charpy impact energy, and elastic-plastic fracture toughness. Additionally, microstructural characterization of the aged samples via electron backscatter diffraction and transmission electron microscopy was performed to better understand the nature of the embrittlement.

## 4:25 PM

**Microstructural and Mechanical Characteristics of Friction Stir Welded ODS Alloys:** *Ramprasad Prabhakaran*<sup>1</sup>; J. Wang<sup>2</sup>; K. Chitrada<sup>3</sup>; W. Yuan<sup>2</sup>; I. Charit<sup>1</sup>; J. Cole<sup>1</sup>; R. Mishra<sup>2</sup>; <sup>1</sup>Idaho National Laboratory; <sup>2</sup>Missouri University of Science and Technology; <sup>3</sup>University of Idaho

Efforts are underway to examine the feasibility of using oxide dispersion strengthened (ODS) alloys for various high temperature applications including advanced nuclear reactors. Conventional fusion welding of ODS alloys causes various undesirable effects, such as coalescence of oxide dispersoids and significant porosity. In this study, MA956 and MA754 alloys were friction stir

welded in a bead-on-plate configuration. Microhardness testing across the weld zone was performed to reveal the microstructural gradient in the weld. Sub-size tensile testing of the base material and stir zone were carried out to evaluate the tensile properties. Higher weld efficiencies have been achieved in both the alloys. Optical microscopy and transmission electron microscopy were used to study the changes in grain size and characteristics of the fine oxide dispersoids across the weld zone.

## 4:45 PM

**Diffusion of Silver and Gold in Ion Irradiated Glassy Polymeric Carbon:** Malek Abunaemeh<sup>1</sup>; *Ibidapo Ojo*<sup>1</sup>; Claudiu Muntele<sup>1</sup>; Daryush Ila<sup>1</sup>; <sup>1</sup>Alabama A&M University

In this study we investigate glassy polymeric carbon (GPC) as an alternative to PyC as a diffusion barrier for fission products in TRISO fuel. Silver diffusion is of particular interest. GPC can maintain dimensional and chemical stability in adverse environment and very high temperatures (up to 3000°C). In this work, we are looking at the diffusion of 5 MeV implanted Ag and Au in GPC. The implantation fluences were chosen such that they would produce an estimated 1 dpa. We used three types of GPC materials, pyrolyzed to 1000, 1500 and 2000°C. We sequentially heat treated and measured the metal implanted GPC, in order to create a series of diffusion profiles from which to extract diffusion coefficients in irradiation damaged and nonirradiated GPC. For measuring the metal distribution we used Rutherford backscattering spectroscopy and the simulation software RUMP.

## 5:05 PM

**Late-Blooming Phase Investigation in an Ion Irradiated Fe-1wt.%Mn Alloy:** *Estelle Meslin*<sup>1</sup>; Bertrand Radigue<sup>2</sup>; Philippe Pareige<sup>2</sup>; Alain Barbu<sup>1</sup>; <sup>1</sup>CEA; <sup>2</sup>CNRS/University of Rouen

The mechanism at the origin of the formation of solute clusters in RPV steels is still subject to debate (irradiation enhanced or irradiation induced). Indeed, excepted for Cu, solute atoms usually present in solute clusters observed in neutron irradiated RPV steels are known to be under-saturated, at least considered separately, but solubility limits in more complex alloys remain unknown. In order to clarify this mechanism, an under-saturated FeMn binary alloy was self-irradiated within the multi-beam facility Jannus in Saclay at 400°C up to 2 dpa and then characterized by atom probe tomography. Experimental procedure and results will be presented.

## 5:25 PM

**The Effects of Stress and Temperature on the Fatigue Crack Growth Behavior and Microstructural Evolution of Alloy 230:** *Jatu Burns*<sup>1</sup>; Megan Frary<sup>1</sup>; <sup>1</sup>Boise State University

Alloy 230, a nickel-based superalloy, is a candidate material for heat exchangers in very high temperature reactors. The heat exchangers are expected to see a wide range of operating conditions, so it is important to understand the effects of both stress and temperature on mechanical behavior and microstructural evolution. We studied crack growth behavior under controlled stress intensity factor near the threshold regime between 650 and 800°C. The tests were performed in using static and cyclic loads with various frequencies and stress ratios. In the different temperature regimes, the damage mechanism is dominated by different phenomena. Electron backscatter diffraction was used to observe the cracking mode and to characterize microstructure and texture at the crack tip. Transgranular cracks were observed from fatigue cracking. In grains near the crack tip, the local orientation spread increased in to as much as 5°, an indication of local deformation.

## 5:45 PM

**High-Temperature Corrosion of YSZ Plasma-Sprayed on Nickel-Alloys in Molten Chloride Salts:** *Oscar Quintana*<sup>1</sup>; J. Ernesto Indacochea<sup>1</sup>; Mark Williamson<sup>2</sup>; Christine Snyder<sup>2</sup>; <sup>1</sup>University of Illinois; <sup>2</sup>Argonne National Laboratory

The objective of this work is to develop advanced structural materials that are strong and stable under conditions typical of pyrochemical processing systems, such as electrolytic reduction, designed for used nuclear fuel recycle. Two structural materials, 316L SS and HAYNES 214, were plasma sprayed with a NiCrAlY metallic bond coat layer, and an 8% Ytria stabilized zirconia top coat layer. One set of coated specimens was submerged for 72 hours in molten LiCl+6 wt.%Li<sub>2</sub>O at 650°C with Ar+10%O<sub>2</sub> gas bubbling at two different flow rates (33ml/min and 3ml/min), and another set was exposed to the vapors, suspended above the molten salt. All tests were carried out in an



argon-atmosphere glovebox. The submerged coated specimens failed while the suspended ones did not. XRD, SEM-EDS detected  $\text{Li}_2\text{ZrO}_3$  and  $\text{Li}_4\text{ZrO}_4$  as well as other oxide phases on the corroded specimens.

### Modeling, Simulation, and Theory of Nanomechanical Materials Behavior: Nanotubes, Soft Materials and Biomedical Applications

*Sponsored by:* The Minerals, Metals and Materials Society, TMS Materials Processing and Manufacturing Division, TMS/ASM; Computational Materials Science and Engineering Committee, TMS; Nanomechanical Materials Behavior Committee

*Program Organizers:* Thomas Buchheit, Sandia National Laboratories; Sergey Medyanik, Washington State Univ.; Douglas Spearot, University of Arkansas; Lawrence Friedman, Penn State University; Edmund Webb, Sandia National Laboratories

Tuesday PM Room: 304  
February 16, 2010 Location: Washington State Convention Center

*Session Chairs:* Markus Buehler, Massachusetts Institute of Technology; Michael Chandross, Sandia National Laboratories

#### 2:00 PM Invited

**Molecular Scale Modeling of Polymer Nanolithography:** *Michael Chandross*<sup>1</sup>; Gary Grest<sup>1</sup>; <sup>1</sup>Sandia National Laboratories

The production of surfaces with controllable/tunable nanostructures over large areas and at throughputs practical for commercial applications can be very difficult. Two processes of recent interest have been step-flash imprint lithography (SFIL) and nanoimprint lithography (NIL) in which nanoscale masks are imprinted into polymeric materials to create features with nm-scale resolution. Empirical approaches are currently the norm for industrial scale-up but are often prohibitively time-consuming and expensive. Modeling and simulation can decrease manufacturing process design cycle time enormously, as has been proven in many industry segments. Here we present our activities specifically with regard to nanopatterning by detailed large-scale simulations of nanolithographical processes in which rigid molds are imprinted into liquid oligomers that are subsequently hardened. We use a generic polymer model that can be applied to both SFIL, in which the oligomers are cross-linked by exposure to UV irradiation, and NIL, in which the liquid is hardened by lowering the temperature below the glass transition. Multiple stamps are inserted into melts of liquid oligomers at a temperature above the glass transition. The melts are either quenched or cross-linked and the systems are equilibrated. Stamps are then either removed at constant velocity to study the effects of stress and adhesion on resulting features, or simply deleted to study the effects in the limit of zero stress. We vary the size and pitch of the stamps in order to study the resolution limits of both methods.

#### 2:30 PM

**Atomistic Simulations of the Nanoindentation of Cyclotrimethylene Trinitramine (RDX) (001) Surfaces:** *Marc Cawkwell*<sup>1</sup>; Kyle Ramos<sup>1</sup>; Daniel Hooks<sup>1</sup>; <sup>1</sup>Los Alamos National Laboratory

Recent nanoindentation studies of cyclotrimethylene trinitramine (RDX) single molecular crystals have provided the first convincing evidence for the homogeneous nucleation of dislocations around the theoretical yield stress of a molecular material [K.J. Ramos, D.E. Hooks, and D.F. Bahr, *Phil. Mag.* (in press)]. Furthermore, the indentation of (001) surfaces suggests a previously unknown slip system is activated. We have undertaken a series of very large-scale molecular dynamics simulations of the nanoindentation of RDX surfaces using an accurate and transferable non-reactive molecular potential for nitramines. These simulations confirm that dislocation loops corresponding to the previously unknown slip system (001)[010] nucleate homogeneously beneath the indenter. We find that the location of the homogeneous nucleation events are best described by a Schmid-like criterion based on the location of the maximum resolved shear stress beneath the tip rather than Miller and Acharya's stress gradient criterion or commonly used Hertzian analyses.

#### 2:50 PM

**Atomistic Simulation Studies of Rotational Effects in Double-Wall Carbon Nanotubes:** *Iman Salehinia*<sup>1</sup>; Sergey Medyanik<sup>1</sup>; <sup>1</sup>WSU

Carbon nanotubes are important building blocks in the design of novel nanomechanical devices. The weak van der Waals interaction between the walls of a double-wall carbon nanotube (DWCNT) allows for an easy slide and rotation of the tubes with respect to one another. This property provides a possibility to construct a new family of mechanical nanodevices where the nanometer scale motion is the relative sliding, rotation or helical bolt-nut motion of nanotube walls. In this work atomistic simulation method is applied to study the transmission between translational and rotational motions (helical motion) in double-wall carbon nanotubes. DWCNTs are classified in several cases and general rules regarding the possibility of bolt-nut behavior are found. It is found that the helical motion is dependent on both the chiralities of the inner and outer tubes. Types of DWCNTs that are the most applicable bolt-nut pairs for being used in nanomechanical devices are identified.

#### 3:10 PM Invited

**Insights into the Mechanical Behaviour of Glassy Polymers through Molecular Dynamic Simulations:** *Sumit Basu*<sup>1</sup>; Dhiraj Mahajan<sup>1</sup>; <sup>1</sup>Indian Institute of Technology Kanpur

In this work we use Molecular Dynamics (MD) simulations of glassy polymers with a view to informing and enriching constitutive models for these materials. Firstly, we discuss effects of sample preparation, sample size and simulation parameters that influence the ability of Molecular Dynamics to simulate realistic deformation behaviour of glassy polymers. We further show that if proper simulation methodologies are employed, MD does provide important insights into various aspects of the mechanical behaviour of polymers. These include their ability to harden remarkably at large strains and aging and rejuvenation. We illustrate that the both these aspects of their mechanical behaviour have important bearing on the mechanics of fracture initiation in these materials. Finally, our MD simulations, coupled with primitive path analyses show that stress induced dis-entanglement takes place in glassy polymers during deformation. Moreover, formation of voids during deformation affect the local entanglement densities in a significant manner.

#### 3:40 PM Break

#### 4:00 PM Invited

**Nanomechanical Properties of Human Vimentin Intermediate Filaments:** *Markus Buehler*<sup>1</sup>; Zhao Qin<sup>1</sup>; <sup>1</sup>Massachusetts Institute of Technology

Intermediate filaments (IFs), in addition to microtubules and microfilaments, are one of the three major components of the cytoskeleton in eukaryotic cells. Here we present the development of a full atomistic molecular model of the vimentin dimer and tetramer, based on a bottom-up molecular dynamics simulation approach. We report an analysis of the behavior of IF dimers and tetramers under mechanical stress, including studies of changing the pulling velocity and a detailed analysis of the deformation and rupture mechanisms. We observe a transition of alpha-helices to beta-sheets under mechanical deformation, as has been observed indirectly in earlier experimental studies in similar materials, enabling the protein filaments to sustain large tensile strain in excess of several hundred percent strain at very large failure strength approaching several nN. We compare our results quantitatively with AFM results of IF stretching, showing good agreement. We also discuss the mechanics of IF networks in cells.

#### 4:30 PM

**Multi-Scale Model for the Extreme Piezoresistivity in Silicone/Nickel Nanostrand Nanocomposites:** *Oliver Johnson*<sup>1</sup>; *George Kaschner*<sup>2</sup>; Thomas Mason<sup>2</sup>; David Fullwood<sup>1</sup>; Brent Adams<sup>1</sup>; George Hansen<sup>3</sup>; <sup>1</sup>Brigham Young University; <sup>2</sup>Los Alamos National Laboratory; <sup>3</sup>Conductive Composites Company, LLC.

Extreme piezoresistivity was discovered in a novel Silicone/Nickel Nanostrand/Nickel Coated Carbon Fiber (Si/NiNs/NCCF) nanocomposite. The three-dimensional structure of this nanocomposite system has been investigated using Focused Ion Beam (FIB) and Scanning Electron Microscopy (SEM). The inter-nanoparticle distance distribution has been established. A novel technique was developed to study the charge transport phenomena responsible for the extreme piezoresistivity in the Si/NiNs/NCCF system using conductive nanoindentation. Using this information, finite element simulations have been developed to investigate the evolution of the inter-nanoparticle distance distribution with bulk material deformation. A quantitative quantum mechanical

# Technical Program

tunneling (QMT)/percolation model has been developed based upon first principles, which bridges the gap between quantum effects at the nanoscopic scale and bulk material response at the macroscopic scale. The predictions of this model are compared to experimental measurements conducted under various environmental conditions.

## 4:50 PM Invited

**Nanomechanical Energy Exchange and Dissipation:** Jeffrey Grossman<sup>1</sup>; P. Alex Greaney<sup>1</sup>; <sup>1</sup>Massachusetts Institute of Technology

We review our recent work employing classical molecular dynamics simulations to understand the details of vibrational energy transfer at the nanoscale, and ways in which the unique behaviors of nanomechanical energy exchange could be utilized for the development of completely novel detection strategies. In addition, we present results from the simulation of dissipation in carbon nanotube resonators, where anomalous dissipation is observed during the ringdown of a flexural mode, leading to variations in the quality factor of more than an order of magnitude.

## 5:20 PM

**Study of Thermo Mechanical Behavior of Plasma Nano Coated TiNi Shape Memory Alloy (SMA) for Biomedical Applications Using Finite Element Method:** Payodhar Padhi<sup>1</sup>; Ramakanta Behuria<sup>2</sup>; <sup>1</sup>Hi-Tech Medical College and Hospital; <sup>2</sup>Konark Institute of Science and Technology

Shape-memory alloys (SMAs) are metals that at a certain temperature revert back to their original shape when being strained. The combination of good biocompatibility, good strength and ductility with the specific functional properties of SMA such as the shape memory effect, damping capacity and superelasticity create a smart material for biomedical applications. Some of the most innovative SMA devices include: the self expanding stents, shape memory staples, vascular filters, orthodontic arch wires and porous implants. In present study the temperature distribution induced during plasma coated was calculated using a two-dimensional finite element model (FEM) in ANSYS, finite element solver. To reduce computation time, a part of the NiTi-coated side affected by the plasma will be modeled. The size of the model could be further reduced using axis of symmetry. The film was simulated using 5-node rectangular shell. The paper studies the thermo mechanical effect of SMA for an expanding stents.

## 5:40 PM

**Spatial Nonlocality and the Viscosity of Polymer Melts toward their Glassy State:** Ruslan Puscasu<sup>1</sup>; Billy Todd<sup>1</sup>; Peter Daivis<sup>2</sup>; Jesper Hansen<sup>1</sup>; <sup>1</sup>Swinburne University of Technology; <sup>2</sup>RMIT University

Once the confinement of fluids approaches molecular dimensions, classical theory must be generalized to allow for local position dependent coefficients. It has been recently shown that for flow fields with high gradients in the strain rate over the with of the real-space kernels nonlocality plays a significant role [Todd et al., Phys. Rev. Lett. 100, 195901 (2008)]. An extended analysis of the exact nonlocal viscous kernel for undercooled polymer melts is presented. We compute the k-space and r-space kernels calculated from the stress and transverse momentum density autocorrelation functions. Functional forms have been found to fit the kernel data. The results show that the kernels have a width of a few molecular diameters which means that the generalized transport coefficients must be used in predicting the flow properties of fluids on length scales where the gradient in the strain rate is of the order of these dimensions (eg in nanofluidics).

## Neutron and X-Ray Studies of Advanced Materials III: Applications of Line Profile Analysis

*Sponsored by:* The Minerals, Metals and Materials Society, ASM International, TMS Structural Materials Division, TMS/ASM: Mechanical Behavior of Materials Committee, TMS: Titanium Committee  
*Program Organizers:* Rozaliya Barabash, Oak Ridge National Laboratory; Jaimie Tiley, Air Force Research Laboratory; Erica Lilleodden, GKSS Research Center; Peter Liaw, University of Tennessee; Yandong Wang, Northeastern University

Tuesday PM Room: 303  
February 16, 2010 Location: Washington State Convention Center

*Session Chairs:* Emil Zolotoyabko, Technion, Israel; Peter Liaw, University of Tennessee Knoxville

## 2:00 PM Keynote

**X-Ray Line Profile Analysis – An Ideal Tool to Quantify Structural Parameters of Nanomaterials:** Michael Zehetbauer<sup>1</sup>; Erhard Schafner<sup>1</sup>; Michael Kerber<sup>1</sup>; Sigrid Bernstorff<sup>2</sup>; Tamas Ungar<sup>3</sup>; <sup>1</sup>University of Vienna; <sup>2</sup>Sincrotrone Trieste S.C.p.A.; <sup>3</sup>Eötvös Lorand University Budapest

For a long time the shift and broadening of Bragg profiles have been used to evaluate internal stresses and coherent domain sizes, i.e. the smallest crystalline region without lattice defects. Modern technology provides both enhanced detector resolution and high brilliance X-ray sources thus allowing measurements with high resolution in space and time. In parallel to the hardware, also diffraction theories have been substantially improved so that the shape of Bragg profiles can be quantitatively evaluated not only in terms of the crystallite size and -distribution, but also in terms of the density, type and arrangement of dislocations, twins and stacking faults. Thus state-of-the-art X-ray line profile analysis enables the thorough characterization especially of nanostructured materials which also contain lattice defects. The method can be also used to prove the existence of dislocations in crystalline material. Examples with nanostructured metals, ceramics, polymers and even molecular crystals like fullerenes are given.

## 2:30 PM Invited

**In-Situ Synchrotron and Neutron Diffraction Studies of Deformation Behaviors at Small Length Scales:** Xun-Li Wang<sup>1</sup>; Sheng Cheng<sup>2</sup>; Alexandru Stoica<sup>1</sup>; Joe Horton<sup>1</sup>; C. T. Liu<sup>3</sup>; Peter Liaw<sup>2</sup>; Liang Zuo<sup>4</sup>; <sup>1</sup>Oak Ridge National Laboratory; <sup>2</sup>University of Tennessee; <sup>3</sup>Hong Kong Polytechnic University; <sup>4</sup>Northeastern University

There have been considerable debates over the deformation mechanisms at small length scales. In-situ synchrotron and neutron diffraction were used to study deformation mechanisms in Ni over a broad range of grain sizes, under both monotonic and cyclic loading conditions. The experimental data show that unlike in coarse-grained metals, where the deformation is dominated by dislocation slip, plastic deformation in nanocrystalline Ni is mediated by grain-boundary activities, as evidenced by the lack of intergranular strain and texture development. For ultrafine-grained Ni, although dislocation slip is an active deformation mechanism, deformation twinning also plays an important role, whose propensity increases with the grain size. This research was supported by U.S. Department of Energy (DOE), Office of Basic Energy Sciences, under Contract DE-AC05-00OR22725 with UT-Battelle, LLC. LZ and XLW thank Natural Science Foundation of China for supporting their collaborative research (No. 50528102).

## 2:50 PM Invited

**Neutron Diffraction and Micromechanics Studies of the Fatigue Crack Deformation Behavior:** Yanfei Gao<sup>1</sup>; Rozaliya Barabash<sup>2</sup>; Lili Zheng<sup>1</sup>; Sooyeol Lee<sup>1</sup>; Hahn Choo<sup>1</sup>; Peter Liaw<sup>1</sup>; <sup>1</sup>University of Tennessee; <sup>2</sup>Oak Ridge National Laboratory

The general deformation characteristics near a fatigue crack tip include a plastic zone in front of the crack tip and a plastic wake left behind, where the cyclic loading and fatigue crack growth lead to a compressive strain. The magnitude and distribution of the compressive strain in this plastic wake depend on the stress multiaxiality, material properties, and crack growth increment in each loading cycle. We compare lattice strain measurements by the neutron diffraction technique and simulations by an irreversible and hysteretic cohesive-



interface model, which is developed to simulate the fatigue crack nucleation and growth. Crystal plasticity simulations have been conducted to relate the macroscopic and lattice strains. Good agreement between micromechanical models and neutron strain measurements has been reached.

### 3:10 PM Invited

#### **Diffraction Line Profile Analysis for the Study of Transformation Kinetics in Nanocrystalline Materials:** *Paolo Scardi*<sup>1</sup>; <sup>1</sup>University of Trento

Diffraction techniques in kinetics studies are mostly employed to identify and quantify phase changes. However, further information can be obtained from the study of the line profiles. This is especially useful when studying the evolution of nanocrystalline and of heavily deformed materials during high temperature kinetics. Modern methods of diffraction profile modeling provide a detailed picture of the nanostructure in terms of crystalline domain size/shape distribution and density of lattice defects, together with the usual information on phase composition. This information can be collected also during the kinetics, by in situ measurements. As data quality is an important issue in line profile studies, the high brilliance and focusing of synchrotron beams are a valuable support to follow fast kinetics. This contribution will show results of line profile analysis in kinetics studies of grain growth in different nanocrystalline systems. Recent advancements in line profile analysis will also be reviewed.

### 3:30 PM Invited

#### **Single-Grain Microstructure from Polycrystalline Specimens:** *Tamas Ungar*<sup>1</sup>; <sup>1</sup>Eötvös University Budapest

X-ray line profile analysis proves to be a powerful method to characterize the microstructure of crystalline materials. In its conventional application it provides data about the average properties of large aggregates of crystallites. Synchrotrons facilitate to extract single-grain or single-crystallite microstructure properties in powder- or polycrystalline specimens. The lecture will deal with the method itself, first results provided by the method and the scientific possibilities offered by the procedure.

### 3:50 PM Invited

#### **Evolution of Microstructure during Tensile Deformation of TWIP Steel: X-Ray Line Profile Analysis:** *Hahn Choo*<sup>1</sup>; *Tamas Ungar*<sup>2</sup>; *Yang Ren*<sup>3</sup>; *Sang-Ho Han*<sup>4</sup>; <sup>1</sup>University of Tennessee; <sup>2</sup>Eotvos University; <sup>3</sup>Argonne National Laboratory; <sup>4</sup>POSCO

The evolution of average grain size, dislocation density, twin density, and crystallographic texture was investigated during the tensile deformation of twinning-induced plasticity (TWIP) steel using high-energy synchrotron x-ray diffraction and line profile analysis. TWIP steel, recently developed by POSCO for automotive applications, exhibits an excellent combination of high strength (about 1 GPa tensile strength) and ductility (about 65% total elongation). In this study, we investigated the volumetric evolution of twin volume fraction and dislocation density as a function of the tensile plastic deformation to further the understanding of the interaction between the twin and dislocation and its influence on hardening and ductility of the TWIP steel.

### 4:10 PM Invited

#### **Neutron Diffraction and EPSC Modeling:** *Bjørn Clausen*<sup>1</sup>; *Donald Brown*<sup>1</sup>; *Carlos Tomé*<sup>1</sup>; *Laurent Capolungo*<sup>2</sup>; *Sean Agnew*<sup>3</sup>; <sup>1</sup>Los Alamos National Laboratory; <sup>2</sup>Georgia Tech-Lorraine; <sup>3</sup>University of Virginia

In-situ neutron diffraction measurements provide volume averaged bulk information about the evolution of internal strain, texture and defect concentration during deformation. The information contained in each diffraction peak originates solely from the sub-set of grains within the polycrystal that has the given lattice plane normal parallel to the scattering vector for the detector. This level of detail is well matched by the EPSC model that is based upon a discrete set of single crystals with an orientation distribution representative of the actual texture of the material. By selecting sub-sets of grains based upon their orientation it is possible to generate average values of elastic strains, weight fractions and dislocation densities from the model that can be directly compared to the peak shifts, peak intensities and peak widths from the diffraction measurements. The two techniques are frequently used in combination to elucidate material properties not probable by other means.

### 4:30 PM Break

### 4:40 PM Invited

#### **Phase Transformation and Tensile Behavior of a Bainite Steel Studied by In Situ Neutron Scattering and Dilatometry:** *Yo Tomota*<sup>1</sup>; *Min-Seo Koo*<sup>1</sup>; <sup>1</sup>Ibaraki University

Bainitic transformation was monitored simultaneously by a dilatometer test and neutron scattering. The changes in lattice constants and volume fractions of bainitic ferrite and the retained austenite were measured by high angle diffraction while the size distribution of bainite lath by small angle scattering. In both cases, the transformation kinetics was estimated from the specimen length change with the dilatometer. These three data show good agreements and hence the detailed mechanism of the bainitic transformation at a very low temperature like 573K resulting in nano-size scaled layer structure with ferrite and carbon enriched austenite was totally discussed. Then, the tensile behavior of the bainite steel was studied by neutron diffraction during tension test. The stress partitioning between ferrite and austenite, i.e., phase strains and among differently hkl oriented grains, i.e., intergranular strains and stress-induced martensitic transformation were found to change with work-hardening.

### 5:00 PM Invited

#### **Line Broadening Analysis of High Resolution X-ray Data:** *I. Noyan*<sup>1</sup>; *Andrew Ying*<sup>1</sup>; *Conal Murray*<sup>2</sup>; <sup>1</sup>Columbia University; <sup>2</sup>IBM Research Division

We report thickness values measured from a set of ideal samples (semiconductor grade silicon-on-insulator thin films) using the Scherrer equation (FWHM and integrated-breadth variants), rocking-curve modeling, thickness fringe analysis, Fourier analysis, the Warren-Averbach method (single peak and multiple-order variants), the Williamson-Hall method as well as from x-ray reflectivity and cross-sectional transmission electron microscopy. We will compare these results and discuss the applicability of these techniques to various types of samples.

### 5:20 PM

#### **Characterization of Pt Nanoparticles by Debye Function Analysis of the X-Ray Diffraction Pattern:** *Kenneth Beyerlein*<sup>1</sup>; *Paolo Scardi*<sup>2</sup>; *Bob Snyder*<sup>1</sup>; <sup>1</sup>Georgia Institute of Technology; <sup>2</sup>University of Trento

One of the most promising and immediate applications of nanoparticles is their use as highly efficient, energy saving catalysts for industrial chemical synthesis. Their efficiency is dependent on the small particle size and in some cases the particle shape. A whole pattern Debye Function Analysis technique of extracting this important microstructure information from the x-ray diffraction pattern will be presented. Platinum nanoparticles prepared by a salt reduction process with sizes ranging from 1-20nm were the focus of this study. Synchrotron diffraction patterns from these particles were analyzed by this Debye approach with the size distribution, particle shape abundance, and faulting densities determined. The results of this analysis will be compared with the quantities obtained by Transmission Electron Microscopy image analysis.

### 5:30 PM Invited

#### **Protein Powder Diffraction and Materials Science:** *Robert Von Dreele*<sup>1</sup>; <sup>1</sup>APS/Argonne National Laboratory

Protein crystallography and materials science might appear to be non-intersecting fields of science, however powder diffraction provides insight into the materials science aspects of crystalline proteins. Surprisingly, proteins provide extremely sharp powder diffraction patterns that are sensitive to sample environment and composition (pH, salt concentration, etc.). Amongst other things, these changes provide a means of extracting sufficient information to partially overcome the extreme peak overlap problem inherent in protein powder patterns. Protein powder patterns also allow examination of protein crystallization, the effect of radiation damage and crystalline phase changes. This talk will review the current status of these and other aspects of this new field. This work was supported by the U.S. Department of Energy, Office of Science, Office of Basic Energy Sciences under contract number DE-AC02-06CH11357.

### 5:50 PM

#### **Quantifying the Evolution of Lattice Strain due to Cyclic Loading in 7075 Aluminum Alloy:** *Jay Schuren*<sup>1</sup>; *Matthew Miller*<sup>1</sup>; *Alex Kazimirov*<sup>2</sup>; <sup>1</sup>Cornell University; <sup>2</sup>Cornell High Energy Synchrotron Source

X-ray diffraction experiments during in-situ cyclic mechanical loading were used to quantify the lattice strain distributions within a polycrystalline

# Technical Program

aluminum alloy (AA7075-T6) at various points in the cyclic loading. By isolating the changes between the lattice strain distributions at different points in the sample's cyclic life we investigated the evolution of the lattice strain distributions as the sample progressed toward fatigue failure. The focus of this presentation will be on a new method for quantifying the image specific experimental resolution, the requirement of a statistically significant population of crystals in each measurement, and the evolution of lattice strain distributions due to cyclic loading in AA7075-T6 undergoing zero-tension macroscopic loading.

## **Pb-Free Solders and Emerging Interconnect and Packaging Technologies: Reliability (II)**

*Sponsored by:* The Minerals, Metals and Materials Society, TMS Electronic, Magnetic, and Photonic Materials Division, TMS: Electronic Packaging and Interconnection Materials Committee

*Program Organizers:* Kwang-Lung Lin, National Cheng Kung University; Sung Kang, IBM; Jenq-Gong Duh, National Tsing-Hua University; Laura Turbini, Research In Motion; Iver Anderson, Iowa State University; Fu Guo, Beijing University of Technology; Thomas Bieler, Michigan State University; Andre Lee, Michigan State University; Rajen Sidhu, Intel Corporation

Tuesday PM                      Room: 204  
February 16, 2010              Location: Washington State Convention Center

*Session Chairs:* Rajen Sidhu, Intel Corp.; Alexandre Kodentsov, Eindhoven University of Technology

### **2:00 PM**

**Impact of Isothermal Aging on Long Term Reliability of Fine Pitch Ball Grid Array Packages with Sn-Ag-Cu Solder Interconnects:** *Tae-Kyu Lee<sup>1</sup>; Weidong Xie<sup>1</sup>; Kuo-Chuan Liu<sup>1</sup>; Thomas R. Bieler<sup>2</sup>; <sup>1</sup>Component Quality and Technology, Cisco Systems; <sup>2</sup>Chemical Engineering and Materials Science, Michigan State University*

The interaction between isothermal aging and long term reliability of fine pitch ball grid array packages with Sn-3.0Ag-0.5Cu (wt%) solder interconnects are investigated. In this study, 0.4mm fine pitch packages with 300/956m diameter Sn-Ag-Cu solder balls are used. Two different die sizes and package substrate surface finishes are selected to compare the internal strain impact and alloy effect during thermal cycling. The samples are isothermally aged and thermal cycled from 0 to 100°C with a 10minute dwell time. Based on weibull plots for each condition, the lifetime of the package reduced approximately 45% with 150°C aging precondition and with longer time for 100°C aged samples. The microstructure evolution is observed during thermal aging and thermal cycling, focused on Sn grain single to multi grain transformation. Different mechanisms after aging in various conditions are observed and their impact on lifetime reduction is discussed.

### **2:15 PM**

**Pb-Free Process Development for Microcircuit Package Assemblies – A University/Industry Design Project Collaboration:** *Mike Powers<sup>1</sup>; Jim Shackelford<sup>2</sup>; Derek Fong<sup>2</sup>; Zi Gwen Kwan<sup>2</sup>; Tammy Leung<sup>2</sup>; Kit-Ying Mak<sup>2</sup>; Enrique Pedron<sup>2</sup>; Raminderdeep Sidhu<sup>2</sup>; Hong-Siang Wei<sup>2</sup>; <sup>1</sup>Agilent Technologies; <sup>2</sup>University of California Davis*

A team of engineering students in the Department of Chemical Engineering and Materials Science at the University of California Davis collaborated on a design project investigation to develop a cost effective process for Pb-free solder assembly of hybrid microcircuit package assemblies employed in test and measurement instruments (a “real” materials design project). The students considered the required materials properties, as dictated by the component assembly design, and how the properties are affected by materials selection and the joining process. The team conducted solder joint strength, Au embrittlement and solder wetting experiments at UC Davis in order to evaluate the process design. The team also conducted process development, including furnace profiling and reliability testing, at Agilent facilities in Santa Rosa, California. Through applied research and testing the student team developed a reliable Pb-free process for solder assembly of the hybrid microcircuit package assembly project vehicle.

### **2:30 PM**

**Reliability Evaluation of Cu-Cored Solder Joints:** *YunSung Kim<sup>1</sup>; Eunsik Kim<sup>2</sup>; Heylim Choi<sup>1</sup>; Jungtak Moon<sup>2</sup>; Heeman Choe<sup>2</sup>; <sup>1</sup>Kookmin University; <sup>2</sup>MK Electron Co*

Recently, copper-cored solder balls have attracted attention in microelectronic packaging community for two main reasons; first, they are known to have enhanced resistance to electromigration failure. Second, Cu-cores in the solder balls can serve as a spacer during reflow and prevent the solder balls from touching each other when the ball size and pitch is very small as in high-density BGA or CSP packages. As little data is available in the literature primarily on the shear strength of Cu-cored solder joints, an extensive study is required to evaluate fully the reliability of Co-cored solder joints both at package- and board-levels. In this study, we are assessing the physical and mechanical properties of the Cu-cored solder joints using several test methods, such as thermal cycling and high-speed ball pull tests to compare to those of conventional Sn-Ag-Cu solder joints.

### **2:45 PM**

**Roles of Service and Materials Parameters on Reliability of Pb-Free, Sn-Based, Solder Joints:** *K.N. Subramanian<sup>1</sup>; Andre Lee<sup>1</sup>; <sup>1</sup>Michigan State University*

Isothermal mechanical testing of single shear-lap specimens of Pb-free, Sn-based, solder joints at various temperatures ranging from -55°C to 150°C indicate different modes of deformation to be dominant in different temperature ranges. These observations also indicated the role of strain-rate on the mode of deformation. Importance of these findings on thermomechanical behavior of high Sn-based solder joints will be discussed along with their implications on testing parameters employed in accelerated thermal cycling tests. Results from repeated thermal shock, thermomechanical fatigue (with different dwell-times at temperature extremes, different heating- rates, and in different temperature ranges), and iso-thermal stress relaxation studies will be presented to illustrate these implications. These findings bring out the critical issues that need to be taken into consideration in designing accelerated thermomechanical test methods for long-term reliability of Sn-based solder joints.

### **3:00 PM**

**Thermal and Mechanical Fatigue Reliability of TiW/Cu and Al/Cu Underbump Metallizations on Glass Substrate:** *Yong Jun Oh<sup>1</sup>; Chul Min Choi<sup>1</sup>; Jae Ho Kim<sup>1</sup>; <sup>1</sup>Hanbat University*

Direct formation of interconnect lines and underbump metallization (UBM) on glass substrates is a promising technique that enables simple and cost-effective sensor chip packaging. In this study, the joint reliability of SnAg solder/UBM(TiW/Cu or Al/Cu)/glass under thermal and bending fatigue cycles is evaluated. The TiW/Cu UBM is fabricated by sputter deposition of TiW onto glass and electroplating of Cu, while the Al/Cu UBM is formed by anodic bonding of glass to Al and electroplating of Cu onto Al. SnAg solder bumps are electroplated on both the UBMs and reflowed at 260°C. The samples are exposed to temperature cycles between -20 and +120°C. The three-point bending test is conducted for rectangular specimens with a dimension of 10×20 mm<sup>2</sup> (L×W) at ambient temperature. The failure mechanisms under thermal and mechanical fatigue are presented from the viewpoint of the strength of each layer and its bonding strength with the joined materials.

### **3:15 PM**

**Accelerated Life Prediction of Electrochemical Ion Migration on ENIG Surface Finish Circuit:** *Won Sik Hong<sup>1</sup>; No Chang Park<sup>1</sup>; <sup>1</sup>Korea Electronics Technology Institute(KETI)*

Electrochemical metallic ion migration(ECM) can be generated by electrochemical reaction between anodic and cathodic electrode on electric circuit in case of existing temperature, humidity and applied voltage, and finally induce to malfunction of electronics due to precipitation of metallic ion in cathode. Thus we have studied failure mechanism and accelerated life prediction method of ECM occurrence. Modified Eyring model which is combined stress model(temperature, humidity, voltage) was utilized to accelerated life prediction model. To obtain temperature and humidity coefficient factors of ECM failure, accelerated life test was conducted by more than f(50%) failure. Failure criterion of insulation resistance was 10E7O. From these results, we have deduced temperature and humidity coefficient factors of acceleration model for predicting ECM failure life. Also electrochemical oxidation and reduction mechanism of ECM were examined by physics-of-failure based



failure analysis. These results would be helpful to predict the life of electronic circuit due to ECM failure.

### 3:30 PM Break

### 3:45 PM

**Space: The Final Frontier for Pb-Free Electronics?:** *David Witkin*<sup>1</sup>; <sup>1</sup>The Aerospace Corporation

While military and aerospace electronics are currently exempt from RoHS prohibitions on Pb in electronics, the Pb-free transition in the consumer electronics industry has influenced exempt industries. Long-term costs of Pb-free interdiction and sourcing of Sn-Pb parts may soon exceed the costs to find an acceptable Pb-free solution for high-reliability systems in harsh usage environments. Space electronics systems are low-volume and high cost. In these systems, solder joints are subjected to multi-year storage times and extensive ground testing before launch, and are not accessible for inspection or repair after launch. The question arises as to whether Pb-free solders well suited to the unique assembly, test, storage and orbit environments are the same as those being pursued for other industries. Using previous reliability testing programs as a guide, Bi-containing Sn-Ag solders were selected for characterization. The microstructural evolution and mechanical properties of Bi-bearing solders were compared to SAC305, exhibiting significant differences.

### 4:00 PM

**Creep Property of Sn-3Ag-0.5Cu-xNi/Au/Ni Joints after Aging:** *Chung-Nan Peng*<sup>1</sup>; *Jeng-Gong Duh*<sup>2</sup>; *Tae-Kyu Lee*<sup>3</sup>; *Kuo-Chuan Liu*<sup>3</sup>; *Michael Tsai*<sup>3</sup>; <sup>1</sup>Department of Materials Science and Engineering, National Tsing Hua University; <sup>2</sup>Department of Materials Science and Engineering, National Tsing Hua University; <sup>3</sup>Interconnect Technology Team Reliability Engineer, Manufacturing Technology Group, CISCO

In BGA packages and flip-chip packages, SnAgCu solder alloys have been regarded as the most promising Pb-free substitutes for the SnPb solder. However, flip chip package solder joints suffer thermomechanical fatigue and creep failures due to the CTE mismatch between silicon die and substrate. In this study, creep tests were conducted on Sn-3Ag-0.5Cu-xNi/Au/Ni ( $x = 0-0.1$  wt.%) joints at 100°C and 150°C, respectively. Various creep parameters, such as global and localized creep strain, variation of creep strain and strain-rate for creep were determined. It was demonstrated that the observed behavior could be well-fitted using creep constants for Sn-3Ag-0.5Cu-xNi/Au/Ni joints in the modified creep power law. In addition, the effect of Ni content in the solder on the grain-orientation-dependent elastic deformation state was also discussed. Microstructure characterization, including EBSD and FE-EPMA analysis, were used to describe the creep behavior of the Sn-3Ag-0.5Cu-xNi/Au/Ni joints.

### 4:15 PM

**Interface Design of Lead-Free Electronic Interconnects:** *K.N. Subramanian*<sup>1</sup>; *Deep Choudhuri*<sup>1</sup>; *Andre Lee*<sup>1</sup>; <sup>1</sup>Michigan State University

Service reliability of lead-free electronic components is significantly affected by the thermal excursions encountered during service. Catastrophic crack that develops from such thermal excursions due to coefficient of thermal expansion mismatches are invariably at the interfaces, especially at the tin/tin grain boundaries or tin/(intermetallic-compound) interfaces, near the solder/substrate interface regions. Keying such interfaces to retard sliding of mating regions, or stitching such mating regions to prevent de-cohesion and dissipate stresses by promoting plastic deformation in tin grains, enhances the reliability of the lead-free electronic interconnects. Reinforcing lead-free solders containing significant amounts of tin with Nano-structured Polyhedral Oligomeric Silsesquioxane (POSS), consisting of Si-O cages with surface active radicals, provides such attributes to enhance the service reliability of interconnects made with them.

### 4:30 PM

**Study of the Impact Performance of Solder Joints by High-Velocity Impact Tests:** *Ning Zhang*<sup>1</sup>; *Yao Shi*<sup>2</sup>; *Fu Yang*<sup>3</sup>; <sup>1</sup>Beijing University of Technology and University of Kentucky; <sup>2</sup>Beijing University of Technology; <sup>3</sup>University of Kentucky

The impact behavior of solder joints were studied using three different high-velocity impact tests of the U-notch Charpy impact test, the No-notch Charpy impact test and a lab-designed drop test. The solder joints were made of five solder alloys, Sn37Pb, Sn3.8Ag0.7Cu, Sn2.0Ag0.7Cu, Sn1.0Ag0.7Cu and Sn0.7Ag0.7Cu (in weight percent), in which the traditional Cu/solder/Cu

butt joint was used. All three impact tests gave the same trend of the impact behavior of the solder joints with the Sn37Pb joints having the highest impact resistance and the Sn3.8Ag0.7Cu joints having the lowest impact resistance. For the lead-free joints, the Sn1.0Ag0.7Cu joints had better impact resistance than the Sn2.0Ag0.7Cu, and the Sn2.0Ag0.7Cu joints better than the Sn0.7Ag0.7Cu. The impact behavior was correlated to the fracture morphologies from the SEM micrographs. The comparison of three cases showed that the No-notch Charpy impact test is a promising method for evaluating the drop performance of solder joints.

### 4:45 PM

**Investigation and Effects of Wafer Bow in Different 3D Stacking Schemes:** *Kuan-Neng Chen*<sup>1</sup>; *Y. Zhu*<sup>2</sup>; *W. W. Wu*<sup>1</sup>; *R. Reif*<sup>3</sup>; <sup>1</sup>National Chiao Tung University; <sup>2</sup>IBM T J Watson Research Center; <sup>3</sup>Massachusetts Institute of Technology

3D stacking technology has become an attractive candidate for future packaging and semiconductor applications. The reliability of this technology is definitely a significant consideration before it can be fully used for products. The reliability of 3D stacking, which is related to the quality of stacking, is highly dependent with wafer bow. Wafer bow, also as known as "wafer warpage", is contributed by materials on the wafer and process steps. When the wafer bow is too large, the stacking quality is affected and thus a reliability issue is occurred. This paper investigated the effects of wafer bow in different 3D stacking schemes, including metal bonding, oxide fusion bonding, and SOI-based layer transfer technology. Fabrication considerations and material selections are discussed for minimizing wafer bow in 3D stacking applications.

### 5:00 PM

**Shear and Bending Fatigue Failure of Lead Free Solder Joint and Fracture Mechanics:** *Huili Xu*<sup>1</sup>; *Woong Ho Bang*<sup>1</sup>; *Choong-Un Kim*<sup>1</sup>; *Tae-Kyu Lee*<sup>2</sup>; *Hongtao Ma*<sup>2</sup>; *Kuo-Chuan Liu*<sup>2</sup>; <sup>1</sup>University of Texas at Arlington; <sup>2</sup>Cisco System Inc.

With continuing miniaturization of packaging structure for electronic devices, the reliability failure at solder joint is becoming of major concern in microelectronic industry. Among many mechanisms leading to solder joint failure, the fracture by cyclic bending, shear, and shock load is particularly concerned. Conventionally, those load conditions rarely contribute to the joint failure; however, with an expansion of mobile electronics combined with compact packaging structure, they are becoming equally problematic to more conventional cyclic thermal load. Consequently, there are growing numbers of research conducted on this subject in recent years, yet understanding on the involved fracture mechanics is still unclear. This paper presents the result of our investigation, both theoretical and experimental, that aim to identify the fracture mechanics active in cyclic bend and shear fatigue and the contributing factors to the fracture at each fatigue mode including type of solder alloy, mechanical constraints, and fatigue conditions.

### 5:15 PM

**Investigating Defects in through-Silicon via (TSV) Chains by Three Dimensional Imaging Reconstruction:** *Alphonse-Marie Kamto Tegueu*<sup>1</sup>; *Robert Morris*<sup>1</sup>; *Gregory Thompson*<sup>1</sup>; *Susan Burkett*<sup>1</sup>; <sup>1</sup>The University of Alabama

Metal filled through-silicon vias (TSVs) allow electronic devices to be connected using a three dimensional approach. This technology is being optimized to address the need for increased functionality and performance. Vias with tapered sidewalls are formed in our laboratory, lined with silicon dioxide, titanium, and copper as insulation, barrier, and seed films, respectively. Vias are then filled with copper by a pulsed electroplating process. The process wafer is attached to a carrier before mechanically thinning the process wafer back side. The base of the vias is exposed from the opposite side and contact pads are formed for testing the electrical resistance of vias chained together. Discontinuity in the via chains can be investigated by a procedure involving multiple polishing and imaging steps along both the diameter and depth of the vias. Three dimensional imaging reconstruction will be described for TSVs as useful method for investigating possible defects or failures.

Tue. PM

# Technical Program

## Phase Stability, Phase Transformations, and Reactive Phase Formation in Electronic Materials IX: Session IV

*Sponsored by:* The Minerals, Metals and Materials Society, TMS Electronic, Magnetic, and Photonic Materials Division, TMS Structural Materials Division, TMS: Alloy Phases Committee

*Program Organizers:* Chih-ming Chen, National Chung Hsing University; Srinivas Chada, Medtronic; Sinn-wen Chen, National Tsing-Hua University; Hans Flandorfer, University of Vienna; A. Lindsay Greer, University of Cambridge; Jae-ho Lee, Hongik University; Kejun Zeng, Texas Instruments; Yee-wen Yen, National Taiwan University of Science and Technology; Wojciech Gierlotka, AGH University of Science and Technology; Chao-hong Wang, National Chung Cheng University

Tuesday PM                      Room: 203  
February 16, 2010              Location: Washington State Convention Center

*Session Chairs:* Wojciech Gierlotka, AGH University of Science and Technology; Clemens Schmetterer, University of Vienna

### 2:00 PM Invited

**High Temperature Lead-Free Solder: Solidification Behavior of (Cu,Ni)-Sn-Zn:** *Hans Flandorfer*<sup>1</sup>; Clemens Schmetterer<sup>1</sup>; Matthieu Froger<sup>1</sup>; Herbert Ipson<sup>1</sup>; <sup>1</sup>University of Vienna

In order to obtain solder joints for e.g. die-attach and BGA (Ball Grid Array) solder spheres, chip-scale package (CSP) and multi-chip modelling (MCM), solder materials with a higher melting regime (> 230 °C) are necessary. The hitherto used high Pb solders (up to 85 % Pb) need to be substituted by lead-free materials. Promising candidates for such lead-free solders are e.g., alloys of the systems Cu-Sn-Zn and Ni-Sn-Zn. Knowledge about these systems is highly important as it provides detailed information to the solidification behavior and formation of intermetallic phases. This is a crucial point for the control of the microstructure and texture of alloys and alloy interfaces. The systems Cu-Sn-Zn and Ni-Sn-Zn have been investigated by means of XRD, DTA and metallography including EPMA techniques. Isothermal sections of Cu-Sn-Zn and Ni-Sn-Zn at various temperatures will be presented here. The resulting phase diagrams are also based on a careful literature assessment.

### 2:25 PM Invited

**Phase Diagrams in Lead-Free Soldering:** *Clemens Schmetterer*<sup>1</sup>; Hans Flandorfer<sup>1</sup>; Herbert Ipson<sup>1</sup>; <sup>1</sup>University of Vienna

During soldering layers of intermetallic compounds (IMCs) are created, which influence the mechanical joint-stability. Knowledge of these IMCs, required to understand their formation, is conveniently summarized by the phase diagram containing the constituents of the solder and the contact material. Within COST Actions 531 and MP0602 emphasis has been placed on the experimental and thermodynamic study several intermetallic systems, like Ag-Cu-Ni-Sn and its subsystems and Ni-P-Sn for conventional soldering, or Sn-Zn and Sn-Au based systems for HT-soldering. Other systems have been studied as well in order to explore many promising systems, but some of these may only find use in niche-applications, e.g. In-Ni-Sn, due to the high price of In. Examples from several systems will be presented in this contribution. The experimental phase diagrams will be compared to thermodynamic assessments based on the COST 531 database. Their relevance for soldering and solder related processes will be shown.

### 2:50 PM

**Phase Equilibria in the Sn-Ni-Zn Ternary System:** *Jaewon Chang*<sup>1</sup>; Sun-Kyoung Seo<sup>1</sup>; Hyuck Mo Lee<sup>1</sup>; <sup>1</sup>KAIST

In the electronic packaging field, the minor addition of Ni and Zn in Sn-based Pb-free solders has been recommended to enhance the mechanical properties of solder joint. In order to thermodynamically evaluate the proper composition level of Ni and Zn as well as to analyze the reaction with the Ni substrate, the thermodynamic data are needed for the Sn-Ni-Zn ternary system. In this study, the phase equilibria of the Sn-Ni-Zn ternary system have been investigated at 473, 773, and 1073K (less than 60 at% Ni). To identify the equilibrium phases, the scanning electron microscopy (SEM), X-ray diffraction (XRD) and electron probe microanalysis (EPMA) were used. On the basis of the experimental data and thermodynamic parameters, the isothermal sections of the Sn-Ni-Zn

ternary system have been modified in consideration of the ternary solubility in the binary compounds.

### 3:10 PM

**Interfacial Reaction between Pure Sn and Cu Foil with Different Cu Grain Sizes:** *Jo Mei Wang*<sup>1</sup>; Jenq Gong Duh<sup>1</sup>; <sup>1</sup>National Tsing Hua University

Cu<sub>6</sub>Sn<sub>5</sub> and Cu<sub>3</sub>Sn were easily formed at the interface between Sn and Cu during reflow and aging process. Thick Cu-Sn compound and Kirkendall voids at the interface would reduce the mechanical strength of solder joints. The IMC growth rate in solder was related to the grain size of Cu foil. In this study, the pure Sn solder was reflowed with the Cu foils with different grain sizes at 250 °C for 1-20 min. It was found out that the Cu foil with small grain size can reduce the IMC growth. In addition, Cu<sub>6</sub>Sn<sub>5</sub> and Cu<sub>3</sub>Sn growth rates were calculated for samples with various Cu grain sizes. The correlation between the grain size and the distribution of Kirkendall voids were also discussed and proposed.

### 3:30 PM

**Interfacial Reactions in the Sn-In-(Zn)/Ag and Sn-In-(Zn)/Ni Couples:** *Ching-feng Yang*<sup>1</sup>; Sinn-wen Chen<sup>1</sup>; <sup>1</sup>National Tsing-Hua University

Sn-In alloys are important low melting-point solders. Ni and Ag are commonly used in electronic products. The dissolution behaviors and intermetallic compound formation of Ag and Ni substrates in the Sn-20In solder with Zn addition up to 5 wt.% upon dissolution are examined at 230°C. The Zn addition in the Sn-20In alloy lowers the solidus and liquidus temperatures, effectively reduces the undercooling, and retards the dissolution rate of Ag substrate. The reaction product in the Sn-In-(Zn)/Ag couple is the  $\xi$  phase when Zn is less than 1 wt.%. When the Zn addition is higher than 1 wt.%, three different Ag-Zn compounds are formed. The reaction product is the Ni<sub>3</sub>Sn<sub>4</sub> phase in the Sn-In-(Zn)/Ni couples when Zn is lower than 2 wt.%. The growth rate of the Ni<sub>3</sub>Sn<sub>4</sub> phase is reduced with Zn addition. When the Zn addition is higher than 2 wt.%, the reaction product changes to the Ni<sub>3</sub>Zn<sub>21</sub> phase.

### 3:50 PM Break

### 4:00 PM Invited

**Enhancement of Heterogeneous Nucleation of  $\beta$ -Sn Phases in Sn-Rich Solders by Adding Minor Alloying Elements with Hexagonal Closed Packed Structures:** Moon Gi Cho<sup>1</sup>; Hyun You Kim<sup>1</sup>; Sun-Kyoung Seo<sup>1</sup>; *Hyuck Mo Lee*<sup>1</sup>; <sup>1</sup>KAIST

The measured undercooling of pure Sn was about 30°C due to the difficulty of nucleating a solid  $\beta$ -Sn phase from a liquid phase. To promote the heterogeneous nucleation of  $\beta$ -Sn phases, the addition of impurity elements to the solders was suggested. Among the impurity elements, alloying elements with hexagonal closed packed (HCP) structures, such as Co, Zn, Ti and Mg, were found effective to enhance heterogeneous nucleation of  $\beta$ -Sn phases in Sn-rich solders. Calculations of the density functional theory indicate that the interfacial energy between  $\beta$ -Sn and Zn was relatively low; furthermore, the surface of Zn (10-11) was estimated to have the lowest interfacial energy with  $\beta$ -Sn phases. Minor alloying elements with HCP crystals are expected to provide more favorable heterogeneous nucleation sites for  $\beta$ -Sn phases.

### 4:25 PM

**Phase Diagram and Thermodynamic Properties of Ag-Cu-In-Sn Quaternary System:** *Wojciech Gierlotka*<sup>1</sup>; Dominika Jendrzyczek-Handzlik<sup>2</sup>; <sup>1</sup>Yuan-Ze University; <sup>2</sup>AGH University of Science and Technology

The Sn-Ag-In alloys are promising lead-free solders. Copper is commonly used as a substrate material and in this case phases relationships and phases stabilities in Ag-Cu-In-Sn quaternary system are very important for electronic industry. The CALPHAD approach was used for thermodynamic modeling of Ag-Cu-In-Sn quaternary system as well as for all the constituents binaries and ternaries systems. Good agreement between calculations and available thermodynamic data was found.

### 4:45 PM

**Interfacial Reaction Effect on Mechanical and Electrical Reliability in Cu/Solder/Cu Bump:** *Myeong-Hyeok Jeong*<sup>1</sup>; Jae-Won Kim<sup>1</sup>; Byunghoon Lee<sup>2</sup>; Kiwook Lee<sup>3</sup>; Jaedong Kim<sup>3</sup>; Hoo-Jeong Lee<sup>2</sup>; Young-Bae Park<sup>1</sup>; <sup>1</sup>Andong National University; <sup>2</sup>Sungkyunkwan University; <sup>3</sup>Amkor Technology Korea

Cu/Solder/Cu bump makes large amount of intermetallic compound and Kirkendall void which can degrade electrical and mechanical reliability. Therefore, it is essential to understand the fundamental growth mechanisms



of IMC and Kirkendall void. And also, their effects on mechanical reliability should be systematically investigated. In this work, we performed kinetic studies on the Cu/Sn/Cu bump structure in order to quantify the amount of intermetallic compound and Kirkendall void by using in-situ annealing and electromigration test in a scanning electron microscope chamber during current stressing conditions with current density of  $2.0 \times 10^4$  A/cm<sup>2</sup> at 125~175oC. Cu<sub>6</sub>Sn<sub>5</sub> and Cu<sub>3</sub>Sn were already formed at interface between Cu bump and solder after reflow. Intermetallic compound growth was significantly enhanced by current stressing where the growth rate follows a linear relationship with stressing time. Finally, their effect on the mechanical reliability of Cu/Sn/Cu bump will be discussed in detail.

### 5:05 PM

**Interaction of Sn-Based Solders with Electroless Nickel Substrates: The Ni-P, Sn-P, and Ni-Sn-P Phase Diagrams:** Clemens Schmetterer<sup>1</sup>; Rajesh Ganesan<sup>1</sup>; Adela Zemanova<sup>2</sup>; Ales Kroupa<sup>2</sup>; Herbert Ipser<sup>1</sup>; Alan Dinsdale<sup>3</sup>; <sup>1</sup>University of Vienna; <sup>2</sup>Institute of Physics of Materials, ASCR; <sup>3</sup>National Physical Laboratory

Electroless nickel substrates contain considerable amounts of phosphorus due to their deposition from aqueous solutions of nickel salts by means of chemical reduction using hypophosphite. In order to understand their reaction with Sn-based solders, a reliable knowledge of the ternary Ni-P-Sn phase diagram is necessary. CALPHAD-type calculations can provide consistent phase diagram information. In the present case experimental phase diagram information was provided for the three title systems. In addition, experimental partial thermodynamic data were obtained for the systems Ni-P and Sn-P, and they were combined with calorimetric measurements of the enthalpy of formation as well as with ab-initio calculations. All these experimental data served as an input into a CALPHAD optimization of the two binary systems Ni-P and Sn-P, and together with available data on the Ni-Sn system, a first attempt was done to extrapolate the ternary Ni-P-Sn system and compare it with the experimental version.

### 5:25 PM

**The Interfacial Reactions of SnAgIn Pb-Free Solders on Cu Substrates:** Yu Yan Jieng<sup>1</sup>; Albert T. Wu<sup>1</sup>; <sup>1</sup>National Central University

Pb-free SnAgIn solder system is an appropriate candidate for its low liquidus temperature that is close to eutectic SnPb solder. Various solder compositions of SnAgIn system were alloyed while the amount of Ag was fixed at 3 wt%. Solders of different compositions were reflowed on Cu substrates at various temperatures for different period of times. Samples were also annealed at 120°C, 150°C and 180°C for prolonged hours for the investigation of solid state aging. The thicknesses of the interfacial compounds, Cu<sub>6</sub>(Sn,In)<sub>5</sub> were calculated, and the kinetics of the growth of compounds is discussed in this paper. ζ-phase particles, solid solution of Ag<sub>4</sub>Sn and Ag<sub>3</sub>In, formed in the solders during reflow and solid state aging. Thermodynamic equilibrium of these phases at various test conditions will be presented.

## Processing Materials for Properties: Light Weight Materials Processing

*Sponsored by:* The Minerals, Metals and Materials Society, TMS Extraction and Processing Division

*Program Organizers:* Brajendra Mishra, Colorado School of Mines; Akio Fuwa, Waseda University; Parituh Bhandhubanyong, National Metal and Materials Technology Center

Tuesday PM Room: 617  
February 16, 2010 Location: Washington State Convention Center

*Session Chairs:* Rachman Chaim, Technion - Israel Institute of Technology; Raman Singh, Monash University

### 2:00 PM Keynote

**Recent Developments in Processing/Structures/Properties Relationships of Titanium Alloys:** Greg Oberson<sup>1</sup>; Sreeramamurthy Ankem<sup>2</sup>; <sup>1</sup>U.S. Nuclear Regulatory Commission; <sup>2</sup>University of Maryland, College Park

While titanium has long been used as a structural material, the 21<sup>st</sup> century will see increasing demand for advanced titanium alloys to meet technological challenges for applications in the aerospace, biomedical, and energy fields,

among many others. Variation of alloying elements and processing conditions of titanium alloys can be used to tailor the microstructures and hence properties such as strength, fracture toughness, creep resistance, corrosion resistance, and biocompatibility. This paper discusses recent findings regarding the effect of processing on microstructure and low-temperature ( $<0.25T_m$ ) creep behavior of single-phase and two-phase titanium alloys. In particular, the role of alloy chemistry, interstitial impurities, and phase morphology will be considered. These findings are useful to predict the creep behavior of presently used titanium alloys and to develop new processing techniques for advanced titanium alloys with enhanced creep resistance.

### 2:30 PM

**Effect of Casting Mould on Mechanical Properties of 6063 Aluminium Alloy:** Wasiu Ayoola; Samson Adeosun<sup>1</sup>; Olujide Sanni<sup>1</sup>; F. Ochulor<sup>1</sup>; <sup>1</sup>University of Lagos

There are various modern processes usually employed in the production of castings vis-a-vis; sand-mould, permanent-mould, die and centrifugal castings. Sand-mould process is known to induce peculiar microstructures depending on average grain size, grain size distribution, grain shape and chemical composition. These affect specific properties such as surface finish, permeability and refractoriness. In this study, the effect of using CO<sub>2</sub> process, permanent mould, cement-bonded sand mould and natural sand mould on the hardness, tensile strength, impact strength and microstructure of cast 6063 Aluminum alloy is examined. The results show that there is significant increase in hardness (33.7BH) and strength (131.23Mpa) of the alloy when natural sand mould is used for its production. Superior impact strength is exhibited in the alloy when permanent mould is used. Keywords: aluminum, casting, mould, mechanical properties, microstructure

### 2:50 PM

**Ignition Characteristics of Aluminum-Nickel Heterostructures Produced by Ultrasonic Powder Consolidation:** Dinc Erdeniz<sup>1</sup>; David Colanto<sup>1</sup>; Gokce Gulsoy<sup>1</sup>; Teiichi Ando<sup>1</sup>; <sup>1</sup>Northeastern University

Al-Ni heterostructures were consolidated from elemental powders and nanoflakes by the application of ultrasonic vibrations to compacts kept under uniaxial loading. This ultrasonic powder consolidation (UPC) technique can produce powder consolidates at room to warm temperatures within a fraction of a second. Consolidation conditions were studied with Al and Ni powders and nanoflakes. The Al-Ni consolidates produced by UPC may be used as local heat sources in different fields of manufacturing. Therefore, their ignition characteristics and heat outputs were also investigated by differential thermal analysis and continuous-heating ignition tests. Results indicate that ignition is preceded by the solid-state reaction  $Al + Ni = Al_3Ni$  which then catalyzes ignition through the formation of eutectic liquid between Al<sub>3</sub>Ni and Al.

### 3:10 PM

**Improved Formability of Normalized Cold Rolled Aluminum 1200 and 1230 Alloys:** Samson Adeosun<sup>1</sup>; Sanmbo Balogun<sup>1</sup>; <sup>1</sup>University of Lagos, Akoka

Annealing of cold rolled aluminium 1xxx alloys at 480°C for 6 hours and stepping down to 420°C for 2 hours produced cups short of the desired height during cupping. Aluminum 1200 and 1230 alloys sheet of 1.2mm thickness have been used for this study. Test samples were subjected to temperatures in the range 400°C – 530°C at 30°C interval with hold time varying from 2 hours to 8 hours and then normalized in natural air. Tensile, cupping and microstructural analyzes were carried out on these samples. In both alloys presence of dendritic structure of Al<sub>3</sub>Fe, fine crystals of α-aluminum and occurrence of well dispersed fine precipitates of Al<sub>12</sub>Fe<sub>3</sub>Si in the matrix caused improved ductility. Good strength with low ear propensity in drawn cups is achieved when AA1200 alloy is normalized at 460°C for 6hrs and AA1230 alloy at 400°C for 6hrs.

### 3:30 PM

**Studies on the Microstructure, Mechanical and High Temperature Wear Behaviour of A356 Alloy with Minor Additions of Copper and Magnesium:** Kori Shivaputrappa<sup>1</sup>; <sup>1</sup>Visvesvaraya Technological University

A356 alloy has wide applications in automotive, marine and other sectors due to its excellent combination of properties such as good fluidity, low coefficient of thermal expansion, high strength-to-weight ratio and good corrosion resistance. In the present study, the effect of copper (Cu) and magnesium (Mg) addition on the microstructure and mechanical behavior of A356 alloy were investigated. Results indicate that, the minor additions of Cu in the range of 0.1-0.5%

Tue. PM

# Technical Program

improves the mechanical properties. This is due to the partial refinement of a-Al dendrites and solid solution strengthening and precipitation hardening. Also, addition of Mg (0.3-0.7%) results in improvements in strength and hardness at the expense of ductility. This improvement is probably due to the conversion of unmodified acicular silicon to lamellar and possibly even a fibrous structure. Similarly, the worn surface study shows that the change in microstructure leads to improvement in tribological properties of A356 alloy.

## 3:50 PM

**Nanoscratch Behavior of Fine and Ultrafine-Grained Bulk Alumina Fabricated by Spark Plasma Sintering:** *Lin Huang*<sup>1</sup>; *Yuhong Xiong*<sup>1</sup>; *Zhihui Zhang*<sup>1</sup>; *Yonghao Zhao*<sup>1</sup>; *Wenlong Yao*<sup>1</sup>; *Amiya Mukherjee*<sup>1</sup>; *Julie Schoenung*<sup>1</sup>; <sup>1</sup>University of California, Davis

Understanding the response of ceramic materials to applied surface scratches is of significant importance for enhancing the finishing fabrication (e.g., grinding and polishing) and the wear resistance of structural ceramic components. Previous studies have indicated that the response is sensitive to grain size. In an effort to systematically evaluate this potential effect, bulk alumina ceramics, with fine and ultrafine-grained microstructures, were fabricated via spark plasma sintering (SPS) and were subjected to variable scratch loads using a Berkovich nanoindenter. The microstructures of residual scratch tracks were characterized using scanning electron microscopy (SEM) and atomic force microscopy (AFM). The effects of different scratch velocities were also investigated. Typical features for both plastic deformation and brittle deformation were observed, and they were further studied using transmission electron microscopy (TEM). Keywords: Alumina; Scratch; Plastic Deformation; Brittle Fracture

## 4:10 PM

**Microstructural Development during Thermo Mechanical Processing of Pipeline Steel:** *Kawunga Nyirenda*<sup>1</sup>; *Hara R. S. Yotam*<sup>1</sup>; <sup>1</sup>The Copperbelt University

Pipeline steels operate under severe conditions such as high pressure and low temperatures and hence require to have high strength and toughness. Good properties can be obtained through understanding of microstructure during thermal mechanic processing. For industrial application, the major changes in microstructure are grain growth and recrystallization. This work looked at recrystallization with a view of determining the upper (T95%) and lower (T5%) limits of recrystallization for an X70 micro-alloyed steel. This was achieved by determining percentage volume of recrystallization and grain aspect ratio.

## 4:30 PM

**Enhanced Performance of Anti-Reflection Functionality by Nano-Sized Structures Fabricated Using Nano-Imprint Lithography:** *Kang-Soo Han*<sup>1</sup>; *Ju-Hyun Shin*<sup>1</sup>; *Heon Lee*<sup>1</sup>; <sup>1</sup>Korea University

As an effective method of increasing its conversion efficiency, the protective layer of solar cells was patterned with a nano-sized moth-eye structure. This pattern with its conical shape and size serves as an anti-reflective layer. To form a pattern on thermoplastic polymer films and glass plates, the hot-embossing method and nano-imprinting method were used, respectively. Moreover, each substrate patterned on both sides was also fabricated to improve the performance of anti-reflection functionality. Due to the enhanced anti-reflection functionality, the transmittance of patterned films and plates were increased. As a result, a solar cell with patterned polymer films and glass plates as a protective layer exhibited higher quantum efficiency and total conversion efficiency than a solar cell with a bare polymer film and a glass plate as a protective layer.

## 4:50 PM

**From Fantasy to Reality: The Development of Silver Bullet Ammunition:** *Kevin Jaansalu*<sup>1</sup>; *Michael Briggs*<sup>1</sup>; <sup>1</sup>Royal Military College of Canada

The silver bullet is an important part of American folklore. Yet when author Patricia Briggs uses a cast silver bullet in her book "Moon Called", fans cry that there is no such thing. There are two parts to developing silver bullet ammunition: first, casting the bullet, and second, loading and firing the bullet. The substitution of silver for lead in bullet casting requires only minor changes in the casting methods to accommodate the higher casting temperatures and heat load. Two interior ballistic codes were used to model the peak chamber pressure and velocity. Two importance factors for small arms are primer performance and bullet resistance forces in the bore. In spite of the scant literature data, modelling captured the essential performance of the silver bullet.

## 5:10 PM

**Research on Microstructure and Mechanical Properties of Low Alloy Cast Steel with High Strength/Low Yield Ratio by TMCP Technology:** *Chi Yu*<sup>1</sup>; *Haitao Zhou*<sup>1</sup>; <sup>1</sup>Qinhuangdao Branch, Northeastern University

The microstructure of an acicular ferrite/bainite dual-phase steel with high strength/low yield ratio was investigated by TMCP technology, with its mechanical properties tested. The results indicate that bainite can be formed in a wide range of cooling rates from 2°X /s to 25°X /s. The different microstructures are obtained under two kinds of cooling rate of as rolled steel, and bainite ferrite microstructure by accelerated cooling has higher strength than granular bainite microstructure after air cooling. Meanwhile, the yield strength of the steel can be up to 635 MPa through TMCP, the ratio of tensile strength to yield strength is 0.78, and the ferrite is benefit to improve the mechanical properties of low carbon microalloyed steel.

## 5:30 PM

**Microstructure Characterization of Joining Dissimilar Materials:** *Oleg Barabash*<sup>1</sup>; *Zhili Feng*<sup>1</sup>; *Mike Miles*<sup>2</sup>; <sup>1</sup>Oak Ridge National Laboratory; <sup>2</sup>Brigham Young University

We present the microstructural analysis results of the joints between the steel sheet DP980 and either aluminum alloy AA5754 or magnesium alloy AZ31B. The joining method is based on the principles of the friction spin welding (SW). Lately this method was widely used for joining different plastic details. Fast rotation of the bit is provided with special equipment. During several second the bit is quickly inserted into the metal with low melting temperature (Al or Mg). Then the top of the bit surface is touching the surface of the steel sheet. Friction forces generate extremely fast heating of the touching surfaces up to hypomelting temperatures and form a high perfection joint. Formation of the joint takes place several seconds. Joint structure was examined by means of optical and electron scanning microscopes. The joint between DP980 and the bit contains extended TMAZ and relatively narrow SZ with intense plastic deformation.

## 5:50 PM

**Low Stress Viscous Creep in a Ti3Al2.5V Tubing Under Internal Pressurization:** *Srikant Gollapudi*<sup>1</sup>; *Indrajit Charit*<sup>2</sup>; *Korukonda Murty*<sup>3</sup>; <sup>1</sup>Defence Metallurgical Research Laboratory; <sup>2</sup>University of Idaho; <sup>3</sup>North Carolina State University

Hoop creep behavior of a thin-walled Ti3Al2.5V tubing studied under closed-end internal pressurization at low stresses of interest to in-service conditions revealed viscous creep behavior. An activation energy close to that for grain boundary diffusion suggested Coble creep mechanism commonly observed in small grain size materials. However, the predicted data were 3 orders of magnitude lower than the experimental strain-rates. The slip bands observed in TEM have a mean spacing of 250 nm and the predictions based on the Spingarn and Nix model of the climb of dislocations at the grain boundaries in the slip bands were noted to be close to the experimental results. This is the first time that the slip band model was found to be operating in the viscous creep regime and further work is needed to find this mechanism in other materials. This work is supported by the National Science Foundation grant #DMR-0412583.



### Solid-State Interfaces: Toward an Atomistic-Scale Understanding of Structure, Properties, and Behavior through Theory and Experiment: Diffusion, Radiation Damage, and Interaction with Point Defects

Sponsored by: The Minerals, Metals and Materials Society, TMS Electronic, Magnetic, and Photonic Materials Division, TMS Structural Materials Division, TMS: Chemistry and Physics of Materials Committee

Program Organizers: Michael Demkowicz, Massachusetts Institute of Technology; Douglas Medlin, Sandia National Laboratories; Emmanuelle Marquis, University of Oxford

Tuesday PM Room: 602  
February 16, 2010 Location: Washington State Convention Center

Session Chair: Y. Mishin, George Mason University

#### 2:00 PM Invited

**Interface Enabled Defects Reduction in Helium Ion Irradiated Cu/V Nanolayers:** *Xinghang Zhang*<sup>1</sup>; Engang Fu<sup>1</sup>; Amit Misra<sup>2</sup>; <sup>1</sup>Texas A&M University; <sup>2</sup>Los Alamos National Laboratory

In nuclear reactors, radiation induced void swelling can cause significant dimensional instability of structural materials and degrade their mechanical properties in the form of embrittlement. Nanostructured composites offer unique opportunity to significantly reduce void swelling via effective annihilation of radiation induced opposite type of point defects. Sputter-deposited Cu/V nanolayer films with individual layer thickness, varying from 1 to 200nm were subjected to helium(He)ion irradiation at room temperature. At a peak dose level of 6 displacements per atom (dpa), the average helium bubble density and lattice expansion decrease significantly with decreasing h. The magnitude of radiation hardening decreases with decreasing layer thickness, and becomes negligible when is 2.5 nm or less. This study indicates that nearly immiscible Cu/V interfaces spaced a few nm apart can effectively reduce the concentration of radiation induced point defects. Consequently, Cu/V nanolayers possess enhanced radiation tolerance, i.e. reduction of void swelling and suppression of radiation hardening after He ion irradiation, compared to monolithic Cu or V.

#### 2:30 PM

**Effects of Solute and Vacancy Segregation on Antiphase Boundary Migration in Fe<sub>3</sub>Al with Stoichiometric and Off-Stoichiometric Composition:** *Yuichiro Koizumi*<sup>1</sup>; Samuel Allen<sup>2</sup>; Masayuki Ouchi<sup>1</sup>; Yoritoshi Minamino<sup>1</sup>; <sup>1</sup>Osaka University; <sup>2</sup>Massachusetts Institute of Technology

Effects of solute and vacancy segregation on migration of 1/2<100> antiphase domain boundaries (APDBs) in Fe<sub>3</sub>Al with Al-concentrations of 24-28at% have been studied by a phase-field method in which inhomogeneous vacancy distribution is taken into account. Fe- and Al-atoms segregate to the APDBs where Al-concentration is respectively smaller and larger than 26at%. Boundary mobilities of APDBs were evaluated by measuring the boundary velocity of shrinking circular APDs at 673 K. The Fe- and Al-segregations both decreased the mobility by solute drag. The more the composition deviates from Fe-26at%Al, the more significant the segregation and the decrease in the boundary mobility are. As the APDs shrink, the APDBs break away from the segregation atmospheres and the mobilities increase. After the breakaway, vacancies segregate at APDBs at lower Al-concentration (<26at%) whereas they are depleted at higher Al-concentration (>26at%). As a result, APDBs exhibit lower mobilities in the case of higher Al-concentration.

#### 2:50 PM

**A First Principles Study of Hydrogen Trapping at Carbides in Steels:** *Sanket Desai*<sup>1</sup>; Neeraj Thirumalai<sup>1</sup>; Peter Gordon<sup>1</sup>; <sup>1</sup>ExxonMobil Research and Engineering

Hydrogen embrittlement of steels is an important problem for the oil and gas industry. Several studies have reported that trapping of hydrogen by strong binding sites in steel can help mitigate hydrogen embrittlement. One type of trapping site suggested by prior studies is the interface between ferrite and carbide (e.g. cementite). Recent experimental studies have indicated that the bulk of the carbides may also trap hydrogen. We examine the atomistic mechanism of hydrogen trapping at carbides through density functional theory. In this talk,

we will discuss our findings on hydrogen trapping in the bulk of carbides and share preliminary studies of trapping at the carbide-steel interface.

#### 3:10 PM

**Mechanisms of Point Defect Migration in CuNb Interfaces:** *Kedarnath Kolluri*<sup>1</sup>; Michael Demkowicz<sup>1</sup>; <sup>1</sup>Massachusetts Institute of Technology

Cu-Nb multilayer nanocomposites exhibit high resistance to radiation damage because Cu-Nb interfaces are strong sinks for radiation-induced defects as well as sites for efficient Frenkel pair recombination. In this presentation, we describe atomistic modeling studies of the mechanisms by which point defects absorbed at Cu-Nb interfaces diffuse. We find that vacancies and interstitials delocalize into jog pairs on Cu-Nb interface misfit dislocations. These defect configurations diffuse by the hopping of individual jogs between misfit dislocation intersections. Defects migrate preferentially along one set of misfit dislocations. The implications of these insights for interface diffusivity and Frenkel pair recombination models are discussed.

#### 3:30 PM

**Molecular Dynamics and Molecular Statics Studies of Cascade Damage in Twist Grain Boundaries in Copper:** *Xian-Ming Bai*<sup>1</sup>; Richard Hoagland<sup>1</sup>; Michael Nastasi<sup>1</sup>; Arthur Voter<sup>1</sup>; Blas Uberuaga<sup>1</sup>; <sup>1</sup>Los Alamos National Laboratory

Molecular dynamics simulations are used to model the defect production due to cascade damage in sigma 5 twist grain boundaries in copper. We have found that the spatial translations result in several different structures for the twist grain boundary. Molecular statics calculations show that these structures have significantly different defect thermodynamics properties (e.g., vacancy and interstitial formation energies) near or at the grain boundaries. For each grain boundary structure, we have performed multiple molecular dynamics simulations to study the statistically averaged number of defects produced as a function of the original distance between the primary knock-on atom and the grain boundary. The correlation between defect thermodynamics and the produced damage is examined. Comparison of radiation damage between twist and tilt grain boundaries is also performed.

#### 3:50 PM

**Radiation Damage and He Solubility at Semi-Coherent Cu/Nb Interfaces:** *Dhriti Bhattacharyya*<sup>1</sup>; Michael Demkowicz<sup>2</sup>; Igor Usov<sup>1</sup>; Richard Hoagland<sup>1</sup>; Amit Misra<sup>1</sup>; <sup>1</sup>Los Alamos National Laboratory; <sup>2</sup>Massachusetts Institute of Technology

Thin films of pure Cu, pure Nb and Cu/Nb multilayered nanocomposites were irradiated with He<sup>+</sup> ions at 33 keV, with a total dose of 10<sup>17</sup>/cm<sup>2</sup>. Implanted He depth profiles were then assessed using Nuclear-Reaction Analysis and radiation damage structures imaged using Transmission Electron Microscopy (TEM). The radiation damage was visible as He-filled bubbles and dislocation loops- both in the 1-2 nm size range. In the case of Cu-Nb multilayers with semicoherent interfaces, it was found from TEM studies that the number of radiation induced defects was much lower, and that the critical He concentration at which bubbles are resolved in TEM was ~5-8%, while this was found to be below the detection limit in the case of pure Cu and Nb. This excellent radiation resistance is attributed to the Cu/Nb interfaces, which act as strong sinks for radiation-induced defects. Research funded by DOE, Office of Basic Energy Sciences.

# Technical Program

## **Solid-State Interfaces: Toward an Atomistic-Scale Understanding of Structure, Properties, and Behavior through Theory and Experiment: Microstructural Evolution**

*Sponsored by:* The Minerals, Metals and Materials Society, TMS Electronic, Magnetic, and Photonic Materials Division, TMS Structural Materials Division, TMS: Chemistry and Physics of Materials Committee

*Program Organizers:* Michael Demkowicz, Massachusetts Institute of Technology; Douglas Medlin, Sandia National Laboratories; Emmanuelle Marquis, University of Oxford

Tuesday PM Room: 602  
February 16, 2010 Location: Washington State Convention Center

*Session Chairs:* Nathan Mara, Los Alamos National Laboratory; Michael Demkowicz, Massachusetts Institute of Technology

### **4:10 PM Invited**

#### **Towards Improved Representations and Maps of the Grain Boundary Character Distribution: Christopher Schuh<sup>1</sup>; Srikanth Patala<sup>1</sup>; <sup>1</sup>MIT**

This talk will summarize our recent efforts to devise new representations of grain boundary misorientation distributions. First, the topology of the rotation group space of misorientations will be discussed, and the minimum number of variables needed to uniquely color the group space determined. This opens the door to a new, more intuitive type of grain boundary character map, in which the grain boundaries in a micrograph can be colored uniquely by their disorientations. Such maps permit a more direct visualization of connectivity among boundaries of various types. Second, a method will be introduced to describe grain boundary misorientation statistics as a continuous function over the fundamental zone of misorientations. This approach resembles that used in the distribution of grain orientation statistics in texture analysis, and makes the representation of grain boundary character distributions both more rigorous and intuitive.

### **4:40 PM**

**Grain Boundary Properties in Three Dimensions: Anthony Rollett<sup>1</sup>; Gregory Rohrer<sup>1</sup>; Jia Li<sup>1</sup>; Sukbin Lee<sup>2</sup>; Moneesh Upmanyu<sup>3</sup>; Michael Groeber<sup>4</sup>; Michael Uchic<sup>4</sup>; Robert Suter<sup>1</sup>; <sup>1</sup>Carnegie Mellon University; <sup>2</sup>Purdue University; <sup>3</sup>Colorado School of Mines; <sup>4</sup>Air Force Research Laboratory**

Current efforts to characterize grain boundary networks in three dimensions are reviewed for both serial sectioning and synchrotron analysis. Results on boundary populations from stereological analysis are compared with analysis of true 3D networks. Correlations of boundary type at triple lines are discussed, including both misorientations and boundary normals. The boundary networks are also analyzed to extract dihedral angles and calculate grain boundary energy as a function of the five-parameter type. The energy anisotropy is compared to theoretical results, where available. Although the energy is generally inverse to the population, there are non-trivial variations from this rule. The measured microstructures also provide instantiations for simulations of properties. The heterogeneity of plastic deformation provides an example of such a microstructure-property relationship.

### **5:00 PM**

**Quantification of Microstructure Variability in Surrogates for Oxide Nuclear Fuels and Its Effects on Local Mechanical Properties: Karin Rudman<sup>1</sup>; Pedro Peralta<sup>1</sup>; Chris Stanek<sup>2</sup>; Kirk Wheeler<sup>1</sup>; Manuel Parra<sup>1</sup>; Darrin Byler<sup>2</sup>; Kenneth McClellan<sup>2</sup>; <sup>1</sup>Arizona State University; <sup>2</sup>Los Alamos National Laboratory**

Grain boundaries (GBs) play an important role in the retention and release of fission gas in oxide fuels. In general, intragranular bubbles tend to grow near boundaries and then move faster across GBs. As shown by recent atomistic simulations, certain GB structures facilitate the movement and release of the gas, while others retain it. This study aims to experimentally characterize misorientation distributions in samples of depleted Urania and Ytria Stabilized Zirconia mixed with Ceria. The samples are characterized using Electron Backscattering Diffraction (EBSD) to determine grain size, grain orientation, and GB misorientation, and Energy Dispersive Spectroscopy to map composition. Microindentation is used along with EBSD to establish correlations between

GB strength and crystallography. The results are used to draw conclusions on the use of these materials as surrogates for mixed oxide (MOX) fuels, and will also inform multiscale simulations of fission gas behavior by providing realistic microstructural information.

### **5:20 PM**

**Fundamental Derivation of Phase Field Equations for Microstructural Evolution in Metals with Defects: Santosh Dubey<sup>1</sup>; Anter El-Azab<sup>1</sup>; <sup>1</sup>Florida State University**

The phase field approach has been extensively used to model mesoscale morphological and microstructural evolution in materials. This approach uses space and time evolution of conserved and non-conserved field variables (order parameters) coupled through the material free energy, to describe nucleation and growth of the microstructure in materials. Most phase field models are phenomenological in scope and they lack a physical justification for using non-conserved order parameters. An attempt has been made to derive the continuum scale kinetic equations for both conserved and non-conserved order parameters from atomistic details using statistical mechanics principles. All model parameters are shown to be linked to the atomistic details of the material. We apply this approach to the problem of void formation in irradiated metals by condensation of vacancies from the matrix, where we also account for the role of interstitials on the processes of void nucleation and growth.

## **Surface Engineering for Amorphous-, Nanocrystalline-, and Bio-Materials: Session IV**

*Sponsored by:* The Minerals, Metals and Materials Society, TMS Materials Processing and Manufacturing Division, TMS: Surface Engineering Committee

*Program Organizers:* Sandip Harimkar, Oklahoma State University; Arvind Agarwal, Florida International University; Sudipta Seal, University of Central Florida; Narendra Dahotre, University of Tennessee

Tuesday PM Room: 604  
February 16, 2010 Location: Washington State Convention Center

*Session Chairs:* Sandip Harimkar, Oklahoma State University; Arvind Agarwal, Florida International University

### **2:00 PM Introductory Comments**

#### **2:05 PM Invited**

**Studies on Plasma Surface Nitriding of Interstitial Free Steel: Manoj Debnath<sup>1</sup>; Jyotsna Dutta Majumdar<sup>1</sup>; Indranil Manna<sup>1</sup>; <sup>1</sup>Indian Institute of Technology Kharagpur**

In the present study, attempts have been made to enhance the surface dependent mechanical (hardness, wear resistance) and electrochemical (corrosion resistance) properties of IF steel by plasma nitriding. Plasma nitriding has been carried out at an applied pressure of 5 mbar using a gas mixture of nitrogen (20 %) and hydrogen (80 %) at 450°C for 1-5 h. The microstructure of the nitrided surface consists of uniformly dispersed globular precipitates of nitrides in the ferrite matrix. The size and volume fraction of the precipitates increases with increase in nitriding time. While  $\gamma$ -Fe<sub>4</sub>N is a common micro-constituent,  $\epsilon$ -Fe<sub>3</sub>N and  $\zeta$ -Fe<sub>2</sub>N also form at high nitriding time. Similarly, prior deformation (20% - 25%) seems to aid formation of  $\epsilon$ -Fe<sub>3</sub>N, besides  $\gamma$ -Fe<sub>4</sub>N. A significant improvement in microhardness and resistance to wear and corrosion has been obtained by plasma nitriding, particularly at 450°C for 5 h after 25% prior cold deformation.

#### **2:25 PM**

**Nucleation and Growth of Diamond Thin Films Deposited by a CO<sub>2</sub> Laser-Assisted Combustion-Flame Method: Travis McKindra<sup>1</sup>; Matthew O'Keefe<sup>1</sup>; <sup>1</sup>Missouri University of Science and Technology**

The deposition of diamond thin films using a CO<sub>2</sub> laser-assisted combustion-flame CVD process was investigated by comparing different wavelengths for deposition times of less than 5 minutes. The laser wavelength was varied based on the resonant absorption of laser energy by gaseous precursors (O<sub>2</sub>/C<sub>2</sub>H<sub>2</sub>/C<sub>2</sub>H<sub>4</sub>), in particular 10.591  $\mu$ m that did not match a resonant absorption (untuned) and 10.532  $\mu$ m that matched a C<sub>2</sub>H<sub>4</sub> molecule resonant frequency (tuned). The film morphology and microstructure was characterized by scanning



electron microscopy (SEM) and scanning transmission electron microscopy (STEM). After one minute of deposition the films were discontinuous. The amount of faceting and particle size was dependent on the laser wavelength. X-ray diffraction (XRD) and micro-Raman spectroscopy were used for phase identification. The diamond component in the films varied with the deposition time and laser wavelength. The largest diamond component and most faceted grains were obtained using the tuned CO<sub>2</sub> laser regardless of time.

### 2:45 PM

**Stress-Driven Surface Instabilities in Ionic Solids Containing Charged Point Defects:** *Steven Henke*<sup>1</sup>; *Anter El-Azab*<sup>1</sup>; *Peter Chung*<sup>2</sup>; <sup>1</sup>Florida State University; <sup>2</sup>U.S. Army Research Lab

Oxides exhibit a wide range of functional characteristics that make them suitable for numerous technological applications. In many of these applications, the oxides phases form epitaxial systems with the underlying support structure, giving rise to internal stresses that affect both surface mass rearrangement and bulk point defect distributions. In oxides, however, point defects can be charged, and their concentrations are also influenced by space charge formation and the associated internal electric fields. We present a continuum model for ionic solids containing charged point defects coupled with elasticity and electrostatics. Using a 3D finite element scheme, we demonstrate the effects of these defects on the film's morphological stability and characterize incipient instabilities in terms of model parameters.

### 3:05 PM

**The Effect of Frequency of Microarc Oxidation on Surface Properties of 7075 Aluminum Alloys:** *Serkan Bozkus*<sup>1</sup>; *Murat Baydogan*<sup>1</sup>; *Huseyin Cimenoglu*<sup>1</sup>; *Eyup Kayali*<sup>1</sup>; <sup>1</sup>Istanbul Technical University

In this study, thick ceramic coatings were fabricated by microarc oxidation on 7075 aluminum alloy in a KOH, Na<sub>2</sub>SiO<sub>3</sub> solution. Micro arc oxidation was performed by using an AC power supply operating in variable frequency between 100 Hz - 167 Hz. Mechanical and physical properties were examined on the surface of the oxide film including hardness, wear resistance and surface roughness. Rockwell C testing was used to compare the relative adhesion characteristics of the oxide film. The unlubricated tribological performance of the coatings was examined using wear system with reciprocating motion against sintered Al<sub>2</sub>O<sub>3</sub> ball. The surface morphology and structure was examined by SEM and X-ray diffractometer. The studied properties of the samples as a function of frequency were discussed.

### 3:25 PM

**Study of the Nanocomposites for Superalloy Thermal Barrier Coatings:** *Shiqiang Qian*<sup>1</sup>; <sup>1</sup>School of Materials Engineering, Shanghai University of Engineering Science

High temperature alloy can be plated on metal bonding coat layer, by magnetron sputtering or electrophoresis, and thermal barrier layer, by high-speed electric or electrophoresis. We can get nanocomposites on alloy by plating metal bonding coat layer first and then thermal barrier layer. The surface morphology, phase composition and element of these two layers can be observed through OM, XRD, SEM. We placed the K17 high temperature alloy into melting sodium chloride at 900° for 1h then air-cooled for 10 minutes and did 15 cycles hot corrosion test. For metal bonding coat layer, magnetron sputtering is better than electrophoresis while for thermal barrier, electrophoresis better than high-speed electric. We found that it has better anti-hot-corrosion performance for nanocomposites through plating NiCrCoAlY, a metal bonding coat layer, by magnetron sputtering and then YSZ, a thermal barrier layer, by electrophoresis on K17 alloy.

### 3:45 PM Break

### 4:00 PM

**Laser Assisted Deposition of AgInSe<sub>2</sub> Films on Si(100):** *Dinesh Pathak*<sup>1</sup>; <sup>1</sup>GNDU, Amritsar, Physics

Laser ablation has attracted special interest for the formation of thin films Compared with other formation technique. A distinctive feature of laser ablation is that it allow high quality and stoichiometry of films of even very complex element material. In this presentation laser ablation of AgInSe<sub>2</sub> chalcopyrite semiconductor will be discussed in which it is difficult to maintain stoichiometry by conventional method. High Quality AgInSe<sub>2</sub> (AIS) films were grown on Si(100) substrates by the ultra-high-vacuum pulsed laser deposition technique from the AIS target synthesized from high-purity materials. The X-ray

diffraction studies of the films show that films are textured in (112) direction. Increase in substrate temperature results in more order structure. It is observed that compositional stoichiometry is maintained to the more extent by PLD technique than other traditional methods like thermal evaporation. The optical studies of the films show that the optical band gap is about 1.20 eV.

### 4:20 PM

**A Novel High Throw Bright Acid Tin Plating of Printed Circuit Boards:** *Xiao Faxin*<sup>1</sup>; *SHEN xiaoni*<sup>1</sup>; <sup>1</sup>Henan University of Science and Technology of China

A novel acid tin plating process produces a bright deposit with excellent throwing power from a sulfate system. Particular attention is placed on the effects of benzylidene acetone, formaldehyde and OP emulsifier on the tin coating and the appropriate concentration of these additives is 0.6 mg/L, 10 mL/L and 15mL/L, respectively. The bright smooth tin layer may be deposited at 1-4 A/dm<sup>2</sup> and 20-45°X in this solution. The throwing power can reach 90% and the deepening plating ability of hole with L/d of 5 is 100%, which shows that this process may be used for rack plating applications of printed circuit boards. The XRD results show that the crystal face is mainly assigned to the (112) face on the deposits. The SEM results show that the appearance is uniform and the grain is superfine. It was also found that vanadium pentoxide greatly enhances the stability of the plating solution.

### 4:40 PM

**A High Speed Electroless Copper Plating Process of Printed Circuit Board from EDTA•2Na-Containing Solution:** *Xiao Faxin*<sup>1</sup>; *Shen Xiaoni*<sup>1</sup>; *Niu Fei*<sup>2</sup>; <sup>1</sup>Henan University of Science and Technology of China; <sup>2</sup>Central South University of China

Electroless copper deposits were plated on printed circuit boards in EDTA•2Na-containing solutions. Particular attention is placed on the effects of a-a'-bipyridine, triethanolamine (TEA) and L-arginine on the copper depositing and the appropriate concentration of these additives is 10 mg/L, 1mL/L and 0.1mg/L, respectively. The smooth and uniform copper coating may be deposited in the pH value of 12.5-13.0 at 20-50°. The depositing rate of this solution, which is up to 6.7µm/h, is much faster than that previously reported. The use of TEA as additive greatly promotes the depositing speed of coating. The XRD results show that the crystal face is mainly assigned to the (111) and (220) face on the deposits. The SEM results show that the appearance is uniform and the grain is superfine. The backlight level of coating in hole with diameter of 1mm achieves 10th grade after plating for 15min.

### 5:00 PM

**Influence of Process Parameters for Electroless Plating Nickel Alloy Nanoparticles on Carbon Fibers:** *Jia Ma*<sup>1</sup>; *Yao Guangchun*<sup>1</sup>; *Bao Li*<sup>1</sup>; *Zhang Xiao*<sup>1</sup>; *Ma Junfei*<sup>1</sup>; <sup>1</sup>Northeastern University

Carbon fibers have been coated with nickel alloy nanoparticles by electroless plating process, with sodium hypophosphite as a reducing agent in an alkaline bath. The effects of process parameters such as catalyzation time, coating time and nickel sulphate concentrations were investigated. The morphology, coating thickness, growth rate, particle-size, phases and element content in the coating layer of the nickel-coated carbon fibers were investigated by scanning electron microscopy (SEM), energy dispersive spectroscopy (EDS), X-ray diffraction (XRD) and ICP, respectively. It has been confirmed that the growth rate and nickel content increase with an increase of nickel sulphate concentrations and coating time. The catalyzation time for 45min, coating time for 20min, bath temperature of 70°, pH of 9, and nickel sulphate concentration of 40g/L is good to get a continuous and uniform coating of nickel alloy nanoparticles on carbon fiber. The average diameter of the nickel alloy nanoparticles has been estimated as 10 nm.

### 5:20 PM

**Synthesis of Nano Porous CO<sub>2</sub> Absorbent for Recycling:** *Sachi Kanta Kar*<sup>1</sup>; *Payodhar Padhi*<sup>2</sup>; <sup>1</sup>Central Tool Room and Training Centre; <sup>2</sup>R&D Centre, Hitech Medical College and Hospital, Bhubaneswar

The absorption of carbon dioxide is a chemical reaction, not a physical one. Carbon dioxide reacts with the sodium hydroxide based absorbent and undergoes a complete chemical change. This change is irreversible; therefore the absorbent cannot be regenerated for reuse. A novel method is used to develop ceramic nano absorbent, which is porous in nature. The material can be reused in cyclic manner. Further it is observed from DSC that the absorbent can withstand high temperature. shows the CO<sub>2</sub> absorbing behavior of this

Tue. PM

# Technical Program

absorbent in various CO<sub>2</sub> concentration atmospheres, as measured with a Thermo gravimetric/Differential Thermal Analyzer (TG/DTA). The absorbent's weight increased around 354°C due to CO<sub>2</sub> absorption, and the reaction was remarkably accelerated around 736°C.

---

## Sustainable Materials Processing and Production: Measuring Sustainability

*Sponsored by:* The Minerals, Metals and Materials Society, TMS Extraction and Processing Division, TMS Light Metals Division, TMS: Recycling and Environmental Technologies Committee, TMS: Education Committee

*Program Organizers:* Christina Meskers, Umicore; Randolph Kirchain, Massachusetts Institute of Technology; Diana A. Lados, Worcester Polytechnic Institute; Markus Reuter, Ausmelt Limited

Tuesday PM                      Room: 2B  
February 16, 2010              Location: Washington State Convention Center

*Session Chair:* Markus Reuter, Ausmelt Ltd

---

### 2:00 PM Introductory Comments

#### 2:05 PM Invited

**Metrology Needs in Sustainability and Materials Performance:** *Richard Ricker*<sup>1</sup>; <sup>1</sup>NIST

Sustainability is an attractive approach to environmental stewardship because it recognizes the importance of continued profitability in maintaining the environment and advancing society. However, the ability of this approach to actually provide benefit will depend entirely on the predictive capability of the full life cycle impact analysis of alternatives. The ability of these models to predict outcomes with acceptable levels of uncertainty will depend on the data used in these models and the appropriateness of the corresponding measurement methods. This presentation will review the on-going effort at NIST to evaluate sustainability metrology needs and examine the role of measures of materials performance and lifetime predictions in these models.

#### 2:30 PM

**Lightweight Materials for the Automotive: Environmental Impact Analysis of the Use of Composites:** *Karel Van Acker*<sup>1</sup>; Ignaas Verpoest<sup>1</sup>; Wim Dewulf<sup>1</sup>; Joost Duflou<sup>1</sup>; <sup>1</sup>K.U.Leuven

The automotive is a sector where energy consumption during the use phase prevails over the production and the end-of-life phase. Therefore, a lot of research and innovations at replacing classical steel parts by lighter materials like light metals and polymer composites. While composites are very attractive for the use phase of cars, their introduction suffers from the limited end-of-life options for composite structures. An extensive life cycle analysis for a reference car design was conducted to study the effects of replacement of conventional steel structures by lightweight carbon fibre composite alternatives. The study also takes second order effects in the design of the car into account. The opportunities and trends of the trend towards more intensive use of carbon-fibre composites in car design are identified. A discussion on the potential of other types of composites for the automotive in terms of sustainability considerations is added.

#### 2:55 PM

**The Challenge of Allocation in LCA: The Case of Open-Loop Recycling:** *Elsa Olivetti*<sup>1</sup>; Anna Nicholson<sup>2</sup>; Jeremy Gregory<sup>1</sup>; Randolph Kirchain<sup>1</sup>; <sup>1</sup>MIT; <sup>2</sup>BIO Intelligence Service

Life cycle assessment (LCA) is used increasingly as a tool to provide quantitative metrics of environmental burden and inform early stage materials selection decisions. One common challenge in LCA stems from allocation of burden when multiple products share some of the same processes. A critical example of this is the partitioning of benefit or burden at product disposition in open-loop recycling scenarios. This work investigates whether the various methods proposed for allocating end-of-life burden lead to different results and explores the trends in allocation method bias for or against particular materials classes. Stylized analyses across a range of materials are presented and allocation methods explored include both economic or value-based as well as mass-based approaches. Results indicate that some methods are more averse to materials with a high ratio between the required secondary and primary

production impact while others are more averse to materials with high primary production impact.

#### 3:20 PM

**Screening-Level Environmental Burden Assessments for Metals Use in Electronics: A Case Study on the U.S. Printed Wiring Board Industry:** *Carl Lam*<sup>1</sup>; Seong-Rin Lim<sup>1</sup>; Oladele Ogunseitan<sup>2</sup>; Julie Schoenung<sup>1</sup>; <sup>1</sup>University of California, Davis; <sup>2</sup>University of California, Irvine

Simple screening-level metric indicator methods have been traditionally used to help identify high environmental burden materials present in electronic product systems for further detailed assessment, development of pollution prevention countermeasures, and general materials selection decision-making with limited environmental information. For this study, metrics for global resource consumption, ecological and human health toxicity (cancer and non-cancer categories) are considered for evaluating the United States printed wiring board (PWB) industry's metals use. Leachable metal quantities are used for the ecological and human health toxicity screening assessments with U.S. EPA's Tool for the Reduction of Chemical and Other Environmental Impacts (TRACI) and U.S. EPA's Risk-Screening Environmental Indicators (RSEI) methodologies. Global resource consumption indicators consider the ratio of PWB metal usage relative to world metal reserve statistics. Sensitivity analyses are performed for variable changes in PWB recycling rate, dynamic reserve quantities and metal leaching ratios.

#### 3:45 PM Break

#### 3:55 PM Invited

**Agent Based Modeling of Large-Scale Socio-Technical Metal Networks:** *I. Nikolic*<sup>1</sup>; Andrew Bollinger<sup>1</sup>; C. Davis<sup>1</sup>; <sup>1</sup>Delft University of Technology

Metals production and consumption networks are complex Large Scale Socio-Technical Systems, consisting of many technical installations, companies operating them, at a global scale, with large environmental impacts. Understanding their dynamics and behavior requires models that are capable of capturing these multiple dimensions. Modeling in the metals domain has traditionally focused on technical and metallurgical aspects. Agent Based Modeling (ABM), a relatively new technique in the metals domain is a tool from the Complex Adaptive Systems field that allows investigation of the change of metals production and consumption networks structure, as they evolve towards a more sustainable state. This paper presents two examples of ABMs of metals networks that illustrate how the modeling technique can be used and the types of insights it offers.

#### 4:20 PM

**Toxicity and Resource Depletion Potentials of Light-Emitting Diodes (LEDs):** *Seong-Rin Lim*<sup>1</sup>; Daniel Kang<sup>2</sup>; Oladele Ogunseitan<sup>2</sup>; Julie Schoenung<sup>1</sup>; <sup>1</sup>University of California, Davis; <sup>2</sup>University of California, Irvine

Light-emitting diodes (LEDs) are regarded as environmentally friendly light sources due to their high energy efficiency and nonuse of mercury. However, various environmental consequences should be additionally investigated to validate the true environmental performance of LEDs because LEDs utilize the III-V semiconductors with toxic and rare materials, such as gallium, indium and arsenic. The objective of this study is to evaluate toxicity and resource depletion potentials of a variety of color LEDs. Leachability tests are performed to investigate whether the LEDs meet waste regulations and to analyze heavy metal contents. Toxicity and resource depletion potentials of the LEDs are evaluated by using the toxicity and resource depletion characterization factors from Life Cycle Impact Assessment (LCIA) methodologies. This study can contribute to identifying diverse environmental impacts of LEDs and providing valuable information for design for environment (DfE), green purchase, and policy making.

#### 4:45 PM

**The Many Aspects of Measuring Sustainability - An Industry Perspective:** *Christina Meskers*<sup>1</sup>; C. Hagemülken<sup>1</sup>; <sup>1</sup>UMICORE Precious Metals Refining

Metals will play a key role in meeting the challenges for the future. The metallurgical industry is an important actor in the transition towards closed product and material life cycles, one of the aspects of a sustainable society. In this role the industry needs to develop "sustainable" production, manufacturing and recycling processes, and to assist material selection. It requires the combination of a holistic, collaborative approach and suitable tools. The former includes looking at the entire life cycle, each stage and the interactions within on



different levels. Furthermore it should include technical, economic, legislative and societal aspects. Suitable tools consider the detail and complexity necessary for analyzing and quantifying phenomena at the macroscopic as well as the microscopic level. Such a transition demands creativity, critical rethinking of existing practices, and possibly radical change or completely new business models. This contribution will explore the practical implications for a materials technology company.

### 5:10 PM

**Substance Flow Analysis of Cobalt in China:** *Xiao Caimei*<sup>1</sup>; Zhong Juya<sup>1</sup>; Guo Xueyi<sup>1</sup>; Tian Qinghua<sup>1</sup>; <sup>1</sup>Central South University

The method of Substance Flow Analysis (abbreviated as SFA) provides a helpful tool for the study of the industrial metabolism of a certain metal within a regional level. Cobalt is one of the important strategic commodities of national economic development in China, the resource utilization and recycling of which are important for the sustainable development of China's economic construction. In this work the flows and inventory of cobalt in China, 2008, were traced with the STAF model, and the situations of production, fabrication and manufacturing, use and waste management in China were introduced. The result revealed that the resource of cobalt in China was so poor that a large amount of cobalt material or cobalt products needed to be imported. Based on the result, several suggestions were proposed in the paper, aiming to contribute important reference information for the industrial metabolism in China.

### 5:35 PM Concluding Comments

## The Vasek Vitek Honorary Symposium on Crystal Defects, Computational Materials Science and Applications: Mechanical Properties

*Sponsored by:* The Minerals, Metals and Materials Society, TMS Materials Processing and Manufacturing Division, TMS/ASM; Computational Materials Science and Engineering Committee  
*Program Organizers:* Mo Li, Georgia Institute of Tech; David Srolovitz, Institute for High Performance Computing, Agency for Science, Technology and Research, Singapore; Adrian Sutton, Imperial College London; Vaclav Paidar, Institute of Physics AS CR vvi; Jeff De Hosson, University of Groningen

Tuesday PM Room: 603  
February 16, 2010 Location: Washington State Convention Center

*Session Chairs:* Takeshi Egami, University of Tennessee; Shao-Ping Chen, Los Alamos National Laboratory

### 2:00 PM Invited

**Rethinking Continuum Plasticity Theory for Crystalline Solids:** *John Bassani*<sup>1</sup>; <sup>1</sup>University of Pennsylvania

Constitutive equations for plastic flow are generally assumed to be associative in the sense that the flow potential is taken to be the yield function. G. I. Taylor recognized as early as 1926 that BCC iron and brass behave quite differently than FCC aluminum and copper. Ample experimental evidence now exists, but not until atomistic simulations became sufficiently refined have we been in a position to rigorously address issues of plastic flow in crystalline solids. Professor Vitek pioneered atomistic simulations of dislocation core structures and their mobility that has led to new understanding. In this lecture, issues that arise at various scales are discussed. Atomistic simulations are used to construct multiscale continuum models. Using homogenization models, the effective behavior of polycrystals is found to generally be of the non-associated flow type. The latter is shown to significantly affect macroscopic deformations and failure mechanisms including cavitation instabilities, sheet necking, and fracture.

### 2:25 PM Invited

**A Comparison of Coulombic and Plastic Shear Faults in Ice:** Narayana Golding<sup>1</sup>; *Erlend Schulson*<sup>1</sup>; Carl Renshaw<sup>1</sup>; <sup>1</sup>Dartmouth College

New experiments at -10 °C on both equiaxed and columnar-grained polycrystals have established unambiguously that ice exhibits two kinds of compressive shear fault. One kind, termed a Coulombic (C) or frictional fault, is oriented at ~ 30° to the direction of shortening and is comprised of a narrow band of microcracks that nucleate prior to terminal failure and then link up to

create the fault. The other, termed a plastic (P) or non-frictional fault, is oriented at ~ 45° (i.e. sub-parallel to planes of maximum shear stress) and is comprised of a band of re-crystallized grains. P-faults form once the degree of triaxial confinement is sufficient to suppress frictional sliding. Both C and P faulting are accompanied by localized heating. These processes appear to operate in rocks and minerals as well, and possibly in ceramics. Their nature will be discussed, and their role in ice-structure interactions will be noted.

### 2:50 PM Invited

**Kinetics of Martensitic Phase Transformation: Molecular Dynamics of Martensitic Phase Transitions:** *Graeme Ackland*<sup>1</sup>; Oliver Kastner<sup>1</sup>; <sup>1</sup>University of Edinburgh

In martensitic phase transformations a crystal phase changes to lower symmetry, typically on cooling. These transitions underlie mechanical behaviour including superelasticity, transformation induced plasticity and shape memory. "Phenomenological theory" relates two crystal structures geometrically, and determines the interfacial "habit" plane while energy minimisation is used to predict microstructures. These approaches are contradictory: the microstructure is determined at the transformation boundary, and cannot "know" whether it will be a global minimiser. Neither theory considers where the atoms go. We introduce interaction potentials which reproduce a martensitic group-subgroup transformation without unphysical metastable states (most previous studies have not). We then model the phase transformation process in 2D and 3D, showing that the "habit" plane is not sharp, and pre-transformation rotations both eliminate the angular momentum problem and trigger the twinning process. Finally, we investigate cycling between two phases, showing how the defect microstructure nucleates subsequent transformation, allowing a reverse shape-memory effect.

### 3:15 PM

**Atomistic Simulations of Hydride Formation and Fracture at the Crack Tip:** *Jun Song*<sup>1</sup>; William Curtin<sup>1</sup>; <sup>1</sup>Brown University

A hydrogen atmosphere is adversely present in many applications involving metals (e.g., Ni). Specially, hydrogen can achieve high concentration at the crack tip. The local crowding of hydrogen at the crack tip may lead to continuous hydride development and consequently greatly influence the fracture behavior. A Coupled Atomistic/Discrete-Dislocation (CADD) multiscale model is then used to explicitly investigate the development of hydride and subsequent fracture process at the crack tip. We clarify both the chemical and mechanical driving forces that lead to the hydride formation. The resultant hydride inhibits the dislocation emission from the crack tip as well as prevents the incoming of dislocations towards the crack tip. Consequently the crack tip is restricted from plastic blunting and brittle cleavage may occur.

### 3:30 PM

**First Principles Calculations of Uranium and Uranium-Zirconium Alloys:** *Benjamin Good*<sup>1</sup>; Benjamin Beeler<sup>1</sup>; Chaitanya Deo<sup>1</sup>; Sergey Rashkeev<sup>2</sup>; Maria Okuniewski<sup>2</sup>; Mike Baskes<sup>3</sup>; <sup>1</sup>Georgia Tech; <sup>2</sup>Idaho National Lab; <sup>3</sup>Los Alamos National Lab

Uranium zirconium (U-Zr) alloys, when used as the fuel matrix in sodium cooled fast nuclear reactors, have a body centered cubic structure that shows a miscibility gap at the temperature of operation. The alloys exhibit a variation in composition under operation with zirconium atoms migrating against the temperature gradient. We examine several systems of U and U-Zr alloys within a density functional theory framework utilizing the Vienna Ab-initio Simulation Package (VASP). We implement a methodology that applies two separate generalized gradient approximations of the exchange-correlation and compare results obtained from the two pseudopotentials. Bulk properties analyzed include the elastic modulus, lattice constant, and the Birch-Murnaghan equation of state for the  $\alpha$ -U,  $\gamma$ -U, and  $\gamma$ -UZr phases. Defect parameters calculated include formation and migration energies of vacancy, interstitial, and substitutional defects for the  $\gamma$ -U and  $\gamma$ -UZr phases. These values are compared to computational and experimental results documented in the literature.

Tue. PM

# Technical Program

## 3:45 PM Break

## 4:05 PM Invited

**Application of Vitek's Relationship between the Plastic Dissipation and Work Expended on Brittle Decohesion to the Understanding of Hydrogen-Induced Intergranular Cracking:** Paul Novak<sup>1</sup>; Rong Yuan<sup>2</sup>; Moshen Dadfarnia<sup>1</sup>; Brian Somerday<sup>3</sup>; *Petros Sofronis*<sup>1</sup>; Robert Ritchie<sup>2</sup>; <sup>1</sup>University of Illinois; <sup>2</sup>University of California-Berkeley; <sup>3</sup>Sandia National Laboratories

Development of a lifetime prediction methodology for failure of materials used for hydrogen containment components is of paramount importance to the planned hydrogen economy. Arguably the most devastating mode of hydrogen-induced degradation is the hydrogen embrittlement of high-strength steels. We present an approach to quantify the effect of hydrogen on the fracture toughness of a low alloy martensitic steel through the use of a statistically-based micromechanical model for the critical local fracture event—the nucleation of a microcrack at a carbide/ferrite interface. We use Vitek's analysis of the relationship between the plastic work accompanying brittle decohesion to calculate the effect of hydrogen on the strength of a carbide/matrix interface. The result is a quantitative description of the interfacial strength in terms of the carbide size and the local hydrogen concentration. The model is used to predict the macroscopic fracture strength as a function of the nominal concentration of hydrogen.

## 4:30 PM Invited

**Breakdown of Relationship between Chemical Bonding and Deformation Behavior in Crystalline Materials:** *Peter Panfilov*<sup>1</sup>; Yuri Gornostyrev<sup>2</sup>; A. R. Kuznetsov<sup>2</sup>; <sup>1</sup>Ural State University; <sup>2</sup>Institute of Metalphysics of the Ural Branch of RAS and CJSC Institute of Quantum Materials Science

According well known paradigm the directed interatomic bonds cause brittleness and poor plasticity, while metallic type of bonds automatically means high plasticity and rupture. This statement is true for majority of crystalline solids, where bonding energy and shear resistance are isotropic and intrinsically coupled. However, there are some cases that do not obey this rule. Refractory FCC-metal iridium exhibits both high plasticity and transgranular cleavage. On the other hand, covalent crystals of titanium dichalcogenides (TiX<sub>2</sub>, X=S, Se, Te) demonstrate brittle fracture together with dislocation plasticity, too. Using complex atomistic approach based on first principle modeling of deformation and fracture mechanisms we examine this paradox behavior. This work is supported by the U.S. Civilian Research and Development Foundation (CRDF) (# RUXO-005-EK-06/BG7305) and the Ministry of Education and Science of the Russia (# 2.2.2.2/5579).

## 4:55 PM

**Transitions of Dislocation Glide to Twinning and Shear Transformation in Shock-Deformed Tantalum:** *Luke Hsiung*<sup>1</sup>; Geoffrey Campbell<sup>1</sup>; James McNaney<sup>1</sup>; <sup>1</sup>Lawrence Livermore National Laboratory

Shock-induced twinning and alpha (bcc) --> omega (hexagonal) phase transition in polycrystal and single-crystal tantalum, which exhibits no clear solid-state phase transformation under hydrostatic pressure conditions, have been observed. Since the domains of deformation twin and omega phase were frequently found in regions containing evenly distributed high-density dislocations without cellular dislocation structures, we suggest that the shock-induced twinning and shear transformation occur as alternative deformation mechanisms to accommodate insufficient dislocation flow resulting from the exhaustion of dislocation multiplication when dynamic recovery processes become largely suppressed under dynamic-pressure conditions. A novel mechanism is proposed to rationalize the transitions of dislocation glide to twinning and shear transformation in shock-deformed tantalum. This work was performed under the auspices of the U.S. Department of Energy by Lawrence Livermore National Laboratory under Contract DEAC5207NA27344.

## 5:10 PM

**Shock Induced Deformation Substructures and Damage in a Copper Bicrystal:** *Ellen Cerreta*<sup>1</sup>; Fang Cao<sup>1</sup>; Irene Beyerlein<sup>1</sup>; Frank Addessio<sup>1</sup>; Carl Trujillo<sup>1</sup>; George Gray<sup>1</sup>; <sup>1</sup>Los Alamos National Laboratory

Controlled shock recovery have been conducted to determine the role of shock pressure and crystal orientation on the substructure and damage evolution of a [100]/[01-1] copper bicrystal. Optical metallography, electron backscatter diffraction (EBSD) and transmission electron microscopy (TEM) were utilized to quantify damage and characterize orientation variation and substructure evolution of post-shock specimens. Dislocation cell structures were displayed

in both grains and the average cell size decreases with increasing shock pressure. Twinning has been observed in [100] grain. The stress and directional dependence of twinning is analyzed in considering the energetically favorable dissociation of dislocations into Shockley partials and the stress-orientation effect on the partial width. The calculated propensities for twinning in the [100] and [01-1] crystals are in good agreement with the experimental observations. Differences in dislocation cell development and twinning based on crystal orientation are linked to observed differences in the damage evolution of incipiently spalled specimens.

## 5:25 PM

**Dislocation Dynamics, Static Shocks and Size Effects:** *Amine Benzerga*<sup>1</sup>; P. J. Guruprasad<sup>1</sup>; <sup>1</sup>Texas A&M University

The plasticity of single crystals of varying size, orientation and initial dislocation content is investigated under compression using discrete dislocation dynamics. Coupling with finite element methods enables rigorous boundary-value problem solutions to be obtained while the physics of dislocation interactions is enhanced through additional rules for dislocation junctions and dynamic sources. By monitoring the evolution of Nye's tensor, maps of geometrically necessary dislocations (GNDs) are generated at desired resolutions and strain levels. The GND contours are thoroughly analyzed for specific pattern recognition with emphasis on potential formation of singularities and "static shocks". The emergence of these patterns is discussed in light of predicted size effects on plastic flow under nominally uniform compressive loading. The analyses provide new insight into the scaling of flow stress with specimen size and also highlight the connection between individual dislocation mechanisms, collective phenomena and overall behavior.

## 5:40 PM

**Computer Simulation of the Peierls Stress, Dislocation Dynamics and Dislocation-Loop Interaction in Alpha-Zirconium:** Hassan Khater<sup>1</sup>; *Anna Serra*<sup>1</sup>; David Bacon<sup>2</sup>; <sup>1</sup>Technical University of Catalonia; <sup>2</sup>The University of Liverpool

Dislocations with Burgers vector  $b = 1/3\langle 11-20 \rangle$  glide preferentially on the first-order  $\{1-100\}$  prism planes in h.c.p. zirconium, yet most of the interatomic potentials developed for this metal result in a preference for slip on the (0001) basal plane. This arises from dissociation of the dislocation core on the (0001) plane due to the relatively low value of the intrinsic basal stacking fault energy. A more recent potential based on ab initio data reverses the order of the  $\{1-100\}$  and (0001) fault energies and is used here to investigate the gamma surface, core structure and Peierls stress for glide of edge and screw dislocations of the two slip systems. Their glide velocity has also been computed as a function of applied shear stress and temperature. The interaction of interstitial dislocation loops with  $1/3\langle 11-20 \rangle\{1-100\}$  edge and screw dislocations has been simulated in order to assess their obstacle strength and reaction mechanisms.

## 5:55 PM

**Multiscale Modeling of Thin Films: Linking Dislocation Dynamics with Macroscopic Mechanical Behavior:** *Ray Fertig*<sup>1</sup>; Shefford Baker<sup>2</sup>; <sup>1</sup>Firehole Technologies; <sup>2</sup>Cornell University

The difficulty in linking macroscopic mechanical behavior in thin films with dislocation-level behavior has hampered multiscale modeling efforts in thin films for many years. Previous research has suggested that knowledge of particular dislocation interactions cannot be readily translated into knowledge of film strength. But in this work, we present a method to unite dislocation dynamics with macroscopic mechanical behavior of thin films. We use dislocation dynamics simulations to statistically characterize the relationship between stress evolution and the behavior of dislocations in films, including specific interactions and interaction strengths. Our novel method applies the knowledge obtained from the simulations to predict not only macroscopic mechanical behavior, but also the types of dislocation interactions that occur, as well as the distribution of stresses.

## 6:10 PM

**Understanding Some of the Microstructural Reasons for the Small-Scale Mechanical Behavior of Directionally Solidified Mo Micropillars:** *E. P. George*<sup>1</sup>; R. I. Barabash<sup>1</sup>; H. Bei<sup>2</sup>; G. E. Ice<sup>2</sup>; <sup>1</sup>Oak Ridge National Laboratory and University of Tennessee, Knoxville; <sup>2</sup>Oak Ridge National Laboratory

When specimen dimensions approach characteristic microstructural length scales (e.g., mean dislocation spacing), interesting mechanical behavior (e.g., "smaller is stronger") is expected and, indeed, found to occur at sizes



of a few tenths to tens of micrometers. Here we discuss how 3D spatially-resolved x-ray microdiffraction can be used to understand the stress-strain response of monocrystalline, directionally-solidified, Mo micropillars. Elastic strain gradients and dislocation densities were measured both in the NiAl-Mo composite containing embedded fibers as well as after the matrix was etched to expose Mo micropillars. The results are discussed in terms of the previously observed mechanical behavior of pillars given different amounts of pre-strain before microcompression. Research sponsored by the Division of Materials Sciences and Engineering, U.S. Department of Energy. XRD was performed on beamline ID-34-E at the Advanced Photon Source supported by the Office of Basic Energy Sciences, U.S. Department of Energy.

### Three-Dimensional Materials Science VI: 3D Representative Volume Elements and Simulated Microstructures

*Sponsored by:* The Minerals, Metals and Materials Society, ASM International, TMS Structural Materials Division, TMS: Advanced Characterization, Testing, and Simulation Committee, ASM-MSCTS: Texture and Anisotropy Committee, TMS/ASM: Phase Transformations Committee

*Program Organizers:* Alexis Lewis, Naval Research Laboratory; Anthony Rollett, Carnegie Mellon University; David Rowenhorst, Naval Research Lab; Jeff Simmons, AFRL; Stuart Wright, EDAX Inc-TSL

Tuesday PM Room: 401  
February 16, 2010 Location: Washington State Convention Center

*Session Chairs:* Alexis Lewis, U S Naval Research Laboratory; Somanth Ghosh, Ohio State University

#### 2:00 PM Invited

**The Role of Representative Volume Elements on Homogenized Material Properties for Heterogeneous Solids:** *Somnath Ghosh*<sup>1</sup>; <sup>1</sup>The Ohio State University

The representative volume element or RVE of material microstructure plays an important role in the analysis of heterogeneous materials like metals and composites. Effective material properties like stiffness and strength depend not only on constituent properties but also on the local microstructural morphology. This is compounded with the evolutionary state of the microstructure for problems involving plasticity and damage. The effect of local morphology is pronounced on failure properties such as fracture toughness and ductility. In this work, a combination of statistical and computational tools will be discussed for identifying the statistically equivalent RVE or SERVE for materials with non-uniform dispersions. Both undamaged microstructures with continuous interfaces and damaging solids will be considered. The final part of this presentation will deal with models for ductility in metallic materials e.g. cast aluminum alloys. The development of a homogenized non-local model of plasticity-damage for ductility from an identified SERVE will be discussed.

#### 2:30 PM

**Dual Grid Approach for Meshing 3D Images:** *Stephen Sintay*<sup>1</sup>; *Anthony Rollett*<sup>1</sup>; <sup>1</sup>Carnegie Mellon University

Utilizing 3D microstructure models as a method of studying microstructure-properties-performance relationships requires representative models of the polycrystalline microstructure. This work focuses on processes for generating statistically representative implicit microstructure models of polycrystalline materials, and extracting explicit geometries from implicit microstructure data. A novel method is presented that uses the centers of mass of linear portions of the dual grid and the partial entity structure boundary representation to explicitly define the interface geometry of the non-manifold, multiple-region microstructure data. The dual grid center of mass method provides a well-defined set of rules that enables a unique smoothed interface to be obtained. An example of statistical microstructure generation for aluminum alloy AA7075-T651 is given, where the distribution of the synthetic microstructure features are well matched EBSD observations. The synthetic aluminum alloy can then be used for physics-based modeling of microstructurally small fatigue cracks, for example.

#### 2:50 PM

**High-Fidelity Hexahedral Mesh Generation for Large 3D Material Microstructures:** *Andrew Geltmacher*<sup>1</sup>; Jin Qian<sup>2</sup>; Wenyan Wang<sup>2</sup>; Yongjie Zhang<sup>2</sup>; Alexis Lewis<sup>1</sup>; Siddiq Qidwai<sup>3</sup>; <sup>1</sup>Naval Research Laboratory; <sup>2</sup>Carnegie Mellon University; <sup>3</sup>SAIC

Improved finite element mesh generation algorithms and tools required for high-fidelity representations (correct topology and accurate geometry) of complex, space-filling specimen geometries in 3D are needed for accurate computational simulations and predictions. Novel octree-based isocontouring methods with pillowing are used to generate non-manifold hexahedral meshes of material microstructure. These meshing tools are used to produce conforming 3D meshes with good mesh quality while controlling local mesh density. Thus, computational efficiency can be increased by producing more accurate 3D geometric interfaces while reducing the total number of elements by varying the mesh density in regions of high gradients. Several different meshes will be evaluated for computational speed and accuracy.

#### 3:10 PM Break

#### 3:30 PM Invited

**Evaluation and Generation of Representative Volume Elements - A Characterization and Modeling Based Approach:** *Stephen Niezgod*<sup>1</sup>; David Turner<sup>1</sup>; David Fullwood<sup>2</sup>; Surya Kalidindi<sup>1</sup>; <sup>1</sup>Drexel University; <sup>2</sup>Brigham Young University

With the advancement of three-dimensional characterization, researchers are building a vast library of digital microstructure maps. A rigorous yet functional representative volume element (RVE) or statistical volume element (SVE) ensemble concept is central to building knowledge (i.e. structure-property-processing relationships) from the vast amount of raw data. Traditional stochastic mechanics RVE approaches are of limited use to the characterization community in determining the appropriate size and number of regions to examine and often lead to RVEs or SVE ensembles that are too large for computationally expensive numerical models such as crystal plasticity FEM. To this end we describe a framework, based on microstructural n-point correlations, to describe the RVE as an optimized minimum set of selected realizations that accurately capture a wide range of effective properties and microstructure metrics of interest. Case studies including 3D polycrystalline microstructures and natural materials such as wood and bone will be presented.

#### 4:00 PM

**Simulations of Realistic Three-Dimensional Multi-Phase Microstructures:** *Arun Gokhale*<sup>1</sup>; Harpreet Singh<sup>1</sup>; Yuxiong Mao<sup>1</sup>; <sup>1</sup>Georgia Institute of Technology

Material microstructures are three-dimensional, stochastic, and they often contain three or more phases (multi-phase). Microstructural features have complex shapes/morphologies, their spatial arrangements are not necessarily uniform-random, and their morphological orientations are frequently partially anisotropic. Current methodologies for microstructure simulations are mostly restricted to single phase or two-phase microstructures, they involve idealized simple particle/feature shapes; uniform-random spatial distribution of microstructural features; and isotropic feature orientations. In this contribution, we present a methodology that enables simulations of realistic three-dimensional multi-phase microstructures where feature shapes/morphologies, spatial arrangement, and feature orientations are statistically similar to those in the corresponding real microstructures. The simulation parameters used for generation of these microstructures can be correlated to the process parameters. The correlations permit generation of a set of "virtual" microstructures that cover a wide range of process conditions. The virtual microstructures can be then implemented in computational models of materials behavior.

#### 4:20 PM

**Synthetic Microstructure Builders for Rare Events:** *Michael Groeber*<sup>1</sup>; Jeff Simmons<sup>1</sup>; Mary Comer<sup>2</sup>; <sup>1</sup>AFRL; <sup>2</sup>Purdue

As the tools for generating synthetic instantiations of microstructure have matured, little emphasis has been paid towards the study of rare events. Microstructure builders to date have been focused on incorporating more and more statistical descriptors that are formed by estimating mean values from the data. This provides valuable inputs for homogeneous property simulations, but is inadequate for flaw-sensitive properties like fracture and fatigue, which are dominated by local behavior. This work will examine the modifications of crystal builders needed to account for large deviations from the mean. Some

Tue. PM

# Technical Program

recent results where limited experimental data are extrapolated to give extreme or other large microstructural deviations suitable for developing a rare event crystal builder will be given.

## 4:40 PM Invited

**Distinguishing Statistical and Representative Volume Elements in Structure-Property Simulations:** *David McDowell*<sup>1</sup>; <sup>1</sup>Georgia Institute of Technology

Modeling metal plasticity associated with dislocation processes occurring over a broad range of length and time scales is among the most challenging scientific problems due to the long range fields in crystalline metals and complexity of many body interactions. This talk will provide a perspective regarding an assessment of the current state-of-the-art, nuances of the role of heterogeneity in modeling microstructure evolution, the development of hierarchical and concurrent multiscale models, and modeling concepts to address the role of grain boundaries in polycrystals. Particular attention is devoted to issues related to computing at the scale of a representative volume element (RVE) size for evolving microstructure that meets requirements of statistical homogeneity and has relevance to problems of interest involving field gradients. These conflicting demands promote the use of multiple realizations of statistical volume elements (SVE) to inform statistical models for evolving microstructure.

## Ultrafine Grained Materials – Sixth International Symposium: Characterization and Computational Modeling

*Sponsored by:* The Minerals, Metals and Materials Society, TMS Materials Processing and Manufacturing Division, TMS Structural Materials Division, TMS/ASM: Mechanical Behavior of Materials Committee, TMS: Nanomechanical Materials Behavior Committee, TMS: Shaping and Forming Committee

*Program Organizers:* Suveen Mathaudhu, U.S. Army Research Laboratory; Mathias Goeken, University Erlangen--Nürnberg; Terence Langdon, University of Southern California; Terry Lowe, Manhattan Scientifics, Inc.; S. Semiati, Air Force Research Laboratory; Nobuhiro Tsuji, Kyoto University; Yonghao Zhao, University of California - Davis; Yuntian Zhu, North Carolina State University

Tuesday PM                      Room: 607  
February 16, 2010                Location: Washington State Convention Center

*Session Chairs:* Yonghao Zhao, University of California - Davis; Scott Mao, University of Pittsburgh; Mahmoud Nili Ahmadabadi, University of Tehran; Malgorzata Lewandoska, Warsaw University of Technology

## 2:00 PM Invited

**Atomistic Simulations of Defect and Microstructure Evolution in Irradiated Nanocrystalline Materials:** *Paul Millett*<sup>1</sup>; *Yongfeng Zhang*<sup>1</sup>; *Michael Tonks*<sup>1</sup>; *Dieter Wolf*<sup>1</sup>; <sup>1</sup>Idaho National Laboratory

One potential application of ultra-fine grained materials is in nuclear energy, in which the abundance of grain boundary (GB) sinks may enhance irradiation tolerance. In this work, molecular dynamics (MD) simulations are used to characterize the emission, diffusion, and annihilation of point defects in nanocrystalline materials to achieve a mechanistic understanding of how these processes evolve under the conditions of high stress, temperature, and irradiation. In particular, we will present results focusing on how GB properties such as structure, diffusion, and migration are affected by on-going point defect nucleation and/or annihilation, and whether GBs sink strengths are infinite or eventually saturate. Finally, deformation behavior including diffusion creep and dislocation plasticity will be analyzed in the presence of irradiation-induced defect structures.

## 2:20 PM

**EBSD Characterization of ECAE Deformed Nb Single Crystals:** *Liang Zhu*<sup>1</sup>; *Hugo R.Z. Sandim*<sup>2</sup>; *Marc Seefeldt*<sup>1</sup>; *Bert Verlinden*<sup>1</sup>; <sup>1</sup>K.U.Leuven; <sup>2</sup>University of Sao Paulo

The evolution of microstructure and local crystallography has been examined in three cylindrical Nb single crystals deformed at room temperature by equal channel angular extrusion (ECAE) to a strain of  $\epsilon=1.15$ . Characterized by orientation imaging microscopy (OIM) and X-ray diffraction (XRD), the

microstructures show a large influence of initial crystallographic orientation on grain subdivision. In crystal I (ID//[11-1], TD//[101]), only a small amount of high angle grain boundaries were formed while crystal II (ID//[-111], TD//[-2-1-1]) displays uniformly spaced coarse parallel sets of large misorientation bands inside the matrix. Crystal III (ID//[-1-1-1], TD//[0-11]) has a large amount of curly structures with curved boundary in transverse section and straight one in longitudinal section. Based on the pole figures measured by OIM, the texture evolution is mainly characterized by the lattice rotation around the transverse direction. The correlations between slip behavior and the initial crystallographic orientation are analyzed.

## 2:35 PM

**Microstructure Evolution through Heavy Compression Aided by Thermodynamic Calculations:** *Farideh Hajiakbari*<sup>1</sup>; *Mahmoud Nili-Ahmadabadi*<sup>1</sup>; *Behrang Poorganji*<sup>2</sup>; *Tadashi Furuha*<sup>2</sup>; <sup>1</sup>Tehran University; <sup>2</sup>Tohoku University

Sever Plastic Deformation techniques such as simple heavy compression is one of the most promising techniques which can produce Ultra Fine Grain (UFG) materials. As a result, the UFG materials exhibited superior mechanical properties, such as high strength and toughness, compared with as-received samples. In this paper, the microstructural evolution of heavy deformed a dual phase bainitic-ferrite steel (Fe-0.22%C-2.03%Si-3%Mn) was estimated by thermodynamic computations. Compression tests were conducted at temperatures of 298K and 573K on wedge and rectangle samples at strain rate of 0.001s<sup>-1</sup>. The specimens were deformed to 40% and 70% of their original thickness. EBSD, SEM and X-Ray diffraction analysis, before and after compression process were performed to verify the thermodynamic calculations. It was found that at 70% compressed samples, at both temperatures; the austenite transformed to the martensite. Additionally, heavy compression resulted in formation of fine grain with high angle grain boundary which confirms grain refinement.

## 2:50 PM

**Prediction of the Stress-Strain Response of the Ultrafine-Grained Nickel Using Multi-Scale Analysis:** *Mihaela Banu*<sup>1</sup>; *Mitica Afteni*<sup>1</sup>; *Alexandru Epureanu*<sup>1</sup>; *Clement Keller*<sup>2</sup>; *Eric Hug*<sup>3</sup>; *Anne-Marie Habraken*<sup>2</sup>; *Laurent Duchene*<sup>2</sup>; <sup>1</sup>University of Galati; <sup>2</sup>Universite de Liege; <sup>3</sup>Universite de Caen

The present paper proposes a multi-scale analysis of the tensile test applied to ultrafine-grained nickel to predict the stress-strain response. The work is divided into (i) nanostructuring of the 3 mm diameter coarse-grained nickel rod to ultrafine-grained nickel using a laboratory-scale SPD process named controlled multidirectional shearing process, (ii) crystallographic analysis of the structure and identification of the crystal plasticity model coefficients, (iii) tensile testing of the ultrafine-grained nickel specimens for obtaining the true stress-strain behavior and (iv) modeling of the tensile test using finite element method coupled with strain gradient and crystal plasticity model. This model uses internal variables the densities of statistically stored dislocations and geometrically necessary dislocations that improves the calculation of the isotropic hardening of the material. The proposed multi-scale analysis gives an accurate prediction of the mechanical behavior of the ultrafine-grained materials that can be further applied to finite element modeling in the microforming processes.

## 3:05 PM Invited

**Fracture Behavior Analysis in Hard-To-Deform Materials during Equal Channel Angular Pressing by the Finite Element Method:** *Hyoung Seop Kim*<sup>1</sup>; *Seung Chae Yoon*<sup>2</sup>; *Taek Soo Kim*<sup>3</sup>; <sup>1</sup>POSTECH; <sup>2</sup>Hyundai HYSCO; <sup>3</sup>KITECH

Equal channel angular pressing (ECAP) uses specially designed channel dies, which enables ECAP to be repeated to produce bulk UFG materials relatively easily. Even if ECAP is a simple technique with less number of variables than any other metal forming processes, it is not easy to process ECAP without fracture of hard-to-deform metallic material due to the accumulation of damage with repeating processing. In this presentation, we investigated the deformation and fracture behavior of pure magnesium using experimental and numerical methods. The finite element method with different ductile fracture models was employed to simulate plastic deformation and fracture behavior of the workpiece. The theoretical approach used in the paper will be useful for the optimum processing design, especially for hard-to-deform materials. This research was supported by a grant from the Center for Advanced Materials Processing (CAMP) of the 21st Century Frontier R&D Program.



3:25 PM

**Micro-Mechanical Modeling of Damage in IF Steel Strengthened by Severe Plastic Deformation:** Nisrin Abdel Al<sup>1</sup>; *Amine Benzerga*<sup>1</sup>; <sup>1</sup>Texas A&M University

The mechanical behavior of interstitial-free (IF) steel strengthened by means of severe plastic deformation is investigated in order to link processing conditions, microstructure and fracture locus in stress space. Equal channel angular extrusion (ECAE) was used to obtain three types of ultra-fine grain microstructures by varying extrusion rate and processing temperature. The strain-hardening behavior was investigated for the three UFG materials as well as the as-received material using round smooth bars whereas the damage behavior was studied using tensile round notched bars with varying notch radii. A micromechanical model that accounts for the three stages of damage accumulation, namely micro-void nucleation, growth and coalescence is used to describe the fracture behavior. This model is essential towards quantification of strength versus ductility in advanced high strength steels as affected by processing conditions. Some difficulties associated with the uncertainties associated with determining model parameters are highlighted and possible remediation outlined.

3:40 PM

**HRTEM and EELS Study on Aluminum Nitride in Nanostructured Al 5083/B4C Metal Matrix Composites:** *Ying Li*<sup>1</sup>; *Zhihui Zhang*<sup>1</sup>; *Rustin Vogt*<sup>1</sup>; *Wei Liu*<sup>1</sup>; *Enrique Lavernia*<sup>1</sup>; *Julie Schoenung*<sup>1</sup>; <sup>1</sup>University of California Davis

The presence of aluminum nitride in nanostructured Al 5083/B4C metal matrix composites fabricated by cryomilling process was studied by high resolution transmission electron microscopy (HRTEM), electron energy loss spectroscopy (EELS) and energy dispersive X-ray spectroscopy (EDX) analysis. Three different types of aluminum nitride structure were identified; in the predominant phase the N atoms occupy the tetragonal interstitial position in the Al lattice. The cubic and hexagonal aluminum nitride particles were also identified. The present results suggest that the aluminum nitride phases were frequently accompanied by O and Mg. Moreover, the aluminum nitride structure was noted to preferentially form in close proximity to boron carbide particles, arguably related to the segregation of N, O, and Mg in the same region. The results suggest the evolution of the aluminum nitride phase from intermediate transitional structures that involved N atoms in the Al lattice.

3:55 PM Break

4:10 PM

**Synergic Effects of Grain Refinement and Precipitation Strengthening:** *Malgorzata Lewandowska*<sup>1</sup>; *Krzysztof Kurzydowski*<sup>1</sup>; *Romuald Dobosz*<sup>1</sup>; <sup>1</sup>Warsaw University of Technology

Grain refinement down to nano-scale range offers a great possibility of grain boundary induced improvement of low temperature strength of a wide selection of metals. However, the strength of nano-sized metals is still well below the theoretical limit of E/30, which implies 2.4 GPa for aluminium. This is due to physical limits in strengthening of metals by grain size refinement alone, due to the inverse Hall-Petch relationship and diversity in grains size. In this situation further increase in mechanical strength of nanostructured metals can be achieved by synergic effects brought about by combination of strengthening mechanisms. In this context the paper describes combined contributions of grain size strengthening and by second phase particles. The results obtained for 7475 aluminium alloy are presented, which show the non-additive character of the two strengthening mechanisms in question. These results are rationalized by Finite Element Model of the plastic deformation of two-phase nano-metals.

4:25 PM

**Influence of Specimen Dimensions and Strain Measurement Methods on the Apparent Ductility of Bulk Nanostructured Materials:** *Yonghao Zhao*<sup>1</sup>; *Troy Topping*<sup>1</sup>; *Yazhou Guo*<sup>2</sup>; *Qiuming Wei*<sup>2</sup>; *Yuntian Zhu*<sup>3</sup>; *Terence G. Langdon*<sup>4</sup>; *Enrique Lavernia*<sup>1</sup>; <sup>1</sup>University of California-Davis; <sup>2</sup>University of North Carolina-Charlotte; <sup>3</sup>North Carolina State University; <sup>4</sup>University of Southern California

Miniature tensile specimens, having various sizes and geometries, are often used to measure the mechanical properties of bulk nanostructured materials. However, these samples are generally too small for use with conventional extensometers so that the strains are usually calculated from the crosshead displacements. This study uses experimental results and finite element modeling

(FEM) to critically evaluate the influence of the specimen dimensions and strain measurement methods on the tensile curves obtained from miniature specimens. Using ultrafine grained and coarse-grained Cu as model materials, the results demonstrate that the values of strain obtained from the crosshead displacement are critically influenced by the specimen dimensions such that the uniform elongation and the post-necking elongation both increase with decreasing gauge length or increasing specimen thickness. The results provide guidance on the optimum procedures for the tensile testing of miniature specimens of both coarse-grained and nanostructured materials.

4:40 PM Invited

**Avoiding Cracks and Inhomogeneities in Billets Processed by ECAP:** *Paulo Cetlin*<sup>1</sup>; *Maria Teresa Aguilar*<sup>1</sup>; *Roberto Figueiredo*<sup>2</sup>; *Terence Langdon*<sup>2</sup>; <sup>1</sup>Federal University of Minas Gerais; <sup>2</sup>University of Southern California

Equal-channel angular pressing (ECAP) is an established technique for producing bulk ultrafine-grained metallic materials. The present paper discusses the occurrence of strain heterogeneities and fracture in billets of the Pb-Sb alloy processed by ECAP and also in aluminum and magnesium alloys. The Pb-Sb alloys are interesting model materials as they are age-hardenable, display dynamic recrystallization at room temperature and soften as a result of the break-down of the as-cast structure. The present work evaluates different processing variables and includes results of experiments and computer simulations of plastic flow. It is shown that pre-deformation of the as-cast material, the decrease of the ECAP strain per pass through the adoption of dies with angles higher than 90° and the heating of the material/die are effective procedures to avoid inhomogeneities and the cracking of billets during ECAP.

5:00 PM

**Multiscale Modeling of Back-Stress Evolution in Equal-Channel Angular Pressing:** *Enze Chen*<sup>1</sup>; *Laurent Duchêne*<sup>2</sup>; *Anne-Marie Habraken*<sup>2</sup>; *Bert Verlinden*<sup>1</sup>; <sup>1</sup>Katholieke Universiteit Leuven, Belgium; <sup>2</sup>FNRS Fonds de la Recherche Scientifique, Université de Liège

Fine-grained materials produced by ECAP exhibit kinematic hardening due to the existence of a back-stress. This paper discusses two different-scale models that are able to describe the kinematic hardening behavior during tensile and compression tests. The investigated material is commercial-purity-aluminum AA1050, processed by ECAP route C. A macroscopic phenomenological Teodosiu-type model is studied first. The initial parameters are identified from a series of mechanical tests. The predicted back-stress saturates quickly and remains constant during the process, which doesn't agree with the increasing trend experimental result. For better prediction, a new dislocation-based composite model is introduced. It is based on Yuri Estrin's dislocation model and adopts a back-stress description from Maxime Sauzay's. Coupled with a Full-constraint Taylor model, it can predict the evolution of the dislocation densities, the cell size, especially the back-stress. This model takes into account the microstructure evolution and gives a better prediction compared to the previous one.

5:15 PM

**Microstructure of Cu and Cu + Zr Samples after ECAP and HPT Deformation Studied by Different Methods:** *Radomir Kuzel*<sup>1</sup>; *Zdenek Matej*<sup>1</sup>; *Milos Janecek*<sup>1</sup>; *Jakub Cizek*<sup>1</sup>; *Milan Dopita*<sup>2</sup>; <sup>1</sup>Charles University in Prague, Faculty of Mathematics and Physics; <sup>2</sup>Institute of Materials Science, TU Bergakademie Freiberg

X-ray diffraction (XRD), transmission electron microscopy (TEM), electron backscatter diffraction (EBSD) and positron annihilation spectroscopy (PAS) were used for microstructural studies of Cu and Cu + Zr samples deformed by equal-channel angular pressing (ECAP), 1-8 passes, and high-pressure torsion (HPT), 1-20 rotations. In addition to grain refinement with the number of ECAP passes, TEM and EBSD revealed also the evolution of grain boundaries from low-angle to high-angle ones. PAS detected the presence microvoids and enabled determination of their size. Because of high dislocation densities (10<sup>15</sup> m<sup>-2</sup>) only XRD could be used for their determination. Both individual diffraction line profile analysis and total diffraction pattern fitting by own newly-developed software revealed changes in densities and dislocation correlations. XRD and EBSD were used for detailed texture measurements also from different sides of ECAP samples. XRD 2D diffraction patterns can easily be used for fast characterization of thermal stability of the microstructure.

Tue. PM

# Technical Program

## 5:30 PM

### Partial Dislocation Nucleation and Travelling in Nanocrystalline Metals:

Scott Mao<sup>1</sup>; Zhiwei Shan<sup>2</sup>; <sup>1</sup>University of Pittsburgh; <sup>2</sup>Hysitron Inc

This talk focuses on partial dislocation dynamics from grain boundary and storage in nc materials through in-situ TEM and in-situ synchrotron tests. It is believed that the dynamics of partial dislocation processes during the deformation of nanocrystalline materials can only be visualized by computational simulations. Here we demonstrate that observations of partial dislocation processes during the deformation of nanocrystalline metals using a combination of in situ tensile straining and high-resolution transmission electron microscopy. In situ synchrotron on nc and micron Ni under hydrostatic stress up to 57Gpa show that peak broadening increases during loading up to 45 Gpa in nc-Ni, which indicates high dislocation density storage, and no clear grain growth or texturing.

## 5:45 PM

### Ultra Fine-Grained Structures Formed in Impact Welding of 6061 Aluminum Alloy and 110 Copper Alloy: Yuan Zhang<sup>1</sup>; Glenn Daehn<sup>1</sup>; Suresh Babu<sup>1</sup>; <sup>1</sup>The Ohio State University

Magnetic pulse welding is an impact-welding process, similar to explosive welding, that produces a metallurgical bond by the oblique impact of two metal solids at high velocity. The violent impact removes surface layers, brings new surfaces together at high strain rates, and produces high strains at strain rates on the order of 10E6 s<sup>-1</sup>. The process is very heterogeneous even at very short length scales. Local melted regions may be present, and there is also extreme grain refinement; the original 40µm grain size can be reduced to the order of 50nm near the AA6061 welded interface and the micro-twinning and micro-band structures present on welded Cu101. Further, there is no trace of the original interface and the impact-welded region typically has higher strength than the base metal. This study will correlate the structure as determined by TEM and EBSD to the local impact process.

## Ultrafine Grained Materials – Sixth International Symposium: Microstructural Evolution

Sponsored by: The Minerals, Metals and Materials Society, TMS Materials Processing and Manufacturing Division, TMS Structural Materials Division, TMS/ASM: Mechanical Behavior of Materials Committee, TMS: Nanomechanical Materials Behavior Committee, TMS: Shaping and Forming Committee

Program Organizers: Suveen Mathaudhu, U.S. Army Research Laboratory; Mathias Goeken, University Erlangen--Nürnberg; Terence Langdon, University of Southern California; Terry Lowe, Manhattan Scientifics, Inc.; S. Semiatin, Air Force Research Laboratory; Nobuhiro Tsuji, Kyoto University; Yonghao Zhao, University of California - Davis; Yuntian Zhu, North Carolina State University

Tuesday PM Room: 606  
February 16, 2010 Location: Washington State Convention Center

Session Chairs: Matthias Goeken, University Erlangen--Nürnberg; Mohammed Haouaoui, Texas A&M University; Joel House, U.S. Air Force Research Laboratory; Indranil Roy, Schlumberger

## 2:00 PM Invited

### Atom Probe Tomography: A New Insight into the Partition and Segregation of Solutes in Ultrafine-Grained and Nanocrystalline Al Alloys: Gang Sha<sup>1</sup>; Xiaozhou Liao<sup>1</sup>; Rimma Lapovok<sup>2</sup>; Ruslan Valiev<sup>3</sup>; Terence Langdon<sup>4</sup>; Simon Ringer<sup>1</sup>; <sup>1</sup>The University of Sydney; <sup>2</sup>Monash University; <sup>3</sup>Ufa State Aviation Technical University; <sup>4</sup>University of Southern California

Severe plastic deformation (SPD) is well known to be effective in modifying materials microstructures and achieving significant refinement in grain size. The large volume of grain boundaries in the ultrafine-grained (UFG) or nanocrystalline materials bear important consequences for the partition and segregation of solutes and are correlated with many important properties of the materials. The quantitative characterization of solute partition and segregation microstructures has been a challenge. The recent development of atom probe tomography (APT) has significantly improved our ability to access atomistic quantitative information about the structure and chemistry of materials. In this contribution, we highlight a methodology in the application of APT to gain

structural and chemical information of grain boundaries, and we summarise our recent results from UFG and nanocrystalline Al alloys. The effect of processing temperature and grain size on the partition and segregation of solutes will be addressed.

## 2:20 PM

### Deformation Induced Grain Growth in Nanostructured Al-Mg Alloy: Zhihui Zhang<sup>1</sup>; Xiaolin Wu<sup>2</sup>; Ying Li<sup>1</sup>; Troy Topping<sup>1</sup>; Yizhang Zhou<sup>1</sup>; Wei Xu<sup>2</sup>; Kenong Xia<sup>2</sup>; Enrique Lavernia<sup>1</sup>; <sup>1</sup>University of California, Davis; <sup>2</sup>University of Melbourne

Deformation induced grain growth in nanostructured materials during thermomechanical processing has been widely reported. However, the governing mechanisms are not well understood. In this study, the microstructural evolution in cryomilled Al-Mg alloy powders (grain size ~25 nm) was studied following equal channel angular pressing (ECAP), and hot extrusion, respectively. For ECAP, the nanostructured powder was directly consolidated at 325°C with a back pressure 50 MPa for 4 passes whereas for extrusion, it was annealed for 24 hours at 400°C (grain size ~100 nm) and then extruded with a ratio 10:1 (grain size ~300 nm). Despite the longer thermal exposure time, the latter sample exhibited a higher yield strength (530 MPa) than the former (470 MPa), indicating the effect of plastic strain on grain growth. The growth process was characterized using TEM and texture measurement. The results showed that grain rotation and coalescence contributed to the observed grain growth.

## 2:35 PM Invited

### Microstructural Evolution during Processing and Deformation of Ultrafine Grain Metals: Marc Meyers<sup>1</sup>; Y.-B. Xu<sup>2</sup>; H. J. Yang<sup>2</sup>; B. K. Kad<sup>1</sup>; <sup>1</sup>UCSD; <sup>2</sup>Institute for Metal Research Chinese Academy of Sciences

The processes of ECAP and high-strain, high strain rate deformation were used to reduce the grain size from the polycrystalline to the ultrafine grain regime in FCC metals. The grain size and morphology resulting from the two processes are similar, the result of close values of the Zener-Hollomon parameters. High-strain, high-strain rate plastic deformation was applied to the ufg structure in forced shear bands. It leads to an increase in grain size due to thermally-induced recrystallization. The microstructural evolution is analyzed with quantitative predictions of grain-size refinement during severe plastic deformation.

## 2:55 PM

### Grain Refinement in Magnesium Alloys Processed by ECAP: Roberto Figueiredo<sup>1</sup>; Terence Langdon<sup>1</sup>; <sup>1</sup>University of Southern California

Equal-channel angular pressing (ECAP) is an effective tool for producing exceptional grain refinement in bulk polycrystalline f.c.c. metals. However, the situation is more complex in h.c.p. metals, as in magnesium alloys, where successful processing generally requires a preliminary grain refinement through an extrusion step prior to processing by ECAP. This paper examines the characteristics of grain refinement in magnesium alloys and the significance of the production of a bi-modal grain distribution.

## 3:10 PM Invited

### Microstructure Evolutions in Ti and Zr by Pressure-Induced Phase Transformation under HPT-Straining: Yoshikazu Todaka<sup>1</sup>; Hiroaki Azuma<sup>1</sup>; Kensyu Irie<sup>1</sup>; Nozomu Adachi<sup>1</sup>; Yuuki Ohnishi<sup>1</sup>; Minoru Umemoto<sup>1</sup>; <sup>1</sup>Toyoashi University of Technology

HPT (high-pressure torsion) process, which is one of severe plastic deformation (SPD) techniques, has an additional unique characteristic: deformation under high pressure. It is well-known that Ti and Zr display three phases as a function of pressure and temperature. At ambient condition these materials stabilize in the hexagonal close-packed  $\alpha$ -phase, and under high pressure at 2 GPa (Ti) and 3 GPa (Zr) at room temperature the  $\alpha$ -phase transforms into the simple hexagonal  $\omega$ -phase. The stabilization of  $\omega$ -phase in Ti and Zr at ambient condition occurred by applying shear deformation in the state of  $\omega$ -phase under HPT process. In this study, HPT-straining was applied to investigate the effects of pressure and shear deformation on the stabilization of  $\omega$ -phase in Ti and Zr. The microstructure, thermal stability and mechanical properties were examined.

### 3:30 PM Invited

#### New Strategies to Overcome the Limits in Refinement by Severe Plastic

**Deformation:** Reinhard Pippan<sup>1</sup>; Anton Hohenwarter<sup>1</sup>; Andrea Bachmaier<sup>1</sup>; <sup>1</sup>Erich Schmid Institute of Materials Science, Austrian Academy of Sciences

The evolution of the microstructure of single-phase materials deformed by SPD shows a relatively uniform behaviour: With increasing strain the size of fragmented crystalline elements decreases until at strains larger than a certain value no further refinement is observed. The minimum grain-size can be affected by deformation temperature, impurities, alloying, the mode of deformation, and strain rate. Even at very low deformation temperatures a grain-size below 30nm cannot be obtained. The aim of the paper is to present different strategies to overcome this limit. The evolution of the microstructure during high pressure torsion (HPT) deformation of different microcomposites and precipitate forming alloys has been investigated. Furthermore, examples for the generation of nanocomposites by means of powder consolidation with HPT will be presented. The possibilities, advantages and disadvantages of the different strategies to overcome the single-phase limit in refinement by SPD by means of a composite like structure will be discussed.

### 3:50 PM Break

### 4:05 PM Invited

#### Strain Path and Microstructure Evolution during Severe Plastic Deformation (SPD) Processing:

Terry McNeley<sup>1</sup>; Juan Garcia-Infanta<sup>2</sup>; Srinivasan Swaminathan<sup>3</sup>; Alexandre Zhilyaev<sup>4</sup>; Fernando Carreno<sup>2</sup>; Oscar Ruano<sup>2</sup>; <sup>1</sup>Naval Postgraduate School; <sup>2</sup>Centro Nacional de Investigaciones Metalurgicas; <sup>3</sup>GE Global Research; <sup>4</sup>Centro Nacional de Investigaciones Metalurgicas and Institute for Metals Superplasticity Problems

A variety of SPD methods have been developed in order to impart exceptionally large strains and produce highly refined deformation-induced microstructures. SPD methods involving monotonic straining will be reviewed and contrasted with techniques that may result in redundant straining. The former comprise accumulative roll bonding (ARB), large strain extrusion machining (LSEM), equi-channel angular pressing (ECAP) by routes A and BA, uni-directional high-pressure torsion (HPT) and friction stir processing (FSP). The latter include ECAP by routes BC and C, and cyclic straining during HPT. In pure metals it is often difficult to distinguish monotonic and redundant strain paths from examination of the refined grains. However, monotonic and redundant strain paths may be readily distinguished in alloys containing non-deforming constituent particles. Results from several studies will be described and the implications in production of homogeneous and refined microstructures will be summarized.

### 4:25 PM

#### Nanoscale Structural Refinement and Deformation Mechanisms in Beta-Type Titanium Alloys:

Mariana Calin<sup>1</sup>; Wei Xu<sup>2</sup>; Jürgen Thomas<sup>1</sup>; Norbert Mattern<sup>1</sup>; Michael Zehetbauer<sup>3</sup>; Jürgen Eckert<sup>1</sup>; <sup>1</sup>IFW Dresden; <sup>2</sup>University of Melbourne; <sup>3</sup>Universität Wien

In recent years, extensive investigations have been carried out to develop  $\beta$ -type Ti-based alloys with a low Young's modulus and high strength for orthopedics applications. In this work, the  $\beta$  phase stability and its effect on the deformation behavior have been investigated for a series of  $\beta$  Ti-Nb and Ti-Nb-Ta-X (X= Zr, In, Ag, Cr) alloys produced by casting. Microstructural evolution was identified upon compressive loading and high pressure torsion for  $\beta$  alloys with different phase stability against  $\beta \rightarrow \alpha'$  martensitic transformation. With increasing the degree of deformation, martensitic transformation and deformation twinning are initially operative followed by slip of dislocations for the less stabilized  $\beta$  Ti alloys, whereas slip is initially operative followed by nanoscale deformation twinning for the relatively stabilized alloys. A pronounced grain refinement of  $\beta$  grains to the nanoscale (50~100 nm) easily occurred in the In- and Ag-containing alloys with low stacking fault energy.

### 4:40 PM

#### Microstructural Evolution during Cryomilling of B4C Reinforced Al Nanocomposite:

Byungmin Ahn<sup>1</sup>; Yuzheng Zhang<sup>1</sup>; Rustin Vogt<sup>2</sup>; Zhihui Zhang<sup>2</sup>; Julie Schoenung<sup>2</sup>; Enrique Lavernia<sup>2</sup>; Steven Nutt<sup>1</sup>; <sup>1</sup>University of Southern California; <sup>2</sup>University of California, Davis

Al matrix nanocomposite powders reinforced by B4C particulate was fabricated by cryomilling. The powders were cryomilled for different times in order to investigate the microstructural evolution during milling. The microstructure was examined using transmission electron microscopy (TEM),

scanning electron microscopy (SEM) and density measurements. Grain size distribution and microvoid content were correlated with powder particle size and shape. Energy dispersive X-ray spectroscopy (EDS) was used to identify intermetallic phases derived from dispersoids and constituent particles. The evolution of oxides, intermetallic phases, microvoids, and grain structure was studied as a function of cryomilling time.

### 4:55 PM

#### Recrystallization of Tantalum Processed by Equal Channel Angular

**Pressing:** Joel House<sup>1</sup>; John Bingert<sup>2</sup>; Philip Flater<sup>1</sup>; James O'Brien<sup>3</sup>; William Hosford<sup>4</sup>; Robert DeAngelis<sup>5</sup>; Richard Harris<sup>1</sup>; <sup>1</sup>Air Force Research Laboratory; <sup>2</sup>Los Alamos National Laboratories; <sup>3</sup>O'Brien and Associates; <sup>4</sup>University of Michigan; <sup>5</sup>University of Florida

The current study examines the effects of severe plastic deformation of commercially pure tantalum by equal channel angular pressing (ECAP) on recrystallization. Round bars 63 mm diameter of tantalum supplied by H.C. Starck and Cabot Supermetals were processed by eight passes through a 135-degree ECAP die with a 180\176 rotation between each pass and then forged into 6.3 mm thick plates. Coupons, sectioned from the plates, were vacuum annealed for one hour at temperatures ranging from 700\176C to 1250\176C. Hardness measurements, optical micrographs, and diffraction data were gathered from the annealing coupons. The hardness data indicated a 150\176C difference in the softening temperature between the two mill products. The diffraction data indicated that the severe plastic deformation reduced the texture banding in the annealed microstructures, but the final annealed microstructures differed significantly between the two mill products.

### 5:10 PM

#### Ultrafine Grain Refinement of Co-29Cr-6Mo Alloys with Considerably Low Stacking Fault Energy during Conventional Hot-Compression

**Deformation:** Akihiko Chiba<sup>1</sup>; Kenta Yamanaka<sup>1</sup>; Manami Mori<sup>1</sup>; Shingo Kurosu<sup>1</sup>; Hiroaki Matsumoto<sup>1</sup>; Yunping Li<sup>1</sup>; <sup>1</sup>Tohoku University

To examine the microstructural evolution during hot compression deformation of Co-29Cr-6Mo alloy, hot compression tests have been conducted at deformation temperatures ranging from 1323 to 1473 K at various strain rates of  $10^{-3}$  -  $10$  s<sup>-1</sup>. The DRX grain size of deformed specimens considerably decreased with increasing Zener-Hollomon parameter at strain rates ranging from  $10^{-3}$  to  $0.1$  s<sup>-1</sup>. Ultrafine grained microstructure with the grain size of approximately  $0.6 \mu\text{m}$  was obtained under deformation at 1323K at  $0.1$  s<sup>-1</sup> from initial grain size of  $40\mu\text{m}$ . The grain refinement to submicrometer scale of Co-Cr-Mo alloys has been achieved with hot deformation by ~60% due to the DRX in which the bulging mechanism is not operative. The ultrafine grains obtained due to the DRX without bulging is closely related to considerably low SFE of the Co-Cr-Mo alloy at deformation temperatures.

### 5:25 PM Invited

#### Effect of Interfaces on Microstructural Evolution and Deformation Behavior of Ultrafine Ag-Cu Lamellar Nanocomposites:

Nathan Mara<sup>1</sup>; Dhriti Bhattacharyya<sup>1</sup>; Irene Beyerlein<sup>1</sup>; David Alexander<sup>1</sup>; Carl Necker<sup>1</sup>; <sup>1</sup>Los Alamos National Laboratory

We have observed unusual mechanical behavior during warm rolling of Ag-Cu nanoscale eutectic. Starting with an Ag-Cu alloy with an eutectic lamellar bilayer thickness of 200 nm, the as-cast rods are rolled to 75% to 95% nominal reduction in thickness. Cu (111) X-ray pole figures from the rolled nanocomposite indicate unexpected texture evolution during rolling of pure bulk Cu from that involving dislocation slip alone. A Visco-Plastic Self-Consistent (VPSC) polycrystal model indicates that both silver and copper deformed by slip and twinning, with the twin fraction reaching over 50%, depending on rolling reduction. We hypothesize that the unusual observation of room temperature deformation twinning in Cu is induced by twinning in Ag, aided by high Ag-Cu interfacial content. Microstructural evolution and mechanical behavior of the nanocomposite were evaluated at different strain levels in an effort to determine the effects of the interface on deformation processes at diminishing length scales.

# Technical Program

## 2010 Functional and Structural Nanomaterials: Fabrication, Properties, Applications and Implications: Synthesis of Nanomaterials III

Sponsored by: The Minerals, Metals and Materials Society, TMS Electronic, Magnetic, and Photonic Materials Division, TMS: Nanomaterials Committee

Program Organizers: David Stollberg, Georgia Tech Research Institute; Nitin Chopra, University of Alabama; Jiyoung Kim, University of Texas - Dallas; Seong Jin Koh, University of Texas at Arlington; Navin Manjoran, Siemens Corporation; Ben Poquette, Keystone Materials; Jud Ready, Georgia Tech

Wednesday AM Room: 214  
February 17, 2010 Location: Washington State Convention Center

Session Chair: Seong Jin Koh, University of Texas at Arlington; Navin Manjoran, Siemens Corporation

### 8:30 AM Introductory Comments

#### 8:35 AM

#### Effect of Milling Parameters on the Structural Stability of Isothermally Heat Treated Nanostructured Al-2.7at. %Ni Mechanically Alloyed Eutectic Powders: Hanadi Salem<sup>1</sup>; Mohy Eldin Raged<sup>1</sup>; <sup>1</sup>American University in Cairo

In the current research optimum milling parameters and energy domains for the synthesis of Nanocrystalline Al-2.7 at.%Ni eutectic alloy was determined. Effect of milling parameters on the eutectic platelets morphology of Al<sub>3</sub>Ni was investigated. Structural stability before and after isothermal heating at temperatures higher than the recrystallization temperature was investigated using a differential scanning calorimeter. TEM and SEM were employed for the characterization of the structural evolution. The average stored energy increased with increasing the milling time, ball-to-powder ratio (BPR) and rotation speed (RPM). The average stored energy recorded for the powders milled at 200RPM for 40 hrs was 16.571 and 42.39J/g for the 5:1 and 10:1 BPR, respectively. The variation in dislocation densities was calculated for the mechanically alloyed powders before and after isothermal heating.

#### 8:55 AM

#### Influence of the Dispersion Mechanism of Nanostructured Al<sub>50</sub>Ni<sub>50</sub> Intermetallic Compound in Al-Matrices on the Consolidation Behavior and Structural Stability: Hanadi Salem<sup>1</sup>; Abdel Hamid Abdel Hamid<sup>1</sup>; <sup>1</sup>American University in Cairo

Fabrication and processing of Aluminum reinforced AlNi intermetallic MMCs with 0, 5, 10% volume fractions was carried out. 99.7% purity Al powder with mean particle size of 15 μm was mixed with mechanically alloyed nanostructured AlNi using either regular mixing or mechanical milling. The AlNi phase was fully formed after 12hrs of milling time, while prolonged milling for 31hrs resulted in a significant change in the powder morphology and produced nanopowders about 2μm in average size and 18nm crystallite size. The mixed powders were consolidated via a combination of cold pressing followed by hot extrusion at 480°C for 1hr using 4:1 reduction ratio. Hardness and tensile properties of the extruded composite powders were characterized. Structural evolution of the milled composite powders was investigated before and after extrusion using optical microscopy and Field Emission Scanning Electron Microscopy. Energy Dispersive Spectroscopy was employed for mapping the Intermetallic dispersion distribution within the matrix.

#### 9:15 AM

#### Fabrication of Aluminum Carbon Nanotube Composites Via High-Energy Milling: Joseph Paras<sup>1</sup>; Ryan Carpenter<sup>1</sup>; Deepak Kapoor<sup>1</sup>; Stephen Bartolucci<sup>1</sup>; Tony Zahrah<sup>2</sup>; Rod Rowland<sup>2</sup>; <sup>1</sup>U.S. Army ARDEC; <sup>2</sup>MATSYS Inc.

Aluminum-Carbon Nanotube systems are of great military interest in the field of high performance, lightweight structural materials. Traditional methodologies for fabricating these composites involve wet mixing through solvents or direct wetting of nanotubes with molten aluminum. The work presented in this paper will focus on producing composites using dry powder mixing methods. Mixtures of aluminum and multiwall carbon nanotubes (MWCNTs) were used to produce nanostructured composite powders via high-energy milling. These powders were then consolidated using an instrumented hot isostatic press (HIP), which allows for real-time monitoring of sample densification. This process

minimizes the exposure of the nanostructured powder to high temperature, and as a result, the microstructure of the final product can be controlled. Imaging of the consolidated pieces show MWCNTs sandwiched between aluminum lamellae, which is evidence of the retention of the nanostructure imparted during the high-energy milling process.

#### 9:35 AM

#### Studies on the Mechanical Properties of Al-Mg-SiO<sub>2</sub> Metal-Matrix Nanocomposite Synthesized by Mechanical Alloying: Nikhil Balachander<sup>1</sup>; Shashank Shekher<sup>1</sup>; Arun Naik<sup>1</sup>; Jatin Bhatt<sup>1</sup>; D.R. Peshwe<sup>1</sup>; <sup>1</sup>VNIT Nagpur

Mechanical Alloying using high-energy ball milling was employed to produce a metal-matrix composite powder of Al-Mg reinforced with amorphous silica particulate. Nano and submicron-sized silica particles embedded in an Al-Mg matrix were obtained. Four different compositions were chosen with varying magnesium content (0.5%, 1%, 2.5%, 5% by weight). No new phases were found in mechanically alloyed Al-Mg-SiO<sub>2</sub> nanocomposite powder. X-ray diffraction analysis showed that magnesium dissolves into the aluminum matrix completely. It was also found that crystallite size decreased and lattice strain increased with progress in mechanical alloying. Scanning electron micrographs indicate a decrease in particle size via plastic deformation and fracture. The powders are compacted to pelletized form by Spark Plasma Sintering for evaluation of mechanical properties. The mechanical properties of this nanocomposite will be discussed with a focus on possible applications in the automotive industry.

#### 9:55 AM Break

#### 10:10 AM

#### Microstructures and Electrochemical Properties of Nanostructured Mg<sub>2</sub>Ni-Based Compound Containing Nb Additives: Maryam Mohri<sup>1</sup>; Seyed Farshid Kashani Bozorg<sup>1</sup>; <sup>1</sup>University of Tehran

High hydrogen capacity of Mg<sub>2</sub>Ni intermetallic compound has made it a candidate material for negative electrode of rechargeable Nickel Metal Hydride batteries. In the present work, two strategies were selected in order to improve its hydrogen absorption kinetic; synthesis of Mg<sub>2</sub>Ni-based nanostructured compound and modification of composition using Nb additives. High energy ball milling of binary and ternary powder mixtures (Mg<sub>1.75</sub>Nb<sub>0.25</sub>Ni and Mg<sub>2</sub>Ni<sub>0.75</sub>Nb<sub>0.25</sub>) was carried out. The effects of milling process and initial compositions on the microstructure milled products were studied employing X-ray diffraction and scanning and transmission electron microscopy. Also, electrochemical measurements of the nanostructured electrodes made from the milled product were measured using an automatic galvanostat. It was found that Mg<sub>1.75</sub>Nb<sub>0.25</sub>Ni has beneficial effect on the formation kinetic of Mg<sub>2</sub>Ni nanocrystallites. Electrode made from the 20h milled product using initial composition of Mg<sub>1.75</sub>Nb<sub>0.25</sub>Ni exhibited a high discharge capacity of ~600mAhg<sup>-1</sup> and relatively longer discharge life.

#### 10:30 AM

#### Influence of Using MgCO<sub>3</sub> and MgO as Initial Materials on the Synthesis of Pure Nanocrystalline Forsterite Powder: F. Tavangarian<sup>1</sup>; R. Emadi<sup>1</sup>; Ehsan Mohammadi Zahrani<sup>2</sup>; <sup>1</sup>Isfahan University of Technology (IUT); <sup>2</sup>The University of British Columbia

Pure nanocrystalline forsterite (Mg<sub>2</sub>SiO<sub>4</sub>) powder was synthesized by mechanical activation technique followed by subsequent annealing. The starting materials were talc (Mg<sub>3</sub>Si<sub>4</sub>O<sub>10</sub>(OH)<sub>2</sub>), magnesium carbonate (MgCO<sub>3</sub>) and magnesium oxide (MgO) powders. To produce forsterite, two mixtures were prepared including talc and magnesium oxide (first mixture) as well as talc and magnesium carbonate powders (second mixture). First, both mixtures were milled by a planetary ball mill, and then annealed at 1000 °C and 1200°C for 1 h. Thermogravimetric (TG) analysis, X-ray diffraction (XRD) and SEM techniques were utilized to characterize synthesized powders. After 5 h of mechanical activation of the first mixture and subsequent annealing at 1000 °C for 1 h, pure nanocrystalline forsterite was synthesized with 40 nm particle size. A pure nanocrystalline forsterite with a particle size equal to 35 nm was obtained after 10 hr ball milling of the second mixture and subsequent annealing at 1000 °C for 1h.



### 10:50 AM

**Development of Colloidal Single-Sized Photoluminescent Quantum Dots with Bandgap Photoluminescence:** *Kui Yu*<sup>1</sup>; Michael Hu<sup>2</sup>; <sup>1</sup>National Research Council Canada; <sup>2</sup>Oak Ridge National Laboratory

Colloidal photoluminescent (PL) semiconductor nanocrystals have attracted significant attention over the past decade for both fundamental science and potential applications. For example, with tunable bandgap across the visible range (~400 nm to ~700 nm) of the electromagnetic spectrum, CdSe quantum dots (QDs) are of particular interest for the fundamental study of photophysics and have great potential in various applications including bio-imaging and bio-labeling. QDs are spherical semiconductor nanocrystals whose excitons are confined in three spatial dimensions, and can thus absorb and emit light size-dependently. Their optical properties, absorption and emission, are size-dependent. Therefore, one colloidal ensemble of regular QDs (RQDs) is fascinating, but with intrinsic difficulties to study: the variation in size leads to inhomogeneous spectral broadening, in addition to homogeneous spectral broadening. This presentation will address our recent advances in the synthesis of colloidal PL semiconductor QDs which are single-sized without inhomogeneous spectral broadening. The single-sized QDs are also termed as magic-sized QDs (MSQDs), including CdS, CdSe, CdTe, CdTeSe, and CdP.

### 11:10 AM Concluding Comments

## Advances in Composite, Cellular and Natural Materials: Functional Composite Materials

*Sponsored by:* The Minerals, Metals and Materials Society, TMS Structural Materials Division, TMS/ASM: Composite Materials Committee

*Program Organizers:* Yuyuan Zhao, The University of Liverpool; David Dunand, Northwestern University

Wednesday AM Room: 305  
February 17, 2010 Location: Washington State Convention Center

*Session Chairs:* Nik Chawla, Arizona State University; Katsuyoshi Kondoh, Osaka University

### 8:30 AM

**Piezoelectric Smart Composites: Electromechanical Properties and Design Maps:** *T Venkatesh*<sup>1</sup>; <sup>1</sup>Stony Brook University

Piezoelectric materials, by virtue of their unique electromechanical characteristics, have been recognized for their potential utility in many applications as sensors and actuators. However, the sensing or actuating functionality of monolithic piezoelectric materials is generally limited. The composite approach to piezoelectric materials provides a unique opportunity to access a new design space with optimal mechanical and coupled characteristics. An analytical model is developed to predict the complete elastic, dielectric and piezoelectric constitutive properties of a general piezoelectric composite, where the constituent phases are elastically anisotropic and piezoelectrically active. Furthermore, through finite-element modeling, a systematic methodology for quantifying the effects of piezoelectric characteristics (i.e., the poling direction), microstructural aspects (i.e., grain-size and phase volume fraction) and geometric features (i.e., size, shape, and distribution of the constituent phases), on the electromechanical response of piezoelectric composites is presented. Strategies for designing unique piezoelectric sensors with enhanced functionality in multiple directions are formulated.

### 8:50 AM

**Ultrahigh Piezoresistive Effect Induced by Field Emission at Sharp Nano-Tips on the Surface of Spiky Spherical Nickel Powders:** *Baoguo Han*<sup>1</sup>; Jinping Ou<sup>1</sup>; <sup>1</sup>Harbin Institute of Technology

The spiky spherical nickel powders with sharp nano-tips on their surface are dispersed into cement-matrix to fabricate nickel powder filled cement-based composites with ultrahigh piezoresistive response. The piezoresistive sensitivities of these composites to compressive stress and strain can reach to 0.19/MPa and 1932.0 respectively. This extremely high piezoresistive effect is attributed to the unique spiky surface morphology of nickel powders. Comparing to the normal smooth spherical nickel particles, the sharp nano-tip on the surface of spiky spherical nickel particles can induce field emission

and tunneling effects, which leads to highly sensitive responses to compressive stress and strain.

### 9:10 AM

**Extreme Piezoresistivity of Silicone/Nickel Nanocomposites for High Resolution Large Strain Measurement:** Oliver Johnson<sup>1</sup>; *George Kaschner*<sup>2</sup>; Thomas Mason<sup>2</sup>; David Fullwood<sup>1</sup>; Tommy Hyatt<sup>1</sup>; Brent Adams<sup>1</sup>; Kevin Cole<sup>1</sup>; George Hansen<sup>2</sup>; <sup>1</sup>Brigham Young University; <sup>2</sup>Los Alamos National Laboratory; <sup>3</sup>Conductive Composites Company, LLC.

A Silicone/Nickel Nanostrand/Nickel Coated Carbon Fiber (Si/NiNs/NCCF) nanocomposite system has been developed for large strain and motion sensing applications. The response of this nanocomposite under various environmental conditions (i.e. temperature, humidity, pressure), strain rates, and cyclic loading has been studied. The useful strain range, resolution, strain rate sensitivity, and fatigue properties of this system have been characterized. The Si/NiNs/NCCF nanocomposite was also adhered to various substrates which were subjected to tensile tests as well as four-point bending tests and traditional strain sensing techniques were used to verify the response of the nanocomposite gauges. This system was found to have an easily calibrated useful strain range of over 30% strain with better than microstrain resolution. These nanocomposite gauges serve as an inexpensive, easily applied after-market alternative to existing large displacement sensing techniques.

### 9:30 AM

**Synthesis and Microstructural Evolution of SiC/Si<sub>3</sub>N<sub>4</sub>/Si<sub>2</sub>N<sub>2</sub>O Nitride Porous Ceramic Composites Processed via HYSYCV D:** *Martin Pech-Canul*<sup>1</sup>; Jose Flores-Garcia<sup>1</sup>; <sup>1</sup>Centro de Investigacion y de Estudios Avanzados del Instituto Politecnico Nacional

The effect of using successive stages of infiltration and different atmosphere types on the microstructural evolution and physical properties of SiC/Si<sub>3</sub>N<sub>4</sub>/Si<sub>2</sub>N<sub>2</sub>O nitride porous ceramic composites was investigated. Composites were processed via solid-gas phase reactions using the hybrid precursor system chemical vapor deposition (HYSYCV D) route. SiCp porous preforms were infiltrated in subsequent stages (S1, S2) according to the following schedule: S1-1 and S1-2 at 1300 °C for 70 min in high purity nitrogen (HPN); S2 at 1350 °C for 120 min in ultra high purity nitrogen (UHPN). The composites were characterized by XRD, SEM and by means of He pycnometry, volume-measurement approach and immersion in Hg using Archimedes's principle. Results show that atmosphere type and stage-processing approach affect the type, morphology and size of the nitrides formed. Stage-infiltration approach allows establishing conditions to control morphology, size (including nanometric size) and distribution of deposited phases, thus determining the properties of the composites.

### 9:50 AM

**Transformation Plasticity in Rare Earth Orthophosphate/Orthovanadate Solid Solutions: Application to Fiber-Matrix Interphases in CMCs:** *Randall Hay*<sup>1</sup>; Geoff Fair<sup>1</sup>; Emmanuel Boakye<sup>2</sup>; Pavel Mogilevsky<sup>2</sup>; Triplicane Parthasarathy<sup>2</sup>; <sup>1</sup>AFRL; <sup>2</sup>UES, Inc.

Oxide-oxide CMC's with rare-earth orthophosphate interphases such as monazite and xenotime have been successfully demonstrated. The major concern for these interphases is the high fiber pull-out stresses, typically ~80 - 200 MPa. An approach to lowering pullout stress involves use of interphases that weaken by transformation plasticity during a -ΔV martensitic phase transformation. The xenotime → monazite martensitic phase transformation for rare-earth orthophosphate/orthovanadate solid-solutions was investigated for transformation plasticity during indentation. The ease of inducing the transformation and the subsequent effect of transformation plasticity on mechanical properties was assessed by the stress-strain behavior and hysteresis during indentation. The transformation extent and accompanying deformation were characterized by FIB and TEM of sections beneath the indents. Characterization was complicated by concerns about transformation of surface layers during polishing, and reversibility of the transformation with time. Processing methods necessary to deposit dense xenotime coatings near the xenotime-monazite phase boundary are discussed.

# Technical Program

## 10:10 AM Break

## 10:30 AM

### **Creep and Fatigue Interactions of Haynes 282 at Elevated Temperatures:**

*Sara Longanbach*<sup>1</sup>; Carl Boehlert<sup>1</sup>; <sup>1</sup>Michigan State University

Superalloys can be considered as composite structures due to the significant strengthening offered by their precipitates. Haynes 282 is a wrought, gamma-prime strengthened nickel-based superalloy intended for use in high temperature structural applications. To investigate processing-microstructure-property relationships, the microstructure and elevated-temperature (760 – 815°C) creep and fatigue behavior were evaluated after processing involving strain-recrystallization treatments. Microstructural evaluation was performed using SEM and EBSD. General high angle boundaries (GHAB), low angle boundaries (LAB), and coincident site lattice boundaries (CSLB) made up 38%, 4% and 58%, respectively, of all the grain boundaries. It is noted that 47% of the boundaries were twins. The creep and fatigue properties of this alloy were compared to those obtained for two solid solution-strengthened superalloys, Haynes 230 and Udimet 188. The Haynes 282 alloy exhibited superior creep resistance. The deformation behavior and mechanisms will be discussed and particular emphasis will be placed on the grain boundary deformation.

## 10:50 AM

### **Oxidation of NixZry/Zr-4 Composite Surfaces:** *Walter Luscher*<sup>1</sup>; Edgar Gilbert<sup>1</sup>; Stan Pitman<sup>1</sup>; <sup>1</sup>Pacific Northwest National Laboratory

Surfaces of Zircaloy-4 (Zr-4) components have been electroplated with nickel (Ni) and thermally treated to form a coherent, exterior layer of NixZry intermetallics. The result is a component with a graded composite surface consisting of discrete intermetallic layers over a Zr-4 substrate that exhibits two distinct stages of oxidation. Oxidation occurs rapidly at first as the intermetallic layer oxidizes, then slows asymptotically to a rate characteristic of the Zr-4 substrate as the intermetallic becomes saturated with oxides. This self-limiting oxidation behavior permits adequate structural integrity and mechanical strength of the substrate to be retained for the anticipated service environment. Microstructural evolution and elemental segregation determined by scanning electron microscopy and energy dispersive x-ray spectroscopy, respectively, correlates with isothermal weight gain data. An analysis of oxidation kinetics was also performed. Hardness and strength were evaluated via microindentation and tensile testing, respectively.

## 11:10 AM

### **Long Term Thermal Stability of Al<sub>2</sub>O<sub>3</sub> Fiber (Sapphire) Reinforced NiAl Composites:** *Jia Song*<sup>1</sup>; Weiping Hu<sup>1</sup>; Günter Gottstein<sup>1</sup>; <sup>1</sup>Institute of Physical Metallurgy and Metal Physics, RWTH Aachen University

The long term thermal stability was tested for NiAl-Al<sub>2</sub>O<sub>3</sub> composites. After the annealing of composites at 700°C and 1100°C for 2000 hours, the NiAl-Al<sub>2</sub>O<sub>3</sub> system showed a good long term chemical stability. However, at such a high temperature, the grain growth and embrittlement took place in polycrystalline NiAl matrix. Besides, the corresponding interfacial shear strength was reduced from 222±50 MPa for the as-fabricated sample to 197±48 MPa and 150±38 MPa for the as-annealed samples at 700°C and 1100 °C respectively. Based on the microstructure changes and interfacial properties, the tensile strength was about 360 MPa for both as-fabricated and as-annealed samples at 700 °C, indicating a tiny change. But the tensile strength of the as-annealed samples at 1100 °C dropped to 170 MPa, 30 MPa lower than the value of 200MPa for the un-annealed one. The possible influences of microstructure and interface structure on mechanical properties are discussed.

## 11:30 AM

### **Synthesis and Deformation Behavior of Metal-Ceramic Nanolaminates:**

*Danny Singh*<sup>1</sup>; Nik Chawla<sup>1</sup>; Guanlin Tang<sup>2</sup>; Yu-Lin Shen<sup>2</sup>; Amit Misra<sup>3</sup>; Krishan Chawla<sup>4</sup>; <sup>1</sup>Arizona State University, School of Mechanical, Aerospace, Chemical, and Materials Engineering; <sup>2</sup>University of New Mexico/Department of Mechanical Engineering; <sup>3</sup>Los Alamos National Lab/CINT; <sup>4</sup>University of Alabama at Birmingham/Department of Materials Science and Engineering

Nanolayered composites are used in a variety of applications such as wear resistant coatings, thermal barrier coatings, optical and magnetic thin films, and biological coatings. Mechanical performance and reliability in all these applications is a key concern. In this talk we present a study of the synthesis, microstructural characterization, and deformation behavior of a nanolaminated metal-ceramic (Al/SiC) system. The nanolayered composite was processed by physical vapor deposition (PVD) using magnetron sputtering. Layer

thickness and morphology were studied using a dual beam focused ion beam (FIB). Mechanical properties such as hardness and modulus were obtained using nanoindentation and micro-compression testing. Nanoscratch testing was conducted to quantify the resistance to wear and to estimate the adhesion strength between layers. Finally the damage mechanisms under various loading conditions were modeled using finite element modeling of the deformation process.

## 11:50 AM

### **Strengthening Behavior of Bilayer and Trilayer Cu-Based Nanocomposites:**

*Aikaterini Bellou*<sup>1</sup>; Nicole Overman<sup>1</sup>; David Bahr<sup>1</sup>; Hussein Zbib<sup>1</sup>; Ioannis Mastorakos<sup>1</sup>; Amit Misra<sup>2</sup>; <sup>1</sup>Washington State University; <sup>2</sup>Los Alamos National Laboratory

The effects of varying chemistry and individual layer thickness on the mechanical properties of Cu-based nanocomposites, of interest for a number of thin film applications, were investigated. Two different sets of samples were used. In the first case the thickness of the individual layers was kept constant at 20 nm while three different stacking sequences were used; Cu/Ni, Cu/Nb and Cu/Ni/Nb. Bulge testing and nanoindentation were utilized to evaluate the mechanical properties and especially the strength of the nanocomposites with the Cu/Nb system showing the higher hardness. The second set of multilayers involved only trilayer Cu/Ni/Nb films where the thickness of the Cu and Ni layers was maintained constant at 5nm while the thickness of the Nb layer ranged from 1 to 4 nm. The strengthening behavior of these films was again evaluated and comparison of the strengthening behavior of the Cu based multilayers with established models will be discussed.

---

## **Alternative Energy Resources for Metals and Materials Production Symposium: Session I**

*Sponsored by:* The Minerals, Metals and Materials Society, TMS Extraction and Processing Division, TMS Light Metals Division, TMS: Energy Committee

*Program Organizers:* Ann Hagni, Geoscience Consultant; Neale Neelameggham, U.S. Magnesium, LLC; Aldo Steinfeld, ETH Zurich; Robert Palumbo, Valparaiso University

Wednesday AM

Room: 310

February 17, 2010

Location: Washington State Convention Center

*Session Chairs:* Ann Hagni, Ann Hagni Consulting, LLC; Robert Palumbo, Valparaiso University

---

## 8:30 AM Introductory Comments

## 8:35 AM Keynote

### **The Global Scramble for Energy and Mineral Resources--Will the Move Towards Alternative Energy Sources Alleviate Our Import Problems?:**

*Vincent Matthews*<sup>1</sup>; <sup>1</sup>Colorado Geological Survey

Mineral and energy resources are being strained to supply increasing demand in established and emerging economies. Prices of natural-resource commodities dramatically escalated between 2003 and 2008 before plunging more steeply in four months, than in four years of the Great Depression. The competition to obtain a share of these natural resources became intense. The U.S. suffered from a shortage of several mineral commodities. From cement, to steel, to petroleum, to rare earth elements; the scramble for a piece of the worldwide pie is in a state the world has never known. The nation is being, and will be, significantly affected by this new world disorder. In addition to importing oil, natural gas, and uranium; the U.S. imports most of its needs for alternative energy technologies. China is taking advantage of the economic downturn to strengthen its position in mineral and energy commodities.

## 9:30 AM

### **Conceptual Process Plant Utility Schemes with Hybrid Energy System:**

*Neale Neelameggham*<sup>1</sup>; <sup>1</sup>US Magnesium LLC

Most of the chemical process plants and metallurgical production facilities already have some sort of co-generation to minimize process energy costs. Use of Alternative energy Production from sun and wind power with storage can become an integral part of a process plant utility. This will facilitate reduced fossil fuel usage, and help minimize thermal emissions. This will be similar to Pollution Control equipment which became essential parts of process plants in



the past 4 decades. Conceptual flow sheets of such a Process utility schemes are presented.

### 9:50 AM

**Advanced Electrochemical Storage R&D at PNNL for Renewable Integration and Utility Applications:** *Zhenguo "Gary" Yang*<sup>1</sup>; Cheng Hung<sup>1</sup>; Daiwon Choi<sup>1</sup>; Gordon Graff<sup>1</sup>; Jianzhi Hu<sup>1</sup>; Soowan Kim<sup>1</sup>; Jun Liu<sup>1</sup>; Xiaochun Lu<sup>1</sup>; Kerry Meinhardt<sup>1</sup>; Vince Sprenkle<sup>1</sup>; John Lemmon<sup>1</sup>; Donghai Wang<sup>1</sup>; Guan-Guang Xia<sup>1</sup>; <sup>1</sup>Pacific Northwest National Laboratory

Growing world energy consumption, environmental concerns over the use of fossil fuels and the resource constraints have spurred great interests in renewable energy from wind and solar. To effectively use the renewable energy and to make it dispatchable, however, demand electrical energy storage (EES). EES is also a useful tool to improve reliability, stability and efficiency of future grids that is expected to be able to provide fuel (i.e. electricity) to plug-in hybrid vehicles. Among the most promising ones are electrochemical storage technologies or batteries that are capable of storing and releasing electrical energy in accordance with the demand. While a number of technologies have been developed or even demonstrated, there remain significant challenges in performance and cost for market penetration. As such PNNL has carried out wide research into advanced materials and EES technologies. This paper will report the efforts and discuss the needs, status and challenges.

### 10:10 AM Invited

**Metal Ferrite Spinel for Solar-Thermal Water Splitting REDOX Cycles:**

*Alan Weimer*<sup>1</sup>; <sup>1</sup>University of Colorado

If H<sub>2</sub> could be obtained cost effectively via the splitting of water using concentrated sunlight, then it's possible to operate a fuel cell using renewable H<sub>2</sub> or to synthesize other fuels based on renewable H<sub>2</sub> for generating electricity (H<sub>2</sub> + CO<sub>2</sub> ==> syngas ==> CH<sub>4</sub>) or for running internal combustion engines (syngas ==> methanol ==> gasoline). Spinel ferrites of the form M<sub>x</sub>Fe<sub>3-x</sub>O<sub>4</sub>, where M generally represents Ni, Zn, Co, Mn, or other transition metals, have been shown to be capable of splitting water according to a two step REDOX solar thermochemical cycle. This presentation will focus on the thermodynamics and thermochemistry of solar-thermal chemical reaction processing with a special emphasis on the splitting of water using metal ferrites of the spinel structure. Experimental results for the REDOX reactions will be presented along with a possible process flow sheet (100,000 kg H<sub>2</sub>/day) and economic analysis (< \$4/gge).

### 11:05 AM

**Solar Thermal Electrolytic Production of Metals from Their Oxides:** *Robert Palumbo*<sup>1</sup>; <sup>1</sup>Valparaiso University

Students and faculty at Valparaiso University launched a solar thermal electrolytic research program focused on the production of metals from their oxides. In this presentation, I describe the thermodynamic argument motivating the research and illustrate the influence of thermal transport processes such as electrolytic ionic conductivity and electrode reaction kinetics on the solar process. From this theoretical frame work, I present our experimental program and latest findings. Specifically, I show the ionic conductivities we established for mixtures of ZnO in Na<sub>3</sub>AlF<sub>6</sub> and in xCaF<sub>2</sub>-y Na<sub>3</sub>AlF<sub>6</sub> mixtures. I describe a 10 kW solar electrolytic reactor that we developed and are using to expose how ionic conductivity and electrode reaction kinetics influence process performance through operating variables and cell design variables. These influences are illustrated through interpretation of current vs. voltage maps as well as current vs. time plots for the electrolysis of ZnO within the temperature range of 1200-1500 K.

### 11:25 AM

**CO<sub>2</sub> Mitigation in Extractive Metallurgical Processes Using Concentrated Solar Energy:** *Aldo Steinfeld*<sup>1</sup>; <sup>1</sup>ETH Zurich

Solar thermochemical processes make use of concentrated solar radiation as the energy source of high-temperature process heat. Considered are the thermal and carbothermal reduction of metal oxides for the production of metals, metal nitrides, and metal carbides. R&D work encompasses fundamental studies on thermodynamics, reaction kinetics, heat/mass transfer, and chemical reactor engineering. Solar reactor prototypes – at the 10 kW power level – are designed, fabricated, modeled, and tested in a high-flux solar furnace, further optimized for maximum solar-to-chemical energy conversion efficiency, and finally scaled-up for industrial applications – at the MW power level – using concentrating solar tower technology.

### 11:45 AM

**Applications of Concentrating Solar Power in Materials Production:** *Daniel Cook*<sup>1</sup>; Jordan Mayorga<sup>1</sup>; Joseph Kopp<sup>1</sup>; Robert Boehm<sup>1</sup>; <sup>1</sup>University of Nevada, Las Vegas

Solar generated power has long been considered a useful energy source only for low-energy density and non-mission critical use, such as providing electricity for residential applications. The success of Concentrating Solar Power (CSP) facilities, such as the 64 MW Nevada Solar-1 near Las Vegas, have demonstrated that solar does have application to high energy density industries such as materials and chemical production. This paper will discuss the current operating configuration of the Solar-1 facility and show how proposed modifications, such as addition of thermal storage and use of liquid salts as the working fluid, can further improve the efficiency and energy production of the plant.

### 12:05 PM

**Radio-Thermionic Induced Reactions on Aluminum Based Materials and Their Correlation with Plasmon Formation and Tribocatalytic Mechanisms:**

*John Elton*<sup>1</sup>; James Cornwell<sup>1</sup>; <sup>1</sup>Protective Systems, Inc.

Thermionic induced reactions and radiation resonance catalysis of aluminum and aluminum oxide materials exposed to microwaves and triboemissions will be described and explained from both a fundamental and practical level. Magnetron operation at distinct operating conditions that generates both plasmon and triboemissive radiation will be explained and the resulting tribochemical and radiation resonance catalytic reactions between aluminum, aluminum oxide, water and graphite will be delineated. The generation of hydrogen from these materials using triboemissive radiation and microwaves will be described, and the application of this methodology for hydrogen based technologies will be discussed.

### 12:25 PM Concluding Comments

## Alumina and Bauxite: Process Improvements and Experiences - Red Side II

*Sponsored by:* The Minerals, Metals and Materials Society, TMS Light Metals Division, TMS: Aluminum Committee, TMS: Aluminum Processing Committee

*Program Organizers:* Carlos Suarez, Hatch Associates Inc; Everett Phillips, Nalco Company

Wednesday AM

Room: 611

February 17, 2010

Location: Washington State Convention Center

*Session Chair:* Shawn Kostelak, Gramercy Alumina

### 8:30 AM Introductory Comments

### 8:40 AM

**Effect of Digesting Conditions on Physical Properties of Diaspore Red Mud:** *Li Bao*<sup>1</sup>; Ting'an Zhang<sup>1</sup>; Zhihe Dou<sup>1</sup>; Guozhi Lv<sup>1</sup>; Xujian Wu<sup>1</sup>; Yongnan Guo<sup>1</sup>; Peiyuan Ni<sup>1</sup>; Jia Ma<sup>1</sup>; <sup>1</sup>Northeastern University

Diaspore, a kind of bauxite ore used to produce alumina, has complicated compositions and un-dense microstructure. The change of physical properties of diaspore is key to kinetic investigation of digesting process. Diaspore particles with the same particle size were digested under different digesting temperatures, times and stirring speeds. Specific surface area, pore volume and pore size of initial diaspore sample and red muds, the insoluble solid products during digesting process, were analyzed by nitrogen adsorption-desorption measurement performed on ASAP 2020 Micromeritics apparatus. Meanwhile, Archimedes principle was employed to measure the densities of samples. The results show that digestion temperature and time bring about greater influence on the physical properties of particle samples than stirring speed.

### 9:10 AM

**Extracting Alumina from Coal Flyash through Sodium Aluminate Solution in Soda-Sintering and Acid-Leaching Process:** *Jilai Xue*<sup>1</sup>; Li Yan<sup>1</sup>; Yun Zhu<sup>1</sup>; <sup>1</sup>University of Science and Technology Beijing

Coal fly-ash containing 40% -50%Al<sub>2</sub>O<sub>3</sub> and 40-50% SiO<sub>2</sub> from power plants is an alternative resource for alumina production. The alumina content in the coal fly-ash was extracted using soda-sintering and aluminate solution

# Technical Program

digesting process in laboratory. The sintering process was investigated using XRD, DTA and SEN-EDS techniques. The analysis showed that NaAlSiO<sub>4</sub> was produced when the ratio of fly ash to Na<sub>2</sub>CO<sub>3</sub> was 1:0.4 at 900°C, and the best leaching efficiency for the sintered NaAlSiO<sub>4</sub> powders was obtained at the ratio 1:0.6. Removal of a glass-like silica layer on the surface of particles containing Al<sub>2</sub>O<sub>3</sub>/SiO<sub>2</sub> in the fly ash. The so made sodium aluminate solutions after purification for removing Si and Fe were used to produce Al(OH)<sub>3</sub> powders in a seeded precipitation process similar to Bayer's. This process can be an independent one or part of an ordinary industrial operation in alumina refining plants.

## 9:40 AM Break

### 10:00 AM

**Improved Performance of Red Mud Settlers at Worsley Alumina:** *Dane Eckart*<sup>1</sup>; John Kildea<sup>2</sup>; Peter Prinsloo<sup>3</sup>; David Nicholson<sup>2</sup>; Everett Phillips<sup>4</sup>; <sup>1</sup>Worsley Alumina Pty Ltd; <sup>2</sup>Nalco Australia Pty Ltd; <sup>3</sup>BHP Billiton; <sup>4</sup>Nalco Company

Efficient operation of the red mud removal system is a key operational goal for at Worsley Alumina. The plant has a series of high rate settlers employed as the primary solid/liquid separation step. Typically these vessels have used a combination of conventional polyacrylate flocculants and hydroximated polymers to deliver the required process targets. As part of a review of process efficiency Worsley has recently undertaken an assessment of Nalco's RRA polymer technology. Replacement of the conventional polyacrylate flocculant with a new RRA flocculant has led to substantial improvements in key process parameters for the vessels. Specifically use of the RRA polymer has resulted in significantly higher underflow solids density and more efficient overflow liquor filtration. Further optimization of the RRA technology has improved unit operation at a lower cost versus conventional product use. Use of the RRA technology is reviewed and further benefits from its use will be discussed.

### 10:30 AM

**Redundancy of Security Filtration:** *Peter-Hans ter Weer*<sup>1</sup>; <sup>1</sup>TWS Services and Advice

Security Filtration in the Bayer alumina refinery aims at controlling the contamination of alumina product by lowering the solids concentration in the decanter / settler overflow to the desired level in the Liquor to Precipitation (LTP). Significant strides have been made in the design of high rate thickeners and their feedwells, and similarly in the preparation of modern synthetic flocculants. Recent technological developments enable achieving solids levels in the bauxite residue settler overflow which are low enough to meet the targeted solids in LTP. This applies to existing refineries as well as to brownfield and greenfield projects. These developments provide an opportunity to lower alumina refinery operating and capital costs by (partly) by-passing or excluding the Security Filtration area. Savings include opex savings up to 8-1.5 \$/tA and, in case of brownfield and greenfield projects, capex savings of 15-25 \$/Annual tA.

### 11:00 AM

**Tricalcium Aluminate Hexahydrate (TCA) Synthesis and Characterization:** *Mamata Mohapatra*<sup>1</sup>; S. Acharya<sup>1</sup>; <sup>1</sup>Institute of Minerals and Materials Technology

Tricalcium aluminate hexahydrate (TCA) is an important filter-aid for Bayer's liquor (BL) polishing in addition to a few other applications. TCA can be prepared by reaction of CaO or Ca(OH)<sub>2</sub> in NaAlO<sub>4</sub> solutions preferably at low temperatures, [NaOH] and [CO<sub>3</sub><sup>2-</sup>], however, various TCA sample properties influence efficiency of controlling the BL impurities. So the preparation of desired TCA samples under the synthetic conditions needs to be ascertained. In this study a synthesis approach for TCA was attempted using Ca(OH)<sub>2</sub> and Al(OH)<sub>3</sub> (gibbsite) at low temperature and [NaOH] under atmospheric pressure. To control the TCA synthesis process and the physicochemical properties further, a few simple surface active agents and ammonia-carbonate releasing reagents are tested. The effect of temperature, particle dispersion, NaOH and time on particle size and morphology, reactant surface coating and TCA product phase formation were analyzed using various analytical techniques. This kinetic study provides some insight into the TCA formation mechanism and interaction of various synthesis parameters influencing the TCA physicochemical properties.

### 11:30 AM

**Effect of Carbide Slag on High Pressure Digestion Properties of Diaspore:** *Wang Bo*<sup>1</sup>; Sun Huilan<sup>1</sup>; Bi Shiwen<sup>2</sup>; <sup>1</sup>Hebei University of Science and Technology; <sup>2</sup>Northeastern University

Carbide slag is one of the industrial waste residue in the production of acetylene, and it pollutes the environment seriously. Carbide slag was used to replace lime as the additive during high pressure digestion of diaspore in this paper. The effect of carbide slag on the digestion and settling properties of diaspore was studied, and the mechanism of carbide slag during the high pressure digestion process was also investigated by XRD, SEM and EDS methods. The results indicated that the alumina relative digestion rate of diaspore could reach 96% when the addition of carbide was 18%. If the additive was lime, its addition was 10% during this digestion rate. The existence of carbide slag could improve the settling properties of the slurry after alumina digestion compared to the addition of lime. The action mechanism indicated that carbide slag could accelerate the formation of sodium-silicon residue during high pressure digestion process.

## Aluminum Alloys: Fabrication, Characterization and Applications: Fatigue and Corrosion

*Sponsored by:* The Minerals, Metals and Materials Society, TMS Light Metals Division, TMS: Aluminum Processing Committee

*Program Organizers:* Subodh Das, Phinix LLC; Steven Long, Kaiser Aluminum Corporation; Tongguang Zhai, University of Kentucky

Wednesday AM

Room: 615

February 17, 2010

Location: Washington State Convention Center

*Session Chair:* Tongguang Zhai, University of Kentucky

### 8:30 AM

**Corrosion-Fatigue Interactions in Hollow AA6XXX Alloy Extrusions:** *Nicholas Nanninga*<sup>1</sup>; Calvin White<sup>2</sup>; <sup>1</sup>NIST; <sup>2</sup>Michigan Technological University

The effect of an aqueous 3.5 wt% NaCl environment on the high cycle fatigue properties of hollow AA6082 and AA6063 extrusions has been evaluated. These two alloys have contrasting extrusion microstructures, with the AA6063 alloy being fully recrystallized, and the AA6082 alloy retaining a fully fibrous core microstructure with a recrystallized surface layer. Both alloys exhibited substantial reductions in their fatigue lives when exposed to the salt solution. The environmental effect on fatigue appears to be primarily associated with pitting and intergranular corrosion, which leads to premature fatigue crack initiation. Fatigue properties were most severely affected at low stress amplitudes (longer fatigue lives), probably as a result of the more extensive pitting and intergranular corrosion that occurred in those specimens.

### 8:50 AM

**Corrosion Fatigue and Stress-Corrosion Crack Growth in Sensitized Al 5083:** *Peter Pao*<sup>1</sup>; Ramasis Goswami<sup>2</sup>; Ronald Holtz<sup>1</sup>; <sup>1</sup>Naval Research Laboratory; <sup>2</sup>SAIC

The corrosion fatigue and stress-corrosion crack growth kinetics of sensitized (175 °C/10 days) and as-received (H131) Al 5083 were investigated. TEM investigations reveal the presence of continuous magnesium-rich β phase (Al<sub>3</sub>Mg<sub>2</sub>) at the grain boundaries in sensitized Al 5083 while in as-received Al 5083-H131 such β phase is absent. The saltwater stress-corrosion cracking threshold of sensitized Al 5083 is significantly lower than that of the as-received Al 5083-H131. While the saltwater corrosion fatigue cracking thresholds of sensitized and as-received Al 5083 are comparable at a low stress ratio, the corrosion fatigue threshold is significantly lower and crack growth rate significantly higher in sensitized Al 5083 than those of as-received Al 5083. The observed fatigue crack growth and stress-corrosion cracking responses are discussed in terms of differences in microstructure and the interplay between stress-corrosion and corrosion fatigue cracking thresholds.



### 9:10 AM

**Environmental Degradation of SCC-Affected Fatigue Life of High-Strength Aluminum Alloys and Prediction Methodology for Remaining Fatigue Life in Aging Aircraft:** *Yoon Jeong*<sup>1</sup>; Hyunjung Lee<sup>2</sup>; Eungeong Lee<sup>2</sup>; Haksu Kim<sup>2</sup>; Cheolju Lee<sup>1</sup>; Sangshik Kim<sup>2</sup>; <sup>1</sup>Korea Aerospace Industries, LTD.; <sup>2</sup>Gyeongsang National University

There is a need to understand the effects of environmental degradation on fatigue and stress corrosion cracking (SCC) behaviors for predicting the remaining life of aging aircraft. In this study, hour-glass type specimens were prepared from aging aircrafts, the parts of which had been in service and stored after retirement, and S-N fatigue tests were conducted and the results were compared to those of pristine specimens. Smooth bar and single edge notch specimens were also prepared, and slow strain rate tests were performed to determine the effect of SCC. The present study demonstrates that the environmental degradation, predominantly corrosion pits, significantly reduces the fatigue life, and the SCC contribution needs to be considered for accurate remaining fatigue life prediction. Based on the fracture mechanics-based SCC data and the actual fatigue data, several prediction methodologies for remaining fatigue life are discussed with quantification of corrosion and modeling of crack propagation.

### 9:30 AM

**Effect of Heat Treatment on Corrosion Behavior of Aluminum-Lithium Alloy 8090:** *Amr Kobeisy*<sup>1</sup>; Ahmed Metwali Abd El-Aziz<sup>1</sup>; Randa Abdel-Karim<sup>2</sup>; Abdel-Aziz Waheed<sup>3</sup>; <sup>1</sup>German University in Cairo; <sup>2</sup>Cairo University; <sup>3</sup>Atomic Energy Authority

Al-Li 8090 alloy was subjected to different retrogression and reaging (RRA) treatments to investigate their effects on the mechanical and corrosion properties in comparison to peak aged (PA) condition. Optical microscopy, scanning electron microscopy, x-ray diffraction, hardness and tensile measurements were used. Stress corrosion cracking and salt spray tests were carried out and results were compared with microstructure and mechanical properties. The RRA 170 and 190 treatments' corrosion resistance have deteriorated in both tests compared to the PA, while the RRA 210 treatment showed the same atmospheric corrosion resistance as PA. However, RRA 210 showed a much lower SCC resistance, even lower than the RRA 170 and 190 treatments. The results have been explained by the anodic dissolution of uneven distributed phases on the grain boundaries. These precipitations created micro-galvanic cells and thus accelerating localized anodic dissolution mechanism. Pitting and intergranular stress corrosion cracking were found to be the corrosion mechanisms.

### 9:50 AM

**Multi-Axial Fatigue Behaviour of A356-T6:** *Matthew Roy*<sup>1</sup>; Yves Nadot<sup>2</sup>; Daan Maijer<sup>1</sup>; <sup>1</sup>The University of British Columbia; <sup>2</sup>Ecole Nationale Supérieure de Mécanique et d'Aérotechnique (ENSMA)

As light castings become commonplace in transportation applications, design tools must capture multi-axial fatigue effects for structural components. In this investigation, uni-axial and multi-axial fatigue tests have been conducted to investigate the fatigue behaviour of A356-T6 casting alloy in the high cycle regime. The step technique was used to determine the fatigue limit at a million cycles for material with different microstructure. Through tension and torsion testing of specimens with artificial defects, the fatigue mechanism is scrutinized and the crack growth rate has been tabulated for using the replica technique. These results are used to discuss the suitability of treating defects as cracks using linear fracture mechanics. For different loading cases, the stress distribution around defects is examined to understand the role of the stress state in the fatigue process. The results are applied to other classical multi-axial fatigue criterion (Crossland and Van Dang), and one based on principal stresses.

### 10:10 AM

**Processing of Ultra-Fine Grain Structure in Aluminium Alloy by Equal Channel Angular Pressing:** Narasimhan Narayani<sup>1</sup>; Prasad Shanmugasandaram<sup>1</sup>; C. K. Gopalakrishnan<sup>1</sup>; R. Hariharan<sup>1</sup>; G. Swarupini<sup>1</sup>; S. Balasivananda Prabhu<sup>1</sup>; <sup>1</sup>Anna University

The paper involves developing nanostructured Al6061 particles, characterizing their unique mechanical properties and microstructure. Equal Channel Angular Pressing (ECAP), a discontinuous process for Severe Plastic Deformation (SPD) is used. The Ultra Fine Grain microstructure of the material is characterized by TEM, SEM and XRD to identify their high angle strain, low angle strain and other strength related properties. A split die of required dimensions to produce

maximum possible strain without causing failure is used for the process. The resulting Aluminium 6061 alloy material can be widely used in aerospace industries where the proposed increase in density and toughness will make a very big impact. Sports, yacht construction, automotive industries also stand to gain out of this project. The characterization will give researchers and industrialists better insight into the mechanical behaviour and properties of Al 6061 processed through ECAP. Suggestions relating to more optimized die design and lubrication aims at making ECAP a more efficient and effective production process for bulk materials.

### 10:30 AM Break

### 10:45 AM

**Fatigue in Friction Stir Welded 7050 Al:** *Ashley Teare*<sup>1</sup>; Adam Hein<sup>1</sup>; Aaron Wilkinson<sup>1</sup>; David Field<sup>1</sup>; Tracy Nelson<sup>2</sup>; <sup>1</sup>Washington State University; <sup>2</sup>BYU

The fatigue life of a friction stir welded 7050 aluminum alloy was investigated. Measurements of grain boundary structure and local texture were made by electron backscatter diffraction to investigate the correlation between local structure and fatigue life. Miniature single edge notch fatigue specimens were machined from various regions of the weld nugget and surrounding thermo-mechanically and heat affected material. These were tested to obtain fatigue life data for local regions in the welded plate. A strong gradient of fatigue behavior was observed with fatigue life being maximized in the weld nugget center and increasingly shorter life for specimens near the advancing and retreating edges of the weld and into the heat affected regions. Local microstructure was observed to play a significant role in fatigue life performance.

### 11:05 AM

**Effects of Multipass Friction Stir Processing on Microstructure and Mechanical Properties of Al-Zn-Mg (7039) Alloy:** *Prashant Soni*<sup>1</sup>; Bhagwati Kashyap<sup>1</sup>; N. Prabhu<sup>1</sup>; A.G. Rao<sup>1</sup>; V. Deshmukh<sup>1</sup>; <sup>1</sup>IIT Bombay

Hot rolled Aluminum 7039 sheets were subjected to Friction Stir Processing (FSP) up to three passes for grain refinement. The grain size was found to decrease from the initial value of 50 μm to 10 μm after two passes in the nugget zone. The number of FSP pass was continued to explore further evolution in microstructure. Precipitate size and distribution were investigated in the nugget zone, thermo-mechanically affected zone and heat affected zone as a function of number of passes and the same were related to its role in the mechanism for grain growth in quasi-single phase system. Tensile tests were conducted at room temperature and elevated temperatures. Hall-Petch type relation was obtained at low temperature whereas the fine equiaxed microstructure of grain size less than 10 μm exhibits superplastic behavior.

### 11:25 AM

**Influences of Tool Pin Profile and Welding Speed on the Formation of Friction Stir Welding of AA7075 and AA5083:** *Reza Behnagh*<sup>1</sup>; Mohammad Kazem Besharati<sup>2</sup>; <sup>1</sup>Tehran University; <sup>2</sup>Department of Mechanical Engineering, Tehran University

Friction stir welding (FSW) process is an emerging solid state joining process in which the material that is being welded does not melt and recast. This process uses a non-consumable tool to generate frictional heat in the abutting surfaces. The welding parameters and tool pin profile play major roles in deciding the weld quality. In this investigation, an attempt has been made to understand the effect of welding speed and tool pin profile on friction stir welding formation of AA7075 and AA5083. Two different tool pin profiles (cylindrical, tapered cylindrical) have been used to fabricate the joints at different welding transverse and rotational speeds. It is found that the threaded tapered cylindrical tool produces mechanically sound and metallurgically defect free welds compared to other tool pin profile.

### 11:45 AM

**Tensile Properties of a Friction Stir Processed Al-Cu 2218 Alloy at Elevated Temperatures and Related Microstructural Characteristics:** *Ssu-Ta Chen*<sup>1</sup>; Truan-Sheng Lui<sup>1</sup>; Li-Hui Chen<sup>1</sup>; <sup>1</sup>Department of Material Science and Engineering, National Cheng Kung University

Tensile properties of extruded Al-Cu 2218 base metal and friction stir processed (FSPed) Al-Cu 2218 specimens at elevated temperatures are carried out in this study. From room temperature to 300°, FSPed specimens exhibit higher tensile yield stress than base metal. The higher yield stress of FSPed specimens is resulted mainly from natural aging and minor from grain-refinement. The advantage of FSPed sample disappears and simultaneously

# Technical Program

accompanies by an increasing total elongation when tensile tests are conducted at 400° and 450°, respectively. To compare with base metal, FSPed specimens have a more pronounced increasing in total elongation. The excellent total elongation of FSPed specimens is a consequence of dynamic recrystallization and grain boundary sliding.

**12:05 PM**

**Effect of Porosity on the High-Cycle Fatigue Properties of 356 Casting Aluminum Alloy:** Young-Jae Lee<sup>1</sup>; Kwang-Jun Euh<sup>2</sup>; Kyu-Sang Cho<sup>3</sup>; *Kee-Ahn Lee*<sup>4</sup>; <sup>1</sup>Center for Advanced Green Materials Technology, Andong National University; <sup>2</sup>Korea Institute of Material Science; <sup>3</sup>Dongyang University; <sup>4</sup>Andong National University

The effect of porosity on the high-cycle fatigue properties of A356 casting aluminum alloys was investigated in this study. The high-cycle fatigue results indicated that the fatigue strength of the 356-T6 (heat-treated) alloy was higher than that of the 356-F (casted) alloys because of the significant reduction in volume fraction of pores by heat treatment. The SEM fractography results showed that porosity affected detrimental effect on the fatigue life: 80% of all tested samples fractured as a result of porosity which acted as the main crack initiation site. It was found that fatigue life decreased as the size of the surface pore increased. A comparison was made between surface pore and inner pore for its effect on the fatigue behavior. The results also showed that the fatigue strength with the inner pores was higher than that of the surface pore. \*This research was supported by Materials Bank Program, Korea.

---

## Aluminum Reduction Technology: Hall-Héroult Cell: Processes Modeling and Aluminium Smelter Modeling

*Sponsored by:* The Minerals, Metals and Materials Society, TMS Light Metals Division, TMS: Aluminum Committee, TMS: Aluminum Processing Committee

*Program Organizers:* Charles Mark Read, Bechtel Corporation; Gilles Dufour, Aluminerie de Deschambault

Wednesday AM      Room: 608  
February 17, 2010      Location: Washington State Convention Center

*Session Chairs:* Marc Dupuis, GéniSim Inc; Daniel Richard, Hatch

---

### 8:30 AM Introductory Comments

**8:40 AM**

**Mathematical Modeling of Aluminum Reduction Cell Potshell Deformation:** *Marc Dupuis*<sup>1</sup>; <sup>1</sup>GéniSim Inc

One of the key component of an aluminum reduction cell design is the potshell design. The potshell must be designed in such a way that it will not deform excessively in operation and will remain as much as possible in elastic deformation mode. Yet, heavy over-designed potshells are very costly hence the importance of producing a close to optimal design where all structural elements are getting their fair share of the total load while being charged close to their elastic limit. Producing such an optimal potshell design would be very time consuming without the extensive usage of modeling tools. Three such tools are presented here in order of complexity, namely: the empty shell, the almost empty shell and the half empty shell ANSYS® based thermo-mechanical models. Results are presented for each model solved both in elastic and plastic modes as well as the CPU time required to solve them.

**9:10 AM**

**The Use of CFD Simulations to Optimise Ventilation of Potrooms:** *André Maarschalkers*<sup>1</sup>; <sup>1</sup>Colt Technology

Ventilation in potrooms has always been a hot issue. Well engineered systems to evacuate the surplus of thermal energy from the potrooms are mandatory, and should be given the attention that they deserve. Insufficient ventilation could lead to overheating of pots with the accompanying problems. Simulations can help in optimising the ventilation and gives better understanding of the behaviour of airflows inside the building. Besides the main focus on productivity, attention should be given to the exposure of operators to HF concentration and high temperatures. A well designed ventilation scheme can help to create a healthy and safe environment for the operators. Airflows outside the building can be

investigated with the same simulation technique, providing information about the spreading of contaminated airflows.

**9:40 AM**

**Safe and Efficient Traffic Flow for Aluminum Smelters:** *Laszlo Tikasz*<sup>1</sup>; Charles Read<sup>1</sup>; Robert Baxter<sup>1</sup>; Rafael Pires<sup>1</sup>; Robert McCulloch<sup>1</sup>; <sup>1</sup>Bechtel

Aluminum smelter design, construction and operation requires: in-depth knowledge of smelter operations; integration of engineering disciplines; process modeling and dynamic simulation expertise. This paper outlines an approach for improving plant configurations by applying Safety by Design and Lean Manufacturing Methods to achieve a safe and efficient plant design that delivers value over the entire life cycle of the plant, from early project definition, through execution and beyond operational start-up. Design steps used to develop the improved layout include activities such as: listing and specifying movements of People, Products and Materials between Customer and Supplier connections, identifying and quantifying traffic-related hazards, developing and comparing alternative solutions that offer a safe and efficient road network, and traffic scheduling for vehicles and pedestrians throughout the Smelter. To demonstrate the method applied, examples from a Plant Traffic Model and comments on typical traffic risks are presented.

**10:10 AM**

**Development and Application of an ANSYS® Based Thermo-Electro-Mechanical Anode Stub Hole Design Tool:** *Marc Dupuis*<sup>1</sup>; <sup>1</sup>GéniSim Inc

At the 2009 TMS conference, we could observe a renewed interest for the optimization of anode stub hole design. This is not surprising considering that we can estimate that the contact resistance voltage drop at the cast iron/anode carbon interface is about 60 mV (assuming 0.1 m<sup>2</sup> of contact surface per stub hole, 3000 A of current per stub and 2 micro-ohm m<sup>2</sup> of the average contact resistance) which translate to 1.2 MM\$ per year of operational cost for a typical modern smelter for that contact resistance alone. Hence, it is easy to understand that there is a good incentive to optimize the stub hole design in order to minimize the cast iron/anode carbon contact resistance voltage drop. For that purpose, the author took advantage of the recent development of ANSYS® contact elements library to develop an ANSYS® version 12.0 based fully coupled TEM anode stub hole design tool.

**10:40 AM Break**

**10:50 AM**

**Effects of High Temperatures and Pressures on Cathode and Anode Interfaces in a Hall-Heroult Electrolytic Cell:** *Lyne St-Georges*<sup>1</sup>; <sup>1</sup>UQAC

This paper deals with the physical modifications occurring at high temperatures and pressures at the interfaces found in the anode and cathode of a Hall-Heroult electrolytic cell. The anode and the cathode are fabricated with carbon blocks, where steel bars are inserted and sealed with cast iron. Consequently, their interfaces are composed of cast-iron and steel and of cast-iron and carbon. For the investigation presented here, an experimental setup was built to heat and load anodic and cathodic samples. A specific attention was put on the samples preparation, to reproduce real cathode/anode sealing conditions. During the heating and the loading of the samples, fluctuations of electrical and thermal contact resistances are observed and related to physical transformation at the interfaces. These transformations could explain the fluctuations of electrical and thermal contact resistances observed and potentially the non-homogeneities of voltage and current distribution occurring in a Hall-Heroult electrolytic cell.

**11:20 AM**

**Design of a Bypass Joint for the Aluminum Reduction Cells:** *Yimy Sarkis*<sup>1</sup>; <sup>1</sup>Morochos JJ C.A.

This paper presents the design of an electrical joint for the by-pass system of 230kA cells of Aluminum Reduction that produce lower values of voltage drop and enhanced ergonomics for the installation, using a FEM code with interface contact elements, thermo-electrical and thermo-mechanical non-linear simulations were conducted, using properties such as thermal expansion and electrical and thermal contact resistance determined by mathematical models that depends on surface roughness and pressure, the first analysis was the study of the current joint's behavior, which determined that contact occurs only at discrete parts of the interface, then the proposed design model that has a system for pressure adjustment to increase contact pressure and distribute it evenly, making better use of the contact area, therefore, the electrical and thermal contact conductance increase, which is reflected in a decrease of temperature



values up to 20,47% and voltage drop up to 36,5%, generating substantial energy savings.

### 11:50 AM

**3D Freeze Shape Study of the Aluminum Electrolysis Cells Using Finite Element Method:** Cui Xifeng<sup>1</sup>; Zhang Hongliang<sup>1</sup>; Zou Zhong<sup>1</sup>; Li Jie<sup>1</sup>; Lai Yanqing<sup>1</sup>; Xu Yujie<sup>1</sup>; Zhang Hehui<sup>1</sup>; Lv Xiaojun<sup>1</sup>; <sup>1</sup>Central South University

A proper shape of the frozen electrolyte on the sidewall is vital for the aluminum reduction cells. Its formation is influenced by sorts of factors. In this paper, the impact of some parameters upon the shape of the side-ledge is assessed based upon a quarter 3-D thermal-electric ANSYS finite element model, which is developed to fulfill the 3-D calculation of side-ledge. The model has been validated using measurements from a 300kA cell. The influence of the parameters, such as the ACD, the anode change, the anode-channel width, the heat preservation situation of the bottom, side and top, and the property of the cathode block are discussed. Various recommendations are correspondingly made to obtain a proper frozen electrolyte layer.

### 12:20 PM Concluding Comments

## Aluminum Reduction Technology: Hall-Héroult Cell: Processes Modeling and Measurements

*Sponsored by:* The Minerals, Metals and Materials Society, TMS Light Metals Division, TMS: Aluminum Committee, TMS: Aluminum Processing Committee

*Program Organizers:* Charles Mark Read, Bechtel Corporation; Gilles Dufour, Aluminerie de Deschambault

Wednesday AM Room: 614  
February 17, 2010 Location: Washington State Convention Center

*Session Chairs:* Nobuo Urata, Alumilab; James Evans, University of California, Berkeley

### 8:30 AM Introductory Comments

### 8:35 AM

**CFD Modelling of Effect of ACD and Anode Size on Alumina Mixing in Aluminium Reduction Cells:** Yuqing Feng<sup>1</sup>; Mark Cooksey<sup>1</sup>; Phil Schwarz<sup>1</sup>; <sup>1</sup>CSIRO Minerals

Aluminium reduction cells have been continuously improved to reduce energy consumption and increase metal production rates, e.g. by reducing anode-cathode distances (ACDs). Line currents have been increased to increase production rates, which often requires larger anodes to maintain an acceptable current density. These changes may have a significant impact on aspects of cell performance such as bath flow and alumina mixing. In previous work, a computational fluid dynamics (CFD) model of bath hydrodynamics in aluminium reduction cell has been developed and validated using water model data and plant measurement. In the present work, the validated CFD model has been extended to study the effect of ACD and anode size on bath flow and alumina mixing in a typical full-scale industrial cell. The relative effect of ACD and anode size has been compared in terms of bath flow, gas layer thickness in the ACD, and alumina mixing kinetics.

### 9:00 AM

**Terminating Anode Effects by Lowering and Raising the Anodes - A Closer Look at the Mechanism:** Jomar Thonstad<sup>1</sup>; Helmut Vogt<sup>2</sup>; <sup>1</sup>Norwegian University Sc. Technology; <sup>2</sup>TFH, University of Applied Sciences

In aluminium cells anode effects are unwanted events, leading to a waste of energy, overheating and emissions of PFC gases that have a high environmental impact. A common way to quench anode effects in prebake cells is to lower and raise the anodes repeatedly, so-called "anode pumping". This method is normally very effective, the anode effect going off when the anodes are in the low position. The actual mechanism has been the subject of some controversy, explanations varying from: (1) the effect of exposing fresh anode surface area, (2) lowering the anode current density by exposing a larger active anode surface area, or (3) making short circuits to the metal pad. Based on a mathematical model the present work discusses the mechanism, focussing on the enhancement of the anode surface area.

### 9:25 AM

**Bath Temperature Inference through Soft Sensors Using Neural Networks:** Fabio Soares<sup>1</sup>; Roberto Limao<sup>2</sup>; Marcos Castro<sup>3</sup>; <sup>1</sup>Exodus; <sup>2</sup>UFPA; <sup>3</sup>Albras

The thermal balance has a direct impact in current efficiency, however its measures are subjected to hardware and human errors, and normally it takes a long time between measures in the same cell. Those kind of process variables have lately been estimated with the aid of soft sensors, which are computational intelligence algorithms used for complex processes modeling. Since they are software based, they are not subjected to hardware failures and can estimate any process variable according to the data history and available plant operation knowledge. With soft sensors, online temperature estimation is possible, allowing plant operators to early detect process abnormalities and plot trends without needing to perform a real measure. A case of a soft sensor for online temperature estimation in an important Brazilian aluminium smelter is presented in this work, since its design through implementation at production, according to a research methodology.

### 9:50 AM

**The Determination of Pot Current Distribution by Measuring Magnetic Fields:** Nobuo Urata<sup>1</sup>; James Evans<sup>2</sup>; <sup>1</sup>Alumilab; <sup>2</sup>UC, Berkeley

A couple of previous papers have suggested that the current distribution in a pot can be determined by measuring magnetic fields, e.g. the distribution of current among the anode rods can be found by placing a magnetic field sensor next to each rod. Because the current distribution can have a significant effect on pot performance, the suggestion is worth analyzing and this has been done by mathematical models in the present paper. One important aspect of such measurements is the effect of fields generated by other currents on the measurement of a particular current, e.g. the effect of currents in adjacent anode rods on the measurement for one rod. It is shown that, with the use of a sufficient number of sensors, it should be possible to de-convolute individual anode currents, and other currents, from the measured field values.

### 10:15 AM Break

### 10:25 AM

**Busbar Circuit Design and Installation for Boosting Already Boosted Pots:** Daniel Champagne<sup>1</sup>; Donald Ziegler<sup>2</sup>; Andre Schneider<sup>1</sup>; Daniel Richard<sup>1</sup>; <sup>1</sup>Hatch; <sup>2</sup>Alcoa

This tight-schedule project was an important milestone in the announced modernization of the Baie-Comeau Smelter plant. In the spring of 2008, an integrated Alcoa-Hatch multidisciplinary team succeeded to install in record time a new booster rectifier circuit for testing prototype pots. A unique feature of this project is that the new circuit is boosting already boosted pots. To emulate the magnetic field that would affect the pots once the whole potline operates at the target amperage, the new circuit includes a split booster input circuit. Also, in order to accommodate changing conditions in the line and two boost rectifiers, a custom-designed variable electrical resistance was also installed to control the current split in the booster input branches. By using available equipment, a very tight timeline was achieved, and the new systems were put in place with the potline running and with no loss-time injury.

### 10:50 AM

**Study of Surface Oscillation of Liquid Aluminum in 168kA Aluminum Reduction Cells with a New Type of Cathode Design:** Wang Ziqian<sup>1</sup>; Feng Naixiang<sup>1</sup>; Peng Jianping<sup>1</sup>; Wang Yaowu<sup>1</sup>; Qi Xiquan<sup>2</sup>; <sup>1</sup>Northeastern University; <sup>2</sup>Northeastern University Engineering & Research Institute Co. Ltd.

The surface oscillation of liquid aluminum in the new type of cathode structure in 168kA aluminum reduction cells was measured by a dynamic detecting system of surface oscillation of liquid aluminum which is designed independently to research the mechanism on energy saving. The measurements show that the cathode convex in the new type of cathode could reduce the velocity of liquid aluminum and could weaken the surface oscillation of liquid aluminum, so the energy consumption could be reduced by decreasing interpolar distance. The surface oscillation of liquid aluminum was not affected by the operation of metal tapping but it was affected greatly by anode changing. After anode changing, the periodic time is changed a little. Typically, the periodic time of liquid aluminum wave in the new type of cathode aluminum reduction cells is 50 s, the average velocity of the liquid aluminum wave is 0.12 m/s, and the wavelength is 6 m.

# Technical Program

11:15 AM

**Modelling and Optimization of Busbar Configuration in Aluminum Electrolysis Cell with Genetic Algorithm:** *Mao Li*<sup>1</sup>; <sup>1</sup>Central South University

Based on the commercial package ANSYS and custom APDL code, a parametrical mathematic model of busbar configuration in aluminum electrolysis cell was proposed. An object function was established based on a simplified magnetohydrodynamic stability criteria, the parameters of busbar configuration model was studied and optimized automatically with genetic algorithm according to the value of custom object function. It is shown that the parametrical busbar configuration model can be established and calculated adaptively to find the optimal busbar configuration, the physical fields of the cell after busbar optimization is also discussed, cell with optimized busbar configuration has shown satisfying distribution of physical fields.

11:40 AM **Concluding Comments**

## **Biological Materials Science: Mechanical Behavior of Biological Materials III: Soft Tissues and Materials**

*Sponsored by:* The Minerals, Metals and Materials Society, TMS Structural Materials Division, TMS: Biomaterials Committee, TMS/ASM: Mechanical Behavior of Materials Committee

*Program Organizers:* John Nychka, University of Alberta; Jamie Kruzic, Oregon State University; Mehmet Sarikaya, University of Washington; Amit Bandyopadhyay, Washington State University

Wednesday AM      Room: 205  
February 17, 2010      Location: Washington State Convention Center

*Session Chairs:* Po-Yu Chen, University of California, San Diego; Roger Narayan, NC State/UNC Chapel Hill

8:30 AM **Invited**

**Using Optical Tweezers to Probe Mechanical Response from Single Molecules to Soft Biological Materials:** *Nancy Forde*<sup>1</sup>; <sup>1</sup>Simon Fraser University

In the past decade, the ability to manipulate and measure forces exerted by single biological molecules has transformed our understanding of their mechanical response, stability, and the mechanisms by which they operate. One of the essential tools in this revolution has been optical tweezers, which use a focused laser beam to “trap” (hold stably in three dimensions) micrometer-sized refractive particles. In this talk, I will briefly describe how optical tweezers work and how they can be used to manipulate and probe the mechanical response of single protein molecules. I will then discuss our work developing the technique of holographic optical tweezers as a microscale tensometer for soft materials, capable of straining and measuring stresses on materials in three dimensions. We are applying these techniques to learn about the molecular basis for mechanical response of the extracellular matrix proteins collagen and elastin.

9:00 AM **Invited**

**Investigating the Structure-Properties Relationship of the Cornea and Sclera:** Brad Boyce<sup>1</sup>; Thao Nguyen<sup>2</sup>; <sup>1</sup>Sandia National Laboratories; <sup>2</sup>Johns Hopkins University

We are developing an integrated experimental and modeling program to investigate the relationship between the structure, mechanical behavior, and physiologic function of the cornea and sclera. Central to the program is an inflation testing method that uses digital image correlation (DIC) to provide a three-dimensional deformation map of the exposed surface of the specimen. We have developed the method for bovine, human, and mouse tissues. Human and mouse experiments compare the anisotropic viscoelastic behavior of tissues of normal and clinically diagnosed glaucoma (human) and induced glaucoma (mouse) eyes. Inflation experiments do not measure directly the stress response of the tissues and require a constitutive and finite element modeling to process the results. For glaucoma, we also apply the models to probe the effects of the measured differences in the properties of the cornea and sclera on the deformation and stress state of the optic nerves.

9:30 AM **Invited**

**Polymer Mechanics Models the Fraction of Cartilage Stress Relaxation Not Caused by Fluid Flow:** *David Fyhrle*<sup>1</sup>; R. June<sup>2</sup>; Corey Neu<sup>3</sup>; Justin Barone<sup>4</sup>; <sup>1</sup>University of California, Davis; <sup>2</sup>University of California, San Diego School of Medicine; <sup>3</sup>Purdue University; <sup>4</sup>Virginia Technological University

Stress relaxation of calf cartilage for less than  $\approx 1$  sec is best modeled using a monodisperse polymer model but for  $\geq 1$  sec (up to 1800 seconds) a combination of elastic response, inviscid fluid flow (KLM model) and a polymer fluid accurately fits the experimental data. Relaxation of polymer fluids is often approximated by the Kolrausch-Williams-Watt (KWW or stretched exponential) function. We derive a new application of the KWW function based on random bonding of linear macromolecules. Analysis of the experimental data demonstrates a transition between relaxation dominated by fluid flow and relaxation dominated by polymer mechanics. The best fit to the experimental data was consistent with our analysis of the random bonding mechanism. The conclusion is that stress relaxation in calf cartilage is well approximated by a KWW function with a shape exponent consistent with the mechanism of relaxation dispersion being random bonding between linear polymers.

10:00 AM

**Stimulated Cellular Response of Novel Hybrid Bimodal Network Elastomers for Soft Tissue Implants:** *Wah Wah Thein-Han*<sup>1</sup>; Jinesh Shah<sup>1</sup>; Devesh Misra<sup>1</sup>; <sup>1</sup>University of Louisiana

In reconstructive surgery, tissue transplantation and/or tissue substitute transplantation approaches are widely used to reconstruct and repair the deformity and defects of human organs. In this regard, we describe here the synthesis and biological property of novel hybrid bimodal network elastomers that are characterized by high strength-high ductility combination and good biocompatibility. Pre-osteoblasts grown on hybrid network were well spread, flat, large in size with rough cell surface, and appeared as a group. In contrast, these features were less pronounced in pure elastomers (e.g. smooth cell surface, not well-spread). Interestingly, immunofluorescence study illustrated distinct fibronectin expression level, stronger vinculin focal adhesion contacts associated with abundant actin stress fibers in pre-osteoblasts grown on the composite compared to silicone rubber, implying enhanced cell-substrate interaction.

10:20 AM **Break**

10:30 AM **Keynote**

**Nanomechanical Properties of Biological Tissues – Pushing the Boundaries of Nanoindentation Testing:** *Michelle Dickinson*<sup>1</sup>; <sup>1</sup>Auckland University

Biological tissues consist of a complex hierarchical architecture at a range of length scales from nano to macro. Each of these components combine to perform diverse mechanical, biological and chemical functions which are ever-changing. Many diseases are not diagnosed until catastrophic failure occurs, such as a broken bone or tendon rupture. However, these may have been preceded by significant microstructural changes which, if detected early can lead to identification of the key contributing failure mechanisms. Nanoindentation testing on these biological materials is becoming more popular. This paper highlights recent work measuring individual components within biological tissues including single osteons in bone, collagen fibrils in vertebrae and calcified deposits on smooth muscle walls. The results show how testing structures at the nanoscale can relate each component to the micro, and bulk properties. By studying healthy and diseased tissues at the nanoscale, a more targeted approach to disease progression/prevention can be pursued.

11:10 AM

**Dynamic Nanoindentation of Articular Cartilage:** Oliver Franke<sup>1</sup>; Mathias Göken<sup>2</sup>; Marc Meyers<sup>3</sup>; Karsten Durst<sup>2</sup>; *Andrea Hodge*<sup>4</sup>; <sup>1</sup>MIT; <sup>2</sup>University of Erlangen; <sup>3</sup>University of California, San Diego; <sup>4</sup>University of Southern California

A technique to study the time-dependant properties of hyaline porcine cartilage under in vitro conditions is presented. The tests were carried out in a wide range of frequencies from 1 Hz to 250 Hz on frozen and fresh samples. While the fresh samples show storage moduli between 3.6 MPa and 8 MPa (for 1 Hz to 20 Hz), freezing lowers the values for the surface region by a factor of 2. The same trend was observed for the loss modulus. Since the classical contact area determination for sharp indenters in viscoelastic materials is expected to be inaccurate a new method is introduced using the same approach used for the pile-up corrected hardness. An internal calibration on the tested material



is required as the values may vary from spot to spot or between samples. It will be shown, how this can be achieved using different loading profiles and frequencies.

### 11:30 AM

**Nanoindentation of Ultrasoft Biological Materials:** *Vinod Nayar*<sup>1</sup>; Andrea Hodge<sup>2</sup>; James Weiland<sup>3</sup>; <sup>1</sup>University of Southern California - Department of Biomedical Engineering; <sup>2</sup>University of Southern California - Department of Aerospace & Mechanical Engineering; <sup>3</sup>University of Southern California - Keck School of Medicine

The methodology and analysis for testing sclera tissue by nanoindentation are presented. Using a Hysitron Triboscope nanoindenter, a reduced modulus of  $31.50 \pm 8.30$  kPa and hardness of  $0.19 \pm 0.09$  kPa were obtained from harvested porcine, posterior-sectioned, sclera in room temperature saline conditions with a load-controlled, flat punch, fluid-cell, sapphire tip. This methodology has significantly improved upon the consistency of previous studies and will allow for further studies of similar ultrasoft biological materials. Previous nanoindentation studies have focused on both hard and soft biological materials, ranging from dentin and cortical bone to arteries and cartilage. In contrast, the sclera tissue is considered an ultrasoft material since it has a reduced modulus less than 1 MPa. The effect of factors including drift monitoring, hydration conditions, spring force corrections, mounting procedures, peak loads, and selection of load functions are also discussed.

### 11:50 AM

**Quantitative Viscoelasticity Measurements of Biological Materials by Atomic Force Acoustic Microscopy:** *Arnaud Caron*<sup>1</sup>; Ansgar Hohmann<sup>2</sup>; Erhard Stupperich<sup>3</sup>; Franz-Günter Sander<sup>2</sup>; Hans-Jörg Fecht<sup>1</sup>; <sup>1</sup>Institute of Micro- and Nanomaterials, University Ulm; <sup>2</sup>Department of Orthodontics, University Ulm; <sup>3</sup>Institute of Microbiology and Biotechnology, University Ulm

Atomic Force Acoustic Microscopy (AFAM) is a resonance spectroscopy technique where a micro-fabricated cantilever beam in contact with a sample surface is excited to its resonance via the injection of ultrasound waves through the investigated sample. The resonance frequencies of a cantilever in contact with a surface sample depends on the contact stiffness  $k^*$  and so on the elastic properties of the sample. Attempts have been made to apply AFAM and related technique such UAFM and SNFHU for imaging the elastic properties of biological materials, however no quantitative measurements using these techniques have been reported yet. In this work we present results on the viscoelasticity of agar gel-samples as measured by AFAM. Agar gel is a good model material to test the ability of AFAM on soft mater. Further we show application examples of AFAM on biological materials (i.e. biofilms and the human periodontal ligament) to investigate their viscoelastic properties.

### 12:10 PM

**Multi-Scale Mechanisms of Osteogenesis Imperfecta Disease in Collagenous Tissues:** *Markus Buehler*<sup>1</sup>; Alfonso Gautieri<sup>1</sup>; Sebastien Uzel<sup>1</sup>; <sup>1</sup>Massachusetts Institute of Technology

Osteogenesis imperfecta is a genetic disorder in collagen characterized by mechanically weakened tendon, fragile bones, skeletal deformities and in severe cases prenatal death. Here we show by a hierarchy of full atomistic and mesoscale simulation that osteogenesis imperfecta mutations severely compromise the mechanical properties of collagenous tissues at multiple scales, from single molecules to collagen fibrils. Mutations that lead to the most severe osteogenesis imperfecta phenotype correlate with the strongest effects, leading to weakened intermolecular adhesion, increased intermolecular spacing, reduced stiffness, as well as a reduced failure strength of collagen fibrils. Our findings provide insight into the microscopic mechanisms of this disease and lead to explanations of characteristic osteogenesis imperfecta tissue features such as reduced mechanical strength and lower cross-link density. The study explains how single point mutations can lead to catastrophic tissue failure at much larger length-scales, and makes a direct links between genetics, mechanical failure, and material properties.

### Bulk Metallic Glasses VII: Fatigue and Corrosion

*Sponsored by:* The Minerals, Metals and Materials Society, TMS Structural Materials Division, TMS/ASM: Mechanical Behavior of Materials Committee

*Program Organizers:* Peter Liaw, The University of Tennessee; Hahn Choo, The University of Tennessee; Yanfei Gao, The University of Tennessee; Gongyao Wang, University of Tennessee

Wednesday AM

Room: 213

February 17, 2010

Location: Washington State Convention Center

*Session Chairs:* D. Gary Harlow, Lehigh University; Annett Gebert, Leibniz-Institute for Solid State and Materials Research IFW Dresden

### 8:30 AM Invited

**A Fracture Mechanics Model of Fatigue Crack Propagation in Bulk-Metallic Glasses:** *Xiaoqing Jin*<sup>1</sup>; *Leon Keer*<sup>1</sup>; *Gongyao Wang*<sup>2</sup>; *Peter Liaw*<sup>2</sup>; <sup>1</sup>Northwestern University; <sup>2</sup>The University of Tennessee

A three-point bending experiment was performed to investigate the fatigue behavior of Zr<sub>50</sub>Cu<sub>40</sub>Al<sub>10</sub> bulk metallic glass (BMG). The fatigue crack growth path as well as both the fine and coarse fatigue striation spacings were measured during the testing. In amorphous alloys, since the crystal defects are absent and plastic flow is mainly confined to the shear bands, their formation could play a significant role in causing fracture. It is postulated that a fatigue crack initiates from the ruptured shear band, and advances conforming to the shear bands along the most favorable direction. A modeling analysis implementing the energy criterion of linear elastic fracture mechanics (LEFM) is developed to explore the proposed fatigue mechanism based on the shear band hypothesis. The present numerical simulation predicts good agreement with the fatigue crack characteristics observed in the experiments.

### 8:50 AM

**Mechanisms of Fatigue Crack Growth in Zr-Based Bulk Metallic Glasses:** *Jamie Kruzic*<sup>1</sup>; *Sarah Philo*<sup>1</sup>; *Maximilien Launey*<sup>2</sup>; <sup>1</sup>Oregon State University; <sup>2</sup>Lawrence Berkeley National Laboratory

Fatigue crack growth rates were measured for Zr<sub>44</sub>Ti<sub>11</sub>Ni<sub>10</sub>Cu<sub>10</sub>Be<sub>25</sub> and Zr<sub>58.5</sub>Nb<sub>2.8</sub>Cu<sub>15.6</sub>Ni<sub>12.8</sub>Al<sub>10.3</sub> bulk metallic glasses (BMGs). Growth rate data overlapped considerably for both. To understand the mechanisms of fatigue crack growth the former BMG was tested in different initial free volume and residual stress states, and in both an ambient air and dry nitrogen environment. Fatigue crack growth rates were relatively unaffected by the initial free volume state. This was attributed to the formation of a fatigue transformation zone of increased local free volume at the fatigue crack tip. When residual thermal tempering stresses from the initial processing were not annealed out, it was found that the fatigue threshold and fracture toughness were both increased due to residual compressive stresses at the sample surfaces suppressing crack growth. Finally, it was found that testing in a dry nitrogen environment significantly increased the fatigue threshold, suggesting a corrosion fatigue mechanism in ambient air.

### 9:00 AM Invited

**Effect of Stress Gradient on Fatigue Strength of Zr-Based Bulk Metallic Glass:** *Yoshikazu Nakai*<sup>1</sup>; *Kohei Fujihara*<sup>1</sup>; *Naoki Sei*<sup>1</sup>; *Kunihiro Ando*<sup>1</sup>; *Bok-Key Kim*<sup>2</sup>; <sup>1</sup>Kobe University; <sup>2</sup>Myongji College

Fatigue strength of notched specimen and smooth specimen of Zr-based bulk metallic glass were conducted under either plane-bending or axial-loading. The fatigue notch factor was almost equal to the elastic stress concentration factor either for plane-bending or for axial loading. It indicates that the effect of stress gradient around notch root is negligible, and the fatigue limit of notched specimen is determined by the stress at the notch root. On the contrary, the fatigue strength and the fatigue limit were lower for the axial-loading than the plane-bending either for notched or smooth specimen. It is considered that the fatigue strength of BMG depends on the cooling rate in the casting process of the material, which is different along the thickness direction, and the fatigue strength of plane-bending reflects the strength at the specimen surface while that of axial-loading is determined by the weakest strength in the thickness direction.

# Technical Program

## 9:20 AM

### Near-Threshold Fatigue Crack Growth in Metallic Glass Matrix

**Composites:** Kombaiah Boopathy<sup>1</sup>; Douglas Hofmann<sup>2</sup>; William Johnson<sup>3</sup>; Upadrasta Ramamurty<sup>1</sup>; <sup>1</sup>Indian Institute of Science; <sup>2</sup>Liquidmetal Technologies; <sup>3</sup>California Institute of Technology

A major drawback in using bulk metallic glasses (BMGs) as structural materials is their extremely poor fatigue performance. One way to alleviate this problem is through the composite route, in which second phases are introduced into the glass to arrest crack growth. In this work, the fatigue crack growth behavior of in-situ reinforced BMGs with crystalline dendrites, which are tailored to impart significant ductility and toughness to the BMG, was investigated. Three composites, all with equal volume fraction of dendrite phases, were examined to assess the influence of chemical composition on the near threshold fatigue crack growth characteristics. Nanoindentation experiments on the constituent phases show that the amorphous matrix is much harder and stiffer as compared to the crystalline dendritic phase. The threshold stress intensity factor range for fatigue crack initiation in composites was found to be enhanced by more than 100%.

## 9:30 AM Invited

### Fracture and Fatigue of Zr- and Ti-Based Metallic Glass In-situ Matrix

**Composites:** Maximilien Launey<sup>1</sup>; Douglas Hofmann<sup>2</sup>; William Johnson<sup>2</sup>; Robert Ritchie<sup>3</sup>; <sup>1</sup>Lawrence Berkeley National Laboratory; <sup>2</sup>California Institute of Technology; <sup>3</sup>University of California Berkeley

The mechanical properties of bulk metallic glasses (BMGs) are often plagued by low fracture and fatigue resistance. Correspondingly, much effort in recent years has been devoted to improving their damage tolerance properties, either through compositional changes or by introducing some degree of microstructure. By matching the microstructural length scales (of a second phase) to mechanical crack-length scales, metallic glass matrix composites demonstrate strongly improved tensile ductility, fracture toughness, and fatigue resistance. These remarkable improvements are explained by the effect of the mechanically soft and ductile second phase, which acts stabilizing against shear localization and critical crack propagation; it results in extensive plastic shielding, which further stabilizes crack growth. The fracture and fatigue behavior of semi-solidly processed Zr- and Ti-based BMG matrix composites with in-situ dendritic phase was examined. Specifically resistance-curve, fatigue crack-growth, and stress-life behavior are here presented in light of the relevant toughening and fatigue mechanisms involved.

## 9:50 AM

### Effects of Laser-Surface Modification on Bending-Fatigue Characteristics of Zr-Based Bulk Metallic Glasses:

**Ritesh Sachan<sup>1</sup>; G.Y. Wang<sup>1</sup>; P.K. Liaw<sup>2</sup>; Ramki Kalyanaraman<sup>1</sup>; <sup>1</sup>University of Tennessee-Knoxville**

For the last two decades, bulk metallic glasses (BMGs) have received attention from material science community because of their unusual characteristics, including high tensile strengths and great elastic limits. Recently, much work has focused on studying the inherent brittleness of BMGs. Here we investigate the surface modification of Zr<sub>50</sub>Cu<sub>30</sub>Al<sub>10</sub>Ni<sub>10</sub> metallic glass by nanosecond pulsed laser irradiation. Surface treatments were performed as a function of laser-energy density, number of pulses, and spatial uniformity of laser beam (i.e., interference irradiation). The resulting surface structure and morphology was investigated by the scanning-electron microscopy (SEM), atomic-force microscopy (AFM), and x-ray diffraction techniques. The resulting surface structure and morphology was correlated with 4-point bending experiments to measure the bending fatigue properties of bar-shaped specimens. A significant change was observed in number of cycles to failure at a constant stress range, suggesting that the surface-laser treatment could help control the fatigue behavior of BMG specimens.

## 10:00 AM Break

## 10:10 AM Invited

### Statistical Aspects of Fatigue for Bulk-Metallic Glasses:

**D. Gary Harlow<sup>1</sup>; Gongyao Wang<sup>2</sup>; Peter Liaw<sup>2</sup>; Yoshihiko Yokoyama<sup>3</sup>; <sup>1</sup>Lehigh University; <sup>2</sup>University of Tennessee; <sup>3</sup>Tohoku University**

The fatigue lives of bulk-metallic glasses (BMG) exhibit large scatter. The primary sources are from manufacturing, microstructure, environment, and loading. Because of the inherent microstructural properties of BMG, experimental testing cannot adequately identify all of the sources and magnitude of the randomness in the fatigue life. Nevertheless, the identification

and significance of these variables are paramount for predicting the fatigue life. The variability associated with differences in fatigue-testing techniques, manufacturing processes, material properties, and chemical compositions are investigated. The statistical characterization of internal inhomogeneities and surface damage, each of which impact fatigue lives, is considered. Three classes of BMG, i.e., Zr, Cu, and Fe based BMG, are examined to study the statistical effect of different microstructures. Also, the statistical influence of cast processing is investigated by considering two different processes. The statistical properties are examined in the context of standard stress and fatigue-life cycles (S-N) response.

## 10:30 AM

### Zr-Base Glass-Forming Film for Fatigue Property Improvements of 316L

**Stainless Steel:** Jinn Chu<sup>1</sup>; Cheng-min Lee<sup>1</sup>; Peter Liaw<sup>2</sup>; <sup>1</sup>Nation Taiwan University of Science and Technology; <sup>2</sup>The University of Tennessee

Effects of 200-nm-thick glass-forming Zr<sub>33</sub>Cu<sub>29</sub>Al<sub>12</sub>Ni<sub>6</sub> sputtered film on four-point bending fatigue properties of 316L stainless steel substrate have been investigated. The fatigue life is found to improve from 4.4x10<sup>5</sup> cycles of uncoated sample to 4.5x10<sup>6</sup> cycles of coated sample under a stress of 750MPa. The life is further increased to >10<sup>7</sup> cycles, more than 22 times, when the film is annealed in supercooled liquid region ( $\Delta T$ ). The improvements in fatigue limit are 700MPa and 750MPa for as-deposited and annealed films, respectively, from 600MPa of uncoated sample. The excellent fatigue properties are attributed to the several factors, such as smooth surface, high film strength and better adhesion between film and 316L stainless steel. The sample surface becomes smooth after coated with the film, and it is further improved after annealing in  $\Delta T$ . As a result, the substrate with the annealed film could have enhanced fatigue properties. Detailed results will be presented.

## 10:40 AM Invited

### Effect of Surface Finishing and Mechanically Induced Defects on the Corrosion of Bulk Metallic Glasses:

**Annett Gebert<sup>1</sup>; <sup>1</sup>Leibniz-Institute for Solid State and Materials Research IFW Dresden**

It is well established that surface reactivity and corrosion behaviour of amorphous alloys is principally determined by various material-dependent factors. It is clearly demonstrated that under real casting and rapid quenching conditions the preparation of absolutely defect-free amorphous alloys is nearly impossible. The paper reports on first systematic studies regarding the effect of different mechanically and chemically generated surface finishing states on the anodic behaviour of Zr-based bulk metallic glasses. It will be demonstrated that depending on the treatment process the active-passive behaviour can be significantly altered. Fundamental studies combining electrochemical and surface analyses with mechanical testing of selected Zr-based bulk glass-forming alloys were conducted. Those clearly revealed that the pitting initiation is dependent on the mechanically induced defect concentration. Pits are pinned to pre-formed shear bands at the sample surface. The stress field of local mechanical defects supports the corrosion process and determines the corrosion damage morphology.

## 11:00 AM

### Fatigue Behavior of Tough Fe-Based Bulk-Metallic Glasses:

**Gongyao Wang<sup>1</sup>; Marios Demetriou<sup>2</sup>; Russell Graves<sup>1</sup>; Peter Liaw<sup>1</sup>; William Johnson<sup>2</sup>; <sup>1</sup>University of Tennessee; <sup>2</sup>California Institute of Technology**

Amorphous steel alloys of composition Fe-(Mo,Ni,Cr)-(C,B)-P with low shear moduli exhibiting high toughness and good glass-forming ability have recently been developed. Specifically, alloy Fe<sub>70</sub>Mo<sub>5</sub>Ni<sub>5</sub>C<sub>5</sub>B<sub>2.5</sub>P<sub>12.5</sub> forms glassy rods 4 mm in diameter, has a shear modulus of 57 GPa, and exhibits notch toughness of 50 MPa $\times$ m<sup>1/2</sup>. In this presentation, results from compression-compression fatigue experiments performed on Fe<sub>70</sub>Mo<sub>5</sub>Ni<sub>5</sub>C<sub>5</sub>B<sub>2.5</sub>P<sub>12.5</sub> in air will be introduced. The applied stress versus cycles to failure (S-N) curve will be presented and compared to other Fe-based and Zr-based bulk-metallic glasses. Moreover, a mechanistic insight into the mechanism governing the fatigue failure in a low-shear-modulus high-toughness Fe-based bulk-metallic glasses will be proposed. The present work is supported by the National Science Foundation (NSF), the Combined Research-Curriculum Development (CRCD) Program, under EEC-9527527 and EEC-0203415, the Integrative Graduate Education and Research Training (IGERT) Program, under DGE-9987548, the International Materials Institutes (IMI) Program, under DMR-0231320.



### 11:10 AM Invited

**Stress-Assisted Corrosion of Cu-Based Bulk Metallic Glass:** Ding Li<sup>1</sup>; Fuqian Yang<sup>1</sup>; Peter K. Liaw<sup>2</sup>; <sup>1</sup>University of Kentucky; <sup>2</sup>University of Tennessee

Using microindentation, the stress-assisted-electrical corrosion of Cu-based bulk metallic glass (Cu<sub>46.25</sub>Zr<sub>45.25</sub>Al<sub>7.5</sub>Er<sub>1</sub>) was studied in a 10 wt% NaCl electrolyte. The microindentation was performed in an indentation load range of 500 mN to 4000 mN to create shear bands over the deformation zone. Electric current of various densities was passed through the indented-bulk metallic glass to evaluate the effect of shear bands on the electrical corrosion of the bulk metallic glass. Surface corrosion (the formation of pits) always initiated from the shear-banding zones, and the size of the corrosion zone grew with the corrosion time surrounding the shear-banding zones. Worm-like structures were formed, and the density of the worm-like structures increased with the current density and the corrosion time.

### 11:30 AM

**Biocompatibility of Zr-Based Bulk Metallic Glasses: Effects of Micro-Alloying and Surface Roughness:** Lu Huang<sup>1</sup>; Zheng Cao<sup>2</sup>; Wei He<sup>2</sup>; Harry Meyer<sup>2</sup>; Peter Liaw<sup>2</sup>; Elena Garlea<sup>4</sup>; Shujie Pang<sup>1</sup>; Tao Zhang<sup>1</sup>; <sup>1</sup>Beijing University of Aeronautics and Astronautics; <sup>2</sup>University of Tennessee, Knoxville; <sup>3</sup>Oak Ridge National Laboratory; <sup>4</sup>Y12 National Security Complex

The present work evaluated the effects of micro-alloying and surface roughness on the biocompatibility of Zr-based bulk metallic glasses (BMGs), and assessed their potential application as an implant material. Ti-6Al-4V alloy was selected as a reference material. Surface properties, including surface composition, surface roughness, and wettability were characterized for all substrates. Bone-forming mouse MC3T3-E1 pre-osteoblastic cells were used to investigate cellular behaviors, including cell attachment, proliferation, and differentiation activities on substrates with different compositions and surface roughness. Cell adhesion and proliferation behaviors were found comparable on all substrates. However, cell differentiation behaviors were found to be influenced by both composition and roughness. A higher differentiation activity was found on BMG samples than on the Ti-alloy. This study concluded that, in addition to their excellent mechanical and electrochemical properties, Zr-based BMGs exhibited a good biocompatibility which made them a competitive candidate to be used as a medical implant material. Acknowledgement: This work was supported by the International Materials Institutes (IMI) program, and the National Natural Science Foundation of China (NSFC). Research at the Oak Ridge National Laboratory SHaRE User Facility was sponsored by the Scientific User Facilities Division, Office of Basic Energy Sciences, U.S. Department of Energy.

### 11:40 AM

**Compression-Compression Fatigue Behavior of Zr-Based Bulk-Metallic Glasses:** Gongyao Wang<sup>1</sup>; P. Liaw<sup>1</sup>; Y. Yokoyama<sup>2</sup>; R. Graves<sup>1</sup>; A. Inoue<sup>2</sup>; <sup>1</sup>University of Tennessee; <sup>2</sup>Institute for Materials Research

Rod Zr<sub>50</sub>Cu<sub>40</sub>Al<sub>10</sub>, Zr<sub>60</sub>Cu<sub>30</sub>Al<sub>10</sub>, and Zr<sub>50</sub>Cu<sub>30</sub>Al<sub>10</sub>Ni<sub>10</sub> (in atomic percent) bulk-metallic glasses (BMGs) were fabricated by an arc-melt tilt-casting technique. Compression-compression fatigue experiments were performed on these zirconium (Zr)-based BMGs in air. The experiments were conducted at a frequency of 10 Hz, using an electrohydraulic machine with an R ratio of 0.1, where  $R = |s|_{min} / |s|_{max}$ ,  $|s|_{min}$  and  $|s|_{max}$  are the applied minimum and maximum absolute stresses, respectively. These samples exhibit high fatigue-endurance limits of over 1,400 MPa, based on the stress range. The results suggested that the fatigue resistance of BMGs can be improved with fabrication technique. A mechanistic understanding of the compression-compression fatigue behavior of these Zr-based BMGs is provided. The present work is supported by the National Science Foundation (NSF), the Combined Research-Curriculum Development (CRCD) Program, under EEC-9527527 and EEC-0203415, the Integrative Graduate Education and Research Training (IGERT) Program, under DGE-9987548, the International Materials Institutes (IMI) Program, under DMR-023132

### 11:50 AM Invited

**Corrosion Behaviors of Fe<sub>41</sub>Co<sub>7</sub>Cr<sub>15</sub>Mo<sub>14</sub>C<sub>15</sub>B<sub>6</sub>Y<sub>2</sub> Bulk Metallic Glass in Sulfuric Acid Solutions:** Jun Shen<sup>1</sup>; <sup>1</sup>Harbin Institute of Technology

The corrosion resistance of Fe<sub>41</sub>Co<sub>7</sub>Cr<sub>15</sub>Mo<sub>14</sub>C<sub>15</sub>B<sub>6</sub>Y<sub>2</sub> bulk metallic glass in sulfuric acid solutions was determined by electrochemical measurement. The passive film formed on the surface of the alloy after immersion in the 0.5 mol/L H<sub>2</sub>SO<sub>4</sub> solution for a week was analyzed by X-ray photoelectron spectroscopy

(XPS). Electrochemical measurements show that the corrosion resistance of the studied alloy in the 1 mol/L H<sub>2</sub>SO<sub>4</sub> solution is superior to stainless steel (SUS 321), and almost the same as Ti6Al4V, indicating that the amorphous alloy studied exhibits excellent corrosion resistance in sulfuric acid solutions.

### Cast Shop for Aluminum Production: Direct Chill and Conveyor Casting

*Sponsored by:* The Minerals, Metals and Materials Society, TMS Light Metals Division, TMS: Aluminum Committee, TMS: Aluminum Processing Committee

*Program Organizers:* John Grandfield, Grandfield Technology Pty Ltd; Pierre Le Brun, Alcan Voreppe Research Center

Wednesday AM

Room: 609

February 17, 2010

Location: Washington State Convention Center

*Session Chair:* Gerd-Ulrich Grün, Hydro Aluminium Deutschland GmbH

### 8:30 AM

**Microsegregation of Direct Chill Ingot of Super High Strength Aluminum Alloy Cast from Heavily Electromagnetically Stirred Melt:** Takateru Umeda<sup>1</sup>; Pramote Thirathipviwat<sup>1</sup>; Mawin Suparadist<sup>1</sup>; Hiromi Nagaumi<sup>2</sup>; <sup>1</sup>Chulalongkorn University; <sup>2</sup>Nippon Light Metal

Low frequency electromagnetic casting (LFEC) applied to Al alloys produces intensive stirring in direct chill (DC) melt, which prevents hot cracking of high strength aluminum alloys never produced by DC. For instance, Al-10%Zn-2.7%Mg-2.3%Cu alloy, of which extruded and heat treated alloy shows 780MPa in tensile strength and 13% in elongation, is available by LFEC because of fine grain size due to heavy stirring and its grain size is small enough, such as  $45 \times 10^{-6}$  m cast into 200 mm diameter billet. Not only to control this new casting well but also to develop alloy designing properly it is necessary to understand solidification behavior microscopically. Therefore, in this report, microsegregation in accordance with solidification progress including formation of various kinds of intermetallic compounds is firstly discussed by both precise experiments and the prediction by using thermodynamic data base. Next solute redistribution is simulated considering back diffusion happened by fine grain size.

### 8:55 AM

**Utilizing Safety Pit Coating Repair Kits to Prevent Production Stoppages:** Alex Lowery<sup>1</sup>; Joe Roberts<sup>2</sup>; <sup>1</sup>Wise Chem LLC; <sup>2</sup>Pyrotek Inc.

Studies have proven that safety pit coatings prevent molten metal explosion from bleed-outs during direct chill casting in an aluminium mills. The safety pit coatings are applied to any substrate that can come into contact with any molten metal at the casting station. Upon repeated exposures the coating surface sacrifices itself upon contact with molten metal to prevent an explosion from occurring. Eventually the coating surface exposes the bare substrate (e.g., concrete, steel, stainless steel). Further studies have shown that a bare spot as small as 4 sq. inches (25.4 sq. cm) in the safety pit coating surface can be an ignition source for a molten metal explosion. Repair of the damaged coating surface was time consuming and commonly disrupted production. Recent introduction have safety pit coating repair kits that enable the quick repair of damaged coating surfaces have minimized and in most instances eliminated any disruption in production.

### 9:20 AM

**Effect of Application of out-of-Phase Electromagnetic Field on Horizontal Direct Chill Casting of 7075 Aluminum Alloy:** Qingfeng Zhu<sup>1</sup>; Zhihao Zhao<sup>1</sup>; Xiangjie Wang<sup>1</sup>; Jianzhong Cui<sup>1</sup>; <sup>1</sup>Key Laboratory of Electromagnetic Processing of Materials, Ministry of Education, Northeastern University

The effect of application of the out-of-phase electromagnetic field in HDC on the process and the metallurgical quality of 7075 alloy ingots was investigated in detail. The results show that when out-of-phase electromagnetic field was applied, the effect of gravity on the HDC casting process was eliminated effectively, the temperature distribution in the pool became more uniform, the cooling difference between upper and bottom surface and depth of sump were decreased, the sump shape was changed to be more symmetric about geometrical center of the mold, the thickness of segregation layer decreased and the surface quality and the microstructures of the ingots were improved,

# Technical Program

the area of feathery grains decreased and the area of equiaxed grains increased, the equiaxed grains were refined and the floating grains eliminated so that the quality of the ingots was improved.

## 9:45 AM

**Next Generation of Almex Direct Chill Tooling Systems:** *Shaun Hamer*<sup>1</sup>; <sup>1</sup>Almex USA Inc.

Almex USA Inc. has introduced the next generation of slab and rolling ingot tooling systems for Direct Chill casting of aluminum alloys. The design is based upon the Almex philosophy of "Safety, Simplicity and Performance". The new systems are a result of extensive thermodynamic, fluid dynamic and metallurgical modeling combined with decades of cumulative design experience and hands-on casting knowledge and understanding. The result is a tooling system with a wide operating window allowing for excellent process and alloy flexibility. Combining this tooling with Almex proprietary casting recipes and practices facilitates the end user with the capability of producing world class slab and rolling ingot with excellent metallurgical properties, high pit recovery and optimum safety for casting of alloys across the entire wrought alloy series. This paper describes the key design features of this new tooling and provides evaluation of the metallurgical and process performance of the system.

## 10:10 AM

**Thermal Assessment of the Casting Operation at IMASA Shop:** Claudio Méndez<sup>1</sup>; César Sánchez<sup>1</sup>; Gabriel Plascencia<sup>1</sup>; Marco Rubio<sup>2</sup>; *David Jaramillo*<sup>1</sup>; <sup>1</sup>CIITEC - IPN; <sup>2</sup>IMASA S.A. de C.V.

A thermal assessment of the semi-continuous casting facility at IMASA shop was conducted. Temperature measurements were carried out in situ as ingots of the 1XXX and 3XXX aluminum alloys series were processed. Simultaneously, the temperature in the cooling water was measured and recorded. With the data collected at the shop, a thermal balance was performed. It was found that there is a significant excess in the amount of water used for heat extraction during the solidification of the ingots. This major finding; lead to conceptualize a more efficient cooling system, since the current cooling system increase the production cost at IMASA. This new cooling system concept is under development and some first results obtained from finite element analysis are presented and discussed in this paper.

## Characterization of Minerals, Metals and Materials: Characterization of PMC's, Composites, Fibers, Polymers, and Organics

*Sponsored by:* The Minerals, Metals and Materials Society, TMS Extraction and Processing Division, TMS Structural Materials Division, TMS/ASM: Composite Materials Committee, TMS: Materials Characterization Committee

*Program Organizers:* Ann Hagni, Geoscience Consultant; Sergio Monteiro, State University of the Northern Rio de Janeiro - UENF; Jiann-Yang Hwang, Michigan Technological University

Wednesday AM Room: 307  
February 17, 2010 Location: Washington State Convention Center

*Session Chairs:* Mingdong Cai, Exova; Jeong Guk Kim, Korea Railroad Research Institute

## 8:30 AM

**Weibull Analysis of Tensile Tested Piassava Fibers with Different Diameters:** Denise Cristina Nascimento<sup>1</sup>; Ludy Motta<sup>1</sup>; *Sergio Monteiro*<sup>1</sup>; <sup>1</sup>State University of the Northern Rio de Janeiro - UENF

Technical and economical advantages in addition to environmental considerations are promoting the substitution of natural fiber for the glass fiber in polymer matrix composites. However, by contrast to the glass fiber uniformity, natural fibers are heterogeneous in their dimensions, especially the cross section measured by the equivalent diameter. It has been found that this variability in diameter can be correlated to different levels of mechanical resistance. In this work, a statistical analysis of tensile strength of piassava fibers using the Weibull methodology was performed. An attempt to correlate the fiber strength, obtained in tensile tests, with the diameter, precisely measured by means of a profile projector, was carried out. The results revealed an inverse dependence between the piassava fiber diameter and corresponding tensile strength. Fracture

tip observation by SEM suggested possible mechanisms that could justify this inverse correlation.

## 8:50 AM

**Thermal Analysis of Curaua Fiber Reinforced Polyester Matrix Composites:** Ailton Ferreira<sup>1</sup>; Ruben Jesus Rodriguez<sup>1</sup>; Felipe Lopes<sup>1</sup>; *Sergio Monteiro*<sup>1</sup>; <sup>1</sup>State University of the Northern Rio de Janeiro - UENF

Natural fiber reinforced polymer composites are gaining attention as an environmentally correct solution to replace glass fiber composites. Among the drawbacks associated with the application of natural fibers, especially those lignocellulosic obtained from plants, the low thermal resistance is a limitation for composites subjected to temperatures above 100°C. The hydrophilic nature of the lignocellulosic fiber causes water evolution at this temperature level, which may introduce pores and flaws in the polymeric matrix of the composites. The objective of the present work was to conduct a thermal gravimetric analysis (TGA) on polymer composites with different amounts of curaua, a strong lignocellulosic fiber. Both TGA and DTA curves were analyzed to determine the effect of the curaua fiber on the thermal resistance of the composites. It was found that not only higher weight loss but also displacement of DTA peaks towards higher temperatures were associated with the curaua fibers in the composites.

## 9:10 AM

**Thermographic Characterization of Damage Evolution in Polymer Matrix Composites:** *Jeongguk Kim*<sup>1</sup>; Sung Cheol Yoon<sup>1</sup>; Jung-Seok Kim<sup>1</sup>; Hyuk-Jin Yoon<sup>1</sup>; Sung-Tae Kwon<sup>1</sup>; <sup>1</sup>Korea Railroad Research Institute

The tensile failure behavior of glass fiber reinforced epoxy polymer matrix composites (PMCs) was characterized using infrared camera. In order to monitor tensile damage evolution of PMC sample, a high-speed infrared camera was used to measure surface temperature changes during tensile testing. Through the thermographic image analysis, crack initiation and propagation were qualitatively monitored. Moreover, the thermographic images provided the information on fracture mode and mechanisms in PMC sample. After tensile testing, the microstructural characterization using SEM was performed on tensile fractured specimens. The SEM characterization results were comparable with in-situ monitored IR camera analysis results. In this investigation, an IR camera and SEM characterization method were used to facilitate a better understanding of damage evolution and failure mode of PMC materials during tensile testing.

## 9:30 AM

**Characterization of the Flexural Properties of Polyester Matrix Composites Reinforced with Continuous Jute Fibers:** *Sergio Monteiro*<sup>1</sup>; Leandro Marques<sup>1</sup>; Kestur Satyanarayana<sup>2</sup>; <sup>1</sup>State University of the Northern Rio de Janeiro - UENF; <sup>2</sup>Federal University of Parana (UFPR)

Engineering applications of natural fibers, especially those obtained from cellulose-containing plants is nowadays considered an environmentally correct alternative to substitute non-recyclable energy-intensive, abrasive and toxic synthetic fibers like the common glass fiber. Composites reinforced with lignocellulosic fibers such as coir, hemp and jute are already on the market. These composites are normally processed for short-cut fibers that do not present the highest mechanical strength as compared to continuous fibers of the same kind. The objective of this work was to study the mechanical behavior, by means of flexural tests, of polyester matrix composites reinforced with continuous jute fibers. Bend tests were conducted in standard specimens with up to 40% of jute. Fracture analysis by SEM displayed the rupture mechanisms. The results showed an improvement in some flexural properties with incorporation of jute fiber. However, a low fiber/matrix interfacial stress was responsible for limitation in the values attained by some properties.

## 9:50 AM

**Charpy Toughness Behavior of Continuous Sisal Fiber Reinforced Polyester Matrix Composites:** Wellington Inácio<sup>1</sup>; Felipe Lopes<sup>1</sup>; *Sergio Monteiro*<sup>1</sup>; <sup>1</sup>State University of the Northern Rio de Janeiro - UENF

Natural fibers obtained from plants are increasingly being applied as polymer composite reinforcement for interior automobile parts such as covers and panels. These parts should be impact resistant and absorb the energy without splitting in sharp pieces during a crash event. Sisal is a strong natural fiber that has not yet been considered for such composites. Therefore, this work investigates the toughness behavior of polyester matrix composites reinforced with up to 40% in volume of long, continuous and aligned sisal fibers by means of Charpy impact



tests. It was found that the addition of sisal fibers results in a marked increase in the absorbed impact energy of the composites. Macroscopic observation of the post-impact specimens and SEM fracture analysis showed that longitudinal rupture through the sisal fiber interface with the polyester matrix is the main mechanism for the remarkable toughness of these composites.

### 10:10 AM

**Evaluation of the Interfacial Strength of Ramie Fibers in Polyester Matrix Composites:** Frederico Margem<sup>1</sup>; Felipe Lopes<sup>1</sup>; Sergio Monteiro<sup>1</sup>; <sup>1</sup>State University of the Northern Rio de Janeiro - UENF

The efficiency by which an applied load is transmitted through the composite structure depends on the strength of the interface between the matrix and the second phase. In fiber reinforced composites, the interfacial shear stress plays a major role in the composite capacity to support the applied load. This interfacial stress can be obtained by means of pullout tests using the fiber embedded to a certain length in a socket of the matrix material. In the present work, pullout tests were performed to evaluate the interfacial stress of ramie, a relatively strong natural fiber, reinforcing polyester matrix composites. The general result permitted to calculate a critical length for the ramie fiber embedded in polyester resin. From this critical length, the value of the interfacial stress was calculated. An interpretation of this result together with SEM observation displayed a relatively weak bond between the ramie fiber and the polyester matrix.

### 10:30 AM

**Patterning Atop Shape Memory Polymers and Their Characterization:** Y. Zhao<sup>1</sup>; Mingdong Cai<sup>2</sup>; Weimin Huang<sup>1</sup>; T. H. Tong<sup>3</sup>; <sup>1</sup>Nanyang Technological University; <sup>2</sup>Exova Group Ltd and Southeast University; <sup>3</sup>Cornerstone Research Group Inc.

The surface morphology of materials is of fundamental importance to many applications (e.g., surface wetting, friction, surface roughness, reflection, drag, adhesion, etc). Various approaches for micro/nano patterning atop polymer surfaces have been proposed in recent years. However, a cost effective technique is still highly in demand. In this paper, we demonstrate a few novel but rather simple and generic approaches for surface micro/nano patterning using shape memory polymers (SMPs). Reversible micro vertical chains, crown shaped protrusion arrays and strip/labyrinth wrinkles atop SMPs are presented. Those novel 3-D surface structures are quantitatively analyzed by scanning electron microscopy and atomic force microscopy.

### 10:50 AM

**Characterization of a Natural Biofoam from the Buriti Palm Tree:** Lucas Costa<sup>1</sup>; Sergio Monteiro<sup>1</sup>; Tammy Portela<sup>1</sup>; Nubia Santos<sup>2</sup>; Cecília Zavaglia<sup>2</sup>; <sup>1</sup>State University of the Northern Rio de Janeiro - UENF; <sup>2</sup>State University of Campinas - UNICAMP

Solid foams are non-fluid porous materials with a large capacity to retain air, which makes them lighter than the water with densities below 0.5 g/cm<sup>3</sup>. These foams are nowadays extensively used in engineering applications such as thermal insulation, packing, lifebuoy, automobile cushion, furniture and many others. Most foam materials are produced by bubbling air through a polymer while in a low viscosity state. The negative side of these synthetic foams is the CO<sub>2</sub> contribution to global warming by means of the energy required for the foaming process. Moreover, as a non-degradable polymer, discarded synthetic foams also contribute to long term water and ground pollution. In this work, a natural foam extracted from the Amazon buriti palm tree is investigated as possible substitute for synthetic foams. The basic physical and mechanical properties of this biofilm were evaluated. Its spongelike structure was characterized by the amount of pores and morphological aspects.

### 11:10 AM

**Characterization of Fibers from Different Parts of the Buriti Palm Tree:** Tammy Portela<sup>1</sup>; Lucas Costa<sup>1</sup>; Felipe Lopes<sup>1</sup>; Sergio Monteiro<sup>1</sup>; <sup>1</sup>State University of the Northern Rio de Janeiro - UENF

Well known lignocellulosic fibers extracted from cultivated plants such as cotton, sisal, jute, coir, hemp, flax and many others have been traditionally used in simple products. These fibers are nowadays, also reinforcing composites for more technological-intensive uses as automobile interior components and civil construction panels. Less known plants like the buriti palm tree can also provide lignocellulosic fibers for composite reinforcement. However, its most commonly used fiber obtained from the leaves was recently found to have low mechanical strength. By contrast, the fibers extracted from the petiole have primarily shown a higher strength. Therefore, the objective of this work was to

make a comparative characterization of the structural aspects as well as technical and mechanical properties of these two different buriti fibers. The structural aspects, both for integer and tensile-ruptured fibers were characterized by SEM. The results revealed significant differences in the microstructure and properties of the investigated fibers.

### 11:30 AM

**Tensile Properties of Epoxy Composites Reinforced with Continuous Curaua Fibers:** Felipe Lopes<sup>1</sup>; Ailton Ferreira<sup>1</sup>; Sergio Monteiro<sup>1</sup>; <sup>1</sup>State University of the Northern Rio de Janeiro - UENF

The curaua is a bush-like plant, similar to the pineapple, native of the Amazon region. Fibers extracted from the curaua leaves are among the strongest lignocellulosic and have been used as composite reinforcement. Characterization of these composites is being carried out for different polymer matrices and mechanical tests. The objective of the present work is to evaluate the tensile properties of composites with a specific epoxy matrix reinforced with different amounts of curaua fibers. Tensile specimens with up to 40% in volume of long, continuous and aligned curaua fibers were room temperature tested in an Instron machine. The fracture was analyzed by SEM. The results showed significant changes in the mechanical properties with the amount of curaua fibers. This was compared to other bend-tested composites with distinct matrices. The fracture analysis revealed a weak fiber/matrix interface, which could be responsible for the comparatively low performance of some properties.

### 11:50 AM

**Characterizing the Mechanical Properties of Wax-Coated Granular Composites:** John Bridge<sup>1</sup>; Michael Peterson<sup>2</sup>; Ryan Beaumont<sup>3</sup>; <sup>1</sup>Maine Maritime Academy; <sup>2</sup>University of Maine; <sup>3</sup>R.M. Beaumont Corporation

Triaxial compression tests at various confining pressures and temperatures, as well as tangent modulus tests using ultrasonic waves, were conducted for wax-coated granular composite materials. This material is used as a surface for Thoroughbred horse racing. The purpose of these tests is to examine how track shear strength and tangent modulus at a range of loads respond to changing temperatures. Previous work has shown that a wide range of operational temperatures are experienced which have been reproduced in the lab. Using differential scanning calorimetry, it is confirmed that these operational temperatures correspond to distinct thermal transition regions for the wax that is used to coat the sand in these surfaces. Preliminary results show that both shear strength and tangent modulus are sensitive to temperature changes with maximum strengths correlating with major DSC wax transition regions.

### 12:10 PM

**Mechanical Behavior of Polyester Matrix Composites Reinforced with Continuous Bamboo Fibers:** Lucas Costa<sup>1</sup>; Sergio Monteiro<sup>1</sup>; Rômulo Loiola<sup>1</sup>; <sup>1</sup>State University of the Northern Rio de Janeiro - UENF

The stem of the bamboo has been traditionally used in simple structural parts such as scaffolding and huts. In spite of the relatively high stiffness the bamboo is limited in terms of engineering application, due to its cylindrical shape. Moreover, as any lignocellulosic material, the direct exposure of the bamboo may cause deterioration. A possible solution for both, the dimensional limitation and weather deterioration is to separate the bamboo fibers from the stem to be applied as polymer composite reinforcement. The objective of this work was to characterize individual bamboo fibers and investigate the flexural mechanical properties of polyester composites reinforced with these fibers. Specimens with up to 30% of continuous and aligned bamboo fibers added to polyester composites were bend-tested until fracture. The results showed improvement in the composite strength with a decreasing tendency for higher amounts of fibers, due to the weak interface developed with the polyester matrix.

# Technical Program

## Computational Thermodynamics and Kinetics: Phase Field, CALPHAD and Other Modeling Techniques

*Sponsored by:* The Minerals, Metals and Materials Society, TMS Electronic, Magnetic, and Photonic Materials Division, TMS Materials Processing and Manufacturing Division, TMS Structural Materials Division, TMS: Chemistry and Physics of Materials Committee, TMS/ASM: Computational Materials Science and Engineering Committee  
*Program Organizers:* Jeffrey Hoyt, McMaster University; Dallas Trinkle, University of Illinois at Urbana-Champaign

Wednesday AM      Room: 308  
February 17, 2010      Location: Washington State Convention Center

*Session Chair:* To Be Announced

### 8:30 AM

**A Phase Field Study on the Growth and the Interaction of  $Ni_4Ti_3$  Precipitates in Niti Shape Memory Alloy:** *Wei Guo*<sup>1</sup>; Ingo Steinbach<sup>1</sup>; Christoph Somsen<sup>2</sup>; Gunther Eggeler<sup>2</sup>; <sup>1</sup>Interdisciplinary Centre for Advanced Materials Simulation (ICAMS), Ruhr-University Bochum; <sup>2</sup>Institut für Werkstoffe, Ruhr-University Bochum

Growth and interaction among  $Ni_4Ti_3$  particles is studied using the multi-phase field method. A special pattern of two precipitates due to the elastic interaction among them is observed. This means that precipitates have strong elastic interaction among each other. It is also found that applied stress has a strong effect on the  $Ni_4Ti_3$  shape. Under a compressive stress along the axis of the disc-shape precipitate, the aspect ratio increases with the applied stress up to around 1. This phenomenon agrees qualitatively with the experimental observation while the sensitivity of the shape on the external stress is largely underestimated in the simulation. The growth kinetics of the precipitate can also be influenced significantly by the applied stress. With the increase of the compressive stress along the axis of precipitate its growth velocity increases notably. All simulation results are compared with experimental observations.

### 8:50 AM

**A Mixed-Mode Model for Precipitation in Al-Mg-Si Alloys:** *Abbas Bahrami*<sup>1</sup>; Alexis Miroux<sup>2</sup>; Jilt Sietsma<sup>1</sup>; Leo Kestens<sup>1</sup>; <sup>1</sup>Materials Science and Engineering Department, Technical University of Delft (TUDelft); <sup>2</sup>Materials to Innovation Institute (M2i)

A modified Kampmann-Wagner numerical (KWN) precipitation model has been developed considering the mixed-mode character of precipitate growth. The  $\eta$ -parameter, which is proportional to the diffusivity of the diffusing alloying element and inversely proportional to the mobility of interface and to the radius of precipitates, is used to implement the character of precipitate growth into the kinetic model. The effects of interfacial energy, diffusivity, and interface mobility on the character and kinetics of precipitation in Al-Mg-Si system have been systematically studied. The results show that the interfacial energy has almost no effect on the precipitation character. However, diffusivity and interface mobility have significant influences on the character of precipitation. The results also show that when the alloying element is interstitial, the alloy is heavily-deformed before ageing, or precipitates are very small with coherent interface, the assumption of mixed-mode growth is more accurate than the assumption of diffusion-controlled growth.

### 9:10 AM

**Thermodynamics, Structural Properties and Transformation Behavior of CoNiGa Alloys from First Principles:** *Raymundo Arroyave*<sup>1</sup>; Anchalee Junkaew<sup>1</sup>; Andres Garay<sup>1</sup>; Arpita Chari<sup>1</sup>; Chun-Wei Yao<sup>1</sup>; <sup>1</sup>Texas A&M University

CoNiGa alloys have been receiving considerable interest due to their high temperature shape memory properties. While there have been many investigations on the mechanical and magnetic behavior of these materials, very little is known about the fundamental microscopic basis for the observed macroscopic behavior. In this work, we discuss the stability of CoNiGa-based structures as a function of composition. Thermodynamic properties of these phases including vibrational, configurational, electronic and magnetic degrees of freedom are taken into account. In addition, we investigate the nature of the martensitic transformation responsible for the observed shape memory behavior. Elastic properties as well as the behavior of phonon modes allows to

elucidate the specific causes for the observed instability of the austenite phase. Linking to CALPHAD methods is done in order to predict the full ternary Co-Ni-Ga phase diagram at arbitrary composition/temperature conditions.

### 9:30 AM

**Pressure-Induced Invar Behavior in Pd3Fe:** *Michael Winterrose*<sup>1</sup>; Matt Lucas<sup>1</sup>; Alan Yue<sup>1</sup>; Itzhak Halevy<sup>1</sup>; Lisa Mauger<sup>1</sup>; Jorge Munoz<sup>2</sup>; Jingzhu Hu<sup>2</sup>; Michael Lerche<sup>3</sup>; Brent Fultz<sup>1</sup>; <sup>1</sup>Caltech; <sup>2</sup>NSLS; <sup>3</sup>HPSynC

Synchrotron x-ray diffraction (XRD) measurements, nuclear forward scattering (NFS) measurements, and density functional theory (DFT) calculations were performed on L12-ordered Pd3Fe. Measurements were performed at 300 K at pressures up to 33 GPa, and at 7 GPa at temperatures up to 650 K. The NFS revealed a collapse of the 57Fe magnetic moment between 8.9 and 12.3 GPa at 300 K, coinciding with a transition in bulk modulus found by XRD. Heating the sample under a pressure of 7 GPa showed negligible thermal expansion from 300 to 523 K, demonstrating Invar behavior. Zero-temperature DFT calculations showed a ferromagnetic ground state and several antiferromagnetic states of comparable energy at pressures above 20 GPa.

### 9:50 AM

**Explaining the Change in Diffusion Mechanism in the Series of  $L1_2$  Phases  $In_2R$  ( $R$ = Rare-Earth):** *John Bevington*<sup>1</sup>; Matthew Zacate<sup>2</sup>; Gary Collins<sup>1</sup>; <sup>1</sup>Washington State University; <sup>2</sup>Northern Kentucky University

Recent experiments revealed a remarkable change in the mechanism of diffusion for atoms on the In-sublattice along a series of  $In_2R$  line compounds having  $L1_2$  structure [Phys. Rev. Lett. 102, 155901 (2009)]. Experiments were carried out on pairs of samples with opposing boundary compositions (slightly In-rich and In-poor). Whereas light lanthanide indides ( $R$ = La, Ce, Pr, Nd) exhibited higher jump frequencies for In-rich samples, heavy lanthanide indides had higher jump frequencies for In-poor samples. Since, at given temperature, R-vacancy (In-vacancy) concentrations can only increase (decrease) monotonically with increasing In composition, it was concluded that the dominant diffusion mechanisms involve R-vacancies (In-vacancies) in the light (heavy) lanthanide indides. To explain this remarkable change in behavior, calculations of point defect energies along the entire lanthanide tri-indide series are being carried out using the full-potential, all-electron program WIEN2k, with results to be reported at the meeting.

### 10:10 AM

**Diffusion of Interstitial and Substitutional Elements in  $\gamma/\gamma'$  Interface in Ni-Al Superalloys: A First Principles Study:** *Priya Gopal*<sup>1</sup>; Peter Wagner<sup>2</sup>; Srinivasan Srivilliputhur<sup>1</sup>; Gregor Mori<sup>2</sup>; <sup>1</sup>University of North Texas, Denton; <sup>2</sup>University of Leoben

Ni-based superalloys possess desirable high-temperature properties including strength, ductility, fracture toughness as well as resistance to creep and oxidation. An important factor for strengthening mechanism is the microstructure of the alloy which consists of ordered  $\gamma'$ -Ni<sub>3</sub>Al precipitates within a  $\gamma$  (Ni-Al) matrix. In addition, a variety of substitutional and interstitial elements like Cr, Ta, Re, Ru, Ti, W, Mo, C, S etc. play a crucial role in strengthening of these alloys. It is thus important to understand the electronic structure and diffusion of these elements. Using density functional theory methods with plane-wave basis sets we determine the partitioning behavior of alloying elements in the interface. We also systematically explore the energetics and kinetics of diffusion of Cr, Mo, C, and O in the bulk and across the  $\gamma/\gamma'$  interface. We use transition state theory combined with nudged elastic band method to determine the transition paths and diffusion activation barriers.

### 10:30 AM Break

### 10:40 AM

**Modelling Ordering Phenomena in Condensed Phases:** *Bo Sundman*<sup>1</sup>; Mauro Palumbo<sup>2</sup>; Suzana Fries<sup>2</sup>; <sup>1</sup>CEA; <sup>2</sup>Ruhr University Bochum

Ordering phenomena are a fascinating theoretical, experimental and applied scientific topic since more than one century. For simple binary system detailed models can be made but for multicomponent system Computational Thermodynamics (CT) is the only methodology that can be applied to combine the acquired knowledge for relevant applications. Guided by theoretical approaches and based on experimental evidence, CT uses simple models which are very powerful in simulations for materials development, in particular the recent successful use of DFT results in the calculation of TCP solution phases. There are no similar theoretical methods to deal with ordering in liquid phases



but models for ordering in liquids are very important. This paper reviews the present models, points out the need of improvements and how they can be used in the recently launched SAPIENS project for a sustainable thermodynamic database.

**11:00 AM**

**Modeling of Phase Separation in Uranium-Zirconium Alloys via Monte Carlo Methods:** Benjamin Beeler<sup>1</sup>; Benjamin Good<sup>1</sup>; Chaitanya Deo<sup>1</sup>; Sergey Rashkeev<sup>2</sup>; Maria Okuniewski<sup>2</sup>; Mike Baskes<sup>3</sup>; <sup>1</sup>Georgia Institute of Technology; <sup>2</sup>Idaho National Laboratory; <sup>3</sup>Los Alamos National Laboratory

U-Zr alloys are used as the fuel matrix in sodium cooled fast nuclear reactors. They have a body centered cubic structure ( $\gamma$  phase) that exhibits a miscibility gap at the temperature of operation. The alloy exhibits a variation in composition under operation with zirconium atoms migrating up the temperature gradient in the high temperature  $\gamma$  phase. We study the two phase evolution of U-Zr using a kinetic Monte Carlo (kMC) simulation which is well suited for studying diffusion-based phase transformations. We utilize an extension of the Ising model that accounts for atom transport through vacancy migration and allows a physically meaningful definition of time. The kMC simulation is linked to first-principles calculations via the implementation of local, composition-dependant values of the migration barrier energy. The short-range order, vacancy diffusion coefficient, and self-diffusion coefficients of uranium and zirconium are determined. The variance of these parameters with temperature and composition is analyzed.

**11:20 AM**

**Thermodynamics Calculation and Phase-Field Simulation of Morphotropic Phase Boundary in (001) BiFeO<sub>3</sub> Thin Films:** Guang Sheng<sup>1</sup>; Jingxian Zhang<sup>1</sup>; Robert Zeches<sup>2</sup>; Jinxing Zhang<sup>2</sup>; Alexander Melville<sup>3</sup>; Jon Ihlefeld<sup>3</sup>; Venkatraman Gopalan<sup>1</sup>; Darrel Schlom<sup>3</sup>; Lane.W Martin<sup>4</sup>; Ramamoorthy Ramesh<sup>2</sup>; Zi-Kui Liu<sup>1</sup>; Long-Qing Chen<sup>1</sup>; <sup>1</sup>The Pennsylvania State University; <sup>2</sup>University of California, Berkeley; <sup>3</sup>Cornell University; <sup>4</sup>Lawrence Berkeley National Laboratory

A strain-driven morphotropic phase boundary was recently observed in (001) BiFeO<sub>3</sub> thin film deposited on YAO and LAO substrates. In this study, we constructed the strain-temperature phase stability diagram for (001) BiFeO<sub>3</sub> thin film using both thermodynamic calculation and phase-field simulations. The tetragonal to distorted rhombohedral phase boundary predicted from thermodynamic analysis is consistent with the density function calculations. The predicted strain diagram and experimental observations are in very good agreement with BiFeO<sub>3</sub> films grown on LAO and YAO with -4.29% and -6.8% strains respectively. The volume fraction changes of different phases as a function of strain from phase-field simulation across the morphotropic phase boundary will be also presented.

**11:40 AM**

**CALPHAD Modeling of the Al-Cr-Ni System Supported by First Principles Calculations:** Wren Chan<sup>1</sup>; Michael Gao<sup>2</sup>; <sup>1</sup>Carnegie Mellon University; <sup>2</sup>National Energy Technology Laboratory

Al, Cr and Ni are among the most important alloying elements in many commercial structural alloys including Ni-based superalloys and steels. However, even today there still lacks thermodynamic description of the complete Al-Cr-Ni ternary system. In this work, this ternary is thermodynamically assessed using the CALPHAD method. Two ternary compounds are reported: hexagonal and high-temperature orthorhombic [J. Alloys Compd. 460 (2008) 299]. Their energies are studied using first principles density functional theory calculations, and are integrated into CALPHAD optimization. The ternary isotherms and liquidus data are taken from the literature. The thermodynamic descriptions of all edge binaries are taken from previous reports. The calculated ternary phase diagram will be compared with available experimental data, and the impact of this work on Ni-based superalloy will be addressed.

**12:00 PM**

**Occupancy Probability of a Sublattice of D0<sub>22</sub>-Ni<sub>3</sub>V in Ni-Al-V System: Determined by Microscopic Phase Field:** Jing Zhang<sup>1</sup>; Houchuang Zhuang<sup>1</sup>; Zheng Chen<sup>1</sup>; <sup>1</sup>Northwestern Polytechnical University

In this paper, a sublattice of D0<sub>22</sub>-Ni<sub>3</sub>V is subdivided into a1 and a2 according to the location they reside. We use an atomic-scale microscopic phase field to study the occupancy probabilities (OP) of a1 and a2, including antisite defect, substitutional defect and phase transition. The results are as follows: Antisite defect (V<sub>a1</sub>, V<sub>a2</sub>) and substitutional defect (Al<sub>a1</sub>, Al<sub>a2</sub>) coexist in both a1 and a2,

and the sequence of OP ranked in magnitude is Ni<sub>a1</sub>, Ni<sub>a2</sub>, V<sub>a2</sub>, Al<sub>a2</sub>, V<sub>a1</sub>, and Al<sub>a1</sub>. The inherent atom (Ni<sub>a1</sub>, Ni<sub>a2</sub>) decline but defects rise with the elevated temperature. At temperature lower than 1150K, part of the being substituted Ni exchanges V on  $\beta$  sublattice and the other dissolves into matrix or enters L1<sub>2</sub> structure, while at temperature higher than 1150K the being substituted Ni together with Ni from matrix enters  $\beta$  sublattice, which accounts for the complicated phase transition from D0<sub>22</sub> to L1<sub>2</sub>.

**12:20 PM**

**Kinetic Monte Carlo Study of Sputter-Induced Morphological Patterns in Alloy Surfaces:** Bharathi Srinivasan<sup>1</sup>; Ramanarayan Hariharaputran<sup>1</sup>; <sup>1</sup>Institute of High Performance Computing

Ion beam sputtering of surfaces gives rise to interesting nanopatterns. In single phase systems, these patterns form as a result of the competition between erosion by ion bombardment and surface diffusion. In the case of alloys, interesting patterns characterized by variation in both surface height and composition are formed because of the composition-dependence of surface diffusion and sputter yield. To study these rich patterns formed on alloy surfaces we have used Kinetic Monte Carlo method. In our study we find that for binary alloys the morphological patterns are accompanied by compositional segregation. We have characterized these patterns as a function of parameters such as flux of the ion beam, temperature, sputter yields and diffusivities of the two species and we present these results in this talk.

### Cost-Affordable Titanium III: Creative Processing and Property Enhancement I

*Sponsored by:* The Minerals, Metals and Materials Society, TMS Structural Materials Division, TMS: Titanium Committee  
*Program Organizers:* M. Ashraf Imam, Naval Research Lab; F. H. (Sam) Froes, University of Idaho; Kevin Dring, Norsk Titanium

Wednesday AM

Room: 618

February 17, 2010

Location: Washington State Convention Center

*Session Chairs:* Curt Lavender, Pacific Northwest National Laboratory; Vasisht Venkatesh, TIMET Inc

**8:30 AM**

**Development Pathways to Low-Cost Engineering Beta Gamma TiAl Alloys:** Young-Won Kim<sup>1</sup>; <sup>1</sup>Development Pathways to Low-Cost Engineering Beta Gamma TiAl Alloys

Gamma (titanium aluminide) alloys possess an attractive combination of low density and high temperature (over 800°C) capability, ideal for hot structures and turbine engine components. Yet, the alloys have not been inserted into aerospace service due to their material and manufacturing limitations, which include processing difficulties requiring costly multi-step forming process and large lamellar grains lowering damage tolerance. To remove or reduce such barriers, we have explored a new class of TiAl-based alloys, called beta gamma, utilizing the beneficial effects of beta solidification on grain refinement and beta phase distribution on processibility. Tests indicate that remarkably improved processibility and machinability, along with required attributes, could be achieved on the composition that would yield a desired phase distribution as a function of temperature. This presentation discusses our ongoing effort in optimizing the beta gamma alloy composition and processing, which will be led to a low-cost viable structural materials technology.

**8:55 AM**

**Microstructure and Mechanical Properties of A' Martensite Type Ti-V-Al Alloy after Cold- or Hot Working Process:** Hiroaki Matsumoto<sup>1</sup>; Hiroshi Yoneda<sup>1</sup>; Kazuhisa Sato<sup>1</sup>; Toyohiko Konno<sup>1</sup>; Akihiko Chiba<sup>1</sup>; <sup>1</sup>Institute for Materials Research, Tohoku University

Ti alloys are widely used for industrial applications due to their excellent mechanical properties combined with low density. In general, Ti alloys are classified as  $\alpha$ ,  $\alpha+\beta$  and  $\beta$  alloys. Quite recently, we have presented new type structural  $\alpha'$  martensite Ti alloys with low Young's modulus, high strength and excellent ductility at room temperature. Microstructural control technique utilizing  $\alpha'$  martensite is not so common in industrial production of Ti alloys. Therefore, there have been few reports concerning the systematic characteristic with martensite ( $\alpha'$  or  $\alpha''$ ) structure. In this work, we examined the microstructure

# Technical Program

and mechanical properties of a' martensite type Ti-V-Al alloy after cold- or hot working process. Then, we found that refined equiaxed ( $\alpha+\beta$ ) microstructure with grain size less than 1  $\mu\text{m}$  was obtained by hot working with starting structure of a' martensite. This result suggests the new type deformation processing utilizing a' martensite in industrial Ti alloys.

**9:20 AM**

**Effect of Oxygen on Phase Precipitation and Mechanical Functionality in Ti-29Nb-13Ta-4.6Zr:** Mitsuo Niinomi<sup>1</sup>; Masaaki Nakai<sup>1</sup>; Toshikazu Akahori<sup>1</sup>; Harumi Tsutsumi<sup>1</sup>; <sup>1</sup>Tohoku University

From the viewpoint of saving resources of rare metals, proper using common metals such as Fe, Si, Cu and Sn or interstitial elements such as O, N, C and H, which have been regarded as impurities in titanium and its alloys, as alloying elements to improve the mechanical functionalities of titanium alloys is becoming more important. Among those elements, oxygen plays very important roles in titanium and its alloys. Solute oxygen in titanium alloys leads to solid solution strengthening, suppressing the precipitation of the athermal omega or orthorhombic martensite phase, enhancing the formation of the alpha-case, etc. The proper using oxygen is effective to improve the mechanical functionalities of titanium alloys. However, the role of oxygen in titanium alloys is still not well understood. Therefore, the effect of oxygen on the mechanical functionalities such as strength-ductility balance, Young's modulus and super elastic behavior in Ti-29Nb-13Ta-4.6Zr was investigated.

**9:45 AM**

**Local Heat Treatment of Titanium Alloys: Microstructure and Mechanical Properties:** Pavlo Markovskiy<sup>1</sup>; <sup>1</sup>G.V. Kurdyumov Institute for Metal Physics, NAS of Ukraine

Local Rapid Heat Treatment (LRHT) based on induction-heating methods can be used to form unique location-specific microstructures and properties in commercial titanium alloys while maintaining the bulk of the material in an initial, non-heat-treated condition. The present work focused on commercial-purity titanium (CP-Ti), Ti-6Al-4V, and TIMETAL-LCB. For each alloy, LRHT was performed using cylindrical specimens of 8 mm diameter that were surface heated to temperatures up to 1000°C at a rate of approximately 400°C/s followed by water quenching. By and large, the treatments produced a significant improvement in tensile and fatigue strength and a decrease in ductility. The source of these changes in properties will be discussed in terms of the evolution of microstructure and phase composition as well as residual stresses formed in surface layers, each of which depended on the specific alloy.

**10:10 AM Break**

**10:25 AM**

**The Relative Contribution of Factors Influencing the Flow and Thermal Fields in Electron Beam Casting of Ti-6Al-4V:** Tao Meng<sup>1</sup>; Daan Maijer<sup>1</sup>; Steven Cockcroft<sup>1</sup>; Riley Shuster<sup>1</sup>; Denis Favez<sup>1</sup>; David Tripp<sup>2</sup>; Stephen Fox<sup>3</sup>; <sup>1</sup>The University of British Columbia; <sup>2</sup>TIMET Morgantown; <sup>3</sup>TIMET Henderson

Electron Beam Cold Hearth Remelting/Melting is a relatively new and cost-effective consolidation technique for titanium alloys. The flow field that develops within the ingot liquid pool in the associated casting process is influenced by several factors including buoyancy, surface tension (Marangoni) phenomena and the decreasing permeability within the mushy zone; the former two tending to drive flow whereas the latter tends to attenuate the flow. In this study, a coupled thermal-fluid flow model of a Ti-6Al-4V electron beam button melting process has been developed to examine the relative contribution of these factors on the temperature distribution, flow field, and pool profile. Additionally, an approximation of the time-dependent electron beam pattern by a time-averaged heat source has been evaluated. It is shown that above a critical pattern repetition frequency, the surface temperature field can be correctly calculated with this time-averaged approximation, thus reducing drastically computation time.

**10:50 AM**

**The Influence of Surface Treatments and Subsequent Annealing on the Fatigue Performance of Ti-6Al-4V for Biomedical Applications:** Milos Janecsek<sup>1</sup>; Jaroslav Fencel<sup>2</sup>; Lothar Wagner<sup>3</sup>; Robert Kral<sup>1</sup>; Josef Strasky<sup>1</sup>; <sup>1</sup>Charles University; <sup>2</sup>Beznoska, Ltd.; <sup>3</sup>Clausthal University of Technology

Alpha-beta titanium alloys, in particular Ti-6Al-4V, are widely used as surgical implant materials for large-sized joint replacements such as artificial

knee, hip and shoulder. Electro-erosion was performed to prepare the surface of the alloy for optimum bone cell growth. However, tensile properties and in particular fatigue performance were found to markedly suffer from this treatment. For example, yield stress, ultimate tensile strength, tensile ductility and fatigue strength were decreased to values unacceptable for biomedical applications. In order to improve these properties, various further treatments including annealing after electro-erosion were conducted. Changes in properties will be correlated with modifications in microstructure as observed by optical microscopy and SEM.

**11:15 AM**

**Microstructure-Properties of Cast Ti-5Al-5Mo-5V-3Cr with Elevated Oxygen Levels:** Edward Chen<sup>1</sup>; D. R. Bice<sup>1</sup>; J. A. Hall<sup>2</sup>; <sup>1</sup>Transition45 Technologies, Inc.; <sup>2</sup>Wah Chang

Alloy Ti-5Al-5Mo-5V-3Cr-0.5Fe (Ti-5553) is an emerging high strength titanium alloy with improved mechanical properties compared with the industry workhorse Ti-6Al-4V. It is primarily targeted for aerospace applications including as airframe structures. All works to date on Ti-5553 have focused on more costly aerospace grades that may not be suitable for non-aerospace applications. For cost sensitive systems such as combat vehicles and armaments, a lower cost Ti-5553 with higher oxygen levels may be preferable. This work evaluates the microstructure-properties of cast Ti-5553 with oxygen levels above the maximum specified in aerospace standards. Casting is chosen here since the ability to produce complex shapes near-net offers additional cost and weight savings over traditionally machined wrought components. Mechanical properties of the "non-aerospace" Ti-5553 castings are discussed in relation to their aerospace grade counterparts, and show outstanding strength and ductility even at elevated oxygen levels. This work was supported by the U.S. Army-ARDEC.

**11:40 AM**

**Elevated-Temperature Fatigue Behavior of Boron-Modified Ti-6Al-4V:** Wei Chen<sup>1</sup>; Carl Boehlert<sup>1</sup>; Jane Howe<sup>2</sup>; Seshacharyulu Tamirisakandala<sup>3</sup>; Daniel Miracle<sup>4</sup>; <sup>1</sup>Michigan State University; <sup>2</sup>Oak Ridge National Lab; <sup>3</sup>FMW Composite Systems Inc.; <sup>4</sup>US Air Force

This work investigated the elevated-temperature fatigue behavior of Ti-6Al-4V (wt.%) modified with 1B. The fatigue response of alloys in four different product forms, namely, ingot casting (IC), IC plus extrusion, powder metallurgy (PM) rolled plate, and PM extrusion, at 455°C and a maximum applied stress range of 250-700 MPa (R=0.1, 5Hz) was compared. The PM alloys exhibited microstructures containing equiaxed grains while the IC alloys contained  $\alpha+\beta$  lath microstructures, which enabled the PM alloys to achieve greater fatigue lives than the IC processed alloys. In both the PM extruded and IC extruded alloys, the TiB whiskers were aligned in the extrusion direction and the  $\alpha$ -phase was strongly textured with the basal plane predominately oriented perpendicular to the extrusion axis. The equiaxed  $\alpha+\beta$  microstructure and the  $\alpha$ - and TiB-phase textures were identified to be responsible for the significantly higher fatigue strength exhibited by the PM extruded alloy compared to the other conditions.

## Electrode Technology for Aluminum Production: Anode Green Mill

*Sponsored by:* The Minerals, Metals and Materials Society, TMS Light Metals Division, TMS: Aluminum Committee

*Program Organizers:* Ketil Rye, Alcoa Mosjøen; Morten Sorlie, Alcoa Norway; Barry Sadler, Net Carbon Consulting Pty Ltd

Wednesday AM

Room: 616

February 17, 2010

Location: Washington State Convention Center

*Session Chair:* Lorentz Lossius, Hydro Aluminium AS

**8:30 AM Introductory Comments**

**8:35 AM**

**Use of Eddy Current Separator in Butts Processing:** Juraj Chmelar<sup>1</sup>; Hogne Linga<sup>1</sup>; <sup>1</sup>Hydro

Installation of Eddy Current Separator in a butts separation line has so far showed very promising potentials in an application in this field of industry. This equipment is able to separate aluminium and iron particles from the crushed



butts. The separator has low maintenance cost and with its simple construction and small dimensions it can easily be installed in a production line. Butts can contain iron (about 0.01 wt%) and aluminium (about 0.003 wt%) particles. The total amounts are not significant, but significant enough for equipment to be damaged, with consequent loss of production, higher maintenance cost and also contamination of produced anodes. The separated aluminium showed above 95 wt% content aluminium and 3.2 wt% iron. The separator treats the +20 mm fraction. Without separation metal pieces will tend to cycle between the cone crusher and the screen until they are worn down to a size passing the upper screen.

### 9:00 AM

**From Technology Development to Successful Start-Up and Operations of Sohar: The Potential of the Bi-Eirich Mixing Line:** François Morales<sup>1</sup>; Magali Gendre<sup>1</sup>; Nigel Backhouse<sup>1</sup>; Berthold Hohl<sup>2</sup>; David Stephenson<sup>2</sup>; Mohammed Al Balushi<sup>3</sup>; <sup>1</sup>Rio Tinto Alcan; <sup>2</sup>Maschinenfabrik Gustav Eirich; <sup>3</sup>Sohar Aluminium

In 2008 a new paste plant comprising an RTA specified Eirich Mixing Cascade EMC was successfully commissioned at Sohar Aluminium. The paper outlines the technological and process developments over the last 15 years leading to this development. The paper starts with the first adaptations of the intensive mixer for use in anode paste mixing, the equipment optimisation to improve paste quality via both laboratory scale trials and small scale industrial trials, the resulting development of the Eirich Mixing Cascade and its initial industrial implementation. Next an overview of the start-up and operations of the Sohar installation is given. This installation consists of two continuous intensive mixers in series producing at rates of up to 36 tonnes per hour. Anode process and quality results from the start up and resulting operation are presented. Finally the paper discusses the further potential development of this type of mixing line.

### 9:25 AM

**New Design of Process Area Based on Math Modelling and Simulation for Buss Kneader Principle in the Application of Green Anode Paste Preparation:** Hans-Ulrich Siegenthaler<sup>1</sup>; Joel Stampfli<sup>1</sup>; <sup>1</sup>Buss AG

The Buss Kneader principle is known in this application for nearly 60 years. A great development step forward could be achieved recently, when all specific process requirements have been analysed with math modelling and simulation. Based on the results the kneader was redesigned allowing a much more intense mixing process with a micro distribution of the pitch. This paper presents the way to the latest state of the developments to mix green anode paste with specific focus on high anode density combined with high production capacities to achieve the processing and economic advantages as requested by the anode producers today and tomorrow.

### 9:50 AM

**AluChemie Back to Benchmark:** Patrick Claudel<sup>1</sup>; Erwin Smits<sup>1</sup>; <sup>1</sup>AluChemie / Rio Tinto Alcan

AluChemie was considered in the 90's to be the benchmark in Anodes but made the wrong strategic choices early 2000 and suffered several customer complaints. A new and rigorous approach in 2007 brought us back as the supplier of choice. Our purpose is to share with our peers the success factors and findings of this first step of our journey for a more efficient anode. The team has first drawn Alchemies' *variation finger print*. This tool clearly identifies priorities and develops low effort solutions very quickly. Encouraged by customer feed back and challenged by the results of the variation analysis, the operational teams created a set of basics rules in order to eliminate the worst practices. Finally, AluChemie established an early warning system to sustain and further improve the level of quality. These 3 elements will be reviewed in detail, illustrated by practical applications and documented findings.

### 10:15 AM Break

### 10:30 AM

**Successful Start up of the Combined Rhodax® and IMC® Processes at the Sohar Smelter:** André Pinoncely<sup>1</sup>; Jean Bigot<sup>2</sup>; Christophe Bouche<sup>3</sup>; <sup>1</sup>Solios Carbone; <sup>2</sup>Rio Tinto Alcan; <sup>3</sup>Fives Solios

In December 2005, Sohar Aluminium Company (Sultanate of Oman) awarded Solios Carbone the turn-key supply of its Green Anode Plant. Upon the successes of the Rhodax® process start up at the Alba line 5, and of the Intensive Mixing Cascade (IMC®) Chinese references, the Sohar anode plant

specified by Aluminium Pechiney Technology was the first opportunity to combine these two breaking through technologies. The first anode was produced in March 2008 and the plant performs today beyond expectations at 36 tph capacity. This paper describes the main features and performance of this new plant and highlights the optimizations which resulted from a close collaboration between all parties. Finally it gives some preview of the 60 tph Green Anode Plant presently under commissioning at the Qatalum smelter in Qatar, becoming soon the next reference of such combined process evolution toward the high capacity requirement of modern smelters.

### 10:55 AM

**Amelios™, A Performance Analysis Tool for Green Anode Plant:** Christophe Bouche<sup>1</sup>; Oussama Cherif Idrissi El Ganouni<sup>2</sup>; André Molin<sup>1</sup>; <sup>1</sup>Solios Carbone; <sup>2</sup>Fives

Stable anode density is crucial to operate reduction cells at peak performance. AMELIOS is a performance analysis tool combining process expertise, mass balance calculation and data mining, developed to improve green anode density stability and plant productivity. It allows quick identification of process deviation root causes to implement corrective actions. Process parameter time series from PLCs are analyzed in real-time to generate reconciled and synchronized anode process data along with KPI allowing an individual anode tracking throughout the process. A statistical analysis of the anode densities identifies the most influent process parameters. The plant breakdown root causes are analyzed to identify the bottlenecks. This information is made available to maintenance, operators and management to improve process transparency and help them to focus on critical equipment, critical process parameters and plant performance objective. A beta version of AMELIOS™ has been in operation in a Green Anode Plant since April 2009.

### 11:20 AM

**Anode Paste Plants: Innovative Solution for Optimum Emission Performances:** Hugues Vendette<sup>1</sup>; <sup>1</sup>Solios Environnement Inc.

Coal tar pitch volatiles (PAHs) emitted during paste mixing and anode forming are traditionally captured via coke dry-scrubbers. In recent years, regenerative thermal oxidizers (RTO) have occasionally been used to reduce the emissions of the PAH lighter fractions. However RTOs have relatively high operating costs and can be subject to plugging and fire hazards due to the building-up of condensed tars. This paper presents a new treatment approach that has recently been implemented in new anode plants where dual treatment systems relying on the use of conventional dry-scrubbers and RTOs were supplied. Low PAH concentration streams from the anode former area are treated using a coke dry-scrubber whereas the higher concentration streams from the paste cooler are treated with the combined action of a coke dry-scrubber followed by a RTO. The combination of these two approaches provides the Owner with high capture/destruction efficiency, lower operating costs and very high reliability.

## General Abstracts: Light Metals Division: Session I

**Sponsored by:** The Minerals, Metals and Materials Society, TMS Light Metals Division, TMS: Aluminum Committee, TMS: Magnesium Committee, TMS: Recycling and Environmental Technologies Committee, TMS: Energy Committee, TMS: Aluminum Processing Committee

**Program Organizers:** Alan Luo, General Motors Corporation; Eric Nyberg, Pacific Northwest National Laboratory

Wednesday AM

Room: 607

February 17, 2010

Location: Washington State Convention Center

**Session Chair:** Alan Luo, General Motors Research & Development Center

### 8:30 AM

**Alcoa Alumina Refinery Secures Future through Reliability Excellence Efforts:** John Kalpoe<sup>1</sup>; Keith Johnson<sup>2</sup>; <sup>1</sup>Suralco Alumina Refinery; <sup>2</sup>Life Cycle Engineering

In 2009 alumina prices plummeted, stock values dropped, the price of raw materials rose, and the partnership between Alcoa and BHP was coming to an end, leaving Alcoa Suralco leadership with some very tough business decisions to make. The refinery manager stated that the implementation of Reliability Excellence (ReX) was the foundation of their survival plan. It was

# Technical Program

this management commitment during the toughest of times that has paid off for Suralco. This paper will cover Suralco's Reliability Excellence journey. The major points will be centered on early challenges, processes, strategy, communication and results. It will show how leadership's commitment, perseverance, and good judgment resulted in a much larger return on investment than expected during a crisis period. This paper will show what Suralco has accomplished in a very tough environment, and how ReX has given them the tools to set a benchmark in their industry.

## 8:50 AM

**Application of ECAP on Commercial Purity Aluminum:** Nilufer Evcimen<sup>1</sup>; Yahya Bayrak<sup>1</sup>; Ahmet Ekerim<sup>1</sup>; <sup>1</sup>Yildiz Technical University

The present study includes determination and optimization of parameters which were effective on achieving sub-micron grain size on commercial purity aluminum to be able to use for industrial processes. Equal Channel Angular Pressing (ECAP)-Conform process was attempted at room temperature on commercial purity aluminum wire samples. Before ECAP process, heat treatments were applied between 320-450/176C for up to 8 h to remove wire texture. Number of passes was increased systematically. For characterization purposes, optical microscope, scanning electron microscope, SEM and transmission electron microscope, TEM were used. Transmission electron microscopy revealed that sub-micron grain size was attained after 11 passes. Mechanical tests such as hardness and tensile test were conducted to characterize the mechanical properties.

## 9:10 AM

**Assessment of Casting Filling by Modelling Surface Entrainment Events Using CFD:** Mark Jolly<sup>1</sup>; Carl Reilly<sup>1</sup>; Nick Green<sup>1</sup>; <sup>1</sup>University of Birmingham

The reliability of cast components is dependent on the quality of the casting process. During this highly transient filling phase the prevention of free surface turbulence and consequential oxide entrainment is critical to assure the mechanical integrity of the component. Past research has highlighted a number of events that lead to entrainment of surface oxides. FLOW-3D, flow structures that result in surface entrainment events have been simulated and an algorithm developed that allows entrainment and defect motion to be tracked. This enables prediction of the quantity and motion of oxide film generated from each event. The algorithm was tested experimentally using real-time X-ray radiography and real metal flows. A quantitative criterion is proposed to assess the damage of each type of event. Complete running systems have also been studied to understand how they could be assessed for quality of filling based on the flows within them.

## 9:30 AM

**Behavior of MgO during Forming and Leaching Process of Calcium Aluminate Slag:** Wang Bo<sup>1</sup>; Sun Huilan<sup>1</sup>; Bi Shiwenz<sup>2</sup>; <sup>1</sup>Hebei University of Science and Technology; <sup>2</sup>Northeastern University

MgO is one of the major impurities in calcium aluminate slag. The existence of MgO will decrease the alumina leaching property of calcium aluminate obviously. The effect of MgO on phase components, crystal structure and alumina leaching property of calcium aluminate slag are studied in this paper by the methods of XRD, EDS and SEM. The results indicate that MgO will be dissolved in 12CaO·7Al<sub>2</sub>O<sub>3</sub> crystal and it causes the expansion of crystal cellular and the increment of interplanar spacing when the content of MgO is lower than 1%. MgO has little effect on alumina leaching ratio of slag under this condition. When the content of MgO is higher than 1%, the compound 20CaO·13Al<sub>2</sub>O<sub>3</sub>·3MgO·3SiO<sub>2</sub> which is difficult to leach is formed and decreases the alumina leaching property of calcium aluminate obviously. After alumina leaching process, the major phase of MgO in red mud is Mg(OH)<sub>2</sub>.

## 9:50 AM

**Effect of Variables on Deposit Characteristics of Aluminum from EMIC-AlCl<sub>3</sub> Ionic Liquid Electrolytes:** Debabrata Pradhan<sup>1</sup>; Ramana Reddy<sup>1</sup>; <sup>1</sup>The University of Alabama

Aluminum alloys were electrorefined from 1-Ethyl-3-methyl-imidazolium chloride (EMIC)-AlCl<sub>3</sub> (60 wt%) ionic liquid electrolyte on copper/aluminum cathodes at 90 ± 3°C. The experiments were carried out to investigate the effect of electrode surface masking, anode and cathode materials, surface roughness of electrodes and deposition time on deposit morphology of aluminum and cathode current density. The deposits were characterized using scanning electron microscope (SEM), energy dispersive spectroscopy (EDS) and X-ray

diffraction (XRD). It was shown that electrode masking plays an important role on deposition characteristics of aluminum rather than other variables. Electrode masking produced non-dendritic deposit even after 25 hours of experiments. Pure aluminum (>99%) was deposited for all experiments with current efficiency of 91-99%.

## 10:10 AM Break

## 10:30 AM

**Effects of Microstructure on Fatigue Crack Growth Behavior of 6061-T6 Wrought Alloys:** Anastasios Gavras<sup>1</sup>; Brendan Chenelle<sup>2</sup>; Diana Lados<sup>1</sup>; <sup>1</sup>Worcester Polytechnic Institute

Fatigue crack propagation of long and small cracks was investigated in wrought 6061-T6 alloys with various grain morphologies. The grain structure was varied using combinations of chemistry, forming, and heat treatment. Low residual stress was ensured during processing to shed light on microstructural effects on crack growth. To evaluate the long and small crack growth behavior of the alloys, compact tension and surface flaw tension specimens were tested at room temperature and constant stress ratio, R=0.1. Microstructure related mechanisms were used to explain the fatigue crack growth behavior at different growth stages. The differences in the near-threshold behavior between long and small cracks were evaluated for each alloy, assessing closure and microstructurally small crack growth effects. Methods for combined closure/microstructure compensation on long crack growth data are provided together with recommendations for their integration in design.

## 10:50 AM

**Electrochemical Characterization of the Al-Mg Foamed Materials in NaCl Solutions:** S. Valdez<sup>1</sup>; S. Casolco<sup>2</sup>; H. Castañeda<sup>3</sup>; <sup>1</sup>UNAM-ICF; <sup>2</sup>ITESM-Puebla; <sup>3</sup>Battelle Memorial Institute

The AlMg-alloy was made by melting Al and Mg ingot pieces in an alumine crucible, kept in a resistance electrical furnace. The molten alloy was poured into steel containers with NaCl crystals, in order to produce the foamed material. After solidification the salt was removed using hot water. The corrosion resistance properties of the material are characterized by electrochemical techniques. The potentiodynamic polarization and electrochemical impedance spectroscopy were used to elucidate the interfacial mechanisms of the alloy when exposed to 3.5% NaCl (reagent grade) at room temperature. The evolution of dissolution under different exposure conditions was used to characterize the corrosion rate in corrosive environment. Key words: Al-Mg alloys, electrochemical characterization, metallic foams.

## 11:10 AM

**Effect of Variables on Deposit Characteristics of Aluminum from EMIC-AlCl<sub>3</sub> Ionic Liquid Electrolytes:** Debabrata Pradhan<sup>1</sup>; Ramana Reddy<sup>1</sup>; <sup>1</sup>The University of Alabama

Aluminum alloys were electrorefined from 1-Ethyl-3-methyl-imidazolium chloride (EMIC)-AlCl<sub>3</sub> (60 wt%) ionic liquid electrolyte on copper/aluminum cathodes at 90 ± 3°C. The experiments were carried out to investigate the effect of electrode surface masking, anode and cathode materials, surface roughness of electrodes and deposition time on deposit morphology of aluminum and cathode current density. The deposits were characterized using scanning electron microscope (SEM), energy dispersive spectroscopy (EDS) and X-ray diffraction (XRD). It was shown that electrode masking plays an important role on deposition characteristics of aluminum rather than other variables. Electrode masking produced non-dendritic deposit even after 25 hours of experiments. Pure aluminum (>99%) was deposited for all experiments with current efficiency of 91-99%.

## 11:30 AM

**Effects of Volume Percent and Aspect Ratio of Short Carbon Fiber on Mechanical Properties of Reinforced Aluminum Matrix Composites:** Yan Pengfei<sup>1</sup>; Yao Guangchun<sup>1</sup>; Shi Jianchao<sup>1</sup>; Mu Yongliang<sup>1</sup>; <sup>1</sup>School of Materials & Metallurgy, Northeastern University

Carbon fiber reinforced aluminum matrix composites have been prepared by stir casting. Al-4 wt%Cu was selected as a matrix. The samples were prepared with four volume fractions (2, 4, 6 and 8) and three aspect ratios (300, 500, and 700). Then the aging treatment was carried out. A tensile test was performed to evaluate the tensile strength of the composites. The results show that when the content of carbon fibers is 6 vol% the tensile strength of composites increases by 78% and 36% after aging treatment. Hardness test shows that the hardness



of the composites increases by 194% and 34%. Moreover, the fracture behavior and crack deflection of composites were investigated using scanning electron microscopy (SEM). The study also shows that the strengthening mechanism depends strongly on fiber volume fraction, aspect ratio and the degree of wetting between fiber and matrix.

### 11:50 AM

**Effective Capital Management – A Case Study:** Joe Petrolito<sup>1</sup>; *Martin Richard*<sup>2</sup>; <sup>1</sup>Hatch; <sup>2</sup>Alcoa

Since 2001, Alcoa's Canada Primary Products division and Hatch Ltd have partnered to supply full EPCM services for their Northeast Region. The region includes three smelters in Quebec, two smelters in the Massena region and one in Iceland. This partnership has resulted in significant improvements in the area of capital allocation and cash flow management. Considerable effort is placed on project readiness to ensure proper forecasting in the interest of avoiding reserving capital and the ensuing opportunity loss. By measuring KPI's such as Project Safety, Cost, Schedule and Technical Performance of completed projects across the region, lessons learned/best practices are easily shared. This relationship has proven particularly beneficial to Alcoa during the present period of low LME markets where flexibility of resources and active project portfolio management has been paramount. The management principles adhered to have helped Alcoa to better control/allocate the reduced amount of available capital.

### General Abstracts: Materials Processing and Manufacturing Division: Microstructure, Characterization, and Modeling

*Sponsored by:* The Minerals, Metals and Materials Society, TMS Materials Processing and Manufacturing Division, TMS/ASM: Computational Materials Science and Engineering Committee, TMS: Global Innovations Committee, TMS: Nanomechanical Materials Behavior Committee, TMS/ASM: Phase Transformations Committee, TMS: Powder Materials Committee, TMS: Process Technology and Modeling Committee, TMS: Shaping and Forming Committee, TMS: Solidification Committee, TMS: Surface Engineering Committee  
*Program Organizers:* Thomas Bieler, Michigan State University; Corbett Battaile, Sandia National Laboratories

Wednesday AM Room: 601  
February 17, 2010 Location: Washington State Convention Center

*Session Chair:* To Be Announced

### 8:30 AM

**Improving Creep Properties through Grain Boundary Engineering:** *Milo Kral*<sup>1</sup>; Daniel Drabble<sup>1</sup>; <sup>1</sup>University of Canterbury

Grain boundary engineering is a promising methodology to improve the properties of many FCC metals and alloys. The aim of the present work was to investigate the feasibility of using grain boundary engineering to improve the high-temperature properties of an austenitic nickel-iron-chromium alloy. Samples of 800H (32%Ni-21%Cr-44%Fe with Al, Ti additions) were 'grain boundary engineered' using a range strain/anneal conditions and then characterized using Electron Backscatter Diffraction (EBSD) analysis. The various processing conditions provided samples with a range of grain size, grain boundary character and grain boundary connectivity. This work has culminated in correlations between the microstructural characteristics and high-temperature material properties such as steady-state creep rate and strength/ductility under typical service conditions.

### 9:10 AM

**Modeling the Anisotropic Properties of Tantalum Taylor Impact Specimens:** *Michael Nixon*<sup>1</sup>; Joel House<sup>1</sup>; Brian Plunkett<sup>1</sup>; Joel Stewart<sup>1</sup>; <sup>1</sup>USAF AFRL

Numerical simulations of the Taylor Impact experiment using commercially pure tantalum were performed with isotropic and anisotropic yield surface descriptions of the mechanical properties within the Elastic-Plastic Impact Code (EPIC version 2006). The anisotropic yield surface representation with strain hardening was based upon calculations using the Visco-Plastic Self Consistent model developed by Tome and Lebensohn. The simulation of the high strain rate plastic deformation assuming different yield surfaces allows the comparison

of the specimen profile geometry to reveal the effects of anisotropy on the mechanical properties under dynamic loading. The numerical simulations were compared to experimental data from a lot of tantalum with a processing history that included Equal Channel Angular Pressing, forging and annealing. Details of the thermo-mechanical processing and the Taylor Impact experiments are reported by House et al (2010).

### 9:30 AM

**Neural Networks Modeling of Mechanical Properties in Medium Carbon Steels:** *N. S. Reddy*<sup>1</sup>; Jae Sang Lee<sup>1</sup>; Yang Mo Koo<sup>1</sup>; <sup>1</sup>GIFT, POSTECH, Pohang, Korea

Neural network (NN) model has been developed for the analysis of the correlation between the mechanical properties and composition and heat treatment parameters of low alloy steels. The input parameters of the model consist of alloy compositions and heat treatment parameters. The outputs of the NN model are mechanical properties. The model can be used to calculate the properties of low alloy steels as a function of alloy composition and heat treatment variables. The individual and the combined influence of inputs on properties of medium carbon steels is simulated using sensitivity analysis. The current study achieved a good performance of the NN model, and the results are in agreement with experimental knowledge. Explanation of the calculated results from the metallurgical point of view is attempted. The developed model can be used as a guide for further alloy development.

### 9:50 AM

**Mathematical Modelling of an Annealing Furnace for Process Control Applications:** *Nick Depree*<sup>1</sup>; James Sneyd<sup>1</sup>; S. Taylor<sup>1</sup>; Mark Taylor<sup>1</sup>; M. O'Connor<sup>2</sup>; John Chen<sup>1</sup>; <sup>1</sup>University of Auckland; <sup>2</sup>New Zealand Steel Ltd.

Dynamic thermal models of a continuous annealing furnace have been developed, with the intention of optimising furnace control in both steady state and changing furnace conditions. The models calculate both strip and furnace temperatures, and strip microstructural changes for all operating conditions. Existing manual control during transient operation results in large amounts of strip receiving incorrect heat treatment and products that do not meet specifications. A 3D finite element model has been constructed which is accurate but computationally expensive, and is used to provide understanding of furnace radiative heat transfer and temperature distribution. A reduced dimensionality model from heat transfer fundamentals with a coupled steel recrystallisation model gives rapid results that can be used to optimise steady state settings or simulate the furnace response during transient conditions. Successful furnace optimisation will provide significant financial and energy savings due to reduced wastage and rework of incorrectly heat treated product.

### 10:10 AM Break

### 10:30 AM

**Dynamic Abnormal Grain Growth in Alpha Iron:** *Phi Thanh*<sup>1</sup>; George Kaschner<sup>2</sup>; J.P. Delplanque<sup>1</sup>; Joanna Groza<sup>1</sup>; <sup>1</sup>UC Davis; <sup>2</sup>Los Alamos National Labs

We investigated dynamic abnormal grain growth (DAGG) in alpha iron in attempt to create centimeter-size grains. We performed strain controlled tensile deformation in the temperature range (TH = 0.4 – 0.6) and strain-rates (10<sup>-7</sup> to 10<sup>-3</sup> s<sup>-1</sup>). Both constant strain-rate and strain-rate jump experiments were performed to induce DAGG. Once abnormally large grains appear, grain boundary mobility is sustained by balancing dislocation generation and annihilation rate by varying strain-rate at temperature.

### 10:50 AM

**A Study on the Behavior of Boron in Low Carbon Steel by Neutron Autoradiography:** *Dong Jun Mun*<sup>1</sup>; Kyung Chul Cho<sup>1</sup>; Eun Joo Shin<sup>2</sup>; Jae Sang Lee<sup>1</sup>; Yang Mo Koo<sup>1</sup>; <sup>1</sup>Pohang University; <sup>2</sup>Korea Atomic Energy Research Institute

It is well known that when trace boron is added to steel, their properties can be considerably improved. It has been shown that the beneficial effect of boron is caused by the segregation of boron at austenite grain boundaries. The distribution behavior of boron in steel such as segregation along the grain boundary and formation of borocarbides or boronitrides is sensitively subject to cooling rate, heat treating temperature, and alloying elements. However, in general, it is well known that a very small amount of boron in steel is hard to be detected with electron spectroscopy because of its low atomic value, so that a special technique is necessary to observe boron distribution in steel. In this

# Technical Program

present study, the segregation and precipitation behavior of boron in austenite phase was mainly studied by means of Neutron Autoradiography method. From those results, the behavior of boron in low carbon steel was discussed.

## 11:10 AM

**Flexure Strength and Hydrothermal Degradation of 3mol% Ytria-Stabilized Zirconia (3Y-TZP): Microwave vs. Conventional Sintering:** *Kirk Wheeler*<sup>1</sup>; *Pedro Peralta*<sup>1</sup>; *Scott Atkin*<sup>2</sup>; <sup>1</sup>Arizona State University; <sup>2</sup>Creative Dental Laboratories

Flexure strength was determined for 3Y-TZP samples sintered in either a microwave or a conventional furnace. Microwaved samples showed an increase in flexure strength (~1490 MPa) compared to samples sintered conventionally (~1380 MPa). This was attributed to a nearly 50% reduction in grain size from ~1.0  $\mu\text{m}$  for conventional samples to ~0.5  $\mu\text{m}$  for microwave samples, as determined via scanning electron microscopy (SEM). In addition, an accelerated ageing test was performed to simulate the degradation of 3Y-TZP in a humid environment. Samples were tested in a steam environment at ~125 °C and ~200 kPa pressure for 75 hrs. A reduction of flexure strength by ~43% was found for conventionally sintered samples while only a ~14% reduction was measured for the microwaved samples. The increased degradation of the conventionally sintered samples can be attributed to an increase in the monoclinic phase as determined by powder x-ray diffraction.

## 11:30 AM

**Novel Pathways to Hydrogen Dissociation and Diffusion on Pd Alloys:** *Heather L. Tierney*<sup>1</sup>; *Ashleigh E. Baber*<sup>1</sup>; *John R. Kitchin*<sup>2</sup>; *E. Charles H. Sykes*<sup>1</sup>; <sup>1</sup>Tufts University; <sup>2</sup>Carnegie Mellon University

This combined scanning tunneling microscopy (STM) and density functional theory (DFT) study shows that individual Pd atoms in an inert Cu matrix are active for the dissociation of hydrogen and subsequent spillover onto Cu sites. The atomic-scale compositions of both Pd/Cu{111} and Pd/Au{111} near-surface alloys were elucidated and H uptake was quantified. Experimental and theoretical results indicated that H spillover was facile on Pd/Cu at 400 K but that the hydrogen diffusion barrier is insurmountable on a Pd/Au sample with the same atomic composition and geometry. These results demonstrate the powerful influence an inert substrate has on the catalytic activity of Pd atoms supported in its surface. While these experiments were performed in ultra-high vacuum, an understanding of the nature of H<sub>2</sub>-surface interactions, including molecular adsorption, dissociation and surface diffusion provides a basis for the development of next-generation energy technologies.

## 11:50 AM

**An Investigation on the Flow Behavior of Metals when Forging Specimens Having Different Cross Sections:** *Bashir Raddad*<sup>1</sup>; <sup>1</sup>University of Alfatrah, Mechanical Department

Experiments were carried out to generate data on cold compression of solid copper and aluminum specimens having different cross section shapes (cylindrical, hexagonal, square and rectangular) and height-to-diameter ratios, between flat dies at two degrees of surface condition (dry or lubricated). Different cross section shapes and surface conditions are expected to create different loading characteristics and modes of deformation during this process. Experimental results showed load/displacement/ curves consisted of many stages: the metal begins to overcome the frictional force at the interface in the first stage and the metal begins to flow after reaching the yield point. This stage is characterized by a steep rate of increase of load. In the second stage, the load was less in the lubricated specimens. And this stage showed the different in load due to the different Ho/Do ratio.

## General Abstracts: Structural Materials Division: Non-Ferrous Materials

*Sponsored by:* The Minerals, Metals and Materials Society, TMS Structural Materials Division, TMS: Advanced Characterization, Testing, and Simulation Committee, TMS: Alloy Phases Committee, TMS: Biomaterials Committee, TMS: Chemistry and Physics of Materials Committee, TMS/ASM: Composite Materials Committee, TMS/ASM: Corrosion and Environmental Effects Committee, TMS: High Temperature Alloys Committee, TMS/ASM: Mechanical Behavior of Materials Committee, TMS/ASM: Nuclear Materials Committee, TMS: Refractory Metals Committee, TMS: Titanium Committee  
*Program Organizers:* Eric Ott, GE Aviation; Robert Hanrahan, National Nuclear Security Administration; Judith Schneider, Mississippi State University

Wednesday AM

Room: 3A

February 17, 2010

Location: Washington State Convention Center

*Session Chair:* To Be Announced

## 8:30 AM

**A Creep Rupture Time Model for Anisotropic Creep-Damage of Transversely Isotropic Materials:** *Calvin Stewart*<sup>1</sup>; *Ali Gordon*<sup>1</sup>; <sup>1</sup>University of Central Florida

Anisotropic creep-damage modeling has become an increasingly important prediction technique in both the aerospace and industrial gas turbine industries. The introduction of tensorial damage mechanics formulations in modeling tertiary creep behavior has lead to improved predictions of the creep strain that develops due to anisotropic grain structures and the induced anisotropy that occurs with intergranular damage. A number of isotropic creep-damage rupture time prediction models have been developed in literature however; few rupture time prediction models for tensorial anisotropic creep-damage are available. In this paper, a rupture time model for anisotropic creep-damage of transversely isotropic materials is derived. Comparison with the associated isotropic formulation and the Larson-miller parameter show improved creep rupture time prediction.

## 8:50 AM

**Comparison of Deformation Mechanisms for Constant Strain Rate and Creep Testing of a Ni-Based Superalloy:** *Hallee Deutchman*<sup>1</sup>; *Raymond Unocic*<sup>2</sup>; *Michael Mills*<sup>1</sup>; <sup>1</sup>The Ohio State University

The effect of microstructure, stress, temperature, and strain rate on deformation mechanisms were investigated under creep and constant strain rate conditions on an advanced, polycrystalline Ni-based disk superalloy. A detailed microstructure characterization aimed at measuring the gamma-prime precipitate size, morphology, distribution as well as grain size and degree of grain boundary serration was performed prior to mechanical testing experiments so that the effects of microstructure can be correlated with the deformation response. Constant load creep tests and constant strain rate tests were performed at the same temperature so that the influence of strain rate on deformation substructure can be assessed. Following mechanical testing, a thorough TEM characterization study was done to determine the operative deformation mechanisms. Mechanisms found included microtwinning and isolated faulting of the gamma-prime precipitates. Funding for this work has been provided by AFOSR through the Metals Affordability Initiative (MAI) program.

## 9:10 AM

**A Combinatorial Approach to Investigate Solid Solution Hardening in Ni-Based Systems by Nanoindentation:** *Oliver Franke*<sup>1</sup>; *Karsten Durst*<sup>2</sup>; *Mathias Göken*<sup>2</sup>; <sup>1</sup>MIT; <sup>2</sup>University of Erlangen

Diffusion couples are used to study the thermodynamics of a wide range of materials. With nanoindentation local mechanical properties in a diffusion zone can be studied with high lateral resolution. The combination of nanoindentation and scanning electron microscopy can be used to investigate solid solution hardening effects of certain alloying elements quickly and efficiently. In this work a study of three alloying elements (Fe, Mo and Ta) in binary Ni-based systems and Ni-NiAl was carried out. After annealing the diffusion zone was characterized using arrays of indents and EDX. For Ni-NiAl, a significant modulus change is observed in the beta-NiAl-regime. In Ni-Mo, Ni-Fe and Ni-Ta, the solid solution hardening effect was studied as they show solubility



over a wide concentration range and the diffusion zone was wide enough to be accessed by nanoindentation. The obtained results can be described by a slight modification of Labusch's model on solid solution hardening.

### 9:30 AM

**Single-Crystal Solidification of New Co-Al-W Base Superalloys:** *Masafumi Tsunekane*<sup>1</sup>; Akane Suzuki<sup>2</sup>; Tresa Pollock<sup>1</sup>; <sup>1</sup>University of Michigan; <sup>2</sup>GE Global Research

Solidification processing of new high-temperature Co-Al-W base single-crystals has been investigated. Single-crystal bars with compositions of Co-9.4Al-10.7W, Co-8.8Al-9.8W-2Ta and Co-7.8Al-7.8W-1.5Ta-4.5Cr were successfully grown with a conventional Bridgman process. Primary dendrite arm spacings in each single-crystal were measured to be about 300  $\mu\text{m}$ . Segregation of constituent elements in the dendritic structure was very limited, compared to nickel-base single-crystals. Partitioning coefficients of each element were calculated to be close to 1 from concentration profiles obtained by EPMA. Polycrystalline starters utilized to initiate single-crystal growth were also investigated to consider the possible effect of back diffusion. Segregation characteristics within the starters were similar to the characteristics of single-crystals. These observations collectively suggest that freckle formation is unlikely to occur during solidification in single-crystals of Co-Al-W base alloys.

### 9:50 AM Break

### 10:10 AM

**Nucleation of Extension Deformation Twins in  $\alpha$ -Ti:** *Leyun Wang*<sup>1</sup>; Yiyi Yang<sup>1</sup>; Martin Crimp<sup>1</sup>; Philip Eisenlohr<sup>2</sup>; Darren Mason<sup>3</sup>; Thomas Bieler<sup>1</sup>; <sup>1</sup>Michigan State University; <sup>2</sup>Max-Planck-Institut für Eisenforschung GmbH; <sup>3</sup>Albion College

Activity of two extension twinning systems,  $\{10\bar{1}2\}\langle 111\rangle$ (T1) and  $\{11\bar{2}1\}\langle 112\bar{6}\rangle$ (T2), is observed in textured polycrystalline  $\alpha$ -Ti. The crystallographic direction of hexagonal c-axes was preferentially aligned with the global tensile direction resulting from 4-point bending. Hence, most grains are in a hard orientation with low Schmid factors for basal and prismatic slip. T1 twinning was observed much more frequently than T2 twinning. The statistically significant correlation of the alignment between T1 twins and active prismatic slip systems, or, alternatively, other T1 twins, in neighboring grains indicates that nucleation of these twins follows from strain compatibility constraints at grain boundaries. Formation of T2 twins is found to require not only high Schmid factors, but is additionally limited to conglomerates of hard-oriented grains. This preferential activation in hard clusters will be discussed. Support was provided by NSF grant DMR-0710570 and DFG grant EI 681/2-1.

### 10:30 AM

**Influence of Grain Boundary Sliding on Diffusion in Yttria Stabilized Tetragonal Zirconia:** *Santonu Ghosh*<sup>1</sup>; Sathya Swaroop<sup>2</sup>; Peter Fielitz<sup>3</sup>; Guenter Borchardt<sup>3</sup>; Atul Chokshi<sup>1</sup>; <sup>1</sup>Indian Institute of Science; <sup>2</sup>VIT University; <sup>3</sup>Technische Universität, Clausthal

Although there have been suggestions of an enhancement in diffusion because of grain boundary sliding, there are no data available to critically evaluate this possibility. High temperature deformation in a superplastic yttria stabilized tetragonal (YTZ) occurs by grain boundary sliding. In the present study creep experiments were conducted on a fine grained 3 mol% yttria stabilized tetragonal zirconia, under conditions associated with superplasticity at 1598 and 1623K. Grain boundary sliding measurements revealed that the grain boundary sliding contribution to the total creep deformation is >75%. Tracer diffusion studies under creep conditions and without load indicate that there is no enhancement in either the lattice or grain boundary diffusivities. The experimental creep data are consistent with an interface controlled diffusion creep model.

### 10:50 AM

**Constitutive Response of Polymers, Filled and Unfilled, as a Function of Temperature and Strain-Rate:** *Eric Brown*<sup>1</sup>; Carl Cady<sup>1</sup>; George Gray III<sup>1</sup>; Mathew Lewis<sup>1</sup>; Dana Dattelbaum<sup>1</sup>; <sup>1</sup>Los Alamos National Laboratory

Recently, interest has been shown concerning the mechanical response of polymers and polymer composites for several reasons. First, evidence has shown that there may be issues with aging and nitroplasticizer uptake. The second area of focus was related to the development of predictive materials models that describe the mechanical behavior of these materials. Accordingly, detailed information about the constitutive response is crucial. Compression

measurements were conducted on these materials as a function of temperature from -55°C to +70°C and strain rate using a specially-designed split Hopkinson pressure bar (strain rate of  $\sim 2800 \text{ s}^{-1}$ ) and quasi-statically (strain rates from  $\approx 0.001$  to  $1 \text{ s}^{-1}$ ) using a hydraulic load frame. The mechanical response of the filled VCE showed a strong dependency on strain rate and was most sensitive to changes in test conditions. The filled foam materials were much less sensitive to changes in temperature or strain rate. The visco-elastic recovery of VCE is seen to dominate the mechanical behavior at temperatures above the glass transition temperature ( $T_g$ ). It also exhibited increasing elastic loading moduli, E, with increasing strain rate or decreasing temperature, which is similar to other polymeric materials and there is a pronounced shift in the apparent  $T_g$  to higher temperatures as the strain rate is increased. Analysis of the filled materials implies damage in the filler material as indicated by a load drop on the stress-strain curve.

### 11:10 AM

**Shape Memory Behavior of an Ultra-Fine Grained Ti-30Ni-20Pd Alloy through Equal Channel Angular Extrusion (ECAE) Processing:** *Rabindra Mahapatra*<sup>1</sup>; Charles Lei<sup>1</sup>; <sup>1</sup>Naval Air Systems Command

The Ti-30Ni-20Pd Alloy (in at.%) was ECAE processed to produce ultra-fine grains of 0.5-1 micro-meter. The effects of ultra-fine grain and alloying with Pd on transition temperature and fracture toughness of the alloy relative to Ni-Ti binary alloy will be presented. The effects of phase transformation and related microstructure on transition temperature behavior of the alloy will be discussed.

### 11:30 AM

**High Temperature Creep-Fatigue Crack Growth Models:** *Jeffrey Evans*<sup>1</sup>; <sup>1</sup>University of Alabama in Huntsville

There are numerous applications in the modern engineering world which involve the use of metals under conditions of cyclic loading in operating conditions that can cause creep and/or environmental interactions with time independent, mechanical fatigue processes. Various approaches for modeling the creep-fatigue crack growth behavior have been proposed to capture the various types of damage that is occurring. These include mechanistic modeling, crack growth modeling using the method of superposition to incorporate time-dependent and cycle-dependent components, and numerical modeling. A number of phenomena have been investigated to obtain a better understanding of the fundamental creep-fatigue crack growth process. The various models and techniques used in modeling the elevated temperature creep-fatigue crack growth process will be reviewed.

## Global Innovations in Manufacturing of Aerospace Materials: The 11th MPMD Global Innovations Symposium: Innovations in Primary and Secondary Forming - Nickel

*Sponsored by:* The Minerals, Metals and Materials Society, TMS Materials Processing and Manufacturing Division, TMS Structural Materials Division, TMS: Shaping and Forming Committee, TMS: High Temperature Alloys Committee  
*Program Organizers:* Deborah Whitis, General Electric Company; Thomas Bieler, Michigan State University; Michael Miles, BYU

Wednesday AM Room: 306  
February 17, 2010 Location: Washington State Convention Center

*Session Chairs:* Dan Sanders, Boeing Corporation; Lee Semiatin, AFRL-RX

### 8:30 AM Invited

**Technical and Manufacturing Innovations Required to Meet Global Aerospace Requirements for the 21st Century:** *Anthony Banik*<sup>1</sup>; <sup>1</sup>ATI Allvac/Allegheny Technologies

The metals industry has reached the 10% mark of the 21st Century. The demand for aerospace materials reached an initial peak at the start of the century spurring a considerable investment in product and process development to meet the demands of this expanding market. Allegheny Technologies is stepping up to this challenge by making substantial investments through a combination of new materials development, advanced modeling capabilities, expanded data acquisition systems, as well as substantial investments in infrastructure. Based on information from the beginning of the century, the expectations for the 21st

# Technical Program

century will be considered in light of the current performance. As a result, the focus for the next steps in the development, melting and conversion of aerospace materials will be discussed from a producer's perspective in meeting the aerospace market demands for higher temperature, extended life and highest value to aircraft OEMs.

## 9:00 AM Invited

**Some Challenges in Current and Future Superalloy Production:** *Lesh Patel*<sup>1</sup>; <sup>1</sup>Special Metals Corp

Nickel Superalloys continue to be the alloys of choice for critical components in a range of industries from Aerospace to traditional and emerging Energy Production systems. Along with the classic challenges of developing alloys which will meet the property requirements of these demanding new applications, materials manufacturers are wrestling with the need for bigger and bigger components in these new systems. This requires different thinking and sometimes new approaches to melting and processing these alloys in order to avoid segregation and other melt related defects in large ingots and also forging and other downstream hot working difficulties. This paper gives some examples and a perspective on these issues.

## 9:30 AM

**Accelerating Insertion of Materials at GE Aviation:** *Deborah Whitis*<sup>1</sup>; *Arturo Acosta*<sup>1</sup>; *Shesh Srivatsa*<sup>1</sup>; *Daniel Wei*<sup>1</sup>; <sup>1</sup>General Electric Company

Material and process development for aircraft engines has, in the past, required long and costly experimental programs, imposing a significant barrier to the insertion and exploitation of new materials and manufacturing processes. With the advent of computer modeling and simulation of materials processing, and the accelerated insertion of materials (AIM) approach, we have begun to provide the tools to industrial materials designers that they need to increase productivity and reduce cost of alloy and process development. This presentation will provide an overview of the implementation of the AIM approach at GE Aviation. The integration of materials models, historical databases, and analysis tools have allowed us to more rapidly downselect new alloys and manufacturing processes, responding quickly to the design requirements of a particular component and engine environment. Current progress in applying these techniques to nickel-based superalloys will be reviewed.

## 9:50 AM

**Constitutive Model of Superplastic and Power-Law Creep Deformation during Isothermal Forging of P/M Alloy René 88DT:** *Wen Tu*<sup>1</sup>; *Tresa Pollock*<sup>1</sup>; <sup>1</sup>University of Michigan

Deformation mechanisms during isothermal compression of P/M alloy René 88DT has been studied. Grain level analysis by electron backscatter diffraction is used to quantify different microstructural phenomena that occur during both superplastic and power-law creep deformation. A constitutive model including all straining mechanisms and concurrent microstructural phenomena has been created to predict the grain structure evolution during isothermal compression. During superplastic deformation at lower strain rates, excess vacancies created at the grain boundaries increase grain boundary mobility causing enhanced grain growth. The quantity of excess vacancy created follows an Avrami solution as a function of temperature and strain rate. During power-law creep deformation at higher strain rates, dynamic recrystallization initiates after a critical local stored deformation. This critical stored energy for dynamic crystallization is measured experimentally as a function of strain rate. Experimental results for grain size are compared to those predicted by the grain structure evolution model.

## 10:10 AM Break

## 10:30 AM

**$\gamma - \gamma' - \delta$  Ternary Eutectic Ni-Base Superalloys Alloys Amenable for Manufacture:** *Yijing Shi*<sup>1</sup>; *Alejandro Rodriguez*<sup>1</sup>; *Mengtao Xie*<sup>1</sup>; *Randy Helmink*<sup>2</sup>; *Mark Hardy*<sup>3</sup>; *Sammy Tin*<sup>1</sup>; <sup>1</sup>Illinois Institute of Technology; <sup>2</sup>Rolls-Royce Corporation; <sup>3</sup>Rolls Royce plc

As one of the most important classes of high-temperature structural materials, Ni-base superalloys are critical to the continued development of high-performance turbine engines for propulsion and power generation. In order to accommodate the increases in engine operating temperatures required for improved performance and efficiency, higher concentrations of refractory alloying elements have been used to enhance the mechanical properties of Ni-base superalloys. However, many of these compositional modifications have also tended to result in the alloy being more difficult to manufacture

into large-scale components using traditional approaches and techniques. The present investigation evaluates the novel Ni-Nb-Cr-Al alloys, based on the pseudo-ternary eutectic  $\gamma - \gamma' - \delta$  system, that exhibit promising physical and mechanical properties for turbine engine applications.

## 10:50 AM

**Microstructure and Properties of Platinum-Group-Metal Modified Nickel-Base Superalloys:** *Adam Pilchak*<sup>1</sup>; *Donald Weaver*<sup>2</sup>; *Donna Ballard*<sup>2</sup>; *S. Semiatin*<sup>2</sup>; <sup>1</sup>Universal Technology Corporation; <sup>2</sup>Air Force Research Laboratory

The addition of platinum-group metals (PGM) to nickel-base superalloys can significantly enhance their oxidation resistance. Thus, these alloys are being developed as candidate materials for metallic thermal protection systems for use at high temperature. In the present work, the microstructure and properties of wrought PGM-modified superalloys were investigated and compared to those of commercially-produced alloys such as Haynes® 230. For this purpose, cast ingots were forged or extruded and subsequently hot-pack rolled to produce sheet and foil. The resulting microstructures were characterized using scanning electron microscopy and electron backscatter diffraction, and elevated-temperature tensile and compressive strengths were measured.

## 11:10 AM

**Modelling the Effect of Initial Heat-Treatment on the Creep of Multi-Modal Nickel Superalloys:** *James Coakley*<sup>1</sup>; *Hector Basoalto*<sup>2</sup>; *David Dye*<sup>1</sup>; <sup>1</sup>Imperial College; <sup>2</sup>QinetiQ

Polycrystalline nickel superalloys used in aero-engine disc applications can often possess a bimodal gamma prime microstructure, for example in NI115 and René 80. During heat treatment and service the gamma prime distribution can evolve, with consequent effects on the creep behaviour. Here a modified LSW coarsening model is presented to model the effect of heat treatment and service conditions on the precipitate distribution. The distribution is then used in a physically-based, phenomenological creep model, based on the work of Dyson and McLean, to predict the effect of heat treatment on the creep behaviour. The results are compared to experiment for creep tests and heat treatments performed on NI115.

## 11:30 AM

**Flow Behavior of Superalloy 945 during High Temperature Deformation:** *Steve Coryell*<sup>1</sup>; *Kip Findley*<sup>1</sup>; *Martin Mataya*<sup>1</sup>; <sup>1</sup>Colorado School of Mines

The demand for improved materials is continuously pushing producers to obtain a fine grain structure and tight restrictions on grain size uniformity in forged superalloy rod. Understanding flow and recrystallization behavior is critical for optimizing forge and annealing practices to meet these requirements. The flow behavior of INCOLOY® alloy 945, a newly developed hybrid of alloys 718 and 925 with a unique combination of strength and corrosion resistance, was performed using uniaxial compression testing at elevated temperatures, characteristic of hot working. Compression was performed at temperatures ranging 950°-1150°C and strain rates ranging 0.001-1.0s<sup>-1</sup>. Flow and peak stresses increased with strain rate and decreasing temperature, shown by the Zener-Holloman relationship. Material constants such as the activation energy for deformation, stress exponents, and strain rate sensitivities were determined as a prerequisite for developing mathematical models for the constitutive behavior of INCOLOY® 945. Possible mechanisms causing distinct flow characteristics will also be discussed.

## 11:50 AM

**Microstructure Based Monotonic Stress-Strain Modeling of R-104 as a Function of Temperature:** *Sujoy Kar*<sup>1</sup>; *Sanjay Sondhi*<sup>1</sup>; *Daniel Wei*<sup>2</sup>; *David Mouret*<sup>2</sup>; <sup>1</sup>GE Global Research; <sup>2</sup>GE Aviation

Nickel based superalloy René 104 is a polycrystalline turbine disk alloy. The stress-strain response of this alloy is dependent on microstructure and the operative damage mechanisms. Deformation mechanisms vary in different temperature regimes and plastic strain levels. The model developed is based on Estrin's dislocation based framework. Equation sets have been adapted to capture different in-elastic hardening and softening mechanisms operative at different temperature regimes for René 104. In the present paper, the details of the monotonic stress-strain model and its predictive capability on different microstructures and at different temperatures will be described.



12:10 PM

**Effects of Temperature, Deformation Strain, and Slow Transfer on the Microstructure and Mechanical Properties of 304L Stainless Steel Forgings:** *Nathan Switzer*<sup>1</sup>; Robert Bergen<sup>2</sup>; Jamie McQueen<sup>1</sup>; James Knutson<sup>1</sup>; <sup>1</sup>Honeywell FM&T; <sup>2</sup>Precision Metal Products, Inc

304L forgings were made in a High Energy Rate Forging (HERF) press at hot working temperatures of 1550°F and 1725°F. Prior to forging, the preform shape had a “mountain” appearance in the side view, with the intent of gathering information about multiple strain levels from a single sample. We also varied the time of transfer between heating furnace, forging press, and water quench. Mechanical testing and microstructural analysis were conducted on final forgings. Intuitively, room temperature yield and ultimate strength increased with deformation strain; however the high deformation strain levels of approximately 1.5 to 2.0 EQPS resulted in decreased strength due to deformation heating. Added transfer time resulted in a slight increase in strength; but at the higher strain levels, deformation softening eliminated the effects of delayed transfer. The deformation process was modeled with ABAQUS coupled thermal-mechanical simulation to predict final shape and properties.

### Hume-Rothery Symposium: Configurational Thermodynamics of Materials: Session V

*Sponsored by:* The Minerals, Metals and Materials Society, TMS Electronic, Magnetic, and Photonic Materials Division, TMS Structural Materials Division, TMS: Alloy Phases Committee, TMS: Chemistry and Physics of Materials Committee  
*Program Organizers:* Chris Wolverton, Northwestern University; Mark Asta, University of California, Davis; Gerbrand Ceder, Massachusetts Institute of Technology (MIT)

Wednesday AM Room: 212  
February 17, 2010 Location: Washington State Convention Center

*Session Chair:* To Be Announced

8:30 AM Invited

**Order-Disorder in the Phase Field Crystal Model:** *Jeffrey Hoyt*<sup>1</sup>; Ken Elder<sup>2</sup>; <sup>1</sup>McMaster University; <sup>2</sup>Oakland University

Over the course of his career, Didier de Fontaine has made several significant advances in the study of phase equilibria, thermodynamics and kinetics of ordering in alloys. In this work we use the ideas of de Fontaine to formulate a phase field crystal model (PFC) that can describe the order-disorder phenomenon. It is shown that a simple extension to the original binary alloy PFC free energy leads to a rich variety of phase diagrams. In addition to a liquid and a high temperature disordered phase, the PFC model can stabilize the BCC based ordered phases B2, B32 or DO<sub>3</sub> depending on the choice of a single length scale parameter. Several applications of the model will be discussed including ordering kinetics, the variation of long range order within the vicinity of dislocations and grain boundaries, and disorder trapping during rapid solidification.

9:00 AM Invited

**Phase Equilibria, Microstructural Evolution and Coarsening Kinetics In “Inverse” Ni<sub>3</sub>Ge (γ’)-Ni(Ge) (γ) Alloys:** *Alan Ardell*<sup>1</sup>; Yong Ma<sup>2</sup>; <sup>1</sup>National Science Foundation; <sup>2</sup>UCLA

The phase boundary separating the γ’ and (γ + γ’) regions of the Ni-Ge phase diagram was established from 700 to 1000 °C in alloys containing 22.0 to 23.5 at.% Ge. “Inverse” γ’ alloys were aged to study the kinetics of the precipitation of the γ phase. The precipitate shapes change from spherical to large non-equiaxed plates as the size increases; coalescence is responsible. γ precipitates are more strongly spatially correlated than γ’ precipitates in normal Ni-Ge alloys and coalesce faster at all volume fractions (f<sub>v</sub>). The γ precipitates grow by diffusion-controlled coarsening with a rate constant k(f<sub>v</sub>) that increases with increasing volume fraction, f<sub>v</sub>. The particle size distributions are broader than the theoretical distribution of the LSW theory in most of the alloys. The kinetics of coarsening of γ precipitates in inverse alloys is much slower than in normal alloys, as expected from chemical diffusion in the two phases.

9:30 AM Invited

**Phase Field Crystals: Atomistic Simulations on Diffusive Timescales:** *Kuo-An Wu*<sup>1</sup>; *Peter Voorhees*<sup>1</sup>; <sup>1</sup>Northwestern University

Phase field crystal models have been used to describe a wide range of phenomena from grain growth to solidification. The strength of the method lies in its ability to follow the atomic scale motion that accompanies a process that occurs on diffusive timescales. As illustrations, we discuss the effects of an applied stress on the stability of a solid-liquid interface and the evolution of grains in crystals. The grain growth simulations show the evolution of the dislocation structure of a grain boundary and the local atomic displacements of atoms near the boundary during grain growth. We find that dislocation reactions play an important role in grain morphology and rotation. The simulations of the stress-driven interfacial instability illustrate the importance of the structure of the solid-liquid interface on the evolution of the instability.

10:00 AM Break

10:30 AM Invited

**Phase Field Modeling of the Martensitic Transition: Intermittent Dynamics and Self-Organized Criticality:** *Alphonse Finel*<sup>1</sup>; *Oguz Salman*<sup>1</sup>; <sup>1</sup>ONERA

Martensitic transformations in shape memory alloys are characterized by large strain misfits between austenite and martensite. The transitions are often athermal, dominated by elastic accommodation, and the dynamics are essentially thermoelastic. We first present a qualitative picture of the physical mechanisms that lead to thermoelasticity. On a macroscopic scale, partial accommodation with finite polytwinned domains, together with internal constraints, is responsible for the thermoelastic behavior. On a finer scale, due to pinning effects, the thermoelastic dynamics consists in a large series of metastable equilibrium states separated by instabilities. Next, using a lagrangian method that incorporates inertia, we present a quantitative analysis of the cubic-to-tetragonal martensitic transition in a Fe-Pd alloy. We show that the dynamics is critically self-organized: it consists in a large series of bursts that display power-law distributions. Finally, we compare our results with a recent experimental investigation of the acoustic emission observed in a Fe68.8Pd31.2 single crystal.

11:00 AM Invited

**Quantitative Phase-Field Simulations of Growth and Coarsening in Polycrystalline Multi-Component and Multi-Phase Materials:** *Nele Moelans*<sup>1</sup>; *Liesbeth Vanherpe*<sup>2</sup>; *Jeroen Heulens*<sup>1</sup>; *Bert Rodiers*<sup>3</sup>; *Bart Blanpain*<sup>1</sup>; *Patrick Wollants*<sup>1</sup>; <sup>1</sup>K.U. Leuven, dept. Materials Science and Engineering; <sup>2</sup>K.U. Leuven, Dept. Computer Science; <sup>3</sup>LMS International

Phase-field modeling has become very important for simulating microstructure evolution. It has been applied to study solidification, precipitation, grain growth, martensitic transformations and many more phenomena. To account for alloy specific properties --such as phase equilibria, interface energy and kinetics, diffusion coefficients, elastic properties, and crystal structure and orientation relationships--, phase-field models rely on experimental measurements and other modeling techniques (e.g. first principles, CALPHAD and molecular dynamics). With a naive model formulation, however, the relations between model parameters and alloy properties are too complicated so that realistic simulations are practically unfeasible for multi-phase, multi-component or polycrystalline alloys. We discuss state-of-the-art phase-field models that can account accurately for the effect of interface and bulk properties on the evolution of grain morphology and solute distribution at the mesoscale. Attention is given to their applicability to multi-component alloys. The capabilities of the models are illustrated using recent simulation results.

11:30 AM

**3D-Microstructures at the Atomic Scale: A Monte Carlo Method with Elastic Interactions:** *Varvenne Celine*<sup>1</sup>; *Alphonse Finel*<sup>1</sup>; *Mathieu Fevre*<sup>1</sup>; *Yann Le Bouar*<sup>2</sup>; <sup>1</sup>ONERA; <sup>2</sup>CNRS

It is well-known that size effects have a great influence both in phase diagrams and microstructure morphology. The choice of an atomic scale study is relevant to describe thin interfaces, which is very common in bulk materials, and to reproduce realistic kinetics of precipitation. Furthermore, it allows a direct link between quantitative interatomic potentials and thermodynamics. An efficient way for this study is to combine the lattice static (LS) formalism with Monte Carlo statistical mechanics: the former allows us to treat elasticity in coherent microstructures and the latter to calculate structural and thermodynamic properties. A particular attention has been devoted to the long

# Technical Program

wavelength limit of the LS and its link with the continuum linear elasticity (as implemented in phase field methods). Moreover, a special effort has been made to have an efficient code, in order to simulate systems large enough to analyse 3D microstructures in ordered binary alloys.

## 11:50 AM Invited

### Effect of Biaxial Strain on Phase Stability and Microstructure Development in Single-Crystal Films: *Long Qing Chen*<sup>1</sup>; <sup>1</sup>Pennsylvania State University

This presentation will discuss the phase transitions and microstructure evolution in thin films. The focus is on the effect of biaxial strains, e.g., from the mechanical constraint by a substrate due to lattice mismatch or thermal mismatch, on phase and microstructure stability. Two types of phase transitions will be considered, namely, ferroic and isostructural phase separation. It is shown that the shifts in the thermodynamic instability temperatures and the nature of phase transitions can be predicted from purely classical thermodynamic analysis. An efficient, full spectral numerical method will be presented for solving the order parameter and composition evolution equations describing the morphological and microstructural evolution in thin films for which the boundary condition along the out-of-plane direction is non-periodic. It is shown that a biaxial strain can drastically change the relative phase stability, volume fractions of differently orientated domains and the domain-wall orientations, as well as compositional distributions.

## Jim Evans Honorary Symposium: Primary and Secondary Production of Metals

*Sponsored by:* The Minerals, Metals and Materials Society, TMS Extraction and Processing Division, TMS Light Metals Division

*Program Organizers:* Ben Li, University of Michigan; Brian G. Thomas, University of Illinois at Urbana-Champaign; Lifeng Zhang, Missouri University of Science and Technology; Fiona Doyle, University of California, Berkeley; Andrew Campbell, WorleyParsons

Wednesday AM Room: 620  
February 17, 2010 Location: Washington State Convention Center

*Session Chair:* Lifeng Zhang, Missouri University of Science and Technology

## 8:30 AM Introductory Comments

### 8:40 AM

#### Low Cost $TiCl_4$ , the Indispensable Compound to Make Titanium: *James Withers*<sup>1</sup>; *J. Laughlin*<sup>1</sup>; *Y. Elkadi*<sup>1</sup>; *A. Putilin*<sup>1</sup>; *R. Loutfy*<sup>1</sup>; <sup>1</sup>MER Corporation

Titanium tetrachloride ( $TiCl_4$ ) is indispensable to make pigment ( $TiO_2$ ) as well as titanium metal by the metallothermic and electrolysis processes. Traditionally ( $TiCl_4$ ) is produced from an ore source as a particulate and carbon in a fluid bed at approximately 1000°C which requires extensive fractionation to purify the  $TiCl_4$ . An alternate process carbothermically treats the ore as very fine particulate provides ore purification and produces a suboxide-carbide ( $TiO_xC_y$ ) as an XRD identifiable compound. The  $TiO_xC_y$  containing both stoichiometric oxygen and carbon can be chlorinated as low as 180°C – 200°C which produces only  $TiCl_4$  in a purified form thus eliminating subsequent fractionation. The lower cost tickle can be used to produce titanium by the standard Kroll process or alternative processing in a re-engineered Kroll process or electrolysis that produces a highly purified powder product. Discussion includes carbothermic reduction, the low temperature  $TiCl_4$  synthesis and titanium produced from the  $TiCl_4$ .

### 9:05 AM

#### The Optimization of the Coke and Agglomerate Quantity in Lead Production in “Water-Jacket” Furnace: *Ahmet Haxhija*<sup>1</sup>; *Egzon Haxhija*<sup>2</sup>; <sup>1</sup>University of Prishtina; <sup>2</sup>American University in Kosovo

Paper contains the analysis of technological process depending on the composition of lead (Pb) in agglomerate, and the theoretical and real rapport of coke consumption per tone of technical lead produced. The findings are based in the work of “Water-jacket” furnace in Trepça. Paper brings the results of theoretical and experimental studying, along with analytical and graphical analyses of regional thermal balance depending on the composition of load, and the coke quantity in load. While analyzing the technological process of technical lead production we have been searching for the growth of technical lead quantity produced depending on lead percentage in agglomerate and the air

that is enclosed in the furnace. Moreover, we aimed to optimize the percentage of lead in agglomerate and the parameters of the process. Simultaneously, keeping the attention to the growth of technical lead produced, the minimization of energy consumption, and the minimization of environment pollution.

### 9:30 AM

#### Wireless Instrumentation of Aluminum Smelting Operatings: *Dan Steingart*<sup>1</sup>; *James Evans*<sup>2</sup>; *Paul Wright*<sup>2</sup>; <sup>1</sup>City College of New York; <sup>2</sup>Wireless Industrial Technologies

Wireless instrumentation has been demonstrated in locations heretofore unfeasible for measurement within aluminum smelters in demonstration and pilot projects over the past five years. Quantities such as heat flux at the shell, duct exhaust temperature and flow rate, individual anode current and bridge position have been correlated with cell potential. With these sensors we have been able to suggest improved pot maintenance schedules, and also predict anode effects almost 90 seconds before the event occurs. In addition to reviewing the data gathered from these wireless devices, this presentation will touch up methods for powering sensors from environmental sources within power plants.

### 9:55 AM Break

### 10:10 AM

#### The Development of Product Microstructure “Morphology Maps” and their Significance in Describing the Decomposition of Solids: *Peter Hayes*<sup>1</sup>; <sup>1</sup>University of Queensland

The decomposition of solids in reactive gas atmospheres has been the subject of numerous studies over a wide range of chemical systems. Whilst significant advances have been made in understanding and describing the influence of gas phase mass transfer on these processes, the key process phenomena and physico-chemical properties of the solid phases determining the product morphologies have remained less well characterised. These product morphologies can, however, be critical in determining the rate limiting reaction mechanisms and the overall rates of reduction. By considering the fundamental processes occurring at the reaction interface the conditions for the formation of various product morphologies are identified, and the methodology and theoretical basis for the development of morphology maps established. The methodology is shown to be general, and can be applied to the analysis of any system involving the decomposition of metal compounds in reactive gas atmospheres.

### 10:35 AM

#### Development and Application of Dynamic Soft Reduction Technology for Continuous Casting Machine: *Cheng Ji*<sup>1</sup>; *Miaoyong Zhu*<sup>1</sup>; <sup>1</sup>Northeastern University of China

Dynamic soft reduction is an effective method to reduce the central segregation and porosity of continuous casting strands. Based on the review of the previous work, the investigation and development of dynamic soft reduction key technologies, such as soft reduction parameters design, on-line prediction of strand solidification end, the dynamic soft reduction control model, and the corresponding process control system, are presented in this paper. The applications in Baosteel Meishan No.2 slab, Panzhihua steel No.2 bloom, and Xingtai steel No. 5 bloom continuous casting machines in China are introduced, and the detail macro structure and center carbon segregation inspection results pre and post the technology application have been demonstrated.

### 11:00 AM

#### Transient Behavior of Inclusion Chemistry, Shape and Structure in Fe-Al-Ti-O Melts: Effect of Titanium/Aluminum Ratio: *Cong Wang*<sup>1</sup>; *Sridhar Seetharaman*<sup>1</sup>; <sup>1</sup>Carnegie Mellon University

The effect of Ti/Al ratio on inclusion behaviors was investigated in aluminum and titanium deoxidized iron melt. When the Ti/Al ratio was maintained at 1/4, titanium-containing oxides exist temporarily after titanium addition, generating little shape change and producing transient stage inclusions with low titanium contents. When the Ti/Al ratio was increased to 1/1, inclusions showed a distinct increase in the titanium content. The transient reaction was accompanied by an irreversible shape change from spherical to irregular. When the Ti/Al ratio in the melt was further increased to 15/1, the inclusion population evolved from spherically-dominant case to irregular ones with the final inclusion chemistry has more titanium. When the Ti/Al ratio in the melt was increased to 75/1, the inclusions evolved towards  $TiO_x$  inclusions, and this is accompanied by a shape change from spherical to irregular. TEM results confirmed the existence of  $Ti_2O$ .



### Magnesium Technology 2010: Cast Alloys, Casting, and Grain Refinement

Sponsored by: The Minerals, Metals and Materials Society, TMS Light Metals Division, TMS: Magnesium Committee

Program Organizers: Sean Agnew, University of Virginia; Eric Nyberg, Pacific Northwest National Laboratory; Wim Sillekens, TNO; Neale Neelameggham, US Magnesium LLC

Wednesday AM Room: 613  
February 17, 2010 Location: Washington State Convention Center

Session Chairs: Mei Li, Ford Motor Company; Norbert Hort, GKSS Research Center

#### 8:30 AM

**Effects of Section Thicknesses on Tensile Properties of Permanent Mould Cast Magnesium Alloy AJ62:** Jonathan Burns<sup>1</sup>; Lihong Han<sup>1</sup>; Henry Hu<sup>1</sup>; Xueyuan Nie<sup>1</sup>; <sup>1</sup>University of Windsor

Applications of high temperature magnesium alloys as structural materials commonly employ high-pressure die-casting processes. Among these magnesium alloys, AJ62 shows great die-castability for automotive engine blocks. However, its potential for use in less expensive, gravity-fed processes that achieve relatively thick sections remains to be demonstrated. Development of such a process will lead to a greater range of applicability for this remarkable alloy. In this study, step-castings of AJ62 were produced in a gravity-fed, permanent mould to understand the mechanical effects of section thickness. Specimens of four varying thicknesses were prepared from respective steps in the castings, and subsequently tested in tension at room temperature. A general degradation of mechanical properties was observed as thickness increased. Evident variations in microstructure for each thickness were also observed via porosity measurements and microstructural analysis. Thereby, an attribution of the changes in mechanical performance to differences in microstructure evolution during solidification can be made.

#### 8:50 AM

**Growth Restriction Factor Effects near the Surface of High Pressure Die Cast Mg-Al Binary Alloys:** Anumalasetty Nagasekhar<sup>1</sup>; Carlos Caceres<sup>1</sup>; Mark Easton<sup>2</sup>; <sup>1</sup>The University of Queensland; <sup>2</sup>Monash University

Solute concentration effects on the grain microstructure at the corner, surface and core regions of the cross-section of high pressure die cast Mg-Al alloys have been evaluated, for Al contents between ~6 and 12 mass%, using electron back scattered diffraction technique. The grain microstructure is bimodal in all cases, but especially at the core, due to the prevalence of large dendritic grains formed in the shot sleeve. The average grain size near the surface and at the corner regions is controlled by the amount of solute in the same way as in quiescent castings. Keywords: Magnesium-aluminum alloys, High pressure die casting, Grain size, Growth restriction factor, Electron back scattered diffraction, AZ91 alloy

#### 9:10 AM

**Strengthening Mechanisms in Mg-Al-Sn Based Alloys:** Shaul Avraham<sup>1</sup>; Alexander Katsman<sup>1</sup>; Menachem Bamberger<sup>1</sup>; <sup>1</sup>Technion- Israel Institute of Technology

New creep resistant and microstructurally stable Mg-Al alloys for elevated temperatures are of both scientific and engineering interest. The presence of Al results in the formation of the creep deteriorating  $\gamma$ -Mg<sub>17</sub>Al<sub>12</sub> at the grain boundaries (GB). The modification of AM50 with Sn (Base) and Ce (Base+Ce) was investigated by computational thermochemistry (CT), microstructural stability tests and creep tests. Microhardness measurements proved the thermal stability of the alloys during prolonged aging at 200°C. The stress exponent for both alloys is typical of dislocation climb controlled creep at low temperatures ( $n=7$ ). The Al<sub>11</sub>RE<sub>3</sub> formation at the GB results in reduced GB sliding and enhanced creep resistance. The Mg<sub>3</sub>Sn fine densely dispersed precipitates formed in the  $\alpha$ -Mg matrix. The enhanced threshold stress is attributed to dislocation-precipitate interaction. The activation energy for creep in the Base+Ce alloy is higher than in the Base alloy and close to the Mg self-diffusion energy.

#### 9:30 AM

**Numerical Simulation and Experimental Study of Squeeze Casting Magnesium Alloy AM50:** Zhizhong Sun<sup>1</sup>; Henry Hu<sup>1</sup>; Alfred Yu<sup>1</sup>; <sup>1</sup>University of Windsor

The heat transfer measurements are rarely performed in squeeze casting. With different applied pressure levels, the heat transfer rate and heat flow patterns becomes more important in squeeze castings. The paper discussed the effect of applied pressures on the solidification and cooling behavior of a cylindrical squeeze casting of magnesium alloy AM50A. Due to high temperature gradient between the molten metal and the steel die, heat flow in boundary layers is affected by partial solidification. The temperature distributions, the cooling curves, the shape and position of the phase front were simulated with the commercial CFD software Flow3D®. The results show that the application of high pressures result in rapid heat transfer across casting/die interface, and consequently increase solidification and cooling rates. To verify prediction, temperature measurements at various locations inside an experimental squeeze casting were performed. Comparisons of the numerical results with the experimental measurements show close agreement.

#### 9:50 AM

**Section Thickness and the Skin Effect in a High Pressure Die Cast Mg-12%Al Alloy:** Kun Yang<sup>1</sup>; Anumalasetty Nagasekhar<sup>1</sup>; Carlos Caceres<sup>1</sup>; <sup>1</sup>The University of Queensland

Microhardness maps of cast-to-shape tensile specimens of rectangular and circular cross-sections have been produced for a range of alloys. In comparison with that at the centre, the hardness is generally higher near the surface and at the corners of the cross-section. The difference in hardness value is accounted for by the coarser solidification microstructure and the concentration of porosity at the casting's core. The evidence indicates the presence of a harder surface layer (or skin) around the periphery of the cross section; however, the harder layer appears patchy, uneven and asymmetrical, questioning the concept of a definable skin which is uniform and continuous in both hardness and depth. Physical reasons for these features of the casting's skin are discussed.

#### 10:10 AM

**Investigations on Microstructure and Properties of Mg-Sn-Ca Alloys with 3% Al Additions:** Fady Elsayed<sup>1</sup>; Tarek Abuleil<sup>1</sup>; Ahmed Abd El-Aziz<sup>2</sup>; Karl Kainer<sup>1</sup>; Norbert Hort<sup>1</sup>; <sup>1</sup>GKSS Forschungszentrum Geesthacht GmbH; <sup>2</sup>Department of Materials Science, German University in Cairo

New magnesium alloys based on the Mg-Sn system have been studied with an emphasis on the Mg-Sn-Ca system due to their attractive property profile. This research work investigates the effect of 3 wt.% Al additions on two selected Mg-Sn-Ca alloys namely the Mg-3Sn-2Ca (TX32) alloy, and the Mg-9Sn-1Ca (TX91) alloy at different temper conditions (F, T4, T6). The aim is to improve room temperature mechanical properties and corrosion resistance. A comparison of experimental results for the new Mg-Sn-Al-Ca (TAX) alloys is performed with their base Mg-Sn-Ca (TX) alloys and explicitly discussed. Al additions were found to have a favourable effect on strength of Mg-Sn-Ca (TX) alloys while they caused rapid decrease in their corrosion resistance. Furthermore the results show a significantly deteriorated corrosion resistance with respect to the addition of Al.

#### 10:30 AM

**Simulation of Stresses during Casting of Binary Magnesium-Aluminum Alloys:** Matthew Pokorny<sup>1</sup>; Charles Monroe<sup>1</sup>; Christoph Beckermann<sup>1</sup>; Z. Zhen<sup>2</sup>; Norbert Hort<sup>2</sup>; <sup>1</sup>University of Iowa; <sup>2</sup>GKSS Research Centre Geesthacht

A viscoplastic deformation model is used to predict thermal stresses and hot tear evolution during casting of binary Mg-Al alloys. The predictions are compared to experiments that allow for the measurement of contraction forces during solidification and cooling. These force measurements, together with estimates from data found in the literature, are used to obtain the high-temperature mechanical properties needed in the deformation model. The coherency and yielding behavior of the semi-solid material during solidification is investigated in detail. The model is then used to predict the hot tears observed in the experiments. The simulation results show good agreement with the measurements. In particular, the hot tear severity is well predicted for a range of alloy compositions and initial mold temperatures.

# Technical Program

**10:50 AM**

**Study on the Microstructure Changes during the In Situ Tensile Processes of as-Cast and Aged Specimens of High-Vacuum Die-Cast Mg-9Al-1Zn Alloy:** Jie Song<sup>1</sup>; *Shou-Mei Xiong*<sup>1</sup>; <sup>1</sup>Tsinghua University

The microstructure and mechanical properties of the as-cast, solution treated and aged specimens of high-vacuum die-cast Mg-6Al alloy was studied, and the precipitation behavior during the aging procedure was also analyzed by using scanning electron microscopy, vickers micro hardness test, differential scanning calorimetry and transmission electron microscopy observation. The  $\beta$ -Mg<sub>17</sub>Al<sub>12</sub> phase of Mg-6Al alloy dissolved in the matrix from the as-cast stage to the solution stage, and then small  $\beta$  particles precipitated from the grain boundaries of the matrix during the aging process. The specimens were aged for different time periods at three different temperatures for better understanding of the precipitation behaviors. The skin regions were more favorable to the precipitation during the aging process than the center ones. Factors influencing the heat treatment and precipitation processes were discussed.

**11:10 AM**

**Structure-Property Relationships for Die-Cast Magnesium Alloys:** *Jeffrey Wood*<sup>1</sup>; J.P. Weiler<sup>1</sup>; J. Jekl<sup>2</sup>; R. Berkmortel<sup>2</sup>; <sup>1</sup>University of Western Ontario; <sup>2</sup>Meridian Technologies, Inc.

This paper summarizes the work performed, as part of a larger project, on a high-pressure die-cast AM60B magnesium alloy component. The ultimate goal of this project is to develop the capability to predict local mechanical properties from the die-casting parameters used during production. However, the variability of mechanical properties throughout a casting due to different local solidification conditions, as is the case in die-cast magnesium alloys, results in the inability to predict local mechanical properties from conventional methods. The work reported here reviews the relationships between local mechanical properties and local microstructural features developed for the die-cast AM60B component, that are applicable to any die-cast magnesium alloy. The results from this work indicate that the yield strength can be predicted from the average grain size through the casting thickness, and the local effective fracture strength from the size and relative location of the largest local area fraction of porosity.

**11:30 AM**

**Grain Refinement of Mg-Al Alloys by Carbon Inoculation:** *Yuanding Huang*<sup>1</sup>; Bin Liu<sup>1</sup>; Okechukwu Anopu<sup>1</sup>; Norbert Hort<sup>1</sup>; Karl Kainer<sup>1</sup>; <sup>1</sup>GKSS Research Center

Grain refinement of magnesium alloys not only reduces the hot tearing and improves their mechanical properties, but also weakens the texture and improves their isotropic properties. In aluminium-free magnesium alloys, the element Zr is an effective nucleants to refine the microstructure and its mechanism of grain refinement is clear. In Al-containing magnesium alloys, the grain refinement by carbon inoculation was considered to be the best approach until now. However, the mechanism of grain refinement is still unclear. After inoculated by carbon or SiC particles, the grain size of as-cast Mg-Al alloys reduces largely. The grain refinement is mainly attributed to the enhanced nucleation of alpha-Mg on the surface of the ternary compound Al<sub>2</sub>MgC<sub>2</sub>. Experimental investigations also confirm that this ternary compound is unstable at room temperature and easily reacts with water to produce most likely the gas CH<sub>4</sub> and the spinel phase MgAl<sub>2</sub>O<sub>4</sub>.

**11:50 AM**

**A Systematic Study of the Grain Refinement of Magnesium by Zirconium:** *Partha Saha*<sup>1</sup>; Katie Lolie<sup>1</sup>; Srinath Viswanathan<sup>1</sup>; Arun Gokhale<sup>2</sup>; Robert Batson<sup>1</sup>; <sup>1</sup>The University of Alabama; <sup>2</sup>Georgia Institute of Technology

Zirconium is well known as an excellent grain refiner for magnesium alloys that do not contain aluminum. While a number of studies on the grain refinement of magnesium alloys by zirconium have been reported in the literature, there is still some uncertainty about the exact mechanism of grain refinement. In this work, a Design of Experiments (DOE) approach was used for a systematic study of the grain refinement of magnesium by zirconium. Variables included the amount of zirconium, the pouring temperature, and the holding time prior to casting. Samples were poured into a special "hockey puck" mold designed to reproduce the conditions in permanent mold casting. Optical metallography and quantitative image analysis were used to measure the resultant grain sizes. The effect of the various factors on the measured grain size and the interaction among the various factors is discussed.

**12:10 PM**

**Grain Refinement of AZ91 Alloy by Addition of Ceramic Particles:** Dmitry Shepelev<sup>1</sup>; Julia Klemf<sup>1</sup>; Menachem Bamberger<sup>1</sup>; *Alexander Katsman*<sup>1</sup>; <sup>1</sup>Technion

The a-Al<sub>2</sub>O<sub>3</sub> and SiC ceramic particles can serve as additives to refine the microstructure of Mg-based alloys. The Mg/a-Al<sub>2</sub>O<sub>3</sub> and Mg/SiC pre-alloys were prepared using the new method developed in the present work. The ceramic particles were inserted into a molten Mg bath through a Mg-nitride layer formed at the surface of the liquid magnesium through which the nitrogen gas is blown. The particles of about 30-nm in size were placed in a porous alumina crucible and vacuum heat treated at 700°C. The liquid Mg penetrated through the porous walls of the crucible. The mixture was cooled to room temperature under a nitrogen atmosphere. The resulting Mg matrix contained about 15wt% evenly distributed particle agglomerates of about 0.5  $\mu$ m. Alloy AZ91 was successfully grain refined using the pre-alloys developed. The grain size of the refined alloy, ~40 $\mu$ m, was about two times smaller than that of the base alloy.

---

## Magnesium Technology 2010: Deformation Mechanisms

*Sponsored by:* The Minerals, Metals and Materials Society, TMS Light Metals Division, TMS: Magnesium Committee

*Program Organizers:* Sean Agnew, University of Virginia; Eric Nyberg, Pacific Northwest National Laboratory; Wim Sillekens, TNO; Neale Neelameggham, US Magnesium LLC

Wednesday AM

Room: 612

February 17, 2010

Location: Washington State Convention Center

*Session Chairs:* Sean Agnew, University of Virginia; Louis Hector Jr, GM R&D Center

---

**8:30 AM**

**The Evolution of In-Grain Misorientation Axes (IGMA) during Deformation of Wrought Magnesium Alloy AZ31:** *Young Chun*<sup>1</sup>; Chris Davies<sup>1</sup>; <sup>1</sup>Monash University

Understanding deformation mechanism is a prerequisite for the development of more formable magnesium alloys. We have developed a novel approach which is based on analysis of in-grain misorientation axes (IGMA) and allows identification of dominant slip system for a large number of grains. Based on this approach we investigated for rolled AZ31 the effects of orientations and temperatures on active deformation mechanisms, including slip, deformation twinning and kink banding. The IGMA analysis suggests that increasing rolling temperature promotes activation of prism  $\langle a \rangle$  slip, which enhances the rollability of the plate favorably oriented for this slip mode. The approach also reveals orientation-dependent occurrence of kink banding and its crystallographic relationship with parent grain. It is concluded that IGMA analysis can be effectively used to study deformation mechanism in hcp metals, and also used as a criterion for substantiating the validity of some crystal plasticity models.

**8:50 AM**

**Influence of Deformation Processing on the Tensile/Compressive Asymmetry in Wrought Mg-3Al-Zn Alloy:** *Ran Liu*<sup>1</sup>; De Liang Yin<sup>1</sup>; Jing Tao Wang<sup>1</sup>; <sup>1</sup>Nanjing University of Science and Technology

Deformation anisotropy in a rolled Mg-3Al-1Zn alloy was investigated by mechanism-based modeling. Orientation factors for each slip and twinning systems in samples with typical rolled texture were conducted to find active deformation system, and the strain incrementals resulted from the activation of these deformation systems were accumulated for strain hardening and geometrical hardening evaluation. Modeling results indicate that the dominating deformation modes in samples with typical rolling texture are basal slip and [10-12] twinning, and the model results correspond quantitatively to the marked mechanical anisotropy of the rolled magnesium alloy.



## 9:10 AM

**Importance of Crystallographic Texture of AZ31B Importance of Crystallographic Texture of AZ31B on Flow Stress Anisotropy and Tension-Compression Asymmetry:** *Majid Al-Maharbi*<sup>1</sup>; David Floey<sup>1</sup>; Ibrahim Karaman<sup>1</sup>; Irene Beyerlein<sup>2</sup>; Ted Hartwig<sup>1</sup>; Laszlo Kecskes<sup>3</sup>; Suveen mathaudhu<sup>3</sup>; <sup>1</sup>Texas A&M University; <sup>2</sup>Los Alamos National Laboratory; <sup>3</sup>U.S. Army Research Laboratory

Crystallographic texture of AZ31B magnesium alloy processed using equal channel angular extrusion (ECAE) was found to play an important role in both flow stress anisotropy and tension-compression (T/C) asymmetry. In order to obtain different crystallographic textures, the alloy was ECAE processed following different conventional and hybrid ECAE routes. A viscoplastic self-consistent (VPSC) crystal plasticity model was employed to predict the texture evolution during ECAE. Despite the dynamic recrystallization taking place during the ECAE processing at 200°C and the continuous grain refinement with the number of ECAE passes, the crystallographic texture was successfully predicted up to four passes. The flow stress anisotropy and T/C asymmetry of the processed samples, were, then predicted using the same VPSC model coupled with a recently developed dislocation-based constitutive hardening law. The ramifications of these predictive capabilities on processing large AZ31B plates using ECAE for target crystallographic textures will be discussed.

## 9:30 AM

**Mechanical Behavior of AZ31 Due to Texture and Microstructure:** *David Foley*<sup>1</sup>; Majid Al-Maharbi<sup>1</sup>; K.T. Hartwig<sup>1</sup>; Ibrahim Karaman<sup>1</sup>; Laszlo Kecskes<sup>2</sup>; Suveen Mathaudhu<sup>2</sup>; <sup>1</sup>Texas A&M University; <sup>2</sup>US Army Research Lab

Achieving high strength in common Mg alloys requires phase, texture, and grain size distribution engineering. In order to understand the potential of SPD to control these parameters and to evaluate the mechanical behavior of the resulting materials, several studies were carried out. In AZ31, specimens were created with fixed texture and varied grain size, illustrating the grain size effect on yield, hardening, and mechanical anisotropy. Samples were also created with varied textures but fixed grain size distribution to evaluate these trends. In ZK60, varied thermomechanical processing has resulted in differing phase morphology and concentration. Finally, notable differences in texture development and microstructural refinement during deformation as well as general processability of these alloys will be discussed.

## 9:50 AM

**Mechanical Anisotropy in Extruded Mg Alloy AM30:** Brian Gerard<sup>1</sup>; Adam Niechajowicz<sup>2</sup>; Zbigniew Gronostajski<sup>2</sup>; *Wojciech Misiolek*<sup>1</sup>; <sup>1</sup>Lehigh University; <sup>2</sup>Wroclaw University of Technology

An industrial magnesium alloy AM30 extrudate was examined for microstructural gradients using metallographic techniques. Additionally, tensile samples were cut from the extrudate at different angles with respect to the extrusion direction. The tensile testing was performed at various high strain rates to study the influence of deformation anisotropy under automobile crash conditions. It was observed that the direction of tensile loading significantly impacted the yielding and fracture behavior as well as the dominant deformation mechanisms. These phenomena can be attributed to the highly anisotropic yielding behavior of magnesium hexagonal close packed crystals combined with a strong extrusion texture. Additionally, voids forming on specific twin planes were shown to significantly contribute to failure, which has been observed previously at low strain rates. The results of these experiments add to the knowledge base for determining the crashworthiness of structural magnesium alloy components.

## 10:10 AM

**Implementation of the Anisotropy of Plastic Flow in Inverse Parameter Calculations of the Deformation Behavior of AZ31 Magnesium Alloy:** Timo Ebeling<sup>1</sup>; *Christian Hartig*<sup>1</sup>; Rüdiger Bormann<sup>1</sup>; <sup>1</sup>Hamburg University of Technology

A better understanding of the texture evolution and anisotropic behavior is needed in order to improve the mechanical properties of magnesium wrought alloys. The approach is an investigation of the deformation mechanisms by model calculations. Therefore, room temperature tensile tests of AZ31 rolled sheets have been performed. The stress-strain behavior and the Lankford-coefficient have been measured. An inverse parameter calculation yielding information about deformation mode activities, texture evolution and mechanical properties was performed using a viscoplastic self-consistent model. Additional to the

macroscopic hardening, the strain dependent Lankford coefficient, which reacts strongly on changes of the yield surface, was introduced into the modeling. The additional experimental input about the anisotropy of plastic flow yields a better insight into the mostly disregarded latent hardening of the deformation modes. It could be shown that the stress-strain behavior, the texture evolution and the Lankford-coefficient were simulated simultaneously under appropriate assumptions about the deformation modes.

## 10:30 AM

**Tensile Mechanical Properties and the Ductile-To-Brittle Transition Behavior of the Mg-Li-Al-Zn Alloy:** *Chung-Wei Yang*<sup>1</sup>; Truan-Sheng Lui<sup>1</sup>; Li-Hui Chen<sup>1</sup>; <sup>1</sup>National Cheng Kung University

The present study focuses on investigating the tensile mechanical properties and failure behaviours of the LAZ1021 Mg-Li alloy. The tensile tests of LAZ1021 specimens were performed at -25°C to 250°C, with a tensile strain rate of  $1.67 \times 10^{-3}$ /s. The XRD analysis results represented that the microstructural characteristics of LAZ1021 was combined with the Mg-rich alpha-phase and the Li-rich beta-phase, and there was less phase composition change after tensile tests at various testing temperatures. The tensile strength and elongations were sensitive to the deformation temperatures. The total elongation was significantly increased from 4% at -25°C to about 55% above 100°C tensile testing temperatures. A significant ductile-to-brittle transition temperature (DBTT) was recognized at about 50°C. The failures, which occurred from brittle fracture with evident cleavage to ductile dimpled ruptures, is related to the transition of slip systems with increasing temperatures and the cavitation between alpha/beta-phase interface.

## 10:50 AM

**The Influence of Sn and Pb Addition on the Tensile Properties of Mg Alloys:** *Wei Gao*<sup>1</sup>; Hongmei Liu<sup>1</sup>; <sup>1</sup>The University of Auckland

A new Mg alloy system containing small amounts of Sn-Pb or Pb-Zr has been developed. These alloys possess exceptionally high ductility with good strength: the elongation reaches 20-28% at room temperature in as-cast state without any heat treatment. This type of cold deformation properties has not been reported with other Mg cast alloys. The small addition of Pb dramatically changed the microstructure of Mg-Sn alloys, forming small/round and well dispersed intermetallic phases. A special microstructure was also found in Mg-Sn-Pb alloy system: equiaxed grain boundaries and dendrite structures cross each other and independently exist in alloys. This microstructure cannot be explained by traditional solidification theories, but may have played an important role in improving ductility of these alloys. The development of this alloy system will open a door for Mg industry that cast alloy plate or sheet can be directly mechanically formed into net-shaped working parts.

## 11:10 AM

**Room Temperature Tensile Anisotropy of Extruded Magnesium Plates:** *Paul Krajewski*<sup>1</sup>; Adi Ben-Artzy<sup>2</sup>; Raj Mishra<sup>1</sup>; <sup>1</sup>General Motors; <sup>2</sup>Rotem Industries

The room temperature tensile behavior of four extruded magnesium plates: AZ31, AM50, ZM21, and AZ61 were evaluated at 0, 45, and 90 degrees to the extrusion direction. The low aluminum content alloys ZM21 and AZ31 exhibited significant anisotropy of ductility and flow strength. The 45 degree to the rolling direction showed the lowest yield strength and a ductility of over 25%. The higher aluminum content materials, AM50 and AZ61 exhibited no anisotropy of yield strength or ductility. EBSD was used to explain the differences in tensile behavior between the low Al and high Al content materials.

## 11:30 AM

**Mechanical Properties and Microstructural Analysis of AXJ530 Magnesium Alloy Reinforced with Alumina Fibers:** Bin Hu<sup>1</sup>; Liming Peng<sup>1</sup>; Bob Powell<sup>2</sup>; Anil Sachdev<sup>2</sup>; *Xiaoqin Zeng*<sup>1</sup>; <sup>1</sup>Shanghai Jiao Tong University; <sup>2</sup>General Motors Corporation

The creep-resistant magnesium alloy AXJ530 was reinforced with 15 volume percent, silica-bonded, Saffil fibers. The optimal squeeze casting parameters for infiltration of the fiber preforms were determined and the effects of reinforcement on the tensile and creep properties of the alloy were determined. Microstructural analysis of the composites, including the interface between the fibers and the AXJ530 matrix, was done. The results are discussed in terms of the shear lag theory for strengthening in composites.

# Technical Program

11:50 AM

**Very High Strain Rate Deformation of AZ31b Mg Alloys Using Split Hopkinson Pressure Bar:** Mehdi Sanjari<sup>1</sup>; Amir Farzadfar<sup>1</sup>; Steve Yue<sup>1</sup>; Elhachmi Essadiqi<sup>2</sup>; <sup>1</sup>McGill; <sup>2</sup>CANMET-MTL

Nowadays, an understanding of strain rate dependence of material behavior is very important. The effects of strain rate on the deformation behavior of cubic materials have been studied extensively. However, high strain rate deformation of hexagonal materials has received relatively little attention. The present study considers the uniaxial compression behavior of as-cast AZ31B alloy at very high strain rates in the wide temperature range. A split Hopkinson pressure bar is used to attain strain rates in the range of 1000s<sup>-1</sup>. The results show that the microstructure is fully recrystallized at 250°C and strain rate of 103 s<sup>-1</sup>. The EBSD measurements show that most grains are oriented such that their c-axis is aligned with the compression direction. At higher strain rates such as 103 s<sup>-1</sup>, the basal poles split toward transverse directions indicating the activation of <c+a> slip systems because of increasing temperature due to more plastic and frictional work.

12:10 PM

**Observation of Non-Basal Slip in Ductile Deformed MgY Alloys:** Igor Schestakow<sup>1</sup>; Stefanie Sandlöbes<sup>1</sup>; Sangbong Yi<sup>2</sup>; Stefan Zaeferrer<sup>1</sup>; <sup>1</sup>Max-Planck-Institut für Eisenforschung GmbH; <sup>2</sup>GKSS-Forschungszentrum - Magnesium Innovation Center (MagIC)

MgY clearly shows an enhanced room temperature ductility compared to pure Mg and other Mg alloys. The presented study of a Mg 3 wt-% Y alloy focuses on understanding the mechanisms for this ductility improvement by slip trace analysis, texture analysis based on electron backscatter diffraction (EBSD) and transmission electron microscopy (TEM). Slip trace analysis on slightly RT-deformed MgY showed slip traces, which are consistent with second-order <c+a>-pyramidal slip. It has been reported that beside non-basal slip, {10-11} {10-12} double twinning might be responsible for the room temperature ductility enhancement. Texture and microstructure analysis of RT-deformed MgY showed, however, that besides double twinning, another texture-weakening deformation mode must be activated. Our TEM investigations showed a significant amount of non-basal dislocations in deformed MgY. The experimental results are discussed focusing on the mechanism effecting the observed activation of non-basal slip in MgY.

## Materials in Clean Power Systems V: Clean Coal-, Hydrogen Based-Technologies, Fuel Cells, and Materials for Energy Storage: SOFC II

*Sponsored by:* The Minerals, Metals and Materials Society, TMS Electronic, Magnetic, and Photonic Materials Division, TMS Structural Materials Division, TMS/ASM: Corrosion and Environmental Effects Committee, TMS: Energy Conversion and Storage Committee

*Program Organizers:* Xingbo Liu, West Virginia University; Zhenguo Yang, Pacific Northwest National Lab; K. Weil, Pacific Northwest National Lab; Mike Brady, Oak Ridge National Lab; Jay Whitacre, Carnegie Mellon University; Ayyakkannu Manivannan, National Energy Technology Laboratory; Zi-Kui Liu, Penn State University

Wednesday AM Room: 211  
February 17, 2010 Location: Washington State Convention Center

*Session Chairs:* Zhenguo "Gary" Yang, Pacific Northwest National Laboratory; Jeffrey Fergus, Auburn University

8:30 AM Invited

**Advanced Novel Interconnect Coatings for Hermetic Sealing and Mitigation of Cr Volatility in Planar SOFC Stacks:** Jung Pyung Choi<sup>1</sup>; Scott Weil<sup>1</sup>; Matt Chou<sup>1</sup>; Jeff Stevenson<sup>1</sup>; Gary Yang<sup>1</sup>; Gordon Xia<sup>1</sup>; <sup>1</sup>Pacific Northwest National Laboratory

Low-cost, chromia-forming ferritic stainless steels have found widespread use in SOFCs, because of their low thermal expansion mismatch in high operating temperature. However, the volatile Cr-containing species, which originate from its oxide scale, can poison the cathode material in the cells and subsequently cause power degradation in the device. To prevent this, a conductive MnCo spinel coating has been developed. However this coating is not compatible with formation of hermetic seals between the interconnect frame component and the

ceramic cell. Thus, a new aluminizing process has been developed to enable durable sealing, prevent Cr evaporation, and maintain electrical insulation between stack repeat units. This paper will present recent progress regarding these novel coatings and discuss some of the compatibility issues that arise when integrating both coatings into the same component.

9:10 AM Invited

**Coating of Dense Oxide Layer on the Fe-Cr Alloys for Interconnects of Solid Oxide Fuel Cells:** Teruhisa Horita<sup>1</sup>; Haruo Kishimoto<sup>1</sup>; Katsuhiko Yamaji<sup>1</sup>; Manuel Brito<sup>1</sup>; Harumi Yokokawa<sup>1</sup>; <sup>1</sup>AIST

Metallic interconnects are considered as interconnects of Solid Oxide Fuel Cells (SOFCs) operated at medium temperatures. The control of oxide scale growth is one of the critical issues for applying the Fe-Cr alloys. A coating of oxides is one candidate and several kinds of coatings have been examined by many authors. The present study adopted pulse laser deposition (PLD) method to deposit a dense (La,Sr)(Co,Fe)O<sub>3</sub> (LSCF) on the Fe-Cr alloys. The oxide scale was formed between LSCF and Fe-Cr alloy. The microstructures, growth rates of oxide scale, and electrical conductivity of growth rate were discussed.

9:50 AM

**Characterization of Mn-Co Electrodeposition for SOFC Interconnect Applications by QCM:** Junwei Wu<sup>1</sup>; Ayyakkannu Manivannan<sup>2</sup>; Randall Gemmen<sup>2</sup>; Xingbo Liu<sup>1</sup>; <sup>1</sup>West Virginia University; <sup>2</sup>National Energy Technology Laboratory

(Mn,Co)<sub>3</sub>O<sub>4</sub> spinel is one of the promising coating for solid oxide fuel cell (SOFC) interconnect application. Electroplating of alloys followed by oxidation offers a cost effective method to produce the desired spinel, and previous long term ASR and interconnect on-cell test which has been proved to be effective for interconnect application. The biggest barrier to Mn/Co co-deposition is the dramatic difference of deposition potentials of Mn (-1.18V) and Co (-0.28V), which makes it quite difficult to co-deposit two metals in thermodynamics aspect. In this work, fundamental aspects of Mn/Co co-deposition will be studied by quartz crystal microbalance (QCM). For comparison, pure Mn, Co depositions are studied as well. For all the depositions, mass gain follows the trend: Co > Mn-Co > Mn. Furthermore, SEM/EDX analysis shows Mn content increases with the applied voltage due to increased contribution to Mn deposition.

10:10 AM Break

10:20 AM Invited

**Interactions between (Mn,Co)<sub>3</sub>O<sub>4</sub> SOFC Interconnect Coating Materials and Chromia:** Jeffrey Fergus<sup>1</sup>; Kangli Wang<sup>1</sup>; Yingjia Liu<sup>1</sup>; <sup>1</sup>Auburn University

Manganese cobalt oxides are promising coating materials for reducing chromium volatilization, and thus the associated cathode poisoning, from interconnect alloys in solid oxide fuel cells (SOFCs). Interaction between this coating and the oxide scale formed on the alloy during fuel cell operation can lead to changes in the coating composition and thus its performance. In this paper, the reaction between manganese cobalt spinel oxides and chromia is described. The reaction product consists of two layers. The layer in contact with chromia has two chromium ions per formula unit, i.e. (Mn,Co)Cr<sub>2</sub>O<sub>4</sub>, and grows by the diffusion of cobalt and manganese from (Mn,Co)<sub>3</sub>O<sub>4</sub>. In addition, chromium dissolves into (Mn,Co)<sub>3</sub>O<sub>4</sub>, which results in a second reaction layer. Both layers form the spinel structure, but there is a distinct difference between the growth mechanisms. When exposed to lower chromia activities, the (Mn,Co)Cr<sub>2</sub>O<sub>4</sub> layer does not form even after long exposure times.

11:00 AM

**Recent Progress in Cathode/Interconnect Contact Materials R&D for SOFCs at PNNL:** Gordon Xia<sup>1</sup>; Zigui Lu<sup>1</sup>; Josh Templeton<sup>1</sup>; Gary Yang<sup>1</sup>; Jeffrey Stevenson<sup>1</sup>; <sup>1</sup>Pacific Northwest National Laboratory

Contact materials for solid oxide fuel cell (SOFC) stacks are necessary for minimizing electrical contact resistances at the interfaces between interconnects and electrodes. In general, the contact materials should be electrically conductive, chemically and thermally stable, and capable to form robust bonds with adjacent SOFC components. At PNNL, we have been carrying out R&D on contact materials for a number of years. Our goal is to develop materials and methods for fabricating cost-effective and high performance contact layers between cathodes and interconnects during SOFC stacks assembling and operation. This paper will present the recent progress in our research and development on cathode/interconnect contact materials.



### 11:20 AM

**The Evolution of Oxide Ridges during Scaling of Fe-22wt%Cr Alloys:** *Jingxi Zhu*<sup>1</sup>; Laura Fernandez Diaz<sup>2</sup>; Gordon Holcomb<sup>2</sup>; Paul Jablonski<sup>2</sup>; Christopher Cowen<sup>2</sup>; David Laughlin<sup>1</sup>; Dave Alman<sup>2</sup>; Sridhar Seetharaman<sup>2</sup>; <sup>1</sup>Carnegie Mellon University; <sup>2</sup>National Energy Technology Laboratory

Oxide ridges were observed to form during the transient stage of the scale evolution in iron alloys containing 22 wt.% Cr at 800°C in dry air. The effect of La (120 and 290 ppm) and Ce (270 and 610 ppm) added during melt-stage processing were investigated. The surface oxidation process was imaged in-situ through a Confocal Scanning Laser Microscope (CSLM) and the results were correlated with post-experiment characterization through FEG-SEM and FIB-SEM combined with 3D reconstruction. It was found that the oxide ridges formed on top of the Cr-oxide scale and overlapped the intersections of the underlying alloy-grain boundaries with the Cr-oxide scale. Ridges were not observed on grain boundaries with misorientation angles less than 10° and consequently it is suggested that the boundaries of the top grains in the alloy serve as bottle necks for transport of Mn.

### 11:40 AM

**The Possibility for IT SOFC Interconnector Material Used to Stainless Steel:** Kee-Do Woo<sup>1</sup>; MinSeok Moon<sup>1</sup>; Eui-pyo Kwon<sup>1</sup>; Myeong-han Yoo<sup>1</sup>; Sang-hyuk Kim<sup>1</sup>; Duck-soo Kang<sup>1</sup>; <sup>1</sup>Chonbuk National University

IT SOFC(intermediate temperature solid oxide fuel cell) has low operating temperature than conventional SOFC system. In this study, the possibility of application of stainless steel as IT-SOFC materials was studied. An oxidation resistance layer on each differently surface treated specimen was investigated by using XRD, and FE-SEM. EDX result of STS430 showed that oxidation thickness of as polished, as received and sand blast samples were about 7.8µm, 12.8µm and 8.8µm, respectively. With increasing the exposed time from 100hr to 400hr, the oxide thickness of as polished, as received and sand blast samples increased to about 41.7µm, 17.7µm and 10.3µm, respectively. As a result, sand blast sample had very stabilized oxide film.

## Modeling of Multi-Scale Phenomena for Batteries: Session I

*Sponsored by:* The Minerals, Metals and Materials Society, TMS Extraction and Processing Division, TMS Materials Processing and Manufacturing Division, TMS/ASM: Computational Materials Science and Engineering Committee

*Program Organizers:* Adrian Sabau, Oak Ridge National Laboratory; Perla Balbuena, Texas A&M University, Artie McFerrin Department of Chemical Engineering; Venkat Subramanian, Tennessee Tech University, Department of Chemical Engineering

Wednesday AM Room: 604  
February 17, 2010 Location: Washington State Convention Center

*Session Chairs:* Adrian Sabau, Oak Ridge National Laboratory; Venkat Subramanian, Washington University

### 8:30 AM Introductory Comments

### 8:35 AM

**Predicting of Surface Morphology Defects in Electrochemical Storage Devices:** *Adrian Sabau*<sup>1</sup>; Nancy Dudney<sup>1</sup>; <sup>1</sup>Oak Ridge National Laboratory

The demand for higher energy and power density batteries has created the need to understand the stability of interfaces and dynamic processes under realistic conditions. In the battery systems, there are regions with sharp composition gradients and reaction interfaces that are paramount to the understanding of the transport phenomena in electrode microstructures. Dendrite formation is a primary failure mechanism in lithium/polymer batteries. Most of the studies on dendrite initiation were based on experimental observations as a function of current, time, and surface features. Recently, it was found that solid electrolyte interphase (SEI) has an important role in dendrite initiation. Computer models could be one efficient tool to explore and understand the life-limiting phenomena in multi-component battery systems, which include SEI role on dendrite initiation. One of the main challenges is to develop new moving boundary models (MBM) for these nano-scale phenomena in order to bridge the multiple length-scale models for traditional MBM and novel interfacial models.

### 9:05 AM

**Continuum and Multi-scale Modeling of Performance Curves and Capacity Fade in Lithium-Ion Batteries:** Ravi Methekar<sup>1</sup>; Venkatsailanathan Ramadesign<sup>1</sup>; Venkat Subramanian<sup>1</sup>; Kejia Chen<sup>2</sup>; Richard Braatz<sup>2</sup>; <sup>1</sup>Tennessee Tech University, Department of Chemical Engineering; <sup>2</sup>University of Illinois at Urbana-Champaign

Mathematical models reported in the literature for capacity fade do not include all postulated mechanisms. Such a mathematical model, although highly desirable, has not been forthcoming due to (1) incomplete understanding of all of the capacity fade mechanisms, (2) lack of knowledge for the values of the model parameters in these mechanisms, (3) difficulties in obtaining these values due to cumulative non-separable effects of individual mechanisms occurring simultaneously, and (4) lack of efficient numerical solvers. A mathematical model reformulation for improving the computational efficiency of continuum models for lithium-ion batteries will be presented. The use of these efficient algorithms to model capacity fade and to identify optimal operational strategies and materials design will be presented. In addition, the development and implementation of a Kinetic Monte Carlo (KMC) and coupled KMC-continuum multi-scale model to quantify the effect of surface-reaction mechanisms and heterogeneity at the solid-electrolyte interface will be presented.

### 9:35 AM

**Diffusion and Phase Transformations in Lithium Ion Battery Anodes from First Principles:** *Jishnu Bhattacharya*<sup>1</sup>; Anton Van der Ven<sup>1</sup>; <sup>1</sup>University of Michigan

Lithium ion battery electrodes consist of intercalation compounds that accommodate Li ions in interstitial sites. Charge-discharge rates and reversibility depend sensitively on diffusion and the kinetics of first-order phase transformations. Here, we study Li diffusion and phase transformation mechanisms in titanates, a class of transition metal oxides that are increasingly considered as promising candidate anodes for high rate batteries. Li-diffusion occurs primarily in the non-dilute regime. Therefore, interactions among Li ions are important in determining diffusion mechanisms and rates. To predict the composition dependence of the Li diffusion coefficients from first-principles, we evaluate Kubo-Green expressions using the cluster expansion technique in kinetic Monte Carlo simulations. We find that diffusion coefficients depend sensitively on Li composition and titanate crystal structure. These calculated diffusion coefficients can then be used in continuum simulations of electrode dynamics. Migration of interfaces during first-order phase transformations will also be discussed.

### 10:05 AM Invited

**The Solid-Electrolyte-Interface Processes in Lithium-Ion Battery by Atomistic Simulations:** *Ken Tasaki*<sup>1</sup>; <sup>1</sup>Mitsubishi Chemical USA

The solid-electrolyte-interface (SEI) processes in lithium-ion battery cells critically affect the battery performance such as the cycle life, the cell life, and the safety; yet, little is understood on the SEI film characteristics, the film formation mechanism and others. In this report, we focus on the SEI processes on the anode electrode side, trying to shed light into their complex nature through atomistic simulations. The SEI film is a heterogeneous system consisting of organic as well as inorganic salts in both amorphous and crystalline phases. This makes atomistic simulations challenging. We show experimental observations for a wide range of salts can be reproduced, at least qualitatively, through relatively simple manipulation of force field parameters based on DFT calculations. The subjects we discuss in our report will include the solubility of SEI film components in organic solvent and the thermodynamics on the Li insertion to graphite.

### 10:50 AM Concluding Comments

# Technical Program

## Modeling, Simulation, and Theory of Nanomechanical Materials Behavior: Physics of Defects, Dislocation Nucleation and Fracture I

Sponsored by: The Minerals, Metals and Materials Society, TMS Materials Processing and Manufacturing Division, TMS/ASM: Computational Materials Science and Engineering Committee, TMS: Nanomechanical Materials Behavior Committee

Program Organizers: Thomas Buchheit, Sandia National Laboratories; Sergey Medyanik, Washington State Univ.; Douglas Spearot, University of Arkansas; Lawrence Friedman, Penn State University; Edmund Webb, Sandia National Laboratories

Wednesday AM Room: 304  
February 17, 2010 Location: Washington State Convention Center

Session Chairs: Sulin Zhang, The Pennsylvania State University; Sergey Medyanik, Washington State University

### 8:30 AM Invited

**Nanoscale Modeling of Fracture:** *W. Curtin*<sup>1</sup>; S. Chakravarthy<sup>1</sup>; <sup>1</sup>Brown University

We apply the plane-strain-dislocation-dynamics (DD)/cohesive-zone (CZ) model to investigate the fracture of high-strength metal alloys bonded to elastic substrates, with application to thermal barrier coatings. In these systems the plastic zone size is on the order of 50nm and the atomistic cohesive zone lengths are sub-nanometer, so that the discreteness of the dislocations may be essential to capturing the toughening mechanisms. We use a new set of methodological tools that overcome computational and conceptual issues associated with prior DD implementations. We then predict the toughness as a function of the internal metal structure (obstacle strengths and spacings) at a fixed macroscopic yield stress, and as a function of the nanoscale cohesive zone parameters. The role of crack-tip dislocation nucleation is also explored. Comparisons of our results to predictions from strain-gradient plasticity are made, with the goal of identifying material features that establish the gradient length scale in this problem.

### 9:00 AM

**Understanding Scaling Relations in Fracture and Mechanical Deformation of Single Crystal and Polycrystalline Silicon by Performing Atomistic Simulations at Mesoscale:** *Hansung Kim*<sup>1</sup>; *Vikas Tomar*<sup>1</sup>; <sup>1</sup>University of Notre Dame

In past, several methods have been developed to overcome the limitation of time scale in atomistic simulations such as molecular dynamics (MD) time acceleration methods, Voter et al. 2002, and Hybrid Monte Carlo method (HMC), Mehlig et al. 1992 and Tomar 2007. However, till now it has not been possible to atomistically investigate meso and micro-scale phenomenon using MD simulations at continuum time scale. In this talk, a new atomistic method is developed to increase time step and size of MD simulations and used to investigate mechanical deformation and dynamic fracture in single crystal and polycrystalline silicon. In this method, dynamic equivalent crystal lattices are generated to represent a classical analogue of the statistical mechanical description of the underlying material. By using the method, we found that the length scale can increase up to 200 times and time scale up to 500 times.

### 9:20 AM

**Effects of Geometry, Mode Mixity, and Temperature on Dislocation Nucleation in Strained Electronics:** *Tianlei Li*<sup>1</sup>; *Jinhaeng Lee*<sup>1</sup>; *Yanfei Gao*<sup>1</sup>; <sup>1</sup>University of Tennessee

Dislocation loops may be nucleated from sharp geometric features in strained micro- and nano-electronic devices. This process is investigated by a dissipative cohesive interface model which treats the dislocation core as a continuous, inhomogeneous lattice slip field. As a representative example, we calculate the critical stress for dislocation nucleation from the edges/corners of a rectangular Si<sub>3</sub>N<sub>4</sub> pad on a Si substrate as a function of geometric parameters such as the length-to-height ratio and the three-dimensional shape of the pad. The shapes of the dislocations are also simulated. An important observation arises from the mode mixity of the singular stress fields near the edge. The relationship between the critical stress intensity factor and the mode mixity can be determined from this explicit model of dislocation nucleation process zone. The dependence of

both critical load and activation energy on modulus mismatch as characterized by Dundurs parameters will be presented.

### 9:40 AM

**Analysis of Generalized Stacking Fault Energy for FCC Fe-Mn Alloys Using Molecular Dynamics Simulation:** *Minho Jo*<sup>1</sup>; *Y. M. Koo*<sup>1</sup>; *S. K. Kwon*<sup>1</sup>; <sup>1</sup>Graduate Institute of Ferrous Technology, Pohang University of Science and Technology

Atomistic calculations for the <112>-generalized stacking fault (GSF) energy curve are performed for various fcc Fe-Mn alloys making use of molecular-dynamics simulations. A modified embedded atom method potential is used to model atomic interactions. The <112>-GSF energy curves are analyzed into stacking fault energy (SFE), unstable stacking fault energy (USFE), twinning fault energy (TFE), and unstable twinning fault energy (UTFE). With the energy terms, we tried to explain various deformation behavior of Fe-Mn system. It is suggested that the difference of USFE and UTFE barriers determines the next procedure after occurring one stacking fault, e.g., twin broadening or additional stacking fault. If USFE is lower than UTFE, additional stacking fault will be induced at different plane regardless of SFE. Otherwise, twin boundary propagates enlarging twin region.

### 10:00 AM Break

### 10:20 AM Invited

**Size Effect on the Fracture Behaviors of Si Nanowires in Tension:** *Wei Cai*<sup>1</sup>; *Keonwook Kang*<sup>1</sup>; <sup>1</sup>Stanford University

We performed Molecular Dynamics (MD) simulations of [1 1 0]-oriented Si nanowires (NWs) described by the modified embedded-atom-method (MEAM) potential under uniaxial tensile loading at a constant strain rate until failure. We found that the brittle or ductile fracture behavior of the NWs depends not only on the temperature but also on the NW diameter. Thick NWs break by crack nucleation and growth on the (110) plane at low temperature (a "brittle" mechanism) and by dislocation-mediated slip on {111} planes at high temperature (a "ductile" mechanism). Surprisingly, NWs with diameter less than 4 nm break by the "brittle" mechanism regardless of the temperature. The observed size and temperature dependence of fracture behavior is explained in terms of the competition between crack and dislocation nucleation from the NW surface.

### 10:50 AM

**Lattice Misorientation Patterns and Strain Gradient Effects in Single Crystals under Spherical Indentation:** *Yanfei Gao*<sup>1</sup>; *B. Larson*<sup>2</sup>; *G. Pharr*<sup>1</sup>; <sup>1</sup>University of Tennessee; <sup>2</sup>Oak Ridge National Laboratory

The ability to quantitatively predict dislocation microstructure and its evolution on mesoscopic length scales is a critical step towards developing a mechanistic understanding of small scale crystal plasticity. The three-dimensional measurements of lattice rotation and elastic strain fields with sub-micron resolution by a x-ray structural microscopy can be used to compute the lattice curvature and the dislocation density tensor. The modeling effort adopts a strain-gradient crystal plasticity theory in which the extra hardening to the slip strength arises from the geometrically necessary dislocations. Experimental/modeling comparisons suggest that when the ratio a/R (with contact radius a and indenter radius R) is less than about 0.2, the lattice rotation pattern is determined primarily by the crystallographic orientations, slip systems, and indenter shape, but is insensitive to the gradient effects. The magnitude of lattice misorientation angle can be estimated from the ratio a/R for spherical indenters or the pyramidal indenter angle.

### 11:10 AM Invited

**Nanoscale Fracture in Graphene:** *Sulin Zhang*<sup>1</sup>; <sup>1</sup>The Pennsylvania State University

The nanoscale fracture of a monolayer graphene is governed by the competition between bond breaking and bond rotation at a crack tip. We were able to precisely control the cracking pathways in atomistic simulations of graphene fracture. This was achieved by utilizing the lattice trapping effect which arises intrinsically due to the discrete nature of crystal lattice. We identified a novel fracture mechanism, involving the fracture paths of alternating bond rotation and rupture. The results demonstrate that mechanical cracking can create strain-engineered fracture edges with atomic-scale morphologies, providing a structural basis of tailoring the electronic properties of graphene either intrinsically or by further functionalizing the edges.



### Neutron and X-Ray Studies of Advanced Materials III: Strain and Dislocation Gradients from Microdiffraction II

*Sponsored by:* The Minerals, Metals and Materials Society, ASM International, TMS Structural Materials Division, TMS/ASM: Mechanical Behavior of Materials Committee, TMS: Titanium Committee  
*Program Organizers:* Rozaliya Barabash, Oak Ridge National Laboratory; Jaimie Tiley, Air Force Research Laboratory; Erica Lilleodden, GKSS Research Center; Peter Liaw, University of Tennessee; Yandong Wang, Northeastern University

Wednesday AM Room: 303  
February 17, 2010 Location: Washington State Convention Center

*Session Chairs:* Dean Haeflner, Argonne National Laboratory; Klaus-Dieter Liss, Australian Nuclear Science and Technology Organisation

#### 8:30 AM Keynote

##### Strain and Dislocation Density in Barium Titanate by Synchrotron and Laboratory X-Ray Diffraction: *Davor Balzar*<sup>1</sup>; <sup>1</sup>University of Denver

Ferroelectrics are attracting much attention because of their growing use by electronics industry. Diffraction provides means of determining both strains (stresses) and defects. We studied microstructural changes upon poling of polycrystalline BaTiO<sub>3</sub> using high-resolution synchrotron x-ray diffraction. We report evidence for a significant increase of defects density with an associated strain-energy increase. This implies that the application of an external poling field generates defects in the structure and increases the internal stress. Possible consequences in both bulk and thin-film applications include accelerated aging and microcracking.

#### 9:00 AM Invited

##### Using X-Ray Microbeams to Measure Complete Strain Tensors from Dislocation Cell Structures in Deformed Cu: *Michael Kassner*<sup>1</sup>; Peter Geantil<sup>1</sup>; Lyle Levine<sup>2</sup>; Bennett Larson<sup>3</sup>; Jon Tischler<sup>3</sup>; <sup>1</sup>University of Southern California; <sup>2</sup>National Institute of Standards and Technology; <sup>3</sup>Oak Ridge National Laboratory

Previous studies by our group produced the first quantitative, spatially resolved measurements of elastic strains from individual dislocation cell walls and cell interiors in heavily deformed metals. The measurements demonstrated that these dislocation structures were under significant, widely varying internal stresses of opposite sign. However, these investigations only measured elastic strains in the axial (deformation) direction. We have now initiated measurements of diffraction line profiles for multiple independent reflections from spatially resolved, submicrometer sample volumes, which make it possible to extract all six elements of the strain tensors from spatially resolved dislocation cell interiors. The experimental and data analysis techniques for these measurements will be described, along with preliminary results. These measurements will provide critical data for validating and guiding the development of detailed dislocation-based simulations and models for dislocation structure evolution.

#### 9:20 AM

##### Microstructure, Mechanical Behavior and Deformation Mechanisms of Nanocrystalline Ni-50wt%Fe: *Steven Van Petegem*<sup>1</sup>; Julien Zimmermann<sup>1</sup>; Stefan Brandstetter<sup>2</sup>; Xavier Sauvage<sup>3</sup>; Marc Legros<sup>2</sup>; Bernd Schmitt<sup>1</sup>; Helena Van Swygenhoven<sup>1</sup>; <sup>1</sup>Paul Scherrer Institut; <sup>2</sup>CEMES-CNRS; <sup>3</sup>University of Rouen

In order to understand the elastic and plastic deformation properties of nanocrystalline metals we have developed an in situ synchrotron x-ray diffraction technique which allows the simultaneous measurement of many diffraction peaks continuously during mechanical testing, providing a direct link between the evolving microstructure and the macroscopic mechanical data. Here we present recent results obtained for electrodeposited Ni-Fe with a nominal iron content of 50%. The microstructure of this alloy is characterized by a narrow grain size distribution with a mean value of 10nm. Uni-axial mechanical tensile tests indicate that Ni-Fe exhibits a transient regime during reloading or after transient testing. This regime is characterized by an upper or lower yield point. Such a yield point is not observed during continuous loading. Furthermore the strain rate sensitivity is relatively low. In-situ x-ray

diffraction experiments reveal a strong relaxation effect during initial loading in the microplastic regime.

#### 9:35 AM Invited

##### X-Ray Diffraction Microscopy Studies of Microstructure Responses: Christopher Hefferan<sup>1</sup>; Shui Fai Li<sup>1</sup>; Ulrich Lienert<sup>2</sup>; Anthony Rollett<sup>1</sup>; Greg Rohrer<sup>1</sup>; *Robert Suter*<sup>1</sup>; <sup>1</sup>Carnegie Mellon University; <sup>2</sup>Argonne National Laboratory

We present progress and future trends in synchrotron high energy x-ray diffraction microscopy studies of microstructure evolution. Differential thermal annealing in high purity aluminum has been observed and compared to predictions of curvature driven grain growth, both on the coarse grained level of the MacPherson-Srolovitz equation and on the level of individual boundary motions. Future work will include the combination of microstructure mapping with 1) tomography to detect and correlate void formation with microstructural features upon strain application and 2) strain tensor measurements to generate maps of ensembles of grains including geometry, neighborhood, and stress states. These measurements will allow validation of polycrystal plasticity models of materials response. Large volumetric data sets can be used as starting states in computations and computed responses compared to experimental observations. The capabilities described are applicable to a wide variety of materials; derived understanding should lead to improved materials design and prediction of properties.

#### 9:55 AM

##### Thermo-Mechanical Processing in a Synchrotron Beam: *Klaus-Dieter Liss*<sup>1</sup>; <sup>1</sup>Australian Nuclear Science and Technology Organisation

Well collimated, high energy X-rays of 90 keV from synchrotron sources have been used to study metals undergoing plastic deformation in-situ, in real time and in the bulk of the materials. The spottiness of poorly illuminated Debye-Scherrer rings showing reflections from individual crystallites is analyzed to obtain grain statistics, mosaic spread and orientation. Upon cold deformation, coarse grained materials show fingerprints of sub-grain formation, grain rotation, grain refinement and the evolution from a single grain into the asymptotic texture. Heating of metals under continuous load drives the observation through the regimes of phase transformation and grain relationships therein, grain coarsening, dynamic recovery and dynamic recrystallization. The paper points out these different phenomena which were observed without precedence.

#### 10:10 AM Invited

##### Correlation of X-Ray Diffraction Examination of Recovery in Cold-Rolled Aluminum with Dynamic Dislocation-Defect Analysis: *Shig Saimoto*<sup>1</sup>; Joyce Cooley<sup>1</sup>; <sup>1</sup>Queen's University

X-ray line-profile analysis tends to become one of model-in and model-out, even for pure metals. One way to delineate contributing effects is to correlate the changes with other complimentary methods during recovery. The role of point defects and their recovery has resulted in a suggestion that examination of the diffuse background scattering can reveal their presence. This methodology was pursued at recovery temperatures below 200 °C where point defects, small loops and stacking fault tetrahedra's are reported to anneal out. Furthermore the applicability of using the typical 2-theta diffraction scanning with K-alpha one and two to qualitatively reveal the recovery process was examined in comparison with the use of a four-bounce monochromator. The results indicate that recovery of the background scattering is related to the presence of geometrically necessary boundaries rather than point defects or loops. This observation suggests copious presence of stacking faults within these boundaries.

#### 10:30 AM Break

#### 10:40 AM Invited

##### FSP-Induced Plastic Deformation and Elastic Strains in Individual Dendrites of the Ni-Based Superalloy from X-Ray Microdiffraction: *Oleg Barabash*<sup>1</sup>; Rozaliya Barabash<sup>1</sup>; Gene Ice<sup>1</sup>; Zhili Feng<sup>1</sup>; <sup>1</sup>Oak Ridge National Laboratory

Spatially-resolved X-ray micro-Laue diffraction and SEM were used to study FSP-induced local structural transformations in the individual dendrites of the Ni-based superalloy near the boundary between the TMAZ and the SZ. Material behavior is distinct in the TMAZ and the SZ. Plastic deformation of individual dendrites with the formation of shear bands takes place in the TMAZ. Bending of the dendrites in the {111} plane and rotation towards <011> pole is observed. Due to dislocations movement and interactions at the FSP-induced

# Technical Program

high temperatures, they rearrange with the formation of small-angle boundaries. Elastic strain and GNDs density tensors within the individual dendrites are determined from the analysis of micro-Laue diffraction. Severe plastic deformation and recrystallization takes place in the SZ. Dendrite structure is completely destroyed in the SZ in contrast to the TMAZ. The formation of the so called "onion rings" structure with the bimodal grain size distribution is found.

## 11:00 AM Invited

**Synchrotron Microdiffraction Analysis of the Microstructure of Cryogenically Treated High Performance Tool Steels Prior to and after Tempering:** *Ning Xu*<sup>1</sup>; *Andrea Gerson*<sup>1</sup>; *Giuseppe Cavallaro*<sup>1</sup>; <sup>1</sup>ACeSSS (Applied Centre for Structural and Synchrotron Studies)

The phase transformation and strain changes within cryogenically (-196°C) treated high performance tool steels (AISI H13) before and after tempering have been examined using both laboratory XRD and synchrotron microdiffraction. The martensitic unit cell was found to have very low tetragonality as expected for low carbon steel. Tempering resulted in the diffusion of excess carbon out of the martensite phase and consequent unit cell shrinkage. On tempering the martensite became more homogeneous for cryogenically treated samples as compared to those had not been tempered. The effect was most pronounced for the rapidly cooled sample which was the least homogenous sample prior to tempering but was the most homogenous sample after tempering. This suggests that considerable degree of disorder due to rapid cryogenic cooling results in the beneficial release of micro-stresses on tempering thus possibly resulting in the improved wear resistance and durability observed for cryogenically treated tool steels.

## 11:20 AM Invited

**Materials Studies Using High-Resolution Laue X-Ray Microdiffraction:** *John Budai*<sup>1</sup>; *Wenjun Liu*<sup>2</sup>; *Jon Tischler*<sup>1</sup>; <sup>1</sup>Oak Ridge National Laboratory; <sup>2</sup>Argonne National Lab

Synchrotron microdiffraction facilities such as the scanning, polychromatic microscope at the Advanced Photon Source (beamline 34ID-E) provide unique opportunities for structural studies of a wide range of advanced materials. At this focused microbeam facility, depth-resolved Laue diffraction patterns are analyzed with automated software, to produce 3-D maps of the local crystal structure, lattice orientation and strain tensor. This talk will illustrate how new spatially-resolved information can be obtained from materials systems ranging from 1-D nanostructures to bulk 3-D polycrystals. For example, studies of luminescent 1-D nanowires have revealed new crystal structures and provided local information such as the preferred growth axes. In 3-D materials, structural investigations have included nondestructive studies of thermal grain growth in polycrystalline aluminum, lattice parameter changes in ferroelectrics and local phase separation in complex manganite crystals. Support at ORNL, UT-Battelle by DOE-BES, Materials Sciences and Engineering Division; UNI-XOR support at APS by DOE-BES.

## 11:40 AM

**Wear Properties of Single Phase Ti Alloys and Surface Damage Characterization by X-Ray Diffraction:** *Eri Miura-Fujiwara*<sup>1</sup>; *Hisashi Sato*<sup>1</sup>; *Gene Ice*<sup>2</sup>; *Yoshimi Watanabe*<sup>1</sup>; <sup>1</sup>Nagoya Institute of Technology; <sup>2</sup>Oak Ridge National Laboratory

Characteristic deformation behavior due to wear in single phase Ti alloys was investigated using a glancing angle powder diffraction method with X-ray microbeam. Wear test was performed by a ball-on-disc test in artificial saliva at 310 K. From the results of our previous study, alpha phase (hcp) peaks and beta phase (bcc) peaks changed in different ways when wear damage was introduced in Ti-6Al-7Nb, alpha + beta Ti alloy for biomedical applications. That is, alpha peaks showed peak broadening and orientation alignment, and beta peaks showed peak broadening and peak shift. Thus, the results infer that diffraction peaks of single phase could behave likewise. In this study, we investigated single alpha or beta phase Ti alloys. Similar peak broadening or peak shifts as alpha + beta Ti alloy were confirmed in commercial purity Ti and Ti-Al-Zr-Mo-Nb alloy after wear test.

## 11:55 AM Invited

**Polychromatic X-Ray Microdiffraction (PXM) Studies of Stress Corrosion Cracking (SCC) in Alloy 600:** *Marina Suominen Fuller*<sup>1</sup>; *Jing Chao*<sup>1</sup>; *N. Stewart McIntyre*<sup>1</sup>; *Sridhar Ramamurthy*<sup>1</sup>; *Leo Lau*<sup>1</sup>; *Roger Newman*<sup>2</sup>; *Anatolie Carcea*<sup>2</sup>; *Renfei Feng*<sup>3</sup>; <sup>1</sup>University of Western Ontario; <sup>2</sup>University of Toronto; <sup>3</sup>Canadian Light Source Inc.

Stress corrosion cracking (SCC) is known as an active degradation mechanism in steam generators used in both CANDU and PWR nuclear reactors. Alloy 600 has been used as the primary steam generator (SG) tubing material and is prone to SCC. To predict the onset of cracking under the SG operating conditions requires that the interplay of mechanical and chemical behaviours of these materials be thoroughly understood. The synchrotron-based Polychromatic X-ray Microdiffraction (PXM) method will be used to follow the strain distributions around cracks in stressed Alloy 600 C-rings exposed to (a) water vapour/hydrogen and (b) caustic environments. Some of the first PXM results from the new VESPERs beamline at the Canadian Light Source in Saskatoon, SK, Canada, will be shown.

## 12:15 PM

**Crystal Distortion Gradient in the Vicinity of a Grain-Boundary in Plastically Deformed Bicrystals:** *Gael Daveau*<sup>1</sup>; *Benoit Devincere*<sup>1</sup>; *Thierry Hoc*<sup>2</sup>; *Odile Robach*<sup>3</sup>; <sup>1</sup>LEM-CNRS/ONERA; <sup>2</sup>MSSMat-Centrale Paris; <sup>3</sup>NRS/CEA-Grenoble

A dislocation density based model [1] developed for fcc single crystal is extended for the simulation of strain hardening of polycrystal materials. Crystal rotation and elastic strain in a strained copper bicrystal were measured by X-ray microdiffraction. Existence of a strain gradient in the vicinity of the grain boundary at low plastic deformation is shown. Dislocation dynamics simulations are used to investigate the influence of dislocation density gradient on the diffraction pattern. From those calculations, a decrease of the dislocation mean free path is defined as a function of the boundary distances. A modified crystal plasticity constitutive law accounting for the influence of grain boundary is proposed. Finally, a comparison between the results of finite elements simulations and experiments is made.[1] Devincere, Hoc, Kubin, Science, 320 (2008) p 1745-1748.

## 12:25 PM

**Grain Rotation and Texture Evolution in Cubic Polycrystals Determined by Synchrotron X-Ray Diffraction:** *Kun Yan*<sup>1</sup>; *Klaus-Dieter Liss*<sup>1</sup>; *Rian Dippenaar*<sup>2</sup>; <sup>1</sup>The Bragg Institute; <sup>2</sup>University of Wollongong

By high energy synchrotron X ray diffraction, the evolution of microstructures during the compression of copper with different grain sizes were traced respectively. The grain refinement and mosaic spread of sub-grain were observed dynamically from the movie of 2D diffraction patterns as well as the diffraction profile broadening, the anisotropic grain orientations were obtained with numerical analysis. Complementary neutron diffraction was employed for the ex-situ texture measurement, which approve the effects of grain rotation on the formation of texture. Relation between lattice strain and grain refinement rate was analyzed with various loading condition. The results fulfill the understanding of the evolution of grain orientation and slip mechanism during compressive deformation.

## 12:35 PM

**2010 JIM International Scholar Award Winner: Development of Coherent X-Ray Diffraction Microscopy and Its Application in Materials Science:** *Yukio Takahashi*<sup>1</sup>; *Y. Nishino*<sup>2</sup>; *T. Ishikawa*<sup>2</sup>; *K. Yamauchi*<sup>1</sup>; *E. Matsubara*<sup>3</sup>; <sup>1</sup>Osaka University; <sup>2</sup>RIKEN SPring-8 Center; <sup>3</sup>Kyoto University

Coherent X-ray diffraction microscopy (CXDM) is a novel technique for reconstructing the electron density distribution of a sample, which has attracted much attention as a new tool for analyzing the nanostructures of metallic materials. CXDM has great potential as a technique for structural studies of metallic materials because it is a nondestructive method and is applicable to samples of micrometer thickness. Until now, we have applied CXDM to the mesoscopic structure analysis of a precipitation-hardened aluminum alloy and to the in-situ observation of electromigration voids in a Cu thin line. Recently, aiming towards the development of higher-resolution CXDM, we have developed a high-resolution CXDM using synchrotron X-rays focused by total reflection mirrors, and have achieved 3 nm resolution. We have successfully reconstructed the three-dimensional electron density distribution of a shape-controlled gold nanoparticle using the high-resolution diffraction microscope.



The present method is the key technology for realizing single-pulse diffractive imaging using X-ray free electron lasers.

### Nuclear Energy: Processes and Policies: Material Behavior

*Sponsored by:* The Minerals, Metals and Materials Society, TMS Structural Materials Division, TMS/ASM: Nuclear Materials Committee, TMS: Public and Governmental Affairs Committee

*Program Organizers:* Brajendra Mishra, Colorado School of Mines; Aladar Csontos, U.S. Nuclear Regulatory Commission; Stuart Maloy, Los Alamos National Laboratory; Jeremy Busby, Oak Ridge National Laboratory; Sue Lesica, U.S. Department of Energy's Office of Nuclear Energy

Wednesday AM Room: 201  
February 17, 2010 Location: Washington State Convention Center

*Session Chairs:* Stuart Maloy, Los Alamos National Laboratory; Jeremy Busby, Oak Ridge National Laboratory

#### 8:30 AM Keynote

**Future of Nuclear Energy Research and Development:** *Sue Lesica*<sup>1</sup>; <sup>1</sup>U.S. Department of Energy's Office of Nuclear Energy

Abstract not available.

#### 9:05 AM

**A Study of the Initial Effects of Irradiation on Nanocluster Stability on ODS Steel:** *Alicia Certain*<sup>1</sup>; Jim Bentley<sup>2</sup>; Michael Miller<sup>2</sup>; Jeremy Busby<sup>2</sup>; Robert Ulfig<sup>3</sup>; Todd Allen<sup>1</sup>; Kevin Field<sup>1</sup>; <sup>1</sup>University of Wisconsin-Madison; <sup>2</sup>Oak Ridge National Laboratory; <sup>3</sup>Imago Scientific Instruments

Oxide dispersion strengthened ferritic/martensitic steels, otherwise referred to as nano-featured alloys (NFAs), are considered for fission and fusion applications for their improved high-temperature properties and the assumed radiation resistance. This paper reports on work aimed at understanding the irradiation performance of NFAs and attempts to determine the current boundaries in studying the very small and complex nanoclusters of this material with advanced imaging and compositional techniques, and to apply these techniques to observe the initial evolution in composition and/or microstructure of the nanoclusters. NFAs were irradiated to low dose with protons in the temperature range of 400-700°C and doses ranging from 1 to 10 dpa. Samples were investigated by energy-filtered TEM, STEM/EDS, and atom probe tomography. The size range (~0.5 nm to 30 nm diameter) and the relative inhomogeneity of the nanocluster distribution make using complimentary analysis techniques essential to a complete understanding of the nanocluster evolution under irradiation.

#### 9:30 AM

**Fracture and Impact Properties of HT-9 Steel Irradiated to High Dose in FFTF:** *Thak Sang Byun*<sup>1</sup>; Stuart Maloy<sup>2</sup>; <sup>1</sup>Oak Ridge National Laboratory; <sup>2</sup>Los Alamos National Laboratory

Fracture and impact properties were investigated for the ACO-3 duct (made of HT-9) irradiated in the Fast Flux Test Facility (FFTF). Small Charpy impact specimens with the dimensions of 3×4×27mm and disk compact tension (DCT) fracture specimens with 12.7mm diameter and 3mm thickness were machined from various positions of the ACO-3 duct that had been irradiated in FFTF up to a total dose of 155 dpa and irradiation temperatures were in the range of 370-510°C. The impact tests were performed in a 25J capacity tester in the temperature range from -50 to 350°C, and the fracture toughness tests performed at room temperature, 250, and the irradiation temperature in a servo-hydraulic testing machine. The ductile-to-brittle transition temperature (DBTT) increased with dose, while the upper shelf energy decreased with dose and reached levels lower than 5J. These data will be summarized and compared to previous fast reactor test data.

#### 9:55 AM

**In-Plane Anisotropy in Microstructure and Mechanical Behavior of Alloy 617 Following High Temperature Aging:** *Kun Mo*<sup>1</sup>; Gianfranco Lovicu<sup>2</sup>; Hsiao-ming Tung<sup>1</sup>; Xiang Chen<sup>1</sup>; James Stubbins<sup>1</sup>; <sup>1</sup>University of Illinois; <sup>2</sup>University of Pisa

Alloy 617 is considered as a leading material used for next generation nuclear power plant, due to its good corrosion resistance and exceptional high-

temperature strength. In the present work, the effects of long-term aging (up to 3000 h) at 900°C and 1000°C on the microstructure and associated mechanical properties were investigated. Specimens from the rolling plane and transverse plane were selected to study the anisotropic effect, which was originally induced by intermetallic inclusions from the hot rolling processing. Microstructure characterization by transmission electron microscope (TEM) and scanning electron microscope (SEM) revealed the precipitation evolution processes for different aging conditions. Precipitate type, size, location and coherency were investigated. Hardness and tensile tests showed that the influence of the in-plane anisotropy was significant during the aging process, which may be attributed to diffusion-controlled coarsening of the precipitates.

#### 10:20 AM Break

#### 10:35 AM

**MaRIE; A Proposed Materials Facility at Los Alamos National Laboratory:** *Mark Bourke*<sup>1</sup>; <sup>1</sup>Los Alamos National Laboratory

Los Alamos National Laboratory is currently engaged in the definition of a facility called MaRIE (Matter-Radiation Interactions in Extremes). It is being conceived as a world class national user facility that will provide unique measurements of material performance under extreme radiation conditions and during dynamic shock events on, among others, materials of relevance to the fission and national security communities respectively. Current objectives include; in situ measurement of materials response in a fast reactor level neutron fluence (with complementary ex situ PIE capabilities), in situ measurements of strain with microstructural spatial resolution and nanosecond temporal resolution during explosive shock events and provision of state of the art synthesis and characterization tools. The concept anticipates the increasing role that control science is expected to play in materials research when compared to observation science. Experimental capabilities are being considered that will most usefully inform models enabled by recent advances in computational capability.

#### 11:00 AM

**Microstructural Evolution in Friction Stir Welded MA956 and 14YWT:** *Michael West*<sup>1</sup>; Bharat K. Jasthi<sup>1</sup>; William J. Arbegast<sup>1</sup>; David T. Hoelzer<sup>1</sup>; <sup>1</sup>South Dakota School of Mines and Technology

Friction stir welding presents a unique opportunity for joining oxide dispersion strengthened (ODS) alloys. This research presents results of friction stir welding the high temperature ODS alloys MA956 and the nanostructured ferritic alloy 14YWT. Studies focus on alternative thermal strategies such as induction preheating as a way of lowering process forces. The effect of process parameters on resulting particle dispersion and microstructure are discussed.

#### 11:25 AM

**The Behavior of Precipitate Strengthened Steels under Irradiation:** *Peter Hosemann*<sup>1</sup>; Erich Stergar<sup>2</sup>; Stuart Maloy<sup>1</sup>; Harald Leitner<sup>2</sup>; Andrew Nelson<sup>1</sup>; <sup>1</sup>LANL; <sup>2</sup>University of Leoben

Oxide dispersion strengthened alloys are known to be radiation tolerant and usable up to high temperature and dose. The key to creating materials with extraordinary radiation tolerance is to allow the created defects to annihilate on defect sinks such as nano precipitates. Here new heats of the alloy 14YWT were made and irradiated using a low energy proton beam. The post irradiation examination results are presented on those materials. Maraging steels are known to form intermetallic precipitates at a proper heat treatment. Here we exposed a Co free maraging steel (Corrax) (aged and not aged) to ion beam irradiation and performed PIE to investigate the effectiveness to reduce radiation damage in the material by these intermetallic particles. Post irradiation nanoindentation showed a hardness increase of the maraging steel to the same level as a 500C heat treatment would achieve.

#### 11:50 AM

**In Situ Synchrotron Study and Computer Modeling of Advanced Nuclear Structural Alloys:** *Meimei Li*<sup>1</sup>; Jonathan Almer<sup>1</sup>; Ken Natesan<sup>1</sup>; David Rink<sup>1</sup>; <sup>1</sup>ANL

Advanced materials are often multi-component alloy systems with many different phases. The development of such complex alloy systems has historically been a long process from initial trials to implementation due to lack of a fundamental understanding of the physical mechanisms controlling mechanical responses. This development process can be significantly shortened with advanced computer simulations tools coupled with advanced experimental techniques. In this paper, we will present recent findings on the applications of

# Technical Program

in situ synchrotron x-ray diffraction to the study of the temporal evolution of structure and phases during high temperature thermo-mechanical processing in advanced ferritic-martensitic steels. Computer modeling by Thermo-Calc was used to calculate phase equilibria and diffusion-controlled precipitation and coarsening kinetics. Experimental data of phase analysis are compared with modeling results to understand the microstructure development under thermo-mechanical conditions and its impact on the development of high-performance structural alloys for advanced nuclear energy applications.

## **Pb-Free Solders and Emerging Interconnect and Packaging Technologies: Alloy Development**

*Sponsored by:* The Minerals, Metals and Materials Society, TMS Electronic, Magnetic, and Photonic Materials Division, TMS: Electronic Packaging and Interconnection Materials Committee

*Program Organizers:* Kwang-Lung Lin, National Cheng Kung University; Sung Kang, IBM; Jenq-Gong Duh, National Tsing-Hua University; Laura Turbini, Research In Motion; Iver Anderson, Iowa State University; Fu Guo, Beijing University of Technology; Thomas Bieler, Michigan State University; Andre Lee, Michigan State University; Rajen Sidhu, Intel Corporation

Wednesday AM Room: 204  
February 17, 2010 Location: Washington State Convention Center

*Session Chairs:* Iver Anderson, Iowa State University; Jenn-Ming Song, National Dong Hwa University

### **8:30 AM Invited**

**Shock Resistant and Thermally Reliable Low Ag SAC Solders Doped with Mn or Ce:** *Ning-Cheng Lee*<sup>1</sup>; Weiping Liu<sup>1</sup>; Adriana Porras<sup>2</sup>; Min Ding<sup>2</sup>; Anthony Gallagher<sup>3</sup>; Austin Huang<sup>4</sup>; Scott Chen<sup>4</sup>; Jeffrey ChangBing Lee<sup>5</sup>; Indium Corporation; <sup>2</sup>Freescale Semiconductor; <sup>3</sup>Motorola Inc; <sup>4</sup>Advanced Semiconductor Engineering Group; <sup>5</sup>IST-Integrated Service Technology Inc

The reliabilities of low Ag SAC alloys doped with Mn or Ce were evaluated under JEDEC drop, dynamic bending, thermal cycling, and cyclic bending test conditions against eutectic SnPb, SAC105, and SAC305 alloys. The Mn or Ce doped low cost SAC105 alloys achieved a higher drop test and dynamic bending test reliability than SAC105 and SAC305, and exceeded SnPb for some test conditions. More significantly, being a slightly doped SAC105, both SACM and SACC matched SAC305 in thermal cycling performance. In other words, the low cost SACM and SACC achieved a better drop test performance than the low Ag SAC alloys plus the desired thermal cycling reliability of high Ag SAC alloys. The mechanism for high drop performance and high thermal cycling reliability can be attributed to a stabilized microstructure, with uniform distribution of fine IMC particles, presumably through the inclusion of Mn or Ce in the IMC.

### **8:55 AM**

**Effects of Co Addition upon Sn-8.8Zn/Cu and Sn-57Bi/Cu Interfacial Reactions:** *Yu-chih Huang*<sup>1</sup>; Sinn-wen Chen<sup>1</sup>; <sup>1</sup>National Tsing Hua University

Eutectic Sn-Zn and Sn-Bi alloys are promising Pb-free solders, and Cu is commonly used in electronic products. Interfacial reactions between Cu substrate and Sn-Zn and Sn-Bi solders are investigated at 230 and 160°C. Two different sizes of solders, 2mg and 2g, added with different amounts of Co (up to 0.5%) are examined. The reaction products in the couples prepared with the two kinds of solders are not changed with the addition of Co, and they are  $\gamma$ -Cu<sub>5</sub>Zn<sub>8</sub> and  $\eta$ -Cu<sub>6</sub>Sn<sub>5</sub> phases, respectively. With and without Co addition, the  $\gamma$ -Cu<sub>5</sub>Zn<sub>8</sub> phase in the Sn-Zn-(Co)/Cu couple is layer structure, and it is found that the growth rate of  $\gamma$ -Cu<sub>5</sub>Zn<sub>8</sub> phase decreases with higher Co addition and smaller sizes of joints. On the other hand, the morphology of  $\eta$ -Cu<sub>6</sub>Sn<sub>5</sub> phase becomes porous with the Co addition. The growth rate of  $\eta$ -Cu<sub>6</sub>Sn<sub>5</sub> increases with higher Co addition, but it decreases with smaller sizes of joints.

### **9:10 AM**

**High-Temperature Lead-Free Solder Alternatives: Possibilities and Properties:** *Vivek Chidambaram*<sup>1</sup>; John Hald<sup>1</sup>; Jesper Hattel<sup>1</sup>; <sup>1</sup>Technical University of Denmark

High-temperature solders have been widely used as joining materials to provide stable interconnections that resist a severe thermal environment and

also to facilitate the drive for miniaturization. High-lead containing solders have been commonly used as high-temperature solders. The development of high-temperature lead-free solders has become an important issue for both the electronics and automobile industries because of the health and environmental concerns associated with lead usage. Unfortunately, limited choices are available as high-temperature lead-free solders. This work outlines the criteria for the evaluation of a new high-temperature lead-free solder material. Furthermore, a list of potential high-temperature lead-free solder alternatives has been proposed. The high-temperature stability of microstructures and mechanical properties of these potential candidate alloys have been extensively reported. Focus has also been given to the property of corrosion resistance. This paper presents the superior characteristics as well as some drawbacks of the various high-temperature lead-free solder alternatives.

### **9:25 AM**

**Improvement of Wettability and Thermal Properties at Bi Based Alloys:** *Minoru Ueshima*<sup>1</sup>; <sup>1</sup>Senju Metal Industry

There is Bi based alloy as candidate to replace Pb-rich alloy because of the high melting point, but Bi is hard to get wet with Copper electrode because it doesn't form any intermetallic compound with Copper. We try to improve the wetting properties of Bi on Cu by addition of small amount of Sn and In. Increase of Sn and In at Bi alloys make the wettability on Cu better, but however the solidus line of the alloys decrease to be 139 centigrade degree. It was found that the addition of Cu and Ag is effective to restrict decreasing the solidus line. In this study, the wetting properties of Bi-xSn and Bi-xIn alloys (x=0.5,1,3,6) on Cu electrode are researched and the soldering process to restrict the decrease of the solidus line at Bi-Sn-Cu alloy is proposed.

### **9:40 AM**

**Liquid Phase Sintered Solders as Thermal Interface Materials for Conventional and High Temperature Electronic Applications:** *Jia Liu*<sup>1</sup>; Paul Rottmann<sup>1</sup>; Shouvik Dutta<sup>1</sup>; Chelliah Nagaraj<sup>2</sup>; Praveen Kumar<sup>1</sup>; Mukul Renavikar<sup>3</sup>; Rishi Raj<sup>2</sup>; Indranath Dutta<sup>1</sup>; <sup>1</sup>Washington State University; <sup>2</sup>University of Colorado; <sup>3</sup>Intel Corp.

Liquid phase sintering (LPS) is utilized to design novel composite solder microstructures for next generation thermal interface material (TIM) applications for high power density devices. Cu-In composites are explored for microelectronic applications (up to 125°C), while Cu-Bi is studied for high temperature power electronics applications (above 270°C). The new LPS solders constitute a majority high melting phase (HMP) in a matrix of a minority low melting phase (LMP), and proffers high conductivity in conjunction with high mechanical compliance. The Cu-In system is susceptible to the formation of interfacial intermetallics, the effects of which on the evolution of sintered density and properties is discussed. The Cu-Bi system is less thermally conductive, but is highly mechanically compliant above the melting point of Bi, making it very attractive as a 'thermal grease' TIM. The mechanical and thermal properties of LPS solder systems with and without LMP melting will be discussed in detail.

### **9:55 AM**

**Development of Sn-Ag-Cu-X Alloys for Electronic Assembly:** *Adam Boesenberg*<sup>1</sup>; Iver Anderson<sup>2</sup>; Joel Harringa<sup>2</sup>; <sup>1</sup>Iowa State University; <sup>2</sup>Ames Laboratory of US DOE

The global electronic assembly community is striving for a robust replacement for Pb-containing solders due to increased environmental regulations. A family of Pb-free ternary solder alloys based on Sn-Ag-Cu (SAC) compositions has shown promise for implementation; but issues in reliability in certain assembly and operating environments have arisen. Elemental (X) additions (Co, Ni, Mn, Zn, Al, Fe) to SAC3595 were analyzed for better understanding of heterogeneous nucleation mechanisms for greater control in joint solidification. Solderability on Cu of down-selected SAC+X alloys (Mn, Zn, Al) was tested using micro-wetting global testing due to concern about increased oxidation during the reflow process. Minimization of the X concentration was investigated in simplified Cu joints by differential scanning calorimetry and joint microstructure analysis to determine undercooling effects and solidification morphology on single and multiple reflow cycles. Supported by Iowa State University Research Foundation and Nihon-Superior, Inc., through Ames Lab contract No. DE-AC02-07CH11358.



### 10:10 AM Break

### 10:25 AM

**On the Mechanism of Retarding Cu<sub>3</sub>Sn Growth by Ni Addition:** *Yi-Wun Wang*<sup>1</sup>; C. Robert Kao<sup>1</sup>; <sup>1</sup>National Taiwan University

The effect of Ni addition to solders reacting with Cu was investigated in order to understand the mechanism of retarding Cu<sub>3</sub>Sn growth. The liquid-solid reaction and solid-state annealing behavior of two high-lead solders, 90Pb10Sn-xNi and 95Pb5Sn-xNi (x=0~0.1 wt.%), was examined. The reflow temperature and time are 350°C and 2 min. The samples were then subjected to solid-state aging at 160°C for 500, 1000 and 2000 hrs. After reflow, Cu<sub>3</sub>Sn formed on the Cu substrate for both solders. However, solid-state annealing produced significantly different reaction products for the two solder compositions. In the case of 90Pb10Sn solder, the Cu<sub>3</sub>Sn and Cu<sub>6</sub>Sn<sub>5</sub> grow after 160°C aging. On the other hand, in the case of 95Pb5Sn solder, only Cu<sub>3</sub>Sn continued to grow after 160°C aging. The experimental results show that the Ni addition to high-lead solder doesn't retard Cu<sub>3</sub>Sn growth. Ni retards the growth of Cu<sub>3</sub>Sn through Cu<sub>6</sub>Sn<sub>5</sub>.

### 10:40 AM

**On the Merits of Transient Liquid Phase Bonding as a Substitute for Soldering with High-Pb Alloys:** *Alexandre Kodentsov*<sup>1</sup>; <sup>1</sup>Eindhoven University of Technology

There is still no obvious replacement for high-lead solder alloys that are in the use today for electronics assembly operations. Experimental and theoretical studies conducted in the framework of the European COST Action MP0602 established two practical routes in which further effort to find a suitable no-lead replacement should be directed. One is to design solders that contain no lead, like Zn-Al and/or Bi-Ag based (near-) eutectic alloys. The other option is to find substitute joining technologies for traditional soldering. It is possible to develop a cost-effective Transient Liquid Phase (TLP) joining process for the fabrication of high-temperature Pb-free interconnections. Through the judicious selection of Sn- or Bi-based interlayer between under bump metallization and substrate pad, transient liquid-phase bonding can be achieved at ~240 or ~270 C, and the resulting joints are capable of service at elevated temperatures.

### 10:55 AM

**Thermal, Mechanical Stability, and Wetting Behavior of Novel Cerium (Ce)-Containing Pb-Free Solders on Cu and Ni-Au Metallization:** *Huxiao Xie*<sup>1</sup>; Ling Jiang<sup>1</sup>; Mukul Renavikar<sup>2</sup>; Nik Chawla<sup>1</sup>; <sup>1</sup>Arizona State University, School of Mechanical, Aerospace, Chemical, and Materials Engineering; <sup>2</sup>Intel/ATTD

Traditional Pb-free solders such as Sn-Ag-Cu (SAC) show relatively low ductility and poor damage tolerance. Our research has shown that SAC-alloy doped with trace amounts of Ce exhibits a substantial improvement in ductility, with a relatively small decrease in strength. These alloys also have better oxidation resistance than other rare earth-containing solders such Lanthanum and Yttrium. In addition to the beneficial bulk and surface properties, it is imperative to understand the long-term thermal and mechanical stability as well as the interaction of Ce-containing SAC solders with most prevalent surface metallizations. As a consequence, microstructural characterization, as well as shear strength of SAC305 and SAC-Ce (0.5 wt. %) on Cu and electroless Ni-Au metallizations were studied in the as-processed and thermally aged conditions. The wetting behavior of SAC and SAC-Ce on Cu was evaluated by measuring the contact angle and spreading area ratio on underlying metallizations.

### 11:10 AM

**Polymers Investigation for 3D IC Stacking Technology:** Cheng-Ta Ko<sup>1</sup>; Wei-Chung Lo<sup>1</sup>; *Kuan-Neng Chen*<sup>2</sup>; Huan-Chun Fu<sup>1</sup>; Zhi-Cheng Hsiao<sup>1</sup>; Yu-Hua Chen<sup>1</sup>; <sup>1</sup>Industrial Technology Research Institute; <sup>2</sup>National Chiao Tung University

3D IC has been generally acknowledged as the next generation semiconductor technology with the advantages of small form factor, high performance, low power consumption, and high density integration etc. The stacked bonding is one of the core technologies to perform 3D interconnection. One emerging approach with high yield and reliability is hybrid bonding, which can achieve interconnection with adhesive serving reinforcement of the mechanical stability between stacked ICs. To develop the metal/adhesive hybrid bonding technology, several polymer materials were evaluated as the adhesive in this research. The material has to basically possess high thermal resistance for well collocation with metal bonding. Analyses such as SAT and shear test were adopted to

evidence the bonding condition and strength. Samples with hybrid scheme were fabricated to perform hybrid bonding and realize the compatibility in whole process. The process conditions and evaluation results of material candidates will be disclosed in the paper.

### 11:25 AM

**Modeling of Reflow Temperatures and Wettability in Lead-Free Solder Alloys Using Hybrid Evolutionary Algorithms:** *Chedtha Puncreobutr*<sup>1</sup>; Gobboon Lohthongkum<sup>2</sup>; Prabhas Chongstittvattana<sup>1</sup>; Boonrat Lohwongwatana<sup>2</sup>; <sup>1</sup>Department of Computer Engineering, Faculty of Engineering, Chulalongkorn University; <sup>2</sup>Department of Metallurgical Engineering, Faculty of Engineering, Chulalongkorn University

When designing new solder alloys, many key performance properties must be considered and optimized, for example, liquidus and solidus temperatures, the reflow-ability, the strength of soldered contacts, wettability and microstructural stability, etc. With more parameters, the optimization process becomes complex and tedious. Hybrid evolutionary algorithms model is proposed as a tool for designing new alloy compositions by optimizing three key aspects: wettability, liquidus and solidus temperatures. The first aspect was investigated using Butler's equation. The liquidus and solidus of Sn-Ag-Cu-Bi-In solders were investigated using CALPHAD. The results were used as training database for genetic programming, an evolutionary algorithm which mimics nature by allowing only superior genetic traits to survive. With three key objectives combined, genetic algorithm was used to identify worthy candidates. Experimental results confirmed that the algorithms were reliable. The model can be extended to other key performance parameters to produce a complete assessment of optimized alloy recipes.

### 11:40 AM

**Effects of Processing and Amount of Co Addition on Shear Strength and Microstructural Development in Sn-3.0Ag-0.5Cu Solder Joint:** *Limin Ma*<sup>1</sup>; Feng Tai<sup>1</sup>; Guangchen Xu<sup>1</sup>; Fu Guo<sup>1</sup>; <sup>1</sup>Beijing University of Technology

Co has been considered as one of the promising alloying elements to improve the strength and reliability of Pb-free solders, due to its high modulus values and good bonding with Sn. The characteristic microstructure and mechanical properties of Sn-3.0Ag-0.5Cu+XCo (X=0, 0.1, 0.2, 0.45 and 1.0 wt. %) solder joint with Cu substrate were investigated. This study was attempted to clarify the effects of different weight fraction of Co addition on solder joint. The change of undercooling degrees and solidifying phases of solder joints were investigated. An exploration of different solder joint fabrication methods, with both solder preforms and solder paste, was also carried out. The interfacial intermetallics layer stability and stress strength of the solder joints were systematically studied and compared with the control samples. The change in mechanical integrity of the solder joints were correlated with the microconstituents in the solidified solder joints.

## Polymer Nanocomposites: Carbon Fibers and Carbon Nanotubes

*Sponsored by:* The Minerals, Metals and Materials Society  
*Program Organizer:* John Zhanhu Guo, Lamar University

Wednesday AM Room: 309  
February 17, 2010 Location: Washington State Convention Center

*Session Chairs:* John Zhanhu Guo, Lamar University; Carla Leer, Applied Sciences, Inc

### 8:30 AM Introductory Comments

### 8:35 AM Keynote

**An Assessment of the Science and Technology of Carbon Nanotube Composites:** *Tsu-Wei Chou*<sup>1</sup>; Erik Thostenson<sup>1</sup>; Limin Gao<sup>1</sup>; <sup>1</sup>University of Delaware

This paper examines the recent advancements in the science and technology of carbon nanotube (CNT)-based fibers and composites. The assessment is made according to the hierarchical structural levels of CNTs used in composites, ranging from 1-D to 2-D to 3-D. At the 1-D level, fibers composed of pure CNTs or CNTs embedded in a polymeric matrix produced by various techniques are reviewed. At the 2-D level, the focuses are on CNT-modified advanced fibers,

# Technical Program

CNT-modified interlaminar surfaces and highly oriented CNTs in planar form. At the 3-D level, we examine the mechanical and physical properties CNT/polymer composites, CNT-based damage sensing, and textile assemblies of CNTs. The opportunities and challenges in basic research at these hierarchical levels have been discussed.

## 9:15 AM

**Hierarchical Nanocomposites Based on Controlled CNT Arrays:** *Wei Chen*<sup>1</sup>; Steven Nutt<sup>1</sup>; <sup>1</sup>University of Southern California

The CVD growth of carbon nanotube arrays with controlled diameter, density, and length on carbon fibers was attained through a freeze-dry assisted catalyst deposition method in this study. Preheating temperature and catalytic solution concentration were proven to be the key parameters in determining CNT diameter and forest density respectively. The hierarchical nano-structure was incorporated into an epoxy matrix through a vacuum bag process and characterized for thermal and mechanical performances.

## 9:35 AM Invited

**Study on Damping Properties of Polyetherimide/Graphite Nano-Platelet Composites:** *Anthony Perugini*<sup>1</sup>; Bin Li<sup>1</sup>; Weihong Zhong<sup>1</sup>; <sup>1</sup>Washington state university

Polyetherimide (PEI)/graphite nano-platelet (GNP, both as-received and chemically treated) composites with 0.5wt% to 3.0wt% GNPs were prepared for damping applications in aerospace structures. The influences of concentration, size, as well as chemical surface treatment of the GNP, on damping properties of the composites, were studied by dynamic mechanical property analyzer. The results show that, the storage modulus of PEI/GNP composites was noticeably improved with only 0.5 wt% GNP loading. The addition of as-received GNPs did not show obvious impact on the energy dissipation of the composites. To improve the interfacial interaction, chemical surface treatments of GNPs were carried out using a silanization method, which could greatly improve the damping properties of the PEI/GNP composites due to the enhanced frictional motion between PEI molecule chains and GNPs, as well as between the interlayers.

## 9:55 AM

**Mechanomodifiable Carbon Nanotube Arrays:** *Markus Buehler*<sup>1</sup>; Steven Cranford<sup>1</sup>; <sup>1</sup>Massachusetts Institute of Technology

Here we present atomistic-based multi-scale simulation studies of a magnetically active array of carbon nanotubes to illustrate the concept of mechanomodifiability. We show that applying external fields, it is possible to change the nanostructure and to induce a desired mechanical response. Direct numerical simulations are reported that illustrate this concept via mechanical testing through nanoindentation. Specifically, the contact stiffness of an array of carbon nanotubes can be changed reversibly from approximately 73 MPa to 910 MPa due to the application of an external field. A hierarchical approach, implemented through coarse grain molecular modeling, is utilized to develop a framework that can successfully collaborate atomistic theory and simulations with material synthesis and physical experimentation, and facilitate the progress of novel mechanomodifiable structural materials. Further studies of modifiable polymer nanotube arrays are presented, and a comparison with experimental results is discussed.

## 10:15 AM Break

## 10:45 AM Invited

**Plasma Coating and Magnetic Alignment of Carbon Nanotubes in Polymer Composites:** *Donglu Shi*<sup>1</sup>; Hoon Sung Cho<sup>1</sup>; Christopher Huth<sup>1</sup>; Jie Lian<sup>2</sup>; <sup>1</sup>University of Cincinnati; <sup>2</sup>Rensselaer Polytechnic Institute

Carbon nanotubes were modified by a novel plasma polymerization method. In this process, ultrathin films of polystyrene were deposited on the surfaces of carbon nanotubes for improved dispersion. A small percent by weight of these surface-coated nanotubes were incorporated into polystyrene to form a polymer nanocomposite. The plasma coating greatly enhanced the interfacial bonding in the polymer matrix. High-resolution transmission-electron-microscopy images revealed an extremely thin film of the polymer layer (~3 nm) at the interface between the nanotubes and matrix. Tensile test results showed considerably increased strength in the coated nanotubes composite while an adverse effect was observed in the uncoated composites. Furthermore, the carbon nanotubes were magnetically aligned in the polymer composites, responsible for a

pronounced anisotropy in mechanical strength. The processing details and mechanical properties of the carbon nanotube composites will be presented.

## 11:15 AM Invited

**Interfacial Interaction among Carbon Nanofibers Reinforced Epoxy Nanocomposites:** *Jiahua Zhu*<sup>1</sup>; Suying Wei<sup>1</sup>; John Zhanhu Guo<sup>1</sup>; <sup>1</sup>Lamar University

Surface functionalized carbon nanofibers (s-CNFs) and as-received CNFs (u-CNFs) with different loadings were dispersed in epoxy monomers, and the rheological and electrical properties were comparatively investigated at different oscillatory frequencies and temperatures. CNFs network structure was formed once the loading exceeds the percolation point, which can be characterized by the change of storage modulus and loss modulus. Results show that the percolation points are strongly related to the surface character of the CNFs, and also the CNFs loading corresponding to the sharp increase of electrical property are found to be well consistent with the rheological percolations. In bulk matrixes, the interfacial strength between the s-CNFs and solid matrixes were greatly improved owing to the covalent bonding arising from the attached amine group on s-CNFs surface and epoxy monomers. Thus, the mechanical and thermal properties are significantly enhanced as compared to the u-CNFs/epoxy nanocomposites. The reinforcing mechanisms are proposed.

## 11:45 AM

**Localized Characterization of Carbon Nanotubes and Carbon Nanotube Reinforced Nanocomposites Using Novel Micromechanical Devices:** *Yogi Ganesan*<sup>1</sup>; Yang Lu<sup>1</sup>; Cheng Peng<sup>1</sup>; Hao Lu<sup>1</sup>; Roberto Ballarini<sup>1</sup>; Boris Jakobson<sup>1</sup>; Jun Lou<sup>1</sup>; <sup>1</sup>Rice University

The knowledge of carbon nanotube (CNT) strength and the fundamental mechanisms that govern mechanical behavior at the nanotube-matrix interface are critical for CNT reinforced nanocomposite development i.e. in order to realize the theoretically and computationally predicted potential of CNTs as reinforcements for high performance composites. In this work, we have developed a simple micro-fabricated device that could be used within an SEM/TEM chamber in order to perform in situ tensile tests of individual CNTs treated with different functional groups and nanoscale CNT pullout experiments using different matrices quantitatively. The insights gained from this research could potentially help engineer superior CNT reinforced nanocomposites by enabling the development of powerful predictive models.

## 12:05 PM

**Quantification of Carbon Nanotube Distribution and Property Correlation in Nanocomposites:** *Srinivasa Bakshi*<sup>1</sup>; Ruben Batista<sup>1</sup>; Arvind Agarwal<sup>1</sup>; <sup>1</sup>Florida International University

Quantification of the quality of distribution is essential in carbon nanotube (CNT) composites since it reflects the homogeneity of the properties. In this work, an attempt is made to quantify the quality of distribution of carbon nanotubes in a metal matrix composite by two methods. Two parameters have been proposed which are complimentary. The first one called Dispersion Parameter (DP) is based on the image analysis technique and is obtained based on the size of CNT cluster while the second one, named the Clustering Parameter (CP) is based on distances between centers of the nanotubes obtained by Delaunay triangulation. The method is applied to compare the distribution of nanotubes in three micrographs of CNT reinforced aluminum composite. A comparison between two quantification techniques is made. Carbon nanotube distribution obtained by image analysis technique is utilized to correlate and account for experimentally obtained elastic modulus values of the nanocomposite by nanoindentation.



### Processing Materials for Properties: Functional Materials Processing

Sponsored by: The Minerals, Metals and Materials Society, TMS Extraction and Processing Division

Program Organizers: Brajendra Mishra, Colorado School of Mines; Akio Fuwa, Waseda University; Paritid Bhandhubanyong, National Metal and Materials Technology Center

Wednesday AM Room: 617  
February 17, 2010 Location: Washington State Convention Center

Session Chairs: Sreeramamurthy Ankem, University of Maryland; Vikas Sinha, UES, Inc.

#### 8:30 AM Keynote

**Melting Behavior of Solid Particles during High Temperature Bath Processing:** Florian Kongoli<sup>1</sup>; Ian McBow<sup>1</sup>; E. O'Brien<sup>1</sup>; S. Llubani<sup>1</sup>; <sup>1</sup>FLOGEN Technologies Inc

In primary smelting as well as in recycling processes the solid remaining materials from several processing units or crashed electronic materials are recycled in order to extract their valuable residual elements. In some actual processes the recycling is done by simply feeding the solid particles into a furnace while the injection of these particles into a bath is also a viable opportunity. In this paper the melting behavior of the slag particles in recycling processes is quantified through an original non-equilibrium physical model that takes into account all the factors that influence the melting behavior of the solid particles such as the slag particle size, temperature, chemical composition and physical properties of both the slag particles and that of the furnace bath as well other physical parameters. The advantages of this physical model related to the increase of efficiency and productivity of these recycling processes are also discussed.

#### 9:00 AM

**Direct Reversal Imprint Lithography of Indium-Tin Oxide (ITO) Nanoparticles for Improvement of Light Extraction Efficiency of GaN Based LED Devices:** Ki-Yeon Yang<sup>1</sup>; Sang-Chul Oh<sup>1</sup>; Kyeong-Jae Byeon<sup>1</sup>; Heon Lee<sup>1</sup>; <sup>1</sup>Korea University

Recently, light emitting diodes (LEDs) has widely used as a light source for LCD back-light, mobile display, indoor lighting source due to low power consumption, long lifetime and thin configuration. In order to develop the highly efficiency GaN based LED devices, a number of researches have been progressed for enhancement of its low light extraction efficiency. For making the most enhancement of light extraction efficiency and applying into industrial process, photonic crystal patterns must be formed by simple process with low process cost. In this study, indium-tin oxide (ITO) nanoparticle (NP) photonic crystal patterns were formed on the ITO/GaN based blue LED substrate by direct reversal imprint lithography. And we confirmed that light extraction efficiency of GaN based blue LED with ITO NP photonic crystal patterns was drastically enhanced in relation to that of the LED without ITO NP photonic crystal patterns through analysis of photo-luminescence and electro-luminescence.

#### 9:20 AM

**Fabrication of Photonic Crystal Patterns on GaN-Based Light-Emitting Diodes to Improve Photon Extraction Efficiency:** Kyeong-Jae Byeon<sup>1</sup>; Eun-Ju Hong<sup>1</sup>; Hyoungwon Park<sup>1</sup>; Kyung-Min Yoon<sup>1</sup>; Joong Yeon Cho<sup>1</sup>; Heon Lee<sup>1</sup>; <sup>1</sup>Korea University

In order to enhance the light extraction of the GaN-based light-emitting diodes (LEDs), various photonic crystal patterns were formed in the LED structure by nanoimprint lithography. Indium tin oxide electrode and p-GaN top cladding layer were patterned with photonic crystals by UV imprinting and dry etching process. Photonic crystal patterns could be uniformly formed on 2 inch whole LED substrate by using a flexible polymer stamp, which can ensure conformal contact between the stamp and LED wafer, during imprinting process. As a result, photoluminescence intensity of the patterned LED was drastically increased by prominent light scattering and light coupling with photonic crystal patterns. And electroluminescence intensity of the patterned LED device was enhanced up to 25% compared to that of the non-patterned LED device. By measuring I-V characteristics of the patterned LED and non-patterned LED devices, electric degradation was analyzed.

#### 9:40 AM

**Indium-Gallium-Zinc-Oxide Based Thin-Film-Transistor for Display Devices:** Sonachand Adhikari<sup>1</sup>; Rajeev Gupta<sup>1</sup>; Deepak<sup>1</sup>; Ashish Garg<sup>1</sup>; <sup>1</sup>Indian Institute of Technology Kanpur

Indium-Gallium-Zinc-Oxide (IGZO), which exhibits higher carrier mobility than a-Si, is more suitable for thin film transistors in backplane of active-matrix flat panel displays. IGZO films deposited by pulsed laser deposition (PLD) or sputtering require preparation of a target by mixing individual oxides and sintering them. Because this process is not yet standardized, considerable variation in optimal composition is reported in literature. We have mixed the three oxides and sintered them under different temperature, time and processing conditions. Based on detailed X-ray diffraction analysis and comparing it with compositional analysis by wet and dry methods, we determined the conditions in which sintering is complete. Using the target thus made, films deposited by PLD under partial pressure of oxygen varying between  $10^{-2}$  -  $10^{-5}$  mbar are characterized for transparency and conductivity. We believe, the variation reported in literature for IGZO composition may be due to inadequate method of preparing the target.

#### 10:00 AM

**Production and Characterization of ASTM F75 Balls Produced by the Uniform-Droplet Spray Process:** Sudesna Roy<sup>1</sup>; Teiichi Ando<sup>1</sup>; <sup>1</sup>Northeastern University

Mono-size droplets of a Co-28wt.%Cr-5wt.%Mo alloy (ASTM F75) were produced by the uniform-droplet spray (UDS) process, a capillary jet breakup process, in diameters ranging from 300  $\mu$ m to 700  $\mu$ m, and characterized for their solidification microstructures. The 700  $\mu$ m droplets all had a well-developed dendritic microstructure, while the 300  $\mu$ m droplets exhibited a microcrystalline microstructure, indicative of dendrite fragmentation, which may take place during the post-recalescence plateau stage. Conditions for dendrite fragmentation, determined with a dendrite fragmentation model and recently developed simulations models for the nucleation and crystallization kinetics of traveling molten droplets, also suggest the occurrence of dendrite fragmentation in the 300  $\mu$ m.

#### 10:20 AM Break

#### 10:30 AM

**Preparation and Characterization of Microfibrous Entrapped Solid Adsorbents for Desulfurization of Liquid Fuels:** David Cocke<sup>1</sup>; Mohammad Islam<sup>1</sup>; Jewel Gomes<sup>1</sup>; Eric Peterson<sup>2</sup>; Morgan Reed<sup>1</sup>; Doanh Tran<sup>1</sup>; Hylton McWhinney<sup>3</sup>; <sup>1</sup>Lamar University; <sup>2</sup>Fluor; <sup>3</sup>Prairie View A&M University

Existing hydrodesulfurization technologies are not competent to reduce the sulfur content of gasoline or diesel to less than 10 ppmw, partly because remaining sulfur compounds in current commercial liquid fuels are thiophenic sulfur compounds. Even if the severity of the reaction is increased at high H<sub>2</sub> pressure and high temperature, it is difficult to reach sulfur removal below 5 ppmw while the olefin content in the fuel is kept unchanged. In this study, we focused on preparation of microfibrous entrapped alumina support particles by impregnation method such as microfibrous entrapped Zn/Al<sub>2</sub>O<sub>3</sub> for desulfurization. As microfibrous agent, glass and silica were used. The structure and the morphology of the porous materials were characterized by XRD, SEM/EDS, XPS, and TGA. The analysis of the porous structure was justified using BET equations, H-K equation and BJH theory, and its physicochemical behaviors was compared with traditional Zn/Al<sub>2</sub>O<sub>3</sub> catalysts.

#### 10:50 AM

**Energy Efficient Sintering of Al/Cu Nanocomposites Using Different Microwave Power Levels:** Shashank Nawathe<sup>1</sup>; W.L.E. Wong<sup>2</sup>; M. Gupta<sup>2</sup>; <sup>1</sup>University of California, Berkeley; <sup>2</sup>National University of Singapore

Pure aluminum and Al/Cu nanocomposites were fabricated by integrating pure aluminum with nano copper reinforcement using powder metallurgy route incorporating energy efficient microwave assisted rapid sintering technique. The composites were subjected to different microwave power levels during the sintering. Microstructural characterization studies revealed the presence of minimal porosity and reasonably uniform distribution of the reinforcement in the nanocomposites. Mechanical characterization revealed that the maximum strength is achieved for composite sintered at 50% power level while the highest ductility is achieved for composite sintered at 30% power level. The best overall combination of mechanical properties assessed in terms of work of fracture was realized in the composite sintered at 100% microwave power level. An attempt

# Technical Program

is made in the present study to correlate the effect of different microwave power levels on the characteristics of the Al/Cu nanocomposites.

## 11:10 AM

**Microstructural Characterization of Shape Memory Alloys for Ferromagnetic Applications:** *F. Khalid*<sup>1</sup>; <sup>1</sup>GIK Institute of Engineering Science and Technology

Ni-Mn-Ga shape memory alloys are employed for applications in actuation and sensing, robotics and aerospace industry. These alloys exhibit ferromagnetic behavior and are capable of demonstrating large reproducible strains in moderate magnetic fields. This work presents a study on the effect of annealing treatment on the microstructure and phases that are evolved in Mn-rich off-stoichiometric compositions of alloys. Microstructural and XRD results revealed martensitic structure at RT in the alloys with Mn=28at% whereas the alloy containing higher Ga (>22at%) revealed austenitic structure at room temperature. Homogenization followed by annealing treatment has shown reduction in segregation, grain growth and formation of ordered structure and consequently its influence on final properties is explained.

## 11:30 AM

**Anisotropic Crystallization of Uniaxially Pressed Mixed Rare Earth-Iron-Boron Alloys:** *Nathaniel Oster*<sup>1</sup>; *Iver Anderson*<sup>2</sup>; *Wei Tang*<sup>2</sup>; *Yaqiao Wu*<sup>2</sup>; *Kevin Dennis*<sup>2</sup>; *Matthew Kramer*<sup>2</sup>; *R. McCallum*<sup>2</sup>; <sup>1</sup>Iowa State University; <sup>2</sup>Ames Lab

Anisotropic nanocrystalline mixed rare earth (MRE) magnet alloy particulate for use in polymer-bonded magnets shows promise for use in high torque electric motors and other applications which require high energy density magnets capable of performing at elevated temperatures. A novel method of forming particulate with the desired microstructure from the amorphous state is presented. Due to processing differences between the proposed method and traditional methods, this technique shows promise for reduction in processing costs. In this study, amorphous MRE-iron-boron alloy particulate was uniaxially pressed during crystallization to induce texture. Texture can be formed because anisotropy in the crystal cell provides preferred growth directions under non-hydrostatic stress. Microstructure and texture are observed through transmission electron microscopy, scanning electron microscopy, and x-ray diffraction. Results will be presented. Supported by DOE-EERE-FCVT Office through Ames Lab contract DE-AC02-07CH11358

## 11:50 AM

**The Effect of Sputtering Parameters on the Phase Formation of Sputtered Tantalum:** *Anahita Navid*<sup>1</sup>; *Andrea Hodge*<sup>1</sup>; <sup>1</sup>University of Southern California

The phase transitions in magnetron sputtered Tantalum as a function of residual stress and internal plasma conditions are presented in this study. The formation of body centered cubic (BCC) and tetragonal tantalum was observed on films deposited on a Si substrate at pressures between 0.3 and 1.4 Pa. The results demonstrate the formation of BCC tantalum at a 0.7 Pa sputtering pressure at various power settings. However, any other sputtering pressure did not yield a BCC structure but rather mixed BCC/tetragonal or a tetragonal phase. The texture and residual stress of both BCC and tetragonal tantalum changed significantly with increasing pressure and film thickness. In addition, the effect of underlayer material on the corresponding phase formation will also be presented for various sputtering pressures.

## 12:10 PM

**TiO<sub>2</sub> Aggregates for Dye-Sensitized Solar Cells Application:** *Qifeng Zhang*<sup>1</sup>; *Xiaoyuan Zhou*<sup>1</sup>; *Christopher Dandeneau*<sup>1</sup>; *Kwangsuk Park*<sup>1</sup>; *Supan Yodyingyong*<sup>1</sup>; *Guozhong Cao*<sup>1</sup>; <sup>1</sup>University of Washington

TiO<sub>2</sub> aggregates were synthesized via a hydrolysis of alkoxide of titanium(IV) in acetic acid aqueous. The aggregates are in submicron size, feature a spherical porous structure, and consist of ~10-nm anatase TiO<sub>2</sub> nanocrystallites. When such aggregates are used in dye-sensitized solar cells, they impart an extremely large internal surface area to the photoelectrode film for dye molecule adsorption, and meanwhile may generate effective light scattering in view of their submicron size that is comparable with the wavelengths of visible light. When compared with the traditional dye-sensitized solar cells, in which the photoelectrode film only comprises TiO<sub>2</sub> nanoparticles, the solar cells based on TiO<sub>2</sub> aggregates show a significant improvement in the light harvesting efficiency and, thus, contribute to the overall conversion efficiency. It is

anticipated that TiO<sub>2</sub> aggregates would have a practical application in the field of solar cells in the future.

## Recycling General Sessions: Metals

*Sponsored by:* The Minerals, Metals and Materials Society, TMS Extraction and Processing Division, TMS Light Metals Division, TMS: Recycling and Environmental Technologies Committee  
*Program Organizer:* Joseph Pomykala, Argonne National Laboratory

Wednesday AM

Room: 206

February 17, 2010

Location: Washington State Convention Center

*Session Chair:* Joseph Pomykala, Argonne National Laboratory

## 8:30 AM

**Preliminary Research on Preparation Al-Si-Ti Alloy with Aluminum Ash as Electrolysis Materials:** *Liu Qingsheng*<sup>1</sup>; *XUE Jilai*<sup>2</sup>; *JING Qingxiu*<sup>1</sup>; <sup>1</sup>Jiangxi University of Science and Technology; <sup>2</sup>University of Science and Technology Beijing

A new method of recycling aluminum ash for preparation Al-Si-Ti alloy was studied in this paper. In the experiment, first the aluminum ash was pretreated by leaching and calcining process, the fine purity and phase of the intermediate oxide powder up to electrolysis demands, then, could be obtained, which was treated by molten salt electrolysis. Finally, the Al-Si-Ti alloy was successfully obtained through electrochemical co-deposition in the cathode shows a typical as-cast microstructure. This new recycling method can produce high quality alloy and may bring remarkable economic and social benefits.

## 8:50 AM

**Effective Utilization of Wastes Generated in the Integrated Aluminium Production - A Review:** *Narasimharaghavan Krishnaswamy*<sup>1</sup>; *Nand Kumar Kshatriya*<sup>1</sup>; *Bibhu Mishra*<sup>1</sup>; *Ramaswamy Jagannathan*<sup>1</sup>; *Durba Khasyap*<sup>1</sup>; <sup>1</sup>Bharat Aluminium Co. Ltd., (A Unit of Vedanta Resources Plc.), BALCO Nagar, Korba

The major wastes generated in the integrated Aluminium process are: Red Mud from the Bayer process, Carbon skimming, Spent Pot Lining from the Aluminium reduction process, Ash from the power plants which give energy to the reduction process and Aluminium dross from the Cast house and Foundry. In this review our recent attempts to recover caustic and the value added minerals from Red Mud, effective recovery of Fluoride salts from the carbon skimming, use of fly ash and red mud in the production of cost effective bricks for construction and our efforts towards reduction in dross generation in Cast House and Foundry has been discussed. Jarosite, the waste from the Zinc industry has been used in the recovery of value added constituents from the red mud.

## 9:10 AM

**Stabilization of Chromium-Based Slags with MgO:** *Hugo Cabrera-Real*<sup>1</sup>; *Antonio Romero-Serrano*<sup>1</sup>; *Beatriz Zeifert*<sup>1</sup>; *Manuel Hallen-Lopez*<sup>1</sup>; <sup>1</sup>IPN

This work investigated the chemical and mineralogical properties of CaO-SiO<sub>2</sub>-CrOx-CaF<sub>2</sub>-MgO slags. Synthetic slags were prepared and the effect of the slag basicity (CaO/SiO<sub>2</sub>) and MgO contents on the stability of the mineralogical species formed was analyzed. The morphology and composition of the slags were analyzed by XRD and SEM-EDS, whilst their chemical stability was evaluated by leaching with an aqueous acetic acid solution. It was found that in slags with CaO/SiO<sub>2</sub> = 1, the main Cr-compound was MgCr<sub>2</sub>O<sub>4</sub> spinel, which forms octahedron crystals. Small amounts of CaCr<sub>2</sub>O<sub>4</sub> and CaCrO<sub>4</sub> were also observed. It was found that increasing the slag basicity from 1 to 2 the compounds MgCr<sub>2</sub>O<sub>4</sub> and CaCr<sub>2</sub>O<sub>4</sub> were formed together with the Cr(V)-containing compound complex Ca<sub>5</sub>(CrO<sub>4</sub>)<sub>3</sub>F which forms hexagonal crystals. The results showed that the highest chromium concentration levels in the leaching liquors corresponded to slags with CaO/SiO<sub>2</sub> = 2, probably owing to the formation of Ca<sub>5</sub>(CrO<sub>4</sub>)<sub>3</sub>F.



### 9:30 AM

**Preparation of Potassium Ferrate by Hypochlorite Oxidation Method:** Guomin Jiang<sup>1</sup>; *Liyuan Chai*<sup>1</sup>; Yunyan Wang<sup>1</sup>; Yude Shu<sup>1</sup>; Min Yue<sup>1</sup>; <sup>1</sup>Central South University

Potassium ferrate is an excellent multifunctional agent for wastewater treatment, but its preparation is crucial. The improved hypochlorite oxidation method was used to prepare potassium ferrate in this study. Iron nitrate, the preferred iron source, was added into hypochlorite solution and then the stabilization agent was added during the purification process of product. The influence of available chlorine content, iron molecular proportion, reaction temperature and reaction time on potassium ferrate preparation was investigated. The optimal condition for potassium ferrate preparation is 15% of available chlorine content, 0.6 of iron molecular proportion, 30° of reaction temperature, 45min of reaction time. The yield of potassium ferrate is about 67% with more than 99% of purity. The structure and performances of the product was characterized by XRD, EDX, SEM, TG and IR and the results show that the prepared product is consistent with the properties of potassium ferrate(VI).

### 9:50 AM Break

### 10:00 AM

**Isotherm and Kinetics Studies of the Biosorption of Cobalt from Aqueous Solutions by Waste Materials:** *Chen Yunmen*<sup>1</sup>; Fan Jingbiao<sup>1</sup>; <sup>1</sup>Jiangxi University of Science and Technology

In the present study, waste materials like pine sawdust and spent grains were investigated to assess their potential for removal of cobalt ion from water by the process of biosorption. The effects of solution pH, reaction time and initial concentration were studied in batch experiments. The removal efficiency of Co(II) by spent grains was higher than that of pine sawdust. The initial removal was rapid and equilibrium was established in less than 90 min. Equilibrium data all agreed well with Freundlich isotherm model for the two metal-biomass sorption processes. Good correlation coefficients were obtained for the pseudo second-order kinetic model. Pine sawdust and spent grains were shown to be promising biosorbents for Co(II) removal from aqueous solutions.

### 10:20 AM

**Novel Technology for Wastewater Treatment by Biologics in Hydrometallurgical Processes of Lead-Zinc:** Qingwei Wang<sup>1</sup>; *Liyuan Chai*<sup>1</sup>; Yunyan Wang<sup>1</sup>; Qingzhu Li<sup>1</sup>; Zhihui Yang<sup>1</sup>; <sup>1</sup>Central South University

Heavy metal-containing wastewater from hydrometallurgical processes of lead-zinc was treated by biologics in a 200 m<sup>3</sup>/h industrial scale experiment. The result shows that Zn concentration declined from 50.28 mg/L~240.81 mg/L to 0.21 mg/L~1.98 mg/L, Pb from 1.00 mg/L~13.47 mg/L to 0.083 mg/L~0.71 mg/L, Cu from 0.24 mg/L~2.38 mg/L to 0.059 mg/L~0.40 mg/L, Cd from 2.12 mg/L~23.47 mg/L to 0.011 mg/L~0.071 mg/L and As from 0.50 mg/L~6.00 mg/L to 0.005 mg/L~0.10 mg/L. The concentrations of the above heavy metals in the treated water were lower than that in Integrated Wastewater Discharge Standard (GB8978-1996) in China. Furthermore, the treated wastewater was recycled and reused in smelter plant. Zinc content in hydrolytic sludge reached up to 34.04%, which indicates that this sludge can be used to recover valuable metals.

### 10:40 AM

**Study on the In-Situ Remediation of Cr-Contaminated Soil by Indigenous Microorganism:** *Shunhong Huang*<sup>1</sup>; <sup>1</sup>Hunan Research Institute of Nonferrous Metals, Changsha

Based on the optimization of culture medium composition and growth conditions and ability of Cr(VI) reduction, the bioremediation of Cr-contaminated soil can be achieved by adding culture medium in soils to stimulate the activity of indigenous microorganism. The optimal condition for the Cr(VI) reduction by indigenous microorganism was 5g glucose and 5g yeast extract per kg soil at 30°C and the ratio of soil and water was 1:1. Under the optimal condition, 92% of total Cr(VI) in soil contaminated by chromium-containing slag heap was removed and water soluble Cr(VI) was completely removed at 4 days.

### 11:00 AM

**The Optimum Condition for Cr(VI) Bioremediation in Soils Contaminated by Chromate Ore Processing Residue:** Changqing Su<sup>1</sup>; *Yonghua Zhu*<sup>1</sup>; Bing Wang<sup>1</sup>; Hangbin Li<sup>1</sup>; Yingping Liao<sup>1</sup>; <sup>1</sup>Central South University

A batch incubation experiment has been carried out to investigate the optimal condition for the microbial remediation of hexavalent chromium (Cr(VI)) in

soils contaminated by chromate ore processing residue (COPR) at Hunan Iron-Alloy Factory in China. The results indicated that glucose and yeast extract was the optimal component of culture medium and the quantities of the above components were 8 g L<sup>-1</sup> and 13 g L<sup>-1</sup>, respectively. The favorable temperature and pH value were 30° and 10.0, respectively. A bioreactor was operated under the optimal condition and water soluble Cr(VI) in soils was reduced from 313 mg kg<sup>-1</sup> Cr(VI) of the initial concentration to below detection limit after 30 h. Thus, there is a large potential to accomplish Cr(VI) bioremediation at the presence of indigenous bacteria by the addition of optimal culture medium in soils contaminated by chromate ore processing residue.

### 11:20 AM

**Thermodynamic Equilibrium of Hydroxyl Complex Ions in Mn2+-H2O System:** Fei Pei<sup>1</sup>; *Yunyan Wang*<sup>1</sup>; Liyuan Chai<sup>1</sup>; <sup>1</sup>Central South University

Pc-pH diagrams and -lnγ±MnSO4-I relationship for activity coefficient and ionic strength of Mn2+-H2O system have been drawn based on the thermodynamic principle of coordination chemistry combined with the Pitzer theory at 298.15K. The diagram of -lnγ±MnSO4-I indicated that -lnγ±MnSO4 increased from 0 up to 1.2147 when I changed from 0 to 0.09, increase of -lnγ±MnSO4 became slowly when I was at 1.00 -1.69, and -lnγ±MnSO4 kept constant when I was at 2.25-4.00. Diagrams of pc-pH illustrated that the minimum solubility of Mn(OH)2(s) increased with I, the pc decreased from 6.5 to 5.5 when I changed from 0 to 4.00; The pH value of the minimum solubility of Mn(OH)2(s) increased from 11.80 to 12.76 when I changed from 0 to 2.89, and pH kept constant with I increasing when I was less than 4.0. There is a simple relationship between the minimum solubility of Mn(OH)2(s) and pH in different I.

## Sustainable Materials Processing and Production: Sustainable Technologies I

*Sponsored by:* The Minerals, Metals and Materials Society, TMS Extraction and Processing Division, TMS Light Metals Division, TMS: Recycling and Environmental Technologies Committee, TMS: Education Committee

*Program Organizers:* Christina Meskers, Umicore; Randolph Kirchain, Massachusetts Institute of Technology; Diana A. Lados, Worcester Polytechnic Institute; Markus Reuter, Ausmelt Limited

Wednesday AM Room: 2B  
February 17, 2010 Location: Washington State Convention Center

*Session Chairs:* Randolph Kirchain, Massachusetts Institute of Technology; Gabrielle Gaustad, Rochester Institute of Technology

### 8:30 AM Introductory Comments

#### 8:35 AM Keynote

**IT and Sustainability: The Power to Transform:** *Joe Johnson*<sup>1</sup>; <sup>1</sup>Cisco Systems, Inc.

The global footprint of the IT sector is estimated to be 2% of worldwide carbon emissions and growing. At the same time, innovative applications of IT have the potential to reduce global emissions many times over this amount. Recent trends, such as broad adoption of video teleconferencing technologies and virtual collaboration tools have validated IT can reduce emissions from other sectors. Opportunities such as smart grids, smart buildings and connected cities aim to apply intelligent networks to manage and reduce energy consumption on a global scale. IT products are also subject to materials restrictions and other eco-regulations which mitigate impacts by shifting environmental focus from production to products. This presentation will review these topics and the transformational capacity of IT to help achieve a sustainable future.

#### 9:00 AM Invited

**'Slag Valorisation', as an Example of High Temperature Industrial Ecology:** *Daneel Geysen*<sup>1</sup>; Peter Jones<sup>1</sup>; Arnout Sander<sup>2</sup>; Yiannis Pontikes<sup>1</sup>; Özlem Cizer<sup>3</sup>; Tom Van Gerven<sup>4</sup>; Marc Craps<sup>5</sup>; Johan Eyckmans<sup>5</sup>; Bart Blanpain<sup>1</sup>; <sup>1</sup>MTM KULeuven; <sup>2</sup>InsPyro; <sup>3</sup>BWK, KULeuven; <sup>4</sup>CIT KULeuven; <sup>5</sup>HUB

Better slag valorisation is part of improving the sustainability of steel, stainless steel and non-ferrous metal production. Besides, it can improve the sustainability of other products and production processes as well. Several slag valorisation routes were studied in the past but not much high value applications

# Technical Program

are implemented yet due to technical, environmental or economic constraints. Granulated Blast furnace steel slag (GBFS) is already used for long in cement production. Its application is very successful. GBFS helps to reduce the CO<sub>2</sub> emissions of the cement production process. Also other slag types have potential but its quality needs to be improved by slightly optimising the metallurgical process. Besides cement, slags can be used in high quality aggregates, slag wool insulation, ceramics and carbon sines. The paper discusses slag valorisation opportunities for different slag types and indicates non-technical limitations and opportunities such as market structures and environmental constraints and benefits.

## 9:25 AM

**Sustainability Study in Selective Laser Sintering – An Energy Perspective:** *Rameshwar Sreenivasan*<sup>1</sup>; David Bourell<sup>1</sup>; <sup>1</sup>The University of Texas at Austin

Additive Manufacturing (AM) processes which include Selective Laser Sintering (SLS) have experienced tremendous growth and development since their introduction over 20 years ago. Characteristic of AM processes is the creation of parts without the use of part-specific tooling. In this study, a sustainability analysis was performed on the SLS process with Nylon-12 using the Environmental and Resource Management Data (ERMD) known as Eco-Indicators. The energy perspective alone was considered and a Total Energy Indicator (TEI) value was calculated using various parameters to quantify process sustainability: process productivity, energy consumption rate, etc. A comparison of TEI values between SLS and other AM processes was made to evaluate sustainability of AM from a broad perspective.

## 9:50 AM Invited

**2010 Vittorio de Nora Award Winner: Designing Crushing and Grinding Circuits for Improved Energy Efficiency:** *Zeljka Pokrajacic*<sup>1</sup>; <sup>1</sup>WorleyParsons Services Pty Ltd – Minerals and Metals

Crushing and grinding, or comminution, circuits are the most energy intensive process of a mineral processing plant. Comminution involves the physical size reduction of an orebody to a particle size sufficient for recovery of the mineral values. However, the comminution process remains inherently inefficient. The inefficiency is a result of the operating nature of comminution devices such as grinding mills, where transfer of energy between grinding media and particles in unconstrained and completely random. New comminution circuit design strategies are presented in this paper. The aim of the new strategies is to improve the overall efficiency of the comminution process and reduce the total energy consumption of a comminution circuit. This paper also explores the financial impact of certain energy efficient strategies using an analysis tool called EcoNomics™. It shows that substantial financial gains can be made by including more efficient technologies and methods in comminution circuit design.

## 10:15 AM Break

## 10:30 AM

**Energy and Environmental Challenges in Aluminium Industry - A Review:** *Narasimharaghavan Krishnaswamy*<sup>1</sup>; Bibhu Mishra<sup>1</sup>; Ramaswamy Jagannathan<sup>1</sup>; <sup>1</sup>Bharat Aluminium Co. Ltd., (A Unit of Vedanta Resources Plc.), BALCO Nagar, Korba

This paper discusses briefly the major reasons associated with the growth and its impact on the energy requirement and Environmental imbalance. A projection based on the present global Alumina and Aluminium requirement indicate a substantial further growth of at least 30% over the next 10 years. It is indicated that the main factors which are likely to influence investments are the environmental factors such as the Climate Change and global response to the growing energy prices and sustainable development. Each of the developed / developing nations must find response to the GHG emissions which will encourage the Aluminium Industry to make an effective contribution to global warming while preserving the international competitiveness of the industry - a challenging task. The efforts shall concentrate on improving energy efficiency in the industry possibly of the order of 25% over the next 10 to 20 years. The developments in this line are discussed.

## 10:55 AM

**Towards Sustainable Material Usage: Investigating Limits to Secondary Aluminum Sinks:** *Gabrielle Gaustad*<sup>1</sup>; Elsa Olivetti<sup>2</sup>; Randolph Kirchain<sup>2</sup>; <sup>1</sup>Rochester Institute of Technology; <sup>2</sup>MIT

For aluminum, substitution of primary with secondary resources decreases energy consumption; this energy advantage creates a strong economic incentive to recycle. Several authors have raised concerns that the current sinks for secondary materials may soon be saturated, impeding subsequent expansion of recycling. This work combines dynamic material flow analysis with optimal batch planning models to quantify the significance and drivers of these pending limits under several scenarios, and thereby explore potential opportunities to increase recycling. An aluminum recycling system case was developed that includes containers and packaging, automotive, and construction products and scraps. System parameters such as accumulation of tramp elements and size of dissipative scrap sinks are explored in the context of changing alloy product demand, lifetime, and collection. Insights drawn from this specific case study could be applied to multi-stakeholder, systemic models.

## 11:20 AM

**Use of Eco Friendly Alternate Refining Flux in Aluminium Cast House - A Step towards Sustainable Development:** *Narasimharaghavan Krishnaswamy*<sup>1</sup>; Mousumi Kar<sup>1</sup>; T. Prabu<sup>1</sup>; Charulata Mathur<sup>1</sup>; Gautam Dey<sup>1</sup>; <sup>1</sup>Bharat Aluminium Co. Ltd., (A Unit of Vedanta Resources Plc.), BALCO Nagar, Korba

The major threat to the sustainability of Aluminium Industry is its significant contribution to global warming by way of generation of non eco-friendly gases during its production cycle from Bauxite to the finished product. Though reduction measures are taken in control and effective recovery of values from pot room gases, efforts in use of environment friendly additives in the final products production line is warranted. In this line, the present paper describes our efforts in the use of a new generation refining flux which apart from helping in effective removal of alkali metals, reduction in inclusions and ensure a better metal cleanliness shall also aide in reduction of abnoxious gases generated during the metal refining process prior to casting. The aim of the current work was to reconcile the practical results with the old generation fluxes used. Further improvements to bring in a better metal cleanliness will also be discussed.

## 11:45 AM

**Sustainable Electrolysis for Electrowinning and Electrorefining of Metals:** *Geir Martin Haarberg*<sup>1</sup>; <sup>1</sup>Norwegian University of Science and Technology

Modern electrolysis technologies can provide possibilities for developing sustainable processes in terms of energy and environment. Laboratory experiments were carried out to study electrodeposition of iron from molten salts and aqueous solutions using an inert oxygen evolving anode to eliminate the emissions of CO<sub>2</sub>. The possibilities of molten salt electrorefining of metallurgical grade silicon to produce solar grade silicon were also investigated. Furthermore the development of an electrochemical route using molten salts for the production of titanium is under investigation. Electrochemical techniques were used to study the electrochemical behaviour of dissolved iron, silicon, and titanium species. Bulk electrolysis was carried out to deposit pure iron, silicon, and titanium. The quality of the deposits was studied by SEM/EDS and XRD analyses.

## 12:10 PM Concluding Comments



## The Vasek Vitek Honorary Symposium on Crystal Defects, Computational Materials Science and Applications: Grain Boundaries and Interface Structure and Properties: Joint Session with Solid-State Interfaces

*Sponsored by:* The Minerals, Metals and Materials Society, TMS Materials Processing and Manufacturing Division, TMS/ASM: Computational Materials Science and Engineering Committee  
*Program Organizers:* Mo Li, Georgia Institute of Tech; David Srolovitz, Institute for High Performance Computing, Agency for Science, Technology and Research, Singapore; Adrian Sutton, Imperial College London; Vaclav Paidar, Institute of Physics AS CR vvi; Jeff De Hosson, Univ of Groningen

Wednesday AM Room: 603  
 February 17, 2010 Location: Washington State Convention Center

*Session Chairs:* Vaclav Paidar, Institute of Physics AS CR vvi; Alan Needleman, University of North Texas; Antonia Antoniou, Georgia Institute of Technology

### 8:30 AM Invited

**The Simulation of Grain Boundaries in Single Component and Multi-Component Systems:** *Adrian Sutton*<sup>1</sup>; Alvin Chua<sup>1</sup>; Nicole Benedek<sup>1</sup>; Lin Chen<sup>1</sup>; Manuel Kurdian<sup>1</sup>; Sebastian von Althaus<sup>2</sup>; Peter Haynes<sup>1</sup>; Kimmo Kaski<sup>2</sup>; Mike Finnis<sup>1</sup>; <sup>1</sup>Imperial College London; <sup>2</sup>Helsinki University of Technology

We show that the removal of atoms is an important mode of relaxation at grain boundaries in silicon and ferromagnetic iron. In silicon it is only when atoms are removed from (001) twist boundaries that new ordered configurations are obtained with lower energies than the disordered states found before. When the same thinking is applied to grain boundaries in strontium titanate we have to include in the free energy of the interface terms involving the chemical potentials of the species present. The existence of three atomic species at these boundaries increases the configurational complexity of these boundaries by astronomical factors, and the possibility of getting trapped at local energy minima is far greater than in single component systems. To overcome these problems we have developed a new computational approach based on a genetic algorithm, and we use ab initio thermodynamics to calculate the free energies.

### 8:55 AM Invited

**Structure and Properties of Metal/Ceramic Interfaces in Materials Systems:** *Manfred Rühle*<sup>1</sup>; <sup>1</sup>MPI for Metals Research

Metal/Ceramic Interfaces (MCI) play an important, sometimes controlling, role for many materials consisting of both, metals and ceramics. The structure of MCIs as well information on bonding across the interface can be obtained by different quantitative TEM techniques. As an example, the shear strength of an MCI can be revealed by a detailed analysis of the displacement field around misfit dislocations adjacent to the MCI. Those studies were initiated by V.Vitek during his sabbatical stay in Stuttgart. (G. Gutekunst, J. Mayer, V. Vitek and M. Rühle, Phil. Mag. A 75 (1997) 1329-1355, 1357-1382) and were recently experimentally as well theoretically in a quantitative way. Results will be reported for specific, artificially grown MCIs (Ni/a-Al<sub>2</sub>O<sub>3</sub>, Cu/a-Al<sub>2</sub>O<sub>3</sub>, Pd/SrTiO<sub>3</sub>, Ni/SrTiO<sub>3</sub>).

### 9:20 AM Invited

**Elastic and Anelastic Interface Properties in Martensitic Transformations:** *Robert Pond*<sup>1</sup>; John Hirth<sup>2</sup>; <sup>1</sup>University of Exeter; <sup>2</sup>Private Individual

A model of the structure of parent-martensite interfaces has been developed based on dislocation theory. Two arrays of defects are generally present in the habit plane; one is an array of disconnections (line defects with dislocation and step character), and the other is produced by crystal defects (slip or twinning) in the martensite crystal. The object of the present paper is to discuss the elastic and anelastic properties of such defect networks. We distinguish between the plasticity induced by motion of the defect network, which is reversible or "anelastic", and the distortions arising due to the elastic fields of the defects in the static state. The former can be represented as an engineering strain expressed in terms of the Burgers vectors of the crystal defects and disconnections and their planes of motion. The latter include short-range coherency strains and small ancillary rotations that modify the orientation relationship of the crystals.

### 9:45 AM

**Response of a  $\Sigma$  11 Asymmetric Tilt Grain Boundary in Copper to an Applied Shear Stress at Finite Temperatures:** *Saryu Fensin*<sup>1</sup>; Mark Asta<sup>1</sup>; Richard Hoagland<sup>2</sup>; <sup>1</sup>University of California, Davis; <sup>2</sup>Los Alamos National Laboratory

We present results of molecular dynamics simulations studying the temperature dependence of the structure and mechanical response to an applied shear stress for an *asymmetric*  $\Sigma$  11 tilt grain boundary in copper. At higher temperatures a disordered liquid-like layer forms at the grain boundary and becomes wider in width as the melting temperature is approached from below. Upon application of shear stress the boundary undergoes incremental normal displacement also known as coupled motion at low temperatures. This behavior is analyzed to determine the atomic mechanisms of the grain boundary motion within the framework of disconnections. With increasing temperature, and associated disordering of the interface structure, the mechanical response switches to that of grain-boundary sliding at the highest temperatures, with more complex behavior being displayed at intermediate temperatures.

### 10:10 AM Break

### 10:30 AM Invited

**Crystal Symmetry and Burgers-Vector Content of Grain Boundaries:** *J. Cahn*<sup>1</sup>; Y. Mishin<sup>2</sup>; <sup>1</sup>National Institute of Standards and Technology; <sup>2</sup>George Mason University

Applied shear stresses can induce glissile motion of planar grain boundaries (GBs) at low temperatures similar to dislocation glide. The coupling of stress to move the GB and deform the volume it traverses depends on the GB's Burgers vector content given by the Frank-Bilby equation (FBE). Because the FBE has multiple solutions, a multiplicity of possible deformation modes and coupling factors are possible for the same GB. The complete set of coupling factors is predicted from the point symmetry of the bi-crystal and the angles which characterize the GB. The results of this analysis are compared with recent experiments and with molecular dynamics simulations.

### 10:55 AM Invited

**Temperature Dependence of Grain Boundary Properties:** *Stephen Foiles*<sup>1</sup>; Elizabeth Holm<sup>1</sup>; David Olmsted<sup>2</sup>; <sup>1</sup>Sandia National Laboratories; <sup>2</sup>Northeastern University

The properties of grain boundaries, such as their energy and mobilities, have been studied extensively over many years. However, the variation of these properties with temperature is still not fully explored. The temperature dependence of the interfacial free energy of a grain boundary in Ni is computed and the correlations between this temperature dependence and that of the elastic constants are explored. Some results on the temperature dependence of the boundary mobility are also presented which indicate that the variations of the mobility with temperature are substantially more complex than a simple Arrhenius type variation. Sandia is a multi-program laboratory operated by Sandia Corporation, a Lockheed Martin Company, for the United States Department of Energy's National Nuclear Security Administration under contract DE-AC0494AL85000.

### 11:20 AM

**Heterophase Segregation on an Atomic Scale: Atom-Probe Tomographic Experiments and First-Principles Simulation:** *David Seidman*<sup>1</sup>; <sup>1</sup>Northwestern University

In multiphase systems heterophase interfacial segregation is ubiquitous and relevant to different physical and mechanical properties of materials at both microscopic and macroscopic length scales. Heterophase interfacial segregation (or depletion) may be either monotonic (unconfined) or non-monotonic (confined): it is rare for an interface to not exhibit segregation (or depletion). We have utilized atom-probe tomography extensively to measure directly Gibbsian interfacial excesses or depletions at heterophase interfaces, using both J. W. Gibbs's and J. W. Cahn's formalisms, for a wide range of systems: nickel-based and aluminum-scandium based alloys, nickel (platinum or rhodium)/silicon interfaces, copper/magnesium oxide and silver/cadmium oxide interfaces produced by internal oxidation of dilute ternary metallic alloys. Atom-probe tomography and atom-probe field-ion microscopy are unique in their ability to measure quantitatively Gibbsian excesses with a minimum amount of data deconvolution. The experimental results are compared with first-principles calculations performed using the Vienna ab initio simulation package for nickel-based alloys.

# Technical Program

11:35 AM

**Full Delineation of Harrison's Diffusion Kinetics Regimes for Grain Boundary Diffusion: A Monte Carlo Study:** *Graeme Murch*<sup>1</sup>; *Irina Belova*<sup>1</sup>; *Thomas Fiedler*<sup>1</sup>; <sup>1</sup>The University of Newcastle

Harrison's classification scheme for the kinetics regimes (A,B and C) for the measurement of grain boundary diffusivities from tracer concentration depth profiles has been very widely accepted. But the locations of the transition points between the various kinetics regimes are very poorly known thereby making detailed analysis of many grain boundary diffusion experiments quite difficult. In this paper, we make use of a recently developed Monte Carlo method that allows the determination of depth profiles in a similar way to that found in experiments. This unique approach allows the transitions between the Harrison kinetics regimes to be readily determined for various well known grain boundary models such as the parallel slab and cubic grain models. The approach is shown to be able to deal with both self-diffusion and impurity diffusion with associated segregation to grain boundaries. The complete map of the Harrison kinetics regimes will be shown.

---

## Thermo-Mechanical Response of Molecular Solids: Multi-Resolution Theory, Simulations, and Experiments: Polymers and Composites

*Sponsored by:* The Minerals, Metals and Materials Society, TMS Electronic, Magnetic, and Photonic Materials Division

*Program Organizers:* Alejandro Strachan, Purdue University; Thomas Sewell, University of Missouri-Columbia; Rodolfo Pinal, Purdue University; Chunyu Li, Purdue University

Wednesday AM      Room: 203  
February 17, 2010      Location: Washington State Convention Center

*Session Chair:* To Be Announced

---

### 8:30 AM Introductory Comments

8:35 AM Invited

**Carbon Nanotube Adhesion: Myths and Magic:** *R. Pipes*<sup>1</sup>; <sup>1</sup>Purdue University

Frictionless interaction of multiwalled carbon nanotubes has been well established, yet the adhesion of carbon nanotubes in bundles and arrays is a major issue in mixing and dispersion. This paper will examine the influence of CNT chirality of adhesion as measured in array flexural AFM experiments and molecular modeling simulations. These observations provide the basis for an adhesion hypothesis that suggests a strong relationship between chirality and the non-bonding adhesion of CNT in both the single and multi-walled geometries.

9:05 AM

**Characterization of Material Response to Indentation Process in Composite**

**Materials:** *Harsha Yejju*<sup>1</sup>; *Alvaro Mendoza*<sup>1</sup>; *Marisol Koslowski*<sup>1</sup>; <sup>1</sup>Purdue University

The difference in bulk matrix properties of polymer and the fiber-matrix interphase region is pronounced at the nanoscale level. Here we present finite elements simulations that show the effect of the variation of the materials properties of this fiber-matrix interphase region. We carry simulations involving high density of fibers aligned in close proximity to each other. We will show the material response to indentation in the fiber-matrix interphase region with multiple fibers in close proximity to each other and the dependence of the material response on the volume of fibers and on the vicinity of the indentation probe.

9:25 AM

**Microstructure Sensitive Design Framework for Elastic-Plastic Multi-Phase Materials:** *Jacqueline Milhans*<sup>1</sup>; *Dongsheng Li*<sup>1</sup>; *Hamid Garmestani*<sup>1</sup>;

<sup>1</sup>Georgia Institute of Technology

In this study, a microstructure sensitive design (MSD) framework for elastic-plastic properties is formulated using 2-point correlation functions. In the past, mechanical behavior predictions have been made for elastic and plastic properties in multiphase materials using correlation functions. This study extends these formulations to predict the elastic-plastic deformation behavior of composite composed by elastic and plastic materials. The formulation is based on solution of the Green's function for elastic-plastic behavior and 2-point correlation

function. Material behavior is predicted by using the 2-point correlation function of a material, which characterizes the morphology and phase volume fraction of the microstructure, and the individual phase properties. These both serve as inputs to the MSD framework, which then predicts the overall behavior of the material. This methodology is applied to a glass-ceramic solid oxide fuel cell (SOFC) seal material, made up of a plastically deforming glass matrix with embedded elastic crystalline needles.

9:45 AM

**Role Loading Conditions on the Mechanical Response of PMMA from Molecular Dynamics:** *Eugenio Jaramillo*<sup>1</sup>; *Alejandro Strachan*<sup>2</sup>; <sup>1</sup>Texas A&M International University; <sup>2</sup>Purdue University

We use molecular dynamics (MD) with the DREIDING force field to characterize the mechanical response of amorphous PMMA including yield and post yield phenomena for various loading conditions. We studied periodic systems with linear dimensions 24 nm and five loading conditions: including pure shear, a series of uniaxial tension deformation with various Poisson's ratios, and isotropic expansion. We find that the pressure-modified von Mises criteria (with critical effective yield stress proportional to hydrostatic pressure) can describe our MD results accurately and with pressure sensitivity in excellent agreement with experiments. The yield stress for zero pressure obtained from MD is about 20% larger than the experimental value due to the large strain rates in the MD simulations. We also study yield criteria in terms of deviatoric and volumetric strain and find that the SIFT can describe our data accurately for deformation paths that involve significant volume expansion.

10:05 AM Invited

**Multiscale Modeling of Polymer Modified Colloidal Suspensions:** *Dmitry Bedrov*<sup>1</sup>; <sup>1</sup>University of Utah

We have applied a multiscale modeling approach to investigate the influence of polymer brush modifications on interactions and rheological properties in dense colloidal suspensions. Specifically, we have investigated polydispersed MgO colloidal suspensions in aqueous solutions modified with poly(ethylene oxide) brushes. The multiscale modeling approach included: a) atomistic explicit solvent molecular dynamics simulations, b) coarse-grained implicit solvent Langevin dynamics (LD) simulations, and c) coarse-grained implicit solvent implicit polymer LD simulations. Each coarse-grained model has been parametrized based on structural and thermodynamic properties obtained from the finer scale simulations.

10:35 AM Break

10:50 AM Invited

**Implications of Dynamic Heterogeneity for Mechanical Behavior of Glassy Polymers:** *Grigori Medvedev*<sup>1</sup>; *James Caruthers*<sup>1</sup>; <sup>1</sup>Purdue University

Existence of dynamic heterogeneities at nano-scale in glass forming materials is well established via a number of experimental techniques. However, existing models of glassy polymer relaxation do not include the dynamic heterogeneity using only the average material properties. Here we report on development of the stochastic constitutive model of glassy materials where the presence of heterogeneities is explicitly acknowledged. This effort is an initial attempt to bridge the gap between traditional molecular simulations and continuum mechanics. Two phenomena are treated: (1) the volume relaxation in response to temperature jumps (2) yield and post-yield behavior in uni-axial tension and compression. The stochastic model predicts volume behavior in a two-step "short anneal" experiment. In the uni-axial constant strain rate experiment the stochastic model predicts yield and post-yield softening and its dependence on the aging time – this is the only constitutive model to-date that predicts, rather than a priori assumes, post-yield softening.

11:20 AM Invited

**Mechanical Properties of Block Copolymer Self-Assemblies:** *Kim Rasmussen*<sup>1</sup>; <sup>1</sup>Los Alamos National Laboratory

We will discuss how self-consistent field theory can be applied to illuminate aspects of the mechanical properties of self-assemblies of block copolymers. Specifically, we will look at how insight into the structure of the physical crosslinking that is responsible for the mechanical properties can be obtained and correlated with observable mechanical properties. Further, we will show how self-consistent field theory methods, can provide direct calculation of the components the tensile and shear moduli that arise from structural properties of the self-assembled materials. Finally, we demonstrate how a generalized self-



consistent field theory for polymer melts that explicitly includes elastic stress and strain fields can be applied to the study of block copolymers melts. This technique allows the calculation of the overall stress profile of the materials and we show that it is the result of the combined effects of chain connectivity across the interface, and the immiscible nature of the monomers.

**11:50 AM**

**Molecular Dynamics Simulations of Crosslinked EPON862/DETDA Polymers:** *Chunyu Li*<sup>1</sup>; *Alejandro Strachan*<sup>1</sup>; <sup>1</sup>Purdue University

Currently, there is a great interest in aircraft industry to use thermosetting polymers as the matrices of composites because of their higher stiffness, higher creep resistance and higher thermal resistance over thermoplastic polymers. These favorite properties come from the 3D crosslinked structures of thermosetting polymers. A fundamental understanding of the structural evolution and the relationship between material properties and molecular structures is essential. Computer simulations provide an attractive substitute technique for better understanding these polymers. The objective of this study is to provide a more comprehensive molecular dynamics (MD) simulation procedure for thermosetting polymers. The system we chose is epoxy resin EPON-862 with curing agent DETDA. In this presentation, we will systematically address the issue of atomic charge distribution and introduce a new effective charge updating approach. The procedure introduced in this paper is expected to be applied to the MD simulations of other thermosetting polymer systems without any difficulties.

**12:10 PM**

**Role of Interface Thermal Boundary Resistance, Straining and Morphology in Thermal Conductivity of a Set of Si-Ge Superlattices and Biomimetic Si-Ge Nanocomposites:** *Vikas Samvedi*<sup>1</sup>; *Vikas Tomar*<sup>2</sup>; <sup>1</sup>University of Notre Dame; <sup>2</sup>Purdue University

Comparison of thermal behavior of superlattices and nanocomposites considering their characteristic structural factors such as periodicity and period length for superlattices, and morphology for nanocomposites, is performed for a set of Si-Ge superlattices and Si-Ge biomimetic nanocomposites using non-equilibrium molecular dynamics (NEMD) simulations at three different temperatures (400 K, 600 K, and 800 K) and at strain levels varying between -10% and 10%. The analysis of interface TBR contradicts the usual notion that each interface contributes equally to the heat transfer resistance in a layered structure. The comparison of thermal behavior of superlattices and nanocomposites indicate that the morphology differences lead to a striking contrast in the phonon spectral density, interfacial thermal boundary resistance, and thermal conductivity. Both compressive and tensile strains are observed to be important factors in tailoring the thermal conductivity of the analyzed superlattices, whereas have very insignificant influence on the thermal conductivity of the analyzed nanocomposites.

**Three-Dimensional Materials Science VI: Novel Tools for 3D Data Acquisition and Analysis - Part I**

*Sponsored by:* The Minerals, Metals and Materials Society, ASM International, TMS Structural Materials Division, TMS: Advanced Characterization, Testing, and Simulation Committee, ASM-MSCTS: Texture and Anisotropy Committee, TMS/ASM: Phase Transformations Committee

*Program Organizers:* Alexis Lewis, Naval Research Laboratory; Anthony Rollett, Carnegie Mellon University; David Rowenhorst, Naval Research Lab; Jeff Simmons, AFRL; Stuart Wright, EDAX Inc-TSL

Wednesday AM Room: 401  
February 17, 2010 Location: Washington State Convention Center

*Session Chairs:* Alexis Lewis, U S Naval Research Laboratory; John Budai, Oak Ridge National Laboratory

**8:30 AM Invited**

**3-D Materials Science using Polychromatic Synchrotron X-Ray Microdiffraction:** *John Budai*<sup>1</sup>; *Jon Tischler*<sup>1</sup>; *Wenjun Liu*<sup>2</sup>; *Anthony Rollett*<sup>3</sup>; <sup>1</sup>Oak Ridge National Laboratory; <sup>2</sup>Argonne National Lab; <sup>3</sup>Carnegie Mellon University

Synchrotron x-ray microdiffraction facilities continue to make progress in providing new techniques for quantitative, 3-D structural studies in

materials science. In particular, we have developed a polychromatic, scanning microdiffraction and microfluorescence beamline with submicron spatial resolution at the Advanced Photon Source. X-ray area detectors such as the one recently implemented on our beamline are capable of collecting raw images at rates exceeding 5 GB/min. Such large datasets require rapid, automated analysis techniques in order to obtain 3-D spatially-resolved lattice, orientation, and strain maps. This presentation will review progress in 3-D Laue micro- and nano-diffraction techniques and will illustrate how nondestructive x-ray microscopy can provide unique measurements in the areas of thermal grain growth and phase separation. The goal of these studies is to provide experimental datasets for comparison with computational theory and modeling. Support at ORNL, UT-Battelle by DOE-BES, Materials Sciences and Engineering Division; UNIXOR support at APS by DOE-BES.

**9:00 AM**

**Applications of a Local-Electrode Atom-Probe (LEAP) 4000X Si for Obtaining Three-Dimensional Chemical Information with Subnanoscale Resolution:** *David Seidman*<sup>1</sup>; <sup>1</sup>Norhwestern University

Results obtained utilizing the first commercial LEAP 4000X Si, installed in the Northwestern University Center for Atom-Probe Tomography in early July 2009, are presented. This instrument utilizes a short wavelength picosecond solid-state laser to dissect specimens on an atomic scale, one atom at a time, at pulse repetition rates of up to 1000 kHz. The LEAP 4000X Si has many unique advantages over earlier versions of LEAP tomographs. Particularly, it has a smaller spot size, significantly improved mass resolution (1/1800 FWHM for Al), and a larger signal-to-noise (S/N) ratio. The smaller spot size produces more localized laser-beam heating, which results in a lower background and improved mass resolution. The larger value of the S/N ratio implies a smaller minimum detectable mass. The 4000X Si is used for analyzing high-strength low-carbon steels, nickel-based and aluminum-scandium-based alloys, silicidation reactions, low-energy implants in silicon, and magnesium oxide layers in magnetic tunnel junctions.

**9:20 AM**

**Partitioning Behavior of Al and Si in FINEMET Nanocrystalline Soft Magnetic Alloys, as Studied by Atom-Probe Tomography:** *Keith Knippling*<sup>1</sup>; *Maria Daniil*<sup>1</sup>; *Matthew Willard*<sup>1</sup>; <sup>1</sup>Naval Research Laboratory

FINEMET is a nanocrystalline soft magnetic material comprised of ~70 vol.% randomly oriented D<sub>0</sub><sub>3</sub> Fe-Si grains (~10 nm) embedded in a residual B- and Nb-rich amorphous matrix. Owing to the small grain size, the magnetocrystalline anisotropy is averaged out by exchange interactions and the alloys possess a unique combination of large magnetization, high permeability, and low core losses. Substituting Al for Fe further decreases the magnetocrystalline anisotropy of the nanocrystals. We employ three-dimensional atom-probe tomography to quantify the phase compositions obtained in a series of (Fe,Si,Al)<sub>87</sub>B<sub>9</sub>Nb<sub>3</sub>Cu<sub>1</sub> alloys. Relationships between the compositions of the nanocrystals and the observed bulk magnetic properties (saturation magnetization and coercivity) are discussed. The wide field-of-view of modern atom-probes now also enables detailed structural analysis, including measurement of grain size, volume fraction, number density, and edge-to-edge intergranular distances directly in three dimensions. We correlate these measurements to structural information obtained by X-ray diffraction and transmission electron microscopy.

**9:40 AM**

**Recent Advances in Atom Probe Tomography for 3D Microstructural Characterization:** *Michael Miller*<sup>1</sup>; <sup>1</sup>ORNL

Atom probe tomography is one of the most direct methods for the characterization of fine scale microstructures, as the technique generates the atomic coordinates and mass-to-charge state and hence the elemental identity of the atoms in the sampled volumes. Recent advances in atom probe instrumentation enable datasets into the billion atom range to be collected. Several statistical methods have been developed to extract important microstructural information of the features present in these data. These data can be directly compared to atomistic models and simulations of the microstructure. A review of the recent major advances in local electrode atom probe (LEAP®) instrumentation and data analysis techniques and the resulting improvements in performance will be presented. Research at the Oak Ridge National Laboratory SHaRE User Facility was sponsored by the Scientific User Facilities Division, Office of Basic Energy Sciences, U.S. Department of Energy.

Wed. AM

# Technical Program

10:00 AM

**Atom Probe Studies on the Segregation of C and N in Fe-17%Mn Steels:** *Jae-Bok Seol*<sup>1</sup>; *Soon-Ki Lee*<sup>2</sup>; *Chan-gyung Park*<sup>3</sup>; <sup>1</sup>POSTECH; <sup>2</sup>POSCO; <sup>3</sup>POSTECH, NCNT

It has been widely known that Fe-17wt.%Mn steels exhibit a good damping capacity, which is caused by the movement of  $\gamma/\epsilon$  interface formed on cooling. Since undesired C and N are often added to the steels during commercial fabrication process, the damping capacity of the steels is deteriorated. However, the effects of C and N on the damping sources have not been understood yet. In the present study, atom probe tomography with tunable laser, high spatial resolution of 2–3 nm, was applied to investigate the exact position and quantitative information of impurity atoms in Fe-17%Mn. The current results have demonstrated that APT techniques have made it possible to identify and quantify the exact state of C and N with three dimensional tomography imaging and composition profile in the atomic scale. The discussion on segregation of C and N at the  $\gamma/\epsilon$  interface and  $\epsilon$  martensite phase will be followed.

10:20 AM Break

10:50 AM

**Correlative Microscopy: 3-D Multiscale Imaging and Modelling:** *Farid Tariq*<sup>1</sup>; *Ralph Haswell*<sup>2</sup>; *Peter Lee*<sup>1</sup>; *David McComb*<sup>1</sup>; <sup>1</sup>Imperial College London; <sup>2</sup>Shell Global Solutions International B.V.

Materials are often inadequately described using 2-D imaging and furthermore their properties can depend on their structure on multiple length scales. In this study several tomographic techniques will be combined to investigate 3-D structure on length scales that span four orders of magnitude. Heterogeneous ceramic catalysts are an ideal system to analyse as they represent a material where functionality is dependant on multiscale flow of molecules through a hierarchical pore structure. Consequently, multiscale characterisation of their structure can provide key insights for future catalyst design. Ceramic catalysts were analysed using (i) synchrotron x-ray microtomography (XMT); (ii) serial sectioning using dual beam focused ion beam (DB-FIB); and electron tomography (ET). Each respective technique provides information at different scale lengths for different volume sizes. Shapes, structures and morphology can be characterised and the structure modelled to provide useful insights into catalyst performance and lifetime.

11:10 AM

**Multi-Scale Characterization of a Ni-Base Single Crystal Turbine Blade:** *Michael Groeber*<sup>1</sup>; *Dennis Dimiduk*<sup>1</sup>; *Chris Woodward*<sup>1</sup>; *Michael Uchic*<sup>1</sup>; *Rebecca Fahringer*<sup>1</sup>; <sup>1</sup>AFRL

Multi-scale modeling of materials dictates the need for multi-scale characterization of structure. Over the past decade, multiple tools for collecting 3D structure information at various scales have matured, but without a concerted effort to link their resultant data. This work will focus on the collection of 3D structure information across multiple scales and the integration of the data into a systems level representation of the material. Specifically, this talk will focus on the experimental collection of the 3D structure information for a Ni-base superalloy turbine blade. The characterization process employed in this study is truly multi-scale in nature and requires the integration of various investigatory techniques. The microstructural features of interest span 3–4 orders of magnitude and are visible after different preparation steps and under different imaging conditions. This presentation will outline the approach necessary to characterize this material at the systems level in a robust fashion.

11:30 AM

**Multi-Length Scale Three Dimensional Characterization of Tantalum Carbide Microstructures:** *Robert Morris*<sup>1</sup>; *Gregory Thompson*<sup>1</sup>; <sup>1</sup>The University of Alabama

Tantalum carbide compounds have been fabricated by either hot-isostatic pressing (HIP), spark plasma sintering (SPS), and vacuum plasma spraying (VPS) of constituent powders. Depending upon the targeted stoichiometry (TaC or Ta<sub>2</sub>C or mixed) and fabrication process, a single or dual phase microstructure can be formed. The duplex microstructure was found to be either acicular grains in HIP processes or laths within equiaxed grains for arc based processing. The microstructures have been analyzed across different length scales. Atom probe tomography has revealed preferential segregation of powder impurities, including iron, to the grain boundaries. STEM-HAADF tomography has revealed that the laths are tens of nm thick and can terminate through mutual intersections. Serial sectioning FIB based techniques reveal the global structure

in which the laths do not necessarily span the entire grain. The collective combination of 3D techniques will describe the formation and stability of tantalum carbide microstructures.

11:50 AM

**ACrystal-Plasticity FEM Study on Effects of Simplified Grain Representation and Mesh Types on Mesoscopic Deformation Heterogeneities:** *Yoon Suk Choi*<sup>1</sup>; *Michael Groeber*<sup>2</sup>; *Dennis Dimiduk*<sup>2</sup>; *Christopher Woodward*<sup>2</sup>; *Michael Uchic*<sup>2</sup>; *Triplicane Parthasarathy*<sup>1</sup>; <sup>1</sup>UES, Inc.; <sup>2</sup>Air Force Research Laboratory

Polycrystalline microstructure-based elastic or elasto-viscoplastic FEM approaches have been a subject of numerous studies since these approaches provide crucial information regarding the development of mesoscopic deformation heterogeneities and its microstructural dependence. However, only few preliminary parametric studies have attempted to clarify and understand numerical artifacts, which might be caused by simplified grain geometries, intractable meshes and ad-hoc RVE selection. The present study systematically investigated the influence of the simplification of grain boundary morphologies and the selection of different mesh types on the distribution of simulated flow heterogeneity across the grain boundary. A bicrystal sphere embedded in a cubic box was utilized to perform the current preliminary parametric study. Simulation results were analyzed using various statistical characterization techniques.

## Ultrafine Grained Materials – Sixth International Symposium: Young Scientist

**Sponsored by:** The Minerals, Metals and Materials Society, TMS Materials Processing and Manufacturing Division, TMS Structural Materials Division, TMS/ASM: Mechanical Behavior of Materials Committee, TMS: Nanomechanical Materials Behavior Committee, TMS: Shaping and Forming Committee

**Program Organizers:** *Suveen Mathaudhu*, U.S. Army Research Laboratory; *Mathias Goeken*, University Erlangen–Nürnberg; *Terence Langdon*, University of Southern California; *Terry Lowe*, Manhattan Scientifics, Inc.; *S. Semiatin*, Air Force Research Laboratory; *Nobuhiro Tsuji*, Kyoto University; *Yonghao Zhao*, University of California - Davis; *Yuntian Zhu*, North Carolina State University

Wednesday AM

Room: 606

February 17, 2010

Location: Washington State Convention Center

**Session Chairs:** *Terry Langdon*, University of Southern California; *Suveen Mathaudhu*, U.S. Army Research Laboratory; *Yuntian Zhu*, North Carolina State University; *Terry Lowe*, Manhattan Scientifics, Inc.

8:30 AM

**Grain Growth Kinetics for an Aluminum Based Nanocomposite:** *Leyla Hashemi-Sadraei*<sup>1</sup>; *Rustin Vogt*<sup>1</sup>; *Zhihui Zhang*<sup>1</sup>; *Ying Li*<sup>1</sup>; *S. Ebrahim Mousavi*<sup>1</sup>; *Enrique Lavernia*<sup>1</sup>; *Julie Schoenung*<sup>1</sup>; <sup>1</sup>University of California, Davis

An aluminum based nanocomposite has been produced by cryomilling powders of aluminum 5083 and boron carbide. This material when consolidated is known to exhibit super-high strength and good stiffness due to the ultrafine grained (UFG) structure of aluminum and incorporation of B<sub>4</sub>C reinforcement, respectively. The thermal stability which is essential for UFG materials has been studied for these nanocomposite powders by annealing at various temperatures for select times. The effect of cryomill-generated second phase particles on thermal stability of UFG aluminum grains was investigated. Further, grain growth kinetics and mechanisms were studied based on the experimental results and existing grain growth equations. For this purpose, grain size values were calculated and compared using several X-ray-based methods in addition to observation with transmission electron microscopy. The results provided a better understanding of grain size calculation techniques and confirmed the expected high thermal stability of this material. (I'd like to be considered for the Young Scientist Session)

8:45 AM

**Influence of High-Pressure Torsion on Hardness of a Supersaturated Al-7136 Alloy:** *Zhi Duan*<sup>1</sup>; *Xiaozhou Liao*<sup>2</sup>; *Megumi Kawasaki*<sup>1</sup>; *Roberto Figueiredo*<sup>1</sup>; *Terence Langdon*<sup>1</sup>; <sup>1</sup>University of Southern California; <sup>2</sup>University of Sydney

The potential for further strengthening of the 7000 series Al alloys using severe plastic deformation makes it attractive to apply high-pressure torsion

(HPT) to the Al-7136 alloy. In addition to HPT processing, different pre-processing was conducted by equal-channel angular pressing including 1 pass at room temperature and 4 passes at 473 K. Hardness contour mapping was used to demonstrate the presence of a complicated microhardness evolution which depended upon the pre-processing as well as the strains imposed in processing. The effect of HPT on the Al-7136 alloy is discussed based on TEM images of the grains and precipitates. It is shown that HPT processing significantly refines the grain size to a minimum size of less than 40 nm in some parts of the sample and promotes grain boundary segregation of excessive alloying elements.

**9:00 AM**

**Microstructural Characterization of Ti-6Al-4V Metal Chips by Focused Ion Beam and Transmission Electron Microscopy:** *Lei Dong*<sup>1</sup>; Judy Schneider<sup>1</sup>; Jane Howe<sup>2</sup>; <sup>1</sup>Mississippi State University; <sup>2</sup>Oak Ridge National Laboratory

It has been reported that chips formed during metal cutting contain nanocrystalline structures. This current study utilizes focused ion beam (FIB) techniques to prepare transmission electron microscopy (TEM) thin foils from various regions and orientations of cut Ti-6Al-4V metal chips to verify the crystalline nature of the chips. Images of the resulting microstructure were obtained via TEM and used to construct a 3-dimensional image. A range of grain sizes and morphologies were observed, which are consistent with an inhomogeneous deformation process. A comparison of the results obtained at different length scales will be presented. Research supported in part by ORNL's SHaRE User Facility, which is sponsored by the Scientific User Facilities Division, Office of Basic Energy Sciences, the U.S. Department of Energy.

**9:15 AM**

**UFG Aluminum Alloy Tested in Dynamic High Temperature Compression:** *Emily Huskins*<sup>1</sup>; K. Ramesh<sup>1</sup>; <sup>1</sup>Johns Hopkins University

Materials with ultra-fine grained (UFG) nanostructures have been of interest for many years due to their improved strengthening over their coarse-grained counterparts. However, these UFG materials also exhibit different strain rate sensitivity and deformation mechanisms, both of which affect the stability of plastic deformation and therefore ultimate failure of the material. Such plastic instabilities may be localized and experience a significant temperature rise due to plastic work during nearly-adiabatic dynamic deformations. However, there are limited studies of the material response of UFG materials at both high temperatures and high strain rates. In this work an UFG aluminum alloy is tested under dynamic compression ( $10^3\text{s}^{-1}$ ) loading at elevated temperatures (298K – 673K). The material response including strain rate sensitivity and thermal softening are discussed.

**9:30 AM**

**Work-Hardening Stages of AA1070 and AA6060 after Severe Plastic Deformation:** *Matthias Hockauf*<sup>1</sup>; Lothar W. Meyer<sup>1</sup>; Ines Schneider<sup>2</sup>; <sup>1</sup>Chemnitz University of Technology; <sup>2</sup>Wehrwissenschaftliches Institut für Werk- und Betriebsstoffe

Based on the concept of work-hardening for f.c.c. metals the commercially pure aluminium AA1070 (soft annealed) and the aluminium alloy AA6060 (peak aged) were investigated. Equal-Channel Angular Pressing (ECAP) was used to introduce very high strains and an ultrafine-grained microstructure. Subsequently compression tests were performed in a wide range of strain rates between 10<sup>-4</sup> and 10<sup>3</sup> s<sup>-1</sup>. The results indicate that strain path and the corresponding dislocation structure is important for the post-ECAP yielding and the following hardening response. Furthermore the precipitates of the AA6060 clearly constrain the interactions of dislocations in work-hardening stage III – causing lower strain rate sensitivity. If compared to the AA1070 they avoid hardening in stage V where an additional rate and temperature depending effect contributes – caused by the interaction of deformation induced vacancies and dislocations.

**9:45 AM**

**Unusual Macro-Structure and Hardness Patterns in Duplex Stainless Steel Processed by High-Pressure Torsion:** *Yang Cao*<sup>1</sup>; Yanbo Wang<sup>1</sup>; Saleh Alhajeri<sup>2</sup>; Xiaozhou Liao<sup>1</sup>; Simon Ringer<sup>1</sup>; Terence Langdon<sup>3</sup>; Yuntian Zhu<sup>4</sup>; <sup>1</sup>The University of Sydney; <sup>2</sup>University of Southampton; <sup>3</sup>University of Southern California; <sup>4</sup>North Carolina State University

We report a surprising observation that double swirl shear strain patterns and local shear vortices form in duplex stainless steel disks processed by high-pressure torsion (HPT). This contradicts our conventional belief that the processing strain only varies with the distance from the disc center. Duplex

stainless steel disks with appropriately the same volume fraction of austenite and ferrite phases were processed using HPT for a series of from 2 to 20 revolutions. The macroscopic shear strain induced by HPT and its evolution were visualized using optical microscopy. Microstructural evolution was characterized using transmission electron microscopy (TEM). Hardness evolution of the two phases was investigated using nanoindentation and the results were correlated with the local structural features observed from TEM.

**10:00 AM**

**Improvement of Strength and Ductility for an AA6065 Aluminium Alloy Achieved by a Combination of Equal-Channel Angular Pressing and Ageing Treatment:** Lothar W. Meyer<sup>1</sup>; *Kristin Hockauf*<sup>1</sup>; Matthias Hockauf<sup>1</sup>; Thorsten Halle<sup>1</sup>; <sup>1</sup>Chemnitz University of Technology

Incited by the aim of improving the strength and preserving a moderate ductility, the promising approach of a combined ECAP (equal-channel angular pressing) and ageing treatment was applied to AA6056, an AlMgSi(Cu)-alloy. In this presentation, the evolution of hardness during post ECAP ageing and the effect of ageing temperature and time on strength and ductility will be discussed. By means of scanning transmission electron microscopy, the underlying microstructural features in terms of grain size and precipitation characteristics of coherent  $\beta''$  and semicoherent Q' precipitates will be presented. It was found that peak-ageing especially at low ageing temperatures is suitable for achieving the desired high-strength combination, whereas – on the expense of some percent in the strengthening- the ductility is best in slightly underaged conditions. Compared to the initial peak-aged condition, an increase in strength of 30%, combined with a moderate ductility of 7% uniform elongation could be achieved.

**10:15 AM Break**

**10:30 AM**

**Aging of an Al-Si-Mg Alloy Processed by ECAP: The Effect of the Initial Microstructure:** *Edgar Garcia-Sanchez*<sup>1</sup>; Edgar Ortiz-Cuellar<sup>1</sup>; Edgar Lopez-Chipres<sup>2</sup>; Martha P. Guerrero-Mata<sup>1</sup>; Rafael Colás<sup>1</sup>; <sup>1</sup>FIME-UANL; <sup>2</sup>Facultad de Química, Universidad Juárez del Edo. de Durango

With the aim to study the second phase particles effect on the grain refinement and mechanical properties in Aluminum alloy, in this work a commercial Al-Mg-Si alloy under various initial microstructural conditions has been deformed at room temperature by multi-pass 90° equal channel angular pressing (ECAP). The alloy after ECAP was aged under different conditions. The post ECAP annealing heat treatments in some cases promote high strengths and relatively high ductility; these were evaluated by means of tensile tests carried out at room temperature. The grain refinement was promoted by the presence of particles as observed by SEM and TEM. With this work was possible to obtain the optimal conditions for processing an Aluminum alloy under SPD and post aging heat treatments improving the mechanical properties.

**10:45 AM**

**Grain Size Effect on the Deformation Mechanisms and Mechanical Properties of Gum Metals:** *Yanbo Wang*<sup>1</sup>; Xiaozhou Liao<sup>1</sup>; Yonghao Zhao<sup>2</sup>; Enrique Lavernia<sup>2</sup>; Ruslan Valiev<sup>3</sup>; <sup>1</sup>The University of Sydney; <sup>2</sup>University of California, Davis; <sup>3</sup>Ufa State Aviation Technical University

Gum Metals are an emerging class of multifunctional titanium alloys with superior mechanical properties including super elasticity, super strength, and superplastic-like cold workability, which arise from their unusual deformation mechanisms. It has been well-established that reducing grain sizes down to the ultrafine-grained (< 1  $\mu\text{m}$ ) and nanocrystalline (< 100 nm) regimes affects significantly the deformation mechanisms of materials, and that this in turn affects mechanical properties of the materials. In this presentation, we will report our investigation results on the effect of grain size reduction on the deformation mechanisms and mechanical properties of Gum Metals. Grain size reduction is achieved via severe plastic deformation. Deformation mechanisms and mechanical properties are investigated using in-situ and ex-situ transmission electron microscopy and hardness test.

**11:00 AM**

**Equal Channel Angular Pressing of Pure Gold:** *Anumalasetty Nagasekhar*<sup>1</sup>; T. Rajkumar<sup>2</sup>; D. Stephan<sup>2</sup>; Y. Tick-Hon<sup>3</sup>; <sup>1</sup>The University of Queensland; <sup>2</sup>Heraeus Materials Singapore Pte Ltd; <sup>3</sup>University of Toronto

Equal channel angular pressing (ECAP) is the most promising severe plastic deformation (SPD) technique for fabrication of bulk ultrafine and nanostructured

# Technical Program

materials, compaction of powders, and mechanical property enhancement of tubular materials. Large variety of materials has been processed through ECAP to fabricate ultrafine and nano structures. In current studies, the precious metal pure gold (99.99% purity) is processed upto twelve ECAP passes via Route Bc (90 degree clock wise rotation between successive passes). The microstructural and mechanical properties changes in the pure gold with increase in ECAP passes have been reported.

**11:15 AM**

**Synthesis of Bulk Nanostructured Cu via Spark Plasma Sintering and High Pressure Torsion of Cryomilled Powders:** *Haiming Wen*<sup>1</sup>; *Yonghao Zhao*<sup>1</sup>; *Osman Ertorer*<sup>1</sup>; *Troy Topping*<sup>1</sup>; *Ruslan Valiev*<sup>2</sup>; *Enrique Lavernia*<sup>1</sup>; <sup>1</sup>University of California at Davis; <sup>2</sup>Ufa State Aviation Technical University

Bulk nanostructured materials can be prepared using a variety of severe plastic deformation methods. These can be grouped into two general categories, discrete powder methods (e.g., cryomilling and cold finger deposition) and solid state transformation methods (e.g., equi-channel pressing). Powder consolidation methods provide benefits, such as control of grain size distribution, resistance against grain growth and scale-up potential; however, some disadvantages include contamination and incomplete particle bonding which can lead to porosity. In this study, we use spark plasma sintering (SPS) and high pressure torsion to synthesize bulk dense nanostructured Cu. The Cu powders, with an average grain size of 20 nm, were prepared via cryomilling in liquid nitrogen. High-pressure SPS is used to prepare bulk NS Cu. In addition, high pressure torsion was used to consolidate dense NS Cu at its super-plasticity regime. Mechanical properties and microstructures are measured and compared with particular emphasis on operative deformation mechanisms. (I'd like to be considered for the Young Scientist Session)

**11:30 AM**

**Continuous High Pressure Torsion:** *Kaveh Edalati*<sup>1</sup>; *Zenji Horita*<sup>1</sup>; <sup>1</sup>Kyushu University

Continuous high pressure torsion (CHPT) was developed as a severe plastic deformation process (SPD) so that the ribbons of high purity Al, Cu and Fe with rectangular cross sections, 0.6mm thickness and 3mm width, were successfully processed by introducing intense strain under high pressure. It is shown that the results of hardness measurements by CHPT are well consistent with those of conventional HPT using disc and ring specimens. Microstructural observations using transmission electron microscopy demonstrate that CHPT can be used as a continuous SPD process for grain refinement.

**11:45 AM**

**Unconventional ECAE Processing of Magnesium Alloys:** *David Foley*<sup>1</sup>; *Majid Al-Maharbi*<sup>1</sup>; *K.T. Hartwig*<sup>1</sup>; *Ibrahim Karaman*<sup>1</sup>; *Hans Maier*<sup>2</sup>; *L.J. Kecskes*<sup>3</sup>; *Suveen Mathaudhu*<sup>3</sup>; <sup>1</sup>Texas A&M University; <sup>2</sup>University of GH Paderborn; <sup>3</sup>US Army Research Lab

While SPD matured as a research area, standard deformation techniques were adopted by groups worldwide. In ECAE/ECAP this includes die angles, processing routes, and workpiece geometries. Although this standardization allows for intra-lab repeatability and understanding, it can influence a researcher's thought process: "What route/temperature is best?" rather than "What microstructure and texture am I seeking and what deformation modes and strain paths do I need to get there?" The researcher's approach becomes especially important in materials with limited slip systems, high mechanical anisotropy, or variable room-temperature phase concentration and morphology. An examination of conventional and unconventional ECAE processing in magnesium alloys will illustrate the importance of customized processing methods for achieving desired textures and microstructures. Hybrid routes, intra-pass temperature variation, and SPD + Rolling allow for greater control over the material's resulting mechanical properties.

**12:00 PM**

**Thermal Stability of Ultrafine Grained 316 Austenitic Stainless Steel:** *Auriane Etienne*<sup>1</sup>; *Bertrand Radiguet*<sup>1</sup>; *Ruslan Valiev*<sup>2</sup>; *Cécile Genevois*<sup>1</sup>; *Jean-Marie Le Breton*<sup>1</sup>; *Philippe Pareige*<sup>1</sup>; <sup>1</sup>GPM UMR CNRS 6634; <sup>2</sup>Institute of Physics of Advanced Materials

Austenitic Stainless steels (ASS) in internal structures of pressurized water reactor are susceptible to irradiation-assisted stress corrosion cracking (IASCC). Even if this complex form of material degradation is still not well understood, only the combination of all irradiation-induced microstructural changes (point defect (PD) and solute clustering, segregation at grain boundaries (GB)...

can lead to IASCC. Since all these changes are essentially due to PD supersaturation, increasing PD annihilation at GB could limit IASCC. A 316 ASS has been nano-structured by high pressure torsion and ion irradiated at 350°C. The evolution of the grain size under the ion irradiation has been measured. However, this evolution may be the result of a combination of thermal and irradiation effects. Thus, the thermal stability of this nano-material was investigated using complementary techniques (transmission electron microscopy, X-ray diffraction and Mössbauer Spectroscopy). Results after thermal ageing between 350 up to 900°C will be presented and discussed.

**12:15 PM**

**A Study of the Thermal Stability of Nano-Twinned Copper:** *Christopher Saldana*<sup>1</sup>; *Sergey Suslov*<sup>1</sup>; *Matthew Hudspeth*<sup>1</sup>; *Eric Stach*<sup>1</sup>; *Srinivasan Chandrasekar*<sup>1</sup>; <sup>1</sup>Purdue University

Inadequate thermal stability has precluded the widespread application of nanostructured materials. The use of conventional stabilization methods has generally only been feasible in multi-component nanostructured systems, leaving single-component systems without an effective route to thermal stabilization. In this study, stabilization in high purity copper is demonstrated through the stability afforded by a dense network of twin boundaries. A range of microstructures, including one dominated by twins, is produced in the copper by carrying out deformation under a wide set of conditions – strain rates varying from 10 to 10<sup>3</sup> per second, strains from 1 to 7 and temperatures as low as cryogenic. Stability of these microstructures is evaluated by microstructure observation, strength measurement and calorimetry. Changes in microstructure and hardness stability, as well as a switchover from grain boundary mediated diffusion to twin diffusion, is demonstrated in the case of heavily twinned copper.

## 2010 Functional and Structural Nanomaterials: Fabrication, Properties, Applications and Implications: Characterization of Nanomaterials

*Sponsored by:* The Minerals, Metals and Materials Society, TMS Electronic, Magnetic, and Photonic Materials Division, TMS: Nanomaterials Committee

*Program Organizers:* David Stollberg, Georgia Tech Research Institute; Nitin Chopra, University of Alabama; Jiyoung Kim, University of Texas - Dallas; Seong Jin Koh, University of Texas at Arlington; Navin Manjooran, Siemens Corporation; Ben Poquette, Keystone Materials; Jud Ready, Georgia Tech

Wednesday PM Room: 214  
February 17, 2010 Location: Washington State Convention Center

*Session Chair:* Nitin Chopra, University of Alabama; Jiyoung Kim, University of Texas - Dallas

**2:00 PM Introductory Comments**

**2:05 PM**

**The Investigation on Internal Structure of Spherical Graphites in Ductile Cast Iron by Transmission Electron Microscopy:** *Ali-Reza Kaini-Rashid*<sup>1</sup>; *Arash Elhami-Khorasani*<sup>1</sup>; <sup>1</sup>Ferdowsi University of Mashhad

Microstructure of cast irons often consists of two totally different phases: Metallic matrix (like steel microstructures), and graphite with semi metallic properties. In the process of preparing the specimens for observing by TEM, maintenance of graphite particles before reaching adequate thinness is not quiet easy. In the present study, by choosing the specific techniques, it has been attempted to maintain the spherical graphites in their primer locations, while reaching extreme thinness. This leads to the ability of having a clear microscopic observation of the graphites' internal structure, especially on the outer layers. Further studies reveal these graphites; consist of a laminar internal structure with a special rotation pattern along crystal planes.

**2:25 PM**

**Selective Placement of Single Nanoparticles of Different Sizes:** *Pradeep Bhadrachalam*<sup>1</sup>; *Seong Jin Koh*<sup>1</sup>; <sup>1</sup>University of Texas at Arlington

For practical applications involving nanoscale building blocks such as nanoparticles, nanotubes, and nanowires, it is necessary to place these building blocks onto desired substrate locations. We demonstrate a new technique for

Wed. PM



precise placement of individual nanoparticles of different sizes onto different target locations on the same substrate. This was done in a self-limiting manner using wet chemistry and CMOS-compatible parallel processing. Au nanoparticles (AuNPs) with  $\approx 20\text{nm}$  and  $\approx 50\text{nm}$  in diameter were used as a model system. This size-selective placement was achieved using electrostatic guiding structures which first guide single  $\approx 50\text{nm}$  AuNPs onto targeted locations and then single  $\approx 20\text{nm}$  AuNPs onto different target locations. Theoretical analysis revealed that the change in the free energy barrier after the placement of a single nanoparticle onto a targeted location is responsible for self-limiting size-selective placement of nanoparticles.

### 2:45 PM

**Activation Energy for Crystallization in Nanocrystalline Exchange Coupled Magnets:** *Matthew Willard*<sup>1</sup>; *Maria Daniil*<sup>2</sup>; *B. Hornbuckle*<sup>3</sup>; *Juan Saavedra*<sup>4</sup>; <sup>1</sup>Naval Research Laboratory; <sup>2</sup>George Washington University; <sup>3</sup>University of Alabama - Tuscaloosa; <sup>4</sup>University of Puerto Rico - Mayaguez

Nanocrystalline soft magnetic alloys have been studied for their excellent magnetic performance. Amorphous materials are processed using the rapid solidification technique melt spinning. The rapidly solidified alloys are isothermally annealed to improve their magnetic performance by partially devitrifying the ribbon samples. To examine the crystallization kinetics, constant heating rate experiments were performed with heating rates varied between 2 and 85°C/min from 50 to 900°C. In this study, the crystallization kinetics of alloys with composition (Fe, Co, Ni)-Zr-B-(Cu) are determined by Kissinger analysis. The thermally activated primary crystallization temperature was observed for each sample at numerous heating rates to provide accurate activation energies. Fe-rich alloys have activation energies (3.0-3.5 eV/atom), while Ni-rich alloys have lower activation energies (2.1-2.5 eV/atom). The reduced activation energy likely results from the more active diffusion in Ni-based alloys and may be a reason for the deteriorated nanocrystalline alloy formation at these compositions.

### 3:05 PM

**Tunneling Spectroscopy of Colloidal Nanoparticles:** *Ramkumar Subramanian*<sup>1</sup>; *Pradeep Bhadrachalam*<sup>1</sup>; *Seong Jin Koh*<sup>1</sup>; <sup>1</sup>The University of Texas at Arlington

For practical applications of nanoparticles such as in nanoelectronics, photonics, and bio-medicine, knowledge of their electronic structure plays a critical role. We demonstrate a new solid-state tunneling spectroscopic technique for individual nanoparticles that not only enables direct probing of the energy levels of a single nanoparticle, but many such measurement units can be fabricated in a single-batch process. Resonant tunneling between the vertically separated electrodes and the nanoparticle placed between these electrodes forms the basis of spectroscopic measurements. Spectroscopic units with  $\approx 7\text{nm}$  CdSe nanoparticles were used as a model system. Current-voltage measurements for these units yielded the energy level spacings and the band gap by numerical differentiation of the I-V plots. These will be compared with measurements using the lock-in method that directly measures differential conductance.

### 3:25 PM

**Grains Size Effect on Density of Geometrically Necessary Dislocations:** *Eduard Kozlov*<sup>1</sup>; *Nina Koneva*<sup>1</sup>; <sup>1</sup>Tomsk State University of Architecture and Building

The scalar density of dislocations can be divided on two components: statistically stored dislocations (SSD) also geometrically necessary dislocations (GND). SSD are braked by rather weak barriers - other dislocations. If at metal or an alloy there are stronger barriers there is accumulation of GND. Density GND is proportional to a deformation gradient. The density of excess dislocations is proportional to curvature-torsion of a crystal lattice or a deformation gradient. In work methods of measurement of density as GND, and excess dislocations are considered. Measurements of these sizes on polycrystals of pure metals, solid solutions and steels are spent. Dependence of GND density on the grain size the size of dislocation fragments and dislocations cells is established. It is shown, that fraction of GND increases when sizes of structural element crushes. At that the general density of dislocations decreases and the density of partial disclinations especially joint disclinations increases.

### 3:45 PM Break

### 4:00 PM

**A Comparative Study of Characterization of CNT Turfs by Means of SEM Analysis and Stereological Techniques:** *H. Malik*<sup>1</sup>; *K. Stephenson*<sup>1</sup>; *D.F. Bahr*<sup>1</sup>; *D.P. Field*<sup>1</sup>; <sup>1</sup>Washington State University

The numerous novel and emerging properties of carbon nanotubes have placed this relatively new breed of technological materials under great focus. For applications in the regime of micro-electro-mechanical systems (MEMS) including electrical and thermal contact switches, and sensors, it is crucial to understand the combined collective behavior of CNT turfs rather than the mechanical properties of a single tube. In this present study, we have investigated the existing correlation between the mechanical behavior of multi-walled carbon nanotube (MWCNT) turfs and stereological parameters. Image analysis techniques using SEM were employed in connection with 2D planar and projected images. Also, stereological measures were incorporated to collect information from projected sections of images. These measures serve as a comprehensive source of information regarding turf density, tortuosity, connectivity, i.e. interaction between individual CNT segments, complexity, nanotopology, etc.

### 4:20 PM

**Nucleation Energetics and Kinetics of Solidification in Nanoscale Metallic Droplets:** *Ritesh Sachan*<sup>1</sup>; *J. Strader*<sup>1</sup>; *H. Krishna*<sup>2</sup>; *A.K. Gangopadhyay*<sup>2</sup>; *R. Kalyanaraman*<sup>1</sup>; <sup>1</sup>University of Tennessee-Knoxville; <sup>2</sup>Washington University

Over the past century, solidification process has been qualitatively investigated by classical nucleation theory. In the present work we discuss nucleation energetics and kinetics by a modified CNT for the solidification of nanoscale elemental metallic droplets of Ag, Co and Ni on as SiO<sub>2</sub> surface. Such nanostructures have important applications in the field of plasmonics, magnetic data storage and catalysis. This theory includes the effect of the density change during solidification and liquid droplet size. Our theory shows strong size-dependent nucleation energetics and kinetics, and that the interface between liquid and vacuum is the most favorable nucleation site. Experimental measurements, of number and size of grains forming within solidified hemispherical metallic droplets, were made for drops prepared by nanosecond pulsed laser-induced melting and self-organization. The experimental results also show strong size-dependence of nucleation rate consistent with our modified CNT theory.

### 4:40 PM

**Preparation, Characterization and Antibacterial Properties of Ag-Doped MgO/TiO<sub>2</sub> Nanoparticles:** *Guoliang Li*<sup>1</sup>; *Peng Bing*<sup>1</sup>; *Liyuan Chai*<sup>1</sup>; *Yajun Gu*<sup>1</sup>; <sup>1</sup>Central South University

Ag-doped MgO/TiO<sub>2</sub> nanoparticles were successfully prepared via hydrothermal precipitation using titanium sulfate, magnesium chloride and silver nitrate as raw materials. The effects of various conditions on the preparation process of the Ag-doped MgO/TiO<sub>2</sub> nanoparticles are investigated. The results showed that the optimal conditions were as follows: pH 9.0, mass ratio of titanium to silver 0.02, mass ratio of titanium to magnesium 2:1, reaction temperature 80°, mass ratio of surfactant to titanium and magnesium 3%, calcination temperature 500°. The as-obtained Ag-doped MgO/TiO<sub>2</sub> nanocomposites were well characterized by X-ray diffraction, scanning electron microscopy and energy dispersive X-ray. The antibacterial experiments exhibit that the composite has a higher antibacterial activity than that of both the Ag-doped TiO<sub>2</sub> nanoparticles and the mechanical mixture of Ag-doped TiO<sub>2</sub> and MgO.

### 5:00 PM

**Synthesis and Performance Study of Sn-Doped Nanometer Rutile TiO<sub>2</sub> Powder:** *Wu Daoxin*<sup>1</sup>; <sup>1</sup>Changsha University of Science and Technology

In this paper, originated from Ti(Bu)<sub>4</sub>, nano-rutile Sn-TiO<sub>2</sub> was synthesized by low temperature hydrolytic process. Then they were characterized by means of X-ray diffraction, UV-vis diffuse reflectance, fluorescence spectrum. Results showed that with the increase of the doped concentration of Sn, the reflectance of DRS decreased accordingly, while the powder's increase in light absorbance. Absorption of light broad to the visible region, which indicated that red shift occurred. The fluorescence spectrum intensity of Sn-TiO<sub>2</sub> increased according to the doped concentration. Sn-TiO<sub>2</sub> change the crystalline form when Calcined at different temperatures: in the low temperature for anatase; as the temperature rising, it transit to rutile, while at 800°, it is almost entirely rutile. With the

# Technical Program

increase of the calcination temperature, the Absorption of DRS increased, while the fluorescence spectrum intensity of Sn-TiO<sub>2</sub> decreased accordingly.

## 5:20 PM Concluding Comments

### Advanced Materials and Fuels Enabling Future Fusion, Fission and Hybrid Reactor Systems: Diagnostics and Structural Materials

*Sponsored by:* The Minerals, Metals and Materials Society, TMS Structural Materials Division, TMS Materials Processing and Manufacturing Division, TMS/ASM: Computational Materials Science and Engineering Committee, TMS/ASM: Corrosion and Environmental Effects Committee, TMS: High Temperature Alloys Committee, TMS/ASM: Nuclear Materials Committee

*Program Organizers:* Joseph Farmer, Lawrence Livermore National Laboratory; Thomas M. Anklam, Lawrence Livermore National Laboratory; Magdalena Serrano de Caro, Lawrence Livermore National Laboratory

Wednesday PM Room: 3A  
February 17, 2010 Location: Washington State Convention Center

*Session Chairs:* Joseph Farmer, Lawrence Livermore National Laboratory; Magdalena Serrano de Caro, Lawrence Livermore National Laboratory

## 2:00 PM Introductory Comments

### 2:05 PM Plenary

**MaRIE (Matter-Radiation Interactions in Extremes): An Experimental Facility Concept:** *Jack Shlachter*<sup>1</sup>; <sup>1</sup>Los Alamos National Laboratory

MaRIE, for matter-radiation interactions in extremes, is Los Alamos National Laboratory's concept for an experimental facility complex which will provide transformational materials solutions to address national security, energy security, and discovery science needs in the coming decades. The historical approach to developing materials with required lifetime and performance characteristics relied heavily on observation and subsequent validation of empirical models. This approach will not be sufficiently timely or cost effective to solve future problems in fusion, fission, or hybrid reactor systems, and it is widely recognized that predictive tools and material fabrication control will be required. MaRIE is being designed to bridge the "micron" gap between atomistic calculations and continuum models, thereby facilitating this paradigm shift. The three components of the facility complex as currently envisioned will be described and include a state-of-the-art synthesis and characterization capability, a multi-probe hall which can subject samples to dynamic shock conditions, and a spallation irradiation environment with in situ diagnostic capability, the latter dedicated to providing access to a radiation region of relevance to fission, fusion, and hybrid systems. The entire MaRIE complex is predicated on a predictive theory, modeling and simulation capability.

### 2:45 PM Invited

**TEM Study of Oxide Nanoparticles in ODS Steels Developed for Radiation Tolerance:** *Luke Hsiung*<sup>1</sup>; *Michael Fluss*<sup>1</sup>; *Joshua Kuntz*<sup>1</sup>; *Bassem El-Dasher*<sup>1</sup>; *William Choi*<sup>1</sup>; *Scott Tumey*<sup>1</sup>; <sup>1</sup>Lawrence Livermore National Laboratory

Many issues remain unsolved for developing ODS steels for fission and fusion applications including the role of fusion relevant helium and hydrogen gases on the deformation and fracture of irradiated material and mechanisms of swelling suppression in ODS steels. To resolve these issues, we plan to investigate microstructural changes of ODS steels driven by ion-beam irradiation. In preparation for the experiments, we are performing high resolution electron microscopy to study ODS steels with an emphasis on oxide/matrix interfacial structure. We will point out the features which may influence the growth and refinement of nano-particles. We will also point to those features that are of interest with respect to the suppression of radiation-induced swelling due to the nano-particles according to the new results obtained from the He+Fe irradiation experiments. This work was performed under the auspices of the U.S. Department of Energy by Lawrence Livermore National Laboratory under Contract DEAC5207NA27344.

### 3:15 PM Invited

**A Small Angle X-Ray Scattering Study of Helium/Nano-Oxide Structure in ODS Steels:** *B. S. El-Dasher*<sup>1</sup>; *J. D. Kuntz*<sup>1</sup>; *M. Caro*<sup>1</sup>; *S. O. Kucheyev*<sup>1</sup>; *T. Van Buuren*<sup>1</sup>; *T. M. Willey*<sup>1</sup>; *A. Kimura*<sup>2</sup>; *J. Farmer*<sup>1</sup>; <sup>1</sup>Lawrence Livermore National Laboratory; <sup>2</sup>Kyoto University

Oxide Dispersion Strengthened (ODS) steels are primary candidate materials in fusion reactor cladding design due to their reduced activation, high temperature strength and creep resistance properties. The presence of nano-oxide features in ODS steels (typically Y<sub>2</sub>O<sub>3</sub>) is primarily responsible for this increased material performance. While experimental evidence indicates that these nano-oxides also act as sinks for Helium bubbles that form during exposure to neutron irradiation, and thereby improving swelling properties, it is not definitive due to the experimental restrictions (i.e. requirement to defocus in the TEM in order to observe voids). In this work, we present results from small angle X-ray scattering (SAXS) experiments performed at the Advanced Photon Source to characterize the nanostructures present in ODS steels implanted with Helium ions. Two types of ODS steels were used in the study, each with differing nano-oxide size distributions, in order to observe how the oxide size distributions affect the resultant He bubbles. We also show that by taking advantage of operating the SAXS beamline in Anomalous mode (ASAXS), further elucidation of the Helium/nano-oxide structure is possible. This work performed under the auspices of the U.S. Department of Energy by Lawrence Livermore National Laboratory under Contract DE-AC52-07NA27344.

### 3:40 PM Break

### 3:50 PM

**Atomic Level Characterization of Advanced Radiation Tolerant Steels:** *Michael Miller*<sup>1</sup>; *D.T. Hoelzer*<sup>1</sup>; *K.F. Russell*<sup>1</sup>; <sup>1</sup>Oak Ridge National Laboratory

The development of radiation tolerant materials for the next generation of advanced reactors requires state-of-the-art microstructural characterization tools to ensure that the microstructure remains stable during exposure to high doses of irradiation at elevated temperatures. Atom probe tomography permits atomic scale characterization of the size, composition, morphology, and number density of nanoscale precipitates as well as quantifying the levels and extent of solute segregation to grain boundaries and dislocations. Examples will be presented of the types of characterizations that are possible to perform on neutron irradiated nanostructured ferritic steels with a local electrode atom probe (LEAP®) in conjunction with a dual beam scanning electron microscope/focused ion beam milling system. This research was sponsored by the Division of Materials Sciences and Engineering and the SHaRE User Facility of the Scientific User Facilities Division in the Office of Basic Energy Sciences, U.S. Department of Energy.

### 4:10 PM Invited

**The Corrosion of Oxide Dispersion Strengthened (ODS) Ferritic Steel in Molten Fluoride Salts:** *Joseph Farmer*<sup>1</sup>; <sup>1</sup>Lawrence Livermore National Laboratory

Oxide dispersion strengthened (ODS) ferritic steel has exceptional high-temperature strength and swells very little during neutron irradiation. This material has already been successfully used as a cladding for high burn-up fission fuel, and is now being considered as a structural material for the construction of fusion, fission, and fusion-fission hybrid reactor systems. This material has been found to undergo corrosion in high temperature molten fluoride salts that may ultimately be used as coolants for fusion and fusion-fission reactor systems. Fluoride salts infiltrate the surface of the alloy, and preferentially dissolve chromium rich phases, as shown in scanning electron micrographs. A special high-temperature electrochemical cell has been developed that has enabled electrochemical impedance spectroscopy (EIS) to be performed at frequencies ranging from 0.001 to 500,000 Hz, and at temperatures of 800C to 1000C. This capability is being used to develop a detailed understanding of the corrosive attack of ODS steel by high temperature fluoride-salt coolants of importance to future generations of fusion reactors. Corrosion models have been developed that account for the frequency dispersion in the observed complex impedance, and have been compared to classic linear networks frequently used to interpret low-temperature impedance data. The techniques that have been developed have enabled in situ measurements of charge transfer kinetics, interfacial capacitance (double layer and passive film) and mass transport rates associated with corrosion. Corrosion resistant coatings for the protection of the ODS



steel are also being investigated, and include alloys of tungsten, vanadium and nickel. Based upon thermo-chemical arguments, these materials should have some immunity to corrosion in such environments.

### 4:35 PM

#### **Magnetic Environment-Dependent Migration Pathways of Point Defects in Fe-Cr Alloys:** *Duc Nguyen-Manh*<sup>1</sup>; Mikhail Lavrentiev<sup>1</sup>; <sup>1</sup>UKAEA

In order to understand point defect properties generated under irradiation and to identify the kinetic pathways of micro-structural evolution in Fe-Cr system, a systematic density functional theory calculations of the activation energy of migration barriers for a vacancy jump at low-energy alloy configurations have been carried out using Nudged Elastic Band methods. We found by using spin-density maps at saddle point configurations that migration energy pathways are very sensitive to the magnetic behavior of the local atomic environments. A comparative study of vacancy migration pathways for modeling of phase separation in Fe-Cr binary using empirical inter-atomic potentials and conventional magnetic cluster expansion techniques demonstrates clearly the need of including of magnetic treatment which has been ignored in all previous kinetic Monte-Carlo simulations. We intend to use the created data base of magnetic environment-dependent migration energies to develop a new algorithm based on magnetic cluster expansion.

### 4:55 PM Invited

#### **Tungsten-Rhenium Super Alloy Development for Ultra High Temperature Space Fission and Fusion Reactors:** Jonathan Webb<sup>1</sup>; Indrajit Charit<sup>2</sup>; <sup>1</sup>Center for Space Nuclear Research; <sup>2</sup>University of Idaho

Tungsten based super alloys containing rhenium show great promise for uses in the space nuclear power and propulsion reactors as well as wall liners in fusion reactors. This paper will discuss previous research programs to develop and characterize tungsten-rhenium alloys and fuel forms. Different fabrication techniques will be discussed as well as material properties such as ductile to brittle transition temperature, tensile strength, super-plasticity and hardness. Historical methods of producing tungsten based fuel forms during the GE-710 and ANL nuclear rocket programs will be discussed as well as in core reactor testing at the Transient Test Reactor (TREAT) at the National Reactor Test Site in Idaho. Lastly a current program to develop tungsten-rhenium alloys at the Idaho National Laboratory along with the Center for Space Nuclear Research and the University of Idaho will be discussed.

### 5:25 PM Invited

#### **Radiation Damage Study in Mo by in situ TEM/Ion Irradiation and Computer Modeling:** *Meimei Li*<sup>1</sup>; Mark Kirk<sup>1</sup>; Pete Baldo<sup>1</sup>; Donghua Xu<sup>2</sup>; Thibault Faney<sup>2</sup>; Brian Wirth<sup>2</sup>; <sup>1</sup>ANL; <sup>2</sup>University of California

This paper presents the experimental data of radiation defects produced during in situ ion irradiation of pure molybdenum with 1MeV Kr ions at the IVEM-Tandem facility. In situ ion irradiation was carried out at 80 and 300C to a wide range of doses at dose rates over three orders of magnitude. Quantitative analysis was made to determine the number density and size distribution of defect clusters as a function of foil thickness, dose, dose rate and irradiation temperature. The experimental findings were compared with the computational data of defect cluster dynamic models using the rate theory. The identical material was previously neutron-irradiated at 80C in the HFIR. A direct comparison of defect microstructure was made to correlate damage between in situ ion and neutron irradiations. The findings showed that in situ ion irradiation provides valuable experimental data that can be used to benchmark computational modeling and simulate neutron damage.

### 5:55 PM Concluding Comments

## **Advances in Composite, Cellular and Natural Materials: Composites and Modelling**

*Sponsored by:* The Minerals, Metals and Materials Society, TMS Structural Materials Division, TMS/ASM: Composite Materials Committee

*Program Organizers:* Yuyuan Zhao, The University of Liverpool; David Dunand, Northwestern University

Wednesday PM

Room: 305

February 17, 2010

Location: Washington State Convention Center

*Session Chairs:* Larry Murr, University of Texas at El Paso; Martin Pech-Canul, Centro de Investigacion y de Estudios Avanzados del Instituto Politecnico Nacional

### 2:00 PM

#### **An Accurate and Efficient Method for Constituent-Based Progressive Failure Modeling of a Woven Composite:** *Ray Fertig*<sup>1</sup>; <sup>1</sup>Firehole Technologies

Accurate modeling of woven composites continues to challenge designers of composite structures. In order to make the problem computationally tractable, finite element modeling efforts usually require homogenization of the composite microstructure, which masks constituent interactions and stresses that actually drive failure. But because failure is a constituent level phenomenon, any general method for predicting initiation and propagation of failure must incorporate constituent behavior. In this paper we propose a computationally efficient method for failure prediction of a composite structure using finite element analysis. The approach requires using multicontinuum mechanics for a three-constituent composite to extract constituent-level stresses from a routine finite element analysis of a composite structure. Failure criteria are then applied at the constituent level to predict constituent failure, after which constituent and composite properties are adjusted. This technique is coupled with a numerically robust progressive failure algorithm to form a robust tool for failure prediction of composite weaves.

### 2:20 PM

#### **Micro-Mechanical Modeling and Simulations Composites Using Reconstructed Three-Dimensional Microstructures:** *Arun Gokhale*<sup>1</sup>; Arun Sreeranganathan<sup>2</sup>; Harpreet Singh<sup>1</sup>; Yuxiong Mao<sup>1</sup>; <sup>1</sup>Georgia Institute of Technology; <sup>2</sup>Stress Engineering Services Inc

Micro-mechanical response of composites depends on the morphology, anisotropy, and spatial arrangement of the reinforcement phase (particles, fibers, whiskers, etc.). Nonetheless, these aspects of the microstructural geometry are frequently ignored in the simulations of the mechanical behavior of composites. Further, most of the simulations are based on two-dimensional (2D) microstructures although real microstructures are three-dimensional (3D). In this contribution, we present simulations of the micro-mechanical behavior of real 3D microstructures of composites that utilize 3D volume segments of real microstructures. For this purpose, high resolution large volume segments of 3D microstructures are reconstructed. These 3D microstructure segments are implemented in the finite elements based simulations of the micro-mechanical response of the composites.

### 2:40 PM

#### **Size Dependent Ductile Failure Analysis of Particle-Reinforced Composites via Finite Element Modeling of Dislocation Punched Zone:** *Yeong Sung Suh*<sup>1</sup>; Yong Bae Kim<sup>1</sup>; Shailendra P. Joshi<sup>2</sup>; K. T. Ramesh<sup>3</sup>; <sup>1</sup>Hannam University; <sup>2</sup>National Singapore University; <sup>3</sup>Johns Hopkins University

A size dependent strength analysis of particle-reinforced composites via finite element modeling of augmented axisymmetric unit cell that includes dislocation punched zone by thermal mismatch between the particle and the matrix. Assuming that there is no particle fracture, the failure may take place either on the matrix-particle interface or in the matrix by ductile failure, depending on the particle size and the volume fraction. Initial study reveals this in such a way that the maximum plastic deformation is observed on the matrix-particle interface or inside the matrix adjacent to the punched zone. More in depth analysis that takes account of interface debonding and damage initiation and evolution in the matrix is in progress. It is expected to show that the failure of the particle-reinforced composites exhibits length scale according

# Technical Program

to the density of the geometrically necessary dislocations formed in the punched zone around the particle.

## 3:00 PM

**SMT Reflow Jig Material Analysis:** *Xin Ma*<sup>1</sup>; <sup>1</sup>Samsung Electronics (Suzhou) Semiconductor Co.Ltd / SESS

Nowadays, composite material is widely used in modern industries. In semiconductor industry, it has taken place of aluminium alloy gradually as surface mount technology (SMT) reflow jig material. The most widely used composite material is scattering glass fiber composite material. But its structural defect is exposed during using. In this paper, the main factors leading failure of scattering glass fiber composite material have been analyzed; the finite element (FE) simulation has been done; and the improvement methods have been proposed. In addition, the thermal and mechanical properties have been tested and been compared with other two composite materials. Conclusion has been received that the composite material with glass fibers cross style waved can avoid the failure of scattering glass fiber composite material. Thus extend the service life of SMT reflow jig and decrease the misalign rate in solder print process.

## 3:20 PM

**Microstructure in Work-Hardened Micro-Truss Materials Given Post-Forming Annealing Treatments:** *Brandon Bouwhuis*<sup>1</sup>; *Uta Klement*<sup>2</sup>; *Glenn Hibbard*<sup>1</sup>; <sup>1</sup>University of Toronto; <sup>2</sup>Chalmers Institute of Technology

Micro-truss cellular materials can be used as structurally efficient cores in light-weight sandwich panels. These sandwich cores have been produced using deformation-forming approaches, which introduce plastic strain into the truss struts. While this imparted strain can be used to strengthen the overall micro-truss core, it also drives recrystallization and grain growth if sandwich panel assembly involves conventional brazing treatments that subject the truss core to elevated temperatures. In addition to losing a potential strengthening mechanism, brazing can also result in the grain size of the annealed microstructure approaching the cross-sectional dimensions of the micro-truss struts. The present study is an examination of the strut microstructures in aluminum alloy and stainless steel micro-truss materials fabricated using a deformation-forming approach, and following a post-fabrication annealing step. These results serve as a guideline for future sandwich panel thermal processing to minimize the reduction of strength due to annealing and detrimental size effects.

## 3:40 PM Break

## 4:00 PM

**Wear Behavior of SiC /Al-Si Alloy Matrix Composites Produced by Squeeze Casting:** *Muna Abbass*<sup>1</sup>; <sup>1</sup>University of Technology, Baghdad

The aim of present work is to study dry sliding wear behavior of the (Al – 12 % Si) matrix alloy reinforced with 5wt% SiC particles. Composite materials were prepared by stir casting using vortex technique and squeeze casting under varying casting pressures from 7.5 to 53 MPa, and mold preheating at temperature (200oC). Microstructure and hardness for prepared composite materials were carried out. Wear tests of type (Pin-on-Disc) were conducted at varying loads from 5 to 20 N under a constant sliding speed of 2.7 m / sec. The results showed that a refinement in the microstructure with increasing the squeeze pressure. Increasing the squeeze pressure resulted in increasing the hardness and decreasing the wear rate. It has been found that the composites produced by squeeze casting have wear resistance higher than that of the stir casting.

## 4:20 PM

**Influence of Heating of Al<sub>2</sub>O<sub>3</sub> Particle with Holding Time Variation to Compactibility of Al/Al<sub>2</sub>O<sub>3</sub> Isotropic Composite:** *Widyastuti*<sup>1</sup>; *Mochamad Zainuri*<sup>1</sup>; *Agita Riani*<sup>1</sup>; <sup>1</sup>ITS Surabaya

Heating of Al<sub>2</sub>O<sub>3</sub> particles is one of the ways to increase the quality of the bonding. In this research, volume fraction Al<sub>2</sub>O<sub>3</sub> are 10, 20, 30, 40% heated on 1100°C and hold on 2, 4, 6 hours. Then, Al and Al<sub>2</sub>O<sub>3</sub> are mixed and compacted by 25kN for 15 minutes. Pre sintering temperature is 200°C for 30 minutes and sintering temperature is 600°C for 2 hours. The result shows that the increasing volume fraction will increase modulus elasticity on 2 and 4 hours but decrease it on 6 hours. The increasing holding time will decrease the value of modulus elasticity. The best volume fraction and holding time of heating process are 40% and 2 hours.

## 4:40 PM

**Effect of Vacuum Degassing on Composites Preparation:** *Che Dehui*<sup>1</sup>; *Yao Guangchun*<sup>1</sup>; *Kang Wei*<sup>1</sup>; *Zhang Xiaoming*<sup>1</sup>; <sup>1</sup>Institute of Materials and Metallurgy, Northeastern University

In processing of preparation of carbon fiber reinforced aluminum matrix composite materials by stirring casting and a vacuum degassing process was used after mixing. The porosity of the composite materials is effectively reduced and therefore the mechanical properties of composites are enhanced. In this paper, the carbon fiber-reinforced A356 alloy matrix composite slurry was degassed in 0.2 Pa vacuum, and the effect of temperature and time on the density of composites were studied. When the temperature is 700°C, degassing 2 min, the porosity of composites reduced to 0.2%. And interface morphology of the composites was characterized by SEM and no hole was found.

## 5:00 PM

**Fabrication of Carbon Nanotube Grown on Al Powders Reinforced Al Matrix Composite:** *Chitoshi Masuda*<sup>1</sup>; *Fumio Ogawa*<sup>2</sup>; *Ryoichi Hirashima*<sup>2</sup>; <sup>1</sup>Waseda University; <sup>2</sup>Graduate School of Waseda University

Carbon nanotubes have very high strength and physical properties. For fabrication of carbon nanotube reinforced composites the agglomeration of carbon nanotubes are very big problem to distribute homogeneously in the matrix. To improve the agglomeration of carbon nanotubes, the carbon nanotubes are grown on the metal powders and mixed with metal powders. In this presentation the carbon nanotubes are tried to be grown on Al powders by CVD method. On the Al powders (average size is about 17µm in diameter) are used and carbon nanotubes are grown in the vacuum chamber by alcohol atmosphere. The fine carbon nanotubes were grown on the Al powders. The diameter of CNT is about 30nm and its length is about 10µm. The Al powders grown by CNT were consolidated by SPS method. The mechanical properties of bulk materials were examined. Moreover, the grown CNTs were checked by TEM and EDX.

## 5:20 PM

**Diffusion of Liquid Media in Vulkanizats:** *Milena Milenova*<sup>1</sup>; *Verjina Aleksandrova*<sup>1</sup>; *Aleksandar Aleksandrov*<sup>1</sup>; *Gunai Halil*<sup>1</sup>; <sup>1</sup>University of Chemical Technologi and Metallurgy- Sofia

The kinetics of the diffusion of aggressive, liquid and industrial mediums in vulcanizers are concerned in the present study in view of further investigation of the influence of diffusion on their deformation and strength characteristics. The penetration is realized through a diffusion i.e. the liquid migrates in the body's volume under the influence of the concentrative gradient. The distribution of the diffusing liquid's concentration in the different points of the body can be described by the so called Fick's second law. The solution depends on the body's form and the initial and border conditions of the particular problem and it is based on the concept average concentration. In our case the calculations showed that for different average concentrations, the diffusion coefficient may vary within close limits and with a sufficient for the engineering practice it may be accepted as a constant.

## Alumina and Bauxite: Bauxite Characterization and Handling

*Sponsored by:* The Minerals, Metals and Materials Society, TMS Light Metals Division, TMS: Aluminum Committee, TMS: Aluminum Processing Committee

*Program Organizers:* Carlos Suarez, Hatch Associates Inc; Everett Phillips, Nalco Company

Wednesday PM

Room: 612

February 17, 2010

Location: Washington State Convention Center

*Session Chair:* Jorge Aldi, Alunorte

## 2:00 PM Introductory Comments

## 2:10 PM

**Reduction Roasting and Fe-Al Separation of High Iron Content Gibbsite-Type Bauxite Ores:** *Guanghui Li*<sup>1</sup>; *Na Sun*<sup>1</sup>; *Jinghua Zeng*<sup>1</sup>; *Zhongping Zhu*<sup>1</sup>; *Tao Jiang*<sup>1</sup>; <sup>1</sup>School of Minerals Processing & Bioengineering; Central South University

Large reserves of high iron gibbsite-type has been found in China, which is characterized as relatively high iron content, but low alumina content and A/S



ratio. Aluminiferous minerals and ferrous minerals are fine or superfine in size, and conjoint and substituted with each other; therefore, physical beneficiation is impracticable due to extremely difficult liberation. In this study, reduction roasting and separation of iron and aluminum has been investigated. The influences of reduction time, roasting temperature and magnetic separation were involved. The results indicate that when process a sample with 31.22% total iron grade and 26.35% alumina, a metallic iron concentrate with 93.3% total iron grade and non-magnetic product with 40% alumina content were obtained. Metallic iron concentrate can be used as steelmaking burden, and alumina can be extracted from the non-magnetic product further.

### 2:40 PM

**Study and Application of an Improved Sintering Process with Pre-Drying of Raw Material Slurries:** *Hengqin Zhao*<sup>1</sup>; *Baozhong Lu*<sup>2</sup>; *Hualong Ma*<sup>1</sup>; <sup>1</sup>Zhengzhou Institute of Multipurpose Utilization of Mineral Resources, CAGS; <sup>2</sup>Shanxi Zhongke PACL Co. Ltd

An improved sintering process to produce alumina was studied. The raw material slurries with proper mass ratio were dried with waste gas of kiln. The temperature of waste gas of kiln was decreased to under 110°C from above 500°C during drying of the slurries. The content of moisture of the slurries was reduced to 5% from 40% through drying process with the waste gas of the kiln. The dried slurries called as dry raw slurries were fed to the kiln and were sintered to the sinter. The aluminate sodium of the obtained sinter was very easy to be leached and leaching rate of alumina and oxide sodium in the obtained sinter reached to up 90% and 95% respectively. According to industrial application after adoption of the improved sintering process, consumption of coal in the sintering can be decreased by 18% than before improvement.

### 3:10 PM

**Bayer Process and Soda-Lime Sintering Process of Special Diasporic Bauxite with High Silica:** *Cao Wenzhong*<sup>1</sup>; *Tian Weiwei*<sup>1</sup>; *Shong Hong*<sup>1</sup>; <sup>1</sup>Environmental and Chemical Engineering Institute, Nanchang University

The bauxite in the eastern region of China is diasporic type with high silica containing about 8-16% SiO<sub>2</sub>. The main silica minerals in the bauxite are kaolinite, chamosite and illite. Technological investigations were carried out based on the Bayer process and a soda-lime sintering process. Sintering and leaching properties of the clinker in the sintering process, and the settling characteristics of the red mud were determined. The presence of high silica causes high bound-soda losses in the red mud in the Bayer process, though a part of silica content in the bauxite was in the form of chamosite. However, the bound-soda losses can be greatly reduced by using soda-lime sintering process. Therefore, it is necessary to study Bayer process, sintering and leaching properties of the special diasporic bauxite with high silica.

### 3:40 PM Break

### 4:00 PM Discussion Time

## Alumina and Bauxite: Industry Trends and Issues

*Sponsored by:* The Minerals, Metals and Materials Society, TMS Light Metals Division, TMS: Aluminum Committee, TMS: Aluminum Processing Committee

*Program Organizers:* Carlos Suarez, Hatch Associates Inc; Everett Phillips, Nalco Company

Wednesday PM Room: 611  
February 17, 2010 Location: Washington State Convention Center

*Session Chair:* Benny Raahauge, FLSmidth Denmark

### 2:00 PM Introductory Comments

### 2:10 PM

**Heat Transfer in the Bayer Process:** *Daniel Thomas*<sup>1</sup>; *Michael Evans*<sup>1</sup>; <sup>1</sup>WorleyParsons

Heat transfer equipment represents a significant portion of Bayer process plant capital and operating costs. Heater operation and maintenance activities can also create potential hazard exposure. Very early flowsheets tended to rely on batch operation and/or direct heat transfer (steam injection), and this still persists to some extent today. There has however been an ever increasing utilisation of indirect heat exchange over the past 100 years. This has been

driven by higher energy costs and enabled by improved heat transfer equipment. This paper presents an historical perspective, explores some heater selection case studies, and looks at future challenges and opportunities.

### 2:40 PM

**Sustainable Bauxite Mining - A Global Perspective:** *Christian Wagner*<sup>1</sup>; *Bauxite & Alumina Committee of the International Aluminium Institute*<sup>1</sup>; <sup>1</sup>International Aluminium Institute

In 2008 the International Aluminium Institute commissioned its fourth sustainable bauxite mining report with the aim to collect global data on the environmental, social and economic impacts of bauxite mining operations and their rehabilitation programmes. The report shows that bauxite mining has become sustainable and land area footprint neutral; it is a relatively small land use operation when compared to most other types of mining. All operations have clearly defined rehabilitation objectives, fully integrated rehabilitation programmes, and written rehabilitation procedures. Almost 80% of the surveyed mines are ISO 14001 certified for environmental management. Bauxite miners are actively engaging with local communities to support development through employment, infrastructure, training and social programmes and compensatory packages. Displacement and resettlement issues are limited for the bauxite mining industry in total, but of high priority at the individual level for the people that need to be displaced and relocated.

### 3:10 PM Break

### 3:30 PM

**The Need for Energy Efficiency in Bayer Refining:** *Lawrie Henrikson*<sup>1</sup>; <sup>1</sup>WorleyParsons

During the recent economic boom, the high Alumina price encouraged rapid expansion of world Alumina refining capacity. The main objective was speed rather than efficiency, so refineries were constructed faster than ever before, especially in China, taking advantage of lucrative profit margins, without much concern for operating cost. However, when the world economy crashed in late 2008, the fall in commodities prices caused a severe profit squeeze at many refineries. The lack of built-in efficiency caused many refineries to wind-back production or commence full shut-down. The main operating cost pressure was energy, even with much lower unit energy costs. This paper examines the key energy efficiency drivers for a refinery, and evaluates the trade-off of capital cost against operating cost, with the expectation of rising long-term energy prices. The option of Brownfields retrofits against Greenfields installations is also discussed.

### 4:00 PM

**A Case for Replication of Alumina Plants:** *Anthony Kjar*<sup>1</sup>; <sup>1</sup>Gibson Crest Pty Ltd

Rising capital costs of one off greenfield projects in many countries as well as a stalled creep capacity increase is a rate limiting step for many alumina producers. A new approach is required to enable Western alumina producers to develop in an economic way increased capacity to match rising demand and not loose further market share to Chinese producers. There are lessons to be learnt from a replication approach. This has been successful for periods of time in gold, coal processing, power stations, and is now being tried in copper processing, nuclear power reactors and in many Chinese developments in nickel, magnesium and aluminium.

Wed. PM

# Technical Program

## Aluminum Alloys: Fabrication, Characterization and Applications: Emerging Technologies

*Sponsored by:* The Minerals, Metals and Materials Society, TMS Light Metals Division, TMS: Aluminum Processing Committee  
*Program Organizers:* Subodh Das, Phinix LLC; Steven Long, Kaiser Aluminum Corporation; Tongguang Zhai, University of Kentucky

Wednesday PM Room: 615  
February 17, 2010 Location: Washington State Convention Center

*Session Chair:* Subodh Das, Phinix LLC.

### 2:00 PM

**Microstructure of Ultrasonic Impact Treated Aluminum 5456-H116:** *Kim Ngoc Tran*<sup>1</sup>; *Elissa Bumiller*<sup>1</sup>; *Lourdes Salamanca-Riba*<sup>2</sup>; <sup>1</sup>Naval Surface Warfare Carderock Division; <sup>2</sup>University of Maryland

The Navy is using ultrasonic impact treatment (UIT) experimentally to treat 5456-H116 in order to mitigate crack initiation and propagation. While UIT has been shown to be promising, the effects of UIT on the properties and microstructure of 5456-H116 are not understood. The Navy is investigating the effects of UIT on 5456-H116 through material characterization and material's property testing. The objective of the work is to develop a fundamental understanding of the mechanisms that cause material property changes. Preliminary work to characterize UIT treated plate is in progress. This work includes x-ray diffraction measurements, surface profilometry, optical microscopy (OM), scanning electron microscopy (SEM) combined with electron backscattering diffraction, and tensile testing. Current work expands the scope to include the evaluation of treated welds. This work includes transmission electron microscopy (TEM), in-situ TEM using a heating stage, ASTM-G67 testing for intergranular corrosion, nanohardness measurements, additional mechanical testing, OM, and SEM.

### 2:20 PM

**Charge Weld Effects in High Cycle Fatigue Behavior of a Hollow Extruded AA6082 Profile:** *Nicholas Nanninga*<sup>1</sup>; *Calvin White*<sup>2</sup>; <sup>1</sup>NIST; <sup>2</sup>Michigan Technological University

Fatigue properties of specimens taken from different locations along the length of a hollow AA6082 extrusion where charge weld properties and the degree of coring are expected to vary have been evaluated. The fatigue strengths of transverse specimens containing charge welds are lower near the front of the extrusion where the charge weld separation is relatively large. The lower fatigue properties of the AA6082 specimens appear to be associated with early overload fatigue failure along the charge weld interface. Coring does not appear to have significantly affected fatigue behavior in either of these alloys.

### 2:40 PM

**Ag Nanoparticles Dispersion on Surface-Modified Al Alloy Porous Body and Their Filtration Properties:** *Young Ik Seo*<sup>1</sup>; *Se Hwan An*<sup>1</sup>; *Dae-gun Kim*<sup>1</sup>; *Kyu Hwan Lee*<sup>2</sup>; *Young Do Kim*<sup>1</sup>; <sup>1</sup>Hanyang University; <sup>2</sup>Korea Institute of Science and Technology

For the water purification and anti-bacterial filters, the combination of the enlarged specific surface area and anti-microbial material is necessary for the filtration efficiency. Because the pore surface acts as an adsorption site with impurities and the anti-microbial material, such as silver nanoparticle, suppresses the proliferation of bacteria. Silver nanoparticle dispersed Al-4wt.% Cu porous body was manufactured by the following manner. The granulated powder was fabricated by low energy ball mill and was compacted under the pressure of 20 MPa for macropore network. After sintering, the sintered body was surface-modified in dilute alkali solution for microporous surface. Subsequently, the surface-modified porous body was immersed in the solution that was synthesizing Ag nanoparticles by polyol process. The scanning electron microscopy (SEM) and transmission electron microscopy (TEM) were employed to investigate the microstructure and phase confirmation. Permeability and filtration characteristics evaluated by specially manufactured device using pure water and artificial waste water.

### 3:00 PM

**Incubation Behavior of Hg-LME in Aluminum:** *Scott Keller*<sup>1</sup>; *Ali Gordon*<sup>1</sup>; <sup>1</sup>University of Central Florida

When high strength aluminum alloys are subjected to liquid metals, physical and chemical reactions ensue resulting in what is known as liquid metal embrittlement (LME). A subset of stress corrosion cracking, LME is exhibited when a liquid metal, e.g. Hg or Ga, comes into intimate contact with a solid metal having significant susceptibility. As mechanical loads are applied, the interaction between the two metals results in a reduction in the flow properties of the solid metal. Several theories have been proposed to identify the underlying microstructural failure mechanism; however, none have been widely accepted. Crack growth experiments on Al 7075-T651 in liquid mercury have been conducted to extend these physically-based theories. Through constant stress intensity factor (SIF) tests, incubation periods were analyzed, providing data for a diffusion-based theory of LME. These mechanical test data, along with metallographic analysis, show that the phenomena of LME is both strongly time- and SIF-dependent.

### 3:20 PM

**Recent Advances in FSW Joining of Sheets on Structural Extruded Profiles:** *Lorenzo Donati*<sup>1</sup>; <sup>1</sup>University of Bologna

Recently industries involved in train, airplane and ship construction increased the use of FSW for replacement of traditional assembly technologies like mechanical fasteners (bolts and rivets) and MIG or TIG welding. The FSW technology is usually applied in joining two sheets in the butt joint configuration. Nevertheless, some industrial applications require the joining of three bodies, usually called T-joint or corner welds. In this work a detailed study on the union of two sheets on an extruded structural profile is presented. The innovative idea presented is related to the opportunity of freely shaping the extruded profile, thus allowing the production of appendix suitable to be used as filler material or clamping system during the FSW stage. Three types of profile shapes were used (simple, with I and T appendix) and, for each condition, optimizations of PIN shape and process parameters were carried out based on tensile tests and microstructural analysis.

### 3:40 PM Break

### 3:55 PM

**Adiabatic Shear Localization of Al-Sc Alloy at Extremely High Strain Rates:** *Woei-Shyan Lee*<sup>1</sup>; *Tao-Hsing Chen*<sup>2</sup>; *Ging-Ting Lu*<sup>1</sup>; <sup>1</sup>Department of Mechanical Engineering, National Cheng Kung University; <sup>2</sup>Center for Micro/Nano Science and Technology, National Cheng Kung University

The adiabatic shear behaviour of aluminum-scandium (Al-Sc) alloy under high strain rates ranging from  $3.0 \times 10^5$  s<sup>-1</sup> to  $6.3 \times 10^5$  s<sup>-1</sup> is studied by using a compressive-type split-Hopkinson pressure bar (SHPB). The results show that both the shear stress and the strain rate sensitivity increase with increasing the strain rate. In addition, it is shown that an adiabatic shear band is formed within the deformed specimens for all values of the strain rate. As the strain rate is increased, the width of the shear band decreases, but the microhardness increases. At a strain rate of  $3.0 \times 10^5$  s<sup>-1</sup>, the fracture surface is characterised by multiple transgranular cleavage fractures. However, for strain rates greater than  $4.5 \times 10^5$  s<sup>-1</sup>, the fracture surface has a transgranular dimple-like characteristic, and thus it is inferred that the ductility of the unweldable Al-Sc alloy improves with increasing the strain rate.

### 4:15 PM

**Effect of Electric Potential on the Evolution of Defect Substructure and Fracture Surface of Aluminum under Creep:** *Sergey Konovalov*<sup>1</sup>; *Oksana Stolboushkina*<sup>1</sup>; *Yurii Ivanov*<sup>2</sup>; *Roman Filipiev*<sup>1</sup>; *Viktor Gromov*<sup>1</sup>; <sup>1</sup>Siberian State Industrial University; <sup>2</sup>Institute of High Current Electronics Siberian Branch of Russian Academy of Science

The investigation of the morphology of the fracture surface and defect substructure, which is formed with creep in the zone of the fracture of the samples of technical pure aluminum are carried out by the methods of scanning and diffraction electron microscopy. It is shown that the structure, which is formed under creep conditions under the potential, is characterized by the higher degree of self-organizing dislocation substructure in the zone of the fracture of samples, in comparison with the samples, destroyed with creep under the normal conditions.



4:35 PM

**Using Artificial Neural Network to Optimize the Bakehardening of AL2024 and AL7075:** *Niloofar Kamkar Zahmatkesh<sup>1</sup>; Kamran Dehghani<sup>1</sup>; Atiyeh Nekahi<sup>1</sup>; <sup>1</sup>Amirkabir University of Technology*

In the present work, the response of two aluminum alloys (Al2024 and Al7075) to strain aging and bake hardening (BH) was investigated. After the primary heat treatments, the direct chilled ingots were subjected to laboratory cold rolling. Various treatments and different testing conditions were used to evaluate the aging and baking behaviors of the mentioned alloys. The different strains were applied so that to attain different dislocation densities required for attaining various aging and baking values. The results show that the higher the strain, the greater the strain aging and bake hardening amounts will be. Experimental data was used for the training of ANN and a multilayer cascade forward back-propagation neural network was designed. The optimization was achieved by minimizing the errors between the predicted values and the ones that were obtained experimentally. The predicted values obtained from the trained ANN are found to be in close agreement with the experimental results.

4:55 PM

**Defects Producing Formation of Microcracks in Aluminum during Electrochemical Charging with Hydrogen:** *Paul Rozenak<sup>1</sup>; <sup>1</sup>Hydrogen Energy Batteries LTD*

The formation of micro-cracks in high purity aluminum during electrochemical charging by hydrogen was studied. The experiments reveal that, in aluminum samples, a wide distribution of hydrogen bubbles on the surface (blisters) and under the surface into the volume, were produced during electrochemical charging. This phenomenon can lead to the formation of micro-cracks in the absence of externally applied stress. Examination of electrochemically charged samples by transmission electron microscopy (TEM) showed micro-cracks with a typically ductile mode of fracture.

### Aluminum Reduction Technology: Hall-Héroult Cell: Process Control

*Sponsored by:* The Minerals, Metals and Materials Society, TMS Light Metals Division, TMS: Aluminum Committee, TMS: Aluminum Processing Committee

*Program Organizers:* Charles Mark Read, Bechtel Corporation; Gilles Dufour, Aluminerie de Deschambault

Wednesday PM Room: 608  
February 17, 2010 Location: Washington State Convention Center

*Session Chair:* Alan Phillips, KTD LLC

### 2:00 PM Introductory Comments

2:10 PM

**Continuous Improvement in Aluminium Reduction Cell Process Performance with the ALPSYS® Control System:** *Sylvain Fardeau<sup>1</sup>; Benoît Sulmont<sup>1</sup>; Philippe Vellemans<sup>1</sup>; Claude Ritter<sup>1</sup>; <sup>1</sup>Rio Tinto Alcan*

Improving cell productivity through increased current generally leads to higher anode current densities, lower bath to amperage ratios and changed cell dynamics. Up-to-date process control is required in order to maintain or improve existing performance under these increasingly challenging conditions. The ALPSYS® control system has been continuously improved to cope with these new constraints. It provides innovative solutions in order to increase cell productivity while moving towards zero anode effects. This paper shows how a large scale deployment of the latest alumina control developments has resulted in a significant reduction of anode effect rate while increasing cell productivity in the Alma smelter. It also shows how the sharing of best practices for anode effect treatment has enabled a halving of anode effect duration in all Alcan AP plants. Hence, even for benchmark cell technology, effective process control can further improve current efficiency while reducing green house gas emissions.

2:40 PM

**A Nonlinear Model Based (NMPC) Control Strategy for the Aluminium Electrolysis Process:** *Steinar Kolas<sup>1</sup>; Stein Wasbø<sup>2</sup>; <sup>1</sup>Hydro; <sup>2</sup>Cybernetica AS*

Important factors for the aluminium industry for succeeding in reducing greenhouse gas emissions and increase energy efficiency is not only the

speed in which the organization is able to utilize new knowledge, but also the development and use of new advanced process control systems. New advanced process control systems imply utilizing state of the art process control systems as e.g. Nonlinear Model Predictive Control (NMPC). Although the conventional control structures are dominating the aluminium industry, several authors have addressed advanced process control structures for controlling the Hall-Héroult process. This includes the adaptive control of alumina addition, 9-Box Matrix Control, LQG Control, Model Predictive Control and control structures involving the Neural network approach. Recently Hydro has been active in developing an NMPC control structure for controlling the Hall-Héroult process. The Hydro NMPC control structure and results from operational practice on Hydro's Hal4e cells is presented.

3:10 PM

**CVG-Venalum Potline Control and Supervisory Integrated System VEN-PCISIS:** *Jose Ramones<sup>1</sup>; Frangil Ramirez<sup>1</sup>; Maria Colmenares<sup>1</sup>; Jesus Larez<sup>1</sup>; Jesus Gonzalez<sup>1</sup>; <sup>1</sup>CVG Venalum*

Profitability of smelters strongly depends on cells performance; therefore efforts are dedicated into increasing production capacity, reducing energy consumption, shifting from raw material providers, testing new anode or cathode designs, and so on. To successfully accomplish these changes, as well as the necessary adjustments on pot operations, companies must be capable of developing control and supervisory systems to handle such challenges. Friendly human machine interface satisfying information handling requirements from cell operators is also needed, so strict monitoring of cells performance can be easily performed on real time. To fulfill these targets, CVG-Venalum developed an aluminum reduction pot control and supervisory integrated system (VEN-PCISIS). The central control unit of VEN-PCISIS is based on a PC-104 standard board, and the supervisory system runs on free-software web technology. Results of VEN-PCISIS during the trial period overpowered existing systems; hence CVG-Venalum management decided replacing former cell control and supervisory systems with the VEN-PCISIS.

3:40 PM Break

3:50 PM

**Efficient Thermal Balance Strategy Developed by CVG Venalum:** *Maria Colmenares<sup>1</sup>; Adela Ruiz<sup>1</sup>; Jesus Imery<sup>1</sup>; <sup>1</sup>CVG Venalum*

Worldwide, in order to keep their businesses as profitable as possible, smelters are aware of the key importance of improving any aspect of their processes, whilst increasing production capacity. This never ending quest, in many cases brings cells at or beyond their former performance limits, which strongly impacts the thermal balance. As a result, developing a control strategy capable of dealing with managerial targets, and yet successfully minimizing bath temperature deviations with a minimum consumption of aluminum fluoride became a very desirable asset. This paper describes the development of a temperature control system using fuzzy logic algorithms. Results obtained during the stage trail in three different aluminum reduction cell technologies were outstanding, with a significant reduction in bath temperature and bath acidity deviations with reduced aluminum fluoride consumption. Nowadays, the system is operating in most of the 905 cells of CVG -VENALUM

4:20 PM

**Usage of Fuzzy Logic as a Strategy for the Aluminium Fluoride Addition in Electrolytic Cells:** *Fabio Soares<sup>1</sup>; <sup>1</sup>Exodus*

This work describes an Intelligent Aluminum Fluoride (AlF<sub>3</sub>) Addition Strategy in Electrolytic Cells, based on Fuzzy Logic concepts, wherein the knowledge retained by process specialists is qualitatively translated into a set of linguistic rules such as: IF < condition > THEN < action >. The usage of a Fuzzy Strategy is justified by its natural capacity of dealing with inaccurate information, along with the absence of a known available dynamic model which takes into account the knowledge acquired by process specialists in Albras for each Cell, instead of using classical methods for modeling the process whose great complexity of the thermodynamic and electromagnetic phenomena involved is a very awkward problem

Wed. PM

# Technical Program

4:50 PM

**Development and Application of a Multivariate Process Parameters Intelligence Control Technology for Aluminum Reduction Cells:** *Yi Xiaobing*<sup>1</sup>; Tian Qinghong<sup>1</sup>; <sup>1</sup>CHALIECO

Everybody knows that the aluminum reduction process has strong interaction multivariate characteristics with limited process observability and responses which are non-linear and vary over a wide range of time scales. Generally saying, the process and control technology developed and used in each aluminum smelter worldwide, which are based on different control philosophy, normally are different from others. This paper emphasizes on the introduction of one advanced multivariate process parameters intelligence control technology developed by CHALIECO GAMI in recent years, and its successful application resulting in significantly higher current efficiency and reduced energy consumption by several large domestic and abroad green-field or modernized smelters.

5:20 PM **Concluding Comments**

---

## Biological Materials Science: Surface Engineering: Biomimetics and Biological Applications

*Sponsored by:* The Minerals, Metals and Materials Society, TMS Structural Materials Division, TMS: Biomaterials Committee, TMS/ASM: Mechanical Behavior of Materials Committee

*Program Organizers:* John Nychka, University of Alberta; Jamie Kruzic, Oregon State University; Mehmet Sarikaya, University of Washington; Amit Bandyopadhyay, Washington State University

Wednesday PM Room: 205  
February 17, 2010 Location: Washington State Convention Center

*Session Chairs:* Marc Meyers, UCSD; Devesh Misra, University of Louisiana

---

2:00 PM **Invited**

**Oxide Wettability:** Jim Ruud<sup>1</sup>; *Molly Gentleman*<sup>2</sup>; <sup>1</sup>GE Global Research; <sup>2</sup>Texas A&M University

Oxides are believed to be hydrophilic because of the strong affinity for hydroxylation at their surfaces. This paper explores the relationship between hydroxylation of oxide surfaces and their resulting wettability. Here we demonstrate that hydroxyls increase the hydrophobicity, or reduce the wettability, of oxide surfaces by reducing the polar component of surface free energy. Using alumina as a model material, increased hydrophobicity with hydroxylation was confirmed experimentally and a correlation between the strength of the hydroxyl-driven hydrophobic response and surface treatment was demonstrated. Additionally an overview of how to design oxides with increased hydrophobicity will be discussed.

2:30 PM

**In situ Biomimetic Ceramic Coatings:** *Jadid Samad*<sup>1</sup>; *John Nychka*<sup>1</sup>; <sup>1</sup>University of Alberta

Biomimetic approaches for the creation of hydrophobic surfaces has generally, like nature, focused upon altering surface morphology to effect changes in wettability. The wetting angle of liquids on solid surfaces depends on rather few variables and nature has optimized the morphology of surfaces, along with their chemistry, to achieve incredible hydrophobicity - recall the lotus leaf. We report on our method to alter the wettability of surfaces of metallic substrates through creation of in situ oxide layers of varying morphology via simple oxidation treatments in air. Changes in wetting angle from over 100 degrees to less than 40 degrees can be achieved through such simple treatments.

2:50 PM

**Surface Modification of Laser Processed Nitinol:** *Sheldon Bernard*<sup>1</sup>; *Susmita Bose*<sup>1</sup>; *Amit Bandyopadhyay*<sup>1</sup>; <sup>1</sup>Washington State University

Nitinol (NiTi) is an equiatomic intermetallic compound of nickel and titanium whose unique mechanical properties contribute to its increasing use as a biomaterial. The objective of this research is to modify the surface of laser processed NiTi via anodization to enhance biocompatibility. Laser Engineering Net Shaping (LENS<sup>TM</sup>) processed fully dense NiTi (50/50 atom%) samples were anodized in 1N sulfuric acid (H<sub>2</sub>SO<sub>4</sub>) electrolyte at three different pHs, 4.5, 2.0 and 1.5. All anodization experiments were performed at 20V and 30°C. Using anodization, we were able to improve the surface wettability by

lowering the contact angle from 32 degrees to less than 5 degrees. The surface free energy was also calculated to show comparable properties to that of cpTi. This presentation will focus on influence of surface morphology on wettability, surface free energy, bone cell-materials interactions and Ni ion release of LENS<sup>TM</sup> processed NiTi.

3:10 PM

**Grain Boundary Grooving and Its Effect on Biological Response:** *Wah Wah Thein-Han*<sup>1</sup>; *Devesh Misra*<sup>1</sup>; *Maresh Somani*<sup>2</sup>; *Pentti Karjalainen*<sup>2</sup>; <sup>1</sup>University of Louisiana; <sup>2</sup>University of Oulu

Metallic materials with sub-micron to nanometer-sized grains provide surfaces that are different from conventional polycrystalline materials because of the large proportion of grain boundaries with high free energy. Grooving of grain boundaries is expected to stimulate biological response. In this regard, we describe the cellular response of grooved grain boundaries in nanogained/ultrafine-grained materials. The improved cellular response is described in terms of initial cell attachment, proliferation, viability, morphology and spread on the nanogained/ ultrafine-grained grooved surface. Furthermore, grooving of grain boundaries demonstrated superior biological properties in terms of immunocytochemistry and protein analysis compared to the ungrooved substrate.

3:30 PM

**Interaction of Ti-Fe Based Alloys with L929 Cells:** *Arnaud Caron*<sup>1</sup>; *Dmitri Louzguine-Luzgin*<sup>2</sup>; *Franz-Günter Sander*<sup>3</sup>; *Akihisa Inoue*<sup>2</sup>; *Hans-Jörg Fecht*<sup>1</sup>; <sup>1</sup>Institute of Micro- and Nanomaterials, University Ulm; <sup>2</sup>WPI Advanced Institute for Materials Research, Tohoku University; <sup>3</sup>Department of Orthodontics, University Ulm

Mechanical testing of Ti-Fe based alloys reveal outstanding properties. In this work we investigate the toxicity of this alloy class on L929 cells by direct cell contact and filter test. These tests give good prediction on the ability of the alloys to be used as dental implants. Before and after toxicity tests, the alloy samples are investigated by scanning electron microscopy and atomic force acoustic microscopy in order to investigate eventual corrosion events on the samples surface after testing.

3:50 PM **Break**

4:00 PM

**Bone Cell Infiltration in Porous Graphitic Surfaces: Influence of Surface Coatings and Nanotube Grafting:** *Sharmila Mukhopadhyay*<sup>1</sup>; *Elizabeth Maurer*<sup>1</sup>; *Saber Hussain*<sup>2</sup>; <sup>1</sup>Wright State University; <sup>2</sup>Air Force Research Laboratory

This investigation aims at understanding the interaction of bone cells with graphite, and the possibility of enhancing their growth into porous scaffolds by surface modification. Graphitic foam samples having interconnected porosity, low density, and controllable thermal and electrical properties have been used for attachment and growth of osteoblast cells. The influence of surface coatings such as collagen and silica has been studied. Additionally, carbon nanotubes have been grafted on these substrates and the subsequent adhesion and proliferation of bone cells through these hierarchical porous structures has been investigated. Biocompatibility studies are done by various cell staining and imaging techniques, as well as mitochondrial functionality assays. Structural and functional evaluation of carbon-bone composites are performed using microscopy, spectroscopy, mechanical and electrical tests. These results indicate that the proliferation and overall functionality of bone cells in porous graphitic scaffolds can indeed be controlled, and significantly improved for use in future implant materials.

4:20 PM

**Bovine Serum Albumin Protein Adsorption and Release on Electrically Polarized Biphasic Calcium Phosphates:** *Mohammad Tarafder*<sup>1</sup>; *Subhadip Bodhak*<sup>1</sup>; *Shashwat Banerjee*<sup>1</sup>; *Amit Bandyopadhyay*<sup>1</sup>; *Susmita Bose*<sup>1</sup>; <sup>1</sup>Washington State University

Calcium phosphates (CP) are widely used in bone tissue engineering due to their compositional similarity with human bone. Our objective here is to investigate adsorption and release behavior of bovine serum albumin (BSA) as a model protein on the positively and negatively poled surfaces of three different biphasic calcium phosphate (BCP) composites. Three different biphasic calcium phosphate composites with different weight percent ratio of hydroxyapatite and  $\beta$ -tricalcium phosphate were prepared and then polarized.



Stored charge density showed the increasing trend with the increasing percent content of HAp in the composites. Bovine serum albumin protein adsorption on the positively-poled surfaces was maximum after 6-hour. BSA release from the positively-poled surfaces was performed for up to 48-hour at 7.4 pH. A decreasing trend in percent release of BSA was observed with the increasing charge density. The presentation will discuss processing and characterization of BCPs and BSA adsorption and release behavior from them.

#### 4:40 PM

**Magnetic Nanoparticle Interactions with Hydroxyapatite:** *Otto Wilson*<sup>1</sup>; Meron Haimanot<sup>1</sup>; <sup>1</sup>Catholic University of America

Enhanced functionality can be imparted to biomaterial implants at the macroscale, microscale, or nanoscale level and can involve a multitude of features related to bioactivity. These factors work together to orchestrate cell function, overall tissue healing, and promote seamless integration of the biomaterial implant into the neighboring tissue. Magnetic nanoparticles (MNPs) were adsorbed onto nanophase hydroxyapatite (HAp) particles to develop magnetically active hydroxyapatite. MNP modified HAp particles were characterized via electrophoretic mobility, particle size analysis, and electron microscopy. The MNPs rapidly adsorbed onto the surface of the HAp via heterocoagulation based interactions. MNP surface modification of HAp imparts magnetic behavior and allows the HAp to be translated in solution via magnetic fields. Applications for this novel HAp in hard tissue engineering will be presented with a focus on mechanically stimulated scaffolds for enhanced cell activity.

#### 5:00 PM

**Solid-Binding Peptide-Based Antibacterial Implants:** *Hilal Yazici*<sup>1</sup>; Mary Rood<sup>1</sup>; Brandon Wilson<sup>1</sup>; Mustafa Gungormus<sup>1</sup>; Candan Tamerler<sup>1</sup>; Mehmet Sarikaya<sup>1</sup>; <sup>1</sup>University of Washington

Implant-associated infections are a primary cause of early implant failures. Prescribed oral antibiotics are not always effective because of the inability to reach the infection site and an increase in bacterial resistance. A novel class of peptides, the antimicrobial peptides (AMPs), is useful mainly because of the difficulty for microorganisms to develop resistance towards them. In the present study, we use a novel bi-functional peptide based approach that exhibits both titanium-binding (TiBP1) antimicrobial (AMP) properties for implant surface functionalization. The efficiency of TiBP1-AMP bi-functional was evaluated both in solution by analyzing bacterial growth using optical density measurement and on the functionalized titanium surface with fluorescence microscopy, scanning electron microscopy analysis at various time points. For example, *Streptococcus mutans* adhesion was reduced on the TiBP1-AMP peptide-based functionalized substrate compared to controls. The approach may be a candidate for the prevention of implant infections. This research is supported by GEMSEC at UW.

#### 5:20 PM

**Development of Anti-Microbial Silver Coating on Stainless Steel:** *Paul DeVasConCellos*<sup>1</sup>; Susmita Bose<sup>1</sup>; Amit Bandyopadhyay<sup>1</sup>; Lewis Zirkle<sup>2</sup>; <sup>1</sup>BRC, Washington State University; <sup>2</sup>Surgical Implant Generation Network (SIGN)

Silver has been utilized for many years as an antimicrobial agent. With an increasing amount of antibiotic-resistant bacteria, silver-coatings and treatments are again being noticed as an effective way to prevent infection. In situations where cost effectiveness is necessary, the use of silver coatings on medical implants could be a valuable addition to help prevent infections. This is especially crucial when surgeries are performed in environments where sanitation is not ensured as well as environments in North American Hospitals. This research presents methods and feasibility of silver coatings on stainless steel (SS) which is a practical material for low cost implants. There are many parameters that can be adjusted for each method to apply silver coatings. In an effort to optimize antimicrobial effectiveness and keep human cell-toxicity to a minimum, we have experimented with various coating parameters and observed their effects on the utility of silver coating on SIGN SS-implants.

### Bulk Metallic Glasses VII: Simulation and Modeling

*Sponsored by:* The Minerals, Metals and Materials Society, TMS Structural Materials Division, TMS/ASM: Mechanical Behavior of Materials Committee

*Program Organizers:* Peter Liaw, The University of Tennessee; Hahn Choo, The University of Tennessee; Yanfei Gao, The University of Tennessee; Gongyao Wang, University of Tennessee

Wednesday PM Room: 213  
February 17, 2010 Location: Washington State Convention Center

*Session Chairs:* Christopher Schuh, MIT; John Lewandowski, Case Western Reserve University

#### 2:00 PM Invited

**Influence of Condensed Bond Enthalpy on Metallic Glass Stability:** *Dan Miracle*<sup>1</sup>; Garth Wilks<sup>2</sup>; Amanda Dahlan<sup>3</sup>; <sup>1</sup>AF Research Laboratory; <sup>2</sup>General Dynamics, Inc.; <sup>3</sup>SOCHE

While empirical guidelines suggest that the enthalpy of mixing influences glass stability, previous work has failed to show a correlation. This work seeks to establish a connection between nearest neighbor bond energy and glass-forming ability through evaluation of interatomic bond enthalpies. An approach to determine bond enthalpies from available thermodynamic data will be briefly described and resulting bond enthalpies will be presented. The number and type of atom bonds that are present in a metallic glass structure are estimated as a function of metallic glass constitution using the efficient cluster packing structural model. By combining these two analyses, we estimate the enthalpy associated with glass formation, and explore correlations with experimental measurements of glass-forming ability.

#### 2:20 PM

**Model Experiments to Mimic Fracture Surface Features in Metallic Glasses:** *Lisa Deibler*<sup>1</sup>; John Lewandowski<sup>1</sup>; <sup>1</sup>Case Western Reserve University

The purpose of this study is to examine how changes in viscosity, specimen geometry, and degree and type of inhomogeneity affect the fracture surface observations on a model of metallic glass fracture. Experiments were conducted on tensile samples of various geometries constructed to contain liquids of different viscosity that were tested at three temperatures. The influence of mixtures, layers, and dispersions of two different viscosity materials on the fracture surface features was also investigated. The observed fracture surfaces of these viscous materials were quantitatively examined to provide a comparison with surface features found in several metallic glasses.

#### 2:30 PM Invited

**Modeling the Mechanical Behavior of Metallic Glasses Using STZ Dynamics:** Eric Homer<sup>1</sup>; *Christopher Schuh*<sup>1</sup>; <sup>1</sup>MIT

Recent advancements in a meso-scale model for the mechanical behavior of metallic glasses have allowed a single modeling technique to bridge the disparate timescales associated with different modes of deformation in a metallic glass, a task which has proven difficult using other modeling approaches. A discussion of the modeling technique, which is based on the shear transformation zone, and its application using finite element analysis and the Kinetic Monte Carlo algorithm are presented. Recent analyses of simulations performed with this technique elucidate the conditions under which spatial and temporal correlations between shear transformation zones lead to different modes of observed macroscopic deformation. These correlation analyses provide some of the first insights into the localized microscopic processes that lead to inhomogeneous deformation analogous to nascent shear banding. Details regarding the extension of the modeling technique to three-dimensional systems and complex loading conditions are discussed.

#### 2:50 PM

**Continuum Model for Bulk Metallic Glass Composites:** *Fadi Abdeljawad*<sup>1</sup>; Mikko Haataja<sup>1</sup>; <sup>1</sup>Princeton University

Recent experimental work has suggested that the problem of catastrophic failure by shear band propagation in Bulk Metallic Glasses (BMGs) can be solved by forming composites with a two-phase microstructure consisting of the glassy BMG matrix phase and a non-percolating, soft crystalline phase. In this talk, we present a continuum model of plastic deformation in two-dimensional BMG composites. The elastic energy density is a periodic nonlinear function of

# Technical Program

the strains, while the structural heterogeneity of the glassy phase is accounted for by defining a quenched, spatially varying random variable that corresponds to the maximum local strain needed to cause a slip event. Simulations of BMGs with various sizes of crystalline domains under simple shear loading show that deformation patterns and mechanical strength are affected by the area fraction and spatial distribution of the crystalline domains, implying a size effect in the strength of BMG composites.

## 3:00 PM Invited

**Deformation and Failure of Glasses at Nanoscale:** *Ju Li*<sup>1</sup>; Erik Bitzek<sup>1</sup>; <sup>1</sup>University of Pennsylvania

Recent experiments on nanoscale amorphous materials have suggested interesting ductility - size scale dependencies (PNAS 104, 11155; PRB 77, 155419). Such size effect may shed light on the connection between plastic deformation and underlying spatio-temporal hierarchies of structural flow defects, the smallest of which is a single shear transformation zone (STZ)  $\sim 1\text{nm}^3$ . A mesoscale computational model (on the same level as discrete dislocation dynamics for crystalline materials) is constructed, which utilizes detailed statistical information about shear transformations, damage accumulations and damage repairs from atomistic simulations. Adjacency to surfaces/interfaces and the loading constraints could have strong effect on the apparent ductility of nanoscale glasses.

## 3:20 PM

**Numerical Deformation Simulations on Bulk Metallic Glasses Using First-Principles Methods:** *Lizhi Ouyang*<sup>1</sup>; Despina Louca<sup>2</sup>; Gongyao Wang<sup>3</sup>; Yoshihito Yokoyama<sup>4</sup>; Peter Liaw<sup>3</sup>; <sup>1</sup>Tennessee State University; <sup>2</sup>University of Virginia; <sup>3</sup>University of Tennessee; <sup>4</sup>Tohoku University

It was found recently that the cyclic fatigue loading causes the local structure changes in Zr-Cu-Al bulk metallic glasses (BMG). To reveal their atomistic origins, we performed numerical fatigue tests on Zr<sub>50</sub>Cu<sub>40</sub>Al<sub>10</sub> and Zr<sub>60</sub>Cu<sub>30</sub>Al<sub>10</sub> (in atomic percent) using first-principles methods. Large periodic models with 600 atoms are constructed for the two metallic glasses using the quenching and annealing technique. The local strain distributions of the deformed models generated by the numerical fatigue loadings are analyzed to identify irreversible structural changes and potential shear-band nucleation sites. The structure evolutions of the two BMGs under numerical cyclic loading are examined and the changes in their pair distribution functions are compared with the experimental results.

## 3:30 PM Break

## 3:40 PM Invited

**Simulating Poisson Ratio Effects on Shear Banding Behavior in Metallic Glasses:** *James Morris*<sup>1</sup>; Takeshi Egami<sup>2</sup>; <sup>1</sup>Oak Ridge National Laboratory; <sup>2</sup>University of Tennessee

Shear banding occurs commonly during deformation of bulk metallic glasses, often leading to failure. Understanding and controlling this phenomenon is important to improving the properties of metallic glasses. Several studies have suggested that an increased Poisson ratio is correlated with improved mechanical properties; for example, the fracture energy can change by three orders of magnitude as the Poisson ratio changes from 0.3 to 0.4 [J. J. Lewandowski et al., Phil. Mag. Letters 85, 77-87 (2005)]. To understand this behavior, we have begun molecular dynamic simulations of glasses under simple shear, using a model with a tunable Poisson ratio. The inhomogeneous shearing behavior is examined as a function of Poisson ratio, temperature, and strain rate. These results are compared with a phenomenological model which predicts the coexistence of two states with distinct viscosities.   
This research was sponsored by the Division of Materials Sciences and Engineering, U.S. Department of Energy.

## 4:00 PM

**Reverse Monte Carlo Simulation of Medium-Range Atomic Order in Bulk Metallic Glass Incorporating Fluctuation Electron Microscopy:** *Jinwoo Hwang*<sup>1</sup>; Paul Voyles<sup>1</sup>; <sup>1</sup>University of Wisconsin Madison

We have investigated medium-range order in Zr-based BMGs using fluctuation electron microscopy (FEM) and Reverse Monte Carlo (RMC) simulation. Initial RMC simulations incorporating FEM and electron diffraction reduced density function (RDF) data showed that including FEM data in RMC more uniquely confines the short to medium-range atomic structure compared to RDF data alone, and that the FEM signal is likely to arise from nanometer-scale planar

order in the structure. However, the MRO in the model was anisotropic due to limitations in the simulation and experiment. Improved FEM data obtained using highly-coherent, variable probe-size nanodiffraction in an aberration-corrected STEM will be presented, as will the results of more isotropic FEM RMC simulations which incorporate approximate chemical information in the form of EAM empirical potentials.

## 4:10 PM

**Reliability of Methods of Computer Simulation of Structure of Amorphous Alloys:** *Mikhail Mendeleev*<sup>1</sup>; Matthew Kramer<sup>1</sup>; <sup>1</sup>Ames Laboratory

There are several computer simulation methods to generate atomic models of glasses. We analyzed advantages and disadvantages of these methods. We took a model created by the MD simulation with a semi-empirical potential as a target system and explored how its structure can be reproduced using different simulation techniques. First, we explored effect of the cooling rate and found that if the cooling rate is  $\sim 10^{13}$  K/s the system has no time to adjust its structure to the change in temperature/density. It was also found that a small model size used in ab initio MD simulations can affect the final structure. Finally we used the target PPCFs to explore a possibility to create the atomic models from diffraction data using the RMC method. We created models with the PPCFs which almost coincided with the target ones but the structure of these models was different from the target structure.

## 4:20 PM Invited

**Connecting Atomic Structure and Plastic Deformation in Zr-Based Bulk Metallic Glasses:** *Paul Voyles*<sup>1</sup>; Jinwoo Hwang<sup>1</sup>; Jonathan Puthoff<sup>1</sup>; Don Stone<sup>1</sup>; <sup>1</sup>University of Wisconsin, Madison

We have recently used broadband nanoindentation creep to measure the volume of shear transformation zones (STZs) in three Zr-Cu-Al alloys in the context of the Johnson-Samwer cooperative shear model of plastic deformation. The STZs occupy 100-300 atomic volumes, which corresponds to spheres 1.5 to 2 nm in diameter. We use fluctuation electron microscopy (FEM) to measure structure at this length scale, which is difficult to access from more conventional techniques. Reverse Monte Carlo simulations incorporating FEM data show that consistency with FEM requires nanoscale regions with pseudo-planar order in the model and constrains the partial pair distribution functions. Higher-quality, variable probe-size FEM data from a new aberration-corrected STEM and hybrid reverse Monte Carlo simulations incorporating EAM potentials for Zr-Cu-Al will be presented.

## 4:40 PM

**Computational Studies on Free Volume and Plastic Flow in Metallic Glasses:** *Joshua Askin*<sup>1</sup>; Ashwini Bharathula<sup>1</sup>; Wolfgang Windl<sup>1</sup>; Katharine Flores<sup>1</sup>; <sup>1</sup>The Ohio State University

Positron annihilation spectroscopy studies reveal a trimodal lifetime distribution corresponding to 3 distinct defect volume ranges in bulk metallic glass structures which evolve in a regular manner with plastic deformation. These volumetrically distinct defects are hypothesized to be inherent interstitial holes, flow defects and nano-scale voids. To test this hypothesis, we developed an electron density model based on radial averaging of ab-initio charge density, [1] which we use to visualize evolution of "free/excess" volume or lower density regions during MD annealing and deformation. Rather than using different cooling rates to control density, a series of voids are injected into the glass structure under constant volume conditions. Under constant-volume annealing, the void redistributes amongst other defects. Under constant-volume shear, strain localization only occurs above a critical void size, indicating a requisite combination of applied shear and available excess volume. References [1] Metallurgical and Materials Transactions A, 39A 2008 1779-1785.

## 4:50 PM

**Structure and Anelastic Relaxation in Metallic Glasses:** *Garth Wilks*<sup>1</sup>; Daniel Miracle<sup>1</sup>; Amanda Dahlman<sup>1</sup>; <sup>1</sup>Air Force Research Laboratory

Variation in the constitution of several metallic glass ribbons are used to probe their deformation activation energy spectra via anelastic bend stress relaxation. The specific effects of vacancy and anti-site defects predicted by the Efficient Cluster Packing model are used to rationalize deviations in spectra between material conditions, particularly the effects that the energy, type, and concentration of such defects contribute to local free volume dilatation and their ability to act as sites for unit shear process nucleation.



### 5:00 PM

#### Avalanches, Size-Effects, and Critical Behavior in Shared Model Metallic Glasses: K. Michael Salerno<sup>1</sup>; Craig Maloney<sup>2</sup>; Mark Robbins<sup>1</sup>; <sup>1</sup>Johns Hopkins; <sup>2</sup>Carnegie Mellon University / Civil & Environmental Engineering

We perform computer simulations of sheared binary Lennard-Jones glasses in 2D at zero temperature and in the limit of small strain rate. The strain energy is released in discrete bursts with a Gutenberg-Richter size distribution. The plastic strain is organized into lines of slip which accumulate during avalanches over a system-size dependent characteristic strain scale  $\Delta\gamma_c$ .  $\Delta\gamma_c$  should give rise to interplay between indentation rate and system size which may be observable in micro-pillar indentation experiments on metallic glasses. Furthermore, we show that the spatial organization of the plastic deformation has a novel kind of fractal geometry, with orientation-dependent scaling exponents. These results further suggest that micro-pillar indentation experiments performed on bulk-metallic glass samples should exhibit a kind of self-organized critical behavior similar to that observed in crystalline samples [1]. [1] Dimiduk, DM, et al. Science 312 (5777). 1188-1190 (2006).

Transformation between crystalline and amorphous phases in the Zr<sub>47</sub>Cu<sub>31</sub>Al<sub>13</sub>Ni<sub>9</sub> metallic glass is studied with the molecular dynamics (MD) simulation to understand atomic stress and strain distributions under uniaxial stress and various heat treatments. In this paper, a molecular model of the Zr-based metallic glass is obtained by sputter MD simulation. Then, a portion of the as-deposited film is used as initial structures for uniaxial tension/compression tests and heat treatment. The discontinuity in volume change upon heating is observed around the T<sub>g</sub> of the metallic glass, and corresponding microstructures are studied. It is found that the uniaxial compression of the glass has superior plasticity than that of its tensile behavior. Atomic stress and strain calculations reveal atomic constitutive relationships to facilitate identification of microstructural changes.

### 5:10 PM Invited

#### Stress and Temperature Induced Phase Transformation in Zr-Based Metallic Glass via Molecular Dynamics Simulation: Yunche Wang<sup>1</sup>; Chun-Yi Wu<sup>1</sup>; Jinn Chu<sup>2</sup>; Yanfei Gao<sup>3</sup>; Peter Liaw<sup>3</sup>; <sup>1</sup>National Cheng Kung University; <sup>2</sup>National Taiwan University of Science and Technology; <sup>3</sup>The University of Tennessee

Transformation between crystalline and amorphous phases in the Zr<sub>47</sub>Cu<sub>31</sub>Al<sub>13</sub>Ni<sub>9</sub> metallic glass is studied with the molecular dynamics (MD) simulation to understand atomic stress and strain distributions under uniaxial stress and various heat treatments. In this paper, a molecular model of the Zr-based metallic glass is obtained by sputter MD simulation. Then, a portion of the as-deposited film is used as initial structures for uniaxial tension/compression tests and heat treatment. The discontinuity in volume change upon heating is observed around the T<sub>g</sub> of the metallic glass, and corresponding microstructures are studied. It is found that the uniaxial compression of the glass has superior plasticity than that of its tensile behavior. Atomic stress and strain calculations reveal atomic constitutive relationships to facilitate identification of microstructural changes.

Transformation between crystalline and amorphous phases in the Zr<sub>47</sub>Cu<sub>31</sub>Al<sub>13</sub>Ni<sub>9</sub> metallic glass is studied with the molecular dynamics (MD) simulation to understand atomic stress and strain distributions under uniaxial stress and various heat treatments. In this paper, a molecular model of the Zr-based metallic glass is obtained by sputter MD simulation. Then, a portion of the as-deposited film is used as initial structures for uniaxial tension/compression tests and heat treatment. The discontinuity in volume change upon heating is observed around the T<sub>g</sub> of the metallic glass, and corresponding microstructures are studied. It is found that the uniaxial compression of the glass has superior plasticity than that of its tensile behavior. Atomic stress and strain calculations reveal atomic constitutive relationships to facilitate identification of microstructural changes.

### 5:30 PM

#### Directional Deformation Memory and Orthogonal Bauschinger Effect in Metallic Glasses: Erik Bitzek<sup>1</sup>; David Rodney<sup>2</sup>; Ju Li<sup>1</sup>; <sup>1</sup>University of Pennsylvania; <sup>2</sup>Institut Polytechnique de Grenoble

In crystalline materials the Bauschinger effect whereby plastic deformation in one direction leads to a different deformation behavior upon re-straining in the opposite direction is well known. In bulk metallic glasses (BMGs) however, no such effect has been reported. Furthermore, as the free-volume model of plastic deformation is inherently isotropic, the accumulation of damage is usually believed to be directionally independent, as long as no shear bands are formed. Here we present results of MD simulations on BMGs which show a directional dependence of the deformation memory: when strained along one axis and then unloaded, the samples show a different deformation behavior depending on whether they are strained again in the same direction, or orthogonal to the initial loading direction. The simulations are compared with recent experiments, and the origin of the orthogonal Bauschinger effect is discussed in terms of the directional properties of the shear transformation zones.

### 5:40 PM

#### Atomistic Simulations to Estimate Plasticity of Cu-Zr Bulk Metallic Glasses: Kyung-Han Kang<sup>1</sup>; Byeong-Joo Lee<sup>1</sup>; <sup>1</sup>POSTECH

Understanding the origin of and thus improving the plasticity is one of the hot issues in the bulk metallic glass (BMG) society. Many reports suggest that plasticity of BMGs may be correlated with several properties such as free volume, short range ordered structure, the ratio of shear modulus to bulk modulus, Poisson's ratio, atomic displacement and viscosity. In this study, a special attention was focused on the evaluation of the correlation between the above mentioned properties and plasticity in the Cu-Zr binary BMGs, by comparing the experimentally reported composition dependence with that of various properties obtained from atomistic calculations based on a modified embedded-atom method (MEAM) interatomic potential. It was found that the free volume and the distribution of short range ordered structures have a

relatively clear correlation with plasticity. The correlation between the plasticity and other individual properties will also be presented.

### Carbon Management and Carbon Dioxide Reduction: Session I

*Sponsored by:* The Minerals, Metals and Materials Society, TMS Light Metals Division, TMS Extraction and Processing Division, TMS: Energy Committee

*Program Organizers:* Subodh Das, Phinix LLC; Brajendra Mishra, Colorado School of Mines; Neale Neelameggham, US Magnesium LLC

Wednesday PM Room: 310  
February 17, 2010 Location: Washington State Convention Center

*Session Chair:* Subodh Das, Phinix, LLC

### 2:00 PM

#### Upcoming Carbon Management Legislations: Impacts and Opportunities for the Global Aluminum Industry: Adam Gesing<sup>1</sup>; Subodh Das<sup>1</sup>; <sup>1</sup>Phinix, LLC

The European Union is planning to include the aluminum industry in its carbon management system in 2013. Additionally, if and when enacted, "The American Clean Energy and Security Act" of 2009 will also force U.S. industries to comply with much debated "carbon cap and trade" system. The Waxman and Markey legislation – along with the Environmental Protection Agency mandate under the Clean Air Act – will specifically include US aluminum industry with CO<sub>2</sub> equivalent sources of more than 25,000 tons per year. This paper will review the carbon management system as it now operates and how it is likely to be applied to the European and American aluminium industry.

### 2:30 PM

#### Cost-Effective Gas Stream Component Analysis Techniques and Strategies for Carbon Capture Systems from Oxy-Fuel Combustion (An Overview): John Clark<sup>1</sup>; Danylo Oryshchyn<sup>1</sup>; Thomas Ochs<sup>1</sup>; Steve Gerdemann<sup>1</sup>; Cathy Summers<sup>1</sup>; <sup>1</sup>National Energy Technology Lab

Limited analysis of combustion gas streams where carbon capture is not of interest is done mainly to ascertain operation parameters. Stringent regulations on acid gases and particulates promote careful flue gas analysis. Unregulated components are typically not analyzed. Typically not more than four points (two in the boiler and one each in the flue and the stack) are sampled. A successful oxy-fuel process with carbon capture and compression is anticipated to require a many as 12 sample points with analysis for water, nitrogen, oxygen, argon, NO<sub>x</sub>, SO<sub>x</sub>, and carbon monoxide. Carbon dioxide captured for beverages produces a high value product and the cost associated with analysis is warranted. However, carbon capture for disposal must keep all costs to a minimum. This paper will compare alternative approaches for cost-effective sampling and analysis of the carbon dioxide product streams from oxy-fuel combustion, through all stages of production through compression and pipeline/vessel delivery.

Limited analysis of combustion gas streams where carbon capture is not of interest is done mainly to ascertain operation parameters. Stringent regulations on acid gases and particulates promote careful flue gas analysis. Unregulated components are typically not analyzed. Typically not more than four points (two in the boiler and one each in the flue and the stack) are sampled. A successful oxy-fuel process with carbon capture and compression is anticipated to require a many as 12 sample points with analysis for water, nitrogen, oxygen, argon, NO<sub>x</sub>, SO<sub>x</sub>, and carbon monoxide. Carbon dioxide captured for beverages produces a high value product and the cost associated with analysis is warranted. However, carbon capture for disposal must keep all costs to a minimum. This paper will compare alternative approaches for cost-effective sampling and analysis of the carbon dioxide product streams from oxy-fuel combustion, through all stages of production through compression and pipeline/vessel delivery.

### 3:00 PM

#### Strategic Approaches for CO<sub>2</sub> Reduction Rate from Fossil Fuel Use in Steel Industry: Malti Goel<sup>1</sup>; <sup>1</sup>INSA

Technology advancements in fossil fuel based energy generation are currently being aimed at minimization of CO<sub>2</sub> emissions. To attain energy security, India must accelerate the pace of economic development, while achieving reduction in CO<sub>2</sub> emissions per unit of energy. It would need access to advanced coal utilization technologies to be demonstrated on indigenous coal characteristics. Of specific importance would be: improvement in coal quality, increasing efficiency of fossil fuel use, and suitability of other CO<sub>2</sub> sequestration technologies for reducing CO<sub>2</sub> footprints. There is need to address related risks and financial burden through adoption of policies and regulations including the issue of open access in energy research. In this paper, seven important areas of strategic plan that need to be pursued for managing CO<sub>2</sub> emissions in energy sector are discussed. A case study from steel industry is presented.

# Technical Program

3:30 PM

## Development of Reverberatory Furnace Using in Copper Scrap Smelting by Reformed Natural Gas: *Mohamed Ahmed Hamad*<sup>1</sup>; <sup>1</sup>CMRDI

Reverberatory furnace which used for smelting of scrap of copper, residual anodes and cathodes from the next stages which carried out in copper after casting from this furnace using wood as a resource of reduction gases such carbon monoxide, hydrogen and methane. That is the problem, using of wood causes the following: (1) Pollution of medium of copper melting (forming soot of smock above furnace) (2) low efficiency in removal of oxygen from copper and more contamination in copper matte causes in rising of heat to remove of it and increasing in cost and time of casing of copper (3) high expensive this problem was solved by using of reformed natural gas as a source of reduction gases (CO+ H<sub>2</sub>).

4:00 PM Break

4:15 PM

## Bauxite Residue Neutralization with Carbon Sequestration: *Luis Venancio*<sup>1</sup>; Emanuel Macedo<sup>2</sup>; Antonio Ernandes Paiva<sup>1</sup>; José Antonio Souza<sup>2</sup>; <sup>1</sup>Federal Institute of Education Science and Technology - Maranhão; <sup>2</sup>Universidade Federal do Pará

The production of alumina from bauxite using the Bayer process generate 1.25 ton of the residue known by red mud and 460 kg of CO<sub>2</sub> per ton of alumina. The direct use of exhaust gases from the alumina refineries to react and neutralize the bauxite residue may allow a double gain: open a wide range of new applications for bauxite residue reducing the reactivity of red mud and sequester approximately 15% or 67 kg of CO<sub>2</sub> per ton of alumina. This paper shows the reaction of a suspension of bauxite residue-water with a simulation of the calcinator exhaust gases of the refinery. The influence of the temperature and the ratio water red mud is also analyzed.

4:45 PM

## Electrochemical Quartz Crystal Microbalance Study on Carbon Dioxide Adsorption in the Presence of Electrosorbed Hydrogen on Cu-Gold Single Crystals: *Maria Salazar-Villalpando*<sup>1</sup>; <sup>1</sup>National Energy Technology Laboratory

Finding areas of CO<sub>2</sub> utilization represents an opportunity to decrease global warming. The electrochemical reduction of CO<sub>2</sub> could represent a form of energy storage. Tests of carbon dioxide adsorption on Cu-Gold single crystals are a preliminary step in the study of CO<sub>2</sub> electrochemical conversion. The electrochemical deposition of Copper is studied with the electrochemical quartz crystal microbalance (EQCM) on a gold substrate. Cu is deposited from acidic sulphate bath. Cyclic voltammograms are obtained to determine electrical potentials for copper deposition on Au-single crystals. Moreover, electrical potentials for products generated between electrosorbed Hydrogen and CO<sub>2</sub> molecules are investigated.

5:10 PM

## The Thermal Gas Processing in Pre-Heating Zone of "Water-Jacket" Furnaces in "Trepça": *Ahmet Haxhijaj*<sup>1</sup>; Egzon Haxhijaj<sup>2</sup>; <sup>1</sup>University of Prishtina; <sup>2</sup>American University in Kosovo

The paper has as a studying object the issue of effective management of gasses' heating and dusts in reducing melting process in lead (Pb) metallurgy. It also analyses the issue related to the usage and recycling of dusts and gasses in all pyro-metallurgical processes of technical lead production. The paper contains the analysis of technological process of separation of humidity, gasses, and dusts of valuable remainders in "Trepça" plant. Paper has the results of theoretical-experimental studying, analytical and graphical of gasses thermal balance depending on height and composition of load, and the coke quantity on load for reducing melt in "Water-Jacket" furnaces. With thermal balance, having into consideration all parameters of heat in entry and exit depending on aforementioned factors we aimed to optimize the parameters of the process, keeping the attention to the minimization of energy consumption, and the overall influence on environment.

5:35 PM

## Oxidation Kinetics of Fe-Cr and Fe-V Liquid Alloys under Controlled Oxygen Pressures: *Haijuan Wang*<sup>1</sup>; Nurni Viswanathan<sup>2</sup>; Seshadri Seetharaman<sup>1</sup>; <sup>1</sup>Royal Institute of Technology(KTH), Sweden; <sup>2</sup>Indian Institute of Technology Bombay, Mumbai, India

The oxidation kinetics of Fe-Cr as well as Fe-V alloys were investigated with CO<sub>2</sub> as the oxidant gas by thermogravimetric analysis (TGA) in the temperature range 1550-1650°. Further, the gas-liquid reaction sequence was monitored by X-ray radiographic observations at 1600°. The results of the TGA experiments show clearly that the oxidation proceeds at a slower rate when pure CO<sub>2</sub> is used as the oxidizer compared with different CO<sub>2</sub>-O<sub>2</sub> mixtures. The post-measurements samples were subjected to chemical analysis, SEM-EDS and XRD analysis. The result indicated that the oxide scale was mainly a spinel phase; the oxidation of iron was found to occur alongside the oxidation of chromium and vanadium. The oxidation was taking place in steps indicated by the changes in the slopes of the thermogram for oxidation as a function of time. In general, rates of oxidation decrease after achieving a maximum value through an initial transient.

## Cast Shop for Aluminum Production: Cast House Productivity and Strip Casting

*Sponsored by:* The Minerals, Metals and Materials Society, TMS Light Metals Division, TMS: Aluminum Committee, TMS: Aluminum Processing Committee

*Program Organizers:* John Grandfield, Grandfield Technology Pty Ltd; Pierre Le Brun, Alcan Voreppe Research Center

Wednesday PM

Room: 609

February 17, 2010

Location: Washington State Convention Center

*Session Chair:* Philippe JARRY, Unité de Recherches Fonderie ALCAN CRV

2:00 PM

## Means of Improving Casthouse Productivity: *Peter Whiteley*<sup>1</sup>; <sup>1</sup>Munimula Technology Pty Ltd

This presentation will deal with ways of improving casthouse productivity by commencing with management issues concerned about product mix, organisation, potroom interface in a smelter context and the fabrication interface in a remelt context, production and maintenance planning, training and culture. Following this introduction, the next matters to be considered are means to maximise asset utilisation by examining a suite of opportunities including process intensivity, debottlenecking, benchmarking, scrap reduction, data logging, trending and use of algorithms, compiling multiple activity charts, identification of root causes of delays and aborts, conducting dynamic simulations, adaption of new technologies, melt loss minimisation, and other ways of improving plant OEE. The presentation will cover smelter based casthouses as well as remelters and scrap based operations, since each have specific challenges and opportunities.

2:25 PM

## Estimating the Production Capabilities of Casthouse Equipment Configuration Options: *Phillip Baker*<sup>1</sup>; <sup>1</sup>Hatch Associates

Operational Casthouses must, above all else, be capable of accepting all primary metal produced by the Potlines so as not to limit the ability of the smelter to produce metal and to provide the most stable operating regime for the reduction cells by allowing consistent metal pad depth. To be effective, Casthouse equipment configurations must accommodate not only the Normal operational state, but also both Repair and Catch-Up scenarios. Hatch has developed a simple first pass methodology for assessing the performance of equipment configuration options for primary aluminium Casthouses in this context.

2:50 PM

## Electrochemical Characterization of TRC 7072AA for Heat Exchangers: *Aziz Dursun*<sup>1</sup>; Beril Corlu<sup>1</sup>; Canan Inel<sup>1</sup>; Murat Dundar<sup>1</sup>; Rasim Erdogan<sup>1</sup>; Mustafa Ürgen<sup>2</sup>; <sup>1</sup>Assan Aluminium; <sup>2</sup>Istanbul Teknik Üniversitesi

We present the results of corrosion potential measurements of DC and TRC cast 7072AA used as a fin material in mechanical heat exchanger applications. The alloys used were continuously cast to two different gauges and Zn, Ti Fe and



Si content, using twin roll casting technology. Optic and electron microscopy with x-ray EDS capability was used to correlate the electrochemical results with microstructure and chemical composition at the surface. It was shown that higher solidification rates developed during twin roll casting at much thinner gauges resulted in much lower corrosion potentials. This in turn made us possible to reduce Zn content to improve the thermal conductivity while maintaining the desired corrosion potential. Unlike Zn and Ti, higher concentrations of Fe and Si added with the purpose of retaining adequate strength at much thinner thicknesses do not have an adverse effect on corrosion potentials.

### 3:15 PM

**Influence of the Cooling Water Temperature on Productivity and Product Quality in Twin Roll Casting with Copper Shells:** *Mark Badowski*<sup>1</sup>; Eduardo Garate<sup>1</sup>; David Armendariz<sup>1</sup>; <sup>1</sup>Hydro Aluminium

The use of twin roll casters for the production of aluminium strip is today widespread. The twin roll casting process offers advantages such as reduced investment and energy costs or a fine grained microstructure. However, the production volume compared to the DC-casting process is limited by the low productivity and restricted alloy range. Utilization of copper shells can increase productivity through improved heat extraction at the solidification interface. Increased heat flux can impact several other parameter like strip profile and mechanical properties. A better understanding of this complex relationship is required to fully utilize the potential of this new technology. The present paper describes operational experiences at Hydro Aluminium INASA obtained with copper shell technology. The productivity and product quality achieved after implementation is compared to previous numerical predictions. The influence of the cooling water temperature is discussed including the productivity and product quality achieved through optimization work.

### 3:40 PM

**The Use of Copper Shells by Twin Roll Strip Casters:** Aldenir Clemente<sup>1</sup>; John Tsiros<sup>2</sup>; Aristeidis Arvanitis<sup>2</sup>; *Dionisis Spathis*<sup>2</sup>; Hans-Gunter Wobker<sup>3</sup>; <sup>1</sup>Castcom Ltda; <sup>2</sup>Hellenic Aluminium Industry SA ( Elval SA); <sup>3</sup>KME Europe

Twin roll casting of aluminum alloys is a well established process, which exists over several decades. The productivity of the process has been largely limited by the heat transfer capability of the steel shells used on the caster rolls. In recent years, developments in the manufacture of shells based on special copper alloys have opened a window for productivity increases and quality improvement. One or both rolls of a caster can be lined with copper shells, to take advantage of the higher thermal conductivity of Cu relative to Fe, which provides for an increased cooling capacity of working rolls. This paper presents a review of the equipment/operation, productivity increase and product/quality performance, by using both copper/copper and copper/steel combination

### 4:05 PM

**A TEM Study of the Microstructures of 3003 and 3003-Zr Alloys Produced by Twin Roll Casting:** *Beril Corlu*<sup>1</sup>; Ozgur Duygulu<sup>2</sup>; Selda Ucuncuoglu<sup>2</sup>; Gizem Oktay<sup>2</sup>; Aziz Dursun<sup>1</sup>; Murat Dunder<sup>1</sup>; <sup>1</sup>Assan Aluminium; <sup>2</sup>TUBITAK MAM

3003 is a typical alloy produced with twin roll casting (TRC) technology for various application of industry. Alloying of 3003 with Zr has been studied for conventional production technique, i.e. DC casting and hot-rolling. However, it has not been investigated for a similar composition solidified at the cooling rate of TRC. In this study, the microstructures of TRC 3003 and ~0.08 wt.% Zr containing TRC 3003 alloys were investigated using optical microscopy (OM), scanning electron microscopy (SEM) and transmission electron microscopy (TEM). For both alloys, the same thermomechanical downstream process was employed, which included a homogenization treatment at an intermediate thickness and a final annealing. Intermetallic particle evolution after the annealing steps was investigated comparatively. Recrystallization temperature of TRC 3003 alloys were significantly altered with the addition of ~0.08 wt.% Zr due to the formation of Zr containing second phase particles.

### 4:30 PM

**Casthouse Design for the Production of Air-Cooled, Low-Profile Aluminium Sows:** *Tom Plikas*<sup>1</sup>; Tony Cesta<sup>1</sup>; Lowy Gunnewiek<sup>1</sup>; Michael Trovant<sup>1</sup>; Rui Santiago<sup>1</sup>; Jean Vanasse<sup>2</sup>; <sup>1</sup>Hatch Ltd.; <sup>2</sup>Aluminerie Alouette Inc.

The Aluminerie Alouette Inc. Smelter in northern Quebec, Canada recently completed a major plant expansion that includes a new casthouse for the continuous production of low-profile aluminium sows using natural air cooling technology. This is a novel concept representing a departure from the traditional

batch, water-cooled casting operations of the past, and has benefits in terms of sow quality, production efficiency, safety, and mould maintenance. The casthouse design presented many challenges: ensuring proper casting and cooling of sows at the correct metal production rate to produce high quality sows, design of the casting machine and moulds to withstand thermal shocks and stresses, developing a ventilation system for effective management of heat released during the casting process, and protection of heat sensitive equipment and instrumentation using radiation shielding. This paper describes how these engineering challenges were met through the use of sound design practice, empirical testing, and computational methods.

### 4:55 PM

**The Measurement of Heat Flow within a DC Casting Mould:** *Arvind Prasad*<sup>1</sup>; John Taylor<sup>1</sup>; Ian Bainbridge<sup>1</sup>; <sup>1</sup>University of Queensland

The heat flow between the molten metal and the mould-wall in DC casting is often assumed to be negligible compared to that due to the sub-mould water cooling. Furthermore, the entire DC casting process is often described based on this assumption. However the assumption of negligible heat transfer in the metal-mould region and its subsequent minimal influence on cast product quality remains unproven. The focus of the present paper is therefore on understanding the heat transfer in the metal/mould wall region. To this end a method for the laboratory measurement of the flow of heat from the metal being cast to the wall of a DC casting mould has been developed. The equipment and methodology are briefly described together with the initial results obtained. The implications of this work for use in simulation models and for the design and operation of DC casting moulds are discussed.

## Characterization of Minerals, Metals and Materials: Characterization of Cu, Zn, Mn, Fe, Au, and Carbon Phases

*Sponsored by:* The Minerals, Metals and Materials Society, TMS Extraction and Processing Division, TMS Structural Materials Division, TMS/ASM: Composite Materials Committee, TMS: Materials Characterization Committee

*Program Organizers:* Ann Hagni, Geoscience Consultant; Sergio Monteiro, State University of the Northern Rio de Janeiro - UENF; Jiann-Yang Hwang, Michigan Technological University

Wednesday PM Room: 307  
February 17, 2010 Location: Washington State Convention Center

*Session Chairs:* Tzong Chen, CANMET-MMSL; Yoshitaro Nose, Kyoto University

### 2:00 PM Introductory Comments

### 2:10 PM

**Ternary Phase Diagram of the Zn-Sn-P System for Fabrication of ZnSnP<sub>2</sub> Compound Semiconductor:** *Yoshitaro Nose*<sup>1</sup>; Noriyuki Tanaka<sup>1</sup>; Tetsuya Uda<sup>1</sup>; <sup>1</sup>Kyoto University

Recently, solar cells using compound semiconductors such as Cu(In,Ga)Se<sub>2</sub> with chalcopyrite structure attract much attention. However, the compounds consist of In and Ga, which are rare elements, and Se with toxicity. We thus focus on ZnSnP<sub>2</sub>, which has also chalcopyrite structure and consists from safe and abundant elements. Additionally, its bandgap varies from 1.66 eV to 1.25 eV. In this study, we try to fabricate ZnSnP<sub>2</sub> based on ternary phase diagram of the Zn-Sn-P system. First, we establish the phase diagram by equilibrium experiments using zinc, tin and their phosphides. At 700 °C, ZnSnP<sub>2</sub> is almost stoichiometry, while its single-phase region ranges to Zn-rich composition at 600 °C. It is also obtained that ZnSnP<sub>2</sub> is stable at higher temperatures than literature data. Some differences with the previously reported diagram of the Sn-Zn-P<sub>2</sub> pseudo-binary system have been clarified and the diagram of the system has been re-constructed.

# Technical Program

2:35 PM

**Microstructure Evolution in Copper-Clad-Steel and Copper-Clad-Aluminum Bimetallic Wires during Drawing Processes:** *Taisuke Sasaki*<sup>1</sup>; Robert Morris<sup>1</sup>; Karen Torres<sup>1</sup>; Gregory Thompson<sup>1</sup>; Y. Syarif<sup>2</sup>; D. Fox<sup>2</sup>; <sup>1</sup>University of Alabama; <sup>2</sup>Fushi Copperweld, Inc.

Bimetallic wires combine the features of dissimilar metals to achieve a cost and/or a performance advantage over solid metal conductors in applications such as battery cables, coaxial cables, and grounding. In high frequency applications, the copper-clad steel provides a high strength alternative and the copper-clad aluminum offers a low weight option. The thermomechanical and microstructure evaluation in these simultaneously co-deformed materials are compared at different drawing stages. In the as-drawn condition, a filamentary granular microstructure forms along the closest packed directions as quantified by SEM-EBSD. The copper sheath also shows deformation twins. The cold worked drawing passes have a corresponding increase in hardness as a function of reduced area per pass. The hardness is lowered with a loss of preferred texture during intermediate heat treatments because of recrystallization. Nanoindentation hardness of the drawn wires has been measured across the bimetallic interfaces and compared to TEM-EDX compositional profiles.

3:00 PM

**OIM Characterization of a Jewelry Gold Alloy Subjected to Small-Charge Explosion:** Chiara Pozzi<sup>1</sup>; John Bingert<sup>2</sup>; Donato Firrao<sup>1</sup>; <sup>1</sup>Politecnico di Torino; <sup>2</sup>Los Alamos National Laboratory

As part of a wider experimental campaign a gold alloy sample was exposed to a blast from 100 g of plastic explosive, at a charge-to-sample distance of 220 mm. From optical microscopy observations, the occurrence of very fine deformation features on the surface exposed to the blast wave was documented. Due to the high deformation rate related to an explosive-generated shock, the occurrence of deformation twinning was suspected. Orientation imaging microscopy was employed to investigate the actual nature of the deformation marks observed by optical microscopy. Results obtained on the post-mortem sample are presented and compared to those of the as-prepared condition.

3:25 PM

**Characterization of Tin-Rich Copper Anodes from Secondary Copper Refineries:** *Tzong Chen*<sup>1</sup>; John Dutrizac<sup>1</sup>; <sup>1</sup>CANMET-MMSL

Copper anodes generated from copper scrap are relatively rich in Sn, Zn and Fe. Because of the presence of oxygen, only trace amounts of Sn are present in solid solution in the copper crystals. Thus, Sn occurs mainly as SnO<sub>2</sub>, Cu-Sn-Ni oxide and Sn-Ni-Zn oxide in the copper anodes, and Zn and Fe occur mainly as minor constituents in the Sn-Ni-Zn oxide and Cu-Sn-Ni oxide. During electrorefining, these oxide species are liberated directly from the copper anodes and report to the anode slimes. The trace amounts of Sn, present in solid solution in the copper crystals, dissolve but reprecipitate as Sn arsenate or a Sb-As-Sn-O phase. Accordingly, high Sn contents in copper anodes do not lead to elevated Sn concentrations in the electrolyte.

3:50 PM

**Study on the Interface Behavior of Ore Powder in the Organic Media:** *Li Dan*<sup>1</sup>; Chen Qiyuan<sup>1</sup>; <sup>1</sup>Central South University

In this paper, pyrite ore powder for the raw materials, acetone, chloroform, cyclohexane, cyclohexanol, toluene, tetrahydrofuran, sodium dodecyl sulfate to organic solvents, n-dodecanethiol as a modifier, study from the dispersion of yellow iron ore body in this organic solvent interface in seven acts. Dispersion in the study, with photographs of law, ultraviolet spectroscopy, oscillation, scanning electron microscopy, and electron spin resonance method in the seven types of pyrite in the organic solvent dispersion of research. The experimental results for the pyrite in sodium dodecyl sulfate in the dispersion of the best, followed by tetrahydrofuran, followed by cyclohexanol, chloroform dispersion of the worst. After pyrite modified with ESR analysis showed that iron ore yellow surface a series of localized paramagnetic state. Samples of the modified scanning electron microscope results show that modified after treatment in n-dodecanethiol smaller lattice.

4:15 PM

**Synthesis of ZnO/TiO<sub>2</sub> and Study on its Photocatalytic Activity:** *Wu Daoxin*<sup>1</sup>; <sup>1</sup>Changsha University of Science and Technology

With Ti(C<sub>4</sub>H<sub>9</sub>O)<sub>4</sub> and Zn(Ac)<sub>2</sub>•2H<sub>2</sub>O used as raw materials, oxalic acid as the complexing agent and anhydrous ethanol as solvent. The ZnO/TiO<sub>2</sub> photocatalytic nanocomposite materials was prepared by Sol-gel method and characterized by

XRD, DRS and FS, and catalyst for photodegradation experiments. The results show that when TiO<sub>2</sub> composite is 40% (mole fraction), calcination temperature is 400°. ZnO/TiO<sub>2</sub> has a good absorption performance, which indicated that red shift occurred. With sunlight as the light source, pH=5.0, catalyst concentration is 1.0mg.L<sup>-1</sup>, concentration of methyl orange is 5.0mg.L<sup>-1</sup>. The result shows that ZnO/TiO<sub>2</sub> powders(40%,400°) has the most photodegradation efficiency, and the degradation efficiency of 96.5% after 4 hours.

4:40 PM Concluding Comments

4:50 PM Question and Answer Period

---

## Cost-Affordable Titanium III: Creative Processing and Property Enhancement II

*Sponsored by:* The Minerals, Metals and Materials Society, TMS Structural Materials Division, TMS: Titanium Committee

*Program Organizers:* M. Ashraf Imam, Naval Research Lab; F. H. (Sam) Froes, University of Idaho; Kevin Dring, Norsk Titanium

Wednesday PM

Room: 618

February 17, 2010

Location: Washington State Convention Center

*Session Chairs:* Mitsuo Niinomi, Toyohashi University of Technology; Rodney Boyer, Boeing Commercial Airplanes

---

2:00 PM

**Rapid Consolidation of Ti-6Al-4V Powders by Transformation Superplasticity:** Bing Ye<sup>1</sup>; Marc Matsen<sup>2</sup>; David Dunand<sup>1</sup>; <sup>1</sup>Northwestern University; <sup>2</sup>The Boeing Company

The densification kinetics of Ti-6Al-4V powders with spherical or angular shapes are compared in uniaxial die pressing experiments between isothermal conditions (at 1020 °C, in the beta-field, where deformation occurs by creep) and during thermal cycling (860-1020 °C, within the range of the alpha-beta phase transformation) of the alloy, where transformation-mismatch superplasticity is activated). Densification kinetics are markedly faster under thermal cycling than under isothermal conditions, as expected from the higher deformation rate achieved under transformation-mismatch plasticity conditions as compared to creep conditions. The densification curves are successfully modeled for both creep and superplastic deformation mechanisms using (i) simple closed-form solutions and (ii) the finite-element method. Densification kinetics, under isothermal and thermal cycling conditions, of Ti-6Al-4V powders containing 5-20 vol.% ceramic particles are also presented.

2:25 PM

**Evaluation of Titanium for Vehicle Fuel Economy and Performance Improvement:** P.K. Mallik<sup>1</sup>; Curt Lavender<sup>2</sup>; Scott Weil<sup>2</sup>; <sup>1</sup>University of Michigan at Dearborn; <sup>2</sup>Battelle - Pacific Northwest National Laboratory

The potential for titanium to decrease the mass of propulsions system in a vehicle have been studied and used to predict the increase in fuel efficiency of a vehicle. The overall efficiency improvement will come not only from titanium substitution but also from downsizing or material substitution of other interacting components resulting in reduced engine friction losses and inertia force reduction in reciprocating and rotating components. Candidate components for titanium have been identified and low cost processing routes have been identified for each component using emerging low cost titanium raw materials and processing routes.

2:50 PM

**Titanium Recycling Process by Disproportionation of Titanium Subchloride in Molten Magnesium Chloride:** *Taiji Oi*<sup>1</sup>; Toru Okabe<sup>1</sup>; <sup>1</sup>The University of Tokyo

In order to establish a new titanium recycling process, the synthesis of TiCl<sub>2</sub> from Ti scrap heavily contaminated with Fe and the production of pure Ti by the disproportionation of TiCl<sub>2</sub> in molten MgCl<sub>2</sub> were investigated. TiCl<sub>2</sub> containing small amount of Fe was synthesized by reacting TiCl<sub>4</sub> with heavily contaminated Ti scrap (Ti-44%Fe-9%Cr-5%Ni) in by utilizing MgCl<sub>2</sub> molten salt as a reaction medium at 1273 K. Ti powder with a purity of over 99% was obtained by the disproportionation of TiCl<sub>2</sub> in molten MgCl<sub>2</sub> at 1273 K. The results of this study showed the feasibility of the new Ti recycling process. The feasibility of a new Ti coating method based on the disproportionation of



TiCl<sub>2</sub> is also discussed from some of the results obtained in the preliminary experiments.

### 3:15 PM

**Modeling Beta-Transus Temperature of Titanium Alloys:** *N. S. Reddy*<sup>1</sup>; Chan Hee Park<sup>2</sup>; Chong Soo Lee<sup>2</sup>; <sup>1</sup>GIFT, POSTECH, Pohang, Korea; <sup>2</sup>Department of Materials Science and Engineering, POSTECH

Beta transus temperature is the basic reference point for treatment in titanium alloys. Therefore, it is desirable to determine this temperature for a given alloy accurately, especially for some near- $\alpha$  alloy whose processing window is narrow. The beta transus is sensitive to chemical composition and the relationships between them are complex and nonlinear. An artificial neural network (ANN) model was developed to simulate the nonlinear relationship between the alloying elements and beta transus temperature. By performing sensitivity analysis on ANN model, the individual and the combined influence of alloying elements on beta transus was achieved. The optimum percentage of composition for the desired beta transus was calculated by using genetic algorithms. The results are in agreement with experimental data. Explanation of the calculated results from the metallurgical point of view is attempted. The model can be used as a guide for further alloy development.

### 3:40 PM Break

### 3:55 PM

**Study of Ti-6Al-4V in Liquid State by Electrostatic Levitation:** *John Li*<sup>1</sup>; Won-Kyu Rhim<sup>1</sup>; William Johnson<sup>1</sup>; <sup>1</sup>Caltech

Some thermophysical properties of liquid Ti-6Al-4V were measured around the melting temperature by the Electrostatic Levitation. The properties include the specific heat, the total hemispherical emissivity, the heat of fusion, the density and the thermal expansion coefficient with 280 ° K of undercooling in liquid state. Over 1661 ~ 1997 ° K the ratio of the constant pressure heat capacity and the total hemispherical emissivity for liquid phase can be expressed by  $C_p / \epsilon_T = 3064 + 0.1291(T - T_m)$  J/kg/K with the melting temperature  $T_m = 1943$  ° K. The heat of fusion has been measured to be 300 kJ/kg. Liquid density over 1661 to 1997 ° K can be expressed by  $d(T) = 4123 - 0.254(T - T_m)^3$ , and the corresponding volume expansion coefficient is  $\alpha = 6.05 \times 10^{-5} \text{ K}^{-1}$  near  $T_m$ .

### 4:20 PM

**Laser Additive Manufacturing of Titanium for Orthopedic Implants:** *James Sears*<sup>1</sup>; Dana Medlin<sup>1</sup>; Jacob Fuerst<sup>1</sup>; <sup>1</sup>South Dakota School of Mines & Technology

Increasing the lifespan of implants by improving fixation of the medical device in bone tissue, through improved osteointegration, can increase patient health and decrease medical costs by reducing the need for revision surgeries on an implant. Initially a scaffolding designed to more accurately match the porosity of cortical bone was deposited on a Ti-6Al-4V substrate with a Nd:YAG laser piped through a 600 $\mu$ m fibre and finely screened Ti-6Al-4V or Ti-15Mo powder in an argon atmosphere. Subsequent testing has been performed using a new M-LAM system that employs a 10  $\mu$ m fiber with six degrees of freedom motion. Using very fine Ti-6Al-4V powder, structured surfaces were deposited onto a like substrate demonstrating surface features as low as 100 $\mu$ m with minimal substrate distortion and a heat affected zone of less than 200 $\mu$ m deep.

### 4:45 PM

**Laser Beam Welding of ATI 425 Titanium:** *Paul Edwards*<sup>1</sup>; Todd Morton<sup>1</sup>; Greg Ramsey<sup>1</sup>; <sup>1</sup>The Boeing Company

Laser Beam Welding of the low cost alloy ATI 425 was performed on 2 mm gage butt joints. This new alloy could be used in place of standard Ti-6Al-4V for a variety of lower cost solutions. Demonstration of its fusion weldability with laser welding is of particular interest because it is a near net shape process, capable of high welding speeds, which will further enable low cost manufacturing options. It was found that ATI-425 could be successfully welded using a fiber laser at speeds over 2 m/min. Results of the laser welding process development along with the resulting metallographic and mechanical property evaluations will be presented.

### 5:10 PM

**Heat Treatments for Friction Stir Welded Ti-6Al-4V:** *Paul Edwards*<sup>1</sup>; Marc Petersen<sup>1</sup>; <sup>1</sup>The Boeing Company

Friction Stir Welding is a solid state joining process which can be used to fabricate near net titanium structures at a reduced cost compared to traditional

manufacturing processes. To date, Friction Stir Welding of titanium 6Al-4V has been demonstrated in butt welds, corner welds, T-welds and complex contour structures from 1.5 to 12 mm in thickness. Heat treatment processes for standard fusion welding techniques in titanium are well established, but the optimal heat treatment for Friction Stir Welded titanium has not been evaluated. In this study, 6 mm thickness titanium 6Al-4V butt welds were subjected to heat treatments ranging from 700 to 900 C. Results of the metallographic analysis for each heat treatment condition will be presented in addition to tensile and fatigue properties.

### Electrode Technology for Aluminum Production: Anode Baking/Anode Properties

*Sponsored by:* The Minerals, Metals and Materials Society, TMS Light Metals Division, TMS: Aluminum Industry Committee

*Program Organizers:* Ketil Rye, Alcoa Mosjøen; Morten Sorlie, Alcoa Norway; Barry Sadler, Net Carbon Consulting Pty Ltd

Wednesday PM

Room: 616

February 17, 2010

Location: Washington State Convention Center

*Session Chair:* Gudrun Saevarsdottir, Reykjavik University

### 2:00 PM Introductory Comments

### 2:05 PM

**On the Logistics of Rebuilding an Anode Baking Furnace while Maintaining Operation:** *Richard Coulombe*<sup>1</sup>; David Machado<sup>1</sup>; John Ferguson<sup>2</sup>; Darren Carle<sup>2</sup>; <sup>1</sup>Hatch and Associates; <sup>2</sup>Portland Aluminium

During 2008, Portland Aluminium Smelter refurbished one of its two anode baking furnaces. The works included replacing the insulation and dense refractory with a new design to allow larger anodes within the existing tub, introducing a new state-of-the-art firing system, replacing the waste gas main and building a new scrubber. This refurbishment was done on-the-run, with ongoing production on three of the four fire trains on the furnace, thereby minimising the quantity of replacement anodes required to maintain smelting operation. This paper will elaborate on the project management, safety aspects and logistics required to achieve a successful rebuild, whilst maintaining baked anode quality.

### 2:30 PM

**Specific Energy Consumption in Anode Bake Furnaces:** *Felix Keller*<sup>1</sup>; *Peter Sulger*<sup>1</sup>; Markus Meier<sup>1</sup>; Dagoberto Schubert Severo<sup>2</sup>; Vanderlei Gusberti<sup>2</sup>; <sup>1</sup>R&D Carbon Ltd.; <sup>2</sup>PCE Ltda.

In anode baking, specific energy consumption is one of the important cost elements. When ordering a new furnace the buyer therefore asks for guarantees regarding specific energy consumption. Typically such guarantees are asked for from the supplier of the process control system. This approach is inappropriate, as will be explained in this document. Specific energy consumption is a function of numerous variables of which most are outside the sphere of influence of the process control system supplier. This document discusses the main factors influencing the specific energy consumption for anode bake furnaces.

### 2:55 PM

**Desulphurisation Control during Anode Baking, Its Impact on Anode Performance and Operational Costs-Alba's Experience:** *Hameed Abbas*<sup>1</sup>; Khalil Khaji<sup>1</sup>; Daniel Sulaiman<sup>1</sup>; <sup>1</sup>Aluminium Bahrain

During year 2006, carbon dusting was noticed in the pots of lines 4 and 5, operating at 335 and 340 kA current. One of the main parameters for carbon dusting in the pots is the CO<sub>2</sub> dust loss which is influenced by the degree of anode desulphurisation which again is dependent on the level of anode baking. Alba developed an approach to optimize the anode baking level to control the desulphurisation of anodes to resolve the carbon-dusting problem. The approach shows that optimization of anode baking could be an effective way to resolve the carbon dusting in pots operating at high kA currents. In addition, there are benefits of reduced natural gas consumption, SO<sub>2</sub> emissions. There is significant impact on the increase in flue wall refractory life. The paper describes the approach, and presents the results of the work on control of anode desulphurisation.

# Technical Program

## 3:20 PM Break

## 3:35 PM

**Development of a New Improved Dry Alumina Scrubber for Emission Control from Anode Bake Furnaces:** *Paulo Douglas Vasconcelos*<sup>1</sup>; *André Mesquita*<sup>2</sup>; <sup>1</sup>Albras Alumínio Brasileiro S.A.; <sup>2</sup>Solve Engenharia Ltda

The alumina-based dry scrubbing for emission control from potrooms in the aluminum industry is nowadays the standard process, and some different technologies are commercially available in the market. However, the presence of tar and SO<sub>2</sub> together the emission of fluorides still represent a challenge for an efficient dry scrubber using alumina as adsorbent. This work presents the development of a new improved alumina-based dry fluidized bed scrubbing for emission control from anode bake furnaces. The development is carried-out from an experimental prototyping testing to a real pilot plant. This system uses a cooling tower, an in-duct initial adsorption process, and a fluidized bed and bag house for secondary and final adsorptive process, in order to assure the desulfurization, and the elimination of tar and fluorides emission. The results from a pilot plant installed at Albras smelter for emission control from an anode bake furnace are presented.

## 4:00 PM

**Baked Anode Density Improvement through Optimization of Green Anode Dry Aggregate Composition:** *Khalil Khaji*<sup>1</sup>; *Hameed Abbas*<sup>1</sup>; <sup>1</sup>Aluminium Bahrain

At Alba, green anodes were manufactured as per the dry aggregate composition recipe given by the technology suppliers. For given set of raw materials, paste plant process and equipment parameters the dry aggregate composition was giving baked anode density of 1.565-1.570 g/cm<sup>3</sup>. Pot rooms gradually increased line current to increase aluminium metal production. Therefore there was need to improve baked anode density, net carbon consumption so that butts thickness at increased line current will be maintained. With in-house research, baked anode density of 1.600 g/cm<sup>3</sup> was achieved. This was achieved by optimization of dry aggregate composition. The paper describes the work done on the optimization of dry aggregate composition and the results achieved over a period of two and half years.

## 4:25 PM

**Characterization of Surface Topography on Carboxy Reactivity Residue:** *Stein Rørvik*<sup>1</sup>; *Lorentz Petter Lossius*<sup>2</sup>; *Hogne Linga*<sup>2</sup>; *Arne Petter Ratvik*<sup>1</sup>; <sup>1</sup>SINTEF Materials & Chemistry; <sup>2</sup>Hydro Aluminium

The ISO 12988-1 method for determining carboxy reactivity of anodes has widespread use in the aluminium industry. In this test, an anode core sample is exposed to CO<sub>2</sub> at 960°C for 7 hours. The relative amount remaining sample and accumulated dust is then measured. Visually, some samples show distinct selective reactivity, but there is currently no quantification of the degree of this selective reactivity (except for its indirect impact on sample weightloss and dust produced). To address this, an apparatus and a method were developed to quantify the surface topography of the tested samples. The method is based on automatically taking a picture-series of a back-lighted sample rotated in small increments using a computer controlled motor. A computer program then applies image analysis to the sample profile in the pictures to create a 3D reconstruction of the surface. This is then compared to carboxy reactivity and other anode properties.

## Federal Funding Workshop

Wednesday PM      Room: 602  
February 17, 2010      Location: Washington State Convention Center

## 4:30 PM

**Materials Research Support at the Office of Basic Energy Sciences:** *John Vetrano*<sup>1</sup>; <sup>1</sup>Program Manager, Division of Materials Science and Engineering, Office of Basic Energy Sciences, Office of Science, Department of Energy

John Vetrano will give an overview of the fundamental materials research activities at the DOE office of Basic Energy Sciences (BES). BES Supports basic research in materials science, chemistry, geo-sciences and biosciences, as well as the construction and operation of nearly two dozen major scientific user facilities, including the nation's large synchrotron radiation light sources, neutron scattering facilities, electron-beam microscopy centers, and nanoscale science

research centers. The major emphasis of the materials science and engineering program at BES is on fundamental experimental and theoretical research that provides the foundations for the discovery and design of new materials with novel functions and properties. Disciplinary areas supported include: Materials physics; condensed matter physics; mechanical behavior; materials chemistry; biomolecular materials; x-ray-, neutron-, and electron-scattering sciences; and related disciplines where the emphasis is on the science of materials. Knowledge gained in the program is aimed at providing the scientific basis for a clean, sustainable, and secure energy future through materials innovation. The presentations will highlight specific new research opportunities, including basic research on nanoscale science, hydrogen economy, solar energy utilization, advanced nuclear energy system, superconductivity, solid-state lighting, and other research areas. Inquiries can be directed to [John.Vetrano@science.doe.gov](mailto:John.Vetrano@science.doe.gov).

## 5:00 PM

**Materials Research Support at the National Science Foundation:** *Alan J. Ardell*<sup>1</sup>; <sup>1</sup>Program Director, Metals and Metallic Nanostructures Division of Materials Research, Directorate of Mathematical and Physical Sciences, National Science Foundation

The NSF/DMR perspective on materials research and education will be presented. NSF invested ~\$400M in FY09, supporting people, ideas, and instrumentation primarily through awards to the nation's colleges and universities: that figure was supplemented by the ARRA allocation of ~\$107M. Apart from DMR, there is also substantial support for materials and materials-related research and education from other programs in NSF. Specific new opportunities – including the 3+ year-old program in biomaterials and the recent SOLAR and EFRI initiatives – will be described. There are also avenues for collaborative research, nationally and internationally, via different types of special funding programs (e.g. MRSEC). The projects supported by the MMN program in FY09, including the impact of the ARRA funds, and the budgetary outlook for FY10 will be described. General information on all the programs in DMR can be found on the DMR Web page: <http://www.nsf.gov/mps/divisions/dmr/>.

## 5:30 PM

**The Technology Innovation Program (TIP): Funding Innovative Research for Critical National Needs:** *Michael A. Schen*<sup>1</sup>; <sup>1</sup>Scientific Advisor to the Director, Technology Innovation Program, NIST

Located at the National Institutes of Standards and Technology (NIST) in Gaithersburg, Maryland, TIP has the purpose to help U.S. businesses, institutions of higher education, and other organizations—such as national laboratories and nonprofit research institutes—support, promote, and accelerate innovation in the United States by funding high-risk, high-reward research in areas of critical national need. This presentation will familiarize participants with the mission, objectives, and methods of the TIP program, provide insights on areas of nation attention being examined by the program, and outline TIP's activities and possible competition for 2010. Information about four areas of possible interest for future TIP solicitations may be found at [http://www.nist.gov/tip/wp\\_cmts/index.html](http://www.nist.gov/tip/wp_cmts/index.html). TIP also has a booth as part of the TMS Annual Meeting where representatives are available for discussion.



### General Abstracts: Electronic, Magnetic and Photonic Materials Division: Session I

*Sponsored by:* The Minerals, Metals and Materials Society, TMS Electronic, Magnetic, and Photonic Materials Division, TMS: Alloy Phases Committee, TMS: Biomaterials Committee, TMS: Chemistry and Physics of Materials Committee, TMS: Electronic Materials Committee, TMS: Electronic Packaging and Interconnection Materials Committee, TMS: Nanomaterials Committee, TMS: Superconducting and Magnetic Materials Committee, TMS: Thin Films and Interfaces Committee, TMS: Energy Conversion and Storage Committee  
*Program Organizers:* Long Qing Chen, Pennsylvania State University; Sung Kang, IBM Corporation; Mark Palmer, Kettering University

Wednesday PM Room: 308  
February 17, 2010 Location: Washington State Convention Center

*Session Chair:* To Be Announced

#### 2:00 PM Introductory Comments

#### 2:05 PM

**Multiferroic Fibers by Electrospinning:** *Shuhong Xie*<sup>1</sup>; *Jiangyu Li*<sup>1</sup>; <sup>1</sup>University of Washington

In this paper, we report a strategy for synthesize multiferroic fibers at nanoscale. Three kinds of multiferroic fibers are synthesized by a sol-gel process and electrospinning, which include composite multiferroic CoFe<sub>2</sub>O<sub>4</sub>-Pb(Zr<sub>0.52</sub>Ti<sub>0.48</sub>)O<sub>3</sub>, NiFe<sub>2</sub>O<sub>4</sub>-Pb(Zr<sub>0.52</sub>Ti<sub>0.48</sub>)O<sub>3</sub>, and single phase BiFeO<sub>3</sub> fibers. After being calcined, the diameters of multiferroic fibers are in the range from 100 to 300 nm. CoFe<sub>2</sub>O<sub>4</sub>-Pb(Zr<sub>0.52</sub>Ti<sub>0.48</sub>)O<sub>3</sub>, NiFe<sub>2</sub>O<sub>4</sub>-Pb(Zr<sub>0.52</sub>Ti<sub>0.48</sub>)O<sub>3</sub> composite nanofibers are obtained by calcined in air. However, pure perovskite BiFeO<sub>3</sub> nanofibers are obtained by using Ar as protective atmosphere. The spinel structure of CoFe<sub>2</sub>O<sub>4</sub>, NiFe<sub>2</sub>O<sub>4</sub> and perovskite structure of Pb(Zr<sub>0.52</sub>Ti<sub>0.48</sub>)O<sub>3</sub>, BiFeO<sub>3</sub> are verified by X-ray diffraction and high resolution transmission electron microscopy. Transmission electron microscopy indicate that multiferroic nanofibers are composed of rather dense nanocrystalline grains with different nanograin size. The piezoresponse force microscopy (PFM) is used to confirm the ferroelectricity of multiferroic nanofibers. Ferromagnetism of multiferroic fibers are also confirmed by vibrating sample magnetometer (VSM) measurement.

#### 2:25 PM

**High-Temperature Thermoelectric Behaviors of Highly Dense Polycrystalline Nonstoichiometry TiO<sub>x</sub> Ceramics:** *Yong Liu*<sup>1</sup>; *Jinle Lan*<sup>2</sup>; *Bo-Ping Zhang*<sup>3</sup>; *Hongmin Zhu*<sup>1</sup>; <sup>1</sup>School of Metallurgical and Ecological Engineering, University of Science and Technology Beijing; <sup>2</sup>State Key Laboratory of New Ceramics and Fine Processing, Department of Materials Science and Engineering, Tsinghua University; <sup>3</sup>School of Materials Science and Engineering, University of Science and Technology Beijing

Polycrystalline nonstoichiometry TiO<sub>x</sub> (x=1.6, 1.7, 1.8 and 1.9) ceramics with high density were prepared by a spark plasma sintering process at 1373 K using TiO<sub>2</sub> and TiO as starting materials. The temperature dependences of the electrical conductivity, Seebeck coefficient, and power factor have been investigated. The results indicate that the electrical conductivity of all the samples is in the range of a semiconductor transport behavior (51 Scm<sup>-1</sup> ~360 Scm<sup>-1</sup>), increases with temperature increasing, and decreases with oxygen content increasing. All samples show high negative Seebeck coefficients (-50 ~ -375 μV/K), reveals that the primary carriers in these ceramic samples are electrons. Power factor of all samples increased with temperature increasing. The obtained TiO<sub>1.6</sub> ceramic shows better thermoelectric properties and the maximum power factor ~5×10<sup>-4</sup> Wm<sup>-1</sup>K<sup>-2</sup> has been obtained at 873K in the air, which can be a promising candidate of n-type material for high-temperature thermoelectric application.

#### 2:45 PM

**Microstructure and Temperature Dependence of Ferroelectric Properties of Bi(Mg<sub>2</sub>ti<sub>3</sub>)-PbTiO<sub>3</sub> Ceramics:** *Seema Sharma*<sup>1</sup>; *D. Hall*<sup>2</sup>; <sup>1</sup>Magadh University; <sup>2</sup>Materials Science Center

Ceramics in the (1-x) Bi(Mg<sub>2</sub>.5Ti<sub>0.5</sub>)O<sub>3</sub>-(x)PbTiO<sub>3</sub> perovskite system with x=0.30, 0.35 and 0.40 have been processed by conventional sintering (9500C) from ceramics powders synthesized by direct solid-state reaction of

the constituent oxides. X-ray diffractograms reveal the transformation of crystal structure from rhombohedral to tetragonal for x=0.35 to 0.40. Ferroelectric hysteresis curves show the transition from ferroelectric to antiferroelectric state with respect to temperature upto 1500C at an applied electric field of 6kV/mm. As the PbTiO<sub>3</sub> content increases in the composition, the ferroelectric curves become less constricted in the central region. This effect is the most pronounced at x=0.40 and is quite expected one, since PbTiO<sub>3</sub> being a ferroelectric material, the curves tend towards the conventional ferroelectric curves. Diffusivity (γ) study of phase transition in these compounds provided values between 1 and 2 indicating the variation of degree of disorderness in the system.

#### 3:05 PM Break

#### 3:35 PM

**Bio-Inspired Methods to Self-Assemble 3D Micro-/Nano-Structures for Energy Harvesting:** *Huan Li*<sup>1</sup>; *Xiaoying Guo*<sup>1</sup>; *K. Jimmy Hsia*<sup>1</sup>; *Ralph Nuzzo*<sup>1</sup>; <sup>1</sup>University of Illinois at Urbana-Champaign

Often used in nature, self-assembly at the micro- and nanoscales is a powerful tool to construct complex 3D structures from planar sheets. Water, among all materials, plays a critical role in many self-assembling processes. In particular, these processes often involve surface phenomena, such as capillary interactions and surface adhesion. In the current work, we demonstrate that mechanics can indeed be a useful tool to help understand surface phenomena-driven self-assembly by considering the self-assembly of a 3-D photovoltaic device made of patterned, thin silicon sheets. A model is developed to identify the mechanisms controlling the behavior of these processes. Critical parameters emerge naturally from the analysis which can be used to guide the device formation and manufacturing of nanoscale components.

#### 3:55 PM

**Monitoring Electrode Degradation in Lithium Ion Batteries Using Acoustic Emission:** *Kevin Rhodes*<sup>1</sup>; *Claus Daniel*<sup>2</sup>; *Nancy Dudney*<sup>2</sup>; *Edgar Lara-Curzio*<sup>2</sup>; <sup>1</sup>University of Tennessee; <sup>2</sup>Oak Ridge National Laboratory

Lithium ion batteries for large scale applications such as vehicles and stationary energy storage face the challenge of being safe, powerful, reliable, and cost effective. To fulfill the requirements and understand failure new characterization techniques must be developed for guidance to new materials with improved performance. Composite electrodes with various types of active materials, including silicon and LiCoO<sub>2</sub>, were charge cycled in lithium ion half cells while monitoring acoustic emission. Both constant current and cycled voltage experiments were performed. Readily identifiable waveforms were recorded that are attributed to the degradation of active materials as observed cycled electrodes by SEM. This technique is being used to guide the development of improved materials capable of higher charge rates and greater cycle life.

#### 4:15 PM

**CuInSe<sub>2</sub>/Si Heterojunctions for Photovoltaic Applications:** *Okechukwu Akpa*<sup>1</sup>; *Shaik Shoieb*<sup>1</sup>; *Kalyan Das*<sup>1</sup>; <sup>1</sup>Tuskegee University

Growth and characterization of CuInSe<sub>2</sub> (CIS) thin films deposited on Si, for the purpose of forming heterojunctions to investigate the suitability of the material system for high efficiency solar cells, is reported here. Deposition was obtained by rf magnetron sputtering using a stoichiometric CIS target. As CIS and Si are closely lattice matched, large grain polycrystalline films were obtained. Rutherford backscattering spectroscopy (RBS) indicated that these CIS films have a composition of Cu<sub>1.05</sub>In<sub>1.04</sub>Se<sub>2.5</sub>. Circular diodes were fabricated and the current-voltage characteristics of these diodes indicated that reasonable quality p-n junctions were obtained. The forward current of these devices increased by three orders of magnitude from 0.003 to 2.65 mA at a bias of 2 V when illuminated with a 75 watt halogen lamp and this strong response to illumination indicates that the material system has a high potential for use as solar cells.

#### 4:35 PM

**The Multi-Level Switching PRAM Device Using Stacked Phase Change Materials Structure:** *Sung-Hoon Hong*<sup>1</sup>; *Heon Lee*<sup>1</sup>; <sup>1</sup>Korea University

Phase change random access memory (PRAM) is considered to be the most promising next generation non-volatile memory. Recently, multi-level switching of PRAM device has been studied for high density memory device. In this study, multi-level switching phase change memory, which has stacked phase change materials (PCMs) structure, was suggested. As stacked PCMs,

# Technical Program

Ge<sub>2</sub>Sb<sub>2</sub>Te<sub>5</sub>/ AgInSbTe, Ge<sub>2</sub>Sb<sub>2</sub>Te<sub>5</sub>/ GeTe, In<sub>2</sub>Se<sub>3</sub>/ Ge<sub>2</sub>Sb<sub>2</sub>Te<sub>5</sub> PCMs were used. The 200nm stacked PCMs structure nano-pillar device was fabricated using NIL and the electrical property was studied using c-AFM connected a pulse generator and voltage source. In case of Ge<sub>2</sub>Sb<sub>2</sub>Te<sub>5</sub>/ GeTe and In<sub>2</sub>Se<sub>3</sub>/ Ge<sub>2</sub>Sb<sub>2</sub>Te<sub>5</sub> PCMs stacked structure PRAM device, multi-level switching was observed.

## General Abstracts: Light Metals Division: Session II

*Sponsored by:* The Minerals, Metals and Materials Society, TMS Light Metals Division, TMS: Aluminum Committee, TMS: Magnesium Committee, TMS: Recycling and Environmental Technologies Committee, TMS: Energy Committee, TMS: Aluminum Processing Committee

*Program Organizers:* Alan Luo, General Motors Corporation; Eric Nyberg, Pacific Northwest National Laboratory

Wednesday PM      Room: 607  
February 17, 2010      Location: Washington State Convention Center

*Session Chair:* Eric Nyberg, Pacific Northwest National Lab

### 2:00 PM

**Enhanced Resistance of Ti-Alloys against Environmental Attack by a Combined Al- and F-Treatment:** *Alexander Donchev*<sup>1</sup>; Michael Schütze<sup>1</sup>; Rossen Yankov<sup>2</sup>; Andreas Kolitsch<sup>3</sup>; <sup>1</sup>DECHEMA; <sup>2</sup>FZD

Titanium alloys cannot be used at elevated temperatures above approximately 500°C because of their limited environmental stability. Several ways have been investigated so far to improve the environmental stability of Ti-alloys e.g. coatings but these attempts in a majority of cases have not been really successful. A new way to improve the performance of these alloys is the combination of Al-enrichment in the surface zone plus additional fluorine treatment. The Al-enrichment leads to the formation of intermetallic phases. These phases improve the oxidation resistance of Ti-alloys but not to a sufficient extent. An additional fluorine treatment on top of the Al-enriched surface leads to the formation of a stable alumina scale due to the fluorine effect. In this paper results from oxidation and other tests performed on Ti-samples without any treatment, with single Al- or F-treatment and with a combination of both are presented and the results are discussed.

### 2:20 PM

**Fabrication of Aluminum Foam with New Stabilizer Composed by Fly Ashes and Short Copper-Coated Carbon Fibers:** *Pei-hong Chen*<sup>1</sup>; Hong-jie Luo<sup>1</sup>; Lei Wang<sup>1</sup>; Yong-liang Mu<sup>1</sup>; <sup>1</sup>Northeastern University

Closed-cell Al foam contained fly ashes and short copper-coated carbon fibers as composite stabilizer was successfully prepared by melt direct foaming process. The scanner at the resolution of 300dpi, SEM and EDX were used to investigate the macro and microstructure of foamed samples. The results show that vertical density gradient is reduced and cell sizes are well-proportioned. Fly-ash particles are located mainly at the edges of cell walls and Plateau borders, and short copper-coated carbon fibers exist inside cell walls. Over a very large number of trials, foam stability is improved greatly by the composite stabilizer consisting of 3.0wt.% copper-coated carbon fibers and 2.0wt.% fly ash particles fibers.

### 2:40 PM

**Fundamental Materials-Design Limits in Ultra Light-Weight Mg-Li Alloys Determined from Quantum-Mechanical Calculations:** *Martin Friak*<sup>1</sup>; William Counts<sup>1</sup>; Dierk Raabe<sup>1</sup>; Joerg Neugebauer<sup>1</sup>; <sup>1</sup>Max Planck Institute for Iron Research

Quantum-mechanical calculations are becoming increasingly useful to engineers interested in designing new alloys because these calculations are able to accurately predict basic material properties only knowing the atomic composition of the material. In this paper, fundamental physical properties (formation energies, elastic constants) of 11 bcc Mg-Li compounds are calculated using density-functional theory (DFT) and compared with experimental data. These DFT-determined properties are in turn used to calculate engineering parameters like (i) specific Young's modulus (Y/rho) or (ii) bulk over shear modulus ratio (B/G) differentiating between brittle and ductile behavior. The engineering parameters are then used to identify alloys that have optimal

mechanical properties for light weight applications. An Ashby map containing Y/rho vs. B/G shows that it is not possible to increase both Y/rho and B/G by changing only the composition or local order of a binary alloy (W. A. Counts et al., *Acta Mater* 57 (2009) 69-76).

### 3:00 PM

**Material Selection for the Lining of Aluminum Holding and Melting Furnaces:** *Andy Wynn*<sup>1</sup>; John Coppack<sup>1</sup>; Tom Steele<sup>1</sup>; <sup>1</sup>Thermal Ceramics

The range of monolithics available for lining Aluminum holding and melting furnaces is extensive and product selection can be confusing. Without appropriate material selection for the furnace lining, furnace performance will be compromised. An understanding of monolithic selection criteria is critical in providing efficient furnaces for processing Aluminum. This paper reviews operating conditions found in all key zones of a typical melting and holding furnace – Belly Band/Lower Wall, Hearth/Ramp (working face), Hearth/Ramp (substructure) and Superstructure. The test methods utilised by many of the large Aluminum producers for product selection are reviewed and areas where these test methods do not necessarily reflect real operating conditions are highlighted. A range of monolithic materials are subjected to a representative program of approval testing. A package of monolithic technologies is proposed that will assist the furnace designer in selecting the best material available for each of the key furnace zones.

### 3:20 PM

**Mechanical Properties and Precipitation Behaviors of Mg-Al-Sn and Mg-Zn-Sn Alloys:** *Toyohiko Konno*<sup>1</sup>; JongBeom Lee<sup>1</sup>; Takahiro Ohya<sup>1</sup>; Hyeon-Taek Son<sup>2</sup>; Haguk Jeong<sup>2</sup>; <sup>1</sup>Tohoku University; <sup>2</sup>Korea Institute of Industrial Technology

In order to develop low-cost Mg alloys, we have examined age-hardening behaviors of Mg-Al-Sn (MAS) and Mg-Zn-Sn (MZS) alloys, with and without Mn addition, by means of a mechanical testing and microstructure characterization using transmission electron microscopy (TEM). For the MAS alloys, the ultimate strength (UTS) of an extruded Mg-9wt%Al-2wt%Sn alloy reached 390MPa. TEM observation indicated that plate-like Mg<sub>17</sub>Al<sub>12</sub> precipitates having Burgers orientation relationship with the matrix are responsible for the strength. This alloy also exhibits age hardening behavior. For example, the peak hardness appears after 15-20 hrs of heat treatment at 473K. On the other hand, the UTS of the MZS alloys are on the order of 300MPa. It was found that the addition of Mn effectively make their grain size small. The precipitates are composed of the Mg<sub>2</sub>Sn and MgZn<sub>2</sub> phases, and interestingly, the former often acts as a nucleation sites for the latter.

### 3:40 PM Break

### 4:00 PM

**Microstructure and Composition Modifications in the Surface Layers of a Mg AZ80 Alloy Induced by Laser Melting:** *Kemin Zhang*<sup>1</sup>; Jianxin Zou<sup>2</sup>; <sup>1</sup>Shanghai University of Engineering Science; <sup>2</sup>University of British Columbia

Laser surface melting has been applied on a cast Mg AZ80 alloy to improve its surface properties. The microstructure and composition modifications encountered in the surface layers were carefully investigated by using SEM, EDX and XRD techniques. The untreated alloy contains coarse grained Mg matrix, large sized Mg<sub>17</sub>Al<sub>12</sub> intermetallic phase at grain boundaries and AlMn particles. Due to the melting followed by rapid solidification and cooling, a layer having graded microstructures and compositions formed. The Mg<sub>17</sub>Al<sub>12</sub> phase was completely dissolved into the melted layer during melting and partially segregated as very fine particles during solidification in inter-dendritic areas. In contrast, the AlMn particles could not be fully dissolved at the bottom of the melted layer owing to their high melting point. The difference in the chemical composition and the thermal history at different depths has a strong impact on the segregation behaviours and hardness distribution in the melted layer.

### 4:20 PM

**Multi Sensor Data Fusion for Aluminium Cell Health Monitoring and Control:** *Håkon Viundal*<sup>1</sup>; Ru Yan<sup>2</sup>; Morten Liane<sup>3</sup>; Bjørn Petter Moxnes<sup>4</sup>; Saba Mylvaganam<sup>5</sup>; <sup>1</sup>Telemark Technological Research and Development Centre (tel-tek); <sup>2</sup>Telemark University College; <sup>3</sup>Hydro, Primary Metal Technology; <sup>4</sup>Hydro Aluminium; <sup>5</sup>Telemark Technological Research and Development Centre (tel-tek) and Telemark University College

The prevailing aluminium electrolysis process demands steady-state conditions within narrow borders, to improve performance with respect to



molten metal production per day, energy usage per kg of aluminium, current efficiency, CO<sub>2</sub> and flour-gas emissions etc. However, only the current and the cell voltage are obtained by on-line measurements. Many bath parameters are manually measured on a daily or even weekly basis. Innovating measurements of the bath temperature, the bath chemistry, the molten metal height and the height of the electrolyte would all be of substantial importance for the control regime. However, combining new measurements and soft sensors for estimating "unavailable" variables would improve both the monitoring and controlling tasks of the aluminium electrolysis process. This paper gives an overview of many online and off-line measurements and reports some new possible measurement scenarios with increasing potential for extensive, fast, efficient and even real-time data fusion. Finally some interesting examples of data fusion examples based on actual plant measurements covering many months are also included.

#### 4:40 PM

**Effect of Copper Coatings on the Interfacial between Short Carbon Fiber and Aluminum Matrix:** *Yan Pengfei*<sup>1</sup>; Yao Guangchun<sup>1</sup>; Shi Jianchao<sup>1</sup>; Mu Yongliang<sup>1</sup>; <sup>1</sup>School of Materials and Metallurgy, Northeastern University

Short carbon fiber reinforced aluminum alloy matrix composites were prepared by stir casting. The fibers were coated copper by electroless plating and then characterized. The microstructure of the composites was observed by Optical Microscope, Scanning Electron Microscope (SEM) and XRD. The results show that copper coating prevents the harmful interfacial reaction between carbon fibers and aluminum matrix, and improves the wettability between the fibers and molten aluminum, and carbon fiber distributes homogenous in the aluminum matrix.

#### 5:00 PM

**Effect of Mg on Microstructure and Mechanical Properties of Copper-Coated Short Carbon Fiber Reinforced Aluminum Alloy Matrix Composite:** *Yan Pengfei*<sup>1</sup>; Yao Guangchun<sup>1</sup>; Shi Jianchao<sup>1</sup>; Mu Yongliang<sup>1</sup>; <sup>1</sup>School of Materials and Metallurgy, Northeastern University

Copper coated short carbon fiber reinforced aluminum alloy matrix composites have been prepared with 0.3-1.5 wt% Mg as alloying addition by stir casting. Effect of Mg on the microstructure and mechanical properties of the composites was investigated. The microstructure was observed by scanning electron microscopy (SEM) and the results show that adding Mg can make the distribution of carbon fibers uniform in the composites, reduce laminated and agglomerated. Tensile test and hardness test were carried out, the results show that the tensile strength and the hardness of the composite is increased by 13% and 8% when Mg content is 0.9 wt%.

### General Abstracts: Materials Processing and Manufacturing Division: Synthesis and Processing

*Sponsored by:* The Minerals, Metals and Materials Society, TMS Materials Processing and Manufacturing Division, TMS/ASM: Computational Materials Science and Engineering Committee, TMS: Global Innovations Committee, TMS: Nanomechanical Materials Behavior Committee, TMS/ASM: Phase Transformations Committee, TMS: Powder Materials Committee, TMS: Process Technology and Modeling Committee, TMS: Shaping and Forming Committee, TMS: Solidification Committee, TMS: Surface Engineering Committee  
*Program Organizers:* Thomas Bieler, Michigan State University; Corbett Battaile, Sandia National Laboratories

Wednesday PM Room: 601  
February 17, 2010 Location: Washington State Convention Center

*Session Chair:* To Be Announced

#### 2:00 PM

**Innovative and Integrated Technologies for the Development of Aeronautic Components:** *Nicola Gramegna*<sup>1</sup>; Franco Bonollo<sup>2</sup>; Emilia Della Corte<sup>1</sup>; Fabio Grosselle<sup>2</sup>; Marco Cocco<sup>3</sup>; <sup>1</sup>ENGINSOFT; <sup>2</sup>University of Padova - DTG; <sup>3</sup>AVIO S.p.A.

The "design innovation program" lies in the development and integration, since the very first steps, of all those aspects related with component life cycle, from manufacturing till end\_of\_life, in order to meet the requirements of a greater product quality, of a more and more comprehensive knowledge about

the component potential, of a cost and TTM (Time To Market) reduction. In particular, the knowledge about the mechanical properties, coming from the manufacturing process, contributes to the improvement of the component performance and reliability, to exploit the synergies of the departments involved in the project and to maximize the suppliers collaboration. In such perspective, light alloy components for aeronautic sector play an important role. Propulsive systems consist of complex and diversified parts that require a structural design in the non-linear and fatigue fields, to be also integrated in the main manufacturing aspects: the casting process and the subsequent heat treatment.

#### 2:20 PM

**Selective Laser Sintering of Magnesium Powder for Fabrication of Compact Structures:** *Ng Chi Chung*<sup>1</sup>; <sup>1</sup>The Hong Kong Polytechnic University

In past decades, considerable research effort has been reported in the area of direct metal laser sintering (DMLS). However, rarely work has previously been found on the laser sintering of magnesium powder. The novelty of the present research lies in the fabrication of compact structures by laser sintering of magnesium powder using a Nd:YAG laser. The laser sintering of single tracks and single layers of magnesium powder were carried out for demonstrating the process feasibility and for examining the influences of several processing parameters (laser power, scan speed and repetition rate) on microstructural characteristics and mechanical properties of the final sintered structures. The experimental results give valuable information about geometrical features and microstructural evolution of magnesium powder under a Nd:YAG laser irradiation, which would facilitate the fabrication and controllability of compact structures by deliberating the associated effect of different processing parameters for fabrication of structural parts in transportation industries.

#### 2:40 PM

**Novel Lead-Free Bronze Bearing Materials Produced by Powder Metallurgy Processing:** *Greg Vetterick*<sup>1</sup>; Iver Anderson<sup>1</sup>; Matthew Besser<sup>2</sup>; <sup>1</sup>Ames Laboratory and Iowa State University; <sup>2</sup>Ames Laboratory

Leaded bronze alloys such as Cu-10Sn-10Pb (wt.%) are utilized effectively in tribological systems that are prone to lubrication starvation. These Cu-based leaded alloys typically exploit the insolubility of Pb in Cu to create soft phase pockets in the microstructure on solidification of a chill casting or a gas atomized powder. Properly distributed throughout the bearing, free Pb provides a low shear solid lubricant for sliding interfaces. However, the toxicity of Pb necessitates the development of alternatives for the soft Pb phase. The current work explores replicating the desirable microstructure of leaded bronze by utilizing powder metallurgy processes. Impregnation of a bronze matrix microstructure with Pb-free soft alloys shows considerable promise as a bearing alloy production method. Microstructural analysis and tribological evaluation of the resulting composite bearings helped verify adequate performance as a Pb-free bearing system. Supported by Sauer-Danfoss Inc. as work for others through Ames Laboratory Contract No. DE-AC02-07CH11358.

#### 3:00 PM

**Microstructural Evolution of Cu, Ni and Al Powder Particles Processed by Cold Spray:** *Yu Zou*<sup>1</sup>; Ahmad Rezaeian<sup>1</sup>; Eric Irissou<sup>2</sup>; Jean-Gabriel Legoux<sup>2</sup>; Jerzy Szpunar<sup>1</sup>; Stephen Yue<sup>1</sup>; <sup>1</sup>McGill University; <sup>2</sup>National Research Council Canada (NRC)

Cold spray is a relatively new coating technology by which coatings can be produced using high-velocity impact of powder particles without significant heating introduced. Micron-sized pure Cu, Ni and Al powder particles were processed by the cold spray, respectively. Microstructural evolutions of these particles were investigated using electron backscatter diffraction and transmission electron microscopy. The results show that non-uniform microstructures with elongated grains/subgrains in the size of microns, equiaxed grains in sub-microns and nanocrystalline grains appear in as-sprayed materials. Moreover, deformation twins in nano-scale are observed in the cold sprayed Cu. Formation of these structures is explained by high strain-rate deformation with the dynamic recovery/recrystallization in the complex thermo-mechanical process during cold spraying.

#### 3:20 PM

**Recent Trends in Cold Spray Technology:** *Julio Villafuerte*<sup>1</sup>; Bert Jodoin<sup>2</sup>; <sup>1</sup>Centerline Windsor Ltd; <sup>2</sup>University of Ottawa

Cold spray, emerged as a practical technology in the 1980's from the Institute of Theoretical and Applied Mechanics of the Russian Academy of Sciences in Novosibirsk. Almost twenty years later, interest on this technology has grown

# Technical Program

exponentially. Today, cold spray is known as a solid-state spraying process where materials are not melted but simply propelled in a supersonic stream against the substrate to produce bonding; the advantage being the ability to produce fully dense deposits that are free of oxidation, tensile residual stresses and other thermal effects inherent to conventional thermal spray. Since the year 2000, a number of commercial cold spray technologies have become available. Today, they can be seen serving in applications including corrosion protection, restoration, repair, additive manufacturing, and others. This paper describes the process working principles, its advantages and challenges. It also presents the state of the art of the technology.

## 3:40 PM Break

## 4:00 PM

### **Introduction of High-Throughput, Commercial Application, Spark Plasma Sintering (SPS) Technology:** *Robert Aalund*<sup>1</sup>; <sup>1</sup>Thermal Technology

Spark Plasma Sintering, and similar, technologies have been used in R&D and academically for compacting advanced ceramics, powder metals, and cermets for more than two decades. And SPS remains a highly sought-after research and development tool, because of its high speed processing, particle bonding attributes, and impressive material properties capabilities. Though there have been some attempts to apply this incredible technology to specific commercial projects, they remain largely unknown and are commonly veiled in a shroud of secrecy. This discussion is about removing the veil and looking closely at several examples of how SPS can be used commercially, today. We will review several equipment processing approaches designed around several types of product, including estimated throughput, operational costs, and tooling design. We will also discuss some of the limitations of SPS with regard to commercial applications.

## 4:20 PM

### **Thermo-Mechanical Behavior of Chemically Bonded Phosphate Ceramic Composites Reinforced with Graphene Nanoplatelets: A Substantial Material Improvement toward Structural Applications:** *H. A. Colorado*<sup>1</sup>; *C. Hiel*<sup>2</sup>; *H. T. Hahn*<sup>3</sup>; <sup>1</sup>University of California, Los Angeles and Universidad de Antioquia; <sup>2</sup>Composite Support and Solutions Inc.; <sup>3</sup>University of California, Los Angeles

Mechanical properties and microstructures of a chemically bonded phosphate ceramic (CBPC) and its composite with 1.0 wt% graphite nanoplatelets (GNPs) reinforcement have been investigated. The GNPs were functionalized by different procedures including acid treatment and dried oxidation. Three different mixing techniques and different process parameters are evaluated. Microstructure was identified by using optical and scanning electron microscopes, x-ray micro tomography, and X-ray diffraction. In addition, weight loss of the resin at room temperature and pH were studied. The microstructure characterization shows that CBPC is a composite itself with several crystalline (wollastonite and brushite) and amorphous phases. SEM and micro tomography show a homogeneous distribution of crystalline phases. Bending strength of the composite material was increased from less than 10 Mpa (reported results) to more than 20MPa.

## 4:40 PM

### **Kinetics of Lamellar Decomposition in U-Nb Alloys:** *Robert Hackenberg*<sup>1</sup>; *Heather Volz*<sup>1</sup>; *Pallas Papin*<sup>1</sup>; *Ann Kelly*<sup>1</sup>; *Robert Forsyth*<sup>1</sup>; *Robert Dickerson*<sup>1</sup>; *Tim Tucker*<sup>1</sup>; <sup>1</sup>Los Alamos National Lab

Lamellar decomposition products result when U-Nb alloys are transformed between about 300C and the 650C monotectoid temperature. The kinetics of these cellular precipitation reactions are of interest since the resulting microstructures give undesirable properties. Detailed kinetic studies of these reactions were undertaken in isothermally transformed U-5.6 wt% Nb and U-7.7 wt% Nb alloys. The volume fractions, growth rates, interlamellar spacings, and phase compositions of the initial discontinuous precipitation as well as the succeeding discontinuous coarsening reactions were investigated via light microscopy, X-ray diffraction, SEM, and TEM. These results will be compared with theory. Attention will be paid to the rates and degrees to which these various aging reactions drive the system toward its final equilibrium state.

## 5:00 PM

### **Synthesis and Microstructure of TiC/TiN Porous Ceramic Composites Processed via HYSYCVD/Direct Nitridation:** *Jose Flores-Garcia*<sup>1</sup>; *Martin Pech-Canul*<sup>1</sup>; <sup>1</sup>Centro de Investigacion y de Estudios Avanzados del Instituto Politecnico Nacional

The effect of varying oxygen content in the nitrogen atmosphere during successive stages of vapor infiltration on the microstructural evolution and physical properties of TiC/TiN porous ceramic composites was investigated. Composites were processed via the hybrid precursor system chemical vapor deposition (HYSYCVD) and direct nitridation (DN) routes. TiCp porous preforms were infiltrated in subsequent stages: S1-1 and S1-2 at 1300°C for 70 min in high purity nitrogen (HPN); S2 at 1350°C for 120 min in ultra high purity nitrogen (UHPN). The composites were characterized by XRD, SEM, He pycnometry, volume-measurement approach and immersion in Hg. The study was complemented with thermodynamic analyses using the FactSage™ program and databases. Results show that the presence of O<sub>2</sub>, NH<sub>3</sub> and silicon-fluoride gaseous species throughout consecutive stages of processing affect the amount, morphology and distribution of TiN formed. Formation of TiN is ascribed to a combined effect of DN and HYSYCVD mechanisms.

## 5:20 PM

### **The Production of BCl<sub>3</sub> Gas from Mechanochemical Reaction Product Containing Elemental Boron and Magnesium Oxide:** *Duygu Agaogullari*<sup>1</sup>; *Ozge Balci*<sup>1</sup>; *Ismail Duman*<sup>1</sup>; <sup>1</sup>Istanbul Technical University

The most preferred method in industrial production of boron trichloride (BCl<sub>3</sub>) is from the carbon containing raw materials such as boron carbide (B<sub>4</sub>C). In the proposed study, boron oxide (B<sub>2</sub>O<sub>3</sub>) was used as a cheap raw material. Firstly, elemental boron powder containing MgO was obtained as a result of mechanochemical synthesis of boron oxide (B<sub>2</sub>O<sub>3</sub>) and magnesium (Mg) powder mixture in a high-energy ball-mill (Spex 8000D Mixer/Mill) with a ball-to-powder weight ratio of 18:1. Then, chlorine gas (Cl<sub>2</sub>) was passed through this intermediate product in a vertical quartz reactor heated to 650-1200°C by a tube furnace with SiC heating element. Cl<sub>2</sub> reacts only with free elemental boron while MgO powder behaves totally inert. Thus, the formation of carbon-containing gaseous compounds (COCl<sub>2</sub>) was prevented and high purity BCl<sub>3</sub> was obtained. Mechanochemically synthesized intermediate products were characterized by XRD and SEM whereas gaseous chlorination products were analyzed by FTIR.

## 5:40 PM

### **Cyclic Oxidation Behavior of Detonation Gun Sprayed Ni-20Cr Coating on a Boiler Steel at 900°C:** *Gagandeep Kaushal*<sup>1</sup>; *Harpreet Singh Saheet*<sup>1</sup>; *Satya Prakash*<sup>1</sup>; <sup>1</sup>RIMT-Institute of Engineering & Technology

Detonation-gun spray technology provides the possibility of producing high quality coatings with significant adherence strength. In this study, Detonation gun spray technique was used to deposit Ni-20Cr coating on a commonly used boiler steel ASTM-SA213-T-22. The specimens with and without coatings were subjected to cyclic oxidation testing at an elevated temperature of 900°C to ascertain usefulness of the coating. Weight change data was evaluated to formulate the kinetics of the oxidation. The uncoated sample suffered intensive spallation along with a significant overall weight gain. The oxidation rate was found to reduce appreciably after the deposition of the coating as the overall weight gain was reduced by 91%. The exposed specimens were characterized by scanning electron microscopy and energy dispersive spectroscopy (SEM/EDS). It was observed that Detonation gun sprayed Ni-20 Cr coating was suitable to provide oxidation resistance to the given steel in the air environment.



### Global Innovations in Manufacturing of Aerospace Materials: The 11th MPMD Global Innovations Symposium: Innovations in Primary and Secondary Forming - Aluminum, Magnesium, and Titanium Aluminides / Innovations in Machining and Joining

*Sponsored by:* The Minerals, Metals and Materials Society, TMS Materials Processing and Manufacturing Division, TMS Structural Materials Division, TMS: Shaping and Forming Committee, TMS: High Temperature Alloys Committee

*Program Organizers:* Deborah Whitis, General Electric Company; Thomas Bieler, Michigan State University; Michael Miles, BYU

Wednesday PM Room: 306  
February 17, 2010 Location: Washington State Convention Center

*Session Chairs:* Ron Wallis, Wyman Gordon; David Furrer, Rolls-Royce

#### 2:00 PM

**Simulating Hot Gas-Pressure Forming of Light Alloy Sheet Materials:** *Eric Taleff*<sup>1</sup>; Louis Hector<sup>2</sup>; Paul Krajewski<sup>2</sup>; <sup>1</sup>The University of Texas at Austin; <sup>2</sup>General Motors Corp.

Superplastic forming and related hot gas-pressure forming technologies are used in the commercial production of light-alloy components for the transportation industries. Recent progress in simulation technologies, particularly the development of improved material constitutive models, provides for accurate predictions of these forming processes. This new capability now makes it possible to better design and optimize forming processes. Improved understanding of material response during hot forming also makes the integration of material design and optimization for light alloys possible. This presentation will summarize advances relevant to simulating the hot gas-pressure forming of aluminum and magnesium sheet materials and suggest how these may be introduced into the integrated computational materials engineering paradigm.

#### 2:20 PM

**Stress Corrosion Behavior of Ti-Al-Nb Intermetallic Alloys Made from Accumulative Roll Bonding and Reaction Annealing:** *Peng Qu*<sup>1</sup>; Mona El-Demellawy<sup>2</sup>; Viola Acoff<sup>1</sup>; <sup>1</sup>The University of Alabama; <sup>2</sup>American University of Cairo

The TiAlNb intermetallic compound has been considered as a potential structural material for the aircraft engine because of its light weight and excellent properties at elevated temperatures. In order to be a candidate material for the turbine engine, the TiAlNb alloy shall meet qualification requirements for the engine cleaning materials. In this paper, a ternary Ti-46Al-9Nb intermetallic alloy (at. %) was produced by accumulative cold roll bonding (ARB) followed by reaction annealing. The stress-corrosion test, which was according to the ASTM standard, was applied to the intermetallic alloy. The preliminary evaluation and metallographic inspection were performed by light microscopy and scanning electron microscopy. Cracks, especially the tension or compression cracks were examined in detail. It is predicted that the TiAlNb alloy in this study will have high stress-corrosion resistance. The relationship between number of ARB cycles and resistance will be evaluated. Key words: Ti-46Al-9Nb; cold roll bonding; stress-corrosion; intermetallics

#### 2:40 PM

**Study on the Asymmetric Cross Rolling of AZ31 Magnesium Alloy:** *Bin Chen*<sup>1</sup>; <sup>1</sup>Shanghai Jiaotong University

The shear strain and its directions were thought to play an important role in severe plastic deformation (SPD). Asymmetric rolling, however, has a shear deformation zone in the middle section of deformation zone. Accordingly, Asymmetric cross rolling, a new rolling method was developed by us. And its experiments have been conducted to investigate its effects on microstructure and mechanical properties of AZ31. The influencing factors such as velocity ratio of rolls, rolling route, rolling temperature were investigated. It was found that the shear strain of asymmetric cross rolling contributes to refinement of grain size. Samples rolled by asymmetric cross rolling have finer grain size than that rolled by common rolling.

#### 3:00 PM

**Fabrication of Dimensionally-Correct Sheet Metal Components Directly from T-6 Aluminum Alloys and Airframe Applications:** Christian Weddeling<sup>1</sup>; Steven Woodward<sup>2</sup>; Bill Carson<sup>3</sup>; *Glenn Daehn*<sup>2</sup>; <sup>1</sup>Technische Universitat Dortmund; <sup>2</sup>Ohio State University; <sup>3</sup>Cutting Dynamics

Aluminum airframe components are commonly produced from heat-treatable aluminum alloys by hydroforming in the soft condition and then heat treating them to the T-6 temper and then manually correcting the shape with hammers. Sometimes several form and anneal cycles are required to create the basic shape. A process is demonstrated wherein components can be made in a single step using a variant of rubber pad forming augmented with an electromagnetic calibration step using an inexpensive disposable electromagnetic actuator. This new process is amenable to single-part flow in the production environment and can dramatically reduce the time required to produce a quantity of parts. High dimensional accuracy is possible and the components maintain the peak-aged materials properties. This presentation will discuss in detail the important process variables.

#### 3:20 PM

**Role of Precipitates in the Actuation Behavior of NiTiPt High Temperature Shape Memory Alloys:** *Shipeng Qiu*<sup>1</sup>; Santo Padula II<sup>2</sup>; Ron Noebe<sup>2</sup>; Raj Vaidyanathan<sup>1</sup>; <sup>1</sup>UCF; <sup>2</sup>NASA GRC

NiTiPt shape memory alloys hold promise in aerospace actuator applications as a result of their higher phase transformation temperatures when compared to binary NiTi. Recently, macroscopic thermomechanical testing has shown that Ni<sub>29</sub>Ti<sub>30</sub>Pt<sub>21</sub> samples aged at 500 °C for 5 h have better dimensional stability and higher work output when compared to non-aged samples. In order to assess the role of the resulting precipitates from the aging treatment on shape memory behavior, in situ neutron diffraction measurements during heating/cooling and mechanical loading were performed on aged and as-received Ni<sub>29</sub>Ti<sub>30</sub>Pt<sub>21</sub> samples. The influence of stoichiometry was additionally investigated by comparable experiments on a Ni<sub>28.5</sub>Ti<sub>30.5</sub>Pt<sub>21</sub> alloy. The role of precipitates in influencing texture evolution and internal strain development along with the phase transformation characteristics during deformation was quantitatively studied. The understanding presented offers new guidelines for processing NiTiPt alloys for high temperature aerospace applications.

#### 3:40 PM Break

#### 3:50 PM Invited

**Analysis and Optimization of Aerospace Machining Processes:** *Liangji Xu*<sup>1</sup>; <sup>1</sup>The Boeing Company

Commercial airframe manufacture has historically been machining intensive as metallic components are shaped into their required forms. Although there is significant movement to employ more composite materials in airframe manufacture, composite use has also driven the need to use more exotic metallic components. Materials such as titanium offer better thermal growth and corrosion characteristics but are more challenging to machine. Due to the high quantity of material that must be removed, it is critical to maintain high material removal rates in machining processes to minimize the manufacturing costs of the airframe parts. Material removal rates are often limited by design limitations of a machine tool, such as the spindle power and servo drive torque, as well as constraints imposed by the dynamic compliance of the machine structure and the cutting tools. Accurate calculation of the cutting forces generated during the machining process is essential in optimizing the process according to a machine tool's capability.

#### 4:20 PM

**Effect of Machining Processes on Low Cycle Fatigue Behavior of a Powder Metallurgy Disk Superalloy:** *Jack Telesman*<sup>1</sup>; Pete Kantzos<sup>2</sup>; Tim Gabb<sup>1</sup>; Louis Ghosn<sup>3</sup>; <sup>1</sup>NASA GRC; <sup>2</sup>Honeywell International; <sup>3</sup>Ohio Aerospace Institute

A study has been performed to investigate the effect of various machining processes on fatigue life of configured low cycle fatigue specimens machined out of a NASA developed LSHR P/M nickel based disk alloy. Two types of configured specimen geometries were employed in the study. To evaluate a broach machining processes a double notch geometry was used with both notches machined using broach tooling. EDM machined notched specimens of the same configuration were tested for comparison purposes. Honing finishing process was evaluated by using a center hole specimen geometry. Comparison testing was again done using EDM machined specimens of the same geometry. The effect of these machining processes on the resulting surface roughness,

# Technical Program

residual stress distribution and microstructural damage were characterized and used in attempt to explain the low cycle fatigue results.

**4:40 PM**

**Investigation a New Method for Produce Favorable Surface Integrity in as Machined Surface of Gamma Titanium Aluminide during HSM Machining:** *Sajjad Kolahdouz*<sup>1</sup>; <sup>1</sup>Tehran Polytechnic ( Amirkabir University of Technology)

Gamma titanium aluminide provides a peerless set of properties that can lead to substantial pay offs in aircraft engine applications. Regarded as a new material, machining of gamma titanium aluminide is much more difficult than machining Ti6Al4V. While there have been many studies on the produce of gamma titanium aluminide intermetallics but studies that report the satisfactory condition when machining this component is restricted due to this reason use this material is limited. In this study HSM (high speed machining) and UHSM (ultra high speed machining) in dry and MQL (minimum quantity lubricant) condition of this component are studied by new tool. After that surface integrity and mechanism of chip formation and micro hardness were studied. These parameters and these results compare with electric discharge machining and grinding and fine polishing.

**5:00 PM**

**Material Flow Forming the Shoulder Flow Zone Using Scroll Shoulder Tool during Friction Stir Welding of Thick Section Aluminum Alloys:** *David Yan*<sup>1</sup>; *Zhan Chen*<sup>1</sup>; *Guy Littlefair*<sup>1</sup>; <sup>1</sup>AUT University

Scroll tool offers advantages of eliminating the tilted tool axis and performing non-linear thick section FSW with a simple machine. However, its shoulder flow zone forming mechanism, determining defect or defect-free weld formation, remains unidentified. A scroll tool was used to FSW thick aluminium plates under different conditions, thereby made a defect, non-defect and 'marker insert' welds for flow pattern investigation. It was observed that a layer-to-layer banded structure appears on the bottom section, but disappears on the top section of shoulder flow zone. Accordingly, shoulder flow zone forming mechanism was suggested. When tool pin is plunged into workpiece, workpiece material is extruded by the pin, and pushed up into the scroll groove forming the pick up material (PUM). During tool moving forward, the central portion of PUM is driven downward by the root portion of pin and then detaches from the tip portion of pin in a layer-to-layer manner.

**5:20 PM**

**Effect of Welding Parameters on the Mechanical and Metallurgical Properties of Friction Stir Spot Welded 2024-T351 Aluminum Alloy:** *Amin Maki*<sup>1</sup>; *Masoud Goodarzi*<sup>1</sup>; *Shahram Kheirandish*<sup>1</sup>; *Mohamad Ali Safarkhanian*<sup>1</sup>; <sup>1</sup>Iran University of Science and Technology

Friction Stir Welding (FSW) is less than fifteen years old and Friction Stir Spot Welding (FSSW) has just recently arrived on the scene. In this investigation, Friction stir spot welding was used to make lap joints on strips of 2024-T351 aluminum alloy sheets. The influence of tool rotational speed and tool holding time on bond formation and tensile shear strength of the resulting joints was determined. The weld microstructures varied significantly depending on tool rotational speed and tool holding time. Metallographic observations were performed by optical microscope. As results showed, wide of stir zone and heat affected zone and Thermo mechanical affected zone, increased by increasing of tool rotational speed and tool holding time. Micro indentation hardness data of base metal (BM), heat affected zone (HAZ), Thermo mechanical affected zone (TMAZ) and SZ were obtained. The HAZ is the softest region and stir zone hardness increased by increasing of tool rotational speed and tool holding time and then decreased. An optimum combination of parameters that maximizes joint strength was identified.

## Hume-Rothery Symposium: Configurational Thermodynamics of Materials: Session VI

*Sponsored by:* The Minerals, Metals and Materials Society, TMS Electronic, Magnetic, and Photonic Materials Division, TMS Structural Materials Division, TMS: Alloy Phases Committee, TMS: Chemistry and Physics of Materials Committee

*Program Organizers:* Chris Wolverton, Northwestern University; Mark Asta, University of California, Davis; Gerbrand Ceder, Massachusetts Institute of Technology (MIT)

Wednesday PM

Room: 212

February 17, 2010

Location: Washington State Convention Center

*Session Chair:* To Be Announced

**2:00 PM Invited**

**Bulk and Surface Properties of Perovskites for Solid Oxide Fuel Cell Cathodes:** *Dane Morgan*<sup>1</sup>; *Yueh-Lin Lee*<sup>1</sup>; <sup>1</sup>University of Wisconsin - Madison

Perovskites are the major class of materials used for modern solid oxide fuel cell (SOFC) cathodes and have the ability to catalyze the oxygen reduction reaction (ORR) on their surfaces and transport oxygen to the electrolyte through their bulk. Their effectiveness as a cathode is therefore intimately tied to their bulk and surface defect thermokinetics. In this talk we discuss some of the challenges and opportunities of using ab initio methods to determine perovskite thermokinetics for SOFC applications. In particular, we focus on LaBO<sub>3</sub> (B=Mn, Fe, Co, and Ni) systems, their deviations from ideal defect behavior, and the impact of these deviations on stoichiometry and kinetics. We also consider how simple descriptors for the ORR can be established with ab initio methods for different SOFC materials.

**2:30 PM Invited**

**Configurational Design of Functional Oxides:** *Hisao Yamauchi*<sup>1</sup>; *Maarit Karppinen*<sup>1</sup>; <sup>1</sup>Helsinki University of Technology

Crystals of functional materials usually possess particular local structures from which the main part of functionality stems. For example, crystals of high-Tc superconductive copper oxides commonly have CuO<sub>2</sub> planes where superconductivity occurs. Even without thorough understanding of the functionality mechanism it is wise to systematically categorize materials of a particular functionality in terms of configurational parameters and design new variants to enhance the functionality. This concept has been useful in extending the frontier of functional materials and successfully applied to HTSC copper oxides: most of them have been grouped into two types of "Homologous Series". Synthesis of the designed "novel material" is another major task in new material research. For the case of copper oxides, most of new members have been realized through ultra-high pressure techniques (since 1993) and filled blanks for possible members. Similar approaches have been applied to other functional materials including high-efficiency oxide thermoelectrics.

**3:00 PM**

**Order and Stability of III-V Semiconductor Surface Alloys at Finite Temperature:** *John Thomas*<sup>1</sup>; *Joanna Mirecki-Millunchick*<sup>1</sup>; *Normand Modine*<sup>2</sup>; *Anton Van der Ven*<sup>1</sup>; <sup>1</sup>University of Michigan; <sup>2</sup>Sandia National Laboratories

The surface structure and composition of III-V semiconductor alloys is of significant importance given the epitaxial synthesis of these materials. We develop a cluster expansion for the coupled substitutional and adsorption/desorption sublattices and apply it, via Monte Carlo, to the As-rich (2×4) reconstructed surface of In<sub>x</sub>Ga<sub>1-x</sub>As/GaAs (001) in order to understand the effects of atomic size mismatch and temperature on surface ordering and stability. We analyze the smooth a2(2×4)-β2(2×4) transition and directly examine the entropy and cation site occupancy in both reconstructions. There exists a strong tendency for compositionally-dependent dimer ordering in a2(2×4) as well as a chemical potential region of stability for a hybrid a2(2×4)-β2(2×4) reconstruction, which drives pronounced composition modulation of surface cation sites. Additionally, we describe new techniques for the prediction of unknown surface structure in III-V compounds and similar systems, with results from a number of binary III-V compounds.



### 3:20 PM

**Stability, Surface Energy and Specific Properties of Al-Based Complex Intermetallics:** Esther Belin-Ferré<sup>1</sup>; Jean Marie Dubois<sup>1</sup>; <sup>1</sup>CNRS Institut Jean Lamour

The stability of Al-based quasicrystals, related complex and simpler compounds depends basically upon Al sp- transition element d hybridization at EF[1]. The electronic structure of bulk specimens drives wetting by water of their surfaces [2]. Electronic structure is investigated using soft X-ray emission spectroscopy that provides partial and local densities of states (DOS) in a compound. From measurements of friction coefficients in vacuum against hard steel for Al-based conventional and complex crystals and quasicrystalline icosahedral Al-Cu-Fe [3] we suggested the DOS at EF is the essential parameter determining friction and solid-solid adhesion in vacuum. Here, we report on DOS and friction measurements for binary Al-TM complex intermetallics focusing at the contribution of d states at EF. 1. E. Belin-Ferré, J. Phys.: Cond. Matter 14 R789 (2002). 2. J.M. Dubois, J. Non Cryst. Sol., 334&335 481 (2004). 3. E. Belin-Ferré and J.M. Dubois, Int. J. Mat. Res. 97 985 (2006).

### 3:40 PM Break

### 4:10 PM Invited

**Simulating Atomic-Scale Phenomena with Colloids:** Frans Spaepen<sup>1</sup>; <sup>1</sup>Harvard School of Engineering and Applied Sciences

Colloids consist of micrometer-size particles in a fluid that interact by central potentials (hard sphere or electrostatic). At large packing fractions they form phases similar to those formed by atoms in condensed matter: liquids, crystals and glasses. Since the colloidal particles are large and slow, they can be tracked in time and in three-dimensional space by confocal microscopy. Colloidal systems, therefore, are highly efficient "analog computers" for the study of the dynamics of complex multiparticle phenomena in condensed matter. A number of examples are presented: crystal nucleation, coherency dislocations in epitaxial growth, indentation of single crystals, and plastic shear of glasses.

### 4:40 PM Invited

**Molecular Dynamics Simulations of Crystallization in Metallic Glasses:** Diana Farkas<sup>1</sup>; <sup>1</sup>Virginia Tech

Model metallic glasses were studied using molecular dynamics simulations, creating them by fast quenching from the liquid temperature range. This talk will present the results of structure relaxation at various temperatures and the response of the glasses to applied strain. The results show that crystallization can be induced by the applied strain. The details of the atomic level configurational changes leading to the crystallization transformation will be discussed.

### 5:10 PM

**Structure in Liquid Alloys Investigated by First-Principles Molecular Dynamics Simulations:** Mark Asta<sup>1</sup>; Haxhimali Tomorr<sup>2</sup>; <sup>1</sup>University of California, Davis; <sup>2</sup>Northwestern University

Throughout his career Professor de Fontaine has made major contributions to the modeling and theoretical understanding of the origins and consequences of configurational short-range order (SRO) in alloy solid solutions. Just as SRO is an important feature of alloy solid solutions, local topological and chemical order in liquid alloys can have important consequences for a number of technologically important processes including crystal nucleation and growth. In this talk we review the insights into liquid alloy structure and dynamics that can be derived within the framework of first-principles molecular-dynamics simulations. We focus on applications to molten Au-Si and Au-Ge alloys, which have received considerable recent interest due to their widespread use as catalysts for semiconductor nanowire growth by the vapor-liquid-solid mechanism. We present results elucidating the nature of the liquid structure and dynamics based on calculated radial distribution functions, bond-angle distributions, common-neighbor analysis, and mean-square displacements.

### 5:30 PM

**Quantum Mechanical Corrections to Simulated Shock Hugoniot Temperatures:** Nir Goldman<sup>1</sup>; Evan Reed<sup>1</sup>; Larry Fried<sup>1</sup>; <sup>1</sup>Lawrence Livermore National Laboratory

We present a straightforward method for the inclusion of quantum nuclear vibrational effects in molecular dynamics calculations of shock Hugoniot temperatures. Using a Grüneisen equation of state and a quasi-harmonic approximation to the vibrational energies, we derive a simple, post-processing method for calculation of the quantum corrected Hugoniot

temperatures. We have used our novel technique on *ab initio* simulations of both shock compressed water and methane. Our results indicate significantly closer agreement with all available experimental temperature data for these two systems. Our formalism and technique can be easily applied to a number of different shock compressed molecular liquids or solids, and has the potential to decrease the large uncertainties inherent in many experimental Hugoniot temperature measurements of these systems.

## Jim Evans Honorary Symposium: Electrochemical Phenomena

*Sponsored by:* The Minerals, Metals and Materials Society, TMS Extraction and Processing Division, TMS Light Metals Division  
*Program Organizers:* Ben Li, University of Michigan; Brian G. Thomas, University of Illinois at Urbana-Champaign; Lifeng Zhang, Missouri University of Science and Technology; Fiona Doyle, University of California, Berkeley; Andrew Campbell, WorleyParsons

Wednesday PM Room: 619  
February 17, 2010 Location: Washington State Convention Center

*Session Chair:* Fiona Doyle, University of California, Berkeley

### 2:00 PM Introductory Comments

### 2:10 PM

**The Application of Electrochemical Techniques to Elucidate the Mechanisms of Copper Chemical Mechanical Planarization (CMP):** Fiona Doyle<sup>1</sup>; Serdar Aksu<sup>2</sup>; Ling Wang<sup>3</sup>; Shantanu Tripathi<sup>4</sup>; Seungchoun Choi<sup>1</sup>; <sup>1</sup>University of California, Berkeley; <sup>2</sup>Solopower, Inc.; <sup>3</sup>Applied Materials; <sup>4</sup>Intel

Chemical mechanical planarization (CMP) is an important unit process in the manufacture of integrated circuits. During CMP of copper metallization lines, electrochemical oxidation phenomena act synergistically with mechanical abrasion to remove copper preferentially from protruding topography. In order to be able to optimize CMP processes, minimize defects, and model the material removal rate for process control, it is desirable to understand the mechanisms at play. Here we discuss various electrochemical studies that we have been used for this purpose, including potentiodynamic tests, in-situ polarization studies, electrochemical quartz crystal microbalance tests, and measurement of passivation kinetics using scratch-repassivation and potential-step chronomamperometry. Electrochemical impedance spectroscopy was used in the latter to distinguish capacitive charging from passivation currents. The mechanisms elucidated by these techniques are discussed, along with a mechanistic tribo-chemical model proposed for CMP.

### 2:35 PM

**Development of Inert Anodes for Electrowinning in Calcium Chloride – Calcium Oxide Melts:** Shuqiang Jiao<sup>1</sup>; Derek Fray<sup>1</sup>; <sup>1</sup>University of Cambridge

There is a need to develop inert anodes for use in calcium chloride-calcium oxide melts. Most metallic alloys severely corrode in these melts and oxide based materials form stable insulating calcium compounds. Anodes could be made from these materials, provided the electronic conductivity can be increased. In the case of calcium titanate, there have been several attempts at doping with lower valent oxides but the increases in electronic conductivity were minor. In this work, a different approach has been adopted which was to form a solid solution with a compound that has an identical structure but is an excellent electronic conductor. Calcium ruthenate is such a compound with a room temperature conductivity of about 1000 ohm<sup>-1</sup> cm<sup>-1</sup>. Solid solutions of calcium ruthenate and calcium titanate were found to act as anodes in calcium chloride-calcium oxide melts, evolving oxygen for over 150 hours with negligible attack.

### 3:00 PM

**Electrochemical Characterization of Nanoparticle Silver Based Zn-AgO Batteries:** Abhinav Gaikwad<sup>1</sup>; Josh Gallaway<sup>1</sup>; Dan Steingart<sup>1</sup>; <sup>1</sup>City College of New York

We examine the use of a nanoparticle silver ink as the basis for alkaline battery electrodes. This ink is intended as bussing material for printed electronic circuits, and despite organic additives, provides expected performance from silver with respect to electrochemical characterization. As the negative

# Technical Program

electrode in a ZnO-KOH electrolyte, it serves as a substrate for plating zinc, and as a positive electrode, it undergoes the  $\text{Ag} \rightarrow \text{Ag}_2\text{O} \rightarrow \text{AgO}$  reaction. The electrochemical behavior and mechanical strength of this material will be characterized within microfluidic channels. Cell configurations and example applications will also be discussed.

## 3:25 PM

**Molten Oxide Electrolysis for Lunar Oxygen Generation Using *in situ* Resources:** Alex Vai<sup>1</sup>; James Yurko<sup>2</sup>; D. H. Wang<sup>3</sup>; Donald Sadoway<sup>1</sup>; <sup>1</sup>Massachusetts Institute of Technology; <sup>2</sup>Electrolytic Research Corporation; <sup>3</sup>22Ti LLC

Molten oxide electrolysis (MOE) is a demonstrated laboratory-scale process for producing oxygen from JSC-1A and other lunar simulants and is being pursued by NASA as a candidate process for lunar oxygen production using *in situ* resources. As part of an investigation to improve the technological readiness of critical subsystems, the technical feasibility of MOE has been studied in a laboratory-scale cell. Under constant current chronopotentiometric conditions, scaleable iridium and iridium-alloy anodes demonstrated a capability for generating more than 1 L of oxygen from a silicate melt at temperatures near 1575°C, drawing current at levels as high as 12A. Cell voltage, gas flow, and gas chromatography data will be shown from the electrolysis experiments. Real-time visual observation of the electrolysis process as well as SEM and EDX characterization of the electrodes and reaction products will be shown. Scale-up considerations for larger size reactors and future work will be discussed.

## 3:50 PM Break

## 4:05 PM

**Leaching of Metal Components from Waste PCBs by Electro-Generated Chlorine in Hydrochloric Acid Solution:** Eun-young Kim<sup>1</sup>; Min-seuk Kim<sup>1</sup>; Jae-chun Lee<sup>1</sup>; Kyoungkeun Yoo<sup>1</sup>; Manoj Kumar<sup>1</sup>; <sup>1</sup>Korea Institute of Geoscience and Mineral Resources (KIGAM)

The leaching behavior of metal components from waste printed circuit boards (PCBs) has been investigated using electro-generated chlorine in hydrochloric acid solution. The experiments were carried out by employing two different reactors: (a) a single reactor facilitated with simultaneous  $\text{Cl}_2$  generation and metals leaching, (b) a separate metal leaching reactor connected with the anode compartment of  $\text{Cl}_2$  generation. Various parameters, viz. current density, chloride concentration, leaching temperature and time, agitation speed have been studied to understand the mechanism of copper leaching using both reactors. Also, two different reactors were compared in terms of leaching efficiency for the application to the recycling of valuable metals from PCBs through hydrometallurgical route.

## 4:30 PM

**Morphology of Zinc Studied under Additive Control within Microfluidic Channels:** Joshua Gallaway<sup>1</sup>; Abhinav Gaikwad<sup>1</sup>; Dan Steingart<sup>1</sup>; <sup>1</sup>City College of New York

The morphology of electrodeposited metal is critical in situations where demanding physical or electrical properties of the resultant metal are required, such as with energy storage in rechargeable battery electrodes, semiconductor patterning, or metal finishing. Morphology is typically controlled by the presence of additives at ppm concentrations, which either alter the deposition mechanism or hinder troublesome side-reactions. Microfluidic electrochemical cells allow quantitative observation of the effect of additives, through rapid *in situ* introduction or removal of the additives under plating conditions. *In situ* monitoring of the electrode surface and current-potential responses reveals real-time electrochemical events in a fashion impossible to achieve in, for example, a typical rotating disk electrode configuration. Millisecond resolution of such transitions allows one to observe time scales of the relevant processes, such as additive adsorption, desorption, or bubble generation. Additionally, the technique requires only small analyte volumes, and provides well-defined hydrodynamics for system modeling and analysis.

## 4:55 PM

**Direct Write Dispenser Printed Energy Storage Devices:** Christine Ho<sup>1</sup>; Jay Keist<sup>1</sup>; Ba Quan<sup>1</sup>; Paul Wright<sup>1</sup>; James Evans<sup>1</sup>; <sup>1</sup>University of California, Berkeley

As electronic devices become smaller in volume and more specialized in functionality, a paradigm shift in energy storage design and manufacture is beginning to emerge and can be realized with the development of simple,

low-cost, solutions-based processing methods to incorporate custom energy buffers directly onto a device. We have been developing the materials and direct write fabrication methods for printing carbon based electrochemical capacitors and zinc batteries directly onto a substrate. Our materials efforts include the optimization of mechanical and ionic transport properties of ionic liquid gel electrolytes, and this has enabled the fabrication of completely printable "solid-state" capacitors and batteries, mitigating manufacturing and packaging concerns. Through a pneumatic dispenser printing system, the energy storage devices can be patterned and integrated directly on-chip. We will also present comprehensive device characterization, including long-term cycling performance and rate behavior.

## Jim Evans Honorary Symposium: Modeling

*Sponsored by:* The Minerals, Metals and Materials Society, TMS

Extraction and Processing Division, TMS Light Metals Division

*Program Organizers:* Ben Li, University of Michigan; Brian G. Thomas, University of Illinois at Urbana-Champaign; Lifeng Zhang, Missouri University of Science and Technology; Fiona Doyle, University of California, Berkeley; Andrew Campbell, WorleyParsons

Wednesday PM

Room: 620

February 17, 2010

Location: Washington State Convention Center

*Session Chair:* Lifeng Zhang, Missouri University of Science and Technology

## 2:00 PM Introductory Comments

### 2:10 PM

**Mathematical Modeling of Spooling/Unspooling Stresses in Electricity Distribution Cables:** James Evans<sup>1</sup>; W. Kinzy Jones, Jr<sup>2</sup>; <sup>1</sup>UC, Berkeley; <sup>2</sup>Amoeba Technologies

Much of the nation's electric power is distributed through underground cables having a central conductor carrying electricity at approximately 12,000 volts. The insulation between the conductor and the ground is only a few millimeters thick and its failure results in expensive cable replacement or occasionally an explosive event injuring, or even killing, passers-by. The insulation is subjected to electromagnetic forces that have been modeled at Berkeley but it is also subject to stresses arising prior to installation in the ground because it is wound on a spool at manufacture and subsequently unwound in the field at placement in service. The paper reports on a finite element analysis, based on measurements of the mechanical properties of the insulation, of stresses that could result in this way and that could contribute to the ultimate failure of the cable.

### 2:35 PM

**Computational Modeling of Heap Leaching Processes:** Mark Cross<sup>1</sup>; Chris Bennett<sup>1</sup>; Diane McBride<sup>1</sup>; A. Hernandez<sup>2</sup>; T. N. Croft<sup>1</sup>; J.E. Gebhardt<sup>2</sup>; <sup>1</sup>Swansea University; <sup>2</sup>Process Engineering Resources Inc

Heap leaching is becoming increasingly popular for the extraction of low grade ores, where copper sulphides and gold/silver/copper complexes are the most common applications, although there are others (e.g. for nickel sulphides). Although the leaching process is simple in concept, it involves what may be characterised as multi-phase reactive thermo-fluid flows in porous media. Hence, the computational modelling of this process in its industrial context is very challenging. It is worth addressing though, because model based simulation tools offer the potential for process optimisation and overall control at a level not conventionally aspired to on plants. In this paper an overview of the work done by the team over a decade is described in the development, validation and industrial deployment of heap leach models for the analysis, simulation and strategic control of plants processing both copper sulphides and gold/silver/copper oxides.

### 3:00 PM

**A T-Ψ Potential Formulation for Numerical Simulation of Induction Heating Processes:** Nagy El-Kaddah<sup>1</sup>; Thinius Natarajan<sup>2</sup>; <sup>1</sup>The University of Alabama; <sup>2</sup>United States Steel Corporation

This paper describes an efficient computational method for 3-D numerical simulation of induction heating processes. It is based on hybrid differential-integral formulation of the current vector potential (T) and reduced magnetic scalar potential (Ψ) of the electromagnetic field. This hybrid formulation confines the solution domain of the open boundary electromagnetic field problem to the



metal, and permits full coupling of electromagnetic and heat transfer aspects of the induction heating process. The governing electromagnetic and heat transfer equations were solved using finite element method. The versatility of the developed algorithm for handling complex geometries and coil configurations is demonstrated by presenting results of numerical simulation of transverse flux induction heating (TFIH) of steel sheets during rolling.

### 3:25 PM

**Modeling on the Cast Start during Steel Continuous Casting Process:** *Yufeng Wang*<sup>1</sup>; Lifeng Zhang<sup>1</sup>; <sup>1</sup>Missouri University of Science and Technology

Serious defects, such as surface longitudinal cracking, inner impurities are frequently found in slabs at the beginning of the first heat casting. During this stage, molten steel is continuously filled into a cavity surrounded by mold walls and dummy bar head. The unstable fluid flow-related phenomena, including the fluctuation of molten steel, the interaction between steel phase and air phase, are the source of quality problems and manufacture accidents. And steel products from this stage are often downgraded or rejected. In order to control the process and reduce the cost, relevant investigations are performed in the current study. A three-dimensional multiphase (gas, molten steel, and mold flux) model is developed for the continuous casting process. Volume of Fluid (VOF) Multiphase method was applied to track the interface between steel phase and air phase.

### 3:50 PM Break

### 4:05 PM

**Improved Computational Modeling of the Flame Spray Pyrolysis Process for Silica Nanopowder Synthesis:** Miguel Olivas-Martinez<sup>1</sup>; *Hong Yong Sohn*<sup>1</sup>; Hee Dong Jang<sup>2</sup>; Terry Ring<sup>1</sup>; <sup>1</sup>University of Utah; <sup>2</sup>Korea Institute of Geoscience and Mineral Resources (KIGAM)

A computational fluid dynamics (CFD) model is presented that couples the fluid dynamics with various processes involving precursor droplets and product particles during the flame spray pyrolysis (FSP) synthesis of silica nanopowder from volatile precursors. The gas-phase processes are modeled by the governing turbulent equations of overall continuity, momentum, energy, and species mass transport. The transport and evaporation of binary liquid droplets are simulated from the Lagrangian viewpoint. The kinetics of particle formation by homogeneous nucleation and growth by Brownian coagulation are accounted for by the population balance. The latter is solved by the quadrature method of moments (QMOM), which makes no prior assumption on the particle size distribution (PSD). Results for the simulation of silica nanopowder synthesis by the gas-phase thermal oxidation of tetraethylorthosilicate in a bench-scale FSP reactor are presented. The effects of the feed rates of dispersion air and precursor solution on the PSD have been evaluated.

### 4:30 PM

**Global and Local Stability of Magnetically-Levitated Droplets:** *Ben Li*<sup>1</sup>; X. Ai<sup>1</sup>; Y. Huo<sup>1</sup>; <sup>1</sup>University of Michigan

This paper presents a numerical study of the global stability of and the local linear and nonlinear magnetically-induced flow instability in a liquid droplet levitated in an alternating magnetic field. The numerical solution of the full 3-D, time harmonic Maxwell equations is obtained using the combined finite element and boundary element method. The computational model, validated for a microwave processing system, is then used to predict the asymmetric electromagnetic forces induced by the induction coils in a liquid droplet. Its global stability and the accompanying temperature distribution are studied using model for various perturbed configurations. The linear and nonlinear flow stabilities of the magnetically-levitated droplet are studied based on the high-order finite difference solution of the Navier-Stokes equations with induced electromagnetic forces. Both linear and nonlinear phenomena are studied and the numerical results are compared with experimental observations.

### 4:55 PM

**Dynamics of Magnetically Levitated Liquid Droplets:** Valdis Bojarevics<sup>1</sup>; *Koullis Pericleous*<sup>1</sup>; Alan Roy<sup>1</sup>; Stuart Easter<sup>1</sup>; <sup>1</sup>University of Greenwich

A number of different methods have been developed, which allow the noncontact electromagnetic levitation of liquid metal droplets to investigate the melting/solidification process and measure the properties of these highly reactive materials. The intense AC magnetic field required to produce levitation in terrestrial conditions, along with the buoyancy and thermo-capillary forces, results in turbulent convective flow within the droplet. The presented numerical

results show that the use of a homogenous DC magnetic field allows the large scale flow to be damped. However the turbulence properties are affected at the same time, leading to a lower turbulent damping. The reduction in the AC field driven flow in the main body of the drop leads to a noticeable thermo-capillary convection at the edge of the droplet, thus affecting the thermal loss and solidification. An alternative method without internal electric currents, using high gradient D.C. magnetic levitation, is analyzed analytically and numerically.

### 5:20 PM

**Magnetically-Damped Flows: Numerical Simulations and Experimental Measurements:** *Ben Li*<sup>1</sup>; X. Bing<sup>1</sup>; Y. Shu<sup>1</sup>; <sup>1</sup>University of Michigan

This paper presents a study on magnetic damping of metal flows with and without the effect of gravity. Comprehensive numerical models are developed for the purpose of simulating electromagnetic and transport phenomena in the media with and without radiative transfer participating. The numerical models are based on the combined continuous and discontinuous finite element solution of the Maxwell equations, radiative transfer equations, Navier-Stokes equations and energy balance equations. Accompany experimental measuring systems were developed where SCN and liquid gallium are used as simulating liquid. Flow measurements were taken by particle velocimetry and hot wire probes for certain configurations. The measurements are compared with the numerical models. With validated models, extensive numerical simulations are conducted to study the magnetic-damping phenomena in various flow configurations for applications in space materials processing applications.

## Magnesium Technology 2010: Effects of Heat Treatment and Casting Process

*Sponsored by:* The Minerals, Metals and Materials Society, TMS Light Metals Division, TMS: Magnesium Committee

*Program Organizers:* Sean Agnew, University of Virginia; Eric Nyberg, Pacific Northwest National Laboratory; Wim Sillekens, TNO; Neale Neelameggham, US Magnesium LLC

Wednesday PM

Room: 613

February 17, 2010

Location: Washington State Convention Center

*Session Chairs:* Elhachmi Essadiqi, CANMET; Zi-Kui Liu, The Pennsylvania State University

### 2:00 PM

**On Mechanical Properties and Microstructures of TTMP Wrought Mg Alloys:** Jack Huang<sup>1</sup>; Amir Arbel<sup>2</sup>; Laura Ligessi<sup>2</sup>; Jesse McCaffrey<sup>1</sup>; Sanjay Kulkarni<sup>1</sup>; J. Jones<sup>2</sup>; Tresa Pollock<sup>2</sup>; *Raymond Decker*<sup>1</sup>; Steve LeBeau<sup>1</sup>; <sup>1</sup>Thixomat; <sup>2</sup>University of Michigan

Thixomat has recently developed a simplistic innovative process for producing high strength wrought Mg sheet cost effectively, the T (Thixomolding) TMP (Thermomechanical Processing) process. The theoretical basis behind this TTMP process is by leveraging the inherent fast cooling nature of the Thixomolding process to produce fine-grained starting sheet stock for the enablement of the high-strain thermomechanical forming step. Recent mechanical property characterization of the TTMP wrought sheets consistently shows tensile yield strength of 300MPa, ultimate tensile strength of 350MPa, and elongation at break of 10% or higher. To further understand the correlation between the enhanced resultant mechanical properties and the deformation mechanism(s) as well as the microstructures of the wrought sheet, we set out to characterize, via microscopic and x-ray diffraction techniques, the grain structures at various stages of the TTMP process. Observations on probable correlation between enhancement of the mechanical properties and microscopic/mechanistic features will be reported.

### 2:20 PM

**The Effect of Thermomechanical Processing on the Tensile and Fatigue Behavior of Thixomolded® AM60:** *Zhe Chen*<sup>1</sup>; B. Kuhr<sup>1</sup>; Alex Ritter<sup>1</sup>; Jack Huang<sup>2</sup>; Ray Decker<sup>2</sup>; Steve LeBeau<sup>2</sup>; Carl Boehlert<sup>1</sup>; <sup>1</sup>Michigan State University; <sup>2</sup>Thixomat

Tensile and fatigue experiments were performed at RT and 150°C on AM60 after three processing treatments: (1) as-thixomolded (as-molded), (2) Thixomolded then thermo mechanically processed (TTMP) and (3) TTMP then

# Technical Program

annealed (annealed). The TTMP procedure resulted in a significantly reduced grain size and a tensile strength greater than twice that of the as-molded material without a debit in elongation-to-failure. The as-molded material exhibited the lowest strength while the annealed material exhibited an intermediate strength but the highest elongation-to-failure (>17%). The as-molded material exhibited the lowest fatigue threshold values and the lowest fatigue resistance. The annealed material exhibited the greatest fatigue resistance and this was suggested to be related to its balance of tensile strength and ductility. Overall the results indicate that TTMP processing of AM60 dramatically improves the mechanical behavior making this alloy attractive for structural applications in the automotive, aerospace, wind energy, and biomedical industries.

## 2:40 PM

**Influence of the Heat Treatment on Mechanical Properties and Microstructure in LPSO Mg-Zn-Y Alloys:** *Masafumi Noda*<sup>1</sup>; Tyuyoshi Mayama<sup>1</sup>; Yoshihito Kawamura<sup>1</sup>; <sup>1</sup>Department of Materials Science, Kumamoto University

Mg-Zn-Y alloys are composed of  $\alpha$ -Mg and LPSO phases. The extruded Mg-Zn-Y alloys are known to have dramatically enhanced strength because the kink deformation occurring in the LPSO phase during plastic deformation. In this present study, the effect of heat treatment on mechanical properties and the thermal stability of microstructure in Mg-Zn-Y extruded alloys were investigated. The elongation of the alloys achieved to about twice while its high strength was retained up to heat treatment temperature of 623 K with no change in the microstructure compared with extruded alloys. On the other hands, yield stress and tensile strength decreases while elongation improves in 623K or more so that  $\alpha$ -Mg phase grain growth. Even at heat treatment temperature of 623 K, it was possible to maintain high strength and thermal stable structure.

## 3:00 PM

**The Effect of Zn Additions on Precipitation Hardening of Mg-Ca Alloys:** *Brian Langelier*<sup>1</sup>; Shahrzad Esmaeili<sup>1</sup>; <sup>1</sup>University of Waterloo

Precipitation hardening can be an effective mechanism for enhancing the strength of magnesium alloys. Calcium is known to provide grain refinement and creep resistance to magnesium casting alloys, and may also be utilized for precipitation hardening through formation of the Mg<sub>2</sub>Ca phase. The hardening effect in binary Mg-Ca alloys is small, but may be significantly improved by the addition of Zn. The effect of Zn on the precipitation hardening behavior of Mg-Ca-(Zn) alloys is characterized with combined differential scanning calorimetry and microhardness measurements, as well as FactSage thermodynamic analysis. Zn additions result in the precipitation of ternary phases, and the refinement of precipitates. Precipitate refinement is attributed to an altered precipitation sequence in the Mg-Ca-Zn alloys. The results of this work show the effectiveness of combined thermal-mechanical and thermodynamic analysis in characterizing the effects of alloying element additions on precipitation hardening in magnesium.

## 3:20 PM

**The Recent Developments in Mg-Sn Based Alloy Thermodynamic Database:** *Manas Paliwal*<sup>1</sup>; Jina Kim<sup>1</sup>; Daehoon Kang<sup>1</sup>; In-Ho Jung<sup>1</sup>; <sup>1</sup>McGill University

Mg-Sn based alloy is one of the most promising Mg alloys for high temperature applications. In order to keep pace with the Mg-Sn alloy development, the Mg-Sn based alloy database has been developed for many years. Thermodynamic calculations based on the accurate thermodynamic database can provide invaluable information for the alloy design such as liquidus/solidus temperature, secondary phase precipitation, heat treatment temperature, etc. In the present study, the recent thermodynamic optimizations for the Mg-Sn-Ca, Mg-Ge-Si, Mg-Ge-Sn, Mg-Pb-Si, Mg-Pb-Sn, Mg-Al-Bi and Mg-Al-Sb ternary systems will be presented. In addition, the applications of the updated thermodynamic database to new Mg-Sn alloy design will be presented.

## 3:40 PM Break

## 4:00 PM

**Influence of Zn Additions on Age Hardening Response and Microstructure of Mg-0.3at.%Ca Alloys:** *Keiichiro Oh-ishi*<sup>1</sup>; Chamini Mendis<sup>1</sup>; Ryuichi Watanabe<sup>2</sup>; Kazuhiro Hono<sup>1</sup>; <sup>1</sup>National Institute for Materials Science; <sup>2</sup>Graduate School, University of Tsukuba

The age-hardening response of creep-resistant Mg-Ca alloys has been known to be improved by the trace addition of Zn. We have investigated the age hardening responses and corresponding microstructures of Mg-0.3Ca-xZn (x =

0.0, 0.1, 0.3, 0.6, 1.0, 1.6 at.%) alloys by hardness test, transmission electron microscopy (TEM), and high-angle annular dark field-scanning transmission electron microscopy (HAADF-STEM). Zn additions up to x = 0.6 lead to enhanced age hardening responses with the highest peak hardness of Hv = 69 for x = 0.6. Further addition of Zn degraded the age hardening responses. The peak aged Mg-0.3Ca-0.6Zn alloy showed finer precipitates than the binary Mg-0.3Ca alloy. HAADF-STEM images revealed that the finely dispersed monolayer G.P. zones with internal ordered structure are the major contributor to the age hardening. Excess addition of Zn resulted in the formation of Ca<sub>2</sub>Mg<sub>6</sub>Zn<sub>3</sub> precipitates suppressing the formation of the ordered G.P. zones.

## 4:20 PM

**Effect of Aging and Thermomechanical Processes in Twin Roll Cast Mg AZ91 Alloy Sheet:** *Ozgur Duyugulu*<sup>1</sup>; Selda Ucuncuoglu<sup>1</sup>; Gizem Oktay<sup>1</sup>; Onuralp Yucel<sup>2</sup>; Ali Arslan Kaya<sup>3</sup>; <sup>1</sup>TUBITAK Marmara Research Center; <sup>2</sup>Istanbul Technical University; <sup>3</sup>Mugla University

6 mm thick and 1500 mm wide magnesium alloy AZ91 sheet was produced by twin roll casting. Sheets were homogenized between 350-475°C for 1-24 h. Afterwards, they were hot rolled down to 1 mm. Age hardening was also performed on twin roll cast AZ91 alloy sheets. Specimens were aged at 100-300°C for up to 100 h. Characterization was performed by light microscope, SEM-EDS, TEM-EDS, EPMA and XRD after twin roll casting and also after each thermomechanical process including aging. Tensile tests were performed for mechanical properties. Moreover, the age-hardening response of Mg AZ91 alloy was examined by micro hardness test.

## 4:40 PM

**Experimental Studies on the As-Cast Microstructure of Mg-Al Binary Alloys with Various Solidification Rates and Compositions:** *Dae Hoon Kang*<sup>1</sup>; Manas Paliwal<sup>1</sup>; Elhachmi Essadiqi<sup>2</sup>; In-Ho Jung<sup>1</sup>; <sup>1</sup>McGill University; <sup>2</sup>CANMET-MTL

As the solidification rate is undoubtedly the most important processing parameter to determine the as-cast microstructure and consequent mechanical properties of alloys, there have been many approaches to clarify qualitatively the effect of solidification rate on segregation and microstructural features. In the present study, the Mg-Al alloys of 3, 6 and 9 wt% Al were cast with different cooling rates, and their as-cast microstructures were examined to determine the influence of cooling rate on the segregation fraction and compositional variation. In addition, a simple kinetic solidification model associated with the thermodynamic database was developed to simulate the as-cast microstructures of Mg-Al alloys.

## 5:00 PM

**Impurity and Tracer Diffusion Studies of Magnesium and Its Alloys:** Sarah Brennan<sup>1</sup>; Andrew Warren<sup>1</sup>; Kevin Coffey<sup>1</sup>; *Yongho Sohn*<sup>1</sup>; Nagraj Kulkarni<sup>2</sup>; Peter Todd<sup>3</sup>; <sup>1</sup>University of Central Florida; <sup>2</sup>University of Tennessee; <sup>3</sup>Oak Ridge National Laboratory

An Integrated Computational Materials Engineering (ICME) approach for optimizing processing routes for Mg-alloys requires reliable thermodynamic and diffusion databases. We are developing a tracer diffusion database using both stable and unstable isotopes for Mg-alloys. Mg and Zn tracer diffusion studies in several polycrystalline Mg-Al-Zn alloys were conducted using the thin film method. Approximately 500 nm thick Mg, and Zn enriched isotopic films were deposited on in-situ RF plasma-cleaned polycrystalline Mg-alloys by DC magnetron sputtering from pure targets. Specimens were then diffusion annealed at various temperatures below 600°C in quartz capsules that were evacuated to 10<sup>-8</sup> torr and backfilled with Ar-H<sub>2</sub> mixtures. Concentration profile of Mg and Zn isotopic diffusion profiles into single phase Mg-Al-Zn alloys was determined by depth-profiling technique using secondary ion mass spectroscopy. The Mg and Zn tracer diffusion coefficients determined as a function of temperature and composition for the various Mg-Al-Zn alloys will be presented and discussed.

## 5:20 PM

**Effect of Alloying and Solidification Rates on Microstructure of Hot Rolled and Annealed Micro-Alloyed Az31 Sheet:** *Elhachmi Essadiqi*<sup>1</sup>; Amjad Javaid<sup>2</sup>; Mahmoud Shehata<sup>2</sup>; Teddy Muller<sup>3</sup>; Stephane Yue<sup>4</sup>; Ravi Verma<sup>5</sup>; <sup>1</sup>CANMET; <sup>2</sup>CANMET; <sup>3</sup>Evry University; <sup>4</sup>McGill University; <sup>5</sup>General Motors

A possible process to produce Mg strip using twin roll casting begins with 3 to 10 mm thick Mg alloys strip that will be hot rolled to sheet with low cost for automotive application. To optimize the as-cast strip thickness, there is a need to



determine the minimum hot rolling reduction of these strips required to produce 1 to 2 mm thick sheet with targeted properties. In this study, as-cast micro-alloyed AZ31 plates with different thicknesses (6 to 18 mm) have been rolled to 1.5 mm thick sheets and annealed. The influence of the as-cast microstructures and micro-alloying on the final hot rolled and annealed microstructure and mechanical properties has been established. The optimum hot rolling reduction required to produce targeted properties has been determined

### 5:40 PM

**Texture and Anisotropy of Continuous Cast (CC) and Direct Chill Cast (DC) AZ31 Magnesium Sheets:** Raj Mishra<sup>1</sup>; Jon Carter<sup>1</sup>; Sooho Kim<sup>2</sup>; <sup>1</sup>GM R&D; <sup>2</sup>GM R&D (retired)

This study compares the microstructure and mechanical properties of CC and DC AZ31 sheets. In O-temper, the grain sizes are homogeneous through the sheet thickness, but the CC sheet has a slightly finer grain size. The c-axes of grains lie normal to the sheet surface with the prism planes distributed nearly randomly. The tensile yield strength values are nearly the same in both materials in the rolling direction (RD) and increase from RD to TD (transverse direction). The flow curves are asymmetric on the sheet plane with YS in compression being ~40% less than that in tension. The ultimate tensile strengths are independent of in-plane orientation and elongation of CC sheet decreases from RD to TD. The compression data in the sheet normal direction (ND) is similar to the tensile data in the RD or TD, but the compression data in RD shows an S-shape, characteristic of twinning.

### Materials in Clean Power Systems V: Clean Coal, Hydrogen Based-Technologies, Fuel Cells, and Materials for Energy Storage: SOFC, PEM and DMFC

*Sponsored by:* The Minerals, Metals and Materials Society, TMS Electronic, Magnetic, and Photonic Materials Division, TMS Structural Materials Division, TMS/ASM: Corrosion and Environmental Effects Committee, TMS: Energy Conversion and Storage Committee  
*Program Organizers:* Xingbo Liu, West Virginia University; Zhenguang Yang, Pacific Northwest National Lab; K. Weil, Pacific Northwest National Lab; Mike Brady, Oak Ridge National Lab; Jay Whitacre, Carnegie Mellon University; Ayyakkannu Manivannan, National Energy Technology Laboratory; Zi-Kui Liu, Penn State University

Wednesday PM Room: 211  
February 17, 2010 Location: Washington State Convention Center

*Session Chairs:* K. Scott Weil, Pacific Northwest National Lab; Rod Borup, Los Alamos National Laboratory

### 2:00 PM

**Kinetics of Oxide Scale Formation on Nicrofer-6025HT at Elevated Temperatures for Advanced Coal Based Power Plants:** Vineet Joshi<sup>1</sup>; Alan Meier<sup>1</sup>; Scott K. Weil<sup>2</sup>; Jens T. Darsell<sup>2</sup>; <sup>1</sup>Alfred University; <sup>2</sup>Pacific Northwest National Laboratories

Oxygen separation membranes for clean coal energy delivery in advanced coal based power plants rely on use of solid state mixed ionic/electronic conductors which operate at temperatures in the range 700-900°C. Nicrofer-6025HT is a nickel based alloy which shows compatibility with these systems. Nicrofer has been proposed as a manifold material to transport the hot gases into these oxygen separation membranes. The present work investigates the kinetics of oxide scale formation on Nicrofer. Electron dispersive spectroscopy, wavelength dispersive spectroscopy and X-Ray photoelectron spectroscopy were used to characterize the oxide scale. It was observed that the oxide scale consisted primarily of two layers, an outer scale of chromium oxide and an alumina scale beneath it.

### 2:20 PM

**Electrochemical Characterizations of Ni-YSZ Electrode in the Thin NiFe Supported Solid Oxide Fuel Cell:** Kyeong Hyun Kim<sup>1</sup>; Young Min Park<sup>2</sup>; Haekyoung Kim<sup>1</sup>; <sup>1</sup>Yeung Nam University; <sup>2</sup>Research Institute of Industrial Science and Technology

Metal-supported solid oxide fuel cells (SOFCs) have been discussed as a next generation SOFC configuration due to good mechanical properties and

thermal shock resistance. NiFe alloy is one of the most promising metallic materials as a supporter because of similar thermal expansion coefficient with the ceramic electrolyte. The thin NiFe supported SOFC, NiFe/Ni-YSZ/YSZ/LSCF, have been successively fabricated through tape casting and co-firing method. In order to study the effects of morphologies and components in anode electrode, the particle size and the composition of Ni and YSZ were controlled. The electrochemical performances will be discussed in terms of the fuel utilization and temperature. The long term stability will also be presented with the electrode morphologies.

### 2:40 PM

**Metal-Supported Solid Oxide Fuel Cell:** Gyeong Man Choi<sup>1</sup>; Hyup Je Cho<sup>1</sup>; Young Min Park<sup>2</sup>; <sup>1</sup>POSTECH; <sup>2</sup>RIST

SOFC (Solid Oxide Fuel Cell) has advantages in efficiency, power density, life time and multifuel capability. However, SOFC is very weak against mechanical or thermal shock due to its inherent brittleness and the low thermal conductivity of the component materials. SOFC is commonly manufactured either in the form of electrolyte-supported or anode-supported type. However, metal-supported SOFC is more promising due to its mechanical strength, thermal shock resistance, and low cost etc.. The high mechanical and thermal strength of the supporting metal compensates the weakness of ceramics and thus strengthens the cell. In this study, we have developed a thin (<~250 μm) metal-supported SOFC using a simple and common co-sintering process. The strong and thin structure gives flexible nature to SOFC. In the presentation, we will discuss the fabrication technique and electrochemical performance. The performance is comparable to or better than the conventional electrolyte- or anode-supported SOFC.

### 3:00 PM Invited

**Development of Niobium Coated Stainless Steels as Bipolar Plate Materials for PEMFC Stacks:** Sung-Tae Hong<sup>1</sup>; K Scott Weil<sup>2</sup>; Yong-Zoo You<sup>1</sup>; <sup>1</sup>University of Ulsan; <sup>2</sup>Pacific Northwest National Laboratory

Niobium (Nb) coated stainless steel (SS) is being developed as a metallic bipolar plate material for PEMFC stacks. Roll boning process has been used to fabricate Nb-clad SS. The result of prior work has shown that the Nb-clad SS is electrochemically viable, exhibiting passivating behavior with current densities that were comparable to non-corrosive noble metals such as Pt. However, during the post-roll annealing process, a brittle interfacial layer may form between the two bonded materials. The brittle interfacial layer may act as an additional design constraint in forming of bipolar plates. Recently, as an alternative of roll bonding process, sputtering has been used to fabricate Nb-sputtered SS as bipolar plate materials for PEMFC stacks. The experimental result shows that the electrochemical properties of the Nb-sputtered SS can be compatible with those of the Nb-clad SS while keeping the thickness of Nb layer a few times thinner than Nb-clad SS.

### 3:40 PM Break

### 3:50 PM Invited

**PEM Fuel Cell Material Durability and Degradation:** Rod Borup<sup>1</sup>; Rangachary Mukundan<sup>1</sup>; John Davey<sup>1</sup>; David Wood<sup>1</sup>; <sup>1</sup>Los Alamos National Laboratory

The durability of polymer electrolyte membrane (PEM) fuel cells is a major barrier to the commercialization for transportation and stationary power applications. Each component and material in the fuel cell has different characteristics, different operational considerations and potentially different durability concerns. Within a PEMFC, the individual components are exposed to an aggressive combination of strong oxidizing conditions, liquid water, strongly acidic conditions, high temperature, high electrochemical potentials, reactive intermediate reaction products, a chemically reducing atmosphere at the anode, high electric current, and large potential gradients. To improve durability, it is important to understand the roles of these various conditions in material degradation processes and work to improve material durability. Topics for discussion will include durability testing methods including accelerated stress testing (AST), the effect of operating conditions on durability, and focus on the various component materials: membranes, electrocatalysts, catalyst supports, gas-diffusion media and bipolar plates.

# Technical Program

## 4:30 PM

**Performance of Micro-DMFCs with Two Kinds of Flow Fields:** *Yuhao Lu Lu<sup>1</sup>; Ramana Reddy<sup>1</sup>; <sup>1</sup>The University of Alabama*

Micro fuel cells have been recognized as promising electrochemical power sources in portable electronic devices due to their safety, high efficiency renewable fuel, and environmental compatibility. Although performance of a micro-DMFC depends on all its components, its behavior is drastically affected by different flow fields fabricated on the end plates. In addition, scaling effects of micro-channels make the flow fields have different performance in micro-DMFCs from conventional DMFCs as well. This study evaluated performance of micro-DMFCs with two kinds of flow fields including single-channel and double-channel serpentine designs. Polarization, electrochemical impedance spectroscopy, and chronoamperometry were employed to obtain the electricity output, resistance, and response time of micro-DMFCs at different conditions, respectively. Results showed that micro-DMFC with double-channel serpentine flow field presented a better performance than single-channel serpentine design. Meanwhile, double-channel design also demonstrated the faster response than single design when the electric load was changed.

## 4:50 PM

**Pre-Oxidized and Nitrided Stainless Steel Foil for Proton Exchange Membrane Fuel Cell Bipolar Plates:** *Michael Brady<sup>1</sup>; Todd Toops<sup>1</sup>; Peter Tortorelli<sup>1</sup>; Heli Wang<sup>2</sup>; John Turner<sup>2</sup>; Harry Meyer<sup>1</sup>; Karren More<sup>1</sup>; Fernando Garzon<sup>3</sup>; Tommy Rockward<sup>3</sup>; Don Gervasio<sup>4</sup>; Francisco Estevez<sup>2</sup>; Jim Rakowski<sup>6</sup>; <sup>1</sup>Oak Ridge National Lab; <sup>2</sup>National Renewable Energy Lab; <sup>3</sup>Los Alamos National Lab; <sup>4</sup>Arizona State University; <sup>5</sup>AGNI-GenCell; <sup>6</sup>ATI Allegheny Ludlum*

Developmental Fe-20Cr-4V alloy and 2205 stainless steel foils were pre-oxidized and nitrided to form low-interfacial contact resistance (ICR), corrosion-resistant surfaces. Promising corrosion resistance for both materials was observed under simulated aggressive anode- and cathode-side bipolar plate conditions. Variation in ICR values were observed for treated 2205 foil, and lower (better) values generally observed for the treated Fe-20Cr-4V. Single-cell, fuel cell testing of stamped and pre-oxidized/nitrided foils was conducted with a repeating cycle of 0.6V (30 min), 0.7V (20 min), 0.5V (20 min) and open-circuit voltage (1 min) out to 1000 h. Benchmark untreated stainless steel foil and machined graphite plates also were evaluated. The pre-oxidized and nitrided Fe-20Cr-4V alloy exhibited the best performance of the examined materials. Post-test analyses of the membrane electrode assemblies (MEAs) by x-ray fluorescence indicated an Fe concentration of only 0.1-0.3 x10<sup>-6</sup> g/cm<sup>2</sup> in the MEAs tested with the pre-oxidized and nitrided Fe-20Cr-4V and graphite plates.

## 5:10 PM

**Effect of Pretreatment and Surface Treatment Conditions on Corrosion Resistance Property in Metallic Bipolar Plate Materials:** *Kee-Do Woo<sup>1</sup>; Min-seok Moon<sup>1</sup>; Eui-pyo Kwon<sup>1</sup>; Sang-hyuk Kim<sup>1</sup>; Duck-soo Kang<sup>1</sup>; Zhiguang Liu<sup>2</sup>; Xiao-peng Wang<sup>1</sup>; <sup>1</sup>Chonbuk National University; <sup>2</sup>Harbin Institute of Technology*

Fuel cell is one of the new energy systems. But fuel cell components are very expensive. Therefore, development of new process or materials for fuel cell components with reduced manufacturing cost has been becoming an important issue in fuel cell industry. The possibility of replacement of the graphite bipolar plate to metallic bipolar plate was studied. In this study, three types of stainless steel were investigated. Electrochemical property of stainless steel that can be used for metallic bipolar plate was investigated in accordance with the conditions of pre-treatment and surface treatments by using Potentiodynamic analyzer. Reaction behaviors of main elements of the stainless steels within similar PEMFC/DMFC (Proton exchange membrane fuel cells/Direct-methanol fuel cells) corrosion condition were investigated by using XRD, ICP and FE-SEM observation. In comparison, austenite base stainless steel has good potentiodynamic value. Corrosion current densities (I<sub>corr</sub>) of STS316, STS304 and STS430 were 3.5~5.2x10<sup>-7</sup>amp/cm<sup>2</sup>, 3.8~5.1x10<sup>-7</sup>amp/cm<sup>2</sup> and 1.9~7.4x10<sup>-6</sup>amp/cm<sup>2</sup>, respectively. Interfacial contact resistance has different behavior between As-polished and As-Received condition on the same material. Normally as-polished has good contact resistance better than as-received condition. Comparison of contact resistance on STS316, as-polished specimen has 31.125(mΩcm<sup>2</sup>) and as-received specimen has 322.925(mΩcm<sup>2</sup>) with compaction pressure approx. 120N/cm<sup>2</sup>.

## Modeling, Simulation, and Theory of Nanomechanical Materials Behavior: Physics of Defects, Dislocation Nucleation and Fracture II

*Sponsored by: The Minerals, Metals and Materials Society, TMS Materials Processing and Manufacturing Division, TMS/ASM: Computational Materials Science and Engineering Committee, TMS: Nanomechanical Materials Behavior Committee*

*Program Organizers: Thomas Buchheit, Sandia National Laboratories; Sergey Medyanik, Washington State Univ.; Douglas Spearot, University of Arkansas; Lawrence Friedman, Penn State University; Edmund Webb, Sandia National Laboratories*

Wednesday PM

Room: 304

February 17, 2010

Location: Washington State Convention Center

*Session Chairs: Harley Johnson, University of Illinois; Douglas Spearot, University of Arkansas*

## 2:00 PM Invited

**Multiple Time Scale Analysis of the Ion Bombardment Surface Instability:** *Harley Johnson<sup>1</sup>; Kallol Das<sup>1</sup>; Nagarajan Kalyanasundaram<sup>1</sup>; Maryam Ghazisaeidi<sup>1</sup>; Jonathan Freund<sup>1</sup>; <sup>1</sup>University of Illinois*

Low temperature ion irradiation of materials often results in nanoscale surface topology modification, ranging from the formation of dots and parallel or perpendicular ripples, to smoothing, depending upon the incident beam angle. Using a combined atomistic and continuum simulation method, we study the origins of the surface instability that gives rise to this interesting phenomenology. Thousands of single ion impacts are first studied at different incidence angles using molecular dynamics (MD). A continuum simulation then incorporates the individual "crater functions" gathered from MD into a model that includes surface diffusion over much longer time scales. We show that local mass redistribution along the surface plays a dominant role in determining the growth rate and orientation of surface features. Finally, we introduce an alternative method for spanning the time scales in the high temperature problem, when the surface is affected not only by sputtering and surface diffusion, but also by recrystallization.

## 2:30 PM

**Stress and Strain near Rough Surfaces and Interfaces:** *Lawrence Friedman<sup>1</sup>; <sup>1</sup>Penn State University*

The importance of surface roughness is well known for strained surfaces and interfaces. Surface roughness can concentrate stress at the micro- and nano-scales; conversely, stress and strain can drive surface roughening such as in Stranski-Krastanow and Volmer-Webber growth. Similar phenomena result for internal surfaces effecting long-range stress fields as well as net interfacial energies with impacts on adhesion and delamination. Here a Green function method is used to calculate stress fields and interfacial energies to arbitrary order in surface and interface roughness. Numerical requirements and limitations are presented along with applications to the stochastic formation of self-assembled quantum dots such as Ge<sub>x</sub>Si<sub>1-x</sub>/Si and thin-film adhesion energies.

## 2:50 PM

**Saddle-Node Scalings during Dislocation Nucleation in Perfect Crystals under Inhomogeneous Loads:** *Asad Hasan<sup>1</sup>; Craig Maloney<sup>1</sup>; <sup>1</sup>Carnegie Mellon University / Civil & Environmental Engineering*

Under sufficiently high loads, dislocations will be nucleated in perfect crystals. An outstanding issue is the prediction of where and under what loads nucleation will occur. Many criteria have been put forward which address this question, some in terms of the local stress field, others in terms of the local tangent stiffness of the material. More recently it has been questioned whether a local criterion can be used at all [1]. We perform molecular dynamics simulations to address these questions. We show that nucleation can be understood in terms of a classical saddle-node bifurcation, during which the velocity of the system concentrates onto a single mode which couples linearly to the applied deformation. These scalings should have important implications for the estimation of the nucleation rate via classical rate theory. [1] R.E. Miller and D. Rodney, J. Mech. Phys. Solids 56 (4) 1203-1223, 2008.



### 3:10 PM

**Phase Stability and Transformations in NiTi from Density Functional Theory Calculations:** *Karthik` Guda Vishnu<sup>1</sup>; Alejandro Strachan<sup>1</sup>; <sup>1</sup>Purdue University*

We used density functional theory to characterize various crystalline phases of NiTi alloys: i) high temperature austenite phase B2, ii) orthorhombic B19, iii) the monoclinic martensite phase B19', and iv) a body centered orthorhombic phase (B33), theoretically predicted to be the ground state. We also investigated possible transition pathways between the various phases and the energetics involved. Interestingly, We predict a new phase of NiTi, denoted B19'', which is involved in the transition between B19' and BCO. B19'' is monoclinic and can exhibit shape memory. We find B19 to be metastable with a 4 meV energy barrier separating it from B19'. We would also like to show our large scale molecular dynamics (MD) simulation results to understand the role of size in martensitic transformation at nano scale.

### 3:30 PM Break

### 3:50 PM Invited

**Coupled Continuum - Density Functional Theory Investigation of Crack-Tip Propagation and Dislocation Nucleation:** *Arun Nair<sup>1</sup>; Derek Warner<sup>1</sup>; Richard Hennig<sup>1</sup>; <sup>1</sup>Cornell University*

Atomic-scale modeling of deformation processes has long been plagued by the challenge of accurately and efficiently describing the complexities of multispecies bonding. In the case of metals, this has led to the majority of the atomistic modeling effort focusing on pure elemental metals in a vacuum, rather than more technologically relevant problems involving alloys with impurities in realistic environments. In an attempt to address this long-standing challenge we have employed a concurrent multi-scale approach that couples an atomistic region whose forces are calculated via Kohn-Sham Density Functional Theory to a continuum region described by linear elasticity. This approach enables us to examine large simulation cell sizes and thus properly account for the long-range elastic fields associated with key defects such as dislocations. This talk will specifically focus on the application of the above method to crack-tip phenomenon in aluminum in the presence of oxygen.

### 4:20 PM

**Modeling of Magnetic Thin Film with Misfit Dislocations:** *Nirand Pisutha-Arnon<sup>1</sup>; Bo Yang<sup>2</sup>; Dong-Hee Lim<sup>1</sup>; Mark Asta<sup>2</sup>; Katsuyo Thornton<sup>1</sup>; <sup>1</sup>University of Michigan; <sup>2</sup>University of California, Davis*

We present multiscale calculations of misfit dislocations to study dislocation energetics and structures within heteroepitaxial Fe films grown on Mo(110) and W(110) substrates. On the atomic level, we calculate the generalized stacking fault energies of the Fe/Mo and Fe/W systems from the density functional theory, which are used as an input to the continuum models. On the continuum level, the Peierls-Nabarro formulation is employed to calculate the elastic field originating from the misfit dislocations within a film of finite thickness. The semi-analytical and numerical methods are used for planar and non planar films. By allowing the dislocation spacing to vary and by including the effect of homogeneous strain, the equilibrium dislocation spacing as a function of film thickness is obtained. We relate these results to the surface instability mechanism and the metastable height observed in the Fe/Mo and Fe/W systems.

### 4:40 PM

**Strain Engineering on Si/Ge Nanoscale Heterostructures:** *Yumi Park<sup>1</sup>; Winnie Tan<sup>1</sup>; Alejandro Strachan<sup>1</sup>; <sup>1</sup>Purdue University*

Strained heterostructures are ubiquitous in microelectronic applications and the ability to control strain is critical to improve their electronic properties. We use molecular dynamics to explore nanopatterning and local amorphization followed by re-crystallization as possible avenues for strain engineering. Nanopatterning of strained Si/Ge/Si heterostructures into 1-D bars leads to transverse strain relaxation in the Ge section due to surface relaxation and we characterize how this relaxation increases with decreasing the bar width (W) and increasing the Ge thickness (H). Local amorphization of Si/Ge nanolaminates also leads to strain relaxation in the direction normal to the crystal/amorphous interface that increases as the height of Si/Ge bi-layer (H) increases and the periodic length of the crystalline/amorphous pattern (W) decreases. In both cases, a full strain relaxation is achieved for roughly square cross section (H≈W) leading to a uniaxial strain state, which is desirable for high-speed electronics.

### 5:00 PM

**Anomalous Dissipation in Single-Walled Carbon Nanotube Resonators:** *Peter Greaney<sup>1</sup>; Giovanna Lani<sup>2</sup>; Giancarlo Cicero<sup>3</sup>; Jeffrey Grossman<sup>1</sup>; <sup>1</sup>Massachusetts Institute of Technology; <sup>2</sup>Ecole Polytechnique; <sup>3</sup>Polytechnic of Torino*

We observe transient anomalous dissipation during molecular dynamics simulation of the ring-down of flexural modes in single-walled carbon nanotube (CNT) resonators. During the anomalous regime the quality factor of the mode can be reduced by more than 95% for tens of picoseconds. The anomalous dissipation is sensitive to the CNT temperature and the energy in the mode, and remarkably increasing the excitation energy in the resonator causes it to decay to zero faster. This counter intuitive phenomenon is analogous to the Mpemba effect in the freezing of water, and as with the Mpemba effect, it implies that the background temperature in the system does not uniquely define its dissipative state. Using a projection algorithm we are able to follow the energy as it dissipates, identifying gateway modes that mediate the dissipation, and a resulting athermal phonon population. The implications for these observations for continuously driven resonators are discussed.

## Neutron and X-Ray Studies of Advanced Materials III: Diffuse Scattering II

*Sponsored by: The Minerals, Metals and Materials Society, ASM International, TMS Structural Materials Division, TMS/ASM: Mechanical Behavior of Materials Committee, TMS: Titanium Committee*  
**Program Organizers:** *Rozaliya Barabash, Oak Ridge National Laboratory; Jaimie Tiley, Air Force Research Laboratory; Erica Lilleodden, GKSS Research Center; Peter Liaw, University of Tennessee; Yandong Wang, Northeastern University*

Wednesday PM

Room: 303

February 17, 2010

Location: Washington State Convention Center

*Session Chairs:* Darren Goossens, Australian national University; Yang Ren, Argonne National Laboratory

### 2:00 PM Keynote

**Monte Carlo Simulation of Disorder in the Ag<sup>+</sup> Fast Ion Conductors Pearceite and Polybasite:** *Richard Welberry<sup>1</sup>; <sup>1</sup>Research School of Chemistry*

The pearceite-polybasite group of minerals (i.e. pearceite, antimonpearceite, arsenopolybasite and polybasite), of general stoichiometry  $[M_6^{TIII}_2S_6][Ag^+Cu^+S_4]$  with  $M=Ag^+, Cu^+$  and  $T=As^{3+}, Sb^{3+}$ , occur relatively commonly in nature. All have recently been shown to exhibit  $Ag^+$  fast ion conduction at rather low temperatures (only slightly above or below room temperature). The average crystal structure determination of these materials shows the positions of the  $Ag^+$  ions to be smeared out or delocalised within sheets in an ordered framework structure comprised of the remaining ions. At the same time, strong and highly structured diffuse scattering has been observed which contains diffuse peaks that are incommensurate with the diffraction peaks of the framework structure. In order to try to understand the origins of the fast ion conduction properties of these materials we have used Monte Carlo computer simulation of a model system to interpret and analyse this observed diffuse scattering.

### 2:30 PM Invited

**Monte Carlo Modelling of Diffuse Scattering from Single Crystals:** *Darren Goossens<sup>1</sup>; Aidan Heerdegen<sup>1</sup>; <sup>1</sup>Australian National University*

Diffuse scattering probes the local ordering in a crystal, whereas Bragg peaks are descriptive of the average long-range ordering. The population of local configurations can be explored by modelling the three-dimensional distribution of diffuse scattering. Local configurations are not constrained by the average crystallographic symmetry so one way of modelling diffuse scattering is by modelling a disordered (short-range ordered) structure and then calculating its diffuse scattering. The structure must contain enough unit cells to give a statistically valid model of the populations of local configurations, and so requirements for a program to model this ordering are very different from programs which model average crystal structures (used to fit the Bragg diffraction). The strategies used to tackle the problem and the way in which they are implemented will be discussed.

# Technical Program

## 2:50 PM Invited

**Phase Transition under High Pressure in Ionic Liquid Based Mixtures:** Hiroshi Abe<sup>1</sup>; Yusuke Imai<sup>1</sup>; Takefumi Goto<sup>1</sup>; Takahiro Takekiyo<sup>1</sup>; Yukihir Yoshimura<sup>1</sup>; <sup>1</sup>National Defense Academy

Room temperature ionic liquids (RTILs) have been big subjects of an environmentally “green” chemistry. Recently, anomalous domain growth was observed in [DEME][BF<sub>4</sub>]-H<sub>2</sub>O mixtures.[1] The anomaly causes superstructure and volume contractions.[2] In this study, we investigate isotope effect in hydrogen/deuterium (H<sub>2</sub>O, DHO and D<sub>2</sub>O) using [DEME][BF<sub>4</sub>]-water mixtures by the simultaneous measurements. Crystallization temperature decreases by isotope effect in deuterium of water. Nucleation process in the mixture is suppressed instead of little water concentrations ( $\cong 1$  mol%). At the same time, anomalous domain growth, superstructure and volume contractions disappear accompanied by the isotope effect of water. [1] Y. Imai, H. Abe, T. Goto, Y. Yoshimura, S. Kushiyama and H. Matsumoto, J. Phys. Chem. B 112, 9841 (2008). [2] Y. Imai, H. Abe and Y. Yoshimura, J. Phys. Chem. B 113, 2013 (2009).

## 3:10 PM Invited

**Synchrotron High-Energy X-Ray Study of Advanced Materials with Nano-Scale Structures:** Yang Ren<sup>1</sup>; Valeri Petkov<sup>2</sup>; Yandong Wang<sup>3</sup>; Zhihua Nie<sup>3</sup>; Dongmei Liu<sup>4</sup>; Peter Liaw<sup>5</sup>; <sup>1</sup>Argonne National Laboratory; <sup>2</sup>Central Michigan University; <sup>3</sup>Beijing Institute of Technology; <sup>4</sup>Northeastern University; <sup>5</sup>University of Tennessee

Materials with nano-scale structures have a broad range of applications and detailed knowledge of their atomic-level structure is essential in order to understand and predict their properties and functionalities. Nano-scale structures include nano-particles, nanocrystalline metals and alloys, nano-size precipitates in bulk samples, nano-twins, defects and local disorders, etc. Synchrotron high-energy x-rays are widely used to study the structure, phase transformation and mechanical properties of nano-materials. Among them, a non-traditional approach based on high-energy x-ray total diffraction and atomic pair distribution function data analysis and structure simulations has been developed to investigate the atomic level structures of nanomaterials, that can be performed in various conditions. In this talk, we will present our recent work in this area, including the principle of the method, experimental facility and scientific results of different nanostructures. (Use of the Advanced Photon Source was supported by the U. S. DOE, Office of Science, under Contract No. DE-AC02-06CH11357.)

## 3:30 PM Invited

**Unlocking the ‘True’ Structure of Complex Materials Using Total Scattering:** Thomas Proffen<sup>1</sup>; <sup>1</sup>Los Alamos National Laboratory

Total scattering is becoming crucial tool to understanding the atomic structure of complex materials. Conventional structure determination based on Bragg scattering and yields the average structure of the material. However, many modern materials owe their properties to defects or their nano-crystalline character makes conventional Bragg analysis difficult or impossible. New neutron and X-ray instrumentation as well as advances in data reduction and modeling software are making total scattering analysis more accessible and add an invaluable characterization tool for complex materials. Recent developments as well as a cross section of recent applications of this technique will be discussed.

## 3:50 PM

**X-Ray Diffraction Investigation of Ferroelectric Constitutive Behavior at Multiple Length Scales:** Goknur Tutuncu<sup>1</sup>; Mesut Varlioglu<sup>1</sup>; Ulrich Lienert<sup>2</sup>; Ersan Ustundag<sup>1</sup>; <sup>1</sup>Iowa State University; <sup>2</sup>Argonne National Laboratory

The complex response of ferroelectrics to electromechanical loading requires rigorous characterization of their internal stresses and texture at multiple length scales to fully appreciate their constitutive behavior. **MACROSCALE:** Lattice strain and domain switching (texture) in polycrystalline BaTiO<sub>3</sub> under electric field and/or mechanical loading were measured along multiple directions simultaneously. It was seen the lattice strain data are highly anisotropic resulting in large differences between hkl-specific strains. In addition, texture analysis suggests non-180° domain switching is tightly coupled with lattice strain evolution. **MESOSCALE:** The 3D-XRD X-ray diffraction technique was employed to probe the constitutive behavior of individual grains of polycrystalline BaTiO<sub>3</sub> under electric field. In addition, domain variants of those grains were identified and their evolution was monitored as a function of applied

field and temperature. 3-D XRD data correlate well with the macroscale results, but also yield valuable information about local variations at the mesoscale.

## 4:05 PM

**Imaging Strains on the Nanoscale with Coherent X-Ray Diffraction Microscopy:** Ross Harder<sup>1</sup>; Loren Beitra<sup>2</sup>; Steven Leake<sup>2</sup>; Marcus Newton<sup>3</sup>; Ian Robinson<sup>2</sup>; <sup>1</sup>Argonne National Lab; <sup>2</sup>University College London; <sup>3</sup>University of Surrey

Nanocrystals are being developed for a great range of applications. Strain on the nanometer scale within these structures has a great impact on their electronic properties. Coherent x-ray diffraction(CXD) microscopy done around the Bragg peaks of nanocrystalline samples have shown remarkable sensitivity to strain within the crystal structure. Recent improvements in CXD instrumentation at the Advanced Photon Source have allowed us to measure CXD patterns around multiple Bragg peaks of isolated nanocrystals of gold and zinc oxide. When each of these Bragg peaks is inverted to direct space the 3D image contains one projection of the distortion of the nanocrystal lattice within the crystal. These separate images have been combined into a fully three-dimensional image of the distortion field of the lattice of the nanocrystals. The full strain tensor of the material in 3D can then be visualized. Our imaging of the strain within nanocrystals will be discussed.

## 4:20 PM Break

## 4:30 PM Invited

**Geometry, Topology and Structure of Amorphous Solids:** Zbigniew Stachurski<sup>1</sup>; Richard Welberry<sup>1</sup>; <sup>1</sup>Australian National University

The understanding of the structure of solids began with the concept of translational symmetry, and has to a large degree come about because of the methods of X-ray crystallography. Frank and Kasper considered the topology of clusters of atoms instead of crystallographic unit cell. They distinguished three cases: (1) Coordination shell atoms make equilateral triangles with the centre. (2) Triangles in coordination shell are equilateral; shell atoms make isosceles triangles with the centre. (3) No requirements on the shape of the triangles within the shell. The third case provides a basis for development of a model of a completely random structure (ideal amorphous solid). A model of Zr-based metallic glass has been constructed and described. Debye x-ray scattering computations can reveal the presence of vacancies and other imperfections. Two new atomic mechanisms are identified as the fundamental means of compositional re-distribution in the alloy.

## 4:50 PM Invited

**In-Situ Neutron Diffraction Study of B2 CoTi and CoZr:** Rupalee Mulyal<sup>1</sup>; James Wollmershauser<sup>1</sup>; Sean Agnew<sup>1</sup>; <sup>1</sup>University of Virginia

Fully-ordered B2 intermetallic compounds, CoTi and CoZr, are examined by in-situ neutron diffraction during compression testing. The results reiterate that the primary slip systems in these materials are  $\langle 100 \rangle \{011\}$ , but also exposed a deformation mechanism transition that helps to explain the anomalous ductility of these compounds. Previous studies revealed kink banding, under some conditions. Preliminary cyclic tension tests carried out on these materials have shown that they exhibit a strong Bauschinger effect, and recent publications in the literature have emphasized a possible connection between “incipient kink banding” and such strong Bauschinger effects. However, preliminary polycrystal plasticity modeling predicts a similarly strong Bauschinger effect in CoZr without the incorporation of a kink banding mechanism, rather intergranular stresses create the effect. Cyclic in-situ neutron diffraction and electron back-scattered diffraction studies of CoTi and CoZr are being used to determine the role of kink banding in the deformation of these materials.

## 5:10 PM

**Influence of Calcium and Strontium Substitution on the Expansion Behaviors and Oxygen Vacancy Concentration of the Lanthanum Ferrite:** David Thomsen<sup>1</sup>; Patrick Price<sup>1</sup>; Ellen Rabenberg<sup>1</sup>; Darryl Butt<sup>1</sup>; <sup>1</sup>Boise State University

X-ray diffraction (XRD) was used to investigate the lattice expansion behavior of La<sub>x</sub>Ca<sub>1-x</sub>FeO<sub>3-d</sub> and La<sub>x</sub>Sr<sub>1-x</sub>FeO<sub>3-d</sub> which are mixed ion conductor. La<sub>x</sub>Ca<sub>1-x</sub>FeO<sub>3-d</sub> and La<sub>x</sub>Sr<sub>1-x</sub>FeO<sub>3-d</sub> samples were made by solid state method from 0 = x = 1. The Bruker AXS D8 Discover high-resolution XRD was used to measure the lattice as a function of temperature. XRD has the ability to isolate the lattice parameter with negligible effect from changing vacancy concentration. By comparison, dilatometry measures bulk thermal expansion,



which includes the effects of vacancies. In theory, the vacancy concentration in the material can be determined from the difference between the two methods of measurement. Substitution of Ca<sup>2+</sup> can influence the thermal expansion both by creating oxygen vacancies and affecting local lattice distortions. Detailed expansion behavior of LaxCa1-xFe3-d and LaxSr1-xFeO3-d as a function of temperature and composition was developed by comparing data from dilatometry and XRD patterns.

### 5:20 PM

**Application of Small Angle Neutron Scattering to Study the Nucleation and Growth Mechanisms of Thin and Thick Films:** *Yong Choi*<sup>1</sup>; B. S. Seong<sup>2</sup>; E. J. Shin<sup>2</sup>; <sup>1</sup>Sunmoon University; <sup>2</sup>KAERI

Small angle neutron scattering was applied to non-destructively analyze microstructure of various thin and thick films for electronic and automobile industries and to study the nucleation and growth mechanisms of the electro-deposited films. Average thickness of nano-sized multi-layers of thin film device was non-destructively evaluated by SANS model. Eco-friendly trivalent chromium layers have nano-sized cracks about 40 nm in size, which decreased with decreasing plating current density and voltage. The micro-size crack with "Calabash shape" is formed by the interconnection of the several nano-sized cracks. A nucleation and growth model of the trivalent chromium layers under pulse current condition was proposed based on the microstructure observation and SANS results.

### 5:35 PM

**Non-Destructive Evaluation of Crack Size and Distribution of Eco-Friendly Trivalent Chromium Deposits for Automobile Industries by Small Angle Neutron Scattering:** *Yong Choi*<sup>1</sup>; Sik C. Kwon<sup>2</sup>; Eun J. Shin<sup>3</sup>; Baik S. Seong<sup>2</sup>; <sup>1</sup>Sunmoon University; <sup>2</sup>KIMS; <sup>3</sup>KAERI

Eco-friendly trivalent chromium layers was prepared in a modified chromium sulfate bath by various electroplating conditions to replace hexavalent hard chromium coating in industrial fields, which microstructure were analyzed by small angle neutron scattering (SANS) and electron microscopy, respectively. The deposit has columnar grains in which chromium clusters and inter-connected cracks existed. Most of nano-size crack in a grain has about 40 nm in size. The crack size was decreased with decreasing plating current density and voltage. The interconnected micro-size crack seems to be "Calabash shape" which is formed by the interconnection of several nano-size cracks. A nucleation and growth model for the pulse plated chromium layer will be proposed based on the SANS and microstructure observation.

### 5:50 PM

**EXAFS Measurements in Fe-Based Magnetostrictive Single Crystals:** *Gavin Garside*<sup>1</sup>; Shamita Shitole<sup>1</sup>; Sivaraman Guruswamy<sup>1</sup>; <sup>1</sup>University of Utah

Magnetostriction is sensitive to the inter-atomic spacing of the magnetic ion core in ferromagnetic materials. Measurements of local inter-atomic distances is of interest to gain an improved understanding of how solutes influence magnetostriction in alpha-Fe-based alloys. Extended x-ray absorption fine structure (EXAFS) measurements were made at the Advanced Photon Source at ANL on Fe-X (where X= Ga, W, and Mo) based single crystals of specific composition and thermal history, that show large magnetostriction. These measurements were made at the K-edges of Fe and the L-edges for W and Mo, to determine the Fe-X, Fe-Fe, and X-X atom distances and short range ordering pair correlations to help understand how Ga, W, and Mo additions modify the magnetostriction of Fe.

## Nuclear Energy: Processes and Policies: Characterization

*Sponsored by:* The Minerals, Metals and Materials Society, TMS Structural Materials Division, TMS/ASM: Nuclear Materials Committee, TMS: Public and Governmental Affairs Committee  
*Program Organizers:* Brajendra Mishra, Colorado School of Mines; Aladar Csontos, U.S. Nuclear Regulatory Commission; Stuart Maloy, Los Alamos National Laboratory; Jeremy Busby, Oak Ridge National Laboratory; Sue Lesica, U.S. Department of Energy's Office of Nuclear Energy

Wednesday PM Room: 201  
February 17, 2010 Location: Washington State Convention Center

*Session Chairs:* Todd Allen, Idaho National Laboratory; Aladar Csontos, US Nuclear Regulatory Commission

### 2:00 PM Keynote

**Characterization of Neutron- and Ion-Irradiated Nano-Structured Ferritic Alloys by TEM:** *James Bentley*<sup>1</sup>; David Hoelzer<sup>1</sup>; <sup>1</sup>Oak Ridge National Laboratory

Nano-structured ferritic alloys (NFA) have outstanding mechanical properties and the potential to be highly resistant to radiation damage through the presence of high concentrations (>10<sup>23</sup> m<sup>-3</sup>) of small (<5 nm) Ti-Y-O nanoclusters (NC). Energy-filtered transmission electron microscopy (EFTEM) is essential for reliable characterization of NC by TEM. Our continuing studies involve characterization of neutron-irradiated specimens, including 12YWT and MA957 irradiated in HFIR to 9 dpa at ~500°C, and in-situ ion irradiations of NFA, including 14YWT, to observe directly the effects of irradiation on individual NC. EFTEM characterization of 14YWT before and after ion irradiation at the Argonne National Laboratory IVEM-Tandem Facility will be supplemented by in-situ irradiation with concurrent EFTEM at the French JANNuS facility. Research supported by the Division of Materials Sciences and Engineering and the SHaRE User Facility of the Scientific User Facilities Division, Office of Basic Energy Sciences, U.S. Department of Energy.

### 2:35 PM

**A Multilab-Multitechnique SANS, APT and TEM Characterization Study of a Reference Nanostructured Ferritic Alloy:** *G. Robert Odette*<sup>1</sup>; Nicholas Cunningham<sup>1</sup>; Yuan Wu<sup>1</sup>; Erin Haney<sup>1</sup>; Emmanuelle Marquis<sup>1</sup>; Peter Hosemann<sup>1</sup>; Eric Stergar<sup>1</sup>; <sup>1</sup>UC Santa Barbara

Future energy systems require structural alloys with outstanding properties that are sustained during long-term service in ultra-severe environments. We are developing a new transformational class of nanostructured ferritic alloys (NFA) that show enormous promise for meeting these challenges. NFA are 12-14 Cr steels that are powder processed by dissolving Y and O by ball milling. These elements precipitate along with Ti during hot consolidation to form an ultra-high density of Y-Ti-O-enriched nano-features (NF), that produce very high strength, are remarkably stable, trap He in fine-scale bubbles and enhance vacancy-self interstitial atom recombination, suppressing severe radiation damage. However, the precise characters of various NF are not yet well understood; they appear to range from complex clusters with Y<sub>2</sub>Ti<sub>2</sub>O - Ti<sub>2</sub>O core-shell shells structures to near stoichiometric complex oxides. This presentation will update progress on a round robin characterization study of a reference NFA by SANS, APT and TEM.

### 3:00 PM

**Characterization of 14YWT As Atomized, Milled and Annealed Powders and Consolidated Alloys:** *Nicholas Cunningham*<sup>1</sup>; Yuan Wu<sup>1</sup>; G. Robert Odette<sup>1</sup>; Erin Haney<sup>1</sup>; <sup>1</sup>UC Santa Barbara

Fourteen Cr nano-dispersion strengthened ferritic alloys, that contain a high density of Y-Ti-O-enriched nano-features (NF), have high strength, are very stable and manifest remarkable radiation damage tolerance. A multi-technique characterization of 14Cr-0.2T-0.3Ti-low to 0.015O powders obtained from Crucible Research (as part of a collaborative study with LANL, ORNL, UC Berkeley and South Dakota School of Mines and Crucible Research) is described. Powders were characterized in the as-atomized, milled, annealed and consolidated conditions using EMPA, SANS, APT, TEM and microhardness methods. Special emphasis was on characterizing the distribution of Y after

# Technical Program

various processing steps and the distribution and character of NF after heat treatment and their relation to the alloy grain size distribution and strength. Inhomogeneous Y distributions in the as-atomized powders are homogenized by milling. Powder annealing and hot consolidation result in high concentrations of NF even in cases with bimodal grain size distributions.

**3:25 PM**

## **Development and Characterization of Radiation Tolerant Nanostructured Ferritic Steels:** *Michael Miller*<sup>1</sup>; David Hoelzer<sup>1</sup>; Kaye Russell<sup>1</sup>; <sup>1</sup>ORNL

The development of advanced materials for future generation power systems requires experimental microstructural characterization of candidate materials to ensure that the microstructure, and hence the properties, remain stable during exposure to high doses of irradiation at elevated temperatures. The atomic level quantification of the microstructural features provided by atom probe tomography enables a fundamental understanding of the nanostructured ferritic steels to be established and provides the necessary scientific background for future regulatory guidelines. The unique stability of 2-4-nm-diameter Ti-O-Y nanoclusters in nanostructured ferritic steels that were exposed to high doses of neutron and ion irradiations will be discussed. This research was sponsored by the Division of Materials Sciences and Engineering and the SHaRE User Facility of the Scientific User Facilities Division in the Office of Basic Energy Sciences, U.S. Department of Energy.

**3:50 PM Break**

**4:05 PM**

## **Characterization of Nano-Scale Particles in Mechanically Alloyed and HIP-ed Oxide Dispersion Strengthened Steels:** *Dhriti Bhattacharyya*<sup>1</sup>; Patricia Dickerson<sup>1</sup>; Peter Hosemann<sup>1</sup>; G. Odette<sup>2</sup>; Michael Nastasi<sup>1</sup>; Amit Misra<sup>1</sup>; Stuart Maloy<sup>1</sup>; <sup>1</sup>Los Alamos National Laboratory; <sup>2</sup>University of California, Santa Barbara

Oxide Dispersion Strengthened (ODS) ferritic steels with a high density of nano-features, also known as Nano-structured Ferritic Alloys (NFAs) have excellent potential to withstand high doses of radiation when used in advanced fission and fusion reactors. The nano-features thought to be responsible for the exceptional radiation damage tolerance in these steels are complex oxides of Y and Ti, the detailed structure and chemistry of which are not fully understood. Two such ODS alloys are: a commercially produced mechanically alloyed steel MA-957 (produced by Special Metals), and a recently developed alloy, U14YWT, which, for this heat, is processed by Hot Isostatic Pressing (HIP). In this work, the authors examine the morphology, crystal structure and chemistry of various kinds of nano-scale oxide particles existing in these alloys and their orientation relationship with the BCC iron matrix using conventional and high-resolution Transmission Electron Microscopy (TEM) and Energy Dispersive X-Ray Spectroscopy (EDX).

**4:30 PM**

## **TEM Characterization of a Monolithic U-Mo Plate-Type Nuclear Fuel:** *Dennis Keiser*<sup>1</sup>; JanFong Jue<sup>1</sup>; Bo Yao<sup>2</sup>; Emmanuel Perez<sup>2</sup>; Yongho Sohn<sup>2</sup>; <sup>1</sup>Idaho National Laboratory; <sup>2</sup>University of Central Florida

The Reduced Enrichment for Research and Test Reactors (RERTR) program is developing low-enriched U-Mo alloy fuels for application in research and test reactors. One type of fuel is a monolithic plate-type fuel where a U-Mo foil is co-rolled with Zr and then encased in 6061 Al cladding. The starting microstructure of the fuel plate after fabrication will impact the performance of the plate in reactor. As a result, a TEM investigation has been performed on as-fabricated fuel plates to determine the phases that developed at the U-Mo/Zr and Zr/6061 Al cladding interfaces during the hot isostatic pressing (HIP) fabrication process. This talk will describe the types of phases that were identified and how these phases can impact the performance of the fuel plate during irradiation. Some actual images of irradiated fuel plates will be presented to demonstrate how different phases behaved during irradiation.

**4:55 PM**

## **Weldability Characteristics of Oxide Dispersion Strengthened Alloys: An Overview:** *Kalyan Chitrada*<sup>1</sup>; Ramprasad Prabhakaran<sup>2</sup>; Jiye Wang<sup>3</sup>; Larry Zirker<sup>2</sup>; Mitchell Meyer<sup>2</sup>; James Cole<sup>2</sup>; Korukonda Murty<sup>4</sup>; Rajiv Mishra<sup>3</sup>; Darryl Butt<sup>5</sup>; Megan Frary<sup>5</sup>; Indrajit Charit<sup>1</sup>; <sup>1</sup>University of Idaho; <sup>2</sup>Idaho National Laboratory; <sup>3</sup>Missouri University of Science and Technology; <sup>4</sup>North Carolina State University; <sup>5</sup>Boise State University

Oxide dispersion strengthened (ODS) alloys are considered an important class of structural materials for various high temperature applications including

advanced nuclear reactors. Conventional fusion welding methods lead to high porosity and agglomerated oxide particles in these alloys deteriorating critical properties of the joint. That is why solid state joining techniques are touted as the potential remedy for the welding issues encountered in these alloys. Research activities in an ongoing research program supported by the DOE (grant # DE-FG07-08ID14925) are highlighted. In this program, friction stir welding and pressure resistance welding have been used to successfully weld various ODS alloys, such as MA956, MA957 and MA754. Microstructural characteristics of the welded alloys are studied using a host of microscopy techniques. Mechanical properties are evaluated using microhardness, miniaturized tensile and shear punch test techniques. Appropriate microstructure-property correlations are developed. An overview of the state-of-the-art based on the published literature is also presented.

**5:20 PM**

## **Multi-Scale Characterizations and Formation Mechanism in an ODS Steel Elaborated by Reactive Ball-Milling and Annealing:** *Mathilde Brocq*<sup>1</sup>; Fabrice Legendre<sup>1</sup>; Bertrand Radiguet<sup>2</sup>; Marie-Hélène Mathon<sup>3</sup>; Fabien Cuvilly<sup>2</sup>; Philippe Pareige<sup>2</sup>; <sup>1</sup>SRMP - CEA; <sup>2</sup>GPM-Université de Rouen; <sup>3</sup>LLB

Oxide dispersion strengthened (ODS) steels are promising structural materials for future nuclear reactors. Indeed they exhibit excellent creep and radiation resistance thanks to a dispersion of complex nanometric oxides. We proposed a new processing route based on reactive ball milling of iron oxide (Fe<sub>2</sub>O<sub>3</sub>), yttria intermetallic (YFe<sub>3</sub>) and iron based alloy. A multiscale characterization including Atom Probe Tomography (APT) and Small Angle Neutron Scattering (SANS) was performed. In as-milled material, Y, Ti and O enriched nanoclusters were observed. From 400°C up to 800°C annealing, the nanocluster density increases while their size remains unchanged. In those synthesis conditions, a new formation mechanism is highlighted. Indeed not only nanocluster nucleation starts during ball-milling but also their number greatly increases thanks to brief and low-temperature annealings. This is not a usual dissolution-precipitation mechanism lead by thermodynamic. As a conclusion another mechanism based on ball-milling property of creating metastable state will be proposed.

## **Pb-Free Solders and Emerging Interconnect and Packaging Technologies: Microstructure, Intermetallics, Whisker(I)**

*Sponsored by:* The Minerals, Metals and Materials Society, TMS Electronic, Magnetic, and Photonic Materials Division, TMS: Electronic Packaging and Interconnection Materials Committee  
*Program Organizers:* Kwang-Lung Lin, National Cheng Kung University; Sung Kang, IBM; Jenq-Gong Duh, National Tsing-Hua University; Laura Turbini, Research In Motion; Iver Anderson, Iowa State University; Fu Guo, Beijing University of Technology; Thomas Bieler, Michigan State University; Andre Lee, Michigan State University; Rajen Sidhu, Intel Corporation

Wednesday PM Room: 204  
February 17, 2010 Location: Washington State Convention Center

*Session Chairs:* John W. Morris, University of California-Berkeley; Andre Lee, Michigan State University

**2:00 PM**

## **A Quantitative Assessment of Microstructural Coarsening of SnAgCu Solders: Effect of Metallization and Thermo-Mechanical History:** *Praveen Kumar*<sup>1</sup>; Zhe Huang<sup>1</sup>; Indranath Dutta<sup>1</sup>; Ganesh Subbarayan<sup>2</sup>; Vikas Gupta<sup>3</sup>; <sup>1</sup>WSU; <sup>2</sup>Purdue University; <sup>3</sup>Texas Instruments

Microstructural coarsening in small Sn-3.8%Ag-0.7%Cu joints attached to Ni bond-pads and bulk solder samples, subjected to various thermo-mechanical histories, was quantitatively characterized. The Ag<sub>3</sub>Sn precipitates coarsened significantly faster in smaller joints as compared to the bulk samples, and the coarsening was more rapid nearer the bond-pads than farther away. This accelerated aging was attributed to the depletion of Cu from the joint samples due to solution/reaction with Ni pads. In addition to precipitate coarsening, the volume fraction of the eutectic-microconstituent also increased due to aging, leading to an accelerated increase in the inter-particle spacing. Based on these observations, we define a thermo-mechanical history dependent effective diffusion distance, on which precipitate spacing within the eutectic depends



linearly. This proffers a single length parameter which may be used to describe in situ evolution of constitutive behavior due to precipitate coarsening during any thermo-mechanical history.

### 2:15 PM

#### **Interfacial Reactions of Sn<sub>3.0</sub>Ag<sub>0.5</sub>Cu Solder with Cu-Mn UBM during Aging:** *Chien-Fu Tseng*<sup>1</sup>; Jenq Gong Duh<sup>1</sup>; <sup>1</sup>National Tsing Hua University

Cu UBM has been widely used as surface finish in the flip chip technology. The major disadvantages of Cu UBM are fast consumption of copper, rapid growth of IMCs and formation of Kirkendall voids. Recently, minor element addition into Cu UBM has been observed to suppress the formation of Cu-Sn IMCs at the interface. In this study, different Mn content (1-20 at.%) were added into Cu UBM by sputtering technique. With higher Mn concentration in Cu-Mn UBM, a new phase, MnSn<sub>2</sub>, was formed between Cu<sub>6</sub>Sn<sub>5</sub> and Cu-Mn UBM. MnSn<sub>2</sub> may be a diffusion barrier to reduce the interfacial reaction and reduce the formation of Kirkendall voids. The detailed mechanism of the IMC formation will be probed and discussed.

### 2:30 PM

#### **Cross-Interaction between Ni and Cu across a High-Lead Solder Joint with Different Solder Volume:** *Chih-Chiang Chang*<sup>1</sup>; C. Robert Kao<sup>2</sup>; <sup>1</sup>National Taiwan University

In this study, the Ni/95Pb5Sn/Cu ternary diffusion couples were used to investigate the solder volume effect on the cross-interaction between Ni and Cu. Experimentally, a high-lead solder layer with thickness of 100 or 400 microns was electroplated over Cu foils. A pure Ni layer (20 microns) was then deposited over the as-deposited high-lead solder surface. The diffusion couples were aged at 150 to 250°C for different periods of time. With this technique, the diffusion couples were assembled without experiencing any high temperature process, such as reflow, which would have accelerated the interaction and caused difficulties in analysis. This study revealed that the massive spalling also occurred in aging state without reflow. The massive spalling started from the formation of the micro-voids. When the micro-void congregated, the intermetallics (Cu<sub>3</sub>Sn) started to spall from the interface. This spalling phenomenon will occur early due to higher aging temperature and smaller solder volume.

### 2:45 PM

#### **Current Stressing Effect on Intermetallic Compound Growth Kinetics in Cu Pillar/Sn Bump:** Myeong-Hyeok Jeong<sup>1</sup>; Jae-Won Kim<sup>1</sup>; Gi-Tae Lim<sup>1</sup>; Byoung-Joon Kim<sup>2</sup>; Kiwook Lee<sup>3</sup>; Jaedong Kim<sup>3</sup>; Young-Chang Joo<sup>2</sup>; *Young-Bae Park*<sup>1</sup>; <sup>1</sup>Andong National University; <sup>2</sup>Seoul National University; <sup>3</sup>Amkor Technology Korea Inc

Cu pillar bump makes large amount of intermetallic compound and Kirkendall void between Cu pillar and solder which can degrade electrical and mechanical reliability. Therefore, it is essential to understand the fundamental growth mechanisms of intermetallic compound and Kirkendall void. In this work, we performed kinetic studies on the Cu pillar/Sn bump structure in order to quantify the amount of intermetallic compound and Kirkendall void by using in-situ annealing and electromigration test in a scanning electron microscope chamber during current stressing conditions with current density of 3.5~7.2x10<sup>4</sup> A/cm<sup>2</sup> at 120~180°. The activation energy values for the growth of Cu<sub>6</sub>Sn<sub>5</sub>, Cu<sub>3</sub>Sn, and total (Cu<sub>6</sub>Sn<sub>5</sub>+Cu<sub>3</sub>Sn) IMC were found to be 0.16, 0.56 and 0.48 eV/atom, respectively. Current density exponent for transition time of IMC during current stressing was estimated to be 2.2. And also, their effects on the electrical reliability of Cu pillar bump during current stressing will be discussed in detail.

### 3:00 PM

#### **Formation and Growth of Intermetallic Compound (Cu<sub>6</sub>Sn<sub>5</sub>) at Early Stages in Lead-Free Soldering:** *Min Soo Park*<sup>1</sup>; Raymundo Arroyave<sup>1</sup>; <sup>1</sup>Texas A&M University

Phase field simulations of Intermetallic compound (IMC) formation and growth during early stages will be performed, considering the interactions between liquid Sn-based solder and copper substrate. The liquid Sn-based solder (L phase) and the copper substrate ( $\alpha$  phase) are considered to be under metastable conditions that eventually lead to the nucleation of Cu<sub>6</sub>Sn<sub>5</sub> IMC ( $\eta$  phase) at the interface between the two substances. The nucleation events are determined by using a classical nucleation theory represented probabilistically through Poisson distribution function. The driving force can be calculated from the Gibb's energies through the CALPHAD approach. Phase field simulations

for nucleation phenomenon at the early stages will be prepared with variation of phases' according to temperatures and L/ $\eta$  interface energies to numerically investigate the possible soldering reactions at the early stages compared with previous works, showing the decomposition of the substrate and the formation and growth (or coalescence) of IMC grains.

### 3:15 PM

#### **Local Mechanical Properties of Cu<sub>6</sub>Sn<sub>5</sub> Intermetallics in Pb-Free Solder Joints by Microcompression Testing of Pillars:** *Ling Jiang*<sup>1</sup>; Nik Chawla<sup>1</sup>; <sup>1</sup>Arizona State University, School of Mechanical, Aerospace, Chemical, and Materials Engineering

A methodology for performing uniaxial compression tests on Cu<sub>6</sub>Sn<sub>5</sub> intermetallics in Pb-free solder joints was used to probe mechanical properties of Cu<sub>6</sub>Sn<sub>5</sub> intermetallics. Focused Ion beam (FIB) was employed to mill Cu<sub>6</sub>Sn<sub>5</sub> pillars in various nodules grown between Sn-rich solder and a Cu substrate. The pillars were tested using a nanoindenter with a flat tip in compression, to determine the stress-strain behavior of the Cu<sub>6</sub>Sn<sub>5</sub> pillars. Young's modulus of Cu<sub>6</sub>Sn<sub>5</sub> intermetallics obtained in uniaxial compression testing was compared with that obtained by nanoindentation. The effect of aspect ratio and taper of pillars on mechanical properties will be discussed. The crystallographic orientation of pillars was examined using electron back-scattered diffraction. The relationship between orientation and mechanical properties of pillars will be discussed.

### 3:30 PM Break

### 3:45 PM

#### **Effects of Minor Ni Doping on Interfacial Reaction and Microstructure Variation in the Cu/Sn-3Ag-0.5Cu-xNi/Au/Ni Sandwich Structure:** *Chi-Yang Yu*<sup>1</sup>; Jenq-Gong Duh<sup>1</sup>; Tae-Kyu Lee<sup>2</sup>; Michael Tsai<sup>2</sup>; Kuo-Chuan Liu<sup>2</sup>; <sup>1</sup>National Tsing Hua University; <sup>2</sup>CISCO

Cu/Sn-3Ag-0.5Cu-xNi/Au/Ni (x= 0, 0.01, 0.05 and 0.1 wt.%) after reflow were aged at 100 oC and 150 oC, respectively, for 500 h. In the consideration of interfacial reaction, the local Ni concentration would affect the formation of intermetallic compounds (IMCs), i.e. (Cu,Ni)<sub>6</sub>Sn<sub>5</sub> and (Ni,Cu)<sub>3</sub>Sn<sub>4</sub>. The behavior of Ni migration before and after aging at different temperature was investigated with the aid of field emission electron probe microanalyzer (FE-EPMA). It was revealed that the morphology and growth rate of IMCs at both Cu and Au/Ni sides were rather different. During the heat treatment, cross-interaction was attributed to the Cu and Ni diffusion from one side to the other side between Cu and Au/Ni substrates. The variation in elemental distribution would cause microstructure evolution in these solder matrixes. In this study, the effects of minor Ni doping on interfacial reaction and microstructure variation in the solid state reaction will be reported.

### 4:00 PM

#### **Mechanical Properties of Interfacial IMCs in Solder Joints Evaluated by Nanoindentation:** *Y.L. Shen*<sup>1</sup>; C. W. Su<sup>2</sup>; J. M. Song<sup>2</sup>; S. Y. Chen<sup>1</sup>; <sup>1</sup>National Taiwan University of Science and Technology; <sup>2</sup>National Dong Hwa University

This study reports the mechanical properties of the intermetallic compounds (IMCs) formed at the interfaces between Sn-Ag-Cu, Sn-Zn solders and the commonly used electronic substrates using nanoindentation. The hardness (H), elastic modulus (E), yield strength (Y) and work hardening exponent (n) were estimated. In view of the reliability under the conditions of drop or creep, strain rate sensitivity (m) and creep stress exponent (CSE) of the interfacial IMCs were also evaluated. Results showed that soft Ag and Au based IMCs exhibited a greater degree of strain rate hardening compared to hard Cu and Ni based IMCs. With respect to creep properties, it could be concluded that the CSE value was in agreement with the work hardening exponent (n) rather than melting temperature or crystal structure. This implies that IMCs with greater dislocation slip resistance exhibited better ability against creep.

### 4:15 PM

#### **Kinetics of Intermetallic Compound Formation at the Interface between Sn-3.0Ag-0.5Cu Solder and Cu-Zn Alloy Substrate:** *Youngmin Kim*<sup>1</sup>; Hee-Ra Roh<sup>1</sup>; Young-Ho Kim<sup>1</sup>; <sup>1</sup>Hanyang University

The interfacial reaction and intermetallic compound (IMC) growth during aging at the Sn-3.5Ag-0.5Cu (SAC)/Cu-Zn interface were investigated. By dipping Cu or Cu-10Zn wires into the molten solder at 260°, the scallop-shaped Cu<sub>6</sub>Sn<sub>5</sub> formed. Then, specimens were aged subsequently at 120°, 150°,

# Technical Program

and 180° up to 2000 h. The typical bi-layer of  $\text{Cu}_6\text{Sn}_5$  and  $\text{Cu}_3\text{Sn}$  formed and numerous microvoids were found at the SAC/Cu interfaces, while no  $\text{Cu}_3\text{Sn}$  and microvoids were observed at the SAC/Cu-Zn interfaces after aging. IMC growth was remarkably depressed on Cu-Zn substrates and this effect was more prominent at higher aging temperature. The parabolic behavior of IMC thickness versus aging time shows the IMC growth is controlled by diffusion. The activation energy for the IMC growth of SAC/Cu-Zn specimens was larger than that of SAC/Cu specimens. This research was supported by the Component Material Technology Development Program of the Ministry of Commerce, Industry, and Energy (MOCIE).

## 4:30 PM

**Sn Whiskers and Grain Boundary Sliding:** *John Osenbach*<sup>1</sup>; <sup>1</sup>LSI Corporation

Grain boundary sliding has been proposed as one possible mechanism for whisker nucleation and growth. Experimental results are presented indicating grain boundary sliding prevents whisker growth rather than promoting whisker growth. It will be shown that these results are consistent with the predictions of a multi-mechanism creep/whisker theory.

## 4:45 PM

**Critical Current Density of Inhibiting the  $(\text{Cu,Ni})_6\text{Sn}_5$  Formation in the Ni-Side of Cu/Solder/Ni Joints:** W.H. Wu<sup>1</sup>; H.L. Chung<sup>1</sup>; C.N. Chen<sup>1</sup>; *Cheng-En Ho*<sup>1</sup>; <sup>1</sup>Yuan Ze University

The Cu/solder/Ni sandwich structure is one of the most common joint configurations used to electrically connect chips to the next packaging level. During joints operation, the Cu can diffuse across the entire solder region and nucleates as an undesired  $(\text{Cu,Ni})_6\text{Sn}_5$  layer over the Ni-side of Cu/solder/Ni. The driving force for this cross-interaction process is known to be the chemical potential gradient. To counterbalance the chemical force-induced Cu flux, an opposite current stressing with various current densities ( $0 - 2 \times 10^4 \text{ A/cm}^2$ ) was examined using a Cu/Sn(50 microns thick)/Ni structure at a fixed specimen temperature, 150 Celsius. Research results clearly indicated the growth of  $(\text{Cu,Ni})_6\text{Sn}_5$  cannot be retarded until a current stressing of near  $10^4 \text{ A/cm}^2$  is applied. This suggests that the critical current density of inhibiting the  $(\text{Cu,Ni})_6\text{Sn}_5$  formation is approximately  $10^4 \text{ A/cm}^2$ . The strong correlation between the  $(\text{Cu,Ni})_6\text{Sn}_5$  growth and current densities will be presented in this study.

## 5:00 PM

**Interfacial Reactions between near Eutectic SnAgCu Solder Alloys and Electrolytic Au/Ni Substrates:** *Mao Gao*<sup>1</sup>; Eric Cotts<sup>1</sup>; <sup>1</sup>Binghamton University

Interfacial reactions during reflow between near eutectic SnAgCu solder and Au/Ni substrates profoundly affect final solder joint microstructure. Reaction products and morphologies are affected not only by time and temperature of anneals, but by small changes in the concentration of the noble metals in the solder. Such dependencies were examined for a range of conditions using differential scanning calorimetry to impose a precise thermal history upon the samples. Quantitative relationships between the growth kinetics of both  $(\text{Cu,Ni,Au})_6\text{Sn}_5$  and  $(\text{Ni,Cu})_3\text{Sn}_4$ , and the initial Cu supply (Cu concentration and solder volume), and the thermal conditions were examined. As previously observed, for high Cu concentrations,  $(\text{Cu,Ni,Au})_6\text{Sn}_5$  initially formed at the SnAgCu/Ni interface. When the Cu concentration in the solder decreased to 0.32% wt.,  $(\text{Ni,Cu})_3\text{Sn}_4$  was observed to form at the  $(\text{Cu,Ni,Au})_6\text{Sn}_5$  /Ni interface. Under certain conditions, the  $(\text{Cu,Ni,Au})_6\text{Sn}_5$  intermetallic layer or  $(\text{Ni,Cu})_3\text{Sn}_4$  was observed to spall at the interface.

## 5:15 PM

**Effect of Ag on the Kirkendall Void Formation in Sn-Ag/Cu Solder Joints:** *Sunghwan Kim*<sup>1</sup>; Jin Yu<sup>1</sup>; <sup>1</sup>KAIST

Sn-Ag solders with varying amount of Ag were reacted with Cu UBM which was electroplated using an additive containing S. After the reflow process, all specimens were isothermally aged at 150 C for varying times. Developments of Kirkendall voids at the joints were investigated using SEM, while variation of the surface chemistry of the joint interfaces were monitored using AES. It was shown that reduction of the Ag content below the eutectic composition allowed more S segregation at the  $\text{Cu}_3\text{Sn}/\text{Cu}$  interface, which is concomitant with larger fraction of Kirkendall voids at the interface. This is consistent with our recent analyses on the effect of sulphide forming element additions to Sn-3.5Ag solder on the Kirkendall void formation (Acta Mater. in press).

## Polymer Nanocomposites: Metals and Other Nanoparticles

*Sponsored by:* The Minerals, Metals and Materials Society  
*Program Organizer:* John Zhanhu Guo, Lamar University

Wednesday PM

Room: 309

February 17, 2010

Location: Washington State Convention Center

*Session Chairs:* Katie Weihong Zhong, Washington State University; Qiang Wang, Institute of Chemical and Engineering Sciences (ICES); Lu Sun, Praxair Electronics

## 2:00 PM Introductory Comments

### 2:05 PM Keynote

**Effect of Particle Size on the Strength of Nanocomposites:** *C. T. Sun*<sup>1</sup>; <sup>1</sup>Purdue University

The particle size effect on the mechanical properties of nanocomposites has not been convincingly established because the quality of particle dispersion in nanocomposites cannot be assured. Thus, it is difficult to decouple the effect of nanoparticle size and its dispersion on the mechanical properties of nanocomposites made from conventional processing methods. Moreover, particle dispersion is also affected adversely as the loading (weight/volume fraction) of nanoparticles increases. In this talk, the effect of particle size on the mechanical properties of polymeric nanocomposites is examined based on experimental results using a processing method to achieve uniform particle dispersion in an epoxy resin. MD simulation and fracture mechanics are used to aid the interpretation of the experimental results. The fracture toughness of the interfacial crack is evaluated experimentally using micron-sized particles and the size effect is then extrapolated to nanoparticles. The results indicate that debonding is unlikely a failure mode in nanocomposites.

### 2:45 PM

**Electrically Conductive Nanocomposites with Thermoplastic Polymers:** *Nathan Hansen*<sup>1</sup>; George Hansen<sup>1</sup>; Greg Sawyer<sup>2</sup>; <sup>1</sup>Conductive Composites Company; <sup>2</sup>University of Florida

Nickel Nanostrands are three dimensional nanostructures with a branching and interconnected geometry, forming a network of metallic nanoscale Faraday cages and three dimensionally percolated networks. As such, the electromagnetic shielding and electrical conductivity properties of polymer nanocomposites using these materials have outstanding properties. Nanostrands are easily dispersed in low viscosity mediums, such as paints and water. However, there have been challenges in dispersing these nanomaterials in highly viscous thermoplastic polymer systems. A novel method of dispersion using jet milled polymer powders allows micron diameter powders to be blended with nanostrand structures. These polymer powders can be dry mixed with nanostrands, or solvated and solution mixed. The resulting conductive powder blend can be used in any commercial thermoplastic polymer process, with composite bulk resistivities of 0.01-0.001 ohm-cm at 10 volume percent filler. Electrical, electromagnetic, percolative, and microanalytical results are presented.

### 3:05 PM

**Effects of Incorporation of Silica and Zirconia Nanoparticles on the Thermal and Thermomechanical Properties of Polymer Nanocomposites:** *Muhammad Sajjad*<sup>1</sup>; Thomas Koch<sup>1</sup>; Sabine Seidler<sup>1</sup>; <sup>1</sup>TU Wien

Hybrid materials of PMMA, Polystyrene & Epoxy consisting of Silica and Zirconia nanoparticles with loadings up to 10 % have been characterized by DSC, TGA, DMA and Nanoindentation techniques. Nanocomposites were prepared via in situ polymerization whereas the dispersibility of the particles in organic media was investigated by DLS, SAXS experiments and TEM. We were able to synthesize polymer systems filled with small particles (22 nm in size), aggregated at nanometer size only, and well dispersed large particles (66 nm in size). The properties of the resulting nanocomposites were generally superior to the pure polymer matrix. Composites with strong interface exhibit profound effect on the ultimate properties as clear from the results of high values of damping, glass transition temperature  $T_g$  and hardness modulus. The enhanced  $T_g$  values observed in the nanocomposites arise from these attractive polymer-nanoparticles interfacial interactions that reduce cooperative segmental



mobility. Composites with weak interface showed essentially no change in Tg and damping or even a decline with filler contents. This reduction is ascribed to the free surfaces at the non wetted interfaces of the matrix and nanoparticles that were not well dispersed. The prepared nanocomposite films exhibited somewhat high hardness, better transparency and good thermal stability. On the other hand, incorporation of the particles did not alter the thermal degradation behaviour of PMMA and Epoxy.

### 3:25 PM

**Electrical Resistance Investigation of Cotton Fabrics after Treating with Polyaniline Solution:** *Cem Gunesoglu*<sup>1</sup>; *Sinem Gunesoglu*<sup>1</sup>; *Suying Wei*<sup>2</sup>; *Zhanhu Guo*<sup>2</sup>; <sup>1</sup>Gaziantep University; <sup>2</sup>Lamar University

The emanating electromagnetic radiation has become serious concerns, not only for increased working quality of devices but also for health. Any protection by textiles needs certain electrical conductivity; however, traditional fibers used in the textile fabrics are electrically insulating materials with a negligible electromagnetic shielding performance. The widely accepted technique is to add conductive fillers into the textile fabrics to manufacture conductive woven or knitted fabrics. However, macrostructure will have large effect on constructional properties like thickness, weight and appearance. Highly conductive textile surface will need micron and nano conductive fillers considering the minimal changes of the fabric properties. This study investigates the usage conductive polymeric nanocomposites such as polypyrrole (PPy) and polyaniline (PANI) to increase the electrical conductivity of textile fabrics. The production and application of the nanocomposites are discussed, conductivity of treated fabrics is obtained by standard four-probe method and physicochemical property changes of the textile are evaluated.

### 3:45 PM Break

### 4:15 PM Invited

**Multifunctional Conductive Nanocomposites: Fabrication, Property Analysis and Applications:** *John Zhanhu Guo*<sup>1</sup>; *Di Zhang*<sup>1</sup>; *Pallavi Mavinakuli*<sup>1</sup>; *Jiahua Zhu*<sup>1</sup>; *Suying Wei*<sup>1</sup>; <sup>1</sup>Lamar University

Both carbon-based and conductive polymer-based conductive nanocomposites will be presented in the talk. The electric conductivity of these two systems is investigated from low temperature to room temperature. The electron transport phenomena will be presented. The magnetic properties of the magnetic nanocomposites are investigated and will be presented. The application for sensors is also presented in the talk.

### 4:40 PM Invited

**Magnetic Properties of Some Polyaniline-Based Magnetic Nano-Composites for EMI Applications:** *Jayanta Banerjee*<sup>1</sup>; *O Perales-Pérez*<sup>2</sup>; *J. Banerjee*<sup>1</sup>; <sup>1</sup>University of Puerto Rico at Mayaguez

Polyaniline(PANI)-based magnetic nano-composites, with Mn-Zn ferrite nano-particles as disperse phase, can be used for EMI shielding applications in electronic devices. In the present paper such PANI composites, having different PANI-Ferrite w/w ratios were prepared under suitable laboratory controlled conditions in order to avoid excessive dissolution of the ferrite and in favor of its dispersion in the polymeric matrix. A particular stoichiometry was chosen because of its highest magnetization value (55emu/g) and susceptibility of 3.645. Using Scherrer's formula the ferrite's average crystallite size was calculated as 10.6 nm. HRTEM, XRD and SQUID analyses confirmed the formation of magnetic nano-composites. The saturation magnetization in the nano-composites varied according to the PANI-Ferrite w/w ratio, without affecting the magnetic susceptibility of the ferrite.

### 5:05 PM

**Effect of Nanometer-Sized Titanium Dioxide on the Piezodielectric Effect of Carbon Fiber Sulphoaluminate Cement Composites:** *Cheng Xin*<sup>1</sup>; *Wang Shoude*<sup>1</sup>; <sup>1</sup>University of Jinan

Carbon fiber sulphoaluminate cement composites prepared by pressing. Its piezodielectric effects with or without nanometer-sized titanium dioxide under uniaxial and cyclic loads were investigated in this paper. The experiment results indicated that nanometer-sized titanium dioxide could improve the sensitivity and repeatability of the piezodielectric effect of carbon fiber sulphoaluminate cement composites. This was related to that nanometer-sized titanium dioxide improved the quantity of the polarization dipole in the carbon fiber sulphoaluminate cement composites.

### 5:25 PM

**Design, Synthesis, and Characterization of Polymer Matrix Nanophosphor Composite Scintillators:** *Meredith Barta*<sup>1</sup>; *Jason Nadler*<sup>1</sup>; *Zhitao Kang*<sup>1</sup>; <sup>1</sup>Georgia Institute of Technology

Polymer matrix nanophosphor composite scintillators are designed, fabricated and characterized for use in a gamma ray detection materials system. Polymer-matrix composite scintillators can be manufactured far more rapidly and easily in a much wider range of geometric configurations compared to conventional single crystals. The durability of these material systems also provides considerable advantages with respect to impact and environmental sensitivity. Recent results indicate that these scintillators can be fabricated using periodic arrays of high phosphor loading regions surrounded by light pipes. Additional results demonstrate the benefits of refractive index matching and near-UV transparency of the polymer matrix.

### 5:45 PM

**Nano-Moldable Polymer-Ceramic Composite:** *Isaac Finger*<sup>1</sup>; <sup>1</sup>University of Florida

Recent advancements in the creation of Group 5b aqueous sol-gels has brought about the discovery of a novel particle generation system incorporating Titanium and Silicon oxides. It has been found that the precipitation of this aqueous particle system with the introduction of a ketonated solvent results in the formation of a ceramic-organic hybrid material. After filtration this material has a temporary plasticity that makes it amenable to molding. We have shown that the molding of this material allows for the reliable reproduction of surface features on the scale of microns. It is shown that the micro-morphologies introduced in the molding process are maintained, with high fidelity, through the calcining and sintering process. Hypotheses on the reactivity and microstructure of the material are presented and possible applications of this material are considered.

### 6:05 PM Concluding Comments

## Processing Materials for Properties: Processing-Microstructure-Properties

*Sponsored by:* The Minerals, Metals and Materials Society, TMS Extraction and Processing Division

*Program Organizers:* Brajendra Mishra, Colorado School of Mines; Akio Fuwa, Waseda University; Paritid Bhandhubanyong, National Metal and Materials Technology Center

Wednesday PM Room: 617  
February 17, 2010 Location: Washington State Convention Center

*Session Chairs:* Ramana Reddy, The University of Alabama; John Moore, Colorado School of Mines

### 2:00 PM Keynote

**Materials Processing Augmentation in Hostile Environments for Hydrocarbon Recovery:** *Rashmi Bhavsar*<sup>1</sup>; *Indranil Roy*<sup>1</sup>; *Christian Wilkinson*<sup>1</sup>; <sup>1</sup>Schlumberger

The rising demand for energy combined with our depleting natural oil and gas reserves has led to oilfield operations being conducted in environments which were formerly considered too harsh. Consequently, there has been a constant demand for improved materials and processes to allow operation in these hostile conditions. Low alloys steels have limited corrosion resistance in CO2 environments and Stainless steels have limited resistance in chlorides, hence nickel based alloys are recommended. Embrittlement, the loss of ductility of a metal due to absorption of H2S or hydrogen, resulting in catastrophic failures, has posed a significant challenge to those designing microstructures capable of surviving such environments. In this presentation, technological advancements in materials from new superalloys, coatings and grain-refined nanocrystalline materials to survive extremes of temperature, pressure and corrosive fluids in the oil and gas industry are highlighted. Surface modifications to refine surface morphology to increase corrosion resistance are also discussed.

# Technical Program

2:30 PM

**Computational and Experimental Investigation into the Oxidation Behavior of HVOF-Sprayed Cryomilled NiCrAlY Bond Coats:** *Kaka Ma<sup>1</sup>; Jianrong Song<sup>2</sup>; Lianmeng Zhang<sup>2</sup>; Julie Schoenung<sup>1</sup>; <sup>1</sup>University of California, Davis; <sup>2</sup>Wuhan University of Technology*

Thermal barrier coating systems (TBCs) have been commonly applied to protect turbine blades against high-temperature corrosion and oxidation. The morphology and the composition of the thermally grown oxide (TGO) layer are known to be crucial to the performance of TBCs. Our previous work has demonstrated that cryomilled NiCrAlY coatings exhibit better oxidation behavior than conventional equivalents. After oxidation, the formation of a uniform alumina layer without the presence of other mixed oxide phases was observed on the surface of the cryomilled coating while the conventional coating exhibited a discontinuous alumina layer as well as mixed oxides consisting of NiO and Ni(Cr,Al)2O4 spinels. In this paper, further investigation into the TGO growth in the HVOF-sprayed conventional/cryomilled NiCrAlY coatings is presented, with a focus on microstructural characterization of both the bond coat and TGO after select heat treatment conditions. The oxidation mechanism is discussed from the thermodynamic perspective using Thermo-calc® modeling.

2:50 PM

**High Thermal Gradient Directional Solidification and Its Application in the Processing of Nickel-Based Superalloys:** *Lin Liu<sup>1</sup>; <sup>1</sup>Northwestern Polytechnical University*

During directional solidification, thermal gradients in front of the liquid-solid interface (G) are important in defining the subsequent cooling rate and the solidification microstructure. An elevated G is frequently demanded, especially in the production of single-crystal superalloys and most metallic materials. In this study, the heat transfer during directional solidification by Bridgman-type directional solidification has been analyzed and a relationship has been established that reflects the effect of alloy properties, process parameters and equipment characteristics on thermal gradients. Based on this relationship, some methods for obtaining high thermal gradients have been developed. By using zone-intensified overheating and liquid-metal cooling, high thermal gradients of up to 800 K/cm were achieved. Application of these methods in the processing of single crystal superalloys indicated that high thermal gradient directional solidification produced more uniform microstructures, less microsegregation and optimized mechanical properties.

3:10 PM Keynote

**In Search of Rapid Processing Routes for CIGS Photovoltaic Absorber Materials:** *Carelyn Campbell<sup>1</sup>; <sup>1</sup>National Institute of Standards and Technology*

Rapid processing of the  $\alpha$ -Cu(In,Ga)Se<sub>2</sub> (CIGS) photovoltaic absorber material is critical for making these solar materials cost-effective. The current processing times must be reduced to less than 2 minutes, while maintaining optimum material properties. Exploration of novel processing routes within this complex system requires combining CALPHAD-based thermodynamic and diffusion mobilities descriptions. Using these multicomponent descriptions enables prediction of reaction pathways for prospective processing sequences. Preliminary thermodynamic and diffusion mobility descriptions for the Cu-In-Ga-Se system will be presented. The diffusion mobility descriptions are derived from both measured unary, binary and ternary tracer, intrinsic and chemical diffusion data and experimentally derived activation energies. The diffusion mobility descriptions are then used to simulate a wide range of model reactions. These simulations provide some insights into potential processing routes with significantly lower processing times.

3:30 PM

**Microstructure and Properties of New Wear Resistant Steel with High Strength and High Toughness:** *Li Hongbin<sup>1</sup>; <sup>1</sup>Baosteel*

A multi-element wear-resistant low-alloy steel with high strength and high toughness was developed. Microstructure, hardness, tensile properties and impact properties were carried out in order to establish a correlation amongst the parameters and to optimize the microstructural features and mechanical properties for superior wear performance. The results show that the optimal microstructure and mechanical properties were got when quenching at 880~910° and tempering at 160~260°. Fine martensite can be obtained, and the hardness is above 500HB, the tensile strength is above 1700MPa, the yield strength is above 1350MPa, the elongation is above 12%, and the impact energy is about

50J. The results obtained have been supplemented through the characteristics of the worn surfaces, subsurface regions, debris and fractured surfaces. These analyses also helped to understand the operative mechanisms of material removal and failure.

3:50 PM

**Enhanced Electrical and Mechanical Properties of the Heat-Treated Cu-Ni-(Si, Ti) Alloys:** *Kwangjun Euh<sup>1</sup>; Seung Zeon Han<sup>1</sup>; Sangshik Kim<sup>2</sup>; Sung Hwan Lim<sup>3</sup>; <sup>1</sup>Korea Institute of Materials Science; <sup>2</sup>Gyeongsang National University; <sup>3</sup>Kangwon National University*

Cu-Ni-Si alloys are extensively used as leadframe and connector materials in the electronic devices due to their high strength. However, the electrical conductivity of Cu-Ni-Si alloy is relatively lower than those of other leadframe alloys such as Cu-Fe-P alloys. In order to increase electrical conductivity of Cu-Ni-Si alloy without deterioration of strength, thermomechanical treatment such as rolling and heat treatment can be one of promising candidate process methods. In this study, small amount of Ti was added to promote precipitation of Ni-Si compounds and heat-treated at the various temperature and time. Electrical and mechanical properties simultaneously increased at the early stage of aging. The microstructures and properties of the aged specimens were comparatively analyzed in order to understand the effect of aging process on the property enhancement of the Cu-Ni-(Si, Ti) Alloys.

4:10 PM

**Preparation and Mechanical Properties of Nanostructured Cryomilled NiCrAlY Alloy Fabricated by Spark Plasma Sintering:** *Jianrong Song<sup>1</sup>; Kaka Ma<sup>2</sup>; Lianmeng Zhang<sup>3</sup>; Julie Schoenung<sup>2</sup>; <sup>1</sup>University of California - Davis and Wuhan University of Technology, China; <sup>2</sup>University of California - Davis; <sup>3</sup>Wuhan University of Technology, China*

NiCrAlY coatings are widely used on turbine blades and vanes for protection against high temperature oxidation and corrosion. Nanostructured cryomilled NiCrAlY powder was consolidated by spark plasma sintering (SPS) to provide bulk samples for in-depth characterization without the microstructural complexities that are generated in thermal sprayed coatings. Heat treatment at select times and temperatures was also carried out. Through microhardness testing, Scanning Electron Microscopy (SEM) and Energy-Dispersive X-ray analysis (EDX), the mechanical properties, microstructure and phase composition of the samples were investigated. The results indicated that there was a strengthening effect in the cryomilled alloy, compared to conventional alloy, because of refinement in the microstructure and the presence of nanostructural features. After heat treatment, the microhardness of the samples decreased, due to changes in the microstructure and phase transformation.

4:30 PM

**Thermal History and Mechanical Behavior of PH13-8Mo Fabricated via LENS®:** *Jonathan Nguyen<sup>1</sup>; Baolong Zheng<sup>1</sup>; Yuhong Xiong<sup>1</sup>; William Hofmeister<sup>2</sup>; John Smugeresky<sup>3</sup>; Yizhang Zhou<sup>1</sup>; Enrique Lavernia<sup>1</sup>; <sup>1</sup>University of California, Davis; <sup>2</sup>University of Tennessee Space Institute; <sup>3</sup>Sandia National Laboratories*

Laser Engineered Net-shaping (LENS®) is a layer additive manufacturing process of near net shape metallic components from computer aided design (CAD) files. Consequently, numerous reheat cycles of previously deposited material are involved which contribute to the microstructural evolution and significantly affect mechanical behavior of LENS® deposited components. Thermocouples and high speed infrared thermal imaging were used to provide insight into the influence of the overall thermal history and molten pool temperature on the resulting microstructure. SEM, TEM, and OM were used to study microstructural changes under various processing conditions. Tensile and microhardness tests were carried out to evaluate the mechanical behavior of LENS® deposited PH13-8Mo. Overall thermal history and molten pool temperatures and their effects on microstructural evolution and resulting mechanical behavior were investigated to better understand the relationships among process parameters, microstructure, and mechanical behavior of LENS® deposited PH13-8Mo components.

4:50 PM

**Transformation Induced Plasticity in Fe-Cr-V-C:** *Uta Kuehn<sup>1</sup>; Jan Romberg<sup>1</sup>; Norbert Mattern<sup>1</sup>; Juergen Eckert<sup>1</sup>; <sup>1</sup>IFW*

On the basis of the Fe84.3Cr4.6Cr4.3Mo4.6V2.2 high speed tool steel, manufactured under relatively high cooling rates and highly pure conditions, a further improvement of the mechanical characteristics by slight modification of



the alloy composition was attempted. For this, the alloy Fe88.9Cr4.3V2.2C4.6 was generated by elimination of Mo. By applying special preparation conditions, a microstructure composed of martensite, retained austenite and a fine network of special carbides was obtained already in the as-cast state. This material exhibits extremely high compression strength of over 5000 MPa combined with large compression strain of more than 25 % due to deformation-induced martensite formation. With this alloy a new class of TRIP assisted steels was found, which shows an extreme mechanical loading capacity.

### 5:10 PM

**Accounting for High Temperature Measurements with Changing Effective Emissivity in PTAW Processing:** *Tonya Wolfe*<sup>1</sup>; Hani Henein<sup>1</sup>; <sup>1</sup>University of Alberta

High temperature measurements of PTAW (plasma transferred arc welding) coatings deposited in-situ are required in order to optimize the process. There is wide interest in obtaining high temperature measurements for other high temperature processes using infrared thermography. However, the reliability of the quantitative data is often in question. Changes in emissivity with temperature, surface condition and phase change challenge the credibility of infrared results. In this paper, the methodology developed and applied to PTAW in order to generate reliable temperature measurements of the surface of the deposit upon cooling after the arc is extinguished, will be described. The methodology applies the coupled use of differential scanning calorimetry, laser reflectance pyrometry, infrared thermography and mathematical modeling.

### 5:30 PM

**The Role of Microtexture on Fatigue Lifetime Variability and Crack Initiation Mechanisms:** *Christopher Szczepanski*<sup>1</sup>; James Larsen<sup>2</sup>; Lee Semiatin<sup>2</sup>; <sup>1</sup>UTC/AFRL; <sup>2</sup>AFRL

Microtexture is known to affect the fatigue behavior of alpha + beta titanium alloys as numerous studies have cited microtextured regions as the fatigue crack initiation sites. To quantify the effect of microtexture on the fatigue behavior of alpha + beta titanium alloys, three different microstructural conditions of Ti-6Al-4V have been produced via distinct thermomechanical processing routes: a duplex microstructure containing microtexture, a beta annealed structure containing microtexture and a duplex microstructure free of microtexture. The impact of sample orientation on fatigue behavior was examined by testing specimens along three different orientations relative to the original plate reference frame; RD, TD, and 45° from the RD. The mechanism of fatigue crack initiation will be discussed with regard to microstructural condition (processing history) and sample orientation. Furthermore, the distributions of fatigue lifetimes will be characterized based on processing condition to determine if the presence of microtexture significantly impacts fatigue lifetime variability.

## Recycling General Sessions: Waste Utilization

*Sponsored by:* The Minerals, Metals and Materials Society, TMS Extraction and Processing Division, TMS Light Metals Division, TMS: Recycling and Environmental Technologies Committee  
*Program Organizer:* Joseph Pomykala, Argonne National Laboratory

Wednesday PM Room: 206  
February 17, 2010 Location: Washington State Convention Center

*Session Chair:* Jeffrey Spangenberg, Argonne National Laboratory

### 2:00 PM

**Analysis of Light Hydrocarbon Gases in the Pyrolysis and Combustion Processes of Waste Tires:** *Joner Alves*<sup>1</sup>; Chuanwei Zhuo<sup>2</sup>; Yiannis Leventidis<sup>2</sup>; Jorge Tenorio<sup>1</sup>; <sup>1</sup>University of Sao Paulo; <sup>2</sup>Northeastern University

The disposal of scrap tires has been a serious environmental problem. The treatment of this waste by pyrolysis and combustion has advantages as landfill releasing and a production of fuel. However, that processes needs a rigid control of emissions. This work presents a study of the light hydrocarbon gases (HC) generated during the burn of waste tire chips in a two-stage laminar-flow horizontal furnace. Different temperatures in the primary and secondary stage of the furnace were tested, was also varied the oxygen/nitrogen percentage during the combustion process. A Gas Chromatograph (Agilent 6890 Series GC-FID/TCD system) was used to separate and characterize the components of the gases

mixture. The results showed the behavior of the gases during the burn of tires, providing valuable information to the control of hydrocarbon emissions.

### 2:25 PM

**Utilization of Brazilian Waste Mica in Preparation of Pigments:** *Shirleny Santos*<sup>1</sup>; Silvia Cristina França<sup>2</sup>; Tsuneharu Ogasawara<sup>3</sup>; <sup>1</sup>COPPE/UFRJ/CETEM; <sup>2</sup>CETEM; <sup>3</sup>COPPE/UFRJ

Muscovite mica crystals lower than 15 mm diameter are discarded as "trash mica" in the mining area in Borborema-Seridó (BRAZIL). This work has the objective of ore dressing and purifying the "trash mica" aimed use it at preparation of pearlescent pigment. The muscovite was dry ground using knives mills and an ultrasound treatment. It was possible to achieve 67% of mica with particle size lower than 100 µm. This product was used in the preparation of brilliant pigments based on muscovite flakes covered with rare earths oxides (CeO<sub>2</sub>, PrO<sub>2</sub>, Ce<sub>0.95</sub>Pr<sub>0.05</sub>O<sub>2</sub>). The pigments were characterized by X-ray Diffraction, Thermal analysis and scanning electronic microscopy. The color of the resulting pigments was analyzed using the CIELAB method and it has showed the following colors: muscovite-CeO<sub>2</sub> – yellow, muscovite-PrO<sub>2</sub> – black and muscovite-Ce<sub>0.95</sub>Pr<sub>0.05</sub>O<sub>2</sub> – orange. Those results have shown that the "trash mica" is suitable for use in the preparation of pigments.

### 2:50 PM

**Effect of Processes in Degraded Decoloration of Frying Oil Treated with Brazilian Clays:** Elaine Araújo<sup>1</sup>; *Edcleide Maria Araújo*<sup>1</sup>; Marcus Vinicius Lia Fook<sup>1</sup>; Sara Verusca de Oliveira<sup>1</sup>; Divânia Ferreira Da Silva<sup>1</sup>; Dayanne Diniz De Souza<sup>1</sup>; <sup>1</sup>Federal University of Campina Grande-UFCG

The process of developing frying characteristics of odor, flavor, color and texture those make the food more attractive to the consumer. During this process, termooxidativas changes occur that alter the quality of oil. Three agents contribute to compromising the quality and modify the structure of frying oil subjected to different temperatures: the humidity, the oxygen and causes to oxidative modification. The oil when frying suffers oxidation process tends to darken, increase the viscosity, increase the formation of foams and develop undesirable flavor and aroma. The aim of this study, through the techniques of kinematic viscosity and acidity content of the effect of bleaching clays Brazilian oil for frying that went through different processes of degraded frying oil treated with Brazilian clays. The results showed that the oils subjected to higher temperatures rose a greater time to clear when compared with those submitted to low temperatures.

### 3:15 PM

**Reuse of Fired Red Ceramic Brick Waste:** *Carlos Mauricio Vieira*<sup>1</sup>; Sergio Monteiro<sup>1</sup>; <sup>1</sup>State University of the North Fluminense

In the county of Campos dos Goytacazes, north of the State of Rio de Janeiro, Brazil, there is a large production of red ceramic, mainly perforated bricks. A percentage of these bricks are damaged during the firing processing and become a red ceramic waste. This work investigates a possible solution to this environmental problem through the mixture of fired brick wastes, up to 20 wt.%, with clay bodies to produce red ceramics. Body samples were initially tested for plasticity by the Atterberg limits. Cylindrical pressed bodies were fired at temperatures varying from 500 to 1100°C. After firing, samples were then tested for linear shrinkage, water absorption and mechanical strength. The results showed that brick waste addition did not changed the workability of the clay and that up to 5 wt.% of waste no detrimental effect occurred on the fired properties at all temperatures.

### 3:40 PM

**Evaluating the Compressive Strength and Microstructure of Recycled Glass Compacts:** *Adele Garkida*<sup>1</sup>; Jiann-Yang Hwang<sup>2</sup>; Xiaodi Huang<sup>2</sup>; Bowen Li<sup>2</sup>; <sup>1</sup>Ahmadu Bello University; <sup>2</sup>Michigan Technological University

Compacts were made using the uniaxial press at 69 MPa from powders of waste drinking glass, fluorescent tubes, laboratory glass and window glass and 5% bentonite as binder. They were sintered at a temperature range of 600°C - 800°C with holding time of two hours. Sufficient fusion of the compacts was established at 700°C. The compressive strengths of these compacts were determined using Instron 4468 Testing Machine. The microstructures of the specimens were observed using a JEOL JSM 820 Scanning Electron Microscope (SEM). The results showed that there was no significant difference in strength among the four types of recycled glass compacts and the maximum compressive strength attained being 61MPa. However the nature of microstructures exhibited incomplete fusion of the glass particles as showed by the presence of pores

# Technical Program

with irregular shapes. These specimens have come very close to the maximum strength of 69 MPa attainable according to ASTM C 126.

## 4:05 PM Break

## 4:20 PM

**Preparation of Building Material Using Elemental Sulfur and Heavy-Metal Containing Slag:** Yanjie Liang<sup>1</sup>; Liyuan Chai<sup>1</sup>; Xiaobo Min<sup>1</sup>; Zhihui Yang<sup>1</sup>; Shaohui Yang<sup>1</sup>; Xi Cao<sup>1</sup>; <sup>1</sup>Central South University

Element sulfur and volatilization kiln slag (VKS) produced by smelter factories were used to produce sulfured building material. The effects of heating mode, material proportion (MS:MWQS), size of waste particles and ratio of aggregate to filler (A/F), on the mechanical properties and leaching toxicities of solidified stuff were investigated. The optimal conditions for the solidification are stepped heating mode, 3:7 ratio of MS to MWQS, particle size less than 150 $\mu$ m and 0.15 ratio of A/F. Under the above optimal conditions, the compressive strength of solidified stuff rises to 35 MPa, and water absorption is up to 4%-6%. Furthermore, when NaOH is applied as an additive in the process of solidification, the concentrations of most heavy metals except Pb<sup>2+</sup> have reached the national leaching toxicity standard. The results of X-ray diffraction reveal that sulfured solidification is due to the physical encapsulation rather than chemical transformation.

## 4:45 PM

**Study on the EMD Residue and Shale for Preparing Solidification Brick:** Wang Jia<sup>1</sup>; Peng Bing<sup>1</sup>; Chai Li Yuan<sup>1</sup>; Zhang Jin Long<sup>1</sup>; Li Guo Liang<sup>1</sup>; <sup>1</sup>Central South University

To employ resource utilization of residue from the electrolytic manganese dioxide (EMD) production, EMD residue combined with shale and fly ash was used as main material to prepare solidification-sintering brick. Compressive strength and leaching toxicity were chosen as main indexes and then the effect of sintering temperature, sintering time, solid waste ratio and cooling process on its mechanical strength and heavy metal solidification effect was studied. Calcined residue had capability of solidifying heavy metal. By optimizing preparation process, with EMD residue proportion no more than 40% the sample brick treated at T=1073~1273K for 3~5h, then cooled by 873K-semi-quench exhibited good performance and accorded with the national standard.

## 5:10 PM

**Experimental Study on the EMD Residue Admixture Cementitious Material:** Wang Jia<sup>1</sup>; Peng Bing<sup>1</sup>; Chai Li Yuan<sup>1</sup>; Zhang Jin Long<sup>1</sup>; Li Guo Liang<sup>1</sup>; <sup>1</sup>Central South University

To employ resource utilization of residue from the electrolytic manganese dioxide (EMD) production. As a substitute for partial gypsum, EMD residue combined with fly ash was added into cement clinker to prepare EMD residue admixture cementitious material. Compressive strength and leaching toxicity were chosen as main indexes in addition to XRD analysis, orthogonal analysis and SEM analysis. The effect of activation means, solid waste ratio, water-cement ratio and maintenance means on its mechanical strength and heavy metal solidification effect was studied. The residue treated by calcination, mechanical-activation and sulphate-activation exhibited good cementing performance. By optimizing preparation process, the sample prepared at residue: gypsum: fly-ash=1:1:1, water-cement ratio=0.3 and maintained at 293k in constant temperature and humidity equipment for 1 day and then in air for 6 days accorded with the slay cement national standard.

## 5:35 PM

**Study of Recycling Aggregates of Concrete Waste in Pervious Concrete:** Prakash Parasivamurthy<sup>1</sup>; Kiran Kumar BV<sup>1</sup>; Veena Jawali<sup>2</sup>; <sup>1</sup>Dayanada Sagar College of Engineering; <sup>2</sup>B.M.S.College of Engineering

Paper aims to study the Recycling of aggregates of concrete waste (CW) in pervious concrete. The size of the aggregate and the proportion of the particles in the coarse aggregate on the properties of the pervious concrete are investigated. The work includes, type, testing and evaluating quality of aggregate made from CW and evaluating effect of replacement of natural aggregate by recycled aggregate in Pervious concrete. The 28-day strength of CW used pervious concrete was about 3% to 11% lower than that of the pervious concrete made of natural aggregate. The infiltration rate of pervious concrete made of CW fall in the range of 70 to 680 liters per minute per square meter. Pervious concrete made of CW can be used in, pedestrian walkways, nature trails and plazas.

It aids in the process of qualifying for LEED Green Building Rating system credits available for using recycled products.

## Solid-State Interfaces: Toward an Atomistic-Scale Understanding of Structure, Properties, and Behavior through Theory and Experiment: Thermal, Electrical, and Thermoelectric Behaviors

*Sponsored by:* The Minerals, Metals and Materials Society, TMS Electronic, Magnetic, and Photonic Materials Division, TMS Structural Materials Division, TMS: Chemistry and Physics of Materials Committee

*Program Organizers:* Michael Demkowicz, Massachusetts Institute of Technology; Douglas Medlin, Sandia National Laboratories; Emmanuelle Marquis, University of Oxford

Wednesday PM

Room: 602

February 17, 2010

Location: Washington State Convention Center

*Session Chair:* Srinivasan Srivilliputhur, University of North Texas

## 2:00 PM Invited

**Theoretical and Simulation-Based Predictions of Grain Boundary Kapitza Resistance in Semi-Conductors:** Sylvie Aubry<sup>1</sup>; Patrick Schelling<sup>2</sup>; Chris Kimmer<sup>3</sup>; Xiaowang Zhou<sup>4</sup>; Reese Jones<sup>4</sup>; <sup>1</sup>Stanford University; <sup>2</sup>University of Central Florida; <sup>3</sup>University of Louisville; <sup>4</sup>Sandia National Laboratories

This talk will present recent theoretical and simulation-based calculations of the thermal conductivity in GaN as well as calculations of the Kapitza conductance in silicon grain boundaries using improved numerical methods such as the direct heat flux, the Green-Kubo and the lattice dynamics methods. A more accurate molecular dynamics calculation of thermal conductivity using the direct heat flux method will be explained and applied to GaN. This method will be compared to the Green-Kubo approach. An improved lattice dynamics approach will also be presented and compared to the direct heat flux method in the case of two different grain boundaries, a low scattering and a high scattering grainboundary in silicon.

## 2:30 PM Invited

**Thermal Conductance of Solid-State Interfaces:** David Cahill<sup>1</sup>; <sup>1</sup>University of Illinois

Rapid progress in the synthesis and processing of materials with structure on nanometer length scales has created a demand for greater scientific understanding of thermal transport in nanoscale devices, individual nanostructures, and nanostructured materials. In this talk, I will emphasize a critical aspect of this growing field: the thermal conductance of interfaces. We have recently advanced the state-of-the-art of time-domain-thermoreflectance (TDTR) measurements of thermal transport and are using TDTR to study i) heat transport by lattice vibrations across individual interfaces with extremely high and low thermal conductance; ii) interfacial heat transport by electrons in metals; and iii) the thermal conductivity of nanoscale multilayers and disordered layered crystals that violate conventional wisdom about the lower-limit to the thermal conductivity of solids.

## 3:00 PM

**Intrinsic Electric Fields in Nanostructured Oxide Ceramics:** Pankaj Nerikar<sup>1</sup>; Christopher Stanek<sup>1</sup>; Susan Sinnott<sup>2</sup>; Simon Phillpot<sup>2</sup>; Blas Uberuaga<sup>1</sup>; <sup>1</sup>Los Alamos National Laboratory; <sup>2</sup>University of Florida

Microstructure plays a central role in influencing the properties of materials that determine their performance. Among the many examples of such properties are the nucleation, growth, and subsequent release of fission gases in nuclear fuels, such as urania, UO<sub>2</sub>. In examining the dependence of fission gas segregation on the structure of symmetric grain boundaries, we have found that, as the spacing between grain boundaries becomes small, an electric field is created across the layers in the ceramic. This field is due to slight distortions in the atomic positions that lead to an asymmetry in the atomic structure. Urania is not unique as other fluorite-structured ceramics also exhibit this field; however, this behavior is not universal. As the bulk of this work relies upon empirical potentials, density functional theory is used to validate the results. We discuss the implications of this field for the structure and behavior of nanostructured ceramics.



3:20 PM

**Schottky Barriers at Interfaces between Transition Metals and Strontium Titanate:** *Matous Mrovec*<sup>1</sup>; Jan-Michael Albina<sup>1</sup>; Bernd Meyer<sup>2</sup>; Christian Elsaesser<sup>1</sup>; <sup>1</sup>Fraunhofer Institute for Mechanics of Materials; <sup>2</sup>University of Erlangen-Nuernberg

A thorough understanding of interfaces between metals and perovskite oxides is crucial for a successful integration of perovskite materials into modern microelectronic devices. In the case of insulating perovskite oxides, the key feature characterizing the interface is a formation of a potential barrier known as the Schottky barrier. In this work, we present a systematic theoretical study of the Schottky barriers for a series of transition-metal/strontium titanate interfaces. The barriers were calculated using the first-principle mixed-basis pseudopotential method based on density-functional theory. The process of interface formation was analyzed in a step-by-step procedure that enables to distinguish between structural and electronic contributions influencing the Schottky barrier height. This decomposition yields not only detailed information about the most relevant quantities that determine the band lineup at the interface but also provides means to validate fundamental assumptions of phenomenological theories, which estimate the Schottky barrier height from few characteristic material parameters.

3:40 PM

**Role of an Interface on the Thermal and Mechanical Characteristics of Heterogeneous Nanocomposites by Correlating Molecular-Quantum Study Focusing on Nanoscale Diffusion and Defect Formation:** *Vikas Samvedi*<sup>1</sup>; Vikas Tomar<sup>2</sup>; <sup>1</sup>University of Notre Dame; <sup>2</sup>Purdue University

Interfaces in nanocomposites make available the option to obtain materials with tailored properties by making microstructural changes. In the present research, atomistic analyses of nanocomposite interfaces have been correlated and supported with quantum calculations based on plane-wave basis sets combined with the density function theory (DFT). The focuses of quantum study is on analyzing the nanoscale diffusion phenomena during the formation of interfaces and on correlating the developed understanding with observed thermal and mechanical properties from atomistic calculations. The nanoscale re-configuration at the interfaces leading to the formation of defects and dislocations at high temperatures is studied to predict the overall thermal and mechanical characteristics of such nanocomposites. Analyses of the effect of straining on the nanocomposite property changes are performed to study it as a promising means to obtain nanocomposites with tailored properties.

4:00 PM

**Interfacial Defect Mechanism in the Precipitation of Tetradymite Plates in Rocksalt-Structured Tellurides:** *Douglas Medlin*<sup>1</sup>; J. Sugar<sup>1</sup>; <sup>1</sup>Sandia National Labs

Controlling the formation and stability of interfaces is important in developing high performance thermoelectric nanocomposites. Here, we consider the transformation mechanism between rocksalt and tetradymite-structured tellurides. Such compounds encompass a wide range of important thermoelectric materials. Our HRTEM observations of tetradymite-structured Sb<sub>2</sub>Te<sub>3</sub> plates within rocksalt structured AgSbTe<sub>2</sub> have identified a defect that can transform the rocksalt phase to the tetradymite phase through a diffusive-glide mechanism. We analyze this mechanism by establishing the geometric properties of the defect-- namely its step height and Burgers vector, which has components both perpendicular and parallel to the interface. Climb of the perpendicular dislocation component removes a metal plane from the rocksalt phase, forming the tellurium double-layer. Glide of the parallel component places the close-packed planes into the correct tetradymite stacking sequence. The defect properties also give the atomic flux requirements for defect motion, which we analyze for different compositions of the two phases.

### Stochastic Methods in Materials Research: Stochastic Methods I: New Algorithms and Model Building

*Sponsored by:* The Minerals, Metals and Materials Society, TMS Materials Processing and Manufacturing Division, TMS/ASM; Computational Materials Science and Engineering Committee  
*Program Organizers:* Richard Hennig, Cornell University; Dallas Trinkle, University of Illinois, Urbana-Champaign

Wednesday PM

Room: 614

February 17, 2010

Location: Washington State Convention Center

*Session Chairs:* Richard Hennig, Cornell University; Dallas Trinkle, University of Illinois Urbana-Champaign

2:00 PM Invited

**Building Effective Models from Sparse but Precise Data:** *Axel van de Walle*<sup>1</sup>; Eric Cockayne<sup>2</sup>; <sup>1</sup>Caltech; <sup>2</sup>NIST

A common approach in materials science is the use of a small number of highly accurate but expensive calculations to generate data to fit the parameters of a less accurate but more computationally tractable "effective model" enabling larger-scale simulations. A typical example is the fit of a simplified energy model to accurate quantum mechanical calculations. Although least-squares minimization is traditionally used for this purpose, it is not commonly recognized that this approach implicitly and incorrectly assumes that the uncertainty lies in the data rather than in the effective model. We demonstrate that the fact that the model is less accurate than the data can be properly taken into account within a Bayesian framework. This approach enables a perfect fit to the input noiseless data, while avoiding the usual artifacts of overfitting and enables the seamless inclusion of physical knowledge into the fitting procedure.

2:30 PM

**Statistical Learning and Materials Informatics:** *Krishna Rajan*<sup>1</sup>; Chang Sun Kong<sup>1</sup>; Prasanna Balachandran<sup>1</sup>; <sup>1</sup>Iowa State University

This presentation explores the application of statistical learning techniques unraveling the complex relationships between structure, bonding and chemistry in inorganic materials -- for example, identifying pathways that demonstrate how parameters describing electronic structure, chemistry and crystal geometry "communicate" with each other to ultimately define properties. We show how by integrating electronic and crystal geometry information into both classification and predictive data mining techniques, one can extract complex rule based design strategies for materials. In this presentation we also discuss how statistical learning techniques can be used to augment more classical approaches to computational based design of materials.

2:50 PM Break

3:10 PM Invited

**Error Estimation in Density Functional Theory:** *Vivien Petzold*<sup>1</sup>; James Sethna<sup>2</sup>; Karsten Jacobsen<sup>1</sup>; <sup>1</sup>Technical University of Denmark; <sup>2</sup>Cornell University

We investigate the use of different statistical approaches for developing new electronic density functionals and for estimating prediction errors of the functionals. The development focuses on generalized gradient functionals with a variable enhancement factor, and the optimization is carried out based on molecular fragmentation energies. The question of overfitting is addressed using bootstrap and the .632 estimator. For the estimation of errors we investigate and compare the use of different model ensembles both using multivariate, regression analysis and other ensembles obtained by optimizing the error prediction. The optimal functional is found to lead to prediction errors considerable smaller than other generalized-gradient functionals and of comparable quality with the computationally much more costly hybrid functionals.

3:40 PM

**Applications of Stochastic Geometry for Statistical Representation, Stereological Characterization, Modeling, and Simulations of Material Microstructures:** *Arun Gokhale*<sup>1</sup>; <sup>1</sup>Georgia Institute of Technology

Material microstructures are stochastic and three-dimensional (3D), and they usually contain features (particles, grain, voids, etc) that are of complex shapes/morphologies. Statistical spatial correlations often exist among

# Technical Program

different microstructural features and their morphological orientations are not always uniform-random. Stochastic geometry provides a powerful basis for statistical representation, characterization, modeling, and simulations of complex 3D microstructures. This contribution will present applications of stochastic geometry for analytical modeling of triple phase boundaries in the microstructures of solid oxide fuel cell cathodes, stereological characterization of 3D microstructures of liquid phase sintered tungsten heavy alloys from lower dimensional manifolds, statistical representations of microstructures of composites using lineal path probabilities and correlation functions, and computer simulations of realistic 3D microstructures of multi-phase materials.

## 4:00 PM

**Fractal Analysis of Microstructural Images for Evaluation of HSLA Steel:** *Mita Tarafder*<sup>1</sup>; I. Chatteraj<sup>1</sup>; S.K. Das<sup>1</sup>; M. Nasipuri<sup>2</sup>; S. Tarafder<sup>1</sup>; <sup>1</sup>National Metallurgical Laboratory; <sup>2</sup>Jadavpur University

Investigation of materials invariably requires usages of high resolution images of material structures for quantification of microstructural features, and subsequent development of correlations with the material properties. Often microstructural images of materials exhibit self similar structures or patterns formed due to network of grain boundaries, presences of precipitates, uneven surface elevations, etc. Microstructural images containing self similar fractal patterns at different length scales or resolutions remain unaffected by translations, rotations, projections and many other operations with regard to images. This makes the fractal analysis a useful technique for quantifying microstructural images by fractal dimension — the non-integer dimensional exponent used for representing non-linear complex phenomena. This paper presents fractal analysis of a set of microstructural images of high strength low alloy (HSLA) steel at various aging conditions and reports that the variation of fractal dimensions identifies the morphological changes occurring in nano-scale due to copper precipitation.

## 4:20 PM Break

## 4:40 PM

**Two Stochastic Mean-Field Polycrystal Plasticity Methods:** *Michael Tonks*<sup>1</sup>; John Bingert<sup>2</sup>; Curt Bronkhorst<sup>2</sup>; Daniel Tortorelli<sup>3</sup>; <sup>1</sup>Idaho National Laboratory; <sup>2</sup>LANL; <sup>3</sup>University of Illinois at Urbana-Champaign

Mean-field polycrystal plasticity methods efficiently determine the resultant stress and texture evolution due to an applied strain. However, the deformation of the individual crystals must be approximated since the crystal topology is not represented. In this work, we develop two models in which the crystal deformations are approximated stochastically. Through comprehensive CPFEM analyses of an idealized tantalum polycrystal, we verify that the velocity gradients tend to follow a normal distribution and surmise that this is due to the crystal interactions. We draw on these results to develop the stochastic Taylor model (STM) and the stochastic no-constraints model (SNCM), which differ in the manner in which the crystal strain rates are prescribed. Calibration and validation of the models are performed using data from tantalum compression experiments. Both models predict the compression textures more accurately than the fully-constrained model (FCM), and the SNCM predicts them more accurately than the STM.

## 5:00 PM

**A Stochastic Continuum Model for Growth and Optimization of Epitaxial Quantum Dot Multilayers:** Chandan Kumar<sup>1</sup>; *Lawrence Friedman*<sup>1</sup>; <sup>1</sup>The Pennsylvania State University

Randomly seeded processes at the nanoscale present both challenges and opportunities for materials fabrication. The fabrication of Nanoscale Epitaxial Self-Assembled Quantum Dots (SAQDs) marries stochastic and deterministic influences to produce technologically useful electronic and photonic nanostructures. In this process, strained semiconductor thin films are deposited epitaxially and then spontaneously form quasi-periodic 3D nanostructures. Typical materials systems include  $\text{Ge}_x\text{Si}_{1-x}/\text{Si}$  and  $\text{In}_x\text{Ga}_{1-x}\text{As}/\text{GaAs}$ . It has been observed that more regularity can be obtained by growing multilayers rather than single films. The fabrication of SAQD multilayers is modeled as space-time white thermal noise passed through a series of linear and non-linear spatial filters, resulting in a sequence of stochastic partial differential equations that are consistent with thermodynamics. Modeling indicates that this sequence can be tuned to produce more ordered structures by varying spacer layer thicknesses. SAQD multilayer fabrication demonstrate the synergy and competition of stochastic and deterministic effects in nanoscale fabrication.

## 5:20 PM

**Monte Carlo Method for Electromagnetic Scattering Incorporating Finite Element Methods to Generate Scatter Sources for Nanoscale Inclusions in Composites:** *Erik Sapper*<sup>1</sup>; Brian Hinderliter<sup>1</sup>; <sup>1</sup>North Dakota State University

Scattering of electromagnetic waves by a composite has a significant impact on its perceived quality, and has been used as a nondestructive measurement surrogate for the health of polymeric composites. Electromagnetic wave scattering is used to estimate flaw size distribution, used as input in calculating fracture failure due to stress concentration. Light scattering from the surface (specular) and reemerging from within a coating (diffuse) is a function of wavelength and the weighted integral of these terms gives the gloss and color of a material, particularly for coatings. Monte Carlo ray tracing is a stochastic computational method used to calculate the transport of electromagnetic waves, with a finite element solution of nanoparticle scattering used to generate a surface source for particles below the geometric limit. A 3-dimensional Monte Carlo/FEA model is being developed, capable of analyzing scattering by composites containing scatterers comparable to or smaller than the wavelength of incident light.

## Sustainable Materials Processing and Production: Sustainability in Education

*Sponsored by:* The Minerals, Metals and Materials Society, TMS Extraction and Processing Division, TMS Light Metals Division, TMS: Recycling and Environmental Technologies Committee, TMS: Education Committee

*Program Organizers:* Christina Meskers, Umicore; Randolph Kirchain, Massachusetts Institute of Technology; Diana A. Lados, Worcester Polytechnic Institute; Markus Reuter, Ausmelt Limited

Wednesday PM

Room: 2B

February 17, 2010

Location: Washington State Convention Center

*Session Chairs:* Diana Lados, Worcester Polytechnic Institute; Adam Powell, Opennovation

## 2:00 PM Introductory Comments

### 2:05 PM Invited

**Appropriate Technology and Sustainability:** *Richard LeSar*<sup>1</sup>; <sup>1</sup>Iowa State University

Sustainability will require more from engineering than the development of technology or structures. Engineering must also take into account the effects of that technology on the integrated social, economic, and environmental processes that constitute our society. Schumacher introduced the powerful concept of an appropriate technology, by which he meant a technology that is appropriate to the environmental, educational, cultural, and economic situation for which it is intended. While the principles of appropriate technology have been most commonly applied in the developing world, they are equally valid, and indeed essential, in the developed world as well. In this talk we will review appropriate technology and discuss its applicability in materials development and use. We will end by presenting a strategy for introducing the concepts and applications of appropriate technology in an engineering curriculum.

### 2:30 PM Invited

**Ceramics for Life in Rural Africa: A TMS Grant Update:** *Nathan Johnson*<sup>1</sup>; Sara Moser<sup>1</sup>; Andrew Havens<sup>1</sup>; <sup>1</sup>Iowa State University

In 2009, TMS awarded \$5,000 to the Iowa State chapters of Materials Advantage and Engineers Without Borders. The collaboration aims to improve the quality of life in Mali by developing clean, safe, and sustainable household technologies that meet basic needs of impoverished families. This grant introduces three technologies into the home: (1) ceramic water filters that remove particulates and bacteria from ground water, (2) materials to construct clean and efficient cooking stoves that reduce indoor air pollution, and (3) bricks to construct houses that do not degrade in the rainy season. A kiln will be constructed in Mali and local artisans trained to support sustainability. The process from scoping the problem, design at Iowa State, and implementation in Mali is a life experience for student engineers to become the leaders that address tomorrow's needs.



### 2:55 PM Invited

#### **Depth through Breadth: Addressing the Grand Challenges of Teaching Sustainability:** Svetlana Nikitina<sup>1</sup>; <sup>1</sup>Worcester Polytechnic Institute

While many question “sustainability” as an intellectual field on the grounds that it is too broad and “undisciplined,” we are able to achieve a good balance between breadth of coverage and depth of inquiry in our team-taught seminar “The Grand Challenges: Sustainable Development for the 21st Century” offered to first year students at Worcester Polytechnic Institute. We strike this balance between breadth and depth by a) problematizing key sustainability issues in class discussions; b) by explicitly exploring the lenses of different disciplines (the historical context, the scientific facts, the engineering interventions and the philosophical foundations of unsustainable behaviors); and c) by offering our students opportunities to pursue a targeted project on specific sustainability issues (vertical gardening, metals recycling on college campus) through which they gain depth of understanding as well as practical exposure to all components of the problem, which puts them on the path of seeking effective solutions.

### 3:20 PM

#### **Engagement is an Essential Skill in the 21st Century:** Dirk van Zyl<sup>1</sup>; <sup>1</sup>University of British Columbia

As part of the North American regional activities during the Mining, Minerals and Sustainable Development Project (MMSD) one project focused on the development of sustainability evaluations at the operations level. Engagement was identified as one of the seven important questions to be addressed. Engineers and scientists employed in the mining, minerals and materials production arenas must understand the importance of stakeholder engagement, both within and outside the operations as it is essential in the ongoing activities required to contribute to sustainable development. After developing the awareness that a social license can only be contemplated if engagement is in place they also have to develop skills in applying it. This presentation will present the business case for engagement as well as an approach to motivate undergraduate mining engineers to embrace it. The presentation will also review some recent and ongoing research to improve the engagement process.

### 3:45 PM Break

### 3:55 PM

#### **Embracing Sustainability in the Materials Engineering Curriculum: Suggestions and Examples to Build Competencies for Today's Materials Engineering Graduate:** Katherine Chen<sup>1</sup>; Linda Vanasupa<sup>1</sup>; Trevor Harding<sup>1</sup>; Blair London<sup>1</sup>; Richard Savage<sup>1</sup>; <sup>1</sup>Cal Poly State University

To better prepare students for the complex, global challenges of the 21st century, the Materials Engineering department at Cal Poly transformed its curriculum through a NSF-departmental level reform grant to embrace sustainability. While basic principles of materials science and engineering are still at the core, there has been a shift in the approach – from scientific analysis to engineering design with realistic constraints. Central tenets to the new curriculum include systems thinking and the role of engineers in society. These themes are introduced the freshmen year and continue throughout the different years in different courses (e.g., Materials Selection of the Lifecycle). Several courses are now project-based and involve teams of students working on design challenges. Real world contexts and realistic design constraints that involve environmental and societal impacts have provided rich learning experiences for students. Essential professional skills, such as teamwork, communication and project management, are developed in the process.

### 4:20 PM

#### **Sustainability and Mineral Resource Utilisation: A Study Guide:** William Rankin<sup>1</sup>; <sup>1</sup>CSIRO Minerals

It is essential that professionals, both technical and non-technical, working in the mineral and metal commodity industries understand the concept of sustainability and its implications for the industry. Undergraduate courses have not done this well in the past. Much has been written in this field, and there have been great advances in understanding. However, much of what has been published is superficial and sometimes misleading, and there is as yet no coherent, single account that can serve as an introduction or overview. This paper presents an outline which can guide readers in developing an understanding of the topic and its relevance to their work. Key references are provided, particularly those accessible on the internet, which will serve to introduce the reader to the important principles and understandings. The guide

should also be useful to academics preparing students to work in the minerals and metal production sectors.

### 4:45 PM Invited

#### **Teaching Design for “Sustainability” on the Basis of Metallurgy and Materials Science:** Markus Reuter<sup>1</sup>; <sup>1</sup>Ausmelt Limited

Metals play a pivotal role in society as their properties impart unique functionality to engineered structures and consumer products. Furthermore, metals are theoretically infinitely recyclable. However, among others, design complicates recycling due creating complex structures that produce impure recyclates, hence forcing dilution by the use of virgin pure metal. Metallurgical smelting ingenuity, good technology and intelligent use of thermodynamics and transfer processes gets metallurgists a far way down the path of creating high recycling rates; it is however the 2nd Law of Thermodynamics that also flags the limitations of recovering all elements. This is also then directly linked to economics of the various process routes. A key issue is the creation of optimal industrial ecological systems (Web of Materials) that maximize the recovery of materials from ores and recyclates within the boundaries of thermodynamics, technology and economics.

### 5:10 PM

#### **Materials and Society Resources on the Teaching Archive of the Materials Digital Library:** Adam Powell<sup>1</sup>; Laura Bartolo<sup>2</sup>; Matthew Krane<sup>3</sup>; Edwin Garcia<sup>3</sup>; Lan Li<sup>2</sup>; <sup>1</sup>Opennovation; <sup>2</sup>Kent State University; <sup>3</sup>Purdue University

MatDL (<http://matdl.org>) provides stewardship of significant content and services to support the integration of research and education in the materials community. Two of its complementary services are: 1) MatForge (<http://matforge.org>) and 2) Teaching Archive (<http://teaching.matdl.org/>), online workspaces for collaborative development of materials simulation/modeling codes as well as core undergraduate materials teaching resources. By offering materials educators convenient access to relevant, shared learning resources based on research, both teaching and learning within materials science and cognate disciplines are positively impacted. This talk will describe MatDL content focused on sustainability. In particular, several of the resources of the Teaching Archive address the issues of sustainability and the impact of materials technology on society.

### 5:35 PM Concluding Comments

## **The Vasek Vitek Honorary Symposium on Crystal Defects, Computational Materials Science and Applications: Crystal Defects and Mechanical Properties**

*Sponsored by:* The Minerals, Metals and Materials Society, TMS Materials Processing and Manufacturing Division, TMS/ASM; Computational Materials Science and Engineering Committee  
*Program Organizers:* Mo Li, Georgia Institute of Tech; David Srolovitz, Institute for High Performance Computing, Agency for Science, Technology and Research, Singapore; Adrian Sutton, Imperial College London; Vaclav Pavidar, Institute of Physics AS CR vvi; Jeff De Hosson, Univ of Groningen

Wednesday PM Room: 603  
February 17, 2010 Location: Washington State Convention Center

*Session Chairs:* Ralf Drautz, Ruhr-Universität Bochum; Petros Sofronis, University of Illinois

### 2:00 PM Invited

#### **Heating Graphene in a Microscope:** Ju Li<sup>1</sup>; Liang Qi<sup>1</sup>; Li Feng<sup>1</sup>; Jianyu Huang<sup>2</sup>; Ping Lu<sup>2</sup>; Feng Ding<sup>3</sup>; Boris I. Yakobson<sup>3</sup>; <sup>1</sup>University of Pennsylvania; <sup>2</sup>Sandia National Laboratories; <sup>3</sup>Rice University

Curvy nanostructures such as carbon nanotubes and fullerenes have extraordinary properties but are difficult to pick up and assemble into devices after synthesis. We have performed experimental and modeling research into how to construct curvy nanostructures directly integrated on graphene, taking advantage of the fact that graphene bends easily after open edges have been cut on it, which can then fuse with other open edges, like a plumber connecting metal fittings. By applying electrical current heating to few-layer graphene inside an electron microscope, we observed the in situ creation of many interconnected,

# Technical Program

curved carbon nanostructures, such as graphene bilayer edges (BLEs), aka “fractional nanotubes”; BLE polygons equivalent to “squashed fullerenes” and “anti quantum-dots”; and nanotube-BLE junctions connecting multiple layers of graphene. The BLEs, quite atypical of elemental carbon, have large permanent electric dipoles of 0.87 and 1.14 debye/Å for zigzag and armchair inclinations, respectively. An unusual, weak AA interlayer coupling leads to a twinned double-cone dispersion of the electronic states near the Dirac points. This entails a type of quantum Hall behavior markedly different from what has been observed in graphene-based materials, characterized by a magnetic field-dependent resonance in the Hall conductivity. Further simulations indicate that multiple-layer graphene offers unique opportunities for tailoring carbon-based structures and engineering novel nano-devices with complex topologies.

## 2:25 PM Invited

**Layer Growth by Ion Bombardment:** *Miklos Menyhard*<sup>1</sup>; Peter Sule<sup>1</sup>; Janos Labar<sup>1</sup>; <sup>1</sup>Research Institute for Technical Physics and Materials Science

Ion bombardment generally causes the mixing of originally sharp interfaces of imbedded particles bilayers etc. We have found special cases, when the ion bombardment results in layer growth. This strange behavior was explained by the strongly asymmetric material transport induced by the ion bombardment. We could show that applying various ion (30 keV Ga<sup>+</sup>, 20 keV Ni<sup>+</sup>) bombardment on Si/Cr and C/Ni bilayers, the transport, induced by the ion bombardment, of Cr and C are order of magnitude larger than those of Si and Ni, respectively. This difference causes layer formations CrSi mixture, and Ni<sub>3</sub>C and Ni mixture for Si/Cr and C/Ni bilayers, respectively. The newly formed layers join to the reminder matrix by sharp interfaces. We attempted to understand the asymmetric mixing by applying MD simulation. Though a reasonable agreement with the experimental data has been found it has not resulted in an understanding of the phenomenon.

## 2:50 PM

**The Strength and Deformation of Gum Metal:** *John Morris*<sup>1</sup>; Eizabeth Withey<sup>1</sup>; Rohini Sankaran<sup>1</sup>; Andrew Minor<sup>1</sup>; Daryl Chrzan<sup>1</sup>; <sup>1</sup>University of California - Berkeley

The name “Gum metal” has been given to a set of β-Ti alloys that, with appropriate preparation, appear to deform by a dislocation-free mechanism involving elastic instability at the limit of strength. We have studied their deformation of these materials through instrumented, in situ compression of nanopillars in high resolution TEM. Interesting results include the following: (1) nanopillars approach ideal strength in the limit of small diameter; (2) there is no significant “size effect” in pillar strength until the diameter falls below 100 nm; (3) the deformation mode is fine-scale, even in pillars of 100 nm size, and involves the growth and micro-rotation of ultrafine domains; (4) the dislocations that are imaged in some tests appear pinned by nanobarriers of uncertain nature; (5) a martensitic transformation to the face-centered orthorhombic “a” phase is sometimes observed, but is an incidental feature of the deformation rather than a significant cause of it.

## 3:05 PM

**Deformation of Precipitate Platelets in High Strength Aluminum Alloys under High Strain-Rate Compression:** K. El-Khodary<sup>1</sup>; William Lee<sup>1</sup>; L. Sun<sup>1</sup>; Bryan Cheeseman<sup>2</sup>; Donald Brenner<sup>1</sup>; *Mohammed Zikry*<sup>1</sup>; <sup>1</sup>North Carolina State University; <sup>2</sup>Army Research Laboratory

The objective of this study is to identify the dominant microstructural and dislocation mechanisms related to the high strength and ductile behavior of high strength aluminum alloys, and how high strain-rate loading conditions would affect the overall behavior. Characterization techniques and specialized microstructurally-based finite-element (FE) analyses based on a dislocation-density based multiple-slip formulation that accounts for an explicit crystallographic and morphological representation of O precipitates and their rational orientation relations was conducted. As the microstructural FE predictions have indicated, and consistent with the experimental observations, the combined effects of different precipitates, acting on different crystallographic orientations, enhance the strength, the ductility, and reduce the susceptibility of 2139-Al to shear strain localization due to dynamic compressive loads.

## 3:20 PM Break

## 3:40 PM Invited

**Physical and Mechanical Properties of Co<sub>3</sub>(Al,W) with the L1<sub>2</sub> Structure:** *Haruyuki Inui*<sup>1</sup>; Norihiko Okamoto<sup>1</sup>; Katsushi Tanaka<sup>1</sup>; Kyosuke Kishida<sup>1</sup>; Takashi Ohashi<sup>1</sup>; <sup>1</sup>Kyoto University

The recent discovery of the stable L1<sub>2</sub>-ordered intermetallic compound, Co<sub>3</sub>(Al,W) coexisting with the solid-solution based on Co with a fcc structure has opened up a pathway to the development of a new class of high-temperature structural material based on cobalt, ‘Co-base superalloys’. However, almost nothing is known about mechanical properties of the constituent L1<sub>2</sub> phase, Co<sub>3</sub>(Al,W). We have investigated some physical and mechanical properties of single crystals and polycrystals of Co<sub>3</sub>(Al,W) with the L1<sub>2</sub> structure. When judged from the values of Poisson ratio, Cauchy pressure and Gh/Bh, the ductility of Co<sub>3</sub>(Al,W) is expected to be sufficiently high so that Co<sub>3</sub>(Al,W) can be used as the constituent phase of ‘Co-base superalloys’. The anomalous temperature dependence of yield stress observed above 700°C is attributed to thermally activated cross-slip of a/2<110> dislocations separated by an APB from octahedral to cube slip planes, as observed in many other L1<sub>2</sub> compounds such as Ni<sub>3</sub>Al.

## 4:05 PM Invited

**Propagation of Shear Transformation Zone at Sound Velocity in Metallic Glass:** *Shin Takeuchi*<sup>1</sup>; Yasushi Kamimura<sup>1</sup>; Takaaki Yoshihara<sup>1</sup>; Keiichi Edagawa<sup>1</sup>; <sup>1</sup>Tokyo University of Science

Molecular dynamics simulation has been performed for a model binary Ni-Y metallic glass produced by melt-quenching and annealing. The stability of dislocations has been examined by introducing edge and screw dislocations with the Burgers vector of 0.2 and 0.5nm, followed by static relaxation. The stress analysis has shown that the stress field around both edge and screw dislocation center almost completely disappears after relaxation. By applying an initial strain larger than 0.04 to the model, a steady plastic flow occurs only above a critical stress of 0.03G (G: shear modulus) by forming localized shear transformation zones with a thickness of 1 to 2nm. However, if a dislocation with b=0.6nm is introduced at the edge of the model under a stress of 0.026G, a continuous shear band propagation occurs at a high speed of sound velocity, so that the stress field of the moving dislocation is not blunted by relaxation.

## 4:30 PM Invited

**Multiscale Models of Dislocation Core Structures in Iron and Copper:** *Nasr Ghoniem*<sup>1</sup>; A. Takahashi<sup>2</sup>; Z. Chen<sup>3</sup>; N. Kioussis<sup>3</sup>; G. Lu<sup>3</sup>; <sup>1</sup>University of California, Los Angeles; <sup>2</sup>Science University of Tokyo; <sup>3</sup>California State University, Northridge

We discuss here a range of multiscale modeling approaches to describe the atomistic structure of dislocation cores in iron. First, we first present a concurrent multiscale approach, where ab initio calculations are directly coupled with MD simulations. Then, we describe a Peierls-Nabarro sequential multiscale modeling approach that is a hybrid of ab initio and continuum methods for the analysis of dislocation cores in three-dimensional configurations. We also present another approach to describe the core structure of screw dislocations in bcc metals, and that is the hybrid ab initio-based Atomic-Row sequential model. These models are applied to the study of the core structures in a number of applications in iron: (1) The effect of Cu and Cr Nano-clusters on dislocation cores in α-Fe; (2) Dislocation interactions with nano-scale Y<sub>2</sub>O<sub>3</sub> Precipitates; (3) Dislocation-precipitate interaction; (4) DFT Calculations of the effects of stress on Self-Interstitial (SIA) rotation; (5) The structure of SIA clusters in iron and copper; (6) SIA cluster core response to applied shear.

## 4:55 PM

**Quantum Monte Carlo Calculations for Point Defects in Silicon:** *Richard Hennig*<sup>1</sup>; W. Parker<sup>2</sup>; K. Driver<sup>2</sup>; J. Wilkins<sup>2</sup>; <sup>1</sup>Cornell University; <sup>2</sup>The Ohio State University

Point defects in silicon have been studied extensively for many years. Nevertheless, there is still no agreement on the formation energies of self-interstitials in silicon with theoretical predictions and experimental measurements ranging from 2-5 eV. To answer the question of the formation energy of Si interstitials we resort to quantum Monte Carlo (QMC) and hybrid density functional techniques. Previous QMC calculations resulted in formation energies for the interstitials of around 5 eV. We present a careful analysis of all the controlled and uncontrolled approximations that affect the defect formation energies in variational and diffusion Monte Carlo calculations. We find that more



accurate trial wave functions for QMC using improved Jastrow expansions and most importantly a backflow transformation for the electron coordinates result in slightly lower interstitial formation energies than previous quantum Monte Carlo calculations in close agreement with hybrid density functional results.

### 5:10 PM

**Modeling of Point Defect Diffusion in Fe-Cr-Ni Alloys Using Ab-initio Based Multi-Scale Approach:** *Samrat Choudhury*<sup>1</sup>; Benjamin Swoboda<sup>1</sup>; Leland Barnard<sup>1</sup>; Julie Tucker<sup>2</sup>; Anton Van der Ven<sup>3</sup>; Todd Allen<sup>1</sup>; Dane Morgan<sup>1</sup>; <sup>1</sup>University of Wisconsin, Madison; <sup>2</sup>Knolls Atomic Power Laboratory; <sup>3</sup>University of Michigan - Ann Arbor

Formation and transport of point defects under irradiation are known to play a significant role in determining the temporal evolution of microstructure and structural properties in Fe-Cr-Ni alloys used in nuclear reactors. In particular, radiation induced segregation (RIS) is a process where point defects migrating to sinks leads to changes in composition near sink boundaries. In this work, we calculate diffusion parameters for both vacancy and interstitial mediated diffusion in dilute and concentrated alloys. The phenomenological ( $L_{ij}$ ) and tracer diffusion coefficients ( $D^*$ ) are calculated based on a multi-frequency approach using ab-initio diffusion energetics for dilute alloys, while a combination of ab initio energetics, cluster expansion formalism and kinetic Monte Carlo approach is used to calculate  $L_{ij}$  and  $D^*$  in concentrated alloys as a function of composition. The diffusion parameters are then used in a rate theory model to predict the evolution of concentration profiles near grain boundaries under irradiation.

### 5:25 PM

**Computing Ab Initio Free Energy Contributions of Point Defects:** *Blazej Grabowski*<sup>1</sup>; Lars Ismer<sup>1</sup>; Tilmann Hickel<sup>1</sup>; Jörg Neugebauer<sup>1</sup>; <sup>1</sup>Max-Planck-Institut für Eisenforschung

A common assumption when computing defect concentrations is that the dominant entropy contribution is due to configurational entropy. Other entropy contributions such as harmonic and anharmonic lattice vibrations are assumed to be second order effects and are computationally expensive to calculate. Thus, such contributions have been rarely considered in defect calculations. With the increasing capability of ab initio approaches to e.g. provide accurate free energies to macroscopic approaches (e.g. CALPHAD), the inclusion of the aforementioned smaller entropy contributions will become more and more important. We have therefore developed a hierarchical scheme to coarse grain the configurations space allowing to efficiently calculate harmonic and anharmonic contributions to vacancy formation [PRB 79, 134106 (2009)]. In the present talk we will discuss the application of this approach to vacancies in aluminum.

### 5:40 PM

**Ab Initio Modeling of Dislocation/Solute Interactions in Mg:** *Joseph Yasi*<sup>1</sup>; Louis Hector<sup>2</sup>; Dallas Trinkle<sup>1</sup>; <sup>1</sup>University of Illinois at Urbana-Champaign; <sup>2</sup>General Motors Technical Center

New lightweight, strong, formable Mg alloys are of considerable interest to the transportation industries for improved fuel economy. Efficient, accurate computational modeling of dislocations and solute interactions with dislocations is essential for the development of meaningful constitutive models of strength. In magnesium, the basal slip system is the most active. Prismatic dislocations are two orders of magnitude stronger than basal dislocations, but mobility is necessary to achieve the five independent slip systems required for forming. The first principles flexible boundary condition method is used to compute  $a$ -type screw, edge, and mixed atomic-scale Mg dislocation geometries in the basal slip system as well as  $a$ -type edge,  $c$ -type screw and  $c$ -type edge in the prismatic slip system. For these dislocations, we calculate solute binding energies for many industrially important solutes by direct substitution in the optimized dislocation cores and also from interaction with local slip and strain in the dislocation cores.

### 5:55 PM

**Embrittlement in Metals: An Atomistic Study of the Hydrogen Enhanced Local Plasticity (HELP) Mechanism:** *Johann von Pezold*<sup>1</sup>; Liverios Lymperakis<sup>1</sup>; Jörg Neugebauer<sup>1</sup>; <sup>1</sup>Max-Planck-Institut für Eisenforschung GmbH

The embrittlement of metals by H is a long-standing problem, whose underlying mechanisms are still largely unclear. In this study we consider the atomistic basis of the HELP mechanism. According to this mechanism

interstitial H shields dislocation-dislocation interactions, resulting in increased dislocation densities and eventually the nucleation of cracks in regions of high H concentrations. Using a combination of density-functional theory calculations, semi-empirical EAM potentials and an effective lattice-gas Hamiltonian we determine the effect of H on the stress field around edge dislocations in fcc metals. Depending on the strength of the H-H interactions, a hydride phase is formed in the vicinity of the dislocation core already at rather modest bulk H concentrations. The formation of this new phase significantly reduces the shear stress along the glide plane of the dislocation, resulting in reduced separations in dislocation pile-ups and eventually in the onset of localised plastic fracture.

### 6:10 PM

**Atomic Scale Study of the Interaction of Point Defects with Edge and Screw Dislocations in Bcc Iron:** *Erin Hayward*<sup>1</sup>; Blas Uberuaga<sup>2</sup>; Chaitanya Deo<sup>1</sup>; Carlos Tome<sup>2</sup>; <sup>1</sup>Georgia Institute of Technology; <sup>2</sup>Los Alamos National Laboratory

Understanding and predicting irradiation creep in structural reactor materials requires a knowledge of physical processes occurring within dislocation cores. Because Linear Elastic theory can not accurately describe core interactions computation with atomistic methods is vital. We perform molecular statics calculations in order to understand the interactions between vacancies and interstitials and line dislocations in bcc iron. These are compared to similar results given by linear elasticity theory. For vacancies and a variety of self-interstitial dumbbell configurations near both edge and screw dislocations, we find significant differences between continuum theory and atomistics. For vacancies some interaction is seen with both edge and screw dislocations where none is predicted. Results for interstitials tended to have a strong dependence on orientation and position about the core. Particularly for the screw, continuum theory misses the tri-fold splitting of the dislocation core which has a large influence on atomistic results.

### 6:25 PM

**Simulation of Tensile Loading of Ag <110> Nanowires with Extremely Slow Strain Rates Using Accelerated Molecular Dynamics:** *Chun-Wei Pao*<sup>1</sup>; Danny Perez<sup>2</sup>; Sriram Swaminarayan<sup>2</sup>; Arthur F. Voter<sup>2</sup>; <sup>1</sup>Research Center for Applied Sciences, Academia Sinica; <sup>2</sup>Los Alamos National Laboratory

Nanowires have unique mechanical and electric properties and are very promising for future nanodevices applications. The mechanical properties of these nanowires are of particular interests because they are very different from their bulk counterparts. Atomistic scale simulations such as molecular dynamics (MD) simulation are the best way to characterize the deformation mechanisms of nanowires. However, due to the time scale limitations of MD simulations, the applied strain rates during typical tensile loading simulations are usually tens of millions times higher than those in real world experiments. Here we present our recent study on the simulation of tensile loading of Ag <110> nanowires using massive parallel-replica dynamics simulation. We are able to reach a time scale of 1 ms and extraction velocity of 1  $\mu\text{m/s}$ , which corresponds to an approximate strain rate of 400/s at room temperature. We observed a lot of interesting new physics, for the first time, with atomistic resolution. We observed that there exists an optimum strain rate which maximizes the ductility of the Ag nanowire: for strain rates higher or lower than this particular strain rate, the nanowire ruptures at smaller applied strains due to kinetic or thermodynamic reasons. We also observed an interesting self-healing behavior in the Ag nanowire investigated. The stacking faults generated along the axis of the nanowire during tensile loading processes vanished upon further loading due to the passing of another partial slip, which makes the nanowire free of defects again and one atomic plane thinner.

### 6:40 PM

**Modeling of Deformation and Microstructure Evolution in Severe Plastic Deformation:** *Hyoung Seop Kim*<sup>1</sup>; <sup>1</sup>POSTECH

The evolution of microstructure and the mechanical properties of severe plastic deformation (SPD) processed materials depend on the plastic deformation behavior during SPD, which is governed mainly by the die geometry, the constitutive behavior of the material itself and the processing conditions. In this study, we describe some of our results of continuum-based modelling and microstructural-based modelling of various SPD processes in order to illustrate the capabilities of the models. Modelling the evolution of microstructural features of misorientation angle using a dislocation cell model during SPD is presented. Of great interest for modelling the effects of SPD on the material

# Technical Program

microstructure is the misorientation angle distribution using a probabilistic description involving distribution functions in terms of a Fokker-Planck equation derived using the Langevin approach. The dislocation cell model is implemented into the finite element method associated with cellular automata, which show realistic features of evolutions of grain size and misorientation.

## The Vasek Vitek Honorary Symposium on Crystal Defects, Computational Materials Science and Applications: Dislocations II

Sponsored by: The Minerals, Metals and Materials Society, TMS Materials Processing and Manufacturing Division, TMS/ASM: Computational Materials Science and Engineering Committee

Program Organizers: Mo Li, Georgia Institute of Tech; David Srolovitz, Institute for High Performance Computing, Agency for Science, Technology and Research, Singapore; Adrian Sutton, Imperial College London; Vaclav Paidar, Institute of Physics AS CR vvi; Jeff De Hosson, University of Groningen

Wednesday PM Room: 604  
February 17, 2010 Location: Washington State Convention Center

Session Chairs: Christopher Woodward, Air Force Research Laboratory; Ladislav Kubin, CNRS

### 2:00 PM Invited

**Atomic-Scale Modelling of Dislocation Interaction with Nanoscale Obstacles:** David Bacon<sup>1</sup>; Yuri Osetsky<sup>2</sup>; <sup>1</sup>University of Liverpool; <sup>2</sup>Oak Ridge National Laboratory

Irradiation of metals with high-energy atomic particles creates nanoscale defect clusters that are obstacles to dislocation glide and can give rise to effects such as hardening and strain localisation. Treatment of these effects in the elasticity theory of dislocations is problematic without information about the atomic mechanisms that occur. Atomic-scale computer simulation can provide details of the influence of stress, strain rate and temperature on the mechanisms. Recent results for dislocations gliding under stress against obstacles in a variety of metals across a range of temperature are classified in this presentation. The effects observed vary from reactions in which the dislocation and obstacle are left unchanged, through ones in which the obstacle is changed but the dislocation is not, to ones in which the obstacle is absorbed temporarily or permanently by the dislocation. Although some processes can be represented within the continuum approximation, others cannot.

### 2:25 PM Invited

**Multiscale Models of Dislocation Core Structures in Iron and Copper:** N. M. Ghoniem<sup>1</sup>; A. Takahashi<sup>2</sup>; Z. Chen<sup>3</sup>; N. Kioussis<sup>3</sup>; G. Lu<sup>3</sup>; <sup>1</sup>University of California, Los Angeles; <sup>2</sup>Science University of Tokyo; <sup>3</sup>California State University, Northridge

We discuss here a range of multiscale modeling approaches to describe the atomistic structure of dislocation cores in iron. First, we first present a concurrent multiscale approach, where ab initio calculations are directly coupled with MD simulations. Then, we describe a Peierls-Nabarro sequential multiscale modeling approach that is a hybrid of ab initio and continuum methods for the analysis of dislocation cores in three-dimensional configurations. We also present another approach to describe the core structure of screw dislocations in bcc metals, and that is the hybrid ab initio-based Atomic-Row sequential model. These models are applied to the study of the core structures in a number of applications in iron: (1) The effect of Cu and Cr Nano-clusters on dislocation cores in Fe-Fe; (2) Dislocation interactions with nano-scale Y2O3 Precipitates; (3) Dislocation-precipitate interaction; (4) DFT Calculations of the effects of stress on Self-Interstitial (SIA) rotation; (5) The structure of SIA clusters in iron and copper; (6) SIA cluster core response to applied shear.

### 2:50 PM

**Is Dislocation Locking Possible without External Stress?:** Bella Greenberg<sup>1</sup>; Mike Ivanov<sup>2</sup>; Alexander Patselov<sup>1</sup>; <sup>1</sup>Institute of Metal Physics, Ural Branch, Russian Academy of Sciences; <sup>2</sup>Kurdjumov Institute of Metal Physics, National Academy of Sciences of Ukraine

The theoretically predicted effect of the self-locking of dislocations actually was detected in Ni<sub>3</sub>(Al, Nb) and TiAl. By the self-locking we mean transformations

of dislocations from glissile to locked configurations at a zero external stress. Experiments included no-load heating after preliminary deformation. Reasons for the self-locking of superdislocations and single dislocations in intermetallics are revealed. By its nature, this process represents the thermally activated flip of a dislocation from a shallow valley to a deep valley of the potential relief. It is the change of the valley depth that stimulates the self-locking of dislocations. The evidences were obtained that the two effects - the anomaly of the yield stress and the self-locking - have the same origin, namely a double-valley potential relief of dislocations. For comparison similar experiments were performed for BCC metals (Armco-Fe and Mo), which have no the  $\sigma_y(T)$  anomaly. The self-locking of dislocations was not observed.

### 3:05 PM

**Brittle-Ductile Behavior and Dislocation Core Structure in Y- and Co-Based B2 Intermetallics:** Oleg Kontsevoi<sup>1</sup>; Yuri Gornostyrev<sup>2</sup>; Arthur Freeman<sup>1</sup>; <sup>1</sup>Northwestern University; <sup>2</sup>Institute of Metal Physics

Recently, a class of ductile rare-earth B2 intermetallics (such as YCu, YAg, YZn) has been discovered. In addition, high ductility was found in CoZr, belonging to a unique group of Co-based B2 CoX intermetallics (X = Ti, Zr, Hf). We present a systematic investigation of the shear, elastic, and cleavage energetics of Co- and Y-based alloys by means of first-principles FLAPW calculations. We identify that the ductility of Co- and Y-based B2 intermetallics has intrinsic origins and is connected with martensitic instability of B2 phase with respect to B19, B27, or B33 transformation. Using the modified Peierls-Nabarro model with ab initio parametrization we investigate the structure of {001} and {110} dislocations and predict that the <100>{011} dislocations have a wide core and split according to  $\mathbf{b} = \mathbf{b}/2 + \mathbf{b}/2$  scheme. This will result in a low Peierls stress, high dislocation mobility and easy plastic relaxation leading to high ductility.

### 3:20 PM Break

### 3:40 PM Invited

**Structure of Random Tilt Boundaries and Dislocation Emission Behavior under Stress:** Diana Farkas<sup>1</sup>; Laura Patrick<sup>1</sup>; Nicklas Floyd<sup>1</sup>; <sup>1</sup>Virginia Tech

In this talk we will present the results of a large scale atomistic study of tensile deformation in a virtual FCC polycrystalline sample with columnar grain structure, 40 nm average grain size and a [110] texture. The grain boundaries analyzed were all pure tilt with random misorientation angles and crystallographic orientation of the grain boundary plane. We analyzed the structure and energetics of these random boundaries and their response to stress. We will report the details of dislocation emission from the different grain boundaries and relate the process to the structural units present in the boundaries. Finally, we will show how dislocation debris accumulates in the sample and the strain can localize in certain grains and grain regions, driven by the particular local structure and orientation of the various grain boundaries.

### 4:05 PM Invited

**Copper Precipitation Strengthening of Iron and Steels. Dislocation Locking Mediated by Phase Instability:** Yuri Gornostyrev<sup>1</sup>; <sup>1</sup>Institute of Metalphysics of the Ural Branch of RAS and CJSC Institute of Quantum Materials Science, Ekaterinburg, Russia

The prediction of the mechanical behavior starting from fundamental microscopic physical principles is challenge problem of materials science. The pronounced strengthening effect of copper precipitates in steels has been studied extensively in the past however the mechanism of this phenomenon are still under debate. To make clear the factors controlling the formation of copper inclusions and strengthening we employ a multiscale modeling approach which involves first principles calculations of the effective interaction parameters, subsequent Monte Carlo simulations of Cu precipitation and molecular dynamic simulations of the dislocation - particle interactions. We show that strengthening effect of copper precipitates caused by dislocation locking due to the phase instability in nanometer-sized bcc Cu-rich precipitates. The experimental features of the mechanical behavior Fe-Cu based alloys are discussed.

### 4:30 PM

**A Peierls Model of Atomic Stick-Slip Frictional Behavior:** Yanfei Gao<sup>1</sup>; <sup>1</sup>University of Tennessee

In atomic friction measurements, the stick-slip behavior critically depends on lattice structures of the two contacting surfaces, sliding direction, contact size, sliding velocity, environmental temperature, to name a few. By representing the



friction as a point mass moving on top of a periodic potential, the Tomlinson approach restricts all the interface atoms to move uniformly, thus unable to explain the effects of lattice incommensurability and many other factors. We attempt to elucidate the atomic-friction mechanisms from the spatiotemporal evolution of interface defects and lattice structure. A Peierls-type framework replaces singular defect model by the inhomogeneous slip field on the interface. Experimental observations, such as structural lubricity, frictional anisotropy, and contact size dependence, can be explained as a consequence of initiation and multiplication of interface dislocations and their interactions with pre-existing interface defects. Drawbacks of the theoretical model are also discussed.

### 4:45 PM

**Atomistic Modeling of Screw Dislocation Mobility in Alpha-Fe:** *Neeraj Thirumalai*<sup>1</sup>; Peter Gordon<sup>1</sup>; Ju Li<sup>2</sup>; Youhong Li<sup>1</sup>; Mikhail Mendelev<sup>3</sup>; Michael Luton<sup>1</sup>; <sup>1</sup>ExxonMobil Research and Engineering; <sup>2</sup>University of Pennsylvania; <sup>3</sup>Ames Laboratory

It is well-known that at low temperatures the flow stress in alpha-Fe exhibits strong temperature dependence. This dependence arises from the motion of screw dislocations, known to be controlled by double-kink nucleation. Previous atomistic studies suggested that this temperature sensitivity is partly a consequence of the polarized core structure of the screw dislocations. However, recent ab initio calculations have shown the core structure of screw dislocations to be compact. We have investigated the kink nucleation pathways that control screw dislocation motion using newly developed interatomic potential for alpha-Fe using Nudged Elastic Band (NEB) and Molecular Dynamics (MD) simulations. In addition, we have also investigated the 2D dislocation motion using ab-initio calculations. In this presentation we will discuss the results of this study and its relevance towards understanding low temperature plasticity in alpha-Fe.

### 5:00 PM

**Atomistically Informed 3D Dislocation Dynamics Simulations of BCC Ta:** *Z. Wang*<sup>1</sup>; Irene Beyerlein<sup>1</sup>; <sup>1</sup>Los Alamos National Laboratory

Screw dislocations in BCC metals have non-planar cores, which split onto multiple planes and lead to high Peierls stresses. Atomistic simulations find that non-driving stress components affect the core structures and thus change dislocation behavior and macroscopic properties[1]. Our three-dimensional dislocation dynamics simulations of BCC Ta have shown that without proper implementation of fundamental atomistic-level dislocation properties, plastic behavior of single crystals cannot be correctly predicted. The anisotropy of Ta is dependent on the non-driving shear stresses on the {110} slip planes non-parallel to the glide plane of screw dislocations, while its tension/compression asymmetry is dependent on the stress components normal to the Burgers vector. Our work clearly demonstrates the importance of passing atomistic knowledge to models at larger length scales in understanding material behavior.[1]. K. Ito, V. Vitek, "Atomistic study of non-schmid effects in the plastic yielding of bcc metals", Phil. Mag. A, 81:1387-1407, 2001

### 5:15 PM

**Atomistic Investigation and Analysis of Dislocation Precipitate Interactions in Al-Cu Alloys:** *Chandra Veer Singh*<sup>1</sup>; Derek Warner<sup>1</sup>; <sup>1</sup>Cornell University

Al-Cu alloys are attractive aerospace materials due to their light weight and strength. The strength of these alloys is primarily controlled by precipitate formation, with the specific type of the precipitate being controlled by the material aging processes. Here we investigate the mechanisms by which a specific and well known class of precipitates, Guinier-Preston (GP) zones, influence plasticity through dislocation interaction. The dislocation-GP zone interaction is found to be either controlled by long range misfit stress fields or short range chemical forces dependent upon the dislocation-GP zone geometry. To best interpret the atomistic simulations in light of experimental literature, we investigate the activation energy barriers for dislocation-GP zone cutting using transition state theory via the finite temperature string method. Specifically, estimates of the yield strength and its rate and temperature dependence extracted from our results are compared to that of underaged Al-Cu alloys.

### 5:30 PM

**Atomistic Simulations of Athermal Cross-Slip at Screw Dislocation Intersections in Face-Centered Cubic Nickel:** *Satish Rao*<sup>1</sup>; Dennis Dimiduk<sup>2</sup>; El-Awady Jafaar<sup>3</sup>; Triplicane Parthasarathy<sup>1</sup>; Michael Uchic<sup>2</sup>; Christopher Woodward<sup>2</sup>; <sup>1</sup>UES Inc.; <sup>2</sup>Air Force Research Laboratory; <sup>3</sup>UTC

The Escaig model for thermally activated cross-slip in Face-Centered Cubic (FCC) materials assumes that cross-slip preferentially occurs at obstacles that

produce large stress gradients on the Shockley partials of the screw dislocations. However, it is unclear as to the source, identity and concentration of such obstacles in single-phase FCC materials. In this manuscript, we describe embedded atom potential, molecular-statics simulations of screw character dislocation intersections with forest dislocations in FCC Ni to illustrate a new mechanism for cross-slip nucleation. The simulations show how such intersections readily produce cross-slip nuclei and thus are preferential sites for spontaneous athermal cross-slip. The energies of the dislocation intersection cores are determined and it is shown that a partially cross-slipped configuration for the intersections is the most stable. In addition, simple 3-dimensional dislocation dynamics simulations accounting for Shockley partials are shown to qualitatively reproduce the atomistically-determined core structures for the same dislocation intersections.

### 5:45 PM

**Dislocation Statistics in FCC Crystals:** *Mamdouh Mohamed*<sup>1</sup>; Jie Deng<sup>1</sup>; Anter El-Azab<sup>1</sup>; <sup>1</sup>Florida State University

This presentation will give an overview of the statistics of dislocations in FCC crystals with the objective of providing closure of the kinetic equations within the framework of density-based models of dislocation dynamics. In this regard, we perform a detailed statistical analysis of dislocation velocity and the resolved shear stress on dislocation segments, and use this analysis to develop a mobility law valid for dislocation density. In addition, we carry out statistical analysis of the spatial and orientation statistics of dislocation and develop analytical correlation formulas suitable for the closure of the kinetic equations governing the density evolution during plastic deformation. The method of dislocation dynamics simulation will be used to conduct numerical simulation of all pertinent statistical measures.

### 6:00 PM

**Modeling of Magnesium <a> and <c+a> Dislocation Cores by First Principles and EAM Potentials:** *Thomas Nogaret*<sup>1</sup>; Joseph A. Yasi<sup>2</sup>; Louis Hector Jr<sup>3</sup>; Dallas Trinkle<sup>2</sup>; William Curtin<sup>1</sup>; <sup>1</sup>Brown University; <sup>2</sup>University of Illinois at Urbana-Champaign; <sup>3</sup>General Motors Technical Center

Magnesium has a poor formability due to its HCP structure: <a> dislocations glide easily in the basal planes, but the pyramidal <c + a> and twinning dislocations, that are required to accommodate the deformation along the <c> axis, have high Peierls stresses. The pyramidal deformation modes are not well understood and constitute a great challenge for material scientists. We performed first principles and EAM potential calculations of gamma surfaces and <a> dislocation core properties in basal and prism planes, and the results were compared. One of the tested EAM potentials was found in good agreement with ab-initio calculations and used to study <c+a> dislocations in pyramidal planes. New low energy <c+a> dislocation core structures were observed and their associated Peierls stresses were calculated at 0K and finite temperature.

## Thermo-Mechanical Response of Molecular Solids: Multi-Resolution Theory, Simulations, and Experiments: Molecular Solids I

*Sponsored by:* The Minerals, Metals and Materials Society, TMS Electronic, Magnetic, and Photonic Materials Division  
*Program Organizers:* Alejandro Strachan, Purdue University; Thomas Sewell, University of Missouri-Columbia; Rodolfo Pinal, Purdue University; Chunyu Li, Purdue University

Wednesday PM Room: 203  
February 17, 2010 Location: Washington State Convention Center

*Session Chair:* Rodolfo Pinal, Purdue University

### 2:00 PM Introductory Comments

#### 2:05 PM Invited

**Shock-Induced Subgrain Microstructures as Possible Homogenous Sources of Hot Spots and Initiation Sites in Energetic Polycrystals:** Julian Rimoli<sup>1</sup>; Ercan Gurses<sup>2</sup>; *Michael Ortiz*<sup>2</sup>; <sup>1</sup>MIT; <sup>2</sup>Caltech

Microscopic defects such as voids are thought to be a prime source of hot-spots in crystalline energetic materials. For instance, the formation of jets during the collapse of voids may result in temperatures and pressures that

# Technical Program

greatly exceed values in the bulk, thereby promoting molecular decomposition. The impact sensitivity of defect-free energetic single crystals is comparatively less well-understood, but dislocation-mediated plasticity suggests itself as an explanation for the observed orientation dependencies. It is well-known that dislocation-mediated plastic deformation is almost universally inhomogeneous at the sub-grain level and exhibits microstructural patterns that include localization of deformation and temperature to slip-lines. We investigate the role of such slip-lines as possible hot-spots for initiation in void-free energetic polycrystals. We account for sub-grain microstructure development by means of an explicit construction that can be shown to be optimal. The construction is integrated into a finite element model to simulate the plate-impact test of PETN.

## 2:35 PM

### **Shear-Induced Disorder in Small Molecule Organic Crystalline Solid Materials: Modeling, Characterization and Relevance in Pharmaceutical Drug Products:** *Peter Wildfong*<sup>1</sup>; <sup>1</sup>Duquesne University

Small molecule organic crystalline solids and polymers used to manufacture composite solid oral drug products are often subject to phase transitions resulting from exposure to high shear mechanical processing. Transformations to the amorphous state can result in unpredictable product performance. Multivariate logistic regression was applied to a library of 23 organic crystalline materials to develop a model that identifies properties correlating with the potential to become completely disordered upon application of intense mechanical shear. The optimum model combined glass transition temperature and molar volume, which predicted disordering potential in complete agreement with experimental observations. Of the materials studied, theophylline (a common bronchodilator) was observed to be susceptible to significant disordering under shear stress. Compaction of this material alone, and in the presence of common excipients resulted in detectable induction of disorder as evaluated by PDF-transformed PXRD data collected from intact tablets. Implications for drug delivery are discussed.

## 2:55 PM

### **Thermo-Mechanical and Spectroscopic (TMS) Analyses of Structural Transformation Produced by Mechanical Processing:** *Derya Cebeci*<sup>1</sup>; *Diana Guzman*<sup>1</sup>; *Dea Herrera*<sup>2</sup>; *Dor Ben-Amotz*<sup>1</sup>; *M. Teresa Carvajal*<sup>1</sup>; <sup>1</sup>Purdue University; <sup>2</sup>Facultad de Farmacia, UAEM

Milling is a method to reduce particle size of materials and it is among the methods used to enhance the dissolution rate and the oral bioavailability of the active pharmaceutical ingredient (API, drugs) with poor aqueous solubility. However, milling brings multiple transformations produced in the API. These transformations and the resulting behavior of certain organic solid materials need a more fundamental understanding. The influence of mechanical stress applied by cryogenic milling of the crystalline organic solids was investigated via thermal, spectroscopic and mechanical analyses. Various model crystalline APIs were cryo-milled followed by characterization using analytical tools such as XRPD, DSC, Raman, DMA and surface analysis by inverse gas chromatography (IGC) to determine the existence of phase transitions phenomena induced during milling. Differences in the behavior between milled, amorphous and crystalline drugs were clearly observed. Selected experimental and theoretical results from this study will be presented and discussed.

## 3:15 PM

### **Microstructural Evolution of Molecular Crystals:** *Lei Lei*<sup>1</sup>; *Marisol Koslowski*<sup>1</sup>; <sup>1</sup>Purdue University

Understanding the mechanisms of deformation of molecular crystals is critical in processing of pharmaceutical products as well as in tailoring key drug properties such as dissolution rate and stability. The process of milling of pharmaceutical materials not only results in particle size reduction but also induces a significant degree of disorder in the material. The increase in disorder as a result of milling can be of two types; either crystal lattice defects or amorphous regions. Here we propose a model to study the transition from a high dislocation density crystal to an amorphous material. In particular we analyze the effect of grain and particle size in this transition with 3D dislocation dynamics simulations.

## 3:35 PM Break

## 3:55 PM

### **Mechanical Response of Pharmaceutical and Explosive Molecular Single Crystals:** *Kyle Ramos*<sup>1</sup>; *Daniel Hooks*<sup>1</sup>; *David Bahr*<sup>2</sup>; <sup>1</sup>Los Alamos National Laboratory; <sup>2</sup>Washington State University

The mechanical response of molecular crystals is important in a variety of applications. Dislocations have been implicated in die compaction affecting the physical integrity and bioavailability of solid dosage pharmaceutical tablets and in initiation mechanisms affecting the sensitivity to detonation of explosives. Nanoindentation investigations of oriented molecular, single crystals have been conducted revealing orientation dependent nucleation of dislocations through load excursion behavior. Atomic force microscopy characterization of the peripheral regions surrounding indentation impressions has allowed direct observation of slip traces and deformation mechanism analysis using zone axis projections. Deformation features indicate the appearance of additional slip modes in terms of cross slip and new slip systems as a function of orientation and indentation load. These observations provide explanations for deformation behavior in terms of compatibility conditions. Experimental data will be presented for exemplary materials from the pharmaceutical and explosive industries.

## 4:15 PM

### **Thermal and Elastic Mechanical Properties of Crystalline 1,3,5-Triamino-2,4,6-Trinitrobenzene (TATB):** *Dmitry Bedrov*<sup>1</sup>; *Oleg Borodin*<sup>1</sup>; *Grant Smith*<sup>1</sup>; *Thomas Sewell*<sup>2</sup>; *Dana Dattelbaum*<sup>3</sup>; *Lewis Stevens*<sup>3</sup>; <sup>1</sup>University of Utah; <sup>2</sup>University of Missouri-Columbia; <sup>3</sup>Los Alamos National Laboratory

TATB is a high-explosive compound that is remarkably insensitive to shock or thermal initiation. Molecular dynamics simulations of TATB crystals were performed using quantum-chemistry-based dipole polarizable and nonpolarizable force fields for hydrostatic pressures up to 10 GPa at 300 K and for temperatures between 200 K and 500 K at atmospheric pressure. The predicted heat of sublimation and room temperature hydrostatic compression curve were found to be in good agreement with available experimental data. The pressure- and temperature-dependent second-order isothermal elastic tensor was determined for temperatures between 200 K and 400 K at normal pressure and for pressures up to 10 GPa on the 300 K isotherm. The results indicate considerable anisotropy in the mechanical response of the triclinic crystal, with modest softening and significant stiffening of the crystal with increased temperature and pressure, respectively. In general, the polarizable potential was found to yield better agreement with available experimental properties.

## 4:35 PM Invited

### **Thermodynamic Stability and Formation of Multicomponent Molecular Crystals:** *Chinmay Maheshwari*<sup>1</sup>; *Rodolfo Pinal*<sup>2</sup>; *Nair Rodriguez-Hornedo*<sup>1</sup>; <sup>1</sup>University of Michigan; <sup>2</sup>Purdue University

Cocrystals offer the advantage of generating solid forms of active pharmaceutical ingredients (APIs) with other molecular components and produce materials with strikingly different and advantageous physicochemical properties such as solubility and stability. Much of the research in this field has focused on the application of supramolecular chemistry concepts to the design of cocrystals while cocrystal formation and structure-property relationships are not well understood. This talk will address phase formation, stability and transformation during the synthesis, processing and use of pharmaceutical cocrystals. A thorough understanding of cocrystal thermodynamics is critical for the development of these materials. Calculation of cocrystal free energies of formation will be presented from thermal analysis of solid phases and solubility behavior of cocrystal and its components.

## 5:05 PM Invited

### **Acoustic and Thermal Responses across the Brillouin Zone:** *Keith Nelson*<sup>1</sup>; <sup>1</sup>Department of Chemistry, MIT

We have developed time-domain methods for optical generation and measurement of longitudinal and shear acoustic waves spanning much of the Brillouin zone, including MHz-GHz frequencies and micron-nanometer wavelengths. These are being applied to the study of viscoelastic behavior and thermal transport in a wide range of materials. Thermal diffusivity measurements are made directly as well, and the results can be compared to the values determined for wavevector-dependent phonon mean free paths. Finally, we have extended the techniques to permit generation of nonlinear acoustic and shock waves whose propagation and evolution can be observed directly.



### Three-Dimensional Materials Science VI: Novel Tools for 3D Data Acquisition and Analysis - Part II

*Sponsored by:* The Minerals, Metals and Materials Society, ASM International, TMS Structural Materials Division, TMS: Advanced Characterization, Testing, and Simulation Committee, ASM-MSCTS: Texture and Anisotropy Committee, TMS/ASM: Phase Transformations Committee

*Program Organizers:* Alexis Lewis, Naval Research Laboratory; Anthony Rollett, Carnegie Mellon University; David Rowenhorst, Naval Research Lab; Jeff Simmons, AFRL; Stuart Wright, EDAX Inc-TSL

Wednesday PM Room: 401  
February 17, 2010 Location: Washington State Convention Center

*Session Chairs:* George Spanos, U S Naval Research Laboratory; Nik Chawla, Arizona State University

#### 2:00 PM Invited

##### X-Ray Synchrotron Tomography for Three Dimensional (3D) Microstructure Visualization and Modeling of Deformation in Metal Matrix Composites:

Jason Williams<sup>1</sup>; Anna Tosas<sup>1</sup>; Zeke Flom<sup>1</sup>; *Nik Chawla*<sup>1</sup>; Francesco de Carlo<sup>2</sup>; <sup>1</sup>Arizona State University, School of Mechanical, Aerospace, Chemical, and Materials Engineering; <sup>2</sup>Argonne National Laboratory/Advanced Photon Source

We report on a novel methodology that addresses the critical link between microstructure and deformation behavior, by using a three-dimensional (3D) virtual microstructure as the basis for a robust model to simulate damage caused by deformation. The approach involves capturing the microstructure by novel and sophisticated x-ray tomography techniques, using an x-ray synchrotron source, followed by image analysis, 3D reconstruction of the microstructure, and incorporation into a powerful finite element modeling code for simulation. We will present a case study based on uniaxial tensile deformation of SiC particle reinforced Al alloy matrix composites. In particular, the damage in the form of particle fracture, interfacial debonding, and void growth will be described. Acknowledgment: Use of the Advanced Photon Source was supported by the U. S. Department of Energy, Office of Science, Office of Basic Energy Sciences, under Contract No. DE-AC02-06CH11357.

#### 2:30 PM

##### Orientation Determination by Laue Diffractometry in a Robomet.3D System: *Abhijeet Budruk*<sup>1</sup>; Clayton Stein<sup>1</sup>; Marc De Graef<sup>1</sup>; <sup>1</sup>Carnegie Mellon University

There is growing interest in 3D microstructural data across a broad range of length scales. Existing focused ion beam (FIB) scanning electron microscope and micro-miller-optical microscope combinations cannot conveniently provide 3D information for large sample volumes (several cubic millimeters or larger) while simultaneously obtaining orientational data. To this end, a high-resolution x-ray Laue camera has been added to a metallographic Robomet.3D system, a custom integration of off-the-shelf components, including a programmable robot arm, a multiprep polishing machine, a sample preparation stage, and an inverted motorized optical microscope. The combined system will automatically acquire serial sectioning images of microstructures along with orientational information through the automated indexing of x-ray Laue diffraction patterns. In addition to sectioning larger volumes, it has the advantage of acquiring orientational data on ceramic as well as metallic samples, as it does not employ charged particles as in the more conventional FIB+OIM configuration.

#### 2:50 PM

##### Utilizing the New Femtosecond Laser Tomographic Sectioning Technique: Reconstruction and Analysis of Low Volume Fraction Titanium Nitride Particles: *McLean Echlin*<sup>1</sup>; Naji Hussein<sup>1</sup>; John Nees<sup>1</sup>; Tresa Pollock<sup>1</sup>; <sup>1</sup>University of Michigan

Rarely occurring inclusion phases can determine fundamental material properties, such as fatigue life and shear strength. A titanium-modified 4330 steel system with low volume fraction (0.02 to 0.07%) titanium nitride inclusions was serial sectioned and reconstructed using a recently developed tomographic technique that utilizes a femtosecond laser to perform the machining steps. This sectioning technique operates in a fully automated mode, with fast removal rates of approximately  $7.5 \times 10^4 \mu\text{m}^3/\text{s}$ , and a minimum slice thicknesses of

50 nm/slice. TiN datasets were collected over unattended 40-48 hour periods, with subsequent segmentation of the image stack taking 3-5 hours. Volume fraction, particle spacing, nearest neighbor distances, and other statistics were compared with mechanically serial sectioned datasets of the same alloy. In Situ spectrographic data collection is also demonstrated as an alternative chemical recognition technique for inclusion phase differentiation.

#### 3:10 PM

##### Three-Dimensional (3D) Visualization and Modeling of Reflow Porosity in Pb-Free Solder Joints by Lab-Scale X-Ray Tomography: *Ling Jiang*<sup>1</sup>; Martha Dudek<sup>1</sup>; Jason Williams<sup>1</sup>; Nik Chawla<sup>1</sup>; Luke Hunter<sup>2</sup>; S.H. Lau<sup>2</sup>; <sup>1</sup>Arizona State University, School of Mechanical, Aerospace, Chemical, and Materials Engineering; <sup>2</sup>XRadia

X-ray tomography is an excellent non-destructive technique for quantifying microstructures in three dimensions (3D). We have used lab-scale x-ray tomography to visualize the microstructure of a Sn-3.9Ag-0.7Cu/Cu solder joints. The system had a high resolution (1  $\mu\text{m}$ ), which was used for visualization of the three-dimensional (3D) characteristics of reflow porosity. The microstructure of the solder joints was visualized using the x-ray microtomography system, followed by monotonic shear and fatigue experiments of the individual joints. The effect of pore fraction, size, distribution and geometry of each individual joint, was then simulated using the finite element method. A comparison between the experiments and simulations will be discussed.

#### 3:30 PM Break

#### 4:00 PM

##### Direct Three Dimensional Characterization of Microstructures in $\alpha/\beta$ - and $\beta$ -Ti Alloys: *Robert Williams*<sup>1</sup>; Daniel Huber<sup>1</sup>; John Sosa<sup>1</sup>; Santhosh Koduri<sup>1</sup>; Vikas Dixit<sup>1</sup>; Peter Collins<sup>1</sup>; Srinivasan Rajagopalan<sup>1</sup>; Hamish Fraser<sup>1</sup>; <sup>1</sup>The Ohio State University

New research tools for the direct 3-D characterization of microstructures have been developed and applied to the characterization of  $\alpha/\beta$ - and  $\beta$ -Ti alloys. The first tool can acquire 3-D datasets using various techniques, including: Optical Microscopy (using the RoboMet-3D™), the Dual Beam-FIB (imaging with either secondary or backscattered electrons), 3D EBSD/OIM (for Ti-based alloys), and Energy Filtered (EFTEM) tomography using (scanning) transmission electron microscopy. The second tool provides an "automated" methodology for 3-D reconstructions through image preprocessing on large image stacks, including alignment of individual images, resulting in the reconstruction of microstructural features. The tool provides for isolation of individual features and their refinement when image preprocessing is inaccurate. These tools, and their application to the direct 3-D characterization of microstructures of  $\alpha/\beta$ - and  $\beta$ -Ti alloys, will be discussed. Support from the Office of Naval Research and the Defense Advanced Research Agency under contract number N00014-05-1-0504 is gratefully acknowledged.

#### 4:20 PM

##### 3D Characterization, Analysis, and Modeling Tools: *George Spanos*<sup>1</sup>; Andrew Geltmacher<sup>1</sup>; <sup>1</sup>Naval Research Laboratory

The objective of this team project has been to develop a set of tools for the generation, quantitative analysis, visualization, and collaborative exchange of experimental and simulated 3D materials microstructure and properties data. The team consists of eight research groups from various universities and laboratories, including a group at the Naval Research Laboratory (NRL) who assembled the team. The suite of tools developed provides materials researchers and designers with 3D materials data and predictive modeling capabilities, and can be categorized under three components. The first two components include experimental tools for generating and analyzing 3D data, and computational "Evolver" modules for predictive modeling and simulation. The final component is a Web-based 3D Materials Atlas and related materials data environment for interactive exchange of 3D materials data between materials researchers and/or designers. This talk will provide an overview of the program, and outline the individual tasks and team members.

#### 4:40 PM

##### D3D Design Research Tools: *Greg Olson*<sup>1</sup>; <sup>1</sup>Northwestern University

A suite of tomographic characterization and analysis tools for quantification of the spatial distribution of multiscale particle dispersions has been integrated with a set of high fidelity 3D simulation tools addressing microstructural evolution governing strength, toughness, shear instability resistance and fatigue

# Technical Program

strength in high-performance steels for naval applications. Atomic-scale LEAP tomographic reconstruction has quantified the obstacle spacing distributions in martensitic steels strengthened by a combination of bcc Cu and M<sub>2</sub>C carbide precipitation. FIB/SEM reconstruction of a shear band cut from an isothermal shear test specimen taken to the onset of shear localization demonstrates an early stage of microvoid formation at TiC particle clusters. Crack tip reconstruction clarifies the relation of primary voids and the pattern of shear localization that accelerates their coalescence, consistent with multiscale simulations and measured correlation of normalized toughness with critical void growth ratio. ONR/DARPA sponsored.

---

## Ultrafine Grained Materials – Sixth International Symposium: Applications and Transitions

*Sponsored by:* The Minerals, Metals and Materials Society, TMS Materials Processing and Manufacturing Division, TMS Structural Materials Division, TMS/ASM: Mechanical Behavior of Materials Committee, TMS: Nanomechanical Materials Behavior Committee, TMS: Shaping and Forming Committee

*Program Organizers:* Suveen Mathaudhu, U.S. Army Research Laboratory; Mathias Goeken, University Erlangen--Nürnberg; Terence Langdon, University of Southern California; Terry Lowe, Manhattan Scientifics, Inc.; S. Semiatin, Air Force Research Laboratory; Nobuhiro Tsuji, Kyoto University; Yonghao Zhao, University of California - Davis; Yuntian Zhu, North Carolina State University

Wednesday PM Room: 606  
February 17, 2010 Location: Washington State Convention Center

*Session Chairs:* Suveen Mathaudhu, U.S. Army Research Laboratory; Yuntian Zhu, North Carolina State University; Terry Lowe, Manhattan Scientific; Judson Marte, GE Global Research

---

### 2:00 PM Awards Presentation

### 2:10 PM Panel Discussion

### 2:30 PM Invited

**Can SPD Techniques Provide Bulk Ultrafine Grained Functional Materials?:** *Michael Zehetbauer*<sup>1</sup>; <sup>1</sup>University of Vienna

The fact that SPD techniques allow processing of bulk ultrafine grained (UFG) materials with advanced mechanical properties suggests to apply them also for bulk *functional* ones, especially in cases where physical properties could be significantly increased already in UFG materials with small dimensions. Some success has been reached in SPD processed bulk shape memory UFG alloys, UFG metals/alloys for hydrogen storage, and UFG magnetic alloys. However, applying SPD for achieving bulk UFG materials with other functional properties like thermoelectric ones, or like such being tunable by electronic interface charging, seems questionable. Alternative processing routes using SPD for consolidation of powder UFG materials from ball milling and other techniques may open some chances here.

### 2:50 PM

**Corrosion and Mechanical Properties of a Steel Processed by SMAT in Contrast to Its Coarse Grained Counterpart:** *Indranil Roy*<sup>1</sup>; Christian Wilkinson<sup>1</sup>; Rashmi Bhavsar<sup>1</sup>; Jian Lu<sup>2</sup>; Yuntian Zhu<sup>3</sup>; Farghalli Mohamed<sup>4</sup>; <sup>1</sup>Schlumberger; <sup>2</sup>The Hong Kong Polytechnic University; <sup>3</sup>North Carolina State University; <sup>4</sup>University of California, Irvine

Corrosion resistance, the ability of a material to mitigate deterioration of its intrinsic properties due to reactions with its environment, especially in H<sub>2</sub>S has been an engineering challenge for the oil and gas industry to extract hydrocarbons. Material selection for oilfield tools is generally dictated by a few available standards, for example, NACE MR 01-75. It has been a constant endeavor to develop and qualify more resistant materials for hostile applications that also comply to these standards. In this presentation we discuss the corrosion and salient mechanical properties of a steel treated by SMAT to produce a gradient of nanocrystalline grains on the alloy's surface, starting from a coarse-grained condition.

### 3:05 PM

**Eutectic Structure from an Amorphous Al<sub>2</sub>O<sub>3</sub>-ZrO<sub>2</sub>-Y<sub>2</sub>O<sub>3</sub> System by Rapid-Quenching Technique for Potential Hybrid Solar Cell Application:** *Young-Hwan Han*<sup>1</sup>; Jondo Yun<sup>2</sup>; Yohei Harada<sup>3</sup>; Taro Makino<sup>3</sup>; Kwang-Ho Kim<sup>1</sup>; Sehun Kwon<sup>1</sup>; Kazuyuki Kakegawa<sup>3</sup>; <sup>1</sup>Pusan National University; <sup>2</sup>Kyungnam University; <sup>3</sup>Chiba University

Rapid-quenched eutectic crystals are known to be finely oriented, particular microstructures with strong bonding between the component phases, which controls and improves the microstructures. Eutectic ceramics have excellent high temperature strength characteristics, creep resistance, oxidation resistance, and thermal stability at 1700°C in air. Al<sub>2</sub>O<sub>3</sub>-based eutectic systems have been studied for use in the emitters of thermophotovoltaic (TPV) generation systems, which emit photons when thermally excited by a heat source. Ternary Al<sub>2</sub>O<sub>3</sub>-ZrO<sub>2</sub>-Y<sub>2</sub>O<sub>3</sub> samples with a eutectic composition were prepared using the rapid-quenching method, with some samples further annealed at 1300°C for 30 min and then slow cooled. The SEM and TEM observations of the ternary samples agreed with the XRD: The rapid-quenched sample was an amorphous phase. Observations showed that the rapid-quenched and annealed sample was completely crystalline with a granular structure and well-defined crystals of 40-60 nm.

### 3:20 PM Invited

**Recycling of Titanium Machining Chips by Severe Plastic Deformation Consolidation:** P. Luo<sup>1</sup>; H. Xie<sup>1</sup>; M. Paladugu<sup>2</sup>; S. Palanisamy<sup>2</sup>; M. S. Dargusch<sup>2</sup>; K. Xia<sup>1</sup>; <sup>1</sup>University of Melbourne; <sup>2</sup>University of Queensland

It has been demonstrated that SPD can be used to consolidate particles of a wide range of sizes from nano to micro into fully dense bulk material with good mechanical properties. SPD consolidation allows processing to be conducted at much lower temperatures and is therefore suitable for particles with highly metastable structures such as nanocrystalline. It is especially useful in the fabrication of multiphase materials including metal matrix nanocomposites. In this investigation, SPD consolidation was applied to recycle Ti machining chips. In particular, the as-received chips were consolidated by equal channel angular pressing at temperatures between 300 and 600°C with the application of a back pressure from 50 to 200 MPa. Fully dense bulk Ti with ultrafine grain sizes was produced, possessing strength comparable or higher than that of commercially pure wrought Ti. It is concluded that SPD consolidation is a promising method for recycling and value-adding of Ti chips.

### 3:40 PM

**Processing of High Temperature Shape Memory Alloy Ni<sub>33.7</sub>Ti<sub>50.3</sub>Pd<sub>16</sub> via Equal Channel Angular Extrusion:** *Mohammed Haouaoui*<sup>1</sup>; Benat Kockar<sup>2</sup>; Kadri C. Atli<sup>1</sup>; Ji Ma<sup>1</sup>; Ibrahim Karaman<sup>1</sup>; <sup>1</sup>Texas A&M University; <sup>2</sup>Hacettepe University

High temperature shape memory alloys (HTSMAs) with phase transformation temperatures above 100°C have wide uses and opportunities for developments in automotive, aeronautical and oil applications. The main issues in HTSMAs are poor cyclic dimensional stability and fatigue life, and poor formability. Equal channel angular extrusion (ECAE) is used to tackle the plasticity problem in these materials by refining the microstructure and eliminating/breaking up detrimental precipitates. We will present the methodology and the appropriate ECAE processing conditions which permit application of high strains to the hard to work Ni<sub>33.7</sub>Ti<sub>50.3</sub>Pd<sub>16</sub> material without causing cracking or shear localization of the workpiece. The processing parameters include the canning material, the dimensions of the can, extrusion temperatures, routes and number of passes. Processing Ni<sub>33.7</sub>Ti<sub>50.3</sub>Pd<sub>16</sub> through route 4E at 425°C proved to increase the dimensional and cyclic stability and decrease the irrecoverable strains. ECAE also increases the fracture toughness by breaking up the brittle precipitates.

### 3:55 PM

**Enabling Near-Net Shaped Forging of Titanium Aerospace Components by Severe Plastic Deformation:** *Judson Marte*<sup>1</sup>; Robin Forbes Jones<sup>2</sup>; <sup>1</sup>GE Global Research; <sup>2</sup>ATI Allvac

Severe plastic deformation technologies enable materials capable of low-temperature superplastic response. This presentation will provide an overview of an ongoing collaborative program between ATI Allvac and GE evaluating the production, characterization, and application of ultrafine-grained titanium. Multi-axis forging (MAF) has been used to produce bulk samples with submicron alpha grain size. Extensive characterization of the microstructure

shows that, after MAF, the beta phase tends to pin alpha, enhancing thermal stability. Deformation properties have been evaluated and used to make finite element models of near-net shape forging processes. Laboratory-scale near-net shape forgings have been produced to demonstrate feasibility and provide material for microstructural and mechanical evaluation, which will also be presented.

#### 4:10 PM Break

#### 4:25 PM Invited

**Improved Recrystallized Microstructures in Nb and Ta:** *K. Ted Hartwig*<sup>1</sup>; Shreyas Balachandran<sup>1</sup>; Suveen Mathaudhu<sup>2</sup>; <sup>1</sup>Texas A&M University; <sup>2</sup>U.S. Army Research Laboratory

Low temperature superconducting wires are made by extrusion and wire drawing. In all cases, uniform deformation of the wire components is crucial for optimum electrical performance of the wire. Non-uniform deformation of the wire components during fabrication often occurs and can lead to mechanically weak regions, increased electrical resistance, and wire fracture. The origin of nonuniform deformation includes a nonuniform and poorly oriented starting microstructure; a remedy to the problem is microstructural refinement and texture control. Grain refinement and a degree of texture control in recrystallized microstructures can be achieved through uniform, oriented and severe plastic deformation (SPD) allied via multipass equal channel angular extrusion combined with recrystallization annealing treatments. Results from work done on pure niobium and pure tantalum for improved filament and diffusion barrier codeformation behavior in Nb<sub>3</sub>Sn filamentary superconductors are given to illustrate the benefits of SPD processing for improved microstructures in recrystallized materials.

#### 4:45 PM

**Deformation Processing of Nanostructured Alloys and Their Application in the Production of Hollow Structures:** *Radik Mulyukov*<sup>1</sup>; Oleg Valiakhmetov<sup>1</sup>; Rafail Galeev<sup>1</sup>; Rinat Safiullin<sup>1</sup>; Aleksey Kruglov<sup>1</sup>; Renat Imayev<sup>1</sup>; Ayrat Nazarov<sup>1</sup>; Victor Ivan'ko<sup>2</sup>; <sup>1</sup>Institute for Metals Superplasticity Problems, Russian Academy of Sciences; <sup>2</sup>CJSC "INNOTEKHPRM"

Principles of production of nanostructured materials by multiple isothermal forging and warm rolling are formulated. The former allows processing of bulk materials with a uniform nanostructure, while the latter transforms these materials into sheet semi-products retaining their nanostructure. On an example of titanium alloys it is demonstrated that technological operations with nanostructured sheet materials such as pressure welding and superplastic forming can be performed at significantly lower temperatures than with sheet materials having conventional fine grains. This opens new possibilities for the fabrication of hollow structures by a combination of pressure welding and superplastic forming. On an example of hollow blades for double-flow aircraft engines the development of a technology for an implementation in the industry is demonstrated. It is shown that the technology proposed provides not only an enhancement of the properties of hollow blades but also makes their production cost, energy and labor effective and ecologically more friendly.

#### 5:00 PM

**Design and Realization of High Strength and High Ductility Metallic Nanomaterials:** *Jian Lu*<sup>1</sup>; Ai Ying Chen<sup>1</sup>; Hoi Lam Chan<sup>1</sup>; Hong Ning Kou<sup>1</sup>; Lin Li Zhu<sup>1</sup>; Hai Hui Ruan<sup>1</sup>; Ka Po Cheung<sup>1</sup>; <sup>1</sup>The Hong Kong Polytech University

Nanocrystalline materials have attracted considerably scientific interests from both academia and industries due to their unique material properties. We summarize the recent development of the high strength and high ductility metallic nanomaterials. The SMAT (surface mechanical attrition treatment) has been combined with other technologies (co-rolling, electro-deposition, pre- and post-heat treatments) for enhancing the yield stress of the materials by 200% to 300% with limited reduction of elongation. The development of different efficient fabrication methods for obtaining nanomaterials with exceptional high strength and high ductility by different toughening strategies will be presented: layered nanostructured stainless steel, high twin density Cu and Fe based metallic nanomaterials. The results obtained using the multiscale experimental (nanoindentation, in-situ SEM) and simulation (MD, crystal plasticity, multimillions elements FEM) tools for investigating the local mechanical behavior of the graded structural materials will be presented.

#### 5:15 PM Invited

**Potential of Severe Plastic Deformation for Producing Bioimplant Materials:** *Yuri Estrin*<sup>1</sup>; <sup>1</sup>Monash University

Several techniques of severe plastic deformation (SPD), notably equal-channel angular pressing as a most developed method, are known to lead to extreme grain refinement in metals and alloys. The ensuing improvement of mechanical properties, including enhancement of fatigue strength, opens up possibilities of downsizing metallic bioimplants or using commercial purity materials, such as CP titanium, instead of alloys, thus eliminating the exposure of the patient to toxic alloying elements. Recent studies conducted in a number of research groups suggest that beside the strengthening effect, SPD processing may lead to improved biocompatibility of the prospective implant materials, such as enhanced cell adhesion and accelerated cell growth. An overview of recent developments in this area will be given, with an emphasis on CP titanium for permanent implant applications and magnesium alloys for temporary, bioresorbable implants.

#### 5:35 PM

**Concluding Comments**

# Technical Program

## 2010 Functional and Structural Nanomaterials: Fabrication, Properties, Applications and Implications: Mechanical Properties of Nanomaterials

*Sponsored by:* The Minerals, Metals and Materials Society, TMS Electronic, Magnetic, and Photonic Materials Division, TMS: Nanomaterials Committee

*Program Organizers:* David Stollberg, Georgia Tech Research Institute; Nitin Chopra, University of Alabama; Jiyoung Kim, University of Texas - Dallas; Seong Jin Koh, University of Texas at Arlington; Navin Manjoran, Siemens Corporation; Ben Poquette, Keystone Materials; Jud Ready, Georgia Tech

Thursday AM                      Room: 214  
February 18, 2010                Location: Washington State Convention Center

*Session Chairs:* Gregory Thompson, University of Alabama; David Stollberg, Georgia Tech Research Institute

### 8:30 AM Introductory Comments

#### 8:35 AM

**Substrate Effect on the Young's Modulus Measurement of TiO<sub>2</sub> Nanoribbons by Nanoindentation:** *Xiaoxia Wu*<sup>1</sup>; Terry T. Xu<sup>1</sup>; <sup>1</sup>University of North Carolina Charlotte

Nanoindentation was conducted on individual TiO<sub>2</sub> nanoribbons laid on different substrates, including 1 nm thick SiO<sub>2</sub> layer on Si, Si(100) and sapphire (0001). The nanoribbons had an average thickness of 30 nm and width of 150 nm. Experiment results showed that substrate has a significant effect on Young's modulus measurement. To further understand the substrate effect, three-dimensional (3D) finite element modeling was carried out to simulate the indentation of nanoribbon-on-substrate systems using the commercial software ABAQUS. Numerical results demonstrated that nanoindentation could measure the intrinsic mechanical properties of the nanoribbon if a suitable substrate was chosen. Otherwise, the Young's modulus of the nanoribbon could be either overestimated or underestimated depending on substrate used. For the TiO<sub>2</sub> nanoribbons, the intrinsic mechanical properties could be obtained from the indentation tests when sapphire (0001) was used as the substrate. The Young's modulus of TiO<sub>2</sub> nanoribbons was determined to be  $375 \pm 25$  GPa.

#### 8:55 AM

**Commercializing Unique Molecular-Scale Surface and Interfacial Coatings:** *Eric Bruner*<sup>1</sup>; <sup>1</sup>Aculon, Inc.

Self-Assembled Monolayers of Phosphonates (SAMP) enable a variety of applications by imparting hydrophobicity, adhesion, or corrosion. SAMPs can impart any of these properties as desired to metals, metal oxides and even some polymer surfaces by drawing on a library of structurally tailored phosphonic acids. The secret to the commercialization is covalent bonding, which creates a uniquely strong attachment between the SAMP and substrate. The SAMP is one approximately 1.5 nm thick. It completely covers the material to which it is applied, and assures total surface coverage regardless of the type or texture of that material. The composition of the SAMP determines the properties it imparts to its substrate. Terminal omega group substituents are chosen to act as reactive handles to covalently bond materials subsequently deposited. Using SAMPs as interfacial coating layers is a powerful tool for solving adhesion issues between dissimilar materials.

#### 9:15 AM

**Fracture Behavior of Co-Rich Nanocrystalline Soft Magnetic Ribbons:** *Maria Daniil*<sup>1</sup>; Paul Ohodnicki<sup>2</sup>; Michael McHenry<sup>2</sup>; Matthew Willard<sup>1</sup>; <sup>1</sup>Naval Research Laboratory; <sup>2</sup>Carnegie Mellon University

(Co,Fe)-based nanocrystalline alloys have good soft magnetic properties at high frequencies and temperatures making them candidates for transformers and inductors. Recently, the fracture toughness of ribbons was found to improve with increased Co-content. In this work, the fracture behavior and mechanical properties of (Co<sub>1-x</sub>Fe<sub>x</sub>)<sub>89</sub>Zr<sub>7</sub>B<sub>4</sub> (x=0-0.7) nanocrystalline ribbons were studied. These ribbons consist of majority hcp-(Co,Fe) for the Co-rich composition x=0, bcc-(Co,Fe) for moderate and higher Fe contents (x=0.05) and grain sizes below 15 nm for all compositions. The relative strain-at-fracture decreases dramatically for x = 0.15, with corresponding brittle fracture surfaces,

no shear banding and high Vickers hardness values. Samples with lower Fe contents show a maximum strain-at-fracture at x=0.025 and 0.05. The brittle ribbons showed smoother fracture surface, very little or no shear bands and very high hardness. The more ductile ribbons exhibit vein patterned fracture surfaces, significant microvoids, extensive shear bands, and lower hardness.

#### 9:35 AM

**Ductility of Bulk Nanostructured Materials:** *Yonghao Zhao*<sup>1</sup>; Yuntian Zhu<sup>2</sup>; Enrique Lavernia<sup>1</sup>; <sup>1</sup>University of California-Davis; <sup>2</sup>North Carolina State University

The limited ductility of bulk nanostructured materials has evolved as one of major hurdles limiting widespread application of these materials, despite their relatively high strength. The low ductility of bulk nanostructured materials is determined by their limited plasticity and deformation mechanisms. In this talk, we will first review microstructure (including grain size, grain size distribution, grain boundary nature, dislocation density and configuration, texture, solid solute and precipitates)-ductility relationship and external factors (including strain rate, temperature, specimen dimensions, processing artifacts and boundary segregation) that influence the ductility of bulk nanostructured materials, and then summarize effective strategies for improving the poor ductility of bulk nanostructured materials. Finally we will report on recent efforts in our laboratories to implement these strategies in nanostructured Cu, Ni, Ti to obtain both high strength and ductility.

#### 9:55 AM

**Evaluation of Fracture Toughness of Carbon Nanotube Reinforced Nano-Aluminum Oxide Via Fractal Approach:** *Abhishek Rishabh*<sup>1</sup>; Kantesh Balani<sup>1</sup>; <sup>1</sup>Indian Institute of Technology Kanpur

Aluminum oxide (Al<sub>2</sub>O<sub>3</sub>) is considered as high temperature ceramic owing to its high hardness and wear resistance at high temperatures. Lately, the secondary reinforcements, such as of carbon nanotubes (CNTs) have shown to enhance the fracture toughness of Al<sub>2</sub>O<sub>3</sub> matrix by 50% - 300%. The grain size transition from nano to micro of Al<sub>2</sub>O<sub>3</sub> (either equiaxed or elongated), porosity content, and CNT reinforcement can play a major role in dictating the elastic modulus and consequent toughening. Fractal approach has been utilized in the current analytic modeling to predict the fracture toughness of Al<sub>2</sub>O<sub>3</sub>-CNT nanocomposites using Mandelbrot fractal geometry with deciding crack pathway. This new approach of considering circumferential crack-path propagation along the CNT surface has shown that experimental fracture toughness values of plasma sprayed Al<sub>2</sub>O<sub>3</sub> - CNT nanocomposites fall within the standard deviation range (or ~2% error) of estimations.

#### 10:15 AM Break

#### 10:30 AM

**Warm Sever Plastic Deformation to Form Nanostructured Surface Layer in IF Steels:** *Mohammad Nasirizadeh*<sup>1</sup>; Kamran Dehghani<sup>1</sup>; <sup>1</sup>Amirkabir University

Warm sever plastic deformation is introduced in the present work as a new technique to form nanostructure layers on the surface of interstitial free (IF) steels. This technique is an easy, practical, simple and low-cost method to carry out the surface SPD. The process was then modeled using FEM to predict the required strain to attain the nanograins on surface of an interstitial free steel. The results show that at 350°C with the brush rotating of 25000 rpm, one is able to attain a strain about 3.6 required to form nanograins by SPD. The formation of nanograins, 50-150nm, was observed within a surface layer of about 45µm thick. TEM, AFM and SEM techniques were used to characterize the nanostructured layers.

#### 10:50 AM

**Bulk Functional Materials Obtained by Shock Waves Compaction of Ultrafine Al and Ti:** *Nikoloz Chikhradze*<sup>1</sup>; Constantin Politis<sup>1</sup>; Mikheil Chikhradze<sup>1</sup>; Akaki Gigineishvili<sup>1</sup>; George Oniashvili<sup>1</sup>; <sup>1</sup>Mining Institute/Georgian Technical University

Investigations of shock wave consolidation processes of nano sized Al and ultra-disperse Ti-powder compositions are discussed. The mixtures of ultra-disperse Ti and nano sized (< 50nm) Al powder compositions were consolidated to full or near-full density by explosive-compaction technology. The emulsion and ammonium nitride based industrial explosives were used for generation of shock waves. To form ultra-fine grained bulk TiAl intermetallics with different compositions, ultra-disperse Ti particles were mixed with nano-crystalline



Al. Each reaction mixture was placed in a sealed container and explosively compacted using a normal and cylindrical detonation set-up. Explosive compaction experiments were performed in range of pressure impulse (5-20 GPA). Structural investigations (SEM) and micro-hardness measurements were used to characterize the intermetallics phase composition and mechanical properties. The results of analysis revealing the effects of the compacting conditions and precursor particles sizes, affecting the consolidation and the properties of this new ultra high performance alloys are discussed.

### 11:10 AM

**Corrosion Rates and Mechanical Properties of Nanocrystalline Materials in Contrast to their Coarse Grained Counterparts:** *Indranil Roy*<sup>1</sup>; Shehreen Dheda<sup>2</sup>; Manuel Marya<sup>1</sup>; Farghalli Mohamed<sup>2</sup>; <sup>1</sup>Schlumberger; <sup>2</sup>University of California, Irvine

Ultrafine grained (UFG) and nanocrystalline (nc)-metals and alloys are known for frequently outperforming their microcrystalline counterparts due to superior mechanical strengths and wear (abrasion) resistance. The performance of UFG and nc-metals and alloys as bulk material for engineering applications in corrosive environments are however less understood. This paper specifically discusses and compares mechanical and electrochemical properties of nc-nickel, its alloys and UFG Al5083 in contrast to their coarse grained counterparts in various brine environments and temperatures. Weight-loss corrosion and pitting are also discussed in relation to micro/nanostructure and compositions.

### 11:30 AM

**Structural Properties of Nanostructured Fe-Co-V Prepared by Mechanical Alloying and Spark Plasma Sintering:** *Baolong Zheng*<sup>1</sup>; Randy Dumas<sup>1</sup>; Asit Biswas<sup>2</sup>; Yizhang Zhou<sup>1</sup>; Kai Liu<sup>1</sup>; Dean Baker<sup>2</sup>; Enrique Lavernia<sup>1</sup>; <sup>1</sup>University of California, Davis; <sup>2</sup>Advanced Powder Solutions, Inc.

FeCo-based soft magnetic materials, having the high saturation magnetization and high Curie temperatures, are ideal for high-temperature applications. Mechanical and magnetic properties of these soft magnetic materials can be further improved by grain size refinement. In this study, nanocrystalline Fe-Co-V soft magnetic alloy powders with an average grain size of 20nm were prepared by severe plastic deformation via high-energy mechanical alloying. XRD analysis showed that bcc-FeCo solid solution was formed after 8 hours of milling. Spark Plasma Sintering (SPS) was used to fabricate bulk nanostructured magnets, whose saturation magnetization, about 229emu/g, is noticeably higher than that of as-milled powders. Characterization techniques including SEM, XRD, DSC, and TEM were used to study the microstructural evolution of both milled powder and SPS consolidated samples under various processing conditions. Magnetic and mechanical properties were measured and further analysis was conducted with emphasis on the relationship among the constitution, processing, microstructure and properties.

### 11:50 AM

**Reticulated Vitreous Carbon Foam Saturated with SiO<sub>2</sub> Aerogel for Heat Insulation Purposes:** *Liping Shi*<sup>1</sup>; Yesheng Zhong<sup>1</sup>; Xiao dong He<sup>1</sup>; Jia Yu<sup>1</sup>; <sup>1</sup>Harbin Institute of Technology

Reticulated vitreous carbon (RVC) foam has a three-dimensional cellular structure with good thermal insulation and low thermal expansion. Aerogels have lots of particular application especially as superinsulation materials because of their nano-size particles and porous distribution. Silica gels were prepared by taking tetraethoxysilane (TEOS) as precursor based on two-step acid-base catalysis method and RVC samples were obtained from polyurethane foam impregnated by furfuryl alcohol under different heat treatment temperature. The heat insulation composites, RVC carbon foam matrix impregnated with SiO<sub>2</sub> aerogel, were processed by multi-solgel method coupled with dipping treatment. The influence of foam porosity and number of saturated SiO<sub>2</sub> aerogel to thermal performance of these composites were investigated by experiments. And the phase composition, microstructure and evolving regularity of this composite were also involved by XRD, EDS and SEM. Besides the mechanical properties and thermal conductivity of carbon foam with and without SiO<sub>2</sub> aerogel were compared and discussed.

### 12:10 PM Concluding Comments

## Advanced Materials and Fuels Enabling Future Fusion, Fission and Hybrid Reactor Systems: Hybrid Fission Fuels

*Sponsored by:* The Minerals, Metals and Materials Society, TMS Structural Materials Division, TMS Materials Processing and Manufacturing Division, TMS/ASM: Computational Materials Science and Engineering Committee, TMS/ASM: Corrosion and Environmental Effects Committee, TMS: High Temperature Alloys Committee, TMS/ASM: Nuclear Materials Committee

*Program Organizers:* Joseph Farmer, Lawrence Livermore National Laboratory; Thomas M. Anklam, Lawrence Livermore National Laboratory; Magdalena Serrano de Caro, Lawrence Livermore National Laboratory

Thursday AM Room: 3A  
February 18, 2010 Location: Washington State Convention Center

*Session Chairs:* Magdalena Serrano de Caro, Lawrence Livermore National Laboratory; Joseph Farmer, Lawrence Livermore National Laboratory

### 8:30 AM Introductory Comments

#### 8:35 AM Invited

**Grain Boundary Structure Effects on Radiation Assisted Segregation and Damage:** *Zhe Leng*<sup>1</sup>; David Field<sup>1</sup>; <sup>1</sup>Washington State University

Ferritic/martentic steels are attractive materials for use as components in nuclear reactors because of their high strength and good swelling resistance. Grain boundary specific phenomena (such as segregation, voiding, cracking, etc) are prevalent in these materials so grain boundary character is of primary importance. Certain types of boundaries are more susceptible to damage whereas others tend to resist radiation damage. If more damage resistant boundaries can be introduced into the structures, this will result in steel that is more resistant to the processes of degradation that prevail in high-temperature, radiation containing environments. We have characterized the grain boundary structure in HT9 steel by electron backscatter diffraction to identify boundaries that are resistant to degradation and those that are more susceptible to damage in extreme environments. It is found that intergranular damage is mitigated by a high fraction of low energy boundaries due to lower diffusivity and less segregation.

#### 9:05 AM

**Materials Behavior under Extreme Conditions: An Aspect from Ab Initio Calculations:** *Fei Gao*<sup>1</sup>; H.Y. Xiao<sup>1</sup>; W.J. Weber<sup>1</sup>; <sup>1</sup>Pacific Northwest National Laboratory

SiC and GaN have attracted extensive theoretical and experimental interest due to their potential applications for electronic devices. GaN and SiC are both covalent materials, but with GaN being more ionic and SiC more covalent. SiC is of additional interest because of its potential technological applications in high-temperature structural components for fission and fusion reactors. Recent progress of studying ion-solid interactions in these materials using first-principles approach is reviewed. Large-scale ab initio simulation methods (up to a few thousand atoms) have been developed for the study of ion-solid interactions in materials, and these methods have been employed to investigate defect properties in SiC and GaN. Relative stabilities of these defects have been determined, and their electronic structures provide insight into the configurations and binding properties of these native defects. Atomic structures, formation energies and binding energies of small clusters (both vacancy and interstitial clusters) have been investigated, and their relative stabilities determined. More recently, ab initio molecular dynamics (AIMD) methods have been used to calculate threshold displacement energies and to simulate the primary damage states for the PKA (primary knock-on atom) energies up to 1 keV in SiC and GaN. These simulations provide important insights into electronic effects on ion-solid interaction processes, and reveal that significant charge-transfer occurs between atoms. The charge variation of the recoil atom can decrease the energy barrier for stable defect formation, and the corresponding dynamics evolution is a charge-assisted process, which is expected to have significant effects on defect creation in covalent and ionic materials. Thousand-atom ab initio simulation provides a feasible path to study low-energy ion-solid interaction, charge transfer and charge-redistribution,

# Technical Program

with first-principle accuracy, in covalent materials. In addition, AIMD methods are used to investigate high-pressure phase transitions in SiC and GaN. These simulations bring a fundamental level of understanding of the wurtzite to rocksalt phase transformation that undergoes inhomogeneous displacements via a tetragonal atomic configuration, and suggest that the transition path may be independent of the presence of d electrons on the cation in GaN. Also the simulated results resolve the discrepancy between experimental observations and theoretical predictions.

## 9:35 AM

**Interatomic Forces in Stainless Steels:** *Graeme Ackland*<sup>1</sup>; Derek Hepburn<sup>1</sup>; <sup>1</sup>University of Edinburgh

Stainless steels, primarily FeNiCr based, remain the materials of choice for many reactor components. Modelling of radiation damage at the atomistic level is required to understand the geometry and dynamics of various defects. Molecular dynamics is still the primary method for obtaining such details, and this in turn relies on interatomic potentials. The FeCrC system is uniquely challenging. In addition to the requirement for describing metallic bonding, which is well achieved using Embedded atoms or similar, the energetics depend on antiferromagnetic frustration (FeCr), covalent bonding and charge transfer (carbon). I will describe how appropriate functional forms can be motivated by first principles calculations of relevant configurations. I will then describe how these can be combined with empirical data to provide an optimised parameterization for particular applications. Finally, I will show some applications.

## 9:55 AM Invited

**Thermo-Mechanical Response of a TRISO Fuel Particle in a Fusion/Fission Engine for Incineration of Weapons Grade Plutonium:** *Magdalena Serrano de Caro*<sup>1</sup>; P. DeMange<sup>1</sup>; J. Marian<sup>1</sup>; A. Caro<sup>1</sup>; <sup>1</sup>Lawrence Livermore National Laboratory

The Laser Inertial Fusion Engine (LIFE) is an advanced energy concept under development at Lawrence Livermore National Laboratory (LLNL). LIFE is a laser-based inertial confinement fusion engine. This engine could drive a subcritical fission blanket. Different fuel blankets are under consideration which include fertile fuel, such as natural and depleted uranium, or fissile fuel like highly-enriched uranium or weapons-grade plutonium (WGPu). WGPu LIFE is an attractive option because it could achieve a burn up of over 99% fraction of initial metal atoms (FIMAs) in less than 10 years lifetime frame. Materials challenges imposed by the intense pulsed flux of 14MeV neutrons produced by the inertial-confinement fusion (ICF) source, will affect the fuel lifetime. Current LIFE engine designs envisage fuel in pebble bed form with TRISO particles embedded in a graphite matrix, and pebbles flowing in fluoride coolant at T~700C. WGPu LIFE engine operating conditions of high neutron fast fluence, high radiation damage, and high Helium and Hydrogen production pose severe challenges for typical TRISO particles. WGPu LIFE fuel reaches 99.97% FIMA after ~9.4 years after a neutron exposure to fast fluence  $F(E > 0.1 \text{ MeV})$  of  $\sim 3.62 \times 10^{22} \text{ n/cm}^2$ . The thermo-mechanical fuel performance code HUPPCO (High burn-Up fuel Pebble Performance COde) currently under development accounts for spatial and time dependence of the material elastic properties, temperature, and irradiation swelling and creep mechanisms. The effects on the thermo-mechanical response of TRISO particles used for incineration of weapons grade in LIFE engine are analyzed. Preliminary results show the importance of developing reliable high-fidelity models of the performance of these new fuel designs and the need of new experimental data relevant to WGPu LIFE conditions.

## 10:25 AM

**The Evolution and Thermal Recovery of Irradiation Effects in Silicon Carbide:** *William J. Weber*<sup>1</sup>; F. Gao<sup>1</sup>; R. Devanathan<sup>1</sup>; Y. Zhang<sup>1</sup>; W. Jiang<sup>1</sup>; <sup>1</sup>Pacific Northwest National Laboratory

Silicon carbide (SiC) is a robust refractory material with potential applications for advanced nuclear energy systems. Experimental and multiscale computational approaches have been integrated to develop fundamental understanding and predictive models of defects, defect production, irradiation damage evolution, and thermal recovery in SiC. In situ ion-beam channeling methods and electron microscopy have been used to study ion-irradiation effects and thermal recovery. Multiscale computation methods have been employed to determine stable defect configurations, defect production, damage efficiency, cascade-overlap effects, close-pair recombination, and defect migration energies

and pathways. These studies show that energetic ion-solid interactions in SiC result primarily in the creation of interstitials, vacancies, antisite defects, and small defect clusters that interact to produce long-range structural disorder. The disordering behavior, volume change, and high-resolution images of damage states obtained experimentally and from molecular dynamic (MD) simulations of cascade overlap are in good agreement. This synergistic integration of experimental and computational efforts is providing atomic-level understanding and necessary parameters to model dynamic defect processes and the evolution of irradiation damage in SiC as a function of time, temperature, and dose rate.

## 10:45 AM Break

## 10:55 AM Invited

**The Synthesis and Sintering of Advanced Fuels:** *Brian Jaques*<sup>1</sup>; Daniel Osterberg<sup>1</sup>; Richard Reavis<sup>1</sup>; A. S. Hamdy<sup>1</sup>; Brian Marx<sup>1</sup>; Darryl Butt<sup>1</sup>; <sup>1</sup>Boise State University

The future of nuclear energy in the U.S. and its worldwide expansion depend greatly on our ability to reduce high level waste while maintaining proliferation resistance. Implicit in the so-called advanced fuel cycle is the need for greater fuel burn-up and consequential use of complex nuclear fuels comprised of fission materials such as Pu, Am, Np, and Cm. Advanced nitride and oxide fuels comprised of ternary and quaternary mixtures of uranium and higher actinides have been considered for applications in advanced nuclear power plants, but there remain many processing challenges. Non- and Low-fertile advanced fuels were synthesized and conventionally sintered in various conditions. The materials were characterized by means of particle size analysis, x-ray diffraction, x-ray photoelectron spectroscopy, electron microscopy, and thermogravimetric techniques.

## 11:25 AM

**Development of a Continuous CVD Process for TRISO Coating of AGR Fuel:** *Clay Richardson*<sup>1</sup>; <sup>1</sup>Babcock and Wilcox

As part of the Department of Energy's Advanced Gas Reactor Fuel program, Babcock & Wilcox has developed a fluidized bed chemical vapor deposition process to deposit a TRISO coating on UCO and UO<sub>2</sub> kernels. These coated kernels will go into irradiation tests in the Advanced Test Reactor at Idaho National Laboratory. This paper reports on the development activities including the furnace design and the furnace runs made to qualify the coating process.

## 11:45 AM

**Interaction of the Fission Product Pd with TRISO Fuel Coatings:** *Yufeng Zhang*<sup>1</sup>; D. Hanks<sup>1</sup>; S. Krause<sup>1</sup>; G. Gajjala<sup>1</sup>; T. Hofmann<sup>1</sup>; L. Weinhardt<sup>1</sup>; M. Bär<sup>1</sup>; C. Heske<sup>1</sup>; <sup>1</sup>Department of Chemistry, University of Nevada, Las Vegas

Tristructural-isotropic (TRISO) nuclear fuel is a key component of high-temperature gas-cooled reactors (HTGR). Typically, SiC is used in the TRISO fuel as the diffusion barrier for both radioactive (fuel) elements and gaseous and metallic fission products, because of its good chemical inertness, high thermal conductivity, and low neutron absorption cross-section. However, it was observed that Pd causes corrosion of the SiC layers in various kernel compositions<sup>1</sup>, and may lead to coating failure of TRISO fuels. ZrC, a more corrosion-resistant material, is studied as an alternative. Thus, it is important to understand the mechanisms of Pd-SiC and Pd-ZrC interaction. So far, most experiments used bulk-sensitive techniques, which cannot provide direct information about the chemical bonding at the Pd/SiC and Pd/ZrC interfaces. X-ray photoelectron spectroscopy (XPS) is widely used in studying metal-semiconductor interfaces, and has proven to be extremely powerful to understand both the electronic and chemical properties of interfaces and contacts. We will present a detailed XPS study of the formation of Pd/SiC and Pd/ZrC interfaces. The results give direct insight into the local chemical environment of the involved elements (i.e., C, Si, Zr, and Pd at the interface), in particular the formation of secondary phases at the interface.

## 12:05 PM Invited

**ZrC Surface Cleaning and Interaction with the Fission Product Ru:** *Stefan Krause*<sup>1</sup>; D. Hanks<sup>1</sup>; Y. Zhang<sup>1</sup>; C. Heske<sup>1</sup>; <sup>1</sup>Department of Chemistry, University of Nevada, Las Vegas

To ensure the safety of TRISO fuel particles, coating layers need to be optimized to encapsulate all fission products in the particle under all possible operating conditions. ZrC is a candidate for a diffusion barrier, and therefore detailed information about the interaction between ZrC and selected fission products is required. We have investigated the surface cleaning of ZrC and the



subsequent interface formation with Ru using photoelectron spectroscopy (XPS, UPS), and x-ray absorption as well as emission spectroscopy (XES, XAS). These methods allow the study of changes in the chemical environment of the atoms in the material surface as a function of preparation conditions and Ru deposition. Furthermore, relative surface composition changes can be monitored precisely. We will discuss experiments and procedures to clean the ZrC substrate from oxides, carbon contaminations, and other manufacturing residues. Furthermore, we will present first experiments in which Ru was deposited on ZrC surfaces.

**12:35 PM Concluding Comments**

### Alumina and Bauxite: Alumina Precipitation

*Sponsored by:* The Minerals, Metals and Materials Society, TMS Light Metals Division, TMS: Aluminum Committee, TMS: Aluminum Processing Committee

*Program Organizers:* Carlos Suarez, Hatch Associates Inc; Everett Phillips, Nalco Company

Thursday AM Room: 611  
February 18, 2010 Location: Washington State Convention Center

*Session Chair:* Patrick James, Alumina Partners of Jamaica - Alpart

**8:30 AM Introductory Comments**

**8:40 AM**

**Study on the Precipitation Kinetics for Improving the Quality of Alumina with Regard to Fines and Attrition Properties:** *Narasimharaghavan Krishnaswamy*<sup>1</sup>; Nand Kumar Kshatriya<sup>1</sup>; Supratim Dasgupta<sup>1</sup>; Ramaswamy Jagannathan<sup>1</sup>; <sup>1</sup>Bharat Aluminium Co. Ltd., (A Unit of Vedanta Resources Plc.), BALCO Nagar, Korba

Hydrate of Alumina is precipitated from a super saturated Aluminate liquor, produced from the digestion of Bauxite ores. The two important properties of Alumina which make it qualify as suitable for pre-baked smelter grade are fines (-325 mesh fraction) and the Alpha content. Though the second parameter to some extent is dependent on the -325 fraction in hydrate, the growth of the alumina hydroxide is dependent on the size distribution of the seed hydrate present during precipitation and the precipitation conditions. Further the effects of the operating parameters on these product parameters are not well understood. From this study it has been found that the particle strength is dependent on the precipitation kinetics, the temperature gradient in the precipitators, seed size, seed ratio and the organic contaminants. It could be observed that the product size (-325 fraction) and the strength improved with fine seed addition compared to the coarser seeds.

**9:10 AM**

**Wet Oxidation of Bayer Liquor Organics: Reaction Mechanisms:** *Jackie Dong*<sup>1</sup>; James Tardio<sup>1</sup>; Joanne Loh<sup>2</sup>; Greg Power<sup>2</sup>; Chris Vernon<sup>2</sup>; Suresh Bhargava<sup>1</sup>; <sup>1</sup>MIT University; <sup>2</sup>CSIRO Minerals

Organic impurities in Bayer liquor cause significant losses in productivity and hence the development of improved processes for removing these impurities from this unique solution is of great interest to the alumina industry. Of the various organics removal processes that have been studied and implemented oxidation processes such as wet air oxidation that do not involve the introduction of foreign species into Bayer liquor have received most interest. The chemistry of wet air oxidation of Bayer organics such as sodium malonate and similar compounds is however poorly understood which has hindered improvements in Bayer liquor wet air oxidation processes. In the work reported here results are presented on the influence of key structural features on the reactivity of common Bayer organics under typical wet air oxidation conditions. Reaction mechanisms that occur in the wet air oxidation of several common Bayer impurities are also discussed using <sup>13</sup>C NMR and kinetics techniques.

**9:40 AM Break**

**10:00 AM**

**The Roles of Adsorption in Hydrate Precipitation:** *Joanne Loh*<sup>1</sup>; Greta Brodie<sup>1</sup>; Fatima Naim<sup>1</sup>; <sup>1</sup>Parker Centre/CSIRO Light Metals Flagship (CSIRO Minerals)

It has been well established that organic compounds with adjacent hydroxyl groups in Bayer process liquor can inhibit gibbsite precipitation by acting as seed

poisons. The degree of inhibition is a function of the number and stereochemistry of the hydroxyl groups. Seed poisons generally adsorb strongly onto hydrate surfaces, implying that surface coverage is the mechanism for yield inhibition. There are examples however of organics that strongly adsorb but do not lead to yield inhibition. There is a possibility that this apparent contradiction may be an artifact of differences in conditions between the adsorption and precipitation experiments. The present work investigates the adsorption and inhibition effects of a range of compounds under strictly similar conditions to clarify the role of adsorption on yield inhibition.

**10:30 AM**

**The Microstructure of Aluminum Hydroxide Powders:** *Yu Haiyan*<sup>1</sup>; Li Wen-cheng<sup>1</sup>; Bi Shiwen<sup>1</sup>; <sup>1</sup>Northeastern University

In this paper, both the foreign and domestic aluminum hydroxide powder products were studied by SEM, XRD, and Raman spectroscopy, and their microscopic structures were also discussed. The results show that the two products are different in three aspects, i.e. the degree of preferential orientation on the (002) crystal plane, the lattice parameters, and the full width at half maximum (FWHM) of Raman peak. The preferential orientation factor, the lattice parameters and the Raman peak FWHM of the domestic product are larger than those of the foreign product. The XRD results indicate that there is no obvious preferential orientation on the (002) crystal plane of the foreign product. The foreign product rather shows preferential growth on a few other crystal planes. Less impurity and defects and better crystallinity possibly contributed to the excellent properties of the foreign product.

### Aluminum Reduction Technology: Hall-Héroult Cell: Raw Materials and Process Control

*Sponsored by:* The Minerals, Metals and Materials Society, TMS Light Metals Division, TMS: Aluminum Committee, TMS: Aluminum Processing Committee

*Program Organizers:* Charles Mark Read, Bechtel Corporation; Gilles Dufour, Aluminerie de Deschambault

Thursday AM Room: 608  
February 18, 2010 Location: Washington State Convention Center

*Session Chair:* Charles Mark Read, Bechtel Corporation

**8:30 AM Introductory Comments**

**8:35 AM**

**Rapid, Non-Destructive Analysis of % Gibbsite in Smelting Grade Alumina:** *Kerrick Dando*<sup>1</sup>; *Neal Dando*<sup>2</sup>; <sup>1</sup>Juniata College; <sup>2</sup>Alcoa

At present, there is no easy-to-use method for performing rapid analysis of gibbsite content in smelting grade alumina (SGA). Such an analysis would help aluminum smelters to distinguish between alumina supplies based on % gibbsite (Al<sub>2</sub>O<sub>3</sub>·3H<sub>2</sub>O), track batch variability and correlate cell performance with SGA quality parameters. This report details the development of a rapid, non-destructive near infrared (NIR) method for the quantitative analysis of weight % gibbsite (Al<sub>2</sub>O<sub>3</sub>·3H<sub>2</sub>O) in smelting grade alumina over the range 0-10 weight %. A sample pre-treatment method was also developed for minimizing the effect of physically adsorbed moisture on the analysis method. The single term linear least squares NIR method developed in this study has a standard error of calibration of 0.27 wt %, a standard error of prediction of 0.50 wt% gibbsite and a method repeatability error (1 standard deviation) of <0.017%.

**9:00 AM**

**Alumina Dissolution Rate as Impacted by Ore Pre-Treatments:** *Xiangwen Wang*<sup>1</sup>; Jack Sorensen<sup>1</sup>; Neal Dando<sup>1</sup>; Weizong Xu<sup>2</sup>; <sup>1</sup>Alcoa, Inc.

Alumina dissolution rate in cryolitic electrolytes has been a subject of intensive study over the last several decades. Alumina dissolution rate can be affected by the physical, morphological and microstructural properties of the ore, as well as the dynamic of the feeding process. In this study, alumina ore samples were subjected to treatments under various temperature conditions. The pretreated ore samples were then studied to characterize their overall dissolution rates. The HF release upon immediate ore contact to molten bath was also measured and correlated with ore pretreatment and stage of alumina ore dissolution. Dissolution mechanisms are proposed based on the dissolution

# Technical Program

rate and observation of morphological/microstructural changes of ore samples and flats/crust formed prior to being dissolved.

## 9:25 AM

**Processing of Anode Cover Material:** Ingo Eick<sup>1</sup>; Bruno Rausch<sup>1</sup>; Juraj Chmelar<sup>2</sup>; Ulrich Kohaupt<sup>3</sup>; <sup>1</sup>Hydro Aluminium Deutschland GmbH; <sup>2</sup>Hydro Aluminium Metal; <sup>3</sup>Steinert Elektromagnetbau GmbH

For high amperage cell the content and consistency of anode cover material (ACM) is essential for an optimal performance. However, ACM is composed partly from recycled material out of various sources from potroom operation contaminated by impurities. In cooperation with Steinert GmbH an approach was established by Hydro to separate impurities from the ACM stream affecting current efficiency and metal quality. Additionally, repair cost for processing equipment will be reduced and the ACM properties improved. Beside magnetic and eddy current separation an industrial solution for inductive sensor sorting has been examined for different sorting sequences applied to various pre-crushed material. The sorting results are strongly affected by the grain sizes and the sorting sequences of the crushed ACM. In average about 1% aluminium and iron and 2-4% carbon weight percentages were found and separated from the samples which sum to 0.2% current efficiency and 1.3 ppm less iron in metal.

## 9:50 AM

**Statistical Investigation and Modeling of Bath Level in Hall-Héroult Cells:** Jayson Tessier<sup>1</sup>; Patrice Doiron<sup>1</sup>; <sup>1</sup>Alcoa Deschambault

Industrially, alumina is produced through the decomposition of alumina (Al<sub>2</sub>O<sub>3</sub>) in metallurgical reactors known as pots. Basically, smelter grade alumina powder has first to be dissolved in an electrolytic bath, which is a molten mixture of cryolite and fluoride salts. Dissolved alumina is then dissociated to produce aluminium. Bath level control is of great importance to smelter operators as it directly affects different key performance indicators related to current efficiency, energy consumption and metal purity. This paper presents an investigation of the variables having an impact on bath level control. It is presented how pot manipulated and state variables and other parameters are statistically linked to bath levels variations. Moreover, different statistical models are used in order to attempt a prediction and forecast of bath level.

## 10:15 AM Break

## 10:25 AM

**In Situ Raman Experimental Study of Ionic Species in Cryolite Melts of Various Composition:** Sergey Vassiliev<sup>1</sup>; Veronika Laurinavichute<sup>1</sup>; Zoya Kuz'minova<sup>1</sup>; Galina Tsirlina<sup>1</sup>; Evgeny Antipov<sup>1</sup>; Alexander Gusev<sup>2</sup>; Dmitry Simakov<sup>2</sup>; <sup>1</sup>Laboratory for Basic Research in Aluminium Production, M.V.Lomonosov Moscow State University; <sup>2</sup>RUSAL

Systematic comparison of Raman spectral behavior for cryolite melts of various cation composition is reported in relation to reactivity of inert anodes for aluminum production.

## 10:50 AM

**In Situ Cell Control:** Michael Schneller<sup>1</sup>; <sup>1</sup>Consultant

Substituting the pseudo-resistance variable ( $R_p$ ) with the more statistically robust predicted voltage variable ( $V_p$ ) can enhance the potline process control tool kit. The predicted voltage variable is able to measure *in situ* bath alumina levels and bath temperatures upon demand. Alumina ore feed rates are based upon the intimate linkage between predicted voltage and bath alumina concentration. Pots are fed ore at a steady state rate to maintain a targeted % Al<sub>2</sub>O<sub>3</sub> concentration which decreases the risk of un-dissolved alumina/bath conglomerate formation. Multiple daily bath temperature predictions employing predicted voltage can promote voltage and bath ratio optimization. The Lomb algorithm is used to detect statistically significant voltage cycling as part of a scheme to partition the total pot noise into components: 1) voltage cycling; 2) overvoltage changes; 3) pseudo-white noise. A judicious selection of noise components modify ore feed and voltage decisions.

## 11:15 AM

**Determination of Cryolite Ratio of Aluminum Electrolytes:** Bingliang Gao<sup>1</sup>; Dan Li<sup>1</sup>; Zhongning Shi<sup>1</sup>; Zhaowen Wang<sup>1</sup>; Bijun Ren<sup>2</sup>; <sup>1</sup>Northeastern University, China; <sup>2</sup>Yichuan Power Group Head Corporation

In aluminum industry, the molar ratio of sodium fluoride to aluminum fluoride is termed as cryolite ratio. Additives, such as MgF<sub>2</sub>, LiF, NaCl, KF, were used to improve the properties of electrolyte. However, these additives make the composition of aluminum electrolyte complex, and difficult in

accurately determining of cryolite ratio. The purpose of our study is to improve this situation, and makes the determination of cryolite ratio more accurate and practical. XRD that commonly used in industrial smelters has big measurement error and poor reproducibility in determining bath ratio of electrolytes containing additives, such as MgF<sub>2</sub>, LiF, NaCl and KF. Therefore, the calibration formula for XRD was derived according to the experimental results, and it is believed that it can reduce errors and improve the accuracy of cryolite ratio determination of bath to some extent.

## 11:40 AM Concluding Comments

## Aluminum Rolling: Session I

*Sponsored by:* The Minerals, Metals and Materials Society, TMS Light Metals Division, TMS: Aluminum Committee  
*Program Organizer:* Kai Karhausen, Hydro Aluminium Deutschland GmbH

Thursday AM Room: 615  
February 18, 2010 Location: Washington State Convention Center

*Session Chairs:* Kai Karhausen, Hydro Aluminium; Gary Parker, Wise Alloys, LLC

## 8:30 AM Introductory Comments

## 8:35 AM

**Integrated through Process Modeling Using a Virtual Platform for Materials Processing by the Example of a Multi-Pass Rolling Process:** Thomas Henke<sup>1</sup>; Markus Bambach<sup>1</sup>; Gerhard Hirt<sup>1</sup>; <sup>1</sup>RWTH Aachen University

Material properties are the basis for the functionality of any final product including rolled aluminum products. The material properties depend on the microstructure of the final product. The evolution of microstructure during the whole production chain is greatly influenced by the process parameters (e.g. pass reduction and temperatures). Therefore an extensive through process prediction of materials properties including microstructure is highly important. Such a prediction requires coupling of different models to a virtual process chain starting from a homogeneous, isotropic and stress-free melt and up to the final product, sometimes even beyond. In this paper, we present a new web-based platform – the Aachen virtual platform for Materials Processing (AixViPMap). This platform combines complex physical material models and application-oriented simulation tools. It comprises a virtual, integrative numerical description of processes and of microstructure evolution along entire production chains. Applications of the platform with respect to hot rolling will be given.

## 8:55 AM

**Aluminium Rolling Simulations Considering Interstep Annealing:** Volker Mohles<sup>1</sup>; <sup>1</sup>RWTH Aachen University

Intended or unintended annealing in between rolling steps can have a significant impact on the rolling process and the material properties even in cases where no recrystallization but only recovery takes place. To consider this recovery effect in computer simulations, a consistent physical model for the work hardening and recovery during rolling steps and the recovery inbetween is needed. In the simulations presented, the dislocation density based three internal variables model 3IVM+ is used. However, like all statistical flow curve models, 3IVM+ must be calibrated to a set of flow curves. In addition, the recovery parameters of this model need a specialized calibration for the recovery periods. As shown, stress relaxation tests can be used for this. They need a special evaluation, but require rather little experimental effort. The simulations are discussed in respect of their present applicability and aspired future development.

## 9:15 AM

**Grain Interactions and Dislocation Density Evolution during Channel Die Compression of Aluminum:** Alankar Alankar<sup>1</sup>; Ioannis Mastorakos<sup>1</sup>; David Field<sup>1</sup>; <sup>1</sup>Washington State University

We study the microstructure evolution of a 2D-quasi single layer of large grain aluminum polycrystals using our dislocation density based 3D-crystal plasticity model. Initial grain structure is mapped onto a FEM mesh and the predictions of spatial distribution of plastic microstrain are compared with the experimental work reported in the literature. Evolution of dislocation density,



crystallite orientations and the Taylor factor are used to compare the predictions with the experimental observations. Local and non-local both effects are considered and are compared with each other.

### 9:35 AM

**Impact of Solute State and Precipitations on the Properties of 8xxx Alloys after Cold Rolling and Recrystallization:** *Galya Lapyeva*<sup>1</sup>; Carmen Schäfer<sup>2</sup>; Kai F. Karhausen<sup>1</sup>; Volker Mohles<sup>2</sup>; Günter Gottstein<sup>2</sup>; <sup>1</sup>Hydro Aluminium Deutschland GmbH, R&D; <sup>2</sup>Institute of Physical Metallurgy and Metal Physics-RWTH Aachen

The mechanical properties of industrially produced 8xxx cold-rolled sheets and the recrystallization during the subsequent heat treatment are strongly related to the thermal processing and rolling conditions (e.g. rolling speed, pass reductions). Depending on the time-temperature processing conditions (e.g. homogenization schedule) of 8xxx alloys various precipitation states are obtained which can cause a strong hindering up to a complete suppression of the recrystallization. The microchemistry in combination with shear amount are therefore the most important material parameters for the manufacturing of material properties. In this contribution, the interaction of different microchemistry states and softening is modelled. The evolution of solute levels and precipitation is hereby predicted for the respective heat treatment using a precipitation model based on the theory of classical nucleation and growth. The recrystallization is modelled by means of a temporal and spatial resolved cellular automaton. The simulation results are discussed with respect to experimental observations.

### 9:55 AM Panel Discussion

### 10:25 AM Break

### 10:40 AM

**Inspection Systems and Data Warehousing of Informaton:** *David Pond*<sup>1</sup>; <sup>1</sup>Automation and Control Technology Inc.

As the Aluminum industry continues to face competition and slower economic times, information is needed to improve efficiency, quality and ultimately management control. On the production floor, the task is to make available the information needed to identify issues in the process, enable quality to determine the overall compliance to standards, certify to the customer that the product ordered was produced to their specifications and to do it efficiently with minimal human resource. The data needed to support operations is many times stored throughout the company in different databases. This dispersed data being reported in different formats from different data sources leads to confusion, extensive conversations about data validity, and distracts the organization, preventing it from focusing on other corporate initiatives. A consolidated single warehouse of information will be presented to mitigate this problem.

### 11:00 AM

**Expert5i - Intelligent Software Solution for Yield Optimization along the Production Line of Aluminium Flat Rolled Products:** *Sigrid Hillebrand*<sup>1</sup>; *Uwe Knaak*<sup>1</sup>; *Reinhard Rinn*<sup>1</sup>; <sup>1</sup>ISRA PARSYTEC GmbH

Surface quality inspection has become state of the art in the production of aluminium flat rolled products. Many production lines in the world for e.g. can end stock, lithographic material, or automotive annealed aluminium are already equipped with surface inspection systems. Inspection systems monitor and document surface defects through the individual coil processing steps, enabling the production managers to react promptly on defects, reduce scrap production, and improve delivered quality. However, surface data alone is not sufficient to optimize processes and production. A huge amount of data at each stage of the aluminium making process is waiting to be utilized for the daily decision making of the production and quality managers. This is how the ISRA Parsytec Enterprise PROduction Management Intelligence software "EPROMI" provides help: It analyzes the available information and generates knowledge-based suggestions for the decision makers to make production and quality decisions and finally ensure yield maximization.

### 11:20 AM

**Possibilities of Laser Measurement for Aluminum Processing:** *Patrick Sonntag*<sup>1</sup>; <sup>1</sup>Nokra GmbH

Effective measurement during processing of aluminum can save cost, time and effort. Implemented in steelworks first, laser measurement is now also applied within aluminum processing lines. Complete dimensions, surface faults, flatness, form faults etc. can be measured at 100% of production within the line. Fault

detection before quality control and optimized usage of production equipment can enhance quality, reduce scrap, and lead to a higher percentage of output with required properties. Everything between "width x depth x height" and a complete "virtual piece of metal" is possible, superseding manual measurement and inspection. Usage of laser measurement in steel and aluminum industries has proven the advantageousness of constant, complete, and objective measurement with systems that fulfil the requirements of measurement equipment capability standards. Application of this technology has the potential to enormously save time, cost, energy and additionally enhance quality in metal processing.

### 11:40 AM Panel Discussion

## Biological Materials Science: Computational Materials Science

*Sponsored by:* The Minerals, Metals and Materials Society, TMS Structural Materials Division, TMS: Biomaterials Committee, TMS/ASM: Mechanical Behavior of Materials Committee

*Program Organizers:* John Nychka, University of Alberta; Jamie Kruzic, Oregon State University; Mehmet Sarikaya, University of Washington; Amit Bandyopadhyay, Washington State University

Thursday AM Room: 205  
February 18, 2010 Location: Washington State Convention Center

*Session Chairs:* Nima Rahbar, University of Massachusetts Dartmouth; Devesh Misra, University of Louisiana

### 8:30 AM Invited

**Molecular Bioassemblies as Mechanical Systems:** *Richard LeSar*<sup>1</sup>; <sup>1</sup>Iowa State University

One of the most intriguing ideas in materials development is to use motor proteins either directly as molecular motors or to provide a means to transport material to desired locations. Modeling and simulation offer a path to increase our understanding of these molecules and, perhaps, to design variations of them that have specific properties. The challenge for modeling and simulation is a familiar one to the materials science community - the length and time scales of importance for the behavior of these molecules span a very large range. At the chemical scale, atomistic simulations are the methods of choice. At the largest scales, one approach is to ignore all atomic-level features and to treat large biomolecules as mechanical systems. In this talk, we will review these mechanical descriptions and discuss an approach to bridge the gap between them and the underlying atomistic nature of the molecules.

### 9:00 AM Invited

**Optimized Design of Porous Titanium for Bio-Medical Applications:** *Alex Turner*<sup>1</sup>; *Nikolas Hrabe*<sup>1</sup>; *Rajendra Bordia*<sup>1</sup>; <sup>1</sup>University of Washington

Stress-shielding has been recognized as a factor in the reduction of hip implant lifetime. In this presentation, we will discuss the simulated performance of a porous titanium implant with a non-uniform distribution of stiffness. The results are based on a two-dimensional finite element model of an implant-bone system. It was found that implants with high stiffness proximally and decreasing stiffness distally provide significant improvements in bone stimulation (measured in terms of strain energy density) in the proximal regions of the femur relative to a conventional fully-dense Ti implant model and an optimized uniformly porous implant model. These results were then confirmed in bone adaptation simulations that measured bone loss following implantation of the various implant models. Other important issues in the development of gradient porosity structures including processing, and relevant mechanical properties will be discussed.

### 9:30 AM

**Numerical Analysis of Tesselated Shark Cartilage in Bending:** *Xiaoxi Liu*<sup>1</sup>; *Mason Dean*<sup>1</sup>; *Adam Summers*<sup>1</sup>; *James Earthman*<sup>1</sup>; <sup>1</sup>University of California, Irvine

A large portion of the skeleton of sharks, skates and rays (Chondrichthyes) is characterized by a tessellated structure, composed of mineralized plates (tesserae) joined by intertesseral ligaments overlaying a soft cartilage core. An understanding of the mechanical advantages provided by this skeletal tissue type has been lacking. An equivalent cross section model was developed to analyze the function of the intertesseral ligaments in regulating the stress

# Technical Program

distribution within the skeletal tissue during bending. The results indicate that this structure distributes more stress to the tesseræ loaded in compression than is distributed to those loaded in tension. This behavior provides plausible advantages for 1) reducing susceptibility to fatigue damage; 2) reducing tearing of the tissue by large tensile stresses and 3) allowing compressive stress to power nutrient flow throughout the unmineralized phase. The present model simulations demonstrate these advantages for a typical geometry and range of ligament properties.

## 9:50 AM

**Binding and Assembly of Material-Specific Peptides on Solid Substrates by Atomic Force Microscopy:** *Christopher So*<sup>1</sup>; Megan Noyes<sup>2</sup>; Ersin Oren<sup>1</sup>; Hakim Meskine<sup>3</sup>; Hilal Yazici<sup>4</sup>; Paul Mulheran<sup>3</sup>; Candan Tamerler<sup>4</sup>; John Evans<sup>5</sup>; Mehmet Sarikaya<sup>1</sup>; <sup>1</sup>University of Washington; <sup>2</sup>University of Michigan; <sup>3</sup>University of Strathclyde; <sup>4</sup>Istanbul Technical University; <sup>5</sup>New York University

Understanding biomineralization and the realization of biology-inspired materials technologies depends on understanding the nature of the chemical and physical interactions between proteins and inorganic material surfaces. Here, we combine high-resolution atomic force microscopy (AFM) and nuclear magnetic resonance (NMR) experiments with both atomistic and molecular-scale simulation methods to understand the binding and assembly process of genetically engineered peptides and their correlation with the symmetry of the solid surface lattice. We use several such material-specific binding peptides (BP) in this study including AuBP, GrBP, and MicaBPs onto Au(111), Graphite(0001) and Mica(111) respectively. Through these methods, we identify putative docking sites where surface-exposed residues align with these crystallographic surfaces. Further, using ex situ time-lapsed AFM results we describe the spatial nucleation and growth mechanisms over large timescales by kinetic Monte Carlo (KMC) coarse-grained simulations used to describe inorganic epitaxial processes. Supported by GEMSEC, an NSF-MRSEC, and NSF-BioMat grants at the UW.

## Bulk Metallic Glasses VII: Mechanical and Other Properties

*Sponsored by:* The Minerals, Metals and Materials Society, TMS Structural Materials Division, TMS/ASM: Mechanical Behavior of Materials Committee

*Program Organizers:* Peter Liaw, The University of Tennessee; Hahn Choo, The University of Tennessee; Yanfei Gao, The University of Tennessee; Gongyao Wang, University of Tennessee

Thursday AM                      Room: 213  
February 18, 2010                Location: Washington State Convention Center

*Session Chairs:* Yanfei Gao, The University of Tennessee; Y. Yokoyama, Institute for Materials Research

## 8:30 AM Invited

**Indentation Creep Behavior of Amorphous Selenium and Amorphous Alloys near the Glass Transition Temperature:** *Yanfei Gao*<sup>1</sup>; Caijun Su<sup>1</sup>; George Pharr<sup>1</sup>; <sup>1</sup>University of Tennessee

The indentation response of a creeping solid can be correlated to its uniaxial response, when replacing the uniaxial stress by indentation pressure and the uniaxial strain rate by an effective strain rate. A general definition of the effective strain rate has been provided by using the Hill-Bower similarity transformation method. A stiffness-based methodology has been developed to study the indentation creep behavior at high temperatures. For amorphous selenium, the dependence of stress exponent and activation volume on the temperature and strain rate agrees with the deformation modes in uniaxial compression tests. The decrease of temperature and the increase of strain rate lead to the decrease of activation volume. A similar observation is also found for amorphous alloys. These results are explained from the strain localization behavior in a rate-dependent solid.

## 8:50 AM

**Crystallization Mechanism in Amorphous Cu-Zr System:** *Ilkay Kalay*<sup>1</sup>; Eren Kalay<sup>1</sup>; Matthew Kramer<sup>1</sup>; Ralph Napolitano<sup>1</sup>; <sup>1</sup>Iowa State University / Ames Laboratory

The Cu-Zr binary system is the basis for many bulk metallic glass and amorphous crystalline composite materials due to its high glass forming ability. However, the prediction and control of the relative phase stability is elusive because of the complex devitrification behavior of the binary alloy. In this current study, best glass forming compositions in Cu-Zr binary alloy were investigated in terms of crystallization kinetics and thermal stability. The isochronal devitrification phase transformation paths were determined using in situ high energy synchrotron X-ray diffraction (HEXRD) experiments. The transformation kinetics and microstructural evolution during isothermal annealing was investigated using transmission electron microscopy (TEM), HEXRD and differential scanning calorimetry (DSC). The mechanism of crystallization accompanied with TEM at different stages of crystallization and the thermal stabilities will be discussed and compared for best glass forming compositions in Cu-Zr binary alloy system. Research supported by U.S. DOE-OS, Ames Laboratory contract No.DE-AC02-07CH11358.

## 9:00 AM Invited

**Tensile Ductility in Metallic Glass:** Z.F. Zhang<sup>1</sup>; F.F. Wu<sup>1</sup>; *Scott Mao*<sup>2</sup>; <sup>1</sup>Shenyang National Laboratory for Materials Science, Institute of Metal Research; <sup>2</sup>University of Pittsburgh

The tensile ductility or brittleness of metallic glasses is strongly dependent on the critical shear offset, which reflects the shear deformation ability of metallic glass. Furthermore, the size effect on the tensile shear deformation of metallic glass can be well understood: with decreasing specimen size smaller than the equivalent critical shear offset, there exists a transition from the unstable shear deformation to the stable shear deformation, which corresponds with the transition from the global brittleness on the millimeter-scale to the large global plasticity and even necking on the millimeter- or sub-millimeter-scale. These results are fundamentally useful to understand the physical nature of tensile shear deformation of various metallic glasses and even to design new metallic glassy materials with good plasticity.

## 9:20 AM

**Crystal Formation at Unusually Low Temperatures:** Joachim Bokeloh<sup>1</sup>; Nancy Boucharat<sup>2</sup>; Harald Roesner<sup>1</sup>; *Gerhard Wilde*<sup>1</sup>; <sup>1</sup>University of Muenster; <sup>2</sup>Research Center Karlsruhe

Nanocrystal formation at extremely high number densities is the key reaction that controls the synthesis of high strength nanostructured Al-rich Al-RE-TM (RE: rare earth, TM: transition metal) alloys. With the benefits of increased stability against coarsening and improved mechanical performance at higher nanocrystal number densities, the origin of the nanocrystal formation and the development of methods to tune the microstructure on the nanometer level have been issues of active research and controversial discussions. While previous results clearly indicated the importance of the as-quenched structure of the glass, a correct description of the kinetics of the underlying nucleation and growth processes from the early to the intermediate stages of nanocrystal formation has not been achieved. Recent results from combined measurements by microcalorimetry, modulation calorimetry and quantitative microstructure analyses provide new insight into the early stages of devitrification of Al-rich metallic glasses, indicating the complex processes that proceed during initial crystal formation

## 9:30 AM Invited

**Evolution of Shear Bands in Bulk Metallic Glass Composite:** *G. Chen*<sup>1</sup>; J. L. Cheng<sup>1</sup>; H. Bei<sup>2</sup>; C. T. Liu<sup>2</sup>; <sup>1</sup>Nanjing University of Science and Technology; <sup>2</sup>Oak Ridge National Laboratory

The evolution of shear bands in Zr-based bulk metallic glass matrix composite at different tensile strain had been tested under uniaxial tension have been investigated. It is found that on the yield point a few slip bands formed first inside the soft  $\beta$ -Zr phase. At this time, there are no shear bands being discovered in the glass matrix. As the deformation increases, the density of slip bands in the  $\beta$ -Zr phase get more. There are shear bands generating from the interface and develop into the glass matrix. The shear bands get more and more till fracture take place.



9:50 AM

**Deformation Mechanisms in Amorphous-Crystalline Nanocomposites:** *Yvonne Ritter*<sup>1</sup>; Karsten Albe<sup>1</sup>; <sup>1</sup>Technische Universität Darmstadt

In order to elucidate the deformation mechanisms present in amorphous-crystalline composites, we have studied different composites consisting of an amorphous  $\text{Cu}_x\text{Zr}_{1-x}$  phase and a crystalline Cu phase by molecular dynamics simulations, employing EAM-potentials to model the atomic interactions. Nanolaminates with alternating glass- and crystal-layers serve as model geometries to investigate the properties of amorphous-crystalline interfaces as well as the effect of geometrical confinement. We find the thickness of the individual layers to have a strong influence on the operating deformation mechanisms, both, in the glass and in the crystalline layers. Additionally, shear-banding in the presence of nanocrystalline-precipitates is studied by deforming a fully 3d-sample containing spherical Cu-crystallites in an amorphous Cu-Zr-matrix in tension. Sample dimensions, glass composition and preparation, as well as the loading conditions are chosen to allow for shear band nucleation despite the absence of stress concentrators like pre-existing notches or an indenter-tip.

10:00 AM Break

10:10 AM Invited

**Dissimilar Mechanical Properties between Various Families of Bulk Metallic Glasses:** *Maria D Baró*<sup>1</sup>; Jordina Fornell<sup>1</sup>; Santiago Suriñach<sup>1</sup>; Weihuo Li<sup>2</sup>; Annett Gebert<sup>3</sup>; Jordi Sort<sup>1</sup>; <sup>1</sup>Universitat Autònoma de Barcelona; <sup>2</sup>Anhui University of Technology; <sup>3</sup>IFW Dresden

The mechanical properties of various families of bulk metallic glasses (BMGs), based on Zr, Ti or rare earths, have been investigated. Although all these alloys share an amorphous structure, their mechanical properties are distinctly different. Namely, while BMGs based on rare-earths fracture before yielding, the Zr-based BMGs show signatures of superplasticity. Moreover, whereas Zr-based and Ti-based BMGs are very hard and exhibit a large Young's modulus, the rare-earth BMGs are relatively soft and show a low Young's modulus. These differences in mechanical behavior can be correlated with the different values of elastic constants and glass transition temperature of the several families of BMGs. Particular emphasis will be given in this presentation to recent results from nanoindentation experiments to shed light on several issues such as the influence of normal stress components acting on the shear plane at yielding, strain rate effects or deformation-induced nanocrystallization.

10:30 AM

**Submicron Scale Measurement of Residual-Stress Profiles in Amorphous Materials by the FIB Incremental Slitting Technique:** *Bartłomiej Winiarski*<sup>1</sup>; Ali Gholinia<sup>1</sup>; Jiawan Tian<sup>2</sup>; Yoshihiko Yokoyama<sup>3</sup>; Peter Liaw<sup>2</sup>; Philip Withers<sup>1</sup>; <sup>1</sup>University of Manchester; <sup>2</sup>The University of Tennessee; <sup>3</sup>Himeji Institute of Technology

Residual-stresses exist in solids in the absence of external forces or due to thermal gradients, thus alter the component performance and promote/inhibit failure processes. There have been numerous efforts to measure residual-stresses in crystalline, amorphous materials and multilayered coatings (e.g. semiconductor devices, MEMS, nuclear materials) at the micron scale. Diffraction and other conventional laboratory methods are robust to evaluate stresses in crystalline matter, however their application to glassy materials is very difficult and often impossible. We present a new technique for mapping residual-stress profiles in amorphous and crystalline materials with high spatial definition. The new sub-micron-scale mechanical-relaxation method uses FEGSEM-FIB incremental slitting and Digital Image Correlation strain analysis to evaluate residual-stresses in surface-severe-plastic-deformed Zr50Cu40Al10 BMG. The calculation algorithm is based on the Unit Pulse Method and is enriched by Tikhonov regularisation and FEA. We demonstrate that the new technique infers residual-stress profiles in amorphous materials with high spatial definition (200-300nm).

10:40 AM

**Heating-Rate-Dependent Crystallization Behavior of a Zr-Based Bulk Metallic Glass:** *Hongqing Sun*<sup>1</sup>; Katharine Flores<sup>1</sup>; <sup>1</sup>The Ohio State University

Pronounced asymmetry has been observed in crystallization of multicomponent bulk metallic glasses (BMGs) when they are heated from glassy state versus cooled from the liquid. Understanding the crystallization mechanisms of different heating and cooling conditions is necessary to enable

novel processing of BMGs, such as laser deposition or joining. In this work, as-cast  $\text{Zr}_{58.5}\text{Cu}_{15.6}\text{Ni}_{12.8}\text{Al}_{10.3}\text{Nb}_{2.8}$  glass specimens were heated to the melting temperature at heating rates of 0.5 ~ 50 K/s. Lower heating rates resulted in the formation of densely packed nano-scale crystals. TEM and EDS analysis indicates that the nanocrystal nucleation is preceded by phase separation. In contrast, higher heating rates result in the formation of micro-scale spherulites. Nucleation was suppressed by rapid heating, allowing growth to dominate the crystallization process. The rapid transformation from glass to spherulite was accomplished without evidence of prior phase separation. Calculation of crystallization activation energies also indicates various mechanisms at different heating rates.

10:50 AM

**Influence of Minor Aluminum Concentration Changes in Zirconium-Based Bulk Metallic Glasses on the Elastic, Anelastic, and Plastic Properties:** *Arnaud Caron*<sup>1</sup>; Rainer Wunderlich<sup>1</sup>; Dmitri Louzguine-Luzgin<sup>2</sup>; Guoqiang Xie<sup>2</sup>; Akihisa Inoue<sup>2</sup>; Hans-Jörg Fecht<sup>1</sup>; <sup>1</sup>Institute of Micro- and Nanomaterials, University Ulm; <sup>2</sup>WPI Advanced Institute for Materials Research, Tohoku University

The Poisson's ratio of Zr-based bulk metallic glasses in the System Zr63-xCu24AlxNi10Co3 was found to exhibit a non-monotonous behavior as a function of x when measured with ultrasound by pulse echo technique. Also from wave propagation velocity measurements at different frequencies, i.e.  $f = 2.25$  MHz and  $f = 10$  MHz, a composition dependent anelastic behavior as a function of x is found, exhibiting a similar non-monotonous behavior. In this work we further investigated the plastic deformation and the creep properties of this glass system in compression tests and by nanoindentation. The plastic strain and the measured creep deformation shows correlation with the Poisson's ratio. We then discuss the anelastic behavior observed while measuring the sound wave propagation velocity in the frame of the thermoelastic damping and the bond reorientation as proposed by Egami. Finally we discuss these effects with regards to X-ray diffraction analysis.

11:00 AM

**Length Scale Effects on Deformation in a Zr-Based Bulk Metallic Glass:** *Ashwini Bharathula*<sup>1</sup>; <sup>1</sup>The Ohio State University

Size effects on plasticity and deformation modes of a Zr-based bulk metallic glass are examined using specimens with diameters ranging from 200 nm – 3.6  $\mu\text{m}$ . Shear banding in micron- and sub-micron-scale testing is more stable than in macro-scale testing because of the smaller ratio of the specimen to load frame stiffness. As the specimen size decreases, smaller but more frequent displacement “pop-in” events are observed with increasing load. A change in deformation mode from discrete displacement pop-ins to more continuous “wavy” deformation in specimens < 300 nm in diameter is observed at low strains. Isolated shear bands are visible via high resolution SEM of specimens where testing was interrupted after the first pop-in. However the total shear offset is insufficient to account for the total plastic strain, suggesting that the wavy deformation includes homogeneous flow. Experimental results will be compared with observations of defect evolution from molecular dynamics simulations.

11:10 AM

**Effects of Ion-Implantation on Surface Properties and Bioactivity of a Nickel-Free Zr-Based Bulk Metallic Glass:** *Lu Huang*<sup>1</sup>; Wei He<sup>1</sup>; Claudiu Muntele<sup>2</sup>; Yoshihiko Yokoyama<sup>3</sup>; Harry Meyer<sup>4</sup>; Daryush Ila<sup>2</sup>; Akihisa Inoue<sup>3</sup>; Tao Zhang<sup>5</sup>; Peter Liaw<sup>1</sup>; <sup>1</sup>University of Tennessee, Knoxville; <sup>2</sup>Alabama A&M University; <sup>3</sup>Tohoku University; <sup>4</sup>Oak Ridge National Laboratory; <sup>5</sup>Beijing University of Aeronautics and Astronautics

The purpose of this study was to investigate the ion-implantation effects on the surface properties and the bioactivity of a nickel-free Zr-based bulk metallic glass (BMG). Polished alloy disks were implanted with Ca and Ar ions, respectively. The stopping and range of ion in matter (SRIM) package was used to simulate the distribution of implanted ions. Surface properties and bioactivity on both treated and untreated samples were characterized and compared. Surface morphology and roughness were examined through atomic force microscopy (AFM). Chemical compositions and depth profiles of the surface layers were obtained using x-ray photoelectron spectroscopy (XPS). The wettability of all substrates was determined by the sessile-drop contact angle method. Corrosion resistance for the untreated alloy was studied in a physiologically-relevant environment. Effects of implantation treatments on cell morphology

# Technical Program

and proliferation behaviors of bone-forming mouse MC3T3-E1 osteoblastic cells seeded on the Zr-based BMGs were investigated. Acknowledgement: This work was supported by the International Materials Institutes (IMI) Program, and the National Natural Science Foundation of China (NSFC). Research at the Oak Ridge National Laboratory SHaRE User Facility was sponsored by the Scientific User Facilities Division, Office of Basic Energy Sciences, U.S. Department of Energy.

---

## Cast Shop for Aluminum Production: Melt Oxidation, Inclusions and Hydrogen

*Sponsored by:* The Minerals, Metals and Materials Society, TMS Light Metals Division, TMS: Aluminum Committee, TMS: Aluminum Processing Committee

*Program Organizers:* John Grandfield, Grandfield Technology Pty Ltd; Pierre Le Brun, Alcan Voreppe Research Center

Thursday AM                      Room: 609  
February 18, 2010                Location: Washington State Convention Center

*Session Chair:* Richard Chandler, Altek-MDY

---

### 8:30 AM

**Formation of the Solid Layer on the Top of Molten Aluminum:** Lucas Nana Wiredu Damoah<sup>1</sup>; Lifeng Zhang<sup>2</sup>; <sup>1</sup>University of Ghana; <sup>2</sup>Missouri University of Science and Technology

The formation of the top solid layer on the molten aluminum in launders during refining and casting, constituting production loss, were experimentally, thermodynamically and kinetically investigated in the current study. The effects of humidity and composition of the metal on the oxide layer were discussed. The thickness of the top thin oxide layer was only 1 - 5  $\mu\text{m}$ , and the rest of the top layer averaging 350  $\mu\text{m}$  were mainly composed of aluminum matrix with MgO clusters, other inclusions and Fe-rich precipitated phases. Two most feasible reactions out of six were determined to be responsible for the formation of the thin oxide layer. The formation mechanism of the whole top layer was proposed. Higher humidity enhanced the oxidation of molten aluminum while lower humidity favored dissolve [Mg] oxidation. Increasing the humidity reduced the thickness of the oxide formed, however, such increases resulted in increased hydrogen content in the molten metal.

### 8:55 AM

**Removal of Solid Inclusions from Molten Aluminium through Ceramic Foam Filtration:** Alma Engelbrecht<sup>1</sup>; <sup>1</sup>Hycast AS

A CFF (ceramic foam filter) is commonly found in aluminium cast houses as a final inline melt treatment step before casting. An analytical model to predict the inclusion removal efficiency of a ceramic foam filter has been derived and verified against practical measurements. The model is based on an analogy to the removal of solid particles from a liquid by means of flotation and consists of a simple exponential function of particle size, filter pore size and filtration depth. However, the effects of the melt flow velocity, total inclusion load and the inclusion particle size amongst that of other factors on the operational performance of the CFF have also been studied. It was found that the behaviour of a CFF becomes unpredictable with respect to any model currently available from the literature for certain conditions. This is especially observed for high flow rates and coarse filters.

### 9:20 AM

**Strategies to Reduce Inclusion Input during Liquid Metal Transportation and Melt Distribution while DC Casting of Al Alloys:** Bernd Prillhofer<sup>1</sup>; Holm Böttcher<sup>1</sup>; Helmut Antrekowitsch<sup>2</sup>; <sup>1</sup>AMAG Casting GmbH; <sup>2</sup>University of Leoben

For the production of high quality rolling ingots, the quality of aluminum melts must be improved along the whole process chain. Furthermore it is absolutely necessary to avoid impurity re-entry after the last melt refinement step in the launder. The inclusion re-entry can be related to oxides, which are generated by surface turbulences in the launder and the melt distribution system of the mould. The most critical phase is the start-up of the DC casting process, which leads to excessive oxide contamination. Finally, the melt distribution bag in the mould has a significant impact on the resulting ingot quality. This paper deals with a reliable methodology to investigate the inclusion input during casting with

ultra sonic testing, PreFil® and metallographic analysis, as well as strategies to reduce inclusion re-entry by improved melt flow in the launder. The paper also includes the presentation of special designs of melt distribution systems.

### 9:45 AM Break

### 10:05 AM

**A New Multi Stage System of Filtration Employing a Cyclone:** John Courtenay<sup>1</sup>; Frank Reusch<sup>2</sup>; <sup>1</sup>MQP Limited; <sup>2</sup>Drache Umwelttechnik GmbH

The development of a new prototype multi stage filter was described at TMS 2009 in which a ceramic foam filter was applied in a first chamber operating in cake mode; grain refiner added in a second chamber and a cyclone deployed in a final chamber to ensure removal of any oxides or agglomerates arising from the grain refiner addition or release events from the foam filter. The first industrial prototype was installed at Trimet Aluminium at Essen in Germany and demonstrated that liquid metal could pass through the cyclone successfully without excessive turbulence or splash. The further development of the prototype based on new water modeling work together with plant trials is described.

### 10:30 AM

**Hazards Associated with the Use of Bone Ash in Contact with Molten Aluminum:** Don Doutré<sup>1</sup>; <sup>1</sup>Novelis Global Technology Centre

Bone ash (calcium hydroxyapatite or simply calcium phosphate) has traditionally been used in the cast house to fill cracks, patch holes and cover "make and break" or moveable joints. It has many attractive attributes including its ease of use, low cost and non-wetting characteristics. Bone ash itself is non-toxic and environmentally benign. However recent evidence indicates that bone ash can be reduced upon contact with aluminum alloys to produce metal phosphides. Metal phosphides can in turn react with water or water vapor to liberate phosphine (PH<sub>3</sub>) a highly dangerous and toxic gas. This paper reviews the observations and experiments that lead to this conclusion and discusses Novelis' search to identify a satisfactory substitute.

### 10:55 AM

**In-Situ Measurement of Dissolved Hydrogen during Low Pressure Die Casting of Aluminium:** Matthew Hills<sup>1</sup>; Mark Henson<sup>1</sup>; Chris Thompson<sup>1</sup>; Barnett Geddes<sup>2</sup>; Carsten Schwandt<sup>3</sup>; R Kumar<sup>3</sup>; Derek Fray<sup>3</sup>; <sup>1</sup>EMC Limited; <sup>2</sup>Foseco; <sup>3</sup>University of Cambridge

Hydrogen based microporosity is the primary source of defects in Low Pressure Die Cast (LPDC) aluminium wheels, and is one of the most difficult to control. The in-situ measurement of dissolved hydrogen in an LPDC holding furnace is challenging and cannot be achieved by conventional methods such as reduced pressure or circulating gas techniques. A new version of the ALSPEK H probe for the electrochemical measurement of hydrogen in molten aluminium has been developed, and is suitable for deployment in sealed environments. This article presents results of testing under LPDC conditions at a commercial foundry. The probe showed good measurement stability, even during the LPDC pressurised cycle, and responded well to changes in the hydrogen level.

### 11:20 AM

**Hycast SIR- A Unique Concept for Inline Melt Refining:** Idar Steen<sup>1</sup>; Erling Myrbostad<sup>1</sup>; Terje Haugen<sup>1</sup>; Arild Håkønsen<sup>1</sup>; <sup>1</sup>Hycast

Hycast AS, a Hydro Aluminium subsidiary, developed in the beginning of this decade a new generation of inline melt refining units (I-60 SIR) for the aluminium industry. A traditional gas fluxing principle combined with a unique design, eliminates disadvantages of the conventional degassing systems available today. The I-60 SIR has shown a remarkable high and stable removal efficiency of hydrogen and inclusions from the molten aluminium. The operational costs are low due to very low process gas (Argon) consumption, a drain free reactor and only 2 rotors in operation for a capacity of more than 65 metric tons per hour. The system is a fully automated either as a stand-alone system or integrated in a superior automation system. Installation and verification in more than 90% of the actual Hydro cast houses has been fulfilled, and the concept is now available for the international market.



### Characterization of Minerals, Metals and Materials: Characterization of Micro-, Nano-, and Thin Films

Sponsored by: The Minerals, Metals and Materials Society, TMS Extraction and Processing Division, TMS Structural Materials Division, TMS/ASM: Composite Materials Committee, TMS: Materials Characterization Committee

Program Organizers: Ann Hagni, Geoscience Consultant; Sergio Monteiro, State University of the Northern Rio de Janeiro - UENF; Jiann-Yang Hwang, Michigan Technological University

Thursday AM Room: 306  
February 18, 2010 Location: Washington State Convention Center

Session Chairs: Ann Hagni, Ann Hagni Consulting, LLC; Toru Okabe, The University of Tokyo

#### 8:30 AM Introductory Comments

##### 8:35 AM

**4-D Microstructural Characterization of Snow and Ice:** *I. Baker*<sup>1</sup>; R. Obbard<sup>1</sup>; S. Chen<sup>1</sup>; R. Lomonaco<sup>1</sup>; K. Aho<sup>1</sup>; G. Troderman<sup>1</sup>; T. Cassano<sup>1</sup>; <sup>1</sup>Dartmouth College

In this presentation we outline the use of modern analytical techniques to characterize the complete 3-D microstructures of ice and snow firn (multi-year snow) as a function of time. Snow metamorphosis was studied by periodically examining fresh snow over a period of one month, while firn from Summit, Greenland was examined every meter from the surface to pore close off at 90 m, i.e. over several hundred years of snow deposition. The characterization utilized a combination of micro X-ray computed tomography from a unit situated in a cold room and cold-stage scanning electron microscopy, including energy dispersive spectroscopy and electron backscattered patterns. This research was supported by the U.S. National Science Foundation Grants OPP-0738975 and OPP-0821056, and U.S. Army Research Office Contact 51065-EV.

##### 9:00 AM

**Characterization of Elastic and Mechanical Properties of Materials by Atomic Force Acoustic Microscopy:** *Arnaud Caron*<sup>1</sup>; Shanker Ram<sup>2</sup>; Siddhartha Das<sup>3</sup>; Hans-Jörg Fecht<sup>3</sup>; <sup>1</sup>Institute of Micro- and Nanomaterials, University Ulm; <sup>2</sup>Materials Science Center, Indian Institute of Technology, Kharagpur; <sup>3</sup>Department of Metallurgical and Materials Engineering, Indian Institute of Technology, Kharagpur

Atomic Force Acoustic Microscopy (AFAM) is a resonance spectroscopy technique where a micro-fabricated cantilever beam in contact with a sample surface is excited to its resonance via the injection of ultrasound waves through the investigated sample. The resonance frequencies of a cantilever in contact with a surface sample depend on the contact stiffness  $k^*$  and thus on the elastic properties of the sample. AFAM can be used as an imaging technique to image the microstructure from the local elasticity changes. Also quantitative investigation of the elastic properties of the single phases constituting the microstructure can be carried out. A new application scope lays in the investigation of the contact damping. Here we show how the contact damping may be related to plasticity events and friction.

##### 9:25 AM

**Nanoindentation Analysis as a Two-Dimensional Tool for Mapping the Mechanical Properties of Complex Microstructures:** *Nicholas Randall*<sup>1</sup>; <sup>1</sup>CSM Instruments

Instrumented indentation (referred to as nanoindentation at low loads and low depths) has now become established for the single point characterization of hardness and elastic modulus of both bulk and coated materials. This makes it a very good technique for measuring mechanical properties of homogeneous materials. However, many composite materials comprise material phases that cannot be examined in bulk form ex-situ (e.g., carbides in a ferrous matrix, calcium silicate hydrates in cements, etc.). The requirement for in-situ analysis and characterization of chemically complex phases obviates conventional mechanical testing of large specimens representative of these material components. This paper will focus on new developments in the way that nanoindentation can be used as a two-dimensional mapping tool for examining the properties of constituent phases independently of each other. This approach

relies on large arrays of nanoindentations (known as grid indentation) and statistical analysis of the resulting data.

##### 9:50 AM

**Characterization of Nanocrystalline CdS:In Thin Films Prepared by the Spray-Pyrolysis Technique:** *Shadia Ikhmayies*<sup>1</sup>; Riyadh Ahmad-Bitar<sup>1</sup>; <sup>1</sup>University of Jordan

Nanocrystalline CdS:In thin films with particle size in the range (3-36 nm) were produced by the spray pyrolysis technique on glass substrates. The films were characterized by investigating their X-ray diffractograms (XRD), scanning electron microscope images (SEM), transmittance curves and photoluminescence (PL) spectra. The size of the nanocrystallites was estimated from XRD diffractograms and then from the hyperbolic band model and the bandgap energies of the nano-particles, which were calculated from the positions of the minima in the first derivative curve of the absorbance. Fine-structured PL spectra confirmed the nanocrystalline nature of the films.

##### 10:15 AM

**Characterization of Nanoscale  $\gamma'$  Precipitates in Ni-Base Superalloys:** *Gopal Viswanathan*<sup>1</sup>; R. Srinivasan<sup>1</sup>; J. Tiley<sup>2</sup>; Soumya Nag<sup>3</sup>; R. Banerjee<sup>3</sup>; Hamish Fraser<sup>1</sup>; <sup>1</sup>The Ohio State University; <sup>2</sup>Air Force Research Laboratory; <sup>3</sup>University of North Texas

Nanoscale primary and secondary precipitates from Rene88 DT, a Ni-base superalloy were characterized for their size, morphology, lattice parameters and chemistry as function of selected cooling rates and aging times both in constrained and unconstrained conditions through advanced analytical techniques that include energy-filtered transmission electron microscopy (EFTEM), synchrotron XRD and 3D atom probe tomography (3DAP). The results will be presented and discussed in detail with particular reference to the coarsening kinetics of  $\gamma'$  precipitates with aging time.

##### 10:40 AM

**Chemical Co-Deposited PbS – CuS Thin Film Characterization: Effect of Annealing:** *Mishark Nnabuchi*<sup>1</sup>; *Chinedu Ekuma*<sup>2</sup>; Israel Owate<sup>2</sup>; <sup>1</sup>Ebonyi State University; <sup>2</sup>University of Port Harcourt

A heterojunction of PbS – CuS thin film has been grown on glass slides by SGT. The films were annealed for 1hr at temperature of 373K and 423K respectively. The optical properties were characterized using a UNICO UV – 2102 PC Spectrophotometer at normal incidence of light in the wavelength range of 200 – 1000nm. The minimum percentage transmittance was observed to be 34% for sample A and 25% for sample B within the same optical region. The band gap energy was determined from the spectra to be 2.05eV for sample A and 1.85eV for sample B which gave a band shift of 0.20eV. It can thus be concluded that the optical properties of the films within the VIS – UV – NIR can find application in solar thermal technology, particularly as antireflection coating, window materials and as good materials for selective solar cell fabrication.

##### 11:05 AM

**Nanosecond Electrical Discharges between Semiconducting Sulfide Mineral Particles in Water:** *Igor Bunin*<sup>1</sup>; Valentine Chanturiya<sup>1</sup>; <sup>1</sup>Research Institute of Comprehensive Exploitation of Mineral Resources RAS

Application of high-voltage nanosecond pulses (HPEMP) to disperse mineral media containing particles (from 10 microns to 1 mm in size) of natural semiconducting sulfide minerals leads to electric field concentration at contacts or gaps between neighboring particles due to transient currents through the particles. As a result, conditions for developing electrical discharges between mineral particles are formed. When powder samples, previously moistened or placed in water, are subjected to electric-pulse treatment, particle-particle discharges occur in water; the nature of these discharges differs from that for air gaps. A model for developing electric discharges between sulfide mineral (pyrite) particles under HPEMP-irradiation in a water medium is considered. The probability of electrical breakdowns of liquid gaps between particles depend strongly on the sulfide conductivity. To disintegrate particles with high conductivity, one has to use shorter pulses with a larger voltage amplitude and shorter leading edge, while low-conductivity particles require longer pulses.

# Technical Program

11:30 AM

**Quantitative Measurement of Volumes for Nanoparticles by High-Angle Annular Dark-Field Scanning Transmission Electron Microscopy:** Helge Heinrich<sup>1</sup>; Biao Yuan<sup>1</sup>; <sup>1</sup>University of Central Florida

A quantitative method to determine sample thicknesses in Transmission Electron Microscopy (TEM) using the Scanning (STEM) mode is introduced. A High-Angle Annular Dark-Field (HAADF) detector collects electrons scattered to high angles. The intensity of the HAADF signal is proportional to the sample thickness and increases with the atomic number. Multilayered samples provided by TriQuint in Apopka (FL) are used for calibration yielding data on the interaction cross section per atom. With Convergent-Beam Electron Diffraction the thickness of these multilayer systems was measured. Multislice simulations in C# .NET 3.5 are used for comparison with experimental results. These calibrations were applied to determine concentration gradients in nanoscale Fe-Pt multilayers as well as thicknesses and volumes of individual Au-Fe, Pt, Au, and Ag nanoparticles. With this method volumes of nanoparticles with known composition can be determined with an accuracy better than 15%.

11:55 AM **Concluding Comments**

12:00 PM **Question and Answer Period**

## Characterization of Minerals, Metals and Materials: Characterization of Refractories, Clays, Concrete, Interfaces, and Thermodynamics

*Sponsored by:* The Minerals, Metals and Materials Society, TMS Extraction and Processing Division, TMS Structural Materials Division, TMS/ASM: Composite Materials Committee, TMS: Materials Characterization Committee

*Program Organizers:* Ann Hagni, Geoscience Consultant; Sergio Monteiro, State University of the Northern Rio de Janeiro - UENF; Jiann-Yang Hwang, Michigan Technological University

Thursday AM                      Room: 307  
February 18, 2010                Location: Washington State Convention Center

*Session Chairs:* Jiann-Yang Hwang, Michigan Technological University; Takashi Nagai, The University of Tokyo

8:30 AM **Introductory Comments**

8:35 AM

**Effect of Cold Working on the Thermal Expansion and Mechanical Properties of Fe-29%Ni-17%Co Low Thermal Expansion Alloy:** Song-Yi Kim<sup>1</sup>; Jung Namgung<sup>2</sup>; Mun-Chul Kim<sup>2</sup>; Kee-Ahn Lee<sup>3</sup>; <sup>1</sup>Center for Advanced Green Materials Technology, Andong National University; <sup>2</sup>RIST; <sup>3</sup>Department of Advanced Material Science and Engineering, Andong National University

The change of thermal expansion and mechanical behavior by cold working and annealing has been investigated in Fe-29%Ni-17%Co low thermal expansion Kovar alloy. Thermal expansion was measured from 25° to 600° with a heating rate of 5°/min by using vacuum differential dilatometer. It was found that thermal expansion coefficient ( $\alpha_{30-400^\circ\text{C}}$ ) slightly decreased and then remarkably increased with increasing reduction ration of cold rolling. Thermal expansion coefficient sharply decreased after annealing heat-treatment. Yield and tensile strengths continuously increased and elongation decreased by cold rolling. Microstructural observation and X-ray diffraction analysis results showed that the phase significantly increased as the reduction ratio increased. The slight decrease of thermal expansion coefficient in the early stage of low reduction ratio could be explained by the destroying short-range ordering and the decreasing of grain size. The correlation between the microstructural cause and invar effect of the low thermal expansion behavior was also discussed.

8:55 AM

**Thermodynamic Measurement of Phosphorus Oxide in Oxide Systems by Double Knudsen Cell Mass Spectrometry:** Takashi Nagai<sup>1</sup>; Masafumi Maeda<sup>1</sup>; <sup>1</sup>The University of Tokyo

Thermodynamic information on alloys and oxides forms a scientific foundation for the development of new technologies for refining steel and alloys. Double Knudsen cell mass spectrometry was used as a new method to investigate thermodynamic properties on metals and alloys. In this method,

more accurate properties can be estimated easily than those by traditional methods, such as chemical equilibrium method, since pressure of gaseous species in equilibrium with specimens can be measured directly. In this study, this method was applied to measure the properties of oxide systems. The thermodynamic properties of calcium phosphates and other phosphates were estimated by measuring the pressures of gaseous phosphorus and phosphorus oxide in equilibrium with specimen by this method. A new de-phosphorization process in iron and steel industry with multi-phase flux can be proposed with these data, and use of harmful elements for environment and waste slag can be reduced in the process.

9:15 AM

**Characterization of Refractories in Gasification Systems Using Post Mortem Analysis and Thermodynamics:** Kyei-Sing Kwong<sup>1</sup>; James Bennett<sup>1</sup>; Rick Krabbe<sup>1</sup>; Hugh Thomas<sup>1</sup>; <sup>1</sup>NETL

Gasification is a process that converts a carbon feedstock into synthesis gas (CO+H<sub>2</sub>). Slagging gasifiers operate at high temperature and pressure and in a corrosive-wear environment from the slag. Cr<sub>2</sub>O<sub>3</sub>-based refractory linings are used to protect the steel vessel that comprises the gasifier from the aggressive gasification environment. Increasing service life of the gasifier is one of the keys for wide spread development of this technology. In support of the goals, research on the gasifier atmosphere, the slag chemistry, the interaction of Cr<sub>2</sub>O<sub>3</sub> refractory with different feedstock mixtures (e.g., coal and petcoke) were characterized by post mortem analysis of bricks from service in gasifiers and thermodynamics simulation of the environment. Examples demonstrating how thermodynamic calculations can explain the post mortem results and make predictions of material interactions will be given. Attention is placed on the possibility of Cr+6 in different feedstock mixtures and operating conditions

9:35 AM

**The Reception of Ceramic Aluminum Silicate Refractories:** Sereda Borys<sup>1</sup>; Irina Krugljak<sup>1</sup>; Alexandr Zherebtsov<sup>1</sup>; <sup>1</sup>ZSEA

The properties, characteristics and phase structure of chamotte refractories produced with the usage of mullitecorund chamotte and caoline have been given. The comparison of new refractory C-45 obtained by us and refractory C-43 produced by traditional method has done. The physical-chemical properties of refractories is reviewed. The visual porosity, density and pore characteristics of given refractories was calculated. It is established that C-45 has the less gas permeability then C-43 that gives melting units more stability. The petrographical microstructures of refractories have been done. The main phase structures and their influence on refractories properties have been observed. It is established that refractories with mullitecorund chamotte adition has more advantages then refractories gained by traditional method and can be applied to melting units.

9:55 AM

**Utilization of Aluminum Slag for the Expansion of Lightweight Concrete:** Xuan Li<sup>1</sup>; Jiann-Yang Hwang<sup>2</sup>; Hee-Joon Jeon<sup>2</sup>; Matthew Andriese<sup>2</sup>; Zheng Zhang<sup>2</sup>; <sup>1</sup>University of Science and Technology Beijing; <sup>2</sup>Michigan Technological University

Aluminum slag is generated when aluminum metals are recycled through a smelting process in the presence of salt. There are small amounts of aluminum metals trapped in the aluminum slag. This research aims at evaluating the use of aluminum slag as an expansion agent for the production of lightweight concrete by taking advantages of the residual aluminum metals in the slag. The research identified key elements of producing lightweight concrete products through utilizing various mixture components including NaOH, CaO, cement, and gypsum. The volumetric expansion rate was investigated and the density and strength of the products were determined. The results show that aluminum slag can be utilized for the production of lightweight concrete products.

10:15 AM

**Characterization of Vitrified Tile Bodies with Kaolinitic Clay and Nepheline-Syenite:** Carlos Mauricio Vieira<sup>1</sup>; Sergio Monteiro<sup>1</sup>; <sup>1</sup>State University of the North Fluminense

This work had for objective to characterize ceramic bodies for vitrified tiles elaborated with the mixture of nepheline-syenite flux and kaolinitic clay. Compositions were prepared with addition of 0, 30 and 50 wt.% of nepheline-syenite to a kaolinitic clay. The firing behavior of the compositions was evaluated by optical dilatometry. Specimens were prepared by uniaxial pressure at 30 MPa followed by firing at 1175°C. The fired specimens were submitted to the



following tests: bulk density, linear shrinkage, three point bending mechanical strength and water absorption. Microstructural analysis was carried out by scanning electron microscopy. The results showed that the formulations with nepheline-syenite have a potential to obtain vitrified ceramic, by significantly decreasing the porosity of the pure clayey ceramic.

**10:35 AM**

**Systematic Study of Bentonitic Clay and Quaternary Ammonium Salts:**

Renata Barbosa<sup>1</sup>; Dayanne Souza<sup>1</sup>; Karine Nóbrega<sup>1</sup>; *Edcleide Araújo*<sup>1</sup>; Tomás Mélo<sup>1</sup>; <sup>1</sup>UFCC

Besides the vantage of the abundance of bentonitic clays in the Brazil and the modification of these clays by surface treatment with quaternary ammonium salts is a simple method. In this work, it was made a previous study with four different ammonium salts and a bentonitic clay. The clay was characterized by cationic exchange capacity, determination content of montmorillonite, X-ray fluorescence and X-ray diffraction. The salts were characterized by Differential Scanning Calorimetry and Thermogravimetry. Then, a salt with thermal stability was selected for organophilization. It was observed that some ammonium salts are more thermally stable than others and with near values of decomposition temperature. The results of DSC and TG indicated that the salts with chloride anion (Cl<sup>-</sup>) decompose first and the salt with bromide anion has more thermal stability. The evidence of the incorporation of the quaternary ammonium salts in the clays structure was seen by XRF and XRD.

**10:55 AM**

**Technological Characterization of Serpentinite Rock from Andorinha**

(Bahia/Brazil): *Aline Maria Teixeira*<sup>1</sup>; João Sampaio<sup>2</sup>; Francisco Garrido<sup>3</sup>; Marta Medeiros<sup>3</sup>; <sup>1</sup>IQ/UFRJ - CETEM; <sup>2</sup>CETEM; <sup>3</sup>IQ/UFRJ

Serpentinite is an ultra basic and metamorphic rock consisting mainly of magnesium, calcium and silicon oxides. The rock under study is a host rock of chromite mine located in Andorinha, BA. The objective of this paper is to evaluate the rock's physical and chemical characteristics to be used as an additional fertilizer of acid soils. After comminution, rock samples were submitted to chemical analysis, XRD, SEM-EDS and TGA. Afterwards, particle size distribution was determined. Result analysis confirms that our rock consists mainly of dolomite, calcite and diopside. According to the result obtained, it can be said that the serpentinite rock has promising applications in agriculture for the correction and additional fertilization of acid soils. However, it is necessary to study the characteristics of the rock such as its dangers and toxicity as well as evaluate them according to the legislation for corrective acidity.

**11:15 AM**

**Properties and Durability of Ready Mix Repair Mortars in Hot Environment:** *Bencha Benabed*<sup>1</sup>; <sup>1</sup>University of Laghouat

The main objective of this work is to study the physical and mechanical properties and durability of ready mix repair mortars. The experimental study was carried out on four types of repair mortars (one hydraulic mortar, a micro-concrete a mortar with latex and a mortar containing fibers and silica fume). The properties of the repair mortars at the fresh and hardened states are analyzed. The effect of humid curing using Hessian regularly humidified, on the mechanical properties in hot and dry environment was also studied. The results of the experimental study showed that the repair mortar containing silica fume gave a better compressive strength in all curing environments. The study showed also the negative effect of hot and dry environment on all types of ready mix repair mortars and demonstrated the importance of humid curing during early age.

**11:35 AM Concluding Comments**

**11:40 AM Question and Answer Period**

**Electrode Technology for Aluminum Production: Preheating and Operational Aspects**

*Sponsored by:* The Minerals, Metals and Materials Society, TMS Light Metals Division, TMS: Aluminum Committee  
*Program Organizers:* Ketil Rye, Alcoa Mosjøen; Morten Sorlie, Alcoa Norway; Barry Sadler, Net Carbon Consulting Pty Ltd

Thursday AM Room: 616  
February 18, 2010 Location: Washington State Convention Center

*Session Chair:* Paulo Douglas Vasconcelos, Albras Alumínio Brasileiro S.A

**8:30 AM Introductory Comments**

**8:35 AM**

**Loss in Cathode Life Resulting from the Shutdown and Restart of Potlines at Aluminum Smelters:** *Alton Tabereaux*<sup>1</sup>; <sup>1</sup>Consultant

The loss in potlife that results from the shutdown of aluminum cells in potlines is primarily due to cathode cooling that occurs in potlines when the amperage is significantly reduced or when the power is interrupted. Cooling cells from 955°C to ambient, 25°C, results in irreversible and non-repairable damage to the cathodes. Cooling ultimately result in the formation of numerous long 'cooling' cracks on the surface of cathode blocks and in the seams between blocks. The impact of uncontrolled vs. controlled shutdown of cells in potlines is discussed. The amount of loss in potlife can be substantially different for potlines at smelters depending upon the circumstance of the cathodes at the time of the potline shutdown as well as the potline restart method.

**8:55 AM**

**Investigation of the Impact of Pre-Heating, Start-Up and Early Operation on Potlife:** *Jayson Tessier*<sup>1</sup>; Carl Duchesne<sup>1</sup>; Gary Tarcy<sup>2</sup>; Claude Gauthier<sup>2</sup>; Gilles Dufour<sup>2</sup>; <sup>1</sup>Laval University; <sup>2</sup>Alcoa Inc

Industrially, aluminium is produced inside metallurgical reactors, known as reduction cells or pots. Given that a few hundreds to a thousand of cells are operated in a smelter and because these pots have a typical life span of 4 to 10 years, replacing and starting pots is almost a common operation in a smelter. Once in place, new cells are pre-heated, started and operated. It is believed that pots experiencing upsets during these steps may give a lower potlife. This study presents a statistical analysis based on 31 started pots from the Alcoa Deschambault smelter. Using different statistical tools, it is demonstrated that enough information is enclosed in the pre-heating, start-up and early operation steps to perform a meaningful potlife prediction, on a pot-to-pot basis, a few weeks after start-up. Prediction results are discussed and the model structure is investigated to find variables having the greatest influence on potlife.

**9:15 AM**

**Evaluation of Mothballing and Subsequent Restarting of Søderberg Cells:** *V.Yu. Buzunov*<sup>1</sup>; V. I. Borisov<sup>1</sup>; Ye.G. Masyutin<sup>1</sup>; D.G. Bolshakov<sup>1</sup>; A.A. Pinayev<sup>1</sup>; <sup>1</sup>RUS-Engineering Ltd.

In view of the latest economic changes, the world aluminium producers have stopped the least cost-effective production capacities, reducing process costs and aluminium supply to the market trying to keep the price at an acceptable level. For choosing a mothballing technology some basic requirements were taken into consideration: - minimum costs on cells shutdown, heating and restart; - minimum influence on the cell's death age. In this paper we present our evaluation of two mothballing methods: the partial and complete metal tapping out from the cathode for vertical stud Søderberg cells.

**9:35 AM**

**Analysis of the Coke Bed Preheating Method for Aluminium Cells:** *Mohamed Ali*<sup>1</sup>; <sup>1</sup>The Aluminium Company of Egypt

Resistor coke bed preheating method is the most common method used in aluminium cells preheating. This was based on typical start-up anode effect as well as typical cathode heat-up rate during preheat and start-up. The drawbacks of this method were studied and modified to give the best performance for cells preheating. These modifications include coke bed thickness, preheating time, using flexible anode connections, fixing cathode carbon blocks and ramming paste sources and adaptation the procedures for preheating. These modifications improved from pot lives, and lowered the electrical energy and

# Technical Program

coke consumption during the preheating process. Also, the effect of workers experience on the performance of preheating was studied.

**9:55 AM**

**The Combined Flame and Aluminum Preheating Method:** Tian Yingfu<sup>1</sup>; Feng Naixiang<sup>2</sup>; Peng Jianping<sup>2</sup>; Wang Yaoyu<sup>2</sup>; Li Jian<sup>3</sup>; <sup>1</sup>Chongqing Tiantai Aluminum Industry Co., Ltd.; <sup>2</sup>Northeastern University; <sup>3</sup>Jianwenyuan Industrial Equipment Company

A combined Flame-Aluminum-Preheating (FAP) method for aluminum electrolysis cells is presented. This preheating process includes two steps. In the first step the aluminum electrolysis cell is preheated to 700~800° by the flame from gas burning, and in the second step about 8 tons of liquid aluminium are poured into the cell, and the cell is then preheated to 950° by electrical heating. The FAP method has been applied successfully in three 168 kA novel cathode cells at the Tiantai aluminum smelter in China. This shows that the FAP method is simple, safe and reliable, and it gives a short preheating time and low energy consumption of 12400 kW·h and gas consumption of 2500 m<sup>3</sup>.

**10:15 AM Break**

**10:30 AM**

**Cell Preheat on Full Line Current at Dubal:** Ali Al Zarouni<sup>1</sup>; Maryam Al Jallaf<sup>1</sup>; Arvind Kumar<sup>1</sup>; K. Alaswad<sup>1</sup>; J. Blasques<sup>1</sup>; <sup>1</sup>DUBAL

Main objective of cathode preheating is to achieve an optimum cathode life by pyrolyzing the bonding pitch and gradually raising the temperature of the lining material close to the normal operating temperature of the cell. The risk of thermal stresses and melt penetration can be minimised by adopting a good preheat and start up procedure. Resistive preheating on full line current was tried out by initially using a mixture of CP coke and graphite and later by using 100% graphite as heat transfer and resistance media. By doing so, resistor material consumption dropped by 93%, preheat energy was reduced by 10%, use of compressed air to cool shunts was eliminated and hardly any skimmings following bath up. The method permits accelerated start up especially in expansion projects and in restarting a potline following power outage. A techno-economic evaluation shows the method contributes to higher productivity at lower cost.

**10:50 AM**

**Optimization of the Anode-Stub Contact: Material Properties of Cast Iron:** Bjarte Oye<sup>1</sup>; Elin Haugland<sup>2</sup>; Jorund Hop<sup>2</sup>; Arne Nordmark<sup>1</sup>; Morten Onsoien<sup>1</sup>; <sup>1</sup>SINTEF; <sup>2</sup>Hydro Aluminium

Contact between the anode and the anode stub is normally made by cast iron. Important parameters are the iron fluidity during casting and the subsequent dimensional changes during cooling and the first heat-up. Three qualities of cast iron were investigated; standard grey iron with and without inoculation, and non-inoculated iron with 0.5 percent added phosphorus. The main contributor to fluidity appeared to be the temperature, as the metal flow when cast from 1350 °C was twice the length found at 1250 °C. Only minor differences were observed between the iron qualities, where the ordinary grey iron performed best. The cooling shrinkage of inoculated iron was lower than for the non-inoculated, probably because of an advantageous graphite structure obtained during the ferrite transition. Only minor differences were observed for the non-inoculated alloys. During the first heating, high phosphorus irons expanded significantly more than the rest at temperatures above 600°C.

**11:10 AM**

**Voltage Drop, Stub-Anode Connection, Cast Iron:** Adel Nofal Adel Nofal<sup>1</sup>; Mohamed Waly<sup>1</sup>; Ahmed Ahmed<sup>1</sup>; Mahmoud Agour<sup>1</sup>; Amr Kandil<sup>1</sup>; Shaher Mohamed<sup>1</sup>; Mohamed Mourad<sup>1</sup>; <sup>1</sup>Aluminium Company of Egypt

This paper studies the influence of the carbon equivalent (CE) of grey iron on the electrical resistance of the stub-anode connection. Three levels of CE were studied i.e. 3.9, 4.3 and 4.5 through changing the Si-content, the effect of increased P-content was also studied. A bench-scale experimental set-up was used to simulate the operating conditions at the steel stub / cast iron collar / carbon anode. The change in microstructure and electrical resistance was measured at temperatures up to 850°C. up to 30 days. The thermal expansion properties of different cast iron grades and of the steel stub were measured using a high precision automatic dilatometer. The electrical resistance at the stub / collar / anode connection was related to both the electrical resistivity of the iron collar and the contact pressure, which was found to depend on the cast iron graphitization favoured by high CE-values.

## General Abstracts: Electronic, Magnetic and Photonic Materials Division: Session II

*Sponsored by:* The Minerals, Metals and Materials Society, TMS Electronic, Magnetic, and Photonic Materials Division, TMS: Alloy Phases Committee, TMS: Biomaterials Committee, TMS: Chemistry and Physics of Materials Committee, TMS: Electronic Materials Committee, TMS: Electronic Packaging and Interconnection Materials Committee, TMS: Nanomaterials Committee, TMS: Superconducting and Magnetic Materials Committee, TMS: Thin Films and Interfaces Committee, TMS: Energy Conversion and Storage Committee  
*Program Organizers:* Long Qing Chen, Pennsylvania State University; Sung Kang, IBM Corporation; Mark Palmer, Kettering University

Thursday AM Room: 308  
February 18, 2010 Location: Washington State Convention Center

*Session Chair:* To Be Announced

**8:30 AM Introductory Comments**

**8:35 AM**

**Chemical Vapor Transport Synthesis and Optical Property of Moo<sub>3</sub> Thin Film:** Young Jung Lee<sup>1</sup>; Chang Won Park<sup>1</sup>; Dae-Gun Kim<sup>1</sup>; *Young Do Kim<sup>1</sup>*; <sup>1</sup>Hanyang University

Transition metal oxides have attention in the industrial application fields of photochromic, electrochromic, sensor, catalyst and electrode for microbatteries. Among them, MoO<sub>3</sub> thin films have been extensively investigated in the electrochromic (EC) device field due to its superior optical properties. Recently, many deposition techniques to deposit Mo oxide thin films have been developed. In this study, new deposition technique for the successful deposition of homogeneous MoO<sub>3</sub> thin films was accomplished through the chemical vapor transport of volatile MoO<sub>3</sub>(OH)<sub>2</sub> during the reduction of MoO<sub>3</sub> powder and subsequent thermal annealing. As annealing commenced, the optical transmittance of the films increased due to enhancement of the crystallinity resulted from oxygen vacancy reduction and increase of the relative density from reduction of porosity. Also, electrochromic property of the annealed MoO<sub>3</sub> thin film was analyzed by intercalation of ions in LiClO<sub>4</sub> dissolved in propylene carbonate (PC) as electrolyte.

**8:55 AM**

**Improved Performance of a Fluorescent Blue Organic Light Emitting Diode with Hole Blocking Materials as Dopants for Transport Layers:** Girija Samal<sup>1</sup>; K. N. Narayanan Unni<sup>1</sup>; Saswat Bharat<sup>1</sup>; *Deepak<sup>2</sup>*; <sup>1</sup>Samtel Color Ltd; <sup>2</sup>Indian Institute of Technology Kanpur

Realizing a highly efficient deep blue organic light emitting diode (OLED) with sufficient life time is the biggest challenge in the fabrication of full color OLED displays. Using hole blocking layers (HBL) has been an established technique to confine excitons or carriers in the recombination region. In the present work, we have doped the hole transport layer (HTL) and electron transport layer (ETL) with two different hole blocking materials and compared the performance of these devices with that of a standard device. Our standard blue OLED demonstrates a current efficiency of 2.3 cd/A. To improve its current efficiency, we have doped the ETL by a hole blocking material (BPhen), which shows no improvement in current efficiency. But, doping the HTL with another hole blocking material (TPBi) has led to current efficiency as high as 4.3 cd/A. The importance of band gap engineering is discussed based on the above studies.

**9:15 AM**

**Luminescence of the GaP:N Long-Term Ordered Single Crystals:** *Sergei Pyszhkin<sup>1</sup>*; John Ballato<sup>2</sup>; Andrea Mura<sup>3</sup>; Marco Marceddu<sup>3</sup>; <sup>1</sup>Academy of Sciences; <sup>2</sup>Clemson University; <sup>3</sup>The University of Cagliari

GaP:N single crystals were prepared by one of the authors (SP) during 1963-1966 using the method of free crystallization from Ga solution. It is known that the characteristic time of the substitution reaction during N diffusion along P sites in GaP:N crystals at room temperature constitutes 15-20 years. Hence, the observations of highly excited luminescence of the crystals made in the sixties and the nineties were then compared with the results obtained in 2009 in closed experimental conditions. The impressive nearly semi-centennial evolution of the GaP:N luminescence observed is interpreted as the result of both volumetric



N impurity ordering and the formation of an ordered bound exciton system at some level of optical excitation. The highly ordered nature of this new host and excitonic lattices increases the radiative recombination efficiency, and makes possible the creation of advanced non-linear optical media for optoelectronic application.

9:35 AM

**Opals, Photonic Band Gap Materials, Pleochroic Refraction, and Monochromatic Lasers:** *Michelle Stem*<sup>1</sup>; <sup>1</sup>University of Texas at El Paso

Opals embody the application of Bragg's Law over visible light. Here, fundamental research was applied to natural opals because they are used to develop photonic band gap (PBG) material templates. Effects from applying two laser wavelengths (532nm and 630-650nm) and tungsten white (580-590nm) to the many types of natural opal were compared. The ranges of many traits of opals includes: opaque to transparent, vibrant to colorless, diffuse to refraction. Because some types of opals (transparent and refraction) exhibit at least partial PBG control, a comparison of refraction and colors refracted relative to incident angles were determined for each photon source. This research determined whether only polychromatic light caused certain opals to refract different wavelengths in different directions or if the monochromatic lasers caused the same opals to have different refraction wavelengths or different directions. Opal-based materials are transforming the computer industry, especially for NOEMS and MOEMS materials.

9:55 AM Break

10:15 AM

**Coercivity Enhancement of Nd-Fe-B Sintered Magnets by Two-Step Sintering:** Se Hoon Kim<sup>1</sup>; Hoon-sup Kim<sup>1</sup>; Jin Woo Kim<sup>1</sup>; Dae-Gun Kim<sup>1</sup>; *Young Do Kim*<sup>1</sup>; <sup>1</sup>Hanyang University

Nd-Fe-B sintered magnets are normally composed of Nd<sub>2</sub>Fe<sub>14</sub>B hard magnet phase as matrix and Nd-rich phase on grain boundary. Many researchers have shown that the coercivity of Nd-Fe-B magnets was sensitive to microstructure, such as the grain boundary phases and grain size, etc. Therefore, modifying a sintering process has been an important method for better homogeneous microstructure. In this study, Nd-Fe-B powder was compacted under magnetic field of 20kOe. After that, the green compact was sintered at 950°C for 4h as first-step and second-step sintering was performed as 1050°C. The microstructure was investigated by TEM and EPMA. Magnetic properties were measured by a B-H tracer. Densification over 99% could be obtained by the two-step sintering of Nd-Fe-B powder under 6μm in Nd<sub>2</sub>Fe<sub>14</sub>B phase and the Nd-rich phase was homogeneously distributed around Nd<sub>2</sub>Fe<sub>14</sub>B phases. Moreover, the two-step sintering process led to uniform grain size distribution which had the improved magnetic properties. This research was supported by a grant from the Fundamental R&D Program for Core Technology of Materials funded by the Ministry of Knowledge Economy, Republic of Korea.

10:35 AM

**Structure and Magnetic Properties of Fe-Co-Ni-Zr-B-Cu Nanocrystalline Soft Magnetic Alloys:** *Keith Knipling*<sup>1</sup>; Maria Daniil<sup>1</sup>; Matthew Willard<sup>1</sup>; <sup>1</sup>Naval Research Laboratory

Nanocrystalline soft magnetic materials possess a unique combination of large magnetization, high permeability, and low core losses. In these materials, nanoscale ferromagnetic grains are exchange-coupled through a surrounding amorphous matrix, minimizing magnetocrystalline anisotropy and improving the magnetic performance. This exchange-coupling is eliminated, however, above the Curie temperature of the intergranular amorphous phase, limiting the maximum service temperature of the alloys. The effect of substituting Co and Ni for Fe in a series of Fe<sub>88-2x</sub>Co<sub>1-x</sub>Ni<sub>x</sub>Zr<sub>7</sub>B<sub>4</sub>Cu<sub>1</sub> alloys (x = 0-22) are presented. Magnetization generally decreases and the coercivity increases with increasing x, whereas the Curie temperature of the amorphous phase increases significantly (from 73°C at x = 0 to 570°C at x = 22). There is thus an optimum composition near x = 5.5 exhibiting excellent soft magnetic properties at 300-500°C. The performance is competitive with extant Co-based alloys but at much lower costs by virtue of the high Fe content.

**General Abstracts: Electronic, Magnetic and Photonic Materials Division: Session III**

*Sponsored by:* The Minerals, Metals and Materials Society, TMS Electronic, Magnetic, and Photonic Materials Division, TMS: Alloy Phases Committee, TMS: Biomaterials Committee, TMS: Chemistry and Physics of Materials Committee, TMS: Electronic Materials Committee, TMS: Electronic Packaging and Interconnection Materials Committee, TMS: Nanomaterials Committee, TMS: Superconducting and Magnetic Materials Committee, TMS: Thin Films and Interfaces Committee, TMS: Energy Conversion and Storage Committee  
*Program Organizers:* Long Qing Chen, Pennsylvania State University; Sung Kang, IBM Corporation; Mark Palmer, Kettering University

Thursday AM Room: 310  
February 18, 2010 Location: Washington State Convention Center

*Session Chair:* To Be Announced

8:30 AM Introductory Comments

8:35 AM

**A Subatomic Particle Electromagnetic Wave Solution In A Simplified Space/Time Environment:** *John Elton*<sup>1</sup>; James Cornwell<sup>1</sup>; <sup>1</sup>Protective Systems, Inc.

The derivation of the electromagnetic wave functions for subatomic particles using Maxwell's equations is described. This solution demonstrates how Heaviside and Dirac Delta functions can be used to solve Maxwell's equations at a point. Fundamental relationships between electromagnetic variables will be discussed and physical constants of selected subatomic particles will be determined. Using these solutions the rest mass of subatomic particles can be represented and the fundamental relationship between energy, rest mass and momentum can be derived.

8:55 AM

**Effect of Electroplating Bath Temperature on Sn Surface Morphology:** *Uttara Sahaym*<sup>1</sup>; Stephanie Miller<sup>2</sup>; M Norton<sup>1</sup>; <sup>1</sup>Washington State University; <sup>2</sup>University of Illinois

The present study documents the effect of electroplating bath temperature on the surface brightness/reflectivity and the evolution of surface morphology of electrodeposited pure Sn films, and its subsequent effect on whisker formation. The brightness/reflectivity of the films increased with increase in temperature. Detailed microstructural analysis of the electroplated Sn films showed that unique pyramid shaped features formed at elevated temperatures (below 85°C) and the underlying surface became increasingly smooth with temperature. The plating temperature also affected the morphology of the whiskers that formed upon aging at room temperature. The whisker diameter increased whereas the size decreased with increase in plating temperature. It was also observed that the diameter and length of each whisker depends on the Sn grain size. The growth mechanisms of pure Sn films and the development surface morphology during electrodeposition at different temperatures will be discussed.

9:15 AM

**Introduction of Digital Field Control System in Skelp Mill, DSP:** *Tapas Kanti Dutta*<sup>1</sup>; Goutam Majumder<sup>2</sup>; Suresh Sarkar<sup>2</sup>; Nilay Gupta<sup>2</sup>; Shaktiveer Singh<sup>1</sup>; <sup>1</sup>RDCIS, SAIL; <sup>2</sup>Durgapur Steel Plant, SAIL

In Skelp mill of Durgapur Steel Plant, the roughing stands consisting of six horizontal stands and three vertical stands (edgers), are driven by DC motors with one common armature voltage. The finishing stands, consisting of five horizontal stands are driven by another common armature voltage. The two armature voltages are generated by two separate thyristor converters. The fields of the motors are controlled to obtain speed regulation. There was no correction of speed drop due to impact of biting and operation of the mill motors over entire speed range could not be achieved. Absence of on-line diagnostics led to increase in downtime in case of mill breakdown. Introduction of this scheme has resulted in faster response (faster speed drop correction), possibility of setting speed over entire speed range, reduction in down time and operator's satisfaction to run the mill.

# Technical Program

9:35 AM

**The Photophysics of a Luminescent Ruthenium Polypyridyl Complex with Pendant  $\beta$ -Cyclodextrin; pH Modulation of Lifetime and Photoinduced Electron Transfer:** *Muath Atme'h*<sup>1</sup>; <sup>1</sup>National University of Ireland

We have conducted detailed photophysical studies on the luminescent host [Ru(bpy)<sub>2</sub>(phen-CD)]<sup>2+</sup>. The complex exhibits a strong pH dependent luminescence, which is attributed to protonation/deprotonation of the secondary amine bridge linking the CD and ruthenium polypyridyl centre. From emission studies, the pK<sub>a</sub> for the amine was determined to be 11.5. [Ru(bpy)<sub>2</sub>(phen-CD)]<sup>2+</sup> forms host guest complexes with AQ and AQC, with association constants of 4,920 ± 560 M<sup>-1</sup> and 14,657 ± 2,200 M<sup>-1</sup>. The anthraquinone guest appears to participate in efficient photoinduced electron transfer from the excited ruthenium polypyridyl centre. The possibility that protonation/deprotonation at the amine linker can be used to modulate electronic communication between the CD and luminophore was explored. However, the rate of photoinduced electron transfer appeared to be relatively insensitive to the state of protonation of the bridge.

9:55 AM

**Materials and Manufacturing Challenges in Hybrid Flexible Electronics:** *Khershed Cooper*<sup>1</sup>; <sup>1</sup>NRL

Flexible electronics is a relatively new field involving electronic or optoelectronic devices on flexible substrates. It is a silicon-based technology necessitating ingenious ways of laying down the brittle silicon and other semiconductors on plastic substrates. Hybrid flexible electronics is an emerging technology of considerable promise. Conformable, foldable, stretchable, rollable and deformable electronic devices are possible. A key ingredient is organics, which opens up the material selection window significantly for the development of semiconductors, dielectrics and other electronic components. However, to advance hybrid flexible electronics, there is a pressing need for research in thin-film organic-inorganic hybrid circuits, devices and systems and high throughput, roll-to-roll manufacturing requiring high resolution and accurate registry. An in-depth understanding of materials behavior and fabrication issues should advance the field greatly so applications such as lighting, photovoltaics, batteries, displays, e-paper, sensors, actuators, RFIDs on flexible substrates can be realized.

10:15 AM Break

10:35 AM

**An Experimental Setup and Procedure for Thermal Resistance Measurements of a Thermal Interface Material:** *Kaustubh Kalkundri*<sup>1</sup>; Frank Andros<sup>1</sup>; Bahgat Sammakia<sup>1</sup>; <sup>1</sup>SUNY at Binghamton

Increasing functionality while concurrent scaling has put demanding requirements on the reliability of silicon devices due to the resultant increase in power dissipation. A test apparatus was developed for steady state thermal resistance measurements of a Thermal Interface Material (TIM) based on Fourier law. The primary objective to develop a measurement system compatible with industry needs for repeatable measurements was realized by using a commercial thermally conductive epoxy adhesive as TIM. Experiments performed determined interface thermal resistance of assembled test samples as a function of their Bond Line Thickness. An uncertainty analysis was performed to find the maximum potential variation in the thermal resistance and emphasize on the selection of appropriate equipment for measurements. It was verified that increasing the heat flow and BLT reduces the uncertainty in interface temperature difference. Furthermore, modeling was used to understand the impact of defects in the TIM interface.

10:55 AM

**Effect of Isothermal Aging and Thermal Cycling on Interfacial IMC Growth and Fracture Behavior of SnAgCu/Cu Joints:** *Xiaoyan Li*<sup>1</sup>; <sup>1</sup>Beijing University of Technology

The growth of IMCs of SnAgCu/Cu solder joint in isothermal aging and thermal cycling, was investigated with the focus on the growth kinetics. The joints were isothermal aged at 125C, 150C and 175C while the thermal cycling was performed on -25C to 125C and -40C to 125C. The tensile strength was evaluated by in-situ tensile test. It was found that the grain size of IMCs increases and their morphology were changed. The thickness of IMCs was found increases with the thermal cycles but the growth rate was less than that of thermal aging. The growth of IMCs was found follows Arrhenius's diffusion model and the corresponding diffusion factor and active energy were obtained.

The tensile strength of the joints decreases with the increase of aging time while the fracture site was moved. The shear strength was found decrease with the increases of the thermal cycles.

11:15 AM

**Magnetic Properties of New Diluted Ferromagnetic Semiconductors Pb<sub>1-x-y</sub>Mg<sub>x</sub>Cr<sub>y</sub>Te:** *Elena Zvereva*<sup>1</sup>; Olga Savelieva<sup>1</sup>; Sergey Ibragimov<sup>1</sup>; Evgeny Slyn'ko<sup>2</sup>; Vasily Slyn'ko<sup>2</sup>; <sup>1</sup>Moscow State University; <sup>2</sup>Institute of Material Science Problems

The temperature and magnetic field dependencies of the magnetization (T=1.8-300 K, B ≤ 7 T) and X-band EPR (f=9.1-9.6 GHz, B ≤ 0.7 T, T=80-400 K) has been studied for novel diluted magnetic semiconductors Pb<sub>1-x-y</sub>Mg<sub>x</sub>Cr<sub>y</sub>Te. It was shown that all samples are ferromagnetic with the Curie temperature up to T=275 K. Magnetic saturation is achieved at magnetic fields higher 5 T. With increasing of the chromium content the magnetic saturation moment increases and achieves 0.2 emu/g. The temperature dependencies of the magnetization M(T) is rather concave type with a broaden maximum at temperature about 115 K. EPR spectra in the paramagnetic phase were satisfactory approximated by a single Dysonian line with the typical linewidth about 600 G. In ferromagnetic phase pronounced distortion and splitting of the EPR spectra on two Dysonian lines were revealed. Temperature dependencies of the effective g-factor and the line width for each absorption line were obtained.

11:35 AM

**Structure and Properties of Metamagnetic Functional Alloys Ni-Mn-In:** *Pnina Ari-Gur*<sup>1</sup>; Michael Morris<sup>1</sup>; Gregory Huizenga<sup>1</sup>; Victor Koledov<sup>2</sup>; Vladimir Shavrov<sup>2</sup>; Vladimir Zolotarev<sup>2</sup>; Alexander Kamantsev<sup>2</sup>; Vladimir Khovailo<sup>2</sup>; Fernando M. Araujo-Moreira<sup>3</sup>; Oscar F. de Lima<sup>4</sup>; <sup>1</sup>Western Michigan University; <sup>2</sup>Kotelnikov' Institute of Radioengineering and Electronics of RAS (Moscow); <sup>3</sup>Universidade Federal de São Carlos (Brazil); <sup>4</sup>Universidade Estadual de Campinas (Brazil)

Metamagnetic Shape Memory Alloys (SMA) Ni-Mn-In demonstrate unique properties of both giant magnetic field-induced strains and giant magnetocaloric effect. This is due to the phenomenon of the thermoelastic martensitic transition, giving rise to shape memory effect, merging with the metamagnetic phase transition from ferro to antiferromagnetic state. In the present work, the samples of metamagnetic SMA Ni-Mn-In were prepared and their structure, magnetic properties and phase transitions studied. The clear thermally-induced shape memory effect has been demonstrated. In situ neutron diffraction tests showed the effect of magnetic-field-induced structure transformation near metamagnetostructural transition temperature.

## General Abstracts: Light Metals Division: Session III

*Sponsored by:* The Minerals, Metals and Materials Society, TMS Light Metals Division, TMS: Aluminum Committee, TMS: Magnesium Committee, TMS: Recycling and Environmental Technologies Committee, TMS: Energy Committee, TMS: Aluminum Processing Committee

*Program Organizers:* Alan Luo, General Motors Corporation; Eric Nyberg, Pacific Northwest National Laboratory

Thursday AM Room: 607  
February 18, 2010 Location: Washington State Convention Center

*Session Chair:* Alan Luo, General Motors Research and Development Center

8:30 AM

**Multistage Fatigue Modeling for Three Wrought Al Alloys:** *Yibin Xue*<sup>1</sup>; <sup>1</sup>Utah State University

Wrought aluminum alloys are primary materials in aerospace and automotive vehicular body structures. Alloying, casting, wrought process, heat-treatment/aging, and final form establish distinct composition, microstructural features, and hardening mechanisms of wrought Al alloys, which also alter fatigue behaviors. Solution treated, age-harden 2xxx, precipitate hardened 6xxx, and solution heat treated, precipitation hardened 7xxx Al alloys, are chosen for multistage fatigue modeling excises. Presumably, all alloys are tempered for the highest achievable strength. The physically motivated mechanistic MultiStage Fatigue (MSF) model are developed for the three alloys based on the static, cyclic, limited fatigue behaviors, and micromechanical simulations. The differences in



fatigue damage incubation mechanisms are identified and incorporated into the MSF model according to the accumulated microplasticity associated with the incubation mechanism. The first-order MSF model developing methodology is proposed and the MSF model predicts fairly coherent upper and lower bounds of fatigue lives in the high cycle fatigue regime.

**8:50 AM**

**Optimized Fatigue Behaviour of Ti-6Al-4V Alloy Components Fabricated by MIM:** *Orley Ferri*<sup>1</sup>; Thomas Ebel<sup>1</sup>; Rüdiger Bormann<sup>1</sup>; <sup>1</sup>GKSS - Research Centre

During the last few years, processing of Ti-6Al-4V alloy powders by Metal Injection Moulding (MIM) has gained increasing interest in research and applications. Nowadays, it is possible to manufacture MIM Ti-6Al-4V alloy components with tensile properties comparable to those of the wrought material. In contrast, the fatigue behaviour of MIM components does not follow the same trend. In order to improve the fatigue behaviour of MIM components, the critical microstructural features and process parameters were identified. The results showed that grain size is more important than remaining porosity and impurity levels. Based on this result, a beneficial microstructure was obtained by adding amorphous boron powder in the range of 0.1 to 0.5 wt.% to Ti-6Al-4V alloy powder during the MIM process. Excellent tensile ( $\sigma_y = 790$  MPa, UTS = 900 MPa,  $\epsilon = 12\%$ ) and fatigue (endurance limit ~ 640 MPa) properties were achieved by adding 0.5 wt.% boron.

**9:10 AM**

**Structural Analysis of Hot Blow Formed Aluminum Center Pillar with Residual Stress Consideration:** *Dongok Kim*<sup>1</sup>; Jinpyeong Kim<sup>1</sup>; Yongmun RYU<sup>1</sup>; <sup>1</sup>KATECH

Hot blow forming has been introduced to automotive industries since it makes super-plastic forming possible for the materials which has been considered to be difficult to form. Although its low production rate due to the limitation of the allowed strain rate is the disadvantage, by applying this process complex shapes of the metal sheet can be achieved in one piece and the absence of weld and rivet can reduce the risk for fatigue damages. However, many studies have carried out the structural analysis without the consideration of residual stress after hot blow forming. In addition, the material properties of aluminum alloys after hot blow forming have not been applied to the analysis. Therefore, in this study, the structural analysis of hot blow formed center-pillar with considering changed material properties and residual stresses has been carried out to achieve more precise prediction of finite element analysis.

**9:30 AM**

**Thermo-Mechanical Characterization of Al-Cu-Mg Composites Reinforced with Diboride Particles:** *Natalia Cortes*<sup>1</sup>; Pilar Barrado<sup>1</sup>; Sergio De Hoyos<sup>1</sup>; Hermes Calderón<sup>1</sup>; Oscar Suárez<sup>1</sup>; <sup>1</sup>University of Puerto Rico-Mayaguez

Aluminum-based composites are being evaluated for aerospace and transportation applications where light weight and appropriate strength at high temperatures are key requirements. The present work focused on the mechanical response of a series of Al matrix composites at room and high temperature. The composite matrix contained 2.5 wt.% Cu and 1 wt.% Mg and was reinforced with different levels of boron (0, 1, 2, 3 and 4 wt.%) forming AlB<sub>2</sub> particles. The specimens, fabricated via gravity casting, were tested using a Thermo-Mechanical Analyzer (TMA) under constant compression loads. This TMA instrumentation also permitted studying creep response of the composites. Our results indicated that even at 300°C higher concentration of diboride particles helped the composite retain high hardness compared to an unreinforced alloy with similar concentrations of Mg and Cu.

**9:50 AM**

**Upgrade and Electrochemical Reduction of TiO<sub>2</sub>-Rich Slag to Titanium:** *Qian Xu*<sup>1</sup>; Ling Sun<sup>1</sup>; Qiu-Shi Song<sup>1</sup>; Wei Xing<sup>1</sup>; Ji-Hong Du<sup>2</sup>; Zheng-Ping Xi<sup>2</sup>; <sup>1</sup>Northeastern University; <sup>2</sup>Northwest Institute for Non-Ferrous Metal Research

An upgraded titania slag with more than 95% mass percent TiO<sub>2</sub> was produced by alkali fusion and acid leaching of TiO<sub>2</sub>-rich slag prepared by electrical furnace smelting. The influence of various experimental conditions on the chemical composition of the upgraded titania slag has been investigated, such as the amount of alkali used, reaction time, HCl concentration for leaching and final pH. The mechanism of the alkali fusion-acid leaching process is studied by X-Ray diffraction and Fourier Transform Infrared spectrometry. The

upgraded titania slag was compacted to the thin pellets, then sintered at 900°, and finally electrochemical de-oxidized to titanium.

**10:10 AM Break**

**10:30 AM**

**Wear Behaviour of the Newly Developed Biomedical Beta Titanium Alloy (Ti-23Nb-0.7Ta-2Zr-1O):** *Sathish Sathyavageswaran*<sup>1</sup>; M. Venkatesh<sup>1</sup>; Geetha Manivasagam<sup>1</sup>; Asokamani Rajamanickam<sup>1</sup>; T.K. Nandy<sup>2</sup>; <sup>1</sup>VIT University; <sup>2</sup>Defence Metallurgical Research Laboratory

In spite of superior mechanical properties such as low modulus of elasticity, high strength to weight ratio and excellent biocompatibility among the biomedical titanium alloys, it suffers from poor wear resistance. The objective of this work is to enhance the wear resistance of the newly developed beta titanium alloy, gum metal (Ti-23Nb-0.7Ta-2Zr-1O) by subjecting it to various heat treatments. These alloys were subjected to  $\alpha$  and  $\beta$  solution treatments and its mechanical properties were measured. Phase analysis was performed using X-ray diffraction technique and microstructural observations were made using scanning electron microscopy. The sliding wear behavior of all these heat treated samples were studied under simulated body fluid (Hank's solution) condition and compared with the conventional Ti-6Al-4V and  $\beta$ -CEZ alloys. The results of the above studies will be discussed in detail in this paper.

**10:50 AM**

**Friction Stir Spot Welding of Magnesium Alloys:** *Qi Yang*<sup>1</sup>; Xiang Li<sup>1</sup>; Ke Chen<sup>1</sup>; <sup>1</sup>Hitachi America, Ltd.

Friction stir spot welding, as a derivative of friction stir welding, has been developed for joining body structures. In the present study, AZ31, AM30, and AM60 magnesium alloys are friction stir spot welded with different material combinations and welding configurations. The effect of process condition on macrostructures, microstructures and strengths of spot welds is investigated. Higher weld strength is obtained at a lower rotation speed. Furthermore, spot welds of dissimilar materials could show higher strength than spot welds of the same materials.

**11:10 AM**

**Study on the Materials of Rolled Al-Mg-Si Alloy Used for the High-Speed Trains:** *Kai Ji*<sup>1</sup>; Guangchun Yao<sup>1</sup>; Yongliang Mu<sup>1</sup>; Guoyin Zu<sup>1</sup>; <sup>1</sup>School of Materials & Metallurgy, Northeastern University

Based on 6082 aluminum alloys, a novel Al-Mg-Si alloy was designed, which possesses strong weldability and corrosion resistance. Through the orthogonal test, effects of adding slight Mg, Mn, Cu and Cr on strong weldability and corrosion resistance was analyzed. The results show that the best composition design of rolled Al-Mg-Si alloy was Mg 1.0%, Si 0.8%, Mn 0.70%, Cu 0.40%, Cr 0.20%. Moreover, the appropriate technology of TIG welding has been found to improve the mechanical properties of the welds due to grain refinement occurring in the fusion zone. The joint efficiency by ER5356 welding wires reached up to 78%. Finally, silicon and copper were concentrated at the dendrite boundaries and a-Al + Si + Al<sub>2</sub>Cu + Mg<sub>2</sub>Si eutectic was observed by optical (OM) and scanning electron (SEM) microscopy. Coarse dimples and voids had been observed in the fractographs. The joints show a transgranular type failure.

**11:30 AM**

**Thermodynamic Design of Ultra-Strong Titanium Alloys Undergoing Plasticity Induced Martensitic Transformations:** *Suresh Neelakantan*<sup>1</sup>; Pedro Rivera-Diaz-del-Castillo<sup>2</sup>; Sybrand van der Zwaag<sup>2</sup>; <sup>1</sup>Materials Innovation Institute/Delft University of Technology; <sup>2</sup>Delft University of Technology

Our previous work has shown that the strength of  $\beta$  titanium alloys can be increased up to 50 % via inducing martensitic transformations under plastic deformation, without compromising on other properties such as ductility. Tailoring such transformations for various alloy compositions and deformation temperatures may be performed with the aid of thermodynamic computations. Inspired by Ghosh and Olson's theory for martensite formation in ferrous systems [*Acta. Met.*, Vol. 42, pp. 3361, 1994], a thermodynamic framework is presented to control Plasticity induced transformations in titanium alloys; and its application in developing novel alloys, subjected to various deformation schemes is presented. The prospects of developing a new family of metastable  $\beta$  alloys displaying improved strength/ductility relationships via plasticity induced transformation effects is outlined.

# Technical Program

## General Abstracts: Materials Processing and Manufacturing Division: Forming and Machining

Sponsored by: The Minerals, Metals and Materials Society, TMS Materials Processing and Manufacturing Division, TMS/ASM: Computational Materials Science and Engineering Committee, TMS: Global Innovations Committee, TMS: Nanomechanical Materials Behavior Committee, TMS/ASM: Phase Transformations Committee, TMS: Powder Materials Committee, TMS: Process Technology and Modeling Committee, TMS: Shaping and Forming Committee, TMS: Solidification Committee, TMS: Surface Engineering Committee  
Program Organizers: Thomas Bieler, Michigan State University; Corbett Battaile, Sandia National Laboratories

Thursday AM Room: 606  
February 18, 2010 Location: Washington State Convention Center

Session Chair: To Be Announced

### 8:30 AM

#### Effect of AWJ Machining Processes on Flexural Properties of CFRP Composites: T. Briggs<sup>1</sup>; M. Ramulu<sup>1</sup>; <sup>1</sup>University of Washington

This paper investigates the dependence of mechanical performance on the manufacturing process chosen to prepare composite material testing specimens. Carbon Fiber Reinforced Plastic (CFRP) specimens have been machined from consolidated plates to testing coupons using abrasive waterjet (AWJ) cutting as well as abrasive diamond saw (ADS) cutting. The extensional and flexural properties of the CFRP composite material system have been experimentally determined through tensile and 3-point bend testing, respectively. The measured, in-plane elastic properties, in addition to micro and macroscopic features, failure loads and damage progression behavior, have been shown to have a correlation to the surface topography induced by the respective post processing operation.

### 8:50 AM

#### A Simple Method for Producing Large Tubular Components of Varying Profiles: Michel Guillot<sup>1</sup>; Augustin Gakwaya<sup>1</sup>; Xavier Elie-dit-Cosaque<sup>1</sup>; <sup>1</sup>Laval University

Aluminum tubes of varying profiles are used for structural components in automobiles, bicycles and many products. Because tubular hydroforming can be very expensive for large components, an alternative technique that can produce many simple shapes (e.g. rectangular, L, ...) without internal pressure is introduced. The technique involves dies which internal geometry is defined such as to provoke during die closing, a forming sequence which result into the desired shape after springback. First, the paper presents this forming technique, tooling and the computational method used to establish the shape of the die and tool motion for a given final geometry. Different shapes are tabulated for AL6061-O and T6 using extruded 50.8mm O.D. tubes. Thereafter, tests are carried out (1) in straight tubes of constant section profiles, (2) in straight tubes of varying section profiles, and (3), in bent tubes of constant section profiles. The resulting components are characterized dimensionally and metallurgically.

### 9:10 AM

#### A Study of Electromagnetic Compression of Thin-Walled Steel and Aluminum Tubes: Anupam Vivek<sup>1</sup>; Keun-Hwan KIM<sup>2</sup>; Glenn Daehn<sup>1</sup>; <sup>1</sup>Ohio State University; <sup>2</sup>POSCO

Electromagnetic forming represents an elegant and efficient way of reducing tube diameter as there is no physical contact with the tube and deformation can be much more stable because of inertial stabilization of buckling. The ease and precision for controlling pressure is a major advantage of this technique and hence small to large tubes can be compressed using the same basic equipment. Velocity, displacement, currents and strains are measured with high accuracy and resolution using advanced instrumentation like Photon Doppler Velocimetry and Rogowski coils. In this work, Steel and Aluminum tubes are electromagnetically compressed and experimental results are compared to a numerical model. The model could not predict the buckling so it is experimentally studied in detail by varying material temper, energy level and pressure rise time. All the experimental and simulation results will be presented and subsequently discussed.

### 9:30 AM

#### Texture Control for Improving Deep Drawability of Cu Bearing New BH Steel: Kyu Hwan Oh<sup>1</sup>; Dong Nyung Lee<sup>1</sup>; Yang Mo Koo<sup>1</sup>; Se Min Park<sup>1</sup>; Sung-il Kim<sup>1</sup>; <sup>1</sup>Graduate Institute of Ferrous Technology, Pohang University of Science and Technology

The deep drawability, e.g., the limiting drawing ratio or the plastic strain ratio, of steel sheets is well known to increase with increasing density of  $\gamma$  fiber ( $\langle 111 \rangle / ND$  with ND denoting the sheet normal direction) component in their textures. Therefore, steel sheets for deep drawing are desired to have as high density of  $\gamma$  fiber component as possible. A thermomechanical process has been developed to increase the  $\gamma$  fiber component in Cu bearing new BH steel manufactured by POSCO. The process comprises the first rolling of about 20% reduction and subsequent annealing at 780°C and the second rolling of about 70% reduction and subsequent annealing at 780°C. The first step process aims at seeding the  $\gamma$  fiber grains, which can grow preferably in the second step process. In this way the density of  $\gamma$  fiber component in the steel sheet substantially increased compared with that in the conventionally processed one.

### 9:50 AM

#### Edge Cracking Characterization and Analysis on Advanced Dual Phase Steels: Xin Wu<sup>1</sup>; <sup>1</sup>Wayne State University

Advanced high strength dual phase steels have been applied for lightweight structures such as automotive bodies. One of the challenges is its sensitivity to edge cracking and the uncertainty to predicting the stamping failure. In this paper material microstructures are characterized, and the edge fracture as a function of material grade, orientation and deformation histories are examined, and the mechanisms responsible for edge fracture is determined. Mechanical analysis is performed using a meso-scale composite model to reflect various dual phase microstructural features and the response to the deformation and fracture.

### 10:10 AM

#### Closure of Cylindrical Voids in a Slab under Plane-Strain Compression: Jong Jin Park<sup>1</sup>; Jae Won Lee<sup>1</sup>; <sup>1</sup>Hongik University

Voids in a slab or an ingot are required to be closed during rolling or forging processes. However, the level of closure depends on the location of a void since the state of stress is inhomogeneous. In the present study, cylindrical voids were assumed to be located along the thickness direction in a slab that was under plane-strain compression along the width, and the closure phenomenon of the voids was investigated by experiment and numerical analysis. It was found that a void is closed through contraction and collapse stages, where it deforms to an ellipse and folds along the major axis, respectively. It was also found that a void is closed when the effective strain reaches a certain value, which in fact depends on the aspect ratio of the cross section of a void but not on its magnitude.

### 10:30 AM Break

### 10:50 AM

#### Springback Correction by Electromagnetic Deformation in Sheet Metal Fabrication: Jianhui Shang<sup>1</sup>; Steve Hatkevich<sup>1</sup>; Larry Wilkerson<sup>1</sup>; Jeremy Westerheide<sup>1</sup>; Allen Jones<sup>1</sup>; <sup>1</sup>American Trim LLC

Springback is caused by the elastic recovery of bending area after unloading. It leads to the deviation of part shape. Therefore, springback control is a key to get the desired shape in sheet metal forming. In this study, electromagnetic forming was applied to springback correction as a second step after bending. Basic principle is to place magnetic impulses at bending area of metal parts to eliminate springback. From this principle, two approaches (direct and indirect approach) were investigated for springback correction of V-shape bent metal parts. The tested materials included Al alloy and high strength steel (HSS). The detailed experiment design and results will be presented here. Overall this study demonstrates the feasibility of springback correction by electromagnetic forming.

### 11:10 AM

#### Microstructure Evolution and Static Re-Crystallization Kinetics of High Manganese Steel at Hot Rolling Conditions: Hyukjin An<sup>1</sup>; Soon Gi Lee<sup>2</sup>; Jong-Kyo Choi<sup>2</sup>; Jae-Sang Lee<sup>1</sup>; Yang-Mo Koo<sup>1</sup>; <sup>1</sup>POSTECH; <sup>2</sup>POSCO

To study the static re-crystallization under the hot rolling conditions of high manganese steel, double compression isothermal tests and multi-pass hot torsion tests were performed. It is important to estimate austenite microstructure depending on hot rolling condition, for controlling final mechanical properties.



It is known that  $T_{nr}$  corresponds to the temperature where re-crystallization starts to be incomplete. But actually the “pancake” structure, the standard no re-crystallization microstructure on rolled microstructure, appears at lower temperature than  $T_{nr}$ . Thus, in order to estimate austenite microstructure, the observed austenite aspect ratio are compared with softening fraction between  $T_{nr}$  and RST (re-crystallization stop temperature) has been designed. No-recrystallization temperature ( $T_{nr}$ ) was measured by using multi-pass continuous cooling torsion tests. RST and RLT (re-crystallization limit temperature) was calculated from softening ratio which is measured by using double deformation tests.

### 11:30 AM

**New High Strength Ductile Bainitic Forging Steels:** *Christoph Keul*<sup>1</sup>; Marcus Urban<sup>2</sup>; Martin Fischer<sup>1</sup>; Gerhard Hirt<sup>2</sup>; Wolfgang Bleck<sup>1</sup>; <sup>1</sup>Institute of Ferrous Metallurgy; <sup>2</sup>Institute of Metal Forming

New alloying and process designs without a secondary heat treatment are necessary to enable an economic production of forged steel components that combine high strength and good toughness. Forging steels containing approx. 0.20%C, 1.5%Si, 1.5%Mn, 1.3%Cr, 0.0025%B, 0.03%Nb, 0.02%Ti have been found adequate to achieve these aims. This alloying concept, combined with an adapted process route, enables a bainitic microstructure which leads to a tensile strength greater than 1200MPa, a total elongation greater than 10% and a toughness bigger than 27J at room temperature. These material properties have been accomplished by a defined deformation/heat treatment concept tested in laboratory and have been verified in industrial scale. The required bainitic microstructure formed either during a continuous or isothermal phase transformation has been characterized on a detailed morphological basis depending on the forging/cooling procedure. Therefore, a quantitative correlation between processing route and resulting mechanical properties is possible.

### 11:50 AM

**Superplastic Blow Forming of Steel and Titanium Alloys for Aerospace Parts:** *Ho-Sung Lee*<sup>1</sup>; Jong-Hoon Yoon<sup>1</sup>; Yeong-Moo Lee<sup>1</sup>; <sup>1</sup>Korea Aerospace Research Institute

By using superplastic blow forming technology, it is possible to form a complex shape in one piece with least amount of waste during machining. The present study constructs an analysis model to predict blow forming behavior of duplex steel and titanium alloy from results of biaxial and uniaxial tension tests. The experimental results show a complex shape was successfully formed from bonded sheets of superplastic metals. The results demonstrate that the developed technology to process design of high temperature blow forming by the finite element method can be applied for near net shape forming of a combustion chamber skin and a cylindrical hollow tank of ramjet engine.

### 12:10 PM

**Cooling Behavior of Lead-Free Bismuth Bronze Produced through the Frozen Mold Casting Process:** *Shuji Tada*<sup>1</sup>; Hiroyuki Nakayama<sup>1</sup>; Toshiyuki Nishio<sup>1</sup>; Keizo Kobayashi<sup>1</sup>; <sup>1</sup>National Institute of Advanced Industrial Science and Technology

Lead-free bismuth bronze castings were produced by several frozen molds. The effect of sand characteristics constructing frozen mold on the cooling behavior of bronze castings was examined. The sand particle characteristics such as higher thermal conductivity, greater grain size and spherical shape increased the cooling rate of castings. The cooling potential of frozen mold relates closely to the behavior of vaporized water. In the frozen mold, the ice near the mold surface contacting to molten metal thaws immediately and changes to vapor just after pouring. Then it blows out from the mold with removing the heat from the casting. Accordingly, the frozen mold which has good air permeability is able to enhance its cooling ability. The structure of lead-free bismuth bronze castings was successfully refined by the frozen mold casting process, which enabled to accelerate the cooling rate of cast products drastically.

### General Abstracts: Structural Materials Division: Environmental Degradation

*Sponsored by:* The Minerals, Metals and Materials Society, TMS Structural Materials Division, TMS: Advanced Characterization, Testing, and Simulation Committee, TMS: Alloy Phases Committee, TMS: Biomaterials Committee, TMS: Chemistry and Physics of Materials Committee, TMS/ASM: Composite Materials Committee, TMS/ASM: Corrosion and Environmental Effects Committee, TMS: High Temperature Alloys Committee, TMS/ASM: Mechanical Behavior of Materials Committee, TMS/ASM: Nuclear Materials Committee, TMS: Refractory Metals Committee, TMS: Titanium Committee  
*Program Organizers:* Eric Ott, GE Aviation; Robert Hanrahan, National Nuclear Security Administration; Judith Schneider, Mississippi State University

Thursday AM Room: 601  
February 18, 2010 Location: Washington State Convention Center

*Session Chair:* To Be Announced

### 8:30 AM

**Phase Field Modeling of Sintering Process in Thermal Barrier Coating Systems:** *Anter El-Azab*<sup>1</sup>; Jie Deng<sup>1</sup>; Karim Ahamed<sup>1</sup>; <sup>1</sup>Florida State University

The development of thermal barrier coating (TBC) systems with well controlled and predictable performance is crucial for making breakthroughs in many high-temperature application areas. Related research and development efforts, however, have been highly experimentally oriented and little modeling effort is being conducted in parallel to understand the complex nature of bonding and failure mechanisms in TBC systems. At the root of these failure mechanisms is the interlayer and surface diffusion driven by high temperature, stress gradients and chemical composition differences between different components of the TBC systems. In this presentation we will discuss the critical aspects of connection between diffusional processes, microstructural and morphological changes and sintering mechanisms in TBC systems, and present phase field modeling results for the densification and porosity changes and inter-layer diffusion in typical TBC systems.

### 8:50 AM

**High-Temperature Cyclic Oxidation of Pd/Pt-Modified NiAl Bond Coats:** *Raghavendra Adharapurapu*<sup>1</sup>; Dan Widrevitz<sup>1</sup>; Jun Zhu<sup>1</sup>; Don Lipkin<sup>2</sup>; Voroman Dheeradhada<sup>2</sup>; Tresa Pollock<sup>1</sup>; <sup>1</sup>University of Michigan; <sup>2</sup>General Electric (GRC)

Oxidation resistant NiAl-based bond coats are an important element of thermal barrier coating systems. A combinatorial approach to investigating the effects of higher order additions to NiAl, including Pt, Pd and Hf, on the oxidation and interdiffusion behavior of the bond coats has been developed. Bond coats with compositions in the range of Ni-(33-39)Al-5Cr-(2-8)Pd/Pt were deposited on RenéN5 substrates. Long-term cyclic-oxidation experiments on Pd/Pt-modified NiAl+Hf at 1100°C revealed similar oxidation kinetics in both type of coatings. While the alumina scales formed on Pd-modified bond coats were slightly thicker than the Pt-modified ones, both exhibited a high resistance to large-scale spalling. Microprobe measurements have also shown that the difference in the penetration depths of Pd and Pt into the substrate are not as large as expected from the higher interdiffusion-coefficient of Pd in NiAl/Ni. SEM and XRD analysis of the oxidation products at various stages of oxidation will be presented.

### 9:10 AM

**Role of TM (TM = Pd, Rh, Ir) on Stability and Oxidation Behavior of Ternary  $\beta$ -NiAl:** *Travis Brammer*<sup>1</sup>; Pratik Ray<sup>1</sup>; Yi Ye<sup>2</sup>; Matthew Kramer<sup>2</sup>; Mufit Akinc<sup>1</sup>; <sup>1</sup>Iowa State University; <sup>2</sup>Ames Laboratory

The drive for greater efficiencies and clean power generation requires the modern day gas turbines to operate at as high a temperature as possible in harsh operating conditions. Controlling oxidation at these elevated temperatures is a prime concern for system lifetime. In our work, we focus on the  $\beta$ -NiAl. Choice of alloying additions for the current work was made using a multi-stage ‘sieving process’ to reduce the large number of potential alloying elements. Initial filtering of the prospective elements was done using extended Miedema model. Promising elements were studied within the framework of

# Technical Program

DFT using VASP to check the role of minor additions on stability. Pd, Rh and Ir were deemed the most suitable for experimental testing. Additionally, the oxidation behavior of NiAl has been analyzed as functions of composition and temperature. The alloys were tested at isothermal temperatures ranging from 1100°C-1300°C, and thermal cycling at 1150°C.

## 9:30 AM

**Investigation of the Stress Corrosion Cracking of Carbon Steel in Fuel Grade Ethanol Environments:** *Lindsey Goodman*<sup>1</sup>; Xiaoyuan Lou<sup>1</sup>; Preet Singh<sup>1</sup>; <sup>1</sup>Georgia Institute of Technology

Recently, there has been much evidence of the phenomenon of stress corrosion cracking (SCC) in steel equipment in the ethanol industry. Research shows the effects of simulated fuel grade ethanol (SFG) and impurities such as water, chlorides, and pH<sub>e</sub> on SCC severity in carbon steel. In this study, carbon steel was exposed to fuel grade ethanol (FGE) to concurrently investigate surface film formation on carbon steel and compositional changes in the FGE environments. Ethanol breakdown can occur over time based on environmental conditions, thus effects of these compositional variations on carbon steel surfaces were investigated. Scanning electron microscopy (SEM), and X-ray diffraction (XRD) were used to characterize the steel surface. Raman spectroscopy was used to characterize both FGE chemical composition and steel surface. Electrochemical behavior of carbon steel in the ethanol environments was evaluated. Experimental results are detailed in the body of the paper.

## 9:50 AM

**Observation and Detection of Corrosion on Aerospace Bearing Steels in Ester Based Lubricants:** *Michael Hurley*<sup>1</sup>; Cole Smith<sup>1</sup>; Darryl Butt<sup>1</sup>; <sup>1</sup>Boise State University

Lubricant degradation or contamination in jet turbine engines is a precursor to corrosion of the bearing materials. Once corrosion is initiated, the eventual outcomes are decreased engine performance, required service, and parts replacement. Characterization of the bearing steel corrosion behavior in the engine environment is elusive since typical electrochemical corrosion measurements are ineffective due to ultra high solution resistance of the lubricating fluid. In this work EIS (Electrochemical Impedance Spectroscopy) and in-situ optical microscopy were utilized in an effort to characterize the corrosion behavior of M50 and P675 bearing steels tested in a range of water and chloride contaminated ester based oils. EIS was found to be sensitive to water contamination levels and relatively insensitive to chloride contamination level and the presence of active corrosion. Further insight in to the corrosion behavior was obtained via optical microscopy of the complex interaction of water, oil, and steel microstructure in-situ.

## 10:10 AM Break

## 10:20 AM

**Assessment of Slag-Aided Deoxidation Process in 3.5CrMo Rotor Steel:** *June-Seong Park*<sup>1</sup>; Chang-Woo Seo<sup>1</sup>; Seonhyo Kim<sup>1</sup>; <sup>1</sup>POSTECH

Refining process of rotor steels by applying slag-aided deoxidation using CaO-CaF<sub>2</sub> flux has been investigated at 1873K. Initial deoxidation rate was faster through increasing CaF<sub>2</sub>/CaO ratio until 1.15. However, experimental results recommended 1:1 to optimum CaF<sub>2</sub>/CaO ratio because excess CaF<sub>2</sub> contents promoted the dissolution of MgO at the crucible. By considering slag-aided deoxidation, the Deoxidation rate is decreased with increment of Fe<sub>2</sub>O. At input of Ca-Si deoxidant for slag deoxidation, Silicon acted not only Ca-carrier and slag reductant, but also affected the direct deoxidation of molten steel. 3% of Ca-Si deoxidant was insufficient in slag with 5% of Fe<sub>2</sub>O. 7% of Ca-Si deoxidant affected adversely by increasing silicon content, and deoxidation rate was similar to input 5%. Thus effective content was 5% of Ca-Si deoxidant.

## 10:40 AM

**Factors Affecting the Environmental Assisted Cracking Behavior of 2205 Duplex Stainless Steel:** *Kevin Chasse*<sup>1</sup>; Di Yang<sup>2</sup>; Preet M. Singh<sup>1</sup>; Richard W. Neu<sup>3</sup>; <sup>1</sup>Georgia Institute of Technology; <sup>2</sup>University of Colorado at Boulder; <sup>3</sup>Georgia Institute of Technology and University of Colorado at Boulder

The reliable performance of duplex stainless steels (DSSs) in chloride- and sulfide-containing solutions is important to many industrial processes. Previous studies have shown that DSSs are susceptible to environmental assisted cracking (EAC) under certain conditions in these solutions; however, the mechanical and electrochemical conditions under which DSSs may become susceptible are not well understood. To elucidate some of these mechanical and electrochemical

conditions, the EAC susceptibilities of a 2205 DSS were evaluated in an acidic-chloride solution and a sulfide-containing caustic solution. Low frequency cyclic tests were performed for a fixed number of cycles, and the crack initiation events were examined after these tests. In the chloride solution, corrosion pits are the preferential sites for crack initiation under cyclic loading. In the sulfide-containing caustic solution, precipitates tend to be the preferential sites for cracks to initiate, especially the ones at or near the interface of the phase boundary and grain boundary. Hydrogen embrittlement (HE) was also found to be a potential form of EAC in this solution at room temperature when a cathodic potential (CP) was applied.

## 11:00 AM

**Hydrogen Embrittlement of a Bainitic Wheel Steel:** *Ren Xuechong*<sup>1</sup>; Liu Fenbin<sup>1</sup>; Su Yanjing<sup>1</sup>; Chu Wuyang<sup>1</sup>; <sup>1</sup>University of Science and Technology Beijing

The slow strain rate tensile (SSRT) test and hydrogen-induced delayed cracking (HIDC) were investigated in a novel bainitic wheel steel. The results showed that hydrogen embrittlement susceptibility of the bainitic wheel steel was really higher than that of ferrite-pearlite wheel steel. The threshold stress intensity factor of hydrogen-induced delayed cracking, K<sub>IH</sub>, decreased exponentially with the increasing of diffusible hydrogen concentration C<sub>0</sub>. And the crack propagating rate can achieve as high as 0.2 mm/min when C<sub>0</sub>=1.6×10<sup>-6</sup>.

## 11:20 AM

**Microstructural and Mechanical Aspects of High Nitrogen Steels at Cryogenic Temperature:** *Zurui Zhang*<sup>1</sup>; Huabing Li<sup>1</sup>; Zhouhua Jiang<sup>1</sup>; Zhen Li<sup>1</sup>; <sup>1</sup>Northeastern University

Charpy V-Notch impact tests of high nitrogen austenitic stainless steels with different nitrogen concentration 0.96, 0.88 and 0.82 (wt. %) from 77K to 293K are processed in this paper. The fracture facets are observed by using scanning electron microscopy (SEM) and transmission electron microscopy (TEM) to reveal the micro fracture mechanism. With increasing the nitrogen content, the ductile to brittle transition temperature (DBTT) increases. The change of fracture patterns of high nitrogen austenitic stainless steels is dimple=>shallow dimple=>mixture of quasi-cleavage facets and dimple=>cleavage facet. Fracture facets with river patterns or tear ridges, along annealing twin boundary and cross the annealing twin plane are observed in this investigation. Critical dislocation density around crack-tip field  $\rho_c=(6\pi\tau_v^2/K_{Ic}^2)^2$  can be used for explaining DBT behavior at cryogenic temperature. Deformation twinning is frequently observed at cryogenic temperature. Crack forms along the coherent twin boundary between twinning and the matrix.

## 11:40 AM

**The Relationship between Sliding-Wear Rate and the Microstructure of AISI 1020 Plain-Carbon Steel:** *Jong Chul Kim*<sup>1</sup>; Jun Ki Park<sup>1</sup>; Sul Ki Yi<sup>1</sup>; *Yong-Suk Kim*<sup>1</sup>; <sup>1</sup>Kookmin University

The relationship between sliding-wear rate and the microstructure of plain-carbon steel (0.2C-0.7Mn-0.05Si) was investigated. The steel was heat treated under various conditions to have different microstructures, and the effect of microstructure on the sliding wear was explored. Dry sliding wear tests of the heat-treated steel were carried out using a pin-on-disk wear tester at a fixed load of 100 N at room temperature. AISI 52100 bearing steel and alumina balls were employed as a counterpart. Tensile properties and hardness of the heat treated steel were evaluated to characterize wear behavior of the steel. The wear rate of the steel heat treated under different conditions did not change significantly with the microstructural variation, though hardness of the steel varied significantly with the microstructure. Effects of the morphology and volume fraction of constituting phases of the microstructure on the wear rate were explored in connection with deformation beneath wearing surface (subsurface-deformation-layer formation).

## 12:00 PM

**Dynamic Tensile Extrusion Behavior of DU and U6NB:** *Carl Trujillo*<sup>1</sup>; George Gray<sup>1</sup>; Ellen Cerrera<sup>1</sup>; Joel Montalvo<sup>1</sup>; Daniel Martinez<sup>1</sup>; <sup>1</sup>Los Alamos National Laboratory

While there have been studies investigating the quasi-static, stress-strain behavior of uranium alloys, there have been few studies that have examined the high strain, high strain rate response of these materials. One way to examine this behavior is through high-rate, tensile extrusion. Using a technique developed at Los Alamos National Laboratory, U6Nb and DU spheres were accelerated to velocities of 550m/s and extruded through a steel die. High speed



photography captured the in-situ extrusion response. Recovered fragments were characterized using optical and electron microscopy. Spheres were fired at temperatures ranging from 25-300C. At quasi-static rates, DU and U6Nb display ductile behavior. However, during high strain rate extrusion, deformation was dominated by shear processes that significantly limited ductility. Comparisons between the temperatures and extrusion rates will be presented. Continuum simulations based on Mechanical Threshold Stress (MTS) models will be performed to provide insight into the dynamic extrusion process.

### Jim Evans Honorary Symposium: Beyond Berkeley Times

*Sponsored by:* The Minerals, Metals and Materials Society, TMS Extraction and Processing Division, TMS Light Metals Division  
*Program Organizers:* Ben Li, University of Michigan; Brian G. Thomas, University of Illinois at Urbana-Champaign; Lifeng Zhang, Missouri University of Science and Technology; Fiona Doyle, University of California, Berkeley; Andrew Campbell, WorleyParsons

Thursday AM Room: 620  
February 18, 2010 Location: Washington State Convention Center

*Session Chair:* Ben Li, University of Michigan

#### 8:30 AM Introductory Comments

#### 8:40 AM

**Contamination Issues – A Contrast in Industries:** *Stanley Siu*<sup>1</sup>; <sup>1</sup>S & V Siu Associates, LLC

Contamination issues in the semiconductor industry have always been a major focus of attention due to its direct impact on device performance and yield. The term “killer defects” is indicative of the seriousness of this issue and sophisticated technologies to detect contaminants have evolved to such a level that contamination and defect detection has become an industry in itself. In the medical device industry contamination has received much less attention, but as devices have become more sophisticated, this issue is beginning to gain more attention. The medical device industry is now venturing into the realm of metrology that has traditionally been the territory of semiconductor processing. Major differences in goals, objectives, and requirements make contamination detection and mitigation a very different and challenging problem and will be highlighted with a case study in this paper.

#### 9:05 AM

**Electrodynamic and Thermal Interaction of Nanoparticles in Hyperthermia Cancer Therapy and Solar Energy Systems:** *Ben Li*<sup>1</sup>; <sup>1</sup>University of Michigan

The paper presents a study on the electrodynamic and thermal interaction of nanoparticles as applied to therapeutic treatment of cancer patients and to development of high efficiency solar energy systems. For these applications, nanoparticles need to have a structure that is tunable to a given frequency of an electromagnetic energy source for resonance absorption and/or scattering. Electrodynamic model is developed based on the analytical and numerical solution of the full 3-D Maxwell equations to determine the tunable resonance absorption as a function of varying structure parameters. The electromagnetic model is then linked to a thermal model, which is based on the solution of combined internal thermal radiation, conduction and convection. Experiments are conducted to validate the electromagnetic and thermal models. Both modeling and experimental results will be presented for the systems under consideration for cancer treatment and solar energy system applications.

#### 9:30 AM

**Metallurgical Design Issues at Cirque du Soleil:** *Daniel Cook*<sup>1</sup>; <sup>1</sup>University of Nevada, Las Vegas

The modern live entertainment industry poses a number of interesting engineering problems in the design and use of large, dynamic, theatrical stage components, which can be on the order of 10s of meters in length and 100s of metric tons in moving mass. A prime example of these types of stage components can be seen at the Cirque du Soleil show Ka. Since show opening in 2005, a number of the components of the Gantry Lift, the main stage system, have needed modification to correct operational issues that arose from the initial design(s). This paper will focus on how mathematical modeling and analysis of

the as-built components has been conducted to correct and improve operation of the stage system. In particular, this paper will describe the static and dynamic structural calculations which have been used as the basis for component redesign to alleviate fatigue failure in the stage system.

#### 9:55 AM

**An Electrochemical Technique for Minimizing Soil and Ground Water Contamination by Heavy Metals Leached from Solid Industrial Wastes:** *Nilesh Shukla*<sup>1</sup>; *Manoj Harbola*<sup>1</sup>; *Kali Sanjay*<sup>2</sup>; *Rajiv Shekhar*<sup>1</sup>; <sup>1</sup>Indian Institute of Technology; <sup>2</sup>Institute of Minerals & Materials Technology

Indiscriminate dumping of solid industrial wastes in un-engineered sites and the consequent soil and water contamination by heavy metals -- dissolved in rain water -- is a major environmental hazard in India. This study addresses an important issue: how do we minimize the rain water assisted transport of toxic heavy metals from solid wastes to the ground water? Preliminary experiments have shown that electrochemical fencing, which uses an electric field to capture the heavy metal ions, is a viable technique for slowing down the rain-assisted transport of heavy metals through soil. Experiments simulating the natural rain fall conditions on a saturated soil covered with a dichromate residue have been carried out. The effect of applied voltage, electrode depth, and electrode configuration on the efficacy of electrochemical fencing has been investigated. A mathematical model that calculates the trajectory of Cr(VI) ions to predict the efficacy of electrochemical fencing has been formulated.

#### 10:20 AM Break

#### 10:35 AM

**Hall Cell MHD Instability: Recent Theoretical Analyses and Experimental Support:** *Donald Ziegler*<sup>1</sup>; <sup>1</sup>Alcoa Primary Metals

We review progress on understanding of MHD instability in Hall cells. Recent theoretical work has shown the existence of other types of instability beyond the classical caused by the vertical component of the magnetic field. In this work, we describe our calculations of one of these instabilities and show evidence from plants that appear to fit the phenomenon described by the theoretical work.

#### 11:00 AM

**Common Modeling Approaches in Displays: Case Studies in Organic Light Emitting Diodes and Plasma Display Panels:** *Deepak*<sup>1</sup>; <sup>1</sup>IIT Kanpur

The design of electronic devices that are based on current flow is commonly described by a drift-diffusion type approach, which received prominence with its use in design of silicon based electronic devices. This paper addresses the use of same approach in displays: the plasma display panels (PDPs) and organic light emitting diodes (OLEDs). While the drift-diffusion approach is the same in both, in PDP, new physics is included through plasma reactions that create the charged and excited species in gas and innovative boundary conditions. In OLEDs, however, the physics is entirely different from inorganic semiconductors due to hopping transport of charges and the excitons that play a prominent role. However, the approach of drift-diffusion is so ubiquitous that attempt is still made to cast the problem in that form. Using these approaches, we demonstrate both the principle of operation and design of devices in PDPs and OLEDs.

#### 11:25 AM

**Modeling Pulsatile Blood Flow in End-to-Side Anastomoses:** *Daniel Cook*<sup>1</sup>; *Christopher Thompson*<sup>2</sup>; <sup>1</sup>University of Nevada, Las Vegas; <sup>2</sup>General Electric

Analysis of the transient, pulsatile blood flow in a simplified anastomosis located between the human aorta and a centrifugal heart assist pump was carried out. Modeling efforts focused on the fluid flow in the anastomosis for junction angles of 60, 75, and 90 degrees at varying heart and pump flow rates. Results from this modeling indicated that higher junction angles produced larger areas of stagnation and shear gradients internal to the fluid, whereas lower junction angles yielded higher shear rates at the arterial wall opposite to the junction.

# Technical Program

## Magnesium Technology 2010: Forming and Welding

Sponsored by: The Minerals, Metals and Materials Society, TMS Light Metals Division, TMS: Magnesium Committee

Program Organizers: Sean Agnew, University of Virginia; Eric Nyberg, Pacific Northwest National Laboratory; Wim Sillekens, TNO; Neale Neelameggham, US Magnesium LLC

Thursday AM Room: 613  
February 18, 2010 Location: Washington State Convention Center

Session Chairs: Amit Ghosh, University of Michigan; Jon Carter, GM R&D

### 8:30 AM

**Test Results and FEA Predictions from Magnesium AZ31 Sheet Beams in Bending and Axial Compression:** *David Wagner*<sup>1</sup>; Stephen Logan<sup>2</sup>; Kathy Wang<sup>3</sup>; Tim Skrzek<sup>4</sup>; <sup>1</sup>Ford Motor Company; <sup>2</sup>Chrysler LLC; <sup>3</sup>General Motors Corp.; <sup>4</sup>Magna Cosma International

Load versus displacement measurements are compared to finite element analysis (FEA) predictions for magnesium AZ31 sheet beams. The beams are two stampings joined with epoxy and rivets. The longitudinal axis of the beams is aligned in the rolling direction in some samples and in the transverse direction in others. Results from quasi-static four-point bend, quasi-static axial compression and high-speed axial compression tests of AZ31 sheet beams show the beam's behavior over a range of loadings and the two orientations. The AZ31 beams exhibit significant material cracking and splitting in all tests. LS-DYNA material model MAT\_124 captures the sheet magnesium AZ31 constitutive behavior over a range of strain rates and accommodates different responses in tension and compression. The boundary conditions in the FEA predictions closely mimic the loading and constraint conditions in the component testing. LS-DYNA explicit FEA predictions of the tests agree to differing degrees with the test results.

### 8:50 AM

**Microstructure and Mechanical Properties of Magnesium Extrusion Alloys AM30 and AZ31:** *Alan Luo*<sup>1</sup>; Joy Forsmark<sup>2</sup>; Xichen Sun<sup>3</sup>; Scott Shook<sup>4</sup>; W.Z. Misiolek<sup>5</sup>; Raj Mishra<sup>1</sup>; <sup>1</sup>General Motors Corporation; <sup>2</sup>Ford Motor Company; <sup>3</sup>Chrysler Group LLC; <sup>4</sup>Timminco Metals; <sup>5</sup>Lehigh University

Magnesium alloy extrusions offer potentially more mass savings compared to magnesium castings in lightweighting vehicle structures applications. The objective of the United States Automotive Materials Partnership (USAMP) "Magnesium Front End Research and Development" (MFERD) project is to evaluate various magnesium alloys for automotive body applications. As a task in the MFERD project, solid and hollow extrusions of AM30 and AZ31 alloys were fully characterized for grain structure and crystallographic texture. Mechanical properties in tension and compression were tested in extrusion, transverse and 45 degree directions. Mechanical properties of magnesium extrusions are generally better than those of conventional die cast alloys. Significant tension-compression asymmetry (different yield strength in tension and compression) and plastic anisotropy (different plastic behavior in different directions) are due to the strong texture developed in the extrusion process.

### 9:10 AM

**Texture Development in a Twin Roll Cast and Warm Rolled ZK60 Magnesium Alloy:** *Hongmei Chen*<sup>1</sup>; Huashun Yu<sup>2</sup>; Suk Bong Kang<sup>3</sup>; Guanghui Min<sup>2</sup>; <sup>1</sup>Jiangsu University of Science and Technology; <sup>2</sup>Shandong University; <sup>3</sup>Korea Institute of Materials Science

The effect of rolling conditions on the microstructure and texture development of twin roll cast ZK60 alloy strip was investigated. Texture of ZK60 Mg alloy sheets were evaluated by X-ray diffraction method in this study. Tensile test was performed to show the influence of the per pass thickness reduction on mechanical properties. The microstructure of ZK60 alloy sheets consisted of fibrous structure with elongated grains and a relatively density of shear bands along the rolling direction which were warm rolled at 350°C with 10%, 30% and 50% thickness reduction per pass. Dynamic recrystallization could be found during the warm rolling process with different per pass thickness reduction. Grain refinement was found to occur during the warm rolling process, producing a finer grain size of which was warm rolled with 50% reduction in single pass rolling at 350°C. This could result in better mechanical properties.

### 9:30 AM

**Cruciform Geometries for Elevated Temperature Biaxial Testing of Mg AZ31B:** *Fadi Abu-Farha*<sup>1</sup>; *Louis Hector Jr*<sup>2</sup>; <sup>1</sup>Pennsylvania State University; <sup>2</sup>GM R&D Center

Plastic deformation of metals is typically characterized with the uniaxial tensile test. However, multiaxial loading in sheet metal forming requires more complex tests such as the controlled biaxial test with cruciform specimens. Efforts have been limited by testing instrumentation complexity, especially at higher-than-ambient temperatures, and specimen designs that preclude plastic strain accumulation in the gauge section. Here, focus is on development of Mg AZ31B cruciform geometries where plastic deformation is achieved in the gauge section. Testing was conducted in a biaxial apparatus capable of multi-rate stretching at temperatures up to 500 °C. Deformation of the gauge section of each specimen during loading to fracture was recorded with digital images at a constant rate. A state-of-the-art digital image correlation algorithm was then applied to compute strain fields from the images. The results provide key insights into the influences of specific geometrical parameters on the degree of deformation-biaxiality in a cruciform specimen.

### 9:50 AM

**Characterization of Continuous-Cast AZ31B Magnesium Alloy Sheets and Lubricants for Warm-Forming - Friction Effects:** *Aashish Rohatgi*<sup>1</sup>; Darrell Herling<sup>1</sup>; Eric Nyberg<sup>1</sup>; <sup>1</sup>Pacific Northwest National Laboratory

Our goal is to understand the inter-relationships between the initial properties of continuous-cast magnesium alloy (AZ31B) sheets and their subsequent formability and post-formed mechanical performance for use in cost-effective, lightweight, automotive body panels. As-received sheets, provided by the AMD 602 team, have been characterized by surface roughness measurements using mechanical and optical profilometry. Microstructural analysis of as-received sheets and formed pans is being performed via optical microscopy, electron backscattered diffraction (EBSD) and microhardness measurements. Mechanical properties of AZ31B pans are being characterized by room-temperature quasi-static tensile tests. Several commercial lubricants are being evaluated by elevated temperature friction tests and will be used to conduct limited dome height (LDH) tests on as-received sheets. This research will identify how starting properties of continuous-cast AZ31B sheets could be controlled to achieve an optimum combination of formability and post-formed mechanical performance to enable their use as a low-cost alternative to conventional wrought AZ31B sheets.

### 10:10 AM Break

### 10:30 AM

**High Strength ZK60 Mg Plate Produced by Grain Refinement and Precipitation during Alternate Biaxial Reverse Corrugation (ABRC) Process and Friction Stir Process (FSP):** *Bilal Mansoor*<sup>1</sup>; *Sibasish Mukherjee*<sup>1</sup>; *Amit Ghosh*<sup>1</sup>; <sup>1</sup>University of Michigan

Under research support by US Army, a process of Alternate Biaxial Reverse Corrugation (ABRC) was explored to impart large severe plastic deformation to ZK60 Mg alloy. This process had previously utilized to strengthen AZ31 Mg and reported elsewhere (Yang and Ghosh). The present results with ZK60 alloy exhibit higher strength (>350 MPa), and retention of adequate ductility (> 7% tensile elongation). The enhanced strength levels are believed to be influenced by a number of precipitates found in this alloy not existing in AZ31 alloy, in addition to grain size strengthening produced by about 1-2 micron grain size. Partial depth penetration into sheet from the top and bottom surfaces of alloy by friction stir process was also examined for this alloy to cause a different form of grain refinement. The strengthening effect in this case was found to be higher.

### 10:50 AM

**Formability of Mg Alloys at Room Temperature:** *D.-W. Kim*<sup>1</sup>; D. H. Kang<sup>2</sup>; S. Kim<sup>3</sup>; G. T. Bae<sup>4</sup>; K. H. Kim<sup>1</sup>; Nack J. Kim<sup>1</sup>; <sup>1</sup>POSTECH; <sup>2</sup>McGill University; <sup>3</sup>General Motors R&D Center; <sup>4</sup>Georgia Institute of Technology

Mg alloys are the lightest commercial alloys developed so far and have great potential for high performance automotive applications. For the application of Mg sheet products, it is necessary for the sheets to be readily formable for making complicated shapes. Therefore, many researches are being carried out to enhance the high temperature formability of Mg alloy sheets. However, further improvement is certainly needed to ensure the room temperature formability of Mg alloys to expand their applications. In the present study, the relationship between the room temperature formability and the microstructural features of



Mg alloys has been investigated. Various Mg alloys with various microstructural features were fabricated by twin-roll casting and their uniaxial tensile properties were correlated with room temperature formability measured by the Erichsen cupping test. It shows that the alloys with larger work hardening capacity have the better formability at room temperature.

### 11:10 AM

#### **Dynamic Blankholder Control for the Enhanced Forming Limit of Magnesium Sheets:** *Wonkyu Bang*<sup>1</sup>; <sup>1</sup>RIST

The deep drawability of magnesium is known to be affected significantly not only by forming temperature and speed, but by blankholder force. Since magnesium alloys typically exhibit very weak strain hardening at the elevated temperature, thinning (instability) can be triggered by small amount of excessive blankholder force. In this study, a servo-controlled blankholder mechanism was implemented to the dies/tools for magnesium warm drawing. As reported in the previous studies of high strength steels and aluminum alloys, improvement of forming limit coupled by lower forming load was reproduced for magnesium warm forming. Cyclic 'clamp-and-release' blankholder motion eased off the resistance of metalflow from flanges to walls, which resulted in smaller stretcher strain and more uniform thickness distribution. By optimizing the control function of blankholder action, the forming limit can be increased by 20% and more.

### 11:30 AM

#### **Joining Magnesium to Steel:** *Yuri Hovanski*<sup>1</sup>; Glenn Grant<sup>1</sup>; Mike Santella<sup>2</sup>; <sup>1</sup>Pacific Northwest National Laboratory; <sup>2</sup>Oak Ridge National Laboratory

Solid state joining methods were utilized to evaluate the joining potential of magnesium alloys to automotive sheet steels. Friction stir welding, friction stir spot welding, and ultrasonic welding techniques were developed to produce structural joints between both cast and wrought magnesium components and coated and uncoated steel sheets. The effects of tool design and process parameters were evaluated. The joint interface was examined, allowing characterization of the resultant mixing and microstructure. Mechanical performance of joints produced using each solid state technology were evaluated and presented.

### 11:50 AM

#### **Accumulative Roll Bonding of Wrought Magnesium Alloy:** *H. Nayaka*<sup>1</sup>; B.S.S. Daniel<sup>1</sup>; G.P. Chaudhari<sup>1</sup>; <sup>1</sup>IIT Roorkee

Accumulative Roll Bonding (ARB) is a severe plastic deformation process, which can produce high strength metal alloys with ultrafine-grained structure. An ultrafine-grained AZ61 magnesium alloy was produced using upto six ARB passes at a rolling temperature of 300°C and upto three passes at a rolling temperature of 270°C. Reduction of 50% was employed for each pass. The mechanical properties are evaluated by micro-hardness tests. The micro hardness values for the as-received AZ61 alloy was found to be 60 VHN and that of six pass ARB sample was 125 VHN. Resulting ultrafine-grained microstructure was characterized by the use of optical microscopy and TEM. DSC analysis was performed to study the thermal stability of the roll-bonded samples.

### 12:10 PM

#### **Mechanical Properties and Corrosion Behavior of Friction Stir Welded Mg/Mg- and Mg/Al-Joints:** *Otmar Klag*<sup>1</sup>; Guntram Wagner<sup>1</sup>; Dietmar Eiffler<sup>1</sup>; <sup>1</sup>Institute of Materials Science and Engineering / University of Kaiserslautern

In this research project the friction stir weldability (FSW) of similar joints of die casted AZ91-Mg-alloy, MRI-Mg-alloys and dissimilar joints between AZ91-Mg-alloy and AA5454-Al-alloy were investigated. In monotonic tensile tests for welds between similar materials tensile strengths at the value of the parent materials were determined. With two-dimensional hardness measurements it could be proved that in the case of the similar joints the FSW-process leads to a decrease of the hardness in the welding zone as a result of the of the inducted thermal energy. But for dissimilar joints an extreme increase of the hardness in the nugget was observed. SEM investigations and EDX element mappings have shown that this is caused by the formation of intermetallic phases particularly positioned as interlayers in the contact area between the Mg- and the Al-alloy. Cracks are predominantly initiated at the intermetallic phases. Furthermore the corrosion behavior of the FSW zone was investigated.

## Magnesium Technology 2010: ICME II and Biomedical Applications

*Sponsored by:* The Minerals, Metals and Materials Society, TMS Light Metals Division, TMS: Magnesium Committee  
*Program Organizers:* Sean Agnew, University of Virginia; Eric Nyberg, Pacific Northwest National Laboratory; Wim Sillekens, TNO; Neale Neelameggham, US Magnesium LLC

Thursday AM Room: 612  
February 18, 2010 Location: Washington State Convention Center

*Session Chairs:* John Allison, Ford Motor Company; Wim Sillekens, TNO Science and Industry

### 8:30 AM

#### **Two- and Three-Dimensional Cellular Automaton Models for Simulating Dendrite Morphology Evolution of Cast Magnesium Alloys:** *Liang Huo*<sup>1</sup>; *Zhiqiang Han*<sup>1</sup>; Baicheng Liu<sup>1</sup>; <sup>1</sup>Tsinghua University

Two- and Three-dimensional cellular automaton (CA) models have been developed for simulating the dendrite morphology evolution of cast magnesium alloys. In the two-dimensional model a hexagonal mesh was used to perform CA calculation to reflect the texture of Mg alloy dendrites, and an orthogonal mesh was used to solve the solute transport equations. In the three-dimensional model the solute transport equation was also solved by using an orthogonal mesh, but the CA calculation was performed using a mesh that is defined by the hexagonal close-packed (HCP) crystal lattice. The growth kinetics of dendrite tips was determined by the difference between local equilibrium composition and local actual composition obtained by solving the solute transport equation. The models were applied to simulate equiaxed dendrite evolution and columnar dendrite growth of AZ91D Mg alloy. Permanent mold step-shaped castings were poured and metallographic examinations were carried out for validating the present models.

### 8:50 AM

#### **Elemental Partitioning and Microstructure of Mg-Al-Ca-Sn Quaternary Alloys:** *Jessica TerBush*<sup>1</sup>; Olivia Chen<sup>1</sup>; J.Wayne Jones<sup>1</sup>; Tresa Pollock<sup>1</sup>; <sup>1</sup>University of Michigan

Creep behavior in cast Mg-Al-Ca-based alloys depends strongly on precipitation and solid solution strengthening in the primary  $\alpha$ -Mg cells. In MRI230D, the presence of Sn is believed to significantly influence the elemental segregation during solidification, which in turn can affect precipitation and solid solution strengthening. The influence of Sn on elemental partitioning during solidification has been systematically investigated for the quaternary Mg-Al-Ca-Sn alloy system using an electron microprobe technique coupled with a Scheil analysis. The addition of less than 1 wt% of Sn to Mg-5Al-3Ca causes an increase in the amount of Al and Ca in the primary  $\alpha$ -Mg phase as compared to AX44 or AXJ530, although the increase is not as dramatic as the one observed in MRI230D. The creep behavior of two Mg-5Al-3Ca-xSn quaternary alloys is compared to that of AXJ530, MRI230D and MRI153M and the role of Sn on microstructure and subsequent creep behavior is described.

### 9:10 AM

#### **Numerical Simulation of Flow-Induced Air Entrapment Defects in the High Pressure Die Casting Process:** *Shuai-Jun Li*<sup>1</sup>; *Shou-Mei Xiong*<sup>1</sup>; Bai-Cheng Liu<sup>1</sup>; Mei Li<sup>2</sup>; John Allison<sup>2</sup>; <sup>1</sup>Tsinghua University; <sup>2</sup>Ford Motor Company

In current paper, a numerical method to predict the air entrapment defects in the high pressure die casting (HPDC) process is presented and the distribution of the entrapped air at the end of filling was represented by the concentration of air in the liquid metal. The time-dependent, incompressible Navier-Stokes equations were firstly solved by a fractional step algorithm to model the fluid flow during the mold filling of HPDC process. The free surfaces were calculated using the volume of fluid method. At each time step, the isolated air bubbles in the liquid metal were found and the pressure of the bubbles was updated using the ideal gas law. The concentration transport equation was applied for the calculation of the air entrapment distribution. X-ray inspection of a step-shape magnesium die casting was performed to verify the air entrapment prediction. The comparison between experimental and numerical results shows a good agreement.

# Technical Program

9:30 AM

**ESPEI: Extensible, Self-Optimizing Phase Equilibrium Infrastructure for Magnesium Alloys:** *Shun-Li Shang*<sup>1</sup>; Yi Wang<sup>1</sup>; Zi-Kui Liu<sup>1</sup>; <sup>1</sup>MaterialsInformatics LLC

In order to store and use previous knowledge of thermodynamics in materials design, we develop a user-friendly, extensible, self-optimizing phase equilibrium computer program for magnesium alloys. This ESPEI program integrates first-principles data, thermodynamic data, parameter evaluation, and automation of phase diagram calculations with graphical user interface (GUI) designed with C-sharp and SQL (structured query language). We established the data infrastructure for storing input data used for thermodynamic modeling and output data for thermodynamic analysis. The storing of experimental data and parameter evaluation processes for phase diagram is unique for ESPEI. In the present work, the features of ESPEI will be demonstrated in the Mg-Al and Mg-Ni systems.

9:50 AM

**Modeling Casting and Heat Treatment Effects on Microstructure in Super Vacuum Die Casting (SVDC) AZ91 Magnesium Alloy:** *Mei Li*<sup>1</sup>; Ruijie Zhang<sup>1</sup>; John Allison<sup>1</sup>; <sup>1</sup>Ford Motor Company

Magnesium applications for the automotive and aerospace industry have received significant attention in recent years due to light-weight and consequent potential to reduce both fuel consumption and green house effect. Canada-China-USA three-country Magnesium Front End R&D (MFERD) program was established to explore the potential applications of magnesium alloys in automotive industry. In this program, the super vacuum die casting (SVDC) process was developed to produce the components. The SVDC offers advantages over conventional high pressure die casting (HPDC) in significantly reducing the air entrapment so that the produced magnesium castings can be heat treated. This paper describes the progress in the development of models to study the effects of casting and heat treatment process on the microstructures in SVDC AZ91 magnesium alloy. The microstructure model combined with property model will provide critical virtual tool in evaluating and optimizing the design and manufacturing process of magnesium alloy castings.

10:10 AM

**First-Principles Study of Ternary Hcp Solid Solution Phases from Special Quasirandom Structures: Application to Mg-Al-X Alloys:** *Dognwon Shin*<sup>1</sup>; Christopher Wolverton<sup>1</sup>; <sup>1</sup>Northwestern University

We have constructed ternary hcp special quasirandom structures (SQSs) whose correlation functions are close to those of the completely random hcp solid solutions. By performing first-principles DFT calculations of these SQSs, we have studied the Hf-Zr-Ti system, which exhibits hcp solubility in the entire composition range, to test the ability of constructed SQSs to mimic random hcp solid solutions. First-principles mixing energies and structural analysis show that our ternary hcp SQSs are capable of accurately predicting the properties of ternary hcp solid solutions. We further apply our ternary hcp SQSs to the Mg-Al-X (X = Si, Ti, Mn, Fe, Zn, and Zr) systems. We use our first-principles ternary mixing energies from SQSs to critically test a commonly used approximation in CALPHAD assessments, namely that of extrapolating ternary solution energetics from the constituent binary systems. We have also studied the effect of atomic vibrations on the mixing energies of hcp solid solutions.

10:30 AM Break

10:50 AM

**Slip and Twinning in Mg Single Crystals:** *Erica Lilleodden*<sup>1</sup>; Gyu Seok Kim<sup>1</sup>; Sangbong Yi<sup>1</sup>; Yuanding Huang<sup>1</sup>; Norbert Huber<sup>1</sup>; <sup>1</sup>GKSS Research Center

There is considerable need to develop mechanism-based material models for the deformation of Mg, due to its strong anisotropy and its importance in the development of lightweight structural materials. Unfortunately constitutive inputs for such models are critically lacking; fundamental studies of the critical stresses and strains and associated deformation mechanisms are needed. Employing the recently exploited method of microcompression testing along with EBSD and TEM characterization, we have investigated the deformation behavior of Mg single-crystals. The ability to obtain test volumes which can be subsequently fully characterized and which are absent of pre-existing twins makes this technique highly attractive. In this presentation, the results from microcompression testing will be discussed in terms of orientation-dependent slip activity and twinning mechanisms, and the role of geometric scale in the associated strain-strain relations.

11:10 AM

**Assessing and Modeling the Impact of Initial Microstructure on Dynamic Recrystallization of Sheets:** *Frederick Polesak*<sup>1</sup>; Paul Krajewski<sup>2</sup>; Babak Ræisina<sup>1</sup>; Sean Agnew<sup>1</sup>; <sup>1</sup>University of Virginia; <sup>2</sup>GM

Samples of distinctly processed alloy AZ31 sheets were deformed in tension under strain rate and temperature conditions typical of warm forming operations. The flow curves, r-values, crystallographic texture, and metallographic observations of the microstructure were used to characterize the dynamic recrystallization behavior. Samples with larger grain sizes are shown to flow at higher stresses and undergo dynamic recrystallization more slowly than the initially fine grained samples. For samples with initially sharp basal textures, the r-value decreases when dynamic recrystallization is active. The crystallographic texture itself shows a distinct evolution during deformation involving extensive dynamic recrystallization from that observed at lower temperatures. These distinctions in r-value and texture evolution are both related to the activities of deformation mechanisms that sustain the strain. Modeling of the material flow and microstructure evolution using a viscoplastic self-consistent code is discussed.

11:30 AM

**Modified AZ80 Magnesium Alloys for Biomedical Applications:** *Muge Erinc*<sup>1</sup>; <sup>1</sup>TNO

Our research focuses on developing cardiovascular stent materials from magnesium alloys that satisfy mechanical and chemical requirements to be used in the human body. High aluminium alloys (7-8.5 wt %) modified with zinc, manganese, rare-earth elements and yttrium are developed by casting and thixomolding. Refining the grain size by forming is essential since zirconium is not biocompatible. It is shown that, finer grain sizes can be achieved by a single extrusion step from a thixomolded structure. Further, chemical homogeneity and solidification structure can be controlled at a higher level by thixomolding. The mechanical performance of the tubes are evaluated by tensile, compressive and torsion tests. The in-vivo biodegradation and potential inflammatory behaviour is analyzed in a mouse model by subcutaneous and intraperitoneal positioning. In-vitro tests are performed in simulated body fluid. It is shown that AE route magnesium alloys produced by thixomolding satisfy criteria concerning mechanical performance, biodegradability and biocompatibility.

11:50 AM

**The Dissolution Behavior of a Mg-Zn-Ca Alloy for Biomedical Applications:** *Michele Manuel*<sup>1</sup>; Harpreet Brar<sup>1</sup>; <sup>1</sup>University of Florida

Traditional metallic-based implantable biomaterials like stainless steel, cobalt-chromium and titanium alloys have been used for many years in structural implants for load bearing applications. These materials are considered permanent in nature and additional surgeries are needed for their removal when used in temporary implant applications like bone fixation devices. Hence, there is a need for metallic-based materials that can provide temporary structural support but yet are biodegradable and bioabsorbable after the healing process. In recent years, there has been an increase in research and development of magnesium-based alloys due to their biodegradable and biocompatible properties. This paper analyzes the dissolution behavior of a magnesium-zinc-calcium alloy in Hank's solution and the effect of surface treatment on the dissolution rate.

12:10 PM

**Controlling the Biodegradation Rate of Magnesium-Based Implants through Surface Nanocrystallization Induced by Cryogenic Machining:** *Z. Pu*<sup>1</sup>; D. Puleo<sup>1</sup>; O.W. Dillon, Jr.<sup>1</sup>; I.S. Jawahir<sup>1</sup>; <sup>1</sup>University of Kentucky

Magnesium alloys are emerging as a new class of biodegradable implant materials for internal bone fixation. They provide good temporary fixation and do not need to be removed after healing, providing the relief to the patients. However, premature failure of these implants often occurs due to high biodegradation rate caused by low corrosion resistance of magnesium alloys in physiological environments. To control biodegradation/corrosion of magnesium alloys, grain refinement on the surface was achieved through machining-induced severe plastic deformation. Liquid nitrogen was used during machining to suppress grain growth. Nanocrystallized layers with various grain size and thickness have been fabricated by controlling the machining conditions. In vitro corrosion tests proved that the nanocrystallized layers enhanced corrosion resistance to different extents, depending on the thickness and grain sizes of the layer. By proper selection of machining conditions, magnesium-based implants with customized biodegradation rates for different medical requirements can be manufactured.



### Materials in Clean Power Systems V: Clean Coal-, Hydrogen Based-Technologies, Fuel Cells, and Materials for Energy Storage: Batteries and Others

*Sponsored by:* The Minerals, Metals and Materials Society, TMS Electronic, Magnetic, and Photonic Materials Division, TMS Structural Materials Division, TMS/ASM: Corrosion and Environmental Effects Committee, TMS: Energy Conversion and Storage Committee  
*Program Organizers:* Xingbo Liu, West Virginia University; Zhenguo Yang, Pacific Northwest National Lab; K. Weil, Pacific Northwest National Lab; Mike Brady, Oak Ridge National Lab; Jay Whitacre, Carnegie Mellon University; Ayyakkannu Manivannan, National Energy Technology Laboratory; Zi-Kui Liu, Penn State University

Thursday AM Room: 212  
 February 18, 2010 Location: Washington State Convention Center

*Session Chairs:* Jeffrey Hawk, U.S. Department of Energy; Xingbo Liu, West Virginia University

#### 8:30 AM Invited

#### Nanostructured Functional Materials for Energy Conversion and Storage: Donghai Wang<sup>1</sup>; <sup>1</sup>Penn State University

The role of nanostructured materials in addressing the challenges in energy has attracted wide attention. Many promising results of nanostructured materials in renewable energy harvesting, conversion and storage have demonstrated the important role of high surface area to maximize the surface activity, and the importance of optimum dimension and architecture, controlled pore channels and alignment of the nanocrystalline phase to optimize transport of electrons, ion and other species for better performance. In my talk, I will present some works on synthesis of nanostructured materials. I will also discuss how such controlled nanostructures can be used in energy conversion and storage and improve device performance for Li-ion batteries and fuel cells. Specifically, the electrochemically active material/graphene hybrid nanostructures have been studied as electrodes in Li ion battery and fuel cells showing superior capacity retention and high rate performance during lithiation/delithiation and enhanced stability as cathode catalysts for PEM fuel cells.

#### 9:10 AM

#### Cathode/Anode Selection and Full Cell Performance for Stationary Li-Ion Battery System: Daiwon Choi<sup>1</sup>; Donghai Wang<sup>2</sup>; Vilayanur Viswanathan<sup>1</sup>; Wu Xu<sup>1</sup>; Ji-Guang Zhang<sup>1</sup>; Gary Yang<sup>1</sup>; Gordon Graff<sup>1</sup>; Jun Liu<sup>1</sup>; <sup>1</sup>Pacific Northwest National Laboratory; <sup>2</sup>Penn State University

Li-ion battery technology is being actively investigated in recent years due to energy and environmental issues. In the past, Li-ion battery is mainly used for portable devices due to its high energy density. However, more research is need in the field of larger scale stationary application which can compliment renewable energy sources like solar or wind power generation. For stationary unlike portable applications, different criteria for Li-ion battery are required since weight and space limitation is less important issue. The more important factor for such application is cost, cycling stability, safety and toxicity. In our work, choice of cathode and anode and its combination in full cell is characterized and presented.

#### 9:30 AM

#### Synthesis, Orientation and Electrochemical Properties of Nanostructured LiMPO<sub>4</sub>(M:Fe, Mn, Co) Cathode for Li-Ion Battery: Daiwon Choi<sup>1</sup>; Donghai Wang<sup>2</sup>; In-Tae Bae<sup>3</sup>; Zimin Nie<sup>1</sup>; Jie Xiao<sup>1</sup>; Wu Xu<sup>1</sup>; Ji-Guang Zhang<sup>1</sup>; Gary Z. Yang<sup>1</sup>; Gordon Graff<sup>1</sup>; Jun Liu<sup>1</sup>; <sup>1</sup>Pacific Northwest National Laboratory; <sup>2</sup>Penn State University; <sup>3</sup>State University of New York at Binghamton

Demands for batteries with higher energy and power densities are ever-increasing due to the growing energy storage needs for current and future portable electronic devices and electrical vehicles. In this regard, olivine structured LiMPO<sub>4</sub> (M: Fe, Mn, Co, Ni) are investigated for alternative cathode materials. However, due to the low intrinsic electronic and ionic conductivity of LiMPO<sub>4</sub> (M: Fe, Mn, Co, Ni), it is difficult to utilize the full theoretical capacity at useful rates. Recent studies clearly indicate the critical importance of LiMPO<sub>4</sub> (M: Fe, Mn, Co) particle morphology to overcome these limitations. In our study, novel molten surfactant based technique has been developed to obtain nano-sized LiMPO<sub>4</sub> (M: Fe, Mn, Co) with improved electrochemical

activity. The particle morphology, orientation and electrochemical properties will be presented and discussed.

#### 9:50 AM Break

#### 10:00 AM

#### GraphiMetal Coatings on High Thermal Conductivity Graphite Foam to Prevent "Dusting" and Facilitate Solder Joining: Ben Poquette<sup>1</sup>; Stephen Kampe<sup>2</sup>; <sup>1</sup>Keystone Materials LLC; <sup>2</sup>Michigan Tech

Keystone Materials, LLC utilizes its patent pending GraphiMetal™ coating process to fully metallize graphite foam in a way that does not close the porosity and leaves fluid/air flow through the foams unhindered. The GraphiMetal™ process is readily scalable and does not utilize rare or cost prohibitive materials that could hinder large scale production. The coating method was initially developed at Virginia Tech in conjunction with Oak Ridge National Laboratory (ORNL) to provide solderability for meso-phase pitch derived graphitic foams for the creation of high thermal conductivity joints in heat exchangers. This process facilitates direct joining of coated foams to other metallic structures using traditional soldering techniques. The uniform metal deposit formed also creates a continuous envelope to prevent "dusting" without negatively affecting foam performance. With this improvement, GraphiMetal™ foam has become a viable material to replace traditional metallic thermal materials in energy storage and recovery systems.

#### 10:20 AM

#### The Effect of Stoichiometry and Sintering Temperature on the Thermoelectric Properties of Titanium Cobaltite: Bipradas Dutta<sup>1</sup>; Sezhan Annamalai<sup>1</sup>; Rudra Bhatta<sup>1</sup>; Ian Pegge<sup>1</sup>; <sup>1</sup>The catholic University of America

Calcium cobaltites exhibit superior thermoelectric efficiency among all ceramic materials. While calcium cobaltites have been studied extensively enough attention has not been paid towards other cobaltites. In the present investigation, the thermoelectric properties of titanium cobaltite, which is a paramagnetic material with spinel structure, have been studied. The samples with three different Ti/Co ratios were sintered from 900 to 1250°C. X-ray diffraction and scanning electron microscopy were utilized to perform phase and microstructural analysis to study the evolution of various phases and microstructure as a result of the change in the Ti/Co ratio as well as the sintering temperature. The effect of such changes on resistivity and Seebeck coefficient are also discussed. Resistivity and Seebeck coefficient of Ti<sub>x</sub>Co<sub>1-x</sub>O<sub>y</sub> were determined in the temperature range of 300 – 700 K. The activation energies for both electrical conduction as well as thermoelectric transport were calculated and discussed to identify the transport mechanisms.

#### 10:40 AM

#### Specialized Metal Coatings Unleash the Potential of High Thermal Conductivity Graphite Foam: Ben Poquette<sup>1</sup>; Stephen Kampe<sup>2</sup>; <sup>1</sup>Keystone Materials LLC; <sup>2</sup>Michigan Tech

In the late 90's, ORNL developed a technique to fabricate high conductivity graphite foam. With its unique properties, this foam has shown promise to revolutionize the performance of many commercial and defense related systems including: thermal management, inert electrodes and catalyst supports, and acoustic signature management. Until recently, low strength, conductive particle dusting, and difficulties in joining have hindered its incorporation into current platforms. A coating technique was developed at Virginia Tech, which allows a strongly adhered, uniform metallic coating to be applied throughout the thickness of graphite foam. These metal coatings have been shown to solve existing short-falls (low strength, dusting, joinability, etc.) as well as lend their properties (magnetic, catalytic, oxidation resistance, etc.) to graphitic foam without significantly affecting the foam's low density. This lightweight, high conductivity material system should lead to considerable improvements in heat exchanger efficiency for industrial and energy cogeneration systems.

#### 11:00 AM

#### Development of Advanced Low-Temperature Sodium Beta-Alumina Batteries: Xiaochuan Lu<sup>1</sup>; Guangang Xia<sup>1</sup>; Kerry Meinhardt<sup>1</sup>; John Lemmon<sup>1</sup>; Vince Sprenkle<sup>1</sup>; Zhenguo Yang<sup>1</sup>; <sup>1</sup>Pacific Northwest National Laboratory

Due to the high round trip efficiency and capability of energy storage for a duration of hours, the sodium β"-alumina battery technologies have gained increasing interests for renewable and utility applications. The batteries are typically fabricated upon a thick tubular β"-alumina electrolyte (> 2 mm) with a relatively high operating temperature (> 300°C) to achieve adequate cell

# Technical Program

performance. Recently, we attempt to develop battery cells constructed on a thinner planar electrolyte. At the meanwhile, research work has been conducted to modify the cathode both the microstructure and composition in such a way that a satisfactory performance can be achieved at a lower temperature. The details of the work the paper will be presented.

---

## Materials in Clean Power Systems V: Clean Coal-, Hydrogen Based-Technologies, Fuel Cells, and Materials for Energy Storage: PEM and Batteries

**Sponsored by:** The Minerals, Metals and Materials Society, TMS Electronic, Magnetic, and Photonic Materials Division, TMS Structural Materials Division, TMS/ASM: Corrosion and Environmental Effects Committee, TMS: Energy Conversion and Storage Committee  
**Program Organizers:** Xingbo Liu, West Virginia University; Zhenguo Yang, Pacific Northwest National Lab; K. Weil, Pacific Northwest National Lab; Mike Brady, Oak Ridge National Lab; Jay Whitacre, Carnegie Mellon University; Ayyakkannu Manivannan, National Energy Technology Laboratory; Zi-Kui Liu, Penn State University

Thursday AM            Room: 211  
February 18, 2010      Location: Washington State Convention Center

*Session Chairs:* Jay Whitacre, Carnegie Mellon University; Guozhong Cao, University of Washington

---

### 8:30 AM

#### Alternative Catalyst Supports Based on Metal Carbides: *Susanne Opalka*<sup>1</sup>;

<sup>1</sup>United Technologies Research Center

Transition metal carbides offer numerous benefits for replacing traditional mesoporous carbon polymer electrolyte membrane fuel cell electrode supports, including good corrosion-resistance and low contact resistance with loaded noble metal catalysts. The oxygen reduction reaction activity and active surface area stability of Pt electrocatalysts loaded on carbide supports, like tungsten carbide, are enhanced by strong electronic Pt-carbide interfacial interactions. The design of strong metal support interactions (SMSI) provides another route to tune catalyst activity, in addition to more traditional approaches of modifying catalyst composition, morphology, and distribution. These SMSI phenomena may result from shifts of: catalyst electron distribution from support electronic donation/withdrawal, electron energy density due to the covalent overlap of support and catalyst electronic orbitals, and energy level broadening from support-catalyst geometric or coordinative interactions. In these regards, atomic modeling will be presented to provide insights into the electronic basis for SMSI phenomena in tungsten carbide supported Pt catalysts.

### 8:50 AM

#### Nanoscale Tantalum Oxide Based Catalysts for PEM Fuel Cell Applications:

*Jin Kim*<sup>1</sup>; Tak-Keun Oh<sup>1</sup>; Yongsoon Shin<sup>1</sup>; K. Scott Weil<sup>1</sup>; <sup>1</sup>Pacific Northwest National Laboratory

One of key barriers in the commercialization of PEM fuel cells is the use of expensive platinum-based catalysts. Even though a lot of efforts have been made to minimize or eliminate platinum in the electrodes of PEMFCs, none of alternative catalysts show satisfactory properties in term catalytic activity and stability. Based on the unique properties of tantalum oxide such as high oxygen reduction onset potential and excellent stability, we developed nanoscale tantalum oxide/carbon composite catalysts for PEMFC cathode. Nanoscale tantalum oxide/carbon composite catalysts exhibited the improvement in catalytic performance compared to commercial tantalum oxide due to increasing triple-phase boundaries where the oxygen reduction reaction occurs. In this study, the electrochemical performance of nanoscale tantalum oxide based catalysts and the effect of dopants on the electrochemical performance of tantalum oxide have been investigated. The detailed results to date will be discussed.

### 9:10 AM Invited

#### Lithium Ion Batteries: Materials Processing and Mechanical Degradation:

*Claus Daniel*<sup>1</sup>; Kevin Rhodes<sup>2</sup>; <sup>1</sup>Oak Ridge National Laboratory and University of Tennessee; <sup>2</sup>University of Tennessee

Lithium ion battery technology is projected to be the leapfrog technology for the electrification of the drivetrain and to provide stationary storage solutions

to enable the effective use of renewable energy sources. Extensive research and development has enhanced the technology to a stage where it seems very likely that safe and reliable lithium ion batteries will soon be on board hybrid electric and electric vehicles and connected to solar cells and windmills. However, safety of the technology is still a concern, service life is not yet sufficient, and costs are too high. New materials processing technology is needed to reduce cost. Mechanical degradation and fatigue behavior has to be better understood in order to provide microstructural solutions to new and advanced energy storage systems. This presentation will give an overview for a materials science community to bundle forces and help solve our energy problem.

### 9:50 AM

#### Low Cost Aqueous Electrolyte Based Energy Storage: Materials and Performance: *Jay Whitacre*<sup>1</sup>; Sangeun Chun<sup>1</sup>; Sanjeev Sharma<sup>1</sup>; Amul Tevar<sup>1</sup>; Andrew Polonsky<sup>1</sup>; <sup>1</sup>Carnegie Mellon University

Cost is the single largest barrier to wide adoption of energy storage technology for high capacity applications. To this end, we have investigated the possibility of processing ubiquitous and inexpensive precursors to make functional electrode materials for electrochemical energy storage. Anode materials include various high surface area carbons and some Si and Ti based oxides, while cathode materials are transition metal oxides. Since the organic electrolytes used in Li-ion systems are expensive (in part due to the requirement for a dry handling environment), we turn to the higher ionic conductivity aqueous electrolyte systems. The talk will explore different electrode options, the performance of some promising devices in different conditions, and likely future development paths.

### 10:10 AM Break

### 10:20 AM Invited

#### Sol-Gel Derived Lithium Iron Phosphate Films for Efficient Lithium-Ion

**Intercalation:** *Yanyi Liu*<sup>1</sup>; *Dawei Liu*<sup>1</sup>; *Qifeng Zhang*<sup>1</sup>; *Betzaida Garcia*<sup>1</sup>; *Guozhong Cao*<sup>1</sup>; <sup>1</sup>University of Washington

In this presentation, we will use sol-gel derived nanostructured LiFePO<sub>4</sub> thin films as an example to demonstrate the significant influences of the micro-, nano-, and crystal structures on lithium ion intercalation properties. In addition, we will also show the impacts of the surface chemistry, impurity or defects on the phase transition and mass and charge transport accompanied to the lithium ion intercalation-extraction processes. With appropriate control of micro-, nano- and crystal structures and surface chemistry, both high specific energy and specific power are readily achieved. For example, at a current density of 100mA/g, LiFePO<sub>4</sub> films demonstrated a lithium-ion intercalation capacity of 250 mAh/g, far exceeding the theoretical storage capacity of conventional LiFePO<sub>4</sub> electrode. The presentation will demonstrate the experimental evidences and articulate the relationship between the processing condition, controlled impurity and defects, micro-, nano-, and crystal structures, and the lithium-ion intercalation properties.

### 11:00 AM

#### A New Material, Li<sub>2</sub>Mn<sub>2</sub>(MoO<sub>4</sub>)<sub>3</sub> for Li-Ion Batteries: Synthesis and

**Characterization:** *K.M. Begam*<sup>1</sup>; S.R.S. Prabaharan<sup>2</sup>; M.S. Michael<sup>3</sup>; <sup>1</sup>Universiti Teknologi PETRONAS; <sup>2</sup>University of Nottingham; <sup>3</sup>SSN Engineering College

The demand for electrically operated devices has led to a variety of energy storage systems amongst which Li-ion batteries substantially impact the areas of energy storage and advanced vehicles. A new polyanion material, Li<sub>2</sub>Mn<sub>2</sub>(MoO<sub>4</sub>)<sub>3</sub> is introduced for use as positive electrode in Li-ion batteries. The new material was prepared following a solution based low temperature protocol and found to crystallize in a single phase structure with high phase purity upon annealing the as-prepared product. Rectangular rod-shaped particles having submicrometre dimension were evident from SEM analysis. As for the electrochemical properties, potentiostatic and galvanostatic cycling tests were conducted. The new material was found to exhibit redox peaks corresponding to the transition metals Mn and Mo indicating the electrochemical reversibility as evidenced from Slow Scan Cyclic Voltammetry (SSCV) studies. The charge-discharge profiles obtained by means of Galvanostatic cycling tests signified removal/reinsertion of lithium in the new materials. Key Words: Polyanions, Lithium batteries



11:20 AM

**Effect of Co Substitution on the Structural and Electrochemical Behavior of Spinel LiMn<sub>2</sub>O<sub>4</sub>:** *Rahul Singhal*<sup>1</sup>; Naba Karan<sup>1</sup>; Rajesh Katiyar<sup>1</sup>; Ram Katiyar<sup>1</sup>; <sup>1</sup>University of Puerto Rico

We have synthesized LiMn<sub>2-x</sub>CoxO<sub>4</sub> (x = 0, 0.03, 0.05, 0.10, 0.25, and 0.50) cathode materials by sol-gel method. The phase pure materials were obtained at an annealing temperature of 875°C for 15 h. The materials were characterized using X-ray diffraction (XRD), scanning electron microscopy (SEM), energy-dispersive analysis by X-ray (EDAX), and micro Raman spectroscopy. The cathodes and coin cells were prepared as reported earlier<sup>1</sup>. The electrochemical behavior of the cathode materials were studied using cyclic voltammetry and charge-discharge characteristics. LiMn<sub>1.97</sub>Co<sub>0.03</sub>O<sub>4</sub> cathode material showed an initial discharge capacity of 133.72 mAh/g, with 89% capacity retention, after 50 charge-discharge cycles. It was found that as the cobalt concentration increases, the discharge capacity decreases gradually. The detailed structural and electrochemical results will be presented during the meeting. References: 1. R. Singhal, M.S. Tomar, S.R. Das, S.P. Singh, A. Kumar, R.S. Katiyar, *Electrochemical and Solid-State Letters*, 10(7) 2007, A163.

11:40 AM

**Mg<sub>3</sub>N<sub>2</sub>-Li-Mg Cermet Anodes for Lithium Based Batteries:** *Alpesh Khushalchand Shukla*<sup>1</sup>; Thomas Richardson<sup>1</sup>; <sup>1</sup>Lawrence Berkeley National Laboratory

Lithium alloys have been considered as attractive candidates to replace graphite in anodes for lithium based batteries, mainly due to their high theoretical capacities. However, these alloys suffer from significant irreversible capacities, poor cyclability and rate capability. In this study, Lithium rich ceramic-metal composites, or cermets, were developed using a simple metathesis reaction were developed and characterized using transmission electron microscopy and electron energy loss spectroscopy. The cermets were prepared by mixing Li<sub>3</sub>N powder with Mg powder and heating them to the melting temperature of the alloy phase. This resulted in a composite which consisted of Mg<sub>3</sub>N<sub>2</sub> particles embedded in a Li or Li-Mg matrix. Cycling experiments were also carried out, and preliminary results showed that the Li-Mg cermets performed better than their alloy counterparts in terms of rate capability and potential relaxation following stripping.

### Modeling, Simulation, and Theory of Nanomechanical Materials Behavior: Nanoindentation and Contact Mechanics

*Sponsored by:* The Minerals, Metals and Materials Society, TMS Materials Processing and Manufacturing Division, TMS/ASM; Computational Materials Science and Engineering Committee, TMS; Nanomechanical Materials Behavior Committee

*Program Organizers:* Thomas Buchheit, Sandia National Laboratories; Sergey Medyanik, Washington State Univ.; Douglas Spearot, University of Arkansas; Lawrence Friedman, Penn State University; Edmund Webb, Sandia National Laboratories

Thursday AM Room: 304  
February 18, 2010 Location: Washington State Convention Center

*Session Chairs:* Dylan Morris, NIST; Lawrence Friedman, NIST

8:30 AM Invited

**Plastic Deformation of Au Particles on a Sapphire Substrate:** Dan Mordehai<sup>1</sup>; Eugen Rabkin<sup>1</sup>; *David Srolovitz*<sup>2</sup>; <sup>1</sup>Technion - Israel Institute of Technology; <sup>2</sup>Yeshiva University

We report a combined experimental/molecular dynamics study of the indentation of faceted Au nanoparticles on a sapphire surface. The particles were created via the agglomeration of a polycrystalline Au film. Indentations were also performed in Au films of similar dimensions. Both simulations and experiment show that the particles are softer than the film and that the deformation behavior is nearly independent of particle size. Deformation is controlled by dislocation nucleation near the indenter, followed by fast dislocation glide toward the surface. Well defined pile-ups were observed near the indents in thin films, while no such pile-ups were observed in the particles. We present a comparison of post-deformation particle shapes from high resolution AFM and the simulations.

9:00 AM

**Effect of Temperature on Nano-scale Asperity Contact and Separation in Au:** *Jun Song*<sup>1</sup>; David Srolovitz<sup>2</sup>; <sup>1</sup>Brown University; <sup>2</sup>Yeshiva University

We performed a series of molecular dynamics simulations of contact and separation of two Au surfaces at different temperatures; one with a single, initially hemispherical asperity and the other flat. We monitor the force between the two surfaces and the symmetry order parameter together with the atomic structure during loading and unloading at each temperature. The pull-off force decreases monotonically with increasing temperature except for an abrupt rise that occurs between T<sub>1</sub>=T<sub>2</sub>. This abrupt rise can be traced to a series of phase transformation in the sample during separation (FCC->HCP->FCC) at elevated temperatures. The FCC->HCP->FCC process transforms the system from the original FCC structure to one that is in a twin orientation relative to the original FCC structure. The new FCC structure has a lower Schmid factor than the original FCC structure and consequently exhibits higher tensile strength.

9:20 AM

**The Strongest Contact and Size Effect in Nanoscale Metal-Metal Contact: Molecular Dynamics Simulation Study:** *Hojin Kim*<sup>1</sup>; Alejandro Strachan<sup>1</sup>; <sup>1</sup>Purdue University

We characterize the tensile strength of the nanoscale contacts formed when two clean platinum asperities are brought together by using large-scale molecular dynamics simulation. Simulation results show that the tensile strength of the nanoscale contacts exhibits significant size effect with a maximum at approximately 5 nm contact size. As we know, it is the first time to appear a "strongest size" in single crystals. This size effect connects with the density of dislocations that are generated during contact closing and opening. A reduction of initial dislocation density (created during contact closing) and an increasing difficulty in the production of dislocations during contact opening cause to weaken strength as size decrease down to 5 nm. The strongest contact occurs when the density of dislocations during closing becomes a minimum and the following strength decrease with decreasing size is due to reduced constraints to mechanical deformation by the slabs.

9:40 AM Invited

**Friction and Adhesion at the Nanoscale:** *Izabela Szlufarska*<sup>1</sup>; Yifei Mo<sup>1</sup>; Yun Liu<sup>1</sup>; <sup>1</sup>University of Wisconsin

Friction and adhesion are particularly important for mechanical performance of nanoscale devices, where surface-to-volume ratio is high. Two major challenges to understanding nanoscale friction are: (i) Macroscopic laws do not apply to nanoscale contacts; (ii) It is not possible to predict friction force because of the complexity of energy dissipation mechanisms involved in sliding (e.g., dislocations, phonons, surface chemistry). This talk will focus on fundamental understanding of nanoscale tribology gained through molecular dynamics (MD) and ab initio methods. MD simulations have been used to determine friction laws in dry nanoscale contacts. Two specific contributions to friction will be discussed: adhesion and adsorbate atoms. Using Si and SiC as model systems, it is shown that adhesion can be controlled by surface strain and chemistry. Hydrogen and deuterium adsorbates on diamond are used to explore dependence of friction on vibrational excitations and on surface coverage.

10:10 AM Break

10:30 AM Invited

**Dislocation Nucleation, Jerky Flow and Size Effects in Nanoindentation:** Wei Wang<sup>1</sup>; Yuan Zhong<sup>2</sup>; Garritt Tucker<sup>2</sup>; Ke Lu<sup>1</sup>; Lei Lu<sup>1</sup>; *David McDowell*<sup>2</sup>; Ting Zhu<sup>2</sup>; <sup>1</sup>Shenyang National Laboratory for Materials Science; <sup>2</sup>Georgia Institute of Technology

Recent results from MD simulations regarding homogeneous and heterogeneous dislocation nucleation in fcc crystals are summarized, with emphasis on non-Schmid effects and reordering processes. It is shown that the activation volume for homogeneous nucleation is on the order of a few b<sup>3</sup> at high stress levels characteristic of nanoindentation. Deeper insight into stochastic jerky plastic flow during nanoindentation of single crystal copper is gained by combining experiments, statistical analyses, and atomistic simulations. The nanoindentation size effect on yield strength arises in concert with extreme value statistics of dislocation sources. Source activation induces a dislocation avalanche and indenter displacement burst, and its probability decreases with the radius of the indenter tip. Our results demonstrate that jerky plastic flow can be caused by the activation of either surface or bulk dislocation sources, with sensitivity to the orientation of the crystal relative to the indentation direction.

# Technical Program

## 11:00 AM

**Assessment of the Hertzian Estimate of Plasticity-Initiating Shear Stresses during Nanoindentation:** Dylan Morris<sup>1</sup>; Li Ma<sup>1</sup>; Lyle Levine<sup>1</sup>; Stefhanni Jennerjohn<sup>2</sup>; David Bahr<sup>2</sup>; <sup>1</sup>NIST; <sup>2</sup>Washington State University

The sudden onset of plasticity during nanoindentation of metals is associated with dislocation nucleation, multiplication, and propagation. The shear stresses responsible for the sudden onset of plasticity are typically estimated from Hertzian contact mechanics. Here, a critical assessment of possible errors and pitfalls in the experimental measurement of plastic-onset stresses is made. The near-apex shape of Berkovich probes – one sharp, and one worn – was measured by scanning probe microscopy. These data were used as “virtual” indentation probes in a 3-dimensional finite-element analysis (FEA) of indentation on <100>-oriented single-crystal tungsten. Experiments were also carried out with those probes on <100>-oriented tungsten. Excellent agreement is found between experimental and FEA force-displacement relationships, but the discrepancies between Hertzian and FEA estimates of the controlling shear stresses are larger than 30%.

## 11:20 AM

**Atomic-Scale Study of Nanoindentation in Iron and Copper:** Yury Osetskiy<sup>1</sup>; Chansun Shin<sup>2</sup>; Roger Stoller<sup>3</sup>; <sup>1</sup>ORNL; <sup>2</sup>Korea Atomic Energy Research Institute

We present results of extensive molecular dynamics study of materials deformation during nanoindentation process in Fe and Cu. We have used different indentation surfaces namely  $\frac{1}{2}\{110\}$  and  $\{100\}$  in Fe and  $\frac{1}{2}\{111\}$  and  $\{100\}$  in Cu and spherical rigid indenters of diameter from 5 to 40 nm at indentation speeds of 2 m/s and 10 m/s in crystals of up to  $1.1 \times 10^8$  atoms. Plastic deformation at early stages or by small size indenter occurred mainly by emission of glissile dislocation loops. Large indenters may create complex three-dimensional structures that affect strongly the deformation process. Dislocation junctions of different structures and mobility were observed and classified from the point of view of their effects to nanoindentation process. A higher indentation loading rate was observed to promote the formation of shear loops on a nucleated circular dislocation in Fe.

## 11:40 AM

**Nanoindentation Simulations to Predict Macroscale Properties of Cement:** Priscilla Fonseca<sup>1</sup>; <sup>1</sup>Northwestern University

The microstructure of cementitious materials determines most of their macroscale properties, such as strength, permeability, shrinkage, and creep. As new types of cement are developed, it becomes important to develop predictive models that connect the microstructure to macroscale behavior. Calcium silicate hydrate (C-S-H), the primary binding phase of concrete, is responsible for macroscale cohesion and durability. This talk presents a numerical model of the nanostructure of C-S-H and its capability to predict macroscale properties. Generated using an autocatalytic growth algorithm, C-S-H as an assemblage of discrete granular particles will be introduced with particle-scale properties such as elastic modulus, friction, and surface charge. Using DEM simulations, macroscale indentation properties of hardened cement paste are quantitatively predicted. This predictive capability suggests that it is possible to numerically determine macroscale properties relating to the durability of concrete for new cement mix designs without engaging in extensive experimental testing.

## Neutron and X-Ray Studies of Advanced Materials III: Diffraction Analysis of Alloys

*Sponsored by:* The Minerals, Metals and Materials Society, ASM International, TMS Structural Materials Division, TMS/ASM: Mechanical Behavior of Materials Committee, TMS: Titanium Committee  
*Program Organizers:* Rozaliya Barabash, Oak Ridge National Laboratory; Jaimie Tiley, Air Force Research Laboratory; Erica Lilleodden, GKSS Research Center; Peter Liaw, University of Tennessee; Yandong Wang, Northeastern University

Thursday AM Room: 303  
February 18, 2010 Location: Washington State Convention Center

*Session Chairs:* Jaimie Tiley, Air Force Research Laboratory; Erica Lilleodden, GKSS Research Center

## 8:30 AM Keynote

**Simulating Realistic Conditions and In-Situ Studies Using Neutron Diffraction:** Ron Rogge<sup>1</sup>; <sup>1</sup>National Research Council

The high penetration of neutrons in most industrial materials permits examining the material's response to external influences throughout its volume. The high penetration also enables relatively straightforward development of sample environments. These can be used for fundamental studies of material response in order to understand the material or guide development of new materials. Other environments may simulate manufacturing conditions in order to evaluate or improve processes and others simulate in-service conditions, which can contribute to fitness-for-service evaluations. A variety of examples will be presented demonstrating each of these.

## 9:00 AM

**Why Neutrons to Study Superalloys?:** Ralph Gilles<sup>1</sup>; Pavel Strunz<sup>2</sup>; Debashis Mukherji<sup>3</sup>; <sup>1</sup>TU Muenchen; <sup>2</sup>Nuclear Physics Institute; <sup>3</sup>TU Braunschweig

Characterization of microstructure in superalloys is predominantly carried out with microscopic methods. Due to the low penetration of X-rays, electrons or light the samples have to be very thin by using transmission methods or the investigation is limited to the surface. Neutrons enable to enlarge the investigated sample volume, both the cross section due to the large size of neutron beams and the thickness up to a few millimeters thanks to the favorable penetration depth. In superalloys, for example in situ measurements at high temperatures are quite often useful. The detection of detrimental phases like TCP phases, or the determination of lattice misfit between precipitate and matrix, demonstrated how worthwhile it is using the non-destructive tools of small-angle neutron scattering and neutron diffraction. Examples will be discussed to show the advantages and the complementarity of neutrons to X-ray and electron radiation. Reference: R. Gilles, Z. Metallkd. 96 (2005), 4, 325-334.

## 9:15 AM

**Determining the Impact of Cooling Rate and Aging Times on Nickel Base Super Alloys Using Calibrated XRD Intensity Ratios which Courses Were Actually Held?:** Jaimie Tiley<sup>1</sup>; R Banerjee<sup>2</sup>; <sup>1</sup>AFRL/RXLM; <sup>2</sup>University of Texas

Determining the volume fraction of gamma prime phases within nickel base superalloys is difficult due to nanometer sized tertiary gamma prime precipitates. This research develops calibration curves based on ordered intensity peaks for different volume fractions of Rene88 gamma prime and gamma powders extracted from bulk material samples. The curves are used to determine volume fractions of bulk samples using synchrotron data. Volume fractions and misfit strains are obtained for water quenched and slow cooled samples aged up to 200 hours at 760°C.

## 9:30 AM Invited

**Deformation Of Shape Memory Alloys Under Biaxial Loading:** Donald Brown<sup>1</sup>; Catherine Tupper<sup>2</sup>; Vaidyanathan Raj<sup>3</sup>; Deniece Korzekwa<sup>1</sup>; Sisneros Thomas<sup>1</sup>; Clausen Bjorn<sup>1</sup>; <sup>1</sup>Los Alamos National Lab; <sup>2</sup>Northwestern University; <sup>3</sup>University of Central Florida

We have made a concerted effort on SMARTS to study shape memory alloys (SMA's) under their operating conditions. This has included the development of sample environments to allow straining measurements at high and low temperatures, in magnetic fields, and under cyclic deformation. Most recently, we have developed the capability to study SMA's under biaxial tensile deformation.



Both UNb and NiTi have been studied in-situ during uniaxial deformation using neutron diffraction techniques. However, applications seldom require uniaxial deformation of SMA's, but rather require more complicated deformation paths. Using hydraulic bulge test and in-situ neutron diffraction experiments, we have examined the strain and texture evolution in both shape memory systems in-situ under biaxial loading conditions. Equivalent through-thickness and membrane strains are compared to both tensile and compressive uniaxial measurements in order to evaluate the deformation mechanisms under the disparate loading conditions.

### 9:50 AM

**In-Situ Observation of Strain Evolution in CP-Ti over Multiple Length Scales:** *Colleen Bettles*<sup>1</sup>; Peter Lynch<sup>2</sup>; Andrew Stevenson<sup>2</sup>; Dacian Tomus<sup>1</sup>; Mark Gibson<sup>2</sup>; Kia Wallwark<sup>3</sup>; Justin Kimpton<sup>3</sup>; <sup>1</sup>ARC Centre of Excellence for Design in Light Metals, Monash University; <sup>2</sup>CSIRO Materials Science and Engineering; <sup>3</sup>Australian Synchrotron

The strain evolution in polycrystalline CP-Ti strip under tension was studied, in-situ and at two length scales, using Synchrotron X-ray diffraction. To establish the bulk material behaviour, experiments were performed at the Australian synchrotron facility. Owing to the relatively large grain size, discontinuous 'spotty' Debye ring patterns were observed, and a peak fitting algorithm was developed to determine the individual spot positions with the necessary precision for strain determination. The crystallographic directional dependence of strain anisotropy during the loading cycle was determined. Strain anisotropy and yielding of individual crystallographic planes prior to the macroscopic yield point were further clarified by in-situ loading experiments performed at the Advanced Light Source. The deviatoric strain accumulation and plastic response were mapped on a grain by grain basis. The onset of microscopic yielding in the grains was identified and correlated with the relative orientation of the grains with respect to the loading direction.

### 10:05 AM

**Influence of Strain Rate on Mechanical Properties and Crystallographic Texture of Hot-Pressed and Rolled Beryllium:** *Thomas Sisineros*<sup>1</sup>; Donald Brown<sup>1</sup>; Bjorn Clausen<sup>1</sup>; Saurabh Kabra<sup>1</sup>; William Blumenthal<sup>1</sup>; <sup>1</sup>Los Alamos National Lab

Plastic deformation of hexagonal metals such as beryllium occurs by a mix of slip and twinning mechanisms. Deformation slip and twinning are controlled by different mechanisms at the atomic scale, and thus respond differently to variations in strain rate. In general, deformation twinning is expected to be favored by high strain rate conditions. Strongly textured and random beryllium samples were deformed at strain rates from 0.0001/sec to 5000/sec. The yield point is strain rate insensitive over 7+ orders of magnitude of strain rate. The hardening, however, is strongly rate dependent. Optical microscopy and neutron diffraction measurement of crystallographic texture were carried out to monitor the evolution of the microstructure and specifically the activity of mechanical twinning as a function of strain rate. The relative roles of the active slip and twin deformation mechanisms are linked to the observed rate dependence of the flow stress.

### 10:15 AM

**In-situ Neutron-Diffraction and Thermal Characterization of Fatigue Behavior:** *E-Wen Huang*<sup>1</sup>; Rozaliya Barabash<sup>2</sup>; Bjorn Clausen<sup>3</sup>; Yee-Lang Liu<sup>4</sup>; Ji-Jung Kai<sup>4</sup>; Wenjun Liu<sup>3</sup>; Gene Ice<sup>2</sup>; Peter Liaw<sup>1</sup>; <sup>1</sup>University of Tennessee; <sup>2</sup>Oak Ridge National Laboratory; <sup>3</sup>Los Alamos National Laboratory; <sup>4</sup>National Tsing-Hua University; <sup>5</sup>Argonne National Laboratory

Cyclic loading and the subsequent temperature evolution of the lattice strain have been investigated with in-situ neutron-diffraction and thermal characterization for a nickel-base alloy. The lattice strain and thermal response to the applied load are investigated as a function of the fatigue cycles. Fatigue damage is observed with bulk hardening, softening, and eventual saturation evident in the diffraction patterns and the thermal-evolution features. An increase in dislocation density is responsible for hardening during the first cycles. The transition to saturation cycles is characterized by the anisotropy of the lattice-strain evolution. Moreover, inhomogeneity of the thermal response and irreversible compression of the lattice planes are observed in the final saturation fatigue cycles. The local fatigue damages are quantitatively studied by the polychromatic X-ray microdiffraction and transmission electron microscopy. The ex-situ results are discussed along with the in-situ measurements. The development of irreversible microstructure are discussed.

### 10:25 AM

**In-situ Neutron Diffraction Experiments as a Guide for Understanding the Microstructure Evolution during Deformation of Complex Materials:** *Steven Van Petegem*<sup>1</sup>; Alexander Evans<sup>1</sup>; Helena Van Swygenhoven<sup>1</sup>; <sup>1</sup>Paul Scherrer Institut

Predicting the development of intra- and intergranular stresses during deformation is a challenging task, especially for materials with a complex microstructure such as advanced steels and multiphase engineering components. A detailed knowledge of these so-called 'microstresses' is of utmost importance for understanding the influence of microstructure exerted on the mechanical properties. Here we present some recent results obtained at POLDI, the Time-Of-Flight diffractometer at SINQ (Paul Scherrer Institut). In particular we focus on the development of microstresses during uni-axial tensile deformation of some multiphase advanced steels. We report on the complex interplay between elastic and plastic anisotropy, which is responsible for the built-up of large residual stresses. Furthermore we demonstrate how in-situ x-ray diffraction can be used as a complementary tool to reveal the role of those phases which are invisible for neutrons because of their low volume fraction and/or chemical nature.

### 10:40 AM

**Real Time Synchrotron Radiography of High Temperature High Cycle Fatigue Crack Growth in Single-Crystal Nickel-Base Superalloys:** *Clinique Brundidge*<sup>1</sup>; Naji Hussein<sup>1</sup>; Erik Hanson<sup>1</sup>; Chris Torbet<sup>1</sup>; Roy Clarke<sup>1</sup>; J. Wayne Jones<sup>1</sup>; Tresa Pollock<sup>1</sup>; <sup>1</sup>University of Michigan

High temperature ultrasonic fatigue experiments were performed at the Advanced Photon Source at Argonne National Laboratory in order to image, in situ, the fatigue crack growth (FCG) in a single-crystal nickel-base superalloy using high brilliance x-ray undulator radiation. A portable ultrasonic fatigue instrument was used to produce a frequency of 20 kHz (R=0.1) with axial loading in the <001> direction. A micro-torch heated samples between 538°C to 982°C. Fatigue cracks emanating from notched samples with a 200µm thickness were observed (through-thickness) with x-ray radiographs taken every thousand cycles over tens of millions of cycles showing micron-by-micron crack growth. Crystallographic cracks propagated along specific planes at temperatures below 760°C and non-crystallographic crack growth became more prevalent as the temperature increased. For well-oriented samples, cracks propagated along {111} slip planes, however, misoriented samples produced crack growth on alternative planes. The influence of cast microstructural features and temperature on FCG will be discussed.

### 10:50 AM

**Evolution of Crystallographic Texture of TRIP Steel under Forming Load Conditions:** *Adam Kreuziger*<sup>1</sup>; Thomas Gnaeupel-Herold<sup>1</sup>; Tim Foecke<sup>1</sup>; <sup>1</sup>National Institute of Standards and Technology

TRIP (Transformation Induced Plasticity) steels are a relatively new multi-phase, high strength, high ductility steel alloy being investigated by the automotive industry to improve fuel economy. In this study, as received TRIP steel sheets are deformed under uniaxial, plane strain and balanced biaxial strain conditions. After deformation the micro-structural properties of the deformed material are investigated using neutron diffraction to determine the phase fractions in the deformed material and how the crystallographic texture evolves as a function of strain for each deformation mode. Using crystallographic theory of martensite (CTM), theoretical predictions for the austenite transformation as a function of texture and stress state are compared to the measured texture.

### 11:05 AM Break

### 11:15 AM

**Software Tools for the Monitoring, Analysis and Interpretation of Engineering Neutron Diffraction Data:** *Seung Yub Lee*<sup>1</sup>; Youngshin Kim<sup>1</sup>; Hyuntae Na<sup>1</sup>; *Ersan Ustundag*<sup>1</sup>; <sup>1</sup>Iowa State University

Proper analysis and interpretation of engineering neutron diffraction (ND) data requires the solution of an inverse problem where experimental data are compared to the predictions of crystallographic and materials models. This process involves numerous parameters, some of which may be highly correlated, and without proper software tools can be rather difficult to handle. As part of the DANSE project (danse.us), we have been developing tools that will not only aid the user in this process, but will also allow real-time monitoring and analysis of data for a more efficient use of beam time. This presentation will also describe tools that perform full experiment simulation. Our ultimate goal is to help

# Technical Program

establish ND data analysis and interpretation on a more rigorous theoretical and computational foundation.

## 11:30 AM

### **Transformation Pathways in High Temperature Shape Memory Alloy Candidates Based on the NiTi, NiMnGa and ZrCu Alloy Systems:** *Mohammed Azeem*<sup>1</sup>; Seema Raghunathan<sup>1</sup>; David Dye<sup>1</sup>; <sup>1</sup>Imperial College

High temperature (>200 °C) shape memory alloys (HTSMAs) would be of great interest, e.g. in aerospace applications. Here, synchrotron X-ray diffraction is used to characterise the evolution of phase assemblage and texture during thermal cycling of several candidate HTSMA systems - NiTi, NiMnGa and ZrCu, in polycrystalline rolled strip. It is shown that Af transformation temperatures in excess of 200°C can readily be achieved but that Mf temperatures in excess of this are harder to achieve. Temperature hysteresis is typically greater than that observed in NiTi. Cyclic stability is also problematic, although there are well-known approaches to mitigate this problem. In Ni<sub>54</sub>Mn<sub>25</sub>Ga<sub>21</sub> a two-step transformation is observed, while in Ni<sub>50</sub>Ti<sub>35</sub>Hf<sub>7.5</sub>Zr<sub>7.5</sub> martensite can be retained on cycling. It is also noted that DSC experimentation alone is a poor guide to behaviour, as it is insensitive to the transformation pathways of the alloys.

## 11:45 AM

### **Martensitic Transformation Induced Plasticity in Nanostructured Steel: A High-Energy X-Ray Diffraction Study:** *Sheng Cheng*<sup>1</sup>; Hahn Choo<sup>1</sup>; Yandong Wang<sup>2</sup>; Xun-Li Wang<sup>3</sup>; Jon Almer<sup>4</sup>; Peter Liaw<sup>1</sup>; Young-Kook Lee<sup>5</sup>; <sup>1</sup>University of Tennessee; <sup>2</sup>Northeast University of China; <sup>3</sup>Oak Ridge National Laboratory; <sup>4</sup>Argonne National Laboratory; <sup>5</sup>Yonsei University

In contrast to the poor tensile behavior in most nanostructured materials, a recently-developed metastable austenite steel was demonstrated with high strength and outstanding tensile ductility, owing to the contribution from transformation-induced plasticity (TRIP) effect. To understand the contribution of the martensitic transformation, an in situ synchrotron X-ray diffraction was conducted. With the analysis of load-partitioning behavior, transformation kinetics, as well as the texture evolution, it is revealed that the martensitic transformation contributed greatly to the plastic deformation in first stage of deformation, while the dislocation-based mechanism mainly contributed to the second stage. Different from the coarse-grained sample, the martensitic transformation was mainly propelled through Lüders band propagation, which was elaborately explored by micro-beam scanning. This work was supported by the National Science Foundation Major Research Instrumentation (MRI) Program (DMR-0421219) and International Materials Institutes (IMI).

## 12:00 PM

### **Mechanical Behavior and Microstructure Evolutions in a Nanocrystalline Ni-Fe Alloy:** *Li Li*<sup>1</sup>; Tamas Ungar<sup>2</sup>; Yandong Wang<sup>3</sup>; Yang Ren<sup>4</sup>; Hahn Choo<sup>1</sup>; Peter Liaw<sup>1</sup>; <sup>1</sup>Department of Materials Science and Engineering, The University of Tennessee; <sup>2</sup>Department of Materials Physics, Eötvös University; <sup>3</sup>School of Materials Science and Engineering, Beijing Institute of Technology; <sup>4</sup>X-Ray Science Division, Argonne National Laboratory

Bulk nanocrystalline Ni-Fe alloy with grain size around 20 nm is rolled to 10%, 20%, and 30% reductions at both room temperature and liquid-nitrogen temperature, respectively. Hardness tests are performed in the prepared samples. Synchrotron high-energy X-ray diffraction and X-ray line profile analysis are applied in the experiments and in data reductions. The microstructure evolutions such as dislocation density, grain size, and twin density are investigated in the above mentioned samples. Temperature effects and deformation level are considered in the deformation study. This study will provide detailed microstructure information for explaining the exhibited mechanical behaviors and unveiling the underlying deformation mechanisms in bulk nanocrystalline Ni-Fe alloy.

## 12:10 PM

### **Neutron Diffraction Study of the Internal Stress and Strain States of a Single Crystal Superalloy under Different Heat Treatment Conditions:** *Erdong Wu*<sup>1</sup>; Guangai Sun<sup>2</sup>; Bo Chen<sup>2</sup>; Sucheng Wang<sup>1</sup>; Thilo Pirling<sup>3</sup>; Darren Hughes<sup>3</sup>; <sup>1</sup>Institute of Metal Research, Chinese Academy of Science; <sup>2</sup>Institute of Nuclear Physics and Chemistry; <sup>3</sup>Institut Laue Langevin

The microstructures of the nickel-based single crystal superalloy vary considerably under different heat-treatment conditions, which strongly affect the high temperature mechanical properties of the superalloy. A neutron diffraction investigation of the lattice mismatches of the  $\gamma$ -matrix and the  $\gamma'$ -precipitate

phases of a superalloy involving thorough examinations of the superlattice of the  $\gamma'$ -precipitates demonstrates that the relevant diffraction contours are strongly indices dependent, and differ significantly for different phases and different microstructures. These contour variations are analyzed to characterize the internal stress and strain states, and associates the microstructures to the high temperature mechanical properties of the superalloy. The correlations between the interphase stress and the intraphase strain induced by the evolution of the  $\gamma'$ -precipitates from the  $\gamma$ -matrix and the relevant lattice-mismatch changes during different heat treatments of the superalloy are revealed and discussed based on the calculation and relevant dislocation modeling of the internal stress and strain states.

## 12:25 PM

### **Understanding the Texture Development during Biaxial Mechanical Loading:** *Ercan Cakmak*<sup>1</sup>; Hahn Choo<sup>1</sup>; <sup>1</sup>Department of Materials Science and Engineering, The University of Tennessee

Fundamental understanding of the evolution of microstructure (intergranular strain, texture, etc.) during biaxial mechanical loading is of significant scientific and technical importance because torsional loading or the combination of torsion and tension/compression loading conditions better represent the realistic manufacturing conditions of most engineering materials compared to simpler uniaxial loading conditions. In this study, texture development during biaxial loading of a model fcc polycrystal is investigated by performing systematic measurements as a function of: (1) loading path (pure torsion with free ends, pure torsion with fixed ends, torsion/tension, torsion/compression as well as pure tension and compression as baseline measurements), (2) applied (shear and normal) strain, and (3) position along the radial direction of the specimen. The experimental results provide a clear understanding of the evolution of texture during biaxial loading by allowing us to deconvolute the various effects of different loading paths on the observed texture components and their interactions.

## 12:35 PM

### **High Pressure Deformation of Zirconium:** *James Wilkerson*<sup>1</sup>; David Weldon<sup>1</sup>; Sven Vogel<sup>1</sup>; Donald Brown<sup>1</sup>; Carlos Tomé<sup>1</sup>; Sébastien Merkel<sup>2</sup>; <sup>1</sup>Los Alamos National Laboratory; <sup>2</sup>Laboratoire de Structure et Propriétés de l'Etat Solide Université de Lille

Uni-axial deformation of pure Zirconium was performed with the D-DIA apparatus at the APS. The transformation from  $\alpha$ -Zr to  $\omega$ -Zr was observed at ~4.5 GPa at room temperature with the applied pressure derived from the unit cell volume of  $\alpha$ -Zr and the known equation of state. A combination of texture analysis of the diffraction data and texture modeling allows to establish the orientation relationship between the two phases for the first time with a large number of grains. After the transformation, the D-DIA apparatus allows to deform the  $\omega$ -Zr and study deformation mechanism such as slip and twinning activities. We will present first results of this study and compare the deformation modes at ~5 and 8-GPa.

## 12:50 PM

### **Modelling and Characterisation of Gamma Prime ( $\gamma'$ ) Evolution in a Nickel-Base Superalloy Using Small-Angle Neutron Scattering:** *David Collins*<sup>1</sup>; Richard Heenan<sup>2</sup>; Howard Stone<sup>1</sup>; <sup>1</sup>University of Cambridge; <sup>2</sup>ISIS Facility, Rutherford Appleton Laboratory

Small angle neutron scattering (SANS) has been used to evaluate the temporal evolution of  $\gamma'$  precipitates in the nickel-base superalloy, RR1000, in situ during a 16 hour heat treatment at 760°C following a supersolvus heat treatment and oil quench. The bimodal distribution of secondary and tertiary  $\gamma'$  was analysed using a specially developed polydispersive model capable of evaluating the scattering curves to obtain precipitate size distributions and volume fractions as a function of time. The results show an increase in volume fraction of secondary  $\gamma'$  at the expense of tertiary  $\gamma'$ , as may be expected from Ostwald ripening, along with the simultaneous coarsening of both distributions. The model was designed to be suitable for high volume fractions of  $\gamma'$ , and for the scattering interaction between precipitates. The initial and final precipitate distributions have been characterised using TEM, and show satisfactory correlation with the SANS data across the scattering vector range.



### Nuclear Energy: Processes and Policies: Material Development

*Sponsored by:* The Minerals, Metals and Materials Society, TMS Structural Materials Division, TMS/ASM: Nuclear Materials Committee, TMS: Public and Governmental Affairs Committee

*Program Organizers:* Brajendra Mishra, Colorado School of Mines; Aladar Csontos, U.S. Nuclear Regulatory Commission; Stuart Maloy, Los Alamos National Laboratory; Jeremy Busby, Oak Ridge National Laboratory; Sue Lesica, U.S. Department of Energy's Office of Nuclear Energy

Thursday AM Room: 201  
February 18, 2010 Location: Washington State Convention Center

*Session Chairs:* Sue Lesica, US Department of Energy; Mark Bourke, Los Alamos National Laboratory

#### 8:30 AM Keynote

**Core Materials Development for Fast Reactors:** *Stuart Maloy*<sup>1</sup>; M. Toloczko<sup>2</sup>; J. Cole<sup>3</sup>; Byun<sup>4</sup>; <sup>1</sup>Los Alamos National Laboratory; <sup>2</sup>Pacific Northwest National Laboratory; <sup>3</sup>Idaho National Laboratory; <sup>4</sup>Oak Ridge National Laboratory

The Advanced Fuel Cycle Initiative is investigating methods of burning minor actinides in a transmutation fuel. To achieve this goal, the fast reactor core materials (cladding and duct) must be able to withstand very high doses (>300 dpa design goal) while in contact with the coolant and the fuel. Thus, these materials must withstand radiation effects that promote low temperature embrittlement, high temperature helium embrittlement, swelling, accelerated creep, corrosion with the coolant, and chemical interaction with the fuel (FCCI). Research is underway that includes determining radiation effects in ferritic/martensitic steels at doses up to 200 dpa, testing and development of liners and coatings to prevent/reduce FCCI, and developing advanced alloys with improved irradiation resistance. A summary and status of these studies will be presented with plans for future research.

#### 9:05 AM

**Developments in Powder Production for Nano-Structured Ferritic Alloys:** *David Hoelzer*<sup>1</sup>; Jim Bentley<sup>1</sup>; Michael Miller<sup>1</sup>; Brian Wirth<sup>2</sup>; Yong Kim<sup>2</sup>; Matt Ferry<sup>3</sup>; Jean Stewart<sup>3</sup>; <sup>1</sup>Oak Ridge National Laboratory; <sup>2</sup>University of California, Berkeley; <sup>3</sup>Crucible Research

Mechanical alloying is commonly used for producing oxide dispersion strengthened (ODS) alloys, including the 14YWT nanostructured ferritic alloy (NFA) containing nanoclusters (NC), since bulk products can be produced from metals and alloys, especially those that have low oxygen solubility. However, a significant problem that adversely affects the mechanical properties of ODS alloys is non-uniformity of oxide dispersions caused by poor mechanical mixing of the oxide and metal or pre-alloyed powders by ball milling. In this study, pre-alloyed Fe powders containing Y and O additions were produced by Ar atomization. The effectiveness that the modified powders have on the uniformity of NC in 14YWT will be presented. This research was sponsored by the Office of Nuclear Energy, Science and Technology and the Division of Materials Sciences and Engineering and the SHaRE User Facility of the Scientific User Facilities Division in the Office of Basic Energy Sciences, U.S. Department of Energy.

#### 9:30 AM

**Growth Kinetics and Phase Development in Diffusion Couples: U-Mo vs. Al-Si:** *Emmanuel Perez*<sup>1</sup>; Dennis Keiser<sup>2</sup>; Yongho Sohn<sup>1</sup>; <sup>1</sup>University of Central Florida; <sup>2</sup>Idaho National Laboratory

Interdiffusion and microstructural development in U-Mo-Al-Si system was examined using solid-to-solid diffusion couples, U-7wt.%Mo, U-10wt.%Mo and U-12wt.%Mo vs. Al, Al-2wt.%Si, Al-5wt.%Si annealed at 550°C for 1, 5 and 20 hours. Microstructural and compositional analyses were carried out by analytical microscopy and spectroscopy. Results were compiled to elucidate the evolution of the interdiffusion layer that develops between the U-Mo and Al-Si alloys. Alloying Si into Al caused a significant reduction in the thickness of the interdiffusion layer. TEM identified UA13, UMo2Al20, U6Mo4Al43 and UA14 phases in the interdiffusion layer for U-Mo vs. Al diffusion couples. When Si was added to the Al, and U-Mo vs. Al-Si diffusion couples were examined, only (U,Mo)(Al,Si)<sub>3</sub> and UMo2Al20 phases were identified by TEM. The

disappearance of U6Mo4Al43 and UA14 phases and/or solutioning of UA13 into (U,Mo)(Al,Si)<sub>3</sub> may be responsible for the slower growth of the interdiffusion zones in the U-Mo vs. Al-Si diffusion couples.

#### 9:55 AM

**Ion Irradiation of an Ultrafine Grained 316 Austenitic Stainless Steel:** *Auriane Etienne*<sup>1</sup>; Bertrand Radiguet<sup>1</sup>; Philippe Pareige<sup>1</sup>; Ruslan Valiev<sup>2</sup>; <sup>1</sup>GPM UMR CNRS 6634; <sup>2</sup>Institute of Physics of Advanced Materials

Austenitic Stainless steels (ASS) in internal structures of pressurized water reactor are susceptible to irradiation-assisted stress corrosion cracking (IASCC). Even if this complex form of material degradation is still not well understood, it's proved that only the combination of all microstructural changes (formation of point defect (PD) clusters, solute clustering, radiation-induced segregation at grain boundaries (GB)...) observed under irradiation can lead to IASCC. Since all these changes are due to PD super-saturation, increasing PD annihilation at sinks, such as GB, could limit IASCC. A 316 ASS was nano-structured by high pressure torsion. To study the effect of irradiation, samples were irradiated with 160keV Fe+ at 350°C. Irradiated samples were studied by transmission electron microscopy to see nano-grain size evolution as well as by atom probe tomography to observe the solute atom distribution evolution. The nanostructure evolution is compared to previous examinations of ion irradiated "large grain" 316 ASS.

#### 10:20 AM Break

#### 10:35 AM

**Radiation Response of High Temperature, Ultrafine-Precipitation-Strengthened Steel:** *Yong Yang*<sup>1</sup>; Todd Allen<sup>1</sup>; <sup>1</sup>University of Wisconsin-Madison

Fast reactor cladding could be improved by increasing the swelling resistance and high temperature strength of an austenitic steel through the inclusion of a high density of nanometer-sized precipitates such as the High Temperature, Ultrafine-precipitation-strengthened Steel (HT-UPS) developed by Oak Ridge National Laboratory. However, the radiation response of the HT-UPS is not well known. In our study, HT-UPS is irradiated with a 2.0MeV proton beam at 300 and 500°C for various doses up to 3 dpa. The irradiation hardening is evaluated using micro-Vickers hardness test, and the irradiation microstructures are examined using the transmission electron microscopy. Specifically, the stability of nano-sized precipitates is studied using the carbon extraction replica technique.

#### 11:00 AM

**Friction Stir Welding of Dispersion-Strengthened Alloy MA754:** *Jiye Wang*<sup>1</sup>; Wei Yuan<sup>1</sup>; Rajiv Mishra<sup>1</sup>; Indrajit Charit<sup>2</sup>; <sup>1</sup>Missouri University of Science and Technology; <sup>2</sup>University of Idaho

Friction stir welding of MA754, an Y2O3 dispersion-strengthened superalloy, were investigated. The research is supported by the DOE through grant # DE-FG07-08ID14925. A tool rotation rate of 1000 rpm and a traverse speed of 50.8 mm per minute were employed with a tungsten carbide tool. Tensile behavior of the nugget was compared with that of parent material at various temperatures. Results indicated that a refinement of grain size during friction stir welding leads to improved ductility without the loss of strength at room temperature.

#### 11:25 AM

**Development of a Simplified Powder Processing Method for Production of Oxide Dispersion Strengthened Ferritic Alloys:** *Joel Rieken*<sup>1</sup>; I. Anderson<sup>2</sup>; M. Kramer<sup>2</sup>; <sup>1</sup>Iowa State University; <sup>2</sup>Ames Laboratory

A simplified powder processing method was used to form an oxide dispersion strengthened ferritic stainless steel microstructure. Precursor ferritic stainless steel powders were oxidized in situ using a newly developed gas atomization reaction synthesis technique. The as-atomized powders contained an ultra thin kinetically favored (i.e., Cr-enriched) surface oxide. This surface layer was used as a vehicle to carry oxygen into the as-consolidated alloy microstructure, where heat treatments were designed to drive oxygen exchange between the less stable prior particle boundary oxide and dissolved Y and other additions. Exchange reactions and subsequent thermal-mechanical processing resulted in nano-metric Y-enriched oxide dispersoids and ultimate strengthening from dislocation sub-structures. Transmission electron microscopy and synchrotron X-ray diffraction helped evaluate the evolution of the alloy microstructure and elevated temperature tensile testing was used to assess the strength of the alloy. Support from the DOE-FE (ARM program) through Ames Laboratory contract no. DE-AC02-07CH11358 is gratefully acknowledged.

# Technical Program

11:50 AM

**Impact of Zirconium Hydride Precipitates on Fracture of Zirconium Alloys:** *Matthew Kerr*<sup>1</sup>; Mark Raymond<sup>2</sup>; Richard Holt<sup>2</sup>; Jonathan Almer<sup>3</sup>; Stephanie Stafford<sup>4</sup>; <sup>1</sup>US Nuclear Regulatory Commission; <sup>2</sup>Queen's University; <sup>3</sup>Argonne National Lab; <sup>4</sup>Kinectrics Inc

Zirconium alloys are of major importance to the nuclear industry, with primary application as a structural material for the in-reactor environment. The formation of brittle hydrides within zirconium alloys results in a degradation of the mechanical properties of the component in which they form. Thus, the rate and characteristics of formation as well as the subsequent impact of these hydrides are critical factors in the determination of zirconium component service life. We have carried out a three part study of hydrides in zirconium using high energy synchrotron x-ray diffraction. Part I characterized the mechanical response of zirconium hydride, in situ within a bulk Zircaloy-2 matrix. Part II studied the near crack tip behavior of un-hydrated Zircaloy-2. Part III characterizes the effect of notch tip hydrides; the aim is to quantify the influence of hydrides on the local notch tip strain field and characterize the internal strains in the hydrides themselves.

## Pb-Free Solders and Emerging Interconnect and Packaging Technologies: Microstructure, Intermetallics, Whisker (II)

*Sponsored by:* The Minerals, Metals and Materials Society, TMS Electronic, Magnetic, and Photonic Materials Division, TMS: Electronic Packaging and Interconnection Materials Committee

*Program Organizers:* Kwang-Lung Lin, National Cheng Kung University; Sung Kang, IBM; Jenq-Gong Duh, National Tsing-Hua University; Laura Turbini, Research In Motion; Iver Anderson, Iowa State University; Fu Guo, Beijing University of Technology; Thomas Bieler, Michigan State University; Andre Lee, Michigan State University; Rajen Sidhu, Intel Corporation

Thursday AM Room: 204  
February 18, 2010 Location: Washington State Convention Center

*Session Chairs:* John. W. Osenbach, LSI Corporation; Sinn-Wen Chen, National Tsing Hua University

8:30 AM

**Effects of Current Density on the Crystallographic Texture of Sn Based Electrodeposited Films Containing Cu and Pb:** *Aaron Pedigo*<sup>1</sup>; Pylon Sarobol<sup>1</sup>; Peng Su<sup>2</sup>; John Blendell<sup>1</sup>; Carol Handwerker<sup>1</sup>; <sup>1</sup>Purdue University; <sup>2</sup>Cisco Systems, Inc

Tin whisker growth is a reliability concern for lead-free electronic systems. Current whisker testing is performed with regards to JEDEC standards but the output from these tests only reports if a film is or is not whisker prone. An understanding of the mechanism of whisker formation is necessary to develop whisker mitigation strategies. Other material properties should be measured to engineer electrolytes and plating processes that decrease the propensity to whisker. In this work, the effects of electrolyte chemistry and current density during plating on texture and hillock and whisker growth were evaluated. Full pole figure analysis was performed using XRD with GADDS. EBSD was also performed to compare local texture to the macroscopic texture. Results show that the addition of Pb in the electrolyte causes drastic changes in crystallographic texture. The texture effects from Pb could be recreated in lead free electrolytes by changing the current density.

8:45 AM

**Interfacial Reaction and Microstructure Variation in the Liquid Reaction of Sn-xAg-Cu Solders on Cu-yZn Substrates:** *Chi-Yang Yu*<sup>1</sup>; Jenq-Gong Duh<sup>1</sup>; <sup>1</sup>National Tsing Hua University

This study aims to investigate the liquid reaction of Sn-xAg-0.5Cu (x= 1 and 3 wt.%) solders on different Cu-yZn (y= 0, 15 and 30 wt.%) substrates at 250 oC for 30 s, 2 and 10 min, respectively. Cu and Zn atoms would dissolve from Cu-xZn substrates into molten solders during reflow. Under this condition, Cu<sub>6</sub>Sn<sub>5</sub> was the dominating intermetallic compound (IMC) formed at the Sn-xAg-Cu/Cu-yZn interface. The composition of the Cu<sub>6</sub>Sn<sub>5</sub> and other IMCs were altered with various solder joints and reflow time. Besides, IMCs growth rate was affected by the Zn concentration at the interface. In addition to interfacial

reaction, the microstructure evolution and phase formation inside the Sn-3Ag-Cu and Sn-1Ag-Cu solders were correlated to the elemental distribution. Based on these results, the interaction between Ag content (x) in solder and Zn content (y) in substrate will be probed and discussed.

9:00 AM

**Interfacial Reaction between Sn-Ag-Cu Solder and Cu Base Metal Using Laser Soldering Process:** *Hiroshi Nishikawa*<sup>1</sup>; Noriya Iwata<sup>1</sup>; Tadashi Takemoto<sup>1</sup>; <sup>1</sup>Osaka University

With the miniaturization of electronic productions and the use of heat sensitive electronic components, the traditional reflow soldering process often has difficulties. As an alternative soldering process, the laser soldering process has been recently proposed. The laser soldering process brings several advantages in terms of localized heating, rapid rise and fall in temperature, non-contact and easily automated process. Therefore, in this study, the characteristics of the laser soldering process were investigated to especially clarify the effect of the heating method on the formation and growth of an intermetallic compound (IMC) at the interface between Sn-Ag-Cu solder and a Cu base metal and the microstructure of the solder after heating. The results show that the rapid rise and fall in temperature strongly affected the IMC at the interface and the IMC thickness for the laser soldering process was thinner than that for the traditional reflow soldering process.

9:15 AM

**Microstructure and Orientation Evolution Study on Sn-Ag-Cu Solder Joints as a Function of Position in Ball Grid Arrays Using Orientation Image Microscopy:** *Tae-Kyu Lee*<sup>1</sup>; Kuo-Chuan Liu<sup>1</sup>; Bite Zhou<sup>2</sup>; Thomas R. Bieler<sup>2</sup>; <sup>1</sup>Cisco Systems, Component Quality and Technology Group; <sup>2</sup>Chemical Engineering and Materials Science, Michigan State University

The microstructure evolution of Sn-Ag-Cu solder alloy joints are observed during thermal cycling, focused on Sn grain orientation in ball grid array (BGA) packages with different die sizes. Thermally cycled BGA packages after various pre-conditions with 196 full array solder joints are used in this study. Each selected package is polished to view the solder joints from the top by using an Orientation Imaging Microscopy. The observations reveal different patterns of single and multi-grained Sn microstructure distribution and Sn c-axis orientation for each solder joint as a function of position in the package depending on their pre-condition and thermal cycle history. The overall percentage of the single grain oriented solder joints is reduced after thermal cycling with a faster rate after 150°C aging condition compared to lower aging temperature. The difference of the distribution of individual grain orientations and evolution of those orientations during thermal cycling are discussed.

9:30 AM

**Stress and IMC Growth in Annealed and Reflowed Sn-Cu Bilayers and Their Relation to Whisker Kinetics:** *Nitin Jadhav*<sup>1</sup>; Gordon Barr<sup>2</sup>; Eric Chason<sup>1</sup>; <sup>1</sup>Brown University; <sup>2</sup>EMC Corporation

Though annealing and reflowing in Pb-free Sn have been recognized as effective methods to impede whisker formation, little is known about the fundamental mechanisms that make them work. We have done studies to understand how different heat treatments (annealing, reflow, and annealing followed by reflow) affect the stress development in the Sn layers and growth and morphology of the intermetallic (IMC), which are the key parameters controlling whisker formation. In order to quantify the nucleation kinetics we have measured the whisker density using an optical method. Our results show how the heat treatment results in IMC formation which is more continuous and uniform compared to the as-deposited sample. This impedes whiskering in two ways: the IMC layer is an effective diffusion barrier that slows down the IMC growth kinetics and the smoother morphology creates less stress in the overlayer for the same volume of IMC as in the as-deposited sample.

9:45 AM

**Nucleation and Solidification of Sn in Pb Free, SnAgCu Solder Joints:** *Babak Arfaei*<sup>1</sup>; Yan Xing<sup>1</sup>; Eric Cotts<sup>1</sup>; <sup>1</sup>Binghamton University

The replacement of eutectic Pb-Sn with near eutectic Sn-Ag-Cu to create Pb free solder joints has provided a number of challenges. Ag and Cu are much less effective than Pb in promoting solidification of Sn, so pronounced undercooling, and thus rapid solidification effects on solder joint microstructure are observed in standard procedures. Furthermore, six-fold, cyclic growth twinning of Sn during solidification from the melt is generally observed in Sn-Ag-Cu solders.



This study examines variations in solder joint microstructure resulting from changes in solidification pathways. The solder impurity content, sample size and solder joint properties, such as substrate metallization, are varied. Both variation of nucleation rates of Sn from the Sn-Ag-Cu melt, and of resultant Sn grain solidification morphologies, are reported. Studies of the failure of Sn-Ag-Cu solder joints are discussed in the context of these different Sn grain morphologies.

### 10:00 AM Break

### 10:15 AM

**Mitigation of the Growth of Tin Whiskers by Surface Treatments:** *Chien-Hao Su*<sup>1</sup>; Albert T. Wu<sup>1</sup>; <sup>1</sup>National Central University

The growth of tin whiskers on lead-free finishes coated on the leadframes is a spontaneous process and contributed by stress generation and relaxation. A protective layer of tin oxide that grown on the surfaces is required for the formation of tin whiskers. The oxide layer prevents the relaxation of stresses that are built up due to the formation of intermetallic compounds. Cracks on the oxide served as weak spots that are essential for the protrusion of whiskers to release the stresses. This paper presents a new approach to mitigate the growth of tin whiskers. The sample surfaces were treated by etchant and polishing to greatly reduce the coherence of oxide. Tin oxide nanoparticles were sprayed on the "clean" surface to deliberately produce weak spots to enhance the relaxation of stresses. The results suggested that many short hillocks instead of long whiskers grown after performing surface treatments.

### 10:30 AM

**Interfacial Reactions of Cu/Sn3.5Ag/Au Solder Joint under Electromigration:** *Tsung-Chieh Chiu*<sup>1</sup>; Kwang-Lung Lin<sup>1</sup>; <sup>1</sup>National Cheng Kung University

In this study, a lead free Cu/Sn3.5Ag/Au solder joint under electromigration of  $2.56 \times 10^3$  A/cm<sup>2</sup> at 100° with various times was investigated. After 480 h of current stressing, the morphology of cathodic Cu electrode became rough which is due to the migration of Cu toward the anode side. The AuSn4 in the solder matrix near the Cu electrode tended to dissolve and released Au in the interfacial Cu6Sn5 to form (Cu,Au)6Sn5. The migration of Sn to the anode resulted in the formation of crack at the (Cu,Au)6Sn5/solder interface. As the Cu at the anode side, the thickness of IMC formed under electromigration is greater than that under isothermal aging. At the Au electrode, four types of IMC including AuSn4, AuSn2, AuSn and Au5Sn were sequentially formed at the interface regardless of the direction of electron flow under electromigration.

### 10:45 AM

**The Relationship between Whisker Growth and Corrosion in Sn-3.0Ag-0.5Cu:** *Keith Sweatman*<sup>1</sup>; Takashi Nozu<sup>1</sup>; J Masuda<sup>1</sup>; Masuo Koshi<sup>1</sup>; Tetsuro Nishimura<sup>1</sup>; <sup>1</sup>Nihon Superior Co., Ltd.

Corrosion has been identified as one source of the compressive stress recognized as a driver of whisker growth in high-tin alloys and in this paper the authors report a study directed at identifying the relationship between the extent of corrosion and whisker growth. Printed circuit coupons with an OSP finish were soldered with Sn-3.0Ag-0.5Cu using wave, reflow, and manual methods with a range of "no-clean" fluxes typical of current commercial practice and exposed for up to 3000 hours to 40°C/95%RH, 60°C/90%RH and 85°C/85%RH. As well as recording the location of whiskers, their density, and length as a function of time, the extent of corrosion of the solder was measured by cross-sectioning. While the environment proved to be the main controlling factor the incidence and growth rate of whiskers was found to vary with the soldering method, the flux type, and the geometry and could be correlated with the concomitant corrosion.

### 11:00 AM

**Corrosion Enhanced Sn Whisker Growth:** *John Osenbach*<sup>1</sup>; H. L. Reynolds<sup>2</sup>; G. Henshall<sup>3</sup>; R. D. Parker<sup>4</sup>; P. Su<sup>5</sup>; <sup>1</sup>LSI Corporation; <sup>2</sup>Sun Microsystems, Inc.; <sup>3</sup>Hewlett-Packard; <sup>4</sup>Delphi Electronics and Safety; <sup>5</sup>Cisco Systems

Sn whisker growth is affected by corrosion. We have found corrosion enhances whisker growth by lowering the effective activation energy for whisker growth. A theory based on excess, non-creep relaxed, oxidation induced strain was developed to explain the corrosion induced energy barrier lowering.

### 11:15 AM

**Back-Stress Induced Single Crystal Hillock Growth in Unpassivated and Nanotwinned Copper Lines under Electromigration at Device Operation Temperature:** *Hsin-Ping Chen*<sup>1</sup>; King-Ning Tu<sup>1</sup>; Lih J. Chen<sup>2</sup>; Chien-Neng Liao<sup>3</sup>; W.W. Wu<sup>3</sup>; <sup>1</sup>UCLA; <sup>2</sup>NTHU; <sup>3</sup>NCTU

Hillock growth has been observed in unpassivated and nanotwinned copper lines under electromigration at normal device operation temperature of 100°C by using ultrahigh vacuum transmission electron microscopy. The formation of hillocks in the anode side implies that electromigration has caused a back-stress and also a localized stress gradient in the Cu line. From TEM analysis, the single crystal hillocks are larger than the grain size in the line and have facets. The growth direction of hillock is random and there is no preferred orientation.

### 11:30 AM

**Microstructure Changes and Physical Properties of the Intermetallic Compounds Formed at the Interface between Sn-Cu Solders and Cu Substrate Due to Minor Additions of Alloying Elements:** *Petr Hrcuba*<sup>1</sup>; Milos Janecek<sup>1</sup>; <sup>1</sup>Charles University Prague

Several Sn-based alloys have been proposed recently as lead-free alternatives of Sn-Pb alloys. Sn-Cu alloy seem to be one of the most promising candidates with several enhanced properties which are achieved by additions of other elements. In this study the influence of alloying elements on the morphology of intermetallic compounds (IMC) formed at the interface of the liquid Sn-Cu solder and Cu substrate has been investigated. Minor additions of alloying elements, in particular Ni and P, were shown to improve soldering as well as other physical properties of the joints. The morphology and composition changes of the IMC layer formed during liquid solder/solid Cu substrate reaction in a wide range of temperatures and reaction times were investigated by scanning electron microscopy and energy dispersive X-ray analysis. The IMC layer growth kinetics is analysed using Arrhenius approach.

### 11:45 AM

**Reaction between Sn and Electroplated Cu Foils with Different Orientation:** *Tzu Sung Huang*<sup>1</sup>; C. Y. Liu<sup>1</sup>; Hua-wei Tseng<sup>1</sup>; Yu-Hsiang Hsiao<sup>1</sup>; Cheng Tze Liu<sup>1</sup>; <sup>1</sup>National Central University

The binary Cu/Sn soldering system is the most important joint system in the current IC packaging. In this thesis, we will study the correlation between the microstructure of Cu substrate (Cu grains size and preferred orientation) and the interfacial reaction (Cu-Sn compound formation and Kirkendall voids distribution). Cu substrates with different orientation are prepared by electroplating, and then reflow solder balls on the electroplated Cu substrates. After that, aged the Sn/Cu samples under 150°. In this investigation, the electroplated Cu were performed by metallurgical examination, XRD and FIB analysis to examine the grain size morphology, preferred orientation and Kirkendall voids distribution. The experimental results indicated that the Cu3Sn thickness of Cu substrate with the (Random) plane is thicker than that with the (111) and (220) planes. In addition, there was almost no Cu3Sn growth in (111) and (220) after 2000 hrs aging.

## Polymer Nanocomposites: Fabrication, Characterization, Modeling and Applications

*Sponsored by:* The Minerals, Metals and Materials Society  
*Program Organizer:* John Zhanhu Guo, Lamar University

Thursday AM Room: 309  
February 18, 2010 Location: Washington State Convention Center

*Session Chairs:* Jiahua Zhu, Lamar University; Wei Chen, University of Southern California

### 8:30 AM Introductory Comments

### 8:35 AM Invited

**Negative Permittivity in Polymer Nanocomposites: Influences of Size Distribution of Carbon Nanofiber Networks:** *Bin Li*<sup>1</sup>; Weihong Zhong<sup>1</sup>; <sup>1</sup>Washington State University

A polymeric "single negative permittivity metamaterial" was successfully fabricated from the non-metallic materials, polyetherimide (PEI) and carbon nanofibers. The determinant structure in the polymer nanocomposites was

# Technical Program

the continuous 3D network composed of imide chains wrapped upon long CNFs (CNF agglomerates), which is equivalent to the thin metallic wires in the J.B.Pendry Model. In this study, the low power ultrasonic treatment was applied to disentangle the large CNF agglomerates and consequently reduce the size of the CNF agglomerates and their related distribution. The results showed that the size of CNF agglomerates exerts strong influence on the occurrence of negative permittivity. A qualitative relationship between size/size distribution and negative permittivity of PEI/CNF nanocomposites was established.

**9:05 AM**

**Crystallization Behavior of Polymer Nanocomposites: Influence of Pressure and Nanoparticles:** *Qiang Yuan*<sup>1</sup>; Jinesh Shah<sup>1</sup>; Juan Chen<sup>1</sup>; Yang Yang<sup>1</sup>; Devesh Misra<sup>1</sup>; <sup>1</sup>University of Louisiana

The objective of the presentation is to elucidate the basic physical mechanisms underlying the evolution of hierarchical structures and phases during pressure-induced crystallization of polymers containing dispersion of nanoparticles. High pressure crystallization enables structural characteristics such as high crystallinity and preferential phase selection in polymer nanocomposites. The phase selection in the polymers is normally dictated by pressure and temperature, however, the introduction of nanoparticles can dramatically alter the kinetics of the formation of the phases via nanoparticle interface driven nucleation. Thus, by controlling pressure and crystallization temperature, a high degree of phase selection and structural control may be achievable, which has profound effect on mechanical properties.

**9:25 AM**

**Effect of Melt Flow Rate on the Properties of Polypropylene/Bentonite Nanocomposites:** Tatianny Alves<sup>1</sup>; Laura de Carvalho<sup>1</sup>; Eduardo Canedo<sup>1</sup>; Pamela Cipriano<sup>1</sup>; Vanize Fernandes<sup>1</sup>; <sup>1</sup>UFCEG

Polymer nanocomposites have several advantages over conventional microcomposites, among which is the fact that similar or better properties can be obtained at very low loadings (1-5%). Layered silicates such as those present in bentonite clays are some of the most useful loads. Melt compounding with organically modified clays is the preferred method to prepare nanocomposites based on non-polar matrices such as polyolefins. In this work, nanocomposites made with two polypropylene homopolymers having very different melt flow rates (10 and 40 g/10min) and 1% local bentonite clay, organofilled with hexadecyl trimethyl ammonium bromide in our laboratories, were prepared by melt compounding in a single-screw extruder fitted with mixing elements. Results show that intercalated structures were obtained with both matrices. A larger increase in interlayer spacing was observed for the compounds made with the more viscous, i.e., lower MFR polymer.

**9:45 AM**

**Synthesis, Structure and Properties of a Novel Hybrid Bimodal Network Elastomer with Inorganic Cross-Links:** *Jinesh Shah*<sup>1</sup>; Qiang Yuan<sup>1</sup>; Juan Chen<sup>1</sup>; Yang Yang<sup>1</sup>; Devesh Misra<sup>1</sup>; <sup>1</sup>University of Louisiana

A novel hybrid bimodal network elastomer was synthesized with high strength-high ductility combination involving utilization of functionalized nanocrystalline titania as short-chain cross-links between neighboring elastomer chains. Silicone rubber is selected as the model elastomer. The short-chain cross-links are acrylic acid functionalized nanocrystalline titania that are an integral component of bimodal network structure of the elastomer. To delineate and separate the effects of functionalization from nanoparticle effects, a relative comparison is made between silicone rubber-titania nanocomposite (i.e. containing dispersion of titania as a reinforcement filler) and silicone rubber-titania hybrid network elastomer (i.e. titania as short chain cross-links). The basic physical mechanisms that govern elastic recovery in hybrid bimodal network elastomer with short chain cross-links of functionalized nanocrystalline inorganic particles are discussed.

**10:05 AM**

**Modification of Nanocrystal-Polymer Composite Electrolyte by Ethelene Glycol for Dye-Sensitized Solar Cell:** *Yang Ying*<sup>1</sup>; Guo Xueyi<sup>1</sup>; <sup>1</sup>Central South University

A quasi-solid-state dye-sensitized solar cell (DSSC) employing poly (ethylene oxide)-poly (vinylidene fluoride) (PEO-PVDF) gel electrolyte was modified by ethanol and glycol. The performance of additive-modified electrolyte was studied by Fourier transform infrared (FTIR), differential scanning calorimetry (DSC) and viscosity measurements. The conductivity of the electrolytes and the corresponding performances of the DSSC were also studied. The experiments

exhibit that 3.1% ethanol modified electrolyte shows an increase of the connected ion transport networks in the electrolyte, leading to an improvement in energy-conversion efficiency from 4.4% (unmodified DSSC) to about 5.3% and an increase in stability from 130 to about 500 hours in room temperature. However, compared to ethanol modification, the same amount of glycol addition into the electrolyte causes little improvement in both conductivity and cell performances. This may be due to the formation of a polymer aggregates in the electrolyte, which inhibits the ion transport in the electrolyte.

**10:25 AM Break**

**10:40 AM**

**Nanoscale Near-Surface Deformation in Polymer Nanocomposites:** *Qiang Yuan*<sup>1</sup>; Jinesh Shah<sup>1</sup>; Yang Yang<sup>1</sup>; Juan Chen<sup>1</sup>; Devesh Misra<sup>1</sup>; <sup>1</sup>University of Louisiana

The objective of the presentation is to elucidate the nanoscale near-surface deformation response of two polymer nanocomposite systems with significant differences in ductility during nanoscratching with a Berkovich indenter. An accompanying objective is to investigate the commonality in surface deformation behavior between nano- and microscale deformation to reinforce the underlying fundamental principles governing surface deformation. An understanding of surface deformation response is accomplished through determination of physical and mechanical properties, structural characterization and electron microscopy analysis of surface deformation tracks and residual plastically deformed structures. The deformation behavior is described in terms of physical and mechanical properties of materials notably percentage crystallinity and elastic recovery.

**11:00 AM Invited**

**Formation and Structural Characterization of Potassium Titanates and the Lattice Potassium Reactivities:** Qiang Wang<sup>1</sup>; Zhanhu Guo<sup>1</sup>; Jong Shik Chung<sup>2</sup>; <sup>1</sup>Lamar University; <sup>2</sup>POSTECH

Potassium titanates (K<sub>2</sub>Ti<sub>2</sub>O<sub>5</sub>, K<sub>2</sub>Ti<sub>4</sub>O<sub>9</sub> and K<sub>2</sub>Ti<sub>6</sub>O<sub>13</sub>) are synthesized by solid state method. Their structures and morphologies are characterized by X-ray diffraction, Raman spectra and scanning electron microscopy. The binding energies of K, Ti and O in potassium titanates are then evaluated by X-ray photoelectron spectroscopy and compared with those in K/TiO<sub>2</sub>. Finally the lattice potassium reactivities are evaluated by NO<sub>2</sub> adsorption and ion exchange in Co(NO<sub>3</sub>)<sub>2</sub> solutions. It is found that the binding energy of K in K<sub>2</sub>Ti<sub>2</sub>O<sub>5</sub> is much higher than those in K<sub>2</sub>Ti<sub>4</sub>O<sub>9</sub> and K<sub>2</sub>Ti<sub>6</sub>O<sub>13</sub>, and because of which, it shows quite different catalytic performances. Compared with other potassium titanates, only K<sub>2</sub>Ti<sub>2</sub>O<sub>5</sub> shows NO<sub>2</sub> adsorption activity and the K in K<sub>2</sub>Ti<sub>2</sub>O<sub>5</sub> is much easier to be exchanged out.

**11:20 AM**

**Catalytic Reduction of Nitrates Using Modified Double Layered Hydroxides:** *Jewel Gomes*<sup>1</sup>; George Irwin<sup>1</sup>; Kamol Das<sup>1</sup>; Manish Rahate<sup>1</sup>; Doanh Tran<sup>1</sup>; David Cocke<sup>1</sup>; <sup>1</sup>Lamar University

Layered Double Hydroxides (LDHs), such as green rust and hydrotalcites, are a group of anion-exchangeable materials containing mixed metal hydroxides similar to brucite. They have relatively weak interlayer bonding compared to cationic clays resulting excellent ability to capture inorganic anionic contaminants, such as nitrates. With the increasing sources of nitrogen and nitrates from natural, agricultural, and man-made activities, nitrate contamination of groundwater is a common problem when surface water comes in contact with any source of nitrate. Existing nitrate (NO<sub>3</sub>-) treatment processes such as distillation, reverse osmosis, and ion exchange, are expensive and have inherent disadvantages. The aim of this study was to investigate the feasibility of catalytic removal of nitrate using modified LDHs formed by impregnation of transition metals. The study also included the characterization of modified LDHs using XRD, FTIR, SEM and Mössbauer spectroscopy. Thermal degradation and flame retardant effect of the nano-LDHs were also studied.

**11:40 AM**

**Molecular Dynamics Simulation of Diffusion of Atmospheric Penetrates in Polydimethylsiloxane (PDMS) and PDMS-Based Nanocomposites:** *Alex Sudibjo*<sup>1</sup>; Douglas Spearot<sup>1</sup>; <sup>1</sup>University of Arkansas

Molecular dynamics simulations are used to study the nanoscale mechanisms associated with diffusion of small atmospheric penetrates in polydimethylsiloxane (PDMS) and PDMS-based nanocomposites with metal nanoparticle inclusions. Specifically, diffusion constants and activation



energies are computed for methane, nitrogen and oxygen penetrates in PDMS and PDMS-based nanocomposites. PDMS is modeled within the molecular dynamics framework using both united-atom and all-atom interatomic potentials; the accuracy of each model and its ability to capture structural aspects of PDMS, including bulk densities and radius of gyration, is evaluated. Diffusion coefficients are computed via mean-squared displacements of the atmospheric penetrates. MD simulations provide a detailed understanding of how penetrate species, temperature, nanoparticle size and distribution influence the diffusion flux through the nanocomposite. These calculations are necessary to interpret experimental results for a MEMS-based corrosion sensor, where metallic nanoparticles are embedded within a PDMS matrix.

### 12:00 PM

**Metalization of Platinum on Polyimide as Counterelectrode for Flexible Dye-Sensitized Solar Cells:** *Sheng-Jye Cherng*<sup>1</sup>; Chih-Ming Chen<sup>1</sup>; <sup>1</sup>National Chung Hsing University

The counterelectrodes of flexible dye-sensitized solar cells (DSSCs) are usually fabricated by sputtering a catalytic platinum (Pt) layer on flexible transparent conductive polymer substrate (ITO/PEN). However, sputtering is not a cost efficient method which restrains its applications. Therefore, development of a low cost method of depositing Pt for DSSCs is an important issue. In this talk, we demonstrate a simple and low cost method of growing Pt nanoparticles on polyimide. Four point probe analysis reveals the nonconductive polyimide becomes electrically conductive after surface metallization of Pt. DSSCs employing the Pt-coated polyimide as the counterelectrodes were assembled and their photovoltaic performances were measured.

### Processing Materials for Properties: Polymers, Ceramics and Glasses

*Sponsored by:* The Minerals, Metals and Materials Society, TMS Extraction and Processing Division

*Program Organizers:* Brajendra Mishra, Colorado School of Mines; Akio Fuwa, Waseda University; Paritid Bhandhubanyong, National Metal and Materials Technology Center

Thursday AM Room: 617  
February 18, 2010 Location: Washington State Convention Center

*Session Chairs:* Stuart Maloy, Los Alamos National Laboratory; Mychailo Toloczko, Pacific Northwest National Laboratory

### 8:30 AM Keynote

**Transparent Ceramics by Spark Plasma Sintering of Oxide Nanopowders:** *Rachman Chaim*<sup>1</sup>; Zhijian Shen<sup>2</sup>; Claude Estournes<sup>3</sup>; <sup>1</sup>Technion - Israel Institute of Technology; <sup>2</sup>Stockholm University; <sup>3</sup>CIRIMAT et Plateforme Nationale CNRS de Frittage Flash

Spark plasma sintering (SPS) was used for superfast densification of ceramic nanopowders. Simultaneous application of pulsed dc currents and load are the necessary conditions for rapid and full densification of ceramic nanopowders by SPS. Nanopowders of MgO, YAG and Y<sub>2</sub>O<sub>3</sub> were densified using SPS at different temperatures, pressures and durations. Nanocrystalline MgO and YAG powders were densified to optical transparency at distinctly different homologous temperatures (0.3T<sub>m</sub> for nc-MgO and 0.7T<sub>m</sub> for nc-YAG). Dense Nd-YAG and Y<sub>2</sub>O<sub>3</sub> specimens were translucent with micrometer grain size. Analysis of the density and grain size evolution versus the SPS parameters showed that densification of these nanopowders proceed either by plastic deformation, grain-rotation coalescence and sliding, aided by softening of the particle surfaces or by accelerated surface diffusion. These may be followed by normal grain growth. The active densification mechanism depends on the changes both in the mechanical and electrical properties of the ceramic with temperature.

### 9:00 AM

**Direct Laser Deposition of Bulk Metallic Glasses:** *Hongqing Sun*<sup>1</sup>; Pete Collins<sup>1</sup>; Hamish Fraser<sup>1</sup>; Katharine Flores<sup>1</sup>; <sup>1</sup>The Ohio State University

Bulk metallic glasses (BMGs) have attracted tremendous attention as structural materials because of their remarkable mechanical properties. However, the critical cooling rates required to produce an amorphous atomic structure limit the dimensions of as-cast BMG components and therefore

restrict their widespread use. As a layer-by-layer additive process with localized heat input and inherently rapid cooling, direct laser deposition provides the potential opportunity to produce non-equilibrium or amorphous structures that exceed the as-cast dimensional limit. In the present work, we use the Laser Engineering Net Shaping (LENS<sup>TM</sup>) process to deposit pre-alloyed Zr-based metallic glass forming powders. A continuous amorphous layer was achieved with optimization of the processing parameters. However, the accumulated heat input during multi-layer deposition results in the crystallization at the bottom of the deposit. To address this, we investigate the thermal history of the deposit and substrate using a combination of finite element modeling and in-situ thermal imaging.

### 9:20 AM

**Microscopic Study of Slags from a Secondary Lead Blast Furnace:** *Fumito Tanaka*<sup>1</sup>; Yusuke Kimura<sup>1</sup>; Mikio Watanabe<sup>2</sup>; <sup>1</sup>Mitsubishi Materials Corp.; <sup>2</sup>Hosokura Metal Mining Co., Ltd.

Hosokura Metal Mining Co., Ltd. processes spent lead-acid battery to produce electrolytic lead, while leaving acceptable influences on the environment. The company derives noticeable competitiveness from proven technologies for operating the blast furnace, which was developed jointly with Mitsubishi Materials Corp. Emerged businesses to recycle various lead-bearing materials have also been enhancing the bullion production. Processing lead-bearing materials, however, impacts on the slag chemistry or energy balance of the blast furnace, thereby misleading the operators occasionally. Microscopic examination of slag samples from the blast furnace revealed the metallurgical cause of the operational difficulties and helped to identify secondary materials whose feeding rate should be optimized. Among impurities included in secondary materials, the present paper will focus on the metallurgical impact of alumina and soda. It will also discuss the furnace controls under the influence of alumina and soda, applying slag chemistry of the state of the art.

### 9:40 AM

**Particle Size Distribution of Natural Montmorillonite Clay Using Dispersion Analysis:** *Morgan Reed*<sup>1</sup>; Gary Beall<sup>2</sup>; David Cocke<sup>1</sup>; Jewel Gomes<sup>1</sup>; <sup>1</sup>Lamar University; <sup>2</sup>Texas State University

The particle size and distribution of suspensions of clays are of considerable interest to many industrial processes including oil-well drilling, environmental abatement, polymer nanocomposites, and nanoflake catalysts. Although exploration of the interactions between montmorillonite clay with water-ethanol mixtures was studied before, particle sizing drew particle attention in the realm of nanotechnology due to particle-particle interaction and its role in distribution and sedimentation. In this study, the particle size was determined by employing a dispersion analyzer utilizing extinction and transmission profiles. The particle size distribution of montmorillonite particles, dispersed in a water-ethanol mixture, was obtained by analyzing the light transmission at a defined constant position with the measured time. This method of analysis was used for its robust accommodation of all types of suspensions with broad size distributions. The competitive behavior between ethanol and water molecules for active sites located at clay particle edges was also discussed considering particle size variation.

### 10:00 AM

**Study of Properties of Spinel, Obtained by Hydrothermal Synthesis:** *Oscar Restrepo*<sup>1</sup>; Leidy Jaramillo<sup>1</sup>; Ernesto Baena Murillo<sup>1</sup>; <sup>1</sup>National University of Colombia

This study provides an analysis of the properties of spinels Fe(1-x)Zn(x)Cr<sub>2</sub>O<sub>4</sub> obtained by hydrothermal synthesis. Experiments were conducted where changes were made to the pH, the concentration of precursor salts and the type of iron salt used. The response variables analyzed were the distribution of phases, color, particle size distribution, chemical composition and shape of particles. The methods used to characterize the spinels obtained were by X-ray diffraction (XRD), UV-VIS-NIR spectroscopy, scanning electron microscopy (SEM), energy dispersion X-ray analysis (EDX) and thermal analysis (DTA/TGA). Results are compared with a commercial product obtained by traditional method of solid state synthesis at high temperature. It is hoped that this study will serve as a technical option for the development of alternate routes for spinels production so as to provide environmental benefits, economic and technology compared to traditional methods.

# Technical Program

10:20 AM

**Research on the Performance of Environment-Friendly MgO-CaO-ZrO<sub>2</sub> Refractories:** *Caiyun Lu<sup>1</sup>*; Min Chen<sup>1</sup>; Jingkun Yu<sup>1</sup>; Zhongqiang Sun<sup>2</sup>; <sup>1</sup>Northeastern University; <sup>2</sup>Northeastern University Institute of Metallurgical Technology Co., Ltd

Considering MgO-Cr<sub>2</sub>O<sub>3</sub> refractories using in the alkaline environment led environmental problems caused by hexavalent chromium pollution, MgO-CaO-ZrO<sub>2</sub> refractories is a new type refractories for substitution of MgO-Cr<sub>2</sub>O<sub>3</sub> refractories using in secondary refining vessels in metallurgical industries for its excellent properties as well as environment-friendly features. In the present work, Micro-ZrO<sub>2</sub> and Nano-ZrO<sub>2</sub> were used as additives applied in MgO-CaO refractories to respectively investigate their improvement on performance of MgO-CaO refractories. The results showed that the densification of the MgO-CaO refractories was appreciably promoted when a small amount of ZrO<sub>2</sub> was added, the thermal shock resistance and slaking resistance of the MgO-CaO refractories could be appreciably improved with a small amount of ZrO<sub>2</sub> addition. The effect of nano-sized ZrO<sub>2</sub> additive on densification, thermal shock resistance and slaking resistance was more obvious than micro-sized one. The Penetration index of MgO-CaO refractories was significant reduced as the amount of nano-sized ZrO<sub>2</sub> additive increased.

10:40 AM Break

10:50 AM

**Synthesis of Spinel by Thermal Spray Flame:** *Oscar Restrepo<sup>1</sup>*; Ernesto Baena Murillo<sup>1</sup>; <sup>1</sup>National University of Colombia

The formation of spinels Fe(1-x)Zn(x)Cr<sub>2</sub>O<sub>4</sub> by thermal spray flame synthesis using iron (Fe<sub>2</sub>O<sub>3</sub>), zinc (ZnO) and chromium (Cr<sub>2</sub>O<sub>3</sub>) oxides as precursors is studied. It is evaluated the influence of two process operating parameters, O<sub>2</sub>/C<sub>2</sub>H<sub>2</sub> ratio and pressure of those combustion gases, by X-ray diffraction (XRD), UV-VIS-NIR spectroscopy, scanning electron microscopy (SEM), energy dispersion X-ray analysis of (EDX) and thermal analysis (DTA/TGA). Changes in reflectance spectra of pigments obtained by this non-conventional method are related to the identified phase transformations, crystallinity and the spatial arrangement of cations. Results are compared with a commercial product obtained by traditional method of solid state synthesis at high temperature. This alternative production method present advantages as efficiency improvement of process and product, because of reductions in energy consumption and byproducts generation, as well as reducing environmental impacts.

11:10 AM

**Novel Forming Techniques in Fabrication of Powder-Based Metals via Current Activated Tip-Based Sintering (CATS):** *D. Elting<sup>1</sup>*; E. Villar<sup>1</sup>; K. Moon<sup>1</sup>; S. Kassegne<sup>1</sup>; K. Morsi<sup>1</sup>; <sup>1</sup>San Diego State University

Bulk powder-based products that are fabricated using spark plasma sintering are completed in significantly shorter times and lower temperatures compared to a conventional sintering process. This paper discusses novel techniques in current activated tip-based sintering (CATS) where current activation is applied "locally" through a conductive tip to a powder bed or compact under the application of a forming pressure. Research includes simple and more complex small-scale artifact fabrication through the CATS process, the variables involved and their optimization, and the implications for macro as well as micro scale pressure assisted manufacturing processes. The processing-manufacturing for property relations is discussed.

11:30 AM

**Effects of Sensitizer Length on Radiation Crosslinked Shape-Memory Polymers:** *Taylor Ware<sup>1</sup>*; Walter Voit<sup>1</sup>; Ken Gall<sup>1</sup>; <sup>1</sup>Georgia Institute of Technology

Poly(methyl acrylate) (PMA) is blended with poly(ethylene glycol) diacrylate (PEGDA) of several molecular weights in various concentrations and exposed radiation. PEGDA sensitizes the radiation crosslinking of PMA. Minimum dosage for gelation decreases from 25.57 kGy for unblended PMA to 2.06 kGy for PMA blended with 10.00 mole% PEGDA. Increasing the length of the blended PEGDA molecule at a constant molar ratio increases the efficacy of the molecule as a radiation sensitizer as determined by the increase in gel fraction and rubbery modulus across dosages. However, at a constant weight ratio of PEGDA to PMA, shorter PEGDA chains sensitize more crosslinking because they have more reactive ends per weight fraction. Sensitized samples of PMA with PEGDA were tested for shape-memory properties and showed shape fixity

of greater than 99%. Samples had a glass transition temperature near 28°C and recovered between 97% and 99% of the induced strain when strained to 50%.

11:50 AM

**Radiation Crosslinked Polyacrylates with Shape Memory:** *Walter Voit<sup>1</sup>*; Taylor Ware<sup>1</sup>; Ken Gall<sup>1</sup>; <sup>1</sup>The Georgia Institute of Technology

Shape-memory polymers (SMPs) are active smart materials with tunable stiffness changes at specific, tailored temperatures. Thermoplastic SMPs lose "memory" properties near melt temperatures and have large residual strains, while network (thermoset) SMPs fully recover, limiting device disfiguration. However the use of thermoset SMPs has been limited in mass-manufacture and commodity applications because low-cost plastics processing techniques like injection molding and blow molding are not possible with network polymers. In this study of thermoset SMPs, beyond adjusting the glass transition temperature (T<sub>g</sub>) between 28 and 60°C and tuning the recoverable force between 0.5 and 13 MPa, a novel manufacturing process, Mnemosynation, is described. The customizable mechanical properties of traditional SMP are coupled with traditional plastic processing techniques to enable a new generation of mass producible plastic products with thermosetting shape-memory properties: low residual strains, tunable recoverable force and adjustable T<sub>g</sub>.

12:10 PM

**Synthesis of Polyamine PET for the Sulfate Ions Removal in Aqueous Solution:** *Haiying Wang<sup>1</sup>*; Liyuan Zhang<sup>1</sup>; Liyuan Chai<sup>1</sup>; Meilan Li<sup>1</sup>; <sup>1</sup>Central South University

Polyamine PET was synthesized by condensation polymerization of epichlorohydrin and triethylenetetramine. FTIR, TG and SEM were used to character the PET product. The sulfate removal performance of PET in aqueous solutions was studied. The results showed that the product had strong thermostability and good sulfate ion removal capability. The sulfate ions adsorption of PET can bring into equilibrium within 30 min and 10 min respectively at neutral and acidic aqueous solutions containing 2.0 g/L sulfate ions. When the reaction maintained 30 min, the sulfate ions removal ratio can reach more than 99.0 % in aqueous solutions with the absorption capacity 180 mg/g or so.

---

## Stochastic Methods in Materials Research: Stochastic Methods II: Property Prediction and Material Design

*Sponsored by:* The Minerals, Metals and Materials Society, TMS Materials Processing and Manufacturing Division, TMS/ASM: Computational Materials Science and Engineering Committee  
*Program Organizers:* Richard Hennig, Cornell University; Dallas Trinkle, University of Illinois, Urbana-Champaign

Thursday AM Room: 614  
February 18, 2010 Location: Washington State Convention Center

*Session Chairs:* Dallas Trinkle, University of Illinois Urbana-Champaign; Richard Hennig, Cornell University

8:30 AM Invited

**Probabilistic Materials Science: Taking AIM:** *Greg Olson<sup>1</sup>*; <sup>1</sup>Northwestern University

The systems approach to computational materials design has expanded in the past decade to encompass the full materials development and qualification cycle. The efficient control of minimum property allowables has demanded a major departure from traditional data-driven empirical statistical methods to a new mechanistic predictive science of probabilistic materials behavior. Under the DARPA-AIM initiative, multidisciplinary tools were integrated within the iSIGHT system to predict microstructure-based property variation resulting from six stages of manufacturing, demonstrating a novel modified Bayesian method in which a mechanism-based probability distribution is calibrated with minimal data by linear transformation. Employing iSIGHT sensitivity analysis tools in early alloy design, the AIM methodology has now been successfully demonstrated in the process optimization and qualification of the new Ferrium S53 corrosion-resistant aircraft landing gear steel. Enhanced models developed under the ongoing ONR/DARPA D3D Digital Structure consortium support process optimization for control of minimum fatigue properties based on distributed microstructure.



### 9:00 AM Invited

**The Application of Bayesian Neural Network Modeling for the Prediction of the Tensile and Fracture Toughness Properties in  $\alpha/\beta$  Titanium Alloys:** *Santhosh Koduri<sup>1</sup>; Vikas Dixit<sup>1</sup>; Peter Collins<sup>1</sup>; Hamish Fraser<sup>1</sup>; <sup>1</sup>The Ohio State University*

The development of novel combinatorial methods based on Bayesian statistics to address the structure property relationships in commercially important materials is a valuable step towards the accelerated maturation of the materials. Non-linear data modeling tools such as neural networks with Bayesian framework have been used to predict the tensile and fracture toughness properties of Ti6Al4V at room temperature. The development of rules - based models necessitates population of extensive database consisting of the information about the composition and microstructural features to train and test the neural network models. These models have been successfully used to isolate the influence of the individual microstructural features on the mechanical properties, consequently guiding the efforts towards the development of more robust phenomenological models. The influence of critical microstructural features on tensile and fracture toughness properties has been investigated using the electron back-scattered diffraction and transmission electron microscopy.

### 9:30 AM

**A Stochastic Simulation Study of the Role of Hierarchy in Crack-Initiating Microstructural Arrangements in Fatigue Lifetime Distribution:** *Sushant Jha<sup>1</sup>; Christopher Szczepanski<sup>1</sup>; James Larsen<sup>2</sup>; <sup>1</sup>Universal Technology Corporation; <sup>2</sup>US Air Force Research Laboratory*

Recent research has revealed that the mean and the lower-tail of fatigue lifetime distribution show disparate rates of response to relevant microstructural and loading variables. This difference in responses, which controls the lifetime variability, is underlined by crack initiation in a hierarchical array of local microstructural arrangements. Here, we employ stochastic simulation to study this hypothesis of fatigue variability. Random, polycrystalline ensembles with given nominal grain size distribution and crystallographic texture were constructed using Voronoi Tessellation. The ensembles were then probed for the incidence of various critical microstructural arrangements. Probabilities of occurrence of such arrangements as a function of the heterogeneity level were calculated and correlated with the experimentally determined crack-initiating microstructural configurations and their frequency of producing failures in a titanium alloy. The effect of varying nominal microstructural attributes as they affect the probability of occurrence of a life-limiting crack-initiation condition was investigated.

### 9:50 AM Break

### 10:00 AM Invited

**Multiscale Design of Solute-Strengthened Aluminum Alloys:** *W. Curtin<sup>1</sup>; G. Leyson<sup>1</sup>; L. Hector<sup>2</sup>; <sup>1</sup>Brown University; <sup>2</sup>GM Technical Center*

The strengthening of alloys by the addition of solutes is well-established across a wide spectrum of metal alloys. The actual predictions of strengthening are based on approximate models of dislocation/solute interactions. Here, we develop a stochastic model for substitutional solute strengthening in fcc alloys, using concepts derived from early work by Labusch wherein the solute strengthening arises from favorable solute concentration fluctuations over some critical length determined by the fluctuations and the interaction energies. We then use first-principles methods to calculate the solute-dislocation interaction energies within the core of an edge dislocation in Al, and use these energies as input into the model to make nearly parameter-free predictions of solute strengthening. A rate-dependent thermal activation model is used to extend the model to finite temperatures and experimental strain-rates. The methodology is applied to Mg, Si, Cu, and Cr solute additions to Al, and the predictions are compared with available experiments.

### 10:30 AM

**Multiscale Entropy Analysis of the Portevin-Le Chatelier Effect in an Al-2.5%Mg Alloy:** *Apu Sarkar<sup>1</sup>; P Barat<sup>2</sup>; P Mukherjee<sup>2</sup>; <sup>1</sup>Bhabha Atomic Research Centre; <sup>2</sup>Variable Energy Cyclotron Centre*

Portevin-Le Chatelier (PLC) effect, observed in many dilute alloys of technological importance, is one of the widely studied metallurgical phenomena. It is a striking example of the complexity of spatiotemporal dynamics resulting from the collective behavior of dislocations. In uniaxial loading with constant imposed strain rate, the effect manifests itself as a series of repeated stress drops in the stress-time curve. The complexity of the PLC effect in Al-2.5%Mg

polycrystalline samples subjected to uniaxial tensile tests is quantified. Multiscale entropy analysis is carried out on the stress time series data observed during jerky flow to quantify the complexity of the distinct spatiotemporal dynamical regimes. It is shown that for the static type C band, the entropy is very low for all the scales compared to the hopping type B and the propagating type A bands. The results are interpreted considering the time and length scales relevant to the effect.

### 10:50 AM

**Using Eigenvalue and Information Theory Analysis to Predict Failure in Plastically Deformed Aluminum Sheet:** *Mark Stouder<sup>1</sup>; Joseph Hubbard<sup>1</sup>; <sup>1</sup>National Institute of Standards and Technology*

A recent study employed two approaches to characterize the apparent structure observed in strain localization maps constructed from surface topography data acquired from deformed aluminum sheet with scanning laser confocal microscopy. One used a conventional two-point autocorrelation analysis, and the other used information theory to analyze the eigenvalue spectrum associated with each strain map. While the results from the ACF analysis proved inconclusive, the information theory-based approach revealed two competing processes: one where the formation of structure is favorable and one where it is not. The crossover point can be regarded as a precursor to failure because once the dominant process shifts, the surfaces become metastable and the application of additional strain produces perturbations that trigger the failure event. The methodology for this approach and the potential impact on models used to predict limiting strains shall be presented and discussed.

### 11:10 AM Break

### 11:20 AM Invited

**Probabilistic Polycrystal Model for Twin Nucleation and Propagation in Zr and Mg:** *Carlos Tome<sup>1</sup>; Irene Beyerlein<sup>1</sup>; Laurent Capolungo<sup>1</sup>; <sup>1</sup>Los Alamos National Laboratory*

This work proposes a probabilistic approach for introducing twin nucleation and propagation effects in plastic deformation simulations of hcp metals. The elements of the model are based on a recent statistical study of twinning in pure Zr and pure Mg. This study provided insight on the correlation between twinning and: grain size, grain orientation, neighbor misorientation, and grain boundary length. A simulation algorithm for the model is proposed and implemented into the Visco-Plastic Self-Consistent (VPSC) polycrystal code. Simulation results for pure polycrystalline Zr and Mg deforming at 76 and 300 K, respectively, are compared to previous results using deterministic twin models and to experimental information about stress-strain response, texture evolution and twin fraction evolution.

### 11:50 AM

**Predicting and Validating the Stochastic Effects of Microstructure on Polycrystal Elasticity and Plasticity:** *Luke Brewer<sup>1</sup>; Corbett Battaile<sup>1</sup>; John Emery<sup>1</sup>; <sup>1</sup>Sandia National Laboratories*

The continuum mechanics necessary to describe the stress concentration and plastic deformation around bolt holes, voids, and crack tips is well developed. However, these continuum-based methods generally treat the material constitutive laws as deterministic functions. They do not include any way of representing the variability found in real materials microstructures; and therefore cannot predict the variability of the component response. We will discuss the early results of our efforts to represent material constitutive laws as probabilistic functions for use in component-level simulations. Brass produced at multiple grain sizes is being used as a model system for studying the change in microstructural variability and its effect on mechanical variability. The experimentally determined microstructures are converted into statistical representations from which many "statistically similar" microstructures can be generated and then are used to generate probabilistic property descriptions. For validation, a combination of in situ microscale experiments with simulations will be presented.

### 12:10 PM

**Modeling Stochastic Interaction between Fatigue Damage Evolution and Random Heterogeneities:** *Yibin Xue<sup>1</sup>; <sup>1</sup>Utah State University*

Cyclic small-crack growth may consume a large portion of fatigue life of certain components under certain cyclic loading conditions. Measurement of fatigue small-crack growth on the surface of smooth or notch specimens has evolved into a mature experimental technique. However, post data processing and

# Technical Program

model correlation for fatigue small-crack growth has not progressed in a parallel manner to the measurement technique. A new physics-based, mathematically precise fatigue small-crack growth modeling method is developed based on a multistage fatigue modeling scheme. The uncertainty in measurement errors and the effects of random variation of microstructural features on the small-crack growth were explored using Monte Carlo (MC) simulations. The stochastic interaction between microstructural features and the fatigue crack front is numerically explored. Fatigue damage incubation life is proven to be an essential quantity, both mathematically and physically. The proposed model is demonstrated using fatigue surface crack growth measurements of a two-phase Ti-alloy.

## Sustainable Materials Processing and Production: Sustainable Technologies II

*Sponsored by:* The Minerals, Metals and Materials Society, TMS Extraction and Processing Division, TMS Light Metals Division, TMS: Recycling and Environmental Technologies Committee, TMS: Education Committee

*Program Organizers:* Christina Meskers, Umicore; Randolph Kirchain, Massachusetts Institute of Technology; Diana A. Lados, Worcester Polytechnic Institute; Markus Reuter, Ausmelt Limited

Thursday AM                      Room: 2B  
February 18, 2010                Location: Washington State Convention Center

*Session Chairs:* Jeffrey S. Spangenberg, Argonne National Laboratory; Tim Skrzek, Magna Cosma Engineering

### 8:30 AM Introductory Comments

#### 8:35 AM

#### Lightweight Structural Concrete Incorporating Volcanic Materials for Sustainable Construction: *Khandaker Hossain*<sup>1</sup>; <sup>1</sup>Ryerson University

This paper presents the development of lightweight concrete (LWC) incorporating pumice aggregate and volcanic ash (VA) based ASTM Type I blended cement (PVAC). Fresh and mechanical properties of LWC mixtures such as slump, air content, compressive strength, tensile strength, density and modulus of elasticity are described. The durability characteristics are investigated by drying shrinkage (DS), water permeability, mercury intrusion porosimetry (MIP), differential scanning calorimetry (DSC) and microhardness tests. The investigation suggests the production of LWCs incorporating blended PVAC and VPA having satisfactory strength/durability characteristics for structural applications. The use of PVAC induces the beneficial effect of reducing drying shrinkage and water permeability as well as refinement of pore structures and better interfacial transition zone (ITZ). Development of such non-expensive and environmentally friendly LWCs with acceptable strength and durability characteristics is extremely helpful for sustainable development and rehabilitation of volcanic disaster areas around the world.

#### 9:00 AM

#### Mechanical and Chemical Development of Alkali Activated Slag Fine Aggregate Concrete by Design of Experiment (DOE): *Alexander Moseson*<sup>1</sup>; *Aaron Sakulich*<sup>1</sup>; *Dana Moseson*<sup>2</sup>; *Ken MacKenzie*<sup>3</sup>; *M Barsoum*<sup>1</sup>; <sup>1</sup>Drexel University; <sup>2</sup>Emerson Resources, Inc.; <sup>3</sup>Victoria University of Wellington

Alkali-activated cements (AACs) are an attractive alternative to ordinary portland cement as they have comparable performance and cost but little CO<sub>2</sub> emission. The development of a ground, granulated, blast furnace slag-cement activated by soda ash (sodium carbonate), with a fine, granular limestone aggregate to form a fine-aggregate concrete will be presented. Mixture DOE was utilized, with analysis of compressive strength, hydraulic properties, and quantitative chemical products (by Rietveld analysis,) yielding valuable models of the system. This allows, amongst other things, a better understanding of mixture-component interactions, and the ability to optimize the system. Models for system responses will be presented and correlated. Successful formulations are hydraulic and cure at room temperature, with strengths as high as 40.7 MPa at 3 days, 64.5 MPa at 28 days and costs as low as ~\$33 USD/tonne for materials.

#### 9:25 AM

#### Dissolution Behavior of Ru into the Na<sub>2</sub>O-SiO<sub>2</sub>-Al<sub>2</sub>O<sub>3</sub> Slag System: *Hiroshi Shuto*<sup>1</sup>; *Toru Okabe*<sup>1</sup>; *Kazuki Morita*<sup>1</sup>; <sup>1</sup>University of Tokyo

Evaluation of dissolution loss of platinum group metals (PGMs) into molten slags is important in their pyrometallurgical recovery process. However, few research have been done on their solubilities into slags. In this study, dissolution behavior of Ru, one of the PGMs, into the Na<sub>2</sub>O-SiO<sub>2</sub>-Al<sub>2</sub>O<sub>3</sub> slag system was investigated. About 1.5g of Na<sub>2</sub>O-SiO<sub>2</sub>-Al<sub>2</sub>O<sub>3</sub> slags and 3g of Ru pellet were placed in Al<sub>2</sub>O<sub>3</sub> crucible, and equilibrated at 1473±2 K in a resistance furnace for 18 hours. Partial pressure of O<sub>2</sub> was controlled to 10<sup>-4</sup>-10<sup>-2.5</sup> atm by flowing a gas mixture of O<sub>2</sub> and Ar. After equilibration, the slag was subjected to chemical analysis to determine the Ru content. The solubility of Ru increases with increasing P<sub>O<sub>2</sub></sub>, and there is a linear relationship between logP<sub>O<sub>2</sub></sub> and log(ppmw Ru), with a slope of about 0.61, suggesting that Ru dissolves into the slags by oxidation as divalent or trivalent.

#### 9:50 AM

#### New Process for Separation and Recovery of Platinum Group Metals: *Tsuyoshi Yukawa*<sup>1</sup>; *Kazuki Morita*<sup>1</sup>; *Toru Okabe*<sup>1</sup>; <sup>1</sup>The University of Tokyo

In order to develop an environmentally-sound materials recycling process, we investigated a new recycling process of platinum group metals (PGMs), particularly Rh, Ru, and Ir. The sustainable recycling process consist of a series of new pretreatment methods and a successive leaching step in aqueous solution without using any harmful oxidizing agent. During pretreatment, PGMs were reacted with Mg at 1193 K to obtain PGM-Mg alloys, which were then chlorinated using CuCl<sub>2</sub> or other chlorination agents in the temperature range of 673–873 K. Finally, the obtained samples were dissolved in aqueous solutions of HCl or NaCl, which are free from strong oxidizer. The experimental results showed that valuable PGMs could be recovered by using a combination of the proposed pretreatment method and subsequent dissolution in HCl or NaCl solution. Currently, studies are underway for developing an effective pretreatment-dissolution combination for the successful recovery of PGMs.

#### 10:15 AM Break

#### 10:25 AM

#### Reductive Leaching Behavior of Valuable Metals from Spent Li-Ion Polymer Battery Cathode Material: *Jingu Kang*<sup>1</sup>; *Jeong-soo Sohn*<sup>2</sup>; *Tae-hyun Kim*<sup>2</sup>; *Young-uk Kim*<sup>1</sup>; *Dong-hyo Yang*<sup>2</sup>; *Shun Myung Shin*<sup>2</sup>; <sup>1</sup>Korea University of Science and Technology (UST); <sup>2</sup>Korea Institute of Geoscience and Mineral Resources (KIGAM)

Commercial trend of cathode material for Li-ion batteries, LiCoO<sub>2</sub>, is changing because of a shortcoming such as high prices, specific capacity having expanded to limit, raw materials falling in short, and not so safe. This study describes the leaching behavior of cobalt, lithium, nickel, and manganese from new type of spent cathode materials of Li-ion polymer battery. For extracting valuable metals from the active material, feasibility studies for leaching test were investigated in different parameters such as concentration of H<sub>2</sub>SO<sub>4</sub>, use of reductive or not, temperature, time, and agitation speed. The composition of powder was 19.8% Co, 7.3% Li, 19.9% Ni, and 18.3% Mn, respectively. Under the best leaching conditions (2.0 mol dm<sup>-3</sup> H<sub>2</sub>SO<sub>4</sub>, 5vol% H<sub>2</sub>O<sub>2</sub>, 40°C, 100 g L<sup>-1</sup> pulp density, 30 min, and 200 rpm), the leaching efficiency of cobalt, lithium, nickel, and manganese was over 99.5%, respectively.

#### 10:50 AM

#### Materialization of Manganese by Selective Precipitation from Used Battery: *Shun Myung Shin*<sup>1</sup>; *Jin-gu Kang*<sup>2</sup>; *Young-Uk Kim*<sup>2</sup>; *Tae-Hyun Kim*<sup>1</sup>; *Soo-Kyung Kim*<sup>1</sup>; *Jeong-Soo Sohn*<sup>1</sup>; <sup>1</sup>Korea Institute of Geoscience & Mineral Resources (KIGAM); <sup>2</sup>Korea University of Science & Technology (UST)

MnO<sub>2</sub> preparation by chemical methods is investigated for possible applications on materialization of manganese from used batteries. A preparation procedure was tested: reductive leaching and precipitation-oxidation by NaClO (single step-CIO). Leaching behavior of valuable metals with sulfuric acid and hydrogen peroxide was investigated in order to interpret the behavior of impurities. For extracting zinc and manganese from the used battery without other impurities such as copper, aluminum, and iron, the leaching tests were carried out. Leaching amount of zinc and manganese were 39.9 g/L and 30.3 g/L, under the leaching conditions at 1.0 mol dm<sup>-3</sup> H<sub>2</sub>SO<sub>4</sub>, 3vol.% H<sub>2</sub>O<sub>2</sub>, 60°C, 100 g L<sup>-1</sup> pulp density, 1h, and 300 rpm. At the same time, the impurities in the leachate were Fe 0.5 ppm, Cu 2 ppm, and Al 1 ppm, respectively. As the result of XRD, we confirmed γ-MnO<sub>2</sub> peaks. The purity of γ-MnO<sub>2</sub> was 57.7% Mn, 0.01% Zn, respectively.



11:15 AM

**Leaching Studies for the Recovery of Metals from the Waste Printed Circuit Boards (PCBs):** *Manis Kumar Jha*<sup>1</sup>; Shivendra<sup>2</sup>; Vinay Kumar<sup>1</sup>; Banshi Dhar Pandey<sup>1</sup>; Rakesh Kumar<sup>1</sup>; Jae-chun Lee<sup>3</sup>; <sup>1</sup>National Metallurgical Laboratory (CSIR), India; <sup>2</sup>Indian Institute of Technology, Kanpur, India; <sup>3</sup>Korea Institute of Geosciences and Mineral Resources, South Korea

In view of recovery/ recycling of metals from PCBs, leaching studies were carried out from the PCBs containing Cu 17.05%, Ni 0.74%, Fe 1.74%, Pb 4.35% and Sn 8.32% using various acids like H<sub>2</sub>SO<sub>4</sub>, HCl and HNO<sub>3</sub>. Sulphuric acid was not found suitable leachant for the dissolution of metals from PCBs. However, hydrochloric acid selectively dissolved tin from the PCBs. The nitric acid was found to be effective lixiviant and 99.99% Cu, Fe, Ni and 36.66% Pb were leached out by 6M HNO<sub>3</sub> at S/L ratio 100 g/L, and 90°C. The kinetic studies carried out with 2M and 4M HNO<sub>3</sub> at 90°C showed “Ash diffusion control dense constant size-spherical particles” model. Similar kinetic model was observed with 6M acid concentration at 75°C. However, with an increase in temperature to 90°C, the kinetic model changed and was found to follow “Film diffusion control dense shrinking spheres”.

11:40 AM **Concluding Comments**

### The Vasek Vitek Honorary Symposium on Crystal Defects, Computational Materials Science and Applications: Grain Boundaries and Grain Boundary Engineering

*Sponsored by:* The Minerals, Metals and Materials Society, TMS Materials Processing and Manufacturing Division, TMS/ASM: Computational Materials Science and Engineering Committee  
*Program Organizers:* Mo Li, Georgia Institute of Tech; David Srolovitz, Institute for High Performance Computing, Agency for Science, Technology and Research, Singapore; Adrian Sutton, Imperial College London; Vaclav Paidar, Institute of Physics AS CR vvi; Jeff De Hosson, University of Groningen

Thursday AM Room: 604  
February 18, 2010 Location: Washington State Convention Center

*Session Chairs:* Kevin Hemker, Johns Hopkins University; Diana Farkas, Virginia Tech

8:30 AM **Invited**

**Modelling and Grain Boundary Engineering for High Performance Photovoltaic Polysilicon:** *Tadao Watanabe*<sup>1</sup>; Kota Kido<sup>2</sup>; Sadahiro Tsurekawa<sup>3</sup>; <sup>1</sup>Visiting Professor, Northeastern University, Shenyang, China, formerly Tohoku University (Sendai, Japan); <sup>2</sup>YKK Corp., Japan; <sup>3</sup>Kumamoto University

Modelling of polycrystalline silicon with desirable grain boundary microstructure has been performed to obtain useful information for future development of polysilicon solar cell with high performance photovoltaic and electric properties by grain boundary engineering, on the basis of our recent experimental studies of structure-dependent electrical properties of individual grain boundaries in polysilicon (e.g. K. Kido, S. Tsurekawa and T. Watanabe; Phil. Mag. Letters, 85 (2005), 41-49). Some recent attempts for Grain Boundary Engineering for high performance polysilicon by such as “unidirectional and rotational solidification processing” T. T. Watanabe, K. Kido and S. Tsurekawa; Mater. Sci. Forum, 558-559 (2007), 845-850) will be introduced, for future development of high performance solar cell polysilicon in the 21st century.

8:55 AM **Invited**

**Atomic Characterization of Grain Boundary Networks in Poly- and Nanocrystalline Materials and Its Application:** *Mo Li*<sup>1</sup>; Tao Xu<sup>1</sup>; <sup>1</sup>Georgia Institute of Technology

While single grain boundaries have been characterized and measured rather routinely for quite some time, following the pioneering work by Vitek, atomic characterization of grain boundary networks in poly- and nano-crystalline environment has been relatively unexplored to date. In this talk, we shall present a systematic method to build digital microstructures featured with the grain boundary networks of different characters. Contrasts to Gibbs' description of the mathematically abstract network, the grain boundary networks on atomic scale consist of topological entities with different dimensions and finite size.

With the method, we could measure the thickness and area of a grain boundary, the length and diameter of a triple junction, and the volume of a vertex point, and their statistical or ensemble averages. Finally, we will show how those entities function in mechanical deformation in nanocrystalline materials, which is a special type of polycrystalline materials.

9:20 AM

**The Role of Microstructure Scale and Morphology on Mechanical Behavior in FCC Metals:** *Remi Dingreville*<sup>1</sup>; Corbett Battaile<sup>2</sup>; Luke Brewer<sup>2</sup>; Elizabeth Holm<sup>2</sup>; <sup>1</sup>Polytechnic Institute of NYU; <sup>2</sup>Sandia National Laboratories

One of the underlying principles of materials science is that materials properties can be deduced from the knowledge of its microstructural features. In particular, the sizes, shapes, orientation, line defects and connectivity of internal attributes are often critical in a material's response. However, many current approaches to simulating mechanical response lack this ability to adequately address so many factors at once. In this presentation, we will address two key aspects of this problem. First, we will present a dislocation-based constitutive model for the deformation of FCC metals in which the effects of the microstructure and its associated length scales are captured by a non-local crystal plasticity formulation. Second we will assess the role of microstructure's morphology by examining and comparing various microstructures (idealized and digitized micrographs) both at the macroscopic scale and the microscopic scale. This survey assesses the fidelity and sensitivity of the numerical model to the microstructural representation.

9:35 AM

**Scale Invariance in Grain Misorientation Distribution:** *Claude Fressengeas*<sup>1</sup>; Benoit Beausir<sup>1</sup>; Nilesh Gurao<sup>2</sup>; Satyam Suwas<sup>2</sup>; Laszlo Toth<sup>1</sup>; <sup>1</sup>University Paul Verlaine - Metz; <sup>2</sup>Indian Institute of Science

Grain misorientation is studied in relation with nearest neighbor's mutual distance using electron back-scattered diffraction measurements. The Misorientation Correlation Function is defined as the probability density for the occurrence of a certain misorientation between pairs of grains separated by a certain distance. Scale-invariant spatial correlation between neighbor grains manifests itself by a power law dependence of the preferred misorientation vs. intergranular distance in various materials after diverse strain paths. The scaling exponent is in the range of  $-2 \pm 0.3$  for high angle grain boundaries. It decreases in the presence of low angle boundaries or dynamic recrystallization, indicating faster decay of correlations. The correlations vanish in annealed materials, or when random assignment of grain pairs is performed. The results are interpreted in terms of lattice incompatibility and continuity conditions at the interface between neighboring grains. Grain size effects on texture development and the implications of such spatial correlations on texture modeling are discussed.

9:50 AM **Break**

10:05 AM **Invited**

**Intermittency and Multiplication-Limited Flow in Microcrystal Deformation:** *Dennis Dimiduk*<sup>1</sup>; Ed Nadgorny<sup>2</sup>; Chris Woodward<sup>1</sup>; Michael Uchic<sup>1</sup>; Satish Rao<sup>3</sup>; Paul Shade<sup>4</sup>; <sup>1</sup>Air Force Research Laboratory; <sup>2</sup>Michigan Technological University; <sup>3</sup>UES, Inc.; <sup>4</sup>UTC, Inc.

Current research seeks methods for coarse graining the ensemble dislocation response, especially when mean-field models fail. The microcompression method for single-crystal materials is contributing to understanding dislocation processes at micrometer scales and below. This work examines attributes of microcrystal deformation including strengthening and intermittency, for Ni and Mo, and LiF in as grown and irradiated conditions. The work examines dislocation mechanisms and dynamic processes for experiments and simulations. The studies suggest common attributes and incomplete interpretations for the observed behavior. They also suggest that a better understanding of both ensemble dislocation behavior and selected atomistic and dislocation core behaviors, as they pertain to dislocation multiplication, are necessary to complete the mechanistic views. One conclusion from the work is that a quantitative understanding of the time-dependent response may not be possible via current microcompression experiments because of the mismatch between time scales for the dislocation response and those for experimental observation.

# Technical Program

## 10:30 AM Invited

### Grain Boundary Plane Engineering: Model Experiments: Pavel Lejcek<sup>1</sup>;

<sup>1</sup>Institute of Physics, AS CR

Recently, new concept of grain boundary plane engineering was proposed emphasizing the effect of the grain boundary plane orientation on the properties of polycrystalline materials (V. Randle, *Acta Mater.* 46 (1998) 1459). It is supposed that optimized polycrystalline material can also be produced by reorientation of the grain boundaries between existing grains during suitable annealing instead of forming completely new microstructure by recrystallization processes (P. Lejcek et al., *Acta Mater.* 51 (2003) 3951). In this contribution we show how the grain boundaries change their orientation from a high energy one to that possessing lower energy during thermal treatment of model samples: (i) bicrystals with free boundary; and (ii) tricrystals with one end of the boundary constrained at the triple junction.

## 10:55 AM

### Molecular Dynamics Simulations of Atomistic Mechanisms for Grain Boundary Migration in [001] Twist Boundaries: Xinan Yan<sup>1</sup>; Hao Zhang<sup>1</sup>;

<sup>1</sup>University of Alberta

Molecular dynamics simulations were performed to characterize atomic motions governing grain boundary migration in a series of twist boundaries. In particular, migrations of a S5, a S13 and a  $\theta=40.23^\circ$  general high angle [001] twist boundaries driven by stored elastic energy in an fcc Ni were investigated. The simulation results showed although four-atom shuffling motions were the predominant atomic motions in S5 twist boundary, they are intrinsic type of atomic motions and the correlation between individual four-atom shuffles are rather random than cascaded, as suggested by previous reports. Moreover, besides the four-atom shuffle, a more generalized cooperative string-like atomic motions was identified in all type of twist boundaries. Such a string-like motions tended to become stronger and more random as grain boundary losing its local symmetry. In addition, the activation energy for grain boundary migration is surprisingly well correlated with the average string length found in these boundaries.

## 11:10 AM

### Ab Initio Investigation of Grain Boundary Cohesion in Al Alloys: Shengjun Zhang<sup>1</sup>; Oleg Kontsevoi<sup>1</sup>; Arthur Freeman<sup>1</sup>; Gregory Olson<sup>1</sup>;

<sup>1</sup>Northwestern University

The embrittling and cohesion-enhancing effects of impurities on a  $\Sigma$  5(012)[100] aluminum grain boundary are investigated by means of the full-potential linearized augmented plane-wave (FLAPW) method with the generalized-gradient approximation (GGA) formula within the framework of the Rice-Wang thermodynamic model. Analysis of the atomic and electronic structures identifies the roles of atomic size and the bonding behavior of the impurity with the surrounding Al atoms. The results show that He, H and Na are strong embrittlers, Zn is a weak embrittler, while Sc, B, Cu and Mg are cohesion enhancers. This work provides a fundamental electronic basis for stress corrosion behavior in Al alloys and provides quantitative parameters for the design of high strength Al alloys. Work supported by the AFOSR (grant No. FA 9550-07-1-0174) and the Ford-Boeing Nanotechnology Alliance at Northwestern.

## 11:25 AM

### Role of Grain Boundary Character Distribution on Dynamic Recrystallization Using Monte Carlo Simulations: Jared Stein<sup>1</sup>; Megan Frary<sup>1</sup>;

<sup>1</sup>Boise State University

Monte Carlo simulations are commonly applied to study microstructural evolution, including abnormal grain growth and recrystallization. Here, Monte Carlo simulations are used to study the effects of grain boundary character distribution on dynamic recrystallization. The initial stored energy is uniformly distributed and a constant strain rate is achieved by incremental increases in stored energy. The simulation tracks the grain size, special boundary fraction, and recrystallization fraction. Recrystallization rates vary with initial special boundary fraction and are compared to kinetic models. Similar to experimental results, a high percentage of grains that nucleate early in the simulation have special-boundary relationships with surrounding grains. As the simulation progresses, the orientation of nuclei becomes nearly random compared to surrounding grains. The simulations also predicted that the final special boundary fraction can be controlled by varying the strain rate. Once correlated

with experimental results, the simulation can be used to investigate and refine hot-deformation processes.

## 11:40 AM

### Development of a Microstructure Sensitive Model Which Shows Dislocation Patterning: Alankar Alankar<sup>1</sup>; Ioannis Mastorakos<sup>1</sup>; David Field<sup>1</sup>;

<sup>1</sup>Washington State University

A dislocation density based crystal plasticity finite element model (CPFEM) is developed for aluminum which tracks dislocation densities on all octahedral slip systems. Based upon the kinematics of crystal deformation and dislocation interaction laws, dislocation generation and annihilation laws are modeled. It is shown that due to local deformation conditions e.g. deformation gradient, strain, and strain rate and orientation of each crystallite in a polycrystal, dislocation densities evolve heterogeneously. Description of dislocation densities is presented in form of pole figures along with evolution of crystallographic texture in idealized plane strain condition. Cross-slip of dislocations is modeled as a probabilistic event. The CPFEM model is calibrated for single slip and multi-slip deformation of pure aluminum using experimental stress-strain curves of pure aluminum single crystal from literature. Dislocation densities evolve as state variables in the model, leading to spatially inhomogeneous dislocation densities that show patterning in the dislocation structures.

## 11:55 AM

### Dislocation Dynamics Simulations of Slip System Interactions and Dislocation Boundary Formation: Benoit Devincere<sup>1</sup>; Grethe Winther<sup>2</sup>;

<sup>1</sup>CNRS-ONERA; <sup>2</sup>Risø National Laboratory

Analysis of fcc single crystal and polycrystal microstructures deformed in tension and rolling has established the combination of active slip systems and their interactions as the main factor controlling the crystallographic directionality of the dislocation boundaries. Five different classes of slip system interactions have been shown to give rise to different types of dislocation boundaries. As a first study, the case of duplex collinear slip is selected to investigate, by DD simulations, the fundamental dislocation mechanisms that control the formation and the stability of planar dislocation boundaries. For this case good agreement is found between the DD simulations of elementary dislocation-dislocation interactions and the experimentally observed dislocation boundary planes in grains/crystals with different crystallographic orientations and slip system activity. The results are promising for more general studies.

## 12:10 PM

### On the Role of Dislocations during the Martensitic Transformation in NiTi Shape Memory Alloys: Gunther Eggeler<sup>1</sup>; Antonin Dlouhy<sup>2</sup>;

<sup>1</sup>Ruhr University Bochum; <sup>2</sup>IPM Brno

NiTi shape memory alloys have fascinating properties. These rely on the martensitic transformation, a diffusionless phase transformation between a high temperature (B2) and a low temperature phase (B19'). Shape memory researchers have always been more interested in crystallography, in martensite variants and in phase transition temperatures than in dislocations. But dislocations are important in three respects. They are created during thermo mechanical processing of NiTi shape memory alloys to adjust certain properties (like tube or wire drawing followed by annealing). They are introduced when a SMA is trained for the two way effect. And they play a role during the martensitic transformation itself where they accommodated internal stresses (lattice invariant accommodation). The present contribution to the Vasek Vitek Honorary Symposium gives an overview on the different areas of overlap between dislocation plasticity and martensitic transformations. It then concentrates on how dislocations multiply during the martensitic transformation in NiTi alloys. And it finally outlines what effect dislocations have on the functional fatigue properties of shape memory alloys. Areas in need of further work are highlighted.

## 12:25 PM

### Disclinations and Deformation of Hierarchically Twinned Martensite: Peter Mullner<sup>1</sup>; Alexander King<sup>2</sup>;

<sup>1</sup>Boise State University; <sup>2</sup>Ames Laboratory

Shape-memory alloys deform via the reorganization of a hierarchically twinned microstructure. Twin boundaries themselves present obstacles for twin boundary motion. In spite of a high density of obstacles, twinning stresses of Ni-Mn-Ga Heusler alloys are very low. Neither atomistic nor dislocation based models account for such low yield stresses. Twinning mechanisms are studied here on a mesoscopic length scale making use of the disclination theory. In a first approach, a strictly periodic twin pattern containing periodic disclination walls with optimally screened stress fields is considered. Strict periodicity implies



that the twin microstructure reorganizes homogeneously. In a second approach, a discontinuity of the density of secondary twins is introduced and modeled as a disclination dipole. The stress required for nucleation of this discontinuity is larger than the stress required for homogeneous reorganization. However, once the dipole is formed, it can move under a much smaller stress in agreement with experimental findings.

### 12:40 PM

**Mesoscale Polycrystal Calculations of Damage Histories in Shock Loaded Metals:** John Bingert<sup>1</sup>; *Davis Tonks*<sup>1</sup>; Veronica Livescu<sup>1</sup>; Curt Bronkhorst<sup>1</sup>; <sup>1</sup>Los Alamos National Lab

Dynamic damage evolution in metals is determined by both the stress loading history and the material microstructure. Important microstructural actors are the crystal grain boundary and twinning networks that directly promote void nucleation and deformation localizations that lead to void nucleation. The role of these networks in shock damage processes will be studied through polycrystal plasticity finite element calculations based on mesoscale microstructure from recovered samples. Results from copper and, possibly, tantalum samples will be addressed. The experimental loading will be the gas gun. The emphasis will be to understand the cause and effect in the damage evolution by supplying the calculated stress and strain histories, which are not measured in experiment. Correlations between void nucleation positions and microstructure will be sought.

### The Vasek Vitek Honorary Symposium on Crystal Defects, Computational Materials Science and Applications: Grain Boundaries, Dislocations and Mesoscopic Modeling

*Sponsored by:* The Minerals, Metals and Materials Society, TMS Materials Processing and Manufacturing Division, TMS/ASM; Computational Materials Science and Engineering Committee  
*Program Organizers:* Mo Li, Georgia Institute of Tech; David Srolovitz, Institute for High Performance Computing, Agency for Science, Technology and Research, Singapore; Adrian Sutton, Imperial College London; Vaclav Paidar, Institute of Physics AS CR vvi; Jeff De Hosson, University of Groningen

Thursday AM Room: 603  
February 18, 2010 Location: Washington State Convention Center

*Session Chairs:* Tadao Watanabe, Visiting Professor, Northeastern University, Shenyang, China, formerly Tohoku University (Sendai, Japan); John Bassani, University of Pennsylvania

### 8:30 AM Invited

**Shear Stresses, Dislocations and Grain Boundaries:** *Kevin Hemker*<sup>1</sup>; <sup>1</sup>Johns Hopkins University

It is well known that shear stresses couple with dislocations and move them. It is also widely accepted that shear stresses can couple to low-angle tilt boundaries and move them. By contrast, high-angle grain boundaries are generally considered to be obstacles to dislocation motion. This talk will start with the effect of dislocation core geometry and non-Schmid stresses on the mobility of dislocations in intermetallic alloys, topics of which Professor Vitek has taught us much. Experiments on nanocrystalline thin films will then be used to highlight the fact that dislocation activity is fundamentally different in nanocrystalline metals and that shear stress-coupled grain boundary migration is manifest in room temperature grain growth and enhanced plasticity.

### 8:55 AM Invited

**The Effect of Segregated Sp-Impurities on Grain-Boundary Embrittlement in Nickel:** *Monika Vsianska*<sup>1</sup>; *Mojmir Sob*<sup>1</sup>; <sup>1</sup>Masaryk University, Faculty of Science

We have studied segregation and embrittling potency of sp-elements in the 3rd, 4th and 5th period (Al, Si, P, S, Ga, Ge, As, Se, In, Sn, Sb and Te) at the S5(210) grain boundary (GB) in fcc nickel and the segregation of these impurities at the (210) free surface (FS). Full relaxation of the geometric configuration of the GB and FS without and with impurities has been performed and the effect of impurities on the distribution of magnetic moments has been analysed. We determined the embrittling potency energy from the difference

between the GB and FS binding energies on the basis of the Rice-Wang model; here a positive/negative value of this quantity means that the solute atom has the embrittling/strengthening effect on the GB. It turns out that all substitutionally segregated impurities studied are GB embrittlors in Ni.

### 9:20 AM

**Multi-Time Scale Modeling of the Annealing of Radiation-Induced Defects at Tilt Grain Boundaries:** *Xian-Ming Bai*<sup>1</sup>; *Arthur Voter*<sup>1</sup>; *Richard Hoagland*<sup>1</sup>; *Michael Nastasi*<sup>1</sup>; *Blas Uberuaga*<sup>1</sup>; <sup>1</sup>Los Alamos National Laboratory

We have used Molecular Dynamics (MD) and Temperature Accelerated Dynamics (TAD) simulations to investigate the annealing of radiation-induced damage near symmetric tilt grain boundaries (GBs) in copper over different time scales. The short-time (picoseconds) defect production stage is modeled by MD, and the resulting damaged structures are used as the input for long-time defect annealing studies in TAD simulations. Our simulations show that the defect annealing behavior in grain boundaries is quite different from that in single bulk crystals. The presence of the grain boundary affects the defect diffusion barriers significantly. The interaction between the grain boundaries and point defects results in new vacancy annealing mechanisms that help anneal the radiation-induced defects, significantly increasing the radiation tolerance of the material.

### 9:35 AM

**Mesoscale Modeling of Particle Strengthened Interfaces:** *Seth Wilson*<sup>1</sup>; *A.D. Rollett*<sup>1</sup>; <sup>1</sup>Carnegie Mellon University

Particle pinning remains the most practical way of controlling grain size and structure in materials. It is also critical to the phenomenon of abnormal grain growth (AGG), which is both a desirable process for certain production processes and an unwanted coarsening in other cases. In many materials, AGG is strongly correlated with temperatures near the solvus, when particles are dissolving. Computational modeling of this phenomenon must accurately reproduce particle-boundary, boundary-solute, and particle-solute couplings, as well as multi-junction constraints and topological transformations, at mesoscopic length scales in 3D, in a single simulation framework. To address this challenge, this work considers a novel modification of the level set method. A description of this modification and simulations demonstrating its versatility will be presented, including an exploration of boundary-particle interaction in the small-particle limit.

### 9:50 AM Break

### 10:10 AM Invited

**Effect of Pre-Melting on Grain Boundary Properties:** *T. Frolov*<sup>1</sup>; *Y. Mishin*<sup>1</sup>; *J. W. Cahn*<sup>2</sup>; <sup>1</sup>George Mason University; <sup>2</sup>National Institute of Standards and Technology

Pre-melting of grain boundaries can affect high-temperature behavior of materials. GB diffusion rates and response of GBs to applied shear stresses are examples of properties that can be strongly affected by GB pre-melting. We apply molecular dynamics simulations to show that these properties can also be used as sensitive probes of the pre-melted state of GBs. The self-diffusion coefficients of GBs and their triple junctions rapidly increase and approach the diffusivity of the bulk liquid phase as GBs develop liquid layers near the bulk melting point. In the same temperature range, the resistance of GBs to sliding rapidly drops to nearly zero, signifying the formation of a liquid layer.

### 10:35 AM Invited

**Molecular Dynamics and Phase-Field-Crystal Studies of Grain Boundary Premelting in bcc Fe and fcc Ni:** *David Olmsted*<sup>1</sup>; *Dorel Buta*<sup>2</sup>; *Ari Adland*<sup>1</sup>; *Mark Asta*<sup>2</sup>; *Alain Karma*<sup>1</sup>; *Stephen Foiles*<sup>3</sup>; <sup>1</sup>Northeastern University; <sup>2</sup>University of California, Davis; <sup>3</sup>Sandia National Laboratories

The premelting of grain boundaries is metallurgically important because of its effects on solidification and on high temperature processing. We have used molecular dynamics (MD) with embedded-atom potentials and the phase field crystal method (PFC) to study the premelting of  $\langle 0 0 1 \rangle$  symmetric tilt boundaries in bcc Fe and fcc Ni. The critical misorientation angles for premelting in the two materials have been bracketed within four degrees for boundaries in MD on both ends of the misorientation range (boundary planes nearer to  $\{1 0 0\}$  and those nearer to  $\{1 1 0\}$ ). A structural transition, distinct from premelting, is observed, both in MD and in PFC, in several of the boundaries, with the transition temperature depending sensitively on misorientation.

# Technical Program

**11:00 AM Invited**

## **Lattice Geometry Effects on Ideal Shear Resistance and Dislocation**

**Mobility:** *Vasily Bulatov*<sup>1</sup>; *Keonwook Kang*<sup>2</sup>; *Wei Cai*<sup>2</sup>; <sup>1</sup>Lawrence Livermore National Laboratory; <sup>2</sup>Stanford University

Over its 75 years dislocation theory has repeatedly appealed to lattice geometry considerations, most notably to Frenkel's equation for the ideal shear resistance and to Vitek's concept of gamma surfaces. These two concepts inspired our recent attempts to relate dislocation mobility and crystal strength to the geometry of host crystal lattice. Based on a large number of accurate atomistic calculations we present two important observations: (1) that the common interpretation of Frenkel's equation relating shear resistance to the inter-planar spacing is incorrect and (2) that lattice resistance to dislocation motion is a discontinuous function of dislocation orientation. Analysis of atomistic calculations data for FCC and BCC model materials reveals that lattice geometry does indeed define both the ideal shear resistance and the line orientation dependence of dislocation mobility, but in ways that contradict the understanding prevailing in the literature. Finally, we describe implications of our findings for crystal shear strength.

**11:25 AM**

## **Applications of $\gamma$ -Surfaces in Phase Field Modelling of Dislocations in Ni-Base Superalloys:**

*Vassili Vorontsov*<sup>1</sup>; *Roman Voskoboinikov*<sup>1</sup>; *Catherine Rae*<sup>1</sup>; <sup>1</sup>University of Cambridge

The "Phase-Field Microelasticity Theory" was used to simulate shearing of  $L_2$  ordered  $\gamma'$  phase precipitates by  $a/2\langle 110 \rangle$  and  $a\langle 112 \rangle$  dislocations. Incorporation of  $\gamma$ -surface data from atomistic simulations into the energy functional allows many complex core structures to be simulated on continuum scale. In addition to the conventional single-plane  $\gamma$ -surface, the concept of a two-plane "effective  $\gamma$ -surface" is introduced into the phase field model. This opens new dissociation pathways for the dislocations, which enables modelling of extrinsic stacking faults that form at elevated temperatures in superalloys. The model successfully demonstrates sensitivity of precipitate shearing mechanisms to variations in stress, precipitate geometry and dislocation character. Further potential applications of the model include its use as a tool, in conjunction with TEM, for measuring stacking fault and APB energies of complex alloy systems. Dislocation mobility during shear can be semi-quantitatively related to  $\gamma$ -surface topography, and input into creep models.

**11:40 AM**

## **Phase Field Modeling of Deformation Mechanisms in Ni-Base Superalloys:**

*Ning Zhou*<sup>1</sup>; *Chen Shen*<sup>2</sup>; *Libor Kovarik*<sup>1</sup>; *Raymond Unocic*<sup>1</sup>; *Michael Mills*<sup>1</sup>; *Yunzhi Wang*<sup>1</sup>; <sup>1</sup>The Ohio State University; <sup>2</sup>GE global

Plastic deformation in superalloys at service temperatures is often controlled by mechano-chemically or displacive-diffusionally coupled mechanisms of dislocation-precipitate interactions. For instance, chemical reordering may couple strongly to dislocation shearing of gamma prime precipitates and govern the rate of deformation. On the other hand, dislocation plasticity can also change the precipitate microstructure in so-called directional coarsening or rafting process. In this presentation, recent efforts in developing modeling approaches by integrating ab initio information such as the generalized stacking fault (GSF) energy with continuum phase field approaches, motivated and focused by experimental characterization, will be discussed. Examples will be presented to demonstrate the quantitative aspects of the microscopic phase field model in predicting critical stress for dislocation dissociation and superlattice extrinsic stacking fault (SESF) shearing of gamma prime precipitates, tension-compression asymmetry, and the effect of re-ordering kinetics on the rate of deformation. The work is supported by AFOSR under MAI program.

**11:55 AM**

## **Phase Field Simulations of Brittle Fracture in Composites with Spatially Varying Elastic Moduli:**

*Rajeev Ahluwalia*<sup>1</sup>; *Weili Cheah*<sup>2</sup>; <sup>1</sup>Institute of High Performance Computing; <sup>2</sup>Institute of Materials Research and Engineering

We perform phase field simulations of fracture in materials that are composites of a hard brittle component and a soft, less brittle component. The motivation of this study is to understand the fracture mechanisms in materials such as bone which are composites of a brittle mineral phase and a soft organic phase. We model this system by a material that has a spatially varying elastic moduli such that one component is hard and brittle where as the other component is soft and relatively less brittle. A phase field model is used to study crack propagation in such materials. It is demonstrated that a crack that initiates from a notch

in the brittle phase stops on reaching the interface between the brittle and the soft phase. On increasing the strain, the crack propagates into the soft phase by branching. These results shed light on the toughening mechanisms in such composite materials.

**12:10 PM**

## **Phase Field Simulations of Elastic Deformation Driven Grain Boundary Migration in Copper:**

*Michael Tonks*<sup>1</sup>; *Paul Millett*<sup>1</sup>; *Dieter Wolf*<sup>1</sup>; <sup>1</sup>Idaho National Laboratory

Deformation can have a large influence on grain boundary migration, altering both the grain growth kinetics and the evolving grain structure. In this work, a phase field grain growth simulation is coupled with a linear elastic stress calculation to model deformation driven grain growth in copper. The model is verified by comparing the predicted behavior to atomic scale simulation results in bicrystals and analytical grain boundary migration expressions. Our simulations indicate that grains oriented such that they have a higher elastic stiffness in the load direction tend to have less stored elastic energy, and therefore tend to grow. The applied load does not change the exponent at which the average grain area grows, but it does alter the steady state grain size distribution and the final orientation distribution.

---

## **Thermo-Mechanical Response of Molecular Solids: Multi-Resolution Theory, Simulations, and Experiments: Molecular Solids II**

*Sponsored by:* The Minerals, Metals and Materials Society, TMS Electronic, Magnetic, and Photonic Materials Division

*Program Organizers:* *Alejandro Strachan*, Purdue University; *Thomas Sewell*, University of Missouri-Columbia; *Rodolfo Pinal*, Purdue University; *Chunyu Li*, Purdue University

Thursday AM

Room: 203

February 18, 2010

Location: Washington State Convention Center

*Session Chairs:* *Alejandro Strachan*, Purdue University; *Chunyu Li*, Purdue University

---

**8:30 AM Introductory Comments**

**8:35 AM Invited**

## **Fundamental Processes in a Prototypical Organic Material: Nitromethane:**

*Donald Thompson*<sup>1</sup>; <sup>1</sup>University of Missouri-Columbia

Molecular organic crystals and liquids are ubiquitous, with usage ranging from drugs to energetic materials. Our understanding of chemical reactions in solids remains rudimentary at best. The main reason for this is that it is not possible to experimentally monitor events within a solid. Nevertheless, progress is being made, thanks in large part to theoretical modeling. Accurate modeling of chemistry requires a good understanding of the underlying fundamental physical processes. We have focused on a prototypical solid with the idea that a thorough understanding of it will help guide studies of more complex solids. We chose nitromethane because of its relatively small size yet complex molecular and crystalline behaviors. We have developed a force field that accurately predicts the structural and thermodynamic properties. We have most recently investigated post-shock behavior, including energy redistribution, in crystalline nitromethane. These and other recent results will be discussed.

**9:05 AM**

## **Elastic Deformation Mechanics of Cellulose Nanocrystals:**

*Xiawa Wu*<sup>1</sup>; *Ryan Wagner*<sup>1</sup>; *Arvind Raman*<sup>1</sup>; *Robert Moon*<sup>2</sup>; *Ashlie Martini*<sup>1</sup>; <sup>1</sup>Purdue University; <sup>2</sup>US Forest Service/ Purdue University

Cellulose nanocrystals (CNC) have great potential for polymer nanocomposite materials. However, a fundamental understanding of the CNC properties and their role in composite property enhancement is not currently available. To address this issue, we are developing atomic force microscopy (AFM) protocols combined with molecular dynamics (MD) and continuum modeling techniques that enable characterization of individual CNCs. AFM can be used to measure topography, pull-off force, stiffness and bending of CNCs, which are then related using the models to physical, chemical, mechanical and deformation properties, respectively. This paper outlines the development of a fully atomistic model of an individual CNC and its validation by comparison of predicted geometric,

energetic, and elastic properties of the material to previous modeling results and experimental measurements.

**9:25 AM**

**Break Down Assessment and Modeling of the Enthalpic Relaxation of Aging Glasses through a Combination of Experiment and Simulation:** Chen Mao<sup>1</sup>; Sai Prasanth Chamarthy<sup>2</sup>; *Rodolfo Pinal*<sup>3</sup>; <sup>1</sup>Xenoport, Inc.; <sup>2</sup>Schering-Plough Research Institute; <sup>3</sup>Purdue University

The calorimetric glass transition encodes a wealth of information about the nature and structural behavior of organic molecular glasses. We present a DSC based investigation on the evolution of the thermal properties of glasses as a function of annealing time. A combination of experimental measurements and theoretical simulations produces a level of detail and accuracy not achievable by either method alone. The approach quantitatively discriminates between the effects of the glass forming properties of the material and the thermal history of the sample, including potential artifacts inherent to the choice of experimental method. Based on this approach, we propose an unambiguous definition of the time scale of the experiment, an important parameter that has remained vaguely defined at best. Using salicin as model compound, we investigate the effect of annealing time and experimental conditions on the evolution of the calorimetric glass transition.

**9:45 AM**

**Transforming Powder Processibility by Particle Surface Engineering:** *Calvin Sun*<sup>1</sup>; <sup>1</sup>University of Minnesota

The manufacturing of pharmaceutical dosage forms is frequently challenged with deficiencies in physico-mechanical properties of constituting molecular solids. There is a pressing need to replace the empirical formulation and process development with scientifically rigorous design and engineering based on a thorough understanding of relevant material properties and processes, a practice frequently termed as quality-by-design (QbD). We will discuss potentials of the QbD approach in overcoming two common problems in powder processing, i.e., flow and compaction. First, we will show that poor flow properties of fine organic powders can be significantly improved by coating with nano-sized material, which serves as both spacers to reduce powder cohesion and ball bearings to reduce friction. We will then show that polymer coating can profoundly improve compaction properties of fine sand. Fine sand coated with polyvinylpyrrolidone (PVP) exhibits excellent tableting performance because of the formation of a three-dimensional bonding network of PVP upon compaction.

**10:05 AM Break**

**10:25 AM**

**Multiscale Coarse-Grain Modeling of Nitromethane and RDX:** *Sergei Izvekov*<sup>1</sup>; Peter Chung<sup>1</sup>; Betsy Rice<sup>1</sup>; <sup>1</sup>U.S. Army Research Laboratory

A recently developed multiscale coarse-graining (MS-CG) method [Izvekov and Voth, *J. Chem. Phys.* 123, 134105 (2005); Noid et al., *J. Chem. Phys.* 128, 244114 (2008)] for obtaining short-ranged coarse-grain (CG) potentials from atomistic level interactions was applied to two conventional energetic materials, nitromethane and cyclotrimethylenetrinitramine (RDX). For nitromethane one-bead and two-bead models fitted to liquid phase simulations at ambient conditions were developed. For RDX, one-bead and four-bead models were derived from crystal and liquid phase simulations to improve transferability of the model across different phases. Performance of resulting models in a simulation of crystal and liquid phases in a broad range of thermodynamic conditions was evaluated against underlying atomistic simulations and experiment. CG models performed reasonably well in a reproduction of various bulk structural and thermodynamic properties, including radial distribution functions, thermal expansion properties, bulk modulus.

**10:45 AM**

**RDX Material Properties Containing Defects:** *Lynn Munday*<sup>1</sup>; Peter W. Chung<sup>1</sup>; Betsy Rice<sup>1</sup>; Santiago Solaris<sup>2</sup>; <sup>1</sup>U.S. Army Research Laboratory; <sup>2</sup>University of Maryland

Orientation-dependent material properties of RDX crystals containing defects are explored using molecular dynamics with Smith's (1999) flexible molecular potential. Defects in energetic materials are of interest due to their role in triggering chemical decomposition of molecules through the development of hot spots. The RDX crystal is known to be approximately orthotropic and this work will explore the effect of crystal defects on these orthotropic material properties.

General types of defects in RDX are known experimentally and from some predictions in literature. We specifically calculate the defect core structures for single dislocations and limited studies with two sessile dislocations to show the substantial effect of the defect orientation on the melting temperature and shock Hugoniot curve.

**11:05 AM Invited**

**Unraveling Shock-Induced Chemistry Using Ultrafast Lasers:** *David Moore*<sup>1</sup>; <sup>1</sup>Los Alamos National Laboratory

The exquisite time synchronicity between shock and diagnostics needed to unravel chemical events occurring in picoseconds has been achieved using a shaped ultrafast laser pulse to both drive the shocks and interrogate the sample via a multiplicity of optical diagnostics. The shaped laser drive pulse can produce well-controlled shock states of sub-ns duration with sub-10 ps risetimes, sufficient for investigation of fast reactions or phase transformations in a thin layer with picosecond time resolution. The shock state is characterized using ultrafast dynamic ellipsometry (UDE) in either planar or Gaussian spatial geometries, the latter allowing measurements of the equation of state of materials at a range of stresses in a single laser pulse. Time-resolved processes in materials are being interrogated using UDE, ultrafast infrared absorption, ultrafast UV/visible absorption, and femtosecond stimulated Raman spectroscopy. Recent results will be presented, and future trends outlined.

**11:35 AM Invited**

**Engineering of the Thermo-Mechanical Response of Molecular Crystals by Solid Solution Impurity Control:** *Daniel Hooks*<sup>1</sup>; <sup>1</sup>Los Alamos National Laboratory

Crystalline molecular solids are widely used as pharmaceutical ingredients, dyes, foods, optical elements, electronic materials, and explosives. In many classes of materials (e.g. metals) knowledge of phase behavior and structure-property relations of multi-component systems are used to enormous advantage in engineering materials for specific uses. This is not generally the case for molecular materials because structure-property knowledge is sparse for single component systems and almost entirely absent for more complex multi-component systems. The interactions that direct intermolecular assembly are so subtle that interpretation of structure-property relations are founded on hindsight rationalization in all but a few cases. We have recently prepared molecular crystals with engineered solid solution behavior. The resulting materials have different phase behavior and mechanical response. Material preparation and property characterization, including resulting phase diagrams and elastic-plastic response will be discussed. Plans to include engineering of more complex multi-component crystal systems will also be described.

# Technical Program

## General Poster Session

Sponsored by: The Minerals, Metals and Materials Society, TMS Electronic, Magnetic, and Photonic Materials Division, TMS Extraction and Processing Division, TMS Light Metals Division, TMS Materials Processing and Manufacturing Division, TMS Structural Materials Division

Program Organizer: Mark Palmer, Kettering University

Mon-Wed PM Room: Exhibit Hall  
February 15-17, 2010 Location: Washington State Convention Center

### 3D Interconnected Calcium Phosphate Scaffolds for Bone-Tissue Engineering: *Mohammad Tarafder*<sup>1</sup>; *Shashwat Banerjee*<sup>1</sup>; *Vamsi Balla*<sup>1</sup>; *Amit Bandyopadhyay*<sup>1</sup>; *Susmita Bose*<sup>1</sup>; <sup>1</sup>Washington State University

Calcium phosphates (CaP) are widely used in bone tissue engineering due to their compositional similarity with human bone and excellent bioactivity. The objective of the present study is to investigate mechanical and biological properties of calcium phosphate based 3D interconnected biodegradable porous scaffold using 3-D ceramic printing technology, one of the solid free-form fabrication (SFF) methods. SFF method allows to fabricate structures with controlled geometry and architecture. It's a layer by layer manufacturing process in which a 3D ceramic scaffold is printed by printing a chemical binder onto powdered calcium phosphates. 3D interconnected porous scaffolds with pre-set dimension and pore size have been successfully made using 550 nm  $\beta$ -tricalcium phosphates. Suitable temperature and layer heights have been optimized. Over 87% sintered density was obtained after sintering the scaffold at 1250°C. Different dopants were also added to investigate their effects on the mechanical and biological properties of these scaffolds.

### A Materials Investigation of the UV Degradation of Eco-Friendly, Polypropylene Polymer Composites with Kenaf Fibers: *Christine Carpenter*<sup>1</sup>; *Katherine Chen*<sup>1</sup>; *Christina Blattner*<sup>1</sup>; *Katie Greenstein*<sup>1</sup>; *Robert Arens*<sup>1</sup>; *Edmund Saliklis*<sup>1</sup>; <sup>1</sup>Cal Poly State University

Eco-friendly composites of recycled polymers and agricultural waste fibers have been developed for commercial markets, and are currently being pursued as thin shell, curvilinear architectural structures and emergency shelters. However, better understanding of the mechanical properties and the degradation mechanisms are imperative for the development of these materials. This study concentrates on polypropylene (PP) homopolymer and co-polymer composites with kenaf fibers. The effect of accelerated weathering was conducted with ultraviolet (UV) radiation (300-350 nm) and humidity to simulate outdoor conditions. Up to 2000 hours of exposure was conducted, and samples were characterized at every 500 hour interval. Tensile tests and four-point bend tests were conducted, and the stiffness of the composites was found to decrease over time, but the homopolymer and copolymer composites had different behaviors. Fourier-Transformed Infrared Spectroscopy (FTIR) revealed that the fibers break down and the cellulose-polypropylene bond weakens as a result of irradiation and moisture cycling.

### A Molecular Dynamics Study of the Tensile Deformation Behavior of Au Nanowires: *Na-Young Park*<sup>1</sup>; *Ho-Seok Nam*<sup>1</sup>; *Pil-Ryung Cha*<sup>1</sup>; *Seung-Cheol Lee*<sup>2</sup>; <sup>1</sup>Kookmin University; <sup>2</sup>Korea Institute of Science and Technology (KIST)

We performed molecular dynamics simulations for the tensile deformation behavior of Au nanowires. Au nanowires have FCC rhombic structures with a  $\langle 110 \rangle$ -crystallographic orientation and with four  $\{111\}$  lateral surfaces. In order to investigate the effect of nanowire dimension and different empirical potentials on the deformation behavior, nanowires with the widths ranging from 4nm to 20nm were considered and three different empirical embedded atom method potentials were considered. All nanowires showed the plastic deformation by twin formation and the migration of twin boundaries which induces the formation of  $\langle 100 \rangle$ -oriented grain along tensile direction and its growth. The yield stress was observed to increase with decreasing nanowire dimension and the change of deformation mechanism was observed between 4nm and 10nm widths. The deformation behavior of nanowires also shows strong dependence on the empirical potentials, which will be also presented in this study.

### A Study of the High Rate Response of Squeeze Cast Magnesium Alloy AZ91: *Phil Gullett*<sup>1</sup>; *Wilburn Whittington*<sup>1</sup>; *Michael Fortier*<sup>2</sup>; <sup>1</sup>Mississippi State University; <sup>2</sup>University of Rochester

The uniaxial compressive response of squeeze cast magnesium alloy AZ91 has been measured for material with different cross-section thicknesses. Samples have been tested at strain rates varying from quasi-static to 4000 s<sup>-1</sup>. The high strain rate tests were performed using a Split-Hopkinson Pressure Bar. Microstructural evaluations were performed before and after testing to correlate the evolution of porosity, grain size distributions, particles size and geometrical distributions, and twin size distributions with mechanical response of the Mg-alloy material.

### A Study on the Microstructure and Mechanical Properties of the Powder Injection Molded WC-8%Co: *Sung-Hyun Choi*<sup>1</sup>; *Kyoung-Rok Do*<sup>1</sup>; *Sang-Dae Kang*<sup>1</sup>; *Kwon-Koo Cho*<sup>1</sup>; *In-Shup Ahn*<sup>1</sup>; <sup>1</sup>Gyeongsang National University

This study was investigated for microstructure and mechanical properties of WC-8%Co alloy system fabricated by PIM process. After WC-8%Co mixed-powder were PIMed, debinding process were carried by 2-steps methods with thermal debinding and solvent extraction. After solvent extraction to eliminate the binder, thermal debinding was examined at the temperature between 250 and 500°C, in the mixed gas atmosphere of N<sub>2</sub> and H<sub>2</sub>. After debinding process, specimens were vacuum-sintered at 1380°C. The transverse rupture strength (TRS) and hardness were measured. The microstructure and phase were observed by XRD, TEM and SEM. In the case of sintered WC-8%Co at 1380°C, the transverse rupture strength of 2000MPa was obtained, and the hardness was 90HRA. The relative density of PIMed WC-8%Co was 99.5%.

### A Study on the Microstructures and Electromagnetic Interference Shielding of Sn-Al-Ni Thin Films: *Hung Fei-Yi*<sup>1</sup>; *Hung Fei-Shuo*<sup>2</sup>; *Chiang Che-Ming*<sup>2</sup>; *Lui Tuan-Sheng*<sup>3</sup>; <sup>1</sup>Institute of Nanotechnology and Microsystems Engineering, Center for Micro/Nano Science and Technology, National Cheng Kung University; <sup>2</sup>Department of Architecture, National Cheng Kung University; <sup>3</sup>Department of Materials Science and Engineering, National Cheng Kung University

Electromagnetic interference (EMI) is a new form of pollution discovered in recent years. The elements Sn and Al not only possess EMI shield efficiency, but also have acceptable costs. In this study, sputtered Sn-Al thin films with Ni doped (1 wt.%) were used to investigate the effect of the crystallization mechanism and film thickness on the electromagnetic interference (EMI) characteristics. In addition, the annealed microstructure, electrical conductivity and EMI of the Sn-Al films and the Ni-doped Sn-Al films were compared. The results show that Sn-Al film increased the electromagnetic interference (EMI) shielding after annealing. For the Ni-doped Sn-Al films with higher Ni atomic concentration, the low frequency EMI shielding could be improved. After annealing, the Sn-Ni and Al-Ni intermetallic compound (IMC) of thin film distributed in the matrix. This metallurgical effect not only enhanced the diffusion of atoms to the grain boundaries, but also promoted the high frequency EMI shielding.

### A Study on the Stress Test of Truck Frames for Freight Trains: *Sung Cheol Yoon*<sup>1</sup>; <sup>1</sup>Korea Railroad Research Institute/Railroad Safety Research and Testing Center

The truck that is used as running equipment for freight train support is a core structural part that supports the load of the car body and that greatly influences the safety of freights and vehicles, as well as their running performance. The running equipment is composed of truck frames, wheels and wheel axles, independent suspensions, and brakes. Among these components, the truck frame supporting the load of the vehicles and freights may be the most important one. This study was carried out to analyze the structure of truck frames and to determine whether they are safe when the maximum vertical load, breaking load, and front and rear loads are applied to them. This was done by subjecting the truck frames to stress tests and then measuring the stress on each of their parts. To measure the stresses based on the results of the structural analysis, strain gages were attached to the surfaces of truck frames. The results of the stress tests showed that truck frames have a safe vehicle load design.

### A Study on the Structural Design of the Car Body of a Locomotive: *Sung Cheol Yoon*<sup>1</sup>; *Jeongguk Kim*<sup>1</sup>; *Myung Yong Kim*<sup>1</sup>; *Kang Youn Choe*<sup>1</sup>; <sup>1</sup>Korea Railroad Research Institute/Railroad Safety Research and Testing Center

This study was carried out to analyze the structure of the car body of a locomotive, and to subject such car body to a load test to determine whether



it is structurally safe when the maximum load is applied to it. The car body of a locomotive is an important structure that must support the locomotive's under frame, bolster, side frame, roof, and main equipment, including the heavyweight machinery and electric equipment installed inside it. Based on the load conditions in accordance with the enforced "Guide to the Safety Standards in Railway Rolling Stock" in the Railroad Safety Act, a structural analysis and a load test were carried out. The load test was carried out by referring to the results of the structural analysis. The results of the load test showed that the car body of a locomotive has a safe and stable load design.

**A Study on the Structure and Mechanical Properties of HSS T42 Steel Using Powder Injection Moulding Method (PIM):** *Kyoung-Rok Do*<sup>1</sup>; Sung-Hyun Choi<sup>1</sup>; Sang-Dae Kang<sup>1</sup>; Su-gun Lim<sup>1</sup>; In-Shup Ahn<sup>1</sup>; <sup>1</sup>School of Nano and Advanced Materials Engineering, I-Cube Center, K-MEM R&D Cluster

High speed steels (HSS) were used as cutting tools and wear parts, because of high strength, wear resistance, and hardness together with an appreciable toughness and fatigue resistance. Conventional manufacturing process for production of components with HSS was used by casting. The powder metallurgy techniques were currently developed due to second phase segregation of conventional process. The Powder injection mould method (PIM) was received attention owing to shape without additional processes. The experimental specimens were manufactured using the PIM with T42 powders and polymer. Polymer degradation temperatures were investigated. Specimens were sintered in vacuum and the N<sub>2</sub>-5% H<sub>2</sub> gases atmosphere at between 1150 and 1240°C. Density and Hardness measurement were examined. Microstructures were investigated by SEM, XRD and TEM. Polymer degradation temperature about optimum condition was found at 450°C. 8.3g/cm<sup>3</sup> density and 55HRC hardness were observed at 1230°C sintering temperature. Carbide microstructures of smaller and well dispersion were observed at 1230°C.

**A Thermo-Kinetic Model and Experimental Analysis of Multiple Passes Laser Phase Transformation Hardening by Using High-Power Direct Diode Laser:** *Soundarapandian Santhanakrishnan*<sup>1</sup>; Radovan Kovacevic<sup>1</sup>; <sup>1</sup>Southern Methodist University

Laser phase transformation hardening (LPTH) based on rapid heating and cooling cycles produces hard and wear-resistant layers at the metallic component. However, a tempered zone is formed in overlapped regions of a large hardened area during multiple passes. This study is focused on the development of a thermo-kinetic model to minimize the softening effect due to tempering by multiple passes. A back tempering model is coupled with the thermal model to predict the hardness distributions across the multiple passes hardened area. A tool steel AISI S7 is hardened by using different levels of laser power (1200 W- 1800 W) with different scanning speeds (5 mm/s- 25 mm/s). The effect of multiple passes on the formation of tempered martensite is studied for different overlapped configurations (1mm – 3 mm). The thermo-kinetic model is validated with the experimental results to optimize the processing parameters for multiple passes laser hardening.

**Aerosol Route Synthesis of Copper Oxide Nanoparticles Using Copper Nitrate Solution:** *Burcak Ebin*<sup>1</sup>; *Ovgu Gencer*<sup>1</sup>; *Sebahattin Gurmen*<sup>1</sup>; <sup>1</sup>Istanbul Technical University

Copper oxide nanoparticles show unique features such as electronic, optical, thermal and magnetic properties depending on particle dimension and high surface to volume ratio. Applications of copper oxide nanoparticles cover a large field from gas sensors to magnetic storage media, solar energy transformation to semiconductors and catalysis. We report preparation of the copper oxide nanoparticles by thermal decomposition of the copper (II) nitrate (Cu(NO<sub>3</sub>)<sub>2</sub>·3H<sub>2</sub>O) based aerosol droplets. We studied the effects of reaction temperature on size, morphology and crystallinity of copper oxide nanoparticles under air atmosphere. Scanning Electron Microscopy (SEM) analyses revealed that nearly 30 nm sized copper oxide spherical nanoparticles were synthesized. Energy Dispersive Spectrometry (EDS) analysis show that the weight ratios of Cu to O are 79.89:20.11 for the all samples which are the same ratio with tenorite. Also, X-ray diffraction (XRD) patterns indicate that obtained nanoparticles have monoclinic crystal structure.

**AlGaAs-Based Optical Device Fabricated on Si Substrate Using Microchannel Epitaxy:** *Shigeya Naritsuka*<sup>1</sup>; *Daisuke Kanbayashi*<sup>1</sup>; Takuya Kawakami<sup>1</sup>; Yuhei Ando<sup>1</sup>; Takahiro Maruyama<sup>1</sup>; <sup>1</sup>Meijo University

Optoelectronic integrated circuits (OEIC) are very promising to meet an increasing demand for high speed and high capable information processing in

telecommunication and computer applications. To realize OEIC, it is mandatorily important to grow dislocation-free GaAs layers on Si substrates. Microchannel epitaxy (MCE) is known as an excellent way to reduce both dislocation density and residual stress in heteroepitaxy [1]. In this paper, AlGaAs-based resonant cavity light emitting diodes (RCLED) are fabricated on the dislocation-free GaAs areas grown on Si substrates using MCE. These LEDs show superior characteristics as good as those fabricated on GaAs substrates. It is also found from a preliminary life test that the LEDs operate more than 300 hours without any degradation. [1] Y. Ujiie, T. Nishinaga, Jpn. J. Appl. Phys, 28 (1989) L337. This work was partly supported by a Grant-in-Aid for Scientific Research on Priority Areas (B) No.18360155 from MEXT in Japan.

**Ambient Temperature Stress Corrosion Cracking of 304L Stainless Steel:** *Swati Ghosh*<sup>1</sup>; Vivekanand Kain<sup>1</sup>; <sup>1</sup>BARC

Effect of plastic deformation induced by cold rolling or surface machining on the susceptibility to Cl-SCC at ambient temperature of 304L SS was investigated in this study. The as received material was (a) solution annealed, (b) cold worked (CW) and (c) surface machined to induce different levels of strain/stresses in the material. Subsequently constant strained samples were produced for each condition and these were exposed to 1M HCl at ambient temperature until cracking occurred. Subsequently the cracked samples were characterized in detail using stereo microscopy, optical microscopy, atomic force microscopy and EBSD. The results obtained highlight for the first time the effect of microstructural changes produced by straining on the mechanism of crack initiation and propagation at ambient temperature in chloride environment.

**Anisotropic Behavior of Rolled AZ31 Magnesium under Quasi-Static and High Rate Loading:** *Phil Gullett*<sup>1</sup>; Matthew Tucker<sup>1</sup>; <sup>1</sup>Mississippi State University

The anisotropic mechanical response of rolled magnesium AZ31B was examined for quasi-static and high rate loading conditions. Strong strain rate dependencies were observed in the compressive yield, hardening rate, ductility and toughness in the normal direction while rate dependence in the rolling and transverse directions was limited to the hardening response. Therefore, the material texture played a significant role in the mechanical response at both quasi-static and high strain rates. In-situ thermal measurements and microstructural evaluations (grain size distributions, particles size and geometrical distributions, and twin size distributions) are correlated to the mechanical response.

**Analysis of Oxide Formation in High Mn Twinning-Induced Plasticity-Aided Steel during Dew-Point Control:** *Woong-Pyo Hong*<sup>1</sup>; *Sung-II Baik*<sup>1</sup>; *Sung-Dae Kim*<sup>1</sup>; *Gyo-Sung Kim*<sup>2</sup>; *Sun-Ho Jeon*<sup>2</sup>; *Kwang Geun Chin*<sup>2</sup>; *Chang-Seok Oh*<sup>3</sup>; *Young-Woon Kim*<sup>1</sup>; <sup>1</sup>Seoul National University; <sup>2</sup>POSCO Technical Research Laboratory; <sup>3</sup>Korea Institute of Materials Science

To improve a wettability of molten Zn in Twin-Induced Plasticity (TWIP)-aided steel, it is necessary to minimize the surface Mn-oxide, which is controlled by dew-point (DP) control. In this study, oxides formations under different DP controlled environment were investigated at the surface of TWIP steel. DP temperatures were changed from 0°C to -60°C in the gas mixture of H<sub>2</sub>/N<sub>2</sub> ratio of 15:85 in volume. Morphologies and the distributions of the Mn-O oxides will be reported from the results of cross-sectional view in scanning transmission electron microscopy. Mn depletion regions were observed with the DP above -20°C and the distribution of the surface oxide dramatically changed in the DP temperature range between -20 and -40°C. Ferrite structures were found in the Mn-depleted region near the surface. Surface and internal oxidation revealed that the fast diffusion path along the grain boundaries of ferrite.

**Annealing Behavior of TiO<sub>2</sub>-Sheathed Ga<sub>2</sub>O<sub>3</sub> Nanowires:** *Chongmu Lee*<sup>1</sup>; *Hyunsoo Kim*<sup>1</sup>; *Changhyun Jin*<sup>1</sup>; *Jina Jun*<sup>1</sup>; *Chanseok Hong*<sup>1</sup>; *Jungwoo Kang*<sup>1</sup>; <sup>1</sup>Inha University

Ga<sub>2</sub>O<sub>3</sub>-core/TiO<sub>2</sub>-shell nanowires have been synthesized by a two step process: thermal evaporation of GaN powder on Au-coated Si substrates and sputter-deposition of TiO<sub>2</sub>. Transmission electron microscopy and X-ray diffraction analysis results reveal that the Ga<sub>2</sub>O<sub>3</sub> cores and the TiO<sub>2</sub> shells are crystalline with monoclinic and tetragonal structures, respectively. Photoluminescence measurements show a red emission peak centered at around 700 nm. Our results also show that coating Ga<sub>2</sub>O<sub>3</sub> nanowires with thin TiO<sub>2</sub> layers can significantly enhance the red emission intensity. The PL peak intensity of the Ga<sub>2</sub>O<sub>3</sub>/TiO<sub>2</sub> coaxial nanowires prepared by sputter-deposition of TiO<sub>2</sub> for 1.5 min on Ga<sub>2</sub>O<sub>3</sub> nanowires and then annealing is about 20 times as high

# Technical Program

as that of Ga<sub>2</sub>O<sub>3</sub> nanowires. X-ray Photoemission spectrometry analysis results suggest that the PL enhancement is attributed to increases in the concentrations of deep levels such as oxygen and titanium interstitials as well as the density of interface states.

**Atomic-Scale Characterization of Grain Boundary Embrittlement in Structural Steels:** *NamSuk Lim*<sup>1</sup>; *JaeBok Seol*<sup>1</sup>; *ChanGyung Park*<sup>1</sup>; *Raghavan Ayer*<sup>2</sup>; *Howie Jin*<sup>2</sup>; *Russell Mueller*<sup>2</sup>; <sup>1</sup>Pohang University of Science & Technology; <sup>2</sup>ExxonMobil Research & Engineering

Intergranular embrittlement of structural steels is characterized by lower impact toughness and is caused by exposure of the steel in the susceptible temperature range, typically around 400°C. This phenomenon is postulated to be associated with preferential grain boundary segregation of solute elements (e.g., S, P). However, direct measurement of atomic segregation has not been possible due to the limitations in characterization methodologies in both spatial and mass resolution. Advances in high-resolution characterization techniques would enable reliable determination of the grain boundary chemistry at near atomic spatial resolution. The present study was performed to determine the grain boundary chemistry in quenched and tempered 4340 steels by Atom Probe Tomography. The presentation will describe the methodology developed to prepare site-specific specimens and characterization results on the grain boundary composition in steels in the as-quenched and quenched and tempered at 400°C.

**Atomistic Study of Dislocation/Vacancy Interactions in bcc Metals:** *Zhiming Chen*<sup>1</sup>; *Matous Mrovec*<sup>2</sup>; *Peter Gumbsch*<sup>1</sup>; <sup>1</sup>Institut für Zuverlässigkeit von Bauteilen und Systemen, Universität Karlsruhe (TH); <sup>2</sup>Fraunhofer-Institute Für Werkstoffmechanik

In the present work we investigate the interaction of  $\frac{1}{2}\langle 111 \rangle$  and  $\langle 100 \rangle$  dislocations with a vacancy in body-centered cubic (bcc) metals tungsten and iron by means of atomistic simulations. Two models with a different level of sophistication have been employed for the description of interatomic interactions -- the empirical Finnis-Sinclair potential, which is a central-force scheme, and the bond-order potential, which is based on the tight-binding theory and is therefore able to describe correctly directional covalent bonds that are crucial for the cohesion and structure of bcc transition metals. In order to study the influence of the vacancy on dislocation mobility, the nudged elastic band method was employed to determine the changes of the energy barrier for the dislocation motion. Our simulations show that the dislocation mobility may be strongly influenced by the presence of vacancies and that the change of the energy barrier depends sensitively on the vacancy position.

**Basic Study on Synthesis of Sphalerite with Low Iron and Oxygen Pressure Acid Leaching of Sphalerite:** *Yan Gu*<sup>1</sup>; *Ting-an Zhang*<sup>1</sup>; *Gouzhi Lv*<sup>1</sup>; *Zhihe Dou*<sup>1</sup>; *Yan Liu*<sup>1</sup>; *Weiguang Zhang*<sup>1</sup>; <sup>1</sup>Northeastern University

Pressure leaching performance of sphalerite was studied using synthesized sphalerite containing low concentration iron as raw material. The zinc element entering into leaching solution as ions and the sulfur entering into slag as elementary substance. Effects of process parameters on leaching rate of sphalerite and conversion rate of sulfur were researched. Results show that the reasonable parameters are particle size -260 mesh, stirring speed 500 rad/min, leaching temperature 150 °C, oxygen partial pressure intensity 1.0 MPa, initial sulfuric acid concentration 150 g/l, leaching time 90 min, solid-liquid ratio 10:1 (ml:g). The leaching rate of the zinc, iron and sulfur can reach above 95%, 33.5% and 65% at this condition. The kinetic study of pressure leaching was studied. Results show that as to zinc leaching process is controlled by surface chemical reaction and follows kinetic law of "shrinking of unreacted core model", and its reaction activation energy is 73.58 kJ/mol.

**Carpenter ACUBE™ 100 an Alternative Copper-Beryllium Alloy for High-Load Bushings and Bearings Applications:** *Rick Frank*<sup>1</sup>; *Karl Heck*<sup>1</sup>; *Joseph Stravinskas*<sup>1</sup>; <sup>1</sup>Carpenter Technology

Carpenter ACUBE™ 100 alloy is a non-magnetic, cobalt-based alloy exhibiting high strength, excellent corrosion resistance, and outstanding wear resistance. Exposure to beryllium dust has been tied to a variety of health hazards. ACUBE 100 is beryllium free, eliminating the health and safety issues associated with beryllium-containing alloys. The ACUBE 100 alloy can be considered as a direct replacement for copper-beryllium alloy to the AMS 4533 specification. Made by premium-melting and processing operations, ACUBE 100 has demonstrated excellent corrosion resistance to salt spray, nitric acid, acetic acid and humidity. Processing by warm working (work strengthen condition)

produces a yield strength of 140 ksi (965 MPa) for use in applications which require superior resistance to galling and wear such as bushings, bearings and other rotating parts that are exposed to corrosive environments and/or subject to high stress and heavy loads.

**Cations Removal from Synthetic Neutral Zinc Leach Solution Using Synthetic Iron Oxide:** *Mamata Mohapatra*<sup>1</sup>; *P. Singh*<sup>2</sup>; *S. Anand*<sup>1</sup>; *B.K. Mishra*<sup>1</sup>; <sup>1</sup>Institute of Minerals and Materials Technology; <sup>2</sup>Murdoch University

Selective separation of heavy metal ions from industrial and waste aqueous solutions is frequently required in hydrometallurgical processing. In recent years many researcher have worked on supported liquid membrane and floatation technique for the removal of Cd(II) from zinc electrolyte solutions. The selectivity of cationic surfactants for anions has been established in several ion floatation experiments including chloride and cyanide metal complexes of Zn(II), Cd(II), Hg(II), and Au(III) investigated foam separation of Cd(II) ions by dodecyl sulfate from aqueous solutions in the presence of electrolytes and found a negative influence of these electrolytes on Cd(II) foam separation. Study of Cd(II) over Zn(II) ions separation in the presence of inorganic ligands by anionic and cationic collectors was also reported. However, no work has been reported on removal of impurities from zinc neutral leach solutions using solid adsorbents. In the present chapter, a synthetic solution of zinc neutral leach (matching with industrial composition) was prepared and the synthetic solid iron oxide/hydroxide samples were used as adsorbents to remove cations from the synthetic solutions. The mixed iron oxide sample was found to be good for Cd(II) removal from neutral leach solution whereas 6-line ferrihydrite and goethite samples showed good adsorption property for nickel and iron removal. A combination of mixed iron oxide and 6-line ferrihydrite/goethite the neutral leach solution can be used for purification of input to zinc electro-winning.

**Comparative Study of Microstructural Characteristics of PM Sintering and Plasma Spraying Coating on a Steel Surface:** *Zhang Jie*<sup>1</sup>; *WANG Maocai*<sup>2</sup>; *ZHAI Yuchun*<sup>1</sup>; <sup>1</sup>Northeastern University; <sup>2</sup>State Key Laboratory for Corrosion and Protection, Institute of Metal Research, Chinese Academy of Sciences

In this paper, a comparative study has been made between microstructural characteristics in coatings prepared by PM sintering and air plasma spray technique. Some interesting results have been achieved. Firstly, wear-resistant coatings can be commonly achieved by these two techniques. Secondly, microstructural morphologies of these two coatings are obviously different, fully dense structure prevails in the PM sintering coating while bedded grain defective structure in the air plasma spray coatings. Thirdly, PM coating possesses finer, much thicker and more homogeneous microstructure than air plasma spray coating.

**Comparison of Stress Corrosion Cracking and Hydrogen Embrittlement Resistance of High Strength Aerospace Alloys:** *David Wert*<sup>1</sup>; *Thomas Werley*<sup>1</sup>; <sup>1</sup>Carpenter Technology Corp.

Historically, stress corrosion cracking and hydrogen embrittlement issues with aerospace high strength structural alloys have been addressed by plating parts using cadmium, chromium, or combinations thereof. However, these surface treatments are not 100% effective, and their application and the disposal of the required plating baths often result in environmental issues. For that reason, new grades have been introduced which can minimize or eliminate the use of these protective surface treatments. This presentation will compare recent results of stress corrosion cracking ( $K_{I_{SCC}}$ ) and hydrogen embrittlement ( $K_{I_{HE}}$ ) testing of 300M, Custom 465® Stainless, Carpenter Ferrium® S53, and Carpenter AerMet® 100 alloys. These results were generated using the RSL™ Rising Step Load Bend Testing System. The data to be presented represents samples held at potentials ranging from open circuit, where the test sample is freely corroding in 3.5% NaCl test solution, to -1.10 V<sub>see</sub>, simulating cathodic charging while being galvanically coupled to zinc.

**Corrosion Behavior of Al-Si-Cr-Ni-Cu Bearing Low Carbon Steel in a Cyclic Dry/Wet Laboratory Test:** *Dongping Zhan*<sup>1</sup>; *Huishu Zhang*<sup>1</sup>; *Songlian Bai*<sup>1</sup>; *Zhouhua Jiang*<sup>1</sup>; <sup>1</sup>Northeastern University

The corrosion behaviors of two designed low carbon steels which bearing of Al-Si-Cr-Ni-Cu elements and Q235 were tested in a cyclic dry/wet environment containing 0.01mol/L NaHSO<sub>3</sub>. Rust layers were observed by optical microscope (OM), scanning electron microscopy (SEM) and XRD. The electrochemical behaviors of the steels were studied on the polarization curves and electrochemical impedance spectroscopy (EIS). The results indicate that the mechanical properties and the corrosion-resistant performances of the designed



steel are better than those of Q235. The annual corrosion rates of the designed steels reduce 41.2% than Q235 at least. There are the enrichments of Cu, Cr, Si and Al in the rust layer close to the matrix, which make the rust layer be more compact and protected. The corrosion currents of the two designed steels are lower than that of Q235, the corrosion potentials and rust layer impedances are higher than that of Q235.

**Corrosion Behavior of Aluminum Matrix Composite (AMCS) Prepared by Atomization:** Muna Abbass<sup>1</sup>; Mohammad Waheed<sup>1</sup>; Ali Faris<sup>1</sup>; <sup>1</sup>University of Technology, Baghdad

In this study, metal matrix composite of an aluminum alloy 7020 reinforced by Al<sub>2</sub>O<sub>3</sub> particles with weight percentages of 5%, 7%, and 10% and its size of (53-75) μm were prepared using molten metal atomization technique. Corrosion behavior of aluminum matrix composite (AMC's) in 3.5% NaCl solution was examined using potentiodynamic polarization measurements. The corrosion rate was found to increase as the temperature was nominally raised from 30°C to 38°C and 45°C for the 10%wt of alumina in atomized AMCS samples in 3.5% NaCl solution. At a temperature of 30°C the corrosion rate was found to rise with increasing percentages of Al<sub>2</sub>O<sub>3</sub> particles for the given atomized samples. This is due to galvanic corrosion between the matrix and reinforcement and the presence of second phases around Al<sub>2</sub>O<sub>3</sub> particles in microstructure of AMCS.

**Cracking near a Hole on a Heat Resistant Alloy Subjected to Thermo-Mechanical Cycling:** Feng-Xun Li<sup>1</sup>; Ki-Ju Kang<sup>1</sup>; <sup>1</sup>Chonnam National University

In a hot section of gas turbine, the turbine blades were protected from high temperature by not only a thermal barrier coating (TBC) but also cooling air fed through internal passages within the blade. The cooling air is then passed through discrete holes in the blade surface, creating a film of cooling air, further protects the surface from the hot mainstream flow. The holes are subjected to stresses due to the lateral growth of the thermally-grown oxide, the thermal expansion misfit between the constituent layers and centrifugal force by high speed revolution, which often results in cracking. In this work, the deformation and cracks occurring near a hole on a heat-resistant alloy subject to thermo-mechanical cycling were investigated. The experiments showed that during thermo-mechanical cycling the cracks occur around the hole depending applied stress level and number of cycles, which could be explained by analytic solution.

**Defect Energetics and Fission Product Transport in ZrC:** Sungtae Kim<sup>1</sup>; Young Ki Yang<sup>1</sup>; Tyler Gerczak<sup>1</sup>; Todd Allen<sup>1</sup>; Dane Morgan<sup>1</sup>; Izabela Szlufarska<sup>1</sup>; <sup>1</sup>University of Wisconsin - Madison

ZrC is being considered as replacement fission product barrier and structural layer to SiC in TRistructural-ISOTopic nuclear fuel. Though the formation and evolution of point defects under irradiation is a major mechanism for degradation in nuclear materials, defect properties of ZrC are largely unknown. Therefore, we have determined the point defect energetics in ZrC using ab initio calculations. The C vacancy and C interstitial defects are shown to be energetically favored over Zr vacancies and interstitials, consistent with the formation of C Frenkel defects under irradiation and the C poor ZrC<sub>x</sub> (x<1) stoichiometry measured experimentally. To understand fission product retention from ZrC TRISO fuel particles, the Ag diffusion coefficients in ZrC are experimentally measured. This work was performed as part of the Deep Burn Project: Transuranic High-Temperature Reactor Fuel Qualification under a subcontract with the Battelle Energy Alliance.

**Deformation Field and Microstructure of Copper in Flat Punch Indentation:** Matthew Hudspeth<sup>1</sup>; T. Murthy<sup>1</sup>; C. Saldana<sup>1</sup>; Srinivasan Chandrasekar<sup>1</sup>; <sup>1</sup>Purdue University

A study has been made of the deformation field in plane strain indentation of OFHC copper with a flat punch. Deformation parameters displacement, velocity, strain rate and strain are estimated in situ from optical images of the indentation by tracking the motion of asperities on the surface of the copper. The measurements have confirmed the presence of a dead metalzone underneath the indenter and have demonstrated the formation and evolution of regions of intense strain rate (e.g. shear banding), consistent with classical indentation theory. Metallographic studies of the regions surrounding the indentation zone have been made by optical and transmission electron microscopy, as well as through nano-indentation. The resulting post-deformation microstructure and its correlation to the measured deformation parameters is studied.

**Deformation in Shock-Loaded Materials:** Veronica Livescu<sup>1</sup>; John Bingert<sup>1</sup>; George Gray III<sup>1</sup>; Davis Tonks<sup>1</sup>; <sup>1</sup>Los Alamos National Laboratory

Understanding the deformation of materials during dynamic loading remains difficult. A material shock-loaded by high-explosive detonation experiences a complex loading path evolving both spatially and temporally, which implies an evolving balance of hydrostatic and deviatoric stresses. Twinning may be a favored deformation mechanism under shock loading conditions and plays an important role in damage nucleation. This work brings experimental evidence on the progression of deformation in shock-loaded materials to inform and constrain future numerical damage models. Results from Electron Backscatter Diffraction (EBSD) analysis and fracture surface measurements will be discussed in relation to deformation and damage nucleation. Aspects of shock obliquity and microstructural interactions during deformation will be presented and the results of quantification of twin density gradients with respect to distance from the detonation point will be discussed.

**Deformation of High Purity Copper Specimens in Compression between Flat and Grooved Dies:** Bashir Raddad<sup>1</sup>; Teahert Al-hashani<sup>2</sup>; Mohiudeen Abdel-Rahman<sup>3</sup>; <sup>1</sup>El-Fateh University; <sup>2</sup>Academy of Graduate Studies - School of Applied Sciences and Engineering Department; <sup>3</sup>Minia University

Experiments were carried out to generate data on cold compression of high purity copper specimens having different height-to-diameter (Ho/Do) ratios (0.5 to 1.5) between two flat dies having various degrees of surface condition (knurled, dry and lubricated) and between grooved dies having different groove numbers (1 to 3). Different Ho/Do ratios, die surface conditions and number of grooved resulted in different loading characteristics and also different modes of deformation. The latter case resulted forward and backward extrusion modes plus the radial flow resulting from ordinary compression. Three shapes of deformed specimen were obtained according to the number of grooves. Load values decreased as Ho/Do increased and friction condition improved. For a fixed load, displacement increased for higher Ho/Do ratio. For a fixed displacement, however, load level decreased as Ho/Do increased. Surface strains were apparently affected by the above variables.

**Dendrite Tip Shape in Pivalic Acid-Ethanol and Succinonitrile-Salol Systems:** Myung-Jin Suk<sup>1</sup>; Young-Min Park<sup>1</sup>; Young-Do Kim<sup>2</sup>; <sup>1</sup>Kangwon National University; <sup>2</sup>Hanyang University

In the present work, dendrite tip shapes are fitted by parabolic function, and the difference of dendrite tip shapes between the pivalic acid(PVA)-ethanol(Eth) and succinonitrile(SCN)-salol systems which are characterized by anisotropic and isotropic solid-liquid interfacial property, respectively, is quantitatively treated using shape parameters. PVA-Eth system shows slightly higher Z/R value than SCN-salol system, their Z/R values lying in the range 2-4. (Z is the distance from the tip beyond which the parabolic fit starts to deviate from the profile, and R the tip radius.) λp is the distance from the tip beyond which side branching starts to appear, and is different for both sides of the 2-dimensional dendrite profile. The difference of λp between both sides of the dendrite is larger for PVA-Eth system than for SCN-salol, implying that the dendrite of PVA-Eth is more nonaxisymmetric than that of SCN-salol.

**Development of In-Situ Mg-Based Bulk Metallic Glass Composites with High Plasticity:** Ka Ram Lim<sup>1</sup>; Eun Soo Park<sup>2</sup>; Won Tae Kim<sup>3</sup>; Do Hyang Kim<sup>1</sup>; <sup>1</sup>Yonsei University; <sup>2</sup>Seoul National University; <sup>3</sup>Cheongju University

Among main engineering metallic alloys, Mg metal has advantages of the lowest specific weight, a large amount of deposits on the earth and its easy recycling ability for the saving of energy and other natural resources. Therefore, high-strength and high-ductility Mg-based alloys have been under intense investigation. Mg-based bulk metallic glasses (BMGs) were found to have good castability as well as high strength. However, the Mg-based BMGs do not exhibit appreciable plastic deformation. In the present study, Mg-Cu-RE (RE = Gd, Y) alloys with excellent glass forming ability were selected as starting compositions. Mg-based BMG composites were fabricated by addition of a metal element (Al, Ag, Zn). The reinforcing phase embedded in Mg-based BMG matrix hinder the propagation of shear bands, hence retarding the emergence of catastrophic failure in BMG matrix. The details on the mechanical properties and deformation mechanism will be discussed.

# Technical Program

**Development of Ultrasonic Techniques for Process Control in Iron and Steel Making:** Jagdish Pandey<sup>1</sup>; Manish Raj<sup>1</sup>; Krishnan Balasubramaniam<sup>1</sup>; Nikhiles Bandyopadhyay<sup>1</sup>; <sup>1</sup>Tata Steel Ltd.

The paper highlights the potential of ultrasonic C scan image analysis system using 5 and 10 MHz focused beam transducers to optimize electromagnetic stirring parameters during continuous casting of steel billets and overall assessment of billet quality including its cleanliness level. The ultrasonic C scan image plot could also reveal columnar and equiaxed grain structure in these billets and the effect of electromagnetic stirring on the change in equiaxed zone could be estimated. This technique also helped in reducing split end and cracking problem during hot rolling of continuously cast billets for thermo mechanically treated steel bars. An attempt was also made to measure viscosity and melting characteristics of mould powder slags used in continuous casting of steel using normal shear wave transducers. The experimental results show the possibility of using such technique for on-line measurement of viscosity and break temperatures of iron making as well as steel making slags/fluxes.

**Dissolution of Platinum from Scrap Automotive Catalytic Converters Using a Combination of HCl+H<sub>2</sub>O<sub>2</sub>:** Candenz Uysal<sup>1</sup>; Serdar Aktas<sup>1</sup>; Eray Kizilaslan<sup>1</sup>; Kelami Sesen<sup>1</sup>; <sup>1</sup>Istanbul Technical University

Dissolution of platinum which is incorporated in automotive catalytic converters is performed through chemical methods. There is a need to develop a cost-effective and environmentally friendly process for platinum dissolution. This poster summarizes research on the possibility of 10 HCl: 1 H<sub>2</sub>O<sub>2</sub> solution to replace aqua regia for the mentioned task. Dissolution of platinum in this solvent was studied as functions of agitation rate, time, liquid/solid mass ratio and the reaction temperature. A comparison of the solvent's efficiency with that of aqua regia was provided at each step. It was demonstrated that 95% dissolution of platinum in catalytic converters could be achieved with 10 HCl: 1 H<sub>2</sub>O<sub>2</sub> solution under moderate experimental conditions, which are easy-to-adopt to the industrial plants.

**Dynamics Research on Leaching Process of Bonded Copper Oxides Strengthened by Mechanical Activation:** Liu Wei<sup>1</sup>; Tang Motang<sup>1</sup>; Tang Zhaobo<sup>1</sup>; He Jing<sup>1</sup>; Yang Shenghai<sup>1</sup>; Yang Jianguang<sup>1</sup>; <sup>1</sup>Central South University

In order to increasing the leaching rate of the bonded copper oxides in the Tang Dan copper mineral of Yunan province of China, the mechanical activation method was used to strengthen the leaching process. The samples were mechanically activated after the free copper oxides were removed. The leaching dynamics research was conducted by leaching the samples unactivated and activated in the system of NH<sub>3</sub>-NH<sub>4</sub>Cl-H<sub>2</sub>O solution. The apparent activation energy of the leaching process of the samples unactivated and activated for 15min and 30min were calculated to be 24.13kJ/mol, 15.40kJ/mol and 14.76kJ/mol, respectively. Granularity distribution and X-ray diffraction analysis indicated that the improving of the leaching effect was the co-contribution of increase of both surface area and imperfection content.

**EDM and AWJ Edge Finishing on Surface Morphology of Hybrid Composite Laminates:** Laxminarayana Pappula<sup>1</sup>; V. Isvilanonda<sup>2</sup>; M. Ramulu<sup>2</sup>; Naga Prasada Rao Boyalapalli<sup>3</sup>; <sup>1</sup>University College of Technology, Osmania University; <sup>2</sup>Department of Mechanical Engineering, University of Washington; <sup>3</sup>Department of Mechanical Engineering, University College of Engineering, Osmania University

Hybrid titanium laminate is the new high strength-light weight material that possesses great potential for high speed and elevated temperature aerospace structural applications. In this research, series of cuts were made on multi-layers hybrid titanium laminates using die sinker electrical discharge machining (EDM) and abrasive waterjet (AWJ) machining processes. It was found that for EDM machining, low power setting resulted in slow cutting rate but smoother surface was achieved. High power EDM cut cause severe melting and rough surface finish. Both EDM conditions generate thermal cracks and heat damages which are detrimental to load bearing capability. AWJ cuts were impressively faster and machined surfaces were relatively smoother than die sinker EDM. Based on extensive optical and scanning microscopic examination of machined surfaces, it is concluded that AWJ is the preferred method to cut hybrid titanium laminate due to faster cut, smaller damage than EDM process.

**Effect of Niobium on Solidification Structure of Gray Cast Iron:** Zhou Wenbing<sup>1</sup>; Zhu Hongbo<sup>1</sup>; Zheng Dengke<sup>1</sup>; Hua Qin<sup>1</sup>; Zhai QiJie<sup>1</sup>; <sup>1</sup>Shanghai University

The effect of niobium on the matrix microstructure has been studied with varied contents of niobium in gray cast iron, and its mechanism is also analyzed. The results show that when the content of niobium is in the range of 0.042~1.48%, the eutectic size is refined, and the lamellar spacing of pearlite is also significantly decreased. Meanwhile, graphite is refined, too.

**Effect of Nitrogen Addition on Isothermal Phase Transformation and Mechanical Properties in Biomedical Co-Cr-Mo Alloys:** Shingo Kurosu<sup>1</sup>; Hiroaki Matsumoto<sup>1</sup>; Akihiko Chiba<sup>1</sup>; <sup>1</sup>Institute for Materials Research, Tohoku University

Effect of nitrogen addition on isothermal phase transformation behavior in a biomedical Co-Cr-Mo alloy without addition of carbon was investigated during aging at temperature between 973 K and 1273 K for up to 90 ks. In the Co-Cr-Mo alloy, phase transformation from fcc to hcp<sub>1</sub> with super-saturation of Cr occurred by massive transformation. With prolonged aging treatment, a lamellar structure consisting of hcp<sub>2</sub> with equilibrium of Cr and  $\sigma$  phases was formed at hcp<sub>1</sub>/hcp<sub>1</sub> boundaries by a discontinuous/cellular reaction, expressed by the reaction equation hcp<sub>1</sub>→hcp<sub>2</sub>+ $\sigma$ . The phase transformation is remarkably changed by addition of nitrogen. In the Co-Cr-Mo-N alloy, the phase transformation from fcc to hcp occurs with a significant long incubation period compared with that in Co-Cr-Mo alloy. Besides, lamellar Cr<sub>2</sub>N precipitates during phase transformation, suggesting that phase transformation of Co-Cr-Mo-N alloy may be dominant by the eutectoid transformation (fcc→hcp+Cr<sub>2</sub>N).

**Effect of Non-Sinusoidal Oscillation Parameters on Liquid Friction and Lubrication near the Meniscus of Slab Continuous Casting Mold:** Xiangning Meng<sup>1</sup>; Miaoyong Zhu<sup>1</sup>; <sup>1</sup>Northeastern University

The extremum equation of liquid friction force in meniscus was solved based on momentum and mass conservation, and a mechanism with consideration of shell deformation for flux consumption was presented, then infiltration time and intensity for estimating consumption were proposed, moreover, effect of oscillation parameters on liquid friction, infiltration time and intensity were analyzed. The results show that liquid flux above free surface is periodically infiltrated into gap between oscillating mold and withdrawing slab by negative pressure caused by widening flux channel from last stage of positive strip time until last stage of negative strip time. Flux consumption increases with decrease of oscillation frequency, and friction force is restricted. Improving amplitude is helpful to welding existed surface cracks, but almost has no effect on flux consumption. Non-sinusoidal oscillation factor has an inverse effect on flux consumption and liquid friction respectively, and it should be a constant for invariable casting conditions.

**Effect of Particle Size on the Microstructure of Rapidly Solidified Hypereutectic Iron Alloy Powder:** Min Yang<sup>1</sup>; Yongxiang Dai<sup>1</sup>; Changjiang Song<sup>1</sup>; Qijie Zhai<sup>1</sup>; <sup>1</sup>Shanghai University

Microstructures of atomized hypereutectic iron alloy powders with different diameters were characterized by X-ray diffraction, optical microscopy and scanning electron microscopy. The phase transformation and eutectic colony melting temperatures of powders with different diameters were measured by using differential scanning calorimetry (DSC). The results show that the as-atomized powders are mainly composed of austenite and a composite microstructure of hard (Fe, Cr)7C<sub>3</sub> carbide, but, ferrite and a composite microstructure of hard (Fe, Cr)7C<sub>3</sub> carbide after annealed. With the increase of the particle size, the phase transformation temperature increases and the eutectic colony melting temperature of powders slightly decreases.

**Effect of Silicon Addition on the Microstructure and Mechanical Properties of Extruded Mg-Zn Alloys:** Hwa Chul Jung<sup>1</sup>; Ji Hoon Hwang<sup>1</sup>; Kwang Seon Shin<sup>1</sup>; <sup>1</sup>Magnesium Technology Innovation Center, Seoul National University

The Mg-Zn alloys have a large age hardening response, stemming from the precipitation of the transition phase ( $\beta'$ ), and consequently offer both good strength and ductility. In the present study, the effect of Si addition was investigated in order to improve room and high temperature mechanical properties of the Mg-6Zn alloy. The precipitation behavior of different phases in the Mg-Zn-Si alloys was examined by thermodynamic simulations using PandatTM software and casting and extrusion experiments. With the addition of Si in Mg-6Zn alloy, the Mg<sub>2</sub>Si phase, which has a high hardness and melting point, was formed. The morphology of coarse Mg<sub>2</sub>Si particles observed in



the as-cast Mg-Zn-Si alloys was modified by the extrusion process, and the tensile properties of the Mg-Zn-Si alloys were significantly improved. It was also found that the double aging treatment after extrusion and solution heat-treatment significantly increased both the yield and tensile strengths of the Mg-Zn-Si alloys.

**Effects of Lamination on Mechanical Behavior of Nano-Structured Aluminum Composite:** *Hala Hassan*<sup>1</sup>; Adel El-Shabasy<sup>1</sup>; John Lewandowski<sup>2</sup>; <sup>1</sup>Ain Shams University, Faculty of Engineering; <sup>2</sup>Case Western Reserve University

A nano-structured Al89Gd7Ni3Fe1 alloy was made from extruding its atomized amorphous powder at different extrusion ratios (ER). The effects of changing the notch radius from fatigue pre-crack to 100  $\mu\text{m}$  on mode I fracture toughness were studied at different test temperatures (e.g. 298K and 498K) and the fracture surfaces were studied with SEM [1]. In addition, laminated specimens (nano-structured Al composite/ Al) were fabricated via co-extrusion to investigate the effects of a laminated structure on smooth bend properties as well as notched properties in both the crack arrestor and crack divider orientations. The laminates were either bi-layer or tri-layer laminates. The addition of a ductile layer to the tensile surface of a nano-composite produced higher bend ductility and notched toughness.[1] H. A. Hassan, J.J. Lewandowski, Materials Science and Engineering A, 497 (2008) pp 212-215.

**Effects of Material and Process Parameters on Final Residual Stress and Distortion Predictions during Welding of Steel:** *Amir Masoud Akbari Pazooki*<sup>1</sup>; <sup>1</sup>TU Delft

It is well known that material properties as well as welding process parameters have a big influence on residual stresses and distortion in welded structures. The main goal of this paper is the analysis of the sensitivity of material properties and process parameters variations on the temperature, stress and strain fields in welding simulations. The properties under investigation are heat conductivity, specific heat capacity, density, Young's modulus, yield strength, thermal expansion, Poisson's ratio, work hardening, process efficiency, heat input and the geometrical parameters of the Goldak heat input model. Two types of steel (DP600 and AISI 316L) are considered. The welding process used in this investigation is Gas Tungsten Arc Welding. All predictions are made by FEM commercial software (Msc.Marc). The final residual stress and distortion in numerical modeling have been validated by experimental measurements such as synchrotron X-Ray diffraction and laser scanning.

**Effects of Mesh Size on Final Residual Stress and Distortion Predictions during Welding of DP600 and AISI 316L Steel Plates:** *Amir Masoud Akbari Pazooki*<sup>1</sup>; <sup>1</sup>TU Delft

Predictions of residual stress and distortion in welding process are two important topics in welding engineering. FEM is a powerful tool for this reason. Selecting a suitable mesh size can influence the final results in prediction of residual stress and distortion. In this paper the effect of different mesh sizes (Density) on the final predictions of residual stress and distortion of 316L and DP600 steel plates in a GTAW process are presented. The simulation results of stress and distortion have been compared with the results of experiments such as synchrotron X-Ray diffraction and laser scanning.

**Effects of Microstructural and Mechanical Length Scales on Fatigue Crack Propagation in Beta-Annealed Ti-6Al-4V:** Thomas Villarreal<sup>1</sup>; Ikshawku Atodaria<sup>1</sup>; Pedro Peralta<sup>1</sup>; <sup>1</sup>Arizona State University

Effects of grain orientation and crack tip strain fields in relation to applied loading and fatigue crack growth kinetics are studied in beta-annealed Ti-6Al-4V. Electron Backscattering Diffraction (EBSD) was used to characterize Compact-Tension (CT) specimens before and after tension-tension fatigue at constant  $\Delta K$ , from 10  $\text{MPa}\cdot\text{m}^{0.5}$  to 20  $\text{MPa}\cdot\text{m}^{0.5}$ , which result in different plastic zone sizes. In-situ loading and Digital Image Correlation (DIC) are used to obtain crack tip strain fields. Taylor and Schmid factor maps from EBSD data and known slip systems for loading cases approximating crack tip behavior are compared to the measured strain fields to understand local heterogeneities. The strain fields are 'integrated' ahead of the crack tips in order to study relationships among these fields, grain orientation and overall crack growth kinetics, and to elucidate the role of the interaction between microstructural and mechanical length scales in fatigue crack propagation in this material.

**Effects of Post-Deformation Annealing Conditions on the Behavior of Lamellar Cementite and the Occurrence of Delamination in High Strength Cold Drawn Pearlitic Steel Wires:** Jung Won Lee<sup>1</sup>; *Ui Gu Kang*<sup>1</sup>; Yong Shin Lee<sup>1</sup>; Kyung Tae Park<sup>2</sup>; Wonjong Nam<sup>1</sup>; <sup>1</sup>Kookmin University; <sup>2</sup>Hanbat University

Wire drawing is one of the most effective way to increase the strength. Suspension bridge is generally required to do galvanizing process to avoid corrosion. At this point, The effects of both annealing temperature and time on mechanical properties and the occurrence of delamination in high strength cold drawn pearlitic steel wires were already investigated. For the low temperature annealing, the carbon dissolution into lamellar ferrite due to strain aging which is known for first and second stage of aging would enhance not only the increase of strength but also the occurrence frequency of delamination. Whereas, as annealing temperatures and annealing time increase further, age softening that includes the break-up, spheroidization of lamellar cementite and recovery of lamellar ferrite starts to operate. Consequently, the reduction of carbon content dissolved in lamellar ferrite would result in the decrease of tensile strength and suppress the occurrence of delamination. The voids formed at the surface of globular cementite particle, which were produced during post-deformation annealing at high temperatures for a long time, would act as one of the origins for delamination during torsion test. This paper provides a major cause to explain the occurrence of delamination behaviour of high strength cold drawn pearlitic steel wires.

**Effects of Thermal Residual Stress and Whisker Network on Neutron Diffraction Patterns for SiC-Alumina Composites during Creep Deformation:** *Juan Kong*<sup>1</sup>; Nikolas Provatas<sup>1</sup>; David Wilkinson<sup>1</sup>; <sup>1</sup>McMaster University

Whisker network deformation inside a creeping matrix must be understood in order to optimize the design of composite materials. Previous modeling suggests that whisker bending is the dominant deformation mechanism in an aligned percolating network. Experiments were done by Quan et al to verify this, using neutron diffraction peak width (FWHM) as a measure of elastic whisker bending, and peak position to monitor average residual thermal stress. These experiments on crept alumina composites containing 20-30vol% of SiC whiskers showed an unexpected decrease of peak width for the  $\langle 111 \rangle$  whisker peak. In this work, we have used finite element method applied to a representative volume element (RVE) with two types of whisker network to simulate the creep and hot pressing processes: 3-D random-oriented-short-fibre unit cell without contact generated by a random sequential adsorption algorithm; and 2-D regularly aligned percolating unit cells

**Effects of Twin on the Mechanical Behavior of Mg Single Crystals:** *Hwa Chul Jung*<sup>1</sup>; Ming Zhe Bian<sup>1</sup>; Nam Kyoung Kwon<sup>1</sup>; Kwang Seon Shin<sup>1</sup>; <sup>1</sup>Magnesium Technology Innovation Center, Seoul National University

The mechanical behavior of HCP metals is strongly influenced by their inherent anisotropic characteristics that originate from the crystal structure. The resolved shear stresses that activate the prismatic, pyramidal and  $\langle c+a \rangle$  slip modes are much greater than those required to initiate the basal slip and tensile twin at room temperature. Therefore, the predominant deformation modes of magnesium at room temperature are the basal slip and tensile twin. While the slip behavior of magnesium alloys has been extensively investigated, research on the twin behavior has been rather limited, even though twinning is an important mode of deformation in HCP metals. The interactions between the dislocations and twin boundaries are important because the deformation-induced twins could act as obstacles to dislocation motion. In this study, effects of twin on deformation and recrystallization behavior of Mg single crystals were systematically investigated by scanning electron microscopy and electron backscattering diffraction (EBSD) analysis.

**EKOLUBE™, the Economical, Eco-Friendly Solution for Sendzimir™ 20Hi Mills:** *Suresh Neelakantan*<sup>1</sup>; Josef Graetz<sup>1</sup>; <sup>1</sup>Magnum Integrated Technologies

Waterbury Farrel™ continues to lead the development of its 20Hi Sendzimir™ mill, with new technologies including As-U-Roll™ Top and Bottom Crown control and advanced 'ZR' housing designs. Now, Waterbury Farrel™ has elevated its ZMill™ technology by designing EKOLUBE™, a new and exciting patented lubrication technology. This new approach to 20 Hi mill lubrication is designed to extend the operating life of backing bearing assemblies, therefore reducing spares, maintenance and downtime costs. As well, it reduces the use of mill lubrication oil consumables, thus significantly reducing mill operating

# Technical Program

costs. The EKOLUBE™, system is available on the Waterbury Farrel™ 20Hi Sendzimir™ ZMill™, and may be retrofitted to all existing 20Hi Mills. The paper presented at this conference will describe the EKOLUBE™ system, which injects precise amounts of pure lubricant into 20Hi backing bearings from a dedicated hardware and automation system. EKOLUBE®, the economical, Eco-friendly solution for Sendzimir™ 20Hi mills.

**Electrical Conductivity Manipulation and Switching Phenomena of PBZT Thin Film by Doping Process:** Jiahua Zhu<sup>1</sup>; Sung Park<sup>2</sup>; John Willis<sup>3</sup>; Max Alexander<sup>3</sup>; *John Zhanhu Guo*<sup>1</sup>; <sup>1</sup>Lamar University; <sup>2</sup>NGC Aerospace Systems; <sup>3</sup>Air Force Research Laboratory

Both chemical and physical doping processes were developed to manipulate the electrical conductivity of the (PBZT) in this work. Protonation with hydrochloride and sulfuric acid significantly enhanced the electric conductivity of PBZT thin film and meanwhile switching phenomenon intrigued by an applied voltage was also observed. The mechanisms for the electrical change and the switching phenomena are investigated and explained from the PBZT molecular structure transformation. Reduction with different metals on protonated PBZT increased the electric conductivity significantly. The behind doping mechanism will be discussed. PBZT nanocomposites doped with conductive nanoparticles and other conductive polymers such as polyaniline and polypyrrole for improving electric conductivity were also discussed. FT-IR, XRD, TGA, EDAX and four-point probe testing were used to better understand the mechanism of doping process.

**Electrochemical Behavior of Ni-Cr Base Alloys in Corrosive Environment:** *Aezeden Mohmaed*<sup>1</sup>; <sup>1</sup>University of Manitoba

The corrosion behavior of two Ni-Cr base alloys is IN600 and IN601 has been evaluated by potentiodynamic polarization in NaCl solution. IN600 has less passivation range in comparison with IN601 is observed. In addition, the passivation current has been found to be higher than that of IN601. Tafel polarization indicates that IN601 is more corrosion resistant than IN600 in different NaCl concentrations.

**Electrochemical Behavior of RuO<sub>2</sub>-IrO<sub>2</sub>-SnO<sub>2</sub>/Ti Electrode under Mild and Forced Conditions:** *Ozgenur Kahvecioglu*<sup>1</sup>; Servet Timur<sup>1</sup>; <sup>1</sup>Istanbul Technical University

Dimensionally stable anode (DSA®) with a ternary coating of RuO<sub>2</sub>-IrO<sub>2</sub>-SnO<sub>2</sub> deposited on a Ti substrate was prepared by polymeric precursor (Pechini) method. The nano-structure, morphology and compositions of the coating were characterized by FESEM, XRD and EDS. Chronopotentiometric studies were carried out at two different current densities: 20 mA cm<sup>-2</sup> (mild condition, MC) and 1000 mA cm<sup>-2</sup> (forced condition, FC). After each application, linear sweep voltammetry (LSV) and cyclic voltammetry (CV) tests were performed to investigate the electrochemical behavior of the electrode. The FESEM microphotographs showed that columnar based needle like nano-particles occurred on the ridges of the roughened surface whereas more smooth and compact morphology was observed for the flat parts of the surface. It was seen that the electrode maintained its electrocatalytic activity for lower current density region and its stability when an anodic current of 1000 mA cm<sup>-2</sup> was applied.

**Electrochemical Impedance Spectroscopy of SEI on Porous SnO<sub>2</sub>/CNT Composite Anode for Lithium Ion Batteries:** *Abirami Dhanabalan*<sup>1</sup>; Xifei Li<sup>1</sup>; Yan Yu<sup>2</sup>; Kevin Bechtold<sup>1</sup>; Chunlei Wang<sup>1</sup>; <sup>1</sup>Florida International University; <sup>2</sup>Max Planck Institute for Solid State Research

Tin oxide based composites have been studied extensively because of the high theoretical specific capacity compared to the commercialized carbon anode. During charge and discharge, solid electrolyte interface (SEI) film is formed at the interface between the electrolyte and anode due to the reaction between the anode and the electrolyte. SEI is a thin lithium ion conductive film which protects the anode from co-intercalation of solvents and consequent exfoliation. It has important influence on the irreversible capacity, cycle performance and stability of Li<sup>+</sup> insertion into anode. In this work, impedance studies were carried out on SnO<sub>2</sub>/CNT anodes prepared by electrostatic spray deposition (ESD). The deposition temperature and concentration of CNT in the composite were also varied. The electrochemical impedance spectroscopy (EIS) test was performed to understand the formation and the change of SEI film on SnO<sub>2</sub>/CNT anode with subsequent cycling. The equivalent circuit was proposed to fit the EIS plots.

**Enhanced Mechanical Properties in Mg-Based Ultrafine Eutectic-Dendrite Composites:** Jong Youn Lee<sup>1</sup>; Tae Eung Kim<sup>1</sup>; Sung Woo Shon<sup>1</sup>; Won Tae Kim<sup>2</sup>; Do Hyang Kim<sup>1</sup>; <sup>1</sup>Yonsei University; <sup>2</sup>Cheongju University

Nano grained materials exhibit a remarkable improvement in strength when compared with conventional coarse-grained alloys. However these materials generally suffer from insufficient plastic strain and reduced toughness during deformation. In the present study, a possible way to fabricate MgSnZn and MgSnCu nanostructure-dendrite composites with enhanced plasticity has been investigated. Our main focus is to investigate systematically the effect of microstructure evolution on mechanical properties. We prepared in-situ bulk samples with ultrafine scale eutectic-dendrite composite structure via an injection casting method. In particular, alloys with compositions near ternary eutectic composition were investigated to design the microstructure with different length scale. In the case of Mg-Sn-Zn alloys, addition of ~7at% Zn in Mg-10.7at%Sn alloy effectively endows larger plastic strain reaching ~over 10% with a reasonably high strength of ~657MPa.

**Enhancing Mineral Beneficiation by High Intensity Power Ultrasound:** *Jagdish Pandey*<sup>1</sup>; Manish Raj<sup>1</sup>; Moni Sinha<sup>1</sup>; Nikhiles Bandyopadhyay<sup>1</sup>; <sup>1</sup>TATA STEEL Ltd.

The paper highlights the attempts made at R & D of Tata Steel Ltd. to reduce impurities from iron ore such as alumina, silica and phosphorous under the influence of high intensity power ultrasound using 20 KHz frequency and 220 Watt power. The laboratory trials indicated 5 minutes treatment time for iron ore slurry containing 1:10 solid/liquid ratio could reduce alumina from 1.72 to 1.12 % and silica from 1.70 to 1.34 % whereas no significant reduction in phosphorous was observed. Scanning Electron Microscope (SEM) micrographs revealed the locations on the surface where the alumina phase in the microstructure detached due to ultrasonic treatment for 5 minutes. The possible reason appears to be the cavitation and streaming under the influence of high intensity power ultrasound. Based on the laboratory results, a pilot scale plant to treat 100 Kg of ore/coal has been set up to implement it in the plant.

**Evaluation of High Energy Milling Behavior of ZnO Powders in Different Milling Conditions:** *Sezen Yakar*<sup>1</sup>; Ahmet Söyler<sup>1</sup>; Burak Özkal<sup>1</sup>; Sebahattin Gürmen<sup>1</sup>; Mustafa Öveçoglu<sup>1</sup>; <sup>1</sup>ITU

In compare to many other techniques, high energy milling is a very effective and simple technique to produce nanocrystalline powders with the possibility of obtaining larger quantities. On the other hand, application of high energy milling is limited because of the contamination problems. In this study, milling behavior of ZnO powder was studied using different equipment including Spex Mixer and planetary ball mill under different milling conditions. Milled powders were characterized via XRD, BET, LPS measurements and SEM observations for the optimization of milling conditions leading nanosized ZnO powders.

**Fabrication and Mechanical Properties of NbC-binders (Co, Ni, Fe) Nano-Composite Consolidated by High Frequency Induction Heated Sintering:** *Kee-Do Woo*<sup>1</sup>; Duck-soo Kang<sup>1</sup>; Sang-hyuk Kim<sup>1</sup>; Seong-bae Park<sup>1</sup>; Na-young Song<sup>1</sup>; In-jin Shon<sup>1</sup>; <sup>1</sup>Chonbuk National University

Recently, high energy mechanical milling (HEMM) has become a popular method to fabricate nanocrystalline due to its simplicity and relatively inexpensive equipment. Many of the metal carbides (WC, NbC, TiC, etc) are very interesting and important for several industrial applications such as abrasive material, cutting tools, wear resistant parts in wire drawing, extrusion and pressing dies and wear-resistant surfaces. Especially, NbC is a very important material with promising properties such as outstanding hardness, good resistance to chemical attack and excellent electronic conductivity. The aim of this study was to fabricate the nano-sized carbide, NbC based material, with 10vol.%binders(Ni, Co and Fe) by using high frequency induction heated sintering(HFIHS) method. The relative densities of the sintered NbC-10vol.%binders(Ni, Co and Fe) composites by using HFIHS, pressure of 80MPa were respectively about 91.26%, 91.90% and 91.26%. The grain size, fracture toughness and hardness of NbC-10vol.%Co were 33nm, 10.5 MPa·m<sup>1/2</sup> and 1409 kg/mm<sup>2</sup>, respectively.

**Fabrication of FeS<sub>2</sub>-Pyrite Cathode by Spray Dryer Methode:** *Sang Dae Kang*<sup>1</sup>; Sung Hyun Choi<sup>1</sup>; Kyung Rok Do<sup>1</sup>; Hyo Jun Ahn<sup>1</sup>; In Sup Ahn<sup>\*\*1</sup>; <sup>1</sup>School of Nano and Advanced Materials Engineering, I-C&D Center, K-MEM R&D Cluster, Gyeongsang National University

A lot of studies about the Li/FeS<sub>2</sub> secondary battery, which has high ion capacity and energetic density. In order to obtain nano size FeS<sub>2</sub> particles, Fe



metal salt solution and sulfur solution were prepared for spray drying. Active carbon and iron die-sulfide were mixed with the ratio of 1/3 and 2/3. The mixture was milled in the planetary ball mill to fabricate carbon coated iron die-sulfide particles. The porous compact for electrode was made by sintering the mixture at the temperature range between 400 and 700°. The microstructure was observed by SEM and phase transformation was analyzed by XRD and TEM. The 60 nm size FeS<sub>2</sub> particles was obtained by spray drying, and the carbon was coated at the surface on the iron sulfide surface homogeneously, and the relative density of 55% was measured at the electrode compact. The capacity of early charge indicated 900mAh/g and formed.

**Fabrication of the Mg/Al Clad Sheet and Its Mechanical Properties:** *Beomsoo Shin*<sup>1</sup>; *Sockyeon Yoon*<sup>1</sup>; *Changseong Ha*<sup>2</sup>; *Seungkwan Yun*<sup>2</sup>; *Donghyun Bae*<sup>1</sup>; <sup>1</sup>Yonsei University; <sup>2</sup>G-Alloy Technology Co., Ltd.

Mg-Zn base alloy clad with the thin Al1050 sheets were fabricated by means of a hot rolling process at 280°C. Microstructure of the interface and mechanical properties of the clad sheets were investigated. After heat treatment at 230°C for 30 min, average 15 µm sizes of grains were developed in the Mg alloy sheet and Mg-rich layer was found to be developed about 2 µm in thickness at the Mg and Al interface. Tensile test was carried out at the initial strain rate range of 1x10<sup>-3</sup>s<sup>-1</sup> ~ 1x10<sup>-4</sup>s<sup>-1</sup> and the temperature range up to 300°C. The clad sheet shows superior elongation to failure not only at room temperature but also at the elevated temperatures compared to the Mg alloy sheets. During the test, few numbers of cracks which provide the formation of necking are developed in the layer.

**Facile Synthesis of Hollow Co<sub>3</sub>O<sub>4</sub> Microspheres by Solution Spray-Oxidation Method and Its Properties as Supercapacitors:** *Guo Qiusong*<sup>1</sup>; *Du Guangrong*<sup>1</sup>; *Guo Xueyi*<sup>1</sup>; <sup>1</sup>Central South University

The hollow Co<sub>3</sub>O<sub>4</sub> microspheres were synthesized by solution spray-oxidation method. The feed solution was prepared by using CoCl<sub>2</sub>•6H<sub>2</sub>O as raw materials, sprayed by using inner mixed air-nozzle and roasted in the erective pipe resistance furnace with compressed oxygen as carrier gas. The as-prepared samples were characterized by FT-IR, XRD and SEM techniques. The results show that the reaction temperature has an important impact on micro-structure and purity during the process of spray and oxidization for cobalt chloride solution, and the hollow Co<sub>3</sub>O<sub>4</sub> microspheres were obtained at 700°. Furthermore, the electrochemical tests show that the electrode prepared by the samples exhibits distinct characteristic of capacitance, the electrochemical capacitive properties of the hollow Co<sub>3</sub>O<sub>4</sub> microspheres were evaluated using cyclic voltammetry and alternating current impedance methods. The capacitive properties depict that the sample Co<sub>3</sub>O<sub>4</sub> by spray-oxidation method is capable of exhibiting excellent capacitive performance in 3.0 mol·L<sup>-1</sup> KOH electrolytes.

**Fast SET Switching Behavior of Nano-Scale AgInSbTe Based Phase Change Memory:** *Sung-Hoon Hong*<sup>1</sup>; *Byeong-Ju Bae*<sup>1</sup>; *Heon Lee*<sup>1</sup>; <sup>1</sup>Korea University

Phase change random access memory (PRAM) is considered to be the most promising next generation non-volatile memory. As a phase change material, Ge<sub>2</sub>Sb<sub>2</sub>Te<sub>5</sub> (GST) material has been mainly used as the phase change material in PRAM cells, however new phase change material should be needed for high density PRAM device because of high operation power. In this study, Ag and In co-doped SbTe based phase change material was used to fabricate phase change memory. It was proved that AgInSbTe material has higher thermal stability than that of GST material by the in-situ measurement of both the temperature dependent X-ray diffraction and sheet resistance. And Fast set speed was proved by measuring a 200nm diameter sized Ag<sub>6</sub>In<sub>5</sub>Sb<sub>59</sub>Te<sub>30</sub> nano-pillar phase change device by means of a conducting atomic force microscope (AFM) connected to a pulse generator and voltage source.

**Fatigue Life Prediction for Notched Structures Using Mechanistic Multistage Fatigue Model:** *Yibin Xue*<sup>1</sup>; *Brian Jordan*<sup>2</sup>; *Mark Horstemeyer*<sup>2</sup>; <sup>1</sup>Utah State University; <sup>2</sup>Mississippi State University

Physically motivated mechanistic MultiStage Fatigue (MSF) model is developed to predict fatigue damage state of structural components under variable and multiaxial loading cases. The MSF model depicts the effects of microstructural features on fatigue damage evolution stages, i.e., incubation, small crack growth, and long crack growth. It allows the assessment of variations in fatigue behaviors associated with random microstructural features and stochastic interference between damage progression and microstructural features. The application of MSF model to notch structures under variable loading cases is realized such that variable loads are reorganized at the notch

root not only as stress, strain or plastic strain but also as supplementary plastic deformation or residual stresses induced by overloads. The MSF model predicts comparable fatigue lives, and upper and lower bounds of notched structure under variable loading for structural health prognosis of an airframe-wing component under various service conditions.

**Fatigue of Hybrid Polymeric Composites on Twisting:** *Nikoloz Chikhradze*<sup>1</sup>; *Levan Japaridze*<sup>2</sup>; *Guram Abashidze*<sup>2</sup>; *Levan Okijava*<sup>3</sup>; <sup>1</sup>Mining Institute/Georgian Technical University; <sup>2</sup>G. Tsulukidze Mining Institute; <sup>3</sup>Zavriev Institute of Building Mechanics and Seismic Stability

In the paper, the results of the testing on twisting of the composites representing an epoxy matrix reinforced by high-strength and high-modulus carbon fiber, basalt and glassy fiber are considered. Reinforcing components were characterized by the following data: linear density of carbon filament 390 tex, of basalt one – 330 tex and of glassy one – 1500 tex. Investigated composites with the corresponding arrangement of each of these reinforcing elements in relation to the product axis is dedicated for the fabrication of the shell and of the spar of wind turbine blade. Composites are prepared by prepreg technology and have the following physical characteristics: density 1.49-1.55 g.cm<sup>-2</sup>, porosity -9,2-9,7%, phase concentration: of matrix 61,1-67,0%, of fibers 38,9-43,0%. Composites, selected for the testing on twisting differed from the composites of other series by larger values of short-term mechanical strength on tension, compression, bending and shearing.

**Finite Element Analysis of Residual Stress of Plasma-Sprayed Coatings on Thick Wall Components Based on Nastran Software:** *Li-Ping Niu*<sup>1</sup>; *Ting-an Zhang*<sup>1</sup>; *Guan-yong Shi*<sup>1</sup>; *Zhi-he Dou*<sup>1</sup>; *Ji-cheng He*<sup>1</sup>; *Xiao-chang Cao*<sup>1</sup>; *Dongping Zhan*<sup>1</sup>; <sup>1</sup>Northeastern University

Residual internal stresses of plasma-spraying lies on different materials and technological parameters, it's hard to study by experimental systematic and most of the experimental methods are ruinous, needs to spend a lot of time and funds. In this paper, residual internal stresses were estimated by mathematical analysis based on finite element analysis. Calculated results of the model shows well agreements with the experimental results of Alumina and tungsten coatings on different matrixes (by plasma-sprayed). The computational results shows that coefficient of thermal expansion, preheating temperature of matrixes and thickness of coating have greater impact on residual internal stresses. Key words: plasma-sprayed, residual stresses, mathematical model, finite element analysis

**Flip Chip Bonding of Sn-58Bi Solder Bumps Formed on Flexible PCB:** *Sehyung Lee*<sup>1</sup>; *Yuesoen Shin*<sup>1</sup>; *Sehoon Yoo*<sup>1</sup>; *Chang -Woo Lee*<sup>1</sup>; <sup>1</sup>Korea Institute of Industrial Technology

Low melting temperature Sn-58Bi solder bumps were formed on the flexible PCB by electrodeposition and joint and reliability properties were evaluated in this study. Diameter of fabricated bumps was 35µm. Flip chip bonding was performed under the temperature of 180° and the bonding force of 40 N. Thermal shock test (TS) was performed with the range from -40 to 85°. The IMC growth thicknesses before and after TS test were 2µm and 5µm, respectively. Shear strengths before and after TS test were 35gf/bump and 20gf/bump, respectively. Shear strength decreased by 40 % after TS compared with that before TS. The mechanism of the microstructural change and bonding strength decrease will be discussed.

**Formation of Different Generations of Gamma Prime Precipitates in Rene 88DT Nickel Base Superalloy:** *Antarikh Singh*<sup>1</sup>; *Junyeon Hwang*<sup>1</sup>; *Soumya Nag*<sup>1</sup>; *Srinivasan Rajagopalan*<sup>2</sup>; *Jaimie Tiley*<sup>3</sup>; *Gopal Viswanathan*<sup>2</sup>; *Hamish Fraser*<sup>2</sup>; *Rajarshi Banerjee*<sup>1</sup>; <sup>1</sup>University of North Texas; <sup>2</sup>The Ohio State University; <sup>3</sup>Air Force Research Laboratory

The compositional and microstructural evolution of different generations of γ' precipitates during the continuous cooling, followed by isothermal aging, of a commercial nickel base superalloy, Rene 88DT, have been characterized by three dimensional atom probe tomography (3DAP) coupled with energy-filtered transmission electron microscopy (EFTEM) studies. After solutionizing in the single γ phase field, during continuous cooling at a relatively slow rate (~ 24°C/min), the first generation primary γ' precipitates, forming at relatively higher temperatures, exhibit near-equilibrium compositions, while the smaller scale secondary γ' precipitates, forming at lower temperatures, exhibit non-equilibrium compositions often consisting of excess Co and Cr, while being depleted in Al and Ti content. Subsequent isothermal aging at 760°C, leads to the composition of the secondary γ' precipitates being driven towards equilibrium.

# Technical Program

The mechanisms associated with the early stages of nucleation and growth of the different generations of these  $\gamma'$  precipitates will be discussed.

**Fracture and Fatigue of Fe-Based Metallic Glass Ribbons:** *Adel El-Shabasy*<sup>1</sup>; Hala Hassan<sup>1</sup>; John Lewandowski<sup>2</sup>; <sup>1</sup>Ain Shams University; <sup>2</sup>Case Western Reserve University

Vickers microhardness indentations, tension and notch toughness tests, as well as controlled static and cyclic strain experiments via bending over mandrels of different diameter have been performed on 30  $\mu\text{m}$  thick Fe78Si9B13 metallic glass ribbons. In addition, Fe-Si-Cr-B ribbon used in magnetic applications has also been tested. For the Fe78Si9B13 ribbons Vickers microhardnesses of  $910 \pm 100$  kg/mm<sup>2</sup> and  $1030 \pm 40$  kg/mm<sup>2</sup> were obtained for the air side and wheel side, respectively. Tensile strengths were  $1640 \pm 35$  MPa. While the notch toughnesses obtained were  $94.5 \pm 5.5$  MPa $\sqrt{\text{m}}$ . The static "bend over mandrel" tests revealed that the ribbons simply deformed via shear banding for mandrel diameters as small as 0.225 mm. Fully reversed flex bending fatigue experiments revealed a fatigue limit of  $\approx 260$  MPa. SEM examination was used to characterize all fracture surface details. These results are discussed in the light of recent work on metallic glass systems. Funds provided by NSF-EGYPT Collaborative Research Program.

**Furnace Pressure Control System:** *Robert Voyer*<sup>1</sup>; <sup>1</sup>Hatch

A efficient furnace pressure control is essential in order to achieve fuel efficiency in casthouse furnaces. Some casthouse teams consider present furnace pressure control technology as unsatisfactory and are experimenting with a variety of methods. During this poster session, Hatch will introduce invention for a new, simple and innovative method to be used for furnace pressure control.

**Glass Forming Ability and Mechanical Properties of Zr-Based Zr-Al-Ni Metallic Glasses:** Yanhui Li<sup>1</sup>; Wei Zhang<sup>2</sup>; Chuang Dong<sup>1</sup>; Jianbing Qiang<sup>2</sup>; Akihiro Makino<sup>2</sup>; Akihisa Inoue<sup>3</sup>; <sup>1</sup>School of Materials Science and Engineering, Dalian University of Technology; <sup>2</sup>Institute for Materials Research, Tohoku University; <sup>3</sup>Tohoku University

Recently, bulk metallic glasses (BMGs) with critical diameter more than one centimeter were discovered in Zr-based Zr-Al-Cu and Zr-Al-Co ternary alloy systems. In this study, aiming to develop new Zr-based BMGs with high glass-forming ability (GFA) and good mechanical properties in Zr-Al-Ni system, the thermal stability, GFA, and mechanical properties of the alloys were systematically investigated. The fully glassy samples with critical diameter above 10 mm were obtained in a wide composition range of present system. The BMGs have a large supercooled liquid region ( $\Delta T_x$ ) and reduced glass transition temperature ( $T_{rg}$ ) more than 70 K and 0.54, respectively. Room compression test revealed that the BMGs exhibit a high yielding strength of 1.7–2 GPa and distinct plastic strain. The BMGs also showed good corrosion resistance in 1 N H<sub>2</sub>SO<sub>4</sub> solution. In addition, the crystallization behavior of the alloys was investigated for understanding their high GFA.

**Grain Boundary Character Distribution and Mechanical Property of an as Cold Rolled High Nitrogen Austenitic Stainless Steel:** Wei Yan<sup>1</sup>; Yin Shan<sup>1</sup>; Ke Yang<sup>1</sup>; Wei Wang<sup>1</sup>; <sup>1</sup>Institute of Metal Research

Grain boundary character distribution and mechanical property of a cold rolled stainless steel with high nitrogen content of 0.66% in weight were studied. The employed cold rolling reductions are 0%, 10% and 20%, respectively. It is shown that both yield strength and ultimate tensile strength were almost linearly increasing with increase of the cold rolling reduction, but uniform elongation was decreased. The high nitrogen steel is found to possess the plastic instability stress (PIS), which is independent of cold working condition. The microstructure deformed by cold rolling was studied by transition electron microscopy (TEM). Electron back scattered diffraction (EBSD) was used to further evaluate the evolution of the grain boundary character distribution, which was caused by the planar slipping of dislocations. The combination of the above two characteristics produced a deeper understanding of the relationship between the deformed microstructure and the mechanical property.

**Heterogeneous Phase Nucleation and Growth in  $\beta$ -Ti Alloys:** *Robert Williams*<sup>1</sup>; Soumya Nag<sup>2</sup>; Arun Devaraj<sup>2</sup>; Peter Collins<sup>1</sup>; Srinivasan Rajagopalan<sup>1</sup>; Rajarshi Banerjee<sup>2</sup>; Hamish Fraser<sup>1</sup>; <sup>1</sup>The Ohio State University; <sup>2</sup>University of North Texas

$\beta$ -Ti alloys exhibit several complex and competing phase transformations, such as the nucleation of the metastable  $\omega$ -phase at low to intermediate

temperatures,  $\beta$ -phase separation at intermediate temperatures and intragranular nucleation and growth of the  $\alpha$ -phase that can be assisted by the  $\omega$ -phase and/or  $\beta$ -phase separation. Through study on the commercial Ti-5553 and model Ti-Mo alloy systems, an attempt is made to understand the stability of the  $\omega$ -phase, and factors governing the nucleation of the  $\alpha$ -phase, at low to intermediate temperatures. Using a combination of (HR)STEM, HRTEM, EELS and 3DAP Tomography, the structure and composition of the  $\omega$  and  $\alpha$  phases are investigated for various alloy compositions and thermal histories. Finally, an attempt is made to rationalize  $\omega$ -assisted  $\alpha$ -nucleation and  $\beta$ -phase separation-mediated nucleation of the  $\alpha$ -phase in  $\beta$ -Ti alloys.

**High Reliability Bonding Process Using Ag-Cu Mixed Nanoparticles:** *Yoshiaki Morisada*<sup>1</sup>; Toru Nagaoka<sup>1</sup>; Masao Fukusumi<sup>1</sup>; Yukiyasu Kashiwagi<sup>1</sup>; Mari Yamamoto<sup>1</sup>; Masami Nakamoto<sup>1</sup>; Hiroyuki Kakiuchi<sup>2</sup>; Yukio Yoshida<sup>2</sup>; <sup>1</sup>Osaka Municipal Technical Research Institute; <sup>2</sup>Daiken Chemical Co.

Low temperature bonding process using Ag-Cu mixed nanoparticles was investigated. Though Cu nanoparticles is expected to be the material for low temperature bonding, the bonding temperature of  $\sim 400^\circ$  and the bonding pressure of  $\sim 20$  MPa are need to obtain good joints. In this study, the bonding temperature and pressure were decreased by addition of the Ag nanoparticles and the bonding strength of the joint reached about 50 MPa at the bonding condition of  $350^\circ$  and 10 MPa. Additionally, the sintered layer of the Ag-Cu mixed nanoparticles showed excellent ion migration resistance.

**Impact Toughness Enhancement of an Electron Beam Welded Ti-6Al-4V Titanium Alloy through Post-Welding Heat Treatment:** *Christophe Buirette*<sup>1</sup>; Julitte Huez<sup>1</sup>; <sup>1</sup>CIRIMAT-ENSIACET

Electron beam welding of Ti-6Al-4V leads to a loss of mechanical properties in the fusion zone such as fatigue or impact toughness. Fast cooling rate and the associated  $\alpha'$  martensitic structure are at the origin of this observation. Various parameters of heat treatment, like soaking time above  $\beta$  transus, cooling rates and stress relieving treatment have been investigated. The analysis of the resulting microstructures associated with impact toughness and tensile tests results allows us to point out the efficiency of each post-weld heat treatment. Moreover these different tests are necessary to investigate the fracture toughness of various microstructure, for a better understanding of damage mechanisms.

**Impacts of Impurities on the Properties of Secondary Al-Si-Cu Alloys:** *Daryoush Emadi*<sup>1</sup>; Musbah Mahfoud<sup>1</sup>; <sup>1</sup>Qatar University

Recycling of aluminum alloys could provide major economic and environmental benefits. In addition to energy savings, increasing the use of recycled metal is also quite important from an ecological standpoint. Therefore, it is essential to identify, develop, and implement technologies that will optimize the benefits of recycling. In recent designs, Al parts have been used in conjunction with other materials, and therefore, tramp or alloying elements from other alloys, such as tin or scandium become trace elements in the recycled Al alloys. The present study discusses the effects of these trace elements on the mechanical properties of secondary 319 alloy in as-cast and heat-treated conditions. Moreover, a new function, Alloy Recycling Index, is discussed as an industry aid to recognizing the relative recyclability of aluminum alloys, with the goal of maximizing the industry contribution to a green environment.

**Improvement of Heat Dissipation in High-Power Light-Emitting Diodes Using Highly Heat Conductive Die-Attach Material:** *Chia-ju Chen*<sup>1</sup>; <sup>1</sup>National Chung Hsing University

In recent years, applications of high-power light-emitting diodes (HP LED) have constantly increased. HP LED requires high current drives than before and then generates much heat. Only 15–20% of the input power converts to light and the rest converts to heat. The heat generated by LED chip must be dissipated to the environment effectively in order to maintain the thermal stability of the LED devices. In this poster, we proposed a novel composite die-attach material for LED packaging. This composite die-attach material is prepared by adding proper amounts of nanosized diamond particles into commercial Sn-3wt.%Ag-0.5wt.%Cu (SAC305) solder paste. Since diamond is a highly heat conductive material with a excellent heat conductivity of 2300 W/mk, its incorporation into the SAC305 solder paste ( $\sim 20$  W/mk) can promote greatly the heat conductive capacity of the die attach materials and thereby dissipates heat more effectively.



**In-Plane Compressive Properties of Hybrid Dyneema®/Carbon Fiber Reinforced Polymer Matrix Composites:** *Shahram Amini*<sup>1</sup>; John Shaw<sup>1</sup>; Michael Rossol<sup>1</sup>; Frank Zok<sup>1</sup>; <sup>1</sup>University of California, Santa Barbara

The principal objective of the study is to investigate the potential performance benefits derived from the addition of high performance polyethylene fibers to carbon fiber reinforced polymer (CFRP) composites. The study focuses specifically on 3D orthogonal weaves with carbon employed for the warp and weft yarns and Dyneema® for the z-yarns. Experiments on a series of composite panels with various volume fractions of z-yarns demonstrate that the retained in-plane compressive strength following impact is indeed enhanced by the presence of the z-yarns. The benefits derive from a reduced propensity for delamination during impact and buckling of the in-plane fibers during subsequent compressive loading. Analogous trends are obtained for open-hole compression. Insights into the failure mechanisms are gleaned from microstructural examinations of impacted specimens as well as in situ full-field strain measurements during compression testing.

**Influence of Cold Working and Grain Size on the Pitting Corrosion Resistance of Ferritic Stainless Steel:** *Zhen Li*<sup>1</sup>; Zhouhua Jiang<sup>1</sup>; Huabing Li<sup>1</sup>; Zuru Zhang<sup>1</sup>; <sup>1</sup>Northeastern University

The influence of cold working and grain size on the pitting corrosion resistance of Fe-Cr-Nb-Mo ferritic stainless steel is investigated using optical microscope and electrochemical methods. The pitting corrosion resistance firstly decreases then increases with increasing the cold-rolling reduction. The number of nucleation site of pitting corrosion increases from 0 to 30% cold-rolling reduction which results in the reduction of pitting potential. However, the increment of pitting potential can be attributed to disappearance of grain boundaries, stacked dislocation and uniform microstructure from 40% to 60% cold-rolling reduction. The recrystallization behavior of the steel with 60% cold-rolling reduction occurs completely after 5 minutes annealing time at 1100°. With prolonging the annealing time, the grain size of the steel grows, and the pitting potential of the steel decrease. The smaller grain size promotes the formation of compact passive film and improves the pitting corrosion resistance.

**Influence of Forming Ratio on Mechanical Properties of Pipe Line:** *Amir Abachi*<sup>1</sup>; Mehdi Naderi<sup>1</sup>; Afshin Erfanfar<sup>1</sup>; Reza Shamloo<sup>1</sup>; <sup>1</sup>Safa Rolling and Pipe Mills Co.

During pipe forming and testing, different layers of plate thickness undergoes in different modes of stress and the competition between the bauschinger effect and strain hardening determines the final properties of the pipe. To investigate the mechanical properties and difference between plate and pipe, tests were carried out on API X52 and X70 line pipe steels. These tests conducted on plate and pipe with different forming ratios. To perform the behavior of plate under different conditions according to forming ratios, a Finite Element simulation used to modeling the response of the material using industrial software based on FEM method. The results show that at a certain forming ratio, the negative difference between plate and pipe properties become positive by elimination of ladders elongation.

**Influence of Shock Prestraining and Texture on the Dynamic-Tensile-Extrusion of High-Purity Zirconium:** *Daniel Martinez*<sup>1</sup>; Carl Trujillo<sup>1</sup>; Joel Montalvo<sup>1</sup>; Victoria Webster<sup>1</sup>; <sup>1</sup>Los Alamos National Laboratory

The mechanical behavior and damage evolution in textured, high-purity zirconium (Zr) is influenced by strain rate, temperature, stress state, grain size, and texture. In particular, texture is known to influence the slip-twinning response of Zr, which directly affects the work hardening behavior at both quasi-static and dynamic strain rates. However, while microstructural and textural evolution of Zr in compression and to relatively low strains in tension has been studied, little is understood about the dynamic, high strain, tensile response of Zr. Here the influence of texture on the dynamic, tensile, mechanical response of high-purity Zr is correlated with the evolution of the substructure. A bullet-shaped sample is impacted into a steel extrusion die using dynamic-tensile-extrusion process. Mechanical Threshold Stress (MTS) modeling will be performed to provide insight into the dynamic extrusion process. Quantitative comparisons between the predicted and measured deformation topologies and extrusion rates will be presented.

**Influence of the Magnesium Addition on the Strength, Ductility and Microstructure of Al-7.4Zn At.% Alloy Artificially Aged at Different Times:** *J. Baron De la Rosa*<sup>1</sup>; A. Garcia H.<sup>1</sup>; B. Campillo<sup>2</sup>; S. Valdez<sup>2</sup>; <sup>1</sup>FQ-UNAM; <sup>2</sup>UNAM-ICF

Microstructural characterization, tension and microhardness tests were carried out in an Al-7.4Zn at.% alloy in order to know the influence of magnesium content. The microstructure was observed by using scanning electron microscopy, in order to study the phases developed by the aged treatment. The mechanical strength and ductility properties, were investigated by using Vickers microhardness measurements, and tensile test pulled to failure at room temperature using an Instron Universal Testing Machine, at a constant crosshead speed with an initial strain rate of  $3 \times 10^{-3} \text{ s}^{-1}$ . Microstructure results show the presence of  $\text{Al}_3\text{Mg}_2$  and  $\text{MgZn}_2$  on the  $\alpha$ -Al matrix for aged samples. In addition, a significant enhancement of the mechanical properties compared to the casting alloy were obtained.

**Influences of Rotational Speed and Welding Speed on the Friction Stir Welding between Copper and 304L Stainless Steel:** *Yousef Imani*<sup>1</sup>; Mohammad kazem Besharati<sup>1</sup>; Reza Abdi<sup>1</sup>; <sup>1</sup>University of Tehran

Dissimilar friction stir welding between 304L stainless steel and commercially pure copper plates with thicknesses of 3 mm was performed. A number of FSW experiments were carried out to obtain the optimum mechanical properties by adjusting the rotational speed and welding speed in the range of 500-1000 rpm and 14-112 mm/min, respectively and with an adjustable offset of the pin location with respect to the butt line. Microstructural analysis has been done to check the weld quality (defective or defect free). Cross-sectioning of the welds for metallographic analysis in planes perpendicular to the welding direction and parallel to the weld crown was also performed. The mechanical properties of the welds were determined using a combination of conventional hardness and tensile testing. From this investigation it is found that the offset of the pin is an essential factor in producing defect free welds in friction stir welding of copper and steel.

**Interfacial Reactions of Pure Sn, Sn-3.0Ag-0.5Cu and Sn-9.0Zn Lead-Free Solders with the Fe-42Ni Substrate:** *Yu-Ping Hsieh*<sup>1</sup>; *Yee-wen Yen*<sup>1</sup>; Chien-Chung Jao<sup>1</sup>; <sup>1</sup>National Taiwan University of Science & Technology

The study investigated the interfacial reactions between Sn, Sn-3.0 wt%Ag-0.5 wt%Cu (SAC) and Sn-9 wt%Zn (SZ) and the Fe-42Ni (Alloy 42) substrate at 240, 255 and 270°. The experimental results indicated that two intermetallic compounds (IMCs) with different surface morphologies were observed in the Sn/Alloy42 couple. However, both they were the FeSn<sub>2</sub> phases. In the SAC/Alloy 42 couples, only the (Fe,Ni)Sn<sub>2</sub> phase was formed at the interface. Three layers structure of IMCs were observed in SZ/Alloy 42 couples and they were the (Ni,Fe)5Zn<sub>21</sub> phases. Two stages of IMC thickness change were found in three couples. The IMC thickness in these couples increased as increasing reaction times and temperatures, and it was proportional to the square root of reaction time. As the results, the interfacial reaction mechanism of them was diffusion controlled.

**Investigation of Possibility to Metallic Interconnector on the IT (Intermediate Temperature) SOFC:** *Kee-Do Woo*<sup>1</sup>; *MinSeok Moon*<sup>1</sup>; *Eui-pyo Kwon*<sup>1</sup>; *Sang-hyuk Kim*<sup>1</sup>; *Duck-soo Kang*<sup>1</sup>; *Myeong-han Yoo*<sup>1</sup>; <sup>1</sup>Chonbuk National University

IT SOFC (intermediate temperature solid oxide fuel cell) has low operating temperature than conventional SOFC system. In this study, the possibility of application of stainless steel as IT-SOFC materials was studied. An oxidation resistance layer on each differently surface treated specimen was investigated by using XRD, and FE-SEM. EDX result of STS430 showed that oxidation thickness of as polished, as received and sand blast samples were about 7.8µm, 12.8µm and 8.8µm, respectively. With increasing the exposed time from 100hr to 400hr, the oxide thickness of as polished, as received and sand blast samples increased to about 41.7µm, 17.7µm and 10.3µm, respectively. As a result, sand blast sample had very stabilized oxide film.

**Investigation of Weldability during Laser Lap Welding of Dissimilar Al Alloys:** *Cheolhee Kim*<sup>1</sup>; *Do-Chang Ahn*<sup>1</sup>; *Namhyun Kang*<sup>2</sup>; <sup>1</sup>KITECH; <sup>2</sup>Pusan National University

Requirements in terms of weight reduction in the automotive industry lead to wide usage of aluminum alloys which have low density and good formability. As various kinds of aluminum alloys are applied to the car body structure, the welding technologies between various combinations of Al alloys are also

# Technical Program

required. The aluminum alloys have high thermal conductivity, high thermal expansion and high affinity for hydrogen so laser welding is one of most preferred joining methods in the automotive industry. This research investigated the overlap welding of dissimilar Al alloy sheets – 5J32 and 6K32. The plates have 1mm thickness, respectively, and a 4kW Yb:YAG disk laser was used as heat source. Al 5J32 and 6K32 have different thermal conductivity and chemical compositions so the arrangement of the plates affected the weld quality of lap welds. The mechanical and metallurgical behaviour of weldment were observed according to the arrangement of the plates.

**Investigation on the Compressive Properties and Microstructural of New Sand Polymer Composite:** Esmail Sadeghi Meresht<sup>1</sup>; Jamshid Aghazadeh<sup>1</sup>; Mohsen Seifi<sup>1</sup>; <sup>1</sup>Amirkabir University of Tehran

The development of new construction materials using recycled plastics is important to both the construction and the plastic recycling industries. This work aimed to reuse the PET bottles waste as a partial additive to sand in mortar compositions in form of Sand Polymeric Composite (SPC) so as to reduce the amount of waste and save the environment from its hazards. The resulting products from the PET mortar compositions give comparable performance against compressive strength. Best conditions for the tested variables with weight proportion of sand to PET were 2 at 250°C temperature with 5 minutes for stiffing time. The results showed maximum compressive strength around 65 MPa. In addition it was observed from scanning electron microscopy fine microstructure and coherency between filler particles of sand and PET polymeric chain and porosity of structure.

**Investigation Surface Faint-Sliver Defects of Cold-Rolling IF Steel Sheets from Slabs Produced by Continuous Casting:** Jian Zhang<sup>1</sup>; Cheng Dengfu<sup>1</sup>; Li Jianquan<sup>2</sup>; <sup>1</sup>Chongqing University; <sup>2</sup>Vanadium Recovery & Steelmaking Plant, Panzhihua New Steel & Vanadium Co.Ltd

Surface faint-sliver defects of cold-rolling IF steel sheets will have a bad effect on the appearance and use of rolled products. In this paper, it is revealed that Al<sub>2</sub>O<sub>3</sub> is the important reason for causing surface faint-sliver defects of cold-rolling IF steel sheets by detecting the inclusion in the strands and analyzing the quality of finished rolled products. Therefore, some methods can be employed to evidently weaken surface faint-sliver defects of cold-rolling IF steel sheets, which include the ladle slag modifier to decrease oxidizability of the ladle slag, high basicity (CaO/SiO<sub>2</sub>) refining slag, controlling chemical composition of slag to increase the absorbency of slag to inclusion, improving the clean of steel liquid, decreasing the amount and size of Al<sub>2</sub>O<sub>3</sub> inclusion and properly increasing the heating time of strand in heating-furnace.

**Investigations of Shock\_Wave Induced SHS Reactions in Ni-Al System:** George Oniashvili<sup>1</sup>; Mikheil Chikhradze<sup>1</sup>; Inga Janelidze<sup>1</sup>; Nikoloz Chikhradze<sup>2</sup>; <sup>1</sup>Institute of Metallurgy and Materials Science; <sup>2</sup>G. Tsulukidze Mining Institute

Intermetallics, obtained in Ni-Al system are attractive materials for high-temperature structural applications. Synthesis of Ni-Al intermetallics using shock wave compaction technology was the interest of several investigations. The ratio of Ni and Al were selected accordance of phase diagram of Al-Ni. The precursors were processed in ball mill for activation of surfaces before compaction. Particles sizes was 40-80µm. The assembly was placed in explosive container and surrounded with explosive materials. The ammonite, Hexogene were used as explosives. Following SC/SHS compacts were recovered in different shapes and prepared for investigations. Ni-Al powders of two different compositions were explosively loaded in cylindrical mode and successfully realized shock-wave induced reactions. The stress components, generated by pressure impulse, propagated along the surface by constant rate velocity have been theoretically calculated. The SEM and X-ray analyses were carried out for investigation of microstructure and phase composition. The porosity was estimated using the optical microscope.

**Joint Strength of Cu-Sn58Bi-Cu Bonding with Cap Bump Thickness Variation:** Yueseon Shin<sup>1</sup>; Sehyung Lee<sup>1</sup>; Jeonghan Kim<sup>1</sup>; Changwoo Lee<sup>1</sup>; Sehoon Yoo<sup>1</sup>; <sup>1</sup>KITECH/Micro-joining center

Cu pillar bumps has been received great attention in ultra fine pitch 3D packaging. Unlike solder bumps which are collapsed after flip chip bonding, Cu pillar maintained original dimension after bonding, therefore, no bridging occur for ultra fine pitch 3D bonding. In this study, Sn-58Bi on Cu pillar bumps were bonded on the Cu pad and the joint properties were investigated. Sn-58Bi solder were formed onto the Cu pillar bumps with electroplating. The diameters of the bumps were 30 µm. Flip chip bonding was performed under the temperature of

180° and the bonding force of 40 N. Shear strength of as-reflowed joint at the cap solder thickness with 5µm was higher than samples with other thickness. In addition, Shear strength decreased with aging time due to IMC growth at the interface.

**Kinetics of Titanium and Chromium Carbides Coating Produced on Structural Steel by Thermo-Reactive Deposition Technique:** Helal Tahirlu<sup>1</sup>; Mosaad Sadawy<sup>1</sup>; Elshan Elshan<sup>1</sup>; Taherli Shirinov<sup>1</sup>; <sup>1</sup>University of Technology

A multi-component diffusion study of titanium and chromium on steel substrate has been studied by pack cementation process. The thickness, structure and hardness of the coated layers have been investigated at different time and temperatures by optical microscopy, X-ray diffraction (XRD) analysis and Vickers micro-hardness tests. The coating layer formed on the steel samples is smooth and compact and well bonded to the steel matrix. The thickness of titanium and chromium carbides layer formed on the steel samples ranged from 20 to 32 µm, depending on temperature and the treatment time. The kinetics of the reaction have also been studied.

**Laser Beam Welding of Haynes 188:** Akin Odabasi<sup>1</sup>; Necip Unlu<sup>1</sup>; Gultekin Goller<sup>1</sup>; Niyazi Eruslu<sup>1</sup>; <sup>1</sup>Istanbul Teknik Universitesi

Haynes 188 (HN-188) is a commonly used Co-Ni-Cr-W superalloy since 1960s (Haynes 188 is a registered trademark of Haynes International, Kokomo, IN, USA). Because of its excellent high temperature strength, good resistance to hot corrosion, and wear resistance, HN-188 has found extensive applications such as afterburner components and combustors. Even the alloy has been investigated previously, new industrial processes such as laser beam applications i.e., laser beam welding, and laser powder deposition, increase the demand on theoretical and experimental knowledge. In this research, laser beam welding characteristics of HN-188 superalloy (2.1 mm thick) were investigated. Two different heat inputs (61.3 J/mm and 90.1 J/mm) and travel speeds (46.5 mm/s and 22.2 mm/s) were applied. The base metal (BM), fusion zone (FZ), heat affected zone (HAZ) and the geometry of weld seams were characterized using optical microscopy (OM) and scanning electron microscopy (SEM). In addition, the welded samples were examined radiographically.

**Lattice Constant Effect on the Deformation Behavior of Mg-Zn-Re Alloys:** Sock Yeon Yoon<sup>1</sup>; Beomsoo Shin<sup>1</sup>; Donghyun Bae<sup>1</sup>; <sup>1</sup>Yonsei University

Since the slip system of the magnesium alloys is significantly limited at room temperature, other deformation modes are imparted during deformation. In this study, we can change the amount of the soluble elements in the matrix by varying the content of the rare-earth in Mg-Zn-Re alloy, thereby developing the alloys having different lattice constants. The alloys are produced under an Argon atmosphere. Lattice parameters are obtained from the X-ray diffraction patterns using the Cohen method. As the amount of the rare-earth element increases, the lattice constants increase in some composition range. These results induce higher flow stress and enhanced twinability when the lattice constant increases. The deformation behavior of the alloy sheets at room and elevated temperature will be presented.

**Local Stress and Strain Analysis of Atomistic Simulations:** Matthew Priddy<sup>1</sup>; Donald Ward<sup>1</sup>; Phil Gullett<sup>1</sup>; <sup>1</sup>Center for Advanced Vehicular Systems, Mississippi State University

Molecular dynamic simulations are used to examine the failure in isolated triple junctions in aluminum. Understanding the state of the material for which voids nucleate is essential in helping to characterize the conditions that facilitate damage at the nanoscale. The simulations are displacement controlled, uniaxial and biaxial deformation with the voids nucleating at or near the triple junction or along a grain boundary. This work evaluates the local stress, local strain, and local triaxiality to better elucidate the state of the material during deformation. Simulation results for various grain orientations and textures are compared.

**Low Temperature Bonding Process Using Cu Nanoparticles:** Toru Nagaoka<sup>1</sup>; Yoshiaki Morisada<sup>1</sup>; Masao Fukusumi<sup>1</sup>; Yukiyasu Kashiwagi<sup>1</sup>; Mari Yamamoto<sup>1</sup>; Masami Nakamoto<sup>1</sup>; Hiroyuki Kakiuchi<sup>1</sup>; Yukio Yoshida<sup>1</sup>; <sup>1</sup>Osaka Municipal Technical Research Institute

Bonding of oxygen-free copper using various sizes of Cu nanoparticles was investigated. The bonding process was conducted in air under the condition of the pressure of 5-20 MPa and the temperature of 300-400°C. The average sizes of Cu nanoparticles were 7.2 nm, 203 nm, and 498 nm, respectively. The joints with Cu nanoparticles (203 nm) showed the highest shear strength among the samples. Since Cu nanoparticles (7.2 nm) should be coated with Cu<sub>2</sub>O before



bonding because of its small size, it was difficult to be sintered. On the other hand, it seems that the size of Cu nanoparticles (498 nm) was too large to be sintered at low temperature of 300–400°C. Cu nanoparticles (203 nm) prevented oxidation and showed low-temperature sintering property. Consequently, it seems that the size of Cu nanoparticles (203 nm) should be suitable for low temperature bonding.

**Magnetic Properties of High-Coercivity Nanocrystalline Pr-Fe-Co-Al-B Bulk Amorphous:** *Lofi Bessais*<sup>1</sup>; <sup>1</sup>CNRS

The Pr-based bulk-amorphous have attracted much attention as they were regarded as promising magnetic materials. In this study our objective is to improve the hard magnetic properties of the bulk amorphous PrFeCoAlB by a controlled nanocrystallization of the as-milled alloys and understand the nature of the entities responsible for this improvement. Besides magnetic measurements, we have carried out structural investigations, HRTEM, and Mössbauer spectroscopy. PrFeCoAlB bulk amorphous shows a coercivity of 8kOe. The controlled nanocrystallization enhances the coercivity to 30kOe and remanent magnetization to 90emu/g. Those values are the highest ever found for annealed bulk amorphous isotropic systems. The grain size for optimal magnetic properties is around 28nm. The high coercivity is explained by several effects: the exchange coupling F-AF, a low dipolar interaction, and a low value of the effective demagnetizing factor. As a consequence, those systems open a route for promising permanent magnet applications.

**Mechanical Properties and Rapid Consolidation of Binderless Nanostuctured Tantalum Carbide from Mechanically Activated Powder by Pulsed Current Activated Sintering:** *In-Jin Shon*<sup>1</sup>; Byung-Ryang Kim<sup>1</sup>; Min-Seok Moon<sup>1</sup>; Kee-Do Woo<sup>1</sup>; Na-Ri Kim<sup>1</sup>; <sup>1</sup>Chonbuk University

Industrial applications of metal carbides are cutting tools, hard coating, and hard constituents in the metal matrix composites for high temperature applications because of their great strength, hardness and melting temperature. Among these carbides, tantalum carbide has a very important and promising properties, such as outstanding hardness, high melting point (3880°), good resistance to chemical attack, thermal shock and oxidation, and excellent electronic conductivity. Highly dense nanostructured TaC with a relative density of up to 96% were obtained within 2 minutes by pulsed current activated sintering under a pressure of 80 MPa. The relative density of TaC increased and the average grain size of TaC decreased with milling time. The hardness and fracture toughness of the dense TaC produced by PCAS were 2076, 1645, 1287 kg/mm<sup>2</sup> and 6.8, 7.6, 8.9 MPa.m<sup>1/2</sup> with milling time for 10, 4, and 1h, respectively.

**Mechanical Properties of the Ti-Nb-X%HA Biomaterials Fabricated by High Frequency Induction Heated Sintering Using High Energy Ball Milled Powders:** *Kee-Do Woo*<sup>1</sup>; Sang-hyuk Kim<sup>1</sup>; Duck-soo Kang<sup>1</sup>; Jung-nam Woo<sup>1</sup>; Xiaopeng Wang<sup>1</sup>; Zhiguang Liu<sup>2</sup>; <sup>1</sup>Chonbuk National University; <sup>2</sup>Harbin Institute of Technology

Ti and Ti based alloy are widely used as biomaterial due to low density, high strength and good biocompatibility. Especially, Ti-6%Al-4%V ELI alloy is one of the most useful biomaterials. But, Ti-6%Al-4%V ELI alloy has been reported that Al leads to Alzheimer's disease and V is classified into toxic material. Also, Ti-6Al-4V ELI alloy is high elastic modulus material than that of bone. Therefore, biomaterial with low elastic modulus and non-toxic characteristics has to be developed. The aim of this study was to fabricate the Ti-Nb-HA composites by high frequency induction heated sintering (HFHS) at 1000° under 60MPa pressure using high energy mechanical milled Ti, Nb and HA powders for 0~8hr. After sintering, the physical and mechanical properties of the Ti-Nb-HA composites have been investigated. As results, relative density and hardness of the sintered Ti-42wt%Nb-(0,10,15)wt%HA composites which milled for 8hr were 94%, 611.7kg/mm<sup>2</sup>, 95%, 865.2kg/mm<sup>2</sup>, 97% and 882.3kg/mm<sup>2</sup>, respectively.

**Mechanical Properties of Consolidate of Nanostructured Niti Alloy by Rapid Sintering:** *In-Jin Shon*<sup>1</sup>; Na-Ri Kim<sup>1</sup>; In-Yoong Ko<sup>1</sup>; Je-Shin Park<sup>2</sup>; Wonbaek Kim<sup>2</sup>; <sup>1</sup>Chonbuk University; <sup>2</sup>Korea Institute of Geoscience and Mineral Resources

NiTi alloy has been used in many areas such as naval, automobile, robotic, nuclear, aerospace, and biomedical applications because of practical shape memory alloy with high strength, ductility, excellent corrosion resistance, wear resistance, and good biocompatibility. NiTi was synthesized from Ni and Ti powder during the high energy ball milling for 10hours. Dense nanostructured

NiTi was consolidated within 2 minutes from the mechanically alloyed powder by pulse current activated sintering under pressure of 80Mpa. The grain size, hardness and fracture toughness of NiTi sintered by pulse current activated sintering were 166nm, 696kg/mm<sup>2</sup> and 7MPa•m<sup>1/2</sup>, respectively.

**Mechanical Strength and Fracture Behavior of Silicon Wafer Based-Solar Cell:** *Jai-Won Byeon*<sup>1</sup>; Bong-Kul Shin<sup>1</sup>; Chang-Yong Hyun<sup>1</sup>; <sup>1</sup>Seoul National University of Technology

During mass production of Si wafer-based solar cell, unexpected fractures have been reported to occur at the substrate Si-wafer or thin film layer. Mechanical and thermal stress induced during the fabrication process cause failure at the defects such as microcrack in Si-wafer and interface between substrate and thin film layer. In this study, the effect of saw damages and thickness of Si wafer as well as fabrication process variables on the strength and fracture behavior of solar cell were investigated. Wafers with different thickness from 200 μm to 100 μm were prepared by chemical etching of as-saw wafer. Fracture strength as a function of thickness of Si wafer was measured by four point bending test of over 50 bending specimens in one wafer. Fracture surface was observed to examine crack initiation site by scanning electron microscopy and non-destructive scanning acoustic microscope. These observations were discussed in relation with measured fracture strength.

**Mechanical Strength Change of Dissimilar Friction Stir Welded Joint between Al and Mg Alloys by Probe Position Variation:** *Yoonki Sa*<sup>1</sup>; Hansur Bang<sup>2</sup>; Heonsun Bang<sup>2</sup>; Yutaka S. Sato<sup>3</sup>; Sehoon Yoo<sup>1</sup>; Changwoo Lee<sup>1</sup>; <sup>1</sup>Korea Institute of Industrial Technology; <sup>2</sup>Chosun University; <sup>3</sup>Tohoku University

Mechanical properties of dissimilar friction stir welding (FSW) joint of Al and Mg alloys were improved by shifting probe position. Significantly high tensile strength of 218.8 MPa, which was 81~87 % of the tensile strength of matrix materials, was achieved when probe position was 0.9 mm shifted toward Al6061 side from the center of the weld. The tensile strength was 182.9 MPa when probe was located at the center and it was 132.3 MPa when the probe was 0.9 mm shifted toward AZ31 from the center. The amount of plastic flow was the highest when probe position was shifted toward Al6061. Finite element analysis indicated that the weld had high and well-distributed temperature on the basis of joint line when the probe position was shifted by 0.9 mm toward Al6061 side. Such thermal characteristics by shifting probe position led to enhance plastic flow and tensile strength.

**Microstructural Characterization of the Composite AlZnAg Clad Coating on AlFe:** S. Casolco<sup>1</sup>; S. Valdez; <sup>1</sup>ITESM-Puebla

The composite material has been clad by the rolling process. A layer of AlZnAg alloy has been coated on both surfaces by an AlFe film. The characterization was carry out by atomic force microscopy (AFM) and scanning electron microscopy (SEM) in both transversal and longitudinal section zone in order to know the surface morphology. The results show a strong mechanical bond between the AlZnAg and AlFe alloys. In addition the composite-clad material has been deformed by tension test and their results shows bands of strain, due to the superplastic deformation and the small grain size

**Microstructural Weak Links for Spall Damage in Polycrystalline Metals:** Leda Wayne<sup>1</sup>; *Pedro Peralta*<sup>1</sup>; Darrin Byler<sup>2</sup>; Christine Tomforde<sup>1</sup>; Stephan Digiacomio<sup>1</sup>; Shima Hashemian<sup>1</sup>; Heber D'Armas<sup>3</sup>; Shengnian Luo<sup>2</sup>; Scott Greenfield<sup>2</sup>; Robert Dickerson<sup>2</sup>; Kenneth McClellan<sup>2</sup>; <sup>1</sup>Arizona State University; <sup>2</sup>Los Alamos National Laboratory; <sup>3</sup>Universidad Simon Bolivar

Correlations between spall damage and local microstructure were investigated using multi- and polycrystalline copper samples via laser-driven plate impacts at low pressures (2-6 GPa). The short pressure pulses (250 ns), allowed isolating microstructural effects on spall damage. Velocity interferometry was used to measure free-surface velocity, to monitor spall failure, and to examine changes on the shock response due to microstructure variability. Electron Backscattering Diffraction was used to relate the presence of porosity to microstructural features such as grain boundaries and triple points. Potential sites for preferred damage nucleation and strain localization were identified in terms of their crystallography via statistical sampling in serial sectioned specimens. Results indicate that terminated twins and grain boundaries with misorientations between 25° and 50° are the preferred locations for intergranular damage localization. Two-dimensional hydrocode simulations based on crystallography and geometry of selected damage sites are used to correlate these variables to the presence of damage.

# Technical Program

**Microstructure and Formation Mechanical of 3D-Meshy SiC/2Cr13 Composite Interface:** *Yu Liang*<sup>1</sup>; *Ru Hongqiang*<sup>1</sup>; <sup>1</sup>Texture of Materials, Ministry of Education, College of Materials and Metallurgy, Northeastern University,

The microstructure, formation mechanism of the matrix and the interface of SiC/2Cr13 composites have been investigated by XRD, EDS attached to SEM. Results showed that the interface included two zones, which are silicon carbide reaction zone (SRZ) and metal reaction zone (MRZ), and the MRZ can be divided two zones, one is the poor chromium zone (PCrZ-MRZ) and the other is rich chromium zone (RCrZ-MRZ). SRZ is mainly composed of the bright matrix of Fe<sub>5</sub>Si<sub>3</sub>Cr<sub>7</sub>C<sub>3</sub>Cr<sub>23</sub>C<sub>6</sub> and Cr<sub>3</sub>Si, and randomly distributed graphite precipitates. RCrZ-MRZ mainly contains Cr<sub>23</sub>C<sub>6</sub>. PCrZ-MRZ is mostly made up of Fe<sub>2</sub>Si. The order of the interface formation is determined by the solidification rate of the material resultant. Cr<sub>23</sub>C<sub>6</sub> in the PCrZ-MRZ casts firstly. Secondly, Fe<sub>2</sub>Si casts in the PCrZ-MRZ. Finally, Fe<sub>5</sub>Si<sub>3</sub> deformed by Fe<sub>2</sub>Si casts in the SRZ. The PCrZ-MRZ hinders the interface reaction by inhibiting the diffusion of Fe atoms from the alloy towards the SRZ.

**Microstructure and Mechanical Properties of Al Based Composite Coatings Produced by the Cold Gas Dynamic Spraying Process:** *Onur Meydanoglu*<sup>1</sup>; *Huseyin Cimenoglu*<sup>1</sup>; *Eyup Kayali*<sup>1</sup>; <sup>1</sup>Istanbul Technical University

In this study, microstructure and mechanical properties (hardness and wear) of Al-B4C composite coatings at various amount of B4C content prepared on structural steel substrate by cold spraying were investigated. Microstructural characterization was performed by XRD, optical and scanning electron microscopes. Hardness values and wear resistances of composite coatings wear measured. It was observed that hardness and wear resistance of composite coatings were higher than that of pure Al coating. Although hardness of coatings increased with increasing amount of B4C content, no significant change was observed in the wear resistances of composite coatings with change of B4C content.

**Microstructure and Phase Evolution of Uranium and Dysprosium Nitrides Formed during Reactive Ball Milling:** *Brian Jaques*<sup>1</sup>; *Daniel Osterberg*<sup>1</sup>; *Cole Smith*<sup>1</sup>; *Patrick Callahan*<sup>1</sup>; *Brian Marx*<sup>1</sup>; *Darryl Butt*<sup>1</sup>; <sup>1</sup>Boise State University

Uranium, dysprosium, and (U<sub>x</sub>, Dy<sub>1-x</sub>) (where X ranges from 0 to 1) metals have been ball milled for different lengths of time in a nitrogen atmosphere. It was found that full conversion of dysprosium metal to DyN occurs in less than 60 minutes and results in a phase pure mononitride, DyN, which has a FCC crystal structure. Ball milling uranium metal in nitrogen results in a phase pure sesquinitride, U<sub>2</sub>N<sub>3</sub>, which has a BCC crystal structure. As the uranium content is decreased to 60 mol% the resultant powder is primarily amorphous. However, when the uranium content reaches 50 mol%, a FCC crystal structure is observed. The temperature and pressure of the milling vessel was recorded as a function of time to gain insight into the kinetics of the nitridation reactions. The resultant materials were characterized by means of x-ray diffraction, electron microscopy, and particle size analysis.

**Microstructure Changes in Primary Recrystallization of Grain-Oriented Silicon Steel by Pulse Current Intermediate Annealing:** *Lihua Liu*<sup>1</sup>; *Qiangqiang Xia*<sup>1</sup>; *Wen Shi*<sup>1</sup>; *Lijuan Li*<sup>1</sup>; *Xueliang Wu*<sup>1</sup>; *Qijie Zhai*<sup>1</sup>; *Wu Zeng*<sup>1</sup>; <sup>1</sup>Shanghai University

The effect of intermediate annealing by pulse current on the grain textures and final magnetic properties of grain-oriented silicon steel sheets produced by one-stage rolling method was investigated. It was found that the texture and microstructure of the sample treated by pulse current are very different from that by conventional annealing treatment. Pulse current annealing, for primary recrystallization, increases the (110) crystal plane to 3 times as strong as that of furnace annealing, and increases the special boundaries with misorientation angles of 20-45°, but has little influence on grain size. Pulse current intermediate annealing improves magnetic properties (B<sub>8</sub>) and enables to reduce the iron loss in oriented silicon steel after secondary recrystallization. In addition, for pulse current intermediate annealing, from primary to secondary recrystallization Goss texture increased 38 times from primary to secondary recrystallization, for pulse current intermediate annealing but for conventional treatment, only increases 22times.

**Microstructure Components and Mechanical Properties of an Acicular Ferrite Pipeline Steel:** *Wei Wang*<sup>1</sup>; *Yin Shan*<sup>2</sup>; *Wei Yan*<sup>2</sup>; *Ke Yang*<sup>2</sup>; <sup>1</sup>Electric Power Research Institute, Guangdong Power Grid Corporation; <sup>2</sup>Institute of Metal Research

Through thermo-mechanical controlled processing (TMCP), the acicular ferrite (AF) microstructures with different phase components were obtained in a pipeline steel, and the relation between AF microstructures and mechanical properties was investigated. The results showed that the effective grain size (EGS) reduced obviously with decreasing finish rolling temperature (FRT), but did not change with cooling rate (CR) and simulated coiling temperature (SCT). Lowering FRT or enhancing CR could increase the percentage of granular bainitic ferrite (GF) and bainitic ferrite (BF). The content of high angle grain boundaries (HAGBs) increased with the decrease of FRT when FRT=800°, then decreased with FRT at 750°. It was found that the higher fraction of HAGBs led to the better low temperature toughness. When fine AF was obtained with high GF and BF content and low quasi-polygonal ferrite (QF) content, the steel could possess good strength and toughness.

**Microstructure Development of Silicon Steel Prepared by Near-Rapid Solidification:** *Xianyong He*<sup>1</sup>; *Quanzhi Sun*<sup>1</sup>; *Lei Wang*<sup>1</sup>; *Qin Peng*<sup>1</sup>; *Qijie Zhai*<sup>1</sup>; <sup>1</sup>Shanghai University

The aim of this work was to have an insight into microstructure development of silicon steel by thin strip continuous casting. The experiments were designed to approximate the solidification conditions of thin strip continuous casting and carried out under controlled laboratory conditions. The thin strip with three different silicon compositions were prepared by vacuum non consumable arc-melting. Based on the experiments of thin strip casting in lab, the cooling rate was determined by different strip thickness. The effects of compositions on the microstructure of silicon steel thin strip are studied. The results show that the microstructure of thin strip with different composition and thickness are composed of dendrite and equiaxed grain. With change of silicon content and strip thickness, the solidification structure and area percent of equiaxed grain varies significantly.

**Microstructures and Four-Point-Bending Fatigue Behavior of Three Kinds of Low-Carbon Steels for Load-Chain Materials:** *Wei Wu*<sup>1</sup>; *Gongyao Wang*<sup>1</sup>; *David Huber*<sup>2</sup>; *Peter Hogan*<sup>2</sup>; *Rodney Reynolds*<sup>2</sup>; *Jules Raphael*<sup>2</sup>; *Peter Liaw*<sup>1</sup>; <sup>1</sup>The University of Tennessee; <sup>2</sup>Columbus McKinnon Corporation

Three kinds of low-carbon steels, 10B22, 4615, and 4720, are used in electric hoists as load-chain materials. The microstructures of these low-carbon steels were observed. Four-point-bending-fatigue tests were conducted on cylindrical specimens to examine the fatigue behaviors of these low-carbon steels at different stress levels. The four-point-bending-fatigue tests were performed at a stress ratio of 0.1 and a frequency of 10 Hz with a sinusoidal waveform. The fatigue results showed that the fatigue-strength of the 10B22 steel was the highest at the reference cycles, 107. However, the fatigue-strength of the 4720 steel is the lowest at the same fatigue life. The fractography was investigated by using scanning electron microscopy (SEM), which indicated that the fatigue cracks initiated from the specimen surface and propagated transgranularly.

**Microstructures and Mechanical Properties of AM60B-based Eco-Mg Alloys:** *Min-Ho Choi*<sup>1</sup>; *Dong-In Jang*<sup>1</sup>; *Shae K. Kim*<sup>1</sup>; <sup>1</sup>Korea Institute of Industrial Technology

This paper focuses on the potential to maintain mechanical properties of CaO added Eco-Mg alloys based on AM60B Mg alloy which has been applied to automobile parts where excellent ductility, toughness, and crashworthiness are required. It has already verified that the mechanical properties of CaO addition of below 0.3wt.% as ingredient into AZ31B and AZ91D Mg alloys can be maintained with refined grain size. CaO does not exist as CaO itself in the solidified state. The purpose of this paper is to investigate the tendency of grain refinement and the change of mechanical properties, esp. elongation for CaO added AM60B Mg alloys with respect to CaO contents, on the basis of non-SF<sub>6</sub> gas processing and maintaining the alloy's process-abilities. CaO added AM60B Mg alloys were manufactured by conventional melting and casting procedure. Each alloy will be investigated through optical microscope, EDS analysis, and hardness and tensile tests.



**Molecular Dynamics Simulation of Au-Rh Precipitates Structure:** *Peihua Jing*<sup>1</sup>; Hyon-Jee Lee<sup>2</sup>; Ian Robertson<sup>3</sup>; Jae-Hyeok Shim<sup>4</sup>; Brian Writh<sup>2</sup>; <sup>1</sup>Structural Integrity Associates; <sup>2</sup>Department of Nuclear Engineering, The University of California; <sup>3</sup>Department of Material Science and Engineering; <sup>4</sup>Korea Institute of Science and Technology,

The strength and creep properties of precipitate strengthened materials are controlled by the interactions of dislocations with obstacles, which depend on precipitate coherency, elastic and thermodynamic properties. In this paper, the molecular dynamics simulations of oversized Au precipitates and undersized Rh precipitates are discussed and analyzed as a function of precipitate radius. For Au precipitates, coherency loss is associated with the defected matrix atoms forming an octahedral structure. Dislocation reaction analysis explains the observed structure of a network of Hirth dislocation and Shockley partial dislocations. As the precipitate size increases, additional Shockley partial dislocation loops emanate from the octahedron. For the undersized Rh precipitates, coherency loss involved an octahedral-type structure in the matrix. However, with increasing Rh precipitate size, the coherency loss transitioned to internal precipitate deformation. Evidently, above a critical size, the excess volume associated with an undersized precipitate allows for significant deformation within the precipitate.

**Modeling the Effect of the Contact Surface Temperature on the Deformation of an Aluminum Pin During A Wear Test:** *Mario Rosenberger*<sup>1</sup>; Elena Forlerer<sup>2</sup>; Carlos Schvezov<sup>1</sup>; <sup>1</sup>Universidad Nacional de Misiones; <sup>2</sup>Comisión Nacional de Energía Atómica

The temperature of the contact surface of aluminum pins increases under dry sliding, the temperature increases the plastic deformation of the subsurface, which moves and places superficial materials on the borders of the pin. A thermal model with asperities on the contact surface was developed to calculate the temperature field of the bulk, which is used in an elasto-plastic model to predict the pin deformation. A three-dimensional model was employed, and temperature dependent mechanical properties were assumed. Loads were applied simulating a test performed in a pin-on-ring machine. A sudden subsurface deformation was observed when the tangential load achieves a well determined value, defined as the critical load. This critical load increases when the temperature diminishes. The results of the model are compared with experiments performed on AA1060 alloys reinforced with 15 % alumina particles. Agreement between predictions and experiments was observed.

**Monitoring Particle Pulverization in Composite Silicon Anodes for Lithium Ion Batteries by Acoustic Emission:** *Kevin Rhodes*<sup>1</sup>; Claus Daniel<sup>2</sup>; Edgar Lara-Curzio<sup>2</sup>; Nancy Dudney<sup>2</sup>; <sup>1</sup>University of Tennessee; <sup>2</sup>Oak Ridge National Laboratory

Due to the brittle nature of Si, extensive particle fracturing occurs during lithiation which leads to capacity fade and eventual failure of the cell. Better understanding of particle degradation due to cycling is paramount to directing future research aimed to improve this material's stability. In this research, acoustic emission (AE) has been used to monitor events occurring within Si/Li foil half cells during both constant current-constant voltage (CCCV) and cyclic voltammetry (CV) tests. CCCV between 50mV-1.3V showed the greatest amount of AE activity on the first Li intercalation with each subsequent cycle delivering progressively fewer emissions. SEM showed deep cracks and particle fractures. When CCCV was limited between 170mV-1.3V significantly fewer emissions were recorded and no notable particle damage was observed. CV testing at 0.05mV/s between gave AE activity only on Li intercalation at low potentials. SEM of these samples shows extensive surface cracking and peeling on the particle surface.

**Neutron Diffraction Measurements of Residual Stresses in Bent Stainless Steel Pipes:** *Mihyun Kang*<sup>1</sup>; Wanchuck Woo<sup>1</sup>; Vyacheslav Em<sup>1</sup>; Hyoung Seop Kim<sup>1</sup>; Sun Ig Hong<sup>1</sup>; Baek-Seok Seong<sup>1</sup>; Kye Hong Lee<sup>1</sup>; <sup>1</sup>KAERI (Korea Atomic Energy Research Institute)

Owing to the extraordinary anti-corrosion and high strength properties, stainless steels have been widely used for the structural materials in nuclear power plants. In many designs and applications, bending of the pipes is inevitable and the residual stresses can be detrimental to the integrity of the end products. In this study, we investigated the distributions of the residual stresses from bent 304 stainless steel pipes using neutron diffraction. A total of four seamless pipes, as-received state (without bending) and bent with the three different bending curvatures (R = 250,500 and 750 mm), have been prepared.

Each pipe specimen was installed in the residual stress diffractometer at HANARO (High-flux Advanced Neutron Application Reactor), KAERI (Korea atomic energy research institute) and the residual stresses were measured at several different locations of pipes. The neutron diffraction results will be also compared to the computational simulation results calculated using the finite element method.

**Numerical Simulation of Alumina Sintering:** *Mohammed Kadhim*<sup>1</sup>; <sup>1</sup>University of Technology

Sintering process has been analysed mathematically by prediction unsteady-state mathematical model in order to give more description and understanding for the mechanism of this process. This includes mass transport phenomena which may occur via diffusion. The spatial and temporal temperature profile with the solid medium has been determined by solving the unsteady state Fourier heat energy transport equation using the explicit finite difference numerical method, which would minimize the solution errors. This has been lead to more realistic determination of temperature distribution within the work-piece. Alumina has been selected as a target to represent nonmetallic material of diverse physical and thermal properties. The average grain size for alumina powder is 0.5  $\mu\text{m}$  with initial compact density 2160 kg/m<sup>3</sup>. These values gave a reliable approach to calculate the porosity and relative strength. The porosity is a function of density and relative strength, so the porosity decreases with increase in the density.

**On the Role of Peierls Stress in the Shock Response of Cubic Metals:** *Neil Bourne*<sup>1</sup>; <sup>1</sup>AWE

The response of four cubic metals to shock loading is reviewed in order to understand the effects of microstructure on continuum response. Experiments are described that link defect generation and storage mechanisms at the mesoscale to observations in the bulk. The behaviours described are linked through description of time-dependent plasticity mechanisms to the final states achieved. Recovered targets displayed dislocation microstructures illustrating processes active during the shock loading process. Lower symmetry metals possess high Peierls stress and thus have higher resistances to defect motion in the lattice under shock loading conditions. These behaviours illustrate the role of defect generation, transport, storage and interaction in determining the response of materials to shock prestraining.

**Oxidation and Ignition Resistances of AM60B-Based Eco-Mg Alloys:** *In-Kyum Kim*<sup>1</sup>; Jung-Ho Seo<sup>1</sup>; Shae K. Kim<sup>1</sup>; <sup>1</sup>Korea Institute of Industrial Technology

This paper focuses on the possibility to improve oxidation and ignition resistances of CaO added Eco-Mg alloys based on AM60B with good elongation, ductility and high-pressure die-castability. It has been already confirmed by the previous studies that the oxidation and ignition resistances of CaO added AZ31 and AZ91 are improved by the small addition of 0.3wt.% CaO. The purpose is to optimize CaO contents not only for improving the oxidation and ignition resistances but also for maintaining the alloy's process-abilities and mechanical properties, esp. elongation, on the basis of non-SF<sub>6</sub> gas processing. Varying amounts of CaO (0.1, 0.3 and 0.5wt.%) were added into AM60B and the prepared alloys were gravity-cast into a metallic mold. The oxidation resistance was examined through TGA. The ignition resistance was examined by DTA under dry air atmosphere. The AES depth profile was performed to evaluate the ignition resistance in terms of surface oxide stability.

**Oxidation Behavior of ZrB<sub>2</sub>-ZrO<sub>2</sub> Composites Prepared by Spark Plasma Sintering:** *Lian Zhang*<sup>1</sup>; Junguo Li<sup>1</sup>; Jianrong Song<sup>1</sup>; Huiping Yuan<sup>1</sup>; Chuanbin Wang<sup>1</sup>; Qiang Shen<sup>1</sup>; <sup>1</sup>Wuhan University of Technology

ZrB<sub>2</sub>-ZrO<sub>2</sub> composites were prepared by spark plasma sintering at 1900° from ZrB<sub>2</sub> powders which were coated by and mixed with ZrO<sub>2</sub>-3mol%Y<sub>2</sub>O<sub>3</sub>, respectively. The composites were then oxidized at 1200° for 240 min and the phase, microstructure and weight change of the samples, before and after oxidation, were investigated. For the samples prepared from the mixed ZrB<sub>2</sub>-ZrO<sub>2</sub> powders, macro-cracks appeared on the sample surface and oxygen diffused rapidly through these cracks, leading to the fast oxidation of ZrB<sub>2</sub> grains. However, the oxidation rate of the composites prepared from coated ZrB<sub>2</sub> powders was decreased remarkably and they showed good resistance to oxidation. The main phase of the coated ZrB<sub>2</sub>-ZrO<sub>2</sub> composites was ZrB<sub>2</sub> with a small amount of t- and m-ZrO<sub>2</sub>, even after oxidation for 4 hours. No crack was discerned on the sample surface, and as a result oxygen diffused hardly through the ZrB<sub>2</sub> grain boundary.

# Technical Program

**Phase Decomposition during Aging in an Al-22wt.%Zn Alloy:** Lizbeth Melo-Maximo<sup>1</sup>; Dulce Melo-Maximo<sup>1</sup>; Susana Lezama-Alvarez<sup>1</sup>; Erika Avila-Davila<sup>2</sup>; Victor Lopez-Hirata<sup>1</sup>; Orlando Soriano-Vargas<sup>1</sup>; Jorge Gonzalez-Velazquez<sup>1</sup>; <sup>1</sup>Instituto Politecnico Nacional (ESIQIE); <sup>2</sup>Instituto Tecnologico de Pachuca

This work shows a study of morphology and growth kinetics of the phase decomposition as well as its effect on the hardening behavior during the aging at 373 and 393 K in an Al-22wt.%Zn alloy. The aging process was analyzed using a solution of the nonlinear Cahn-Hilliard equation by the explicit finite difference method. Besides, the aging process was studied by XRD, TEM and Vickers hardness of the aged Al-22wt.%Zn alloy. The numerical simulation results showed the supersaturated solid solution decomposed spinodally into a mixture of Al- and Zn-rich phases after aging. Simulation and TEM results showed that the morphology of the decomposed phases was irregular and interconnected and it changed to rounded particles as aging progressed. The increase in hardness is related directly to the formation of the decomposed phases during aging of this alloy.

**Plasma-Polymerization of Hexamethylcyclotrisiloxane Using Atmospheric Pressure Dielectric Barrier Discharge:** Gi Taek Kim<sup>1</sup>; Yoon Kee Kim<sup>1</sup>; <sup>1</sup>Hanbat National University

In this work, we have tried to deposit organosilicon layers from hexamethylcyclotrisiloxane (HMCTSO) using helium DBD generated by 30 kHz AC at atmospheric pressure. The compositions of organosilicon layers have been controlled from SiOC to SiO<sub>2</sub> by changing flow rates of the carrier gas and oxygen. The O<sub>2</sub>/HMCTSO-He carrier gas flow ratios ranged from 1:2 to 1:20 and the coatings have been grown with deposition rates in the range from 200nm/min to 800nm/min. The coatings exhibit Si-O bonding and Si-CH<sub>3</sub> bonding. The Si-O bonding was increased with the O<sub>2</sub>/HMCTSO-He carrier gas flow ratio and finally, silicon to oxygen ratios are approximately 1:2 with some incorporated carbon. We will discuss the effects of the composition of source gases on the surface morphologies and bonding structures of the films.

**Prediction of Rapid Solidification Nanosize Structure for Aluminium Alloys:** S. Valdez<sup>1</sup>; <sup>1</sup>UNAM-ICF

The purpose is to develop a principle based on kinetic and thermodynamic solidification theory in order to predict the rapid solidification nanosize structures to be applied at aluminium alloys. Thermodynamic considerations are based in the thickness of the solidified layer, which must be known in order to calculate the heat flux per unit time to the chill substrate. Considering that the cooling condition in melt spinning is controlled by the melt/substrate interface (Newtonian cooling). In addition, the equilibrium phase diagram has been used as well as assumptions based in the Scheil Solidification Model. For rapid solidification theory, is considered that the Local equilibrium exists at the solid/liquid interface, No diffusion in the solid phases, Uniform liquid composition and No density difference between solid and liquid.

**Preparation and Characterization of Nanocrystalline Silver Particles:** Burcak Ebin<sup>1</sup>; Elif Yazici<sup>1</sup>; Sebahattin Gurmen<sup>1</sup>; Burak Ozkal<sup>1</sup>; <sup>1</sup>Istanbul Technical University

Silver particles are widely used as antibacterial/microbial agent in medical, cosmetic, textile and marine sectors. They are also an important substance of conductive inks, paste, sensors and various electronic devices due to their physicochemical properties that can be controlled by size in nanoscale. In this research, nanocrystalline Ag particles were prepared by ultrasonic spray pyrolysis (USP) method using silver nitrate aqueous solution. The dependence of morphology, particles and crystalline sizes to the carrier gas (H<sub>2</sub>, N<sub>2</sub> and air) were investigated under 1.0 l/min gas flow rate, 0.1M precursor concentration, 600°C reaction temperature and 1.3 MHz ultrasonic frequency conditions. Scanning electron microscopy (SEM), energy dispersive spectroscopy (EDS) and X-ray diffraction (XRD) were used to investigate size, morphology and crystal structure of particles. It was observed that nanocrystalline spherical Ag particles obtained in all conditions with crystalline sizes are nearly 39 nm which are calculated by Scherrer equation.

**Preparation of Iridium Fine Particle by the Effect of Grinding Additive, NaCl:** Young Jin Kim<sup>1</sup>; Youngsan Ham<sup>1</sup>; Jaeryeong Lee<sup>1</sup>; <sup>1</sup>Kangwon National University

Grinding of the mixture, Ir(Iridium) and NaCl(Sodium chloride), was carried out for the preparation of Ir fine powders. For the Grinding for only Ir, the structure of Ir was defected and also the abrasion from the pot and balls was

input the ground mixture due to the intensive grinding. On the case of grinding with NaCl, the crystalline of Ir was kept and the abrasion was suppressed considerably. The fine Ir with a size of 1~3 μm can be prepared by the washing process for the ground with mixture.

**Pressureless Sintering of Al<sub>2</sub>O<sub>3</sub>-SiC Nano Composites and Effect of Additives on Sintering Temperature:** H.R. Rezaie<sup>1</sup>; <sup>1</sup>Iran University of Science and Technology

Al<sub>2</sub>O<sub>3</sub>-SiC nano composite ceramics were prepared by pressureless sintering with or without the addition of Y<sub>2</sub>O<sub>3</sub>, MgO and TiO<sub>2</sub> as sintering aids. The effects of these compositional variables on sintering rate and final density were investigated. The addition of 5 vol.% SiC to Al<sub>2</sub>O<sub>3</sub> hindered densification. In contrast, the addition of Y<sub>2</sub>O<sub>3</sub>, MgO and TiO<sub>2</sub> to Al<sub>2</sub>O<sub>3</sub>-5% SiC nanocomposites improved densification. Al<sub>2</sub>O<sub>3</sub> and SiC nano powders that were produced separately by sol gel method in previous work were used in this part as starting materials. Green bodies were obtained by uniaxial pressing of 200 MPa. Pressureless sintering was carried out in a nitrogen atmosphere at 1600°C and 1630°C. Maximum density (97%) was achieved at 1630°C. Vickers hardness 18GPa after sintering at 1630°C. Scanning electron microscopy revealed that the SiC particles were located predominantly to the interior of the matrix grains and well distributed throughout the compositemicrostructures.

**Process Modeling for Synthesis of Metal Matrix Nanocomposites:** Payodhar Padhi<sup>1</sup>; Biranchi Dash<sup>2</sup>; <sup>1</sup>Hi-Teh Medical College & Hospital; <sup>2</sup>Konark Institute of Science & Technology

The present study models the processing of metal matrix nanocomposites in a solidification rout, where the dispersion of nano ceramic particles in the liquid aluminum melt during the cavitation process. High-intensity ultrasound is used for mixing, dispersing and deagglomeration of the fine particles in the liquids. The model simulates the effect of pressure shock wave generated as a result of periodic collapsing of bubbles at a location on particle distribution within adjacent agglomerate of nano-particles. This model will demonstrate the phenomenon of deagglomeration and dispersion. In the model a combination of Eulerian multiphase and turbulence model will be used which solves a set of momentum and continuity equations for each phase. Coupling is achieved through the pressure and interphase exchange coefficients. The distribution of nano ceramic particles in the melt liquid during the process of metal matrix nanocomposites has been studied.

**Producing of Composite Layer of TiO<sub>2</sub>/Al5083 via Friction Stir Processing:** Reza Behnagh<sup>1</sup>; Mohamm Kazem Besharati<sup>2</sup>; <sup>1</sup>Tehran University; <sup>2</sup>Department of Mechanical Engineering, Tehran University

Friction stir processing is a solid state process to modify microstructure and mechanical properties of sheet metals and as-cast materials. In this process stirring action of the tool causes the material to intense plastic deformation that yields a dynamical recrystallization. In this study the effect of FSP and process parameters on hardness, and microstructure of Al5083 has been investigated. Also by using of FSP, composite layer of TiO<sub>2</sub>/Al5083 has been produced. Results show that, FSP leads to finer and homogenized grain structure, as well as increased hardness, strength, toughness, and elongation of material. The composites produced by FSP have uniformly distribution of TiO<sub>2</sub> particles between the grains of base metal.

**Production of Boron Fiber in a CVD Reactor:** Selim Ertürk<sup>1</sup>; Ismail Duman<sup>1</sup>; <sup>1</sup>Istanbul Technical University

Boron fibers are special yarns, having a diameter of 100-130 microns that are produced by chemical vapor deposition (CVD) process on tungsten filament (φ 10-15 microns) as the core material. A glass reactor used as CVD medium (30 cm length and 10 mm ID / 12 mm OD) was designed to investigate the optimum production conditions of boron fiber production by the reaction of borontrichloride and hydrogen gases. Reaction temperature is controlled by heating the tungsten substrate (wire) via mercury-indium amalgam. An FT-IR spectrophotometer is connected to the exhaust of the reactors to perform online chemical analysis of the effluent gas mixture. Experiments were carried out at atmospheric pressure and at a reaction temperature range of 800-1250 °C with different inlet reactant concentrations. According to production conditions, mechanical and chemical properties of the boron fibers were investigated.



**Production of Porous, Intermetallic Titanium Aluminide Reinforced Titanium Matrix Composites by Powder Metallurgy Method:** Aydin Bicer<sup>1</sup>; Eyup Kayali<sup>1</sup>; Huseyin Cimenoglu<sup>1</sup>; <sup>1</sup>Istanbul Technical University

In this study, intermetallic titanium aluminide reinforced titanium matrix composites were produced by conventional powder metallurgy method (i.e cold pressing and sintering). Composites produced directly from titanium (70wt%) and aluminum(30wt%) powder mixtures provided porosity (37%) consist of micropores formed by intermetallic transformation in the microstructure, while involving high compressive strength values (69MPa). In the present study porosities were increased by putting volatile polymer powders into mixture as additive and presintering at volatilizing temperature. When volatilizing (presintering) process performed, pores with same particle size took place of polymer powders in addition to smaller pores formed by intermetallic transformation during liquid phase sintering process at 700°C. Due to having two types of pores which have different particle size also provided an advantage of allowing interconnection. The structure was not only highly porous but also had remarkable compressive strength (23MPa) to maintain that sufficient porosity (63%).

**Production of Titanium Carbide Reinforced Titanium Matrix Composites via Powder Metallurgy Method:** Burak Karaduman<sup>1</sup>; Onur Meydanoglu<sup>1</sup>; Huseyin Cimenoglu<sup>1</sup>; Eyup Kayali<sup>1</sup>; <sup>1</sup>Istanbul Technical University

In this study titanium carbide reinforced titanium matrix composites were produced by conventional powder metallurgy method. Titanium powders were mixed with graphite powders at different compositions. Composites produced directly from titanium and graphite powder mixtures provided high amount of porosity in the microstructure, while involving high hardness values. In the present study porosities were eliminated by a two step process. As the first step bulk titanium carbide was produced from titanium and graphite powder mixture. In the second step porosity free titanium matrix composites were produced by utilizing the mixture of titanium carbide and titanium powders. In order to determine the effect of hot pressing on microstructure titanium and graphite mixtures were hot pressed at 1300C under vacuum conditions. Microstructural examinations, hardness measurements and wear tests were conducted on composites. Although relative densities of composites decreased, higher hardness values and wear resistances were obtained as titanium carbide content increased.

**Properties and Performance of Composites Based on Superrefractories Cements:** Ilyoukha Nickolai<sup>1</sup>; Timofeeva Valentina<sup>1</sup>; <sup>1</sup>Academic Ceramic Center

Superrefractories cements (1800-2700°C) is a new refractory insulating material and objective of this work is to enlarge our knowledge about this new product and to search solutions for problems the industry is facing. Based on this target, we realized several test to find answers to important questions about the application of this product in severe industrial conditions and to analyze how this material performs in high temperatures. High temperature composites and coatings based on superrefractories cements are meant to protect units from influence of temperature more than 2000°C and used for manufacturing monolithic lining, crucibles used in the melting of pure metals, including alloys on rare-earth elements, for closing one of ceramic modules of fire wall, in refractory lining of quartzglasstanks, petrochemistry reactors, H<sub>2</sub>, furnaces, carbon reactors in burial of radiation wastes by extreme environments. Key words: composites materials, properties, performances, cements reactors, temperature.

**Properties and Rapid Consolidation of Nanostructured Ti from Mechanically Activated Ti and TiH<sub>2</sub> By High Frequency Induction Heated Sintering:** In-Jin Shon<sup>1</sup>; Na-Ri Kim<sup>1</sup>; In-Yong Ko<sup>1</sup>; Je-Shin Park<sup>2</sup>; Wonbaek Kim<sup>2</sup>; <sup>1</sup>Chonbuk University; <sup>2</sup>Korea Institute of Geoscience and Mineral Resources

Titanium has a good deformability, high hardness, high biocompatibility, excellent corrosion resistance and low density. Due to these attractive properties, it has been used in many industrial applications. Dense nanostructured Ti was sintered from mechanically activated Ti and TiH<sub>2</sub> powders by the high frequency induction heated sintering under pressure of 80Mpa, respectively. TiH<sub>2</sub> powder was decomposed to Ti during the sintering. The hardness of Ti increased and the average grain size of Ti decreased with increasing milling time. The average grain sizes of Ti sintered from Ti powder and TiH<sub>2</sub> powder milled for 5hrs were about 17nm, 28nm, respectively. The hardness and fracture

toughness of Ti sintered from Ti powder and TiH<sub>2</sub> powder milled for 5hrs were 504kg/mm<sup>2</sup>, 567kg/mm<sup>2</sup> and 7MPa•m<sup>1/2</sup>, 7MPa•m<sup>1/2</sup>, respectively.

**Properties and Rapid Consolidation of Nanostructured Tasi<sub>2</sub> from Mechanically Synthesized Powder by High Frequency Induction Heating:** In-Jin Shon<sup>1</sup>; Seung-Myoung Chae<sup>1</sup>; In-Yong Ko<sup>1</sup>; Jin-Kook Yoon<sup>2</sup>; Kee-Do Woo<sup>1</sup>; <sup>1</sup>Chonbuk University; <sup>2</sup>Korea Institute of Science and Technology

TaSi<sub>2</sub> has an attractive combination of properties, including high melting temperature, high modulus, high oxidation resistance in air, and a relatively low density. To improve on its mechanical properties, the approach commonly utilized has been the addition of a second phase to form composite and to make nanostructured materials. Nanopowder of TaSi<sub>2</sub> was synthesized from Ta and 2Si powder during the high energy ball milling for 20hrs. Dense nanostructured TaSi<sub>2</sub> was consolidated by high frequency induction heating within 2 minutes from mechanically synthesized powders of TaSi<sub>2</sub>. Highly dense TaSi<sub>2</sub> with relative density of up to 98% was consolidated under simultaneous application of a 80 MPa pressure and the induced current. The average grain sizes of TaSi<sub>2</sub> were about 33 nm. The average hardness and fracture toughness values obtained were 1330 kg/mm<sup>2</sup> and 3.3 MPa•m<sup>1/2</sup>, respectively.

**Qualitative Analysis of Temperature Evolution in Railway Brake Disc:** Jeongguk Kim<sup>1</sup>; Sung-Tae Kwon<sup>1</sup>; Sung Cheol Yoon<sup>1</sup>; Byung Choon Goo<sup>1</sup>; <sup>1</sup>Korea Railroad Research Institute

In order to analyze the degradation mechanism of brake disc, the qualitative analysis of surface temperature changes on railway brake disc was conducted using a high-speed infrared camera. The infrared camera employed for this investigation has max speed of 380 Hz. The braking tests with the railway brake disc were performed with a full scale dynamometer, and the high-speed infrared camera was used to monitor surface temperature changes on the brake disc during the braking test. Through the analysis of thermographic monitoring images, the temperature evolution with different braking speeds was qualitatively evaluated, and the results showed the initial thermal bands on brake disc was formed at relatively low braking speed, and the localized hot spots were observed at the braking speed of 180 km/h. In this paper, the qualitative investigation results on the temperature evolution of railway brake disc was summarized and presented.

**Quality and Productivity Improvements for Wire and Cable Industry:** Kiran Manchiraju<sup>1</sup>; <sup>1</sup>Southwire Company

Abstract: Significant quality and productivity improvements can be made to wire and cable products if porosity is detected and eliminated during the casting of copper rod. A system that detects porosity, during the continuous casting (CC) of copper bar has been developed. This system uses an infrared red camera that measures surface temperature as the copper bar exits the casting wheel and after cooler. A statistical algorithm that uses the temperature profile from the IR camera has been developed that reveals the existence or absence of porosity within the CC bar. The temperature profile is curve fitted to an nth degree polynomial and is then evaluated by analyzing the residuals at peak temperatures. Using the procedures advanced above, bar porosity less than 1/8th of an inch in diameter have been detected at the Southwire Carrollton facility.

**Quality Control of the Refining Process at Electron Beam Melting and Development and Implementation of Engineering Support System for Process Modeling and Control:** Elena Koleva<sup>1</sup>; Georgi Mladenov<sup>1</sup>; Idilia Batchkova<sup>2</sup>; Kamen Velev<sup>2</sup>; Vania Vassileva<sup>1</sup>; Katia Vutova<sup>1</sup>; <sup>1</sup>Institute of Electronics - Bulgarian Academy of Sciences; <sup>2</sup>University of Chemical Technology and Metallurgy

The behavior of various impurities in the crystallized ingots and the evaporated base metal losses at Electron Beam Melting and Refining (EBMR) of Ti, Cu and some refractory metals are analyzed. Experimental kinetic dependencies of impurity concentrations are estimated. Simulation of the thermal processes is used for some parameter estimation at EBMR. Statistical methods are applied for the quality improvement of the obtained ingots. Optimization of the EBMR regime conditions is performed aiming improving the quality of the obtained ingots (including the variations and the repeatability of the results) and minimization of base metal evaporation losses. The developed Engineering Support System (ESS) for EBMR plant is briefly described. The system is intended to integrate and organize the knowledge for the EBMR, to serve modeling, control system design and simulation of EBMR and complementary

# Technical Program

production processes (either continuous or discrete) connected to the industrial needs for efficiency, adaptability, flexibility and reconfigurability.

**Quality of Slab Ingots and Heavy Plates Produced by a 40t ESR Furnace:** *Xin Geng*<sup>1</sup>; Zhouhua Jiang<sup>1</sup>; <sup>1</sup>Northeastern University

The research on the refining and solidification in a large bifilar ESR furnace for production of slabs up to 40t are performed. The gross segregation experiments were carried out to check the uniformity of components of heavy plates in different position. The slab ingots were rolled to heavy plates, and then the impact toughness and tensile properties of heavy plates produced by an ESR furnace for slab products with different position were compared with that of heavy plates produced by a conventional process. The suitable refining and solidification process was obtained during the ESR for slab ingots. Adjusting taper of the mold and using CaF<sub>2</sub>-CaO-Al<sub>2</sub>O<sub>3</sub>-SiO<sub>2</sub>-MgO slag are necessary to improve surface quality of the ESR slab. The gross segregation results show that the heavy plates produced by ESR furnace exhibits excellent uniformity. And the mechanical properties of the heavy plates are superior to that of conventional materials.

**Rapid Consolidation of Nanocrystalline 2Fe-Al<sub>2</sub>O<sub>3</sub> Composite from Mechanically Alloyed Powders by Pulsed Current Activated Sintering:** *In-Jin Shon*<sup>1</sup>; Dong-Mok Lee<sup>1</sup>; Na-Ra Park<sup>1</sup>; Na-Ri Kim<sup>1</sup>; Je-Shin Park<sup>2</sup>; Wonbaek Kim<sup>2</sup>; <sup>1</sup>Chonbuk University; <sup>2</sup>Korea Institute of Geoscience and Mineral Resources

Metal matrix composites combine metallic properties (ductility and toughness) with ceramic characteristics (high strength and modulus), leading to greater strength in shear and compression and to higher service temperature capabilities. The attractive physical and mechanical properties that can be obtained with metal matrix composites, such as high specific modulus, strength-to-weight ratio, fatigue strength, and temperature stability and wear resistance, have been documented extensively. Nano-powders of Fe and Al<sub>2</sub>O<sub>3</sub> were synthesized from Fe<sub>2</sub>O<sub>3</sub> and 2Al powders by high energy ball milling. Nanocrystalline 2Fe-Al<sub>2</sub>O<sub>3</sub> composite was consolidated by pulsed current activated sintering (PCAS) method within 2 minutes from mechanically alloyed powders of Al<sub>2</sub>O<sub>3</sub> and 2Fe. The average grain sizes of Fe and Al<sub>2</sub>O<sub>3</sub> in the composite were 150 nm and 86 nm, respectively. The average hardness and fracture toughness values obtained were 1202 kg/mm<sup>2</sup> and 12 MPa·m<sup>1/2</sup>, respectively.

**Rapid Solidification of FeAlCr-B2 Intermetallic Compounds - Microstructure and Mechanical Behavior:** *Roberto Rodriguez-Diaz*<sup>1</sup>; Julio Juarez-Islas<sup>2</sup>; Jesus Arenas-Alatorre<sup>3</sup>; <sup>1</sup>Facultad de Quimico-Metalurgica UNAM; <sup>2</sup>IIM\_UNAM; <sup>3</sup>Instituto de Fisica - UNAM

This work presents microstructural characterization of a melt-spun intermetallic compound Fe<sub>40</sub>Al<sub>5</sub>Cr (% at.), produced by rapid solidification employing the melt spinning technique at different wheel speeds. Microstructure and structure features in ribbons were characterized by optical and scanning electron microscopy (SEM), x-ray diffraction analyses (XRD) Transmission electron microscopy (TEM) and EDS technique was employed to perform point and scan line chemical analyses. Micro hardness Vickers measurements as well as tensile tests at room temperature were applied to ribbons. The grain size of rapidly solidified Fe<sub>40</sub>Al<sub>5</sub>Cr ribbons suffered a drastic reduction as compared with those alloys in as-cast state. Grain size of as-spun ribbons decreased as the wheel speed or cooling rate increased. Hardness measurements revealed a softening in rapidly solidified FeAlCr ribbons as compared with FeAl alloys and tensile test exhibited a (transgranular + intergranular) mode of fracture, reaching up to 3 % of elongation in FeAlCr alloys.

**Recovery of Metallic Values from Spent Li Ion Secondary Batteries:** *Serdar Aktas*<sup>1</sup>; Derek Fray<sup>2</sup>; Jo Fenstad<sup>2</sup>; Odn Burheim<sup>2</sup>; Ercan Acma<sup>1</sup>; <sup>1</sup>Istanbul Technical University; <sup>2</sup>University of Cambridge

Recovery of metallic values from spent Li ion batteries by a precipitation technique using ethanol was investigated. Cobalt was recovered in two steps. During the first step, 92% of the cobalt was recovered as CoSO<sub>4</sub> by the use of ethanol at a volume ratio of 3 : 1. In the second step, the remaining cobalt was precipitated as cobalt hydroxide by increasing the pH value with the addition of lithium hydroxide. Lithium, which remained in the solution, was then recovered as lithium sulphate with up to 90% recovery efficiency by the addition of ethanol at a 3 : 1 volume ratio. It was found that the ethyl alcohol was capable of removing water ligands from cations, resulting in the precipitation of metals as metal sulphate monohydrate. It was shown that metals could be precipitated

separately by the ethanol/sulphate precipitation technique depending on their concentrations present in the solution.

**Removal of Phosphorus from High-Phosphorus Iron Ores by Selective HCl Leaching Method:** *Wentang Xia*<sup>1</sup>; Xingyu Chen<sup>2</sup>; Zhengde Ren<sup>1</sup>; Ailiang Chen<sup>2</sup>; Yifeng Gao<sup>1</sup>; Tongguo Wang<sup>1</sup>; <sup>1</sup>Chongqing University of Science and Technology; <sup>2</sup>Central South University

The selective HCl leaching method was used to remove phosphorus from high-phosphorus iron ores. The hydroxyapatite in high-phosphorus iron ores was converted into soluble phosphate during the process of HCl leaching. The effects of reaction time, particle size, hydrochloric acid concentration, reaction temperature, liquid-solid ratio and stirring speed on the dephosphorization rate were studied. The results showed the dephosphorization ratio can exceed 98% on the conditions of reaction time 30-45 min, particle size 0.074-0.104 mm, hydrochloric acid concentration 2.5mol/L, reaction temperature 25°, liquid-solid ratio 5/1 and stirring speed 150-250r/m. After dephosphorization reaction, the content of phosphorus in iron ore accorded completely with requirement of steel production.

**Rhodium Recovery from Spent Rhodium Plating Solutions:** *Bihter Zeytuncu*<sup>1</sup>; Serdar Aktas<sup>1</sup>; Hakan Morcali<sup>1</sup>; Onuralp Yucel<sup>1</sup>; <sup>1</sup>Istanbul Technical University

In this study, recovery of rhodium from spent rhodium plating solutions via cementation was investigated. Rhodium, a member of the platinum group metals, is used for decorative purposes, and in most cases is preferred to silver since it does not tarnish under moderate conditions unlike silver. For recovery experiments, fine metallic aluminum, zinc and iron powders were employed, and their recovery efficiencies were compared to each other. It was found that increasing temperature plays an important role in the recovery of rhodium as well as in the reaction time. When the same amount of cementator was employed zinc was found to be more successful in attaining higher recovery efficiencies than aluminum and iron, which can be attributed to the fact that aluminum and iron are more prone to oxidation than zinc powder. It was shown that these three cementators are capable of precipitating rhodium from spent plating solutions quite effectively.

**Rotary Ultrasonic Drilling of Al<sub>2</sub>O<sub>3</sub> Ceramic Material:** *Naga Prasada Rao Boyalappalli*<sup>1</sup>; Laxminarayana Pappula<sup>2</sup>; M. Ramulu<sup>3</sup>; <sup>1</sup>Department of Mechanical Engineering, University College of Engineering, Osmania University; <sup>2</sup>University College of Technology, Osmania University; <sup>3</sup>Department of Mechanical Engineering, University of Washington

Ultrasonic Machining (USM) can effectively machine hard and brittle materials such as ceramics but it has the disadvantage of a low material removal rate. It was found in this study that the material removal rate can be substantially increased by applying a rotating motion to the work piece during machining. The increase in material removal rate can be four times greater than the rate achieved without rotation (conventional USM). Polynomial models of the resulting material removal rate and tool wear rate were made. The relationship between parameters and response was examined. Optimum parameters for maximum material removal rate and for minimum tool wear rate were also found. The Taguchi method was used in combination with regression analysis to find robust process parameters that would satisfy the objective of reducing the influence of noise factors by controlling the controllable factors thereby maximizing MRR and minimizing TWR.

**Scrap Modified Alloy Design of Wrought Aluminum Alloy:** *Myoung-Gyun Kim*<sup>1</sup>; <sup>1</sup>Research Institute of Industrial Science and Technology (RIST)

Saving of resource and energy is very important for establishing the sustainable environment. The developments of materials processing and recycling for light metals, especially, aluminum alloys, are very useful for the materials and energy saving in various industries. Because aluminum scrap, in particular, contains iron-containing parts, such as bolt, nut, etc., in remelting or recycling aluminum scrap, it is essential to develop the technique removing iron in aluminum melts. It is well known that the intermetallic-AlFeSi phase that forms needle shape during the solidification of aluminum alloys is detrimental to extrusion properties owing to increasing of extrusion pressure. In this study, we are going to modified alloy design wrought (5000, 6000, 7000 base) aluminum alloy using aluminum scrap. To develop scrap modified alloy design of wrought aluminum alloy, both computer simulation and experimental results are discussed.



**SEM Analysis of Worn Carbon Cathodes in Industrial Aluminium Electrolysis Cells:** *Øyvind Østrem*<sup>1</sup>; Christian Rosenkilde<sup>2</sup>; <sup>1</sup>Norwegian University of Science and Technology; <sup>2</sup>Norsk Hydro ASA

Wear of the carbon cathode is the main limiting factor for the life span of aluminium electrolysis cells. The wear profile is often very uneven with areas in the middle of the cell showing little wear while at the sides and edges the cathode can be worn down to the current collector bars. A more even wear could give a prolongation of the life span by several years, which obviously can be a significant economic advantage. This work focuses on microscopy analysis of surface samples of cathodes in industrial aluminium electrolysis cells. The objective is to thoroughly study the metal cathode interphase to determine if there are visible differences in the surface from areas with little wear compared to the surface from areas with more wear. Any differences, together with the surface study itself, may give indications to what wear mechanisms the carbon cathode is subjected to during aluminium electrolysis.

**Silver Recovery from Silver-Rich Photographic Processing Solutions by Copper:** *Bihter Zeytuncu*<sup>1</sup>; Hakan Morcali<sup>1</sup>; Serdar Aktas<sup>1</sup>; Onuralp Yucel<sup>1</sup>; <sup>1</sup>Istanbul Technical University

The present study investigates silver recovery from silver-rich photographic processing solutions by copper. The effects of various reaction parameters on silver recovery efficiency were studied in detail. Parameter optimization was also carried out. The possibility of recovering silver with more than 99% efficiency was demonstrated under both air and argon atmospheres. In the latter case, more than 99% recovery efficiency was achieved at an agitation rate of 875 rpm for 8 minutes. When cementation was carried out under air, the silver recovery efficiency decreased with increasing time, and agitation rate. This decrease can be attributed to the redissolution of cemented silver back into the solution. In addition, the solution pH was demonstrated to influence the efficiency of silver recovery by copper.

**Silver Recovery from Waste Radiographic Films Using Different Methods:** *Hakan Morcali*<sup>1</sup>; Serdar Aktas<sup>1</sup>; Onuralp Yucel<sup>1</sup>; <sup>1</sup>Istanbul Technical University

A chemical processing scheme was adopted to recover silver from waste radiographic films. The films were subjected to 1 M nitric acid solution for 3.5 hours at 80°C. The silver nitrate solution was then treated by two different methods. The first involved cementation with iron and zinc powders. These cementators were compared to each other with respect to purity of the final product and the recovery efficiency. The second method was sodium hydroxide precipitation. The treatment with Fe and Zn powders resulted in the formation of metallic silver in just one step; silver oxide obtained via NaOH precipitation was subsequently treated by two different methods: a treatment with a mixture of glucose and NaOH to yield metallic silver, and a heat treatment, in which Ag<sub>2</sub>O was converted to silver at 500°C. With the exception of the powder produced by glucose reduction, all the other powders would easily find industrial application.

**Simulation of Dislocation Interaction with Precipitates:** *Peihua Jing*<sup>1</sup>; Hyon-Jee Lee<sup>2</sup>; Jae-Hyeok Shim<sup>3</sup>; Ian Robertson<sup>4</sup>; Brian Wirth<sup>2</sup>; <sup>1</sup>Structural Integrity Associates; <sup>2</sup>Department of Nuclear Engineering, The University of California, Berkeley; <sup>3</sup>Korea Institute of Science and Technology; <sup>4</sup>Department of Material Science and Engineering, The University of California, Berkeley

Molecular Dynamics (MD) simulations of an edge dislocation interacting with several obstacles have been analyzed in terms of the partial dislocation reactions using Thompson tetrahedron notation. These include an oversize {100} platelet and a self-interstitial [001] loop, and the results provide a basis to understand the interaction between an edge dislocation and non-coherent precipitates. In all cases, the MD simulations reveal more complicated interactions between the dislocation and non-coherent precipitates than theoretically anticipated. For an oversized Au precipitate, the interaction involves a combination of Orowan looping plus absorption and subsequent dragging of a dislocation loop segment. For an undersized in-coherent Rh precipitates, numerous Shockley partial dislocation loops were nucleated at the precipitate – matrix interface as the dislocation approached, thereby significantly increasing the obstacle strength.

**Simultaneous Synthesis and Consolidation of Nanostructured Ti-ZrO<sub>2</sub> from Mechanically Activated Powders by High Frequency Induction Heated Combustion:** *In-Jin Shon*<sup>1</sup>; Seung-Myoung Chae<sup>1</sup>; Je-Shin Park<sup>2</sup>; Wonbaek Kim<sup>2</sup>; Kee-Seok Nam<sup>3</sup>; <sup>1</sup>Chonbuk University; <sup>2</sup>Korea Institute of Geoscience and Mineral Resources; <sup>3</sup>Korea Institute of Materials Science

Interest in cermet of Ti-ZrO<sub>2</sub> has increased significantly in recent years because of their potential application as aeronautical and automotive materials. This combination of metal and ceramic has good properties, such as adequate creep resistance at high temperature, low density, excellent oxidation and corrosion resistance, good wear resistance and high hardness. Dense nanostructured Ti-ZrO<sub>2</sub> composite was synthesized by high frequency induction heated combustion synthesis (HFHCS) method within 2 minutes in one step from mechanically activated powders of TiO<sub>2</sub> and Zr. Highly dense Ti-ZrO<sub>2</sub> with relative density of up to 99% was simultaneously synthesized and consolidated under application of a 80 MPa pressure and the induced current. The average grain sizes of Ti and ZrO<sub>2</sub> in the composite were 26 nm and 21 nm, respectively. The hardness and fracture toughness of the composite were 1041 kg/mm<sup>2</sup> and 10 MPa.m<sup>1/2</sup>, respectively.

**Sintering Behaviors of ZrC Nanoparticle Dispersed Tungsten Based Composites:** *MinKyung Kim*<sup>1</sup>; HyunJu Choi<sup>1</sup>; DongHyun Bae<sup>1</sup>; <sup>1</sup>Yonsei University

ZrC/W composites have been received a growing attention for aerospace applications requiring ablation resistance, creep resistance and toughness at extremely high temperature (= 2000°C); ZrC particles could be turned into ZrO<sub>2</sub> layers at high temperature and the oxide layer could effectively hinder the oxidation of tungsten. In this study, ZrC/W composites have been fabricated using mechanical milling and sintering. Planetary ball milling has been used to disperse ZrC particles in the tungsten powders. As milling was processed, the brittle ZrC particles could be fragmented to be hundreds nanometer-sized and homogeneously distributed in the tungsten powders. By controlling the sizes of tungsten powders in the range from 1 μm to 20 μm, the distribution of ZrC particles in the composites was observed. The effects of the particle morphology on the sintering process will be also discussed.

**Sintering Densification and Microstructural Characterization of Mechanical Alloyed Fe-Mn-Si Based Powder Metal System:** *Ahmet Söyler*<sup>1</sup>; Burak Özkal<sup>1</sup>; Leandru Bujoreanu<sup>2</sup>; <sup>1</sup>ITU; <sup>2</sup>"Gh. Asachi" Technical University from IASI

In this study sintering behaviour of Fe-Mn-Si based powder metal system were investigated using vertical dilatometer. Grain size refinement of key target composition alloys performed via mechanical alloying by taking advantage of high energy milling equipment. Both powder state and sintered state phases were characterized via XRD studies and effect of mechanical alloying time against sintering densification of Fe-Mn-Si based powder metal system were investigated for the different sintering regimes and atmospheres.

**Sintering Kinetics of SPS Tungsten and Tungsten-Ceria Cermets:** Jeffrey Perkins<sup>1</sup>; Kyle Knori<sup>1</sup>; *Darryl Butt*<sup>1</sup>; <sup>1</sup>Boise State University

The spark plasma sintering (SPS) method was used to consolidate tungsten powders and tungsten-ceria powders. Sintering temperatures, dwell times, pressures, and ceria content were varied to study the densification kinetics and grain growth kinetics of these parts. The sintering kinetics was evaluated based on the densities, porosities, grain sizes, and sintering displacement rates of the parts. The growth of tungsten grains was inhibited by small additions of ceria, and larger additions of ceria had a limited effect on tungsten grain growth. No diffusion was observed between the tungsten and the ceria. At higher temperatures, ceria was reduced during sintering, causing pores to be formed in the resulting microstructure. Based on the kinetics data, potential sintering mechanisms of tungsten and tungsten-ceria in SPS are proposed.

**Small Punch Creep of Service-Exposed SUS 316 HTB Superheater Tubes of Fossil Boilers:** *Maribel Saucedo-Muñoz*<sup>1</sup>; Shin-Ichi Komazaki<sup>2</sup>; Toshiyuki Hashida<sup>3</sup>; Toru Takahashi<sup>3</sup>; Victor Lopez-Hirata<sup>1</sup>; Tetsuo Shoji<sup>3</sup>; <sup>1</sup>Instituto Politecnico Nacional (ESIQIE); <sup>2</sup>Muroran Institute of Technology; <sup>3</sup>Tohoku University

The creep properties for a SUS 316 HTB austenitic stainless steel were evaluated by using the small-punch creep test at 650°C and loads of 234, 286, 338, 408 and 478 N, and at 700°C and loads of 199 and 234 N. The creep curves, determined by means of the small punch creep test, were similar to those obtained from a conventional uniaxial creep test. That is, they exhibited

# Technical Program

clearly the three creep stages. The width of secondary creep stage and rupture time  $t_r$  decreased with the increase in testing load level. This difference in creep resistance was explained based on the difference in the creep deformation and/or fracture mechanism. It was also found that the ratio between the load of small-punch creep test and the stress of uniaxial creep test was about one for having the same value of creep rupture life.

**Some Recent Research Work on the Hot Processing of Engineering  $\gamma$ -TiAl Alloys:** *Yuyong Chen*<sup>1</sup>; *Yanfei Chen*<sup>1</sup>; *Shulong Xiao*<sup>1</sup>; *Fantao Kong*<sup>1</sup>; *Jing Tian*<sup>1</sup>; <sup>1</sup>Harbin Institute of Technology

TiAl alloys have attracted a major effort in lightweight structural components for aerospace and automotive applications because of their favorable properties of high specific strength and temperature capability over the past 20 years. The paper outlines some recent research work on the hot processing of engineering TiAl alloys through ingot metallurgy technology including investment casting and sheet rolling at our laboratory. Ingots and castings of TiAl alloys are prepared by ISM in a water cooling copper crucible. TiAl blades and rudder frame work were successfully produced by investment casting using a newly developed ceramic mold. And Ti-43Al-9V-0.3Y sheets were obtained with hot rolling of canned forged TiAl alloys in  $\alpha+\gamma$  zone. Some concerns in producing the TiAl castings and sheets will be summarized.

**Spark Plasma Sintering of Next Generation Nuclear Materials:** *Daniel Osterberg*<sup>1</sup>; *Jeff Perkins*<sup>1</sup>; *Matt Luke*<sup>1</sup>; *Brian Jaques*<sup>1</sup>; *Michael Hurley*<sup>1</sup>; *Darryl Butt*<sup>1</sup>; <sup>1</sup>Boise State University

Spark plasma sintering (SPS) has been employed in various materials systems as a novel consolidation method for nuclear materials. SPS has recently seen a broad range of applications and it is considered a potential efficient and cost effective alternative to traditional consolidation methods. Use of SPS for oxide and nitride nuclear fuel fabrication, high level waste reprocessing, radioisotope heat sources, and powder metallurgy has been investigated. Specific materials of interest include Uranium oxide and nitrides, Tungsten cermets, and Nickel alloys.

**Step-Wise Exothermic Reactions in Cold-Rolled Ni/Al, Ti/Al, and Ta/Al Multilayer Foils:** *Laszlo Kecskes*<sup>1</sup>; *Anthony Roberts*<sup>1</sup>; *Nathan Wingate*<sup>1</sup>; *Bradley Klotz*<sup>2</sup>; *Xiaotun Qiu*<sup>3</sup>; *Jiaping Wang*<sup>4</sup>; <sup>1</sup>US Army Research Laboratory; <sup>2</sup>Dynamic Science Inc; <sup>3</sup>Arizona State University; <sup>4</sup>Tsinghua University

Exothermic reactions in cold-rolled Ni/Al, Ti/Al, and Ta/Al reactive multilayer foils were investigated. To understand conditions approaching combustion synthesis reactions, the cold-rolled samples were heated to temperatures above 1000°C in a differential scanning calorimeter. During heating, a series of endo- or exothermic peaks were noted; corresponding to a multi-step process, the relative positions, widths, and amplitudes of the peaks were found to be indicative of a stepwise reaction. Subsequent to obtaining the total calorimetric heat output for a given heating rate, samples were also heated to each peak temperature to identify the intermediate reaction product and evolution of the microstructure from reactants to steady state products. Scanning electron microscopy showed that lower temperature peaks corresponded to aluminum-rich intermetallics, while higher temperature peaks corresponded to conversion of these intermetallics to the nominal composition. Differences in the stepwise reaction mechanisms, as dictated by the underlying intermixing processes, are described.

**Structural and Magnetic Properties of Nanocrystalline Fe-Si-Ni Powders Produced by Mechanical Alloying:** *Maryam Yazdanmehr*<sup>1</sup>; <sup>1</sup>Technical University of Delft (TuDelft)

Structural and magnetic properties of nanocrystalline Fe-Si-Ni powders produced by mechanical alloying have been studied. The samples with different chemical compositions and milling times were characterized by X-ray diffraction (XRD) and scanning electron microscope (SEM). The alloy powders with average grain size 8–19 nm were synthesized by milling for 35–100 h. Increasing the mechanical alloying time results in the decreasing of both Coercivity and crystallite size. Maximum saturation magnetization and minimum coercivity were obtained at the composition of Fe85Si10Ni5 after 70 h milling.

**Structural and Morphological Characterization of Composites of Nylon 6/Ferrite NiFe<sub>2</sub>O<sub>4</sub>:** *daniella bezerra*<sup>1</sup>; *Patricia Costa Fernandes*<sup>1</sup>; *Taciana Regina De Gouveia*<sup>1</sup>; *edcleide Maria araujo*<sup>1</sup>; *Ana Cristina Figueiredo Melo Costa*<sup>1</sup>; <sup>1</sup>UFCCG

In this work, summed up powder NiFe<sub>2</sub>O<sub>4</sub> by the combustion reaction, which was added to a thermoplastic polymer (nylon 6) in order to obtain a composite. The powder was characterized by XRD, nitrogen adsorption by BET and SEM. The ferrite powder was incorporated into the polymer matrix of nylon 6, using a Haake internal mixer Blücher at a temperature of 240°C and 60rpm in concentrations of 30 and 60wt%. The composites of nylon 6/NiFe<sub>2</sub>O<sub>4</sub> were characterized by: XRD and SEM. At both concentrations observed characteristic diffraction peaks of the ferrite and nylon 6. The morphology of composites show that the concentration of 60% of NiFe<sub>2</sub>O<sub>4</sub> showed more clusters and large pores, which was expected due to higher amount of particles. The concentration of 30%, the particles are dispersed, leading to formation of clusters, but smaller than for the composites with concentration of 60%.

**Structure and Thermal Oxidation Properties of RuAl and Ru-Al-Ti Alloys Prepared by Mechanical Alloying:** *Marlene Clisson*<sup>1</sup>; *Julie Gaudet*<sup>1</sup>; *Lionel Roué*<sup>1</sup>; *Daniel Guay*<sup>1</sup>; <sup>1</sup>INRS

RuAl remain amongst the most efficient materials for high temperature applications in aggressive environments. In this study, nanocrystalline RuAl was prepared by ball milling from elemental Al and Ru powders using both steel and WC crucible and balls. In both cases, RuAl is formed (B2 structure) and pollution by Fe and WC increases with milling time. In the case of pollution by Fe, these atoms are dissolved in the cubic structure of RuAl, while a composite is formed in the case of WC. Thermal gravimetric analysis under pure O<sub>2</sub> atmosphere shows that oxidation of RuAl(Fe) is initiated at 380°C. In comparison, the oxidation of RuAl prepared with WC crucible (1 at.% WC) starts at 465°C. The addition of 5 at.% WC to the initial Ru + Al powder mixture yields to a composite whose oxidation is not initiated before 494°C. The origin of this effect will be discussed.

**Study of Metal-Oxide Composites Prepared by Ball Milling and Evaluated as Inert Anodes for Aluminum Production:** *Sébastien Helle*<sup>1</sup>; *Boyd Davis*<sup>2</sup>; *Daniel Guay*<sup>1</sup>; *Lionel Roué*<sup>1</sup>; <sup>1</sup>INRS EMT; <sup>2</sup>Kingston Process Metallurgy Inc.

In a previous study, we have shown that monophased Cu<sub>x</sub>Ni<sub>85-x</sub>Fe<sub>15</sub> alloys can be synthesized by high energy ball milling. Alloys with 60 < x < 85 gave stable potential at 0.5 A/cm<sup>2</sup> during 20h of electrolysis in low temperature (700°C) KF-AlF<sub>3</sub> electrolyte. The best result in terms of aluminum purity (0.2wt.% Cu) was obtained for the Cu<sub>65</sub>Ni<sub>20</sub>Fe<sub>15</sub>. In this study, further work was performed to improve the corrosion resistance of the electrode and the purity of the produced aluminium. For that purpose, small amount (5 and 15wt.%) of various oxides (Cu<sub>2</sub>O, CuAlO<sub>2</sub>, CuAl<sub>2</sub>O<sub>4</sub>) were added to pre-milled Cu<sub>65</sub>Ni<sub>20</sub>Fe<sub>15</sub> to prepare a composite. To achieve this, CuAlO<sub>2</sub> and CuAl<sub>2</sub>O<sub>4</sub> were first prepared by mixing copper oxide and alumina via ball milling and heating the resulting material to initiate the reaction. The oxidation at 700°C of the composites was studied and compared to the metal. Finally, 20h aluminium electrolysis tests were conducted in low-temperature KF-AlF<sub>3</sub> electrolyte.

**Study on Magnetic-Gravity Combination Separation and Acid Leaching of a High Phosphorus Fine Hematite:** *Tao Jiang*<sup>1</sup>; *Lin Yang*<sup>1</sup>; *Yufeng Guo*<sup>1</sup>; <sup>1</sup>Central South University

Process mineralogy of an Inner Mongolia iron ore was investigated. The results indicated that the iron ore mainly included hematite, a few magnetite and limonite, and the gangues mainly were quartz, secondly Montmorillonite, Spessartite and so on. The dissemination size of primary valuable minerals was fine and uneven distribution. In this work, a method was developed to solve the problem of low recovery of magnetic-gravity separation combined process. An iron concentrate with 61.18% Fe grade and 65.84% recovery could be obtained by low-intensity magnetic separation-High-intensity separation-screening classification-gravity separation combined process. However, the content of phosphorus was highly to 0.510%. The iron concentrate was leached by acid to remove the phosphorus, the content of phosphorus of final iron concentrate was decreased to 0.117%. The iron grade of leached concentrate was increased to 62.93% and total iron recovery of that was reached 64.16%.

**Study on Visible Light Photocatalytic Performance of Nano Tungsten Trioxide:** *Wu Daoxin*<sup>1</sup>; <sup>1</sup>Changsha University of Science and Technology

Photocatalytic technology is a new environment for energy technology, it has low energy consumption, simple operation, mild reaction conditions, reducing



the secondary pollution, etc., and get more and more attention. And tungsten trioxide is an important photocatalytic material, its band gap energy of 3.2eV, less than 500 nm can absorb sunlight. Tungsten trioxide thin films are widely used in electrochromic, solar energy conversion and degradation of pollutants. In this paper, sodium tungstate as raw materials, was used to get tungsten trioxide with nano-sol synthesis. tungsten trioxide samples were characterized XRD (X-ray diffraction), DRS (diffuse reflectance UV-Vis), FS (fluorescent). methyl orange degradation products as the goal, with in the visible light conditions, nano-three-oxide photocatalytic properties were studied, The results show that with the sol-method, tungsten trioxide carried out on methyl orange photocatalytic read its absorbance. It has been showed that the Nano tungsten trioxide has been better properties in the visible band.

**Surface Treatment of Materials by Low Energy High Current Pulsed Electron Beam under Evaporating Mode:** *Kemin Zhang*<sup>1</sup>; <sup>1</sup>Shanghai University of Engineering Science

The interaction of Low energy high current pulsed electron beam (LEHCPEB) with materials has recently received enormous attention for surface treatment. The LEHCPEB irradiation induces dynamic temperature fields in the surface of the treated materials, giving rise to superfast heating, melting and even evaporating followed by rapid solidification. In the present contribution, the potential of the technique for structure and composition modifications associated with the use of the pulsed electron beam under “evaporating” condition are highlighted. It is shown that the LEHCPEB induced evaporation accounts for the formation of special surface morphology and composition modifications in the treated materials. As a result of these modifications, the corrosion resistance of the treated materials can be significantly improved.

**Synthesis of Ag/ZnO Nanocomposite Particles by Ultrasonic Spray Pyrolysis Method:** *Sebahattin Gurmen*<sup>1</sup>; *Burcak Ebin*<sup>1</sup>; <sup>1</sup>Istanbul Technical University

Ag/ZnO nanocomposites have drawn interest because Ag and ZnO are extremely attractive materials to be investigated at the nanoscale due to size- and shape-dependent catalytic, antibacterial, optical and electrical properties which promising various applications for both of them. Combination of their features in nanometer size possesses unique properties and, therefore, offers new technologies and business opportunities. In this research, Ag/ZnO nanocomposite particles were prepared by ultrasonic spray pyrolysis (USP) method using silver nitrate and zinc nitrate aqueous solution in desired concentration under constant air flow rate at 800°C furnace temperature. Then samples were structurally characterized by X-ray diffraction (XRD), scanning electron microscope (SEM) and energy dispersive spectroscopy (EDS). The results show that Ag/ZnO nanocomposite particles in spherical morphology were obtained successfully. Also, it was observed that nanocrystal size of Ag and ZnO in the nanocomposite particles are nearly 36 and 34 nm, respectively which are calculated by Scherrer equation.

**Synthesis of Nanostructured Materials for High-Voltage, High-Energy-Capacity Cathode of Li-Ion Batteries:** *Chunhu Tan*<sup>1</sup>; *Bob Liu*<sup>1</sup>; *Timothy Lin*<sup>1</sup>; <sup>1</sup>Aegis Technology Inc.

There is a great interest in developing energy storage systems based on more advanced lithium ion battery technology. One of the key technologies of such Li-ion batteries is the more advanced cathode material with properties like high energy capacity, good cyclability, enhanced safety and low cost. This presentation is on the development of a novel class of LiMPO<sub>4</sub>/C (M = Co, Fe) nanocomposite for high-performance cathodes aimed to provide high voltage, high capacity, high charging/discharging rate, excellent stability and low cost. With the support from one ongoing DoE SBIR project, Aegis has established the capability in development and large scale production of advanced electrode materials for high performance Li-ion batteries. The latest results including the establishment of a cost-effective, scalable synthesis process, the influence of key processing parameters on the morphology and sizes of the resultant LiMPO<sub>4</sub> particles, and electrochemical tests will be presented.

**Temperature and Stress Effects on Cathodic Hydrogen Charging of High-Strength Line-Pipe Steels:** *John Roubidoux*<sup>1</sup>; *F.J. Sanchez*<sup>2</sup>; *B. Mishra*<sup>1</sup>; *D.L. Olson*<sup>1</sup>; <sup>1</sup>Colorado School of Mines

The effects of temperature and stress(strain)on cathodic hydrogen charging of high-strength line-pipe steels(X52,X70,and X80)in the presence of a strong and uniform magnetic field will be described.It was experimentally demonstrated that the diffusible hydrogen content in steel is strongly influenced by magnetic

induction. The room temperature measurements present both enhanced hydrogen ingress,as well as pitting and cracking behavior. This observation suggests both cathodic and anodic involvement in the magnetocorrosion situation. The elevated temperature experiments were performed to report rate coefficients and apply activated complex theory these electrochemical results. To test the effects of stress on cathodic hydrogen charging of high-strength line-pipe steels,hydrogen charged tensile samples were strained with and without a magnetic field. These observations may have significant implication to hydrogen-cracking susceptibility from magnetic remanence resulting from Magnetic Flux Leakage(MFL) pigging operations on higher strength line pipe steels. These results will be discussed and a comprehensive model will be presented to offer more insight into this behavior.

**Temporal Evolution of A Ni-Al-Cr Superalloy with a Dilute Ruthenium Addition:** *Yang Zhou*<sup>1</sup>; *Dieter Isheim*<sup>1</sup>; *Gillian Hsieh*<sup>1</sup>; *David Seidman*<sup>1</sup>; <sup>1</sup>Northwestern University

The temporal evolution of a Ni-10.0 Al-8.5 Cr-2.0 Ru at.% alloy aged at 1073 K is investigated using transmission electron microscopy and atom-probe tomography. The gamma-prime-precipitate morphology is spheroidal until 256 h of aging, which is attributed to the Ru addition. The temporal evolution of the gamma-prime-precipitate average radius, volume fraction and number density was investigated and compared to the predictions of classical coarsening models. Contrary to the common belief that refractory additions decelerate the coarsening kinetics, the addition of Ru accelerates the concentration evolution of the gamma-prime- and gamma- phases, which achieve equilibrium values after 0.25 h. The Ru decreases the partitioning of Ni, while increasing the partitioning of Al and Cr at long times. Ruthenium is also responsible for accelerating the partitioning of Ni, Al and Cr. The interfacial width of the gamma-prime/gamma interface is different for each alloying element.

**Tensile Deformation Behavior of Zr-Based Bulk Metallic Glass Composite with Different Strain Rate:** *Kyu-Sik Kim*<sup>1</sup>; *Ji-Sik Kim*<sup>2</sup>; *Hoon Huh*<sup>3</sup>; *Kee-Ahn Lee*<sup>4</sup>; <sup>1</sup>Center for Advanced Green Materials Technology, Andong National University; <sup>2</sup>Department of Advanced Materials Science and Engineering, Kyungpook National University; <sup>3</sup>Department of Mechanical Engineering, KAIST; <sup>4</sup>Advanced Materials Science and Engineering, Andong National University

Tensile deformation behavior with different strain rate was investigated. Zr<sub>56.2</sub> Ti<sub>13.8</sub> Nb<sub>3.0</sub> Cu<sub>6.9</sub> Ni<sub>3.6</sub> Be<sub>12.5</sub> (bulk metallic glass composite possessed crystal phase which was called β-phase, dendrite shape, mean size of 20~30μm and occupied 25% of the total volume) was used in this study. Maximum tensile strength was obtained as 1.74GPa at strain rate 10<sup>2</sup> s<sup>-1</sup> and minimum strength was found to be 1.6GPa at 10<sup>-1</sup> s<sup>-1</sup>. And then, maximum plastic deformation showed narrow width local plastic deformation at the strain rate of 5x10<sup>2</sup> s<sup>-1</sup> and represented 1.75%, though minimum plastic deformation showed 0%. In the specific range of strain rate, relatively higher plastic deformation and lower ultimate tensile strength were found with lots of shear bands. The fractographical observation after tensile test indicated that wide range of vein like pattern on the fracture surface was well developed especially in the above range of strain rate.

**Tensile Failure Analysis of Railway Steels Using Infrared Thermography NDE Technique:** *Jeongguk Kim*<sup>1</sup>; *Sung Cheol Yoon*<sup>1</sup>; *Sung-Tae Kwon*<sup>1</sup>; <sup>1</sup>Korea Railroad Research Institute

Several different types of railway steels, which are employed for railway vehicle parts such as wheel axle, bogie frame, bolster, and coupler, were introduced to characterize the tensile properties. The tensile specimens were prepared from the actual railway vehicle parts, which were used for over 20 years. During the tensile testing, an infrared camera was used to monitor damage evolution in terms of surface temperature measurements. A qualitative image analysis was conducted to explain failure mode and mechanisms in different railway steel samples based on infrared thermographic images obtained during tensile testing. Moreover, the microstructural characterization using scanning electron microscope (SEM) was performed to correlate the mechanical failure mode with thermographic results. The SEM characterization results were comparable with in-situ monitored IR camera analysis results.

**The Effect of Different Heat Treatment Cycles on Controlled Surface Graphitization in CK45 Steel:** *Ali-Reza Kiani-Rashid*<sup>1</sup>; *Yaser Hamed*<sup>2</sup>; <sup>1</sup>Ferdowsi University of Mashhad; <sup>2</sup>Sharif University of Technology, Tehran

Controlled graphitization has become known as a practical method for improvement of wear resistance and machining properties in steels. In this

# Technical Program

paper, the effect of heat treatment on microstructure of Ck45 steel has been investigated. Austenitising was carried out at 920°C for 5 hours. Besides, isothermal transformation was conducted at 750°C in the time range of 1-20 hours. The microstructure of the steel considerably changes by this heat treatment process which exhibits the effects of temperature, appropriate austenitising duration and isothermal transformation. Conducted experiments show a suitable distribution of semi-spherical graphite particles especially on the surface of the steel. Also, analyses demonstrate that the amount of formed graphite in the austenitising temperature 920°C is more than graphite in single heat treatment temperature of 750°C.

**The Effect of Calcium on Preventing Grain Growth of Al-Zn-Mg Aluminium Alloy:** *Sung Yong Shim*<sup>1</sup>; Dae Hwan Kim<sup>1</sup>; Yeong Hwa Kim<sup>1</sup>; In Sang Jeong<sup>1</sup>; In Shup Ahn<sup>1</sup>; Su Gun Lim<sup>1</sup>; <sup>1</sup>K-MEM R&D Cluster, i-Cube Center, Gyeongsang National University

In order to preventing coarsened grain during reheating treatment of thixo-forming process, the effect of calcium on coarsening grain of Al-Zn-Mg Al alloy in the reheating process was investigated. When calcium was added in aluminum alloy, the formed Al<sub>2</sub>Ca phase performed grain-boundary pinning, which enabled the reheating process for Thixo-forming to reduce grain growth. In this present, Al-Zn-Mg Al alloys contained calcium (0.3, 0.5 and 0.8 mass %) were fabricated and their microstructures with increasing holding time were observed by optical microscope and scanning electron microscope. The reheating temperature considered as liquid fraction of 10 and 20% was selected by differential thermal analysis and we examined reheating behavior at 600 and 615°. Increasing holding time, the grain growth was inhibited in all alloys except calcium free alloy. What's clear is that calcium contents are able to effectively form fine and equiaxed grain via reheating process at desired temperatures.

**The Effect of Frequency of Microarc Oxidation on Surface Properties of 7075 Aluminum Alloys:** *Serkan Bozkus*<sup>1</sup>; Murat Baydogan<sup>1</sup>; Huseyin Cimenoglu<sup>1</sup>; Sabri Kayali<sup>1</sup>; <sup>1</sup>Istanbul Technical University

In this study, thick ceramic coatings were fabricated by microarc oxidation on 7075 aluminum alloy in a KOH, Na<sub>2</sub>SiO<sub>3</sub> solution. Micro arc oxidation was performed by using an AC power supply operating in variable frequency between 100 Hz - 167 Hz. Mechanical and physical properties were examined on the surface of the oxide film including hardness, wear resistance and surface roughness. Rockwell C testing was used to compare the relative adhesion characteristics of the oxide film. The unlubricated tribological performance of the coatings was examined using wear system with reciprocating motion against sintered Al<sub>2</sub>O<sub>3</sub> ball. The surface morphology and structure was examined by SEM and X-ray diffractometer. The studied properties of the samples as a function of frequency were discussed.

**The Effect of Polymer Structures, Nanoparticle Loadings and Nanoparticle Surface Treatment on the Dynamic Shear Rheological Behaviors of Polydimethylsiloxane (PDMS):** *Atarsingh Yadav*<sup>1</sup>; Sameer Pallavkar<sup>1</sup>; Thomas Ho<sup>1</sup>; John Zhanhu Guo<sup>1</sup>; <sup>1</sup>Lamar University

Rheological study of two different types of polydimethylsiloxane (PDMS), low molecular weight (4200, hydroxy terminated) and high molecular weight (139,000, trimethyl siloxy terminated), was investigated under certain range of shear rates to illustrate the viscosity and shear stress variations as a function of shear rate. The shear rate for LMW is 0.1 s<sup>-1</sup> to 1200 s<sup>-1</sup> and 0.1 s<sup>-1</sup> to 200 s<sup>-1</sup> for HMW. The investigation was carried out at different temperatures (25°C, 50°C and 70°C). The nanoparticle surface adsorption was used to interpret the observed rheological behavior phenomenon. The effect of Fe<sub>2</sub>O<sub>3</sub> nanoparticle loading and surface treatment with surfactants such as LMW PDMS and oleic acid on the rheological behaviors of PDMS will be presented in this presentation.

**The Effects of Nickel in Oxide Layers on the AZ91 Mg Alloys Synthesized by Plasma Electrolytic Oxidation:** Dong H. Shin<sup>1</sup>; Ki R. Shin<sup>1</sup>; In J. Hwang<sup>1</sup>; Dong H. Lee<sup>1</sup>; Bongyoung Yoo<sup>1</sup>; <sup>1</sup>Hanyang University

Recently, adding metal ions into electrolyte for plasma electrolytic oxidation (PEO) process to improve the functionality of passivation layer has been widely researched. In this study, Ni ions was incorporated into electrolytes in PEO process, by which the corrosion resistance was enhanced. In addition, the color could be changed from conventional gray to dark brown color, which could be one of the option to improve the appearance of Mg alloy when it is used as a housing of electrical applications. It is also observed that the growth

rate of oxide layer increased by nickel ion in electrolyte, and the content of Ni in oxide layer was confirmed as 7.4 at.% when ~350 V was applied.

**The Estimation of the Characteristic of Trivalent Chromium Coated Layer According to the Plating Conditions:** *Beomsuck Han*<sup>1</sup>; Siyoung Sung<sup>1</sup>; <sup>1</sup>Korea Automotive Technology Institute

The Directive on the restriction of the use of certain hazardous substances (RoHS) in electrical and electronic equipment was adopted by the European Union. This directive restricts the use of six hazardous materials in the manufacture of various types of electronic and electrical equipment. Hexavalent chromium is a main substance of regulated element. Trivalent chromium baths have environmental and health advantages. We are developing a functional trivalent chromium plating bath using a chromium chloride as a replacement for commercial hexavalent chromium plating bath. We make an estimation of the characteristic of coated layer according to the each plating condition using a commercial software (Plating Master). We confirm the characteristic of the practice coated layer.

**The Structure Dependence of Rolling Contact Fatigue Damage around Small Cracks for Tempered Martensitic Steel by Electron Backscatter Diffraction Analysis:** *Satoshi Morooka*<sup>1</sup>; Yutaka Yamaji<sup>1</sup>; Osamu Umezawa<sup>1</sup>; <sup>1</sup>Yokohama National University

Electron backscatter diffraction (EBSD) analysis has been employed to study local deformation gradient resulted from rolling contact fatigue on a SCM420H martensitic steel tempered at 723K. The fatigue tests were carried out for the specimens involving an artificial hole. The highest damaged region was developed in the specimen interior of about 100 micrometer in depth, where some grains rotated along <111> axis. Cracks were found beneath the region produced in which strain gradient was developed. Misorientation typically near grain boundary were detected in the region and resulted in the localized strain incompatibility near grain boundary. Severe localized plastic deformation at crack-tip may cause dynamic recrystallized fine grains along cracks.

**Thermal Oxidation of Titanium Wires:** *Tanmay Engineer*<sup>1</sup>; Adriel Apter<sup>1</sup>; Michael Hurley<sup>1</sup>; Darryl Butt<sup>1</sup>; <sup>1</sup>Boise State University

With the objective of growing TiO<sub>2</sub> micro and nanotubes using thermal treatments, the oxidation behavior of pure titanium wires (100 to 2000 μm) was investigated from 800-1200°C in both ambient air, and Ar-20%O<sub>2</sub>. In order to derive an oxidation kinetics model for cylindrical geometry, oxide thickness, phase distribution, and morphology were assessed as a function of time and temperature. At higher temperatures, the oxidation mechanism was observed to be complex with larger diameter wires showing formation of distinguishable multilayers of different Ti oxides. The smaller diameter wires formed tubular structures with a compact outer-oxide layer and a porous oxide core. The oxidation rate was observed to be higher in air than that in Ar-20%O<sub>2</sub>. At lower temperatures, a thin monolayer of TiO<sub>2</sub> over alpha-Ti core was observed. In conjunction with micro-structural characterization and dimensional measurements, platinum marker experiments were carried out to illustrate the mechanisms of oxidation.

**Thermal Tensioning during Welding of DP600 Steel Plates:** *Amir Masoud Akbari Pazooki*<sup>1</sup>; <sup>1</sup>TU Delft

Welding often results in a combination of different deformation modes. Thermal tensioning describes a group of techniques to redistribute welding induced residual stresses and thereby mitigate distortion. In this paper a review is given of systems applied in practice. The second part of the paper focuses on Transient Thermal Tensioning by means of additional heating sources attached to the welding torch. Although the technique is already applied in practice, the physical background is not yet fully understood and there is potential for improvement and optimization. In this paper experimental and simulation results of transient thermal tensioning during welding of DP600 steel plates are presented and compared. The influence of process parameters such as the power of the heaters and the position of the heaters with respect to the weld centre line and the welding torch on the final residual stress pattern is also discussed.

**Three Dimensional Carbon Nanotube Photovoltaics:** *Jack Flicker*<sup>1</sup>; Jud Ready<sup>2</sup>; <sup>1</sup>Georgia Institute of Technology; <sup>2</sup>Georgia Tech Research Institute

Although photovoltaic technology has been around for over fifty years, the use of a nanostructured, three dimensional morphology in these types of devices has occurred only relatively recently. We introduce a three dimensional photovoltaic device with carbon nanotube pillars coated with photoactive

materials to create a solar cell. The extra dimensionality of this cell added by the nanotubes has been theorized to increase the relative energy generated over planar cells by up to four times. The energy increase is due to an increase in the interactions between photons and the photoactive material as the sun is at an off normal angle to the cell substrate. Prototypes of these cells have been made and, although suffering from a low overall efficiency, do show an increased energy production in the same manner that theory predicts when the light source is at an off normal angle.

#### **Thermographic Detection of Artificial Flaws in Polymer Matrix Composite**

**Panel:** Jeongguk Kim<sup>1</sup>; Sung Cheol Yoon<sup>1</sup>; Jung-Seok Kim<sup>1</sup>; Hyuk-Jin Yoon<sup>1</sup>; <sup>1</sup>Korea Railroad Research Institute

The thermographic detection of artificial flaws on epoxy polymer matrix composites (PMCs) was performed using the infrared thermography method with a high-speed infrared camera. The pulsed thermography with flash lamp was used for the integrity evaluation of PMC panel. The spherical artificial flaws with different diameters and depths were prepared from the panel of glass fiber reinforced epoxy polymer matrix composites. In this investigation, the pulsed thermography was employed to develop a nondestructive evaluation tool for the detection of flaws in PMC panel.

**Transient Oxidation and Grain Boundary Characteristics:** Jingxi Zhu<sup>1</sup>; Laura Fernandez Diaz<sup>1</sup>; Gordon Holcomb<sup>2</sup>; Paul Jablonski<sup>2</sup>; Christopher Cowen<sup>2</sup>; David Laughlin<sup>1</sup>; Sridhar Seetharaman<sup>1</sup>; <sup>1</sup>Carnegie Mellon University; <sup>2</sup>National Energy Technology Laboratory

Oxide ridges were observed to form during the transient stage oxidation of the scale evolution in iron alloys containing 22 wt% Cr that have been held at 800°C in dry air. The post-oxidation characterization through DualBeam® system (focus ion beam and electron beam) combined with 3D reconstruction revealed that the oxide ridges formed on top of the Cr-oxide scale overlapped the intersections of the underlying alloy-grain boundaries with the Cr-oxide scale. Combining the alloy grain boundary characteristics extracted from orientation imaging with SEM characterization, it is found that ridges differ in size with different underlying grain boundaries of different disorientation, which suggests that there is a correlation between the grain boundary diffusivity and grain boundary characteristics.

#### **Transient Thermal Tensioning during Welding of AISI 316L and DP600 Steel Sheets:** Amir Masoud Akbari Pazooki<sup>1</sup>; <sup>1</sup>TU Delft

Thermal tensioning describes a group of techniques to redistribute welding induced residual stresses and thereby mitigate distortion. In these techniques, different cooling or heating strategies are applied during welding. In this paper experimental and simulation results of transient thermal tensioning during welding of stainless steel (AISI 316L) and dual phase steel (DP 600) are presented and compared. For the numerical simulation Finite Element Analysis 3-D models and extended bar-models have been developed. The influence of process parameters such as the power of the heaters and the position of the heaters with respect to the weld centre line and the welding torch on the final residual stress pattern is also discussed.

**Transition Metal Oxide-Doped BaTiO<sub>3</sub> Thin Films Prepared by R.F. Magnetron Sputtering:** W. Z. Chang<sup>1</sup>; J. P. Chu<sup>1</sup>; S. F. Wang<sup>2</sup>; C. H. Wu<sup>1</sup>; <sup>1</sup>National Taiwan University of Science and Technology; <sup>2</sup>National Taipei University of Technology

The perovskite phase BaTiO<sub>3</sub> (BTO) is a promising candidate for use as a dielectric in next-generation dynamic random access memory (DRAM) due to its numerous good properties. This presentation reports the effects of transition metal oxide (TMO)-doped BTO thin films with thickness of ~200nm fabricated by r.f. magnetron sputtering on Pt (130nm)/Ti (70nm)/SiO<sub>2</sub> (200nm)/Si substrate. Eventually, the metal-insulate-metal (MIM) structure is post-annealing at temperatures up to 650C. The dielectric constants of pure and doped BTO thin films are found to increase with increasing annealing temperature, while they decrease with increasing TMO content. The TMO dopant is also effective to reduce leakage current compared to the pure BTO. This may be attributed to the substitution of cation of TMO in the B site of BTO lattice which might have behaved as the electron acceptor to prevent electrons to pass through.

**Twinning during the Tensile Deformation of a TWIP Steel:** Yongfeng Shen<sup>1</sup>; Yandong Wang<sup>2</sup>; Liang Zuo<sup>3</sup>; Xin Sun<sup>1</sup>; R. Lin Peng<sup>4</sup>; <sup>1</sup>Pacific Northwest National Lab; <sup>2</sup>School of Materials Science and Engineering Beijing Institute of Technology; <sup>3</sup>Key Laboratory for Anisotropy and Texture of Materials (Ministry of Education), Northeastern University; <sup>4</sup>Department of Mechanical Engineering, Linkoping University

The twinning process and deformation mechanism were investigated by both in-situ tensile test using the synchrotron-based high energy X-ray diffraction (HEXRD) and postmortem TEM observations for a hot-rolled TWIP steel (Fe-20Mn-3Si-3Al). The results clearly showed that the twinning process occurred during the tensile deformation, leading to an increase amount of special grain boundary and optimization of grain boundary structure. The twinning process was facilitated by the crystal with a misorientation of {111}, {222}, {220} and {311}. Interactions between twin boundary and dislocation as well as twin boundary were responsible for the strain hardening during tensile testing. The interactions between primary twins and secondary twins resulted in an additional hardening, enhanced the plasticity in the later stage of deformation. The present strain value of 38% is still less than that of conventional counterpart, which can be due to the fine grain size (~5 μm) in the as-prepared specimen.

**Water Modeling Study on the Behavior of Inclusions in a Gas-Stirred Ladle with Two Tuyere:** Shu-guo Zheng<sup>1</sup>; Xiang-yang Chen<sup>1</sup>; Jian-dong Hu<sup>1</sup>; Miao-yong Zhu<sup>1</sup>; <sup>1</sup>Northeastern University

The effects of time, flowrate and mode of gas bubbling on inclusion removal in a 140 ton gas-stirred ladle with two tuyeres were investigated by choosing emulsion drops simulated as inclusions in a water model, and the effect of argon blowing by one tuyere and two tuyere on the inclusion removal was also studied. The results show that most of the inclusions can be removed within eight minutes and all the inclusions which had the possibility to be removed almost disappeared from the system in twenty-eight minutes. There was both an optimal gas flowrate for the inclusion removal with the high and the low gas flowrates, which was explained by discussing the mechanism of inclusion removal. Argon blowing by one tuyere seemed to be more efficient for inclusion removal within six minutes gas blowing than argon blowing by two tuyeres, in contrast, in the further course of blowing, argon blowing by two tuyeres were more efficient. The mode of gas bubbling with firstly larger gas flowrate and then smaller flowrate seemed to be efficient for inclusions removal. Furthermore, it had been found that the inclusion removal was in exponential relationship with gas blowing time.

# Index

## A

- Aalund, R ..... 303  
 Aaram, S ..... 149  
 Abachi, A ..... 384  
 Abashidze, G ..... 382  
 Abbas, H ..... 298, 299  
 Abbass, M ..... 12, 47, 287, 378  
 Abd El-Aziz, A ..... 262  
 Abdel-Karim, R ..... 242  
 Abdel-Rahman, M ..... 378  
 Abdel Al, N ..... 234  
 Abdel Hamid, A ..... 237  
 Abdeljawad, F ..... 292  
 Abdi, R ..... 384  
 Abdullah, S ..... 88  
 Abe, H ..... 313  
 Abedrabbo, S ..... 196  
 Abel, P ..... 74  
 Abeykoon, A ..... 166  
 Abouie, M ..... 168  
 Abu-Farha, F ..... 353  
 Abuleil, T ..... 262  
 Abunaemeh, M ..... 61, 217  
 Acharya, S ..... 241  
 Ackelid, U ..... 152  
 Ackland, G ..... 230, 335  
 Acma, E ..... 391  
 Acoff, V ..... 304  
 Acosta, A ..... 259  
 Adachi, N ..... 235  
 Adams, B ..... 218, 238  
 Adams, D ..... 151  
 Adams, J ..... 182  
 Adams, R ..... 75  
 Addressio, F ..... 231  
 Adedokun, S ..... 137  
 Adel Nofal, A ..... 345  
 Adeosun, S ..... 119, 224  
 Adharapurapu, R ..... 350  
 Adhikari, S ..... 274  
 Adland, A ..... 147, 372  
 Adler, S ..... 215  
 Afonona, V ..... 10  
 Afteni, M ..... 233  
 Agaogullari, D ..... 15, 303  
 Agarwal, A ..... 27, 74, 123, 175, 227, 273  
 Aghazadeh, J ..... 385  
 Agnew, S ..... 22, 23, 56, 106, 107, 108,  
 ..... 157, 159, 211, 212, 220, 262,  
 ..... 263, 308, 313, 353, 354, 355  
 Agour, M ..... 345  
 Agrawal, D ..... 71  
 Aguaze, J ..... 161  
 Aguilar, M ..... 234  
 Aguirre, M ..... 124  
 Ahamed, K ..... 350  
 Ahluwalia, R ..... 165, 373  
 Ahmad-Bitar, R ..... 195, 342  
 Ahmed, A ..... 87, 345  
 Ahn, B ..... 81, 236  
 Ahn, D ..... 384  
 Ahn, H ..... 381  
 Ahn, I ..... 375, 376, 381, 395  
 Ahn, K ..... 42, 196  
 Aho, K ..... 342  
 Ahuja, S ..... 146  
 Ai, X ..... 308  
 Aich, S ..... 124, 146  
 Aikin, R ..... 48  
 Aithal, K ..... 12  
 Ajayan, P ..... 75, 82  
 Akahori, T ..... 253  
 Akatyeva, K ..... 10  
 Akbari Pazoooki, A ..... 47, 380, 395, 396  
 Akinc, M ..... 173, 350  
 Akiyama, K ..... 192  
 Akpa, O ..... 300  
 Akre, J ..... 15  
 Aksu, S ..... 306  
 Aktas, S ..... 379, 391, 392  
 Al-hashani, T ..... 378  
 Al-Jassim, M ..... 42, 196  
 Al-Maharbi, M ..... 78, 80, 264, 283  
 Alamdari, H ..... 97  
 Alankar, A ..... 86, 337, 371  
 Alaswad, K ..... 138, 345  
 Al Balushi, M ..... 254  
 Albe, K ..... 61, 141, 340  
 Albina, J ..... 322  
 Albinmousa, J ..... 211  
 Aldi, J ..... 287  
 Aleksandrov, A ..... 287  
 Aleksandrova, V ..... 287  
 Alexander, D ..... 236  
 Alexander, M ..... 381  
 Alfantazi, A ..... 42, 123  
 Alhajeri, S ..... 282  
 Ali, M ..... 344  
 Al Jallaf, M ..... 138, 345  
 Allard, B ..... 97  
 Allen, S ..... 226  
 Allen, T ..... 270, 314, 326, 362, 378  
 Allendorf, M ..... 143  
 Allison, B ..... 35  
 Allison, J ..... 106, 125, 354, 355  
 Alman, D ..... 109, 266  
 Al Maqbali, S ..... 88  
 Almer, J ..... 39, 66, 115, 186, 270, 361, 363  
 Almosilhy, A ..... 172  
 Aloe, M ..... 105  
 Alonso, E ..... 177  
 Alptekin, G ..... 160  
 Al Reyami, A ..... 138  
 Alsaran, A ..... 131  
 Alsem, D ..... 202  
 Alterach, M ..... 75  
 Altman, K ..... 190  
 Alvarez, D ..... 173  
 Alves, J ..... 320  
 Alves, T ..... 365  
 Alvin, M ..... 93, 145  
 Alwan, A ..... 47  
 Al Zarouni, A ..... 138, 345  
 Amara, H ..... 103  
 Ambrosini, A ..... 143  
 Amini, S ..... 384  
 Amooorzaei, M ..... 188  
 An, H ..... 349  
 An, K ..... 64  
 An, S ..... 289  
 Anand, S ..... 377  
 Ande, C ..... 19  
 Anderoglu, O ..... 181  
 Anderson, I ..... 25, 66, 116, 124, 152,  
 ..... 154, 168, 185, 221, 271,  
 ..... 275, 302, 315, 362, 363  
 Anderson, P ..... 62  
 Anderson, T ..... 195  
 Ando, D ..... 160  
 Ando, K ..... 246  
 Ando, T ..... 224, 274  
 Ando, Y ..... 376  
 Andrews, M ..... 169  
 Andrews, R ..... 82  
 Andriese, M ..... 343  
 Andros, F ..... 347  
 Angioletti-Uberti, S ..... 104  
 Angirash, M ..... 88  
 Angoua, B ..... 214  
 Ankem, S ..... 224, 274  
 Anklam, T ..... 285, 334  
 Annamalai, S ..... 356  
 Anopuo, O ..... 159, 263  
 Anselmo, G ..... 145  
 Antipov, E ..... 337  
 Antolin, N ..... 165  
 Antoniou, A ..... 84, 134, 278  
 Antrekowitsch, H ..... 36, 341  
 Anyalebechi, P ..... 58, 59, 110, 162, 215  
 Apel, M ..... 86, 102  
 Apelian, D ..... 124  
 Apisarov, A ..... 189  
 Appaji, A ..... 215  
 Appleby-Thomas, G ..... 49  
 Apter, A ..... 395  
 Aracena, A ..... 156, 209  
 Araújo, C ..... 145  
 Araújo, E ..... 320, 344, 393  
 Araujo-Moreira, F ..... 347  
 Arbegast, W ..... 270  
 Arbel, T ..... 308  
 Ardell, A ..... 260  
 Ardell, J ..... 299  
 Arenas-Alatorre, J ..... 391  
 Arens, R ..... 375  
 Ares, A ..... 58, 75, 124  
 Arfaei, B ..... 363  
 Argyropoulos, S ..... 210  
 Ari-Gur, P ..... 10, 74, 347  
 Arkanti, K ..... 137  
 Armendariz, D ..... 296  
 Arola, D ..... 190  
 Arroyave, R ..... 29, 251, 316  
 Arvanitis, A ..... 296  
 Ashby, M ..... 83  
 Ashtana, A ..... 46  
 Askin, J ..... 293  
 Asta, M ..... 19, 50, 51, 52, 103, 104, 154,  
 ..... 207, 260, 278, 305, 306, 312, 372  
 Astashynski, V ..... 176  
 Atamanenko, T ..... 143  
 Atambo, D ..... 216  
 Atkin, S ..... 257  
 Atli, K ..... 331  
 Atmeh, M ..... 347  
 Atodaria, I ..... 380  
 Atzmon, M ..... 38  
 Aubry, S ..... 173, 321  
 Averbach, R ..... 31, 62, 147, 148  
 Avila-Davila, E ..... 389  
 Avraham, S ..... 262  
 Ayas, C ..... 113  
 Ayer, R ..... 195, 377  
 Aynibal, F ..... 15  
 Ayoola, W ..... 119, 224  
 Azeem, M ..... 361  
 Azhari, C ..... 35  
 Azizi-Alizamini, H ..... 21  
 Azuma, H ..... 235

## B

- Baars, D ..... 121  
 Baated, A ..... 68  
 Babaghorbani, P ..... 188



Babakhani, A.....	70	Bang, H.....	386	Bei, H.....	62, 63, 64, 101, 113, 171, 231, 339
Baber, A.....	257	Bang, J.....	117	Beitra, L.....	313
Babu, S.....	235	Bang, W.....	42, 159, 169, 222, 354	Belin-Ferré, E.....	306
Bache, M.....	205	Banik, A.....	258	Bell, W.....	105
Bachmaier, A.....	236	Banoth, L.....	146	Bellon, P.....	31, 62, 147
Bachurin, D.....	27	Banovic, S.....	85	Bellou, A.....	239
Backhouse, N.....	254	Bansal, R.....	101	Belokon, Y.....	145
Bacon, D.....	174, 231, 327	Bansiddhi, A.....	120	Belonoshko, A.....	125
Badowski, M.....	296	Banu, M.....	233	Belova, I.....	28, 279
Bae, B.....	382	Bao, L.....	16, 240	Belt, C.....	201
Bae, D.....	186, 382, 385, 392	Bao, Y.....	12, 158	Ben-Amotz, D.....	329
Bae, G.....	24, 353	Bär, M.....	335	Ben-Artzy, A.....	108, 159, 264
Bae, I.....	356	Barabash, O.....	225, 268	Benabed, B.....	344
Bae, J.....	24, 49	Barabash, R.....	25, 62, 63, 64, 114, 121, 166, 219, 231, 268, 312, 359, 360	Benedek, N.....	278
Baena Murillo, E.....	366, 367	Baram, M.....	73	Beneduce Neto, F.....	208
Baggash, I.....	138	Barat, P.....	368	Bengtson, A.....	44
Bahr, D.....	72, 151, 239, 284, 329, 359	Barbato, C.....	187	Benito Páramo, J.....	181
Bahrami, A.....	251	Barbee, T.....	128	Benjiang, Q.....	145
Bai, G.....	156	Barber, R.....	79	Bennett, C.....	307
Bai, S.....	377	Barbosa, N.....	60, 112, 163, 216	Bennett, J.....	343
Bai, X.....	226, 372	Barbosa, R.....	344	Benson, D.....	49
Baik, S.....	376	Barbu, A.....	217	Bentley, J.....	270, 314, 362
Baily, S.....	83	Barkhordarian, G.....	80	Benzerge, A.....	46, 165, 231, 234
Bainbridge, I.....	296	Barnard, L.....	326	Bequette, D.....	201
Baiocchi, F.....	25	Barnett, M.....	213	Bergen, R.....	260
Bajaj, D.....	190	Barnett, S.....	21, 215	Bergström, T.....	194
Bajaj, S.....	29	Barney, E.....	91	Berkmortel, R.....	263
Bajvani Gavanluei, A.....	69	Baró, M.....	340	Bernard, J.....	211
Bakai, A.....	39	Barone, J.....	245	Bernard, S.....	14, 291
Bakai, S.....	39	Barr, G.....	363	Berne, X.....	138
Bakavos, D.....	47	Barrado, P.....	348	Berneder, J.....	36
Baker, A.....	105	Barry, J.....	88	Bernstorff, S.....	219
Baker, D.....	334	Barsoum, M.....	369	Berry, C.....	123
Baker, F.....	161	Barta, M.....	318	Bertolini, M.....	45
Baker, I.....	18, 48, 75, 342	Barth, H.....	190	Besharati, M.....	242, 384, 389
Baker, P.....	295	Bartlett, L.....	111	Bessais, L.....	386
Baker, S.....	231	Bartolo, L.....	324	Besser, M.....	66, 302
Baker, W.....	100	Bartolucci, S.....	237	Bettles, C.....	360
Bakshi, D.....	138	Baruah, T.....	166	Bevington, J.....	251
Bakshi, S.....	273	Baserinia, A.....	106	Beyerlein, I.....	80, 194, 231, 236, 264, 328, 368
Balachander, N.....	237	Baskes, M.....	19, 230, 252	Beyerlein, K.....	220
Balachandran, P.....	322	Basoalto, H.....	259	Beygelzimer, Y.....	180
Balachandran, S.....	332	Bassani, J.....	230, 372	Bezerra, D.....	393
Balakrishnan, A.....	119	Bassler, K.....	166	Bezerra, E.....	17
Balan, P.....	30	Bastie, P.....	178	Bhadrachalam, P.....	283, 284
Balani, K.....	333	Basu, S.....	218	Bhagat, R.....	44, 96
Balasubramaniam, K.....	379	Batchkova, I.....	390	Bhandhubanyong, P.....	69, 119, 171, 224, 274, 318, 366
Balbuena, P.....	266	Batista, R.....	273	Bharadwaj, M.....	145
Balci, O.....	303	Batson, R.....	263	Bharat, S.....	345
Baldo, P.....	286	Battaille, C.....	46, 179, 256, 302, 349, 368, 370	Bharathula, A.....	293, 340
Baldock, R.....	208	Bauer, G.....	166	Bhargava, S.....	82, 336
Balla, V.....	13, 14, 375	Baxter, R.....	86, 243	Bhat, R.....	182, 183
Ballard, D.....	259	Baydogan, M.....	124, 228, 395	Bhat, V.....	161
Ballarini, R.....	114, 273	Bayles, R.....	199	Bhatt, J.....	11, 237
Ballato, J.....	345	Bayliss, C.....	87	Bhatta, R.....	356
Balle, F.....	86	Bayrak, Y.....	255	Bhattacharjee, S.....	11
Balogh, L.....	79	Beall, G.....	366	Bhattacharya, J.....	266
Balogun, S.....	119, 224	Bearne, G.....	75	Bhattacharya, S.....	185
Balzar, D.....	268	Beaudoin, A.....	21	Bhattacharyya, D.....	84, 174, 226, 236, 315
Bambach, M.....	337	Beaumont, R.....	250	Bhattacharyya, S.....	41
Bamberger, M.....	262, 263	Beausir, B.....	370	Bhavsar, R.....	318, 331
Bammann, D.....	56, 66, 107	Bechtold, K.....	381	Bhesetti, C.....	25
Ban, Y.....	139	Becker, C.....	82, 95, 202	Bi, Y.....	16
Bandhyopadhyay, A.....	191	Beckermann, C.....	262	Bian, J.....	111
Bandyopadhyay, A.....	13, 14, 37, 84, 89, 119, 134, 139, 172, 190, 245, 291, 292, 338, 375	Bednarcik, J.....	39	Bian, M.....	380
Bandyopadhyay, N.....	40, 379, 381	Bedrov, D.....	279, 329	Bice, D.....	101, 253
Banek, M.....	97	Beeler, B.....	230, 252	Bicer, A.....	390
Banerjee, J.....	318	Beer, A.....	24, 160, 213	Bichara, C.....	103
Banerjee, R.....	17, 72, 342, 359, 382, 383	Begam, K.....	357	Bieler, T.....	21, 25, 28, 46, 49, 66, 100, 116, 117, 121, 151, 168, 205, 221, 256, 258, 271, 302, 304, 315, 349, 363
Banerjee, S.....	14, 191, 291, 375	Behnagh, R.....	242, 389		
		Behuria, R.....	219		

# Index

Biener, J	84	Bourke, M	270, 362	Burkett, S	222
Biener, M	84	Bourne, N	49, 388	Burns, J	217, 262
Biermann, D	206	Bouvard, C	107	Busby, J	270, 314, 362
Bigot, J	254	Bouvard, D	70	Buslaps, T	65
Bing, H	54	Bouwhuis, B	287	Buta, D	50, 372
Bing, P	284, 321	Bouzemmi, W	97	Butler, B	182, 183
Bing, X	308	Bower, A	116	Butt, D	17, 59, 313, 315, 335, 351, 387, 392, 393, 395
Bingert, J	120, 187, 236, 297, 323, 372, 378	Bowers, R	85	Buzunov, V	344
Birat, J	142	Boyapalli, N	379, 391	Bv, K	321
Biol, Y	146, 196	Boyce, B	45, 60, 81, 99, 150, 202, 245	Byeon, J	386
Birosca, S	22, 205	Boyce, D	62	Byeon, K	274
Biswas, A	334	Boyer, R	297	Byler, D	227, 386
Bitzek, E	46, 293, 294	Boyle, K	106, 163	Byrd, D	152
Bjarno, O	88	Bozkaya, D	120, 172	Byun	362
Bjorn, C	359	Bozkus, S	228, 395	Byun, T	60, 270
Blaesing, J	115	Braatz, R	266		
Blanco, E	53, 209	Bradford, M	63	<b>C</b>	
Blank, J	148	Brady, M	57, 109, 160, 214, 265, 310, 311, 356, 357	Caballero, F	40
Blanpain, B	58, 260, 276	Braga, P	136	Cabrera-Real, H	275
Blasques, J	138, 345	Brammer, T	173, 350	Cabrera Marrero, J	181
Blattner, C	375	Branco, M	38	Caceres, C	262
Blavette, D	78	Brandstetter, S	268	Cady, C	48, 49, 258
Blawert, C	108, 158	Brar, H	355	Caffarey, M	125
Bleck, W	172, 350	Brasileiro, M	17	Cagin, T	29
Blendell, J	363	Brennan, S	309	Cahill, D	43, 321
Bligh, R	85	Brenner, D	325	Cahn, J	52, 278, 372
Blumenthal, W	360	Brewer, L	60, 179, 368, 370	Cai, J	130, 183
Bm, G	93	Bridge, J	250	Cai, M	137, 194, 249, 250
Bm, S	93	Briggs, M	225	Cai, W	61, 267, 373
Bo, W	85, 241, 255	Briggs, T	349	Caimei, X	230
Bo, Z	54	Brigmon, R	93, 123	Cakmak, E	64, 361
Boakye, E	238	Brito, M	265	Calderón, H	348
Bodde, S	139	Brock, J	114	Calin, M	236
Bodhak, S	14, 119, 291	Brocq, M	59, 73, 315	Caliste, D	173
Boehlert, C	66, 239, 253, 308	Broderick, S	208	Callahan, P	127, 387
Boehm, R	240	Brodie, G	336	Campbell, A	22, 55, 105, 156, 210, 261, 306, 307, 352
Boesenberg, A	271	Brodu, B	200	Campbell, C	319
Boettinger, W	51, 147	Broek, S	87	Campbell, D	40
Böhner, A	131	Brokhorst, C	323, 372	Campbell, G	231
Bojarevics, V	210, 308	Brooks, G	149, 210	Campillo, B	384
Bokeloh, J	154, 339	Brothers, A	141	Campillo-Illanes, B	15
Bollinger, A	229	Brown, D	49, 164, 167, 220, 359, 360, 361	Campion, M	31
Bolshakov, D	344	Brown, E	258	Canedo, E	365
Bonadiman, R	26	Browne, D	101	Cang, X	188
Bondarchuk, V	149	Bruce, R	198	Cao, A	46, 61
Bonollo, F	302	Brundidge, C	100, 360	Cao, B	128, 129
Boopathy, K	247	Brunelli, M	166	Cao, D	13
Booth-Morrison, C	28	Bruner, E	74, 94, 333	Cao, F	74, 231
Booty, M	196	Brush, L	125	Cao, G	275, 357
Borbely, A	65	Buchheit, T	61, 113, 165, 218, 267, 311, 358	Cao, P	148
Borchardt, G	258	Buchholz, A	194	Cao, Q	91
Borchers, C	131	Buchovecky, E	116	Cao, W	58, 85, 86
Bordia, R	14, 134, 338	Budai, J	269, 280	Cao, X	35, 321, 382
Borges, A	136	Budruk, A	330	Cao, Y	282
Borges, M	177	Buehler, M	34, 83, 100, 218, 246, 273	Cao, Z	20, 135, 248
Borisov, V	344	Buehrig-Polaczek, A	158, 212	Capdevila-Montes, C	144
Borkar, T	27	Buelters, O	111	Capolungo, L	194, 220, 368
Bormann, R	207, 264, 348	Buffiere, J	22, 179	Caputo, G	10
Borodin, O	329	Buhr, A	105, 201	Carcea, A	269
Borup, R	310	Buirette, C	383	Cardona, C	95
Borys, S	119, 145, 343	Bujoreanu, L	392	Cardoso, I	26, 203
Bose, S	13, 14, 84, 89, 119, 172, 191, 291, 292, 375	Bulatov, V	373	Carle, D	298
Botelho, J	200	Bulovic, V	151	Carlson, B	75
Böttcher, H	341	Bumiller, E	289	Carmichael, C	70
Böttger, B	86	Bunin, I	342	Caro, A	19, 62, 335
Boucharat, N	180, 339	Burakovsky, L	125	Caro, M	285
Bouche, C	254	Burek, M	99	Caron, A	246, 291, 340, 342
Boucher, P	88	Burheim, O	391	Caron, F	194
Bouler, J	191	Burke, P	108	Carpenter, C	112, 375
Boulianne, R	88	Burkes, D	60, 61		
Bourell, D	277				



Carpenter, R	133, 237	Chateigner, D	65	Choi, G	310
Carre, A	86	Chattoraj, I	323	Choi, H	116, 186, 221, 392
Carreno, F	236	Chaudhari, G	130, 354	Choi, J	20, 265, 349
Carreon, H	144	Chaudhary, R	55	Choi, M	53, 387
Carson, B	304	Chawla, K	239	Choi, S	163, 306, 375, 376, 381
Carter, J	24, 160, 310, 353	Chawla, N	34, 117, 238, 239, 272, 316, 330	Choi, W	28, 178, 285
Carter, W	122	Chbihi, A	78	Choi, Y	146, 151, 281, 314
Caruthers, J	279	Che-Ming, C	375	Chokshi, A	258
Carvajal, M	329	Cheah, W	373	Chongstitvattana, P	272
Casolco, S	255, 386	Cheeseman, B	325	Choo, H	38, 39, 64, 90, 140, 181, 191, 219, 220, 246, 292, 339, 361
Cassano, T	342	Chelikowsky, J	43	Chopra, N	10, 33, 82, 133, 183, 237, 283, 333
Castañeda, H	255	Chelliah Machavallavan, N	116	Chou, M	265
Castro, M	244	Chen, A	332, 391	Chou, T	272
Castro, W	145	Chen, B	304, 361	Chou, Y	122
Castro-Ceseña, A	140	Chen, C	68, 69, 117, 118, 126, 169, 170, 223, 317, 366, 383	Choudhary, B	164
Castro-Colin, M	166	Chen, D	16	Choudhuri, D	222
Caton, M	109	Chen, E	101, 234, 253	Choudhury, S	326
Cavalcante, D	17	Chen, G	171, 339	Christodoulou, J	50
Cavallaro, G	269	Chen, H	136, 170, 195, 207, 215, 353, 364	Christodoulou, L	50
Cawkwell, M	178, 218	Chen, I	139, 170	Chrzan, D	113, 150, 325
Cawthorne, S	19	Chen, J	60, 138, 212, 256, 365	Chu, J	91, 170, 175, 247, 294, 396
Cebeci, D	329	Chen, K	58, 63, 118, 143, 161, 168, 184, 222, 266, 272, 324, 348, 375	Chu, K	198
Ceder, G	52, 103, 154, 207, 208, 260, 305	Chen, L	12, 40, 91, 111, 122, 242, 252, 261, 264, 278, 300, 345, 346, 364	Chu, M	49
Celikin, M	160	Chen, M	38, 141, 192, 367	Chua, A	278
Celine, V	260	Chen, O	354	Chuang, A	39
Cerreta, E	49, 231, 351	Chen, P	90, 139, 140, 245, 301	Chuang, C	91
Cerri, E	36	Chen, R	25	Chuang, H	26
Certain, A	270	Chen, S	68, 85, 117, 121, 125, 170, 223, 230, 242, 271, 316, 342, 363	Chuang, T	117
Cesta, T	296	Chen, T	289, 296, 297	Chulist, R	181
Cetinel, S	38	Chen, W	103, 149, 169, 253, 273, 364	Chumbimuni-Torres, K	90
Cetlin, P	234	Chen, X	15, 98, 189, 209, 270, 391, 396	Chumbley, S	154
Cha, D	33, 83	Chen, Y	18, 28, 68, 91, 117, 178, 180, 184, 272, 393	Chun, D	161
Cha, P	375	Chen, Z	48, 252, 305, 308, 325, 377	Chun, I	133
Cha, W	49	Chenelle, B	47, 255	Chun, S	118, 357
Chada, S	68, 117, 170, 223	Cheng, J	339	Chun, Y	263
Chae, S	390, 392	Cheng, S	219, 361	Chung, H	317
Chai, L	18, 276, 284, 321, 367	Cheng, Y	118	Chung, J	365
Chaim, R	224, 366	Chepushtanova, T	162	Chung, P	228, 374
Chaka, A	113	Cherif Idrissi El Ganouni, O	254	Chung, Y	172
Chakrabarti, S	120	Cherng, S	366	Churaman, W	82
Chakraborty, M	146	Chernovich, I	176	Ci, L	75
Chakravarthy, S	267	Chertkov, G	120	Cicero, G	312
Chakravartty, J	81	Cheung, K	332	Ciftja, A	72
Challa, A	133	Chevy, J	178	Cimenoglu, H	124, 228, 387, 390, 395
Chamarthy, S	374	Chiang, T	167	Cipriano, P	365
Champagne, D	244	Chiannng, T	115	Ciulik, J	71
Champoux, P	88	Chiba, A	236, 252, 379	Cizek, J	234
Chan, E	130	Chi Chung, N	302	Cizer, Ö	276
Chan, H	332	Chidambaram, V	271	Clark, J	294
Chan, L	77	Chikhradze, M	333, 385	Clark, M	148
Chan, S	195	Chikhradze, N	333, 382, 385	Clarke, R	360
Chan, V	128	Chin, K	376	Claudel, P	254
Chan, W	252	Chinella, J	35, 85	Clausen, B	164, 220, 360
Chandler, R	341	Chitrada, K	217, 315	Clement, P	135
Chandrasekar, S	30, 283, 378	Chiu, C	56	Clemente, A	296
Chandrasekaran, S	121	Chiu, T	364	Clisson, M	393
Chandross, M	77, 218	Chiu, Y	67, 169	Clos, R	115
Chang, C	316	Chmelar, J	253, 337	Clouet, E	27, 126
Chang, H	142	Cho, H	72, 273, 310	Cloutier, B	86
Chang, J	223	Cho, J	183, 274	Coakley, J	259
Chang, S	132, 184	Cho, K	23, 24, 81, 243, 256, 375	Cocco, M	302
Chang, W	396	Cho, M	67, 223	Cochran, J	121
Chang, Y	12, 85, 101, 117, 159	Cho, S	55	Cockayne, E	322
Chang-chun, X	189	Choe, H	221	Cockcroft, S	106, 253
Chanturiya, V	342	Choe, K	375	Cocke, D	215, 216, 274, 365, 366
Chao, J	144, 269	Choi, C	221	Cockeram, B	70, 71, 120, 172
Chappell, D	95	Choi, D	240, 356	Coffey, K	309
Chari, A	251			Coker, E	143
Charit, I	60, 61, 112, 217, 225, 286, 315, 362			Colakoglu, C	216
Chartrand, P	97, 213			Colanto, D	224
Chason, E	116, 146, 363			Colás, R	282
Chasse, K	351				

# Index

Cole, J	217, 315, 362
Cole, K	238
Colliex, C	72
Collins, D	361
Collins, G	19, 103, 251
Collins, J	45
Collins, P	16, 18, 96, 127, 330, 366, 368, 383
Colmenares, M	290
Colorado, H	303
Comer, M	127, 232
Compton, C	121
Cong, D	167
Conklin, B	145
Conner, D	38
Conrad, E	114
Contescu, C	161
Cook, D	240, 352
Cook, R	202
Cooksey, M	201, 244
Cooley, J	268
Cooper, C	175
Cooper, K	347
Coppack, J	301
Coral-Escobar, E	12
Cordill, M	151
Corlu, B	295, 296
Cornwell, J	240, 346
Corona, E	151
Cortes, N	348
Coryell, S	259
Costa, J	26
Costa, L	16, 250
Costine, A	135
Côté, P	88
Cotts, E	317, 363
Coulombe, M	97
Coulombe, R	298
Coulter, K	160
Counts, W	43, 301
Courtenay, J	143, 341
Couvrat, M	59
Cowen, C	110, 266, 396
Cox, A	71
Cox, M	135
Cozzoli, D	10
Cranford, S	273
Craps, M	276
Creuziger, A	360
Crimp, M	28, 258
Croft, M	74
Croft, N	157
Croft, T	307
Crooks, R	21
Cross, M	157, 307
Crossa Archiropoli, U	41
Crouse, C	35
Cserhati, C	176
Csik, A	176
Csontos, A	270, 314, 362
Cui, H	11, 13
Cui, J	193, 248
Cui, Y	200
Cunningham, N	314
Cupid, D	22, 101
Curran, L	82
Curtarolo, S	207
Curtin, W	230, 267, 328, 368
Cuvilly, F	59, 73, 315
<b>D</b>	
D'Armas, H	386
Da Costa, G	122
Dadfarnia, M	231
Daehn, G	235, 304, 349
Daemen, L	120
Dahlman, A	90, 91, 292, 293
Dahlman, J	90
Dahmen, U	173
Dahotre, N	27, 74, 123, 158, 175, 227
Dai, Q	136
Dai, Y	60, 379
Daivis, P	219
Dalili, N	26
Damaskin, A	186
Damoah, L	341
Damodaran, A	147
Dan, L	297
Dandeneau, C	275
Dando, K	336
Dando, N	86, 88, 336
Daniel, B	354
Daniel, C	123, 300, 357, 388
Daniil, M	280, 284, 333, 346
Danoix, F	15
Danoix, R	15
Dantas, A	10
Dantzig, J	166
Daoxin, W	284, 297, 393
Daphalapurkar, N	129
Darbandi, P	121
Dargusch, M	331
Darling, K	79, 182, 183
Darsell, J	110, 310
Das, G	93
Das, K	215, 216, 300, 311, 365
Das, S	11, 35, 76, 85, 100, 101, 136, 145, 187, 241, 289, 294, 323, 342
Das Gupta, R	34
Dasgupta, S	336
Dash, B	389
Dashwood, R	44, 96
da Silva, A	15
Da Silva, D	320
Dattelbaum, D	258, 329
Dauskardt, R	45, 99, 100, 150, 151, 202
Daveau, G	269
Davey, J	310
David, S	88
Davidchack, R	197
Davies, C	78, 263
Davila, J	124
Davis, B	23, 24, 57, 200, 213, 393
Davis, C	229
Davis, M	136
Dawson, P	62
Daymond, M	65, 363
De, P	80, 204
Deal, A	182, 183
Dean, J	45
Dean, M	338
DeAngelis, R	120, 236
Debnath, M	175, 227
de Carlo, F	330
de Carvalho, L	365
Decker, R	308
Dedrick, D	143
Dedyukhin, A	189
Deepak	274, 345, 352
De Fontaine, D	52
De Gouveia, T	393
De Graef, M	14, 127, 195, 330
Dehghani, K	13, 137, 290, 333
Dehm, G	151
DeHoff, R	95
De Hosson, J	27, 74, 76, 125, 126, 177, 230, 278, 324, 327, 370, 372
De Hoyos, S	348
Dehui, C	176, 287
Deibler, L	292
Delagnes, D	15
Delahanty, T	81
De la Rosa, J	384
Delette, G	202
Del Genio, C	166
de Lima, O	347
DellaCorte, C	74
Della Corte, E	302
DeLorme, R	23, 213
Delorme, R	24
Delplanque, J	59, 198, 256
DelRio, F	202
DeLucca, J	25
DeMange, P	335
Demetriou, M	140, 247
DeMint, A	60
Demircan, O	214
Demirci, K	196
Demirhan, O	15
Demkowicz, M	72, 114, 122, 173, 226, 227, 321
Demura, M	161
Deng, G	29
Deng, J	165, 328, 350
Dengfu, C	59, 385
Dengke, Z	379
Dennis, K	275
Denoirjean, A	167
Deo, C	230, 252, 326
de Oliveira, S	320
DePari, L	107
Depree, N	256
Deqing, Z	55
Dera, P	63
Derezinski, S	109
Dernell, W	13
Desai, S	226
Desai, V	12
Deshmukh, V	242
DeSilva, J	44, 45
De Silva, L	187
De Souza, D	320
Deutschman, H	257
Deutsch, T	42
Devanathan, R	335
Devaraj, A	17, 383
DeVasConCellos, P	13, 292
Devincere, B	177, 269, 371
DeVoe, K	14
Dewulf, W	229
Dey, G	277
Dhanabalan, A	381
Dheda, S	334
Dheeradhada, V	350
Diaz, S	90
Diaz-Ortiz, A	52
Dick, A	27, 29, 208
Dickerson, P	84, 174, 315
Dickerson, R	303, 386
Dickinson, M	245
DiDomizio, R	182
Didomizio, R	183
Dieringa, H	159
Difffoot-Carlo, N	14



Digiaco, S.....	386	Dufour, G.....	86, 87, 88, 138, 188, 243, 244, 290, 336, 344	El-Demellawy, M.....	304
Dillion, S.....	77	Dugger, M.....	203	El-Desouky, A.....	132
Dillon, Jr., O.....	355	Duh, J.....	25, 26, 66, 116, 118, 168, 221, 222, 223, 271, 315, 316, 363	El-Kaddah, N.....	307
Dillon, S.....	122	Dulyaphant, P.....	13	El-Khodary, K.....	325
di Michiel, M.....	65	Duman, I.....	15, 303, 389	El-Shabasy, A.....	380, 383
Dimiduk, D.....	113, 151, 281, 328, 370	Duman, S.....	134	Elam, J.....	93
Dimitrovska, A.....	26	Dumas, R.....	334	Elangovan, S.....	143
Ding, F.....	324	Dumortier, P.....	86	Elder, K.....	260
Ding, H.....	192	Dunand, D.....	11, 34, 36, 83, 103, 120, 134, 135, 180, 185, 186, 238, 286, 297	Eldin Raged, M.....	237
Ding, M.....	271	Duncan, K.....	214	Elhami-Khorasani, A.....	283
Ding, R.....	205, 206	Dundar, M.....	295, 296	Elie-dit-Cosaque, X.....	349
Ding, S.....	141	Dupas, N.....	88	Elkadi, Y.....	44, 45, 261
Ding, W.....	56, 211, 212	Dupuis, C.....	194	El Kadiri, H.....	107, 211
Ding, Y.....	63	Dupuis, M.....	243	Elsaesser, C.....	126, 322
Dingreville, R.....	179, 370	Durgamahanty, S.....	82	Elsamadicy, A.....	61
Dinsdale, A.....	224	Durst, K.....	245, 257	Elsayed, F.....	262
Dippenaar, R.....	269	Dursun, A.....	295, 296	Elshan, E.....	385
Dittrick, S.....	14	Duscher, G.....	175	Elstnerova, P.....	140
Diver, R.....	143	Dutrizac, J.....	297	Elting, D.....	367
Divinsky, S.....	180	Dutta, B.....	356	Elton, J.....	240, 346
Dixit, V.....	16, 127, 330, 368	Dutta, I.....	67, 116, 271, 315	Em, V.....	388
Djambazov, G.....	55	Dutta, S.....	271	Emadi, D.....	383
Dlouhy, A.....	186, 371	Dutta, T.....	346	Emadi, R.....	237
Dmowski, W.....	39, 91	Dutta Majumdar, J.....	124, 175, 227	Emery, J.....	368
Do, K.....	375, 376, 381	Dutton, R.....	49	Emmerich, H.....	50, 102, 103, 120, 153, 206, 207
Dobatkin, S.....	130, 131	Duval, P.....	178	Ene, C.....	73
Dobosz, R.....	234	Duygulu, O.....	296, 309	Engelbrecht, A.....	153, 341
Doernberg, E.....	207	Duz, V.....	96	Engl, T.....	72
Dogan, O.....	121	Dye, D.....	44, 64, 96, 205, 259, 361	Engineer, T.....	395
Dohner, A.....	75	Dziociol, K.....	65	England, L.....	45
Doiron, P.....	337	<b>E</b>		Enser, J.....	36
Domgin, F.....	55	Earthman, J.....	182, 338	Entelmann, W.....	57
Donati, L.....	136, 289	Easter, S.....	308	Entemeter, D.....	69
Donchev, A.....	301	Eastman, J.....	114	Epureanu, A.....	233
Dong, C.....	383	Easton, M.....	160, 206, 262	Erdemir, A.....	74
Dong, J.....	211, 336	Ebacher, V.....	190	Erdeniz, D.....	224
Dong, L.....	282	Ebel, T.....	348	Erdogan, M.....	98
Dong, T.....	170	Ebeling, T.....	264	Erdogan, R.....	295
Dong, Y.....	156	Ebin, B.....	376, 389, 394	Erfanfar, A.....	384
Donner, W.....	166	Ebrahimi, F.....	22, 101	Erinc, M.....	355
Dopita, M.....	234	Echeverria, M.....	12	Ertorer, O.....	31, 130, 283
Dotson, M.....	53	Echlin, M.....	330	Ertürk, S.....	389
Dou, Z.....	16, 240, 377, 382	Eckart, D.....	241	Eruslu, N.....	385
Doughty, G.....	44	Eckert, J.....	39, 103, 120, 140, 191, 236, 319	Esaka, H.....	26, 78
Doutre, D.....	341	Eckert, S.....	55	Eskin, D.....	143
Downey, J.....	53, 104, 155, 208	Edagawa, K.....	28, 325	Esmaili, S.....	86, 309
Doyle, F.....	22, 55, 105, 156, 210, 261, 306, 307, 352	Edalati, K.....	79, 283	Espana, F.....	84, 172
Drabble, D.....	256	Edwards, P.....	298	Esper, F.....	10
Drault, R.....	52, 76, 126, 324	Edwin, I.....	164	Essadiqi, E.....	162, 265, 308, 309
Drelich, J.....	53, 92, 104, 155, 208	Efrem, V.....	49	Esteves-Alcazar, F.....	15
Dreyer, C.....	107	Efstathiou, C.....	62	Estevez, F.....	311
Dreyssé, H.....	208	Egami, T.....	38, 39, 125, 230, 293	Estournes, C.....	366
Drezet, J.....	106	Eggeler, G.....	16, 186, 251, 371	Estrin, Y.....	56, 131, 165, 332
Dring, K.....	44, 45, 96, 148, 198, 199, 252, 297	Ehrke, J.....	36	Etienne, A.....	283, 362
Driscoll, K.....	75	Eichlsteder, W.....	157	Euh, K.....	243, 319
Driver, K.....	325	Eick, I.....	337	Evans, A.....	106, 360
Druschitz, A.....	85	Eiffler, D.....	86, 92, 354	Evans, G.....	210
Druschitz, E.....	85	Eiken, J.....	102	Evans, J.....	35, 37, 210, 244, 258, 261, 307, 339
Dryepont, S.....	110	Eisenlohr, P.....	28, 258	Evans, M.....	288
Du, J.....	135, 348	Eizenberg, M.....	170	Evans, N.....	110
Du, Q.....	102	Ekerim, A.....	255	Evcimen, N.....	255
Duan, Z.....	18, 281	Ekuma, C.....	342	Everett, R.....	195
Dubey, D.....	190	El-Awady, J.....	113	Evteev, A.....	28
Dubey, S.....	198, 227	El-Azab, A.....	164, 165, 198, 227, 228, 328, 350	Eyckmans, J.....	276
Dubois, J.....	306	El-Aziz, A.....	242	<b>F</b>	
Ducastelle, F.....	103	El-Bitar, T.....	172	Faber, K.....	115
Duchene, L.....	233, 234	El-Dasher, B.....	285	Fabritius, H.....	140
Duchesne, C.....	344			Fafard, M.....	97
Dudek, M.....	330			Fahringer, R.....	281
Dudney, N.....	266, 300, 388			Fair, G.....	238
Duflou, J.....	229				

# Index

Fan, J	141	Finnis, M	104, 278	Fu, H	272
Fan, L	167	Fiory, A	196, 197	Fu, W	87
Fan, X	209	Fiot, L	138	Fuchs, B	14
Faney, T	286	Firrao, D	40, 48, 92, 144, 174, 297	Fuerst, C	213
Fang, J	11	Fischer, F	151	Fuerst, J	298
Fang, S	199	Fischer, M	350	Fugetsu, B	185
Fang, Z	199	Fister, T	114	Fujihara, K	246
Farahany, S	188	Fjeld, A	157	Fujita, K	192
Faraji, M	41	Flandorfer, H	68, 117, 170, 223	Fukuda, H	158
Fardeau, S	290	Flater, P	120, 236	Fukusumi, M	383, 385
Faris, A	378	Fleer, M	86	Fullwood, D	218, 232, 238
Farkas, D	61, 306, 327, 370	Flicker, J	33, 395	Fultz, B	19, 103, 155, 251
Farmer, J	285, 334	Fliflet, A	198	Fuoss, P	114
Farrow, A	49	Floey, D	264	Furár, I	74
Farzadfar, A	265	Flom, Z	330	Furrer, D	205, 304
Fathi, M	42, 123	Flores, K	40, 90, 175, 190, 191, 204, 293, 340, 366	Furu, E	149
Fathi Doost, H	92	Flores-Garcia, J	238, 303	Furu, J	194
Fauchais, P	167	Floyd, N	327	Furuhara, T	233
Favez, D	106, 253	Fluss, M	285	Furuta, T	80
Favilla, P	75	Foecke, T	85, 360	Fuwa, A	69, 119, 171, 224, 274, 318, 366
Faxin, X	176, 228	Foiles, S	20, 61, 95, 278, 372	Fyhrie, D	245
Fechner, D	108	Foley, D	78, 79, 80, 264, 283		
Fecht, H	128, 141, 181, 246, 291, 340, 342	Foley, R	85	<b>G</b>	
Fedyayev, A	136	Foltz, J	18	Gabb, T	304
Fei, H	117	Fonda, R	47, 179, 195	Gabbitas, B	148
Fei, N	228	Fong, D	114, 221	Gagne, J	88
Fei-Shuo, H	375	Fong, H	37, 38, 191	Gaies, J	36
Fei-Yi, H	184, 375	Fonseca, P	359	Gaikwad, A	306, 307
Fein, A	57	Fook, M	320	Gaines, L	177
Felicelli, S	66, 162	Forbes Jones, R	331	Gaither, M	202
Fell, D	94	Forcade, R	52	Gajjala, G	335
Fenbin, L	351	Forde, N	245	Gakwaya, A	349
Fencel, J	253	Forlerer, E	388	Galeev, R	332
Feng, C	199	Fornell, J	340	Gali, A	70
Feng, L	215, 324	Forsik, S	163	Galinski, H	73
Feng, Q	11	Forsmark, J	353	Gall, K	367
Feng, R	63, 269	Forsyth, R	303	Gallagher, A	271
Feng, Y	244	Fortier, M	375	Gallagher, M	79, 182
Feng, Z	47, 65, 172, 225, 268	Forwald, K	104	Galloway, J	306, 307
Feng-qi, D	189	Foster, B	191	Gallego, N	161
Fensin, S	278	Foulk, J	202	Gan, M	93, 209
Fenstad, J	391	Fox, D	297	Ganesan, R	224
Fergus, J	265	Fox, S	106, 253	Ganesan, Y	46, 273
Ferguson, J	114, 298	Fragoudakis, R	111	Ganfeng, T	189
Fernandes, P	393	Franca, S	136, 187, 320	Gangopadhyay, A	284
Fernandes, V	365	Frank, R	377	Ganguli, S	120
Fernandez Diaz, L	266, 396	Franke, M	153	Gansert, R	199
Ferreira, A	249, 250	Franke, O	245, 257	Gao, B	12, 108, 139, 337
Ferreira, H	17	Franklin, J	188	Gao, C	96
Ferreira Neto, J	208	Franz, H	40	Gao, F	147, 171, 334, 335
Ferri, O	348	Frary, M	59, 77, 217, 315, 371	Gao, L	272
Ferris, K	22, 23	Fraser, H	16, 17, 18, 72, 73, 96, 127, 151, 330, 342, 366, 368, 382, 383	Gao, M	121, 252, 317
Ferry, M	362	Fray, D	34, 44, 71, 148, 306, 341, 391	Gao, W	264
Fertig, R	231, 286	Free, M	52, 98	Gao, X	16
Feuerstein, J	191	Freeman, A	104, 327, 371	Gao, Y	38, 63, 66, 90, 140, 191, 219, 246, 267, 292, 294, 327, 339, 391
Fevre, M	260	Freitas, I	203	Garate, E	296
Fiedler, T	279	Fressengeas, C	69, 178, 370	Garay, A	29, 251
Field, D	86, 94, 187, 242, 284, 334, 337, 371	Freund, J	311	Garcia, B	357
Field, F	75, 177	Friak, M	27, 103, 120, 126, 140, 301	Garcia, E	324
Field, K	270	Frick, T	111	Garcia, H	175
Fielitz, P	258	Fried, L	306	Garcia-Hinojosa, A	15
Figueiredo, R	234, 235, 281	Friedman, L	61, 113, 165, 218, 267, 311, 323, 358	Garcia-Infanta, J	236
Figueiredo Melo Costa, A	393	Fries, S	154, 251	Garcia-Mateo, C	40
Filidore, A	187	Froes, F	44, 96, 148, 198, 252, 297	Garcia-Matech, E	282
Filipiev, R	289	Froger, M	223	García H., A	384
Finch, J	17	Frolov, T	19, 94, 122, 372	Gardin, P	55
Findley, K	259	Frost, L	143	Garg, A	145, 274
Fine, M	167, 172	Fu, B	122	Garkida, A	104, 320
Finel, A	260	Fu, E	226	Garlea, E	248
Finger, I	318			Garmestani, H	24, 206, 279
Fink, M	207				
Finklea, H	214				



Garrett, W.....	119	Gnäupel-Herold, T.....	74	Gromov, V.....	289
Garrido, F.....	15, 186, 344	Goeken, M.....	29, 78, 80, 128, 130, 180, 182, 233, 235, 281, 331	Gronostajski, Z.....	264
Garside, G.....	314	Goel, M.....	294	Gronsky, R.....	123
Garzon, F.....	311	Göken, M.....	131, 245, 257	Gross, M.....	51
Gates, R.....	202	Gokhale, A.....	144, 145, 214, 232, 263, 286, 322	Grosse, A.....	75
Gaudet, J.....	393	Goksu, O.....	98	Grosselle, F.....	302
Gaune-Escard, M.....	163	Golding, N.....	230	Grossman, J.....	219, 312
Gaustad, G.....	276, 277	Goldman, N.....	306	Groza, J.....	89, 184, 198, 256
Gauthier, C.....	344	Gollapudi, S.....	225	Gruber, D.....	116
Gautieri, A.....	246	Goller, G.....	385	Grün, G.....	248
Gavras, A.....	203, 255	Golubic, T.....	200	Gu, C.....	78
Gaytan, S.....	134, 152	Golumbskie, W.....	187	Gu, S.....	189
Gazawi, A.....	131	Gomes, J.....	215, 216, 274, 365, 366	Gu, Y.....	284, 377
Gazder, A.....	78	Gong, J.....	206	Guan, P.....	38
Geantil, P.....	63, 268	Gong, X.....	202	Guang-qiang, L.....	172
Gebert, A.....	246, 247, 340	Gonzalez, J.....	290	Guangchun, Y.....	176, 201, 228, 255, 287, 302
Gebhardt, J.....	307	Gonzalez-Velazquez, J.....	389	Guangping, Z.....	139
Geddes, B.....	341	Goo, B.....	390	Guangrong, D.....	382
Gee, S.....	169	Gooch, J.....	60	Guay, D.....	200, 393
Geier, G.....	143	Good, B.....	230, 252	Guda Vishnu, K.....	312
Geiss, R.....	99	Goodarzi, M.....	305	Gudbrandsen, H.....	71
Geltmacher, A.....	179, 232, 330	Goodman, L.....	351	Guebels, C.....	198
Gemmen, R.....	265	Goodwin, W.....	145	Gueijman, S.....	58
Genau, A.....	136	Goosens, D.....	312	Guenther, R.....	207
Gencer, O.....	376	Goossens, D.....	312	Guerrero-Mata, M.....	282
Gendre, M.....	254	Gopal, P.....	251	Guilian, R.....	123
Genevois, C.....	122, 283	Gopalakrishnan, C.....	242	Guillen-Bonilla, H.....	82
Geng, X.....	391	Gopalan, V.....	252	Guillot, M.....	47, 349
Gennaro, P.....	152	Gordon, A.....	257, 289	Gullett, P.....	375, 376, 385
Gentleman, M.....	291	Gordon, P.....	29, 226, 328	Gulsoy, B.....	14, 127
George, E.....	63, 70, 101, 113, 231	Gornostyrev, Y.....	27, 231, 327	Gulsoy, G.....	224
Gerard, B.....	264	Gosslar, D.....	207	Gumbsch, P.....	27, 126, 377
Gerberich, W.....	17, 114	Goswami, R.....	188, 241	Gunderov, D.....	78
Gerbeth, G.....	55	Goto, S.....	131	Gunesoglu, C.....	318
Gerczak, T.....	378	Goto, T.....	313	Gunesoglu, S.....	318
Gerdemann, S.....	148, 294	Gottstein, G.....	182, 239, 338	Gungormus, M.....	38, 191, 292
Germann, T.....	62, 174	Goutiere, V.....	194	Gunnewiek, L.....	296
Gers, H.....	36	Goyel, S.....	22, 101	Günyüz, M.....	124
Gershenson, M.....	88	Grabowski, B.....	208, 326	Guo, F.....	25, 66, 68, 116, 168, 221, 271, 272, 315, 363
Gerson, A.....	269	Graetz, J.....	380	Guo, H.....	141, 214, 215
Gerstmayr, G.....	157	Graf, M.....	172	Guo, J.....	85, 86, 272, 273, 317, 318, 364, 381, 395
Gervasio, D.....	311	Graff, G.....	240, 356	Guo, L.....	167
Gesing, A.....	108, 294	Gramegna, N.....	302	Guo, M.....	58
Geysen, D.....	276	Gramlich, M.....	114	Guo, W.....	251
Ghasemi, H.....	46	Gran, H.....	97	Guo, X.....	133, 300
Ghasemi-Nanasa, H.....	129	Granasy, L.....	102	Guo, Y.....	16, 30, 52, 209, 234, 240, 393
Ghazisaeidi, M.....	174, 311	Grande, T.....	97, 149	Guo, Z.....	318, 365
Gheno, T.....	110	Grandfield, J.....	143, 157, 193, 213, 248, 295, 341	Guo Liang, L.....	321
Gholinia, A.....	340	Grant, D.....	199	Gupta, C.....	81
Ghoniem, N.....	325	Grant, G.....	110, 354	Gupta, M.....	274
Ghosh, A.....	31, 130, 205, 353	Grantham, J.....	211	Gupta, N.....	346
Ghosh, G.....	167, 172	Graves, R.....	247, 248	Gupta, R.....	160, 171, 182, 274
Ghosh, S.....	93, 232, 258, 376	Gravouil, A.....	179	Gupta, V.....	315
Ghosn, L.....	304	Gray, A.....	115	Gurao, N.....	370
Gianola, D.....	45, 46	Gray, G.....	49, 121, 231, 258, 351, 378	Gurevich, S.....	188
Gibala, R.....	43	Greaney, P.....	219, 312	Gurmen, S.....	376, 389, 394
Gibson, J.....	23	Green, N.....	157, 255	Gürmen, S.....	381
Gibson, L.....	34, 83	Greenberg, B.....	327	Gurses, E.....	328
Gibson, M.....	160, 360	Greenfield, S.....	386	Guruprasad, P.....	165, 231
Gierlotka, W.....	68, 117, 170, 223	Greenstein, K.....	375	Gururajan, M.....	180
Gigineishvili, A.....	333	Greenwood, M.....	95	Guruswamy, S.....	314
Gilbert, E.....	239	Greer, A.....	68, 90, 102, 117, 170, 223	Gusberti, V.....	298
Gilles, R.....	66, 359	Greer, J.....	99	Gusev, A.....	337
Gitanjali G.....	196	Gregory, J.....	229	Guzman, D.....	329
Gittard, S.....	123	Grelia, A.....	15	Guzonias, D.....	92
Glaeser, A.....	123	Grest, G.....	218	Gwaze, M.....	75
Glavicic, M.....	205	Gripenberg, H.....	194	Gwynne, B.....	56
Gleiter, H.....	141	Gröbner, J.....	158, 212		
Glicksman, M.....	50, 102, 153, 195, 206	Groeber, M.....	127, 227, 232, 281		
Gludovatz, B.....	71	Groebner, J.....	56		
Glynn, M.....	152	Groger, R.....	77, 177		
Gnaeupel-Herold, T.....	360				

# Index

## H

Ha, C	382	Harding, T	324	Henager, C	147
Ha, H	48	Hardy, M	259	Henao, H	155
Ha, S	68	Hariharan, R	242	Henein, H	106, 128, 186, 320
Haarberg, G	45, 71, 96, 277	Hariharaputran, R	51, 252	Henke, S	228
Haataja, M	41, 76, 95, 292	Harimkar, S	27, 74, 123, 175, 227	Henke, T	337
Habraken, A	233, 234	Harlow, D	246, 247	Hennies, W	10
Hackenberg, R	303	Harringa, J	271	Hennig, R	312, 322, 325, 367
Hackett, M	112	Harris, R	120, 236	Henrickson, L	288
Hackney, S	161	Hart, G	52, 207	Henry, J	112
Hadaway, J	187	Hartig, C	207, 264	Henshall, G	364
Haddadi, F	47	Hartvigsen, J	143	Henson, M	341
Haeffner, D	186, 268	Hartwig, K	78, 79, 80, 264, 283, 332	Hepburn, D	335
Hagelüken, C	229	Hartwig, T	264	Herlach, D	51, 102, 153
Hagni, A	15, 40, 92, 144, 194, 239, 249, 296, 342, 343	Harvey, W	86	Herling, D	353
Hahn, H	185, 303	Hasan, A	311	Hernandez, A	307
Haimanot, M	292	Hasegawa, T	151	Hernandez-Garcia, A	15
Haines, C	133	Hashemi-Sadraei, L	281	Hernandez-Garcia, S	56
Haixin, Z	11	Hashemian, S	386	Hernquist, M	21
Haiyan, Y	336	Hasheminasari, M	94	Herrera, D	329
Hajiakbari, F	233	Hashida, T	392	Herring, J	143
Håkonsen, A	341	Hassan, H	380, 383	Heske, C	335
Hald, J	271	Haswell, R	281	Heulens, J	260
Hale, L	114	Hatada, N	18	Hewertson, R	201
Halevy, I	251	Hatcher, N	104	Hibbard, G	287
Halil, G	287	Hatkevich, S	349	Hickel, T	29, 208, 326
Hall, D	300	Hattar, K	60	Hiel, C	303
Hall, G	101	Hattel, J	271	Higashida, K	79
Hall, J	253	Haugen, T	341	Highland, M	114
Halle, T	282	Haugland, E	345	Hild, F	179
Hallen-Lopez, M	275	Haupt, T	108	Hild, S	140
Halloran, J	100	Hausöl, T	131	Hildeman, G	71, 72
Ham, Y	389	Havens, A	323	Hilgraf, P	135
Hamaguchi, M	200	Hawk, J	58, 356	Hillebrand, S	338
Hamdy, A	335	Hawkes, G	143	Hills, M	341
Hamed, Y	93, 394	Haxhijaj, A	209, 261, 295	Hinderliter, B	323
Hamel, S	21	Haxhijaj, E	209, 261, 295	Hiraga, K	22
Hamer, S	249	Hay, R	238	Hirakawa, T	185
Hammad, M	295	Hayamizu, Y	37	Hirano, T	161
Hammerschmidt, T	76	Hayden, S	114	Hirashima, R	287
Han, B	36, 238, 395	Hayes, P	155, 261	Hirata, G	90, 140
Han, C	100	Haynes, P	278	Hirt, G	337, 350
Han, G	54	Hayward, E	326	Hirth, J	62, 95, 181, 278
Han, J	67	He, A	26	Hirvela, J	86
Han, K	225	He, B	115	Hjortstam, O	194
Han, L	262	He, H	98	Hnilova, M	37, 38
Han, M	66	He, J	204, 382	Ho, C	118, 307, 317
Han, S	220, 319	He, Q	210	Ho, T	395
Han, Y	331	He, W	123, 248, 340	Hoagland, R	62, 174, 181, 226, 278, 372
Han, Z	354	He, X	20, 334, 387	Hoc, T	269
Handwerker, C	25, 168, 363	He, Y	162	Hockauf, K	282
Haney, E	314	Hebert, R	40, 180	Hockauf, M	180, 282
Hanks, D	335	Hecht, U	102, 207	Hodge, A	18, 81, 84, 128, 146, 245, 246, 275
Hanlummyuang, Y	113	Heck, K	377	Hoelzer, D	270, 285, 314, 315, 362
Hanna, M	41	Hector, L	23, 106, 107, 108, 177, 304, 326, 368	Hoffelner, W	60, 112, 163, 164, 216
Hanrahan, R	48, 203, 257, 350	Hector Jr, L	107, 263, 328, 353	Hoffmann, A	71
Hansen, G	218, 238, 317	Heenan, R	361	Hoffmann, T	94
Hansen, J	219	Heerdegen, A	312	Hofmann, D	140, 186, 247
Hansen, N	81, 317	Hefferan, C	268	Hofmann, M	66
Hanson, E	360	Hefiti, L	206	Hofmann, T	335
Hao, H	25	Hegazy, A	172	Hofmeister, C	81
Hao, X	152	Hehui, Z	244	Hofmeister, W	59, 319
Hao, Y	12	Heidloff, A	152	Hogan, P	387
Haouaoui, M	235, 331	Heilig, M	158, 171, 212	Hogan, R	143
Haq, S	137	Heilmaier, M	181	Hohenwarter, A	29, 236
Harada, Y	331	Hein, A	104, 242	Hohl, B	254
Harbola, M	352	Heinl, P	14	Hohmann, A	246
Harcuba, P	364	Heinrich, H	343	Holcomb, G	266, 396
Harder, B	115	Heinz, W	151	Holder, H	125
Harder, R	313	Heldt, L	40	Holland-Moritz, D	51, 153
		Helle, S	200, 393	Holm, E	20, 77, 81, 94, 95, 278, 370
		Helminck, R	259	Holt, R	363
		Hemker, K	100, 370, 372	Holtz, R	188, 241



Holy, V	166	Huang, Q	156	Inostroza, C	75
Holzer, I	21	Huang, S	167, 276	Inoue, A	90, 141, 192, 193, 248, 291, 340, 383
Homborgsmeier, E	57	Huang, T	364	Inoue, J	204
Homer, E	292	Huang, W	137, 250	Inui, H	325
Hong, C	376	Huang, X	81, 104, 155, 320	Ipser, H	223, 224
Hong, E	274	Huang, Y	54, 141, 159, 182, 213, 263, 271, 355	Iqbal, G	214, 215
Hong, H	115, 167	Huang, Z	54, 89, 150, 166, 212, 315	Irie, K	235
Hong, S	49, 300, 310, 382, 388	Hubbard, C	66	Irissou, E	70, 152, 302
Hong, W	221, 376	Hubbard, J	368	Irwin, G	216, 365
Hong, Z	288	Huber, D	16, 330, 387	Irzhak, A	10
Hong-liang, Z	189	Huber, N	355	Isheim, D	172, 394
Hong-Xu, C	216	Hubert, J	103, 120	Ishida, T	69
Hongbin, L	319	Hudspeth, M	30, 283, 378	Ishikawa, T	269
Hongbo, Z	379	Huey, H	198	Islam, M	274
Hongliang, Z	189, 244	Huez, J	383	Islam, Z	166, 167
Hongqiang, R	42, 387	Hug, E	233	Isler, D	146
Hono, K	309	Hugenschmidt, C	66	Ismer, L	326
Hooks, D	218, 329, 374	Hughes, D	361	Isvilanonda, V	379
Hop, J	345	Huh, H	394	Ivan'ko, V	332
Höppel, H	131	Huilan, S	85, 241, 255	Ivanisenko, Y	128, 180, 181
Horbach, J	51	Huizenga, G	347	Ivanov, M	327
Horita, T	214, 265	Hull, A	113	Ivanov, Y	289
Horita, Z	79, 80, 283	Humadi, H	19	Ivashishin, O	78, 149
Horky, J	80	Humphrey, E	195	Ivey, D	26, 168
Hornbuckle, B	284	Humphreys, N	157	Iwata, N	363
Horstemeyer, M	23, 211, 382	Hunang, J	83	Izvekov, S	374
Horstemeyer, S	107	Hünert, D	57		
Hort, N	108, 158, 159, 212, 213, 262, 263	Hung, C	240	<b>J</b>	
Horton, J	219	Hunter, L	330	Jaansalu, K	225
Hosemann, P	60, 270, 314, 315	Huo, L	354	Jablonski, P	110, 148, 266, 396
Hosford, W	120, 236	Huo, Y	308	Jackson, B	44, 96
Hosokawa, A	17	Hurley, M	351, 393, 395	Jackson, J	69
Hossain, K	369	Huskins, E	129, 282	Jackson, M	96, 127
Hou, T	15	Hussain, S	291	Jacobs, P	74
Hou, X	98	Husseini, N	330, 360	Jacobsen, K	322
Houbaert, Y	15	Hutchinson, N	40	Jacobson, A	166
House, J	120, 235, 236, 256	Huth, C	273	Jadhav, N	116, 363
Hovanski, Y	110, 354	Hwang, I	158, 395	Jafaar, E	328
Howe, J	253, 282	Hwang, J	15, 40, 53, 72, 92, 104, 105, 142, 144, 155, 161, 194, 208, 249, 293, 296, 320, 342, 343, 379, 382	Jaffe, J	147
Howell, R	111	Hwang, W	170	Jagannathan, R	275, 277, 336
Hoyt, J	19, 43, 50, 94, 147, 197, 251, 260	Hyatt, T	238	Jahed, H	211
Hrabe, N	14, 134, 338	Hyun, C	386	Jahja, A	42
Hsia, K	133, 300	Hyun, S	68	Jain, P	121
Hsia, Y	170, 195			Jak, E	155
Hsiao, V	100	<b>I</b>		Jalil, J	47
Hsiao, Y	118, 364	Iadicola, M	85	James, P	336
Hsiao, Z	142, 272	Ibragimov, S	347	Jamseh, M	124
Hsieh, G	394	Ice, G	63, 116, 231, 268, 269, 360	Janda, M	142
Hsieh, Y	384	Idris, M	188	Janecek, M	32, 234, 253, 364
Hsiung, L	231, 285	ihlefeld, J	252	Janelidze, I	385
Hsu, Y	16	Iida, O	69	Jang, C	217
Hu, B	212, 264	Ikhmayies, S	194, 195, 342	Jang, D	38, 99, 109, 387
Hu, H	262	Ila, D	61, 217, 340	Jang, E	68
Hu, J	240, 251, 396	Ilavsky, J	166, 167	Jang, H	308
Hu, L	85, 105	Ilbahi, A	128	Jang, J	90, 91, 92, 161
Hu, M	238	Im, J	78	Janissek, P	177
Hu, W	239	Imai, H	158, 185	Janssens, K	164
Hu, X	35, 87, 108, 139	Imai, Y	313	Jao, C	384
Hu, Y	54, 92	Imam, M	44, 96, 148, 198, 199, 252, 297	Japaridze, L	382
Hu, Z	184, 197	Imani, Y	384	Jaquerod, C	106
Hua, H	215	Imayev, R	332	Jaques, B	335, 387, 393
Hua, J	215	Imery, J	88, 290	Jaramillo, D	249
Hua, Q	15	Imhoff, S	192	Jaramillo, E	279
Hua, S	99	Imrie, W	188	Jaramillo, L	366
Hua, Z	11, 134, 135, 201	Inácio, W	249	Jarry, P	295
Huabing, L	48	Inal, K	211	Jasthi, B	270
Huang, A	271	Indacochea, J	217	Javid, A	309
Huang, D	20, 54, 209	Inel, C	295	Jawahir, I	355
Huang, E	360	Inman, D	44, 96	Jawali, V	321
Huang, J	33, 45, 46, 90, 91, 181, 308, 324			Je, J	24
Huang, L	39, 225, 248, 340			Jeanclaude, V	69
Huang, M	24				

# Index

- Jekl, J ..... 263  
 Jen, A ..... 38  
 Jendrzeczyk-Handzlik, D ..... 223  
 Jennerjohn, S ..... 359  
 Jensen, D ..... 179  
 Jensen-Holm, C ..... 84  
 Jensrud, O ..... 199  
 Jeon, H ..... 343  
 Jeon, S ..... 376  
 Jeong, H ..... 301  
 Jeong, I ..... 395  
 Jeong, J ..... 22, 53  
 Jeong, M ..... 68, 223, 316  
 Jeong, Y ..... 183, 242  
 Jepson, P ..... 70, 120, 172  
 Jha, M ..... 142  
 Jha, S ..... 109, 203, 368  
 Ji, C ..... 261  
 Ji, H ..... 159  
 Ji, K ..... 12, 348  
 Jia, Q ..... 83, 173  
 Jia, R ..... 100, 151  
 Jia, W ..... 321  
 Jia Ming, Z ..... 138  
 Jian, L ..... 345  
 Jian, P ..... 55  
 Jianchao, S ..... 255, 302  
 Jiang, F ..... 39, 40  
 Jiang, G ..... 215, 276  
 Jiang, H ..... 117, 141  
 Jiang, J ..... 40, 91  
 Jiang, L ..... 213, 272, 316, 330  
 Jiang, T ..... 53, 54, 92, 104, 155, 156, 208, 209, 287, 393  
 Jiang, T ..... 15, 52, 209  
 Jiang, W ..... 335  
 Jiang, Y ..... 12, 158, 202  
 Jiang, Z ..... 92, 204, 351, 377, 384, 391  
 Jianguang, Y ..... 18, 379  
 Jianping, P ..... 189, 244, 345  
 Jianquan, L ..... 385  
 Jiao, S ..... 96, 306  
 Jie, L ..... 98, 150, 189, 244  
 Jie, Z ..... 377  
 Jieng, Y ..... 224  
 Jilai, X ..... 275  
 Jin, C ..... 376  
 Jin, H ..... 86, 100, 101, 377  
 Jin, L ..... 211, 213  
 Jin, S ..... 204  
 Jin, X ..... 189, 246  
 Jing, H ..... 18, 379  
 Jing, P ..... 388, 392  
 Jing, T ..... 180  
 Jingbiao, F ..... 276  
 Jingyang, L ..... 42  
 Jin Long, Z ..... 321  
 Jiricny, V ..... 210  
 Jo, M ..... 267  
 Jo, T ..... 216  
 Jodoin, B ..... 302  
 Johansen, J ..... 97  
 Johanson, S ..... 167  
 Johansson, J ..... 128  
 Johnson, A ..... 34  
 Johnson, F ..... 66  
 Johnson, H ..... 311  
 Johnson, J ..... 276  
 Johnson, K ..... 254  
 Johnson, N ..... 323  
 Johnson, O ..... 218, 238  
 Johnson, W ..... 67, 140, 186, 247, 298  
 Jolly, M ..... 201, 255  
 Jonas, J ..... 213  
 Jones, A ..... 349  
 Jones, D ..... 22, 23  
 Jones, I ..... 49, 205, 206  
 Jones, J ..... 308, 354, 360  
 Jones, Jr, W ..... 307  
 Jones, P ..... 276  
 Jones, R ..... 321  
 Jonnalagadda, K ..... 100  
 Joo, S ..... 30, 31  
 Joo, Y ..... 316  
 Jordan, J ..... 35  
 Jordon, B ..... 382  
 Jordon, J ..... 23, 211  
 José, D ..... 143  
 Joshi, S ..... 286  
 Joshi, V ..... 310  
 Joung, S ..... 31  
 Ju, J ..... 38  
 Juarez-Islas, J ..... 391  
 Judson, J ..... 87  
 Jue, J ..... 61, 315  
 Jun, J ..... 376  
 Jun, X ..... 145  
 June, R ..... 245  
 Jun fei, M ..... 201, 228  
 Jung, C ..... 36  
 Jung, H ..... 23, 162, 379, 380  
 Jung, I ..... 193, 213, 309  
 Jung, S ..... 25, 26, 68  
 Junkaew, A ..... 251  
 Juya, Z ..... 230
- K**
- Kabir, M ..... 178  
 Kabra, S ..... 360  
 Kacar, T ..... 37  
 Kad, B ..... 235  
 Kadhim, M ..... 388  
 Kadjo, J ..... 70  
 Kaftelen, H ..... 186  
 Kahvecioglu, O ..... 381  
 Kai, J ..... 360  
 Kai, L ..... 176, 189  
 Kai, W ..... 142  
 Kain, V ..... 376  
 Kainer, K ..... 32, 159, 213, 262, 263  
 Kaini-Rashid, A ..... 70, 283  
 Kakegawa, K ..... 331  
 Kakeshita, T ..... 167  
 Kakiuchi, H ..... 383, 385  
 Kalashnikov, V ..... 10  
 Kalay, E ..... 154, 339  
 Kalay, I ..... 339  
 Kalidindi, S ..... 179, 232  
 Kalkundri, K ..... 347  
 Kalpoe, J ..... 254  
 Kalyanaraman, R ..... 175, 247, 284  
 Kalyanasundaram, N ..... 311  
 Kamantsev, A ..... 347  
 Kamikawa, N ..... 81  
 Kamimura, Y ..... 28, 325  
 Kamineni, P ..... 159  
 Kamkar Zahmatkesh, N ..... 13, 94, 137, 290  
 Kammerhofer, C ..... 29  
 Kampe, S ..... 105, 356  
 Kamto Tegueu, A ..... 222  
 Kanbayashi, D ..... 376  
 Kandil, A ..... 345  
 Kang, B ..... 93, 145, 214, 215  
 Kang, D ..... 193, 229, 266, 309, 311, 353, 381, 384, 386  
 Kang, J ..... 162, 369, 376  
 Kang, K ..... 84, 134, 267, 294, 373, 378  
 Kang, M ..... 388  
 Kang, N ..... 384  
 Kang, S ..... 25, 33, 66, 67, 116, 168, 221, 271, 300, 315, 345, 346, 353, 363, 375, 376, 381  
 Kang, U ..... 31, 380  
 Kang, Y ..... 162, 213  
 Kang, Z ..... 318  
 Kangjian, S ..... 138  
 Kano, K ..... 200  
 Kantzos, P ..... 304  
 Kao, C ..... 26, 67, 169, 272, 316  
 Kao, P ..... 142  
 Kao, T ..... 170  
 Kapelle, B ..... 45  
 Kaplan, W ..... 73, 122  
 Kapoor, D ..... 133, 237  
 Kapoor, M ..... 172  
 Kapoor, R ..... 80, 81  
 Kar, M ..... 277  
 Kar, S ..... 228, 259  
 Karaduman, B ..... 390  
 Karakaya, I ..... 98  
 Karaman, I ..... 78, 80, 130, 137, 183, 264, 283, 331  
 Karan, N ..... 358  
 Karcher, C ..... 162  
 Karhausen, K ..... 337, 338  
 Karjalainen, P ..... 128, 291  
 Karkin, I ..... 27  
 Karkina, L ..... 27  
 Karl, J ..... 16  
 Karma, A ..... 147, 372  
 Karppinen, M ..... 305  
 Karthik, S ..... 32  
 Kaschner, G ..... 218, 238, 256  
 Kashani Bozorg, S ..... 237  
 Kashiwagi, Y ..... 383, 385  
 Kashyap, B ..... 242  
 Kashyap, S ..... 89  
 Kaski, K ..... 278  
 Kasprzak, W ..... 188  
 Kassegne, S ..... 59, 132, 367  
 Kassner, M ..... 63, 81, 268  
 Kastner, O ..... 230  
 Katgerman, L ..... 143  
 Katiyar, R ..... 358  
 Kato, H ..... 91, 193  
 Kato, T ..... 157  
 Katoh, Y ..... 60  
 Katragadda, S ..... 202  
 Katsman, A ..... 262, 263  
 Kaufman, M ..... 145  
 Kaushal, G ..... 303  
 Kawakami, M ..... 96  
 Kawakami, T ..... 376  
 Kawalla, R ..... 172  
 Kawamura, Y ..... 213, 309  
 Kawasaki, M ..... 69, 80, 81, 281  
 Kaya, A ..... 309  
 Kayali, E ..... 124, 228, 387, 390  
 Kayali, S ..... 395  
 Kayihan, A ..... 196  
 Kazimirov, A ..... 220  
 Ke, J ..... 67  
 Kearns, V ..... 83  
 Kecskes, L ..... 78, 79, 80, 129, 183, 264, 283, 393  
 Keer, L ..... 246  
 Keiser, D ..... 60, 61, 315, 362



Keist, J	307	Kimura, A	285	Kolluri, K	114, 173, 226
Keller, C	233	Kimura, Y	366	Kolmogorov, A	76
Keller, F	298	King, A	371	Komatsu, N	200
Keller, R	99	King, P	121	Komazaki, S	392
Keller, S	289	Kingsbury, D	117	Komiyama, S	146
Kellogg, G	143	Kinney, C	168	Kondoh, K	158, 185, 238
Kelly, A	49, 303	Kinsella, M	50	Koneva, N	284
Kelly, M	182	Kioussis, N	325	Kong, C	322
Kempf, B	111	Kipouros, G	108, 158	Kong, F	393
Kennedy, F	75	Kirchain, R	124, 176, 177, 229, 276, 277, 323, 369	Kong, J	380
Kennedy, J	177	Kirchheim, R	122, 131	Kongoli, F	171, 274
Kennedy, M	45, 99, 150, 151, 202	Kirk, M	286	Kongstein, O	71
Keralavarma, S	46	Kirka, M	101	Konno, T	22, 252, 301
Kerber, M	219	Kiselkov, D	134	Konovalov, S	289
Kerr, J	134	Kishida, K	325	Kontsevoi, O	104, 327, 371
Kerr, M	65, 112, 363	Kishimoto, H	265	Koo, M	220
Kerscher, T	52	Kitchin, J	57, 257	Koo, Y	28, 256, 267, 349
Keshavarz, Z	24	Kiyotani, K	69	Kopp, J	240
Kesler, M	22, 101	Kizilaslan, E	379	Korfmacher, H	176
Kestens, L	251	Kjar, A	288	Körmann, F	208
Keul, C	350	Kjos, O	45, 96	Korzekwa, D	359
Khajeh, E	180	Klag, O	354	Korzhenevskii, A	166
Khaji, K	298, 299	Klassen, I	51, 153	Koseki, T	204
Khaleel, M	163	Klassen, R	99	Koshi, M	364
Khalid, F	275	Klaus, G	158, 212	Koslowski, M	279, 329
Khalifa, H	140	Klement, U	287	Kostelak, S	240
Khan, K	120	Klemf, J	263	Koster, M	92
Khan, M	119	Klett, C	85	Kostorz, G	166
Kharicha, A	157	Klier, E	182	Kotula, P	81, 127
Khasyap, D	275	Klingelhöffer, H	57	Kou, H	332
Khatayevich, D	38	Klotz, B	182, 393	Kountouriotis, Z	55
Khater, H	231	Knaack, J	193	Kovacevic, R	26, 105, 376
Khatibi, G	80	Knaak, U	338	Kovarik, L	16, 145, 178, 204, 373
kheirandish, s	305	Knipling, K	47, 195, 280, 346	Kozachakov, H	140
Khiev, S	127	Knori, K	392	Kozeschnik, E	20, 21
Khisamov, R	33	Knutson, J	260	Kozlov, A	56
Khovailo, V	347	Ko, C	272	Kozlov, E	284
Kiani-Rashid, A	41, 93, 111, 195, 394	Ko, I	10, 386, 390	Krabbe, R	343
Kido, K	370	Ko, Y	29, 31, 79, 117, 128, 129	Krajewski, P	23, 75, 108, 159, 160, 264, 304, 355
Kiggans, J	148	Kobas, M	167	Kral, K	33
Kildea, J	241	Kobayashi, K	350	Kral, M	88, 256
Kim, B	10, 22, 246, 316, 386	Kobayashi, T	116	Kral, R	253
Kim, C	41, 42, 93, 114, 115, 146, 169, 196, 222, 384	Kobeisy, A	242	Kramer, M	66, 95, 154, 173, 275, 293, 339, 350, 362
Kim, D	23, 24, 30, 142, 191, 192, 216, 217, 289, 345, 346, 348, 353, 378, 381, 395	Koch, C	130, 171, 182	Krane, M	324
Kim, E	116, 221, 307	Koch, D	94	Kranzmann, A	57
Kim, G	185, 355, 376, 389	Koch, H	36	Kraus, L	129
Kim, H	20, 24, 30, 31, 159, 223, 233, 242, 267, 310, 326, 346, 358, 376, 388	Koch, T	317	Krause, S	335
Kim, I	388	Kockar, B	331	Kreller, C	215
Kim, J	10, 26, 33, 68, 82, 83, 99, 117, 133, 169, 183, 184, 213, 221, 223, 237, 249, 283, 309, 316, 333, 346, 348, 351, 357, 375, 385, 390, 394, 396	Kockegey-Lorenz, R	201	Kripesh, V	25
Kim, K	24, 26, 49, 68, 183, 310, 331, 349, 353, 394	Kodentsov, A	170, 221, 272	Krishna, B	134
Kim, M	33, 83, 169, 217, 307, 343, 375, 391, 392	Koduri, S	96, 127, 330, 368	Krishna, H	284
Kim, N	10, 24, 30, 49, 353, 386, 390, 391	Koehler, M	207	Krishna Balla, V	84
Kim, S	20, 22, 24, 48, 55, 68, 109, 157, 204, 211, 217, 240, 242, 266, 310, 311, 317, 319, 343, 346, 349, 351, 353, 369, 376, 378, 381, 384, 386, 387, 388	Koehler, T	36	Krishnamurthy, R	41
Kim, T	233, 369, 381	Koerner, C	14	Krishnaswamy, N	275, 277, 336
Kim, W	23, 24, 142, 192, 378, 381, 386, 390, 391, 392	Koh, S	10, 33, 82, 133, 183, 237, 283, 284, 333	Kritboonyarit, P	13
Kim, Y	24, 64, 92, 145, 216, 217, 221, 252, 286, 289, 316, 345, 346, 351, 360, 362, 369, 376, 378, 389, 395	Kohaupt, U	337	Kronenberg, T	86
Kimmer, C	321	Kohkonen, K	47	Krost, A	115
Kimpton, J	360	Köhler, M	136	Kroupa, A	224
		Kohli, S	25	Krug, M	36
		Koide, J	200	Krugljak, I	343
		Koike, J	146, 160	Kruglov, A	332
		Koizumi, Y	226	Kruglyak, I	119
		Kokenyesi, S	176	Krumdick, G	41, 93, 146, 196
		Kolahdouz, S	305	Kruzic, J	13, 37, 89, 139, 190, 245, 246, 291, 338
		Kolas, S	290	Kshatriya, N	275, 336
		Koledov, V	10, 347	Kubin, L	177, 327
		Kolesnikov, Y	162	Kucheyev, S	285
		Koleva, E	390	Kuehn, U	103, 319
		Koley, G	35	Kühn, U	120
		Kolitsch, A	301		

# Index

- Kuhr, B ..... 66, 308  
 Kukimoto, Y ..... 116  
 Kulakov, M ..... 199  
 Kulkarni, N ..... 309  
 Kulkarni, R ..... 88  
 Kulkarni, S ..... 308  
 Kumar, A ..... 138, 345  
 Kumar, C ..... 323  
 Kumar, D ..... 30  
 Kumar, G ..... 38, 141, 142  
 Kumar, K ..... 121  
 Kumar, M ..... 53, 307  
 Kumar, N ..... 32, 80  
 Kumar, P ..... 67, 271, 315  
 Kumar, R ..... 341, 370  
 Kumar, S ..... 25, 75, 121, 124, 158, 203  
 Kumar, V ..... 53, 138, 370  
 Kumar Jha, M ..... 53, 370  
 Kuntz, J ..... 285  
 Kunz, M ..... 63, 168  
 Kuo, C ..... 117  
 Kuramoto, S ..... 80, 150  
 Kurdian, M ..... 278  
 Kurmanaeva, L ..... 100, 128, 181  
 Kurosu, S ..... 236, 379  
 Kurtz, R ..... 60  
 Kurumlu, D ..... 186  
 Kurzydowski, K ..... 20, 107, 234  
 Kuz'minova, Z ..... 337  
 Kuzel, R ..... 32, 64, 196, 234  
 Kuzmitski, A ..... 176  
 Kuznetsov, A ..... 231  
 Kvasov, N ..... 176  
 Kvithyld, A ..... 71, 193  
 Kwan, Z ..... 221  
 Kwon, E ..... 266, 311, 384  
 Kwon, J ..... 204  
 Kwon, N ..... 380  
 Kwon, O ..... 55  
 Kwon, S ..... 146, 249, 267, 314, 331, 390, 394  
 Kwon, Y ..... 159, 206  
 Kwong, K ..... 343  
 Kyeong, J ..... 23, 24
- L**
- Labar, J ..... 325  
 Lados, D ..... 47, 124, 176, 203, 229, 255, 276, 323, 369  
 Lahlouh, B ..... 196  
 Lai, Y ..... 67, 169  
 Laine, J ..... 55  
 Laird, B ..... 51, 197  
 Lam, C ..... 229  
 Lamas, D ..... 124  
 Lambert, S ..... 211  
 Lammi, C ..... 47, 203  
 Lan, J ..... 300  
 Lancon, F ..... 173  
 Lang, D ..... 176  
 Langdon, T ..... 29, 78, 80, 81, 128, 130, 180, 182, 183, 233, 234, 235, 281, 282, 331  
 Langelier, B ..... 309  
 Lani, G ..... 312  
 Lapovok, R ..... 56, 78, 131, 235  
 Laptyeva, G ..... 338  
 Lara, L ..... 14  
 Lara-Curzio, E ..... 300, 388  
 Larez, J ..... 290  
 Laribou, H ..... 69  
 Larouche, A ..... 106  
 Larsen, J ..... 109, 203, 320, 368  
 Larsen, S ..... 97  
 Larson, B ..... 63, 267, 268  
 Lashmore, D ..... 34  
 Lau, L ..... 269  
 Lau, S ..... 330  
 Lau, T ..... 178  
 Laughlin, D ..... 266, 396  
 Laughlin, J ..... 44, 45, 261  
 Launey, M ..... 186, 190, 246, 247  
 Lauridsen, E ..... 179, 180  
 Laurinavichute, V ..... 337  
 Laux, B ..... 101  
 Lavender, C ..... 96, 110, 252, 297  
 Lavernia, E ..... 30, 31, 42, 130, 142, 181, 187, 192, 234, 235, 236, 281, 282, 283, 319, 333, 334  
 Lavoie, P ..... 97  
 Lavrentiev, M ..... 286  
 Law, C ..... 214  
 Lawler, H ..... 161  
 Le, N ..... 163  
 Leake, S ..... 313  
 Leau, W ..... 170  
 LeBeau, S ..... 308  
 Lebeuf, M ..... 97  
 Le Bouar, Y ..... 260  
 Le Breton, J ..... 283  
 Lebreton, J ..... 59, 73  
 Le Brun, P ..... 143, 193, 248, 295, 341  
 Lebyodkin, M ..... 178  
 Lechner, R ..... 166  
 Lee, A ..... 25, 66, 68, 116, 168, 221, 222, 271, 315, 363  
 Lee, B ..... 20, 68, 184, 223, 294  
 Lee, C ..... 29, 30, 31, 79, 117, 129, 175, 205, 242, 247, 298, 376, 382, 385, 386  
 Lee, D ..... 115, 349, 391, 395  
 Lee, E ..... 242  
 Lee, G ..... 55  
 Lee, H ..... 67, 68, 115, 157, 163, 217, 223, 225, 242, 274, 300, 350, 382, 388, 392  
 Lee, I ..... 68  
 Lee, J ..... 22, 25, 28, 31, 33, 53, 68, 109, 117, 118, 169, 170, 183, 223, 256, 267, 271, 301, 307, 349, 370, 380, 381, 389  
 Lee, K ..... 20, 29, 36, 158, 223, 243, 289, 316, 343, 388, 394  
 Lee, M ..... 33, 62, 83  
 Lee, N ..... 271  
 Lee, P ..... 55, 96, 104, 144, 281  
 Lee, R ..... 130  
 Lee, S ..... 49, 64, 115, 140, 150, 157, 219, 227, 281, 349, 360, 375, 382, 385  
 Lee, T ..... 26, 48, 117, 168, 169, 221, 222, 316, 363  
 Lee, W ..... 180, 289, 325  
 Lee, Y ..... 26, 66, 243, 305, 345, 350, 361, 380  
 Leer, C ..... 272  
 Lefstad, M ..... 199  
 Lega, P ..... 10  
 Legendre, F ..... 59, 73, 315  
 Legoux, J ..... 70, 302  
 Legros, M ..... 268  
 Legut, D ..... 126  
 Lei, C ..... 21, 258  
 Lei, L ..... 329  
 Lei, M ..... 123  
 Leisk, G ..... 161, 204  
 Leitner, H ..... 270  
 Lejcek, P ..... 371  
 Lekakh, S ..... 58  
 Lemiale, V ..... 165  
 Lemmon, J ..... 240, 356  
 Leng, Z ..... 334  
 Leo, P ..... 36  
 Leonhardt, T ..... 71  
 Lerche, M ..... 251  
 LeSar, R ..... 323, 338  
 Lesica, S ..... 270, 314, 362  
 Lesuer, D ..... 80, 82  
 Leung, T ..... 221  
 Leuthold, J ..... 180  
 Levchenko, E ..... 28  
 Levendis, Y ..... 320  
 Levi, K ..... 100, 151  
 Levine, L ..... 63, 113, 268, 359  
 Levy, O ..... 207  
 Lewandoska, M ..... 233  
 Lewandowska, M ..... 234  
 Lewandowski, J ..... 91, 292, 380, 383  
 Lewis, A ..... 77, 127, 179, 232, 280, 330  
 Lewis, D ..... 195  
 Lewis, J ..... 123, 186  
 Lewis, M ..... 258  
 Leyson, G ..... 368  
 Lezama-Alvarez, S ..... 389  
 Li, B ..... 22, 34, 40, 55, 105, 109, 129, 150, 156, 201, 210, 228, 261, 273, 306, 307, 308, 320, 352, 364  
 Li, C ..... 279, 280, 328, 373  
 Li, D ..... 24, 89, 206, 248, 279, 337  
 Li, F ..... 378  
 Li, G ..... 54, 92, 155, 156, 208, 284, 287  
 Li, H ..... 110, 133, 208, 276, 300, 351, 384  
 Li, J ..... 20, 46, 72, 77, 79, 92, 98, 101, 156, 162, 199, 227, 293, 294, 298, 300, 324, 328, 388  
 Li, L ..... 62, 181, 324, 361, 387  
 Li, M ..... 27, 76, 125, 143, 159, 177, 230, 245, 262, 270, 278, 286, 324, 327, 354, 355, 367, 370, 372  
 Li, N ..... 46, 181  
 Li, Q ..... 15, 28, 52, 92, 155, 156, 276  
 Li, R ..... 39  
 Li, S ..... 12, 141, 268, 354  
 Li, T ..... 34, 113, 267  
 Li, W ..... 84, 98, 133, 188, 340  
 Li, X ..... 35, 85, 89, 133, 161, 167, 185, 343, 347, 348, 381  
 Li, Y ..... 16, 30, 31, 42, 92, 130, 142, 181, 187, 192, 234, 235, 236, 281, 328, 383  
 Li, Z ..... 15, 111, 137, 210, 351, 384  
 Lian, J ..... 273  
 Liane, M ..... 301  
 Liang, L ..... 11, 135, 201  
 Liang, S ..... 169  
 Liang, Y ..... 42, 321, 387  
 Liangxing, J ..... 98  
 Liao, C ..... 364  
 Liao, H ..... 137  
 Liao, X ..... 97, 181, 183, 187, 235, 281, 282  
 Liao, Y ..... 48, 276  
 Liaw, P ..... 17, 25, 38, 39, 40, 62, 64, 90, 91, 114, 140, 142, 166, 167, 175, 181, 191, 192, 219, 246, 247, 248, 268, 292, 293, 294, 312, 313, 339, 340, 359, 360, 361, 387  
 Liebesfeld, J ..... 36  
 Lienert, U ..... 62, 64, 268, 313  
 Lifson, M ..... 214  
 Ligiski, L ..... 308  
 Lilleodden, E ..... 25, 62, 64, 114, 166, 219, 268, 312, 355, 359  
 Lim, A ..... 76  
 Lim, D ..... 24, 312



Lim, G	316	Longanbach, S	239	Ma, X	287
Lim, H	24	Lookman, T	77	Ma, Y	260
Lim, J	24, 216	Lopes, F	16, 249, 250	Maarschalkerwaard, A	243
Lim, K	191, 192, 378	Lopez, F	144	MacDowell, A	190
Lim, N	377	Lopez, M	49, 90	Macedo, E	295
Lim, S	229, 319, 376, 395	Lopez-Chipres, E	282	Machado, D	298
Lima, J	136	Lopez-Hirata, V	389, 392	Machai, C	206
Limao, R	244	Lorentsen, O	86	MacKenzie, K	369
Limarga, A	127	Lorenz, N	51	Maddox, B	49
Limodin, N	179	Lossius, L	200, 253, 299	Madison, J	100, 179
Lin, C	118, 170	Lou, J	46, 75, 82, 109, 133, 273	Madshus, S	97
Lin, J	94	Lou, X	351	Maeda, M	53, 104, 105, 343
Lin, K	25, 66, 67, 116, 168, 221, 271, 315, 363, 364	Louca, D	39, 293	Maekawa, K	199
Lin, M	15, 118	Louhenkilpi, S	55	Mahajan, D	218
Lin, P	142	Loutfy, R	44, 45, 96, 261	Mahapatra, R	258
Lin, T	11, 30, 394	Louzuigne, D	90	Mahboubi, F	94
Lin, Y	26, 67, 69, 139	Louzuigne-Luzgin, D	141, 291, 340	Mahdipoor, M	94
Linares, X	168	Lovato, M	48	Mahesh, K	93
Lindsay, S	87	Love, D	25	Maheshwari, C	329
Ling, Z	212	Lovicu, G	270	Mahfoud, M	383
Linga, H	253, 299	Lowe, T	29, 78, 80, 128, 130, 180, 182, 233, 235, 281, 331	Maier, H	183, 283
Linger, D	148	Lowengrub, J	134, 197	Maier, V	131
Lingyun, Y	209	Lowery, A	197, 248	Maijer, D	106, 180, 242, 253
Lin Peng, R	167	Lu, B	288	Maire, E	17
Liou, W	118	Lu, C	29, 367	Major, R	17
Lipkin, D	350	Lu, G	289, 325	Majumder, G	346
Lipp, E	170	Lu, H	82, 98, 99, 105, 133, 143, 273	Mak, K	221
Liqing, C	145	Lu, J	141, 193, 331, 332	Makaya, A	192
Liss, K	268, 269	Lu, K	131, 358	Maki, A	305
Littlefair, G	48, 305	Lu, L	358	Makino, A	383
Liu, B	101, 106, 263, 354, 394	Lu, M	84	Makino, T	331
Liu, C	17, 48, 118, 171, 200, 219, 339, 364	Lu, P	51, 324	Mali, S	128
Liu, D	98, 115, 313, 357	Lu, X	240, 356	Malik, H	284
Liu, E	167	Lu, Y	34, 46, 133, 273, 311	Malik, S	113
Liu, F	189	Lu, Z	265	Mallick, P	158
Liu, G	131, 194	Lucas, M	103, 251	Mallik, P	297
Liu, H	209, 264	Ludwig, A	157	Maloney, C	294, 311
Liu, J	35, 91, 116, 129, 240, 271, 356	Ludwig, O	105	Maloy, S	60, 270, 314, 315, 362, 366
Liu, K	26, 117, 168, 169, 221, 222, 316, 334, 363	Ludwig, W	179	Maltais, J	87
Liu, L	319, 387	Luganov, V	162	Manchiraju, K	390
Liu, M	54, 79	Lui, T	12, 242, 264	Mancosu, R	26
Liu, Q	26, 98, 168, 215	Luke, M	59, 393	Mandal, S	51
Liu, R	263	Lukes, J	188	Mandavgane, S	11
Liu, W	30, 63, 116, 121, 211, 234, 269, 271, 280, 360	Lukitsch, M	212	Mangu, R	82
Liu, X	29, 57, 70, 109, 110, 111, 160, 202, 214, 265, 310, 338, 356, 357	Luo, A	56, 106, 212, 254, 301, 347, 353	Manivannan, A	57, 109, 160, 214, 265, 310, 356, 357
Liu, Y	13, 46, 85, 91, 99, 105, 135, 137, 159, 169, 171, 265, 300, 357, 358, 360, 377	Luo, H	11, 83, 109, 135, 185, 301	Manivasagam, G	348
Liu, Z	18, 43, 57, 84, 109, 160, 214, 252, 265, 308, 310, 311, 355, 356, 357, 386	Luo, J	45, 46, 94, 197	Manjooran, N	10, 33, 82, 133, 183, 237, 283, 333
Livescu, V	372, 378	Luo, P	331	Mann, J	34
Li Yuan, C	321	Luo, S	62, 199, 386	Manna, I	146, 175, 227
Llubani, S	274	Luo, W	11	Mansoor, B	353
Lo, W	272	Luo, Y	98	Manuel, M	211, 355
Locatelli, J	194	Luscher, W	239	Mao, C	374
Lodin, J	194	Luton, M	328	Mao, H	63
Löffler, J	192	Lutterotti, L	65	Mao, J	139
Logan, S	353	Lv, D	139	Mao, S	45, 46, 61, 233, 235, 339
Lograsso, T	185	Lv, G	16, 240, 377	Mao, X	54
Loh, J	135, 336	Lv, L	54	Mao, Y	83, 139, 144, 232, 286
Lohthongkum, G	272	Lymperakis, L	140, 326	Mao, Z	28
Lohwongwatana, B	272	Lynch, P	360	Maocai, W	377
Loiola, R	250	<b>M</b>		Mara, N	62, 84, 173, 174, 227, 236
Lolies, K	263	Ma, D	64, 140	Marathe, G	180
Lomonaco, R	342	Ma, E	39, 78, 79, 129	Marcano, D	57
London, B	324	Ma, H	38, 169, 222, 288	Marceddu, M	345
Long, M	16	Ma, J	11, 16, 134, 135, 201, 204, 228, 240, 331	Marchand, P	88
Long, S	11, 35, 85, 136, 187, 241, 289	Ma, K	319	Marcoux, A	87
Long, Z	85, 187	Ma, L	272, 359	Margem, F	250
		Ma, N	195	Marian, J	335
		Ma, Q	107	Marin, E	56, 107
				Marinica, M	27, 126
				Markovsky, P	253

# Index

Marks, J.....	87	McDowell, D.....	177, 203, 233, 358	Militzer, M.....	21, 95
Marques, L.....	249	McGrath, M.....	110	Miller, A.....	49
Marquis, E.....	72, 122, 173, 226, 227, 314, 321	McHenry, M.....	333	Miller, D.....	202
Marshall, P.....	194	McIntyre, N.....	269	Miller, J.....	100, 143
Marte, J.....	182, 183, 331	McIntyre, S.....	63	Miller, M.....	17, 18, 40, 48, 62, 73, 144, 207, 220, 270, 280, 285, 315, 362
Marthinsen, K.....	194	McKay, B.....	143, 153	Miller, R.....	70, 163
Martin, C.....	70, 119, 202	McKenna, I.....	180	Miller, S.....	346
Martin, D.....	133	McKindra, T.....	227	Millett, J.....	49
Martin, L.....	252	McKinney, S.....	200	Millett, P.....	133, 164, 198, 233, 373
Martin, O.....	138	McKittrick, J.....	90, 139, 140	Mills, K.....	55
Martin, P.....	151	McMahon, C.....	76	Mills, M.....	16, 17, 145, 178, 204, 257, 373
Martin-Cortés, G.....	10	McNaney, J.....	231	Min, C.....	216
Martinez, A.....	45, 96	McNelly, T.....	236	Min, G.....	353
Martinez, D.....	351, 384	McNulty, I.....	180	Min, X.....	321
Martinez, E.....	134, 152	McQueen, H.....	36	Minamino, Y.....	226
Martinez, L.....	134, 152	McQueen, J.....	260	Minchenya, V.....	162
Martinez, O.....	41	McWhinney, H.....	274	Minggang, W.....	145
Martini, A.....	373	Medeiros, M.....	15, 186, 344	Mingolo, N.....	41
Martins, G.....	53	Medina, F.....	134, 152	Minor, A.....	150, 173, 325
Maruyama, T.....	376	Medlin, D.....	72, 122, 173, 226, 227, 298, 321, 322	Minville, R.....	88
Marx, B.....	335, 387	Medvedev, G.....	279	Miracle, D.....	90, 91, 253, 292, 293
Marya, M.....	171, 334	Medyanik, S.....	61, 62, 113, 165, 218, 267, 311, 358	Mirecki-Millunchick, J.....	305
Mascarenhas, O.....	200	Mei, J.....	152, 153	Mirihanage, W.....	101
Mason, D.....	258	Meier, A.....	310	Mirnezami, M.....	17
Mason, T.....	218, 238	Meier, M.....	298	Miroux, A.....	251
Mastorakos, I.....	86, 163, 239, 337, 371	Meijer, M.....	138	Mishin, Y.....	19, 28, 94, 122, 226, 278, 372
Masuda, C.....	185, 287	Meinhardt, K.....	356	Mishra, B.....	69, 94, 119, 162, 171, 208, 212, 224, 270, 274, 275, 277, 294, 314, 318, 362, 366, 377, 394
Masuda, J.....	364	Meinhardt, K.....	240	Mishra, M.....	124
Masyutin, Y.....	344	Melnyk, C.....	199	Mishra, R.....	23, 24, 32, 80, 204, 211, 212, 213, 217, 264, 310, 315, 353, 362
Mataya, M.....	259	Melo, R.....	190	Mishra, S.....	171
Matej, Z.....	64, 196, 234	Mélo, T.....	344	Misiolok, W.....	107, 264, 353
Mathaudhu, S.....	29, 57, 78, 79, 80, 128, 130, 135, 180, 182, 183, 233, 235, 264, 281, 283, 331, 332	Melo-Maximo, D.....	389	Misra, A.....	46, 62, 174, 181, 226, 239, 315
Mathon, M.....	315	Melo-Maximo, L.....	389	Misra, D.....	128, 191, 245, 291, 338, 365
Mathur, A.....	200	Melville, A.....	252	Misra, M.....	143
Mathur, C.....	277	Melzer, C.....	36	Missalla, M.....	85
Matoy, K.....	151	Mendeleev, M.....	44, 293, 328	Mitchell, J.....	89
Matsen, M.....	297	Méndez, C.....	249	Mittal, S.....	11
Matson, D.....	161, 204	Mendis, C.....	309	Miura-Fujiwara, E.....	269
Matsubara, E.....	269	Mendoza, A.....	279	Miwa, K.....	192
Matsumoto, H.....	236, 252, 379	Menezes, R.....	17	Mladenov, G.....	390
Matsuo, H.....	96	Meng, T.....	106, 253	Mo, K.....	270
Matsushita, M.....	193	Meng, X.....	379	Mo, Y.....	358
Matsutani, T.....	69	Menyhard, M.....	325	Moat, R.....	205
Matsuyama, A.....	96	Merkel, S.....	361	Modine, N.....	305
Matteis, P.....	92, 144	Merwade, M.....	197	Moelans, N.....	260
Mattern, N.....	39, 191, 236, 319	Meskers, C.....	124, 176, 229, 276, 323, 369	Moeslang, A.....	60
Matthews, D.....	126	Meskine, H.....	339	Mogilevsky, P.....	238
Matthews, V.....	239	Meslin, E.....	217	Mohamed, F.....	181, 182, 331, 334
Mauger, L.....	19, 251	Mesquita, A.....	299	Mohamed, M.....	165, 328
Maung, K.....	182	Methekar, R.....	266	Mohamed, S.....	345
Maurer, E.....	291	Meydanoglu, O.....	387, 390	Mohammad, I.....	185
Mavinakuli, P.....	318	Meyer, B.....	322	Mohammadi Zahrani, E.....	42, 123, 237
Mayama, T.....	309	Meyer, H.....	248, 311, 340	Mohammad Mirzaie, M.....	137
Mayorga, J.....	240	Meyer, L.....	282	Mohanty, G.....	32
Maziasz, P.....	110	Meyer, M.....	315	Mohanty, J.....	203
Mazumdar, D.....	210	Meyers, M.....	49, 90, 139, 235, 245, 291	Mohapatra, M.....	241, 377
Mazumder, J.....	41, 46	Meyyappan, M.....	183	Mohapatra, S.....	143
McBow, I.....	274	Miao, X.....	55	Mohles, V.....	337, 338
McBride, D.....	157, 307	Miceli, P.....	114	Mohmaed, A.....	381
McCabe, R.....	194	Michael, J.....	60	Mohney, S.....	170
McCaffrey, J.....	308	Michael, M.....	357	Mohri, M.....	237
McCallum, R.....	275	Michael, N.....	41, 42, 93, 146, 196	Mohri, T.....	52
McClellan, K.....	164, 216, 227, 386	Michel, C.....	82	Molin, A.....	254
McColskey, D.....	161	Michiuchi, M.....	204	Molodova, X.....	182
McComb, D.....	73, 281	Michler, J.....	150	Momeni, K.....	46
McConnell, R.....	105	Middlemas, M.....	121	Momtaf, A.....	99
McCulloch, B.....	86	Mikhailovskij, I.....	39	Mondal, A.....	71
McCulloch, R.....	243	Milenova, M.....	287	Mönig, R.....	45
McCune, R.....	106, 157, 158	Miles, M.....	21, 47, 49, 100, 151, 205, 225, 258, 304		
McDonald, R.....	21, 135	Milans, J.....	279		



Monroe, C	262	Mukherji, D	66, 359	Nandy, T	348
Monsen, B	200	Mukhlis, R	149	Nanninga, N	40, 241, 289
MONTALVO, J	351, 384	Mukhopadhyay, S	184, 291	Nanstad, R	112
Montavon, G	167	Mukhter, A	131	Napolitano, R	147, 154, 339
Monteiro, S	15, 16, 40, 92, 144, 194, 249, 250, 296, 320, 342, 343	Mukunda, P	12	Narasimhan, N	13, 18
Monteiro-Riviere, N	93	Mukundan, R	310	Narasimhan, S	74
Montgomery, J	24	Mulay, R	313	Narayan, R	41, 93, 123, 146, 196, 245
Montoya-Davila, M	12	Mulheran, P	339	Narayanan TSN, S	75, 124
Moody, N	114, 151	Mulholland, M	18, 207	Narayani, N	242
Moon, J	116, 221	Mulki, S	81	Narendranath, N	12
Moon, K	59, 132, 367	Muller, T	309	Naritsuka, S	376
Moon, M	266, 311, 384, 386	Mullner, P	371	Nascimento, D	249
Moore, R	373	Mulyukov, R	33, 332	Naser-Zoshki, H	41, 195
Mooney, A	186	Mun, D	256	Nasipuri, M	323
Moore, D	374	Munday, L	374	Nasirizadeh, M	333
Moore, J	94, 119, 318	Munoz, D	138	Nastasi, M	226, 315, 372
Moraes, J	136	Munoz, J	103, 251	Natarajan, T	307
Morales, F	254	Munroe, P	42, 48, 75	Natesan, K	270
Morales, M	65	Muntele, C	61, 217, 340	Nath, S	130
Morales, R	56	Mura, A	345	Navid, A	146, 275
Moran, J	82	Murashkin, M	79	Nawathe, S	274
Moran-Lazaro, J	82	Murch, G	28, 279	Nayak, B	208
Moras, A	86, 88	Murphy, C	45	Nayak, S	128
Morcali, H	391, 392	Murr, L	134, 152, 286	Nayaka, H	354
Mordehai, D	358	Murray, B	147	Nayar, V	246
Mordi, G	184	Murray, C	220	Nazari, A	92
More, K	311	Murthy, T	378	Nazarov, A	33, 332
Moreno, H	216	Murthy, B	181	Nazarov, K	33
Morgan, D	44, 305, 326, 378	Murty, K	112, 225, 315	Necker, C	236
Morgan, E	190	Musil, J	64, 196	Needleman, A	76, 278
Mori, G	157, 251	Musinski, W	203	Neelakantan, S	348, 380
Mori, M	236	Muthukumar, S	12	Neelameggham, N	22, 56, 106, 108, 142, 157, 159, 211, 212, 239, 262, 263, 294, 308, 353, 354
Morimitsu, M	52	Myers, B	128	Nees, J	330
Morisada, Y	383, 385	Myers, D	96	Nekahi, A	137, 290
Morita, K	369	Mylvaganam, S	301	Neklyudov, I	39
Morooka, S	395	Myrbostad, E	341	Nele, M	187
Morrall, J	154, 165	<b>N</b>		Nelson, A	270
Morri, A	144	Na, H	64, 360	Nelson, K	329
Morris, D	60, 112, 163, 216, 358, 359	Na, L	117	Nelson, L	52
Morris, J	113, 150, 168, 293, 315, 325	Naab, F	158	Nelson, P	177
Morris, Jr., J	113	Nadakuduru, V	131, 148	Nelson, T	242
Morris, M	347	Naderi, M	384	Nemoto, N	68
Morris, R	222, 281, 297	Nadgorny, E	370	Nerikar, P	73, 321
Morsi, K	59, 132, 367	Nadler, J	318	Neu, C	245
Mortarino, G	144	Nadot, Y	242	Neu, R	351
Morton, T	298	Nag, S	17, 72, 342, 382, 383	Neugebauer, J	27, 29, 103, 104, 120, 140, 208, 301, 326
Morva, I	142	Nagai, T	53, 104, 105, 343	Neves, G	17
Morvová, M	142	Nagaoka, T	383, 385	Newhouse, R	19, 103
Moser, S	323	Nagaraj, C	271	Newman, R	269
Moseson, A	369	Nagasekhar, A	30, 211, 262, 282	Newton, M	313
Moseson, D	369	Nagaumi, H	248	Ng, H	106
Moss, S	166	Naidoo, K	157	Ngai, E	38
Moss, W	130	Naik, A	237	Nguyen, J	59, 319
Motang, T	18, 379	Naim, F	336	Nguyen, L	114, 169
Motta, L	249	Nair, A	312	Nguyen, T	31, 245
Mourad, M	345	Naixiang, F	13, 189, 244, 345	Nguyen, V	157
Mourer, D	204, 259	Nakagawa, T	68	Nguyen-Manh, D	126, 286
Mousavi, S	281	Nakai, M	253	Ni, P	16, 240
Moxson, V	96	Nakai, Y	246	Ni, S	183
Mrovec, M	126, 322, 377	Nakamori, Y	211	Nicholson, A	229
Mu, Y	11, 135, 185, 301, 348	Nakamoto, M	383, 385	Nicholson, D	241
Mubarak, A	40	Nakayama, H	350	Nichtova, L	64, 196
Mueller, A	79	Nakayama, K	192	Nickolai, I	390
Mueller, R	195, 377	Nam, H	375	Nicola, L	165
Muhlstein, C	45	Nam, K	10, 392	Nie, J	160, 212
Mujun, L	59	Nam, S	24	Nie, X	262
Mukai, T	212, 213	Nam, W	31, 380	Nie, Z	167, 313, 356
Mukherjee, A	79, 225	Nambu, S	204	Niechajowicz, A	264
Mukherjee, K	172	Namgung, J	343	Nieh, T	90, 175
Mukherjee, P	368	Namgung, S	29, 31, 79, 129		
Mukherjee, S	353				

# Index

Niehoff, T.....	201	Ogunseitan, O.....	229	<b>P</b>	
Niendorf, T.....	183	Ogura, K.....	142	Packard, C.....	151
Niezgoda, S.....	179, 232	Oh, C.....	48, 376	Padap, A.....	130
Niinomi, M.....	253, 297	Oh, J.....	92	Padhi, P.....	219, 228, 389
Nikitina, S.....	324	Oh, K.....	49, 349	Padilla, H.....	81
Nikles, D.....	184	Oh, S.....	274	Padilla, R.....	53, 156, 209
Nikolaeva, E.....	189	Oh, T.....	357	Padron, I.....	197
Nikolic, I.....	229	Oh, Y.....	221	Padula, S.....	145
Nikolic, S.....	155	Oh-ishi, K.....	309	Padula II, S.....	304
Nikolov, S.....	140	Ohashi, T.....	325	Paidar, V.....	27, 76, 125, 177, 230, 278, 324, 327, 370, 372
Nili Ahmadabadi, M.....	129, 233	Ohnishi, Y.....	235	Paital, S.....	123
Ning, X.....	96	Ohodnicki, P.....	333	Paiva, A.....	295
Ningileri, S.....	85	Ohriner, E.....	70	Pakzad, A.....	46
Ninomiya, N.....	211	Ohya, T.....	301	Pal, U.....	109
Nishikawa, H.....	363	Oi, T.....	297	Paladugu, M.....	331
Nishimura, T.....	185, 364	Ojo, I.....	61, 217	Palafox-Hernandez, J.....	51
Nishino, Y.....	269	Ojo, V.....	137	Palanisamy, S.....	331
Nishio, T.....	350	Okabe, T.....	297, 342, 369	Palauqui, J.....	14
Niu, L.....	382	Okamoto, N.....	325	Palberg, T.....	51, 153
Niu, Q.....	98, 215	Okijava, L.....	382	Paliwal, M.....	309
Niu, X.....	66	Oktay, G.....	296, 309	Pallavkar, S.....	395
Nix, W.....	150	Okubo, T.....	51	Palmer, M.....	300, 345, 346, 375
Nixon, M.....	256	Okuniewski, M.....	230, 252	Palsson, H.....	86
Niyomwas, S.....	96	Okuyama, N.....	200	Palumbo, M.....	251
Nnabuchi, M.....	342	Olbricht, J.....	57	Palumbo, R.....	239, 240
Nóbrega, K.....	344	Olevsky, E.....	139	Pan, D.....	101
Noda, M.....	309	Olivas-Martinez, M.....	308	Pan, X.....	154
Noebe, R.....	145, 304	Olivetti, E.....	176, 229, 277	Pan, Z.....	129
Nogaret, T.....	328	Olmsted, D.....	278, 372	Pandey, A.....	35
Noldin, J.....	143	Olson, D.....	69, 119, 171, 212, 394	Pandey, B.....	370
Nordmark, A.....	345	Olson, G.....	195, 330, 367, 371	Pandey, J.....	40, 379, 381
Northover, S.....	198	Oniashvili, G.....	333, 385	Panfilov, P.....	231
Norton, G.....	72	Ono, T.....	192	Pang, S.....	248
Norton, M.....	346	Onsoien, M.....	345	Panov, A.....	136, 186
Nose, Y.....	18, 296	Opalka, S.....	357	Pantleon, K.....	114, 115
Novak, P.....	231	Oppedal, A.....	107	Pantsyrny, V.....	122
Novitskaya, K.....	140	Oren, E.....	37, 339	Pao, C.....	326
Noyan, I.....	220	Orlov, D.....	131	Pao, P.....	188, 199, 241
Noyes, M.....	339	Orlova, Y.....	199	Papanikolaou, S.....	28, 178
Nozu, T.....	364	Ortiz, M.....	328	Papin, P.....	49, 303
Nunn, S.....	148	Ortiz-Cuellar, E.....	282	Pappula, L.....	379, 391
Nunner, G.....	143	Oryshchyn, D.....	294	Paradies, A.....	175
Nutt, S.....	236, 273	Osborne, W.....	72	Paras, J.....	133, 237
Nuzzo, R.....	300	Ose, S.....	88	Parasivamurthy, P.....	321
Nyberg, E.....	22, 56, 57, 96, 106, 108, 157, 159, 211, 212, 254, 262, 263, 301, 308, 347, 353, 354	Osen, K.....	45, 71	Pareige, P.....	59, 73, 217, 283, 315, 362
Nychka, J.....	13, 37, 89, 139, 190, 245, 291, 338	Osenbach, J.....	25, 317, 363, 364	Parga, C.....	173
Nyirenda, K.....	225	Osetskiy, Y.....	174, 359	Parga, J.....	53
Nyland, G.....	87	Osetsky, Y.....	327	Park, B.....	20
		Oshiumi, N.....	52	Park, C.....	145, 183, 281, 298, 345, 377
<b>O</b>		Oster, N.....	275	Park, E.....	40, 378
O'Brien, E.....	274	Osterberg, D.....	335, 387, 393	Park, H.....	274
O'Brien, J.....	120, 143, 236	Österle, W.....	57	Park, J.....	36, 38, 84, 162, 191, 192, 349, 351, 386, 390, 391, 392
O'Connor, M.....	256	Østrem, Ø.....	392	Park, K.....	275, 380
O'Donnell, R.....	165	Osuna, T.....	80	Park, M.....	316
O'Keefe, M.....	169, 227	Oswald, K.....	157	Park, N.....	10, 221, 375, 391
Obasi, G.....	205	Ott, E.....	48, 148, 203, 257, 350	Park, S.....	349, 381
Obbard, R.....	342	Ott, R.....	66	Park, Y.....	68, 223, 310, 312, 316, 378
Oberson, G.....	60, 112, 119, 163, 216, 224	Ou, J.....	238	Parker, G.....	337
Ocelik, V.....	126	Ou, Y.....	123	Parker, R.....	25, 364
Ocelik, V.....	74	Ouchi, M.....	226	Parker, W.....	325
Ochs, T.....	294	Ourdjini, A.....	188	Paromova, I.....	186
Ochulor, F.....	119, 224	Ouyang, L.....	293	Parra, M.....	227
Oda, M.....	185	Ovecoglu, M.....	186, 381	Parra Garcia, M.....	164
Odabasi, A.....	385	Overman, N.....	239	Parson, N.....	188
Oder, G.....	57	Owate, I.....	342	Parthasarathy, T.....	238, 281, 328
Odette, G.....	60, 112, 314, 315	Oye, B.....	345	Patala, S.....	227
Ofzidani, I.....	161	Ozavar, S.....	59	Patel, L.....	259
Ogasawara, T.....	320	Ozkal, B.....	134, 381, 389, 392	Patel, M.....	59
Ogawa, F.....	185, 287	Özkan, S.....	99	Patel, P.....	97
		Ozolins, V.....	154		



Pathak, D.....	228	Pippan, R.....	29, 71, 129, 236	Pu, Z.....	355
Patrick, L.....	327	Pirayesh, H.....	89	Puckett, J.....	176
Patselov, A.....	327	Pires, R.....	243	Puleo, D.....	355
Pattabhiraman, H.....	11	Pirling, T.....	361	Pun, G.....	28
Patterson, B.....	95	Pisutha-Armond, N.....	312	Puncreobutr, C.....	144, 272
Patzer, G.....	108	Pitchure, D.....	161	Purcek, G.....	130, 131, 137
Pawlek, R.....	188	Pitman, S.....	239	Puscasu, R.....	219
Payton, E.....	17	Plascencia, G.....	249	Pusztai, T.....	102
Peaslee, K.....	111	Pledger, B.....	160	Puthoff, J.....	293
Pech-Canul, M.....	12, 238, 286, 303	Pleydell-Pearce, C.....	205	Putilin, A.....	261
Pedigo, A.....	363	Plikas, T.....	296	Pyshkin, S.....	345
Pedron, E.....	221	Plunkett, B.....	256	Pyzalla, A.....	65
Pegg, I.....	356	Podmaniczky, F.....	102		
Pei, F.....	276	Pokorny, M.....	262	<b>Q</b>	
Pei, Y.....	126	Pokrajcic, Z.....	277	Qi, L.....	324
Pekguleryuz, M.....	160	Pol, V.....	120	Qi, X.....	138, 139
Pellin, M.....	93	Polesak, F.....	23, 355	Qi-feng, G.....	189
Pelton, A.....	162, 213	Politis, C.....	333	Qian, D.....	82
Peng, C.....	46, 133, 222, 273	Pollak, I.....	127	Qian, J.....	232
Peng, L.....	56, 212, 264	Pollock, T.....	100, 179, 258, 259, 308, 330, 350, 354, 360	Qian, L.....	152
Peng, Q.....	213, 387	Polonsky, A.....	357	Qian, M.....	102, 199, 206
Peng, R.....	396	Pomykala, J.....	275, 320	Qian, S.....	42, 228
Peng, S.....	118	Pond, D.....	338	Qiang, J.....	383
Peng, T.....	212	Pond, R.....	278	Qiao, D.....	39
Peng, Z.....	104	Pontikes, Y.....	276	Qiao, J.....	141
Pengfei, Y.....	255, 302	Poole, W.....	21, 102, 188	Qidwai, M.....	179
Perales-Pérez, O.....	318	Poorganji, B.....	233	Qidwai, S.....	232
Peralta, P.....	117, 164, 216, 227, 257, 380, 386	Pope, D.....	76	QiJie, Z.....	379
Pereloma, E.....	78	Popov, A.....	78	Qin, C.....	141
Perepezko, J.....	50, 102, 153, 172, 192, 206	Poquette, B.....	10, 33, 82, 133, 183, 237, 283, 333, 356	Qin, H.....	379
Peretti, M.....	148, 151	Porras, A.....	271	Qin, Z.....	218
Perez, D.....	174, 326	Portela, T.....	250	Qing, X.....	156
Perez, E.....	315, 362	Portillo, B.....	173	Qinghong, T.....	291
Pericleous, K.....	55, 210, 308	Pouchon, M.....	60	Qinghua, T.....	230
Perkins, J.....	392, 393	Pougis, A.....	131	Qingsheng, L.....	275
Persson, K.....	208	Poulsen, H.....	62	Qingxiu, J.....	275
Perugini, A.....	273	Poulsen, S.....	179, 180	Qiu, G.....	209
Peshwe, D.....	11, 237	Pourboghra, F.....	121	Qiu, S.....	98, 192, 304
Peter, D.....	16	Powell, A.....	108, 109, 323, 324	Qiu, X.....	393
Peter, W.....	148, 149	Powell, B.....	212, 264	Qiusong, G.....	382
Petersen, M.....	298	Powell, C.....	57	Qiyuan, C.....	297
Peterson, E.....	274	Power, G.....	135, 336	Qu, J.....	171
Peterson, M.....	250	Powers, M.....	221	Qu, P.....	304
Peterson, R.....	201	Pozas, D.....	82	Quach, D.....	184
Petford-Long, A.....	195	Pozas-Zepeda, D.....	82	Quan, B.....	307
Petkov, V.....	313	Pozzi, C.....	174, 297	Quek, J.....	198
Petrolito, J.....	256	Prabhakaran, R.....	60, 61, 217, 315	Quek, S.....	165
Petrov, M.....	140	Prabaharan, S.....	357	Queennec, X.....	213
Petrusenko, Y.....	39	Prabhu, B.....	13, 30	Quinn, G.....	202
Petter Moxnex, B.....	301	Prabhu, N.....	242	Quinta da Fonseca, J.....	21, 205
Pettifor, D.....	52, 76, 125, 126	Prabhu, S.....	242	Quintana, O.....	217
Petukhou, Y.....	176	Prabu, T.....	277		
Petzold, V.....	322	Pradhan, D.....	255	<b>R</b>	
Phadke, S.....	33	Prahl, U.....	172	Raabe, D.....	140, 301
Pharr, G.....	113, 267, 339	Prakash, D.....	205	Raahauge, B.....	84, 288
Phatak, C.....	195	Prakash, S.....	196, 303	Rabenberg, E.....	17, 313
Phillion, A.....	106	Prangnell, P.....	47, 182	Rabkin, E.....	56, 358
Phillips, A.....	290	Prasad, A.....	296	Rachlitz, R.....	36
Phillips, E.....	84, 135, 186, 240, 241, 287, 288, 336	Prasad, Y.....	159	Rack, H.....	44, 78, 79, 199
Phillips, P.....	17, 204	Preuss, M.....	21, 22, 205	Rack, P.....	175
Phillipot, S.....	321	Price, P.....	17, 140, 313	Raddad, B.....	257, 378
Philo, S.....	246	Priddy, M.....	385	Radeker, W.....	72
Picard, D.....	97	Prillhofer, B.....	193, 341	Radetic, T.....	173
Pierce, C.....	35	Prillhofer, R.....	36	Radiguet, B.....	59, 73, 217, 283, 315, 362
Pikart, P.....	66	Prinsloo, P.....	241	Radis, R.....	20
Pilchak, A.....	81, 259	Prive, D.....	88	Radmilovic, V.....	123
Pinal, R.....	279, 328, 329, 373, 374	Priyadarshini, B.....	146	Rae, C.....	373
Pinayev, A.....	344	Proffen, T.....	313	Rae, P.....	48
Pinoncely, A.....	254	Provatas, N.....	95, 188, 380	Raeisia, B.....	23, 107, 355
Pint, B.....	58, 109, 110	Proville, L.....	178	Raghavendra, K.....	87
Pipe, L.....	46				
Pipes, R.....	279				

# Index

Raghunathan, S	44, 361	Reichert, H	103	Rodriguez, R	16, 249
Rahate, M	216, 365	Reif, R	222	Rodriguez-Baracaldo, R	181
Rahbar, N	190, 338	Reilly, C	255	Rodriguez-Diaz, R	391
Rahman, S	215	Remmert, J	120	Rodriguez-Hornedo, N	329
Raj, M	40, 379, 381	Ren, B	337	Roesner, H	180, 339
Raj, R	116, 271	Ren, I	142	Roessler, D	46
Raj, S	134	Ren, Y	39, 91, 167, 220, 312, 313, 361	Rogge, R	359
Raj, V	359	Ren, Z	188, 391	Roh, H	316
Raja, H	13	Renavikar, M	271, 272	Rohan, P	157
Rajagopalan, S	17, 72, 73, 330, 382, 383	Renshaw, C	230	Rohatgi, A	353
Rajamanickam, A	348	Restrepo, O	165, 366, 367	Rohrer, G	77, 122, 227, 268
Rajan, K	32, 208, 322	Rethoré, J	179	Rokkam, S	164, 198
Rajaputra, S	82	Rettenmayr, M	111, 207	Rolandi, M	37
Rajgarhia, R	174	Reusch, F	341	Rolim, D	203
Rajkumar, T	282	Reuter, M	124, 125, 176, 229, 276, 323, 324, 369	Rollett, A	14, 77, 85, 94, 127, 179, 227, 232, 268, 280, 330, 372
Rakowski, J	311	Reyes, J	82	Rolseth, S	71
Ram, S	342	Reyes-Gomez, J	82	Romberg, J	319
Ramachandran, M	96	Reynolds, H	364	Romero, T	60
Ramadass, A	197	Reynolds, R	387	Romero-Serrano, A	275
Ramadesign, V	266	Rezaeian, A	152, 302	Rong, Y	111
Ramalingam, G	11	Rezaie, H	389	Rood, M	292
Ramamurthy, S	269	Rhamdhani, M	149	Roos, B	45
Ramamurti, R	123	Rhim, W	298	Root, J	187
Ramamurty, U	247	Rhodes, K	300, 357, 388	Roriguez, F	88
Raman, A	373	Rhym, Y	118	Rørvik, S	299
Raman, J	88	Riani, A	287	Rosalie, J	212, 213
Ramesh, K	100, 129, 282, 286	Rice, B	374	Rose, D	88
Ramesh, R	252	Richard, D	243, 244	Rosefort, M	36
Ramirez, F	290	Richard, M	256	Rosenberger, M	75, 124, 388
Ramirez, G	209	Richards, V	58, 110	Rosenkilde, C	392
Ramirez, J	113	Richardson, C	335	Rösler, J	101
Ramirez Lopez, P	55	Richardson, T	358	Ross, J	87
Ramones, J	290	Richardson, T	358	Rossiter, J	211
Ramos, K	218, 329	Richter, G	45	Rossol, M	384
Ramsey, G	298	Ricker, R	160, 161, 229	Roth, R	177
Ramulu, M	349, 379, 391	Ridgway, M	123	Roth, S	39, 167
Ramuni, V	128	Rieger, T	111	Rottler, J	95
Randall, N	342	Rieken, J	152, 362	Rottmann, P	271
Rankin, W	324	Riella, H	177	Roubidoux, J	69, 394
Rao, A	242	Riley, D	28	Roué, L	200, 393
Rao, K	45	Rimoli, J	328	Rounaghi, A	111
Rao, M	155	Ring, T	308	Rounaghi, S	41
Rao, R	186	Ringer, S	183, 235, 282	Roux, S	179
Rao, S	113, 328, 370	Ringnalda, J	73	Roven, H	30, 79, 193
Raoufi, M	94	Rink, D	270	Rowenhorst, D	77, 127, 179, 180, 195, 232, 280, 330
Raphael, J	387	Rinn, R	338	Rowland, R	237
Rapheal, G	158	Rios, O	22, 101	Roy, A	308
Rashkeev, S	230, 252	Rios, P	195	Roy, I	235, 318, 331, 334
Rasmussen, K	279	Rishabh, A	333	Roy, M	194, 242
Ratke, L	136, 207	Ritchie, R	139, 186, 190, 202, 231, 247	Roy, S	274
Ratvik, A	149, 200, 299	Ritter, A	66, 308	Rozak, G	70, 120, 172
Rausch, B	337	Ritter, C	138, 290	Rozas, R	51
Ravindra, N	41, 42, 93, 146, 196, 197	Ritter, Y	340	Rozenak, P	64, 290
Ray, P	173, 203, 350	Rivera-Diaz-del-Castillo, P	163, 198, 348	Ruan, H	332
Raynova, S	148	Rivero, R	196	Ruano, O	236
Read, C	86, 87, 138, 188, 243, 244, 290, 336	Ro, Y	28	Rubio, M	249
Read, D	99	Roach, S	106	Rudman, K	227
Reade, N	108	Robach, O	269	Ruehle, M	278
Ready, J	10, 33, 82, 133, 183, 237, 283, 333, 395	Robbins, M	294	Rugg, D	205
Reddy, N	28, 256, 298	Roberts, A	393	Ruiz, A	290
Reavis, R	335	Roberts, C	94	Ruiz, M	53, 156, 209
Rebak, R	112	Roberts, J	197, 248	Rundman, K	40
Reddy, K	71	Robertson, I	388, 392	Russell, K	18, 48, 144, 285, 315
Reddy, R	96, 119, 142, 198, 255, 311, 318	Robinson, A	61	Russo Spena, P	92
Redkin, A	189	Robinson, B	148	Rutlin, J	97, 149
Reed, E	306	Robinson, I	313	Ruud, J	291
Reed, M	274, 366	Robson, J	182	Ryabov, D	210
Reedy, E	151, 202	Rockward, T	311	Rye, K	87, 97, 149, 200, 253, 298, 344
Reggiani, B	136	Rodiers, B	260	Ryu, Y	348
Reglitz, G	180	Rodney, D	90, 178, 294		
Reiber, H	51	Rodriguez, A	259		
		Rodriguez, F	124		



### S

Sa, Y	117, 386
Saavedra, J	284
Sabau, A	148, 266
Sabbadini, S	152
Sachan, R	175, 247, 284
Sachdev, A	75, 144, 212, 264
Sachs, C	140
Sadawy, M	385
Sadeghi Meresht, E	385
Sadler, B	97, 149, 200, 253, 298, 344
Sadoway, D	307
Saevarsdotir, G	86, 298
Safarkhanian, M	305
Safiullin, R	332
Saglam, C	59
Saha, P	263
Saha, S	44
Sahaym, U	346
Saheet, H	303
Sahoo, M	188
Saida, J	193
Saigal, A	111, 161, 204
Saimoto, S	268
Sajjad, M	317
Sakai, T	69, 211
Sakidja, R	172
Sakulich, A	369
Sakurai, H	116
Sakurai, T	192
Salamanca-Riba, L	195, 289
Salazar-Villalpando, M	295
Saldana, C	182, 283, 378
Salehnia, I	165, 218
Salem, H	237
Salerno, K	294
Saliklis, E	375
Salishchev, G	205
Saliwan-Neumann, R	57
Salleo, A	33
Salman, O	260
Samad, J	291
Samajdar, I	81
Samal, G	345
Samaras, M	60, 164
Samarov, V	148
Sammakia, B	347
Samonds, M	85
Sampaio, J	15, 186, 344
Sampson, E	79, 199
Samudrala, R	37
Samvedi, V	280, 322
Sánchez, C	249
Sanchez, F	394
Sanchez, J	52
Sand, U	194
Sandala, R	21
Sander, A	276
Sander, F	246, 291
Sanders, D	205, 258
Sandim, H	233
Sandlöbes, S	265
Sangid, M	27
Sanjari, M	265
Sanjay, K	352
Sankaran, R	325
San Marchi, C	161
Sanni, O	224
Sano, T	23
Santafe, H	16
Santala, M	123
Santana, L	17
Santella, M	354
Santhanakrishnan, S	105, 376
Santiago, R	296
Santos, N	250
Santos, R	186
Santos, S	320
Saotome, Y	141
Sapper, E	323
Saray, O	130, 131, 137
Sargent, G	205
Sarikaya, M	13, 37, 38, 89, 139, 190, 191, 245, 291, 292, 338, 339
Sarkar, A	81, 368
Sarkar, S	346
Sarkis, Y	243
Sarobol, P	363
Sasaki, H	53
Sasaki, T	297
Sastri, B	142
Sathyavageswaran, S	348
Sato, H	269
Sato, K	252
Sato, M	141
Sato, Y	97, 386
Satyanarayana, K	249
Saucedo-Muñoz, M	392
Sauvage, X	78, 122, 268
Savage, R	324
Save, S	87
Savelieva, O	347
Savvakin, D	149
Sawyer, G	317
Saxena, A	174
Scardi, P	220
Scattergood, R	130
Scavino, G	144
Schade, D	168
Schaefer, J	61
Schäfer, C	338
Schaffer, G	199
Schafner, E	219
Schafrik, R	50
Scheller, P	210
Schelling, P	321
Schen, M	299
Scheriau, S	129
Schestakow, I	265
Schimmel, G	111
Schlieter, A	103, 120
Schlom, D	252
Schmetterer, C	223, 224
Schmid-Fetzer, R	50, 56, 102, 153, 158, 206, 207, 212
Schmidt, T	193
Schmidtmeier, D	105
Schmitt, B	268
Schmitz, G	73
Schnapp, D	36
Schneider, A	244
Schneider, I	282
Schneider, J	38, 48, 203, 257, 282, 350
Schneider, W	103
Schneller, M	337
Schnitzlbaumer, J	36
Schoenfeld, B	167
Schoenung, J	30, 59, 129, 130, 225, 229, 234, 236, 281, 319
Schöning, C	149
Schöpe, H	51, 153
Schramm, J	140
Schroeder, S	199
Schroers, J	38, 141, 142, 191
Schroth, J	75
Schubert Severo, D	298
Schuh, C	90, 183, 227, 292
Schulson, E	230
Schulte, A	58
Schulz, W	57
Schumacher, P	143, 153
Schuren, J	220
Schuster, B	129, 183
Schütze, M	301
Schvezov, C	58, 75, 124, 388
Schwandt, C	34, 44, 341
Schwarz, P	244
Schwen, D	147, 148
Scott, S	86
Seal, S	27, 74, 123, 175, 227
Sears, J	44, 96, 148, 151, 152, 298
Sediako, D	160, 188
Sedlmayr, A	45
Seefeldt, M	233
Seelam, U	80
Seetharaman, S	163, 261, 266, 295, 396
Sehitoglu, H	27
Sei, N	246
Seidler, S	317
Seidman, D	18, 28, 36, 103, 122, 207, 278, 280, 394
Seif, M	61
Seifert, H	22, 101
Seifi, M	385
Seiser, B	76
Sekar, A	30
Sekkingstad, A	149
Sekunowo, O	119
Selvaraj, P	18
Semiatin, L	205, 258, 320
Semiatin, S	29, 78, 80, 128, 130, 180, 182, 233, 235, 259, 281, 331
Senkov, O	91
Senthil Kumaran, S	12
Seo, C	351
Seo, J	22, 388
Seo, S	67, 223
Seo, Y	289
Seol, J	145, 281, 377
Seong, B	314, 388
Sepehrband, P	86
Serebryany, V	131
Serizawa, A	73, 207
Serna, L	127
Serna, S	15
Serra, A	174, 231
Serrano de Caro, M	285, 334, 335
Sesen, K	379
Seshadri S.K.	75
Sethna, J	28, 178, 322
Setyawan, A	193
Sevik, C	29
Sewell, T	279, 328, 329, 373
Sha, G	183, 235
Shackelford, J	89, 221
Shade, P	151, 370
Shah, J	128, 245, 365
Shah, M	21
Shahandeh, S	21
Shahbazian-Yassar, R	46
Shaily, B	69
Shamloo, R	384
Shan, Y	383, 387
Shan, Z	45, 79, 99, 150, 202, 235
Shang, J	212, 349

# Index

Shang, S	355	Shoieb, S	300	Smetana, J	25
Shankar, M	130, 183	Shoji, T	392	Smith, C	88, 351, 387
Shanmugam, J	30	Sholl, D	160	Smith, G	329
Shanmugasandaram, P	13, 18, 242	Shon, I	10, 381, 386, 390, 391, 392	Smith, P	187
Shao, S	62	Shon, S	381	Smits, E	254
Shapovalov, V	96	Shook, S	353	Smugeresky, J	59, 319
Sharma, S	300, 357	Shoude, W	318	Snead, M	37
Sharon, J	100	Shridas, N	137	Sneyd, J	256
Sharp, L	125	Shu, Y	276, 308	Snyder, B	220
Shartal, K	158	Shuigen, W	59	Snyder, C	217
Shavrov, V	10, 347	Shukla, A	358	So, C	38, 339
Shaw, J	384	Shukla, N	352	So, Y	28
Shaw, L	45	Shukralla, M	87	Soares, F	244, 290
Shayesteh, P	111	Shuster, R	106, 253	Sob, M	126, 372
Shayesteh-Zeraati, A	41, 195	Shute, C	128	Soboyejo, W	190
Shechtman, D	160	Shuto, H	369	Sofie, S	214
Shehata, M	309	Sickels, K	200	Sofronis, P	231, 324
Sheikh-Ali, A	29, 173	Sidhu, M	88	Sohal, M	143
Shekhar, C	124	Sidhu, R	25, 66, 116, 168, 221, 271, 315, 363	Sohn, H	53, 308
Shekhar, R	352	Siegel, N	143	Sohn, J	369
Shekhar, S	130, 183	Siegenthaler, H	254	Sohn, S	142
Shekher, S	237	Sietsma, J	251	Sohn, Y	81, 115, 309, 315, 362
Shelyakov, A	10	Siewert, T	161	Sokolov, M	60
Shen, C	92, 373	Sigler, D	75	Sokolowski, J	108
Shen, H	204	Sik Lee, J	31	Solak-Gok, O	53
Shen, J	248	Siljan, O	149	Solanki, K	56
Shen, Q	388	Sillekens, W	22, 56, 106, 108, 157, 159, 211, 212, 262, 263, 308, 353, 354	Solaris, S	374
Shen, Y	239, 316, 396	Silva, A	10	Solheim, A	149
Shen, Z	366	Silva, F	34, 186	Somani, M	128, 291
Sheng, G	252	Silva, O	26, 203	Somekawa, H	212, 213
Shenghai, Y	18, 379	Sim, J	68	Somerday, B	231
Shepelev, D	263	Simakov, D	337	Somerman, M	37, 191
Sherburne, M	113	Simko, S	158	Somsen, C	251
Sherby, O	82	Simmons, J	20, 77, 127, 179, 198, 232, 280, 330	Son, H	301
Shet, S	42, 196	Simpson, M	155	Sondhi, S	259
Shevchenko, D	157	Singh, A	72, 175, 212, 213, 382	Song, C	379
Shevchenko, S	78	Singh, C	328	Song, G	158
Shi, D	273	Singh, D	239	Song, J	116, 169, 170, 230, 239, 263, 271, 316, 319, 358, 388
Shi, F	98	Singh, H	144, 196, 232, 286	Song, K	23
Shi, G	382	Singh, J	81	Song, L	16, 82
Shi, J	12	Singh, P	70, 351, 377	Song, N	381
Shi, L	334	Singh, R	16, 70, 96, 120, 123, 171, 182, 224	Song, Q	348
Shi, Q	92	Singh, S	196, 346	Song, S	90
Shi, R	102	Singh, V	33, 82, 197	Song, T	123
Shi, S	161	Singhal, R	358	Song, Y	97, 216
Shi, W	12, 33, 387	Sinha, M	381	Soni, P	242
Shi, Y	25, 91, 222, 259	Sinha, V	120, 274	Sonnemann, G	176
Shi, Z	13, 108, 139, 158, 337	Sinnott, S	73, 321	Sonntag, P	338
Shi-wen, L	189	Sintay, S	232	Sopian, K	35
Shim, J	388, 392	Siquieri, R	102, 207	Sopu, D	141
Shim, S	395	Sisneros, T	164, 360	Sorensen, J	336
Shimasaki, S	157	Siu, S	352	Sorhuus, A	87, 88
Shimokawa, T	79	Sivaramakrishnan, S	31	Soriano-Vargas, O	389
Shin, B	382, 385, 386	Sizek, H	50	Sorlie, M	97, 149, 200, 253, 298, 344
Shin, C	359	Sket, F	65	Sort, J	340
Shin, D	29, 31, 79, 129, 158, 355, 395	Skipper, C	204	Sosa, J	16, 96, 127, 330
Shin, E	256, 314	Skirde, S	88	Sossaman, T	172
Shin, H	83	Skorpenske, H	64	Soucy, G	97
Shin, J	153, 186, 225	Skripnyuk, V	56	Souza, D	344
Shin, K	23, 158, 379, 380, 395	Skrotzki, B	57	Souza, J	295
Shin, S	49, 369	Skrotzki, W	181	Söyler, A	381, 392
Shin, Y	357, 382, 385	Skszek, T	353, 369	Spaepen, F	40, 50, 102, 153, 206, 306
Shinozuka, K	26, 78	Skybakmoen, E	45, 149	Spangenberg, J	320, 369
Shirai, S	105	Slade, S	108, 157	Spanos, G	77, 188, 195, 330
Shirazi, H	129	Slagnes, S	149	Spathis, D	296
Shirinov, T	385	Slamovich, E	214	Spatschek, R	147
Shishegar, H	93	Slifka, A	161	Spearot, D	61, 113, 165, 174, 218, 267, 311, 358, 365
Shitole, S	314	Sloutskin, E	51	Specht, E	65
Shivaputrapa, K	224	Sluiter, M	19, 43, 154	Spolenak, R	63, 216
Shivendra	370	Slyn'ko, E	347	Spowart, J	35, 120, 179
Shiwen, B	85, 241, 255, 336	Slyn'ko, V	347		
Shlachter, J	285				



Sprague, A.....	95	Sturm, D.....	181	Syarif, Y.....	297
Sprenkle, V.....	240, 356	Su, C.....	276, 316, 339, 364	Sykes, B.....	168
Squatrito, R.....	144	Su, L.....	29	Sykes, E.....	257
Sreenivasan, R.....	277	Su, P.....	363, 364	Syn, C.....	82
Sreeranganathan, A.....	286	Su, S.....	147	Synkov, S.....	180
Srinivasan, B.....	252	Su, Z.....	84	Szczepanski, C.....	203, 320, 368
Srinivasan, k.....	18	Suarez, C.....	84, 135, 186, 240, 287, 288, 336	Szluafarska, I.....	358, 378
Srinivasan, M.....	113	Suárez, O.....	348	Szpunar, J.....	302
Srinivasan, R.....	342	Subbarayan, G.....	168, 315		
Srivastava, A.....	133	Subbarayan, S.....	30	<b>T</b>	
Srivastava, C.....	184	Subramanian, K.....	66, 68, 116, 221, 222	Tabachnikova, E.....	128
Srivatsa, S.....	259	Subramanian, P.....	182, 183	Tabereaux, A.....	138, 344
Srivilliputhur, S.....	17, 19, 251, 321	Subramanian, R.....	284	Tada, S.....	350
Srolovitz, D.....	27, 76, 125, 165, 177, 230, 278, 324, 327, 358, 370, 372	Subramanian, V.....	266	Tahirlu, H.....	385
St-Georges, L.....	243	Subramanya Sarma, V.....	181	Tai, F.....	272
Stach, E.....	283	Sudibjo, A.....	365	Takagi, M.....	69
Stachurski, Z.....	313	Suganuma, K.....	68, 116	Takahashi, A.....	325
Stafford, S.....	363	Sugar, J.....	322	Takahashi, T.....	392
Stal, R.....	194	Sugawara, M.....	96	Takahashi, Y.....	269
Stampfli, J.....	254	Sugui, T.....	145	Takamatsu, Y.....	26
Stanek, C.....	73, 227, 321	Suh, Y.....	286	Takano, C.....	208
Stanford, M.....	74	Suk, M.....	378	Takats, V.....	176
Stanford, N.....	213	Sulaiman, D.....	298	Takei, R.....	158
Stauffer, D.....	17	Sule, P.....	325	Takekiyo, T.....	313
Stechel, E.....	143	Sulger, P.....	298	Takemoto, T.....	363
Steele, T.....	301	Sulmont, B.....	290	Takenaka, T.....	96
Steen, I.....	341	Summers, A.....	338	Takeuchi, S.....	325
Stein, C.....	330	Summers, C.....	294	Taktak, B.....	37
Stein, J.....	371	Sun, C.....	317, 374	Taleff, E.....	304
Steinbach, I.....	251	Sun, G.....	361	Talling, R.....	64, 205
Steinfeld, A.....	239, 240	Sun, H.....	175, 340, 366	Tamerler, C.....	37, 38, 191, 292, 339
Steingart, D.....	261, 306, 307	Sun, J.....	79	Tamirisakandala, S.....	253
Stem, M.....	346	Sun, L.....	34, 317, 325, 348	Tamura, N.....	63, 168
Stender, P.....	73	Sun, N.....	54, 287	Tamura, T.....	192
Stephan, D.....	282	Sun, P.....	187	Tan, C.....	394
Stephens, E.....	96	Sun, Q.....	387	Tan, S.....	170, 195, 196
Stephenson, C.....	198	Sun, X.....	155, 161, 353, 396	Tan, W.....	312
Stephenson, D.....	254	Sun, Y.....	75, 147, 200	Tanaka, F.....	366
Stephenson, G.....	114	Sun, Z.....	58, 262, 367	Tanaka, K.....	325
Stephenson, K.....	284	Sundaram, P.....	14	Tanaka, M.....	79
Stergar, E.....	270, 314	Sundararajan G.....	74	Tanaka, N.....	296
Steurer, W.....	167	Sundara Raman S, G.....	75	Tancret, F.....	191, 205
Stevens, L.....	329	Sundman, B.....	251	Tang, G.....	239
Stevenson, A.....	360	Sung, H.....	49	Tang, L.....	145
Stevenson, J.....	265	Sung, S.....	36, 395	Tang, S.....	71
Stewart, C.....	257	Suo, B.....	34	Tang, T.....	211
Stewart, J.....	256, 362	Suominen Fuller, M.....	269	Tang, W.....	168, 275
StJohn, D.....	153, 206	Suparadist, M.....	248	Tangstad, M.....	72
Stoica, A.....	64, 219	Suri, J.....	180	Taniguchi, S.....	157
Stoica, M.....	39	Suriñach, S.....	340	Tannenbaum, J.....	93, 145
Stolboushkina, O.....	289	Suryanarayana, C.....	80	Tao, N.....	131
Stoldt, C.....	82, 202	Susila, P.....	181	Tao, X.....	35
Stollberg, D.....	10, 33, 82, 133, 183, 237, 283, 333	Suslov, S.....	283	Tarafder, M.....	93, 291, 323, 375
Stoller, R.....	60, 174, 359	Suss, A.....	136, 186	Tarafder, S.....	93, 323
Stone, D.....	293	Suter, R.....	227, 268	Tarcy, G.....	344
Stone, H.....	361	Sutou, Y.....	146, 160	Tardio, J.....	336
Stoost, C.....	143	Sutton, A.....	27, 76, 125, 177, 230, 278, 324, 327, 370, 372	Tariq, F.....	281
Storm, R.....	96	Sutton, M.....	166	Tasaki, K.....	266
Stoudt, M.....	368	Suwanpinij, P.....	172	Tassa, O.....	152
Stover, A.....	49	Suwas, S.....	370	Taupin, V.....	178
Strachan, A.....	279, 280, 312, 328, 358, 373	Suzuki, A.....	258	Tavangarian, F.....	237
Strader, J.....	175, 284	Swaminarayan, S.....	326	Tavazza, F.....	113
Strasky, J.....	253	Swaminathan, S.....	236	Taylor, J.....	296
Stravinskias, J.....	377	Swamy, N.....	16	Taylor, M.....	136, 256
Streiffer, S.....	114	Swamy, R.....	152	Taylor, R.....	52
Stroeve, P.....	184	Swaroop, S.....	258	Taylor, S.....	256
Strunz, P.....	359	Swarupini, G.....	242	Tayon, W.....	21
Stubbins, J.....	270	Sweatman, K.....	364	Tazibt, A.....	69
Stukowski, A.....	61	Swenson, H.....	48	Teare, A.....	242
Stumphy, B.....	31	Switzer, N.....	260	Tedenac, J.....	171
Stupperich, E.....	246	Swoboda, B.....	326	Tegze, G.....	102

# Index

Teixeira, A	344	Tomorr, H	306	Tutuncu, G	313
Telesman, J	304	Tomota, Y	220	<b>U</b>	
Templeton, J	265	Tomus, D	360	Ubertalli, G	48
Teng, Z	17, 167	Tong, C	118	Uberuaga, B	73, 226, 321, 326, 372
Tenorio, J	320	Tong, P	39	Uchic, M	151, 227, 281, 328, 370
Terai, T	167	Tong, T	250	Ucuncuoglu, S	296, 309
TerBush, J	354	Tonks, D	372, 378	Uda, T	18, 296
ter Weer, P	241	Tonks, M	164, 233, 323, 373	Uddin, S	17
Tessier, J	337, 344	Tönnies, D	91	Ude, A	35
Tevar, A	357	Toops, T	311	Udofot, B	10, 184
Tewari, A	144	Topping, T	31, 130, 142, 181, 192, 234, 235, 283	Udovic, T	91
Thackray, R	41	Torabi, S	134, 197	Udyansky, A	104
Thadhani, N	35	Torbet, C	360	Ueda, M	211
Thanh, P	198, 256	Toroian, D	140	Ueshima, M	271
Thein-Han, W	191, 245, 291	Torres, K	297	Uggowitz, P	36, 192
Thess, A	162	Tortorelli, D	323	Ugle, R	59
Thevoz, P	105	Tortorelli, P	311	Uglov, V	176
Thirathipviwat, P	248	Torvanger, K	194	Uk, H	175
Thirumalai, N	29, 226, 328	Tosas, A	330	Ulfig, R	270
Thirunavukkarasu, S	88	Toth, G	102	Ulrich, G	70
Thiyagarajan, P	167	Toth, L	131, 165, 370	Um, H	68
Thomas, B	22, 55, 105, 156, 210, 261, 306, 307, 352	Tóth, L	78	Umeda, J	158, 185
Thomas, D	288	Tran, D	274, 365	Umeda, T	248
Thomas, H	343	Tran, K	289	Umemoto, M	235
Thomas, J	236, 305	Tran, T	75, 89, 198	Umezawa, O	395
Thomas, M	50	Trembly, J	160	Ungar, T	79, 181, 219, 220, 361
Thomas, S	359	Trenkler, J	166	Unlu, N	186, 385
Thomas, W	101	Trifonov, V	136	Unni, K	345
Thompson, C	114, 115, 341, 352	Trinkle, D	19, 43, 94, 147, 161, 174, 177, 197, 251, 322, 326, 328, 367	Uno, K	52
Thompson, D	373	Tripathi, S	306	Unocic, R	178, 204, 257, 373
Thompson, G	122, 184, 222, 281, 297	Tripp, D	106, 253	Unuvar, C	119
Thomsen, D	17, 313	Trivedi, R	153	Upadhyaya, A	71
Thomson, C	114	Troderman, G	342	Upmanyu, M	227
Thonstad, J	244	Trong, S	16	Urata, N	244
Thornton, D	128	Trovant, M	296	Urban, I	57
Thornton, K	128, 179, 215, 312	Truan-Sheng, L	375	Urban, M	350
Thostenson, E	272	Trujillo, C	231, 351, 384	Urgen, M	99, 146
Threrujirapapong, T	185	Trunov, M	176	Ürgen, M	295
Tian, J	340, 393	Tsai, C	116	Usami, N	69
Tian, S	111	Tsai, M	67, 193, 222, 316	Usov, I	226
Tichy, G	178, 181	Tsai, T	91	Ustundag, E	64, 313, 360
Tick-Hon, Y	282	Tsakiropoulos, P	41, 173	Uyar, F	14, 179
Tiejun, C	55	Tsao, C	192	Uysal, C	379
Tierney, H	257	Tschöpe, K	149	Uzel, S	246
Tieu, K	29	Tseng, C	26, 316		
Tikare, V	95	Tseng, H	364	<b>V</b>	
Tikasz, L	243	Tsirlina, G	337	Vai, A	307
Tiley, J	25, 62, 64, 72, 101, 114, 166, 219, 268, 312, 342, 359, 382	Tsiros, J	296	Vaidyanathan, R	304
Timmel, K	55	Tsuji, N	29, 78, 80, 128, 130, 180, 182, 233, 235, 281, 331	Vainik, R	143
Timoney, C	34	Tsunekane, M	258	Valdez, S	255, 384, 386, 389
Timur, S	99, 381	Tsurekawa, S	370	Valentina, T	390
Tin'ghaev, P	189	Tsutsumi, H	253	Valenzuela, J	53
Tin, S	259	Tu, G	12	Valenzuela-Díaz, F	10
Tischler, J	63, 116, 268, 269, 280	Tu, K	66, 67, 122, 168, 169, 364	Valette, S	167
Tkacheva, O	189	Tu, W	259	Valiakmetov, O	332
Todaka, Y	235	Tucker, G	177, 358	Valiev, R	31, 78, 79, 181, 235, 282, 283, 362
Todaro, I	144	Tucker, J	168, 217, 326	Valone, S	174
Todd, B	219	Tucker, M	376	Van Acker, K	229
Todd, I	41	Tucker, T	303	Van Aken, D	58, 110, 111
Todd, P	309	Tulk, E	65	Vanasse, J	296
Tokar, V	208	Tumey, S	285	Vanasupa, L	324
Toledo Filho, R	34	Tung, H	270	Van Buuren, T	285
Toloczko, M	60, 362, 366	Tupper, C	359	van den Bergh, M	81
Toloui, M	95	Turbini, L	25, 66, 116, 168, 221, 271, 315, 363	Van der Biest, O	58
Tomar, V	93, 190, 267, 280, 322	Turchi, P	29	Van der Giessen, E	113, 165
Tombolato, L	140	Turk, B	160	Van der Ven, A	43, 155, 266, 305, 326
Tome, C	95, 194, 326, 368	Turner, A	338	van der Zwaag, S	163, 348
Tomé, C	220, 361	Turner, D	232	van de Walle, A	104, 154, 322
Tomesani, L	136, 144	Turner, J	42, 196, 311	Van Gerven, T	276
Tomforde, C	386	Turski, M	213		



Vangolu, Y.....	131	Vsianska, M.....	372	Webb, E.....	61, 113, 147, 165, 218, 267, 311, 358
Vanherpe, L.....	260	Vutova, K.....	390	Webb, J.....	286
Van Petegem, S.....	62, 63, 268, 360	<b>W</b>		Weber, T.....	167
Vansickle, S.....	190	Wachs, D.....	60, 61	Weber, W.....	334, 335
Van Swygenhoven, H.....	62, 63, 268, 360	Wachsmann, E.....	214	Webster, M.....	74
Van Vechten, T.....	34	Wäger, P.....	176	Webster, V.....	384
Van Vliet, K.....	72, 178	Wagner, C.....	288	Weckman, D.....	106
van Zyl, D.....	324	Wagner, D.....	353	Wedde, G.....	87, 88
Varlioglu, M.....	313	Wagner, G.....	86, 92, 354	Weddeling, C.....	304
Varma, S.....	173, 215	Wagner, L.....	253	Wee, D.....	161
Varnik, F.....	51	Wagner, M.....	16	Weertman, J.....	128
Varyukhin, V.....	180	Wagner, P.....	251	Wegst, U.....	139
Vasconcelos, P.....	299, 344	Wagner, R.....	373	Wei, C.....	49
Vassileva, V.....	390	Wagoner Johnson, A.....	83, 89	Wei, D.....	204, 259
Vassiliev, S.....	337	Waheed, A.....	242	Wei, H.....	221
Vaughan, G.....	39	Waheed, M.....	378	Wei, K.....	287
Vaynman, S.....	172	Wain, N.....	152	Wei, L.....	18, 379
Väyrynen, P.....	55	Walker, M.....	188	Wei, Q.....	129, 174, 234
Vecchio, K.....	140	Wallis, R.....	304	Wei, S.....	273, 318
Velev, K.....	390	Wallwark, K.....	360	Wei, Y.....	46, 61
Vellemans, P.....	290	Waly, M.....	345	Weihmuller, L.....	101
Venancio, L.....	295	Wan, A.....	208	Weihns, T.....	49
Vendette, H.....	86, 254	Wang, B.....	276	Weil, K.....	57, 109, 110, 160, 214, 265, 310, 356, 357
Venkatasurya, P.....	128	Wang, C.....	68, 117, 170, 223, 261, 381, 388	Weil, S.....	265, 297, 310
Venkatesh, M.....	348	Wang, D.....	240, 307, 356	Weiland, J.....	246
Venkatesh, T.....	185, 238	Wang, F.....	169	Weiler, J.....	263
Venkatesh, V.....	252	Wang, G.....	38, 39, 90, 108, 111, 140, 167, 191, 246, 247, 248, 292, 293, 339, 387	Weimer, A.....	240
Ventelon, L.....	27, 126	Wang, H.....	34, 42, 114, 173, 196, 199, 295, 311, 367	Weinberger, C.....	61
Vera, M.....	53, 124	Wang, J.....	13, 26, 46, 62, 90, 95, 113, 117, 128, 129, 144, 181, 217, 223, 263, 315, 362, 393	Weinhardt, L.....	335
Verbrugge, M.....	75	Wang, K.....	26, 118, 168, 265, 353	Weiss, B.....	80
Verlinden, B.....	233, 234	Wang, L.....	11, 28, 61, 63, 66, 94, 134, 135, 201, 258, 301, 306, 387	Weissmüller, J.....	100
Verma, B.....	203	Wang, M.....	66, 180	Weitz, D.....	51
Verma, R.....	309	Wang, P.....	98, 107	Weiwei, D.....	13
Vernon, C.....	336	Wang, Q.....	137, 141, 212, 276, 317, 365	Weiwei, T.....	288
Verpoest, I.....	229	Wang, R.....	190	Wejrzanowski, T.....	20
Vetrano, J.....	299	Wang, S.....	55, 71, 212, 361, 396	Welberry, R.....	312, 313
Vetterick, G.....	302	Wang, T.....	208, 391	Welch, B.....	87
Victoria, M.....	164	Wang, W.....	15, 16, 42, 98, 232, 358, 383, 387	Welcing, A.....	19
Vidu, R.....	184	Wang, X.....	40, 64, 65, 91, 219, 248, 311, 336, 361, 386	Weldon, D.....	361
Vieira, C.....	320, 343	Wang, Y.....	25, 39, 50, 62, 64, 72, 102, 114, 133, 156, 166, 167, 178, 183, 200, 210, 219, 268, 272, 276, 282, 294, 308, 312, 313, 355, 359, 361, 373, 396	Welk, B.....	18
Villafuerte, J.....	302	Wang, Z.....	13, 87, 97, 108, 139, 174, 328, 337	Wells, M.....	102, 106, 188
Villar, E.....	367	Wanning, L.....	48	Wen, H.....	283
Villarreal, T.....	380	Ward, D.....	385	Wen, W.....	11, 13
Vinogradov, A.....	90	Ward, M.....	152	Wen, X.....	85, 137
Viswanathan, G.....	72, 73, 342, 382	Ware, T.....	367	Wen, Y.....	20, 139, 198
Viswanathan, N.....	295	Warner, D.....	114, 312, 328	Wen-cheng, L.....	336
Viswanathan, S.....	263	Warren, A.....	309	Wenbing, Z.....	379
Viswanathan, V.....	356	Warren, J.....	51, 147	Wenzhong, C.....	288
Vitek, V.....	76	Warwick, J.....	205	Werley, T.....	377
Viumdal, H.....	301	Wasbø, S.....	290	Wert, D.....	377
Vivek, A.....	349	Wasekar, N.....	74	West, J.....	33
Vleugels, J.....	58	Watanabe, M.....	366	West, M.....	270
Vo, N.....	31, 62	Watanabe, R.....	309	Westerheide, J.....	349
Vogel,.....	171	Watanabe, T.....	370, 372	Wette, P.....	51, 153
Vogel, S.....	120, 361	Watanabe, Y.....	269	Wheeler, B.....	203
Vogt, H.....	244	Watkins, T.....	66	Wheeler, D.....	51
Vogt, R.....	30, 130, 234, 236, 281	Watkowski, J.....	25	Wheeler, K.....	164, 216, 227, 257
Voit, W.....	367	Watson, K.....	87	Wheeler, R.....	120, 151
Volkert, C.....	45, 91	Way, J.....	160	Whipple, D.....	201
Volkova, O.....	210	Wayne, L.....	386	Whitacre, J.....	57, 109, 160, 214, 265, 310, 356, 357
Voller, V.....	156	Weaver, D.....	259	White, B.....	35
Volz, H.....	49, 303			White, C.....	241, 289
von Alfthan, S.....	278			White, P.....	125
Von Dreele, R.....	220			Whiteley, P.....	193, 295
von Pezold, J.....	27, 104, 326			Whitis, D.....	21, 49, 100, 151, 205, 258, 259, 304
Voorhees, P.....	21, 179, 180, 260			Whittington, W.....	375
Vorontsov, V.....	373			Wicker, R.....	134, 152
Voskoboinikov, R.....	373			Widrevitz, D.....	350
Voter, A.....	126, 174, 226, 326, 372			Widyastuti.....	287
Voyer, R.....	194, 383			Wilde, G.....	154, 180, 339
Voyles, P.....	192, 293				
Vratna, J.....	32				

# Index

- Wildfong, P. .... 329  
Wilkerson, J. .... 361  
Wilkerson, L. .... 349  
Wilkins, J. .... 325  
Wilkinson, A. .... 206, 242  
Wilkinson, C. .... 318, 331  
Wilkinson, D. .... 17, 127, 380  
Wilks, G. .... 90, 91, 292, 293  
Wilks, T. .... 213  
Willaime, F. .... 27, 126  
Willard, M. .... 280, 284, 333, 346  
Willey, T. .... 285  
Williams, F. .... 84  
Williams, J. .... 18, 81, 117, 204, 330  
Williams, R. .... 17, 83, 330, 383  
Williamson, M. .... 217  
Williamson, S. .... 76  
Willis, J. .... 381  
Wilson, B. .... 38, 292  
Wilson, I. .... 34  
Wilson, J. .... 215  
Wilson, O. .... 89, 292  
Wilson, S. .... 372  
Wind, S. .... 84  
Windl, W. .... 90, 165, 293  
Wingate, C. .... 187  
Wingate, N. .... 393  
Winiarski, B. .... 340  
Winning, M. .... 179  
Winterrose, M. .... 251  
Winther, G. .... 371  
Wirth, B. .... 163, 286, 362, 392  
Wise, S. .... 134  
Withers, J. .... 44, 45, 96, 148, 261  
Withers, P. .... 205, 340  
Withey, E. .... 150, 325  
Withey, P. .... 157  
Witkin, D. .... 222  
Witusiewicz, V. .... 102  
Wobker, H. .... 296  
Wolf, A. .... 135  
Wolf, D. .... 164, 198, 233, 373  
Wolfe, T. .... 69, 320  
Wolk, J. .... 195  
Woll, A. .... 114  
Wollants, P. .... 260  
Wollmershauser, J. .... 164, 313  
Wolverton, C. .... 43, 52, 103, 154,  
..... 207, 260, 305, 355  
Wombles, R. .... 200  
Wong, C. .... 187  
Wong, W. .... 70, 274  
Woo, J. .... 386  
Woo, K. .... 10, 266, 311, 381, 384, 386, 390  
Woo, W. .... 65, 388  
Wood, D. .... 310  
Wood, J. .... 263  
Woodfield, A. .... 148  
Woodward, C. .... 20, 100, 104, 113, 177,  
..... 198, 281, 327, 328, 370  
Woodward, S. .... 304  
Wright, N. .... 68  
Wright, P. .... 261, 307  
Wright, S. .... 77, 127, 179, 232, 280, 330  
Wright, W. .... 90  
Writh, B. .... 388  
Wrobel, J. .... 107  
Wu, A. .... 67, 224, 364  
Wu, C. .... 170, 294, 396  
Wu, D. .... 51, 198  
Wu, E. .... 133, 361  
Wu, F. .... 339  
Wu, G. .... 117, 212  
Wu, H. .... 18, 43, 48  
Wu, J. .... 265  
Wu, K. .... 85, 260  
Wu, L. .... 98, 215  
Wu, M. .... 170, 195  
Wu, P. .... 26  
Wu, S. .... 137  
Wu, W. .... 118, 122, 222, 317, 364, 387  
Wu, X. .... 16, 18, 48, 78, 129, 152, 153,  
..... 199, 235, 240, 333, 349, 373, 387  
Wu, Y. .... 56, 185, 275, 314  
Wu, Z. .... 123  
Wunderlich, R. .... 340  
Wurster, S. .... 71  
Wuyang, C. .... 351  
Wynn, A. .... 301
- X**
- Xi, Z. .... 348  
Xia, G. .... 240, 265, 356  
Xia, K. .... 199, 235, 331  
Xia, Q. .... 387  
Xia, W. .... 54, 391  
Xianghua, L. .... 145  
Xiao, B. .... 111  
Xiao, C. .... 172  
Xiao, H. .... 334  
Xiao, J. .... 156, 356  
Xiao, S. .... 393  
Xiao, Z. .... 201, 228  
Xiao-jun, L. .... 150, 189  
Xiaobing, Y. .... 291  
Xiaodan, L. .... 11  
Xiaodong, Y. .... 138  
Xiaojun, L. .... 98, 244  
Xiaoming, Z. .... 287  
Xiaoni, S. .... 176, 228  
Xiaowu, L. .... 139  
Xie, B. .... 156  
Xie, C. .... 156  
Xie, G. .... 90, 141, 340  
Xie, H. .... 199, 272, 331  
Xie, M. .... 259  
Xie, S. .... 128, 300  
Xie, W. .... 221  
Xifeng, C. .... 244  
Xin, C. .... 318  
Xin, H. .... 54, 215  
Xing, D. .... 142  
Xing, W. .... 348  
Xing, Y. .... 363  
Xinyan, Y. .... 42  
Xiong, J. .... 83  
Xiong, S. .... 263, 354  
Xiong, Y. .... 59, 225, 319  
Xiquan, Q. .... 189, 244  
Xu, B. .... 15, 187  
Xu, C. .... 214  
Xu, D. .... 169, 286  
Xu, G. .... 25, 66, 68, 272  
Xu, H. .... 200, 222  
Xu, J. .... 71  
Xu, L. .... 169, 304  
Xu, N. .... 269  
Xu, Q. .... 101, 348  
Xu, R. .... 167  
Xu, T. .... 333, 370  
Xu, W. .... 199, 235, 236, 336, 356  
Xu, X. .... 210  
Xu, Y. .... 11, 13, 161, 235
- Xu, Z. .... 158  
Xue, J. .... 97, 98, 99, 150, 162,  
..... 189, 200, 215, 216, 240  
Xue, X. .... 35, 83  
Xue, Y. .... 347, 368, 382  
Xuechong, R. .... 351  
Xuemei, W. .... 55  
Xueyi, G. .... 230, 365, 382
- Y**
- Yablinsky, C. .... 204  
Yadav, A. .... 395  
Yakar, S. .... 381  
Yakobson, B. .... 273, 324  
Yakushev, R. .... 134  
Yamaji, K. .... 265  
Yamaji, Y. .... 395  
Yamamoto, K. .... 31  
Yamamoto, M. .... 383, 385  
Yamamoto, O. .... 134  
Yamamoto, T. .... 112  
Yamamoto, Y. .... 110, 148, 149  
Yamanaka, K. .... 236  
Yamasaki, T. .... 192  
Yamauchi, H. .... 305  
Yamauchi, K. .... 269  
Yan, D. .... 48, 305  
Yan, H. .... 98  
Yan, K. .... 269  
Yan, L. .... 117, 240  
Yan, M. .... 199  
Yan, R. .... 301  
Yan, W. .... 383, 387  
Yan, X. .... 371  
Yan, Y. .... 15, 42, 196  
Yan-qing, L. .... 150, 189  
Yang, B. .... 312  
Yang, C. .... 12, 118, 223, 264  
Yang, D. .... 351, 369  
Yang, F. .... 25, 89, 108, 145, 222, 248  
Yang, G. .... 265, 356  
Yang, H. .... 235  
Yang, J. .... 188  
Yang, K. .... 262, 274, 383, 387  
Yang, L. .... 393  
Yang, M. .... 379  
Yang, Q. .... 348  
Yang, R. .... 40  
Yang, S. .... 108, 169, 321  
Yang, T. .... 26  
Yang, W. .... 63, 210  
Yang, Y. .... 19, 20, 28, 52, 61, 85, 87,  
..... 92, 101, 193, 258, 362, 365, 378  
Yang, Z. .... 57, 98, 109, 160, 214, 240,  
..... 265, 276, 310, 321, 356, 357  
Yanjing, S. .... 351  
Yanjun, W. .... 42  
Yankov, R. .... 301  
Yanli, J. .... 189  
Yanqing, L. .... 98, 189, 244  
Yanyan, B. .... 59  
Yao, B. .... 81, 315  
Yao, C. .... 251  
Yao, G. .... 11, 12, 134, 135, 159, 185, 201, 348  
Yao, K. .... 192  
Yao, W. .... 225  
Yaowu, W. .... 189, 244  
Yaoyu, W. .... 345  
Yap, Y. .... 46  
Yasi, J. .... 326, 328  
Yavari, A. .... 39, 90, 192



Yazdanmehr, M	393	Yuchun, Z	11, 377	Zhang, Y	13, 54, 83, 92, 129, 141, 155, 156, 165, 188, 232, 233, 235, 236, 335
Yazici, E	389	Yue, A	251	Zhang, Z	30, 31, 34, 42, 130, 134, 142, 171, 201, 225, 234, 235, 236, 281, 339, 343, 351, 384
Yazici, H	292, 339	Yue, M	276	Zhao, F	150
Yazzie, K	117	Yue, S	70, 152, 265, 302, 309	Zhao, H	288
Ye, B	297	Yue-yuan, L	216	Zhao, J	43
Ye, J	151, 173, 193	Yueying, W	175	Zhao, L	161
Ye, Y	350	Yuezhong, D	13	Zhao, M	25
Yeager, J	151	Yujie, X	244	Zhao, X	31
Yeh, J	193	Yukawa, T	369	Zhao, Y	11, 29, 30, 31, 34, 78, 80, 83, 84, 128, 130, 134, 180, 181, 182, 185, 187, 225, 233, 234, 235, 238, 250, 281, 282, 283, 286, 331, 333
Yeju, H	279	Yumaguzin, Y	33	Zhao, Z	111, 212, 248
Yen, Y	68, 117, 118, 170, 223, 384	Yun, J	331	Zhaobo, T	18, 379
Yexiang, L	98	Yun, S	382	Zhen, Z	262
Yi, D	13, 188	Yun-long, L	189	Zheng, B	192, 319, 334
Yi, F	192	Yunnen, C	276	Zheng, D	15
Yi, J	180	Yurko, J	307	Zheng, H	46
Yi, S	32, 265, 351, 355	<b>Z</b>		Zheng, L	219
Yim, T	68	Zacate, M	251	Zheng, S	396
Yin, D	263	Zacherl, D	105, 201	Zheng, W	92
Yin, H	162	Zaefferer, S	117, 265	Zheng, X	43
Yin, J	84	Zahrah, T	105, 237	Zheng, Y	162
Yin, L	163	Zaikov, Y	189	Zhenrong, L	145
Yin, W	129	Zainuri, M	287	Zherebtsov, A	119, 145, 343
Yin, Z	84	Zaky Farahat, A	172	Zhilyaev, A	236
Ying, A	220	Zander, D	123, 158, 212	Zhong, C	37
Ying, Y	365	Zarif, M	153	Zhong, K	317
Yingfu, T	189, 345	Zavaglia, C	250	Zhong, W	34, 273, 364
Yip, S	178	Zberg, B	192	Zhong, Y	334, 358
Yodyingyong, S	275	Zbib, H	163, 239	Zhong, Z	74, 244
Yokokawa, H	265	Zbib, M	72	Zhong-liang, T	150
Yokoyama, Y	39, 192, 247, 248, 293, 339, 340	Zeches, R	252	Zhonggang, Z	145
Yoneda, H	252	Zehetbauer, M	80, 219, 236, 331	Zhongliang, T	189
Yongliang, M	255, 302	Zeifert, B	275	Zhou, B	15, 117, 168, 363
Yoo, B	92, 158, 395	Zelger, C	36	Zhou, C	157
Yoo, J	24, 30	Zelicourt, M	138	Zhou, H	225
Yoo, K	22, 307	Zemanova, A	224	Zhou, M	208
Yoo, M	266, 384	Zen, H	69	Zhou, N	102, 178, 373
Yoo, S	117, 382, 385, 386	Zeng, J	287	Zhou, P	67, 134
Yook, W	142	Zeng, K	25, 68, 117, 170, 223	Zhou, Q	123
Yoon, D	217	Zeng, P	20	Zhou, S	147
Yoon, E	30	Zeng, Q	136	Zhou, W	15
Yoon, H	249, 396	Zeng, T	200	Zhou, X	114, 156, 275, 321
Yoon, J	10, 68, 350, 390	Zeng, W	387	Zhou, Y	28, 42, 192, 235, 319, 334, 394
Yoon, K	274	Zeng, X	56, 159, 212, 264	Zhouhua, J	48
Yoon, S	30, 233, 249, 375, 382, 385, 390, 394, 396	Zeytuncu, B	391, 392	Zhou, Y	142
Yoshida, Y	383, 385	Zhai, J	83	Zhu, H	96, 300
Yoshihara, T	325	Zhai, Q	15, 379, 387	Zhu, J	97, 98, 99, 150, 200, 215, 216, 266, 273, 318, 350, 364, 381, 396
Yoshimura, Y	313	Zhai, T	11, 35, 71, 85, 136, 137, 187, 241, 289	Zhu, L	233, 332
Yotam, H	225	Zhan, C	109	Zhu, M	56, 261, 379, 396
You, T	116	Zhan, D	204, 377, 382	Zhu, Q	248
You, Y	310	Zhan, Y	46, 133	Zhu, S	160
Young, D	110	Zhang, B	106, 300	Zhu, T	358
Young, G	112, 217	Zhang, D	25, 130, 131, 148, 318	Zhu, Y	29, 78, 80, 128, 130, 180, 181, 182, 183, 187, 222, 233, 234, 235, 240, 276, 281, 282, 331, 333
Young, M	186	Zhang, F	85	Zhu, Z	287
Yousef-Sani, M	41	Zhang, G	12, 13	Zhuang, H	252
Yousefiani, A	182	Zhang, H	11, 13, 159, 371, 377	Zhucheng, H	54, 209
Youssef, K	130	Zhang, J	16, 59, 75, 110, 133, 191, 199, 202, 252, 356, 385	Zhuo, C	320
Yu, A	169, 262	Zhang, K	152, 153, 301, 394	Zhuokun, C	176
Yu, C	225, 316, 363	Zhang, L	20, 22, 55, 105, 142, 143, 156, 210, 261, 306, 307, 308, 319, 341, 352, 367, 388	Ziaei, M	70
Yu, H	56, 215, 353	Zhang, M	72	Ziegler, D	244, 352
Yu, J	109, 204, 317, 334, 367	Zhang, N	222	Zigler, A	140
Yu, K	238	Zhang, P	211	Zikry, M	325
Yu, Q	79	Zhang, Q	275, 357	Zimmerman, J	114
Yu, X	121	Zhang, R	66, 355	Zimmermann, E	190
Yu, Y	381	Zhang, S	214, 267, 371		
Yuan, B	343	Zhang, T	16, 35, 39, 99, 240, 248, 340, 377, 382		
Yuan, H	101, 388	Zhang, W	65, 70, 141, 377, 383		
Yuan, L	209	Zhang, X	16, 46, 99, 135, 181, 226		
Yuan, Q	365				
Yuan, R	231				
Yuan, W	23, 80, 204, 217, 362				
Yucel, O	59, 216, 309, 391, 392				

# Index

---

Zimmermann, J .....	268
Ziqian, W .....	244
Zirker, L .....	315
Zirkle, L .....	292
Zok, F .....	384
Zolotorev, V .....	347
Zolotoyabko, E.....	64, 219
Zondlo, J .....	214
Zope, R .....	166
Zou, G .....	83, 173
Zou, J .....	143, 301
Zou, Y .....	302
Zrnik, J .....	128, 129, 131
Zschack, P.....	63
Zu, G .....	12, 348
Zumbilev, A.....	115
Zumbilev, I.....	115
Zuo, L .....	219, 396
Zvereva, E.....	347

# TMS

## **Who We Are**

The Minerals, Metals & Materials Society (TMS) is the professional organization encompassing the entire range of materials science and engineering, from minerals processing and primary metals production to basic research and the advanced applications of materials. The Society's broad technical focus covers light metals; electronic, magnetic and photonic materials; extraction and processing; materials processing and manufacturing; and structural materials.

## **Our Members**

Included among TMS professional members are metallurgical and materials engineers, scientists, researchers, educators and administrators who work in industry, government and academia, as well as students. They hail from more than 70 countries on six continents.

## **Our Mission**

The mission of TMS is to promote the global science and engineering professions concerned with minerals, metals and materials. The Society works to accomplish its mission by providing technical learning and networking opportunities through interdisciplinary and specialty meetings; continuing education; publications, including four journals and proceedings; and its Web site.

**To learn more, visit [www.tms.org](http://www.tms.org) or [www.materialstechnology.org](http://www.materialstechnology.org).**

## **TMS**

184 Thorn Hill Road

Warrendale, PA 15086-7514 USA

Telephone: (724) 776-9000 • (800) 759-4TMS

Fax: (724) 776-3770

E-mail: [tmsgeneral@tms.org](mailto:tmsgeneral@tms.org)



# Corporate Sponsors





# TMS 2011

## 140th Annual Meeting & Exhibition

***SAVE THE DATE!***  
***February 27 - March 3***  
***San Diego Convention Center***  
***San Diego, California***

The brightest minds and leading industry professionals in the materials world gather at this international forum every year to present and exchange the latest technical advancements.

Nearly 4,000 attendees representing more than 68 countries bring a variety of technical interests and experience to this dynamic conference!

Symposium Proposals in the following areas are now being accepted:

- **Aluminum and Magnesium**
- **Advanced Characterization and Modeling**
- **Electronic Materials**
- **High Performance Structural Materials**
- **Materials and Society**
- **Materials Processing and Production**
- **Nanoscale and Amorphous Materials**

Visit the [www.tms.org/TMS2011](http://www.tms.org/TMS2011) for more information or to submit proposals or abstracts!

